AUTOMATION AND REMOTE CONTROL

Volume 21 (1960)

BLANK
PAGE

AUTHOR INDEX

1960

Abdullaev, A. Estimates, Based on Usage, of the Service Life of Contact Apparatus - 175
Abdullaev, A. A. and I. A. Nabiev. Automatic Telemetry System for Oil-Well Flow - 183
Agababyan, M. M., see Sarkisyan, E. P. - 563
Aizerman, M. A., L. A. Gusev, L. I.Rozonoer, I. M. Smirnova, and A. A. Tal'. Finite Automata. I. - 156
Aizerman, M. A., L. A. Gusev, L. I. Rozonoer, I. M. Smirnova, and A. A. Tal'. Finite Automata II. - 248
Aizerman, M. A., L. A. Gusev, L. I. Rozonoer, I. M. Smirnova, and A. A. Tal'. On Methods for Realizing a Finte Automaton whose Cyclical Nature is Determined by the Variation of the Input State - 1126
Alimov, Yu. I. Lyapunov Functions for Relay Control Systems - 500
Andreev, N. I. Determining Pulse System Optimum Weighting Function which Ensures the Extreme of a Functional - 322
Andreeva, E. A. Calculation of Static Characteristics of "Nozzle-Baffle" Elements - 691
Andryushchenko, V. A. Electrets and the Prospects of Their Use in Automation. (Survey) - 93
Anisimov, I. A., see Aronovich, V. V. - 575
Aronovich, V. V., I. A. Anisimov, M. I. Lyudmirskii, and R. S. Patushinskaya. Control of Chemical Production Processes by Indicators of Product Quality - 575

Baikovskii, V. M. On the Noise Immunity of the Discrete-Incremental Method of Information Transmission - 239
Bamdas, A. M., V. A. Kulinich, V. A. Somov, V. A. Suchkov, S. V. Shapiro, A. O. Shmidt, and Ku Shen-ku. New Electromagnetic Executive Organs for Automatic Control Systems - 639
Baranova, V. S. and A. A. Pervozvanskii. Parametric Phenomena in the Simplest Continuous Extremal Control Systems - 881
Barashin, E. A. An Estimate of the Maximum Deviation for a Given Trajectory - 945
Barbashin, E. A. Estimating the Mean Square Deviation from a Given Trajectory - 661
Baverman, E. M. Certain Problems in the Design of Machines which Classify Objects According to an Identifying Feature which is not Specified A Priori - 971
Belya, K. K. On the Stability of the Periodic Motion of Piecewise Linear Automatic Control Systems - 799
Belaya, T. P. An Investigation of Some Types of Matrix Decoders with a Relay Output - 924
Belyavskii, V. F. and Yu. M. Shamaev. Designing Circuits which Contain Cores with Rectangular Hysteresis Loop Characteristics - 838
Berezovets, G. T. and Chou, Ching-leng. Experimental Investigation of Rubber-Fabric Membrane Characteristics - 224
Blokh, A. Sh. Equivalent Transformations of Sequential Machines - 1057
Blokh, Z. Sh. Transient Responses in Control Systems with Lags - 493
Bogomolov, V. N. Contactless DC Automatic Potentiometer with a Transformer Based on the Hall Effect - 90
Boguslavskii, I. A. On Unbiased Estimates of Signals which Depend Nonlinearly on Unknown Parameters - 27
Boguslavskii, I. A. On a Drive Scheme with a Given Equation of Motion - 236
Bol'shakov, I. A., see Tikhonov, V. I. - 765
Boyarchenkov, M. A. and M. A. Rozenblat. Reversive (Duodirectional) Magnetic DC Amplifiers of Increased Efficiency - 1066
Brik, V. A. Error Accumulation Digital Computations - 412
Burovoi, I. A. and S. V. Emel'yanov. On the Control of Certain Industrial Processes by Means of Minimum Changes of the Controlling Inputs - 810
Butkovskii, A. G. and A. Ya. Lerner. The Optimal Control of Systems with Distributed Parameters - 472

Chang Jen-wei. Stability of a Controlled System with Two Nonlinear Elements - 897
Chang Jen-wei. The Stability of a Certain Nonlinear Controlled System - 1047
Cherepanov, A. I. Analysis of a Two-Position Compensating Control System under Constant Prolonged Disturbances - 215
Cherepanov, A. I. Letter to the Editor - 384
Chernetskii, V. I. An Interpolation Method for Analyzing Automatic Control System Accuracy under Random Stimuli - 333
Chilikin, M. G. and I. I. Petrov. Scientific and Engineering Problems of Automated Electric Drives During the Current Seven-Year Period - 107
Chinaev, P. I. On the Principles of Synthesizing Automatic Systems with Many Controlled Quantities - 529
Ching-leng, Chou, see Berezovets, G. T. - 224

Chugin, Yu. I. Noise Stability of a Frequency Telemetering System for Weak Pulse Noise - 62

Dashevskii, L. N., see Glushkov, V. M. - 617
Dekabrun, I. E., N. P. Kozlov, and I. M. Krassov. Electromagnetic Control-Element Dynamics - 348
Dekabrun, L. L. On Amplifiers of Error Signals of Electrical Automatic Control Systems - 71
Devyatov, B. N. Determination of Dynamic Characteristics of Chemical Engineering Apparatus as Well as the Relevant Criteria of Persistence and Controllability - 544
Diligenskii, S. N. Differentiation of Slowly Varying Signals - 353
Doganovskii, S. A. Automatic Operating Mode Optimization of a Class of Systems with Respect to Statistical Performance Criteria - 779
Dubnikov, E. E., see Gadzhiev, M. Yu. - 936
Dzhelyalov, A. R., see Gadzhiev, M. Yu. - 936

Emel'yanov, S. V. and A. I. Fedotova. Constructing Optimal Second-Order Automatic Control Systems Using Limiting Values of Control Loop Element Gains - 37
Emel'yanov, S. V., see Burovoi, I. A. - 810
Eskin, M. G. Automatic Control of the Turbine Drilling Process by Means of Adaptive Systems - 552

Fedotova, A. I., see Emel'yanov, S. V. - 37
Fel'dbaum, A. A. Statistical Theory of Gradient Systems of Automatic Optimization for Objects with Quadratic Characteristics - 111
Fel'dbaum, A. A. Dual Control Theory I - 874
Fel'dbaum, A. A. Dual Control Theory II - 1033
Fialko, G. M. Use of Electrothermal Isodrome Devices for the Interconnected Control of Production Processes - 568
Fitsner, L. N. Two Types of Optimum-Extremal Systems - 786

Gadzhiev, M. Yu., F. B. Gul'ko, A. R. Dzhelyalov, E. E. Dubnikov, V. D. Kazakov, I. A. Litovchenko, K. B. Norkin, and N. L. Prokhorov. The Seventh Scientific-Technical Conference of Young Scholars of the Institute of Automatics and Remote Control of the Academy of Sciences of the USSR - 936
Gashkovets, I. and N. P. Vasil'eva. Questions of Stability of Operation of Closed (or Lengthy) Schemes Constructed of Certain Types of Logical Elements - 628
Glushkov, V. M., L. N. Dashevskii, and A. I. Nikitin. Use of Electronic Computers for Bessemer Process Automation - 617
Gol'traf, V. I. Hydraulic Servomotor Motion in Automatic Control Systems with a Jet Amplifier - 863
Gordon, M. M. Complex Automation of an Open-Hearth Furnace with Gas Heating - 596
Gorskaya, N. S. Effect of Rate Feedback on Loaded Relay Servomechanism Dynamics - 416
Gul'ko, F. B., see Gadzhiev, M. Yu. - 936
Gusev, L. A., see Aizerman, M. A. - 156
Gusev, L. A., see Aizerman, M. A. - 248
Gusev, L. A., see Aizerman, M. A. - 1126
Gusev, M. I. Determining the Effect of Regular Signal Dynamics in the Statistical Linearization Method - 1093
Gutovskii, I. G. Selection of the Most Suitable Circuit for a Photoelectric Fluxmeter - 989
Guzenko, A. I. Plotting Logarithmic Frequency Responses for Servosystems with Combined Control - 1101

Il'in, V. A. On the Reliability of Schemes for Connecting Dispersed Objects - 364
Il'in, V. A. Remote Control of Several Objects Located at Different Places - 826

Karibskii, V. V. On the Errors of an Interpolating Device for a Given Circular Motion - 220
Kazakevich, V. V. Theory of Ideal Models of an Extremal Controller - 338
Kazakov, I. E. The Dynamics of Self-Adaptive Systems with Extremal Continuous Adjustment of the Compensating Network in the Presence of Random Disturbances - 1040
Kazakov, V. D., see Gadzhiev, M. Yu. - 936
Kazakov, V. D. and O. P. Kuznetsov. List of Foreign Works Published in 1958 on the Theory of Relay Actions and Finite Automata - 941
Kerbnikov, F. I. The Theory of a Magnetic Modulator with Crossed Fields and a Fundamental Frequency Output - 1062
Khokhlov, V. A. Forced Periodic Motion of a Hydraulic Actuating Mechanism with a Positional Load - 654
Kilin, F. M. Transient and Steady-State Processes in an Automatic Range Finder. II. Range Finder with an Operational Amplifier - 146
Kislov, B. D. Reduced Equivalent Amplification Factor of a Nonlinear Element in the Presence of Noise - 804
Kislyakov, V. S. Application of the Krylov-Bogolyubov Method of Constructing Asymptotic Approximations to the Investigation of Systems with Lags - 307
Kislyakov, V. S. Foundations for the Application of the Harmonic Linearization Method to an Investigation of Periodic Oscillations in Systems with Lag - 1051
Klempner, K. S., see Vasil'ev, A. G. - 169
Klubnikin, P. F. Investigation of a Servosystem with an Electromagnetic Induction Clutch which Operates with Low Null Currents - 678
Klubnikin, P. F. On Synthesizing Control Programs in Systems that Include a Digital Computer - 1106
Kochanov, N. S. The Relationship between Linear Systems' Transient Responses and Their Laplace Transforms - 12

Kogan, B. Ya. On Methods of Simulating Rational-Fraction Transfer Functions without the Use of Differentiating Elements - 47
Kosharskii, B. D. Dynamic Characteristics of a "Jet Amplifier—Servomechanism" System - 701
Kozlov, G. D. The Effect of Nonuniformity of Magnetization on the Static Characteristic of Cores I - 80
Kozlov, G. D. Effect of Magnetization Irregularity on the Static Characteristics of Cores II - 744
Kozlov, N. P., see Dekabrun, I. E. - 348
Krasovskii, A. A. On the Theory of Two-Channel Follow-up Systems with a Relay Component in the AC Circuit - 911
Krassov, I. M., see Dekabrun, I. E. - 348
Krassov, I. M., L. I. Radovskii, and B. G. Turbin. An Approximate Determination of Jet Reaction in a "Nozzle-Flapper" Hydraulic Amplifier - 1091
Krassov, I. M., L. I. Radovskii, and B. G. Turbin. The Effect of the Characteristics of an Electrical Control Element on the Choice of the Parameters for a Hydraulic Amplifier - 1171
Kryuchkov, V. V. Automation and Centralization of a Copper Mine - 610
Kulikov, S. V. A Voltage Defection Pickup Based on Semiconductor Elements - 284
Kulinich, V. A., see Bamdas, A. M. - 639
Kurakhtanov, G. I., see Zavolokin, A. K. - 635
Kurdyukov, K. P. On the Question of Relay-Contact Device Reliability - 366
Ku Shen-ku, see Bamdas, A. M. - 639
Kuznetsov, O. P., see Kazakov, V. D. - 941

Landa, P. S. On the Stability of Servo-Controlled Systems with Random Stimuli - 23
Landa, P. S. and S. P. Strelkov. On the Stability of an Aileron Control System Disturbed by Turbulence - 953
Leonov, Yu. P. and L. N. Lipatov. A Statistical Method for Determining Dynamic Characteristics of Industrial Objects in the Presence of Noise and for Analyzing Infralow-Frequency Random Processes - 119
Leonov, Yu. P. The Problems of Shaping Filters and Optimal Linear Systems - 467
Lerner, A. Ya., see Butkovskii, A. G. - 472
Letov, A. M. Analytical Controller Design - 303
Letov, A. M. Analytic Controller Design - 389
Letov, A. M. Analytical Controller Design III - 458
Levin, S. M. and L. G. Manusevich. A Vector Method for Calculating One Class of Control Systems - 962
Lipatov, L. N., see Leonov, Yu. P. - 119
Lipman, R. A. and M. V. Ol'shvang. A Transistorized Magnetic Amplifier - 755
Litovchenko, I. A. On a Problem of Optimum Control - 791
Litovchenko, I. A., see Gadzhiev, M. Yu. - 936
Lueck, W. A New Method of Spectral Measurements by Means of Photosensitive Layers - 762
Lyudmirskii, M. I., see Aronovich, V. V. - 575

Malkina, O. G. Rectified Voltage Regulator - 372
Manusevich, L. G., see Levin, S. M. - 962
Maslov, A. A. and Yu. G. Purlov. A Universal Function Generator Based on the Principle of Quadratic Approximations - 164
Maslov, A. A. A Three-Channel Multiplier with Frequency Division of the Signals - 1150
Matveev, P. S. Determination of the Optimal Impulsive Response Function in the Presence of Internal Noise - 198
Matyas, J. Letter to the Editor - 1016
Matyash, I. and Ya. Shilkhanek. A Generator of Random Processes from their Given Spectral Density Matrices - 18
Miller, E. V. Contactless Semiconductor Switching Elements - 728
Mirenskii, M. S. Calculation and Construction of Induction Clutches - 736
Mironov, V. D. Development of Apparatus for the Automatic Control of Boiler Aggregates - 584
Miroshnichenko, G. P. On the Autooscillations of a Dynamic Table Platform - 204
Monastyrshin, G. I. Processing Experimental Frequency Characteristics - 294
Morosanov, I. S. Investigation of the Periodic Behavior of Relay Systems with Extremum Regulation - 668
Morosanov, I. S. Effect of Fluctuations on Extremal Relay Systems under Self-Oscillation Conditions - 884
Moslov, A. A. Survey and Classification of Multiplying Devices - 1000

Nabiev, I. A., see Abdullaev, A. A. - 183
Nadzhafova, G. A. The Maximum Dynamic Characteristic Values of Servomechanism Components of Servosystems I - 685
Nechaev, G. K. Stabilizing the Temperature of Heated Thermistors - 376
Nelepin, R. A. Theory of Certain Indirect Control Systems with Several Essential Nonlinearities - 478
Nikitin, A. I., see Glushkov, V. M. - 617
Norkin, K. B., see Gadzhiev, M. Yu. - 936
Novikov, A. I. Exponential Converters with a Logarithmic Transformation Law - 714
Novoselov, V. S. Investigation of Probability Stability Using Example of Automatic Control of Aircraft Course - 462
Novosel'tsev, V. N. Optimal Processes in Second-Order Pulse-Relay Systems - 394
Ol'shvang, M. V., see Lipman, R. A. - 755
Ostianu, V. M. On Binary Signal Corrector Schemes - 426

Patushinskaya, R. S., see Aronovich, V. V. - 575

Perfil'ev, G. L. New Method and Universal Measuring Device for Active Inspection on Metal-Cutting Machines - 622
Pervozvanskii, A. A. Continuous Extremum Control Systems in the Presence of Random Noise - 673
Pervozvanskii, A. A., see Baranova, V. S. - 881
Petrov, I. I., see Chilikin, M. G. - 107
Petrov, Yu. P. Optimal Frequency Control of Asynchronous Electric Motors - 232
Polonnikov, D. E. Wide-Band Decision (Operational) Amplifiers - 1161
Popov, V. S. Use of Heater Resistances for Current and Voltage Stabilization - 381
Posdeev, A. D. On Choosing the Optimum Number of Pole Pairs and the Main Dimensions of Electromagnetic Slipping Clutches with Massive Steel Armatures - 844
Pospelov, D. A. Synthesis of Circuits whose Operation is Described by Boolean Time Functions - 997
Pozin, N. V. On the Interference Resistance of Pulse-Time and Pulse-Width Telemetering Subjected to Strong Fluctuation Noise - 930
Prokhorov, N. L., see Gadzhiev, M. Yu. - 936
Prouza, L. Note on the Properties of a Simple Extrapolator with a "Switch" - 91
Pshenichnikov, A. M. Choice of Frequency Range for Industrial Pulse-Frequency Telemetry System Devices - 361
Pul'er, Yu. M. Transformer Distance Transmission by Means of Two Phase Contactless Induction Potentiometers - 722
Pupkov, K. A. Method of Investigating the Accuracy of Essentially Nonlinear Automatic Control Systems by Means of Equivalent Transfer Functions - 126
Purlov, Yu. G., see Maslov, A. A. - 164
Pyatnitskii, G. I. The Effect of Stationary Random Processes on Automatic Control Systems Containing Essentially Nonlinear Elements - 328
Pyatnitskii, G. I. The Action of Random Processes on Discontinuous Control Systems - 405
Pyshkin, I. V. Processes of Finite Duration in Pulse-Width Systems - 141

Radovskii, L. I., see Krassov, I. M. - 1091
Radovskii, L. I., see Krassov, I. M. - 1171
Rastrigin, L. A. Extremal Control by the Method of Random Scanning - 891
Razumikhin, B. S. The Application of Lyapunov's Method to Problems in the Stability of Systems with Delay - 515
Rodin, R. N., see Rosenbauli, O. B. - 1083
Roginskii, V. N. and Shestakov, V. I. On the Book "Elements of Structural Synthesis of Relay Control Circuits" - 767
Roginskii, V. N. Reply to V. I. Shestakov's Critical Review of the Book "Elements of Structural Synthesis of Relay Control Circuits" by V. N. Roginskii - 771
Rosenbauli, O. B., and R. N. Rodin. Designing Circuits for Stabilizing Compound Electric Drives which Use a Special Three-Winding Transformer - 1083
Rostkovskaya, S. E., see Sot-skov, B. S. - 439
Rotach, V. Ya. Determination of Parameters of Combined Linear Control Systems - 858
Rozenblat, M. A., see Boyarchenkov, M. A. - 1066
Rozenvasser, E. N. The Reduction of Nonlinear Control System Equations to Their Simplest Form - 9
Rozenvasser, E. N. On the Accurate Determination of Periodic Regimes in Sectionally Linear Control Systems - 902
Rozonoer, L. I., see Aizerman, M. A. - 156
Rozonoer, L. I., see Aizerman, M. A. - 248
Rozonoer, L. I., see Aizerman, M. A. - 1126
Rubinovich, Ya. I. Synthesizing Control Systems with Monotonically Decreasing Gains by the Root-Locus Method - 31
Rudnitskii, B. E. Determining the Transfer Functions for Certain Systems with Varying Parameters - 1115
Rukhadze, V. A., see Zasedatelev, S. M. - 646
Ryabov, Yu. A. The Application of the Method of Small Parameters in the Investigation of Systems of Automatic Control with Delay - 507

Saakyan, P. S., see Sarkisyan, E. P. - 563
Safris, L. V. Certain Questions in the Theory of Magnetic Amplifiers Loaded by DC Drives - 273
Sarkisyan, E. P., M. M. Agababyan, and P. S. Saakyan. Adaptive Automatic Control for Obtaining Aluminum by the Electrolytic Process Using a Computing Device - 563
Shamson, A. S. A Paper-Making Machine as an Object of Control and Some Ways Toward its Complex Automation - 602
Shapiro, S. V., see Bamdas, A. M. - 639
Shestakov, V. I., see Roginskii, V. N. - 767
Shilkhanek, Ya., see Matyash, I. - 18
Shimanov, S. N. On the Theory of Oscillations of Quasi-Linear Systems with Constant Lags - 490
Shiniberov, L. P. Determination of the Interval of Positiveness of the Real Frequency Characteristic from the Graph of the Transient Response - 292
Shirokorad, B. V. On Steady-State Modes in Automatic Control Systems - 316
Shkilkhanek, Ya. On the Simulation of Linear Systems with n Stationary Random Input Processes without the Use of Random Function Generators - 451
Shmidt, A. O., see Bamdas, A. M. - 639
Shubin, A. B. 10-Channel Automatic Electronic-Relay Optimizer - 432
Smirnov, A. M. On the Dynamic Characteristics of Hydraulic Couplings - 920
Smirnova, I. M., see Aizerman, M. A. - 156
Smirnova, I. M., see Aizerman, M. A. - 248
Smirnova, I. M., see Aizerman, M. A. - 1126
Smolyar, L. I., see Volgin, L. I. - 816

Somov, V. A., see Bamdas, A. M. - 639
Sot-skov, B. S. and S. E. Rostkovskaya. Reliability Characteristics of Resistors and Condensers - 439
Sribner, L. A. Determination of Magnetic Conductance with Geared Stator and Rotor - 75
Strelkov, S. P., see Landa, P. S. - 953
Subbotina, G. V. Work of the All-Moscow Seminar on Magnetic Automation Components - 1018
Subbotina, G. V. and I. S. Trefilova. List of Literature on Magnetic Components for Automation, Remote Control, and Computer Technology for 1959 - 1019
Suchkov, V. A., see Bamdas, A. M. - 639
Sun Tszyan'. Optimal Control of a Nonlinear System - 2
Suponitskii, A. P. and V. D. Urin. Transistorized Relay Networks - 1144
Syuzyumova, E. M. Some Questions Concerning Coordinated Control Systems - 521

Tal', A. A., see Aizerman, M. A. - 156
Tal', A. A., see Aizerman, M. A. - 248
Tal', A. A., see Aizerman, M. A. - 1126
Tel'ksnis, L. A. Determination of the Second-Order Moments of Various Coordinates of Automatic-Control Systems by the Use of Electronic Analog Computers - 153
Teverovskii, V. I. On One Particular Case of a Sampled-Data System with Variable Parameters which Change by Jumps - 42
Tikhonov, V. I. Phase-Lock Automatic Frequency Control Operation in the Presence of Noise - 209
Tikhonov, V. I. and I. A. Bol'shakov, An Error in the Article "Effect of Fluctuations on the Simplest Parametric Systems" - 765
Tishchenko, N. M. Contactless Magnetic Time Relays - 850
Tolchan, A. Ya. On Constructing Bridge Circuits by the Short-Circuit Method - 54
Tovstukha, T. I. The Effect of Random Noise on the Steady-State Operation of a Step-Type Extremal System for an Object with a Parabolic Characteristic - 398
Trefilova, I. S., see Subbotina, G. V. - 1019
Tsypkin, Ya. Z. Estimating the Effect of Quantization by Level on the Processes in Automatic Digital Systems - 195
Tulin, A. S. Generalized Proportionality Conditions of Electromagnetic Systems (Geometry of Electromagnetic Systems) - 259
Turbin, B. G., see Krassov, I. M. - 1091
Turbin, B. G., see Krassov, I. M. - 1171

Udalov, N. P. An Approximate Calculation of the Transients in a Thermistor Circuit - 933
Urin, V. D., see Suponitskii, A. P. - 1144

Vasil'ev, A. G., I. S. Zhitomirskii, and K. S. Klempner. Reliability Criteria for Automatic Relays Devices with Radioactive Emitters - 169
Vasil'eva, N. P., see Gashkovets, I. - 628
Vasilevskii, Yu. A. The Use of Hall Pickups in Magnetic Heads - 279
Veller, V. N. Methods of Increasing Reliability and Response Speed of Steam Turbine Control - 589
Venchkovskii, L. B. Analysis of Noise in an 0.4/6 kv Power Network - 832
Vershinin, V. D. Controlling a Servodrive Using One Null Indicator which Performs the Functions of Two Null Indicators - 979
Vershinin, V. D. A Vacuum-Tube Network for Summing Signals - 1111
Vitenberg, M. I. Relay Winding Overheating and Heat Transmission Coefficient as Functions of Ambient Air Temperature - 266
Vitkov, M. G. Taking the Weak Surface Effect into Account in Switching the Magnetic State of a Ferromagnetic Plate - 984
Vlasov, N. P. A Method for Obtaining Transfer Functions of Automatic Control Systems Operating on Alternating Current - 538
Volgin, L. I. and L. I. Smolyar. Servomechanism-Compensation by Using Discrete Calculating Devices - 816

Yang Hsi-zeng. Determination of Maximum Error of a Binary Multiplier - 709
Yuferova, E. K. Digital Computation Elements, Based on the Principal of Integrating Voltage Pulses - 821

Zakrevskii, A. D. A Visual-Matrix Method for Minimizing Boolean Functions - 255
Zarenin, Yu. G. Regarding the Theory of Third-Order Linear Systems - 290
Zasedatelev, S. M. and V. A. Rukhadze. Design of Transducers with Force Compensation - 646
Zavolokin, A. K. A Numerical-to-Electrical Converter - 179
Zavolokin, A. K. and G. I. Kurakhtanov. On One Method of Constructing Analog-to-Digital Transformers - 635
Zdrok, A. G. On the Design of Magnetic Amplifiers Operating with Single-Phase and Three Phase Semiconductor Rectifiers on an Active Load and a Counter-Emf. - 443
Zdrok, A. G. Application of Transistors in Circuits of Vibrational Voltage Regulators - 1075
Zhitomirskii, I. S., see Vasil'ev, A. G. - 169

EDITORIAL BOARD OF AVTOMATIKA I TELEMEKHANIKA

M. A. Aizerman
L. A. Charikhov
V. A. Il'in
V. V. Karibskii
M. P. Kostenko
S. P. Krasivskii
V. S. Kulebakin
A. M. Letov
(Assoc. Editor)
B. N. Petrov
N. N. Shumilovskii
V. V. Solodovnikov
B. S. Sotskov
V. A. Trapeznikov
(Editor in Chief)
Ia. Z. Tsypkin
G. M. Ulanov
(Corresp. Secretary)

Automation and Remote Control

A translation of Avtomatika i Telemekhanika, a publication of the Academy of Sciences of the USSR

Russian Original Dated January, 1959

Vol. 21, No. 1, pp. 1-106

August, 1960

CONTENTS

	PAGE	RUSS. PAGE
Optimal Control of a Nonlinear system. Sun Tszyan'	2	3
The Reduction of Nonlinear Control System Equations to Their Simplest Form. E. N. Rozenvasser	9	15
The Relationship between Linear Systems' Transient Responses and Their Laplace Transforms. N. S. Kochanov	12	20
A Generator of Random Processes from Their Given Spectral Density Matrices. I. Matyash and Ya. Shilkhanek	18	29
On the Stability of Servo-Controlled Systems with Random Stimuli. P. S. Landa	23	36
On Unbiased Estimates of Signals which Depend Nonlinearly on Unknown Parameters. I. A. Boguslavskii	27	42
Synthesizing Control Systems with Monotonically Decreasing Gains by the Root-Locus Method. Ya. I. Rubinovich	31	48
Constructing Optimal Second-Order Automatic Control Systems Using Limiting Values of Control Loop Element Gains. S. V. Emel'yanov and A. I. Fedotova	37	56
On One Particular Case of a Sampled-Data System with Variable Parameters which Change by Jumps. V. I. Teverovskii	42	64
On Methods of Simulating Rational-Fraction Transfer Functions without the Use of Differentiating Elements. B. Ya. Kogan	47	72
On Constructing Bridge Circuits by the Short-Circuit Method. A. Ya. Tolchan	54	82
Noise Stability of a Frequency Telemetering System for Weak Pulse Noise. Yu. I. Chugin	62	93
On Amplifiers of Error Signals of Electrical Automatic Control Systems. L. L. Dekabrun	71	106
Determination of Magnetic Conductance with Geared Stator and Rotor. L. A. Sribner	75	112
The Effect of Nonuniformity of Magnetization on the Static Characteristics of Cores. I. G. D. Kozlov	80	119
Contactless DC Automatic Potentiometer with a Transformer Based on the Hall Effect. V. N. Bogomolov	90	135
Note on the Properties of a Simple Extrapolator with a "Switch." L. Prouza	91	137
Electrets and the Prospects of Their Use in Automation. (Survey). V. A. Andryushchenko	93	139
LETTERS TO THE EDITOR		
A Note to a Paper of Yu. S. Sobolev, "On the Absolute Stability of Certain Controlled Systems," [1]	96	143
CHRONICLE		
Seminar on the Engineering Applications of Mathematical Logic (1958-1959)	98	145
BIBLIOGRAPHY		
A List of Literature on Magnetic Elements of Automation, Remote Control, and Computing Technology for 1958	101	149

EDITORIAL BOARD OF AVTOMATIKA I TELEMEKHANIKA

M. A. Aizerman
L. A. Charikhov
V. A. Il'in
V. V. Karibskii
M. P. Kostenko
S. P. Krasivskii
V. S. Kulebakin
A. M. Letov
(Assoc. Editor)
B. N. Petrov
N. N. Shumilovskii
V. V. Solodovnikov
B. S. Sotskov
V. A. Trapeznikov
(Editor in Chief)
Ia. Z. Tsypkin
G. M. Ulanov
(Corresp. Secretary)

Automation and Remote Control

A translation of Avtomatika i Telemekhanika, a publication of the Academy of Sciences of the USSR

Russian Original Dated February, 1960

Vol. 21, No. 2 **October, 1960**

CONTENTS

	PAGE	RUSS. PAGE
Scientific and Engineering Problems of Automated Electric Drives During the Current Seven-Year Period. M. G. Chilikin and I. I. Petrov	107	161
Statistical Theory of Gradient Systems of Automatic Optimization for Objects With Quadratic Characteristics. A. A. Fel'dbaum	111	167
A Statistical Method for Determining Dynamic Characteristics of Industrial Objects in the Presence of Noise and for Analyzing Infralow-Frequency Random Processes. Yu. P. Leonov and L. N. Lipatov	119	180
Method of Investigating the Accuracy of Essentially Nonlinear Automatic-Control Systems by Means of Equivalent Transfer Functions. K. A. Pupkov	126	191
Processes of Finite Duration in Pulse-Width Systems. I. V. Pyshkin	141	201
Transient and Steady-State Processes in an Automatic Range Finder. II. Range Finder with an Operational Amplifier. F. M. Kilin	146	209
Determination of the Second-Order Moments of Various Coordinates of Automatic-Control Systems by the use of Electronic Analog Computers. L. A. Tel'ksnis	153	220
Finite Automata. I. M. A. Aizerman, L. A. Gusev, L. I. Rozonoer, I. M. Smirnova, and A. A. Tal'	156	224
A Universal Function Generator based on the Principle of Quadratic Approximations. A. A. Maslov and Yu. G. Purlov	164	237
Reliability Criteria for Automatic Relay Devices with Radioactive Emitters. A. G. Vasil'ev, I. S. Zhitomirskii, and K. S. Klempner	169	245
Estimates, Based on Usage, of the Service Life of Contact Apparatus. A. Abdullaev	175	254
A Numerical-To-Electrical Converter. A. K. Zavolokin	179	260
Automatic Telemetry System for Oil-Well Flow. A. A. Abdullaev and I. A. Nabiev	183	266
BIBLIOGRAPHY	189	271

EDITORIAL BOARD OF AVTOMATIKA I TELEMEKHANIKA

M. A. Aiserman
L. A. Charikhov
V. A. Il'in
V. V. Karibskii
M. P. Kostenko
S. P. Krasivskii
V. S. Kulebakin
A. M. Letov
(Assoc. Editor)
B. N. Petrov
N. N. Shumilovskii
V. V. Solodovnikov
B. S. Sotskov
V. A. Trapeznikov
(Editor in Chief)
Ia. Z. Tsypkin
G. M. Ulanov
(Corresp. Secretary)

Automation and Remote Control

A translation of Avtomatika i Telemekhanika, a publication of the Academy of Sciences of the USSR

Russian Original Dated March, 1960

Vol. 21, No. 3, pp. 195-302 November, 1960

CONTENTS

	PAGE	RUSS. PAGE
Estimating the Effect of Quantization by Level on the Processes in Automatic Digital Systems. Ya. Z. Tsypkin	195	281
Determination of the Optimal Impulsive Response Function in the Presence of Internal Noise. P. S. Matveev	198	286
On the Autooscillations of a Dynamic Table Platform. G. P. Miroshnichenko	204	293
Phase-Lock Automatic Frequency Control Operation in the Presence of Noise. V. I. Tikhonov	209	301
Analysis of a Two-Position Compensating Control System under Constant Prolonged Disturbances. A. I. Cherepanov	215	310
On the Errors of an Interpolating Device for a Given Circular Motion. V. V. Karibskii	220	317
Experimental Investigation of Rubber-Fabric Membrane Characteristics. G. T. Berezovets and Chou Ching-leng	224	323
Optimal Frequency Control of Asynchronous Electric Motors. Yu. P. Petrov	232	333
On a Drive Scheme with a Given Equation of Motion. I. A. Boguslavskii	236	340
On the Noise Immunity of the Discrete-Incremental Method of Information Transmission. V. M. Baikovskii	239	344
Finite Automata. II. M. A. Aizerman, L. A. Gusev, L. I. Rozonoér, I. M. Smirnova, and A. A. Tal'	248	359
A Visual-Matrix Method for Minimizing Boolean Functions. A. D. Zakrevskii	255	369
Generalized Proportionality Conditions of Electromagnetic Systems (Geometry of Electromagnetic Systems). A. S. Tulin	259	374
Relay Winding Overheating and Heat Transmission Coefficient as Functions of Ambient Air Temperature. M. I. Vitenberg	266	384
Certain Questions in the Theory of Magnetic Amplifiers Loaded by DC Drives. L. V. Safris	273	393
The Use of Hall Pickups in Magnetic Heads. Yu. A. Vasilevskii	279	402
A Voltage Deflection Pickup Based on Semiconductor Elements. S. V. Kulikov	284	409
Regarding the Theory of Third-Order Linear Systems. Yu. G. Zarenin	290	417
Determination of the Interval of Positiveness of the Real Frequency Characteristic from the Graph of the Transient Response. L. P. Shiniberov	292	420
Processing Experimental Frequency Characteristics. G. I. Monastyrshin	294	422
INFORMATION		
The ÉMU-8 Electronic Analog Computer	301	429

EDITORIAL BOARD OF
AVTOMATIKA I
TELEMEKHANIKA

M. A. Aizerman
L. A. Charikhov
V. A. Il'in
V. V. Karibskii
M. P. Kostenko
S. P. Krasivskii
V. S. Kulebakin
A. M. Letov
(Assoc. Editor)
B. N. Petrov
N. N. Shumilovskii
V. V. Solodovnikov
B. S. Sotskov
V. A. Trapeznikov
(Editor in Chief)
Ia. Z. Tsypkin
G. M. Ulanov
(Corresp. Secretary)

Automation and Remote Control

A translation of Avtomatika i Telemekhanika, a publication of the Academy of Sciences of the USSR

Russian Original Dated April, 1960

Vol. 21, No. 4 **November, 1960**

CONTENTS

PAGE RUSS. PAGE

Analytical Controller Design. A. M. Letov 303 436
Application of the Krylov-Bogolyubov Method of Constructing Asymptotic Approximations to the Investigation of Systems with Lags. V. S. Kislyakov 307 442
On Steady-State Modes in Automatic Control Systems. B. V. Shirokorad 316 456
Determining Pulse System Optimum Weighting Function Which Ensures the Extreme of a Functional. N. I. Andreev 322 465
The Effect of Stationary Random Processes on Automatic Control Systems Containing Essentially Nonlinear Elements. G. I. Pyatnitskii 328 474
An Interpolation Method for Analyzing Automatic Control System Accuracy under Random Stimuli. V. I. Chernetskii 333 481
Theory of Ideal Models of an Extremal Controller. V. V. Kazakevich 338 489
Electromagnetic Control-Element Dynamics. I. E. Dekabrun, N. P. Kozlov, and I. M. Krassov 348 506
Differentiation of Slowly Varying Signals. S. N. Diligenskii 353 513
Choice of Frequency Range for Industrial Pulse-Frequency Telemetry System Devices. A. M. Pshenichnikov 361 525
On the Reliability of Schemes for Connecting Dispersed Objects. V. A. Il'in 364 530
On the Question of Relay-Contact Device Reliability. K. P. Kurdyukov 366 533
Rectified Voltage Regulator. O. G. Malkina 372 542
Stabilizing the Temperature of Heated Thermistors. G. K. Nechaev 376 548
Use of Heater Resistances for Current and Voltage Stabilization. V. S. Popov 381 555
Letter to the Editor. A. I. Cherepanov 384 558

[This issue of AVTOMATIKA I TELEMEKHANIKA contained an article commemorating the 90th anniversary of the birth of V. I. Lenin. Since that article did not discuss either the present state of Soviet research in automation or its historic development, and as a matter of fact, contained no information of scientific interest, it was omitted from the translation.]

EDITORIAL BOARD OF
AVTOMATIKA I
TELEMEKHANIKA

M. A. Aizerman
L. A. Charikhov
V. A. Il'in
V. V. Karibskii
M. P. Kostenko
S. P. Krasivskii
V. S. Kulebakin
A. M. Letov
(Assoc. Editor)
B. N. Petrov
N. N. Shumilovskii
V. V. Solodovnikov
B. S. Sotskov
V. A. Trapeznikov
(Editor in Chief)
Ia. Z. Tsypkin
G. M. Ulanov
(Corresp. Secretary)

Automation and Remote Control

A translation of Avtomatika i Telemekhanika, a publication of the Academy of Sciences of the USSR

Russian Original Dated May, 1960

Vol. 21, No. 5, pp. 385-454 **December, 1960**

CONTENTS

	PAGE	RUSS. PAGE
Ya. Z. Tsypkin. Lenin Prize Laureate	385	I
Analytic Controller Design. II. A. M. Letov	389	561
Optimal Processes in Second-Order Pulse-Relay Systems. V. N. Novosel'tsev	394	569
The Effect of Random Noise on the Steady-State Operation of a Step-Type Extremal System for an Object with a Parabolic Characteristic. T. I. Tovstukha	398	575
The Action of Random Processes on Discontinuous Control Systems. G. I. Pyatnitskii	405	585
Error Accumulation in Digital Computations. V. A. Brik	412	595
Effect of Rate Feedback on Loaded Relay Servomechanism Dynamics. N. S. Gorskaya	416	601
On Binary Signal Corrector Schemes. V. M. Ostianu	426	615
10-Channel Automatic Electronic-Relay Optimizer. A. B. Shubin	432	624
Reliability Characteristics of Resistors and Condensers. B. S. Sot-skov and S. E. Rostkovskaya	439	633
On the Design of Magnetic Amplifiers Operating with Single-Phase and Three Phase Semiconductor Rectifiers on an Active Load and a Counter-Emf. A. G. Zdrok	443	639
On the Simulation of Linear Systems with n Stationary Random Input Processes without the Use of Random Function Generators. Ya. Shilkhanek	451	652

INFORMATION

	PAGE	RUSS. PAGE
Bureau of the Presidium of the Academy of Sciences of the USSR	453	655

EDITORIAL BOARD OF
AVTOMATIKA I
TELEMEKHANIKA

M. A. Aiserman
L. A. Charikhov
V. A. Il'in
V. V. Karibskii
M. P. Kostenko
S. P. Krasivskii
V. S. Kulebakin
A. M. Letov
(Assoc. Editor)
B. N. Petrov
N. N. Shumilovskii
V. V. Solodovnikov
B. S. Sotskov
V. A. Trapeznikov
(Editor in Chief)
Ia. Z. Tsypkin
G. M. Ulanov
(Corresp. Secretary)

Automation and Remote Control

A translation of Avtomatika i Telemekhanika, a publication of the Academy of Sciences of the USSR

Russian Original Dated June, 1960

Vol. 21, No. 6 December, 1960

CONTENTS

PAGE RUSS. PAGE

The Approaching First Congress of the International Federation of Automatic Control 455 657
A Message from the President of the IFAC. 457 659
Analytical Controller Design. III . A. M. Letov 458 661
Investigation of Probability Stability Using Example of Automatic Control of Aircraft Course. V. S. Novoselov 462 666
The Problem of Shaping Filters and Optimal Linear Systems. Yu. P. Leonov 467 674
The Optimal Control of Systems with Distributed Parameters. A. G. Butkovskii and A. Ya. Lerner . 472 682
Theory of Certain Indirect Control Systems with Several Essential Nonlinearities. R. A. Nelepin . . 478 692
On the Theory of Oscillations of Quasi-Linear Systems with Constant Lags. S. N. Shimanov 490 706
Transient Responses in Control Systems with Lags. Z. Sh. Blokh 493 710
Lyapunov Functions for Relay Control Systems. Yu. I. Alimov 500 720
The Application of the Method of Small Parameters in the Investigation of Systems of Automatic Control with Delay. Yu. A. Ryabov 507 729
The Application of Lyapunov's Method to Problems in the Stability of Systems with Delay. B. S. Razumikhin 515 740
Some Questions Concerning Coordinated Control Systems. E. M. Syuzyumova 521 749
On the Principles of Synthesizing Automatic Systems with Many Controlled Quantities. P. I. Chinaev 529 761
A Method for Obtaining Transfer Functions of Automatic Control Systems Operating on Alternating Current. N. P. Vlasov 538 772
Determination of Dynamic Characteristics of Chemical Engineering Apparatus as Well as the Relevant Criteria of Persistence and Controllability. B. N. Devyatov 544 779
Automatic Control of the Turbine Drilling Process by Means of Adaptive Systems. M. G. Éskin . . . 552 791
Adaptive Automatic Control System for Obtaining Aluminum by the Electrolytic Process Using a Computing Device. É. P. Sarkisyan, M. M. Agababyan, and P. S. Saakyan 563 806
Use of Electrothermal Isodrome Devices for the Interconnected Control of Production Processes. G. M. Fialko 568 812
Control of Chemical Production Processes by Indicators of Product Quality. V. V. Aronovich, I. A. Anisimov, M. I. Lyudmirskii, and R. S. Patushinskaya 575 821
Development of Apparatus for the Automatic Control of Boiler Aggregates. V. D. Mironov 584 833
Methods of Increasing Reliability and Response Speed of Steam Turbine Control. V. N. Veller . . . 589 840
Complex Automation of an Open-Hearth Furnace with Gas Heating. M. M. Gordon 596 849
A Paper-Making Machine as an Object of Control and Some Ways Toward its Complex Automation. A. S. Shamson 602 857

CONTENTS (continued)

	PAGE	RUSS. PAGE
Automation and Centralization of a Copper Mine. V. V. Kryuchkov	610	867
Use of Electronic Computers for Bessemer Process Automation. V. M. Glushkov, L. N. Dashevskii, and A. I. Nikitin	617	877
New Method and Universal Measuring Device for Active Inspection on Metal-Cutting Machines. G. L. Perfil'ev	622	884
Questions of Stability of Operation of Closed (or Lengthy) Schemes Constructed of Certain Types of Logical Elements. I. Gashkovets and N. P. Vasil'eva	628	892
On One Method of Constructing Analog-to-Digital Transformers. A. K. Zavolokin and G. I. Kurakhtanov	635	902
New Electromagnetic Executive Organs for Automatic Control Systems. A. M. Bamdas, V. A. Kulinich, V. A. Somov, V. A. Suchkov, S. V. Shapiro, A. O. Shmidt, and Ku Shên-ku	639	907
Design of Transducers with Force Compensation. S. M. Zasedatelev and V. A. Rukhadze	646	918
Forced Periodic Motion of a Hydraulic Actuating Mechanism with a Positional Load. V. A. Khokhlov	654	929

INFORMATION

International Federation of Automatic Control (IFAC) and Its First Congress	658	934

Automation and Remote Control

A translation of Avtomatika i Telemekhanika, a publication of the Academy of Sciences of the USSR

EDITORIAL BOARD OF AVTOMATIKA I TELEMEKHANIKA

D. I. Ageikin
M. A. Aizerman
A. B. Chelyustkin
(*Assoc. Editor*)
E. G. Dudnikov
N. Ya. Festa
V. A. Ilin
A. G. Iosuf'yan
V. V. Karibskii
A. V. Khramoi
B. Ya. Kogan
V. S. Kulebakin
S. A. Lebedev
A. Ya. Lerner
A. M. Letov
(*Assoc. Editor*)
V. S. Malov
B. N. Petrov
Yu. P. Portnov-Sokolov
B. S. Sotskov
A. A. Tal'
(*Corresp. Secretary*)
V. A. Trapeznikov
(*Editor in Chief*)
Ya. Z. Tsypkin
G. M. Ulanov
A. A. Voronov
S. V. Yablonskii

Vol. 21, No. 7 Russian Original Dated July, 1960 **February, 1961**

CONTENTS

PAGE RUSS. PAGE

Estimating the Mean Square Deviation from a Given Trajectory. E. A. Barbashin. 661 941
Investigation of the Periodic Behavior of Relay Systems with Extremum Regulation. I. S. Morosanov. 668 951
Continuous Extremum Control Systems in the Presence of Random Noise. A. A. Pervozvanskii. 673 958
Investigation of a Servosystem with an Electromagnetic Induction Clutch Which Operates with Low Null Currents. P. F. Klubnikin. 678 964
The Maximum Dynamic Characteristic Values of Servomechanism Components of Servosystems. I. G. A. Nadzhafova. 685 973
Calculation of Static Characteristics of "Nozzle-Baffle" Elements. E. A. Andreeva. 691 982
Dynamic Characteristics of a "Jet Amplifier – Servomechanism" System. B. D. Kosharskii 701 997
Determination of Maximum Error of a Binary Multiplier. Yang Hsi-zeng. 709 1007
Exponential Converters with a Logarithmic Transformation Law. A. I. Novikov. 714 1015
Transformer Distance Transmission by Means of Two Phase Contactless Induction Potentiometers. Yu. M. Pul'er. 722 1026
Contactless Semiconductor Switching Elements. E. V. Miller. 728 1035
Calculation and Construction of Induction Clutches. M. S. Mirenskii. 736 1046
Effect of Magnetization Irregularity on the Static Characteristics of Cores. II. G. D. Kozlov 744 1057
A Transistorized Magnetic Amplifier. R. A. Lipman and M. V. Ol'shvang. 755 1073
A New Method of Spectral Measurements by Means of Photosensitive Layers. W. Lueck. . 762 1084

LETTERS TO THE EDITOR

An Error in the Article "Effect of Fluctuations on the Simplest Parametric Systems" by V. I. Tikhonov. I. A. Bol'shakov 765 1088

DISCUSSION

On the Book "Elements of Structural Synthesis of Relay Control Circuits" by V. N. Roginskii. V. I. Shestakov 767 1090
Reply to V. I. Shestakov's Critical Review of the Book "Elements of Structural Synthesis of Relay Control Circuits" by V. N. Roginskii. V. N. Roginskii. 771 1094

Erratum. 775 1098

Automation and Remote Control

A translation of Avtomatika i Telemekhanika, a publication of the Academy of Sciences of the USSR

EDITORIAL BOARD OF AVTOMATIKA I TELEMEKHANIKA

D. I. Ageikin
M. A. Aizerman
A. B. Chelyustkin
(Assoc. Editor)
E. G. Dudnikov
N. Ya. Festa

V. A. Ilin
A. G. Iosuf'yan
V. V. Karibskii
A. V. Khramoi
B. Ya. Kogan
V. S. Kulebakin
S. A. Lebedev

A. Ya. Lerner
A. M. Letov
(Assoc. Editor)
V. S. Malov
B. N. Petrov
Yu. P. Portnov-Sokolov
B. S. Sotskov

A. A. Tal'
(Corresp. Secretary)
V. A. Trapeznikov
(Editor in Chief)
Ya. Z. Tsypkin
G. M. Ulanov
A. A. Voronov
S. V. Yablonskii

Vol. 21, No. 8 Russian Original Dated August, 1960 March, 1961

CONTENTS

	PAGE	RUSS. PAGE
The Mechanization and Automation of Production – The General Line of Development of Industry. Results of the June Plenum of the Central Committee of the Communist Party of the Soviet Union	777	1101
Automatic Operating Mode Optimization of a Class of Systems With Respect to Statistical Performance Criteria. S. A. Doganovskii	779	1105
Two Types of Optimum-Extremal Systems. L. N. Fitsner	786	1115
On a Problem of Optimum Control. I. A. Litovchenko.	791	1122
On the Stability of the Periodic Motion of Piecewise Linear Automatic Control Systems. K. K. Belya	799	1134
Reduced Equivalent Amplification Factor of a Nonlinear Element in the Presence of Noise. B. D. Kislov	804	1141
On the Control of Certain Industrial Processes by Means of Minimum Changes of the Controlling Inputs. I. A. Burovoi and S. V. Emel'yanov	810	1149
Servomechanism-Compensation by Using Discrete Calculating Devices. L. I. Volgin and L. I. Smolyar	816	1158
Digital Computation Elements, Based on the Principal of Integrating Voltage Pulses. E. K. Yuferova	821	1165
Remote Control of Several Objects Located at Different Places. V. A. Il'in	826	1173
Analysis of Noise in an 0.4/6 kv Power Network. L. B. Venchkovskii	832	1181
Designing Circuits Which Contain Cores With Rectangular Hysteresis Loop Characteristics. V. F. Belyavskii and Yu. M. Shamaev	838	1188
On Choosing the Optimum Number of Pole Pairs and the Main Dimensions of Electromagnetic Slipping Clutches With Massive Steel Armatures. A. D. Posdeev	844	1198
Contactless Magnetic Time Relays. N. M. Tishchenko	850	1206
Determination of Parameters of Combined Linear Control Systems. V. Ya. Rotach	858	1218
Hydraulic Servomotor Motion in Automatic Control Systems With a Jet Amplifier. V. I. Gol'traf	863	1224

Automation and Remote Control

A translation of Avtomatika i Telemekhanika, a publication of the Academy of Sciences of the USSR

EDITORIAL BOARD OF AVTOMATIKA I TELEMEKHANIKA

D. I. Ageikin
M. A. Aizerman
A. B. Chelyustkin
(Assoc. Editor)
E. G. Dudnikov
N. Ya. Festa

V. A. Ilin
A. G. Iosuf'yan
V. V. Karibskii
A. V. Khramoi
B. Ya. Kogan
V. S. Kulebakin
S. A. Lebedev

A. Ya. Lerner
A. M. Letov
(Assoc. Editor)
V. S. Malov
B. N. Petrov
Yu. P. Portnov-Sokolov
B. S. Sotskov

A. A. Tal'
(Corresp. Secretary)
V. A. Trapeznikov
(Editor in Chief)
Ya. Z. Tsypkin
G. M. Ulanov
A. A. Voronov
S. V. Yablonskii

Vol. 21, No. 9 Russian Original Dated September, 1960 **April, 1961**

CONTENTS

	PAGE	RUSS. PAGE
Results of the First Congress of the International Federation of Automatic Control (IFAC)	867	1229
Dual Control Theory. I. A.A. Fel'dbaum	874	1240
Parametric Phenomena in the Simplest Continuous Extremal Control Systems. V.S. Baranova and A.A. Pervozvanskii	881	1250
Effect of Fluctuations on Extremal Relay Systems under Self-Oscillation Conditions. I.S. Morosanov	884	1254
Extremal Control by the Method of Random Scanning. L.A. Rastrigin	891	1264
Stability of a Controlled System with Two Nonlinear Elements. Chang Jên-wei	897	1272
On the Accurate Determination of Periodic Regimes in Sectionally Linear Automatic Control Systems. E.N. Rozenvasser	902	1279
On the Theory of Two-Channel Follow-up Systems with a Relay Component in the AC Circuit. A.A. Krasovskii	911	1293
On the Dynamic Characteristics of Hydraulic Couplings. A.M. Smirnov	920	1306
An Investigation of Some Types of Matrix Decoders with a Relay Output. T.P. Belaya	924	1311
On the Interference Resistance of Pulse-Time and Pulse-Width Telemetering Subjected to Strong Fluctuation Noise. N.V. Pozin	930	1320
An Approximate Calculation of the Transients in a Thermistor Circuit. N.P. Udalov	933	1323

CHRONICLE

The Seventh Scientific-Technical Conference of Young Scholars of the Institute of Automatics and Remote Control of the Academy of Sciences of the USSR. M.Yu. Gadzhiev, F.B. Gul'ko, A.R. Dzhelyalov, E.E. Dubnikov, V.D. Kazakov, I.A. Litovchenko, K.B. Norkin, and N.L. Prokhorov	936	1326

BIBLIOGRAPHY

List of Foreign Works Published in 1958 on the Theory of Relay Actions and Finite Automata. V.D. Kazakov and O.P. Kuznetsov	941	1332

Automation and Remote Control

A translation of Avtomatika i Telemekhanika, a publication of the Academy of Sciences of the USSR

EDITORIAL BOARD OF AVTOMATIKA I TELEMEKHANIKA

D. I. Ageikin
M. A. Aizerman
A. B. Chelyustkin
(Assoc. Editor)
E. G. Dudnikov
N. Ya. Festa
V. A. Ilin
A. G. Iosuf'yan
V. V. Karibskii
A. V. Khramoi
B. Ya. Kogan
V. S. Kulebakin
S. A. Lebedev
A. Ya. Lerner
A. M. Letov
(Assoc. Editor)
V. S. Malov
B. N. Petrov
Yu. P. Portnov-Sokolov
B. S. Sotskov
A. A. Tal'
(Corresp. Secretary)
V. A. Trapeznikov
(Editor in Chief)
Ya. Z. Tsypkin
G. M. Ulanov
A. A. Voronov
S. V. Yablonskii

Vol. 21, No. 10 Russian Original Dated October, 1960 **April, 1961**

CONTENTS

	PAGE	RUSS. PAGE
An Estimate of the Maximum Deviation for a Given Trajectory. E. A. Barbashin	945	1341
On the Stability of an Aileron Control System Disturbed by Turbulence. P. S. Landa and S. P. Strelkov	953	1352
A Vector Method for Calculating One Class of Control Systems. S. M. Levin and L. G. Manusevich	962	1365
Certain Problems in the Design of Machines Which Classify Objects According to an Identifying Feature Which is Not Specified A Priori. É. M. Braverman	971	1375
Controlling a Servodrive Using One Null Indicator Which Performs the Functions of Two Null Indicators. V. D. Vershinin	979	1387
Taking the Weak Surface Effect into Account in Switching the Magnetic State of a Ferromagnetic Plate. M. G. Vitkov	984	1393
Selection of the Most Suitable Circuit for a Photoelectric Fluxmeter. I. G. Gutovskii	989	1401
Synthesis of Circuits Whose Operation is Described by Boolean Time Functions. D. A. Pospelov	997	1410
Survey and Classification of Multiplying Devices. A. A. Moslov	1000	1414
Letter to the Editor. J. Matyáš	1016	1433
Work of the All-Moscow Seminar on Magnetic Automation Components. G. V. Subbotina	1018	1435
List of Literature on Magnetic Components for Automation, Remote Control, and Computer Technology for 1959. G. V. Subbotina and I. S. Trefilova	1019	1436

Automation and Remote Control

A translation of Avtomatika i Telemekhanika, a publication of the Academy of Sciences of the USSR

EDITORIAL BOARD OF AVTOMATIKA I TELEMEKHANIKA

D. I. Ageikin
M. A. Aizerman
A. B. Chelyustkin
(Assoc. Editor)
E. G. Dudnikov
N. Ya. Festa

V. A. Ilin
A. G. Iosuf'yan
V. V. Karibskii
A. V. Khramoi
B. Ya. Kogan
V. S. Kulebakin
S. A. Lebedev

A. Ya. Lerner
A. M. Letov
(Assoc. Editor)
V. S. Malov
B. N. Petrov
Yu. P. Portnov-Sokolov
B. S. Sotskov

A. A. Tal'
(Corresp. Secretary)
V. A. Trapeznikov
(Editor in Chief)
Ya. Z. Tsypkin
G. M. Ulanov
A. A. Voronov
S. V. Yablonskii

Vol. 21, No. 11 Russian Original Dated November, 1960 May, 1961

CONTENTS

	PAGE	RUSS. PAGE
Dual Control Theory. II . A. A. Fel'dbaum	1033	1453
The Dynamics of Self-Adaptive Systems with Extremal Continuous Adjustment of the Compensating Network in the Presence of Random Disturbances. I. E. Kazakov	1040	1465
The Stability of a Certain Nonlinear Controlled System. Chang Jên-wei	1047	1475
Foundations for the Application of the Harmonic Linearization Method to an Investigation of Periodic Oscillations in Systems with Lag. V. S. Kislyakov	1051	1481
Equivalent Transformations of Sequential Machines. A. Sh. Blokh	1057	1490
The Theory of a Magnetic Modulator with Crossed Fields and a Fundamental Frequency Output. F. I. Kerbnikov	1062	1497
Reversive (Duodirectional) Magnetic DC Amplifiers of Increased Efficiency. M. A. Boyarchenkov and M. A. Rozenblat	1066	1503
Application of Transistors in Circuits of Vibrational Voltage Regulators. A. G. Zdrok	1075	1514
Designing Circuits for Stabilizing Compound Electric Drives which Use a Special Three-Winding Transformer. O. B. Rosenbaum and R. N. Rodin	1083	1525
An Approximate Determination of Jet Reaction in a "Nozzle-Flapper" Hydraulic Amplifier. I. M. Krassov, L. I. Radovskii, and B. G. Turbin	1091	1536
Determining the Effect of Regular Signal Dynamics in the Statistical Linearization Method. M. I. Gusev	1093	1539
Plotting Logarithmic Frequency Responses for Servosystems with Combined Control. A. I. Guzenko	1101	1547
On Synthesizing Control Programs in Systems that Include a Digital Computer. P. F. Klubnikin	1106	1554
A Vacuum-Tube Network for Summing Signals. V. D. Vershinin	1111	1560

Automation and Remote Control

A translation of Avtomatika i Telemekhanika, a publication of the Academy of Sciences of the USSR

EDITORIAL BOARD OF AVTOMATIKA I TELEMEKHANIKA

D. I. Ageikin
M. A. Aizerman
A. B. Chelyustkin
(Assoc. Editor)
E. G. Dudnikov
N. Ya. Festa
V. A. Ilin
A. G. Iosuf'yan
V. V. Karibskii
A. V. Khramoi
B. Ya. Kogan
V. S. Kulebakin
S. A. Lebedev
A. Ya. Lerner
A. M. Letov
(Assoc. Editor)
V. S. Malov
B. N. Petrov
Yu. P. Portnov-Sokolov
B. S. Sotskov
A. A. Tal'
(Corresp. Secretary)
V. A. Trapeznikov
(Editor in Chief)
Ya. Z. Tsypkin
G. M. Ulanov
A. A. Voronov
S. V. Yablonskii

Volume 21, No. 12 Russian Original Dated December, 1960 July, 1961

CONTENTS

	PAGE	RUSS. PAGE
Determining the Transfer Functions for Certain Systems with Varying Parameters. B. E. Rudnitskii	1115	1565
On Methods for Realizing a Finite Automaton whose Cyclical Nature is Determined by the Variation of the Input State. M. A. Aizerman, L. A. Gusev, L. I. Rozonoér, I. M. Smirnova, and A. A. Tal'	1126	1576
Transistorized Relay Networks. A. P. Suponitskii and V. D. Urin	1144	1595
A Three-Channel Multiplier with Frequency Division of the Signals. A. A. Maslov	1150	1601
Wide-Band Decision (Operational) Amplifiers. D. E. Polonnikov	1161	1613
The Effect of the Characteristics of an Electrical Control Element on the Choice of the Parameters for a Hydraulic Amplifier. I. M. Krassov, L. I. Radovskii, and B. G. Turbin	1171	1623
Lev Semenovich Gol'dfarb (Obituary). The Editors	1175	1627
A List of Literature on Mathematical Simulation (Analog Computers) For 1958	1176	1629
Author Index – Volume 21 (1960)	1197	
Tables of Contents for Volume 21 (1960)	1202	

BLANK
PAGE

OPTIMAL CONTROL OF A NONLINEAR SYSTEM

Sun Tszyan'

(Moscow)

(Translated from: Avtomatika i Telemekhanika, Vol. 21, No. 1, pp. 3-14, January, 1960)
Original article submitted May 26, 1959

The paper considers transient responses, optimal as concerns speed of response, in control systems containing a rotary amplifier and a dc motor. The motor's excitation voltage is considered as a second independent control parameter. Methods are suggested for the synthesis of an optimal controlling device. An example is given of the synthesis of simplified second- and third-order systems.

Electrical control and regulation systems containing rotary amplifiers and dc motors have found wide application. The various systems in use today are ordinarily constructed on the basis of the linear theory. Control of the motor is effected on the side of the rotary generator's control winding, wherein the controlling signals are proportional to a combination of the error (the discrepancy between input and output) and its derivatives. The motor's excitation voltage is ordinarily fixed. These systems can also contain other connections, introduced for the purpose of compounding or compensation. In all these systems, the signal applied to the rotary generator's control winding is the sole control parameter. However, a second possible control parameter – the motor's excitation voltage – exists in these systems. With a variable motor excitation voltage, the system can manifest better quality indications, for example, higher speeds of response.

A system with two control parameters is nonlinear, as will become obvious in the sequel. The analysis and synthesis of such optimal systems are very difficult variational problems. Today, the problem of synthesizing such optimal systems can be solved on the basis of the work of L. S. Pontryagin, V. G. Boltyanskii, and R. V. Gamkrelidze [1-3]. In these works, the variational maximum principle is proven to be a necessary condition for optimality of control. However, in many cases, the maximum principle, in conjunction with other information about a system, permits one to solve completely the problem of synthesizing an optimal system.

1. Equation of System Motion

We consider the electrical control system containing a rotary amplifier whose block schematic is shown on Fig. 1. With the nomenclature used on this figure, we can write the following system of equations:

$$\begin{aligned} &\frac{dX_1}{dt} = \zeta\Omega, && J\frac{d\Omega}{dt} = k_3 I_a I_e + M_{st}, \\ &T_1\frac{dI_c}{dt} + I_c = k_1 U_1, && T_2\frac{dI_e}{dt} + I_e = k_2 U_2, \\ &T_3\frac{dE_g}{dt} + E_g = k_4 I_c, && E_g - c\Omega I_e = I_a R_a. \end{aligned} \tag{1}$$

Here, ζ, k_1, k_2, k_3, and k_4 are constant gains, T_1, T_2, and T_3 are the time constants of the rotary amplifier's control winding, in the motor's excitation winding and in the transverse circuit of the rotary amplifier, respectively. In our further transformations of system of equations (1) we shall made the following assumptions: the load's static torque is small in comparison with the load's inertia; time constant T_1 of the rotary amplifier's control winding is small in comparison with T_3. System (1) will then, after some transformation and after conversion to dimensionless units, have the following form:

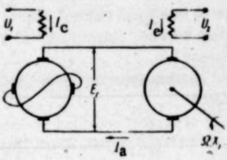

Fig. 1.

$$\begin{aligned} &\frac{dx}{dt} = \zeta_0\omega, && \frac{d\omega}{dt} = \frac{\eta}{1-\mu} i_e e_g - \omega i_e^2, \\ &\frac{de_g}{dt} = -\beta_1 e_g + \beta_1 u_1, && \frac{di_e}{dt} = -\beta_2 i_e + \beta_2 u_2. \end{aligned} \tag{2}$$

In these equations,

$$x = \frac{X_1}{X_{1\max}}, \quad e_g = \frac{E_g}{E_{g\max}}, \quad i_e = \frac{I_e}{I_{e\max}},$$

$$i_a = \frac{I_a}{I_{a\,nom}}, \quad \omega = \frac{\Omega}{\Omega_{nom}}, \quad u_1 = \frac{U_1}{U_{1\max}},$$

$$u_2 = \frac{U_2}{U_{2\max}}, \quad \beta_1 = \frac{T_{em}}{T_3}, \quad \beta_2 = \frac{T_{em}}{T_2},$$

$$T_{em} = \frac{JR_a}{k_3 C I_{e\max}^2}, \quad \eta = \frac{E_{g\max}}{E_{g\,nom}} > 1,$$

$$\mu = \frac{I_{a\,nom} R_a}{E_{g\,nom}} < 1.$$

The time t in system (2) of equations is also dimensionless; as the basic quantity we take the electromechanical time constant T_{em}. For convenience, we retain the previous notation for time.

In actual systems there are four essential limitations: limitations on the control and excitation voltages u_1 and u_2, limitations on armature current, and limitations on the motor's rotational speed. The last two are limitations on coordinates of the system. The analysis and synthesis of optimal systems when limitations on coordinates are taken into account are complicated mathematical problems requiring special study. However, the coordinate limitations in practice are quite simple. In many cases, quite simple considerations permit one to find the optimal processes with coordinate limitations taken into account [5]. In this paper we shall only consider limitations on the controlling parameters, as the case most studied from the point of view of the variational calculus. In relative units, the limitations imposed on u_1 and u_2 are expressed by the following inequalities:

$$|u_1| \leqslant 1, \quad 0 < \lambda \leqslant u_2 \leqslant 1. \tag{3}$$

The lower limit for the motor excitation voltage λ is defined by the condition that the motor not enter a separation mode of operation for small static loads.

We shall investigate the optimal transient responses in the processing of original errors. In this case, the magnitude of an original error does not effect the structure of the optimal controlling portion. When the input stimulus varies linearly in time, the problem is solved analogously, but a more complicated structure (design) is obtained since, in this case, the velocity at which the input stimulus varies will enter into the equation of motion. Let the input stimulus be $g(t) = A_0$, where A_0 is an arbitrary constant. We introduce new coordinates, related to the old coordinates in the following way:

$$x_1 = A_0 - x, \quad x_2 = \frac{dx_1}{dt} = -\zeta_0\omega,$$
$$x_3 = -e_g, \quad x_4 = i_e. \tag{4}$$

By substituting the new coordinates in Eqs. (2), we get the definitive system of equations:

$$\frac{dx_1}{dt} = x_2, \quad \frac{dx_2}{dt} = \alpha x_3 x_4 - x_2 x_4^2,$$
$$\frac{dx_3}{dt} = -\beta_1 x_3 - \beta_1 u_1, \quad \frac{dx_4}{dt} = -\beta_2 x_4 + \beta_2 u_2. \tag{5}$$

Expressions (3) for the limitations on u_1 and u_2 also hold for equations in the new coordinates.

2. Optimal Processes and Optimal Equations

Let the initial state of the system be given, i.e., at the initial moment of time let the four coordinates of system of equations (5) be given. It is required to choose controls $u_1(t)$ and $u_2(t)$ which will take the system to the null state in minimal time. We first consider the phase space X of system (5). Each point of this space, called a representative point, defines one state of the system. The system's null state is characterized by the point with coordinates $\{0, 0, 0, \gamma\}$, where $\gamma (0 < \lambda < \gamma < 1)$ is some fixed number. The system's motion will be considered as a trajectory of the representative point $\{x_1, x_2, x_3, x_4\}$ in phase space X. The general point in X is denoted by the letter x.

Limitations (3) form a closed rectangle U on the control plane, whose coordinates axes are u_1 and u_2. The control vector with coordinates u_1 and u_2 we shall denote by the letter u. A vector function u(t) is called admissible if all its values lie in U. In the sequel we shall assume that u(t) is an admissible piecewise-smooth function with no more than a finite number of first-order discontinuities. Each such fixed control uniquely defines one continuous trajectory which passes through the given initial point in phase space.

With this notation, the system of equations in (5) can be replaced by one vector equation

$$\frac{dx}{dt} = f(x) + Bu. \tag{6}$$

Here, B is the rectangular matrix

$$B = \begin{pmatrix} 0 & 0 \\ 0 & 0 \\ -\beta_1 & 0 \\ 0 & \beta_2 \end{pmatrix}.$$

The optimal control problem can be formulated as follows: In phase space X the point x(0) is given, and it is required to find an admissible control $u(t) = \{u_1(t), u_2(t)\}$ which will carry point x(0) over into null point $\xi_0 = \{0, 0, 0, \gamma\}$ in minimal time.

In accordance with the theorems of the maximum principle [3], we set up the system of differential equations which is adjoint to system (5) with the new variables $\psi = \{\psi_1, \psi_2, \psi_3, \psi_4\}$:

$$\frac{d\psi_1}{dt} = 0, \quad \frac{d\psi_2}{dt} = -\psi_1 + x_4^2\psi_2,$$
$$\frac{d\psi_3}{dt} = -\alpha x_4 \psi_2 + \beta_1 \psi_3, \tag{7}$$
$$\frac{d\psi_4}{dt} = (2x_2x_4 - \alpha x_3)\psi_2 + \beta_2\psi_4.$$

Here, ψ is a covariant vector whose components are computed by the usual formula

$$\frac{d\psi_i}{dt} = -\sum_{\alpha=1}^{n} \frac{\partial f_\alpha}{\partial x_i} \psi\alpha \quad (i = 1, 2, 3, 4).$$

We now set up the Hamiltonian function, which is here the scalar product of the vector ψ by the velocity vector dx/dt. We denote by H the Hamiltonian function:

$$H(x, \psi, u) = \left(\psi, \frac{dx}{dt}\right)^{*} = \psi, f(x) + Bu) =$$
$$= (\psi, f(x)) + (\psi, Bu). \tag{8}$$

---

[*] We shall use parentheses to denote the scalar product of two vectors.

With this notation, we formulate the necessary condition for the optimality of control u(t) in the following way [3]. Let u(t) be an optimal control and x(t) the corresponding optimal trajectory. There then exists a nonzero continuous vector function $\psi(t)$ such that

$$H(\psi(0),\ x(0),\ u(0)) \geqslant 0,$$

the functions $\psi(t)$, x(t), and u(t) satisfy systems (5) and (7) of equations, so that along the trajectory, at any moment of time, the Hamiltonian function is a maximum with respect to u, i.e.,

$$H(\psi(x),\ x(t),\ u(t)) = \sup_{u\in U}(\psi(t),\ f(t)+Bu)$$

and

$$H(\psi(t),\ x(t),\ u(t)) = \text{const} \geqslant 0. \qquad (9)$$

We note that the quantity in the first parentheses in the rightmost member of (8) does not depend on u. Consequently, the expression in the second parentheses attains a maximum simultaneously with Hamiltonian function H. The necessary condition for optimality leads to the condition

$$(\psi(t),\ Bu(t)) = \sup_{u\in U}(\psi(t),\ Bu). \qquad (10)$$

We now write (10) in expanded form:

$$(\psi,\ Bu) = -\psi_3(t)\beta_1 u_1 + \psi_4(t)\beta_2 u_2.$$

If an optimal control exists, it is easily seen that it is defined by the following relationships:

$$u_1(t) = -\operatorname{sign}\psi_3(t),$$
$$u_2(t) = \begin{cases} 1 \text{ for } & \psi_4(t) > 0, \\ \lambda \text{ for } & \psi_4(t) < 0. \end{cases} \qquad (11)$$

This means that if the optimal control exists, it consists of a certain number of intervals, in each of which u_1 and u_2 assume one of their limiting values.

Controls u_1 and u_2 change their values by a jump each time $\psi_3(t)$ and $\psi_4(t)$ pass through zero. This is the state of affairs in all nonlinear systems where the controlling parameters enter linearly and if the corresponding components of the covariant vector do not vanish identically in any finite interval of time.

We now give the solution of system (7) of equations for the vector $\psi(t)$

$$\psi_1(t) = \psi_{10} = \text{const},$$

$$\psi_2(t) = e^{\int_0^t x_4^2(\tau)\,d\tau}\left[\psi_{20} - \psi_{10}\int_0^t e^{-\int_0^\tau x_4^2(s)\,ds}\,d\tau\right],$$

$$\psi_3(t) = e^{\beta_1 t}\left[\psi_{30} - \alpha\int_0^t x_4(\tau)\,\psi_2(\tau)\,e^{-\beta_1\tau}\,d\tau\right],$$

$$\psi_4(t) = e^{\beta_2\tau}\left[\psi_{40} + 2\int_0^t (x_2(\tau)\,x_4(\tau) - \alpha x_3(\tau))e^{-\beta_2\tau}\,d\tau\right]. \qquad (12)$$

It is clear from (12) that $\psi_3(t)$ goes through zero no more than once. Consequently, if $x_4(t)$ does not change sign, $\psi_3(t)$ goes through zero not more than twice and, in the general case, $u_1(t)$ consists of three intervals.

These consequences are useful for the solution of the synthesis problem. To be assured of the possibility of constructing an optimal system, it is nice to know the following theorem on the existence of optimal controls: For each point of the phase space given by (5), there exists an optimal control which takes this point to the point $\xi_0 = \{0,\ 0,\ 0,\ \gamma\}$ in minimal time.

The proof of this theorem for the system of (5) can easily be carried through by modifying the well-known scheme of the proof of the similar theorem for linear systems which has been given by R. V. Gamkrelidze [2]. This may be done because the nonlinearity in (5) enters only into the coefficients of the corresponding equations.†

Concrete analysis shows that one can expect the optimal control in our case to be unique.‡ This means that, for a given point of phase space, there exists a unique control which takes this point over into point ξ_0 in minimal time. We shall make use in the sequel of the existence and uniqueness theorems for optimal controls.

3. Some Properties of the Field of Optimal Trajectories

In this section we give a brief presentation of some of the properties of optimal trajectories. As was stated earlier, we can assume existence and uniqueness of the optimal controls for the system being studied, i.e., for any point of phase space there exists a unique optimal trajectory joining the given point to the null point ξ_0. To each point of phase space there corresponds just one duration of the optimal transient response. The time T is a single-valued function of the phase-space points. We now consider the set S_T of points with the same duration of the optimal transient response. All these points lie on some hypersurface with equation

$$T(x_1,\ x_2,\ x_3,\ x_4) = C. \qquad (13)$$

The entire space is filled by the optimal trajectories. In the direction of point ξ_0 these trajectories can only converge, not diverge. On each optimal trajectory from a remote point there lies only one point which is in the set S_T.

---

† The theorem on the existence of optimal controls is proved in [7] for nonlinear nonstationary systems with linear controls and for certain additional limitations.

‡ What we have in mind here are the concrete constructions of optimal processes on planes and in three-dimensional space. So far as the author knows, the literature contains no proof of the existence theorem for an arbitrary nonlinear system.

It may be proved** that the point set S_T is a closed convex hypersurface. Moreover, this hypersurface is everywhere continuous and almost everywhere differentiable, i.e., except for a set of points of "area" (measure) zero, there is a tangent plane at every point of S_T. Following A. Ya. Lerner [5], we call S_T an isochrone. All points inside S_T have a duration of the transient response less than T. An isochrone continuously widens with increasing time. As $T \to \infty$, S_T fills the entire finite phase space.

The function $T(x_1, x_2, x_3, x_4)$ forms a scalar potential field in phase space. Equation (13) defines an equipotential hypersurface. Since hypersurface S_T is differentiable almost everywhere, field T generates a vector gradient field, which is the field of external normals to hypersurface (13). One may easily remark the relationship between the field of external normals and the covariant vectors ψ, which is noted in L. S. Pontryagin's maximum principle. It turns out that the vector ψ forms a vector field in phase space X, with the exception of the set of points of the space where the hypersurface S_T is not differentiable. This can be written in the form of a vector equation

$$\operatorname{grad} T(x_1, x_2, x_3, x_4) = \sigma(x_1, x_2, x_3, x_4)\,\psi(x_1, x_2, x_3, x_4), \tag{14}$$

where σ is some function of the points of space X.

Equation (14) gives rise to several partial differential equations which, in some of the simplest cases, can be integrated, giving the function T in explicit form. It may also be shown that there is a continuous dependence of the optimal control on the original position of the point,†† i.e., points which are close in phase space have "close" optimal controls. This fact was established for linear systems by F. M. Kirillova in [6].

4. The Synthesis of an Optimal Controlling Device

As is well known, the task of synthesis reduces to the finding of the optimal control in the form of a function of the points of phase space $u_i(x_1, x_2, x_3, x_4)$ $(i = 1, 2)$ or, what amounts to the same thing, to finding the switching hypersurface for the controls u_1 and u_2 since, according to expression (11), the optimal control has the form of a relay function. If the optimal control functions cannot be found exactly by analytic means, then the switching hypersurface can be found approximately. Optimal trajectories always consist of a finite number of segments of curves of four families, corresponding to the controls $u_1 = \pm 1$ and $u_2 = 1, \lambda$. With this, the entire space is divided into regions, in each of which u_1 and u_2 have definite values. The boundaries of these regions are also the switching hypersurface. Two methods can be proposed for finding the switching hypersurfaces approximately. In the first method, one sets up, on an analog computer, a model whose time runs in the reverse direction of system (5). Then, all the optimal trajectories leaving point ξ_0 will have the reverse direction. We also construct the conjugate model in accordance with system of equations (7), but with time t replaced by −t. We then connect these two models as in Fig. 2. Since each initial condition $\psi(0)$ defines one optimal trajectory, we can, by giving various values of $\psi(0)$, obtain a set of optimal trajectories. With this, the pulse generator sends a command at the moments of switching of u_1 and u_2 which causes the recorder to write the values $\{x_1, x_2, x_3, x_4\}$. Thanks to the linearity of Eqs. (7) in ψ_i $(i = 1, 2, 3, 4)$, $\psi(0)$ can be chosen so as to satisfy the condition:

$$\psi_{10}^2 + \psi_{20}^2 + \psi_{30}^2 + \psi_{40}^2 = 1.$$

For each trajectory we record the times of switching and the corresponding system coordinates at the moment of switching. By continuing this for a sufficient number of times, we obtain an approximate representation of the switching hypersurface in the form of a table. Using the tabular data, one can carry out the synthesis of the optimal controlling device by the method cited in [9].

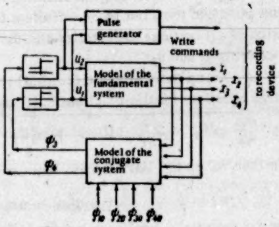
Pulse generator
Write commands
u_2
u_1
Model of the fundamental system
x_1
x_2
x_3
x_4
to recording device
ψ_3
ψ_4
Model of the conjugate system
ψ_{10} ψ_{20} ψ_{30} ψ_{40}

Fig. 2

If it is impossible to measure the system's parameters with sufficient accuracy, it is then advantageous to use another method for the determination of the optimal control function, wherein one uses the relationship between the gradient field of the duration of the optimal transient response and the vector field of the function $\psi(x_1, x_2, x_3, x_4)$. The isochrones for various durations of the optimal transient response can be constructed approximately by means of a machine of the type of the automatic optimizer which was developed under the direction of A. A. Fel'dbaum at the Institute of Automation and Remote Control of the Academy of Sciences, USSR. The algorithm for solving this problem on the automatic

---

** The proof of the following assertion, which we omit here, depends essentially on the specific features of nonlinear system (5), and is therefore of a concrete, nongeneral character. It is different from the well-known proof for linear systems.

†† A continuous dependence here has the mathematical meaning of continuity of the norm. If $u^1(t)$ and $u^k(t)$ are two optimal controls which take points ξ^1 and ξ^k to the null point then, as ξ^k tends to ξ^1, the integral $\int_0^T [u^1(t)-u^k(t)]^2 dt$ tends to zero, where $T = \max(T_1, T_k)$.

optimizer was developed by R. L. Stakhovskii. By constructing the isochrone hypersurfaces we can, using Eqs. (14), determine the distribution of the signs of the functions $\psi_3(x_1, x_2, x_3, x_4)$ and $\psi_4(x_1, x_2, x_3, x_4)$, and thereby find the switching hypersurface.

For certain limiting cases, when the order of Eqs. (5) can be lowered, the synthesis problem can also be solved analytically. We give below the results of synthesis for two limiting cases: for the case when the generator's time constant and the motor's excitation winding time constant are negligibly small in comparison with the electromechanical constant, and for the case when only the second of these can be neglected. In the first case, we can substitute $\beta_1 = \infty$ and $\beta_2 = \infty$ in system of equations (5). The equations will then have the form:

$$\frac{dx_1}{dt} = x_2, \qquad \frac{dx_2}{dt} = -u_2^2 x_2 - \alpha u_1 u_2. \quad (15)$$

As before, the limitations imposed on the system have the form given in (3). For this limiting case, the maximum principle turns out to be sufficient for the determination of all optimal trajectories and the switching lines of controls u_1 and u_2.

We now set up the conjugate (adjoint) system of differential equations for the functions $\psi_1(t)$ and $\psi_2(t)$:

$$\frac{d\varphi_1}{dt} = 0, \qquad \frac{d\varphi_2}{dt} = -\varphi_1 + u_2^2\varphi_2. \quad (16)$$

We then set up the Hamiltonian function:

$$H(x, \varphi, u) = \varphi_1 x_2 + \varphi_2(-u_2^2 x_2 - \alpha u_1 u_2). \quad (17)$$

For the essentially nonlinear system (15), it is not known, in general, if there is an optimal control for any arbitrary initial conditions and, if there is one, whether or not it is unique. But, since system of equations (15) is a limiting case of system (5), one may expect that system (15) also possesses these properties. The results of the synthesis substantiate this assumption.

We now write the solution of system of equations (16):

$$\varphi_1(t) = \varphi_{10} = \text{const},$$

$$\varphi_2(t) = e^{\int\limits_0^t u_2^2(\tau)\,d\tau}\left[\varphi_{20} - \int\limits_0^t \varphi_{10} e^{-\int\limits_0^\tau u_2^2(s)\,ds}\,d\tau\right]. \quad (18)$$

We notice that $\psi_2(t)$ cannot change sign more than once. We now turn our attention to the Hamiltonian function (17). Within the parentheses there, α is a positive number and u_2 is always positive. Then, in accordance with the requirement of the maximum principle,

$$u_1 = -\operatorname{sign}\varphi_2(t). \quad (19)$$

To elicit the optimal law for control $u_2(t)$, we rewrite the Hamiltonian function in another form:

$$H(x, \varphi, u) = \varphi_1 x_2 + \varphi_2\left[-x_2\left(u_2 + \frac{\alpha u_1}{2x_2}\right)^2 + \frac{\alpha^2 u_1^2}{4x_2}\right]. \quad (20)$$

Let us consider separately the two possible cases.

a) $\psi_2(t) < 0$. In this case, $u_1 = 1$. For $x_2 > 0$, u_2 must assume its greatest value, equal to unity. On the lower half-plane, where $x_2 < 0$, the optimal control u_2 is defined as follows:

$$u_2 = \begin{cases} 1, & \text{if } \left|\frac{\alpha}{2x_2}\right| \geqslant 1, \\ \frac{\alpha}{2x_2}, & \text{if } \lambda \leqslant \left|\frac{\alpha}{2x_2}\right| \leqslant 1, \\ \lambda, & \text{if } \left|\frac{\alpha}{2x_2}\right| \leqslant \lambda. \end{cases} \quad (21)$$

b) $\psi_2(t) > 0$, $u_1 = -1$. On the upper half-plane, where $u_2 > 0$, the optimal control u_2 is defined by the expression

$$u_2 = \begin{cases} 1 & \text{for } \frac{\alpha}{2x_2} \geqslant 1, \\ \frac{\alpha}{2x_2} & \text{for } \lambda \leqslant \frac{\alpha}{2x_2} \leqslant 1, \\ \lambda & \text{for } \frac{\alpha}{2x_2} \leqslant 1. \end{cases}$$

On the lower half-plane, $u_2 = 1$.

It is thus clear that in the general case u_1 consists of two intervals, in each of which u_1 assumes the value 1 or −1. Control u_2, which is the motor excitation, consists of four intervals. In one of these intervals, u_2 continuously sweeps through the segment $[\lambda, 1]$. On the succeeding segment u_2 can only assume its maximum value, 1, since otherwise the function H would not be a maximum at the endpoint, where $x_1 = x_2 = 0$. It may be noticed that, at the origin of coordinates, only two curves, from the different half-planes, pass. These two curves comprise the final segments of all optimal trajectories. We denote them by L_1 and L_1' (Fig. 3). On line L_1 control $u_1 = -1$ and on line L_1', control $u_1 = 1$. Analogous relationships lead us to the conclusion that ψ_2 changes sign on lines L_1 and L_1'. Generalizing what has been said, we conclude that the phase plane is divided into six regions (Fig. 3). Lines L_1 and L_1' divide the phase plane into two half-planes; in the left half-plane $u_1 = -1$ and, in the right one, $u_1 = 1$. Moreover, there is a strip in each half-plane, bounded by the lines Γ_1 and Γ_2 in the left half-plane and the lines Γ_1' and Γ_2' in the right one. If the initial point x(0) is in the third quadrant then the optimal trajectory rises upward with controls $u_1 = -1$ and $u_2 = 1$. Meeting line Γ_1, u_2 begins to vary in accordance with the law $u_2 = \alpha / 2x_2$. On leaving this strip, u_2 takes its minimum value, λ; when the trajectory meets line L_1', u_1 changes sign and u_2 jumps to its maximum value

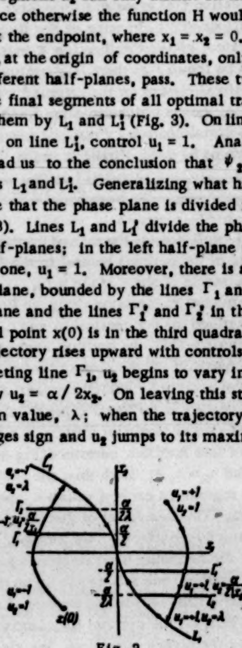

Fig. 3

after which the trajectory follows line L_1' to the origin of coordinates. The transient response and the laws of change of the controls with time are shown on Fig. 4.

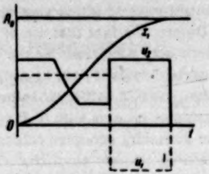

Fig. 4

We now consider the other case, when $\beta_2 = T_{em}/2 = \infty$, and β_1 is finite. In this case, we have the following system of differential equations

$$\frac{dx_1}{dt} = x_2, \quad \frac{dx_2}{dt} = \alpha x_3 u_2 - x_2 u_2^2,$$
$$\frac{dx_3}{dt} = -\beta_1 x_3 - \beta_1 u_1. \qquad (22)$$

The adjoint system of equations for the vector ψ will be

$$\frac{d\phi_1}{dt} = 0, \quad \frac{d\phi_2}{dt} = -\phi_1 + u_2^2\phi_2,$$
$$\frac{d\phi_3}{dt} = 0 - \alpha u_2\phi_2 + \beta_1\phi_3. \qquad (23)$$

The solution of this system is:

$$\phi_1(t) = \phi_{10} = \text{const},$$

$$\phi_2(t) = \left[-\phi_{10}\int_0^t e^{-\int_0^t u_2^2(s)\,ds}\,d\tau + \psi_{20}\right] e^{\int_0^t u_2^2(s)\,ds},$$

$$\psi_3(t) = \left[-\alpha\int_0^t u_2(\tau)\,\phi_2(\tau)\,e^{-\beta_1\tau}d\tau + \psi_{30}\right] e^{\beta_1 t}. \qquad (24)$$

We can conclude from expressions (24) that, by virtue of the constancy of $\psi_1(t)$ along the given trajectory, $\psi_2(t)$ cannot change its sign more than once. Since $u_2(t)$ is assumed to be always positive, then $\psi_3(t)$, in the general case, does not change sign more than twice. The Hamiltonian function is

$$H(x, \psi, u) = \qquad (25)$$
$$= \phi_1 x_2 + \phi_2(\alpha x_3 u_2 - x_2 u_2^2) + \phi_3(-\beta_1 x_3 - \beta_1 u_1).$$

For the Hamiltonian function to be maximal with respect to u_1, it is necessary that u_1 vary in accordance with the law

$$u_1 = -\operatorname{sign}\phi_3.$$

Thus, in general (in accordance with the remark made earlier), optimal control $u_1(t)$ consists of three intervals, in each of which u_1 assumes one of its boundary values. To determine the character of control $u_2(t)$, we rewrite the Hamiltonian function (25) in the following equivalent form:

$$H(x, \phi, u) = \phi_1 x_2 +$$
$$+ \phi_2\left[-x_2\left(u_2 - \frac{\alpha x_3}{2x_2}\right)^2 + \left(\frac{\alpha x_3}{2x_2}\right)^2 x_2\right] + \qquad (25')$$
$$+ \phi_3(-\beta_1 x_3 - \beta_1 u_1).$$

We consider separately the following cases.

1) $x_2 > 0$, $x_3 > 0$. When $\psi_2 < 0$, the Hamiltonian function H, according to (25'), attains a maximum for

$$u_2 = \begin{cases} 1, & \text{if } \dfrac{\alpha x_3}{2x_2} < \dfrac{1+\lambda}{2}, \\ \lambda, & \text{if } \dfrac{\alpha x_3}{2x_2} > \dfrac{1+\lambda}{2}. \end{cases}$$

When $\psi_2 > 0$, H is a maximum for

$$u_2 = \begin{cases} 1, & \text{if } \dfrac{\alpha x_3}{2x_2} \geqslant 1, \\ \dfrac{\alpha x_3}{2x_2}, & \text{if } \lambda \leqslant \dfrac{\alpha x_3}{2x_2} \leqslant 1, \\ \lambda, & \text{if } \dfrac{\alpha x_3}{2x_2} \leqslant \lambda. \end{cases}$$

2) $x_3 > 0$, $x_2 < 0$. In this case, the conditions for a maximum for H will be: $u_2 = \lambda$ for $\psi_2 < 0$ and $u_2 = 1$ for $\psi_2 > 0$.

3) $x_3 < 0$, $x_2 < 0$. The corresponding conditions are written as follows:

for $\psi_2 > 0$,

$$u_2 = \begin{cases} 1, & \text{if } \dfrac{\alpha x_3}{2x_2} < \dfrac{1+\lambda}{2}, \\ \lambda, & \text{if } \dfrac{\alpha x_3}{2x_2} > \dfrac{1+\lambda}{2}; \end{cases}$$

for $\psi_2 < 0$,

$$u_2 = \begin{cases} 1, & \text{if } \dfrac{\alpha x_3}{2x_2} \geqslant 1, \\ \dfrac{\alpha x_3}{2x_2}, & \text{if } \lambda \leqslant \dfrac{\alpha x_3}{2x_2} \leqslant 1, \\ \lambda, & \text{if } \dfrac{\alpha x_3}{2x_2} \leqslant \lambda; \end{cases}$$

4) $x_3 < 0$, $x_2 > 0$. In this region, H attains a maximum if

$$u_2 = \begin{cases} 1 & \text{for } \phi_2 < 0, \\ \lambda & \text{for } \phi_2 > 0. \end{cases}$$

On the basis of the discussion given, we can, in general, construct all the optimal trajectories in phase space. However, this necessitates a great deal of computational work. The structure of the switching surfaces for both controlling parameters is quite complicated.

The construction of these surfaces is an independent problem for investigation. Here, we speak only of certain features of the optimal transient responses in the system described by Eqs. (22).

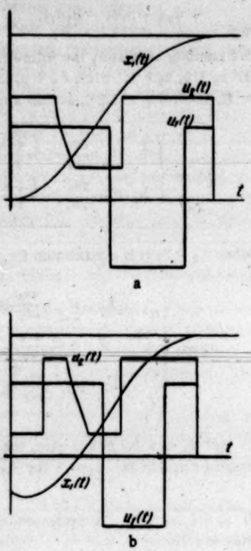

Fig. 5

Figure 5a gives the optimal transient response for zero initial conditions. Here, control $u_1(t)$, as it must, consists of three intervals. Control $u_2(t)$ has the same form as the corresponding control in the previous case. The difference amounts only to this: that the moment when u_2 switches from a minimum to a maximum does not coincide with the moment when u_1 is switched, but occurs later.

A completely different picture is obtained if the initial conditions are nonzero. As shown in Fig. 5b, for certain initial conditions, u_2 varies by a significantly more complicated law than in the case of the process with zero initial conditions.

CONCLUSIONS

The maximum principle of L. S. Pontryagin is a very powerful means for solving the problem of synthesizing control systems which give optimal speeds of response. Despite the fact that use of this principle leads only to necessary conditions for the optimality of controls, in certain cases it can, in conjunction with other information, provide sufficient information to permit the designing of systems with high speeds of response.

The generally accepted scheme for a control system containing a rotary amplifier with fixed motor excitation voltage is not the best one. It is more advantageous to introduce a variable excitation voltage whose law of variation can be exactly computed for a given system. By using the maximum principle, one can effect an exact synthesis of an optimal controlling device which makes the system best, in the sense of speed of response.

LITERATURE CITED

[1] V. G. Boltyanskii, R. V. Gamkrelidze, and L. S. Pontryagin, "On optimal process theory," Doklady Akad. Nauk SSSR 110, 1 (1956).

[2] R. V. Gamkrelidze, "Theory of optimally fast processes in linear systems," Izvest. Akad. Nauk SSSR, Ser. Matem. 22, 4 (1958).

[3] L. S. Pontryagin, "Optimal control processes," Usp. Matem. Nauk 14, 1, 85 (1959).

[4] A. A. Fel'dbaum, "On the synthesis of optimal systems by means of phase space," Avtomat. i Telemekh. 16, 2 (1955).

[5] A. Ya. Lerner, "On the limiting speed of response of automatic control systems," Avtomat. i Telemekh. 15, 6 (1954).

[6] F. M. Kirillova, "On the validity of the posing of one optimal control problem," Izvest. Vysshikh Ucheb. Zavedenii, Ser. Matem. 4 (1958).

[7] N. N. Krasovskii, "On a problem of optimal control of nonlinear systems," Prikl. Matem. i Mekh. 23, 2 (1959).

[8] R. Bellman, "On the bang-bang control processes," Quarterly Appl. Math. 14, 1 (April, 1956).

[9] Sun Tszyan', "Synthesis of the controlling portion of an optimally fast servo system," Avtomat. i Telemekh. 20, 3 (1959).‡‡

---

‡‡ See English translation.

THE REDUCTION OF NONLINEAR CONTROL SYSTEM EQUATIONS TO THEIR SIMPLEST FORM

E. N. Rozenvasser

(Leningrad)

(Translated from: Avtomatika i Telemekhanika, Vol. 21, No. 1, pp. 15-19, January, 1960)
Original article submitted May 29, 1959

Formulas are given for linear transformations which take the equations of direct control systems to single *n*th-order differential equations. Use of this transformation allows one to shorten the computations required in carrying out certain calculations for control systems, for example, for determining the autooscillations in the case of piecewise-linear characteristics.

1. We shall consider the system of differential equations

$$x_k = \sum_{\alpha=1}^{n} b_{k\alpha} x_\alpha + h_k f(\sigma,\ t) \quad (k = 1,\ 2,\ \ldots,\ n),$$

$$\sigma = \sum_{s=1}^{n} j_s x_s, \tag{1}$$

where $b_{k\alpha}$, h_k, and j_s are constants, and $f(\sigma,\ t)$ is some nonlinear function.

The characteristic polynomial of the linear portion of system (1) will be written in the form

$$D(\lambda) = |\lambda\delta_{k\alpha} - b_{k\alpha}| = \lambda^n + f_1\lambda^{n-1} + \ldots + f_n \tag{2}$$

($\delta_{k\alpha}$ is a Kronecker delta).

We now introduce the determinants $H_s(\lambda)$ ($s = 1,\ 2,\ \ldots,\ n$) which are obtained by replacing the *s*th column of determinant (2) by the column $\{H\}$ whose components are the number h_k. If we expand the determinants in powers of λ, we shall have

$$H_s(\lambda) = \sum_{k=1}^{n} h_{sk}\lambda^{n-k}. \tag{3}$$

We introduce the additional notation

$$M(\lambda) = \sum_{s=1}^{n} j_s H_s(\lambda) = \sum_{l=1}^{n} m_l \lambda^{n-l}. \tag{4}$$

We consider, in addition to (1), the system of equations

$$D(p)\,y = f(\sigma,\ t),\quad \sigma = M(p)\,y, \tag{5}$$

where D and M are the polynomials of (2) and (4) and *p* is the symbol for differentiation.

Let

$$y' = \frac{dy}{dt},\quad y'' = \frac{d^2y}{dt^2},\ \ldots,\quad y^{(n-1)} = \frac{d^{n-1}y}{dt^{n-1}}$$

and the determinant composed of the numbers h_{sk} be nonzero. Then, we have the relationship

$$x_i = \sum_{s=1}^{n} h_{is}\, y^{(n-s)}. \tag{6}$$

We now consider the columns

$$\{U_1\} = \{H\}, \tag{7}$$

$$\{U_2\} = B\{U_1\},\ \ldots,\ \{U_n\} = B^{n-1}\{H\} = B\{U_{n-1}\},$$

where B is the matrix whose components are the numbers $b_{k\alpha}$.

We denote by Δ_n the determinants consisting, respectively, of the columns $\{U_1\},\ \{U_2\},\ \ldots,\ \{U_n\}$, and by Δ_n^s the algebraic complement of the element of the *s*th row and *n*th column of determinant Δ_n.

If we then solve system (6) for *y* and its derivatives, we get

$$y^{(n-k)} = \sum_{\alpha=1}^{n} m_{k\alpha} x_\alpha \tag{8}$$

where

$$m_{n\alpha} = \frac{\Delta_n^\alpha}{\Delta_n} \quad (\alpha = 1,\ 2,\ \ldots,\ n), \tag{9}$$

and the remaining quantities, m_{ps}, are defined by the recursion formulas

$$m_{ps} = \sum_{\alpha=1}^{n} m_{p+1,\alpha} b_{\alpha s}. \tag{10}$$

The derivations of formulas (6), (8), (9), and (10) are given in the Appendix.

2. For solving various control problems which relate to systems of the form of (1), it is convenient to make direct use of Eqs. (5) since, in every case, the computational work connected with the analysis of Eqs. (5) is simpler. As was noted earlier, Eqs. (5) can be written immediately if one knows the coefficients of the characteristic equation of linearized system (1) for $f(\sigma) = c\sigma$.

The subsequent transition from Eqs. (5) to the original system (1) is made by means of (6), and presents no difficulty.

In particular, let us consider the question of determining the autooscillations in system (1) in the case of a piecewise-linear characteristic. In system (1), let

$$f(\sigma, t) = f(\sigma) = a_i\sigma + b_i \quad \text{for} \quad \sigma_{i-1} < \sigma < \sigma_i, \tag{11}$$

where the σ_k are given. Then the corresponding system (5) will have the form:

$$\left[D(p) - a_i M(p)\right] y - b_i = 0$$

$$\text{for} \quad \sigma_{i-1} < M(p)\, y < \sigma_i. \qquad (12)$$

With this, the search for continuous periodic solutions of system (1) reduces to the search for periodic solutions of Eqs. (12) which are continuous up to the (n-1)th derivative inclusive.

If we give ourselves the type of periodic mode of operation and then find the general solutions of the corresponding linear Eqs. (12) on each segment of variation of σ, we can, by matching up the solutions, construct a system of transcendental equations for the determination of the autooscillation period and the time of motion on each portion of the nonlinear characteristic. The matching-up method does not differ from the methodology presented in [1] as applied to system (1). However, the use of (12) significantly shortens the computational work involved in matching up and setting up the equations for the periods since, as is known [2], setting up the general solution of Eqs. (12) and its derivatives on each of the segments is much simpler than setting up the general solution of the original system (1).

One can also seek the periodic solutions of Eqs. (12) directly in the form of trigonometric series by the method, for example, proposed by L. A. Gusev [3].

However, in the given case, there exists an essential simplification. In [3], following M. A. Aizerman and F. R. Gantmakher [4], the author uses the derived equation of the form

$$D(p)\,\sigma - M(p)\, f(\sigma) = 0, \qquad (13)$$

which was obtained from (1) by differentiation followed by elimination of unknowns. With this there are periodic solutions of Eq. (13) for definite conditions which relate the discontinuities of the derivatives of σ and $f(\sigma)$ at the moments of switching (saltus conditions). In [3], the saltus conditions were given in the form

$$\{\sigma\}_{q1} = U_q \{\sigma\}_{q2} - V_q, \qquad (14)$$

where $\{\sigma\}_{q1}$ is a column with values $\sigma - m_n b_q/(f_n - a_q m_n)$, $\sigma, \ldots, \sigma^{(n-1)}$ at time $t_q - 0$, $\{\sigma\}_{q2}$ is the same column at time $t_q + 0$, t_q is the time of the qth switching, U_q is a constant matrix, and V_q is a constant column.

By virtue of what has previously been said, the use of (13) as the derived equation allows one to replace the saltus conditions by the conditions of continuity of y, y', . . . , $y^{(n-1)}$ at the moments of switching. If, for this, we set up the conditions analogous to (14), we shall have

$$U_q = E, \quad V_q = \left| \begin{matrix} \dfrac{b_q}{f_n - q_q m_n} - \dfrac{b_{q+1}}{f_n - a_{q+1} m_n} \\ 0 \\ \cdot \\ \cdot \\ \cdot \\ 0 \end{matrix} \right| \qquad (15)$$

where E is the unit matrix.

For (15), Eqs. (27) of [3], which are used for the elimination of the arbitrary constants, are essentially simplified. Since the switchings occur for definite values of

$$\sigma_q = \sigma_{q\,\text{giv}} \qquad (16)$$

then, by eliminating the arbitrary constants, we arrive at equations for the periods which are analogous to Eqs. (30) of [3]:

$$\sigma_q(t_1, t_2, \ldots, t_h) = \sigma_{q\,\text{giv}} \qquad (q = 1, 2, \ldots, h). \qquad (17)$$

where $t_1, \ldots, t_h$ are the moments of switching.

If the times t_i are found, it is then easy to find y(t), y'(t), . . . , $y^{(n-1)}(t)$, after which, using (6), all the $x_i(t)$ are found. If Eq. (13) were used as the derived equation then, after finding the periodic solution $\sigma(t)$, the quantities $x_i(t)$ could only be found by integrating the corresponding system of linear inhomogeneous equations obtained from (1) by setting $\sigma = \sigma(t)$.

What has been presented here may also be used for finding the forced oscillations of system (1) for the case of piecewise-linear characteristics.

APPENDIX

Derivation of the Basic Formulas

For simplicity, we shall assume that the roots of equation $D(\lambda) = 0$: $\lambda = \lambda_\rho$ ($\rho = 1, 2, \ldots, n$) are simple, and also that, for each ρ, an m is found such that

$$H_m(\lambda_\rho) \neq 0.$$

Then, by introducing new variables z_ρ by the formulas

$$x_k = \sum_{\rho=1}^{n} \frac{H_k(\lambda_\rho)}{D'(\lambda_\rho)} z_\rho, \quad z_\rho = \frac{1}{H_m(\lambda_\rho)} \sum_{k=1}^{m} D_{km}(\lambda_\rho)\, x_k, \qquad (18)$$

where $D_{km}(\lambda)$ is the algebraic complement of the kth row and mth column of determinant (2), we take system (1) to the canonical form of A. I. Lur'e:

$$\dot{z}_\rho = \lambda_\rho z_\rho + f(\sigma), \quad \sigma = \sum_{\rho=1}^{m} \frac{M(\lambda_\rho)}{D'(\lambda_\rho)} z_\rho. \qquad (19)$$

On the other hand, system (5) also reduces to the form of (19) by means of the transformation:

$$z_\rho = \sum_{\alpha=1}^{n} B_{\alpha n}(\lambda_\rho)\, y^{(n-\alpha)}, \quad y^{(n-\alpha)} = \sum_{\rho=1}^{n} \frac{\lambda_\rho^{n-\alpha}}{D'(\lambda_\rho)} z_\rho, \tag{20}$$

where the $B_{\alpha n}(\lambda)$ are polynomials of the form

$$B_{1n} = 1, \quad B_{2n} = f_1 + \lambda,$$
$$B_{3n} = (f_1 + \lambda)\lambda + f_2, \ldots, B_{kn}\lambda = B_{k-1,\,n}\lambda + f_{k-1}. \tag{21}$$

By taking (18), (20), (21), and (3) into account, we can get

$$x_k = \sum_{l-1}^{n} p_{k\alpha} y^{(n-\alpha)}, \tag{22}$$

where the numbers $p_{k\alpha}$ are written in the form

$$p_{k\alpha} = \sum_{l=1}^{n} h_{kl}\pi_{l\alpha}, \tag{23}$$

where

$$\pi_{ls} = \sigma_{n-l+s-1} + f_1\sigma_{n-l+s-2} + \cdots + f_{s-1}\sigma_{n-l}$$
$$(1 \leqslant l \leqslant n,\ 1 \leqslant s \leqslant n), \tag{24}$$

and the quantities σ_k are defined by the relationships

$$\sigma_k = \sum_{\rho=1}^{n} \frac{\lambda_\rho^k}{D'(\lambda_\rho)}. \tag{25}$$

By taking into consideration the well-known equations for sums of the form of (25) [2]

$$\sigma_k = 0 \quad (k = 0, 1, \ldots, n-2),$$
$$\sigma_{n-1} = 1, \tag{26}$$

we obtain

$$\pi_{ls} = \begin{cases} 0 & \text{for} \quad l > s, \\ 1 & \text{for} \quad l = s. \end{cases} \tag{27}$$

Now, let $s \geq l + 1$. Then by virtue of (26) we have

$$f_{s-2}\sigma_{n-l-1} + \cdots + f_n\sigma_{s-l-1} = 0.$$

If we add this to (24), we find that

$$\pi_{ls} = \sigma_{n-l+s-1} + f_1\sigma_{n-l+s-2} + \cdots + f_n\sigma_{s-l-1}.$$

If we now take the identity

$$\frac{\lambda_\rho^{s-l-1}}{D'(\lambda_\rho)} D(\lambda_\rho) \equiv 0$$

and sum over all ρ, we get

$$\pi_{ls} = 0 \quad \text{for} \quad s > l. \tag{28}$$

We obtain (6) from (22), (23), (27), and (28). Formulas (9) can be obtained directly by solving system (6) for y, y', . . . , $y^{(n-1)}$ and then carrying out certain simplifications. Relationships (10) are obtained in the following way. From (18) and (20) we have that

$$m_{k\alpha} = \sum_{\alpha=1}^{n} \frac{\lambda_\rho^{n-k} D_{\alpha m}(\lambda_\rho)}{D'(\lambda_\rho) H_m(\lambda_\rho)}. \tag{29}$$

We set up the sum

$$\sum_{\alpha=1}^{n} b_{\alpha s} m_{k\alpha} = \sum_{\alpha=1}^{n}\sum_{\rho=1}^{n} \frac{\lambda_\rho^{n-k} b_{\alpha s} D_{\alpha m}(\lambda_\rho)}{D'(\lambda_\rho) H_m(\lambda_\rho)}.$$

By reversing the order of summation and by taking into account the equation [5]

$$\sum_{\alpha=1}^{n} b_{\alpha\beta} D_{\alpha\gamma}(\lambda_\rho) = \lambda_\rho D_{\beta\gamma}(\lambda_\rho),$$

we obtain (10).

LITERATURE CITED

[1] M. A. Aizerman and F. R. Gantmakher, "On the determination of the periodic modes in nonlinear dynamic systems with piecewise-linear characteristics," Prikl. Matem. i Mekh. 5 (1956).

[2] A. I. Lur'e, Operational Calculus [in Russian] (Gostekhizdat, 1951).

[3] L. A. Gusev, "The determination of the periodic modes in automatic control systems which contain nonlinear elements with piecewise-linear characteristics," Avtomat. i Telemekh. 19, 10 (1958).*

[4] M. A. Aizerman, Lectures on Automatic Control Theory [in Russian] (Fizmatgiz, 1958).

[5] A. I. Lur'e, Some Nonlinear Problems of Automatic Control Theory [in Russian] (Gostekhizdat, 1951).

---

* See English translation.

THE RELATIONSHIP BETWEEN LINEAR SYSTEMS' TRANSIENT RESPONSES AND THEIR LAPLACE TRANSFORMS

N. S. Kochanov

(Leningrad)

(Translated from: Avtomatika i Telemekhanika, Vol. 21, No. 1, pp. 20-28, January, 1960)
Original article submitted April 23, 1959

Methods are considered for the determination of discrete values of a linear system's transient response from its given Laplace transform, and for finding the Laplace transform from equally spaced given values of the transient response. These methods do not require that the roots of algebraic equations be computed.

Posing of the Problem

In solving the problem of analyzing the transient responses in linear systems with lumped parameters, great difficulty arises because of the necessity of calculating the roots of algebraic equations in order to make the transition from the transform of a time-domain function to the time-domain function itself.

The use of the methods of calculating the transient responses from frequency characteristics in such problems involves a significant amount of computation and graphical construction.

There is thus great interest in numerical methods of calculating transient responses which would allow one, in many cases, to compute quite simply discrete values of the transient response without determining the roots of the characteristic equation, and without graphical constructions.

Among these methods are the approximate operator method of G. S. Pospelov [1] and the similar methods discussed in the foreign literature [2, 3].

The practical use of these methods is significantly limited by the fact that, to obtain sufficiently high accuracy of the computations, one must choose a small discrete step, which leads to a corresponding increase in the amount of computational work, since the computations are carried out with constant steps.

With this, to determine discrete values of transient responses, one must carry out the expansion of several fractions in series.

The distinguishing features of the method proposed in the present work are the use of recursion formulas for the computations, and the use of a method for doubling the discrete step.

In the solution of the problem of synthesizing linear systems with lumped constants, the first question that arises is the determination of the transform of a given function of time. With this, due to the condition of physical realizability of such systems, the transform sought must be a rational fraction.

Thus, the second task of the present paper is the finding of methods for the determination of the Laplace transforms of functions of time in the form of exponential polynomials which approximate the given time-domain characteristics.

Transforms of Transient Responses

We shall consider impulsive responses, or regular parts of transient responses, which provide Laplace transforms in the form of rational fractions

$$\overline{F}(p) = \frac{b_0 p^{n-1} + b_1 p^{n-2} + \cdots + b_{n-1}}{p^n + a_1 p^{n-1} + a_2 p^{n-2} + \cdots + a_n}. \qquad (1)$$

The expansion of these fractions in negative powers of p will have the form:

$$\overline{F}(p) = \frac{s_0}{p} + \frac{s_1}{p^2} + \frac{s_2}{p^3} + \cdots + \frac{s_k}{p^{k+1}} + \cdots \qquad (2)$$

The coefficients s_k, which are the initial values of the function F(t) and its derivatives, satisfy the recursion relationship

$$s_{n+i} + a_1 s_{n-1+i} + a_2 s_{n-2+i} + \cdots + a_n s_i = 0$$

$$(i = 0, 1, 2, \ldots). \qquad (3)$$

This relationship is obtained from the equation

$$p^n + a_1 p^{n-1} + a_2 p^{n-2} + \ldots + a_n = 0 \qquad (4)$$

by using the following systems of correspondences:

$$1 = p^0 \to s_0, \quad p \to s_1, \quad p^2 \to s_2, \ldots, p^i \to s_i, \ldots \qquad (5)$$

If the transient response is characterized by the system of discrete values $F_0, F_1, F_2, \ldots, F_{2n-1}, \ldots$, corresponding to equally spaced values of the argument t, then one can set up the series

$$\overline{F}(m) = \frac{F_0}{m} + \frac{F_1}{m^2} + \frac{F_2}{m^3} + \cdots + \frac{F_{2n-1}}{m^{2n}} + \cdots, \qquad (6)$$

where $m = e^{p\tau}$ and τ is the discrete step.

By converting this series to a continued fraction [4], one can find a fraction which converges to this series:

$$\bar{\Phi}(m) = \frac{B_0 m^{n-1} + B_1 m^{n-2} + \cdots + B_{n-1}}{m^n + A_1 m^{n-1} + A_2 m^{n-2} + \cdots + A_n}. \quad (7)$$

The expansion of this fraction by negative powers of m will coincide with series (6) up the term F_{2n-1}/m^{2n} inclusive, if 2n terms were used in converting the series to a continued fraction.

The following terms of this expansion will give the equally-spaced values of that nth-order exponential polynomial which, at the points $F_0, F_1, F_2, \ldots, F_{2n-1}$, assumes the given values.

If the equally spaced values $F_0, F_1, F_2, \ldots, F_{2n-1}$ are values of some nth-order exponential polynomial then by expanding fraction (7) in negative powers of m, one can compute the exact values of this exponential polynomial, $F_{2n}, F_{2n+1}, F_{2n+2}, F_{2n+3}, \ldots$

For this, the equally spaced values of the function under consideration can be computed by means of the recursion formula

$$F_{n+i} + A_1 F_{n-1+i} + A_2 F_{n-2+i} + \cdots + A_n F_i = 0$$

$$(i = 0, 1, 2, 3, \ldots), \quad (8)$$

which is obtained from the equation

$$m^n + A_1 m^{n-1} + A_2 m^{n-2} + \cdots + A_n = 0 \quad (9)$$

by using the following table of correspondences:

$$m^0 \to F_0, \quad m \to F_1,$$

$$m^2 \to F_2, \ldots, m^i \to F_i, \ldots \quad (10)$$

Thus, one can solve the problem of extrapolating an exponential polynomial given 2n equally-spaced values.

This fact allows one to develop a sufficiently simple method of calculating transient responses by means of recursion formulas.

Method of Constructing a Recursion Equation for Equally Spaced Values of a Time-Domain Function

Recursion equation (8), as was mentioned, can be obtained by means of Eq. (9). The coefficients of this equation, $A_1, A_2, \ldots, A_n$, are expressed, as is well known, in terms of its roots $e^{pk\tau}$:

$$A_1 = -(e^{p_1\tau} + e^{p_2\tau} + \cdots + e^{p_n\tau}),$$
$$A_2 = [e^{(p_1+p_2)\tau} + e^{(p_1+p_3)\tau} + \cdots + e^{(p_{n-1}+p_n)\tau}],$$
$$\cdots\cdots\cdots\cdots\cdots$$
$$A_n = (-1)^n e^{(p_1+p_2+\cdots+p_n)\tau}.$$

It follows from this that coefficient A_n of this equation can be exactly determined by coefficient a_1 of Eq. (4):

$$A_n = e^{-a_1\tau}.$$

However, the other coefficient cannot be determined in such fashion. For their computation, therefore, we use an approximate method.

If we express the relationship between parameters p and m in the form of an approximate formula

$$p \approx \frac{2}{\tau} \frac{m-1}{m+1},$$

then, after substituting this relationship in Eq. (4), we can obtain an Eq. (9) which is valid for sufficiently small τ.

To increase the size of the discrete step, we transform this equation. The coefficients of Eq. (9) are combinations of the roots $e^{pk\tau}$. By setting up the analogous combinations of the squares of these roots, $e^{2pk\tau}$, we obtain an equation with a double step.

The coefficients of the new, transformed equation are set up by the method, known in algebra, which was employed by N. I. Lobachevskii for solving algebraic equations of high degree:

$$\begin{aligned} A_1^{(1)} &= A_1^2 - 2A_2, \\ A_2^{(1)} &= A_2^2 - 2A_1A_3 + 2A_4, \\ &\cdots\cdots\cdots\cdots \\ A_{n-1}^{(1)} &= A_{n-1}^2 - 2A_{n-2}A_n, \\ A_n^{(1)} &= A_n^2. \end{aligned} \quad (11)$$

We thus obtain the equation for the double step

$$m^{2n} + A_1^{(1)} m^{2n-2} + A_2^{(1)} m^{2n-4} + \cdots + A_n^{(1)} = 0.$$

From this, the recursion formula follows

$$F_{2n+i} + A_1^{(1)} F_{2n-2+i} +$$

$$+ A_2^{(1)} F_{2n-4+i} + \cdots + A_n^{(1)} F_i = 0.$$

By using this method of doubling the step several times, we can increase the discrete step by factor of 4, 8, 16, etc., without decreasing the accuracy of the recursion formula.

With this, the given method can be applied both at the beginning and during the course of the computation of the transient characteristics, thus allowing, on the one hand, a sufficient accuracy of the recursion formula to be obtained and, on the other hand, a significant reduction in the amount of computational work to be realized.

The initial equally spaced values of the time-domain function sought, these being necessary for the use of recursion formulas, may be first of all computed by means of the series

$$F(t) = s_0 + s_1 t + s_2 \frac{t^2}{2!} + s_3 \frac{t^3}{3!} + \cdots,$$

which is obtained by expanding the given function in negative powers of p. With this, in order to simplify the computations, one can use equispaced function values for both positive and negative t, i.e., compute F(τ) and F(−τ), F(2τ), and F(−2τ), etc.

Example of the Computation of Transient Responses

We illustrate the method of computing transient responses by the example of an electrohydraulic servo system acted on by a unit step function.*

In this case, the Laplace transform of the function has the form:

$$\overline{F}(p) = \frac{0.0035\,p^2 + 0.37\,p + 9.5}{p\,[p^4 + 103\,p^3 + 3065\,p^2 + 149250\,p + 1081500]}$$

By separating the pole of the function for p = 0, we get

$$\overline{F}(p) = \frac{1}{1081500}\left\{\frac{9.5}{p} - \overline{F}_1(p)\right\},$$

where

$$\overline{F}_1(p) = \frac{9.5\,p^3 + 978.5\,p^2 + 25332.25\,p + 1017720}{p^4 + 103\,p^3 + 3065\,p^2 + 149250\,p + 1081500}.$$

The computation of the curve of the transient response will be carried out for the function $\overline{F}_1(p)$. If, in the system's characteristic equation

$$p^4 + 103\,p^3 + 3065\,p^2 + 149250\,p + 1081500 = 0$$

we make the substitution

$$p = \frac{2}{\tau}\,\frac{m-1}{m+1},$$

then, for the step τ = 0.005, we shall have

$$m^4 - 3.5263\,m^3 + 4.6615\,m^2 - 2.7283\,m + 0.5937 = 0.$$

By employing the method of doubling the step, we get

$$m^8 - 3.1118\,m^6 + 3.6754\,m^4 - 1.9086\,m^2 + 0.3525 = 0.$$

Thus, the recursion formula for the step τ = 0.01 will have the form:

$$F_{4+i} =$$

$$= 3.1118\,F_{3+i} - 3.6754\,F_{2+i} + 1.9086\,F_{1+i} - 0.3525\,F_i.$$

We determine the initial values of the function sought by means of the series

$$F_1(t) = 9.5 - 1892.5\,t^2 - 1712\,t^3 + 11221\,t^4.$$

We have $F_0 = 9.500$, $F_1 = 9.309$, $F_2 = 8.731$, and $F_3 = 7.760$. Further computations are carried out then by means of the recursion formulas for the step τ = 0.01 and also for 2τ = 0.02 and 4τ = 0.04:

$$F_{2(4+i)} = 2.3325\,F_{2(3+i)} - 2.3352\,F_{2(2+i)} + \\ + 1.0516\,F_{2(1+i)} - 0.1243\,F_{2i},$$

$$F_{4(4+i)} = 0.770\,F_{4(3+i)} - 0.796\,F_{4(2+i)} + \\ + 0.525\,F_{4(1+i)} - 0.0155\,F_{4i}.$$

The results of these computations are given in the table.

The values obtained are close to the values computed by other methods (cf. the graph on page 50 of the book by V. V. Solodovnikov et al., Frequency Methods of Constructing Transient Responses using Tables and Nomograms.) This accuracy can be increased if the initial discrete step is decreased.

This example shows the efficacy of the method of doubling the step since, for computing this same curve of the transient response with about the same accuracy using the other approximate methods cited at the beginning of this paper, a significantly greater number of points would have to be computed.

Method of Determining the Denominator of the Transform of an Approximating Function

We now pose the problem of determining the Laplace transform of an exponential polynomial used to approximate a given time-domain characteristic of a system.

The first step in the solution of this problem will be the determination of the denominator of the fraction expressing the transform being sought.

Let the given time-domain characteristic be approximated by an exponential polynomial for 2n equally spaced interpolation points. Then, function (7) can be found for the given equispaced values of the time-domain characteristic. Using this function, we can determine any number of equally spaced values of the exponential nth-order polynomial which assumes the given values at the selected interpolation points.

It is necessary for this that the function found be expanded in negative powers of m, or that recursion formula (8) be employed.

These equally spaced values can be used for the determination of the coefficients of the system's characteristic equation

$$p^n + a_1 p^{n-1} + a_2 p^{n-2} + \cdots + a_n = 0.$$

---

* This example was borrowed from the book by V. V. Solodovnikov, Yu. I. Topcheev, and G. V. Krutikova, Frequency Methods of Constructing Transient Responses using Tables and Nomograms [in Russian] (Gostekhizdat, 1955).

Table of Values of the Function F(t), Computed from the Formula

$$F(t) = \frac{1}{1081500}\,(9.5 - F_1(t))$$

t	0.00	0.01	0.02	0.03	0.04	0.05	0.06	0.08	0.10
$F(t)\cdot 10^6$	0.000	0.177	0.711	1.608	2.752	4.010	5.232	7.189	8.016
t	0.12	0.16	0.20	0.24	0.28	0.32	0.36	0.40	0.44
$F(t)\cdot 10^6$	7.733	6.236	6.918	8.858	8.998	7.956	8.419	8.978	9.086

If we use approximate formulas for the relationship between the parameters m and p which give convergent fractions for the logarithm, for example,

$$p \approx \frac{2}{\tau}\frac{m-1}{m+1},\quad p \approx \frac{3}{\tau}\frac{m^2-1}{m^2+4m+1},$$

$$p \approx \frac{4}{\tau}\frac{(m-1)(m^2+4m+1)}{(m+1)(m^2+10m+1)},$$

and substitute them in the sought system's characteristic equation, we then obtain, after some transformations,

$$m^n + A_1^* m^{n-1} + A_2^* m^{n-2} +$$

$$+ \cdots + A_{n-1}^* m + A_n^* = 0,$$

or

$$m^{2n} + D_1 m^{2n-1} + D_2 m^{2n-2} +$$

$$+ \cdots + D_{2n-1} m + D_{2n} = 0,$$

or

$$m^{3n} + G_1 m_{3n-1} + G_2 m^{3n-2} +$$

$$+ \cdots + G_{3n-1} m + G_{3n} = 0.$$

By using these equations and the table of correspondences given in (10), we can set up the recursion relationships connecting a definite number of equipspaced values of the exponential polynomial sought. Thus, we can obtain

$$F_{n+i} + A_1^* F_{n-1+i} + A_2^* F_{n-2+i} +$$

$$+ \cdots + A_{n-1}^* F_{1+i} + A_n^* F_i = 0,$$

or

$$F_{2n+i} + D_1 F_{2n-1+i} + D_2 F_{2n-2+i} +$$

$$+ \cdots + D_{2n-1} F_{1+i} + D_{2n} F_i = 0,$$

or

$$F_{3n+i} + G_1 F_{3n-1+i} + G_2 F_{3n-2+i} +$$

$$+ \cdots + F_{3n-1} F_{1+i} + G_{3n} F_i = 0.$$

By means of these recursion formulas, one can determine the unknowns $a_2, a_3, \ldots, a_n$ which enter into the coefficients $A_k^* \mid D_k, G_k \mid$. We note that coefficient a_1 equals

$$a_1 = -\frac{1}{\tau}\ln|A_n|.$$

For example, for the interpolation of a given time-domain characteristic, let there be used a second-order exponential polynomial which is defined by the four equispaced values F_0, F_1, F_2, and F_3. Then, the function $\overline{\Phi}(m)$ will have the form:

$$\overline{\Phi}(m) = \frac{B_0 m + B_1}{m^2 + A_1 m + A_2}.$$

By means of this function, we can determine F_4, F_5, etc. Then, for the determination of the coefficients of the second-order characteristic equation

$$p^2 + a_1 p + a_2 = 0$$

by using the approximate equality

$$p \approx \frac{3}{\tau}\frac{m^2-1}{m^2+4m+1}$$

we obtain the following equation:

$$\frac{9}{\tau^2}(F_{4+i} - 2F_{2+i} + F_i) +$$

$$+ a_1\frac{3}{\tau}(F_{4+i} + 4F_{3+i} - 4F_{1+i} - F_i) +$$

$$+ a_2(F_{4+i} + 8F_{3+i} + 18F_{2+i} + 8F_{1+i} + F_i) = 0,$$

where

$$a_2 = -\frac{1}{\tau}\ln|A_2|.$$

For characteristic equations of higher order, the coefficients are determined from a system of linear equations.

Method of Determining the Numerator of the Transform

The determination of the transform's numerator can be carried out by means of series whose coefficients are the initial values of the approximating function sought and its derivatives, or by the initial moments of this function.

We consider the series obtain by expanding the function $m\overline{\Phi}(m)$ in negative powers of m:

$$m\overline{\Phi}(m) =$$

$$= F_0 + \frac{F_1}{m} + \frac{F_2}{m^2} + \cdots + \frac{F_{2n-1}}{m^{2n-1}} + \frac{F_{2n}}{m^{2n}} + \cdots$$

The coefficients of this series are equispaced values of the exponential polynomial being sought.

If we expand the function $m^{-k} = e^{kp\tau}$ in a series and regroup terms, we get

$$\tau e^{p\tau}\overline{\Phi}(e^{p\tau}) =$$

$$= \left(F_0 + \sum_{i=1}^{\infty} F_i\right)\tau - p\sum_{i=1}^{\infty} i\tau^2 F_i + \frac{p^2}{2!}\sum_{i=1}^{\infty} i^2\tau^3 F_i - \cdots =$$

$$= \tau c_0 - pm_1 + \frac{p^2}{2!}m_2 - \frac{p^3}{3!}m_3 + \cdots$$

Here, m_1, m_2, and m_3 are the initial moments of the function.

It is easily seen that the sums entering into the given expansion are approximate expressions for the initial moments as defined by the trapezoidal quadrature formula.

Thus, we shall have

$$\overline{F}(p) \approx \tau\left(c_0 - \frac{F_0}{2}\right) - pm_1 + \frac{p^2}{2!}m_2 - \frac{p^3}{3!}m_3 + \cdots$$

An analogous representation can be obtained by first carrying out an expansion of the functions $e^{kp\tau}$ in the numerator and denominator of the fraction for $m\overline{\Phi}(m)$ and the expanding this fraction in positive powers of p, i.e.,

$$\tau e^{p\tau}\overline{\Phi}(e^{p\tau}) = \tau\frac{(B_0 + B_1 + \cdots + B_{n-1}) - p\tau[nB_0 + (n-1)B_1 + \cdots + B_{n-1}] + \cdots}{(1 + A_1 + \cdots + A_n) - p\tau[n + (n-1)A_1 + \cdots + A_{n-1}] + \cdots} =$$

$$= \tau c_0 - pm_1 + \frac{p^2}{2!}m_2 - \frac{p^3}{3!}m_3 + \cdots$$

It should be mentioned that the accuracy of the computations of the initial moments by such a method is higher, the higher the order of the moment.

While this assertion can be rigorously proven, it is better to illustrate it by a simple example.

Let it be required to determine the initial moments of the function e^{-t}. For this purpose, we expand the transform of the function in positive powers of p:

$$\frac{1}{p+1} = 1 - p + p^2 - p^3 + p^4 - \cdots$$

We now consider the interpolation of the given function by two points, t = 0 and t = 1. The function $\tau m\overline{\Phi}(m)$ will then have the form

$$\frac{m\tau}{m - 0.36788} = \frac{\tau e^{p\tau}}{e^{p\tau} - 0.36788}.$$

If we expand this function in positive powers of p we get

$$\tau e^{p\tau}\overline{\Phi}(e^{p\tau}) = 1.58198 - 0.92068p + 0.99615p^2 -$$

$$- 1.00108p^3 + 1.00012p^4 - \ldots \quad (\tau = 1).$$

By comparing the coefficients of the two expansions we easily see that the accuracy in the determination of the moments rapidly increases with increasing order of the moment, even for a significantly large discrete step.†

To determine the exact values of the lower-order moments, we can find an approximating fraction for the segment of the series whose coefficients are accurately defined, and expand this fraction in decreasing powers of p. By extending the expansion of this fraction, we can find the initial values of the function sought, plus those of its derivatives.

The method given permits the determination, with very high accuracy, of both the numerator and denominator of the first fraction expressing the transform of the approximating function sought.

To determine the fraction which approximates a segment of a series, one can also use the denominator of the fraction obtained by the method of the previous paragraph.

Thus, one can obtain the series

$$\overline{F}(p) = m_0 - m_1 p + m_2\frac{p^2}{2!} - m_3\frac{p^3}{3!} + \cdots$$

---

† The initial moments are proportional to the corresponding coefficients of the series.

The coefficients of the numerator of the Laplace transform are determined from the coefficients of this series:

$$b_{n-1} = a_n m_0,$$
$$b_{n-2} = -a_n m_1 + a_{n-1} m_0,$$
$$b_{n-3} = a_n \frac{m_2}{2!} - a_{n-1} m_1 + a_{n-2} m_0,$$
$$\cdots\cdots\cdots\cdots$$

Example. Let it be required to determine the Laplace transform for the exponential polynomial which is characterized by the values

$$F_0 = 0, \quad F_1 = 1, \quad F_2 = 1, \quad F_3 = 0.75 \quad \text{for} \quad \tau = 1.$$

Solution. For the given equispaced values, we construct the series

$$\overline{F}_1(m) = \frac{1}{m^2} + \frac{1}{m^3} + \frac{0.75}{m^4} + \cdots,$$

for which we determine the approximating second-order fraction:

$$\overline{\Phi}(m) = \frac{1}{m^2 - m + 0.25}.$$

By using the method presented earlier, we find the denominator of the transform, in the form

$$Q(p) = p^2 + 1.3863\,p + 0.4793.$$

To determine the numerator of the transform, we use the expansion

$$\frac{e^p}{0.25 - e^p + e^{2p}} =$$

$$= 4 - 12\,p + 26\,p^2 - 50\,p^3 + 90.167\,p^4 - 156.1\,p^5 + \cdots,$$

by means of which we find the zeroth-order initial moment: $m_0 = 4.18$.

The final solution of the problem is the expression

$$\overline{F}(p) = \frac{2.0034}{p^2 + 1.3863\,p + 0.4793}.$$

The exact transform of the initial function has the form:

$$\overline{F}(p) = \frac{2}{p^2 + 1.3863p + 0.4804} \rightarrow 2te^{-0{,}6931t}.$$

In conclusion, we note that this same problem could be solved by computing moments of sufficiently high order.

In particular, by using the moments of second, third, fourth, and fifth order, we get

$$\overline{F}(p) = \frac{2.0025}{p^2 + 1.3836\,p + 0.47907}.$$

CONCLUSION

1. The possibility was demonstrated of calculating transient responses by means of recursion formulas obtained on the basis of an approximate formula for the differentiation operator and the application of the method of doubling the discrete step.

The method of calculating transient responses presented here is highly accurate.

2. A method was presented of determining the Laplace transform corresponding to an exponential polynomial by interpolating the given time-domain characteristic for equally spaced points. This method can be used for finding the Laplace transforms of functions which are given graphically.

LITERATURE CITED

[1] G. S. Pospelov, Fundamentals of Automation [in Russian] (Izd. Zhukovskii VVIA, 1954).

[2] R. Boxer and S. Thaler, "A simplified method of solving linear and nonlinear systems," Proc. I.R.E. No. 1, (1956).

[3] R. Boxer, "A note on numerical transform calculus, Proc. I.R.E. No. 10 (1957).

[4] A. A. Markov, "Lectures on continued fractions," in: Collected Works on the Theory of Continued Fractions and the Theory of Functions Deviating Least from Zero [in Russian] (Gostekhizdat, 1948).

A GENERATOR OF RANDOM PROCESSES FROM THEIR GIVEN SPECTRAL DENSITY MATRICES

I. Matyash and Ya. Shilkhanek

(Pardubitse, Czechoslovakia)

(Translated from: Avtomatika i Telemekhanika, Vol. 21, No. 1, pp. 29-35, January, 1960)
Original article submitted July 20, 1959

A method is described for constructing a generator of n stationary random processes with arbitrary matrices of rational spectral densities, using a minimal number of uncorrelated white noise generators and stable linear filters. The transfer functions of these filters are determined by a very simple method from the given spectral densities. The method is illustrated by an example for the case when n = 3.

Analog computers are frequently used for the analysis and synthesis of automatic control and regulation systems which are acted upon by random functions of time. For this, the inputs to the computer must be random functions which correspond to the input random functions of the actual system.

In this paper we shall consider only stationary random functions (processes) whose proper and mutual spectral densities are rational-fractional functions of the variable $s = j\omega$. In practice it is necessary to replace the experimentally determined spectral densities by approximating rational functions. Methods of implementing such approximations are described in the literature (cf., for example, [1, 2]).

To study actual systems by means of analog computers (modeling devices), it is necessary to generate random processes with given spectral densities. The generation of one stationary random process with a given proper spectral density is described, for example, in [2]. In [3] a method is given for reproducing two processes with given proper and mutual spectral densities. However, with this method one can obtain two random processes with given spectral densities only in special cases

In the present paper we present a general method for generating any number n of stationary random processes with arbitrary proper and mutual spectral densities.

Generation of One Random Process

The generator's block schematic (cf. [2]) is shown in Fig. 1, where Q_1 is a white noise generator (a process with unit spectral density) and F_{11} is a filter with transfer function $Y_{11}(s)$.

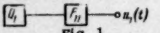

Fig. 1.

The condition that the output signal $u_1(t)$ be a process with the given density ${}^1G_{11}(s)$ is written in the form

$$ {}^1G_{11}(s) = Y_{11}(s)\, Y_{11}(-s). \qquad (1)$$

Since ${}^1G_{11}(s)$ is a spectral density, there exists just one function $A_1(s)$ which does not have poles and zeros in the right half-plane and such that the following equation holds

$$A_1(s)\, A_1(-s) = {}^1G_{11}(s) \qquad (2)$$

(cf. [1, 2, 4]). By comparing this with (1), we obtain the well-known result (cf. [2])

$$Y_{11}(s) = A_1(s), \qquad (3)$$

wherein $Y_{11}(s)$ is the transfer function of a stable linear filter with minimal phase.

For the generation of several processes, it is sometimes necessary to construct a filter with nonminimal phase. If we connect in series with the filter whose transfer function is $A_1(s)$ a filter which varies only in phase, and whose transfer function has the form:

$$H_1(s) = \frac{f(s)}{f(-s)}, \qquad (4)$$

where f(s) is a polynomial then, obviously, the following relationship holds

$$|H_1(s)|^2 = H_1(s)\, H_1(-s) = 1, \qquad (5)$$

i.e., the spectral density of the output process is not changed.

Thus, the transfer function $Y_{11}(s)$ of filter F_{11} can be written in the general form:

$$Y_{11}(s) = A_1(s)\, H_1(s), \qquad (6)$$

where $H_1(s)$ is any function of the form of (4) such that the function $A_1(s)H_1(s)$ is the transfer function of a stable filter.

Generation of n Random Processes

Spectral densities of the random processes. We shall denote by ${}^1G_{ik}(s)$ (i, k = 1, 2, . . . , n) the given proper and mutual spectral densities of the random processes $u_1(t)$, $u_2(t)$, . . . , $u_n(t)$. The functions ${}^1G_{ik}(s)$ denote the mutual spectral density of the processes $u_i(t)$ and $u_k(t)$. The functions ${}^1G_{ik}(s)$ form the matrix of spectral densities $\| {}^1G_{ik}(s) \|$ (i, k = 1, 2, . . . , n) [5].

From the self-evident relationship

$$ {}^1G_{ki}(s) = {}^1G_{ik}(-s) \qquad (s = j\omega) \qquad (7) $$

we obtain

$$ {}^1G_{ki}(s) = {}^1G^{*}_{ik}(s), \qquad (8) $$

where the symbol $*$ denotes the complex conjugate quantity. Consequently, the spectral density matrix $\|{}^1G_{ik}(s)\|$ is a Hermitian matrix. It is completely defined by its $n(n+1)/2$ elements ${}^1G_{ik}(s)$ ($i = 1, 2, \ldots, n$; $k = 1, i+1, \ldots, n$).

The Appendix describes several properties of the spectral density matrix which are used in this paper.

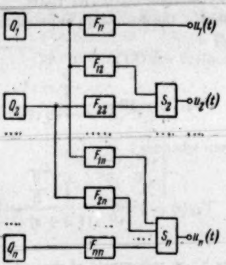

Fig. 2.

Block schematic of the generator. The block schematic of the generator of n random processes is shown in Fig. 2. It consists of n uncorrelated (for example, statistically independent) white noise generators $Q_1, Q_2, \ldots, Q_n$ (generators of uncorrelated processes with unit spectral densities), $n(n+1)/2$ stable linear filters F_{ik} ($i = 1, 2, \ldots, n$; $k = i, i+1, \ldots, n$) with transfer functions $Y_{ik}(s)$ and $n-1$ adders S_k ($k = 2, 3, \ldots, n$). Process $u_1(t)$ is found at the output of filter F_{11}, while process $u_k(t)$ ($k = 2, 3, \ldots, n$) is found at the output of adder S_k.

In order that the generator's output signals $u_1(t)$, $u_2(t), \ldots, u_n(t)$ be the processes with the given spectral density matrix $\|{}^1G_{ik}(s)\|$ ($i, k = 1, 2, \ldots n$), it is necessary (cf., for example, [6]) that the following conditions hold:

$$
\begin{aligned}
&{}^1G_{11}(s) = Y_{11}(s)\,Y_{11}(-s),\\
&{}^1G_{12}(s) = Y_{12}(s)\,Y_{11}(-s),\\
&{}^1G_{22}(s) = Y_{12}(s)\,Y_{12}(-s) + Y_{22}(s)\,Y_{22}(-s),\\
&\ldots\ldots\ldots\ldots\ldots\ldots\ldots\ldots
\end{aligned}
$$

i.e., in general,

$$ {}^1G_{ik}(s) = \sum_{j=1}^{i} Y_{jk}(s)\,Y_{ji}(-s) $$

$$ \begin{pmatrix} i = 1, 2, \ldots, n \\ k = i, i+1, \ldots, n \end{pmatrix}. \qquad (9) $$

The problem thus reduces to determining the transfer functions $Y_{ik}(s)$ of the stable linear filters F_{ik} ($i = 1, 2, \ldots, n$; $k = i, i+1, \ldots, n$) such that system of equation (9) holds.

Determination of the transfer functions $Y_{ik}(s)$. From (9), by setting $i = 1$, we obtain

$$ {}^1G_{1k}(s) = Y_{1k}(s)\,Y_{11}(-s) \quad (k = 1, 2, \ldots, n). \qquad (10) $$

For $k = 1$, Eq. (10) is identical with (1). Consequently, in accordance with formula (6),

$$ Y_{11}(s) = A_1(s)\,H_1(s). \qquad (11) $$

By using (10), we find the functions $Y_{1k}(s)$ in the form

$$ Y_{1k}(s) = \frac{{}^1G_{1k}(s)}{A_1(-s)}\,H_1(s) \qquad (k = 1, 2, \ldots, n). \qquad (12) $$

The function $H_1(s)$, of the form given in (4), is such that all the $Y_{1k}(s)$ ($k = 1, 2, \ldots, n$) are transfer functions of stable filters. We obtain a function $H_1(s)$ of the least degree if, for the null points of $H_1(s)$ [the roots of the polynomial $f(s)$], we choose the set of poles in the right half-plane of the expressions ${}^1G_{1k}(s)/A_1(-s)$ (each pole being chosen with the maximum multiplicity in these expressions). This completely determines the function $H_1(s)$ [cf. (4)].

To compute the transfer functions $Y_{ik}(s)$ ($i > 1$), we define the auxiliary functions ${}^{r+1}G_{ik}(s)$ ($r = 1, 2, \ldots, n-1$) by the formula

$$ {}^{r+1}G_{ik}(s) = {}^1G_{ik}(s) - \sum_{j=1}^{r} Y_{jk}(s)\,Y_{ji}(-s) $$

$$ \begin{pmatrix} i = r+1, \ldots, n \\ k = i, \ldots, n \end{pmatrix}. \qquad (13) $$

These functions obviously satisfy the recursion relationship

$$ {}^{r+1}G_{ik}(s) = {}^rG_{ik}(s) - Y_{rk}(s)\,Y_{ri}(-s). \qquad (14) $$

After substituting (13) in (9) we obtain, for $r + 1 = i$,

$$ {}^iG_{ik}(s) = Y_{ik}(s)\,Y_{ii}(-s) $$

$$ (k = i, i+1, \ldots, n). \qquad (15) $$

For $k = i$ we obtain from this

$$ {}^iG_{ii}(s) = Y_{ii}(s)\,Y_{ii}(-s). \qquad (16) $$

If follows from (16) that the function ${}^1G_{ii}(s)$ ($i = 2, 3, \ldots, n$) must be real and nonnegative:

$$ {}^iG_{ii}(s) \geqslant 0 \qquad \begin{pmatrix} s = j\omega \\ i = 2, 3, \ldots, n \end{pmatrix}. \qquad (17) $$

It is proven in the Appendix that conditions (17) are met if the functions ${}^1G_{ik}(s)$ form a spectral density matrix.

Since formula (16) has the form of (1), we define the functions $Y_{ii}(s)$ in accordance with formula (6) by the method described earlier:

$$Y_{ii}(s) = A_i(s)\, H_i(s)\,, \tag{18}$$

where the functions $A_i(s)$ are defined by the equations

$$A_i(s)\, A_i(-s) = {}^iG_{ii}(s) \tag{19}$$

just as $A_1(s)$ of (2), and the $H_i(s)$ are as yet undetermined functions of the form of (4).

By substituting (18) in (15), we get

$$Y_{ik}(s) = \frac{{}^iG_{ik}(s)}{A_i(-s)} H_i(s)$$

$$\begin{pmatrix} i = 1, 2, \ldots, n \\ k = i, i+1, \ldots, n \end{pmatrix}. \tag{20}$$

The functions $H_i(s)$ are defined by the conditions that all the $Y_{ik}(s)$ ($k = i, i+1, \ldots, n$) be the transfer functions of stable filters [analogously to the function $H_1(s)$].

Formulas (20) define all the transfer functions $Y_{ik}(s)$ ($i = 1, 2, \ldots, n$; $k = i, i+1, \ldots, n$). In practice, one first computes transfer functions $Y_{1k}(s)$ from the given functions ${}^1G_{1k}(s)$ ($k = 1, 2, \ldots, n$), then determines the auxiliary functions ${}^2G_{ik}(s)$ from (14), then computes from these the transfer functions $Y_{2k}(s)$ ($k = 2, 3, \ldots, n$), etc. In general, the functions ${}^{r+1}G_{ik}(s)$ are determined step by step from the ${}^rG_{ik}(s)$ by formula (14). Transfer functions $Y_{r+1,k}(s)$ are computed from these by formulas (20).

Example. As an illustration, we use the example of the generator of three random processes whose spectral densities are given in the form

$${}^1G_{11}(s) = \frac{2 - s^2}{4 - s^2}\,, \qquad {}^1G_{12}(s) = \frac{s^2}{(3+s)(2-s)}\,,$$

$${}^1G_{13}(s) = \frac{2 - s^2}{(3+s)(2-s)}\,, \qquad {}^1G_{22}(s) = \frac{-2s^2 + 2s^4}{(2-s^2)(9-s^2)}\,,$$

$$G_{23}(s) = \frac{-2s + 2s^2}{9 - s^2}\,, \qquad {}^1G_{33}(s) = \frac{4 - 2s^2}{3 - s^2}\,.$$

It follows from (12) that

$$Y_{11}(s) = \frac{\sqrt{2} + s}{2 + s} H_1(s)\,,$$

$$Y_{12}(s) = \frac{s^2}{(3+s)(\sqrt{2} - s)} H_1(s)\,,$$

$$Y_{13}(s) = \frac{\sqrt{2} + s}{3 + s} H_1(s)\,.$$

From the stability conditions we obtain, based on what has been presented earlier,

$$H_1(s) = \frac{\sqrt{2} - s}{\sqrt{2} + s}\,.$$

By this, transfer functions $Y_{1k}(s)$ ($k = 1, 2, 3$) are completely determined.

From formula (14) we now compute the functions ${}^2G_{ik}(s)$:

$${}^2G_{22}(s) = \frac{-s^2}{9 - s^2}\,, \qquad {}^2G_{23}(s) = \frac{-2s + s^2}{9 - s^2}\,,$$

$${}^2G_{33}(s) = \frac{(2 - s^2)(15 - s^2)}{(3 - s^2)(9 - s^2)}\,.$$

From these, by (20), we obtain

$$Y_{22}(s) = \frac{s}{3 + s} H_2(s), \qquad Y_{23}(s) = \frac{2 - s}{3 + s} H_2(s).$$

Consequently, we can set $H_2(s) = 1$. This then determines functions $Y_{22}(s)$ and $Y_{23}(s)$.

Finally, the following expression for ${}^3G_{33}(s)$ follows from (14)

$${}^3G_{33}(s) = 10 \frac{\frac{9}{5} - s^2}{(3 - s^2)(9 - s^2)}\,.$$

From whence

$$Y_{33}(s) = \sqrt{10}\, \frac{\sqrt{\frac{9}{5}} + s}{(\sqrt{3} + s)(3 + s)}\,.$$

The block schematic of the generator of the three random processes desired is shown in Fig. 3.

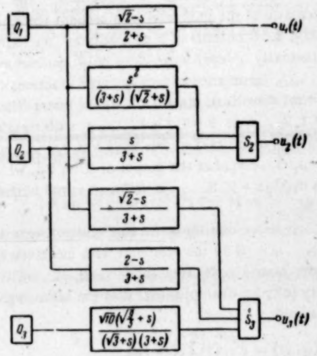

Fig. 3.

CONCLUSIONS

The method herein described for generating any number n of stationary random processes from a given matrix of rational spectral densities is a general method. It permits one to construct a generator of random processes from any matrix of rational spectral densities.

One easily convinces oneself that the generator contains the least number (n) of white noise generators Q_i and the least number ($n(n+1)/2$) of linear filters F_{ik}.

(In [3] there was described a generator of two processes which consisted of three white noise generators and three filters.)

The generator's functional schematic (Fig. 2) allows the transfer functions $Y_{ik}(s)$ of the filters F_{ik} to be computed in a very simple way from the given spectral densities [cf. formulas (20)].

APPENDIX

Certain Properties of Spectral Density Matrices

For brevity, we shall formulate these properties in the form of theorems. From these properties one can derive results which are important for the construction of the random process generators described in this paper.

Theorem 1. The functions ${}^{r+1}G_{ik}(s)$ ($i = r + 1, \ldots, n$; $k = 1, \ldots, n$) of Eq. (13) are defined by the relationships

$$
{}^{r+1}G_{ik}=\frac{\begin{vmatrix} {}^1G_{11}\ldots{}^1G_{1r}\,{}^1G_{1k} \\ \ldots\quad\ldots\quad\ldots \\ {}^1G_{r1}\ldots{}^1G_{rr}\,{}^1G_{rk} \\ {}^1G_{i1}\ldots{}^1G_{ir}\,{}^1G_{ik} \end{vmatrix}}{\Delta_r}, \tag{21}
$$

where

$$
\Delta_r=\begin{vmatrix} {}^1G_{11}\ldots{}^1G_{1r} \\ \ldots\quad\ldots\quad\ldots \\ {}^1G_{1r}\ldots{}^1G_{rr} \end{vmatrix}. \tag{22}
$$

Proof. From (14), we get that

$$
{}^{r+1}G_{ik}=\frac{\begin{vmatrix} {}^rG_{rr}\,{}^rG_{rk} \\ {}^rG_{ir}\,{}^rG_{ik} \end{vmatrix}}{{}^rG_{rr}}. \tag{23}
$$

The assertion of our theorem is proven by the method of complete induction. It follows from (23) that (21) is valid for $r = 1, 2, \ldots$ We assume that (21) is valid for all $r \leq m-1$. For $r = m$, we obtain from (23) that

$$
{}^{m+1}G_{ik}=\frac{\begin{vmatrix} {}^mG_{mm} & {}^mG_{mk} \\ {}^mG_{im} & {}^mG_{ik} \end{vmatrix}}{{}^mG_{mm}}. \tag{24}
$$

By assumption, we can assert the relationship

$$
{}^mG_{mm}=\frac{\Delta_m}{\Delta_{m-1}} \tag{25}
$$

from whence

$$
\frac{\Delta_m}{\Delta_{m-1}}\,{}^{m+1}G_{ik}=\begin{vmatrix} {}^mG_{mm} & {}^mG_{mk} \\ {}^mG_{im} & {}^mG_{ik} \end{vmatrix}. \tag{26}
$$

From Sylvester's determinant identity we get

$$
\begin{vmatrix} {}^mG_{mm}\,{}^mG_{mk} \\ {}^mG_{im}\,{}^mG_{ik} \end{vmatrix}=\frac{1}{\Delta_{m-1}}\cdot\begin{vmatrix} {}^1G_{11} & \ldots & {}^1G_{1m} & {}^1G_{1k} \\ \ldots & & \ldots & \ldots \\ {}^1G_{m1} & \ldots & {}^1G_{mm} & {}^1G_{mk} \\ {}^1G_{i1} & \ldots & {}^1G_{im} & {}^1G_{ik} \end{vmatrix}. \tag{27}
$$

By comparing (26) and (27) we immediately obtain the equation

$$
{}^{m+1}G_{ik}\,\Delta_m=\begin{vmatrix} {}^1G_{11} & \ldots & {}^1G_{1m} & {}^1G_{1k} \\ \ldots & & \ldots & \ldots \\ {}^1G_{m1} & \ldots & {}^1G_{mm} & {}^1G_{mk} \\ {}^1G_{i1} & \ldots & {}^1G_{im} & {}^1G_{ik} \end{vmatrix} \tag{28}
$$

which proves the theorem.

Corollary of Theorem 1. By virtue of (21), we have the equation

$$
{}^rG_{rr}=\frac{\Delta_r}{\Delta_{r-1}} \qquad (r=2, 3, \ldots, n). \tag{29}
$$

Consequently, conditions (17) can be written in the form

$$
\frac{\Delta_r}{\Delta_{r-1}}\geqslant 0 \qquad (r=2,3,\ldots,n). \tag{30}
$$

Theorem 2. A necessary and sufficient condition for the matrix $\| {}^1G_{ik} \|$ ($i, k = 1, \ldots, n$) to be a spectral density matrix is that it be a nonnegative Hermitian matrix.

For the proof, cf. [5] and [7].

Theorem 3. A necessary and sufficient condition that a Hermitian matrix be nonnegative is that all its principal minors be nonnegative.

For the proof, cf., for example, [8].

Theorem 4. If $\| {}^1G_{ik} \|$ ($i, k = 1, 2, \ldots, n$) is a spectral density matrix then, for any $r = 2, 3, \ldots, n$, the matrix $\| {}^rG_{ik} \|$ ($i, k = r, r + 1, \ldots, n$) [cf. (21)] is also a spectral density matrix.

Proof. The validity of the following inequality is a consequence of theorem 3:

$$
\Delta_r \geqslant 0 \qquad (r=1,2,\ldots,n). \tag{31}
$$

From Sylvester's determinant identity, one easily proves that all the principal minors of matrix $\| {}^rG_{ik} \|$ are nonnegative. We then obtain the assertion of theorem 4 by using theorems 2 and 3.*

Corollary of Theorem 4. If all the matrices $\| {}^rG_{ik} \|$ ($r = 2, 3, \ldots, n$) are spectral density matrices, then inequalities (17) and (30) hold. It suffices for this, by theorem 4, that matrix $\| {}^1G_{lk} \|$ be a spectral density matrix. It follows from this that, using the method described in this paper, one can construct a generator of random stationary processes with any arbitrary matrix of rational spectral densities.

---

* The validity of theorem 4 follows directly from (13), since it is easy to determine the random processes for which the spectral density matrix is the matrix $\| {}^rG_{ik} \|$ ($i, k = r, \ldots, n$).

LITERATURE CITED

[1] V. V. Solodovnikov, Introduction to the Statistical Dynamics of Automatic Control Systems [in Russian] (Gostekhizdat, 1952).

[2] J. H. Laning and R. H. Battin, Random Processes in Automatic Control (McGraw-Hill, N. Y., 1956).

[3] O. J. M. Smith, Feedback Control Systems (McGraw-Hill, N. Y., 1958).

[4] N. Wiener, Extrapolation, Interpolation, and Smoothing of Stationary Time Series (John Wiley & Sons, N. Y., 1949).

[5] A. M. Yaglom, "Introduction to the theory of stationary random functions," Uspekhi Mat. Nauk 7, 5 (1952).

[6] V. S. Pugachev, Theory of Random Functions and Their Application to Problems of Automatic Control [in Russian] (Gostekhizdat, 1957).

[7] H. Cramer, "On the theory of stationary random processes," Ann. Math. 41, 1 (1949).

[8] F. R. Gantmakher, Matrix Theory [in Russian] (Gostekhizdat, 1954).

[9] J. Silhanek and J. Matyas, "Generator skupiny n nahodnych procesu s predepsanymi vlastnimi a vzajemnymi spektralnimi hustotami," Ceskoslovenska patentni prihlaska cis. PV 3962-59.

ON THE STABILITY OF SERVO-CONTROLLED SYSTEMS WITH RANDOM STIMULI

P. S. Landa

(Moscow)

(Translated from: Avtomatika i Telemekhanika, Vol. 21, No. 1, pp. 36-41, January, 1960)
Original article submitted April 13, 1959

Excitation conditions are found for servo systems containing nonlinear backlash-type elements. The probability of excitation of such a system when noise is present is computed as a function of time.

Due to feedback paths, both designed and parasitic, and also to the various types of nonlinear elements, automatic control systems which are stable for small oscillations can be excited by large disturbances. Such systems with rigid excitation have, for even relatively small fluctuating stimuli, a finite probability of being excited to autooscillation during a given time interval. Therefore, the solution of the problem of computing this probability is of significant interest for the rational choice of the parameters of such systems.

The problem posed may be solved comparatively simply in the case when the object of control is an oscillatory system with one degree of freedom, and the controlling organ contains some nonlinear element, for example, backlash, dry friction, etc.

In this paper we use, as an example, the system whose block schematic is shown in Fig. 1. The dotted line denotes the additional feedback path between the controlled object's motion and the control organ in this system. The character of this feedback is defined by the coefficient β which, in general, can be complex. For simplicity we shall consider β to be real, but the method is easily generalized to the case when β takes on complex values.

We shall assume that the controlling stimulus g(t) varies very slowly in comparison with the system's natural frequency of oscillation. It may then be neglected in writing the system's equations. With this, the system under consideration, as is clear from Fig. 1, is described by the following equations:

$$\ddot{x} + 2\delta\dot{x} + \omega^2 x = kz_1 - \omega^2\zeta(t),$$
$$\dot{z} = b\varepsilon, \quad \varepsilon = \beta x - z, \; z_1 = f(z), \qquad (1)$$

where $\zeta(t) = -\omega^2\zeta_1(t)/k$ is a stationary random function with zero mean and f(z) is the backlash characteristic (Fig. 2).

We also assume that

$$b \gg \delta, \qquad (2)$$

i.e., the servo motor's time constant is small in comparison with the natural time of the controlled object.

If a = 0 (no backlash), the system becomes linear and the following conditions for oscillatory instability can easily be written for it:

$$\beta < 0, \quad k > \frac{2\delta\omega(1+\alpha^2)}{|\beta|\alpha} = k_0, \qquad (3)$$

where $\alpha = \omega/b$ (with this, the excitation is soft).

If a ≠ 0, the system becomes stable for small oscillations about the equilibrium position. However, for definite values of k, even if conditions (3) do not hold, rigid excitation of oscillations is possible in the system.

In this case, we shall find the excitation conditions and the system's steady-state oscillations in the absence of noise, and also the probability of system excitation as a function of time and of the magnitude of the noise.

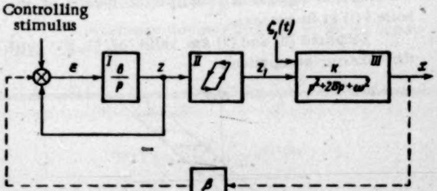

Fig. 1. Block schematic of a servo system. I is a servo motor of the hydraulic amplifier type, II is a nonlinear element of the backlash type, and III is the controlled object.

For this, we use the method presented in [1, 2], and we write the contracted equations for the amplitude and phase of the oscillations, wherein we define the latter in the following way:

$$x = A\cos(\omega t + \varphi), \quad \dot{x} = -A\omega\sin(\omega t + \varphi). \qquad (4)$$

By virtue of assumption (2), we can express the coordinate z in terms of A and φ:

$$z = \frac{\beta}{\sqrt{1+\alpha^2}} A\cos(\omega t + \varphi + \psi), \qquad (5)$$

where

$$\phi = \operatorname{arc\,tg}(-\alpha).$$

By substituting (4) in (5) and expanding the function f(z) = F(t) in a Fourier series in t, we obtain equations in the coordinates (variables) A and φ:

$$\dot{A} = -\delta A - \frac{k\beta C}{2\omega\sqrt{1+\alpha^2}} A \sin\chi + \xi, \qquad (6)$$

$$\dot{\varphi} = -\frac{k\beta C}{2\omega\sqrt{1+\alpha^2}} \cos\chi + \frac{\xi'}{A}; \qquad (7)$$

Here, we have introduced the following notation:

$$C = \begin{cases} 0 & \text{for } \dfrac{\beta A}{\sqrt{1+\alpha^2}} \leqslant a, \\ \dfrac{1}{\pi}\sqrt{(u^2-1)^2+v^2} & \text{for } \dfrac{\beta A}{\sqrt{1+\alpha^2}} \geqslant a, \end{cases}$$

$$\operatorname{tg}\chi = \alpha\pi \frac{F_\alpha(u)}{v+\alpha(u^2-1)}, \quad u = 1 - 2\frac{a\sqrt{1+\alpha^2}}{|\beta| A},$$

$$v = \frac{3\pi}{2} - \arcsin u + u\sqrt{1-u^2},$$

$$F_\alpha(u) = \begin{cases} 0 & \text{for } \dfrac{\beta A}{\sqrt{1+\alpha^2}} \leqslant a, \\ \dfrac{1}{\alpha\pi}(\alpha v + 1 - u^2) & \text{for } \dfrac{\beta A}{\sqrt{1+\alpha^2}} \geqslant a, \end{cases}$$

ξ and ξ' are δ-correlated random functions with zero means and correlation function $K(\tau) = 2\lambda^{-1}\delta(\tau)$, where $\lambda^{-1} = \omega^2\kappa(\omega)/4$; $\kappa(\omega)$ is half the spectral density of the noise $\zeta(t)$ at frequency ω.

Equations (6) and (7) are valid (cf. [1, 2]) with the following assumptions.

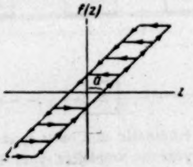

Fig. 2.

1. The oscillations in the system are almost harmonic, i.e., A and φ slowly vary during the period. This requirement corresponds to the condtions:

$$\frac{\delta}{\omega} < 1; \qquad \frac{k|\beta|}{\omega^2(1+\alpha^2)} < 1,$$

$$\begin{cases} \sqrt{\overline{\zeta^2}} < A_0 & \text{for } \tau_{\text{cor}} \geqslant \dfrac{2\pi}{\omega}, \\ \sqrt{\omega\kappa(\omega)} < A_0 & \text{for } \tau_{\text{cor}} < \dfrac{2\pi}{\omega}, \end{cases} \qquad (8)$$

where A_0 is the amplitude of the unstable limiting cycle and τ_{cor} is the correlation time of the noise $\zeta(t)$.

2. The correlation time of the noise is small in comparison with the system's relaxation time, i.e.,

$$\tau_{\text{cor}} < \frac{1}{\delta} \text{ and } \tau_{\text{cor}} < \frac{\omega(1+\alpha^2)}{k|\beta|}.$$

Since the right side of Eq. (7) does not depend on φ, this expression can be considered as the correction to the system's frequency of oscillations:

$$\Delta\omega = -\frac{k\beta C}{2\omega\sqrt{1+\alpha^2}}\cos\chi + \frac{\xi'}{A}.$$

The presence of the random stimulus in the right side leads only to fluctuations of the frequency about the mean value

$$\omega_0 = \omega + \Delta\omega_{\text{me}},$$

where

$$\Delta\omega_{\text{me}} = -\frac{k\beta C}{2\omega\sqrt{1+\alpha^2}}\cos\chi.$$

By virtue of conditions (8), $\Delta\omega_{\text{me}} \ll \omega$.

To answer the question of system stability, it suffices to investigate only Eq. (6), since it does not depend on φ.

With no noise present, the magnitudes of the limiting cycles are determined from the equations

$$\frac{k\beta}{2\omega\sqrt{1+\alpha^2}} C \sin\chi = -\delta$$

or

$$F_\alpha(u) = -\frac{2\omega\delta(1+\alpha^2)}{k\beta\alpha}. \qquad (9)$$

The graph of the function $F_\alpha(u)$ as a function of u for various values of α is given on Fig. 3. The function $F_\alpha(u)$ has an extremum at the point $u_0 = \alpha/\sqrt{(1+\alpha^2)}$, equal to $F_\alpha(u_0) > 1$. Consequently, as is clear from the graph, limiting cycles are possible with the conditions

$$\beta < 0, \quad k > \frac{2\omega\delta(1+\alpha^2)}{|\beta|\alpha F_\alpha(u_0)} = \frac{k_0}{F_\alpha(u_0)}.$$

The points of intersection of the line defined by the right member of Eq. (9) with the curve $F_\alpha(u)$ give the amplitudes of the unstable and stable limiting cycles, where the left point corresponds, as is easily shown, to the unstable cycle.

If $k > k_0$, which corresponds to the condition for excitation of oscillations in the absence of noise, then there is no steady-state stable mode for the system. If, however, $k_0/F_\alpha(u_0) < k < k_0$ then, with backlash in the system, it is possible to have autooscillations with stationary amplitude whose excitation occurs rigidly. Using the method suggested by R. L. Stratonovich (cf. [1, 2]) for the approximate solution of the Fokker-Planck equation, we compute the probability of system excitation when it is stimulated by a random force.

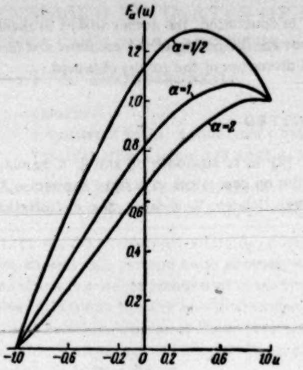

Fig. 3.

It is necessary for this to impose additional conditions on the magnitude of the random stimulus:

$$\frac{1}{\sqrt{\lambda\delta}} < A_0, \quad \frac{1}{\sqrt{\lambda K}} < A_0, \tag{10}$$

where

$$K = -\left.\frac{\partial^2 U(A)}{\partial A^2}\right|_{A=A_0},$$

$$U(A) = \delta\frac{A^2}{2} - \frac{2k\alpha a^2}{\omega|\beta|}\int\frac{F_\alpha(u)}{(1-u)^2}\,du.$$

We now write the corresponding Fokker-Planck equation for the amplitude's distribution density w(A,t):

$$\frac{\partial w}{\partial t} = -\frac{\partial G}{\partial A}, \tag{11}$$

where

$$G = -\left[\delta + \frac{k\beta\alpha F_\alpha(u)}{2\omega(1+\alpha^2)}\right]Aw + \frac{1}{\lambda A}w - \frac{1}{\lambda}\frac{\partial w}{\partial A}.$$

As follows from [2], the probability of system excitation at time $\tau \leq t$ equals $q(t) = 1 - e^{-\gamma/2t}$, where

$$\gamma = G_0|_{A=A_0},$$

$$G_0 = -\left[\delta + \frac{k\beta_\alpha F_\alpha(u)}{2\omega(1+\alpha^2)}\right]Aw_0 + \frac{1}{\lambda A}w_0 - \frac{1}{\lambda}\frac{dw_0}{dA},$$

and, as $w_0(A)$, one can take as an approximation the steady-state solution of the Fokker-Planck equation with zero boundary conditions:

$$\frac{dG_0}{dA} = 0,$$

$$w_0(A_0) = 0, \quad \int_0^{A^0} w_0(A)\,dA = 1. \tag{12}$$

By virtue of the zero boundary condition, we obtain the simple expression for γ:

$$\gamma = -\frac{1}{\lambda}\left.\frac{dw_0}{dA}\right|_{A=A_0}.$$

Since, due to conditions (10), we consider the noise to be quite small, we can assume that the effect of the zero boundary condition on the course of the distribution density $w_0(A)$ is limited to a narrow region close to the boundaries characterized by the inequality $\Delta A < \sqrt{1/\lambda K}$. It is natural to assume that, outside of this region, $w_0(A)$ coincides with the steady-state solution of Eqs. (12), w(A), which satisfies the condition that it vanishes at infinity.

As one easily convinces oneself by direct substitution in (12),

$$w(A) = CAe^{-\lambda U(A)}.$$

The normalizing constant C can be computed approximately by using conditions (10):

$$C^{-1} = \int_0^{A_0} Ae^{-\lambda U(A)}\,dA \approx \frac{1}{\lambda\delta}.$$

Based on what has been said earlier, we can set

$$w_0(A) = w(A)\,w^*(A), \tag{13}$$

where $w^*(A)$ is a correction factor, equal to zero for $A = A_0$ and equal to unity for $A_0 - A > 1/\sqrt{\lambda K}$.

By substituting (13) in (12), we obtain the equation for $w^*(A)$:

$$\frac{d}{dA}\left(w\frac{dw^*}{dA}\right) = 0 \tag{14}$$

with the conditions

$$w^*(A_0) = 0, \quad w^*(A) = 1 \text{ for } A_0 - A > \frac{1}{\sqrt{\lambda K}}. \tag{15}$$

We also note that

$$\left.\frac{dw_0}{dA}\right|_{A=A_0} = w(A_0)\left.\frac{dw^*}{dA}\right|_{A=A_0} = -\lambda\gamma.$$

We can now write the first integral of Eq. (14):

$$w(A)\frac{dw^*}{dA} = -\lambda\gamma.$$

To determine the magnitude of γ, we use conditions (15):

$$w^*(A)\Big|_{A_0-A>\sqrt{\frac{1}{\lambda K}}} = C^{-1}\lambda\gamma\int_{A_0}^{A}\frac{1}{A}e^{\lambda U(A)}\,dA \approx$$

$$\approx \gamma\frac{1}{\delta A_0}\sqrt{\frac{\pi}{2\lambda K}}\,e^{\lambda U(A_0)} = 1.$$

From whence

$$\gamma = \delta A_0\sqrt{\frac{2\lambda K}{\pi}}\,e^{-\lambda U(A_0)},$$

where

$$K = \frac{a\alpha k}{A_0\omega\sqrt{1+\alpha^2}}\left.\frac{dF_\alpha(u)}{du}\right|_{A=A_0}.$$

Thus, the probability of system excitation during any given interval of time is completely determined. Knowing it, we can easily compute the average time during which the system is excited. It equals $t_{av} = 2/\gamma$.

SUMMARY

1. The presence of backlash can lead to undesirable system excitation.
2. The excitation is rigid.

3. Even for low noise, one can cite a time interval during which the system is excited with probability arbitrarily close to unity.

In conclusion, the author wishes to thank Prof. S.P. Strelkov for the posing of the problem and for the very useful discussion of the results obtained.

LITERATURE CITED

[1] R. L. Stratonovich, "Self-excited oscillator synchronization in the presence of noise," Radiotekh. i Elektron. 4 (1958).

[2] R. L. Stratonovich and R. S. Landa, "Noise stimulus on generators with rigid excitation," Izvest. Vysshikh Uchebn. Zavedenii, Ser. Radiofizika 1 (1959).

ON UNBIASED ESTIMATES OF SIGNALS WHICH DEPEND NONLINEARLY ON UNKNOWN PARAMETERS

I. A. Boguslavskii

(Moscow)

(Translated from: Avtomatika i Telemekhanika, Vol. 21, No. 1, pp. 42-47, January, 1960)
Original article submitted April 2, 1959

A method is presented which, in many cases, allows one to use linear theory for obtaining, in the presence of noise, an unbiased estimate of a signal which depends nonlinearly on unknown parameters.

In [1-4], the problem of obtaining, in the presence of noise, an optimal, in some sense or other, estimate of a signal which is a linear function of unknown parameters was solved. In many cases of practical importance, the signal is a nonlinear function of these parameters. The general solution of the corresponding nonlinear problem was obtained by V. S. Pugachev.*

However, there is a definite practical interest in artificial ways of effectively solving the problem in certain cases by using the well-known linear methods of statistical dynamics. One such method is presented below. The method allows one, for example, to implement sufficiently simply an unbiased filtering of a random process whose signal satisfies a nonlinear differential equation of a definite type with unknown initial conditions. The method can be used for smoothing, without dynamic errors, the coordinates and velocity of Sputniks and cosmic rockets during their unpowered flight phases, etc.

Description of the Method

A random process Z(t) is observed, its form being

$$Z(t) = \Phi(c_1, c_2, \ldots, c_n, t) + m(t),$$

where Φ is the signal, the c_k are random parameters, and m(t) is the noise.

Let it be possible to give a transformation I which takes Φ to a function of the form $\sum_{k=1}^{n} c_k W_k(t)$ with the $W_k(t)$ known a priori, and a transformation II which, when applied to the result of an application of transformation I, leads back to the function Φ. In addition, we shall assume that the random process $Z_1(t)$ which results from the application of transformation I to Z(t), may be presented approximately in the form

$$Z_1(t) = \sum_{k=1}^{n} c_k W_k(t) + m_1(t),$$

where $m_1(t)$ is a random noise process whose correlation function can be expressed in terms of the probability characteristics of the noise m(t).

Then, a scheme for obtaining an unbiased estimate of the signal can be constructed in the following manner.

1. We apply transformation I to Z(t).
2. We apply $Z_1(t)$ to the input of an optimal unbiased filtering link, constructed in accordance with the well-known linear methods on the basis of the data on the functions $W_k(t)$ and the correlation function of the noise $m_1(t)$; after the selected memory time T of the link, we obtain at its output the function $\sum_{k=1}^{n} c_k W_k(t)$ with a decreased random error.
3. We apply transformation II to the output of this link.

The realization of the sequence of operations just described allows one to construct, with time lag T, the function $\Phi(c_1, c_2, \ldots, c_n, t)$ without dynamic errors and with decreased random errors only if transformation II insignificantly "increases" the noise at the output of the optimal linear link.

Let it be known that the signal Φ satisfies a nonlinear differential equation of the form

$$a_0(t)\frac{d^n\Phi}{dt^n} + a_1(t)\frac{d^{n-1}\Phi}{dt^{n-1}} + \cdots + a_n(t)\Phi = F[t, \Phi] \tag{1}$$

with unknown initial conditions

$$c_1 = \Phi(0), \quad c_2 = \Phi^{(1)}(0), \ldots, c_n = \Phi^{(n-1)}(0).$$

Because of the presence of the function F(t, Φ) in the right member of (1), the signal in the case under consideration is a nonlinear function of the unknown parameters $c_1, c_2, \ldots, c_n$. It follows from (1) that

$$\Phi(c_1, c_2, \ldots, c_n, t) = \sum_{k=1}^{n} c_k W_k(t) + \int_0^t W(t, \tau) F[\tau, \Phi]\, d\tau, \tag{2}$$

where $W_k(t)$ is the solution of the homogeneous equation

$$a_0(t)\frac{d^n W_k}{dt^n} + a_1(t)\frac{d^{n-1} W_k}{dt^{n-1}} + \cdots + a_n(t) W_k = 0$$

with initial conditions

$$W_k^{(m)}(0) = \begin{cases} 0 & \text{for} \quad m \neq k, \\ 1 & \text{for} \quad m = k, \end{cases}$$

and W(t, τ) is the impulsive response of the corresponding linear dynamic link.

---

* In a paper given February 16 and March 2, 1959, at the seminar on probabilistic methods in automatic control theory of the Institute of Automation and Remote Control of the Academy of Sciences of the USSR.

It is clear from (2) that transformation I should be defined by the relationship

$$Z_1(t) = Z(t) - \int_0^t W(t,\tau)\,F[\tau, Z(\tau)]\,d\tau, \qquad (3)$$

and transformation II by the relationship

$$Z_2(t) = Z^*(t) + \int_0^t W(t,\tau)\,F[\tau, Z(\tau)]\,d\tau, \qquad (4)$$

where $Z^*(t)$ denotes the result of optimal unbiased filtering of the process $Z_1(t)$. After time T, given by the solution of the optimization problem, $Z_2(t)$ will differ from $\Phi(c_1, c_2, \ldots, c_n, t)$ only by a random error.

As a rule, one can approximately set $m_1(t) \approx m(t)$ only if the link with impulsive response $W(t, \tau)$ possesses essential filtering properties, and $F[t, \Phi]$ is of the same order as Φ. Analogously to what has been presented, one can obtain an unbiased estimate of the result of applying any given linear operator S to the function Φ.

In this case

$$Z_2(t) = Z^*(t) + S\left\{\int_0^t W(t,\tau)\,F[\tau, Z(\tau)]\,d\tau\right\},$$

where $Z^*(t)$ is the optimal unbiased estimate, after time lag T, of the function $S\left\{\sum_{k=1}^{n} c_k W_k(t)\right\}$.

We note that, for a given function $\Phi(c_1, c_2, \ldots, c_n, t)$, the corresponding nonlinear differential equation can be found by eliminating the parameters c_k from the following system of n + 1 algebraic equations:

$$\begin{aligned} \Phi &= \Phi(c_1, c_2, \ldots, c_n, t), \\ \frac{d\Phi}{dt} &= \Phi_t'(c_1, c_2, \ldots, c_n, t), \\ \frac{d^n\Phi}{dt^n} &= \Phi_t^{(n)}(c_1, c_2, \ldots, c_n, t). \end{aligned}$$

However, a direct application of the transformations of (3) and (4) can only be used for obtaining an unbiased estimate in the case when the nonlinear portion of the differential equation obtained depends only on Φ and t.

By using the Jacobian of the functions $\Phi, \Phi_t', \ldots$ with respect to $c_1, c_2, \ldots$, one can obtain an analytic expression for the condition cited.

For n = 1, this condition is always met. Thus, if for example,

$$\Phi = \frac{c}{c+t},$$

then

$$\frac{d\Phi}{dt} = -\frac{c}{(c+t)^2} \quad \text{and} \quad t\frac{d\Phi}{dt} + \Phi = \Phi^2.$$

If, to the method presented, one adds the optimally determined derivatives of the function $Z_1(t)$, one can then, in conjunction with the method of successive approximation, obtain an unbiased estimate even when the nonlinear portion is a function of the derivatives of the function Φ.

Obtaining an unbiased estimate by the scheme presented above does not require that a nonlinear differential equation be solved. Therefore, in the example to be considered below, the use of the scheme allows a concrete engineering problem to be solved in an uncomplicated way.

Determination of the Smoothed Values of the Elements of a Sputnik's Trajectory

We now construct a methodology for determining, without dynamic errors, the smoothed values of the position and velocity of a Sputnik. For brevity we shall consider the problem in a plane; taking nonplanar motion into account for the smoothing engenders no difficulties.

Let x and y be the coordinates of the Sputnik with respect to a rectangular coordinate system passing initially through the center of the earth but not rotating with it. If one neglects the atmospheric braking of the Sputnik and the effect of the nonsphericity of the earth, then x and y satisfy the nonlinear differential equations

$$\ddot{x} = -gR^2 \frac{x}{(x^2+y^2)^{\frac{3}{2}}}, \qquad (5)$$

$$\ddot{y} = -gR^2 \frac{y}{(x^2+y^2)^{\frac{3}{2}}}, \qquad (6)$$

where R is the radius of the earth; g = 9.81 meters/sec^2.

Therefore, x(t), for example, is described by the formula

$$x(t) = x(0) + \dot{x}(0)\,t - \int_0^t \frac{gR^2(t-\tau)\,x(\tau)}{[x^2(\tau)+y^2(\tau)]^{\frac{3}{2}}}\,d\tau \qquad (7)$$

or by the formula

$$x(t) = x(0)\cos\omega t + \frac{\dot{x}(0)}{\omega}\sin\omega t -$$
$$-\frac{1}{\omega}\int_0^t \sin\omega(t-\tau)\,x(\tau)\left\{\frac{1}{[x^2(\tau)+y^2(\tau)]^{\frac{3}{2}}} - \frac{1}{R^3}\right\}d\tau, \qquad (8)$$

where $\omega = \sqrt{g/R}$.

In formula (8) the portion of the signal which depends linearly on the nonlinear parameters x(0) and $\dot{x}(0)$ is separated more completely than in formula (7). However, the effectiveness of the filtering turns out to be practically the same, whether (7) is used or (8). We may therefore use formula (7) which provides a simpler form of the linear operator which implements optimal unbiased filtering of the result of transformation I. Let the following random process be observed

$$Z_x(t) = x(t) + m_x(t),$$

where $m_x(t)$ is the random error in measuring the coordinate $x(t)$ by terrestrial radar (radio) and optical means.

It follows from (7) that transformation I is defined by the relationship

$$Z_{x1}(t) = Z_x(t) + \int_0^t \frac{gR^2(t-\tau)Z_x(\tau)}{[Z_x^2(\tau) + Z_y^2(\tau)]^{\frac{3}{2}}}\,d\tau, \quad (9)$$

and transformation II by the relationship

$$Z_{x2}(t) = Z_x^*(t) - \int_0^t \frac{gR^2(t-\tau)Z_x(\tau)}{[Z_x^2(\tau) + Z_y^2(\tau)]^{\frac{3}{2}}}\,d\tau. \quad (10)$$

The nub of the problem under consideration is that, in the given case, the function $W(t, \tau)$ does not possess the filtering properties [with the use of (7) or (8), $W(t, \tau)$ equals, respectively, $t-\tau$ or $\sin\omega(t-\tau)/\omega$]. Therefore, the dispersion of the noise $m_{x1}(t)$ contained in $Z_{x1}(t)$ increases without bound in the course of time.

However, if T is limited by some value completely admissible for practical purposes (cf. the Appendix), then $m_{x1}(t)$ coincides in practice with the noise $m_x(t)$. Therefore, with the known correlation function of the noise $m_x(t)$, it is easy to construct a scheme which takes $Z_{x1}(t)$ to $Z_x^*(t)$, which is the optimal unbiased filtering of the random process whose signal is a linear function of time.

In the case of the limitation on T already mentioned, transformation II does not in practice decrease the efficiency of this filtering.

In an analogous way, one carries out the unbiased filtering of the random errors arising in the measurement of coordinate y. If it is necessary to find $V_x(t)$ and $V_y(t)$, the projections of the Sputnik's velocity vector, then transformation I, as before, is described by relationship (9), and transformation II takes the form

$$V_x(t) = V_x^*(t) - \int_0^t \frac{gR^2 Z_x(\tau)}{[Z_x^2(\tau) + Z_y^2(\tau)]^{\frac{3}{2}}}\,d\tau,$$

where $V_x^*(t)$ is the result of unbiased optimal differentiation of random process $Z_{x1}(t)$.

If the lack of sphericity of the earth is taken into account, the smoothing scheme remains unchanged only if the constant g in the formula is replaced by a function of x and y, defined by well-known relationships of potential theory. To take into account the braking of the Sputnik by the atmosphere, one must add, to the right members of Eqs.(5) and (6) and, certainly, to the integrands in (9) and (10), terms which depend, not only on x and y, but also on V_x and V_y. The forms of these terms are known if we know the density of the atmosphere as a function of x and y, and the drag coefficient as a function of V. With this, the smoothing method is somewhat complicated, it being required to use successive approximations, and may be laid out in the following way. First, using the method given above, wherein the braking force is not taken into account, we find V_x and V_y with some dynamic error. The values of V_x and V_y found are used to construct terms in which this force is taken into account, these terms being added to the integrands in (9) and (10), after which the process is repeated, resulting in new, more accurate values of V_x and V_y. By carrying out this process several times, we obtain V_x and V_y practically without dynamic errors, and with random errors defined, for limited T, on the basis of the random errors of the optimal differentiation. We may note that frequently one need not use successive approximations but may, instead of V_x and V_y, use the results of numerical differentiation with specially chosen increments of the observed quantities Z_x and Z_y.

The method can also be used, without change, for obtaining smoothed values of the coordinates and the projections of the velocity of cosmic rockets (space probes) describing complicated paths under the influence of the gravitational fields of earth and several other heavenly bodies. In this case, the right members of Eqs. (5) and (6) contain terms which depend on x, y and on the current value of t, these terms taking into account the variations in the coordinates of these bodies with respect to the earth during the course of the smoothing process.

APPENDIX

We denote by $\Delta(t)$ the random component contained in the integral terms of formulas (9) and (10) due to the presence of the random errors $m_x(t)$ and $m_y(t)$ and, by $\sigma_\Delta^2(t)$, we denote its dispersion.

We assume that, in practice, the magnitude of $x^2 + y^2$ is several orders of magnitude greater than the quantity $2(xm_x + ym_y) + m_x^2 + m_y^2$. Thus,

$$\Delta(t) \approx \int_0^t \frac{gR^2(t-\tau)m_x(\tau)}{[x^2(\tau) + y^2(\tau)]^{\frac{3}{2}}}\,d\tau$$

and

$$\sigma_\Delta^2(t) \leqslant \frac{g^2}{R^2}\int_0^t\int_0^t (t-\tau_1)(t-\tau_2)\,\varphi_x(\tau_1, \tau_2)\,d\tau_1\,d\tau_2, \quad (11)$$

where $\varphi_x(t_1, t_2)$ is the correlation function of random error $m_x(t)$.

We assume that

$$\varphi_x(t_1, t_2) = \sigma_0^2 e^{-\gamma|t_1 - t_2|}.$$

It follows from (11) that, in this case

$$\sigma_\Delta(t) \leqslant \sigma_0 \frac{g}{R}\sqrt{\frac{2}{3\gamma}t^3 - \frac{1}{\gamma^2}t^2 - \frac{2}{\gamma^3}te^{-\gamma t} + \frac{2}{\gamma^4}(1 - e^{-\gamma t})}. \quad (12)$$

For definiteness, we set $\gamma = 1\ \text{sec}^{-1}$, and we shall assume that, in constructing the scheme for the optimal unbiased filtering which takes $Z_{x1}(t)$ to $Z_x(t)$, and for computing σ_x^2, the dispersion of the noise at the output of this scheme, we can ignore $\Delta(t)$ ($m_x(t) \approx m_{x1}(t)$), if

$$\sigma_\Delta(t) < 0{,}1\ \sigma_0. \qquad (13)$$

It follows from (12) that (13) holds for $t < 1900$ sec. In this case, the optimal circuit's impulsive response is easily found, and

$$\sigma_x^2 = \sigma_0^2 \frac{24 + 24\gamma T + 8\gamma^2 T^2}{24 + 24\gamma T + 8\gamma^2 T^2 + \gamma^3 T^3}, \qquad (14)$$

where T is the memory of the optimal circuit and σ_x^2 is the dispersion of the noise contained in $Z_x^*(t)$.

It follows from (12) and (14) that the addition of an integral term in correspondence with formula (10) to the output of the optimal circuit does not, in practice, increase the random error, if $t = T < 500$ sec. Therefore, the memory of the optimal circuit should be defined by the conditions

$$T = t \quad \text{for} \quad t < 500 \text{ sec},$$
$$T = 500 \text{ sec} \quad \text{for} \quad t \geqslant 500 \text{ sec}.$$

In this case, formula (14) can be used to define the dispersion of the random error in the smoothed coordinates of the Sputnik.

Starting with time t = 500 sec, the lower limit of the integrals in the right members of formulas (9) and (10) should be replaced by t-500.

It is shown analogously that this same choice of T allows one to neglect $\Delta(t)$ in the determination of V_x also. Then, the impulsive response of the optimal differentiating circuit is easily found, and σ_V^2, the dispersion of the random error in the determination of the projections of the Sputnik's velocity, is described by the relationship

$$\sigma_V^2 = \sigma_0^2 24\gamma^2 \frac{2 + \gamma T}{24\gamma T + 24\gamma^2 T^2 + 8\gamma^3 T^3 + \gamma^4 T^4}. \qquad (15)$$

If, for example, we choose $\sigma_0 = 1$ km, we get from (14) and (15) that, after 200 sec of receiving information from the Sputnik, one can find its coordinates and the projections of its velocity without dynamic error, and with random errors characterized by the quantities $\sigma_x = 200$ m and $\sigma_V = 1.7$ m/sec.

LITERATURE CITED

[1] V. S. Pugachev, Theory of Random Functions and Their Applications to Problems of Automatic Control (Gostekhizdat, 1957).

[2] V. S. Pugachev, "The determination of optimal systems by arbitrary criteria," Avtomat. i Telemekh. 19, 6 (1958).†

[3] V. V. Solodovnikov, Introduction to the Statistical Dynamics of Automatic Control Systems [in Russian] (Gostekhizdat, 1952).

[4] J. H. Laning and R. H. Battin, Random Processes in Automatic Control [Russian translation] (IL, 1958).

---

† See English translation.

SYNTHESIZING CONTROL SYSTEMS WITH MONOTONICALLY DECREASING GAINS BY THE ROOT-LOCUS METHOD

Ya. I. Rubinovich

(Moscow)

(Translated from: Avtomatika i Telemekhanika, Vol. 21, No. 1, pp. 48-55, January, 1959)
Original article submitted May 11, 1959

We consider a periodically connected control system which contains a link whose gain decreases monotonically with time. We introduce the concept for the quasi-majorant closed control system for which, using the root-locus method, we choose a correcting circuit.

Posing of the Problem

We assume that the control process lasts for time T, after which the control system returns to its initial state, and the process is again repeated when the controlled object is subjected to the same, or to an analogous, perturbing movement.

In the general case, the open-loop control circuit consists of two series-connected links: link I with transfer function

$$G(s)=\frac{\prod\limits_{i=1}^{m}(s+z_i)}{\prod\limits_{i=1}^{n}(s+p_i)}, \tag{1}$$

where n ≥ m, and the p_i lie in the left half of the s plane, and link II, whose variable gain decreases monotonically with time in accordance with the law

$$K_1(t)=\frac{K_0}{(t+a)^r}. \tag{2}$$

The quantity r lies within the limits $1 \le r \le 4$, and depends on the telecontrol method being used.

To simplify the analysis, we replace link II by link II*, whose gain varies in accordance with the law

$$K_1^*(t)=Ae^{-\frac{t}{\tau}}. \tag{3}$$

The coefficients A and τ are so chosen than $K_1(0) = K_1^*(0)$ and $K_1(T) = K_1^*(T)$. Then

$$A=\frac{K_0}{a^r}, \qquad \tau=\frac{T}{\ln\left(1+\frac{T}{a}\right)^r}$$

and

$$K_1^*(t)=\frac{K_0}{a^r}\exp\left[-\frac{t}{T}r\ln\left(1+\frac{T}{a}\right)\right]. \tag{4}$$

It follows, from the properties of exponential functions, that

$$K_1^*(t) > K_1(T) \text{ for } 0 < t < T.$$

The system thus obtained, consisting of links I and II*, will be quasi-majorant* with respect to the initial system with link II.

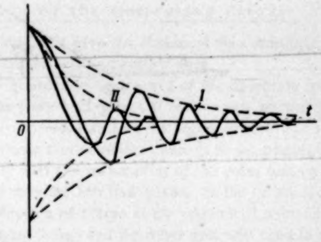

Fig. 1

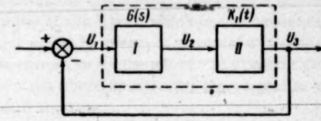

Fig. 2

Since function G(s) has no poles in the right half-plane, the closed-loop system with link II* (Fig. 2) will also be quasi-majorant with respect to the closed-loop system with link II.

If a signal $U_1(t)$ is applied to the input of link I of the open-loop system then, at the output of link II*, one obtains the signal $U_3(t)$, whose Laplace transform has the form:

$$U_3(s)=AG\left(s+\frac{1}{\tau}\right)U_1\left(s+\frac{1}{\tau}\right). \tag{5}$$

Thus, the exponentially decreasing gain is equivalent, in the open-loop system, to a shift to the left by the amount $1/\tau$ of all the zeros and poles of the transfer function and of the disturbing stimulus. It is obvious that, if the zeros and poles of the disturbing stimulus are

---

* A system will be called quasi-majorant with respect to another system if the envelope of the first system's transient response completely contains the transient response curve of the second (given) system. For example, the system which gives the transient response corresponding to curve I on Fig. 1 is quasi-majorant with respect to the system giving curve II for its transient response.

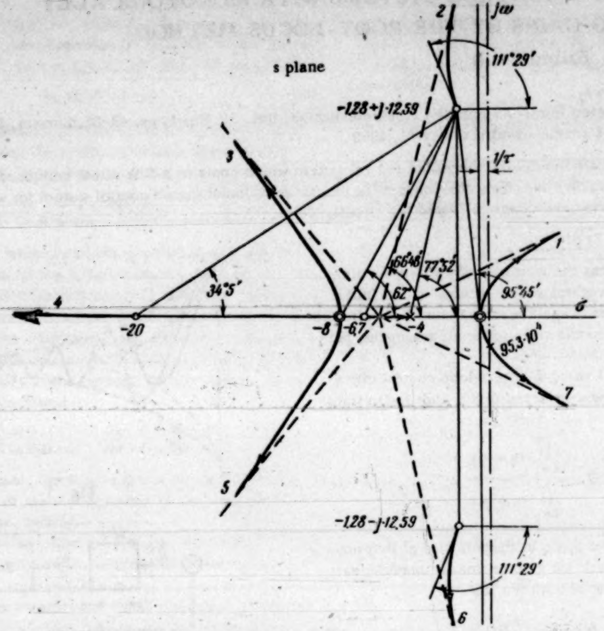

Fig. 3. O is a simple pole, ʘ is a double pole, and × is a simple zero.

shifted to the right by the same quantity, $1/\tau$, then the curve of $U_3^*(t)$ which one obtains in this case will be quasi-majorant with respect to curve $U_3(t)$ corresponding to Eq. (5). The system with open-loop transfer function $AG(s + 1/\tau)$ will, after closing the loop by a feedback path, be quasi-majorant with respect to the initial system (Fig. 2). Therefore, one can make certain estimates of stability and transient response quality for the initial system by investigating the quasi-majorant system obtained.

We use the following concrete example for showing the method of synthesizing such control systems.

Let link I's transfer function have the following form:

$$G(s) = \frac{(s+z_1)}{s^2(s+p_1)(s+p_2)^2(s+p_3)(s^2+2\zeta\omega_n s+\omega_n^2)}, \tag{6}$$

where $z_1 = 4$, $p_1 = 6.7$, $p_2 = 8$, $p_3 = 20$, $\zeta = 0.101$ and $\omega_n = 12.65$/sec.

The gain of link II varies in accordance with the following law:

$$K_1(t) = \frac{K_0}{t+a}, \tag{7}$$

where $K_0 = 2 \cdot 10^5$ and $a = 0.2$ sec. Operation time is $T = 10$ sec.

It is necessary to so choose a series-connected correcting circuit that, after closing the loop with a feedback path, one obtains a relative damping coefficient† for the system of not less than 0.2 for any pair of complex poles.

Root Motion Analysis of the Closed-Loop System

We draw the positions of the zeros and poles of function G(s) on the complex $s = (\sigma + j\omega)$ plane (Fig. 3). The arrows on the curves show the direction of motion of the poles as K_{syst} increases.

If the system is closed by a negative feedback path (Fig. 2) then, as the system gain K_{syst} increases from zero to infinity, the roots of the closed-loop system's characteristic equation (the poles of the closed-loop system) will move from the poles of the open-loop system to its zeros.

We now construct the trajectories of the roots as they move. The rules for constructing such trajectories have been published in the literature [1-5], so that we shall use them here without proof. As is well known, the number of individual trajectory branches tending to infinity equals the difference

---

† By the relative damping coefficient we understand the damping coefficient which corresponds to the presence of just one pair of complex poles.

q = (number of finite poles) –
– (number of finite zeros).

In our example, there will be seven such branches. For a sufficiently large gain K, these trajectory arms tend to asymptotes which start at one point on the real axis and form, with that axis, angles equal to ± [180°/ q + + i • 360°/ q], where i = 0, 1, 2, 3, . . . , etc.

We find the coordinate of the point of intersection of the asymptotes by the formula

$$s_1 = \frac{\Sigma(\text{poles}) - \Sigma(\text{zeros})}{q} =$$

$$= \frac{(-6.7 - 2.8 - 20 - 2\cdot 1.28) - (-4)}{7} = -5.89$$

and we draw the asymptotes at the angles (Fig. 3)

$$\theta_1 = \pm\frac{180^\circ}{7} = \pm 25^\circ 42',$$

$$\theta_3 = \pm\left(25^\circ 42' + \frac{360^\circ}{7}\cdot 2\right) = \pm 128^\circ 30',$$

$$\theta_2 = \pm\left(25^\circ 42' + \frac{360^\circ}{7}\right) = \pm 77^\circ 6',$$

$$\theta_4 = \pm\left(25^\circ 42' + \frac{360^\circ}{7}\cdot 3\right) = \pm 180^\circ.$$

All portions of the real axis lying to the left of an odd-numbered root (zero or pole), where the roots are counted starting from the far right, are parts of trajectories. We thus find that the pole at point s = −6.7 moves along the real axis to the zero at point s = −4, and the pole at point s = −20 tends to infinity along the real axis towards the left.

We now determine the slope of the trajectory starting from the pole s = −1.28 + 12.59j. To do this, we join this pole with the remaining roots and poles. The slope angle sought, θ, is found from the relationship

Σarg(vectors from zeros) – Σarg(vectors from poles) – θ° = 180° ± n · 360°.

In our case,

$$77^\circ 52' - [90^\circ + 2\cdot 95^\circ 45' + 66^\circ 48' +$$

$$+ 2\cdot 62^\circ + 34^\circ 5'] - \theta^\circ = 180^\circ + n\cdot 360^\circ,$$

$$\theta^\circ = -428^\circ 31' - 180^\circ \pm n\cdot 360^\circ = -248^\circ 31'$$

$$\text{or} \quad -111^\circ 29'.$$

We can now easily construct approximate trajectories of the roots' motion, as was done on Fig. 3. If all the curves are shifted to the left by the amount

$$\frac{1}{\tau} = \frac{\ln\left(1 + \frac{T}{a}\right)}{T} = \frac{\ln 51}{10} = 0.393$$

or, equivalently, the imaginary axis is shifted to the right by this amount, we obtain the root locus of the quasi-majorant system (Fig. 3).

A system with a constant gain will be unstable for any value of that gain, since the double pole at the origin will immediately enter into the right half-plane.

The quasi-majorant system becomes unstable for $K_{syst} \geq 95.3 \cdot 10^4$, as one may verify by determining the value of the gain for which the pole moving along arm I intersects the shifted imaginary axis. For this, we take the product of the lengths of the vectors from the poles to the point of intersection and divide this by the product of the lengths of the vectors from the zeros to this same point.

Choice of the Correcting Circuit

We first give the choice of the correcting circuit for a system with a constant gain.

In order to keep arm I of the trajectory from entering the right half-plane, it is necessary to introduce a zero on the real axis on the segment from 0 to s = − 6.7. The closer this additional zero is to the origin, the more sharply will the trajectories of the poles turn up from the origin into the left half-plane. In the limiting case, the introduction of a zero at the origin will neutralize one of the poles there, and the other pole will tend to the zero at the point s = − 4 along the real axis. The introduction of a zero at the origin means the introduction of a pure derivative of the signal, which can be accomplished in practice either by means of a special differentiating amplifier circuit, or by the use of tachometer generators in the cases where the circuit's input signal is in the form of a shaft rotation.

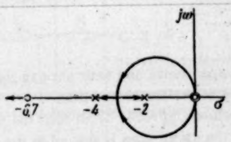

Fig . 4

For the realization of a zero on the real axis by a passive RC circuit, it is desirable that the zero not be too close to the origin. We shall introduce a zero at the point $s = -z_1^{*} = -2$. Then, an approximate sketch of the motion of the root in the neighborhood of the origin takes the form shown in Fig. 4.

For realizing this zero by means of a series-connected passive RC network, it is necessary that the transfer function of the correcting circuit have the form:

$$G_2(s) = \frac{(s + z_1^{*})}{(s + p_1^{*})} \frac{p_1}{z_1^{*}}.$$

It is desirable to choose the pole p_1^{*} sufficiently far from the origin so that the component of system behavior attributable to it will be rapidly damped. However, it is undesirable to remove it too far, since the

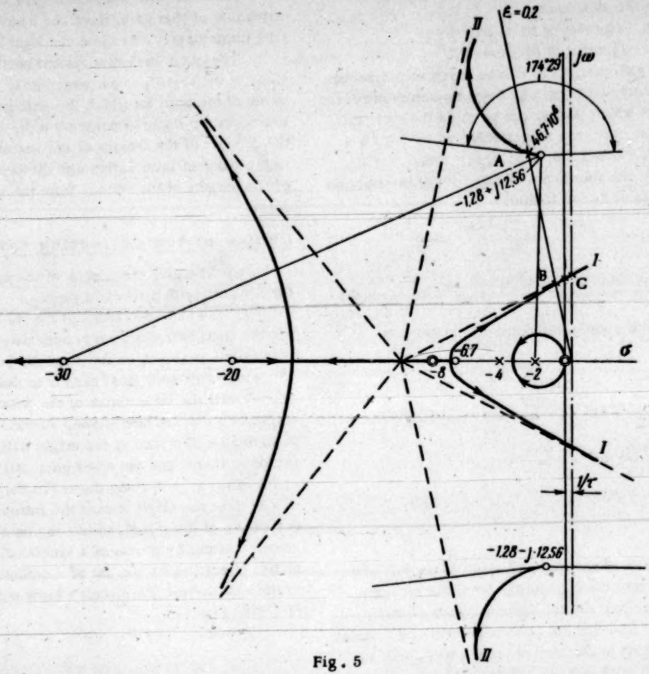

Fig. 5

requisite capacitance and resistance in the network would be difficult to realize in practice.

We choose $p_1^* = 30$. With this, the point of intersection of the asymptotes is shifted to the left by the amount $(p_1^* - z_1^*)/7 = (30-2)/7 = 4$.

The slopes of the asymptotes do not change. By again joining the pole and zero introduced with the point $s = -1.28 + 12.59j$, we find the additional rotation of the trajectory starting from the pole:

$\Delta\theta^\circ = \arg(\text{vector from } z_1^*) - \arg(\text{vector from } p_1^*) =$
$= 86^\circ 45' - 23^\circ 45' = 63^\circ$.

The root locus takes the form shown on Fig. 5. We now determine for what gain the poles of the closed-loop quasi-majorant system will lie on the intersections of the line of constant damping coefficient, $\xi = 0.2$, with trajectories I and II.

For point A we get

$$K_{\text{syst}} = \frac{30.6 \cdot 22 \cdot 14^2 \cdot 13.6 \cdot 13.1^2 \cdot 25 \cdot 4 \cdot 1}{13 \cdot 12.9} = 46.7 \cdot 10^6;$$

for point B

$$K_{\text{syst}} = \frac{29.8 \cdot 20 \cdot 8.72^2 \cdot 7.6 \cdot 4.7^2 \cdot 8.1 \cdot 9.2}{5.8 \cdot 4.8} = 20.5 \cdot 10^6.$$

At the boundary of stability of the quasi-majorant system (point C)

$$K_{\text{syst}} = \frac{30.8 \cdot 21 \cdot 9.8^2 \cdot 8.7 \cdot 5^2 \cdot 17.7 \cdot 7.8}{6.8 \cdot 5.6} = 49 \cdot 10^2.$$

For the quasi-majorant system, the required gain is

$$K_{\text{syst}} = \frac{p_1^*}{z_1^*} \frac{K_0}{a} = \frac{30}{2} \frac{2 \cdot 10^5}{0.2} = 15 \cdot 10^6.$$

Thus, the introduction of the correcting circuit provides system stability, but does not give the necessary damping coefficient.

We note that the introduction of zeros and poles on the real axis does not, in general, have much effect on the displacement of the complex poles when the gain is small, since they will be translated in a small neighborhood of the point $s = -1.28 \pm 12.59j$. Consequently, the sole means of obtaining the necessary damping coefficient is to eliminate these poles, which can be done by a correcting circuit with zeros at the points cited.

We thus obtain the following desirable transfer function for the correcting circuit:

$$G_2(s) = \frac{(s+2)\,(s^2 + 2\xi\omega_n s + \omega_n^2)\,15 p_2^* p_3^*}{(s+30)\,(s+p_2^*)\,(s+p_3^*)\,\omega_n^2}.$$

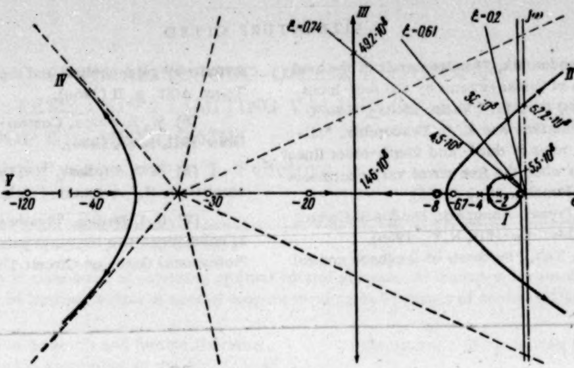

Fig. 6.

The poles at the points $-p_2^*$ and $-p_3^*$ are introduced in order to obtain a passive network realizable by capacitances and resistances. As a rule, these should be chosen further to the left than the original zeros and poles, in order that the components in the transient response introduced by them be rapidly damped. In addition, the introduction of these poles moves the point of intersection of the asymptotes to the left, which increases the system's stability.

We choose $p_2^* = 40$ and $p_3^* = 120$. Then, the open-loop circuit thus obtained will have the following transfer function:

$$G_{\text{syst}}(s) =$$

$$= \frac{K_{\text{syst}}\ (s+2)(s+4)}{s^2 (s+6.7)(s+8)^2 (s+20)(s+30)(s+40)(s+120)}.$$

The magnitude of K_{syst} for the quasi-majorant system (with the correcting circuit) will equal

$$K_{\text{syst}} = \frac{15 p_2^* p_3^*}{\omega_n^2} \frac{K_0}{a} = \frac{15 \cdot 40 \cdot 120}{12.65^2} \cdot \frac{2 \cdot 10^5}{0.2} = 4.5 \cdot 10^8.$$

The root locus of the closed-loop system is shown on Fig. 6. The values of the gains are given directly on the curves. The relative damping coefficient of any pair of complex poles is greater than 0.2. With this, the pair of poles on arm III of the trajectory provides a component of the transient response which is rapidly damped and has small oscillation. The poles on arm I provide a component which is small in magnitude (due to the proximity of the zeros at points -2 and -4) and which is slowly damped.

The roots on arms IV and V give very rapidly damped terms and do not have any practical effect on the system's transient response or frequency characteristic. Thus, the system obtained completely satisfies the requirements posed.

When the poles $-1.28 \pm 12.59j$ are not exactly compensated, there arises a slowly damped, rapidly oscillating, component of insignificant amplitude whose magnitude equals the residues at these poles, i.e., is proportional to the magnitude of the dipole obtained in this case [3, 5].

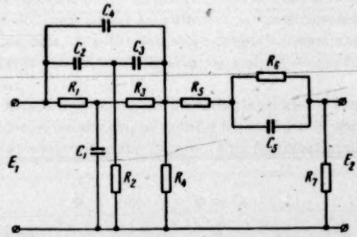

Fig. 7. R_1 = 11.6 kohm, R_2 = 1.1 kohm, R_3 = 23 kohm, R_4 = 11.3 kohm, R_5 = 22.5 kohm, R_6 = 832 kohm, R_7 = 17.7 kohm, C_1 = 2.5 μf, C_2 = 22 μf, C_3 = 1.1 μf, C_4 = 0.0725 μf, C_5 = 0.6 μf.

The correcting function is implemented by the network shown in Fig. 7. The synthesis of this network from the given function $G_2(s)$ was carried out by Dasher's method [7]. To connect the network in the circuit, it is necessary to equalize the gains of the network and of the function $G_2(s)$ since, for dc, $G_2(0) = 1$ and the network gives $E_2/E_1 = 0.005$. Consequently, it is necessary to connect in the circuit an amplifier with gain equal to

$$K_a = \frac{1}{0.005} = 200.$$

LITERATURE CITED

[1] K. F. Teodorchik, "Fundamentals of the analysis and correction of linear systems by the root-locus (natural frequencies) method," Vestn. MGU 4 (1957).

[2] G. A. Bendrikov and K. F. Teodorchik, "Migration laws of the roots of third- and fourth-order linear algebraic equations when the free terms vary continuously," Avtomat. i Telemekh. 16, 3 (1955).

[3] John G. Truxal, Automatic Feedback Control System Synthesis (McGraw-Hill, N.Y., 1955).

[4] V. C. M. Yeh, "Synthesis of feedback control systems by gain-contour and root-contour methods," Trans. AIEE, p. II (1956).

[5] W. R. Evans, Control-System Dynamics. (McGraw-Hill, N.Y., 1954).

[6] S. P. Strelkov, "On the general theory of linear amplifiers, II," Avtomat. i Telemekh. 10, 4 (1949).

[7] B. J. Dasher, "Synthesis of RC transfer functions as unbalanced two terminal pair networks," Trans. IRE Professional Group on Circuit Theory (1952).

CONSTRUCTING OPTIMAL SECOND-ORDER AUTOMATIC CONTROL SYSTEMS USING LIMITING VALUES OF CONTROL LOOP ELEMENT GAINS

S. V. Emel'yanov and A. I. Fedotova

(Moscow)

(Translated from: Avtomatika i Telemekhanika, Vol. 21, No. 1, pp. 56-63, January, 1960)
Original article submitted June 20, 1959

The possibility is considered of obtaining optimal control processes in second-order automatic control systems with the use of limiting values of control loop element gains by means of nonlinear "key"-type correcting devices.

Recently, both in domestic and foreign literature, ever greater attention has been given to the questions of improving the quality of automatic control systems by means of the introduction of nonlinear transformers (function generators) which realize desirable control laws [1-10].

A significant number of works are devoted to the synthesis and realization of nonlinear control laws which provide for the flow of optimal transient responses in automatic control systems when there are limitations imposed on one or several of the systems' coordinates [11-18]. However, the question of constructing optimal automatic control systems using limiting values of control loop element gains has occupied comparatively little space.

The purpose of the present paper is to determine the control law (and also its realization) with which one can obtain optimal transient responses in second-order linear automatic control systems using limiting values of the systems' transmission coefficient.

For the systems under consideration here, we shall understand by optimal transient responses those transient responses which, for unit jump disturbances, have no overshoot, wherein the time during which the value of the controlled coordinate is less than some previously given constant value is minimal.

1. Construction of Optimal Transient Responses of Second-Order Automatic Control Systems Using Limiting Values of Transmission Coefficients

We consider a linear second-order automatic control system (Fig. 1) whose transmission coefficient is bounded.

The equations of the system's links can be written in the following form:

the equation of the object being controlled

$$T_a \dot{x} + \rho x = -\mu + f(t); \tag{1}$$

the equation of the executive mechanism

$$T_s \dot{\mu} = \xi; \tag{2}$$

the equation of the forcing device

$$x - g(t) = \varphi; \tag{3}$$

the equation of the summing device

$$\xi = K\varphi + T\dot{\varphi}.$$

Here, $\underline{x}$ is the relative deviation of the controlled coordinate, φ is the relative change of the error signal, μ is the relative deviation of the controlling organ, $1/\rho$ is the object's static transmission coefficient, T_a/ρ is the time constant of the object of control, T_s is the integration constant of the executive mechanism, K is the gain of the error signal amplifier, T is the differentiator's time constant, ξ is the summing device's output quantity, f(t) is the external disturbance and g(t) is the forcing stimulus.

After elimination of the variables $\underline{x}$ and μ from Eqs. (1)-(3), we obtain, by setting f(t) = g(t) = 0, the differential equation of the system's free (natural) oscillations.

$$\ddot{\varphi} + 2h\dot{\varphi} + \omega_0^2\varphi = 0.$$

Here,

$$2h = \frac{\rho}{T_a} + \frac{T}{T_a T_s}, \quad \omega_0^2 = \frac{K}{T_a T_s}. \tag{4}$$

In the automatic control system under consideration, let the coefficients T_a, T_s, and ρ be some constant numbers which depend on the design peculiarities of the object and the controller, and let the gains K and T be variable within the limits

$$-K_0 \leqslant K \leqslant K_0, \quad -T_0 \leqslant T \leqslant T_0,$$

where K_0 and T_0 are the limiting values of the actual system's gains.

It is required to determine the sequence of changes of the gains K and T during the flow of the transient response which is necessary for obtaining an optimal transient response in the system for stepwise changes in the magnitude of the disturbing stimulus f(t) or of the forcing function (stimulus) g(t). In other words, it is required to determine the nonlinear control law and its realization

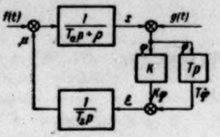

Fig. 1

for obtaining an optimal transient response in the automatic control system under investigation.

It is convenient to carry out the synthesis of a nonlinear control law for the class of systems under consideration by means of the phase plane method. Then, the problem posed is the construction of the automatic control system's phase plane which images the sequence of variations of the coefficients (structure) of the system during the transient response for various initial conditions.

The various combinations of signs of the coefficients K and T give four different system structures:

1) $K > 0, \quad T > 0$;
2) $K > 0, \quad T < 0$;
3) $K < 0, \quad T > 0$;
4) $K < 0, \quad T < 0$.

For the first case, the equation describing the free oscillations will have the form:

$$\ddot{\varphi} + 2h\dot{\varphi} + \omega_0^2\varphi = 0. \tag{5}$$

After the elimination of time from Eq. (5), we obtain the image of the transient response on the φ, $\dot{\varphi}$ plane.

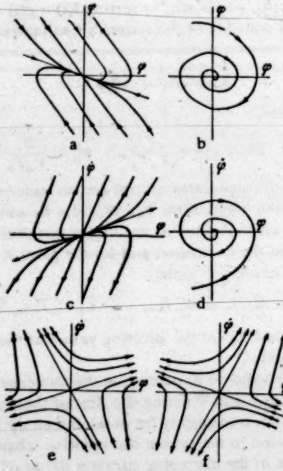

Fig. 2.

For $\omega_0^2 > h^2$, the equation of the phase trajectories will be the equation of the family of helices spiraling into the origin [6] (Fig. 2b):

$$(\dot{\varphi} + h\varphi)^2 + (\omega_0^2 - h^2)\varphi^2 = \\ = c \exp \frac{2h}{\sqrt{\omega_0^2 - h^2}} \quad \operatorname{arc\,tg} \frac{\dot{\varphi} + h\varphi}{\sqrt{\omega_0^2 - h^2}\,\varphi} \tag{6}$$

where $\underline{c}$ is a constant.

For $\omega_0^2 < h^2$, the equation of the phase trajectories will be the equation of a family of deformed parabolas tangent to the line $\dot{\varphi} = -q_1\varphi$ at the origin [11] (Fig. 2a):

$$\dot{\varphi} + q_1\varphi = c_1(\dot{\varphi} + q_2\varphi)^{\frac{q_1}{q_2}}. \tag{7}$$

Here,

$$q_1 = -h + \sqrt{h^2 - \omega_0^2},$$
$$q_2 = -h - \sqrt{h^2 - \omega_0^2},$$

and c_1 is a constant.

For the second case (if $T > \rho T_s$), the equation of the system's free oscillations will be

$$\ddot{\varphi} - 2h\dot{\varphi} + \omega_0^2\varphi = 0. \tag{8}$$

For $\omega_0^2 > h^2$, the phase trajectories are spirals starting from the origin (Fig. 2d) and, for $\omega_0^2 < h^2$, we obtain a family of parabola-like curves on the phase plane but, as it moves along any of the integral curves, the representative (image) point will move ever further from the equilibrium position (Fig. 2c).

In the third case, the equation of the free oscillations has the form:

$$\ddot{\varphi} + 2h\dot{\varphi} - \omega_0^2\varphi = 0. \tag{9}$$

The equation of the phase trajectories will be the equation of a family of deformed hyperbolas (Fig. 2e) [11]:

$$c_2(\dot{\varphi} - \varphi q_2')^{q_2'}(\varphi + \varphi q_.')^{q_1'} = 1. \tag{10}$$

Here, c_2 is a constant,

$$q_1' = -h + \sqrt{h^2 + \omega_0^2}, \quad q_2' = -h - \sqrt{h^2 + \omega_0^2}.$$

The equations of the asymptotes to the hyperbolas have the form:

$$\dot{\varphi} = -q_1'\varphi, \quad \dot{\varphi} = -q_2'\varphi. \tag{11}$$

And, for the fourth case, the equation of the system's free oscillations is written in the form

$$\ddot{\varphi} - 2h\dot{\varphi} - \omega_0^2\varphi = 0. \tag{12}$$

The equation of the phase trajectories will also be the equation of a family of deformed hyperbolas analogous to (10). These intervals will have other slopes for the asymptotes (Fig. 2f). For this family of curves, the asymptote equations are

$$\dot{\varphi} = -q_1^{*}\varphi, \quad \dot{\varphi} = -q_2^{*}\varphi. \tag{13}$$

Here,

$$q_1^{*} = h + \sqrt{h^2 + \omega_0^2}, \quad q_2^{*} = h - \sqrt{h^2 + \omega_0^2}.$$

We now determine the sequence of changes of the system's structure for which the image point will so move to the origin that the transient response will be optimal with respect to the controlled coordinate.

In the automatic control system under consideration, let there be applied a disturbing stimulus f(t) of the unit step type, which is equivalent to the presence of some nonzero initial conditions, specifically, $\dot{\varphi} = \varphi_0$, $\varphi = 0$. It is easily seen from a consideration of the phase trajectories (Fig. 2) that, for the image point to proceed to the equilibrium position with minimal deviation of the error φ during the duration of the transient response, with these initial conditions it must move in the region $\varphi\dot{\varphi} > 0$ along phase trajectories corresponding to an automatic control system with positive values of the coefficients K and T (Fig. 2a,b). With any other combination of signs for K and T, the image point would either move away from the equilibrium position (Fig. 2c,e,f) or have a large maximum deviation of the error φ during the transient response (Fig. 2d).

After the error signal reaches its maximum value ($\varphi = \varphi_{\max}$, $\dot{\varphi} = 0$) this discrepancy should be liquidated as soon as possible. In order that this requirement be met, the phase plane for $\varphi\dot{\varphi} < 0$ must be so constructed that, for given initial conditions, the area under the integral curve will be maximal, since it is well known that, in this portion of the phase plane, the duration of the control is inversely proportional to the area under the integral curve.

In order for the response to occur without overshoot, one of the components of the integral curve to be synthesized must pass through the origin in this region of the phase plane and, in order for the area under the integral curve to be maximal, it is necessary that the slope of this phase trajectory be as large as possible.

It is clear, from a consideration of the phase sketches (Fig. 2), that there are trajectories passing through the origin in the required portion of the phase plane for three different combinations of signs of K and T (Fig. 2a,e,f). It is easily remarked that the greatest slope of the null phase trajectory corresponds to the structure of the system with a positive value of the differentiator's time constant T and a negative gain K of the error signal (Fig. 2e).

As follows from Eqs. (9) and (11), the equation of such a phase trajectory has the form: $\dot{\varphi} = -q_2^{*}\varphi$. Here, $q_2^{*} = -h - \sqrt{h^2 + \omega_0^2}$.

The second component of the integral curve should be so chosen that the image point will travel from position $\varphi = \varphi_{\max}$, $\dot{\varphi} = 0$ along the null phase trajectory chosen by us with the largest possible value of the coordinate $\dot{\varphi}$. This also makes it possible to obtain the greatest area under the integral curve. From this point of view, those phase trajectories are most suitable which correspond to the unstable structural scheme with a positive value of K and a negative value of T (Fig. 2c and d).

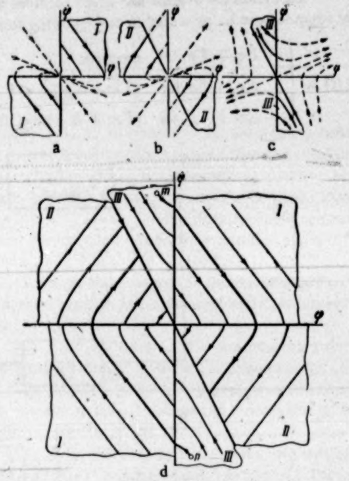

Fig. 3.

The process of constructing the phase "portrait" for obtaining an optimal transient response in the system is shown in Fig. 3a,b,c, and d.

Thus, the phase portrait of the optimal control system can be presented in the form of a three-sheeted phase surface (Fig. 3d).* The first sheet corresponds to the phase plane satisfying the condition $\varphi\dot{\varphi} \geq 0$ (Fig. 3a) and Eq. (5) for the free oscillations. The second sheet corresponds to the portion of the phase plane which satisfies the condition $(T_j\dot{\varphi} + K_j\varphi)\varphi < 0$ (Fig. 3b).

The constant coefficients T_j and K_j are so chosen that the boundary of the sheet, corresponding to the equation

$$T_j\dot{\varphi} + K_j\varphi = 0,$$

coincides with the phase trajectory described by the equation $\dot{\varphi} = -q_2^{*}\varphi$, where $q_2^{*} = -h - \sqrt{h^2 + \omega_0^2}$ (Fig. 2e), and passing through the origin.

The third sheet corresponds to the phase plane satisfying the condition $(T_j\dot{\varphi} + K_j\varphi)\varphi \leq 0$ (Fig. 3c). The boundary of the sheet, corresponding to the equation $T_j\dot{\varphi} + K_j\varphi = 0$ is common to the second and third sheets.

---

* The method of multisheeted phase surfaces, as applied to automatic control systems, has been worked out in [18-20].

Thus, it is clear from an analysis of the phase planes constructed, that the optimal control system changes its structure three times during the transient response when the system operates in the stabilization mode, and twice when the system operates in the tracking mode. In both cases, the disturbing action is taken to be in the form of unit jumps.

The nonlinear control law which provides this shift of structure can be presented in the following form:

$$\xi(t)=\begin{cases} K\varphi+T\dot{\varphi} & \text{for}\quad \varphi\dot{\varphi}\geqslant 0,\\ K\varphi-T\dot{\varphi} & \text{for}\quad (T_j\dot{\varphi}+K_j\varphi)\,\dot{\varphi}<0,\\ -K\varphi+T\dot{\varphi} & \text{for}\quad (T_j\dot{\varphi}+K_j\varphi)\,\varphi\leqslant 0.\end{cases}\qquad (14)$$

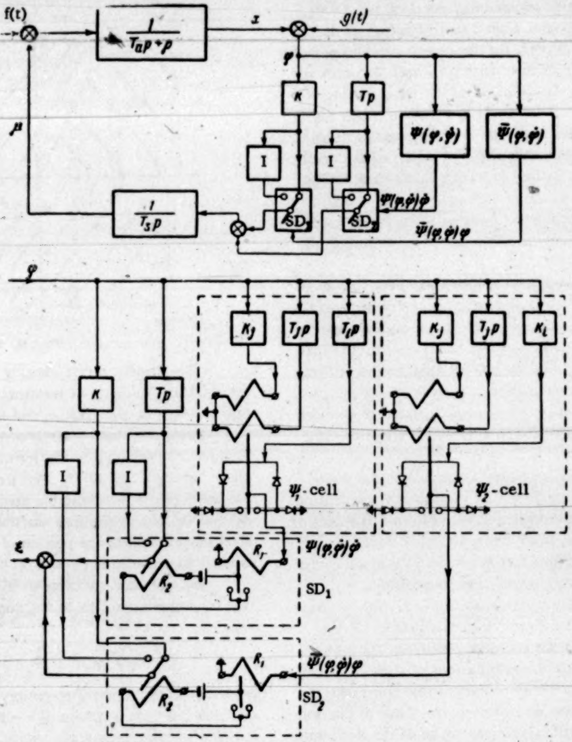

Fig. 4.

2. Realization of the Optimal Control Law

For the automatic control system to have the phase portrait shown in Fig. 3, it must contain a nonlinear correcting device which realizes the optimal control law given by (14). It follows from expression (14) that the nonlinear link must contain a switching device which varies the signs of the error signal and its derivative during the transient response as a function of their signs and relationships.

For the realization of this control law, we us a nonlinear "key"-type correcting device consisting of two monotypic Ψ-cells [4] (Fig. 4).

The first Ψ_1-cell passes the signal $\dot{\varphi}$ only under the condition $(T_j\dot{\varphi}+K_j\varphi)\dot{\varphi}\leq 0$, and the second Ψ_2-cell passes signal φ under the condition that $(T_j\dot{\varphi}+K_j\varphi)\varphi\leq 0$. The static characteristics of these nonlinear devices are shown in Fig.5.†

The signal from the output of these Ψ-cells acts on switching devices SD_1 and SD_2, consisting of the relay

---

† The nonlinear coefficients $\Psi(\varphi,\dot{\varphi})$ and $\bar{\Psi}(\varphi,\dot{\varphi})$ in the hatched portions of the $\varphi\dot{\varphi}$ plane equal the constant coefficients T_1 and K_1, respectively. In the nonhatched portions they equal zero.

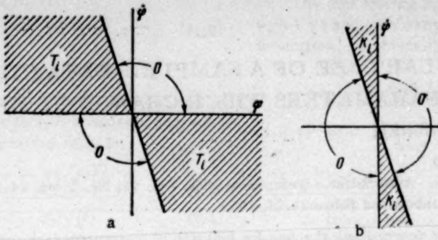

Fig. 5.

set R_1 and R_2. These devices provide the necessary changes in the signs of the error and its derivative by means of the inverter I.

The coefficients K_j and T_j of the correcting device are chosen on the basis of the relationship

$$\frac{K_j}{T_j} = h + \sqrt{h^2 + \omega_0^2}.$$

The connection between these coefficients and the system's parameters is defined by the following equation

$$\frac{K_j}{T_j} = \frac{T_s p + T}{2T_a T_s} + \sqrt{\frac{(T_s p + T)^2 + 4KT_a T_s}{4T_a^2 T_s^2}}. \quad (15)$$

Generally speaking, coefficients T_i and K_i can be chosen arbitrarily as functions of the dead zones of relays R_1 and R_2.

LITERATURE CITED

[1] V. V. Petrov, Investigation of a Pneumohydraulic Autopilot Servomechanism [in Russian] Dissertation (IAT AN SSSR, 1948).

[2] G. Lewis, "The use of nonlinear feedback for improving transient responses in automatic control systems," [Russian translation] Voprosy Raketnoi Tekhniki 4 (1954).

[3] G. M. Ostrovskii, "The use of nonlinear correcting devices in second-order automatic control systems," Avtomat. i Telemekh. 17, 11 (1956).‡

[4] V. A. Maslennikov, "Qualitative control of a neutral object by an astatic controller," Avtomat. i Telemekh. 17, 2 (1956).‡

[5] S. V. Emel'yanov, "A method for obtaining complex control laws using only the error signal or the controlled coordinate and its first derivative," Avtomat. i Telemekh. 18, 10 (1957).‡

[6] Automatic Control Fundamentals, [in Russian] ed. V. V. Solodovnikov (Mashgiz, 1954).

[7] I. Flügge-Lotz and C. F. Taylor, "Synthesis of a nonlinear control system," Trans. IRE, PG AC-1 (May, 1956).

[8] I. Flügge-Lotz and W. S. Wunch, "On a nonlinear transfer system," Journ. Appl. Phys. 26 (April, 1955).

[9] J. M. L. Janssen and J. C. Vermeulen, Behandlung zweier Regalungsprobleme mit Hysteresis und Reibung nach der Methode der Beschreibungsfunktion Nichtlineare Regelungs Forgange, Vortrage, (Munich, 1955).

[10] A. M. Letov, "Conditionally stable controlled systems (on one class of optimal controlled system)," Avtomat. i Telemekh. 18, 7 (1957).‡

[11] N. N. Bogolyubov and Yu. A. Mitropol'skii, Asymptotic Methods in Nonlinear Oscillation Theory [in Russian] (Mashgiz, 1955).

[12] A. A. Fel'dbaum, "The simplest relay systems of automatic control," Avtomat. i Telemekh. 10, 4 (1949).

[13] A. A. Fel'dbaum, "Optimal processes in automatic control systems," Avtomat. i Telemekh. 14, 6 (1953).

[14] A. A. Fel'dbaum, "On synthesizing optimal systems by means of phase space," Avtomat. i Telemekh. 16, 2 (1955).

[15] A. Ya. Lerner, "Improving the dynamic properties of automatic compensators by means of nonlinear connections, I and II," Avtomat. i Telemekh. 13, 2 and 4 (1952).

[16] A. Ya. Lerner, "On the limiting speed of response of automatic control systems," Avtomat. i Telemekh. 15, 6 (1954).

[17] V. V. Petrov and V. Yu. Rutkovskii, " Some questions in the construction of circuits and the choice of characteristics of fast-acting servomechanisms," in: Automatic Control and Computing Technology [in Russian], collected papers edited by V. V. Solodovnikov (Mashgiz, 1959) 2nd ed.

[18] V. V. Petrov and G. M. Ulanov, "Community of the skipping, vibration, and optimal modes of the class of servomechanisms," [in Russian]. Doklady Akad. Nauk SSSR 112, 3 (1957).

[19] V. V. Petrov and G. M. Ulanov, "Theory of the two simplest control systems," Avtomat. i Telemekh. 11, 5 (1950).

[20] V. V. Petrov, Mnoholistove a nektere trojrozmerne i lohy dynamiky nelinearnich servomechanismu souhrn praci o aut omatisaci, (Prague, 1957).

---

‡ See English translation.

ON ONE PARTICULAR CASE OF A SAMPLED-DATA SYSTEM WITH VARIABLE PARAMETERS WHICH CHANGE BY JUMPS

V. I. Teverovskii

(Dnepropetrovsk)

(Translated from: Avtomatika i Telemekhanika, Vol. 21, No. 1, pp. 64-71, January, 1960)
Original article submitted February 26, 1959

A method is given for determining the transfer function of a sampled-data system with periodically varying parameters in the particular case when the system is comprised of a series connection of a first-order link with variable parameters and links with constant parameters.

Among systems with variable parameters, a special place is occupied by systems whose parameters vary periodically at the pulse repetition frequency, remaining constant during the pulses and in the intervals between pulses, and changing by jumps at the boundaries of these time segments. Works by F. M. Kilin, E. A. Rozenman, and others have been devoted to these systems. A method for designing such systems in the general case was given in [1]. This method leads to cumbersome computations. In [2] Ya. Z. Tsypkin presented a simple method for investigating first-order systems.

The attempt is made in the present work to design sampled-data systems with periodically varying parameters for the very important particular case when only one root of the characteristic equation changes. As will be shown, this means physically that the system consists of a series connection of a first-order link with variable parameters and a system with constant parameters.

1. The First-Order Link*

We consider a link described by the equation

$$(q-q_0)\,x(\bar{t}) = -kq_0 f(\bar{t}). \qquad (1.1)$$

Here and in the sequel we shall use the dimensionless variables $\bar{t} = t/T$, $q = pT$ $(p = d/dt)$, where T is the repetition period of the input pulses.

The parameters q_0 and $\underline{k}$ are variable, and are subject to the following relationships:

$$\left.\begin{aligned} q_0 &= q_1 \\ k &= k_1 \end{aligned}\right\} \text{ for } n \leqslant t \leqslant n+\gamma,$$

$$\left.\begin{aligned} q_0 &= q_1' \\ k &= k_1' \end{aligned}\right\} \text{ for } n+\gamma < \bar{t} < n+1.$$

Here, $n = 0, 1, 2, \ldots$, $\gamma = \tau/T$, τ is the duration of the input pulses,

$$f(\bar{t}) = f[n] \quad \text{for} \quad n \leqslant \bar{t} \leqslant n+\gamma$$

and

$$f(\bar{t}) = 0 \quad \text{for} \quad n+\gamma < \bar{t} < n+1.$$

By solving Eq. (1.1) for the interval $(n, n+\gamma)$ with initial condition x[n] and for the interval $(n+\gamma, n+1)$ with initial condition $x[n+\gamma]$, and by also taking into account that no jump in the initial conditions occurs at the boundary of the intervals cited, we obtain the difference equation

$$x[n+1] = \\ = k_1 f[n]\left(1-e^{q_1\gamma}\right)e^{q_1'(1-\gamma)} + x[n]\,e^{q_1\gamma + q_1'(1-\gamma)}. \qquad (1.2)$$

If we take the discrete Laplace transform of Eq.(1.2 taking into account the lead theorem and the condition x(0) = 0 [3], we obtain

$$X^*(q) = k_1\frac{\left(1-e^{q_1\gamma}\right)e^{q_1'(1-\gamma)}}{e^q - e^{q_{1\,\mathrm{av}}}}\,F^*(q), \qquad (1.3)$$

where $X^*(q)$ and $F^*(q)$ are the discrete Laplace transform of the step functions x[n] and f[n], respectively, and

$$q_{1\,\mathrm{av}} = q_1\gamma + q_1'(1-\gamma).$$

Consequently, the transfer function of the first-orde sampled-data system with variable parameters has the form:

$$W^*(q) = k_1\frac{\left(1-e^{q_1\gamma}\right)e^{q_1'(1-\gamma)}}{e^q - e^{q_{1\,\mathrm{av}}}}. \qquad (1.4)$$

We now determine the impulsive response of system (1.4) at an arbitrary moment of time.

Letting $\bar{t} - n = \varepsilon$, we get

$$w[n,\varepsilon] = k_1\left(e^{-q_1\gamma} - 1\right)e^{q_{1\,\mathrm{av}}n}e^{q_1\varepsilon} \qquad (0 \leqslant \varepsilon \leqslant \gamma,\ \ n > 0), \qquad (1.5)$$

$$w[n,\varepsilon] = k_1\left(1-e^{q_1\gamma}\right)e^{q_{1\,\mathrm{av}}n}e^{q_1'(\varepsilon-\gamma)} \qquad (\gamma < \varepsilon < 1, n > 0), \qquad (1.6)$$

$$w[0,\varepsilon] = k_1\left(1-e^{q_1\varepsilon}\right) \qquad (0 \leqslant \varepsilon \leqslant \gamma). \qquad (1.7)$$

---

* The investigation of such links was provided in [2].

$$w[0, \varepsilon] = k_1 (1 - e^{q_1\gamma}) e^{q_1'(\varepsilon-\gamma)}$$

$$(\gamma < \varepsilon < 1). \qquad (1.8)$$

2. The Second-Order System

We now consider the second-order system consisting of a series connection of the link with variable parameters and a link with constant parameters (Fig. 1):

$$(q - q_{10}) x_1(\bar{t}) = - k q_{10} f(\bar{t}),$$

$$(q - q_2) x(\bar{t}) = - q_2 x_1(\bar{t}). \qquad (2.1)$$

Here, q_2 = const, $q_{10} = q_1$, and $k = k_1$ when $n \leq \bar{t} \leq n + \gamma$, $q_{10} = q_1'$ and $K = k_1'$ when $n + \gamma < \bar{t} < n + 1$.

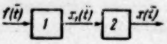

Fig. 1.

We now determine the impulsive response of the system described by Eqs. (2.1).

In this case, the input to link 2 with constant parameters is signal $x_1(\bar{t})$, the impulsive response of link 1 with variable parameters [cf. Eqs. (1.5)-(1.8)]:

$$(q - q_2) w_2[n, \varepsilon] = - q_2 w_1[n, \varepsilon]. \qquad (2.2)$$

The solution is carried out for the time interval (n, n + 1).

The result of solving Eq. (2.2) with initial condition $w_2[n]$ is

$$w_2[n + \gamma] = k_1 (e^{-q_1\gamma} - 1) \frac{q_2}{q_1 - q_2} (e^{q_2\gamma} - e^{q_1\gamma}) \times$$

$$\times e^{q_1 a v^n} + w_2[n] e^{q_2\gamma}.$$

By now solving Eq. (2.2) with initial condition $w_2(n + \gamma)$ and then carrying out some elementary transformations, we obtain the following difference equation:

$$w_2 \, n + 1] = w_2[n] e^{q_2} -$$

$$- k_1 (e^{-q_1\gamma} - 1) \frac{q_2}{q_1 - q_2} (e^{q_2(1-\gamma)+q_1\gamma} - e^{q_2}) e^{q_1 a v^n} -$$

$$- k_1 (1 - e^{q_1\gamma}) (e^{q_1'(1-\gamma)} - e^{q_2(1-\gamma)}) \frac{q_2}{q_1' - q_2} e^{q_1 a v^n}. \qquad (2.3)$$

As is well known, one gives the name operator, or transfer function, of a sampled-data system to a series of the form

$$W^*(q) = \sum_{n=1}^{\infty} w[n] e^{-qn} \quad \text{for} \quad w(0) = 0, \qquad (2.4)$$

where w[n] is the impulsive response of the corresponding continuous system.

It may be easily shown that

$$\sum_{n=1}^{\infty} w[n+1] e^{-qn} = e^q \sum_{n=1}^{\infty} w[n] e^{-qn} - w[1]. \qquad (2.5)$$

Indeed, by making the substitution n = k - 1, we get

$$\sum_{n=1}^{\infty} w[n+1] e^{-qn} = e^q \sum_{k=2}^{\infty} w[k] e^{-qk}.$$

By adding and subtracting w[1] in the right member, we obtain (2.5).

If we multiply both sides of Eq. (2.3) by e^{-qn} and then sum them over n from 1 to infinity, taking into account (2.5) and the equality [3], we get

$$\sum_{n=1}^{\infty} e^{\alpha n} e^{-qn} = \frac{e^{\alpha}}{e^q - e^{\alpha}},$$

$$W_2^*(q) = k_1 \frac{\left[(1 - e^{-q_1\gamma})(e^{q_2(1-\gamma)+q_1\gamma} - e^{q_2}) \frac{q_2}{q_1 - q_2} + (e^{q_1\gamma} - 1) \frac{q_2}{q_1' - q_2} (e^{q_1'(1-\gamma)} - e^{q_2(1-\gamma)})\right] e^{q_1 a v}}{(e^q - e^{q_2})(e^q - e^{q_1 a v})} + \frac{w_2[1]}{e^q - e^{q_2}}; \qquad (2.6)$$

$w_2[1]$ is determined analogously to $w_2[n + 1]$ on the basis of expressions (1.7) and (1.8), account being taken of the fact that $w_2(0) = 0$.

As the result, we obtain

$$w_2[1] = k_1 \frac{q_2 (q_1 - q_2) e^{q_1 a v} - q_1 (q_1' - q_2) e^{q_2} + q_2 (q_1' - q_1) e^{q_1\gamma + q_2(1-\gamma)}}{(q_1 - q_2)(q_1' - q_2)} + \frac{(q_2 - q_1)(q_2 e^{q_1'(1-\gamma)} - q_1' e^{q_2(1-\gamma)})}{(q_1 - q_2)(q_1' - q_2)}. \qquad (2.7)$$

By taking (2.7) into account, we obtain the final expression for $W_2^*(q)$:

$$W_2^*(q) = k_1 \frac{b_1 e^q + b_0}{(e^q - e^{q_2})(e^q - e^{q_1 a v})}, \qquad (2.8)$$

where

$$b_0 = e^{q_2 + q_1 a v} + \frac{q_2 e^{q_2 + q_1'(1-\gamma)} - q_1 e^{q_1 a v + q_2(1-\gamma)}}{q_1 - q_2}; \qquad (2.9)$$

$$b_1 = \frac{w_2[1]}{k_1}. \qquad (2.10)$$

If the system is astatic and its linear portion has a transfer function of the form

$$W_a(q) = \frac{-kq_{10}}{(q-q_{10})\,q}, \qquad (2\ 11)$$

it is then easily seen that the corresponding discrete transfer function can be obtained by passing to the limit:

$$W^*_a(q) = \lim_{q_2 \to 0}\left[-\frac{1}{q_2}W^*_2(q)\right]. \qquad (2.12)$$

By carrying out some elementary transformations, we get

$$W^*_a(q) = k_1\frac{[(\dot{q}'_1-q_1)(1-e^{q_1\gamma}) + q_1(e^{\dot{q}'_1(1-\gamma)} - e^{q_1\mathrm{av}}) + \gamma q_1 q'_1]\,e^q}{q_1 q'_1 (e^q - e^{q_1\mathrm{av}})(e^q-1)} + \frac{q'_1(e^{q_1\mathrm{av}} - e^{\dot{q}'_1(1-\gamma)} - \gamma q_1 e^{q_1\mathrm{av}})}{q_1 q'_1 (e^q - e^{q_1\mathrm{av}})(e^q-1)}. \qquad (2.13)$$

In the very important particular case when $\gamma \ll 1$, the expression for $W^*(q)$ is significantly simplifed. By taking into account that $e^{q_i\gamma} \approx 1 + q_i\gamma$ (if $|q_i\gamma| \ll 1$), we get

$$W^*_2(q) = k_1\frac{\gamma q_1 q_2 (e^{q_1} - e^{q_2})e^q}{(q'_1-q_2)(e^q - e^{q_1\mathrm{av}})(e^q - e^{q_2})}. \qquad (2.14)$$

3. A System of Arbitrary Order with One Variable Root of the Characteristic Equation

Let there be given a system of arbitrary order r. One of the roots of the system's characteristic equation is variable, all the roots being assumed to be simple. It may then be shown that the system takes the form of a series connection of a variable link 1 and a constant portion 2 which is described by an equation of order (r-1).

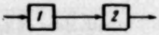

Fig. 2.

The transfer function of link 1 (Fig. 2) is

$$W_1(q) = -k_1\frac{q_{10}}{q-q_{10}}, \qquad (3.1)$$

where q_{10} is the variable root, assuming the values of q_1 and q_1^*.

The transfer function of the constant portion 2 is

$$W_{r-1}(q) = \frac{P(q)}{Q(q)}, \qquad (3.2)$$

where P(q) and Q(q) and polynomials in q, the order of P(q) being less than the order of Q(q).

Then,

$$W_{r-1}(q) = \frac{P(q)}{Q(q)} = \sum_{k=1}^{r-1}\frac{P(q_k)}{Q'(q_k)}\frac{1}{q-q_k} = \sum_{k=1}^{r-1}\frac{c_k}{q-q_k}, \qquad (3.3)$$

where q_k are the roots of the equation $Q(q) = 0$, $Q'(q_k) = dQ(q)/dq\,|_{q=q_k}$.

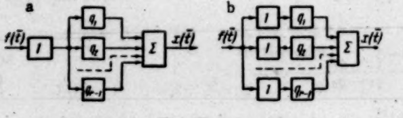

Fig. 3.

On the basis of (3.3), the block diagram of the system may be given as shown on Fig. 3 a.†

On Fig. 3 a, $q_1, q_2, \ldots, q_{r-1}$ denote the links whose transfer functions are the terms of sum (3.3); Σ is a summing device.

Obviously, the processes in the system are not changed if the block schematic is varied so as to take the form shown in Fig. 3 b. But, it is clear from Fig.3 b, that an rth-order system with variable parameters can be given in the form of a parallel connection of r-1 second-order systems and, consequently, the discrete transfer function of such a system has the form:

$$W^*(q) = \sum_{k=1}^{r-1} c_k W^*_k(q), \qquad (3.4)$$

where

$$W^*_k(q) = -\frac{1}{q_k}\frac{b_{1k}e^q + b_{0k}}{(e^q - e^{q_1\mathrm{av}})(e^q - e^{q_k})},$$

$$b_{1k} = \frac{q_1(q_k - q'_1)e^{q_k} + q_k(q'_1 - q_1)e^{q_k(1-\gamma)+q_1\gamma}}{(q_1-q_k)(q'_1-q_k)} + \frac{q_k(q_1-q_k)e^{q_1\mathrm{av}} + (q_1-q_k)(q'_1 e^{q_k(1-\gamma)} - q_k e^{\dot{q}'_1(1-\gamma)})}{(q_1-q_k)(q'_1-q_k)}$$

$$b_{0k} = e^{q_1\mathrm{av}+q_k} + \frac{q_k e^{q_k+\dot{q}'_1(1-\gamma)} - q_1 e^{q_1\mathrm{av}+q_k(1-\gamma)}}{q_1-q_k}. \qquad (3.5)$$

If $q_k = 0$, then expression (2.13) can be used for computing $W^*_k(q)$.

If $\gamma \ll 1$, then $W^*_k(q)$ can be computed by formula (2.14) by replacing q_2 by q_k in its right member and dividing by $(-q_k)$.

---

† A similar representation of the schematic is given in [1].

Up till now, we have assumed that the first link is a simple inertial one. If, however, the transfer function of this link has the form:

$$W_1(q) = k_1 \frac{q + \alpha}{q + \beta}, \tag{3.6}$$

where k_1, α, and β are variable parameters, then the link may be presented in the form of a parallel connection of an inertial link and an ideal amplifier with variable parameters:

$$W_1(q) = k_1 - k_1 \frac{\beta - \alpha}{q + \beta}. \tag{3.7}$$

Since the input to the variable system is $f(\bar{t})$ at times $n + \gamma < \bar{t} < n + 1$, varying the amplifier parameters does not affect the process, and the discrete transfer function of the second-order system whose first link has a transfer function of the form (3.7) is obtained in the form of a difference of the discrete first-order transfer function corresponding to the second link, but multiplied by k_1, and the discrete transfer function of the second-order system whose first link has a transfer function of the form $k_1(\beta - \alpha)/(q + \beta)$.

Thus, for a sampled-data system with periodically varying parameters, it is sufficiently simple to determine the discrete transfer function which has constant parameters (in the case when only one root of the characteristic equation varies). It is particularly simple to obtain the expression when the pulses are of short duration ($\gamma \ll 1$).

In conclusion, we consider an example of the application of the method presented above.

4. Transient Response in a Radar Range Finder

The range finder's operation is based on the comparison of the position of the pulse reflected from the target with the position of a pair of special selector pulses – semistrobe S and the translation of S after the translation in time of the echo pulse EP.

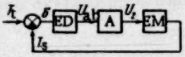

Fig. 4.

The block schematic of the range-finder is given in Fig. 4.

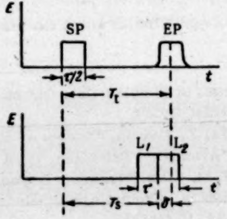

Fig. 5.

The scheme shown does not, of course, represent the contemporary state of radar technology, but is very convenient as an example of the application of the method presented here.

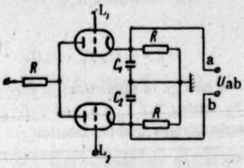

Fig. 6.

The nomenclature used on Fig. 4 is as follows: ED is the error discriminator, A is an amplifier, EM is the executive mechanism, T_t is the temporal position of the middle of the echo pulse from the target with respect to the sonde pulse SP, and T_s is the position of the semistrobe boundary (Fig. 5). The ED processes the voltage proportional to the quantity $\delta = T_t - T_s$. We now consider one discriminator circuit (Fig. 6).

Tubes L_1 and L_2 are normally cut off, and are opened by the semistrobes. If the center of the EP coincides with the boundary of a semistrobe, the charges taken by capacitors C_1 and C_2 during a period are equal, and $U_{ab} = 0$.

If the EP is displaced relative to the semistrobes, the charges taken by C_1 and C_2 are unequal, and $U_{ab} \neq 0$.

It is easily seen that the error discriminator parameters are different when the semistrobes are present from what they are when the semistrobes are absent.

Strictly speaking, the system under consideration is a system with pulse-width modulation (PWM). But with low porosity $\gamma = \tau/2T_r$ (τ is the total length of the semistrobes and T_r is the repetition period of the sonding pulses) and if the condition $\tau/2 \ll T_c$ holds (T_c is the time constant of the charging of capacitors $C_1 = C_2 = C$), one can replace the system with PWM by a system with pulse-amplitude modulation with a constant pulse duration equal to $\tau/2$. Moreover, the time for switching the discriminator parameters is defined by the duration of the semistrobes $\tau/2 = \text{const}$.

From what has been said above, we obtain the following equations for the discriminator.

$$(T_c p + 1) U_{ab} = k_1 \frac{R}{R + R_1} \delta \quad \text{for} \quad nT_r \leqslant t \leqslant nT_r + \frac{\tau}{2} \tag{4.1}$$

and

$$(T_p p + 1) U_{ab} = 0 \quad \text{for} \quad nT_r + \frac{\tau}{2} < t < (n + 1) T_r \tag{4.2}$$

Here, $k_1 = 4E/\tau$, E is the amplitude of the echo pulse at the discriminator's input,

$$T_c = \frac{CRR_1}{R + R_1} \approx CR_1, \quad T_p = RC.$$

The amplifier and the executive mechanism are links with constant parameters. Their equations are, respectively,

$$U_2 = k_2 U_{\text{ab}}, \tag{4.3}$$

$$(T_M p + 1)\, p T_s = k_3 U_2. \tag{4.4}$$

We now go to dimensionless parameters.

By letting $T_r / T_p = a_1$ and $T_c / T_p = \alpha$, we obtain the discriminator's transfer function:

$$W_1(q) = k_1 \frac{(1-\alpha')\,\frac{a_1}{\alpha'}}{q + \frac{a_1}{\alpha'}}, \tag{4.5}$$

where $\alpha' = \alpha$ for $n \le \bar{t} \le n + \gamma$ and $\alpha' = 1$ for $n = \gamma < \bar{t} < n + 1$.

The transfer function of the amplifier and the EM takes the form

$$W_2(q) = \frac{k_2 k_3 T_r \; a_2}{(q + a_2)\, q} = k_2 k_3 T_r \left(\frac{1}{q} - \frac{1}{q + a_2}\right). \tag{4.6}$$

By taking into account that $\gamma \ll 1$ and using formula (2.14), we obtain the transfer function of the open-loop sampled-data system in the form

$$W^*(q) = k_1 k_2 k_3 T_r\,(1-\alpha)\,\frac{\gamma}{\alpha}\left[\frac{(1-e^{-a_2})\,e^q}{(e^q - e^{-a_{1\,\text{av}}})(e^q - 1)} - \frac{a_1 (e^{-a_1} - e^{-a_2})\,e^q}{(a_2 - a_1)(e^q - e^{-a_2})(e^q - e^{-a_{1\,\text{av}}})}\right].$$

where

$$a_{1\,\text{av}} = \frac{a_1}{\alpha}\gamma + a_1(1-\gamma) \approx a_1\left(1 + \frac{\gamma}{\alpha}\right).$$

After some elementary transformations, we finally obtain

$$W^*(q) = k\,\frac{\left(1 - \frac{a_1 e^{-a_2} - a_2 e^{-a_1}}{a_1 - a_2}\right) e^{2q} + \left(e^{-(a_1 + a_2)} - \frac{a_1 e^{-a_2} - a_2 e^{-a_1}}{a_1 - a_2}\right) e^q}{(e^q - e^{-a_{1\,\text{av}}})(e^q - e^{-a_2})(e^q - 1)}. \tag{4.7}$$

If the transfer function of the open-loop sampled-data system has the form:

$$W^*(q) = k\,\frac{B_2 e^{2q} + B_1 e^q}{A_3 e^{3q} - A_2 e^{2q} + A_1 e^q - A_0},$$

then, starting from the analogy of the Nyquist criterion, one can show that the following inequality must hold in order that the closed-loop system be stable:

$$k < \left|\frac{A_0^2 + A_1 A_3 - A_0 A_2 - A_3^2}{A_0 B_2 + A_3 B_1}\right|. \tag{4.8}$$

For the given case, inequality (4.8) takes the form

$$k < \frac{(1 - e^{-(a_2 + a_{1\,\text{av}})})(e^{-a_2} + e^{-a_{1\,\text{av}}} - e^{-(a_2 + a_{1\,\text{av}})})}{e^{-(a_2 + a_{1\,\text{av}})}\left(1 - \frac{a_1 e^{-a_2} - a_2 e^{-a_1}}{a_1 - a_2}\right) + e^{-(a_1 + a_2)} - \frac{a_1 e^{-a_2} - a_2 e^{-a_1}}{a_1 - a_2}}. \tag{4.9}$$

If $a_2 \ll 1$ and $a_1 \ll 1$, which corresponds to $T_p \gg T_r$ and $T_M \gg T_r$, then inequality (4.9) simplifies to

$$k < \frac{(1 - e^{-a_{1\,\text{av}}})(1 - e^{-a_{1\,\text{av}}} + a_2 e^{-a_{1\,\text{av}}})}{a_1}. \tag{4.10}$$

If the condition $a_{1\,\text{av}} \ll 1$ also holds, then condition (4.9) takes the form:

$$k < \frac{a_2 a_{1\,\text{av}} + a_{1\,\text{av}}^2}{a_1}. \tag{4.11}$$

In conclusion, the author wishes to express his gratitude to Ya. Z. Tsypkin for his aid in the preparation of this paper.

LITERATURE CITED

[1] F. M. Kilin, "Transient responses and steady-state processes in sampled-data systems with variable parameters which change by jumps," Avtomat. i Telemekh. 18, 12 (1957).‡

[2] Ya. Z. Tsypkin, Theory of Sampled-Data Systems [in Russian] (Fizmatgiz, 1958).

[3] Ya. Z. Tsypkin, Transient Responses and Steady-State Processes in Sampled-Data Circuits [in Russian] (Gosénergoizdat, 1951).

[4] Ya. Z. Tsypkin, "Theory of discontinuous control, I, II," Avtomat. i Telemekh. 10, 3 and 5 (1949).

[5] F. M. Kilin, "Transient responses and steady-state processes in automatic range-finders," Avtomat. i Telemekh. 19, 10 (1958).‡

---

‡ See English translation.

ON METHODS OF SIMULATING RATIONAL-FRACTION FUNCTIONS WITHOUT THE USE OF DIFFERENTIATING ELEMENTS

B. Ya. Kogan

(Moscow)

(Translated from: Avtomatika i Telemekhanika, Vol. 21, No. 1, pp. 72-81, January, 1960)
Original article submitted June 2, 1959

Methods of simulating rational-fraction transfer functions without the use of differentiating elements when the original differential equations contain constant and variable coefficients are compared. It is asserted that the minimum number of operational amplifiers required is n + 3, where n is the order of the differential equation. For simplicity of the circuit and for the minimum amount of preliminary calculation, the method of combining derivatives is preferable for constant coefficients, whereas the method of going over to the equivalent system of first-order equations is preferable when the coefficients are variable.

In the investigation of automatic control and regulation systems by means of electronic analog computers, the necessity frequently arises of reproducing rational-fraction transfer functions of the form

$$W(s) = \frac{b_m s^m + b_{m-1} s^{m-1} + \cdots + b_1 s + b_0}{s^n + a_{n-1} s^{n-1} + \cdots + a_1 s + a_0}, \quad (1)$$

where

$$m \leqslant n,$$

and $b_m, b_{m-1}, \ldots, b_1, b_0$ and $a_{n-1}, a_{n-2}, \ldots, a_1, a_0$ are given constant coefficients.

Transfer functions of this type are obtained, for example, from the approximate representation of lags by a Padé series, the synthesis of correcting circuits, and a number of problems in the statistical dynamics of automatic control systems.

The use of differentiators in the setups for these transfer functions is proscribed because of the sharp amplification of the noise which is always found in the output signals of operational amplifiers, the representation of the right members as given functions of time being possible only in a very limited number of cases when the law of change of the input signal is known beforehand.

Various methods of reproducing these transfer functions using only integrating and adding elements are known from the literature [1-4]. These methods can be reduced to four basic ones:

1) direct integration;

2) decomposition of the transfer function into simpler ones (method of structure transformation);

3) decomposition into first-order equations;

4) combination of derivatives.

In the literature, these methods were not compared among themselves, and some of them were mentioned only superficially. It is also of interest to establish the possibility of extending them to the case when the coefficients of the differential equation giving rise to (1) are given functions of time.

1. Method of Direct Integration

It is convenient to consider this method in terms of the simple example of the equation

$$_3y''' + a_2y'' + a_1y' + a_0y =$$
$$= b_0x + b_1x' + b_2x'' + b_3x'''$$

with given constant coefficient a_0, a_1, a_2, and a_3, and b_0, b_1, b_2, and b_3, initial conditions $y(0)$, $y'(0)$, and $y''(0)$, and a disturbance x whose dependence on time is not given beforehand.

We solve the initial equation for the difference of the highest derivatives:

$$a_3y''' - b_3x''' =$$
$$= -(a_2y'' - b_2x'') - (a_1y' - b_1x') - (a_0y - b_0x).$$

By introducing the symbolic integration operator $\int dt = 1/p$, $\int\int dt\, dt = 1/p^2$, etc., we obtain

$$a_3y - b_3x = -\frac{1}{p}(a_2y - b_2x) -$$
$$- \frac{1}{p^2}(a_1y - b_1x) - \frac{1}{p^3}(a_0y - b_0x). \quad (2)$$

In order to retain the initial values of the coefficients a_0, a_1, a_2, a_3, b_0, b_1, b_2, and b_3 in the setup of the problem, we add the term $-(a_2-1)y$ to the right and left sides of expression (2). The result is

$$y = -\frac{1}{p}(a_2y - b_2x) - \frac{1}{p^2}(a_1y - b_1x) -$$
$$- \frac{1}{p^3}(a_0y - b_0x) + b_3x - (a_3 - 1)y. \quad (3)$$

Expression (3) allows the structural scheme (block schematic) of the setup to be given directly. Indeed, if we denote by the new variable z_1 the sum of all the terms in (3) which contain the symbol for integration, we obtain the equation

$$y = z_1 + b_3x - (a_3 - 1)\,y. \tag{4}$$

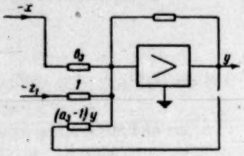

Fig. 1.

The quantity y, in correspondence with (4), can be formed by means of an adder, as shown on Fig. 1. It should be mentioned that such a method for isolating y gives a stable setup only in case $a_3 > 1$. If $a_3 < 1$, it is necessary to divide all the coefficients by a_3 as a preliminary step. With this, there is no longer the necessity of introducing the term $(a_3-1)y$ and, in the problem setup, there appear the new values of the coefficients:

$$\frac{a_2}{a_3},\quad \frac{a_1}{a_3},\quad \frac{a_0}{a_3};\quad \frac{b_0}{a_3},\quad \frac{b_1}{a_3},\quad \frac{b_2}{a_3},\quad \frac{b_3}{a_3}.$$

For the further construction of the scheme, we determine the value of the product pz_1:

$$pz_1 = -(a_2y - b_2x) - \frac{1}{p}(a_1y - b_1x) - \frac{1}{p^2}(a_0y - b_0x).$$

By introducing the notation

$$z_2 = -\frac{1}{p}(a_1y - b_1x) - \frac{1}{p^2}(a_0y - b_0x),$$

we get

$$pz_1 = -(a_2y - b_2x) + z_2. \tag{5}$$

Consequently, it is necessary to add an integrator to the schematic of Fig. 1. By continuing similarly, we arrive at the expression

$$pz_2 = -(a_1y - b_1x) + z_3, \tag{6}$$

where

$$pz_3 = -(a_0y - b_0x),\quad z_3 = -\frac{1}{p}(a_0y - b_0x).$$

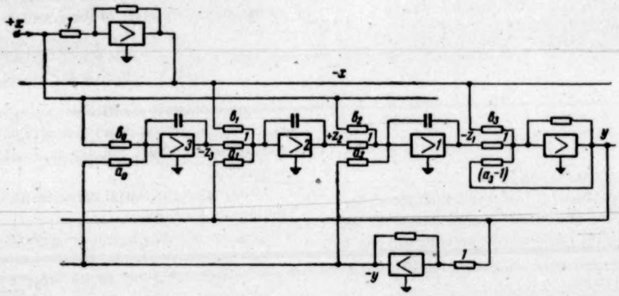

Fig. 2.

Equations (4), (5), and (6) lead directly to the setup shown on Fig. 2. For m = n, the total number of blocks required here is n + 3. For m < n, one can obviously dispense with the output adder, so that the number of blocks will be n + 2.

The initial conditions for integrators 1, 2, and 3 can be computed by giving the relationships for z_1, z_2, and z_3 in the form

$$z_1(0) = a_3y(0) - b_3x(0),$$

$$z_2(0) = a_3y'(0) - b_3x'(0) + a_2y(0) - b_2x(0),$$

$$z_3(0) = a_3y''(0) - b_3x''(0) + a_2y'(0) - b_2x'(0) + a_1y(0) - b_1x(0).$$

The regularities apparent in the relationships given allow one to write directly the relationships for the initial conditions for the kth integrator:

$$z_k(0) = z_{n-j} = \sum_{1}^{n-j}\left[a_{(i+j)}y^{(i-1)}(0) - b_{(i+j)}x^{(i-1)}(0)\right], \tag{7}$$

where j = n − k, i = 1, 2, 3, . . .

The basic advantage of the method just considered is that the setup is implemented from the original coefficients, and the computation of the initial conditions is carried out with comparative simplicity.

2. Decomposition of the Transfer Function into Simpler Ones

The basis of this method is that any transfer function W(s) can be considered as the transfer function of some single-loop system with negative feedback, in which the forward path has transfer function $W_1(s)$ and the feedback path has transfer function $W_2(s)$. The conditions imposed on the functions W_1 and W_2 are that the numerator of the first may not contain terms with s, and the numerator of the second may be a polynomial in s which is of degree one less than the polynomial in the numerator of W(s).

Indeed, let

$$W(s) = \frac{R(s)}{P(s)} = \frac{W_1(s)}{1 + W_1(s)\,W_2(s)}. \tag{8}$$

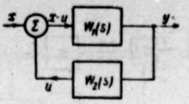

Fig. 3.

The block schematic of the connection of $W_1(s)$ and $W_2(s)$ is given in Fig. 3.

Let

$$W_1(s) = \frac{y(s)}{x(s) - u(s)} = \frac{1}{Q_1(s)},$$

$$W_2(s) = \frac{u(s)}{y(s)} = \frac{Q_2(s)}{Q_3(s)}. \tag{9}$$

We now find the conditions which must be satisfied by $Q_1(s)$, $Q_2(s)$, and $Q_3(s)$ so that Eq. (8) may be valid:

$$\frac{R(s)}{P(s)} = \frac{Q_2(s)}{Q_1(s)\,Q_2(s) + Q_3(s)}, \tag{10}$$

whence

$$R(s) = Q_2(s), \quad P(s) = Q_1(s)\,Q_2(s) + Q_3(s). \tag{11}$$

It follows from conditions (11) that the degree of polynomial $Q_1(s)$ must be equal to the difference of the degrees of polynomials $P(s)$ and $R(s)$, and from (9) and (10) that the degree of polynomial $Q_3(s)$ must be one less than the degree of polynomial $R(s)$. By using these special characteristics, we can write the general form of the polynomials $Q_1(s)$ and $Q_3(s)$:

$$Q_1(s) = \sum_{i=0}^{n-m} l_i s^i, \quad Q_3(s) = \sum_{i=0}^{m-1} m_i s^i, \tag{12}$$

where l_i and m_i are constants to be determined.

For example, let $R(s) = b_0 + b_1 s + b_2 s^2 + b_3 s^3$ and $P(s) = a_0 + a_1 s + a_2 s^2 + s^3$. Then, in accordance with (12), we obtain

$$Q_1(s) = l_0, \quad Q_2(s) = b_0 + b_1 s + b_2 s^2 + b_3 s^3,$$

$$Q_3(s) = m_0 + m_1 s + m_2 s^2.$$

To determine the values of l_0, m_0, m_1, and m_2, we substitute the values found for Q_1, Q_2, and Q_3 in (11). The result is

$$a_0 + a_1 s + a_2 s^2 + s^3 = l_0 b_3 s^3 + (l_0 b_2 + m_2) s^2 +$$

$$+ (l_0 b_1 + m_1) s + l_0 b_0 + m_0,$$

whence the coefficients sought will be

$$l_0 = \frac{1}{b_3}, \quad m_0 = a_0 - \frac{b_0}{b_3},$$

$$m_1 = a_1 - \frac{b_1}{b_3}, \quad m_2 = a_2 - \frac{b_2}{b_3}.$$

Thus,

$$W_1(s) = \frac{1}{l_0}, \quad W_2(s) = \frac{m_0 + m_1 s + m_2 s^2}{b_0 + b_1 s + b_2 s^2 + b_3 s^3}.$$

In its turn, $W_2(s)$ can be presented as

$$W_2(s) = \frac{W_{11}(s)}{1 + W_{11}(s)\,W_{22}(s)},$$

where

$$W_{11}(s) = \frac{1}{n_0 + n_1 s}, \quad W_{22}(s) = \frac{c_0 + c_1 s}{m_0 + m_1 s + m_2 s^2}.$$

To determine the unknown coefficients we use, based on (11), the relationship

$$b_0 + b_1 s + b_2 s^2 + b_3 s^3 =$$

$$= (n_0 + n_1 s)(m_0 + m_1 s + m_2 s^2) + (c_0 + c_1 s).$$

By equating coefficients, we get

$$c_0 = b_0 - \left(b_2 - b_3 \frac{m_1}{m_2}\right) \frac{m_1}{m_2},$$

$$c_1 = b_1 - \left[b_3 \frac{m_0}{m_2} + \frac{m_1}{m_2}\left(b_2 - b_3 \frac{m_1}{m_2}\right)\right],$$

$$n_0 = \frac{b_2 - b_3 \dfrac{m_1}{m_2}}{m_2}, \quad n_1 = \frac{b_3}{m_2}.$$

We now decompose $W_{22}(s)$ into the simpler components:

$$W_{22}(s) = \frac{W_{111}(s)}{1 + W_{111}(s)\,W_{222}(s)},$$

$$W_{111}(s) = \frac{1}{q_0 + q_1 s}, \quad W_{222}(s) = \frac{r_0}{c_0 + c_1 s}.$$

We determine the coefficients r and q from the relationship

$$m_0 + m_1 s + m_2 s^2 = (q_0 + q_1 s)(c_0 + c_1 s) + r_0,$$

whence

$$q_1 = \frac{m_2}{c_1}, \quad q_0 = \left(m_1 - \frac{c_0}{c_1} m_2\right) \frac{1}{c_1},$$

$$r_0 = m_0 - \left(m_1 - m_2 \frac{c_0}{c_1}\right) \frac{c_0}{c_1}.$$

Thus, the problem leads to the setup of the following system of equations:

$$\begin{aligned} y &= \frac{1}{l_0}(x - u), \\ (n_0 + n_1 s)\,u &= y - u_1, \\ (q_0 + q_1 s)\,u_1 &= u - u_2, \\ (c_0 + c_1 s)\,u_2 &= r_0 u_1. \end{aligned} \tag{13}$$

The block schematic and the setup which correspond to this system of equations are given in Figs. 4 and 5. The initial conditions for the new variables u, u_1, and u_2 can be found from the given initial conditions by means of system (13). As follows from Fig. 5, this method gives a setup requiring a large number of integrators in comparison with the method of direct integration. In addition, a comparatively large amount of time must be expended on the computation of the coefficients of the transformed equations.

3. Decomposition of the Initial Inhomogeneous nth-Order Equation into a System of n Inhomogeneous First-Order Equations

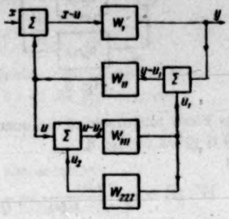

Fig. 4.

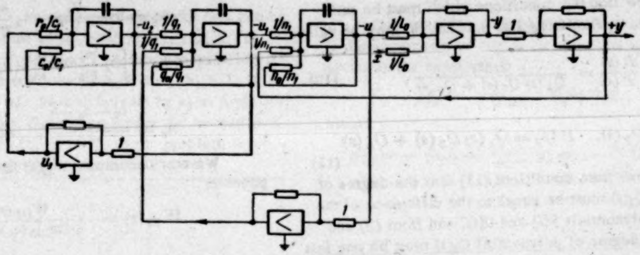

Fig. 5.

While this decomposition is not unique, the best results are given by the method described in [3], according to which the linear differential equation with constant coefficients

$$\frac{d^n y}{dt^n} + a_{n-1}\frac{d^{n-1}y}{dt^{n-1}} + \ldots + a_1\frac{dy}{dt} + a_0 y =$$
$$= b_0 x + b_1\frac{dx}{dt} + \ldots + b_{n-1}\frac{d^{n-1}x}{dt^{n-1}} + b_n\frac{d^n x}{dt^n} \quad (14)$$

can be presented in the form of a system of linear first-degree differential equations:

$$\begin{aligned} y &= y_1 + \alpha_n x, \\ \frac{dy_1}{dt} &= y_2 + \alpha_{n-1}x, \\ &\ldots\ldots\ldots \\ \frac{dy_{n-1}}{dt} &= y_n + \alpha_1 x, \\ \frac{dy_n}{dt} &= -a_{n-1}y_n - a_{n-2}y_{n-1} - \\ &- \ldots - a_1 y_2 - a_0 y_1 + \alpha_0 x. \end{aligned} \quad (15)$$

Indeed, by eliminating $y_1, y_2, \ldots, y_n$ from the last equation of system (15), we arrive at an equation of the form

$$\frac{d^n y}{dt^n} + a_{n-1}\frac{d^{n-1}y}{dt^{n-1}} + \ldots + a_1\frac{dy}{dt} + a_0 y = \alpha_n\frac{d^n x}{dt^n} +$$
$$+ (\alpha_{n-1} + \alpha_n a_{n-1})\frac{d^{n-1}x}{dt^{n-1}} +$$
$$+ \ldots + (\alpha_1 + a_{n-1}\alpha_2 + \ldots + a_1\alpha_n)\frac{dx}{dt} +$$
$$+ (\alpha_0 + \alpha_1 a_{n-1} + \ldots + \alpha_{n-1}a_1 + \alpha_n a_0)\,x. \quad (16)$$

In order that Eqs. (15) and (16) be identical, it is necessary that the values of the new coefficients α_i satisfy the following equations:

$$\begin{aligned} b_0 &= \alpha_0 + \alpha_1 a_{n-1} + \alpha_2 a_{n-2} + \ldots + \alpha_{n-1}a_1 + \alpha_n a_0, \\ b_1 &= \alpha_1 + \alpha_2 a_{n-1} + \ldots + a_{n-1}a_2 + \alpha_n a_1, \\ b_2 &= \alpha_2 + \ldots + \alpha_{n-1}a_3 + \alpha_n a_2, \\ &\ldots\ldots\ldots\ldots\ldots\ldots \\ b_{n-1} &= \alpha_{n-1} + \alpha_n a_{n-1}, \\ b_n &= \alpha_n. \end{aligned} \quad (16a)$$

The block schematic for the system of equations (15) is constructed in the form shown on Fig. 6a. The total number of blocks required is n + 3. The coefficients α_0, $\alpha_1, \ldots, \alpha_n$ are easily computed on the basis of (16a) by successively substituting the values of α_1, starting with $\alpha_n = b_n$. The initial conditions for the new variables y_1, $y_2, \ldots, y_n$ are determined by means of system of equations (15) from the given $y(0)$, $y^{(1)}(0), \ldots y^{n-1}(0)$

and $\quad x(0),\ x^{(1)}(0),\ x_0^{(2)}(0), \ldots, x^{(n-1)}(0).$

As an example, we consider the reproduction of the transfer function

$$W(s) = \frac{s^2 - \frac{6}{\tau}s + \frac{12}{\tau^2}}{s^2 + \frac{6}{\tau}s + \frac{12}{\tau^2}},$$

approximating the transfer function of a lag link, $e^{-s\tau}$, by a Padé series for $\mu = \nu = 2$ [6]. Here, $n = 2$, $a_0 = 12/\tau^2$, $a_1 = 6/\tau$, $a_2 = 1$, $b_0 = 1/\tau^2$, $b_1 = -6/\tau$, and $b_2 = 1$.

On the basis of (15), the equivalent system of equations is written in the form

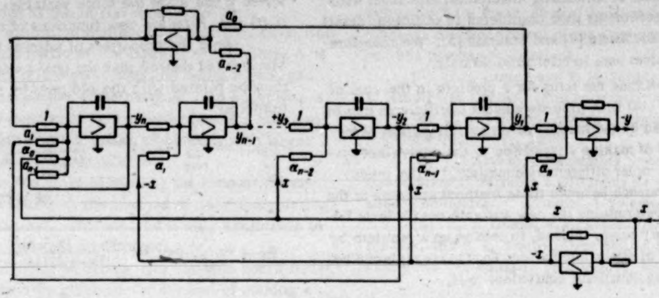

Fig. 6a.

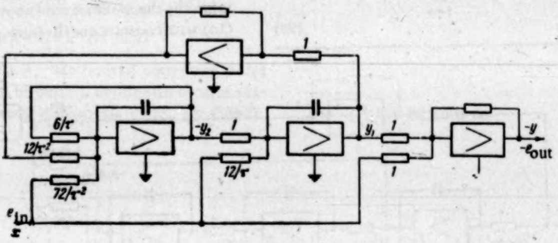

Fig. 6b.

$$\frac{dy_2}{dt} = -a_1 y_2 - a_0 y_1 + \alpha_0 x,$$

$$\frac{dy_1}{dt} = y_2 + \alpha_1 x, \quad y = y_1 + \alpha_2 x,$$

where y corresponds to the output signal e_{out} and x to the input signal e_{in}. Based on what has gone before, the coefficients α_0, α_1 and α_2 will be

$$\alpha_2 = b_2 = 1, \quad \alpha_1 = b_1 - a_1 = -\frac{12}{\tau}, \quad \alpha_0 = \frac{72}{\tau^2}.$$

The setup is shown on Fig. 6 b.

4. The Method of Combining Derivatives

We separate initial Eq. (14) into two by introducing the new variable

$$u = \frac{x}{p^n + a_{n-1}p^{n-1} + \ldots + a_1 p + a_0}. \tag{17}$$

As the result, we get

$$y = b_n \frac{d^n u}{dt^n} + b_{n-1}\frac{d^{n-1}u}{dt^{n-1}} + \ldots + b_1 \frac{du}{dt} + b_0 u. \tag{18}$$

Expression (17) can be rewritten in differential form:

$$\frac{d^n u}{dt^n} + a_{n-1}\frac{d^{n-1}u}{dt^{n-1}} + \ldots + a_1\frac{du}{dt} + a_0 u = x. \tag{19}$$

To establish the setup on the computer, it is initially necessary to "set up" Eq. (19) by the method of reducing the order of the derivatives and thereafter forming the desired variable y in the form of a sum of derivatives with respect to u with the proper coefficients. The values of the derivatives $d^i u/dt^i$ are obtained directly from the corresponding outputs of the integrators for the solution of Eq. (19). Some simplification of the setup is achieved if $d^n u/dt^n$ is eliminated from Eq. (18) by substituting its value from Eq. (19). The result is the set of equations

$$\frac{d^n u}{dt^n} + a_{n-1}\frac{d^{n-1}u}{dt^{n-1}} + \ldots + a_1\frac{du}{dt} + a_0 u = x,$$

$$y = (-b_n a_{n-1} + b_{n-1})\frac{d^{n-1}u}{dt^{n-1}} + \ldots + (-b_n a_1 + b_1)\frac{du}{dt} + (-b_n a_0 + b_0)u + b_n x.$$

For m = n = 3, the block schematic of the setup for these equations is shown in Fig. 7. In the general case, n + 3 operational blocks are needed in the setup. It is not necessary to carry out laborious computations to determine the coefficients for the setup.

5. Methods of Simulating Differential Equations with Variable Coefficients

Methods of simulating differential equations with variable coefficients were considered in sufficient detail by Laning and Battin [3] and Matyash [5]. We therefore limit ourselves here to brief remarks only.

Establishing the setup for a problem in the case of solving Eq. (14) with time-dependent coefficients can be implemented by the method of direct integration or by the method of making a transition to the equivalent system of first-order differential equations.* The fundamental difference between these methods amounts to the method of determining the new variable coefficients for the equations' setup. Indeed, in setting up a problem by the method of direct integration, Eq. (14) is replaced by the following equations, equivalent to it,

$$\sum_{j=0}^{n}(-1)^{j}(\alpha_{j}\ y)^{(j)} = -\sum_{j=0}^{m}(-1)^{j}(\beta_{i}x)^{(j)}, \tag{20}$$

where y and x are the same variables as in (14), but $\alpha_j(t)$ and $\beta_j(t)$ are new functions of time.

Using the properties of adjoint linear operators, Matyash [5] showed that the new variable coefficients must be related with the old ones by the following relationships:

$$\beta_{m-k} = \sum_{i=0}^{k}(-1)^{(m-i)}\frac{(m-i)!}{(m-k)!\,(k-i)!}b_{m-i}^{(k-i)}$$

$$(k = 0, 1, 2, \ldots, m).$$

$$\alpha_{n-k} = \sum_{i=0}^{k}(-1)^{n-i}\frac{(n-i)!}{(n-k)!\,(k-i)!}a_{n-i}^{(k-i)}$$

$$(k = 0, 1, 2, \ldots, n).$$

The block schematic for the setup of Eq. (20) is obtained by the methods used above for differential equation (14) with constant coefficients, with the sole difference that, at the proper places, dividers of the variable coefficients are connected for the establishment of $\beta_{m-k}(t)$ and $\alpha_{n-k}(t)$.

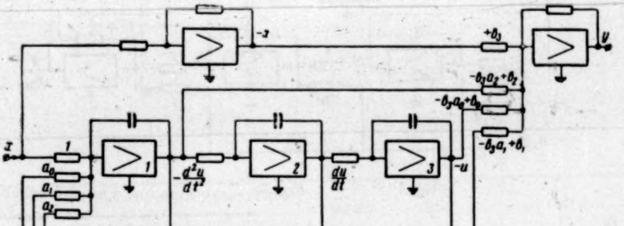

Fig. 7.

The transition to an equivalent system of first-order differential equations is made exactly the same as in the case of constant coefficients, but here the new coefficients, $\alpha_n(t), \alpha_{n-1}(t), \ldots, \alpha_0(t)$, must be considered as some functions of time. The determination of these functions of time in terms of the original variable coefficients can be performed on the basis [3] of the recursion formulas

$$\alpha_0(t) = b_0(t),$$

$$\alpha_i(t) = b_i(t) - \sum_{k=0}^{i-1}\sum_{r=0}^{i-k} C_{n+r-i}^{n-i}a_{i-k+r}(t)\frac{d^r\alpha_k(t)}{dt^r}.$$

It follows from a comparision of the two methods considered that the transition to an equivalent system of first-order differential equations requires less computational work, since the original variable coefficients $a_j(t)$ enter into the setup in untransformed form. In solving a problem by the method of direct integration, one has to recompute all the variable coefficients entering into the equation actually set up.

SUMMARY

The comparison of the methods considered for simulating rational-fraction transfer functions allows the following conclusions to be drawn.

1. Reproduction of rational-fraction transfer functions and the differential equations which give rise to them by means of electronic analog computers without differentiating elements can be implemented by several methods. For nonzero initial conditions, one must also

---

* The methods of decomposing transfer functions into simpler ones and of combining derivatives are invalid here, since they lead to an interchange of differential operators which, with variable coefficients, is inadmissible.

know the values of the independent variable and its first (n-1) derivatives at the initial moment of time.

2. The minimum number of operational amplifiers in the block schematic of the setup is n + 3, where n is the order of the differential equation being set up, and does not depend on the setup method. An exception is the method of decomposing a transfer function into simpler ones, which leads to block schematics with larger numbers of operational amplifiers.

3. From the point of view of the amount of preliminary work required, the method of combining derivatives is the simplest. This method is only applicable to problems with constant coefficients.

4. For solving problems with variable coefficients, preference should be given to the method of making a transition to an equivalent system of first-order differential equations as requiring the least amount of additional computational work.

LITERATURE CITED

[1] A. K. Ganulich, "Methods of correcting distortions in the simulation of certain automatic control systems," [in Russian], Trudy Zhukovskii VVIA, 553 (1955).

[2] D. Mitchell, "The technology of using analog computes," in: Proceedings of the Session of Analog Computers in the Proceedings of the Conference at Cranfield in 1951 [Russian translation].

[3] J. H. Laning and R. H. Battin, Random Processes in Automatic Control [Russian translation] (IL, 1958).

[4] C. L. Johnson, Analog Computer Techniques (McGraw-Hill, N.Y., 1956).

[5] I. Matyash, "Programing linear differential equations with variable coefficients for their solution by analog computers," Avtomat. i Telemekh. 20, 7 (1959).†

[6] V. V. Gurov, V.M. Evseev, B. Ya. Kogan, A.A. Maslov, and F. E. Tranin, Type ÉMU-8 Electronic Analog Computer [in Russian] (Fil. VINITI, Moscow, 1957).

---

† See English translation.

ON CONSTRUCTING BRIDGE CIRCUITS BY THE SHORT-CIRCUIT METHOD

A. Ya. Tolchan

(Moscow)

(Translated from: Avtomatika i Telemekhanika, Vol. 21, No. 1, pp. 82-92, January, 1960)
Original article submitted April 18, 1959

Net structure is proposed as the general representation of bridge circuits. On the basis of an analysis of complete nets, sufficient grounds for the possibility of constructing bridge circuits by the short-circuit method are deduced.

The problem of constructing, from an existent circuit's structural formula F(a,b,. . . , w), the bridge circuit equivalent to it is a very urgent one, since a significant gain in number of circuit elements might thereby be obtained in many cases. One of the methods of carrying out such constructions is well known under the name of the short-circuit method [1].

Practical application of this method is limited by the circumstance that, in the majority of cases, the parts of the circuit necessary for the construction are missing from the original structural formula F(a, b, . . . , w) [1].

In connection with this, the necessity arises of investigating the conditions under which use of this method is possible, as well as the methods of transforming the original structural formula to a form more convenient to use.

To investigate bridge circuits in the general case, it is convenient to present them in the form of a "complete net" as shown on Fig. 1. A complete net is a rectangular net with one element connected in each side of each mesh (elemental grid rectangle), where there are equal numbers of meshes in each file (row) in any given direction. All the nodes of its two opposite sides are connected to the input and output nodes.

The sides of the meshes are conventionally called longitudinal and lateral, depending on whether they are parallel or perpendicular to the input and output terminal buses. This nomenclature is also extended to the individual elements, depending on the side of the mesh they are connected in.

Longitudinal series of elements are called rows while lateral ones are called columns. Initial elements are denoted by I and final ones by F. The denotation of the remaining elements is in accordance with Fig. 1, and the numeration of rows and columns is from left to right and from top to bottom (not counting the rows of the initial and final elements).

The nodes of the net are denoted by $\alpha_{i,n}$, where i is the number of the longitudal elements' row and n the number of the lateral elements' column at the intersection of which the node is to be found.

Each planar bridge circuit can be converted (transformed) to a complete net. For this, all elements connected between two series-parallel nodes are replaced by one element; full rows and columns of longitudinal and lateral elements are then made up by adding elements equal to zero in places where gaps initially appeared, and elements equal to unity at places where conducting lines initially appeared. This transformation is not single-valued but among the variants of the resulting complete nets there is always a variant such that there are no zeros in the first or last rows of longitudinal elements. To obtain this variant, it suffices to begin the transformation by filling in these rows with elements occurring in the original planar scheme. Several examples of such a transformation are given in Fig. 2.

Conversely, from a net with a sufficient number of columns and rows of longitudinal and lateral elements, one may obtain any planar scheme, if part of the elements reduce to zero or to unity, and certain elements, where necessary, are replaced by series-parallel connections of a number of elements.

For nonplanar circuits, analogously, the general form of a bridge structure is a complete space lattice. Each of its facets (or of its cross sections parallel to any facet) is a complete planar net such as those considered above. Each cell of the lattice is a cube in each edge of which one element is connected. All the nodes of two opposite facets of the lattice are joined to the input and output nodes. Its conversion to a nonplanar circuit and vice versa are carried out by methods analogous to those described for plane nets.

All further exposition will deal exclusively with planar circuits and plane nets. The question of extending the conclusions derived from a consideration of plane nets to nonplanar circuits and to space lattices requires special consideration.

Relationships which exist in a complete net are valid in all cases when the individual elements equal zero or unity, i.e., are valid for any bridge circuit. Indeed, zero and unity are particular values which a circuit element may assume.

For the analysis of a complete net, we use a special "table of correspondences." Let t be a row of longitudinal elements and s be a column of lateral elements in a net.

Each column in a table is headed by one of the initial elements I_n, and each row by a final element F_p. In the cell of the table at the intersection of column I_n and row F_p, we write the full structural formula of the circuit joining nodes α_{in} and α_{tp}, denoted by us as Π_{np}. As a preliminary step, this circuit must be presented (for example, by a successive expansion by initial and final elements) in the form of a sum of circuits, each consisting of series connections of elements only. In the sequel, we shall call each such component circuit entering into Π_{np} an elementary circuit, and denote it by π_{np}.

Any bridge circuit presents itself, in the most general form, as some middle portion $f(a_{ij}, b_{mn})$ connected to input and output nodes via initial and final elements (Fig. 3 a). It is essential here that there be no isolated parallel circuits in the middle portion which are connected to the input and output nodes. This circumstance is used in the short-circuit method, where one initially seeks a middle portion of the circuit which is connected to the output node via all the final elements and is connected to the input node via one of the initial elements. After this, one seeks the points for connecting the remaining initial elements to the middle portion [1].

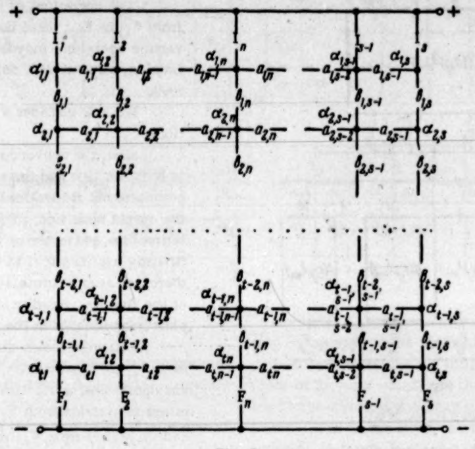

Fig. 1.

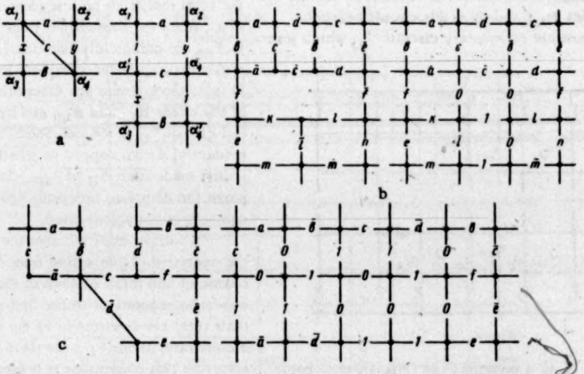

Fig. 2.

In the most general case, the decomposition of a bridge circuit by initial and final elements must give a set of parallel circuits, each of which is a middle portion, $f(a_{ij}, b_{mn})$ joined to the input node via one initial element and to the output node via one final element (Fig. 3 b).

This suggests that, among the elementary circuits into which any two of the full parallel circuits mentioned above may be decomposed, there must be elements similar in content, and differing only in the placement of the points at which the initial and final elements are connected to the middle portions and the elements themselves.

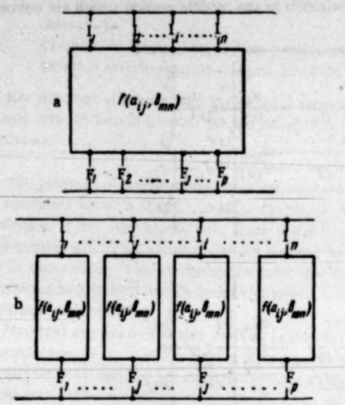

Fig. 3.

Analysis of a Complete Net

Let there be given some complete net, namely, a two-terminal network with s columns of lateral elements and t rows of longitudinal elements. Let Π_{ij} be the circuit joining nodes $\alpha_{1,i}$ and $\alpha_{t,j}$, this circuit being the sum of all the possible elementary circuits π_{ij} which join these nodes.

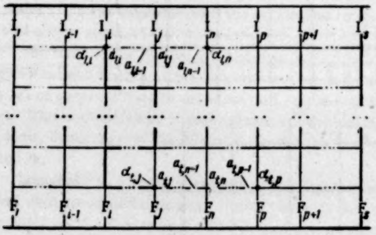

Fig. 4.

Theorem. If, in a complete net (Fig. 4), one choose any pair of nodes, $\alpha_{1,i}$ and $\alpha_{t,j}$, some other pair of nodes, $\alpha_{1,n}$ and $\alpha_{t,p}$, and then, in some elementary circuit π_{ij} of Π_{ij}, one replaces the elements in it which come from the set of longitudinal elements connected in the first row between nodes $\alpha_{1,i}$ and $\alpha_{1,n}$ and in the tth row between nodes $\alpha_{t,j}$ and $\alpha_{t,p}$ by all the elements of this set lacking in it, then the newly obtained elementary circuit will be some circuit π_{np} of Π_{np}.

On Fig. 4, only those nodes and elements mentioned in the theorem are noted. One of the possible circuits π_{ij} is shown in heavy lines.

In the sequel, we shall call such an operation the "operation of converting from π_{ij} to π_{np}" for two pairs of nodes from the first and tth rows. If this operation is carried out for all circuits π_{ij} of Π_{ij}, this is then the "operation of converting from Π_{ij} to Π_{np}".

The operations of converting from π_{ij} to π_{nj} and from π_{ij} to π_{ip}, these being particular cases of the conversion operation, may be considered as conversion operations in, respectively, only the first and only in the tth rows.

We now consider a number of preliminary propositions.

First, the conversion operation occurs analogously in both the first and the tth rows, since the structure of a complete net is identical on both the input node side and the output node side. This means that all conditions, relationships, and results of the conversion operation in the first row are identical to those in the tth row. We shall therefore always formulate propositions henceforth in terms of the first row, bearing in mind that they are also completely applicable to the tth row.

It may be shown that the operation of converting from π_{ij} to π_{np} actually breaks down into two independent operations, which can be carried out in either order: either conversion from π_{ij} to π_{nj}, i.e., in the first row, and thereafter from π_{nj} to π_{np}, i.e., in the tth row or, conversely, initially from π_{ij} to π_{ip}, i.e., in the tth row and then from π_{ip} to π_{np}, i.e., in the first row. Indeed, the final results for both sequences of operations are identical, since the conversions from π_{ij} to π_{nj} and from π_{ip} to π_{np} are completely identical, from the point of view of the makeup of the group of elements to be converted. In fact, these groups are determined only by the positions of the nodes $\alpha_{1,i}$ and $\alpha_{1,n}$ and by the behavior of the initial circuit π_{ij} in the neighborhood of the first row which, evidently, do not depend on whether or not the conversion is first made from π_{ij} to π_{ip}. One can clearly use this to prove the complete independence of the order of the two component operations cited.

It follows from this that the character and result of the operation of converting from π_{ij} to π_{np} depend on the character and result of each of the individual component conversion operations in the first and tth rows which, in their turn, are determined by the behavior of the original elementary circuit π_{ij} near the first and the tth rows separately. This means that it is meaningful to differentiate the forms of the elementary circuits in the net by the character of their behavior close to the first (tth) row.

From this point of view, two cases are theoretically possible, while we shall formulate with respect to the first row only.

1. The original elementary circuit π_{ij} is so situated in the net that, once having started out from one node of the first row of longitudinal elements, it never again passes through any node of this row which is comprised in the set of nodes situated between $\alpha_{1,i}$ and $\alpha_{1,n}$, including

$\alpha_{1,n}$ (Fig. 5a,b,c). We remark that the elementary circuit can pass arbitrarily often through the remaining nodes of the first row.

2. The original elementary circuit π_{1j} is so situated in the net that, once having started out from one node of the first row of longitudinal elements, it again passes, at least once, through nodes of this row which are comprised in the set of nodes situated between $\alpha_{1,1}$ and $\alpha_{1,n}$, including $\alpha_{1,n}$ (Fig. 5 d,e).

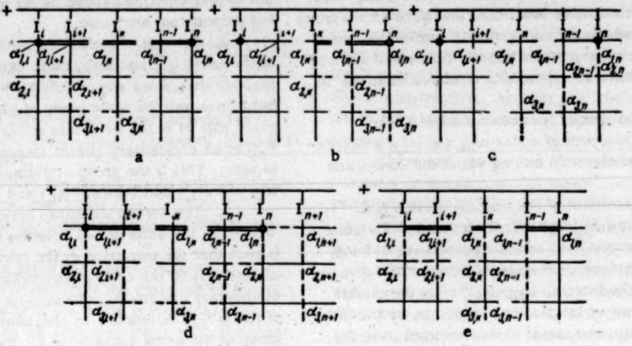

Fig. 5.

We now show that, in these two cases, the conversion operation in the first row from π_{1j} to π_{nj} does in fact lead from π_{1j} to π_{nj}. The graphical proof of this is shown on Fig. 5 where, to avoid encumbering the figure, no elements are shown in the sides of the net's meshes. These latter are understood to be present. Only the nodes occurring in the path of the elementary circuit are notated. The dashed lines represent the initial elementary circuit, while those of its parts which pass through elements participating in the conversion operation are shown by solid lines. Double solid lines denote the circuit paths through the remaining elements in the group subject to conversion. Thus, the results of this operation are clearly visible.

There are obviously three possible diverse circuits for the first case, mentioned above, of the behavior of the original elementary circuit in the neighborhood of the first row. The conversion operations for them are treated in Fig. 5 a,b, and c, from which it is clear that these operations indeed lead to π_{nj}.

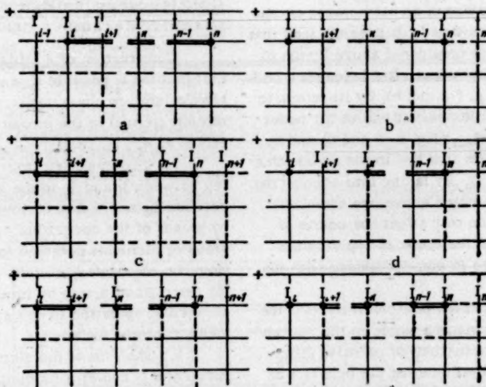

Fig. 6.

We must consider two diverse circuits (Fig. 5d and e) for the second case cited above, finding that in both of them the conversion operation leads to π_{nj}, although with the addition of a closed contour.

In order to extend this proof to the general case of the theorem, we first consider which special features of the behavior of the original circuit in the net affect the course and the result of the operation of converting from π_{ij} to π_{nj}. With this, we shall take into account the group of elements in which the conversion is carried out, the make-up of the subgroups of elements (discarded and added) and the absence or appearance of closed contours in series with π_{nj}.

Among the special features considered are:

1) the placement of nodes $\alpha_{1,i}$ and $\alpha_{1,n}$ which define the group of elements among which the conversion is carried out;

2) the placement of the node $\alpha_{1,k}$ via which π_{ij} leaves the first row of longitudinal elements, by which the subgroups of discarded and added elements are defined;

3) the presence or absence of a return of π_{ij} to one of the nodes in the interval $\alpha_{1,i}-\alpha_{1,n}$ after the circuit leaves the first row of longitudinal elements, by which is determined the appearance of closed contours in series with π_{nj}.

It is also essential that the behavior of π_{ij} in the middle portion of the net in no way affects the course of the operation of conversion from π_{ij} to π_{nj} and, as was stated earlier, that this operation occurs independently in the first and the tth rows.

By taking these data into account, we conclude that all the possible variants of the behavior of an elementary circuit in the neighborhood of the first row, from the point of view of the character of the conversion operation and its results, lead to the two cases considered above. This becomes obvious from a consideration of Fig. 6, where all possible variants of the behavior of an elementary circuit close to the first row are represented. It is easily seen that they differ from the two cases considered above by the direction of the circuit's path in the net after it leaves a node in the interval $\alpha_{1,i}-\alpha_{1,n}$ (Fig. 6 a and b), by its returns to the first row of longitudinal elements at one of the nodes outside of the interval $\alpha_{1,i}-\alpha_{1,n}$ (Fig. 6 c and d) and by the number of its returns to the first row in the nodal interval $\alpha_{1,i}-\alpha_{1,n}$ (Fig. 6 e and f). By taking into account the essential special features presented above, we establish that all these differences in no way affect the course of the conversion operation, and the result of applying this operation to them will also be in correspondence with the theorem given above.

Finally, it is obvious that all possible variants of the course of the elementary circuit as a whole in the net can be given as the different combinations of pairwise different variants of these two general cases of the behavior of a circuit in the vicinity of the first and of the tth row, in conjunction with an arbitrary behavior in the remaining portion of the net. But, since the theorem is valid for all variants of these two cases, it is then valid for all forms of elementary circuits which are possible in a net.

Corollary. In presenting the corollary, we shall deal only with full nets, bearing in mind that it can be extended to any bridge circuit as a particular case of a net.

For some net, let a table of correspondences analogous to that described above be set up. Then, the following propositions are valid.

1. Between the elementary circuits of any two cells of the table I_iF_j and I_nF_p, there exists such an interrelationship that, from any circuit π_{ij} by a conversion carried out in one and the same group of elements common to the given pair of cells, we obtain either one of the circuits π_{np} or an elementary circuit longer than π_{np}, i.e., equal to zero. This is the group of elements connected between $\alpha_{1,i}$ and $\alpha_{1,n}$ and between $\alpha_{t,j}$ and $\alpha_{t,p}$.

2. The interrelationship between the elementary circuits of the cells of two columns I_i and I_n of this table is such that the transition in the rows from the elementary circuits π_{ij} of the cells of one column of the table to the elementary circuits π_{nj} of the cells of the other column of the table corresponds to the conversion in the one group of elements common to all the rows. In this group there appear the elements which are connected between $\alpha_{1,i}$ and $\alpha_{1,n}$ in the first row of longitudinal elements.

3. The connection between the elementary circuits of two rows F_j and F_p of the table is such that transition in the column from the elementary circuits of the cells of one row to the elementary circuits of the cells of the other row corresponds to the conversion in the group of elements which are common to all columns, this group containing elements connected between $\alpha_{t,j}$ and $\alpha_{t,p}$ in the tth row.

Sufficient Grounds for the Possibility of Constructing Bridge Circuits by the Short-Circuit Method

Construction of a bridge circuit by the short-circuit method is possible if, and only if, the following interrelationships characterize the individual elementary circuits (terms) in the circuit's original structural formula F(I, F, a, b, . . . , w).

1. The transition from the elementary circuits passing between I_i and F_j to the elementary circuits passing between I_n and F_j can be implemented, for given i and n, by means of the conversion operation in one and the same group of elements common for any j, and the transition from the elementary circuits passing between I_i and F_p, for given j and p, can be implemented by means of the conversion operation in one and the same group of elements common for any i.

2. The sum of the elementary circuits passing between any I_i and F_j must contain all the circuits necessary for the construction of the bridge circuit which is equivalent to this sum.

It is necessary to convince ourselves that the holding of these two conditions is sufficient for the construction of the bridge circuit by the short-circuit method. It is obvious that the holding of the second condition allows one to construct the bridge circuit of the middle portion f(a_{ij},

b_{IIIn}) (cf. Fig. 3 a), and the holding of the first condition guarantees the possibility of seeking such nodes in this middle portion that, upon their being connected to all initial and final elements, they will form the bridge circuit sought.

Practical Investigation of the Possibility of Constructing a Bridge Circuit by the Short-Circuit Method

Let there be given the structural formula $F(a, b, \ldots, w)$ of the circuit, the bridge circuit variant of which it is necessary to construct.

In order to verify the possibility of employing the short-circuit method, one must:

a) determine the complete group of initial and final elements;

b) set up the table of correspondences;

c) convince oneself that the make-up of the elements in all the cells of the table is identical;

d) verify that the aforementioned sufficient conditions hold, wherein the second condition is verified only for an arbitrary one of the table's cells.

If these conditions do not hold immediately for the original structural formula, one may then introduce, in the table's cells, additional elementary circuits which are equal to zero (containing mutually inverse elements or containing completely one of the pre-existing elementary circuits in the particular cell) and certain elements of the individual elementary circuits can be repeated.

When the necessary conditions have finally been met, the table obtained may be considered as the result of expanding the bridge circuit sought by initial and final elements where, in any cell I_iF_j of the table, are to be found all the elementary circiuts by which the corresponding complete circuit Π_{ij} can be expanded.

Starting from this, we construct, for any arbitrarily chosen cell of the table, its partial bridge circuit Π_{ij}, which we then join to the initial and final nodes via I_j and F_j. On the circuit thus obtained we then find the nodes which, when the remaining initial and final elements are connected to them, allow the elementary circuits of the remaining cells of the table to be realized.

However, the use of this methodology leads simply and rapidly to the desired result only in those rare cases when the bridge circuit sought contains no repeated elements and no mutually inverse elements. In the overwhelming majority of actual cases, bridge circuits contain both repeated elements and mutually inverse elements, as a result of which the initial structural formula lacks a significant portion of the elementary circuits necessary for the construction. Another part of these circuits is present in altered form due to the repetition of identical elements.

Therefore, for the use of this methodology, it is necessary to employ special means and an additional construction condition.

This latter condition is suggested by the fact that, generally speaking, there is no unique bridge circuit equivalent to some series-parallel circuit. However, in analogy with the usual requirement that a circuit be realized with the minimum number of elements, one can propose a universal requirement on the construction of bridge circuits, to wit, that there be a minimum number of repeated identical elements.

It seems reasonable to consider the methodology treated above, together with the additional means of construction, in terms of a concrete example.

Let there be given some structural formula for a circuit whose bridge variant must be constructed:

$$
\begin{aligned}
F = {} & a\{b(\bar{g}l + m) + c(ehl + gm) + \\
& + l[e + h(\bar{e} + \bar{g})] + m(e\bar{g} + h)\} + \\
& + b\{l(eh + \bar{e}) + m[h(e\bar{g} + g) + \bar{e}\bar{g}]\} + \\
& + c\{l[g(eh + \bar{e}) + \bar{g}h] + hm\} = ab\bar{g}l + \\
& + abm + acehl + acgm + ael + a\bar{e}hl + \\
& + a\bar{g}hl + ae\bar{g}m + ahm + behl + b\bar{e}l + \\
& + be\bar{g}hm + bghm + b\bar{e}\bar{g}m + \\
& + cegl + c\bar{e}gl + c\bar{g}hl + chm.
\end{aligned}
$$

TABLE 1

	a_I	b_I	c_I
l_F	$b\bar{g}+ceh+e+\bar{e}h+\bar{g}h$	$eh+\bar{e}+a\bar{g}$	$egh+\bar{e}g+\bar{g}h$
m_F	$b+cg+e\bar{g}+h$	$\bar{e}gh+gh+\bar{e}\bar{g}$	h

This initial structural formula contains 42 elements in grouped form. Other variants of the grouping do not provide any significant gain in the number of elements necessary. After multiplying out the parentheses, we obtain a structural formula in the form of a sum of 18 elementary circuits.

Without stopping to seek the initial and final elements, methods of finding which are described in detail in the literature [1], we state that the initial elements are a, b and c and that the final elements are l and m. We denote them by a_I, b_I, c_I, l_F, and m_F.

We now set up the table of correspondences (Table 1), writing in it successively the elementary circuits from the structural formula (without the initial and final elements).

A scan of the terms in the individual cells of the table by make-up of elements and make-up of individual terms shows that the bridge circuit being sought must contain both mutually inverse elements and repetitions. This means, that the construction problem now entails dealing with the minimum number of repeated elements and mutually inverse elements which are present in the original structural formula.

TABLE 2

	a_I	h	b_I	g	c_I
l_F	$e+\bar{e}h+\bar{g}ha+g\bar{g}hh_1+$ $+aegh_1$		$eh+\bar{e}+a\bar{g}+g\bar{g}h_1+$ $+aeghh_1$		$egh+\bar{e}g+\bar{g}h_1+aehh_1+$ $+ag\bar{g}$
$\bar{g}$					
m_F	$e\bar{g}+ha+\bar{e}\bar{g}h+ghh_1+$ $+aeg\bar{g}h_1$		$e\bar{g}h+\bar{e}\bar{g}+gh_1+a+$ $+aeg\bar{g}hh_1$		$h_1+ag+eg\bar{g}h+\bar{e}g\bar{g}+$ $+ae\bar{g}hh_1$

From this point of view, it follows from a comparison of terms in the cells $a_I l_F$ and $a_I m_F$ with the remaining ones that the repeated elements b and c (b_I and b, c_I and c) must appear in the circuit being sought. It is easily remarked that the shift of the elementary circuits $ab\bar{g}l$, acehl, abm, and acgm to the cells, respectively, $b_I l_F$, $c_I l_F$, $b_I m_F$, and $c_I m_F$, i.e., taking as the initial elements in these circuits, not a_I, but b_I and c_I, allows one to deal with the repeated element a (a_I and a) only (Table 2). With this, the make-ups of the cell elements become identical (taking into account the possibility of repetition of the initial element of cells $a_I l_F$ and $a_I m_F$) except for $\bar{g}$, which does not appear everywhere.

A comparision of cells $b_I l_F$ and $b_I m_F$ (Table 2), which contain the greatest numbers of terms, leads to the conclusion that the group of elements in which conversion is to be carried out for the cells of rows l_F and m_F consists of $\bar{g}$.

In the corresponding pairs of cells of rows l_F and m_F, we verify that this correspondence of terms holds, adding the deficiencies if they equal zero. A comparison of the cells of columns a_I and b_I leads to the acceptance of h as the sole element of the group in which conversion is carried out in columns a_I and b_I, with the condition that element a repeats, since otherwise a term equal to unity would appear in cell $b_I m_F$. Element h is also repeated (h and h_1) (Table 2).

In Table 2, all the added elementary circuits either contain mutually inverse elements or are longer ($a_I ghh_1 m_F$) than those already in the circuit ($a_I ahm_F$). In Table 2, all the added elements, circuits, and subscripts are given in boldface type.

Analogously, by considering the circuits of the table's cells $b_I l_F$ and $c_I l_F$, and $b_I m_F$ and $c_I m_F$, we find the most probable makeup of the group of elements to be converted, namely, g, for the cells of columns b_I and c_I.

We then fill all cells of the table until complete correspondence of all terms is attained. Now, the make-up of elements in the circuits of all the table's cells is the same for all, namely, a, e, $\bar{e}$, g, $\bar{g}$, h, and h_1. After this, we construct the equivalent bridge circuit for the elementary circuits of one of the table's cells, with the purpose of obtaining the middle portion of the bridge circuit being sought. In general, this construction could have been carried out earlier, without complete correspondence, i.e., when the first of the sufficient conditions for the possibility of constructing a bridge circuit was unfulfilled. This construction sometimes allows one to determine the make-up of the group of elements in which conversion is carried out. Thus, we consider the cell $b_I l_F$ of the table, since it contains the shortest elementary circuit. For this, we shall consider that elements h and g are connected in the first, and g in the last, row of longitudinal elements, since they enter into the groups of elements in which conversion is carried out.

In the general case, this construction must be carried out by a method analogous to the one presented here.

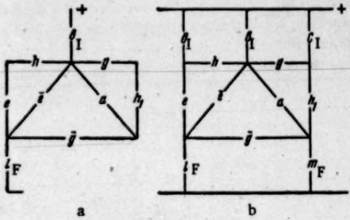

a b

Fig. 7

However, in the majority of cases, the number of terms in the table's cells is small, and this construction can be carried out from the information obtained from all the cells' elementary circuits. Thus

$$f_{b_I l_F} = eh + \bar{e} + a\bar{g} + g\bar{g}h_1 + aeghh_1$$

and the equivalent bridge circuit is represented on Fig. 7 a. In it, one easily determines the nodes for connecting the remaining initial and final elements, since one already knows the elements of the first and last rows of the circuit which are connected between these nodes. The final bridge circuit is shown on Fig. 7 b.

By considering the different elementary circuits of the scheme obtained, we convince ourselves that it is equivalent to the original structural formula F.

We note that there are, in the table, elementary circuits ($aegh_1$, $aeghh_1$, etc.) which consist of a somewhat shorter circuit from the same cell plus a closed contour (agh_1) abutting the first or last row of longitudinal elements. This is in complete agreement with the theorem proved earlier; such a circuit, naturally, does not violate equivalence. It should be added that, in seeking the group of elements in which conversion is to be carried out for the circuits of some pair of cells, it is ordinarily a good first move to consider a group which is contained completely in at least one term of each cell, and which is completely absent from a least one term.

To convince oneself of the truth of this regularity, it suffices to recall that among the elementary circuits of any cell there will always be a circuit of the form shown in Fig. 5 a, as well as a circuit of the form shown in Fig. 5 c.

When there are mutually inverse elements in this group, the rule given is false. The rule can also be violated in other cases of special locations of mutually inverse elements.

LITERATURE CITED

[1] M. A. Gavrilov, Switching Circuit Theory [in Russian] (Izdatelstvo AN SSSR, 1950).

NOISE STABILITY OF A FREQUENCY TELEMETERING SYSTEM FOR WEAK PULSE NOISE

Yu. I. Chugin

(Moscow)

(Translated from: Avtomatika i Telemekhanika, Vol. 21, No. 1, pp. 93-105, January, 1960)
Original article submitted April 28, 1959

The noise stability of a telemetering frequency receiver is investigated for pulse noise of arbitrary duration. The threshold of noise stability and the optimal deviation frequency are determined.

The noise stability of the various forms of modulation have been most fully investigated (both theoretically and experimentally) for the case of fluctuation noise. Questions of noise stability for pulse noise, for frequency modulation in particular, have been treated with insufficient completeness in the literature.

In a number of the works devoted to this question, the treatment was mainly qualitative [1, 2]. There are works which contain incorrect initial assumptions [3] (as shown in [4]). There is definite interest inhering in the investigation of δ - function type noise in FM receivers which was given in [4, 5], but the action of such noise, so far from the actual noise encountered, very inadequately discloses the phenomena which occur in the receiver, and so the results thus obtained have a limited domain of applicability.

In the present paper we present the investigation of the effect of weak pulse noise of arbitrary duration on a frequency receiver. The results of the analysis are used for calculating the noise stability of a frequency telemetering system. The use of a narrow band output device allows one to use, as the criterion of noise stability of the telemetering system, the reduced mean-square error, defined as the ratio of the effective noise voltage V_n at the receiver's output to the maximum voltage of the output signal obtained by varying the signal frequency from $-\omega_d$ to $+\omega_d$, where ω_d is the maximum deviation frequency. The noise voltage V_n can be determined by the energy spectrum of the pulse noise at the discriminator's output. If a sequence of random noise pulses act at the receiver's input, then the phase φ_0 of the carrier frequency at the moment when a noise pulse acts can be considered a random variable, and the result of the noise's action at the discriminator's output can be considered a random pulsed process.

1. Reduced Mean-Square Error at the Receiver's Output

By definition, the magnitude of the reduced error at the output of the frequency receiver (Fig. 1) with pulse noise equals

$$\delta = \frac{V_n}{2U_{\max}}, \qquad (1)$$

where $U_{\max}$ is the maximum voltage of the receiver's output signal, equal to ω_d (for an ideal discriminator with characteristic slope of $s = 1$), V_n is the noise voltage at the receiver's output, defined as $V_n = \sqrt{P_n}$, where

$$P_n = \frac{1}{2\pi}\int_0^\infty W(\omega)\,K(\omega)\,d\omega \qquad (2)$$

is the noise power at the receiver's output, $W(\omega)$ is the energy spectrum of the sequence of random noise pulses at the discriminator's output and $K(\omega)$ is the frequency characteristic of output filter F_2.

We now determine δ for an ideal and for a bell-shaped form of the output filter's frequency characteristic.

a. The Ideal Filter Form

By substituting in (2) the value of $W(\omega)$ obtained in Appendix II (formula II.16) and then integrating, we obtain the noise power at the output of a filter with pass band 0 to F_f and $K(\omega) = 1$:

$$P_n = 0.425\,\frac{m\omega_f^3}{\omega_0^2}\left(\frac{U_n}{U_s}\right)^2 \Phi_I. \qquad (3)$$

Here,

$$\Phi_I = 1 - 3\left[\frac{2}{\alpha^2}\cos\alpha + \left(\frac{1}{\alpha} - \frac{2}{\alpha^3}\right)\sin\alpha\right]\times$$

$$\times\cos(\omega_0 + \lambda\omega_d)\tau -$$

$$-\frac{3\pi}{2}\left(\frac{\lambda\omega_d}{\Delta\omega}\right)\left[\left(-1 + \frac{6}{\alpha^2}\right)\times\right.$$

$$\left.\times\cos\alpha + 3\left(\frac{1}{\alpha} - \frac{2}{\alpha^3}\right)\sin\alpha\right]\frac{\sin(\omega_0 + \lambda\omega_d)\tau}{\Delta\omega\tau},$$

U_s is the amplitude of the sinusoidal signal at the receiver's input, U_n is the amplitude of the noise pulse at the receiver's input, τ is the duration of the noise pulse, $\underline{m}$ is the average number of pulses per second, λ is the transmitted parameter, varying from −1 to +1, ω_0 is the mean frequency of the input filter, $\alpha = \omega_f\tau$, $\omega_f = 2\pi F_f$, and $\Delta\omega = 2\pi\Delta f$.

By substituting the values of $V_n = \sqrt{P_n}$ and $U_{\max}$ in formula (1), we obtain the expression for the reduced

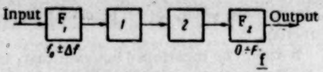

Fig. 1. Block schematic of the frequency receiver. F_1 is the input filter, 1 is a limiter, 2 is the discriminator, and F_2 is the output filter.

mean-square error at the output of a receiver with ideal output filter in the form

$$\delta_I = 0.33 \frac{\sqrt{m}\, \omega_f^{3/2}}{\omega_d \omega_0} \frac{U_n}{U_s} \sqrt{\Phi_I}. \qquad (4)$$

As follows from (II.17), the magnitude of the systematic error at the receiver's output equals zero.

On the basis of (I.12) and (I.13), formula (4) can be written in the form

$$\delta_I = 0.37 \frac{\sqrt{m}\, \omega_f^{3/2}}{\omega_d \omega_0} \left(\frac{A_0}{U}\right) e^{-\frac{\pi}{8}\left(\frac{\lambda\omega_d}{\Delta\omega}\right)^2} \sqrt{\Phi_I}, \qquad (5)$$

where A_0 is the maximum amplitude of the transient response at the output of the input filter to a voltage jump (or to a noise pulse of long duration, where the transient responses to the noise's leading and trailing edges do not overlap) and U is the signal amplitude at the filter's output.

The expression for Φ_1 is simplified if $\alpha \leq 2.5$. In this case,

$$\xi_1 = \frac{2}{\alpha^2}\cos\alpha + \left(\frac{1}{\alpha} - \frac{2}{\alpha^3}\right)\sin\alpha \approx \frac{1}{3} - \frac{1}{10}\alpha^2,$$

$$\xi_2 = \left(-1 + \frac{6}{\alpha^2}\right)\cos\alpha + 3\left(\frac{1}{\alpha} - \frac{2}{\alpha^3}\right)\sin\alpha \approx$$

$$\approx \frac{1}{5}\alpha^2 - \frac{1}{42}\alpha^4.$$

If $\alpha > 10$, then $\xi_1 \approx \sin\alpha/\alpha$ and $\xi_2 \approx -\cos\alpha + 3\sin\alpha/\alpha$. It is clear from formula (4) that the magnitude of the reduced error increases linearly with increasing amplitude of the noise pulses U_n and decreases with increasing mean signal frequency ω_0 and maximum deviation frequency ω_d. The error depends very little on the bandwidth of the input filter (the third term in the expression for Φ_I is small in comparison with unity). For $\lambda = 0$, $\delta \neq \varphi(\Delta f)$. The relationship of the error to the noise duration is expressed in a complicated manner. Formula (4), as follows from its derivation, is valid under the conditions when the maximum amplitude of the transient response to pulse noise at the input filter's output $B_{max}(t)$ does not exceed the amplitude of the signal $U(k_{max} = B_{max}(t)\, U \leq 1)$.

b. The Bell-Shape Filter Form

By carrying out the analogous computation for the bell-shaped form of the output filter's frequency characteristic

$$K(\omega) = e^{-\frac{\pi}{8}\left(\frac{\omega}{\omega_f}\right)^2}$$

we obtain the following formula:

$$P_n = \frac{2.3 m \omega_f^3}{\omega_0^2}\left(\frac{U_n}{U_s}\right)^2 \Phi_b, \qquad (6)$$

where

$$\Phi_b = 1 - e^{-\frac{2}{\pi}\alpha^2}\left(1 - \frac{4}{\pi}\alpha^2\right)\cos(\omega_0 + \lambda\omega_d)\tau -$$

$$- \frac{\pi}{2}\left(\frac{\lambda\omega_d}{\Delta\omega}\right) e^{-\frac{2}{\pi}\alpha^2} \cdot \frac{4\alpha^2}{\pi}\left(3 - \frac{4\alpha^2}{\pi}\right)\frac{\sin(\omega_0 + \lambda\omega_d)\tau}{\Delta\omega\tau},$$

$$\delta_b = 0.76 \frac{\sqrt{m}\cdot \omega_f^{3/2}}{\omega_d \omega_0}\left(\frac{U_n}{U_s}\right)\sqrt{\Phi_b}, \qquad (7)$$

or

$$\delta_b = 0.85 \frac{\sqrt{m}\, \omega_f^{3/2}}{\omega_d \Delta\omega}\left(\frac{A_0}{U}\right) e^{-\frac{\pi}{8}\left(\frac{\lambda\omega_d}{\Delta\omega}\right)^2} \sqrt{\Phi_b}. \qquad (8)$$

2. Dependence of the Error on the Duration of the Noise Pulses

Figure 2 gives the square of the reduced mean-square error, computed from formulas (4) and (7) as a function of the noise duration for the ideal and bell-shaped output filter forms, respectively,

$$\phi_I = 0.33 \frac{\sqrt{m}\,\omega_f^{3/2}}{\omega_d \omega_0}\left(\frac{U_n}{U_s}\right), \quad \phi_b = 2.3\phi_I, \quad \frac{\lambda\omega_d}{\Delta\omega} < 1.$$

It is clear from Fig. 2 that the curve for the relationship of the error and $\alpha = \omega_f\tau$ has the character of a modulated high-frequency oscillation. The high-frequency component depends on the relationship of the noise duration and the signal's frequency, i.e., on $\cos(\omega_0 + \lambda\omega_d)\tau$, and the envelope of the error variation curve depends on the relationship of the noise duration and the pass band of the output filter (on α).

As α increases, the error tends to a constant value, determined by the action on the receiver of the two pulse edges independently. The laws of variation of the error as a function of noise duration are similar for the ideal and the bell-shaped form of the output filter but, in the case of the bell-shaped form, the error's high-frequency component decays much more rapidly.

It follows from formulas (4) and (7) that, for a definite duration of the noise pulse [for $(\omega_0 + \lambda\omega_d)\tau = \pi$)], the magnitude of the error is a maximum, and equals

$$\delta_{I\max} = 0.466 \frac{\sqrt{m}\,\omega_f^{3/2}}{\omega_d \omega_0}\left(\frac{U_n}{U_s}\right), \qquad (9a)$$

$$\delta_{B\max} = 2.3\delta_{I\max}. \qquad (9b)$$

For very long durations of the noise, when $\alpha \to \infty$ (in practice, even for $\alpha > 30$),

$$\delta_{I_{\alpha\to\infty}} = 0.33 \frac{\sqrt{m}\,\omega_f^{3/2}}{\omega_d \omega_0}\left(\frac{U_n}{U_s}\right), \qquad (10a)$$

$$\delta_{B_{\alpha\to\infty}} = 2.3\,\delta_{I_{\alpha\to\infty}}. \qquad (10b)$$

It is clear from (9) and (10) that $\delta_{\max} = \sqrt{2}\,\delta_{\alpha\to\infty}$. This relationship is self-evident since, by definition, $\delta \equiv \sqrt{P_n}$ and, as follows from physical considerations, $P_{n\max} = 2P_{n\,\alpha\to\infty}$.

If the noise pulse has a duration much less than the period of the high-frequency carrier, i.e., if $\omega_0\tau \ll 1$, and the noise may be approximated by delta functions, then

$$\delta I_{\omega_0\tau<1} = 0.233\,\frac{\sqrt{m}\,\omega_f^{3/2}}{\omega_d}\left(\frac{U_n\tau}{U_s}\right), \tag{11a}$$

$$\delta b_{\omega_0\tau<1} = 2.3\,\delta I_{\omega_0\tau<1}. \tag{11b}$$

As follows from Fig. 2 and from formulas (4) and (7), the influence of the phase relationships (of the high frequency) on the magnitude of the error exists, not only in the case when the transient responses from the leading and trailing edges of the noise pulse overlap [as follows from (1.13) for $\sqrt{\beta}\tau < 4$], but also in the case when these transient responses have a significant separation between them, i.e., in the case when, for all practical purposes, they do not overlap.

It should be mentioned however that, in actual conditions, due to the instability of the duration of the noise pulses (this instability being of significant magnitude when the durations are long), an averaging of the error within the limits of variation of the noise pulses $\Delta\tau$ can occur and for $\Delta\tau > (0.5/f_0)$, the averaged error will be close to $\delta_{\alpha\to\infty}$. In practice, one frequently has to do with noise pulses of unknown duration. In these cases, it is most reasonable to carry out the computations for the worst case (i.e., for that duration of the noise which maximizes the error). From formulas (9a) and (9b), one can determine the maximum error (for the critical τ) which is possible when the full bandwidth of the input filter is used, when $\omega_d = \Delta\omega - \omega_f = \text{const}$, with the conditions that the transient responses from the individual noise pulses at the output of filter F_1 do not overlap and that $m \to 2\Delta f$ and $k_{\max} \to 1$. If these conditions hold (cf. II.15), formulas (9a) and (9b) will have the form:

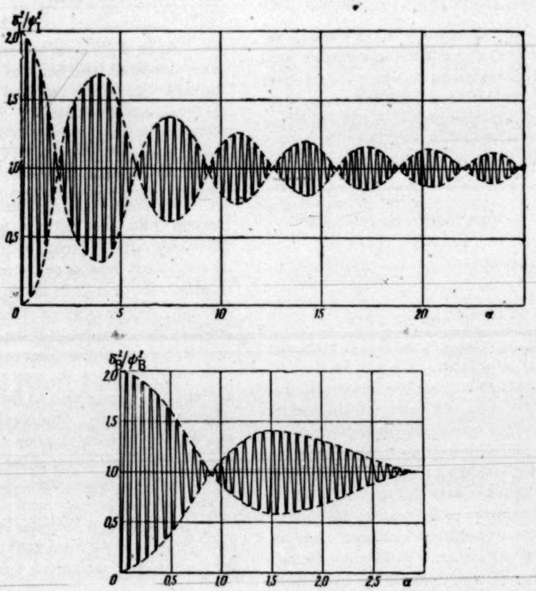

Fig. 2.

$$\delta^{\bullet}_{I\max} \leqslant \frac{0.1}{(\gamma-1)\sqrt{\gamma}}, \tag{12a}$$

$$\delta^{\bullet}_{b\max} \leqslant \frac{0.23}{(\gamma-1)\sqrt{\gamma}}, \tag{12b}$$

where $\gamma = \Delta\omega/\omega_f = \Delta f/F_f$. For telemetry systems, one ordinarily has $\gamma \geq 5$ and, as follows from (12), $\delta^{\bullet}_{I\max} \leq 1.1\%$ and $\delta^{\bullet}_{B\max} \leq 2.5\%$. The maximum error obtainable in the very worst conditions, cited above, is thus relatively small.

It is clear from the formulas given above that the error quantities $\delta_{\max}$, $\delta_{\alpha\to\infty}$, $\delta_{\omega_0\tau\ll1}$ and $\delta^{\bullet}_{\max}$ are

2.3 times greater for the bell-shaped form of the output filter than for the case of the ideal filter form.

It is necessary to note that the taking off experimentally of the function $\delta = \varphi(\tau)$ gives rise to technical difficulties related to the necessity of a high stability of τ, particularly for large values of f_0 but, nonetheless, the character of the curves of Fig. 2 was substantiated experimentally.

3. Noise Stability Threshold for Noise Pulses

As was stated earlier, the formulas for the reduced mean-square error are valid for $k_{max} = B_{max}(t)/U \leq 1$. Since the theoretical analysis of the case when $k_{max} > 1$ gives rise to mathematical difficulties, noise stability under these conditions was investigated experimentally. Figure 3 shows the function $\delta_{max} = \varphi(k_{max})$, taken off experimentally for the following values of the parameters: $\tau = 15.5$ msec, $m = 17$, $f_0 = 1$ kc, $2\Delta f = 150$ cps, $F_f = 2$ cps, $\gamma = 0$. The dashed line gives the same relationship computed from the theoretical formula (9b). It is clear from Fig. 3 that, for $k_{max} < 1$, the error is of small magnitude (less than 0.1%) and increases linearly with increasing k_{max}, a rapid growth in the error occurring for $k_{max} > 1$. The experimental results bear out the assertion of [1] that the condition $k_{max} = 1$ corresponds to the threshold of noise stability for frequency modulation for pulse noise. For the condition to hold that $k_{max} \leq 1$ (the equal sign corresponds to the noise stability threshold), the following conditions must be met [cf. formulas (II.13)-(II.15)]:

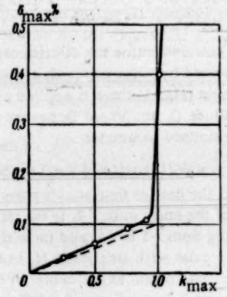

Fig. 3.

1) For the duration of the noise pulses much less than one period of the high frequency, i.e., for $\omega_0\tau \ll 1$,

$$\frac{U_n}{U_s}\Delta\omega\tau \leqslant 0.75;$$

2) for virtual nonoverlapping of the transient processes from the leading and trailing edges of the individual noise pulses, i.e., for $\Delta f\tau > 0.8$,

$$\frac{U_n}{U_s}\frac{\Delta\omega}{\omega_0} \leqslant 0.75;$$

3) for overlapping of the transient responses from the edges of the noise pulses and a doubled total reaction,

$$\frac{U_n}{U_s}\frac{\Delta\omega}{\omega_0} \leqslant 0.375.$$

4. Optimal Deviation Frequency for Pulse Noise

Figure 4 shows the curves for the relationship of the maximum error (for the critical duration of the noise pulses)

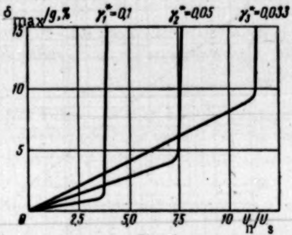

Fig. 4.

and the ratio U_n/U_s at the receiver input for various values of $\gamma = \Delta f/F_f$, constructed on the basis of theoretical (with $k_{max} < 1$) and experimental (for $k_{max} > 1$) data (the sharp bends in the curves correspond to the condition $k_{max} = 1$):

$$g = \frac{17.5\sqrt{m}\,\omega_f^{3/2}}{\omega_d\Delta\omega}, \gamma^* = \gamma\frac{\omega_f}{\omega_0}.$$

It is clear from Fig. 4 that, if it be required to provide a small error for a large amount of noise (small δ_{max}/g), then it is advisable to work with large values of γ, since this error will be attained for the greatest amount of noise.

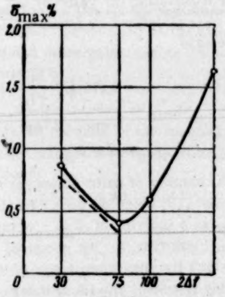

Fig. 5.

However, if δ_{max}/g is large, it is then more advantageous to reduce the input filter's bandwidth (reduce γ). Thus, for constant U_n/U_s, there exists an optimal pass band of the input filter and, consequently, an optimal deviation frequency for which the mean-square error at the receiver's output will be minimal. The determination of the conditions corresponding to the optimal deviation frequency was carried out experimentally. Figure 5 shows the function $\delta_{max} = \varphi(2\Delta f)$, obtained experimentally for τ = 35.5 msec, m = 17, f_0 = 1 kc, F_f = 2 cps, and k_{max} = = 1 for $2\Delta f$ = 80 cps. The dashed line gives the theoretical function, constructed from formula (9b). It is obvious from Fig. 5 that the minimum error occurs for $k_{max} = 1$. The value of the optimum pass band can thus be defined from expressions (II.13)-(II.15).

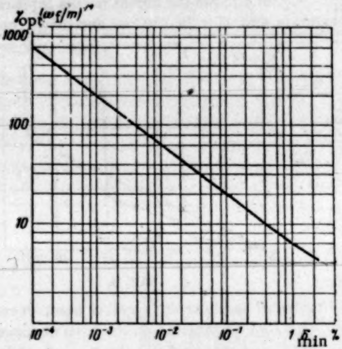

Fig. 6.

The optimal deviation frequency will equal $\omega_{d\ opt} = \Delta\omega_{opt} - \omega_f$ and, for small ω_f, $\omega_{d\ opt} \approx \Delta\,\omega$. The presence of the optimal deviation frequency for $k_{max} = 1$ also follows from the curves of Figs. 3 and 4, if one takes into account the sharply increasing error for $k_{max} > 1$.

Knowing $\omega_{d\ opt}$, one can determine the least value of error possible for a given ratio U_n / U_s at the receiver input. By substituting the value of $\omega_{d\ opt} = \Delta\,\omega_{opt} - \omega_f$, where $\Delta\,\omega_{opt}$ is defined by formula (II.15), in (9a) and (9b), we obtain

$$\delta_{I\,min} = \frac{0.175\sqrt{\frac{m}{\omega_f}}}{(\gamma_{opt} - 1)\,\gamma_{opt}}, \tag{13a}$$

$$\delta_{b\,min} = 2.3\,\delta_{I\,min}. \tag{13b}$$

If the number of noise pulses per second $m \to 2\Delta f$, then formulas (13) coincide with formulas (12). Figure 6 shows γ_{opt} as a function of δ_{min}, obtained from formula (13b). It is clear that, for the choice of the optimal pass band for which the maximum range of the action of the telemetering system is provided, it suffices to know the system's error, its speed of response (the quantity ω_f), and the average number of noise pulses per unit time. After γ_{opt} has been chosen, it is necessary to verify the condition of nonoverlap of the transient responses from the individual noise pulses at the input filter's output, since the formulas obtained are rigorously valid only for this condition. The question of the receiver's noise stability when this condition of nonoverlap is violated requires additional investigation.

SUMMARY

1. With operation of a frequency receiver of a telemetering system under conditions of weak noise pulses of arbitrary duration (without special noise-protection measures having been taken), when the maximum amplitude of the transient response to the noise does not exceed the signal amplitude ($k_{max} < 1$), the reduced mean-square error at the receiver's output depends slightly on the input filter's bandwidth, decreases with increasing maximum deviation frequency, and depends on the duration of the noise pulses in a complicated way.

2. With frequency modulation and noise pulses, there exist a threshold of noise stability and an optimal value of deviation frequency, both occurring when k_{max} = = 1. The conditions under which $k_{max} \leq 1$ are defined by formulas (II.13)-(II.15).

3. The maximum value of the error (for the critical duration of the noise pulses), obtained for complete employment of the input filter's bandwidth and with the condition of nonoverlap of the transient responses to individual noise pulses at the input filter's output and the conditions that $k_{max} \to 1$ and $\gamma \geq 5$, does not exceed 1.1% for an ideal characteristic of the output filter and 2.5% for a bell-shaped characteristic.

4. For $k_{max} > 1$, the error exceeds the admissible one for telemetry, and it is necessary to take special measures to limit the noise pulses.

APPENDIX I

Discriminator's Output Voltage with Noise Pulses Acting on the Receiver

We now determine the discriminator's output voltage engendered by noise pulses if, at the frequency receiver's input (Fig. 1) there is applied a sinusoidal signal with amplitude U_s and whose frequency depends linearly on the transmitted parameter λ:

$$u = U_s \cos[(\omega_0 + \lambda\omega_d)\,t + \varphi_0]. \tag{I.1}$$

where φ_0 is the carrier frequency's phase at the moment of action of the noise pulse, λ is the transmitted parameter, varying from -1 to +1, and there simultaneously acts a noise pulse with amplitude U_n and duration τ. By placing the time origin at the center of the noise pulse, we can present it in the form of a difference of two dc voltage jumps, one of which acts at time $t = -\tau/2$, the other at time $t = \tau/2$. When one voltage jump acts on input filter F_1, the filter's output voltage can be given as

$$u_s = A(t)\cos\omega_0 t. \tag{I.2}$$

where A(t) is the voltage envelope of the transient response.

Using the principle of superposition for the action of two jumps, i.e., the noise pulse, we can write the filter's output voltage as

$$u_n = A\left(t + \frac{\tau}{2}\right)\cos\omega_0\left(t + \frac{\tau}{2}\right) - A\left(t - \frac{\tau}{2}\right)\cos\omega_0\left(t - \frac{\tau}{2}\right).$$

We give this expression in the form

$$u_{\mathrm{n}} = B(t)\cos[\omega_0 t + \theta(t)]. \qquad (I.3)$$

where B(t) is the voltage envelop of the transient response engendered by the noise pulse of duration τ; $\theta(t)$ is the phase of the transient response voltage,

$$B(t) = \left[A^2\left(t+\frac{\tau}{2}\right) + A^2\left(t-\frac{\tau}{2}\right) - 2A\left(t+\frac{\tau}{2}\right)A\left(t-\frac{\tau}{2}\right)\cos\omega_0\tau\right]^{\frac{1}{2}}. \qquad (I.4)$$

$$\theta(t) = \operatorname{arctg}\frac{A\left(t+\frac{\tau}{2}\right) + A\left(t-\frac{\tau}{2}\right)}{A\left(t+\frac{\tau}{2}\right) - A\left(t-\frac{\tau}{2}\right)}\operatorname{tg}\frac{\omega_0\tau}{2}. \qquad (I.5)$$

The resulting voltage from signal and noise at the output of filter F_1 will equal

$$U_{\mathrm{p}} = U\cos[(\omega_0 + \lambda\omega_{\mathrm{d}})t + \varphi_0] + B(t)\cos[\omega_0 t + \theta(t)] = S\cos[\omega_0 t + \psi(t)], \qquad (I.6)$$

where U is the signal amplitude at the filter's output.

The phase of this oscillation is

$$\psi(t) = \operatorname{arctg}\frac{U\sin(\lambda\omega_{\mathrm{d}}t + \varphi_0) + B(t)\sin\theta(t)}{U\cos(\lambda\omega_{\mathrm{d}}t + \varphi_0) + B(t)\cos\theta(t)}. \qquad (I.7)$$

The deviation of the frequency of the resulting oscillation from the mean frequency ω_0 is determined by the time derivative of the function $\psi(t)$, i.e., by the magnitude of $d\psi/dt$, and the deviation of the frequency of this oscillation from the signal's frequency (equal to $\omega_0 + \lambda\omega_{\mathrm{d}}$) is defined by the expression $\Delta\omega_{\mathrm{r}}(t) = d\psi/dt - \lambda\omega_{\mathrm{d}}$.

By differentiating, we obtain

$$\Delta\omega_{\mathrm{r}}(t) = \frac{-\frac{dk}{dt}\sin\gamma}{1+k^2+2k\cos\gamma} - \left(\lambda\omega_{\mathrm{d}} - \frac{d\theta}{dt}\right)\frac{k^2 + k\cos\gamma}{1+k^2+2k\cos\gamma}, \qquad (I.8)$$

where

$$k = k(t) = \frac{B(t)}{U}, \qquad \gamma = \lambda\omega_{\mathrm{d}}t + \varphi_0 - \theta(t).$$

For k < 1, the fractions in (I.8) can be expanded in simple series:

$$\frac{\sin\gamma}{1+k^2+2k\cos\gamma} = \sum_{n=1}^{\infty} k^{n-1}\sin n\gamma,$$

$$\frac{k^2 + k\cos\gamma}{1+k^2+2k\cos\gamma} = \sum_{n=1}^{\infty} k^n\cos n\gamma.$$

With this, formula (I.8) is written in the form

$$\Delta\omega_{\mathrm{r}}(t) = (-1)^n\left\{\frac{dk}{dt}\sum_{n=1}^{\infty}k^{n-1}\sin n\gamma - \left(\lambda\omega_{\mathrm{d}} - \frac{d\theta}{dt}\right)\sum_{n=1}^{\infty}k^n\cos n\gamma\right\}. \qquad (I.9)$$

By assuming an ideal frequency discriminator, i.e., one whose output voltage is directly proportional to the deviation of the frequency from the mean value ω_0:

$$u_{\mathrm{out.\,d}} = s(\omega - \omega_0), \qquad (I.10)$$

we get from (I.9) that the discriminator's output voltage, when noise pulses act on the receiver's input, will equal

$$u_{\mathrm{out}}(t) = s\Delta\omega_{\mathrm{r}}(t). \qquad (I.11)$$

In what follows, we shall assume the slope of the discriminator's characteristic to be s = 1. For the case of a bell-shaped frequency characteristic $C(\omega)$ of input filter F_1

$$C(\omega) = C_0 e^{-\frac{\pi}{2}\frac{(\omega-\omega_0)^2}{(2\Delta\omega)^2}}, \qquad (I.12)$$

where $\Delta\omega = 2\pi\Delta f$ and $2\Delta f$ is the bandwidth; the voltage envelope of the transient response at the filter's output when a dc voltage of magnitude U_{n} acts at the input is determined by the formula [6]

$$A(t) = A_0 e^{-\beta t^2} = \frac{\sqrt{8}}{\pi}U_{\mathrm{n}}C_0\frac{\Delta\omega}{\omega_0}e^{-\frac{2}{\pi}\Delta\omega^2 t^2}. \qquad (I.13)$$

APPENDIX II

Energy Spectrum of a Sequence of Noise Pulses at the Discriminator Output

The expression for the energy spectrum of the sequence of noise pulses appearing at the discriminator's output when random noise pulses act at the receiver's input has the form [7]:

$$W(\omega) = 2m\,|F(\omega)|^2, \qquad (II.1)$$

where $|F(\omega)|$ is the modulus of the spectral density of an individual noise pulse and m is the average number of pulses per second.

The spectral density of an individual noise pulse

$$F(\omega) = \int_{-\infty}^{\infty} u_{\mathrm{out}}(t)e^{-i\omega t}dt \qquad (II.2)$$

can be written in the form

$$F(\omega) = A(\omega) - iB(\omega) = |F(\omega)|\,e^{-\eta(\omega)}, \qquad (II.3)$$

where

$$A(\omega) = \int_{-\infty}^{\infty} u_{\mathrm{out}}(t)\cos\omega t\,dt, \quad B(t) = \int_{-\infty}^{\infty} u_{\mathrm{out}}(t)\sin\omega t\,dt, \qquad (II.4)$$

and $u_{\mathrm{out}}(t)$ is defined by formula (I.11).

By substituting the value of $u_{out}(t)$ in (II.4) and computing the integrals, we obtain the expressions for the real and imaginary parts of the spectral density in the form

$$A(\omega) = \sum_{n=1}^{\infty} A_n(\omega) = \sum_{n=1}^{\infty} \frac{(-1)^n \omega}{n} \int_{-\infty}^{\infty} \left[\frac{B(t)}{U}\right]^n \sin n\,[\lambda\omega_d t + \varphi_0 - \theta(t)] \sin \omega t\, dt, \tag{II.5}$$

$$B(\omega) = \sum_{n=1}^{\infty} B_n(\omega) = \sum_{n=1}^{\infty} -\frac{(-1)^n \omega}{n} \int_{-\infty}^{\infty} \left[\frac{B(t)}{U}\right]^n \sin n\,[\lambda\omega_d t + \varphi_0 - \theta(t)] \cos \omega t\, dt.$$

By carrying out a number of trigonometric transformations, and by taking into account, as follows from (I.3), that

$$B(t)\cos\theta(t) = \left[A\left(t+\frac{\tau}{2}\right) - A\left(t-\frac{\tau}{2}\right)\right]\cos\frac{\omega_0\tau}{2},$$

$$B(t)\sin\theta(t) = \left[A\left(t+\frac{\tau}{2}\right) + A\left(t-\frac{\tau}{2}\right)\right]\sin\frac{\omega_0\tau}{2}, \tag{II.6}$$

we get, for $A(\omega)$ and $B(\omega)$, that

$$A(\omega) = \sum_{n=1}^{\infty} A_n(\omega) = \sum_{n=1}^{\infty} [A_{2n-1}(\omega) + A_{2n}(\omega)], \tag{II.7}$$

where

$$A_{2n-1}(\omega) = \frac{(-1)^{2n-1}\omega \sin(2n-1)\varphi_0}{2n-1} \left[\int_{-\infty}^{\infty} \left[\frac{B(t)}{U}\right]^{2n-1} \cos(2n-1)\theta \cos(2n-1)\lambda\omega_d t \sin\omega t\, dt + \right.$$

$$\left. + \int_{-\infty}^{\infty} \left[\frac{B(t)}{U}\right]^{2n-1} \sin(2n-1)\theta \sin(2n-1)\lambda\omega_d t \sin\omega t\, dt\right],$$

$$A_{2n}(\omega) = \frac{(-1)^{2n}\omega \cos 2n\varphi_0}{2n}\left[\int_{-\infty}^{\infty} \left[\frac{B(t)}{U}\right]^{2n} \cos 2n\theta \sin n\lambda\omega_d t \sin\omega t\, dt - \int_{-\infty}^{\infty} \left[\frac{B(t)}{U}\right]^{2n} \sin 2n\theta \cos 2n\lambda\omega_d t \sin \omega t dt\right],$$

$$B(\omega) = \sum_{n=1}^{\infty} B_n(\omega) = \sum_{n=1}^{\infty} [B_{2n-1}(\omega) + B_{2n}(\omega)], \tag{II.8}$$

where

$$B_{2n-1}(\omega) = -\frac{(-1)^{2n-1}\omega \cos(2n-1)\varphi_0}{2n-1}\left[\int_{-\infty}^{\infty} \left[\frac{B(t)}{U}\right]^{2n-1} \cos(2n-1)\theta \sin(2n-1)\lambda\omega_d t \cos\omega t\, dt - \right.$$

$$\left. - \int_{-\infty}^{\infty} \left[\frac{B(t)}{U}\right]^{2n-1} \sin(2n-1)\theta \cos(2n-1)\lambda\omega_d t \cos\omega t\, dt\right],$$

$$B_{2n}(\omega) = -\frac{(-1)^{2n-1}\omega \sin 2n\varphi_0}{2n-1}\left[\int_{-\infty}^{\infty} \left[\frac{B(t)}{U}\right]^{2n} \cos 2n\theta \cos 2n\lambda\omega_d t \cos\omega t\, dt + \int_{-\infty}^{\infty} \left[\frac{B(t)}{U}\right]^{2n} \sin 2n\theta \sin 2n\lambda\omega_d t \cos\omega t\, dt\right].$$

It follows from (II.7) and (II.8) that, after averaging over the phase angle φ_0 for its equiprobable values, one obtains the following valid relationships

$$\overline{[A(\omega)]^2} = \sum_{n=1}^{\infty} \overline{[A_n(\omega)]^2}, \quad \overline{[B(\omega)]^2} = \sum_{n=1}^{\infty} \overline{[B_n(\omega)]^2},$$

since $\overline{\sin n\varphi_0 \cos l\varphi_0} = 0$, $\overline{\sin k\varphi_0 \sin l\varphi_0} = 0$ and $\overline{\cos k\varphi_0 \cos l\varphi_0} = 0$.

With this, the energy spectrum of (II.1) can be written in the form

$$W(\omega) = 2m \sum_{n=1}^{\infty} \overline{|F_n(\omega)|^2}, \tag{II.9}$$

where $\overline{|F_n(\omega)|^2} = \overline{[A_n(\omega)]^2} + \overline{[B_n(\omega)]^2}$.

We now express the values of $B(t)^n \cos n\theta(t)$ and $B(t)^n \sin n\theta(t)$ in terms of their values for $n = 1$ (II.6), substitute them in the expressions for $A_n(\omega)$ (II.7) and $B_n(\omega)$ (II.8) and then integrate. In finding $[A_n(\omega)]^2$ and $[B_n(\omega)]^2$ and substituting in these expressions the values of A_0, β, and C_0 / U, defined in accordance with (I.12) and (I.13) by the formulas

$$A_0 = \frac{\sqrt{8}\, U_n C_0 \Delta\omega}{\pi\omega_0}, \quad \beta = \frac{2\Delta\omega^2}{\pi}, \quad \frac{C_0}{U} = \frac{e^{\frac{\pi}{8}\left(\frac{\lambda\omega_d}{\Delta\omega}\right)^2}}{U_s},$$

we get that the following real relationships hold for telemetering systems in which $\omega_{max} / \Delta\omega = \omega_f / \Delta\omega \leq 0.2$ and $\omega_d \leq \Delta\omega - \omega_f$:

$$|\overline{F_1(\omega)}|^2 = 4\left(\frac{\omega}{\omega_0}\right)^2 \left(\frac{U_n}{U_s}\right)^2 \left\{1 - \cos(\omega_0 + \lambda\omega_d)\tau \cos\omega\tau - \frac{\pi}{2}\left(\frac{\lambda\omega_d}{\Delta\omega}\right)\left(\frac{\omega}{\Delta\omega}\right) \sin(\omega_0 + \lambda\omega_d)\tau \sin\omega\tau\right\} \qquad (II.10)$$

$$|\overline{F_2(\omega)}|^2 = 4\left(\frac{\omega}{\omega_0}\right)\left(\frac{U_n}{U_s}\right)^2 \left[\frac{1}{\pi^2}\left(\frac{\Delta\omega}{\omega_0}\right)^2 \left(\frac{U_n}{U_s}\right)^2\right] \left\{1 - \cos 2(\omega_0 + \lambda\omega_d)\tau \cos\omega\tau + \right.$$

$$+ \frac{\pi}{2}\left(\frac{\lambda\omega_d}{\Delta\omega}\right)\left(\frac{\omega}{\Delta\omega}\right) \sin 2(\omega_0 + \lambda\omega_d)\tau \sin\omega\tau - 4e^{-\frac{\beta\tau^2}{2}}\left[\cos(\omega_0 + \lambda\omega_d)\tau \cos\frac{\omega\tau}{2} + \right.$$

$$\left.\left. + \frac{\pi}{2}\left(\frac{\lambda\omega_d}{\Delta\omega}\right)\left(\frac{\omega}{\Delta\omega}\right) \sin(\omega_0 + \lambda\omega_d)\tau \sin\frac{\omega\tau}{2}\right] + 2e^{-\beta\tau^2}\right\}, \qquad (II.11)$$

$$|\overline{F_3(\omega)}|^2 = 4\left(\frac{\omega}{\omega_0}\right)\left(\frac{U_n}{U_s}\right)^2 \left[\frac{2.38}{\pi^4}\left(\frac{\Delta\omega}{\omega_0}\right)^4 \left(\frac{U_n}{U_s}\right)^4\right] \left\{1 - \cos 3(\omega_0 + \lambda\omega_d)\tau \cos\omega\tau - \right.$$

$$\left. - \frac{\pi}{2}\left(\frac{\lambda\omega_d}{\Delta\omega}\right)\left(\frac{\omega}{\Delta\omega}\right) \sin 3(\omega_0 + \lambda\omega_d)\tau \sin\omega\tau\right\}. \qquad (II.12)$$

Formulas (II.10)-(II.12) are valid for $k_{max} = B(t)_{max}/U < 1$. We now determine the maximum value of $U_n \Delta\omega / U_s \omega_0$ for which the condition $k_{max} < 1$ holds.

The signal amplitude at the output of filter F_1

$$U = U_s C(\omega) = U_s C_0 e^{-\frac{\pi}{2}\frac{(\omega-\omega_0)^2}{(2\Delta\omega)^2}}$$

has its maximum value for $\omega - \omega_0 = \lambda\,\omega_d = \omega_d$. Since $\omega_d = \Delta\omega - \omega_f \approx \Delta\omega$ (for small ω_f), then $U_{min} = 0.677\, U_s C_0$.

If $\omega_0 \tau \ll 1$ then, as follows from (II.4), $B(t)_{max} = A_0 \omega_0 \tau$ and, for the condition $k_{max} < 1$ to hold, it is necessary that the following inequality hold

$$\frac{U_n}{U_s}\Delta\omega\tau < 0.75. \qquad (II.13)$$

If the transient responses from the leading and trailing edges of the individual noise pulses virtually do not overlap, which occurs, as follows from (I.13), for $\sqrt{\beta}\,\tau > 4$, then $B(t)_{max} = A_0$ and, in order for the inequality $k_{max} < 1$ to hold, it is necessary that the following condition be met

$$\frac{U_n}{U_s}\frac{\Delta\omega}{\omega_0} < 0.75. \qquad (II.14)$$

When the transient responses from the noise pulse edges do overlap, i.e., when $\sqrt{\beta}\,\tau < 4$ and when, for definite values of noise pulse duration, the responses may overlap in phase and the total reaction be doubled, one must assume that $B(t)_{max} = 2A_0$. Then, to obtain the condition that $k_{max} < 1$, one must have the relationship

$$\frac{U_n}{U_s}\frac{\Delta\omega}{\omega_0} < 0.375. \qquad (II.15)$$

By taking into account that condition (II.15) must hold for $0 < \sqrt{\beta}\,\tau < 4$, we obtain the following formulas for the coefficients of expressions (II.10)-(II.12)

$$\nu_1 = 1, \quad \nu_2 = \frac{1}{\pi^2}\left(\frac{\Delta\omega}{\omega_0}\right)^2 \left(\frac{U_n}{U_s}\right)^2 < 0.0143,$$

$$\nu_3 = \frac{2.38}{\pi^4}\left(\frac{\Delta\omega}{\omega_0}\right)^4 \left(\frac{U_n}{U_s}\right)^4 \leqslant 0.000487.$$

For $\sqrt{\beta}\,\tau > 4$ and condition (II.14) being met,

$$\nu_1 = 1, \qquad \nu_2 = 0.057, \qquad \nu_3 = 0.00768.$$

From the values obtained for the ν, it is clear that, with an accuracy sufficient for our purposes, we can set

$$|\overline{F(\omega)}|^2 \approx |\overline{F_1(\omega)}|^2,$$

since

$$|\overline{F_1(\omega)}|^2 \gg |\overline{F_2(\omega)}|^2 \gg |\overline{F_3(\omega)}|^2.$$

Thus, the energy spectrum of the sequence of noise pulses at the discriminator output for $\omega_{max}/\Delta\omega = \omega_f/\Delta\omega \leq 0.2$ and $k_{max} = B(t)_{max} / U < 1$ is defined by the equation

$$W(\omega) \approx 2m\,|\overline{F_1(\omega)}|^2, \qquad (II.16)$$

where $\overline{|F_1(\omega)|}^2$ is found from formula (II.10)

The constant (dc) component of the sequence of noise pulses at the discriminator [7]

$$U_{\text{const}} = mF(0), \qquad \text{(II.17)}$$

equals zero, it following from (II.5) that $F(0) = A(0) - iB(0) = 0$.

Due to the absence of the constant component of (II.17), the discrete portion of the energy spectrum of the sequence of noise pulses at the discriminator output (consisting, in the general case, of a discrete and a continuous portion) will equal zero, and formula (II.1), defining the spectrum's continuous portion, will be valid, for equiprobable values of φ_0, both for chaotic and for periodic trains of noise pulses.

LITERATURE CITED

[1] R. D. Maurice, "V. H. F. broadcasting: Reduction of impulsive interference in f.m. reception," Electronic and Radio Engineer 34, new ser., 8 (1957).

[2] J. C. Tellier, "An analysis of the behavior of limiter-discriminator f. m. detectors in the presence of impulse noise," Proc. of National Electronics Conference (Chicago) 3 (1947).

[3] M. K. Zinn, "Transient response of an f.m. receiver," Bell System Techn. J. 27, 4 (1948).

[4] V. M. Sidorov, "The action of weak pulse noise on receivers of frequency modulated oscillations," Radiotekhnika 13, 3 (1958).

[5] L. B. Venchkovskii and Yu. I. Chugin, Actual Noise Stability of Frequency Receivers and the Statistical Characteristics of Noise, [in Russian] (Proc. IAT AN SSSR, 1957).

[6] S. I. Evtyanov, Transient Responses in Receiver-Amplifier Circuits [in Russian] (Svyaz'izdat, 1948).

[7] I. S. Gonorovskii, Radio Signals and Transient Phenomena in Radio Circuits [in Russian] (Svyaz'izdat, 1954).

ON AMPLIFIERS OF ERROR SIGNALS OF ELECTRICAL AUTOMATIC CONTROL SYSTEMS

L. L. Dekabrun
(Moscow)

(Translated from: Avtomatika i Telemekhanika, Vol. 21, No. 1, pp. 106-111, January, 1960)
Original article submitted February 16, 1959

A new principle of designing synchronous detector circuits is presented which permits a significant lowering in the magnitude of the lag* introduced in the transmission of a signal by amplifiers of slowly varying voltage. The circuits permit the broadening of the domain of applicability of such amplifiers in automatic control systems where amplifiers with galvanic connections cannot provide high accuracy.

A qualitative analysis is given of the lag introduced by amplifiers in existing synchronous detection circuits.

The simplest amplifiers of error signals in automatic control systems are amplifiers with galvanic connections. Their disadvantage is that the drift of the output voltage [1, 2] and the indeterminacy of the initial state determine the limits of the accuracy with which the system can maintain a given value of the controlled quantity. Amplifiers with preliminary transformation of error signal voltages to ac carrier-frequency voltages [3] allow the system accuracy to be increased by at least two orders of magnitude and, with very good regulation, even higher, although in theory there is also drift in these amplifiers [4]. However, such amplifiers transmit signals with significant lag which, in some cases, can lead to a loss of system stability.

The "inertia" of amplifiers with transformed input voltages has received little treatment in the literature [5]. Below, we give an approximate quantitative estimate of this quantity, and present a significantly less "inertial" principle for designing such amplifiers.

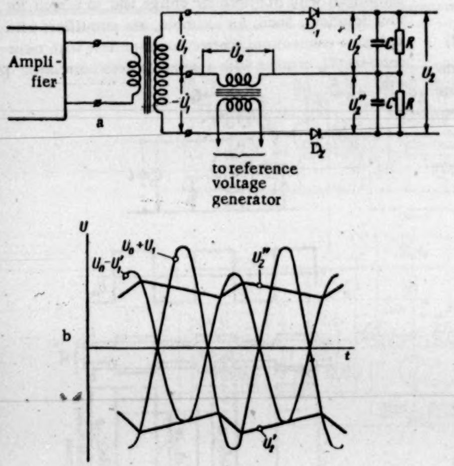

Fig. 1.

The lag in amplifiers with transformed input voltage is induced by the filters which smooth the voltage at the output of the synchronous detector circuit following the amplifiers. Figure 1 a shows one of the widely used synchronous detector circuits; Fig. 1 b shows a somewhat simplified graph of the output voltages U_2' and U_2'' of each section of this circuit. The difference of these voltages constitutes the output voltage U_2 of the synchronous detector and amplifier as a whole.

For adequate smoothing of the output voltage, it is necessary that the following condition hold

$$T_0 < \tau, \tag{1}$$

where T_0 is the period of the carrier frequency voltage off which the transformer of the input voltage operates and $\tau = RC$ is the smoothing filter's time constant. When condition (1) holds, the dc component of voltage U_2 will have the magnitude

$$U_{20} = 2U_1\left(1 - \frac{T_0}{2\tau}\right), \tag{2}$$

and the relative magnitude of the pulsation is found from the formula

$$\varepsilon = \frac{(U\text{pulse})_{\max}}{U_{20}} \doteq \frac{\frac{T_0}{\tau}}{2\left(1 - \frac{T_0}{2\tau}\right)}. \tag{3}$$

Figure 2 shows U_{20} and ϵ as functions of the smoothing filter's time constant.

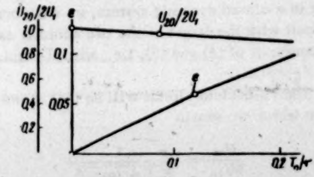

Fig. 2.

---

* In this paper, we understand by the terms "lag" and "inertia" a sum of factors which give rise to any distortion, other than scale-factor changes, of the output signal as compared to the input signal.

The transient response of the synchronous detector (and, consequently, of the amplifier as a whole), i.e., its reaction to an abrupt change in amplitude of the detected voltage U_1, is a complicated function of the circuit parameters and of time. By simplifying the outlines, we can show that

a) for an abrupt decrease of U_1, the fall of the output voltage will follow a law close to an exponential one with a time constant somewhat larger than

$$\tau_f = RC; \qquad (4)$$

b) for an abrupt increase in U_1, the rise of the output voltage will follow a law close to an exponential one with a time constant somewhat larger than

$$\tau_r = \frac{RR_1}{R + R_1} C. \qquad (5)$$

Here, R_1 is the resulting resistance of the circuit through which the condenser charges (the resistance of the diode, the transformer, etc.).

The rise and fall of the output voltage do not follow purely exponential laws because, in the given circuit, they are not continuous processes, e.g., with rising voltage, the condensers only charge during fractions of the positive half-periods while, during the rest of the time, they discharge through their load resistances.

We now construct the amplitude and phase frequency characteristics of the amplifier, with the assumption that its input voltage, i.e., the error signal voltage, varies harmonically

$$U_{in} = U_M \cos \omega_1 t. \qquad (6)$$

For a given frequency ω_0 of the modulating voltage, the frequency ω_1 of the input voltage must lie within the limits of

$$0 \leqslant \omega_1 \leqslant (0.1 \div 0.2)\omega_0, \qquad (7)$$

since otherwise the amplifiers's modulating device could not transmit the form of the input voltage with sufficient accuracy [3]. With this, the detected voltage U_1 will be a sinusoid with variable amplitude

$$U_1 = (U_M \cos \omega_1 t) \sin \omega_0 t. \qquad (8)$$

For estimating the possibilities of using the amplifier in a closed dynamic system, we shall consider its circuit with the larger of the two actually existing time constants of (4) and (5), i.e., with the time constant τ_f = RC.

The equivalent circuit will be that shown on Fig. 3, from which we obtain

$$\frac{U_{20}}{kU_{in}} = \frac{1}{\sqrt{1 + (\omega_1 \tau_f)^2}}, \qquad (9)$$

$$\operatorname{tg} \psi = -\omega_1 \tau_f. \qquad (10)$$

Here, k is the over-all gain and ψ is the phase shift of the amplifier's output voltage with respect to its input voltage.

Figure 4 shows the amplitude and phase frequency characteristics of the amplifiers computed by these formulas. The parameter of the characteristics is the relative time constant of the detector's smoothing circuit, $\beta = T_0/\tau$. These characteristics are universal, being valid for all forms of synchronous detector circuits, including the so-called fast-acting variants of [6]. It is clear from the curves of Fig. 4 that, for good smoothing, the amplifier's output voltage reacts only to very slow changes in the input voltage, while even in this region, i.e., the region of very small values of ω_1, the phase shift of the output voltage with respect to the input voltage retains a significant size. These disadvantages of amplifiers with transformers oblige one to search for new solutions. Such, for example, are amplifiers with galvanic connections, corrected amplifiers with transformers [7], circuits with automatic zero correction [8], etc.

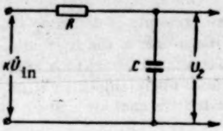

Fig. 3.

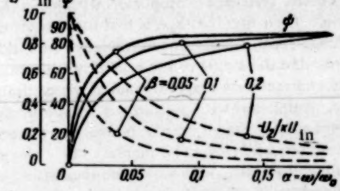

Fig. 4.

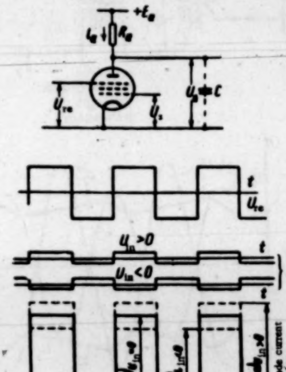

Fig. 5.

The "inertia" of an amplifier with transformation of the input voltage can be significantly decreased if the smoothing of the output voltage is implemented, not by means of accumulators of energy (on the circuit of Fig. 1, the capacitor C is such an accumulator of energy), but by the filling of the "holes" between the pulses of output voltage by pulses obtained from a detection circuit. If the transforming device transforms the input voltage to rectangular pulses (as, for example, in the case of transformation by means of a contact chopper) and the reference voltage also has the form of rectangles, one could then theoretically get rid of the smoothing condensers at the output. Figure 5 shows the block schematic of a synchronous detector and the graphs characterizing its operation in the case when the reference and the detected voltages have the form of rectangular pulses. We assume that there is a second such circuit, operating on the same load resistance R_a but at those intervals of time when the first circuit is cut off by the reference voltage, i.e., the operating cycle of the second circuit is shifted by π with respect to the operating cycle of the first circuit. Then, in the ideal case, the output voltage (the voltage on load R_a) will have no pulsations. Figure 6 gives the functional block schematic of an amplifier with a transformer of the input voltage and an inertialess two-cycle synchronous detector, while Fig. 7 gives the graphs which characterize its operation. The difficul-

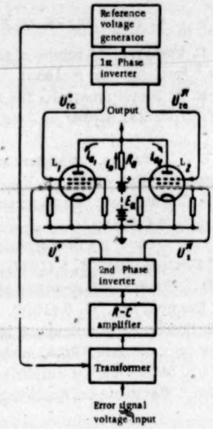
Reference voltage generator
1st Phase inverter
U^{0}_{re}
Output
U^{π}_{re}
L_1
i_{a_1}
i_a
R_a
i_{a_2}
L_2
E_a
U^{0}_{1}
U^{π}_{1}
2nd Phase inverter
R-C amplifier
Transformer
Error signal voltage input

Fig. 6.

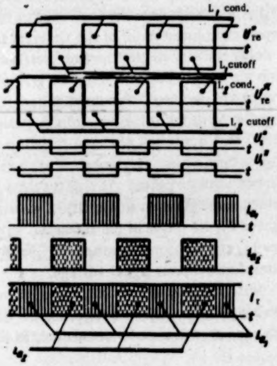
L_1 cond.
U^{0}_{re}
t
L_1 cutoff
L_2 cond.
U^{π}_{re}
t
L_2 cutoff
U^{0}_{1}
t
U^{π}_{1}
t
i_{a_1}
t
i_{a_2}
t
i_1
t
i_{a_1}
i_{a_2}

Fig. 7.

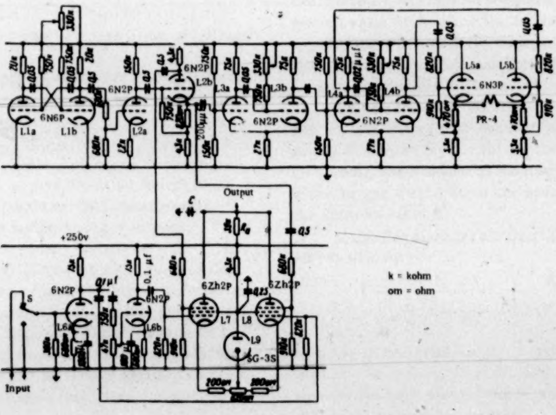
6N6P
L1a
L1b
6N2P
L2a
6N2P
L2b
L3a
L3b
6N2P
L4a
L4b
6N2P
L5a
L5b
6N3P
PR-4
Output
C
R_a
0.5
+250v
6N2P
S
L6a
0.1 μf
6N2P
L6b
6Zh2P
6Zh2P
L7
L8
L9
SG-3S
200om
200om
Input
k = kohm
om = ohm

Fig. 8.

ties related to the realization of this principle have to do, principally, with the accuracy of synchronization of the operating cycles, and with the accuracy of matching the characteristics of the two channels. Figure 8 shows a circuit which is one of the possible variants of the solution to this problem. The basis of the circuit is a two-cycle synchronous detector (tubes L_7 and L_8) analogous to that considered above. The circuit's rhythm of operation is given by the independently driven multivibrator $L_{1a}L_{1b}$ in whose circuit there is the capability of tuning symmetric cycles. The reference voltage of the synchronous detection circuit is formed by amplifier-limiter L_{2a} and split by phase-inverter L_{2b}. The contact transformer of the error signal voltage, implemented by polarized relay PR-4, is connected at the output of the symmetric cathode follower $L_{5a}L_{5b}$. The adjustment of the equality of the intervals of open and closed states of the contacts is regulated by the delay time of single flip-flop oscillator $L_{4a}L_{4b}$, from which the controlling pulses for the grid of the cathode follower are obtained. Synchronization of the input voltage pulses with the reference voltage pulses is so performed, that triggering of single flip-flop oscillator $L_{4a}L_{4b}$ is carried out with some lag with respect to the reference voltage pulses. The delay time is established by means of regulation single flip-flop oscillator $L_{3a}L_{3b}$, triggered by the edges of the reference voltage pulses. Tubes L_{6a} and L_{6b} form an amplifier-phase-inverter for the transformed error signal voltage.

With inexact adjustment, there are some pulsations in the amplifier's output voltage, for the smoothing of which capacitor C must be connected, as shown with a dashed line on the circuit diagram. However, even with comparatively inexact adjustment, to attain smoothing of the output voltage in the given circuit which is comparable with the smoothing obtained in the ordinary synchronous detector circuits, there is required a time constant of the smoothing circuit which is less than the usual one by several tens.

The gain of the system shown on Fig. 8 is about 400. To increase the gain, it is necessary to include one or more amplifying stages before the circuit of phase-inverter $L_{6a}L_{6b}$.

LITERATURE CITED

[1] C. Verhagen, "A survey of the limits in dc amplification," Proc. IRE No. 5 (1953).

[2] M. A. Bonch-Bruevich, The Use of Electronic Tubes in Experimental Physics [in Russian] (Gostekhizdat, 1955).

[3] L. L. Dekabrun, Amplifiers and Voltage Supplies [in Russian] (MIFI, 1958).

[4] S. C. Hutcheon, "Dc to ac converter circuits," Proc. IRE 104C, 6 (1957).

[5] F. H. Krentz, "Transfer function of dc chopper amplifier," Electron. Eng. 76, 9 (1957).

[6] D. L. Davis, "A fast-acting phase-conscious indicator," Electron. Eng. 75, 9 (1956).

[7] E. Goldberg, "Stabilization of wide-band dc amplifier for zero and gain," RCA Review 11, 20 (1950).

[8] M.N. McFadden, "Dc amplifier with zero input correction," Electronic and Radio Engineering 10, 10 (1957).

DETERMINATION OF MAGNETIC CONDUCTANCE WITH GEARED STATOR AND ROTOR

L. A. Sribner

(Odessa)

(Translated from: Avtomatika i Telemekhanika, Vol. 21, No. 1, pp. 112-118, January, 1960)
Original article submitted May 28, 1959

A method is considered for the calculation of magnetic conductance for a geared stator and rotor, with flux leakage being taken into account. Functional relationships are established for the determination both of the total magnetic conductance and of the coefficients which take into account flux leakage.

The method developed can be used for designing electric hammers, geared inductive transducers, pitch and pulsed motors, and other electromagnetic systems, and also for the computation of the flux pulsation in the teeth of electrical machines with geared rotors and stators.

In contemporary technology, broad use is made of various electromagnetic mechanisms with moving and immovable geared portions.

The computation of the magnetic circuits of such mechanisms is virtually untreated in the literature. Ordinarily, for computing the magnetic conductance of an air gap, it is recommended that one use awkward graphical methods. The greatest difficulty is presented by the accounting for flux leakages. If one knows the magnetic conductance with flux leakages taken into account, the problem is significantly simplified. An extensive literature [1-3] is devoted to computational methods for this case.

The flux leakage in certain mechanisms with geared rotors and stators is large, and sometimes exceeds significantly the basic flux. In some of these mechanisms the flux leakage is almost constant [4], but it varies sharply in the overwhelming majority of the cases. Sometimes, Carter's formula [5, 6] is used for calculating leakage fluxes, but for small air gaps its use gives understated results.

In the present paper we present a formula for calculating the magnetic conductance of an air gap for geared stators and rotors.

Definition of the Fictitious Air Gap

We shall agree to give the name "rotor" to the moving part of a magnetic circuit, independently of whether its motion is reciprocating or rotational. The nonmoving part of the circuit we call the stator. The flux between the teeth of the stator and rotor we shall call the basic magnetic flux. The magnetic fluxes in the grooves, in the face ends, and through the ribs of the teeth we shall call the leakage fluxes. It must be said at once that, in many cases (for example, in electrical machines), the leakage flux is not a parasitic flux, but is added to the useful basic flux. However, even in this case, we shall call it a leakage flux.

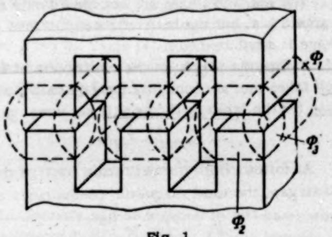

Fig. 1.

There are the following leakage fluxes between the stator and rotor teeth (Fig. 1): 1) lateral leakage flux Φ_1; 2) face end leakage flux Φ_2; 3) leakage flux through the ribs of the teeth Φ_3; 4) the leakage flux of the coil, i.e., the leakage flux through the air around the coil.

The leakage flux of the coil is constant for practical purposes, and may be computed by multiplying the greatest value of the basic flux by the coefficient $\sigma = 0.05$ to 0.2. The coefficient σ depends on the design characteristics of the magnetic circuit. In the sequel, we shall not consider the leakage flux of the coil.

We now introduce the concept of the fictitious air gap δ'. For this we shall consider the air gap to be uniformly distributed (by considering the rotor and stator to be smooth), and a change in the magnetic conductance of the air gap will be taken into account by a change in the fictitious air gap.

If the flux leakages are ignored, then the fictitious air gap will equal

$$\delta' = \frac{\delta_0}{\frac{a}{t}\left(1 - \frac{l}{a}\right)} = \frac{\delta_0}{0.5\left(1 - \frac{l}{a}\right)}, \quad (1)$$

where δ_0 is the actual air gap, a is the width of the teeth, $t = 2a$ is the pitch of the teeth, i.e., the total width of the tooth plus the groove, and l is the relative shift of the rotor and stator teeth.

We now consider how one may take leakage fluxes into account with the determination of the fictitious air gap δ'. For simplicity of the reasoning, we shall assume that the rotor teeth are against the stator teeth, i.e., that $l = 0$.

The magnetic conductance of the basic flux on unit tooth length equals

$$g = \frac{\mu_0 S}{\delta_0} = \frac{\mu_0 a}{\delta_0}, \qquad (2)$$

where μ_0 is the magnetic permeability of air and S is the area through which the basic flux passes. In our case, $S = a$.

Moreover, the flux leakages induce additional magnetic conductance. This conductance, per unit tooth length, equals

$$g_1 = k_1 \frac{\mu_0 2a}{\delta_0}. \qquad (3)$$

The leakage fluxes are not closed only through the area $S = a$, but the magnetic conductance of the leakage is attributed to it.

In formula (3), k_1 is the coefficient of leakage which takes into account that the equivalent air gap $\delta_{0\,\text{equ}}$ for the leakage fluxes will not equal gap δ_0:

$$\delta_{0\,\text{equ}} = \delta_0/k_1.$$

As follows from the definition itself of the fictitious air gap, the total magnetic conductance equals

$$g_t = \frac{\mu_0 2S}{\delta'} = \frac{\mu_0 2a}{\delta'}. \qquad (4)$$

On the other hand, the total magnetic conductance is

$$g_t = g + g_1.$$

By substituting the values of the conductances from formulas (2), (3), and (4), we get that

$$\frac{\mu_0 2a}{\delta'} = \frac{\mu_0 a}{\delta_0} + k_1 \frac{\mu_0 2a}{\delta_0}, \qquad (5)$$

or, after some transformations,

$$\delta' = \frac{\delta_0}{0.5 + k_1}.$$

If the rotor teeth are shifted relative to the stator teeth, i.e., if $l \neq 0$, then, by taking formula (1) into account, we get

$$\delta' = \frac{\delta_0}{0.5\left(1 - \frac{l}{a}\right) + k_1}. \qquad (6)$$

Taking into Account the Magnetic Conductance of the Lateral Flux Leakage

The coefficient which takes into account the magnetic conductance of the lateral (side) flux leakage depends, in addition to everything else, on the shift of the rotor teeth relative to the stator teeth. We shall therefore first determine it for the case when the rotor teeth are against the stator teeth.

It is clear from expression (3) that the computation of the coefficient of side leakage $k_s = k_1$ reduces to the computation of the magnetic conductance of the lateral leakage per unit length $g_s = g_1$, since the remaining quantities of expression (3) are already known.

If we assume that the magnetic lines of forces are semicircles, then the conductance equals [2]

$$g_1 = \frac{\mu_0}{\pi} \ln\left[1 + \frac{2a}{\delta_0}\right]. \qquad (7)$$

If they are assumed to be semi-ellipses, then [2]

$$g_1 = \frac{\mu_0}{\pi} \ln\left[1 + 2\,\frac{a + \sqrt{a^2 + a\delta_0}}{\delta_0}\right]. \qquad (8)$$

If they are considered to consist of four portions of circles and straight lines, we then obtain [2]

$$g_1 = \frac{\mu_0}{\pi} \ln\left[1 + \frac{\pi a}{\delta_0}\right]. \qquad (9)$$

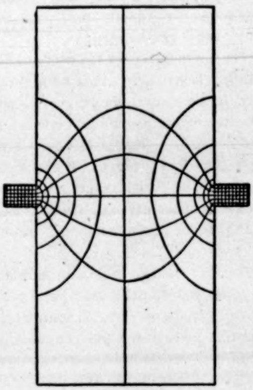

Fig. 2.

We now consider what form the actual lines of force might have. On Fig. 2, we have constructed the outlines of the magnetic field in the grooves for the groove depth equal to its width. For this construction, the steel surface was taken as an equipotential surface which, in the given case, is completely admissible, even for comparatively large values of induction.

It is clear from Fig. 2 that the magnetic lines of force differ significantly from semicircles or parts of ellipses. Moreover, for various values* of x, the magnetic lines of force are described by different equations and, for $x = a$, reduce to straight lines. In this case, the mean length of the magnetic lines of force equals approximately $l_x = 3x + \delta_0$; for small x the length is $l_x > 3x + \delta_0$ and, for large x, $l_x < 3x + \delta_0$ and, for increasing x, approximates to the value $l_x = 2x + \delta_0$.

---

*We denote by x the distance between the magnetic lines of force and the beginning of the groove for equipotential surfaces equally spaced from the teeth.

The area through which the magnetic flux passes is not constant, but varies per unit length from 0.5 to 1.5a, there being a corresponding change in the area of the elementary force tubes from 0.5 to 1.5 dx; in the mean, this area equals dx.

The estimates given are also approximately valid for other relationships of the size of the air gap and the teeth dimensions.

By substituting these mean values of length and area of the elementary force tubes in the formula for computing magnetic conductance, we get

$$g_s = g_1 = \mu_0 \int_0^a \frac{dx}{3x + \delta_0} =$$

$$= \frac{\mu_0}{3} \left| \ln (3x + \delta_0) \right|_0^a = \frac{\mu_0}{3} \ln \left(1 + \frac{3a}{\delta_0}\right). \qquad (10)$$

Finally, we take the following formula which gives the results coinciding most exactly with experimental results:

$$g_s = \frac{\mu_0}{\pi} \ln \left(1 + \frac{3a}{\delta_0}\right). \qquad (11)$$

From expressions (3) and (11), we obtain the expression for the coefficient of lateral (side) leakage

$$k_s = \frac{\delta_0 \ln \left(1 + \frac{3a}{\delta_0}\right)}{\pi a}. \qquad (12)$$

We now consider how the coefficient of lateral conductance varies as the rotor teeth are shifted (displaced) with respect to the stator teeth.

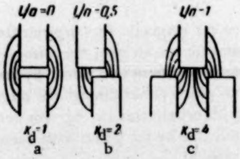

Fig. 3.

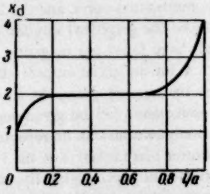

Fig. 4.

Let the rotor teeth be displaced relative to the stator teeth by half a tooth (Fig. 3 b). In this case the conductance $g_1 = \mu_0 \int_0^a dx/l_x$ will be twice as large as in the case with nondisplaced teeth (Fig. 3 a), since here the length of the magnetic lines of force is twice as small. Consequently, the coefficient of side conductance will be twice as large here. The coefficient of side (lateral) conductance will be exactly the same if there are teeth only on the stator, the rotor being smooth, or conversely.

We now consider the case when the rotor teeth are against (opposite) the stator grooves (Fig. 3 c). Here, the coefficient of lateral conductance will be twice as large as in the previous case, i.e., four times larger than for nondisplaced teeth. We take the variation of the coefficient of lateral displacement into account by introducing a coefficient of teeth displacement k_d, which is defined by the graph of Fig. 4. This graph was constructed with experimental results being taken into account, these results showing that the curve of the magnetic flux of such electromagnetic mechanisms is a straight line when the teeth displacement lies within the limits of $l/a = 0.2$ to 0.7 and, for larger and for smaller values of l/a, becomes curved. Analogous curves of the flux were also given by Yasse [4] (for two teeth).

The formula for determining the fictitious air gap takes the following form:

$$\delta' = \frac{\delta_0}{0.5\left(1 - \frac{l}{a}\right) + k_d k_s}. \qquad (13)$$

This formula can be applied in all cases when there are narrow and long grooves. If the grooves are only on the rotor, or only on the stator, then the coefficient k_s must be doubled, whereby it no longer depends on the position of the rotor. Then, the formula is written in the following form:

$$\delta' = \frac{\delta_0}{0.5 + k_s}. \qquad (14)$$

For electrical machines, formulas (13) and (14) give results which coincide closely with those computed by Carter's formula [7].

Further Refinement of the Formula for Determining the Fictitious Air Gap

Formula (13) gives incorrect results for short grooves. In this case it is necessary to take into account the face leakage flux and the leakage flux through the ribs of the teeth.

The coefficient of face end leakage can be computed analogously to the coefficient of lateral leakage, assuming the depth of the grooves to be significantly greater than the width, but the active depth equal to the groove width.

The length of the magnetic lines of force can be taken equal to $l_x = 3.5x \pm \delta_0$, on the average, and the cross section of an elementary magnetic force tube per unit length equal, on the average, to approximately dx.

The magnetic conductance of the face end flux leakage equals

$$g_f = \mu_0 \int_0^a \frac{dx}{l_x} = \mu_0 \int_0^a \frac{dx}{3.5x + \delta_0} =$$

$$= \frac{\mu_0}{3.5} |\ln (3.5x + \delta_0)|_0^a = \frac{\mu_0}{3.5} \ln \left(1 + 3.5 \frac{a}{\delta_0}\right), \quad (15)$$

from whence we obtain, for the coefficient of face end conductance,

$$k_f = \frac{\delta_0 \ln \left(1 + 3.5 \frac{a}{\delta_0}\right)}{3.5a} \frac{a}{b} = \frac{\delta_0 \ln \left(1 + 3.5 \frac{a}{\delta_0}\right)}{3.5b}, \quad (16)$$

where b equals the groove length.

As the rotor teeth are displaced relative to the stator teeth, the coefficient of face end conductance, i.e., the leakage flux through the face end, just as with the basic flux, decreases linearly.

We now take into account the conductance of the teeth ridges. If one equates the conductance of the ridges with the conductance of the face end, it is then easily calculated that the coefficient of ridge flux for undisplaced teeth equals $0.6k_f$. When the rotor teeth are opposite the stator grooves, this coefficient is doubled, since the flux contains an angle twice as large. We assume that the coefficient of flux leakage through a ridge varies linearly as the rotor teeth as shifted with respect to the stator teeth (although, in actuality, it varies in accordance with a more complicated law).

The formula for calculating the fictitious air gap when one takes into account the coefficients of face end flux leakage and ridge flux leakage takes the following form:

$$\delta' = \frac{\delta_0}{\left(1 - \frac{l}{a}\right)(0.5 + k_f) + 0.6k_f\left(1 + \frac{l}{a}\right) + k_d k_s}, \quad (17)$$

where k_s and k_f are defined by formulas (12) and (16).

Taking the Reluctance of the Magnetic Circuit into Account

Formula (17) makes it possible to calculate the magnetic conductance of an air gap with the flux leakages taken into account. However, for small air gaps δ_0, the reluctance of the magnetic circuit becomes commensurable with the reluctance of the air gap, and must therefore be taken into account.

As is well known, for ferromagnetic materials the dependence on ampere-turns of the magnetic flux is nonlinear, and is given by the magnetization curve. Consequently, the magnetic circuit's reluctance is not constant, but depends on the ampere-turns applied.

It is simplest to take the magnetic circuit's reluctance into account graphically. For this, we decompose the magnetic circuit into a series of portions (segments) such that the cross-section of the magnetic circuit will be invariant on each segment. For each portion one constructs, from the magnetization curve for the given type of steel, the magnetization curve of the segment multiplied by the value of induction from the first curve on the segment's cross section, and the field strength (specific ampere-turns) on the segment's length.

Thereafter, one constructs the magnetization curve of the entire magnetic circuit, adding up, for arbitrary values of magnetic flux, the ampere-turns of the segments of the magnetic circuit.

After this, it is necessary to construct the dependence of the magnetic flux on the ampere-turns for the air gap. For this, we give ourselves the ampere-turns iw and compute the magnetic flux Φ_0 in the air gap under the assumption that the magnetic circuit's reluctance equals zero:

$$\Phi_0 = \frac{iw}{\delta'} \mu_0 S, \quad (18)$$

where S is the area of the air gap.

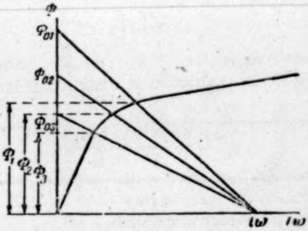

Fig. 5.

Since the magnetic flux depends linearly on the ampere-turns for the air gap, the corresponding graph can be constructed from two points by drawing the straight line which passes through the origin and through the point with coordinates iw, Φ_0. For convenience, we construct this line by the points with coordinates iw, 0, and 0, Φ_0 (Fig. 5).

Then, the point of intersection of the magnetic circuit's magnetization curve and the line for the air gap will also be the graphical solution of the problem, i.e., we shall have found the magnetic flux of the magnetic system Φ for the given ampere-turns. If the flux is divided by the ampere-turns, the quotient will be the magnetic conductance for the given conditions.

Such computations can be repeated for various shifts of the rotor teeth relative to the stator teeth, i.e., for various fictitious gaps. Naturally, the magnetization curve of the magnetic circuit will not thereby be varied.

The data thus obtained can be employed in the design of all the possible electromagnetic devices.

The magnitude of the magnetic conductance and its variations as a function of the displacement of the rotor teeth relative to the stator teeth can be converted to terms of forces, moments (torques), or inductions, depending on the purpose for which the device being designed is intended.

In conclusion, the author wishes to thank L. K. Shrago for reading the manuscript and for making a number of valuable comments.

LITERATURE CITED

[1] A. Ya. Bulov, Fundamentals of Electrical Apparatus Construction [in Russian] (Gosénergoizdat, 1946).

[2] B. S. Sotskov, Elements of Automation and Remote Control Apparatus [in Russian] (Gosénergoizdat, 1950).

[3] G. K. Roters, Electromagnetic Mechanisms [in Russian] (Gosénergoizdat, 1949).

[4] E. Yasse, Electromagnets [in Russian] (Gosénergoizdat, 1934).

[5] A. I. Moskvitin, "On the conductance of a gap with opened grooves on stator and rotor," Izvest. Akad. Nauk SSSR, Otd. Tekh. N. 1 (1941).

[6] A. I. Moskvitin, Reciprocating Electrical Machines [in Russian] (Izd. AN SSSR, 1950).

[7] Carter, Air gap induction, El. World and Eng., 38 (1901).

THE EFFECT OF NONUNIFORMITY OF MAGNETIZATION ON THE STATIC CHARACTERISTICS OF CORES. I

G. D. Kozlov

(Moscow)

(Translated from: Avtomatika i Telemekhanika, Vol. 21, No. 1, pp. 119-134, January, 1960)
Original article submitted June 4, 1959

The effect of nonuniformity of magnetization on the static characteristics of cores is considered. The computations are given for the limiting magnetization polarity reversal loop of a core, the symmetric and biased magnetization polarity reversal loops, and the "basic magnetization curve".

Recently, in various branches of automation, remote control, and computing technology, wide use has been made of magnetic amplifiers employing cores with complicated forms of magnetic circuits (magnetic circuits with variable cross sections, ramified or multibranched magnetic circuits, etc.). Among the magnetic devices with ramified magnetic circuits are the "transfluxers" which can be used as decoders, logical elements, memory devices without destructive read-out, etc. The magnetization of the magnetic circuit in such devices occurs nonuniformly, and is fundamentally conditioned by the geometric form and the dimensions of the magnetic circuit, and also by the physical position of the magnetizing windings. In [1, 2] was considered the question of taking into account the effect of nonuniform core magnetization on its static characteristics, the present work being a development of the earlier ones. In [1, 2], the authors determine the magnitude of the magnetic induction of a toroidal core as a function of the field strength, B = f(H). With this, the field strength, is taken, in [1], relative to the mean core radius $R = (R_0 + R_1)/2$ and, in [2], relative to the mean harmonic radius $R_h = (R_0 - R_1/ \ln(R_0/R_1)$.* From our point of view, one can more simply and more graphically derive conclusions by using the relationship B = f(F) instead of B = f(H), where F is the number of ampere-turns of the magnetization. The advantage of introducing such a relationship is particularly clearly seen when one takes into account the nonuniformity of magnetization in a multibranched magnetic circuit, where the relationship B = f(H) loses its meaning, since it is not known relative to which length of lines of force the field strengths are defined.

The present work is devoted to accounting for the effect of nonuniformity of core magnetization on its static characteristics for various core geometries and for various modes of magnetic polarity reversal. In this portion of the work, all the basic relationships are derived for toroidal magnetic circuits when they undergo complete, and partial, reversal of their magnetic polarity.

Basic Statements

The hysteresis loops of all magnetic material can, with sufficient accuracy, be presented by two forms of idealized hysteresis loops (Figs. 1 and 2). Each form of loop corresponds to a definite group of materials. Within each group, the materials can be distinguished from each other by the following parameters; b_s, the saturation induction; b_p, the induction at the beginning of magnetic polarity reversal; h_s the saturation field

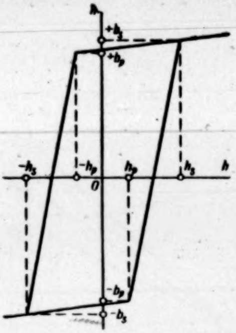

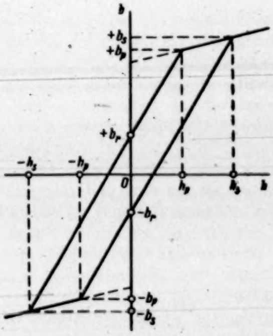

Fig. 2.

---

* Publishers' note – "o" and "i" are "outside diameter" and "inside diameter," respectively.

strength; h_p the field strength at the beginning of magnetic polarity reversal. Such idealized material hysteresis loops permit one to determine, not only qualitatively, but also quantitatively, the effect of nonuniformity of core magnetization on its static characteristics. The process of magnetic polarity reversal of a core presents itself as the reversal of magnetic polarity of individual concentric layers of material lying one within the other. The reversal of magnetic polarity begins with the inner levels, when the induced field strength becomes greater than the quantity h_p. The reversal of magnetic polarity ceases when the magnitude of the field strength reaches the value h_s.

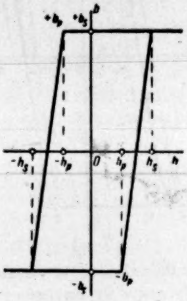

Fig. 3.

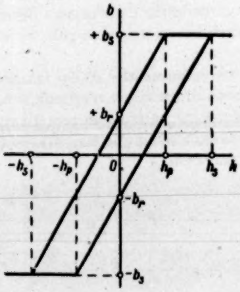

Fig. 4.

For simplicity, we shall consider the material hysteresis loops shown on Figs. 3 and 4, for which the ascending and descending arms of the hysteresis loops are expressed mathematically as follows:

For the case of Fig. 3,

$$b = \frac{2b_s}{h_s - h_p}\left(h - \frac{h_s + h_p}{2}\right), \tag{1}$$

$$b = \frac{2b_s}{h_s - h_p}\left(h + \frac{h_s + h_p}{2}\right); \tag{2}$$

for the case of Fig. 4,

$$b = \frac{2b_s}{h_s + h_p}\left(h - \frac{h_s - h_p}{2}\right), \tag{3}$$

$$b = \frac{2b_s}{h_s + h_p}\left(h + \frac{h_s - h_p}{2}\right). \tag{4}$$

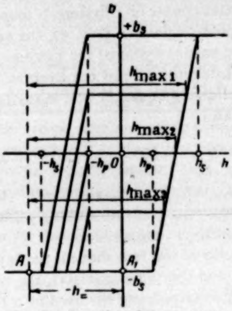

Fig. 5. Family of symmetric cycles of a hysteresis loop.

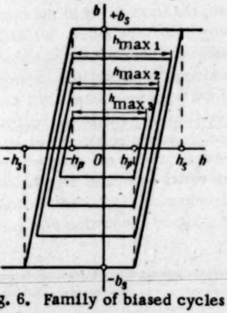

Fig. 6. Family of biased cycles of a hysteresis loop.

For the consideration of the process of reversal of a material's magnetic polarity, we shall henceforth assume that the ascending and descending arms are symmetric and have the same slope in the partial hysteresis loops as the arms of the limiting hysteresis loop. This assertion is borne out to a significant degree by the experimental data provided in the literature. We shall therefore assume that the characteristic slope of the material, $b = f(h)$, is constant for the ascending and descending arms, and equal to $2b_s/(h_s - h_p)$ (for the case of Fig. 3) independently of the form of the hysteresis loop by which the process of magnetic polarity reversal occurs. The quantity h_p remains constant both for symmetric and for biased partial cycles of a hysteresis loop (Figs. 5 and 6). This permits the ascending and descending arms of the family of symmetric cycles of a hysteresis loop (Fig. 5) to be described by the following equations:

$$b = \frac{2b_s}{h_s - h_p}\left(h - \frac{h_{\max} + h_p}{2}\right), \tag{5}$$

$$b = \frac{2b_s}{h_s - h_p}\left(h + \frac{h_{\max} + h_p}{2}\right). \qquad (6)$$

Here, $h_{\max}$ is the maximum value of the magnetizing field strength.

In reversing a material's magnetic polarity by biased partial cycles of a hysteresis loop, when the initial working point is point A (Fig. 6), the ascending arm of the biased partial cycle of the hysteresis loop coincides with the ascending arm of the limiting hysteresis loop, but the following equation will actually hold for the descending arm

$$b = -b_s - \frac{2b_s}{h_s - h_p}(h' - h_{\max}'), \qquad (7)$$

where $h'_{\max} = h_{\max} - h_=$ and $h' = h - h_=$ is the value of the field strength if the working point is translated to A_1 (Fig. 6).

In spite of the fact that all the layers of a core are of one and the same material, the core as a whole has its magnetic polarity reversed by a loop which differs from the material's hysteresis loop. The explanation of this is that, for one and the same number of ampere-turns, the inner layer of the core has a greater field strength than the outer. We shall therefore distinguish henceforth between terms which relates to the material (limiting hysteresis loop, family of symmetric cycles of the hysteresis loop, etc.) and terms referring to the core (limiting magnetic polarity reversal loop, symmetric magnetic polarity reversal loop family, etc.).

For determining the magnetic polarity reversal loop of an entire core, one uses the concept of the mean magnetic induction [1, 2]. We define the magnitude of the mean magnetic induction of a core by the equation

$$B = \frac{1}{R_0 - R_1}\int_{R_1}^{R_0} b\,dR, \qquad (8)$$

where R_0 and R_1 are the core's outer and inner radius and $\alpha = R_0/R_1$ is the ratio of the radii.

To find the relationship $B = f(F)$, we substitute the transformed Eqs. (1)-(7) in Eq. (8).

The Core's Magnetic Characteristics

Depending on the maximum number of magnetizing ampere-turns $F_{\max}$, the core will have different modes of magnetic polarity reversal, defining the form of the function $B = f(F)$.

We initially consider the operation of a core in the mode of its limiting magnetic polarity reversal loop, if the materials's hysteresis loop has the form shown on Fig. 3.

a) Magnetic Polarity Reversal by the Limiting Loop ($F_{\max} \geq \alpha F_s$)

Figure 7 shows the construction of the core's limiting magnetic polarity reversal loop in terms of the coordinates B and F. We denote by the lines aa_1 and cc_1 the ascending and descending arms of the hysteresis loops for the inner and outer layers of the material, respectively. The values of F_p and F_s define the ampere-turns of the inner layer's magnetic polarity reversal and saturation, respectively. The values of αF_p and αF_s serve similarly for the outer layer. In considering Fig. 7, one may note that the values of the ampere-turns for the beginning and the end of the magnetic polarity reversal for different core layers do not coincide. For a given magnetic material and for different core geometries, one can consider three cases of core induction variation when the core has its magnetic polarity reversed along its limiting loop.

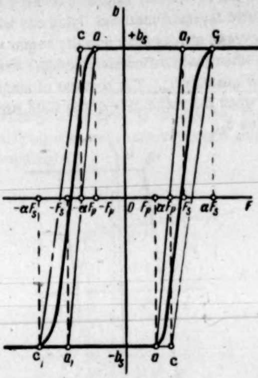

Fig. 7.

For the determination of the function $B = f(F)$, i.e., the magnitude of the core's magnetic induction as a function of the magnetizing ampere-turns, it is necessary to substitute, in Eq. (8), Eqs. (1) and (2), transformed to the form:

$$b = \frac{2b_s}{F_s - F_p}\left(F\frac{R_1}{R} - \frac{F_s + F_p}{2}\right), \qquad (9)$$

$$b = \frac{2b_s}{F_s - F_p}\left(F\frac{R_1}{R} + \frac{F_s + F_p}{2}\right). \qquad (10)$$

In the first case (Fig. 7), the core's geometry is such that $\alpha F_p < F_s$, i.e., the beginning of the material's magnetic polarity reversal along the outer perimeter occurs sooner that the saturation of the material along the inner perimeter. This case is optimal, since the function $B = f(F)$, for such a core geometry, is linear on a significant portion.

For this case, the following condition must hold

$$\alpha < \frac{h_s}{h_p} \qquad (11)$$

or

$$\alpha < \frac{F_s}{F_p}. \qquad (12)$$

To determine the function B = f(F), we substitute Eqs. (9) and (10) in Eq. (8). For different values of F, the function B = f(F) has segments with different characters of variation.

First segment. For the values $-F_{max} \leq F \leq F_p$,

$$B_1 = \frac{1}{R_0 - R_1} \int_{R_1}^{R_0} -b_s dR, \quad B_1 = -b_s. \tag{13}$$

Second segment. For the values $F_p \leq F \leq \alpha F_p$,

$$B_2 = \frac{1}{R_0 - R_1}\left[\int_{R_1}^{R} \frac{2b_s}{F_s - F_p}\left(F\frac{R_1}{R} - \frac{F_s + F_p}{2}\right) dR + \right.$$

$$\left. + \int_{R}^{R_0} -b_s dR \right]$$

(here, $R = R_1 F/F_p$ is the radius dividing the core into two parts, in one of which the process of magnetic polarity reversal has already begun, while in the other it has not).

$$B_2 = \frac{1}{\alpha - 1}\frac{b_s}{F_s - F_p}\left[2F\left(\ln\frac{F}{F_p} - 1\right) - \right.$$

$$\left. - F_s(\alpha - 1) + F_p(\alpha + 1)\right]. \tag{14}$$

Third segment. For the values $\alpha F_p \leq F \leq F_s$,

$$B_3 = \frac{1}{R_0 - R_1} \int_{R_1}^{R_0} \frac{2b_s}{F_s - F_p}\left(F\frac{R_1}{R} - \frac{F_s + F_p}{2}\right) dR,$$

$$B_3 = \frac{1}{\alpha - 1}\frac{b_s}{F_s - F_p}\left[2F\ln\alpha - (F_s + F_p)(\alpha - 1)\right]. \tag{15}$$

Fourth segment. For the values $F_s \leq F \leq \alpha F_s$,

$$B_4 = \frac{1}{R_0 - R_1}\left[\int_{R_1}^{R} b_s dR + \right.$$

$$\left. + \int_{R}^{R_0} \frac{2b_s}{F_s - F_p}\left(F\frac{R_1}{R} - \frac{F_s + F_p}{2}\right) dR\right]$$

(here, $R = R_1 F/F_s$ is the radius dividing the core into two parts, in one of which saturation has already occurred, while it has not in the other),

$$B_4 = \frac{1}{\alpha - 1}\frac{b_s}{F_s - F_p}\left[2F\left(1 + \ln\frac{\alpha F_s}{F}\right) - \right.$$

$$\left. - F_s(\alpha + 1) - F_p(\alpha - 1)\right]. \tag{16}$$

Fifth segment. For the values $\alpha F_s \leq F \leq F_{max}$ and for the reverse variation of F to value zero,

$$B_5 = \frac{1}{R_0 - R_1} \int_{R_1}^{R_0} b_s dR, \quad B_5 = b_s. \tag{17}$$

For negative ampere-turns of magnetization, the function B = f(F) is determined analogously.

By increasing the quantity α ($\alpha = R_0/R_1$), we obtain a second case, when $\alpha F_p = F_s$. This case is characterized by the absence of a linear portion of the function B = f(F) on the ascending and descending arms of the magnetic polarity reversal loop.

A further increase in α leads to the third case, when $\alpha F_p > F_s$. With this, the function B = f(F) has linear portions when the core has its magnetic polarity reversed in the narrow ring extending from the inner layers to the outer ones. In these last two cases, the limiting magnetic polarity reversal loops are determined by the same method as in the first case. For purposes of comparison, Fig. 8 shows the limiting magnetic polarity reversal loops for the first, second, and third cases of values of α:

$$\alpha = 0.75\frac{h_s}{h_p}, \quad \alpha = \frac{h_s}{h_p}, \quad \alpha = 1.5\frac{h_s}{h_p}$$

(curves I, II, III, respectively).

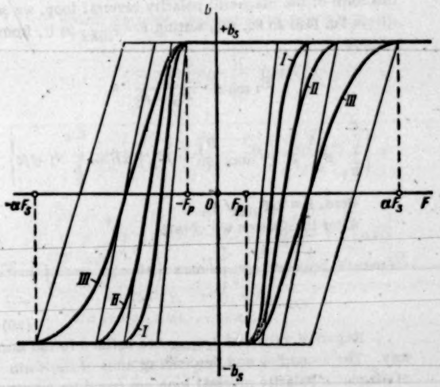

Fig. 8.

b. Magnetic Polarity Reversal by a Symmetric Loop ($F_{max} < \alpha F_s$)

When the maximum value of the magnetizing ampere-turns is inadequate for the magnetic polarity reversal of all the layers of the core material by the limiting hysteresis loop, the core will have its magnetic polarity reversed by symmetric loops. In connection with the circumstance that the individual layers of core material will have their magnetic polarities reversed by different symmetric cycles of the hysteresis loop, the mean maximum variation of the induction of the entire core B_{max} will be less than b_s. For the determination of the symmetric magnetic polarity reversal loops, it is necessary to determine, in addition to the ascending and descending arms of the magnetic polarity reversal loop, the value of $\pm B_{max}$. As a function of the value of F_{max}, the symmetric magnetic polarity reversal loops will differ, not only in magnitude, but also by configuration, where this configuration will also depend on the core's geometry.

We consider only the first case, where $\alpha F_p < F_s$. With further increase in α, the picture does not change qualitatively. To determine the function B = f(F) for symmetric magnetic polarity reversal loops, it is necessary that Eqs. (5) and (6) be transformed to:

$$b = \frac{b_s}{F_s - F_p}\left[(2F - F_{max})\frac{R_1}{R} - F_p\right], \tag{18}$$

$$b = \frac{b_s}{F_s - F_p}\left[(2F + F_{max})\frac{R_1}{R} + F_p\right]. \tag{19}$$

As a function of the size of F_{max}, the symmetric magnetic polarity reversal loops will have three forms.

First Form of the Symmetric Magnetic Polarity Reversal Loops ($F_p < F_{max} \le \alpha F_p$)

To determine B_{max} of the function B = f(F) for this form of the magnetic polarity reversal loop, we substitute Eq. (18) in Eq. (8), setting $F = F_{max}$ in it, from whence

$$B_{1\,max} = \frac{1}{R_0 - R_1} \times$$

$$\times \left\{\int_{R_1}^{R} \frac{b_s}{F_s - F_p}\left(F_{max}\frac{R_1}{R} - F_p\right) dR + \int_{R}^{R_0} 0 \cdot dR\right\}.$$

Here, $R = R_1 F_{max}/F_p$.

After integration we obtain

$$B_{1\,max} = \frac{1}{\alpha - 1}\,\frac{b_s}{F_s - F_p}\left[F_{max}\left(\ln\frac{F_{max}}{F_p} - 1\right) + F_p\right]. \tag{20}$$

Negative values of $B_{1\,max}$ are defined in the same way. The ascending and descending arms of this form of magnetic polarity reversal loop are found by substituting Eqs. (18) and (19) in Eq. (8).

By knowing the ascending and descending arms, and also $\pm B_{1\,max}$, one can construct the entire magnetic polarity reversal loop.

First segment. For values of $-F_{max} \le F \le F_p$,

$$B_1 = -B_{1\,max}. \tag{21}$$

Second segment. For values of $F_p \le F \le F_{max}$,

$$B_2 = \frac{1}{R_0 - R_1}\left\{\int_{R_1}^{R} \frac{b_s}{F_s - F_p} \times\right.$$

$$\times \left[(2F - F_{max})\frac{R_1}{R} - F_p\right] dR +$$

$$\left. + \int_{R}^{R_1} -\frac{b_s}{F_s - F_p}\left(F_{max}\frac{R_1}{R} - F_p\right) dR + \int_{R_1}^{R_0} 0 \cdot dR\right\}.$$

Here,

$$R = R_1\frac{F}{F_p}, \quad R_1 = R_1\frac{F_{max}}{F_p}.$$

After integration, we get

$$B_2 = \frac{1}{\alpha - 1}\,\frac{b_s}{F_s - F_p}\left[2F\left(\ln\frac{F}{F_p} - 1\right) + \right.$$

$$\left. + F_{max}\left(1 - \ln\frac{F_{max}}{F_p}\right) + F_p\right]. \tag{22}$$

Third segment. For values of $-F_p \le F \le F_{max}$,

$$B_3 = B_{1\,max}. \tag{23}$$

For negative values of F, the corresponding portions of the function B = f(F) are determined analogously.

Second Form of the Symmetric Magnetic Polarity Reversal Loops ($\alpha F_p \le F_{max} \le F_s$)

We first determine B_{max} of the function B = f(F) for this form of the magnetic polarity reversal loop:

$$B_{2\,max} = \frac{}{R_0 - R_1}\int_{R_1}^{R_0} \frac{b_s}{F_s - F_p}\left(F_{max}\frac{R_1}{R} - F_p\right) dR$$

or

$$B_{2\,max} = \frac{b_s}{F_s - F_p}\left(\frac{\ln\alpha}{\alpha - 1}F_{max} - F_p\right). \tag{24}$$

We now determine the ascending and descending arms of the function B = f(F) for this form of the magnetic polarity reversal loop.

First segment. For values of $-F_{max} \le F \le F_p$,

$$B_1 = -B_{2\,max}$$

Second segment. For values of $F_p \le F \le \alpha F_p$,

$$B_2 = \frac{1}{R_0 - R_1}\left\{\int_{R_1}^{R} \frac{b_s}{F_s - F_p} \times\right.$$

$$\times \left[(2F - F_{max})\frac{R_1}{R} - F_p\right] dR -$$

$$\left. - \int_{R}^{R_0} \frac{b_s}{F_s - F_p}\left(F_{max}\frac{R_1}{R} - F_p\right) dR\right\}.$$

Here, $R = R_1 F/F_p$.

After integration, we get

$$B_2 = \frac{1}{\alpha - 1}\,\frac{b_s}{F_s - F_p}\left[2F\left(\ln\frac{F}{F_p} - 1\right) - \right.$$

$$\left. - F_{max}\ln\alpha + F_p(\alpha + 1)\right]. \tag{25}$$

Third segment. For values of $\alpha F_p \le F \le F_{max}$,

$$B_3 = \frac{1}{R_0 - R_1} \times$$

$$\times \int_{R_1}^{R_0} \frac{b_s}{F_s - F_p} \left[(2F - F_{\max}) \frac{R_1}{R} - F_p \right] dR,$$

$$B_3 =$$

$$= \frac{1}{\alpha - 1} \frac{b_s}{F_s - F_p} [(2F - F_{\max}) \ln \alpha - F_p (\alpha - 1)]. \quad (26)$$

__Fourth segment.__ For values of $-F_p \leq F \leq F_{\max}$,

$$B_4 = B_2 \max.$$

For negative values of F, the descending arm is determined analogously.

Third Form of the Symmetric Magnetic Polarity Reversal Loops ($F_s \leq F_{\max} \leq \alpha F_s$)

We determined $B_{\max}$ of the function B = f(F) for this form of the magnetic polarity reversal loop:

$$B_{3\max} = \frac{1}{R_0 - R_1} \left[\int_{R_1}^{R_1} b_s \, dR + \right.$$

$$\left. + \int_{R_1}^{R_0} \frac{b_s}{F_s - F_p} \left(F_{\max} \frac{R_1}{R} - F_p \right) dR \right].$$

Here, $R_1 = R_1 F_{\max}/F_s$.
Integration gives

$$B_{3\max} = \frac{1}{\alpha - 1} \frac{b_s}{F_s - F_p} \times$$

$$\times \left[F_{\max} \left(1 + \ln \frac{\alpha F_s}{F_{\max}} \right) - F_s - F_p (\alpha - 1) \right]. \quad (27)$$

We now determine the ascending and descending arms of the function B = f(F) for this form of magnetic polarity reversal loop.

__First segment.__ For the values $-F_{\max} \leq F \leq F_p$,

$$B_1 = -B_3 \max.$$

__Second segment.__ For values $F_p \leq F \leq \alpha F_p$,

$$B_2 = \frac{1}{R_0 - R_1} \left\{ \int_{R_1}^{R_1} \frac{2b_s}{F_s - F_p} \left(F \frac{R_1}{R} - \frac{F_s + F_p}{2} \right) dR + \right.$$

$$+ \int_{R_1}^{R} \frac{b_s}{F_s - F_p} \left[(2F - F_{\max}) \frac{R_1}{R} - F_p \right] dR +$$

$$\left. + \int_{R}^{R_0} - \frac{b_s}{F_s - F_p} \left(F_{\max} \frac{R_1}{R} - F_p \right) dR \right\}.$$

Here, $R_1 = R_1 F_{\max}/F_p$ and $R = R_1 F/F_p$. After integration, we obtain

$$B_2 = \frac{1}{\alpha - 1} \frac{b_s}{F_s - F_p} \left[2F \left(\ln \frac{F}{F_p} - 1 \right) - \right.$$

$$\left. - F_{\max} \left(1 + \ln \frac{\alpha F_s}{F_{\max}} \right) + F_s + F_p (\alpha + 1) \right]. \quad (28)$$

__Third segment.__ For values of $\alpha F_p \leq F \leq F_s$,

$$B_3 = \frac{1}{R_0 - R_1} \left\{ \int_{R_1}^{R_1} \frac{2b_s}{F_s - F_p} \left(F \frac{R_1}{R} - \frac{F_s + F_p}{2} \right) dR + \right.$$

$$\left. + \int_{R_1}^{R_0} \frac{b_s}{F_s - F_p} \left[(2F - F_{\max}) \frac{R_1}{R} - F_p \right] dR \right\}.$$

Here, $R_1 = R_1 F_{\max}/F_s$.
Integration gives

$$B_3 = \frac{1}{\alpha - 1} \frac{b_s}{F_s - F_p} \left[2F \ln \alpha - \right.$$

$$\left. - F_{\max} \left(1 + \ln \frac{\alpha F_s}{F_{\max}} \right) + F_s - F_p (\alpha - 1) \right]. \quad (29)$$

__Fourth segment.__ For values of $F_s \leq F \leq F_{\max}$,

$$B_4 = \frac{1}{R_0 - R_1} \left\{ \int_{R_1}^{R} b_s dR + \right.$$

$$+ \int_{R}^{R_1} \frac{2b_s}{F_s - F_p} \left(F \frac{R_1}{R} - \frac{F_s + F_p}{2} \right) dR +$$

$$\left. + \int_{R_1}^{R_0} \frac{b_s}{F_s - F_p} \left[(2F - F_{\max}) \frac{R_1}{R} - F_p \right] dR \right\}.$$

Here, $R = R_1 F/F_s$ and $R_1 = R_1 F_{\max}/F_s$.
After integration, we obtain

$$B_4 = \frac{1}{\alpha - 1} \frac{b_s}{F_s - F_p} \left[2F \left(1 + \ln \frac{\alpha F_s}{F} \right) - \right.$$

$$\left. - F_{\max} \left(1 + \ln \frac{\alpha F_s}{F_{\max}} \right) - F_s - F_p (\alpha - 1) \right]. \quad (30)$$

__Fifth segment.__ For values of $F_{\max} \leq F$ and $-F_p \leq F \leq F_{\max}$,

$$B_5 = B_3 \max.$$

For negative values of F, the descending arm is found analogously.

By giving various values of $F_{\max}$ we can, by Eqs. (20), (24), and (27), compute the "basic magnetization curve." Figure 9 gives the computed family of symmetric magnetic polarity reversal loops and the "basic magnetization curve."

c) Magnetic Polarity Reversal by a Biased Loop ($F_= \geq \alpha F_s$)

We now consider the mode of magnetic polarity reversal where, at the initial position, all of the core material is magnetized by saturation $F_{=} \geq \alpha F_s$ (Fig. 6 for $h_{=} \geq h_s$). In this mode, the magnetization proceeds by the ascending arm of the limiting magnetic polarity reversal loop and returns to the original state by the descending arm of a biased loop. We shall consider the character of the variation of the function B = f(F) only for the reverse magnetic polarity reversal (the return). For the determination of the function B = f(F), it is necessary to transform Eq. (7) to the form

$$b = -b_s - \frac{2b_s}{F_s - F_p}\left(F' - F_{\max}\right)\frac{R_1}{R}. \qquad (31)$$

Here, $F' = F - F_{=}$ are the ampere-turns for magnetization (after compensation of the constant magnetizing ampere-turns, the working point moves from A to A_1); $F'_{\max} = F_{\max} - F_{=}$.

As in the case of symmetric magnetic polarity reversal loops, the biased loops, as a function of the value of $F'_{\max}$, will have various magnitudes and configurations. We shall therefore distinguish the individual forms of the biased magnetic polarity reversal loops.

First Form of the Biased Magnetic Polarity Reversal Loops ($F_p \leq F'_{\max} \leq \alpha F_p$)

We substitute Eq. (31) in Eq. (8). The function B = = f(F) on the descending arm of a biased magnetic polarity reversal loop will have individual functional segments, determined by the magnitude of F'.

First segment. For values of $-F_p \geq F' \leq F'_{\max}$,

$$B_1 = B_{\max}.$$

Second segment. For values of $-F_p \leq F' \leq -F'_{\max}$.

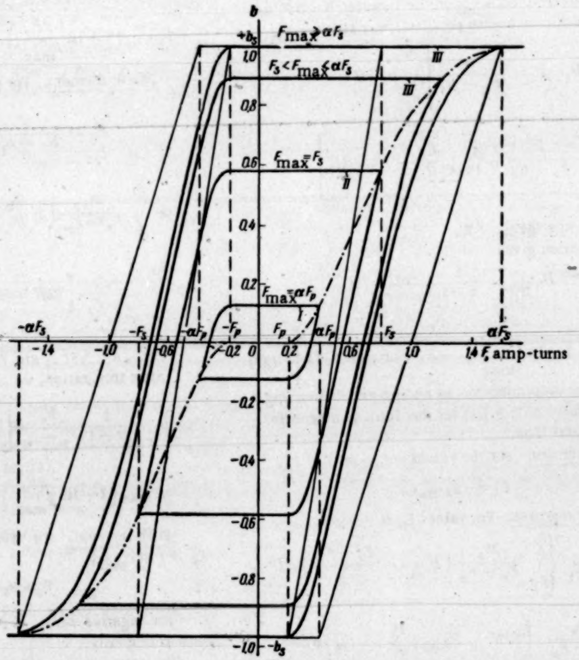

Fig. 9. Family of symmetric magnetic polarity reversal loops and the "basic magnetization curve" computed for the values α = 2, $F_p = 0.2$ ampere-turns, $F_s = 0.8$ ampere-turns. I is the first form of the magnetic polarity reversal loop; II and III are the second and third forms, respectively.

$$B_2 = \frac{1}{R_0 - R_1} \times$$

$$\times \left\{ \int_{R_1}^{R} \left[-b_s - \frac{2b_s}{F_s - F_p} (F' - F'_{\max}) \frac{R_1}{R} \right] dR + \right.$$

$$+ \int_{R}^{R_1} \frac{2b_s}{F_s - F_p} \left(F'_{\max} \frac{R_1}{R} - \frac{F_s + F_p}{2} \right) dR +$$

$$\left. + \int_{R_1}^{R_0} -b_s dR \right\}.$$

Here, $R = R_1 F'/F_p$ and $R_1 = R_1 F'_{\max}/F_p$.
Integration gives

$$B_2 = \frac{1}{\alpha - 1} \frac{b_s}{F_s - F_p} \left[2F' \left(1 - \ln \frac{F'}{F} \right) + \right.$$

$$+ 2F'_{\max} \left(\ln \frac{F'_{\max}}{F_p} - 1 \right) -$$

$$\left. - (F_s - F_p)(\alpha - 1) \right]. \qquad (32)$$

Third segment. For values of $-F'_{\max} \leq F' \leq -F_{\max}$,

$$B_3 = -b_s.$$

Second Form of the Biased Magnetic Polarity Reversal Loops ($\alpha F_p \leq F'_{\max} \leq F_s$)

First segment. For values of $-F_p \geq F' \leq F'_{\max}$,

$$B_1 = B_{\max}.$$

Second segment. For values of $-F_p \leq F' \leq -\alpha F_p$,

$$B_2 = \frac{1}{R_0 - R_1} \left\{ \int_{R_1}^{R} \times \right.$$

$$\times \left[-b_s - \frac{2b_s}{F_s - F_p} (F' - F'_{\max}) \frac{R_1}{R} \right] dR +$$

$$\left. + \int_{R}^{R_0} \frac{2b_s}{F_s - F_p} \left(F'_{\max} \frac{R_1}{R} - \frac{F_s + F_p}{2} \right) dR \right\}.$$

Here, $R = R_1 F'/F_p$; $R_1 = R_1 \frac{F'_{\max}}{F_p}$.
After integration we get

$$B_2 = \frac{1}{\alpha - 1} \frac{b_s}{F_s - F_p} \left[2F' \left(1 - \ln \frac{F'}{F_p} \right) + \right.$$

$$\left. + 2F'_{\max} \ln \alpha - F_s (\alpha - 1) - F_p (\alpha + 1) \right]. \qquad (33)$$

Third segment. For values of $-\alpha F_p \leq F' \leq -F'_{\max}$,

$$B_3 = \frac{1}{R_0 - R_1} \times$$

$$\times \int_{R_1}^{R_0} \left[-b_s - \frac{2b_s}{F_s - F_p} (F' - F'_{\max}) \frac{R_1}{R} \right] dR$$

or

$$B_3 = \frac{1}{\alpha - 1} \frac{b_s}{F_s - F_p} \times$$

$$\times \left[(2F'_{\max} - 2F') \ln \alpha - (F_s - F_p)(\alpha - 1) \right]. \qquad (34)$$

Fourth segment. For values of $-F'_{\max} \leq F' \leq -F_=$,

$$B_4 = -b_s.$$

Third Form of the Biased Magnetic Polarity Reversal Loops ($F_s \leq F'_{\max} \leq \alpha F_s$)

First segment. For values of $-F_p \leq F' \leq \alpha - F_p$,

$$B_1 = B_{\max}.$$

Second segment. For values of $-F_p \leq F' \leq \alpha - F_p$,

$$B_2 = \frac{1}{R_0 - R_1} \times$$

$$\times \left\{ \int_{R_1}^{R_1} - \frac{2b_s}{F_s - F_p} \left(F' \frac{R_1}{R} - \frac{F_s + F_p}{2} \right) dR + \right.$$

$$+ \int_{R_1}^{R} \left[-b_s - \frac{2b_s}{F_s - F_p} (F' - F'_{\max}) \frac{R_1}{R} \right] dR +$$

$$\left. + \int_{R}^{R_0} \frac{2_s}{F_s - F_p} \left(F'_{\max} \frac{R_1}{R} - \frac{F_s + F_p}{2} \right) dR \right\}.$$

Here, $R = R_1 F'/F_p$ and $R_1 = R_1 F'_{\max}/F_s$. Integration gives

$$B_2 = \frac{1}{\alpha - 1} \frac{b_s}{F_s - F_p} \left[2F' \left(1 - \ln \frac{F'}{F_p} \right) + \right.$$

$$+ 2F'_{\max} \left(1 + \ln \frac{\alpha F_s}{F'_{\max}} \right) -$$

$$\left. - (F_s - F_p)(\alpha + 1) \right]. \qquad (35)$$

Third segment. For values of $-\alpha F_p \leq F' \leq -F_s$,

$$B_3 = \frac{1}{R_0 - R_1} \times$$

$$\times \left\{ \int_{R_1}^{R_1} - \frac{2b_s}{F_s - F_p} \left(F' \frac{R_1}{R} - \frac{F_s + F_p}{2} \right) dR + \right.$$

$$\left. + \int_{R_1}^{R_0} \left[-b_s - \frac{2b_s}{F_s - F_p} (F' - F'_{\max}) \frac{R_1}{R} \right] dR \right\}.$$

Here, $R_1 = R_1 F'_{\max}/F_s$.
After integration we obtain

$$B_3 = \frac{1}{\alpha - 1} \frac{b_s}{F_s - F_p} \left[-2F' \ln \alpha + \right.$$

$$\left. + 2F'_{\max} \left(1 + \ln \frac{\alpha F_s}{F'_{\max}} \right) - F_s (\alpha + 1) + F_p (\alpha - 1) \right]. \qquad (36)$$

Fourth segment. For values of $-F_s \le F' \le -F'_{\max}$,

$$B_4 = \frac{1}{R_0 - R_1}\left\{\int_{R_1}^{R} -b_s dR \; - \right.$$

$$-\int_{R}^{R_1} \frac{2b_s}{F_s - F_p}\left(F'\frac{R_1}{R} - \frac{F_s + F_p}{2}\right) dR +$$

$$\left. + \int_{R_1}^{R_0}\left[-b_s - \frac{2b_s}{F_s - F_p}(F' - F'_{\max})\frac{R_1}{R}\right] dR\right\}.$$

Here, $R = R_1F'/F_s$ and $R_1 = R_1F'_{\max}/F_s$.

Integration gives

$$B_4 = \frac{1}{\alpha - 1}\frac{b_s}{F_s - F_p}\left[-2F'\left(1 + \ln\frac{\alpha F_s}{F'}\right) + \right.$$

$$\left. + 2F'_{\max}\left(1 + \ln\frac{\alpha F_s}{F'_{\max}}\right) - (F_s - F_p)(\alpha - 1)\right]. \tag{37}$$

Fifth segment. For values of $-F'_{\max} \le F' \le -F_=$,

$$B_5 = -b_s.$$

Figure 10 shows the family of biased magnetic polarity reversal loops.

By giving different values to $F_= \ge \alpha F_s$, we can compute the family of static characteristics $B = f(F, F_=)$ (Fig. 11).

Taking into account the nonuniformity of core magnetization as it affects its static characteristics when the material has a hysteresis loop of another form (for example, Figs. 1 and 3) can be done in an analogous fashion. Figure 12 shows the limiting magnetic polarity reversal loop of a core whose material has the hysteresis loop shown in Fig. 3.

CONCLUSIONS

On the basis of what has been presented here, we may draw the following conclusions.

1. When the material's hysteresis loop has the form shown on Fig. 2 or on Fig. 3, the core's magnetic characteristic, B = f(F), can be obtained in analytic form.

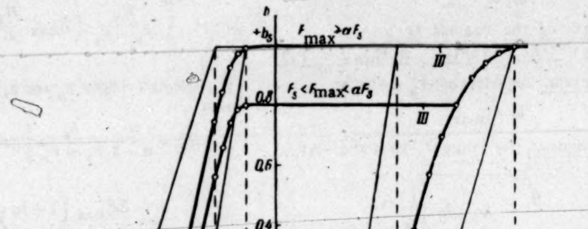

Fig. 10. Family of biased magnetic polarity reversal loops computed for the values $\alpha = 2$, $F_p = 0.2$ ampere-turns, $F_s = 0.8$ ampere-turns, $F_= = \alpha F_s$ = 1.6 ampere-turns.

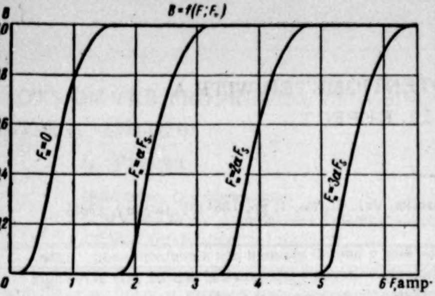

Fig. 11.

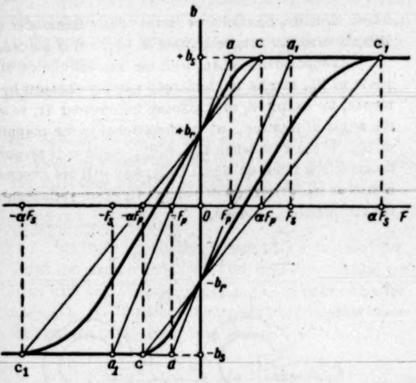

Fig. 12.

2. The form of a core's magnetic characteristic depends on its geometric relationships. There exist three cases of geometric relationships for cores which entail discrepancies in the forms of the magnetic characteristics (Figs. 7 and 8). For $\alpha F_p < F_s$ (the first case), the magnetic polarity reversal loop is characterized by linear segments on the ascending and descending arms. In this case, the outer layers of the core begin to reverse their magnetic polarity until saturation of the inner layers. For $\alpha F_p = F_s$ (the second case), the magnetic polarity reversal loop is characterized by an absence of linear portions on the ascending and descending arms. In this case, at the moment when reversal of the outer layer's magnetic polarity begins, the inner layer is already saturated. For $\alpha F_p > F_s$ (the third case), there is a broadening of the core's magnetic polarity reversal loop. In this case, the core's inner layers have become saturated even before reversal of the outer layers' magnetic polarity has begun. Linear portions of the ascending and descending arms of the magnetic polarity reversal loops are obtained due to the reversal of magnetic polarity of the material in a narrow toroidal sector, beginning at the moment when the inner layers saturate and continuing until the beginning of the reversal of the outer layers' magnetic polarity.

3. The form of the core's magnetic characteristic is also determined by the magnitude of the maximum ampere-turns for magnetization. When the magnitude of the magnetization ampere-turns is inadequate for complete magnetic polarity reversal of the entire core, the core's magnetic polarity is reversed by partial loops. In the modes of core magnetic polarity reversal by symmetric and biased partial loops, there are, as a function of the maximum magnetizing ampere-turns, three forms of loops, differing by their configurations and their dimensions (Figs. 9 and 10). The first loop form, when $F_p < F_{max} \le \alpha F_p$, is characterized by the fact that $\Delta B \ll 2b_s$, and also by the nonlinearity of the function $B = f(F)$ on the ascending and descending arms of the magnetic polarity reversal loop. In this case, only the inner layers have their magnetic polarity reversed. The second loop form, when $\alpha F_p < F_{max} \le F_s$, is characterized by the presence of a linear segment on the ascending and the descending arms of the magnetic polarity reversal loop, and by a larger ratio of $\Delta B / 2b_s$ than in the first case. In this case, the magnitude of the magnetizing ampere-turns is sufficient to reverse the magnetic polarity of the entire core, but inadequate for the saturation even of the inner layers. The third loop form, when $F_s < F_{max} \le \alpha F_s$, is characterized by the fact that all the core's layers have their magnetic polarity reversed, but not all are saturated. With this, the partial loops approximate to the form of the limiting core magnetic polarity reversal loop. All three magnetic polarity reversal loop forms have the same law of variation of the nonlinear segments on the ascending and descending arms.

4. The analytical methods presented can be conveniently employed also for other forms of material hysteresis loops. As an example, Fig. 12 shows the construction of a core's limiting magnetic polarity reversal loop for the material hysteresis loop shown on Fig. 3.

The taking into account of the effect of nonuniformity of core magnetization on its static characteristics for more complicated forms of the material's hysteresis loop, and also the experimental part of the work using ramified cores, will be considered in the second part of the present work.

LITERATURE CITED

[1] R. W. Roberts and R. J. Van Nice, "Influence of ID/OD ratio on static and dynamic magnetic properties of toroidal cores, Trans. AIEE, vol. 74, pt. I (1955).

[2] M. A. Rozenblat, "The dependence of the static characteristics of toroidal cores on their geometric dimensions," Avtomat. i Telemekh. 19, 8 (1958). †

---

† See English translation.

CONTACTLESS DC AUTOMATIC POTENTIOMETER WITH A TRANSFORMER BASED ON THE HALL EFFECT

V. N. Bogomolov

(Leningrad)

(Translated from: Avtomatika i Telemekhanika, Vol. 21, No. 1, pp. 135-136, January, 1960)
Original article submitted June 29, 1959

The circuit is presented for a dc potentiometer lacking a normal element and a contact system. The potentiometer indications are virtually independent of supply voltage oscillations and depend only very slightly on the ambient temperature. Two identical Hall emf transducers are used as a transformer and as a source of compensating emf.

Automatic dc potentiometers are widely used today. In such potentiometers, the dc voltage $U_{\text{in}=}$ to be measured is compensated by a battery voltage, controlled by a normal element, until the difference becomes sufficiently small. Ordinarily, this difference is transformed to ac by a vibrapack, amplified, and then applied to a motor which moves the compensator's slide wire. The disadvantages of such circuits are the presence of the contact transformer, the slide wire with sliding contacts and the normal element. If a transformer based on the Hall effect [1] is used, then one contact element will be replaced by a contactless one. However, nothing is thereby changed in the remainder of the circuit, since the contact slide wire and the normal element remain. By using a Hall-effect transformer, it is nonetheless possible to construct a completely contactless potentiometer, in which there is no longer a necessity for a normal element, if one uses, for the compensation of the Hall emf, an identical transducer which is placed in a constant magnetic field and supplied by the line voltage.

The superiority of such a potentiometer over the ordinary ones consists in its greater mechanical stability, its greater reliability, simplicity, and length of serviceable life.

The circuit of this potentiometer is shown on the accompanying figure. The input dc signal $U_{\text{in}=}$ is immediately transformed to an ac signal $U_{x\sim}$ by the transformer based on the Hall effect, with transmission factor K_1. With this,

$$U_{x\sim} = K_1 U_{\text{in}=}.$$

If one takes into account that K_1 depends both on the temperature, t°, and on the supply (line) voltage U_s, then one may write

$$U_{x\sim} = K_1(t^\circ, U_s)\, U_{\text{in}=} = A f_1(t^\circ)\, f(U_s)\, U_{\text{in}=}.$$

To compensate this alternating emf, one uses the voltage U_c, obtained from an identical transducer, but one immersed in a constant magnetic field and supplied from the line. The RC network is used to shift the phase of U_c by 90°. With this, one may also write

$$U_c = K_2(t^\circ)\, U_s = B f_2(t^\circ)\, f(U_s)\, H,$$

where K_2 is the transmission factor of this transducer and H is the constant magnetic field in which it is placed.

Compensation at ac, with the correct choice of phase of U'_c, can be implemented without contacts by means, for example, of a rotating transformer Tr, in which the angle of rotation, α, is proportional to the magnitude of U'_c. In the case when $U_{x\sim} = U'_c$, angle α is proportional to the input dc signal $U_{\text{in}=}$, and will not depend either on the variations of voltage U_s or on variations of the temperature. Indeed,

$$\frac{U_{x\sim}}{U_{c\sim}} = \frac{A f_1(t^\circ)}{B H f_2(t^\circ)} U_{\text{in}=}.$$

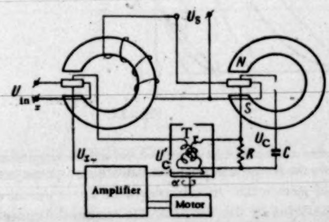

In the case of equality of the temperature dependencies, $f_1(t^\circ)$ and $f_2(t^\circ)$, the ratio just given depends only on $U_{\text{in}=}$ and, consequently, the transformer's angle of rotation α also depends only on $U_{\text{in}=}$. For transducers cut from one rod of germanium, $f_1(t^\circ)$ can differ from $f_2(t^\circ)$ by one to two percent which, in the temperature range of 70° and for a dependency $f(t^\circ)$ equal to 0.4%, gives an error at 1°C [2] for any angle α of rotation of 0.3 to 0.6%. This means that one can, with such a potentiometer, register a measured signal with a temperature error of 0.6% independently of the magnitude of the signal itself.

LITERATURE CITED

[1] V. N. Bogomolov, N. S. Nikolaenko, and V. P. Fedotov, "A transformer of dc to ac based on the Hall effect," Pribory i Tekh. Éksp. No. 2 (1959).*

[2] Collection: Germanium [Russian translation] ed. by D. A. Petrov (IL, 1955).

---

* See English translation.

NOTE ON THE PROPERTIES OF A SIMPLE EXTRAPOLATOR WITH A "SWITCH"

L. Prouza

(Pardubitse, Czechoslovakia)

(Translated from: Avtomatika i Telemekhanika, Vol. 21, No. 1, pp. 137-138, January, 1960)
Original article submitted March 23, 1959

A theorem is proven which relates the properties of a simple extrapolator with a "switch" with lag present with the properties of an extrapolator without lag.

In [1] there was considered the stability of a simple extrapolator with a "switch." The transfer function of the continuous linear portion of such an extrapolator has the form:

$$Y(q) = e^{-\tau q}\left(\frac{\alpha}{q} + \frac{\beta}{q^2}\right) \tag{1}$$

and depends on the lag time τ. We shall now prove a theorem, of which theorem 1 of [1] is a particular case, and shall then consider several applications of it.

General Theorem

Let there be an extrapolator with a "switch" for which the transfer function of the continuous linear portion, with suitable normalization [1], is defined by formula (1). We introduce the generalized impulse transfer function of the open-loop system

$$Y^*(e^q, \varepsilon) = \sum_{n=0}^{\infty} y(n+\varepsilon)\, e^{-nq}, \tag{2}$$

where $y(t) = L^{-1}Y(q)$, $y(0) = 0$, $0 \leq \varepsilon \leq 1$ [2, 3].

Let τ vary in the interval (0,1). One easily convinces oneself that, for $\varepsilon \leq \tau$

$$Y^*(e^q, \varepsilon) = Y_1^*(e^q, \varepsilon) =$$

$$= \frac{[(\alpha - \beta\tau) + \beta(1+\varepsilon)]\, e^q - (\alpha - \beta\tau) - \beta\varepsilon}{(e^q - 1)^2} \tag{3}$$

and, for $\varepsilon > \tau$

$$Y^*(e^q, \varepsilon) = Y_2^*(e^q, \varepsilon) = Y_1^*(e^q\varepsilon) + (\alpha - \beta\tau) + \beta\varepsilon. \tag{4}$$

From (3) and (4) we obtain the ordinary impulse transfer function

$$Y^*(e^q) = Y_1^*(e^q, 0) = e^{-q}Y_2^*(e^q, 1) =$$

$$= \frac{[(\alpha - \beta\tau) + \beta]\, z - (\alpha - \beta\tau)}{(z-1)^2}. \tag{5}$$

Here, we have used the notation $e^q = z$.

Theorem 1 (auxiliary). Let two extrapolators be given, the first with parameters α_1, β_1, and τ_1 and the second with parameters

$$\alpha_2 = \alpha_1 - \beta_1\tau_1, \qquad \beta_2 = \beta_1, \qquad \tau_2 = 0. \tag{6}$$

Then $Y^*(z)$ is identical for the two of them.

The proof follows immediately from the form of expression (5).

Theorem 2. All properties which depend only on transfer function (5) are identical for extrapolators whose parameters are related by relationships (6).

Theorem 2 is an obvious corollary of theorem 1.

Applications

It is clear that theorem 1 of [1] on the deformations of the region of stability is only a particular case of theorem 2.

In [4], one defined the error of tracking a "circular maneuver" for an extrapolator with $\tau = 0$ as a quantity proportional to the expression

$$E = \left|\frac{1}{1 + Y^*(e^{j\lambda})}\right| \tag{7}$$

[cf. [4], formula (30)]. Whence, by theorem 2, it is clear that, for an extrapolator with $\tau > 0$, it suffices to write $\alpha - \beta\tau$ instead of α in formulas (31), (32), and (33) in [4] in order to obtain the expression for the error for $\tau > 0$.

Further, in [4] there was defined a coefficient of error damping for the extrapolation of a unit velocity jump for $\tau = 0$, starting from the formula

$$E^*(z) = \frac{X^*(z)}{1 + Y^*(z)} \tag{8}$$

(cf. formula (8) in [4]), where $X^*(z) = z/(z-1)^2$. It follows from (8) and theorem 2 that the curves of constant damping coefficient (cf. [4], Fig. 4) for $\tau = 0$ are deformed as τ varies in the interval (0, 1) in accordance with relationships (6).

Further, let the noise coefficient of the extrapolator be defined by the formula (cf., for example, formula (53) in [5])

$$\sigma^2 = \frac{1}{2\pi}\int_{-\pi}^{\pi}\left|\frac{Y^*(e^{j\lambda})}{1 + Y^*(e^{j\lambda})}\right|^2 d\lambda. \tag{9}$$

It is clear that expression (9) is identical for parameters related by relationships (6). By computing (9) (for example, by the method described in [6] or by formula (56) in [5]), we obtain, in the general case

$$\sigma^2 = \frac{2(\alpha - \beta\tau)^2 + \beta[(\alpha - \beta\tau) + 2]}{(\alpha - \beta\tau)[4 - 2(\alpha - \beta\tau) - \beta]}. \qquad (10)$$

If we denote $\alpha - \beta\tau = A$, then the minimum of σ^2 for given β and τ is attained for

$$A = \sqrt{\beta} - \frac{\beta}{2}. \qquad (11)$$

Formula (11), for $\tau = 0$, is given in [7]. It is clear from (10) that σ^2 tends to infinity on two sides of the triangle of stability. On the third side, corresponding to $\beta = 0$, σ^2 is defined by the formula

$$\sigma^2 = \frac{A}{2 - A}. \qquad (12)$$

Formula (12) can be derived from formula (86) in [5] where the case of an extrapolator with one integrator is considered in detail.

CONCLUSION

By means of relationships (6), one can, as a function of τ, transform not only the region of stability (theorem 1 in [1]), but other characteristics of the extrapolator system with "switch" considered here as well.

LITERATURE CITED

[1] L. Prouza, "On the stability of one extrapolating device," Avtomat. i Telemekh. 20, 4 (1959).*

[2] V. P. Perov, "Synthesis of sampled-data circuits and systems with sampled-data feedback," Avtomat. i Telemekh. 18, 12 (1957).*

[3] Ya. Z. Tsypkin, Transient and Steady-State Processes in Sampled-Data Circuits [in Russian] (Gosénergoizdat, 1951).

[4] J. Sklansky, "Optimizing the dynamic parameters of a track-while-scan system," RCA Rev. No. 2 (June, 1957).

[5] Ya. Z. Tsypkin, "Designing discontinuous control systems for stationary random stimuli," Avtomat. i Telemekh. 14, 4 (1953).

[6] G. W. Johnson, "Statistical analysis of sampled-data systems," Convent. Rec. IRE Wescon, pt. 4 (1957).

[7] A. H. Benner and R. Drenick, "An adaptive servo system," Convent. Rec. IRE, pt. 4 (1955).

---

* See English translation.

ELECTRETS AND THE PROSPECTS OF THEIR USE IN AUTOMATION (Survey)

V. A. Andryushchenko

(Leningrad)

(Translated from: Avtomatika i Telemekhanika, Vol. 21, No. 1, pp. 139-142, January, 1960)
Original article submitted April 7, 1959

The paper considers the present state of the question of electrets, which are the electrical analogs of magnets, and provides certain practical directions of their use as elements of automatic devices.

The creation of cheaper, more economical, relatively simple in design, and convenient to use automatic systems requires the use of new materials which possess new physical properties. Such a material is the "electret," which is little known in practice.

An electret is the electrical analog of a magnet. This is a dielectric possessing "constant" electrification with opposite charges at the ends.

The first specimens of electrets studied were mixtures of wax and gum whose congealing had occurred in a strong constant electrical field. The disk-shaped electrets thus prepared possess negative charges on the side turned to the anode and a positive charge on the opposite side. If an electret is bifurcated along a neutral line, then two electrets are obtained. Removal of an upper layer of an electret by scraping or shearing does not disturb the electret's properties.

Until today, essentially organic materials have been used for obtaining electrets: wax, gum, hydrocarbons, solid acids, alcohol, etc.

Inorganic materials (glass, porcelain, ceramics, etc.) have been little studied from the point of view of obtaining electrets from them, and the information thus far obtained about them has been contradictory.

TABLE

Material	$MgTiO_3$	$ZnTiO$	$BaO \cdot 4TiO_2$	Bismuth titanate	$CaTiO_3$	$SrTiO_3$	Strontium bismuth titanate	$BaTiO_3$
ε	16	22	28	80	150	175	750	1200

Electrets of inorganic materials have a higher rigidity and thermal stability than electets prepared of organic materials, and can have very diverse dielectric permeabilities (cf. the appended table).

For the preparation of electrets from organic materials there is no particular sense in increasing the temperature of the dielectric very much above the melting point. However, it is very important that the mass be completely converted to the liquid state before being placed in the electric field.

For the preparation of electrets, one ordinarily uses, as the electrodes for the electrization process, tin foil which is easily removed from the surface of the congealed specimens. It turned out that, with a congealed mixture of wax and gum, sufficiently good electrets could be obtained even in the absence of an external polarizing field. In this case, the size of the charge on the poles was 60 to 70% of the charge appearing on electrets obtained from placement in a polarizing field.

The electrets' properties depend, to a certain extent, on the magnitude of the electric field strength.

Once the field strength has reached a magnitude of 10 to 12 kw/cm, further increase of it does not induce any increase in the charge. This is explained by the circumstance that the electrical field on the electret surfaces reaches the maximum size which can exist in air for these gradients, i.e., about 5 CGSE/cm^2. Further increase of the field strength leads to ionization of the air molecules, and discharge commences. There is a corresponding limiting value to the possible density of the charge on the electret's surfaces. For normal atmospheric pressure, temperature, and humidity, the charge density cannot exceed $3 \cdot 10^{-5}$ coul/m^2. With increasing pressure the charge density also increases and, in regions of low pressure, the charge density is proportional to the pressure.

Electrets prepared from organic materials are decomposed by fusion. The quantity of electricity obtained by measuring the current flowing through the external circuit during the time of fusion does not depend on the time elapsed between polarization and fusion. It is almost directly proportional to the strength of the polarizing electrical field. The experimentally obtained maximum current with fusion attained a magnitude of about 10^{-8} amp/cm^2. When all of the specimen of the electret had passed into the liquid state, the current ceased.

For storage, electrets of organic material are sealed. In a humid atmosphere the electret's charge drops sharply, but is reestablished on drying.

In the P. N. Lebedev Institute of Physics of the Academy of Sciences, USSR, the following mode of polarization was used for obtained electrets from inorganic material: The specimen was placed in an electrical field of 20 kw/ cm strength, maintained at room temperature for 30 minutes, and then the temperature was raised to 200°C during 2 hours, after which the specimen was kept at this temperature for another 2 hours, and then the temperature was lowered to 60 to 80°C. The surfaces of the specimens and the electrodes (brass disks were used for the latter) were carefully polished.

The dimensions and the configurations of the specimens can be diverse. The magnitude of the field strength and the seasoning temperature for polarization are limited by the material's stability with respect to thermal disruption. Electrets of inorganic material can be stored either with or without sealing. The charges of electrets of organic and inorganic materials are retained for periods of years. The basic disadvantage of electrets today is the instability of their charge.

We turn now to photoelectrets, which were discovered in 1937 by the Bulgarian academician G. Nadjanoff.

As specimens, sulfur flakes (monocrystalloid or polycrystalloid) were used, these being polished to mirror smoothness by silk moistened with kerosene. A constant voltage of 470 v/ cm was applied to a specimen, and the specimen, after three minutes of remaining in darkness, was exposed to a light of 6000 lux during 12 minutes, after which it was sealed and stored in darkness. The measurement of a photoelectret's charge was carried out by means of its depolarization with repeated illumination. A photoelectret can retain its charge for several days.

Illumination of a photoelectret at low temperatures (−80 to −100°C) leads only to its partial discharge, and complete depolarization occurs only as the result of increasing the specimen's temperature to the temperature at which its polarization occurred. Heating of a photoelectret without simultaneous illumination does not give rise to a discharge of current large enough to be measured, although the total charge on the photoelectret is somewhat decreased. The state of the polarized specimen just described may be called thermophotoelectret.

We now consider instruments (based on electrets) which are elements of automatic systems, or which execute functions of an automatic device.

Figure 1 shows a telephone circuit. If one speaks into microphone A, the sound waves start membrane 1 oscillating. The distance between it and electret 2 will change. As the membrane approaches the electret, the charge induced on it will increase and, as the membrane moves further away, the charge will decrease. These variations of charge induce currents in the telephone circuit which lead to acoustical vibrations of membrane 5 and receiver B. On Fig. 1, 3 is the immovable microphone electrode and 4 is the receiver coil.

One can create ac and dc generators using electrets. A dc generator is shown on Fig. 2 a. During an oscillatory swing of the upper electrode, when the electrodes are close key K_1 will make, i.e., seal the electrodes and key K_2 will break. The charge induced on the electrode by the short circuit will, as the latter moves away, be applied to the plates of condenser C; with this, key K_2 closes and key K_1 opens. By repeating this operation many times, one can charge the condenser up to a potential whose value will be limited only by the breakdown voltage of dielectric e between the condenser plates. In practice, the condenser was charged up to 5 kv.

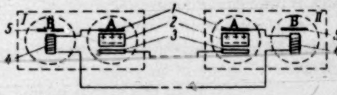

Fig. 1.

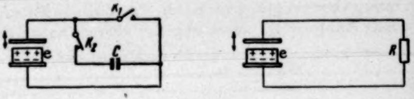

a

b

Fig. 2.

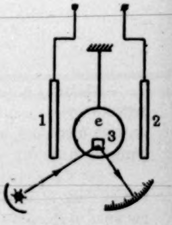

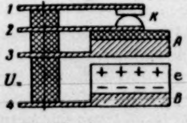

Fig. 3.

Fig. 4.

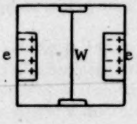

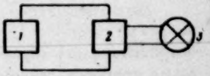

Fig. 5.

Fig. 6.

An ac generator (Fig. 2 b) is obtained by connecting resistor R in the electrical circuit. With oscillatory motion of the electrodes at a frequency of f = 100 cps, an ac current of 10^{-6} amp passes through load R; the effective power on the load in this case equals $P = 10^{-5}$ to 10^{-6} w.

An electrostatic relay based on the use of electrets, and shown schematically in Fig. 3, operates in the following way: As some constant voltage is applied to terminals 3 and 4, the upper electrode A is attracted to electret e attached to immovable electrode B. This causes contacts K to open. Thus, the relay will close or open (depending on the design) a second circuit connected to terminals 1 and 2.

If an electret is suspended on a thread between two metallic electrodes (Fig. 4) on which a charge has been placed, then the electrostatic fields of electrodes 1 and 2 and electret e will interact, turning the electret at a definite angle which is proportional to the charge on the electrodes. A small mirror 3 is fastened to the electret, by means of which mirror readings are made. The instrument, consequently, is a type of mirror galvanometer, in which an electret replaces a moving coil.

In a string voltmeter (Fig. 5) charged to the potential to be measured, wire W is placed between two electrets e which move against each other and have opposite charges. Since electrets change the magnitude of their charge in a radioactive field, after whose removal the charge is again reestablished, then one may judge the degree of radioactivity of a given field as a function of the electret's decrease in charge.

Photoelectrets can be used for danger signaling (Fig. 6). When photoelectret 1 is depolarized, current flows to device 2 which lights signal lamp 3.

Electrets can be used in electronic tubes for applying grid bias, and also in cathode-ray tubes for controlling the electron beam, and also in other instruments where only an electrostatic field is required.

Recently, there has been talk of using electrets in the memory devices of electronic computers.

The theoretical possibility of using electrets is based on the fact that the charges placed on the dielectric's surfaces do not spill over but, as it were, "stick." With this, if an electron falls on an electret's positive pole, it compensates the electret's charge in the given place.

If one could succeed in making an electret in the form of a fine long tape, on one side of which positive charges were placed, with negative charges on the other side, then one could "write," on such an electret tape, a series of definite pulses, using an electron beam. Such a tape, moved past another electron beam, could deflect it in correspondence with the variations in intensity of the first beam.

SUMMARY

The use of electrets in automatic devices allows:

1) the creation of new elements for automatic devices based on the physical properties of electrets;

2) simple design implementation of block schematics of automatic devices;

3) simplification of electric power suplies for automatic devices;

4) decreasing the weight and size of automatic devices.

LITERATURE CITED

[1] "Electrets," in: Problems of Modern Physics, ed. 17 [Russian translation] (IL, 1951).

[2] V. G. Nazarov, "Electrets and their use in electrical engineering," Élektrichestvo 7 (1954).

[3] A. N. Gubkin, "On the question of phenomenological theory of electrets," Zhur. Exptl. i Teoret. Fiz. 27, 9 (1957).

[4] A. N. Gubkin and G. I. Skanavi, "New electrets from inorganic dielectrics," Zhur. Exptl. i Teoret. Fiz. 32, 1 (1957).

[5] A. N. Gubkin and G. I. Skanavi, "Production and properties of new electrets from inorganic dielectrics," Izvest. Akad. Nauk SSSR, Ser. Fiz. 22, 3 (1958).

[6] I. S. Zheludev and V. M. Fridkin, "On photoelectronic and thermoelectronic states in multicrystalloid sulfur," Izvest. Akad. Nauk SSSR, Ser. Fiz. 22, 3 (1958).

[7] B. P. Sukhov, "Electrets," Nauka i Zhizn' 9 (1958).

[8] M. Eguchi, "Effects of electric forces in a permanent electret, Japan J. Phys. 1, 1 (1922).

[9] G. Nadjanoff, "Über eine Art von Elektreten: Photoelektreten,"Physik Z. Sowjetunion 36 (1938).

[10] A. Gremant, "The use of electrets in electrical instruments," Rev. Sci. Instr. 11 (1940).

[11] F. Gutmann, "The electret," Rev Modern Phys. 20 (1948).

[12] L. A. Freedman and L. A. Rosenthal, "Apparatus for the study of electrets," Rev. Sci. Inst. 21 (1950).

[13] Kato Kiyoe, "On the electrets," Natural Science Report of the Ocharomizu University, No. 2 (1955).

LETTERS TO THE EDITOR

A NOTE TO A PAPER OF YU. S. SOBOLEV, "ON THE ABSOLUTE STABILITY OF CERTAIN CONTROLLED SYSTEMS," [1]

(Translated from: Avtomatika i Telemekhanika, Vol. 21, No. 1, pp. 143-144, January, 1960))

In [1], the following theorem was actually proven (below, we retain the symbology and the formula numeration used in [1]).

If, for system (2), satisfying limitations "a"-"e", one can cite a positive definite function $r^2 = V(x_1, \ldots, x_n)$ not depending on h_k ($k = n-m+1, \ldots, n$), whose total derivative with respect to time is, by virtue of (2), negative definite for any $h_k \in (0, +\infty)$, then system (1), satisfying conditions "a"-"e", is absolutely stable.

In fact, in case r^2 depends on h_k, inequality (5) holds, in general, only for sufficiently small h_k ($k = n-m+1, \ldots, n$), and inequality (6) holds only for sufficiently large h_s and sufficiently small h_p. Therefore, there might not exist a system of values of h_k for which both inequalities (5) and (6) would be valid simultaneously. In exactly the same manner, it is impossible to assert anything as to the simultaneous holding of inequalities (7) or (9).

In the case of a linear system (2), the Routh-Hurwitz conditions do not guarantee the presence of a Lyapunov function, mentioned in the conditions of the theorem proven in [1]. We consider, for example, the equation

$$a_3 \frac{d^2x}{dt^2} + a_2 \frac{dx}{dt} + a_1 x = -\varphi(\sigma), \quad \sigma = b_2 \frac{dx}{dt} + b_1 x \tag{I}$$

($\varphi(\sigma)$ is a class A function).

Following [1], we replace (I) by the equation

$$a_3 \frac{d^2x}{dt^2} + a_2 \frac{dx}{dt} + a_1 x = -h\left(b_2 \frac{dx}{dt} + b_1 x\right), \; h \in (0, +\infty),$$

from which we go to the system

$$\dot{x}_1 = x_2,$$
$$\dot{x}_2 = -\frac{a_2 + hb_2}{a_3} x_2 - \frac{a_1 + hb_1}{a_3} x_1. \tag{II}$$

According to the Routh-Hurwitz conditions, the trivial solution of system (I) is asymptotically stable, at least for

$$a_1, a_2, a_3, b_1 > 0, \; b_2 \geqslant 0. \tag{III}$$

We now show that, among the systems (II) satisfying (III), there are such for which it is impossible to construct a positive definite function $V(x_1, x_2) = \sum_{ij=1}^{2} \alpha_{ij} x_i x_j$ with coefficients α_{ij} which do not depend on $\underline{h}$, whose complete derivative with respect to time, dV/dt, by virtue of this system would be negative definite for all $h \in (0, +\infty)$.

Indeed,

$$-0.5 \frac{dV}{dt} = \alpha_{12} \frac{a_1 + hb_1}{a_3} x_1^2 +$$
$$+\left(\alpha_{12} \frac{a_2 + hb_2}{a_3} + \alpha_{22} \frac{a_1 + hb_1}{a_3} - \alpha_{11}\right) x_1 x_2 +$$
$$+\left(\alpha_{22} \frac{a_2 + hb_2}{a_3} - \alpha_{12}\right) x_2^2$$

and the necessary and sufficient conditions that dV/dt be negative definite have the form:

$$\alpha_{22} \frac{a_2 + hb_2}{a_3} - \alpha_{12} > 0, \tag{IV}$$

$$\alpha_{12} \frac{a_1 + hb_1}{a_3} \left(\alpha_{22} \frac{a_2 + hb_2}{a_3} - \alpha_{12}\right) -$$
$$-\frac{1}{4}\left(\alpha_{12} \frac{a_2 + hb_2}{a_3} + \alpha_{22} \frac{a_1 + hb_1}{a_3} - \alpha_{11}\right)^2 > 0$$
$$h \in (0, +\infty). \tag{V}$$

For the holding of (IV) it is necessary ($h \to 0$) that $\alpha_{22} a_2 / a_3 - \alpha_{12} \geq 0$ and, for (V) ($h \to +\infty$), that $-(\alpha_{12} b_2 - \alpha_{22} b_1) = 0$, such that for systems (II)-(III), in which $b_2 a_2 - b_1 a_3 < 0$, (IV)-(V) may not hold for any $h \in (0, +\infty)$.

Thus, the theorem of Yu. S. Sobolev [1] is inadequate for solving the problem posed in [2] of comparing theories of absolute stability.

Yu. I. Alitov

LITERATURE CITED

[1] Yu. S. Sobolev, "On the absolute stability of certain controlled systems," Avtomat. i Telemekh. 20, 4 (1959).*

[2] A. M. Letov, The Stability of Nonlinear Controlled Systems [in Russian] (Gostekhizdat, 1955).

---

* See English translation.

Dear Editor

We became acquainted with the paper of Yu. S. Sobolev, "On the absolute stability of certain controlled systems," published in number 4 of your journal for 1959. This paper gave rise to a number of remarks, which we provide forthwith.

In the first part of the paper [formulas (1)-(9)], Yu. S. Sobolev proves the following assertion: If there exists a positive definite function $r^2(x_1, x_2, \ldots, x_n)$, not depending on the numbers h_k, whose derivative, by virtue of system (2) is negative definite for all $0 < h_k < \infty$, then the derivative of r^2, by virtue of system (1), is also negative definite. This assertion is obvious, and gives rise to no objections. Further (cf. the fine print, formulas (10)-(12)), the generally known properties of linear systems with constant coefficients are adduced, after which (cf. the normal print up to section 2) the incomprehensible assertion is made: "the existence of a function r^2 whose total derivative, by virtue of system (1), is negative definite, is guaranteed by the Routh-Hurwitz conditions." It is not clear what is meant by the Routh-Hurwitz conditions in the general case for systems (1) and (2).

In examples 1 and 2, Yu. S. Sobolev writes that, "according to what was proven above, the region of absolute stability (13) coincides with the region of asymptotic stability. . . of system . . . (14), where $h \in (0, +\infty)$." It is possible to deduce from this that Yu.S. Sobolev believes, in particular, that the following assertion has been proven: The region of absolute stability of a system described by the set of equations

$$\dot{x}_k = \sum_{\alpha=1}^{n} b_{k\alpha} x_\alpha + n_k f(\sigma),$$

$$\sigma = \sum_{s=1}^{n} j_s x_s, \quad \sigma f(\sigma) > 0, \qquad \text{(A)}$$

where $b_{k\alpha}$, j_s, and n_k are constants, coincides with the region of asymptotic stability of system (A) in which one sets $f(\sigma) = h\sigma$ for all $h > 0$.

As is well known, this assertion is untrue (cf., for example, the book of V.A. Pliss, Some Problems of Stability of Motion as a Whole). The author's error consists in the following. It is tacitly assumed that system (A), in which $f(\sigma) = h\sigma$, always has a Lyapunov function which does not depend on h.

In connection with this, it is impossible to consider as proven this assertion in section 2 of Yu. S. Sobolev's paper.

E. N. Rozenvasser and V. A. Pliss

CHRONICLE

SEMINAR ON THE ENGINEERING APPLICATIONS OF MATHEMATICAL LOGIC (1958-1959)[*]

(Translated from: Avtomatika i Telemekhanika, Vol. 21, No. 1, pp. 145-148, January, 1960)

In the fall semester of 1958 and the spring semester of 1959, the seminar on the engineering applications of mathematical logic continued its work under the direction of Lecturer V. I. Shestakov. Taking part in the seminar were scientific workers, teachers, and engineers of a number of research institutes and universities, including the Institute of Automation and Remote Control, the Laboratory for Information Transmission Systems, the Department of Applied Mathematics of the Academy of Sciences, USSR, and the Moscow State University. There were 13 sessions of the seminar in all, in which 11 papers were presented and discussed; of these, 10 contained original results and one was a tutorial paper.

Part of the papers touched on general questions of mathematical logic, arising, to be sure, from the requirements of the engineering applications of mathematical logic but having, perhaps, an independent theoretical value. Such were the papers of A. D. Talantsev, G. N. Povarov, and the tutorial paper of V. P. Goncharov.

A. D. Talantsev read two papers. In the first of them, "On the use of several logical operators for the analysis and synthesis of schemes containing differentiating circuits," presented Oct. 2, 1958, A. D. Talantsev dealt with the questions of the analysis and synthesis of potential-pulse circuits in which differentiating circuits entered. He proposed an essentially new algebraic-logical method for investigating such circuits. The basis of the method is the definition of special operators, the application of which to the "and" and "or" functions allowed one to derive relationships forming interesting analogies with the formulas of mathematical analysis.

It was shown in the paper how the relationships derived could be used for the simplification of circuits containing differentiating circuits. The concept of "covariance" of logical functions was introduced, this concept being related to the substantive meaning of the operators introduced; this concept can sometimes be used for transforming circuits. The exposition of the new concepts was illustrated by the example of a logical circuit for recognizing the direction of motion of a quantized scale for a digital control system for a milling machine.

The second paper of A. D. Talantsev, "On the analysis and synthesis of certain electrical circuits by means of special logical operators", was given on Jan. 16, 1959. In this paper there was developed (with account being taken of remarks made by M. L. Tsetlin and V. I. Shestakov) a new method of investigating electrical circuits which was first presented by A. D. Talantsev on Oct. 2, 1958. Specifically, there was derived an expansion formula for $dF(x_1, x_2, \ldots, x_n)$, where F is an arbitrary Boolean function of n variables. The relationship obtained for dF lies beyond the boundaries of Boolean algebra. Further, there were defined the concepts of potential and of pulse logical variables, the concept of a homogeneous potential-pulse circuit, and the potential-pulse form describing such a circuit. The problem was posed of "integrating" potential-pulse forms, and a general method of "integrating" these forms was given. In conclusion, the example was considered of "integrating" the forms describing a circuit which recognizes the direction of motion of a quantized scale.

The work of A. D. Talantsev was published in the journal Avtomatika i Telemekhanika 20, 7 (1959).[**]

G. N. Povarov gave three papers at the seminar. On Oct. 31, 1958, in the paper "On group invariance of Boolean functions," G. N. Povarov considered the group $\mathfrak{T}_n$, transforming monotypic Boolean functions to other such functions. The concept was introduced of the invariance of Boolean functions with respect to subgroups of group $\mathfrak{T}_n$ as well as the concept of regions of invariance of Boolean functions with respect to subgroups of group $\mathfrak{T}_n$.

G. N. Povarov showed that the regions of invariance comprise a Boolean algebra, and form a structure dually homomorphic to the structure of the subgroups of group $\mathfrak{T}_n$; to the conjugate subgroups correspond monotypic regions of invariance. Results were given of an investigation of a type of region of invariance $D(\mathfrak{S}_n)$ with respect to the group $\mathfrak{S}_n \subset \mathfrak{T}_n$ of permutations of arguments of Boolean functions. Also investigated were the types of regions of invariance contained in $D(\mathfrak{S}_n)$. The study of regions of invariance is important for the theory of switching circuits, since it enables one better to understand the types of regularity characteristic of simple circuits. A brief exposition of the work was then published in Russian in the "Annalele Stuntifice ale Universitatu Al. I. Cuza" din Iasi" (Rumanian People's Republic) 4, 1, 39-44 (Sept. 1, 1958).

In the next paper, to which two seminar sessions were devoted (Feb. 27 and Mar. 6, 1959), "An abstract algebraic theory of cumulative nets,"[***] G. N. Povarov presented a mathematical theory developed by him, of indirect interactions in control, communications, and planning nets of a very wide class, including various switching circuits, radio communications nets and wire networks, transportation networks, target networks, etc.

---

[*] The proceedings of the seminar prior to October, 1958, were presented Avtomat. i Telemekh. 18, 10 (1957) and 20, 1 (1959) [See English translation of 1959 issue].

[**] See English translation.

[***] In the invitations to this session of the seminar, this paper of G. N. Povarov had the name, "On one mathematical method of investigating operations."

The central concept of the theory is the general combinatorial concept of a cumulative net, which is why G. N. Povarov calls this the theory of cumulative nets. The idea of a cumulative net is analogous to the idea of a normalized graph, but more complicated. It characterizes a definite type of indirect interaction, and the interactions characteristic of the enumerated control, communications, and planning nets. The generality of the treatment is provided by the use of the theory of numeroids [the concept of numeroids was introduced by G. N. Povarov in a paper printed in the journal Uspekhi Matematicheskikh Nauk, 11, 5(71), 195-202,1956].

A cumulative net on the numeroid N is defined as a system $\{M, \|a_{ij}\|, \{P_n\}\}$, consisting of a set $M = \{1, 2, \ldots, p\}, p^2$, a matrix $\|a_{ij}\|$ on N and the sequence of sets $P_n \subseteq \sum_{r=2}^{n+1} M^r$, where $n = 1, 2, \ldots, P_1 = M^2$, and $P_n \subseteq P_{n+1}$ for all n. The matrix $\|a_{ij}\|$ is called the primitive connectivity of the net, and the matrix $\|a_{ij}^{(n)}\|$, where

$$a_{kl}^{(n)} = \sum_{ki_1i_2\ldots i_{r-1}l \in P_n} a_{ki_1}a_{i_1i_2}\ldots a_{i_{r-1}l},$$

is called the nth-degree connectivity of the net, and the sequence $\{\|a_{ij}^{(n)}\|\} = \|a_{ij}^{(1)}\|, \|a_{ij}^{(2)}\|, \ldots$ is the evolution of the net's connectivity. The analysis of a cumulative net consists in finding $\{\|a_{ij}^{(n)}\|\}$ from $\|a_{ij}\|$ for known M and $\{P_n\}$. The interpretation of these quantities is that $\|a_{ij}\|$ is the measure of the immediate interaction between elements of M, $\|a_{ij}^{(n)}\|$ is the measure of indirect interaction via not more than n-2 intermediate elements, and $\{\|a_{ij}^{(n)}\|\}$ is the successive development of indirect interaction. $\{P_n\}$ ("the development of the net") defines the method of combining immediate interactions into indirect ones.

G. N. Povarov also spoke of the matrix methods he had developed for the analysis of various cumulative nets; he investigated such properties of cumulative nets as equivalence, stability, the presence of feedback, etc. G. N. Povarov showed that the theory of cumulative nets allows one to reduce to one framework the results of many authors working on the questions of the analysis of control, communications, and planning nets and analogous problems, in particular, the results obtained in these domains by B. I. Aranovich, A. G. Lunts, O. Plekhi, A. Shimbel, Z. Prikhar, G. Frobenius, and others, and also previous results of G. N. Povarov himself relative to the theory of switching circuits and communications networks.

The third paper of G. N. Povarov, "Phenomenological and juridical aspects of logic in connection with the logical problems of engineering," given on May 15, 1959, contained opinions on the convenience and naturalness of the interpretation of logical algebra in switching theory and in other branches of engineering as an algebra of events, and not as an algebra of judgments (propositions).

On May 29, 1959, V. P. Goncharov presented the contents of a paper by Zemanek, "Solving the equations of switching algebra," printed in the journal Archiv der Elektrischen Übertragung 12, 1,35-44 (Stuttgart, 1958). The paper considered methods of finding inverse Boolean functions and solving the equations of Boolean algebra. Zemanek denotes a Boolean function by y_Z^n, where z is the decimal ordinal number of the function, corresponding to the binary representation of the constituent units entering into the given function, and n is the number of Boolean variables.

For the finding of inverse Boolean functions, a new notation was introduced in the paper: P and !. P can assume either the value 0 or the value 1, i.e., it corresponds to an "indifferent" state, but $\bar{P}$ always takes the value opposite to that of P; rules of action are defined for P. ! means that it is impossible to obtain a solution. Although Zemanek states in the paper that no rules of action will be introduced for !, it follows from Zemanek's reasoning, as pointed out by V. I. Shestakov in the discussion of the paper, that he has implicitly introduced certain rules of action for the sign !. In considering various cases of finding inverse functions, Zemanek presents a schematic representation of two of them; in these schemes, the sign P represents an arbitrarily closed or open key. Further, Zemanek considers the equation

$$y_{Z1}^{n+1}(x_i, y) = y_{Z2}^{n+1}(x_i, y),$$

where $i = 1, 2, \ldots, n$ and $y = y_Z^n$ is the unknown Boolean function. This equation is transformed to the following:

$$yy_{I1}^n + \bar{y}y_{N1}^n = yy_{I2}^n + \bar{y}y_{N2}^n,$$

where

$$y_{I1}^n = y_{Z1}^{n+1}(x_i, 1), \quad y_{N1}^n = y_{Z1}^{n+1}(x_i, 0),$$

and y_{I_2} and y_{N_2} is the similar notation for

$$y_{Z2}^{n+1}(x_i, y).$$

From this, Zemanek obtains the solution for the initial equation:

$$y_Z^n = !\,(y_{I1} \not\equiv y_{I2})(y_{N1} \not\equiv y_{N2}) + \\ + O(y_{I1} \not\equiv y_{I2})(y_{N1} \equiv y_{N2}) + 1\,(y_{I1} \equiv y_{I2})(y_{N1} \not\equiv y_{N2}) + \\ + P(y_{I1} \equiv y_{I2})(y_{N1} \equiv y_{N2}),$$

where $\equiv$ is the equivalence sign and $\not\equiv$ is the sign of its negation.

This solution contains all possible values of the Boolean function being sought. Zemanek showed the application of the method developed by him to the solution of equations in Boolean algebra.

The paper of Zemanek is, so far as is known, the first attempt to give an algebraic representation for the general solution of equations in Boolean algebra.

In the other portion of the papers there were treated various questions of the analysis and synthesis of switching circuits. Such were the papers of Yu.L. Sagalovich, B. Yu. Pil'chak and V. D. Kazakov.

On Oct. 17, 1958, Yu. L. Sagalovich gave the paper "On the number of types of symmetric contact (1,k)-poles." The author recalled that contact (1, k)-poles realize the basic sequence of functions of n variables, and he considers them as coinciding correctly to the numbering of the output poles (terminals). The number of different (1,k)-poles equals the number of combinations $m = C_{\mu}^{k}$, where $\mu = 2^{m}-2$. On all m (1,k)-poles one can carry out the operation of substituting variables and (or) inverting (negating) some of them. The set of these operations forms a group G of order $2^n n!$. (1,k)-poles are considered to be of one type if they are obtained from each other by operations from the group G.

Using the methods of the theory of group representations, the author found the number, $N_{n,k}$, of types of (1,k)-poles of n variables:

$$N_{n,\,k} = \frac{1}{2^n n!} \Sigma\, n_c \chi_c,$$

where n_c is the number of elements of class C of group G, χ_c is the character of class C in the representation of group G by substitution matrices of order m. To determine χ_c, one seeks the cyclical structure of the substitutions of degree m induced in the group G by the elements of class C.

B. Yu. Pil'chak, during two seminar sessions (Nov. 21 and Nov. 28, 1958), spoke on, "The synthesis of quasinonrepeated contact circuits." She gave this name to circuits in which there are connected to each relay not more than one make, and not more than one break, contact. These circuits are synthesized by the method of superposition of subcircuits. The subcircuits are isolated by a method which is a generalization of the method of B. A. Trakhtenbrot which he suggested for finding subcircuits of nonrepeated circuits. B. Yu. Pil'chak introduced the concepts of K-conductance and K-realizability, and suggested the formula for K-conductance. These formulas and concepts are necessary for the synthesis of circuits by the superposition method, and are generalizations of the ordinary concepts of conductance, realizability, and conductance formulas.

On April 17, 1959, V. D. Kazakov gave his paper, "Finding the maximum number of simple implicants of an arbitrary symmetric logical function of n variables." The speaker first recalled that, in the majority of methods for the minimization of logical functions and, consequently, of switching circuits, it is necessary to seek minimal equivalents of the original function which consist of some set of simple implicants of the initial function. For the mechanization of this search for minimal equivalents, it is necessary to know the greatest number of simple implicants I_{max} which can appear with one arbitrarily chosen function of n logical variables; the memory of the minimizing device must be constructed on the basis of such a greatest number I_{max}.

After this, V. D. Kazakov presented the method he had developed for determining the greatest number I_{max} of simple implicants of an arbitrary symmetric function of n variables. He showed that, for such functions, I_{max} is found by the formulas

$$\max\,[C_n^{\alpha} C_{\alpha}^{\beta}] + 2C_n^{\frac{n-\alpha-1}{2}} \quad (\text{ for even } \; n-\alpha-1),$$

$$\max\,[C_n^{\alpha} C_{\alpha}^{\beta}] + C_n^{\frac{n-\alpha}{2}} + C_n^{\frac{n-\alpha-2}{2}} \quad (\text{ for odd } \; n-\alpha-1),$$

where n is the number of variables in the original function, and α and β are quantities for definite values of which the product $C_n^{\alpha}\, C_{\alpha}^{\beta}$ of numbers of combinations becomes maximal. The formulas just given are approximate ones ; V. D. Kazakov also obtained an exact formula, but it is very cumbersome. V. D. Kazakov determined the form of the functions having I_{max} simple implicants, and computed, by the method suggested, the value of I_{max} for n = 1, 2, . . . , 20.

The papers of V. R. Telesnin and B. Ya. Falevich were devoted to the descriptions of new contactless circuits, for whose synthesis mathematical logic was employed.

On December 19, 1958, V. R. Telesnin gave the paper, "The use of magnetic matrices for information processing," in which a device was presented which was destined for both the storage and the processing of information. The basis of this device is a plane magnetic matrix used for a memory device. The total number of active elements is no larger than in matrices designed only for information storage. For the processing of information, there were introduced two special rows to which information could be transmitted from the ordinary rows of the memory device in direct, or complemented, code. Such a device has the capability of realizing any logical functions of the arguments written in the places (bit-positions) of all the rows. The addition of four more special rows allowed the realization of addition, subtraction, and multiplication of the numbers written in the matrice's rows.

On Jan. 30, 1959, B. Ya. Falevich, in the paper, "Electronic machines for games of "wolves and sheep," spoke of the schematic implementation, begun under his direction, of the substantive algorithm he had found for this game.

The algorithm presented by the author is not the very simplest.

Many of the papers gave rise to lively discussion.

V. P. Goncharov

BIBLIOGRAPHY

A LIST OF LITERATURE ON MAGNETIC ELEMENTS OF AUTOMATION, REMOTE CONTROL, AND COMPUTING TECHNOLOGY FOR 1958*

(Translated from: Avtomatika i Telemekhanika Vol. 21, No. 1, pp. 149-158, January, 1960)

1. General Questions. Terminology, Bibliography

"Magnetic amplifier bibliography 1951-1956," Commun. and Electronics, No. 39, pp. 613-627 (November, 1958).

"Magnetic amplifier bibliography 1957-1958," Appl. Sub-Committee of the AIEE Magnetic Amplifier Committee.

"Proposed standards for core test methods for toroidal magnetic amplifier cores," Commun. and Electronics No. 38, pp. 524-535 (1958).

"Proposed standard terms and definitions for magnetic amplifiers," Commun. and Electronics No. 38, pp. 429-431 (1958), 3 figs., 1-title bibl.; disc. pp. 431-432, 5-title bibl.

H. F. Storm, "Recommended symbols for magnetic amplifier papers," Proc. C.M.A. (1958), Los Angeles: AIEE, pp. 62-66 (1958), 5 tables.

"Terms and definitions for magnetic amplifiers," Commun. and Electronics No. 38, pp. 429-437 (1958).

2. Ferromagnetic Materials. Cores

a) Magnetic Materials

A. Braginski, "Magnetic materials," [in Polish], Elektronika 5, 1-2, 3-41 (1958).

W. J. Carr, "Theory of ferromagnetic anisotropy," Phys. Rev. 108, pt. 2, 5, 1158-1163 (1957), 1 table.

C. W. Chen, "Temperature dependence of magnetic properties of silicon-iron," J. Appl. Phys. 29, 9, 1337-1343 (1958).

P. F. Davis, "An electrical analogue of magnetic domains," Brit. J. Appl. Phys. 28, 1, 19-20 (1957).

H. C. Fiedler et al., "Magnetic properties of cube textured silicon-iron magnetic sheet," J. Appl. Phys. 29, 3, 363-365 (1958).

J. F. Fritz and J. J. Clark, "Effects of temperature on magnetic properties of nickel-iron alloys," El. Manufacturing, 62, 5, 135-139 (1958).

D. I. Gordan et al., "Radiation effects in magnetic materials," Nucleonics 16, 73-77 (1958).

"Ferrite cores for magnetic memory matrices," [in German]. Archiv der Elektrischen Ubertragung 12, 6 (1958).

H. B. Harms, "An experimental study of magnetic materials for use in ultrahigh-temperature electronic transformers," Commun. and Electronics, No. 36, pp. 181-184 (1958), 8 figs., 2-title bibl.

C. Heck, "Magnetic materials and their use in electronics and communications engineering," [in German] ETZ-A 79, 23, 932-934 (1958), 31 figs.

C. Heck and H. Repiser, " Ferrites with rectangular hysteresis loops, and the testing of the memory properties," [in German] Radio Mentor No. 2, pp. 107-110 (1957).

C. P. Lascaro and A. L. Long, "Effect of high intensity radiation on electronic parts and materials," El. Manufacturing 62, 3, 119-121, 306 (1958), 5 tables, 4-title bibl.

D. H. Martin, "Magnetism in materials," Wireless World 64, pp. 28-30 (Jan. 1958); (February, 1958), pp. 70-74; (March, 1958), pp. 126-131; (April, 1958), pp. 178-180.

"Materials used in radio and electronic engineering. 5. Magnetic materials," J. Brit IRE 18, 449-464, (1958), 1 fig., 9 tables, 91-title bibl.

"A new power ferrite for flyback transformers by Allen-Bradley," Electronics 31, 28 (1958).

G. G. Palmer et al., "Magnetic properties and associated microstructure of zinc-bearing square-loop ferrites," J. Amer. Ceram. Soc. 40, 8, 256-262 (1957), 13 figs, 13-title bibl.

R. H. Pry and C. P. Bean, "Calculation of the energy loss in magnetic sheet materials using a domain model," J. Appl. Phys. 29, 3, 532-539 (1958).

H. Reinboth, The Technology and Applications of Magnetic Materials, [in German] (VEB Verlag Technik, Berlin, 1958) 379 pp.

V. H. Richter, "Ferromagnets with rectangular hysteresis loops, and their applications," [in German] Elektrotechnik Nos. 15/16, 93-96 (1958), 12 figs.

R. Skorski, "Annealing iron and steel (0.45%) in a magnetic field," [in Czech.], Prace Inst. Mech. 6, 21, 32 (1957).

Z. Tischer, "Magnetically soft materials on the basis of nonferrous metals," [in Czech.], Slaboproudy Obz. 19, 5, 329-337 (1958), 23 figs, 2 tables.

Z. Tischer, "Expression for the rectangularity of magnetically soft materials," [in Czech.], Slaboproudy Obz. 19, 10, 653-657 (1958), 18 figs., 6-title bibl.

A. Villachon, "Alloys with rectangular hysteresis loops," [in French], L'Onde El. 37, 360, 259-261 (1957).

J. L. Walter, "Magnetic properties of cube textured transformer sheet," J. Metals, pp. 509-511 (August, 1958).

G. W. Wiener and K. Detert, "Cube oriented magnetic sheet. A major advance in magnetic materials," J. Metals, pp. 507-508 (August, 1958).

H. P. Wijn and H. Heide, "Pulse-response properties of rectangular-loop ferrites," Proc. IRE, B-104, Suppl. 7, pp. 422-427 (1957), 10 figs., 7-title bibl.

b) Magnetization Processes and Dynamic Characteristics of Ferromagnetic Materials (Dissipation, Eddy Currents, Viscosity, etc.)

R. C. Barker, "Magnetization in tape wound cores," Proc. C.M.A. (1958), Los Angeles, AIEE, pp. 1-46 (1958), 34 figs., 1 table, 43-title bibl.

T. C. Chen and A. Papoulis, "Terminal properties of magnetic cores," Proc. IRE 46, pt. 1, 5, 839-849 (1958),

R. L. Conger, "Thin film magnetization reversal studies," Proc. C.M.A. (1958), Los Angeles, AIEE, pp. 444-453 (1958), 7 figs., 5-title bibl.

G. C. Feth, "Core-reset functions in magnetic-amplifier analysis. I. A core-reset function. II. Determination of amplifier performance," Commun. and Electronics No. 38, pp. 503-519 (1958).

K. Ganzhorn, "Computing rectangular hysteresis loops in ferrites," [in German], Z. angew. Phys. 10, 4 169-172 (1958).

A. V. Kienlin, "Toward an elucidation of the question of magnetic aftereffects in ferrites caused by electron diffusion," [in German], Z. angew Phys. 9, 5, 245-250 (1957).

E. W. Lee, "Eddy-current losses in thin ferromagnetic sheets," Proc. IEE 105 C, 8, 337-342 (1958), 4 figs., 24-title bibl.

R. E. Morgan, "Reactions of bistable B-H loops on magnetic amplifiers," Commun. and Electronics No.39, pp. 586-590 (1958), 14 figs., 7-title bibl.

T. D. Rossing and V. J. Korkowski, "Switching properties of permalloy cores of varying coercivity," Appl. Phys 29, 3, 479-480 (1958).

T. D. Rossing et al., "The switching characteristics of 4-79 permalloy cores with different anneals," IRE Trans. Electronic Computers, EC-7, 3, 228-231 (1958), 8 figs.

T. D. Rossing and S. M. Rubens, "Effect of a transverse field on switching rates of magnetic memory cores," J. Appl. Phys. 29, 8, 1245-1247 (1958), 4 figs., 4-title bibl.

J. E. Wolf, "Influence of excitation frequency and waveform on squareness ratio of toroidal tape cores," Proc. C. M. A. pp. 94-112 (1958), 39 figs.

c) Physical Design and Technology of Preparation of Cores

R. E. Ball, "The effects of core variations on production quantities of magnetic amplifiers," Proc. C.M.A. (1958), Los Angeles, AIEE pp. 87-93 (1958), 5 figs. 3-title bibl.

C. Cook, "Some aspects of the design of toroidal inductors," T.M. C. Tech. J. 8, 3, 124-139 (1958).

G. J. Duncan and M. M. Felger, "Properties of electrical insulation at ultrahigh temperatures," Applic. and Ind. 77, pt. 2, 39, 300-305 (1958).

"Here's how magnetic amplifier design will be affected by tape wound core standarization," Electronics, Engineering Edition 31, 5, 59 (1958).

"High speed versatile toroid winders for production or laboratory," Electronics, Engineering Edition 31, 11, 275 (1958).

"How to make a magnetic core that's really small?" Electronics, Engineering Edition 31, 3, 44 (1958).

J. W. Kallender, "Designing minimum weight magnetic cores," El. Manufacturing 61, 2, 118-123 (1958), 3 figs.

T. Konorinskii, "Designing wound cores for communications devices," [in Polish] Przeglad Telekomunikacyjny 1 , 1-7 (1958), 23 figs., 14-title bibl.

"Magnetic Metals Company processes tape wound centricores to provide thermal stability," Electronic Industries No. 3, p. 163 (1958).

D. W. Moore, "The preparation of magnetic films by high vacuum evaporation," Proc. C.M.A. (1958), Los Angeles, AIEE, pp. 278-295 (1958), 12 figs.

T. R. Nisbet, "Optimum design of power transformers and saturable reactors. Part I." Electronic Design, p. 4 (April, 1958).

"Now wind subminiature toroids automatically," Electronics, Engineering Edition 31, 11, 190 (1958).

F. T. Parr, "Organosilicon compounds as insulation for miniature power transformers for high temperature operation," Proc. Electronic Components Symposium, pp. 246-253 (1957).

A. C. Sim, "Nomogram for air-gap design," Electronic and Radio Engr. 35, 7, 250-251 (1958), 1-title bibl.

"Tape wound cores. Bobbin cores," Electronics, Engineering Edition 31, 19, 125 (1958).

"Toroidal coil winder," Instr. and Automation, 32, 7, 1240 (1958), 1 fig.

"Toroidal components," Electronic Industries and Tele-Tech. No. 1, p. 116 (1958).

3. General Questions in the Theory of Nonlinear Magnetic Circuits (General Methods for Computing Circuits with Steel, Ferroresonance, etc.)

S. A. Abbas and D. L. Critchlow, "Calculation of flux patterns in ferrite multipath structures," IRE Nat. Convention Rec. 6, 4, 263-267 (1958), 10 figs.

J. Kryze, "The use of the duality principle for the transfiguration of magnetic circuits," [in Czech.], Elektrotechn. Obzor 47, 3, 130-133 (1958), 19 figs, 8-title bibl.

H. W. Lord, "An equivalent circuit for transformers in which nonlinear effects are present," Proc. C.M.A. (1958), Los Angeles, AIEE, pp. 296-308 (1958), 18 figs., 1-title bibl., 1 table.

A. S. Mostafa and M. I. El-Karaksi, "Subharmonics in iron-cored reactor oscillatory circuits," Commun. and Electronics No. 35, pp. 104-113 (1958).

S. Oshima et al., "Analysis of parametrically excited circuits – parametron and magnetic amplifiers," J. Inst. Electr. Commun. Engrs. of Japan 41, 10, 3-5 (1958).

H. F. Storm, "Applications of nonlinear magnetics. Part I," Electronic Design 6, 4 (1958); Part II – 6, 6, 44-47, 4 figs., 12-title bibl.; Part III – 6, 8, 62-65, 5 figs. 17-title bibl.; Part IV – 6, 10, 60-63, 5 figs, 29-title bibl.

F. G. Wesby, "Electromagnetic fields in a ferromagnetic medium with particular reference to harmonic distortion due to hysteresis," Proc. IEE, 105 C, 7, 218-229 (1958).

4. Magnetic Amplifiers. Survey and Applications

a) Survey

"Control" Standard Reactors, Catalog S-10, R-10, T-10, Control–a division of Magnetics, Inc., Butler, Pennsylvania, U.S.A. (1958).

L. A. Finzi, "Introducing young engineers to the appreciation of magnetic amplifier problems," Commun. and Electronics No. 35, pp. 119-126 (1958), 8 figs, 20-title bibl.; Elec. Eng. 77, 11, 1035-1037 (1958), 1-title bibl.

M. Frank and J. R. Walker, "High-temperature magnetic amplifiers," Electronic Components Symposium (Chicago, 1957), pp. 186-193 (1957).

W. A. Geyger, " Application of magnetic amplifiers in industrial instrumentation and control," Trans. IRE, 4, pt. PGIE 5, 4, 23-36 (1958).

H. B. Harms, "Magnetic materials in ultrahigh temperature electronic transformers," Elec. Eng. 77, 5, 408-412 (1958), 12 figs, 2-title bibl.; Commun. and Electronics No. 36, pp. 181-184 (1958), 8 figs, 2-title bibl.

H. B. Harms et al. "Ultrahigh temperature (500°C) miniaturized power transformers and inductors," Proc. Electronic Components Symposium, pp. 177-185 (1957).

W. G. Harvey, "Magnetic amplifier design principles and some applications," L. S. E. Engng. Bull. 5, 1, 1-13 (1958), 22 figs, 4-title bibl.

"High stability magnetic amplifiers," Process Control and Automation 5, 11, 11 (1958).

H. Hill and F. M. Kinney, "Magnetic amplifier selection by nomograph," El. Manufacturing 62, 4, 80-81, 282, 284, 286 (1958), 2-title bibl.

J. D. Kopsho, "A synchronous power converter for high-efficiency magnetic amplifiers," Proc. STC on Mag. Amp. T-98, pp.8 (August, 1957).

A. Krausz, "Application of magnetic amplifiers in aircraft electrical systems," Proc. NEC 13, 926-933 (1957), 7 figs, 3-title bibl.

K. Kuhnert, "The role of magnetic amplifiers in industrial control" [in French], Instrum. et Labs. 5, 9-18, (1958), 20 figs.

A.Lang, "Magnetic amplifiers – reliable elements of automation" [in German], Automatik 13, 8, 201-206 (1958), figs. 14-26, 14-title bibl.

A. Lang, "New applications of magnetic amplifiers" [in German], Scientia Electr. 4, 3, 61-68 (1958).

C. K. Leonard, "High-frequency temperature-stable magnetic amplifiers," Proc. C.M.A. (1958), Los Angeles, AIEE, pp. 405-413 (1958), 11 figs.

"Low-level preact magnet amplifiers," Electronics No. 13, pp. 92 (1958).

"Magnetic amplifier low-level unit," Electronics, Engineering Edition 31, 11, 208 (1958), 1 fig.

"Magnetic amplifiers and transductors," Control 1, 4 (1958).

"Magnetic amplifiers feature variable gain," Electronics, Business Edition 31, 2, 41-42 (1958), 1 fig.

E. W. Miesner, "Magnetic amplifiers and controlling and regulating devices for electric motors" [in German], Elektrotechnik 39, 44, 361-364 (1957).

A. G. Milnes, "Transistors versus magnetic amplifiers," Power Eng. pp. 88-89 (December, 1958).

J. W. S. Payne, "The performance and application of magnetic amplifiers," Students Quart. J. 28, 112, 173-179 (1958).

L. Pun, "On the simulation of certain industrial systems by small electric motors," [in French], Automatisme 3, 12, 461-468 (1958), 15 figs.

D. A. Ramsay and B. W. Glover, "British magnetic amplifier developments," El. Manufacturing 62, 56-62 (July, 1958), 19 figs., 9-title bibl.

R. W. Spenser and T. H. Bonn, "Magnetic amplifier circuits with feedback," U.S. patent, class 307-88; No. 2812449; 11/5/1957.

L. W. Stammerjohn, "Magnetic amplifiers: basic principles and applications," Bell Labs. Rec. 36, 1, 16-21 (1958), 7 figs.

J. C. Taylor and Ch. L. Wyman, "Transistor circuits alter magnetic amplifier frequency response," El. Manufacturing 62, 2, 90-91 (1958), 8 figs., 16-title bibl.

"Transistor-magnetic amplifier for servomotor control," Electronics, Engineering Edition 31, 27, 122 (1958).

R. Zadsinski, "Universal characteristics of magnetic amplifiers " [in Polish], Archiwum automatyki i telemechaniki 3, 1-2, 17-35 (1958), 8 figs., 9-title bibl.

b) Application in Servo Systems and for Controlling Electric Machines

E. Bernard, "The control of two-phase motors by magnetic amplifiers" [in French], Automatisme 3, 2, 71-75 (1958), 7 figs, 3-title bibl.

H. C. Bourne et al., "Dynamic operation of magnetic amplifiers for feedback control systems," Electronics

Research Lab., U. of Calif., Berkeley, Scientific rept. No. 4, p. 27 (May, 1957).

K. M. Chigrwin, "Aircraft switching-type static inverter supplying rotating machines," Applic. and Ind. No. 39, pp. 334-335 (November, 1958).

H. E. Darling, "Magnetic amplifiers for process control," El. Design 29, p. 3 (October, 1958).

"A dc instrument with magnetic amplifiers" [in German], Elektrotechn. Anz. 74, 6, 142 (1957).

Mitio Fuzdzisava, "Controlling a paper-cutting machine by magnetic amplifiers," Avtomatika 3, 2, 54-58 (1958).

N. F. Horton and H. J. Tyler, "Magnetic amplifier everspeed trip devices (West. Electric Corp.). 5/17/1952. U.S. patent, No. 2760149; 8/21/1956.

G. B. Houck, "Transistor magnetic amplifier circuit", (General Precision Lab. Inc.), U.S. patent, class 179-171, No. 2,819,352; 1/7/1958.

Cigasi Kobajacy and Kanjitiro Morita, "A G-D device controlled by a magnetic amplifier," Japanese patent, class 55c, No. 211, No. 5011, 6/26/1956.

F. Kummel, "Stabilization of a control system with magnetic amplifiers," [in German, Regelungstechnik 6, 6, 209-217 (1958).

P. Lamorlette, "Control equipment for a dc generator" [in French], French patent, class 12-6, No. 1128660; 1/9/1957.

G. Loocke, "Problems in the control and regulation of electric drives (G-D system)" [in German], Energie 10, 5, 198-203 (1958).

H. G. Lott, "Use of magnetic amplifier for braking of 3-phase asynchronous motors," AEG Mitt. 47, 1-2, 19-23 (1957).

R. Mathieson, "Electric drives at consett," Control 1, 5, 235-239 (1958), 7 figs.

V. Nemec, "Synchronous generators with automatic contactless control," [in Czech.], Elektrotechnik 12, 7 225-228 (1957), 11 figs, 5-title bibl.

E. M. Ostaseski, "Amplistats in control," Automatic Control 6, 4, 41-43 (1957), 3 figs.

K. Raedle, "The use of rectifiers and magnetic amplifiers in metallurgy" [in French], Bull. Sci. AIM 71, 2, 89-116 (1958).

S. J. Reisman and E. H. Bowman, "A power method of measuring the torque-producing output of a magnetic amplifier driving one phase of a two-phase servo motor," Commun. and Electronics No. 39, pp. 584-586 (1958), 3 figs.

A. Straughen, P. P. Biringer, and G. R. Slemon, "Three-phase induction motor control using static-frequency doublers," Commun. and Electronics No. 36 (1958).

N. E. Strom, "The speed regulation of small dc machines by means of transductor-controlled rectifiers," ASEA Journal 31, 3, 40-43 (1958). 6 figs.

M. E. Wright, "Press power drive system at Philadelphia Bulletin," Print. Equipm. Engr. 87, 9, 76-80, 112, 113 (1957), 4 figs.

E. Zucker, "Unique ac hoists speed production," El. Digest 27, 3, 55-56, 58 (1958).

c) Use in Controllers and Stabilizers of Current and Voltage

"A complete line of magnetic voltage regulators," Electronics 31, 29 (1958).

W. E. Cronquist, "A simple high-performance magnetic amplifier generator voltage regulator," Proc. STC on Mag. Amp. T-98, p. 245 (August, 1957).

I. K. Dortort, "Current-balancing reactors for semiconductor rectifiers," Commun. and Electronics No. 38, pp. 452-456 (1958).

L. Gador, "Transformer voltage regulator" [in Czech.], Meres es Automatika No. 1, 1-12, (1958), 5 figs.

H. V. Hjermstad and J. T. Keefe, "Static-magnetic regulated dc power supplies," El. Manufacturing 62, 110-113, 270 (1958).

O. Hora, "A Ferroresonant voltage stabilizer" [in Czech], Automatisace No. 5, 157-162 (1958), 15 figs, 7-title bibl.

M. A. Johansson, "A new supply-voltage regulator of transductor type," ASEA Journal 31, 3, 37-40 (1958), 6 figs.

K. King, "Improvements relating to electric control apparatus," English patent, class 40/4, No. 752340; 7/11/1956.

"A magnetic amplifier-regulator" [in German], Regelungstechnik 6, 7, 272-273 (1958), 3 figs.

M. J. Mulhern, "Regulating circuit for energizing variable resistance loads," U.S. Patent, class 315-106, No. 2822507; 2/4/1958.

d) Use in Measuring Devices

H. E. Darling, "DC transformer has continuous adjustable ratio," El. Des. 5, p. 4 (March, 1958).

W. A. Geyger, "Magnetic-amplifier-operated ink recorders," Commun. and Electronics No. 38, pp. 457-471 (1958), 43-title bibl.

A. R. Hamilton, "A magnetic amplifier control circuit for a thermal conductivity vacuum gauge," 4th Nat. Sympos. on Vacuum Technology Trans. (Boston, 1957), pp. 112-114 (1958).

J. McFarlane and M. J. Harris, "The control of flux waveforms in iron testing by the application of feedback amplifier techniques," Proc. IEE 8, 22, 105A, 395-405 (1958).

H. W. Patton, "Magnetic integrating amplifiers. Their design and application," Proc. C.M.A. (1958), Los Angeles, AIEE, pp. 267-277 (1958), 9 figs. 5-title bibl.

A. S. Watson, "An improved transductor dc ammeter," El. Energy 2, 7, 275-281 (1958).

E. V. Weir, "Magnetic amplifier circuit using complex feedback," U.S. patent, class 323-89, No. 2817807; 12/24/1957.

e) Other Applications

A. O. Adams, "Magnetic-amplifier-operated relays for aircraft and missiles," Electronic Industries 17, 12, 12, 72-74, 153 (1958).

P. W. Covert and E. V. Weir, "A transductor summation system for strip plater," Proc. NEC 13, 934-942 (1957), 8 figs., 3-title bibl.

"New stepping switches for power transformers based on the operational principle of a magnetic amplifier" [in German] ETZ-A 79, 23, 934 (1958).

C. L. Hogan, "Magnetoelectric induction devices," U.S. patent, class 333-32, No. 2811697; 19/29/1957.

O. Hora, "The use of heat-sensitive chokes and transformers" [in Czech], Automatisace No. 3, 78-82 (1958), 10 figs., 6-title bibl.

R. V. Hubner, "The use of saturated reactors for controlling mercury rectifiers," [in German], ETZ-A 79, 15, 530-532 (1958), 5 figs.

W. E. Jewett and P. L. Schmidt, "A more stable three-phase transistor-core power inverter," Proc. C.M.A. (1958) Los Angeles, AIEE, pp. 348-362 (1958), 11 figs., 4-title bibl.

J. Maroz, "Magnetic amplifier detects open fuses," Electronics 31, 29, 86- 87 (1958), 1 fig.

B. A. Mazzeo, "A low-level, high accuracy dc magnetic amplifier," El. Manufacturing 62, 5, 106-110 (1958), 12 figs.

W. F. Nesbitt, "Obtaining optimum performance from a magnetic thermocouple amplifier, " Trans. IRE, PGIE-6, pp. 101-114 (1958).

"New annunciator system for generating stations," Westinghouse Engr. No. 1, p. 11 (1958).

A. Newton, "Saturable variable inductor," U.S. patent, class 336-155, No. 2826748; 3/11/1958.

D. L. Plette and J. W. Butler, "Some applications of magnetic amplifiers in aircraft protective systems," Applic. and Ind. 34, 427-433 (January, 1958), 16 figs. 2-title bibl.

R. P. Putkovich and T.M. Corry, "Application of saturable core in transistor power converters," Proc. NEC 14, 874-883 (1958), 10 figs., 7-title bibl.

A. Rose, "Magnetic-core dividers for I.T.V. (Industrial television) sync generators," Electronics 31, 15, 76-77 (1958).

N. R. Schuh, "Frequency-sensitive control device," West. Electrical Corp., 10/15/1953; U. S. patent, No. 2757320; 6/31/1956.

H. E. Thomas, "Saturable reactors fire radar magnetrons," Electronics 31, 19, 72-75 (1958).

P. K. Tien and H. A. Suhl, "Traveling-wave ferromagnetic amplifier," Proc. IRE 46, 700-706 (April, 1958).

C. C. Voice, "Magnetic amplifier drives gyro indicator," Electronics 31, 7, 114-117 (1958), 6 figs., 4-title bibl.

5. Magnetic Amplifiers. Theory, Circuits, Calculations

a) Books, Monographs, Dissertations

G. M. Ettinger, Magnetic Amplifiers (Methuen and Co., London, 1957) issue 2, p. 102.

E. H. Frost-Smith, "The Theory and Design of Magnetic Amplifiers (Chapman and Hall, Ltd., London, 1958) p. 487, 151 figs., 57-title bibl.

S. Platt, Magnetic Amplifiers. Theory and Application (Prentice-Hall, Inc. Englewood Cliffs, N. J., 1958) p. 238.

b) Nonsequential Magnetic Amplifiers (Single-Cycle)

R. E. Anderson, "Magnetic amplifier design. I. The core. II. The windings," Commun. and Electronics No. 36, pp. 160-175 (May, 1958); El. Engng. 77, 5, 394-395 (1958), 3 figs.

E. Bernard and E. Pio, "A contribution to the study of magnetic amplifier operation," [in French], C.R. Acad. Sc. 248, 394-397 (1959).

H. H. Britten, "Characteristics of magnetic amplifiers utilizing square-loop core material and square-wave supply voltage," Commun. and Electronics No. 39, pp. 590-598 (1958), 11 figs., 3-title bibl., discussion.

L. W. Buechler and W. F. Schmidt, "Magnetic amplifier system," U.S. patent, class 323-89, No. 2807776; 9/24/1957.

D. P. Chandler and R. W. Downing, "Elimination of magnetic-amplifier control circuit inductance," Commun. and Electronics No. 39, pp. 550-556 (November, 1958), 18 figs., 1 table, 11-title bibl., disc. pp. 556-558, 4-title bibl.; Proc. STC on Magn. Amp. T-98, p. 21 (August, 1957).

E. L. Clarke "Auto. self-excited transductors. A nonmathematical approach," Instrument Practice 12, 10, 1093-1100 (1958), 20 figs., 2-title bibl.

C. Delgrosso and G. Sacco , "Methods of modifying the dynamic response of magnetic amplifiers," Electrotecnica 44, 6, 318-330 (June, 1957).

J. P. Eckert, "Bipolar output carrier magnetic amplifier," U.S. patent, class 307-88, No. 2808520; 10/1/1957.

J. P. Eckert and T. H. Bonn, "Carrier-type magnetic amplifier with a feedback circuit," U. S. patent, class 307-88, No. 2830198; 4/8/1958.

G. M. Ettinger, "Some aspects of half-wave magnetic amplifiers," Proc. IRE 105B, 21, 237-248 (1958).

E. H. Frost-Smith, "Fast-response magnetic amplifiers," Control 1, 4, 176-182 (1958), 9 figs., 7-title bibl.

E. L. Gardner, "Magnetic amplifier," U.S. patent, class 179-171, No. 2812391; 11/5/1957.

B. W. Glover, "Magnetic amplifiers with half-cycle response," El. Energy 2, 1, 2-9 (1958); 2, 2, 58-64 (1958).

J. C. R. Heydenrych, "A note on the design of transductors for maximum power transfer," Trans. S. African Inst. Elec. Engrs. 48, pt. 12, 370-377 (1957).

R. M. Hubbard, "Block-diagram method of analysis applied to the saturable reactor," Commun. and Electronics, No. 35, pp. 57-65 (March, 1958).

R. M. Hubbard and M. M. Bishop, "A comprehensive study of magnetic amplifier design. Part I. A practical design method. Part II. Toroidal-core dimensional ratios as a factor in magnetic amplifier design," Proc. STC on Mag. Amp. T-98, p. 121 (August, 1957); Commun. and Electronics No. 39, p. 562-583, 15 figs., 3 tables, 3-title bibl.

W. Jentsch, "Average value of magnetic flux and inertia of magnetic amplifiers" [in German], Regelungstechnik 6, 1, 9-14 (1958).

R. H. Kelsall, J. Sherlock, and J. M. Foye, "Improvements relating to saturable core reactance devices," English patent, class 40(4), No. 753356; 7/26/1956.

E. Levi, "New amplifiers for automatic control of active dc leads," IRE Nat. Convention Rec. 6, 6, 216-222 (1958).

M. Mamon, "High speed magnetic amplifiers," Electr. Design News. 3, 9, 48-51 (1958), 5 figs., 3-title bibl.

W. L. Marks, "Bistable Ramey magnetic amplifiers," El. Energy 2, 6, 218-221 (1958).

D. L. Mc Murtrie, "Magnetic amplifier circuits – a classification of half-wave and full-wave nonreversible and reversible self-saturating circuits," Proc. C.M.A. (1958), Los Angeles, AIEE, pp. 67-86 (1958), 22 figs., 4-title bibl., 3 tables.

R. E. Morgan, "A new control amplifier using a saturable current transformer and a switching transistor," Commun. and Electronics No. 39, pp. 557-562 (November, 1958), 15 figs., 4-title bibl., disc.

J. Nagy, "Basic principles in designing magnetic amplifiers" [in Czech.], Meres es Automatika No. 1, 6-9 (1958), 7 figs., 3-title bibl.

K.C. Parton, "Improvements in or relating to magnetic amplifier arrangements," English patent, class 40/4, No. 753363; 7/25/1956.

E. Pio, "Investigation of magnetic amplifiers with self-saturation" [in French], Automatisme 3 (1958), in five parts: I: No. 2, pp. 63-70, 18 figs.; II: No. 4, pp. 144-149, 32 figs.; III: No. 6, pp. 218-244, 50 figs.; IV: No. 8, pp 293-298, 58 figs.; V: No. 11, pp. 430-438, 76 figs., 11-title bibl.

T. J. Pula, "Volt-second transfer efficiency in fast response magnetic amplifiers. Part I. No. 2, Reg. and control," Proc. STC on Mag. Amp. T-98, p. 107 (August, 1957).

(Continued in the following number (21, 2) of this journal.)

SCIENTIFIC AND ENGINEERING PROBLEMS OF AUTOMATED ELECTRIC DRIVES DURING THE CURRENT SEVEN-YEAR PERIOD

M. G. Chilikin and I. I. Petrov

The far-reaching plan for the development of the national economy of the USSR in the period 1959-1965, put forth at the Twenty-first Congress of the Communist Party of the Soviet Union, envisions an all-around increase in the productivity of national labor on the basis of a strengthening of its electrical sinews and the automation of production. The electrical motive power available determines the degree to which production is mechanized, since the basic and principal form of the prime mover for operating machinery is the electric drive. The productivity of labor depends directly on its electrification (i.e., on the electric motive power available to it): over the past ten years, the productivity of industry in the USSR increased by about the same percentage as its electrification.

By an electric drive we understand a complex device which transforms electrical energy to mechanical energy, and which provides electrical control of the transformed mechanical energy. In this connection, the future development of electric drives must be directed to the implementation of all forms of motion without the use of any mechanical means in achieving these purposes (rotary and reciprocating motion; prolonged discontinuous variable and tracking motion; with fixed speed, and with speeds which change sharply, which vary continuously in accordance with a given law, or which change arbitrarily). The development of electric drives must provide for the broadening of their functions in the automatic control and regulation of the operating machines of technological aggregates (control of the starting, reversing, and braking of operating machines; maintaining constancy of speed, torque and power; program control of operating machines, etc.).

The science of electric drives derives basically from the work of Soviet scientists and, today, this branch of technical knowledge has taken definitive shape in the form of an independent section of applied electrical engineering. In the Soviet Union there has been created, and introduced into industry, a system of electric drives of a high technological level. However, the total volume of research work carried out by research and planning institutes, by higher educational institutions, by the design offices of enterprises and other organizations is still insufficient. There remain unsolved many problems concerning electric drives which are of great significance for the country's national economy.

Among the unsolved problems, the first that should be mentioned is the creation of controlled economical ac electric drives. Of particular significance here are the questions of developing simple and reliable systems of frequency control for ac electric motors and, in particular, of creating ac supplies with controlled frequency. Here, special attention must be given to the development and investigation of static-frequency transformers using ionic, electronic, and semiconductor technologies.

The situation is somewhat better with the development of controlled ac electric drives with choke control. In the last few years there have been created, and introduced into industry, a number of such electric drives, and the scientific and engineering methods for designing them have been adequately developed. However, the domain of possible applicability of electric drives with choke control has been somewhat overestimated, which sometimes leads to incorrect choices in selecting the type of electric drive for productive machines. Thus, for example, on insufficient grounds, a choked electric drive was used for excavators of medium productivity, which led to their uneconomical and unreliable performance. Special resolutions of the State Scientific-Engineering Committee of the Soviet Ministers of the USSR recommended that the production of excavators with such electric drives be halted, and that they be replaced by controlled dc electric drives. The attempt to use choked electric drives for materials-handling vehicles was also adjudged unsuccessful. Seemingly, it is necessary to find reasonable limits of applicability of choke-controlled electric drives, taking into account their relatively low energy efficiency for tight and prolonged control of production-machine speed, and the peculiarities of these machine's load characteristics.

Also requiring further investigation are the questions of the dynamics of choked electric drives, with the nonlinearities of their individual elements taken into account, and also the question of electric-drive heating as the load varies cyclically.

In connection with the intensification of productive processes, the necessity arises for developing electric drives with asynchronous short-circuited electric motors designed for production mechanisms with partial starts and reverses. However, this question remains unsolved. In the near future there must be created, based on normally manufactured asynchronous short-circuited electric motors, a modification of the electric motor with a heat-insulating base and with an extended motor, designed for a high frequency of switching in, and there should also be developed a methodology for designing electric drives with partial starts and reverses. With this, particular attention should be given to the transient responses in electric drives, and to the question of their heating.

There has been an improvement recently in the status of the investigations into the operating properties of ac electric drives supplied from autonomous supplies of commensurable power. Even here, however, there remain many problems in connection with increasing the power of asynchronous electric motors supplied from individual generators. The questions as to the dynamics of the processes transpiring in such electric drives deserve particular attention.

It is also going to be necessary to investigate the questions related to the use of synchronous electric motors for uncontrolled (operating at constant speed) and controlled (operating with variable speed) industrial electric drives. The transition to circuits with direct starting of synchronous motors and starting with permanently connected exciters led to a certain broadening of the domain of applicability of synchronous motors. However, despite their specific properties and their high energy efficiency, synchronous motors have still not been as widely used as they should be. Still, a wide dissemination of synchronous electric motors for drives of operational machines can significantly increase the power factor of electrical stands and provide a high rigidity of electric-drive mechanical characteristics within a wide range of speeds. The use of motors with rotary stators permits the problem of synphasing a synchronous shaft to be solved, etc. There might, therefore, be great interest in works devoted to elucidating new domains of applicability of synchronous electric motors, and to the investigation of new automatic control systems for synchronous electric drives, operating both with constant and, especially with variable speeds of rotation. In particular, interest inheres in the questions of the economic speed control of synchronous electric motors with frequency control, and in questions of automatic excitation control of electric motors for drives with impact loads. Also necessary are further investigation of the transient responses in synchronous electric drives and the development of a scientific method of calculating these processes.

Many problems in the domain of controlled dc electric drives also require solution. In the widely used "motor-generator" (M-G) systems, only dc motors with parallel excitation are used, these being less liable to torque overheating than motors with series and with hybrid excitation. The use of power semiconducting rectifiers, connected in the series-excitation winding circuit, permits one to create new types of M-G systems with improved dynamic characteristics. Analogous systems can also be created by supplying the motor from controlled mercury-arc rectifiers (CMR).

Significant success has been achieved in the development and dissemination of electric drives with ionic transformers (for controlled nonreversible drives). An essential improvement of the dynamic characteristics of an M-G drive system has been attained by the use of controlled mercury-arc rectifiers for the excitation of the system's machine. However, the development and dissemination of such systems have been carried out extremely slowly.

Great difficulties ensue when a CMR-M system is used for reversible electric drives. In this connection, great interest inheres in the question of further development and investigation of an automatic control system for an ionic electric drive, where the ionic transformer must be considered as an element of the over-all control system. These systems must possess a high energy factor, permit operation in the rectifying and inverting modes, be fast-acting, and have little control power.

Development and investigation are required for ionic-drive systems, increasing the power factor for tight speed control, and also for systems for the automatic control of the power factor of ionic aggregates for the purpose of providing the very best conditions for supplying electricity to enterprises.

Recently, magnetic amplifiers have been finding increasing application in electric drives. They are used in "magnetic amplifier – motor" electric drive systems, in M-G systems for generator excitation control, for line control by mercury-arc rectifiers, and also as industrial amplifying links.

The employment of semiconductor amplifiers has also been broadened, these being used advantageously in the form of preamplifier stages in conjuction with rotary and magnetic amplifiers. However, the domain of application of these new types of amplifiers has still not been defined sufficiently clearly. It is necessary to carry out a resolute replacement of rotary amplifiers in electric-drive systems by the more reliable and long-lasting magnetic and semiconductor amplifiers.

Simultaneously, it is necessary to work on the creation of power semiconductor rectifiers for "semiconductor amplifier – motor" electric-drive systems, and also for the control of generator excitation in M-G systems. The new means of automation (rotary and magnetic amplifiers, semiconductor and electronic devices) allow the creation of highly efficient electric-drive control systems, providing the maximum usage of the machines, the accurate maintaining of a given trajectory of motion, etc. Of particular significance here are the so-called optimal systems in which, given limitations on trajectory, speed, acceleration, or heating, there is attained a minimum time of execution of the drive mechanism's operating function.

The investigation of the transient responses in such essentially nonlinear systems presents significant difficulty. Today we are completely capable of solving these complicated tasks by the method of mathematic modeling using analog and digital computers. However, for the creation of automated electric-drive systems, these capabilities are used very weakly. This is explained, on the one hand, by the insufficient quantities of such machines at the disposal of research and planning organizations and, on the other hand, by the shortage of scientific and engineering cadres familiar with the methods of mathematical modeling. The preparation of such cadres is unsatisfactory in the higher institutions of learning which turn out engineers with the "electric drive" specialty. Until now, all the textbooks on electric drives have been based on the classical methods of investigation and do not expound, in adequate measure, the more modern methods, including the methods of mathematical and physical modeling. The laboratory courses in the educational institutions do not provide work with computers. In connection with this, the important problems requiring solution are: equipping research and educational institutes, planning-designing, and other organizations with analog and digital computer-models; improving the knowhow of the scientific and engineering cadres in the domains of mathematical and physical modeling; further developing of research work on the study of transient responses in complex systems of automated electric drives, constructed with the use of the new means of automation, and on the synthesis of the modern, essentially nonlinear, systems which provide optimal electric-drive transient responses; modernization of the university courses in "electric drives" and the related disciplines in the direction of developing in them the more modern methods of theoretical and experimental investigation of electric drives; the creating, in the near future, of manuals and textbooks on electric drives which are designed to make the transition from the older methods of studying electric-drive dynamics to the newer ones, including the methods of mathematical and physical modeling.

Certain problems in the domain of multimotor electric drives are also not solved. Thus, further investigation is required of electric shaft systems with variable speed ratios of the individual elements, for mass-production-line electric drives. It is necessary to develop a theory of the nonsteady-state processes in electric drives with friction coupling between the motors, and to investigate questions of oscillation damping in electric shaft systems with frequency transformers and dual-source machines. There has yet to be created a generalized theory for multimotor electric drives with electrical connections, providing a constant tension on the material being processed, for aggregates with continuous technological processes.

Insufficient attention has been given to the production, and to the use in automated electric drives, of the various electromagnetic clutches, including those with ferromagnetic packing. Nonetheless, their use could lead to the creation of a rational electric-drive system, particularly in cases where it is necessary to have smooth starting of the drive, acceleration of large inertial masses, control of torque, speed, etc. They can also play the roles, in automated electric drive systems, of brake dynamometer, position indexer, torque limiter, etc. Today, electromagnetic clutches are comparatively widely used only in machine-stand construction. It is necessary to translate the experience in machine-stand construction to other branches of the national economy, and to carry out a number of investigative tasks, directed toward the explication of the possibilities of constructing rational electric-drive systems with electromagnetic clutches for diverse productive mechanisms.

During many years, various branches of industry, and particularly the machine-building industry, have put forward the problem of creating electric drives with rotary-reciprocating and vibratory motion. Unfortunately, this problem is still unsolved for practical purposes. Research organizations must necessarily increase the exploratory work in the domains of creating reciprocating electric motors, and of constructing autooscillatory systems with simple control systems for the amplitude and frequency of the vibrations.

Of great interest in both the theory and the practice of electric drives might be an investigation of systems containing elastic links. Today, all system elements are considered to be ideally solid bodies, and therefore the phenomena and processes in which elastic deformations play a part are not taken into consideration. The deformations of elastic links lead, in many cases, to significant errors. It would thus be of great advantage to develop general methods of analyzing automatic-control systems containing elastic links, and to solve the problem of synthesizing electric drives and their control systems for mechanisms with elastic links.

Despite the significant development of this theory in recent years, certain questions in the theory of electric-drive heating are still unsolved. Thus, further investigation is needed of the heating processes of ac motors in normal condtions of use, including the asymmetric mode of supply of three-phase asynchronous electric motors. Also requiring further development are the questions of electric-motor heating in transient responses and for cyclical loads, with account being taken of insulation aging. Work should also be continued on the direct use of heat-conduction equations for the thermal computations for electric-drive motors.

There are also many questions in the domain of microdrives to be resolved. This domain is little studied but, at the same time, this energetically evolving. In the next few years, millions of electric motors will be required for microdrives. In connection with this, there is necessary a further development of the questions of creating economical systems of actual microdrives, of increasing their reliability and noiselessness in use, and also the accuracy and speed of response of microdrives as used in the devices of automation.

The modern electric drive plays a very large role in systems of automated productive processes. The particularly essential question is that of program control of the electric drives of individual productive mechanisms and aggregates. Today, a certain measure of success has been achieved in the introduction of program-control systems for a number of metal-working stands, in the screw-down devices of reversible rolling mills, in the electric drives of charging systems for blast furnaces, etc. However, the general state of work in the areas of creating and disseminating program control systems is unsatisfactory. In these systems, the new means of automation - semiconducting and magnetic elements - are used with inadequate completeness, and one finds little reflection of the recent achievements in the area of creating self-adjusting and self-learning systems. As a rule, the programmed systems in use today have a rigidly given program, which does not always answer to the required technological-economical indicators of the process under conditions of nonconstant external disturbances. The use of devices providing automatic program correction in correspondence with changes in an aggregate's external operating conditions would permit the creation of an automatic-control system which would establish the most efficient mode of operation

A significant obstacle to the widespread introduction of automatic control by mechanisms supplied with electric drives is the inadequacy of existing position transducers of the machines' individual organs and of the material to be processed, and also the inadequacy of manufactured relay-contact apparatus which allows only a limited number of switchings in. Thus, the number of contact operations on an automatic machine-stand line reaches tens of thousands, and sometimes even hundreds of thousands, per hour, which sharply reduces the reliability of electric control systems. In this connection, great importance inheres in the development of new types of contactless automatic control devices which use highly reliable semiconducting and magnetic elements.

Insufficient use is made, in control schemes with drives in production lines, of electric apparatus used for communciations devices. It is necessary to practice a wider use of this apparatus which has small dimensions and increased reliability.

For the purpose of accelerating the large-scale use of modern automatic-control systems by electric drives, it becomes necessary to accelerate the utilization, in the electrical industry's standard assemblies, of new control systems, including digital and programmed devices, and also complex control systems for standard electric drives.

The enumeration of problems in the domain of electric drives which has been given here is far from exhaustive, and contains only the first-priority problems.

STATISTICAL THEORY OF GRADIENT SYSTEMS OF AUTOMATIC OPTIMIZATION FOR OBJECTS WITH QUADRATIC CHARACTERISTICS

A. A. Fel'dbaum

(Moscow)

(Translated from: Avtomatika i Telemekhanika, Vol. 21, No. 2, pp. 167-179, February, 1960)
Original article submitted June 12, 1959

The paper formulates the problem of investigating gradient systems of automatic optimization in the presence of random factors. Methods are given for determining the steady-state error and estimating the duration of the transient response for gradient systems with several input variables. The results are illustrated by examples of systems with one and with two variables.

INTRODUCTION

The near future will be marked by a significant development of self-adjusting (adaptive) systems. Great value, therefore, inheres in the development of a theory of automatic serach, which is the basic process in such systems, and which differs essentially from the process of error liquidation in automatic-control systems. One of the classes of adaptive systems which promises to be of importance practically is that of automatic optimization systems. We present below the theory of one of the forms of such systems.

The problem of an automatic optimization system consists of automatically finding and maintaining a minimum of some quantity y with, generally speaking, additional conditions imposed. The quantity y is a function of the variables u_i:

$$y = y(u_1, u_2, \ldots, u_m). \tag{1}$$

The process of automatic search for a minimum is slowed when there is random noise present, and the minimum itself will be determined, and maintained, with some error under these circumstances. The duration of the transient response of the search process, and the steady-state error, are the fundamental symptomatic indicators of the system's process.

The most general problem consists of synthesizing such a controlling portion which will implement the best (in some sense) process of automatic search. We shall consider below the more restricted problem of determining the indicators of the process for a given controlling portion, and also of choosing the optimal values of this portion's parameters.

In the automatic serach for a minimum, tentative movements are made – "experiments" with the object, as it were – and thereafter the operational movement is made on the basis of an analysis of the results of the tentative trial motions. Various combinations of operationa and trial movements are possible. In the sequel, we consider systems of the discrete type in which, during one cycle, a series of trial steps is taken, and then followed by an operational step; in the following cycle, there is again taken a series of trial steps followed by an operational step, etc.

Figure 1 shows an example of an automatic optimization system. Here, C is the controlling portion; at the output of part F_0 of object 0 there is the quantity y which must be minimized. It is joined, in part F of the object, by an error z. At the object's input, the controlling quantities u_i are joined by random-noise quantities, z_{0i}. The sums thus obtained

$$x_i = u_i + z_{0i} \tag{2}$$

are applied to the input of part F_0 of the object. In carrying out trials on the ith input variable, one adds to the quantity x_i the quantity $+\alpha_{0i}$ in the first trial interval and $-\alpha_{0i}$ in the second trial interval. Thus, a trial consists of two intervals. If the total number of input variables is m, the entire cycle is composed of 2m intervals. We shall assume that the variations of the object's input quantities require the expenditure of no time, but that the carrying out of an "experiment," as a result of which the quantity y appears at the object's output, requires some time interval of constant duration.

The presence of the noise z_{0i} at the input gives rise to a random displacement of the minimum point y in the space $u_1, u_2, \ldots, u_m$, which imitates a slow "drift" of the characteristics, which occurs in actual objects. It is possible to set $z_{0i} = \gamma_i n$, where n is discrete time or the number of cycles ($n = 0, 1, 2, \ldots$) and the γ_i are random variables. The noise z at the object's output (for example, in a measuring block) is a random noise of comparatively high frequency. We shall suppose that the increments of these quantities are independent random variables with known distribution law $\psi(v)$, zero mean value and finite dispersion σ^2. Such a form for the noise was introduced for these systems in [1].

The Markov Process in a Gradient System of Automatic Optimization

Let the dependence of the output y^* of portion F_0 of the object on the input quantities x_k^* be described by the formula

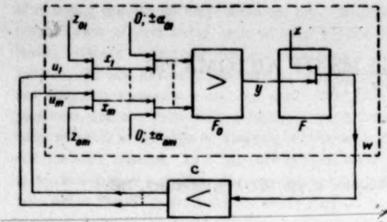

Fig. 1.

$$y' = \sum_{i,k=1}^{m} b'_{ik} x'_i x'_k + \sum_{k=1}^{m} c'_{ik} x'_k + d'. \tag{3}$$

By applying a linear transformation to each variable separately, we can take this formula to the form

$$y = f(x_1, \ldots, x_m) = \sum_{i,k=1}^{m} b_{ik} x_i x_k, \tag{4}$$

where $b_{ik} = b_{ki}$. We shall assume that quadratic form (4) is positive definite. Then y has a unique minimum at the origin of coordinates.

During the ith pair of intervals, whose ordinal numbers within the cycle are j and j + 1, where j = 2i − 1, measurements are made of the quantity y. We denote the values of the quantities x_i in the jth interval by $x_i^{(j)}$, and the value of y by $y^{(j)}$ In the first interval of the ith pair, there is the quantity $x_i^{(j)} + \alpha_{0i}$ at the ith input, while the second interval finds the quantity $x_i^{(j+1)} - \alpha_{0i}$ at this input.

After these two intervals, we determine the difference

$$\Delta_i y_n = f(x_{1,n}^{(j)}, \ldots, x_{i,n}^{(j)} + \alpha_{0i}, \ldots, x_{m,n}^{(j)}) - f(x_{1,n}^{(j+1)}, \ldots, x_{i,n}^{(j+1)} - \alpha_{0i}, \ldots, x_{m,n}^{(j+1)}). \tag{5}$$

The subscripts n denote that the measurements were made in the nth cycle. The corresponding quantity at the output of controlling portion C (Fig. 1) is defined by the expression

$$\Delta_i w_n = \Delta_i y_n + \Delta_i z_n = \Delta_i y_n + v_i. \tag{6}$$

The gradient method consists of this: that after a series of trials, as a result of which one determines the direction of the gradient of the quantity y – the vector with components $\partial y / \partial x_i \cong \Delta_i y_i$, the operational step is taken in this direction. Obviously, the increments of the quantities $u_{i,n+1} - u_{i,n}$, where n is discrete time, must be proportional to the quantities $\Delta_i w$, found in the nth cycle:

$$u_{i,n+1} - u_{i,n} = -\alpha_i (\Delta_i w_n) = -\alpha_i (\Delta_i y_n + v_i). \tag{7}$$

By taking into account (2) and (5), and the formula $z_{0i} = \gamma_i n$, we find that

$$x_{i,n+1} = x_{i,n} + \gamma_i - \alpha_i [f(x_{1,n}^{(2i-1)}, \ldots, x_{i,n}^{(2i-1)} + \alpha_{0i}, \ldots, x_{m,n}^{(2i-1)}) - f(x_1^{(2i)}, \ldots, x_i^{(2i)} - \alpha_{0i}, \ldots, x_m^{(2i)}) + v_i] \tag{8}$$

Here, we have denoted $x_{i,n}^{(1)}$ simply by $x_{i,n}$. Since

$$x_i^{(j)} = \widehat{x_i^{(1)}} + \gamma_i \frac{j-1}{2m} = x_i + \gamma_i \frac{i-1}{m},$$

$$x_i^{(j+1)} = x_i + \gamma_i \frac{2i-1}{2m}, \tag{9}$$

then

$$x_{i,n+1} = x_{i,n} + \gamma_i - \alpha_i \Big[f\Big(x_1 + \gamma_1 \frac{i-1}{m}, x_2 + \gamma_2 \frac{i-1}{m}, \ldots, x_i + \gamma_i \frac{i-1}{m} + \alpha_{0i}, \ldots, x_m + \gamma_m \frac{i-1}{m}\Big) - f\Big(x_1 + \gamma_1 \frac{2i-1}{2m}, \ldots, x_i + \gamma_i \frac{2i-1}{2m} - \alpha_{0i}, \ldots, x_m + \gamma_m \frac{2i-1}{2m}\Big) + v_i \Big]. \tag{10}$$

For brevity, we denote $x_{i,n} = \xi_i$ and $x_{i,n+1} = x_i$; we introduce the vector x in the m-dimensional space Ω_x, the vector ξ with coordinates ξ_i in the space $\Omega_\xi = \Omega_x$ and the vector γ with coordinates γ_i and the vectors ξ_{0i}, again in space Ω_x. Then (10) can be rewritten in the form

$$x_i = \xi_i + \gamma_i - \alpha_i \Big\{ f\Big(\xi + \alpha_{0i}\xi_{0i} + \gamma \frac{i-1}{m}\Big) - f\Big(\xi - \alpha_{0i}\xi_{0i} + \gamma \frac{2i-1}{2m}\Big) + v_i \Big\}. \tag{11}$$

We now take the form of function f(x) [cf., (4)] into account. By substituting (4) in (10) or (11), we obtain after some transformation,

$$x_i = \gamma_i - \alpha_i r_i + \sum_{j=1}^{m} A_{ij} \xi_j + B_i, \tag{12}$$

where

$$A_{ij} = \delta_{ij} + \frac{\alpha_i}{m} \sum_{\substack{k=1 \\ k \neq i}}^{m} b_{kj} \gamma_k + \alpha_i b_{ji} \Big(\frac{\gamma_i}{m} - 4\alpha_{0i} \Big),$$

$$B_i = \frac{4i-3}{2m} \alpha_i \Big\{ \frac{1}{2m} \sum_{\substack{j,k=1 \\ j,k \neq i}}^{m} b_{jk} \gamma_j \gamma_k + \Big(\frac{\gamma_i}{m} - 2\alpha_{0i} \Big) \sum_{\substack{j=1 \\ j \neq i}}^{m} b_{ji} \gamma_j + b_{ii} \gamma_i \Big(\frac{\gamma_i}{2m} - 2\alpha_{0i} \Big) \Big\}. \tag{13}$$

Here, $\delta_{ij} = 1$ for i = j and $\delta_{ij} = 0$ for $i \neq j$; i.e., δ_{ij} is a Kronecker delta.

The sequence $x_{i,n}$ (n = 0, 1, 2, . . .), or the vector x_n, is a random Markov process (cf. [2,3]) since the probability distribution for x_{n+1} depends on the value of x_n.

Initially, let the γ_i be fixed quantities. In view of the independence of the γ_i and the v_i, we can compute the distribution $W(\gamma)$ for γ at any subsequent stage. Further, let the v_i now be all zero. We first investigate the convergence of the automatic search process when the random noises are lacking. Equation (12) can be rewritten as:

$$\mathbf{x} = A\xi + \mathbf{B}, \tag{14}$$

where A is the matrix with elements A_{ij}, and B is the vector with coordinates $\gamma_i + B_i$. If the system converges to a steady state x_{ste}, then this latter state may be found from the equation

$$x_{ste} = A x_{ste} + B. \tag{15}$$

Let E be the unit matrix, and let the inverse $(E-A)^{-1}$ of the matrix E-A exist. Then

$$x_{ste} = (E - A)^{-1} B. \tag{16}$$

We consider the differences

$$x_{n+1} - x_{ste} = \Delta_{n+1}, \quad x_n - x_{ste} = \Delta_n. \tag{17}$$

If follows, from (14), (16), and (17) that

$$\Delta_{n+1} = A\Delta_n. \tag{18}$$

The necessary and sufficient conditions for the convergence of the search process, i.e., for the holding of the condition $\Delta_n \to 0$ as $n \to \infty$, are the inequalities

$$|\lambda_k| < 1, \tag{19}$$

where the λ_k (k = 1, . . . , m) are the roots of the characteristic equation $|A - E\lambda| = 0$ of the matrix A. As is well known, these inequalities reduce to condtions of the Routh-Hurwitz type. We shall assume that these conditions are satisfied.[•] With this, the speeds γ_i can not be arbitrary; the vector γ must lie within a certain region Ω_γ of the m-dimensional space.

We turn now to the general equation, in which random noise is present. Let the transition probability from the point $\xi = \{x_{1,n}, x_{2,n}, \ldots, x_{m,n}\}$ in the interval $x_i \leq x_{i,n+1} \leq x_i + dx_i$ (i = 1, . . . , m) equal $\varphi(\xi, x)$. $dx_1 \ldots dx_m = \varphi(\xi, x)\, d\Omega_x$, where $d\Omega_x = dx_1, \ldots, dx_m$.

Then, $p_{n+1}(x)$, the probability density that x_{n+1} appear in the interval $x_i \leq x_{i,n+1} \leq x_i + dx_i$ (i = 1, . . . , m), is defined by the formula

$$p_{n+1}(x) = \int_{-\infty}^{+\infty} \cdots \int_{-\infty}^{+\infty} \varphi(\xi, x)\, p_n(\xi)\, d\xi_1 \ldots d\xi_m = \\ = \int_{\Omega_\xi} \varphi(\xi, x)\, p_n(\xi)\, d\Omega_\xi, \tag{20}$$

where $d\Omega_\xi = d\xi_1, \ldots d\xi_m$. If this linear integral transformation has a fixed point to which the sequence $p_n(x)$ tends, then by denoting

$$P(x) = \lim_{n \to \infty} p_n(x), \tag{21}$$

we may find this function from the linear integral equation

$$P(x) = \int_{\Omega_\xi} (\xi, x) P(\xi)\, d\Omega_\xi. \tag{22}$$

We find $\varphi(\xi, x)$, assuming now that the γ_i are fixed. From (12) we get

$$v_i = \frac{1}{\alpha_i}\left[\gamma_i - x_i + \sum_{j=1}^{m} A_{ji}\,\xi_j + B_i\right]. \tag{23}$$

The conditional probability that $x_{i,n+1}$ is found in the interval $x_i \leq x_{i,n+1} \leq x_i + dx_i$ if $x_{j,n} = \xi_j$ (j = 1, . . . , m) equals $\psi(v_i)\, dx_i/\alpha_i$, where the v_i are determined from (23). Since, for different x_i, the v_i are independent, we have that

$$p(\xi, x) = \prod_{i=1}^{m} \frac{\psi(v_i)}{\alpha_i} = \prod_{i=1}^{m} \frac{1}{\alpha_i} \psi\left\{\frac{1}{\alpha_i}\left[\gamma_i - x_i + \right.\right. \\ \left.\left. + \sum_{j=1}^{m} A_{ij}\,\xi_j + B_i\right]\right\}. \tag{24}$$

Determination of the Indicators of the Automatic Search Process

We now find the mathematical expectation of the random variable y_n, by which we understand the arithmetic mean over the nth cycle:

$$M[y_n] = \int_{\Omega_x} \frac{1}{2m} \sum_{i=1}^{m} \left[f\left(x + \alpha_{0i}\,\xi_{0i} + \gamma\frac{i-1}{m}\right) + \right. \\ \left. + f\left(x - \alpha_{0i}\,\xi_{0i} + \gamma\,\frac{2i-1}{2m}\right)\right] p_n(x)\, d\Omega_x. \tag{25}$$

We consider separately the expression in the square brackets. By substituting (2) for f(x) we obtain, after some transformations,

$$\frac{1}{2m}\sum_{i=1}^{m}\left[f\left(x + \alpha_{0i}\,\xi_{0i} + \gamma\frac{i-1}{m}\right) + f\left(x - \alpha_{0i}\,\xi_{0i} + \gamma\frac{2i-1}{2m}\right)\right] = \\ = \sum_{j,k=1}^{m} b_{jk}\, x_j x_k + \left(1 - \frac{1}{2m}\right) \sum_{j,k=1}^{m} b_{jk}\, \lambda x_{j\,k} + C, \tag{26}$$

where

$$C = \frac{\frac{2}{3}\,(m+1)(4m-7) + 5}{8m^2} \sum_{j,k=1}^{m} b_{jk}\gamma_j\gamma_k + \\ + \frac{1}{m}\sum_{i=1}^{m} b_{ii}\,\alpha_{0i}^2 - \frac{1}{2m^2}\sum_{i,j=1}^{m} b_{ij}\,\alpha_{0i}\,\gamma_j. \tag{27}$$

Therefore,

$$M[y_n] = \int_{-\infty}^{\infty} \cdots \int_{-\infty}^{\infty} \left\{\sum_{j,k=1}^{m} b_{jk}\, x_{j,n}\, x_{k,n} \right. \\ \left. + \left(1 - \frac{1}{2m}\right) \sum_{j,k=1}^{m} b_{jk}\, x_{j,n}\, \gamma_k + C\right\} + \\ p_n(x_{1,n}; x_{2,n}; \ldots; x_{m,n})\, dx_{1,n}\, dx_{2,n} \ldots dx_{m,n} \tag{28}$$

or

$$M[y_n] = \sum_{j,k=1}^{m} b_{j,k} \int_{\Omega_x} x_j x_k\, p_n(x)\, d\Omega_x + \\ + \left(1 - \frac{1}{2m}\right) \sum_{j,k=1}^{m} b_{jk}\,\gamma_k \int_{\Omega_x} x_j\, p_n(x)\, d\Omega_x + C, \tag{29}$$

[•] The stability conditions for continuous gradient systems, derived in [6], have well-known similarities to those given above for $\gamma_i = 0$.

since

$$\int\limits_{\Omega_x} p_n(\mathbf{x})\, d\Omega_x = 1.$$

We introduce the notation

$$I_{jk,\,n} = \int\limits_{\Omega_x} x_j x_k\, p_n(\mathbf{x})\, d\Omega_x,$$

$$J_{j,\,n} = \int\limits_{\Omega_x} x_j\, p_n(\mathbf{x})\, d\Omega_x \qquad (30)$$

Then,

$$M[y_n] = \sum_{j,\,k=1}^{m} b_{jk} I_{jk,\,n} + \left(1 - \frac{1}{2m}\right) \sum_{j,\,k=1}^{m} b_{jk} \gamma_k J_{j,\,n} + C. \qquad (31)$$

Equations (30) for the integrals can be found from (20). We multiply both members by $x_j x_k d\Omega_x$ and integrate over Ω_x. Then, $I_{jk,\,n+1}$ appears in the left member of the equation, and the expression takes the form:

$$I_{jk,\,n+1} = \int\limits_{\Omega_x} x_j x_k \Big[\int\limits_{\Omega_\xi} \varphi(\xi, \mathbf{x})\, p_n(\xi)\, d\Omega_\xi\Big] d\Omega_x =$$

$$= \int\limits_{\Omega_x} x_j x_k \Big[\int\limits_{\Omega_\xi} \prod_{i=1}^{m} \frac{\psi(v_i)}{\alpha_i}\, p_n(\xi)\, d\Omega_\xi\Big] d\Omega_x. \qquad (32)$$

We now reverse the order of integration, and change from the variables $x_1, x_2, \ldots, x_m$ to the new integrand variables $v_1, v_2, \ldots, v_m$. Since $dx_i = -\alpha_i dv_i$, and the change in sign of the differential compensates for the changes in the signs of the limits of integration, we then find, by letting $d\Omega_v = dv_1 \ldots dv_m$, that

$$I_{jk,\,n+1} = \int\limits_{\Omega_\xi} p_n(\xi) \Big[\int\limits_{\Omega_v} \sum_{i=1}^{m} \psi(v_i)\, (\gamma_j - \alpha_j v_j + \sum_{\nu=1}^{m} A_{j\nu} \xi_\nu + B_j)\, (\gamma_k - \alpha_k v_k + \sum_{\nu=1}^{m} A_{k\nu} \xi_\nu + B_k)\, d\Omega_v\Big] d\Omega_\xi = \int\limits_{\Omega_\xi} p_n(\xi)\, L_{jk}\, d\Omega_\xi. \quad (33)$$

We now consider the interior integral L_{jk} included within the square brackets. By expanding the parentheses in it, we obtain

$$L_{jk} = \int\limits_{-\infty}^{+\infty} \cdots \int\limits_{-\infty}^{+\infty} \Big[\prod_{i=1}^{m} \psi(v_i)\Big] [\alpha_k \alpha_j v_k v_j + v_j (-\alpha_j \gamma_k - \alpha_j \sum_{\nu=1}^{m} A_{k\nu} \xi_\nu - \alpha_j B_k) +$$

$$+ v_k (-\alpha_k \gamma_j - \alpha_k \sum_{\nu=1}^{m} A_{j\nu} \xi_\nu - \alpha_k B_j) + \qquad (34)$$

$$+ (\gamma_j \gamma_k + \gamma_k B_j + \gamma_j B_k + B_k B_j) + (\gamma_j + \gamma_k) \sum_{\nu=1}^{m} (A_{k\nu} + A_{j\nu})\, \xi_\nu + (B_j + B_k) \sum_{\nu=1}^{m} (A_{k\nu} + A_{j\nu})\, \xi_\nu + \sum_{\mu,\,\nu=1}^{m} A_{k\nu} A_{j\mu}\, \xi_\mu \xi_\nu]\, dv_1, \ldots, dv_m.$$

Now, we take into account that

$$\int\limits_{-\infty}^{+\infty} \psi(v_i)\, dv_i = 1, \qquad \int\limits_{-\infty}^{+\infty} v_i\, \psi(v_i)\, dv_i = 0, \qquad (35)$$

and denote the dispersion of the noise at the output by

$$\sigma^2 = \int\limits_{-\infty}^{+\infty} v_i^2\, \psi(v_i)\, dv_i. \qquad (36)$$

By taking (35) and (36) into account, we may rewrite (34) in the form

$$L_{jk} = \delta_{jk} \alpha_k^2 \sigma^2 + (\gamma_j \gamma_k + \gamma_j B_k + \gamma_k B_j + B_k B_j) + \sum_{\nu=1}^{m} [(\gamma_j + B_j) A_{k\nu} + (\gamma_k + B_k) A_{j\nu}]\, \xi_\nu + \sum_{\mu,\,\nu=1}^{m} A_{k\nu} A_{j\mu}\, \xi_\mu \xi_\nu. \qquad (37)$$

By substituting (37) in (33), we obtain

$$I_{jk,\,n+1} = \delta_{jk} \alpha_k^2 \sigma^2 + (\gamma_j \gamma_k + \gamma_j B_k + \gamma_k B_j + B_j B_k) + \sum_{\nu=1}^{m} [(\gamma_j + B_j) A_{k\nu} + (\gamma_k + B_k) A_{j\nu}]\, J_{\nu,\,n} + \sum_{\mu,\,\nu=1}^{m} A_{k\nu} A_{j\mu}\, I_{\mu\nu,\,n}. \qquad (38)$$

It is possible to write $m(m+1)/2$ such equations for determining $I_{jk,\,n+1}$ from $I_{\mu\nu,\,n}$. The $\underline{m}$ quantities $J_{\nu,\,n}$ ($\nu = 1, \ldots, m$) also appear in these equations. These latter quantities can be found from (20) in an analogous way. Indeed, by multiplying this expression by $x_{j,\,n+1} d\Omega_x$ and integrating over Ω_x, we arrive at the formula

$$J_{j,\,n+1} = \int\limits_{\Omega_x} x_j \Big[\int\limits_{\Omega_\xi} \varphi(\xi, \mathbf{x})\, p_n(\xi)\, d\Omega_\xi\Big] d\Omega_x =$$

$$= \int\limits_{\Omega_x} x_j \Big[\int\limits_{\Omega_\xi} \prod_{i=1}^{m} \frac{\psi(v_i)}{\alpha_i}\, p_n(\xi)\, d\Omega_\xi\Big] d\Omega_x = \qquad (39)$$

$$= \int\limits_{\Omega_\xi} p_n(\xi) \Big[\int\limits_{\Omega_x} x_j \prod_{i=1}^{m} \frac{\psi(v_i)}{\alpha_i}\, d\Omega_x\Big] d\Omega_\xi = \int\limits_{\Omega_\xi} p_n(\xi)\, L_j\, d\Omega_\xi.$$

With this,

$$L_j = \int\limits_{\Omega_x} x_j \prod_{i=1}^{m} \frac{\psi(v_i)}{\alpha_i}\, d\Omega_x = \int\limits_{-\infty}^{\infty} \cdots \int\limits_{-\infty}^{\infty} \prod_{i=1}^{m} \psi(v_i)\, (\gamma_j - \alpha_j v_j + \sum_{\nu=1}^{m} A_{j\nu} \xi_\nu + B_j)\, dv_1 \ldots dv_m = \gamma_j + \sum_{\nu=1}^{m} A_{j\nu} \xi_\nu + B_j. \qquad (40)$$

By substituting (40) in (39), we find that

$$J_{j,\,n+1}=\int\limits_{\Omega_\xi} p_n(\xi)\,(\gamma_j+\sum_{\nu=1}^{m}A_{j\nu}\xi_\nu+$$

$$+B_j)\,d\Omega_\xi=(\gamma_j+B_j)+\sum_{\nu=1}^{m}A_{j\nu}J_{\nu,\,n}. \qquad (41)$$

Using (41), we can determine $J_{j,\,n+1}$ from the $J_{\nu,\,n}$, and then substitute the result in (38). The presence of the noises v_i is completely unreflected in (41). For $v_i = 0$, the distribution densities reduce to unit pulse functions, but (41) remain unchanged by this. Therefore, the necessary and sufficient conditions for convergence for the sequence $J_{\nu,n}$ as $n \to \infty$ remain the same inequalities (19). The sequence of second moments $I_{jk,\,n}$ of the distribution also converges for $v_i \neq 0$.

In fact, the presence of the noise v_i in (38) is reflected by the additive terms $\delta_{jk}\,\alpha_k^2\,\sigma^2$. For $\sigma^2 = 0$ (absence of noises v_i), conditions (19) are necessary and sufficient for convergence of the sequence $I_{jk,n}$. It is obvious that the presence of the additional terms $\delta_{jk}\,\alpha_k^2\sigma^2$ only changes the steady-state value, but has no effect on the fact of convergence, since the transformation matrix of the $I_{jk,\,n}$ [cf. (38)] depends only on the A_{jk}. Therefore, inequalities (19), when random noises v_i are present, also guarantee convergence of the first and second moments and, consequently, convergence of the sequence $M[y_n]$ [cf. (31)].

We set

$$I_{jk}=\lim_{n\to\infty}I_{jk,\,n};\quad J_j=\lim_{n\to\infty}J_{j,\,n};$$

$$\eta=\lim_{n\to\infty}M\,[y_n]. \qquad (42)$$

It follows, from (31), (38), and (41), that the quantities I_{jk}, J_j, and η are defined by (43), (44), and (45):

$$I_{jk}=\delta_{jk}\,\alpha_k^2\sigma^2+(\gamma_j\gamma_k+\gamma_jB_k+\gamma_kB_j+B_jB_k)+$$

$$+\sum_{\nu=1}^{m}[(\gamma_j+B_j)\,A_{k\nu}+(\gamma_k+B_k)\,A_{j\nu}]\,J_\nu+$$

$$+\sum_{\mu,\,\nu=1}^{m}A_{k\nu}A_{j\mu}I_{\mu,\,\nu}\quad (j,\,k=1,\,\ldots,\,m). \qquad (43)$$

$$J_j=(\gamma_j+B_j)+\sum_{\nu=1}^{m}A_{j\nu}J_\nu\ (j=1,\,\ldots,\,m). \qquad (44)$$

$$\eta=\sum_{j,\,k=1}^{m}b_{jk}\,I_{jk}+\left(1-\frac{1}{2m}\right)\sum_{j,\,k=1}^{m}b_{jk}\,\gamma_k\,J_j+C. \qquad (45)$$

Thus, the problem of determining the mathematical expectation η of the quantity y in the steady-state mode is solved. A consequence of (43), (44), and (45) is that the error is defined only by the dispersion σ^2 of the noise, and does not depend on the form of the function ψ (v). This property is a consequence of the quadratic characteristic of the object. The mathematical expectation of the deviations from the minimum (in the given case, $y_{\min} = 0$) in the steady state may be considered as a certain measure of the error in this mode. As for the duration of the transient response, its mathematical expectation may also serve as its measure. This criterion was introduced in [4].

However, another measure turns out to be simpler – not the mathematical expectation of the duration of the transient response, but the duration of the transient response for the mathematical expectation, which is not the same thing. Consider the dependence of $M[y_n]$ on n [cf. (31)]. This is a transient response in some equivalent discrete system which may be studied by the ordinary methods, for example by frequency methods, integral methods, etc. In the simple cases (cf., below), one can obtain an expression for the duration of the transient response in such equivalent systems.

If the vector γ is not fixed, but has some probability distribution $W(\gamma)$, we may then, by denoting $d\Omega_\gamma = d\gamma_1 \ldots d\gamma_m$, average the values of η over Ω_γ in accordance with the formula

$$\eta_{av}=\int\limits_{\Omega_\gamma}\eta W(\gamma)\,d\Omega_\gamma. \qquad (46)$$

It may be more advantageous for computational purposes to use (45), where the maximum expected values of the γ_i are substituted.

Example of a Simplest System (m = 1)

We illustrate the use of the formulas obtained by the example of a simple system with one input variable. We set

$$\alpha_1=\alpha,\ \alpha_{01}=\alpha_0,\ x_1=x,\ \xi_1=\xi,\ \gamma_1=$$
$$=\gamma,\ b_{11}=b,\ B_1=B,\ A_{11}=A.$$

In this case, (19) for search stability takes the form $|A| < 1$ or, in accordance with (13),

$$|A|=|1-4\alpha\alpha_0b+\alpha\gamma b|<1. \qquad (47)$$

It is clear from this that the speed γ must not go beyond certain limiting values, i.e., $\gamma_1 \leq \gamma \leq \gamma_2$, where $(\gamma_1, \gamma_2) > 0$.

Equation (45) takes the form

$$\eta=bI_{11}+\frac{b\gamma}{2}J_1+b\left(\alpha_0^2-\gamma\frac{\alpha_0}{2}+\frac{\gamma^2}{8}\right). \qquad (48)$$

The integrals I_{11} and J_1 are determined from (43) and (44), which are rewritten in the form

$$I_{11}=\alpha^2\sigma^2+(\gamma+B)^2+2A\,(\gamma+B)+A^2I_{11}, \qquad (49)$$

$$J_1=\gamma+B+AJ_1. \qquad (50)$$

Here, in accordance with the second of Eqs. (13),

$$B=-\alpha b\gamma\frac{1}{2}\left(2\alpha-\frac{\gamma}{2}\right)=\alpha b\gamma\left(\frac{\gamma}{4}-\alpha_0\right). \qquad (51)$$

From these expressions, we find that

$$J_1=\frac{\gamma+B}{1-A},\ I_{11}=\frac{\alpha^2\sigma^2+(\gamma+B)^2}{1-A^2}+2A\,\frac{(\gamma+B)^2}{(1-A)(1-A^2)} \qquad (52)$$

The transient response is determined by (31), (38), and (41), which take the following form:

$$\eta_n = bI_{11,n} + b\left(\alpha_0^2 - \frac{\gamma\alpha_0}{2} + \frac{\gamma^2}{8}\right) + \frac{b\gamma}{2} J_{1,n},$$
$$I_{11,n+1} = \alpha^2\sigma^2 + (\gamma + B)^2 + 2A(\gamma + B) J_{1,n} + A^2 I_{11,n}.$$
$$J_{1,n+1} = \gamma + B + AJ_{1,n}. \tag{53}$$

We set

$$A_0 = \alpha_0 \sqrt{\frac{b}{\sigma}}, \quad \delta = \gamma \sqrt{\frac{b}{\sigma}}, \quad k = \alpha\alpha_0 b, \quad \varepsilon = \frac{\eta}{\sigma}. \tag{54}$$

Then, after substitution of the values of I_{11} and J_1 from (49) and (50), (48) assumes the form

$$\varepsilon = \left(A_0 - \frac{\delta}{4}\right)^2 + \left(\frac{\delta}{k}\right)^2 \frac{1}{\left(4 - \frac{\delta}{A_0}\right)^2} +$$
$$+ \left(\frac{k}{A_0}\right)^2 \frac{1}{1 - \left(1 - 4k + \frac{k\delta}{A_0}\right)^2}. \tag{55}$$

We rewrite stability condition (47) in the form

$$\left|1 - 4k + k\frac{\delta}{A_0}\right| < 1.$$

$$\text{Если } j = 1 - 4k + k\frac{\delta}{A_0}, \text{ то } k\left(4 - \frac{\delta}{A_0}\right) = \tag{56}$$
$$= 1 - j = q.$$

If $j = 1 - 4k + k\frac{\delta}{A_0}$, then $k(4 - \frac{\delta}{A_0}) = 1 - j = q$.

In a stable system, $-1 < j < 1$ and $0 < q < 2$. The boundary of stability is reached for

$$K_{bo} = \frac{2}{4 - \delta/A_0} \tag{57}$$

The other boundary is obtained from the condition that $k > 0$, i.e.,

$$4 - \frac{\delta}{A_0} > 0. \tag{58}$$

Thus, the region of stability has the form shown in Fig. 2.

As an example, let us set $\delta = 0.2$. For this value, and by giving A_0, we find from (55) the minimal value $\epsilon_{\min}$ as a function of k. Let it be attained for $k = k_{opt}$ (Fig. 3). If we trace the curve $\epsilon_{\min} = \epsilon_{\min}(A_0)$ (Fig. 4a) and the curve $k_{opt} = k_{opt}(A_0)$ (Fig. 4b), we can find the minimum possible value of the steady-state error $\epsilon_{\min\min}$ and the values of the parameters A_0 and k which correspond to it. It is clear from Fig. 4 that $\epsilon_{\min\min} \approx 0.3$, $A_0 = 0.4$, and $k = 0.15$.

The optimal parameter values depend on the fact that for very large steps the error increases due to the significant deviations from the minimum; however, for very small steps the system can not compensate the effect of the "drift" γ of the characteristics, thanks to which the error again increases. One easily convinces oneself that for $\gamma = 0$, the optimal values of α and α_0 are infinitesimally small and, in the limit, the error ϵ tends to zero.

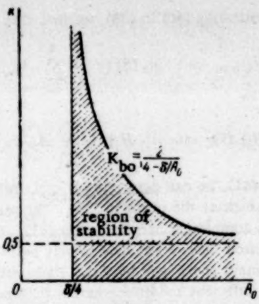

Fig. 2.

We now find the duration of the transient response where, for simplicity, we limit ourselves to the case when $\gamma = 0$. Then from (51) and (53), we find that $B = 0$ and

$$\eta_n = bI_{11,n} + b\alpha_0^2, I_{11,n+1} = \alpha^2\sigma^2 + A^2 I_{11,n}, A = 1 - 4k. \tag{59}$$

The steady-state values turn out to be

$$I_{11} = \frac{\alpha^2\sigma^2}{8k(1 - 2k)}, \quad \eta = \frac{b\alpha^2\sigma^2}{8k(1 - 2k)} + b\alpha_0^2. \tag{60}$$

Since

$$I_{11,n} = \alpha^2\sigma^2 + A^2 I_{11,n-1} = \alpha^2\sigma^2 + A^2[\alpha^2\sigma^2 + A^2 I_{11,n-2}] = \cdots$$
$$\cdots = \alpha^2\sigma^2[1 + A^2 + \cdots + A^{2(n-1)}] + A^{2n} I_{11,0} =$$
$$= \alpha^2\sigma^2 \frac{1 - A^{2n}}{1 - A^2} + A^{2n} I_{11,0} = I_{11}(1 - A^{2n}) + A^{2n} I_{11,0}, \tag{61}$$

the difference

$$\theta_n = \eta_n - \eta = b(I_{11,n} - I_{11}) = bA^{2n}(I_{11,0} - I_{11}). \tag{62}$$

It may be that at the initial moment $I_{11,0} < I_{11}$, if the initial value of x is, for example, at the origin of coordinates. However, if we assume that the system is significantly distant from the steady-state position at the initial moment of time, we can assume that $I_{11,0} - I_{11} > 0$. Then, the quantity θ_n tends to zero with increasing n, while remaining positive. We now find the discrete time n_0 after whose expiration the following relationship is valid:

$$\frac{\theta_n}{\lambda} \leqslant 1, \tag{63}$$

where the constant $\lambda \ll 1$ is some admissable threashold.

It follows from (60), (62), and (63), that

$$n_0 = \frac{1}{2} \frac{\ln \lambda (I_{11} + \alpha_0^2) - \ln (I_{11,0} - I_{11})}{\ln A} \tag{64}$$

The quantity n_0 serves as a measure of the duration of the transient response in the system.

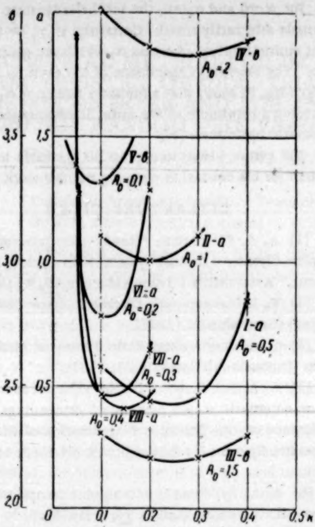

Fig. 3.

Example of a System with Two Variables (m = 2)

Let the object's equation have the form:

$$y = x_1^2 + 2\beta x_1 x_2 + x_2^2. \tag{65}$$

For $|\beta| < 1$, the unique minimum of the function y is found at the origin of coordinates. This case corresponds to m = 2, $b_{11} = b_{22} = 1$, and $b_{12} = \beta$ in the general formulas. We further set $\gamma_1 = 0$, $\alpha_1 = \alpha_2 = \alpha$, $\alpha_{01} = \alpha_{02} = \alpha_0$, $\alpha_1\alpha_{01} = \alpha_2\alpha_{02} = k$. Then, from (13), we find that

$$A_{11} = A_{22} = 1 - 4k, \quad A_{12} = A_{21} = -4\beta k. \tag{66}$$

Equation (45) takes the form:

$$\eta = I_{11} + 2\beta I_{12} + I_{22} + \alpha_0^2. \tag{67}$$

and I_{11}, I_{12}, and I_{22} are found from (43), which can be written in the following forms:

$$\begin{gathered} I_{11} 8k(1-2k) + 8\beta k(1-4k) I_{12} - 16\beta^2 k^2 I_{22} = \alpha^2\sigma^2, \\ I_{11} 4\beta k(1-4k) + 8k(1-2k-2\beta^2 k) I_{12} + I_{22} 4\beta k(1-4k) = 0 \\ -16\beta^2 k^2 I_{11} + 8\beta k(1-4k) I_{12} + I_{22} 8k(1-2k) = \alpha^2\sigma^2. \end{gathered} \tag{68}$$

In these equations, the quantities I_{11} and I_{22} enter in identical fashion, as was to be expected. We set

$$8\beta k(1-4k) = D, \quad 8k(1-2k-2\beta^2 k^2) = E. \tag{69}$$

Then, solving (68), we find that

$$I_{11} = I_{22} = \frac{\alpha^2\sigma^2 E}{E^2 - D^2}, \quad I_{12} = \frac{\alpha^2\sigma^2 D}{D^2 - E^2} \tag{70}$$

and, as follows from (67),

$$\eta = \frac{2\alpha^2\sigma^2(E - \beta D)}{E^2 - D^2} + \alpha_0^2. \tag{71}$$

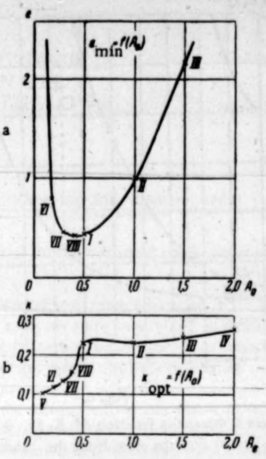

Fig. 4.

We now introduce the relative error from the random noise (for this, we assume that $\alpha_0\alpha = k$)

$$\frac{\eta - \alpha_0^2}{\left(\frac{\sigma}{\alpha_0}\right)^2} = \frac{2k^2(E - \beta D)}{E^2 - D^2} = \theta(k, \beta). \tag{72}$$

By substituting the values of E and D from (69), we find that

$$\theta(k, \beta) = \frac{k(1-2k)}{4} \times$$

$$\times \frac{1-\beta^2}{(1-2k)^2 - 4\beta^2 k(1-2k) + 4\beta^4 k^2 - \beta^2(1-4k)^2}. \tag{73}$$

We find the stability conditions from the characteristic equation $|A - E\lambda| = 0$, or

$$\begin{vmatrix} A_{11} - \lambda & A_{12} \\ A_{21} & A_{22} - \lambda \end{vmatrix} = 0. \tag{74}$$

By substituting the values of A_{ij} here, we arrive at the equation

$$(1 - 4k - \lambda)^2 - 16\beta^2 k^2 = 0, \tag{75}$$

whose roots are

$$\lambda_{1,2} = (1 - 4k) \pm 4\beta k. \tag{76}$$

The search is stable if $|\lambda_{1,2}| < 1$. It follows from this that k must be found within the limits

$$0 < k < \frac{1}{2(1 + |\beta|)}. \tag{77}$$

For a given k, the quantity β may vary within the limits

$$|\beta| < \frac{1}{2k} - 1. \tag{78}$$

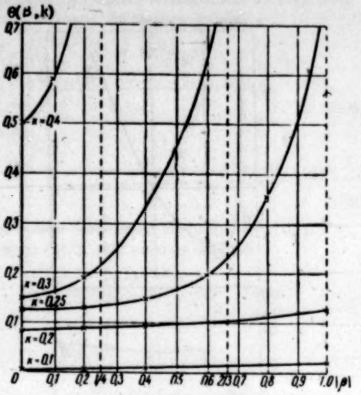

Fig. 5.

Figure 5 shows the function $\theta(\beta, k)$. It is clear from the graphs that the error from the random noise, generally speaking, increases with increasing $|\beta|$. Indeed, for $\beta = 0$ the lines y = const on the (x_1, x_2) plane are concentric circles. With increasing $|\beta|$, they become ellipses whose axes are turned by 45° with respect to the coordinate axes. The greater $|\beta|$ is, the more "elongated" these ellipses become, which worsens the conditions for minimum search and increases the steady-state error from the random noise.

For $\alpha \to 0$ and $\alpha_0 \to 0$, the total steady-state error can be made arbitrarily small. Certainly, if $\gamma_1 \neq 0$, there exist optimal values of α and α_0 which are greater than zero. The essential dependence of the error on α_0 and α (or k) (Fig. 5) shows that automatic tuning of α_0 and α, providing a minimum of the error, is advantageous in automatic optimizers [5].

The author wishes to express his gratitude to B. M. Levitan for his counsel in carrying out this work.

LITERATURE CITED

[1] A. A. Fel'dbaum, "Steady-state processes in the simplest discrete extremal systems with random noise present," Avtomatika i Telemekhanika, 20, 8 (1959).†

[2] V. I. Romanovskii, Discrete Markov Chains [in Russian] (Gostekhizdat, 1947).

[3] T. A. Sarymsakov, Basic Theory of Markov Processes [in Russian] (Gostekhizdat, 1954).

[4] A. A. Fel'dbaum, "On the effect of random factors on automatic search processes," Proceedings of the Conference on the Theory and Application of Discrete Automatic Systems [in Russian] (IAT AN SSSR, Moscow, 1958).

[5] A. A. Fel'dbaum, "An automatic optimizer," Avtomatika i Telemekhanika 19, 8 (1958). †

[6] A. A. Krasovskii, "The dynamics of continuous extremal control systems," Izvest. Akad. Nauk, OTN, Energetika i avtomatika No. 3 (1959).

---

† See English Translation

A STATISTICAL METHOD FOR DETERMINING DYNAMIC CHARACTERISTICS OF INDUSTRIAL OBJECTS IN THE PRESENCE OF NOISE AND FOR ANALYZING INFRALOW-FREQUENCY RANDOM PROCESSES

Yu. P. Leonov and L. N. Lipatov
(Moscow)

(Translated from: Avtomatika i Telemekhanika, Vol. 21, No. 2, pp. 180-190, February, 1960)
Original article submitted August 3, 1959

The paper deals with a computer for the computation of estimates of certain statistical characteristics of stationary random functions and of linear objects' characteristics.

In the experimental investigation of the dynamic characteristics of controlled industrial objects by the method of determining an object's reaction to standard stimuli, the presence of "noise" limits, to a significant extent, the accuracy of the estimates of the high-frequency characteristics.

The investigated object itself is frequently a source of "noise." In a number of cases (for example, in the chemical industry), the "noise" level is so high, and the requirements on the technological regime so rigid, that the investigation of the dynamics of such an object by means of sufficiently large standard stimuli becomes impossible.

Today, one of the methods of investigating the dynamics of industrial objects under their actual working conditions is a statistical method, based on the correlation analysis of realizations of the input and output quantities, with the condition that these quantities, as well as the investigated object's dynamic characteristics, are stationary. The basic difficulty in analyzing industrial systems by statistical methods is that these methods require a large expenditure of labor in carrying out the computational work, in particular, in computing correlation functions or spectral densities.

With the aim of decreasing the volume of computational work, special instruments for statistical analysis were developed, both in the USSR and abroad. The instruments developed can be divided into two groups on the basis of their method of recording results:

a) recording on magnetic tape,
b) recording on paper.

There are a number of special features in the technical characteristics of instruments of the first and the second type. Instruments that record on magnetic tape are superior to instruments that record on paper as regards speed of processing statistical data; but under commutation conditions, or in the presence of magnetic fields, they are surpassed by the latter in reliability and in simplicity of use. Moreover, instruments that record on magnetic tape are designed, as a rule, for the processing of comparatively high-frequency random processes. From this point of view, it might sometimes be more convenient, in investigating the dynamics of industrial objects, to use records obtained on ruled (graph) paper.

Computers of such type, developed in the USSR and the Amsler company, were constructed on mechanical principles. Multiplication and integration in these instruments are implemented mechanically with elements which complicate preparation and increase the instrument's cost. Moreover, the existing instruments which record on paper are designed for narrowly circumscribed goals, i.e., for the computing of correlation functions, while the problem of investigating the dynamics of industrial objects requires a more complete statistical analysis.

Below, we describe an instrument for the statistical investigation of the dynamic characteristics of objects in the presence of noise, and for the analysis of infralow-frequency random processes. Considered also are the possibilities of using such an instrument for estimating statistical characteristics, weight-function parameters and for the determination of objects' frequency characteristics by statistical methods.

Instrument Capabilities and Their Uses

The instrument permits an operation of the following form to be applied to the functions $x(t)$ and $y(t)$:

$$R_{yx}(\tau, T) = \frac{1}{T}\int_0^T x(t)\,y(t-\tau)\,dt. \qquad (1)$$

1. Computing Estimates of Correlation Functions and Dispersions

Expression (1) is an estimate of the cross-correlation function of the random processes $X(t)$ and $Y(t)$. Thus, the instrument allows one to obtain estimates of cross-correlation functions. This is an unbiased estimate which converges in the mean to the true correlation function as $T \to \infty$.

If one sets $X(t) = Y(t)$, then (1) gives an estimate of the autocorrelation function of the process $X(t)$ and, in particular, for $\tau = 0$ we obtain an estimate of the dispersion.

2. Computing Coefficients of Fourier Series

If it is necessary to compute the coefficients of the Fourier series for an arbitrary function $x(t)$, then one should choose, in (1), $y(t) = \cos \omega_k t$ and $\tau = 0$. For this, a realization of $x(t)$ in the given interval $(0,T)$ is written on the graph paper. The realization is reproduced in the form of a voltage on potentiometer brushes, supplied from a sine-wave generator which produced voltages of the form $\sin(2\pi k/T)$ $(k = 1,2, \ldots)$.

3. Computing Estimates of Spectral–Density Functions

If $x(t)$ is a realization of the stationary random process $X(t)$, then the value of the spectral density at the point ω_k is computed on the basis of (1)

$$M[a_k^2] = \frac{2}{T}\int_0^T R_{xx}(\tau)\cos\omega_k\tau\, d\tau + 0\left(\frac{1}{T^2}\right) \quad (2)$$

$$a_k = \frac{2}{T}\int_0^T x(t)\cos\omega_k t\, dt. \quad (3)$$

If the interval $(0,T)$ is sufficiently large, then

$$M[a_k^2] = \frac{\pi}{T}G_{xx}(\omega_k) + 0\left(\frac{1}{T^2}\right), \quad (4)$$

where $G_{xx}(\omega_k)$ is the spectral density of the random process $X(t)$.

The value of the dispersion $M[a_k^2]$ is computed approximately, starting from a finite number of realizations of the process $X(t)$.

4. Determination of Frequency Characteristics by Statistical Methods

Even with a significant noise level, statistical methods permit one to find an estimate of the frequency characteristics of an object at whose input a harmonic oscillation of known frequency and amplitude is applied. Such a method is based on the following relationships.

Let there be three signals:

$$f_1(t) = D\cos\omega t,$$

$$f_2(t) = B\sin(\omega t + \theta) + n(t)$$

and

$$f_3(t) = D\sin\omega t,$$

where $f_1(t)$ is the signal at the object's input, $f_2(t)$ is the signal at the object's output which includes the reaction $B\sin(\omega t + \theta)$ to stimulus $f_1(t)$ and the "noise" $n(t)$, with the condition that $M[n(t)] = 0$.

It is then easily verified that

$$R_{3,2}(0) = \lim_{T\to\infty}\frac{1}{T}\int_0^T f_3(t)\, f_2(t)\, dt = \frac{1}{2}BD\cos\theta, \quad (5)$$

$$R_{1,2}(0) = \lim_{T\to\infty}\frac{1}{T}\int_0^T f_1(t)\, f_2(t)\, dt = \frac{1}{2}BD\sin\theta. \quad (6)$$

On the basis of (5) and (6) we get

$$A = \frac{2}{D^2}\sqrt{R_{1,2}^2(0) + R_{3,2}^2(0)},\ \theta = \arctan\frac{R_{1,2}(0)}{R_{3,2}(0)}, \quad (7)$$

where $A = B/D$ is the value of the amplitude characteristic at frequency ω, and θ is the value of the phase characteristic at the same frequency.

It is easily seen that $R_{3,2}(0)$ and $R_{1,2}(0)$ are estimates of the correlation functions for $\tau = 0$. These estimates are increasingly accurate, the larger the time of integration T.

It is essential to mention that the computation of the integrals must be carried out for the function $f_2(t)$ for $t \geq t_1$, where t_1 is the time after which the natural motions of the system will, for all practical purposes, have ceased.

The instrument described in this paper permits one to execute the enumerated mathematical operations on the estimates of frequency characteristics. A scheme for taking off frequency characteristics by the statistical method is shown in Fig. 1.

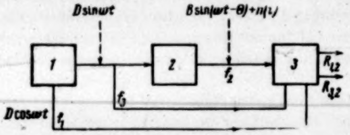

Fig. 1. 1 is a sine and cosine generator; 2 is the object; 3 is the computer.

The signal from the servosystem, which continuously reads the realization $f_2(t)$ of the random process under investigation, is applied to potentiometers which are supplied from the sine-cosine generator. The quantities thus obtained, $f_2(t)\sin\omega t$ and $f_2(t)\cos\omega t$, are applied to integrating motors. The indications of the counters on the motors' shafts correspond to the quantities $R_{3,2}(0)$ and $R_{1,2}(0)$.

5. Estimating the Parameters of Linear Objects' Weight Functions

Sometimes, to simplify a problem, one takes a rough general form of an object's transfer function; it is then necessary to determine its coefficients. As previously, we assume that there is "noise" in the object, and, consequently, we can only determine estimates of the desired parameters on the basis of recordings of the signals at the input and output of the object being investigated.

We shall consider here a method of estimating the moments of the object's weight function by means of the instrument described, for the case of objects with monotonic transient responses* (the reactions of such objects to unit disturbances are monotonic functions of time).

Industrial objects with monotonic transient responses occur quite frequently. In order to describe, in the first approximation, the weight function of such an object, one need estimate only several parameters.

---

*The method considered here can also be extended to the case of nonmonotonic transient responses.

Let $k(t)$ be the object's weight function. By the zeroth-order moment of the function $k(t)$ we mean the number

$$\alpha_0 = \int_{-\infty}^{+\infty} k(t)\,dt. \tag{8}$$

Since $\alpha_0 = \Phi(j\omega)|_{\omega=0}$, where $\Phi(j\omega)$ is the object's frequency characteristic, α_0 is then the static gain.

By the nth-order moment we mean the number

$$\alpha_n = \int_{-\infty}^{+\infty} t^n k(t)\,dt \qquad (n = 0, 1, \ldots). \tag{9}$$

For objects with monotonic transient responses, the weight function is completely determined, under sufficiently general conditions, by giving its moments. We note that for such objects the weight function obviously possesses the properties of a probability-density function, and the frequency characteristic possesses the properties of a characteristic function. For a complete analogy, we should introduce the normalized weight function

$$\bar{k}(t) = \frac{1}{\alpha_0} k(t) \tag{10}$$

and, correspondingly,

$$\bar{\alpha}_n = \int_{-\infty}^{+\infty} t^n \bar{k}(t)\,dt \qquad (n = 0, 1, 2, \ldots). \tag{11}$$

Then, the analogs of the mathematical expectation and the dispersion will be the quantities

$$\bar{\alpha}_1 = \frac{\alpha_1}{\alpha_0} \tag{12}$$

and

$$\bar{\alpha}_{20} = \frac{\alpha_2}{\alpha_0} - \left(\frac{\alpha_1}{\alpha_0}\right)^2 = \bar{\alpha}_2 - (\bar{\alpha}_1)^2. \tag{13}$$

The quantities α_0, $\bar{\alpha}_1$ and $\bar{\alpha}_{20}$ turn out to be very useful in the investigation of objects, and these quantities are frequently sufficient for the description, in a first approximation, of an object's functioning. These quantities have the following physical meanings: α_0 is the object's static gain; $\bar{\alpha}_1$ is the average lag of the transient response; $\bar{\alpha}_{20}$ characterizes the distortion of the input signal.

If the object possesses a pure lag, and does not distort the form of its input signals, its weight function then obviously has the form:

$$k(t) = \delta(t - T), \tag{14}$$

where T is the lag and $\delta(t)$ is a Dirac delta function.

Then, on the basis of (8), (11), and (13), we obtain $\alpha_0 = 1$, $\alpha_1 = \bar{\alpha}_1 = T$, and $\bar{\alpha}_{20} = 0$.

For an object with the weight function

$$k(t) = \frac{1}{T_1} e^{-(t-T)\frac{1}{T_1}} \tag{15}$$

we have

$$\alpha_0 = 1, \bar{\alpha}_1 = T + T_1 \text{ and } \bar{\alpha}_{20} = T^2 + 2TT_1 + 2T_1^2. \tag{16}$$

This weight function corresponds to an object consisting of a series connection of a pure delay link and an aperiodic link. We note that, on the basis of (16), we can easily compute the time constant T_1 and the true lag T of the object as functions of the average lag $\bar{\alpha}_1$ and of $\bar{\alpha}_{20}$.

Now, let $k(t)$ be the weight function of an object consisting of two series-connected links with weight functions $k_1(t)$ and $k_2(t)$.

Then,

$$k(t) = \int_{-\infty}^{+\infty} k_1(t - \tau) k_2(\tau)\,d\tau, \tag{17}$$

and for the transfer functions

$$\Phi(s) = \Phi_1(s)\,\Phi_2(s), \tag{18}$$

where

$$\Phi_i(s) = \int_{-\infty}^{+\infty} e^{-st} k_i(t)\,dt \qquad (i = 1, 2),$$

we have

$$\Phi(s) = \int_{-\infty}^{+\infty} \left[1 - st + \frac{s^2t^2}{2!} - \ldots +\right] k(t)\,dt = \alpha_0 - \alpha_1 s + \frac{\alpha_2 s^2}{2!} - \ldots + . \tag{19}$$

On the basis of (18) and (19) we have, by equating coefficients of like powers of s,

$$\begin{aligned} \alpha_0 &= \gamma_0\beta_0, \\ \alpha_1 &= \gamma_0\beta_1 + \gamma_1\beta_0, \\ \alpha_2 &= \gamma_0\beta_2 + 2\gamma_1\beta_1 + \gamma_2\beta_0, \end{aligned} \tag{20}$$

from which it follows that

$$\begin{aligned} \bar{\alpha}_1 &= \bar{\gamma} = \bar{\beta}_1, \\ \bar{\alpha}_{20} &= \bar{\gamma}_{20} + \bar{\beta}_{20}, \end{aligned} \tag{21}$$

where γ_n and β_n are the moments of the functions $k_1(t)$ and $k_2(t)$, and $\bar{\gamma}_n$ and $\bar{\beta}_n$ are the moments of the normalized functions $\bar{k}_1(t)$ and $\bar{k}_2(t)$ [Cf. (10)].

We now consider the expression

$$R_{yx}(t) = \int_0^T k(t)\,R_{yy}(t - \tau)\,d\tau. \tag{22}$$

We assume here that T in (22) is chosen sufficiently large. By analogy with (20), we can write

$$\begin{aligned} a_0 &= \alpha_0 b_0, \\ a_1 &= b_0\alpha_1 + b_1\alpha_0, \\ a_2 &= b_0\alpha_2 + 2b_1\alpha_1 + b_2\alpha_2, \end{aligned} \tag{23}$$

where

$$a_n = \int\limits_{-\infty}^{+\infty} \tau^n R_{yx}(\tau)\, d\tau \tag{24}$$

and

$$b_n = \int\limits_{-\infty}^{+\infty} \tau^n R_{yy}(\tau)\, d\tau = 2\int\limits_{0}^{\infty} \tau^n R_{yy}(\tau)\, d\tau \; (n = 0, 2, 4, \ldots). \tag{25}$$

Since $R_{yy}(\tau)$ is an even function, we have

$$a_1 = b_0\alpha_1,$$

$$a_3 = b_0\alpha_2 + b_2\alpha_0. \tag{26}$$

Thus, the problem of estimating the α_n reduces to estimating the moments a_n and b_n of the corresponding correlation functions, and to the solution of the system of algebraic equations (26).

The instrument considered below allows the moments a_n and b_n to be estimated. We consider the estimate of the a_n.

On the basis of (24), we can write, starting from the record of a realization on the interval $(t-T_2, t)$,

$$a_n^* = \frac{1}{T_2}\int\limits_{-b}^{a} \tau^n\, d\tau \int\limits_{t-T_2}^{t} x(u)\, y(u-\tau)\, du. \tag{27}$$

The inaccuracy of the estimate in (27) is related to two circumstances: first, the infinite limits in (24) are replaced by finite ones in (27) and, secondly, instead of the cross-correlation function $R_{yx}(\tau)$, we used its estimate, obtained by an averaging operation on the finite interval $(t-T_2, t)$.

It is necessary to bear in mind that the moment of time $\underline{t}$ in (27), at which one can begin averaging to obtain the estimate of the correlation function, must be chosen subject to the condition that $t_0 \geq T$, where T is the object's "memory" (duration of the transient response). With this, t = 0 is taken as the moment when the system begins to operate.

By reversing the order of integration in (27), we get

$$a_n^* = \frac{1}{T_2}\int\limits_{t-T_2}^{t} x(u)\, du \int\limits_{-b}^{a} (\tau)^n y(u-\tau)\, d\tau =$$

$$= \int\limits_{t-T_2}^{t} \Big[x(u)\int\limits_{0}^{a} (\tau)^n y(u-\tau)\, d\tau +$$

$$+ y(u)\int\limits_{0}^{b} (-\tau)^n x(u-\tau)\, d\tau\Big]\, du. \tag{28}$$

An estimate in the form of (28) can be computed in the following way. The realization y(t), written on one strip of paper, is read off in the form of a voltage and applied to a model, where one has chosen a system with finite memory $\underline{a}$ [with weight function $(\tau)^n$]. The voltage at the model's output is applied to a potentiometer whose moving contact is moved in accordance with the law x(t). The voltage at the potentiometer's output is applied to an integrating motor. The number of rotation of the motor gives the first term in (28); the second term is computed analogously.

The functional block diagram for the instrument which computes these estimates is shown in Fig. 2. For estimating the moments of the correlation function in (28), it is necessary to set

$$x(t) = y(t),$$

and then

$$b_n^* = \frac{2}{T_2}\int\limits_{t-T_2}^{t} y(u)\, du \int\limits_{0}^{a} \tau^n y(u-\tau)\, d\tau \; (n = 0, 2, 4, \ldots).$$

The conditions for choosing $\underline{a}$, $\underline{b}$, and $\underline{T_2}$ such that the estimates of the moments a_n and b_n will be sufficient-

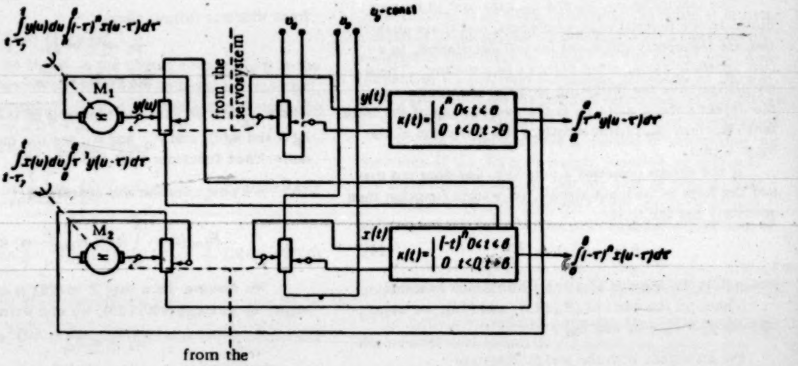
$\int_{t-T_2}^{t} y(u)du \int_0^b (-\tau)^n x(u-\tau)d\tau$
M₁
y(u)
from the servosystem
a_0
a_0
a_0-const
y(t)
$\kappa(t) = \begin{vmatrix} t^n & 0<t<a \\ 0 & t<0, t>a \end{vmatrix}$
$\int_0^a \tau^n y(u-\tau)d\tau$
$\int_{t-T_2}^{t} x(u)du \int_0^a \tau^n y(u-\tau)d\tau$
M₂
x(t)
$\kappa(t) = \begin{vmatrix} (-t)^n & 0<t<b \\ 0 & t<0, t>b \end{vmatrix}$
$\int_0^b (-\tau)^n x(u-\tau)d\tau$
from the servosystem

Fig. 2.

ly accurate are easily obtained if the functions $R_{xy}(t)$ and $R_{xx}(\tau)$ are known [1]. A more detailed discussion of the questions involved in the choice of a, b, and T_2 may be found in [5].

Description of the Instrument

The instrument's functional-block schematic is shown in Fig. 3, and its outside view is shown in Fig. 4. The instrument is constructed physically of two blocks. In the first block are mounted the servosystem (reading), the tape-handling mechanism, and the multiplication potentiometer.

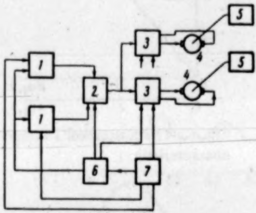

Fig. 3. 1 is a reading device (servosystem); 2 is a multiplier; 3 is a power amplifier; 4 is an integrating motor, 5 is a rotation counter; 6 is a stabilized power supply and 7 is a control panel.

The operation of the servosystem is based on the principle of tracing by a photohead along the edge of a curve drawn on the graph paper. (By the edge of a curve we mean the boundary between the black and white regions.) The photohead consists of a photoimpedance, which is the sensitive element, and a small light bulb.

The photoimpedance is placed on the front side, and the light bulb on the internal side, of the graph-paper strip. The photoimpedance is connected in one of the arms of the servosystem's bridge circuit. The bridge circuit is supplied from a transformer.

Depending on whether the illuminated area of the photoimpedance is increased or decreased, its impedance will decrease or increase, causing a signal of the proper phase to be applied to the input of the phase-sensitive amplifier, made up of twin triodes in a bridge circuit.

The servosystem is executed on the basis of programing device RU5-01 (02). The block schematic of the servosystem's mock-up was changed, permitting the instrument's dynamic characteristics to be increased, i.e., the servosystem's processing speed was increased from 12 to 100 mm/sec.

Depending on the phase of the input signal to a reversible two-phase induction motor, whose control winding is connected in the amplifier's cathode circuit and which is turned in the proper direction, the carriage on which the photohead is mounted will move so as to decrease the imbalance in the bridge circuit.

At the moment when the program's edge covers that portion of the light-sensitive layer of the photoimpedance for which the bridge circuit is balanced, the error signal will equal zero.

Synchronous motors serve as the tape-handling mechanism of the instrument. A realization is carried separately on two reels of graph paper. Reading is implemented separately by the two reading servosystems. Such a kinematic scheme allows the lag τ to be established comparatively simply and within broad limits. The

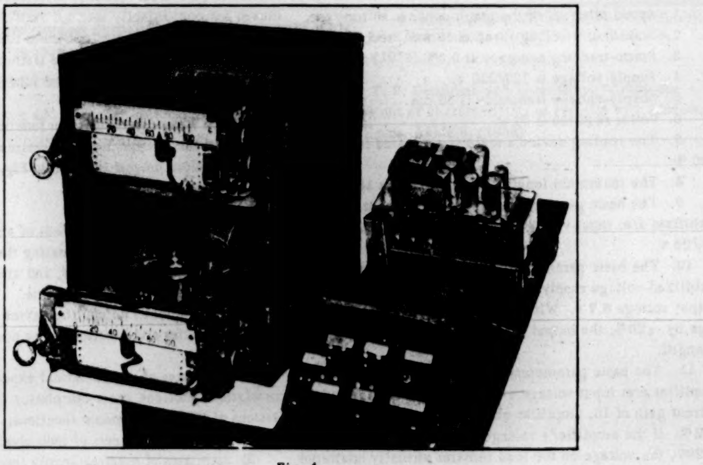

Fig. 4

speeds of the tape-handling drives are synchronized. Multiplication is affected by potentiometers, of which there are two pairs. The moving contacts of the paired potentiometers are rigidly connected to each other.

The resistance ratio of the multiplication potentiometers was designed to be 1:20, for the purpose of avoiding the distortions of their characteristics caused by the loading of one potentiometer by the other. The potentiometers are made up of bridge circuits for the compensation of the voltages corresponding to the mathematical expectations of the random functions.

In this block, the mechanism for reversing the tape-handling drives is also mounted. The second block contains:

1) two ferroresonant voltage stabilizers with two half-period rectifiers and filters;

2) two semiconductor stabilized-voltage sources based on Zener pedestal diodes, used for supplying the multiplication potentiometers;

3) two semiconductor phase-sensitive power amplifiers for controlling the integrating motors, whose inputs are the multiplication potentiometers' output circuits;

4) two integrating motors with rotation counters;

5) the control panel.

The control panel is used for starting, reversing, and stopping the instrument. Instrument stopping is also effected by limit switches on the tape-handling mechanisms. When the limit switches operate, the tape-handling mechanism and integrating motors, whose windings are shorted, are disconnected. The limit switches operate when an index from the pencil on the graph paper hits the transducer of the limit switch. Execution of the various computational tasks on the instrument is implemented by various combinations of its elements.

Technical Characteristics

1 Speed of travel of the graph paper is 15 mm/sec.

2. Maximum tracking speed is 10 mm/sec.

3. Static-tracking accuracy is 0.5%.

4. Supply voltage is 127/220 v.

5. Supply-voltage frequency is 50 cps.

6. Power required is 30 w.

7. The reading device's scale is graduated from 0 to 100 %.

8. The maximum length of graph paper is 16 m.

9. The basic parameters of the ferroresonant voltage stabilizer are: input voltage 12 v, and output voltage 22/25 v.

10. The basic parameters of the semiconductor stabilized-voltage supply are: input voltage 22 v, and output voltage 8.7 v. With variations of the input voltage by ±20%, the output voltage remains virtually unchanged.

11. The basic parameters of the phase-sensitive power amplifier are: input voltage ± 6.7 v, output voltage ± 16 v, current gain of 10, amplifier characteristic linear to within 2%. If the amplifier's voltage supply varies from -10 to 20%, the voltage on the load remains virtually unaltered.

Experimental Characteristics

Figure 5 shows the curve for the number $\underline{n}$ of rotations of the integrating motor during 30 seconds as a function of the voltages u_2 and u_1 at the inputs of the amplifier and motor respectively.

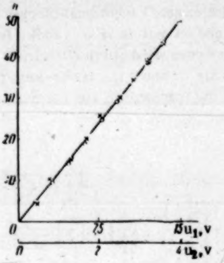

Fig. 5. The instrument's integral characteristic.

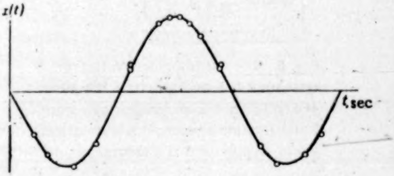

Fig. 6

Figure 6 shows the results of applying operator (1) to the function $\sin(\omega t + \theta)$, it being known that the form of this curve is invariant (as $T \to \infty$) with respect to transformation (1). Consequently, sinusoidal (or cosinusoidal) curves are conveniently used for verifying the instrument's accuracy. The small circles denote the ordinates of the curve computed by means of the instrument. As is clear, the deviation of the experimental function from the computed one does not exceed 4%.

Figure 7 shows a correlation function computed with the help of the instrument. The realization of the corresponding random process is shown in Fig. 8.

Conclusions

This work considered methods of analyzing low-frequency random processes, estimating the parameters of objects in the presence of noise, and also described an instrument for solving such problems.

The instrument's computing device permits the following quantities and functions to be computed automatically:

1) estimates of mathematical expectations, autocorrelation functions, cross-correlation functions and dispersions of stationary random functions;

2) Fourier coefficients of individual realizations;

3) estimates of spectral-density functions;

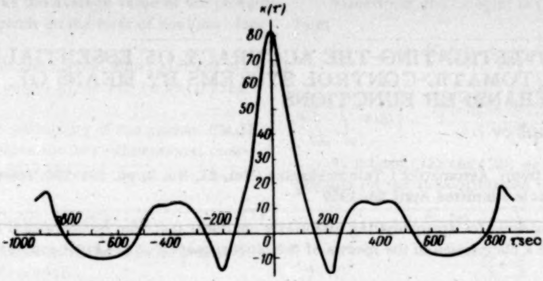

Fig. 7

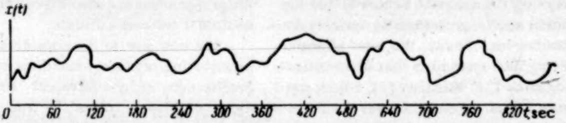

Fig. 8

4) estimates of systems' frequency characteristics;

5) estimates of weight-function moments.

The instrument developed is very simple to use, and is very reliable. These two qualities make it particularly convenient for use in the analysis of industrial objects, and also nicely distinguish it from electronic computing devices with complex circuitry and low reliability.

Among the superior features of this instrument is its capability of using realizations written on paper, since widely used industrial apparatus permits recording on paper tape.

Among the disadvantages of the instrument is the large amount of time necessary for an analysis.

LITERATURE CITED

[1] J. H. Laning and R. H. Battin, Random Processes in Automatic Control [in Russian] (IL, 1958).

[2] H. M. Paytner, Modern Computational Theories and Their Applicability [in German] (Munich, Oldenburg, 1956).

[3] V. S. Pugachev, Theory of Random Functions and Its Application to Automatic Control Problems [in Russian] (Gostekhizdat, Moscow, 1957).

[4] Yu. P. Leonov and L. N. Lipatov, "Mock-up of an instrument for the statistical investigation of the dynamic characteristics of objects in the presence of noise, and for the analysis of infra-low-frequency random processes," Joint Proceedings of the IAT AN SSSR and TsNIIKA (1958).

[5] T. P. Goodman and R. Hillsley, "Continous measurement of characteristics of systems with random input," Trans. ASME 8, (1958).

METHOD OF INVESTIGATING THE ACCURACY OF ESSENTIALLY NONLINEAR AUTOMATIC-CONTROL SYSTEMS BY MEANS OF EQUIVALENT-TRANSFER FUNCTIONS

K. A. Pupkov
(Moscow)

(Translated from: Avtomatika i Telemekhanika, Vol. 21, No. 2, pp. 191-200, February, 1960)
Original article submitted April 29, 1959

A method is considered for approximating essentially nonlinear functions by equivalent frequency characteristics on the basis of a comparison of the spectra of the random process at the input and at the output of the nonlinear element.

One of the complicated problems in automatic-control theory is that of analyzing the dynamic accuracy and the forced motions of closed nonlinear automatic systems acted on by random disturbances. Today, the most effective method for investigating such systems is that of statistical linearization, developed by I. E. Kazakov [1], which starts from the representation of inertialess nonlinear elements by constant equivalent coefficients. This coefficient is most simply defined by one or another of two assumptions and, with this, two values are obtained for the coefficient.

Definition of the coefficient by the condition that the dispersions at the output of the true nonlinear element and of the equivalent linear one be equal leads to the expression

$$k_1^{(1)} = \frac{\sigma_y}{\sigma_x}, \tag{1}$$

where σ_x is the mean-square deviation of the random function at the input of the nonlinear element and σ_y is the mean-square deviation at its output.

The definition of the coefficient starting from the requirement that the mean-square difference between the true and the approximating random functions be a minimum leads to an expression of the form

$$k_1^{(2)} = \frac{R_{yx}(\tau v)}{\sigma_x^2}, \tag{2}$$

where $R_{yx}(\tau)$ is the cross-correlation function of the random processes at the nonlinear element's input and output.

In both cases, the nonlinear element's transfer factor by average value is defined as the ratio of the mathematical expectations at the output and input of this element:

$$k_0 = \frac{m_y}{m_x}, \tag{3}$$

where m_x and m_y are the mathematical expectations of the random processes at the nonlinear element's input and output respectively.

Approximation by the coefficients in (1) and (2) gives good results with the condition that a narrow-band filter stands beyond the nonlinear element. These coefficients are conveniently used only in the analysis of the operational accuracy of simple automatic-control systems which do not contain complicated filters in their structure since, in this case, the representation of the true spectral content of the random process in the nonlinear system is lost. This latter circumstance also makes the synthesis of optimal nonlinear systems difficult.

We turn now to the consideration of a method of approximating nonlinear functions by equivalent frequency coefficients, or by equivalent "transfer" functions, which more completely mirror the true outlines of the random process's passage through the nonlinearity.

This method allows one to compute, with as great an accuracy as desired, the dispersion of any coordinate of a nonlinear system, and opens up a path for the synthesis of optimal filters.

An equivalent frequency-transfer factor for a nonlinear element is defined as the square root of the ratio of the spectral densities of the random process at the input and output:

$$K(\omega, \sigma_x, m_x) = \sqrt{\frac{S_{\text{out}}(\omega)}{S_{\text{in}}(\omega)}}, \tag{4}$$

where $S_{\text{in}}(\omega)$ is the spectral density of the random process at the nonlinear element's input, and $S_{\text{out}}(\omega)$ is that at its output.

Naturally, $K(\omega, \sigma_x, m_x)$ is also a function of σ_x and m_x, and depends on the type of nonlinear characteristic.

For the determination of the frequency characteristic, it is necessary to know the spectral density of the process at the output. We assume that we know the two-dimensional-distribution law and the correlation function of the random process at the input of the nonlinear element, where the distribution law is a normal one.

For a stationary random process, the correlation function (the autocorrelation function) is defined by the expression

$$R_x(\tau) = \int_{-\infty}^{\infty} \int_{-\infty}^{\infty} x_1 - m\ )(x_2 - m_x) W_2(x_1\ x_2, \tau)\, dx_1, dx_2,$$

where $W_2(x_1, x_2, \tau)$ is the random process's two-dimensional probability density.

We now consider the nonlinear functional dependency

$$y = f(x). \tag{6}$$

The autocorrelation function $R_y(\tau)$ at the nonlinear element's output will be the average value of the product $y(t)y(t+\tau)$, which depends on the form of nonlinear function (6).

If the values of the input signal equal $x(t)$ and $x(t+\tau)$, then the values of the output signal will be $f[x(t)]$ and $f[x(t+\tau)]$.

Consequently, the probability of the product $f[x(t)]\, f[x(t+\tau)]$ will determine the two-dimensional probability density $W_2(x_1, x_2, \tau)$.

The mean value

$$M\{f[x(t)]\, f[x(t+\tau)]\} \tag{7}$$

is the autocorrelation function of the random process at the nonlinear element's output.

Expression (7) can be written in the alternative form

$$R_y(\tau) = \int_{-\infty}^{\infty}\int_{-\infty}^{\infty} f(x_1)\, f(x_2)\, W_2(x_1, x_2, \tau)\, dx_1\, dx_2, \tag{8}$$

where

$$x_1 = x(t), \quad x_2 = x(t+\tau).$$

In (8), the random process is taken to have zero mean value.

For the computation of the integral in (8), we approximate the nonlinear function of (6) by rectilinear segments and, for $W_2(x_1, x_2, \tau)$, we use Cramer's expansion by terms of orthogonal Hermite polynomials [2].

The Cramer expansion has the form:

$$\frac{1}{\sqrt{1-\rho^2}} \exp\left[-\frac{\rho^2 x_1^2 + \rho^2 x_2^2 - 2\rho x_1 x_2}{2(1-\rho^2)}\right] = \sum_{\nu=0}^{\infty} \frac{H_\nu(x_1)\, H_\nu(x_2)}{\nu!}\rho^\nu, \tag{9}$$

where $\rho = \frac{R(\tau)}{R(0)}$ is the normalized autocorrelation function, and $H_\nu(x)$ ($\nu = 1, 2, 3, \ldots$) are orthogonal Hermite polynomials.

For the two-dimensional normal probability-density function, we get

$$\frac{1}{2\pi\sqrt{1-\rho^2}} \exp\left[-\frac{\rho^2 x_1^2 + \rho^2 x_2^2 - 2\rho x_1 x_2}{2(1-\rho^2)}\right] \times \exp\left[-\frac{x_1^2 + x_2^2}{2}\right] = \exp\left[-\frac{x_1^2 + x_2^2}{2}\right] \sum_{\nu=0}^{\infty} \frac{H_\nu(x_1)\, H_\nu(x_2)}{2\pi\nu!}\rho^\nu \tag{10}$$

or

$$\frac{1}{2\pi\sqrt{1-\rho^2}} \exp\left[-\frac{x_1^2 + x_2^2 - 2\rho x_1 x_2}{2(1-\rho^2)}\right] = \exp\left[-\frac{x_1^2 + x_2^2}{2}\right] \sum_{\nu=0}^{\infty} \frac{H_\nu(x_1)\, H_\nu(x_2)}{2\pi\nu!}\rho^\nu. \tag{11}$$

We now normalize the random variable $\underline{x}$ with respect to the mean square value σ, i.e., we set $\xi_1 = x_1/\sigma_1$ and $\xi_2 = x_2/\sigma_2$.

In the sequel, we can take $\sigma_1 = \sigma_2 = \sigma$, since the random process is stationary.

Sometimes, the integral in (8) can be written in the form

$$R_y(\tau) = \frac{1}{2\pi\sqrt{1-\rho^2}} \times \int_{-\infty}^{\infty}\int_{-\infty}^{\infty} \exp\left[-\frac{\xi_1^2 + \xi_2^2 - 2\rho\xi_1\xi_2}{2(1-\rho^2)}\right] f(\sigma\xi_1)\, f(\sigma\xi_2)\, d\xi_1 d\xi_2. \tag{12}$$

By joining (11) and (12), we obtain the following expression for the autocorrelation function:

$$R_y(\tau) = \frac{1}{2\pi\nu!} \sum_{\nu=0}^{\infty} \rho^\nu \times \int_{-\infty}^{\infty}\int_{-\infty}^{\infty} f(\sigma\xi_1)\, f(\sigma\xi_2)\, e^{-\frac{\xi_1^2+\xi_2^2}{2}} H_\nu(\xi_1)\, H_\nu(\xi_2)\, d\xi_1\, d\xi_2. \tag{13}$$

The double integral in (13) decomposes into the product of two simple ones. Then (13) may be given in the form:

$$R_y(\tau) = \sum_{\nu=0}^{\infty} a_\nu^2 \rho^\nu, \tag{14}$$

where

$$a_\nu = \frac{1}{\sqrt{2\pi\nu!}} \int_{-\infty}^{\infty} f(\sigma\xi)\, H_\nu(\xi)\, e^{-\frac{\xi^2}{2}}\, d\xi. \tag{15}$$

The orthogonal Hermite polynomials are defined by the relationship

$$\left(\frac{d}{d\xi}\right)^\nu e^{-\frac{\xi^2}{2}} = (-1)^\nu H_\nu e^{-\frac{\xi^2}{2}} \tag{16}$$

and equal, for various values of ν, respectively:.

$$\begin{gathered} H_0(\xi) = 1, \; H_1(\xi) = \xi, \; H_2(\xi) = \xi^2 - 1, \\ H_3(\xi) = \xi^3 - 3\xi, \; H_4(\xi) = \xi^4 - 6\xi^2 + 3, \\ H_5(\xi) = \xi^5 - 10\xi^3 - 15\xi. \end{gathered} \tag{17}$$

Thus, the autocorrelation function at the nonlinear element's output can be determined by computing the series in (14). This series is absolutely convergent, since $\rho(\tau)$ is a bounded function, and the coefficients a_ν decrease at the rate $1/\nu$:.

If the nonlinear device's characteristic is an antisymmetric function, then (14) contains only odd terms of the expansion

$$R_y(\tau) = a_1^2\rho + a_3^2\rho^3 + a_5^2\rho^5 + \cdots \tag{18}$$

If this function is odd, but not symmetric, then all the terms of the series are retained. With this, the coefficient a_0^2 equals the square of the mean value at the output which results from the lack of symmetry.

In this case, the autocorrelation function for the centered random process will be defined by

$$R_y^0(\tau) = \sum_{\nu=1}^{\infty} a_\nu^2 \rho^\nu. \tag{19}$$

From a known autocorrelation function, we obtain the spectral density by a Fourier transformation.

We may now turn to the definition of the equivalent frequency transfer factor. For the determination of this coefficient, it turns out that it suffices to know the a_ν and the spectral densities of the powers of the autocorrelation function at the nonlinear element's input.

Then, by the definition of (4), $K(\omega, \sigma_x, m_x)$ will have the form:

$$K(\omega, \sigma_x \; m_x) = \frac{1}{\sigma} \sqrt{\sum_{\nu=1}^{\infty} a_\nu^2 b_\nu}, \qquad (20)$$

where

$$b_\nu = \frac{S^\nu(\omega)}{S_{\text{in}}(\omega)}, \quad S^\nu(\omega) \div \rho^\nu(\tau).$$

For example, for correlation functions and spectral densities of the form

$$\rho_x(\tau) = e^{-\beta|\tau|}, \quad S_x(\omega) = \frac{2\beta}{\omega^2 + \beta^2} \qquad (21)$$

the coefficients b_ν equal:

$$\begin{aligned} b_1 &= 1, \\ b_2 &= 2\frac{\omega^2 + \beta^2}{\omega^2 + 4\beta^2} \\ b_3 &= 3\cdot\frac{\omega^2 + \beta^2}{\omega^2 + 9\beta^2}, \\ b_4 &= 4\frac{\omega^2 + \beta^2}{\omega^2 + 16\beta^2}, \\ b_5 &= 5\frac{\omega^2 + \beta^2}{\omega^2 + 25\beta^2}, \\ &\ldots\ldots\ldots\ldots \end{aligned} \qquad (22)$$

In this case, the transfer coefficient equals

$$K(\omega, \sigma_x, m_x) =$$

$$= \frac{1}{\sigma_x}\sqrt{a_1^2 + 2a_2^2\frac{\omega^2 + \beta^2}{\omega^2 + 4\beta^2} + 3a_3^2\frac{\omega^2 + \beta^2}{\omega^2 + 9\beta^2} + \cdots} \qquad (23)$$

In accordance with (14), the coefficients a_ν^2 are proportional to the dispersions, and may be computed for the standard essential nonlinearities.

In the given case, the transfer factor by mean value is defined by the expression

$$k_0(m_x, \sigma_x) = \frac{km_x - a_0}{m_x}, \qquad (24)$$

where k is the slope of the nonlinear characteristic at the working point.

We now consider (20) in more detail. If we assume that the spectral densities at the nonlinear element's input and output have the same form, then the coefficients $b_\nu = 1$. As a result, we get the transfer coefficient

$$K(\sigma_x, m_x) = \frac{1}{\sigma_x}\sqrt{\sum_{\nu=1}^{\infty} a_\nu^2} \equiv k_1^{(1)}, \qquad (25)$$

which corresponds to equivalent transfer factor (1), computed by the first approximation method, since

$$\sum_{\nu=1}^{\infty} a_\nu^2 = \sigma_y^2.$$

If we take only the first term of the series, we obtain the transfer factor

$$K(\sigma_x, m_x) = \frac{a_1}{\sigma_x} \equiv k_1^{(2)}, \qquad (26)$$

which corresponds to the equivalent coefficient in (2), computed by the second approximation method.

If we neglect all the coefficients a_ν except a_1, this means physically that we are not taking into account the components of the random process due to the nonlinear transformation.

Thus, (25) and (26) serve as the mathematical bases for the two methods of statistical linearization of nonlinear functions.

We now turn to the consideration of the equivalent "transfer" function for a nonlinear element. Taking into consideration that the equivalent frequency-transfer factor is taken as the ratio of spectral densities, which are even functions of frequency, we present it in the form of a product of complex conjugate factors:

$$K^*(j\omega, \sigma_x, m_x)K(j\omega, \sigma_x, m_x) = K^2(\omega, \sigma_x, m_x). \qquad (27)$$

By choosing the zeroes and poles in the upper half of the complex plane, we obtain the following expression for the equivalent "transfer" function:

$$K(j\omega, \sigma_x, m_x) = k_{\text{st}}\frac{(T_1 j\omega + 1)(T_3 j\omega + 1)\ldots}{(T_2 j\omega + 1)(T_4 j\omega + 1)\ldots}, \qquad (28)$$

where the value of

$$k_{\text{st}} = \frac{1}{\sigma_x}\sqrt{a_1^2 + \frac{1}{2}a_2^2 + \frac{1}{3}a_3^2 + \cdots} \qquad (29)$$

is found from (23) for $\omega = 0$; T_1, T_2, T_3,... are time constants, and are functions of the coefficients a_ν, and of the form of the spectral density at the input, for which $T_1 > T_2$, $T_3 > T_4$, etc.

The coefficient in (29) has a value lying between the values of the coefficients in (25) and (26), and can give as accurate a value as desired for the computation of the dispersion in a nonlinear system.

However, this fact holds in the case when, at the input of the nonlinear element, there acts a random process with a spectral density in the form of "white" noise, or with a frequency band which exceeds the pass band of the linear filter which follows the nonlinearity. In all other cases, it is desirable, in analyzing dynamic accuracy, to use the equivalent "transfer" function of (28).

Since (20), (28), and (29) have been obtained in the form of series, it suffices for practical computations to limit oneself to five, and sometimes even three, terms of the expansion.

It is obvious that, both for the computation of equivalent transfer factors and for the determination of the equivalent "transfer" function, it is necessary to know the coefficients a_ν, defined by the integral in (15). These coefficients are functions of the dispersion of the input random process, and depend on the form of the nonlinear function.

The computational formulas for the a_ν may be given for any nonlinear characteristic.

Let us consider the methodology of computing the a_ν. In (15) the nonlinear function $f(\sigma\,\xi)$ enters, complicating the computation of the integral, so that we approximate this function by rectilinear segments. Then, the integral of (15) may be easily computed by using tables of the incomplete gamma function and of the χ^2 probability function [3].

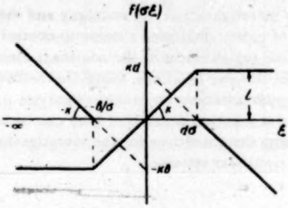

Fig. 1.

We illustrate this methodology by an example. We take a nonlinearity of the limitation type, as shown in Fig. 1, and write the general expression for the a_ν, which has the form:

$$a_\nu = \frac{k\sigma}{\sqrt{2\pi\nu!}} \int_{0^\bullet}^{\infty} \xi H_\nu(\xi)\, e^{-\frac{\xi^2}{2}}\, d\xi +$$

$$+ \frac{k}{\sqrt{2\pi\nu!}} \int_{\frac{d}{\sigma}}^{\infty} (d - \sigma\xi) H_\nu(\xi)\, e^{-\frac{\xi^2}{2}}\, d\xi +$$

$$+ \frac{k\sigma}{\sqrt{2\pi\nu!}} \int_{-\infty}^{\nu} \xi H_\nu(\xi)\, e^{-\frac{\xi^2}{2}} d\xi +$$

$$+ \frac{k}{\sqrt{2\pi\nu!}} \int_{-\infty}^{-\frac{b}{\sigma}} (-b - \sigma\xi)\, H_\nu(\xi)\, e^{-\frac{\xi^2}{2}}\, d\xi. \qquad (30)$$

In the integrands of (30) there appear powers of the variable which depend on the order of the polynomials in (16).

These integrals may be reduced to the tabulated ones:

$$\int_0^{\chi} \xi^n e^{-\frac{\xi^2}{2}}\, d\xi = \sqrt{2}^{\,n-1}\left(\frac{n-1}{2}\right)!\,[1 - P(\chi^2,\ n+1)] \qquad (31)$$

or

$$\frac{1}{2^{\frac{n-2}{2}}\,\Gamma\left(\frac{n}{2}\right)} \int_{\chi}^{\infty} \xi^{n-1} e^{-\frac{\xi^2}{2}}\, d\xi = P(\chi^2,\ n). \qquad (32)$$

The function $P(\chi^2, n)$ is a function of two arguments for which tables have been computed (Cf. [2]).

In the given case, the quantity χ is defined as

$$\chi = \frac{d}{\sigma}, \qquad (33)$$

where

$$d = h \pm m_x.$$

For the nonlinear characteristic shown in Fig. 1,

$$\chi_1 = \frac{h - m_x}{\sigma_x} = \frac{d}{\sigma_x},$$

$$\chi_2 = \frac{-h - m_x}{\sigma_x} = -\frac{b}{\sigma_x}.$$

Then,

$$a_0 = L\left\{\frac{1}{2}\left[\left|\frac{h-m}{h}\right| P(\chi_1^2,\ 1) - \frac{h+m}{h} P(\chi_2^2,\ 1)\right] + \right.$$
$$\left. + \frac{1}{\sqrt{2\pi}}\frac{\sigma}{h}\left[-P(\chi_1^2,\ 2) + P(\chi_2^2,\ 2)\right]\right\},$$

$$a_1 = L\left\{\frac{\sigma}{h}\left[1 - \frac{1}{2}\left(P(\chi_1^2,\ 3) + P(\chi_2^2,\ 3)\right)\right] + \right. \qquad (34)$$
$$+ \frac{1}{\sqrt{2\pi}}\frac{m}{h}\left[P(\chi_2^2,\ 2) - P(\chi_1^2,\ 2)\right] +$$
$$\left. + \frac{1}{\sqrt{2\pi}}\left[P(\chi_1^2,\ 2) + P(\chi_2^2,\ 2)\right]\right\}$$

etc.

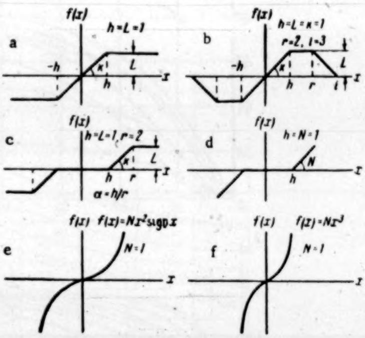

Fig. 2.

Using (34), set up for the nonlinear characteristics shown in Fig. 2, we have calculated and constructed the graphs for the normalized coefficients $a_{n\nu}$ which are given in the Appendix in Figs. 3-28. The parameter m on the graphs has the scale of the quantity x/σ.

In computing the coefficients a_ν from these graphs, it is necessary to take the following relationships into account:

1) for nonlinearities of the limitation type (Fig. 2,a and b),

$$a_\nu = a_{n\nu} L$$

2) for dead zones with limitations (Fig. 2, c),

$$a_\nu = a_{n\nu}\frac{L}{1-\alpha}, \qquad \alpha = \frac{h}{r},$$

3) for dead zones, cubic parabolas and antisymmetric quadratic parabolas (Fig. 2,d,e and f),

$$a_\nu = a_{n\nu} N$$

Example. In conclusion, we give the example of the determination of the equivalent "transfer" function for a nonlinearity of the cubic-parabola type of Fig. 2,f.

Let.

$$N=1, \quad S_{\text{in}}(\omega)=\frac{2\beta}{\omega^2+\beta^2}, \quad \sigma_x=1{,}5, \quad \beta=10, \tag{35}$$

$$K(j\omega,\sigma_x,m_x)=\frac{1}{\sigma_x}\sqrt{a_1^2+\frac{a_3^2}{3}}\;\frac{\sqrt{\dfrac{a_1^2+3a_3^2}{3\beta^2(3a_1^2+a_3^2)}}\,j\omega+1}{\dfrac{1}{3\beta}\,j\omega+1}$$

or

$$K(s,\sigma_x,m_x)=k_{\text{st}}\,\frac{T_1s+1}{T_2s+1}, \qquad s=j\omega,$$

where

$$K_{\text{st}}=\frac{1}{\sigma_x}\sqrt{a_1^2+\frac{a_3^2}{3}}=2{,}25\sqrt{11},$$

$$T_1=\sqrt{\frac{a_1^2+3a_3^2}{3\beta^2(3a_1^2+a_3^2)}}=0{,}1\sqrt{\frac{3}{11}}.$$

$$T_2=\frac{1}{3\beta}=\frac{1}{30}.$$

Then,

$$K(s,\sigma_x,m_x)=7{,}5\,\frac{0{,}0524s+1}{0.0333\,s+1}. \tag{36}$$

The investigation of the accuracy and the forced motions of closed nonlinear automatic-control systems leads to the replacement of the nonlinear elements by equivalent transfer functions, using the method of successive approximations for graphicoanalytic methods. The transfer function considered here can be used for determining the conditions for the investigation of stability of nonlinear systems.

APPENDIX

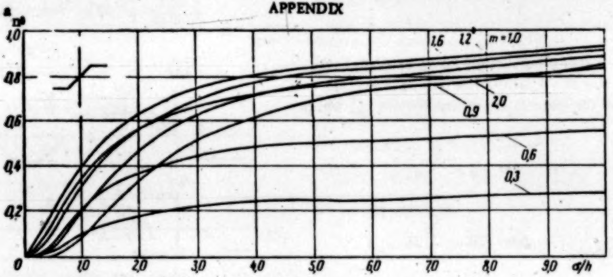

Fig. 3.

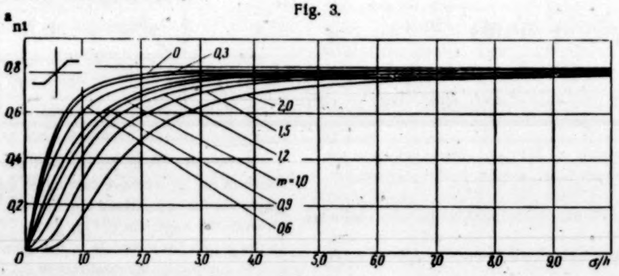

Fig. 4.

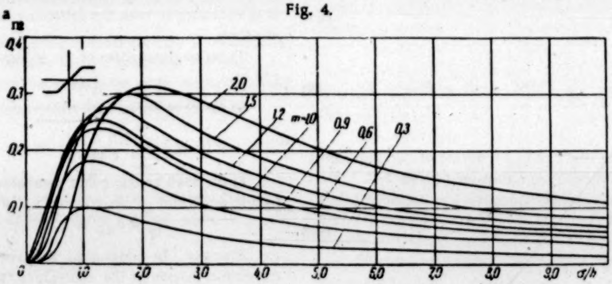

Fig. 5.

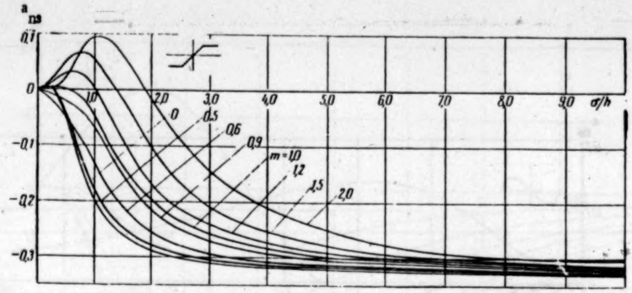

Fig. 6.

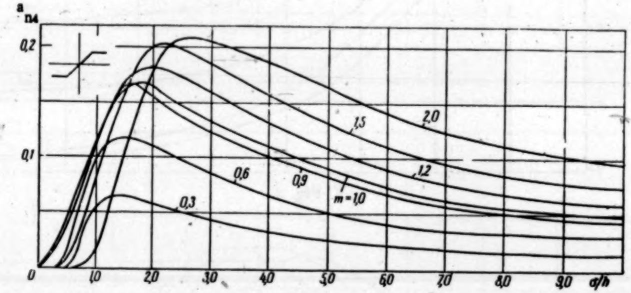

Fig. 7.

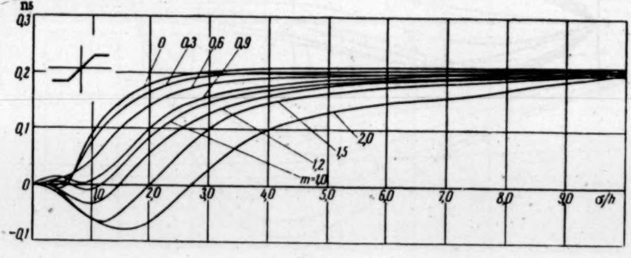

Fig. 8.

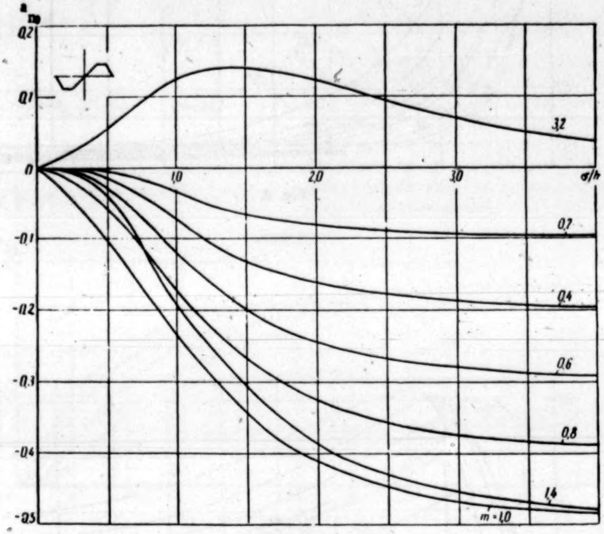
a
n0
0,2
0,1
0
-0,1
-0,2
-0,3
-0,4
-0,5
1,0
2,0
3,0
σ/h
3,2
0,2
0,4
0,6
0,8
1,4
m=1,0

Fig. 9.

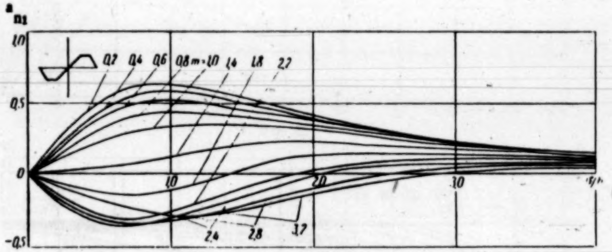
a
n1
1,0
0,5
0
-0,5
1,0
2,0
3,0
σ/h
0,2
0,4
0,6
0,8
m=1,0
1,4
1,8
2,2
2,4
2,8
3,2

Fig. 10.

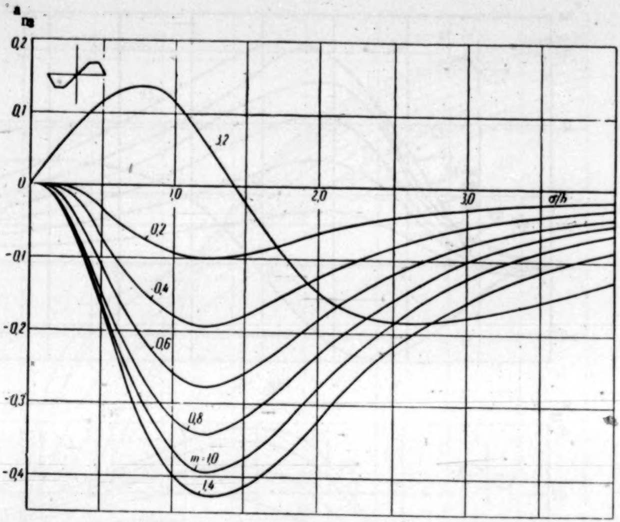

a_{ns}
0,2
0,1
0
-0,1
-0,2
-0,3
-0,4
1,0
2,0
3,0
σ/h
3,2
0,2
0,4
0,6
0,8
m=1,0
1,4

Fig. 11.

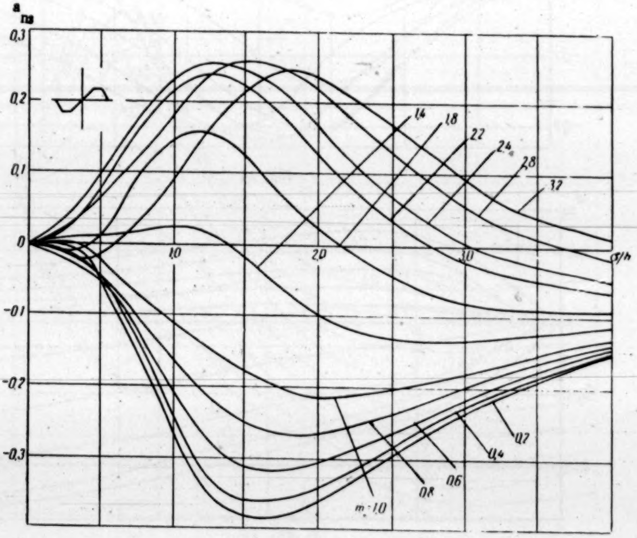

a_{ns}
0,3
0,2
0,1
0
-0,1
-0,2
-0,3
1,0
2,0
3,0
σ/h
1,4
1,8
2,2
2,4
2,8
3,2
0,7
0,4
0,6
0,8
m=1,0

Fig. 12.

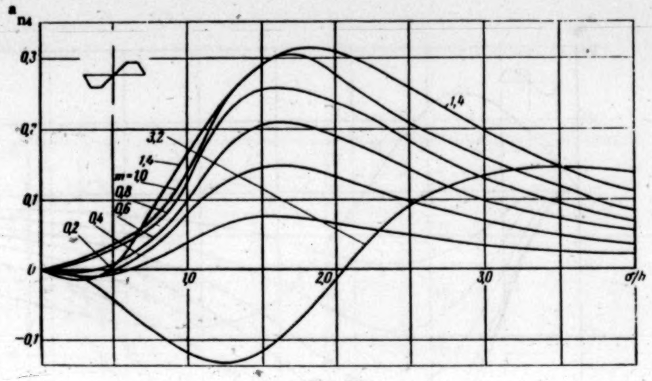

Fig. 13.

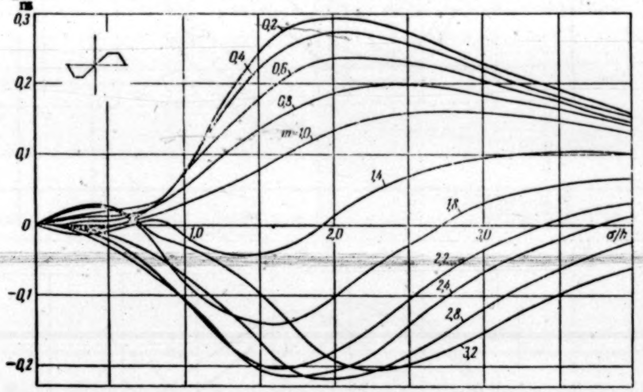

Fig. 14

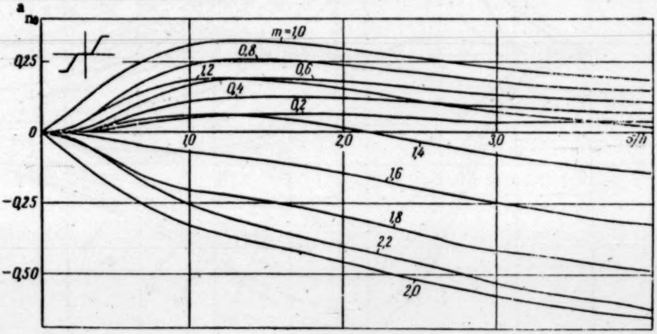

Fig. 15

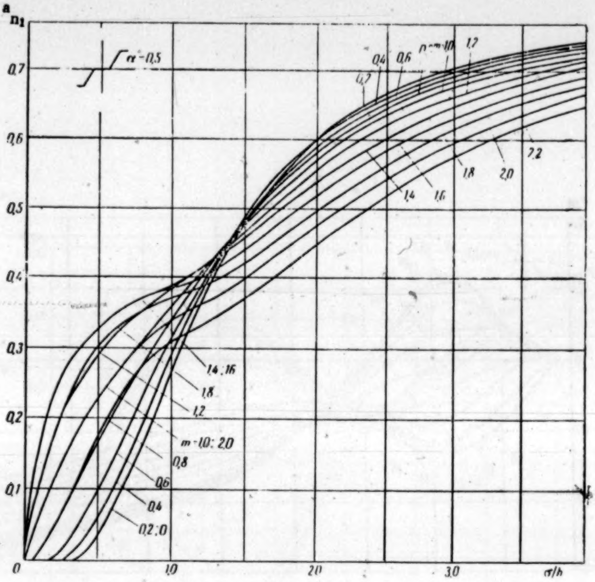
a_{n1}
α=0,5
0,7
0,6
0,5
0,4
0,3
0,2
0,1
0
1,0
2,0
3,0
σ/h
0,2
0,4
0,6
m=1,0
1,2
1,4
1,6
1,8
2,0
2,2
1,4; 1,6
1,8
1,2
m=1,0; 2,0
0,8
0,6
0,4
0,2; 0

Fig. 16

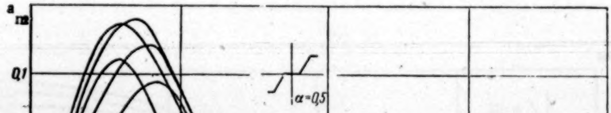
a_{n2}
0,1
0
-0,1
-0,2
1,0
2,0
3,0
σ/h
α=0,5
0,2
0,4
0,6
0,8
m=1,0
1,2
1,4
1,6
1,8
2,0
2,2

Fig. 17

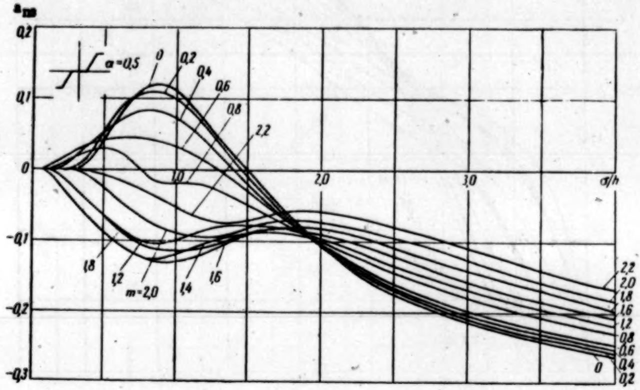

a m3
0,2
0,1
0
-0,1
-0,2
-0,3
α = 0,5
0
0,2
0,4
0,6
0,8
2,2
1,0
2,0
3,0
σ/h
1,8
1,2
m = 2,0
1,4
1,6
2,2
2,0
1,8
1,6
1,2
0,8
0,6
0
0,4
0,2

Fig. 18

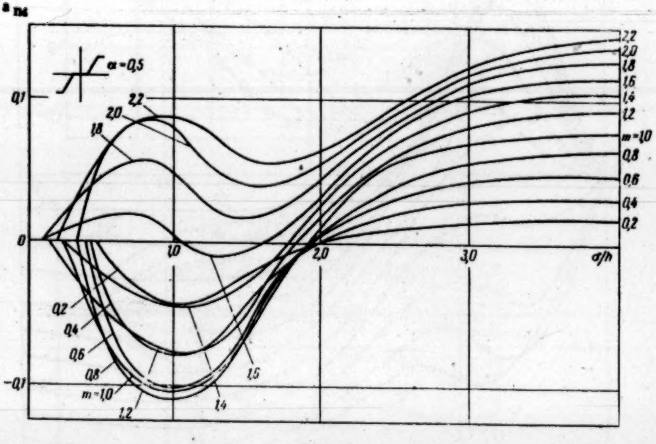

a m4
0,1
0
-0,1
α = 0,5
2,2
2,0
1,8
1,6
1,4
1,2
m = 1,0
0,8
0,6
0,4
0,2
2,0
2,2
1,8
1,0
2,0
3,0
σ/h
0,2
0,4
0,6
0,8
m = 1,0
1,2
1,4
1,6

Fig. 19

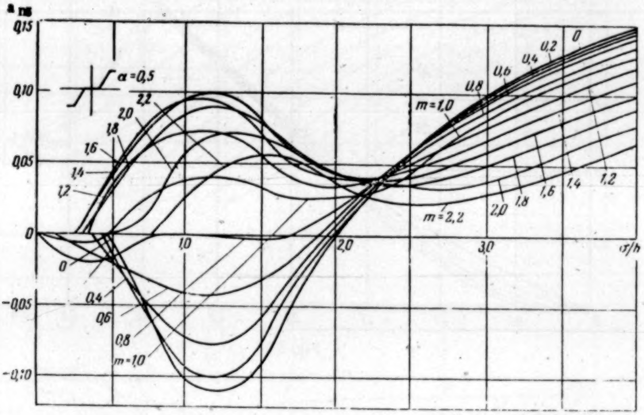

a ns
0,15
0,10
0,05
0
-0,05
-0,10
1,0
2,0
3,0
σ/h
α = 0,5
2,2
2,0
1,8
1,6
1,4
1,2
0
0,4
0,6
0,8
m = 1,0
0,2
0,4
0,6
0,8
m = 1,0
m = 2,2
2,0
1,8
1,6
1,4
1,2

Fig. 20

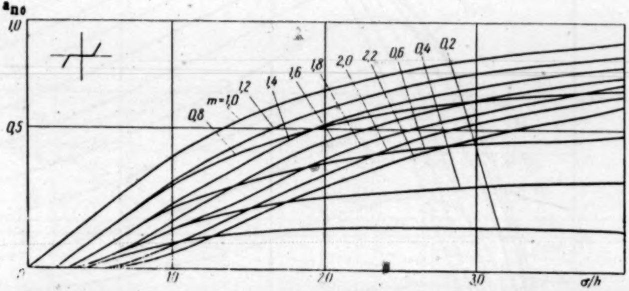

a no
1,0
0,5
0
1,0
2,0
3,0
σ/h
m = 1,0
0,8
1,2
1,4
1,6
1,8
2,0
2,2
0,6
0,4
0,2

Fig. 21

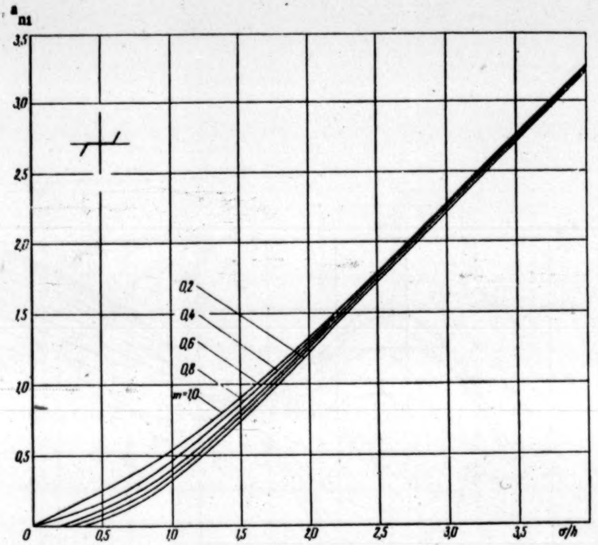

a n1
3,5
3,0
2,5
2,0
1,5
1,0
0,5
0
0,5
1,0
1,5
2,0
2,5
3,0
3,5
σ/h
0,2
0,4
0,6
0,8
m=1,0

Fig. 22

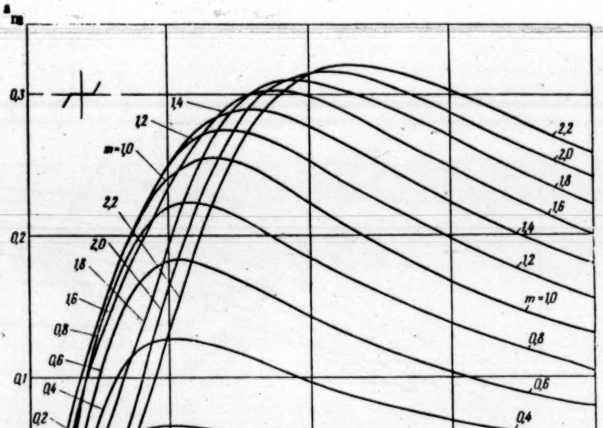

a n2
0,3
0,2
0,1
0
1,0
2,0
3,0
σ/h
1,4
1,2
m=1,0
2,2
2,0
1,8
1,6
0,8
0,6
0,4
0,2
2,2
2,0
1,8
1,6
1,4
1,2
m=1,0
0,8
0,6
0,4
0,2

Fig. 23

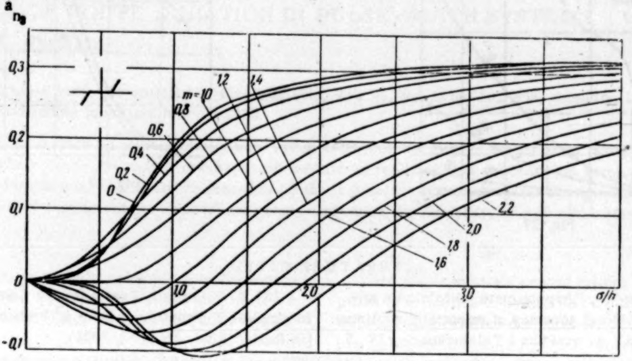

Fig. 24

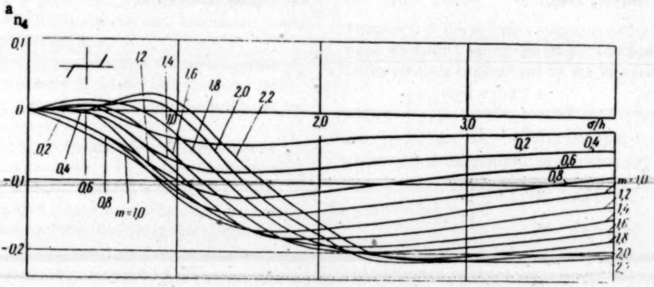

Fig. 25

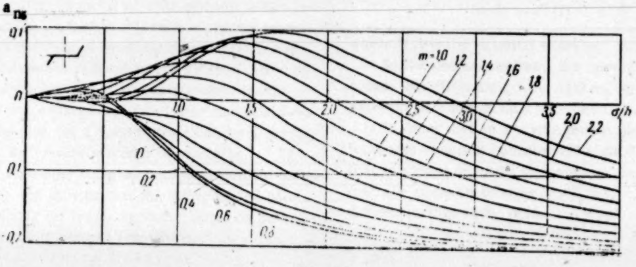

Fig. 26

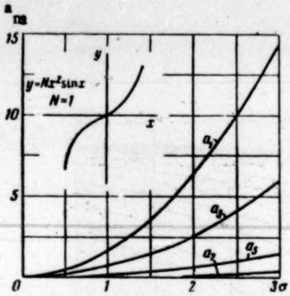

Fig. 27

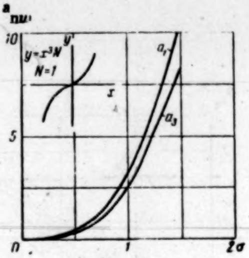

Fig. 28

LITERATURE CITED

[1] I. E. Kazakov, "Approximate probabilistic analysis of the operational accuracy of essentially nonlinear automatic systems," Avtomatika i Telemekhanika **17**, 5 (1956). *

[2] H. Cramer, Mathematical Methods of Statistics [Russian translation] (IL, 1948).

[3] E. E. Slutskii, Tables for the Computation of the Incomplete Γ-Function and the χ^2 Probability Function [in Russian] (Izd. AN SSSR, 1950).

---

* See English translation.

PROCESSES OF FINITE DURATION IN PULSE-WIDTH SYSTEMS

I. V. Pyshkin

(Moscow)

(Translated from: Avtomatika i Telemekhanika, Vol. 21, No. 2, pp. 201-208, February, 1960)
Original article submitted July 18, 1959

Equations are derived for pulse-width systems which determine the form of the transient responses which terminate in a finite time. For second-order systems, methods of realizing such processes are given. It is suggested that the complicated nonlinearities necessary for the realization of such processes be replaced by linear elements. Results of experiments on a model are given, confirming the possibility of such replacements.

Today, much attention is being given to those optimal processes which terminate in a finite and, moreover, a minimal interval of time. In particular, such types of processes may be realized in relay and in pulse systems.

The duration of such a transient response is determined by the order of the differential equation of the system's continuous portion [1, 2]. Finite-duration processes in pulse-amplitude systems with amplitude limitations were considered in [3, 4].

The present work is devoted to the investigation of finite-duration processes in pulse-width systems, where the pulse height is given, and the duration is limited by the repetition interval.

In order that the transient response terminate at some point of discrete time, t = *l* T, it is necessary that, at this moment, the error quantity and its first (n-1) derivatives, inclusive, equal zero, where n is the order of the differential equation describing the system's continuous portion. These conditions may be satisfied by the proper choice of the n durations of the pulses which act on the system up to the moment of time t = *l* T($l \geq n$). Thus, with a limited external stimulus, the transient response can terminate after n cycles of the pulsed (sampled-data) element, just as in sampled-data systems with amplitude modulation. We shall call such a process an n-cycle one. The problem of investigating a transient response of finite duration reduces to the determination of the form of this process and of its realization. In this work we derive the equations which define the indicators of such a process and, for a system described by a second-order equation, we present methods of realizing it. Experiments on a type MN-7 analog computer confirmed the results obtained, and showed that the complicated nonlinearities necessary for realizing finite-duration processes may be replaced by simple amplifiers.

Conditions for Finite Duration

We shall consider a control system which is comprised of a continuous portion and a pulse (sampled-data) element which carried out pulse-width modulation (Fig. 1) Let the continuous portion, which contains an integrating link, be described by a differential equation of the form

$$a_n z^{(n)}(t) + a_{n-1} z^{(n-1)}(t) + \cdots + a_1 z'(t) = y(t), \quad (1)$$

where z(t) is the system's output quantity and y(t) is the pulse element's output quantity. The operation of this latter element is described by the expression

$$y(t) = \begin{cases} k_p \operatorname{sign} \sigma(kT) \\ \quad \text{for } kT < t < kT + T\Omega[\sigma(kT)], \\ 0 \text{ for } kT + T\Omega[\sigma(kT)] < t < kT + T, \end{cases} \quad (2)$$

where σ(t) is the controlling stimulus and

$$\Omega(\sigma) = \begin{cases} \frac{1}{\varkappa}|\sigma| \text{ for } & |\sigma| < \varkappa, \\ 1 \quad \text{for} & |\sigma| > \varkappa. \end{cases} \quad (3)$$

It is clear from (2) and (3) that the pulse element is characterized by three parameters: the repetition interval T, the gain k_p and the sensitivity κ.

At the output of the comparator we shall have the quantity

$$x(t) = F(t) - z(t), \quad (4)$$

where F(t) is the external stimulus.

In the ordinary system, the controlling signal σ(t) equals this difference, i.e., σ(t) = x(t). We assume the external stimulus to be a step function.

In order that an n-cycle process occur in the system for a step-function stimulus of height B, it is necessary that the input quantity to the pulse element σ(t) at the discrete moments of time, 0, T, 2T, .., (n-1)T assume definite values σ(0), σ(T), ..., σ(nT-T) such that, at

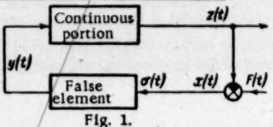

Fig. 1.

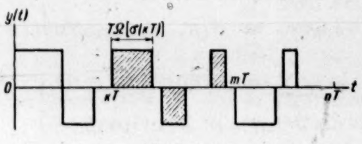

Fig. 2.

time t = nT, the system's output quantity $z(t)$ take the value β and its derivatives, up to and including the (n-1)-th, vanish. Thus, the input quantity y(t) of the continuous portion is a sequence of n rectangular pulses (Fig. 2) whose durations are determined from the conditions for a finite duration of the process:

$$z(nT) = \beta, \quad z^{(j)}(nT) = 0 \quad (j = 1, 2, \ldots, n-1). \tag{5}$$

We now express the $z^{(j)}(mT)$ (j = 0,1,2,...,n-1) in terms $z^{(j)}(kT)$ (j = 0,1,2,..,n-1), where m and k are arbitrary numbers, with n ≥ m > k ≥ 0. It is obvious that the quantities $z^{(j)}(mT)$ can be found as the reaction of the continuous portion to the sequence of rectangular pulses shown hatched on Fig. 2, with initial conditions $z^{(j)}(kT)$ (j = 0,1,2,...,n-1).

If we apply the Lapace transform [5] to (1) with the initial conditions given above, and solve the expression thus obtained with respect to the transform of the output quantity, i.e., with respect to Z(p), we find that

$$Z(p) = \sum_{i=0}^{n-1} A_i(p) z^{(i)}(kT) + K(p) Y_{km}(p),$$

where

$$A_i(p) = \frac{a_{i+1} + a_{i+2}p + \cdots + a_n p^{n-i-1}}{a_1 p + \cdots + a_n p^n},$$

$$K(p) = \frac{1}{a_1 p + \cdots + a_n p^n},$$

and $Y_{km}(p)$ is the transform of the hatched portion of the sequence of rectangular pulses (Fig. 2),

$$Y_{km}(p) = k_p \sum_{i=k}^{m-1} \operatorname{sign}[\sigma(iT)] e^{-pT(i-k)} \frac{1 - e^{-pT\Omega[\sigma(iT)]}}{p}.$$

Using the well-known rules [5] for finding the transforms of the derivatives, we get

$$L\{z^{(j)}(t)\} = \sum_{i=0}^{n-1} B_{ji}(p) z^{(i)}(kT) + \\ + k_p p^j K(p) \sum_{i=k}^{m-1} \operatorname{sign}[\sigma(iT)] e^{-pT(i-k)} \frac{1 - p^{-pT\Omega[\sigma(iT)]}}{p}, \tag{6}$$

where

$$B_{ji}(p) = \begin{cases} p^j \dfrac{a_{i+1} + a_{i+2}p + \cdots + a_n p^{n-i-1}}{a_1 p + \cdots + a_n p^n} & \text{for } j \leqslant i, \\ -p^{j-i-1} \dfrac{a_1 p + \cdots + a_i p^i}{a_1 p + \cdots + a_n p^n} & \text{for } j > i. \end{cases} \tag{7}$$

If we go from (6) to the time-domain function for t = =(m-k)T, we obtain the relationship connecting the quantity $z(t)$ and its derivatives at time t = mT with the quantity $z(t)$ and its derivatives at time t = kT.

$$z^{(j)}(mT) = \sum_{i=0}^{n-1} L^{-1}\{B_{ji}(p)\}_{t=(m-k)T} z^{(i)}(kT) + \\ + k_p \sum_{i=k}^{m-1} \operatorname{sign}[\sigma(iT)] \{h^{(j)}(mT - iT) - \\ - h^{(j)}(mT - iT - T\Omega[\sigma(iT)])\}, \tag{8}$$

where $h^{(j)}(t)$ is the jth derivative of the transient-response function of the system's continuous portion.

This last expression is necessary for us in our investigation of second-order systems. Here, we shall make use of it in order to express analytically the conditions for finite duration of transient response (5) for a system of any order. By setting m = n and k = 0 in (8), and by taking into account that $z^{(j)}(0) = 0$ (j = 0,1,2,..,n-1), we find that

$$k_p \sum_{i=0}^{n-1} \operatorname{sign}\sigma(iT) \{h(nT - iT) - \\ - h(nT - iT - T\Omega[\sigma(iT)])\} = \beta, \\ \sum_{i=0}^{n-1} \operatorname{sign}\sigma(iT) \{h^{(j)}(nT - iT) - \\ - h^{(j)}(nT - iT - T\Omega[\sigma(iT)])\} = 0 \\ (j = 1, 2, \ldots, n-1). \tag{9}$$

In order for an n-cycle process to be realized, the controlling stimuli $\sigma(t)$ must assume, at times 0,T,2T,..., (n-1)T, the values defined by (9). These equations are transcendental so that, just as in the case of relay systems, it is impossible, in the general case, to solve them for the $\sigma(iT)$ (i = 0,1,2,..,n-1) or to state a general method for realizing such a process. We therefore limit ourselves in the sequel to the consideration of special cases, specifically, to second-order systems.

Second-Order Systems

Let the continuous portion be described by the differential equation

$$T_1 z''(t) + z'(t) = ky(t).$$

By comparing this expression with (1), we note that

$$n = 2, \quad a_2 = \frac{T_1}{k}, \quad a_1 = \frac{1}{k}, \quad K(p) = \frac{k}{p(T_1 p + 1)},$$

from whence

$$h(t) = L^{-1}\left\{\frac{1}{p} K(p)\right\} = L^{-1}\left\{\frac{k}{p^2(T_1 p + 1)}\right\} = \\ = k\left[t - T_1\left(1 - e^{-\frac{t}{T_1}}\right)\right], \tag{10}$$

$$h'(t) = k\left(1 - e^{-\frac{t}{T_1}}\right). \tag{11}$$

If we take the inverse Laplace transform [5] of (7), we find that

$$L^{-1}\{B_{00}(p)\} = L^{-1}\left\{\frac{\frac{1}{k} + \frac{T_1}{k} p}{\frac{1}{k} p + \frac{T_1}{k} p^2}\right\} = 1[t], \tag{12}$$

$$L^{-1}\{B_{01}(p)\} = L^{-1}\left\{\frac{\frac{T_1}{k}}{\frac{1}{k} p + \frac{T_1}{k} p^2}\right\} = T_1\left(1 - e^{-\frac{t}{T_1}}\right), \tag{13}$$

$$L^{-1}\{B_{10}(p)\} = L^{-1}\{0\} = 0, \tag{14}$$

$$L^{-1}\{B_{11}(p)\} = L^{-1}\left\{p \frac{\frac{T_1}{k}}{\frac{1}{k} p + \frac{T_1}{k} p^2}\right\} = e^{-\frac{t}{T_1}}. \tag{15}$$

If we substitute (10) and (11) in (9) for n = 2, and carry out some elementary transformations, we can write the conditions for finite duration in the following form:

$$\operatorname{sign}\sigma(T)\left(e^{\frac{T}{T_1}\Omega[\sigma(T)]}-1\right)+ \\ +\operatorname{sign}\sigma(0)\left(e^{\frac{T}{T_1}\Omega[\sigma(0)]}-1\right)e^{-\frac{T}{T_1}}=0 \tag{16}$$

and, by virtue of (16),

$$x(0)=\beta=kk_pT\operatorname{sign}\sigma(T)\,\Omega[\sigma(T)]+ \\ +kk_pT\operatorname{sign}\sigma(0)\,\Omega[\sigma(0)]. \tag{17}$$

In accordance with (3), the parenthesized terms in (16) will be greater than zero and, in order that the left member of (16) equal zero, it is necessary that the quantities σ(T) and σ(0) have opposite signs. With this taken into account, we solve (16) for Ω[σ(T)] and substitute the expression thus obtained in (17). The result is

$$x(0)=N_0[\sigma(0)]=kk_pT\operatorname{sign}\sigma(0)\Big\{\Omega[\sigma(0)]- \\ -\frac{T_1}{T}\ln\left(e^{-\frac{T}{T_1}+\frac{T}{T_1}\Omega[\sigma(T)]}-e^{-\frac{T}{T_1}}+1\right)\Big\}, \tag{18}$$

Where the function Ω[σ(0)] is defined by (3). The inverse relationship, i.e.,

$$\sigma(0)=N_0^{-1}[x(0)], \tag{19}$$

is the relationship sought between the error x(t) and the input function σ(t) of the pulse element at time t = 0.

At time t = T, the relationship between x(T) and σ(T) has a different form. To find it, we use (8) for k=1 and m = n = 2, in which we substitute (10)-(15)for t = (m-k)T = T. If we substitute the values thus obtained for z(2T) and z'(2T), expressed in terms of z(T) and z'(T), in conditions (5) for finite duration, and solve the equations obtained with respect to z(T) and z'(T), we get

$$z(T)=\beta-kk_pT\operatorname{sign}\sigma(T)\times \\ \times\left\{\Omega[\sigma(T)]-\frac{T_1}{T}\left(e^{\frac{T}{T_1}\Omega[\sigma(T)]}-1\right)\right\}=\beta-N_1[\sigma(T)], \tag{20}$$

$$z'(T)=-kk_p\operatorname{sign}\sigma(T)\left(e^{\frac{T}{T_1}\Omega[\sigma(T)]}-1\right)= \\ =-N_2[\sigma(T)]. \tag{21}$$

By noting that, for β = const, x(T) = β -z(T) and x' (T) = -z'(T), we find from these expressions that x(T)= N₁ [σ (T)], x'(T) = N₂[σ(T)], or

$$\sigma(T)=N_1^{-1}[x(T)], \tag{22}$$

$$\sigma(T)=N_2^{-1}[x'(T)]. \tag{23}$$

Relationships (22) and (23) define the relationship between the values of the controlling function and the error, or the velocity of the error, at time t = T. It follows from (19), (22), and (23) that the output quantity of the controlling device can be given by the following two methods:

$$\sigma(t)=\begin{cases}N_0^{-1}[x(0)] & \text{for } t=0,\\ N_1^{-1}[x(T)] & \text{for } t=T\end{cases} \tag{24}$$

and

$$\sigma(t)=\begin{cases}N_0^{-1}[x(0)] & \text{for } t=0,\\ N_2^{-1}[x'(T)]=-N_2^{-1}[z'(T)] & \text{for } t=T.\end{cases} \tag{25}$$

In the intervals between the cycle times (the discrete time moments), σ (t) can assume arbitrary values.

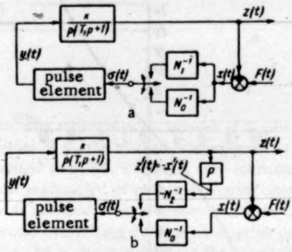

Fig. 3.

In accordance with (24) or (25), the controlling device is comprised of two nonlinear elements and a relay, which switches the error signal from one nonlinear element to the other (Fig. 3, and b). Realization (24) (Fig. 3, a) is worse than realization (25) (Fig. 3, b) since, if the external stimulus varies, not by jumps but arbitrarily, then at time t = T the comparator's output quantity in the first case will not correspond to a two-cycle process, and the system will not process in two cycles that stimulus which was measured for t = 0. In the second case (25) (Fig. 3,b), at cycle time t = T, control is effected by the velocity of the system's output quantity, and on this the variations of the external stimulus have no influence.

Example. As a numerical example, we consider a system in which the continuous portion is described by the differential equation

$$Z''+Z'=y(t),$$

i.e., T_1 = 1 sec, k = 1 and the pulse element has the following parameters: k_p = 20v, κ = 20v and T = 1 sec.

To this system, we apply the second variant of the realization of a finite-duration process. By substituting the parameter values given above for the continuous portion and the pulse element in Expressions (18) and (21), and by taking (3) into account, we find that

$$x(0)=N_0[\sigma(0)]= \\ =\begin{cases}\sigma(0)-20\operatorname{sign}\sigma(0)\ln\left(0{,}368\,e^{\frac{|\sigma(0)|}{20}}+0{,}632\right)\\ \qquad\qquad\text{for } |\sigma(0)|<20,\\ 10{,}3\operatorname{sign}\sigma(0) \qquad \text{for } |\sigma(0)|>20,\end{cases}$$

$$-Z'(T)=N_2[\sigma(T)]= \\ =\begin{cases}20\operatorname{sign}\sigma(T)\left(e^{\frac{|\sigma(T)|}{20}}-1\right) & \text{for } |\sigma(T)|<20,\\ 34{,}4\operatorname{sign}\sigma(T) & \text{for } |\sigma(T)|>20.\end{cases}$$

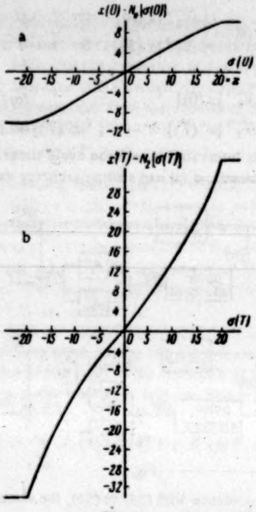

Fig. 4.

The graphs of the relationships $x(0) = N_0[\sigma(0)]$ and $-Z'(T) = N_2[\sigma(T)]$ are given on Fig. 4, a and b. For the realization of a two-cycle process with nonlinearities inverse to these, it is necessary to use control by the scheme shown in Fig, 3,b in the system.

It turned out, with empirical investigation on a model, that these nonlinearities can be replaced by amplifiers which roughly approximate them. It is clear with this that the saturation zone can be ignored, since the pulse element itself, according to (3), possesses saturation for values of the input signal $\sigma(t)$ which correspond to the onset of saturation in the nonlinearities N_0 and N_2. Thus, in the given example, the nonlinearities $N_0^{-1}[x(t)]$ and $N_2^{-1}[-Z'(t)]$, shown in Fig. 3,b can be replaced by amplifiers with gains approximately equal to 2.5 and 0.6 respectively.

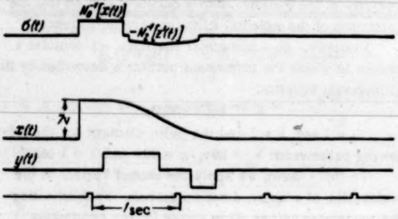

Fig. 5a.

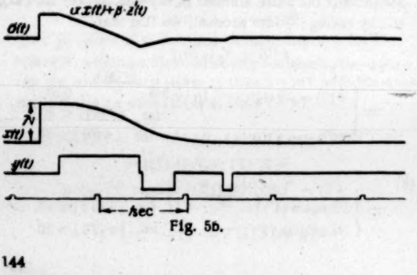

Fig. 5b.

Figure 5,a shows the oscillogram of the transient response of a finite-duration process in the system for a stimulus $F(t) = \beta \cdot 1[t] = 7v$, from which it is clear that the transient response terminates after two cycles of the pulse element, while the ordinary process continues for approximately six cycles. By using the standard linear-correction methods, for example, the introduction of derivative control, one can significantly improve the transient response, but this improved response will last longer than two cycles (Fig. 5,b).

In conclusion, we make several remarks about the behavior of such systems for large amplitudes of the external stimuli. From the oscillograms shown in Fig. 6,a and b, it is clear that, for $\beta = 15v$, the duration of the finite-duration transient response (Fig. 6,a) is comparable with the duration of the response in the system for which the relationship between stimulus magnitude and error velocity was selected in the very best way (Fig. 6,b). Thus, the method presented above for the realization of a two-cycle process becomes of little effect when the stimuli are large.

Equation (18) gives the relationship between the quantity which the system can process within two cycles, and the relative duration of the first corresponding pulse $\Omega[\sigma(0)]$, which cannot be greater than unity. Thus, the maximum amplitude of the external stimulus which the system can process in two cycles is determined by (18) for $\Omega[\sigma(0)=1$, i.e.,

$$x_{0\ \max} = kk_p T\left[1 - \frac{T_1}{T}\ln\left(2 - e^{-\frac{T}{T_1}}\right)\right]. \tag{26}$$

In our numerical example, $x_{0\ \max} = 10.3$. For $F(t) = \beta > x_{0\max}$, the system processes $x_{0\max}$ during the first two cycles and, during the next two cycles, the quantity $\beta - x_{0\ \max}$. If this latter quantity is less than x_0 max, the process terminates after four cycles, otherwise it continues for even longer. Figure 7,a shows the approximate form of such a transient response. As is clear from this figure, the response consists of a series of two-cycle processes. In this case, even the introduction of a simple combination of the quantity and its derivatives can result it an improved transient response. This, however, occurs only for $\beta > x_{0\max}$.

It follows from (26) that the magnitude of $x_{0\max}$ is proportional to the repetition period T. If $\beta > x_{0\ \max}$, then, to obtain an even shorter finite-duration process, it is necessary that the first pulse not terminate at time t = T, but continue even longer, i.e., the system must operate as if the repetition period were 2T, not T. The approximate form of such a process is shown on Fig. 7,b. The dashed lines on Fig. 7,a and b show the variations of the

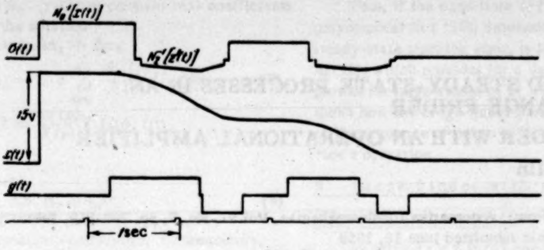

Fig. 6a.

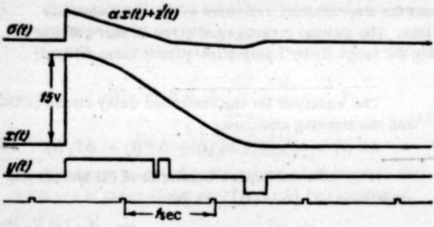

Fig. 6b.

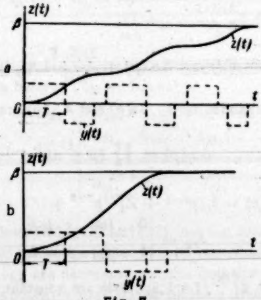

Fig. 7.

quantity y(t). The total duration of the first and second, and also the third and fourth, pulses can be determined from the same expressions as in the case when $\beta < x_{0\,\max}$ if, in them, one substitutes 2T instead of T. For even greater values of β, the system must operate as if the repetition period were 3T, 4T, etc., as β increases.

For the realization of such still shorter transient responses, it is necessary that the controlling device incorporate several controlling devices, similar to those shown on Fig. 3, a and b, but designed for the repetition periods T, 2T, 3T, 4T, etc. as a function of the maximum possible value of the external stimulus. The switching of one or another of the controlling devices into the system must be implemented as a function of the magnitude of the initial error x(0), which equals the external stimulating step β, and may be implemented by means of some supplementary device.

LITERATURE CITED

[1] A. A. Fel'dbaum, "Optimal processes in automatic control systems," Avtomatika i Telemekhanika 14, 6 (1953).

[2] Ya. Z. Tsypkin, "Theory of discontinuous control. III, " Avtomatika i Telemekhanika 11, 5 (1950).

[3] N. N. Krosovskii, "On one optimal control problem," Prikl. matem. i mekh. 21, 5 (1957).

[4] R. E. Kalman, "Design of a self-optimizing control system," Trans. ASME 80, 2 (1958).

[5] M. N. Kontorovich, Operational Calculus and Transient Processes in Electrical Circuits [in Russian] (Gostekhizdat, 1952).

TRANSIENT AND STEADY-STATE PROCESSES IN AN AUTOMATIC RANGE FINDER

II. RANGE FINDER WITH AN OPERATIONAL AMPLIFIER

F. M. Kilin

(Leningrad)

(Translated from: Avtomatika i Telemekhanika, Vol.21, No. 2, pp. 209-219, February, 1960)
Original article submitted June 16, 1959

The dynamic properties of a range finder with an operational amplifier, including an integrating and an inertial link, are considered. In the general case, the investigation of the processes in a range finder with an operational amplifier, if with this one takes into account the step-function variations of the time-separator parameters, leads to cumbersom mathematical computations. The general investigation given in part I of this work [1] and the equations therein obtained for estimating the range finder's properties permit these difficulties to be avoided.

1. Properties of the Range Finder with an Operational Amplifier When It Is Investigated as a Continuous Automatic-Control System

An estimate of the effect of noise on a range finder of the simplest construction, not containing any operational amplifier, was given in [2]. In the present work, we start from the general-range-finder theory presented in [1]. Application of this theory to practically important concrete designs permits their dynamic properties to be estimated comparatively simply. We shall not treat the passage of random signals through the range finder in this paper.

In [1] we found the conditions under which the investigation of the processes in the range finder can be reduced to the investigation of processes in the continuous system described by (I.38)*. We shall assume here that these conditions are met†. We take a definite structure for the operational amplifier, for example, one for which (I.38) take the following form.

The equations for the time separator and the operational amplifier are

$$
\begin{gathered}
(D + a_{11}) U_1(t) = \frac{2K_0 E_s}{\tau_{10} T} \Delta\alpha(t), \\
a_{21} U_1(t) + (D + a_{22}) U_2(t) = 0, \qquad (1) \\
a_{31} U_1(t) + a_{32} U_2(t) + (D + a_{33}) U_3(t) = 0, \\
\dots\dots\dots\dots\dots\dots\dots\dots \\
\sum_{m=1}^{r-1} a_{rm} U_m(t) + (D + a_{rr}) U_r(t) = 0.
\end{gathered}
$$

The parameter a_{11} appertains to the time separator, and is expressed in terms of the time constants τ_{10} and τ_{11} by

$$a_{11} = \frac{\frac{\alpha}{\tau_{10}} + \frac{T-\alpha}{\tau_{11}}}{T}. \qquad (2)$$

The equations for the controlled delay circuit (CDC) and the tracking error are

$$\Delta\vartheta(t) = \sigma U_r(t), \quad \Delta\alpha(t) + \Delta\vartheta(t) = \Delta\vartheta_1(t). \qquad (3)$$

If we take the Lapace transforms of (1) and (3) and solve them for $L\{\Delta\alpha(t)\}$, we get

$$L\{\Delta\alpha(t)\} = \frac{\Delta a(p)}{X(p)} L\{\Delta\vartheta_1(t)\} - \sigma \sum_{k=1}^{r} \frac{A_{rk}(p) U_k(0)}{X(p)}, \qquad (4)$$

where

$$X(p) = \Delta a(p) + \frac{2\sigma K_0 E_s}{\tau_{10} T} A_{r1}(p). \qquad (5)$$

In expanded form, $\Delta a(p)$ and $A_{rk}(p)$ are given by

$$
\begin{gathered}
\Delta a(p) = \prod_{k=1} (p + a_{kk}), \\
A_{rk}(p) = \delta_{rk} p^{r-1} + Z_1^{(rk)} p^{r-2} + \dots + Z_{r-1}^{(rk)}, \qquad (6) \\
\delta_{rk} = \begin{cases} 0 & \text{for} \quad r \neq k, \\ 1 & \text{for} \quad r = k, \end{cases}
\end{gathered}
$$

where the $Z_j^{(rk)}$ $(j = 1, 2, \dots, r-1)$ are constant real coefficients.

The form of the operator function $X(p)$, defined by (5), depends on the structure of the element A_{r1}. In its expanded form, the expression for $A_{r1}(p)$ is given as

$$
A_{r1}(p) = (-1)^{r+1} \begin{vmatrix} a_{21}, & p + a_{22}, & 0, \dots, 0 \\ a_{31}, & a_{32}, & p + a_{33}, \dots, 0 \\ \dots & \dots & \dots \\ a_{r1}, & a_{r2}, & a_{r3}, \dots, a_{r,\,r-1} \end{vmatrix} =
$$

$$= Z_1 p^{r-2} + Z_2 p^{r-3} + \dots + Z_{r-1}, \qquad (7)$$

---

*The Roman numeral I in parentheses means that the formula numeration refers to part I of the given work.

† Cf. [1], section 9 and (I.44).

where the Z_j ($j = 1,2,\ldots,r-1$) are constant real coefficients.

We introduce the notation

$$\Delta\alpha = \Delta\alpha_1 + \Delta\alpha_2,$$

$$L\{\Delta\alpha_1(t)\} = -\sigma\sum_{k=1}^{r}\frac{A_{rk}(p)}{X(p)}U_k(0), \tag{8}$$

$$L\{\Delta\alpha_2(t)\} = \frac{\Delta a(p)}{X(p)}L\{\Delta\vartheta_1(t)\}.$$

We assume that

$$\Delta\vartheta_1(t) = \eta_s t^s, \tag{9}$$

where the η_s are constant coefficients. Consequently,

$$L\{\Delta\alpha_2(t)\} = s!\,\frac{\eta_s\Delta a(p)}{p^{s+1}X(p)}. \tag{10}$$

If the range finder is a stable system, then, for the steady-state mode, we obtain

$$\Delta\alpha_1 = 0,$$

$$\Delta\alpha_2(t) = s!\;\eta_s\sum_{k=0}^{s}\frac{G_k}{(s-k)!}t^{s-k},$$

$$G_k = \frac{1}{k!}\left[\frac{d^k}{dp^k}\frac{\Delta a(p)}{X(p)}\right]_{p=0}. \tag{11}$$

For large values of t, the greatest influence on the accuracy of range-finder operation will be manifested by the term

$$\Delta\alpha_{20}(t) = \eta_s G_0 t^s,\ G_0 = \frac{\prod\limits_{k=1}^{r} a_{kk}}{\prod\limits_{k=1}^{r} a_{kk} + \frac{2\sigma K_0 E_s}{\tau_{10}T}A_{r1}(0)}. \tag{12}$$

On the basis of (7), we have

$$A_{r1}(0) = (-1)^{r+1}\begin{vmatrix} a_{21}, & a_{22}, & 0, & \ldots, & 0 \\ a_{31}, & a_{32}, & a_{33}, & \ldots, & 0 \\ . & . & . & . & . \\ a_{r1}, & a_{r2}, & a_{r3}, & \ldots, & a_{r,\,r-1} \end{vmatrix} \tag{13}$$

It follows from (12) and (13) that the steady-state accuracy of the range finder will be increased if the coefficients a_{kk} are decreased and the quantity $A_{r1}(0)$ is increased. According to (13), the increase of $A_{r1}(0)$ can be achieved by means of the operational amplifier parameters a_{jk} for which $j \neq k$.

To see more graphically how the coefficients a_{kk} ($k = 1,2,\ldots,r$) affect tracking accuracy, we consider the case when the following equalities hold

$$a_{ii} = 0 \quad (i = r-\rho+1,\ r-\rho+2,\ \ldots,\ r). \tag{14}$$

For this case, in the steady state, we get

$$\Delta\alpha_2(t) = s!\;\eta_s\sum_{k=0}^{\nu}\frac{G_{\nu k}}{(\nu-k)!}t^{\nu-k},\quad \nu = s-\rho. \tag{15}$$

The coefficients $G_{\nu k}$ are found from the formulas

$$G_{\nu k} = \frac{1}{k!}\left[\frac{d^k}{dp^k}\frac{\Delta a_\rho(p)}{X(p)}\right]_{p=0},\ \Delta a_\rho(p) = \prod_{k=1}^{r-\rho}(p + a_{kk}). \qquad 16)$$

Thus, if the conditions of (14) hold, the degree of the polynominal in t (15), determining the magnitude of the steady-state tracking error, is lower by ρ units than that in (11), which provides for a decrease in the rate of error growth for large values of t. Formula (12) graphically shows how the range-finder parameters and the parameters of the sequence of pulses affect the accuracy of the device's operation.

2. Range Finder with a Simple-Integration Operational Amplifier

By setting $r = 2$ in (1) and (3), we obtain the equations for the range finder with the simplest operational amplifier:

$$\begin{gathered}(D + a_{11})U_1(t) = \frac{2K_0E_s}{\tau_{10}T}\Delta\alpha(t),\\ a_{21}U_1(t) + (D + a_{22})U_2(t) = 0,\end{gathered} \tag{17}$$

$$\Delta\vartheta(t) = \sigma U_2(t), \qquad \Delta\alpha(t) + \Delta\vartheta(t) = \Delta\vartheta_1(t).$$

We shall be interested only in the component $\Delta\alpha_2$. We assume that the translation of the return pulses from the object is described by the function

$$\Delta\vartheta_1(t) = \begin{cases}0 & \text{for } t \leqslant 0,\\ \eta_0 + \eta_1 t & \text{for } t > 0,\end{cases} \tag{18}$$

where η_0 and η_1 are constants.

By solving (17) with (18) taken into account, we obtain the expression for $\Delta\alpha_2(t)$:

$$\Delta\alpha_2(t) = \eta_0\left[G_0 + \sum_{k=1}^{2}S_k e^{\mu_k t}\right] + \tag{19}$$

$$+\ \eta_1\left[G_0 t + G_1 + \sum_{k=1}^{2}\frac{S_k}{\mu_k}e^{\mu_k t}\right].$$

The coefficients G_k and S_k are found, respectively, from the formulas

$$G_0 = \frac{a_{11}a_{22}}{X_2},\ G_1 = -\frac{2\sigma K_0E_s a_{21}(a_{11} + a_{22})}{\tau_{10}TX_2^2}, \tag{20}$$

$$S_k = \frac{\Delta a(\mu_k)}{\mu_k X'(\mu_k)} \quad (k = 1, 2),$$

where

$$X'(\mu_k) = \left\{\frac{d}{dp}X(p)\right\}_{k=\mu_k}. \tag{21}$$

Here,

$$\begin{gathered}X(p) = p^2 + X_1p + X_2,\quad X_1 = a_{11} + a_{22},\\ X_2 = a_{11}a_{22} - \frac{2\sigma K_0E_s}{\tau_{10}T}a_{21}.\end{gathered} \tag{22}$$

The parameters μ_1 and μ_2 are the roots of the characteristic equation

$$X(\mu) = 0.$$

If the range finder is a stable system, then, for the steady state, (19) takes the simple form:

$$\Delta\alpha_2(t) = G_0[\eta_0 + \eta_1 t] + \eta_1 G_1. \tag{23}$$

The function $\Delta \vartheta_1(t)$ is related to the function $R(t) = R_0 = R_1 t$ which describes the motion of the object with respect to the radar set. This relationship is expressed by

$$\Delta\vartheta_1(t) = \frac{2R(t)}{c},$$

where c is the velocity of propagation of electromagnetic waves.

Consequently, (23) can be rewritten in the form:

$$\Delta\alpha_2(t) = \frac{2G_0}{c}[R_0 + R_1 t] + \frac{2R_1 G_1}{c}. \tag{24}$$

The value of $\Delta\alpha_2$ corresponds to an error in the radius

$$\Delta R(t) = \frac{c\Delta\alpha_2(t)}{2} = G_0[R_0 + R_1 t] + R_1 G_1. \tag{25}$$

If there are very limited possibilities for decreasing the rate of error growth in the range-finder with a simple amplifier, such limitations do not exist in the given scheme. It follows from (19), (20), and (24) that, if a_{22} tends to zero, one can attain an arbitarily small value for the quantity $2G_0R_1/c$ which characterizes the rate of growth of the error. For $a_{22} = 0$, when the operational amplifier becomes a straight integrator, the following relationships hold:

$$X_2 = -\frac{2\sigma K_0 E_3 a_{21}}{\tau_{10}T}, \quad G_0 = 0, \quad G_1 = \frac{a_{11}}{X_2},$$

i.e., for the steady state, (24) in the given case takes the form:

$$\Delta\alpha_2 = -\frac{R_1 a_{11}\tau_{10}T}{\sigma K_0 E_3 a_{21} c}. \tag{26}$$

To guarantee stability of operation, one must give a positive value to the parameter X_2, i.e., $X_2 > 0$ or $a_{21} > 0$.

According to (26), when $a_{22} = 0$ the tracking error in the steady state is proportional to a_{11}, the parameter of the time separator. The value of this parameter is chosen in accordance with the conditions which guarantee reliable operation of the time separator. As shown by (2), to decrease parameter a_{11} it is necessary to increase both time constants τ_{22} and τ_{11}, which is not always possible. Thus, even if the translations of the return pulses follow (18), the range finder now under consideration has essential disadvantages. In it, the tracking accuracy is limited by the possibilities of decreasing parameter a_{11} of the time separator.

Parameter a_{11} also imposes limitations on the character of the range finder's transient response. In fact, for s = 2, $a_{22} = 0$ and a given value of a_{11}, there remains at our disposal just the one variable parameter a_{21}, which is related to X_2 by the equation

$$X_2 = -\frac{2\sigma K_0 E_3}{\tau_{10}T} a_{21}. \tag{27}$$

In view of the fact that the device is described by a second-order differential equation, it is necessary to have at least two variable parameters. The presence of only one of them entails this, that for $X_2 > a_{11}^2/4$, the roots of the characteristic equation assume complex values, and the tracking system goes into a mode of damped oscillation. With this, the lower the value of a_{11}, the lower the values of X_2 for which this transition occurs. From this point of view, it is well to have a large value of a_{11}, which may be obtained by decreasing the time constants τ_{22} and τ_{11} (and not increasing them, as was required above).

To decrease the steady-state error, it is required to give a large value to the quantity X_2. However, for large values of X_2, the oscillatory process will be characterized by an inadmissibly large overshoot. This is shown by the example, given in the Appendix, of the given range-finder scheme.

Structure of an Operational Amplifier Providing Changes in the Range-Finder's Dynamic Properties

It was previously shown that an increase of the parameter X_2 leads to an oscillatory transient response with a large overshoot. This imposes a limitation on the choice of values for X_2. It also limits the possibilities of decreasing the tracking error in the transient and steady states. We now show that such limitations, and to a large degree, also appear when an operational amplifier with multiple integration is connected in the range finder; due to these limitations, the effectiveness of employing such an amplifier in similar devices is significantly decreased. We now write the characteristic equation of (5) in expanded form. By setting $a_{ii} = 0$ (i = 2,3,..,r) in (5), we get

$$\Delta a(p) = p^{r-1}(p + a_{11}), \tag{28}$$

$$X(p) = p^r + X_1 p^{r-1} + \dots + X_{r-1}p + X_r = 0. \tag{29}$$

The coefficients X_k are found from the formulas

$$X_1 = a_{11},$$

$$X_k = \frac{2\sigma K_0 E_3}{\tau_{10}T} Z_{k-1} \quad (k = 2, 3, \dots, r). \tag{30}$$

In their turn, the quantities $Z_1, Z_2, \dots, Z_r$ are determined from (6) in terms of the operational amplifier's parameters a_{jk} (j = 2,3,...,r; k = 1,2,...,j).

In the case under consideration, the operational-amplifier implements an s-fold integration. With this, the quantity s is related to r by the equation s = r-1.

The character of the transient response depends on the roots of characteristic equation (29). If it is possible to vary, within wide limits, all the coefficients X_k of (29), this will thereby provide the necessary conditions for changing the character of the tracking system's transient response. These possibilities are easily established, on the basis of (30).

Since the coefficients $X_2, X_3, \dots, X_r$ depend on the operational amplfier's parameters, they admit variations within quite broad limits. This can not be said, however, of coefficient $X_1 = a_{11}$, the magnitude of which is determined by the parameter a_{11} of the time separator. As has already been stated, the possibilities of varying this parameter are limited.

On the other hand, the coefficients X_k may be expressed as follows:

$$X_1 = \sum_{k=1}^{r} M_k,$$

$$X_2 = M_1 \sum_{k=2}^{r} M_k + M_2 \sum_{k=3}^{r} M_k + \cdots + M_{r-1} M_r, \tag{31}$$

$$\cdots\cdots\cdots\cdots\cdots\cdots$$

$$X_r = M_1 M_2 \ldots M_r.$$

Here,

$$M_k = -\mu_k \quad (k = 1, 2, \ldots, r) \tag{32}$$

Consequently,

$$a_{11} = \sum_{k=1}^{r} M_k = \sum \operatorname{Re} M_k. \tag{33}$$

Thus, if it is necessary to improve the transient response by increasing the real parts of the roots μ_k then, according to (33), it is necessary to increase the value of parameter a_{11}. In the case of multiple roots,

$$M = M_1 = M_2 = \cdots = M_r$$

Formula (33) takes the simplier form: $a_{11} = rM$, or $a_{11} = (s+1)M$, i.e., it is required to provide a greater value for the parameter a_{11}, the greater the multiplicity s of integration in the operational amplifier and the greater the necessary magnitude of the quantity M.

The basic disadvantage of the scheme under consideration is that it is not possible in practice to provide the variation in the time separator's parameter a_{11} which is required for improving the transient response in the automatic range finder. We now show that this disadvantage is eliminated if we use a different operational-amplifier scheme, for example, one for which the processes are described by the equations:

$$\begin{gathered}
(D + a_{11}) U_1(t) = \frac{2K_0 E_s}{\tau_{10} T} \Delta\alpha(t), \\
a_{21} U_1(t) + (D + a_{22}) U_2(t) = 0, \\
a_{31} U_1(t) + a_{32} U_2(t) + (D + a_{33}) U_3(t), \\
\cdots\cdots\cdots\cdots\cdots\cdots \\
\sum_{k=1}^{r-1} a_{rk} U_k(t) + (D + a_{rr}) U_r(t) = 0, \\
\sum_{k=1}^{r} a_{r+1,k} U_k(t) + U_{r+1}(t) = 0.
\end{gathered} \tag{34}$$

Equations (34) can be obtained from (1) by adding

$$U_{r+1} = -\sum_{k=1}^{r} a_{r+1,k} U_k,$$

which expresses the simple amplification of the signals U_k with gains proportional to the coefficients $a_{r+1,k}$, with summation of the results. For (34) we find

$$\begin{gathered}
\Delta a(D) = \prod_{k=1}^{r} (D + a_{kk}), \; A_{r+1,1}(D) = \\
= Z_0' D^{r-1} + Z_1' D^{r-2} + \cdots + Z_{r-2}' D + Z_{r-1}'.
\end{gathered} \tag{35}$$

The equations for the controlled delay circuit and the tracking error when the operational amplifier described by (34) is connected in the device are written in the form

$$\Delta\vartheta(t) = \sigma U_{r+1}(t), \; \Delta\alpha(t) + \Delta\vartheta(t) = \Delta\vartheta_1(t). \tag{36}$$

Taking the Laplace transforms of (34) and (36), and solving them for $L\{\Delta\alpha(t)\}$, we obtain

$$\begin{gathered}
L\{\Delta\alpha_1(t)\} = -\sigma \sum_{k=1}^{r} \frac{A_{r+1,k}(p)}{X(p)} U_k(0), \\
L\{\Delta\alpha_2(t)\} = \frac{\Delta a(p)}{X(p)} L\{\Delta\vartheta_1(t)\}, \\
\Delta\alpha_1 + \Delta\alpha_2 = \Delta\alpha.
\end{gathered} \tag{37}$$

For $a_{ii} = 0$ $(i = 2, 3, \ldots, r)$, we have

$$\begin{gathered}
\Delta a(p) = p^{r-1}(p + a_{11}), \\
X(p) = p^r + X_1 p^{r-1} + X_2 p^{r-2} + \cdots + X_r, \\
X_1 = a_{11} + \frac{2\sigma K_0 E_s}{\tau_{10} T} Z_0', \\
X_k = \frac{2\sigma K_0 E_c}{\tau_{10} T} Z_{k-1}' \quad (k = 2, 3, \ldots, r).
\end{gathered} \tag{38}$$

Here, all the coefficients $X_1, X_2, \ldots, X_r$ depend on the operational amplifier's parameters. Consequently, it is not required to vary the parameter a_{11} in changing from one mode of operation to another, since this transition may be effected by a corresponding change of the operational amplifier's parameters. When an operational amplifier of the type described by (34) is used, the parameter a_{11} is not profitably increased, as was required in the examples given earlier, but, conversely, should be decreased, since the steady-state error is the lower, the smaller the value of a_{11}.

4. Automatic Range Finder with Double Integration Operational Amplifier

In using an operational amplifier with a double integration, the processes of which are described by (34), the automatic range finder's equations are written in the form

$$\begin{gathered}
(D + a_{11}) U_1(t) = \frac{2K_0 E_s}{\tau_{10} T} \Delta\alpha(t), \\
a_{21} U_1(t) + (D + a_{22}) U_2(t) = 0, \\
a_{31} U_1(t) + a_{32} U_2(t) + (D + a_{33}) U_3(t) = 0, \\
a_{41} U_1(t) + a_{42} U_2(t) + a_{43} U_3(t) + U_4(t) = 0, \\
\Delta\vartheta(t) = \sigma U_4(t), \\
\Delta\alpha(t) + \Delta\vartheta(t) = \Delta\vartheta_1(t).
\end{gathered} \tag{39}$$

We shall be interested below only in the component $\Delta\alpha_2$. Taking the Laplace transform of (39), we get

$$L\{\Delta\alpha_2(t)\} = \frac{\Delta a(p)}{X(p)} L\{\Delta\vartheta_1(t)\}. \quad (40)$$

Here, $\Delta a(p) = (p + a_{11})(p + a_{22})(p + a_{33})$,

$$X(p) = p^3 + X_1p^2 + X_2p + X_3,$$

$$X_1 = a_{11} + a_{22} + a_{33} + \varepsilon Z'_0,$$

$$X_2 = a_{11}(a_{22} + a_{33}) + a_{22}a_{33} + \varepsilon Z'_1, \quad (41)$$

$$X_3 = a_{11}a_{22}a_{33} + \varepsilon Z'_2,$$

$$\varepsilon = \frac{2\alpha_0K_0E_c}{\tau_{10}T}.$$

The coefficients Z'_0, Z'_1 and Z'_2 are found from the equations

$$Z'_0 = -a_{41},$$

$$Z_1 = a_{21}a_{42} + a_{31}a_{43} - a_{41}(a_{22} + a_{33}), \quad (42)$$

$$Z'_2 = a_{31}a_{22}a_{43} + a_{21}(a_{33}a_{42} - a_{32}a_{43}) - a_{41}a_{22}a_{33}.$$

We set

$$\Delta\vartheta_1(t) = W_1t + \frac{1}{2}W_2t^2, \ R(t) = R_1t + \frac{1}{2}R_2t^2 \quad (43)$$

or

$$\Delta\vartheta_1(t) = \frac{2R(t)}{c} = \frac{2R_1}{c}t + \frac{R_2}{c}t^2, \quad (44)$$

where c is the velocity of propagation of electromagnetic waves. The function R(t) describes the translation of the object with respect to the radar set.

Going to the time-domain function corresponding to (40) while taking (44) into account, we find, for the steady state,

$$\Delta\alpha_2(t) = \frac{2R_1}{c}f_1(t) + \frac{R_2}{c}f_2(t),$$

$$f_1(t) = G_{10}t + G_{11}, \quad (45)$$

$$f_2(t) = \frac{G_{20}}{2!}t^2 + \frac{G_{21}}{1!}t + G_{22}, \quad (t > t_0),$$

where t_0 is the quantity defining the duration of the transient response.

The coefficients G_{1k} and G_{2k} are found from the formulas

$$G_{ik} = \frac{1}{k!}\left\{\frac{d^k}{dp^k}\frac{\Delta a(p)}{X(p)}\right\}_{p=0} \quad (i = 1, 2). \quad (46)$$

If we set $a_{22} = a_{33} = 0$, we obtain

$$f_1(t) = 0, \ f_2 = \frac{2a_{11}}{X_2}. \quad (47)$$

The most favorable conditions for increasing tracking accuracy occur when $a_{22} = a_{33} = 0$, when the operational amplifier acts simply as a double integrator.

Appendix

Example 1. To determine the transient response and the magnitude of the steady-state tracking error for the following automatic range-finder data: pulse-repetition frequency F = 500 $\sec^{-1}$, duration of the return pulses from the object $\alpha = 2 \cdot 10^{-6}$ sec, length of the tracking pulses $\alpha_0 = 3 \cdot 10^{-6}$ sec, $K_0E_3 = 60$v, $\tau_{10} = 2 \cdot 10^{-4}$ sec, $\tau_{11} = \infty$, the operational amplifier is an integrator, i.e., $a_{22} = 0$. The object moves relative to the radar set with a constant velocity of $R_1 = 300$m/sec.

In correspondence with (2), we find that

$$a_{11} = \frac{\alpha}{T\tau_{10}} = 5 \sec.^{-1}, \ T = \frac{1}{F} = 0{,}002 \text{ sec}$$

The computational results are given in the first table:

The table fives the steady-state values of $\Delta\alpha_2$ and ΔR. In addition, we have computed the values of the roots μ_1 and μ_2, from which one may derive a representation of the character of the transient response in the tracking system. The table also gives the values of the quantities

$$\rho_1T = |\operatorname{Re}\mu_1T|, \quad \rho_2T = |\operatorname{Re}\mu_2T|,$$

$$\varphi T = |\operatorname{Im}\mu_1T| = |\operatorname{Im}\mu_2T|, \quad (48)$$

from which one may judge if (I.44) hold, as they do in the example under consideration.

As we can see, for $a_{11} = 5 \sec^{-1}$, there ensues a damped oscillatory mode when $X_2 > 6.25 \sec^{-2}$. Figure 1 shows a graph of the transient response for the case when $X_2 = 16.12 \sec^{-2}$ and $X_2 = 45.73 \sec^{-2}$. The first case corresponds to the roots $\mu_{1,2} = 2.5 \pm i\pi$, the second to the roots $\mu_{1,2} = 2.5 \pm i2\pi$.

For $X_2 = 16.12 \sec^{-2}$, the overshoot reaches approximately 24%; as the result of this, the maximum error reaches 105m and, in the steady-state, 93m. For $X_2 = 45.73 \sec^{-2}$, the overshoot reaches a significant size - about 69%. Transient responses with such overshoots are inadmissible.

We note in conclusion that the tracking error must not exceed $|\Delta\alpha| < \alpha_0$. If $|\Delta\alpha| \geq \alpha_0$, the return pulses from the object fall beyond the limits of the tracking pulses, and normal operation of the range finder is disrupted. From this point of view, the mode of operation with $X_2 = 2.25 \sec^{-2}$ can not actually exist.

Example 2. To determine the transient response and the steady-state tracking error of an automatic range finder with one integrator for the following data: F = 500 $\sec^{-1}$, $\alpha = 2 \cdot 10^{-6}$ sec, $\alpha_0 = 3 \cdot 10^{-6}$ sec, $\tau_{10} = 10^{-4}$ sec, $\tau_{11} = \infty$; $R_1 = 300$m/sec.

This example differs from the previous one in that the time constant τ_{10} has half the value it previously did. Determining the value of the parameter a_{11}, we find that

$$a_{11} = \frac{F\alpha}{\tau_{10}} = 10 \sec^{-1},$$

the increased value of a_{11} creating more favorable conditions for improving the transient response. Figure 1 shows the graph of the transient response for $X_2 = 50 \sec^{-2}$ For this value of X_2, the overshoot is about 7%, i.e., is significantly less than in the case with $X_2 = 45.73 \sec^{-2}$, considered in Example 1.

X_2, sec $^{-2}$	μ_1, sec $^{-1}$	μ_2, sec $^{-1}$	ρ_1T	ρ_2T	φT	$\Delta\alpha_2$, sec	ΔR, м
2,25	−0,5	−4,5	0,001	0,009	0	$4 \cdot 10^{-6}$	600
5,25	−1,5	−3,5	0,003	0,007	0	$1,9 \cdot 10^{-6}$	285
6,25	−2,5	−2,5	0,005	0,005	0	$1,6 \cdot 10^{-6}$	240
10,25	$-2,5+i2$	$-2,5-i2$	0,005	0,005	0,004	$0,98 \cdot 10^{-6}$	147
15,25	$-2,5+i3$	$-2,5-i3$	0,005	0,005	0,006	$0,66 \cdot 10^{-6}$	100
16,12	$-2,5+i\pi$	$-2,5-i\pi$	0,005	0,005	0,006	$0,62 \cdot 10^{-6}$	93
45,73	$-2,5+i2\pi$	$-2,5-i2\pi$	0,005	0,005	0,013	$0,22 \cdot 10^{-6}$	33

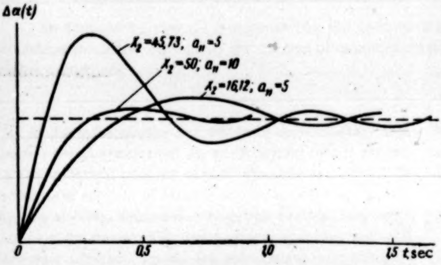

Fig. 1.

Example 3. To determine the parameters of the operational amplifier with a double integrator which provides equal values for all the roots of the characteristic equation, and to find the steady-state tracking error in the region $\Delta\alpha \lesssim 0.1\,\alpha$ as the object moves relative to the radar set with a constant acceleration of $\ddot{R}_2 = 3g = 30 \text{m/sec}^2$. The automatic range-finder data are: $F = 400 \text{sec}^{-1}$, $\alpha = 10^{-6}$-sec, $KE_3 = 60$v, $\sigma = 0.5 \cdot 10^{-6}$ sec/v. The computations are carried out for two cases: a) $\tau_{10} = 2 \cdot 10^{-4}$sec, $\tau_{11} = \infty$; b) $\tau_{10} = 2 \cdot 10^{-3}$sec, $\tau_{11} = \infty$.

The steady-state error is determined from the formula

$$\Delta\alpha = \Delta\alpha_2 = \frac{2R_2 a_{11}}{cX_3}. \tag{49}$$

The inequality $|\Delta\alpha| \geq 0.1\,\alpha$ will hold if

$$X_3 \geqslant X_{30} = \frac{2R_2 a_{11}}{0,1\,\alpha c} = \frac{2R_2 F}{0,1 c\tau_{10}}. \tag{50}$$

In finding the numerical value of X_{30} for cases "a" and "b", we get

$$X_{30} = \begin{cases} 4\,\dfrac{1}{\text{sec}^3} & \text{for} \quad \tau_{10} = 2 \cdot 10^{-4}\,\text{sec} \\ 0,4\,\dfrac{1}{\text{sec}^3} & \text{for} \quad \tau_{10} = 2 \cdot 10^{-3}\,\text{sec}. \end{cases}$$

We now determine the operational amplifier's parameters for the value $X_3 = 1.5X_{30}$. For this, we compute the value of ϵ in (41). By substituting numerical values, we get

$$\varepsilon = \begin{cases} 120\,\dfrac{1}{\text{sec}} & \text{for} \quad \tau_{10} = 2 \cdot 10^{-4}\,\text{sec} \\ 12\,\dfrac{1}{\text{sec}} & \text{for} \quad \tau_{10} = 2 \cdot 10^{-3}\,\text{sec}. \end{cases}$$

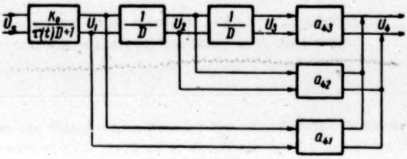

Fig. 2.

τ_{10}, sec	a_{41}	a_{42}	a_{43}
$2 \cdot 10^{-4}$	−0,03	0,08	−0,05
$2 \cdot 10^{-3}$	−0,20	0,18	−0,05

For the case of multiple roots, we have $\mu_1 = \mu_2 = \mu_3 = -M$. For this, the coefficients X_1, X_2, and X_3 are related to M by the equations

$$X_1 = 3M, \qquad X_2 = 3M^2, \qquad X_3 = M^3. \tag{51}$$

In the given example, the magnitude of M is found from

$$M = \sqrt[3]{15\,X_{30}} \approx \begin{cases} 1,82 \text{ sec}^{-1} & \text{for} \quad X_{30} = 4 \quad \text{sec}^{-3}, \\ 0,85 \text{ sec}^{-1} & \text{for} \quad X_{30} = 0,4 \text{ sec}^{-3}. \end{cases}$$

On the basis of (41) we have

$$\begin{gathered} a_{11} + a_{22} + a_{33} + \varepsilon Z_0' = 3M, \\ a_{11}(a_{22} + a_{33}) + a_{22}a_{33} + \varepsilon Z_1' = 3M^2, \\ a_{11}a_{22}a_{33} + \varepsilon Z_2' = M^3. \end{gathered} \tag{52}$$

By substituting $a_{22} = a_{33} = 0$ in Eqs. (42) and (52), and then substituting the values of Z'_0, Z'_1, and Z'_2 from (42) and (52), we get

$$\begin{gathered} a_{41} = \frac{a_{11} - 3M}{\varepsilon}, \quad a_{31}a_{43} + a_{21}a_{42} = \frac{3M^2}{\varepsilon}, \\ a_{21}a_{32}a_{43} = -\frac{1,5\,X_{30}}{\varepsilon}. \end{gathered} \tag{53}$$

We have at our disposal six variable parameters of the operational amplifier, these being related to M and X_{30} by the three equations of (53). Consequently, three of the six parameters can be given arbitrary values. For example, by setting $a_{21} = a_{32} = 1$, $a_{31} = 0$, we get

$$\begin{gathered} a_{41} = \frac{a_{11} - 3M}{\varepsilon}, \quad a_{42} = \frac{3M^2}{\varepsilon}, \\ a_{43} = -\frac{1,5\,X_{30}}{\varepsilon} = -\frac{1,5\,R_2}{0,1\sigma c K_0 E_3}. \end{gathered} \tag{54}$$

The structure of the time separator and the operational amplifier for the given case reduce to the scheme shown in Fig. 2. This scheme deserves attention, since its technological implementation is comparatively simple.

The results of the computations using (54) are given in the second table.

LITERATURE CITED

[1] F. M. Kilin, "Transient and steady-state processes in an automatic range finder. I. Description of the device's operation, and the use of the apparatus of step-functions for analyzing the processes in the indicator," Avtomatika i Telemekhanika 19, 10 (1958)‡.

[2] I. N. Amiantov and V. I. Tikhonov, "Effect of fluctuations on the operation of an automatic range finder," Avtomatika i Telemekhanika 19, 4 (1958)‡.

---

‡ See English translation.

DETERMINATION OF THE SECOND-ORDER MOMENTS OF VARIOUS COORDINATES OF AUTOMATIC-CONTROL SYSTEMS BY THE USE OF ELECTRONIC ANALOG COMPUTERS*

L. A. Tel'ksnis

(Vil'nyus)

(Translated from: Avtomatika i Telemekhanika, Vol. 21, No. 2, pp. 220-223, February, 1960)

Original article submitted September 29, 1959

An engineering method is presented for the determination of second-order moments of various coordinates of automatic-control systems by the method of canonical representations of random functions, using electronic analog computers.

In the investigation and design of contemporary automatic-control systems (ACS), an important role is played by the statistical analysis of their dynamic accuracy. The taking into account of random factors is necessary in designing aircraft, automatic-navigation devices, ship-roll dampers, for determining radar-system accuracy and artillery-gear accuracy, for solving information-processing problems, for designing modern drilling equipment, coal-mining machines, automobile suspension systems, etc.

Analytical methods of determing second-order moments of various ACS variables [1-3], due to the large volume of complicated analytical computations and transformations they entail, can be used in engineering calculations only for solving the most elementary problems.

The method of physical simulation of random processes, using electronic analog computers for ACS statistical analysis [3] can be used only for the solution of a narrow class of stationary problems.

The methods of mathematical simulation of random processes, using electronic computers [2, 3], although they theoretically permit one to solve stationary and nonstationary problems of ACS statistical analysis, are very cumbersome to use in practice because of the large amount of complicated analytical computation and transformation which must be carried out in the preparation of the solution as well as in the solution process itself.

For the creation of a practical method of computing second-order moments of various ACS coordinates, it is advantageous to use the canonical representation of random functions [1, 6]

$$X(t) = \sum_{\nu=1}^{\infty} V_\nu x_\nu(t), \tag{1}$$

where the V_ν are the random, mutually uncorrelated coefficients of the canonical expansion, with dispersions D_ν, and the $x_\nu(t)$ are the canonical expansion's nonrandom coordinate functions.

Thanks to the introduction of the concept of normalized coordinate functions

$$x_\nu^*(t) = D_\nu^{\frac{1}{2}} x_\nu(t) \tag{2}$$

one can obtain expressions for the second-order moments of various ACS coordinates which are readily amenable to computation by uncomplicated special-purpose electronic computers. We now write these expressions:

a) for the output dispersion

$$D_y(t) = \sum_{\nu=1}^{\infty} y_\nu^{*2}(t); \tag{3}$$

b) for the output correlation (autocorrelation) function

$$K_y(t, \tau) = \sum_{\nu=1}^{\infty} y_\nu^*(t)\, y_\nu^*(\tau); \tag{4}$$

c) for the cross-correlation function of the input and output variables at a given moment of time

$$D_{xy}(t) = \sum_{\nu=1}^{\infty} x_\nu^*(t)\, y_\nu^*(t); \tag{5}$$

d) for the cross-correlation function of the input and output variables

$$K_{xy}(t, \tau) = \sum_{\nu=1}^{\infty} x_\nu^*(t)\, y_\nu^*(\tau). \tag{6}$$

Here, y_ν^* (t) is the solution of the differential equation

$$L(p, t)\, y_\nu^*(t) = M(p, t)\, x_\nu^*(t) \quad (\nu = 1, 2, \ldots), \tag{7}$$

and the expressions

$$L(p, t) = \sum_{i=0}^{n} a_i p^i, \quad M(p, t) = \sum_{j=0}^{m} b_j p^j,$$

$$p \equiv \frac{d}{dt}, \; m < n,$$

are the operators of the differential equation which describes the automatic-control system being investigated.

By using Relationships (3) - (6), one can construct a computer for the statistical analysis of an ACS which makes it possible to determine the second-order moments

---

*This paper was given at the All-Union Conference on Computational Mathematics and Computational Technology, at Moscow in 1959

† On the computation of normalized coordinate functions, Cf. [6].

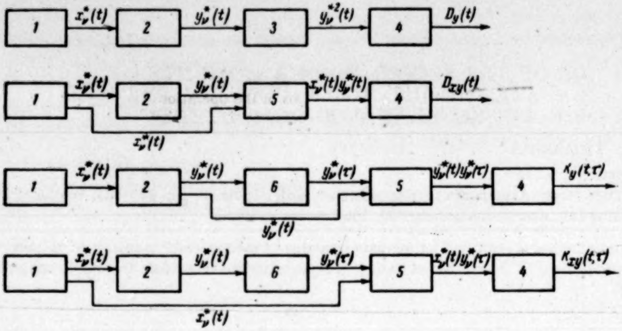

Fig. 1

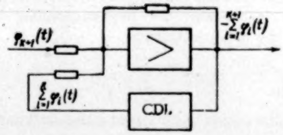

Fig. 2 Principal diagram of special adder.

of various coordinates of the ACS as it is acted on by random disturbances, basing the calculations solely on regular signals, namely, normalized coordinate functions.† Such a device is a special-purpose automatic electronic analog computer. Figure 1 shows the block diagram for a computer designed to determine second-order moments. It contains the following basic blocks: 1 is the block for the memory and for the program control of the computation, 2 is the electronic model of the ACS being investigated, 3 is a squaring device, 4 is a specialized adder, 5 is a multiplier, 6 is a device for introducing delays. The devices used in the computer for squaring, multiplying and introducing delays are standard functional blocks used in electronic simulation [4]. The memory and control block allows input of information (normalized coordinate functions $x_\nu^*(t)$ and the program for controlling the computation) which is written on magnetic tape. For solving (7), the electronic model of the investigated ACS is used. Summation of the series is implemented by means of a special adder (Fig. 2), which is a dc amplifier, operating as a scale amplifier, with additional feedback in the form of a controlled delay line (CDL).

It takes several minutes, on the average, to compute the output dispersion or the cross-correlation function of the ACS's input and output variables on such a machine. It takes some tens of minutes to determine the output autocorrelation function and the ACS's output variable.

Example. As an example, we consider the problem of determining the dispersion of the output coordinate ψ of an ACS during the transient response, when random disturbances act on it. The equations of the system, consisting of object plus controller, are written in the form:

$$\begin{aligned} \omega &= \dot{\psi}, \\ \omega &= a_1\omega - a_2\beta - a_3\delta + X(t) \\ \dot{\beta} &= \omega + a_4\beta + a_5\delta, \\ \dot{\delta} &= \frac{1}{T}\left[i(\psi + \mu\omega)\right] - \delta. \end{aligned} \tag{8}$$

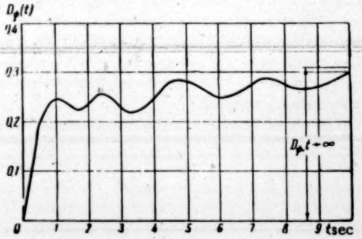

Fig. 3. Curve of the dispersion of the output coordinate ψ of the ACS described by differential equations (8).

Calculation of the dispersion $D_\psi(t)$ of the ACS's output coordinate ψ for $0 \le t \le T = 10$ sec, when the random disturbance $X(t)$ with correlation function $K_x(t,\tau) = \exp(-|t-\tau|)$ acts on it, was implemented in accordance with the block schematic (the first line thereof) shown on Fig. 1. With this, ten terms of the canonical representation of the random disturbance $X(t)$ [6] were taken into account. The time for the computation was 110 sec. Figure 3 gives the curve for the dispersion $D_\psi(t)$.

What has been presented here shows that the use of canonical representations of random disturbances, electronic models of the system being investigated, and additional uncomplicated electronic computing hardware make it possible to find, quite simply from the point of view of engineering practice, the second-order moments of various coordinates of a broad class of automatic-control systems.

LITERATURE CITED

[1] V. S. Pugachev, Theory of Random Functions and Its Application to Automatic Control Problems [in Russian] (Gostekhizdat, 1957).

[2] J. H. Laning and R. H. Battin, Random Processes in Automatic Control [Russian translation] (IL, 1958).

[3] A. M. Batkov, "The solution of one class of nonstationary problems of the statistical dynamics of automatic control systems using electronic analog computers," Dissertation [in Russian] (1958).

[4] B. Ya. Kogan, Electronic Analog Computers and Their Use in the Investigation of Automatic Control Systems [in Russian] (Gostekhizdat, 1958).

[5] I. E. Kazakov, "Approximate probabilistic analysis of the operational accuracy of essentially nonlinear automatic systems," Avtomatika i Telemekhanika 17, 5 (1956). ‡

[6] L. A. Tel'ksnis, "Expansion of random functions in canonical series using electronic analog computers," Trudy Akademii Nauk LitSSR, Ser B 4 (20) (1959).

---

‡ See English translation.

FINITE AUTOMATA. I

M. A. Aizerman, L. A. Gusev, L. I. Rozonoér,
I. M. Smirnóva, and A. A. Tal'
(Moscow)

(Translated from: Avtomatika i Telemekhanika, Vol. 21, No. 2, pp. 224-236, February, 1960)
Original article submitted June 10, 1959

The views of the authors are presented on the basic content and problem areas of the theory of finite automata and on the interrelationships of this theory with the theory of relay-contact circuits; also considered are the possible ways of realizing finite automata.

INTRODUCTION

As soon as it became clear that the propositional calculus was adequate for the technical problems related to the investigations of many relay (switching) devices [1-3], the abstract concept of the "nonsequential switching circuit" was formulated. For many switching circuits, such an abstraction turned out to be natural, and the propositional calculus became the basic mathematical apparatus for analyzing and synthesizing within the limits of this abstraction. However, this abstraction turned out to be inadequate, even for many important switching circuits, since it gave, in principle, no possibility of considering circuit operation in time, and only by artificial methods can be used for solving certain problems in the theory of such circuits.

The desire to introduce time ("sequentiality") into consideration explicitly, and to find an adequate mathematical apparatus for the description of circuits operating through time went beyond the limits of application of solely algebraic, logical operations (the propositional calculus).

"Motion" in such devices was given by special formulas and tables (Cf., for example, [3-7]), by geometric forms (motion of a representative point along the vertices of multidimensional cubes, or along the nodes of some graph or another) (Cf., for example, 4,6-9]) and, finally, by integer recursive functions (Cf., for example, [9-14]). In these works, account was taken, to a greater or lesser degree, of the peculiar features of some concrete method or other of technically realizing logical operations (in particular, the specific features of relay contact technology), i.e., essentially, the soil was prepared for the introduction of new, broader abstractions. It gradually became understood that what was at issue was the isolating of a specific class of dynamic systems*, and that systems constructed of elements having, not two, but an arbitrary, though finite, number of possible states had to be encompassed by these new abstractions.

While, in ordinary dynamic systems, the space and time coordinates have continua for their domains, the basic idiosyncrasy of this special class of dynamic systems is that their time has a countable set for its domain, while their coordinates have finite sets for theirs.

As these abstractions were developed, various names were given to them: logical nets [10], generalized nerve nets [15, 16], finite automata [16], nonprimitive circuits [14], sequential machines [18, 19], robots [17] etc.

The authors prefer the name finite automata for these abstractions.

Certainly, not all switching devices (i.e., those exhibiting relay functioning) are encompassed by these abstractions. For example, the abstraction "finite automata" is not adequate for systems containing devices in which the coordinates are chosen from finite sets, while the time has a continuum for its domain, although these are relay devices. On the other hand, the abstraction "finite automata" corresponds organically to all relay contact circuits which are devoid of such devices. But with certain natural idealizations, many other important technical devices also correspond to it, for example, machine-stand automata, mass-production lines, various digital machines, automata for piecework production, certain abstract models of nervous systems (for example, the nerve nets of McCulloch and Pitts), etc.

2. Basic Definitions and Terminology

As was said earlier, a finite automaton is a special type of dynamic system. The first characteristic of this class of dynamic system is that, in describing its actions, only discrete moments of time are of importance, the intervals between these moments (which, in general, are of unequal duration) being called cycles of the finite automaton's operation. Let p be one of these moments ("the present moment"), and let $p-1, p-2, \ldots, 2, 1, 0$ be the series of preceding moments of time. In this notation, 0 corresponds to the initial moment of automaton operation. We assume that some conditions or other are given which unambiguously define the decomposition of the time axis into cycles†.

---

* In this sense, the older abstraction - the nonsequential relay contact circuit - corresponded to a static system.

In the general case, the dynamic systems under consideration are subject to external stimuli. In the sequel, these stimuli will be called inputs.

Definition. A finite automaton is a dynamic system which, at the discrete moments of time under consideration, satisfies the following conditions.

1. At each of these moments of time, the system can be in just one of a possible finite number k of states.

2. At these moments of time, the system's inputs are also restricted to be chosen from a finite number r of possible states.

3. At any of the moments of time considered, the state of the system is uniquely defined by the state of the system and the state of the input at the previous moment of time.

To distinguish one automaton state from another, we assign a different symbol to each of the k possible states. We denote these symbols by $\kappa_1, \kappa_2, \ldots, \kappa_k$. We call the set of these symbols, denoted by $\{\kappa\}$, the alphabet of the states. Analogously, we write the symbols $\rho_1, \rho_2, \ldots, \rho_r$ for the input states. They form the automaton's input alphabet $\{\rho\}$‡.

We denote by $\kappa(t)$ and $\rho(t)$ the symbols for the automaton state and, input respectively, at time t. Then, by virtue of point 3 in the definition of the finite its operation is described by the recursion formula

$$\varkappa(p) = F[\varkappa(p-1), \rho(p-1)], \tag{1}$$

where F is a single-valued function which puts a definite symbol from the state alphabet into correspondence with each pair of symbols, one of which is chosen from the state alphabet, the other from the input alphabet.

Thus, the abstraction introduced by the concept of "finite automata" singles out a class of systems whose processes are described, not by differential equations, nor yet by difference equations of general form, but by specific equations of the type given in (1). The theory of finite automata concerns the general properties of such a type of system. Therefore, from the point of view of this theory, all systems are identical whose descriptions, with the applicable idealizations, reduce to an equation of type (1) with the same function F in the right member. Moreover, automata described by equations of type (1) with different functions F in their right members can still turn out to be equivalent, in a definite sense, to one another (Cf. section 4 below).

In the actual systems subsumed under the heading of "finite automata," a change of state of an automaton can, in some cases, be taken directly as being the result of the system's operation. In other cases, the automaton has an "output," whose state is uniquely determined by the automaton's state, but is not identical with it**.

Of course, in a finite automaton, the number of possible output states may, but in general does not, coincide with k. Let the output have l ($l \leq k$) states. We write each of the possible output states by a symbol $\lambda\{\lambda_1, \lambda_2, \ldots, \lambda_l\}$, which we call the output alphabet. Then, to describe the operation of an automaton with outputs, (1) must be supplemented by the "instantaneous" relationship

$$\lambda(p) = \Phi[\varkappa(p)], \tag{2}$$

which puts a symbol from the output alphabet into correspondence with each symbol from the state alphabet.

Equation (1) can be given by Table 1, which we call the fundamental table of the finite automaton.

TABLE 1

	$\varkappa_1$	$\varkappa_2$	…	$\varkappa_k$
ρ_1	$\varkappa_3$	$\varkappa_5$	…	$\varkappa_3$
ρ_2	$\varkappa_1$	$\varkappa_k$	…	$\varkappa_6$
⋮	⋮	⋮		⋮
ρ_r	$\varkappa_4$	$\varkappa_5$	…	$\varkappa_3$

This table is set up in the following way: a cell of the table is defined by giving one symbol each from the $\{\rho\}$ and $\{\kappa\}$ alphabets; by taking these symbols to represent matters at time p-1, i.e., by considering them to represent $\rho(p-1)$ and $\kappa(p-1)$, we determine $\kappa(p)$ from (1); we assign the value of $\kappa(p)$ thus determined to this cell.

If the automaton has outputs, then (2) defines the table of correspondences between κ and λ (Table 2).

TABLE 2

$\varkappa$	$\varkappa_1$	$\varkappa_2$	$\varkappa_3$	$\varkappa_4$	$\varkappa_5$	…	$\varkappa_k$
λ	λ_2	λ_4	λ_1	λ_3	λ_l	…	λ_6

---

† It may be assumed, for example, that the continuous time axis is previously divided in some manner into cycles which depend neither on the automaton's operation nor on its external stimuli. In other cases, the moment when a new cycle begins can be taken as the moment when some change in the automaton's input occurs. Finally, the cycles may be defined in such manner that the beginning of a new cycle will also depend on the state of the automaton, or on its output (Cf. part II of the present paper, to be published in the next number of this journal).

‡ In particular, one can number the automata and input states. Then, the state and input alphabets would be comprised of sets of numbers, 1,2,...,k and 1,2,...,r. Such alphabets might be convenient in investigations of individual automata. They are inconvenient in those cases when automata are joined, one to another, since the same symbol here, say the number 3, would apply to states and inputs of different automata.

** For example, in an automaton used for sending alarm signals, the important thing is not its state at each moment, but only whether this state does or does not correspond to an alarm signal.

Together with the finite automaton's fundamental table (Table 1), we shall consider an infinite tape (Table 3), characterizing, for a given initial state and a given sequence of input symbols, the sequence of appearance of state symbols as determined by (1) (or, what amounts to the same thing, as determined by Table 1).

TABLE 3

t	0	1	2	3	4	...
ρ	ρ_1	ρ_3	ρ_5	ρ_r	ρ_2	...
κ	κ_4	κ_1	κ_k	κ_5	κ_1	...

On this tape, each moment of time t is put into correspondence with a ρ and a κ. We call it the state tape.

A triple of symbols, κ(p-1), ρ(p-1) and (p), such as shown on Table 3 by the heavy lines, and chosen for any p, is related internally by (1). We call such a triple a triad.

TABLE 4

t	1	2	3	4	5	...
ρ	ρ_1	ρ_3	ρ_5	ρ_r	ρ_2	...
λ	λ_2	λ_2	λ_5	λ_l	λ_2	...

In cases when the system is defined by (1) and (2) (or by Tables 1 and 2), we shall also consider the automaton's output tape (Table 4), in which each moment of time t is put into correspondence with a pair of symbols ρ and λ.

We take particular note of the case when the input state does not change with time - automata of such type are called autonomous. For an autonomous automaton, (1) has the form:

$$\kappa(p) = F[\kappa(p-1),\ \rho(0)], \qquad (3)$$

where $\rho(0)$ is a time-invariant symbol which can be considered as a parameter.

The operation of an autonomous automaton can be illustrated by a graph.

We place k points on a plane, assigning to each point one symbol corresponding to one of the automaton's possible states. Equation (3) then defines the sequence of changes of state, i.e., the directed transitions from point to point. These directions can be indicated by arrows. It is easily seen that, in general, several arrows can lead to the same point. From a given point, however, at most one, and possible no arrows may lead.

The set of k points, together with the arrows as just described, is called the graph of the autonomous finite automaton.

In a nonautonomous automaton, there can be r input states. Therefore, by fixing and by leaving thenceforth invariant the input state, one can organize r different autonomous automata from a given nonautonomous automaton, each of the autonomous automata having its own graph. The set of these r graphs completely characterizes the nonautonomous automaton. Figure 1 shows an example of such a set, comprised of three graphs; a state table (Table 5) corresponds to this automaton.

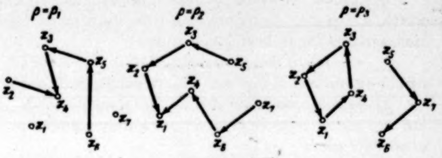

Fig. 1

TABLE 5

	κ_1	κ_2	κ_3	κ_4	κ_5	κ_6	κ_7
ρ_1	κ_1	κ_4	κ_4	κ_4	κ_3	κ_5	κ_7
ρ_2	κ_1	κ_1	κ_2	κ_1	κ_3	κ_4	κ_6
ρ_3	κ_4	κ_1	κ_2	κ_3	κ_7	κ_6	κ_6

3. The General Problems Arising in Connection with the Introduction of the Abstraction "Finite Automata"

Although the abstraction of "finite automata," as this term was introduced in section 2, is a far-reaching one, there arose with its introduction [i.e., with the isolating of the class of systems described by (1), or by (1) + (2)] a number of problems, equally important for all actual systems for which this concept is adequate.

One of these problems, that of the representation of events in finite automata, was solved (inefficiently, it is true) by Kleene's theorems [16] (Cf. also [19-21]).

This is not the sole problem, and a number of important problems in finite automata theory are today not only unsolved, but not even rigorously formulated. These problems arise principally in connection with the fact that both the state tape and the automaton's output tape are infinite. It is therefore meaningless to say that these tapes are "given." All that may be given are algorithms which permit, in a finite number of steps, choosing of the symbol from given alphabets which must be written in an arbitrary cell of the tape.

We denote by A_ρ and A_κ the algorithms corresponding to the upper (ρ) and lower (κ) rows of the state tape, and by A_ρ and A_λ the analogous algorithms for the output tape. From this point of view, a finite automaton, defined by (1) or by (1)+(2) (i.e., by Table 1 or Tables 1 and 2), is essentially an operator which establishes the relationships between algorithms A_ρ and A_κ, or between A_ρ and A_λ.

In connection with this, no scientific problems arise in the task of analysis, i.e., in the task of determining, for a given automaton, the algorithm A_κ (or A_λ) from A_ρ and conversely, and here one may only speak of developing more or less convenient ways of implementing the operations defined by the "finite automaton" operators.

Matters are otherwise when the tape algorithms are given (i.e., A_ρ and A_κ, or A_ρ and A_λ) and it is required to synthesize the automaton (i.e., to construct (1)).

We first consider the case when it is required to synthesize the automaton from the given algorithms A_ρ and A_κ. It is clear that this problem cannot always be solved, since the tape defined by algorithms A_ρ and A_χ may contain triads which are mutually contradictory.

We call two triads contradictory if, in these triads, the symbols $\rho(p-1)$ and $\kappa(p-1)$ are identical, but the symbols for $\kappa(p)$ are different. For example, the pairs of triads

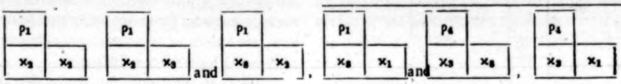

are contradictory, while the pairs of triads

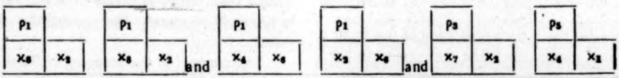

are noncontradictory.

Each cell of Table I contains one symbol. Therefore, the existence of contradictory triads is incompatible with Table 1, i.e., it contradicts the single-valuedness of the function F in (1).

Thus arises the first problem: knowing the algorithms A_ρ and A_κ, to find an algorithm for recognizing their "noncontradictoriness," i.e., the absence of contradictory triads on the state tape.

This problem may be formulated precisely, as follows. We are given the recursive functions $\kappa(p)$ and $\rho(p)$, each of which can assume a finite number of values. It is required to construct a recursive functional $\Psi[\kappa(p), \rho(p)]$ (Cf. [23] Chap. 9) which equals unity on those functions $\kappa(p)$ and $\rho(p)$ for which there exists the function $F(u,v)$, defined on the finite set constituting the domain of u and v such that, for any p, the relationship $\kappa(p) = F[\kappa(p-1), \rho(p-1)]$ holds, and which equals zero otherwise. If, as may be assumed, the problem as formulated is algorithmically unsolvable, the necessity then arises of posing the more restricted tasks of determining a recursive functional Ψ on the functions $\kappa(p)$ and $\rho(p)$ which lie in a more restricted class than the class of all the recursive functions which assume the given number of values.

Although the automaton's state tape is infinite, the numbers r and k are finite, so that the total number of different triads on the tape is also finite. After the question of the "noncontradictoriness" of the algorithms is resolved, there arises a second problem: for given "noncontradictory" algorithms A_ρ and A_κ, to find an algorithm for seeking all the different triads contained on an infinite state tape. The solution of this problem would immediately permit one to fill in all or some of the cells of Table 1, and to define the automaton with an exactitude to within the cells which remained unfilled and could be filled in arbitrarily.

In the case when a finite number of state tapes is given, and it is required to find an automaton which reproduces all these tapes, no new problem arises, since the algorithm for observing contradictions and the algorithm for determining all the different triads may be applied to each tape in turn. New problems arise only when the number of state tapes is infinite.

The matter is significantly more complicated when it is required to synthesize an automaton from its output tape. Here the additional problem arises: knowing the algorithms A_ρ and A_λ, to determine k, i.e., the number of states which must be realized in the automaton, and to find the function Φ in (2), i.e., from the given output tape to construct a noncontradictory state tape.

It is precisely problems of this type which are most interesting in practice, since the requirements on the automaton to be synthesized are ordinarily given directly in "input-output" terms.

It is necessary to mention that the general problem of synthesizing finite automata from given operating conditions has thus far not been precisely formulated. The difficulty of a rigorous posing of this problem stams from the following. In the majority of questions arising in practice, the automaton must transform a given infinite class of input sequences into a required class of output sequences. Up to now, however, there has been developed no sufficiently general and convenient mathematical apparatus in terms of which an adequate description of these infinite classes of sequences could be given. In the present case, a description in terms of sets of tables [15] is unsatisfactory, since the original (verbal) given conditions of operation are posed in other ("logical") terms (closer to the language developed in [22]), while no algorithm has been established for making the transition from the language of sets of tables to the "logical" language.

All algorithmic problems of this nature vanish, and the synthesis problem becomes much easier, in the case when the automaton's tapes are finite.

4. Mappings of Finite Automata and Their Equivalence

In considering an automaton with outputs, we previously used the "instantaneous" relationship of (2).

This relationship can be considered as a rule for transforming state symbols to output symbols. An abstract device which realizes (2) is called a symbol transformer. There is, of course, an analogous symbol transformer at the automaton's input; it will transform the symbols of some external stimulus alphabet to symbols of the automaton's input alphabet.

We now assume that two automata are given: automaton A, operating with input alphabet $\{\alpha\}$ and with state alphabet $\{a\}$, and automaton B, with input alphabet $\{\beta\}$ and state alphabet $\{b\}$. We further assume that there are two symbol transformers: one of them (the input transformer) transforms the symbols $\{\alpha\}$ to $\{\beta\}$, and the second (output) transforms symbols $\{b\}$ to $\{a\}$.

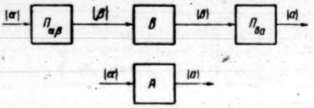

Fig. 2

We now consider the system consisting of the input symbol transformer, automaton B and the output symbol transformer (Fig. 2). This combined system has inputs from the alphabet $\{\alpha\}$ and outputs from the alphabet $\{a\}$, the same as automaton A††.

If we can choose input and output symbol transformers such that, for any sequence of input symbols from alphabet $\{\alpha\}$ and for any initial state of automaton, A, there would exist an initial state of automaton B such that there would appear, at the output of the combined system (automaton B and the two transformers), the same sequence of symbols from the alphabet $\{a\}$ as the sequence of state symbols in automaton A, then we shall say that automaton B is a mapping of automaton A (or that automaton A is mapped onto automaton B).

We symbolize this fact by:

$$A \subseteq B \quad \text{or} \quad B \supseteq A.$$

If simultaneously

$$A \subseteq B \quad \text{and} \quad A \supseteq B,$$

then the automata A and B will be said to be equivalent, and we symbolize this circumstance by $A \asymp B$.

We now give a precise definition of the concept of mapping.

The automaton A ($\{a\}$, $\{\alpha\}$) is mapped onto automaton B ($\{b\}$, $\{\beta\}$) (and automaton B is a mapping of automaton A) if, to each pair (a_i, α_j) of symbols from the alphabets $\{a\} = \{a_1, \ldots, a_k\}$ and $\{\alpha\} = \{\alpha_1, \ldots, \alpha_r\}$, one can set up a correspondence of such a pair ($\{b_i\}$, $\{\beta_j\}$) of sets of symbols from the alphabets $\{b\} = \{b_1, \ldots b_n\}$ and $\{\beta\} = \{\beta_1, \ldots, \beta_m\}$ such that, if

$$F_A(a_i, \alpha_j) = a_s, \tag{4}$$

then, for any symbols $b_{q_i} \in \{b_i\}$ and $\beta_{p_j} \in \{\beta_j\}$ the following condition holds

$$\tag{5}$$

Here, F_A and F_B are the functions in the left bers of equations of the type of (1) for automata A and B respectively.

Two equivalent automata do not differ practically from one another – their differences are external, consisting only in the methods chosen for coding the automata states and inputs. In spite of this, two equivalent automata can be described by completely different equations of type (1). Even the variables in these equations may be taken from different alphabets. Thus, for example, two automata with identical numbers of states and inputs, differing only by the notation of the states and the inputs, i.e., the alphabets from which the symbols are taken and the manner in which these are associated with states and inputs, are known to be equivalent, although the equations of type (1) for them are different.

If $A \subseteq B$, but $A \not\asymp B$, this means that there exists a symbol transformer by means of which automaton B can be "forced" to operate like automaton A, but not conversely.

The concept of the mapping of finite automata, and of their equivalence, is closely related to the topological peculiarities of their graphs.

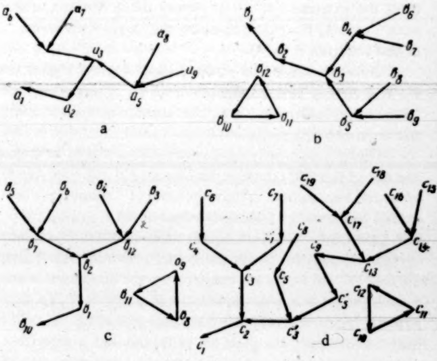

Fig. 3

As an example, we consider the graphs of the four autonomous finite automata, given in Fig. 3. The automata of Fig. 3, b, and c are equivalent, since they differ only by the nomenclature of the states. The automaton of Fig. 3a, is mapped onto each of the automata of Fig. 3, b, and c. This becomes clear by supposing that a transformer is placed at the output of the automaton of Fig. 3,b which places each symbol b_i ($i = 1,\ldots,8$) into correspondence with any of the a_i ($i = 1,\ldots,8$).

---

†† To be sure, such a combined system might not be a finite automaton, since its output symbol at time p might not be uniquely determined by its output and input symbols at time p-1. We shall assume that the combined system under consideration is a finite automaton.

All three of the automata thus far considered are mapped onto the automaton of Fig. 3,d. The output transformer which it is necessary to append to the automaton of Fig. 3,d for it to operate the same as the automaton of Fig. 3,b must place each of the symbols c_i into correspondence with b_i for $i = 1,2,6,7,8,9,10,11$, and 12. Symbols c_3 and c_3' are made to correspond with the same symbol b_3, symbols c_4 and c'_4 with b_4 and symbols c_5 and c''_5 with b_5. In addition, symbols $c_{13}, c_{14},\ldots,c_{20}$ are placed into correspondence with any of the symbols $b_1,\ldots,b_{12}$.

The problem now arises: knowing the fundamental tables of two automata, or their equations of type (1), to determine whether these automata are equivalent, or whether one of them is mapped onto the other ‡‡. In other words, it is required to find criteria for the mappings and equivalences of automata.

The concept of equivalence of automata, and of their mappings, allows one to introduce the concept of the abstract aggregating (assembly) of finite automata, i.e., of assembling a finite automaton from standard elementary automata.

5. Abstract Assembly of a Finite Automaton

We now consider a device with $\underline{s}$ input wires $u_1,\ldots,u_s$ and $\underline{n}$ generalized coordinates $x_1,\ldots,x_n$. At the times $0,1,2,3,\ldots,p$, each input and each coordinate may have only one of a finite number of values, which we shall symbolize by symbols from some alphabets. At any moment of time, each coordinate is determined uniquely by the values of all or some of the inputs and coordinates at the preceding moment of time.

The operation of such a device is described by the recursion relationships

$$x_i(p) = f_i[x_1(p-1),\ldots,x_n(p-1);$$

$$u_1(p-1),\ldots,u_s(p-1)]\ (i = 1,\ldots,n) \qquad (6)$$

or, in vector form,

$$x(p) = f[x(p-1),\ u(p-1)]. \qquad (7)$$

If an x_i can have χ_i different values ($i = 1,\ldots,n$), then the vector $x(p)$ can have $k = \prod_{i=1}^{n} \chi_i$ different values. We call the vector $\underline{x}$ the state of the device being considered, and we choose its $\underline{k}$ values from the symbols $\kappa_1,\ldots,\kappa_k$ of the alphabet $\{\kappa\}$. Analogously, the input vector $\underline{u}$, with $r = \prod_{j=1}^{s} \xi_j$ values (where ξ_j is the number of values of u_j) is called the input state, and we relate its values to the symbols $\rho_1,\ldots,\rho_r$ of the alphabet $\{\rho\}$. With this notation, (7) reduces to (1), which means that the device just described is a finite automaton.

Equations (6) can also be understood as another form of equation of the type (1). Different equations of type (6) can correspond to one and the same equation of type (1), but they all describe the processes in equivalent automata.

In the definition of a finite automaton, given in section 2, and in the equation of type (1) which corresponded to it, we had to do only with automata states and inputs. Now, in making the transition to equations of type (6), we introduced coordinates and input wires (input lines). We shall call the transition from (1) to the equivalent (6) a choice of structure for the finite automaton, and (6) will be called its abstract structure (AS). A technical device which, with the suitable idealizations, is described by equations of type (6), will be called a technical realization of the automaton's structure.

Let there now be given several systems of equations of type (6), each of which is the abstract structure of a corresponding automaton. Each of these systems of equations has its own coordinate and input-line alphabets.

We now introduce into the discussion symbol transformers, each with several input lines and one output. The symbols from the transformer's output alphabet appear at its output at the same instant that the symbols from their respective alphabets are applied to the input lines.

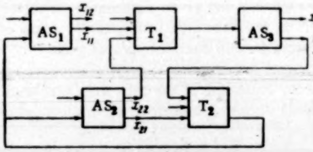

Fig. 4

We use transformers as means for the interconnection of AS (as, for example, on Fig. 4), choosing them in such manner that the corresponding AS alphabets and transformers are properly linked. We call such a set of AS, interconnected via symbol transformers, a net. The coordinates of the net are comprised of all the generalized coordinates x_i of all the AS, including those not applied to any transformer. The net's input lines are both the AS input lines on which no transformer acts, and the transformer input lines on which no AS coordinate acts.

In order to obtain the equations for a net, it is necessary to use the given equations for the transformers for eliminating from the systems of equations of type (6) the corresponding variables for the AS input lines, replacing them by the AS coordinates and the variables of the transformers' input lines. As the result, the net as a whole is also described by a system of recursion relationships of

---

‡‡ Certainly, what we have in mind here is not the trivial solution, obtained by the exhaustive trial of all meaningful correspondences of symbols.

$x(p-1)$				$u(p-1)$				$\kappa(p-1)$	$\rho(p-1)$	$\kappa(p)$	$x(p)$			
x_1	x_2	…	x_n	u_1	u_2	…	u_s				x_1	x_2	…	x_n
		…				…							…	
		…				…							…	
⋮	⋮	…	⋮	⋮	⋮	…	⋮	⋮	⋮	⋮	⋮	⋮	…	⋮

TABLE 6

type (6), i.e., the net itself is the abstract structure of some finite automaton.

From what has been said, it follows that a finite automaton can be constructed from other finite automata by joining them in a net. The question naturally arises as to the possibility of creating a set of automata, or even all meaningful automata, from a small collection of original automata – "elements." Such construction of automata we call abstract assembly. The technological value of this concept is obvious.

The introduction of the concept of abstract assembly leads immediately to the posing of the following problems: to construct algorithms which answer the question as to the possibility of constructing nets from a given set of AS and transformers, these nets being mappings (in the sense of section 4) of given automata, and to specify an algorithm for the efficient implementation of this construction.

A set of AS and transformers from which one can construct nets mapping any given automaton is called a complete set. The problem then immediately arises of determining criteria for the completeness of a set.

A complete set which is very important for technology is the set consisting of the following elements: a) a binary delay element, described by the following equation

$$x(p) = z(p-1)$$

where $\underline{x}$ and $\underline{z}$ are given in an alphabet which contains only two symbols (for example, 0 and 1); b) some set of logical elements which permits the realization of any logical function (this set may consist for example, of conjunction, disjunction and negation elements).

From this set, a net which is the mapping of any finite automaton can be constructed. Indeed, let a finite automaton be given by Eq. (1), i.e., let the function F and the alphabets $\{\kappa\}$ and $\{\rho\}$ be given.

We choose two numbers $\underline{n}$ and $\underline{s}$ such that the conditions $2^n \geq k$ and $2^s \geq \underline{r}$ are satisfied. We introduce the variables $x_1,\dots,x_n$ and $u_1,\dots,u_r$, where each of these variables assumes only the values 0 and 1.

We consider Table 6. On its left side are enumerated all possible combinations of all values of $x_1,\dots,x_n$, $u_1,\dots,u_s$, i.e., Table 6 has 2^{n+s} rows. Each different combination of variables $x_1,\dots,x_n$ is placed in correspondence with its own symbol from the alphabet $\{\kappa\}$. Since the number of these symbols is $\underline{k} \leq 2^n$, there may remain combinations $x_1,\dots,x_n$ for which the alphabet $\{\kappa\}$ cannot supply symbols different from other symbols already used. We assign arbitrary previously used symbols from $\{\kappa\}$ to these combinations $x_1,\dots,x_n$.

We proceed analogously with the combinations of variables $u_1,\dots,u_s$, designating them by symbols from $\{\rho\}$. We write the selected symbols from $\{\kappa\}$ and $\{\rho\}$ in the corresponding row of columns κ (p-1) and ρ(p-1) of Table 6.

Thus, to each set of variables $x_1,\dots,x_n$; $u_1,\dots u_s$ there corresponds a pair of symbols from the alphabets $\{\kappa\}$ and $\{\rho\}$. By taking these pairs of symbols as standing for κ(p-1) and ρ(p-1), we find κ(p) from (1), and write these values in the corresponding rows of column κ(p) of Table 6. We can then immediately fill up the right side of Table 6, since we have already related a definite combination of values $x_1,\dots,x_n$ with each symbol from $\{\ \}$ ***

The table thus constructed determined the value of all xi at time $\underline{p}$ from the given x_i and u_j at time p-1, i.e., it gives $\underline{n}$ logical recursion relationships of the type of (6):

$$x_i(p) = L_i[x_1(p-1),\dots,x_n(p-1);\ u_1(p-1),\dots,u_s(p-1)] \quad (i=1,\dots,n). \tag{8}$$

For any combination of values of the variables, the values of all the functions L_i are read off from Table 6.

It is easily seen that the obtained equations (8) are the abstract structure of an automaton which maps the original automaton which was given by an equation of type (1).

Each equation in (8) can be realized in the form of an elementary one-cycle lag, with equation

$$x_i(p) = z_i(p-1) \qquad (i = 1,\dots,n), \tag{9}$$

and a logical instantaneously acting transformer

$$z_i = L_i(x_1,\dots,x_n;\ u_1,\dots,u_s) \quad (i = 1,\dots,n), \tag{10}$$

which, in the given case, is also a transformer of the coordinate x_i and input u_j symbols to input z_k symbols of the lag of (9). In the given special case, all the symbols x_i, u_j, and z_k are chosen from the same alphabet, namely, $\{0, 1\}$. The entire set of equations (8) is a net composed of $\underline{n}$ lags of the form (9) and $\underline{n}$ transformers of the

---

*** If $k < 2^n$ and if several combinations, $x_1,\dots,x_n$ were related to one and the same symbol of $\{\kappa\}$, then we choose any one of them in any case when the corresponding symbol arises.

form (10). Since any logical transformer is realized from the set of logical elements given by us in the conditions of the problem, this shows that this set of logical elements, supplemented by a delay element, is a complete set of the elements necessary for constructing any automaton.

It can be shown analogously that a set of elements allowing any function of q-valued logic ($q > 2$) to be reproduced, and supplemented by a delay element of the form of (9), wherein the input and output assume values from a q-symbol alphabet, also comprises a complete set.

In this section we first used the concept of a delay element. This concept requires the following additional elucidation.

When any symbol from the input alphabet is applied to the input of delay element (9), the corresponding symbol from the output alphabet appears at its output after a one-cycle delay. It was stated, at the very beginning of this paper, that the cycles could be nonuniform, and that the division of the time axis into cycles was uniquely determined by some additional conditions. So long as we had to do with abstract structure and abstract assembly, i.e., essentially with the replacement of (1) by equations of the form (6), this circumstance was of no significance since in (1) and (6) the sequentiality (i.e., the character of the variation of the argument p) was considered as given. In using the complete sets, described above, for the technological realization of automata, it is assumed that the automata contain special devices – sequencing transducers which, in correspondence with given conditions, process the signals for cycle beginning and apply them to delay elements. This stimuli of the delay elements are not external in the sense in which the term "external stimuli" was used above; they are not encoded by symbols from $\{\rho\}$ in setting up (1), and are not germane to the stimuli u_j in (6). Therefore, even an autonomous automaton may contain these stimuli, which are essential only for the technological realization, and are not taken into consideration when one deals with abstract structure or abstract assembly.

LITERATURE CITED

[1] V. I. Shestakov, "Some mathematical methods for constructing and simplying two-terminal class-A electrical circuits," Dissertation [in Russian] (Scientific-Research Institute of Physics, Moscow State Univ, 1938).

[2] C. E. Shannon, "A symbolic analysis of relay and switching circuits," Trans. AIEE 57 (1938).

[3] M. A. Gavrilov, Switching Circuit Theory [in Russian] (Izd. AN SSSR, 1950).

[4] D. A. Huffman, "The synthesis of sequental switching circuits," Franklin Inst. 257, 3, 4 (1954).

[5] V. N. Roginskii, Elements of Structural Synthesis of Relay Control Circuits [in Russian] (Izd. AN SSSR, 1959).

[6] R. Higonnet and R. Grea, Logical Study of Electrical Circuits and Binary Systems [in French] (Paris, 1955).

[7] S. H. Caldwell, Switching Circuits and Logical Design (New York, 1948).

[8] W. R. Ashby, Introduction to Cybernetics [Russian translation] (IL, 1959).

[9] N. E. Kobrinskii and B. A. Trakhtenbrot, "On constructing a general theory of logical nets," Collection: Logical Investigations [in Russian] (Izd. AN SSSR, 1959).

[10] A. W. Burks and J. B. Wright, "Theory of logical nets," Proc. IRE 4 (1953).

[11] B. A. Trakhenbrot, "On the operators realized in logical circuits," Doklady Akad. Nauk SSSR 112, 6 (1957).

[12] A. W. Burks and H. Wang, "The logic of automata," Assoc. Comp. Mach. 4, 2, 3 (1957).

[13] Yu. Ya. Bazilevskii, "Questions in the theory of time-dependent logical functions," Collection: Questions in the Theory of Mathematical Machines, No. 1 [in Russian] (Fizmatgiz, 1958).

[14] M. L. Tsetlin, "On nonprimitive circuits," Collection: Problems of Cybernetics, No. 1 [in Russian] (edited by A. A. Lyapunov) (Inoizdat, Moscow, 1956).

[15] U. S. McCulloch, W. Pitts, Logical computing of ideas pertaining to nerve activities. Collection: Automata Studies [in Russian] (edited by A. A. Lyapunov) (Inoizdat, Moscow, 1956).

[16] S. C. Kleene, "representation of events in nerve nets and finite automata," Collection: Automata Studies [Russian translation] (edited by A. A. Lyapunov) (Moscow, 1956).

[17] J. T. Culbertson, "Some uneconomical robots," Collection: Automata Studies [Russian translation] (edited by A. A. Lyapunov) (Inoizdat, Moscow, 1956).

[18] E. F. Moore, "Gedanken-experiments on sequential machines," Collection: Automata Studies [Russian translation] (edited by A. A. Lyapunov) (Inoizdat, Moscow, 1956).

[19] I. M. Copi, C. Elgot and J. B. Wright, "Realization of events by logical nets." Assoc. Comp. Mach. 5, 181, 2 (1958).

[20] Yu. T. Medvedev, "On the class of events admitting representation infinite automata," Collection: Automata [in Russian] (edited by A. A. Lyapunov) (Inoizdat, Moscow, 1956).

[21] B. A. Trakhenbrot, "The synthesis of logical nets whose operators are described by means of the single-argument predicate calculus," Doklady Akad. Nauk SSSR 118, 4 (1958).

[22] M. D. Davis, Computability and Unsolvability McGraw-Hill, New York, 1957).

[23] D. D. Aufenkamp, S. Seshu, and F. E. Khon, "Theory of nets," Mathematical collection of Translations of Foreign Papers [Russian translation] 3, 3 (1959).

[24] D. D. Aufenkamp and F. E. Khon, "The analysis of sequential machines," Mathematical Collection of Foreign Papers [Russian translation] 3, 3 (1959).

[25] D. D. Aufenkamp, "The analysis of sequential machines," Mathematical Collection of Foreign Papers [Russian translation] 3, 6 (1959).

A UNIVERSAL FUNCTION GENERATOR BASED ON THE PRINCIPLE OF QUADRATIC APPROXIMATIONS

A. A. Maslov and Yu. G. Purlov
(Moscow)

(Translated from: Avtomatika i Telemekhanika, Vol. 21, No. 2, pp. 237-244, February, 1960)
Original article submitted July 21, 1959

Methods are presented for quadratic approximations for functions given either analytically or graphically. Simple formulas and relationships are derived for finding the rule for argument partitioning. For obtaining a quadratic relationship, a variant of a diode element is considered.

The paper describes the circuit of a universal function generator using quadratic approximations and capable of being implemented in the form of an attachment to a type ÉMU-8 analog computer.

Universal diode-function generators [1-5] based on the principle of piecewise-linear approximations are widely used in modern electronic analog computers for reproducing various nonlinear functions.

When it is necessary to reproduce a function with a comparatively large range of variation of the absolute magnitude of the first derivative, function generators of this type require the use of a large number of diode elements, which complicates the circuit and increases the error. In addition, discontinuities in the value of the first derivative of the reproduced function are introduced which, in many cases, is highly undesirable.

The disadvantages just cited can, to a large extent, be removed if nonlinear functions are approximated by segments of curves, in particular, by segments of parabolas [6-8].

However, the use of quadratic approximations entails a significant increase in the amount of computational work necessary to determine the partitioning along the argument axis, which has resulted in work being carried out to develop simplified analytic and graphical methods of calculating functions, and a variant of a universal function generator, based on the principle of quadratic approximations, has been developed.

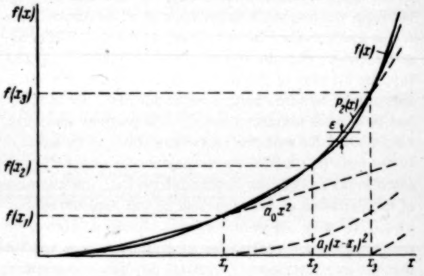

Fig. 1

Method of Piecewise-Quadratic Approximation of Nonlinear Functions

The problem of the piecewise-quadratic approximation of a nonlinear function f(x) amounts to the finding of a number of fixed argument values $x_1, x_2, x_3,$ which provides a second-order approximation polynomial with vertices $f(x_1), f(x_2), \ldots$

$$P_2(x) = a_0 + a_1 x + \sum_{i=1}^{n} b_i (x - x_i)^2,$$

where

$$b_i = \begin{cases} 0 & \text{for} \quad x \leqslant x_i, \\ B_i = \text{const} & \text{for} \quad x > x_i, \end{cases}$$

to the curve f(x) to be reproduced such that, on the entire interval of argument variation, the absolute error of the approximation function does not exceed some previously given value ϵ (Fig. 1).

With respect to the function f(x), it is assumed that it is single-valued and continuous on the given interval of argument variation, and that it has a continuous second derivative everywhere on that interval with the possible exception of a finite number of first-order discontinuities.

For quadratic interpolation, the remainder term in Newton's interpolation formula has the form [9, 10]:

$$R(x) = \frac{f'''(\xi)}{3!}(x - x_1)(x - x_2)(x - x_3),$$

where $f'''(\xi)$ is the value of the reproduced function's third derivative at some point ξ inside the interval (x_1, x_3). The modulus of the error R(x) has its maximum value when $f'''(\xi)$ and the expression $|(x-x_1)(x-x_2)(x-x_3)|$ simultaneously attain their maxima:

$$|R(x)|_{\max} = \frac{|f'''(\xi)|_{\max}}{3!}|(x - x_1)(x - x_2)(x - x_3)|_{\max}.$$

We introduce the new variable $u = (x-x_1)/(x_3-x_1)$ and let $k = (x_2-x_1)/(x_3-x_1)$ and $h = x_3-x_1$.

Then,

$$|R(u, k)|\max = \frac{|f'''(\xi)|\max}{3!}\,|u(u-1)(u-k)|\max h^3.$$

The function $u(u-1)(u-k)$, in the region of variable variation $0 \leq u \leq 1$, $0 \leq k \leq 1$, attains its greatest value, equal to 4/27, at the points ($u=1/3$, $k=1$) and ($u=2/3$, $k=0$).

Thus, for this worst case, we have

$$R(u\ \ k)\ \max = \frac{4h^3|f'''(\xi)|\max}{27\cdot 3!} = \frac{2h^3|f'''(\xi)|\max}{81}.$$

By assuming that $\max|R(u,k)| \leq \epsilon$, we obtain the expression for determining the length of the partition segment $h = x_3 - x_1$ in the form

$$h \approx 3{,}43\sqrt[3]{\frac{\varepsilon}{|f'''(\xi)|\max}}.$$

The worst case was taken in estimating the approximation error. In the general case, a more accurate consideration is very difficult. Experiment shows that, for a wide class of frequently arising functions, we may consider that

$$h = 4\sqrt[3]{\frac{\varepsilon}{|f'''(\xi)|_{\max}}}.$$

Example. It is required to reproduce the function $f(x) = x^3 \cdot 10^{-4}$ in the domain $0 \leq x \leq 100$. We find the law of argument partitioning when the approximation error is taken as $\epsilon = \pm\ 0.35$.

The third derivative of the given function equals the constant quantity $6 \cdot 10^{-4}$. Therefore, all the segments will be the same, and equal to

$$h_k \doteq 4\sqrt[3]{\frac{0{,}35\cdot 10^4}{6}} = 33{,}6.$$

The total number of partition segments is three.

If the function f(x) is given graphically, then the threefold graphical differentiation necessary for the computation of the value of $f'''(\xi)$ is very difficult, and entails large errors. In this case, a graphical method should be used to determine the law of argument partitioning. This method is based on the replacement of a quadratic approximation to the given function f(x) with error ϵ by a piecewise-linear approximation to the first derivative f'(x) with error ϵ'. The problem reduces to the finding of the relationship $\epsilon' = \varphi(\epsilon, x)$. Figure 2 shows one segment of the quadratic second-order approximation polynomial $P_2(x)$. For $x = x_1$, $x = x_2$ and $x = x_3$, the function f(x) to be reproduced and the polynomial $P_2(x)$ have the common points:

$$f(x_1) = P_2(x_1),$$
$$f(x_2) = P_2(x_2), \quad f(x_3) = P(x_3).$$

The greatest error of approximation occurs when $x = x'$ and $x = x''$. It is obvious that for this

$$f'(x') = P_2'(x'), \quad f'(x'') = P_2'(x'').$$

In Fig. 3 there has been constructed the derivative $f(x)$ of the given function, as well as the derivative $P'_2(x)$ of the approximating polynomial. The errors ϵ'_1, ϵ'_2, and ϵ'_3 occur respectively for $x = x_1$, $x = x_2$, and $x = x_3$.

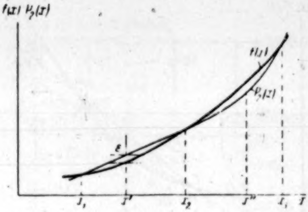

Fig. 2

From the approximation conditions, it follows moreover that

$$S_{ABC} = S_{CDE} = S_{DEF} = S_{FGK} = |\varepsilon|.$$

At the point $x = x'$, the angle between $f'(x)$ and $P'_2(x)$ on the left, α_-, is not greater than the angle on the right, α_+: $\alpha_+ = \alpha_- + \Delta\alpha$, where $\Delta\alpha \geq 0$.

By replacing the curve $f_2(x)$ by straight lines on the segments AC and CE we find, from the equality of the areas $S_{\Delta ABC} = S_{\Delta CDE} \approx |\epsilon|$, that $\epsilon'_1 \leq \epsilon'_2$.

Analogously, we can convince ourselves that $\epsilon'_3 \geq \epsilon'_2$.

We now consider F'(x) on the segment x', x''. Here there is a one-sided linear approximation. Therefore, [11],

$$\varepsilon'_2 \leqslant \frac{A_k(x'x'')^2}{8},$$

where A_k is the maximum value of the third derivative $f'''(x)$ in the interval $x'x''$.

By assuming that point x_2 divides segment $x'x''$ in the ratio l, we find that

$$\varepsilon'_1 \leqslant \frac{A_k(x'x'')^2}{8}l^2 \leqslant \varepsilon'_2 l^2,$$
$$\varepsilon'_2 \leqslant \frac{A_k(x'x'')^2}{8}(1-l)^2 \leqslant \varepsilon'_1(1-l)^2.$$

Thus,

$$\varepsilon = \frac{1}{2}S_{CFE} \approx \frac{1}{2}\left(S_{\Delta CEF} + S_{\Delta CER} + S_{\Delta EFO}\right) =$$
$$= \frac{x'x''}{2\cdot 2}\left[\varepsilon'_2 + l^3\varepsilon'_2 + (1-l)^3\varepsilon'_2\right] =$$
$$= \frac{x'x''}{4}\varepsilon'_2(3l^2 - 3l + 2).$$

From whence

$$\varepsilon'_2 = \frac{4\varepsilon}{x'x''(3l^2 - 3l + 2)}.$$

The expression in the denominator assumes its minimum value for $l = 1/2$. With this, $\epsilon'_2 \leq 16\,\epsilon/5a$, where $a = x'x''$. This last formula gives the connection between the given error ϵ and the tolerance margin ϵ' and size of a.

In reproducing various functions, the lengths of neighboring partition intervals differ little from one another. Therefore, by measuring the quantity a on a constructed segment, we find from the last formula what the tolerance will be for the following segment. Inside the tolerance band ϵ', constructed with respect to $f(x)$, we carry out a

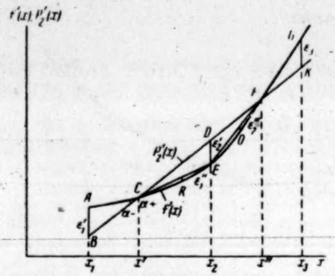

Fig. 3

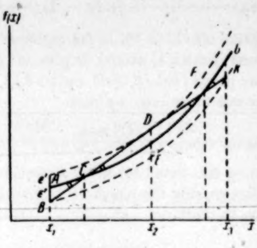

Fig. 4

two-sided linear approximation, as a result of which we find the size of the following partition interval.

It is easily shown that, with such a method of partitioning, the actual error will not be larger than the admissible approximation error ϵ. Indeed, let the admissible error ϵ' be computed from the previous segment. To determine the size of the partitioning segment, we construct the tolerance band with respect to f'(x) (Fig. 4). We then carry out a two-sided linear approximation.

Since ACB ≤ DCE, DFE≤ GFK, then $S_{\Delta ABC} \leq S_{\Delta CDE} \leq \epsilon$ and $S_{\Delta FGK} \leq S_{\Delta FDE} \leq \epsilon$, i.e., with this we obtain a certain underestimate of the length of the partition interval, which leads only to a decrease in the error of approximation of the nonlinear function f(x) to be reproduced.

As the second derivative f''(x) increases, the curvature of the function f(x) also increases and, consequently, the lengths of the segments of the argument partition decrease. So that the magnitude of the error, defined by the previous segment, not exceed the tolerance on the given interval, the partitioning should be carried out from large segments to small ones, i.e., on the side of an increasing second derivative f''(x).

For the finding of the first segment, we may recommend a simplified method of successive approximations, shown on Fig. 5 for the function $f(x) = x^3 \cdot 10^{-4}$, where the graphical construction of the first segment is given. Letting the magnitude of $a_1 = 20$v, we construct the tolerance margin $\epsilon'_1 = 16\ \epsilon/5a_1 = 0.16\,\epsilon$, and we then carry out a piecewise linear approximation. We obtain the quantity $a_2 > a_1 = 20$. We construct the new tolerance margin $\epsilon'_2 = 16\ \epsilon/5a_2$, and carry out a piecewise linear approximation which determines a_3. It is obvious that the optimal length of the segment will be $a_1 \leq a_3 \leq a \leq a_2$. As the interval length varies within these limits, the maximum actual error ϵ'_1 decreases from ϵ'_1 to ϵ'_2, varying along a certain curve AB which is close to being a straight line. At the same time, the admissible error varies along a hyperbola which passes through points C and D, which correspond to the maximum values of ϵ'_1 for $a_1 = 20$ and $a_2 = 24$. If we now replace the hyperbola by the straight line CD we find, on Fig. 5., the point 0 of intersection which, with an accuracy sufficient for a graphical method, gives the magnitude of the error ϵ' for the first and second intervals of the argument partitioning.

Circuit of the Quadratic Diode Element

For obtaining segments with quadratic dependencies in the present work, we used the diode element represented on Fig. 6, a [8]. To the diode are applied input vol-

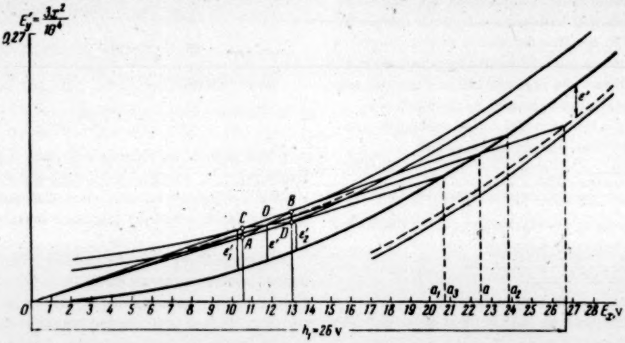

Fig. 5

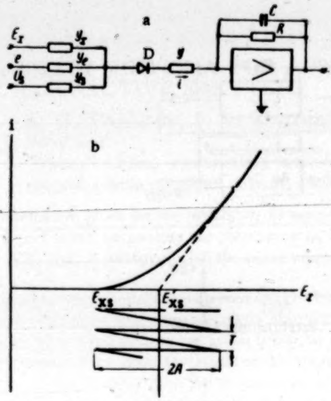

Fig.6

tage E_x, reference voltage e and high-frequency sawtooth voltage U_s. The diode element's transconductance characteristic is determined by the conductance Y.

If the high-frequency voltage U_s is not applied to the diode, the dependence of the current i on the input quantity E_x has the form shown on Fig. 6,b by the dotted line. For $E_x = E'_{xs} = eY_e/Y_x$, diode D is opened, and thereafter the current i increases proportionately to input voltage E_x.

If a sawtooth voltage of amplitude A is applied to the diode via Y_s, the diode will open for lower values of the input voltage:

$$E_x = E_{xs} = e\frac{Y_e}{Y_x} - A\frac{Y_s}{Y_x}.$$

By using the principle of superposition, we find the average value of the diode element's current:

$$i_{av} = \begin{cases} 0 & \text{for } E_x \leqslant E_{xs}, \\ \dfrac{Y}{YAY_0Y_s}(Y_xE_x - Y_ee + Y_s A)^2 & \text{for } E_x > E_{xs}. \end{cases}$$

Here,

$$E_{xs} = e\frac{Y_e}{Y_x} - A\frac{Y_s}{Y_x},$$

$$Y_0 = Y_x + Y_e + Y_s + Y.$$

For getting a sawtooth voltage, a generator circuit, shown on Fig. 7, was developed. A blocking generator was executed based on triode V_1, while pentode V_3 was used as a discharge tube. Charging condenser C_1 is connected in the anode circuit of V_3. During the blocking process, the condenser is charged up to the potential U_{max} close to the anode voltage. Tube V_1 is cut off and condenser C_1 discharges through tube V_3. Because of the current-stabilizing action of the pentode, the discharge of C_1 occurs linearly. As soon as the voltage becomes equal to $U_{C_1} = U_{unb.V_1}$, tube V_1 opens and the blocking process repeats. The generated voltage is applied to the grid of cathode follower V_2. Part of the output voltage is tapped off by the voltage divider formed by resistors R_2, R_3, and R_4, and is applied to the cathode of V_3. The magnitude of the positive feedback can be controlled by resistor R_3, thus varying, within very wide limits, the linearity of the output voltage.

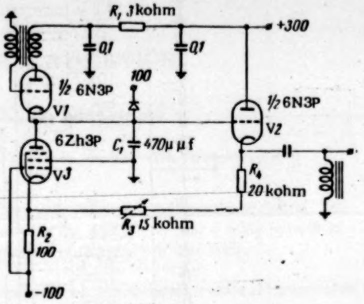

Fig 7

To stabilize the sawtooth amplitude, we use a reference voltage of +100v, limiting the growth of potential on capacitor C_1. The frequency of the generated voltage is determined by the capacitance of condenser C_1 and by the magnitude of the anode current of pentode V_3.

With the nominal values shown on Fig. 7, the circuit provides a generated sawtooth voltage of frequency 25 kcps and output voltage amplitude of 90v. With line-voltage variations of ± 10%, the sawtooth amplitude varies by ± 5%.

Complete Function-Generator Circuit and Its Technical Characteristics

Vacuum tube diodes type 6Kh2P were used as the function generator's diode elements. The transition to vacuum tubes resulted from the great difficulties which arose when germanium diodes were used, due to their low back impedance and their instability under various temperature conditions.

The functional schematic of the universal diode-function generator is given in Fig. 8. In it are included two operational amplifiers A_1 and A_2. Applied to the diode elements DE are a high-frequency sawtooth voltage and a reference voltage from a low-ohmic divider. The low-ohmic divider is executed in the form of individual sections, each of which consists of six wire resistances: r_1 = 60 ohm, r_2 = 120 ohm, r_3 = 240 ohm, r_4 = 420 ohm, r_5 = 840 ohm and r_6 = 1680 ohm. For setting up the law of argument partitioning, part of these resistances are short-circuited by means of a twelve-position switch with inserts in its panel. The total impedance of the low-ohmic dividers is always so chosen that a current of 16.7 ma flows through them. With this, the increment of the argument between the switching points of any neighboring diode elements is con-

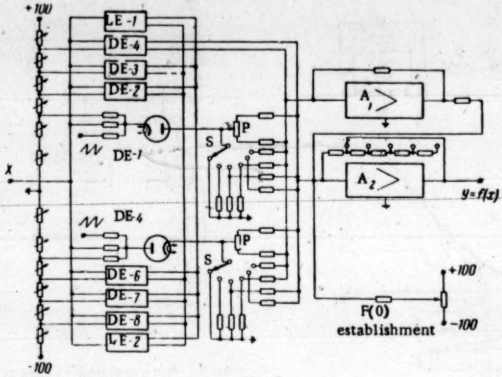

Fig. 8

trolled in the limits of 0 to 56v, varying by discrete steps of 1 volt.

In the function generator, there are eight quadratic diode elements, for which the switching voltage can be controlled, and two linear elements LE, made up of passive-resistor circuits, with switching voltages by zero. By applying the voltage after the diodes, either directly to A_2 or through sign-inverter A_1, we can obtain increments of the function's slopes in all four quadrants. The magnitude of these increments can be controlled discretely and smoothly by, respectively, switch S and potentiometer P (Fig. 8).

The function generator's complete circuit also contains an assembly for establishing the function's initial value.

SUMMARY

1. The function generator constructed in accordance with the principle of quadratic approximations has the following basic advantages in comparison with function generators, in which piecewise-linear approximations are used.

a) A significant reduction in the number of segments of the argument partitioning which are necessary to reproduce the function with the same error. This permits one to simplify the universal function-generator's circuit, to decrease markedly the number of vacuum tubes, to ease significantly the set-up of the functions and the adjustments of the generator.

b) The function generator provides smooth reproduction of functions, and eliminates discontinuities in the first derivative.

2. With this, the universal function generator constructed on the basis of the principle of quadratic approximation possesses the following disadvantages.

a) The device's pass band is determined by the sawtooth generator's frequency which, due to technical difficulties, can not be made higher than 30 to 50 kcps. Therefore, the function generator cannot have a larger band than 1 kcps.

b) The sawtooth voltage has a high-frequency component, so that the mounting block requires careful screening.

Despite these disadvantages, the circuit developed for the universal function generator can find practical employment in electronic models and in various computing devices.

LITERATURE CITED

[1] B. Ya. Kogan, Electronic Computers and Their Use in Investigating Automatic Control Systems [in Russian] (Gostekhizdat, 1957).

[2] A. A. Maslov, "Diode-function generators of a specialized type, based on semiconducting elements," Collection: Works on Automation and Remote Control [in Russian] (1958).

[3] A. D. Talantsev, "Designing diode function generators," Avtomatika i Telewekhanika 17, 2 (1956). •

[4] V. V. Gurov, V. M. Evseev, B. Ya. Kogan, A. A. Maslov, and F. E. Tranin, The Type EMU-8 Electronic Analog Computer [in Russian] (VINITI AN SSSR, 1957).

[5] L. V. Medvedev, A. A. Fel'dbaum, and L. N. Fitsner, "A nonlinear transformer with one input," Avtomatika i Telemekhanika 18, 10 (1957). •

[6] A. A. Fel'dbaum and A. I. Manukhin, "Nonlinear function generator with quadratic approximation," Author's Certificate No. 98096 (1952).

[7] L. N. Fitsner, "A function generator," Author's Certificate No. 119713 x prior. (Feb. 22, 1957).

[8] R. A. Bruns, "An improved diode-function generator for analog computers," Memo 20-113, Jet Propulsion Lab. (Pasadena, 1956).

[9] V. L. Goncharov, Interpolation Theory and Approximation of Functions [in Russian] (Gostekhizdat, 1954).

[10] Sh. E. Mikeladze, Numerical Methods of Mathematical Analysis [in Russian] (Gostekhizdat, 1954).

[11] N. E. Kobrinskii, Analog Computers [in Russian] (Gostekhizdat, 1954).

RELIABILITY CRITERIA FOR AUTOMATIC RELAY DEVICES WITH RADIOACTIVE EMITTERS

A. G. Vasil'ev, I. S. Zhitomirskii and K. S. Klempner
(Khar'kov)

(Translated from: Avtomatika i Telemekhanika, Vol. 21, No. 2, pp. 245-253, February, 1960)
Original article submitted July 17, 1959

Criteria are given for the reliability of automatic relay devices with sources of radioactive emission. The relationship is given connecting the parameters of the relay devices with the probability that a relay remain in a given state and, in addition, with the mean number of "false" transfers of the relay in unit time.

Calculated relationships were given in [1] which allow one to choose the minimum necessary activity of emitters in relay devices from the given limits on the admissible number of standard deviations of the operating utilization of the detector from the threshold level. In the work just cited, one limited oneself, in dealing with the statistical characteristics of the process, to an approximate representation of the potential distribution at the integrator relay's output as a Poisson distribution, or as a Gaussian distribution close to a Poisson one. The recommendations based on these considerations turn out to be of practical utility in determining the parameters of ordinary industrial relay devices. However, in many relay devices in which high reliability or speed of action are required, the accuracy of the computations based on the methodology of [1] may turn out to be inadequate.

Moreover, in the methodology given, the reliability of a device's operation was given only by the probability of a relay's remaining in the proper states. For many devices, in addition to this criterion, it is of great practical value to use, as a reliability criterion, the mean number of "false" transfers to be expected in unit time.

In the present work we render more exact the limits of applicability of the first approximation of [1] for various values of relay parameters. Methods are given for the numerical calculation of reliability to any desired degree of accuracy. Reliability is defined in terms of the probability of "false" relay transfers. Methods are given for the computation of the mean number of "false" transfers in unit time to any desired degree of accuracy. Grapl are given for the determination of reliability from the probability of remaining in a "false" state, and the number of "false" transfers for various combinations of the parameters of relay devices.

As was shown in [2] and [3] the characteristic distribution function of the random variable

$$x = \frac{V}{V_0} \tag{1}$$

for a Poisson distribution of the frequency of the applied signal n(t) and reaction function Φ(t) of the device has the form:

$$\vartheta(\lambda) = \exp\left\{ \int_{-\infty}^{T} \left[e^{i\lambda\Phi(T-t)} - 1 \right] n(t)\, dt \right\}. \tag{2}$$

From (2) we immediately obtain the expression for the cumulants of the distribution

$$k_\mu = \int_{-\infty}^{T} \Phi^\mu (T-t)\, n(t)\, dt. \tag{3}$$

We shall consider devices in which an RC network is used an the integrator. Then, the reaction function will have the form:

$$\Phi(t) = e^{-\frac{t}{RC}}. \tag{4}$$

In (1), V is the potential at the RC network's output and V_0 is the increment of potential at the RC network's output at the moment when a pulse is applied. In the steady state, V_0 is a constant. During transient responses, V_0 remains practically constant if the pulse amplitude is very much greater than the size of V_0 over its entire range of variation during the transient response. This condition holds with sufficient accuracy in all relay devices which operate as velocity measurers with linear scales.

A direct use of (2) for calculating a probability density and a distribution function would lead to extremely cumbersome computations. We shall consider two series expansions for the desired probability density p(x) and the distribution function F(x), one of which is useful for large values of

$$\nu = nRC, \tag{5}$$

and the other for small values of ν.

It was shown, in [2, 3] that, as $\nu \to \infty$, the desired distribution tends to a normal one. For computing the correction to the normal distribution, Rice suggested the use of a series first introduced by Edgeworth (an expansion in terms of the derivatives of the normalized density of a normal distribution). For the probability density, this series has the form:

$$\begin{aligned} p(x) = \frac{1}{k_2^{1/2}} \Bigg[& \varphi\left(\frac{x-k_1}{k_2^{1/2}}\right) - \frac{1}{3!}\frac{k_3}{k_2^{3/2}}\varphi^{(3)}\left(\frac{x-k_1}{k_2^{1/2}}\right) + \\ & + \frac{1}{4!}\frac{k_4}{k_2^{2}}\varphi^{(4)}\left(\frac{x-k_1}{k_2^{1/2}}\right) + \\ & + \frac{10}{6!}\frac{k_3^2}{k_2^{3}}\varphi^{(6)}\left(\frac{x-k_1}{k_2^{1/2}}\right) - \frac{1}{5!}\frac{k_5}{k_2^{5/2}}\varphi^{(5)}\left(\frac{x-k_1}{k_2^{1/2}}\right) - \\ & - \frac{35}{7!}\frac{k_3k_4}{k_2^{7/2}}\varphi^{(7)}\left(\frac{x-k_1}{k_2^{1/2}}\right) - \frac{280}{9!}\frac{k_3^3}{k_2^{9/2}}\varphi^{(9)}\left(\frac{x-k_1}{k_2^{1/2}}\right) + \ldots \Bigg], \end{aligned} \tag{6}$$

and, for the distribution function,

$$F(x) = 0{,}5 + \Phi\left(\frac{x-k_1}{k_2^{1/2}}\right) - \frac{1}{3!}\frac{k_3}{k_2^{3/2}}\varphi^{(2)}\left(\frac{x-k_1}{k_2^{1/2}}\right) + \frac{1}{4!}\frac{k_4}{k_2^{2}}\varphi^{(3)}\left(\frac{x-k_1}{k_2^{1/2}}\right) + \frac{10}{6!}\frac{k_3^2}{k_2^3}\varphi^{(5)}\left(\frac{x-k_1}{k_2^{1/2}}\right) - \frac{1}{5!}\frac{k_5}{k_2^{5/2}}\varphi^{(4)}\left(\frac{x-k_1}{k_2^{1/2}}\right) - \frac{35}{7!}\frac{k_3k_4}{k_2^{7/2}}\varphi^{(6)}\left(\frac{x-k_1}{k_2^{1/2}}\right) - \frac{280}{9!}\frac{k_3^3}{k_2^{9/2}}\varphi^{(8)}\left(\frac{x-k_1}{k_2^{1/2}}\right) + \ldots \tag{7}$$

In using the Edgeworth series, the greatest difficulty is in computing the distribution cumulants in the case when n is not constant. If the velocity of counting does not depend on time, then

$$k_\mu = \int_{-\infty}^{T} e^{\frac{\mu(t-T)}{RC}} n(t)\,dt = \frac{nRC}{\mu} = \frac{\nu}{\mu} \tag{8}$$

and the solution is essentially simplified.

We shall consider such relay devices for which the relative fraction of the time spent in a stationary state is quite large. Then, any consideration of the reliability of the relay's operation can be reduced to a consideration of its reliability in the stationary states.* For this case, (6) and (7) are written in the form

$$p(x) = \frac{0{,}5}{\sqrt{\nu}}\Phi_1\left(\frac{z}{\sqrt{2}}\right) - \frac{0{,}0278}{\nu}\Phi_4\left(\frac{z}{\sqrt{2}}\right) + \frac{0{,}00520}{\nu^{3/2}}\Phi_5\left(\frac{z}{\sqrt{2}}\right) + \frac{0{,}00617}{\nu^{3/2}}\Phi_7\left(\frac{z}{\sqrt{2}}\right) - \frac{0{,}000834}{\nu^2}\Phi_6\left(\frac{z}{\sqrt{2}}\right) - \frac{9{,}87\cdot 10^{-5}}{\nu^2}\Phi_8\left(\frac{z}{\sqrt{2}}\right) - \frac{3{,}58\cdot 10^{-6}}{\nu^2}\Phi_{10}\left(\frac{z}{\sqrt{2}}\right) + \ldots, \tag{9}$$

$$F(x) = 0{,}5 + \Phi(z) - \frac{0{,}0278}{\sqrt{\nu}}\Phi_3\left(\frac{z}{\sqrt{2}}\right) + \frac{0{,}00522}{\nu}\Phi_4\left(\frac{z}{\sqrt{2}}\right) + \frac{0{,}000773}{\nu}\Phi_6\left(\frac{z}{\sqrt{2}}\right) - \frac{0{,}000832}{\nu^{3/2}}\Phi_5\left(\frac{z}{\sqrt{2}}\right) - \frac{1{,}15\cdot 10^{-4}}{\nu^{3/2}}\Phi_7\left(\frac{z}{\sqrt{2}}\right) - \frac{4{,}20\cdot 10^{-6}}{\nu^{3/2}}\Phi_9\left(\frac{z}{\sqrt{2}}\right) + \ldots, \tag{10}$$

where

$$\Phi(z) = \frac{1}{\sqrt{2\pi}}\int_0^z e^{-\frac{V^2}{2}}\,dV \tag{11}$$

is a normalized Laplace function, $\Phi_n(z/\sqrt{2})$ is a derivative of the error probability integral and

$$z = \frac{x-k_1}{k_2^{1/2}} \tag{12}$$

is the multiplicity of the standard deviation.

It is easily shown [1,4] that

$$x = n_0RC, \tag{13}$$

$$k_1 = nRC, \tag{14}$$

$$k_2^{1/2} = \sqrt{\frac{nRC}{2}}. \tag{15}$$

After substituting (13)-(15) in (12), we get

$$z = \frac{2RC(n_0-n)}{\sqrt{2RCn}}, \tag{16}$$

where n_0 is the relay's operation threshold, i.e., the counting speed for which both relay states are equally probably. It is obvious that for the states in the absence of a controlled object on the control line (state 1) the magnitude of n will exceed n_0, and these states will be characterized by negative values of z. For the other state (state 2), the quantity z will be positive.

The essential disadvantage of (9) amd (10) is their nonuniform convergence. These series obviously have poor convergence for large values of z and small values of ν. For $\nu = 0$, the distribution function degenerates to the Heaviside unit function $\eta(x)$:

$$\eta(x) = \begin{cases} 0 & \text{for } x < 0, \\ 1 & \text{for } x \geqslant 0. \end{cases} \tag{17}$$

Therefore, for large z and small ν, it is meaningful to use expansions based on the function $\eta(x)$.

One is led to this type of expansion by a method analogous to that used by Maslov and Povzner [5].

As one may easily convince oneself, the desired probability density p(x) is the solution of the equation

$$\frac{\partial u}{\partial y} = \int_0^1 \frac{u(x-x', y) - u(x, y)}{x'}\,\nu\left(\ln x' + \frac{T}{RC}\right)dx' \tag{18}$$

with initial conditions

$$u(x, 0) = \eta(x) \tag{19}$$

and for the parameter value y = 1.

For y = 1, the distribution function F(x) also coincides with the solution of (18), but with the initial conditions

$$u(x, 0) = \eta(x). \tag{20}$$

With initial conditions (20), the solution of (18) can be obtained either by the methods of finite differences, or in the form of a series

$$F(x) = e^A[\eta(x)] = \eta(x) + A[\eta(x)] + \frac{1}{2!}A^2[\eta(x)] + \ldots + \frac{1}{m!}A^m[\eta(x)], \tag{21}$$

where the letter A denotes the integral operation

$$A[u(x)] = \int_0^1 \frac{u(x-x') - u(x)}{x'}\,\nu\left(\ln x' + \frac{T}{RC}\right)dx'. \tag{22}$$

The convergence of (21) is also nonuniform. For small x, the series converges rapidly, and it is meaningful to use it. For large x, it is more convenient to use finite-differences methods.

---

* A criterion for reliability of relay operation during the transient response could be the probability of just one transfer during the response time.

Computing the distribution function by some method or other, we can find the average time that the relay remains in a given state.

In addition, as has been stated, it is necessary to compute the mean number of "false" transfers per unit time. For an inertialess relay, this problem leads to the determination of the number of intersections of the current potential value with the potential value V_n for which the relay changes state. For state 1, $|\bar{V}| > |V_n|$, and the problem reduces to finding the number of intersections coming down from above ($S\downarrow$). For state 2, $|\bar{V}| < |V_n|$, it is necessary to compute the number of intersections going up from below ($S\uparrow$).

The general formula, well known in the literature [6], for finding the stated quantity ("mean number of blips") requires, for its practical use, a tremendous amount of computation.

In our case, finding the expression for the mean number of intersections poses no difficulty.

We consider a small interval of dimensionless time $\tau = t/RC$, $(\tau, \tau + \Delta\tau)$. The average number of intersections of some level x_0, both coming down from above and going up from below, in this interval is an infinitesimal quantity of the order of $\Delta\tau$. As is known [6], this quantity can be replaced, with an accuracy of second-order infinitesimals in $\Delta\tau$, by the probability $P_{\tau,\Delta\tau}$ of one intersection going up from below and the probability $P_{\tau,\Delta\tau}$ of one intersection coming down from above. Our aim is to find the following limits:

$$S^{\uparrow} = \lim_{\Delta\tau\to 0} \frac{1}{\Delta\tau} P^{\uparrow}_{\tau,\Delta\tau}, \tag{23}$$

$$S^{\downarrow} = \lim_{\Delta\tau\to 0} \frac{1}{\Delta\tau} P^{\downarrow}_{\tau,\Delta\tau}.$$

Thus, the quantities $P^{\uparrow}_{\tau,\Delta\tau}$ and $P^{\downarrow}_{\tau,\Delta\tau}$ can be found with an accuracy of second-order infinitesimals in $\Delta\tau$.

Each of the realizations of the process under consideration increases by a unit jump when a pulse is applied, and decays exponentially in the intervals between pulses.

A realization of the process can intersect the level x_0 from above to below if, and only if, the quantity $x(\tau)$ at time τ lies between the limits x_0 and $x_0e^{\Delta\tau}$ and, in the time interval τ, $\tau + \ln(x/x_0)$, no pulse is applied. Thus,

$$P^{\downarrow}_{\tau,\Delta\tau} = \int_{x_0}^{x_0e^{\Delta\tau}} p(x)\left(1 - \nu(\tau)\ln\frac{x}{x_0}\right)dx \approx x_0 p(x_0)\,\Delta\tau, \tag{24}$$

where the last equality holds with the accuracy required.

It immediately follows from (24) that

$$S^{\downarrow} = x_0 p(x_0). \tag{25}$$

If we now make the transition from dimensionless time to ordinary time, and take (1), (9), and (12)-(16) into account, we obtain the definitive formula

$$S^{\downarrow} = n_0 p(x). \tag{26}$$

Intersection of level x_0 from below upwards is possible if, and only if, $x(\tau)$ lies between x_0-1 and x_0 and a pulse is applied during an interval less than $\ln[x/(x-1)]$. This means that

$$\begin{aligned} P^{\uparrow}_{\tau,\Delta\tau} = \nu(\tau)\,\Delta\tau \int_{(x_0-1)e^{\Delta\tau}}^{x_0} p(x)\,dx + \nu(\tau)\, \times \\ \times \int_{x_0-1}^{(x_0-1)e^{\Delta\tau}} p(x)\ln\frac{x}{x_0-1}\,dx \approx \\ \approx \nu(\tau)\,\Delta\tau \int_{x_0-1}^{x_0} p(x)\,dx. \end{aligned} \tag{27}$$

Whence,

$$S^{\uparrow} = \nu(\tau) \int_{x_0-1}^{x_0} p(x)\,dx = \nu(\tau)\,[F(x_0) - F(x_0 - 1)]. \tag{28}$$

For values of $x_0 \gg 1$ (this corresponds, as is easily seen, to $n_0RC \gg 1$), we can set

$$S^{\uparrow} = \nu(\tau)\,p(x_0). \tag{29}$$

After simple transformations, we finally obtain†

$$S^{\uparrow} = np(x). \tag{30}$$

Starting from what has been presented, we can write the expression for the average blip duration. For state 1 we get

$$T^{\downarrow} = \frac{F(x)}{n_0 p(x)}, \tag{31}$$

and for state 2

$$T^{\uparrow} = \frac{1 - F(x)}{np(x)}. \tag{32}$$

It is of interest to find the expressions for the distribution of durations in "false" states and for the distribution of the number of "false" intersections. This is a complicated problem, and will not be treated in the present work. At the same time, for example, it is easily seen that, with the condition

$$\frac{1}{S^{\downarrow}} > T^{\downarrow} \quad \text{or} \quad \frac{1}{S^{\uparrow}} > T^{\uparrow} \tag{33}$$

the distribution of the number of "false" intersections is close to a Poisson distribution.

We now consider concrete results of computations based on the method presented here.

There is great interest in determining the quantities $1 - F(x)$, $F(x)$, $S^{\downarrow}$, $S^{\uparrow}$, $T^{\downarrow}$, $T^{\uparrow}$ for a wide interval of values of ν and $\underline{z}$.

Of practical interest are the solutions for large values of $\underline{z}$, corresponding to automation and control systems in which "false" transfers lead to very undesirable consequences, and for small ν. Such solutions are obtained effectively by means of computers, using the method presented above [(17)-(22)].

---

† For reliability characteristics based on the number of "false" intersections, one can also use functions of S which take on values from 0 to 1, for example, $P(S) = 1/(1+S)$.

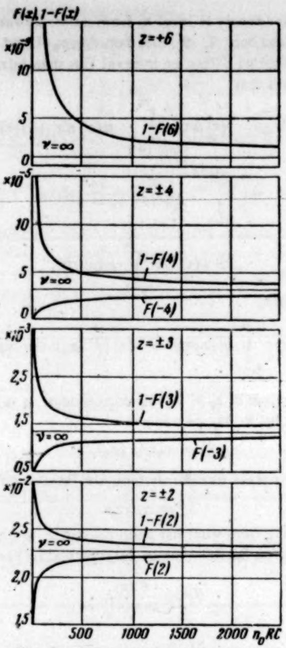

Fig. 1. Values of the probability of the potential remaining in a "false" state.

For widely used relay devices working with low values of z and large values of ν, one can use the Edgeworth series (9) and (10) for the direct computation of the quantities listed above. The values of $\Phi_n(z/\sqrt{2})$ are computed by means of Hermite polynomials:

$$\Phi_n\left(\frac{z}{\sqrt{2}}\right) = (-1)^{n-1} 2^{\frac{n-1}{2}} \frac{2}{\sqrt{\pi}} e^{-\frac{z^2}{2}} H_{n-1}(z). \qquad (34)$$

Figure 1 shows the values of the quantities F(x) and 1-F(x) for several values of z and $n_0RC \ll 2500$. These quantities equal the mean relative time the potential remains in a "false" state for, respectively, state 1 and state 2. The computations were made with all the terms actually written above in (10). For convenience in comparing the results with those previously obtained [1], the product n_0RC has been laid out along the axis of abscissas, being defined, as follows from (5) and (16), by the expression

$$n_0RC = \nu + 2\sqrt{\frac{\nu}{2}}. \qquad (35)$$

The first two terms in (10) do not depend on ν, and give a solution in a Gaussian approximation ($\nu = \infty$). As is clear from Fig. 1, in determining the relative time spent in a "false" state, the deviation from the Gaussian approximation is the larger, the larger is z and the smaller is the product n_0RC.

It should be mentioned that, for state 1, the computations carried out in the Gaussian approximation lead to an increase in the actual reliability of state 1 in comparison with the given value. With this, the value of the minimum necessary activity of the radiation source of 1 is somewhat overstated. In connection with this, as is clear from Fig. 1, the reliability of state 2 will be lower than that which follows from the computations in the Gaussian approximation, from whence the value of the limiting admissible activity of the radiation source turns out to be somewhat overstated. However, in devices in which the controlled object provides a significant attenuation of the emission, the magnitude of the limiting admissible activity significantly exceeds the value of the minimum necessary activity, as is clear from the calculations made in [1]. For these devices, one need not take into account, in calculating source activity, the deviations from the Gaussian approximation for state 2.

The deviations changing, by an order of magnitude, $0.5-\Phi(z)$ occur at $z = \pm 2$ for $n_0RC \overset{\sim}{<} 10$, at $z = \pm 3$ for $n_0RC \overset{\sim}{<} 30$ and at $z = \pm 4$ for $n_0RC \overset{\sim}{<} 50$. Therefore, the Gaussian approximation, as was already noted [1], encompasses a wide circle of problems, but is inadequate when one deals with devices designed for high reliability (large z), high speed of response (low RC) in conjunction with high sensitivity of the relay to radiation (small n_0).

At $z = -6$, the magnitude of $F(-6)$ is $(0.2 \text{ to } 0.5)10^{-9}$ for values of n_0RC from 500 to 2500. In calculating the value of $F(-6)$ for $n_0RC < 500$, the number of terms written in (10) turned out to be inadequate.

The table gives the upper limits on the error of computing the quantities 1-F(x) and f(x), using all the terms actually written in (10). The errors are stated to within 1%. As is clear from the table, the error in computing the relative time in a "false" state falls with decreasing ν and with increasing z.

The accuracy of the determination of the number of "false" transfers is determined by the accuracy of determining the quantity p(x), as is clear from (26) and (30). The accuracy of computing the quantities $S\downarrow$ and $S\uparrow$ varies in approximately the same manner as that for the relative duration of the relay in a "false" state (Cf. the table).

For various values of z and RC, Fig. 2 shows the number of "false" intersections of potential per unit time as a function of n_0. At $z = 6$, the number of terms of (9) taken into account permit the computations to be made only for relatively large values of n_0RC. For example, the computations give $S\uparrow \approx \text{const} \approx 2 \cdot 10^{-8}$ for $z = 6$, $RC = 50$ and $n_0 < 200$.

As is clear from Fig. 2, the number of intersections $S\downarrow$ and $S\uparrow$ do not equal each other for the same multiplicity of the standard deviation. This is particularly apparent for large values of z.

TABLE Error in Computing the Relative Time the Potential Remains in a "False" State

ν	Error less than δ_z, %							
	z							
	+2	−2	+3	−3	+4	−4	+6	−6
10	0	1	2	90	11	448		
20	0	0	1	8	6	325		
50	0	0	0	2	3	47		
100	0	0	0	0	1	9	28	
200	0	0	0	0	1	2	18	
500	0	0	0	0	0	1	8	148
1000	0	0	0	0	0	0	4	32
2500	0	0	0	0	0	0	2	6
5000	0	0	0	0	0	0	1	2

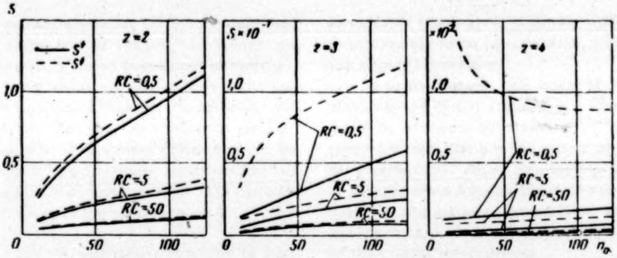

Fig. 2. Average number of "false" intersections of the potential per unit time.

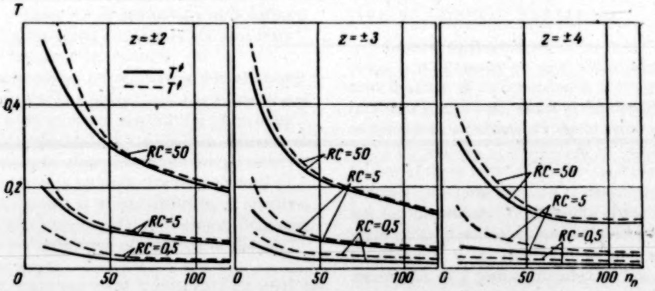

Fig. 3. Average time of "false" intersections.

Figure 3 shows the average time the potential remains in a "false" state for various values of z, n_0 and RC, calculated by (31) and (32).

It should be mentioned that the inertia of the electrical (for example, lamps or bells in the anode circuit of power amplifier relays) or electromechanical relay output (electromechanical relay) can lead to a certain lack of coincidence of the relative time the relay contacts (lamps, bells) remain in a "false" state as compared with the values computed by the method presented above.

On the one hand, a sufficiently inertial output at relay operation will not react on intersections less than some value T_0, determined by this inertia. On the other hand, relays with long release times will lead to a drawing out of the time that the relay device remains in a "false" state after the "false" intersection of the potential has terminated.

With respect to "false" relay transfers, it may be remarked that their number can be somewhat less than the number of "false" intersections of potential, due both to intersections lasting less than T_0 and to the appearance of more than one intersection while the contacts are to be found in a "false" state. These circumstances act to increase the relay's reliability, defined in terms of number of intersections, but limit its speed of response to a well-known extent.

Based on the results given above, one can calculate the relative duration of relay contacts in "false" states and the number of "false" contact transfers for concrete relays with known characteristics. Since the number of known relay types is very large, this question requires special consideration.

In conclusion, the authors wish to thank L. K. Tatochenko for the great interest shown in the present work, and for a number of very useful comments.

LITERATURE CITED

[1] A. G. Vasil'ev and K. S. Klempner, "On computing reliability of automatic gamma-relay devices," Avtomatika i Telemekhanika 20, 2 (1959).

[2] S. O. Rice, "Theory of fluctuating noise," Collection: Theory of Electric Signal Transmission in the Presence of Noise [Russian translation] (IL, 1953).

[3] V.I. Bunimovich, "Effect of the fluctuations and signal voltages on a nonlinear system," J. Physics 10, 1 (1946).

[4] A. G. Vasil'ev and K. S. Klempner, "Computing the parameters of radioactive relays," Avtomatika i Telekhamika 20, 3 (1959). ‡

[5] K. V. Maslov and A. Ya. Povzner, "On the infinitesimal operators of one class of Markov processes," Theoriya veroyatnostei i ee primeneniya 3, 1 (1958).

[6] V. I. Bunimovich, Fluctuation Processes in Radio Receivers [in Russian] (Sovetskoe Radio Press, 1951).

---

‡ See English translation.

ESTIMATES, BASED ON USAGE, OF THE SERVICE LIFE OF CONTACT APPARATUS

D. A. Abdullaev

(Tashkent)

(Translated from: Avtomatika i Telemekhanika, Vol. 21, No. 2, pp. 254-259, February, 1960)
Original article submitted April 15, 1959

The region of useful life of contact apparatus is determined as a function of its modes of operation and of the given admissible number of transfers. Starting from the service life, we estimate the increment of use expenditure per element.

Hitherto, relay contact apparatus has been widely used in systems for automation, remote control, communication, etc. The breakdowns (out-of-order conditions) of individual elements and blocks† which are unavoidable under conditions of use require significant time for the detection and replacement of the faulty element. As a rule, the system must stand idle during this. The system's idle time can be reduced to a minimum by the opportune determination and replacement of the element or block at fault. On the other hand, this measure eliminates the possibility of faulty system operation.

It is well known that the probability of failure of the electromechanical (receiving) portion of a relay element is very much less than the probability of failure of its contacts [1]. This allows one to estimate, with a definite degree of accuracy, the useful state of an element from the probability of failure of its contacts.

A general methodology for estimating the reliability of operation of contacts in a given circuit as a function of such factors as contact pressure, possibilities of sparking or arcing, changes in the form of the contacts' surfaces and other physical reasons for their breakdown are given in [1, 2]. The essential obstacle to using this methodology in usage computations is that it is very difficult, in practice, to determine the data necessary for the computations and, consequently, for the estimation of the state of the contracts during their usage.

The method, described by N. Taylor [3] (the marginal checking method), for inspecting allows one to detect elements which are on the point of breaking down and to replace them. However, this method has been developed as applied to electronic apparatus. Its practical use for the estimation of contact apparatus is not worthwhile, since it entails superfluous operations.

The common feature of these methods is that testing and verifying of element states must be carried out directly at the location where the elements are mounted or by removing them which, in many cases, can turn out to be impossible or inadmissible in practice.

It follows from this that it would be of interest to develop a method for the indirect estimate of the state of contact apparatus. Such a method, which would permit one to determine, if only approximately, the length of serviceable life a given element, would make it possible to replace elements in good time, without detriment to the system's operation.

In actual systems, the modes of operation of different elements and blocks are diverse. Therefore, their breakdowns do not occur simultaneously. If the conditions imposed are such that a given system must operate properly for a period of H years, then the replacement of elements or blocks before the expiration of this period entails an increase in the material expenditure, a "use" expenditure in the given case. It is of interest to estimate the variation of these latter expenditures.

Admissible Duration of Continuous Operation of Contact Apparatus

In order to replace an element at the breakdown point, it is necessary to know beforehand what the admissible duration of its operation is in the given mode of work. It is well known that, under given conditions and modes of operation, an element's useful service life is determined by the number of transfers of its contacts [1]. Since failure of these latter is a random phenomenon, one of the principal problems amounts to determining the distribution law for the probability of failure of the contacts of an element under given conditions. We note that certain authors, for example, V. A. Moroz [4], in their works start with the assumption of a normal distribution law.

In this work we shall adopt the convention that, on the basis of tests and statistical data on the operation of elements whose mode of operation is given by the parameters and structure of the scheme under consideration, we shall have determined the distribution law of the probability of contact failure, and that from this we shall have found the admissible number of transfers of the latter, N_{adm}.

If we start from this condition, then we can determine the admissible duration of continuous operation of an element for a given speed of transfer of its contacts during a call cycle. For electromagnetic elements, this is

---

† By the term "block" in the present paper, we understand a set of elements implementing a definite function and which are found under identical operating conditions.

$$T_{\text{adm}} = \frac{N_{\text{adm}}}{v \cdot 3600} \text{ hr}, \qquad (1)$$

where v is the speed of contact transfers, in units of $\sec^{-1}$.

Definite types of reed frequency elements, in the process of signal reception, transfer the contacts in each period of current (voltage) oscillation, coinciding with their natural frequency (Cf., for example, [5]). If oscillations of frequency f, to which the frequency element is tuned, exist during time t, then the total number of contact transfers during this time will be ft. Consequently,

$$T_{\text{adm}} = \frac{N_{\text{adm}}\tau}{3600\, ft} \text{ hr}, \qquad (2)$$

where τ is the period of a call cycle, cycle, in seconds ‡.

Thus, the admissible duration of continuous operation of a reed element depends both on its natural tuned frequency, and on the time during which the signal exists.

Domain of Proper Operation of Contact Apparatus

If a given circuit element operates N_c times during one call cycle with transfer velocity v, then the duration of its continuous operation with transferring contacts will equal

$$T_c = \frac{N_c}{3600 v} \text{ hr}, \qquad (3)$$

We assume that n_h call cycles are made during one hour. Then, the time of continuous element operation during one hour is defined by the expression

$$T_h = \frac{n_h N_c}{3600\, v} \text{ hr}, \qquad (4)$$

Multiplying (4) by the number of hours in a year, we obtain the time of proper element operation during one year:

$$T_y = \frac{n_h N_c}{3600\, v} 8760 \text{ hr}, \qquad (5)$$

From the design conditions, the useful life of the system must be not less than H years. During this period, the element under consideration must be found in the mode of continuous operation during

$$T' = HT_y = \frac{Hn_h N_c}{3600\, v} 8760 \text{ hr}, \qquad (6)$$

where H is a dimensionless quantity expressing a quantity of years.

With the condition that

$$\frac{T_{\text{adm}}}{T'} \geqslant 1, \qquad (7)$$

the given element operates properly until the end of the proposed time of proper functioning of the entire system. It is therefore not necessary to replace it. Otherwise, replacement would be necessary.

By substituting (1) and (6) in (7), we get

$$\frac{N_{\text{adm}}}{8760\, Hn_h N_c} \geqslant 1. \qquad (7')$$

Whence,

$$n_h N_c \leqslant \frac{N_{\text{adm}}}{8760\, H}. \qquad (8)$$

The left member of (8) is the number of transfers of the element in one hour. We call it the hourly intensity of the element's operation, and we use the notation

$$Q = n_h N_c.$$

Then, (8) can be given in the form

$$Q \leqslant \frac{N_{\text{adm}}}{8760\, H}. \qquad (8')$$

Thus, we have established the possibility of proper element operation with a given N_{adm} as a function of the intensity of its operation. The appended figure gives the curve for $Q = \varphi(H)$, constructed from the condition of equality of the left and right members of (8'). It is therefore a boundary line: the region below it characterizes proper operation, and the upper region characterizes improper functioning of the element during the given period H. It should be mentioned that the character of variation of the curve $Q = \varphi(H)$ coincides with the character described by Feugel for the experimental reliability characteristic as a function of time [6]. This confirms the correctness of the initial premises of our analysis.

In a similar way, we can obtain the expression for estimating the useful life of reed frequency elements (Cf. the Appendix)

$$Q \leqslant \frac{N_{\text{adm}}}{8760\, H}\left(\frac{\tau}{t}\right). \qquad (9)$$

It follows from this that, to increase the useful life of a reed element, tuned to frequency f, it is necessary to shorten the signal's transmission time t. This is possible only if the speed of response of the element itself is increased.

Estimating the usage state of contact apparatus by the method presented here is most effective in the case of mass-produced devices, since the value of N_{adm}, established just once on an experimental basis for individual elements and blocks, can be used as a basic parameter for all the apparatus produced in the same production run.

Influence of Useful Life of Apparatus on Its "Use" Expenditure

The economic efficiency of employing a system is usually estimated by the time taken to recoup its costs [7]

$$T = \frac{\Sigma K}{E_y}, \qquad (10)$$

---

‡ Here we have in mind parallel transmissions of frequency-indication pulses.

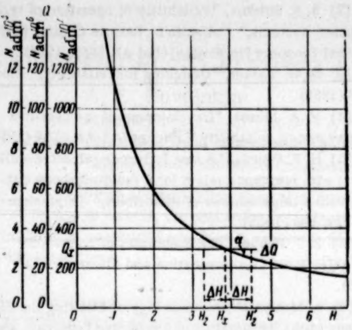

Boundary of the proper functioning characteristic of a relay contact element.

where Σ K is the total expenditure and E_y is the annual saving.

The total expenditure, together with the one-shot initial capital outlay and the wage fund for the personnel, includes deductions for amortization and maintenance, i.e., operating costs ("use" expenditures), a variable quantity which depends on maintenance and replacement periods of the system's individual elements and blocks.

Operating costs per element, in monetary units, we denote by K_A/A, where A is the total number of contact elements in the system. As a percentage of the sum of costs,[**] this quantity amounts to

$$K_A^{\bullet} = \frac{K_A \Sigma K}{A \cdot 100}. \tag{11}$$

By substituting the value of ΣK from (10), we obtain

$$K_A^{\bullet} = \frac{K_A}{100\,A}\,T E_y, \tag{11'}$$

whence,

$$T = \frac{K_A^{\bullet} A \cdot 100}{K_A E_y}. \tag{a}$$

The condition for proper apparatus functioning during the time taken to recoup the system's cost is

$$T \leqslant H_x, \tag{12}$$

where H_x, for a given mode of element operation, is determined from the proper curve of $Q = \varphi(H)$. We assume that

$$T = H_x \pm \Delta H.$$

Obviously, element replacement is necessary if it is the plus sign which stands before ΔH. We now analyze how the quantity $K_A^{\bullet}$ varies with this.

From the figure, we have

$$\frac{\Delta Q}{\Delta H} = \tan\alpha \tag{13}$$

or

$$\frac{dQ}{dH} = \tan\alpha.$$

Bearing in mind the condition for the construction of the curves $Q = \varphi(H)$, we find from (8') that

$$\frac{dQ}{dH} = -\frac{N_{adm}}{H^2 \cdot 8760}. \tag{14}$$

By substituting the value of tan α in (13), we get

$$\Delta H = -\frac{\Delta Q H^2 \cdot 8760}{N_{adm}}. \tag{15}$$

If we adopt the convention that the values of $K_A^{\bullet}$ determined from (11') correspond to $H_x \geq T$ then, for $H_x < T$, the magnitude of the operating costs is expressed by the formula

$$K_{A1}^{\bullet} = \frac{K_A}{100\,A}\,E_y H \left(1 + \frac{\Delta Q H}{N_{adm}}\,8760\right). \tag{16}$$

The relative increment of operating costs per element, as a function of the mode and intensity of its operation, is defined by the expression

$$\Theta = \frac{K_{A1}^{\bullet}}{K_A^{\bullet}} = 1 + \frac{\Delta Q H}{N_{adm}}\,8760. \tag{17}$$

We can, by a similar method, obtain the expression for the case when reed elements are used

$$\Theta = 1 + \frac{\Delta Q H}{N_{adm}}\left(\frac{t}{\tau}\right) 8760. \tag{18}$$

SUMMARY

1. The curves $Q = \varphi(H)$ for a system's individual elements and blocks allow timely replacement of elements on the verge of breakdown, and thereby reduce to a minimum the system's down time.

2. The expressions obtained permit the approximate estimation of and, if necessary, the correction of, initially assumed values for, the operating costs as applied to apparatus operating in identical conditions.

The development of a method for estimating the system as a whole is the subject of a special investigation.

The author takes this opportunity to express his profound gratitude to B. S. Sotskov for posing the problem and for giving his attention to its solution.

Appendix

Derivation of Expression (9)

The numbers of transfers of a frequency element during one call cycle is

$$N_c = ft.$$

If the given object is called n_h times an hour, then the total number of transfers of the element's contacts which participate in the selection of the given object, is

$$N_h = n_h N_c = n_h f t. \tag{19}$$

It is obvious that the quantity $n_h t = T_h$ is the duration of continuous transfer of the element's contacts during one hour. From (19),

---

[**] As in Russian. The correct percentage should be $\frac{K_A \cdot 100}{A \Sigma K}$ – Publisher.

$$T_h = \frac{N_c n_h}{f \cdot 3600} \text{ hr.} \tag{20}$$

The time of continuous transfer of the element's contacts during one year is

$$T_y = \frac{N_c n_h}{f \cdot 3600} \, 8760 \text{ hr} \tag{21}$$

Furthermore,

$$T' = HT_y = \frac{HN_c n_h}{f \cdot 3600} \, 8760 \text{ hr} \tag{22}$$

By denoting $Q = N_c n_h = ftn_h$, and dividing (22) by (2), we obtain (9)

$$Q < \frac{N_{adm}}{H \cdot 8760} \left(\frac{\tau}{t} \right).$$

LITERATURE CITED

[1] B. S. Sotskov, "On criteria for estimating electromechanical relays," Avtomatika i Telemekhanika 18, 3 (1957).††

[2] B. S. Sotskov, "Reliability of operation of relay elements' contacts," Collection: Remote Control in the National Economy [in Russian] (Izd AN SSSR, 1956).

[3] N. H. Taylor, "Designing for reliability," Proc. IRE 6 (1956).

[4] V. A. Moroz, "Development of the questions of relay circuit reliability," Otchet IAT AN SSSR (1950).

[5] H. F. Frundt, "A new full-code selective-call system with resonance relays for a radiotelephony network with a large number of subscribers, Telefunken-Ztg. 22, 108 (1955).

[6] E. F. Feugel, The economics of component parts selection. Communication and Electronics, 35, (1958).

[7] B. M. Lyzlov, Methodology of Eliciting the Efficiency of the Automation of Productive Processes, and also the Introduction of Automatic Inspection, Signalling and Remote Control [in Russian] (Izdatelstvo MIKhM, Moscow, 1956).

---

†† See English translation.

A NUMERICAL-TO-ELECTRICAL CONVERTER

A. K. Zavolokin

(Moscow)

(Translated from: Avtomatika i Telemekhanika, Vol. 21, No. 2, pp. 260-265, February, 1960)
Original article submitted September 2, 1959

The block diagram is described of a transducer which converts numerical quantities to proportional values of voltage or current, the conversion being based on the principle of an intermediate transformation to time intervals. The converter's operation is analyzed, and some general considerations relating to the design of such devices are given.

For the purpose of transforming numerical quantities to voltages or currents proportional to them, one can, in many cases, make very effective use of the principle of intermediate transformation of the numbers to time intervals. Below we describe a device based on this principle. Its operation is characterized by this, that in each transformation cycle one counter is used to develop two successive signals whose durations are such that the time for the entire cycle remains invariant while the duration of one of the signals is proportional to the value of the input quantity. This signal is used for modulating a stabilized dc voltage or current. After being smoothed, the duration-modulated voltage (current) is converted to the electrical equivalent of the numerical quantity.

To elucidate the principle of operation, we consider the block diagram shown in Fig. 1. It consists of the output register of a computer (triggers T'_1-T'_n), gates for uncomplemented code (g_1-g_n), gates for complemented code (g'_1-g'_n), a counter (triggers with counter inputs T_1-T_n), controlling trigger T, key K and smoothing device SD. The rectangles with the sketches of the bipolar pulses in them in Fig. 1 denote differentiating networks. One of the pulses in each rectangle has a stroke through it. This means that the pulses of this polarity will not henceforth be used.

The converter's operation is comprised of two cycles. In the first cycle, via gates g_1-g_n, the code for the number N to be converted is written in parallel in the counter. Pulses continuously applied to the counter's input with frequency f are added to the number written there, so that the counter is returned to its zero state at some moment of time. At this moment, an overflow pulse is emitted by its last stage (trigger T_n). The emission of the overflow pulse terminates the first cycle of operation.

At the beginning of the second cycle, the overflow pulse reverses the state of trigger (flip-flop) T, opening key K. Simultaneously with the key's opening, a signal from the differentiating network is applied to gates g'_1-g'_n, by means of which the number N is again written in the counter, but this time in complemented code. Input pulses again are added into the counter until it is reset to zero. At the moment when the counter returns to its zero state, a second overflow pulse is emitted, transferring T to its original state. This leads to the closing of the key and to the writing of the number N in uncomplemented form in the counter. After this, the aforementioned two-cycle process is repeated.

It is easily seen that the duration $\bar{\tau}$ of the first cycle is linearly related to the number $\bar{N}$, the complement of the number N, namely

$$\bar{\tau} = \frac{\bar{N} + 1}{f}. \tag{1}$$

The equality just written is the mathematical expression of a well-known property of an n-place counter, staticizing input pulses in the number system, with radix b, which has been adopted. This property is formulated as follows. If some number is staticized in a counter, then the counter will be returned to its zero state after one adds to it a series of input pulses, the number of which would bring the counter total to b^n (i.e., the number of pulses is the 10's complement in the decimal system, the 2's complement in the binary system). This added number equals the complement of the given number (i.e., its 9's complement in the decimal system, its 1's complement in the binary system) plus one. Therefore, $\bar{\tau}$ can be defined as the product of $(\bar{N}+1)$ by the size of the interval between two neighboring input pulses.

As an example, we consider two special cases, when the numerical quantity to be converted, expressed in the binary system, has its maximum and minimum values. If $N = 0$ ($\bar{N} = 2^n - 1$), then the number written in the counter in the first cycle will equal zero. Consequently, the overflow pulse appears at the counter's output after 2^n input pulses, i.e., in the given case $\bar{\tau} = 2^n/f$. If the number to be transformed has its maximum value, that is, $N = 2^n - 1$ ($\bar{N} = 0$), then all the counter triggers will be in their "1" state at the beginning of the first cycle, and the application of the first input pulse will lead to the emission of the overflow pulse, i.e., for this case, $\bar{\tau} = 1/f$. We may show analogously that for any intermediate value, the magnitude of $\bar{\tau}$ is determined in accordance with (1).

The number written in the counter at the beginning of the second cycle equals $\bar{N}$. Therefore, the duration τ of the second cycle can be obtained from the expression

$$\tau = \frac{N + 1}{f}. \tag{2}$$

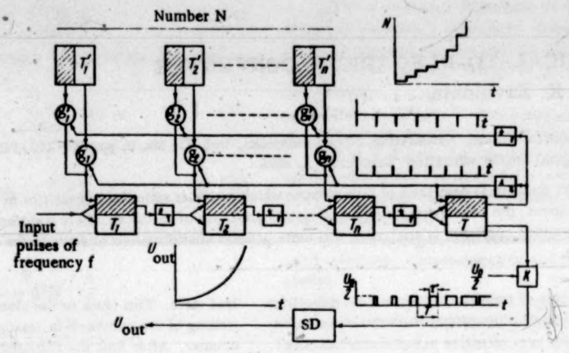

Fig. 1

On the basis of (1) and (2), the time T of a complete cycle, equal to the sum $\bar{\tau} + \tau$, is defined as

$$T = \frac{\overline{N} + N + 2}{f}. \qquad (3)$$

On the other hand, it is well known that the addition of an n-place binary number N to its complement $\overline{N}$ results in a constant which is independent of the absolute magnitude of N, namely:

$$N + \overline{N} = 2^n - 1 \qquad (4)$$

Consequently,

$$T = \frac{2^n + 1}{f}. \qquad (5)$$

On the basis of (5) and (2), we can draw the very important conclusion: in a converter executed in accordance with the block diagram of Fig. 1, the duration of a full cycle (composed of the two part cycles) does not depend on the value of the numerical quantity N to be converted. With this, each cycle consists of two part cycles; the duration of one of them, corresponding to the open state of key K, is a linear function of the number N.

The key K is connected in series in a current generator circuit, or in parallel to a dc voltage generator. In the first case, there will be at the smoothing device's input, duration-modulated current pulses and, in the second case, voltage pulses. Depending on which quantity is smoothed, the numerical quantity will be converted either to current or to voltage. For the sequel, this difference is immaterial so that, for the sake of definiteness, we shall assume that the number is converted to a voltage. Figure 2,a shows the curve of voltage variation at the smoothing device's input as a function of time u = f(t).

The output voltage U_{out} of the smoothing device is proportional to the mean value of the input voltage. If we denote the modulated dc voltage by $U_0/2$, we can write

$$U_{out} = \frac{U_0}{2}\frac{\tau}{T}. \qquad (6)$$

Or, taking (2) and (5) into account,

$$U_{out} = \frac{U_0}{2^{n+1} + 2}(N + 1). \qquad (7)$$

It is clear from (7) that the value of U_{out} is strictly proportional to the converted numerical quantity N. The constant term connected with the "1" in the parenthetical expression (N+1) can always be compensated, either by writing the number N-1, instead of N, in the computer's output register, or by biasing U_{out} by the quantity $U_0/(2^{n+1}+2)$.

Depending on the concrete requirements, the smoothing device can be executed in various ways. In particular, it may turn out to be advantageous to use the corresponding filters, special electronic devices or even simply pointer instruments indicating the average value of voltage (current). A consideration of all the possible practical variants

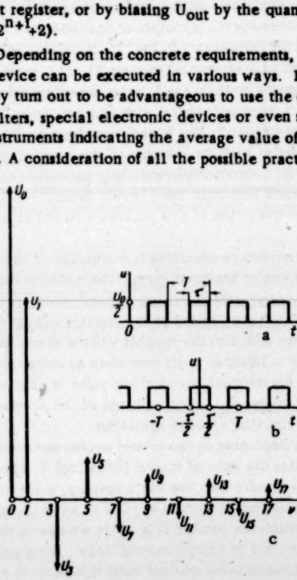

Fig. 2. The curve for u = f(t) and the frequency spectrum for θ = 0.5.

of the smoothing device is not part of our present task. It is relevant here to cite only several general considerations which should be kept in mind in designing it. For this, it is first necessary to look into the magnitude of the individual harmonic components of the curve u = f(t).

In accordance with the converter's principle of operation, u = f(t) for a given N is a periodic function. At any of its points it satisfies the Dirichlet condition, and may be expanded in a trigonometric series. We choose the origin of coordinates as is shown in Fig. 2,b. In this case, the function is an even one and, when expanded in a Fourier series, will have, in addition to the constant term defined by (6), only cosinusoidal terms. With this, the amplitude of the ν th harmonic U_ν is computed as the coefficient in the Fourier series

$$U_\nu = \frac{2}{T}\int\limits_{-T/2}^{+T/2} f(t)\cos\frac{2\pi}{T}\nu t\,dt. \tag{8}$$

If we bear in mind that the function f(t) has the constant value of $U_0/2$ in the interval $(-\tau/2+0) \leq t \leq (\tau/2-0)$ and equals zero in the intervals $-T/2 \leq t \leq (-\tau/2-0)$ and $(\tau/2+0) \leq t \leq T/2$, we can write Expression (8) in the form

$$U_\nu = \frac{U_0}{T}\int\limits_{-\tau/2}^{+\tau/2} \cos\frac{2\pi}{T}\nu t\,dt. \tag{9}$$

By carrying out the integration in (9), we get

$$U_\nu = \frac{U_0}{\pi\nu}\sin\pi\nu\frac{\tau}{T}. \tag{10}$$

By denoting the duty factor, equal to the ratio τ/T, by θ we can write

$$U_\nu = \frac{U_0}{\pi\nu}\sin\pi\nu\theta. \tag{11}$$

If we differentiate (11), we arrive at the expression

$$\frac{dU_\nu}{d\theta} = U_0\cos\pi\nu\theta. \tag{12}$$

Equating the right member of (12) to zero:

$$U_0\cos\pi\nu\theta = 0, \tag{13}$$

we can find the values of θ which correspond to maximum values of U_ν from the condition

$$\nu\theta = \frac{k}{2}, \tag{14}$$

where k is any odd integer.

It must be mentioned that not all solutions which satisfy (14) should be taken into consideration. In fact, it is clear from (2) and (5) that

$$\theta = \frac{N+1}{2^n+1}. \tag{15}$$

Since N is included in the interval

$$0 \leqslant N \leqslant 2^n - 1,$$

then

$$\frac{1}{2^n+1} \leqslant \theta \leqslant \frac{2^n}{2^n+1}. \tag{16}$$

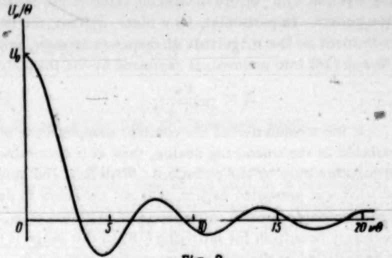

Fig. 3

Consequently, only those solutions of (14) have physical meaning for which the value of θ, for a given ν, satisfy (16). In particular, for $\nu = 1$, only the one value of θ equal to 0.5 is meaningful; for $\nu = 3$, the three values of θ, equal to 1/6, 1/2, and 5/6; for $\nu = 5$, the five values of θ equal to 0.1, 0.3, 0.5, 0.7, and 0.9, etc. It is characteristic of all this that there exists a unique value of θ, equal to 0.5, for which the peak voltage of all the harmonics, including the first, is a maximum. This can be confirmed by setting $\theta = 0.5$ in (14). After this substitution, we obtain the equation

$$\nu = k, \tag{17}$$

which is satisfied for any odd ν. Therefore, the computations of the admissible pulsations at the output of the smoothing device should be carried out for the case $\theta = 0.5$, which is the most disadvantageous from the point of view of the size of the harmonic component. The frequency spectrum for this case, constructed on the basis of (6) and (11), is given in Fig. 2,c.

Figure 3 shows the envelope of the frequency spectrum for any physically meaningful values of ν and θ. Here, the quantity U_ν/θ has been laid out along the axis of ordinates, instead of U_ν, and the product $\nu\theta$, instead of ν, has been taken as the independent variable. As a result of these replacements, we can use one graph to show, in general form, the relationships between ordinal number of harmonic, magnitude of the individual components' amplitudes and the duty factors, which are proportional to the number N to be converted. The graph was constructed on the basis of (11), which can be written in the form

$$\frac{U_\nu}{\theta} = U_0\frac{\sin\pi\nu\theta}{\pi\nu\theta}. \tag{18}$$

The harmonic components cause pulsations at the output of the smoothing device. In its turn, the size of the admissible pulsations is closely connected with the accuracy of the converter's operation. Indeed, if it is necessary to convert a numerical quantity into a voltage proportional to it, this then means that, over the entire range of variation of θ, the absolute error Δ at the smoothing device's output must not exceed the quantity which corresponds to one unit. In other words, Δ must be less than the fraction $1/b^n$ of the maximum value of the constant component. In particular, for a binary system, the requirement on the magnitude of the absolute error, taking (6) and (16) into account, is expressed by the inequality

$$\Delta < \frac{U_0}{2^{n+1}+2}. \qquad (19)$$

If the attenuation of the constant component is invariable in the smoothing device, then Δ is determined in practice only by the pulsations. With this, and based on what was presented earlier, it is not necessary to design the device for the entire range of variation of θ. The necessary condition for satisfying (19) in this range is that it be satisfied at the point corresponding to $\theta = 0.5$.

In practical designing, it should be kept in mind that the speed of a concrete converter, for given f and n, is almost completely determined by the frequency properties of the smoothing device. These, in turn, depend on the device's form, circuit and parameters. With this, as the maximum number of significant places of the numerical-quantity converter decreases, the requirements on the permissible pulsations at the smoothing device's output, in correspondence with (19), relax sharply, which permits a significant increase in speed of action. The speed of the converter can also be increased by decreasing the duration T of a complete cycle which, as is clear from (5), is inversely proportional to the frequency f of the input pulses. But increasing f leads to the use of higher-frequency elements. Therefore, one should significantly increase the frequency of the input pulses only after one has exhausted the possibilities of increasing speed of action by improving the frequency properties of the smoothing device.

Among the advantages of the converter herein described are its simplicity, its lack of precision elements or assemblies, requiring fine adjustment, the ease of executing the device with transistor or ferro-transistor elements, the absence of special requirements on frequency stability of the input pulses, or on the duration of a complete cycle. This latter advantage is due to the fact that any variation of frequency automatically leads to an inversely proportional variation both of τ and of T and, in accordance with (6), thus has no effect on the magnitude of U_{out}.

AUTOMATIC TELEMETRY SYSTEM FOR OIL-WELL FLOW

A. A. Abdullaev and I. A. Nabiev
(Baku)

(Translated from: Avtomatika i Telemekhanika, Vol. 21, No. 2, pp. 266-270, February, 1960)
Original article submitted October 3, 1959

The basis for establishing the correct operating conditions for exploiting oil wells is the measurement, and taking account of, the quantity of oil and water extracted from the wells.

An optimal technological mode of operation of a well can only be established where there is sufficient information concerning the well's output and its variations under various operating modes. Variations in the output of fluid, observed by measurements, allow the necessary measures to be taken to guarantee normal well operation.

In the southern petroleum regions of the Soviet Union, flow measurements are made by grouped measuring stands. The use of such stands permits a sizeable shortening of the pipelines on the fields. At these stands, measurement of well flow is carried out manually. This increases the staffs of the fields, does not allow frequent measurements to be made (the measurers work on one shift) and does not permit systematic observation of well flow. Moreover, manual measurement of well flow retards the transition to complex automation and remote control of the fields.

In the present paper we describe a system of automatic telemetry of oil-well flow, developed at the Research and Planning Institute (NIPI) "Neftekhimavtomat."

The system developed for the automatic measurement of oil-well flow permits the measurement of oil and water flow individually from a well, with transmission of the readings to a control point and their recording on special cards. This system is one of the basic devices (assemblies) of the system of complex automation and remote (central) control of oil fields, developed jointly with the Institute for Automation and Remote Control (IAT) of the AN SSSR and the All-Union Petroleum Research Institute. In 1957, on the fourth field of the "Ordzhonikidzeneft' " oil-field management, workers of the fields and of the NIPI equipped 24 wells with this system, these wells being still successfully exploited today.

Figure 1 shows the control desk (a) and a measuring stand (b). Each measuring trap (measuring tank) serves eight wells (the number of wells can be increased).

Figure 2 shows the scheme of the system for the automatic telemetering of oil-well flow based on grouped measuring stands. Each such stand is equipped with distributor valves with pneumatic-membrane executive mechanisms (MEM) 8, a manometer 17, and position signaller (PS) 21.

To measure the flow of any well, it is necessary to switch it from the common collector to a measuring tank. This is implemented by applying compressed gas to the MEM of the given well. With this, the well is switched from common collector 10 to measuring tank 5, the MEM distributor valves are controlled by the pneumatic stepping distributor (PSD) which has 16 positions; eight of these correspond to a connection of a well to the measuring tank, and eight to an empty measuring tank. Details as to the position of the PSD are obtained by means of the pneumoelectric transformer 21. The PSD drive is a bellows mechanism.

When compressed gas is fed to the chamber of the PSD's bellows mechanism, the PSD is switched from the given position to the following one. The supply of compressed gas to the bellows mechanism is implemented by electropneumatic valve 16. When this latter receives an electric impulse, it sends gas to the bellows mechanism's chamber, thereby switching the PSD. In addition to the eight valves which switch the wells from the common collector to the measuring tank, there is common valve 7 for controlling the measuring tank's drain line. The MEM of this valve is subject to combined control: by the PSD and by electropneumatic valve (EPV) 20. The MEM of the valve on the drain line is maintained in the closed state during the period when a well is connected to the measuring tank by means of the PSD and, after the well is disconnected from the measuring tank, by means of EPV 20. To control the emptying of the measuring tank, zero-level indicator 6 is connected in its lower portion and, to signal overflow of the measuring tank, trouble indicator 14 is connected in. Compressed gas, obtained from the same measuring tank, is used to supply all the system's pneumatic elements. For the pressure stabilization and cleaning of the gas, the system contains pressure reducer 18 and filter 19. Measurement of the oil and water levels in the measuring tank is implemented by level transducer 1 with two floats, 3 and 4, inside of which constant magnets are placed. One of the floats rests on the "water-oil" dividing level, the other rests on the oil level. The floats freely move along the vertical brass tube (or a tube of some other nonmagnetic material) inside of which is to be found indicator 2, set in motion by the transducer's synchronous motor.

Control of the automated measuring tank's operation, and implementation of the interconnections between the stand's individual elements is carried out by relay apparatus, located in the measuring tank's electrical block 13. At the central (control) point is to be found the control console, including program device 25, program-device commutator 26, relay apparatus 28, providing automatic system operation, fixed frequency generator 29, flow recorder 30, and array 27 of signal lamps, keys and knobs.

The program device automatically gives the time for filling the measuring tanks by the output of each well in accordance with a previously established central control program within the limits of 10 minutes to 4 hrs, at 10 min intervals. The time for filling is established by the position of a contact pin on the program device commutator for each well individually. The programing device is built around stepping selectors. An individual stepping selector is assigned to each measuring tank.

The relay apparatus, consisting of several assemblies, connects the basic blocks and elements of the central control point, and provides automatic cyclic operation of the entire measuring system. The output recorder is a number-printing device for recording the serial number of the measuring tank, the well and the levels of oil and water. The electronic frequency generator is a two-channel one. There are 12 fixed frequencies in each channel.

In the system, a frequency method is used for selecting the objects (measuring tanks), and for transmission of

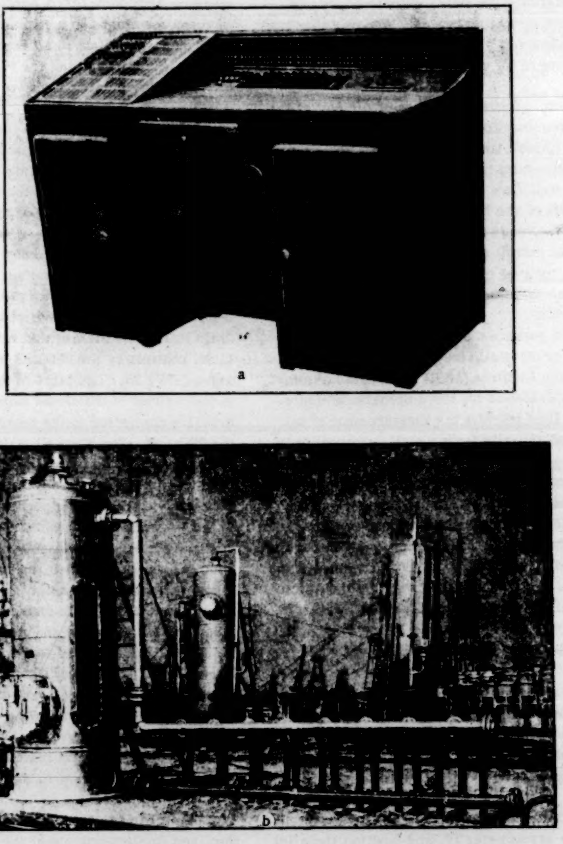

Fig. 1

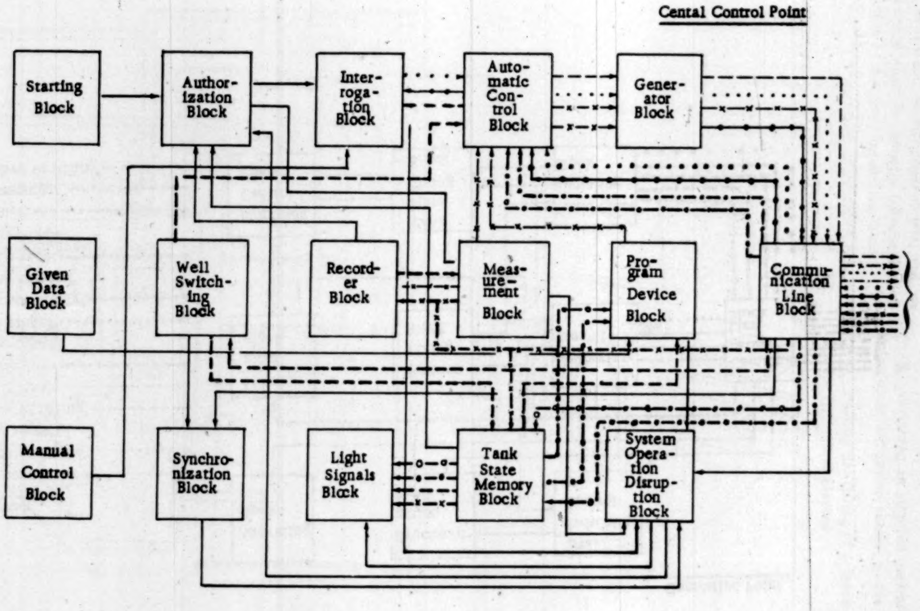
Cental Control Point
Starting Block
Authorization Block
Interrogation Block
Automatic Control Block
Generator Block
Given Data Block
Well Switching Block
Recorder Block
Measurement Block
Program Device Block
Communication Line Block
Manual Control Block
Synchronization Block
Light Signals Block
Tank State Memory Block
System Operation Disruption Block

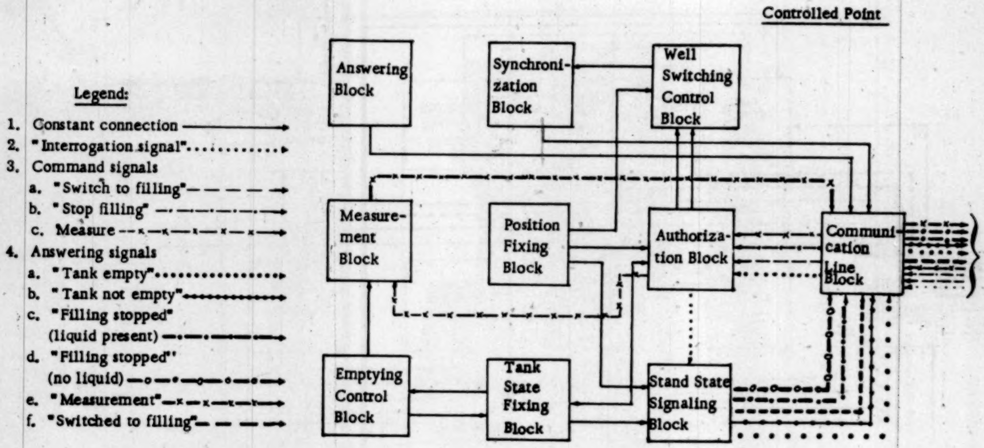

Controlled Point
Legend:
1. Constant connection
2. "Interrogation signal"
3. Command signals
a. "Switch to filling"
b. "Stop filling"
c. Measure
4. Answering signals
a. "Tank empty"
b. "Tank not empty"
c. "Filling stopped" (liquid present)
d. "Filling stopped" (no liquid)
e. "Measurement"
f. "Switched to filling"
Answering Block
Synchronization Block
Well Switching Control Block
Measurement Block
Position Fixing Block
Authorization Block
Communication Line Block
Emptying Control Block
Tank State Fixing Block
Stand State Signaling Block

Fig. 3

the measurement signals, a pulse-time method of selection.

A given measuring stand is a continuously acting complex system, since each of the 12 measuring tanks comprising the system is, as it were, an independent unit, and has a closed operating cycle which is virtually independent of the state and operation of the other measuring tanks.

The system's functioning can be decomposed into several operations.

1. Interrogation as to the state of all the measuring tanks (periodically, at short intervals of from 2 to 5 minutes) with the aim of observing measuring tanks which are emptied subsequent to a prior measurement.

2. Switching an emptied measuring tank, observed during an interrogation period, to the filling mode.

3. Halting the filling of a measuring tank after the time for filling has elapsed.

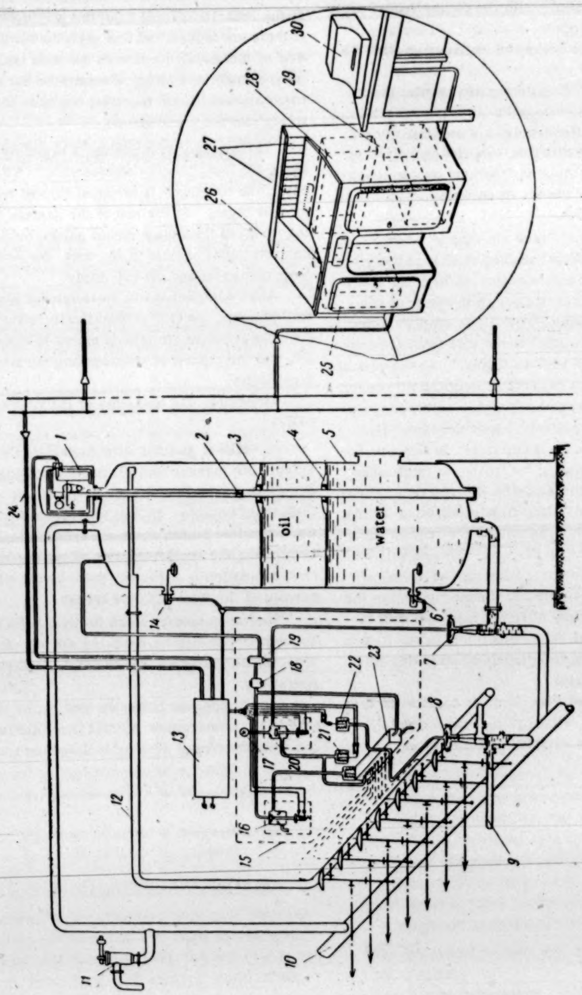

Fig. 2

4. Measuring and recording the results.

5. Switching to the emptying mode after completion of the measurement cycle.

Figure 3 shows the block schematic of the central control point and one of the 12 controlled points of the system of automatic telemetering of oil-well output. We shall consider the operation of the system as shown on the block diagram in accordance with the technological cycle of measuring oil-well output.

For convenience, we begin the explanation with the interrogation cycle.

At the beginning of the interrogation cycle, the interrogation block sends interrogation signals over the line, i.e., signals of 12 fixed frequencies are successively sent over the line. Each measuring tank has its own fixed selection frequency. Each frequency selects its corresponding measuring tank, which sends its answering signal back to the central control point.

If the answering signal "tank not empty" is received, the interrogation block ceases sending signals to the given tank, and switches to the interrogation of the next tank's state. This terminates interrogation of the state of the given tank. If the answering signal "tank empty" is received, then the order is sent over the line from the central control point, "switch tank to filling." At the controlled point, by means of the pneumatic stepping distributor, the next well in turn is switched from the common collector to the measuring tank, and filling of the tank begins.

The time that each well is connected to the measuring tank, i.e., the time alloted for filling, is established beforehand on the program device by the dispatcher (central controller). After the filling time established for the given well has elapsed, the program device sends a signal over the line to halt filling of the tank. This signal, by means of the pneumatic stepping selector and valve, effects switching of the well from the measuring trap to the common collector. The flow of liquid from the well to the measuring tank ceases. The filled tank awaits its turn to be measured. With this, the process of preparing for a flow measurement terminates.

It should be mentioned that, in those cases when the well does not supply fluid, although the measuring tank was in the fill state for the established time, after the well is switched from the measuring tank an answering signal, "filling stopped" (no fluid) is sent. This signal is fixed at the central control point and, when it again is time to interrogate the given tank, it is set up to be filled from the following well.

A measuring tank filled with liquid remains in that state until the recorder is released from operation. As soon as the recorder is freed from the previous measurement and if there are tanks filled and ready to be measured, the process of measuring the flow in the next tank begins. The measurement and fixing of results of the measurement is implemented by one recorder, common to all the tanks entering into the given system.

The measurement process is begun by the order, sent along the line, "begin measurement." At the controlled point, the transducer is switched in, and the measurement process begins. At the end of the process, the recorder, having received the measurement pulses, prints on a special card the serial number of the tank, the well and the well's output of water and oil separately.

After completing the measurement process at the controlled point, the tank automatically switches to emptying, i.e., the liquid in the tank is routed to the common collector, and the process of interrogating the state of the next tank begins.

Thereafter, the operation of the system repeats cyclically.

In addition to automatic operation, the system is equipped for manual control, manual calling of tanks and out-of-sequence flow measurement of any well, at the dispatcher's option. Both at the central control and at the controlled points, there are synchronization blocks, controlling the synchronization of system operation. If synchronization is disrupted, these blocks signal the dispatcher of the trouble in the system.

There is a special block for fixing the disruptions in the system's operation, notifying the dispatcher of the character of the disruption if such occurs, and preventing false operations.

In the apparatus presently used in the system for the automatic measurement of well flow, the recorder is a specially developed device for the given system.

BIBLIOGRAPHY

LIST OF LITERATURE ON MAGNETIC ELEMENTS IN AUTOMATION, REMOTE CONTROL, AND COMPUTING TECHNOLOGY FOR 1958 (continued)*

(Translation from: Avtomatika i Telemekhanika Vol. 21, No. 2, pp. 271-278, February, 1960)

I. Romano, "Magnetic amplifier principles," Rev. Generale de l'electricite 67, 4, 233-244 (1958)

A. P. Rosenstein, "The transactor: a self-saturated transformer. I". Commun. and Electronics 36, 129-142 (1958).

M. A. Ruggles, "The effect of capacitance on cross-conduction in half-wave bridge magnetic amplifiers," Proc. STC on Mag. Amp., T-98, 97 (1957).

H. Schierholt, "Designing simple magnetic amplifiers," Elektronik 11, 7, 11, 337-340 (1958).

W. F. Schmidt, "Self-saturating reactor circuit," USA patent, class 323-89, No. 2807775, Sept. 24, 1957

"Single-stage magnetic amplifier for educational and experimental purposes," Flectro Methods LTD of Stevenage (Saxton way Stevenage, Herts).

P. Siskind, "Voltage-controlled magnetic amplifier," USA patent, class 323-89, No. 2813246, Nov. 12, 1957.

F. Stanciulescu, "Determination of the output and the input-output characteristics of magnetic amplifiers under complex loads," [in Rumanian]. Autom. si electronica 1, 6, 249-256, 11 figs., 6 title-bibliographies (1957).

R. D. Torrey, "Voltage biasing of magnetic amplifiers," USA patent, class 307-88, No. 2814734, Nov. 26, 1957.

J. N. VanScoyoc, "Magnetic amplifier," USA patent, class 323-89, No. 2794165, May 28, 1957.

J. R. Walker and M. Frank, "Design methods for magnetic amplifiers and saturable reactors," Wayne Fngineering Research Inst., Detroit, Mich. 60, (Suppl. No. 1 to WADC Technical Rept. 56-281, AD 110431) (May, 1957).

J. R. Walker, "Magnetic amplifier design," Fl. Design News 3, 1, 36-49 (1958).

S. D. Warner, "A bridge-type high-gain magnetic amplifier for use at high temperatures," Proc. C. M. A. (1958), Los Angeles; AIEE 363-369, 6 fig, 2 bibl. (1958).

P. Willems, "Dynamic behavior of magnetic anplifiers," Revue E. 2, 7, 185-193, 10 figs., (1958).

c) Two-Cycle Magnetic Amplifiers

C. L. Boyajian, "High-efficiency push-pull magnetic amplifier and its use as a dc shunt motor drive," Commun. and Electronics 39, 545-550 (1958) 10 figs., 6 bibls., Proc. STC on Mag. Amp., T-98, 35, August, 1957.

W. A. Geyger, "The effective feedback factor of self-balancing magnetic amplifiers," Commun. and Electronics 35, 66-69 (1958).

W. A. Geyger, "Self-balancing flux-gate magnetometers," Commun. and Electronics 36, 213-216 (1958).

I. M. Horowitz, "Magnetic amplifiers," USA patent, class 179-171, No. 2817717, Dec. 24, 1957.

D. L. McMurtrie and J. P. Ward, "Triggering in the reversible half-wave magnetic amplifier," Commun. and Electronics 39, 598-605 (1958) 15 figs. 17 bibls., Proc. STC on Mag. Amp., T-98, 78, August, 1957.

Z. H. Meiksin, "Comparative study of magnetic servo-amplifiers," Proc. C. M. A. (1958) Los Angeles, AIEE 156-178, 18 figs. 3 tables, 9 bibls, (1958).

A. G. Milnes, "High-efficiency push-pull magnetic amplifiers with transistors as switched rectifiers," Commun. and Electronics 37, 327-330, 5 figs., 7 bibls., discussion 330-331, 1 fig. (1958).

R. Willheim, "Improvements in and relating to magnetic amplifiers," English patent, class 40/4/, No. 794427, May 7, 1958.

d) Multistage Amplifiers

H. T. Carden and A. D. Cawdery, "The cascading of half-wave bridge magnetic amplifiers," El. Energy 2, 10, 394-396, 6 figs., 2 bibls., (1958).

R. M. Hubbard, "Shunt-coupled magnetic amplifier circuits," Proc. C. M. A. (1958) Los Angeles, AIEE 388-404, 10 figs., 15 bibls., 1 table (1958).

G. E. Lynn, "A fast-response full-wave magnetic amplifier," Commun. and Electronics 35, 37-44, 8 figs., 8 bibls. (1958).

S. Weissman, "Two-stage magnetic amplifier," USA patent, class 179-171, No. 2809241, Oct. 8, 1957.

e) Multiphase Amplifiers

E. S. Friedlander, "Improvements in or relating to polyphase magnetic amplifier arrangements," English patent, class 40/4/, No. 744990, Feb. 15, 1956.

C. H. Grace, "Generalized transfer characteristics for 3-phase magnetic amplifiers with inductive loads," Proc. STC on Mag. Amp., T-98, 169, August 1957.

W. A. Moore, "New techniques in designing three-phase magnetic amplifiers," Proc. STC on Mag. Amp.,

---

*For the initial portion, Cf. Avtomatika i Telemekhanika No. 1 (1960).
See English translation.

T-98, 177 August, 1957.

f) AC and High-Frequency Amplifiers

D. W. Grant, "Magnetic amplifier circuits," (Bell Telephone Labs) June 28, 1955, USA patent, class No. 2782269, Feb. 19, 1957.

H. J. Gray, "Investigations of magnetic amplifiers with feedback," Trans. IRE Electronic Computers 7, 3, 213-217, 8 figs., 2 tables (1958).

R. E. Jackson, "The use of magnetic amplifiers at high frequencies", Proc. C. M. A. (1958) Los Angeles, AIEE 454-464, 8 figs, 3 bibls., (1958).

E. W. Lehtonen and E. A. Cronauer, "Controlled magnetic amplifiers," Commun. and Electronics 38, 476-480 (1958), Proc. STC on Mag. Amp., T-98, 8, August, 1957).

D. L. Watrous and J. D. Hamden, "Evaluation of 4-10 kc amplistat design techniques," Proc. NEC 14, 862-873 (1958).

R. L. White, "How to design pulse magnetic amplifiers. Part I. Design," El. Design 20, 4 (1958); Part II. Logic Circuits. El. Design 3, 2 (1958).

6. Magnetic Voltage Amplifiers. Modulators. Sondes (Magnetometers)

D. W. Boensel, "Theory and operation of a cross-field magnetic modulator," Proc. C. M. A. (1958) Los Angeles, AIEE 370-387, 18 figs., 2 tables, 4 bibls., (1958).

A. C. Brown, "Magnetic amplifier modulator," USA patent, class 332-51, No. 280953, Oct. 8, 1957.

R. Elsner and L. Pungs, "The magnetic ring modulator and demodulator," Nachrtech Z. 10, 436-438 (1957).

B. W. Jalbert, "An analysis of the operation of the magnetic second-harmonic modulator," Proc. C. M. A. (1958) Los Angeles AIEE 319-334, 8 figs., 3 bibls., (1958),

D. Lipkin, "Modified pulse-type transverse magnetic amplifier with progressive signal growth," USA patent, class 307-88, No. 2814733, Nov. 26, 1957.

"Magnetic modulators," General Magnetics. Electronics 31, 11, 209 (1958).

W. McMurray, "Analog division circuit," Proc. C. M. A. (1958) Los Angeles, AIEE 113-129, 16 figs., 3 bibls., (1958).

F. Slater, "Frequency modulation by inductance variation: a magnetically stable ferrite modulator," J. Brit. IRE 18, 189-204 (1958).

B. W. Talbert, "An analysis of the operation of the magnetic second-harmonic modulator," Proc. STC on Mag. Amp 319-334 (1958).

F. Voelker, "Magnetometer makes continuous measurements," Electronics 31, 11, 152-154 (1958).

G. Wennerberg, "Magnetic modulator systems," USA patent, class 323-56, No. 2790948, Apr. 4, 1957.

7. Discrete (Digital) Magnetic Elements

a) Books and Dissertations

b) Surveys and Applications of Digital Elements in Control Systems and Computers

C. J. Adams and R. E. Cooper, "Pulse-type logic-element industrial control," Proc. NEC 13, 898-913, 15 figs., 1 appendix (1957).

D. A. Alexander, "Toroidal transformer for an analogue system of machine-tool control", J. Brit. IRE 11, (1958),

I. Amram, H. Guillon and B. Olliver, "Frequency dividers based on delay lines. Application to arithmetic coding," L'Onde Electrique 38, 377-379, 633-640, 16 figs., 19-title bibls., (1958).

E. K. Aschmoneit, "The 'twister', a new magnetic memory element," Elektronik 7, 10, 301-304, 10 figs., 3-title bibls., (1958).

J. Auricoste and H. L'homme, "Logical magnetic circuits: application to digital computers and control systems," LIOnde Electrique 38, 372, 217-224, 17 figs., (1958).

A. H. Bobeck and H. Andrew, "A new storage element suitable for large-sized memory arrays. The Twistor," Bell. System Tech. J. 36, 7, 1319-1340 (1957).

A. H. Bobeck and R. S. Title, "The twistor - its use in a memory array," Proc. C. M. A. (1958) Los Angeles AIEE 234-242, 14 figs., 4 bibls., (1958).

A. C. Brown, R. S. Cole and W. N. Honeyman, "Some applications of ferrites to microwave switches, phasers, and isolators," Proc. IRE 46, 4, 722-727 (1958).

S. W. Brown, "The application of magnetic amplifiers to electronic times," Proc. C. M. A. (1958) Los Angeles, AIFE 130-157, 30 figs., (1958).

"Core-diode type magnetic shift register assemblies," Electronic Industries and Tele-Tech. 1, 56 (1958).

H. D. Crane, "A high-speed logic system using only magnetic elements and connecting wire", Proc. C. M. A. (1958) Los Angeles, AIEE 464-482, 16 figs., 4 bibls., (1958).

"Cypak for industry," Westinghouse Engineer, Annual Engineering Review of the year 1957, 14-15, 1 fig., (1958).

M. Dumaire, H. Jeudon and M. Lilamand, "Logical circuits using magnetic cores and application," Proc. C. M. A. (1958) Los Angeles, AIEE 243-266, 16 figs., 9 bibls., (1958).

S. Franck, "A new electrical counter with ferrite cores," Elektrotech. Z. 79A, 313-315 (1958).

E. Franklin and J. B. James, "Magnetic memory scaling system," Nuclear Power 3, 24, 186 (1958).

J. A. Fusca, "Ferrite cores perform logic functions," Aviation Week 69, 19, 83-92 (1958).

U. F. Gianola, "Nondestructive memory employing a domain-oriented steel wire," J. Appl. Phys. 29, 5, 849-853 (1958).

U. F. Gianola and T. H. Crowley, "Magnetic networks for performing logic," Proc. C. M. A. (1958) Los Angeles, AIEE 425-433, 9 figs., (1958).

B. T. Goda, "A line-printer memory utilizing magnetic cores," Computer and automation 7, 8, 12-13 (1958).

B. T. Goda, W. R. Johnston, S. Markowitz, and R. Stuart-Williams, "All-transistor magnetic core memories," Proc. C. M. A. (1958) Los Angeles, AIEE 222-233, 14 figs., (1958).

B. T. Goda, S. Markowitz and E. Jacobi, "A line-printer memory utilizing magnetic cores," Computers and automation 7, 8, 12-13, 2 figs., (1958).

K. Gosslan, "A magnetic memory device with cores, its construction and theory of operation," Regelungstechnik, 6, 9, 315-319, 9 figs., 10-title bibls., (1958).

W. E. Guenther, D. Noreen and J. H. McNeill, "Design considerations of a static logic annunciator," Proc. NEC 13, 914-925, 9 figs., (1957).

G. J. Hess, "Static control for wood chip chemical digester for the paper industry," Elec. Engng 77, 11, 1024-1029, 13 figs., (1958).

E. W. Hogue, "Magnetic amplifiers for digital computers," Elec. Mfg., 61, 5, 150-151, 6 figs., (1958).

A. D. Holt, "The application of square hysteresis-loop materials in digital computer circuits," Electronic Engng. 30, 362, 196-199 (1958).

K. Hong, "Magnetic-drum components for high-storage density," Commun. and Electronics 39, 667-672, 12 figs., 24 bibls., (1958).

H. W. Katz, "High-frequency ferrite delay line for phase modulation," Electronic Components Symposium (Chicago) 55-58 (1957).

J. Kielsohn and G. Smoliar, "Synchronization of a magnetic computer," Proc. East. Joint Computer Conf., T-92, 90-93, 6 figs., (1957).

N. F. Lockhart, "Logic by ordered flux changes in multipath ferrite cores," IRE Nat. Convention Res., 4, 268-278 (1957).

J. L. Lowrance, "Magnetic saturable-core timing device," Commun. and Electronics 37, 393-397, 9 figs., 5 bibls., (1958).

"Magnetic amplifiers for digital computers," Instrum. Practice 12, 5, 518-520 (1958).

"Magnetic amplifiers for digital computers," Nat. Bur. Standards Tech. News Bull. 42, 4, 77-78, 6 figs., 1 bibls., (1958).

W. L. Marks, "Magnetic amplifier digital techniques," El. Energy 2, 4, 125-129 (1958).

D. W. Moore, "Evaporated magnetic films," Collection: Electronic Components Symposium, 240-245 (Chicago 1957).

V. L. Newhouse, N. R. Kornfield and M M. Kaufman, "A transistorized ferrite plate memory," Proc. NEC 13, 641-652, 11 figs., 3 bibls., (1957).

R. M. Nolan, "Computer component has reliable inert materials," Missiles and Rockets 4, 25, 26-29 (1958).

D. L. Pierce, "Application of static switching in the steel industry," Iron and Steel Engineer 11, 113-125 (1957).

J. A. Rajchman, "Magnetics for computers, A survey of the state of the art in 1958," Proc. C. M. A. (1958) Los Angeles, AIEE 179-221, 23 figs., 39 bibls., (1958).

J. A. Rajchman, G. R. Briggs and A. W. Lo, "Transfluxor-controlled electroluminescent display panels," Proc. IRE 46, 11, 1808-1824, 23 figs., 3 tables, 9 bibls., (1958).

J. A. Rajchman, and H. D. Crane, "Current steering in magnetic circuits," Ire Trans. Electronic Computers, EC-6, 1, 21-30 (March 1957).

J. Reiner, "Magnetic cores for airborne digital computers," Proc. NEC 13, 653-665, 14 figs., (1957).

J. L. Rosenfeld, "Magnetic core pulse-switching circuits for standard packages," IRE Trans. Electronic Computers, EC-7, 3, 223-227, 10 figs., 6 bibls., (1958).

E. L. Rudisill, "Static control of machine operation by small magnetic-amplifier Switches, performing AND, OR, NOT, MEMORY, and DELAY functions," Machine Design 20, 12-127, 15 figs., (1958).

L. Russel, "Diodeless magnetic-core logical circuits," IRE Nat. Convention Rec. 4, 106-114 (1957).

W. B. Saunders, "Magnetic memory circuits employing biased magnetic binary cores," USA patent, class 340-174, No. 2781503, Feb. 12, 1957.

W. F. Schmidt, "Multibranch magnetic amplifier with beneficially interrelated magnetic path (Vickers, Inc.) Apr. 19, 1937, USA patent No. 2778987, Jan 22, 1957.

G. Smoliar and J. Keilsohn, "Synchronization of a computer," Electronic Design 6, 5, 64-65. 6 figs. (1958).

N. Soubies-Camy, "Logical algebra applied to binary technology," in two parts: I, Automotisme 3, 7, 266 (1958); II, Automotisme 3, 8, 303-310, 22 figs. (1959).

H. F. Storm, "Applications of nonlinear magnetics," Commun. and Electronics 37, 380-388, 16 figs., 82 bibls., (1958).

H. Tellefsen and S. Alessio, "Application of magnetic core logic to industrial controls," IRE Nat. Convention Rec. pt. 6, 283-293 (1958).

R. L. Van Allen, "Time-interval generation with transistor switches and magnetic cores," Proc. NEC 14 (1958).

c) Elements in the Form of Magnetic Amplifiers with Feedback

A. Aronowitz, "A transient analysis of a bistable magnetic amplifier," Microwave Research Inst., Polytechnic Inst. of Brooklyn, N. W., 44, Rept. NR-592-57 (1957).

R. W. Durkee, "Basic magnetic switching," Elec. Mfg. 58, 10, 102-106, 276, 278, 280 (1956).

B. Ferranti, "Improvements in or relating to bistable electric apparatus including saturable core inductors," Enblish patent, class 40/4/, No. 778190, Aug. 3, 1957.

E. H. Frei, S. Shtrikman, and D. Treves, "The bistable behavior of the magnetic transductor," Brit. J. Appl.

Phys. 9, 10, 394-395, 4 figs., 7 bibls., (1958).

K. Fukui, K. Onose, K. Habara, and M. Kato, "Multi-apertured parametron," J. Inst. Electr. Commun. Engrs. Japan 41, 2, 4-5, 1 fig., (1958).

D. Katz, "Magnetic amplifiers: bistate operation and application," Bell Labs Record 36, 8, 294-297, 5 figs., (1958).

R. M. Nolan, "Magnetic unit using extremely low power," Missiles and Rockets 4, 23, 39 (1958).

R. W. Spencer, "Magnetic amplifier flip-flop circuit," USA patent, class 307-88, No. 2834893, May 13, 1958.

d) Hysteresis Elements

"A ferrite to remember," Electronic Engng. 30, 370, 55 (1958).

D. B. Erb, "High-speed magnetic switches for memory matrices," Electronic Components Symposium 43-54 (Chicago) (1957).

"Ferroxcube for computers."

U. F. Gianola, "Switching in rectangular loop ferrites containing air gaps," J. Appl. Phys. 29, 7, 1122-1124 12 figs., 2 bibls., (1958).

D. H. Schaefer, "Magnetic-core event counter for earth satellite memory," Elec. Engng. 77, 1, 52-56, 11 figs., 3 bibls., (1958).

e) Ferroresonant Elements

W. E. Proebster, "Ferroresonant switching circuits," Proc. C.M.A. (1958) Los Angeles, AIEE 434-443, 10 figs., 12 bibls., (1958).

f) Transistor-Magnetic Elements

W. J. Dunnet and A. G. Lemack, "A new transistor-magnetic core bilogical computer element," Automat. Control 32-39, 17 figs., 12 bibls., 2 tables.

8. Magnetic Generators and Frequency Transformers

H. Domheim, "Parallel operation of rectifiers with anode chokes," Elektronische Rundschae 9, 315-318, 8 figs., 2 title-bibliographies (1958).

R. W. Kulterman, F. W. Neilson and W. B. Benedick, "Pulse generator based on high shock demagnetization of ferromagnetic material," J. Appl. Phys. 29, 500-501 (1958).

K. Kurutz, "Static frequency tripler and its industrial use," Electrotechnika 50, 3, 99-105 (1957).

G. R. Slemon and P. P. Biringer, "Equivalent-circuit approach to the analysis and design of magnetic frequency triplers," Proc. C.M.A. (1958) Los Angeles, SIEE 335-347, 7 figs., 4 bibls., (1958).

J. E. Sunderlin and M. L. Weinberg, "Magnetic pulse generators," Elec. Mfg. 61, 5, 139-143, 5 figs., 4 bibls., 1 table (1958).

N. L. Weinberg, "Analysis of nonresonant charging circuit for magnetic pulse generator," Commun. and Electronics 37, 271-277, 10 figs., 5 bibls., (1958).

B. M. Wolfframm, "Variations of pulse width in magnetic pulse modulators," Proc. C.M.A. (1958) Los Angeles, AIEE, 309-318, 10 figs., 2 bibls., 1 table (1958).

9) Magnetic Measurements, and Methods of Testing Magnetic Elements

I. Bady, "Measurement of losses of magnetic materials at high inductions at frequencies up to 100 Mc," J. Appl. Phys. 29, 3, 393-394 (1958).

B. Barron, "Measuring phase of distorted signals," Control Engng 11, 115, 117, 5 figs., (1958).

H. Bromberg and P. J. Karttunen, "A ferrometer for the determination of the ac magnetization curve and the iron losses of small ferromagnetic sheet samples," Proc. IEE 8, pt. 105A, 22, 375-384 (1958).

T. H. Bonn, R. D. Torrey, and F. Bernstein, B-H tester measures memory core parameters," Electronics, Engineering Edition 31, 3, 76-80, 10 figs., 3 bibls., (1958).

J. K. Choudhury and P. C. Sen, "Magnetic measurements with the bridged-T network," J. Sci. Instr. 35, 4, 145-146 (1958).

G. M. Clarke, "Coils for magnetic fields. I. Thermal aspects," Electronic and Radio Engr. 35, 8, 298-306 (1958) II. Weight aspects. 9, 340-344.

D. Drechsel, "An instrument for testing ferrites with rectangular hysteresis loops," Nachrichtentechnik 8 352-360, 26 figs., 6 title-bibliographies (1958).

R. Falker and E. E. Huckinger, "Magnetic measurement on ferrite pi-section cores for the output transformer of horizontal deviation," Elektronische Rundschar 8, 270-274, 8 figs., 7 title-bibliographies (1958).

J. R. Freeman, "Pulse testing of magnetic cores," El Eq. 7 (1958).

W. Frings, "An electronic circuit for measuring the characteristics of ferromagnetic materials," Instrumentenkunde 66, 2, 19-25 (1958).

H. L. Goldstein, "Observation of transients in the series-connected saturable reactor with high-impedance control source," Proc. C. M. A. (1958) Los Angeles, AIEE 47-61, 22 figs., 11 bibls., 1 tables (1958).

C. E. Goodell, "Integrator-amplifier for core measurements," Electronics 31, 7, 110-113 (1958).

C. D. Graham, "Method for measuring saturation magnetization in ring samples," J. Appl. Phys. 29, 1, 68-70 (1958).

R. D. Harrington and R. C. Powell, "High-frequency magnetic permeability measurements using torodial coils," Proc. IRE 46, 784 (1958).

W. P. Harris, and I. L. Cooter, "Improved bridge method for the measurement of core losses in ferromagnetic materials at high flux densities," J. Res. Nat. Bur. Standards, 509-516 (1958).

I. S. Jacobs and P. E. Lawrence, "Measurement of magnetic fields," Rev. Sci. Instr. 29, 8, 51-52, 3 figs., (1958).

H. Lachowicz et al. "Equipment measuring magnetic properties of switch-cores with rectangular hysteresis loop," Archiwuna Elektrotechn. 7, 4, 735-740 (1958).

J. McFarlane, P. Milne and J. K. Darby, "Direct-reading iron-loss testing equipment for single sheets, single strips, and test squares," Proc. IEE, 8, part 105A, 22, 385-394 (1958).

B. L. Miller, "Calibration of ballistic galvanometers for magnetic measurements," Am. J. Phys. 26, 2, 129-130 (1958). "Proposed standards for core test methods for toroidal magnetic amplifier cores," Commun. and Electronics. 38, 524-535 (1958).

M. J. Swan, "A permeameter controller for magnetic measurements," J. Sci. Instr. 35, 9, 344-346 (1958).

R. E. Thomkins, L. H. Stauffer and A. Kaplan, "New magnetic core loss comparator," J. Appl. Phys. 29, 3, 502-503 (1958).

S. Yamaguchi, "Magnetic analysis with electron beams," Z. angew. Phys. 1, 3, 138-140 (1958).

Compiled by G. V. Subbotina and I. S. Trefilova

BLANK
PAGE

ESTIMATING THE EFFECT OF QUANTIZATION BY LEVEL ON THE PROCESSES IN AUTOMATIC DIGITAL SYSTEMS

Ya. Z. Tsypkin

(Moscow)

Translated from Avtomatika i Telemekhanika, Vol. 21, No. 3, pp. 281-285, March, 1960
Original article submitted July 28, 1959

An estimate is given of the effect of the level-quantization interval in automatic digital systems whose continuous portions contain both constant and variable parameters.

INTRODUCTION

In automatic digital systems (ADS) at least one quantity is subject to quantization by level and by time. The quantization process consists in fixing previously given discrete levels at discrete moments of time. Level-quantization interval σ_z is determined by the accuracy, and time-quantization interval T by the speed of action, of the digital devices which belong to the automatic system.

The effect of the time-quantization interval was studied earlier [1,2]. An estimate of the effect of the level-quantization interval was made in [3] on the basis of the canonical forms of equations. Due to this, the results of the estimation process were obtained in an unnecessarily complicated form. Moreover, it is not possible to concur with all the conclusions of [3].

Below, we present a simple way of estimating the effect of the level-quantization interval which is not related to the canonical forms of equations, and which is valid for ADS with constant and with variable parameters.

1. Equivalent Scheme of an ADS

We consider the ADS scheme shown on Fig. 1. The functional schematic of the device (AD) for analog-to-digital conversion (Fig. 2, a) may be presented in the form of a series connection of a pulse element and a relay element with a multistep characteristic (Fig. 2,b).

In its turn, the relay element can be presented in the form of a parallel connection of an amplifying element with gain k = 1 and a nonlinear element (Fig. 2, c) whose characteristic Ψ equals the difference between a linear and the relay characteristic.

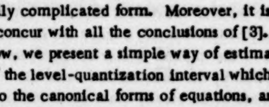

Fig. 1.

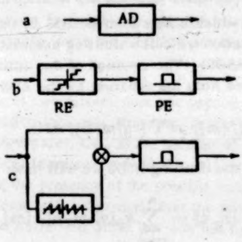

Fig. 2.

By using this representation of the AD converter, we can replace the ADS scheme by the equivalent scheme of a limiting sampled-data system in which the effect of the level quantization is taken into account by the stimuli applied to it via the nonlinear element with characteristic Ψ. In Fig. 3, a, this system is represented as a sampled-data system with a linear feedback path; on Fig. 3, b, the feedback path is included in the limiting system.

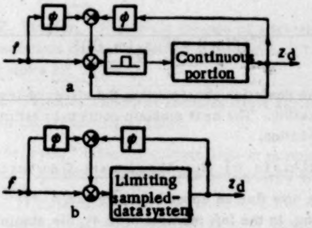

Fig. 3.

We denote the impulse characteristic of the closed linear sampled-data system, which can also contain variable parameters, by $k_c[n, m, \epsilon]$. Methods of determining $k_c[n, m, \epsilon]$ were described in [4]. If there are no variable parameters, then

$$k_c[n, m, \varepsilon] = k_c[n - m, \varepsilon]. \tag{1.1}$$

By using the impulse characteristic, we can write the equation of the ADS of Fig. 3, b in the form

$$z_d[n, \varepsilon] = \sum_{m=0}^{n} k_c[n, m, \varepsilon]\{[\Psi(f[m]) - \Psi(z_d[m, 0])] + f[m]\}. \tag{1.2}$$

2. Deviations Engendered by Level Quantization

A system which differs from an ADS by its absence of level quantization we call a limiting automatic sampled-data system (ASDS). The equation of the limiting ASDS can be obtained from the equation for the ADS (1.2) by setting in it

$$\Psi(f[m]) \equiv \Psi(z_d[m, 0]) \equiv 0. \tag{2.1}$$

Thus, for the limiting ASDS we will have

$$z_s[n, \varepsilon] = \sum_{m=0}^{n} k_c[n, m, \varepsilon] f[m] \tag{2.2}$$

or

$$z_s[n, \varepsilon] = \sum_{m=0}^{n} k_c[n, n - m, \varepsilon] f[n - m]. \tag{2.3}$$

The difference between $z_d[n, \epsilon]$ and $z_s[n, \epsilon]$, defining the effect of level quantization, may be presented on the basis of (1.2) and (2.2), in the form

$$\delta z[n, \varepsilon] = z_d[n, \varepsilon] - z_s[n, \varepsilon] = \sum_{m=0}^{n} k_c[n, m, \varepsilon] \{\Psi(f[m]) - \Psi(z_d[m, 0])\}. \tag{2.4}$$

The deviation characterizes the effect of level quantization. The next problem consists in estimating this deviation.

3. Estimate of the Maximum Deviation

We now find an upper bound for $|\delta z[n, \epsilon]|$. By replacing, in the left member of (2.4), the absolute magnitude of the sum by the sum of the absolute magnitudes, we get

$$|\delta z[n, \varepsilon]| \leqslant \sum_{m=0}^{n} |k_c[n, m, \varepsilon]| \{|\Psi(f[m])| + |\Psi(z_d[m, 0])|\}. \tag{3.1}$$

But the difference between the linear and the relay characteristics or, what amounts to the same thing, between the nonquantized and the quantized quantities, may not, in absolute magnitude, exceed half the quantization interval $\sigma/2$. Therefore,

$$|\Psi(f[m])| \leqslant \frac{\sigma}{2}, \quad |\Psi(z_d[m, 0])| \leqslant \frac{\sigma}{2}. \tag{3.2}$$

By using these inequalities, and replacing the left member of (3.1) by the maximum value, we obtain

$$\max|\delta z[n, \varepsilon]| \leqslant \sum_{m=0}^{n} |k_c[n, m, \varepsilon]| \sigma \tag{3.3}$$

or, after replacing the variable of summation m by $n-m$,

$$\max|\delta z[n, \varepsilon]| \leqslant \sum_{m=0}^{n} |k_c[n, n - m, \varepsilon]| \sigma. \tag{3.4}$$

On the basis of (1.1), for an ADS with constant parameters we obtain from (3.3) and (3.4), respectively,

$$\max|\delta z[n, \varepsilon]| \leqslant \sum_{m=0}^{n} |k_c[n - m, \varepsilon]| \sigma \tag{3.5}$$

or

$$\max|\delta z[n, \varepsilon]| \leqslant \sum_{m=0}^{n} |k_c[m, \varepsilon]| \sigma. \tag{3.6}$$

Thus, the process' maximum deviation engendered by level quantization does not exceed the sum of the absolute values of the impulse characteristic of the limiting ASDS multiplied by the quantization interval.

An estimate of the steady-state deviation is found from (3.4), (3.6) if the limit of summation n tends to ∞.

For an ADS with constant parameters, the estimate of the steady-state deviation is the greatest possible one.

This estimate corresponds to the maximum possible accumulation in the limiting ASDS for stimuli which are modulus-limited, and is the discrete analog of the accumulation problem of B. V. Bulgakov.

4. Comparison of Some Properties of the Limiting ASDS and the ADS

If a step function stimulus

$$f[n] = \begin{cases} 1 & \text{for} \quad n \geqslant 0, \\ 0 & \text{for} \quad n < 0, \end{cases}$$

is applied to the limiting ASDS, its reaction is determined by its time or, more accurately, by its transient characteristic. By using (2.3), for example, we can present the transient characteristic $h[n, \epsilon]$ in the form

$$h[n, \varepsilon] = z_s[n, \varepsilon] = \sum_{m=0}^{n} k_c[n, n - m, \varepsilon]. \tag{4.1}$$

The steady-state characteristic will be

$$h_{\mathrm{ste}}[n, \varepsilon] = \sum_{m=0}^{\infty} k_{\mathrm{c}}[n, n-m, \varepsilon]. \tag{4.2}$$

It is a function of n and ϵ. For an ADS with constant parameters,

$$h_{\mathrm{ste}}[n, \varepsilon] = h(\varepsilon) = \sum_{m=0}^{\infty} k_{\mathrm{c}}[m, \varepsilon] \tag{4.3}$$

is a function of ϵ only. If the ASDS is designed to reproduce the stimuli applied to it then, in general,

$$h_{\mathrm{ste}}[n, \varepsilon] = h(\varepsilon) \leqslant 1. \tag{4.4}$$

We assume that the impulse characteristic of the limiting ASDS, $k_c[n, n-m, \epsilon]$, for given n and ϵ and arbitrary m, is nonnegative, i.e.,

$$k_{\mathrm{c}}[n, n-m, \varepsilon] \geqslant 0, \tag{4.5}$$

so that we shall have, from (3.4) and (4.1),

$$\max|\delta z[n, \varepsilon]| \leqslant \sum_{m=0}^{n} k_{\mathrm{c}}[n, n-m, \varepsilon]\sigma = h[n, \varepsilon]\sigma. \tag{4.6}$$

Thus, in this case the maximum deviation at the given moment of time which is engendered by the level quantization does not exceed the quantity equal to the product of the quantization interval by the value of the characteristic at that same moment of time.

The estimate of the steady-state deviation will have the form

$$\max|\delta z_{\mathrm{ste}}[n, \varepsilon]| \leqslant \sum_{m=0}^{\infty} k_{\mathrm{c}}[n, n-m, \varepsilon]\sigma = h_{\mathrm{ste}}[n, \varepsilon]\sigma. \tag{4.7}$$

Let us consider in somewhat more detail an ADS with constant parameters. For it, the [(4.5)] that $k_c[m, \epsilon] \geq 0$ is equivalent to the condition that $h[n, \epsilon]$ be monotonic for ϵ = const. By taking into account that $h[n, \epsilon] \leq h_{ste}[n, \epsilon] = h(\epsilon)$, we find that

$$\max|\delta z[n, \varepsilon]| \leqslant h[n, \varepsilon]\sigma < h_{\mathrm{ste}}[n, \varepsilon]\sigma = h(\varepsilon)\sigma \tag{4.8}$$

or, by taking (4.4) into account,

$$\max|\delta z[n, \varepsilon]| \leqslant \sigma. \tag{4.9}$$

Thus, for a monotonic characteristic, the deviation due to level quantization does not exceed the quantization interval. In this case, and only in this case, we can deduce the stability of the ADS from the stability of the limiting ASDS. If the characteristic is not monotonic, i.e., the impulse characteristic changes sign, the sum of the absolute values of the impulse characteristic may significantly exceed unity, and instead of (4.6) we shall therefore have

$$\max|\delta z[n, \varepsilon]| \leqslant \alpha\sigma. \tag{4.10}$$

where $\alpha > 1$. Under these conditions, it is possible to have, in an ADS with constant parameters, an autooscillatory mode with an "amplitude" not exceeding $\alpha\sigma$. The greater the oscillation of the characteristic $h[n, \epsilon]$ for ϵ = const, i.e., the greater the oscillation of the limiting ASDS, the greater will be the "amplitude" of the autooscillatory modes possible in the ADS.

Thus, in spite of the assertion made in [3], it is, strictly speaking, impossible in this case to conclude that the ADS is stable from the fact that the limiting ASDS is stable.

The result just derived does not depend on the size of the quantization interval. However, as the quantization interval σ decreases, i.e., as the number of places in the digital devices increases, $\max|\delta z[n, \epsilon]|$ will increase and, despite the presence of the possible autooscillations, their amplitude will be so small that the processes in the ADS and the ASDS will differ less and less from each other.

The estimates given above allow one to determine the maximum quantization interval for which the difference of the processes in the ADS and the ASDS will not exceed a given magnitude.

LITERATURE CITED

1. Ya. Z. Tsypkin, "Frequency method of analyzing discontinuous control systems," Avtomatika i Telemekhanika 19, 1 (1958).
2. Ya. Z. Tsypkin, Theory of Sampled-Data Systems [in Russian] (Fizmatgiz, 1958).
3. J. E. Bertram, "Effect of quantization in sampled-feedback systems," Applications and Industry No. 38 (1958).
4. G. P. Tartakovskii, "Stability of linear sampled-data systems with variable parameters," Radiotekhnika i Élektronika 2, 1 (1957).

DETERMINATION OF THE OPTIMAL IMPULSIVE RESPONSE FUNCTION IN THE PRESENCE OF INTERNAL NOISE

P. S. Matveev

(Moscow)

Translated from Avtomatika i Telemekhanika, Vol. 21, No. 3, pp. 286-292, March, 1960
Original article submitted May 8 , 1959

The problem of determining the optimal transfer function [1, 2] is generalized to the cases when the input stimuli are applied to n different elements of a servosystem and to systems with variable parameters.

In [1, 2] a solution was given to the problem of determining the optimal impulsive response function for cases when input stimuli are applied to two different elements of a servosystem. The aim of the present work is to generalize the results obtained in [1, 2] to the case when the stimuli are applied to n elements of a servosystem, and to systems with variable parameters.

1. Determination of the Impulsive Response Function in the Class of Systems with Constant Parameters

We assume that the servosystem has n elements to which stimuli are applied, whereby a controlling signal

$$y(t) = g(t) + m(t), \tag{1}$$

is applied to one basic element, where g (t) is a given function of time, with

$$g(t) = \sum_{i=0}^{r} g_i t^i, \tag{2}$$

and m (t) is a stationary random function.

In addition, noise n(t), in the form of a stationary random function, is superimposed on the controlling signal. To the remaining n−1 elements of the servosystem (Fig. 1), stimuli are applied in the form of stationary random functions $u_1(t), u_2(t), \ldots, u_{n-1}(t)$. We assume for simplicity that m(t), n(t), $u_1(t), u_2(t), \ldots, u_{n-1}(t)$ have zero mean values and are mutually uncorrelated. We also assume that the transfer functions $W_1(p), W_2(p), \ldots, W_{n-1}(p)$ [or the corresponding impulsive response functions $b_1(t), b_2(t), \ldots, b_{n-1}(t)$] are known. What is not known is the transfer function $W_c(p)$ (impulsive response function) of the correcting device. We initially determine the optimal impulsive response function k(t) of the closed system from which, by using well-known methods [2, 3], we can easily determine the transfer function $W_c(p)$ of the correcting device . The problem may be formulated in the following way: from given correlation functions $R_m(\tau), R_n(\tau), R_{u_1}(\tau), R_{u_2}(\tau), \ldots, R_{u_{n-1}}(\tau)$ [spectral densities $S_m(\omega), S_n(\omega), S_{u_1}(\omega), S_{u_2}(\omega), \ldots, S_{u_{n-1}}(\omega)$], given duration T of the transient response, given reproduction operator H(p), error coefficients C_i and transfer functions $W_1(p), W_2(p), \ldots, W_{n-1}(p)$, to find the impulsive response function k(t) such that the mean-square error will be a minimum.

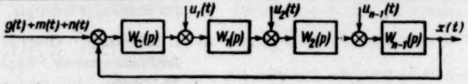

Fig. 1.

It is easily shown that the scheme shown on Fig. 2, for n = 3, is equivalent to the scheme of Fig. 1. This scheme will be used for the subsequent argument. Then [4], the system's output quantity can be written in the following way :

$$x(t) = \int_0^T [g(t-\tau) + m(t-\tau) + n(t-\tau)]\, k(\tau)\, d\tau -$$

$$- \int_0^T k(\tau)\, d\tau \int_{-\infty}^{\infty} b_1(\sigma)\, d\sigma \int_{-\infty}^{\infty} u_1(t-\tau-\sigma-\mu)\, b_2(\mu)\, d\mu - \tag{3}$$

$$-\int_0^T k(\tau)\,d\tau \int_{-\infty}^{\infty} u_2(t-\tau-\sigma)\,b_2(\sigma)\,d\sigma + \int_{-\infty}^{\infty} b_1(\tau)\,d\tau \int_{-\infty}^{\infty} u_1(t-\tau-\sigma)\,b_2(\sigma)\,d\sigma$$

$$+\int_{-\infty}^{\infty} u_2(t-\tau)\,b_2(\tau)\,d\tau,$$

where

$$k(\tau) = N(t) + \sum_{j=0}^{q} E_j\,\delta^{(j)}(t) + \sum_{j=0}^{q} \delta^{(j)}(t-T) \qquad (0 < t < T). \tag{4}$$

Let the ideal system be required to reproduce at its output the signal

$$h(t) = H_g(p)\,g(t) + H(p)\,m(t), \tag{5}$$

where

$$H(p) = \sum_{i=0}^{r} \frac{H_i}{i!} p^i, \quad H_g(p) = H(p) - \sum_{j=0}^{r} \frac{C_j}{j!} p^j \qquad (i \neq j). \tag{6}$$

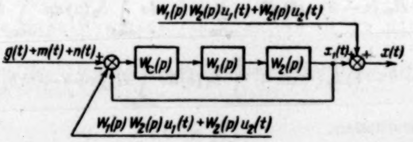
$W_1(p)\,W_2(p)\,u_1(t)+W_2(p)\,u_2(t)$
$g(t)+m(t)+n(t)$
±
−
$W_C(p)$
$W_1(p)$
$W_2(p)$
$x_1(t)$
+
+
$x(t)$
$W_1(p)\,W_2(p)\,u_1(t)+W_2(p)\,u_2(t)$

Fig. 2

Here, for convenience, we have introduced the operator $H_g(p)$ which simultaneously takes into account the operation of reproducing g(t) and the errors with which it is reproduced.

Then the reproduction error can be written in the form

$$\varepsilon(t) = h(t) - x(t).$$

If it now be required that the mean error of reproduction equal zero, then [2, 4, 5] we are led to limitations of k(t) of the form

$$\mu_\nu = (-1)^\nu \int_0^T \tau^\nu k(\tau)\,d\tau \qquad (\nu = 0, 1, 2, \ldots, r) \tag{7}$$

or

$$H_i = (-1)^\nu \int_0^T \tau^i k(\tau)\,d\tau, \quad -C_j = (-1) \int_0^T \tau^j k(\tau)\,d\tau \qquad (j \neq i = 0, 1, 2, \ldots, r). \tag{8}$$

If (8) holds, the reproduction error can be written in the following way:

$$\varepsilon(t) = \int_{-\infty}^{\infty} m(t-\tau)\,\varkappa(\tau)\,d\tau - \int_0^T k(\tau)\,d\tau\,[m(t-\tau) + n(t-\tau) -$$

$$-\int_{-\infty}^{\infty} b_1(\sigma)\,d\tau \int_{-\infty}^{\infty} u_1(t-\tau-\sigma-\mu)\,b_2(\mu)\,d\mu - \int_{-\infty}^{\infty} u_2(t-\tau-\sigma)\,b_2(\sigma)\,d\sigma\Big] - \tag{9}$$

$$-\int_{-\infty}^{\infty} b_1(\tau)\,d\tau \int_{-\infty}^{\infty} u_1(t-\tau-\sigma)\,b_2(\sigma)\,d\sigma - \int_{-\infty}^{\infty} u_2(t-\tau)\,b_2(\tau)\,d\tau,$$

where

$$\varkappa(t)=\frac{1}{2\pi}\int_{-\infty}^{\infty}H(j\omega)e^{j\omega t}\,d\omega.$$

Further, by using the same arguments as in [2, 4, 5, 6], we obtain the necessary and sufficient condition for the minimum average value of the square of (9), when (7) holds, in the form of an integral equation

$$\begin{gathered}\int_0^T\Big[R_m(\tau-\theta)+R_n(\tau-\theta)+\int_{-\infty}^{\infty}b_1(\sigma)d\sigma\int_{-\infty}^{\infty}b_2(\mu)\,d\mu\int_{-\infty}^{\infty}b_1(\lambda)\,d\lambda\\ \times\int_{-\infty}^{\infty}R_{u_1}(\tau+\sigma+\mu-\theta-\lambda-\eta)\,b_2(\eta)\,d\eta+\\ +\int_{-\infty}^{\infty}b_2(\sigma)\,d\sigma\int_{-\infty}^{\infty}R_{u_2}(\tau+\sigma-\theta-\lambda)\,b_2(\lambda)\,d\lambda\Big]k(\theta)\,d\theta=\\ =\int_{-\infty}^{\infty}R_m(\tau-\theta)\varkappa(\theta)\,d\theta+\int_{-\infty}^{\infty}b_1(\sigma)\,d\sigma\int_{-\infty}^{\infty}b_2(\mu)\,d\mu\int_{-\infty}^{\infty}b_1(\theta)\,d\theta\int_{-\infty}^{\infty}R_{u_1}(\tau+\sigma+\\ +\mu-\theta-\lambda)\,b_2(\lambda)\,d\lambda+\int_{-\infty}^{\infty}b_2(\sigma)d\sigma\int_{-\infty}^{\infty}R_{u_2}(\tau+\sigma-\theta)\,b_2(\theta)\,d\theta+\sum_{i=0}^{r}\gamma_i\tau^i,\end{gathered}\tag{10}$$

where the γ_i are Lagrange multipliers.

We now introduce the notation

$$\begin{gathered}R^*_{u_1}(\tau-\theta)=\int_{-\infty}^{\infty}b_1(\sigma)\,d\sigma\int_{-\infty}^{\infty}b_2(\mu)\,d\mu\int_{-\infty}^{\infty}b_1(\lambda)\,d\lambda\times\\ \times\int_{-\infty}^{\infty}R_{u_1}(\tau+\sigma+\mu-\theta-\lambda-\eta)\,b_2(\eta)\,d\eta,\end{gathered}\tag{11}$$

$$R^*_{u_2}(\tau-\theta)=\int_{-\infty}^{\infty}b_2(\sigma)\,d\sigma\int_{-\infty}^{\infty}R_{u_2}(\tau+\sigma-\theta-\lambda)\,b_2(\lambda)\,d\lambda.\tag{12}$$

With the use of the notation of (11) and (12), (10) can be presented in the following form:

$$\begin{gathered}\int_0^T[R_m(\tau-\theta)+R_n(\tau-\theta)+R^*_{u_1}(\tau-\theta)+R^*_{u_2}(\tau-\theta)]\,k(\theta)\,d\theta=\\ =\int_{-\infty}^{\infty}R_m(\tau-\theta)\varkappa(\theta)\,d\theta+R^*_{u_1}(\tau)+R^*_{u_2}(\tau)+\sum_{i=0}^{r}\gamma_i\tau^i\quad(0\leqslant\tau\leqslant T).\end{gathered}\tag{13}$$

Equation(13) does not differ in form from the integral equations obtained in [2, 4, 5, 6] and, therefore, the same methods of solution may be used for the determination of k(t). Obviously , integral equation (13) is easily generalized to the case of n inputs. For this, integral equation (13) can be written in the form

$$\begin{gathered}\int_0^T[R_m(\tau-\theta)+R_n(\tau-\theta)+R^*_{u_1}(\tau-\theta)+R^*_{u_2}(\tau-\theta)+\\ +\ldots+R_{u_{(n-1)}}(\tau-\theta)]\,k(\theta)\,d\theta=\int_{-\infty}^{\infty}R_m(\tau-\theta)\varkappa(\theta)\,d\theta+\\ +R^*_{u_1}(\tau)+R^*_{u_2}(\tau)+\ldots+R^*_{u_{(n-1)}}(\tau-\theta)+\sum_{i=0}^{r}\gamma_i\tau^i\quad(0\leqslant\tau\leqslant T).\end{gathered}\tag{14}$$

If the correlation function $R_m(\tau)+R_n(\tau)+R^*_{u_1}(\tau)+\ldots+R^*_{u(n-1)}(\tau)$ corresponds to a rational-fraction spectral density

$$S(\omega)=\frac{a_0+a_1\omega^2+\ldots+a_k\omega^{2k}}{b_0+b_1\omega^2+\ldots+b_l\omega^{2l}}=\frac{M(\omega)M^*(\omega)}{L(\omega)L^*(\omega)}, \tag{15}$$

then, by using the same arguments as in [5], we can shown that the impulsive response function is defined by the expression *

$$\begin{aligned}k(t)=\sum_{i=0}^{r}A_i t^i+\sum_{i=1}^{2k}B_i e^{\lambda_i t}+\sum_{j=0}^{q}E_j\delta^{(j)}(t)+\sum_{j=0}^{q}D_j\delta^{(j)}(t-T)+\\+L(p)L^*(p)M^{-1}(p)M^{*-1}(p)\Big[\int_{-\infty}^{\infty}R_m(t-\tau)\times(\tau)\,d\tau+\\+R^*_{u_1}(t)+R^*_{u_2}(t)+\ldots+R^*_{u_{(n-1)}}(t)\Big]\quad(0\leqslant t\leqslant T),\end{aligned} \tag{16}$$

where $q=l-k-1$ and $L(p)$ and $M(p)$ equal $L(\omega)$ and $M(\omega)$ for $p=j\omega$, which are easily determined from the spectral density of (15).

The unknowns A_i, B_i, E_j, D_j in (16) are determined as in [5]. Further, by the usual methods [3], the transfer function of the closed system was determined and later, also, the transfer function of the correcting device.

2. Determination of the Impulsive Response Function in the Class of Systems with Variable Parameters

We assume that the system (Fig. 3) is acted upon by stationary random noise $n(t)$ and signal $y(t)=g(t)+m(t)$ consisting of the given function of time

$$g(t)=\sum_{i=0}^{r}g_i t^i, \tag{17}$$

where the g_i are unknown coefficients and the t^i are known functions of time, plus the stationary random function $m(t)$. To the system's second element there is applied a disturbing stimulus in the form of the stationary random function $u(t)$.

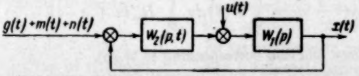

Fig. 3.

The problem solved below may be formulated as follows: from given correlation functions $R_m(\tau)$, $R_n(\tau)$, and $R_u(\tau)$ (spectral densities) and given object transfer function $W_1(p)$, to find the servosystem's impulsive response function such that the system will provide an exact reproduction of $g(t)$ at each moment of time $t>0$ and a minimum dispersion of the random process at the system's output at each moment of time.

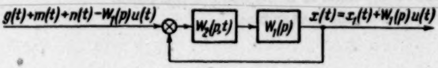

Fig. 4.

It may be shown that the scheme of Fig. 4 is equivalent to that shown on Fig. 3. Henceforth, the scheme of Fig. 4 will be used.

The reproduction error of the system (Fig. 3) can be given in the form

$$\begin{aligned}\epsilon(t)=g(t)+m(t)-x(t)=[1+W_1(p)W_2(p,t)]^{-1}[g(t)+m(t)-Q(t)]-\\-[1+W_1(p)W_2(p,t)]^{-1}W_1(p)W_2(p,t)n(t),\end{aligned} \tag{18}$$

where

$$Q(t)=W_1(p)u(t).$$

The reproduction error of the system given by Fig. 4 may be written in the form

---

* An analogous generalization can also be made for the case when $g(t)$ is a harmonic function [4].

$$\begin{aligned}\varepsilon_1(t) &= g(t) + m(t) - Q(t) - x_1(t) = \\ &= [1 + W_1(p) W_2(p, t)]^{-1} [g(t) + m(t) - Q(t)] - \\ &- [1 + W_1(p) W_2(p, t)]^{-1} W_1(p) W_2(p, t) n(t).\end{aligned} \tag{19}$$

By comparing (18) and (19), we find that $\epsilon(t) = \epsilon_1(t)$ and, consequently, just as in [4, 7], the reproduction error can be written in the form

$$\begin{aligned}\varepsilon(t) &= g(t) + m(t) - Q(t) - x(t) = g(t) + m(t) - Q(t) - \\ &- \int_{-\infty}^{t} [g(\tau) + m(\tau) - Q(\tau) + n(\tau)]\, k(t, \tau)\, d\tau \quad (t > \tau).\end{aligned} \tag{20}$$

The requirement that there be no bias, i.e., zero dynamic error, leads to $r + 1$ conditions of the form

$$t^i = \int_0^t \tau^i k(t, \tau)\, d\tau. \tag{21}$$

If (21) holds, the expression for the error has the form

$$\varepsilon(t) = m(t) - Q(t) - \int_{-\infty}^{t} [m(\tau) - Q(\tau) + n(\tau)]\, k(t, \tau)\, d\tau. \tag{22}$$

It may be shown [7] that the necessary and sufficient condition for a minimum mean value of the square of (22) amounts to this–that the impulsive response function $k(t, \tau)$ satisfy the integral equation

$$\begin{aligned}&\int_{-\infty} [R_m(\tau - \theta) + R_n(\tau - \theta) + R_Q(\tau - \theta)]\, k(t, \theta)\, d\theta \\ &\qquad = \sum_{i=0}^{r} \gamma_i \tau^i + R_m(t) + R_Q(t),\end{aligned} \tag{23}$$

where

$$R_Q(\tau - \theta) = \int_{-\infty}^{\infty} b(\sigma)\, d\sigma \int_{-\infty}^{\infty} R_u(\tau + \sigma - \theta - \lambda)\, b(\lambda)\, d\lambda, \tag{24}$$

and $b(\tau)$ is the impulsive response function corresponding to $W_2(p)$.

For the class of stationary processes for which spectral density corresponding to $R_m(\tau) + R_n(\tau) + R_Q(\tau)$ can be given in the form of (15), the solution of (23) can be written [7] in the following form:

$$\begin{aligned}k(t, \tau) &= \sum_{i=1}^{k} B_i(t) e^{\lambda_i \tau} + \sum_{i=0}^{r} A_i(t) \tau^i + \sum_{j=0}^{q} E_j \delta^{(j)}(t - \tau) \\ &+ L(p) L^*(p) M^{-1}(p) M^{*-1}(p) [R_m(t) + R_Q(t)] \quad (t > \tau).\end{aligned} \tag{25}$$

The rest of the argument is the same as in Section 1 of this paper.

In conclusion, we consider two simple examples.

Example 1. Let

$$S_{u_1}(\omega) = N^2, \quad S_{u_2}(\omega) = \frac{2\alpha M^2}{\omega^2 + \alpha^2}, \quad W_1(p) = \frac{k_1}{p + \tau_1}, \quad W_2 = \frac{k_2}{p + \tau_2},$$

$$H(p) = H_g(p) = 1, \quad g(t) = g_0 + g_1 t.$$

Then [3],

$$S^*_{u_1}(\omega) = |W_1(j\omega)|^2 |W_2(j\omega)|^2 S_{u_1}(\omega) = \frac{k_1^2 k_2^2 N^2}{(\omega^2 + \tau_1^2)(\omega^2 + \tau_2^2)},$$

$$S^*_{u_2}(\omega) = |W_2(j\omega)|^2 S_{u_2}(\omega) = \frac{2\alpha k_2^2 M^2}{(\omega^2 + \tau_2^2)(\omega^2 + \alpha^2)},$$

$$S(\omega) = S^*_{u_1}(\omega) + S^*_{u_2}(\omega) = \frac{k_2^2}{\omega^2 + \tau_2^2}\left[\frac{(2\alpha M^2 + k_1^2 N^2)\omega^2 + 2\alpha\tau_1^2 M^2 + 2\alpha^2 k_1^2 N^2}{(\omega^2 + \alpha^2)(\omega^2 + \tau_1^2)}\right].$$

On the basis of (16), the impulsive response function will have the form

$$k(t) = A_0 + A_1 t + B_1 e^{\lambda_1 t} + B_2 e^{\lambda_2 t} + E_0 \delta(t) + E_1 \delta'(t) + D_0 \delta(t-T) + \\ + D_1 \delta'(t-T) + L(p) L^*(p) M^{-1}(p) M^{*-1}(p) [R^*_{u_1}(t) + R^*_{u_2}(t)],$$

where

$$M(p) M^*(p) = k_2^2 [-(2\alpha M^2 + k_1^2 N^2) p^2 + 2\alpha \tau_1^2 M^2 + 2\alpha^2 k_1^2 N^2],$$

$$L(p) L^*(p) = (\tau_2^2 - p^2)(\alpha^2 - p^2)(\tau_1^2 - p^2)$$

and λ_1 and λ_2 are the roots of the equation $M(\lambda) M^*(\lambda) = 0$.
The expressions for $R^*_{u_1}(t)$ and $R^*_{u_2}(t)$ are determined from (11) and (12).

Example 2. Let

$$g(t) = g_0 + g_1 t, \quad S_u(\omega) = N^2, \quad W_1(p) = \frac{k_1}{p+\tau}.$$

Then,

$$S^*_u(\omega) = |W_1(j\omega)|^2 S_u(\omega) = \frac{k_1^2 N^2}{\omega^2 + \tau^2}.$$

On the basis of (25), we have

$$k(t, \tau) = A_0(t) + A_1(t)\tau + E_0(t)\delta(t-\tau) + D_0(t)\delta(t-\tau) \\ + L(p) L^*(p) M^{-1}(p) M^{*-1}(p) R^*_u(t),$$

where

$$M(p) M^*(p) = k_1^2 N^2, \quad L(p) L^*(p) = \tau^2 - p^2.$$

LITERATURE CITED

1. M. Pelegren, Statistical Design of Servosystems [Russian translation] (IL 1957).
2. P. S. Matveev, Method of Synthesizing Correcting Devices for Servosystems with Given Requirements on Quality Dynamic Accuracy in the Presence of Noise. Dissertation [in Russian] (1958).
3. V. V. Solodovnikov, Introduction to the Statistical Dynamics of Automatic Control Systems [in Russian] (Gostekhizdat, 1952).
4. P. S. Stimuli, Method of Determining the Optimal Impulsive Response function for One Class of Stimulii, Avtomatika i Telemekhanika 20, 1 (1959).
5. V. V. Solodovnikov and P. S. Matveev, Synthesis of Correcting Devices for Servo Systems in the Presence of Noise with Given Requirements on Dynamic Accuracy, Avtomatika i Telemekhanika 16, 3 (1955).
6. L. A. Zadeh and S. R. Ragazzini, "An extension of Wiener's Theory of Prediction," J. Appl. Phys. 21, No.7 (1950).
7. A. M. Batkov, "Analysis and synthesis of linear automatic control systems by the use of analog computers," Automatic Control and Computing Technology [in Russian] (Mashgiz, 1958).
8. P. S. Matveev, "Synthesis of correcting devices for servosystems in the presence of noise," Avtomatika i Telemekhanika, 20, 6 (1959).
9. N. Wiener, Extrapolation, Interpolation and Smoothing of Stationary Time Series (John Wiley, New York, 1949).

ON THE AUTOOSCILLATIONS OF A DYNAMIC TABLE PLATFORM

G. P. Miroshnichenko

(Moscow)

Translated from Avtomatika i Telemekhanika, Vol. 21, No. 3, pp. 293-300, March 1960
Original article submitted December 1, 1959

Determined in this paper are several properties of the motion of the platform of a single-axis dynamic table with an asynchronous motor with a tubular rotor, as well as the conditions under which autooscillations will arise when there is dry friction in the bearings.

In the design and testing of autopilots, one uses tables, that is, dynamic models comprised of a device with a platform on which the autopilot's sensitive element is placed. The platform turns about its center of mass in accordance with the aircraft's law of motion.

Tables may be divided into two classes.

a) Tables whose drives work like a servosystem at whose input a signal from an electronic computer is applied. The errors of such tables, given a small coefficient of friction, are basically determined by the inertia of the drive and the platform.

b) Tables which operate on the principle of dynamic similarity. The output element of such a table is the platform on which torques act which are proportional to the aerodynamic torques acting on the aircraft. The coefficient of similarity equals the ratio of the inertial torques relative to the corresponding axes of the platform (with the autopilot's sensitive element mounted on it) and the aircraft. In this case, the platform's moment of inertia is, in some scale, the aircraft's moment of inertia. The table's viscous friction can be taken into account by the proper decrease of the aerodynamic damping. In this case, the table's errors are principally determined by the presence of dry friction, which may introduce significant distortions in the simulation of certain modes, for example, motion at high altitudes where the damping is small.

Therefore, the study of the effect of friction and of other factors causing distortions in dynamic similarity, including the autooscillations to be studied here, is of practical interest, the more so since tuning of the coefficient of static stability a_2 is carried out by measuring the frequency of the platform's autooscillations.

A single-axis mechanical dynamic table was used by Oppelt [1]. The theory of such tables was developed by him.

In the present paper, the nonlinear problem is solved by a method similar to that of A. A. Andronov.

The single-axis dynamic table is represented by a mathematical two-dimensional model leading, in one case, to Milne's equation and, in the other to Liénard's equation.

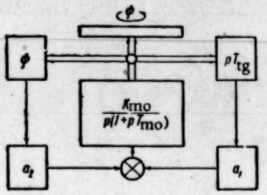

Fig. 1.

The table (Fig. 1) consists of a platform turned by an asynchronous motor with a tubular rotor whose transfer function (if the motor is considered as a linear link) is $k_{mo}/p(1 + pT_{mo})$, where k_{mo} and T_{mo} are the motor's gain and time constant, equal to the aircraft's time constant, and p is the Laplace operator.

On the motor's shaft are fitted the slider of potentiometer ψ and a tachometer generator with gain k_{tg}. The signals are applied to the motor's control winding via dividers a_2 and a_1 and a summing device. However, in actuality the motor has a nonlinear characteristic. In the absence of any signal to the control winding, with a sufficiently weak impulse about its axis, the rotor slowly turns and stops (due to the dry friction), and for a sufficiently strong impulse, the rotor begins to rotate more rapidly. For certain values of a_1 and a_2, after a shock (an impulse about the rotor's axis) there is set up an autooscillation whose frequency can be varied by varying a_2.

For investigating the autooscillation, one must find the nonlinear motor equation.

The adjustment of the table (Fig. 1) under the system to be studied consists of a sequential regulation of the table parameters to quantities defined by the equations of motion of the aircraft relative to the axis under consideration.

Let us consider, in the Liénard plane $\{\psi, \omega\}$, where $\omega = \dot{\psi}$, the phase trajectory and its mathematical expressions, which correspond to the nontrivial steady-state platform modes. It is known [2] that, for a two-dimensional system, such modes can only be periodic.

We denote by I the total moment of inertia of the platform and load with respect to the motor axis, by M_{ro} the rotational torque applied to the motor's rotor and by $M_{fr}(\omega)$ the dry frictional torque in the bearings and platform reducer. By using Newton's second law, we can write the platform's equation of motion in the form

$$I\dot{\omega} = M_{ro} + M_{fr}. \qquad (1)$$

If we express the dry frictional torque in terms of the platform's weight G and the constant frictional coefficient with respect to the motor's axis $k > 0$, we get

$$M_{fr}(\omega) = \begin{cases} -kG & \text{for } \omega > 0, \\ M_{ro} & \text{for } \omega = 0, \\ kG & \text{for } \omega < 0. \end{cases} \qquad (2)$$

By applying a signal depending on ω to the motor's control winding, we can obtain the artificial damping torque $a_1\omega$, where a_1 is the damping coefficient. A torque depending on ω also arises as the result of the voltage induced in the control winding when the rotor moves, from viscous friction in the bearing, from air friction of the rotating parts, etc.

By denoting this torque by $f(\omega)\omega$, and by ignoring the lag in the motor's control winding, we write the expression for the rotational torque:

$$M_{ro} = [a_1 + \varphi(\omega)]\,\omega + a_2\psi, \qquad (3)$$

where $a_1 > 0$ and $a_2 > 0$, and the function $\varphi(\omega)$ is even, bounded and continuous, together with its first two derivatives, in each finite segment $\{\omega_1, \omega_2\}$.

It has been experimentally established that there exists an angular platform velocity ω_0 such that

$$\varphi(\omega) < 0 \text{ for } |\omega| < \omega_0,\ \varphi(\omega) =$$

$$= 0 \text{ for } |\omega| = \omega_0,\ \varphi(\omega) > 0 \text{ for } |\omega| > \omega_0. \qquad (4)$$

Moreover, $\varphi(\omega)$ does not decrease for $\omega > 0$ and does not increase for $\omega < 0$.

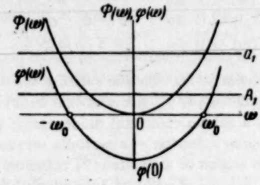

Fig. 2.

By adding and subtracting $\varphi(0)$ in (3), and by denoting [(Fig. 2)] $\Phi(\omega) \equiv \varphi(\omega) - \varphi(0)$, $A_1 \equiv a_1 + \varphi(0)$, we obtain

$$M_{ro} = [A_1 + \Phi(\omega)]\,\omega + a_2\psi. \qquad (5)$$

It is essential to note that the function $\Phi(\omega)$ is even and positive-definite, i.e., $\Phi(\omega) > 0$ for $\omega \neq 0$ and $\Phi(0) = 0$. At the same time, $A_1 > 0$ for $|a_1| > |\varphi(0)$ $A_1 < 0$ for $|a_1| < |\varphi(0)|$ and $A_1 > \varphi(0)$ since $a_1 > 0$.

By substituting (5) in (1), we get

$$I\dot{\omega} + [A_1 + \Phi(\omega)]\,\omega + a_2\psi = M_{fr}(\omega). \qquad (6)$$

The investigation of (6) breaks down into two cases:

1) $A_1 \geq 0$, i.e., $a_1 \geq -\varphi(0)$, $(a_1 \geq 0)$;

2) $A_1 < 0$, i.e., $a_1 < -\varphi(0)$.

Case I. ($A_1 \geq 0$). If, with this, $M_{fr}(\omega) \equiv 0$, then (6) reduces to a form considered by Milne [3] and Sansone [4].

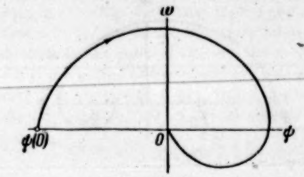

Fig. 3.

We now consider the phase trajectory for $M_{fr}(\omega) \equiv 0$. If $D = A_1^2 - 4Ia_2 \geq 0$, then the solution $\psi \equiv \psi(t)$, $[\psi(0) \neq 0]$ cannot have more than one zero in the time interval $t[0, \infty]$, which corresponds to a stable node (Fig. 3).

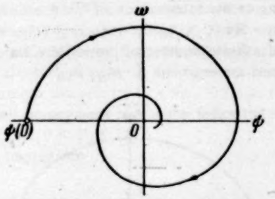

Fig. 4.

In the opposite case for $D < 0$, all solutions oscillate, and the phase trajectory corresponds to a stable focus (Fig. 4). With this, if we denote neighboring zeros of $\psi(t)$ by t_s and t_{s+1}, $t_s < t_{s+1}$, then the Milne-Sansone inequality holds:

$$t_{s+1} - t_s \leqslant \frac{2(\pi - \alpha_0)}{\nu},$$

where $\nu^2 = -D/4I^2 > 0$ and α_0 is an arc between 0 and $\pi/2$ such that $\tan\alpha_0 = \nu I/A_1$.

Consequently, if $T_0 = 2\pi/\nu$ is the period of the platform's free oscillations for $\Phi(\omega) \equiv 0$, and $T = t_{s+1} - t_{s-1}$ is the period of free oscillations for $\Phi(\omega) \neq 0$ then, since $t_{s+1} - t_{s-1} \leq 2(t_{s+1} - t_s)$, we obtain the inequality

$$T \leqslant T_0\left(1 - \frac{\alpha_0}{\pi}\right). \qquad (7)$$

For example, for $a_1 = -\varphi(0)$ (i.e., for $A_1 = 0$), $\alpha_0 = \pi/2$, and the period T satisfies the obvious relationship $T < T_0$, since the case $T = T_0$ occurs only for $\Phi(\omega) \equiv 0$.

We now consider the phase trajectory corresponding to (6) for $M_{fr} \neq 0$. Motion is possible if the angle of the platform's initial position $\psi(0)$, $[\psi = 0]$ lies outside the angle of stagnant dry friction — the segment

$\{-\psi_{fr}, \psi_{fr}\}$, where $\psi_{fr} = KG/a_2$, that is, if $|\psi(0)| > \psi$. In this case, for constructing the trajectory we can use (6), in which the point $\{-\psi_{fr}, 0\}$ is chosen for the origin of coordinates for the upper half-plane (since for $\omega > 0$, $-\psi_{fr} = \text{const}$) and, for the lower half-plane, the point $\{\psi_{fr}, 0\}$ is chosen (since for $\omega < 0$, $\psi_{fr} = \text{const}$).

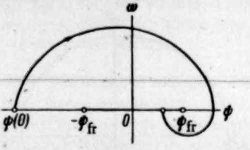

Fig. 5.

Then, on the basis of [3] and [4], in the case $D \geq 0$ the trajectory (Fig. 5) will consist of not more than two pieces, the second of which abuts the segment $(-\psi_{fr}, \psi_{fr})$. The initial conditions will be the point $\{\psi(0) + \psi_{fr}, 0\}$ for the upper piece and the point $\{\psi(t_1) - \psi_{fr}, 0\}$ for the lower piece, where t_1 is the moment of time corresponding to the intersection of the ψ axis by the trajectory. For $D < 0$, the trajectory (Fig. 6) will consist of a finite number of pieces, the last one of which abuts the segment $\{-\psi_{fr}, \psi_{fr}\}$.

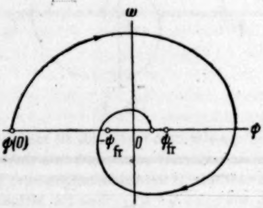

Fig. 6.

For each piece of the trajectory in the case under consideration ($M_{fr}(\omega) \neq 0$), (7) is valid. Consequently, the dry friction does not change the period T of free oscillations, but increases the decrement of damping in such fashion that the radius vector ρ ($\rho^2 = \psi^2 + \omega^2$) during one period T is additionally decreased by the amount $2\psi_{fr}$. Thus, if the radius vector is decreased by $\Delta\rho_{M_{fr}=0}$ for $M_{fr}(\omega) \equiv 0$, then for $M_{fr}(\omega) \neq 0$, it is decreased by $\Delta\rho_{M_{fr} \neq 0} = \rho_{t=T} - \rho_{t=0} = \Delta\rho_{M_{fr}=0} - 2\psi_{fr}$.

From the last relationship (for arbitrary D) and from the Archimedean axiom follows the finitude of the number of previously mentioned arcs, the last of which abuts the segment $\{-\psi_{fr}, \psi_{fr}\}$

Case 2. ($A_1 < 0$). If we introduce into (6) the function

$$F(\omega) = \frac{1}{\mu}[A_1 + \Phi(\omega)]\,\omega,$$

where μ is the angular frequency of the undamped free oscillations, $\mu^2 = a_2/I$, we get

$$\dot{\omega} + \mu F(\omega) + \mu^2\psi = \frac{1}{I} M_{fr}(\omega). \tag{8}$$

For $M_{fr} \equiv 0$ we obtain, by differentiating (8),

$$\ddot{\omega} + \mu f(\omega)\,\dot{\omega} + \mu^2\omega = 0, \tag{9}$$

where

$$f(\omega) \equiv F\frac{\partial F}{\partial \omega} \equiv \frac{1}{\mu}[a_1 + \varphi(\omega) + \varphi'(\omega)\,\omega].$$

For sufficiently small ω, $\omega\varphi'(\omega) \approx 0$ and

$$f(\omega) = \frac{1}{\mu}[a_1 + \varphi(\omega)], \tag{10}$$

but with our condition that $-\omega_0 < \omega < \omega_0$, $\varphi(\omega) < 0$.

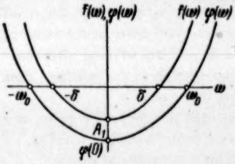

Fig. 7.

Since $A_1 = a_1 + \varphi(0) < 0$, and $\varphi(\omega)$ is continuous, then, for neighboring values of ω, $a_1 + \varphi(\omega) < 0$ and, consequently, $f(\omega) < 0$ for some ω (Fig. 7).

Since, by our assumptions, $\varphi(\omega)$ and $\varphi'(\omega)$ are continuous and bounded, $f(\omega)$ is continuous and satisfies the Lipschitz condition (guaranteeing existence and uniqueness) and, moreover since $\varphi(\omega)$ satisfies (4), then $f(\omega)$, for increasing ω, intersects the axis of abscissas at some point δ and, for decreasing ω, at the point $-\delta$, i.e.,

$$\begin{aligned} f(\omega) &< 0 \text{ for } \quad -\delta < \omega < \delta, \\ f(\omega) &= 0 \text{ for } \quad \omega = \delta, \quad \omega = -\delta \\ f(\omega) &> 0 \text{ for } \quad -\delta > \omega > \delta. \end{aligned} \tag{11}$$

Consequently, the function satisfies the Sansone-Massera condition [4, 6], asserting that to (9) there corresponds a unique nontrivial mode, stable according to the Lyapunov criterion — a periodic solution — a cycle whose region of attraction [7] coincides with the entire $\{\omega, \dot{\omega}\}$ plane with the exception of the origin of coordinates.

From whence it follows [5] that the homogeneous equation corresponding to (8):

$$\dot{\omega} + \mu F(\omega) + \mu^2\psi = 0 \tag{12}$$

also has a unique nontrivial mode — a stable cycle. The phase trajectory of (10) contains a cycle which intersects an arbitrary half-line — the ray $\overline{OA}$ — in the unique point B (Fig. 8).

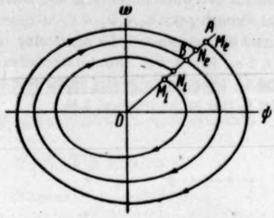

Fig. 8.

Let M_i be an interior point of the segment $\overline{OB}$ of ray $\overline{OA}$. Then the trajectory passing through M_i at time $t = t_0 = 0$ intersects $\overline{OB}$ in the point N_i at time $t' > 0$, where $\overline{ON_i} > \overline{OM_i}$. The last inequality follows from Bendixon's theorem [8]. Analogously, if M_e is an exterior point of ray $\overline{OA}$, i.e., $\overline{OM_e} > \overline{OB}$, then the trajectory defines another point N_e, where $\overline{OM_e} > \overline{ON_e}$.

We consider the phase trajectory of (8) for a sufficiently small coefficient k of dry friction. We assume that the stagnant angle segment $\{-\psi_{fr}, \psi_{fr}\}$ – lies inside the region bounded by the arcs of trajectory $\overset{\frown}{M_iN_i}$ and by the segment $\overline{M_iN_i}$. As in the first case, each trajectory consists of a segment, or segments, lying in the upper ($\omega > 0$) and lower ($\omega < 0$) half-planes. The equations of these segments are led to the form of (10) by changing the variable ψ – translating the origin of coordinates to the point $\{\psi_{fr}, 0\}$ for the transition from the upper to the lower half-plane, and to the point $\{0, -\psi_{fr}\}$ for the converse transition. We assume that the friction angle $2\psi_{fr}$ is so small that the interior $\overset{\frown}{M_iN_i}$ and exterior $\overset{\frown}{M_eN_e}$ trajectories are so little deformed, that the inequalities $\overline{OM_i} < \overline{ON_i}$ and $\overline{OM_e} > \overline{ON_e}$ retain their validity.

Since the continuous dependency of the trajectory on the initial conditions is retained, each point of the closed segment $\overline{M_iM_e}$ can be put into correspondence with a point of segment $\overline{N_iN_e}$, lying strictly interior to $\overline{M_iM_e}$. On the basis of the Bolya-Brauer theorem [9], with such a correspondence there is at least one point of the segment $\overline{M_iM_e}$ which corresponds to itself. It defines the periodic mode described by (9) for sufficiently small k. However, it is impossible to assert in this case that such a mode w be unique. This is borne out by the following example:

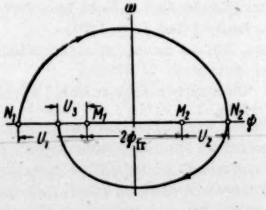

Fig. 9.

Let there exist an interval of variation of the angular velocity $\{-\Omega_0, \Omega_0\}$ such that $\Phi(\omega) = 0$ for $|\omega| < |\Omega_0|$. We then consider the trajectory defined by the equation

$$I\omega + A_1\omega + a_2\psi = M_{fr}(\omega) \tag{13}$$

and passing at time $t = t_0 = 0$ through the point $\{-(U_1 + \psi_{fr}), 0\}$ (Fig. 9), where $U_1 > 0$ and $\psi_{fr} = kG/a_2$.

At time $t_1 = T_0/2 > 0$, the trajectory intersects the axis of abscissas in the point $\{U_2 + \psi_{fr}\ 0\}$. Here, $T_0 = 2\pi/\nu$ is the period of the platform's free oscillations.

Solving (13), we get $U_2 + 2\psi_{fr} = U_1 \exp(-A_1\pi/2I\nu)$, where $A_1 = a_1 + \varphi(0) < 0$, $\nu = \frac{\sqrt{-D}}{2I}$ and $D = A_1^2 - 4Ia_2 < 0$. Whence, $U_2 = U_1 \exp\left(-\frac{\pi A_1}{\sqrt{-D}}\right) - 2\psi_{fr}$.

Motion is possible for $U_2 > 0$, i.e., for

$$U_1 \exp\left(-\frac{\pi A_1}{\sqrt{-D}}\right) > 2\psi_{fr}$$

or

$$U_1 > 2\psi_{fr} \exp\left(\frac{\pi A_1}{\sqrt{-D}}\right).$$

Since the laws of motion in the upper ($\omega > 0$) and lower ($\omega < 0$) half-planes are identical with respect to their own centers of rotation, M_1 (for $\omega > 0$) and M_2 (for $\omega < 0$), it is then necessary and sufficient that, for the representative point of the trajectory moving in the lower half-plane and passing through the point $\{U_2 + \psi_{fr}, 0\}$ at time $t_1 = T_0/2$ to fall on segment $\overline{N_1M_1}$, the following two inequalities hold: $0 < U_3 < U_2$.

From the inequality

$$U_3 = U_2 \exp\left(-\frac{\pi A_1}{\sqrt{-D}}\right) - 2\psi_{fr} =$$

$$= \left[U_1 \exp\left(-\frac{\pi A_1}{\sqrt{-D}}\right) - 2\psi_{fr}\right] \exp\left(-\frac{\pi A_1}{\sqrt{-D}}\right) - 2\psi_{fr} < U_1$$

follows

$$U_1 < \frac{2\psi_{fr}}{\exp\left(-\frac{\pi A_1}{\sqrt{-D}}\right) - 1}.$$

From the inequality $U_3 > 0$ follows

$$U_2 > \frac{2\psi_{fr}}{\exp\left(-\frac{\pi A_1}{\sqrt{-D}}\right)} \quad \text{or} ,$$

$$U_1 > \frac{2\psi_{fr}\left[1 + \exp\left(\frac{\pi A_1}{\sqrt{-D}}\right)\right]}{\exp\left(-\frac{\pi A_1}{\sqrt{-D}}\right)}.$$

Whence.

$$\frac{1 + \exp\left(\frac{\pi A_1}{\sqrt{-D}}\right)}{\exp\left(-\frac{\pi A_1}{\sqrt{-D}}\right)} 2\psi_{fr} < U_1 < \frac{1}{\exp\left(-\frac{\pi A_1}{\sqrt{-D}}\right) - 1} 2\psi_{fr}. \tag{14}$$

For $U_1 > \dfrac{2\psi_{\mathrm{fr}}}{\exp\left(-\dfrac{\pi A_1}{\sqrt{-D}}\right)-1}$ the representative point falls on the segment $\{-\psi_{\mathrm{fr}}, \psi_{\mathrm{fr}}\}$, and motion ceases.

For $U_1 < \dfrac{1+\exp\left(\dfrac{\pi A_1}{\sqrt{-D}}\right)}{\exp\left(-\dfrac{\pi A_1}{\sqrt{-D}}\right)}$ the representative point falls on the ray defined by the inequality $\psi < -(U_1 + \psi_{\mathrm{fr}})$; the system will oscillate.

From the single-valuedness and continuous dependency on the initial conditions of the solution of (13) there flows the existence of a nontrivial steady-state mode-cycle with fixed frequency $f = \nu/2\pi$ and with oscillation spread of $\Psi = |\psi_{\min}| + |\psi_{\max}|$, where

$$|\phi_{\min}| = U_1 + \phi_{\mathrm{fr}} = \frac{2\phi_{\mathrm{fr}}}{\exp\left(-\dfrac{\pi A_1}{\sqrt{-D}}\right)-1} + \phi_{\mathrm{fr}},$$

$$|\phi_{\max}| = U_2 + \phi_{\mathrm{fr}} = \frac{2\phi_{\mathrm{fr}}}{1+\exp\left(\dfrac{\pi A_1}{\sqrt{-D}}\right)} - \phi_{\mathrm{fr}}.$$

From whence,

$$\Psi = \frac{2\psi_{\mathrm{fr}}\left[\exp\left(-\dfrac{2\pi A_1}{\sqrt{-D}}\right)+1\right]}{\exp\left(-\dfrac{2\pi A_1}{\sqrt{-D}}\right)-1}. \qquad (15)$$

This mode is unstable in the strong sense, according to the Lyapunov criterion, i.e., both on the interior and the exterior sides of the region, the orbits of this mode are limited. The topological picture of the interior portion of the domain is a set of trajectories consisting of a finite number of rays, the last one of which abuts the resting segment $\overline{M_1M_2}$. The exterior side consists of trajectories swept out with the cycle's orbits.

In the example considered, it is natural to assume that, for sufficiently large values of the distance R of the representative point from the origin of coordinates ($R^2 = \psi^2 + \omega^2$), there will appear additional dissipative torques applied to the table's platform. The mathematical form of these torques can be found if we start from the assumption that coefficient A_1 of viscous friction in (13) varies as a function of R according to the law

$$A_1 = \begin{cases} a_1 + \varphi(0) < 0 & \text{for} \quad R < \frac{1}{2}\Psi + \varepsilon, \\ E > 0 & \text{for} \quad R \geqslant \frac{1}{2}\Psi + \varepsilon, \end{cases}$$

where ϵ and E are certain fixed positive numbers.

We consider two trajectories (Fig. 10), the first of which passes through point S_1, $\overline{S_1N_1} = \epsilon$, at time $t = t_0 = 0$ and the second through point S_2 for decreasing time parameter t, i.e., for $t < 0$. These trajectories define two points $\overline{S_1}$ and $\overline{S_2}$, where point $\overline{S_1}$ lies to the left of point S_1, and point $\overline{S_2}$ lies in the interval S_2N_1.

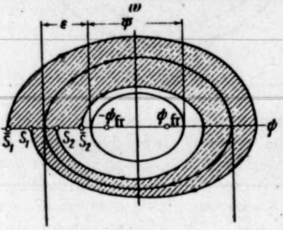

Fig. 10.

Based on what has been said, we conclude that there exists a periodic mode which lies in the hashed portion of the figure. Since all the $R < \Psi/2 + \epsilon$ define points lying on trajectories swept out with unstable orbits, and since all $R > \Psi + \epsilon$ define points corresponding to damped motion ($A_1 > 0$), then $R = \Psi + \epsilon$ defines a point lying on the trajectory corresponding to a stable cycle with spread $\Psi_1 = \Psi + 2\epsilon$ and frequency f.

The author wishes to thank B. V. Shirokorad for his aid in the preparation of this paper.

LITERATURE CITED

1. F. Oppelt, "Airplane navigation for straight-line flights," Luftfahrtforschung 14, 4/5 (1938).
2. V. V. Nemytskii, "On steady-state modes in three-dimensional autonomous dynamic systems," Vestnik MGU, Ser. Matem. No. 1 (1957).
3. W. E. Milne, "Damped vibrations," Univ. Oregon Publ. 2, No. 2 (1923).
4. G. Sansone, Ordinary Differential Equations. 2 [Russian translation] (IL, 1954).
5. I. M. Babakov, Theory of Oscillations [in Russian] (Gostekhizdat, 1958).
6. L. L. Massera, "On a theorem of G. Sansone on Lienard's equation," Boll. unione matematica Italiana 4, 3, 9 (1954).
7. V. I. Zubov, The Method of A. M. Lyapunov and Its Use [in Russian] (Izd. LGU, 1957).
8. J. Bendixon, "On the curves defined by differential equations," Acta Math. 24 (1901).
9. J. Brauer, "On mappings of manifolds," Math. Annalen (1912).

PHASE-LOCK AUTOMATIC FREQUENCY CONTROL OPERATION IN THE PRESENCE OF NOISE

V. I. Tikhonov

(Moscow)

Translated from Avtomatika i Telemekhanika, Vol. 21, pp. 301-309, March, 1960
Original article submitted May 20, 1959

It is established, by means of the two-dimensional Fokker-Planck equation, that due to external and internal fluctuations the mean frequencies of the fundamental and the synchronized generators in a standard phase-lock automatic frequency control scheme do not equal each other. An approximate method is suggested for computing the mean difference of the generators' frequencies and its dispersion.

INTRODUCTION

In [1] there was considered the effect of noise on the operation of a simplified circuit of a phase-lock automatic frequency control scheme (a phase-locked oscillator, henceforth denoted by PLO) in which the low-frequency filter was considered to be ideal. In this work, the circuit was described by a nonlinear first-order differential equation.

In actual PLO circuits, one may use, as a low-frequency filter, either a low-frequency amplifier or a series-connected RC network. The voltage from this latter filter is applied to a reactive tube.

If it is possible to approximate the low-frequency amplifier's frequency characteristic by the frequency characteristic of the RC network, then the operation of the PLO scheme will be described by the two equations [1]

$$\dot{\varphi} = \Delta_0 - su + \dot{\psi}, \tag{1}$$

$$RC\dot{u} + u = \frac{1}{2}\mu A_2 [(A_1 + E_l)\sin\varphi - E_s\cos\varphi]. \tag{2}$$

We now adopt the following nomenclature:

$$\varphi = \Phi_2 - \Phi_1, \ \dot{\psi} = \dot{\theta}_2 - \dot{\theta}_1, \ \Delta_0 = \omega_{l_0} - \omega_0; \tag{3}$$

μ is the transformation coefficient of the phase detector, $\underline{s}$ is the reactive tube's transconductance, ω_{l0} is the mean frequency of the locked (synchronized) generator for $u(t) = 0$. With this, the expressions for the oscillations of the fundamental and the locked generators take the form

$$\begin{aligned} u_f(t) &= A_1 \cos\Phi_1 = A_1\cos(\omega_0 t + \theta_1), \\ u_l(t) &= A_2 \sin\Phi_2 = A_2 \sin(\omega t + \theta_2), \end{aligned} \tag{4}$$

where A_1 and A_2 are constant amplitudes, ω_0 and ω are the mean frequencies, $\theta_1(t)$ and $\theta_2(t)$ are the random phases of the generators' oscillations, resulting from the noise of the generators' tubes and the impedance losses of their elements. The normal fluctuation noise n(t), whose spectral density is symmetric about frequency ω_0, is described in the form of a quasi-harmonic oscillation

$$n(t) = E(t)\cos(\omega_0 t + \theta), \ E_l(t) = E(t)\cos(\theta - \theta_1),$$
$$E_s(t) = E(t)\sin(\theta - \theta_1). \tag{5}$$

By differentiating (1) with respect to time, and then substituting the expressions for $\underline{\dot{u}}$ from (2) and for $\underline{u}$ from (1), we obtain

$$\ddot{\varphi} + \alpha\dot{\varphi} + \alpha\Delta\sin\varphi = \alpha\Delta_0 + \xi(t, \varphi), \tag{6}$$

where

$$\alpha = \frac{1}{RC}, \qquad \Delta = \frac{1}{2}\mu s A_1 A_2, \quad \xi(t, \varphi) =$$
$$= \ddot{\psi} + \alpha\dot{\psi} + \frac{\alpha\Delta}{A_1}(E_s\cos\varphi - E_l\sin\varphi).$$

Nonlinear second-order differential equation (6), with a specific random function in the right member, describes the operation of a PLO scheme when one has taken into account the natural instability of the generators' frequencies and the presence of fluctuation noise in the fundamental generator's channel.

It should be mentioned that the investigation of (6) is of interest apart from its connection with the concrete problem being considered here. Such equations describe many physical systems. Thus, for example, an analogous equation holds for a pendulum acted upon by random disturbances and, under certain conditions, for a gyroscope as well [2].

The basic purpose of the present paper is to compute the mean difference $\overline{\dot{\varphi}}$ of the fundamental and locked generators' frequencies, which is of the greatest practical interest. Here and in the sequel, a superscript bar denotes the operation of averaging over the set of different realizations.

The Two-Dimensional Fokker-Planck Equation

We use the Fokker-Planck equation to solve our problem. It is well known [3] that for the investigation of the behavior of a system with time constant τ_s on which there acts a stationary random disturbance $\zeta(t)$ with correlation time $\tau_c \ll \tau_s$, one can use the apparatus of Markov processes and, in particular, the Fokker-Planck equation. By the correlation time we understand the quantity $\tau_c = \int_{-\infty}^{\infty} |R_\zeta(\tau)|\, d\tau$, where $R_\zeta(\tau)$ is the autocorrelation function of $\zeta(t)$.

We assume that this condition holds for the system described by the differential equation

$$\ddot{x} = F(\dot{x},\ x,\ \zeta(t)), \tag{7}$$

If we consider, instead of the nonlinear differential equation (7), the equivalent system of two first-order equations $\dot{x} = y$, $\dot{y} = F(y, x, \zeta(t))$, we may then, by employing the usual procedure [4, 5], find that the two-dimensional probability density $w_2(\dot{x}, x, t)$ for $\underline{x}$ and $\underline{\dot{x}}$ must satisfy the following two-dimensional Fokker-Planck equation:

$$\dot{w}_2 = -\dot{x}\frac{\partial w_2}{\partial x} - \frac{\partial}{\partial \dot{x}}\left\{\left(\overline{F} + \int\limits_{-\infty}^{0} K\left[\frac{\partial F}{\partial \dot{x}},\ F_\tau\right] d\tau\right) w_2\right\} + $$
$$+ \frac{\partial^2}{\partial \dot{x}^2}\left\{w_2 \int\limits_{-\infty}^{0} K\,[F,\ F_\tau]\,d\tau\right\}. \tag{8}$$

Here, in computing $\overline{F}$ and the integrand correlation functions, denoted by the symbol K, the arguments $\underline{x}$ and $\underline{\dot{x}}$ are considered fixed.

In seeking the solution of (8), it is necessary to add to it the initial and boundary conditions, which are determined by the physics of the concrete problem. Certainly, the probability density $w_2(\dot{x}, x, t)$ must satisfy the normalization condition. By giving some distribution, $w_2(\dot{x}, x, t_0) = w_{20}(\dot{x}, x)$, at some initial moment, we then find, by solving (8), the subsequent deformation of this distribution for $t > t_0$. If the random functions $x(t)$ and $\dot{x}(t)$ can assume all possible values between plus and minus infinity then, as the boundary conditions, one should use the convergence of the probability density to zero as $x, \dot{x} \to \pm\infty$, i.e., $w_2(\pm\infty, \pm\infty, t) = 0$. If the random functions $x(t)$ and $\dot{x}(t)$ assume values which are limited to a certain region, then it is necessary to seek the solution of (8) only in this region. In the problem we are considering, (6), we shall use, as the boundary condition, the condition that the probability density be periodic in φ.

If we limit consideration to a stationary solution of (8), when the probability density w_2 does not depend explicitly on time, i.e., $\dot{w}_2 = 0$, we then obtain the following Fokker-Planck equation for the stationary state:

$$\frac{\partial^2}{\partial \dot{x}^2}\left\{w_2 \int\limits_{-\infty}^{0} K\,[F,\ F_\tau]\,d\tau\right\} - \frac{\partial}{\partial \dot{x}}\left\{\left(\overline{F} + \int\limits_{-\infty}^{0} K\left[\frac{\partial F}{\partial \dot{x}},\ F_\tau\right] d\tau\right) w_2\right\} - \dot{x}\frac{\partial w_2}{\partial x} = 0. \tag{9}$$

As applied to (6), it is now necessary to set

$$F = \alpha\Delta_0 - \alpha\dot{\varphi} - \alpha\Delta\sin\varphi + \xi(t,\ \varphi), \quad x = \varphi. \tag{10}$$

We now compute the individual quantities which enter into (9). It can be shown [6] that

$$\overline{\xi(t,\ \varphi)} = \overline{\ddot{\Psi}} + \alpha\overline{\dot{\Psi}} + \frac{\alpha\Delta}{A_1}\left(\overline{E}_s\cos\varphi - \overline{E}_l\sin\varphi\right) = 0.$$

Therefore,

$$\overline{F} = \alpha\Delta_0 - \alpha\dot{\varphi} - \alpha\Delta\sin\varphi,$$

$$K\,[F,\ F_\tau] = \overline{[F - \overline{F}]\,[F_\tau - \overline{F}_\tau]} = \overline{\xi(t,\ \varphi)\,\xi(t + \tau,\ \varphi)} =$$

$$= \overline{[\ddot{\psi} + \alpha\dot{\psi} + \frac{\alpha\Delta}{A_1}(E_s\cos\varphi - E_l\sin\varphi)][\ddot{\psi}_\tau + \alpha\dot{\psi}_\tau + \frac{\alpha\Delta}{A_1}(E_{s\tau}\cos\varphi - E_{l\tau}\sin\varphi)]} =$$

$$= \overline{\ddot{\psi}\ \ddot{\psi}_\tau} + 2\alpha\,\overline{\dot{\psi}\ \ddot{\psi}_\tau} + \alpha^2\,\overline{\dot{\psi}\ \dot{\psi}_\tau} + \left(\frac{\alpha\Delta}{A_1}\right)^2\sigma^2 r(\tau),$$

where it is assumed that the correlation function of the noise $n(t)$ has the form

$$k_n(\tau) = \sigma^2 r(\tau)\cos\omega_0\tau.$$

From (10) we also have

$$\frac{\partial F}{\partial \dot{\varphi}} = -\alpha, \qquad \frac{\partial F}{\partial \dot{\varphi}} - \frac{\overline{\partial F}}{\partial \dot{\varphi}} = 0, \qquad K\left[\frac{\partial F}{\partial \dot{\varphi}},\ F_\tau\right] = 0$$

By substituting the individual quantities in (9), we obtain the following definitive form of the Fokker-Planck equation which describes the stationary operating mode in the PLO system under consideration:

$$K_2\frac{\partial^2 w_2}{\partial \dot{\varphi}^2} - \frac{\partial}{\partial \dot{\varphi}}\{(\alpha\Delta_0 - \alpha\dot{\varphi} - \alpha\Delta\sin\varphi)\,w_2\} - \dot{\varphi}\frac{\partial w_2}{\partial \varphi} = 0. \tag{11}$$

Here,

$$K_2 = \int_{-\infty}^{0} \{\overline{\ddot{\psi}\ \ddot{\psi}_\tau} + 2\alpha\,\overline{\dot{\psi}\ \ddot{\psi}_\tau} + \alpha^2\,\overline{\dot{\psi}\ \dot{\psi}_\tau} + \left(\frac{\alpha\Delta}{A_1}\right)^2 \sigma^2 r(\tau)\}\, d\tau. \tag{12}$$

Second-order partial differential Eq. (11) is linear and of parabolic type. Its general solution depends on two arbitrary constants, which are defined by the condition that the probability density be normalized and be periodic in φ, i.e.,

$$\int_0^{2\pi}\int_{-\infty}^{\infty} w_2(\dot{\varphi}, \varphi)\, d\dot{\varphi}\, d\varphi = 1, \quad w_2(\dot{\varphi}, \varphi + 2\pi) = w_2(\dot{\varphi}, \varphi). \tag{13}$$

An exact solution of (11) for (13) exists only in the particular case when the initial mistuning of the generators equals zero: $\Delta_0 = 0$. We easily convince ourselves that the solution of the equation

$$K_2 \frac{\partial^2 w_2}{\partial \dot{\varphi}^2} + \frac{\partial}{\partial \dot{\varphi}} \{(\alpha\dot{\varphi} + \alpha\Delta \sin\varphi)\, w_2\} - \dot{\varphi}\, \frac{\partial w_2}{\partial \varphi} = 0, \tag{14}$$

satisfying (13) has the form

$$w_2(\dot{\varphi}, \varphi) = \sqrt{\frac{\alpha}{2\pi K_2}}\, \frac{1}{2\pi I_0\left(\frac{\alpha^2\Delta}{K_2}\right)} \exp\left[-\frac{\alpha\dot{\varphi}^2}{2K_2} + \frac{\alpha^2\Delta}{K_2}\cos\varphi\right], \tag{15}$$

where $I_0(z)$ is a Bessel function of zero order and imaginary argument.

From (15) we find the one-dimensional probability density for the frequency difference $\dot{\varphi}$:

$$w(\dot{\varphi}) = \int_{-\pi}^{\pi} w_2(\dot{\varphi}, \varphi)\, d\varphi = \sqrt{\frac{\alpha}{2\pi K_2}} \exp\left(-\frac{\alpha\dot{\varphi}^2}{2K_2}\right). \tag{16}$$

From this we easily obtain

$$\overline{\dot{\varphi}} = 0,\ \sigma^2_{\dot{\varphi}} = \overline{\dot{\varphi}^2} = \frac{1}{\alpha} K_2 \int_{-\infty}^{0} \left\{RC\, \overline{\ddot{\phi}\ddot{\phi}_\tau} + \frac{1}{RC}\, \overline{\dot{\phi}\dot{\phi}_\tau} + \frac{1}{RC}\left(\frac{\Delta\sigma}{A_1}\right)^2 r(\tau)\right\} d\tau. \tag{17}$$

In many practical cases one can neglect the generators natural fluctuations in comparison with the external noise. Then, the basic role in (17) will be played by the last term in the integrand.

Thus, if the initial mistuning of the generators at the moment when the PLO is switched in is zero, then the average frequencies of the fundamental and locked generators remain equal to each other during PLO operation, and the dispersion of the frequency difference $\sigma^2\dot{\phi}$, as is obvious from (17), increases with increasing intensity of the external noise σ^2 and the generators' natural fluctuations, and decreases with increasing time constant of the RC filter. These results are comprehensible physically.

In the sequel we shall consider approximately the cases when, in (11), the initial mistuning of the generators is different from zero ($\Delta_0 \neq 0$).

Approximate Method of Solving the Fokker-Planck Equation

It is difficult to find a solution in compact form of (11) which satisfies (13). Below, we present an approximate method of solving (11).

We shall seek a solution in the form of a series:

$$w_2(\dot{\varphi}, \varphi) = \sum_{n=0}^{\infty} w^{(n)}(\dot{\varphi})\, L_n(\varphi), \tag{18}$$

where the functions $L_n(\varphi)$ are to be defined, and

$$w(\dot{\varphi}) = \exp\left(-\frac{\alpha\dot{\varphi}^2}{2K_2}\right). \tag{19}$$

By direct differentiation, we easily convince ourselves that the following recursion formulas are valid for the derivatives of the function $w(\dot{\varphi})$:

$$\dot{\varphi} w^{(n)}(\dot{\varphi}) = -\frac{1}{\alpha} K_2 w^{(n+1)}(\dot{\varphi}) - n w^{(n-1)}(\dot{\varphi}) \quad (n = 0, 1, 2, \ldots). \tag{20}$$

By substituting the expression for $w_2(\dot{\varphi}, \varphi)$ from (18) in (11), then using (20) and collecting similar terms, we obtain

$$\frac{1}{\alpha}K_2\sum_{n=0}^{\infty} w^{(n+1)}(\dot{\varphi})\,L_n'(\varphi) - \alpha(\Delta_0 - \Delta\sin\varphi)\sum_{n=0}^{\infty} w^{(n+1)}(\dot{\varphi})\,L_n(\varphi) =$$
$$= \alpha\sum_{n=0}^{\infty} n w^{(n)}(\dot{\varphi})\,L_n(\varphi) - \sum_{n=0}^{\infty} n w^{(n-1)}(\dot{\varphi})\,L_n'(\varphi)$$

or

$$\sum_{n=0}^{\infty} w^{(n+1)}(\dot{\varphi})\,L_n'(\varphi) - \frac{\alpha^2}{K_2}(\Delta_0 - \Delta\sin\varphi)\sum_{n=0}^{\infty} w^{(n+1)}(\dot{\varphi})\,L_n(\varphi) =$$
$$= \frac{\alpha^2}{K_2}\sum_{n=0}^{\infty} n w^{(n)}(\dot{\varphi})\,L_n(\varphi) - \frac{\alpha}{K_2}\sum_{n=0}^{\infty} n w^{(n-1)}(\dot{\varphi})\,L_n'(\varphi). \qquad (21)$$

By equating coefficients of like orders of the derivatives $w^{(n)}(\dot{\varphi})$, we obtain the following system of differential equations for the definition of the $L_n(\varphi)$:

$$\begin{aligned}
&L_1'(\varphi) = 0,\\
&L_0'(\varphi) - \frac{\alpha^2}{K_2}(\Delta_0 - \Delta\sin\varphi)\,L_0(\varphi) = \frac{\alpha^2}{K_2}L_1(\varphi) - 2\frac{\alpha}{K_2}L_2'(\varphi),\\
&L_1'(\varphi) - \frac{\alpha^2}{K_2}(\Delta_0 - \Delta\sin\varphi)\,L_1(\varphi) = 2\frac{\alpha^2}{K_2}L_2(\varphi) - 3\frac{\alpha}{K_2}L_3'(\varphi),\\
&L_2'(\varphi) - \frac{\alpha^2}{K_2}(\Delta_0 - \Delta\sin\varphi)\,L_2(\varphi) = 3\frac{\alpha^2}{K_2}L_3(\varphi) - 4\frac{\alpha}{K_2}L_4'(\varphi),\\
&\cdots\cdots\cdots\cdots\cdots\cdots\cdots\cdots\cdots\cdots\cdots\cdots\cdots\cdots
\end{aligned} \qquad (22)$$

In general,

$$L_{n-1}'(\varphi) - \frac{\alpha^2}{K_2}(\Delta_0 - \Delta\sin\varphi)\,L_{n-1}(\varphi) = n\frac{\alpha^2}{K_2}L_n(\varphi) - (n+1)\frac{\alpha}{K_2}L_{n+1}'(\varphi).$$

We may suggest the following order for solving (22). The equations are solved successively, starting with the first, whereby, in solving each successive equation, we ignore the last terms in the right member, containing derivatives of higher-order functions $L_n(\varphi)$.

For an approximate estimate of the value of the mean frequency difference of the generators, we shall henceforth limit ourselves to computing the first two functions, $L_0(\varphi)$ and $L_1(\varphi)$. From the first equation of (22) we have that $L_1 = c = \text{const.}$ By neglecting the term containing $L_2'(\varphi)$ in the second equation, we obtain the following differential equation for defining $L_0(\varphi)$:

$$L_0'(\varphi) - \frac{\alpha^2}{K_2}(\Delta_0 - \Delta\sin\varphi)\,L_0(\varphi) = \frac{\alpha^2}{K_2}c.$$

The solution of this equation, as we easily convince ourselves, can be written in the form

$$L_0(\varphi) = c\frac{\alpha^2}{K_2}\exp(D_0\varphi + D\cos\varphi)\int_{\varphi_0}^{\varphi}\exp(-D_0\gamma - D\cos\gamma)\,d\gamma,$$

where φ_0 is some arbitrary constant and

$$D_0 = \frac{\alpha^2\Delta_0}{K_2}, \quad D = \frac{\alpha^2\Delta}{K_2}. \qquad (23)$$

Thus, in our approximation, we obtain the following solution of (11):

$$w_2(\dot{\varphi}, \varphi) = w(\dot{\varphi})\,L_0(\varphi) + w'(\dot{\varphi})\,L_1(\varphi) =$$
$$= c\frac{\alpha}{K_2}\exp\left(-\frac{\alpha\dot{\varphi}^2}{2K_2}\right)\left\{-\dot{\varphi} + \alpha\exp(D_0\varphi + D\cos\varphi)\int_{\varphi_0}^{\varphi}\exp(-D_0\gamma - D\cos\gamma)\,d\gamma\right\}. \qquad (24)$$

To satisfy the condition for periodicity (13), it is necessary that the following equation hold:

$$\exp(D_0\varphi + 2\pi D_0 + D\cos\varphi)\int_{\varphi_0}^{\varphi+2\pi}\exp(-D_0\gamma - D\cos\gamma)\,d\gamma =$$
$$= \exp(D_0\varphi + D\cos\varphi)\int_{\varphi_0}^{\varphi}\exp(-D_0\gamma - D\cos\gamma)\,d\gamma.$$

From this equation, the following relationship derives:

$$\int_{\varphi_0}^{\varphi} \exp(-D_0\gamma - D\cos\gamma)\,d\gamma = \frac{\exp(2\pi D_0)}{1-\exp(2\pi D_0)} \int_{\varphi}^{\varphi+2\pi} \exp(-D_0\gamma - D\cos\gamma)\,d\gamma, \tag{25}$$

which permits the arbitrary constant φ_0 to be eliminated.

To determine the second arbitrary constant c, we use the normalization condition

$$\int_0^{2\pi}\int_{-\infty}^{\infty} w_2(\dot{\varphi},\varphi)\,d\dot{\varphi}d\varphi = c\alpha\sqrt{\frac{2\pi\alpha}{K_2}}\,\frac{\exp(2\pi D_0)}{1-\exp(2\pi D_0)}\int_0^{2\pi}\exp(D_0\varphi + D\cos\varphi)\,d\varphi \times$$
$$\times \int_{\varphi}^{\varphi+2\pi} \exp(-D_0\gamma - D\cos\gamma)\,d\gamma = 1. \tag{26}$$

It can be shown [1, 7] that

$$J = \int_0^{2\pi}\exp(D_0\varphi + D\cos\varphi)\,d\varphi \int_{\varphi}^{\varphi+2\pi} \exp(-D_0\gamma - D\cos\gamma)\,d\gamma =$$
$$= 4\pi^2\exp(-\pi D_0)\,|I_{iD_0}(D)|^2,$$

where $I_{i\nu}(z)$ is a Bessel function of imaginary order and imaginary argument. Therefore, we obtain from (26)

$$c = \frac{1}{4\pi\alpha^2}\sqrt{\frac{K_2}{2\pi\alpha}}\,\frac{1-\exp(2\pi D_0)}{\exp(\pi D_0)}\,|I_{iD_0}(D)|^{-2} \tag{27}$$

By using (25) and (27), we can write the approximate expression for the probability density in its definitive form:

$$w_2(\dot{\varphi},\varphi) = \sqrt{\frac{1}{2\pi\alpha K_2}}\,\frac{1-\exp(2\pi D_0)}{4\pi^2\exp(\pi D_0)}\,|I_{iD_0}(D)|^{-2}\exp\left(-\frac{\alpha\dot{\varphi}^2}{2K_2}\right)\times$$
$$\times\left\{-\dot{\varphi} + \alpha\frac{\exp(2\pi D_0)}{1-\exp(2\pi D_0)}\exp(D_0\varphi + D\cos\varphi)\int_{\varphi}^{\varphi+2\pi}\exp(-D_0\gamma - D\cos\gamma)\,d\gamma\right\}. \tag{28}$$

It is easily verified that this formula goes over into the exact formula (15) for zero initial mistuning ($D_0 = 0$). This attests to the fact that the suggested approximate method of solving the Fokker-Planck equation gives logically-noncontradictory results.

By integrating (28) over φ and $\dot{\varphi}$ between the proper limits, we obtain the one-dimensional probability densities for, respectively, $\dot{\varphi}$ and φ:

$$w(\dot{\varphi}) = \left\{\sqrt{\frac{\alpha}{2\pi K_2}} - \dot{\varphi}\sqrt{\frac{2\pi}{\alpha K_2}}\,\frac{1-\exp(2\pi D_0)}{4\pi^2\exp(\pi D_0)}\,|I_{iD_0}(D)|^{-2}\right\}\exp\left(-\frac{\alpha\dot{\varphi}^2}{2K_2}\right). \tag{29}$$

$$w(\varphi) = \frac{1}{4\pi^2}\exp(\pi D_0)\,|I_{iD_0}(D)|^{-2}\exp(D_0\varphi + D\cos\varphi)\int_{\varphi}^{\varphi+2\pi}\exp(-D_0\gamma - D\cos\gamma)\,d\gamma. \tag{30}$$

The last formula for the probability density of φ coincides in form with that obtained in [1]. The difference consists in this, that here the coefficients D_0 and D depend on the low-frequency filter's passband [cf. (23)]. This fact also gives us some confidence that, in taking only the first two functions in (22) into account, we obtain results which are in qualitative agreement with those obtained in [1].

By using (29), we find the average difference of the generators' frequencies and the dispersion of this difference:

$$\overline{\dot{\varphi}} = \overline{\omega} - \omega_0 = \frac{K_2}{2\pi\alpha^2}\,\frac{\exp(2\pi D_0)-1}{\exp(\pi D_0)}\,|I_{iD_0}(D)|^{-2} = \Delta_0\,\frac{\operatorname{sh}\pi D_0}{\pi D_0}\,I_{iD_0}(D)\,|^{-2},\ \sigma^2_{\dot{\varphi}} \approx \frac{1}{\alpha}K_2. \tag{31}$$

For $D_0 = 0$, these formulas coincide with (17).

Particular Examples

Let the external noise n(t) be obtained as the result of the action of a sufficiently wide-band fluctuation on a narrow-band oscillatory loop with resonant frequency ω_0 and, consequently, let the noise have correlation function

$$k_n(\tau) = \sigma^2 e^{-\beta|\tau|} \cos \omega_0 \tau.$$

We assume that we may ignore the natural instability of the frequencies of the fundamental and locked generators in comparison with the noise n(t). Then,

$$K_2 = \left(\alpha\Delta \frac{\sigma}{A_1}\right)^2 \int\limits_{-\infty}^{0} e^{\beta\tau}\, d\tau = \frac{1}{\beta}\left(\alpha\Delta \frac{\sigma}{A_1}\right)^2.$$

By substituting this value of K_2 in (23) and (31), we get

$$D_0 = \frac{\beta\Delta_0}{\Delta^2}\left(\frac{A_1}{\sigma}\right)^2, \quad D = \frac{\beta}{\Delta}\left(\frac{A_1}{\sigma}\right)^2,$$

$$-\Delta = \frac{1}{2}\mu s A_1 A_2, \; \sigma^2_{\dot\varphi} = \frac{\alpha}{\beta}\Delta^2\left(\frac{\sigma}{A_1}\right)^2. \qquad (32)$$

In the given concrete case, D_0 and D do not depend on α. With this, as is clear from (32) and (31), the dispersion of the frequencies' difference depends on α, but the average discrepancy of the frequencies does not depend on α. This last result is seemingly a consequence of the approximate solution of (11). Recently, A. G. Zhuravlev showed that, although the term containing $L_2(\varphi)$ in (18) for the probability density does not of itself give a correction to the mean frequency difference, its being taken into account does result in the function $L_0(\varphi)$ assuming a different form:

$$L_0(\varphi) = C\frac{\alpha}{K_2}\frac{\exp(2\pi D_0)}{1-\exp(2\pi D_0)}\exp \times$$
$$\times (D_0\varphi + D\cos\varphi)\int\limits_{\varphi}^{\varphi+2\pi}(\alpha - \Delta\cos\gamma)\times \qquad (33)$$
$$\times \exp(-D_0\gamma - D\cos\gamma)\, d\gamma.$$

We now make some numerical estimates. It is known [8] that, in the absence of noise, the maximum voltage at the phase detector's output can not exceed twice the magnitude of the least of the applied voltages. We replaced the phase detector by a device implementing multiplication of the voltages $u_f(t)$ and $u_l(t)$. In accordance with what has been said, for $A_2 > A_1$, the maximum value of the voltage at the multiplier's output is determined by the relationship

$$U_{\max} = \frac{1}{2}\mu A_1 A_2 < 2A_1.$$

We take $u_{out} \approx 0.5U_{\max}$, i.e., $\mu A_1 A_2 / 2 \approx A_1$. Whence $\mu \approx 2/A_2$ and $\Delta \approx sA_1$.

The parameters of the PLO scheme are so chosen that stable operation is guaranteed. As follows from [9], for $\Delta_0/\Delta \lesssim 0.6$, stability is guaranteed if the following inequality holds:

$$\sqrt{\frac{1}{RC\Delta}} \geqslant \frac{\pi}{4}\frac{\Delta_0}{\Delta}. \qquad (34)$$

Let $A_1 \approx 1$v, s = 0.1 kg/v, $\alpha = 20\ \text{sec}^{-1}$, $\beta = 300\ \text{sec}^{-1}$, $\Delta_0/\Delta = 0.5$. With these parameters, Ineq. (34) holds and, simultaneously, the conditions hold for the applicability of the Fokker-Planck equation. Then, $\Delta \approx sA_1 = 100$ cps, $D_0 = 1.5\,(A_1/\sigma)^2$, $D = 3\,(A_1/\sigma)^2$ and $\sigma^2_{\dot\varphi} \approx 700(\sigma/A_1)^2$. By using the graphs of I. G. Akopyan, given in [1], we get

$$\bar\omega - \omega_0 \approx 35\text{cps}, \; \sigma_{\dot\varphi} \approx 36\text{ cps for } \left(\frac{A_1}{\sigma}\right)^2 \approx 0.7,$$

$$\bar\omega - \omega_0 \approx 10\text{cps}, \; \sigma_{\dot\varphi} \approx 18\text{ cps for } \left(\frac{A_1}{\sigma}\right)^2 \approx 2.0.$$

From what has been considered above, we may draw the following conclusions:

1. From (32) and the quantitative estimates adduced, it is clear that, when the conditions hold for the applicability of the Fokker-Planck equation ($\alpha \ll \beta$), the mean frequency difference and its mean square decrease as the ratio A_1/σ increases. For sufficiently small signal-to-noise ratios, the average frequency difference may turn out to be significantly less than the mean square value, and it is necessary to take it into account.

2. When stability condition (34) holds, a decrease of the time constant RC provides a shorter duration of the PLO's transient response, but the dispersion of the frequency difference is thereby increased. Therefore, the requirements of short establishment time and high noise immunity are, in a very definite sense, contradictory.

In conclusion, I wish to thank R. L. Stratonovich for his interest in the present work.

LITERATURE CITED

1. V. I. Tikhonov, "Influence of noise on phase-locked oscillator operation," Avtomatika i Telemekhanika 20, 9 (1959).
2. N. N. Bogolyubov and Yu. A. Mitropol'skii, Asymptotic Methods in Nonlinear Oscillation Theory [in Russian] (Fizmatgiz, 1958).
3. P. I. Kuznetsov, R. L. Stratonovich, and V. I. Tikhonov, "Correlation function in the theory of Brownian motion," Zhur. Eksp. i Teor. Fiz. 26, 2 (1954).
4. Wang Ming-chen and G. E. Uhlenbeck, On the theory of the Brownian motion, Rev. Mod. Phys. 17, No. 2-3 (1945).
5. H. A. Kramers, "Brownian motion in a field of force and the diffusion model of chemical reactions," Physics 7, No. 4 (1940).
6. V. I. Tikhonov, "Effect of natural fluctuations on self-excited oscillator operation," Vestnik MGU 2, 53 (1957).
7. R. L. Stratonovich, "Self-excited oscillator synchronization in the presence of noise," Radiotekhnika i Élektronika 3, 4 (1958).
8. M. R. Kaplanov and V. A. Levin, Phase-Lock Automatic Frequency Control [in Russian] (Gosénergoizdat, 1956).
9. Yu. N. Bakaev, "Investigation of inertial systems of television synchronization," Radiotekhnika i Élektronika 3, 2 (1958).

ANALYSIS OF A TWO-POSITION COMPENSATING CONTROL SYSTEM UNDER CONSTANT PROLONGED DISTURBANCES

A. I. Cherepanov

(Pert')

Translated from Avtomatika i Telemekhanika, Vol. 21, No. 3, pp. 310-316, March, 1960
Original article submitted October 28, 1959

It is shown that the simplified graphico-analytic method developed in [1] for computing the processes in a two-position regulator may be employed for analyzing the processes in two-position compensating control systems [2] under constant prolonged disturbances.

In [2] of this author there was described a new method for improving the quality of the processes in a two-position regulator by the use of a special relay-type correcting device. The basic advantage of this method in comparison with prior ones [3, 4, 5, 8] is that, with essentially reduced amplitude of controlled quantity oscillations, of temperature for example, it provides the minimum increase in the required number of switchings of the object's heater in and out of the system, computed on the basis of a nonsymmetric mode of operation.

It should be mentioned that, at the present, of all the types of two-position compensating controllers, those with thermoelectric correcting (compensating) devices have been most widely used [6, 7].

However, electromechanical correcting devices have certain advantages: e.g., such devices can be used both in regulators which employ some electrical means of measuring the controlled parameter and in many industrial two-position regulators of dilatometric, bimetallic, or magnometric types which use some nonelectric means of measuring the controlled quantity. Moreover, the use of an electromechanical correcting device permits the employment of the regulator's measuring portion for measuring or recording the true temperature in the object. When a thermoelectric device is used, it is necessary to have an additional intrument for this purpose, since the action of the device distorts the output signal of the measuring portion.

Simple formulas were obtained in [2] for calculating the correcting device's adjustment parameters and the basic parameters of the compensating control process in the steady state. It was noted in [2] that the character of the possible disturbances in the system should be taken into account in choosing the correcting device's parameters.

In the present paper we provide an analysis of the processes with disturbances in a two-position control system with an electromechanical correcting device. The possibility is demonstrated of the existence in such a system of complex periodic motions, somewhat similar to those considered in [5, 8]. Recommendations are given for the choice of the adjustment parameters of the correcting device which will provide the very best quality processes given the disturbances.

As in [2], the analysis is made by means of a simplified graphico-analytic method of calculating the two-position controller's processes [1], thanks to which the formulas obtained are simple, and may be used without difficulty for engineering computations.

By the adjustment parameters of the correcting device we shall understand the following quantities: t_0t_1 is the duration of the make state of contact K-1, t_{bre} is the duration of the break state of contact K-1, $t_{bre} = t_1t_2$, t_{mak} is the total duration of the make state of contact K-1 during one disk rotation, $t_{mak} = t_0t_1 + t_0t_3 - t_1t_2$, t_{ro} is the time for one complete disk rotation, $t_{ro} = t_0t_3$.

1. Pulse Repetition Period as a Function of the Load

The distinguishing feature of a two-position control system with an electromechanical correcting device is that the repetition period of the pulses of heat admission to the object, for invariant adjustment parameters, depends on the load. This is achieved due to the use in the device of two controlling disks, one of which switches in the flow of energy to the object at a definite previously specified time while the other disk returns the first disk to its initial position in the time following a positive deviation of the parameter from its given value*. With this, if the magnitude of the energy efflux changes within certain limits, for example, if it increases, then the new switching in of the relay's motor would occur somewhat earlier than for the previous value of the efflux. The pulses switching in the influx would have the same duration, but their repetition frequency would increase, and the correction process would not be disrupted.

Figure 1, a shows the graph of the process in a two-position controller with compensation, where the influx multiplicity is $n_1 = 8$, and the degree of correction is $k = 2.86$. In Fig. 1 and in the sequel, we adopt the nomemclature: $\Delta\vartheta$ is the deviation of the controlled parameter (temperature), $\Delta\vartheta'$ is the deviation of the object's controlled temperature with compensation

---

* For a more detailed description of the correcting device's operation, cf. [2].

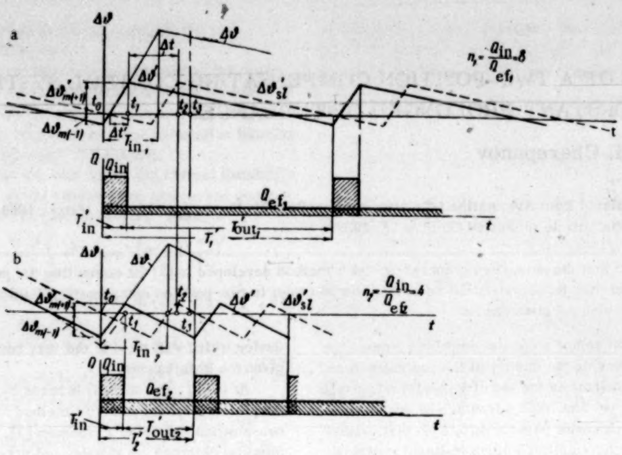

Fig. 1.

(correction), $\Delta\vartheta_{se}$ is the temperature deviation of the sensitive element with compensation, $\Delta\vartheta'_{m(+)}$ is the positive amplitude of the deviation with compensation, $\Delta\vartheta_{m(-)}$ is the negative deviation amplitude. Q_{in} is the influx of heat, Q_{ef} is the efflux of heat, T_{in} is the duration of switching in for control without correction, T'_{in} is the duration of switching in when the corrective device is used, T_{out} is the duration of switching out, T is the period of oscillation, t_0 is the moment of switching in, t_1 is the moment of switching the influx off when correction is used, t_2 is the moment of the new making of controlling contact K-1, t_3 is the moment of disk cessation, Δt is the system's lag time, $\Delta t'$ is the residual lag time when correction is used.

Figure 1,b shows the control process in the same system when the heat efflux is increased twofold, i.e., for $n_2 = 4$. As is clear from the graph, the correction process is not disrupted. The duration of switching in of the heater, T'_{in}, remains as before. The duration of switching out T'_{out_1} is decreased, and becomes equal to T'_{out_2}. The positive amplitude of the deviation is also decreased. The negative deviation amplitude $\Delta\vartheta_{m(-)}$ increases, as with ordinary two-position controllers. The period of influx switching in is shortened to T'_2. The total amplitude of the oscillations, $\Delta\vartheta_{m(+)} + \Delta\vartheta_{m(-)}$ is somewhat decreased.

It may be seen from a comparison of Fig. 1, a and b that the degree of correction k became larger in the second case: k = 6.2.

We now find the dependence of the variation in the degree of correction k on the magnitude of the influx multiplicity n for a constant (given) duration of switching in T'_{in}. As is known [2],

$$k = \frac{\Delta t}{\Delta t'}. \tag{1}$$

The quantity $\Delta t'$ can be expressed in terms of the duration of switching in T'_{in} and the influx multiplicity n by use of the formula [2]

$$T'_{in} = \Delta t' \frac{Q_{in}}{Q_{in} - Q_{ef}} + (\Delta t - \Delta t') \frac{Q_{ef}}{Q_{in} - Q_{ef}}. \tag{2}$$

From (2) we obtain

$$\Delta t' = T'_{in} - \Delta t \frac{1}{n-1}. \tag{3}$$

By substituting (3) in (1), we find that

$$k = \frac{\Delta t}{T'_{in} - \Delta t \frac{1}{n-1}}. \tag{4}$$

From (4) one can calculate the degree of correction for various values of influx multiplicity n and switching in duration T'_{in}.

Equation (4) shows that, for some value of n, the denominator vanishes and k becomes infinite.

This value of n will be, in some sense, a critical one; we denote it by n_{cr}†. Obviously,

$$n_{cr} = 1 + \frac{\Delta t}{T'_{in}}. \tag{5}$$

When the influx multiplicity has the value n_{cr}, the temperature in the object during the given time T'_{in} rises exactly to the given limit. For values of n less than n_{cr}, the temperature in the object during the switching in time T'_{in} does not attain the given value, and the normal course of the correction process is disrupted.

---

† In [2] n_{cr} has a different connotation.

For the case shown on Fig. 1,a, the calculated value of $n_{cr} = 3$. On Fig. 1,b, the dashed line represents the temperature variations in the object for this value $n = 3$. The calculated value of n_{cr} is well borne out by the graph.

Thus, in the system under consideration, the repetition period of the influx switching-in pulses depends on the load, and the correction process flows normally only for influx multiplicities greater than the critical value.

For values of influx multiplicity $n < n_{cr}$, the normal course of the correction process is disrupted, and there arise complex periodic temperature oscillations in the system, examples of which are considered in the following section.

2. Complex Periodic Motions

As was shown in the previous section, the correction process can proceed normally for disturbances up to some value n_{cr}. With this, as the disturbance increases (the value of n decreases) there will be an increase of the negative amplitude and a decrease of the positive amplitude. The given condition ($n > n_{cr}$) for the guarantee of normal correction process is necessary but not sufficient. As is clear from Figs. 2, 3, and 4, it is necessary, for the normal flow of the correction process, that the following additional conditions be met:

$$t_2 > T_{in}, \quad t_{ro} < T'. \tag{6}$$

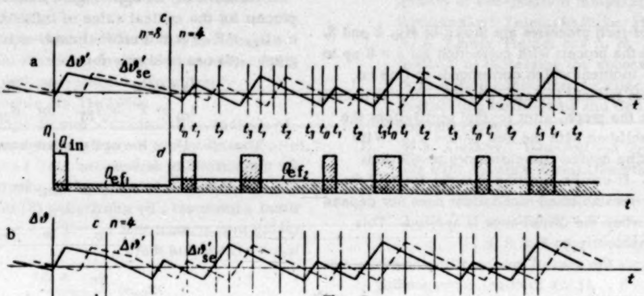

Fig. 2.

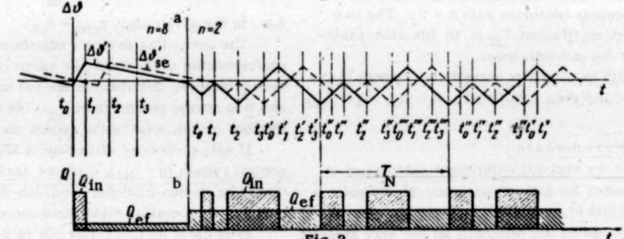

Fig.3.

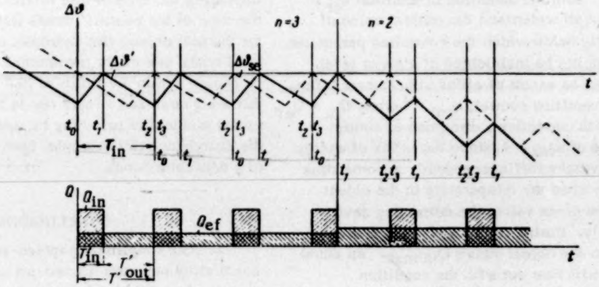

Fig. 4.

If the correcting device's parameters, selected so as to permit processing of the greatest possible disturbances be so chosen that inequalities (6) are transgressed for values of _n_ higher than n_{cr}, then complex periodic motions, similar to those considered in [5, 8], will arise in the system.

Examples of such processes are shown in Fig. 2 and 3. Figure 2,a shows the process with correction for n = 8 up to line cd. At the moment which corresponds to line cd, and instantaneous twofold increase of efflux (n = 4) occurs. As is clear from the graph, after several oscillations the process is reestablished with the new period T_N. With this, the correcting device completes two revolutions during a period. It can be assumed that the form of the postdisturbance-reestablished oscillations does not depend on the moment when the disturbance is applied. This is confirmed graphically on Fig. 2, b.

Figure 3 shows the control process with correction up to line ab for n = 8. At the moment corresponding to ab, a disturbance is applied (a fourfold increase in heat efflux) and the process continues with n = 2. The new period of complex oscillations T_N is, in this case, somewhat less than in the previous case.

Thus, complex oscillations occur in the system if one of the following conditions is not met: $n > n_{cr}$, $t_2 > T_{in}$, $t_{ro} < T'$.

3. Optimal Parameters

We now seek the optimal adjustment parameters of the correcting device for a given accuracy of control (degree of correction _k_), starting from the condition that the correction process not be disrupted for the very greatest disturbance, i.e., from the condition of minimal n_{cr}.

By n_{cm} we shall understand the critical value of influx multiplicity below which the controlled parameter (temperature) can not be maintained at a given level. This occurs due to an excess of efflux of heat over influx. For ordinary two-position control, $n_{cm} = 1$ when $Q_{in} = Q_{ef}$. For regulation with correction, disruption of control occurs for a value of $n_{cm} > 1$, since the influx of energy to the object is switched off independently at some time t_{bre}. In the case when the temperature in the object remains below the given value, the correcting device works continuously. During one rotation, the amount of heat applied to the object equals $Q_{in}t_{mak}$. An equal quantity of heat will flow out with the condition

$$Q_{in}t_{mak} = (t_{bre} + t_{mak})\overline{Q}_{ef},$$

where $\overline{Q}_{ef}$ is the critical value of heat efflux. If $Q_{ef} > \overline{Q}_{ef}$, then the temperature does not rise to the given level.

From whence we find n_{cm} as

$$n_{cm} = \frac{Q_{in}}{\overline{Q}_{ef}} = \frac{t_{mak} + t_{bre}}{t_{mak}} = 1 + \frac{t_{bre}}{t_{mak}}.$$

It is clear that $t_{mak} = t_{ro} - t_{bre}$. We finally obtain

$$n_{cm} = 1 + \frac{t_{bre}}{t_{ro} - t_{bre}} \tag{7}$$

or

$$n_{cm} = \frac{f}{f-1}, \quad \text{where} \quad f = \frac{t_{ro}}{t_{bre}}.$$

We have (5) for n_{cr}. Figure 4 shows the control process for the critical value of influx multiplicity $n = n_{cr} = 3$. For this critical case, as is clear from the graph, (6) can hold only for

$$\begin{aligned} t_2 &= T_{in} && \text{for } n_{cr}, \\ t_{ro} &= T' = T_{in} && \text{for } n_{cr}. \end{aligned} \tag{8}$$

Thus, (8) gives the optimal adjustment parameters for the correcting device.

We now find the value of n_{cm} for the case of optimal adjustment. By substituting (8) in (7), and by taking into account that $t_{ro} = T'_{in} + t_{bre}$ and that $t_{bre} = \Delta t$, we find that

$$n_{cm} = \frac{T'_{in} + \Delta t}{T'_{in}}, \tag{9}$$

i.e., in the given case, $n_{cm} = n_{cr}$.

The correcting device's adjustment parameters corresponding to (8) should be taken in those cases when very protracted disturbances are not observed in practice and _n_ is always greater than n_{cr}. We note that complex motions cannot arise in the system under these conditions.

If very protracted disturbances are possible in the control system ($n < n_{cr}$), then the device's parameters should be chosen from the condition that the system be capable of processing these disturbances.

As is clear from (8), this can be achieved by increasing the time of disk rotation t_{ro} or by decreasing the time of the contact's break state t_{bre}. In practice, for thermal objects (for example, of the dessicator hood type), one might recommend that the rotation time be chosen within the limits of (0.6 to 0.7)T', since with this are guaranteed a rapid rise in temperature at the initial moment of switching in, and good processing of the disturbance (for example, upon opening the door of a dessicator hood).

CONCLUSIONS

1. The simplified graphico-analytic theory of calculating processes in two-position controllers may be used for the analysis of processes with disturbances in two-position controller systems with time correction.

2. The distinguishing feature of the two-position control system with an electromagnetic correcting device is that the pulse repetition period (the mark-space ratio) depends on the load.

3. Under definite conditions, complex periodic motions of the controlled quantity (temperature) arise in the system.

4. With optimal adjustment parameters of the correcting device, normal course of the correction process is guaranteed for the very greatest disturbances.

LITERATURE CITED

1. A. A. Kampe-Hemm, Two-position Control Dynamics [in Russian] (Gosénergoizdat, 1955).
2. A. L. Cherepanov, "On improving the quality of two-position control," Avtomatika i Telemekhanika 19, 5 (1958).
3. A. A. Kampe-Hemm, "Correcting devices with differential switching in of thermocouples, and their use with two-position controllers," Priborostroenie No. 11 (1956).
4. A. A. Kampe-Hemm, "Comparative analysis of several improved methods of two-position control," Avtomatika i Telemekhanika, 17, 8 (1956).
5. A. S. Alekseev, "Two-position temperature controllers with advance zones," Collection: In Commemoration of Aleksandr Aleksandrovich Andronov [in Russian] (Izd. AN SSSR, 1955).
6. A. A. Kampe-Hemm, "The use of thermoelectric isodrome correcting devices for improving the quality of two-position temperature control," Avtomatika i Telemekhanika, 19, 5 (1958).
7. A. A. Kampe-Hemm and A. N. Trusov, "Simple methods of increasing the accuracy of two-position temperature controllers," Collection: Heat-Engineering Instruments and Controllers. 3 [in Russian] (1956).
8. A. S. Alekseev, Two-Position Temperature Controllers with Advance Zones. Dissertation [in Russian] (Gor'kii, 1954).

ON THE ERRORS OF AN INTERPOLATING DEVICE FOR A GIVEN CIRCULAR MOTION

V. V. Karibskii

(Moscow)

Translated from Avtomatika i Telemekhanika, Vol. 21, No. 3, pp. 317-322, March, 1960
Original article submitted July 7, 1959

An algorithm for a digital interpolating device for a given circular motion is described. A theoretical investigation of the interpolation errors is given. A brief description of the device's circuit is provided.

Today, in various domains of technology, the necessity arises of so controlling an object that it moves along a given trajectory. Frequently this is implemented by means of sampled-data servosystems. Each system controls the motion corresponding to one coordinate and, at each input pulse, there results a translation by unit length in the scale chosen, this length being called the value of the pulse. The pulses for each coordinate axis must be distributed in accordance with a given trajectory of the object's motion. Distribution of the pulses is ordinarily implemented by means of special digital computers.

In the present paper we consider the design principles, and estimate the errors, of a device of this type which provides motion along a circle.

The equation for a circle centered at the origin has the form

$$x^2 + y^2 = R^2, \qquad (1)$$

where x and y are the current coordinate values and R is the circle's radius.

We assume that the motion begins at point A with coordinates x = 0, y = R (Fig. 1), and must proceed clockwise about the circle.

We now find the value of x^2 for which the coordinate y is decreased by unity, i.e., becomes equal to y−1, for which we substitute the new value of the coordinate y in (1):

$$x_1^2 = R^2 - (y-1)^2.$$

By taking into account that y = R, we get $x_1^2 = 2R-1$.

Analogously, we can find the values of $x_2^2, x_3^2, \ldots, x_k^2$ for which there are corresponding changes of the coordinate y by 2, 3, . . ., k units. Knowing these values, we can find the corresponding differences, which will have the form

$$\begin{aligned} x_1^2 &= 2R-1, \\ x_2^2 - x_1^2 &= 2R-3, \\ &\ldots\ldots\ldots\ldots \\ x_k^2 - x_{k-1}^2 &= 2R-(2k-1) \quad (k = 1, 2, 3, \ldots). \end{aligned} \qquad (2)$$

Based on the formulas obtained, we can suggest the following method of constructing a circle. First, we must vary the coordinate x until the value of x_1^2 equals 2R-1 and, as soon as this happens, we must change y by one unit, after which we change the coordinate x until the difference $x_2^2-x_1^2$ becomes equal to 2R-3, at which time we again change y by one unit, etc. It is obvious that, in this case, the approximation error is nowhere larger than unity. However, due to the discreteness of the system's operation, such a method is not implementable, since translations of less than the value of a pulse are impossible. Consequently, R and the quantity x_k^2 are integers. However, the quantity x_k may be expressed by a noninteger at points where y_k is expressed by an integer, and conversely. We shall, therefore, in moving from point A, vary coordinate x by unity and then compute the value of x^2. As soon as the coordinate x reaches the integral value x_{i-m} for which the condition $x_{i-m}^2 \geq 2R-1$ holds, we change coordinate y by unity and determine whether the condition holds that

$$\Delta_1 = x_{i-m}^2 - (2R-1) \geqslant 2R-3.$$

If so, then a unit increment of coordinate x at the given point of the circle corresponds to an increment of coordinate y greater than, or equal to, two units. Therefore, coordinate y should be changed by one unit, the quantity $\Delta_2 = x_{i-m}^2 - (2R-1) - (2R-3)$ computed, and the condition $\Delta_2 \geq (2R-5)$ verified etc. Such operations are carried out until the condition $\Delta_k < 2R-[2(k+1)-1]$ begins to hold. As soon as this happens, we again change coordinate x by unity and then compute the increment of x^2 obtained, with account being taken of the residue, i.e., in this case $x_{i+1-m}^2 - x_{i-m}^2 + \Delta_k$ where $x_{i+1-m} - x_{i-m} = 1$. If now the following condition holds:

$$x_{i+1-m}^2 - x_{i-m}^2 + \Delta_k \geqslant 2R - [2(k+1)-1], \qquad (2')$$

then coordinate y should be changed by one unit, and the process just described should be repeated. The sequence of actions described above and (2') comprise the algorithm in accordance with which the scheme described at the end of this paper operates. In this case, naturally, coordinate y will be changed by one unit somewhat later than the time when x reaches a value corresponding to a one-unit change of y, rather than simultaneously. As a result, the circle will be approximated by a broken line with an error. We now estimate this error. For this, we prove that, with the method chosen, varying the magnitude of $\underline{x}$ by unity at any point x_l in the interval $0< x < R/\sqrt{2}$ cannot give rise to a change of the quantity $x^2_{l+1}-x^2_l$ greater than what is necessary to change $\underline{y}$ by one unit.

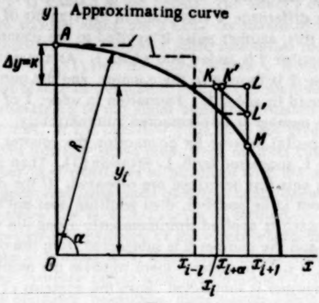

Fig. 1.

A. With motion along an approximating curve in accordance with the method we have adopted, let the moving point reach point K (Fig. 1) where, at this moment, coordinate $\underline{x}$ is changed by x_l units and coordinate $\underline{y}$ by $\underline{k}$ units. Then, a subsequent increment of coordinate $\underline{x}$ by one unit engenders the increment

$$x_{i+1}^2 - x_i^2 = 2x_i + 1. \tag{3}$$

For coordinate y_l to be changed by one unit, with the condition that $\Delta_k = 0$ at point K, it is necessary that the following equation hold:

$$x_{i+1}^2 - x_i^2 = 2R - [2(k+1) - 1]. \tag{4}$$

It follows from this that for all relationships of $\underline{x}$ and $\underline{y}$ which satisfy the condition

$$2R - (2k+1) \geqslant 2x_i + 1, \tag{5}$$

an increment of one unit in coordinate $\underline{x}$ will give rise to an increment of coordinate $\underline{y}$ equal to or less than unity if, at these points, it can be assumed that $\Delta_k = 0$. After transformation, (5) assumes the form

$$R - k \geqslant x_i + 1 \tag{6}$$

or, taking into account that $y_l = R-k$,

$$y_i \geqslant x_{i+1}. \tag{7}$$

For $\underline{x}$ equal to y_l, a unit increment of coordinate $\underline{x}$ engenders, for $\Delta_k = 0$, a unit increment of coordinate $\underline{y}$, which corresponds to an angle of 45 degrees, or $x = R/\sqrt{2}$. In other words, for motion from point A to point K, each unit change of coordinate $\underline{x}$ engenders a smaller variation in $\underline{y}$. Only, when, as the result of successive variations of $\underline{x}$ by unity, coordinate $\underline{x}$ becomes equal to coordinate $\underline{y}$ at the preceding point does the coordinate $\underline{y}$ also change by unity.

B. We now determine the maximum possible deviation of the approximating curve along the axis of ordinates from the given circle in the interval $0 < x < R/\sqrt{2}$, with account being taken of the Δ_k. Let the motion begin at point A (Fig. 1) and be directed clockwise, with the coordinate $\underline{x}$ being given a unit increment. By virtue of what has already been proved, each unit increment of coordinate $\underline{x}$ requires a variation of coordinate $\underline{y}$ by a quantity less than unity.

However, in accordance with the method chosen for constructing the circle, this change does not occur until the resulting increment of x^2 satisfies the condition $x^2 \geq 2R-1$. This means that, for such a value of $\underline{x}$, the deviation along the axis of ordinates of the approximating curve from the given one is $\delta_y \geq 1$. Let such a point, where the condition $x^2 > 2R-1$ holds, be the point with abscissa x_{l-m}. Then, at the point x_{l-m-1} where $x_{l-m}-x_{l-m-1} = 1$, $\delta_y < 1$. But by virtue of the fact that on this segment a unit increment of coordinate $\underline{x}$ cannot engender an increment of coordinate $\underline{y}$ by more than unity, the transition from point x_{l-m-1} to point x_{l-m} can increase δ_y by at most unity. Thus, the resulting error along the axis of ordinates can lie within the limits $0 \leq \delta_y < 2$. It should be kept in mind that, after transition to the point with coordinates (x_{l-m}, y_{l-m}), there occurs a change of $\underline{y}$ by unity, and δ_y becomes less than unity.

By an analogous argument we can successively check each value of $\underline{x}$ in the given interval, coming to the same conclusion each time.

We now consider the very worst case. Let the moving point be at point K with coordinates (x_l, y_l) such that the next increment of coordinate $\underline{x}$ by unity engenders the incrementation of $\underline{y}$ by unity for $\Delta_k = 0$, i.e., $x^2_{l+1}-x^2_l = 2R-(2k+1) = 2y_l-1$, where $\underline{k}$ is the number of units by which coordinate $\underline{y}$ was changed at the moment of transition to point K. We assume that, at the moment of transition to point K, the total accumulated increment is $x^2_l-x^2_{l-l}$, where x_{i-l} is the abscissa of the point at which the last change of $\underline{y}$ occurred, or that the magnitude of the residual Δ_k. If we hit point K after the latest change by unity of coordinate $\underline{y}$ rather than $\underline{x}$, had the maximum possible value $\Delta_{k\ max}$. In accordance with the algorithm for the operation of the scheme, $\Delta_{k\ max}$ must, at point K, be at least one unit less than $2y_l-1$, i.e., must satisfy the equation $\Delta_{k\ max} = 2y_l-2$.

In making the transition from point K to point L, the residual $\Delta_{k\ max}$ increases by $2y_l-1$, as a result of which coordinate $\underline{y}$ changes by unity and executes a transition to point L'. However, the residual at point L', $\Delta_{k+1} = \Delta_{k\ max}$, turns out to be larger than the quantity, $2(y_l-1)-1$, necessary for changing the ordinate of point L' by unity. As a result of this, a transition occurs to point M, and the following residual is formed:

$$\Delta_{k+2} = 2y_i - 2 - 2(y_i - 1) + 1 = 1.$$

A third change of coordinate $\underline{y}$ by unity can only occur for the condition $2(y_l-2)-1 = 1$, i.e., for $y_l = 3$.

By taking (7) into account, we can write $x_{l+1} \leq y_l = 3$. It follows from this that variation of coordinate $\underline{y}$ at point L by three units in succession is only possible for $R = \sqrt{2}\, x_{l+1} \leq 3\sqrt{2}$. For all values of $R > 3\sqrt{2}$, change of coordinate y at point L can occur only by two units. For large R ($R \approx 100$), the magnitude of $2(y_l-2)-1 \gg 1$ and, by neglecting unity in comparison with $2(y_l-2)-1$, we can assume that in the worst case the change of coordinate y is by exactly two units, and point M lies on the circle. Thus, the maximum error, equal to two, will be at point L.

If the order of applying incrementation is somewhat varied, this error can be reduced to unity. For this, we shall first carry out all the computations and then, when it becomes clear that a unit incrementation in y must occur, we execute it simultaneously with the incrementation in x which was giving rise to it. In the actual scheme, this leads to motion at an angle of 45 degrees from point K to point L' (Fig. 1). As a result, the error in coordinate y, equal to δ_y, will everywhere be less than unity. The expression for x in terms of y which is obtained from the equation of the circle coincides with the expression for y in terms of x. Therefore, all the argument already given for x is also valid for y within the limits of variation of angle α from 0 to 45°, i.e., for variation of α within the limits $R \geq x \geq R/\sqrt{2}$, and the approximating curve is symmetric about the line passing through the first quadrant at a 45° angle. At the limits of the interval $0 < x \leq R/\sqrt{2}$, the radial error at any point x will equal

$$\delta_R = \sqrt{(\sqrt{R^2 - x^2} + \delta y)^2 + x^2} - R. \qquad (8)$$

The error δ_y equals the difference between the true value y corresponding to a given x and the next larger integer if y itself is not an integer.

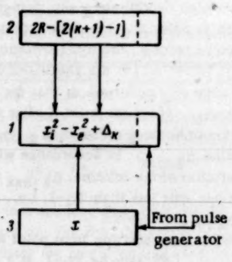

Fig. 2.

Figure 2 shows the simplified block schematic of the interpolating computer which operates in accordance with the principles described above. The circuit consists of counter 3, to which quantity x is fed, adder 1 which stores the current value of the difference $x^2_i - x^2_l + \Delta_k$, and adder 2 which stores the current value of 2R-[2(k+1)-1]. The dashed lines on Fig. 2 mark off the adders' least significant places. If the motion is clockwise, starting from point A (Fig. 1) then, before operations commence, the counter and adder 1 are set to zero and the number 2R-1 is placed in adder 2. Then, from the pulse generator, one pulse is applied to the x counter, storing a "1" in the counter and in adder 1. From the contents of the adder 1 the number 2R-1 is subtracted and, if the difference formed in adder 1 is negative, the number 2R-1 is added to it, and one pulse is applied along the x axis. The sign of the difference is staticized in the sign bit of adder 1. After this, another pulse is applied to the counter, and the number 3 is added into adder 1. As a result, the number 2 is formed in the counter, and the number 4 (2^2) is formed in adder 1. Formation in adder 1 of the square of the number is implemented automatically, thanks to a special scheme for connecting the counter with adder 1, suggested by B. L. Ermilov [1]. Then the arithmetic acts just described are repeated. If the difference turns out to be positive, then addition does not occur, one pulse each is applied simultaneously along the x and y axes, and the number 2 is subtracted from the contents of adder 2, i.e., in adder 2 there remains the number 2R-3. This number is subtracted from the contents of adder 1 and, if the difference is positive, then another pulse is applied along the y axis, and the number 2 is again subtracted from the contents of adder 2, etc., until the difference becomes negative. As soon as the difference does become negative, addition again ensues, and the next pulse is applied from the pulse generator to the counter, etc.

If motion begins from some arbitrary point with coordinates [x_0, y_0], then the initial establishment of values must be the following: in the counter the number x_0 is established, in adder 1 the number $x_0^2 - R^2 + y_0$, and, in adder 2, the number $2y_0 - 1$, where y_0, is the value of y corresponding to the value x_0 and rounded off to the next higher integer.

For processing the complete circle, the initial established values and the direction of motion along the axes are changed in making the transition from one quadrant to the next.

Thus, by means of addition and subtraction, comparisons are made in the scheme proposed of the quantities

$x^2_{j+1} - x^2_j + \Delta k$ with the quantities $2y_j - 1$, where x_j and y_j are the coordinates of any point of the approximating broken line. In a comparison the indication (sign of the difference) is developed which is used for controlling the distribution of the generator pulses along the x and y axes in correspondence with the given law of motion (circular). With such a computational algorithm for circular motion there occurs a variation of the path velocity by a factor of $\sqrt{2}$ which, in the majority of cases, is admissible. Moreover, by using velocity feedback, one can so control the frequency of the pulse generator that the velocity can be kept constant and equal to a given value. (For a more detailed description of the scheme, cf. [2].)

The scheme suggested by B. L. Ermilov [3] operates by such a mathematical algorithm, but with the use of another computational algorithm, the mathematical algorithm not being described in general form. The scheme of B. L. Ermilov consists of two counters and one adder of the accumulative type. Pulses from the generator are applied to the x axis and to the input of one of the counters, forming the quantity x in it; with this, the quantity x^2 is formed in the adder. The adder's overflow pulses are applied along the y axis. By means of the second counter, each overflow pulse introduces the quantity $2^n-(2y_j-1)$ into the adder, where n is the number of places in the adder, adding this number to the number remaining in the adder after transmission of the overflow unit. If the overflow pulse does not give rise to a second overflow pulse then, from the first counter, the number $2x-1$ continues to be added with the arrival of each generator pulse until overflow again occurs, whereby since $x = 1, 2, 3, \ldots, x^2$ is formed.

Since, on the segments of the circle where the coordinate x is close to R, there are emitted $\sqrt{2R-1}$ successive overflow pulses with the frequency of the scheme's elements' operation, there occurs a sharp change in the path velocity. Indeed, the generator's frequency must be approximately $\sqrt{2R-1}$ times less than the frequency of the overflow pulses so that $\sqrt{2R-1}$ overflow pulses can be disseminated between any two generator pulses. As a result, motion at the beginning of the processing of a quadrant of the circle (from 90 to 45°) will occur with a velocity smaller by a factor of $\sqrt{2R-1}$ than that at the end. Such a sharp variation of path velocity in cases when the device is designed to guide a cutting tool is inadmissible. It should be mentioned that control of the path velocity by variation of the generator frequency is not possible in the scheme given, since the frequency of the overflow pulses does not depend on the generator frequency.

SUMMARY

1. For constructing a circle, we use the derived formula $x^2_{j+1} - x^2_j + \Delta_k \geqslant 2R - [2(k+1) - 1]$.

2. In constructing a circle in accordance with the computational algorithm suggested, there occurs no accumulation of errors, and one obtains an absolute radial approximation error δ_R which is less than one unit in the chosen scale.

3. The scheme suggested makes it possible to control path velocity by varying the pulse generator's frequency.

LITERATURE CITED

1. B. L. Ermilov, "Certain types of digital function generators," paper given at the Conference on the Theory and Application of Discrete Automatic Systems [in Russian] (Moscow, 1958).
2. V. V. Karibskii, "An interpolating device for giving circular motion," Priborostroenie 2 (1960).
3. B. L. Ermilov, "Sampled-data device for the automatic control of circular motion," Claim No. 604342/26 of Aug. 19 (1958).

EXPERIMENTAL INVESTIGATION OF RUBBER-FABRIC MEMBRANE CHARACTERISTICS

G. T. Berezovets and Chou Ching-leng

(Moscow)

Translated from Avtomatika i Telemekhanika, Vol. 21, No. 3, pp. 323-332, March, 1960
Original article submitted September 3, 1959

The results are given of an experimental investigation of rubber-fabric membrane characteristics, these membranes being used in pneumoautomation devices.

1. Aim and Methodology of the Investigation

Modern pneumoautomation devices, designed for the regulation and control of various continuous productive processes, are constructed on the principle of force compensation.

As one of their basic physical elements, these devices usually contain either bellows or rubber-fabric membranes. The pneumatic instruments of unified aggregate systems (UAS), produced domestically, as well as the instruments of the majority of foreign companies—Moore, Sunvic, Taylor, Bristol, Brown, Electroflo, DRD, etc. are constructed with membranes. The membranes delimit the individual pneumatic chambers inside the instruments, and it is on the membranes that forces from the compressed air in these chambers are balanced.

Such indicators of quality of operation of modern pneumatic devices as their accuracy and sensitivity, as well as their static and dynamic characteristics, depend to a large extent on the properties and characteristics of their membranes.

There are many works in the literature on the investigation of metallic membranes, but there are only a few works [1-4] devoted to the investigation of rubber-fabric membranes. In connection with this, and because precisely these rubber-fabric membranes have attained their greatest dissemination in pneumatic devices for the control and regulation of productive processes, the necessity for a more careful investigation of these membranes arose.

The membranes investigated had plane and conic profiles (Fig. 1, a and b), prepared from brand 1520 caprone, from glass cloth and TD cloth covered with brand 44-9 rubber, and also included corrugated membranes of AM-93 rubber, used in UAS instruments (Fig. 1, c).

The experimental investigation was to determine the following characteristics:

1) the dependence of the membrane's effective area on its travel, $F_e = f(S)$;

2) the dependence of the membrane's effective area on the pressure drop across it, $F_e = f(\Delta p)$;

3) the membrane's hysteresis.

In addition, we determined the effect of the membrane's geometry, of the dimensions of its rigid center, and of the material's quality on the course of the characteristics $F_e = f(S)$ and $F_e = f(\Delta p)$, investigated the stability of membrane operation, and determined the possible skewing of the membrane which might arise during its operation.

The experiments were carried out on stands specially developed for this purpose, in which atmospheric pressure acted on one side of the membrane and, on the other side, compressed air or a vacuum, the magnitudes of which were controlled.

The forces arising from the pressure drops acting on the membranes were equalized by weights attached to the membranes' rigid centers. The membrane characteristics were taken off for the following weight sizes: 0.540, 0.728, 4.62, 8.85, 13.09, and 17.32 kg. A cathetometer measured the membrane displacements.

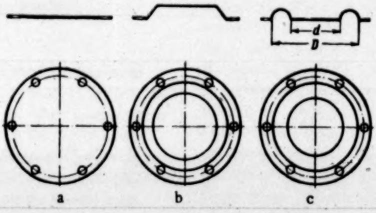

Fig. 1. Forms of the membranes investigated.

For measuring skewing, pressure was introduced into a chamber over the membrane, with a long pointer attached to the membrane's rigid center on the load side. Membrane skewing was determined by the position of the end of the pointer fixed to a scale under the pointer. The scale was a uniform lattice of concentric circles and radial lines. Angles were read off from the radial lines, while the displacement of the pointer's end from the center was read off from the concentric circles.

The magnitude of the membranes' effective area was computed from the formula

$$F_e = \frac{G}{\Delta p},$$

where F_e is the magnitude of the effective area in cm^2, G is the size of the weight placed at the membrane's rigid center, in kg, and Δp is the pressure drop across the membrane, in kg / cm^2.

For the testing of the plane and conical membranes we used rigid centers of two sizes: d = 20 mm and d = 45 mm; the diameter D of the seals of these membranes was the same for all, and equal to 60 mm. A corrugated membrane (Fig. 1, c) was tested with a rigid center d = 45 mm and a value of D equal to 62 mm.

EXPERIMENTAL RESULTS

Stability of Membrane Characteristics and Membrane Skewing

The characteristic $F_e = f(S)$, for new membranes, was only stabilized after the membrane had operated under pressure for several hours. The characteristics of one and the same membrane, in an unchanged set-up, may be repeated only in the case when they are taken off, one after another, without any interruption in membrane operation. Membrane characteristics taken off after an interruption in operation are initially unstable, but then, after some time, are stabilized and begin to coincide with each other; but they almost never coincide exactly with the characteristics taken off before the interruption. The difference between these effective area characteristics can reach 10 to 12 %.

With a readjustment of the membrane, the characteristics taken off before and after the readjustment never coincide. As the pressure drop acting on the membrane becomes larger, the characteristics become more stable.

In investigating membrane skewing, it was observed that they are unstable, but depend basically on the membrane's positioning and, particularly, on the presence of nonconcentricity between the membrane's rigid center and the seal's circle.

Figure 2 shows part of the scale plus the graphs of the motion of the end of the pointer for two different positionings of one and the same membrane. The solid line shows the course of the pointer as the pressure in the chamber over the membrane was increased (forward travel), and the dashed lines show it for decreasing pressure (reverse travel). It was established that the skewing angle between the plane of the flapper, fixed on the membrane's rigid center, and the plane of the nozzle's face end, which this flapper must cover, can oscillate, for different membranes, from 0.5° to 1.5°.

Investigation of Plane Membranes

A comparison of the characteristics $F_e = f(S)$, taken off for membranes prepared of caprone, glass cloth, and TD cloth, led to the following conclusions:

a) the membranes of TD cloth possessed the greatest hysteresis; for them, the relative magnitude of the maximum hysteresis per effective area ΔF_h can reach 18 %, while for membranes of glass cloth, having minimum hysteresis, it was about 7 to 8 % (computing ΔF_h

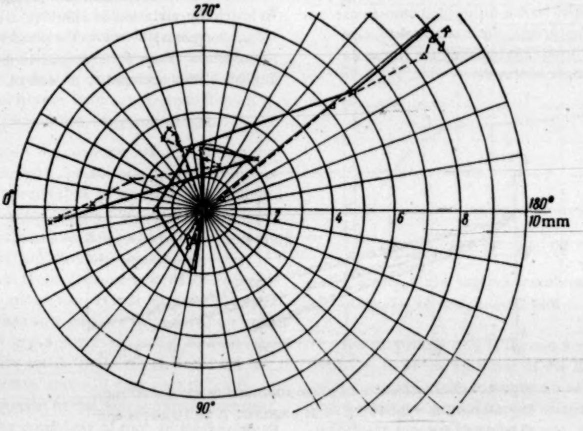

Fig. 2. Graphs characterizing the skewing of a membrane's rigid center.

as the maximum absolute value of the hysteresis divided by the maximum value of effective area $F_{e\ max}$ for forward travel of the membrane);

b) for one and the same pressure drop on the membrane (i.e., for one and the same value of F_e), the least travel was observed in glass cloth membranes; the travels of membranes of caprone and TD cloth were almost identical, and were larger than the travels of glass cloth membranes.

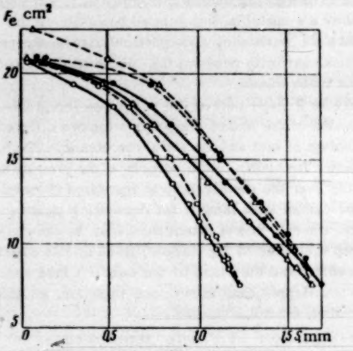

Fig. 3. Characteristics of plane membranes for d = 45 mm, D = 60 mm, G = 0.540 kg. Solid lines are for forward travel, dashed lines for reverse travel; ● is caprone, △ is TD cloth, ○ is glass cloth.

A comparison of plane membrane characteristics (Figs. 3 and 4) with large (d = 45 mm) and small (d = 20 mm) rigid centers leads to the following conclusions:

a) for large rigid centers, the characteristics are nonlinear, while for small centers they are linear for almost the entire length of travel;

b) with small centers, the hysteresis per area equals 1.6 to 2%, i.e., is much less than for membranes with large centers, in which it may oscillate between 7 and 18%;

c) when the rigid center is decreased, the membrane travel is increased, but not by the same amount: in caprone membranes this increase is about 53% of the travel for d = 45 mm and, for glass cloth membranes, about 23%;

d) as the diameter of the rigid center is varied from 45 to 20 mm, or as its area varies from 16.2 to 3.2 cm², the maximum effective area F_e (with S = 0) is varied, for all the membranes, approximately from 21 to 12 cm².

Figure 5 shows the characteristics $F_e = f(S)$ for plane caprone membranes with a large rigid center (d = 45 mm), taken off for weights of different magnitudes.

By considering the characteristics obtained, one can establish the following regularities in their behavior:

1. The larger the weight, i.e., the greater the initial value of the drop necessary for the membrane to begin to move, the greater is the steepness of the characteristic $F_e = f(S)$ as the pressure drop thereafter increases, i.e., the less does the effective area change over the course of the membrane's travel.

This is explained by the circumstance that, with a large weight, there is a large pressure drop across the membrane even before it begins to move, under the action of which pressure drop the membrane's free surface is deformed, forming a semispherical crimp. With a further increase in pressure drop, a motion begins which is analogous to the motion of a crimped (corrugated) membrane.

The formation of crimps in plane membranes occurring under the action of a pressure drop (thanks to which the variation of effective area as a function of travel decreases) increases the possibility of using plane membranes. Thus, for example, in the regulators of the English Sunvic company, instead of using doubled

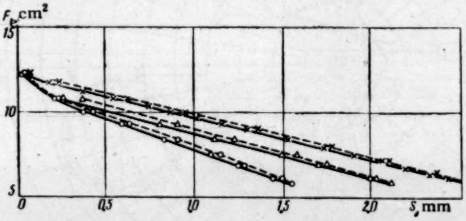

Fig. 4. Characteristics of plane membranes for d = 20 mm, D = 60 mm, G = 0.540 kg. × is caprone, △ is TD cloth and ○ is glass cloth.

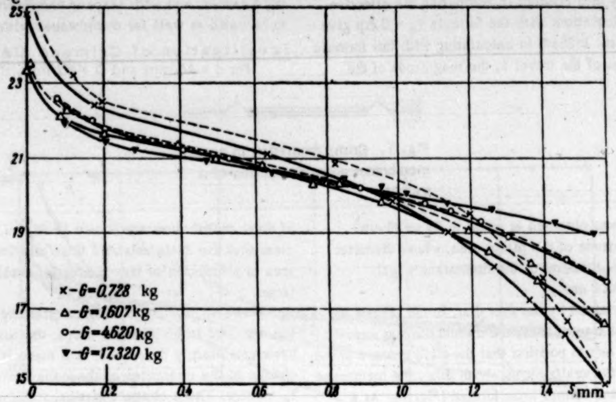

Fig. 5. Plane caprone membrane characteristics, taken off for different weights. d = 45 mm, D = 60 mm.

corrugated membranes with atmospheric pressure between them, as is done in the UAS blocks, doubled plane membranes are used, with the pressure between them being obtained from the supply channel. Since the supply pressure is necessarily greater than the pressure in any of the regulator chambers, crimps are always formed under the action of this pressure.

2. The greater the size of the weight, the less the hystersis per area ΔF_h : if ΔF_h = 3.6 % for a weight G = 0.728 kg, then ΔF_h = 0.2% for G = 4.62 kg and, for G = 8.85 kg, it vanishes completely.

The decrease in hysteresis observed for increase in weight is explained by this, that the internal frictional force which engenders the phenomenon of hysteresis becomes vanishingly small in comparison with the forces generated in the membrane from the pressure drop on it which is necessary to equalize the given weight.

3. Figure 6 shows the characteristic $F_e = f(\Delta p)$ for a caprone membrane with d = 45 mm and D = 60 mm, constructed for different values of travel S[*]. It is clear from the graphs that the effective area varies only for small values of pressure drop, after which, with increasing pressure drop, it remains virtually constant.

This means that if the displacement of the membrane is severely limited, i.e., if it is virtually clamped into the position when it is initially established for values of travel of S = 0.4 to 0.8 mm then, as the pressure drop across the membrane varies within the limits of 0.1 to 1 kg/cm^2, the effective area will vary very insignificantly. The explanation of this fact is very important, since it opens up the possibility of such an establishment of initial membrane position in devices for which deviations of effective membrane area should be minimal.

Investigation of Membranes with Conic Profiles

In the investigation of membranes with conic profiles, it was established that, with small weights

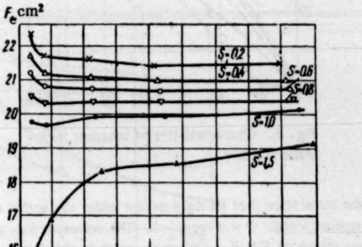

Fig. 6. Plane caprone membrane characteristics. d = 45 mm, D = 60 mm.

---

[*] The magnitude of S is figured from the neutral position, in which the plane of the rigid center coincides with the plane of the membrane's seal. An increase in the travel S corresponds to a displacement of the membrane upward from the neutral position.

(G = 0.540 g), it was necessary to take the membrane's natural rigidity into account in computing the effective area, since calculations with the formula $F_e = G/\Delta p$ give incorrect results. Indeed, in calculating with this formula for small values of the travel S, the magnitude of the effective area was obtained as equal to 30 to 35 cm², while the magnitude of the piston area, whose diameter would equal the diameter of the membrane's seal, equalled only 28.8 cm².

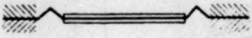

Fig. 7. Crimp formation in conical membranes under the action of a weight.

This is explained by the fact that, in the process of taking off the characteristics, the membrane was so established in its initial position that the rigid center's plane coincided with the seal's plane. With this, the membrane was deformed, and crimps were formed (Fig. 7). As a result, a force Q arose, resulting from the membrane's inherent rigidity, which counteracted the weight G applied to the membrane.

An experiment was specially carried out to determine the inherent rigidity of conical and corrugated membranes, in which the free membrane was gradually loaded, and the translation S of its rigid center under the action of the applied weight Q was recorded. The corresponding graphs are shown on Fig. 8. Curves C and D on this figure correspond to different samples of glass cloth conical membranes.

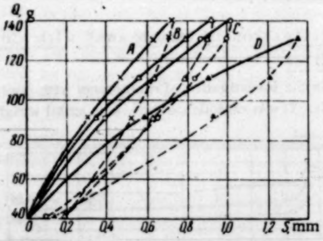

Fig. 8. Characteristics of inherent membrane rigidity.

It is clear from these graphs that, for small weights, the force Q becomes commensurable with the magnitude of the weight G, so that the computation of the effective area in this case can be carried out with the formula $F_e = (G-Q)/\Delta p$.

All the fundamental regularities observed in the testing of plane membranes, both with respect to the behavior of the characteristics $F_e = f(S)$ and $F_e = f(\Delta p)$ for different weights and for different diameters of the rigid center, and with respect to hysteresis, turned out to be valid as well for membranes with conical profiles.

Investigation of Crimped UAS Membranes

For d = 45 mm and D = 62 mm, the characteristics of these membranes are shown in Fig. 9, from which it is clear that the hysteresis and the variation of effective area as a function of travel are, for small weights, very large.

However, for large weights (starting with G = 4.62 kg), i.e., for large pressure drops, the amount of hysteresis sharply decreases, and there is a simultaneous change in the character of the behavior of characteristic $F_e = f(S)$. These characteristics, starting with a travel of about S = 0.45 mm, become practically linear and, what is particularly important, steep.

The magnitude of a UAS membrane's effective area strongly depends on the position of the rigid center with respect to the plane of the membrane's seal. This is particularly apparent for small weights. Figure (10) shows the characteristics of a UAS membrane for d = 45 mm and D = 62 mm, taken off for weights of G = 0.540 kg and G = 17.32 kg, and for various distances h of the membrane's rigid center from the seal plane. Characteristics A correspond to the neutral position, when h = 0; characteristics B correspond to h = -2 mm, i.e., to a position of the membrane below the neutral position, and characteristics C correspond to the position when h = 2 mm, i.e., the membrane is above the neutral position.

For UAS membranes we investigated the hysteresis as a function of the travel (Fig. 11). This confirmed the conclusion, given in [3], that the hysteresis decreases with decreasing travel.

In Fig. 8, given earlier, the characteristics Q = f (S) were given, from which the inherent membrane rigidity can be determined.

Characteristic A corresponds to the case when the UAS membrane is loaded on the side of crimp concavity, and characteristic B to the case when the load is on the convex side.

From a comparison of these characteristics it is clear that the membrane possesses different rigidity, depending on which side of the crimp the force is acting, specifically, the rigidity is greater in the case when the force acts on the crimp's concave side.

SUMMARY

From the experimental results, we may draw the following conclusions:

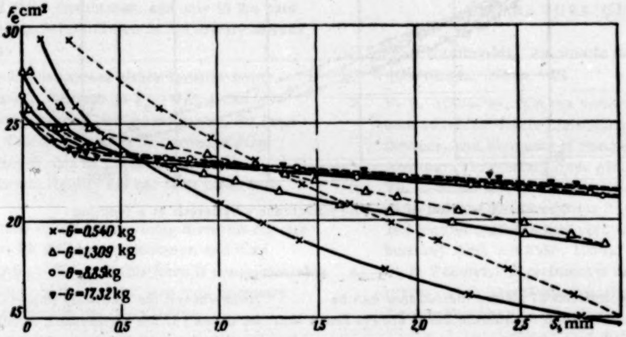

Fig. 9. Characteristics of UAS membranes, taken off for various weights. D = 62 mm, d = 45 mm.

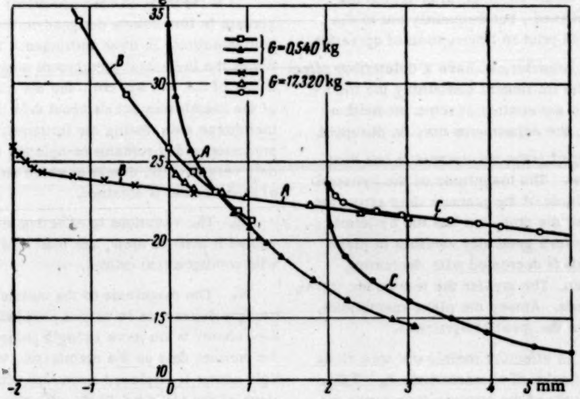

Fig. 10. UAS membrane characteristics, taken off for various positions of the UAS membrane with respect to the plane of the seal.

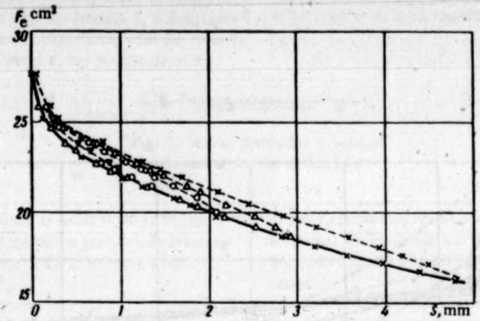

Fig. 11. Variation of the UAS membrane's hysteresis as a function of the travel.

1. The characteristics of all the membranes can be stable only in the case when the membrane is always found under pressure. With large pressure drops, the characteristics are more stable than with small ones. Interruptions in membrane operation lead to a confusion of its characteristics which are then, after protracted operation, again stabilized, but frequently not to the same value which held prior to interruption of operation.

Such membrane behavior can have a deleterious effect on the operation of the instrument containing the membrane and used for the automation of some productive process: for example, the adjustments may be disrupted.

2. The hysteresis of plane membranes is less than that of corrugated ones. The magnitude of the hysteresis depends on the magnitude of the pressure drop across the membrane: the greater the drop, the less the hysteresis; with large drops, hysteresis generally vanishes in plane membranes. Hysteresis is decreased with decreasing membrane rigid center. The greater the membrane travel, the greater its hysteresis. Among the plane membranes, those of TD cloth have the greatest hysteresis.

3. The variation in effective membrane area along its travel, i.e., the behavior of characteristic $F_e = f(S)$, depends on the magnitude of the pressure drop across the membrane. For a given membrane travel, the greater the drop, the less the variation in the membrane's effective area.

4. The effective membrane area varies as a function of the drop; the less the drop, the greater this variation. However, starting with a drop of about 0.15 kg/cm², further increases in it lead to virtually no changes in effective area, i.e., it may be considered constant. This last statement is valid both for plane and for conical and corrugated membranes.

From whence the following important conclusion may be drawn: if the membrane's travel is limited, then its effective area will be constant for all practical purposes for variations of the pressure drop on it within the limits of 0.15 to 1 kg/cm².

It is precisely in such conditions that membranes operate in instruments designed on the principle of force compensation. In these instruments, the pressure drop across the individual membranes might vary within the limits of 0.2 to 1 kg/cm², and the static translation of the membranes equals about 0.05 mm. The effective membrane area, during the instrument's operating processes, either remains completely unchanged or changes only very slightly, thanks to which an increased accuracy of such devices is obtained.

5. The variations in effective area, both with travel and with pressure drop, are least of all in UAS membranes with semispherical crimps.

6. The magnitude of the membrane's effective area strongly depends on its initial establishment; this dependency is the more strongly pronounced, the less the pressure drop on the membrane. When the membrane's rigid center is displaced downward with respect to the plane of the seal (h< 0) the effective area increases in comparison with the case when the membrane is in the neutral position (h = 0) and, when the displacement is upward (h > 0), it decreases.

In connection with this, the accuracy of the initial placement of the membranes in UAS instruments plays an important role, since by it one determines the deviation of the effective area of one membrane from another. In isodrome regulators, for example, this is inadmissible, since it might lead to the appearance of residual nonuniformities.

7. Experiment showed that the formula usually given in the literature for calculating effective membrane area,

$$F_e = \frac{\pi}{12}(D^2 + Dd + d^2),$$

which does not take into account the variation in area as a function of travel and pressure drop, can be used only for determining the value of F_e for zero or very small travels of plane membranes, and only in the case when the membrane is established in the strictly neutral position (h = 0).

8. Calculating membrane characteristics from experimental data by the formula $F_e = G/\Delta p$ can be done only for large weights and, consequently, for large pressure drops. Calculations for small pressure drops give incorrect results, due to the fact that the membrane's inherent rigidity has not been taken into account.

The magnitude of the force arising from this rigidity is not a constant for different membranes, and may reach a magnitude of 300_g. If this force is commensurable with the magnitude of the weight, it is then necessary to take it into account in the calculations.

9. In certain devices of pneumoautomation as, for example, lead blocks, where there are not very stringent requirements on the invariance of membrane effective area, doubled corrugated membranes can be replaced by doubled plane membranes with supply pressure between them.

LITERATURE CITED

1. V. L. Lossievskii, Automatic Regulators [in Russian] (Oborongiz, 1944).
2. V. V. Afanas'ev, "On the variations of effective area of rubber-fabric membranes," Systems, Devices, and Elements of Pneumohydraulic Automata [in Russian] (Izd. AN SSSR, 1959).
3. Yu. L. Mach and S. P. Stepanov, "The investigation of membrane characteristics," Systems, Devices, and Elements of Pneumohydraulic Automata [in Russian] (Izd. AN SSSR, 1959).
4. V. P. Temnyi, "Experimental determination of rubber-fabric membrane rigidity," Avtomatika i Telemekhanika 17, 11 (1956).

OPTIMAL FREQUENCY CONTROL OF ASYNCHRONOUS ELECTRIC MOTORS

Yu. P. Petrov

(Leningrad)

Translated from Avtomatika i Telemekhanika, Vol. 21, No. 3, pp. 333-339, March, 1960
Original article submitted November 25, 1959

The question is investigated as to which law should be followed in controlling voltage and frequency in asynchronous electric motors so as to provide optimal transient responses. The optimal control laws are derived for various requirements on the character of the transient response for the case when the impedance moment depends linearly on the rotational velocity*.

For those stands where it is possible arbitrarily to vary the frequency of the voltage supplying the executive asynchronous electric motors, the problem arises as to which law the frequency should be varied by so as to provide optimal motor operation in the transient states. Electric drives can be divided into two basic groups as a function of the requirements imposed on the character of their transient responses.

Electric drives of the first group must provide maximum translation of the executive mechanism in a given time for given values of initial and final rotational velocities. Electric drives of the second group must provide maximum change of rotational velocity of the executive mechanism in a given time.

As examples of the first group of electric drives, one may take traction motors while, as examples of the second group, one can adduce electric starting motors.

Optimal control laws, as we shall see below, will be different for the different groups of electric drives.

We shall start from the basic equation of electric drive dynamics:

$$M_{\mathrm{mo}} - M_{\mathrm{i}} = J\,\frac{dn}{dt}, \qquad (1)$$

where M_{mo} is the motor's rotational torque, M_l is the impedance torque, depending on rotational velocity, and J is the moment of inertia about the motor shaft of the motor and drive.

We now introduce relative units. As the unit rotational torque we take the maximum (tilting) torque M_{max}, corresponding to critical slipping; as the unit of rotational speed we take n_s, the synchronous velocity for the supply line's maximum frequency; as the time unit we take T_M, the mechanical time constant, numerically equal to the time for accelerating the drive zero up to the synchronous velocity for a constant rotational torque equal to the maximum; as the unit of current frequency in the rotor, we take f_{cr}, the critical frequency corresponding to tilting slipping; for the unit of current we take I_{cr}, the rotor current for critical slipping.

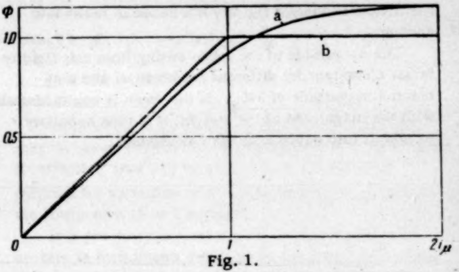

Fig. 1.

The relative units will be : for motor rotational torque, $M = M_{\mathrm{mo}}/M_{\mathrm{max}}$, for impedance moment, $\mu = M_l/M_{\mathrm{max}}$, for time $\tau = t/T_M$, for rotor rotational speed, $\nu = n/n_s$, for rotor current frequency, $\omega = f_{\mathrm{rot}}/f_{\mathrm{cr}}$, for current $i = I/I_{\mathrm{cr}}$ and, for stator frequency, $f = f_{\mathrm{st}}/f_{\mathrm{max}}$.

We make the following assumptions:

1. We shall replace the true motor magnetization curve a by the piecewise-linear curve b, consisting of two segments (Fig. 1).

2. We shall not take into account the electromagnetic transient response (the free component in the rotor current).

In relative units, the dynamics equation (1) takes the following form:

$$M - \mu = \frac{d\nu}{d\tau}. \qquad (2)$$

The rotational torque M and the heat dissipation in the rotor Q will be expressed by the formulas

$$M = \frac{2\Phi^2\omega}{1+\omega^2}, \qquad (3)$$

$$Q = \int_0^\tau \frac{2\Phi^2\omega^2}{1+\omega^2}\,d\tau \qquad (4)$$

---

* The basic propositions of this paper were presented on Sept. 29, 1958 at the All-Union Conference on the Theory and Applications of Discrete Automatic Systems (Section on Optimal System Theory).

where Φ is the motor's magnetic flux in relative units :

$$\Phi = \frac{\Phi_{\text{mo}}}{\Phi_{\text{max}}}.$$

The yield of electric drives of the first group will be proportional to the integral

$$\Delta\alpha = \int_0^\tau \nu d\tau, \tag{5}$$

and that of the second group to the integral

$$\Delta\nu = \int_{\nu_1}^{\nu_2} d\nu = \int_0^\tau \nu' d\tau. \tag{6}$$

In seeking an optimal control law, we should take into account the limitations imposed by the properties of the electric motors. The most important of these is the limitation of heating : the temperature of the winding must not exceed a limiting admissible value. Since the thermal transient responses in a motor flow much more slowly than the mechanical transient responses (heating time constants are measured in minutes [2]), one can ignore the heat emission during the start-up and braking times. With heat emission ignored, the heating limitation on the quantity of heat which can be generated in the rotor in a given time, i.e.,

$$\int_0^\tau \frac{2\Phi^2\omega^2}{1+\omega^2} d\tau \leqslant Q_0. \tag{7}$$

With complete use of motor heating, (7) goes over into an equality. Steel saturation introduces a limitation on magnetic flux. With the assumptions we have made, this limitation, in relative units, is written in the form

$$0 \leqslant \Phi \leqslant 1. \tag{8}$$

Finally, the motor's rotational speed is limited by the supply line's maximum frequency

$$\nu \leqslant \nu_{\text{max}} \tag{9}$$

and, for $\mu = 0$,

$$\nu_{\text{max}} = 1.$$

Optimal Control Law for Electric Drives of the First Group

The optimal control problem for electric drives of the first group is formulated mathematically as follows : to find $\omega = \omega(\tau)$ and $\Phi^2 = \Phi^2(\tau)$ which maximize (5) for a given value of (4), for given relational equations (2) and (3) and given limitations (8) and (9). This is the general Lagrange problem of variational calculus, complicated by the fact that only one-sided variation is admissible here. Consequently [1], the functions sought, $\omega(\tau)$ and $\Phi^2(\tau)$, must :

1) either be extremal, i.e., satisfy the Euler equations

$$\frac{\partial F}{\partial \nu} - \frac{d}{d\tau}\frac{\partial F}{\partial \nu'} = 0, \quad \frac{\partial F}{\partial \omega} - \frac{d}{d\tau}\frac{\partial F}{\partial \omega'} = 0, \quad \frac{\partial F}{\partial \Phi^2} - \frac{d}{d\tau}\frac{\partial F}{\partial \Phi^{2\prime}} = 0$$

for the auxiliary function F :

$$F = \frac{2\Phi^2\omega^2}{1+\omega^2} - \lambda_0\nu + \lambda\left(\nu' + \mu - \frac{2\Phi^2\omega}{1+\omega^2}\right), \tag{10}$$

where λ_0 and λ are Lagrange multipliers, with λ_0 constant and λ a function of τ ;

2) or be boundary curves, i.e., satisfy (8) or (9) with the equality signs;

3) or, finally, may consist of extremal segments plus segments of boundary curves.

We turn now to the search for extremals.

The first Euler equation leads to the expression

$$\lambda\frac{d\mu}{d\nu} - \lambda_0 = \frac{d\lambda}{d\tau}, \tag{11}$$

from which, for $\mu = \mu_0 + k\nu$, we will have

$$\lambda = \frac{\lambda_0}{k} - C_1 e^{k\tau}, \tag{12}$$

and, for the most important case when $\mu = \mu_0 = \text{const}$,

$$\lambda = C_2 - \lambda_0\tau. \tag{13}$$

The second Euler equation, after some transformation, is written in the form

$$\frac{2\omega}{1-\omega^2} = \lambda. \tag{14}$$

We note particularly that (14) does not contain Φ and is valid for any magnetic flux (in addition to the trivial case $\Phi = 0$).

To find the control law for magnetic flux, we use the third Euler equation.

By differentiation of F with respect to Φ^2, we get

$$\frac{\partial F}{\partial \Phi^2} = \frac{2\omega^2}{1+\omega^2} - \lambda\frac{2\omega}{1+\omega^2}. \tag{15}$$

By substituting the value of λ from (14) in (15) , we convince ourselves that $\partial F / \partial \Phi^2$ can not vanish and, consequently, $\Phi^2(\tau)$ which maximizes integral (5) can not be extremal, but is a boundary curve, i.e., $\Phi = 1$.

The optimal voltage control law is a control such that, with account taken of the voltage drop in the stator winding, the magnetic flux will be maintained constant.

The optimal laws of current frequency variation in the rotor will be :

for $\mu = \text{const}$,

$$\frac{2\omega}{1-\omega^2} = C_2 - \lambda_0\tau; \tag{16}$$

for $\mu = \mu_0 + k\nu$

$$\frac{2\omega}{1-\omega^2} = \frac{\lambda_0}{k} - C_1 e^{k\tau}. \tag{17}$$

For constant magnetic flux, the law of rotor frequency variation also determines the optimal law of variation of the motor's rotational torque as a function of time. By knowing the motor's torque and its mechanical time constant, we determine the rotor's speed of rotation and, thereby, the optimal law for supply frequency variation.

This law will be valid until the rotor's speed of rotation reaches its limiting value, bounded by (9). After reaching this limiting speed, one must transfer

Since the extremals must, at the junction point, coincide with the boundary curves tangent to them [1], then the equalitites $M = \mu$ and $d\nu/d\tau = 0$ must hold for the transition points.

Optimal Control Law for Electric Drives of the Second Group

The problem of optimal control for electric drives of the second group is formulated mathematically as follows: to find $\omega(\tau)$ and $\Phi^2(\tau)$ which maximize (6) for a given value of (4), for given relational equations (2) and (3) and given limitation (8). Thus, the optimal control problem for electric drives of the second group is analogous to that for those of the first group, with the sole difference that the auxiliary function will now have the form

$$F_1 = \frac{2\Phi^2\omega}{1+\omega^2} - \lambda_0 \nu' + \lambda\left(\nu' + \mu - \frac{2\Phi^2\omega}{1+\omega^2}\right). \quad (18)$$

The first Euler equation is now written in the form

$$\lambda \frac{d\mu}{d\nu} = \frac{d\lambda}{d\tau}. \quad (19)$$

The second Euler equation will be

$$\frac{1}{1-\omega^2} = \lambda.$$

From the third Euler equation, with account taken of (8), we get, just as for electric drives of the first group, that the magnetic flux, for optimal control, must be maintained constant ($\Phi = 1$). For $\mu = \mu_0 + k\nu$ we obtain, from (19) and (14), the expression for the optimal control law for the current frequency in the rotor:

$$\frac{2\omega}{1-\omega^2} = C_3 e^{k\tau}. \quad (20)$$

It follows from this that the rotational torque must increase as the drive starts up. For k = 0, i.e., for μ = const, it follows from (20) that ω = const. Thus, we arrive at the important conclusion that, for constant impedance torque, the optimal control law for electric drives of the second group amounts to maintaining constant current frequency in the rotor, and consequently, constancy of the rotational torque. With this, the drives rotational speed will vary linearly and, consequently, the supply frequency must also vary as a linear function of time [6].

On the basis of the duality principle of variational calculus [1], all the optimal laws derived by us from the assumptions that the quantity of heat was given, and that it was required to provide the greatest translation (or change of speed), will also remain valid for the case when the translation and the time are given, and it is required to provide minimum dissipation. The same laws also remain valid when the time of translation and the heat dissipation are given, and it is required to provide the minimum time of translation.

The optimal control laws for asynchronous electric motors have great similarity to the optimal laws for dc motors [3-5]. If we compare the dependence of rotational torque on time for optimal control, then the optimal control law for dc motors turns out to be the limiting case of the optimal law for asynchronous motors with the condition that the latter's maximum torque tends to infinity. In an optimally controlled asynchronous motor, the frequency in the rotor is always less than critical, and the rotational torque is less than maximal.

It should also be mentioned that the maximum torque of an optimally controlled asynchronous motor is larger than the maximum torque of a motor with a constant voltage on its terminal, since for critical slipping, due to the voltage drop in the stator winding, the motor's magnetic flux is less than the nominal value. With optimal control, when the magnetic flux is maintained constant, the maximum torque is 1.5 to 2 times greater than what is stated in the catalogs.

Figure 2 shows an example of optimal control for a motor in which critical slipping equals 0.2, the maximum torque multiplicity (for complete magnetic flux) equals 5, the mechanical time constant is $T_M = 1.82$ seconds, the impedance torque is constant and equal to the nominal value, and the electric drive falls in the first group.

Determination of the Coefficients in the Extremal Equations

We had found the extremal equations in a general form. For practical use of the optimal control laws found, it is necessary to know, in each concrete case, the coefficients in the extremal equations as functions of the given electric-drive parameters.

We consider electric drives of the first group, with constant impedance torques. Extremal (16) is known,

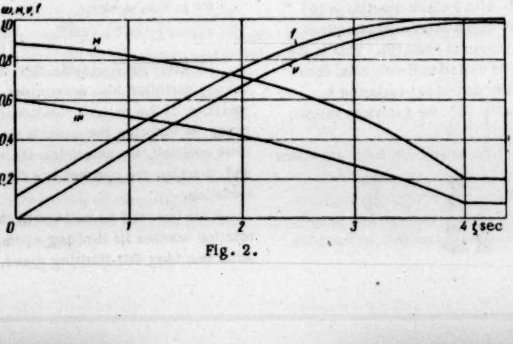

Fig. 2.

from control by extremals (16) or (17) to control by boundary curves, i.e., it is necessary to maintain $\nu = \nu_{max}$ and $M = \mu$ and, consequently, ω = const. and we now derive useful auxiliary formulas. By carrying out a change of variables in (2), (3), and (4) on the basis of (16), and then integrating, we get

$$\nu_2 - \nu_1 = \frac{2}{\lambda_0}\left[\frac{1}{1-\omega^2}\right]_{\omega_2}^{\omega_1} - \mu\tau, \tag{21}$$

$$Q = \frac{2}{\lambda_n}\left[\frac{\omega}{1-\omega^2} - \operatorname{arc\,tanh}\omega\right]_{\omega_2}^{\omega_1}. \tag{22}$$

We recall the self-evident formula

$$\nu = f - s_{cr}\,\omega, \tag{23}$$

where f is the stator frequency in relative units and s_{cr} is the critical slipping.

By using these formulas one can, on the basis of the given parameters of the electric drive and the characteristics of the transient response, find the coefficients in the extremal equations. For the example given, let it be required that the electric motor with critical slipping s_{cr} and impedance torque μ_0 start the drive, within time T_0, from initial speed $\nu_1 = 0$ to speed ν_2, corresponding to stator frequency $f = 1$. The dissipation during starting time T_0 must not exceed Q_0. The electric drive falls in the first group and, consequently, the optimal control problem is to provide maximum translation in time T_0. We know extremal (16). We determine the coefficients C_2 and λ_0 which appear in (16). We start by determining rotor frequency ω_2, corresponding to the end of the start-up period. From the equation

$$\frac{2\omega_2}{1+\omega_2^2} = \mu_0$$

we find ω_2, after which, from (23), we find $\nu_2 = 1 - s_{cr}\omega_2$.

Now, (21) and (22) give us a system of two equations for determining the two unknowns ω_1 and λ_0:

$$\nu_2 = \frac{2}{\lambda_0}\left[\frac{1}{1-\omega^2}\right]_{\omega_2}^{\omega_1} - \mu_0 T_0,$$

$$Q_0 = \frac{2}{\lambda_0}\left[\frac{\omega}{1-\omega^2} - \operatorname{arc\,tanh}\omega\right]_{\omega_2}^{\omega_1}.$$

Knowing ω_1, we determine the coefficient $C_2 = 2\omega_1/(1-\omega_1^2)$ in (16).

SUMMARY

1. For the frequency control of asynchronous motors, there exists an optimal control law of frequency as a function of time which provides maximum yield of the electric drive for given limitations on heating.

2. The optimal control law depends on the conditions imposed on the electric drive, and on the law of variation of the impedance torque. For electric drives of the first group, the optimal control law will be given by (17) and, for those in the second group, by (20). The voltage control law is the same for both groups, and amounts to maintaining the constancy of the motor's magnetic flux.

LITERATURE CITED

1. M. Lavrent'ev and L. Lyusternik, Fundamentals of Variational Calculus. 1 [in Russian] (ONTI, 1935).
2. L. A. Syromyatnikov, Operating Modes of Asynchronous Electric Motors [in Russian] (Gosénergoizdat, 1955).
3. K. L. Kozhevnikov, "Motor current diagrams for auxiliary mechanisms of rolling mills," Élektrichestvo No. 6 (1956).
4. E. A. Rozenman, "On optimal transient responses in systems with power limitations," Avtomatika i Telemekhanika 18, 6 (1957).
5. E. A. Rozenman, "On the limiting speed of response of servosystems with limitations on power, torque, and speed of the executive element," Avtomatika i Telemekhanika 19, 7 (1958).
6. A. A. Bulgakov, Frequency Control of Asynchronous Electric Motors [in Russian] (Izd. AN SSSR, 1955).

ON A DRIVE SCHEME WITH A GIVEN EQUATION OF MOTION*

I. A. Boguslavskii

(Moscow)

Translated from Avtomatika i Telemekhanika, Vol. 21, No. 3, pp. 340-343, March, 1960

Original article submitted May 15, 1959

A method is presented for the construction of a drive scheme with a given equation of motion wherein operational amplifiers are not employed.

In designing an automatic control system controlled by disturbances (cf. [1]) and also in various modelling schemes, it is frequently necessary to have a drive with a given equation of motion. This means that the drive's output coordinate x(t) (angular velocity, or angular displacement of the drive's output axis) must be related to the input coordinate f(t) (for example, with the arbitrarily varying angle of rotation of a potentiometer slider) by a given differential equation of the form

$$\sum_{k=0}^{n} a_k \frac{d^k x(t)}{dt^k} = \sum_{k=0}^{m} b_k \frac{d^k f(t)}{dt^k}. \qquad (1)$$

The problem just formulated is easily solved under the following conditions:

1) if the drive is shunted by a total feedback path for angle or for angular velocity such that the servosystem thus obtained follows, with high static and dynamic accuracy, the output coordinate x(t) by some input voltage u(t) and, consequently,

$$x(t) = ku(t), \qquad (2)$$

where k is a scale factor;

2) if, using operational amplifiers, one constructs an electronic scheme in which the output voltage u(t)** is related to the input f(t) by the equation obtained by replacing x(t) by ku(t) in (1).

However, in certain conditions of industrial usage, an electronic scheme may turn out to be inapplicable due to its complex voltage supply, zero drift of the operational amplifiers, etc. It is therefore advantageous to consider the possibility of replacing an electronic operational circuit by one composed of passive R and C elements (resistors and capacitors) which is free from the disadvantages mentioned above. However, a circuit of passive elements can be used directly only in solving certain special types of differential equations. For example, even for an equation which describes a simple oscillatory link, an RC circuit, as is well known, does not permit an accurate solution. In addition, the direct use of a circuit of passive elements (even in those cases where this is theoretically possible) is inconvenient in that a change in the coefficients of (1) requires, as a rule, a change in the parameters of all the passive elements. We shall show that a circuit with passive elements can be freed of the disadvantages cited if a voltage proportional to x(t) is applied to certain of its links. In this case, the drive, together with the basic direct negative feedback, is shunted by several indirect feedback paths (Fig. 1), and thus participates directly in the solution of (1). The servo amplifier which directly controls drive operation does not fall into the category of operational amplifiers due, for example, to the completely different requirements on gain stability.

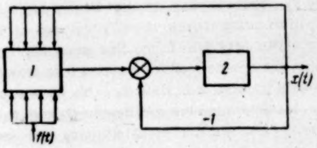

Fig. 1. 1 is the circuit of passive elements, 2) is the drive.

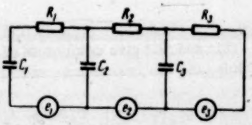

Fig. 2.

For simplicity, we present the proposed principle for drive design in the case when (1) has the form

$$(p^3 + a_2p^2 + a_1p + a_0)\,x(t) = \\ = (b_2p^2 + b_1p + b_0)\,f(t), \qquad (3)$$

where the a_i and b_i are given constant coefficients and p = d/dt.

---

*The material in this paper is contained in the author's paper at the Second All-Union Conference on Automatic Control Theory.

**Note that "u(t)" is used for both input and output voltage [translator's note].

In the general case, the circuit design is carried out analogously.

We consider the electric circuit (Fig. 2) in which the R_i and C_i are constant resistors and capacitors, chosen from technical considerations, and the e_i are certain voltage sources with zero internal impedance. In analyzing the circuit, for example, by the method of loop currents, we find that u, the voltage taken off capacitor C_1, satisfies the equation

$$(p^3 + A_2p^2 + A_1p + A_0)u = (B_2p^2 + = \tag{4}$$
$$= B_1p + B_0)e_1 + (D_1p + D_0)e_2 + C_0e_3,$$

where the A_i, B_i, D_i, and C_0 are constants, easily expressed in terms of the circuit parameters.

We require the holding of (2) and of the conditions

$$e_1 = \frac{1}{k}[k_{x1}x(t) + k_{f1}f(t)], \tag{5}$$

$$e_2 = \frac{1}{k}[k_{x2}x(t) + k_{f2}f(t)], \tag{6}$$

$$e_3 = \frac{1}{k}[k_{x3}x(t) + k_{f3}f(t)], \tag{7}$$

where the k_{xi} and k_{fi} are certain positive or negative constants, defined successively by the relationships

$$A_2 - B_2k_{x1} = a_2, \tag{8}$$
$$A_1 - B_1k_{x1} - D_1k_{x2} = a_1, \tag{9}$$
$$A_0 - B_0k_{x1} - D_0k_{x2} - C_0k_{x3} = a_0, \tag{10}$$

$$B_2k_{f1} = b_2, \tag{11}$$
$$B_1k_{f_1} + D_1k_{f_2} = b_1, \tag{12}$$

$$B_0k_{f_1} + D_0k_{f_2} + C_0k_{f_3} = b_0. \tag{13}$$

By a direct substitution of e_1, e_2, and e_3 in (4), we easily convince ourselves that, if (5)-(13) hold, x(t) and f(t) satisfy the original (3) and, consequently, the construction just described solves the problem posed. As was previously stated, (2) holds as the result of constructing a high-quality system for following x(t) by the voltage u(t). If x(t) is the angular velocity of the output shaft's rotation then, to realize (5), (6), and (7), with the shaft, in addition to the tachometer generator of the direct feedback path, there must be connected three dc tachometer generators whose output voltages are divided by special potentiometers in accordance with the coefficients k_{xi} and then introduced into the proper places in the circuit (Fig. 3). In addition, to the axis rotating to the angle f(t) there must be attached the sliders of three potentiometers with insulated voltage supplies and output voltage dividers operating in correspondence with coefficients k_{fi}. The practical values of R_1, R_2, and R_3 in Fig. 3 are not less than the order of the large divider impedances shunted by the internal impedances of the tachometer generators. Therefore, A_i, B_i, and C_i can be determined without the internal impedances of the voltage supplies being taken into account.

If x(t) is the angular rotation of the output shaft, then to it, in addition to the potentiometer of the direct feedback path, there are connected the sliders of three potentiometers with insulated voltage supplies and with the corresponding dividers. We emphasize that, for any change in the coefficients of (3), the parameters of the passive circuit (the quantities R_i and C_i) are not changed. When there are new values of the k_{xi} and the k_{fi}, only the positions of the divider sliders are subject to change. In an analogous manner, by the use of a passive circuit composed of n series-connected RC networks, n + 1 mutually insulated voltage supplies proportional to x (t), n insulated voltage sources proportional to f(t), and the corresponding number of dividers, one can construct a drive with equation of motion (1) for n > m. By having several circuits of passive elements and several drives with the corresponding number of insulated voltage sources proportional to their output coordinates, one can, by applying portions of these voltages to various points of the circuit, construct a system of drives with given

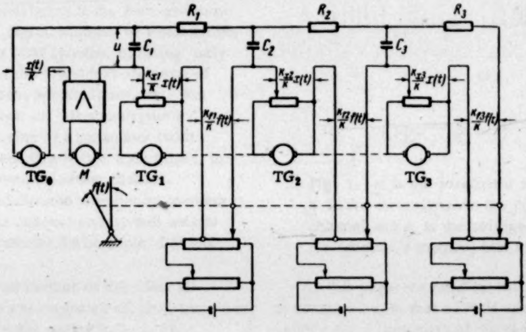

Fig. 3.

interrelationships of the equations of motion. The method described also applies, in an uncomplicated way, to the case when coefficients a_i and b_i of (1) are given functions of time, differentiable a definite number of times. For example, in (3) let $a_0 = a_0(t)$, $a_1 = a_1(t)$, and $a_2 = a_2(t)$.

Then, coefficients k_{xi} in (5)-(7) should be considered as unknown functions of time. As a simple verification, we show that x(t) will satisfy (1) for variable a_i if the functions $k_{xi}(t)$ are successively determined from the following relationships :

$$A_2 - B_2 k_{x1} = a_2(t),$$

$$A_1 - B_1 k_{x1} - 2B_2 \frac{dk_{x1}}{dt} - D_1 k_{x2} = a_1(t),$$

$$A_0 - B_0 k_{x1} - B_1 \frac{dk_{x1}}{dt} - B_2 \frac{d^2 k_{x1}}{dt^2} - D_0 k_{x2} - D_0 \frac{dk_{x2}}{dt} - C_0 k_{x3} = a_0(t).$$

If we , by using the proper elements, move the sliders of the dividers in accordance with the laws $k_{x1}(t)$, $k_{x2}(t)$, and $k_{x3}(t)$, we can implement the realization of a drive with equation of motion (3) for variable $a_0(t)$, $a_1(t)$ and $a_2(t)$.

The static accuracy of the solution of (1) by the drive is determined by the stability of the coefficient $\underline{k}$ in (2), the stability of the values of the R_i and C_i, and by the accuracy of positioning the dividers' sliders for the formation of coefficients k_{xi} and k_{fi}. The dynamic accuracy of the solution of (1) by the drive will be the higher, the wider is the frequency passband of the drive's servosystem, providing for the holding of (2), as compared with the bandwidth of the fundamental frequencies of the solution of Eq. (1).

LITERATURE CITED

1. V. S. Kulebakin, "On the basic problems and methods of increasing the quality of automatic control systems," in Proceedings of the Second All-Union Conference on Automatic Control Theory. 2 [in Russian] (Izd. AN SSSR, 1955).

ON THE NOISE IMMUNITY OF THE DISCRETE-INCREMENTAL METHOD OF INFORMATION TRANSMISSION

V. M. Baikovskii

(Moscow)

Translated from Avtomatika i Telemekhanika, Vol. 21, No. 3, pp. 344-358, March, 1960
Original article submitted August 28, 1959

The potential noise immunity (noise stability) of discrete-incremental modulation (DIM) with fluctuation noise is determined. Comparisons are made of the noise immunity of pulse-code modulation (PCM), deltamodulation(DM) and DIM. It is shown that, in a number of cases, the noise immunity of DIM is higher than of PCM and DM.

INTRODUCTION

In remote action telemetry systems, the communications channel is the most essential element, and determines the entire construction and, often, the accuracy of the system. This is true of telemetering apparatus in energy systems and gas and oil pipelines where it is necessary to transmit a series of parameters over distances of up to hundreds of kilometers. This is also characteristic of radiotelemetric systems, widely used in aviation for controlling various moving objects (including those used in space explorations), etc.

In designing such telemetry systems, the form of signal and the type of modulation are selected, not only from considerations of the best construction of the transforming devices, but also as a function of the channel's noise level and other characteristics.

Recently, many designers have been turning to discrete methods of transmitting data which, distinguished by their high equipment accuracy, permit high noise immunity to be attained. These methods acquire particular value from the broad development of digital technology.

Certain forms of discrete modulation had already been frequently considered as applied to communications problems. Pulse-code modulation is the first, and most highly developed, of the digital methods of transmission. There are many different PCM systems, differing only by the implementation of the individual elements of the apparatus: transformers, accumulators, etc. But there is one thing common to all these systems: the complete instantaneous value of a parameter (with account being taken of quantization) is transmitted, in coded form, along the communication channel.

There later appeared discrete modulation methods in which the signal in the channel corresponds only to the increment of the parameter, for example, DM and delta-PCM.

Recently, still another method of this class for transmitting information was suggested—digital-incremental modulation ("incremental coding") [1, 2, 3]. Incremental coding arose in connection with the desire to increase the efficiency of transmitting data along a channel by exploiting the statistical properties of the information to be transmitted. If the assumption in PCM is that each successive parameter value is not related to the previous one, in DIM the design is based on the assumption that there is a comparatively peaked (at least, nonflat) correlation function for the information.

The DIM operating principle is clearly elucidated in Fig. 1. The basic difference between this modulation method and those of PCM and DM is that here a signal is sent through the channel only at the moments when the measured quantity passes through a quantization level. If it stays within the limits of one quantization step, then no signal appears. Thus, transmission occurs irregularly: the more slowly the information changes, the more rarely are pulses sent through the channel.

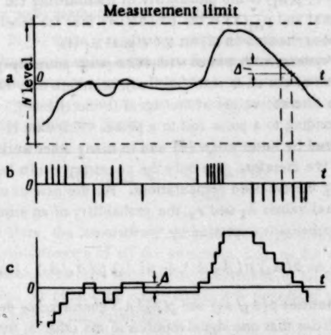

Fig. 1. a is the parameter to be transmitted b is the error signal in the communications channel, and c is the voltage at the output of the receiver's memory block.

In this paper we consider the noise immunity of DIM as compared with that of PCM and DM. As criteria for judging noise immunity of discrete telemetry systems, we adopt here the mathematical expectation of the error (the mean error) and the dispersion of the error (the squared mean-square error). We have obviously made the assumption that the error's probability distribution function is sufficiently completely characterized by its first two moments.

Potential DIM Noise Immunity for One Particular Case

To estimate the effect of fluctuation noise on a discrete system for information transmission, it is convenient to use V. A. Kotel'nikov's theory of potential noise immunity. It consists essentially of the following:

Let the set of signals $\{A(t)\}$ be used for transmission. When signal $A_i(t)$ is sent, then, due to the action of noise, the following total quantity is applied to the receiver:

$$X(t) = A_i(t) + W(t), \qquad (1)$$

where W(t) is a normal fluctuation oscillation. Depending on the value of X(t), the receiver identifies it with (or assimilates it to) one of the possible signals $A_j(t)$ of $\{A(t)\}$ with some probability of error. The potential noise immunity defines the probability of signal distortion as the result of the action of noise, for reception by an ideal receiver.

An ideal receiver is characterized as one for which this probability of incorrect reproduction will be the least for a given form of signal (given energy) and a definite specific energy (per unit bandwidth) of the fluctuation noise. In other words, the ideal receiver reproduces the information, corresponding to that signal, which maximizes the expression

$$p(A_i)\, p_{A_i}(X). \qquad (2)$$

Here, $p(A_i)$ is the probability of transmitting the ith signal and $p_{A_i}(X)$ is the probability that the receiver reproduces the sum in (1) as the signal $A_i(t)$.

In systems with DM or with PCM (with pulse-by-pulse reception of the code combinations), there are only two possible discrete values of the signal in the channel, corresponding to a pulse and to a pause. This case is considered by Kotel'nikov [4] and in many other works [5, 6]. We therefore give only the necessary results here, omitting the detailed computations. For the case of only two signal values A_1 and A_2, the probability of an error in transmission is expressed by the formula

$$p_{\text{dis}} = p(A_1)\, p(A_2/A_1) + p(A_2)\, p(A_1/A_2). \qquad (3)$$

The quantities $p(A_1/A_2)$ and $p(A_2/A_1)$ characterize the probabilities that one signal transfers to the other as the result of the action of fluctuation noise. In correspondence with [4], they equal

$$p(A_2/A_1) = V(\alpha_{21}), \quad p(A_1/A_2) = V(\alpha_{12}), \qquad (4)$$

where

$$V(x) = \frac{1}{\sqrt{2\pi}} \int_x^{\infty} e^{-\frac{z^2}{2}}\, dz,$$

and

$$\alpha_{21} = \alpha + \frac{1}{2\alpha} \ln \frac{p(A_1)}{p(A_2)}, \quad \alpha_{12} = \alpha + \frac{1}{2\alpha} \ln \frac{p(A_2)}{p(A_1)}.$$

Thus, the potential noise immunity is defined by the two quantities :$p(A_1)/p(A_2)$ —the ratio of the a priori probabilities of the two signals—and the quantity α, which characterizes the ratio of the mean energy difference of these signals to the specific energy of the noise, i.e.,

$$\alpha = \sqrt{\frac{1}{2\sigma^2} \int_{-\frac{T}{2}}^{+\frac{T}{2}} [A_1(t) - A_2(t)]^2\, dt}. \qquad (5)$$

Here, T is the signal duration and σ is the specific energy of the noise (intensity), which is defined so that

$$\overline{W^2(t)} = \int_0^{\infty} \sigma^2(\omega)\, d\omega. \qquad (6)$$

Since the quantity to be transmitted in telemetry is always bounded by definite limits, then, on the average, over a sufficiently long interval of its variation, one can consider the appearances of pulses and pauses for DM and PCM to be equiprobable.

Consequently,

$$p(A_1) = p(A_2) = \frac{1}{2}, \qquad (7)$$

$$\alpha_{12} = \alpha_{21} = \alpha.$$

As a result, we obtain

$$p(A_1/A_2) = p(A_2/A_1) = V(\alpha). \qquad (8)$$

Discrete-incremental modulation differs from the foregoing in that the signal can assume three values. In the channel appear the values +1 or −1 when the measured quantity goes through a quantization level and the value 0, if the quantity does not go beyond the bounds of one quantization step. Thus, there are the signals $A_1(t) = +1$, $A_2(t) = 0$ amd $A_3(t) = -1$, with probabilities $p(A_1)$, $p(A_2)$ and $p(A_3)$. With this, and for the same reasons as for (7), we can assume that $p(A_1) = p(A_3)$ and, moreover, that $p(A_2) > p(A_1) = p(A_3)$, since only in this case is DIM meaningful.

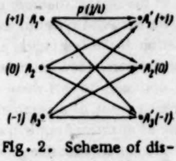

Fig. 2. Scheme of discrete channel (DIM).

The scheme for a channel with discrete-incremental modulation is shown in Fig. 2. According to this scheme, the probability of error for DIM may be found from the formula

$$p_{\text{er}} = \sum_{i=1}^{3} \sum_{j=1}^{3} p(A_i)\, p(A_j/A_i) \quad (i \neq j). \qquad (9)$$

The values of the probabilities $p(A_j/A_i)$ depend on which pulse signs are used for transmission.

In its general form, the problem is difficult to solve even with three signals. It is impossible to find an expression for the probability of distortion in a simple and graphic form, convenient for computations and for comparisons with the analogous expressions for other systems. We therefore consider one simple special case of signal transmission by DIM, and we then show that the results obtained can be used for an approximate estimate of noise immunity in a number of other cases.

We assume that to signals $A_1(t)$ and $A_3(t)$ there correspond identical video pulses of different polarity. Let their transmission be implemented by the so-called synchronous method, i.e., the pulses can be applied to the channel only at regular time intervals, or multiples thereof. Therefore, the intervals between pulses are multiples of some quantity T_{min} chosen, just as in DM, from the condition that there be reproduced the portion of the information with the greatest steepness (the overshoot). In this case, the analysis of noise immunity (cf. the Appendix) allows us to construct, for the ternary channel characterized by the scheme of Fig. 2), the matrix of transition probabilities:

$$\begin{array}{c|ccc|} & A_1' & A_2' & A_3' \\ A_1 & 1-V(\alpha') & V(\alpha')[1-V(\alpha''')] & V(\alpha')V(\alpha''') \\ A_2 & V(\alpha'') & 1-2V(\alpha'') & V(\alpha'') \\ A_3 & V(\alpha')V(\alpha''') & V(\alpha')[1-V(\alpha''')] & 1-V(\alpha') \end{array} \qquad (10)$$

To determine the mathematical expectation and the dispersion of the error, it is necessary to find the "value" or the weight of each individual error ξ_{ij}. The "value" of an error for discrete-incremental modulation is easily determined if we turn back to Fig. 1.

When, under the action of noise, signal A_2 goes over to A_1, or A_3 goes over to A_2, the step function voltage in the receiver will be changed by quantity Δ, i.e., for $(A_2 \to A_1)$ and $(A_3 \to A_2)$, $\xi = +1$ and, analogously, for $(A_2 \to A_3)$ and $(A_1 \to A_2)$, $\xi = -1$. If $(A_3 \to A_1)$ or $(A_1 \to A_3)$, then $\xi = \pm 2$.

Since it was accepted that signals A_1 and A_3 are equiprobable, the system of signals is symmetric, and the average of the error equals zero:

$$MU_{er} = \sum_{i=1}^{3}\sum_{j=1}^{3} p(A_i)\,p(A_j/A_i)\,\xi_{ij} = 0 \qquad (i \neq j). \qquad (11)$$

According to probability theory,

$$D\xi = M(\xi - M\xi)^2.$$

Thus, taking into account that $M\xi = 0$, we find that

$$DU_{er} = \Delta^2 D\xi = \Delta^2 M\xi^2. \qquad (12)$$

By using (9), we find that

$$DU_{er} = \Delta^2\{2p(A_2)V(\alpha'') + 2p(A_1)V(\alpha')[1 - V(\alpha''')] + 8p(A_1)V(\alpha')V(\alpha''')\}. \qquad (13)$$

We now introduce the concept of the probability p_n of a transition of the quantity to be transmitted through a quantization level. Obviously, this quantity depends on the character of the variation of the parameter to be transmitted. The steeper the correlation function, the smaller is the value of p_n. From what was said above, it follows that $p_n = 2p(A_1)$. By keeping in mind that $p(A_2) = 1 - 2p(A_1)$, and by denoting $p(A_2)/p(A_1) = K$, we obtain the final expression for the dispersion of the error for DIM:

$$DU_{er} = \Delta^2 p_n[KV(\alpha'') + V(\alpha') + 3V(\alpha')V(\alpha''')]. \qquad (14)$$

It follows from (14) that the noise immunity of this type of modulation is connected with the statistical properties of the ensemble of possible communications. An analysis of this dependence was given in [2].

On the Approximate Estimate of Noise Immunity of DIM in the General Case

It is obvious that, in addition to the one considered other methods of DIM transmission can be used. However, of all the possible methods, the only interesting ones from the practical point of view are those which are characterized by small values of the probabilities $p(A_1/A_3)$ and $p(A_3/A_1)$.

The determination of an exact analytical expression for noise immunity for each case in even this limited class poses mathematical difficulties.

In [4] there was given a method for the approximate estimation of noise immunity for the transmission of several discrete signals. It is based on the theorem that the probability P of at least one of m possible outcomes B_i lies within the limits

$$p(B_i)_{\max} \leqslant P \leqslant \sum_{k=1}^{m} p(B_i). \qquad (15)$$

Here, the lower limit corresponds to the complete interrelationship of all the outcomes, i.e., to the case when one outcome implies the occurrence of all the others. To obtain the upper limit, it is necessary that the outcomes be incompatible.

As applied to DIM, this inequality takes the form

$$\sum_{i=1}^{3} p(A_i)\,p^*(A_j/A_i)_{\max} \leqslant p_{dis} \leqslant \sum_{i=1}^{3}\sum_{j=1}^{3} p(A_i)\,p^*(A_j/A_i), \qquad (16)$$

where each $p^*(A_j/A_i)$ is determined, in accordance with (4), for each pair of signals without taking account of the others.

We considered several methods of transmission: for example, sending, for the signals $A_1(t)$ and $A_3(t)$, radio pulses with orthogonal frequencies, unipolar orthogonal video pulse, etc. Analysis showed that, for identical p pulse energy, the bounds on the error given by (16) for many methods of DIM transmission virtually coincided with those obtained in the case considered above. With this, the upper and lower bounds are so close that the region of error has the form of a very narrow ribbon (Fig. 3). By keeping this in mind, we can assume that the value of the error found for synchronous transmission of different polarity pulses characterizes, with adequate accuracy, the noise immunity of a number of other forms of DIM transmission. Therefore, in making our subsequent comparisons of noise immunity for the three forms of modulation, we shall use (14) to define the error with DIM (the dashed line on Fig. 3).

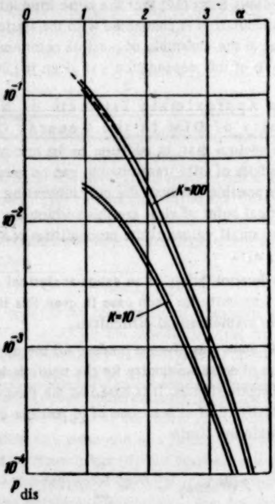

Fig. 3.

It was previously noted that the noise immunity of DIM is determined on the basis of the probabilities of suppression or of formation of false signals $A_1(t)$ and $A_3(t)$ (since $A_2(t) = 0$).

If we therefore replace the "ternary" ideal receiver by two, one of which receives $A_1(t)$ and $A_2(t)$ while the other receives $A_3(t)$ and $A_2(t)$, then the noise immunity will differ very little from the potential value. Computations show that the error arising with this is negligibly small. By taking this into account, we have the possibility, in making approximate estimates of noise immunity for DIM in many cases, to consider two identical binary channels separately. It is obvious that such an approach simplifies the selection of the most efficient methods of transmitting and receiving, and eases system design.

Comparison of Systems' Noise Immunity

For the comparisons, it is necessary to obtain expressions for the dispersion and mathematical expectation of the error for DM and PCM. With deltamodulation, the transition of one signal to the other in the channel (suppression of a pulse or the emergence of a false one) gives rise to a variation in the step function voltage in the receiver by the amount 2Δ. The error voltage with this can be expressed in the form $U_{er} = 2\Delta\xi$, where ξ is a random variable which assumes the values + 1 and − 1. Since these values are equiprobable, the mathematical expectation of the error equals zero:

$$MU_{\text{er}} = 2\Delta M\xi = 0 \qquad (17)$$

The dispersion of the error may be determined as

$$DU_{\text{er}} = 4\Delta^2 D\xi; \qquad (18)$$

since $M\xi = 0$, then $D\xi = M\xi^2$.

For deltamodulation,

$$M\xi^2 = 1\frac{1}{2}p(A_1/A_2) + 1\frac{1}{2}p(A_2/A_1). \qquad (19)$$

By taking (8) into account, we obtain

$$D\xi = V(\alpha). \qquad (20)$$

Thus, for DM

$$DU_{\text{er}} = 4\Delta^2 V(\alpha). \qquad (21)$$

In the case of code modulation, the value of the error depends on which pulse in the code group will be distorted. The value of each individual pulse with ordinal number k in a code group of n pulses is found from the formula

$$N_k = 2^{k-1}\Delta. \qquad (22)$$

Therefore, the error voltage is determined as

$$U_{\text{er}} = \sum_{k=1}^{n} 2^{k-1}\Delta\xi. \qquad (23)$$

Here the random variable, when noise acts, takes the values + 1 and − 1 and, otherwise, the value zero.

Exactly as in the previous case, we find that $MU_{\text{er}} = 0$ and

$$DU_{\text{er}} = D\sum_{k=1}^{n} 2^{k-1}\Delta\xi = \sum_{k=1}^{n} (2^{k-1})^2\Delta^2 D\xi. \qquad (24)$$

After some transformation, we find the formula for the dispersion of the error in the case of PCM:

$$DU_{\text{er}} = \frac{2^{2k}-1}{3}\Delta^2 V(\alpha). \qquad (25)$$

A) The case of a given average transmitter power. We now consider the conditions under which the systems' noise immunity should be compared.

1. We assume that there is no filtering of the signal in the receiver, but simply its recording by a sufficiently

fast-acting reproducing device. We therefore carry out the comparison by using (14), (21), and (25).

2. We assume that all the systems are designed for transmitting information with identical upper-frequency bounds F_u.

3. We assume that the quality of transmission is identical for identical numbers of levels of partitioning, i.e., that the discreteness errors Δ are equal.

4. We assume that the mean transmitter power P_{av} and noise level σ are the same for all cases.

5. We assume that the bandwidth and, consequently the duration of the pulses in the channel, is identical for all the systems.

For simplicity, we shall assume that the pulses are rectangular. With this, the signal energy entering into Formula (6) will equal $P_p\tau$ (here, P_p is the transmitter's pulse power).

Then, for the quantity α we obtain the expression

$$\alpha = \frac{1}{\sigma}\sqrt{\frac{P_p}{2}}\,\tau = \frac{1}{\sigma}\sqrt{\frac{P_{av}}{2}}\,T_t \tag{26}$$

for code and deltamodulation, and the expression

$$\alpha = \frac{1}{\sigma}\sqrt{\frac{P_p}{2}}\,\tau = \frac{1}{\sigma}\sqrt{\frac{P_{av}}{2}}\,T_{av} \tag{27}$$

for discrete-incremental modulation.

Here, the quantity T_{av} is the average duration of the time interval between neighboring pulses. It depends on the statistics of the information to be transmitted and, obviously, is related to p_n. Finding this relationship analytically in the general case entails mathematical difficulties, so that the magnitude of T_{av} is determined from the corresponding distribution, taken off experimentally from recordings of information typical of the given telemetry system.

The implementation of this investigation for several parameters subject to telemetering in industry, in energetics in particular [2], showed that the distribution of the intervals between moments when the parameter changed levels is close to a Poisson distribution. Indeed, if it be assumed that the transition probability p_n on the time segment $\Delta t = T_{min}$ depends on the length of this segment, i.e., $p_n = p_0\Delta t$, and is unrelated to the behavior of the process on the remaining segments, then this distribution will be described by the expression

$$H(t) = p_0 e^{-p_0 t}\Delta t, \tag{28}$$

and the magnitude of T_{av} can be found from the formula

$$T_{av} = \int_0^\infty t p_0 e^{-p_0 t}\,dt = \frac{1}{p_0}. \tag{29}$$

Since we have agreed that $p_n = p_0 T_{min}$, then

$$T_{av} = \frac{T_{min}}{p_n}. \tag{30}$$

In order to express the repetition period in terms of the quantity F_u for code modulation, we use the well-known relationship

$$f_t = 2F_u. \tag{31}$$

The pulse repetition frequency, in the case of delta-modulation, is chosen, as was mentioned earlier, from considerations of reproducing the maximum slope in the information to be transmitted $|dS(t)/dt|_{max}$. Just as in (7) and (8), we use the simplified expression

$$|\Delta| \approx \left|\frac{dS(t)}{dt}\right|_{max} T_t = \Omega_u T_t. \tag{32}$$

Thus, the repetition period for DM, or T_{min} for DIM, will equal

$$T_{IDM} = T_{min} = \frac{\Delta}{2\pi F_u}. \tag{33}$$

On the basis of what has been said earlier, we can write the expressions defining the quantity α for all three forms of modulation:

$$\alpha_{DM} = \frac{1}{\sigma}\sqrt{\frac{P_{av}}{2F_u}}\sqrt{\frac{\Delta}{\pi}}, \tag{34}$$

$$\alpha_{PCM} = \frac{1}{\sigma}\sqrt{\frac{P_{av}}{2F_u}}\sqrt{\frac{1}{2\lg_2\frac{1+\Delta}{\Delta}}}, \tag{35}$$

where $\lg_2[(1+\Delta)/\Delta] = n$ is an integer;

$$\alpha_{DIM} = \frac{1}{\sigma}\sqrt{\frac{P_{av}}{2F_u}}\sqrt{\frac{\Delta}{2\pi}(k+2)}. \tag{36}$$

Figure 4 shows the curves which characterize the potential noise immunity of the three forms of modulation considered, for two different values of Δ. It is clear from the figure that, for a given mean transmitter power,

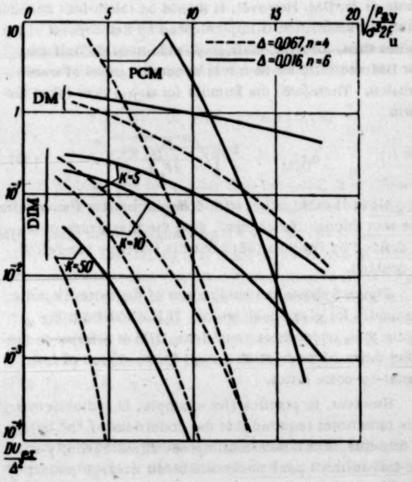

Fig. 4.

the noise immunity of a system with discrete-incremental modulation is always better than in a system with delta-modulation, and only sometimes worse than the noise immunity of a system with PCM. With this, pulse-code modulation turns out to have higher noise immunity than DIM for large numbers of levels to be transmitted and high transmitter power. For small signal-to-noise ratios, conversely, the dispersion of the error is less when DIM is used.

B) The case of given peak pulse power. We now compare the modulation forms we have been considering when the transmitter's peak power is given, retaining all the other conditions assumed under paragraph A.

In this case, (26) and (27) are changed. If we denote by q the mark-space ratio of the pulses, then these expressions will have the form:

$$\alpha_{\text{PCM}} = \frac{1}{\sigma}\sqrt{\frac{P_{\text{p}}}{2F_{\text{u}}\,q^2\lg\dfrac{1+\Delta}{\Delta}}}, \qquad (37)$$

$$\alpha_{\text{DM}} = \frac{1}{\sigma}\sqrt{\frac{P_{\text{p}}\Delta}{2F_{\text{u}}\,q\pi}}. \qquad (38)$$

As for the value of α_{DIM}, we must consider two cases:

a) when the duration of the pulses and the interval $T_{\min}$ are rigidly related to the quantity q ;

b) when the following conditions are imposed on the pulse duration:

$$\tau \leqslant \frac{T'_{\text{av}}}{q} \text{ and } \tau \leqslant T_{\min}$$

In the first case, the magnitude of τ will be the same as for DM. However, it should be taken into account that, if transmission is implemented by heteropolar video pulses then, for DIM, their amplitude must be half that for DM and PCM for identical dynamic ranges of transmission. Therefore, the formula for α_{DIM} now takes the form

$$\alpha_{\text{DIM}} = \frac{1}{\sigma}\sqrt{\frac{P_{\text{p}}}{2F_{\text{u}}q}\,\frac{\Delta}{4\pi}}. \qquad (39)$$

Now, if radio pulses with different carrier frequencies are sent through the channel, then the magnitude of α_{DIM} is defined by Formula (38), but the system's bandwidth is doubled.

Figure 5 shows the comparison of the system's noise immunity for given peak power. It is clear from the figure that, under these conditions, DIM is inferior to the other forms of modulation except in the region of low signal-to-noise ratios.

However, in practice (for example, in radiotelemetry) it is sometimes required that the conditions of "b" hold. In this case, limitations are imposed simultaneously on the transmitter's peak power and on its average power, but the pulse duration is not strictly given (except that $\tau \leq T_{\min}$). With this, the magnitude of α_{DIM} can be found from the formula

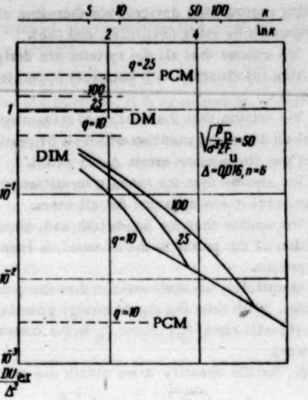

Fig. 5.

$$\alpha_{\text{DIM}} = \frac{1}{\sigma}\sqrt{\frac{P_{\text{p}}}{2F_{\text{u}}}\,\frac{\Delta}{4\pi}\,\frac{(K+2)}{2q}}. \qquad (40)$$

Thus, by increasing the duration of the pulses, one can improve the noise immunity of transmission and, simultaneously, reduce the required channel bandwidth. Broadening of the pulses is possible up to the point when the quantity (K + 2)/2q becomes equal to unity, after which the magnitude of α_{DIM} must remain constant. The improvement of the noise immunity of DIM as a function of K for various admissible mark-space ratios is shown in Fig. 6 .

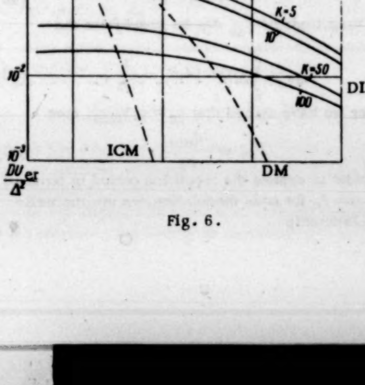

Fig. 6.

SUMMARY

1. The theory of potential noise immunity allows one to estimate the telemetering error with fluctuation noise for the discrete-incremental method of information transmission. An accurate and, at the same time, sufficiently simple expression for the probability of distortion with DIM could be found for only one special case—synchronous transmission of heteropolar pulses. However, this expression can be used for an approximate estimate of the error in a number of other cases.

2. If the signal-to-noise ratio is not very small and the probabilities $p(A_1/A_3)$ and $p(A_3/A_1)$ are much less than the remaining transition probabilities, then a communications channel with DIM may be considered as two individual binary channels, and transmission and reception methods can be chosen in correspondence with this.

3. Noise immunity of DIM is immediately related to the statistics of the messages to be transmitted: the greater the slope of the correlation function, the smaller the probability of error

4. The comparison of the noise immunity of the discrete systems* showed that, for given average power, DIM is always better than DM, and is inferior to PCM only for high signal-to-noise ratios and large numbers of quantization levels.

5. For given peak power and pulse duration, DIM has a practical noise immunity which is comparable to that of DM and significantly worse than for PCM.

For a given mark-space ratio, a gain can be achieved only at the cost of widening the pulses.

APPENDIX

Computation of the Transition Probability Matrix for DIM with Synchronous Transmission of Heteropolar Pulses

We determine the noise immunity for the given particular case of transmission with three discrete signals. For this we return to the basic propositions of the theory of potential noise immunity and to the definition of the ideal receiver which was given previously. We recall that, by Kotel'nikov's theorem, a signal which is limited to the time T and whose energy is lumped into some frequency band F may be completely characterized by a finite number 2FT of its values. These values are considered as the coordinates of the signal vector in a multidimensional space. The length of the vector is determined by the signal's average power, and equals

$$\sqrt{\sum_{r=1}^{2FT} a_r^2} = \sqrt{\overline{A^2(t)}}. \qquad (A.1)$$

Here, the a_r are the signal values at 2FT points uniformly distributed in time. Analogously, the fluctuation noise is represented by a random vector of length

$$\sqrt{\frac{\sigma^2}{2T}\sum_{l=1}^{2FT} \theta_l}, \qquad (A.2)$$

where θ_l is a normal random variable for which

$$p(z < \theta < z + dz) = \frac{dz}{\sqrt{2\pi}} e^{-\frac{z^2}{2}} \qquad (A.3)$$

The terminus of the total vector, corresponding to the oscillation X(t) can, with some probability, fall at various points of space. Therefore, the problem of the receiver is the correct identification of the received signal X(t) with that one of the signals which was transmitted during time T. Thus, the receiver's design principle is characterized by some division or other of the entire signal space into regions of correct reception of each of the signals $A_i(t)$.

In particular, for an ideal receiver, the configuration of the regions is so determined that it must reproduce the signal with the maximum value of the probability described by (2). With transmission of $A_i(t)$, the probability that signal X(t) falls in region dv of the 2FT-dimensional space equals

$$p_{A_i}(X) = \frac{dv}{\left(\sqrt{\frac{\pi}{T}}\sigma\right)^{2FT}} \times$$

$$\times \exp\left(-\frac{T}{\sigma^2}\overline{[X(t) - A_i(t)]^2}\right). \qquad (A.4)$$

Therefore, the ideal signal, in receiving oscillation X(t), will reproduce that signal for which the quantity

$$\frac{T}{\sigma^2}\overline{[X(t) - A_j(t)]^2} - \ln p(A_j) \qquad (A.5)$$

will be minimal.

Thus, when signal $A_i(t)$ of n possible signals is sent, the ideal receiver correctly reproduces the information corresponding to this signal if n-1 inequalities of the following form hold:

$$T\,\overline{[X(t) - A_i(t)]^2} - \sigma^2 \ln p(A_i) \leqslant$$

$$\leqslant T\,\overline{[X(t) - A_j(t)]^2} - \sigma^2 \ln p(A_j). \qquad (A.6)$$

If at least one inequality does not hold, then distortion arises. Analogous conditions are valid for all n signals.

There are the signals $A_1(t) = +1$, $A_2(t) = 0$ and $A_3(t) = -1$. Signal $A_2(t)$ is found at the origin of coordinates, and the radius vectors corresponding to signals $A_1(t)$ and $A_3(t)$ are equal in modulus and oppositely directed. The boundaries between the signal regions are two parallel planes, perpendicular to these radius vectors and symmetrically located with respect to the origin of coordinates (Fig. 7).

---

* We recall that the comparisons made were valid for messages in which the distribution of the intervals between pulses in the channel was close to a Poisson distribution.

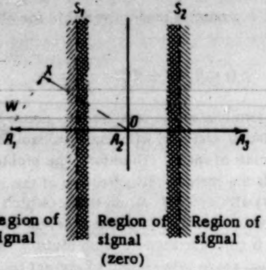

Fig. 7.

It is easily seen that, for distortion of signal $A_1(t)$, it suffices to violate just the one inequality

$$T\,\overline{[X(t)-A_1(t)]^2}-\sigma^2\ln p(A_1)<$$
$$\leqslant T\,\overline{[X(t)-A_2(t)]^2}-\sigma^2\ln p(A_2), \qquad (A.7)$$

since it is only possible to pass from the region of signal $A_3(t)$ to that of $A_1(t)$ by going through the region of signal $A_2(t)$.

We consider the inequality inverse to that of (A.7). By using (1), we may write

$$T\,\overline{[W(t)+A_1(t)-A_1(t)]^2}-\sigma^2\ln p(A_1)\geqslant$$
$$\geqslant T\,\overline{[W(t)+A_1(t)-A_2(t)]^2}-\sigma^2\ln p(A_2) \qquad (A.8)$$

or

$$T\,\overline{W^2(t)}\geqslant T\,\overline{W^2(t)}+2T\,\overline{W(t)\,[A_1(t)-A_2(t)]}+$$
$$+T\,\overline{[A_1(t)-A_2(t)]^2}-\sigma^2\ln\frac{p(A_2)}{p(A_1)}. \qquad (A.9)$$

By then taking into account that, in our case, $A_2(t)=0$, we use (2.60) of [1]:

$$\overline{W(t)\,A(t)}=\frac{\sigma}{\sqrt{2T}}\sqrt{\overline{A^2(t)}}\;\theta. \qquad (A.10)$$

Here, θ is the normal random variable of (A.3). After some transformation we obtain

$$0\geqslant\sigma\sqrt{2T}\sqrt{\overline{A^2(t)}}\;\theta_1+T\,\overline{A_1^2(t)}-\sigma^2\ln\frac{p(A_2)}{p(A_1)}. \qquad (A.11)$$

The probability that this inequality holds is $V(\alpha')$, so that

$$P_{\text{dis}}(A_1)=V(\alpha'). \qquad (A.12)$$

It is obvious here that

$$\alpha'=\frac{\sqrt{T\,\overline{A_1^2(t)}}}{\sigma\sqrt{2}}-\frac{\sigma}{\sqrt{2}\sqrt{T\,\overline{A_1^2(t)}}}\ln\frac{p(A_2)}{p(A_1)} \qquad (A.13)$$

By substituting $\alpha=\dfrac{\sqrt{T\,\overline{A_1^2(t)}}}{\sigma\sqrt{2}}$ and $\dfrac{p(A_2)}{p(A_1)}=K$,

we find

$$\alpha'=\alpha-\frac{1}{2\alpha}\ln K. \qquad (A.14)$$

Distortion of signal $A_2(t)$ corresponds to the holding of the inequalities

$$T\,\overline{[X(t)-A_2(t)]^2}-\sigma^2\ln p(A_2)\geqslant$$
$$\geqslant T\,\overline{[X(t)-A_1(t)]^2}-\sigma^2\ln p(A_1),$$
$$T\,\overline{[X(t)-A_2(t)]^2}-\sigma^2\ln p(A_2)\geqslant$$
$$\geqslant T\,\overline{[X(t)-A_3(t)]^2}-\sigma^2\ln p(A_3). \qquad (A.15)$$

It is easily shown that the probability of each inequality holding is the same for all, and equals

$$p(A_3/A_2)=p(A_1/A_2)=V(\alpha''), \qquad (A.16)$$

where

$$\alpha''=\alpha+\frac{1}{2\alpha}\ln K, \qquad (A.17)$$

and the probability

$$P_{\text{dis}}(A_2)=2V(\alpha''). \qquad (A.18)$$

Due to the symmetry of the system of three signals, we have

$$P_{\text{dis}}(A_3)=P_{\text{dis}}(A_1).$$

We can thus obtain the expression for the probability of error with discrete-incremental modulation in this particular case.

Since

$$P_{\text{er}}=\sum_{i=1}^{3}p(A_i)\,P_{\text{dis}}(A_i), \qquad (A.19)$$

then

$$P_{\text{er}}=2p(A_1)\,V(\alpha')+2p(A_2)\,V(\alpha''). \qquad (A.20)$$

Equation (A.20) characterizes the probability of distortion as a whole. For us to compute the errors, it is necessary to know the transition probabilities of each signal to the two others separately. For this, we consider in more detail the transmission of signals $A_2(t)$ and $A_3(t)$. Let signal $A_2(t)$ be transmitted. The probability that the ideal receiver reproduces precisely signal $A_2(t)$ at its output equals the probability of the simultaneous holding of the inequalities

$$p(A_1)\exp\left(-\frac{T}{\sigma^2}\,\overline{[X(t)-A_1(t)]^2}\right)\leqslant$$
$$\leqslant p(A_2)\exp\left(-\frac{T}{\sigma^2}\,\overline{[X(t)-A_2(t)]^2}\right),$$
$$p(A_3)\exp\left(-\frac{T}{\sigma^2}\,\overline{[X(t)-A_2(t)]^2}\right)\leqslant$$
$$\leqslant p(A_3)\exp\left(-\frac{T}{\sigma^2}\,\overline{[X(t)-A_3(t)]^2}\right). \qquad (A.21)$$

The probability that the first of these hold was already found earlier (A.12).

We consider the second inequality. We rewrite it in the form

$$T\,\overline{[X(t)-A_2(t)]^2}-\sigma^2\ln p(A_2)\leqslant$$
$$\leqslant T\,\overline{[X(t)-A_3(t)]^2}-\sigma^2\ln p(A_3). \qquad (A.22)$$

After multiplying out the parentheses and cancelling, we have

$$2T\,\overline{W(t)\,A_1(t)}+\overline{T\,A_1^2(t)}-\sigma^2\ln\frac{p(A_3)}{p(A_1)}\leqslant$$
$$\leqslant 2T\,\overline{W(t)\,[A_1(t)-A_3(t)]}+T\,\overline{[A_1(t)-A_3(t)]^2}. \qquad (A.23)$$

By taking into account that $|A_1(t)| = |A_3(t)|$ and $p(A_1) = p(A_3)$, we can write

$$2T\,\overline{W(t)\,A_1(t)}\leqslant 2T\,\overline{W(t)\,[A_1(t)-A_3(t)]}+$$
$$+3T\,\overline{A_1^2(t)}+\sigma^2\ln K. \qquad (A.24)$$

We now use Formula (A.10). Then,

$$\sqrt{2T}\sqrt{\overline{A_1^2(t)}}\,\theta_1\leqslant 2\sqrt{2T}\sqrt{\overline{A_1^2(t)}}\,\theta_{13}+$$
$$+3T\,\overline{A_1^2(t)}+\sigma^2\ln K. \qquad (A.25)$$

For the case considered, the quantities θ_1 and θ_{13} are equal, since they are the projections of one and the same vector on one and the same line. With this in mind, we obtain the inequality

$$0\leqslant 2\sqrt{2T}\sqrt{\overline{A_1^2(t)}}\,\theta_1+3T\,\overline{A_1^2(t)}+\sigma^2\ln K. \qquad (A.26)$$

The probability that this holds equals

$$1-V(\alpha'''), \qquad (A.27)$$

where

$$\alpha'''=3\alpha+\frac{1}{2\alpha}\ln K. \qquad (A.28)$$

The probability that the two inequalities in (A.21) hold simultaneously equals the product of the partial probabilities, i.e.,

$$p(A_2/A_1)=V(\alpha')\,[1-V(\alpha''')]. \qquad (A.29)$$

The probability of reproducing signal $A_3(t)$ instead of $A_1(t)$ is defined by the inequalities

$$p(A_1)\exp\left(-\frac{T}{\sigma^2}\overline{[X(t)-A_1(t)]^2}\right)<$$
$$<p(A_3)\exp\left(-\frac{T}{\sigma^2}\overline{[X(t)-A_3(t)]^2}\right),$$
$$p(A_2)\exp\left(-\frac{T}{\sigma^2}\overline{[X(t)-A_2(t)]^2}\right)\leqslant$$
$$\leqslant p(A_3)\exp\left(-\frac{T}{\sigma^2}\overline{[X(t)-A_3(t)]^2}\right). \qquad (A.30)$$

Since the regions of signals $A_3(t)$ and $A_1(t)$ do not have common boundaries, the first inequality should be replaced by the inequality

$$p(A_1)\exp\left(-\frac{T}{\sigma^2}\overline{[X(t)-A_1(t)]^2}\right)\leqslant$$
$$<p(A_3)\exp\left(-\frac{T}{\sigma^2}\overline{[X(t)-A_3(t)]^2}\right). \qquad (A.31)$$

After transformations analogous to those given above, we find† that

$$p(A_3/A_1)=V(\alpha')\,V(\alpha'''). \qquad (A.32)$$

Since $p(A_2/A_3)$ and $p(A_1/A_3)$ have the same value, it is then easy, from the data obtained, to construct the matrix of transition probabilities (10).

LITERATURE CITED

1. V. M. Baikovskii, R. R. Vasil'ev, and A. M. Petrovskii, "Application of the methods of information theory to the analysis and design of certain industrial telemetry systems," Otchet IAT AN SSSR (1956).
2. V. M. Baikovskii, "Discrete-incremental method of transmitting information in telemetering systems," Collection: Automatic Control [in Russian] (Izd AN SSSR, 1960).
3. J. Mass, "An incremental remote position control system," National Telemetering Conference (London, May, 1955).
4. V. A. Kotel'nikov, Theory of Potential Noise Immunity [in Russian] (Gosénergoizdat, 1956).
5. S. V. Borodich, "On the noise immunity of communications with pulse-code modulation," Radiotekhnika No. 5 (1949).
6. N. F. Zyuzev, "Noise immunity of deltamodulation for fluctuation noise," Trudy LKVVIA No. 136 (1955).
7. A. M. Petrovskii, "A method of computing noise immunity of a pulse communications system under fluctuation noise," Avtomatika i Telemekhanika 15, 2 (1954).
8. A. A. Kharkevich, Outlines of General Communication Theory [in Russian] (Gostekhizdat, 1954).

---

† Generally speaking, this can be obtained from simpler considerations, by taking into account (A.29) and that

$$P_{\text{dis}}\ (A_1)=p(A_2/A_1)+p(A_3/A_1).$$

FINITE AUTOMATA.II*

M. A. Aizerman, L. A. Gusev, L. I. Rozonoér,
I. M. Smirnova, and A. A. Tal'
(Moscow)

Translated from Avtomatika i Telemekhanika, Vol. 21, No. 3, pp. 359-368, March, 1960

In the second part of this work we continue the exposition of the authors' point of view on finite automata, the problems in the theory of finite automata, and the interrelationships of this theory with the ordinary theory of switching (in particular, relay contact) circuits. The general problem is posed of constructing automata operating in one time scale (i.e., with one partitioning of the continuous time axis into discrete points) from elements which operate in a different time scale. As examples of this type of system, we consider abstract neurons (neurons of the type proposed by McCulloch and Pitts) and neuron nets. Relay contact and, more generally, switching circuits are then simply one possible technical realization of abstract neuron nets.

6. Realizations of Automata Operating in a Given Time Scale from Automata Operating in a Different One

In the first part of this work it was assumed that both an automaton as a whole and all of the elements of which the automaton was assembled operate in one and the same time scale (the term "sequentiality" was used previously). As applied to the last remarks of section 5, related to technical realization, this meant, for example, that all the delay elements simultaneously received signals denoting the appearance of the next cycle (i.e., next moment of discrete time) from one and the same cycle transducer.

Here we shall be interested in the more general problem of constructing automata which operate in one time scale from automata operating in a different one.

We consider automaton A, defined by the equation

$$\varkappa(p) = F[\varkappa(p-1), \rho(p-1)], \qquad (1)$$

for which there is given partitioning of the time axis into cycles t = 0,1,2,..., p,..., defining the time scale T, and we construct a tape L of the states of this automaton which arise for some initial automaton state $\kappa(0) = \kappa_0$ and for some sequence of inputs $\rho = \rho(t)$. We transform this tape in the following way. From the sequence t = 0, 1, 2,..., p,..., we choose some increasing sequence of values of time $t_0, t_1, t_2, \ldots, t_i, \ldots$, and we pick out from the original tape those columns ρ, κ which correspond to the moments of time $t_0, t_1, \ldots t_i, \ldots$. The sequence of these columns, written in correspondence with the sequence of moments of time $t_0, t_1, \ldots, t_i, \ldots$, forms some new tape L^*. Still one more transformation may be carried out on tape L^* by recoding all the symbols written in row "κ"†. The recoding amounts to this, that all symbols from the $\{\kappa\}$ alphabet which appear on tape L^* are divided into groups, and each group is put into correspondence with some new symbol (which, in particular, may again be a symbol from the $\{\kappa\}$ alphabet). The symbols within any given group are not distinguished from each other, and one and the same new symbol corresponds to each of them. By replacing the symbols in column "κ" of tape L^* by the corresponding new symbols, we obtain tape L'.

It may certainly happen that there are contradictory triads on tapes L^* and L', although there were none on tape L. It is important to note that even if there are contradictory triads on tape L^*, it is possible that, thanks to the recoding, there will be none on tape L'. If there are contradictory triads on tape L', then this tape cannot be the state tape of any finite automaton. But if L' contains no contradictory triads, then it could have been obtained as the result of the operation of some finite automaton, operating in time scale T', defined by the sequence of moments of time $t_0, t_1, \ldots, t_i, \ldots$

We now assume that, for each possible state tape L of automaton A, it is possible to stipulate a sequence of moments of time $t_0, t_1, \ldots, t_i, \ldots$ and a method of recoding‡ such that the transformed tape L' would not contain contradictory triads. With this, let there be no contradictory triads even among the set of all the triads contained in the entire collection of transformed tapes. Then this set of transformed tapes can be considered as the set of state tapes of one and the same new finite automaton A', operating in the new time scale T'[**]. The alphabet $\{\kappa'\}$ of states of automaton A' is defined by the accepted method of recoding and contains, as is readily understandable, a number of symbols less than, or equal to, the number of symbols in alphabet $\{\kappa\}$. The alphabet $\{\rho'\}$ of inputs of automation A' is composed of all or some of the symbols of alphabet $\{\rho\}$. By numbering the moments of time $t = t_0, t_1, \ldots$ by the series of natural numbers $0, 1, \ldots, i, \ldots$ and by introducing the new time variable $t' = 0, 1, 2, \ldots, p', \ldots$, we can present the operation of the new automaton A' by an equation of the form

---

* For the first portion of this work, cf. Avtomatika i Telemekhnika No. 2 (1960).

† The symbols in row "ρ" will not be recoded although, to be sure, this is possible.

‡ For different tapes it is admissible to choose different sequences of time and different methods of coding (for example, the sequence of moments $t_0, t_1, \ldots, t_i, \ldots$ may be determined by the sequence of inputs $\rho(t)$ for which the given tape L was obtained; for an example of this type, see section 7 below). As a particular case, the sequence $t_0, t_1, \ldots, t_i, \ldots$ and the method of coding may be chosen independently of the appearance of any given tape.

$$\varkappa'(p') = F'[\varkappa'(p'-1), \rho'(p'-1)],$$

where $p' = i$ if $p = t_i$.

The problem of constructing a given automaton A', operating in time scale T', from elements operating in time scale T reduces to the realization, based on these elements, of an automaton A which, although operating itself in time scale T, may nonetheless be used, with some coding system and with the proper choice of a "new time", as the automaton A', operating in time scale T'. Automaton A' may be represented as consisting of automaton A and a special "reading" device. This device records, for each state tape L of automaton A, the moments of time $t_0, t_1, \ldots, t_i, \ldots$, reads the symbols for the state and inputs of automaton A at these moments of time, and puts out the notation for these symbols in the adopted coding system[††]. In contradistinction to the cycle transducer which was discussed at the end of section 5, the reading-coding device just described in no way acts on the elements of automaton A.

Automata thus constructed, operating in time scale T', must themselves serve as elements for the construction of nets (section 5), mapping automata operating in the new time scale.

The transition from automaton A to the new automaton A' was implemented by transforming discrete time t to t' and alphabet $\{\kappa\}$ to $\{\kappa'\}$. As was stated earlier, because of the possibility of contradictory triads making an appearance, not each such transformation translates a finite automaton into another finite automaton. The problem arises as to what sort of transformation of discrete time, in conjunction with a recoding of symbols, does not take the device under consideration out of the class of finite automata. Closely related to this question is the question as to which class of device the aforementioned reading-coding device belongs to, and whether it is itself a finite automaton.

We note in conclusion that the contents of sections 5 and 6 reduce to the determination of different structures which are maps of one and the same automaton. What we are saying, essentially, is that different structures, thanks to recoding of states and transformations of time, may be mappings of equivalent automata.

7. Two Methods of Constructing Automata by Transforming Time Scales

Let there be a set of elements, consisting of arbitrary instantaneously acting binary logical transformers and of one-cycle delay element symbols from the alphabet $\{0,1\}$. We assume for simplicity that the cycles are defined by a partition of the continuous time axis into identical intervals of duration τ. It is required to construct, from this set, an automaton forming a given automaton A':

$$\varkappa(p') = F[\varkappa(p'-1), \rho(p'-1)] \qquad (2)$$

with alphabets $\{\kappa\}$ and $\{\rho\}$, operating in a time scale defined by a partitioning of the time axis into identical intervals of length $l\tau$ (l 0– is an integer), i.e., into an l-fold decelerated time scale.

It was shown in section 5 that a net, mapping any given automaton of any time scale T', can be constructed from a set containing any logical transformers and from delay elements of the same time scale T'. We are now given logical transformers and delay elements in time scale T. The problem thus reduces to the construction, from delay elements in time scale T, of delay elements in time scale T'.

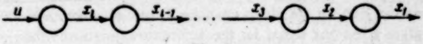

Fig. 1.

[**] A time scale is defined, not by giving a concrete partitioning of the time axis into equal or unequal intervals, but by giving a method which permits such a partitioning to be made in each concrete case. Thus, for example, the statement that each change of the input state means the beginning of a new cycle (i.e., defines a new discrete moment of time) thereby also determines the time scale, since for each concrete giving of the sequence of inputs it permits one to carry out a definite partitioning of the time axis into cycles.

Earlier, before there was any discussion of transformations of time scales, this remark would have been meaningless.

[††] Since, for different tapes of automaton A (i.e., for different inputs and states of the automaton), different sequences of moments of time $t_0, t_1, \ldots t_i, \ldots$ and different coding methods are permitted, then this device must, generally speaking, obtain signals as to the inputs and states of automaton A at each moment of time $t = 0, 1, 2, \ldots, p, \ldots$

This device is intended, essentially, for the representation of events. Specifically, it represents some event characterizing the operation of automaton A (for example, each change of state of A's input, the appearance of some state in automaton A itself, etc.) by putting out a reading signal at the moment when the event transpires.

For this purpose, we join l delay elements, operating in time scale T, in series so as to form a delay line (Fig. 1), which is described by the recursion formulas

$$
\begin{aligned}
x_1(p) &= x_2(p-1),\\
x_2(p) &= x_3(p-1),\\
&\cdots\cdots\\
x_l(p) &= u(p-1).
\end{aligned}
$$

By eliminating from these relationships all the x_l except x_1, we obtain, for the delay line as a whole,

$$x_1(p) = u(p-l).$$

The delay line's output at time sl is uniquely determined by the input at time $(s-1)l$. Therefore, if we set $t' = s$ for $t = sl$, then such a delay line may be considered as a delay element operating in time scale T'.

We now construct an automaton by the assembly method (section 5) but now, instead of delay elements in time scale T, we connect, in each instance, a delay line as just described. The automaton thus constructed will operate in time scale T. But if we read the input symbols of this automaton, and the output of each delay line, only every $l\tau$ seconds, then we shall obtain the required automaton, operating in the time scale we require.

The reading-coding device of which we spoke earlier can, in the given case, be a time counter , which gives a reading signal for the automaton inputs and the delay lines' outputs every $l\tau$ seconds; here, coding is implemented automatically since only the delay lines' outputs are read, by virtue of which those states of automaton A which are not differentiated by the states of the terminal elements of all the delay lines are therewith lumped into one group.

We consider one particular case of the problem of realizing an automaton, operating in a given time scale, by means of an automaton operating in another time scale. This case is of interest in its own right, since it plays a basic role in the understanding of certain important technological methods of realizing finite automata in general, and switching circuits in particular.

We consider some automaton A, given by (1). At time t_0, let the input assume the state denoted by symbol ρ^0, and let the input state thereafter remain unchanged until time t_1. During the entire time $t_0 \le t \le t_1$, the automaton operates as an autonomous automaton, and its changes of state occur in correspondence with the equation

$$\varkappa(p) = F[\varkappa(p-1), \rho^0], \qquad t_0 < p \leqslant t_1. \qquad (3)$$

We now assume that, for each ρ^0, there exists a number $\underline{s}$ such that :

a) this autonomous automaton is decremented, i.e., its graph is such that, from any initial state, it can reach one of several possible equilibrium states [i.e., a state which, by virtue of (3), is transformed into itself] within a finite number $\underline{h}$ ($h \le s$) of cycles, and

b) the following change of the automaton's input occurs only after the automaton has reached an equilibrium state, i.e., $t_1 - t_0 \ge s$.

At time $t = t_1$, input state ρ^0 is changed to ρ^1, which then remains unchanged until time $t = t_2$. There is then formed a new autonomous automaton

$$\varkappa(p) = F[\varkappa(p-1), \rho^1], \qquad t_1 < p \leqslant t_2,$$

about which we make the same two assumptions. Once again, after a time less than $t_2 - t_1$, the automaton reaches an equilibrium state, which may differ from the previous one. At time $t = t_2$, input ρ^1 is changed to ρ^2, etc.

We assume that the automaton's inputs and states are read only at the moments $t_0, t_1, t_2, \ldots, t_i, \ldots$, when the input states change. It is not necessary here to recode the states.

Tape L', written by the corresponding "reading" device,

t	t_0	t_1	t_2	...
ρ	ρ^0	ρ^1	ρ^2	...
$\varkappa$	$\varkappa(t_0)$	$\varkappa(t_1)$	$\varkappa(t_2)$	...

does not contain contradictory triads, as is easily seen.

Therefore, tape L' can be considered, for any input sequence $\rho^0, \rho^1, \rho^2, \ldots$, as the result of the operation of the new automaton A', operating in time scale T' which is defined by the moments at which the inputs change. Serving as the states of automaton A' are the equilibrium states of the autonomous automata formed from automaton A for fixed (sustained) inputs.

It is immediately evident that the operation of automaton A' is completely independent of the time scale of automaton A. It is important only that automaton A operate sufficiently rapidly, i.e., that equilibrium is attained in it before a new cycle commences in automaton A'.

8. Abstract Neurons and Neuron Nets

The name "abstract neuron" is given to an element with a finite number of input lines and one output line, the states of which can be denoted by symbols from the alphabet $\{0, 1\}$; the symbol at the output is uniquely defined by the symbols at the inputs τ seconds previously, where τ is a given number.‡‡

Thus, a neuron is a combination of logical transformers and delay elements with lag time τ. The specific feature of neurons is that the logical transformers and delay elements cannot be distinguished from each other.

---

‡‡ The term "neuron" for these abstract elements is used for historical reasons, and is only slightly related to the physiological meaning of the term.

A neuron may be considered as an elementary finite automaton in which only two states are possible whereby, with a fixed input, an equilibrium state is reached in one cycle (the time between cycles is τ seconds).

Neurons are connected to each other, forming neuron nets. For the formation of a net, the states of several or all input lines of the neurons from some set are immediately identified with the output states of some neurons from the same set. In contradistinction to the nets treated in section 5, neuron nets do not contain symbol transformers, and the original elements are not any automata, but automata of a very special form, namely, neurons.

The logical functions which can be realized by one neuron can be most diverse. But in neurons of a given type only a completely concrete set of logical functions may be realized. By setting up a net from neurons of a given type, this net having one output line and several input lines, one can extend the set of realizable logical functions, in the sense that the state at the output of such a net will be a logical function of the input states, but with a delay, not of τ, but of $l\tau$ seconds, where l is an integer. We now assume that, for any logical function whatever, one can, from neurons of a given type, construct a net which realizes this function in not more than $\zeta\tau$ seconds. The least value of ζ which satisfies this condition will be called the index of the neuron. The number ζ depends on the logical capabilities of the neurons from which the net was set up. •••

It follows from what has been presented that, from neurons with a finite index ζ, one can construct any logical transformer but, in contradistinction to the transformers studied in previous sections, these will not be instantaneously acting: up to $\zeta\tau$ seconds will be required to implement a logical transformation.

A neuron net is a particular case of a net in the sense of section 5, so that any neuron net is therefore a finite automaton. The time scale of this finite automaton is determined by the partitioning of the continuous time axis into equal intervals of duration τ. Obviously, if one is considering the operation of an automaton in such a time scale, then neurons with index $\zeta > 1$ do not constitute a complete set. Indeed, in such a time scale it is impossible to construct from neurons even the simplest automaton.

$$\varkappa(p) = L[\varkappa(p-1), u(p-1)],$$

where L is a logical function for the realization of which more than one cycle is required (if $\zeta > 1$ then, by definition, such a function L exists).

Now, if the time scale is defined by a partitioning of the time axis into identical intervals equal or greater than $\zeta\tau$, then any automaton may be constructed from neurons with index ζ. In fact, any logical function is realized within $\zeta\tau$ seconds, as well as (by the use of feedback paths) a system of equations of the form

$$\varkappa_i(p') = L_i[\varkappa_1(p'-1), \dots, \varkappa_n(p'-1);$$
$$u_1(p'-1), \dots, u_s(p'-1)] \quad (i=1, \dots, n),$$

where $p' = s$ if $p = s\zeta$, i.e., an abstract structure which is the mapping, as was shown in section 5, of any finite automaton of time scale p'.

By using automata operating in such a "uniform" time scale $\zeta\tau$, we can construct, from neurons, automata operating in other time scales. On the basis of the arguments given in sections 5-7, we can now give at least two methods for realizing such automata.

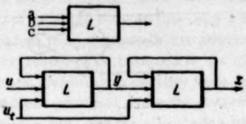

Fig. 2.

First method. From neurons with finite index ζ we can construct delay elements for the time defined by the externally supplied special cycle signals u_t. Figure 2 shows an example of a circuit of such elements, with input u and output x. The transformers L shown on the circuit realize the following logical function with a delay $l\tau$ (where $l \leq \zeta$):

$$z = (a \,\&\, \bar{c}) \vee (b \,\&\, c).$$

In correspondence with this, the equations which describe the delay elements have the form

$$x(p) = [y(p-l) \,\&\, u_t(p-l)] \vee [x(p-l) \,\&\, \bar{u}_t(p-l)],$$
$$y(p) = [u(p-l) \,\&\, u_t(p-l)] \vee [y(p-l) \,\&\, \bar{u}_t(p-l)],$$

Correct operation of the scheme shown can be guaranteed in the case when the new cycle signal u_t lasts for l old cycles and, moreover, if input u does not change before signal u_t is applied. Figure 3 shows the changes in time of all the net coordinates for certain given changes in u and u_t. Figure 4 shows an example of a McCulloch-Pitts neuron net which realizes a delay element for a time defined by synchronizing input u_t.

From such delay elements and from logical transformers which, as was shown above, are constructed from the same neurons, one may construct any finite automaton, operating at a tempo defined by synchronizing input u_t.

••• It is certainly possible that $\zeta = \infty$, or that there exist logical functions which, in general, cannot be realized by neurons of the given type.

The McCulloch-Pitts neuron has index 2, since no more than 2τ seconds is required to realize any complete normal form in a net constructed of McCulloch-Pitts neurons.

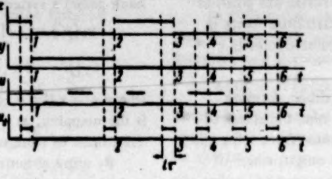

Fig. 3.

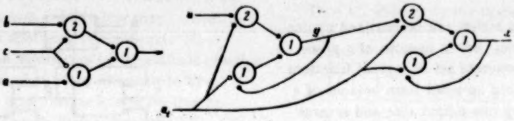

Fig. 4.

Second method . If it is necessary to construct an automaton whose time scale is defined by the changes in the input states, then one may use, in neuron circuits, the method of constructing automata from the equilibrium states of the corresponding autonomous automata (cf. section 7). Certainly, the first method is the more general; it is also valid in the given case, when the signals u_t are engendered by each change of input states in the automaton.

9. Relay Contact Circuits as Finite Automata

In the consideration of relay contact circuits there arise many important technological and scientific problems related to the peculiar features of this branch of technology. The problems alluded to will be briefly stated at the end of the present section. We, however, will not be interested here in these problems, however important they may be for the construction of actual relay contact circuits.

Here, we consider relay contact circuits only from the point of view of their special features which permit their assimilation to finite automata and which permit the use of the methods of the theory of finite automata in the construction of relay contact circuits. Therefore, we shall henceforth in this section consider an idealized model of a relay circuit.

By a relay we understand a device with a finite number of input lines and one output †††, and which satisfies the following two requirements :

a) each of the input lines and the output may have only two states, denoted by zero or unity;

b) the output state is some logical function of the states of the input lines with some time lag τ .

For example, in ordinary electromechanical relays with one winding, each relay has one input (the presence or absence of current in the winding) and realizes a logical function of one variable of the type " yes" (normally open relay contacts) or "no" (normally closed relay contacts). The lag of τ seconds is due to the relay's operating time.

In using relays with several windings, each relay has several inputs, and the character of the logical functions realized (with a delay of τ seconds) in the relays is determined by the special characteristics of the windings.

Individual relays are combined in a relay circuit by means of electrical circuits (contact circuits). These circuits define all or several inputs to relays as logical functions of the states of relay contacts and of contacts whose states depend on external stimuli . These logical functions are realized virtually instantaneously in practice. Therefore, the contact circuits play the role of the instantaneously acting logical transformers.

From what has been presented it follows that a relay is an ordinary neuron, the value of whose index ζ depends on which logic can be realized by means of one relay. A relay circuit differs from a neuron net only in its capability of being used as an instantaneously acting transformer. This difference is inessential, since the essential fact for a neuron net is that its time scale, as an automaton, is predetermined by the time τ — the neurons' lag.

Therefore, relay circuits are finite automata of the "neuron net" type, and everything presented in sections 6 and 7 applies to relay circuits as well. In particular, the two methods given in section 7 for constructing finite automata which operate in time scales different from the neurons' natural time scale, also define two possible ways of constructing relay circuits which map an arbitrary finite automaton whose time scale differs from the natural time scale of the relay circuit, as defined by the relays' time lag. Both these methods are used for synthesizing relay circuits. The first of these (with the construction of delay elements) is used most frequently in the construction of the so-called cyclical circuits. However, it is clear from section 7 that this method is a general one, valid for the relay realization of any finite automaton. As an example, Fig. 5 shows the schematic realization of a delay element for the time defined by synchronizing signal u_t, constructed from ordinary electromechanical relays. The second method, using the equilibrium states of the corresponding autonomous automata, is actually used in almost all sequential circuits.

---

††† Or two outputs, one of which is the negation of the other.

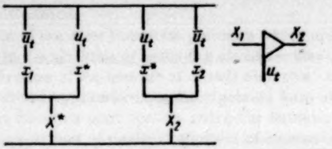

Fig. 5.

Although relay circuits are one of the possible methods of technically realizing finite automata, specific analytical and synthesizing techniques are applied to them. This specificity is due, in particular, to the fact that the lag times in different relays of one circuit are not identical. Therefore, the time axis cannot be partitioned beforehand into equal cycles, thanks to which the analysis and synthesis of relay circuits requires that one obtain additional information which is not forthcoming from finite automata theory. Moreover, the differences in relay operating times might lead to relay competitions.

Also specific are the minimization problems which arise in the synthesis of relay contact circuits (for example, minimization of the number of contacts, windings, etc. Thus, relay circuits pose their own problems which do not arise in the general theory of finite automata. To our way of thinking, the aim of relay circuit theory consists of studying such types of specific problems and of general methods for the technical realization of finite automata by relay circuits of some type or other.

Since finite automata theory began to be crystallized as an independent scientific discipline only very recently, it is natural that part of the general questions which are important for the understanding of finite automata in general were developed within the purview of relay circuit theory. Due to this, there is ordinarily no distinction made between the general questions bearing on finite automata theory and the questions specific to relay realizations.

The development of the theory of logical devices naturally led to the introduction into consideration of abstract "finite automata" and to the splitting off of finite automata theory as an independent scientific discipline.

10. Concluding Remarks

In designing concrete automatic devices, it is necessary to distinguish several independent steps.

Design begins with the analysis and idealization of the operations which the automatic device must execute. If this idealization leads to a formulation of the operating conditions in terms of discrete time and a finite set of variables, each of which may assume only a finite number of values, then the possibility arises of seeking the automatic device to be designed in the class of finite automata. With this possibility there is closely related a problem subsumed under the general problem of representing events, and the elucidation of what may and may not be implemented by finite automata.

If this question is answered in the affirmative, there arises the second problem, namely, by which equation of type (1) may one describe the finite automaton which satisfies the conditions posed , i.e., what are the tapes of this automaton and of what triads do they consist. This problem relates to the problem of the abstract synthesis of a finite automaton from its given operating conditions.

Even within boundaries of abstract consideration, one may cite a number of ways of realizing automata. One and the same automaton may be made, for example, from elements implementing functional transformations of two-valued or of multi-valued logic, with the use of special delay devices for externally given cycles or without their use if the equilibrium states in abstract neuron nets are employed, etc. The choice among the theoretically different ways of realizing an automation is related to the choice of the automaton's structure, to its abstract assembly.

This entire group of questions comprises the contents of the general theory of finite automata.

Each technical realization of a finite automaton gives rise to its own scientific problems, requires its own methods of analysis and synthesis, the taking into account of the technical special features of the actual apparatus, the economic and other requirements on the design or the circuit.

The application of finite automata theory ends as soon as one has chosen the structure or the net, i.e., as soon as one has written the equations of type (6) of the first part of the present work .

For the problem of the technical realization, the equations of type (6), or any of their equivalents, are the initial data, and the aim here is the engineering choice of design or circuit which is optimal in some sense (technical or economical).

Certainly, the boundaries between the problems of finite automata theory and the problems of technical realization are not well-defined.

Even in the choice of an abstract structure, one has to take into account the requirements and the special features of the technical realization. But this "infiltration" of technical requirements into the abstract considerations does not impede the detachment of the general theory from the very important, but specific, problems.

A VISUAL-MATRIX METHOD FOR MINIMIZING BOOLEAN FUNCTIONS

A. D. Zakrevskii

(Tomsk)

Translated from Avtomatika i Telemekhanika, Vol. 21, No. 3, pp. 369-373, March, 1960
Original article submitted April 25, 1959

A semiintuitive method is presented for the minimization of Boolean functions which is based on the use of certain properties of visually perceived information. The method is applicable to the minimization of arbitrary Boolean functions with up to 10 to 12 variables, and is particularly effective for the minimization of incompletely defined functions.

One of the most important problems which must be solved in the synthesis of switching circuits— the minimization of the number of circuit elements – is ordinarily solved by transforming the algebraic form of Boolean functions until one has arrived at formulas which are superpositions of minimal numbers of elementary functions.

The difficulties which arise in minimizing arbitrary Boolean functions increase catastrophically fast as the number n of arguments increases, so that a number of methods become inapplicable in practice even for $n > 6$.

The increase in the number of arguments of the function to be minimized may be compensated for either by restricting the class of functions to be considered or by increasing the speed of solution of the minimization problem by using modern computing technology. The realization of these possibilities is the main subject of a large number of published works [1-17].

A common characteristic feature of the contents of a large part of these works is the algorithmization of the process of minimizing Boolean functions. Significantly less attention has been given to the development of methods based on the use of certain properties of the human perception of information which are difficult to translate into algorithms. Despite this, just such methods are necessary for manual minimization of Boolean functions.

The original information on Boolean functions must be presented in compact and readily perceivable form. Since the basic "memory device" for manual minimization is the two-dimensional sheet of paper, the most compact form of representing information in this case will be a two-dimensional—matrix—form. Matrix forms for presenting Boolean functions were used by O. Plekhl' [10], A. Svoboda [18], M. Karnaugh [19] and others.

In these methods, the elements of information concerning the Boolean functions are the functions' values given by sets of elements in two-dimensional space, placed into a single-valued correspondence with the sets of values of the variables. The order of the mutual spatial arrangement of the elements, a matter of indifference in an algorithmic approach, plays an essential role for the visual perception of the matrix by a human being. An advantageous choice of such a mutual spatial disposition of elements, i.e., such a method of coding the spatial elements by sets of values of the variables, is one for which the properties of the Boolean functions which are of interest to us in trying to carry out minimization, would be readily eye-catching.

In the method suggested by A. Svoboda for minimizing Boolean functions, the potential possibilities for minimizing a Boolean function, as represented by a matrix, are expressed by the periodicity properties of that representation. With large numbers of variables, one has to do with the superposition of periodic representations with different periods which is difficult to preceive visually as a whole. In connection with this, A. Svoboda uses lattices (grids), corresponding to the individual variables, by means of which one successively isolates the portions of the matrix which correspond to definite values of these variables.

In the author's opinion, it is easier to perceive visually the symmetry properties of the representation, which gives the possibility of using the superiority of Gestalt perception of the original information, thus dispensing with cards and leading to the successive analysis of the individual portions of the representation.

The visual matrix method of minimizing Boolean functions which the author proposes is semialgorithmic, semiintuitive, so that its practical implementation is required in order to elucidate its superiorities over other methods.

It should be remembered that, for a large number of arguments, due to the complexity of the problem, the minimization of a Boolean function in the general case is considered to be successfully implemented if it has led to a sufficiently minimal algebraic form (i.e., strictly speaking, to a form which is sufficiently close to the absolutely minimal one).

An arbitrary Boolean function $f(x_1, x_2, \ldots x_n)$ can be given by a matrix (α_{ik}) whose binary elements α_{ik} are the function values, while the subscripts i, k are its arguments. The pairs of values of i, k are put into a one-to-one correspondence with the sets of values of the arguments $x_1, x_2, \ldots x_n$, whereby the arguments are, for convenience, divided into two sets of as close to equal size as possible. Values of the arguments which enter into one of these parts code the values of $\underline{i}$, the values of the remaining arguments code the values of $\underline{k}$. O. Plekhl' and A. Svoboda coded the natural number $i, \bar{k}$ by a positional binary code with weight 2^j for the $\underline{j}$th place (bit).

For coding the rows and columns of the matrix which represents the Boolean function to be minimized, we shall use a symmetric Gray code which, as will be shown, has certain superiorities over other codes.

Unit ("1") values of a Boolean function will be represented by dots in the corresponding matrix elements, blank elements will correspond to zero function values, and blackened matrix elements will attest that the function is not defined on the sets of argument values corresponding to these elements. The set of all elements thus marked will be called the representation of the function.

TABLE 1

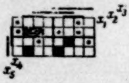

Example 1. Table 1 represents the Boolean function which takes the value "1" on the sets* 00000, 00010, 11011, 01110, 10100, 10110, 00111, is not defined on the sets 10010, 11010, 10001, 01101, 11111 and takes the value "0" on the remaining sets. One may consider that Table 1 represents all $2^5 = 32$ Boolean functions which are defined on all the sets but differ in their values on the sets 10010, 11010, 10001, 01101, and 11111.

We note that when the number of variables does not exceed four, the method suggested here coincides with the method of M. Karnaugh [19] (cf. also [8, 20]), but loses its similarity as the number of variables increases (in Karnaugh's method functions of six variables are represented in three-dimensional space while, for the representation of functions of five variables, Richards [8] suggests carrying out a diagonal decomposition of the elements in the tables representing functions of four variables, etc.).

Let $y = f(f_1, f_2, \ldots, f_m)$ be a Boolean function whose arguments are functions of the binary variables $x_1, x_2, \ldots, x_n$. In order to express $\underline{y}$ as a function of $x_1, x_2, \ldots, x_n$, it suffices to find, for each set of values of $x_1, x_2, x_3, \ldots, x_n$, the corresponding values of $f_1, f_2, \ldots, f_m$ and then to determine the value of $\underline{y}$ corresponding to these latter values.

This permits the easy implementation of operations on Boolean functions by means of their matrix forms, represented by tables on tracing paper. The sheets of tracing paper are laid on each other, the function values in the corresponding elements are compared and, in the corresponding element of the result matrix, the resulting value is noted.

The given method is not only applicable to manual computations; by using bit-wise logical operations, one can easily program it for computers.

TABLE 2

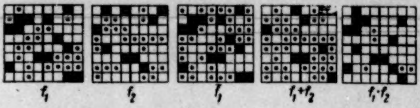

Example 2. Table 2 gives the matrix representations of the incompletely defined functions f_1 and f_2 of six variables, as well as the results of certain operations on them.

Note 1. The character of the representation matrices does not depend on the method of coding their elements if this method is the same for all the interacting matrices, so that the coding was not given here.

Note 2. In obtaining the matrix for f_1 it was supposed that the inverse (negation) of an undefined value of a binary variable is also an undefined value.

We begin the consideration of the method of minimizing Boolean functions with a comparatively simple case—obtaining the minimal disjunctive form (m.d.f.), while assuming that, in the general case, the function to be minimized is not defined on all the sets of argument values.

In general, obtaining the m.d.f. makes it easier to find other minimal forms, although it may turn out that, in making the transition from the m.d.f. to another form, this latter will not be absolutely minimal.

An algorithm which solves completely the problem posed was described by Yu. I. Zhuravlev [7], but it entails scanning variants, which leads to a very lengthy computational procedure, that hinders its practical employment.

Using the terminology of [7], we shall denote by an interval of the $\underline{k}$th rank a set of matrix elements corresponding to the conjunction of $\underline{k}$ variables, some of which may enter with a negation sign.

We now define the rules for isolating intervals.

TABLE 3

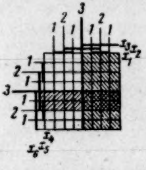

---

* By a set we mean a conjunction of argument values, for example the set 01000 corresponds to the values $x_1 = 0, x_2 = 1, x_3 = x_4 = x_5 = 0$.

1. Vertical lines in the table which separate elements corresponding to different values of x_1 we shall call axes of symmetry of the first rank; lines separating elements corresponding to different values of x_2 we shall call axes of symmetry of the 2nd rank, etc. We apply an analogous nomenclature to the table's horizontal lines (cf. Table 3).

2. A set of elements which form a band of elements of width 2^r , the central line of which is axis of symmetry of the rth rank, shall be called a zone of symmetry of this axis. (The hatched boxes on Table 3 indicate zones for the first rank horizontal axis and second rank vertical axis.)

3. Each element in the table for a Boolean function of n variables is an nth-rank interval.

A set of two kth-rank intervals is an interval of the (k-1)th rank if the intervals are symmetric with respect to some axis of symmetry and are found completely within its zone of symmetry.

We remark that, since the minimum width of a band of symmetry equals two, it follows that two series of elements forming a rectangle are always intervals; analogously, four series of elements forming a square are always intervals.

The task of obtaining the minimal disjunctive form of a Boolean function reduces to finding such a decomposition of the function representative into intervals for which the sum of the ranks of all the intervals will be minimal. The decomposition is obtained by such a covering by intervals of all the table elements corresponding to unit function values for which interval intersections are admitted, and covering by intervals of elements on which the function is undefined, but not admitting the covering of elements which correspond to zero function values.

Example 3. To find the m.d.f. of the function

$$f(a, b, c) = ab + bc + \bar{a}c.$$

TABLE 4

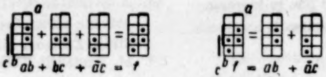

a

b

TABLE 5

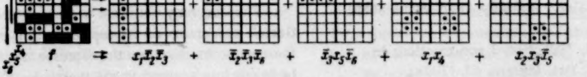

By successively marking with dots the elements of the intervals which correspond to the conjunctions ab, bc, and $\bar{a}c$, we obtain the representation of the function (cf. Table 4, a).

From the visual perception of the representation it becomes obvious that the advantageous decomposition of the representation is into the two intervals corresponding to the conjunctions ab and $\bar{a}c$ (Table 4, b). Thus easily do we obtain the m.d.f. of the original function $f(a, b, c) = ab + \bar{a}c$.

The special convenience of the visual method comes to the fore in the minimization of incompletely defined functions.

Example 4. To find the m.d.f. of the function whose representation is shown in Table 5.

The series of coverings of the representation by intervals is shown in Table 5, given only to elucidate the decomposition principle, since in practice one of the original matrices can be avoided by successively covering the representation by intervals and by blackening the elements which fall in intervals. With a little practice, one can carry out the decomposition of the representation mentally.

The result of the decomposition gives the m.d.f. of the function to be minimized.

$$f = x_1\bar{x}_2\bar{x}_3 + \bar{x}_2\bar{x}_3\bar{x}_6 + \bar{x}_3x_5\bar{x}_6 + x_1x_4 + x_2x_3\bar{x}_5.$$

As this example shows, the visual estimate of the representation permits one to find the optimal variant of the incompletely defined function more rapidly than may be done with algebraic methods [6].

In certain cases, the algebraic form of the original Boolean function which contains a minimal number of variable symbols may be obtained in the form of a product of two disjunctive forms.

TABLE 6

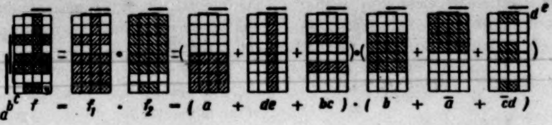
d
b
c
e
$f = f_1 \cdot f_2 = (a + de + bc) \cdot (b + \bar{a} + \bar{c}d)$

Example 5. (Taken from R. K. Richards' book [8], page 70.) To find the minimal algebraic form of the Boolean function $f = ab + a\bar{c}d + bc + bde + a\bar{d}e + \bar{c}de$. The function's representation is given as the intersection of two other representations, f_1 and f_2, easily decomposed into intervals (Table 6). The final result, $f = (a + bc + de)(b + a + cd)$, contains nine variable symbols.†

The material herein presented allows the following conclusions to be drawn:

1. The matrix representation of Boolean functions in which the matrix rows and columns are coded by the variables' values in a Gray code has the convenience of immediate visual perception of certain properties of the function represented, the correct estimate of which is necessary in the finding of the optimal way to minimize. Visual analysis of the representation allows one to estimate the possibilities of minimization presented by the representation by degrees of regularity of the representation's elements, the criterion for which is the symmetry of the elements' mutual positioning.

2. Being intuitive to a certain extent, the visual matrix method of minimizing Boolean functions was designed for using certain properties, difficult to render in algorithmic form, of visual perception, thus allowing, without recourse to computing technology, the implementation of complicated transformations of the original function for its minimization. With a little practice, the minimization of Boolean functions of five or six variables may easily be done mentally (if the representation of the function is in front of one's eyes), while making notes on the representation elements during the minimization process allows one to increase the number of variables up to ten or twelve.

LITERATURE CITED

1. M. A. Gavrilov, Theory of Relay Contact Circuits [in Russian] (Izd. AN SSSR, 1950).
2. V. I. Shestakov, "The algebra of two-terminal networks, constructed exclusively from two-terminal constituents (A—circuit algebra)," Zhur. Tekh. Fiz. 11, 6 (1941).
3. G. N. Povarov, "Mathematical theory of synthesizing contact (1, k)-poles," Doklady Akad. Nauk SSSR 100, 5 (1955).
4. S. V. Yablonskii, "Functional constructions in k-valued logic," Inst. Matem. 51 (1958).
5. E. K. Voishvillo, "Method of simplifying truth function expressions," Nauchn. Dokl. Vyssh. Skoly. Filosophskie Nauki No. 2 (1959).
6. V. N. Roginskii, "Taking unused states into account in synthesizing relay contact circuits," Avtomatika i Telemekhanika 15, 3 (1954).
7. Yu. I. Zhuravlev, "On the separability of subsets of the vertices of an n-dimensional unit cube," Trudy Inst. Matem. 51 (1958).
8. R. K. Richards, Arithmetic Operations in Digital Computers (Van Nostrand, Princeton, 1955).
9. "Synthesis of electronic computing and control circuits" (Harvard Computation Laboratory, 1951).
10. O. Plekhl, Electromechanical Switching and Switching and Switching Apparatus [in Russian] (Énergoizdat, 1959).
11. C. E. Shannon, "The synthesis of two-terminal switching circuits," Bell Syst. Tech. J. 28, 1(1949).
12. W. V. Quine, "The problem of simplifying truth functions," Am. Math. Monthly 59, 8 (1952).
13. E. W. Veitch, "A chart method for simplifying truth functions," Proc. Assoc. Comput. Mach. No. 2 and 3 (1952).
14. E. J. McCluskey, "Minimization of Boolean functions," Bell Sys. Tech. J. 35, 6 (1956).
15. B. Harris, "An algorithm for determining minimal representation of a logic function," Trans. IRE EC-6 2 (1957).
16. J. P. Roth, "Algebraic topological methods for the synthesis of switching systems. I," Trans. Am. Math. Soc. 88, 2 (1958).
17. G. Epstein, "Synthesis of electronic circuits for symmetric functions," Trans. IRE EC-7, 1 (1958).
18. A. Svoboda, "Grafico-mechanicke pomůcky uzivane při analise a synthese kontaktovych obvodů," Stroje Zpracov. inform. 4 (1956).
19. M. Karnaugh, "The map method for synthesis of combinatorial logic circuits," Trans. AIEE 72, Part I (1953).
20. N. B. Acred, "Control circuits design," Electronic Eng. 29, No. 358 (1957).

---

† This is one symbol fewer than in Richards' result, attesting to the fact that the solution of this problem is indeed a puzzle.

The economy obtained is a consequence of the Gestalt perception of the representation which allows the connection between the representation elements to be taken into account in the search for the optimal variant of its decomposition.

GENERALIZED PROPORTIONALITY CONDITIONS OF ELECTROMAGNETIC SYSTEMS

(GEOMETRY OF ELECTROMAGNETIC SYSTEMS)

A. S. Tulin

(Moscow)

Translated from Avtomatika i Telemekhanika, Vol. 21, No. 3, pp. 374-383, March, 1960
Original article submitted November 5 , 1959

Questions of proportionality of electromagnetic devices are propounded. Geometric regularities, related to the conditions of rational use of electromagnetic energy, are used. As a result, there are found many optimal configurations from which, in correspondence with the technical and economic requirements, the actual configuration is chosen in each specific instance.

In devices which use electromagnetic energy, the basic design element is the electromagnetic system, which is a ferromagnetic magnetic circuit with one or several windings.

The electromagnetic system of an electromagnetic device is a function of the device's purpose. Thus, for example, there are electromagnetic systems for transformers, chokes, magnetic amplifiers, relays, and other electromagnetic mechanisms, among which can be included electrical machines.

Despite the variety of the physical forms taken by electromagnetic systems, they have something in common, which speaks for the efficacy of a generalized consideration of the fundamental regularities which are valid for all electromagnetic devices.

For this generalized consideration of electromagnetic systems, we use the fact that any electromagnetic system is some geometric figure whose absolute and relative dimensions are determined by the physical laws concerning the use of electromagnetic energy.

We are justified in calling the set of questions as to the geometry and physics of electromagnetic systems the "geometry of electromagnetic systems ."

Basic Postulates of the Geometry of Electromagnetic Systems

Questions as to the geometry of electromagnetic systems in their generalized form have not yet been treated in the literature, so that it is necessary to first consider certain postulates and, for convenience of exposition, to introduce some terms from electromagnetic system theory.

First of all, it is necessary to introduce the concept of the absolute magnitude of an electromagnetic system.

The necessity for this arises in all cases when it is required to compare different electromagnetic systems among themselves. Such comparisons can be made with sufficient simplicity if the electromagnetic systems to be compared are completely similar. In all other cases, this comparison gives rise to well-known difficulties.

We shall henceforth take, as the absolute magnitude of an electromagnetic system, the sum of the volumes of its active materials, i.e., the sum of the volumes of its windings and magnetic circuit. With this, any change in the dimensions of the electromagnetic system without any concomitant change in the sum of the volumes of its active materials will be considered as a change of its relative dimensions with retention of its absolute magnitude. Conversely, we shall consider that a change in an electromagnetic system's absolute magnitude corresponds to a change wherein all linear dimensions change while the conditions of geometric similarity are retained. Finally, if a change in the dimensions of an electromagnetic system is not accompanied by a retention of the conditions of geometric similarity and, simultaneously, the sum of the volumes does not remain a constant, we shall then consider that, in this case, both the absolute magnitude and the relative dimensions of the electromagnetic system have changed.

As the relative linear dimensions of an electromagnetic system, we take its linear dimensions divided by a fixed one of them.

Corresponding to the concepts of absolute magnitude and relative dimensions of an electromagnetic system are the concepts of the absolute and relative parameters of this system. As the relative (or reduced) parameters we take the absolute parameters divided by the absolute magnitude of the electromagnetic system. With this, if the parameters which interest us are proportional to the first powers of linear dimensions, then their reduction will be implemented by a division by the cube root of the sum of the first powers of the active materials' volumes. For a quadratic dependency, the aforementioned sum will be raised to the second power , etc.

By using the fact that the parameters of electromagnetic devices can be reduced to an arbitrary number of turns of their windings, we shall consider their windings to be reduced to the one-turn form. In this case, instead of the cross section and length of a circuit's winding, we shall consider its mean length and total cross section, with account taken of the corresponding space factor.

Naturally, all parameters of electromagnetic systems are the corresponding functions of the geometric dimensions of these systems and of the properties of the active materials. For convenience of exposition, we shall henceforth, instead of such expressions as "a geometric function of the magnetic circuit's magnetic conductance," use "the magnetic circuit's geometric conductance," "the geometric impedance of the winding," and also "geometric coefficient. . ." or "geometric constant. . .," etc.

The nonlinearity of ferromagnetic materials ordinarily introduces significant complication into the theory of elemectromagnetic devices, but it is not mandatory to take these nonlinearities into account in the theory of the geometry of electromagnetic systems. The explanation of this is that the geometry of electromagnetic systems is concerned with the regularities imposed on the relative (or reduced) parameters, in the aforementioned sense, of electromagnetic systems, and these reduced parameters do not depend on the properties of any material. As will become clear in the sequel, the materials' properties, while having no infleunce on the choice of relative dimensions of electromagnetic systems, influence completely its absolute dimensions.

We should make particular mention of the questions in our generalized consideration of electromagnetic systems which deal with the classification of systems into those with closed or with open magnetic circuits. Thus, for example, a transformer has a closed, and an electromagnetic relay an open, magnetic circuit.

The author initially will consider all electromagnetic systems in the closed magnetic circuit mode (the mode of a short-circuited magnetic circuit). The transition from closed to open magnetic circuits does not render it necessary to change the optimal geometric relationships obtained when considering closed magnetic circuit modes. The proof of this assumption in particular cases of electromagnetic system employment engenders no particular difficulty, and is in good agreement with experience.

The consideration of proportionality of electromagnetic systems with closed magnetic circuits eliminates the necessity of taking magnetic flux leakage into account, which also simplifies the problem.

The reduction of windings to one turn and the ignoring of flux leakage lead to an equivalence between current and ampere-turns, and also between magnetic flux and flux linkages.

Energetic Bases of Electromagnetic Systems

The use of electromagnetic energy in any electromagnetic device is related to the property of the electromagnetic system of accumulating energy obtained from a source of electric current. This energy is then partially or completely utilized, and is partially converted to a source of supply or is lost in the form of various energy dissipations.

As the characteristic of this property of electromagnetic systems, we can use the quantity of accumulated energy divided by the power used in maintaining the static state of the energy stored in the system. To find this parameter we shall use regularities which exist for dc circuits, but it should be kept in mind with this that the parameter in which we are interested does not depend on the nature of the current.

As is well-known, when the windings of an electromagnetic system are connected to a dc source, a transient response ensues for which the following equation is valid:

$$ui\,dt = i^2 r\,dt + i\,d\psi. \tag{1}$$

Equation (1) shows that all the energy from the source consists of two parts, one of which is consumed in thermal losses in the windings, while the other serves to change the system's magnetic state. At the termination of the transient response, the current and the magnetic flux assume constant values. The energy which continues to be supplied from the source is now consumed solely by the thermal losses in the windings. These losses determine the power which goes to maintain the static state of electromagnetic energy accumulated in the electromagnetic system during the transient response. This power, defined in terms of the steady-state value of current I and the electric conductance g_M of the windings, equals

$$P = \frac{I^2}{g_M}. \tag{2}$$

The quantity of electromagnetic energy stored in the electromagnetic system during the transient response is defined by the expression

$$W_L = \int_0^I i\,d\psi. \tag{3}$$

To find the differential magnetic flux which appears in Expression (3), we use the well-known dependency which exists between the magnetizing force of magnetic flux and magnetic conductance. With this, and also using (2), we obtain

$$W_L = \frac{1}{2} P g_M g_c, \tag{4}$$

from whence

$$\frac{W_L}{P} = \frac{1}{2} g_M g_c = kG_M G_c, \tag{5}$$

where G_M and G_c are the geometric conductances of, respectively, the windings and the closed magnetic circuit, and k is a proportionality factor which takes into account the adopted units of measurement, the space factors of the winding cross section and the magnetic circuit, the specific conductance and permeability of the materials of the windings and the magnetic circuit, and other quantities relating the windings' electric conductance and the magnetic circuit's magnetic conductance with the geometric dimensions of the electromagnetic system.

By dropping the factor k from (5), we obtain a function of the electromagnetic system's geometric dimensions which characterizes this system's property of accumulating electromagnetic energy. With this, we obtain

$$\gamma = G_{\text{м}} G_{\text{c}} = \frac{S_{\text{м}} S_{\text{c}}}{L_{\text{м}} L_{\text{c}}}. \tag{6}$$

Here, S_M and S_c are the cross sections of the winding and of the magnetic circuit, and L_M and L_c are their mean lengths.

As is clear from (6), to improve the properties of electromagnetic systems, it is necessary, in choosing their geometric dimensions, to attempt to increase the product of the cross sections of the winding and magnetic circuit, and to decrease the product of their lengths. This is the basic law of the theory of electromagnetic systems. However, (6) cannot be used for comparing different electromagnetic systems among themselves, since the quantity defined by this formula depends not only on the relative, but also on the absolute, dimensions of the electromagnetic systems. To eliminate the dependence on absolute quantities, we use the relative value of the parameter of interest to us. We obtain with this

$$\xi = \frac{1}{\sqrt[3]{Q^3}} \frac{S_{\text{м}} S_{\text{c}}}{L_{\text{м}} L_{\text{c}}}, \tag{7}$$

where Q is the sum of the volumes of the active materials, i.e., the absolute magnitude of the electromagnetic system.

In the theory of the geometry of electromagnetic systems, (7) is one of the fundamentals. In the sequel, this formula will be used for the analysis of the proportionalities of the geometric forms of electromagnetic systems. The parameter defined by (7) is called the "geometric constant" of the electromagnetic system.

The introduction of the concept of the geometric constant into the analysis of proportionality of electromagnetic systems allows geometric function (6) of any electromagnetic device to be presented in the form of two factors, one of which is determined by relative, the other by absolute, dimensions of the electromagnetic

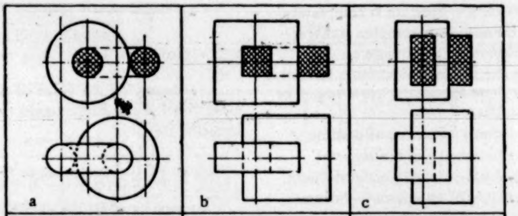

Fig. 1. Certain possible geometric forms of electromagnetic systems.

system, i.e., in the case of the geometric function given by (6), we shall have

$$\gamma = \xi \sqrt[3]{Q^2}. \tag{8}$$

As is obvious, for a given magnitude of the electromagnetic system's geometric function γ, to decrease the expenditure of active materials, i.e., to decrease the quantity Q, it is necessary to try to maximize the geometric constant ξ.

However, it should be taken into account with this that the prices of the materials of the windings and of the magnetic circuit are different, so that it is necessary to attempt to realize, not an absolute decrease in the sum of the volumes of the windings and the magnetic circuit, but a reduction of the total cost of the electromagnetic system's active materials.

Linkages of Geometric Dimensions of Electromagnetic Systems

Electromagnetic systems, in their geometric aspect, are complicated figures which consist of linkages of simpler figures of windings and magnetic circuits.

Linkage between windings and magnetic circuits may be simple or complex. In a simple linkage, the entire aperture of the magnetic circuit is filled by the winding's cross section, and the winding's aperture is completely filled by the magnetic circuit. In a complex linkage, between winding and magnetic circuit there remain certain spaces, filled by the surfaces of winding insulation or by other windings, or these spaces, for some reason or another, may remain unfilled.

As examples, Fig. 1 shows a number of possible geometric forms of simply-linked electromagnetic systems. Certainly, any simply-linked geometric form, with any permissible unfilling of an aperture, becomes a figure with a complex linkage.

For this purpose, as an example, we consider the geometric form of an electromagnetic system as shown in Fig. 2.

As is clear, the given form has four dimensions, the absolute values of which are denoted by a, b, d, and e.

To obtain relative dimensions, we relate all the remaining dimensions to one selected absolute dimension. For example, as such a fundamental dimension, we take the width a of the magnetic circuit's aperture. In this case, the relative dimensions of height, width of core section, and magnetic circuit thickness will equal, respectively,

$$\frac{b}{a} = c, \qquad \frac{d}{a} = m, \qquad \frac{e}{a} = k.$$

With the notation chosen the cross sections and lengths of the windings and magnetic circuit will equal

$$S_{\text{M}} = a^2 c, \quad S_{\text{c}} = a^2 mk, \tag{9}$$

$$L_{\text{M}} = 2a(m + k + 2), \quad L_{\text{c}} = 2a(m + c + 1). \tag{10}$$

Knowing the cross sections and the lengths, we determine the volumes of the windings and magnetic circuits and then, by adding these volumes, we find the quantity which we have called the absolute magnitude of the electromagnetic system. For this, we get

$$Q = 2a^3 [c(m + k + 2) + mk(m + c + 1)]. \tag{11}$$

To determine the value of the parameter which we have taken as the fundamental one, we solve the last equation for a:

$$a = \sqrt[3]{\frac{Q}{2[c(m + k + 2) + mk(m + c + 1)]}}. \tag{12}$$

We now have all the data necessary for determining, by (7), the geometric constant of the electromagnetic system under consideration. This constant equals

$$\xi = \frac{mck}{(m + k + 2)(m + c + 1)\sqrt[3]{16^2 [c(m + k + 2) + mk(m + c + 1)]^2}}. \tag{13}$$

In our task here, we do not enter into an analysis of all the possible geometric forms of electromagnetic systems. We limit ourselves just to a consideration of a method of analysis which is applicable, with the proper specifications being made, to the analysis of any form and of any type of linkage.

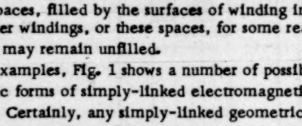

Fig. 2. Geometric form of a three-core electromagnetic system.

The problem of finding the optimal proportions of electromagnetic systems does not have a unique solution. In each particular case it is necessary to take into account the concrete conditions of use of electromagnetic energy and the economic requirements. This bears first of all on the ratio of the volumes of the electromagnetic system's active materials. By bearing this fact in mind, we should seek, not the general case of the maximum of the geometric constant of (13), but its particular cases, each of which corresponds to some previously given ratio of the aforementioned volumes. With the notation we have adopted, the ratio of the volume of the magnetic circuit to that of the windings equals

$$\frac{Q_{\text{c}}}{Q_{\text{M}}} = \frac{mk(m + c + 1)}{c(m + k + 2)}. \tag{14}$$

By solving this last equation for one of the relative dimensions, and then substituting the value obtained in (13), we would have the capability, by computing the partial derivatives with respect to the relative dimensions, to determine the optimal values of these dimensions, which would correspond to the maximum geometric constant for the previously given constant ratio of the volumes of the active materials. However, this path to a solution leads to significant complexity, so that we shall solve this problem by finding the maximum of the

TABLE 1

m	0.0	0.25	0.5	1.0	1.5	2.0	3.0	10.0	15.0
k	3.0	3.0	2.84	3.0	3.16	3.45	3.9	6.95	10.0
c	0.5	1.0	1.3	2.0	2.67	3.36	4.7	15.0	22.0
Q_c, %	0.0	24.4	36.5	50.0	58.0	63.5	71.0	86.5	90.5
$\xi \cdot 10^3$	0.0	2.76	4.48	4.78	4.85	4.55	4.12	2.2	1.51

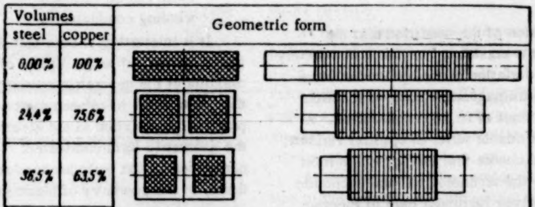

Fig. 3. Series of optimal geometric forms of three-core electromagnetic systems for various ratios of winding and magnetic circuit volumes.

geometric constant of interest to us for a constant value of one of the relative dimensions, which is equivalent to the condition that the ratio of the volumes be constant, although the magnitude of this ratio itself is not given explicitly in this case. As the constant quantity, we take the relative dimension m, since the ratio of the winding and magnetic circuit volumes depends most heavily on this dimension.

By analyzing (13) for an extremum by the method of partial derivatives, we obtain the following optimal values of the relative dimensions k and c for a constant value of dimension m:

$$k=\frac{m+2}{4}\left[1+\sqrt{1+\frac{24c}{m(m+c+1)+c}}\right], \quad (15)$$

$$c=\frac{m+1}{4}\left[1+\sqrt{1+\frac{24mk}{m+k+2+mk}}\right]. \quad (16)$$

Joint solution of (15) and (16) leads to cumbersome computation, so that we solve this problem by the method of successive approximations. The results are given in Table 1, where we also give the volume of the magnetic circuit as a percentage of the total volume of active material plus the corresponding maximum of the geometric constant for the electromagnetic system of the form under consideration.

Thus, the imposition of the condition that the geometric constant be a maximum leads to a completely definite regularity of variation of the optimal relative dimensions of the electromagnetic system as functions of the ratio of the volumes of its active materials. As a result, we obtain a continuous series of optimal variants, from which one should choose that variant which most completely answers to the technological and economic requirements of each given particular case of electromagnetic system usage.

As an illustration of the regularities obtained, Fig. 3 shows a series of forms of the type of electromagnetic system considered. All the sketches on the figure are drawn to scale and are in accordance with the condition that the geometric constant be a maximum. The order in which the sketches are placed on the figure takes into account the ratio of the volumes of active materials for a constant value of their sum. The limits of the series show the sketches with limiting ratios of their dimensions. On the top are shown the sketches corresponding to zero magnetic circuit volume and, on the bottom, those corresponding to zero winding volume.

Knowing the optimal ratios of the dimensions, there is no difficulty in determining all the parameters of electromagnetic systems for any ratio of the volumes of the active materials. Thus, for example, the curves of Fig. 4 show, as functions of the ratio of the volumes of active materials, the relative geometric conductances of the windings and magnetic circuit as well as their product, i.e., the geometric constant of the electromagnetic system under consideration.

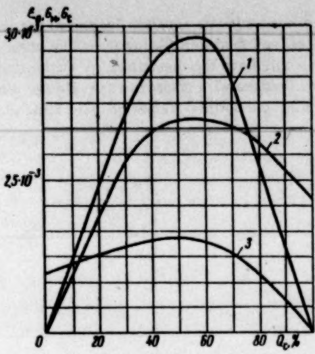

Fig. 4. Geometric conductance of windings and magnetic circuit plus the geometric constant of a three-core electromagnetic system as functions of the ratio of winding and magnetic circuit volumes. 1 is the geometric constant, 2 is the magnetic circuit conductance, and 3 is the winding conductance.

It is interesting to note that the geometric ratios which correspond to the regions of the maximum of the maxima of the geometric constant (Figs. 3 and 4) are the ratios which have been most widely used in the practical application of the electromagnetic systems of the geometric form considered. This substantiates the correctness of the basic assumptions we have made for the theory of the geometry of electromagnetic systems.

TABLE 2

Sketch on figure	Form coefficient $\times 10^3$	Sketch on figure	Form coefficient $\times 10^3$
1. a	3.40	1. e	6.70
1. b	2.46	1. f	5.00
1. c	3.62	1. g	8.00
1. d	4.85	1. h	6.40

The method presented here for the analysis of optimal geometric proportions is applicable to any geometric form of electromagnetic systems. Thus, for example, the author carried out the corresponding analysis of all the sketches given in Fig. 1. Omitting similarities, we give only the value of the maximum of the maxima of the geometric constant for each of these sketches. The results appear in Table 2. The maximum of the maxima of the geometric constant may serve as the characteristic of the form of an electromagnetic system, for which reason we call this parameter the "form coefficient" of an electromagnetic system.

Economics of Electromagnetic Systems

In choosing some variant from the series of optimal design variants of an electromagnetic system (cf., for example, Fig. 3) for some particular case, one must take into account, not only technological, but also economic requirements.

Thus, economic considerations, while having no effect on the general regularities of the geometry of electromagnetic systems, have an effect, in each particular case, on the system's geometric proportions. It should be kept in mind with this, that the basis of the economic influence is the difference in prices of the winding and of the magnetic circuit materials of the electromagnetic system. With identical prices per unit volume of these materials, the economic requirements would cease to be operative.

The cost of an electromagnetic system, defined by the costs of its active materials, equals

$$A = Q_M t_M + Q_c t_c, \tag{17}$$

where Q_M and Q_c are the winding and magnetic circuit volumes, and t_M and t_c are the unit volume costs of, respectively, the windings and the magnetic circuit.

The ratio of unit volume cost of winding to that of magnetic circuit equals

$$t_0 = \frac{t_M}{t_c}. \tag{18}$$

By introducing the coefficient

$$n = \frac{Q_M}{Q_M + Q_c} = \frac{Q_M}{Q}, \tag{19}$$

and by taking (18) into account, we transform Expression (17) to the form

$$A = Qt_c[n(t_0 - 1) + 1]. \tag{20}$$

By dividing (20) by Qt_c, we obtain the relative cost of the electromagnetic system, i.e.,

$$A_0 = \frac{A}{Qt_c} = n(t_0 - 1) + 1. \tag{21}$$

As is clear, the relative cost when the prices of the active materials are equal (i.e., for $t_0 = 1$) is unity, and does not depend on the ratio of the volumes of these materials. In this case, the optimum variant of the electromagnetic system to use is that one which corresponds to the maximum geometric constant. When these prices are not equal, a change in the ratio of the volumes of active materials changes both the geometric constant of the electromagnetic system and its cost. In this case, to choose the optimum variant of electromagnetic system to be used, one should aim at the minimum ratio of the relative cost to the geometric constant, i.e.,

$$A_\xi = \frac{A_0}{\xi} = \frac{n(t_0 - 1) + 1}{\xi}. \tag{22}$$

Thus, for example, from the data of Table 1, if no account is taken of differences in active material costs, i.e., for $t_0 = 1$, the optimal variant of the electromagnetic system to use is the one for which the winding volume is 42 % of the total volume of active materials. If the price of the winding material is, for example, 20 times as high as the magnetic circuit material, then from the data of Table 1 and from (22), we find that the optimal variant for this case is the one where the winding volume is 24% of the total volume of active material in the electromagnetic system.

What has already been said sufficiently adumbrates the principal interrelationships which exist between geometric proportions and the economics of electromagnetic systems.

Conclusion

In this paper we touched on only the most general postulates of the theory of the geometry of electromagnetic systems. In the future, by basing ourselves on these regularities, we can find optimal relationships for standard electromagnetic devices: transformers, electromagnetic relays, magnetic amplifiers, induction relays, chokes, electrical machines, etc.

As the final goal, the consideration of any configuration of the electromagnetic system of any electromagnetic device should allow one to obtain a continuous series of optimal variants of the configuration considered, the sequence of these variants being determined by the ratio of the volumes of windings and magnetic circuit. The study of such a series provides the capability of establishing the interdependencies of the relative dimensions and the technical-economic parameters which are of decisive value in choosing the physical design of the electromagnetic device from this series in each specific case.

RELAY WINDING OVERHEATING AND HEAT TRANSMISSION COEFFICIENT AS FUNCTIONS OF AMBIENT AIR TEMPERATURE

M. I. Vitenberg

(Leningrad)

Translated from Avtomatika i Telemekhanika, Vol. 21, No. 3, pp. 384-392, March, 1960
Original article submitted November 30, 1959

The paper deals with relay winding overheating and heat transmission coefficient as functions of ambient air temperature. Empirical formulas are derived for determining the magnitude of relay winding overheating and relay heat transmission coefficient.

1. Winding Overheating

The excess of relay winding temperature over the ambient medium's temperature is ordinarily determined under normal conditions for an air temperature of +20°C. However, relays are frequently used under conditions where there are large oscillations of the ambient temperature – from -60 to +60°C – and special types of relays are used at temperatures up to +125°C and higher.

As is well known, with a raising of the winding temperature the heat transmission coefficient (specific heat transmission) increases, since heat transmission by convection depends on a fractional power of the overheating temperature, while heat transmission by radiation is proportional to the difference of the fourth powers of the absolute temperatures of the winding and of the ambient air. Therefore, with identical magnitudes of power dissipation, overheating of a relay winding is decreased as the ambient air temperature increases.

The working life of relay insulation is determined by the greatest magnitude of the working temperature. Consequently, it is necessary to know, as accurately as possible, the relay winding overheating for the highest ambient air temperature. Measurement of relay winding overheating with increased temperature is ordinarily carried out experimentally in a thermostat, for which a great deal of time is required. Moreover, these measurements are usually distinguished by their low accuracy, due to the significant relative errors in

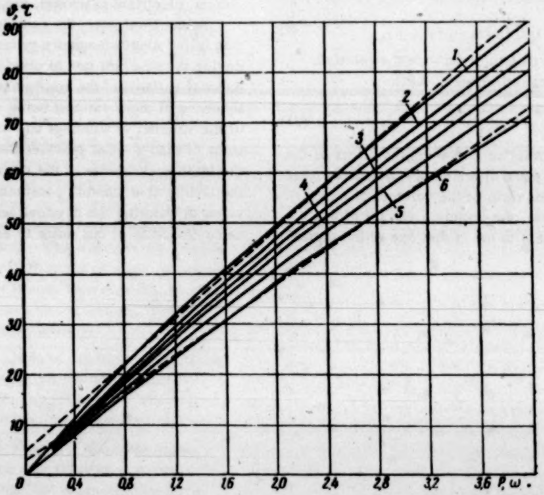

Fig. 1. 1 — θ_0 = 21° C, 2 — θ_0 = 44°C, 3 — θ_0 = 65° C, 4 — θ_0 = 84° C. 5 — θ_0 = 105° C, 6 — θ_0 = 141° C.

determining the winding overheating temperature for an increased temperature of the ambient air.

Thus , for example, with ambient temperature of 100°C and winding overheating temperature of 30°C, an error of 2% (2°C) , in measuring the temperatures of winding and air gives a relative error of about 13% in determining the temperature of the relay winding overheating.

Relay winding overheating temperature can be found more accurately by analytical means.

Figure 1 gives curves showing excess of relay winding temperature over ambient temperature as a function of the power applied for small-size-type RMU relay, taken off experimentally for various ambient temperatures up to +141°C .

The measurements were carried out in a 500-watt dessicator with automatic temperature regulation within the limits of +30 to +200°C with an error no greater than ± 3 % . The working chamber of the dessicator had a diameter of 300 mm and a length of 290 mm.

The dimensions of the relay types tested were: for type RMU, 24.7 x 38.5 x 41 mm, for type RÉS10, 11.1 x x 16.5 x 26 mm and, for type RKN, 25.6 x 56.5 x 97 mm.

The relay weights were: for type RÉS10, 6 g, for type RMU, 70 g and, for type RKN, 290 g.

The relay specimens had wire windings with brand PÉTKM heat-resistant insulation. The winding temperatures were measured by a copper-constantan thermocouple. To eliminate heat leakage at the relay supports, the relays were suspended by a fine wire in the center of the dessicator.

The ventilation apertures of the dessicator were tightly covered by asbestos plugs, and were used for the outlet of the conductors and the thermocouple.

The air temperature in the dessicator was also measured by a thermocouple, which was placed at the level of the specimen relay at a distance of about 30 mm from it. As protection against direct radiation, the thermocouple's junction on the relay's side was shielded by a small fragment of white paper. For each value of supplied power, the relay was immersed for not less than an hour in the given ambient temperature. The actual temperature oscillations in the dessicator did not exceed 2 %. It is clear from Fig. 1 that, in the limits of overheating temperature from 20 to 70°C, the curves differ very little from the straight lines drawn with dashes (the error does not exceed ± 1°C). In Fig. 1, the dashed straight lines are shown only for the extreme curves, so as not to complicate the figure.

In the aforementioned limits, the relay winding overheating curves can be approximated by the formula

$$\vartheta = a + bP, \tag{1}$$

where a is the amount of overheating intercepted by the straight line on the axis of ordinates, and b is the tangent of the slope of this line.

TABLE 1

Ambient temperature θ_0 °C	a, °C	b, °C/ω
21	4.7	21.7
44	4.3	20.9
65	3.8	20.4
84	3.6	19.3
105	3.2	18.6
141	2.8	17.2

The values of the quantities a and b for relay type RMU for different values of ambient air temperature, determined graphically from Fig. 1, are given in Table 1.

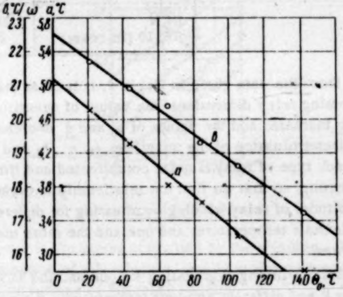

Fig. 2.

From the data of this table, the dependencies of a and b on the ambient temperature were constructed, as shown in Fig. 2. These dependencies are straight lines, which can be expressed by the formulas

$$a = a_0 - c\theta_0, \tag{2}$$

$$b = b_0 - d\theta_0, \tag{3}$$

where a_0 and b_0 are the values of a and b for an ambient temperature of 0°C , and c and d are the tangents of the slopes of these lines.

By substituting in (1) the values of a and b from (2) and (3), we obtain a general expression for determining the relay winding overheating temperature as a function of the supplied power and the ambient temperature :

$$\vartheta = a_0 - c\theta_0 + (b_0 - d\theta_0) P. \tag{4}$$

This formula gives sufficient accuracy only in the limits of overheating values from 20 to 70°C, which are the ones most frequently occurring .

The largest errors are obtained at the initial portion of the curve, for overheating temperatures less than 20°C. The accurate determination of such overheating temperatures ordinarily has no practical value.

From Fig. 2 we find the values of quantities a_0, c , b_0, and d for relay type RMU : a_0 = 50.7°C, c= 0.0175 , b_0 = 22.54°C/watt and d = 0.038.

Consequently, for type RMU relay, winding overheating is expressed by the following formula:

$$\vartheta = 5{,}07 - 0{,}0175\,\theta_0 + (22{,}54 - 0{,}038\,\theta_0)\,P. \tag{4a}$$

By an analogous procedure, we found the values of the quantities a_0, c, b_0, and d for miniaturized type RÉS10 relay (without cover) and normal type RKN relay.

The values of these quantities are given in Table 2.

TABLE 2

Relay type	S_k, cm²	a_0, °C	c	b_0, °C/cm	d
RÉS10 (without cover)	3.2	6,3	0.0171	71.6	0.126
RMU	22.6	5,07	0.0175	22.54	0.038
RKN	60.2	8,36	0.0238	8.85	0.0167
RÉS10 (in cover)	3.2	3,52	—0.006	91.5	0.103

From the data given in Table 2, it is clear that, with increasing relay dimensions, the values of quantities b_0 and c increase, and the values of b_0 and d decrease.

Determination of the quantities a_0, c, b_0, and d for each type of relay is quite complicated and time-consuming, so that we find the relationship between the magnitudes of relay winding overheating for different ambient air temperatures and one and the same magnitude of power.

Relay winding overheating for one and the same power P and different ambient temperatures θ_{01} and θ_{02} will equal

$$\vartheta_1 = a_0 - c\theta_{01} + (b_0 - d\theta_{01})\,P \text{ and}$$

$$\vartheta_2 = a_0 - c\theta_{02} + (b_0 - d\theta_{02})\,P,$$

from which we find the following expression for relay winding overheating for ambient temperature θ_{02}:

$$\vartheta_2 = \vartheta_1 - (c + Pd)(\theta_{02} - \theta_{01}) = \vartheta_1\,[1 - \beta\,(\theta_{02} - \theta_{01})], \tag{5}$$

where

$$\beta = \frac{c + Pd}{\vartheta_1}.$$

Table 3 gives the values of the temperature overheating coefficient β for various values of power in the winding, and the corresponding relay winding overheating temperatures of relay types RMU, RÉS10 and RKN for these values of power and for ambient temperature +20°C, computed by means of (4) and (6).

Figure 3 shows the curves, constructed from the data of Table 3, of the temperature overheating coefficient β as a function of the winding overheating temperature of these types of relays for $\theta_0 = +20°$C. For comparative purposes, the dashed line of Fig. 3 shows the approximate curve for type RÉS10 relay (with cover). It follows from Fig. 3 that the curves for the coefficient β for relay types RMU and RÉS10 (without cover) virtually coincide, and the value of coefficient β for type RKN relay is about 10 % larger.

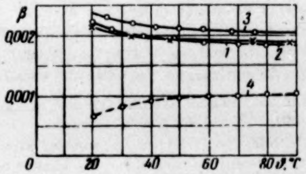

Fig. 3. 1) Relay type RMU; 2) relay type RÉS10 without cover; 3) relay type RKN, 4) relay type RÉS10 in cover.

Type RÉS10 relay, protected by a thin aluminum cover, has a coefficient β of about half the size, due to the poor thermal contact between the relay's magnetic

TABLE 3

Relay type								
RMU			RÉS10 (without cover)			RKN		
P, ω	β	ϑ, °C	P, ω	β	ϑ, °C	P, ω	β	ϑ, °C
0.7	0.00219	19.86	0.2	0.00214	19.77	2	0.00229	24.92
1.0	0.00209	26.5	0.4	0.002005	33.58	3	0.00221	33.43
1.5	0.00199	37.4	0.6	0.001955	47.4	4	0.00216	41.95
2.0	0.00194	48.29	0.8	0.00193	61.22	5	0.00213	50.46
2.5	0.00190	59.22	1.0	0.001905	75.03	6	0.0021	59.0
3.0	0.00188	70.1	1.2	0.001895	88.86	7	0.00208	67.5
						8	0.00207	76.01

circuit and the cover (the relay's pedestal is made of plastic). With air-tight relays having thick steel covers and fastened to a metallic base (pedestal), the magnitude of coefficient β is about the same as for relays unprotected by covers, since the winding of an air-tight relay generally has good thermal contact with the magnetic circuit and with the cover. As the relay winding overheating temperature varies within the limits of 20 to 70°C [the limits of applicability of (4)], the size of coefficient β varies comparatively little (by not more than ± 10 %).

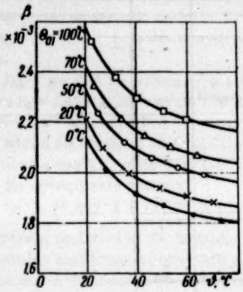

Fig. 4.

The magnitude of coefficient β depends on the initial temperature of the ambient air. Figure 4 gives the curves for the coefficient β as a function of winding overheating for various ambient air temperatures for type RMU relay. By means of these curves, the curves shown on Fig. 5 of coefficient β as a function of ambient air temperature for various heating temperatures were constructed. The curves of Fig. 5, for β within the limits of 0 to 100°C, are practically straight lines, so that coefficient β as a function of initial ambient air temperature with average overheating temperature ($\vartheta = 40°C$) can, for small-size relays (without covers), be expressed by the formula

$$\beta = (1.91 + 0.0036\theta_{01})\,10^{-3}. \qquad (6)$$

Consequently, with a constant magnitude of power, if one knows the winding overheating temperature of small-size relays (without covers) for the ambient temperature θ_{01}, one can, with an accuracy sufficient for practical purposes, determine the overheating of these relays' windings for another ambient temperature θ_{02} by means of the formula

$$\vartheta_2 \approx \vartheta_1\,[1 - (1.91 + 0.0036\,\theta_{01})\,10^{-3}\,(\theta_{02} - \theta_{01})]. \qquad (7)$$

If the initial ambient temperature is θ_{01} = 20°C, then

$$\vartheta_2 \approx \vartheta_1\,[1 - 0.00198\,(\theta_{02} - 20)]. \qquad (7a)$$

Thus, with an increase of ambient air temperature by 10°C (within the limits of 0 to 100°C), the winding overheating of the relay (without cover), for one and the same value of power, is decreased by about 2%.

Measurements carried out on different types of relays showed that this formula is also valid for higher temperatures of the ambient air (up to 140°C).

2. Heat Transmission Coefficient

The magnitude of the average (nominal) heat transmission coefficient of windings of electromagnetic relays and dc apparatus can be determined from the experimental data by means of the formula [1]

$$q_1 = \frac{P}{\vartheta S_k}, \qquad (8)$$

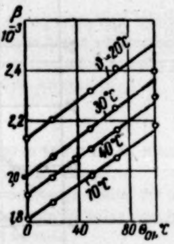

Fig. 5.

where P is the power consumed by the winding, ϑ is the overheating of this winding, and S_k is the computed cooling surface of the relay winding.

Figure 6 gives the experimental curves which show the mean heat transmission coefficient of the winding of a type RMU relay as a function of its overheating for various ambient temperatures. Within the limits of an overheating temperature of 20 to 70°C, these curves differ very little from straight lines. The large scattering of points for overheating values less than 20°C is explained by the inaccuracy of measurements of small temperature drops.

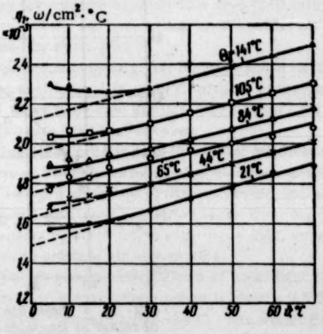

Fig. 6.

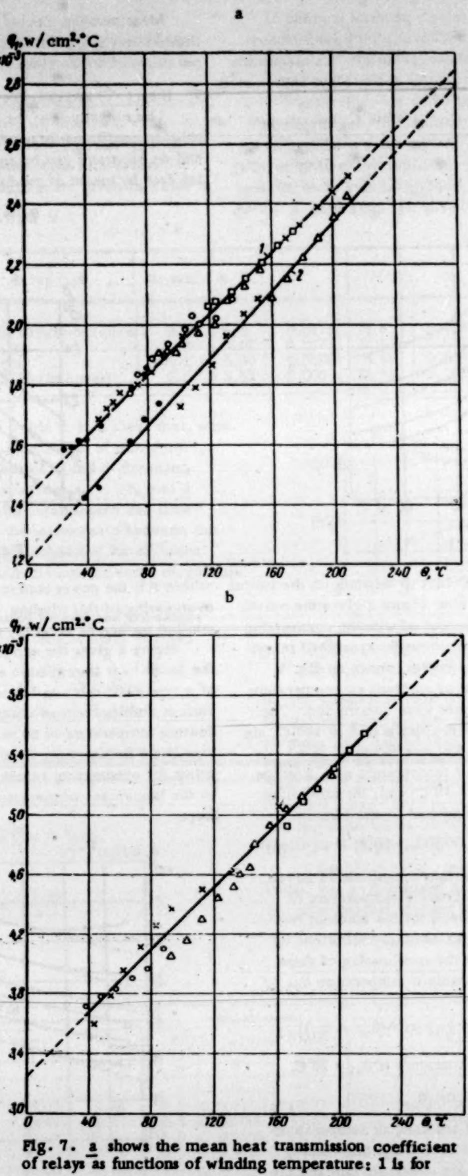

Fig. 7. a shows the mean heat transmission coefficient of relays as functions of winding temperature; 1 is for relay type RMU and 2 is for relay type RKN; b shows the same thing for relay type RÉS10 (without cover).

To elucidate the relationship between relay winding heat transmission and temperature, Fig. 7 shows the constructed relationship of the average heat transmission coefficient of relay windings and the temperature of these windings. Within the limits of 30 to 210°C, this relationship is virtually a linear one which may be expressed by the formula

$$q_1 = q_0 + e\theta = q_0 + e(\theta_0 + \vartheta), \qquad (9)$$

where q_0 is the magnitude of the heat transmission coefficient, intercepted on the axis ordinates by the extension of the straight line, and $\underline{e}$ is the tangent of the slope of this line.

From Fig. 7 we find the values of q_0 and $\underline{e}$ for type RMU relay : $q_0 = 1.422 \times 10^{-3}$ w/cm²/°C and $e = 0.00507 \times 10^{-3}$ w/cm²/°C².

Thus, within the limits of 30 to 210°C, the mean heat transmission coefficient for type RMU relay is expressed by the approximate formula

$$q_1 = (1.422 + 0.00507\,\theta)\,10^{-3}. \qquad (9a)$$

The greatest deviation of the individual values of heat transmission coefficient of type RMU relay from the straight line does not exceed 2.2%. The values of q_0 and $\underline{e}$ for relay types RMU, RÉS10, and RKN are given in Table 4.

TABLE 4

Relay type	q_0, w/cm²·°C	e, w/cm²·°C
RÉS10 (without cover)	$3.24 \cdot 10^{-3}$	$0.01965 \cdot 10^{-3}$
RMU	$1.422 \cdot 10^{-3}$	$0.00507 \cdot 10^{-3}$
RKN	$1.198 \cdot 10^{-3}$	$0.00567 \cdot 10^{-3}$
RÉS10 (in cover)	$2.77 \cdot 10^{-3}$	$0.0045 \cdot 10^{-3}$

The magnitude of the mean heat tramission coefficient for different temperatures θ_1 and θ_2 of the relay winding will be $q_1' = q_0 + e\theta_1$ and $q_1'' = q_0 + e\theta_2$, from which we find the following expression for the mean heat transmission coefficient of the relay winding for temperature θ_2:

$$q_1'' = q_1' + e(\theta_2 - \theta_1) = q_1'[1 + \gamma(\theta_2 - \theta_1)], \qquad (10)$$

where

$$\gamma = \frac{e}{q_1'}. \qquad (11)$$

Figure 8 shows the curves of the transmission coefficient of the mean heat transmission coefficient γ as a function of winding temperature for relay types RMU, RÉS10 , and RKN, computed by means of Formulas (9a) and (11).

It follows from Fig. 8 that the curves of $\gamma = \gamma(\theta)$ for small-size relay types RMU and RÉS10 (without cover) differ very little from each other, and that the value of coefficient γ for type RKN relay is about 25% larger. Type RÉS10 relay, protected by an aluminum cover, has a value of coefficient γ which is about half the size.

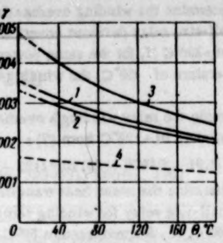

Fig. 8. 1) Relay type RMU; 2) relay type RÉS10 without cover; 3) relay type RKN; 4) relay type RÉS10 in cover.

In the limits of 20 to 160°C for θ, these curves differ very little from straight lines.

In the aforementioned limits, the coefficient as a function of temperature for relay type RMU may be expressed by the formula[1]

$$\gamma = (3.45 - 0.0079\,\theta_1)\,10^{-3}. \qquad (12)$$

Thus, if we know the magnitude of the heat transmission coefficient of small-size type RMU relays (without cover) for winding temperature θ_1, we can, with an accuracy sufficient for practical purposes, determine the heat transmission coefficients of these relays for other winding temperatures θ_2 (in the limits of 20 to 160°C) from the following approximate formula :

$$q_2 \approx q_1\,[1 + (3.45 - 0.0079\,\theta_1)\,10^{-3}\,(\theta_2 - \theta_1)]. \qquad (13)$$

If the initial winding temperature is $\theta_1 = 50$°C, then

$$q_2 \approx q_1\,[1 + 0.00306\,(\theta_2 - 50)]. \qquad (13a)$$

Formula (13a) shows that with a 10°C increase in winding temperature of small-size type RMU relays (without cover), the heat transmission coefficient is increased by about 3%.

We find analogously that the increase in heat transmission coefficient with a 10°C increase in temperature is 2.87 % for relay type RÉS10 (without cover) and 1.5% for relay type RÉS10 in its cover.

Thus, our work has established that overheating temperature of windings of small-size electromagnetic relays (weights up to 300 g) without covers, and also airtight relays with good heat elimination from the windings, is decreased by about 0.2 % with $\theta_{01} = 20$°C for a 1°C increase in ambient air temperature.

The temperature coefficients of mean heat transmission coefficient of these relays is about + 0.3 %/°C for winding temperatures of +50°C. The winding overheating temperature of relays protected by thin covers having poor thermal contact with the windings, is decreased by about a 1%/°C rise in ambient temperature.

Examples

1. We determine the winding overheating temperature of a small-size relay (without cover) for ambient temperature of +125°C if, for the same power and for ambient temperature of +25°C, the winding overheating was 50°C.

We determine the relay winding's overheating with ambient temperature of +125°C from (7):

$$\vartheta_{125} \approx 50\,[1-(1.91+0.0036\times 25)\,10^{-3}\,(125-25)] = 40°\mathrm{C}.$$

2. We determine the mean heat transmission coefficient of a small-size relay for winding temperatures of 40 and of 100°C, if, for temperature 50°C, the heat transmission coefficient equals 1.5×10^{-3} w/cm²/°C.

We determine the relay's heat transmission coefficient by (13):

$$q_{40} \approx 1.5\times 10^{-3}\,[1+(3.45-0.0079\times 40)\,10^{-3}\,(40-50)] = 1.45\times 10^{-3}\ \mathrm{w/cm^2\cdot °C}$$

and

$$q_{100} \approx 1.5\times 10^{-3}\,[1+(3.45-0.0079\times 100)\,10^{-3}\,(100-50)] = 1.7\times 10^{-3}\ \mathrm{w/cm^2\cdot °C}$$

LITERATURE CITED

1. M. I. Vitenberg, "Determination of winding heating of electromagnetic relays," Avtomatika i Telemekhanika 19, 11 (1958).

CERTAIN QUESTIONS IN THE THEORY OF MAGNETIC AMPLIFIERS LOADED BY DC DRIVES

L. V. Safris

(Rostov-on-Don)

Translated from Avtomatika i Telemekhanika, Vol. 21, No. 3, pp. 393-401, March, 1960

Original article submitted November 2, 1959

Equations are derived which characterize the basic modes and peculiarities of operation of a saturated-reactor magnetic amplifier loaded by a dc drive. A simplified method of designing such an amplifier is given.

Introduction

The operation of a magnetic amplifier loaded by a dc motor (MA-M) has its peculiar features. They stem from the fact that the motor, as an energy consumer, presents itself as an impedance and a variable counter-emf whereby, with amplifier control, there is an action on this emf. The presence of the amplifier leads, naturally, to a change in the drive's characteristics. In [1], individual questions in the analysis of such schemes were touched on for one special case. In [2], certain design approaches were adduced. At the same time, there is interest in establishing general regularities characterizing the operation of an MA-M system when its elements are connected in accordance with the scheme of Fig. 1. In the present paper we attempt to fill this void partially. We note that the analogous problem, as applied to a rotary amplifier, and also for the case when control of asynchronous motors is implemented by means of magnetic amplifiers, received consideration in [3-5].

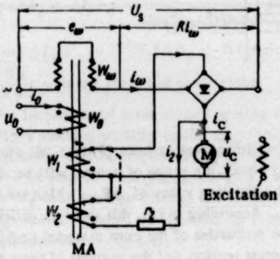

Fig. 1.

As the basis of our investigation, we take the linearization method described in [6, 7]. This method turns out to be particularly effective if one may make the two following assumptions: a) the characteristics of simultaneous core magnetization by constant and variable fields may be approximated by straight line segments ; b) the load curve, expressing the dependency between the variable component of the saturated reactor emf and the load voltage can be replaced by a straight line.

On the strength of the first assumption, we shall suppose that, for amplifier operation, we shall use a linear domain of the magnetization characteristic of the cores, which are made of material of sufficiently high quality. Under these conditions, the increment of the mean value of the working windings' ac current ΔI_ω can be found from the expression [6]

$$\Delta I_\omega = S\Delta I_0 + \frac{\Delta E_\omega}{R_i}. \tag{1}$$

Here, I_0 is the control current, E_ω is the mean value of the ac windings' emf, S is the slope of the characteristic, and R_i is the amplifier's internal impedance. The last two parameters are defined as follows:

$$S = \sigma \frac{W_0}{W_\omega}, \tag{2}$$

$$R_i = \frac{\omega\mu_i W_\omega^2 Q}{l}. \tag{3}$$

W_0 is the number of turns in the control winding, W_ω is the number of turns in the ac winding, Q is the active cross section of the two cores, l is the mean length of the magnetic circuit, $\sigma = \frac{\partial H_\omega}{\partial H_0}$, $\mu_i = \frac{\partial B_\omega}{\partial H_\omega}$, H_0 is the constant (monotonic) component of the magnetic-field strength, H_ω is the "mean" value of the variable component of the magnetic-field strength :

$$H_\omega = \frac{W_\omega I_\omega}{l}, \tag{4}$$

and B_ω is the "mean" value of the variable component of the magnetic induction:

$$B_\omega = \frac{E_\omega}{\omega W_\omega Q}. \tag{5}$$

The second assumption derives from the following considerations. It was established in [8] that, with amplifier operation on the counter-emf, the load curve, as a function of material quality, can deviate from the straight line on both sides.

By taking this circumstance into account, as well as the fact that it is desirable to obtain simple graphic expressions, in the first instance mirroring the qualitative side of the phenomena, we shall assume that $E_\omega = U_s - (E_C + RI_\omega)$ and, consequently,

$$-\Delta E_\omega = \Delta E_C + R\Delta I_\omega. \qquad (6)$$

Here, U_s is the mean value of the supply voltage, E_C is the motor's counter-emf, R is the equivalent active impedance of the ac circuit. Figure 2 gives a geometric interpretation of these assumptions. The family of magnetization curves $H_\omega = f_1(H_0, B_\omega)$ is replaced by the dashed-line parallel segments. The linear domain is marked by the coordinates of points 1 and 2 (B_1, H_1 and B_2, H_2). In correspondence with (6), the increments of voltage and emf drops occurring in the system are represented by segments (ab, bc, ce, etc.) whose projections on the axis of abscissas sum arithmetically to emf E_ω.

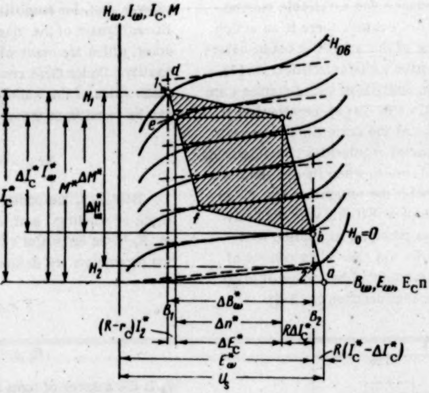

Fig. 2.

Coefficients of Control and Rigidity

We adopt the nomenclature that $K_C = \partial n/\partial I_0$ for M = const is the control coefficient, and $K_r = -\partial M/\partial n$ for I_0 = const is the rigidity coefficient. Here, n is motor speed and M is the torque developed by the motor.

We first consider the case when there is no feedback, and we assume that each conducting arm of the rectifier bridge can be replaced by a constant resistance r / 2. The back impedances will be considered infinite.

If we take into account the generally known expressions for dc motors with independent excitation,

$$M = C_M I_C, \qquad (7)$$

$$E_C = C_E n, \qquad (8)$$

we can write (6) in the following way:

$$-\Delta E_\omega = \Delta n C_E + R\frac{\Delta M}{C_M}. \qquad (9)$$

Here, $I_C = I_\omega$ is the motor armature's current, $R = r_C + r_a + r_1$, r_C is the impedance of the armature winding and motor brushes, r_1 is the impedance of the amplifier's ac winding.

By substituting (7), (8), and (9) in (1), we obtain

$$\Delta n = \frac{k}{C_E}\Delta I_0 - \frac{\Delta M}{C_M C_E}(R_i + R) =$$

$$K_C \Delta I_0 - \frac{1}{K_r}\Delta M, \qquad (10)$$

where

$$k = SR_i.$$

It follows immediately from (9) that, all other things being equal, the range of control will be determined by the limiting value of ΔE_ω, which we denote by ΔE_ω^*. According to (5), this latter quantity depends on the properties of the core material (ΔB_ω^* in Fig. 2), its cross section, and the number of turns of the working winding. Since ΔB_ω^* is a constant for a given material, an increase of ΔE_ω^* may be attained by increasing Q and W_ω. Simultaneously, as is clear from (3), R_i will also be increased, which implies an increase in K_C and a decrease in K_r. In view of these circumstances, it is frequently not possible to create an amplifier which, operating in the scheme under consideration, can satisfactorily provide the necessary values of control range and coefficient, and also the rigidity of the mechanical characteristics. We now show that a system in which the amplifier is used with feedback is free of such a disadvantage.

Effect of Feedback on K_c and K_r

a) Current feedback. Since, in addition to the ampere-turns $W_0 \Delta I_0$, the ampere-turns $W_1 \Delta I_c$ (Fig. 1) also take part in core magnetization, we then obtain, by adding the proper term to (10),

$$\Delta n = \frac{k}{C_E}\left(\Delta I_0 + \frac{W_1}{W_0}\Delta I_c\right) - \frac{\Delta M}{C_M C_E}(R_i + R), \quad (11)$$

where $R = r_c + r_a + r_i + r_1$. By taking (7) into account, we obtain, after some simple transformations,

$$\Delta n = \frac{k}{C_E}\Delta I_0 - \frac{\Delta M}{C_M C_E}[R_i(1 - \beta_1 S) + R]. \quad (12)$$

Here, $\beta_1 = W_1 / W_0$ is the feedback coefficient, W_1 and r_1 are, respectively, the number of turns and the impedance of the current feedback winding.

The expression $R_i(1-\beta_1 S)$ can be considered as the equivalent internal impedance of the amplifier with positive current feedback, the magnitude of which can be varied within broad limits by the proper choice of β_1. This statement is well known from the general theory of amplifiers with feedback [9].

Thanks to this, we can obtain the necessary values for K_r, including the value which provides (at least theoretically) absolute rigidity of the mechanical characteristics. The control coefficient does not depend on the current feedback.

b) Voltage feedback. Change of the control coefficient can be obtained by introducing voltage feedback. For this purpose, we use a winding with number of turns W_2, connected in parallel with the motor via resistor r_2. The increment of feedback current will be $\Delta I_2 = \frac{\Delta E_c + \Delta I_c r_c}{r_2}$. and the corresponding ampere-turns are $\Delta I_2 W_2 = W_0 \beta_2 (\Delta E_c + \Delta I_c r_c)$. Here, $\beta_2 = \frac{W_2}{W_0 r_2}$ — is the feedback coefficient.

The increment of total current passing through the amplifier's working winding equals $\Delta I_\omega = \Delta I_c + \Delta I_2$. Magnetization will be implemented by the positive feedback of ampere-turns $W_0 \Delta I_0 + W_2 \Delta I_2$. Since the current ΔI_2 does not flow through the motor's armature winding, the component $r_c \Delta I_2$ should be subtracted from the right member of (6), i.e.,

$$-\Delta E_\omega = \Delta E_c + R\Delta I_c + (R - r_c)\Delta I_2. \quad (13)$$

By substituting this last expression in (1) and by taking (7) and (8) into account, we find that

$$\Delta n = \frac{k\Delta I_0}{C_E(1 - \beta_2 k + a)} - \frac{\Delta M}{C_E C_M}\frac{[(R_i + R) - (\beta_2 k - a) r_c]}{(1 - \beta_2 k + a)}, \quad (14)$$

where

$$a = \frac{R_i + R - r_c}{r_2}, \qquad R = r_i + r_a + r_c.$$

Frequently, $r_c(\beta_2 k - a) \ll R_i + R$. Then, we can conclude from (14) that the introduction of positive voltage feedback leads to an increase in K_c and a decrease in K_r. The stability of motor speed will be even worse than with the absence of feedback. With negative feedback, the inverse phenomena will be observed. If $|\beta_2| \rightarrow \infty$, then $K_r \rightarrow \frac{1}{r_c}$.

c) Combined Feedback. It is clear from an analysis of the two forms of feedback considered that their properties complement each other to a certain extent, and that their joint use must give the very best results. This is an immediate consequence of the following expression, obtained on the basis of the same considerations and methods which we used previously:

$$\Delta n = \frac{k\Delta I_0}{C_E\left[1 - k\left(\beta_2 + \frac{\beta_1}{r_2}\right) + a\right]} - \frac{\Delta M}{C_E C_M}\frac{\left\{R_i + R - k\left[\beta_1\left(1 + \frac{r_c}{r_2}\right) + \beta_2 r_c\right] + a r_c\right\}^*}{\left[1 - k\left(\beta_2 + \frac{\beta_1}{r_2}\right) + a\right]}. \quad (15)$$

Here, $R = r_i + r_a + r_1 + r_c$. In deriving (15), it was taken into account that the increment of the total constant component of magnetizing force equals $W_0 \Delta I_0 + W_1 \Delta I_c + (W_1 + W_2)\Delta I_2$, and that ΔE_ω is defined by (13).

The relationships $r_c \ll r_2$, $\beta_1 \ll r_2 \beta_2$, $(\beta_2 k - a) r_c \ll R_i + R$ are frequently valid. In this case, (15) can be simplified to

$$\Delta n = \frac{k\Delta I_0}{C_E(1 - \beta_2 k + a)} - \frac{\Delta M}{C_E C_M}\frac{R_i(1 - \beta_1 S) + R}{(1 - \beta_2 k + a)}. \quad (16)$$

By the proper choices of β_1 and β_2, one can attain the necessary values of both the control coefficient and the rigidity coefficient. From this point of view, combined feedback is the most advantageous.

Transient Responses

We first consider the case when there is no feedback. The law of variation of motor speed during the transient response may be found by jointly solving (9) and (10) (written for instantaneous values) and the following equations:

$$\Delta u_0 = r_0 \Delta i_0 + W_0 Q \frac{d(\Delta B_0)}{dt}, \quad (17)$$

---

* The terms β_1/r_2 and r_c/r_2 will be missing if one connects winding W_2 as shown by the dashed line in Fig. 1, which is advantageous for $\beta_2 < 0$.

$$W_0 Q \Delta B_0 = \frac{W_0^2 Q}{l} \mu_c \Delta i_0 - \frac{\nu}{\omega} \frac{W_0}{W_\omega} \Delta e_\omega, \qquad (18)$$

$$\Delta M = \Delta M_0 + m\Delta n + J \frac{d(\Delta n)}{dt}. \qquad (19)$$

Here, u_0 is the voltage applied to the input of the controlling winding, r_0 is the control circuit's impedance, B_0 is the constant (monotonic) component of magnetic induction. Some explanation should be given a propos of the last equations. Expression (17) derives from Kirchhoff's second law for the control circuit; (18) was borrowed from [6, 7]. Henceforth, to simplify the problem, bearing in mind that the cores are of good quality, we shall assume that $\mu_c = 0$, and we shall denote $\nu W_0 / \omega W_\omega$ by T. Equation (19) expresses Newton's law of motion with the assumption that the static impedance torque of the productive mechanism has two components, one of which is constant (ΔM_0) and the second of which is directly proportional to the speed ($m\Delta n$). On the basis of the equations enumerated, we get

$$\tau_{el}\tau_{mec}\delta \frac{d^2(\Delta n)}{dt^2} + \left[\tau_{el}\left(1 + \frac{m\delta}{K_r}\right) + \right. \qquad (20)$$

$$\left. + \tau_{mec}\right] \frac{d(\Delta n)}{dt} + \left(1 + \frac{m}{K_r}\right) \Delta n = K_c \Delta I_0 - \frac{\Delta M_0}{K_r}.$$

Here,

$$\tau_{el} = \frac{K_c T C_E}{r_0}, \quad \tau_{mec} = \frac{J}{K_r},$$

$$\Delta I_0 = \frac{\Delta U_0}{r_0}, \quad \delta = \frac{R K_r}{C_E C_M}.$$

Finding the solution of (20) poses no difficulty. For a qualitative estimate of the possible results, we consider the following particular cases: $\tau_{el} = 0$, $\tau_{mec} \neq 0$, and $\tau_{el} \neq 0$, $\tau_{mec} = 0$. Correspondingly, we obtain the equations

$$\tau_{mec} \frac{d(\Delta n)}{dt} + \left(1 + \frac{m}{K_r}\right) \Delta n = K_c \Delta I_0 - \frac{\Delta M_0}{K_r}$$

and

$$\tau_{el} \left(1 + \frac{m\delta}{K_r}\right) \frac{d(\Delta n)}{dt} +$$

$$+ \left(1 + \frac{m}{K_r}\right) \Delta n = K_c \Delta I_0 - \frac{\Delta M_0}{K_r}.$$

In the first case, the time to establish the number of revolutions is determined by the quantity $\frac{\tau_{mec}}{1 + \frac{m}{K_r}} = \frac{J}{K_r + m}$, which will be quite large, since, in the absence of feedback, K_r is small.

In the second case, the duration of the transient response depends principally on the amplifier lag, and will be characterized by the quantity

$$\frac{K_c T C_E}{r_0} \frac{1 + \frac{mR}{C_M C_E}}{1 + \frac{m}{K_r}}.$$

In investigating transient responses with feedback present, we should, instead of (10), use (16), adding to the latter the terms $W_1 Q d(\Delta B_0)/dt$ and $W_2 Q d(\Delta B_0)/dt$, taking into account the appearance of the corresponding emf, in each of the feedback windings. It was proved in [6] that these emf's can be neglected in the case of current feedback and active load. We assume that this may be done in the present case, bearing in mind the qualitative nature of our estimate. Under these conditions we may, to elucidate the effect of the feedback, use (20), in which the values for K_c and K_r are chosen from (16). It is easily comprehended that an increase in K_r due to positive current feedback or to negative voltage, feedback gives rise to a decrease in τ_{mec} and, consequently, to an acceleration of the transient response. Positive voltage feedback increases K_c and, consequently, τ_{el} as well. However, if r_0 is also simultaneously increased, maintaining the condition $U_0 I_0$ = const, then τ_{el} will be decreased. Thus, with the assumptions we have made, all forms of feedback are advantageous, in the sense of accelerating the transient response.

We note that if $K_r < 0$, then $\tau_{mec} < 0$ and the term with $d(\Delta n)/dt$ may become negative. In this case, the system exhibits a static instability, the assumption of linearity is unrealistic, and autooscillations will arise in the system, as we have observed in experiments.

Several Remarks Regarding Nonlinearity of Mechanical Characteristics

When low-quality cores are used, the two assumptions made will not hold. In this case, it is impossible to consider the coefficients S and R_1 (1) as constants, where their maximum corresponds to a linear domain. With such cores, the load curve cannot be approximated by a straight line, as the second assumption required. In this case, a more suitable approximation is $E_\omega^2 = U_s^2 - (E_c + RI_\omega)^2$, by virtue of which $-dE_\omega = (dE_c + RdI_\omega)(E_c + RI_\omega) / E_\omega$. By denoting $(E_c + RI_\omega) / E_\omega = \alpha$, $R_1 / \alpha = R_{1\alpha}$ and $k/\alpha = k_\alpha$, we can find that

$$dn = \frac{k_\alpha}{C_E} dI_0 - \frac{dM}{C_M C_E} (R_{i\alpha} +$$

$$+ R) = K_c dI_0 - \frac{dM}{K_r}. \qquad (10')$$

Thus, K_c and K_r will depend on the values of α, S, and R_1 which, in their turn, are determined by the choice of the working point. The common structure of (10) and (10') allows the basic propositions of the analysis provided earlier to be extended to the given case also, of course, in the neighborhoods of each working point.

We now explain the influence of S and R_1 on the linearity of the mechanical characteristics: For this purpose, we determine the relative variation of the rigidity coefficient due to the variation of the internal impedance and of the slope, respectively on dR_1 and dS.

Using the expression for K_r from (10), we find that

$$\frac{dK_r}{K_r} \approx -\frac{dR_1}{R_1}.$$

In the absence of feedback, the linearity of the mechanical characteristic will be determined by the constancy of R_1. In the case of positive current feedback

$$\frac{dK_r}{K_r} = -\frac{(1-\beta_1 S)\,dR_1 - \beta_1 R_1 dS}{R_1(1-\beta_1 S)+R}.$$

If

$$|R_1(1-\beta_1 S)+R| - \quad \text{then}$$

$$K_r \to \infty \text{ and } \frac{dK_r}{K_r} \to \infty.$$

Increasing the rigidity by means of current feedback leads to a sharp manifestation of nonlinearity in the mechanical characteristics. Finally, as was shown earlier, with negative voltage feedback, K_r converges monotonically to its limit $1/r_c$ if $|\beta_2| \to \infty$. In this case, dK_r/K_r will converge to zero. Consequently, negative voltage feedback allows the mechanical characteristic to be linearized and, therefore, is frequently used in combination with positive current feedback. This assertion is confirmed, in particular, by the data of the experimental investigation given in [2].

Design Considerations

The order followed in designing amplifiers will be different, depending on the problem posed and the data originally given, which must be sufficient and which must be compatible. The consideration of all the questions related to design goes beyond the limits of the present work. Here, we limit ourselves to illustrating how the expressions given earlier may be employed in design work.

Let there be given the nominal parameters and operating mode of the motor, $M^\bullet$, $I^\bullet_c$, C_M, $n^\bullet$, the voltage on the brushes $U^\bullet_c$, r_c, and C_E, the limiting variation of torque and number of rotations $\Delta M^\bullet$ and $\Delta n^\bullet$, the core parameters $\mu_1, \sigma, B_1, B_2, H_1,$ and H_2 or the corresponding family of magnetization curves from which these parameters may be determined, and the necessary values of the coefficients K_c and K_r.

We now determine the required volume of cores. This will be used in the best way if, in the process of operation, there are attained the largest admissible values (in the limits of the linear domains) of magnetic induction B_2 and magnetic-field strength H_1. By taking this circumstance into account, we find, on the basis of (5) and (13), that

$$\frac{\Delta E^\bullet_c + R\Delta I^\bullet + (R-r_c)\,\Delta I^\bullet_2}{\omega W_\omega \Delta B^\bullet_\omega} = Q, \qquad (21)$$

where $\Delta B^\bullet_\omega = B_2 - B_1$. The components of the voltage drop given in the left member of (21) are represented in Fig. 2 by the following segments: the increase in motor emf $\Delta E^\bullet_c$, by segment ce; the voltage drop across all the active impedances due to the increase in drive current $R\Delta I_c^\bullet$, by segment bc; voltage drop due to the current of the voltage feedback $(R-r_c)\,\Delta I^\bullet_2 \approx (R-r_c)\,I^\bullet_2$ – by segment ed. Since $I^\bullet_\omega = I^\bullet_c + I^\bullet_2$ (Fig. 2) then from (4), we find that

$$\frac{(I^\bullet_c + I^\bullet_2)\,W_\omega}{H_1} = l. \qquad (22)$$

It is assumed for this that the inequality $(I^\bullet_c - \Delta I^\bullet_c)\,W_\omega \geqslant H_2 l$ always holds.

Equations (21) and (22) permit the calculation of the active volume of the cores $V = Ql$ if one knows, in addition to the original data, the values of R and $I^\bullet_2$, i.e., essentially, r_1, r_a, r_1, and r_2. Resistance r_a depends on the rectifier properties and may be found by well-known methods. Amplifier efficiency and volume of copper depend on resistances r_1, r_1, and r_2. Their values can be varied within well-known limits. We assume roughly that $r_i \approx r_1 \approx r_c$, $r_2 \approx (5-10)\frac{U^\bullet_c}{I^\bullet_c}$ and, consequently, $I^\bullet_2 \approx (0{,}2 \text{ to } 0{,}1)\,I^\bullet_c$. We note that the core volume, found in accordance with (21) and (22) is minimal from the point of view of guaranteeing the magnetic mode. The possibilities of spacing the windings must be verified by additional well-known methods.

By knowing the value of V, we can determine Q or l by giving either the cross section or the mean length of the magnetic circuit. For different ratios of Q/l, we obtain different-size apertures and, to a certain degree, different operating conditions for the cores. The question as to the optimal ratio of Q/l requires a special investigation. As a first approximation, it is advantageous to start with the data given in the table below, obtained on the basis of the recommendations found in [10]:

$V/2$, cm^3	1.0	2.0	10	20	30	60	100	300
$Q/2l$, cm	0.02	0.035	0.05	0.075	0.1	0.15	0.2	0.3

By selecting the value of Q, we find from (21) the number of turns W_ω, and from (3) the magnitude of R_1. Then, using (15), we should determine β_1, β_2, and S for the given K_c and K_r. Since there are three unknowns, one of them should be given, since the necessary control coefficient can be obtained by virtue either of the proper value of W_0 or of W_2. When internal feedback is used, $\beta_1 S \approx 1$. Then, β_2 and S are determined uniquely. Finally, we calculate the supply voltage by the formula $U_s = \omega W_\omega Q B_2 + (I^\bullet_c - \Delta I^\bullet_c) R + (U^\bullet_c - \Delta E^\bullet_c)$, the meaning of which is clear from Fig. 2, on which the particular case is shown when $\Delta E^\bullet_c \approx U^\bullet_c$.

SUMMARY

The analysis of the equations obtained for the MA-M system leads to the following conclusions:

1. When there is no feedback, it is not possible to provide a satisfactory operating mode of the MA-M

system. Introduction of current and voltage feedback can have an effect on the rigidity of the mechanical characteristics and on the control coefficient. The best results can be obtained with the concurrent employment of the aforementioned forms of feedback.

2. Feedback permits the acceleration of the transient response and the linearization of the mechanical characteristics.

3. The expressions obtained may be used for a first-approximation design of an amplifier in accordance with the methodology presented.

LITERATURE CITED

1. R. Kh. Bal'yan, "Push-pull magnetic amplifiers with dc outputs," Avtomatika i Telemekhanika 17, 2 (1956).
2. A. B. Rosenbauli and L. N. Selivokhin, "Construction of the characteristics of a dc drive with choke control," Elektrichestvo No. 10 (1958).
3. S. Ya. Dunaevskii, "On the range of speed control in a motor-generator system with a rotary amplifier," Vestnik elektroprom No. 8 (1951).
4. A. A. Sirotin, "An engineering method of calculating the characteristic of an independently excited motor in systems for the automatic maintenance of speed," Elektrichestvo No. 12 (1954).
5. A. G. Ivakhnenko, Automatic Speed Control of Low Power Asynchronous Motors [in Russian] (Izd AN Ukr SSR, 1953).
6. L. V. Safris, "Designing a magnetic amplifier with linearized magnetization characteristics," Trudy Rostov. Inst. Inzh. Zh.-d. Transporta No. 20 (Transzhelkorizdat, 1956).
7. L. V. Safris, "On the question of transient responses in magnetic amplifiers inductively loaded via rectifiers," Avtomatika i Telemekhanika 19, 3 (1958).
8. N. A. Kaluzhnikov, "On the design of choked magnetic amplifiers, connected on a single-phase rectifier bridge," Avtomatika i Telemekhanika 19, 3 (1958).
9. G. S. Tsykin, Negative Feedback and Its Applications [in Russian] (Svyaz'izdat, 1940).
10. M. A. Rozenblat and O. A. Sedykh, "General principles in the construction production planning of toroidal cores for magnetic amplifiers," Otchet Instituta Avtomatiki i Telemekhaniki AN SSSR (1957).

THE USE OF HALL PICKUPS IN MAGNETIC HEADS

Yu. A. Vasilevskii

(Moscow)

Translated from Avtomatika i Telemekhanika, Vol. 21, No. 3, pp. 402-408, March, 1960
Original article submitted March 4, 1959

This paper reports on the development and experimental investigation of magnetic reading heads based on the Hall effect. The heads have the property that their emf is proportional to the residual carrier flux, in contradistinction to the usual induction-type reading heads in which the emf is proportional to the velocity of flux change. The heads can operate both with magnetic tape and with carriers in the form of drums or disks.

In ordinary magnetic heads for reading or reproducing magnetic recording, there occurs a differentiation of the signal stored on a ferromagnetic carrier. With this, there appear distortions in the amplitude and phase frequency characteristics of the reproduction channel which hinder correct transmission of the signal. Exceptions are sinusoidal signals which, in the given case, do not undergo changes in form if the system is linear. However, even for them there are serious limitations in the range of low audio and infraaudio frequencies.

It is not always possible to tolerate this disadvantage of induction heads, despite their great superiority in other respects. Therefore, there were developed a number of designs of the so-called flux-sensitive heads of the servo system type, whose output emf's are proportional, not to the velocity of change, but to the magnitude of the residual carrier flux. The best known of these are the magnetomodulation head whose operating principle is analogous to a magnetic amplifier (sonde) of the second harmonic type, and the electrobeam head, based on a tube with magnetic deflection of the beam.

The flux-sensitive heads to be considered below, based on the Hall effect, are further developments in this direction. Their operating principle amounts to this, that the residual carrier flux, by means of a magnetic circuit, is applied to a Hall pickup, with the result that at the pickup's output there is generated an emf which is proportional to the magnitude of this flux.

One design of such a head is shown schematically on Fig. 1, a; an over-all view of it is shown in Fig. 1, b. Used in it is an ordinary ring-shaped magnetic circuit, for example, from standard head V-01. The dimensions of core 1 are as follows: length of the leading (reading) slit d_1 = 45 microns; length of the trailing slit d_t = 0.28 mm; outside diameter of the core D_0 = 25 mm; inside diameter D_1 = 18 mm. Height of the core assembly is h = 7 mm. The given design is intended to operate with magnetic tape 2 of width 6.35 mm, although it can also operate with a magnetic drum. The Hall pickup 3 is established in the leading slit of the magnetic circuit. Semiconductor pickups of n-type germanium (n-Ge) were used, with dimensions of 6 × 3 × 0.18 mm.

The Hall pickup has a dc supply. The selection of the magnitude of the current turned out to have an essential influence on the head's signal-to-noise ratio. We used the following method to determine the optimum current magnitude. On the carrier there was recorded a sinusoidal signal with a frequency of 125 cps (carrier speed of motion was 38.1 cm/sec) and with a magnitude of residual flux Φ_C = 300 millimaxwells. For the carrier used, this level was about 10 db lower than the saturation level. The pickup's Hall electrodes were supplied directly at the high-ohmic input of the amplifier circuit. Since the pickup's inherent noise is independent, within broad limits, of the magnitude of the signal, the signal-to-noise ratio was determined as the ratio of the indication of

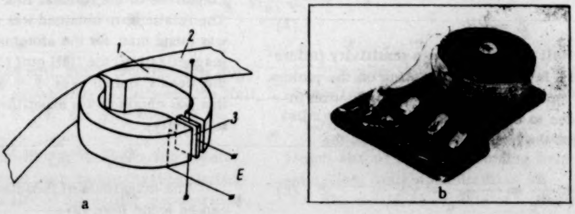

Fig. 1.

the instrument at the output of the amplifier circuit at the time of carrier motion to the instrument's indication for a motionless carrier. This ratio was taken off as a function of the magnitude of the current supplied to the pickup. As a result, it was found that the optimum magnitude of this current for the head under consideration was 8 ma. With such a current, and for an amplifier circuit passband of 20 to 6000 cps, the signal-to-noise ratio was 20.4 db; for a passband of 75 to 150 cps, this ratio was 33.2 db and, for a passband of 25 to 100,000 cps, it equaled 17 db. To eliminate pickup from the constant poles, the current supply circuit for the pickup was carefully screened. A thermal regimen corresponding to the pickup's optimal supply current and to an ambient temperature on the order of 25°C provided prolonged stable operation of the head. For example, the pickup was supplied with current continuously for 48 hours. With this, the operation of the head was periodically verified. No operating changes were observed.

The magnitude of the emf generated by the pickup when it is acted upon by the carrier's magnetic field is related to the head's sensitivity. As a preliminary measure, we found the character of the calculated dependency of the head's sensitivity on the parameters of its magnetic circuit and on the so-called voltage sensitivity of the Hall pickup [1].

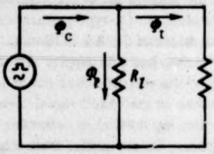

Fig. 2. Simplified equivalent schematic of the head's magnetic circuit. R_l is the reluctance of the leading (reading) slit, R_t is the reluctance of the trailing slit, and Φ_C is the carrier's residual flux.

In a first approximation, the equivalent schematic of the head's magnetic circuit has the form shown in Fig. 2. The emf at the pickup's output may be given as

$$E = \gamma B, \tag{1}$$

where γ is the Hall pickup's voltage sensitivity (microvolts / gauss) and B is the induction acting on the pickup. In our case, B is the average value of the induction in the trailing slit due to the residual carrier flux Φ_C.

We determine the head's sensitivity from the formula

$$\eta = \frac{E}{\Phi_c} = \frac{E}{B}\,\frac{B}{\Phi_c} = \gamma\nu, \tag{2}$$

where ν is a coefficient defined by the parameters of the head's magnetic circuit:

$$\nu = \frac{\Phi_t}{\Phi_c S_t} = \frac{1}{S_t + d/R_l},$$

S_t is the cross section of the flux in the trailing slit, R_l is the reluctance of the leading slit, i.e.,

$$\eta = \frac{\gamma}{S_t + d/R_l}.$$

In the general case, Φ_C is, with certain limitations, an arbitrary function of the space coordinates related to the carrier, and B and E are functions of time corresponding to it.

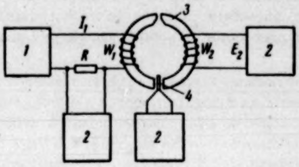

Fig. 3. Scheme for measuring the Hall pickup's sensitivity, with the pickup located in its operating position between the halves of the head's core. 1 is a generator, 2 is a vacuum tube voltmeter, 3 is the head's core, and 4 is the Hall pickup.

The pickup's voltage sensitivity was determined experimentally as shown in Fig. 3. The head's core had two windings: magnetizing winding W_1 and measuring winding W_2. The measure of magnetic induction in the core was taken to be the magnitude of the voltage induced in winding W_2. The ratio of the measured magnitude of the Hall emf E to the corresponding value of induction B gave the mean value of the pickup's voltage sensitivity $\gamma = 116$ microvolts/gauss from whence, for the parameters of the magnetic circuit previously enumerated, we found the computed sensitivity of the head:

$$\eta = 204\ \mu v / \mu sec$$

The experimental value of the head's sensitivity was determined by measuring the emf at the pickup's output and seeking the dependency of the emf on the magnitude of the residual flux for an 8 ma supply current. The relationship obtained was close to a linear one. It was found that, for the aforementioned intensity of magnetization, the Hall emf (the equivalent value) at the head's output was E = 52 microvolts. From this was obtained the experimental value of the head's sensitivity:

$$\eta_{exp} = \frac{52}{0.3} = 173\ \mu v / \mu sec$$

The magnitude of induction B in the trailing slit can be found from (2):

$$B = \frac{\eta}{\gamma}\,\Phi_{\text{н}} = 0.45 \text{ gauss}$$

On the basis of the dynamic range of 20.4 db, found earlier, the head's sensitivity threshold corresponds to a value of induction of

$$B_{\min} = \frac{0.45}{10^{20.4/20}} = 4.3 \cdot 10^{-2} \text{ gauss}$$

The head's frequency characteristic, obviously, is determined by the frequency characteristics of the two factors in (2). The frequency characteristic of the voltage sensitivity γ was measured by the circuit of Fig. 3 for a constant value of induction B = 3 gauss within the frequency limits of 20 to 200,000 cps. It was found that, within these limits, the voltage sensitivity does not depend on frequency.

In a pickup placed in a variable magnetic field, there is induced an induction emf which is added geometrically to the Hall emf. However, the induced emf can be easily compensated by the proper placement on the core of one of the conductors joining the Hall electrodes to the amplifier circuit. The optimum compensation is chosen as that giving the minimum deviation of the instrument in the circuit of the Hall electrodes at the highest operating frequency. On the basis of the system's linearity and the applicability of the principle of superposition, one can use still another method of isolating the Hall emf from the geometric sum of the two emf's : with the current supplying the pickup switched in, one measures (without compensation) the total emf, after which, with the current switched off, one measures the induced emf. Their geometric difference gives the Hall emf. By such a method, results were obtained which coincided closely with the previous ones until the induced emf exceeded the Hall emf by a factor of more than 3 or 4 . This latter method is effective when the Hall pickups are used as pickups for geometric sums or differences of stimuli, one of which is proportional to the frequency.

The frequency characteristic of coefficient ν is determined by the magnetic and geometric parameters of the core such as, for example, the slit and the frequency-dependent losses, and is not characteristic of the given head .

Since, in the range considered, the pickup sensitivity does not depend on frequency, the head's frequency characteristic is simultaneously the frequency characteristic of the induction in the trailing slit.

The head's experimentally obtained frequency characteristic is shown in Fig. 4. The signal was recorded at a constant writing current but at different frequencies, with a speed of carrier motion of 38.1 cm/sec. Some lifting of the characteristic in the low-frequency range is related to the length of the head contact with the carrier. The fall of the characteristic in the high-frequency range is explained both by slit phenomena and by certain other peculiar characteristics of magnetic recording.

On the other hand, since the Hall emf may be defined in practice as the geometric difference of the total emf and the induced emf, this is confirmed by the form of the proportional dependency (1) between the Hall emf E and the induction B, i.e., the head possesses the property of flux sensitivity.

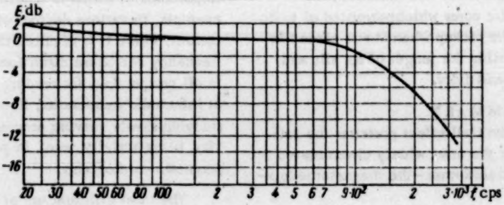

Fig. 4.

This latter was illustrated by the following experiments. Recording was read from an immovable carrier. The magnetization intensity of the carrier corresponded to :

1) a sinusoidal signal with a recording wavelength of 16 mm;

2) a pulse signal with a dipole recording length of 10 mm (recording from zero to saturation; a mark-space ratio of 2);

3) a rectangular signal with a dipole recording length also of 10 mm (recording from saturation to saturation; mark-space ratio of 2).

The carrier, by means of a micrometric device, was drawn past the head for a definite distance and then stopped, after which a sensitive galvanometer measured the voltage on the head's Hall electrodes.

The point of reading initiation coincided with the beginning of the recording, for which the initial portion of the recording was made visible by precipitating on the carrier a powder of carbonyl iron from a heptane suspension. As a result of this, there was shown the synphasing of the carrier's surface residual flux and the voltage on the head's Hall electrodes.

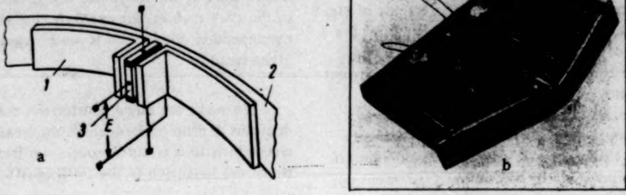

Fig. 5. 1 is the core, 2 is the carrier, 3 is the pickup.

We should mention one further trial head design, shown in Fig. 5, a and b. The head's magnetic circuit is open, and the Hall pickup is placed in the reading slit whose length is about 0.35 mm. The design has extended pole shoes (the length of each shoe is 25 mm) and is intended to read recording of long wavelengths. A simplified equivalent schematic of the head's magnetic circuit can be obtained if, in Fig. 2, one sets $R_t = \infty$. As should be expected, with the same pickup, this design has greater sensitivity and a correspondingly better dynamic range than the first design. At a frequency of 40 cps, the increase in sensitivity is about 4 db.

Other heads based on the Hall effect which were investigated differed from the two types considered here only by the core configurations and materials; for example, we used ferrite cores which permitted us to do without insulation of the pickup when it was placed in the slit, thereby decreasing the length of the slit and increasing the head's sensitivity.

SUMMARY

A head based on the Hall effect possesses the following advantages over the most widely disseminated type of flux-sensitive transformer—the magnetomodulation head.

1. It permits simplification of the electrical reading scheme.

2. It possesses sensitivity to the direction of the carrier field, i.e., to the polarity of the signal.

3. It can operate in a broad frequency range, in particular, for frequencies of the order of 100 kcps and higher. In this case it is advantageous to use a ferrite magnetic circuit.

4. With heads based on the Hall effect, the danger of random erasure or magnetization of the carrier is excluded.

5. Phase distortion of the signal is virtually eliminated.

6. The requirements on head shielding are reduced.

7. Simplicity of design and small dimensions are provided.

This last quality effectively distinguishes the head based on the Hall effect from the other well-known flux-sensitive head—the head of the electron-beam type.

The Hall pickup is an inductionless transformer, which eases the shielding of such a head in comparision with an ordinary induction head of equal sensitivity.

A head based on the Hall effect may be useful in many cases of special uses of magnetic recording, the importance of which is continuously growing; for example, in various devices of automation and remote control, where it is required to read pulses with minimal frequency and phase distortions; in geology, particularly in oil prospecting, for reading processes which change at infraaudio frequencies; in medicine and biology, for studying slowly varying processes related to brain activity, heart activity, etc., in particular, for reading magnetic cardiograms.

The most efficient use of heads based on the Hall effect is in the frequency range from fractions of a cps to about 100 cps, and for carrier speeds up to 4 to 5 cm/sec, i.e., in those cases where induction heads are practically ineffectual. The basic disadvantage of a head with a Hall pickup for sound reproduction is the relatively small dynamic range. There exist the following ways of improving the dynamic range and other indicators of head quality:

1. Improvement of the technology of preparing Hall pickups, the quality of processing the surfaces and contacts.

2. The use of Hall pickups with non-current-carrying contacts.

3. The use, for pickups, of materials with higher Hall constants.

4. Reduction of the length of the slit in which the Hall pickup is established, which introduces the particular requirement to reduce the width of the pickup. There is interest, in this connection, in film pickups of materials with high voltage sensitivity. These latter can be mounted in the form of a thin film of thickness of 10 to 100 micrometers on the face surface of a ferrite core.

5. The use of magnetic recording carriers with high values of residual flux.

6. Operation with high levels of carrier magnetization, for example, with levels corresponding to the magnetic saturation of the carrier, as occurs in the majority of special applications of magnetic recording.

In conjunction with this, it should be mentioned that, in many cases of special uses of magnetic recording, only a twofold increase of signal over noise is sufficient.

LITERATURE CITED

1. A. R. Regel', Semiconductor Measurers of Magnetic-Field Strength [in Russian] (LDNTP, Leningrad, 1956).

A VOLTAGE DEFLECTION PICKUP BASED ON SEMICONDUCTOR ELEMENTS*

S. V. Kulikov

(Moscow)

Translated from Avtomatika i Telemekhanika, Vol. 21, No. 3, pp. 409-416, March, 1960
Original article submitted August 19, 1959

A description is given of a voltage deflection pickup implemented by semiconductor elements — silicon base diodes, transistors, and thermoimpedances. A design methodology is proposed, and calculated relationships and experimental results are given.

General Remarks

The voltage deflection pickup considered in this paper is designed for use in systems for stabilizing voltage or any quantity which is transformed to a voltage. The special feature of the voltage deflection pickup, shown in Fig. 1 and 2, is its implementation by semiconductor elements. This provides its small weight and size (Fig. 2), reliability, heightened resistance to vibration and shock, and length of useful life .

Type D 810 silicon base diodes D_1 and D_1', connected in opposite arms of bridge D_1-R_p-R_{11}-D_1'-R_{12}, execute the function of voltage calibration. The voltage to be regulated, E_{reg}, is applied to one of the bridge's diagonals via ballast resistor R_{13}. Connected to the other diagonal of the bridge is a preamplifier of silicon transistors T_1-P102, T_1'-P102, whose output current controls the relay power amplifier, implemented by germanium transistors T_2, T_2'-P13A, T_3 and T_3'-P4D. Thermoimpedances R_{T_1} and R_{T_2} are used to compensate the temperature variations in the scheme.

To obtain, in load impedances R_3 and R_3', a signal whose average value would be a continuous function of the input signal for a limited range of variation of the latter, one should connect, instead of resistors R_5 and R'_5, condensers C_1 and C'_1 (shown by dashed lines in Fig. 1),which would provide self-excitation, i.e., the principle of vibration linearization is used. Pulse-width modulation is used in the scheme for deviations of the controlled voltage.

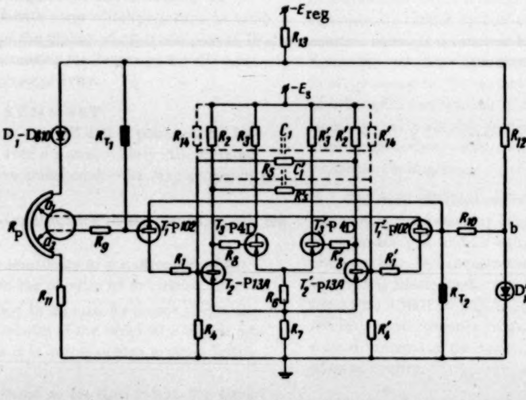

Fig. 1. Simplified schematic of the voltage deflection pickup . $R_1 = R'_1 = 1.2$ kohm; $R_2 = R'_2 = 3.3$ kohm; $R_3 = R'_3 = 100$ ohm; $R_4 = R'_4 = 5.6$ kohm; $R_5 = R'_5 = 15$ kohm; $R_6 = 5$ ohm; $R_7 = 5$ ohm; $R_8 = R'_8 = 1$ kohm; $R_9 = 0$; $R_{10} = 200$ ohm; $R_{11} = 1920$ ohm; $R_{12} = 2100$ ohm; $R_p = 542$ ohm; $R_{a_1-a_2} = 210$ ohm; $R_{a_1} = 40$ ohm ; $R_{13} = 395$ ohm .

---

* The results of the investigation described in this paper were discussed in the April, 1959 seminar of the Laboratory of Automation and Remote Control Elements of the IAT AN SSSR .

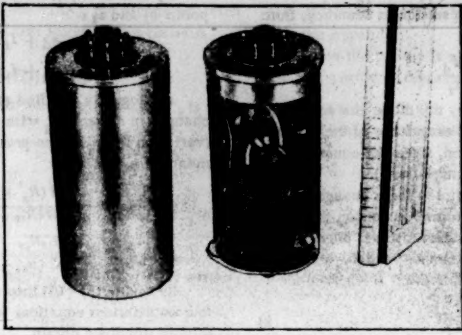

Fig. 2. Outside view of the voltage deflection pickup.

Posing of the Problem

The problem raised in this paper is the presentation of an engineering method of designing the voltage pickup. Relationships are derived which, for given regulated voltage E_{reg}, source voltage E_3 and load resistances R_3 and R'_3, allow one to determine the remaining circuit parameters for which feasibility of the circuit and its stability under temperature variations would be guaranteed.

In addition, a generalized method is propounded for the analysis of transistor switching circuits.

Method of Investigation

Thanks to the fact that silicon transistors in the cutoff region have insignificant current flowing through the base-collector junction ($I_{CO} \leq 1 \mu a$), it is possible to design the bridge together with the thermoimpedances R_{T_1} and R_{T_2}, and to implement the additional impedances R_9 and R_{13} separately.

In designing the bridge, the nonlinear base diodes D_1 and D'_1, after the piecewise-linear approximation of their volt-ampere characteristics, are given as "conditionally autonomous" dipoles with emf's E_d and E'_d and with impedances R_d and R'_d (Fig. 3).

The high-ohmic thermoimpedances R_{T_1} and R_{T_2} are presented as current sources I_{T_1} and I_{T_2}.

As a result, we obtain the replacement scheme, shown in Fig. 4, for the bridge. It is calculated by the methods of the linear theory of electrical circuits.

By considering the outputs of transistors T_1 and T'_1 as current sources (in the equilibrium state the currents virtually equal zero), one can compute the relay stages of transistors T_2, T'_2, T_3 and T'_3 separately. The design of the latter is implemented from the conditions of transistor cutoff and saturation, with account taken of temperature variations.

For the computation of the circuit's sensitivity (cf. the Appendix), we introduce the concept of a "conditionally autonomous three-pole," allowing one to take into account the nonlinear properties of the transistor and, at the same time, to use a generalized method of designing linear electrical circuits.

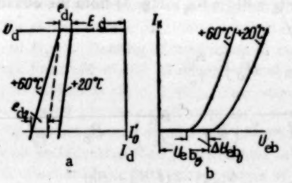

Fig. 3. Volt-ampere characteristics for determining parameters. a is for the silicon base diodes, b is for the silicon transistors.

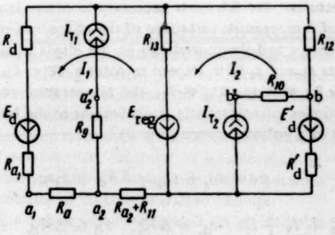

Fig. 4. Equivalent replacement scheme of the nonlinear bridge.

Designing the Nonlinear Bridge

Use of type D808-813 base diodes shows that, for the greatest stability, their operating current I_0 must be of the order of 5 ma.

The magnitude of currents I_{T_1} and I_{T_2} on the circuit of Fig. 4 are determined, with sufficient accuracy, from the equation

$$I_T = \frac{E_d}{R_T}, \tag{1}$$

where E_d is the emf defined by the diode characteristics (Fig. 3), $E_d < E'_d$; R_T is the magnitude of the thermoresistor (the subscript is omitted, since the equation is valid for both diodes and thermoresistors).

The thermoresistors are chosen large enough so that, first of all, operation of the thermoresistors on the linear portion of the volt-ampere characteristic is provided [1] and, secondly, the thermoresistors R_{T_1} and R_{T_2} can be replaced by current sources. This latter is realized for the condition

$$I_0 \geqslant 10 I_T. \tag{2}$$

By neglecting the components of I_T in the bridge, we can find the resistances R_{12}, R_{13} and $R = R_{11} + R_a + R_{a_1} + R_{a_2}$ ($R_p = R_a + R_{a_1} + R_{a_2}$, Fig. 1) from the equations

$$R_{12} = R'_d + \frac{E'_d}{I_0}, \tag{3}$$

$$R = 2\left(R'_d + \frac{E'_d}{I_0}\right) - R_d - \frac{E_d}{I_0}, \tag{4}$$

$$R_{13} = \frac{E_{reg} - 2(I_0 R'_d + E'_d)}{2I_0}, \tag{5}$$

where R'_d is the diode's dynamic impedance.

The remaining unknown resistances, R_a , R_{a_1}, R_{a_9}, and $R_{a_{10}}$, are determined from the conditions of equilibrium of the circuit for normal and for elevated temperatures. For this, it is necessary to determine the effect of temperature variations of the characteristics of the diodes and thermoresistors on the displacement of points a_1 and a_2 with respect to point b (Fig. 4).

For $R_d \ll R$ and $R'_d \ll R_{12}$, the temperature variation of the diodes' characteristic is equivalent to the introduction of a voltage source (Fig. 3)

$$e_d = e_{d_1} + e_{d_2} = \Delta E_d + I'_1 r_d, \tag{6}$$

where

$$I'_0 = I_0 + I_T + i_T, \quad e_{d_1} = \Delta E_d, \quad r_d = \Delta R_d, \quad i_T = \Delta I_T.$$

Using the principle of superposition, we determine the effect of temperature variations of the diodes' characteristic from the matrix equation

$$\begin{bmatrix} i_1 \\ i_2 \end{bmatrix} = \begin{bmatrix} R + R_{13} & -R_{13} \\ -R_{13} & R_{13} + R_{12} \end{bmatrix}^{-1} \begin{bmatrix} -e_d \\ +e_d \end{bmatrix}, \tag{7}$$

where i_1 and i_2 are the increments of currents I_1 and I_2 (Fig. 4).

Solving (7), we get

$$i_1 = \Delta I_1 = \frac{(R_{12} + R_{13})\, e_d - R_{13} \dot{e}_d}{R(R_{12} + R_{13}) + R_{12} R_{13}}. \tag{8}$$

By means of (8), we determine the displacements of points a_1 and a_2 :

$$\Delta U'_{ba_2} = \dot{e}'_d + i_1 (R - R_a - R_{a_1}),$$
$$\Delta U'_{ba_1} = \dot{e}'_d + i_1 (R - R_{a_1}). \tag{9}$$

Analogously, we find the displacements due to changes in current I_{T_1} with the condition that $R \gg R_p$ (variation in I_{T_2} has no practical effect on the displacements of a_1 and a_2) :

$$\Delta \dot{U}_{ba_2} = -\frac{R(R_a + R_{a_1})(R_{12} + R_{13})}{R(R_{12} + R_{13}) + R_{12} R_{13}} i_{T_1};$$

$$\Delta \dot{U}_{ba_1} = \frac{R_a R_{12} R_{13} - R_{a_1} R (R_{12} + R_{13})}{R(R_{12} + R_{13}) + R_{12} R_{13}} i_{T_1}. \tag{10}$$

By taking (8)-(10) into account, one can set up the four equilibrium equations for the two temperatures, by solving which we obtain

$$R_8 = \frac{I_{T_1}(\Delta U_{eb_0} + \Delta U'_{eb_0}) + i_{T_1}(U_{eb_0} + U'_{eb_0})}{I_{T_1} i_1 + I_0 i_{T_1}},$$

$$R_9 = \frac{(I_0 - I_{T_1})(\Delta U_{eb_0} + \Delta U'_{eb_0}) - (i_1 + i_{T_1})(U_{eb_0} + U'_{eb_0})}{I_{T_1} i_1 + I_0 i_{T_1}},$$

$$R_{a_1} = \frac{r_1^2 (U'_0 i_{T_1} - \dot{U}_0 I_{T_1})}{(r_1^2 I_0 - r_2^2 I_{T_1})\, i_{T_1} + (r_1^2 i_1 + r_2^2 i_{T_1})\, I_{T_1}},$$

$$R_{10} = \frac{(r_2^2 I_{T_1} - r_1^2 I_0)\, \dot{U}_0 - (r_1^2 i_1 + r_2^2 i_{T_1})\, U'_0}{(r_1^2 I_0 - r_2^2 I_{T_1})\, i_{T_1} + (r_1^2 i_1 + r_2^2 i_{T_1})\, I_{T_1}}, \tag{11}$$

where

$$r_1^2 = R(R_{12} + R_{13}) + R_{12} R_{13},$$
$$r_2^2 = R(R_{12} + R_{13}),$$
$$U'_0 = I_0 R - E'_d - U'_{eb_0} - I_{T_1} \frac{R_{12} R_{13}}{r_1^2} R_a,$$
$$\dot{U}_0 = -i_1 R - \dot{e}'_d + \Delta U'_{eb_0} - i_{T_1} \frac{R_{12} R_{13}}{r_1^2} R_a;$$

U_{eb_0} , U'_{eb_0} , ΔU_{eb_0} and $\Delta U'_{eb_0}$ are the threshold voltages and their increments , defined for the corresponding triodes T_1 and T'_1 from Fig. 3, b.

As is obvious from (11), for certain special values of the parameters on the right, the magnitudes of resisters R_9, R_{a_1} and R_{10} may turn out to be zero.

Design of Relay Stages (Switching Circuits)

The design of relay stages from transistors T_2, T'_2, T_3 and T'_3 leads to the determination of resistances $R_2 = R'_2$, $R_4 = R'_4$, $R_5 = R'_5$, R_6, R_7, and $R_8 = R'_8$ for known load resistances $R_3 = R'_3$ and supply voltage E_3 . The six unknown resistances are found from the cutoff and saturation conditions of transistors T_2, T'_2, T_3 and T'_3 [2] and from two auxiliary relationships, the first of which expresses the condition that there be no shunting of the relay amplifier's input

$$R_4 \geqslant 10 R_{in} \tag{12}$$

(R_{in} can be set at 500 ohm for P13A), the second of which is the condition of insignificant losses in bias resistors R_6 and R_7:

$$10(R_6 + R_7) \leqslant R_3. \tag{13}$$

The cutoff condition for transistors T_2 and T'_2 is written in the form

$$I_{co_2} R_4 \leqslant \frac{E_s R_7}{R_3 + R_6 + R_7}, \tag{14}$$

where I_{co_2} is the temperature collector current of transistor T_2.

The cutoff condition for transistors T_3 and T'_3, neglecting the emitter current I_{e_2} of triode T_2 in resistors R_6 and R_7, is defined by

$$I_{co_3} R_8 \leqslant \frac{E_s R_6}{R_3 + R_6 + R_7}. \tag{15}$$

The saturation condition for triodes T_2 and T'_2, neglecting I_{co_3} and I_{e_2} in R_7, is written

$$\frac{r_a (r_c^3 - r_b^2 R_5) I_{co_2}}{R_5 E_s} \leqslant R_6 R_2 + R_8 (R_3 + R_6) - r_b^2 \left(\frac{R_7}{R_4} + \frac{R_3 + R_6}{\beta_2 R_2}\right), \tag{16}$$

where

$$r_a = R_3 + R_6 + R_7,$$
$$r_b^2 = R_2 R_5 + R_2 R_8 + R_5 R_8,$$
$$r_c^3 = R_2 R_5 R_8,$$

β_2 is the current transmission coefficient of the base of transistor T_2, and I_{c_2} is the saturation current of the collector of transistor T_2.

The saturation condition for transistors T_3 and T'_3 is defined by the inequality

$$\frac{E_s}{\beta_3 (R_3 + R_6 + R_7)} - I_{co_3} \leqslant I_{b_3}, \tag{17}$$

where I_{b_3} is the base current of transistor T_3. We give this condition in expanded form:

$$r_b^2 \left(\frac{E_s}{\beta_3} - I_{co_3} r_a\right) \leqslant E_s (R_3 R_5 + R_6 R_2) - I_{co_2} R_2 R_5 r_a. \tag{17'}$$

By taking , in (14)-(17), the value of I_{co} which corresponds to the heightened temperature, we can arrive at equalities. A huge increase in the right members of (14)-(17) leads to a lowering of the circuit's sensitivity (cf. the Appendix).

When the pickup is used in the autooscillatory mode, the half-period of the autooscillation, with the conditions

$$R'_{14} = R'_{14} = \infty, \quad R_7 = 0, \quad R_1 = R'_1 = \infty$$

may be found approximately from the formula

$$T = \frac{CE_s}{I_{co_1} + I_{co_2}} \left[\frac{R_2 R_6 + R_3 R_8 + R_6 R_8}{(R_2 + R_8)(R_3 + R_6)}\right], \tag{18}$$

where I_{co_1} is the collector current of transistor $T_1(T'_1)$ at equilibrium, the deviations from which are approximately proportional to the relatively small deviations of the regulated voltage E_{reg}.

Experimental Investigation

The voltage-deviation pickup, designed in accordance with the formulas given above for the case of E_{reg} = 24 v and E_s = 27 v, was subjected to experimental investigation. The pickup's basic parameters are given in the caption of Fig. 1. Testing of the pickup in the temperature range from +20 to +60 °C showed that it reacted reliably to deviations of ± 1 volt. The output current in loads R_9 and R'_9 in the cutoff state for a temperature of +60 °C did not exceed 1 ma. The circuit operated reliably on an inductive load (a differential electromagnetic mechanism). With output stages of transistors P4D, the circuit was capable of a switching power of 200 w. The results of an investigation of the pickup in the proportional mode for a self-excitation frequency of 50 cps are shown in Fig. 5.

Conclusions

The theoretical and experimental investigation provided gives a foundation for concluding that the voltage deviation pickup constructed of semiconducting elements was efficiently developed. The essential advantages of the pickup described —its small weight and dimensions, the increased resistance to shock and vibration, the long useful service life, inherent in semiconducting elements—permit the expanding of the domain of applicability of voltage deviation pickups.

The author wishes to express his gratitude to B. S. Sotskov for his valuable advice on the execution of the present work.

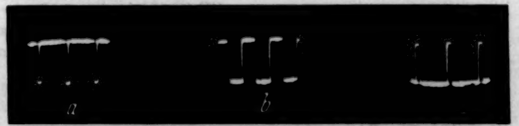

Fig. 5. Oscillograms of pickup output voltages with self-excitation. a is for E_{reg} = 24−0.15 v, b is for E_{reg} = 24 v, and c is for E_{reg} = = 24 + 0.15 v.

APPENDIX

Calculating the Sensitivity of a Relay Scheme

The sensitivity of a relay circuit is defined by the threshold values of controlling current for which the circuit transfers (operates).

In relay schemes constructed of transistors, the currents and voltages on the electrodes of these latter vary within such wide limits that there appear essential nonlinearities in the transistors' properties (cutoff region, saturation and nonlinear active region). However, for a broad class of transistor relay schemes, for definite threshold values of controlling current, it is not necessary to know in detail the nonlinear characteristics of the transistors. It suffices to know the characteristics in the neighborhoods of isolated points, corresponding to the moments of circuit transition points on the boundaries between the cutoff and saturation regions on the one hand, and the active region, on the other.

A nonlinear transistor can be presented as a linear "conditionally autonomous" three-pole (a four-pole with a short-circuited side) for the regions of cutoff and saturation, and also for two (or more) segments of the active region, for example, for the initial (close to the cutoff region) and for the final (close to the saturation region) segments.

Indeed, the behavior of a transistor for constant current in any form of connection (with common emitter, base, collector) is completely described by two nonlinear equations.

For the correspondingly chosen dependent and independent variables, there are six possible variants (systems) of equations. For example, for a circuit with a common emitter, the equations for the dependent base and collector currents have the form

$$I_b = Y_1(U_{eb}, U_{ec}), \quad I_c = Y_2(U_{eb}, U_{ec}),$$

where I_b is the base current, I_c is the collector current U_{eb} is the emitter-base voltage and U_{ec} is the emitter-collector voltage.

On any of the aforementioned segments (in the neighborhood of a point,), one can expand both functions in a Taylor series for two variables, and drop the terms for higher-order derivatives. For example , for the initial portion of the active domain,

$$I_b = \frac{\partial Y_1}{\partial U eb}(U_{eb} - U_{ebI}) + \frac{\partial Y_1}{\partial Y ec}(U_{ec} - U_{ecI}) +$$
$$+ Y_1(U_{ebI}, U_{ecI}), I_c = \frac{\partial Y_2}{\partial U_{eb}}(U_{eb} - U_{ebI}) +$$
$$+ \frac{\partial Y_2}{\partial U_{ec}}(U_{ec} - U_{ec\,I}) + Y_2(U_{ebI}, U_{ecI})$$

or

$$I_b = Y_{11I}U_{eb} + Y_{12I}U_{ec} + Y_{10I},$$
$$I_c = Y_{21I}U_{eb} + Y_{22I}U_{ec} + Y_{20I},$$

where Y_{11I} , Y_{12I}, Y_{21I} , and Y_{22I} are the nonautonomous transistor parameters for the transistor as a four-pole system of conductances for the initial active segment,

$$Y_{10I} = Y_1(U_{ebI}\ \ U_{ecI}) - (Y_{11I}U_{eb\,I} + Y_{12I}U_{ecI}),$$
$$Y_{20I} = Y_2(U_{eb\,I}\ \ U_{ecI}) - (Y_{21I}U_{eb\,I} + Y_{22I}U_{ec\,I})$$

are the "conditionally autonomous" parameters of the transistor as a four-pole for the initial active segment.

By using the well-known relationships for nonautonomous and autonomous parameters [3], one can rewrite the parameters obtained in any system of parameters and for any scheme for connecting the transistor. The parameters for the remaining segments are determined analogously.

A "conditionally autonomous" three-pole can be presented in the form of a nonautonomous three-pole (core) with external autonomous dipoles. Such a representation permits the use of the well-developed methods of analyzing schemes with nonautonomous multipoles [4].

By experimental measurements or by determining from static characteristics the aforementioned transistor parameters, one can replace the circuit of Fig. 1 by an equivalent linear replacement circuit including, together with dipoles, multipole elements and sources. The order of circuit design is as follows: For the first step, one determines the transmission coefficient of the portion of the circuit from E_{reg} to the output of the preamplifier R_1 and R'_1 may be grounded). The second step consists of the determination of the value of collector current of triode $T_1(T'_1)$ which is necessary to operate the relay output stages. For this, the transistors are replaced by "conditionally autonomous" three-poles. As a preliminary step, one determines the collectors' saturation currents, and removes outside the three-pole core the autonomous two-poles. Thereafter, the replacement circuit is constructed.

To determine one (negative) threshold value of the current applied to the input of triode T_2, it is sufficient to determine the magnitude of it for which the base current of cutoff triode T_2 becomes equal to the boundary base current at the beginning of the active portion; the value of this last current is determined from the triode's forward transmission characteristic.

To determine the second (positive) threshold value of current applied to the input of triode T_2, it is first necessary to find the value of base current of triode T_2 for which saturation of triode T'_2 occurs. For this, after disconnecting and grounding the left end of feedback resistor R_6 (Fig. 1), one sets up the matrix of conductances [Y] (or of impedances [Z]) by the method presented in [4]. By a well-known formula, one determines the current transmission factor from the base of T_2 to load R'_2:

$$K_I = \frac{\Delta_{12}}{\Delta_{22} + R'_2\Delta},$$

where Δ is the determinant of matrix [Y], and Δ_{12} and Δ_{22} are cofactors of the determinant [subscript 1 refers to the input (base of T_2) and subscript 2 refers to the output]. After this, one can determine the base current of triode T'_2 which corresponds to saturation of T'_2, and thereafter one finds the threshold value of the input current.

In our case, the problem is essentially simplified, since the circuit is symmetric and is controlled only by negative values of the input current, i.e., only one value of threshold current is determined.

We note that the method presented permits one to take into account the effect on relay sensitivity, not only of the transistors' nonlinearities, but also the temperature variations of their parameters. For this, it is necessary to know the transistor characteristics in the operating temperature range.

LITERATURE CITED

1. B. S. Sotskov, "Thermistors and their use in circuits," Avtomatika i Telemekhanika 7, 1 (1948).
2. B. N. Kononov and L. P. Stepanenko, "Scaler circuits built with semiconducting triodes," Atomnaya énergiya No. 4 (1957).
3. É. V. Zelyakh, Fundamentals of the General Theory of Linear Electric Circuits [in Russian] (Izd AN SSSR, 1951).
4. V. P. Sigorskii, Methods of Analyzing Electric Circuits with Multipole Elements [in Russian] (Izd AN Ukr SSR, 1958).

REGARDING THE THEORY OF THIRD-ORDER LINEAR SYSTEMS

Yu. G. Zarenin

(Kiev)

Translated from Avtomatika i Telemekhanika, Vol. 21, No. 3, pp. 417-419, March, 1960
Original article submitted September 28, 1959

The frequency properties of linear third-order systems are considered. The possible types of frequency characteristics are defined and the relationships which uniquely determine their form are found. The results of the investigation are illustrated by diagrams.

Many automatic control systems can be described by linear third-order differential equations with constant coefficients. In spite of this, the theory of third-order systems is still not completely worked out. In particular, there has not yet been obtained an exhaustive solution to the problem of investigating the frequency properties of these systems. The literature is lacking in statements concerning the possible types of amplitude-frequency characteristics for these systems, as well as any information as to how one might determine the exact number of extremal points of these characteristics (not to mention their coordinates), if the coefficients of the system's differential equation are known. Here, we attempt to fill this void.

The investigation of the amplitude-frequency characteristics of third-order systems is divided into three stages.

a) Determine the possible types of these characteristics. As the basis for classifying amplitude-frequency characteristics, it is convenient to take the number of their extremal points.

b) Elucidate the relationships by means of which one might analytically determine, from the form of the system's differential equation, the type of its frequency characteristic.

c) Define the abscissas of the extremal points of the system's amplitude-frequency characteristic in terms of the coefficients of its differential equation.

We write the differential equation of a third-order linear system in the form

$$(Ap^3 + Bp^2 + Cp + D)\varphi = \psi, \tag{1}$$

where p is the differentiation operator, φ is the instantaneous value of some physical quantity at the system's output which is of interest to us, ψ is the instantaneous value of the signal applied to the input and A, B, C, D are constant coefficients.

To obtain the simplest possible relationships in the sequel, it is convenient [1] to divide both sides of (1) by the coefficient of the highest-order derivative. Denoting the new coefficients thereby obtained by $\underline{a}$, $\underline{b}$, $\underline{c}$, and $\underline{d}$, we can write

$$(p^3 + ap^2 + bp + c)\varphi = d\psi. \tag{2}$$

With this, the equation of the amplitude-frequency characteristic has the form

$$K(\omega) = \left|\frac{d}{H(j\omega)}\right| = \frac{d}{\sqrt{(c - a\omega^2)^2 + (b\omega - \omega^3)^2}}. \tag{3}$$

The number of its extremal points equals the number of positive real roots of the first derivative with respect to ω of the radicand in the denominator of (3). After a single differentiation of this expression, we obtain a fifth-order polynomial which contains no free term; corresponding to this one may assert that the first extremum of a third-order system's frequency characteristic lies on the axis of ordinates. In addition to the root $\omega = 0$, the polynomial under consideration has four pairwise conjugate roots. By considering all these roots to be real, we arrive at the conclusion that the maximum possible number of extremal points of the system's amplitude-frequency characteristic equals three. The minimum number of extrema, realized in the case when all four of the aforementioned roots are imaginary, equals one.

Thus, for a third-order system only three types of frequency characteristics are possible (Fig. 1). The dashed lines show frequency characteristics which are, hypothetically, theoretically possible but which, in practice, are not realizable.

Let us consider in more detail the roots of the first derivative of the radicand expression. By differentiating this expression, and introducing the notation

$$b^2 - 2ac = N \text{ and } 2b - a^2 = R, \tag{4}$$

we obtain the polynomial

$$3\omega^5 - 2R\omega^3 + N\omega = 0, \tag{5}$$

the roots of which equal

$$\omega_1 = 0, \ \omega_{2,3,4,5} = \pm\frac{1}{\sqrt{3}}\sqrt{R \pm \sqrt{R^2 - 3N}}. \tag{6}$$

Discarding the roots less than zero, we obtain the abscissas of the extremal points of the system's amplitude-frequency characteristic:

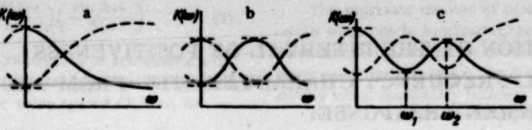

Fig. 1.

$$\omega_1 = 0, \quad \omega_2 = \frac{1}{\sqrt{3}}\sqrt{R+\sqrt{R^2-3N}} \text{ and } \omega_3 = \frac{1}{\sqrt{3}}\sqrt{R-\sqrt{R^2-3N}}. \tag{7}$$

The following conclusions derive from Expressions (7).

1. If N < 0 then, independently of the sign of R, frequency ω_3 is imaginary and ω_2 is real. The system's amplitude-frequency characteristic is a curve with two extrema—at the frequencies $\omega = \omega_1 = 0$ and $\omega = \omega_2$ (Fig. 1, b).

2. For N > 0 and R < 0, both frequencies ω_2 and ω_3 are imaginary. The amplitude-frequency characteristic has only one extremum —at the frequency $\omega = \omega_1 = 0$ (Fig. 1, a). The amplitude-frequency characteristic has the same form in the case when N > 0 and R > 0 but $R^2 < 3N$.

3. Frequencies ω_2 and ω_3 are both real only if the conditions N > 0, R > 0, and $R^2 > 3N$ all hold. With this, the amplitude-frequency characteristic has the form of a curve with extrema at the frequencies ω_1, ω_2, and ω_3 (Fig. 1, c).

The conclusions just drawn, together with (7), exhaust the problem of investigating the frequency properties of third-order systems.

For the practical use of these results, it is very convenient to employ a diagram with coordinates N and R (Fig. 2), on which the various hatchings indicate the regions corresponding to systems with various types of amplitude-frequency characteristics. Similar to those, like the well-known Vyshnegradskii diagram [1], which permit one, without solving equations, to judge of the stability and character of the transient response of a third-order system, the diagram of Fig. 2 gives a representation of its amplitude-frequency characteristic.

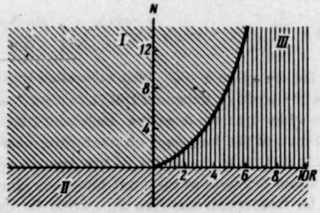

Fig. 2. I is the region of one extremum, II is the region of two extrema, and III is the region of three extrema.

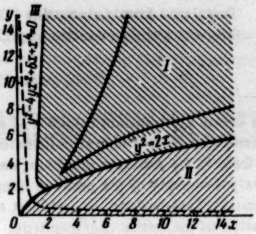

Fig. 3. I is the region of one extremum, II is the region of two extrema, and III is the region of three extrema.

It is interesting to note that the juxtaposition of the diagram proposed by us with the Vyshnegradskii diagram (Fig. 3) graphically illustrates the relationship between the character of a third-order system's transient response and the form of its amplitude-frequency characteristic.

This relationship is implicitly contained in the relationships obtained by Vyshnegradskii and in the relationships given in the present work and, if necessary, could easily be elucidated analytically.

LITERATURE CITED

1. I. A. Vyshnegradskii, "On direct-acting regulators," D. K. Maksvell, I. A. Vyshnegradskii, and A. Stodola, Theory of Automatic Control (the Linearized Problem) [in Russian] (Izd AN SSSR, 1949).

DETERMINATION OF THE INTERVAL OF POSITIVENESS OF THE REAL FREQUENCY CHARACTERISTIC FROM THE GRAPH OF THE TRANSIENT RESPONSE

L. P. Shiniberov

(Leningrad)

Translated from Avtomatika i Telemekhanika, Vol. 21, No. 3, pp. 420-421, March, 1960
Original article submitted April 20, 1959

If one knows the transient response of a closed automatic control system to a unit step stimulus, then one may find from it, by a simple graphical construction, the boundary frequency of the positive interval of the real frequency characteristic ω_p without a detailed determination of the entire characteristic.

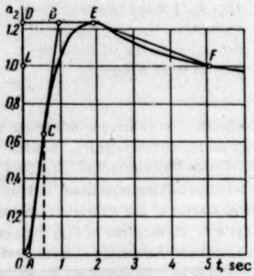

Fig. 1. Determination of ω_p from the graph of the transient response.

We assume that the curve of Fig. 1 is the transient response referred to for the output coordinate $\alpha_2 = f(t)$. On the figure we draw two auxiliary lines: line DE parallel to the axis of abscissas from the axis of ordinates to the maximum point of the transient response, and line AB, coinciding with the majority of points on the ascending (increasing) part of the transient response curve, from the axis of abscissas to line DE. We bisect line AB and find the value of time t_m which corresponds to the midpoint of this line (point C). Then, the boundary frequency of the positive interval can be determined from the formula

$$\omega_p = \frac{\pi}{2t_m}. \tag{1}$$

In the example given, $\omega_p = \pi/2(0.5) = 3.14\ \text{sec}^{-1}$, which is close to the true value of $\omega_p = 3.20\ \text{sec}^{-1}$.

We now prove the validity of the result obtained.

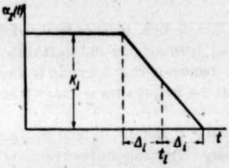

Fig. 2. Typical trapezoidal transient response.

We divide the curve of the transient response, given in Fig. 1, into three parts: 1) the unit step transient response $+1(t)$; 2) the positive trapezoid DEFL lying above the function $+1(t)$ with altitude $K_1 = DL$; 3) the negative trapezoid DBAO with altitude $K_2 = -OD$. From these trapezoidal characteristics it is possible to find the real frequency characteristic of the automatic control system. If we denote the elements of the trapezoidal characteristic as was done in Fig. 2, then in the given case the system's real frequency characteristic $R(\omega)$ will be expressed by the formula [1]

$$R(\omega) = \sum_{i=1}^{2} \left[K_i - \omega K_i t_i \left(\frac{\cos t_i \omega}{t_i \omega} \right) \left(\frac{\sin \Delta_i \omega}{\Delta_i \omega} \right) \right] + 1. \tag{2}$$

For the value $\omega = \omega_p$, this expression must vanish. Since the positive trapezoid DBEFL is always several times wider than the negative trapezoid DBAO, the maximum of the frequency characteristic constructed from it will lie in the region of low frequencies, and it will affect the form of the total frequency characteristic only for frequencies less than ω_p, while for frequencies close to ω_p or larger than ω_p, it will have a constant value, equal to K_1.

This means mathematically that, for frequencies $\omega > 5/t_1$, the term $\omega K_1 t_1 (\cos t_1 \omega / t_1 \omega)(\sin \Delta_1 \omega / \Delta_1 \omega)$ in (2) can be ignored, since it is significantly smaller than $0.1K_1$. Thus, in the neighborhood of frequency ω_p, the real frequency characteristic, when account is taken of the fact that $K_1 + K_2 + 1 = 0$, will be approximately expressed by the formula

$$R(\omega) = -\omega K_2 t_2 \left(\frac{\cos t_2\omega}{t_2\omega}\right)\left(\frac{\sin \Delta_2\omega}{\Delta_2\omega}\right). \qquad (3)$$

The curve for $R(\omega)$ constructed in accordance with (3) will pass through zero for the first time for $\cos t_2\omega / t_2\omega = 0$, which occurs for the value $t_2\omega = \pi/2$, i.e., for

$$\omega = \frac{\pi}{2t_m}, \quad \text{since} \quad t_2 = t_m$$

As is clear, the frequency $\omega = \pi/2t_m$ is the boundary frequency of the positive interval, i.e., (1) is valid.

The value of ω_p thus obtained may serve as an estimate of the cutoff frequency ω_c of the system's logarithmic amplitude characteristic since, as is well known, the logarithmic amplitude characteristic intersects the frequency axis for the values [2]

$$\omega_c = (0.55 - 0.7)\,\omega_p. \qquad (4)$$

The suggested method of determining ω_p gives good results when one is considering transient responses, either determined experimentally or stated as desirable, of power servo systems which are distinguished by comparatively small oscillatory indices; $M = 1.1$ to 1.4.

For other transfer functions, the error reaches 15 to 20 %, and this method can be used only for an approximate estimate of ω_p.

LITERATURE CITED

1. V. V. Solodovnikov, Introduction to the Statistical Dynamics of Automatic Control System [in Russian] (Gostekhizdat, 1952).

2. A. V. Fateev, Fundamental Linear Automatic Control Theory [in Russian] (Gosénergoizdat, 1954).

PROCESSING EXPERIMENTAL FREQUENCY CHARACTERISTICS

G. I. Monastyrshin

(Moscow)

Translated from Avtomatika i Telemekhanika, Vol. 21, No. 3, pp. 422-428, March, 1960
Original article submitted May 20, 1959

For recording forced oscillations, loop oscillographs are ordinarily used, recording both the stimulus and the reaction of the element. In those cases where the oscillations do not have a perfectly sinusoidal form, oscillogram processing is carried out by means of a harmonic analyzer which separates out the harmonic component of the reaction which has the same frequency as the stimulus; for brevity, we shall henceforth call it simply the reaction's harmonic component.

Figure 1 gives a set of oscillograms of a servo drive's oscillations, established under the action of sinusoidal stimuli of various frequencies and constant amplitudes. On these oscillograms, U is the stimulus and V is the servo drive's reaction. The oscillograms also bear the reaction's harmonic component. The cross on each oscillogram marks the maximum deviation of the servo drive's oscillation from the given harmonic component. We note that, in the example given, not only the sinusoidal character of the oscillation is disrupted, but, as is clear from Fig. 1, its periodicity is also disturbed to a certain extent, so that in the cases of Fig. 1, c and d the harmonic analysis is carried out over an interval of several (two) periods of the stimulus.

The results of the measurements are collected in the table, where ω_i is the angular frequency of the harmonic stimulus, A_i is the stimulus amplitude, B_i is the amplitude of the reaction's harmonic component, φ_i is the phase shift between the stimulus and the reaction's harmonic component and ΔB_i is the maximum deviation of the reaction from its harmonic component.

We remark that the table can be obtained without the intermediary of an oscillograph by means of direct measurements using the method cited in [1].

In what follows we shall not deal with any concrete form of the deviations of the forced oscillations from their harmonic components, but shall deal with the study abstractly, assuming that any character of these deviations is possible with limitations on the modulus of the ΔB_i. Corresponding to such a treatment, the forced oscillations are characterized, not by lines, but by the bands included between two sinusoids, equidistant from the harmonic component of the oscillation, and separated from it by the maximum deviation marked on the oscillograms.

By considering the reaction's harmonic component as the projection of the polar vector $\bar{B}_i$, we can interpret the deviations of actual oscillations from their harmonic components as the projections of an auxiliary vector $\Delta\bar{B}_i$, limited in modulus.

i	ω_i, sec.$^{-1}$	A_i, mm	B_i, mm	φ_i, degrees	ΔB_i, mm
1	3.123	31.0	20.95	— 47°20′	3
2	6.148	31.0	13.83	— 74°03′	4
3	12.45	31.0	7.36	—101°46′	3
4	25.13	31.0	3.61	—138°08′	5

If we abstract from the concrete definiteness of the rotation of this auxiliary vector we obtain, instead of the end of the vector $\bar{B}_i$, a circular smear with radius ΔB_i.

The vector interpretation allows one to note that when $\Delta B_i \ll B_i$ (for our purposes, it suffices in practice if $\Delta B_i < 0.5\,B_i$) the ratio $\Delta B_i : B_i$ is determined approximately both by the maximum relative variation of the harmonic component's amplitude and by the maximum variation of its phase (measured in radians) for which the harmonic oscillations will remain within the limits of the smear defined earlier or, what amounts to the same thing, within the limits of the forced oscillations' bands. In this sense, instead of the lines of the frequency, amplitude and phase characteristics, one can consider the bands of the amplitude and phase characteristics. Figure 2 shows such bands, constructed from the oscillograms of Fig. 1. In the neighborhood of the frequency 4 cps, the bands of the phase characteristic are not bounded, due to the fact that the condition on the smallness of ΔB_i does not hold.

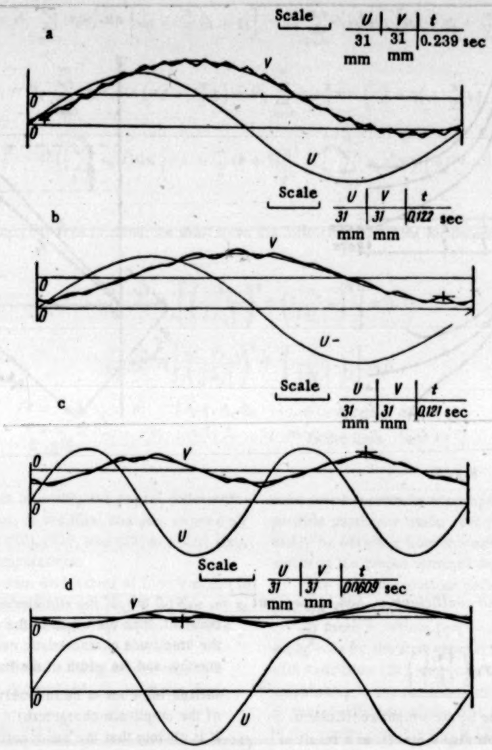

Fig. 1.

In using an element's experimental frequency characteristic, it may turn out to be advantageous to define the system by the differential equation corresponding to these characteristics [2-6]. For example, the problem arises in mathematical modelling of setting up the scheme which reproduces the frequency characteristics.

We assume that the linear differential equation defined by the experimental frequency characteristics has the form

$$\sum_{k=0}^{n} a_k U^{(k)} = \sum_{k=0}^{m} b_k V^{(k)}, \qquad (1)$$

where the $U^{(k)}$ are the stimulus and its derivatives, and the $V^{(k)}$ are the reaction and its derivatives.

As represented on the oscillograms, the stimulus U_1 and the reaction's harmonic component V_1 may be written in the form

$$U_1 = A_1 \sin \omega_1 t, \qquad (2)$$

$$V_1 = B_1 \sin (\omega_1 t + \varphi_1). \qquad (3)$$

To determine the numerical values of the coefficients a_k and b_k of (1), we use the approximate equation obtained by substituting (2) and (3) in (1):

$$\sum_{k=0}^{n} a_k A_1 \omega_1^k \sin\left(\omega_1 t + \frac{\pi}{2} k\right) \approx \sum_{k=0}^{m} b_k B_1 \omega_1^k \sin\left(\omega_1 t + \varphi_1 + \frac{\pi}{2} k\right). \qquad (4)$$

To provide a graphic representation, we denote the left and right members of (4) by polar vectors $\overline{R}_1$ and $\overline{S}_1$ (Fig. 3).

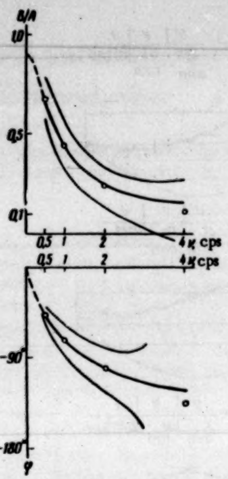

Fig. 2.

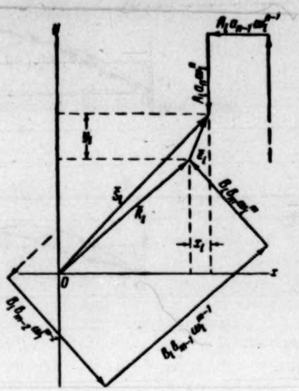

Fig. 3.

To find the unknown coefficients a_k and b_k, we start from the condition

$$\min \sum_i p_i \left(\frac{|\bar{\varepsilon}_i|}{|\bar{R}_i|} \right)^2, \tag{5}$$

where $\bar{\varepsilon}_i = \bar{S}_i - \bar{R}_i$ and the p_i are weight coefficients.

It is easily seen from Fig. 3 that if, as a result of seeking the values of the coefficients of (1), the vectors $\bar{\varepsilon}_i$ lie within the limits of certain circular smears whose radii are in the same ratios to the moduli of vectors $\bar{R}_i$ as the ΔB_i are to the B_i, then the forced oscillations defined by (1), with the values found for the coefficients, lie within the limits of the bands considered earlier.

In correspondence with this, by setting the requirements on the accuracy of the approximation of the frequency characteristics, and omitting the arbitrary coefficient of proportionality, we establish the weight coefficients:

$$p_i = \left(\frac{B_i}{\Delta B_i} \right)^2. \tag{6}$$

If in (6), instead of the quantities ΔB_i, which depend on the frequency of the forced oscillations, we use the quantity $\max \Delta B_i$ and omit the constant factor thereby entailed, then

$$p_i = B_i^2. \tag{7}$$

With this, if the stimulus amplitude is taken to be constant, then the width of the corresponding band of the amplitude characteristic ceases to depend on frequency, and the width of the band of the phase characteristic turns out to be inversely proportional to the value of the amplitude characteristic (for sufficiently small ΔB_i). It is obvious that the bands corresponding to (6) lie inside the bands defined by (7).

We note that (5) for $|\bar{\varepsilon}_i| \ll |\bar{R}_i|$, as may be observed from Fig. 3, is equivalent to the condition

$$\min \sum_i p_i (\Delta_i^2 + \delta_i^2), \tag{8}$$

where the Δ_i are the absolute deviations of the phase characteristic of (1) from the experimental one, measured in radians, and the δ_i are the relative deviations of the amplitude characteristic of (1) from the experimental.

For what follows, it is advantageous to give (5) in the form

$$\min \sum_i p_i \left[\left(\frac{x_i}{|\bar{R}_i|} \right)^2 + \left(\frac{y_i}{|\bar{R}_i|} \right)^2 \right]. \tag{9}$$

where x_i and y_i are the projections of vector $\bar{\varepsilon}_i$.

It is easily seen that

$$x_i = A_i \sum_{k=0}^{n} a_k \omega_i^k \sin\left[\omega_i t + \frac{\pi}{2}(k+1)\right] - B_i \sum_{k=0}^{m} b_k \omega_i^k \sin\left[\omega_i t + \varphi_i + \frac{\pi}{2}(k+1)\right], \tag{10}$$

$$y_i = A_i \sum_{k=0}^{n} a_k \omega_i^k \sin\left(\omega_i t + \frac{\pi}{2}k\right) - B_i \sum_{k=0}^{m} b_k \omega_i^k \sin\left(\omega_i t + \varphi_i + \frac{\pi}{2}k\right), \tag{11}$$

$$\bar{R}_i|^2 = A_i^2\left(\left\{\sum_{k=0}^{n} a_k \omega_i^k \sin\left[\omega_i t + \frac{\pi}{2}(k+1)\right]\right\}^2 + \left[\sum_{k=0}^{n} a_k \omega_i^k \sin\left(\omega_i t + \frac{\pi}{2}k\right)\right]^2\right). \tag{12}$$

With (10), (11), and (12) kept in mind, we shall have the following equations for determining the coefficients sought:

$$\begin{gathered}\frac{\partial}{\partial a_k}\sum_i p_i\left[\left(\frac{x_i}{|\bar{R}_i|}\right)^2 + \left(\frac{y_i}{|\bar{R}_i|}\right)^2\right] = 0, \\ \frac{\partial}{\partial b_l}\sum_i p_i\left[\left(\frac{x_i}{|\bar{R}_i|}\right)^2 + \left(\frac{y_i}{|\bar{R}_i|}\right)^2\right] = 0 \\ \begin{pmatrix} k = 1, 2, \ldots, n; & l = 0, 1, 2, \ldots, m \text{ in the case } a_0 = 1 \\ k = 0, 1, 2, \ldots, n; & l = 1, 2, \ldots, m \text{ in the case } b_0 = 1 \end{pmatrix}.\end{gathered} \tag{13}$$

Since the quantities following the partial differentiation signs in (13) do not, in the final analysis, depend on t, one can set t = 0 in (10), (11), and (12) as a first step, thus simplifying the computations.

If (1) does not contain derivatives of U or V then (13) will be linear since, in the first case, $|\bar{R}_i| = A_i$ (we set a_0 equal to unity) and, in the second, $|\bar{R}_i| \approx |\bar{S}_i| \doteq B_i$ (we set b_0 equal to unity).

Otherwise, the coefficients being sought can, to a first approximation, be determined, for example, from the condition

$$\min \sum_i |\bar{s}_i|^2. \tag{14}$$

To render more exact the solution thus obtained one might determine the quantities $|\bar{R}_i|$ graphically from the vector diagram or by (12) for t = 0 and the numerical values of the coefficients of the first approximation, where for the differentiation of the fractions in (13), one differentiates only the numerator (as in the case when the denominator does not depend on the parameter with respect to which the differentiation is being performed), which is possible if the numerator is sufficiently small with respect to the denominator.

Omitting the detailed computations, we give the final expressions determining the coefficients of the equation

$$\begin{aligned} U + a_1\dot{U} + a_2\ddot{U} + a_3U^{(3)} + a_4U^{(4)} + a_5U^{(5)} = \\ = b_0V + b_1\dot{V} + b_2\ddot{V} + b_3V^{(3)} + b_4V^{(4)} + b_5V^{(5)}. \end{aligned} \tag{15}$$

In terms of this example, we consider the structure of the formulation which permits one to obtain the analogous formulas for any more complicated case. The case considered apparently encompasses all practically possible particular cases. All these particular cases may easily be obtained from the one considered by simply omitting the proper terms of the expressions provided.

The normal equations defining the coefficients of (15) are given by (16).

In these equations, $p_i k_i^2 = 1$ (it is also possible to set $k_i^2 = 1$) for the first approximation in correspondence with condition (14), and may thereafter be determined graphically in the rendering more accurate of the solution by the coefficients of the first approximation by means of the vector diagram ($k_i^2 = |\bar{R}_i|^{-2}$) or by

$$\begin{aligned} k_i^2 = A_i^{-2}[(a_1\omega_i - a_3\omega_i^3 + a_5\omega_i^5)^2 \\ + (1 - a_2\omega_i^2 + a_4\omega_i^4)^2]^{-1}. \end{aligned} \tag{17}$$

For simpler cases it suffices, in (16), to delete the columns, and the rows symmetric with them about the principal diagonal in the matrix of the unknown coefficients, for the coefficients of the higher derivatives which are lacking in (15). The corresponding terms in (17) are also omitted. In the particular case when there are no derivatives in the left member of (15), there remain only the last six columns of the left side of (16) and, correspondingly, only the six last equations $k_i^2 = A_i^{-2}$, and the problem is significantly simplified. If there are no derivatives in the right member of (15), it is then advantageous to change the problem slightly, setting $b_0 = 1$ and taking a_0 as an unknown. In this case, the simplified normal equations obtained from (16) are analogous to the preceding ones if one first makes the following changes in (16): the b_k are replaced by the

$$
\begin{array}{rrrrrrrrrrrcl}
+a_1 \sum_i c_i\omega_i^2 & & -a_3 \sum_i c_i\omega_i^4 & & +a_5 \sum_i c_i\omega_i^6 & -b_0 \sum_i d_i\omega_i & -b_1 \sum_i e_i\omega_i^2 & +b_2 \sum_i d_i\omega_i^3 & +b_3 \sum_i e_i\omega_i^4 & -b_4 \sum_i d_i\omega_i^5 & -b_5 \sum_i e_i\omega_i^6 & = & 0 \\
& a_2 \sum_i c_i\omega_i^4 & & -a_4 \sum_i c_i\omega_i^6 & & +b_0 \sum_i e_i\omega_i^2 & -b_1 \sum_i d_i\omega_i^3 & -b_2 \sum_i e_i\omega_i^4 & +b_3 \sum_i d_i\omega_i^5 & +b_4 \sum_i e_i\omega_i^6 & -b_5 \sum_i d_i\omega_i^7 & = & \sum_i c_i\omega_i^2 \\
-a_1 \sum_i c_i\omega_i^4 & & +a_3 \sum_i c_i\omega_i^6 & & -a_5 \sum_i c_i\omega_i^8 & +b_0 \sum_i d_i\omega_i^3 & +b_1 \sum_i e_i\omega_i^4 & -b_2 \sum_i d_i\omega_i^5 & -b_3 \sum_i e_i\omega_i^6 & +b_4 \sum_i d_i\omega_i^7 & +b_5 \sum_i e_i\omega_i^8 & = & 0 \\
& -a_2 \sum_i c_i\omega_i^6 & & +a_4 \sum_i c_i\omega_i^8 & & -b_0 \sum_i e_i\omega_i^4 & +b_1 \sum_i d_i\omega_i^5 & +b_2 \sum_i e_i\omega_i^6 & -b_3 \sum_i d_i\omega_i^7 & -b_4 \sum_i e_i\omega_i^8 & +b_5 \sum_i d_i\omega_i^9 & = & -\sum_i c_i\omega_i^4 \\
a_1 \sum_i c_i\omega_i^6 & & -a_3 \sum_i c_i\omega_i^8 & & +a_5 \sum_i c_i\omega_i^{10} & -b_0 \sum_i d_i\omega_i^5 & -b_1 \sum_i e_i\omega_i^6 & +b_2 \sum_i d_i\omega_i^7 & +b_3 \sum_i e_i\omega_i^8 & -b_4 \sum_i d_i\omega_i^9 & -b_5 \sum_i e_i\omega_i^{10} & = & 0 \\
-a_1 \sum_i d_i\omega_i & +a_2 \sum_i e_i\omega_i^2 & +a_3 \sum_i d_i\omega_i^3 & -a_4 \sum_i e_i\omega_i^4 & -a_5 \sum_i d_i\omega_i^5 & +b_0 \sum_i f_i & & -b_2 \sum_i f_i\omega_i^2 & & +b_4 \sum_i f_i\omega_i^4 & & = & \sum_i c_i \\
-a_1 \sum_i e_i\omega_i^2 & -a_2 \sum_i d_i\omega_i^3 & +a_3 \sum_i e_i\omega_i^4 & +a_4 \sum_i d_i\omega_i^5 & -a_5 \sum_i e_i\omega_i^6 & & +b_1 \sum_i f_i\omega_i^2 & & -b_3 \sum_i f_i\omega_i^4 & & +b_5 \sum_i f_i\omega_i^6 & = & -\sum_i d_i\omega_i \\
a_1 \sum_i d_i\omega_i^3 & -a_2 \sum_i e_i\omega_i^4 & -a_3 \sum_i d_i\omega_i^5 & +a_4 \sum_i e_i\omega_i^6 & +a_5 \sum_i d_i\omega_i^7 & -b_0 \sum_i f_i\omega_i^2 & & +b_2 \sum_i f_i\omega_i^4 & & -b_4 \sum_i f_i\omega_i^6 & & = & -\sum_i e_i\omega_i^2 \\
a_1 \sum_i e_i\omega_i^4 & +a_2 \sum_i d_i\omega_i^5 & -a_3 \sum_i e_i\omega_i^6 & -a_4 \sum_i d_i\omega_i^7 & +a_5 \sum_i e_i\omega_i^8 & & -b_1 \sum_i f_i\omega_i^4 & & +b_3 \sum_i f_i\omega_i^6 & & -b_5 \sum_i f_i\omega_i^8 & = & \sum_i d_i\omega_i^3 \\
-a_1 \sum_i d_i\omega_i^5 & +a_2 \sum_i e_i\omega_i^6 & +a_3 \sum_i d_i\omega_i^7 & -a_4 \sum_i e_i\omega_i^8 & -a_5 \sum_i d_i\omega_i^9 & +b_0 \sum_i f_i\omega_i^4 & & -b_2 \sum_i f_i\omega_i^6 & & +b_4 \sum_i f_i\omega_i^8 & & = & \sum_i e_i\omega_i^4 \\
-a_1 \sum_i e_i\omega_i^6 & -a_2 \sum_i d_i\omega_i^7 & +a_3 \sum_i e_i\omega_i^8 & +a_4 \sum_i d_i\omega_i^9 & -a_5 \sum_i e_i\omega_i^{10} & & +b_1 \sum_i f_i\omega_i^6 & & -b_3 \sum_i f_i\omega_i^8 & & +b_5 \sum_i f_i\omega_i^{10} & = & -\sum_i d_i\omega_i^5
\end{array}
$$

where $c_i = p_i k_i^2 A_i^2$; $d_i = p_i k_i^2 A_i B_i \sin\varphi_i$; $e_i = p_i k_i^2 A_i B_i \cos\varphi_i$; $f_i = p_i k_i^2 B_i^2$. (16)

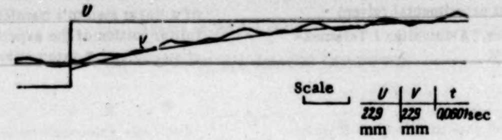

Fig. 4.

a_k and the a_k are replaced by the b_k and, in the expressions for the coefficients c_i, d_i, e_i, and f_i, A_i is replaced by B_i, B_i is replaced by A_i, φ_i is replaced by $-\varphi_i$ and the k_i^2 are defined as B_i^{-2}. One should then retain the six last equations and, correspondingly, the six last columns of the left members of these equations, determining the p_i by (6) or (7).

If, as a result of the computation of the coefficients of (15), the difference between its frequency characteristics and the experimental ones, defined by the harmonic components of the actual oscillations, turns out to be sufficiently small - for example, significantly less than the possible deviations inside the previously defined bands of the forced oscillations - we shall then consider that the problem of determining the linear equation which approximates the experimental frequency characteristics has been successfully solved.

In the concrete example considered, given by Figs. 1 and 2 and by the table, we are investigating an equation of the form

$$U + a_1\dot{U} = b_0 V + b_1\dot{V}, \tag{18}$$

for which we shall have the normal equations

$$\begin{gathered}
a_1 \sum_i p_i k_i^2 A_i^2 \omega_i^2 - \\
- b_0 \sum_i p_i k_i^2 A_i B_i \omega_i \sin\varphi_i - b_1 \sum_i p_i k_i^2 A_i B_i \omega_i^2 \cos\varphi_i = 0. \\
- a_1 \sum_i p_i k_i^2 A_i B_i \omega_i \sin\varphi_i + b_0 \sum_i p_i k_i^2 B_i^2 = \\
= \sum_i p_i k_i^2 A_i B_i \cos\varphi_i, \\
- a_1 \sum_i p_i k_i^2 A_i B_i \omega_i^2 \cos\varphi_i + \\
+ b_1 \sum_i p_i k_i^2 B_i^2 \omega_i^2 = - \sum_i p_i k_i^2 A_i B_i \omega_i \sin\varphi_i
\end{gathered} \tag{19}$$

Setting the p_i by (6) and taking, in correspondence with (17),

$$k_i^2 = A_i^{-2}(a_1^2\omega_i^2 + 1)^{-1} \tag{20}$$

we obtain, as the result of computing the first and second approximations and the corresponding rounding,

$$a_1 = -0.034, \quad b_0 = 1.11, \quad b_1 = 0.325.$$

The corresponding frequency characteristic is given in Fig. 2. The circles on the figure mark the experimental points, while the heavy lines show the results of the approximation.

It should not be overlooked that the frequency characteristics considered can not determine all the properties of the actual element. Due to this, the question as to the use of such a type of characteristics, and the equations approximating them, can form the subject of a concrete study.

For the example considered, Fig. 4 shows the reaction to a unit step function stimulus, obtained from (18) by computing the values of the coefficients, and the analogous reaction of the actual servo drive.

It may happen that, in practice, one does not succeed in obtaining a sufficiently small error of approximation of the experimental frequency characteristics. For example, these errors may remain beyond the limits of the experimentally defined bands of the forced oscillations. In this case, the question as to the possibility of using the results of the approximation can be decided by fixing the band of the forced oscillations in correspondence with the approximation errors obtained.

We note that a treatment analogous to that presented here is also possible in the case when the experimental results are free from nonlinear deviations, and only measurement errors distort them.

LITERATURE CITED

1. K. V. Zakharov and V. K. Svyatodukh, "An instrument for determining frequency characteristics of nonlinear systems," Avtomatika i Telemekhanika 20, 12 (1959).

2. L. A. Galin, "Determining an instrument's differential equation on the basis of testing for forced oscillations," Prikl. Matem. i Mekhan. No. 10 (1946).

3. G. L. Rabkin, B. A. Mitrofanov, and Yu. O. Shterenberg, "On the determination of the numerical values of the coefficients of the transfer functions of linearized links and systems from experimental frequency characteristics," Avtomatika i Telemekhanika 16, 5 (1955).

4. G. I. Monastyrshin, "Mathematical processing of an experiment for the investigation of an automatic control system," Collection: Questions in Automatic Control Theory [in Russian] (Oborongiz, 1956).

5. A. A. Kardashov and L. V. Karnyushin, "Determining system parameters from experimental (given) frequency characteristics," Avtomatika i Telemekhanika 19, 4 (1958).

6. E. E. Dubnikov, "Determination of the coefficients of a linear system's transfer function from the initial portion of the experimental amplitude-phase characteristic," Avtomatika i Telemekhanika 20, 5 (1959)

INFORMATION

THE ÉMU-8 ELECTRONIC ANALOG COMPUTER

As the result of the work on improving electronic analog computers and their elements which has been carried on at the Institute for Automation and Remote Control of the Academy of Science of the USSR in conjunction with a collective under the direction of G. N. Grigor'yan, there has been created a new electronic analog computer, type ÉMU-8, production of which has already begun.

Domain of Application of Type ÉMU-8 Electronic Analog Computer

The type ÉMU-8 electronic analog computer is designed for the investigation of linear and nonlinear dynamic systems. Structurally, it is a general-purpose computer capable of real-time operation (joined with elements of actual apparatus) with accelerated and retarded solution processes within the limits of its passband. The computer can be used to greatest effect in the solution of technological problems where the error in giving the original parameters is sufficiently large (from 5 to 10%).

Among these problems may be listed:

1) investigation of the dynamics of automatic control and regulation systems (automated systems, missile control, boiler aggregate regulation, steam turbine control, various automated electric drives, etc.);

2) certain problems of nuclear physics and technology;

3) investigation of combustion processes in internal-combustion engines;

4) investigation of transient responses in complicated electrical circuits;

5) investigations in the area of nonlinear mechanics.

Brief Technical Characteristics of the ÉMU-8*

The ÉMU-8 computer consists of individual building blocks each of dimensions 450 x 460 x 320 mm. Each building block can provide the solution of linear and nonlinear differential equations up to second-order, inclusive.

---

* For more detailed technical characteristics of the computer plus its functional schematic, see Vestnik Akademii Nauk No. 7 (1958).

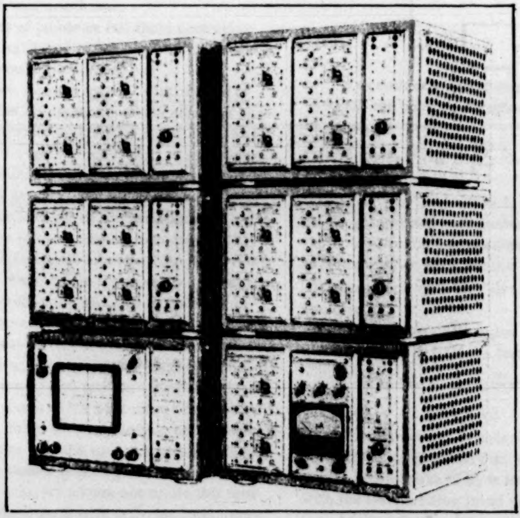

while the standard package of building blocks provides solutions of differential equations up to tenth-order, inclusive. Plug-in units permit the execution of the following mathematical operations: multiplication and division of two independent variables, multiplication by a constant factor, differentiation, integration, reproduction of various nonlinear functions and standard nonlinearities.

The character of the mathematical operations executed is determined by the type of plug-in units, which allows operational amplifiers to be used economically.

By choosing several building blocks with the necessary variants of plug-in units, one can solve problems of various complexity.

In the standard package, five building blocks are used.

Six block indicators are connected to each package to provide visual observation of problem solution.

Each building block is designed in the form of a completely independent instrument, and may be connected directly to a 220v line. The power requirement of each block is about 160w.

Line production of the computer was organized in 1960. The wholesale price of a package is 135,000 rubles.

Bureau of Factory Information

ANALYTICAL CONTROLLER DESIGN. I

A. M. Letov

(Moscow)

Translated from Avtomatika i Telemekhanika, Vol. 21, No. 4, pp. 436-441, April, 1960
Original article submitted December 23, 1959

A solution is presented for the problem of analytical controller design in accordance with a given optimizing functional. The solution is given for the open region of definition of the system's differential equations. The cases of closed regions are worked out in Parts II and III of the present work, which are to be published in succeeding numbers of this journal.

1. Two Classes of Problems in Optimal System Theory

The construction of optimal systems leads to the solution of the allied mathematical problems, which are divided into two classes. The first of these is comprised of those problems which are related to the determination and calculation of the undisturbed modes of motion. Here, one has to do with those programs of automatic control for which the given undisturbed motion possesses the requisite extremal properties. We shall call such systems optimal with respect to control mode.

Systems for which the concept of optimality connotes the arrival at a given state in minimal time we shall find it convenient to call brachistochrone.

In the other class of problems fall those controllers which guarantee the existence of given properties of the disturbed motions (transient processes).

We shall call such systems optimal with respect to transient response. The set consisting of the object of control, the optimal programming element, and the optimal controller comprises an optimal automatic control system. In both cases the optimization problem can be treated as a two-point boundary problem, for the solution of which one may apply all the methods of the variational calculus and, in particular, the latest methods, developed in [1-7]. However, certain differences do exist between these two classes of problems. Thus, in the first case, the problem's solution is obtained in the form of a known function of time, which then becomes the basis for the design of the programming elements. In the second case, the analytical form of the control law appears as some function of the original coordinates of the control system, i.e., the problem consists of the construction of the controller's differential equation. Of course, the process of analytic controller construction is nothing else than the synthesis process. In particular, the synthesis process is here given the same meaning as in [1-5]. However, we choose not to use this term since many other authors use it with differing interpretations. On the other hand, the equivalent terminology "analytic construction" must suggest itself more strongly to engineers, since this terminology implies merely the search, by means of the tools of mathematical analysis, for the form of the controller's differential equation which will answer to the accepted criterion of optimality. In the present paper we consider the problem of the analytical construction (design) of optimal systems which are defined in open regions. In the succeeding papers we shall deal with the same problem as formulated for closed regions.

2. Initial Posing of the Analytical Design Problem

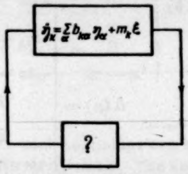
$\dot{\eta}_k = \sum_\alpha b_{k\alpha}\eta_\alpha + m_k\xi$
?

We consider a closed controlled system (cf. Fig. 1) in which the object's disturbed motion is given by the set of equations

$$g_k = \dot{\eta}_k - \Big(\sum_\alpha b_{k\alpha}\eta_\alpha + m_k\xi\Big) = 0 \qquad (2.1)$$

$$(k = 1, \ldots, n)$$

in the generalized coordinates η_k, while the equation of the controller for the coordinate ξ remains unknown. For definiteness, we shall assume that all the $b_{k\alpha}$ and m_k are given constants on which no restraints have as yet been imposed.

Let N be the open region in which (2.1) are given; any conditions in N of the form

$$\eta_1(0) = \eta_{10}, \ldots, \eta_n(0) = \eta_{n0}, \quad \xi(0) = \xi_0, \qquad (2.2)$$

$$\eta_1(\infty) = \ldots = \eta_n(\infty) = \xi(\infty) = 0$$

we shall call natural boundary conditions of the problem. They mean simply this, that whatever the transient response which arises in N, it must terminate, for t = ∞, with the system being found at the origin of coordinates.

As the criterion for system optimality, we choose the integral

$$I(\xi) = \int_0^\infty V\,dt \qquad (2.3)$$

of the positive definite quadratic form

$$V = \sum_k a_k \eta_k^2 + c\xi^2. \tag{2.4}$$

We shall seek such continuous functions $\xi, \eta_1 \ldots \eta_n$ (class C_1) with continuous first derivatives which give the integral in (2.3) a minimum value. The existence and uniqueness of the solution of this problem were proven in [7]. We now give ourselves the task of determining the form of this solution as well as the possibilities of using it for the purpose of an analytic design. The integral $I(\xi)$ is a functional defined on class C_1 of functions, and its value characterizes the integral of the squared error, weighted by the constants a_k and c, which the system will have in the course of the transient response lasting until t • = ∞. The problem consists in writing in analytic form

$$F(\dot{\xi}, \xi, \eta_1, \ldots, \eta_n) = 0 \tag{2.5}$$

the control law which, in conjunction with (2.1), will form a stable system and will guarantee the existence of a minimum for the integral in (2.3).

3. Solution of the Problem

We are dealing with the Lagrange variational problem, the procedures for the solution of which are very well known. Specifically, we first set up the function

$$H = V + \sum_k \lambda_k g_k, \tag{3.1}$$

where the λ_k are arbitrary multipliers.

Then,

$$\frac{\partial H}{\partial \dot{\eta}_k} = \lambda_k, \quad \frac{\partial H}{\partial \eta_k} = 2a_k\eta_k - \sum_\alpha \lambda_\alpha b_{\alpha k}; \quad \frac{\partial H}{\partial \dot{\xi}} = 0,$$
$$\frac{\partial H}{\partial \xi} = 2c\xi - \sum_\alpha m_\alpha \lambda_\alpha. \tag{3.2}$$

The equations of the variational problem have the form

$$\dot{\lambda}_k = -\sum_j b_{jk}\lambda_j + 2a_k\eta_k, \quad 0 = 2c\xi - \sum_j m_j\lambda_j. \tag{3.3}$$

To these, (2.1) should be adjoined.

The further steps in the procedure for analytic design (excluding singular cases) are as follows:

1. The equations of the variational problem must be solved jointly for the functions η_k and λ_k.

Let

$$\Delta(\mu) = \begin{vmatrix} b_{11} - \mu, \ldots, & b_{1n}, & \frac{m_1^2}{2c}, \ldots, & \frac{m_1 m_2}{2c} \\ \cdots & \cdots & \cdots & \cdots \\ b_{n1}, \ldots, & b_{nn} - \mu, & \frac{m_n m_1}{2c}, \ldots, & \frac{m_n^2}{2c} \\ 2a_1, \ldots, & 0, & -b_{11} - \mu, \ldots, & -b_{n1} \\ \cdots & \cdots & \cdots & \cdots \\ 0, \ldots, & 2a_n, & -b_{1n}, \ldots, & -b_{nn} - \mu \end{vmatrix} \tag{3.4}$$

be the system's characteristic determinant. It is easily proven that, if $\mu_1, \ldots, \mu_n$ are simple roots of the equation $\Delta(\mu) = 0$, then the numbers $-\mu_1, \ldots, -\mu_n$ are also simple roots. We assume that $\mu_1, \ldots, \mu_n$ are simple roots, $\mathrm{Re}\,\mu_k \neq 0$, and the roots are numbered in accordance with the inequalities

$$\mathrm{Re}\,\mu_k < 0 \quad (k = 1, \ldots, n). \tag{3.5}$$

This latter step is always possible by virtue of the aforementioned property of determinant (3.4). The general solution of the equations of the problem will consist of a linear combination of exponential functions of the form $c_k e^{\mu_k t}$ and $c_{n+k} e^{-\mu_k t}$ $(k = 1, \ldots, n)$, and will contain 2n arbitrary constants

$$c_1, \ldots, c_n, c_{n+1}, \ldots, c_{2n}.$$

2. By virtue of (2.2)• at infinity we set

$$c_{n+k} = 0 \ (k = 1, \ldots, n)$$

where the constants c_k can be chosen from the initial conditions. However, this operation is not necessary.

3. In the remaining 2n formulas which define the functions $\eta_1, \ldots, \eta_n, \lambda_1, \ldots, \lambda_n$, we eliminate the n functions of time $c_k e^{\mu_k t}$, as a result of which we find that

$$\lambda_j = \sum_\alpha \Delta_{j\alpha}\eta_\alpha \quad (j = 1, \ldots, n), \tag{3.6}$$

where the $\Delta_{j\alpha}$ are completely defined constants.

4. We substitute the values found for the λ_j in the last equation of (3.3), thus finding the controller's equation

$$\xi = p_1\eta_1 + p_2\eta_2 + \ldots + p_n\eta_n. \tag{3.7}$$

It remains to verify that (3.7), in conjunction with the initial equations (2.1), forms a stable† automatic control system. This verification is easily carried out. Indeed, the optimal system found has a general solution which is a linear combination of the exponential functions $c_k e^{\mu_k t}$ $(k = 1, \ldots, n)$. Consequently, the numbers μ_k $(k = 1, \ldots, n)$ are the roots of the characteristic equation of system (2.1), (3.7). We obtained ideal controller (3.7) with rigid feedback and with an infinitely fast servomotor [8]. Thus, we arrive at the conclusion that functionals like (2.3) lead to controllers which can not be realized.

4. Possible Generalizations of Functional (2.3)

We now consider an indefinite quadratic form such as

$$T = \sum_k \sum_j c_{kj}\eta_k\eta_j + \xi^2 \qquad (4.1)$$

and repeat the formulation of the Lagrange problem for the functional

$$I(\xi) = \int_0^\infty (T + V)\, dt.$$

The value of the functional $I(\xi)$ characterizes the integral of the squared position and velocity errors which the system will have in the course of the transient response lasting until $t^* = \infty$.

We remark that the solution of the problem may be simplified by eliminating the derivatives $\dot\eta_k$ in accordance with the original equations. It is reasonable, therefore, to consider first the simpler functional of the form

$$I(\xi) = \int_0^\infty (V + \dot\xi^2)\, dt. \qquad (4.2)$$

The computation will differ from the foregoing only in that now the expression $\partial H/\partial \dot\xi = 2\ddot\xi$ and does not equal zero. Therefore, instead of the last equation of (3.3), we get

$$2\ddot\xi = 2c\xi - \sum_j m_j\lambda_j. \qquad (4.3)$$

This equation, in conjunction with (2.1) and the first n equations of (3.3), solves the given problem. The solution procedure reduces to the implementation of the following operations:

1. The equations of the problem must be solved for the functions η_k, λ_k and ξ.

Let

$$\overline{\Delta}(\mu) = \begin{vmatrix} b_{11}-\mu, \ldots, & b_{1n}, & 0, \ldots, & 0, & m_1 \\ \cdots & \cdots & \cdots & \cdots & \cdots \\ b_{n1}, \ldots, & b_{nn}-\mu, & 0, \ldots, & 0, & m_n \\ 2a_1, \ldots, & 0, & -b_{11}-\mu, \ldots, & -b_{n1}, & 0 \\ \cdots & \cdots & \cdots & \cdots & \cdots \\ 0, \ldots, & 2a_n, & -b_{1n}, \ldots, & -b_{nn}-\mu, & 0 \\ 0, \ldots, & 0, & -m_1, \ldots, & -m_n, & 2c-\mu^2 \end{vmatrix} \qquad (4.4)$$

be the system's characteristic determinant. As in the case of (3.4), it possesses the property that $\overline{\Delta}(\mu) = \overline{\Delta}(-\mu)$. Therefore, the equation $\Delta(\mu) = 0$ will have the roots $\mu_1, \ldots, \mu_{n+1}$ (which we assume to be simple), with the property enunciated by (3.5), plus the roots $-\mu_1, \ldots, -\mu_{n+1}$. The system's general solution will consist of a linear combination of exponential functions of the form $c_k e^{\mu_k t}$ and $c_{n+1+k} e^{-\mu_k t}$ ($k = 1, \ldots, n+1$) and will contain $2n+2$ arbitrary constants.

2. By virtue of (2.2) at infinity we set $c_{n+1+k} = 0$ ($k = 1, \ldots, n+1$). The remaining constants can be determined from the initial conditions.

3. We now take the solution found for the function ξ. In the $n+2$ formulas found for the functions $\eta_1, \ldots, \eta_n$, ξ and $\dot\xi$, we eliminate the functions of time $c_1 e^{\mu_1 t}, \ldots, c_{n+1} e^{\mu_{n+1} t}$, as a result of which we find the controller's equation

$$\dot\xi = \sum_\alpha p_\alpha \eta_\alpha - r\xi. \qquad (4.5)$$

Here, the p_α and r are completely defined constants, determined in the course of implementing the enumerated operations. In conjunction with (2.1), (4.5) forms a stable optimal system. The stability, as in the previous case, is a consequence of the fact that the numbers $\mu_1, \ldots, \mu_{n+1}$ are roots of the optimal system's characteristic equation.

In contradistinction to the solution of Section 3, we obtained a linear controller with a limited variable servomotor speed. Such controllers can be realized if the region N is sufficiently small. The analytic design procedure in the case when the motion of the system is in a closed region N, when the optimal solution can be found on the region's boundary, will be considered in the subsequent papers.

5. Examples

For a first-order system, the equations of the variational problem will be

$$\dot\eta = b\eta + m\xi, \quad \dot\lambda = -b\lambda + 2a\eta, \quad 2\ddot\xi = 2c\xi - m\lambda. \qquad (5.1)$$

To these there correspond the characteristic equation

$$\mu^4 - (b^2 + c)\mu^2 + am^2 + cb^2 = 0 \qquad (5.2)$$

and the solution

$$\eta = c_1 e^{\mu_1 t} + c_2 e^{\mu_2 t},$$

$$\xi = \frac{\mu_1 - b}{m} c_1 e^{\mu_1 t} + \frac{\mu_2 - b}{m} c_2 e^{\mu_2 t}, \qquad (5.3)$$

$$\dot\xi = \frac{\mu_1(\mu_1 - b)}{m} c_1 e^{\mu_1 t} + \frac{\mu_2(\mu_2 - b)}{m} c_2 e^{\mu_2 t}.$$

The controller's equation has the form

$$\begin{vmatrix} 1 & 1 & \eta \\ \dfrac{\mu_1 - b}{m} & \dfrac{\mu_2 - b}{m} & \xi \\ \dfrac{\mu_1(\mu_1 - b)}{m} & \dfrac{\mu_2(\mu_2 - b)}{m} & \dot\xi \end{vmatrix} = 0$$

or, in expanded form,

$$\dot{\xi} = -\frac{(\mu_1 - b)(\mu_2 - b)}{m}\eta + (\mu_1 + \mu_2 - b)\xi. \quad (5.4)$$

For a second example, we consider the second-order system

$$\dot{\eta}_1 = b_{11}\eta_1 + b_{12}\eta_2 + m_1\xi, \quad \dot{\eta}_2 = b_{21}\eta_1 + b_{22}\eta_2 + m_2\xi. \quad (5.5)$$

To obtain the equations of the yariational problem, we must append

$$\begin{aligned} \dot{\lambda}_1 &= -b_{11}\lambda_1 - b_{21}\lambda_2 + 2a_1\eta_1, \\ \dot{\lambda}_2 &= -b_{12}\lambda_1 - b_{22}\lambda_2 + 2a_2\eta_2, \\ 2\ddot{\xi} &= 2c\xi - m_1\lambda_1 - m_2\lambda_2. \end{aligned} \quad (5.6)$$

The characteristic equation has the form

$$\bar{\Delta}(\mu) = \begin{vmatrix} b_{11} - \mu, & b_{12} & 0, & 0, & m_1 \\ b_{21}, & b_{22} - \mu, & 0, & 0, & m_2 \\ 2a_1 & 0, & -b_{11} - \mu, & -b_{21}, & 0 \\ 0, & 2a_2, & -b_{12}, & -b_{22} - \mu, & 0 \\ 0, & 0, & -m_1, & -m_2 & 2c - 2\mu^2 \end{vmatrix} = 0.$$

Let μ_1, μ_2, and μ_3 be the three roots for which $\mathrm{Re}\,\mu_s < 0$. We then have

$$\begin{aligned} \eta_1 &= \sum_{s=1}^{3} \Delta_1(\mu_s) e^{\mu_s t} c_s, \quad \eta_2 = \sum_{s=1}^{3} \Delta_2(\mu_s) e^{\mu_s t} c_s, \\ \xi &= \sum_{s=1}^{3} \Delta_5(\mu_s) e^{\mu_s t} c_s, \quad \dot{\xi} = \sum_{s=1}^{3} \mu_s \Delta_5(\mu_s) e^{\mu_s t} c_s. \end{aligned} \quad (5.8)$$

Here, Δ_1, Δ_2, and Δ_5 are the minors of the first, second, and fifth elements of the first row of the determinant in (5.7). It is obvious that the equation sought for the optimal controller will have the form

$$\begin{vmatrix} \Delta_1(\mu_1) & \Delta_1(\mu_2) & \Delta_1(\mu_3) & \eta_1 \\ \Delta_2(\mu_1) & \Delta_2(\mu_2) & \Delta_2(\mu_3) & \eta_2 \\ \Delta_5(\mu_1) & \Delta_5(\mu_2) & \Delta_5(\mu_3) & \xi \\ \mu_1\Delta_5(\mu_1) & \mu_2\Delta_5(\mu_2) & \mu_3\Delta_5(\mu_3) & \dot{\xi} \end{vmatrix} = 0. \quad (5.9)$$

The author sincerely thanks E. A. Barbashin and N. N. Krasovskii for their active participation in the discussions of the present problem, and for their helpful suggestions.

LITERATURE CITED

1. L. S. Pontryagin, "Some mathematical problems arising in connection with the theory of optimal automatic control systems. Basic problems of automatic regulation and control," Proceedings of the Session of the AN SSSR on the Scientific Problems of the Automation of Production [in Russian] (Izd. AN SSSR, 1957).
2. N. N. Krasovskii, "Concerning optimal control theory," Avtomatika i Telemekhanika 18, No. 11 (1957). ‡
3. R. V. Gamkrelidze, "Concerning optimal process theory," Doklady Akad. Nauk SSSR 116, No. 1 (1957).
4. N. N. Krasovskii, "On one optimal control problem," Prikl. Matem. i Mekh. 21, No. 5 (1957).
5. N. N. Krasovskii, "On one problem in the optimal control of nonlinear systems," Prikl. Matem. i Mekh. 23, No. 2 (1959).
6. R. Bellman, Dynamical Programming (Princeton University Press, 1957).
7. R. Bellman, J. Glicksberg, and O. Gross, "Some aspects of the mathematical theory of control processes," Report 313, RAND Corporation (1958).
8. A. M. Letov, Stability of Nonlinear Controlled Systems [in Russian] (Gostekhizdat, 1955).

---

*For the given case, the boundary condition for the function ξ is superfluous.

† The author wishes to thank M. A. Aizerman for the advice which permitted him to avoid an erroneous judgment on this property, which was contained in the first version of the paper.

‡ See English translation.

APPLICATION OF THE KRYLOV - BOGOLYUBOV METHOD OF CONSTRUCTING ASYMPTOTIC APPROXIMATIONS TO THE INVESTIGATION OF SYSTEMS WITH LAGS*

V. S. Kislyakov

(Moscow)

Translated from Avtomatika i Telemekhanika, Vol. 21, No. 4, pp. 442-455, April, 1960
Original article submitted July 4, 1959

The present paper treats of the application of the Krylov-Bogolyubov method of constructing asymptotic approximations to the investigation of linear and nonlinear systems with lags. The effectiveness of this application of the method is illustrated by the example of the investigation of the Minorsky equation.

Introduction

Today, as an effective instrument for the approximate investigation of nonlinear instruments, one may use the widely disseminated method developed by N. M. Krylov and N. N. Bogolyubov [1] for the construction of asymptotic approximations. This method, in a simplified variant (when only first approximations are considered), is called the harmonic balance method [2].

The nub of the asymptotic method of Krylov and Bogolyubov as applied, for example, to a nonlinear differential equation of the form

$$\ddot{x} + \omega^2 x = \varepsilon f(x, \dot{x}), \qquad (1)$$

where ϵ is a small positive parameter, reduces to the search for the general solution of this equation in the form of a formal series expansion in powers of the small parameter ϵ:

$$x = A\cos\psi + \varepsilon u_1(A, \psi) + \varepsilon^2 u_2(A, \psi) + \ldots, \qquad (2)$$

in which $u_1(A, \psi)$, $u_2(A, \psi)$,.... are periodic functions with period 2π. An additional condition is imposed on the functions u_1, u_2,..., which is expressed by the absence of the first harmonics in the Fourier expansions of these functions.

As a first approximation to the solution of (1), we take the expression

$$x = A\cos\psi, \qquad (3)$$

in which the amplitude A and the phase angle ψ are defined by the equations

$$\dot{A} = \varepsilon D_1(A), \quad \dot{\psi} = \omega + \varepsilon B_1(A). \qquad (4)$$

The coefficients $D_1(A)$ and $B_1(A)$ in (4) are defined as the first (fundamental) harmonics of the expansion of the nonlinear function in a Fourier series:

$$D_1(A) = -\frac{1}{2\pi\omega}\int_0^{2\pi} f(A\cos\psi, -A\omega\sin\psi)\sin\psi\, d\psi, \qquad (5)$$

$$B_1(A) = -\frac{1}{2\pi\omega A}\int_0^{2\pi} f(A\cos\psi, -A\omega\sin\psi)\cos\psi\, d\psi. \qquad (6)$$

As a second approximation to the solution of (1), we take the expression

$$x = A\cos\psi + \varepsilon u_1(A, \psi), \qquad (7)$$

in which A and ψ are defined by the equations

$$\begin{aligned} \dot{A} &= \varepsilon D_1(A) + \varepsilon^2 D_2(A), \\ \dot{\psi} &= \omega + \varepsilon B_1(A) + \varepsilon^2 B_2(A), \end{aligned} \qquad (8)$$

and u_1 is defined by the formula

$$u_1 = -\frac{1}{\omega^2}\sum_{n=2}^{\infty}\frac{g_n(A)\cos n\psi + h_n(A)\sin n\psi}{n^2 - 1}, \qquad (9)$$

where $g_n(A)$ and $h_n(A)$ are coefficients of the Fourier series:

$$\begin{aligned} g_n(A) &= \frac{1}{2\pi}\int_0^{2\pi} f(A\cos\psi, -A\omega\sin\psi)\cos n\psi\, d\psi, \\ h_n(A) &= \frac{1}{2\pi}\int_0^{2\pi} f(A\cos\psi, -A\omega\sin\psi)\sin n\psi\, d\psi, \end{aligned} \qquad (10)$$

and the coefficients $D_2(A)$ and $B_2(A)$ in (8) are defined by the corresponding formulas (cf. [2]).

As a third approximation to the solution of (1) we take the expression

$$x = A\cos\psi + \varepsilon u_1(A, \psi) + \varepsilon^2 u_2(A, \psi) \text{ etc.} \qquad (11)$$

In automatic control systems (ACS) one is frequently most interested in the so-called stationary (steady-state) oscillations. This is related to the fact that all nonstationary oscillations, after a quite rapid transient response, approximate to steady-state oscillations and, almost immediately after the initiation of an oscillatory process, this process can be considered as being stationary. A stationary mode, as is well known, is characterized by a constant amplitude, i.e., such that the derivative of the amplitude with respect to time is zero. For the system described by (1), the steady state is defined by the condition

---

*Some results of this paper were briefly presented at the Sixth Scientific-Engineering Conference of Junior Scientists on Automatic Control of the IAT AN SSSR (Jan. 19-21, 1959) and, synoptically, at a seminar on differential-difference equations at Moscow State University (May 28, 1959).

$$\dot{A} = \varepsilon D_1(A) + \varepsilon^2 D_2(A) + \ldots = 0. \tag{12}$$

The method under consideration, i.e., the Krylov-Bogolyubov method of constructing asymptotic approximations, can be successfully employed, as will be shown below, for differential equations with lagging arguments. With this, the Krylov-Bogolyubov method, when combined with the Routh-Hurwitz criterion, turns out to be a simple and effective means both for finding the steady-state periodic mode and for determining the boundary of the region of stability of the controlled system with lags described by linear and quasi-linear differential equations with lagging arguments. The present paper is based on [3], in which there is contained the foundation for the method of approximate computations of periodic solutions of differential equations with lagging arguments, as well as on the results of simulation studies. The foundation for the possibility of using the asymptotic methods of Krylov and Boglyubov for the investigation of systems with lags will be given in the second part of the present paper.

1. Equivalent Linearization of Nonlinear Oscillatory ACS with Lags by the Krylov-Bogolyubov Method

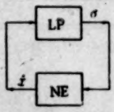

Fig. 1. Block schematic of an ACS with lags. LP is the linear portion and NE is the nonlinear element with lags.

We consider an ACS consisting, in the general case, of a linear portion and a nonlinear element with lags (Fig. 1). The equation of the linear portion may, in general, be arbitrary† while the equation of the nonlinear element has the form

$$\dot{x}(t) = f[\sigma(t-\tau)]. \tag{1.1}$$

An equation of the form of (1.1), in which the lag enters into the argument of the nonlinear function, may be treated, in particular cases, as the equation describing the executive organ of an ACS. In this case, the function $f[\sigma(t-\tau)]$ represents the acting generalized lagged force engendered by the executive organ in accordance with the value of the argument $\sigma(t-\tau)$, where τ is a positive constant which characterizes the temporal delay. In each controlled system, the argument σ expresses the total (sum) pulse (signal) formed in accordance with the control law adopted for the problem. It is assumed that the function $f[\sigma(t-\tau)]$ lies in a subclass A' of class A of functions [4], i.e., satisfies conditions of the form

$$f[\sigma(t-\tau)] = 0 \quad \text{for} \quad \sigma(t-\tau) = 0;$$

$$\left[\frac{df[\sigma(t-\tau)]}{d\sigma(t-\tau)}\right]_{\sigma(t-\tau)=0} \geqslant k > 0,$$

$$\sigma(t-\tau)\varphi[\sigma(t-\tau)] > 0$$

$$\text{for} \quad \sigma(t-\tau) \neq 0,$$

where $\varphi[\sigma(t-\tau)] = f[\sigma(t-\tau)] - k\sigma(t-\tau)$, and $\underline{k}$ is a given constant. This function also satisfies the Dirichlet conditions in the control range $2|\bar{\sigma}|$, and can be presented in the form of a linear portion and a small nonlinear correction:

$$f[\sigma(t-\tau)] = k\sigma(t-\tau) + \varepsilon\varphi[\sigma(t-\tau)], \tag{1.2}$$

where $\varepsilon(\varepsilon \ll 1)$, introduced by means of the substitution $\bar{x}(t) = \varepsilon x(t)$, is a small parameter.

We now find a linear element which is equivalent, in a first approximation, to the nonlinear element of (1.1). We write the differential equation of the linear element in the form

$$\dot{x}(t) = a_1(A)\sigma(t) + a_2(A)\dot{\sigma}(t), \tag{1.3}$$

where $a_1(A)$ and $a_2(A)$ are the amplitude-dependent coefficients of the linear element.

It is required to determine the values of the coefficients $a_1(A)$ and $a_2(A)$ and to resolve the question of the physical interpretation of equivalent formula (1.3). For this we can use the standard electrical engineering concepts of active and reactive power. The active power developed by the executive organ during one period of oscillation corresponding, in the given case, to average power, will equal the work of the force $f[\sigma(t-\tau)]$ during a period T of oscillation, divided by the magnitude of T, i.e.,

$$\frac{1}{T}\int_0^T f[\sigma(t-\tau)]\,\dot{\sigma}(t)\,dt. \tag{1.4}$$

The reactive power will equal

$$\frac{1}{T}\int_0^T f[\sigma(t-\tau)]\,\dot{\sigma}\left(t-\frac{T}{4}\right)dt. \tag{1.5}$$

We now show that the value of the coefficient $a_1(A)$ can be obtained by equating the reactive powers of the nonlinear and the linear elements, and that the value of the coefficient $a_2(A)$ can be obtained by a corresponding equating of the active powers. Thus, in accordance with (1.5) and presenting $f[\sigma(t-\tau)]$ in the form of (1.2), we obtain

---

† The Krylov-Bogolyubov method permits the linearization of a system's nonlinear element independently of the other system parameters.

$$\frac{1}{T}\int_0^T f[\sigma(t-\tau)]\,\dot{\sigma}\left(t-\frac{T}{4}\right)dt =$$

$$= \frac{k}{T}\int_0^T \sigma(t-\tau)\,\dot{\sigma}\left(t-\frac{T}{4}\right)dt +$$

$$+ \frac{\varepsilon}{T}\int_0^T \varphi[\sigma(t-\tau)]\,\dot{\sigma}\left(t-\frac{T}{4}\right)dt. \qquad (1.6)$$

We assume, in a first approximation, that the quantity $\sigma(t)$, during the time interval $T = 2\pi/\omega$, varies harmonically:

$$\sigma(t) = A\cos\omega t, \quad \dot{\sigma}(t) = -A\omega\sin\omega t. \qquad (1.7)$$

By substituting the quantity in (1.7) into (1.6) for the reactive power, and introducing the new independent variable $\psi = \omega t$, we get

$$\frac{1}{T}\int_0^T f[\sigma(t-\tau)]\,\dot{\sigma}\left(t-\frac{T}{4}\right)dt = \frac{A^2 k\omega}{2}\cos\omega\tau +$$

$$+ \frac{\varepsilon A\omega}{2\pi}\int_0^{2\pi} \varphi[A\cos\omega(t-\tau)]\cos\psi\,d\psi. \qquad (1.8)$$

By substituting the quantity defined by (1.3) into (1.5) for the reactive power, and by taking (1.7) into account, we have

$$\frac{1}{T}\int_0^T a_1(A)\,\sigma(t)\,\dot{\sigma}\left(t-\frac{T}{4}\right)dt -$$

$$- \frac{1}{T}\int_0^T a_2(A)\,\dot{\sigma}(t)\,\dot{\sigma}\left(t-\frac{T}{4}\right)dt = \frac{a_1(A)\,A^2\omega}{2}. \qquad (1.9)$$

From a comparison of (1.8) and (1.9) we obtain the value of coefficient $a_1(A)$:

$$a_1(A) = k\cos\omega\tau -$$

$$- \frac{\varepsilon}{\pi A}\int_0^{2\pi} \varphi[A\cos\omega(t-\tau)]\cos\psi\,d\psi. \qquad (1.10)$$

In exactly the same fashion, by substituting $f[\sigma(t-\tau)]$, in the form of (1.2), in (1.4) for the active power, we get

$$\frac{1}{T}\int_0^T f[\sigma(t-\tau)]\,\dot{\sigma}(t)\,dt = \qquad (1.11)$$

$$= \frac{k}{T}\int_0^T \sigma(t-\tau)\,\dot{\sigma}(t)\,dt + \frac{\varepsilon}{T}\int_0^T \varphi[\sigma(t-\tau)]\,\dot{\sigma}(t)\,dt.$$

By substituting the quantity (1.7) in (1.11), we obtain

$$\frac{1}{T}\int_0^T f[\sigma(t-\tau)]\,\dot{\sigma}(t)\,dt = -\frac{kA^2\omega\sin\omega\tau}{2} -$$

$$- \frac{\varepsilon A\omega}{2\pi}\int_0^{2\pi} \varphi[A\cos\omega(t-\tau)]\sin\psi\,d\psi. \qquad (1.12)$$

By substituting in (1.4) for the active power, the quantity defined by (1.3), and by taking (1.7) into account, we have

$$\frac{1}{T}\int_0^T a_1(A)\,\sigma(t)\,\dot{\sigma}(t)\,dt + \frac{1}{T}\int_0^T a_2(A)\,\dot{\sigma}^2(t)\,dt =$$

$$= \frac{A^2\omega^2 a_2(A)}{2}. \qquad (1.13)$$

From a comparison of (1.12) and (1.13) we obtain the value of coefficient $a_2(A)$:

$$a_2(A) = -\frac{k\sin\omega\tau}{\omega} - \frac{\varepsilon}{\pi A\omega}\int_0^{2\pi} \varphi[A\cos\omega(t-\tau)]\sin\psi\,d\psi. \qquad (1.14)$$

The method of determining the equivalent coefficients $a_1(A)$ and $a_2(A)$ by (1.10) and (1.14) can be called the power principle, or the energetic balance principle for a nonlinear element with lags. It is easily shown (cf. the Appendix) that, when the harmonic balance principle is applied in the case when n = 1, one can obtain the values themselves of the coefficients. In accordance with (A.8) and (A.9), (1.10) and (1.14) can be given in the form

$$a_1(A) = \left(k + \frac{\varepsilon g_1(A)}{A}\right)\cos\omega\tau - \frac{\varepsilon h_1(A)}{A}\sin\omega\tau, \qquad (1.15)$$

$$a_2(A) = -\left(k + \frac{\varepsilon g_1(A)}{A}\right)\frac{\sin\omega\tau}{\omega} - \frac{\varepsilon h_1(A)}{A\omega}\cos\omega\tau, \qquad (1.16)$$

where $g_1(A)$ and $h_1(A)$ are the coefficients of the nonlinear function's Fourier series expansion for the case n = 1.

2. Determination of the Steady-State Periodic Mode Parameters in Systems with Time Lags

As the first example of the use of the Krylov-Bogolyubov method of asymptotic approximations, we consider a system described by an ordinary first-order linear differential equation with constant coefficients and lagging argument:

$$x + kx(t-\tau) = 0. \qquad (2.1)$$

Equation (2.1) was investigated by Schmidt [5] by means of a rigorous method for extracting the roots of the so-called transcendental function ‡. Schmidt showed that (2.1) possesses a periodic solution of the form

$$x = c_1\cos\omega t + c_2\sin\omega t, \qquad (2.2)$$

where c_1 and c_2 are arbitrary constants, with the condition that ω is defined by means of the equation

$$\omega = k = \frac{1}{\tau}\left(\frac{\pi}{2} \pm 2\pi n\right) \quad (n = 0, 1, 2, \ldots) \qquad (2.3)$$

---

‡ E. Schmidt considered the transcendental function

$$l(\omega) = i\omega - k\exp(-i\omega\tau) = -k\cos\omega\tau + i(\omega + k\sin\omega\tau). \qquad (2.1a)$$

In his notation, instead of k, τ, ω in (2.1) and (2.1a), there stand λ, h, ν.

By the Krylov-Bogolyubov method, the coefficients a_1 and a_2 of the equivalent system, defined by (1.15) and (1.16), will equal for the example under consideration, ($\epsilon = 0$):

$$ {}_1 = k\cos\omega\tau, \quad a_2 = \frac{-k\sin\omega\tau}{\omega}, \tag{2.4}$$

and the system's equivalent equation has the form

$$\left(1 - \frac{k\sin\omega\tau}{\omega}\right)\dot{x} + k\cos\omega\tau\, x = 0. \tag{2.5}$$

A periodic solution of (2.5) occurs with the conditions that

$$1 - \frac{k\sin\omega\tau}{\omega} = 0, \qquad k\cos\omega\tau = 0. \tag{2.6}$$

As is easily seen, (2.3) follows from this. Thus, the first approximation gives a result which coincides quantitatively with the exact solution of the ordinary linear differential equation with lagged argument which is being considered.

As a second example of the use of the Krylov-Bogolyubov method, we consider the questions connected with the search for the steady-state periodic mode (autooscillation) which occurs under certain conditions in nonlinear oscillatory systems with artifically introduced damping. The system is described by the so-called Minorsky** differential equation

$$\ddot{y}(t) + 2r\dot{y}(t) + \omega_0^2 y(t) + 2q\dot{y}(t-\tau) = \rho\dot{y}^3(t-\tau). \tag{2.7}$$

where r, ω_0 and q are positive constants and ρ is a small positive constant. By considering ρ to be sufficiently small, we set

$$\rho = \varepsilon\nu$$

and present (2.7) in the form of a system of two equations:

$$\dot{y} = z. \quad \dot{z} = -2rz - 2qz(t-\tau) - \omega_0^2 y + \varepsilon\nu z^3(t-\tau). \tag{2.8}$$

On the basis of the theorem on existence and uniqueness proven by Krasovskii†† [3], one can assert that, if the quasi-linear system (2.8) has a periodic solution for $\epsilon=0$ (the so-called generating solution) $y(t,0)$ then, if the condition $|\epsilon| < \epsilon_0$ holds, where ϵ_0 is some positive constant, there exists a unique periodic solution $y(t,\epsilon)$.

We start initially with the periodic solution for $\epsilon = 0$ (the generating solution), defined by the system of equations

$$\dot{y} = z. \quad z = -2rz - 2qz(t-\tau) - \omega_0^2 y. \tag{2.9}$$

By defining the coefficients a_1 and a_2 of the equivalent system by (1.15) and (1.16) (for the case $\epsilon = 0$), we obtain the following equality:

$$2qz(t-\tau) = a_1 z(t) + a_2\dot{z}(t) = 2q\cos\omega\tau\, z(t) - \frac{2q\sin\omega\tau}{\omega}z(t). \tag{2.10}$$

By substituting the value of $2qz(t-\tau)$ in (2.9), we get

$$\dot{y} = z. \quad \dot{z} = -b_1 z - b_2 y. \tag{2.11}$$

where

$$b_1 = \frac{2r + 2q\cos\omega\tau}{1 - \frac{2q\sin\omega\tau}{\omega}}. \quad b_2 = \frac{\omega_0^2}{1 - \frac{2q\sin\omega\tau}{\omega}}.$$

The characteristic equation of (2.11) has the form

$$D(\lambda) = \begin{vmatrix} -\lambda & +1 \\ -b_2 & -b_1 - \lambda \end{vmatrix} = 0 \tag{2.12}$$

or

$$\lambda^2 + b_1\lambda + b_2 = 0. \tag{2.13}$$

Equation (2.13) is an ordinary algebraic equation, and one may apply to it the familiar classical formulas of the theory of linear oscillations, in particular, the Routh-Hurwitz stability criterion. By this criterion, the system described by characteristic (2.13) will lie on the boundary of stability and will manifest undamped periodic oscillations in case

$$R = \Delta_{n-1} = b_1 = 0, \tag{2.14}$$

where Δ_{n-1} is the (n-1)th Hurwitz determinant.

Condition (2.14) occurs when

$$R = 2r + 2q\cos\omega\tau = 0. \tag{2.15}$$

The frequency of the periodic oscillations is defined by the formula

$$\omega^2 = \frac{\omega_0^2}{1 - \frac{2q\sin\omega\tau}{\omega}}. \tag{2.16}$$

By eliminating q from (2.15) and (2.16), we find that

$$\operatorname{tg}\omega\tau = -\frac{\omega^2 - \omega_0^2}{2r\omega}. \tag{2.17}$$

It is easily seen that the periodic solution of (2.13) occurs under the following conditions:

$$\operatorname{tg}\omega\tau < 0. \quad \cos\omega\tau < 0 \tag{2.18}$$

or

$$\frac{\pi}{2} + 2\pi n \leqslant \omega\tau < \pi + 2\pi n \quad (n = 0, 1, 2, \ldots) \tag{2.19}$$

In case of equality, $\omega\tau = \pi + 2\pi n$, the frequency ω of the periodic oscillations either coincides with, or is a multiple of, the natural frequency ω_0 of the system, and the phenomenon of resonance supervenes.

The frequency of the periodic oscillations is determined by a graphic solution of transcendental (2.17), and must satisfy (2.19). The amplitude A is an arbitrary constant, as is ordinarily the case when linear systems are being considered. It should be mentioned that, in the example under consideration, an arbitrarily small delay $\tau > 0$ may give rise to periodic oscillations in a system described by (2.9). In the case when $\tau = 0$, no periodic oscillations exist in the system described by (2.9) for any combination of the coefficients since, by our assumptions, the coeffi-

---

**An equation of the form of (2.7) was investigated by Minorsky [6,7], and then by Pinney [9], as related to the search for periodic oscillations.

†† Independently of Krasovskii, an analogous theorem was proven by Khalanai [10].

cients ω_0, $\underline{r}$, $\underline{q}$ are positive nonzero numbers.

We now determine the periodic solution of (2.8) for $\epsilon \neq 0$. As a first approximation, we give the periodic solution in the form

$$y = A\cos\omega t, \tag{2.20}$$

where the amplitude A and the frequency ω are determined from the solution of the equation obtained from (2.8) by use of the Krylov-Bogolyubov method of equivalent linearization. Determining the coefficients of the equivalent system from (1.15) and (1.16), we have the following equations:

$$\rho z^3(t-\tau) = a_3 z(t) + a_4 \dot{z}(t) = \frac{3}{4}\rho A^2 \cos\omega\tau z(t) - \frac{3}{4}\rho A^2 \frac{\sin\omega\tau}{\omega}\dot{z}(t). \tag{2.21}$$

By substituting the values of $2qz(t-\tau)$ and $\rho z^3(t-\tau)$ in (2.8), we get

$$\dot{y} = z.\quad \dot{z} = -b_3 z - b_4 y. \tag{2.22}$$

where

$$b_3 = \frac{2r + \cos\omega\tau\left(2q - \frac{3}{4}\rho A^2\right)}{1 - \frac{\sin\omega\tau}{\omega}\left(2q - \frac{3}{4}\rho A^2\right)}.$$

$$b_4 = \frac{\omega_0^2}{1 - \frac{\sin\omega\tau}{\omega}\left(2q - \frac{3}{4}\rho A^2\right)}.$$

In this case, the system's characteristic equation will be

$$D(\lambda) = \begin{vmatrix} -\lambda & +1 \\ -b_4 & -b_3 - \lambda \end{vmatrix} = 0 \tag{2.23}$$

or

$$\lambda^2 + b_3\lambda + b_4 = 0. \tag{2.24}$$

For fixed values of the amplitude A, characteristic equation (2.24) is an ordinary algebraic equation, to which we apply the Routh-Hurwitz stability criterion. By this criterion, the system described by (2.24) will lie on the boundary of stability, and periodic oscillations will occur in it if

$$R(A) = \Delta_{n-1} = b_3 = 0. \tag{2.25}$$

which occurs for

$$R(A) = 2r + \cos\omega\tau\left(2q - \frac{3}{4}\rho A^2\right) = 0. \tag{2.26}$$

With this, the frequency of the periodic oscillations is determined by the formula

$$\omega^2 = \frac{\omega_0^2}{1 - \frac{\sin\omega\tau}{\omega}\left(2q - \frac{3}{4}\rho A^2\right)}. \tag{2.27}$$

By eliminating $2q - 3\rho A^2/4$ from (2.26) and (2.27), we find

$$\operatorname{tg}\omega\tau = -\frac{\omega^2 - \omega_0^2}{2r\omega}. \tag{2.28}$$

The expression for the amplitude is determined from (2.26):

$$A = \left[\frac{8(r + q\cos\omega\tau)}{3\rho\cos\omega\tau}\right]^{1/2}. \tag{2.29}$$

Equations (2.28) and (2.29) must satisfy (2.19) and, moreover, the condition

$$q\,|\cos\omega\tau| > r \qquad \left(\text{for}\ \ q > \frac{3}{8}\rho A^2\right). \tag{2.30}$$

which, if satisfied, makes (2.29) physically meaningful (A is real).

The joint solution of (2.28) and (2.29) is most easily begun with a determination of the frequency ω of the steady-state periodic oscillations, specifically, with a graphic solution of transcendental equation (2.28). For this, we present (2.28) in the form of two terms:

$$\operatorname{tg}\omega\tau = \frac{\omega_0^2}{2r\omega} - \frac{1}{2r}\omega. \tag{2.31}$$

the first term of which is the equilateral hyperbola $\xi_1 = \omega_0^2/2r\omega$ with the ξ and ω axes for asymptotes, and the second term is the straight line $\xi_2 = \omega/2r$, with slope $-1/2r$. Using algebraic addition of the ordinates of these two curves for fixed values of ω_0 and $\underline{r}$, we obtain the sum curve (Fig. 2), whose intersections with the tangent curve in the second, sixth, etc. quadrants define the frequencies of the steady-state oscillations of which, if the graph is to be believed, there is an infinite set. However, it is easily shown that not all, but only a strictly finite number $\underline{n}$, of the frequencies obtained from the graphic solution of (2.28) satisfy (2.30) and, consequently, (2.29). Indeed, it is clear from Fig. 2 that, as the ω_i tend to infinity ($i = 2,3,\ldots,n,\ldots$), where we understand by ω_i the frequencies obtained from the intersections of the tangent curves with the curve in the sixth, tenth, etc. quadrants, $\tan\omega_i\tau \to \infty$. With this, $\cos\omega_i\tau \to 0$ and, for any frequency ω_{n+1}, there can occur a violation of (2.30), i.e., the condition of physical realizability of (2.29) no longer holds. Thus, as a first approximation to the solution of (2.7), we obtain the expression‡‡

$$y(t) = \sum_{s=1}^{n} A_s \cos\omega_s t. \tag{2.32}$$

in which the amplitudes A_s ($s = 1,2,\ldots,n$) are determined from (2.29) and the frequencies corresponding to them, which satisfy (2.28) and (2.29), are determined from the graphic solution of (2.28).

As a second approximation to the solution of (2.7), neglecting quantities of the order of smallness of ρ^2, we get the expression

$$y(t) = \sum_{s=1}^{n} A_s \cos\omega_s t + \rho\sum_{s=1}^{n} u_1(A_s, \psi_s). \tag{2.33}$$

where u_1 is defined by a formula analogous to (9):

$$u_1 = -\frac{1}{\omega^2}\sum_{n=2}^{\infty} \frac{\bar{g}_n(A)\cos n\psi + \bar{h}_n(A)\sin n\psi}{n^2 - 1}. \tag{2.34}$$

---

‡‡The proof that every solution y(t) can be given in the form of a sum of partial solutions is carried out in the second part of this paper.

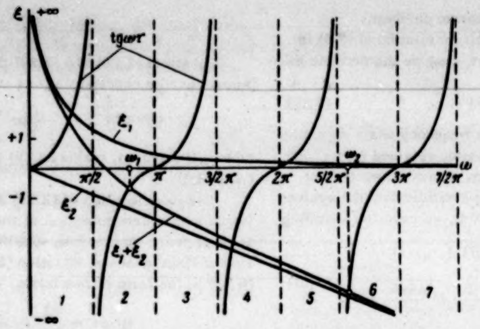

Fig. 2. Graphic solution of transcendental equation (2.28).

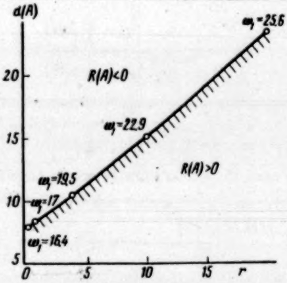

Fig. 3. Boundary of the stability region of system of equations (2.22) in the r, d(A) plane.

and $\bar{g}_n(A)$ and $\bar{h}_n(A)$ are defined by (A.8) and (A.9). In our case,

$$u_1 = \frac{1}{32} A^3 \frac{\cos 3\omega (t - \tau)}{\omega^2}. \tag{2.35}$$

Then, the second approximation has the form

$$y(t) = \sum_{s=1}^{n} A_s \cos \omega_s t + \frac{\rho}{32} \sum_{s=1}^{n} \frac{A_s^3 \cos 3\omega_s (t - \tau)}{\omega_s^2}$$

etc. (2.36)

3. Construction of the Boundaries of the Stability Region for the System of Equations (2.22) and the Investigation of Stability of the Steady-State Periodic Mode (Auto-Oscillation)***

In our example, the boundary of the stability region, as was already stated, is defined by the condition

$$R(A) = 2r + \cos \omega\tau \left(2q - \frac{3}{4} \rho A^2\right) = 0 \quad (\cos \omega\tau < 0). \tag{3.1}$$

By introducing the notation $d(A) = q - 3\rho A^2/8$ and $k(\omega) = 1/|\cos \omega\tau|$, we construct the boundary of the stability region in the r, d(A) plane. This boundary is some curve whose equation may be written in the form

$$d(A) = k(\omega) r. \tag{3.2}$$

For the fixed values $\omega_0^2 = 20$, $\tau = 0.1$ sec, the boundary of the stability region is shown in Fig. 3. It divides the r, d (A) plane into the region of stability, where $R(A) > 0$, and the region of instability, where $R(A) < 0$. Since d(A) is a function of amplitude, each fixed value of A has its own representative point. Therefore, the oscillations corresponding to boundary points of the system's parameter values, defined by (3.1), may be stable for certain values of A and unstable for other amplitude values. The oscillations on the boundary of the region will be stable if

$$\left(\frac{dR(A)}{dA}\right)_{R(A)=0} > 0, \tag{3.3}$$

and unstable if this expression is negative.

In analogy with the criterion for determining safe and dangerous boundaries due to Bautin [11], we may assume that the boundary is dangerous "in the small" if the following inequality holds in its neighborhood:

$$\left(\frac{dR(A)}{dA}\right)_{A\to 0} < 0. \tag{3.4}$$

If this expression is positive, then the boundary is safe "in the small". Dangerous and safe portions of the boundary

***In investigating the stability of the steady-state oscillatory mode, we take the amplitude $A_1 = A$ of the fundamental harmonic into account, but ignore the amplitudes A_i $(i = 2,3,\ldots)$ as being small high-frequency quantities.

are separated from each other by bifurcation points which are characterized by the condition

$$\left(\frac{dR(A)}{dA}\right)_{R(A)=0} = 0. \tag{3.5}$$

Bautin's idea may easily be generalized to the case of stability "in the large", i.e., for A→ ∞. Mathematically, this may be determined as follows. The boundary of stability of the system is safe "in the large" if the following inequality holds:

$$\left(\frac{dR(A)}{dA}\right)_{A\to\infty} > 0. \tag{3.6}$$

If the inverse inequality holds, then the boundary is dangerous "in the large".

Since, for nonlinear systems with lags R(A) depends not only on amplitude but also on the frequency of oscillation, then (3.3) can be rewritten in the form

$$\left(\frac{dR(A)}{dA}\right)_{R(A)=0} = \left(\frac{\partial R(A)}{\partial A}\right)_{R(A)=0} + \left(\frac{\partial R(A)}{\partial \omega}\right)_{R(A)=0} \frac{d\omega}{dA} > 0. \tag{3.7}$$

For the example under consideration, we have

$$\left(\frac{dR(A)}{dA}\right)_{R(A)=0} = -\frac{3}{2}A\rho\cos\omega\tau - \tau\sin\omega\tau\left(2q - \frac{3}{4}\rho A^2\right)\frac{d\omega}{dA},$$

$$\frac{d\omega}{dA} = \frac{3\omega\rho A\sin\omega\tau}{2\left[\left(2q - \frac{3}{4}\rho A^2\right)(\sin\omega\tau + \omega\tau\cos\omega\tau) - 2\omega\right]}, \tag{3.8}$$

where

$$\sin\omega\tau = \frac{\omega^2 - \omega_0^2}{\omega\left(2q - \frac{3}{4}\rho A^2\right)}, \tag{3.9}$$

$$\cos\omega\tau = -\frac{2r}{2q - \frac{3}{4}\rho A^2}. \tag{3.10}$$

By substituting the values of (3.9) and (3.10) in (3.8), we get

$$\left(\frac{dR(A)}{dA}\right)_{R(A)=0} = \frac{3\rho A\left[\omega^2(4r^2\tau + 2r) + 2r\omega_0^2 + \tau(\omega^2 - \omega_0^2)^2\right]}{2\left(2q - \frac{3}{4}\rho A^2\right)\left[\omega^2(2r\tau + 1) + \omega_0^2\right]}. \tag{3.11}$$

The point A = 0 is a bifurcation point, since

$$\left(\frac{dR(A)}{dA}\right)_{A\to 0} = 0. \tag{3.12}$$

The oscillation is stable in the small, since the quantity dR(A)/dA remains positive as A→ 0. According to Bautin [11], the boundary is "safe" in the small. The point A→ ∞ is also a bifurcation point since

$$\left(\frac{dR(A)}{dA}\right)_{A\to\infty} = -0. \tag{3.13}$$

Thus the question of the stability or instability of the oscillations for A → ∞ remains an open one, and requires a more detailed consideration, i.e., investigation of higher approximations and taking into account of oscillations of the form $A_i \cos\omega_i t$ (i = 2,3,...,n). This investigation does not lie within the scope of the present paper.

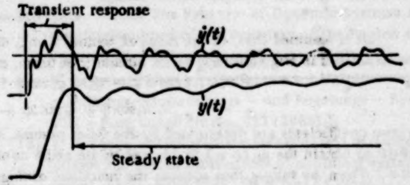

Fig. 4. Oscillogram of the steady-state periodic process in a nonlinear system with lags.

In conclusion, we compare our results with those obtained by Minorsky [6-8]. This latter author considered the appearance of self-excited oscillations in dynamic systems which were described both by linear and by nonlinear differential equations with lagged arguments of the form of (2.7), i.e., essentially linear and nonlinear problems. In considering linear problems, the author arrived at the conclusion that there exist an infinite number of frequencies of self-excited oscillations. In practice, however, in his words, only the basic frequency of the self-excited oscillations is ordinarily observed, which he also considers in his investigation of nonlinear problems. It was shown in the present work that in an autonomous dynamic system described by (2.7) there may exist, not only the fundamental self-excitation frequency, but higher frequencies as well, although their number is strictly finite. The periodic solutions are obtained in the form of sums of series of small parameters, and an estimate of the degree of approximation can always be obtained from the remainder term. Use of the Krylov-Bogolyubov method, in conjunction with the Routh-Hurwitz criterion, allows one to consider, moreover, the boundary of the region of stability of (2.7) and to determine its "dangerous" and "safe" segments. It should be mentioned that the theoretical results obtained from the investigation of the Minorsky equation by means of the Krylov-Bogolyubov asymptotic method were confirmed by simulating the system under consideration on an electronic analog computer. Figure 4 shows the oscillogram of the steady-state periodic process (autooscillation) arising on the boundary of stability of the system considered.

The author wishes to express his deep gratitude to A. M. Letov and Ya. Z. Tsypkin for a number of valuable remarks which have been incorporated in the present work.

APPENDIX

Equivalent Linearization of a Nonlinear Element with Lags by the Harmonic Balance Method

Let the function of the nonlinear element to be linearized have the form

$$F = \varphi\,[\sigma\,(t-\tau)]. \tag{A.1}$$

while its argument σ varies harmonically:

$$\sigma\,(t) = A\cos\omega t = A\cos\psi. \tag{A.2}$$

It is assumed that, in the range of control $2|\,\bar{\sigma}\,|$, the function F satisfies the Dirichlet conditions and may be expanded in trigonometric series without free term, of the form

$$\begin{aligned} F = \varphi\,[A\cos\omega\,(t-\tau)] &= \bar{g}_1\cos\psi + \bar{g}_2\cos 2\psi + \cdots + \bar{g}_n\cos n\psi + \cdots \\ \ldots &+ \bar{h}_1\sin\psi + \bar{h}_2\sin 2\psi + \cdots + \bar{h}_n\sin n\psi + \cdots, \end{aligned} \tag{A.3}$$

whose coefficients are determined by the Euler process, in which both members of (A.3) are multiplied by $\cos n\psi d\psi$ to obtain the $\bar{g}_n$ ($n = 1, 2, \ldots$), and by $\sin n\psi d\psi$ to obtain the $\bar{h}_n$ ($n = 1, 2, \ldots$), and then integrated from 0 to $+2\pi$. Then, by taking into account the functions' orthogonality properties, we get

$$\bar{g}_n = \frac{1}{\pi}\int\limits_0^{2\pi}\varphi\,[A\cos\omega\,(t-\tau)]\cos n\psi\,d\psi. \tag{A.4}$$

$$\bar{h}_n = \frac{1}{\pi}\int\limits_0^{2\pi}\varphi\,[A\cos\omega\,(t-\tau)]\sin n\psi\,d\psi. \tag{A.5}$$

We give $\sin n\psi$ and $\cos n\psi$ in the form

By substituting the expressions thus obtained in (A.4) and (A.5), we get

$$\bar{g}_n = \frac{\cos n\omega\tau}{\pi}\int\limits_0^{2\pi}\varphi\,[A\cos\psi]\cos n\,d\psi - \frac{\sin n\omega\tau}{\pi}\int\limits_0^{2\pi}\varphi\,[A\cos\psi]\sin n\psi\,d\psi, \tag{A.6}$$

$$\bar{h}_n = \frac{\cos n\omega\tau}{\pi}\int\limits_0^{2\pi}\varphi\,[A\cos\psi]\sin n\psi\,d\psi + \frac{\sin n\omega\tau}{\pi}\int\limits_0^{2\pi}\varphi\,[A\cos\psi]\cos n\psi\,d\psi \tag{A.7}$$

or

$$\bar{g}_n = g_n\cos n\omega\tau - h_n\sin n\omega\tau. \tag{A.8}$$

$$\bar{h}_n = h_n\cos n\omega\tau + g_n\sin n\omega\tau. \tag{A.9}$$

where g_n and h_n are the ordinary coefficients of the Fourier series for the nonlinear function without lags. We now substitute (A.8) and (A.9) in (A.3) and group terms with identical Fourier series coefficients. By using the theorem concerning sines and cosines of a doubled angle, we obtain

$$\begin{aligned} F = \varphi\,[A\cos\omega\,(t-\tau)] = g_1\cos\omega\,(t-\tau) + g_2\cos 2\omega\,(t-\tau) + \cdots + h_1\sin\omega\,(t-\tau) + \\ + h_2\sin 2\omega\,(t-\tau) + \cdots \end{aligned} \tag{A.10}$$

In the sequel we shall use either the form in (A.3) or the form in (A.10). Let the nonlinear element be given in the form of (1.2) and the equation of the equivalent linear element be written in the form of (1.3). We use the harmonic balance principle to determine $a_1(A)$ and $a_2(A)$. By substituting (A.2) in (1.2) and taking into account only the fundamental (first) harmonic of the oscillation, we get

$$\begin{aligned} f\,[A\cos\omega\,(t-\tau)] &= kA\cos\omega\,(t-\tau) + \varepsilon\bar{g}_1\cos\psi + \varepsilon\bar{h}_1\sin\psi = \\ &= Ak\,(\cos\psi\sin\omega\tau + \sin\psi\sin\omega\tau) + \varepsilon\bar{g}_1\cos\psi + \varepsilon\bar{h}_1\sin\psi, \end{aligned} \tag{A.11}$$

where g_1 and h_1 are the coefficients of the trigonometric series defined for the case n = 1 by (A.8) and (A.9). We now compare the oscillation of (A.11) with the oscillations obtained by substituting (A.2) in (1.3). From a comparison of the coefficients of the sines and cosines we obtain two equations for determining the unknown coefficients a_1 and a_2:

$$a_1\,(A)\,A = Ak\cos\omega\tau + \varepsilon\bar{g}_1, \quad -a_2\,(A)\,A\omega = Ak\sin\omega\tau + \varepsilon\bar{h}_1. \tag{A.12}$$

From whence

$$a_1\,(A) = \left(k + \frac{\varepsilon\bar{g}_1}{A}\right)\cos\omega\tau - \frac{\varepsilon h_1}{A} - \sin\omega\tau, \tag{A.13}$$

$$a_2\,(A) = -\left(k + \frac{\varepsilon h_1}{A}\right)\frac{\sin\omega\tau}{\omega} - \frac{\varepsilon h_1}{A}\cos\omega\tau. \tag{A.14}$$

LITERATURE CITED

1. N. M. Krylov and N. N. Bogolyubov, Introduction to Nonlinear Mechanics [in Russian] (Izd. AN USSR, 1937)
2. N. N. Bogolyubov and Yu. A. Mitropol'skii, Asymptotic Methods in Nonlinear Oscillation Theory [in Russian] (Fizmatgiz, 1958).
3. N. N. Krasovskii, "On periodic solutions of differential equations with time lags," Doklady Akad. Nauk SSSR 114, No. 2 (1957).
4. A. M. Letov, Stability of Nonlinear Controlled Systems [in Russian] (Gostekhizdat, 1955).
5. E. Schmidt, "Über eine Klasse linearer funktionaler Differentialgleichungen," Math. Annalen 70 (1911).
6. N. Minorsky, "Self-excited mechanical oscillations," J. Appl. Phys. 19 (1948).
7. N. Minorsky, "Self-excited oscillations in systems possessing retarded actions," Proceedings of the Seventh International Congress of Applied Mechanics 4 (1948).
8. N. Minorsky, "Self-excited oscillations in dynamical systems possessing retarded actions," Trans. ASME 64 (1942).
9. E. Pinney, Ordinary Difference – Differential equation (1959).
10. A. Khalanai, "Some qualitative questions in the theory of differential equations with lagged arguments," Rev. Math. Pures et Appliquées 11 (1957).
11. N. N. Bautin, The Behavior of Dynamic Systems in the Neighborhood of the Boundary of the Region of Stability [in Russian] (Gostekhizdat, 1949).
12. K. Magnus, "Uber ein Verfahren zur Untersuchungen nichtlinearer Schwingungs – und Regelungs – Systeme," VDI – Forschungsheft No. 451 (1955).
13. E. P. Popov, "Approximate investigation of autooscillations and forced oscillations of nonlinear systems," Izvest. Akad. Nauk SSSR, OTN No. 5 (1954).
14. K. Magnus, "Stationaure Schwingungen in nichtlinearen dinamischen Systemen mit Totzeiten," Ingenieur – Archiv. 24, No. 5 (1956).

ON STEADY-STATE MODES IN AUTOMATIC CONTROL SYSTEMS*

B. V. Shirokorad

(Moscow)

Translated from Avtomatika i Telemekhanika, Vol. 21, No. 4, pp. 456-464, April, 1960
Original article submitted December 12, 1959

The present paper discusses certain basic concepts and methods of automatic control system (ACS) theory which are related to the existence of steady-state modes of autonomous systems with the coexistence of several independent frequencies.

We limit ourselves to the consideration of the broadest class of autonomous ACS, the properties of which are described by a system of ordinary differential equations, given in the Cauchy form:

$$x = f_k(x_1, x_2, \ldots, x_n) \qquad (k = 1, 2, \ldots, n), \quad (1)$$

where the right member lies in some previously given class of functions, defined in a fixed region G, and does not explicitly contain the time parameter t.

Such systems were called dynamic by Birkhoff [1].

Lyapunov [2] called each (undisturbed) solution of (1) (following Routh's example) a steady-state solution with respect to the initiation of disturbance†. Subsequently, however, it turned out that such a general term was inconvenient, and it fell into desuetude. It developed that it was more convenient to apply the term "steady-state modes" to the more specialized motions of (1) which correspond to stable equilibrium positions (or points of rest). In the investigation of an ACS a basic role is played by the problem of determining the steady-state modes (for example, resting points, periodic, almost periodic, and the most general recurring [1] motions) which are stable with respect to other, transient, motions which approximate to these steady-state motions (control quality). All other motions (for example, generation or autooscillation of missile steering, generation of incorrect alignment of the autonomous contour of a power drive or steering mechanism) turn out to be undesirable, and they are considered from the point of view of the necessity for finding the limitation to be imposed on the ACS which will prevent their appearance in the operating modes (from whence the interest in the tuning of the controller's transfer ratio, the determination of the possible external noise conditions, etc.).

The introduction of the concept of the steady-state mode was an obvious step for linear or for two-dimensional nonlinear ACS with continuous right members of (1), but this was definitely not so for two-dimensional ACS with discontinuous right members, and even less so for multidimensional nonlinear ACS. For these, other fundamental concepts also seemed unclear, concepts such as establishment (of the steady-state mode), roughness (of adjustment), physical realizability, and others.

It was known even in A. Poincaré's time that the two-dimensional system (1) with continuous right members could have, in the phase plane (in the given case, in the velocity plane of A. Liénard), only two forms of steady-state modes: an equilibrium position with one state, or a periodic mode with many states.

If the right members of the two-dimensional system are discontinuous, then oscillatory motions of a new type, not converging to those mentioned above, might appear (for example, such motions appear in the systems treated in [3,4]).

In multidimensional systems described by (1), even with continuous right members, guaranteeing the existence (for t from - ∞ to + ∞) of a unique and continuous dependence of the solution on the initial conditions, there might appear very complicated oscillatory modes, with the coexistence of several, and even infinitely many, incommensurable frequencies.

No mention was made of the existence of such modes even in such fundamental textbooks as [5-7]. Moreover, Teodorchik [8] asserted‡ that, in many cases, one of the frequencies must, in the course of time, dominate over the others, such that after the lapse of some time the (established) mode will be nonetheless periodic (i.e., in actual systems, almost periodic modes do not exist).

Such circumstances led to an incorrect estimate of the value of studying the aforementioned modes in designing ACS. In particular, the problem of uncovering the very simplest of them – the almost periodic ones – in an ACS in the case n ≥ 3 was completely undeveloped, although the properties of such modes in differential equations were described by such authors as Poincaré, d'Anjou, Hayashi, Nemytskii [9], and others.

The etiology of the longstanding incorrect opinion as to the nonexistence of actual steady-state modes with many states of a more complicated nature than periodic ones is related to a very essential factor having to do with experimental observations, as well as to the widespread use of the harmonic balance method without account being taken of its domain of permissible applicability. The fact of the matter is that, in making our observations, we cannot distinguish between, for example, periodic and almost periodic steady-state modes, since the accuracy of the instruments and the intervals of observation time are quite limited. These individually noncharacterizeable steady-state modes present themselves to us phenomenologically as recurrent motions, i.e., those which were introduced into consideration as the most general motions by Birkhoff [1] in 1928. They are characterized by the property that, for each $\epsilon > 0$, there exists its own interval of observation T such that any trajectory of duration T of the recurrent steady-state mode will contain in its ϵ-envelope all the trajectories (as time varies from $-\infty$ to $+\infty$). Thus, an operator taking an observation during a time interval greatly exceeding T will always touch upon a "diffuse cycle" (a periodic mode with noise).

---

*Presented at the All-Moscow Seminar on Nonlinear ACS Methods of March 18, 1959, and at the First All-Union Session of Mechanics of January 29, 1960.

†Lyapunov assumed that the f_k were analytic functions.

‡However, his proofs suffered from mathematical incorrectness.

However, from the heuristic point of view, it is not at all a matter of indifference whether we have to do with a periodic steady-state mode, distorted by random noise or, for example, with an almost periodic mode. In the first case, an analytic investigation of the ACS is possible; in the second case, such an investigation is frequently impossible for the reasons previously cited.

Not only Birkhoff but, in the 1930's, Andronov **, spoke of the importance of investigating almost periodic steady-state modes. Finally, Aizerman [10] came out convincingly in defense of the physical reality of these steady-state modes and the necessity of studying them analytically for designing ACS.

1. Definition and Internal Properties of Dynamic Systems

We preface the more graphical explication and illustrations by a somewhat abstract definition of the dynamic system given by (1) and by a description of certain of its properties, borrowed from topological dynamics [11]. This digression allows an exact mathematic formulation to be given, but does not impair the understanding of the following simpler material.

Let X be a topological space of certain elements $x \in X$, which we shall call a phase space, and let the x be phases (points). Further, let T be a topological group of elements $t \in T$ (such that every pair $t_1, t_2 \in T$ is put into correspondence with a third element $t_3 \in T$). We call T the time group, with moments t. In X we define a transformation F which puts each point $x \in X$ into correspondence with another point of X which we denote by $xF \in X$. The topological product XT is mirrored by the transformation F in X, i.e., each pair (x,t), where $x \in X$ and $t \in T$, corresponds to a point (x,t)F. Descriptively (axiomatically), we define the topological transformation group, denoted briefly by the triplet (X,T,F), which satisfies the following axioms:

1. Identity axiom. In the group T there exists an initial moment of time $0 \in T$ (0 need not be a number) such that the pair t and 0 corresponds to t, and the pair (x,0) is put into correspondence, by transformation F, with the point (x,0)F = x.

2. Homomorphism axiom. If the pair t_1, $t_2 \in T$ corresponds to $t_3 \in T$, then $[(x, T_1)F, t_2]F = (x, t_3)F$.

3. Continuity axiom. The transformation F is one-to-one and continuous (i.e., topological).

If X is a metric space with metric ρ, and the moments of time $t \in T$ are real numbers then, in accordance with the continuity axiom, (x,t)F is a continuous function of the collection (x,t), i.e., for each $t \in T$ and a given pair of numbers $\epsilon > 0$ and $x \in X$ there exists another pair of numbers $\delta = \delta(x,t) > 0$ and $\tau = \tau(x,t)$ such that, for any $y \in X$ and $t_1 \in T$ such that $\rho(x,y) < \delta$ and $|t - t_1| < \tau$, the following inequality holds: $\rho[(x,t)F, (y,t_1)F] < \epsilon$.

By a trajectory (motion) we mean the geometric locus of the images of the fixed point $x \in X$ under the transformation F, corresponding to all the $t \in T$.

If, for all $t \in T$ the transformation F takes the set $I \subset X$ into itself, then I is called an invariant. For example, a singular point (a rest or equilibrium state), each trajectory, the set of all trajectories passing through all the limit points of a fixed almost periodic trajectory (in the case of a metric space X, cf. below), are invariant sets.

It is easily seen that the triplet (I,T,F) satisfies the three axioms given above and, consequently, is itself a topological transformation group (with the induced topology of X).

A nonempty closed invariant set I is called minimal (I_{min}) if it does not contain an invariant set as a proper subset. In the example given above, the invariant set of almost periodic trajectories is minimal.

If, on I_{min}, the invariant J is defined with respect to the points $t \in T$ then we say that I_{min} possesses J-internal stability.

Each trajectory (or resting point) possesses a natural (trivial) invariant: the transformation F takes it into itself for all $t \in T$.

Turning now to the other side, we consider metric invariants. For this we assume that X is a metric space with the metric ρ, and the moments of time $t \in T$ are real numbers. The set I_{min} has S-internal stability (in the sense of Franklin [12]) if, for any pair $\epsilon > 0$ and $x \in I_{min}$ there exists $\delta = \delta(\epsilon, x) > 0$ such that, for each $y \in I_{min}$ lying in the δ-neighborhood of x [i.e., for $\rho(x,y) < \delta$], there will hold, for all moments of time $t \in T$ (i.e., for $-\infty < t < +\infty$

$$\rho[(\dot{x}, t)F, (y, t)F] \leqslant \varepsilon. \tag{2}$$

If, moreover, I_{min} is bounded, i.e., there exists a phase $y \in X$ such that, for each $x \in I_{min}$, $\rho(x, y) < \text{const} < +\infty$, then, by means of the Vitali covering theorem, it is easily proven that in this case δ will depend only on ϵ, and $I_{\min}$ will represent a recurrent motion (in the sense of G. D. Birkhoff [1]), i.e., for each pair $\varepsilon > 0$ and $x \in I_{\min}$ there will exist a $\tau_* = \tau_*(\varepsilon, x) > 0$ such that, for any other pair $t_0, t \in T$ one finds a number $\tau = \tau(t) \in (t_0 - \tau_*, t_0 + \tau_*)$, for which

---

**This latter was communicated to the author by El'shin who consulted with Andronov during those years.

$$\rho[(x, t)F, (x, \tau)F] < \varepsilon. \quad (3)$$

Then, a fortiori, $I_{\min}$ will consist of L-internal stable trajectories (in the sense of Lagrange), i.e., there will exist a $y \in X$ such that, for each fixed $x \in I_{\min}$ and all $t \in T$

$$\rho[(x, t)F, y] < \text{const} < +\infty. \quad (4)$$

Each recurrent trajectory is P-internally stable, meaning that it possesses the local recurrence property (repeatability) in contradistinction to the integral property of (3) (in the sense of Poisson [1]). i.e., for any pair $\varepsilon, \tau > 0$ and any $x \in I_{\min}$ there exist two moments of time, $t_1 < -\tau$ and $t_2 > \tau$ for which

$$\rho[(x, t)F, x] < \varepsilon. \quad (5)$$

The converse is not true. It does not follow from the P-internal stability given by (5) that the trajectory is recurrent, as given by (3).

Since a continuous function on a closed set is uniformly continuous, it follows from the continuity axiom and Vitali's covering theorem, that a closed trajectory (cycle) has S-internal stability and, consequently, presents a recurrent motion.

Markov [13] showed that each bounded S-internally stable $I_{\min}$ consists of almost periodic trajectories, i.e., trajectories such that each of their components is a Bohr almost periodic function, i.e., is expanded in a trigonometric series

$$\sum_{i=1}^{\infty} (a_i \sin \omega_i t + b_i \cos \omega_i t), \quad (6)$$

where the a_i and b_i are constants, and the numbers ω_i need not be integers (in contradistinction to Fourier series).

The following property holds for an almost periodic trajectory $(x,t)F$. For any $\epsilon > 0$ there exists a $\tau_* = \tau_*(\epsilon) > 0$ such that, for each $t_0 \in T$ in the semi-interval $[t_0, t_0 + \tau_*]$ there exists at least one number τ (the so-called almost-period with respect to ϵ) for which

$$\rho[(x, t+\tau)F, (x, t)F] \leqslant \varepsilon \quad (7)$$

for all $t \in T$.

In particular, if (7) holds for $\epsilon = 0$, then the trajectory is called periodic (a cycle) with period τ. In this case, all the ω_i $(i = 1,2,\ldots)$ in (6) will be integers.

We note that dynamic ACS (1) may not satisfy the three enumerated axioms. For example, let X be the ordinary n-dimensional Euclidean space, T the set of real numbers, and $\varphi(x)$ a continuous decreasing function such that $\varphi(x_0) < 0$ for some $x_0 > 0$. Then, the trajectory defined by the equation $\dot{x} = \varphi(x)$ does not exist (i.e., can not be continued) for $t < \int_{x_0}^{+\infty} dx / \varphi(x) < 0$, if this latter integral exists.

It is known that each L-internally stable trajectory (1) can be continued.

A trajectory of the type in (1) that can be continued and is uniformly continuous in t is S-internally stable since, in this case, for each $\epsilon > 0$ there exists a $\delta = \delta(\epsilon) > 0$ such that (7) holds for $0 < \tau < \delta$ and any t.

Local continuity in t is a necessary but not a sufficient condition for S-internal stability. For example, the trajectory $y = 1/(1-x)$ of the system $\dot{x} = 1$, $\dot{y} = -1/(1-x)^2$ which passes through the point (0,1) for $t = 0$ does not possess S-internal stability.

We mention still one more important circumstance. A trajectory of type (1) which can not be continued is necessarily unbounded. The converse is not true. There exist trajectories which are simultaneously S-internally stable and L-internally unstable. Tricomi [14] first encountered such motions in a rotor (armature) of a synchronous motor which lagged the stator's rotating magnetic field by the angle θ, the motion being described by the equation

$$\ddot{\theta} + A\dot{\theta} + B\sin\theta = C. \quad (8)$$

where $A > 0$, $B > C > 0$. The law of this motion is defined by the continuous periodic function $\vartheta = \vartheta(t)$ with period τ:

$$0 = \vartheta + \frac{2\pi}{\tau}t. \quad (9)$$

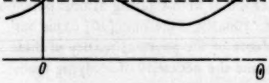

Fig. 1

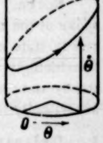

Fig. 2

Fig. 1. Slipping mode of an asynchronous motor's rotor.

Fig. 2. Cylindrical phase plot of an asynchronous motor's rotor slippage.

On the phase (velocity) Liénard $\{\theta, \dot{\theta}\}$ plane, this law takes the form of the unbounded curve shown in Fig. 1.

This law of motion also has another geometric interpretation. On a phase cylinder (Fig. 2), it is given by a closed curve (a cycle) with elliptical form, and is bounded.

The dual interpretation just given has a curious meaning. According to Nemytskii's classification [9], each bounded S-internally stable and (simultaneously) asymptotically stable (external, in the sense of A. M. Lyapunov) trajectory represents a steady-state mode. Consequently, in the sense of Nemytskii, the mode given by (9)[††], depending on the choice of the coordinate system, is simultaneously both steady-state and not steady-state.

[††] It is known that the mode of (9) is asymptotically stable in the sense of Lyapunov.

2. Definition of the Steady-State Mode

We assume *a priori* that, in topological space X, a limiting operation is defined, and that the group T is a well-ordered set of elements ‡‡.

Let I_{min} be embedded in the open region U. The set of points $\underline{x}$ which lie in U but do not lie in I_{min} is called the open envelope of I_{min}, and is denoted by $U(I_{min})$.

If there exists a $U(I_{min})$ such that, for each of its points, there is an increasing sequence $t_i \in T$ $(i = 1, 2, \ldots)$

$$t_1 < t_2 < \ldots < t_n < \ldots \tag{10}$$

such that

$$(x.\, t_n)F \to I_{min} \quad \text{for} \quad n \to +\infty. \tag{11}$$

then I_{min} is called orbitally asymptotically stable (in the sense of Poincaré) in the positive direction. In this case, $U(I_{min})$ is called the domain of attraction of I_{min}.

Correspondingly, one speaks of a negative direction, if the sequence in (10) is a decreasing one.

If there exist simultaneously two sequences, one increasing and the other decreasing, one says that I_{min} is simply orbitally asymptotically stable.

If, moreover, there exists a point $y \in I_{min}$ such that, in addition to (11), there holds the relationship

$$(x.\, t_n)F \to (y.\, t_n)F \quad \text{for} \quad n \to +\infty. \tag{12}$$

then one says that I_{min} is asymptotically stable in the sense of A. M. Lyapunov [in, respectively, the positive, negative, and in both directions where, in the latter case, one says that I_{min} is unconditionally asymptotically stable (in the sense of G. Dirichlet)].

If the space X is a metric one, then the definitions just given assume their ordinary meanings***.

Each mode of motion which is an internally and orbitally asymptotically stable (externally) I_{min} is called a steady-state mode. The corresponding process of establishing the steady state is defined by the limiting process of (11) in the sense of the topology of X.

Each I_{min} of steady-state modes has a domain of attraction. For example, such domains do not exist for any invariant set of motions defined by the equation $\ddot{x} + x = 0$.

Nemytskii [9] showed that the presence of a domain of attraction in an almost periodic mode essentially simplifies its structure. Thus, for example, each asymptotically stable (in the sense of Lyapunov) steady-state mode of a three-dimensional system is either an equilibrium position (with one state) or a periodic mode or an almost periodic mode (with many states) having not more than two independent frequencies. The images of these motions in phase space are, respectively, a point, a closed curve, and an irrational toroidal winding. Whether the analogous suppositions hold for n-dimension systems, for n>3, is not yet known, but is probable.

The domain of attraction of an almost periodic steady-state mode can not keep its trajectories isolated. An infinite set of trajectories passing through the limit points of these almost periodic trajectories will also be embedded in the domain of attraction. All these trajectories will also be almost periodic, with the same frequencies as the first one. The trajectory of a periodic steady-state mode can be unique in its domain of attraction.

We note in conclusion that Nemytskii [9], following Franklin [12], insists that each steady-state mode must be S-internally stable. He starts from the condition that "if at some moment of time two states were neighboring, it must follow that in the future these states must remain neighboring, since otherwise the mode under investigation either would have in the past, or will have in the future, some tendency to development consisting of a separation of these two states from each other, which would render it impossible to speak of a steady-state mode". These words seem essentially unconvincing and unclear, so that the development in time must be understood only from the point of view of the limitation given in (2).

Since every motion in time is a development, then each temporal invariant may, with equal justification, be taken as an indication of nondevelopment (in the meaning defined by him), stationary nature, or establishment in time. The choice of some temporal invariant or another must be determined, not by subjective conceptions, but by the objective problem which supervenes in the concrete investigation of an ACS. On this score, one could give many convincing examples from practice.

3. On Certain Methods of Investigating Almost Periodic Steady-State Modes in an ACS

The simplest method of investigation is a modification of Minorsky's approximate "stroboscopic" method [16], well-known in nonlinear mechanics, this method being a further development of the principle introduced into science in 1883 by A. Gulden and Linstedt [17]†††. The limits of applicability of the "stroboscopic" method were determined by Urabe [18].

For greater clarity we demonstrate this method by the example of a four-dimensional ACS without, however, lessening the generality.

We turn to the example of a "blind" winged missile, circling (without lateral banking) at a constant altitude under the action of residual voltage U (of a hysteresis magnetic or "zero drift" vacuum tube amplifier).

---

‡‡The topological transformation group (X,T,F) is a semi-ordered set if T is well-ordered [11].

***We note that, in the monograph of Zubov [15], orbital stability, as given by (11), is called stability in the sense of Lyapunov, which can lead to misunderstandings. For example, for an isolated orbit of a heavenly body (a Sputnik moving in accordance with Kepler's law in a conservative central force field $\ddot{\eta} = -\mu r/|r|r^2$ (where $\underline{r}$ is the vector of the body and μ is the gravitational constant), the orbit is unstable in the sense of Lyapunov and orbitally stable.

†††Their work also served as the starting point for the development of the results of Krylov and Bogolyubov.

In the particular case, the missile equations can be put in the form

$$\ddot{\beta} + c_1\dot{\beta} + c_2\beta + c_3\delta = 0. \qquad (13)$$
$$\dot{\psi} = \dot{\beta} + c_4\beta$$

(where c_1, c_2, c_3, and c_4 are positive numbers, and β, ψ and δ are the angles of lateral slipping, course, and rudder deviation from the neutral position), while the autopilot equations are

$$\dot{\delta} = f(\sigma), \quad \sigma = i(\dot{\beta} + \nu\beta - U) - \delta. \qquad (14)$$

where $f(\sigma)$ is the piecewise-smooth velocity characteristic of the steering mechanism [$\sigma f(\sigma) > 0$ for $\sigma \neq 0$, $f(0) = 0$], $i > 0$ is the autopilot's rigid feedback coefficient and $\nu > 0$ is the transfer ratio of the accelerometer for lateral linear acceleration.

We assume a priori that oscillations are observed in the system, and that the conditions for applying the "stroboscopic" method are satisfied ‡‡‡. We may then set

$$\beta = \beta_0 + x(t)\sin nt + y(t)\cos nt, \quad \sigma = z(t)\sin nt, \qquad (15)$$

where $\beta_0 = c_3 U/(c_3\nu + c_2/i)$. n is angular frequency, and x(t), y(t), and z(t) are slowly varying functions of time (in relation to the period $2\pi/n$).

On the basis of the previously given theorem of V. V. Nemytskii [9], the state equilibrium positions and the periodic modes of the $\{x,y,z\}$ phase space of the stroboscopic projections of the hyperplanes of the $\{\beta, \dot{\beta}, \delta\}$ phase space of (13)-(14) completely define all the bounded steady-state modes (possessing S-internal stability) of (13)-(14) [owing to the degeneration of (13), since the second equation does not depend on the first]. A study of the three-dimensional (induced) system of equations in the $\{x,y,z\}$ phase space can be carried out by the methods presented in [19-25] and others. However, there are as yet no effective methods for determining the domains of attraction (except for what was presented in [23]).

It so happens that, under certain conditions, the $\{x,y,z\}$ phase space contains a unique stable cycle. It is then easily seen that the cylindrical $\{\beta, \dot{\beta}, \delta, \psi\}$ phase space of (13)-(14) will contain a unique (bounded) steady-state almost periodic mode with two coexisting independent frequencies n and $c_4\beta_0$, so long as the latter are incommensurable.[1]

This same result is attained by the (exact) method of the topological product, the essence of which is as follows.

By well-known topological methods [23] one proves the existence of a stable oscillatory mode in $\{\beta, \dot{\beta}, \delta\}$ phase space.

The cylindrical $\{\beta, \dot{\beta}, \delta, \psi\}$ phase space is considered as the topological product of the $\{\beta, \dot{\beta}, \delta\}$ hyperplane and the $\{\psi\}$ circle. By this we arrive at the result given above

It should be mentioned that the topological product method has thus far been applied only to those ACS whose equations are either degenerate, or reduce in some fashion to those groups of which one, at least, is amenable to the application of one of the methods of investigation given in [19-25].

The author wishes to express his gratitude to V. V. Nemytskii and M. I. Fl'shin for their comments, reflected in the present work.

LITERATURE CITED

1. G. D. Birkhoff, Collected Mathematical Papers (Am. Math. Soc., 1950).
2. A. M. Lyapunov, Collected Works: The General Problem of Stability of Motion [in Russian] (1892) (Izd. AN SSSR, 1956) Vol. 2.
3. A. S. Alekseev, "Two-position temperature controller with leading zones," In Commemoration of A. A. Andronov [in Russian] (Izd. AN SSSR, 1955).
4. I. B. Chelpanov, "Oscillations of systems containing relays with leading characteristics," Prikl. Matem. i Mekh. 22, No. 1 (1958).
5. B. V. Bulgakov, Oscillations [in Russian] (Gostekhizdat, 1954).
6. A. A. Andronov, A. A. Vitt, and S. E. Khaikin, Theory of Oscillations [in Russian] (State Phys.-Math. Lit. Press, 1959).
7. I. M. Babakov, Theory of Oscillations [in Russian] (Gostekhizdat, 1958).
8. K. F. Teodorchik, "Laws of coexistence of frequencies in weak auto-oscillatory systems," Izvest. Akad. Nauk SSSR, OTN No. 3 (1946); Vestnik MGU No. 10 (1946).
9. V. V. Nemytskii, "On the nature of steady-state modes in multidimensional dynamic systems," Proc. Third All-Union Meth. Conference [in Russian] (Izd. AN SSSR, 1956).
10. M. A. Aizerman, "The problem of determining periodic modes in automatic control systems," Proc. of the Second All-Union Conference on the Theory of Automatic Regulation. 1, (Izd. AN SSSR, 1956).
11. W. H. Gottshalk and G. A. Hedlund, Topological Dynamics (Am. Math. Soc. 1955).
12. P. Franklin, "Almost periodic recurrent motions," Math. Z. 30 (1929).
13. A. A. Markoff, "Stabilität im Liapounoffschen sinne und Fastperiodizität," Math. Z 36 (1933).
14. F. Tricomi, "Integrazione di un equazione differenziale presentatasi in Elettrotecnica," Annali della Scuola Normale Superiore di Pisa, II, ser. II (1933).
15. V. I. Zubov, The Methods of A. M. Lyapunov and Their Application [in Russian] (Izd. Leningrad Univ., 1957).
16. N. Minorsky, Comp. Rend. Sci. 228, 60 (1949); 231, 1417 (1950); 232, 1060, 2179 (1951); of the Franklin Inst. p. 147-165 (1953); J. Phys. et Radium 18, 121-130 (1957); Bull. SFM No. 13, p. 1-12.
17. A. Linstedt, Beitrag zur Integration der Differentialgleichungen der Storungstheorie (Petersburg and Leipzig, 1883).

---

‡‡‡For example, in the particular case when $f(\sigma) \equiv A\sigma + B\sigma^3$, where the constants A > 0 and |B| are sufficiently small.

[1] If the $\{\beta, \dot{\beta}, \delta, \psi\}$ space is considered as being Euclidean, then an almost periodic mode turns out to be unbounded, i.e., it will not be steady-state in the sense of Nemytskii (as in the example of Tricomi given earlier).

18. M. Urabe, "Reduction of periodic system to autonomous one by means of one-parameter group of transformations," J. Sci. Hiroshima Univ. 20, No. 1 (1956).

19. K. O. Friedrichs, On Nonlinear Vibrations of Third-Order Studies on Nonlinear Vibration Theory (Inst. for Math. and Mech., New York Univ., 1946)

20. G. Colombo, "Sull-Equazione differenziale non lineare del terzo ordine di un circuito oscillante triodio," Rend. Sem. Math. della Univ. di Padova 20 (1950).

21. L. L. Rauch, Oscillation of a Third-Order Nonlinear Autonomous System (Contributions to the Theory of Nonlinear Oscillations. Princeton, 1950).

22. V. A. Pliss, "The investigation of one system of three differential equations," Doklady Akad. Nauk SSSR 117, (1957).

23. B. V. Shirokorad, "On the existence of cycles outside the conditions of absolute stability of three-dimensional systems," Avtomatika i Telemekhanika 19, No. 10 (1958)[*].

24. É. M. Vaisbort, "On the existence of periodic solutions, and on the over-all boundedness of the solutions, of systems of ordinary third-order differential equations," Izv. Vyssh. Uch. Zaved. No. 11 (1959).

25. M. A. Aizerman and F. R. Gantmakher, "Problem of determining the periodic modes in nonlinear dynamic systems with piecewise-linear characteristics," Prikl. Matem. i Mekh. 20, No. 3 (1956); "On the stability of periodic motions," Prikl. Matem. i Mekh. 22, No. 6 (1958).

---

[*] See translation.

DETERMINING PULSE SYSTEM OPTIMUM WEIGHTING FUNCTION WHICH ENSURES THE EXTREME OF A FUNCTIONAL

N. I. Andreev

(Kharkov)

Translated from Avtomatika i Telemekhanika, Vol 21, No. 4 pp. 465-473, April, 1960
Original article submitted October 17, 1959

A method is described for finding the optimum pulse system which ensures an extreme of a sufficiently general criterion in the form of a functional I = Φ($I_1,\ldots,I_{n+1}$), where Φ is a known function, and I_i are quadratic functionals of the weighting function of the system.

The methods for the determination of the optimum linear pulse systems minimizing the mean-square-error at its output are given in [1,2]. The least mean-square-error criterion seems a suitable choice in many cases when selecting a dynamic system. In practice, however, when evaluating and comparing various pulse systems one often encounters cases where the most suitable criterion is a more complex probability characteristic of the accuracy of the system operation. A characteristic of this type may be, for example, the probability P of the system error not exceeding by numerical value a certain given quantity c. In a specific case the probability P may usually be expressed in terms of mathematical expectation and variance of the separate components of the error, the components having different distributions. (When the components of the system error also depend on one another the moments due to their correlation should also be considered. For example, if the error of the system is composed of the sum of mathematical expectation a and a random component normally distributed with variance σ^2, then

$$P = \frac{1}{\sqrt{2\pi}\sigma}\int_{-c}^{c}\exp\left[-\frac{(a+x)^2}{2\sigma^2}\right]dx = I(a^2, \sigma^2). \qquad (1)$$

In the case when the mathematical expectation of the error is a, and the first random component Z_1 of the error is distributed normally with variance σ^2, and the second random component Z_2 has a rectangular distribution within the interval from -b to +b, and Z_1 and Z_2 are independent, then

$$P = \frac{1}{\sqrt{2\pi}2b\sigma}\int_{-c}^{c}\left\{\int_{-b}^{b}\exp\left[-\frac{(a+y+x)^2}{2\sigma^2}\right]dx\right\}dy = I(a^2, \sigma^2, b^2). \qquad (2)$$

In the often encountered case when the quantity c is small, (1) and (2) assume a simpler form:

$$P \approx \frac{\sqrt{2}c}{\sqrt{\pi}\sigma}\exp\left[-\frac{a^2}{2\sigma^2}\right], \qquad (1a)$$

$$P \approx \frac{c}{\sqrt{2\pi}\sigma b}\int_{-b}^{b}\exp\left[-\frac{(a+y)^2}{2\sigma^2}\right]dy. \qquad (2a)$$

The quantities a^2, σ^2, b^2 are quadratic [3,4,6] functionals of the system weighting function. In a more general case a^2, σ^2, b^2 also depend parametrically on time. Consequently, even the optimum system which at any given moment of time is extreme depends on time and is thus nonstationary.

We shall assume henceforth that the criterion I for selecting the optimum system is a given function Φ of n + 1 quadratic functionals I_i (i = 1,..., n + 1) which in turn depend on the weighting function of the pulse system. The problem of determining the optimum linear pulse system according to the I criterion is formulated in the same way as in [3,5] when determining the optimum linear system of a continuous type.

We assume that there is a method of finding an optimum weighting function $k_0[n,m,\epsilon]$* of a pulse system with given time of the transient process and such that the function will ensure the extreme of the quadratic functional

$$I_{\text{II}} = \theta_1 I_1(k[n,\ m,\ \varepsilon]) + \ldots + \theta_n I_n(k[n,\ m,\ \varepsilon]) + I_{n+1}(k[n,\ m,\ \varepsilon]) \qquad (3)$$

for arbitrary values of the parameters θ_i. A method is sought to determine the optimum weighting function $k^*[n,m,\epsilon]$ with the same transient process time interval, and such that it will ensure the extreme of the functional

$$I = I(k[n,\ m,\ \varepsilon]) = \Phi(I_1, \ldots, I_{n+1}). \qquad (4)$$

The time is here expressed in integral units [1,2]. The time in conventional units is obtained from the integral units as follows: t = nT + mT + εT at any moment of time, t = mT at the discrete values of time. The quantity T is the pulse sampling period, otherwise the control time interval of the pulse system, and ε varies from 0 to 1.

---

*The weighting function $k[n,m,\epsilon]$ of a pulse system with variable parameters of the equivalent (reducible) continuous part expresses its response at the moment t = n + m + ε to a unit impulse applied to the input at the moment t = n – 0.

The problem is solved at an arbitrary moment of time regarded as a parameter.

The difference between the formulations of this problem and of [3,5] lies in the latter continuous case being the optimum system in the class of all the possible linear systems with the same given duration of the transient process; and in our problem the optimum system is selected from the class of pulse linear systems with given pulse sampling period as well as duration of transient process. All the pulse system weighting functions with a given pulse sampling period form a linear manifold (which also holds good for weighting functions of continuous linear systems)[†]. Therefore, all the derivations and proofs obtained in [3,5] for linear systems of continuous type could be repeated by replacing everywhere "linear system" (of continuous type) with "pulse system" (with given pulse sampling period). We just state the fundamental result without reproducing the derivations.

The necessary conditions which must be fulfilled by the weighting function $k^\circ[n,m,\epsilon]$ ensuring the extreme of the functional I are:

a) The function k° should ensure the extreme of the functional I_{II}, i.e., it is required that:

$$k^\circ = k_0[n, m, \varepsilon, \theta_1, \dots, \theta_n]\,|_{\theta_i=\theta_{i0}}; \tag{5}$$

b) The following should be valid:

$$\left.\frac{\partial I\,(k_0\,[n, m, \varepsilon, \theta_1, \dots \theta_n]}{\partial\theta_i}\right|_{\theta_j=\theta_{j0}} \tag{6}$$

$$(i, j = 1, \dots, n).$$

or (a special case) the condition below must be fulfilled:

$$\frac{\partial\Phi\,[I_1(k^\circ), \dots I_{n+1}(k^\circ)]}{\partial I_l} = 0 \qquad (l = 1, \dots n+1).$$

which illustrates the fact that the function Φ reaches its extreme within the domain of variability of the I_i functionals. This special case is usually of no practical importance.

The condition a) enables one to reduce the complex task of determining the function k° at which the extreme of I occurs to a less complex one of finding k_0 at which the extreme of I_{II} occurs. Determining the function $k_0 = k_0[n,m,\epsilon,\theta_1, \dots, \theta_n]$ is the principal stage in the solution of our problem. Once the function $k_0[n,m,\epsilon, \theta_1, \dots, \theta_n]$ has been obtained explicitly for arbitrary values of the parameters θ_i, it is easy to determine the values of the parameters $\theta_i = \theta_{i0}$ satisfying the condition b)[‡]. Where only approximations to the function are obtained, the values of the parameters $\theta_i = \theta_{i0}$ are also evaluated approximately, for example, graphically. As long as the number n of the parameters θ_i remains small, the determination of the values θ_{i0} is fairly straightforward and easy. This is why the determination of the weighting function $k_0[n,m,\epsilon,\theta_1, \dots, \theta_n]$ ensuring the extreme of I_{II} should have primary attention. Methods of determining k_0 with data given in other forms have been sufficiently developed [6, 7 and others]. The functionals I, I_i, I_{II} obtained when investigating the pulse systems differ from the corresponding functionals I, I_i, I_{II} obtained when examining the continuous linear systems (the integrals in the latter case correspond to sums in the former one).

In the case of a pulse system, the determination of k_0 can be reduced to the solution of linear algebraic equations [1,2]. As is known, in the continuous case k_0 is determined as a solution of a certain linear integral equation. The actual form of the equations depends in both cases on the way in which the data are given.

We shall consider one method of determining the optimum weighting function of a pulse system from the criteria (1a). Let on the input of the pulse system be impressed a useful signal $X[n, \epsilon]$ which can be represented as a sum of a known nonrandom continuous function $x[n,\epsilon]$ and a random function $X^\circ[n,\epsilon]$ distributed normally with xero mean and correlation function $R_x[n-m, n-l]$. The interference $Z[n,\epsilon]$ also occurs at the input; it is a random function normally distributed with zero mean and correlation function $R_z[n-m, n-l]$. In order to simplify the subsequent exposition, it is assumed that interference and signal are not correlated, that is, $M[XZ] = 0$. The pulse system at the output is given by the function $HX[n,\epsilon]$, where H is a linear operator. The time of the system transient process is equal to N.

In this case the error is equal to

$$E[n, \varepsilon] = \left\{\sum_{m=0}^{N} x[n-m]\,k[n-m, m, \varepsilon] - Hx[n, \varepsilon]\right\} + \tag{7}$$

$$+\left\{\sum_{m=0}^{N} X^\circ[n-m]\,k[n-m, m, \varepsilon] - HX^\circ[n, \varepsilon]\right\} + \sum_{m=0}^{N} Z[n-m]\,k[n-m, m, \varepsilon]$$

(the effect of initial conditions being neglected).

In the expression (7) the first term represents the mathematical expectation a of the error, the second and the third term being random components of the error.

[†] A set of M is called linear manifold when its elements satisfy the following rules: when k_1 and k_2 belong to M, then $a_1k_1 + a_2k_2$ also belongs to M, whatever the arbitrary numbers a_1, a_2.

[‡] It was shown in [3, 5] that in order to determine $\theta_i = \theta_{i0}$ one can utilize another condition:

$$\frac{\partial I}{\partial I_j} \Big/ \frac{\partial I}{\partial I_{n+1}} = \theta_j \quad (j = 1, \dots, n).$$

instead of condition b).

We denote by I_1 the variance of the error:

$$I_1 = \sigma^2 = M[(E-a)^2] = \sum_{l=0}^{N}\sum_{m=0}^{N} R_z[n-m, n-l]\,k[n-m, m, \varepsilon]\,k[n-l, l, \varepsilon] + \\ + \sum_{l=0}^{N}\sum_{m=0}^{N} R_x[n-m, n-l]\,k[n-m, m, \varepsilon]\,k[n-l, l, \varepsilon] - \\ - 2\sum_{l=0}^{N} HR_x[n-l, n+\varepsilon]\,k[n-l, l, \varepsilon] + HHR_x[n+\varepsilon, n+\varepsilon]. \tag{8}$$

In the last but one term, the operator H on the correlation function R_x operated with respect to its second argument.

We denote by I_2 the square of the mathematical expectation of the error E:

$$I_2 = a^2 = (M[E])^2 = \left\{\sum_{m=0}^{N} x[n-m]\,k[n-m, m, \varepsilon] - Hx[n, \varepsilon]\right\}^2. \tag{9}$$

The functional I_{II} in this case takes the form

$$I_{II} = \theta_1 I_1 + I_2. \tag{10}$$

Bearing in mind what was stated previously, one has to find a weighting function $k_0[n, m, \epsilon, \theta_1]$ which will ensure the extreme of the functional (10). The necessary condition satisfied by such a function k_0 is [6,8] the vanishing of the first variation of the functional I_{II}

$$\left.\frac{dI_{II}\{k[n, m, \varepsilon, \theta_1] + \Delta\varkappa[n, m, \varepsilon]\}}{d\Delta}\right|_{\Delta=0} = 0 \tag{11}$$

for any weighting function κ of a pulse system with pulse sampling period T and time N of the transient process.

We rewrite the expression for the quadratic functional $I_{II}[k + \Delta\kappa]$ in the expanded form

$$I_{II}[k + \Delta\varkappa] = I_{II}[k] + 2\Delta D_1 + \Delta^2 D_2. \tag{12}$$

where

$$D_1 = \sum_{l=0}^{N} \varkappa[n-l, l, \varepsilon]\left\{\sum_{m=0}^{N} k[n-m, m, \varepsilon, \theta_1](\theta_1 R_z[n-m, m-l] + \right. \\ + \theta_1 R_x[n-m, n-l] + x[n-l]\,x[n-m]) - x[n-l]\,Hx[n, \varepsilon] - \\ \left. - \theta_1 HR_x[n-l, n+\varepsilon]\right\},$$

$$D_2 = \sum_{l=0}^{N}\sum_{m=0}^{N} \varkappa[n-l, l, \varepsilon]\,\varkappa[n-m, m, \varepsilon](\theta_1 R_2[n-m, n-l] + \\ + \theta_1 R_x[n-l, n-m] + x[n-m]\,x[n-l]).$$

It follows from (11) and (12) that

$$\sum_{l=0}^{N} \varkappa[n-l, l, \varepsilon]\left\{\sum_{m=0}^{N} k[n-m, m, \varepsilon, \theta_1](\theta_1 R_z[n-m, n-l] + \right. \\ + \theta_1 R_x[n-m, n-l] + x[n-l]\,x[n-m]) - \theta_1 HR_x[n-l, n+\varepsilon] - \\ \left. - x[n-l]\,Hx[n, \varepsilon]\right\} = 0. \tag{13}$$

In order that (13) be valid for an arbitrary function κ from the admissible class, it is necessary that the relation given below be valid:

$$\sum_{m=0}^{N} k[n-m, m, \varepsilon, \theta_1](\theta_1 R_z[n-m, n-l] + \theta_1 R_x[n-m, n-l] + \\ + x[n-l]\,x[n-m]) - \theta_1 HR_x[n-l, n+\varepsilon] - x[n-l]\,Hx[n, \varepsilon] = 0 \\ (l = 0, 1, \ldots, N). \tag{14}$$

To prove it, let us assume that the relation (14) is not valid for certain $l = l_1$, $0 \leq l_1 \leq N$; the parameters n, ϵ, θ_1 are assumed constant. When $l = l_1$ the left-hand side of (14) is equal to some $S \neq 0$. Knowing that κ is an arbitrary function, we choose κ in the following way:

$$\varkappa[n-l_1, l_1, \varepsilon] = 1, \ \varkappa[n-l, l, \varepsilon] = 0 \qquad (l \neq l_1).$$

But if κ is chosen in this way, (13) is not true. Consequently, our assumption has been proved to be wrong.

The relation (14) is also a sufficient condition for the function $\underline{k}$ to minimize I_{II} when $\theta_1 \geq 0$. It follows, namely, from (12) that, when $\underline{k} = \underline{k}_0$ satisfies (14), then $I_{II}[k_0+\varkappa] = I_{II}[k_0] + D_2$, where $D_2 \geq 0$.

It follows that $I_{II}[k_0+\varkappa] \geqslant I_{II}[k_0]$ for an arbitrary κ, which is what we had to prove.

The values $\theta_1 < 0$ are, as a rule, of no practical importance.

The solution $k_0[n,m,\epsilon,\theta_1]$ of the simultaneous linear algebraic equations (14) must be substituted in (8) and (9) to obtain the relations $a^2 = a^2(\theta_1)$, $\sigma^2 = \sigma^2(\theta_1)$; subsequently, by using (1a), it is easy to obtain P as a function of θ_1. Then the value $\theta_1 = \theta_{10}$ corresponding to the maximum of P is found from $dP(\theta_1)/d\theta_1 = 0$. The optimum weighting function of a pulse system is in our case: $k^* = k_0[n,m,\epsilon,\theta_{10}]$; the greatest value of probability – which points to the optimum system – is $P_0 = P(\theta_{10})$.

The conditions which ensure the extreme of the functional I actually occurring at k^* are not considered in the present paper. For pulse systems these conditions can be formulated analogously to those in [5] for continuous systems.

When dealing with a complex problem the main difficulty lies in solving the simultaneous equations (14) or similar equations. In a number of special cases of a similar character, the simultaneous equations can be solved exactly [1]. In the general case, the solving of such or similar equations can be accomplished by means of various approximate methods. The method of the steepest descent [4,6] appears to be particularly appropriate. We shall also apply it directly to determine the extreme of the quadratic functional I_{II}. (A description is given of the main features of this method when it is utilized to find the minimum of the functional I_{II}.

Let the selection of the first approximation of $k[n-m, m, \epsilon] = k_1[n-m, m, \epsilon]$, based on arbitrary considerations. We find next the direction of the gradient in the normed space of functions $k[n-m, m, \epsilon]$, that is, the direction along which the functional I_{II} decreases most steeply. The norm of a function $\underline{k}$ is defined by

$$\|k[n-m, m, \varepsilon]\| = \sum_{m=0}^{N} k^2[n-m, m, \varepsilon]. \qquad (15)$$

The function $\kappa_1[n-m, m, \epsilon]$, which corresponds to the direction of the gradient, should ensure the extreme of the quantity

$$\left.\frac{dI_{II}(k_1[n-m, m, \varepsilon] + \Delta\varkappa_1[n-m, m, \varepsilon])}{d\Delta}\right|_{\Delta=0} \qquad (16)$$

under the condition

$$\sum_{m=0}^{N} \varkappa_1^2[n-m, m, \varepsilon] = 1. \qquad (17)$$

It follows that this function should also ensure the unconditional extreme of the expression

$$\left.\frac{dI_{II}(k_1[n-m, m, \varepsilon] + \Delta\varkappa_1[n-m, m, \varepsilon])}{d\Delta}\right|_{\Delta=0} + \qquad (18)$$
$$+ \mu \sum_{m=0}^{N} \varkappa_1^2[n-m, m, \varepsilon],$$

with μ being the Lagrange multiplier whose value can be found from the constraint (17) (in our problem the multiplier does not appear to be real and therefore is not found from the condition (17)). Bearing in mind that I_{II} is a quadratic functional one is able to write down

$$I_{II}(k_1[n-m, m, \varepsilon] + \Delta\varkappa_1[n-m, m, \varepsilon]) = \qquad (19)$$
$$= I_{II}[k_1] + 2\Delta A_1 + \Delta^2 A_2,$$

where A_1, A_2 depend only on κ_1 and κ_2 but do not depend on Δ, A_1 being of the form

$$A_1 = \sum_{m=0}^{N} B_1[n-m, m, \varepsilon]\, L\varkappa_1[n-m, m, \varepsilon].$$

The expression $B_1[n-m, m, \epsilon]$ here depends only on k_1, but not on κ_1; L is a linear transformation (on κ_1) operator. It is easy to see that in the case often encountered in practice, when $L\kappa_1 = \kappa_1$, the necessary condition for the extreme of the functional (18) is, with an accuracy of up to multiplier μ, of the form

$$\varkappa_1[n-m, m, \varepsilon] = B_1[n-m, m, \varepsilon]. \qquad (20)$$

As the second approximation of the function $\underline{k}$ one takes

$$k_2 = k_1 + \Delta_1\varkappa_1,$$

where κ_1 is given by (20) and Δ_1 is obtained from the condition that when $\Delta = \Delta_1$ then the function $\phi(\Delta) = I_{II}(k_1 + \Delta\varkappa_1)$ reaches its minimum (its extreme). Then $\kappa_1 = B_1$. It follows from (9) that $\Delta_1 = -(A_1 / A_2)$.

The third and subsequent approximations are determined by applying analogous considerations. The evaluation of successive approximations can easily be programmed for a digital computer.

The described method can also be applied to evaluate the extreme of the I functional. Now the determination of $\kappa_l[n-m, m, \epsilon]$ is somewhat more involved (in the expression $\left.\frac{dI}{d\Delta}\right|_{\Delta=0} = \sum_{i=0}^{n+1} \frac{\partial I}{\partial I_i} \left.\frac{dI_i}{d\Delta}\right|_{\Delta=0}$ one has to evaluate also the derivatives $\frac{\partial \Phi}{\partial I_i}$ when $k = k_l$) and the procedure of finding the consecutive values $\Delta_1, \Delta_2, \ldots,$ becomes appreciably more difficult because of the difficulty of determining the extreme of the generally complex function $\xi(\Delta) = I(k_l + \Delta \kappa_l)$. However, in this case it is not indispensable to determine the values of the parameters $\theta_i = \theta_{i0}$ which were introduced only as an artifice. In each individual case one has to decide whether one should try to find directly the extreme of I or whether to find first the weighting function which will ensure the extreme of I_{II} at various values of the parameters θ_i and subsequently determine the values $\theta_i = \theta_{i0}$.

In the specific case when the functional I_{II} is given by (8), (9) and (10), A_1 and A_2 are expressed by means of k_1 and κ_1 as follows:

$$A_1 = \sum_{l=0}^{N} \Big\{ \sum_{m=0}^{N} k_1 [n-m, m, \varepsilon] (\theta_1 R_z [n-m, n-l] + \theta_1 R_x [n-m, n-l] + $$

$$+ x[n+l]\, x[n-m]) - \theta_1 H R_x [n-l, n+\varepsilon] - x[n-l]\, Hx[n, \varepsilon] \Big\} \varkappa_1 [n-l, l, \varepsilon],$$

$$A_2 = \sum_{l=0}^{N} \sum_{m=0}^{N} (\theta_1 R_z [n-m, n-l] + \theta_1 R_x [n-m, n-l] + x[n-m]\, x[n-l]) \times$$

$$\times \varkappa_1 [n-l, l, \varepsilon]\, \varkappa_1 [n-m, m, \varepsilon],$$

$$\varkappa_1 = B_1 = \sum_{m=0}^{N} k_1 [n-m, m, \varepsilon] (\theta_1, R_z [n-m, m, \varepsilon] + \theta_1 R_x [n-m, m, \varepsilon] +$$

$$+ x[n-l]\, x[n-m]) - \theta_1 H R_x [n-l, n, \varepsilon] - x[n-l]\, Hx[n, \varepsilon],$$

$$\Delta_1 = -\frac{A_1}{A_2} = -\frac{\sum_{l=0}^{N} \varkappa_1^2 [n-l, l, \varepsilon]}{A_2} = -\frac{\sum_{l=0}^{N} B_1^2 [n-l, l, \varepsilon]}{A_2}.$$

As a rule, the method of steepest descent implies a rapid convergence. In each case the speed of convergence depends on the starting element k_1 as well as on the form of the functional taken as the norm of the function k. The starting element k_1 should be taken such that its norm be finite.

Example. Let useful signal X and interference Z be impressed on the input of a linear pulse system. The useful signal may be represented in the form $X = vt + X^{\circ}$, where X° is a random variable with a large variance, v a given quantity, and t the time.

The interference behaves as a stationary random process of normal distribution with the following characteristics: its mathematical expectation $M[Z] = 0$, its correlation function $R_z(\tau) = e^{-\alpha|\tau|}$. The variables X and Z are independent.

It is required to determine the weighting function of the pulse system with duration N = 1 of the transient process (the pulse sampling period is T) which would ensure maximum probability that the extrapolation error

$$E = X[n + \varepsilon + \varepsilon_e] - (X[n] + Z[n])\, \kappa [n, 0, \varepsilon] - \\ - (X[n-1] + Z[n-1])\, k[n-1, 1, \varepsilon] \tag{21}$$

shall not exceed by numerical value a small quantity c. The probability of $|E| \leq c$, with c small, is found from the formula (1a).

The weighting function k selected is subjected to the restriction

$$k[n, 0, \varepsilon] + k[n-1, 1, \varepsilon] = 1, \tag{22}$$

which is feasible, since variable X° must have a large variance. It is known that the condition (22) produces nonstability of the xero order. Taking into account the initial data in our example and (22), we shall pick k in the class of stationary weighting functions. Consequently, $k = k[m, \epsilon]$ and (22) becomes

$$k[0, \varepsilon] + k[1, \varepsilon] = 1. \tag{22a}$$

Expression (21) can be rewritten in this case as

$$E = X^{\circ} + vT(n + \varepsilon + \varepsilon_e) - X^{\circ} - vTnk[0, \varepsilon] - \\ - vT(n-1)\, k[1, \varepsilon] - Z[n]\, k[0, \varepsilon] - \\ - Z[n-1]\, k[1, \varepsilon] = vT(\varepsilon + \varepsilon_e) + vTk[1, \varepsilon] - \\ - Z[n]\, k[0, \varepsilon] - Z[n-1]\, k[1, \varepsilon],$$

where $\epsilon_e T$ is the extrapolation time.

We determine a^2, σ^2, and I_{II}:

$$a^2 = (M[E])^2 = v^2 T^2 (\varepsilon + \varepsilon_e + k[1, \varepsilon])^2, \tag{23}$$

$$\sigma^2 = M[(E-a)^2] = k^2[0, \varepsilon] + \\ + 2e^{-\frac{\alpha}{T}} k[0, \varepsilon]\, k[1, \varepsilon] + k^2[1, \varepsilon], \tag{24}$$

$$I_{II} = \theta_1 \sigma^2 + a^2 = \theta_1 (k^2[0, \varepsilon] + \\ + 2e^{-\frac{\alpha}{T}} k[0, \varepsilon]\, k[1, \varepsilon] + k^2[1, \varepsilon]) + \\ + v^2 T^2 (\varepsilon + \varepsilon_e + k[1, \varepsilon])^2. \tag{25}$$

It is necessary to find function k_0 minimizing I_{II} under the condition (22a). This function should ensure the unconditional minimum of the functional

$$'' = I_{II} + 2\gamma_0 (k[0, \varepsilon] + k[1, \varepsilon]), \tag{26}$$

where γ_0 is a Lagrange multiplier which can be determined from (22a). To determine k_0 we utilize (14) which in our case can be written as

$$\theta_1 k[0,\varepsilon] + \theta_1 e^{-\frac{\alpha}{T}} k[1,\varepsilon] = -\gamma_0,$$

$$\theta_1 e^{-\frac{\alpha}{T}} k[0,\varepsilon] + (\theta_1 + v^2T^2)\, k[1,\varepsilon] = -\gamma_0 - v^2T^2(\varepsilon + \varepsilon_e). \tag{27}$$

Solving the simultaneous equations (27) and (22a) we obtain

$$k_0[0,\varepsilon] = \frac{\theta_1 e^{-\frac{\alpha}{T}}[\gamma_0 + v^2T^2(\varepsilon + \varepsilon_e)] - \gamma_0(\theta_1 + v^2T^2)}{\theta_1\left(\theta_1 - \theta_1 e^{-2\frac{\alpha}{T}} + v^2T^2\right)},$$

$$k_0[1,\varepsilon] = \frac{\gamma_0\theta_1\left(e^{-\frac{\alpha}{T}} - 1\right) - v^2T^2(\varepsilon - \varepsilon_e)}{\theta_1\left(\theta_1 - \theta_1 e^{-2\frac{\alpha}{T}} + v^2T^2\right)}, \tag{28}$$

$$\gamma_0 = \frac{\theta_1\left[\theta_1\left(1 - e^{-2\frac{\alpha}{T}}\right) + v^2T^2\right] + v^2T^2(\varepsilon + \varepsilon_e)\left(1 - \theta_1 e^{-\frac{\alpha}{T}}\right)}{2\theta_1\left(e^{-\frac{\alpha}{T}} - 1\right) - v^2T^2}.$$

Formulas (28) enable one to determine the function k_0 when the values of ε and θ_1 are given. By keeping constant the value of the standardized time ε, one should find k_0 for several values of $\theta_1 \geq 0$ and determine subsequently the function $P = P(\theta_1)$; it is easy then to evaluate the value $\theta = \theta_{10}$ which corresponds to the maximum of P.

CONCLUSION

The presented method of finding the optimum pulse system ensuring the extreme of I seems to be more laborious when compared with the method of finding the pulse system ensuring the minimum of the mean-square error of the system, but basically, both methods are equally complex. The criterion I is sufficiently general; it can be utilized when selecting automatic control systems designed for various purposes. This method can also be used in the selection of optimum nonlinear systems [9].

LITERATURE CITED

1. V.P. Perov, Statistical Synthesis of Pulse Networks [in Russian] (Soviet Radio, 1959).
2. Ya. Z. Tsypkin, The Theory of Pulse Networks [in Russian] (Fizmatgiz, 1958).
3. N. I. Andreev, "The determination of optimum dynamic system by the criterion of extreme of a functional of a particular form," Avtomatika i Telemekhanika 18, No. 7 (1957).**
4. L. V. Kontorovich, "Functional analysis and applied mathematics," Uspekhi Matem. Nauk 3, No. 6 (1948).
5. N. I. Andreev, "A theory of determining an optimum dynamic system," Avtomatika i Telemekhanika 19, No. 12 (1958).**
6. S. G. Mikhlin, The Problem of Quadratic Functional [in Russian] (Gostekhizdat, 1952).
7. V. S. Pugachev, The Theory of Random Functions and Its Application to Problems of Automatic Control [in Russian] (Gostekhizdat, 1957).
8. M. A. Lavrent'ev and L. A. Lyusternik, A Course in Calculus of Variation [in Russian] (Gostekhizdat, 1950).
9. N. I. Andreev, "A general condition for the extreme of a given function of mean-square error and of the square of mathematical expectation of error of a dynamic system," Avtomatika i Telemekhanika 20, No. 7 (1959).**

**See English translation.

THE EFFECT OF STATIONARY RANDOM PROCESSES ON AUTOMATIC CONTROL SYSTEMS CONTAINING ESSENTIALLY NONLINEAR ELEMENTS

G. I. Pyatnitskii

(Moscow)

Translated from Avtomatika i Telemekhanika, Vol. 21, No. 4, pp. 474-480, April, 1960
Original article submitted June 22, 1959

A method of calculating nonlinear automatic control systems under the action of stationary random processes is proposed. The method presented is a generalization of the method of statistical linearization and allows one to take into account the distortion of the spectrum of a random process by nonlinear elements.

At the present time the statistical calculation of automatic control systems containing essentially nonlinear elements is accomplished by the method of statistical linearization [1]. In essence this method consists in replacing a nonlinear element by an amplifier equivalent to it in some sense. The method is fairly simple and therefore is widely applicable in practice.

However, this method may never be considered completely justified, since the replacement of a nonlinear element by a linear amplifier does not take into consideration the distortion of the signal spectrum by the nonlinear element, and this distortion may in some cases prove to have a significant influence on the action of the system.

In this paper a more systematic approach to the problem of the statistical calculation of nonlinear systems is presented, in which the method of statistical linearization appears as the first approximation to the solution of the problem. As a consequence, one may estimate the applicability of the method of statistical linearization to a definite class of automatic control systems. The method presented may thus be considered a generalization and development of the ordinary method of statistical linearization.

1. Formulation of the Problem

We consider a system with feedback shown schematically in the figure. It contains one nonlinear element 1 with so-called standard characteristics [2]. All the remaining links are assumed to be linear with constant parameters. Any system containing one nonlinear element may be brought into such a form.

Suppose link 2 has weight function $g(t)$ and frequency characteristic $G(\omega)$, and the link consisting of 2 and 3 in series has weight function $k(t)$ and frequency characteristic $K(\omega)$.

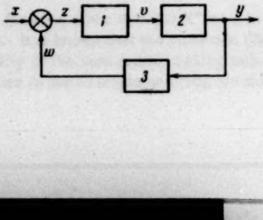

We suppose the input to the system to be a Gaussian stationary random process $x(t)$; let m_x be the mathematical expectation, and σ_x^2 and $R_x(\tau)$ the variance and correlation function of the input process.

The problem consists in calculating the variance σ_y^2 and mathematical expectation m_y of the system's output process $y(t)$.

The process $z(t)$ represents the difference between the input process $x(t)$ and the process $w(t)$, which appears as a result of $z(t)$ acting through the nonlinear element and the succeeding linear elements. The presence of the nonlinear element leads to the fact that the distribution law for the random process at its output will necessarily not be Gaussian. However, the process is "normalized" by passing through the linear elements, so that the distribution law for the process $w(t)$ will be nearer to normal than the distribution law for the process at the output of the nonlinear element. Considering that the process $z(t)$ consists of the normal process $x(t)$ and the "normalized" process $w(t)$, one may assume that the distribution law $z(t)$ will be near normal. Proceeding from this, we make the assumption that the process $z(t)$ possesses a normal two-dimensional distribution law.

This assumption provides the possibility of solving the problem posed comparatively simply, since it is well known how normal fluctuations are transformed by a nonlinear element [2]. A similar assumption is made also in the method of statistical linearization.

2. Formation of the Basic Equation

Let $R_z(\tau)$ and $R_w(\tau)$ be correlation functions for processes $z(t)$ and $w(t)$, respectively, and $R_{zw}(\tau)$ and $R_{wz}(\tau)$, the mutual correlation functions for these processes.

We have the following equation:

$$R_x(\tau) = R_z(\tau) + R_w(\tau) + R_{zw}(\tau) + R_{wz}(\tau). \quad (1)$$

We shall find expressions for $R_w(\tau)$, $R_{zw}(\tau)$ and $R_{wz}(\tau)$ in terms of $R_z(\tau)$.

The normal two-dimensional distribution law for the process z(t) at $m_z = 0$ may be put into the form of a series [3,4]

$$f(z, z_\tau) = \frac{1}{\sigma_z^2} \sum_{n=0}^{\infty} \frac{\rho_z^n(\tau)}{n!} \Phi^{(n+1)}\left(\frac{z}{\sigma_z}\right) \Phi^{(n-1)}\left(\frac{z_\tau}{\sigma_z}\right), \tag{2}$$

where $\rho_z(\tau) = R_z(\tau)/\sigma_z^2$, $\Phi(x)$ is the probability integral defined by

$$\Phi(x) = \frac{1}{\sqrt{2\pi}} \int_{-\infty}^{x} e^{-\frac{t^2}{2}} dt, \tag{2'}$$

and $\Phi^{(n)}(x)$ is the nth derivative of this probability integral with respect to x.

Let the characteristic of the nonlinear element, that is, the connection between the output v(t) and input z(t) of the nonlinear element be given by the relation

$$v = F(z). \tag{3}$$

Characteristics for a different type of nonlinear element are introduced in [1].

Using (2) and (3), one may calculate the mathematical expectation and correlation function of the process v(t) at the output of the nonlinear element [2]:

$$m_v = \int_{-\infty}^{\infty} F(z + m_z)\, d\Phi\left(\frac{z}{\sigma_z}\right), \tag{4}$$

$$R_v(\tau) = \sum_{n=1}^{\infty} \eta_n^2 \frac{\rho_z^n(\tau)}{n!}, \tag{5}$$

where

$$\eta_n = \int_{-\infty}^{\infty} F(z + m_z)\, d\Phi^{(n)}\left(\frac{z}{\sigma_z}\right). \tag{6}$$

The correlation function $R_w(\tau)$ may be written in the form

$$R_w(\tau) = \int_0^\infty \int_0^\infty k(\alpha) k(\beta) R_v(\tau - \alpha + \beta)\, d\alpha\, d\beta$$

or, considering (5),

$$R_w(\tau) = \sum_{n=1}^{\infty} \frac{\eta_n^2}{n!} \int_0^\infty \int_0^\infty k(\alpha) k(\beta) \rho_z^n(\tau - \alpha + \beta)\, d\alpha\, d\beta. \tag{7}$$

Analogously, for $R_{zw}(\tau)$ and $R_{wz}(\tau)$ we have the expressions

$$R_{zw}(\tau) = -\sigma_z \eta_1 \int_0^\infty k(\alpha) \rho_z(\tau + \alpha)\, d\alpha \tag{8}$$

and

$$R_{wz}(\tau) = -\sigma_z \eta_1 \int_0^\infty k(\alpha) \rho_z(\tau - \alpha)\, d\alpha. \tag{9}$$

Substituting (7), (8), and (9) into (1), we obtain an integral equation for $\rho_z(\tau)$:

$$\begin{aligned} &\sigma_z^2 \rho_z(\tau) - \eta_1 \sigma_z \int_0^\infty k(\alpha) [\rho_z(\tau + \alpha) + \rho_z(\tau - \alpha)]\, d\alpha + \\ &+ \eta_1^2 \int_0^\infty \int_0^\infty k(\alpha) k(\beta) \rho_z(\tau - \alpha + \beta)\, d\alpha\, d\beta + \\ &+ \sum_{n=2}^{\infty} \frac{\eta_n^2}{n!} \int_0^\infty \int_0^\infty k(\alpha) k(\beta) \rho_z^n(\tau - \alpha + \beta)\, d\alpha\, d\beta = \sigma_x^2 \rho_x(\tau). \end{aligned} \tag{10}$$

The equation obtained is nonlinear, since it contains a power of the function $\rho_z(\tau)$ higher than first. However, the nonlinear terms contain the factor $\eta_n^2/n!$ which, as an immediate calculation shows, is small in comparison to unity and is less that η_1^2. This circumstance allows us to apply the known method of expansion in powers of small parameters to the solution of (10). Such parameters in this case are $\eta_n^2/n!$. But it is not convenient to expand in powers of these parameters, since the number of them is infinite. Hence, it is more suitable by far to proceed in the following manner. We introduce the factor μ^n in front of the terms of the sums in the left portion of (10) and expand in powers of μ. From here on the solution proceeds according to the usual rules. Finally, one sets μ equal to one in the resulting expression. This may be done, because it is not necessary to consider μ to be a small quantity (in comparison with unity), since $\eta_n^2/n!$ are the small parameters.

3. Solution of the Integral Equation

Taking the above into consideration, we rewrite (10) in a somewhat modified form. We transfer the sum with the nonlinear terms to the right side and adjoin the factor μ^n before the terms of this sum:

$$\begin{aligned} &\sigma_z^2 \rho_z(\tau) - \sigma_z \eta_1 \int_0^\infty k(\alpha) [\rho_z(\tau + \alpha) + \rho_z(\tau - \alpha)]\, d\alpha + \\ &+ \eta_1^2 \int_0^\infty \int_0^\infty k(\alpha) k(\beta) \rho_z(\tau - \alpha + \beta)\, d\alpha\, d\beta = \\ &= \sigma_x^2 \rho_x(\tau) - \sum_{n=2}^{\infty} \mu^n \frac{\eta_n^2}{n!} \int_0^\infty \int_0^\infty k(\alpha) k(\beta) \rho^n(\tau - \alpha + \beta)\, d\alpha\, d\beta. \end{aligned} \tag{11}$$

We represent the solution to (11) in the form of a series:

$$\rho_z(\tau) = \sum_{m=0}^{\infty} \mu^m \rho_m(\tau). \tag{12}$$

Substituting (12) into (11), we obtain

$$\sum_{m=0}^{\infty}\mu^m \Big\{\sigma_z^2\rho_m(\tau) - \eta_1\sigma_z\int_0^{\infty} k(\alpha)\,[\rho_m(\tau+\alpha) + \rho_m(\tau-\alpha)]\,d\alpha + \\ + \eta_1^2\int_0^{\infty}\!\!\int_0^{\infty} k(\alpha)\,k(\beta)\,\rho_m(\tau-\alpha+\beta)\,d\alpha\,d\beta\Big\} = \sigma_x^2\rho_x(\tau) - \\ - \sum_{n=2}^{\infty}\;\sum_{m_1,\,\dots,\,m_n=0}^{\infty} \mu^{n+m_1+m_2+\,\dots\,+m_n}\frac{\eta_n^2}{n!}\int_0^{\infty}\!\!\int_0^{\infty} \rho_{m_1}\rho_{m_2}\rho_{m_3}\cdots\rho_{m_n}\,k(\alpha)\,k(\beta)\,d\alpha\,d\beta. \tag{13}$$

Now it is necessary to equate terms with equal powers of μ on the right and left sides. As a result we obtain a system of equations allowing us to determine successively the functions $\rho_m(\tau)$, expressing each in terms of the preceding. For concise notation we shall consider the left side of (11) as some linear integral operator L acting on the function $\rho_z(\tau)$:

$$L\rho_z(\tau) = \sigma_z^2\rho_z(\tau) - \sigma_z\eta_1\int_0^{\infty} k(\alpha)\,[\rho_z(\tau+\alpha) + \rho_z(\tau-\alpha)]\,d\alpha + \\ + \eta_1^2\int_0^{\infty}\!\!\int_0^{\infty} k(\alpha)\,k(\beta)\,\rho_z^n(\tau-\alpha+\beta)\,d\alpha\,d\beta. \tag{14}$$

Considering this, we obtain the following system of equations:

$$L\rho_0(\tau) = \sigma_x^2\rho_x(\tau), \tag{15}$$

$$L\rho_1(\tau) = 0, \tag{16}$$

$$L\rho_2(\tau) = -\frac{\eta_2^2}{2!}\int_0^{\infty}\!\!\int_0^{\infty} k(\alpha)\,k(\beta)\,\rho_0^2(\tau-\alpha+\beta)\,d\alpha\,d\beta, \tag{17}$$

$$L\rho_3(\tau) = -\frac{\eta_3^2}{3!}\int_0^{\infty}\!\!\int_0^{\infty} k(\alpha)\,k(\beta)\,\rho_0^3(\tau-\alpha+\beta)\,d\alpha\,d_\beta, \tag{18}$$

$$L\rho_4(\tau) = -\frac{\eta_4^2}{4!}\int_0^{\infty}\!\!\int_0^{\infty} k(\alpha)\,k(\beta)\,\rho_0^4(\tau-\alpha+\beta)\,d\alpha\,d\beta - \frac{\eta_2^2}{2!}\int_0^{\infty}\!\!\int_0^{\infty} 2\rho_2\rho_0 k(\alpha)\;k(\beta)\,d\alpha\,d\beta, \tag{19}$$

$$L\rho_5(\tau) = -\frac{\eta_5^2}{5!}\int_0^{\infty}\!\!\int_0^{\infty} k(\alpha)\,k(\beta)\,\rho_0^5\,d\alpha\,d\beta - \\ - \frac{\eta_3^2}{3!}\int_0^{\infty}\!\!\int_0^{\infty} k(\alpha)\,k(\beta)\,3\rho_0^2\rho_2\,d\alpha\,d\beta - \frac{\eta_2^2}{2!}\int_0^{\infty}\!\!\int_0^{\infty} k(\alpha)\;k(\beta)\,2\rho_0\,\rho_3\,d\alpha\,d\beta. \tag{20}$$

This system of equations may be easily solved by Fourier analysis. If we introduce the notation

$$S_m(\omega) = \int_{-\infty}^{\infty} \rho_m(\tau)\,e^{-i\omega\tau}d\tau, \tag{21}$$

then, taking the Fourier transform of (15)-(20), and performing simple transformations, we obtain the following expressions for $S_m(\omega)$:

$$S_0(\omega) = \frac{1}{|\sigma_z - \eta_1 K(i\omega)|^2} \sigma_x^2 S_x(\omega), \tag{22}$$

$$S_1(\omega) \equiv 0, \tag{23}$$

$$S_2(\omega) = -\frac{|K(i\omega)|^2}{|\sigma_z - \eta_1 K(i\omega)|^2} \frac{\eta_2^2}{2} \frac{1}{2\pi} \int\limits_{-\infty}^{\infty} S_0(\nu) S_0(\omega - \nu)\, d\nu, \tag{24}$$

$$S_3(\omega) = -\frac{|K(i\omega)|^2}{|\sigma_z - \eta_1 K(i\omega)|^2} \frac{\eta_3^2}{3!} \frac{1}{(2\pi)^2} \int\limits_{-\infty}^{\infty} S_0(\nu_1) S_0(\nu_2) S_0(\omega - \nu_1 - \nu_2)\, d\nu_1 d\nu_2, \tag{25}$$

$$S_4(\omega) = -\frac{|K(i\omega)|^2}{|\sigma_z - \eta_1 K(i\omega)|^2} \Bigg[\frac{\eta_2^2}{2!} \frac{1}{2\pi} \int\limits_{-\infty}^{\infty} 2 S_2(\nu) S_0(\omega - \nu)\, d\nu + \tag{26}$$

$$+ \frac{\eta_4^2}{4!} \frac{1}{(2\pi)^3} \int\limits_{-\infty}^{\infty} S_0(\nu_1) S_0(\nu_2) S_0(\nu_3) S_0(\omega - \nu_1 - \nu_2 - \nu_3)\, d\nu_1 d\nu_2 d\nu_3 \Bigg],$$

$$S_5(\omega) = -\frac{|K(i\omega)|^2}{|\sigma_z - \eta_1 K(i\omega)|^2} \Bigg[\frac{\eta_2^2}{2!} \frac{1}{2\pi} \int\limits_{-\infty}^{\infty} 2 S_0(\nu) S_3(\omega - \nu)\, d\nu +$$

$$+ \frac{\eta_3^2}{3!} \frac{1}{(2\pi)^2} \int\limits_{-\infty}^{\infty} 3 S_0(\nu_1) S_0(\nu_2) S_2(\omega - \nu_1 - \nu_2)\, d\nu_1 d\nu_2 + \tag{27}$$

$$+ \frac{\eta_5^2}{5!} \frac{1}{(2\pi)^4} \int\limits_{-\infty}^{\infty} S_0(\nu_1) S_0(\nu_2) S_0(\nu_3) S_0(\nu_4) S_0(\omega - \nu_1 - \nu_2 - \nu_3)\, d\nu_1 d\nu_2 d\nu_3 d\nu_4 \Bigg].$$

. . . .

Here $K(i\omega)$ is the frequency characteristic of the serially joined links 2 and 3 (see the figure), corresponding to the weight function $k(t)$.

Considering that

$$\rho_m(\tau) = \frac{1}{2\pi} \int\limits_{-\infty}^{\infty} S_m(\omega) e^{i\omega\tau} d\omega. \tag{28}$$

and also bearing (12) in mind, we obtain for $\rho_z(\tau)$ the expression

$$\rho_z(\tau) = \frac{1}{2\pi} \int\limits_{-\infty}^{\infty} \sum_{m=0}^{\infty} S_m(\omega) e^{i\omega\tau} d\omega. \tag{29}$$

The functions $S_m(\omega)$ entering into (29) depend on the values m_z and σ_z, which are unknown beforehand. It is necessary to calculate them. We obtain the first equation for the determination of m_z and σ_z from (29):

$$\sigma_z^2 = \frac{1}{2\pi} \int\limits_{-\infty}^{\infty} \sigma_z^2 \sum_{m=0}^{\infty} S_m(\omega)\, d\omega. \tag{30}$$

Since the mathematical expectation m_x of the input process is constant, one may write the following equation for the mathematical expectation of the process $z(t)$:

$$m_z = \frac{m_x}{1 + k_0 \chi(m_z, \sigma_z)}\,. \tag{31}$$

where k_0 is the amplification coefficient of the system, and $\chi = m_y / m_z$ is determined by (4). Equation (31) is a second equation for determining m_z and σ_z. Similar equations are also obtained by the method of statistical linearization. For systems whose linear parts are described by differential equations of higher order, the following method of solution of (30) and (31) is usually employed.

For the initial values of m_z and σ_z one may take any quantities, let us say m_x and σ_x. Setting them into the right sides of (30) and (31), we obtain m_{z1} and σ_{z1}, in general different from m_{z0} and σ_{z0}. Then the values m_{z1} and σ_{z1} obtained should again be substituted into the right sides of (30) and (31), after which the new m_{z2} and σ_{z2} are obtained. This process is to be continued until upon a substitution, results are obtained which coincide with zero-order accuracy with the results of the preceding substitution. We note that the procedure of substitution consists in calculating the functions $S_m(\omega)$ from (22) - (27) for given values of m_z and σ_z, thereafter calculating (30), as well as (31). Practical calculation by the method of statistical linearization shows that a similar procedure of solving the equation allows a sufficiently rapid calculation of m_z and σ_z.

After m_z and σ_z are calculated, and also $\eta_1(m_z, \sigma_z)$, $\eta_2(m_z, \sigma_z)$ and so on, the variance of the process y(t) at the output is easily calculated, by using (7) for $\tau = 0$, and substituting the weight function $g(\sigma)$ of link 2 in the straight circuit, for $k(\sigma)$. Taking the Fourier transform, we obtain the following relation:

$$\sigma_y^2 = \frac{1}{2\pi} \int_{-\infty}^{\infty} |G(i\omega)|^2 \Big\{ \eta_1^2 S_z(\omega) + \frac{\eta_2^2}{2!} \frac{1}{2\pi} \int_{-\infty}^{\infty} S_z(\nu) S_2(\omega - \nu)\, d\nu + \\ + \frac{\eta_3^2}{6} \frac{1}{(2\pi)^2} \int_{-\infty}^{\infty} S_z(\nu_1) S_z(\nu_2) S_z(\omega - \nu_1 - \nu_2)\, d\nu_1\, d\nu_2 + \ldots \Big\}. \tag{32}$$

where $S_z = \sum_{m=0}^{\infty} S_m(\omega)$ for the calculated values m_z and σ_z.

We return to (22). It represents an equation for the calculation of the spectral density of the process at the input to the nonlinear element by the method of statistical linearization. Hence, the method of statistical linearization is obtained as the first approximation to a more complete solution to the problem. The functions $S_m(\omega)$ for $m > 0$ are further approximations. Since they contain the parameters $\eta^2/2!$, $\eta^3/3!$, etc., which under definite conditions are negligible, the further approximations under these conditions carry but small contributions in forming the spectral density, and the method of statistical linearization gives the correct solution. However, there may occur conditions under which one may not neglect the further approximations, and then the method of statistical linearization yields an invalid solution. This may occur, for example, when the spectrum of the signal x(t) is essentially concentrated in a neighborhood of the frequency ω_0, and the linear link has a resonance at the frequency $2\omega_0$ or $3\omega_0$, and so on. In order to clarify these conditions, it is necessary to carry out numerical calculations for different specific cases. Such a calculation may be accomplished simply with contemporary computing machines.

CONCLUSION

In this paper it is shown that under the assumption on normal distribution of a random process at the input to a nonlinear element, the problem of calculating the dispersion at the output of a system with feedback containing a nonlinear element may be solved more accurately than may be done using only the method of statistical linearization.

The method of statistical linearization is obtained as the first approximation in the approach to the solution of the problem presented, and consequently, the possibility arises of being able to test its applicability in different cases.

The calculations by the formulas given may be carried out with the aid of contemporary computational techniques.

In conclusion, I take this opportunity to thank R. L. Stratonovich deeply for valuable counsel and direction given by him in connection with this paper.

LITERATURE CITED

1. I. E. Kazakov, "Approximate probabilistic analysis of the accuracy of essentially nonlinear automatic systems," Avtomatika i Telemekhanika 17, No. 5 (1956).*
2. I. M. Amiantov and V. I. Tikhonov, "The effect of normal fluctuation on standard nonlinear elements," Izvest. Akad. Nauk SSSR, OTN No. 4 (1956).
3. G. Kramer, Mathematical Methods of Statistics [Russian translation] (IL, 1948).
4. V. I. Bunimovich, Fluctuational Processes in Radio-Receiving Apparatuses [in Russian] (Sovetskoe Radio, 1951).

---

* See C. B. translation.

AN INTERPOLATION METHOD FOR ANALYZING AUTOMATIC CONTROL SYSTEM ACCURACY UNDER RANDOM STIMULI

V. I. Chernetskii

(Leningrad)

Translated from Avtomatika i Telemekhanika, Vol. 21, No. 4, pp. 481-488, April, 1960
Original article submitted December 23, 1959

An approximate method is suggested for constructing the solution of a system of ordinary differential equations containing random functions and random variables, and formulas are derived for the computation of the moments. The method is a development of certain ideas of Chebyshev [1].

INTRODUCTION

In designing or, when necessary, in improving an automatic control system, the problem arises of analyzing the accuracy of control when one takes into account random disturbances acting on the system.

The systems of differential equations which describe the operation of an automatic control system with random stimuli are, in the general case, nonlinear:

$$\frac{dY_i}{dt} = F_i(t, Y_1, Y_2, \ldots, Y_n, X_1(t), X_2(t), \ldots, X_l(t), \lambda_1, \lambda_2, \ldots, \lambda_s). \qquad (1)$$
$$t = 0, \quad Y_i(0) = y_{i0} \quad (i = 1, 2, \ldots, n).$$

where the Y_i are parameters characterizing the control process, $X_1(t), X_2(t), \ldots, X_l(t)$ are random functions of time whose probability characteristics are assumed to be given, and $\lambda_1, \lambda_2, \ldots, \lambda_s$ are random variables whose probability characteristics are also assumed to be given.

The initial conditions ($t = 0$, $Y_i(0) = y_{i0}$) are also random variables with known probability characteristics. The functions F_i ($i = 1, 2, \ldots, n$) are such that there exists a unique solution of system (1) for each choice of random initial conditions, random variables $\lambda_1, \ldots, \lambda_s$ and random functions $X_1(t), X_2(t), \ldots, X_l(t)$.

Ordinarily, to analyze accuracy of a control system, the nonlinear differential equations are replaced, with certain assumptions, by linear ones, and then one uses the quite well developed methods for analyzing the accuracy of linear systems with random stimuli present [2,3]. Of all the existing linearization methods, the most practical in the given case is Kazakov's statistical linearization method [4,5].

In [6,7], for the analysis of accuracy of nonlinear systems with random stimuli, there were presented quite general theoretical methods which could serve as starting points for the construction of engineering methods and, in the simplest cases, for engineering calculations as well. Thus, in [7], Dostupov put forward an engineering method for analyzing the accuracy of nonlinear control systems with random stimuli, this method being a development of Pugachev's method which assumes the use of the latest computing technology.

In the present work we present a new approximate method for analyzing the accuracy of an automatic control system with random stimuli, wherein the use of electronic computers is also assumed, but where the method is based on other principles than those of [6,7] and does not require that one solve an auxiliary system of algebraic equations, as is the case in [7].

1. Posing of the Problem

If we use the canonical expansions of the random functions $X_1(t), X_2(t), \ldots, X_l(t)$ and limit ourselves to a finite number of terms in these expansions, we may approximately replace system (1) of differential equations by a system of the form

$$\frac{dY_i}{dt} = F_i(t, Y_1, Y_2, \ldots, Y_n, \lambda_1, \lambda_2, \ldots, \lambda_m). \qquad (2)$$
$$t = 0, \quad Y_i(0) = y_{i0} \quad (i = 1, 2, \ldots, n).$$

which contains only random variables in the right members, thus significantly simplifying the investigation.

All the assumptions made relative to (1) remain in force for this new system. Moreover, without reducing the generality, one may assume that the initial conditions are not random, since otherwise one could attain such a position by a linear change of variables, which would only entail an increase in the number of random variables entering the right members of (2).

The random variables $\lambda_1, \lambda_2, \ldots \lambda_m$ will be assumed to be independent, which is also not a very rigid requirement, since in many practical cases one may attain this state by means of a linear transformation of these quantities. As the probability characteristics of the random variables, there are given the distribution densities $P_1(\lambda_1), P_2(\lambda_2), \ldots, P_m(\lambda_m)$, for which there exist moments of every order, i.e., $\int \lambda_j^k P_j(\lambda_j)\, d\lambda_j = m_j^{(k)}$, where the $m_j^{(k)}$ are certain constants for any k and j ($k = 0, 1, 2, \ldots$; $j = 1, 2, \ldots, m$).

Since, by assumption, there exists a unique solution of (2) for each choice of the random variables $\lambda_1, \lambda_2, \ldots, \lambda_m$, which are independent parameters of this system, then the solution of system (2) can be given in the form of certain functions of time and the random variables $\lambda_1, \lambda_2, \ldots, \lambda_m$:

$$Y_i = Y_i(t, \lambda_1, \lambda_2, \ldots, \lambda_m) \qquad (i = 1, 2, \ldots, n). \quad (3)$$

For the set of functions in (3), which are solutions of (2) for any values of the random variables $\lambda_1, \ldots, \lambda_m$, we shall assume the existence of the second moments, i.e.,

$$M[Y_i^2] = \int_{\Delta} \ldots \int Y_i^2(t, \lambda_1, \lambda_2, \ldots, \lambda_m) \prod_{j=1}^{m} P_j(\lambda_j)\, d\lambda_j = K_i \qquad (i = 1, 2, \ldots, n). \quad (4)$$

where the K_i are constants and Δ is the range of values of the random variables $\lambda_1, \ldots, \lambda_m$, and is an m-dimensional finite or infinite parallelopiped.

We choose some set of numbers $\{\mu_{1k_1}, \mu_{2k_2}, \ldots, \mu_{mk_m}\}$ ($k_1 = 0, 1, 2, \ldots, q$; $k_2 = 0, 1, 2, \ldots, q$; $k_m = 0, 1, 2, \ldots, q$) which represents $(q+1)^m$ points in region Δ.

Let a known solution of (1) be computed at each of the aforementioned points:

$$y_i(t, \mu_{1k_1}, \mu_{2k_2}, \ldots, \mu_{mk_m}) \qquad (i = 1, 2, \ldots, n) \quad (5)$$

$$(k_1 = 0, 1, 2, \ldots, q;\ k_2 = 0, 1, 2, \ldots, q;\ \ldots;\ k_m = 0, 1, 2, \ldots, q).$$

It is required, from the given set (5) of solutions of (2), to construct the functions

$$Y_{iq}(t, \lambda_1, \lambda_2, \ldots, \lambda_m) \qquad (i = 1, 2, \ldots, n), \quad (6)$$

which are sufficiently accurate approximations to the solution and, from the functions in (6), to construct the simplest possible formulas for computing the solution's probability characteristics.

1. Probability Principle for Constructing Approximate Solutions

One of the most general principles for construction of the functions in (6) is the principle of minimum probability for each fixed q.

In the case under consideration, this principle may be formulated as follows: from among the set of all the functions $\widetilde{Y}_{iq}(t, \lambda_1, \lambda_2, \ldots, \lambda_m)$, constructed on the basis of the functions $y_i(t, \mu_{1k_1}, \mu_{2k_2}, \ldots, \mu_{mk_m})$, we choose a function such that

$$P[|\widetilde{Y}_{iq} - Y_i(t, \lambda_1, \lambda_2, \ldots, \lambda_m)| > \varepsilon] = \min \qquad (i = 1, 2, \ldots, n) \quad (7)$$

for each fixed q, where $\epsilon > 0$ is any arbitrarily small given number; the symbol P[...] denotes the probability that the inequality within the square brackets actually holds.

If the probability in (7) tends to zero as q increases, one has convergence in probability, which is ordinarily written in the form of a limiting equality,

$$\lim_{q\to\infty} P[|\widetilde{Y}_{iq}(t, \lambda_1, \lambda_2, \ldots, \lambda_m) - Y_i(t, \lambda_1, \lambda_2, \ldots, \lambda_m)| > \varepsilon] = 0 \quad (i = 1, 2, \ldots, n). \quad (8)$$

Instead of the minimum probability principle, one may use the computationally simpler principle of the minimum of the second moment of the difference between the exact and the approximate solutions:

$$M[(\widetilde{Y}_{iq} - Y_i)^2] = \int_{\Delta} \ldots \int (\widetilde{Y}_{iq} - Y_i)^2 \prod_{j=1}^{m} P_j(\lambda_j)\, d\lambda_j = \min \qquad (i = 1, \ldots, n). \quad (9)$$

Indeed, according to Chebyshev's inequality,

$$P[|\widetilde{Y}_{iq} - Y_i| > \varepsilon] < \frac{M[(\widetilde{Y}_{iq} - Y_i)^2]}{\varepsilon^2}. \quad (10)$$

It follows from Chebyshev's inequality that, if

$$\lim_{q\to\infty} M[(\widetilde{Y}_{iq} - Y_i)^2] = 0, \quad (11)$$

then there will be convergence in probability.

If the function $\widetilde{Y}_{iq}$ is chosen from the class of all possible m-dimensional polynomials of degree q, then the problem of minimizing the second moment is, in theory, easily solved.

Indeed, by virtue of the assumptions as to the weight functions, for each function $P_j(\lambda_j)$ ($j = 1, 2, \ldots, m$) there exists [9] a system, unique to within a common factor, of orthogonal polynomials $H_{j0}, H_{j1}, H_{j2}, \ldots$, i.e., such that

$$\int_{a_j}^{b_j} H_{ji}(\lambda_j)\, H_{jk}(\lambda_j)\, P_j(\lambda_j)\, d\lambda_j = \begin{cases} 0 & \text{for} \quad i \neq k, \\ C_{ij}^2 & \text{for} \quad i = k, \end{cases}$$

where the numbers a_j and b_j can be infinite.

Let

$$Y_i^{(F)} = \sum_{n_1 n_2 \ldots n_m} a_{in_1 n_2 \ldots n_m}(t) \prod_{j=1}^{m} H_{jn_j}(\lambda_j). \quad (12)$$

where

$$a_{in_1 n_2 \ldots n_m}(t) = \frac{\int_{\Delta} \ldots \int Y_i \prod_{j=1}^{m} H_{jn_j}(\lambda_j)\, P_j(\lambda_i)\, d\lambda_j}{\int_{\Delta} \ldots \int \prod_{j=1}^{m} H_{jn_j}^2(\lambda_j)\, P_j(\lambda_j)\, d\lambda_j} \quad (13)$$

$$(n_1, n_2, \ldots, n_m = 0, 1, 2, \ldots).$$

From the theory of Fourier series we know that the minimum of the integral in (9) in the class of all possible m-dimensional polynomials of degree q is furnished by segments of the Fourier series for the functions Y_i ($i = 1, 2, \ldots, n$), i.e., the polynomials

$$Y_{iq}^{(F)} = \sum_{n_1 n_2 \ldots n_m} a_{in_1 n_2 \ldots n_m}(t)$$

$$\prod_{j=1}^{m} H_{jn_j}(\lambda_j) \quad \begin{pmatrix} n_1 = 0, 1, 2, \ldots, q \\ n_2 = 0, 1, 2, \ldots, q \\ \cdot\ \cdot\ \cdot\ \cdot\ \cdot\ \cdot\ \cdot\ \cdot\ \cdot \\ n_m = 0, 1, 2, \ldots, q \end{pmatrix}. \tag{14}$$

However, the problem we have posed can be considered solved only theoretically since, for the computation of the m-fold integrals entering into (14), there are only $(q + 1)^m$ points at which the values of the integrands may be assumed to be known.

If the solution of (2) can be presented exactly in the form of m-dimensional polynomials in the random variables $\lambda_1, \lambda_2, \ldots, \lambda_m$ of degrees not exceeding the number $\underline{q}$, then the problem as posed can be solved exactly by means of Lagrange interpolating polynomials.

In fact, in this case, from the given $(q + 1)^m$ interpolation nodes, one can construct, using the Lagrange interpolation formula for the m-dimensional case [8], an m-dimensional polynomial of degree not exceeding $\underline{q}$:

$$Y_{iq} = \sum_{k_1 k_2 \ldots k_m} y_i(t, \mu_{1k_1}, \mu_{2k_2}, \ldots, \mu_{mk_m}) \tag{15}$$

$$\prod_{j=1}^{m} \frac{\omega_{j,q+1}(\lambda_j)}{\omega'_{j,q+1}(\mu_{jk_j})(\lambda_j - \mu_{jk_j})}$$

$$(i = 1, 2, \ldots, n)\,(k_1 = 0, 1, 2, \ldots, q;$$

$$k_2 = 0, 1, 2, \ldots, q; \ldots; k_m = 0, 1, 2, \ldots, q).$$

coinciding identically with the solution of (2), where

$$\omega_{j,q+1}(\lambda_j) =$$

$$= (\lambda_j - \mu_{1k_j})(\lambda_j - \mu_{2k_j}) \ldots (\lambda_j - \mu_{mq_j}); \quad \omega'_{j,q+1}(\mu_{jk_j})$$

is the derivative, computed for $\lambda_j = \mu_{jk_j}$.

However, the case more frequently arises in the applications when the solution can be given in the form of m-dimensional polynomials of degree $\underline{q}$ only approximately, and the interpolation polynomials of (15), therefore, will in general be only approximations whose closeness, in some sense or other, to the solution of (2) depends on the choice of the interpolation nodes.

Since the interpolation nodes can be chosen arbitrarily, it is then necessary to so manage this choice that the second moments of the difference between the solution and the approximation to it in the form of interpolation polynomials be, for each fixed q, as close as possible to their minimum values attainable in the class of all possible m-dimensional polynomials of degree $\underline{q}$, and so that the approximation, in the form of interpolation polynomials, converge in probability to the exact solution of (2).

If one chooses as the $(q + 1)^m$ interpolation nodes all possible combinations of roots of the orthogonal polynomials $H_{j,\, q+1}(\lambda_j)(j = 1, 2, \ldots, n)$ of degree q + 1, which may always be done since the roots of these polynomials are real, different, and lie in the intervals of orthogonality, then these requirements can, to a known degree, be satisfied [9].

In this case, the interpolation polynomials which are the approximate solution may be written in the form

$$\widetilde{Y}_{iq} = \sum_{k_1 k_2 \ldots k_m} y_i(t, \mu_{1k_1}, \mu_{2k_2}, \ldots, \mu_{mk_m})$$

$$\prod_{j=1}^{m} \frac{H_{j,q+1}(\lambda_j)}{H'_{j,q+1}(\mu_{jk_j})(\lambda_j - \mu_{jk_j})} \tag{16}$$

$$(i = 1, 2, \ldots, n) \quad (k_1 = 0, 1, 2, \ldots, q;$$

$$k_2 = 0, 1, 2, \ldots, q; \ldots; k_m = 0, 1, 2, \ldots, q);$$

$$H_{j,q+1}(\lambda_j) = (\lambda_j - \mu_{1kj})(\lambda_j - \mu_{2kj}) \ldots (\lambda_j - \mu_{mk_j});$$

$H_{j,q+1}(\mu_{jk_j})$ is the derivative, computed for $\lambda_j = \mu_{jk_j}$; the numbers μ_{jk_j} satisfy the algebraic equations

$$H_{j,q+1}(\mu_{jk_j}) = 0 \qquad (j = 1, 2, \ldots, m).$$

It can be shown that the construction of the interpolation polynomial by (16) with the thus chosen interpolation nodes, which we shall for brevity henceforth call Chebyshev type nodes, is equivalent to the construction of the segment of the Fourier series from the $(q + 1)^m$ first terms if, in computing the coefficients of the expansion, one uses a Gauss type formula for mechanical quadrature corresponding to weights equal to the given probability density functions. Since Gauss type mechanical quadrature formulas are the quadrature formulas with the highest degree of algebraic accuracy then, in general, it is impossible to give a set of $(q + 1)^m$ interpolation nodes from which one could construct an m-dimensional polynomial of degree $\underline{q}$ lying closer to the segment of Fourier series (14), from the point of view of minimizing the integral in (9), than the polynomial constructed from the Chebyshev type nodes.

As was established earlier [cf. (11)], to prove convergence in probability it suffices to establish a limiting equality to zero of the second moment of the difference between the exact and the approximate solutions.

In the given case,

$$\lim_{q \to \infty} \int \underset{\Delta}{\cdots} \int (Y_i - \overline{Y}_{iq})^2 \prod_{j=1}^{m} P_j(\lambda_j)\, d\lambda_j =$$

$$= \int \underset{\Delta}{\cdots} \int Y_j^2 \prod_{j=1}^{m} P_i(\lambda_j)\, d\lambda_j -$$

$$- 2 \lim_{q \to \infty} \int \underset{\Delta}{\cdots} \int \widetilde{Y}_i Y_{iq}$$

$$\prod_{j=1}^{m} P_j(\lambda_j)\, d\lambda_j + \lim_{q \to \infty} \int \underset{\Delta}{\cdots} \int \widetilde{Y}_{iq}^2 \prod_{j=1}^{m} P_j(\lambda_j)\, d\lambda_j = 0, \tag{17}$$

if

$$\lim_{q \to \infty} \int \underset{\Delta}{\cdots} \int \widetilde{Y}_{iq}^2 \prod_{j=1}^{m} P_j(\lambda_j)\, d\lambda_j = \int \underset{\Delta}{\cdots} \int Y_i^2 \prod_{j=1}^{m} P_j(\lambda_j)\, d\lambda_j \tag{18}$$

and

$$\lim_{q \to \infty} \int \underset{\Delta}{\cdots} \int Y_i \widetilde{Y}_{iq} \prod_{j=1}^{m} P_j(\lambda_j)\, d\lambda_j = \int \underset{\Delta}{\cdots} \int Y_i^2 \prod_{j=1}^{m} P_j(\lambda_j)\, d\lambda_j. \tag{19}$$

By substituting, in (18), the expanded expression for the interpolation polynomial, and by taking into account the orthogonality of the polynomials $H_{j,q+1}(\lambda_j)$, we obtain, after a number of transformations,

$$\lim_{q\to\infty} \int \underset{\Delta}{\cdots} \int \widetilde{Y}^2_{iq} \prod_{j=1}^{m} P_j(\lambda_j)\, d\lambda_j = \tag{20}$$

$$= \lim_{q\to\infty} \sum_{k_1k_2\ldots k_m} y_i(t, \mu_{1k_1}, \mu_{2k_2}, \ldots, \mu_{mk_m}) \prod_{j=1}^{m} \rho_{jk_j}$$

$$(i = 1, 2, \ldots, n)\,(k_1 = 0, 1, 2, \ldots. q;$$

$$k_2 = 0, 1, 2, \ldots, q; \ldots; \quad k_m = 0, 1, 2, \ldots, q),$$

where $\rho_{jk_j} = \int\limits_{a_j}^{b_j} \frac{H_{j,q+1}(\lambda_j)(P_j(\lambda_j)\, d\lambda_j}{H'_{j,q+1}(\mu_{jk_j})(\lambda_j - \mu_{jk_j})}$ are Christoffel numbers.

Formula(20) is a Gauss type mechanical quadrature formula with weights $\prod_{j=1}^{m} P_j(\lambda_j)$ for computing the integral $\int \underset{\Delta}{\cdots} \int Y_i^2 \prod_{j=1}^{m} P_j(\lambda_j)\, d\lambda_j$.

It is well known* that the mechanical quadrature process converges for any Riemann-integrated function if the domain of integration is bounded. If the region is unbounded,the same state of affairs can be attained if, in constructing the interpolation polynomial, one does not take into consideration nodes which lie at a sufficiently great distance from the origin of coordinates, a process which can only have a beneficial effect in calculations with electronic computers (since cases of overflow are avoided).

Since (19) follows from (18), it can be asserted that, when the solution of (2) is such that the second moments in (4) exist, then the interpolation process constructed on Chebyshev type nodes tends in probability to the solution of this system.

3. Calculated Formulas for Computing the Moments

The approximate formulas for computing the moments are obtained from the ordinary formulas expressing these moments in general form if, in these formulas, the exact solution of (2) is replaced by approximate ones in the form of interpolation polynomials constructed from Chebyshev type nodes.

We now obtain the formulas for computing the first- and second-order moments:

$$M[Y_i(t, \lambda_1, \lambda_2, \ldots, \lambda_m)] = \int \underset{\Delta}{\cdots} \int Y_i \prod_{j=1}^{m} P_j(\lambda_j)\, d\lambda_j \approx$$

$$\approx \int \underset{\Delta}{\cdots} \int \widetilde{Y}_{iq} \prod_{j=1}^{m} P_j(\lambda_j)\, d\lambda_j \qquad (i = 1, 2, \ldots, n).$$

$$M[Y_i(t_1, \lambda_1, \lambda_2, \ldots, \lambda_m)\, Y_k(t_2, \lambda_1, \lambda_2, \ldots, \lambda_m)] \approx$$

$$\approx \int \underset{\Delta}{\cdots} \int \widetilde{Y}_{iq}(t_1, \lambda_1, \lambda_2, \ldots, \lambda_m)\, \widetilde{Y}_{kq}(t_2, \lambda_1, \lambda_2, \ldots, \lambda_m) \tag{21}$$

$$\prod_{j=1}^{m} P_j(\lambda_j)\, d\lambda_j$$

$$(i = 1, 2, \ldots, n; \quad j = 1, 2, \ldots, n).$$

By substituting in these formulas the expanded expressions for $\widetilde{Y}_{iq}$ and $\widetilde{Y}_{iq}$ and carrying out a number of transformations, we get

$$M[Y_i] \approx \sum_{k_1k_2\ldots k_m} y_i(t, \mu_{1k_1}, \mu_{2k_2}, \ldots, \mu_{mk_m}) \prod_{j=1}^{m} \rho_{jk_j}.$$

$$M[Y_i(t_1, \lambda_1, \lambda_2, \ldots, \lambda_m)\, Y_k(t_2, \lambda_1, \lambda_2, \ldots, \lambda_m)] \approx$$

$$\approx \sum_{k_1k_2\ldots k_m} y_i(t, \mu_{1k_1}, \mu_{2k_2}, \ldots, \mu_{mk_m})$$

$$y_k(t_2, \mu_{1k_1}, \mu_{2k_2}, \ldots, \mu_{mk_m}) \prod_{j=1}^{m} \rho_{jk_j}$$

$$(i = 1, 2, \ldots., n; \quad j = 1, 2, \ldots, n)$$

$$(k_1 = 0, 1, 2, \ldots, q; \quad k_2 = 0, 1, 2, \ldots, q; \ldots;$$

$$k_m = 0, 1, 2, \ldots, q).$$

where the ρ_{jk_j} are Christoffel numbers.

The approximate formulas for computing higher-order moments have an analogous form.

In computing the moments of the solution of (2) by (21), it is most convenient to determine the functions $y_i(t, \mu_{1k_1}, \mu_{2k_2}, \ldots, \mu_{mk_m})$ $(i = 1, 2, \ldots, n)$ by numerical methods, carrying out the computations on electronic digital computers, since the accuracy of analog computers is, in many cases, inadequate; moreover, the final computations by (21) equally require discrete (digital) technology. The Chebyshev type nodes and the Christoffel numbers $\rho_{jk_1}, \rho_{jk_2}, \ldots, \rho_{jk_m}$ are computed from the given probability density functions. However, in many practical cases this is not necessary, since one can use prepared tables [10] of roots of orthogonal polynomials and the Christoffel numbers corresponding to these polynomials.

For example, let the random variable λ_j be distributed normally, $P_j(\lambda_j) = \frac{1}{\sqrt{2\pi}\sigma_{\lambda_j}} \exp\left[-\frac{(\lambda_j - \overline{\lambda}_j)^2}{2\sigma^2_{\lambda_j}}\right]$. We set

*From the Steklov-Polya theorem.

$\lambda_j = \bar{\lambda}_j + x\sigma_{\lambda_j}\sqrt{2}$. The distribution density of the random variable x will be $P(x) = e^{-x^2}/\sqrt{\pi}$. The Chebysnev-Hermite polynomials

$$H_n(x) = \left(-\frac{1}{2}\right)^n e^{x^2} \frac{d^n}{dx^n}[e^{-x^2}]$$

form a system of polynomials which are orthogonal on the interval $(-\infty, \infty)$.

Let $x_{k,\,q+1}^{q+1}$ $(k = 0, 1, 2, \ldots, q)$ be the roots of the Chebyshev- Hermite polynomial of degree q + 1. In this case, the Chebyshev type interpolation nodes and the Christoffel numbers are computed by the formulas

$$\lambda_{jk_j} = \bar{\lambda}_j + x_k^{(q+1)}\sigma_{\lambda_j}\sqrt{2}$$

$$(k = 0, 1, 2, \ldots, q),$$

$$\rho_{jk_j} = \int\limits_{-\infty}^{\infty} \frac{H_{q+1}(x)\,P(x)\,dx}{H'_{q+1}(x_k^{(q+1)})\,(x - x_k^{(q+1)})} = \rho_k^{(q+1)} \tag{22}$$

$$(k = k_j).$$

For uniform distributions on the intervals $[a_j, b_j]$, the Chebyshev type nodes and the Christoffel numbers are computed by the formulas

$$\lambda_{jk_j} = \frac{b_j - a_j}{2}\,x_k^{(q+1)} + \frac{b_j + a_j}{2}$$

$$(k = 0, 1, 2, \ldots, q), \tag{23}$$

$$\rho_{jk_j} = \rho_k^{(q+1)} = \int\limits_{-1}^{1} \frac{U_{q+1}(x)\,dx}{U'_{q+1}(x_k^{(q+1)})\,(x - x_k^{(q+1)})},$$

where $U_{q+1}(x) = \frac{(q+1)!}{(2q+2)!}\frac{d^{q+1}}{dx^{q+1}}(x^2 - 1)^{q+1}$ is the Legendre polynomial of degree q + 1 and the (k = 0, 1, 2,..., q) are its roots.

Since the method proposed here, for q = 1, gives a linear approximation to the solution of (2), it can be used in that case as one of the possible linearization methods which does not require that the equations of system (2) be transformed.

CONCLUSIONS

The method presented here can be used in the investigation of the accuracy of operation of an automatic control system described by a system of ordinary differential equations for which, with given initial conditions and for any choice of the random variables entering into the system's right members, there exists a unique solution with finite second moments. Thus, the method can also be used for the investigation of systems with essentially nonlinear characteristics.

In conclusion, the author wishes to express his deep appreciation for the friendly aid, valuable advice, and comments, which were advanced during the discussion of certain questions touched upon in the present paper, to E. P. Popov, V. I. Zubov, I. Ya. Diner, A. A. Sveshnikov and A. D. Maksimov.

Example. An automatic control system is described by equations of the form

$$\frac{dY}{dt} + Y^2 = (\lambda + 1)^2, \quad t = 0, \quad Y(0) = 0,$$

where λ is a random variable with zero mathematical expectation, and dispersion $M[\lambda^2] = 0.01$;

$$P(\lambda) = \frac{1}{\sqrt{2\pi}\,0{,}1}\,e^{-\frac{\lambda^2}{0{,}02}}.$$

It is required to determine the mathematical expectation and dispersion of the output coordinate Y.

By using (21) and (22) and making use of tables [10], we find that, for q = 1, M[Y] = 0.949 and D[Y] = 0.0164, while for q = 2, M[Y] = 0.964 and D[Y] = 0.0123.

The exact solution, obtained by solving the given equation with the given initial conditions, is that

M[Y] = 0.963, D[Y] = 0.0123.

Thus, in the given example, for q = 2 the approximate values of the mathematical expectation and the dispersion, computed by the interpolation method, coincide with the exact values to within one unit in the third decimal place.

LITERATURE CITED

1. P. L. Chebyshev, Complete Collected Works, Mathematical Analysis. 2 (1947), 13 (1948) [in Russian] (Izd AN SSSR).
2. V. V. Solodovnikov, Introduction to the Statistical Dynamics of Automatic Control Systems [in Russian] (Gostekhizdat, 1952).
3. J. H. Laning and R. H. Batten, Random Processes in Automatic Control [Russian translation] (IL, 1958).
4. I. E. Kazakov, "Approximate probabilistic analysis of accuracy of operation of essentially nonlinear systems," Avtomatika i Telemekhanika 17, No. 5 (1956)†.
5. E. P. Popov, "On estimating the quality of nonlinear automatic systems with random noise," Avtomatika i Telemekhanika 20, No. 10 (1959).†
6. V. S. Pugachev, Theory of Random Functions and Its Application to Automatic Control Problems [in Russian] (Gostekhizdat, 1958).
7. B. G. Dostupov, "Approximate determination of the probabilistic characteristics of the output coordinates of nonlinear automatic control systems," Avtomatika i Telemekhanika 18, No. 11 (1957)†.
8. V. I. Zubov, Mathematical Methods of Investigating Automatic Control Systems [in Russian] (Sudpromgiz, 1959).
9. I. P. Natanson, Constructive Theory of Functions [in Russian] (Gostekhizdat, 1949).
10. V. I. Krylov, Approximate Computation of Integrals [in Russian] (Fizmatgiz, 1959).

† See English translation.

THEORY OF IDEAL MODELS OF AN EXTREMAL CONTROLLER*

V. V. Kazakevich

(Moscow)

Translated from Avtomatika i Telemekhanika, Vol. 21, No. 4, pp. 489-505, April, 1960
Original article submitted July 6, 1959

By means of the theory of point transformations, an analysis is made of the operation of an extremal control system with a commutator. In the discussion, no essential limitations are imposed on the form of the nonlinearities. The existence of a limiting cycle is proven, and the character of its establishment is determined; the possibility of multiple oscillations, and the conditions for their generation, are investigated. The effect of asymmetry on the extremal function is determined, and an estimate of the accuracy of controller operation is made.

Existing automatic control systems solve the problem of maintaining a controlled quantity either constant or else changing in accordance with a previously prescribed law (in the case of so-called "programmed" control).

After a disturbing factor has acted, the controlled quantity changes its value, and the automatic controller must, by means of its action on the controlling parameter, take it to some given level in some interval of time.

If the problem to be solved by the automatic controller consists in maintaining a given program, then the control system just sketched is theoretically valid for its solution. Thus, for example, we have the problems of maintaining the number of rotations of a machine's principal shaft, steam or gas pressure in a trunk, voltage or current in a circuit, the problem of maintaining a given ratio of components, etc.

However, as technology developed, a number of problems arose which differed in principle from those just cited, these being the problems of the automatic search for, and maintaining of, extremal values of the controlled quantity, either at its upper or its lower boundary.

Such problems arise in the most diverse domains of technology (aviation, motor design, etc.).

Naturally, such problems can be solved only approximately by the ordinary control systems.

Several years ago the author of the present paper developed the automatic control principle which solves these problems, the principle which one may call that of extremal control.

Some of the questions in the theory of operation of extremal controllers were already considered previously by the author [1,2].

In the present paper, using the methods of point transformation theory, we investigate the operation of one of the extremal control schemes.

1. Principle of Operation of the Extremal Controller

In view of the fact that the form of the functional relationship between the controlled and the controlling quantities is not known and, moreover, varies in the course of time by a completely unknown law, to give this relationship in advance is not possible.

It is in relation to this that the idea of introducing an artificial disturbance is made basic to the principle of operation of the extremal controller.

All the motions arising in the system as a result of this disturbance are divided into two classes: a) the class of admissible motions, b) the class of inadmissible motions.

To the class of admissible motions are assigned all those which move the controlled quantity closer to the required extremum or boundary, while the motions which take the controlled quantity further away are assigned to the class of inadmissible motions.

By means of a special device, the direction of the process is verified, and if this direction causes the controlled quantity to approach the required extremum, then the disturbance is accepted; if the quantity moves away from the extremum, then the sign of the disturbance is reversed, and motion in the required direction then commences.

To provide stability of control, the variations of the controlled quantity during the establishment process are carried out nonmonotonically.

Basic to the scheme is a special device which provides selectivity in choosing an admissible disturbance and which transfers the motion from the class of inadmissible motions to that of admissible ones. This device is a relay which takes into account the direction (sign) of the velocity of the disturbed motion. It is because of this that we shall henceforth call it a signum-relay.

The signum-relay is made up of lever 2b (Fig. 1) friction-coupled to the axis of indicating instrument 1a which measures the controlled quantity p, so that the lever is dragged along by the pointer as p varies.

However, lever 2b can move only within the limits of a certain zone between contacts 2c and 2d. This will be called the insensitivity zone. As the pointer of the instrument moves to one side or the other, lever 2b will touch one of the contacts (2c or 2d) and will stop, while the pointer will continue its motion.

---

* This work was first published in the Trudy TsIAM in 1949; it is reprinted here without change.

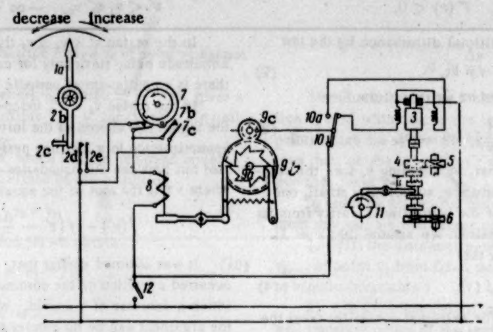

In addition to the signum-relay, the following basic elements enter into the extremal controller scheme (Fig. 1):

1. The instrument which measures the controlled quantity.

2. Reversible device 10 which is connected to the organ which acts on the controlling parameter.

3. A contact device (a commutator) which provides the periodic character of the artificial disturbance.

If the controlled quantity, whose extremum the controller seeks, depends on several parameters, then these latter are switched in by turn by means of device 4-5-6 in such manner that, during the control time for one of the parameters, the remaining ones either remain free, or are kept constant, or are varied in accordance with a given program.

Control is effected in the following manner. We assum that the controller is not switched in; then, the position of pointer 1a will not be changed (under the assumption that natural disturbances are absent), i.e., the parameter v, acting on the quantity p, does not change. With this, let it be assumed that the quantity p does not attain a maximum.

We now switch in knife switch 12. This starts the rotation of motor 3 (to one side or the other) and commutator disk 7.

With this, let the change of parameter v give rise to a decrease of p. With this, instrument pointer 1a, in rotating counterclockwise, drags along lever 2b which, after traversing part of the insensitivity zone, closes contacts 2d and 2e which causes the operation of electromagnet 8 and stepping mechanism 9 which reverse motor 3 and change the direction of parameter v. Thanks to this, the quantity p increases and, if the rotational speed of the disk of contact devic 7 is sufficiently small, the quantity p attains an extremum and begins to move about a maximum.

To eliminate the possibility that the stimuli of disturbing forces would disrupt controller operation, contact device 7 (a commutator) was introduced.

Let the permissible deviation of parameter v from the value v_0 which corresponds to a maximum be some Δv. Then, the number of rotations of disk 7 is so chosen that, during one rotation, the change in the quantity v due to the action of motor 3 does not exceed Δv.

If, with such a choice for the number of rotations of disk 7, there now begins the action of disturbing forces, then two cases are possible:

a) The effect of the disturbance on either side is greater than the effect of variations in v. In this case, changes in v from increasing p cease when $v_1 - \Delta v \leq v \leq v_1 + \Delta v$, where v_1 corresponds to the beginning of the disturbance.

b) The effect of the disturbance on either side is less than the effect of variations in v. In this case, control proceeds normally until one reaches the value of $v^* + \Delta v$ (for disturbances which increase p) or $v^* - \Delta v$ (for the opposite case), where v^* is the quantity attainable in the absence of disturbing forces.

If the rotational speed of the commutators can not be considered small, and if a number of other design requirements do not hold, then the value of v^* attainable by the controller may differ from the optimal value v_0.

2. Investigation of the Establishment Process in the Extremal Controller

An extremal controller is a special nonlinear oscillatory system with one, two, or more degrees of freedom as a function of the character of the idealization.

With a number of far-reaching simplifications, in many cases the motion of the controlled system in the absence of external disturbances, i.e., for fixed values of v (in other words, with the extremal controller switched out), may be described by a linear differential equation

$$\frac{dp}{dt} = f(v) - p. \tag{1}$$

We shall assume that the function $f(v)$ is continuous in the interval $-\infty < v < +\infty$ and

$$f'(v_0) = 0, \quad f''(v) < 0.$$

We introduce the artificial disturbance by the law

$$v = kt. \tag{2}$$

Equation (1) may then be written in the form

$$\frac{dp}{dv} = \frac{1}{k}[f(v) - p]. \tag{3}$$

It is clear from (3) that, by choosing k, i.e., the velocity of the artificial disturbance, sufficiently small, one can make the deviation of the controlled quantity from its static value as small as desired. We assume that $k \ll 1$; with this, we may consider that

$$p = f(v). \tag{4}$$

With this condition, the extremal controller takes the form of a system with one degree of freedom. We denote by δ the magnitude of the signum-relay's insensitivity zone, and by Δt the commutator time (the size of the artificial disturbance's period).

Then, $\Delta v = k\Delta t$ is the quantity by which the argument v can change during the commutator time. We shall assume that, for the value $v = v_1$, the commutator operates and reversal occurs, after which the argument begins changing in one direction or the other.

We now show that the entire line of initial values is divided into a number of regions, where this decomposition depends on the relationship of δ and Δv, and also on the sign of k. The character of the control process is essentially different for each of these regions.

We shall later have occasion to use the following, almost self-evident lemma: if the continuous function $p = f(v)$ satisfies the condition $f'(v_0) = f''(v) < 0$ for $v \leq v_0$ then, for each pair of values v_a and v_b such that $v_a < v_b \leq v_0$, the following inequalities hold:

a) if we are given two numbers C_1 and C_2 $(0 < C_1 \leq C_2)$, then

$$f(v_b) - f(v_b - C_1) < f(v_a) - f(v_a - C_2), \tag{5}$$

b) if we are given numbers d_1 and d_2 such that

$$f(v_a) - f(v_a - d_1) = f(v_b) - f_1(v_b - d_2), \tag{6}$$

then

$$d_1 < d_2 \tag{6a}$$

and

$$v_a - d_1 < v_b - d_2. \tag{6b}$$

The proofs of these inequalities are given in the Appendix.

We shall consider the initial value $v \leq v_0$, assuming that reversal to a decreasing argument occurs for the value $v = v_1$. We assume that there exists a $v' < v_0$ such that

$$f(v') - f(v' - \Delta v) = \delta. \tag{A}$$

This can always be achieved by choosing a sufficiently small Δv or a sufficiently large δ.

We now show that, if (A) holds, the semiline of initial values $v_1 \leq v_0$ can be partitioned into the two regions:

$$v' < v_1 \leqslant v_0, \quad -\infty < v_1 < v'.$$

In the region $v' < v_1 \leq v_0$ the motion is stable, the amplitude being stationary for each initial value (i.e., there is a continuum of periodic motions).

In the region $v_1 < v'$, independently of which point of the region was chosen as the initial value, there occurs an approximation to a limiting periodic motion which is carried out between the boundaries of $v^* - \Delta v/2 \leq v \leq v^*$, where v^* is the root of the equation

$$f(v^*) - f\left(v^* - \frac{\Delta v}{2}\right) = \delta. \tag{B}$$

It was assumed earlier that, at the value $v = v_1$, there occurred operation of the commutator and reverser, after which a decrease of v ensued. With this, the decrease of the argument can be no greater than Δv: if the signum-relay operates, then the variation of the argument will be less than Δv, while if it does not operate the variation of the argument will equal Δv.

As a consequence of the decrease of the argument, the quantity p begins to decrease.

We now show that, if $v_1 < v'$ then, with a decrease of v by a certain definite amount a $(0 < a < \Delta v)$ given by (7) down to a value $v_2 = v_2(v_1)$, the signum-relay must operate; the controlled quantity will thereby decrease by the amount δ.

Indeed, the quantity a is defined by the condition that, with a decrease of the argument v by a, the insensitivity zone be traversed, i.e., that p be decreased by δ:

$$f(v_1) - f(v_1 - a) = \delta \tag{7}$$

or

$$f(v_1) - f(v_2) = \delta, \tag{7a}$$

where $v_2 = v_1 - a$.

We use the lemma at this point. By comparing (7) with (A), we note that (6a) holds if we take

$$v_1 = v_a, \quad v' = v_b, \quad a = d_1, \quad \Delta v - d_2;$$

consequently, $a < \Delta v$.

At the moment of operation of the signum-relay,

$$v = v_2 = v_1 - a.$$

Immediately after this, the argument begins to increase, continuing to do so until the next operation of the commutator.

The increase of the argument is by the quantity $\Delta v - a = \Delta v - (v_1 - v_2)$. At the moment of the next operation of the commutator, the argument has reached the value

$$v_3 = v_2 + [\Delta v - (v_1 - v_2)] = 2v_2 + \Delta v - v_1. \tag{8}$$

After this, the control cycle starts repeating.

Thus, as the result of one complete control cycle, the point v_1 on the axis of abscissas is translated to the point v_3 and, correspondingly, the point p_1 of the curve $p = f(v)$, with abscissa v_1, is translated to point p_3, with abscissa v_3.

It will be shown below that the image v_3 of point v_1 cannot leave the region $v < v'$.

Consequently, (8), where v_2 is defined by (7a), gives a transformation of the semiline $v_1 < v'$ into itself. We call this the transformation T.

The invariant points, which remain unmoved under this transformation, are defined by the condition

$$v_3 = v_1. \tag{9}$$

On the basis of (9) and (8) we obtain

$$v_2 = v_1 - \frac{\Delta v}{2} \tag{10}$$

or

$$a = \frac{\Delta v}{2}.$$

If we eliminate a from (7) by means of this last equation, and denote by v^* an invariant point, we obtain the following formula for determining v^*:

$$f(v^*) - f\left(v^* - \frac{\Delta v}{2}\right) = \delta. \tag{B}$$

3. The Establishment Process in the Extremal Controller

We now discuss the question as to the character of the establishment process, as well as the number of invariant points which satisfy Eq. (B).

After commutator operation, there begins the decrease of v down to the value of v_2, in accordance with the equation

$$v_2 = v_1 - a, \tag{8a}$$

where a is defined by (7).

With the reaching of the value $p = f(v_2)$, the signum-relay operates, and the argument begins increasing up to the value

$$v_3 = v_2 + (\Delta v - a) = v_1 - a + (\Delta v - a). \tag{8b}$$

It follows from (8b) that the value of v_3 will exceed v_1 if the difference $\Delta v - a$ is greater than a; for the entire range of values of v_1 in which this is the case, transformation T will translate every point of this region to the right.

If, in some region of values of v_1, the difference $\Delta v - a$ is less than a, then transformation T will here translate each point of this region to the left.

The condition $\Delta v - a > a$ leads to the inequality $\Delta v/2 > a$, while the condition $\Delta v - a < a$ leads to the inequality $\Delta v/2 < a$.

We consider the two cases $v_1 < v^*$ and $v^* < v_1 < v'$.

The quantity a is defined by (7). We compare it with (B) and note that the right members of (7) and (B) are identical. Consequently, in the case $v_1 < v^*$, the conditions of the lemma are met, if we take $v_1 = v_a$, $v^* = v_b$, $a = d_1$ and $\Delta v/2 = d_2$ but, in this case, we have, according to (6),

$$a < \frac{\Delta v}{2}. \tag{11a}$$

If we now consider the case when $v^* < v_1 < v'$, then the conditions of the lemma hold under the assumptions that

$$v^* = v_a, \quad v_1 = v_b, \quad a = d_2, \quad \frac{\Delta v}{2} = d_1. \tag{11b}$$

In this case,

$$a > \frac{\Delta v}{2}.$$

Thus, transformation T shifts all the points of the semiline $v_1 < v'$ which lie to the left of v^* to the right, and all points which lie to the right of v^* to the left. It thus follows that, on the semiline $v < v^*$ there is just the one immovable point v^*.

In order to determine the character of the establishment process, we must clear up still two more questions.

1. Will the distances ρ_1 of the successive images v_3, v_5,... of point v_1 from fixed point v^* decrease, increase, or remain invariable?

2. Are there conditions under which transformation T will translate points of the semiline $v < v'$ lying to the left of v^* into the region lying to the right of v^* and, conversely, can it translate points lying to the right of v^* into the region lying to the left of v^*?

We first prove that, no matter what point $v_1 < v^*$ we choose, its image v_3 will not leave the region $v < v'$.

Indeed, if the point lies to the right of v^* and to the left of v' then, as was proven earlier, transformation T translates it to the left; consequently, it can not move from the region $v^* < v_1 < v'$ into the region $v > v'$

If, now, the point lies to the left of v^* then, by comparing (7) and (B), we see that, on the basis of (6b) of the lemma, $v_1 - a < v^* - \Delta v/2$; consequently,

$$v_3 = v_1 - a + (\Delta v - a) < v^* - \frac{\Delta v}{2} + (\Delta v - a) = \tag{8c}$$

$$= v^* + \frac{\Delta v}{2} - a.$$

But $a > 0$ and, therefore, by strengthening the inequality we get

$$v_3 < v^* + \frac{\Delta v}{2}. \tag{12}$$

We now compare (A) and (B). On the basis of (6b) of the lemma, we conclude that

$$v^* - \frac{\Delta v}{2} < v' - \Delta v \quad \text{or} \quad v^* + \frac{\Delta v}{2} < v'. \tag{13}$$

Thus, we always have $v_3 < v'$.

We now prove that, with successive applications of transformation T, the successive images v_3, v_5,... always approach closer to v^*. Let the distances of points $v_i (i = 1,2,\ldots)$ from v^* be

$$\rho_i = v^* - v_i. \tag{14}$$

We form the function a':

$$a' = v^* - \frac{\Delta v}{2} - v_1 + a. \tag{15}$$

It is easily seen that

$$\rho_1 - a' = \frac{\Delta v}{2} - q. \tag{16}$$

To determine the character of the establishment process, it is necessary to consider the two cases: $\rho_1 > 0$ and $\rho_1 < 0$.

We first consider the case $\rho_1 > 0$. In this case $v_1 < v^*$. It was determined earlier that, for $v_1 < v^*$, $\Delta v/2 \geq a$.

Consequently, from (16),

$$\rho_1 - a' > 0 \quad (\rho_1 > 0).$$

Moreover, it was shown earlier that, if $v_1 < v^*$, then $v^* - \Delta v/2 > v - a$ and, consequently, $a' > 0$.

Therefore, a' can vary within the limits

$$\rho_1 > a' > 0 \tag{17a}$$

We now rewrite (8), taking (16) into account:

$$v_3 = v_1 + 2\left(\frac{\Delta v}{2} - a\right) = \tag{8d}$$

$$= v^* - \rho_1 + 2(\rho_1 - a') = v^* + \rho_1 - 2a'.$$

By bearing in mind that, on the basis of (14), for $i = 3$

$$v_3 = v^* - \rho_3, \tag{14a}$$

and by comparing (14a) and (8d), we obtain

$$\rho_3 = 2a' - \rho_1. \tag{C}$$

By taking (17a) into account, it is simple to conclude from (C) that ρ_3 can vary within the limits $-\rho < \rho_3 < \rho_1$. Whence

$$|\rho_3| < \rho_1 \quad (\rho_1 > 0). \tag{18a}$$

We turn now to the case when $\rho_1 < 0$, whereby $v' > v_1 > v^*$. In this case, $\Delta v/2 - a < 0$ and $v^* - \Delta v/2 < -v_1 - a$. Consequently, $a' < 0$ and $\rho_1 - a' < 0$.

It follows from this that a' can vary within the limits

$$\rho_1 < a' < 0. \tag{17b}$$

From whence, on the basis of (C), we conclude that

$$|\rho_3| < |\rho_1| \quad (\rho_1 < 0). \tag{18b}$$

It follows from (18a) and (18b) that, for any values $v_1 < v'$,

$$|\rho_3| < |\rho_1|. \tag{18}$$

It is thus shown that no matter where the point v_1 lies on the semiline $v < v'$, we always have $|\rho_3| < |\rho_1|$ i.e., repeated iteration of transformation T shifts its image ever closer to v^*. In other words, for any value of $v_1 < v'$, the extremal control process approximates to the limiting motion of period $\tau = \Delta v/k$, in which the argument changes periodically, with the same period τ, within the limits $v^* - \Delta v/2 \leq v \leq v^*$, and the corresponding controlled quantity p varies within the limits

$$f\left(v^* - \frac{\Delta v}{2}\right) \leqslant p \leqslant f(v^*).$$

Having (C), we can easily find the condition for which image v_3 of point v_1 turns out to be on the same side of the invariant point as v_1.

For this condition to be met, ρ_3 must keep the same sign as ρ_1.

We consider, as previously, the two cases: $\rho_1 > 0$ and $\rho_1 < 0$. Let $\rho_1 > 0$. Since, with this, we also have $a' > 0$ then, from (C), it follows that $\rho_3 > 0$ if

$$2a' > \rho_1; \tag{19a}$$

Now let $\rho_1 < 0$, for which $a' < 0$; consequently, $\rho_3 < 0$ if

$$|2a'| > |\rho_1|. \tag{19b}$$

Both conditions (19a) and (19b) reduce to the one:

$$\phi = |2a'| - |\rho_1| > 0. \tag{20a}$$

Thus, if the function $\phi > 0$, transformation T moves the image of point v_1 to the invariant point v^* while keeping it on the same side of v^*; if

$$\phi < 0, \tag{20b}$$

then the image of point v_1 is shifted by transformation T to v^* while simultaneously transferring over to the other side of v^*. If

$$\phi = 0 \tag{20c}$$

then image v_3 coincides with invariant point v^*, and the further successive images remain immovable.

Condition (20a) gives that property of the function $p = f(v)$ for which ρ_3 retains the sign of ρ_1. One may also give the boundaries for the point v_1 such that its image may not under any conditions coincide with v^*. These boundaries are defined by the condition that $\rho_3 \neq 0$.

Let $\rho_1 > 0$. We have from (16) that

$$a' = \rho_1 - \frac{\Delta v}{2} + a. \tag{16a}$$

On the basis of (C), the condition being sought reduces to the inequality $2a' > \rho_1$, i.e.,

$$2\left(\rho_1 - \frac{\Delta v}{2} + a\right) > \rho_1,$$

from whence

$$\rho_1 > \Delta v - 2a. \tag{21a}$$

But if $v_1 < v^*$, then a can vary within the limits $0 < a < \Delta v/2$. Therefore, if $\rho_1 > \Delta v$, then (21a) always holds. With this, $v_1 = v^* - \rho_1 = v^* - \Delta v$.

Now let $\rho_1 < 0$. With this, $v' > v_1 > v^*$ and the number a can vary within the limits

$$\frac{\Delta v}{2} < a < \Delta v.$$

The condition sought reduces to the inequality $2a' < \rho_1$ from whence, on the basis of (16a),

$$\rho_1 < \Delta v - 2a. \tag{21b}$$

Condition (21b) will be met if $\rho_1 < \Delta v - 2\Delta v = -\Delta v$. With this, $v_1 = v^* - \rho_1 > v^* + \Delta v$. Thus, if v_1 is at a distance from v^* whose modulus is greater than Δv, then the image of point v_1 cannot, under any conditions, coincide with v^*.

We now consider the case when $v_1 > v'$. As before, let a decrease of v commence after commutator operation; the decrease of v can continue either until the signum-relay operates or, failing that, until the commutator operates.

In the case under consideration ($v_1 > v'$) the signum-relay does not operate, since the controlled quantity p can change, with a decrease of the argument by Δv, only by the amount m, which is less than the insensitivity zone width δ.

This quickly follows from the lemma. Indeed, $m = f(v_1) - f(v_1 - \Delta v)$.

From a comparison with (A) we note that $v' < v_1 < v_0$ and the variations of the argument are identical; consequently, on the basis of part "a" of the lemma, $m < \delta$. Therefore, the reversal from an increase in v will occur, not by operation of the signum-relay, but by operation of the commutator, which will occur at the value $v_2 = v_1 - \Delta v$.

After commutator operation, the argument increases up to the value $v_3 = (v_1 - \Delta v) + \Delta v = v_1$. After this, there is again a reversal to decreasing v, operation of the signum-relay, but by operation of the commutator, since the signum-relay does not operate, reversal, etc.

Consequently, one full control cycle translates each initial value which lies in the region $v' < v < v_0$ into itself; there is a continuum of stationary amplitudes.

In other words, if the control process starts from a value of v lying in the region $v' < v < v_0$, then there will occur periodic oscillations of period $\tau = 2\ \Delta v/k$ for periodic variations of the argument within the limits $v_1 - \Delta v \geq v \geq v_1$ and a corresponding variation of the controlled quantity within the limits of $f(v_1 - \Delta v) \leq p \leq f(v_1)$.

Until now we have considered all the points of the semiline $v \leq v_0$ except the point $v = v'$, defined by (A).

All the values considered for $v = v_0$ correspond to definite actual oscillatory processes which occur in the extremal controller. This cannot be said of the initial value $v_1 = v'$.

In fact, according to (A), after a reversal to decreasing v occurs for the value v', the controlled quantity changes by δ for a change of argument of exactly Δv.

But with this there must simultaneously occur two actions: reversal due to signum-relay operation, and reversal due to commutator operation.

Such simultaneous operations have no real meaning. One might think that to this there would correspond a switching out of the entire reversing device; this is not admissible, despite the small probability that (A) holds. In practice, even if the initial value turns out to be equal to v', one must provide operation either of the commutator or of the signum-relay. Consequently, it would be possible to assign the value of v' to one of the regions.

We now consider controller operation if the initial value is $v > v_0$. If we assume that, after commutator operation initially, there occurs an increase of the argument then, by assuming that there exists a $v'' > v_0$ such that

$$f(v'') - f(v'' + \Delta v) = \delta,$$

we can transfer over all the results obtained for $v \leq v_0$ to the case when $v \geq v_0$. Instead of transformation T we shall have transformation T', given by the formula

$$v_3 = 2v_2 - \Delta v - v_1,$$

where v_2 is defined by the formula $f(v_1) - f(v_2) = \delta$.

Consequently, in this case one can partition the semiline of initial values $v \geq v_0$ into two regions: $v_0 \leq v_1 < v''$ and $v'' < v_1$. The value of v'' is defined as the root of (A').

In the region $v_0 \leq v_1 < v''$ the motion is stable, there being a continuum of periodic motions.

In the region $v'' < v_1$ there occurs an approximation to a limiting periodic motion, in which the argument varies periodically with period $\tau = \Delta v/k$ between the limits $v'^{*} \leq v \leq v'^{*} + \Delta v/2$, where v'^{*} is the root of the equation

$$f(v'^{*}) - f\left(v'^{*} + \frac{\Delta v}{2}\right) = \delta.$$

In order to exhaust completely all the possibilities which can ensue for values of Δv and δ for which there exist $v = v'$ and $v = v''$, it is necessary to discard the supposition that, at the moment when the controller is switched in, the commutator necessarily is operated by a decrease of the controlled quantity p.

We note first of all, that if the initial value of v_1 for which the commutator operates on an increase in the controlled quantity is at a distance from v_0 equal to or greater than Δv, then this case leads to that already considered if one takes account, not of the value v_1, but of the value $v_1' = v_1 \pm \Delta v$ ("+" for $v_1 < v_0$ and "-" for $v_1 > v_0$).

In fact, with this the following operation of the commutator will occur for a decrease of $p = f(v)$, which is a case already considered; the behavior of the controlled system will thus depend on whether v_1' lies in the region $v' < v_1 < v''$ or in the region $v_1 < v'$ and $v_1' > v''$.

In the first case, there is a continuum of periodic motions; in the second case, there are either periodic motions about v^{*} and v'^{*} if, respectively, $v_1' = v^{*}$ or $v_1' = v'^{*}$, or an approximation to these limiting motions.

There still remains for consideration the case when the initial value of v_1 for which the commutator operates on an increase of the controlled quantity is separated from v_0 by a distance less than Δv. Let

$$v_1 = v_0 + b > v_0 \qquad (0 < b < \Delta v).$$

It is easily seen that, with a decrease of p from the maximum value $p = f(v_0)$, which will occur with decreasing v, down to the value $p = f(v_1 - \Delta v)$, the signum-relay does not operate, since the change in p, $\delta p = f(v_0) - f(v_0 - \Delta v)$ will be less than δ. Consequently, the following commutator operation occurs for the value:

$$v_2 = v_0 + b - \Delta v < v_0, \quad v_0 - v_2 = \Delta v - b < \Delta v.$$

After commutator operation, there begins an increase of v from the value v_2 to the value

$$v_3 = v_2 + \Delta v = v_0 + b - \Delta v + \Delta v = v_0 + b = v_1.$$

With the attainment of $v_3 = v_1$, there occurs a new operation of the commutator, and the cycle begins to repeat. Consequently, one full control cycle will transfer the initial value of v_1 into itself, i.e., there is a continuum of periodic motions. The case when $v_1 = v_0 - b$, $0 < b < \Delta v$, reduces to what has just been considered if one begins the investigation with the following operation of the commutator.

Thus, the partitioning of the line of initial values, $-\infty < v_1 < +\infty$, into regions depends on which side the argument begins to vary on at the moment when the controller is switched in.

Case A. If commutator operation gives rise to a decrease in v, then the v_1 line is divided into three regions:

region L_1
$$v_1 < v'. \tag{22'}$$

region L_2
$$v' < v_1 < v'' + \Delta v. \tag{22''}$$

region L_3
$$v'' + \Delta v < v_1. \tag{22'''}$$

Case B. If commutator operation gives rise to an increase in v, the regions are shifted to the left, and are the following:

region L_1'
$$v_1 < v' - \Delta v, \tag{23'}$$

region L_2'
$$v' - \Delta v < v_1 < v''. \tag{23''}$$

region L_3'
$$v'' < v_1. \tag{23'''}$$

In the first and third regions there occur approximations to the limiting periodic motions while, in the second region, there is a continuum of periodic motions.

4. Effect of Variations of the Parameters Δv and δ

We have thus far assumed that Δv and δ have values such that there exist numbers $v' < v_0$ and $v'' > v_0$.

We now drop this limitation and consider the influence of changes in the parameters Δv and δ.

Let there exist real values of v' and v''. We shall fix $\Delta v = \Delta_1 v$ and we shall vary δ.

The decomposition into regions L_1, L_2, and L_3 depends on the character of the real roots of (A) and (A').

It is easily seen that, as δ_1 increases, the points v' and v'' move further away from v_0 while, for decreasing δ_1, the points v' and v'' move closer to v_0. For some definite values $\delta = \delta_1$ and $\delta = \delta_2$, the points v' and v'' coincide with v_0; the values of these are determined, respectively, from the expressions

$$f(v_0) - f(v_0 - \Delta v) = \delta_1. \tag{24}$$
$$f(v_0) - f(v_0 + \Delta v) = \delta_2.$$

Simultaneously with the change of position of the points v' and v'' on the line there is a change of position of the invariant points v^* and v^*_1, defined by (B) and (B'). These points move away from v_0 with increasing δ and approach v_0 for decreasing δ. Suppose that they coincide with v_0 for the values $\delta = \delta_3$ and $\delta = \delta_4$, defined by (25):

$$f(v_0) - f\left(v_0 - \frac{\Delta v}{2}\right) = \delta_3. \tag{25}$$
$$f(v_0) - f\left(v_0 + \frac{\Delta v}{2}\right) = \delta_4.$$

It is obvious that $\delta_3 < \delta_1$ and $\delta_2 < \delta_4$. We consider the case when the curve $p = f(v)$ is symmetric about the line $v = v_0$. Then, $\delta_1 = \delta_2$ and $\delta_3 = \delta_4$. Let $\delta_3 < \delta < \delta_1$. Consequently, there exists no v' which satisfies (A). Let $f(v_0) - f(v_0 - a_1) = \delta$ and consequently, $a_1 < \Delta v$. Therefore, operation of the signum-relay occurs to the left of v_0 if the initial value lies to the right of v_0 in the region L_1 [Condition (26)].

With this, the regions of (22) are deformed, and assume the forms:

region L_1
$$v_1 < v_0 + \Delta v - a. \tag{26'}$$

region L_2
$$v_0 + \Delta v - a_1 < v_1 < v_0 + a_1. \tag{26''}$$

region L_3
$$v_0 + a_1 < v_1. \tag{26'''}$$

We shall continue to decrease δ. If $\delta = \delta_3$, i.e., if v^* coincides with v_0, then $a_1 = \Delta v/2$; then,

$$v_0 + \Delta v - a_1 = v_0 + \frac{\Delta v}{2}, \quad v_0 + a_1 = v_0 + \frac{\Delta v}{2}.$$

Consequently, region L_2 shrinks to a point. There remain two regions. Region L_1 : $v_1 < v_0 + \Delta v/2$; region L_3: $v_0 + \Delta v/2 < v_1$.

With still greater decrease of δ, the motion loses its simple character and becomes a multiple motion.

It may be shown that the mode of multiple oscillations is not effective in practice here, since oscillations are possible with this that have greater amplitudes than the simple oscillations.

It is therefore meaningful to decrease δ and to increase Δv until v^* gets close to v_0, but not beyond that; this is the more advantageous since, generally speaking, it is quite difficult to obtain a small δ, but a decrease in Δv is very desirable from the point of view of increasing the stability of the control mode with respect to external disturbances.

We have been changing δ with Δv held fixed. It is easily seen that an increase in Δv acts analogously to a decrease in δ.

We can consider the case of asymmetry analogously.

5. Consideration of a Concrete Problem

Let the function $p = f(v)$ have the form

$$p = -v^2. \tag{27}$$

We shall consider initially a value of $v_1 > v_0 = 0$. If Δv and δ are given, then the magnitude of v^* is defined by the equation

$$f(v^*) - f\left(v^* - \frac{\Delta v}{2}\right) = \delta; \tag{28}$$

from which, based on (27),

$$v^* = \frac{\Delta v}{4} - \frac{\delta}{\Delta v} \qquad (v^* \leqslant 0).$$

Equation (28) is meaningful when $\delta \geq \Delta v^2/4$. Region (A) is isolated by the boundaries v' and $v_0 = 0$, where v', in accordance with (A), is defined by the formula

$$v' = \frac{\Delta v}{2} - \frac{\delta}{2\Delta v} \qquad (v' \leqslant 0). \tag{29}$$

We now determine the character of the establishment process in accordance with (20a) and (20b). The character of the process we are seeking depends on the sign of the expression $\psi = |2a'| - |\rho_1|$. We now construct this function. According to (14),

$$a' = \left(v^* - \frac{\Delta v}{2}\right) - (\delta_1 - a),$$

where $\underline{a}$ is the root of (7).

From (7) we obtain the quadratic equation in $\underline{a}$:

$$a^2 - 2v_1 a - \delta = 0;$$

from whence

$$a = v_1 + \sqrt{v_1^2 + \delta}.$$

(The plus sign is chosen so that $a > 0$.)

Consequently,

$$a' = \left(\frac{\Delta v}{4} - \frac{\delta}{\Delta v} - \frac{\Delta v}{2}\right) - \left[v_1 - \left(v_1 + \sqrt{v_1^2 + \delta}\right)\right|$$

Further,

$$\rho_1 = v^* - v_1 = \left(\frac{\Delta v}{4} - \frac{\delta}{\Delta v} - v_1\right).$$

Inequality (20a) takes the form

$$\phi = \pm\left[-\frac{3}{4}\Delta v - \frac{\delta}{\Delta v} + v_1 + 2\sqrt{v_1^2 + \delta}\right| > 0.$$

(The plus sign is taken for $v_1 < v^*$, the minus sign for $v_1 > v^*$; this expression is meaningful for $\delta \geq \Delta v^2/4$.

It is easily shown that this expression cannot be satisfied for any arbitrary v_1. It follows from this that it is impossible to choose values of Δv and δ such that the approximation to v^* occurs for any v_1 on one side only. However, for certain regions of values of Δv and δ, one can cite such a point $v_1 = v_u \neq v^*$ whose image v_3 coincides with the invariant point v^*.

In fact, it follows from (20c) that this point is defined by the condition that $\psi = 0$.

Whence,

$$v_1 = \frac{-\left(\frac{3}{2}\Delta v + \frac{2\delta}{\Delta v}\right) \pm \left(\frac{4\delta}{\Delta v} - 3\Delta v\right)}{6}.$$

The minus sign defines the invariant point v^*. The plus sign gives the point v_u sought:

$$v_u = \frac{3}{4}\Delta v + \frac{1}{3}\frac{\delta}{\Delta v}. \tag{30}$$

Formula (30) gives a negative value of v_u for $\delta < 2.25\Delta v^2$, while it follows from (28) that v^* has a minus sign [the condition for applicability of (28)] if $4\delta > \Delta v^2$.

Consequently, the values of v_u are meaningful in the region

$$0.25\Delta v^2 < \delta < 2.25\Delta v^2. \tag{31}$$

We now consider the entire v_1 line, and construct the regions of initial values given by (23) and (26). So long as there exist values $v' < v_0 = 0$, i.e., so long as $\delta > \Delta v^2$ [this follows from (29)], the line of initial values is partitioned into the following three regions (22):

1) region L_1

$$v_1 < \frac{\Delta v}{2} - \frac{\delta}{2\Delta v};$$

2) region L_2

$$\frac{\Delta v}{2} - \frac{\delta}{2\Delta v} < v_1 < \frac{\delta}{2\Delta v} - \frac{\Delta v}{2} + \Delta v = \frac{\delta}{2\Delta v} + \frac{\Delta v}{2};$$

3) region L_3

$$\frac{\delta}{2\Delta v} + \frac{\Delta v}{2} < v_1.$$

If δ is included in the interval $0.25\,\Delta v^2 < \delta < \Delta v^2$, then the line of initial values is partitioned into the regions of (26) [where the quantity a_1 is defined by the condition $f(v_0) - f(v_0 - a_1) = \delta$, but $v_0 = 0$, and, consequently, $a_1 = \sqrt{\delta}$]:

1) region L_1

$$v_1 < v_0 + \Delta v - \sqrt{\delta};$$

2) region L_2

$$v_0 + \Delta v - \sqrt{\delta} < v_1 < v_0 + \sqrt{\delta};$$

3) region L_3

$$v_0 + \sqrt{\delta} < v_1.$$

As δ decreases from $\delta = \delta_1 = \Delta v^2$ to $\delta = 0.25\Delta v^2$, region L_2 decreases and, for $\delta = 0.25\,\Delta v^2$, shrinks to a point. With further decreases in δ, the motion becomes multiple.

Returning to (31), we note that, in the region of values $\delta > 2.25\,\Delta v^2$, there occurs an asymptotic approach to periodic motions (if v_1 is chosen in regions L_1 or L_3); in the region of (31) the establishment process can be either asymptotic or finite; in the region of $\delta < 0.25\Delta v^2$, there are multiple oscillations.

The character of the possible motions in the system under consideration depends on the two essential parameters Δv and δ.

Figure 2 shows the Δv, δ parameter plane.

In the region bounded by the arc of the parabola $\Delta v^2 = \delta$ and the positive δ semiaxis, there is a rigid excitation mode with a decomposition of the initial values in accordance with the domains of (22).

In the region between the arcs of the parabolas $\Delta v^2 = 4\delta$ and $\Delta v^2 = \delta$, there are rigid modes with decomposition in accordance with the regions of (26).

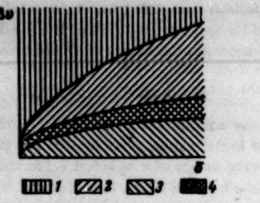

Fig. 2. 1 is the multiple oscillatory mode, 2 is the rigid mode, with decomposition into the regions of (26), 3 is the asymptotic approach to a periodic motion (the decomposition into the regions of (22)), 4 is the finite and asymptotic establishment processes (decomposition into the regions of (22)).

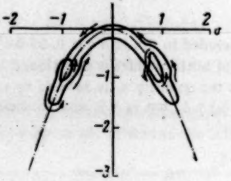

Fig. 3.

The asymptotic approximation to periodic motion occurs in the region bounded by the arc of the parabola $9\Delta v^2 = 4\delta$ and the positive δ semiaxis.

The region $\Delta v^2 > 4\delta$ is characterized by the presence of a multiple oscillatory mode.

Figure 3 shows the phase diagram of the multiple periodic oscillations for $\Delta v = 3$ and $\delta = 1$.

Figure 4 shows the development of the multiple periodic oscillations in time (curve I), where the axis of abscissas is laid out with time in the scale of $1/k$. This same figure gives the development (curve II) in time of the simple periodic oscillations for the limiting value of $\Delta v = 2$ for the chosen value of $\delta = 1$. It is clear, from a comparison of curves I and II, that the multiple oscillations are less suitable, since their amplitudes are greater than those of the simple oscillations.

In conclusion, we consider the question of the influence of the system's parameters on the inaccuracy of the extremal control operation. By "inaccuracy of operation" we shall understand the difference between the value v_0 of the argument corresponding to the true extremal value of the controlled quantity and the limiting value v^* which can be attained as a result of the extremal controller's action.

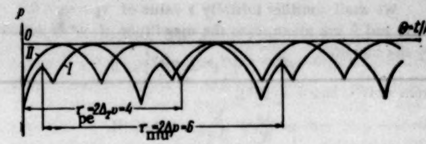

Fig. 4.

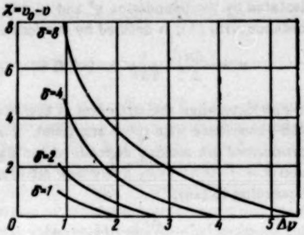

Fig. 5

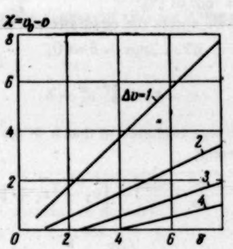

We denote this difference by χ:

$$\chi = v_0 - v^* = \frac{\delta}{\Delta v} - \frac{\Delta v}{4}. \tag{32}$$

Expression (32) is meaningful so long as $\chi \geq 0$, since the case $\chi < 0$ corresponds to the case when the motion becomes multiple, and when (28) can therefore not be applied.

Figure 5 gives graphs of the quantity χ as a function of Δv for different fixed values of δ. It is clear from this figure that each value of δ has its corresponding value of $\overline{\Delta v}$ for which the inaccuracy χ vanishes. With decreasing Δv the inaccuracy increases, this increase not being very large for values of Δv close to $\overline{\Delta v}$; for significant decreases in Δv the magnitude of χ begins to increase more rapidly since, in (32), the first, hyperbolic-type, term begins to play a predominant role.

Figure 6 gives graphs of the quantity χ as a function of δ for different fixed values of Δv. This function is given by a family of straight lines with slopes greater than zero.

A comparison of Figs. 5 and 6 shows that the increases in δ have a lesser effect on the increase of the inaccuracy than do decreases in Δv.

Appendix

Lemma. If the continuous function $p = f(v)$ satisfies the conditions $f'(v_0) = 0$, $f''(v) < 0$ for $v \leq v_0$ then, for each pair of values v_a and v_b ($v_a < v_b \leq v_0$), the following inequalities hold:

a) if there are given two numbers c_1 and c_2 ($0 < c_1 \leq c_2$), then

$$f(v_b) - f(v_b - c_1) < f(v_a) - f(v_a - c_2); \tag{5}$$

b) if there are given two numbers d_1 and d_2 such that

$$f(v_a) - f(v_a - d_1) = f(v_b) - f(v_b - d_2), \tag{6}$$

then

$$d_1 < d_2 \tag{6a}$$

and

$$v_a - d_1 < v_b - d_2. \tag{6b}$$

Proof. We first note that, since $f''(v) < 0$ then, for decreasing v_1, the function $f'(v)$ increases monotonically.

First, we prove (5).

a) We assume initially that $v_a < v_b - c_1$; in this case, the intervals $v_a - c_2 \leq v \leq v_a$ and $v_b - c_1 \leq v \leq v_b$ are nonintersecting.

With this,

$$[f'(v)]_{v < v_a} > [f'(v)]_{v > v_b - c}. \tag{33}$$

Further,

$$f(v_b) - f(v_b - c_1) = \Delta P_1 = \int_{v_b - c_1}^{v_b} f'(v)\, dv, \tag{34a}$$

$$f(v_a) - f(v_a - c_2) = \Delta P_2 = \int_{v_a - c_2}^{v_a} f'(v)\, dv. \tag{34b}$$

On the basis of (33), and bearing in mind that $c_1 \leq c_2$, we conclude that $\Delta P_1 < \Delta P_2$.

b) We now assume that $v_a > v_b - c_2$. In this case, the intervals $v_a - c_2 \leq v \leq v_a$ and $v_b - c_1 \leq v \leq v_b$ partially intersect each other; with this, the segment $v_b - c_1 \leq v \leq v_a$ is common to both intervals. Consequently, on this segment, the changes in the function $f(v)$ will also be identical.

It remains to compare the changes of the function $f(v)$ on the intervals $v_a - c_2 \leq v \leq v_b - c_1$ and $v_a \leq v \leq v_b$. But, for these intervals, we have case "a". Consequently, here also $\Delta P_1 < \Delta P_2$. Thus, (5) is proven.

Now we prove (6a).

We fix the quantity c_1 in the left member of (5), introducing the notation $c_1 = d_2$. We now, in the right member of (5), change c_2 (denoting it by d_1) in such fashion that the inequality becomes an equality.

Since, in (34b), $f'(v)$ retained its sign over the entire interval of integration, the quantity defined by the integral in (34b) can be decreased only by decreasing the length of this interval, whereby, on the basis of (33), equality can be reached only for $d_1 < d_2$.

As for (6b), it is obvious.

LITERATURE CITED

1. V. V. Kazakevich, On Extremal Control (Dissertation) [in Russian] (MVTU, 1944).
2. V. V. Kazakevich, "Investigation of nonlinear processes in an extremal controller," Tekhnicheskii otchet TsIAM, No. 1896 (1948).

ELECTROMAGNETIC CONTROL-ELEMENT DYNAMICS

I. E. Dekabrun, N. P. Kozlov, and I. M. Krassov

(Moscow)

Translated from Avtomatika i Telemekhanika, Vol. 21, No. 4, pp. 506-512, April, 1960
Original article submitted June 30, 1959

The equation of motion is derived for a rotary type electromagnetic control element, and a comparison is made with experimental results.

In automatic control and regulation systems, extensive use has been made of electric controlling elements in which electrical quantities are transformed to mechanical ones. Such elements (electromagnetic and electrodynamic) are used in remote control systems, in electrohydraulic servomechanisms and in other devices of automation technology.

Despire the widespread usage of electric controlling elements, their dynamics are still insufficiently explicated. The existing works [1] in this area treat only individual questions, and lack a general character.

In the present paper we consider the dynamics of an electromagnetic polarized controlling element, since it is the most widely used type.

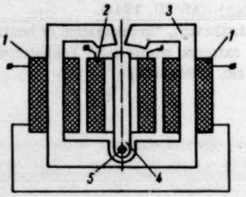

Fig. 1

A schematic drawing of the electromagnetic control element is shown in Fig. 1, where 1 is the excitation coil (superposed magnetization), 2 is the control coil, 3 is the magnetic circuit, 4 is the armature, and 5 is the output shaft. When a controlling signal is applied to coil 2, output shaft 5 is rotated by a definite angle.

We now write the general form of the equation of motion for the electromagnetic control element's armature:

$$J\ddot{\theta} = M_{\mathrm{d}} - M_1 . \tag{1}$$

Here, J is the armature's moment of inertia, θ is the armature's angle of rotation, M_d is the driving torque, and M_1 is the impedance torque of the armature's motion.

The driving torque, equal to

$$M_{\mathrm{d}} = PR \tag{2}$$

(where P is the force engendering the armature rotation and R is the radius of application of the force), depends on the current flowing in the control coil.

The impedance torque is made up of the load torque M_L, the friction torque in the bearings M_F and the damping torque M_v.

In considering the operation of an electromagnetic control element in any actual control scheme, it is necessary to take into account both the form of the load and the frictional force in the bearings arising when an external force is applied to the armature axis [2]. For investigating the dynamics of an inherently electromagnetic control element removed from any control scheme (and these may be very diverse), there is the possibility of not taking the load on the control element's armature into account. In this case, the impedance torque will be determined by the friction in the bearings under the action of the armature's own weight, and by the damping which arises when the armature moves within the surrounding air, i.e.,

$$M_1 = Qrf \operatorname{sign} \dot{\theta} + kq\dot{\theta}, \tag{3}$$

where Q is the armature's weight, r is the radius of the armature shaft, f is the coefficient of friction in the bearings, k is a proportionality factor, and q is the coefficient of viscous friction.

By substituting (2) and (3) in (1), we get

$$J\ddot{\theta} = PR - Qrf \operatorname{sign} \dot{\theta} - kq\dot{\theta}. \tag{4}$$

The work expended in moving the control element's armature, as in every polarized electromagnetic system, is carried out at the expense of two energy sources: the controlling (working) and the polarizing sources. In the general case, the force acting on the armature of the system under consideration can be presented in the form of a sum of three forces [3]

$$P = P_1 + P_2 + P_3,$$

where P_1 is the component due to the polarizing source (or sources), which exists whether or not there is current in the control winding, P_2 is the component due to the controlling (working) source (or sources), P_3 is the component arising from the interaction of the magnetic fluxes of the controlling and polarizing sources which actually determines the direction of armature motion.

For the case when the polarizing and working sources are coils, these components equal

$$P_1 = \Sigma \frac{(i_{\mathrm{e}} w_{\mathrm{e}})^2}{2} \frac{dG_{\mathrm{e}}}{dy}, \quad P_2 = \Sigma \frac{(i_{\mathrm{c}} w_{\mathrm{c}})^2}{2} \frac{dG_{\mathrm{c}}}{dy},$$

$$P_3 = \Sigma \frac{i_{\mathrm{e}} w_{\mathrm{e}} i_{\mathrm{c}} w_{\mathrm{c}}}{2} \frac{dG_{\mathrm{ec}}}{dy},$$

where i_e and i_c are the currents flowing in the excitation and control coils, respectively, w_e and w_c are the number of turns in the excitation and control coils, G_e is the circuit's conductance with respect to the magnetic flux of the excitation coil, G_c is the circuit conductance with respect to the control coil's magnetic flux, G_{ec} is the circuit conductance determining the magnitude of the portion of the excitation coil's magnetic flux in the control winding, y is the linear deviation of the armature from the neutral position*.

As is obvious from these expressions, only the sign of the third component is determined by the polarity of the current in the control winding. The summation signs in all these expressions are indicative of the fact that polarized systems, as a rule, have complicated configurations of magnetic circuits with several controlling and polarizing sources.

The system under consideration is a differential one. In it (Fig. 1) there are two excitation coils on the arms of the magnetic circuit, and one control coil on the cross piece. With no controlling signal present, the electromagnet's armature is acted upon by the forces generated by the first and second excitation coils. In this case, the component P_1 is the sum of these two forces, and equals

$$P_1 = \frac{(i_1 w_1)^2}{2}\frac{dG_1}{dy} + \frac{(i_2 w_2)^2}{2}\frac{dG_2}{dy}, \qquad (5)$$

where G_1 and G_2 are the circuit's conductances with respect to the magnetic fluxes of the first and second excitation coils, respectively, i_1, i_2 and w_1, w_2 are the currents and numbers of turns in the first and second excitation coils, respectively.

Since the coils are identical ($w_1 = w_2 = w_e$) and are connected in series ($i_1 = i_2 = i_e$), the expression may be rewritten in the form

$$P_1 = \frac{(i_e w_e)^2}{2}\left(\frac{dG_1}{dy} + \frac{dG_2}{dy}\right). \qquad (6)$$

The second component P_2, generated by the control coil, can be expressed by the formula

$$P_2 = \frac{(iw)^2}{2}\frac{dG}{dy}, \qquad (7)$$

where i and w are the current and number of turns in the control coil, G is the circuit conductance with respect to the magnetic flux of the control coil.

The third component, created by the interaction of the two counter-directed magnetic fluxes of the first and second excitation coils with the magnetic flux of the control coil, equals

$$P_3 = \frac{iwi_e w_e}{2}\left(\frac{dG_{2c}}{dy} - \frac{dG_{1c}}{dy}\right), \qquad (8)$$

where G_{1c} and G_{2c} are the conductances which determine the magnitude of the magnetic fluxes in the control coil which correspond to the first and second excitation coils.

In order to express P_1, P_2, and P_3 in terms of the controlling element's parameters, we use its replacement circuit (Fig. 2). Figures 3 and 4 show the nomenclature of the basic design parameters of the control element. With this nomenclature, we can write that the impedances of the left and right air gaps equal, respectively,

$$R_{P1} = \frac{\delta}{(c-y)d}, \qquad R_{P2} = \frac{\delta}{(c+y)d}, \qquad (9)$$

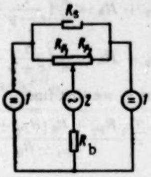

Fig. 2. 1 is the excitation winding's mmf, 2 is the control winding's mmf.

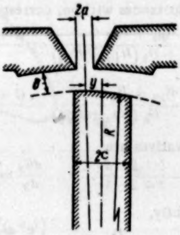

Fig. 3. Basic design parameters of the electromagnetic control element.

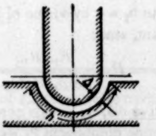

Fig. 4. Design parameters of the armature's bearing portion.

and that the air gap between the bearing and the armature equals

$$R_b = \frac{\delta}{ld}, \qquad (10)$$

where c = b - a, $l = hk_1$, $k_1 = \delta/\Delta$, d is the armature thickness.

We take $R_s = \infty$, and calculate a number of auxiliary quantities:

$$R_{P1} + R_{P2} = \frac{2c\delta}{(c^2 - y^2)d}.$$

$$R_{P1} - R_{P2} = \frac{2y\delta}{(c^2 - y^2)d}.$$

---

*We consider small angular deviations of the armature, within the limits of ± 1 degree.

$$R_{P1}R_{P2}=\frac{\delta^2}{(c^2-y^2)d^2}.$$

$$R_{P1}R_{P2}+R_\delta(R_{P1}+R_{P2})=\frac{\delta^2}{(c^2-y^2)d^2}\left(1+\frac{2c}{l}\right).$$

$$R_{P1}+R_\delta=\frac{\delta}{d}\left(\frac{1}{c-y}+\frac{1}{l}\right).$$

$$R_{P2}+R_\delta=\frac{\delta}{d}\left(\frac{1}{c+y}+\frac{1}{l}\right).$$

To determine P_1 we first find

$$R_1=\frac{1}{G_1}=\frac{R_{P1}R_{P2}+R_\delta(R_{P1}+R_{P2})}{R_{P2}+R_\delta}. \qquad (11)$$

$$R_2=\frac{1}{G_2}=\frac{R_{P1}R_{P2}+R_\delta(R_{P1}+R_{P2})}{R_{P1}+R_\delta}.$$

The conductances will be, correspondingly,

$$G_1=\frac{R_{P2}+R_\delta}{R_{P1}R_{P2}+R_\delta(R_{P1}+R_{P2})}=\frac{(l+c+y)(c-y)d}{(l+2c)\delta}. \qquad (12)$$

$$G_2=\frac{R_{P1}+R_\delta}{R_{P1}R_{P2}+R_\delta(R_{P1}+R_{P2})}=\frac{(l+c-y)(c+y)d}{(l+2c)\delta}.$$

and their derivatives are

$$\frac{dG_1}{dy}=-\frac{l+2y}{l+2c}\frac{d}{\delta}. \qquad \frac{dG_2}{dy}=\frac{l-2y}{l+2c}\frac{d}{\delta}; \qquad (13)$$

Consequently,

$$P_1=-\frac{2(i_e w_e)^2 d}{(l+2c)\delta}y. \qquad (14)$$

The minus sign shows that component P_1 is directed opposite to the translation y.

Component P_2 = 0 by virtue of the fact that the conductance is constant, since

$$R_0=\frac{1}{G}=R_\delta+\frac{R_{P1}R_{P2}}{R_{P1}+R_{P2}}=R_\delta+\frac{\delta}{2cd} \qquad (15)$$

and its derivative dG/dy equals zero.

To determine component P_3 we should find the expressions for G_{1C} and G_{2C}. For this, we sketch the replacement circuit (Fig. 5) and determine which portion of the fluxes engendered by each excitation coil will flow through the control coil. The action of each excitation coil will be considered separately. Based on Ohm's laws and Kirchhoff's laws, we get

$$G_{1C}=\frac{R_{P2}}{R_{P1}R_{P2}+R_\delta(R_{P1}+R_{P2})},$$

$$G_{2C}=\frac{R_{P1}}{R_{P1}R_{P2}+R_\delta(R_{P1}+R_{P2})}. \qquad (16)$$

Consequently,

$$G_{2C}-G_{1C}=\frac{R_{P1}-R_{P2}}{R_{P1}R_{P2}+R_\delta(R_{P1}+R_{P2})}. \qquad (17)$$

After substituting of the impedance values, we get

$$G_{2C}-G_{1C}=\frac{2dly}{\delta(l+2c)}, \qquad (18)$$

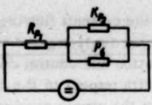

whence

$$\frac{d(G_{2C}-G_{1C})}{dy}=\frac{2ld}{\delta(l+2c)}. \qquad (19)$$

Consequently,

$$P_3=iwi_e w_e\frac{ld}{\delta(l+2c)}. \qquad (20)$$

Thus, the general expression for the force will have the form

$$P=P_3+P_1 \qquad (21)$$

or

$$P=iwi_e w_e\frac{ld}{\delta(l+2c)}-\frac{2(i_e w_e)^2 d}{\delta(l+2c)}y. \qquad (22)$$

As is clear from this expression, the component P_1 of the force on the armature acts as a spring, rotating the armature after cessation of the action of the controlling signal to the original position. It may therefore be called an electrical spring.

Figure 6 shows the family of static characteristics M = f(θ) for various currents i in the control winding, these curves having been obtained experimentally. These graphs substantiate the correctness of our computations.

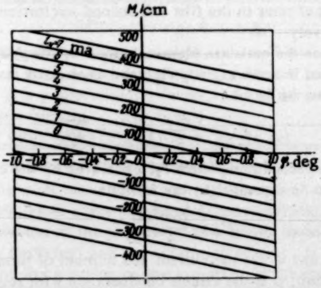

Fig. 6. Static characteristics of the electromagnetic control element.

For small angles of rotor deviation, we may assume that

$$y=\theta R. \qquad (23)$$

Then,

$$P=\frac{iwi_e w_e ld}{\delta(l+2c)}-\frac{2(i_e\omega_e)^2 Rd}{\delta(l+2c)}\theta \qquad (24)$$

or

$$P=Ai-B\theta, \qquad (25)$$

where

$$A=\frac{wi_e w_e ld}{\delta(l+2c)}, \quad B=\frac{2(i_e w_e)^2 Rd}{\delta(l+2c)}.$$

By substituting the expression obtained for the force P in (4), we obtain

$$J\ddot{\theta} = (Ai - B\theta)R - kq\dot{\theta} - Qrf\,\mathrm{sign}\,\dot{\theta}$$

or

$$\frac{J}{AR}\ddot{\theta} + \frac{kq}{AR}\dot{\theta} + \frac{B}{A}\theta + \frac{Qfr}{AR}\,\mathrm{sign}\,\dot{\theta} = i.$$

By going over to dimensionless symbols, we get the equation describing the armature motion in the following form:

$$m\ddot{\varphi} + \gamma\dot{\varphi} + \beta\varphi + \alpha\,\mathrm{sign}\,\dot{\varphi} = I, \qquad (26)$$

where

$$m = \frac{J\delta\,(l + 2c)\,\theta_m}{i_e w_e dlwRi_m}, \quad \gamma = \frac{kq\delta\,(l + 2c)\,\theta_m}{i_e w_e dlwRi_m}, \quad \beta = \frac{2i_e w_e R\theta_m}{lwi_m},$$

$$\alpha = \frac{\theta rf\delta\,(l + 2c)\,\theta_m}{i_e w_e dlwRi_m}, \quad \varphi = \frac{\theta}{\theta_m}, \quad I = \frac{i}{i_m},$$

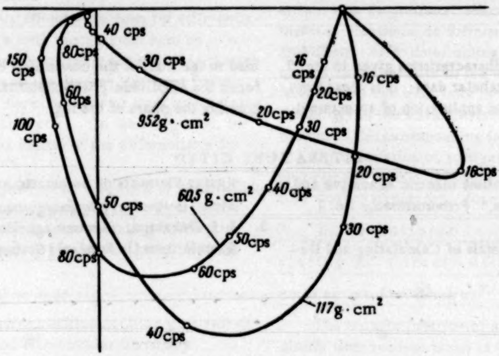

Fig. 7. Experimental amplitude-phase characteristics.

θ_m and i_m are the basic magnitudes of the angle of deviation and the control current.

In (26), the term α sign $\dot{\varphi}$, characterizing the friction in the bearings, is a negligibly small quantity, since the armature axis is supported in ball bearings and operates with flood lubrication. In view of this, the motion of the controlling device's armature can be described by an equation of the form

$$T_2^2\ddot{\varphi} + T_1\dot{\varphi} + \varphi = \frac{1}{\beta}I \qquad (27)$$

where

$$T_2^2 = m/\beta, \quad T_1 = \gamma/\beta.$$

Expression (27) is the usual form for writing the equation of a second-order oscillatory link. Its transfer function can be given in the following form:

$$W(p) = \frac{1}{\beta\left(T_2^2 p^2 + T_1 p + 1\right)}. \qquad (28)$$

The form of the frequency characteristic of such a link is widely known, but the data which characterize the frequency characteristic of an actual electromagnetic controlling device are of definite interest.

The amplitude and phase frequency characteristics of a type REP electromagnetic controlling device were recorded for a controlling current of i = 2 ma and for different inertial loads on the armature axis (for different moments of inertia)†. The armature's inherent moment of inertia J equalled 60.5 g · cm². The table presents the data obtained for a control current of i = 2 ma; the basic magnitude of armature angular rotation was taken to be $\theta_m = 0.4°$. The basic value of control current was taken to be $i_m = 2$ ma.

The quantity N in the table is the ratio of the dimensionless amplitude of armature angle of rotation to the dimensionless control current, i.e.,

$$N = \frac{\theta_a}{\theta_m} \Big/ \frac{i}{i_m},$$

and the quantity ψ is the lag phase.

---

† The experiments were carried out by L. P. Levin, G. Yu. Chubarova, and G. M. Val'kova.

Frequency, cps	Moment of inertia g · cm^2								
	60,5			117			952		
	θ_a, deg	N	ψ, deg	θ_a, deg	N	ψ, deg	θ_a, deg	N	ψ, deg.
16	0.376	0.94	13	0.44	1.11	15	0.64	1.6	24
20	0.372	0.93	20	0.48	1.2	30	0.32	0.8	35
30	0.376	0.94	30	0.53	1.33	42	0.124	0.31	55
40	0.40	1.0	46	0.53	1.33	75	0.05	0.126	85
50	0.42	1.06	60	0.32	0.8	90	0.04	0.1	108
60	0.44	1.11	70	0.16	0.4	110	0.028	0.07	120
80	0.396	0.99	90	0.08	0.2	140	0.02	0.05	150
100	0.20	0.5	110	0.05	0.126	160	0.014	0.035	180
150	0.12	0.3	140	0.025	0.063				

The amplitude-phase characteristics given in Fig. 7 were constructed from the tabular data. It is clear from these characteristics that the application of an external load to the shaft of the controlling element's armature deforms the amplitude-phase characteristic by way of increasing the phase of the lag.

LITERATURE CITED

1. Yu. M. Pul'er, "Contactless electric executive and logometric mechanisms," Priborostroenie No. 1 (1957).
2. B. S. Sotskov, Fundamentals of Calculating and Designing Elements of Automatic and Remote Control Devices [in Russian] (Gosénergoizdat, 1953).
3. I. E. Dekabrun, Electromagnetic Polarized Relays and Transformers [in Russian] (Gosénergoizdat, 1959).

DIFFERENTIATION OF SLOWLY VARYING SIGNALS

S. N. Diligenskii

(Moscow)

Translated from Avtomatika i Telemekhanika, Vol. 21, No. 4, pp. 513-524, April, 1960
Original article submitted August 31, 1959

The paper considers methods of differentiating slowly varying electrical signals with respect to time, taking into account the nonlinearities inherent in actual devices, as well as methods of replacing the differentiation operation by a determination of the increments of the input quantity during fixed intervals of time.

Posing of the Problem

In the present work we consider methods for differentiating slowly varying signals with spectra from zero up to several cps. In such a frequency spectrum the signal derivative will be small, and the receiving devices will have finite sensitivities. Therefore, the differentiator must provide amplification of the signal derivative. On the other hand, for slowly varying signals, the inertia of the differentiator itself has a lower value.

It is convenient to open the investigation of possibilities of differentiating slowly varying signals by comparing the frequency characteristics of the corresponding differentiating device with the frequency characteristics of an ideal differentiator

$$\Phi_{id}(j\Omega) = T_{d.id}\, j\Omega,$$

where $T_{d.id}$ is the derivative coefficient (time constant) of the ideal differentiator and Ω is circular frequency.

On the basis of such a comparison one can establish, for the real differentiator, a working range of frequency characteristic in which its distortion will not exceed some established quantity. We adopt the convention in this work that the difference of the phase frequency characteristics of the ideal and the real differentiators $\Delta\varphi$ shall not exceed 20°, and that the ratio of the ordinates of the amplitude frequency characteristics lie within the limits of 0.8 to 1.2. The derivative coefficient T_d of the real differentiator is bounded. Therefore, in addition to the working range of the frequency characteristic, the magnitude of T_d for the given differentiator is determined.

All differentiating devices can be divided into two types: differentiators in which the operation of differentiation is modeled (analog differentiators) and differentiators in which the operation of differentiation is replaced by the determination of the increment of the input quantity during finite intervals of time (we agree to call such devices discrete differentiators). For the differentiation of slowly varying signals, discrete differentiators turn out to be competitive with analog differentiators.

Analog Differentiators

In this section we shall consider two basic types of electronic differentiators, designed for the differentiation of dc signals, and an electric differentiator in the form of a servosystem with proportional velocity control. The basic elements of electronic dc differentiators are RC circuits[*] and amplifiers. After determining the working range of the frequency characteristics in the linear treatment of these differentiators, one must take into account the effect of nonlinearities in the static characteristics of amplifiers and motors on the corresponding frequency characteristics.

Differentiation of ac signal envelopes by means of passive circuits is, due to large errors, efficacious only for rapidly varying signals (cf., for example, [1]).

A. Differentiator in the Form of a Differentiating RC Circuit with an Amplifier Connected at Its Output[†]

The transfer function of an inherently differentiating circuit with account taken of the impedance of the leakage condenser[‡] is written in the form

$$\frac{\bar{U}_{out}(p)}{\bar{U}_{in}(p)} = \frac{Tp + R/R_{le}}{Tp + 1 + R/R_{le}}, \tag{1}$$

where T = RC is the time constant (coinciding with the derivative coefficient when the amplifier is not connected in), R/R_{le} is the ratio of the circuit's active impedance to the impedance of the leakage condenser, $\bar{U}_{in}(p)$ and $\bar{U}_{out}(p)$ are the transforms of the input and output voltages, respectively.

In Fig. 1 there are constructed the relative amplitude and the phase frequency characteristics. The upper boundary of the working range of the frequency characteristics is due to the presence in (1) of the aperiodic link (in accordance with the conditions adopted earlier for the phase frequency characteristic, $(\Omega T)_{max} = 1$). The lower boundary of the working range is due to the static term in the ampli-

---

[*] In differentiating slowly varying signals, an RC circuit is more convenient than an RL circuit since, by means of an RC circuit, one can easily obtain a larger time constant for a lower sensitivity to noise.

[†] An RC differentiator is described, for example, in [2].

[‡] To increase the time constant one uses a condenser with a large capacity, in which the leakage impedance can be commensurable with R.

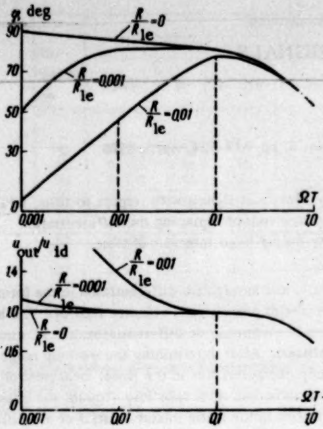

Fig. 1. Phase frequency and relative amplitude frequency characteristics of a differentiating RC link.

fier's transfer function. With this, the magnitude of $(\Omega T)_{min}$, as is clear from the phase frequency characteristics constructed for various R/R_{le}, decreases proportionately to the decrease in R/R_{le}. However, for each type of condenser there exists an absolute magnitude of Ω_{min} which depends only on the coefficient of impedance of the leakage condenser $k_{le} = R_{le}C$.

By substituting $C = k_{le}/R_{le}$ in (1) we obtain

$$\frac{\overline{U}_{out}(p)}{\overline{U}_{in}(p)} = \frac{R/R_{le}(k_{le}p+1)}{R/R_{le}k_{le}p+1+R/R_{le}}. \tag{2}$$

It is clear from (2) that, for low frequencies, the effect of the static term on the transfer function depends only on the magnitude of k_{le}. For example, for $\Delta\varphi = 20°$ and $k_{le} = 3000$ μf·meg, $\Omega_{min} = 0.001$ cps.

It is clear from (1) that the differentiating circuit's time constant coincides with the derivative coefficient. To increase this latter, we connect an amplifier to the differentiating circuit's output.

If we assume that the amplifier has a linear static characteristic, then the derivative coefficient is increased by a factor of $\underline{k}$, where $\underline{k}$ is the amplifier's gain**.

The size of $\underline{k}$ is limited by the increase, at the amplifier's output, of parasitic signals due to internal noise, and also by the decrease in range of variation of the input signal corresponding to the linear portion of the amplifier's static characteristic.

The effect of internal noise on the working range of the frequency characteristic can be estimated by the ratio y_p of the parasitic signal u_p††, as a fraction of the input signal, to the maximum value of the useful signal during one period (for $u_{in}(t) = B \sin \Omega t$):

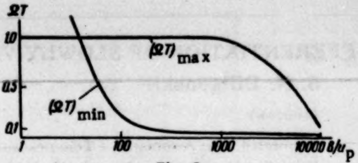

Fig. 2.

$$y_p = \frac{u_p}{B}\frac{1}{\Omega T}. \tag{3}$$

where B is the amplitude of the input signal.

On the other hand, for operation on the linear portion of the amplifier's static characteristic, it is necessary that the following inequality hold for $u_{in.1}$

$$B\Omega T \leqslant u_{in.1}. \tag{4}$$

The aforementioned peculiarities of amplifier operatio will not affect differentiator operation if, in the given frequency range, as B varies within given limits, y_p remains much less than unity and satisfies (4). Figure 2 shows the graphs constructed for $(\Omega T)_{min} = f_I(B/u_p)$ and $(\Omega T)_{max} = f_I(B/u_p)$ for $y_p = 0.05$ and $u_{in.1}/u_{lp} = 1000$ (for k = 1000). It is clear from these graphs that, because of the limitation on the magnitude of $(\Omega T)_{min}$ and the limits of variation of the input signal's amplitude, one can increase the derivative coefficient only by a factor of 1000.

B. Differentiator in the Form of an Amplifier with Aperiodic Feedback

This differentiating device consists of an amplifier, shunted by an aperiodic feedback path, and a subtraction block in which the input signal is subtracted from the amplifier's output signal (Fig. 3). The subtraction block is included so as to eliminate dc components from the amplifier's output signal. If the amplifier's characteristics

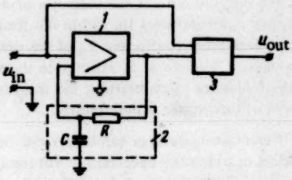

Fig. 3. Block schematic of a differentiator in the form of an amplifier with aperiodic feedback. 1 is the amplifier, 2 is the aperiodic feedback link, and 3 is the subtraction block.

**It is assumed that the amplifier's input impedance is much greater than the RC circuit's output impedance.

†† We understand by u_p an averaged value of the parasitic signal, the magnitude of which depends on the amplifier circuit.

are assumed to be linear, then the transfer function of such a system will have the form

$$\frac{\overline{U}_{\text{out}}(p)}{\overline{U}_{\text{in}}(p)} =$$

$$= \frac{(1+k_1)k}{(k+k_1+k)}\left(\frac{T}{1+k_1}p+1\right)\frac{1}{\frac{Tp}{k+k_1+1}+1} - 1, \qquad (5)$$

where $k_1 = R/R_{\text{in.a}}$ and $R_{\text{in.a}}$ is the amplifier's input impedance.

From (5) one may show that, to eliminate the dc component from u_{out}, k and k_1 must satisfy the relationship

$$k_1 = \frac{1}{k-1}. \qquad (6)$$

By substituting k_1 from (6) in (5), we get

$$\frac{\overline{U}_{\text{out}}(p)}{\overline{U}_{\text{in}}(p)} = \frac{(k-1)^2}{k^2}\,Tp\left(\frac{Tp}{k+k/(k-1)}+1\right)^{-1} \qquad (7)$$

Figure 4 gives the amplitude and phase frequency characteristics of the system. It is clear from these graphs that, as k increases, the magnitude of $(\Omega T)_{\max}$ increases. However, in the given case, the derivative coefficient equals the time constant of the RC circuit. From the expressions $k_1 = R/R_{\text{in.a}}$, $k_1 = 1/(k-1)$, and $T = RC$ for $k \gg 1$, we can obtain

$$T \approx \frac{R_{\text{in. a}}}{k}C. \qquad (8)$$

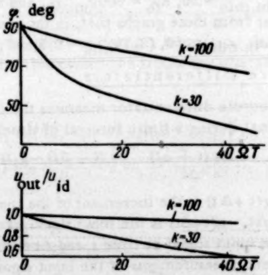

Fig. 4. Phase frequency and relative amplitude frequency characteristics of the differentiator in the form of an amplifier with aperiodic feedback.

Thus, as k increases, T decreases. This decrease can be compensated by increasing the capacity of the condenser until R_{1e} becomes commensurable with $R_{\text{in.a}}$. In practice, even for an amplifier with $R_{\text{in.a}}$ = 10 meg, for k = 100 and C = 500 μf, T = 50 sec. Thus, in a linear system there is a limitation on the size of T_p. From whence, the magnitude of $(\Omega T)_{\max}$ in practice equals 40.

In a linear system no limitation on $(\Omega T)_{\min}$ was obtained, since the dc component due to the condenser leakage was compensated here in the subtraction block. However, in practice the subtraction block has a finite accuracy in implementing the operation of subtraction. We assume that the error with this comprises 0.1% of the dc component of u_{in} ‡‡. As in the previous case, we define the ratio

$$y_s = \frac{0.001}{\Omega T}. \qquad (9)$$

If, as before, we set $y_s = 0.05$, we get that $(\Omega T)_{\min} = 0.02$.

The upper boundary of the working range does not depend on the amplitude of the input signal if $u_{\text{in,1}}/B \geq 1$, where this holds for any frequency***.

C. Servosystem with Proportional Velocity Control as a Differentiating Device

The simplified schematic of the servosystem with proportional velocity control is shown in Fig. 5a. The system consists of electronic amplifier 1, low-power motor 2 controlled by the electronic amplifier, reducer 3, and feedback position transducer 4. In a first approximation, we assume that all links of the system have linear characteristics, and that the time constants of the amplifier and motor may be neglected †††. We write the equations of such a system in the form:

$$u_{\text{m}} = k_{\text{a}}\varepsilon. \qquad (10)$$

$$v = k_{\text{m}}u_{\text{m}} \qquad (11)$$

$$v_{\text{r}} = \frac{v}{k_{\text{r}}}. \qquad (12)$$

$$\overline{U}_{\text{fb}}(p) = k_{\text{fb}}\frac{\overline{V}_{\text{r}}(p)}{p}. \qquad (13)$$

$$\varepsilon = u_{\text{in}} - u_{\text{fb}} \qquad (14)$$

where ϵ is the error signal, u_d is the voltage on the control winding, v is the motor speed prior to the reducer, v_r is the motor speed after the reducer, $\overline{V}_r(p)$ is the transform of v_r, $\overline{U}_{\text{fb}}(p)$ is the transform of the feedback position voltage, u_{in} is the input signal voltage, k_a is the amplifier gain, k_r is the reduction factor, k_{fb} is the position feedback gain, showing the change in u_{fb} for one rotation.

From (10)-(14) we obtain

$$\frac{\overline{V}(p)}{k_{\text{a}}k_{\text{m}}} = \frac{Tp}{Tp+1}\overline{U}_{\text{in}}(p), \qquad (15)$$

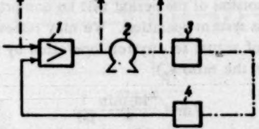

Fig. 5a.

---

‡‡ It is obvious that, for k = 100, the amplifier's background noise will be less than the error from subtraction.

*** This can be verified by defining the signal at the amplifier's input as the difference between $u_{\text{in}} = B\sin\Omega t$ and the feedback signal.

††† The permissibility of this last assumption will be explained below.

where $\bar{U}_{in}(p)$ is the transform of $u_{in}(t)$, $\bar{V}(p)$ is the transform of $v(t)$ and $T = k_r/k_a k_m k_{fb}$.

Expression (15) coincides in form with (1) for the case when $R/R_{1e} = 0$. For the measurement of slowly varying signals, as was established earlier, the value of T should be chosen large (for $R/R_{1e} = 0$). Therefore, for low-power motors, the coefficient $k_r/k_a k_m k_{fb}$ will be larger than the electrical and electromechanical time constants; the working range of frequency characteristics can be found from Fig. 1 (for $R/R_{1e} = 0$, $(\Omega T)_{min} = 0$, $(\Omega T)_{max} \approx 1$).

As the servosystem's output signal, one may use ϵ, u_m, and $\underline{v}$ (a voltage proportional to $\underline{v}$). Measurement of ϵ is equivalent to the case of a passive RC network with an ideal capacitor, while measurement of u_m and $\underline{v}$ is equivalent to the case when an amplifier is connected at the output of the RC network.

The dynamics of the actual servosystem differ from those of the linear system principally because of the nonlinearities of the static motor characteristics and free play in the reducer. It was shown in [3] that the function $v = F(u_m)$ for low-power asynchronous motors has the form

$$\frac{v}{v_{max}} = \frac{2\,\dfrac{u_m - u_{st}}{u_{m.\,max}}}{1 + \dfrac{u_m - u_{st}}{u_{m.\,max}}} \qquad (16)$$

where v_{max} is the maximum motor speed, $u_{m.max}$ is the maximum voltage on the control winding, u_{st} is the voltage corresponding to starting.

For $u_m \ll u_{m.max}$, (16) can be approximated by (11). As shown by experiments, (16) is valid as u_m varies within the limits of $u_{m.min} \leq u_m \leq u_{m.max}$. By $u_{m.min}$ we understand a quantity somewhat larger than u_{st}. The starting voltage is determined by the starting torque, which depends on the load on the motor shaft. The load torque, in its turn, depends on the friction in the bearings, which is not a strictly constant quantity. Therefore, the motor shaft can turn continuously, starting with some velocity v_{min} which we agree to call the minimum velocity of continuous rotation.

If the voltage on the motor winding lies within the limits of $u_{st} \leq u_m \leq u_{m.min}$ there then occurs a discontinuous mode of motor operation. For $u_{in} = B \sin \Omega T$, a definite portion of the period will be comprised of discontinuous system operation. We may reflect this idiosyncrasy of actual servosystem operation by the ratio y_m (similar to the ratio y_p):

$$y_m = \frac{u_{in.\,min}}{B} \frac{1}{\Omega T} \qquad (17)$$

where $u_{in.min}$ is the voltage at the amplifier input which corresponds to $v_{m.min}$; (17) is analogous in form to (3) but, in practice, $u_{in.min}$ is significantly larger than u_p.

For input signals with shallow slopes, the free play in the reducer manifests itself in the servosystem. Because of the presence of the free play, as the sign of the slope of $u_{in}(t)$ changes, the speed of the motor will not correspond to the slope of the input signal during the time that the free play is being taken up. It can be shown (cf. Appendix 1) that the ratio of the motor speed at the moment when the free play has been taken up to the maximum speed during the period (for $u_{in}(t) = B \sin \Omega t$) equals

$$y_f = 1.65 \left(\frac{m_f k_{fb}}{B}\right)^{\frac{2}{3}} \frac{1}{\sqrt[3]{\Omega T}} \qquad (18)$$

where m_f is the free play in the first stage of the reducer.

The upper limit to the working range can be given in the form of (4), where by $u_{in.1}$ we shall understand u_{in} corresponding to the boundary of approximation of nonlinear relationship (16) by the linear static characteristic of (11).

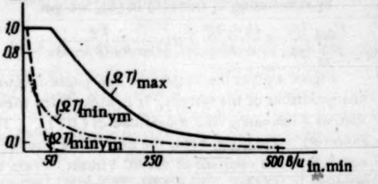

Fig. 5b.

Figure 5b shows the curves constructed for $(\Omega T)_{min}$[‡‡‡] and $(\Omega T)_{max}$ as functions of $B/u_{in.min}$ for $y_m = y_f = 0.05$, $u_{in.1}/u_{in.min} = 50$, $k_{fb} = 500 u_{in.min}$ and $m_f = 0.0001$. It is clear from these graphs that, in the range $20 \leq B/u_{in.min} \leq 50$, $(\Omega T)_{min} \approx 0.5$ and $(\Omega T)_{max} \approx 1$.

Discrete Differentiators

A discrete differentiator measures the increment of the input signal during a finite interval of time:

$$\frac{\Delta g(t + \Delta t)}{\Delta t} = \frac{g(t + \Delta t) - g(t)}{\Delta t}. \qquad (19)$$

where $\Delta g(t + \Delta t)$ is the increment of the input signal at time $t + \Delta t$, $g(t + \Delta t)$ is the input signal at time $t + \Delta t$, $g(t)$ is the input signal at time $\underline{t}$, and Δt is the time interval between measurements of the input signal.

A discrete differentiator may be constructed either on the principle of quantized input signal $g(t)$ or on the principle of quantized time. In measuring the speed of change of a slowly varying input signal, Δg will be small, so that it is more convenient in practice to use the second principle (the value of Δt can be chosen arbitrarily).

The dynamic characteristics of discrete differentiators[1] depend on the method of measuring the increments of the input signal. One can cite two basic methods of measuring Δg:

[‡‡‡] In correspondence with (17) and (18), two curves are given for $(\Omega\ T)_{min}$. For a given value of $B/u_{in.min}$, the lower boundary of the frequency characteristic corresponds to the larger ordinate.

[1] It is understood that we are speaking of discrete differentiators with quantized time.

1. Comparison of the instantaneous values of $g(t+\tau)$ and $g(t)$, where τ is a fixed interval between two measurements [cf. (19)].

In (19) we replace the continuous argument t by the discrete argument $n\tau$ (n corresponds to the moments at which Δg is measured). Then, letting $g(t) = B \sin \Omega t$, we obtain

$$\frac{\Delta g_1(n\tau+\tau)}{B\tau} = \frac{1}{\tau}\left[\sin \Omega (n+1)\tau - \sin \Omega n\tau\right]. \quad (20)$$

By transforming (20), we find that

$$\frac{\Delta g_1(n\tau+\tau)}{B\tau} = \frac{2}{\tau}\sin\frac{\Omega\tau}{2}\cos\left(\Omega n\tau+\frac{\Omega\tau}{2}\right). \quad (21)$$

Expression (21) can be considered as the system's frequency characteristic for a discrete argument. This means physically that (21) shows the difference $\Delta g_1/B\tau$ from the ideal derivative only for the moments of time $n\tau$. The relative amplitude and phase frequency characteristics are given in Fig. 6 (curve 1). As the argument of the frequency characteristics, we have here chosen $\Omega\tau$. It is clear from these graphs that the working range of relative values of $\Omega\tau$ has just the upper boundary of $(\Omega\tau)_{max} \approx 0.6$.

2. Comparison of the results of integrating the input signal over the intervals of time $[t, t+\tau]$ and $[t+\tau, t+2\tau]$, respectively:

$$\frac{\Delta g_2}{B\tau} = \frac{1}{\tau}\left[\int_{t+\tau}^{t+2\tau} g(t)\,dt - \int_{t}^{t+\tau} g(t)\,dt\right]. \quad (22)$$

As in the previous case, it is assumed that $g(t)$ varies sinusoidally. We obtain the frequency characteristic in the form

$$\frac{\Delta g_2(\varphi+2\Omega\tau)}{B\tau} = \frac{4}{\Omega\tau}\sin^2\frac{\Omega\tau}{2}\cos(\varphi+\Omega\tau), \quad (23)$$

where φ is the current value of the argument (analogous to $n\tau$ in number 1 above).

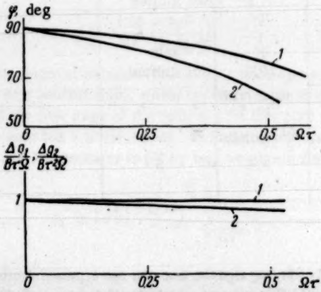

Fig. 6. Phase frequency and relative amplitude frequency characteristics of discrete differentiators. 1 is for a discrete differentiator of the first type, 2 is for a discrete differentiator of the second type.

The relative amplitude and phase frequency characteristics are given in Fig. 6 (curve 2)[2]. It is clear from them that the upper boundary of the working range has been lowered, and that $(\Omega\tau)_{max} \approx 0.45$.

It is clear from (21) and (23) that the derivative coefficient (for small $\Omega\tau$) equals, respectively, 1 and τ[3]. In the first case, T_d can be increased only by connecting an amplifier at the output of the discrete differentiator and, in the second case, at the cost of increasing τ. However, connecting an amplifier reduces the working range (cf. above), and increasing τ decreases Ω_{max} (Fig. 6). Moreover, implementing the necessary operations to determine increments on the basis of analog technology leads to large errors. For example, in the discrete differentiators described in [4-6], there will be large dc components at the output due to the nonideal nature of the elements. The transition to digital technology, as will be shown below, retains the working range of the frequency characteristics with an arbitrarily large derivative coefficient.

We consider a discrete digital differentiator. To measure the results of integrations over the interval τ, it is convenient to present the input signal $g(t)$ in the form of frequencies of trains of pulses (pulse-frequency modulation):

$$f(t) = f_0 + lg(t), \quad (24)$$

where f_0 is the minimum frequency, corresponding to $f(t) = 0$, and is the slope of the analog-digital transformation[4].

Figure 7 shows the block schematic of a discrete digital differentiator. The transformation corresponding to (24) is implemented in device 1. As a reversible counter for the differentiation of slowly varying signals, one may use the low-power pulsed step-by-step motor 2. In switching phase, the rotor of such a motor is rotated by one and the same angle $\Delta\varphi$. The use of a pulsed motor, in addition to simplifying the counter scheme, permits the implementation of a digital-analog transformation by means of inductive transducer 3. The intervals of addition and subtraction are given by synchronous motor 4. The control scheme in 5 provides: a) switching of motor phase

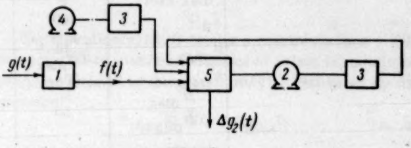

Fig. 7.

---

[2] In Fig. 6, the relative amplitude frequency characteristic was constructed in the dimensionless units $\Delta g_2/B\tau^2\Omega$ instead of $\Delta g_2/B\tau\Omega$.

[3] One can convince oneself of this by expanding $\sin(\Omega\tau/2)$ in a series and retaining just the first term of the expansion.

[4] Such a transformation can be implemented either by means of a special device or by the use of transducers with digital outputs.

with frequency $f(t)$; b) reversal of the direction of phase switching upon transition from addition to subtraction; c) transmission to the differentiator's output of the measured increment of the input signal; d) reset of the system to its initial state.

We now consider what the conditions are which must be satisfied by the digital differentiator's parameters in order to provide the necessary working range of the frequency characteristic (Ω_{min} to Ω_{max}).

The integration time τ can be found, for a given upper boundary of the working range of the frequency characteristic, from the phase frequency characteristic of an ideal discrete differentiator in which $(\Omega\tau)_{max}$ equals 0.45 (Fig. 6, curve 2):

$$\tau = \frac{0.45}{\Omega_{max}}. \qquad (25)$$

In a digital system, Δg will be expressed in the form of some number m of pulses. The general expression for m, as well as the expressions for m_{min} and m_{max} for a given frequency Ω and amplitude B in the case of a sinusoidal input signal, are derived in Appendix 2. The quantity m_{min} characterizes the minimum accuracy in measuring Δg over one period of signal variation. By considering m_{min} to be a given quantity, we obtain from (A.10), after substituting the value of τ from (25), $\Omega = \Omega_{min}$ and $B = B_{min}$, the expression for

$$l = \frac{8m_{min}}{B_{min}}\Omega_{max}\left(\frac{\Omega_{max}}{\Omega_{min}}\right)^2. \qquad (26)$$

With this, the maximum number of pulses necessary to make the transformation from digital form to analog will equal, on the basis of (A.11), $m_{max} = (2B_{max}/B_{min}) \times m_{min}(\Omega_{max}/\Omega_{min})^2$.

Finally, by taking into account the optimal relationship between f_0 and IB(cf., Appendix 2), we find from (A.12) the expression for the maximum capacity of the counter:

$$n_{max} = \frac{8B_{max}}{B_{min}}m_{min}\left(\frac{\Omega_{max}}{\Omega_{min}}\right)^2.$$

Of all the parameters of the digital differentiator, it is the quantity m_{max} which may be limited in practice since, with increasing m_{max} for a given type of digital differentiator, there is a decrease in the magnitude of $\Delta\varphi$ which, in practice, has a lower limit. Therefore, for given m_{min} and m_{max}, a digital differentiator has a bounded working range. For example, $\Omega_{max}/\Omega_{min} = 22$ for $m_{min} = 3$, $m_{max} = 10{,}000$ and $B_{max}/B_{min} = 5$.

In contradistinction to the second type of discrete differentiator which was considered earlier, in the given digital differentiator T_d depends, not only on τ, but also on the proportionality factor between the angle of rotation of the transducer's shaft and the change in voltage at the output of the induction transducer. Here, the proportionality factor does not depend on the working range, and T_d may in fact be made as large as desired.

Comparison of Dynamic Characteristics of Differentiating Devices

The results of a comparison of the three types of analog differentiating devices and the digital discrete differentiator are presented in the following table

	RC network plus ampl.	Ampl. with aperiodic feedback:	Servo system	Digital differentiator
Ω_{min} 1/sec	0,001	0.001	$\frac{0.4}{T}$	Not limited
Ω_{max} 1/sec	$\frac{1}{T}$	0.8	$\frac{1}{T}$	20 Ω_{min}
T_d/T	1000	100	1000	Not limited
B_{max}	$\frac{u_{in.1}}{\Omega T_{max}}$	$u_{in.1}$	$u_{in.1}$	" "
B_{min}	$20u_p$	$20\ u_p$	$20\ u_{in.min}$	" "
$\frac{B_{max}}{B_{min}}$	50	50	2.5	5

It is clear from the table that only the servosystem and discrete digital type differentiators have no limit on the smallness of the quantity Ω_{min}. In the digital differentiator, moreover, the derivative coefficient can be made arbitrarily large. The sole superior feature of the analog differentiator is its greater simplicity vis-a-vis the digital system. However, for the differentiation of slowly varying signals, one can use a pulsed motor in the digital differentiator, which significantly simplifies the entire system.

Summary

Analog differentiating devices with large working ranges (an amplifier at the output of an RC network, or an amplifier with aperiodic feedback) have a limited magnitude of Ω_{min} and of the derivative coefficient. In an electromagnetic differentiator, the quantity Ω_{min} can be made arbitrarily small, and $\Omega_{max}/\Omega_{min}$ can be made less than in electronic differentiators, but the derivative coefficient is of the same order of magnitude.

It is advantageous to construct discrete differentiators in the form of digital systems. A digital differentiator permits one to have an arbitrarily small value of Ω_{min} and an arbitrarily large derivative coefficient.

Appendix 1

For simplicity of computation, we assume that the motor characteristic $v = F(u_m)$ is linear. The free play in the reducer manifests itself when the sign of the input signal's slope changes. We now determine the motor speed at the moment when the free play has all been taken up, given a sinusoidal input signal:

$$v_f = k_a k_m B(1 - \cos \Omega t_f) \approx k_a k_m B \frac{\Omega_f^2 t_f^2}{2}, \qquad (A.1)$$

where v_f is the motor speed at the moment when the free play has all been taken up. Knowing the shaft rotation angle φ_f corresponding to taking up of the free play for a given reducer transfer number, we can, by integrating (A.1) and solving the resulting equation for t_f, determine this quantity in the form

$$t_f = \sqrt[3]{\frac{6\varphi_f}{k_y k_f B\Omega^2}}. \qquad (A.2)$$

By substituting (2) in (1), we find the expression for v_f in terms of φ_f:

$$v_f = k_a k_m B \cdot 1{,}65 \left(\frac{\varphi_f \Omega}{k_y k_m B}\right)^{\frac{2}{3}} \qquad (A.3)$$

We now find the ratio of the maximum speed during one period at a given frequency to the velocity v_f:

$$y_f = \frac{1.65}{\Omega T}\left(\frac{\varphi_f \Omega}{k_a k_m B}\right)^{\frac{2}{3}} \qquad (A.4)$$

The angle of rotation for free play take-up can be presented as a product $m_f k_r$, where m_f corresponds to the free play in the first stage of the reducer (the free play in the other stages has a lower value). By multiplying the numerator and denominator in (4) by k_{fb}, we obtain finally

$$y_f = 1.65\left(\frac{m_f k_{fb}}{B}\right)^{\frac{2}{3}} \frac{1}{\sqrt[3]{\Omega T}}. \qquad (A.5)$$

Appendix 2

The length of the period between two neighboring pulses for a sinusoidal input signal with arbitrary initial phase $\varphi\,[g(t) = B\sin(\Omega t + \varphi)]$ is defined by the equation

$$\int_0^{T_i} [f_0 + lB\sin(\Omega t + \varphi)]\,dt = 1, \qquad (A.6)$$

where T_i is the length of the ith period.

By integrating (A.6) we get

$$f_0 T_i - \frac{lB}{\Omega}\cos(\Omega T_i + \varphi) + \frac{l}{\Omega}\cos\varphi = 1.$$

We now find the expression defining the number $\underline{n}$ of accumulated pulses during the interval $[\varphi, \varphi + \tau]$:

$$f_0 T_1 - \frac{lB}{\Omega}\cos(\Omega T_1 + \varphi) + \frac{lB}{\Omega}\cos\varphi = 1,$$

$$f_0 T_2 - \frac{lB}{\Omega}\cos(\Omega T_1 + \Omega T_2 + \varphi) + \frac{lB}{\Omega}\cos(\varphi + \Omega T_1) = 1, \qquad (A.7)$$

. . . .

$$f_0 T_n - \frac{lB}{\Omega}\cos(\Omega T_1 + \ldots + \Omega T_n + \varphi)$$

$$+ \frac{lB}{\Omega}\cos(\varphi + \Omega T_1 + \ldots + \Omega T_{n-1}) = 1,$$

$$f_0 \sum_i^n T_i - \frac{lB}{\Omega}\cos\left(\Omega\sum_i^n T_i + \varphi\right) + \frac{lB}{\Omega}\cos\varphi = n,$$

$$f_0 \tau - \frac{lB}{\Omega}\cos(\Omega\tau + \varphi) + \frac{lB}{\Omega}\cos\varphi = n.$$

One may show analogously that, during the interval $[\varphi + \tau, \varphi + 2\tau]$, there will, in the general case, be accumulated $(n + m)$ pulses:

$$f_0 \tau - \frac{lB}{\Omega}\cos(2\Omega\tau + \varphi) + \frac{lB}{\Omega}\cos(\varphi + \Omega\tau) = n + m. \qquad (A.8)$$

By subtracting (A.7) from (A.8), we get

$$m = \frac{lB}{\Omega}\,[2\cos(\Omega\tau + \varphi) - \cos(2\Omega\tau + \varphi) - \cos\varphi]. \qquad (A.9)$$

For $\varphi = 3\pi/2$, the number $\underline{m}$ is a minimum:

$$m_{min} = \frac{4lB}{\Omega}\sin^2\frac{\Omega\tau}{2}\sin\Omega\tau \approx lB\tau(\Omega\tau)^2. \qquad (A.10)$$

For $\varphi = \pi$, $\underline{m}$ is maximum. The approximate maximum value of $\underline{m}$ is

$$m_{max} \approx lB\tau(\Omega\tau). \qquad (A.11)$$

Correspondingly, (A.7) attains a maximum for $\varphi = \pi/2$. The approximate maximum number of pulses accumulated during one interval of integration may be estimated by the expression

$$n_{max} \approx \tau(f_0 + B_{max} l). \qquad (A.12)$$

The counter will be used optimally if, for a given $\underline{n}$, the quantity m_{min} is maximal. It can be shown that the ratio m_{min}/n, found from (A.10) and (A.7), will be maximal as $lB/f_0 \to 1$.

LITERATURE CITED

1. D. E. Polonnikov and Yu. N. Bogolyubov, "The AUS electronic differentiator," Otchet IAT AN SSSR (1954)
2. N. I. Davydov, "Electronic differentiator," Priborostroenie No. 2 (1958).

3. Yu. S. Chechet, Controlled Asychronous Motors with Tubular Rotors [in Russian] (Gosenergoizdat, 1955).
4. D. G. Scorgie, "Lead networks utilizing a saturable core memory," Appli. and Ind. 71, No. 18 (1952).
5. F. A. Grigoryan, "Four-terminal network with rectifiers for obtaining ac voltage envelopes and recording motor shaft rotational speed," Izvest. Akad. Nauk. Arm. SSR 9, No. 8 (1956).
6. K. S. Zaitsev, "New type of broad-band ac differentiator for automatic control systems," Avtomatika No. 4 (1957),

CHOICE OF FREQUENCY RANGE FOR INDUSTRIAL PULSE-FREQUENCY TELEMETRY SYSTEM DEVICES

A. M. Pshenichnikov

(Moscow)

Translated from Avtomatika i Telemekhanika, Vol. 21, No. 4, pp. 525-529, April, 1960
Original article submitted November 17, 1959

The paper considers the effect of frequency range of pulse-frequency telemetry system devices on the errors and noise resistance of transmission, speed of action, and receiver dynamics.

The following factors influence the choice of frequency range of pulse-frequency telemetry system devices:

1) telemetry error as a function of frequency range;

2) noise resistance of signal transmission along the communications channel, and the effect of noise from the 50 cps power supply;

3) indicating instrument dynamics and speed of system action;

4) bandwidth of the secondary channel.

1. Telemetry Error as a Function of Frequency Range

As a function of the ratio of the frequencies which correspond to zero value and to the nominal value of the measured parameter, the error α in transforming this parameter to a proportional frequency in the transmitter gives rise to the telemetry error [1]

$$\alpha_{te} = \frac{\alpha}{1 - f_0/f_N}. \quad (1)$$

where f_0 and f_N are the frequencies corresponding to the zero value and to the nominal value, respectively, of the parameter being measured.

Analogously, the error β arising in the receiver when the frequency is transformed to a proportional current gives rise to the error

$$\beta_{te} = \frac{\beta}{1 - f_0/f_N}. \quad (2)$$

The ratio of the errors is

$$\frac{\alpha_{te}}{\alpha} = \frac{\beta_{te}}{\beta} = \frac{1}{1 - f_0/f_N}. \quad (3)$$

The figure shows the relationship of the ratio of errors, α_{te}/α or β_{te}/β, to f_0/f_N. As is obvious from (3) and from the graphs on the figure, the telemetering error decreases as the ratio f_0/f_N decreases.

2. Noise Resistance of Signal Transmission along the Communications Channel and the Effect of Noise from the 50 cps Power Supply

With weak fluctuation noise, the error is determined by the distortion of the pulse edges of the transmitted signals. This error, as a rule, is a very small quantity.

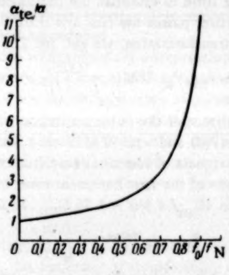

Dependence of the ratio of the telemetering errors to the ratio of the frequencies corresponding to the zero value and to the nominal value of the parameter being measured.

An analysis of the noise resistance of telemetry signal transmission along a channel with weak fluctuation noise, based on the theory of potential noise resistance, was made by V. A. Kashirin and G. A. Shastova [2]. However, in considering pulse-frequency modulation with a constant mark-space ratio PFM II, the authors of [2] analyzed the transmission of triangular pulses with amplitude $2U_m$. The transmission of triangular pulses negates all the advantages of PFM II, and does not correspond to actual conditions.

The noise resistance of PFM II to fluctuation noise can be determined by expanding rectangular pulses in a Fourier series. The pulse frequency in PFM II can be presented in the following manner as a function of the measured parameter λ:

$$f(\lambda) = f_i + \frac{\Delta f}{2}\lambda, \quad (4)$$

where f_i is the mean pulse frequency, and $\Delta f/2 = (f_N - f_0)/2$ is the frequency deviation.

The expression for a rectangular signal of amplitude $2U_m$, after expansion in a Fourier series, can be written in the form

$$A(\lambda, t) = U_m + \frac{4U_m}{\pi}\left[\sin 2\pi\left(f_1 + \frac{\Delta f}{2}\lambda\right)t + \right. \tag{5}$$

$$\left. + \frac{1}{3}\sin 6\pi\left(f_1 + \frac{\Delta f}{2}\lambda\right)t + \dots\right].$$

The mean square error in transmitting the parameter λ_0 due to fluctuation noise is defined by the expression [2]

$$\delta_{\text{me. sq}}(\lambda) = \frac{\sigma}{2\sqrt{2}\sqrt{\int\limits_0^T \left[\frac{\partial A(\lambda, t)}{\partial\lambda}\right]^2_{\lambda=\lambda_0} dt}}, \tag{6}$$

where σ is the specific intensity of the noise in $v(\text{cps})^{1/2}$ and T is the time to establish the indication.

If the filter passes the first and third harmonics then, after some transformation, we get, for $T \gg 2\pi/f_1$,

$$\delta_{\text{me. sq}}\,\text{PFM} = \frac{0.186\,\sigma}{U_m \Delta f T^{3/2}}. \tag{7}$$

Comparisons of the noise resistance with frequency modulation (FM) and with PFM II must necessarily be carried out for signals of identical amplitudes. With this, the amplitude of the first harmonic must be considered equal, not to $4U_m/\pi$ but $\sim 1.15\ U_m$. In this case,

$$\delta_{\text{me. sq}}\,\text{PFM} = \frac{0.22\,\sigma}{U_m \Delta f T^{3/2}}. \tag{8}$$

For the same amplitude, the error with FM is (cf., [2])

$$\delta_{\text{me. sq}}\,\text{FM} = \frac{0.28\,\sigma}{U_m \Delta f T^{3/2}}. \tag{9}$$

Consequently, if the use of filters provides transmission of the first and third harmonics, with PFM II, then with this the mean square error from fluctuation noise will be less than with FM with filters of the same passband. Low-frequency pulse-frequency systems for transmitting first and third harmonics require the same (and sometimes a smaller) frequency range than the existing frequency telemetry systems.

N. V. Pozin [3] carried out a determination of the error with PFM due to the relatively strong noise when the basic signal distortions are due to the breakdown into pulses and pauses, formulas being derived for approximate determinations of the mean and the mean square errors as functions of the probability of a unit distortion, the filter passband $2F_{pb}$, the frequencies corresponding to the zero and nominal values of the measured parameter, and the establishment time of the indicating instrument:

$$\delta_{\text{me}} = \frac{2P}{\Delta f^2}\left[\left(\frac{F_{pb}}{2} - f_0\right)^2 - \left(f_N - \frac{F_{pb}}{2}\right)^2\right], \tag{10}$$

$$\delta_{\text{me. sq}} = \sqrt{\frac{2P}{T\Delta f^3}\left[\left(\frac{F_{pb}}{2} - f_0\right)^2 - \left(f_N - \frac{F_{pb}}{2}\right)^2\right]}, \tag{11}$$

where P is the probability of unit distortion.

The minus sign between the parenthetical expressions in (10) and (11) is due to the fact that, with PFM II, the subcarrier frequency filter must pass at least the third harmonic and, consequently, $F_{pb} \geq 3 f_N$. This latter determines the choice of the frequency range for PFM II. Otherwise, the probability of unit distortion would not be the same for all pulse durations, as was assumed [3] in the derivation of (10) and (11).

The table gives the results of computing δ_{me} and $\delta_{\text{me.sq}}$ for the telemetry devices of the pulse-frequency devices of TsLEM Mosenergo, IAT AN SSSR and TsNIIKA for operation with filters of passbands of 40 cps (developed by IAT AN SSSR), 80 and 140 cps (telegraph filters), starting from the assumption that the formulas for determining δ_{me} and $\delta_{\text{me.sq}}$, to a first approximation, reproduce the state of affairs when the transition is made from PFM II to FM [3].

In the table, P_{40}, P_{80}, and P_{140} denote, respectively, the probability of unit signal distortion for filter passbands of 40, 80, and 140 cps, with identical signal voltages in all cases.

It is clear from the tabulated data that, for the standard telegraph filters, the very best frequency range of those considered is the range from 4 to 20 cps.

In addition to the considerations already mentioned, the noise from the 50 cps power supply (line) has an effect on the choice of frequency range for the devices of frequency and pulse-frequency telemetry systems. The presence of the frequencies of 25, 50, and 100 cps in the frequency range leads to a strengthening of the effect of noise from the power supply on the operation of the receiving device in the neighborhood of the points cited. In the transmission of the telemetered quantity at a frequency of 25 cps there appears, at the receiving side after some nonlinear transformations, a component of the first harmonic of the industrial frequency (50 cps) which is essentially influenced by the power supply.

Since it is desirable to have the ratio f_0/f_N as low as possible, so as to provide accuracy of transmission, one should choose, for the devices of pulse-frequency telemetry systems, a nominal frequency less than 25 cps. If one takes into account the possible oscillations of the line frequency (under trouble conditions, the frequency in energy systems falls to 46 cps) and the fact that, in using standard telegraph filters with 140 cps pass bands, it is desirable to transmit the third harmonic, then one should take, as the very best nominal frequency, one approximately equal to 20 cps.

3. Dynamics of the Indicating Instrument and the System's Speed of Action

The least (zero) frequency of teletransmission is determined by the highest frequency of variation of the measured parameter, F_m, and, for analog reception, by the indicating instrument dynamics. Since industrial telemetry devices are used, basically, for the measurement of relatively slowly flowing processes, the condition

$$f_0 \geqslant 2F_m, \tag{12}$$

Error	Filter pass-band, cps	Frequency range		
		$f_0=1$ cps $f_N=10$ cps (TsLEM Morénergo) $T=4$ sec	$f_0=5$ cps $f_N=15$ cps (IAT AN SSSR) $T=4$ sec	$f_0=4$ cps, $f_N=20$ cps (TsNIIKA) $T=4$ sec
δ_{me}	40	$2\,P^{40}$	P_{40}	$1.06\,P_{40}$
$\delta_{me.\,sq.}$	40	$0.235\sqrt{P_{40}}$	$0.16\sqrt{P_{40}}$	$0.13\sqrt{P_{40}}$
δ_{me}	80	$6.5\,P_{80}$	$4\,P_{80}$	$2\,P_{80}$
$\delta_{me.\,sq}$	80	$0.424\sqrt{P_{80}}$	$0.316\sqrt{P_{80}}$	$0.177\sqrt{P_{80}}$
δ_{me}	140	$13.1\,P_{140}$	$10\,P_{140}$	$5.75\,P_{140}$
$\delta_{me.\,sq}$	140	$0.8\sqrt{P_{140}}$	$0.5\sqrt{P_{140}}$	$0.27\sqrt{P_{140}}$

flowing from Kotel'nikov's theorem, is always met in practice. Thus, the zero (null) frequency is determined by the indicating instrument's dynamics.

The practical behavior of a pointer indicating electromagnetic galvanometer, measuring mean current of a condenser (or transformer) receiver, becomes completely satisfactory for frequencies at the receiver input of 4 to 5 cps (current pulses of frequencies from 8 to 10 cps flow through the instrument).

The speed of action of a telemetry device is defined as both the time to establish the frequency at the transmitter's output and as the time necessary to transform the frequency to a new indication of the indicating device (for analog reproduction) or, again, as the time necessary to translate the frequency to code (for digital reproduction). In the very fastest transmitter, the maximum time for establishing the output frequency will be when the signal changes from its nominal value to its null value. This time is defined by the formula

$$T_1 \leqslant \frac{1}{2f_0}. \qquad (13)$$

The speed of a telemetering system with analog reception is defined as the time to establish the indication of the indicating instrument and, for a frequency range of 4 to 20 cps, is about 4 seconds.

For digital reproduction, the time necessary to translate the frequencies into code is determined by the receiver error β_{te} and by the frequencies corresponding to the zero value and the nominal value of the measured parameter.

With simple pulse counting,

$$T_2 = \frac{100}{\beta_{te}\%\,(f_N - f_0)}. \qquad (14)$$

With a doubled frequency and a transformation of PFM II to PFM I (pulse-frequency modulation with constant pulse duration),

$$T_2 = \frac{50}{\beta_{te}\%\,(f_N - f_0)}. \qquad (15)$$

4. Secondary Channel Bandwidth

As was mentioned earlier, when signals are transmitted by PFM II, the subcarrier frequency filter must pass at least the third harmonic. However, it is possible to use transmitting and receiving devices of a pulse-frequency telemetry system with narrow-band filter, passing only the first harmonic of the nominal frequency. With this, teletransmission in a large part of the frequency range will be implemented, not by PFM II, but by FM. In this case, thanks to the narrow-band filters, the signal-to-noise ratio at the receiver input will be reduced.

In the devices with secondary compression used today, the narrowest secondary channel is a subchannel of an 80 cps width. Since the receiving device of pulse-frequency telemetry provides normal operation when a sinusoidal signal whose frequency is of the order of 20 cps is applied to its input, telemetry devices with such stations will operate reliably.

Summary

1. Decreasing the f_0/f_N ratio lowers the requirements placed on the accuracy of transforming dc (voltage) to frequency and on the inverse transformation of frequency to current.

2. Increasing the frequency range, f_N to f_0, for the same filter passband, first decreases the mean square error for weak and for strong noise and, second, decreases the conversion (coding) time when digital reproduction is used.

3. The highest teletransmission frequency for PFM II is determined by the noise from the 50 cps line and by the existing standard telegraph filters. For filters with a 140 cps passband, it is desirable to transmit the signal's third harmonic. The highest frequency is about 20 cps.

4. The lowest (null) frequency with analog reproduction is determined by the indicating instrument's dynamics, and is about 4 to 5 cps.

5. For a nominal teletransmission frequency of the order of 20 cps, a telemetering device can operate with the use of any telegraphic filter.

LITERATURE CITED

1. V. S. Malov, Frequency Systems of Telemetering [in Russian] (MEI, 1950).
2. V. A. Kashirin and G. A. Shastova, "Noise resistance to telemetry signal transmission along a channel with fluctuation noise," Avtomatika i Telemekhanika 19, No. 8 (1958).*
3. N. V. Pozen, "On the noise resistance of pulse-frequency telemetry," Avtomatika i Telemekhanika 19, No. 19 (1958).*

*See English translation.

ON THE RELIABILITY OF SCHEMES FOR CONNECTING DISPERSED OBJECTS

V. A. Il'in

(Moscow)

Translated from Avtomatika i Telemekhanika, Vol. 21, No. 4, pp. 530-532, April, 1960
Original article submitted July 27, 1959

The paper considers the reliability of schemes for the parallel and series connection of a remote control system's executive points in a communications line. The domain of applicability for each of these schemes is shown.

In [1], the reliability of various remote control line structures for dispersed objects was considered. As a development of this work, we consider here the reliability of schemes for connecting the executive points in communications lines. The choice of some connection scheme or another determines, to a significant degree, the structure, and significantly affects the structural reliability, of remote control systems with dispersed objects (oil and gas industries, pipelines, irrigation systems, transportation, mines and factories, cities' communal economies, etc.). To a certain extent, this also applies to automated systems.

Figures 1, 2, and 3 show schemes for parallel, series, and mixed connections of a group of $\underline{m}$ dispersed executive points (EP) to a common communications bus via distributive devices D which might be parts of the EP's. In a scheme of the mixed type, the individual distributive devices implement, for example, only the functions of switching devices (Fig. 3). Analogous schemes are also used for radio channels.

The executive points on Fig. 1 are connected in parallel via the distributive devices D to a common communications line which joins them to the central point (CP). In many cases, the distributive devices are executed in the form of matching transformers. The parallel connection scheme (Fig. 1) is employed in remote control systems with either frequency or temporal separation of the signals.

With series connections (Fig. 2), the communications line is divided into a chain of segments which are connected in series via the distributive devices D.

In one of the simplest remote control systems with dispersed switching [2], each distributive device contains relay contacts, connected in series in the line, and disconnecting the remaining parts of the system in one of the relay positions. When a series of selection pulses is transmitted, the "next" link is connected to the line at each cycle, and the line is "selected" successively in time.

In remote control systems with dispersed objects, if these systems operate in accordance with the scheme of Fig. 2 and are constructed of contactless elements with rectangular hysteresis loops, the distributive devices are executed in the form of transformers.

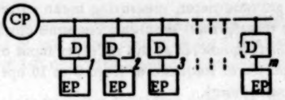

Fig. 1

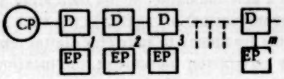

Fig. 2

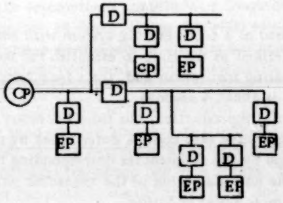

Fig. 3

With a series connection, each distributive device can also implement the function of signal amplification, similar to what takes place in radio relay lines with the same connection scheme.

We now consider the reliability of systems with parallel and with series connections of the EP's in the communications line. Such connection schemes are the fundamental ones.

We make the following assumptions.

1. All distributive devices in one and the same system (scheme) are identical. For each of them there exists a probability of a short-circuited input or output, P_{sc}, and a probability P_{opc} of an opened circuit, for example, from

a winding blowout. The probabilities P_{sc} and P_{opc} for a given EP are mutually independent, and do not depend on the probabilities of short circuits or open circuits of the other EP's.

The probabilities P_{sc} and P_{opc} of a nonoperative state of a given distributive device are related to the mean frequencies of failure due to short circuits f_{sc} and due to open circuits f_{opc} by the following expressions:

$$\bar{f}_{sc} = \frac{P_{sc}}{\bar{T}_{sc}} \text{ and } \bar{f}_{opc} = \frac{P_{opc}}{\bar{T}_{opc}}.$$

Here, $\bar{T}_{sc}$ and $\bar{T}_{opc}$ are the mean nonoperating times of a given distributive device due, respectively, to short circuits and to open circuits during the period of time between maintenance cycles;

$$\bar{T}_{sc} = \frac{1}{n} \lim_{n \to \infty} \sum_{i=1}^{n} T_{i\,sc}, \quad \bar{T}_{opc} = \frac{1}{n} \lim_{n \to \infty} \sum_{i=1}^{n} T_{i\,opc}$$

where n is the number of faults (failures).

2. The communications line itself is considered to be absolutely reliable. Such an assumption simplifies the analysis and can not change the character of the results in any essential way since, when account is taken of the probabilities of short circuits and open circuits in identical links of the line, there is only an increase in the corresponding P_{sc} and P_{opc}.

Then, for schemes with parallel and with series connections, the probability of system failure due to short circuiting of the distributive devices to ground or to the second conductor in a two-conductor line, without taking account of failures due to open circuits, will be expressed by the formula

$$P = 1 - (1 - P_{sc})^m$$

For $mP_{sc} \ll 1$,

$$P \approx mP_{sc}.$$

The probability of a nonoperative state of an object in a system due to open circuits in the distributive devices when parallel connections are employed (Fig. 1) is $P = P_{opc}$, since the open circuiting of any distributive device disrupts the operation only of the EP connected to it.

For a scheme with series connections (Fig. 2), the mean probability of a nonoperative state of an object in the system due to open circuits in the distributive devices, without account being taken of faults due to short circuits, will be

$$P = 1 - \frac{1}{m} \sum_{i=1}^{m} (1 - P_{opc})^{n_i},$$

where n_i is the number of objects connected between the CP and the ith distributive device ($n_1 = 1$) and, for $mP_{opc} \ll 1$, will be

$$P = \frac{m+1}{2} P_{opc}.$$

If an open circuit in a distributive device disrupts only the operation of the EP connected to it in a parallel-connected scheme, the same open circuit in a series-connected scheme will cause failure of an average of $(m+1)/2$ EP's.

It also follows from the expressions obtained that the probabilities of an object's nonoperative state due to a short circuit in a distributive device in systems with parallel and with series connections are equal to each other when the probabilities of short-circuited distributive devices are equal. However, in a parallel-connected scheme, the probability of a nonoperative state of the system due to a short circuit in the distributive devices or in the EP's can be decreased to an arbitrarily small quantity by connecting the EP's to the line via cutouts or limiters similarly to what is done in connecting electric energy users to a power line, or radio relay points to a radio relay network.

For frequency systems of remote control, and for systems which use exponential transformers [3] for the time separation of signals, the EP apparatus is comparatively simple in parallel-connected schemes.

If existing systems of remote control with time separation of signals are connected in accordance with the scheme of Fig. 1, it is necessary to have, at each EP, a one-terminal set (incomplete in many cases) which is frequently unreasonable (for a small number of signals on one EP).

The series-connected scheme can be realized in remote control systems with time separation of signals with contact distributed switches [2] or in contactless systems with elements with rectangular hysteresis loops.

Such systems, even when constructed from contactless elements, have significantly less structural reliability, as our analysis shows.

Frequency systems of remote control can also be constructed in accordance with the series-connected scheme (Fig. 2), but this is unreasonable, in connection with the lower structural reliability of such systems.

The use of series-connected schemes, from the point of view of reliability, may be justified principally in those cases when it is necessary to amplify signals at given points of the line, or it is necessary to switch groups of EP's in communications lines with tree structures, if the solution of such problems gives rise to difficulties when parallel-connected schemes are used.

LITERATURE CITED

1. V. A. Il'in, "On the structure of remote control lines for dispersed objects," Avtomatika i Telemekhanika 18, No. 7 (1958).*

2. V. N. Silaev, "Remote control devices for dispersed objects," Automation and Remote Control [in Russian] (Izd. AN SSSR, 1958).

3. V. A. Il'in, "Design principles for contactless remote control systems with exponential transformers," Avtomatika i Telemekhanika 20, No. 4 (1959).*

---

*See English translation.

ON THE QUESTION OF RELAY-CONTACT DEVICE RELIABILITY

K. P. Kurdyukov

(Moscow)

Translated from Avtomatika i Telemekhanika, Vol. 21, No. 4, pp. 533-541, April, 1960
Original article submitted February 12, 1958

Methods are considered for increasing the reliability of operation of relay-contact devices by means of spare elements. A new method is suggested for sequential circuits which allows the device's reliability to be increased with the minimum number of spare relays.

In recent years the questions of reliability of electrical devices have received great attention. With this, the problem of increasing reliability is solved by two routes. The first of these is the increase of strength and durability of the elements entering into devices, the replacement of contact elements by contactless ones, for example, by semiconducting and magnetic elements, etc. The second route, independent of the first, is the wide use of stand-by elements, assemblies and blocks, i.e., the use of back-up.

In these cases, the operating parts of the apparatus or of its individual blocks, or even individual elements, are supplied with reserves which are either switched into operation automatically when the basic set fails or operate constantly in parallel with it. Such reserve elements are "redundant," since their introduction adds no new functions to the device.

As an example of the use of the back-up method of increasing reliability, one may adduce the automatic track blocking circuit of the Moscow subway in which, as is well known, a type DSR relay is connected in parallel for every two tracks.

In the engineering and scientific literature devoted to the questions of stand-by capability, one considers principally the reliability of radioelectronic apparatus, constructed from contactless elements and used in a number of special domains, for example, in computing technology, in radio relay communications, for the control of moving objects, etc. In correspondence with the purpose of such apparatus, there arises the requirement that it operate without failures during some interval of time, so that here reliability is defined as the probability that, in the course of a definite time interval, the device will correctly carry out its function.

In industrial devices for automation and remote control, one ordinarily considers a device to be sufficiently reliable if a random failure of its elements does not entail an incorrect functioning which leads to an unsafe state of the object. Operational failures in these cases are considered as "protective", and are ordinarily accompanied by either a blocking device and an alarm indication of the fault, or a transfer of the device to a safer state. Thus, for example, when a railway element fails in the automatic blocking circuit, a red light signal automatically appears, requiring that the train stop.

However, as is understandable, each such case of protective failure disrupts the continuity of the technological process. With the modern tendency to intensify production, it becomes important to increase the reliability and unceasing operation of industrial automation and remote control devices.

In the present paper we consider several questions in the construction of reliable relay-contact devices which permit a single failure to occur without disruption of operation. The principles to be considered in the sequel may be extended also to contactless devices using relay-acting (switching) elements.

The effect achieved when the ordinary method of parallel back-up [1] is used can be illustrated by the example of the simplest relay-contact circuit (Fig. 1a), whose function is to close circuit a-b when relay A1 is excited.

We denote the probability of correct closure of the relay contact by $p(A) = p$, and the probability of the event that circuit a-b will be closed by $p(a\text{-}b)$. In the given case, $p(a\text{-}b) = p$.

Connecting relay A2 in parallel to relay A1 (simple back-up) and connecting the contacts of relay A1 and A2 in parallel (Fig. 1,b) increases the probability of correct closure of circuit a-b up to the value $p(a\text{-}b) = 2p-p^2$, i.e., for $1-p \ll 1$, increases the reliability by almost one order.

Conversely, a series connection of the contacts of relays A1 and A2 (Fig. 1c) lowers the probability of closure of circuit a-b to the value $p(a\text{-}b) = p^2$.

Figure 1 d-f, also gives several variants of the simplest schemes for the two- and three-fold back-up of relay A1, and the corresponding values of the probability of closure of circuit a-b. To determine the expressions for the probabilities, it was assumed that all the relays A1, A2, A3, and A4 were monotypic, as were their contacts, that the probability of contact closure was the same for all, and that cases of incorrect operation were statistically independent.

<table>
<tr><th rowspan="2"></th><th rowspan="2">Relay winding connection</th><th rowspan="2">Contact connection</th><th colspan="2">Probability</th></tr>
<tr><th>Closed circuit a-b</th><th>Open circuit a-b</th></tr>
<tr><td>a</td><td>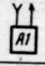 </td><td>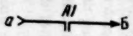 </td><td>$p(a-b)=p$</td><td>$q(a-b)=1-p$</td></tr>
<tr><td>b</td><td>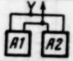 </td><td>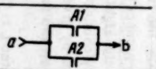 </td><td>$p(a-b)=1-(1-p)^2=2p-p_2$</td><td>$q(a-b)=(1-p)^2=1-2p+p^2$</td></tr>
<tr><td>c</td><td>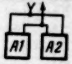 </td><td>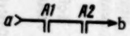 </td><td>$p(a-b)=p^2$</td><td>$q(a-b)=1-p^2$</td></tr>
<tr><td>d</td><td>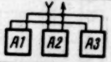 </td><td>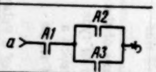 </td><td>$p(a-b)=[1-(1-p)^2]p=2p^2-p^3$</td><td>$q(a-b)=1-2p^2+p^3$</td></tr>
<tr><td>e</td><td>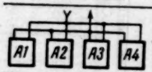 </td><td>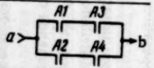

a
A1
A3
A2
A4
b

</td><td>$p(a-b)=1-(1-p^2)^2=2p^2-p^4$</td><td>$q(a-b)=(1-p^2)^2=1-2p^2+p^4$</td></tr>
<tr><td>f</td><td>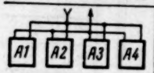 </td><td>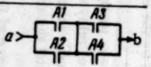

a
A1
A3
A2
A4
b

</td><td>$p(a-b)=[1-(1-p)^2]^2=4p^2-4p^3+p^4$</td><td>$q(a-b)=1-[1-(1-p)^2]^2=1-4p^2+4p^3-p^4$</td></tr>
</table>

Fig. 1.

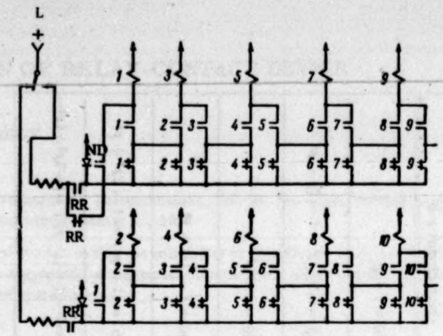

Fig. 2

As is obvious from these examples, by paralleling the corresponding number of relays (with multiple back-up) and by properly connecting their contacts in a circuit which is equivalent in its operation to the action of one contact (or any other more complicated structure), one can attain any previously given degree of reliability, even with the use of elements which are themselves of low reliability. Of course, such back-up leads to a significant increase in complexity and cost of the devices, and to a large expenditure of circuit elements.

For sequential relay-contact circuits, a more economical back-up, which may be called "combined", is possible. The essence of this back-up amounts to this, that the back-up elements, the number of which, as a rule, is less than the number of the basic elements, back each of the basic elements up at that moment (cycle) when the operation of the entire device is determined by the operation of this basic element.

We consider this new back-up method in terms of the example of a centralized control relay distributor of type DVK-3 – DVK-3a. The functional schematic of such a distributor is shown in Fig. 2, and the sequence of its actions is given in Table 1 [2]. One easily convinces oneself that a fault in any one of the counter relays 1-10, or of their contacts, causes the distributor to cease operation, as well as a fault in the action of the entire one-terminal set (and, if this one-terminal set is the central control point, the entire system fails).

We isolate, in Table 1, those cycles which would be terminal points, completing each distributor step, i.e., cycles 0,3,6,9,12,15, etc., and we write the state of the distributor at each of these cycles in the form of a binary number. We adopt the convention that an excited relay state will be denoted by a "1", an unexcited state by a "0". Table 2 gives the sequence of these binary numbers, which completely characterizes the sequence of operations of the distributor relays and which mirrors, by the corresponding binary numbers, their states at each step. Thus, for example, the fifteenth cycle of Table 1 corresponds to the binary number 000001000010 (the fifth cycle of Table 2), while the eighteenth corresponds to 000010000000.

By considering this table of binary numbers as a set defined by given combinations of relay states, and considering all the rest of the set of binary numbers which are not

TABLE 1 Sequence of Operations of a Relay Distributor L is the line relay, RR is the receiving relay.

Relay	Cycles of circuit operation																					etc.
	1	2	3	4	5	6	7	8	9	10	11	12	13	14	15	16	17	18	19	20	21	
RR				+																		
L	+			−			+			−			+			−			+			
1		+				−																
2					+				−													
3								+				−										
4											+				−							
5														+				−				
6																	+				−	
7																				+		
8																						
9																						
10																						

TABLE 2 Sequence of Distributor Operations, Given in the Form of a Table of Binary Numbers

Cycles	Circuit elements											
	10	9	8	7	6	5	4	3	2	1	L	RR
0	0	0	0	0	0	0	0	0	0	0	0	0
1	0	0	0	0	0	0	0	0	0	1	1	1
2	0	0	0	0	0	0	0	0	1	0	0	0
3	0	0	0	0	0	0	0	1	0	0	1	0
4	0	0	0	0	0	0	1	0	0	0	0	0
5	0	0	0	0	0	1	0	0	0	0	1	0
6	0	0	0	0	1	0	0	0	0	0	0	0
7	0	0	0	1	0	0	0	0	0	0	1	0
8	0	0	1	0	0	0	0	0	0	0	0	0
9	0	1	0	0	0	0	0	0	0	0	1	0
10	1	0	0	0	0	0	0	0	0	0	0	0
11	0	0	0	0	0	0	0	0	0	0	1	0

TABLE 3 Distances between Relay State Combinations at Each Cycle of Distributor Operation

Cycle numbers	Cycle numbers										
	0	1	2	3	4	5	6	7	8	9	10
0		3	1	2	1	2	1	2	1	2	1
1	3		4	3	4	3	4	3	4	3	4
2	1	4		3	2	3	2	3	2	3	2
3	2	3	3		3	2	3	2	3	2	3
4	1	4	2	3		3	2	3	2	3	2
5	2	3	3	2	3		3	2	3	2	3
6	4	4	2	3	2	3		3	2	3	2
7	2	3	3	2	3	2	3		3	2	3
8	1	4	2	3	2	3	2	3		3	2
9	2	3	3	2	3	2	3	2	3		3
10	1	4	2	3	2	3	2	3	2	3	

written in the table as distortions of these combinations, one can try to use, for constructing self-correcting circuits, the same methods which were developed for constructing self-correcting codes, also described by binary numbers which are tabulated in analogous fashion [3,4].

It is well known that, for the construction of error-free codes, it is necessary to create redundant elements of the combinations, and thereby to achieve the result that the code combinations differ from each other by a sufficient number of bits ("distance" between combinations). Thus, to construct a code for the correction of unitary errors, it is necessary that the code combinations differ from each other by at least three bits.

We now extend these propositions to the given combination of relay states. Table 3 gives the values of the "distances" between the combinations of relay states (the binary numbers of Table 2) for the distributor of the circuit in Fig. 2, from which it is clear that, in a number of cases, this condition is not satisfied, so that it is required to introduce auxiliary elements in the combinations (relays) to provide the requisite redundancy.

The number of auxiliary relays can be determined from the well-known expression of Hamming

$$2^{n_0} \leqslant \frac{2^n}{n+1},$$

where n_0 is the number of basic relays in the circuit and n is the total number of relays, including the auxiliary ones.

The value of $m = n - n_0$, i.e., the number of auxiliary relays, can be found from the following table, set up in accordance with this formula:

$n_0 =$	1	2	3	4	5	6	7	8	9	10	11	12
$n =$	3	5	6	7	9	10	11	12	13	14	15	16
$m =$	2	3	3	3	4	4	4	4	4	4	4	4

In the case under consideration, it turns out to be sufficient to add four auxiliary relays. Connecting these relays in the over-all operation of the distributor can be implemented in various ways with the same condition that repeated combinations not occur. As is well known, the number of nonrepeating combinations with this will equal 2^n, i.e., the number of arrangements which differ from each other in at least one place. It is most convenient to construct the table of auxiliary relay operations such that, at each cycle, the minimum number of auxiliary relays, i.e., one relay, will change state. This condition is satisfied by, for example, the Gray code [5], used in a somewhat different form for constructing Table 4, giving the operation of auxiliary relays I-IV. One easily convinces oneself that, with this, the distance between the binary numbers of the combinations of relay states at different cycles of distributor operation in no case is less than three, which is the requirement imposed.

We now consider three cases of constructing self-correcting circuits for relay counters.

1. Circuits for self-correction it there appears, in a binary number characterizing an operate cycle of a given relay, a zero instead of a one (for example, if a prior counter relay did not close its contact in the same operate circuit of the given relay).

2. The same, but for the appearance of a one in the binary number instead of a zero (for example, for the sealing of a contact of the prior relay).

3. The same, but for the appearance in a binary number of a zero instead of a one, or a one instead of a zero.

In the first case, to provide for operation of the given next counter relay, its operate circuit, passing through normally open contacts of the previous counter relay, must be backed up by the contacts of that auxiliary relay which also changed its state at the previous cycle (a normally open contact if it were excited, and a normally closed contact if it were unblocked).

In the second case, protection from a false operation on an incorrect cycle due to a random closing of a contact of a previous relay is attained by introducing into the operate circuit of the given relay the contacts of three auxiliary (back-up) relays which do not change their state at the given cycle, and the combination of whose states at the given cycle differs by the state of at least one relay from

TABLE 4 Binary Numbers for Operation of the Distributor with Auxiliary Relays

Cycles	Basic relays of the distribution circuit												Auxiliary relays				Back-up circuit contacts			
	10	9	8	7	6	5	4	3	2	1	Л	НД	IV	III	II	I	IV	III	II	I
0	0	0	0	0	0	0	0	0	0	0	0	0	0	0	0	0				
1	0	0	0	0	0	0	0	0	0	1	1	1	0	0	0	1	NC	NC	NC	—
2	0	0	0	0	0	0	0	0	1	0	0	0	0	0	1	1	NC	NC	—	NO
3	0	0	0	0	0	0	0	1	0	0	1	0	0	0	1	0	NC	NC	NO	—
4	0	0	0	0	0	0	1	0	0	0	0	0	0	1	1	0	NC	—	NO	NC
5	0	0	0	0	0	1	0	0	0	0	1	0	0	1	0	0	NC	NO	—	NC
6	0	0	0	0	1	0	0	0	0	0	0	0	1	1	0	0	—	NO	NC	NC
7	0	0	0	1	0	0	0	0	0	0	1	0	1	0	0	0	NO	—	NC	NC
8	0	0	1	0	0	0	0	0	0	0	0	0	1	0	1	0	NO	NC	—	NC
9	0	1	0	0	0	0	0	0	0	0	1	0	1	0	1	1	NO	NC	NO	—
10	1	0	0	0	0	0	0	0	0	0	0	0	1	0	0	1	NO	NC	—	NO

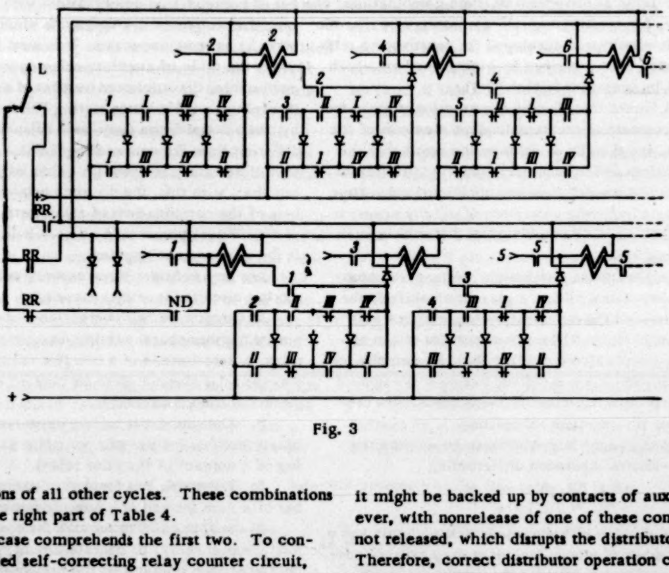

Fig. 3

the combinations of all other cycles. These combinations are given in the right part of Table 4.

The third case comprehends the first two. To construct a protected self-correcting relay counter circuit, it is necessary to create as many back-up operate circuits as there are series contacts of basic and auxiliary relays in the basic operate circuits. Certainly, the contacts of these back-up circuits can be joined by the use of diode elements, as shown in Fig. 3.

It is necessary to dwell on the cut-off relay circuits. As is clear from the scheme of Fig. 2, the blocking and cut-off circuits of the counter relays of an ordinary relay distributor are interconnected, and pass in series through inherently normally open contacts and normally closed contacts of the relay of the next higher ordinal number. For the case of nonclosure of this normally closed contact, it might be backed up by contacts of auxiliary relays. However, with nonrelease of one of these contacts, the relay is not released, which disrupts the distributor's operation. Therefore, correct distributor operation can be achieved only by separating the relays' locking and cut-off circuits, whereby the release of the relays is implemented, not by means of the supply circuit, but by counter flows in the relays' second windings (active unlocking). With this method, unlocking of a given counter relay is obtained by means of the operate circuit of the next relay of the same parity (i.e., even or odd, respectively), and may therefore be identified with it, the differentiation being only by the state of the forcing element, and the cycles on which they are used.

Figure 3 shows the circuit for connecting several of the basic counter relays of a self-correcting distributor, con-

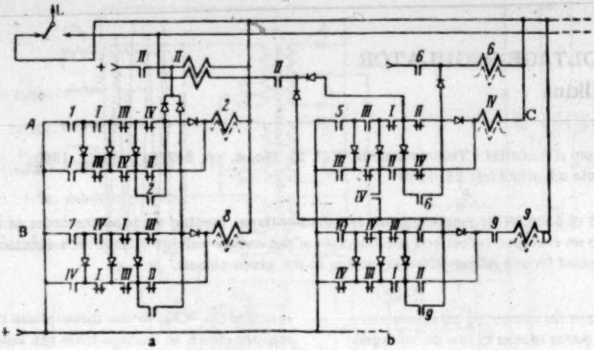

Fig. 4. a is the operate circuit of relay II, b is the release circuit of relay II; A is the operate circuit of relay 2, B is the operate circuit of relay 8, C is the operate circuit of relays 6 and IV, D is the release circuit of relay 9.

structed in accordance with Table 4 and with the conditions to be given now.

As was stated earlier, auxiliary relays I-IV are connected analogously to the basic counter relays in that, at the corresponding cycles of distributor operation, they operate or are released simultaneously with the basic relays. Since auxiliary relays I and II operate and release twice during an operate cycle of the distributor, one then uses for them the binary number of such circuits, as is shown in Fig. 4 for auxiliary relay II.

The difference in the circuits for the basic and the auxiliary relays stems from the fact that there is used, in one of the back-up circuits for operating a basic relay, a proper contact of that auxiliary relay which must also operate (or release) on the same cycle. To obtain coherent operation both of the basic and of the auxiliary relay by this back-up circuit, this circuit is so separated for the basic and the auxiliary relay that the winding of the auxiliary relay is supplied only after the basic relay has operated.

Such a relay distributor provides correct operation for any single fault, i.e., for the failure of any one element, either basic or auxiliary. The distributor's output circuit must, of course, be constructed like an operate circuit, i.e., it must be backed up.

Thus, increasing by almost an order the reliability of distributor operation is attained most economically by adding four relays only, instead of the ten necessary for parallel back-up. It should be mentioned that, according to Hamming's formula, four auxiliary relays can provide back-up for 15 basic relays.*

Using the same principle, one may construct multiple relay contact circuits in which are corrected double, triple, etc. errors, i.e., which will provide correct operation for simultaneous failures of two, three, etc. relays, at the expense of a corresponding increase in redundancy.

LITERATURE CITED

1. E. F. Moore, and C. E. Shannon, "Reliable circuits using less reliable relays," J. Franklin Inst. 261-262, No. 2-3 (1956).
2. F. I. Marushko, "The DVK-3a and DVK-3 centralized control systems," Collected Papers on the New Signal Centralization and Blocking System and Communications Technology [in Russian](Transzheldorizdat, 1955).
3. A. A. Kharkevich, An Outline of General Communication Theory [in Russian] (Gostekhizdat, 1955).
4. R. W. Hamming, "Error detecting and error correcting codes," Collected Papers (subject not given) edited by A. M. Petrov [Russian translation] (Il, 1956).
5. Fundamentals of Automatic Control.2 [in Russian] (edited by V. V. Solodovnikov) (Mashgiz, 1959), Chap. 2.

---

* This last sentence is factually (and mathematically) incorrect, as are the data of Table 3 on page 369. The maximum number of basic relays for which four auxiliary relays will suffice is not 15, but 11 [Publisher's note].

RECTIFIED VOLTAGE REGULATOR

O. G. Malkina

(Moscow)

Translated from Avtomatika i Telemekhanika, Vol. 21, No. 4, pp. 542-547, April, 1960
Original article submitted July 21, 1959

A new variation of a circuit for regulating low rectified-voltage feeding loads on the order of hundreds of watts is discussed. As an example, curves and oscillograms of the output voltage change as a function of the load change are presented for a regulator wired according to the given circuit.

The use of transistors for computing machines and other devices requires power sources of low dc voltages. These voltages may be obtained by lowering and rectifying the ac power line voltage. The use of ac sources means that filters and voltage regulators must be built. The ac source can be ether single- or three-phase.

One of the advantages of using rectified voltages from three-phase ac sources is that the ripple on the output is less; this simplifies and eases the filter requirements of the voltage regulator. The voltage regulators considered in the article are designed for loads on the order of hundreds of watts, and use saturable reactors for regulation. These regulators permit ac line voltage fluctuations of ± 5-10%, a temperature change of the surrounding medium from -30 to +50°C, and continuous control of the regulated voltage over a range of ±20-25%.

The fluctuations of the regulated voltage are less than ±0.5-1.5% for this type of regulator, and the full regulation time for a step change of load from 100% to 50% and, conversely, from 50% to 100% of the nominal value does not exceed 5-15 msec.

The circuit diagram of the regulator is shown in Fig. 1.

The regulator consists of the following basic elements:

1. Saturable reactors $\overline{Ch}_1$ - $\overline{Ch}_3$, made with an external feedback winding W_0 and one control winding W_y, shunted by the capacitance C_y in order to eliminate the effect of the inductive emf of even harmonics. The reactors can also be made with an internal feedback winding.
2. The three-phase transformer Tr (or three single-phase transformers).
3. Power rectifiers B_1-B_6.
4. The filter, consisting of choke $\overline{Ch}_f$ and capacitances C_{f_1} and C_{f_2}.
5. The meter-amplifier element which, in its turn, consists of: a) voltage divider made of resistances R_1-R_3, and R_2-R_4; b) Zener reference diodes V_{c_1} and V_{c_2}, type D809 or D810; c) rectifiers B_7-B_{10}, type D7D-D7Zh; d) junction transistors Q_1, Q_2, and Q_3 (type P4B); e) resistances R_5, R_6, and R_7, which limit the currents in the control winding and transistors Q_1 and Q_3.

The ac of the three-phase power line, at a 400 cps frequency, is connected through three single-phase saturable reactors $\overline{Ch}_1$-$\overline{Ch}_3$, to the three-phase transformer. The stepped-down ac voltage from the secondary windings of the transformer is rectified by rectifiers B_1-B_6, the variable component is filtered out by the filter ($\overline{Ch}_f$, C_{f_1} and C_{f_2}), and the resultant dc is fed to the load.

In this case, the saturable reactors operate as single-phase magnetic amplifiers, working into a variable load resistance. A simplified equivalent circuit diagram of the load windings of such an amplifier is shown in Fig. 2a.

Commercial transformers have an insignificant leakage reactance, and the quantities x_1 and x'_2 can be neglected. If the load resistance is large, it is also possible to neglect the choke resistance (r_{ch}), and primary and secondary winding resistance (r_1 and r'_2) and the core loss resistance (r_0). Therefore, the simplified equivalent circuit diagram of the load windings of the magnetic amplifier corresponds to the circuit shown in Fig. 2b, for no-load on the regulator.

The amplitude of the output voltage U_{out} will be determined, in this case, by the relation between the choke (magnetic amplifier) reactance x_{ch}, and the transformer reactance x_0. The relation chosen between x_{ch} and x_0 and the given value of the regulated voltage determine the transformation ratio of the transformer.

When the transformer is loaded, $R^1_H \ll x_0$, and the simplified equivalent circuit of the load windings of the saturable reactor corresponds to the circuit shown in Fig. 2c.

The regulation of the output voltage in this type of regulator is based on the fact that the reactance of the saturable reactor x_{ch} depends on the magnitude of the dc excitation ampere-turns.

The main excitation of the circuit is caused by the load current, that is, by the ampere-turns of the feedback winding, which has a coefficient somewhat less than unity (this coefficient can even be equal to unity). The load current is minimum at no-load, and is determined by the currents of the voltage dividers R_1+R_3 and R_2+R_4, and the resistance x_{ch} is maximum (in the circuit of Fig. 2b).

At maximum load, x_{ch} is minimum (in the circuit of Fig. 2c), and the change in x_{ch} due to load current compensates for the change in the output voltage due to the change in the voltage drop across the circuit resistance $R = r_{ch} + r_1 + r_2$.

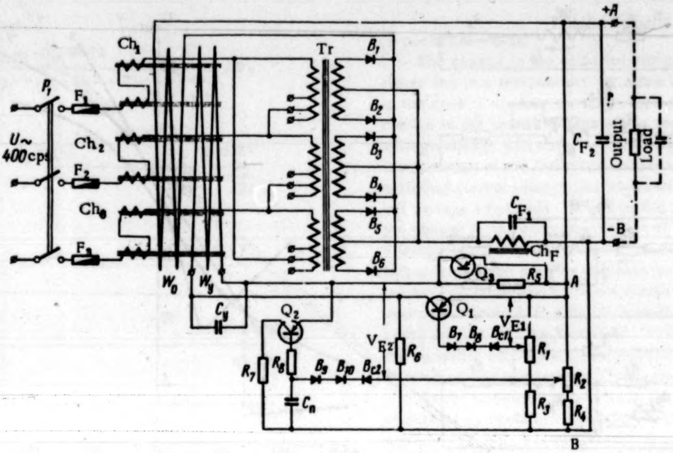
Ch1
P1
F1
U~
400cps
Ch2
F2
Ch0
F3
W0
Wy
Cy
Tr
B1
B2
B3
B4
B5
B6
+A
CF2
Output
Load
CF1
ChF
-B
Q3
RS
A
Q1
VE1
B7
B8
Bc1
R1
R2
R3
R4
B
Q2
VE2
R6
R7
R8
B9
B10
Bc2
Cn

Fig. 1

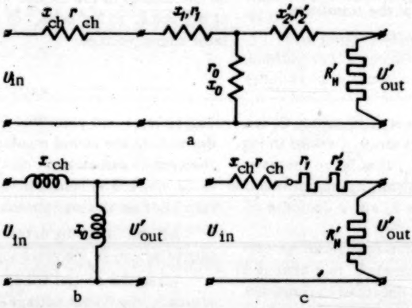
xch rch
x1,r1
x'2,r'2
Uin
r0
x0
R'H
U'out
a
xch
Uin
x0
U'out
b
xch rch
r1
r'2
Uin
R'H
U'out
c

Fig. 2. Simplified equivalent circuit diagram of the load windings of a single-phase saturable reactor at different loads.

The dc excitation of the saturable reactors is caused not only by the ampere-turns of the feedback winding W_0, but also by the ampere-turns of the control winding W_y. The latter is used to get better stabilization of the output voltage, and to control the amplitude of the regulated voltage over a range of ± 20-25%.

The direction and amplitude of the current in the control winding depend on the states of transistors Q_1 and Q_2 in the metering element.

Voltage reference diodes (B_{c_1} and B_{c_2}) are wired in the base circuit of each transistor (Q_1 and Q_2). Therefore, the circuit in the transistor base will, in practice, flow only when the voltage between the moving arm of the divider and the emitter of the given transistor (U_{e_1} or U_{e_2}) is greater than the sum voltage of the reference diode (U_{r_1} or U_{r_2}) and the rectifiers ($U_{v(7-8)}$ or $U_{v(9-10)}$). The greater the difference in the voltages mentioned, the greater the base current of the transistor will be, and the greater the collector current.

When both transistors are cut off, the circuit diagram of the control winding will be practically analogous to the circuit shown in Fig. 3a. The ampere-turns of the control winding in this case assist the excitation action of the feedback winding, and by the same token, cause additional decrease of the reactance x_{ch}.

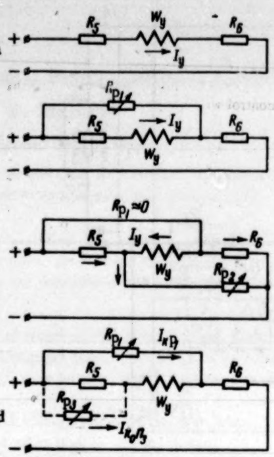

Fig. 3. Simplified equivalent-circuit diagrams of the control winding of the saturable reactor for different states of the transistors in the metering element.

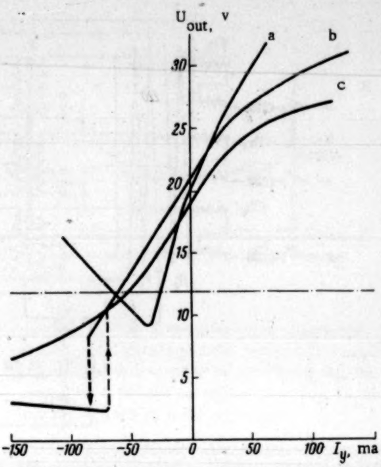

Fig. 4. Dependence of the output voltage of the regulator on the current in the control winding. a) for R_H = 30 ohms, b) 4.2 ohms, c) 1.2 ohms, d) minimum value of the regulator output voltage.

A change in the collector current of transistor Q_1 is equivalent to a change in the resistance R_{p_1}, shown in Fig. 3b. A decrease in the resistance R_{p_1}, that is, an increase in the collector current of this transistor, causes an increase in the voltage drop across resistance R_6 and a decrease of the current in the control winding.

When transistor Q_1 is fully on, the change in the collector current in transistor Q_2 is equivalent to a change in resistance R_{p_2}, shown in Fig. 3c. A decrease in resistance R_{p_2} will cause an increase of an opposing current in the control winding, and therefore these ampere-turns will cause a relative increase in the reactance x_{ch}.

The use of feedback with a coefficient approaching unity ensures an abrupt change in the reactance x_{ch}, and consequently, in the output voltage, when the current in the control winding is changed.

The change in the output voltage of the regulator as the current in the control winding is changed is shown in Fig. 4; the control winding of this regulator has been disconnected from the metering element, and connected to an independent source of dc.

It can be seen from Fig. 4 that to change the output voltage of the given regulator from 12 to 25 v across a load resistance of 30 ohms, it is sufficient to change the control current from -25 to +25 ma, and from -50 to +50 ma for small load resistances. There are 70 turns on the control winding of the reactors of the given regulator. It can also be seen from Fig. 4 that a negative control current exceeding 50 ma is not permitted in this type of regulator. In order to hold the output regulated voltage at 25 v, for example, the control current must be altered within the limits of 22 to 52 ma, and to hold this voltage at 20 v, the control current must be altered between -6 to +8 ma.

All the foregoing determines the choice of the resistances R_5 - R_7 in the metering element.

When the control winding is connected to the metering element, the output voltage is stabilized because a change in the output voltage due to a variation in the load, or power line voltage, causes the base current of a transistor to change; this, in turn, alters the control current so as to counteract the output voltage change.

In principle, it is not possible to compensate completely for the voltage deviation by changing the current in the control winding, since there must always be some voltage difference to cause a new value of the control current. However, the output voltage is maintained quite accurately due to the large amplification factor.

Some curves of the dependence of the output voltage on the load change are shown in Fig. 5 for one of the regulators of the type discussed in this paper. These dependencies are given for different ac source voltages.

The amplitude of the regulated output voltage of this type of regulator is determined by the position of the moving arms of the voltage dividers, which consist of resistances R_1, R_3, and R_2, R_4.

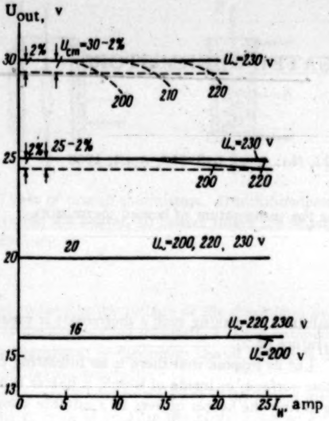

Fig. 5.

The currents in the dividers are significantly greater than the base currents of the transistors; therefore the dividers are only slightly loaded.

The voltage obeys the relation

$$U_{out} = U_{E1}\frac{R_1 + R_3}{R_{x'}},$$

for the first divider, where R_x is the resistance of the divider from point A to the moving arm.

Since the voltage U_{e_1} can be greater under regulation than the sum of the voltages $U_{r_1} + U_{V(7-8)}$ by only a very small amount, an increase in the resistance R_x (that is, a movement of the arm of the divider) will cause a decrease in the output voltage amplitude

The regulated output voltage can be lowered by moving the arm of the first divider from point A to point B, but only to a value which does not require a change in the direction of the current flow in the control winding. Further reduction of the output voltage can be realized by moving the arms of both voltage dividers. For finer control, regulation of the output voltage must be accomplished by moving the arms and the voltage dividers simultaneously, so that the resistance ratios of the dividers

$$\frac{R_1 + R_3}{R_x} \text{ and } \frac{R_2 + R_4}{R_{x_2}}$$

do not differ much.

The change in the collector currents of junction transistors due to a temperature variation leads to a decrease in the control winding current, which in turn causes a change in the output voltage of the regulator. The output voltage change will cause a corresponding variation in the base currents of the transistors, which compensates for the collector current change and practically restores the output voltage amplitude. But when the regulator is heated, the change in the collector current of the transistor due to a temperature increase must be less than the initial collector current, so that the decrease in the transistor base current can compensate for the increase in the collector current. Transistor Q_3 (Fig. 1) is used to prevent ΔI_C from being greater than the initial I_C. With no base connection, the collector current of Q_3 is minimum, and its increase depends on the temperature of the environment.

As the temperature increases, the collector current change of Q_1 leads to a decrease in the control winding current (Fig. 3d), but an increase in the collector current of Q_3, conversely, causes an increase in the control winding current. Thus, the collector current change in Q_3 in this case compensates for the change in the collector current of Q_1.

The output voltage change for a regulator wired according to the circuit discussed is shown on oscillograms (Fig. 6) for various load changes.

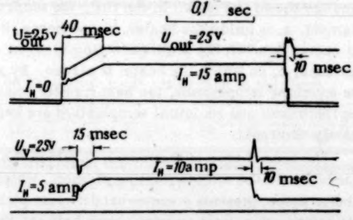

Fig. 6. a) Output voltage change for load current changes from zero to 15 amp and from 15 amp to zero, b) output voltage change for a load current change from 5 to 10 amp, and from 10 to 5 amp.

The recovery time obtained for this particular regulator is not a limit for this type of regulator.

STABILIZING THE TEMPERATURE OF HEATED THERMISTORS

G. K. Nechaev

(Kiev)

Translated from Avtomatika i Telemekhanika, Vol. 21, No. 4, pp. 548-554, April, 1960
Original article submitted October 12, 1959

An analytic method of calculating circuits for stabilizing the temperature of heated thermistors used in time delay apparatus is presented.

At present, a number of methods of obtaining time delay with electrical circuits are used. Circuits using the thermal inertia of thermistors are convenient due to their simplicity, reliability, and ability to give long time delays reaching dozens of minutes. However, these circuits are sensitive to a temperature change of the surrounding medium; this limits their use.

In order to eliminate this dependence on the external temperature, Udalov [1] proposed that heated thermistors be used, whose temperature was regulated in a simple manner by changing the current of the heater.

It must be noted that not all heated thermistors are suitable for this use. Two types of heated thermistors exist; they are shown in Fig. 1. In the first, the semiconducting element, a, is inside the heater, b, and hence, heat transfer occurs between the semiconducting element and the envelope, c, on which the heater is placed. By stabilizing the envelope temperature, the heat transfer conditions of the thermistor and its initial temperature are held approximately constant.

The second type of thermistor, in which the heater is placed inside the semiconducting element, which has a tubular shape, presents a somewhat different picture. In this construction, heat transfer occurs between the semiconducting element and the medium; a temperature change of the latter cannot be compensated for by changing the heater current with the aid of the proposed circuit. Only the temperature of the thermistor can be stabilized. Analysis shows that this condition is not sufficient to maintain the delay transient constant when a circuit with the thermistor is turned on, if the temperature of the surrounding medium changes. Consequently, the second type of thermistor will not do for the circuit being considered.

The operation of the circuit can also be made independent from the temperature of the medium by means of thermostation of the thermistor. However, this method is applicable only in those cases where the thermostat is simple in construction. A heated thermistor of the first type can be considered as a microthermostat, inside of which the temperature can be stabilized within certain limits. By analogy, it is possible to make a small-sized thermostat, and place a direct-heated thermistor in it. The possibility of making such a thermostat is mentioned in the literature [2,3].

Let us suppose that there is an insulating cylinder on whose surface, or inside of which, a heater is placed. By regulating the heater current in a suitable manner, the temperature inside the cylinder can be held constant when the medium temperature changes within certain limits. It should be noted that the temperature inside the thermostat must be higher than the temperature of the surrounding medium.

Two satisfactorily simple circuits for controlling the temperature can be proposed; these are shown in Figs. 2 and 3, in which the thermistor acts as the sensing element. In these circuits, R_T is the thermistor in the regulator circuit, $\underline{r}$ is a linear resistance, r_H is the heater resistance, R_{TC} is the semiconducting element of the heated thermistor, and r_b is the barretter. The circuit using the barretter has the advantage over the circuit of Fig. 2, in that it is independent of supply voltage fluctuations, but such a circuit requires somewhat greater power than the circuit with the linear resistance.

The circuit works in the following manner. At a low temperature of the medium, the thermistor resistance has a considerable magnitude, the current in it is small, and a large amount of power is liberated in the heater. As the temperature of the medium is raised, the current in R_T increases, and by the same token, the current in, and power liberated by the heater decrease. Consequently, it is essential to choose the parameters of the circuit so that as the temperature of the medium changes, the temperature inside the thermostat or heated thermistor will remain within given limits.

It has been experimentally established that the heat transfer between the thermistor or thermostat and the surrounding medium follows Newton's formula well within the operating temperature range

$$P = F\alpha(T_T - T_0) = H(T_T - T_0) = K(T - T_0), \tag{1}$$

where P is the power dissipated by the thermistor or thermostat into the surrounding medium, F is the area of the external surface of the thermistor or thermostat, α is the surface heat emission coefficient, H is the overall dissipation factor of the thermistor, T_T and T_0 are the temperatures of the

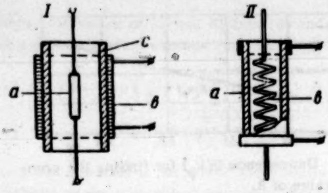

Fig. 1. Types of heated thermistors. I) semiconducting element inside the heater, II) heater inside the semiconducting element.

thermostat surface or the surface of the thermistor heater, and that of the surrounding medium, T is the temperature inside the thermostat or thermistor heater, and K is the over-all heat transfer constant.

Temperature T will be constant if the power dissipated by the resistance r_H is equal to the power emitted by the thermistor or thermostat into the surrounding medium:

$$P_H = I_H^2 r_H = K(T - T_0). \tag{2}$$

If the semiconducting or thermostated element liberates a certain power, it is considered to be a deduction from the computed value of P_H when calculations are made. In time relay circuits, the semiconducting element is ordinarily unexcited before the main circuit is turned on, and thus it is not necessary to account for this power.

Consequently, the power P_H should be a linear function of the medium temperature T_0. The proposed circuits permit one to obtain a dependence $P_H(T_0)$ which is nearly linear in the static mode. In order to have this, it is essential that the curve $P_H(T_0)$ assume values at a number of points in the temperature range which correspond to a linear dependence of $P(T_0)$, that is, so that the difference $\Delta P = P(T_0) - P_H(T_0)$ is zero at these points.

Let us take three such points, which correspond to the limits of the temperature range and its center, as shown in Fig. 4. The curve $P_H(T_0)$ must have an inflection point in order to intersect $P_0(T_0)$ at points 1, 2, and n. This means that d^2P_H/dT_0^2 must be zero at the given point n. Let us consider this condition for the proposed circuit.

For the circuit of Fig. 2, the power liberated in r_H, is determined by the expression

$$P_H = U^2 r_H \frac{P_T^2}{[R_T(r + r_H) + rr_H]^2}, \tag{3}$$

where U is the power supply voltage of the circuit.

Then

$$\frac{d^2P_H}{dT_0^2} = 2U^2 rr_H \tag{4}$$

$$\left\{\frac{[(R_T')^2 + R_T R_T''][R_T(r + r_H) + rr_H] - 3(r + r_H)R_T(R_T')^2}{[R_T(r + r_H) + rr_H]^4}\right\},$$

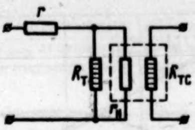

Fig. 2. Circuit for controlling the temperature of a heated thermistor.

whence,

$$\frac{rr_H}{r + r_H} = \frac{R_T[2(R_T')^2 - R_T''R_T]}{(R_T')^2 + R_T''R_T}. \tag{5}$$

The temperature dependence of the thermistor is defined by the expression

$$R_T = R_{T_H}\exp\left(\frac{B}{T} - \frac{B}{T_H}\right) = \gamma R_{T_H}, \tag{6}$$

where R_{T_H} is the thermistor resistance at temperature T_H, and B is a constant defining the properties of the semiconductor from which the thermistor is made.

Then

$$R_T' = -\frac{B}{T^2}R_T,$$
$$R_T'' = \frac{B}{T^4}(B + 2T)R_T. \tag{7}$$

Putting expression (7) into formula (5), we get

$$\frac{rr_H}{r + r_H} = \frac{R_{T_p}}{2}\frac{B - 2T_p}{B + T_p} = R_{T_p}\gamma. \tag{8}$$

The expression for P_H is written in the form

$$P_{H1} = \frac{U^2R_{T_1}^2 r_H}{[R_{T_1}(r + r_H) + rr_H]^2}, \quad P_{H2} = \frac{U^2R_{T_2}^2 r_H}{[R_{T_2}(r + r_H) + rr_H]^2} \tag{9}$$

for temperatures of the medium T_1 and T_2, corresponding to the limits of the working range.

The ratio $\frac{P_{H1}}{P_{H2}}$ must be equal to the ratio P_1/P_2, which is computed or determined in the ordinary manner.

Consequently,

$$k_p = \frac{P_1}{P_2} = \frac{P_{H1}}{P_{H2}} = \frac{R_{T_1}^2\left[R_{T_2} + \frac{rr_H}{r + r_H}\right]^2}{R_{T_2}\left[R_{T_1} + \frac{rr_H}{r + r_H}\right]^2}. \tag{10}$$

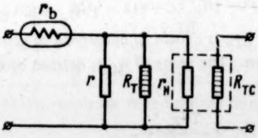

Fig. 3. Circuit for controlling the temperature of a heated thermistor with a barretter.

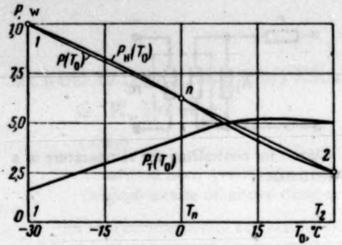

Fig. 4. Dependence of the powers P, P_H, and P_T on the temperature of the surrounding medium.

Then, according to expressions (8) and (10), we get

$$k_p=\left[\frac{R_{T_1}(R_{T_2}+\gamma R_{T_p})}{R_{T_2}(R_{T_1}+\gamma R_{T_p})}\right]^2=\left[\frac{\varepsilon_1(\varepsilon_2+\gamma\varepsilon_p)}{\varepsilon_2(\varepsilon_1+\gamma\varepsilon_p)}\right]^2, \qquad (11)$$

where

$$R_{T_к}=R_{T_н}\exp\left(\frac{B}{T_к}-\frac{B}{T_н}\right)=R_{T_н}\varepsilon_к.$$

The unknown B, which characterizes the thermistor, can be determined from (11). But since this equation is exponential, and is not analytically solved for B, then the curve $k_p(B)$ is plotted, and B, corresponding to a given k_p, is determined from it. Then the resistances r and r_H are determined. However, there is only one expression, (8), which relates these quantities. The second equation can be obtained from the condition of maximum efficiency of the circuit at one of the points in the temperature range. The circuit efficiency is defined by the expression

$$\eta=\frac{P_н}{P}=\frac{R_т^2 r_н}{(R_т+r_н)[R_т(r+r_н)+rr_н]} \qquad (12)$$

where P is the power needed by the whole circuit.

The quantity r, corresponding to a maximum η, is determined from the equality $d\eta/dr_H = 0$:

$$r=\frac{r_н^2 R_т}{R_т^2-r_н^2}. \qquad (13)$$

T_p is chosen as the temperature at which the efficiency is maximum. Then the equation for determining r is obtained from (8) and (13):

$$(1-\gamma^2)r^2-\gamma R_{T_p}(2-\gamma)r-\gamma^2R_{T_p}^2=0. \qquad (14)$$

The quantity R_{T_p} is chosen to correspond to existing types of thermistors. The value of r_H is defined by the expression

$$r_н=\frac{\gamma R_{T_p} r}{r-\gamma R_{T_p}}. \qquad (15)$$

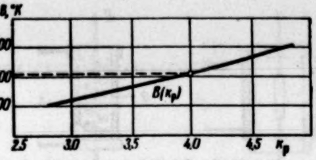

Fig. 5. Dependence $B(k_p)$ for finding the computed value of B.

Then the power supply voltage of the circuit is determined. The power, liberated in r_H at the temperature T_p is found from the formula

$$P_{н.p}=\left[\frac{Ur_н}{R_{T_p}(r+r_н)+rr_н}\right]^2R_{T_p} \qquad (1$$

or after transformation,

$$P_{н.p}=\frac{U^2r_н}{(r+r_н)^2}\left(\frac{1}{1+\gamma}\right)^2. \qquad (17$$

Next the supply voltage is determined:

$$U=(r+r_н)(1+\gamma)\sqrt{\frac{P_{н.p}}{r_н}}. \qquad (18$$

The next step in the calculation is to determine the maximum power dissipated in the thermistor. The power liberated in the thermistor is defined by the expression

$$P_т=\left[\frac{Ur_н}{R(r+r_н)+rr_н}\right]^2R_т. \qquad (19$$

R_T is found from the condition $dP_T/dT = 0$; it corresponds to maximum P_T:

$$R_{T_м}\doteq\frac{rr_н}{r+r_н}=\gamma R_{T_p}. \qquad (20$$

Then

$$P_{т.\max}=\frac{U^2r_н}{4r(r+r_н)} \qquad (21$$

The temperature corresponding to $P_{T\max}$ is found from (8) and (20):

$$T_м=\frac{BT_p}{T_p\ln\gamma+B}. \qquad (22)$$

If T_M proves to be outside of the working temperatur range, the maximum P_T is taken as that for temperature T_2.

To conclude the computation, the maximum static error of the circuit is determined. In order to do this, the temperature at which $\Delta P = P(T_0) - P_H(T_0)$ has extreme values is found. The expression

$$2U^2R_тR_т'rr_н^2=-K[R_т(r+r_н)+rr_н]^3. \qquad (23)$$

is found from the condition $d(\Delta P)/dT_0 = 0$.

Putting the values of R_T and R_T^{+} from (6) and (7) into (23), we get the equation necessary to find T_{OM}:

$$2\frac{U^2 r_H^2 r}{K} = \frac{T_{OM}^2}{B} \frac{\left[R_{T_H} \exp\left(\frac{B}{T_H} - \frac{B}{T_{OM}}\right)(r + r_H) + r r_H\right]^3}{\left[R_{T_H} \exp\left(\frac{B}{T_H} - \frac{B}{T_{OM}}\right)\right]^2}. \quad (24)$$

Since this equation is not solved analytically for T_{OM}, one is obliged to use a graphical method. The maximum static error of the circuit is found from the formula

$$\Delta T_M = \frac{P_H(T_{OM})}{K} - (T - T_{OM}). \quad (25)$$

Let us examine the computation for a circuit with a barretter. It is characterized by constancy of the current flowing through the barretter. This current is defined by the expression

$$I = U_{12}\frac{R_T(r + r_H) + r r_H}{R_T r_H r}. \quad (26)$$

The power liberated in r_H will be

$$P_H = I^2\left[\frac{R_T r}{R_T(r + r_H) + r r_H}\right]^2 r_H. \quad (27)$$

By analogy with the foregoing, an expression similar to (8) corresponds to the condition for obtaining an inflection point on the curve $P_H(T_0)$. If $r = \infty$ in the circuit, we get from (8)

$$r_H = \gamma R_{T_p}. \quad (28)$$

It is possible only in rare cases to make a circuit which will fulfill this condition. By connecting a resistance r in the circuit, one can change the total current and make it equal to the nominal current of the barretter.

The quantity B of the required thermistor is determined from the given ratio of the powers at the edges of the temperature range.

This ratio corresponds to (11) for the first circuit.

If the temperature of the heated thermistor is regulated, then r_H is the given quantity. Choosing a value for R_{T_p}, we find r:

$$r = \frac{\gamma R_{T_p} r_H}{r_H - \gamma R_{T_p}}. \quad (29)$$

The power voltage for the circuit is determined from the values of the lower limit of barretration and from the nominal current of the barretter:

$$U = I\left[\frac{R_{T_1}(r + r_H) + r r_H}{R_T r r_H}\right] + U_{L.B.} \quad (30)$$

In this expression, the thermistor resistance is taken at the lower limit of the temperature range. When the thermistor temperature is raised, the operating point on the volt-ampere characteristic of the barretter will be shifted to the middle of the barretration zone.

The power liberated in the thermistor will be

$$P_T = I^2 R_T\left[\frac{r r_H}{R_T(r + r_H) + r r_H}\right]^2. \quad (31)$$

The amount of thermistor resistance which corresponds to $P_{T\max}$ is determined by an expression similar to (20). The maximum power liberated in the thermistor will be

$$P_{T_M} = I^2\frac{r r_H}{4(r + r_H)}. \quad (32)$$

Hence, the parameters of all the elements in the circuit can be determined. In order to illustrate the method presented, the calculation of the circuit shown in Fig. 2 is presented as an example.

Example. Compute the circuit elements of the temperature regulator of a heated thermistor operating in the temperature range from $\theta_{\theta_1} = -30$, to $\theta_{\theta_2} = +30$°C. The temperature of the semiconducting element $\theta = 50$°C. The power dissipated by the heater at -30°C is $P_{H_1} = 10$ watts.

It is assumed that the best transfer between the thermistor and the medium obeys Newton's formula.

Let us find the power dissipated by the thermistor at temperatures $\theta_{\theta_2} = 30$°C and at $\theta_{\theta p} = 0$°C:

$$P_{H2} = P_{H1}\frac{\theta - \theta_{02}}{\theta - \theta_{01}} = 2.5 \text{ w},$$

$$P_{L.L.} = P_{H1}\frac{\theta - \theta_p}{\theta - \theta_{01}} =$$

$$= 6.25 \text{ w and } k_p = \frac{P_{H1}}{P_{H2}} = 4.$$

Table 1

B,° K	2500	3000	3500
k_p	2,83	3,92	4,8

In order to determine B corresponding to $k_p = 4$, the function $k_p(B)$ is computed from (11) in some range of change in B. The results of the calculation are presented in Table 1.

Having plotted a curve through these points (Fig. 5), we find from it that B = 3025°K, corresponding to $k_p = 4$. We will take a thermistor having $R_{20} = 20$ ohms at $T_H = 293$°K.

Then the values of the thermistor resistance at three points in the temperature range will be

$$R_{T_1} = 165 \text{ ohms} \quad R_{T_2} = 14.2 \text{ ohms} \quad R_{T_p} = 42.8 \text{ ohms}$$

Using (8), we find

$$\gamma = 0.376.$$

The quantity r = 38.5 ohms is found from (14), written in the form

$$r^2 - 30.5\,r - 305 = 0.$$

The heater resistance is determined from (15):

$$r_H = 27.8 \text{ ohms}.$$

The power circuit voltage is computed from (18):

$$U = 43.3 \text{ volts}.$$

Table 2

θ_e, °C	—30	—15	0	15	30
ε	8.25	3.97	2.14	1.17	0.71
P, w	10.0	8.13	6.25	4.38	2.5
P_{H}, w	9.9	8.22	6.25	4.24	2.58
P_{T}, w	1.65	2.86	4.05	5.13	5.0
θ, °C	49.2	50.8	50.0	48.8	50.6

The maximum power dissipated in the thermistor will be $P_{T\max} = 5.13$ w, according to (21).

The thermistor resistance which corresponds to $P_{T\max}$ is found from (20):

$$R_{T_M} = 16.1 \text{ ohms}.$$

The temperature corresponding to R_{T_M} is found from (22): $T_M = 287$°K or 14°C.

The quantities P_H and P_T, and the temperature of the semiconducting element of the heated thermistor are determined on the basis of resistance values, the temperature dependence $R_T(T)$, and U. The results of the calculations are shown in Table 2.

The data of Table 2 confirm the correctness of the proposed method of calculation, and show that such a circuit can be successfully used for regulating the temperature of the semiconducting element in a heated thermistor.

LITERATURE CITED

1. N. P. Udalov, "Stabilizing the temperature of the working body of a heated thermistor," Avtomatika i Telemekhanika 19, No. 11 (1958).*

2. G. A. Becker, C. B. Green, and G. L. Pearson, "Properties and uses of thermistors – thermally sensitive resistors," Elec. Eng. (Nov. 1946).

3. G. K. Nechaev, Thermistors in Temperature Control [in Russian] (Gostekhizdat, Ukr. SSR, 1959).

---

*See English translation.

USE OF HEATER RESISTANCES FOR CURRENT AND VOLTAGE STABILIZATION

V. S. Popov

(Leningrad)

Translated from Avtomatika i Telemekhanika, Vol. 21, No. 4, pp. 555-557, April, 1960

Original article submitted October 8, 1959

A new type of electrical stabilizer with metal heater resistance is considered and analyzed. Results of experimental investigation are given, and technical characteristics are noted.

Bridge stabilizers with nonlinear resistances – incandescent lamps, thermistors, and barretters – are widely used as low-power electric current stabilizers [1].

Bridge stabilizers have a number of advantages – simplicity, wide frequency response, and the absence of moving parts. On the other hand, such instruments have a comparatively low stabilization coefficient; furthermore, they cannot be used in circuits where the load and the supply source are commoned.

In the stabilizer developed by the author the basic advantages of bridge stabilizers are retained, and the stabilization coefficient is increased. The stabilizer is suitable for applications in circuits where the load and the supply source are commoned.

The stabilizer consists of a shunt and a metallic resistance with indirect heating. The heater resistance is represented by a platinum heater in a glass insulating tube, around which a platinum spiral is wrapped (Fig. 1). The heater and spiral are placed in an unevacuated brass container serving to protect the heater resistances from mechanical damage. The diameter of the heater is usually within the limits of 10 to 50 μ; the inner diameter of the insulating tube is approximately double that of the heater. The diameter of the spiral wire varies within the range of 5 to 30 μ. The heater resistance is attached to a socket from a type 6N8S radio tube.

The time constant τ of the heater resistances as a function of heater and spiral dimensions is within the limits 0.03 to 0.80 sec.

As indicated by the investigation, the variation of the spiral resistance R_1 with concurrent action of the heating current I and the current flowing directly through the spiral I_s is of the form

$$R_1 = R_{10} + cI^\alpha + c_1 I_s^\beta, \qquad (1)$$

where R_{10} is the initial resistance of the sensing element (spiral), c and c_1 are constants depending upon the configuration of the heater resistance, α and β are constants within wide limits independent of the lay of winding and of the spiral diameter.

For platinum heaters $\alpha \approx 2.2$, where the temperature rise of the heater due to the heating current is within the

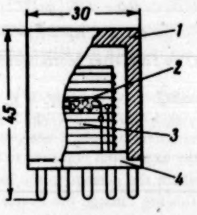

View without cover

Fig. 1. Metallic resistance with indirect heater. 1) Cover; 2) heater resistance; 3) compensating resistance; 4) socket.

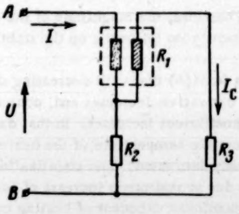

Fig. 2. Circuit diagram of the stabilizer.

limits of 40 to 400°. For heater resistances with nichrome or constantan heaters, $\alpha \approx 1.7$ under the same conditions.

With a platinum spiral, $\beta \approx 2.0$ under the condition that the temperature rise of the spiral due to the current flowing through it does not exceed 20°. With increasing temperature β does increase somewhat.

The arrangement of the stabilizer with heater resistance is shown in Fig. 2.

The relationship between current I_s in the load R_3 and the heating current I is of the form

$$I_s = I \frac{R_2}{R_1 + R_2 + R_3}. \tag{2}$$

Differentiating (2) while taking (1) into account, we obtain

$$\frac{dI_s}{dI} = \frac{R_2 (R_1 + R_2 + R_3) - I R_2 \left(\alpha c I^{\alpha-1} + c_1 \beta I_s^{\beta-1} \frac{dI_s}{dI} \right)}{(R_1 + R_2 + R_3)^2} \tag{3}$$

From that, we find, after rearrangement,

$$\frac{dI_s}{dI} \left(1 + \frac{c_1 \beta I_s^{\beta}}{R_1 + R_2 + R_3} \right) = \frac{R_2 [(R_1 + R_2 + R_3) - \alpha c I^{\alpha}]}{(R_1 + R_2 + R_3)^2}.$$

Equating the expression obtained to zero, we obtain the condition where the current in the load is independent of the current flowing through the heater*:

$$R_1 + R_2 + R_3 = \alpha\ I^{\alpha}. \tag{4}$$

In this manner the condition for stabilization will appear when the resistance increase of the spiral due to the heating current, multiplied α times, is equal to the sum of the resistances of the spiral, load, and shunt.

We will determine the conditions for the stabilization coefficient of the stabilizer to be a maximum. For that purpose we determine the conditions for a minimum of the second derivative d^2I_s/dI^2 in the operating sector of the stabilizer characteristic, that is, in the region where the first derivative dI_s/dI is equal to zero.

Differentiating equation (3) and setting the first derivative equal to zero, we obtain, after a number of rearrangements,

$$\frac{d^2 I_s}{dI^2} = \frac{R_2 (1 - \alpha)}{I (R_1 + R_2 + R_2) \left[1 + \frac{c_1 \beta I^{\beta}}{R_1 + R_2 + R_3} \right]}. \tag{5}$$

The expression $\frac{c_1 \beta I_s^{\beta}}{R_1 + R_2 + R_3}$ is considerably less than unity. Therefore, the magnitude of the current stabilized has practically no influence on the stabilization coefficient.

It follows from (5) that with decreasing shunt resistance R_2 the second derivative decreases and, consequently, the stabilization coefficient increases. In that case, according to (4), the operating temperature of the heater resistance is simultaneously decreased. The stabilization coefficient also increases, due to resistance increase of load R_3, decrease of the nonlinear exponent of heating current α, and increase of the current stabilized; but in that case the operating temperature of the heater resistance increases, and its overload capacity decreases.

According to (4) a higher load resistance is permissible for larger values of the nonlinear exponent α; the power output of the stabilizer increases simultaneously. Therefore, a platinum wire, which has a higher nonlinear exponent than nichrome wire, is used as a heater in the stabilizer.

It was shown by the experimental investigation of a number of stabilizers devised using various metallic heater resistances that, with an increase of the heater current, the load current initially increases, and, thereafter, after reaching some maximum value, decreases. This is due to current redistribution between the load and the shunt as a result of intense resistance increase of the spiral.

The stabilization coefficient of stabilizers is, on the average, equal to 50 for a 10% change in the heating (stabilizing) current, and about 30 for a 20% change of the stabilizing current.

The resistance of the platinum heater increases significantly upon increase of heater current. Consequently, on varying the voltage applied to the heater, the resistance of the latter changes in such a fashion as to oppose a change of the heater current. As a result the stabilizer will be less sensitive to variations of terminal voltage U_{AB} than to heater-current variations.

The table shows the relationship between the load current I_s and the voltage U, transmitted to the terminals of a stabilizer with heater resistances of the platinum heater being of 50μ in diameter and a platinum spiral with wire diameter of 24 μ, with R_2 equal to 1.0 ohm, R_3 equal to 5.0 ohms, and at an ambient temperature t of 20 and 40°.

As can be seen from the table, the stabilization coefficient of a voltage stabilizer is about 70 for a 20% change in the voltage.

The load current decreases when the ambient temperature changes as a result of resistance increase of the spiral and of the heater. For current stabilization, as well as for voltage stabilization, this error can be almost fully compensated for by winding part of the shunt resistance R_2 with copper.

For current stabilizers the copper resistance is 30% of the total in R_2, and for voltage stabilizers is 50%. The compensating copper resistance, wound on a small plate, is located in the same container as the heater resistance (Fig. 1).

During ambient-temperature changes the region of stabilization is somewhat displaced. This is caused by the fact that whenever the ambient temperature increases, the condition for stabilization (4) is disturbed – resistance R_1 increases, and the heating current within the voltage stabilizer decreases slightly. The temperature error of stabilizers does not exceed 0.2% per 10°.

To protect the stabilizers from large overloads, safety fuses made of platinum wire of a diameter equal to approximately 0.8 of the heater diameter should be connected in series with the heater.

---

*In satisfying equation (4) the expression $\frac{c_1 \beta I_s^{\beta}}{R_1 + R_2 + R_3} \ll 1$.

$t = 20°$

U. v	0.5	1.0	1.2	1.3	1.4	1.5	1.6	1.7	1.8	1.9	2.0
I_{c_3} ma	9.20	13.20	13.85	14.02	14.17	14.23	14.25	14.25	14.24	14.20	14.12

$t = 40°$

U. v	1.3	1.4	1.5	1.6	1.7	1.8	1.9	2.0
$I_{\text{э}}$ ma	13.80	14.00	14.10	14.20	14.22	14.22	14.22	14.21

The stabilizers developed are suitable for stabilization of direct current and alternating current (voltage), in the frequency region of from a few cycles to several hundred kilocycles, without wave-form distortion.

As compared with thermistors, the stabilizer with heater resistance has far lower inertia, higher stability, and insignificant temperature error.

A significant advantage of the stabilizer is that it will, after an interruption in operation, reestablish, with a high degree of accuracy, previous values of stabilized current (voltage). It was shown by an investigation of three months' duration that the voltage change at the stabilizer terminals will not exceed + 0.15% of the initial value.

The main advantages of the stabilizer are simplicity, the presence of a commoned point between the load and the supply source, and a high stabilization coefficient.

LITERATURE CITED

1. I. G. Gol'dreer, Voltage Stabilizers [in Russian] (Gosenergoizdat, 1952).

LETTER TO THE EDITOR

Translated from Avtomatika i Telemekhanika Vol. 21, No. 4, p. 558, April, 1960

The work of the author [1] cites new equations for basic parameters of the two-point regulation process with a new time correction method. The conclusion is drawn on the basis of introduction of the concept of residual delay $\Delta t'$ so that the method of calculation approaches the method laid out in [2]. However, for practical calculation of a system with the proposed method of correction, it is expedient to express the equations for the regulation process parameters directly in terms of given values Q_{in}, Q_{out}, C, Δt, and T'_{on}. The time of starting the heat influx into the object T'_{on} is rigorously given by the correction device. In that case the equations will be as follows:

$$\Delta\vartheta'_{m(+)} = \frac{T'_{on}(Q_{in} - Q_{out}) - \Delta t Q_{out}}{C}, \tag{1}$$

$$\Delta\vartheta'_{m(-)} = \Delta\vartheta_{m(-)} = -\Delta t \frac{Q_{out}}{C}. \tag{2}$$

The full amplitude of autooscillation

$$\Delta\vartheta'_m = \Delta\vartheta'_{m(+)} + \Delta\vartheta'_{m(-)} = T'_{on} \frac{Q_{in} - Q_{out}}{c}, \tag{3}$$

$$T'_{off} = T'_{on} \frac{Q_{in} - Q_{out}}{Q_{out}} = T'_{on}(n-1), \tag{4}$$

$$T' = T'_{on} + T'_{off} = T'_{off} \frac{Q_{in}}{Q_{out}} = T'_{on} n. \tag{5}$$

Equations (1) to (5) given can be obtained from equations (1) to (5) of [1], if it is considered that

$$\Delta t' = T'_{on} - \Delta t \frac{Q_{out}}{Q_{in} - Q_{out}}.$$

In addition to the concept of degree of correction k, introduced in [1], it is also expedient to introduce a second degree of correction k_1, which represents the relationship of full oscillation amplitudes of the process without correction to the amplitudes of the process with correction, that is,

$$k_1 = \frac{\Delta\vartheta_m}{\Delta\vartheta'_m}.$$

It is apparent that

$$k_1 = \frac{\Delta t}{T'_{on}} \frac{Q_{in}}{Q_{in} - Q_{out}} = \frac{\Delta t}{T'_{on}} \frac{n}{n-1}.$$

Expressing the full period of autooscillations in the system with correction in terms of a new degree of correction k_1 and a power of influx n, we obtain

$$T' = \frac{\Delta t n^2}{(n-1)k_1}.$$

The curves of the relationship between the autooscillation period T' and a power of the influx n for $\Delta t = 1$, and at various values of the degree of correction k_1 will be of a form coinciding with the curves in Fig. 3 of [1].

LITERATURE CITED

1. A. I. Cherepanov, "Improvement of quality of two-point regulation," Avtomatika i Telemekhanika 19, No. 5 (1958).*
2. A. A. Kampe-Nemm, Dynamics of Two-point Regulation [in Russian] (Gosenergoizdat, 1955).

---

*See English translation.

Ya. Z. Tsypkin

LENIN PRIZE LAUREATE

On April 22, 1960, the Committee for the Lenin prize in the domain of science and technology for the Soviet Ministers of the Union of Soviet Socialist Republics awarded the Lenin prize to Doctor of Mechanics. Professor Yakov Zalmanovich Tsypkin for his work on the theory of sampled-data and relay automatic systems, presented in the monographs, Transient and Steady-State Processes in Sampled-Data Circuits, Theory of Relay Systems of Automatic Control, Theory of Sampled-Data Systems, published during the years 1951-1958.

The editorial board of the journal Avtomatika i Telemekhanika (Automation and Remote Control) warmly congratulates Yakov Zalmanovich Tsypkin for his high honor, and wishes him further creative successes.

The V. I. Lenin prize for works on the theory of relay and sampled-data systems was awarded by the director of the laboratory of the Institute for Automation and Remote Control of the Academy of Sciences of the USSR to Professor Yakov Zalmanovich Tsypkin, member of the editorial board of the journal Avtomatika i Telemekhanika (Automation and Remote Control) and doctor of engineering science.

For the first time, a cycle of theoretical works in the domain of automation has received the highest award. The Institute for Automation and Remote Control of the AN SSSR (Academy of Sciences of the USSR) is rightfully proud that the works singled out for the Lenin prize were executed by one of its leading scientific workers.

The editorial board of the journal Avtomatika i Telemekhanika (Automation and Remote Control) is particularly pleased to state that works of Ya. Z. Tsypkin, awarded this high honor, were published in this journal, starting in 1948.

The biography of Lenin prize laureate Ya. Z. Tsypkin is a typical biography of a young Soviet scientist and patriot of our fatherland.

Ya. Z. Tsypkin's first steps as a scientist were connected with the investigation of continuous control systems. The concept of degree of stability, suggested by him in conjunction with P. V. Bromberg [1, 4, 5, 8, 18, 48], entered into automatic control theory and was widely disseminated in the international literature. His following works were devoted to the dynamics of automatic control systems when lags were taken into account. Ya.Z. Tsypkin developed, and applied to the analysis of stability of these systems, frequency methods [4, 6, 7, 8]. The results which he obtained in this area underlay his doctoral dissertation, "Systems with lagging feedback," [9].

The methods developed by. Ya. Z. Tsypkin for investigating systems with lags received broad recognition, both in the Soviet Union and abroad. It is appropriate to recall here that, in evaluating the work of this period, Academician A. A. Andronov characterized Ya. Z. Tyspkin as one of the most vigorous and promising scientists working in the domain of control theory in the USSR.

The tremendous development of computing technology and radioelectronics in the postwar years engendered a heightened interest in discrete devices for control and communications, in particular, in relay, sampled-data and digital devices. Ya. Z. Tsypkin is one of the first scientists to have properly appreciated the importance of this trend and, more than ten years ago, he applied himself to the development of a general theory of discrete automatic systems. His first work in this direction dates back to 1948 [10].

The fundamentals of sampled-data system theory were first presented by him in [12, 13, 15]. The generality of the developed theories of sampled-data systems was not inferior to the generality of theories of continuous systems. In 1951, Ya. Z. Tsypkin published a monograph on sampled-data circuits, Transient and Steady-State Processes in Sampled-Data Circuit [17]. In [20] there was developed a frequency method of analyzing discontinuous control systems which allowed one to establish in which cases sampled-data control improves the system's dynamic properties as compared to continuous control. A further series of works were devoted to the effect of random stimuli [22], of pulse shapes [33], of forcing actions [40] and of nonlinearities [23, 38] on the dynamic properties of sampled-data systems.

Starting in 1956, he extended sampled-data system theory to cover systems with digital computing devices [39, 44, 46, 47, 49, 50, 51].

The enumerated works were widely used by various organizations, designers, developers, investigators and users of sampled-data systems. The developed theory of sampled-data systems entered into the VUZ (university) curriculum and into courses for advanced engineering [45]. It was widely used and further developed in a number of works by Soviet and foreign scientists.

In 1958, Ya. Z. Tsypkin published the fundamental monograph, Theory of Sampled-Data Systems, [52] which is devoted to the analysis and synthesis of sampled-data systems and contains the fundamental general theory of sampled-data automatic systems, applied in various domains of technology. Together with sampled-data systems, relay systems were investigated by him in a number of works. In the theory of relay systems, Ya. Z. Tsypkin developed general and precise methods of investigation, superficially similar to linear methods but, at the same time, applicable to this class of essentially nonlinear systems. These methods permitted the investigation of various modes of operation in relay systems, the comparison of types of circuits and the development of new, advanced schemes. These works [16, 19, 23, 27, 29, 31] were summarized in the monograph, Theory of Relay Systems of Automatic Control [34].

The monographs of Ya. Z. Tsypkin, and many of this papers, were published in the German Democratic Republic, China, Poland, Rumania, Czechoslovakia, England, France, the German Federal Republic, the United States of America, and Japan, and were given as papers at international congresses [43, 46, 50, 51].

It is necessary to mention the characteristic traits of the creative style of Ya. Z. Tsypkin – clarity and explicitness in posing the problem, simplicity and elegance of the method of investigation, tense and concentrated purposefulness.

It is no coincidence that his last monographs constitute three important successive steps in the solution of a single problem, that of creating a general theory of discrete automatic systems.

Ya. Z. Tsypkin devoted much attention and work to the question of preparing a professional cadre. He is widely known as a superb lecturer. His lectures on automatic control theory have been very popular [14, 21, 28, 45, 54].

Under Ya. Z. Tsypkin's editorship, the fundamental foreign works on automatic control have been translated and published here (McColl, Fundamental Theory of Servomechanism (1947); Lauer, Lesnick, and Matson, Servomechanism Fundamentals (1948); James, Nichols, and Phillips, Theory of Servomechanisms (1949); Flugge-Lotz, Phase Plane Method in Relay System Theory, 1959; and others).

Under Ya. Z. Tsypkin's direction, a large number of dissertations were executed, comprising a broad circle of questions in radio engineering, electronics and automatic control.

Professor Ya. Z. Tsypkin is an important Soviet scientist, creator of a unified theory of sampled-data and relay automatic systems which has found wide practical application and has obtained world-wide recognition.

LIST OF THE BASIC SCIENTIFIC WORKS OF YA. Z. TSYPKIN

1. "On the degrees of stability of linear systems," Izvest. Akad. Nauk SSSR, Otd. tekn. nauk No. 12 (1945). (in conjunction with P. V. Bromberg).
2. "Stability of linear systems with feedback," Radiotekhnika No. 5 (1946).
3. "Stability criterion of linear systems with feedback," Zhur. Tekh. Fiz. No. 6 (1946).
4. "Stability of automatic frequency control systems with account taken of delay effects," Radiotekhnika Nos. 7-8 (1946).
5. "Degree of stability of linear systems" Trudy NISO, Izd. BNT MAP No. 9 (1946). (in conjunction with P. V. Bromberg).
6. "Stability of systems with lagged feedback," Avtomatika i Telemekhanika 7 Nos. 2-3 (1946).
7. "On klystron theory," Radiotekhnika No. 1 (1947).
8. "Degree of stability of systems with lagging feedback," Avtomatika i Telemekhanika 8, No. 3 (1947).
9. "Systems with lagging feedback," Trudy NISO, Izd. BNT Map No. 24 (1947).
10. "Stability and degree of stability of discontinuous control systems," Avtomatika i Telemekhanika 9, No. 2 (1948).
11. "Stability of one class of automatic control systems with distributed parameters," Avtomatika i Telemekhanika 9, No. 3 (1948).
12. "Theory of discontinuous control, I. Equations and characteristics of discontinuous control systems," Avtomatika i Telemekhanika 10, No. 3 (1949).
    Teoria a sistemiov discontinuituuna. I. Probleme de automatizare (Acad. Rep. Popul. Romane, Bukuresti, 1954).
13. "Theory of discontinuous control, II. Stability of discontinuous control systems," Avtomatika i Telemekhanika 10, No. 5 (1949).
    Teoria a sistemiov discontinuituuna. II. Probleme de automatizare (Acad. Rep. Popul. Romane, Bukuresti, 1954).
14. "Stability criterion for linear automatic control systems," VNITO – Priborostroeniya (Mashgiz, 1949).
15. "Theory of discontinuous control, III. Transient responses," Avtomatika i Telemekhanika 11, No. 5 (1950).
    Teoria a sistemiov discontinuituuna. III. Probleme de automatizare (Acad. Popul. Romane, Bukuresti, 1954).
16. "Stability and autooscillations in relay systems of automatic control," Trudy Leningradskoi VVIA No. 32 (1950).
17. Transient and Steady-State Processes in Sampled-Data Circuits [in Russian] (Energoizdat, 1951; Kharbin, 1959). Differenzengleichungen der Impuls- und Regeltechnik (Belin Verlag Technik, 1956).
18. "On the upper bound of the degree of stability of single-loop systems," Avtomatika i Telemekhanika 13, No. 4 (1952).
19. "Forced oscillations of relay systems of automatic control," Avtomatika i Telemekhanika 13, No. 5 (1952).
20. "Frequency methods for analyzing discontinuous control systems," Avtomatika i Telemekhanika 14, No. 1 (1953).
    Frequency Method of Analyzing Intermittent Regulating Systems. Frequency Response (ed. by R. Oldenburger (New York, MacMillan Co., 1956).
21. Lectures on Automatic Control Theory. "Stability of automatic control systems" (Izd. VZEI, 1953, 1956, 1958).
22. "Designing discontinuous control systems for stationary random stimuli," Avtomatika i Telemekhanika 14, No. 4 (1953).
23. "On the stability of periodic motions in relay systems," Avtomatika i Telemekhanika 14, No. 5 (1953).
24. "Influence of the parameters of nonlinear automatic control systems on stability and autooscillations," Trudy VZEI No. 3 (1954).
25. "Stability criteria for nonlinear automatic control systems," Fundamentals of Automatic Control [in Russian] (Mashgiz, 1954) chapter. 10.
    Stabilitatskriterien fur selbsttatige Regelungssysteme. Grundlagen der selbsttatigen Regelung. 1 (Berlin Verlag Technik, 1959; Munchen/, R. Oldenbourg Verlag, 1959).
26. "Basic theory of sampled-data control systems," Fundamentals of Automatic Control [in Russian] (Mashgiz, 1954) chapter 19.
    Grundlagen der Theorie fur Systeme mit Impulsregelung. Grundlagen der selbsttätigen Regelung. 1 (Berlin Verlag Technik, 1959; Munchen R. Oldenbourg Verlag, 1959).
27. "Frequency methods of investigating autooscillations and forced oscillations in relay systems of automatic control," Fundamentals of Automatic Control [in Russian] (Mashgiz, 1954) chapter 27.
    Frequenzmethode zur Analyse der Selbstschwingungen und erzwingenen Schwingungen in Relaisregelungssystemen. Grundlagen der selbsttätigen Regelung. 2 (Berlin Verlag Technik, 1959; München R. Oldenbourg Verlag, 1959).

28. Lectures on Automatic Control Theory: "Introduction to automatic control theory." [in Russian (Izd. VZEI, 1954, 1959).

29. "Frequency methods of investigating periodic modes in relay system of automatic control," In Commemoration of A. A. Andronov [in Russian] (Izd. AN SSSR, 1955).

30. "On the asymptotic properties of multiloop automatic control systems," Trudy VZEI No. 5 (1955).

31. "On the theory of relay systems of automatic control," Proceedings of the Second All-Union Conference on Automatic Control Theory [in Russian] (Izd. AN SSSR, 1955).

32. "On designing nonlinear discontinuous control systems," Proceedings of the Second All-Union Conference on Automatic Control Theory [in Russian] (Izd. AN SSSR, 1955).

33. "On taking pulse forms into account in discontinuous control systems," Avtomatika i Telemekhanika 16, No. 5 (1955).

34. Theory of Relay Systems of Automatic Control [in Russian] (Gostekhizdat, 1955).
Theorie der Relaissysteme des automatischen Regelungs München R. Oldenbourg Verlag, 1958; Berlin Verlag Technik, 1958).
Translated into Japanese (Tokyo, 1960).
Theorie des asservissements a relair (Paris Dunod, 1960).

35. Lectures on Automatic Control Theory. "Stability of automatic control systems." (Izd. VZEI, 1955, 1957, 1959).

36. "On computing limiters' amplitude characteristics," Radiotekhnika No. 12 (1955).

37. "On the connection of the equivalent complex gain of a nonlinear element with its characteristic," Avtomatika i Telemekhanika 17, No. 4 (1956).
"Uber den Zusammenhang zwischen der Kennlinie eines nichtlinearen Gliedes und seiner Beschreibungsfunktion," Regelungstechnik 6, No. 8 (1958).

38. "Calculating the processes in nonlinear discontinuous control systems," Avtomatika i Telemekhanika 17, No. 6 (1956).

39. "On automatic control systems containing digital computers," Avtomatika i Telemekhanika 17, No. 8 (1956).

40. "Investigation of steady-state processes in sampled-data servosystems," Avtomatika i Telemekhanika 17, No. 12 (1956).

41. "On the connection between the spectra of amplitude-modulated pulse sequences and their envelopes," Trudy VZEI No. 7 (1957).

42. "Construction of the transient response in automatic control systems from the characteristics of their individual links," Trudy VZEI No. 7 (1957). (in conjunction with L. N. Gol'denberg).

43. "Stabilization of relay systems of automatic control," [in Russian] Conveguo Internationale sui Problemi Dell' Automatismo, Milano, 8-13 April, 1956 (Roma, 1958) vol. 1.

44. "Correction of sampled-data automatic regulation and control systems," Avtomatika i Telemekhanika 18, No. 2 (1957).

45. Lectures on Automatic Control Theory: "Elements of sampled-data control theory," [in Russian] (Izd. VZEI, 1957, 1960).

46. "On the synthesis of sampled-data automatic regulation and control systems. [in Russian] Regelungstechnik moderne theorie und ihre Verwendbarkeit (München, 1957).

47. "Present state and problems in the development of the theory of discrete automatic systems," Proceedings of the Sessions of the AN SSSR on the Scientific Problems of Automating Production, Oct. 15-20, 1956 [in Russian] (1957) Vol. 2.

48. Uber die obere Grenze des Stabilitatsgrades von I-, P-, PI-, PD-, PID-Reglern," Regelungstechnik 5, No. 2 (1957).

49. "Certain questions in the synthesis of automatic sampled-data systems," Avtomatika No. 1 (1958).

50. "Certain questions in discrete automatic system theory," [in Russian] Proceedings of the Computers in Control Systems Conference, Atlantic City, AIEE (1958).

51. "Sampled-data automatic systems with extrapolating devices," Avtomatika i Telemekhanika 19, No. 5 (1958).
"Impulsowe uklady automatyki z uszadzeniami ekstrapolujacymi," Aschiwum Automatiki i Telemechaniki 3, No.4 (1958).

52. Theory of Sampled-Data Systems [in Russian] (Fizmatgiz, 1958).

53. "Eliminating the effect of lags on the dynamics of nonlinear sampled-data systems," Doklady Akad. Nauk SSSR 124, No. 4 (1959).
Uber die Beseitigung der Einflusses von Totzeit auf die dynamischenEigenschaften von nichtlinearen Impulsregel System," Regelungstecknik No. 6 (1959).

54. Lectures on Automatic Control Theory: "Automatic control systems for random disturbances." [in Russian] (Izd. VZEI, 1959).

55. "Frequency characteristics of relay automatic systems, Avtomatika i Telemekhanika 20, No. 12 (1959).

56. "Discrete automatic systems, their theory and perspective developments," Proceedings of Conference on Theory and Applications of Discrete Automatic Systems [in Russian](1960).

57. "Lag compensation in automatic sampled-data systems," Proceedings of the Conference on Theory and Applications of Discrete Automatic Systems [in Russian](1960).

58. "On some peculiarities and capabilities of automatic sampled-data systems," Izvest. Akad. Nauk SSSR, Otd. tekhn. nauk, Énergetika i avtomatika No. 2 (1960).

ANALYTIC CONTROLLER DESIGN. II

A. M. Letov
(Moscow)

Translated from Avtomatika i Telemekhanika Vol. 21, pp. 561-568, May, 1960
Original article submitted December 23, 1959

The solution is presented for the problem of analytic controller design in correspondence with a given optimizing functional. The solution is given for a closed region which contains the boundary of excursion of the controlling organ.

1. Optimal Systems, Defined in a Closed Region

Essential in all automatic control systems is the limitation on the excursion of the controlling organs ξ:

$$|\xi| \leqslant \bar{\xi} \tag{1.1}$$

on the limitation on the magnitude of the velocity of this excursion

$$|\dot{\xi}| \leqslant \bar{f}, \tag{1.2}$$

where $\bar{\xi}$, f are positive numbers.

With such limitations, the system becomes essentially nonlinear, since the presence of the equality sign in (1.1) and (1.2) permits the system to remain on the boundary of the region $\bar{N}$ of its definition. This region is closed. Moreover, it is impossible here to seek an optimal solution to the problem among functions of the class C_1, since there can be discontinuities on the boundary of the function which solves the problem. By taking into account what has just been said, we formulate the following variational problem.

We consider a closed system to be controlled, in which the disturbed motion of the controlled object is given by the equations

$$g_k = \dot{\eta}_k - \left(\sum_{\alpha} b_{k\alpha}\eta_\alpha + m_k\xi\right) = 0 \quad (k = 1, \ldots, n). \tag{1.3}$$

The notation in (1.3) has the same meaning as in [1]. It is assumed that (1.3), in conjunction with the controller equations being sought, are defined in the closed region $\bar{N}$, characterized by (1.1). In this region there are given the sole boundary conditions

$$\begin{gathered}\eta_{10} = \eta_1(0), \ \ldots, \ \eta_n(0) = \eta_{n0}, \ \xi(0) = \xi_0; \\ \eta_1(\infty) = \ldots = \eta_n(\infty) = \xi(\infty) = 0\end{gathered} \tag{1.4}$$

They mean simply this: that no matter what transient response arises in $\bar{N}$, it must terminate, for $t^* = \infty$, with the system at the origin of coordinates.

As the criterion of optimality, we take the integral

$$I = \int_0^\infty V dt, \tag{1.5}$$

where V is the positively defined quadratic form

$$V = \sum_k a_k\eta_k^2 + c\xi^2. \tag{1.6}$$

We shall search for such continuous functions ξ, η_1, ..., η_n in Class C (permitting, generally speaking, discontinuities of the first derivatives) which minimize the integral in (1.5).

The problem just formulated belongs to the class of the so-called discontinuous problems of the calculus of variations. To solve such problems there exist various methods of the classical variational calculus, as well as newer methods, presented in the works cited in [1]. Here we shall use the methods of the classical variational calculus, supplemented by a nonlinear transformation which, in optimal problems of the first class [1], was used in [2].*

2. Solution of the Problem

We consider the case when the limitation is as in (1.1), and we set

$$\xi = \varphi(\zeta). \tag{2.1}$$

We define the function $\varphi(\zeta)$ as

$$\varphi(\zeta) = \begin{cases} +\bar{\xi} & \text{for} \quad \zeta \geqslant \zeta^*, \\ \varphi(\zeta) & \text{for} \quad |\zeta| < \zeta^*, \\ -\bar{\xi} & \text{for} \quad \zeta \leqslant -\zeta^*, \end{cases} \tag{2.2}$$

where ζ^* is a given positive number and $\varphi(\zeta)$ is any continuous function whose derivative is continuous for $|\zeta| < \zeta^*$, and which is equal to zero for $\zeta = 0$. In particular, such a condition is satisfied by the function $\varphi(\zeta) = \xi \sin \zeta$ for $\zeta^* = \pi/2$ (Fig. 1).

Transformations (2.1) and (2.2) translate the closed region $N(\xi, \eta_1, \ldots, \eta_n)$ into the open region $\bar{N}(\zeta, \eta_1, \ldots, \eta_n)$ and permit one to use the well-known methods of variational calculus for the solution of ordinary Lagrange problems. The only special feature of this solution is that one must verify that the Weierstrass-Erdmann conditions hold at all points of discontinuity of the derivatives. To begin the solution of the problem, we set

---

* The author's attention was called to the transformation by I. A. Litovchenko, to whom the author expresses his gratitude.

$$H = V + \sum_k \lambda_k \left[\dot{\eta}_k - \sum_\alpha b_{k\alpha}\eta_\alpha - m_k\varphi(\zeta)\right]. \tag{2.3}$$

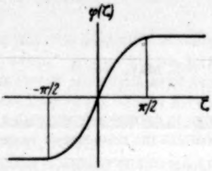

Fig. 1.

On the basis of (2.3), we find that

$$\frac{\partial H}{\partial \dot{\eta}_k} = \lambda_k, \qquad \frac{\partial H}{\partial \eta_k} = 2a_k\eta_k - \sum_\alpha \lambda_\alpha b_{\alpha k},$$

$$\frac{\partial H}{\partial \dot{\zeta}} = 0, \qquad \frac{\partial H}{\partial \zeta} = \left[2c\varphi(\zeta) - \sum_\alpha m_\alpha\lambda_\alpha\right]\frac{\partial\varphi}{\partial\zeta}.$$

The equations of the problem have the form

$$\dot{\eta}_k = \sum_\alpha b_{k\alpha}\eta_\alpha + m_k\varphi(\zeta),$$

$$\dot{\lambda}_k = -\sum_\alpha b_{\alpha k}\lambda_\alpha + 2a_k\eta_k, \tag{2.4}$$

$$0 = \left[2c\varphi(\zeta) - \sum_\alpha m_\alpha\lambda_\alpha\right]\frac{\partial\varphi}{\partial\zeta}.$$

They coincide to within the factor $\partial\varphi/\partial\zeta$ with the equations [(2.1) and (3.3)] of the analogous problem for the open region N(ξ, η_1, ... , η_n) which was formulated in [1].

Therefore, in addition to the solution obtained in [1] for the open region, we should consider the new solution which corresponds to the equation

$$\frac{\partial\varphi}{\partial\zeta} = 0. \tag{2.5}$$

By virtue of the definition given by (2.2), we set

$$\varphi(\zeta) = \pm\bar{\xi} \quad \text{for} \quad |\zeta| \geqslant \zeta^*. \tag{2.6}$$

This latter means that the optimal solution passes over the boundary of the region $\bar{N}$ (ξ, η_1, . . . , η_n).

For interior points of the region, the solution found has the form [1]

$$\xi = \sum_{\alpha=1}^{n} p_\alpha\eta_\alpha. \tag{2.7}$$

Thus, the equation of the controller which corresponds to the functional of (1.5) is written as

$$\xi = \begin{cases} \sum_\alpha p_\alpha\eta_\alpha & \text{for} \quad \left|\sum_\alpha p_\alpha\eta_\alpha\right| < \bar{\xi}, \\ +\bar{\xi} & \text{for} \quad \sum_\alpha p_\alpha\eta_\alpha \geqslant \bar{\xi}, \\ -\bar{\xi} & \text{for} \quad \sum_\alpha p_\alpha\eta_\alpha \leqslant -\bar{\xi}. \end{cases} \tag{2.8}$$

Obviously, this equation corresponds to an ideal nonlinear controller with an infinitely large servomotor speed.

The question of the stability of system (1.3), supplied with the controller defined by (2.8), should be considered separately. It is the subject-matter of an independent problem. As was shown in [1], for a deviation $|\Sigma p_\alpha\eta_\alpha| < \bar{\xi}$, stability is guaranteed; for a deviation $|\Sigma p_\alpha\eta_\alpha| \geqslant \bar{\xi}$ a special investigation is required, leading to the construction of the region of attraction, the boundary of which necessarily lies beyond the limits of $|\Sigma p_\alpha\eta_\alpha| = \bar{\xi}$. Various cases can occur here. Thus, in example 1 of paper [1], where n = 1, b_{11} = b, m_1 = m and, $\eta_1 = \eta$, we had the system of equations

$$\dot{\eta} = b\eta + m\xi,$$

$$\xi = \begin{cases} +\bar{\xi} & \text{for} \quad -\frac{k+b}{m}\eta \geqslant \bar{\xi}, \\ -\frac{k+b}{m}\eta & \text{for} \quad \left|1-\frac{k+b}{m}\eta\right| < \bar{\xi}, \\ -\bar{\xi} & \text{for} \quad -\frac{k+b}{m}\eta \leqslant -\bar{\xi}, \end{cases} \tag{2.9}$$

where the number k is defined by the formula

$$k = +\sqrt{b^2 + \frac{m^2 a}{c}}. \tag{2.10}$$

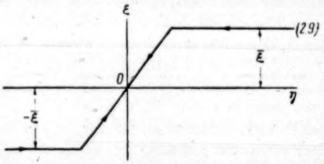

Fig. 2.

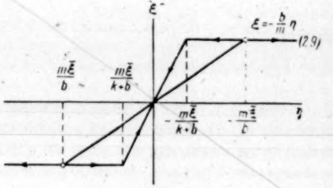

Fig. 3.

Figures 2 and 3 show the system's phase plane for the cases m, b < 0 and m < 0, b > 0. In the first case, the curve $\xi = \xi(\eta)$ (2.9) is the sole integral curve by which the representative point returns to equilibrium for any η_0; in the second case, the system's stability is guaranteed only for $|\eta_0| < -\frac{m\bar{\xi}}{b}$. The features are analogous in the two other cases, in which $m > 0$, $b \gtrless 0$.

It is of interest to note that the choice of sufficiently small weight constants in the function of (1.5) permits an arbitrarily close approach to a relay characteristic of the optimal controller :

$$\xi = \bar{\xi}\,\mathrm{sign}\left(-\frac{k+b}{m}\eta\right). \tag{2.11}$$

However, the execution of the limiting transfer itself requires additional discussion.

3. Possible Generalizations of the Functional of (1.5)

We now consider the case of optimizing a functional of the form

$$I(\xi) = \int_0^\infty (V + \dot{\xi}^2)\,dt. \tag{3.1}$$

In accordance with transformation (2.1), we have

$$I = [\varphi(\zeta)] = \int_0^\infty \left[\sum_k a_k\eta_k^2 + c\varphi^2(\zeta) + \left(\frac{\partial\varphi}{\partial\zeta}\dot{\zeta}\right)^2\right]dt.$$

The boundary conditions remain as before, i.e., (1.4). We set

$$H = \Sigma a_k\eta_k^2 + c\varphi^2(\zeta) + \left(\frac{\partial\varphi}{\partial\zeta}\dot{\zeta}\right)^2$$

$$+\sum_k \lambda_k\left[\dot{\eta}_k - \sum_\alpha b_{k\alpha}\eta_\alpha - m_k\varphi(\zeta)\right]. \tag{3.2}$$

Since

$$\frac{\partial H}{\partial\dot{\zeta}} = 2\left(\frac{\partial\varphi}{\partial\zeta}\right)^2\dot{\zeta},\ \frac{\partial H}{\partial\zeta} = \left[2c\varphi(\zeta) + 2\frac{\partial^2\varphi}{\partial\zeta^2}\dot{\zeta}^2\right]\frac{\partial\varphi}{\partial\zeta} -$$

$$-\sum_k \lambda_k m_k\frac{\partial\varphi}{\partial\zeta}.$$

then the equations of the variational problem will have the form

$$\dot{\eta}_k = \sum_\alpha b_{k\alpha}\eta_\alpha + m_k\varphi(\zeta),$$

$$\dot{\lambda}_k = -\sum_\alpha b_{\alpha k}\lambda_\alpha + 2a_k\eta_k, \tag{3.3}$$

$$\frac{d}{dt}\left[2\left(\frac{\partial\varphi}{\partial\zeta}\right)^2\dot{\zeta}\right] = \left[2c\varphi(\zeta) + 2\frac{\partial^2\varphi}{\partial\zeta^2}\dot{\zeta}^2 - \sum_k\lambda_k m_k\right]\frac{\partial\varphi}{\partial\xi}.$$

Consider the last of these equations. After some obvious simplifications, we find that

$$2\left[\frac{\partial\varphi}{\partial\zeta}\ddot{\zeta} + \frac{\partial^2\varphi}{\partial\zeta^2}\dot{\zeta}^2\right]\frac{\partial\varphi}{\partial\zeta} = \left[2c\varphi(\zeta) - \sum_k m_k\lambda_k\right]\frac{\partial\varphi}{\partial\zeta} \tag{3.4}$$

Therefore, (3.3) should be considered for the two cases

$$\frac{\partial\varphi}{\partial\zeta} = 0, \tag{3.5}$$

when the system's motion occurs on the boundary of region $\bar{N}$, and

$$2\left[\frac{\partial\varphi}{\partial\zeta}\ddot{\zeta} + \frac{\partial^2\varphi}{\partial\zeta^2}\dot{\zeta}^2\right] = 2c\varphi(\zeta) - \sum_k m_k\lambda_k, \tag{3.6}$$

when the system's motion takes place on the interior points of region $\bar{N}$. In the first case we have the solution

$$\varphi(\zeta) = \pm\bar{\xi} \quad \text{for} \quad |\zeta| \geqslant \zeta^*. \tag{3.7}$$

In the second case, since $\frac{\partial\varphi}{\partial\zeta}\dot{\zeta} = \frac{d}{dt}\varphi(\zeta)$, Eq. (3.6) reduces to the form

$$2\ddot{\varphi} = 2c\varphi - \sum_k m_k\lambda_k. \tag{3.8}$$

In conjunction with the first 2n equations of (3.3), this determines the controller equation

$$\dot{\xi} = \sum_\alpha p_\alpha\eta_\alpha - r\xi. \tag{3.9}$$

It is essential to note that, inasmuch as Eqs. (3.3) of the variational problem coincide exactly with (2.1) and (3.3) of [1], the equation just found, (3.9), coincides exactly with (4.5) of [1].

On the $\xi, \eta_1, \ldots, \eta_n$ phase space we sketch the two hyperplanes

$$\sum p_\alpha\eta_\alpha = \pm r\bar{\xi}. \tag{3.10}$$

Then, the controller equation being sought will be written as

$$\dot{\xi} = \begin{cases} +\bar{\xi} & \text{for} \quad \dfrac{\Sigma p_\alpha\eta_\alpha}{r} \geqslant \bar{\xi}, \\ \Sigma p_\alpha\eta_\alpha - r\xi & \text{for} \quad \left|\dfrac{\Sigma p_\alpha\eta_\alpha}{r}\right| < \bar{\xi}, \\ -\bar{\xi} & \text{for} \quad \dfrac{\Sigma p_\alpha\eta_\alpha}{r} \leqslant -\bar{\xi}. \end{cases} \tag{3.11}$$

4. The Weierstrass-Erdmann Conditions

To complete the investigation of the necessary conditions for the existence of an optimal solution of the analytic design problem, one should convince oneself that the Weierstrass-Erdmann conditions hold at the nodal points of function ξ.

In the case when one is considering a functional of the form of (3.1), these conditions reduce to the holding of the following equalities:

$$\frac{\partial H^+}{\partial \dot{\eta}_k} = \frac{\partial H^-}{\partial \dot{\eta}_k}, \qquad \frac{\partial H^+}{\partial \dot{\zeta}} = \frac{\partial H^-}{\partial \dot{\zeta}} \qquad (k = 1, \ldots, n), \tag{4.1}$$

$$H^+ - \sum_k \left(\frac{\partial H}{\partial \dot{\eta}_k} \dot{\eta}_k \right)^+ - \left(\frac{\partial H}{\partial \dot{\zeta}} \zeta \right)^+ = H^- - \sum_k \left(\frac{\partial H}{\partial \dot{\eta}_k} \dot{\eta} \right)^- - \left(\frac{\partial H}{\partial \dot{\zeta}} \zeta \right)^- . \tag{4.2}$$

Here, H is the function in (2.3) or in (3.2), and the "+" and "-" signs denote that the computation of the corresponding functions is carried out to the left or to the right of the nodal points of function ξ.

One easily convinces himself that, if the first n conditions of (4.1) hold, which reduce to the equations

$$\lambda_k^+ = \lambda_k^- \qquad (k = 1, \ldots, n), \tag{4.3}$$

then the two remaining conditions are also satisfied for any functions $\xi, \eta_1, \ldots, \eta_n$ of class C. As for (4.3), it can always be satisfied, as is easily verified, if the optimal system is stable.

Thus, in the example considered in Section 2, the solutions for the optimal controller in the case when have the form $|\xi| \geqslant \bar{\xi}$

$$\begin{aligned} \eta &= c_1 e^{bt} \mp \frac{m\bar{\xi}}{b}, \\ \lambda &= c_2 e^{-bt} \mp \frac{2am}{b^2} \bar{\xi} + \frac{ac_1}{b} e^{bt}, \end{aligned} \tag{4.4}$$

and, in the case when $|\xi| < \bar{\xi}$

$$\begin{aligned} \eta &= \bar{c}_1 e^{-kt} + \bar{c}_2 e^{kt}, \\ \lambda &= \frac{2c}{m^2} [-(k+b) \bar{c}_1 e^{-kt} + (k-b) \bar{c}_2 e^{kt}], \\ \xi &= \frac{1}{m} [-(k+b) \bar{c}_1 e^{-kt} + (k-b) \bar{c}_2 e^{kt}]. \end{aligned} \tag{4.5}$$

From the conditions on the left end (for t = 0)

$$\eta_0 = c_1 \mp \frac{m\bar{\xi}}{b}; \qquad \xi_0 = \pm \bar{\xi}. \tag{4.6}$$

From the conditions on the right end (for t = ∞),

$$\bar{c}_2 = 0. \tag{4.7}$$

The continuity conditions at the nodal points are

$$\bar{c}_1 = c_1 e^{bt_\bullet} \mp \frac{m\bar{\xi}}{b}; \quad -\frac{k+b}{m} \bar{c}_1 = \pm \bar{\xi}. \tag{4.8}$$

The single condition of (4.3) has the form

$$c_2 e^{-bt_\bullet} \mp \frac{2am\bar{\xi}}{b^2} + \frac{ac_1}{b} e^{bt_\bullet} = -\frac{2c}{m^2} (k+b) \bar{c}_1. \tag{4.9}$$

The last equation of (4.1) and (4.2) reduce to identities.

Equations (4.6), (4.7), and (4.9) define the constants c_1, $\bar{c}_7$, and c_2; (4.8) define c_1 and the time $t_\bullet$, corresponding to the nodal point of function ξ. We, hence, find that

$$\pm \frac{k}{b} \frac{m\bar{\xi}}{k+b} = \left(\eta_0 \pm \frac{m\bar{\xi}}{b} \right) e^{bt_\bullet}. \tag{4.10}$$

It is easily established that, for m < 0 and b < 0, (4.10) is solvable for $t_\bullet > 0$ for any $|\eta_0| \geqslant \left| -\frac{m\bar{\xi}}{k+b} \right|$; if this latter inequality does not hold, the system does not go beyond the boundary $|\xi| = \bar{\xi}$ and no nodal point exists. In the case when m < 0 and b > 0, the equation has a solution with respect to $t_\bullet > 0$ for any η_0 which satisfy the inequality

$$\left| -\frac{m\bar{\xi}}{k+b} \right| \leqslant |\eta_0| \leqslant \left| -\frac{m\bar{\xi}}{b} \right|$$

This is again the case shown on Figs. 2 and 3. The analogous features also occur for the other combinations of signs of m and b.

If the functional of (3.1) is used as the criterion of system optimality, then the Weierstrass-Erdmann conditions also are met. Indeed, the solution of the system for $|\xi| = \bar{\xi}$ is as follows:

$$\begin{aligned} \eta &= c_1 e^{bt} \mp \frac{m\bar{\xi}}{b}, \quad \xi = \bar{\xi}, \\ \lambda &= c_2 e^{-bt} \mp \frac{2am\bar{\xi}}{b^2} + \frac{ac_1}{b} e^{bt}. \end{aligned} \tag{4.11}$$

With the boundary conditions at infinity taken into account, the solution of the system for $|\xi| < \bar{\xi}$ is

$$\begin{aligned} \eta &= \bar{c}_1 e^{\mu_1 t} + \bar{c}_2 e^{\mu_2 t}, \\ \xi &= \frac{\mu_1 - b}{m} \bar{c}_1 e^{\mu_1 t} + \frac{\mu_2 - b}{m} \bar{c}_2 e^{\mu_2 t}, \\ \lambda &= -\frac{2a}{\mu_1 + b} \bar{c}_1 e^{\mu_1 t} - \frac{2a}{\mu_2 + b} \bar{c}_2 e^{\mu_2 t}. \end{aligned} \tag{4.12}$$

We find from the initial conditions that

$$\eta_0 = c_1 \mp \frac{m\bar{\xi}}{b}, \quad \xi_0 = \bar{\xi}. \tag{4.13}$$

The continuity conditions for the functions ξ and η at the nodal points are

$$\bar{\xi} = \frac{\mu_1 - b}{m} \bar{c}_1 + \frac{\mu_2 - b}{m} \bar{c}_2, \quad c_1 e^{bt_\bullet} \mp \frac{m\xi}{b} = \bar{c}_1 + \bar{c}_2. \tag{4.14}$$

The Weierstrass-Erdmann conditions reduce to the holding of the two equalities·

$$\lambda^+ = \lambda^-, \quad \left[\left(\frac{\partial \varphi}{\partial \zeta} \right)^2 \dot{\zeta} \right]^+ = \left[\left(\frac{\partial \varphi}{\partial \zeta} \right)^2 \dot{\zeta} \right]^- \tag{4.15}$$

or, what amounts to the same thing, to the equalities:

$$c_2 e^{-bt_\bullet} \mp \frac{2am\bar{\xi}}{b^2} + \frac{ac_1}{b} e^{bt_\bullet} = -\frac{2a}{\mu_1 + b} \bar{c}_1 - \frac{2a}{\mu_2 + b} \bar{c}_2,$$

$$\mu_1 (\mu_1 - b) \bar{c}_1 + \mu_2 (\mu_2 - b) \bar{c}_2 = 0.$$

Equation (4.13) defines the constant c_1; from (4.14) we find that

$$\bar{c}_1 = \frac{1}{\mu_2 - \mu_1}[(\mu_2 - b)\eta^* - m\bar{\xi}],$$
$$\bar{c}_2 = \frac{1}{\mu_2 - \mu_1}[\mu\bar{\xi} - (\mu_1 - b)\eta^*], \quad (4.17)$$

where $\eta^* = \eta(t_*)$. The first equation of (4.16) defines the constant c_2, the second defines the moment of time t_* when the system passes through the nodal point. This last equation, in correspondence with (4.17), takes the form

$$m\bar{\xi}(\mu_1 + \mu_2 - b) = (\mu_1 - b)(\mu_2 - b)\eta^*. \quad (4.18)$$

This last equation means that, at the nodal point, the servomotor speed must vanish, as was also the case with (5.4) of [1].

LITERATURE CITED

[1] A. M. Letov, "Analytic controller design. I," Avtomatika i Telemekhanika 21, No. 4 (1960). †

[2] A. Miele, Aeronat. Sci. 24, No. 2 (1957).

† See English translation.

OPTIMAL PROCESSES IN SECOND-ORDER PULSE-RELAY SYSTEMS

V. N. Novosel'tsev

(Moscow)

Translated from Avtomatika i Telemekhanika Vol. 21, No. 5, pp. 569-574, May, 1960
Original article submitted December 4, 1959

The problem of finding the optimal control law in pulse-relay second-order systems is considered.

Let there be given a physical system which is described by the n-dimensional vector $x_i(t)$ and let the position of the representative point in n-dimensional phase space at the initial moment of time be defined by $x_i(0)$. The representative point must be translated to the given point ξ_i. The process will have been completed after time T, and will be optimal if no other process provides for the attainment of ξ_i in a time less than T.

The optimal control problem for systems described by differential equations of the form

$$\frac{dx_i}{dt} = \varphi_i(x_i, u_l, t) \qquad (i = 0, 1, \ldots, n;\ l = 0, 1, \ldots, r) \tag{1}$$

has been widely investigated in a number of works [1, 2].

In this posing of the problem, time is continuous, and one imposes limitations of the following type on the controlling quantities u_l:

$$|u_l| \leqslant N_l. \tag{2}$$

In [3] the analogous problem is solved for systems described by finite difference equations

$$x_i([k+1]h) - x_i(kh) = \Big[\sum_{j=1}^{n} a_{ij}x_j(kh) + \sum_{l=1}^{r} q_{il}u_l(kh) + f_i(kh)\Big]h. \tag{3}$$

In this problem, time is discrete, t = kh (k = 0,1, . . .) for an arbitrarily chosen h, and conditions of the following type are imposed on the controlling quantities:

$$|u_l(kh)| \leqslant N. \tag{4}$$

Such a system was investigated in [4].

The system of second-order finite difference equations which we consider in this paper, these equations describing planar motion, has the form

$$\begin{aligned} x([k+1]h) - x(kh) &= y(kh)h, \\ y([k+1]h) - y(kh) &= u(kh)h, \end{aligned} \tag{5}$$

where x, y are the point coordinates on the phase plane and u is the point acceleration (controlling action). The behavior of the points is considered under the limitation

$$|u_k| = \text{const}. \tag{6}$$

In this case (a pulse-relay system), it is required to determine the control law $\{u_k^0\}$ which allows the initial point (x_0, y_0) to be translated to the origin of coordinates of phase space in the least possible number of steps K^0. The time here, as in (3), is discrete but, in contradistinction to (1) and to (3), the values of the controlling quantities are also discrete.

The optimal control problem for a system with (5), which we shall solve in the present work, can be classified as a simple number-theoretical problem. It should be mentioned that problems of this type will continue to arise with ever greater frequency in connection with the use of discrete computer technology in automatic control.

It seems advisable to sketch briefly our plan for finding the optimal control law for such a problem. We first find the optimal control law for initial points of the form $(n^2, 0)$, for which we shall use the results of the work of N. N. Krasovskii [3] (the corresponding expressions for the number of steps K^0 and for the control law $\{u^0\}$ can be easily and immediately obtained). We then construct the optimal control for all the integral points of the x axis, x > 0, and we show that the optimal trajectories completely fill up the region of the (x,y) plane defined by the expressions $0 \leq x \leq y(y-1)/2$, $y < 0$. Finally, we shall show that the optimal trajectories of all the other integral points of the (x, y) plane pass through one of the points already considered on the x axis in one of the half planes x > 0 or x < 0. On the basis of the optimal control law obtained, we shall construct an optimal switching line. At the end of this paper we shall discuss questions related to the nonsinglevaluedness of the control law obtained.

We turn now to the solution of the problem, to be carried out in accordance with the plan just given.

The solution obtained in [3] for a second-order system with (4) renders it possible, for a given h, to choose an optimal value of $|u_k|$ which depends on x_{i0} and ξ_i, but does not depend on the number k of steps, and to determine the unique moment for changing the sign of the controlling action (corresponding to a transition from a type N to a P-trajectory [1]).

The peculiar feature of our problem, when (4) been replaced by (6), is that, generally speaking, for a constant modulus of point acceleration, the sign of this acceleration changes more than once during the control process.

Indeed, we consider a point lying on the x axis at a distance x_0 from the origin of coordinates. Let x and y be changed for integer steps, i.e., $|u_k| = 1$, $h = 1$. If $|u_k| = a$ and $h = b$, where $a, b \neq 1$, this leads only to a corresponding change in the scales of the process. In accordance with [3], when (4) holds, K^0 is defined as the least integer which satisfies the inequality

$$\frac{K^2h^2}{4} \geqslant x_0.$$

Replacement of (4) by (6) entails only the change of the inequality sign to an equality sign, i.e.,

$$\frac{K^2h^2}{4} = x_0. \tag{7}$$

In order that (7) have integer solutions in K, it is necessary that x_0 be a perfect square, i.e., $x_0 = n^2$. For such points of the x axis, the optimal control law of [3] remains valid, it taking, in the given case, the form

$$u^0(kh) = -\operatorname{sign}\left[\frac{K^0}{2} - k\right],$$

$$K^0 = 2\sqrt{x_0} = 2n. \tag{8}$$

In the case of (6), for all the remaining points of the x axis, it is not possible to reach the origin of coordinates with a single switching of the acceleration's sign.

We limit ourselves initially to a consideration, for such points, of the half-plane $x > 0$, and to the requirement that one attain in the least number of steps some neighborhood of the origin of coordinates consisting, for example, of the two points (0,0) and (1,0). We define the position of the point on the x axis by the distance p:

$$x_0 = n^2 + p,$$

where

$$0 < p \leqslant 2n + 1.$$

Since the chosen neighborhood is characterized by $y_{K^0} = 0$ then, for $y_0 = 0$, we have the equation

$$\sum_{u_i > 0} u_i = -\sum_{u_j < 0} u_j \quad (i, j = 1, 2, \ldots, K^0), \tag{9}$$

i.e., the neighborhood of zero may be reached only in an even number of steps. It can be shown that

$$K^0 = \begin{cases} 2n, & \text{if} \quad p = 1 \\ 2n + 2, & \text{if} \quad p = 2, 3, \ldots, 2n + 1. \end{cases} \tag{10}$$

In fact, for a zero initial velocity, the path taken by the point in $2n$ steps is maximal for the choice of $u_0(kh)$, according to (8), and is equal to n^2. With this, the point is at the distance p from the origin of coordinates, so that, for $p = 1$, the point falls in the neighborhood of the origin of coordinates, and (8) defines its optimal control law. When (9) is taken into account, for $p \neq 1$, the magnitude of K^0 cannot be less than $2n + 2$.

We now assume that the optimal control law has the form:

$$u_k^0 = -\operatorname{sign}\left[\frac{K^0}{2} - k - 1\right] - 2\delta_{kz},$$

$$\delta_{kz} = \begin{cases} 1 & \text{for} \quad z = k \\ 0 & \text{for} \quad z \neq k \quad (k = 1, 2, 3, \ldots, K^0), \end{cases} \tag{11}$$

where K^0 is defined by (10).

Now we show that one can choose a z corresponding to an optimal control.* As the end point for an even $p = 2l$, we choose the point $x_{K^0} = 1$; for $p = 2l + 1$, let such a point be $x_{K^0} = 0$ ($l = 1, 2, \ldots$). Then z must be so chosen that, for any parity of p ($p \neq 1$), the following equation holds:

$$S_{K^0} + E\left[\frac{p}{2}\right] - E\left[\frac{p-1}{2}\right] = n^2 + p,$$

where S_{K^0} is the path taken by the system during the control process in K_0 steps; $E(\alpha)$ denotes the integral part of α. At the same time, by adding the segments of path taken by the system for the controlling actions of (11), we obtain

$$S_{K^0} = n^2 + 2[2n - 1 - (z - 1)] - 1.$$

By comparing the two last formulas, we obtain the expression for z:

$$z = K^0 - E\left[\frac{p+1}{2}\right]. \tag{12}$$

Consequently, if z is defined by (12), then (11) defines the optimal control law.

The optimal law just obtained is easily extended to any integral point of the phase half plane $x > 0$. In fact, the initial points $x_0 = \operatorname{sign} y_0$ for $x_0 \geq y_0(y_0-1)/2$ (the boundary of this region is the N-trajectory which terminates in the origin of coordinates, i.e., $x_0 = y_0(y_0-1)/2$) lie on one of the optimal trajectories considered. One easily convinces himself that at least one optimal trajectory passes through each point of this region. This follows from the fact that the optimal control law, up until the first switchings (i.e., for $k \leq K^0/2-1$), does not depend on p. The points $\operatorname{sign} x_0 = \operatorname{sign} y_0$ and $\operatorname{sign} x_0 = -\operatorname{sign} y_0$, with the condition that $x_0 < y_0(y_0-1)/2$, are taken over into the case just considered after y_0 steps $u_k = -\operatorname{sign} x_0$ in the right-and left-hand planes respectively. It is easily seen that the "initial translation" of points moving along P- or N-trajectories are also optimal. If necessary, the optimal control law can be written for arbitrary initial conditions. For example, for the case of initial points defined by the conditions

$$\operatorname{sign} x_0 = -\operatorname{sign} y_0, \quad x > {}^1/_2\, y_0(y_0 - 1) \quad (p \neq 1),$$

$$K^0 = 2(n + 1) - |y_0|,$$

$$u_k^0 = -\operatorname{sign}[n - |y_0| - k] - 2\delta_{kz},$$

---

* We adopt the convention that sign 0 = 1.

we have

$$z = K^0 - E\left[\frac{p+1}{2}\right] - |y_0|,$$

$$p = x_0 + {}^1/_2\, y_0(y_0+1) - n^2.$$

The control law just found corresponds to a translation of points to the neighborhood of zero, but it is easily verified that if K^0 remains invariant, and for any number of switchings, if (9) is met then the parity of S_k is unchanged. Therefore, the law that translates the point directly to the origin of coordinates must be supplemented by two steps (when $u_{K^0+1} = -u_{K^0+2} = 1$) to all the trajectories which terminate in the point (1,0). Then, the optimal control law, in the form of (11 and (12), will be valid for all points and, for all p, we shall have $K^* = 2n + 2$.

The control law in the form of (11) and (12) allows us to find the optimal switching line.

We consider the phase half-plane $x > 0$ and the half-line $y = y^*$ on it. It is obvious that the optimal stimulus for all points with integral coefficients on the half-line $y = y^* > 0$ will be $u^0 = -\text{sign}\, x = -1$. Now let $y^* < 0$ and $v = |y^*|$ (Fig. 1). The line under consideration intersects the N-trajectory $x = v(v-1)/2$ at point $\{a[v(v-1)/2, y^*]\}$. Then, for all points with coordinates $0 \leq x \leq v(v-1)/2$; $y = y^*$, we have that $u^0 = \text{sign}\ x = +1$. It remains to consider the points $x > v(v-1)/2$, $y = y^* > 0$. We select an interval of the x axis which contains $2v + 1$ points $v^2 \leq x_0 < (v+1)^2$. For all points, according to (10), $K^0 = 2v^2 + 2$ (in the sense of a translation to the neighborhood of the origin of coordinates) and (11), it is required that $u^0 = \text{sign}\ x = 1$, since a point of such a segment falls on the line after v steps. For points on the x axis such that $x_0 \geq (v+1)^2$, the first change of sign occurs on the step whose ordinal number is known to be greater than v, and for these points $u^0 = -\text{sign}\ x$. Thus, for $y_0 = -v$, the optimal control is these points $u^0 = -\text{sign}\ x$. Thus, for $y_0 = -v$, the optimal control is

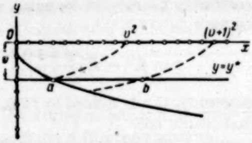

Fig. 1.

$$u^0 = \begin{cases} -\,\text{sign}\, x_0, & \text{if} \quad x \geqslant b, \\ +\,\text{sign}\, x_0, & \text{if} \quad x < b. \end{cases}$$

The abscissa of point b is obviously equal to $v(v-1)/2 + (2v+1) = (v+1)(v+2)/2$. Since the argument did not depend on the choice of v, one may assert that the expression just found defines the optimal switching line on the half-plane $x > 0$.

By carrying out an analogous argument for the half-plane $x < 0$, we can obtain the complete expression for the optimal switching line:

$$u^0 = \begin{cases} -1, & \text{if} \quad x \geqslant f(v, x), \\ +1, & \text{if} \quad x < f(v, x), \end{cases} \tag{13a}$$

where $v = |y|$,

$$f(v, x) = \begin{cases} f_1(v) = \dfrac{(v+1)(v+2)}{2}, & \text{if} \quad x > 0, \\ f_2(v) = \dfrac{v(v+3)}{2}, & \text{if} \quad x < 0. \end{cases} \tag{13b}$$

In the half-plane $x < 0$, to retain the "≥" and "<" signs unchanged, the switching line must be translated by unity toward the y axis.

The switching line just obtained is optimal in the sense that the representative point is translated either to the origin of coordinates or to a neighborhood of it.

The optimal control law, which we have found in the form of (11) and (12), is not unique. We now show that it is possible to define other forms of the control law. We consider the control of points on an expanse of $2n + 2$ steps. A control for which the sign of the stimulus is constant (for example, a negative stimulus) on the first $n + 1$ steps ($i = 1, 2, \ldots, n+1$) and, for $i = n+2, \ldots, 2n+2$, the sign is reversed, we shall call a "canonical" control. With canonical control, there are $(n+1)^2$ points on the path. Since, according to (9), the numbers of steps with "+" and with "−" signs are equal, then all possible controls can be obtained from the canonical one by permutations of signs pairwise between both sign-invariant portions. If, for example, we change the signs of the two terms with ordinal numbers m_1 and m_2

$$1 < m_1 \leqslant n+1,\ n+2 \leqslant m_2 \leqslant 2n+2,$$

then the points passed through on the path will be fewer than with the canonical control, and will be defined by the expression

$$S_{2n+2} = (n+1)^2 - 2(m_2 - m_1) \tag{14}$$

If the initial point is defined by the conditions $x = n^2 + p$, $y = 0$, then we can obtain the expression for its "optimal" control laws by equating $S_{2n+2} = n^2 + p$. From this, we obtain the relationship for m_1 and m_2:

$$m_2 - m_1 = \frac{2n-p}{2}. \tag{15}$$

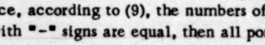

Fig. 2.

In this work, we fixed the value of $m_1 = n + 1$, and m_2 varied as a function of p. Such an approach made it possible to obtain the optimal switching line.

A typical form of controlling stimulus is illustrated on Fig. 2. Here, $x_0 = -19$ and $y_0 = 0$.

Figure 3 shows the optimal trajectory for the point ($x_0 = 12$, $y_0 = 0$) which corresponds to n = 3 and p = 3. Trajectory 1 is formed in accordance with optimal switching line 3, and trajectory 2 (dashed lines) is obtained from the control of (15) for $m_1 = n$.

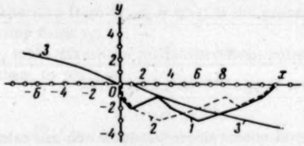

Fig. 3.

Figure 4 shows one of the simplest variants of a realization of an optimal control system using switching lines. The system's action is based on the determination of the mutual positioning of the representative point and the switching line in the half-plane where x > 0.

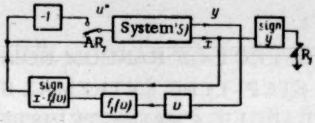

Fig. 4.

LITERATURE CITED

[1] H. S. Tsien, Engineering Cybernetics (McGraw-Hill, N. Y., 1954).

[2] A. A. Fel'dbaum, "On the synthesis of optimal systems using phase space," Avtomatika i Telemekhanika 16, No. 2 (1955).

[3] N. N. Krasovskii, "On one optimal control problem," Prikl. Matem i Mekh. No. 5 (1957).

[4] R. E. Kalman, Optimal nonlinear control of saturating systems by intermittent action. IRE Wescon Convention Record 1, (1957) Part 4.

THE EFFECT OF RANDOM NOISE ON THE STEADY-STATE OPERATION OF A STEP-TYPE EXTREMAL SYSTEM FOR AN OBJECT WITH A PARABOLIC CHARACTERISTIC

T. I. Tovstukha
(Moscow)

Translated from Avtomatika i Telemekhanika Vol. 21, No. 5, pp. 575-584, May, 1960
Original article submitted October 21, 1959

The optimal parameters of the controlling portion of the extremal system under consideration are calculated. These parameters must be determined from estimates of the deviations from the minimum characteristics in the steady state.

It is shown that, in the particular case of uniformly distributed noise increments, it is most advantageous to operate with small steps, to be determined below.

1. Posing of the Problem

In this paper we consider the case of a step-type extremal system whose object has a parabolic characteristic $y = x^2$. The system's task is the automatic search for, and maintenance of, the minimum of the characteristic. The following posing of the problem, as well as the notation, are the same as in [1] of A. A. Fel'dbaum. All quantities are considered at discrete moments of time $t = nT$ ($n = 0, 1, 2, \ldots$), where T is the time between two successive working steps, or the duration of one cycle. Figure 1 is a block schematic of the extremal system under consideration; O is the object of control, its input and output being related by the function

$$y[n] = x^2[n]. \tag{1}$$

Random noise z[n] acts at the object's output. The noise increments $v = z[n + 1] - z[n]$ are assumed to be statistically independent quantities with probability density $\rho(v)$ and zero mean value. The noise z[n] can be identified, for example, with the random noise in the measuring block of an actual system. Slow shifts of the characteristic, or input noise of the object, will not be considered here. The action of noise retards the automatic search for the minimum of the object's characteristic, where the minimum itself is determined with a certain error.

The actual object output, which can be measured, is the sum of the output y[n] and the random noise, i.e., the quantity

$$w[n] = y[n] + z[n]. \tag{2}$$

The quantity w[n] is applied to the input of the controlling portion of the system C.

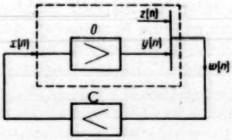

Fig. 1

The search for a minimum is implemented by means of successive cycles; each cycle includes a test to determine the direction of motion toward a minimum, and a working operation which implements this motion. The controlling portion, with its testing motions, disturbs the object's regimen. In the system under consideration, at the beginning of each half cycle, the object's input x [n] receives a stepwise increment of $(\Delta x)_1 = a$ (at the beginning of the cycle) and $(\Delta x)_2 = -a$ (in the middle of the cycle). At the object's output, at the end of each half cycle, one measures the corresponding disturbances $w_1 = y_1 + z_1$ and $w_2 = y_2 + z_2$ and compares them. Thus, one determines the direction of motion toward a minimum, or the sign of the working step (the magnitude of the working step, as of the test step, is a):

$$\begin{aligned} \Delta x[n] &= -a \operatorname{sign} \Delta w[n], \\ \Delta w[n] &= w_1 - w_2. \end{aligned} \tag{3}$$

It is possible with this to make a false step, on moving away from the minimum, since the quantity w is made up of the true output of the object plus noise. If one know the distribution law of the noise increments, $\rho(v)$, then the probability of a false step from the point x equals

$$p(x) = P\{v > \Delta y\},$$

where $\Delta y = y_1 - y_2$, $v = z_1 - z_2$, or

$$p(x) = \int_{-\infty}^{-|\Delta y|} \rho(v)\, dv. \tag{4}$$

The probability of a correct step (one directed toward the minimum) from point x equals

$$q(x) = 1 - p(x).$$

Possible neighboring points $\underline{x}$ are at a distance equal to the working step $\underline{a}$ from each other. We renumber the possible discrete states of the system, assigning the subscript zero to the state which corresponds to the minimum of the characteristic, i.e.,

$$x = ia \qquad (i = -\infty, \ldots, -1, 0, 1, \ldots, \infty). \tag{5}$$

We introduce the notation: $p_i = p(x_i)$ is the probability of a false step from x_i, $q_i = q(x_i)$ is the probability of a correct step from x_i.

If p_{jk} is the transition probability from point x_j to point x_k then, in our case,

$$p_{k,\,k+1} = \begin{cases} p_k & (k > 0), \\ q_k & (k < 0), \end{cases}$$
$$p_{k,\,k-1} = \begin{cases} q_k & (k > 0), \\ p_k & (k < 0), \end{cases}$$
$$p_{k,\,l} = 0 \qquad (l \neq k-1,\ k+1). \tag{6}$$

Thus, the process of seeking a minimum can be considered as a discrete Markov process.

We denote by the "weight" of state x_i the mean value of the object's outputs for the two tests, using the notation $(\overline{\Delta y})_i$ for this quantity. In correspondence with (1) and (5),

$$(\overline{\Delta y})_i = a^2(i^2 + 1) \qquad (i = 0, \pm 1, \pm 2, \ldots). \tag{7}$$

The difference of the values of $\underline{y}$ in the test, $\Delta y =$ $= y_1 = y_2$, is defined as

$$(\Delta y)_i = 4ia^2 \qquad (i = 0, \pm 1, \pm 2, \ldots). \tag{8}$$

The probabilities of false and of correct steps from state x_i are

$$p_i = \int_{-\infty}^{-4|i|a^2} \rho(v)\,dv, \qquad q_i = 1 - p_i. \tag{9}$$

The steps from the minimum, both at the point $x_{+1} = a$ and at the point $x_{-1} = -a$ are false, with a probability of $p_0 = 1/2$.

For convenience and clarity of the exposition, we can construct an equivalent scheme of the discrete Markov process [2]. Such a scheme is shown in Fig. 2. The points on it represent the possible states of the system. The arrows show the transitions from state to state. The probabilities of these transitions are shown. Z is the operator for translation in time, showing that the transition is carried out during a working cycle.

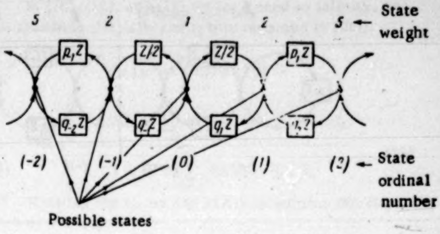

Fig. 2

We denote by $P_i[n]$ the probability that the system is in state x_i at time $t_n = nT$. Then, the mathematical expectation of the output quantity is

$$M_n[y] = \sum_{i=-\infty}^{\infty} (\overline{\Delta y})_i P_i[n] = a^2 \sum_{i=-\infty}^{\infty} (i^2 + 1) P_i[n]. \tag{10}$$

It is necessary to determine $\lim\limits_{n\to\infty} M_n[y]$, if this limit exists, and also to find the $\underline{a}$ for which this limit is a minimum.

The case of an extremal control system with the piecewise-linear characteristic $y = |x|$ was devoted in work [1]. It was shown there that, in the steady state, the minimum value of the mean error in $\underline{y}$ corresponds to a step of size $a \approx 0$ for normally or uniformly distributed output noise.

2. Determination of the Mathematical Expectation and the Dispersion of the Object's Output Variable in the Steady State

We write the equations for the probabilities of the system's states:

$$\begin{aligned}
&\ldots\ldots\ldots\ldots\ldots\ldots\ldots\ldots\ldots \\
&P_{-2}[n] = P_{-3}[n-1]\,q_3 + P_{-1}[n-1]\,p_1, \\
&P_{-1}[n] = P_{-2}[n-1]\,q_2 + P_0[n-1]\,\tfrac{1}{2}, \\
&P_0[n] = P_{-1}[n-1]\,q_1 + P_1[n-1]\,q_1, \\
&P_1[n] = P_2[n-1]\,q_2 + P_0[n-1]\,\tfrac{1}{2}, \\
&P_2[n] = P_3[n-1]\,q_3 + P_1[n-1]\,p_1, \\
&\ldots\ldots\ldots\ldots\ldots\ldots\ldots\ldots\ldots
\end{aligned} \tag{11}$$

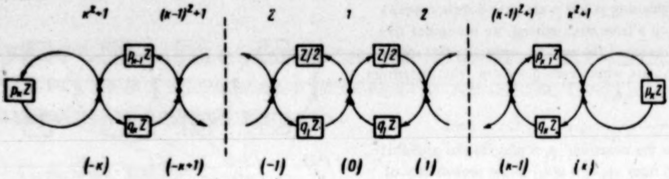

Fig. 3

We have taken into account here that, in correspondence with (9), $p_i = p_{-i}$ and $q_i = q_{-i}$.

We now consider the finite system of 2k + 1 states, shown on Fig. 3. The equations of such system are written in the form

$$
\begin{aligned}
P_{-k}[n] &= P_{-k+1}[n-1]\,p_{k-1} + P_{-k}[n-1]\,p_k,\\
P_{-k+1}[n] &= P_{-k+2}[n-1]\,p_{k-2} + P_{-k}[n-1]\,q_k,\\
&\dots\dots\dots\dots\dots\dots\\
P_{-2}[n] &= P_{-1}[n-1]\,p_1 + P_{-3}[n-1]\,q_3,\\
P_{-1}[n] &= P_0[n-1]\,\frac{1}{2} + P_{-2}[n-1]\,q_2,\\
P_0[n] &= P_{-1}[n-1]\,q_1 + P_1[n-1]\,q_1,\\
P_1[n] &= P_0[n-1]\,\frac{1}{2} + P_2[n-1]\,q_2,\\
P_2[n] &= P_1[n-1]\,p_1 + P_3[n-1]\,q_3,\\
&\dots\dots\dots\dots\dots\dots\\
P_{k-1}[n] &= P_{k-2}[n-1]\,p_{k-2} + P_k[n-1]\,q_k,\\
P\ [n] &= P_{k-1}[n-1]\,p_{k-1} + P_k[n-1]\,p\,.
\end{aligned}
\tag{12}
$$

We consider the limiting system for n → ∞, assuming that the $\lim\limits_{n\to\infty} P_i[n] = r_i$ exists. In this case,

$$
\begin{aligned}
r_{-k} &= r_{-k+1}p_{k-1} + r_{-k}p_k,\\
r_{-k+1} &= r_{-k+2}p_{k-2} + r_{-k}q_k,\\
&\dots\dots\dots\dots\\
r_{-2} &= r_{-1}p_1 + r_{-3}q_3,\\
r_{-1} &= r_0\,\frac{1}{2} + r_{-2}q_2,\\
r_0 &= r_{-1}q_1 + r_1q_1,\\
r_1 &= r_0\,\frac{1}{2} + r_2q_2,\\
r_2 &= r_1p_1 + r_3q_3,\\
&\dots\dots\dots\dots\\
r_{k-1} &= r_{k-2}p_{k-2} + r_kq_k,\\
r_k &= r_{k-1}p_{k-1} + r_kp_k.
\end{aligned}
\tag{13}
$$

It is obvious that

$$\sum_{i=-k}^{k} r_i = 1. \tag{14}$$

We always have 2k + 2 equations in 2k + 1 unknowns. We consider the system of the first 2k equations of (13) and (14), and we determine the r_i which satisfy this system. It will easily be shown that they also satisfy the last equation of (13).

If we also take into account that, by virtue of symmetry, $r_i = r_{-i}$, we shall consequently consider the system

$$
\begin{aligned}
r_0 &= 2r_1q_1,\\
r_1 &= r_0\,\frac{1}{2} + r_2q_2,\\
r_2 &= r_1p_1 + r_3q_3,\\
&\dots\dots\dots\dots\\
r_{k-1} &= r_{k-2}p_{k-2} + r_kq_k\\
r_0 &+ 2\sum_{i=1}^{k} r_i = 1.
\end{aligned}
\tag{15}
$$

We shall successively express all the r_i in terms of r_1:

$$
\begin{aligned}
r_0 &= 2q_1r_1,\\
r_2 &= r_1\,\frac{p_1}{1}\,\frac{1}{q_2}\,,\\
r_3 &= r_1\,\frac{p_1}{1}\,\frac{p_2}{q_2}\,\frac{1}{q_3}\,.\\
&\dots\dots\dots\dots
\end{aligned}
$$

It is easily shown that, in general,

$$r_i = r_1p_1\lambda_2\lambda_3\dots\lambda_{i-1}\zeta_i \qquad (2 \leqslant i \leqslant k), \tag{16}$$

where

$$\lambda_m = \frac{p_m}{q_m}, \quad \zeta_m = \frac{1}{q_m} \quad (m = 1, 2, \dots, k). \tag{17}$$

By substituting, in the last equation of (15), the expression for r_0 from the first equation and the expression for r_i from (16), we obtain

$$r_1 = \frac{1}{2\left(1 + q_1 + \sum\limits_{i=2}^{k} p_1\lambda_2\lambda_3\dots\lambda_{i-1}\zeta_i\right)}\,. \tag{18}$$

The value of r_0 is defined in terms of r_1 from the first equation of (15)

$$r_0 = 2r_1q_1. \tag{19}$$

It is easily verified that the thus determined r_i satisfy the last equation of (13), i.e., the one we didn't consider. Thus, the state probabilities in the steady state are completely given by (16)-(19).

We now turn back to (10). We need to determine the magnitude of the mathematical expectation in the steady state, i.e.,

$$\lim_{n\to\infty} M_n[y] = a^2 \sum_{i=-\infty}^{\infty} (i^2+1)\, r_i. \qquad (20)$$

In (16), (18), and (19) we let k tend to infinity, and we substitute the values of r_i thus obtained in (20):

$$M[y] = \lim_{n\to\infty} M_n[y] =$$

$$= a^2 \frac{1 + 2\zeta_1 + \sum\limits_{i=2}^{\infty} (i^2+1)\, \lambda_1\lambda_2 \ldots \lambda_{i-1}\zeta_i}{1 + \zeta_1 + \sum\limits_{i=2}^{\infty} \lambda_1\lambda_2 \ldots \lambda_{i-1}\zeta_i}. \qquad (21)$$

Knowing the r_i, we can easily determine the dispersion of the quantity y:

$$D[y] = \sum_{i=-\infty}^{\infty} (\overline{\Delta y})_i^2 r_i - M^2[y] =$$

$$= a^4 \left\{ \frac{\zeta_1 + \sum\limits_{i=2}^{\infty} i^4 \lambda_1\lambda_2 \ldots \lambda_{i-1}\zeta_i}{1 + \zeta_1 + \sum\limits_{i=2}^{\infty} \lambda_1\lambda_2 \ldots \lambda_{i-1}\zeta_i} + 2\frac{M[y]}{a^2} - 1 \right\} - M^2[y]. \qquad (22)$$

3. The Case of a Uniform Distribution Law for $\rho(v)$

In this particular case, the computations of M[y] and D[y] by (21) and (22) are easily reduced to numerical results. Let (cf., Fig. 4, a)

$$\rho(v) = \begin{cases} \dfrac{1}{2\eta} & (|v| \leqslant \eta), \\ 0 & (|v| > \eta). \end{cases} \qquad (23)$$

In correspondence with (9), the probabilities of false and correct steps are found from the formulas

$$p_i = \begin{cases} \dfrac{1}{2} - i\dfrac{4a^2}{2\eta} & \left(i < \dfrac{\eta}{4a^2}\right), \\ 0 & \left(i > \dfrac{\eta}{4a^2}\right); \end{cases} \qquad (24)$$

$$q_i = \begin{cases} \dfrac{1}{2} + i\dfrac{4a^2}{2\eta} & \left(i < \dfrac{\eta}{4a^2}\right), \\ 1 & \left(i > \dfrac{\eta}{4a^2}\right) \end{cases} \quad (i = 0, 1, \ldots).$$

We denote by k the integral part of the expression $(\eta - 4a^2)/4a^2$, $\eta = 4a^2 k + \beta$, $\gamma = \beta/4a^2$ (Fig. 4,b)

Then, from (21),

$$M[y] = a^2 \frac{1 + 2\zeta_1 + \sum\limits_{i=2}^{k+1} (i^2+1)\, \lambda_1\lambda_2 \ldots \lambda_{i-1}\zeta_i}{1 + \zeta_1 + \sum\limits_{i=2}^{k+1} \lambda_1\lambda_2 \ldots \lambda_{i-1}\zeta_i},$$

where λ_m and ζ_m are determined from (17), with account being taken of (24).

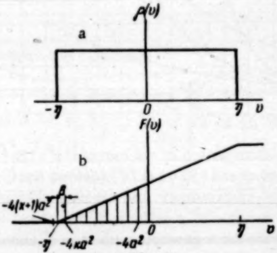

Fig. 4

To simplify the computations, we shall consider, not all a, but only those for which

$$\frac{\eta}{4a^2} = m, \qquad (25)$$

where m is an integer.

We easily obtain from (20), (23), and (24) (cf., the appendix)

$$M[y] = \begin{cases} \dfrac{\eta}{8} + a^2 & \left(\dfrac{\eta}{4a^2} > 1\right), \\ 1.5a^2 & \left(\dfrac{\eta}{4a^2} \leqslant 1\right). \end{cases} \qquad (26)$$

Here, since M[y] is a continuous function of a, $\eta/4a^2$ can take any value, either integral or fractional.

We compute the dispersion D[y] analogously (cf., the appendix)

$$D[y] = \begin{cases} \dfrac{\eta}{16}\left(\dfrac{\eta}{2} - a^2\right) & \left(\dfrac{\eta}{4a^2} > 1\right), \\ \dfrac{a^4}{4} & \left(\dfrac{\eta}{4a^2} \leqslant 1\right), \end{cases} \qquad (27)$$

or we compute the mean-square deviation

$$\sigma[y]=\begin{cases}\frac{1}{4}\sqrt{\eta\left(\frac{\eta}{2}-a^2\right)} & \left(\frac{\eta}{4a^2}>1\right),\\ \frac{a^2}{2} & \left(\frac{\eta}{4a^2}<1\right).\end{cases} \tag{28}$$

The dependence of M[y] and σ[y] on a for several different values of η is given on Fig. 5. For a comparison on the same graph, we give the dependence of the mathematical expectation and the mean-square dispersion on the size of the working step for the case of the piecewise-linear characteristic $y = |x|$, considered in [1], for the same noise distribution law. The corresponding computations are given in the appendix.

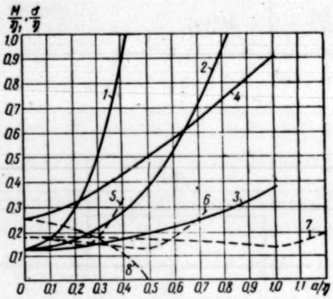

Fig. 5. Comparison of the curves $(M/\eta)(a/\eta)$ (solid lines) and $(\sigma/\eta)(a/\eta)$ (dashed lines) for parabolic characteristic and modulus characteristic in the case of a uniform distribution: curves 1 and 5 are for a parabola with $\eta = 4$, curves 2 and 6 are for a parabola with $\eta = 1$, curves 3 and 7 are for a parabola with $\eta = 0.25$, curves 4 and 8 are for the modulus.

It is clear from the graphs that, for the characteristic $y = x^2$, the optimal (from the point of view of simultaneous smallness of the mathematical expectation and the dispersion) working step a is close to a = 0. A small increase of the step decreases the mean-square deviation insignificantly, but increases the mathematical expectation of the output. In the modulus case, $y = |x|$, it is better to make the step larger than for the relationship $y = x^2$ since, for the modulus, an increase in the step (for small values of the step a) gives an insignificant increase of M[y] accompanied by a decrease of the dispersion.

In conclusion, the author wishes to thank A. A. Fel'dbaum for posing the given problem and for his useful advice. Thanks also to S. Ya. Raevskii for discussing the results obtained.

APPENDIX

1. Determination of the Mathematical Expectation and the Dispersion of the Output Variable for Uniformly Distributed Noise

By substituting (25) in (24) we get

$$p_i=\begin{cases}\frac{1}{2}-\frac{i}{2m} & (i<m),\\ 0 & (i\geqslant m);\end{cases}\qquad q_i=\begin{cases}\frac{1}{2}+\frac{1}{2m} & (i<m),\\ 1 & (i\geqslant m).\end{cases} \tag{I}$$

We find from (21), for m > 1,

$$M[y]=a^2\frac{1+2\zeta_1+\sum_{i=2}^{m}(i^2+1)\lambda_1\lambda_2\ldots\lambda_{i-1}\zeta_i}{1+\zeta_1+\sum_{i=2}^{m}\lambda_1\lambda_2\ldots\lambda_{i-1}\zeta_i},$$

where λ_l and ζ_l are determined from (17) with account being taken of (I).

After some transformations, we obtain the expression

$$M[y]=a^2\frac{2\sum_{i=0}^{m}(i^2+1)\frac{m!^2}{(m-i)!(m+i)!}-1}{2\sum_{i=0}^{m}\frac{m!^2}{(m-i)!(m+i)!}-1}.$$

We let $A(m)=\sum_{i=0}^{m}\frac{1}{(m-i)!(m+i)!}$. Then, since

$$\sum_{j=0}^{2m}\frac{(2m)!}{j!(2m-j)!}=2^{2m} \text{ then } A(m)=\frac{2^{2m-1}}{(2m)!}+\frac{1}{2m!^2},$$

and the denominator of M[y] is written as

$$2m!^2\frac{1}{2}\left[\frac{2^{2m}}{(2m)!}+\frac{1}{m!^2}\right]-1=\frac{2^{2m}m!^2}{(2m)!}.$$

We now consider the numerator of M[y]

$$2\sum_{i=0}^{m}(i^2+1)\frac{m!^2}{(m-i)!(m+i)!}-1=$$

$$=2m!^2(m^2+1)\sum_{i=0}\frac{1}{(m-i)!(m+i)!}-$$

$$-2m!^2\sum_{i=0}^{m}\frac{m^2-i^2}{(m-i)!(m+i)!}-1=\frac{2^{2m-1}m!^2}{(2m)!}(m+2).$$

Whereupon $M[y] = a^2(m + 2)/2$ for $m > 1$.

By taking into account that $m = \eta/4a^2$, we obtain finally,

$$M[y]=\frac{\eta}{8}+a^2 \text{ for } \frac{\eta}{4a^2}>1.$$

For m = 1, we easily get from (21) and (24) that $M[y] = 1.5a^2$; the same result is also obtained for noninteger m less than unity.

The dispersion is computed from (22), with account being taken of (24), (25), and (26).

$$D[y] = a^4 \left\{ \frac{\zeta_1 + \sum_{i=2}^{m} i^4 \lambda_1 \lambda_2 \ldots \lambda_{i-1} \zeta_i}{1 + \zeta_1 + \sum_{i=2}^{m} \lambda_1 \lambda_2 \ldots \lambda_{i-1} \zeta_i} + 2 \frac{M[y]}{a^2} - 1 \right\} - M^2[y],$$

where, as before, λ_l and ζ_l are determined from (17) with account being taken of (I).

We transform the first term in the braces. Then we denote it by B(m). It is easily taken to the form

$$B(m) = \frac{2 \sum_{i=0}^{m} i^4 \frac{m!^2}{(m-i)!(m+i)!}}{2 \sum_{i=0}^{m} \frac{m!^2}{(m-i)!(m+i)!}}.$$

The denominator is the same as in the analogous expression for M[y], andequals $2^{2m} m!^2 : (2m)!$.

We now consider the series in the numerator.

$$\sum_{i=0}^{m} \frac{i^4}{(m-i)!(m+i)!} = m^4 A(m) -$$

$$- (2m^2 - 2m + 1) A(m-1) + A(m-2).$$

By substituting this expression in B(m) we get

$$B(m) = \frac{m(3m-1)}{4}.$$

It is obvious that all these formulas are valid for m > 1.

Finally, for m > 1 ($\eta / 4a^2 > 1$), we find that

$$D[y] = \frac{\eta}{16} \left(\frac{\eta}{2} - a^2 \right).$$

For all $\eta / 4a^2 \leq 1$, we immediately obtain from (22) and (24) that

$$D[y] = \frac{1}{4} a^4$$

2. Mathematical Expectation and Dispersion of the Output Variable for a Uniform Distribution Law in the Case of a Piecewise-Linear Object Characteristic

For the case when the object characteristic is y = |x|, the general expression for the mathematical expectation of the output is found in [1]. We recall that

$$(\overline{\Delta y})_i = (i + \delta_{i,0}) a, \qquad (i = 0, 1, \ldots), \qquad \delta_{i,0} = \begin{cases} 1, \text{ if} & i = 0, \\ 0, \text{ if} & i \neq 0; \end{cases}$$

$$|(\overline{\Delta y})_i| = 2a; \; p_i = p = \int_{-\infty}^{-2a} \rho(v)\, dv;$$

$$r_1 = \frac{1}{2\left(q + \frac{1}{1-\lambda}\right)}; \qquad r_0 = 2qr_1; \qquad r_i = r_1 \lambda^{i-1},$$

where

$$\lambda = \frac{p}{q}; \qquad M[y] = a \frac{q + \frac{1}{(1-\lambda)^2}}{q + \frac{1}{1-\lambda}}.$$

In the case of the uniform distribution of (23)

$$p = \begin{cases} \frac{1}{2} - \frac{a}{\eta} & \left(\frac{1}{2} > \frac{a}{\eta}\right), \\ 0 & \left(\frac{1}{2} \leqslant \frac{a}{\eta}\right); \end{cases} \qquad q = \begin{cases} \frac{1}{2} + \frac{a}{\eta} & \left(\frac{1}{2} > \frac{a}{\eta}\right), \\ 1 & \left(\frac{1}{2} \leqslant \frac{a}{\eta}\right); \end{cases}$$

$$\frac{M[y]}{\eta} = \begin{cases} \frac{4\left(\frac{a}{\eta}\right)^2 + \frac{a}{\eta} + \frac{1}{2}}{4\frac{a}{\eta} + 2} & \text{for} \quad \frac{a}{\eta} < \frac{1}{2}, \\ \frac{a}{\eta} & \text{for} \quad \frac{a}{\eta} \geqslant \frac{1}{2}. \end{cases}$$

We compute the dispersion

$$- a^2 \left[\frac{q + \frac{1}{(1-\lambda)^2}}{q + \frac{1}{1-\lambda}} \right]^2 =$$

$$D[y] = \sum_{i=-\infty}^{\infty} (\overline{\Delta y})_i r_i - M^2[y] = a^2 \frac{q + \sum_{i=1}^{\infty} i^2 \lambda^{i-1}}{q + \frac{1}{1-\lambda}} =$$

$$= a^2 \frac{q\lambda(1-\lambda^2) + \lambda}{(1-\lambda)^4 \left(q + \frac{1}{1-\lambda}\right)^2}.$$

By substituting p and q, we get

$$D[y] = \begin{cases} \frac{\eta^2}{4} \frac{\frac{1}{4} + \frac{a}{\eta} - 3\left(\frac{a}{\eta}\right)^2}{\left(1 + 2\frac{a}{\eta}\right)^2} & \text{for} \quad \frac{a}{\eta} < \frac{1}{2}, \\ 0 & \text{for} \quad \frac{a}{\eta} \geqslant \frac{1}{2}; \end{cases}$$

$$\frac{\sigma[y]}{\eta} = \begin{cases} \frac{1}{2} \frac{\sqrt{\frac{1}{4} + \frac{a}{\eta} - 3\left(\frac{a}{\eta}\right)^2}}{1 + 2\frac{a}{\eta}} & \text{for} \quad \frac{a}{\eta} < \frac{1}{2}, \\ 0 & \text{for} \quad \frac{a}{\eta} \geqslant \frac{1}{2}. \end{cases}$$

LITERATURE CITED

[1] A. A. Fel'dbaum, "Steady-state processes in the simplest discrete extremal system in the presence of random noise," Avtomatika i Telemekhanika 20, No. 8 (1959).*

[2] R. W. Sittler, System Analysis of Discrete Markov Processes. IRE Trans. of Circuit Theory, vol CT-3, No. 4 (Dec., 1956).

---

* See English translation.

THE ACTION OF RANDOM PROCESSES ON DISCONTINUOUS CONTROL SYSTEMS

G. I. Pyatnitskii
(Moscow)

Translated from Avtomatika i Telemekhanika Vol. 21, No. 5, pp. 585-594, May, 1960
Original article submitted April 13, 1959

Questions of the statistical calculations of discontinuous (sampled-data) control systems are considered, these systems being acted upon by stationary random processes. We also consider one particular case when a nonstationary random process acts. It is shown that the method of statistical linearization can be used for the approximate calculation of nonlinear systems in the same form in which it is used for the calculation of continuous nonlinear systems.

INTRODUCTION

Today there is a heightened interest in sampled-data, or discontinuous, control systems. These include systems containing sampled-data elements of one form or another [1, 2], extrapolating devices [3, 4], and digital computers [5, 6].

Discontinuous control systems are superior to continuous ones in those cases when it is necessary to control a slowly varying process, since they require less energy for their operation.

Sampled-data systems can successfully be employed, and are employed, for the purpose of measurement, particularly telemetry; with this, they may easily be made multichannel devices.

Sampled-data systems can be used for the control of several objects by means of the same apparatus which a continuous system must use to control just one object.

The use of digital computers in control systems transforms them into discontinuous control systems since, by their nature, digital machines have to do with discrete information, with digits. Control systems with digital devices are very flexible since, by a simple change of program, they can be made capable of solving their problem under different conditions.

Discontinuous control systems of a quite broad class can be described from a single point of view. In this class fall those systems whose behavior is determined by the values of the input signals at discrete equispaced moments of time.

In [7] a method is given for describing the operation of sampled-data elements with arbitraty pulse forms. The essence of the method is that the actual sampled-data element is presented in the form of a series connection of ideal sampled-data elements which process pulses in the form of Dirac δ-functions (following one another at equally spaced moments of time with norms equal to the values of the element's input signal at the corresponding moments of time) and which form a link which transforms the δ-pulses to pulses of the necessary forms. The shaping link is linear, and is described by a certain weight function and transfer function.

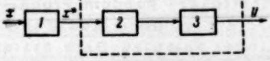

Fig. 1.

The series connection of the sampled-data element with a linear system forms a linear sampled-data circuit. The shaping link with the linear portion of the circuit forms the equivalent continuous portion (ECP) of the circuit (Fig. 1). The transfer function of the ECP is, obviously, the product of the transfer functions of the shaping link and the linear continuous portion of the circuit, and the weight function of the ECP is the convolution of the weight functions of the shaping link and the continuous portion.

If x(t) is the signal acting on the sampled-data circuit's input y (t) is the output signal and g(t) is the weight function of the ECP then, in the steady state of the circuit, the following relationship holds::

$$y(k\Delta t+\varepsilon\Delta t)=\sum_{n=-\infty}^{k} x(n\Delta t)\,g[(k-n)\Delta t+\varepsilon\Delta t]. \tag{1}$$

Here, the time $\underline{t}$ is given in the form $t = k\Delta t + \epsilon\Delta t$, where $\underline{k}$ is an integer, $\epsilon<1$ and Δt is the interval ~~of dis~~creteness (quantization).

Application of the discrete Laplace transform [1] to (1) gives

$$Y^{*}(p,\ \varepsilon)=G^{*}(p,\ \varepsilon)\,X^{*}(p), \tag{2}$$

where Y^{*}, G^{*}, and X^{*} are the transforms of y, g, x, respectively. For example,

$$G^{*}(p,\ \varepsilon)=\sum_{m=0}^{\infty} g(m\Delta t+\varepsilon\Delta t)\,e^{-pm\Delta t}.$$

By analogy with continuous systems, $G^*(p, \epsilon)$ is called the transfer function of the sampled-data circuit. It may be shown that $G^*(p, \epsilon)$ is related to the transfer function (in the usual sense) of the ECP, $G(p)$ by the relationship [8]

$$G^*(p, \varepsilon) = \frac{1}{\Delta t} \sum_{m=-\infty}^{\infty} G\left(p + i\frac{2\pi m}{\Delta t}\right) e^{\varepsilon\Delta t\left(p+i\frac{2\pi m}{\Delta t}\right)}. \tag{3}$$

If p is replaced by $i\omega$, one obtains the frequency characteristic of the sampled-data circuit, which may be interpreted as the ratio of the output signal to the input signal if the input signal is a function of the form $e^{i\omega n\Delta t}$.

Relationships (1) and (2) also hold for systems with feedback, except that, instead of $G^*(p, \epsilon)$ in (2), the system's transfer function enters and, instead of $g(t)$ in (1), the properly defined weight function of system enters.

In the sequel, a time-domain function will always be denoted by a lower-case Latin letter, while its transform will be denoted by the corresponding upper-case letter; to distinguish discrete from continuous transforms, the discrete transforms will always be marked with a star.

1. Stationary Random Processes with Discrete Arguments and Their Actions on Linear Sampled-Data Systems

For the following exposition we shall need certain results from the theory of stationary (in the broad sense) random processes with discrete arguments. This theory is presented in great detail in the book of J. L. Doob [9]. In [10], the theory of discrete random processes is applied to a probabilistic computation of sampled-data systems. In contradistinction to [10], we shall here take as basic the spectral representation of stationary processes given in [9].

Each stationary random process $x(n\Delta t)$ with zero mathematical expectation, permits of a spectral representation

$$x(n\Delta t) = \frac{\Delta t}{2\pi} \int_{-\pi/\Delta t}^{\pi/\Delta t} e^{i\omega n\Delta t} du(\omega), \tag{4}$$

where the random process $u(\omega)$ has orthogonal increments, i.e.,

$$M\left[du(\omega_1)\overline{du(\omega_2)}\right] = \begin{cases} 0 & \text{for} \quad \omega_1 \neq \omega_2; \\ \dfrac{\Delta t}{2\pi} dF(\omega) & \text{for} \quad \omega_1 = \omega_2 = \omega. \end{cases} \tag{5}$$

Here, M is the symbol for mathematical expectation, and a superscript bar denotes the complex conjugate.

The correlation function of a discrete process can be represented in the form

$$R(n\Delta t) = \frac{\Delta t}{2\pi} \int_{-\pi/\Delta t}^{\pi/\Delta t} e^{i\omega n\Delta t} dF(\omega). \tag{6}$$

The function $F(\omega)$ [the same function as in (5)] is called the spectral function of the process, and its derivative with respect to ω, i.e., $S^*(\omega) = F'(\omega)$, is called the spectral density.

The spectral density can be presented in the form of a Fourier series whose coefficients are the values of the correlation function

$$S^*(\omega) = \sum_{n=-\infty}^{\infty} R(n\Delta t)\, e^{i\omega n\Delta t}. \tag{7}$$

It follows from (7) that the spectral density of a discrete process is a periodic function of ω with a period of $2\pi/\Delta t$.

A discrete random process may be obtained from a continuous one if one consider its values at discrete, equally spaced, moments of time.

If $x(t)$ is a continuous stationary random process, then its values for $t = n\Delta t$ comprise a stationary discrete process. Let $S(\omega)$ be the spectral density of the continuous process. The spectral density $S^*(\omega)$ of the discrete process obtained from it can be computed by means of the relationship [11]

$$S^*(\omega) = \frac{1}{\Delta t} \sum_{m=-\infty}^{\infty} S\left(\omega + \frac{2\pi m}{\Delta t}\right), \tag{8}$$

which is easily obtained from (7).

If the stationary random process $x(n\Delta t)$, which can be presented in the form of (4), acts on the input of some linear sampled-data system with constant parameters, then the system's steady-state output, i.e., after damping of the transient response in the system, can be computed by taking account of (1) and (4). The output process will have the spectral representation

$$y(k\Delta t + \varepsilon\Delta t) = \frac{\Delta t}{2\pi} \int_{-\pi/\Delta t}^{\pi/\Delta t} e^{i\omega k\Delta t} G^*(i\omega, \varepsilon)\, du(\omega), \tag{9}$$

where $G^*(i\omega, \epsilon)$ is the system's frequency characteristic.

It follows from (9), when (5) is taken into account, that the output process' correlation function is

$$R_y(n\Delta t, \varepsilon\Delta t) = \frac{\Delta t}{2\pi} \int_{-\pi/\Delta t}^{\pi/\Delta t} e^{i\omega n\Delta t} S_y^*(\omega)\, d\omega. \tag{10}$$

where $S_y^*(\omega)$ is the spectral density of the process y, related to the spectral density of process $x(n\Delta t)$ by the relationship

$$S_y^*(\omega, \varepsilon) = |G^*(i\omega, \varepsilon)|^2 S_x^*(\omega). \tag{11}$$

The dispersion of the process y can obviously be computed from the formula

$$\sigma_y^2(\varepsilon) = \frac{\Delta t}{2\pi} \int_{-\pi/\Delta t}^{\pi/\Delta t} |G^*(i\omega, \varepsilon)|^2 S_x^*(\omega)\, d\omega. \tag{12}$$

Formulas (10) and (12) were obtained from [10].

We turn nowto (8). It immediately follows from it th that the ideal sampled-data element transforms the high-frequency region of the spectrum to a low-frequency one. This leads to the consequence that the introduction of a sampled-data element into a continuous system increases the random errors. This fact is seen particularly clearly in the following example.

Let there be some continuous system, and let there act on it a stationary random process x(t) with spectral density S(ω). Let the system's frequency characteristic K(iω) be such that for | ω | > ω_0, its modulus is so small that the dispersion of the output process can be computed by the formula

$$\sigma_C^2 \approx \frac{1}{2\pi} \int_{-\omega_0}^{\omega_0} S(\omega) \,|\, K(i\omega)\,|^2 \, d\omega. \tag{13}$$

Let us now connect this system to some sampled-data element whose pulse repetition period Δt satisfies the inequality

$$\Delta t < \frac{\pi}{\omega_0},$$

The dispersion of the output random process from the sampled-data circuit thus obtained is computed from (12). With the assumptions made relative to K(iω) and Δt, the frequency characteristic of such a circuit will, according to (3), be

$$G^*(i\omega, \varepsilon) = \frac{1}{\Delta t} F(i\omega)\, K(i\omega)\, e^{i\omega\varepsilon\Delta t}, \tag{14}$$

where F(iω) is the frequency characteristic of the sampled-data element's shaping link.

We assume that over the entire frequency range where | K(iω) | still differs markedly from zero, | F(iω)| / Δt differs little from unity. In fact, this assumption can be satisfied by choosing either a low-frequency part or a sufficiently small Δ t, because | F(iω)| / Δt → 1 for ω → 0 and differs greatly from unity only close to the frequencies ω = ± π/ Δt.

Starting from this, we can write the following expression for the dispersion at the sampled-data circuit's output:

$$\sigma^2 \approx \frac{1}{2\pi} \int_{-\pi/\Delta t}^{\pi/\Delta t} |\, K(i\omega)\,|^2 \sum_{m=-\infty}^{\infty} S_x\left(\omega + \frac{2\pi m}{\Delta t}\right) d\omega. \tag{15}$$

By comparing (15) with (13), and taking into account that $\omega_0 < \pi/\Delta t$, we can infer that $\sigma_S^2 > \sigma_C^2$.

2. Action of a Nonstationary Signal on a Linear Sampled-Data System

Let a nonstationary signal of the following form act on a linear sampled-data system

$$\xi(t) = r(t)\, x(t), \tag{16}$$

where x(t) is a stationary random process and r(t) is a function of time.

The output process can be found by (1):

$$y(k\Delta t + \varepsilon\Delta t) = \sum_{n=-\infty}^{k} \xi(n\Delta t)\, g\,[(k-n)\,\Delta t + \varepsilon\Delta t]. \tag{17}$$

The process ξ (nΔt) can obviously be presented in the form

$$\xi(n\Delta t) = r(n\Delta t)\, \frac{\Delta t}{2\pi} \int_{-\pi/\Delta t}^{\pi/\Delta t} e^{i\omega n\Delta t} du(\omega). \tag{18}$$

By substituting (18) in (17) we get

$$y(k\Delta t + \varepsilon\Delta t) = \frac{\Delta t}{2\pi} \int_{-\pi/\Delta t}^{\pi/\Delta t} du(\omega)\, e^{i\omega k\Delta t} \sum_{m=0}^{\infty} r\,[(k-m)\,\Delta t]\, g\,(m\Delta t + \varepsilon\Delta t)\, e^{-i\omega m\Delta t}. \tag{19}$$

Expression (19) is the spectral representation of the output process. It is a nonstationary process, since k enters into the integrand, and not only into the exponential factor.

We obtain the dispersion of the process y in the following form.

$$\sigma_y^2(k, \varepsilon) = \frac{\Delta t}{2\pi} \int_{-\pi/\Delta t}^{\pi/\Delta t} d\omega S_x^*(\omega) \left| \sum_{m=0}^{\infty} r\,[(k-m)\,\Delta t]\, g\,(m\Delta t + \varepsilon\Delta t)\, e^{-i\omega m\Delta t} \right|^2. \tag{20}$$

We consider two particular cases:

1. Let r(t) be a linear function of time:

$$r(t) = a + bt. \tag{21}$$

Then,

$$\sum_{m=0}^{\infty}[a+b(k-m)\Delta t]\,g[(m+\varepsilon)\Delta t]\,e^{-i\omega m\Delta t}=$$

$$=(a+bk\Delta t)\,G^*(i\omega,\ \varepsilon)+ib\frac{d}{d\omega}G^*(i\omega,\ \varepsilon).$$

If the system's frequency characteristic $G^*(i\omega,\ \epsilon)$ is presented in the form

$$G^*(i\omega,\ \varepsilon)=P(\omega)\,e^{i\varphi(\omega)},$$

then, for the square of the modulus of the sum under the integral sign in (20), we obtain the expression

$$P^2[(a+bk\Delta t)+b\varphi']^2+b^2P'^2,$$

where the "prime" denotes differentiation with respect to ω.

We obtain the following final expression for the dispersion:

$$\sigma_y^2(k,\ \varepsilon)=\frac{\Delta t}{2\pi}\int_{-\pi/\Delta t}^{\pi/\Delta t}d\omega S_x^*(\omega)\,\{P^2[(a+bk\Delta t)+$$

$$+b\varphi']^2+b^2P'^2\}. \qquad (22)$$

For computations by (22), it is necessary to differentiate the modulus and phase frequency characteristics with respect to ω. These operations may be implemented graphically.

2. Let

$$r(t)=e^{at}. \qquad (21a)$$

In this case,

$$\sum_{m=0}^{\infty}e^{\alpha(k-m)\Delta t}g[(m+\varepsilon)\Delta t]\,e^{im\omega\Delta t}=e^{\alpha k\Delta t}G^*(\alpha+i\omega,\ \varepsilon)$$

and, consequently,

$$\sigma_y^2(k,\ \varepsilon)=e^{2\alpha k\Delta t}\frac{\Delta t}{2\pi}\int_{-\pi/\Delta t}^{\pi/\Delta t}d\omega S_x^*(\omega)\,|G^*(\alpha+i\omega,\ \varepsilon)|^2. \qquad (23)$$

In order to compute the dispersion by this formula, it is necessary to reconstruct the system's frequency characteristic, since the presence of α would change all the time constants of the system's continuous part.

A formula analogous to (23) for the case of continuous systems was obtained by V. S. Krapivin [12].

Computations by the formulas obtained can be carried out in the case when the function f(t) is neither linear nor exponential. For this, it is necessary that r(t), in the neighborhood of the moment of time t_0 of interest, can be approximately presented in the form of a linear or exponential function. The size of this neighborhood can be estimated on the basis of the sum entering into (20). It must be such that the magnitude of the quantity under the summation sign outside of this neighborhood be so small that it would be possible to neglect it; at the same time, inside the neighborhood, r(t) must differ only slightly from a straight line or an exponential.

By using general relationship (20), one can compute the dispersion in cases when r(t) varies by a more general law than (21) or (21a).

3. Action of a Stationary Random Process on a Sampled-Data System which Contains a Nonlinear Element

We assume that the stationary random process of the form

$$x(n\Delta t+\varepsilon\Delta t)=\frac{\Delta t}{2\pi}\int_{-\pi/\Delta t}^{\pi/\Delta t}e^{i\omega n\Delta t}Q^*(\omega,\ \varepsilon)\,du(\omega) \qquad (24)$$

acts on some continuous linear system with weight function k(t). The steady-state output process can be presented in the form

$$y(m\Delta t+\eta\Delta t)-\sum_{m=0}^{\infty}\Delta t\int_0^1 x[(m-n)\Delta t+$$

$$+\varepsilon\Delta t]\,k[n\Delta t+(\eta-\varepsilon)\Delta t]\,d\varepsilon. \qquad (25)$$

By substituting (24) therein, we obtain the spectral representation of the output process

$$y(m\Delta t+\eta\Delta t)=\frac{\Delta t}{2\pi}\int_{+\pi/\Delta t}^{\pi/\Delta t}du(\omega)\,e^{im\omega\Delta t}P^*(\omega,\ \eta), \qquad (26)$$

where

$$P^*(\omega,\ \eta)=\Delta\int_0^1 K^*(\omega,\ \eta-\varepsilon)\,Q^*(\omega,\ \varepsilon)\,d\varepsilon, \qquad (27)$$

$$K^*(\omega,\ \eta-\varepsilon)=\sum_{m=0}^{\infty}k[m\Delta t+(\eta-\varepsilon)\Delta t]\,e^{-i\omega m\Delta t}. \qquad (28)$$

We now consider the sampled-data circuit shown on Fig. 2. This circuit contains a nonlinear element. Such an element might be, for example, a relay element, an element with a limited linear zone, and other elements

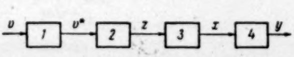

Fig. 2. Nonlinear sampled-data circuit. 1 is an ideal sampled-data element, 2 is a linear link, 3 is a nonlinear element, 4 is a linear link.

[13]. At the circuit's input acts a stationary random process $v(t) = m_v + v_0(t)$, where m_v is the mathematical expectation of the process $\underline{v}$ and $v_0(t)$ is a process with zero mathematical expectation. By using the results of section 1, we can easily find the spectral representation and, consequently, the correlation function $R_z(n\Delta t, \epsilon\Delta t)$ of the process $\underline{z}$ at the nonlinear element's input. It is also easy to compute the mathematical expectation m_z of the process $\underline{z}$. We shall assume that the process $v(t)$ is normally distributed. In this case, the correlation function $R_x(n\Delta t, \epsilon\Delta t)$ of the process $\underline{x}$ at the nonlinear element's output can be presented in the form of a series [14]

$$R_x(n\Delta t,\ \varepsilon\Delta t) = \sum_{l=1}^{\infty} \frac{a_l}{l!} \rho_z^l (n\Delta t,\ \varepsilon\Delta t). \tag{29}$$

Here, $\rho_z = R_z/\sigma_z^2$, σ_z^2 is the dispersion of process $\underline{z}$, and a_l are coefficients which depend on σ_z and m_z. In its turn, the mathematical expectation m_x of process $\underline{x}$ can be presented in the form

$$m_x = \chi(\sigma_z,\ m_z)\, m_z. \tag{30}$$

A simple and elegant method of calculating the coefficients a_l and χ, based on the use of the δ-function, is presented in [14].

For an element with a limited linear zone,

$$\chi = \frac{b}{a}\left\{1 + \frac{\sigma_z}{m_z}\left[\frac{a - m_z}{\sigma_z}\left(1 - \Phi\left(\frac{a - m_z}{\sigma_z}\right)\right) - \varphi\left(\frac{a - m_z}{\sigma_z}\right) - \right.\right.$$

$$\left.\left. - \frac{a + m_z}{\sigma_z}\left(1 - \Phi\left(\frac{a + m_z}{\sigma_z}\right)\right) + \varphi\left(\frac{a + m_z}{\sigma_z}\right)\right]\right\},$$

$$a_l = \sigma_z^2 \frac{b^2}{a^2}\left[\Phi^{(l-1)}\left(-\frac{a + m_z}{\sigma_z}\right) - \Phi^{(l-1)}\left(\frac{a - m_z}{\sigma_z}\right)\right]^2,$$

where $\underline{a}$ is the magnitude of the element's linearity zone, $\underline{b}$ is the limitation level and b/a is the slope of the linear part of the element's characteristic.

For a relay element,

$$\chi = \frac{1}{m_z} b\left[2\Phi\left(\frac{m_z}{\sigma_z}\right) - 1\right],$$

$$a_l = 4b^2\left[\Phi^{(l)}\left(-\frac{m_z}{\sigma_z}\right)\right]^2,$$

where $\underline{b}$ is the signal level at the relay element's output.

Here, everywhere $\Phi(x) = \frac{1}{\sqrt{2\pi}} \int_{-\infty}^{x} e^{-\frac{t^2}{2}} dt$,

and $\Phi^{(l)}(x)$ is the lth derivative of $\Phi(x)$ with respect to $\underline{x}$; $\varphi(x) = \Phi'(x)$.

The spectral density of process $\underline{x}$, starting from (29), can obviously be given in the form of a series

$$S_x^{\bullet}(\omega,\ \varepsilon) = a_1 S_z^{\bullet}(\omega,\ \varepsilon) + \sum_{l=2}^{\infty} \frac{a_l}{l!} \frac{1}{\sigma_z^{(2l+2)}} S_z^{\bullet(l)}(\omega,\ \varepsilon), \tag{31}$$

where $S_z^{\bullet}(\omega, \epsilon)$ is the spectral density of process $\underline{z}$, and $S_z^{\bullet}(l)$ is the lth-order spectrum of the function $S_z^{\bullet}(\omega, \epsilon)$.

Tables 1 and 2 give the values of the coefficients $a/l!$ for an element with a limited linearity zone and a relay element for $a = b = 1$, for various values of m_z and σ_z.

It is clear from the tables that in the overwhelming majority of the cases there holds the inequality $a_l/l! \ll a_1$, for $l = 2, 3, \ldots$ Thus, the terms with $l \geq 2$ in (31) can be ignored.

We turn back now to Fig. 2. Let link 2 have weight function $g(t)$ and link 4, weight function $k(t)$. Then the spectral density of process $\underline{z}$ will be

$$S_z^{\bullet}(\omega,\ \varepsilon) = |G^{\bullet}(i\omega,\ \varepsilon)|^2 S_v^{\bullet}(\omega). \tag{32}$$

As a consequence of what has already been said about $S_x^{\bullet}(i\omega, \epsilon)$, we have that

$$S_x^{\bullet}(\omega,\ \varepsilon) \approx a_1 |G^{\bullet}(i\omega,\ \varepsilon)|^2 S_v^{\bullet}(\omega). \tag{33}$$

TABLE 1

m_z	σ_z	a_1	$a_2/2$	$a_3/6$	$a_4/24$
0	0.5	0.2220	0	0.00194	0
0	1.0	0.4640	0	0.03900	0
0	2.0	0.5860	0	0.08270	0
0.5	0.5	0.1760	0.0070	0.00272	0.00001
0.5	1.0	0.3900	0.0248	0.02280	0.00754
0.5	2.0	0.5540	0.0118	0.06950	0.00916
1.0	0.5	0.0625	0.0198	0	0.00167
1.0	1.0	0.2270	0.0594	0.00194	0.01310
1.0	2.0	0.4650	0.0494	0.03900	0.02650

TABLE 2

m_z	σ_z	a_1	$a_2/2$	$a_3/6$	$a_4/24$
0	0.5	0.6360	0	0.1060	0
0	1.0	0.6360	0	0.1060	0
0	2.0	0.6360	0	0.1060	0
0.5	0.5	0.2340	0.1170	0	0.03910
0.5	1.0	0.4950	0.0620	0.0495	0.03910
0.5	2.0	0.5970	0.0177	0.0865	0.01340
1.0	0.5	0.0116	0.0233	0.0175	0.00194
1.0	1.0	0.2340	0.1170	0	0.03910
1.0	2.0	0.4950	0.0620	0.0465	0.03910

From this we find that the approximate spectral representation of the process x has the form

$$x(n\Delta t + \varepsilon\Delta t) = \frac{\Delta t}{2\pi} \int\limits_{-\pi/\Delta t}^{\pi/\Delta t} e^{i\omega n\Delta t} \sqrt{a_1} G^{*}(i\omega,\ \varepsilon)\, du(\omega), \tag{34}$$

where $u(\omega)$ is the spectral process of $v_0(n\Delta t)$.

Process x acts on the input of linear link 4. We find the spectral representation of process y at the circuit's output in the form of (26).

By taking into account that, in the given case, $Q^{*}(i\omega,\ \varepsilon)$ is $\sqrt{a_1}\ G^{*}(i\omega,\ \varepsilon)$, we obtain

$$P^{*}(\omega,\ \eta) = \frac{1}{\Delta t} \sum_{n=-\infty}^{\infty} \sqrt{a_1} K\left(i\omega + i\frac{2\pi n}{\Delta t}\right) G\left(i\omega + i\frac{2\pi n}{\Delta t}\right) e^{i\eta\Delta t\left(\omega + \frac{2\pi n}{\Delta t}\right)} \tag{35}$$

This expression is the frequency characteristic of the circuit in the case when the nonlinear element is replaced by an amplifier with gain equal to $\sqrt{a_1}$.

By using the representation of the nonlinear element in the form of a linear amplifier, we can easily calculate the probabilistic characteristics of the system with feedback. It is assumed for this that the process at the nonlinear element's input is normal. Such a method of calculating continuous systems is known as the method of statistical linearization, developed by L. E. Kazakov [13].

Thus, the statistical linearization method is also applicable to sampled-data systems. The computational methods for the discrete case are no different from those used in the continuous case, which are well-known. The coefficient $\sqrt{a_1}$ is computed for different types of nonlinear elements in [13].

CONCLUSIONS

In this paper we considered a number of questions dealing with the statistical computations of discontinuous control systems. We took as fundamental the spectral representation of stationary random processes with discrete arguments.

Starting from the relationship between the spectrum of a continuous process and that of the discrete process related to it, we found that under the same conditions the dispersion at the output will be larger in the sampled-data system than in the continuous system equivalent to it. This is a consequence of the fact that the sampled-data element transforms the high-frequency part of the input process spectrum into a low-frequency region.

The formulas obtained for the dispersion at the output of stationary systems permit the computations to be carried out in the cases when nonstationary processes act.

An investigation of the question of the action of a stationary process on a discrete system containing a nonlinear element led to the conclusion that the statistical linearization method is applicable to the discrete case, the computational methodology remaining the same as in the case of continuous systems.

LITERATURE CITED

[1] Ya. Z. Tsypkin, Transient and Steady-State Processes in Sampled-Data Circuits [in Russian] (Gosenergoizdat, 1951).

[2] Fundamentals of Automatic Control (edited by V. V. Solodovnikov) [in Russian] (Mashgiz, 1955).

[3] Ya. Z. Tsypkin, "Sampled-data automatic systems with extrapolating devices," Avtomatika i Telemekhanika 19, No. 5 (1958).*

[4] S. S. Ermakov and E. M. Esipovich, "Methodology for setting up the transfer functions of sampled-data

systems containing extrapolating devices," Avtomatika i Telemekhanika 19, No. 5 (1958).*

[5] W. K. Linvill and J. M. Salzer, "Analysis of automatic systems containing digital computers," [Russian translation of American original: Proc. IRE 41, 7 (1953)], Frequency Methods in Automation (edited by Batkov) [in Russian] (IL, 1958).

[6] J. M. Salzer, "Frequency analysis of digital computers operating in real time, [Russian translation of American original: Proc.IRE 42, 2 (1954)], Frequency Methods in Automation [in Russian] (IL, 1958).

[7] Ya. Z. Tsypkin, "On taking pulse forms into account in discontinuous control systems," Avtomatika i Telemekhanika 16, No. 5 (1955).

[8] Ya. Z. Tsypkin, Theory of Relay Systems of Automatic Control [in Russian] (Gostekhizdat, 1955).

[9] J. L. Doob. Stochastic Processes [Russian translation] (IL, 1957).

[10] Ya. Z. Tsypkin, "Designing discontinuous control systems for stationary random stimuli," Avtomatika i Telemekhanika 14, No. 4 (1953).

[11] L. T. Kuzin, "Some questions in the synthesis of sampled-data servosystems with stationary random stimuli," Automatic Control and Computing Technology, 1 (edited by Solodovnikov) [in Russian] (Mashgiz, 1958).

[12] V. S. Krapivin, "Probabilistic characteristics of linear automatic control systems for nonstationary disturbances," Scientific Works of the N. E. Zhukovskii VVIA. 1 [in Russian] (1954).

[13] L. E. Kazakov, "Approximate probabilistic analysis of the accuracy of operation of essentially nonlinear automatic systems," Avtomatika i Telemekhanika 17, No. 5 (1956).*

[14] I. N. Amiantov and V. I. Tikhonov, "Action of normal fluctuations on standard nonlinear elements," Izvest. Akad. Nauk SSSR, Otd. Tekh. Nauk No.4 (1957).

---

* See English translation.

ERROR ACCUMULATION IN DIGITAL COMPUTATIONS

V. A. Brik

(Moscow)

Translated from Avtomatika i Telemekhanika Vol. 21, No. 5, pp. 595-600, May, 1960
Original article submitted December 26, 1959

The paper describes a method, based on diffusion theory, of estimating the errors of computing devices used in automatic control systems, as well as special-purpose and general-purpose digital computers. An investigation is made of the errors of cyclical computational processes, in which the successively accumulated elementary errors can be considered as independent random variables with an approximately normal distribution density.

Digital computing devices which solve recursive difference equations [1] are used in automatic control systems. In the operation of these devices, the computations are implemented cyclically, wherein the results of the previous cycle, or cycles, are the input data for the following cycle. For this, it is desirable to have the results obtained after each cycle. Recursive computational processes with output of intermediate data also arise frequently in the solution of various problems on general-purpose or special-purpose computers, for example, in computing tables of some function or other by recursion formulas.

With each computational cycle there ordinarily arise errors which gradually accumulate. This accumulation can occur either quite regularly or randomly. If the successively arising errors are virtually statistically independent, then they may be estimated by the use of probabilistic methods [2, 3]. The possibility of using these methods can be established [3] after an analysis of the statistical properties of the table of successive errors.

In many cases, the process of error accumulation amounts to the addition, to some total error which determines the quality of the entire solution and which exists prior to the given cycle, of an error resulting from the given cycle.

If the error attributable to the given cycle is the result of the effect of several independent sources of error (for example, rounding errors after several multiplications), then the resulting error of the cycle may have a probability density close to normal. Ordinarily, the mean value of the error in a cycle is zero. The dispersion σ^2 of the cycle's error is computed from an analysis of the table of successive errors of the cycles.

If one is given some limit a > 0 which must not be exceeded by the absolute magnitude of the total error Δ_n then, if the conditions stated above are met (addition of the successive errors of the cycles, statistical independence of these errors), the process of error accumulation can be considered as the random walk (diffusion) of a point between two absorbing barriers (Fig. 1). The ordinal numbers of the successive cycles are laid out along the axis of abscissas on Fig. 1. The total error after the nth cycle is the sum of the individual cycle errors.

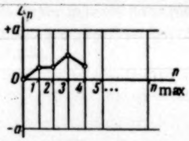

Fig. 1. Diffusion process with two absorbing barriers.

$$\Delta_n = \sum_{i=1}^{n} \delta_i.$$

The random walk begins at the point $\Delta_0 = 0$ (it is assumed that the initial data are given exactly). We shall assume that all the increments δ_i are independent random variables with identical normal distributions with dispersion σ^2 and zero mean value.

We now find the probability $P_0(n)$ that, in n cycles, the random walk will go beyond the barriers at least once.*

For a given n, the probability density of the random variable Δ_n has the form

$$f(x,\ n) = \frac{1}{\sqrt{n\sigma^2}\sqrt{2\pi}} \exp\left(-\frac{x^2}{2n\sigma^2}\right). \qquad (1)$$

Using the reflection method [4, 6], we can introduce a modified "distribution density"

$$f_1(x,\ n) = \sum_{s=-\infty}^{s=+\infty} (-1)^s \frac{1}{\sqrt{n\sigma^2}\sqrt{2\pi}} \exp\left\{-\frac{(x-2as)^2}{2n\sigma^2}\right\}, \qquad (2)$$

characterizing the probability distribution law of the complex event

$$f_1(x,\ n)\,dx = P\{x \leqslant \Delta_n \leqslant x + dx;\ |\Delta_i| < a\}\ (i = 1, 2, \ldots, n-1).$$

---

* For the case of continuous n, the problem, in a more general form, was solved by Bartlett [4, 5].

With this, consequently,

$$\int_{-a}^{a} f_1(x,\ n)\,dx = P\{|\Delta_n| < a;$$

$$|\Delta_i| < a\} \quad (i = 1,\ 2,\ \ldots,\ n-1).$$

$$\int_{-a}^{a} f_1(x,\ n)\,dx = P\{|\Delta_i| < a\} \qquad (i = 1,\ 2,\ \ldots,\ n).$$

The probability of interest to us, $P_0(n)$, equals

$$P_0(n) = 1 - \int_{-a}^{a} f_1(x,\ n)\,dx. \tag{3}$$

After some transformations, we can obtain from (2) and (3) that

$$P_0(n) = 4\sum_{s=0}^{\infty} F\left\{\frac{-a(2s+1)}{\sigma\sqrt{n}}\right\}(-1)^s =$$

$$= 4\left\{F\left(\frac{-a}{\sigma\sqrt{n}}\right) - F\left(\frac{-3a}{\sigma\sqrt{n}}\right) + F\left(\frac{-5a}{\sigma\sqrt{n}}\right) - \ldots\right\}, \tag{4}$$

where

$$F(u) = \int_{-\infty}^{u} \frac{1}{\sqrt{2\pi}} \exp\left(-\frac{z^2}{2}\right) dz.$$

$P_0(n)$, as a function of a/σ and n, computed by (4), is shown on Fig. 2.

The method of estimating the error consists in finding such a value of a that, for a given number of cycles n and a dispersion σ^2 of the maximum possible error D_n (D_n is the maximum of all the Δ_i, $i = 1, 2, \ldots, n$), $P_0(n)$ will equal some definite, sufficiently small, quantity α (for example, $\alpha = 10^{-2}$, 10^{-3} or 10^{-4}). Thus, α is the confidence level for which

$$-D_n < \Delta_i < D_n \quad (i = 1,\ 2,\ \ldots,\ n).$$

The dependence of D_n/σ on n for different α is shown in Fig. 3 on a semilogarithmic scale.

The graphs of Fig. 3 answer the question as to the practical limits of the errors Δ_i ($i = 1, 2, \ldots, n$) for a known dispersion σ^2 of the elementary errors (cycle errors). These graphs can be used for estimating the errors of any computing process in which there occurs accumulation (addition) of statistically independent successive errors with mean zero, dispersion σ^2, and a distribution close to a normal.

We now make an estimate of the error of computing the coordinates of successive equally spaced points on a

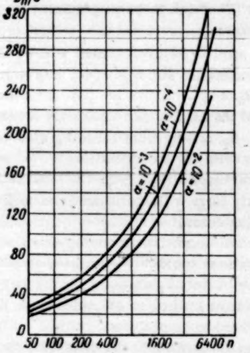

Fig. 3. Dependence of the maximum error D_n, divided by the mean-square deviation of the increment σ, on the number of cycles n and on the quantity α.

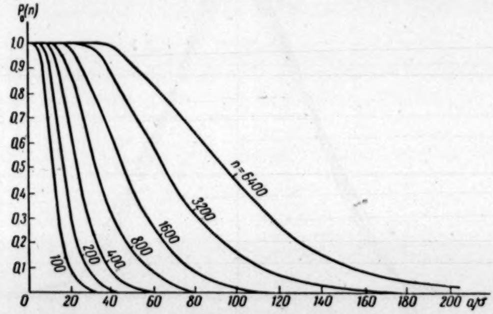

Fig. 2. The probability $P_0(n)$ of going beyond the barriers as a function of the number of cycles n and of the ratio of the distance to the barriers a to the mean-square deviation of the increment σ.

circle (with center at the origin) by means of the recursion formulas

$$x(n+1) = x(n)\cdot(1 - 2^{-2k-1}) \mp y(n)\cdot 2^{-k},$$

$$y(n+1) = y(n)\cdot(1 - 2^{-2k-1}) \pm x(n)\cdot 2^{-k},$$

which are obtained from the formulas

$$x(n+1) = x(n)\cos\omega \mp y(n)\sin\omega,$$

$$y(n+1) = y(n)\cos\omega \pm x(n)\sin\omega$$

after the substitutions

$$\cos\omega \approx 1 - 2^{-2k-1},\quad \sin\omega \approx 2^{-k}, \qquad (5)$$

where $\underline{k}$ is a positive integer and ω is a constant angular increment. This algorithm is used in a special-purpose computer [7] which prepares programs for automatic milling machines.

The error to be investigated will be the deviation of the current radius $R_i = \sqrt{x^2(i) + y^2(i)}$ from the initial radius $R_0 = \sqrt{x^2(0) + y^2(0)}$ over the entire circumference of the circle. We shall only investigate the errors $\Delta R_i = R_i - R_0$ arising from rounding after multiplication (in binary form) by the quantities 2^{-2k-1} and 2^{-k}. The methodical error arising from the substitution in (5), for sufficiently large $\underline{k}$ (larger than three to five), is small and may be neglected.

We shall denote the rounding errors arising from the multiplications $x(n)2^{-2k-1}$, $y(n)2^{-k}$, $y(n)2^{-2k-1}$, and $x(n)2^{-k}$ by $\xi_1(n)$, $\xi_2(n)$, $\xi_3(n)$, and $\xi_4(n)$, respectively, where an error leading to an increase of the radius will be considered to be positive.

It can be shown that the error of a cycle equals

$$\delta_i = R_i - R_{i-1} \approx [\xi_1(i-1) + \xi_2(i-1)]\cos\beta + [\xi_3(i-1) + \xi_4(i-1)]\sin\beta,$$

where

$$\beta = \operatorname{arctan}\frac{y(i)}{x(i)}.$$

We shall assume that the computer operates in fixed point, that $|x| < 1$, $|y| < 1$, and that the machine uses an N-bit word after the binary point. A statistical analysis of the successive errors ξ, carried out for the given problem, showed that for $R_0 > 2^{-N+4k+2}$, i.e., for sufficiently large N, all the quantities $\xi_1(n)$, $\xi_2(n)$, $\xi_3(n)$, $\xi_4(n)$ are statistically independent, and successive values do not depend on preceding ones. It turned out, with this, that they have a uniform distribution density p(z) (Fig. 4). The dispersion of such a distribution equals $2^{-2N}/12$, and the dispersion of the random variables $\delta_i = R_i - R_{i-1}$, the sum of the four independent random variables, equals

$$\sigma^2 = 2\frac{2^{-2N}}{12}\cos^2\beta + 2\frac{2^{-2N}}{12}\sin^2\beta = \frac{2^{-2N}}{6}.$$

The graphs of the distribution density p(z) of the quantity δ_i for various β, computed by a convolution integral, are shown on Fig. 5. Also constructed on the figure is the density curve for a normal distribution with the same dispersion. This curve differs slightly from the others, so that one can consider that all the δ_i are normally distributed with dispersion $2^{-2N}/6$.

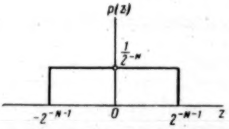

Fig. 4. Distribution density of the quantity ξ (n).

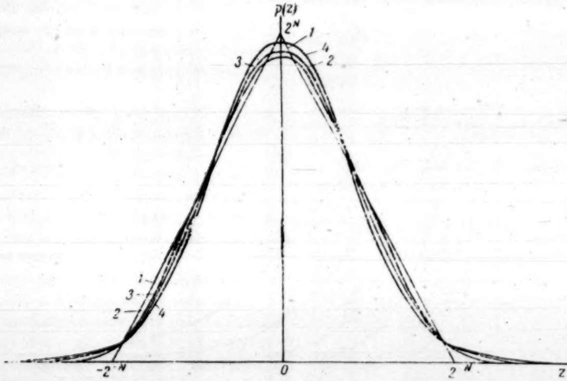

Fig. 5. Distribution density of the increment δ_i for various β: 1 is for $\beta = m\pi/2$; 2 is for $\beta = m\pi/2 \pm \pi/4$; 3 is for $\beta = m\pi/2 \pm \pi/8$, m = 0, 1, 2, 3; 4 is a normal distribution.

k	3	4	5	6	7	8	9	10
n	50	100	200	400	800	1600	3200	6400

The number of cycles n for the complete circle, equal approximately to $\pi 2^{k+1}$, changes by a factor of two when k changes by unity (cf., the table).

By using the graphs given on Fig. 3, one can determine the dependence of D_n on k. For example, for $k = 7$ and for a selected $\alpha = 10^{-3}$ the maximum error

$$|\Delta R_i|\,\max = \Big|\sum_{j=1}^{i} \delta_j\Big|_{\max} = D_n \;\; (i = 1, 2, \ldots, n)$$

equals approximately $(40)2^{-N}$. It is of interest to compare this value with the (theoretically) maximum possible error ΔR_n. Since the maximum value of $R_i - R_{i-1}$, for different β, varies from 2^{-N} to $\sqrt{2}\cdot 2^{-N}$ and, on the average, equals $(1.3)2^{-N}$, then the theoretically possible error ΔR_n equals $1.3n2^{-N} = (1040)2^{-N}$, which is 26 times the value obtained for D_n.

Instead of using graphs to determine D_n, one can use the well-known tables of the function $y = F(u)$. By substituting α instead of $P_0(n)$ and D_n instead of a in (4), and by discarding all except the first term, we get the equation

$$\alpha = 4F\left(\frac{D_n}{\sigma\sqrt{n}}\right).$$

Knowing α, σ, and n, we can easily determine D_n from the tables.

The simplification of (4) just given is admissible for $D_n/\sigma\sqrt{n}$, greater than 1 to 1.5 since, with this, the sum of the discarded terms, as a fraction of the first term, does not exceed 0.01 to 0.00005. For small $P_0(n)$ (or α), this condition is always met.

In about the same way, one can estimate the accumulated errors in those cases when the normal distribution of the independent variables δ_i has a nonzero mean.

LITERATURE CITED

[1] Ya. Z. Tsypkin, Theory of Sampled-Data Systems [in Russian] (Fizmatgiz, 1958).

[2] A. S. Householder, Fundamentals of Numerical Analysis [Russian translation] (IL, 1956).

[3] L. Lukaszewicz, "Accumulation of Errors in Approximate Calculations," Bulletin L'academie polonaise des sciences, serie des sci. math. abstr. et phys. 6, No. 4 (1958).

[4] M. S. Bartlett, "The large-sample theory of sequential tests," Proceedings of the Cambridge Philosophical Society 42, No. 3 (1946).

[5] M. S. Bartlett, Introduction to the Theory of Random Processes [Russian translation] (IL, 1958).

[6] S. Chandrasekhar, "Stochastic problems in physics and astronomy," [Russian translation of American original: Rev. Mod. Phys. 15, No. 1 (1943)] (IL, 1947).

[7] V. A. Brik, "Digital computing devices," Proceedings of the Conference on the Theory and Application of Discrete Automatic Systems [in Russian] (Izd. AN SSSR, 1960).

EFFECT OF RATE FEEDBACK ON LOADED RELAY SERVOMECHANISM DYNAMICS

N. S. Gorskaya
(Moscow)

Translated from Avtomatika i Telemekhanika Vol. 21, No. 5, pp. 601-614, May, 1960
Original article submitted May 28, 1959

The effect of velocity feedback on the free oscillations of a loaded relay servomechanism is considered. The servomechanism's linear portion is described by a complete second-order equation. The investigation is carried out by the point method, using the theory of point transformations [1].

The dependence of the amplitude and time of the autooscillations' half periods on the system's parameters, including the velocity feedback coefficient, is determined.

1. Introduction and Posing of the Problem

The investigation of the dynamics of relay servomechanisms whose linear parts are described by complete second-order equations, has been carried out until now for the cases when the servomechanism's controlling element has a symmetric nonlinear characteristic. In [2-5] there were considered servomechanisms with Z-shaped or looped characteristics and, in [6], characteristics with loops and insensitive zones.

Few works have been published [7] in which consideration is given to unsymmetric looped characteristics of loaded-servomechanism controlling elements.

Some automatic control systems use electrical servomechanisms in which, by means of special relay circuits, there is implemented a charge in direction of the velocity by the switching of the supply voltage of an independently-excited motor from 24 to 48 v. To decrease the static error due to static friction, the servomechanisms are implemented in the form of autooscillatory systems. The autooscillations arise due to the unsymmetric characteristic of the controlling relay, which has one normally closed contact. In the servomechanism whose schematic is shown in Fig. 1, both direct and velocity (position and rate) feedback are employed.

2. Equations of Motion

As is clear from Fig. 1, the total voltage applied to the circuit is

$$\Delta U = U_{fb} - U_{fb} - U_{vf}, \qquad (1)$$

where U_{in} is the input signal voltage, U_{fb} is the (direct) feedback voltage and U_{vf} is the velocity feedback voltage (from the tachometer generator 4).

Controlling relay R_1, connected in the tube's anode circuit, has two working contacts $1R_1$ and $2R_1$. With no

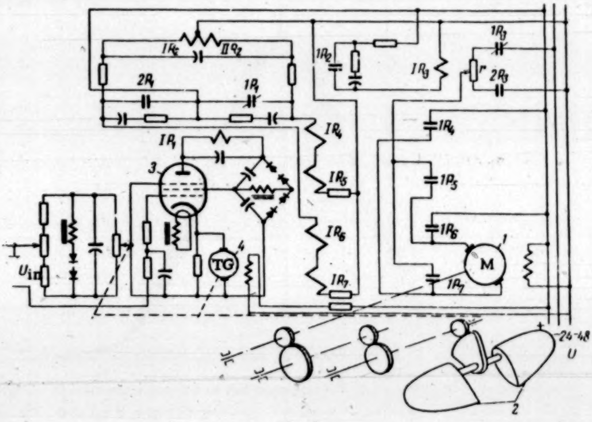

Fig. 1.

current in relay winding $1R_1$ (with negative grid bias), the relay closes contact 1R by means of a spring. With a positive grid bias, anode current will flow through the tube, causing relay R_1 to operate and closing contact $2R_1$. In this case, when contact $1R_1$ closes, current relays R_4 and R_5 and distributor relay R_2 are simultaneously in action. If contact $2R_1$ closes, then current relays R_6 and R_7 and distributor relay R_2 will be simultaneously in action. It is necessary to mention that, with zero signal on the input, relay R_1 operates with a frequency of 20 cps. With this, relay R_2 closes its working contact $1R_2$ with the doubled frequency 40 cps, since it is switched-in twice as frequently as the current relays. When relay R_2 operates, its armature touches contact $1R_2$ and switches in coil $1R_8$ of current relay R_8. Operation of current relays R_4 and R_5 leads to a rotation of motor 1 in one direction, while operation of relays R_6 and R_7 cause it to turn in the other direction. By its operation, relay R_8 switches the motor armature from the 24 v source to the 48 v source. When the winding of relay $1R_8$ is disconnected, its contact $1R_8$ closes the motor armature circuit on that side of resistor r which is connected to part of the 24 v storage battery.

When relay R_8 operates, its contact $2R_8$ closes the motor armature circuit to the other part of resistor r, which is connected to the full voltage of the 48 v storage battery. With no input signal, the motor will still be rotated by virtue of the absence of a neutral position for relay R_1. With zero input signal, the process of switching relay R_2 occurs so rapidly that the contact portion of relay R_8, due to its own inertia, cannot operate, and relay R_8 remains unconnected. With this, current relays R_4, R_5 or R_6,R_7 operate, feeding 24 v to the motor armature. In this case, steering organ 2, set into motion by the servomechanism, will oscillate with a frequency of 20 cps and an amplitude of about 0.5°. When a command is applied, the contact of relay $2R_1$ is closed. In this case, the duration of the closure is sufficient to allow relay R_2, and then relay R_3, to operate. In operating, relay R_3 applies 48 v to the motor armature. With this, the motor will execute the command with maximal speed and torque. Thanks to the presence in the circuit of the tachometer generator feedback, the operation of relay R_1 will be accelerated. With this, the motor will be switched to 24 volts upon reaching the position given by the input signal. This will preclude the arising of a lengthy oscillatory process.

We now consider the servomechanism's free oscillations, i.e., its motion for $U_{in} = 0$. The error equation of (1) can be given in the form

$$\Delta U = -K_\alpha \alpha - K_\Omega \Omega_1, \tag{2}$$

where α is the angle of rotation of the reducer's output axis, Ω_1 is the motor's angular rotational velocity, K_α and K_Ω are proportionality factors.

The speed of the reducer's output shaft is related to the motor velocity by the relationship $\Omega = \Omega_1/K_r = d\alpha/dt$, where K_r is the reduction coefficient.

The equation of the electronic amplifier can be given in the form

$$U_a = K_a \Delta U, \tag{3}$$

where U_a is the voltage at the amplifier's output and K_a is the gain.

The equation of the relay block has the form

$$U = \Psi[U_a] = |U|\, F(U_a), \tag{4}$$

where U is the voltage applied to the motor circuit.

We take the motor's voltage supply to be constant and equal to 48 v, i.e., we do not take into account the action of the scheme for switching the supply voltage. Such an assumption significantly simplifies the solution of the problem without leading to any essential errors in the investigation, since it is based on the fact that switching of the supply voltage to 24 v occurs close to zero error, and turns out to be essential only for the autooscillatory mode. Consequently, in calculating the autooscillation parameters, it is necessary to consider the motor's supply voltage as equal to 24 v, while for the investigation of the system's transient motions one should take the supply voltage as equally 48 v.

The nonlinear function $F(U_a)$ is shown in Fig. 2, where $\left(\varepsilon + \frac{\delta}{2}\right)$ and $\left(\varepsilon - \frac{\delta}{2}\right)$ are the operate and release voltages, respectively, for the relays.

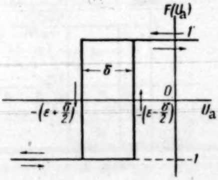
$F(U_a)$
1
δ
0
$-(\varepsilon+\frac{\delta}{2})$
$-(\varepsilon-\frac{\delta}{2})$
U_a
-1

Fig. 2.

The equation for the motor's electrical circuit, if one neglects the armature's inductance, looks as follows:

$$U = IR + C_e\Omega_1, \tag{5}$$

where I is the armature current, R is the active impedance of the armature winding, $E_l = C_e\,\Omega_1$ is the motor's counter-emf and C_e is the motor constant.

If we take the load torque M_L to be proportional to the angle of rotation of the reducer's output axis α, i.e., $M_L = K_L\alpha$, then the equation of motor motion can be given in the form

$$J_{re}\frac{d\Omega}{dt} = C_M I K_r - K_L\alpha, \tag{6}$$

where C_M is the motor constant and J_{re} is the moment of inertia, referred to the reducer's output axis. By eliminating from (2)-(6) all the variables except $U_1 = K_a K_\alpha \alpha$, we get

$$A\frac{d^2U_1}{dt^2} + B\frac{dU_1}{dt} + CU_1 = -F\left(U_1 + D\frac{dU_1}{dt}\right), \tag{7}$$

where

$$A = \frac{J_m R}{|U| C_M K_r K_\alpha K_a}, \quad B = \frac{C_e K_r}{|U| K_\alpha K_a},$$

$$C = \frac{R K_L}{|U| C_M K_r K_\alpha K_a}, \quad D = \frac{K_\Omega K_r}{K_a}.$$

We introduce the following dimensionless parameters:

$$t^* = \sqrt{\frac{C}{A}}\, t, \; x = CU_1, \; h = \frac{B}{2\sqrt{AC}},$$

$$k = D\sqrt{\frac{C}{A}}, \; \mu_\varepsilon = C\varepsilon, \; \Delta = C\delta. \tag{8}$$

Equation (7), written in dimensionless quantities, has the form

$$\frac{d^2x}{dt^{*2}} + 2h\frac{dx}{dt^*} + x = -\Phi\left(x + k\frac{dx}{dt^*}\right). \tag{9}$$

The function $\Phi(\sigma)$, where $\sigma = x + k\,dx/dt^*$, is shown on Fig. 3. This function is described by the equation

$$\Phi(\sigma) = \begin{cases} 1 \text{ for } \sigma \geqslant \mu_\varepsilon - \frac{\Delta}{2}, & \text{if } \Phi(\sigma_0) = 1, \\ -1 \text{ for } \sigma \leqslant \mu_\varepsilon + \frac{\Delta}{2}, & \text{if } \Phi(\sigma_0) = -1, \end{cases} \tag{10}$$

where σ_0 is the initial condition at time t = +0.

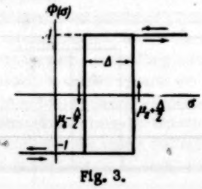
$\Phi(\sigma)$
1
Δ
σ
$\mu_\varepsilon - \frac{\Delta}{2}$
$\mu_\varepsilon + \frac{\Delta}{2}$
-1

Fig. 3.

Figure 4 shows the block schematic of the servomechanism scheme described by (9). Thus, the system is characterized by four essential parameters h, k, μ_ε, and Δ.

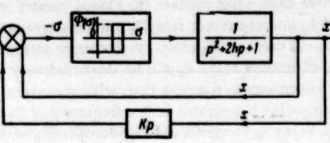
$-\sigma$
$\Phi(\sigma)$
σ
$\frac{1}{p^2+2hp+1}$
x
x
$\dot{x}$
Kp

Fig. 4.

3. The Phase Plane

By setting $dx/dt^* = \dot{x} = y$, we write the equation of motion (9) in the form

$$\dot{x} = y, \quad \dot{y} + 2hy + x = -\Phi(x + ky). \tag{11}$$

We now consider the structure of the servomechanism's phase space. It follows, from the system of equations in (11), that the phase space of the system being investigated is a two-sheeted phase plane. On sheet I the system's motion is described by the differential equations

$$\dot{x} = y, \quad \dot{y} + 2hy + x = -1. \tag{12}$$

On sheet II,

$$\dot{x} = y, \quad \dot{y} + 2hy + x = 1. \tag{13}$$

From the system of equations (12) and (13), it follows that the system's equilibrium states are found at the points x = − 1, y = 0 and x = 1, y = 0, which are stable foci (if h < 1) on stable nodes (if h > 1). Since, in actual systems, $\left|\mu_\varepsilon \pm \frac{\Delta}{2}\right| < 1$ and $\mu_\varepsilon > \frac{\Delta}{2}$, then the representative point, moving along a sheet of the phase plane, always reaches the switching line, never falling on a point

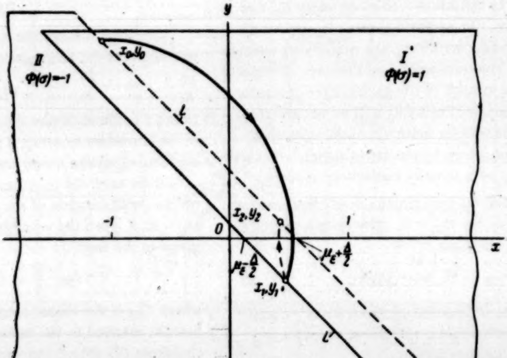
y
II
$\Phi(\sigma)=-1$
I
$\Phi(\sigma)=1$
x_0, y_0
l
x_2, y_2
-1
0
1
x
$\mu_\varepsilon - \frac{\Delta}{2}$
$\mu_\varepsilon + \frac{\Delta}{2}$
x_1, y_1
l'

Fig. 5.

of rest. For the purpose of system stabilization, the damping coefficient k is ordinarily chosen to be positive. The motion of the representative point along the two-shetted phase plane occurs in the following manner. While moving along sheet $I\ [\Phi(x+ky)=1]$ (Fig. 5), the representative point, during some interval of time, falls on the line $L\left(\sigma=\mu_\varepsilon+\frac{\Delta}{2}\right)$ from the line $L_1\left(\sigma=\mu_\varepsilon-\frac{\Delta}{2}\right)$.

The system's phase space is not symmetric, since its equilibrium states are found at points on the axis y = 0 which are unsymmetrically placed with respect to the point $x=\mu_\varepsilon$, $y=0$.

4. Point Transformation

The problem of seeking limiting cycles and of investigating the partitioning of the phase space leads to the study of the point transformation of line L into itself. This point transformation T is defined as $T=S^+S^-$ Transformation S^+ corresponds to a transition of the representative point, lying on line L, to a point lying on line L_1, and transformation S^- corresponds to a transition of the representative point lying on line L_1 to a point lying on line L. We shall find the analytic expressions for the transformations S^+ and S^-.

Sheet I of the Phase Plane $I\ [\Phi(\sigma)=-1]$

The case of small damping (h < 1). If, at time $t^*=0$, the representative point begins its motion from point (x_0, y_0) of line L (cf., Fig. 5) and, during the time interval $t^*=t_1$, arrives at point (x_1, y_1) of line L_1, then the analytic expression for transformation S^+, in the form of a correspondence function $u_1=u_1(v)$, in the case when h < 1, will have the form

$$u_1=\frac{\left(1+\mu_\varepsilon+\frac{\Delta}{2}\right)\cos w_1t_1-\left(1+\mu_\varepsilon-\frac{\Delta}{2}\right)e^{ht_1}}{\left(k-2h+\frac{1}{k}\right)\sin w_1t_1}w_1+$$

$$+\frac{\left(1+\mu_\varepsilon+\frac{\Delta}{2}\right)(h-k)}{k-2h+\frac{1}{k}}+\mu_\varepsilon+\frac{\Delta}{2}$$

$$v=\frac{-\left(1+\mu_\varepsilon-\frac{\Delta}{2}\right)\cos w_1t_1+\left(1+\mu_\varepsilon+\frac{\Delta}{2}\right)e^{-ht_1}}{\left(k-2h+\frac{1}{k}\right)\sin w_1t_1}w_1+ \tag{14}$$

$$+\frac{\left(1+\mu_\varepsilon-\frac{\Delta}{2}\right)(h-k)}{k-2h+\frac{1}{k}}+\mu_\varepsilon-\frac{\Delta}{2},$$

where $w_1^2=1-h^2$, $u_1=x_0$, $v=x_1$, and t_1 is a parameter. It follows from (14) that

$$\frac{dv}{du_1}=\frac{f_1(t_1)}{f_2(t_1)},$$

where

$$f_1(t_1)=w_1\left(1+\mu_\varepsilon-\frac{\Delta}{2}\right)-\left(1+\mu_\varepsilon+\frac{\Delta}{2}\right)$$

$$(w_1\cos w_1t_1+h\sin w_1t_1)\,e^{-ht_1},$$

$$f_2(t_1)=-w_1\left(1+\mu_\varepsilon+\frac{\Delta}{2}\right)+\left(1+\mu_\varepsilon-\frac{\Delta}{2}\right)$$

$$(w_1\cos w_1t_1-h\sin w_1t_1)\,e^{ht_1},$$

$$\frac{d^2v}{du_1^2}=\frac{(k-2h+1/k)\,f_3(t_1)\sin^3 w_1t_1}{f_2^3(t_1)}, \tag{15}$$

where

$$f_3(t_1)=-\frac{2h}{w_1}\left[(1+\mu_\varepsilon)^2-\frac{\Delta^2}{4}\right]\sin w_1t_1+$$

$$+\left(1+\mu_\varepsilon-\frac{\Delta}{2}\right)^2e^{ht_1}-\left(1+\mu_\varepsilon+\frac{\Delta}{2}\right)^2e^{-ht_1}.$$

If the initial conditions are changed on sheet I, i.e., if x_0 and y_0 are changed, the representative point will be translated along sheet I during different time intervals.

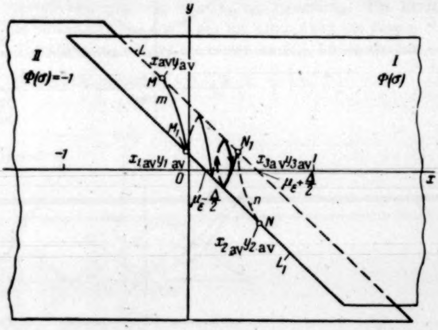

Fig. 6.

The transition time t_1 for the movement of the representative point from line L to line L_1 by a trajectory lying on sheet I and not going off on line L, i.e., the transition time along the "cylindrical" surface, lies in the interval $(0, t_{1s})$. The time T_{1s} is defined by the condition that trajectory m and line L be tangent at the point $M(x_{av}, y_{av})$ (cf., Fig. 6)

$$w_1\left(1+\mu_\varepsilon-\frac{\Delta}{2}\right)-\left(1+\mu_\varepsilon+\frac{\Delta}{2}\right)$$

$$(w_1\cos w_1t_{1s}+h\sin w_1t_{1s})\,e^{-ht_{1s}}=0. \tag{16}$$

The coordinates x_{av} and y_{av} of point M are also defined by the condition that trajectory m and line L be tangent:

$$x_{\text{av}} = -k\frac{\left(1+\mu_\varepsilon+\frac{\Delta}{2}\right)}{k-2h+\frac{1}{k}} + \mu_\varepsilon + \frac{\Delta}{2},\quad y_{\text{av}} = \frac{1+\mu_\varepsilon+\frac{\Delta}{2}}{k-2h+\frac{1}{k}}. \tag{17}$$

The transition time along a trajectory in sheet I and going off the L varies continuously from t_{1s} to π/w_1 as x_0 varies. An investigation of the function $v = v(u_1)$ for the case when $h < 1$ is given in Appendix I. The curve $v = v(u_1)$, given by the parametric equations (14) and (15), is defined for all t_1 from 0 to π/w_1. It is clear, from an analysis of the phase plane, that from the entire set of arms of the curve there should be retained only those arms which satisfy the following limits of coordinate variation:

$$u_1 \text{ from } \mu_\varepsilon + \frac{\Delta}{2} \text{ to } -\infty, \qquad v \text{ from } x_{1\,\text{av}} \text{ to } \infty.$$

The curves $v = v(u_1)$ for values of system parameters such that $h < 1\left|\mu_\varepsilon \pm \frac{\Delta}{2}\right| < 1$ are given in Fig. 7.

The case of large damping ($h > 1$). The transformation S^+ in the form of a correspondence function $u_1 = u_1(v)$, for the case when $h > 1$, has an analytic expression which may be obtained from (14) by replacing w_1, $\sin w_1t_1$ and $\cos w_1t_1$ by, respectively, w, $\sinh wt_1$ and $\cosh wt_1$, where $w^2 = h^2-1$. In the case when $h > 1$, the transition time along a trajectory in sheet I which goes off line L varies within the interval (t_{1s}, ∞). The time t_{1s}, in the case when $h > 1$, has an expression which may be obtained from (16) by replacing w_1, $\sin w_1t_1$ and $\cos w_1t_1$ by, respectively, $w \sinh wt_1$ and $\cosh wt_1$. For the case when $h > 1$, the coordinates x_{av} and y_{av} are expressed, as in the case for $h < 1$, by (17). An investigation of the function $v = v(u_1)$ for the case when $h > 1$ is given in Appendix I. The limits of variation of u_1 and v are the same as in the case when $h < 1$. The curves of $v = v(u_1)$ for values of the parameters $h > 1, \left|\mu_\varepsilon \pm \frac{\Delta}{2}\right| < 1$ are given in Fig. 8.

h close to zero

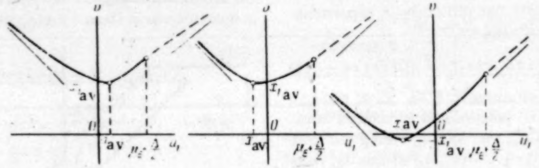

h close to unity

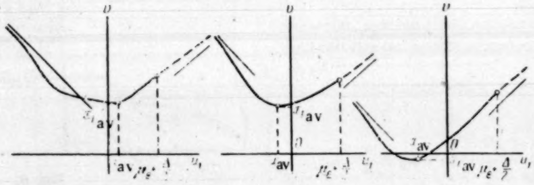

Fig. 7.

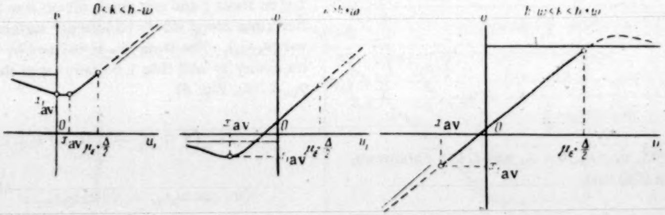

Fig. 8.

Sheet II of the Phase Plane [$\Phi(\sigma) = 1$]

The case of small damping (h < 1). If the representative point, at time $t^* = 0$, begins its motion from point (x_1, y_1) on line L_1 (Fig. 5) and, after a time interval $t^* = t_2$, arrives at the point (x_2, y_2) of line L, then the transformation S^- in the form of a correspondence function $u_2 = u_2(v)$ in the case h < 1 has an analytic expression which can be obtained from (14) by replacing v, u_1, t_1 and μ_ϵ by, respectively, $-u_2$, $-v$, t_2 and $-\mu_\epsilon$, where $u_2 = x_2$, $v = x_1$ and t_2 is a parameter.

The transition time t_2 for the movement of the representative point from line L_1 to line L along a trajectory in sheet II which does not leave line L_1 lies in the interval $(0, t_{25})$. The transition time by a trajectory in sheet II which leaves line L_1 varies continuously from t_{25} to π / w_1 as x_1 varies. The time t_{25}, defined by the condition that trajectory n and line L_1 be tangent at the point $N(x_{2av}, y_{2av})$, has an expression, in the case when h < 1, which can be obtained from (16) by replacing μ_ϵ and t_{15} by, respectively, $-\mu_\epsilon$ and t_{25}. The coordinates x_{2av} and y_{2av} in the case h < 1 and in the case h > 1 have expressions which can be obtained from (17) by replacing x_{av}, y_{av}, and μ_ϵ by, respectively, $-x_{2av}$, $-y_{2av}$ and $-\mu_\epsilon$.

Investigation of the correspondence function $u_2 = u_2(v)$ in the case h < 1 can be carried out in analogy with that of the function $v = v(u_1)$ in the case when h < 1, which is given in Appendix, I, by replacing v, u_1, μ_ϵ, t_1, t_{15} and t_{11} by, respectively, $-u_2$, $-v$, $-\mu_\epsilon$, t_2, t_{25} and t_{22}.

From an analysis of the phase plane (Fig. 5), it is clear that of the entire set of arms of the curve $u_2 = u_2(v)$, there should remain only those arms which satisfy the following limits of coordinate variation:

u_2 from x_{3av} to $-\infty$, v from x_{1av} to ∞.

Curves of $u_2 = u_2(v)$ for system parameter values $h < 1$, $\left|\mu_\epsilon \pm \frac{\Delta}{2}\right| < 1$ are shown on Fig. 9. Also shown on Fig. 9 are curves $u_1 = u_1(v)$ for system parameter values $h < 1$, $\left|\mu_\epsilon \pm \frac{\Delta}{2}\right| < 1$.

The case of large damping (h > 1). The transformation S^- in the form of a correspondence function $u_2 = u_2(v)$ in the case h > 1 has an analytic expression which can be obtained from (14) by replacing v, u_1, μ_ϵ, w_1, t_1, sin w_1t_1 and cos w_1t_1 by, respectively, $-u_2$, $-v$, $-\mu_\epsilon$, w, t_2, sinh wt_2 and cosh wt_2. In the case h > 1, the time t_{25} has an expression which can be obtained from (16) by replacing μ_ϵ, w_1, t_{15}, sin s_1t_{15} and cos w_1t_{15} by, respectively, $-\mu_\epsilon$, w, t_{25}, sinh wt_{25} and cosh wt_{25}

Investigation of the function $u_2 = u_2(v)$ in the case h > 1 can be carried out in analogy to the investigation, given in Appendix II, of the function $v = v(u_1)$ in the case h > 1 by replacing v, u_1, μ_ϵ, t_1, t_{15}, t_{13} and t_{14} by, respectively, $-u_2$, $-v$, $-\mu_\epsilon$, t_2, t_{25}, t_{23} and t_{24}. The limits of variation of u_2 and v are the same as in the case h < 1. The curves $u_2 = u_2(v)$ are shown on Fig. 10 for system parameter values $h > 1$, $\left|\mu_\epsilon \pm \frac{\Delta}{2}\right| < 1$.

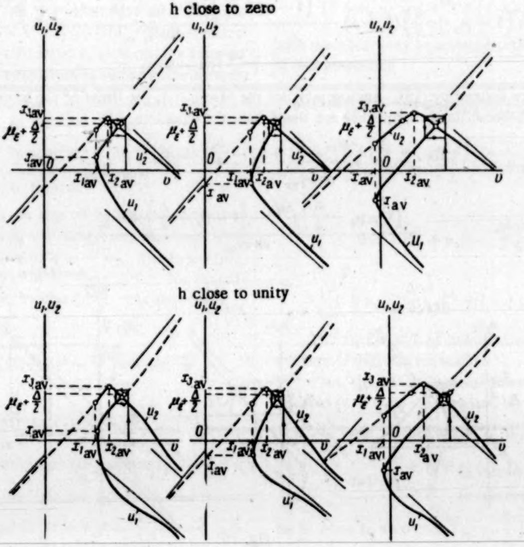

Fig. 9.

Figure 10 also shows curves of $u_1 = u_1(v)$ for system parameter values $h > 1$, $\left|\mu_\varepsilon \pm \frac{\Delta}{2}\right| < 1$.

System Autooscillations

It follows, from the diagrams of point transformation shown in Figs. 9 and 10 for the parameter values $h \neq 1$, $\left|\mu_\varepsilon \pm \frac{\Delta}{2}\right| < 1$, that for these system parameters, the curves of the correspondence function $u_1 = u_1(v)$ and $u_2 = u_2(v)$ must always have one point of intersection in the first quadrant. Consequently, there exists one stable limiting cycle, i.e., there are always autooscillations in the system.

These autooscillations can be established with the presence of a skipping mode (cf., Fig. 6). On the "cylindrical surface" between lines L and L_1, points MN_1NM_1 mark out the region in which a skipping mode occurs. From the conditions that the curves $u_1 = u_1(v)$ and $u_2 = u_2(v)$ intersect, in the case $h < 1$, we find the times t_{1a} and t_{2a} of the half periods of autooscillation in the case when $h < 1$. These conditions are written in the form

$$\begin{gathered}
\frac{\left(1+\mu_\varepsilon+\frac{\Delta}{2}\right)e^{-ht_{1a}}-\left(1+\mu_\varepsilon-\frac{\Delta}{2}\right)\cos w_1t_{1a}}{\sin w_1 t_a}\,w_1+2(h-k)= \\
=\frac{\left(1-\mu_\varepsilon-\frac{\Delta}{2}\right)e^{ht_{2a}}-\left(1-\mu_\varepsilon+\frac{\Delta}{2}\right)\cos w_1 t_{2a}}{\sin w_1 t_{2a}}\,w_1, \\
\frac{\left(1+\mu_\varepsilon+\frac{\Delta}{2}\right)\cos w_1 t_{1a}-\left(1+\mu_\varepsilon-\frac{\Delta}{2}\right)e^{ht_{1a}}}{\sin w_1 t_{1a}}\,w_1+2(h-k)= \\
=\frac{\left(1-\mu_\varepsilon-\frac{\Delta}{2}\right)\cos w_1 t_{2a}-\left(1-\mu_\varepsilon+\frac{\Delta}{2}\right)e^{-ht_{2a}}}{\sin w_1 t_{2a}}\,w_1
\end{gathered} \tag{18}$$

The amplitude of velocity autooscillation y is expressed, in the case when $h < 1$, by the equation $y_a = \frac{y_0 - y_1}{2}$ or

$$\begin{gathered}
y_a=\frac{1}{2k\left(k-2h+\frac{1}{k}\right)}\left[-\frac{\left(1+\mu_\varepsilon+\frac{\Delta}{2}\right)\cos w_1 t_{1a}-\left(1+\mu_\varepsilon-\frac{\Delta}{2}\right)e^{ht_{1a}}}{\sin w_1 t_{1a}}\,w_1-\right. \\
-\left(1+\mu_\varepsilon+\frac{\Delta}{2}\right)(h-k)-\frac{\left(1-\mu_\varepsilon+\frac{\Delta}{2}\right)\cos w_1 t_{2a}-\left(1-\mu_\varepsilon-\frac{\Delta}{2}\right)e^{ht_{2a}}}{\sin w_1 t_{2a}}\,w_1- \\
\left.-\left(1-\mu_\varepsilon+\frac{\Delta}{2}\right)(h-k)\right],
\end{gathered} \tag{19}$$

where t_{1a} and t_{2a} are defined by (18). Analogously, for the case $h > 1$, the times of the autooscillation half periods t_{1a} and t_{2a} and the autooscillation amplitude are found from the equations

$$\begin{gathered}
\frac{\left(1+\mu_\varepsilon+\frac{\Delta}{2}\right)e^{-ht_{1a}}-\left(1+\mu_\varepsilon-\frac{\Delta}{2}\right)\operatorname{ch} wt_{1a}}{\operatorname{sh} wt_{1a}}\,w+2(h-k)= \\
=\frac{\left(1-\mu_\varepsilon-\frac{\Delta}{2}\right)e^{ht_{2a}}-\left(1-\mu_\varepsilon+\frac{\Delta}{2}\right)\operatorname{ch} wt_{2a}}{\operatorname{sh} wt_{2a}}\,w,
\end{gathered} \tag{20}$$

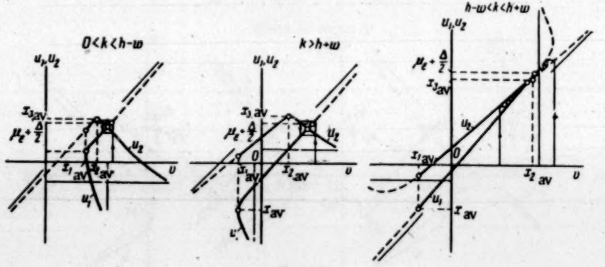

Fig. 10

$$\frac{\left(1+\mu_\varepsilon+\frac{\Delta}{2}\right)\operatorname{ch} wt_{1a}-\left(1+\mu_\varepsilon-\frac{\Delta}{2}\right)e^{ht_{1a}}}{\operatorname{sh} wt_{1a}}w+2(h-k)=$$

$$=\frac{\left(1-\mu_\varepsilon-\frac{\Delta}{2}\right)\operatorname{ch} wt_{2a}-\left(1-\mu_\varepsilon+\frac{\Delta}{2}\right)e^{-ht_{2a}}}{\operatorname{sh} wt_{2a}}w;$$

$$y_a=\frac{1}{2k\left(k-2h+\frac{1}{k}\right)}\left[-\frac{\left(1+\mu_\varepsilon+\frac{\Delta}{2}\right)\operatorname{ch} wt_{1a}-\left(1+\mu_\varepsilon-\frac{\Delta}{2}\right)e^{ht_{1a}}}{\operatorname{sh} wt_{1a}}w-\right.$$

$$-\left(1+\mu_\varepsilon+\frac{\Delta}{2}\right)(h-k)-\frac{\left(1-\mu_\varepsilon+\frac{\Delta}{2}\right)\operatorname{ch} wt_{2a}-\left(1-\mu_\varepsilon-\frac{\Delta}{2}\right)e^{ht_{2a}}}{\operatorname{sh} wt_{2a}}w- \qquad (21)$$

$$\left.-\left(1-\mu_\varepsilon+\frac{\Delta}{2}\right)(h-k)\right].$$

SUMMARY

With a looped relay characteristic of its controlling element, a loaded servomechanism whose linear portion is described by a complete second-order equation tends to an autooscillatory mode of operation for any parameter values satisfying the follow relationships:

$$h \neq 1, \quad \left|\mu_\varepsilon \pm \frac{\Delta}{2}\right| < 1, \quad k > 0.$$

The author wishes to thank N. A. Fufaev and A. S. Alekseev for their valuable advice and comments in their reading and correcting of the manuscript.

Appendix I

Investigation of the Function v = v(u₁) for the Case When h < 1

The function $v = v(u_1)$, for the case when $h < 1$, is defined by expression (14). We determine the signs of the derivatives dv/du_1 and d^2v/du_1^2 by (15). The derivative dv/du_1 is greater than zero when t_1 varies in the interval $(0, t_{1s})$ and is less than zero when t_1 varies in the interval $(t_{1s}, \pi/w_1)$ since

$$f_1(t_1)\begin{cases}<0 & \text{in interval } (0,\ t_{1s}),\\ >0 & \text{in interval } (t_{1s},\ \pi/w_1).\end{cases}$$

$$f_2(t_1)<0 \quad \text{in interval } (0,\ \pi/w_1).$$

We now determine the sign of the second derivative. The sine of the angle w_1t_1 will be greater than zero when t_1 varies in the interval from 0 to π/w_1. The expression $k-2h+1/k$ is greater than zero, since $h < 1$. We investigate the sign of the function $f_3(t_1)$ [5]. The derivative $f_3'(t_1)$ equals

$$f_3'(t_1)=h\left\{-2\left[(1+\mu_\varepsilon)^2-\frac{\Delta^2}{4}\right]\cos w_1t_1+\right.$$

$$\left.+\left(1+\mu_\varepsilon-\frac{\Delta}{2}\right)^2e^{ht_1}+\left(1+\mu_\varepsilon+\frac{\Delta}{2}\right)^2e^{-ht_1}\right\}.$$

Since, by the conditions of the problem $\left|\mu_\varepsilon \pm \frac{\Delta}{2}\right| < 1$ then, for $\cos w_1t_1 < 0$, the function $f_3'(t_1) > 0$, and for $\cos w_1t_1 < 0$, the expression $\left[(1+\mu_\varepsilon)^2-\frac{\Delta^2}{4}\right]\cos w_1t_1 > 0$ and in the undetermined inequality

$$2\left[(1+\mu_\varepsilon)^2-\frac{\Delta^2}{4}\right]\cos w_1t_1 \vee$$

$$\left(1+\mu_\varepsilon-\frac{\Delta}{2}\right)^2e^{ht_1}+\left(1+\mu_\varepsilon+\frac{\Delta}{2}\right)^2e^{-ht_1}$$

both members may be squared without changing the sign of the inequality

$$4\left[(1+\mu_\varepsilon)^2-\frac{\Delta^2}{4}\right]^2\cos^2 w_1t_1 \vee \left(1+\mu_\varepsilon-\frac{\Delta}{2}\right)^4e^{2ht_1}+$$

$$+2\left[(1+\mu_\varepsilon)^2-\frac{\Delta^2}{4}\right]^2+\left(1+\mu_\varepsilon+\frac{\Delta}{2}\right)^4e^{-2ht_1}$$

or

$$0<4\left[(1+\mu_\varepsilon)^2-\frac{\Delta^2}{4}\right]^2\sin^2 w_1t_1+$$

$$+\left[\left(1+\mu_\varepsilon-\frac{\Delta}{2}\right)^2e^{ht_1}+\left(1+\mu_\varepsilon+\frac{\Delta}{2}\right)^2e^{-ht_1}\right]^2.$$

This is, the sign of indetermined inequality $\vee$ is the sign of definite inequality <.

Thus, $f_3'(t_1)$ is greater than zero for all t_1. In the interval $(0, \pi/w_1)$ there exists, for h close to unity and $\left|\mu_\varepsilon \pm \frac{\Delta}{2}\right| < 1$, such a $t_1 = t_{11}$ that $f_3(t_{11}) = 0$ and

$$f_3(t_1)\begin{cases}<0 & \text{in interval } (0,\ t_{11}),\\ >0 & \text{in interval } (t_{11},\ \pi/w_1).\end{cases}$$

for h close to zero and $\left|\mu_\varepsilon \pm \frac{\Delta}{2}\right| < 1$, the function

$f_3(t_1)$ is less than zero in the interval $(0, \pi / w_1)$. Consequently, the second derivative d^2v/du_1^2 can take the following signs:

$$\frac{d^2v}{du_1^2}=\begin{cases} >0 \text{ at } (0, \pi/w_1) \text{ for } h, \sim 0 \ \left|\mu_\varepsilon \pm \frac{\Delta}{2}\right|<1, \\ \left.\begin{matrix} >0 \text{ at } (0, t_{11}) \\ <0 \text{ at } (t_{11}, \pi/w_1) \end{matrix}\right\} \text{ for } h, \sim 1 \ \left|\mu_\varepsilon \pm \frac{\Delta}{2}\right|<1. \end{cases}$$

For $t_1 \to 0$, the function $v \to \infty$ and $u_1 \to \infty$, but the derivative dv/du_1 tends to unity. For $t_1 \to 0$, the function $v = v(u_1)$ approximates to the asymptote

$$v = u_1 - \frac{\Delta}{k(k-2h+1/k)}.$$

For $t_1 \to \pi/w_1$, the functions $v \to \infty$ and $u_1 \to -\infty$, but the derivative tends to $-e^{-\pi h/w_1}$. The function $v = v(u_1)$, for $t_1 \to \pi/w_1$, tends to the asymptote

$$v = -e^{-\pi h/w_1} u_1 + \frac{(2h-k)(1+e^{-\pi h/w_1})}{k-2h+1/k} + \frac{\left(\mu_\varepsilon + \frac{\Delta}{2}\right)e^{-\pi h/w_1} + \mu_\varepsilon - \frac{\Delta}{4}}{k(k-2h+1/k)}.$$

Appendix II

Investigation of the Function $v = v(u_1)$ for the Case When $h > 1$

The function $v = v(u_1)$ and its derivatives dv/du_1 and d^2v/du_1^2 are defined by expressions which may be obtained from (14) and (15) by replacing w_1, $\sin w_1t_1$ and $\cos w_1t_1$ by w, $\sinh wt_1$ and $\cosh wt_1$, respectively.

We determine the sign of the derivative dv/du_1. The function $f_1(t_1)$ is less than zero for $0 < t_1 < t_{1s}$ and greater than zero for $t_{1s} < t_1 < \infty$, since $f_1(0) < 0$ and, for $t_1 = t_{1s}$, the function $f_1(t_{1s}) = 0$ and $f_1'(t_{1s}) > 0$. The function $f_2(t_1)$ is less than zero in the interval $0 < t_1 < \infty$, since $f_2(0)$ and $f_2'(t_1) = -(1 + \mu_\varepsilon - \Delta/2)e^{ht_1} \cosh wt_1 < 0$. Consequently, the derivative dv/du_1 is greater than zero in the interval $0 < t_1 < t_{1s}$ and less than zero in the interval $t_{1s} < t_1 < \infty$.

We determine the sign of the derivative d^2v/du_1^2. For $t_1 > 0$, the function $\sinh wt_1$ is greater than zero. The function $f_3(t_1)$, for t_1 equal to zero, is negative. For t_1 equal to t_{1s}, the function $f_3(t_1)$, equal to

$$\frac{(-\operatorname{ch}^2 wt_{1s}+1)\left[(1+\mu_\varepsilon)^2-\frac{\Delta^2}{4}\right]}{w \operatorname{ch} wt_{1s} + h \operatorname{sh} w t_{1s}},$$

is also less than zero and, for $t_1 = \infty$, equals infinity. Moreover, the derivative $f_3'(t_1)$, for $t_1 = 0$, equal $hw\Delta^2$ and is positive. Further, the derivative $f_3'(t_1)$ equals zero for $t_1 = t_{13}$ and $t_1 = t_{14}$, whereby

$$\left(1+\mu_\varepsilon+\frac{\Delta}{2}\right)e^{wt_{13}} = \left(1+\mu_\varepsilon-\frac{\Delta}{2}\right)e^{ht_{13}}$$

and

$$\left(1+\mu_\varepsilon+\frac{\Delta}{2}\right)e^{-wt_{14}} = \left(1+\mu_\varepsilon-\frac{\Delta}{2}\right)e^{ht_{14}},$$

where $t_{14} < t_{13}$. Since the function $f_3(t_1)$ for $t_1 = t_{14}$ equals $\left[(1+\mu_\varepsilon)^2-\frac{\Delta^2}{4}\right](h+w)e^{-wt_{14}}[1-e^{2wt_{14}}]$, and is less than zero, then $f_3(t_1)$ changes sign only once for some $t_{15} > t_{1s}$. In the case when $h > 1$, the expression $\left(k-2h+\frac{1}{k}\right)$ is positive for $0 < k < h - \sqrt{h^2-1}$ or $k > h + \sqrt{h^2-1}$, and is negative for

$$h-\sqrt{h^2-1} < k < h+\sqrt{h^2+1}.$$

It thus follows from the analysis made that the derivative d^2v/du_1^2 may assume the following signs:

$$\begin{aligned} >0 \text{ for } &\begin{cases} 0<k<h-w \quad \text{or} \quad k>h+w & \text{for } 0<t_1<t_{13}, \quad t_{1s}<t_1<t_{15}, \\ h-w<k<h+w & \text{for } t_{15}<t_1<\infty; \end{cases} \\ <0 \text{ for } &\begin{cases} 0<k<h-w \quad \text{or} \quad k>h+w & \text{for } t_{15}<t_1<\infty, \\ h-w<k<h+w & \text{for } 0<t_1<t_{1s} \quad t_{1s}<t_1<t_{15}. \end{cases} \end{aligned}$$

For $t_1 \to 0$, the functions $v \to \infty$ and $u_1 \to \infty$, for $0 < k < h-w$ or $k > h+w$, and $v \to -\infty$ and $u_1 \to -\infty$ for $h-w < k < h+w$. The derivative dv/du_1 tends to unity for $t_1 \to 0$. For $t_1 \to 0$, the function $v = v(u_1)$ approximates to the asymptote $v = u_1 - \Delta/k(k-2h+1/k)$. For $t_1 \to \infty$, the function u_1 tends to ∞ for $h-w < k < h+w$ and to $-\infty$ for $0 < k < h-w$ or $k > h+w$, and the function

$$v \to \frac{-k-\left(\mu_\varepsilon-\frac{\Delta}{2}\right)(h+w)+(h-w)+\left(\mu_\varepsilon-\frac{\Delta}{2}\right)\frac{1}{k}}{k-2h+1/k}.$$

For $t_1 \to \infty$, the function $v = v(u_1)$ approximates to the asymptote

$$v = \frac{-k-\left(\mu_\varepsilon-\frac{\Delta}{2}\right)(h+w)+(h-w)+\left(\mu_\varepsilon-\frac{\Delta}{2}\right)\frac{1}{k}}{k-2h+1/k}$$

LITERATURE CITED

[1] A. A. Andronov and S. E. Khaikin, Theory of Oscillations [in Russian] (ONTI, 1937).

[2] J. Flugge-Lotz, "Über Bewegungen eines Schwingers unter dem Einfluss von Schwarz - Weiss - Regelungen," ZAMM, 25/27, No. 4 (1947).

[3] J. Flugge-Lotz, and K. Klotter, "Über Bewegungen eines Schwingers unter dem Einfluss von Schwarz-Weiss - Regelungen," ZAMM 28, No. 11/12 (1948).

[4] J. Flugge-Lotz, Discontinuous Automatic Control (Princeton University Press, Princeton, New Jersey, 1953).

[5] V. S. Boyarinov and N. N. Leonov, "On the theory of one relay system," Avtomatika i Telemekhanika 19, No. 2 (1958).*

[6] N. S. Gorskaya, "Dynamics of an electric relay servomechanism whose load varies in proportion to the travel," Avtomatika i Telemekhanika 19, No. 6 (1958).*

[7] A. S. Alekseev, "Two-position temperature controller with a leading zone," In Commemoration of A. A. Andronov [in Russian] (Izd. AN SSSR, 1955).

[8] N. A. Fufaev, "Theory of electromagnetic interruptors," In Commemoration of A. A. Andronov [in Russian (Izd. AN SSSR, 1955).

---

* See English translation.

ON BINARY SIGNAL CORRECTOR SCHEMES

V. M. Ostianu
(Moscow)

Translated from Avtomatika i Telemekhanika Vol. 21, No. 5, pp. 615-623, May, 1960
Original article submitted January 8, 1959

Brief descriptions are given of the methods of constructing and correcting signal systems which were developed by M. A. Gavrilov [1, 2, 3], R. R. Varshamov [4, 5], and R. W. Hamming [6]. The structural formulas of the corrector scheme for each of the correction methods described are found. Corrector schemes are contrived.

One of the methods of providing for correct transmission of discrete signals entails the use of a corrector, which may be connected anywhere in the transmission channel.

We shall assume that the correctors are built of diodes and relay-contact elements.

Every discrete signal can be presented in the form of sequences of zeroes and ones. The number of binary digits (bits) in a signal is called its length. There are 2^n different signals of length n. In this set, one defines the concept of the distance between any pair of codes α and β as the number of noncoincident bits in them, i.e.,

$$\rho(\alpha, \beta) = \sum_{i=1}^{n} \alpha_i - \beta_i |,$$

where $\alpha = (\alpha_1, \alpha_2, \ldots, \alpha_n)$ and $\beta = (\beta_1, \beta_2, \ldots, \beta_n)$.

It is well known [6, 3] that, in a system capable of correcting d errors (i.e., d simultaneous inverted bits), the distance between any two codes in the system must be not less than 2d + 1.

Various methods of constructing such signal systems and implementing error correction are known [4-7]. Here, we shall consider only three of them.

Gavrilov's method of signal correction. Let a set N of working signals be so constructed that any two elements of N are separated by a distance not less than D = 2d + 1. There is established such a correspondence between the signals in N and the set M of all 2^n signals that each signal α in N corresponds to the same signal α in M and that all signals $\alpha' \in M$, whose distance from $\alpha \in M$ is not greater than d correspond to the same signal $\alpha \in N$. Then, instead of correcting the signal α', one can require that each α' be executed as the signal α which corresponds to it

This is a convenient method in that it can be realized for correcting any number of errors d that is desired.

Hamming's method for signal construction and correction. This method is applicable for the correction of single errors only. The construction of the set N is carried out according to definite rules, and signal correction (i.e., error detection) reduces to the verification that these rules are satisfied.

Let it be required to construct a set N of working signals which contains not more than k signals. There is then a number l which satisfies the inequality $k \leq 2$. Then, from the relationship

$$2^t - t - 1 \geqslant l \geqslant 2^{t-1} - (t-1) - 1$$

t is determined, and the signal length is found to be $n = l + t$. t bits of the signal (specifically, reading from left to right, the first, second fourth, eight, sixteenth, etc., i.e., the bits in positions $2^0 = 1$, $2^1 = 2$, $2^2 = 4, \ldots, 2^{t-1}$) are called the check bits, while the remaining l bits are the information bits. The information bit positions are filled by all the possible combinations of zeroes and ones. The check bit positions are filled in accordance with the following rules.

In bit position $2^0 = 1$ there is placed a bit which will give a sum of zero modulo two to the bits in positions $2q + 1$ $(q = 0, 1, \ldots)$.

In bit position $2^1 = 2$ there is placed a bit which will give a sum of zero modulo two to the bits in positions $4q + 2$ and $4q + 3$ $(q = 0, 1, \ldots)$.

In bit position $2^2 = 4$ there is placed a bit which will give a sum of zero modulo two to the bits in positions $8q + 4$, $8q + 5$, $8q + 6$, and $8q + 7$ $(q = 0, 1, \ldots)$.

In general, in bit position 2^i there is placed a bit which will give a sum of zero modulo two to the bits in positions $2^{i+1}q + 2^i$, $2^{i+1}q + 2^i + 1, \ldots, 2^{i+1}q + 2^{i+1} - 1$ $(q = 0, 1, \ldots)$.

We now give an example of the construction of the set N by Hamming's method. Let k = 4, then $l = 2$, t = 3, and n = 5. The signals of set N are given in Table 1.

It is easily verified that the distance between any two signals is not less than 3.

Error-checking is executed by verifying the rules for the construction of set N. All three verifications are made; if the results of the verifications are denoted by the letters ξ, ζ and η, respectively, then the bit position in error in the signal is given by the binary number $\xi \zeta \eta$ (if one takes 1 = 100. . .0, 2 = 010. . .0, 4 = 00100. . . 0). For example,

TABLE 1

Bit position	1	2	3	4	5
Position weight	2^0	2^1	2^2	2^3	2^4
α_1	0	0	0	0	0
α_2	1	0	0	1	1
α_3	1	1	1	0	0
α_4	0	1	1	1	1

if the signal sent were α_3 = (11100) and the signal received were α_3' = (11101), then $\xi = 1$, $\zeta = 0$ and $\eta = 1$. The bit position of the error is given by the number $\xi\zeta\eta$, equal, in this case, to 101 = 5.

Varshatov's method for signal construction and correction. The set N of working signals is so constructed that its elements form an additive group with respect to the operation of bit-by-bit addition modulo two, i.e., with respect to the operation defined by the relationship

$$a \dotplus b = (a_1 \dotplus b_1, a_2 \dotplus b_2, \ldots, a_n \dotplus b_n),$$

where a = $(a_1, a_2, \ldots, a_n)$, b = $(b_1, b_2, \ldots, b_n)$ and the sign "$\dotplus$" is to be understood as addition modulo two.

Varshamov [4, 5] developed a methodology for constructing such sets N for any given code distance D. We limit ourselves here to just a brief description of this methodology.

Let it be required to construct a set N of signals containing not less than k elements. We determine the least integer l satisfying the relationship $k \leq 2^l$. We then find the least integer t satisfying the relationship

$$1 + C^1_{n-1} + C^2_{n-1} + \ldots + C^{D-2}_{n-1} < 2^t.$$

Then, $n = l + t$.

The first l bits in the signal are the information bits, the remaining t bits being the check bits.

The construction is executed as follows. One first constructs a unit matrix of l rows and l columns, to which one appends a second matrix of l rows and t columns. With this, the rows of this latter matrix must satisfy the following conditions: the number of ones in each row is not less than D-1; the number of ones in each sum (modulo two) of any two rows is not less than D-2 and, in general, the number of ones in each sum (modulo two) of any i rows is not less than D-i, where i assumes the values i = = 1, 2, . . . , D-1..

The set of l signals thus constructed is called a basis. The entire set of working signals is comprised of the set of basis signals plus all the possible sums (modulo two) of any 2,3,. . . , l basis signals (including the sum of any signal with itself, i.e., the null signal).

Example. Let k = 4 and D = 3, so that l = 2. We now determine t. For D = 3, we get

$$2^t - t - 1 \geqslant l$$

From this, t = 3 and, consequently, n = 5. We construct the unit matrix and append to it a matrix of two rows and three columns, in each row of which there is not less than two ones, the sum of these two rows containing not less than one "1"

10 011
01 111

The set N is made up of the two basis signals, their sum (modulo two) and the null signal. It is given in Table 2 (and coincides with the signals given in Table 1).

TABLE 2

α_1	00 000
α_2	10 011
α_3	11 100
α_4	01 111

R. R. Varshamov developed [5] a method for correcting d errors if the system of working signals has a code distance of D = 2d + 1. We limit ourselves here to a description of the method for correcting unitary errors, i.e., the case when D = 3.

Let there be received some signal α.

If follows, from the method of constructing the set N, that the information bits of all elements of N exhaust all the 2^l different sequences of binary numbers. Therefore, for each received signal there can be found, among the elements of set N, one element whose information bits coincide with the information bits of signal α. We denote this signal by β. We compare their check bits. It can happen that their check bits coincide exactly, i.e., $\alpha \equiv \beta$, and this means that the transmitted signal was received without distortion (error).

As was shown by the author of the method, if a unitary error changes one of the check bits of the transmitted signal, then the check bits of signal α will differ by one bit from the corresponding bits of signal β, where the bit position of the error is the bit position of the noncoinciding bit. If the unitary error changed one of the information bits of the transmitted signal, then the check bits of signal α will differ from the same bits of signal β by more than one bit, i.e., $\alpha \dotplus \beta = \gamma$.

With this, the information bits of γ will all be zero, and there will be more than one "one" among the check bits. To determine the bit position of the error, one seeks, among the signals of set N, a signal with the same check bits as γ (as was shown in [6], if the transmitted signal underwent no more than one distortion, then such a signal must of necessity be found). We denote it by δ. γ and δ differ by just one bit. The position of the latter gives the position of the error in signal α.

We give an example. Let the signal α_2 = (10011) be transmitted. We assume that the signal α = (10010) is received, i.e., that an error distorted the last check bit. From the table we find the unique signal α_2 with the same information bits as in α. Their check bits differ in one place (bit position). The position of the differing bits is the fifth one; consequently, the error distorted the fifth bit, which was in fact the case.

We now assume that the same signal α_2 was transmitted, but that the error distorted its second bit, i.e., $\alpha = (11011)$. From Table 2 we find the unique signal $\sigma_3 = (11100)$ with the same information bits as α. Their check bits differ in three positions. We then compute the sum $\alpha \dotplus \beta = \gamma = (00111)$.

In Table 2 there is a signal δ whose check bits would be the sequence 111. Obviously, $\delta = \alpha_4$. By comparing the information bits of γ and δ, we convince ourselves that the second bits do not coincide, i.e., that the error distorted the second bit, which was in fact the case.

With some modifications, this method can be extended to correct any number of simultaneous errors.

Synthesis of the correctors. We now determine the structure of the corrector for each method of correction implementation.

If each bit of a signal is simulated by the contact of some relay, then the signal itself will be simulated by the constituent units.

The corrector schemes are relay devices at whose inputs are applied distorted or correct signals from the constructed system of working signals and at whose outputs appear only correct signals (the distorted signals will have been corrected by the corrector). It is very important in this connection that the number of (simultaneous) errors in the signals be matched by the code distances.

It is obvious that such devices must be nonsequential. With identical systems of working signals, identical sets of constituents are applied to the correctors' input, and the circuits, in which one and the same set of elements operate, can be made identical. Therefore, the correctors' schemes can also be made identical, despite the fact that the sequences of operations to be executed by them are different. Obviously, this assertion is valid for any n and d.

We illustrate its validity by the example wherein n = 5 and d = 1.

Corrector for the Gavrilov method. We write the states of relays X_1, X_2, X_3, X_4, and X_5, corresponding to the signals of Table 2:

$$\begin{aligned}
&\alpha_1 - \bar{x}_1\bar{x}_2\bar{x}_3\bar{x}_4\bar{x}_5,\\
&\alpha_2 - x_1\bar{x}_2\bar{x}_3x_4x_5,\\
&\alpha_3 - x_1x_2x_3\bar{x}_4\bar{x}_5,\\
&\alpha_4 - \bar{x}_1x_2x_3x_4x_5.
\end{aligned}$$

We write all the signals at unit distance from α_1, α_2, α_3, and α_4, denoting them, respectively, by

$$\alpha_1^{\mathrm{I}}, \alpha_1^{\mathrm{II}}, \alpha_1^{\mathrm{III}}, \alpha_1^{\mathrm{IV}}, \alpha_1^{\mathrm{V}}, \alpha_2^{\mathrm{I}}, \alpha_2^{\mathrm{II}}, \ldots, \alpha_4^{\mathrm{V}}:$$

$$\begin{array}{llll}
\alpha_1^{\mathrm{I}} - \bar{x}_1\bar{x}_2\bar{x}_3\bar{x}_4\bar{x}_5; & \alpha_2^{\mathrm{I}} - \bar{x}_1\bar{x}_2\bar{x}_3x_4x_5; & \alpha_3^{\mathrm{I}} - \bar{x}_1x_2x_3\bar{x}_4\bar{x}_5; & \alpha_4^{\mathrm{I}} - \bar{x}_1x_2x_3x_4\bar{x}_5;\\
\alpha_1^{\mathrm{II}} - \bar{x}_1x_2\bar{x}_3\bar{x}_4\bar{x}_5; & \alpha_2^{\mathrm{II}} - x_1x_2\bar{x}_3x_4x_5; & \alpha_3^{\mathrm{II}} - x_1\bar{x}_2x_3\bar{x}_4\bar{x}_5; & \alpha_4^{\mathrm{II}} - \bar{x}_1x_2x_3\bar{x}_4x_5;\\
\alpha_1^{\mathrm{III}} - \bar{x}_1\bar{x}_2x_3\bar{x}_4\bar{x}_5; & \alpha_2^{\mathrm{III}} - x_1\bar{x}_2x_3x_4x_5; & \alpha_3^{\mathrm{III}} - x_1x_2\bar{x}_3\bar{x}_4\bar{x}_5; & \alpha_4^{\mathrm{III}} - \bar{x}_1x_2\bar{x}_3x_4x_5;\\
\alpha_1^{\mathrm{IV}} - \bar{x}_1\bar{x}_2\bar{x}_3x_4\bar{x}_5; & \alpha_2^{\mathrm{IV}} - x_1\bar{x}_2\bar{x}_3\bar{x}_4x_5; & \alpha_3^{\mathrm{IV}} - x_1x_2x_3x_4\bar{x}_5; & \alpha_4^{\mathrm{IV}} - \bar{x}_1\bar{x}_2x_3x_4x_5;\\
\alpha_1^{\mathrm{V}} - \bar{x}_1\bar{x}_2\bar{x}_3\bar{x}_4x_5; & \alpha_2^{\mathrm{V}} - x_1\bar{x}_2\bar{x}_3x_4\bar{x}_5; & \alpha_3^{\mathrm{V}} - x_1x_2x_3\bar{x}_4x_5; & \alpha_4^{\mathrm{V}} - x_1x_2x_3x_4x_5.
\end{array}$$

We shall denote the corrector's outputs by Y_i (the state of the i th output coincides with the undistorted state of the i th input).

Output Y_1 must be high (must carry voltage) if the second (α_2) or third (α_3) signal was transmitted or if any of the signals at unit distance from α_2 or α_3^{I} was applied to the corrector input.

We denote by c_2 the sum of the constituents corresponding to α_2 and α_2^{I}, α_2^{II}, α_2^{III}, α_2^{IV}, α_2^{V}, and, by c_3, the sum of the constituents corresponding to α_3, α_3^{I}, α_3^{II}, α_3^{III}, α_3^{IV}, and α_3^{V}.

$$\begin{aligned}
c_2 &= \bar{x}_1\bar{x}_2\bar{x}_3x_4x_5 + x_1x_2\bar{x}_3x_4x_5 + x_1\bar{x}_2x_3x_4x_5 +\\
&+ x_1\bar{x}_2\bar{x}_3\bar{x}_4x_5 + x_1\bar{x}_2\bar{x}_3x_4\bar{x}_5 + x_1\bar{x}_2\bar{x}_3x_4x_5, +\\
+ c_3 &= \bar{x}_1x_2x_3\bar{x}_4\bar{x}_5 + x_1\bar{x}_2x_3\bar{x}_4\bar{x}_5 + x_1x_2\bar{x}_3\bar{x}_4\bar{x}_5 +\\
&+ x_1x_2x_3x_4\bar{x}_5 + x_1x_2x_3\bar{x}_4x_5 + x_1x_2x_3\bar{x}_4\bar{x}_5, \qquad (1)
\end{aligned}$$

which gives us

$$F_{(Y_1)} = c_2 + c_3. \qquad (2)$$

By introducing the analogous notation for c_4

$$\begin{aligned}
c_4 = {} & \bar{x}_1x_2x_3x_4x_5 + x_1x_2x_3x_4x_5 +\\
& + \bar{x}_1\bar{x}_2x_3x_4x_5 + \bar{x}_1x_2\bar{x}_3x_4x_5 +\\
& + \bar{x}_1x_2x_3\bar{x}_4x_5 + \bar{x}_1x_2x_3x_4\bar{x}_5 \qquad (1')
\end{aligned}$$

and by reasoning the same as in the derivation of $F_{(Y_1)}$, we get

$$\begin{aligned}
F_{(Y_2)} &= c_3 + c_4,\\
F_{(Y_3)} &= c_3 + c_1,\\
F_{(Y_4)} &= c_2 + c_4,\\
F_{(Y_5)} &= c_2 + c_4.
\end{aligned} \qquad (2')$$

Corrector for the Hamming method. The corrector must execute three verifications. Let the result of each of these be recorded by the auxiliary relays Z_1, Z_2, and Z_3. Then

$$\begin{aligned}
F_{(Z_1)}' = x_1 \oplus x_3 \oplus x_5 = {} & x_1x_3x_5\\
& + \bar{x}_1\bar{x}_3x_5 + x_1\bar{x}_3\bar{x}_5 + \bar{x}_1x_3\bar{x}_5,
\end{aligned}$$

$$F_{(Z_2)} = x_2 \otimes x_3 = x_2\bar{x}_3 + \bar{x}_2 x_3,$$
$$F_{(Z_3)} = x_4 \oplus x_5 = x_4\bar{x}_5 + \bar{x}_4 x_5. \qquad (3)$$

The circuit comprised of $\bar{z}_1\bar{z}_2\bar{z}_3$ indicates an absence of errors, the circuit $z_1z_2z_3$ indicates that an error occurred in the second bit, $\bar{z}_1z_2z_3$ indicated that an error occurred in the third bit, etc. On the basis of such arguments, we can arrive at the functional schematic shown on Fig. 1. Such a scheme was developed in practice and was described in [8]* but, due to the presence of feedback in it (from relay Z_1 to relay X_j), its operation is unstable. To eliminate the instability of circuit operation, one can transform it in the following way: at the circuit's outputs we supply the states of the input elements and the corresponding corrections to them, obtained by means of the auxiliary relay. Then, the action functions for the input circuits are written as follows:

$$\begin{aligned}
F_{(Y_1)} &= x_1(\bar{z}_1\bar{z}_2\bar{z}_3 + \bar{z}_1z_2\bar{z}_3 + \bar{z}_1\bar{z}_2z_3 + z_1z_2\bar{z}_3 + z_1\bar{z}_2z_3) + \bar{x}_1z_1\bar{z}_2\bar{z}_3,\\
F_{(Y_2)} &= x_2(\bar{z}_1\bar{z}_2\bar{z}_3 + z_1\bar{z}_2\bar{z}_3 + \bar{z}_1\bar{z}_2z_3 + z_1z_2\bar{z}_3 + z_1\bar{z}_2z_3) + \bar{x}_2\bar{z}_1z_2\bar{z}_3,\\
F_{(Y_3)} &= x_3(\bar{z}_1\bar{z}_2\bar{z}_3 + z_1\bar{z}_2\bar{z}_3 + \bar{z}_1z_2\bar{z}_3 + \bar{z}_1\bar{z}_2z_3 + z_1\bar{z}_2z_3) + \bar{x}_3z_1z_2\bar{z}_3,\\
F_{(Y_4)} &= x_4(\bar{z}_1\bar{z}_2\bar{z}_3 + z_1\bar{z}_2\bar{z}_3 + \bar{z}_1z_2\bar{z}_3 + z_1z_2\bar{z}_3 + z_1\bar{z}_2z_3) + \bar{x}_4\bar{z}_1\bar{z}_2z_3,\\
F_{(Y_5)} &= x_5(\bar{z}_1\bar{z}_2\bar{z}_3 + z_1\bar{z}_2\bar{z}_3 + \bar{z}_1z_2\bar{z}_3 + \bar{z}_1\bar{z}_2z_3 + z_1z_2\bar{z}_3) + \bar{x}_5z_1z_2z_3.
\end{aligned} \qquad (4)$$

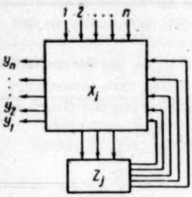

Fig. 1.

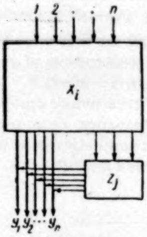

Fig. 2.

The functional schematic of such a corrector is shown on Fig. 2.

If the corrector is constructed in accordance with the structural formulas (3) and (4), then the corrector will contain three auxiliary relays, in addition to the five basic ones, and will be a two-cycle circuit.

Since we established that, in principle, the corrector is a nonsequential device, we carry out a number of transformations of structural formulas (4), specifically: we replace the letter z_1 in them by the corresponding circuit paths of contacts x_j from (3). As a result of such substitutions, using the notation of (1), (1'), we obtain structural formulas (2), (2').

Corrector for the Varshamov method. The noncoinciding check bits in the received signal α and the signal from N with the same information bits as in α will be simulated by relays Z_1, Z_2, and Z_3. Relay Z_1, consequently, must be switched on if, when signal α is applied, one of the following four conditions holds: relays X_1 and X_2 do not operate and relay X_3 does operate; relays X_1 and X_3 do operate and relay X_2 does not; relays X_1 and X_2 do operate and relay X_3 does not; relays X_1 and X_3 do not operate and relay X_2 does, i.e.,

$$F_{(Z_1)} = \bar{x}_1\bar{x}_2x_3 + x_1\bar{x}_2x_3 + x_1x_2\bar{x}_3 + \bar{x}_1x\,\bar{x}\,. \qquad (5)$$

By analogous reasoning, we can obtain the action functions for relays Z_2 and Z_3:

$$F_{(Z_2)} = \bar{x}_1\bar{x}_2x_4 + x_1\bar{x}_2\bar{x}_4 + x_1x_2x_4 + \bar{x}_1x_2\bar{x}_4,$$
$$F_{(Z_3)} = \bar{x}_1\bar{x}_2x_5 + x_1\bar{x}_2\bar{x}_5 + x_1x_2x_5 + \bar{x}_1x_2\bar{x}_5. \qquad (5')$$

If only some one relay Z is activated, then the error occurred in the check bits where, if relay Z_1 is activated, then the first check bit should be corrected, i.e., Y_3 must have voltage on it if relay X_3 is switched off, and conversely, and all the other outputs must be under voltage if the corresponding X relays are switched in. If only relay Z_2 is activated, then the output Y_4 is in the privileged position and , if the single relay Z_3 is activated, then this position will be held only by the output Y_5.

It is easily remarked that an error in the first information bit of any signal will lead to a noncorrespondence in the second and third check bits, i.e., relays Z_2 and Z_3 must be activated simultaneously. It is also easily verified that an error in the second information bit of any signal leads to a noncorrespondence of all three check bits, i.e., relays Z_1, Z_2, and Z_3 must be activated simultaneously. And, finally, if there are no errors in the signal, then there will be no noncorrespondences in the check bits, i.e., all the Z relays will be inactivated.

---

* In the circuit drawings certain annoying misprints occurred: in circuit (a) $\bar{x}_1$ should appear instead of x_1, and x_1 should appear instead of $\bar{x}_1$.

All that has been said so far can be written in the form of the following table:

If	$z_1\bar{z}_2\bar{z}_3$	then	$Y_1=x_1$	$Y_2=x_2$	$Y_3=\bar{x}_3$	$Y_4=x_4$	$Y_5=x_5$
If	$\bar{z}_1z_2\bar{z}_3$	then	$Y_1=x_1$	$Y_2=x_2$	$Y_3=x_3$	$Y_4=\bar{x}_4$	$Y_5=x_5$
If	$\bar{z}_1\bar{z}_2z_3$	then	$Y_1=x_1$	$Y_2=x_2$	$Y_3=x_3$	$Y_4=x_4$	$Y_5=\bar{x}_5$
If	$\bar{z}_1z_2z_3$	then	$Y_1=\bar{x}_1$	$Y_2=x_2$	$Y_3=x_3$	$Y_4=x_4$	$Y_5=x_5$
If	$z_1z_2z_3$	then	$Y_1=x_1$	$Y_2=\bar{x}_2$	$Y_3=x_3$	$Y_4=x_4$	$Y_5=x_5$
If	$\bar{z}_1\bar{z}_2\bar{z}_3$	then	$Y_1=x_1$	$Y_2=x_2$	$Y_3=x_3$	$Y_4=x_4$	$Y_5=x_5$

One can conclude from the table that

$$\begin{aligned}
F_{(Y_1)} &= x_1(z_1\bar{z}_2\bar{z}_3+\bar{z}_1z_2\bar{z}_3+\bar{z}_1\bar{z}_2z_3+z_1z_2z_3+\bar{z}_1\bar{z}_2\bar{z}_3)+\bar{x}_1\bar{z}_1z_2z_3,\\
F_{(Y_2)} &= x_2(z_1\bar{z}_2\bar{z}_3+\bar{z}_1z_2\bar{z}_3+\bar{z}_1\bar{z}_2z_3+\bar{z}_1z_2z_3+\bar{z}_1\bar{z}_2\bar{z}_3)+\bar{x}_2z_1z_2z_3,\\
F_{(Y_3)} &= x_3(\bar{z}_1z_2\bar{z}_3+\bar{z}_1\bar{z}_2z_3+\bar{z}_1z_2z_3+z_1z_2z_3+\bar{z}_1\bar{z}_2\bar{z}_3)+\bar{x}_3z_1\bar{z}_2\bar{z}_3,\\
F_{(Y_4)} &= x_4(z_1\bar{z}_2\bar{z}_3+\bar{z}_1\bar{z}_2z_3+\bar{z}_1z_2z_3+z_1z_2z_3+\bar{z}_1\bar{z}_2\bar{z}_3)+\bar{x}_4\bar{z}_1z_2\bar{z}_3,\\
F_{(Y_5)} &= x_5(z_1\bar{z}_2\bar{z}_3+\bar{z}_1z_2\bar{z}_3+\bar{z}_1z_2z_3+z_1z_2z_3+\bar{z}_1\bar{z}_2\bar{z}_3)+\bar{x}_5\bar{z}_1\bar{z}_2z_3.
\end{aligned} \qquad (6)$$

The functional schematic of such a corrector coincides with the one given on Fig. 2.

By eliminating contacts of the Z_i relays on the basis of (5) and (5'), and by using the notation of (1) and (1'), we also arrive at (2) and (2').

The synthesis of the corrector circuit can be executed in the following way. We construct the (1,3)-terminal network which realizes the conductances c_2, c_3, and c_4. Then, by means of diode networks, we realize the function of $F_{(Y_1)}$, $F_{(Y_2)}$, $F_{(Y_3)}$, $F_{(Y_4)}$, and $F_{(Y_5)}$.

The corresponding circuit is shown on Fig. 3.

In the general case, to synthesis a scheme for any n, it is convenient to construct a (1,p)-terminal network† with a diode network instead of a (1,n) -terminal network if, in the system of working signals, there are many in which the sign "1" arises in the same bit positions.

With this, the number of diodes R does not exceed Q:

$$Q = 2[2^p - (p+1)], \qquad (7)$$

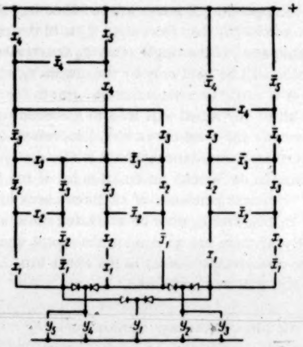

Fig. 3.

whereby R = Q if one of the n functions $F_{(Y_1)}$, $F_{(Y_2)}$, . . ., $F_{(Y_n)}$, for example, $F_{(Y_l)}$, is the sum of the aforementioned p functions, i.e.,

$$F_{(Y_l)} = c_1 + c_2 + \ldots + c_p, \qquad (8)$$

and all the remaining functions are all the possible logical consequences of applying (8). (Obviously, in this case, $n-1 = 2^p-2$).‡

To convince ourselves of this, we use the method of mathematical induction, first noting that, to construct each new output from two existing ones, two diodes are required (Fig. 4).

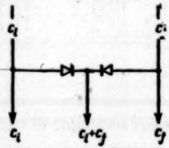

Fig. 4.

We first consider the case $n + 1 = 2^p$. We convince ourselves of the correctness of formula (7) for $p = 2(n=3)$. In this case

$$F_{(Y_1)} = c_1 + c_2, \quad F_{(Y_2)} = c_1, \quad F_{(Y_3)} = c_2$$

and

$$Q = 2[2^2 - (2+1)] = 2(4-3) = 2,$$

which is in accord with the actual facts (Fig. 4).

We now assume that (7) is valid for some p > 2, and we prove its validity for p + 1.

---

† Here, p is the number of different Boolean functions c_1, c_2, . . . , c_p entering into the expressions $F_{(Y_i)}$ (i = 1, 2, . . . , n), each of which is the sum of the constituent units corresponding to some working signal and all of its distorted variants.

‡ We exclude from the number of all the consequences the two trivial ones: 0, and the function $F_{(Y_l)}$ itself.

Let there be given p + 1 outputs, and let it be necessary to obtain from them all possible outputs by interconnecting the primordial p + 1. We assume that, from p outputs, we have already obtained all their possible outputs (their number will be $C_p^1 + C_p^2 + C_p^3 + \ldots + C_p^p$) and that we have used $2[2^p-(p+1)]$ diodes for this. We shall connect the (p+1)'th output with each of these outputs, using two diode elements for each of these connections. With this, we shall use

$$2\,[C_p^1 + C_p^2 + C_p^3 + \ldots + C_p^p] = 2^p\,(2^p - 1)$$

diodes.

Consequently, we shall use a total of

$$2\,(2^p - 1) + 2\,[2^p - (p+1)] = 2\,(2^{p+1} - [(p+1)+1])$$

diodes, q.e.d.

If $n + 1 < 2^p$, then the number of connections and the number of diode elements used will be smaller.

It should be mentioned that the assumption that the correctors be realized by relay contact circuits is not an essential one. In [9] there was presented a method of synthesizing correctors from contactless elements by structural formulas of the form of (2) and (2').

LITERATURE CITED

[1] M. A. Gavrilov, "Signal construction with a combined usage of pulse signs," Avtomatika i Telemekhanika 17, No. 12 (1956).

[2] M. A. Gavrilov and G. A. Shastova, "Basic questions of signal construction and noise resistance theory in remote control devices," Proceedings of the Session of the AN SSSR on Scientific Problems in the Automation of Production (Oct. 15-20, 1956). 4 [in Russian] (Izd. AN SSSR, 1957).

[3] M. A. Gavrilov, "Present state and basic problems of research work in the domain of remote control," Remote Control in the National Economy [in Russian] (Izd. AN SSSR, 1956).

[4] R. R. Varshamov, "Estimate of the number of signals in error-correcting codes," Doklady Akad. Nauk SSSR 117, No. 5 (1957).

[5] R. R. Varsamov, "Construction of error-correcting codes and estimate of the number of signals therein contained," Transaction of the A. S. Popov Research Society (edited by V. I. Siforov) (Izd. AN SSSR, 1958), No. 1.

[6] R. W. Hamming, "Error detecting and error correcting codes," Bell System Tech. J. 26, No. 1 (1950).

[7] D. Slepian, "A class of binary signaling alphabets," Bell System tech. J. 35, No. 1 (1956).

[8] V. M. Ostianu, "On certain questions in signal theory, and circuits for realizing decoders for self-correcting signals," Proceedings of the Session of the AN SSSR on Scientific Problems in the Automation of Production (Oct. 15-20, 1956). 4 [in Russian] (Izd. AN SSSR, 1957).

[9] M. A. Gavrilov, V. M. Ostianu, V. N. Rodin, and B. L. Timofeev, "Realization of discrete corrector circuits," Doklady Akad. Nauk SSSR 123, No. 6 (1958).

10-CHANNEL AUTOMATIC ELECTRONIC-RELAY OPTIMIZER

A. B. Shubin
(Moscow)

Translated from Avtomatika i Telemekhanika Vol. 21, No. 5, pp. 624-632, May, 1960
Original article submitted January 5, 1959

A description is given of a 10-channel automatic electronic-relay optimizer. The operational part of the optimizer consists of electronic operational amplifiers, while the controlling portion is comprised of relays and stepping switches.

The optimizer is designed to operate with electronic analog computers and is used to obtain solutions to complicated variational problems, and problems of finding extrema. An example of problem solution by means of the optimizer is given.

Certain problems in finding extrema cannot be solved analytically, either because analytic expressions of the functions are not known, or because these expressions are too complicated. This is particularly the case for the problems related to the finding of extrema of functions of many variables. In actual systems, or in systems simulated on analog computers, one can, by giving increments to the individual variables, easily determine partial derivatives and, consequently, gradients of a function. By moving either in the direction of the gradient or in a directly opposite direction, one can find a maximum or a minimum of a function. The processes of automatically determining partial derivatives and of moving in the direction of the gradient can be implemented by means of the so-called automatic optimization systems. If, from the conditions of the problem, certain boundaries are imposed on the variables then, as was shown in [1], the determination of an extremum lying on a boundary is possible in this case.

The theoretical considerations bearing on the automatic search process were presented in [1, 2]. A complete electronic variant of an optimizer was described in [3].

Below there is given a description of an electronic-relay instrument which executes automatic search for extrema. For brevity, we shall henceforth call this instrument an optimizer. Participants in the design and adjustment of the optimizer were I. N. Bocharov, A. V. Kalinina, R. I. Stakhovskii, and the author of the present paper.

The optimizer permits one to find the extremum of a function of many variables (up to 10) with the presence of limitations (boundaries).

The function whose extremum is to be sought, as well as the function which is bounded, are applied to the optimizer in the form of dc voltages whose range of variation is ±100 v. The optimizer can operate with objects which continuously output the value of the function whose extremum is being sought, as well as with objects which output the function value only at certain moments of time (for example, after solution on an electronic analog computer).

The optimizer can be divided into two parts: the operational part and the controlling part. The basic computing portions of the automatic optimizer are the electronic analog blocks. The output voltages $x_1, x_2, \ldots, x_{10}$ are formed on dc integrators; the range of variation of the output voltages is ± 100 v. The size of the trial step, applied for the determination of the partial derivatives, is regulated within the limits of 0 to 15 v. The choices just cited are related to the circumstance that the optimizer is basically designed to operate with electronic analog computers and, with such choices for the computing (operational) part, matching of the optimizer with analog computers is executed with extreme simplicity. The accuracy of the operations effected by the computer and the optimizer is of the same order of magnitude in all cases. The accuracy with which the extremum is determined depends on the character of the problem to be solved. For a test object, which was the sum of the moduli of the ten variables $Q = k\sum_{i=1}^{10} |x_i|$, the maximum relative error in determining Q_{extr} was 1%.

The optimizer's controlling portion analyzes the data applied to the optimizer and analyzes the state of the optimizer itself and, as a function of the information obtained, carries out some switching or other. Relays and stepping switches are the basic elements of the controlling portion. Adequate operation of such a controlling block is possible for frequencies of the synchronizing pulses up to 5 cps, i.e., it requires about 0.2 sec to apply the trial increments and to remember (store) the partial derivatives. Such a speed of operation is completely sufficient for operation with ordinary electronic computers which are also relay-controlled.

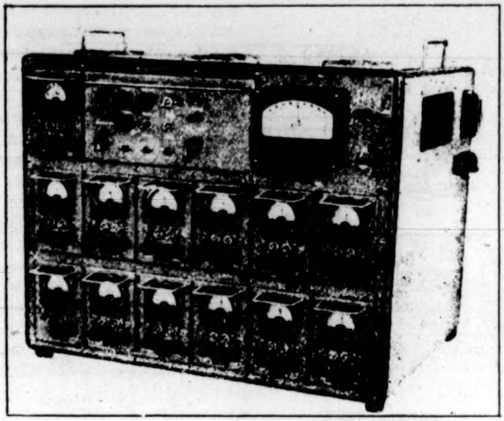

Fig. 1.

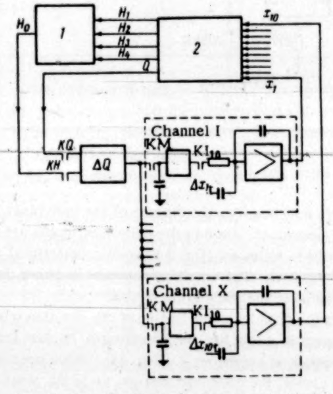

Fig. 2. 1 is the block for forming limitations, 2 is the object.

An exterior view of the optimizer is shown on Fig. 1. The optimizer design incorporates, in one chassis, the controlling block, the limitations block, the ΔQ block, the test block and 10 channel blocks. The front panel of the optimizer is comprised of the front panels of the individual blocks, on which are provided the necessary devices for manual control and testing of the instrument. The dimensions of the optimizer, without the power supply, are 650 × 500 × 450 cm.

Operational Portion

Figure 2 shows the functional schematic of the optimizer's operational portion. The theory of operation amounts to the following: the quantity Q, whose extremum is sought, is applied to the ΔQ block. This block remembers the function and determines its variation. We assume, that, in the ΔQ block, there has been remembered the value of the function for some values of $x_1, x_2, \ldots, x_{10}$; if we now give a trial increment Δx_{1t} to the first variable then, at the output of the ΔQ block we obtain the increment of the function $\Delta Q_1 \approx (\partial Q/\partial x_1)\Delta x_{1t}$, i.e., a quantity which is proportional to the partial derivative of the function with respect to the first variable. Simultaneously with the application of the trial increment, contact KM_1 closes, and storage of the quantities $\pm(\partial Q/\partial x_1)\Delta x_{1t}$ occurs in the memory link of channel 1.

After this, a trial increment is applied to the second variable, etc., up to the tenth variable. At the end of the cycle, there have been stored in the channels' memory links the quantities which are proportional to the partial derivatives, or components of the function's gradient. Upon simultaneous closure, at time t_s, of contacts KI_1, KI_2, . . . , KI_{10}, the integrators receive the increments

$$\Delta x_{1r} = \pm \frac{\partial Q}{\partial x_1} \Delta x_{1t} k t_s \,,$$

$$\Delta x_{2r} = \pm \frac{\partial Q}{\partial x_2} \Delta x_2 \, k t_s \qquad \text{etc.}$$

The trial increments Δx_t and the integration constants k are identical in all the channels, so that the operating variations of the variables (the working steps) are proportional to the components of the gradient. After a working step, one can repeat the determination of the gradient and carry out a new working step along the new gradient; in this case, the search is carried out by the gradient method. After the working step one can determine the sign of the function's change and, if this change

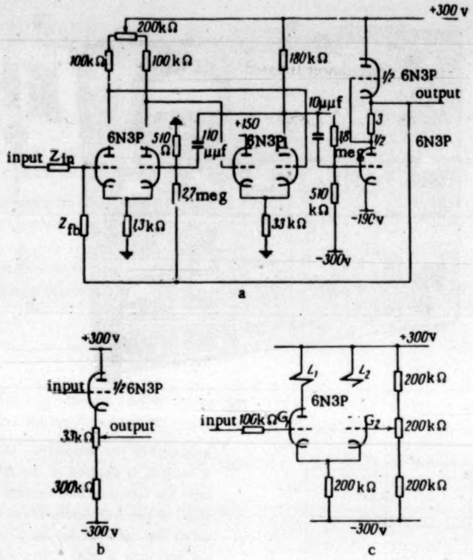

Fig. 3.

occurred in the proper direction, then the working step along the previous gradient may be repeated until such time as the increment changes sign, i.e., until such time as a partial extremum in the direction of the previous gradient is reached. This method of search is called the method of steepest descent. There are a number of switches on the controlling block whose positions correspond to the various search methods.

If limitations are imposed on the system's coordinates i.e., if some function $H_0(x_1, x_2, \ldots, x_{10})$ must not exceed a given value, then the search for an extremum is executed in the following manner. Optimization of the function Q proceeds until the function H_0 goes beyond the limits of the admissible region; with this, there is automatically switched to the input of the ΔQ block, not the function Q whose extremum is sought, but the bounded function H_0. In this case, $x_1, x_2, \ldots, x_{10}$ are so changed that they move out of the region of limitation. After the region of limitation has been left, the process of finding an extremum of function Q is continued. If an extremum is found either on the boundary or inside the region of limitation, there then occurs an oscillation about the boundary and, in the process of these oscillations, the optimizer finds the true extremum or a conditional extremum on the boundary.

We now consider the circuits of the individual blocks of the optimizer. Used in the optimizer blocks are standard cathode followers (Fig. 3 b) and dc operational amplifiers (Fig. 3 a). The amplifiers operate in either the amplification or the integration modes.

In the ΔQ block, the storing of the function whose extremum is sought and the obtaining of its next increment occur on condenser C_1 (Fig. 4a). When contact R_m is closed, the condenser charges up to the potential Q_0 while, when the contact is opened and Q varies, the following voltage is formed at the output of the cathode followers:

$$\Delta Q = (Q - Q_0)\, k_{tc},$$

where k_{tc} is the cathode follower's transfer coefficient.

The function increment obtained from the cathode follower is amplified and applied to the channels' memory links. There are inverters at the input of the ΔQ block which are switched in to the input Q by toggle switch T_{QI} and to input H_0 by toggle switch T_{HI}. This makes it possible to change the signs of the partial derivatives $(\partial Q/\partial x_i)\Delta x_{it}$ and $(\partial H_0/\partial x_i)\Delta x_{it}$, and thereby to carry out either minimization or maximization.

Figure 4b gives the functional schematic for one channel. Storage of the partial derivative occurs on condenser C_2 upon operation of storage relay R_m, i.e., upon closure of contact KM. In order that the charge on the condenser not be decreased when connected in to the integrator's input, the voltage is taken off from it by means of the cathode follower. The cathode follower is based on tube 6 N 3P which has low grid current; the change in the condenser's charge due to grid current does not exceed 0.1 v/ min. To eliminate potential leakage from condensers C_2 and C_3 (and also from condenser C_1 in the ΔQ block) as well as a fatigue effect, polystyrene MPGT condensers of 1 μf capacity are used in the optimizer.

The output voltages $x_1, x_2, \ldots, x_{10}$ are supplied from the dc amplifier-integrators. The amplifier has high gain, uses tube 6N3P in its first stage, and the operating mode of its first stage is chosen so as to minimize grid current. Integrating capacitor C_3 is connected in the amplifier's feedback path.

Application of the trial step is implemented by means of condenser C_4. Upon closure of contact RR at the integrator input, a step voltage U_{ts} is applied via the condenser. As is known, the integrator is an amplifier under these conditions, so that the following increment appears at the integrator output.

$$\Delta x_t = U_{ts}\,\frac{C_4}{C_3}.$$

Upon opening of contact RR there is a voltage step of the opposite sign, and the increment Δx_t is tapped off.

The working changes of the output voltages $x_1, x_2, \ldots, x_{10}$ (the working steps) occur upon operation of step relay R_s, i.e., upon closure of contact KI. With this, the integrator input, via a resistor of 1 meg, is connected to the output of the cathode follower, the voltage on which is proportional to the partial derivative with respect to these variables. Thus, the output voltages receive increments proportional to the partial derivatives.

The initial conditions on the integrators are established by connecting toggle switch T_2 to the channel block. With this, the capacitance of the feedback path is shunted by a resistance and, at the integrator's input, a voltage from a divider is applied.

The circuit for forming the limitation H_0 is given in Fig. 4c. The circuit includes an amplifier with four inputs. There is a vacuum-tube diode at each input. Thus, the circuit gives the sum of only the positive voltages H_i which is just the bounded function H_0. The function to be limited is applied to the limitation indication circuit in the indicator block.

The circuit for indicating limitiations (similar to the circuit used for indicating partial minima and indicating the final solution) is shown on Fig. 3c. The circuit works as follows. In the differential stage's anode circuit there are connected the windings of the polarized relay RP-4. The windings are connected toward each other. On one of the grids, G_2, the constant voltage U_0 is applied, while on the second grid, G_1, the voltage U to be compared is applied. If $U > U_0$, then the current in winding L_1 is greater than that in winding L_2, and the polarized relay is found in one of its positions. For $U < U_0$, the relay is transferred to its other position. Such a circuit allows one to fix the transition of a voltage through any threshold level with an accuracy of about 0.5 v; the hysteresis of the circuit is less than 0.1 v.

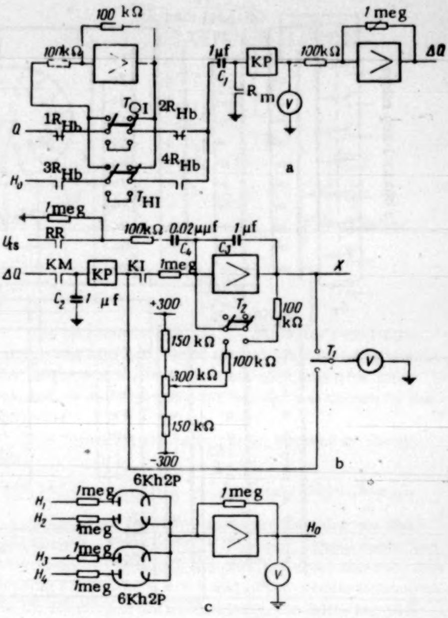

Fig. 4.

Controlling Block

The controlling block is comprised of a stepping switches, relays and switches of various types of operation (Fig. 5).

The first stepping switch SSI executes successive switching in of the memory relays of the channels and, by the Gauss-Seidel method, also executes the individual switching of the channels' step relays. Simultaneously with the switching of the channels' memory relays, the trial increments for the variables are supplied. Thus, as SSI moves along commutator segments 2-11, the gradient is determined for the function whose extremum is being sought. When on the first commutator segment, SSI applies voltage to SSII, causing execution of the operations of working-step implementation and determination of the change in the function during the working steps. With the Gauss-Seidel method, these operations are possible on seg-

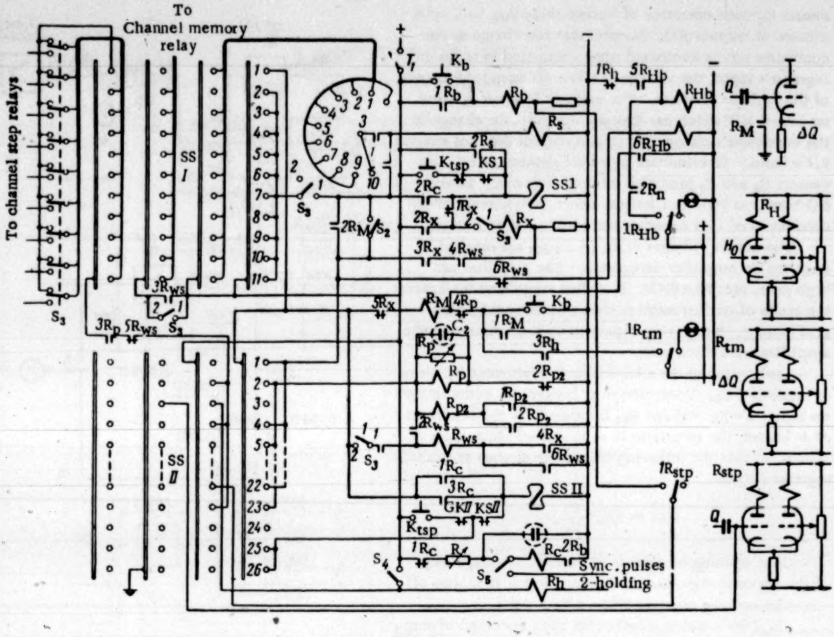

To
Channel memory
relay
To channel step relays
S3
SS
I
SS
II
3Rws
3Rp
5Rws
S3
S3
1Rh
5RHb
RHb
Q
RM
ΔQ
6RHb
2Rn
1RHb
RH
H0
Kb
1Rb
Rb
Rs
2Rs
Ktsp
KS1
2Rc
SS1
1Rx
2Rx
Rx
3Rx
4Rws
6Rws
2RM
S2
T1
5Rx
RM
4Rp
Kb
1RM
C2
Rp'
3Rh
Rp
2Rp2
1Rp2
Rp2
2Rp2
2Rws
Rws
4Rx
6Rws
1Rtm
Rtm
ΔQ
1Rc
3Rc
GKII
KSII
SS II
Ktsp
1Rc
R'
Rc
2Rb
Sync. pulses
2-holding
Rh
S4
S5
1Rstp
Rstp
Q

Fig. 5.

ments 2-11, while commutator segment of stepping switch SSI is passed over by shunt running.

Various relays implement the following basic functions:

1. Start relay R_b, when the start button is pushed, switches in cycle relay R_c.

2. Cycle relay R_c operates upon the reception of a sync pulse from the synchronization block, and transfers SSI or SSII to the following commutator segment, i.e., implements transfer from one operation to the following one. For the optimization of continuous objects, the relay is transferred to the autooscillatory mode by toggle switch S_5.

3. Relay R_s, for shortening the variables cycle, switches SSI to shunt running in order to pass rapidly over the commutator segments which correspond to unused channels.

4. Step relays R_p and R_{p2} provide the required delay to the working step. This delay is determined by condenser C_2 and resistor R_s.

5. The minimum relay R_M operates when a partial (relative) minimum is reached. After the storage operation, relay R_M, by its own contact $2R_M$, switches SSI to gradient determination. The operation of gradient determination must also be executed when the instrument is started and upon input or output of limitations. In the first case, relay R_M is switched on by a normally open contact of the start button and, in the second case, by a special contact $6R_{Hb}$ of limitation blocking (holding) relay R_{Hb}. This contact is closed only in the periods when the relay is transferring from one state to another.

6. Holding relay R_h operates after the termination of a working step. At this moment there is implemented the analysis of the increment of the function whose extrumum is being sought, contact $3R_h$ is closed and the minimum relay is switched to the circuit for minimum indication.

Contact $1R_h$ releases relay R_{Hb}, and contact $2R_h$ switches the limitation holding relay to the limitation indication circuit. After release of R_h, the state of relay R_{Hb} depends on the state of relay R_H at the moment of holding, and remains unchanged until the following operation of relay R_h.

For the optimization of functions obtained after a solution on an analog computer, it is necessary that the holding relay operate at the moment when there is a value of the function to be optimized available at the computer. For this, 2-holding is used.

For an extremum search using the Gauss-Seidel method, the memory relays in the channels are connected-in via the commutator segments of SSI and contact $3R_{ws}$

of the working step relay. To switch this relay in, there is auxiliary relay R_x. Relay R_x operates simultaneously with SSI. Thus, when SSI transfers to the following segment, i.e., when the optimization cycle for the previous variable terminates, relay R_X is found in the operated state. Since contact $4R_x$ is closed, then simultaneously with the operation of R_p working step relay R_{ws} operates and, by its contact $3R_{ws}$, it connects in the memory relay in the corresponding channel; the operation of partial derivative determination then ensues. Contact $5R_{ws}$ cuts out the channel working step relay. Simultaneously relay R_{ws}, by contact $4R_{ws}$, cuts out relay R_x. At the time of the following working step, contact $4R_x$ will be open, relay R_{ws} will not operate, so that a working step will be executed, etc. With the Gauss-Seidel method, the channels' working step relays are opened by switch S_3, and the working step is executed for one of the channels.

The switches have the following basic functions: T_1 applies voltage to the circuit; the closed position of switch S_2 corresponds to search by the gradient method, i.e., after each working step the determination of a new gradient is made; S_3 switches of optimizer from operation by the gradient method to operation by the Gauss-Seidel method; S_4 switches in 2-holding (secondary holding) for discrete objects; S_5 connects the cycle relay to a source of external pulses; S_6 reduces the number of variables for optimization.

Solution of a Problem by Means of the Automatic Optimizer

In addition to the solution of problems without limitations, such as the automatic approximation of a given curve [3], the optimizer permits the solution of complicated problems with limitations.

The problem arose of finding the optimal control program for a motor-generator system such that, during a given time τ, the motor would make the maximum number of rotations from the moment of starting to the moment of stopping, while observing the limitations imposed on the system's internal coordinates.

As the first step, it was assumed that the motor's excitation current remains constant. An approximate linearized system of equations for the object has the form:

$$T_1 \frac{dE_g}{dt} + E_g = kU_1,$$

$$E_g - c\Omega I_{em} = I_a R_a, \quad \frac{dX}{dt} = \xi_0 \Omega.$$

Here, U_1 is the voltage applied to the generator's excitation winding, E_g is the generator's emf, I_a is the motor's armature current, I_{em} is the motor's excitation current, Ω is the angular velocity of the motor shaft, X is the angle of rotation of the output shaft, connected by a reducer to the motor shaft, R_a is the resistor of the circuit of the motor armature and the generator armature.

The circuit set up on the analog computer to simulate the given differential equations is shown on Fig. 6a.

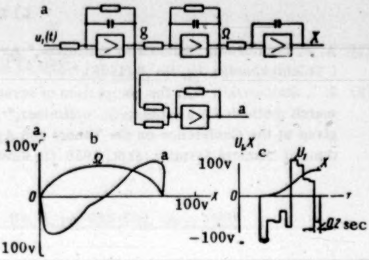

Fig. 6.

The program for varying the generator's excitation voltage was supplied from a special synchronizing block. The program was divided into ten identical time intervals and, in each interval, the voltage was chosen by the optimizer.

The following limitations were imposed on the system:

$$|U_1| \leqslant U_{1\,\max} \quad |I_a| \leqslant I_{a\,\max} \quad |\Omega| \leqslant \Omega_{\max}.$$

In the given problem, it was required that the final conditions $\Omega_{end} = 0$ and $E_g = 0$ be met. These conditions derive from the posing of the problem, since the complete stopping of the motor at the end of the process is required. For the meeting of these conditions, the following additional limitations were imposed:

$$\Omega_{end} \leqslant 0 \text{ and } E_{g\,end} \leqslant 0.$$

After starting of the system from null initial conditions, the optimizer automatically found the optimal program. In the majority of cases, the maximum X lay at the point of intersection of the boundaries of limitation:

$$\Omega_{end} \leqslant 0 \quad E_{g\,end} \leqslant 0, \quad I_a \leqslant I_{a\,\max}.$$

The optimal processes found by the optimizer are shown on Fig. 6, b and c.

CONCLUSIONS

The automatic multichannel optimizer is an instrument allowing one to solve variational problems and problems of finding extrema of functions of many variables.

The given optimizer was designed basically to operate with electronic analog computers with relay control. However, the principles on which the instrument is based can be used for creating optimizers to operate with actual objects. It is possible to have optimization of actual objects carried out in two time scales, i.e., rapid finding of extrema on an analog computer and a subsequent transfer of the results to the actual object.

LITERATURE CITED

[1] A. A. Fel'dbaum, "Automatic optimizer," Avtomatika i Telemekhanika 19, No. 8 (1958).*

[2] R. L. Stakhovskii, "On the comparison of several search methods for an automatic optimizer," Paper given at the Conference on the Theory and Applications of Discrete Systems, Sept. 1958 [in Russian].

[3] R. L. Stakhovskii, "Multichannel optimizer for solving variational problems," Avtomatika i Telemekhanika 20, No. 11 (1959).*

---

* See English translation.

RELIABILITY CHARACTERISTICS OF RESISTORS AND CONDENSERS

B. S. Sotskov and S. E. Rostkovskaya
(Moscow)

Translated from Avtomatika i Telemekhanika Vol. 21, No. 5, pp. 633-638, May, 1960
Original article submitted August 7, 1959

Methods are considered for the presentation of reliability characteristics of resistors and condensers as functions of ambient air temperature and power dissipation or applied voltage.

The reliability of constant carbon resistors, among the most widely used elements of different systems, depends on the physicochemical processes occurring both within the conducting layer and on its surface. Therefore, the reliability of resistor operation is determined, to a large degree, by the choice of materials, the design, and the technology of manufacture. In addition, the reliability of resistor operation also depends on the correctness of the selection of its operating regimen and on external conditions.

In designing circuits containing resistors and condensers, one must know how to determine their reliability under given conditions of use, which may be characterized by the ambient temperature θ_X, dissipated power P_X, voltage U_X and length of serviceable life T. For this end, it is convenient to introduce characteristics which give the connections between reliability and the parameters which define the conditions of use. The consideration of these connections comprises the subject matter of the present paper.

1. By considering the breakdowns of resistors to be random events, we have that the number of operational failures during time interval dt will be the larger, the greater is the number N of resistors, i.e.,

$$-dN = cNdt. \tag{1}$$

It follows from this that

$$\ln N = -ct + \ln k \quad \text{or} \quad N = ke^{-ct}.$$

Since $N = N_0 = k$ for $t = 0$, then

$$N = N_0 e^{-ct} \quad \text{or} \quad \frac{N}{N_0} = p = e^{-ct}.$$

Here, N is the number of existing elements (resistors) at time t: $N/N_0 = p$ is the reliability of action of the set of N_0 elements at time t; $c = 1/\tau$ is the reliability factor (the relative speed of breakdown).

Experimental data substantiate the foregoing dependence of element reliability on time for the fundamental portion of the characteristic $p = N/N_0 = f(t)$ (segment AB on Fig. 1). Deviations occur only in the initial period, when the unconditioned elements go out of order, and after point B when, due to accelerated aging and to other irreversible changes, the element breakdown rate begins to accelerate.

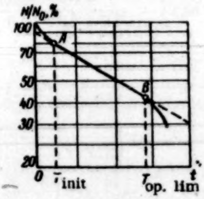

Fig. 1

Point B determines the length of serviceable life T for the given conditions of operation.

We now consider the dependence of the coefficient c on the resistor's heating temperature θ_X.

The velocity of change of material during the reaction process is defined by the equation

$$-\frac{dn}{dt} = \alpha n,$$

where n is the quantity of material at the moment of time under consideration and α is the constant velocity of the reaction.

From the equation given it follows that

$$\frac{dn}{n} = -\alpha\, dt,$$

i.e.,

$$\ln n = -\int_0^T \alpha\, dt,$$

or, for α = const,

$$\ln \frac{n}{n_0} = -\alpha T.$$

The dependence of the constant reaction speed on temperature is determined, according to Arrhenius, by the formula

$$\alpha = A_k \exp\left(-\frac{B}{273° + \theta_x}\right),$$

where A_k and B are constants and $(273 + \theta_X)$ degrees is

the absolute temperature.

Consequently,

$$\ln\frac{n}{n_0} = -A_k \exp\left(-\frac{B}{273^\circ + \theta_x}\right)T.$$

We find from the last expression that

$$T = \left[\frac{1}{A_k}\ln\frac{n_0}{n}\right]\exp\left(\frac{B}{273^\circ + \theta_x}\right)$$

or

$$T = T_\infty \exp\left(\frac{B}{273^\circ + \theta_x}\right).$$

If $\theta_x \lesseqgtr 273^\circ\,\mathrm{C}$, then

$$\frac{T}{T_0} = \frac{T}{T_\infty}\,\frac{\exp\left(\frac{B}{273^\circ + \theta_x}\right)}{\exp\left(\frac{B}{273^\circ + \theta_0}\right)} =$$

$$= \exp\left(-\frac{B\,(\theta_x - \theta_0)}{(273^\circ + \theta_x)\,(273^\circ + \theta_0)}.\right)$$

If $\theta_x \ll 273^\circ\,\mathrm{C}$, then

$$T = T_\infty \exp\left(\frac{B}{273^\circ + \theta_x}\right) =$$

$$= T_\infty \exp\left(\frac{B}{273^\circ\left(1 + \frac{\theta_x}{273^\circ}\right)}\right) \approx$$

$$\approx T_\infty \exp\frac{B}{273^\circ}\exp\left(-\frac{B}{273^2}\theta\right) =$$

$$= T_a \exp\left(-\beta\theta_x\right),$$

or

$$T = T_0 \exp\left[-\beta\left(\theta_x - \theta_0\right)\right],$$

$$T_a = T_\infty \exp\frac{B}{273^\circ}.$$

$$\beta = \frac{B}{273^2},\ T_0 = T_a \exp\left(-\beta\theta_0\right).$$

By denoting by s_0 the amount of material in one resistor, we get that $n = s_0N$ and, consequently $-s_0dN/dt = s_0N\alpha$ or $-dN/dt = N\alpha$.

By comparing the last equation with Eq. (1), we get that $\alpha = c$. We denote by c_0 the value of $\underline{c}$ which corresponds to θ_0; we then find that

$$\frac{c}{c_0} = \frac{A_k \exp\left(-\frac{B}{273^\circ + \theta_x}\right)}{A_k \exp\left(-\frac{B}{273^\circ + \theta_0}\right)} =$$

$$= \exp\left(\frac{B\,(\theta_x - \theta_0)}{(273^\circ + \theta_x)\,(273^\circ + \theta_0)}\right) \tag{2}$$

The value of the temperature θ_x is determined as the sum

$$\theta_x = \theta_{0x} + R_tP_x, \tag{3}$$

where θ_{0x} is the ambient temperature, R_t is the thermal impedance for heat transfer from the surface to the ambient medium and P_x is the power dissipated in the electrical impedance.

By substituting from (3) to (2), and by denoting by c_N the value of $\underline{c}$ for the nominal load P_N and the admissible temperature $\theta_{0x} = \theta_{0N}$, we get

$$\frac{c}{c_N} = \exp\frac{B\left[\theta_{0x} - \theta_{cN} + R_tP\ \left(\frac{P_x}{P_N} - 1\right)\right]}{(273^\circ + \theta_{0x} + R_tP_x)\,(273^\circ + \theta_{0N} + R_tP_N)}.$$

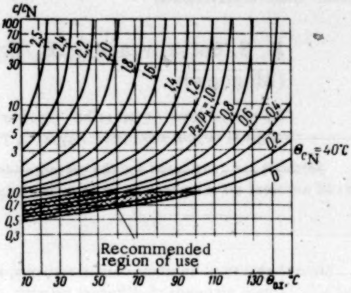

Fig. 2

Figure 2 shows the function c/c_N for one type of resistor. This function is also the characteristic $c/c_N = f(\theta_{0x}, P_x)$ for the resistor.

The quantities B, R_t and c_N are obtained by processing experimental data. The value θ_{0N} corresponds to the maximum permissible temperature for the nominal load $P_x = P_N$.

It should be kept in mind that the values of B, R_t, and c_N vary somewhat as functions of the type and the nominal resistance. However, for determining resistor reliability in the process of designing a scheme, it suffices to estimate the average value of reliability for a given type of resistor. Such averaged values of c_N and B are given in the following table.

If the limiting admissible value for the resistor temperature is $\theta_{x\,\max}$, then the magnitude of the admissible power dissipation equals $P_x = (\theta_{x\,\max} - \theta_{0x})/R_t$.

Figure 3 shows the function $P_x = f(\theta_x)$.

The value of $\theta_{0x} = \theta_{\mathrm{nom}} = \theta_{xN}$ is chosen from the condition limiting the relative variation of the resistance $\Delta R/R = f(\theta_x)$ for $\theta_{0x} = \theta_{xN}$, and should be a value which is achievable technologically or which is determined from the given conditions of use.

The method of choosing the value of $P_{\mathrm{nom}} = P_N$ consists of this: that knowing the length of useful life T_0 and the temperature θ_0 corresponding to it, we give a value to the admissible service life T. Then, based on the foregoing, we obtain

$$P_N = \frac{1}{R_t}\left[\frac{B}{\frac{B}{273^\circ + \theta_0} + \ln\frac{T}{T_0}} - (273^\circ + \theta_{0x})\right].$$

With the condition that the value of $\underline{c}$ remain invariant, the limiting value $\theta_{0x} = \theta_{x\,\max}$ is determined if we set $P_x = 0$, i.e.,

$$\theta_{x\,\max} = \theta_{0x} = \frac{B}{\frac{B}{273^\circ + \theta_0} + \ln\frac{T}{T_0}} - 273^\circ.$$

Type of resistor	Nominal power in W	Admissible limiting temperature θ_{max}, in °C	Limiting ambient temperature θ (for $P = P_N$), in °C	Thermal impedance R_t, in °C/w	c_k (mean value), hr^{-1}	β
VS — 0.12 (ULM — 0.12)	0.12	130	180	350		
VS — 0.25	0.25	130	95	140		
VS — 0.5	0.5	130	85	90	$1.0 \cdot 10^{-3}$	0.13—0.18
VS — 1.0	1.0	130	65	65		
VS — 2.0	2.0	130	70	45		
VS — 5.0	5.0	130	35	19		
VS — 10.0	10.0	130	50	8		
VS per spec.	0,12—10,0	110	40	70		
MLT — 0.5	0.5	130	70	50		
MLT — 1.0	1.0	130	—	—	$1.7 \cdot 10^{-3}$	0.11—0.12
MLT — 2.0	2.0	130	—	—		

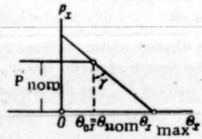

Fig. 3

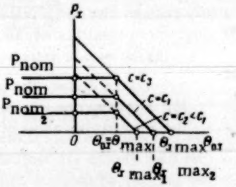

Fig. 4

Conversely, by giving various values: $c = c_1$, $c = c_2$, c c_3, . . . , we obtain various magnitudes of $\theta_{x\ max}$. This makes it possible to define P_N for a given θ_N = const (Fig. 4). The graph of Fig. 4 is another form of the same characteristic $c/c_0 = f(\theta_{0x}, P_x)$ which relates the change of reliability to the change of temperature of the ambient medium and to the change of power dissipation P_x.

The value of the thermal impedance can be found from the formula

$$R_t = \frac{1}{\mu S + 2\lambda S_0 / l_0},$$

where μ is the total heat transfer coefficient, S is the cooling surface, λ is the thermal conductivity of the current leads and S_0 and l_0 are their cross section and length. The expression for the heat transfer coefficient is written in the form

$$\mu = \mu_1 + b\frac{(273^\circ + \theta_x)^4 - (273^\circ + \theta_{0x})^4}{\theta_x - \theta_{0x}},$$

where μ_1 is the heat transfer coefficient due to gas heat conduction and convection. It should be kept in mind that the value of μ_1 varies with changes in p_{h_x}, the pressure of the air surrounding the resistor, by the law

$$\mu_{1h_x} = \mu_{1h_0}\sqrt{\frac{p_{h_x}}{p_{h_0}}},$$

where p_{h_0} is air pressure at sea level. The magnitude of μ_1 also depends on the temperature difference $\theta_x - \theta_{x_0} = \Delta\theta$. The relationship can be expressed approximately by the formula

$$\mu_1 = \mu_{10}(\Delta\theta)^m,$$

where μ_{10} corresponds to the temperature difference $\Delta\theta = 1$°C.

Thus, the value of the nominal power is determined from the expression

$$P'_N = (\theta_{x_{max}} - \theta_N)\left\{S\left[\mu_{10}(\Delta\theta)^m\sqrt{\frac{p_{h_x}}{p_{h_0}}} + b\frac{(273^\circ + \theta_{x\ max})^4 - (273^\circ + \theta\ )^4}{\theta_{x_{max}} - \theta_N}\right] + 2\lambda\frac{S_0}{l_0}\right\}.$$

It follows from this expression that the value of the nominal power must vary somewhat as a function of the air pressure and the value of $\theta_N = \theta_{x\,max} - \theta_N$. It will also depend on the mounting, since l_0 and μ_{10} also vary with this.

The foregoing table gave the values of R_t and c_N for a number of standard resistors, and also gave the permissible temperature of the ambient medium, the value of which changes for resistors of different power ratings.

2. In the case of condensers, it is necessary in estimating the reliability of the finished articles, to take into account both the effect of temperature and the effect of voltage.

The useful life of paper condensers, determined by the aging of the insulation, as a function of the temperature θ_x, is expressed by the formula

$$T_{x0} = T_0 \exp\left[-\beta_n(\theta_x - \theta_0)\right], \tag{4}$$

where β_n is a coefficient which depends on the form of the insulation.

On the other hand, for dielectric aging in the presence of an electric field, we have the empirical relationship

$$\varepsilon = AT^{-n} = \frac{A}{T^n}, \tag{5}$$

where ε is the electric field strength, T is the length of useful life and A is a constant.

By taking into account that $U = \epsilon d$ we get that $U = AdT^{-n}$, where d is the thickness of the dielectric. For condensers with paper insulation, $n \approx 0.2$.

For two different voltages U_x and U_{x0} we have that

$$\left(\frac{U_x}{U_{x0}}\right)^{1/n} = \frac{T_{x0}}{T_x}.$$

In order to take into account the influence both of U_x and of θ_x, we write the ratio T_{x0}/T_x in the form

$$\frac{T_{x0}}{T_x} = \frac{T_0}{T_x}\frac{T_{x0}}{T_0}.$$

Then,

$$\left(\frac{U_x}{U_{x0}}\right)^{1/n} = \frac{T_0}{T_x}\exp\left[-\beta_n(\theta_x - \theta_0)\right],$$

i.e.,

$$\ln\frac{U_x}{U_{x0}} = -n\ln\frac{T_x}{T_0} - n\beta_n(\theta_x - \theta_0). \qquad (6)$$

If the number of condensers remaining in service for $U_x = \text{const}$ and $\theta_x = \text{const}$ is defined by the relationship

$$p = \frac{N}{N_0} = \exp\left(-c_k T_x\right)$$

or

$$\ln p = \ln\frac{N}{N_0} = -c_k T_x,$$

then, by giving some value of p, one can easily determine the value of length of useful life which corresponds to it:

$$T_x = -\frac{\ln p}{c_k}. \qquad (7)$$

By substituting the value of T_x in (6), we get

$$\ln\frac{U_x}{U_{x0}} = -n\ln\left[-\frac{\ln p}{c_k T_0}\right] - n\beta_n(\theta_x - \theta_0). \qquad (8)$$

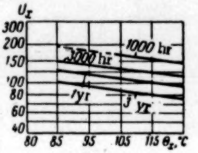

Fig. 5

Figure 5 gives the given characteristic, defined by (6), allowing one to relate the length of useful life T_x to the admissible values of the voltage U_x and the temperature θ_x.

ON THE DESIGN OF MAGNETIC AMPLIFIERS SINGLE-PHASE AND THREE-PHASE SEMICONDUCTOR RECTIFIERS ON AN ACTIVE LOAD ANDOPERATING WITH A COUNTER-EMF

A. G. Zdrok
(Moscow)

Translated from Avtomatika i Telemekhanika Vol. 21, No. 5, pp. 639-651, May, 1960
Original article submitted January 7, 1960

Methods are presented for the transfiguration of single-phase and three-phase rectifier bridges to equivalent loads, and graphicoanalytic methods are considered for determining the characteristics of saturated reactor magnetic amplifiers operating on active loads and counter-emf's.

Circuits for automatic current stabilizers in charging devices are given, and anexample of determining a magnetic amplifier's basic parameters is considered.

Semiconductor rectifiers, in conjunction with magnetic amplifiers, allow the construction of compact automatic control devices. Such devices are widely used for controlling the speed of a motor's rotation by varying the voltage applied to the armature, for charging storage batteries, etc. [1-4]. Setups with magnetic amplifiers and semiconductor rectifiers are increasingly superceding electronic and ionic tubes with grid control.

The currents and voltages at the input and output of rectifier circuits are different, in the majority of cases. The relationships between them vary with changes in the circuit's operating mode (sinusoidal) voltage or sinusoidal current at the rectifier input, etc.) and also with changes in the form of the load (active load, inductive load, counter-emf, etc.). It is usually quite difficult to find the relationships between the input and output currents and voltages, as well as to design the magnetic amplifiers operating in such circuits.

In this paper we present graphicoanalytic methods for determining the characteristics of saturated reactor magnetic amplifiers which operate with single-phase and three-phase semiconductor rectifiers, these methods being based on the transfiguration of the rectifier scheme to a load which is equivalent to it. All other rectifier schemes can be dealt with similarly to the schemes to be considered here.

Magnetic Amplifier Operation with Single-Phase Rectifier Bridge

With operation of a magnetic amplifier on an active load, supplied with rectified current, the instantaneous, average and effective currents at the input and output of the rectifier bridge are all equal to one another, as are the corresponding values of voltage. These relationships are considered for the case of ideal rectifiers, for the absolute magnitudes of the instantaneous values and the average values over a half-period. If the voltage at the rectifier inputs is sinusoidal, then the relationship between the voltage's average value and effective value, as well as the relationship between the analogous current quantities, are constant and equal to 0.9. Therefore, the design of such a circuit engenders no difficulty.

Significant difficulty is engendered in the design of a circuit for rectifier operation on a counter-emf since, in this case, the relationships between the mean and effective values of current and voltage differ from each other, and do not remain constant under variations of the circuit's mode of operation (for example, for sinusoidal voltage and sinusoidal current on the rectifier inputs).

Figure 1 shows the variation of voltages and currents for the operation of a single-phase rectifier bridge on a counter emf for the modes of sinusoidal voltage (Fig. 1a) and sinusoidal current (Fig. 1b) on the rectifier inputs. Here, u and i are the instantaneous values of voltage and current on the rectifier inputs, u_d is the instantaneous value of voltage at the rectifier bridge's output and E is the value of the counter-emf.

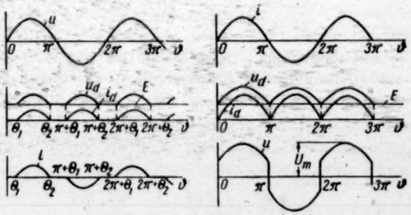

a b

Fig. 1.

In the mode of sinusoidal voltage on the rectifier inputs, the angles θ_1 and θ_2 are defined by the following relationships [1]:

$$\sin \theta_1 = \frac{E}{U_m}, \quad \theta_2 = \pi - \theta_1, \tag{1}$$

where U_m is the amplitude of the voltage applied to the rectifier bridge.

We denote by β_i the ratio of the mean value of rectified current I_d to the effective value of current I at the input of the rectifier bridge, i.e.,

$$\beta_i = \frac{I_d}{I}, \tag{2}$$

and, by β_u, the analogous relationship for voltage, i.e.,

$$\beta_u = \frac{U_d}{U}. \tag{3}$$

With a sinusoidal voltage at the input of a single-phase rectifier bridge, the coefficients β_i and β_u have the following values [1]:

$$\beta_i = 0.9, \quad \beta_u = 0.9 \text{ for } \frac{E}{U_m} = 0, \tag{4a}$$

$$\beta_i = 1.41, \quad \beta_u = 1 \quad \text{for} \quad \frac{E}{U_m} \approx 1. \tag{4b}$$

In order to obtain the analogous values of β_u for the mode of sinusoidal current at the rectifier inputs, we make use of the curves of current and voltage (Fig. 1b). The variation in the voltage u at the rectifier inputs can, with this, be presented by the following relationship:

$$u = E + (U_m - E) \sin \vartheta,$$

$$0 \leqslant \vartheta \leqslant n\pi \quad (n = 1, 3, 5, \ldots). \tag{5}$$

Since $|u| = |u_d|$, then the expression for the rectified voltage will have the same form as in (5), with the sole difference that n = 1, 2, 3, . . .

According to (5), the mean value of the voltage at the rectifier output will equal

$$U_d = E + \frac{1}{\pi}\int_0^{\pi} (U_m - E) \sin \vartheta =$$

$$= E + \frac{2}{\pi}(U_m - E). \tag{6}$$

The effective value of the voltage at the rectifier input is

$$U = \sqrt{E^2 + \frac{(U_m - E)^2}{2}}. \tag{7}$$

By substituting (6) and (7) in (3) we obtain, after some transformations, the expression for the coefficient β_u for the mode of sinusoidal current at the rectifier inputs:

$$\beta_u = \frac{\frac{E}{U_m} + \frac{2}{\pi}\left(1 - \frac{E}{U_m}\right)}{\sqrt{\left(\frac{E}{U_m}\right)^2 + \frac{\left(1 - \frac{E}{U_m}\right)^2}{2}}}. \tag{8}$$

For a sinusoidal current at the input of a single-phase rectifier bridge, the coefficients β_u and β_i have the following values:

$$\beta_u = 0{,}9 \quad \text{for} \quad \frac{E}{U_m} = 0, \tag{9a}$$

$$\beta_u = 1 \quad \text{for} \quad \frac{E}{U_m} = 1, \tag{9b}$$

$$\beta_i = 9 \quad \left(0 \leqslant \frac{E}{U_m} \leqslant 1\right). \tag{9c}$$

Due to the inconstancy of the coefficients β_u and β_i for a variable ratio of E/U_m, and also for sinusoidal current and sinusoidal voltage at the rectifier inputs, it is much more convenient, in designing the circuit, to use the replacement circuit with an equivalent active load r_e instead of the rectifier bridge.

For operation on a counter emf we have

$$U_d = E + I_d r, \tag{10}$$

where r is the active impedance in series with the counter-emf E (if the rectifier output is connected to the armature circuit of a motor or to a storage battery, then r is the active impedance of the armature winding or the battery's internal impedance).

The rectified voltage U_d can also be expressed in terms of the resistance r_d':

$$U_d = I_d r_d', \tag{11a}$$

where, in accordance with (10)

$$r_d' = \frac{E}{I_d} + r. \tag{11b}$$

The power applied to the rectifier bridge equals

$$P = UI. \tag{12}$$

By substituting (2) and (3) in (12), and taking (11a) into account, we get

$$P = I_d^2 \frac{r_d'}{\beta_u \beta_i}. \tag{13}$$

We introduce the concept of the equivalent load impedance r_e, and express the power P in terms of it

$$P = I^2 r_e, \tag{14}$$

where $r_e = U/I$.

By substituting (2) in (14), we get

$$P = I_d^2 \frac{r_e}{\beta_i^2}. \tag{15}$$

By equating (13) and (15), we obtain the definitive expression for the equivalent impedance r_e in the form

$$r_e = \frac{\beta_i}{\beta_u} r_d'. \tag{16}$$

Figure 2 shows the circuit for a single-phase rectifier bridge operating on a counter-emf (a) and its equivalent circuit with active impedance r_e(b). Such a transfiguration of rectifiers with counter-emf to an equivalent active impedance significantly simplifies the circuit design if a

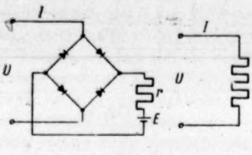

Fig. 2.

magnetic amplifier is connected in series with this impedance. For example, if one ignores the losses in the steel of the magnetic amplifier's cores, then the following equation will be valid for the fundamental harmonics of the voltages and currents (in order to simplify the notation, the subscripts for the fundamental harmonics have been suppressed in this and the following equations):

$$U_L^2 + I^2(r_e + r_{ma})^2 = U^2, \tag{17}$$

where U_L is the fundamental harmonic of the effective value of the inductive component of the voltage across the terminals of the magnetic amplifier's working winding $w_\sim$, U is the fundamental harmonic of the effective value of the source voltage, r_{ma} is the resistance of working winding $w_\sim$ of the magnetic amplifier.

By expressing the voltage and current in terms of the magnetic induction and magnetic field strength we obtain after some uncomplicated transformations,

$$\frac{B_m^2}{B_{m0}^2} + \frac{H^2}{H_0^2} = 1, \tag{18}$$

where

$$B_m = \frac{U_L}{4.44 f w_\sim S}, \quad B_{m0} = \frac{U}{4.44 f w_\sim S};$$

$$H = \frac{w_\sim I}{l}, \quad H_0 = \frac{w_\sim I_{\max}}{l} = \frac{w_\sim U}{l(r_e + r_{ma})}. \tag{19}$$

Here, l and S are the average length and cross-section of the magnetic amplifier's magnetic circuit and I_{max} is the maximum current, corresponding to $U_L = 0$.

Equation (18) is the equation of an ellipse with its center at the origin and with semiaxes B_{m0} and H_0. By joining such an ellipse with the characteristics $B_m = f(H, H_=)$, we easily obtain the magnetic amplifier characteristics we are seeking. A graphicoanalytic method of obtaining magnetic amplifier characteristics is explained in more detail in [5].

The magnitude of the resistance r_e which enters into the expression for the magnetic field strength H_0 depends on the ratio of the coefficients B_I/B_u. For example, for a sinusoidal voltage, according to (4a) and (4b), we have: for $E/U_m = 0$, $r_e = r'_d$; for $E/U_m \approx 1$, $r_e = 1.41r'_d$. For sinusoidal current, according to (9a), (9b), and (9c), we have: for $E/U_m = 0$, $r_e = r'_d$; for $E/U_m = 1$, $r_e = 0.9r'_d$.

Thus, in determining the characteristics of a magnetic amplifier by conjoining the magnetic characteristics $B_m = f(H, H_=)$ with the equation of an ellipse, (18), three limiting cases can be found (Fig. 3): $E/U_m = 0$, i.e., there is a purely active load ($r_e = r'_d = r_l$, where r_l is the load resistance); $E/U_m \approx 1$, i.e., the load is a counter-emf. Here there can be either $r_e = 0.9r'_d$ or $r_e = 1.41r'_d$.

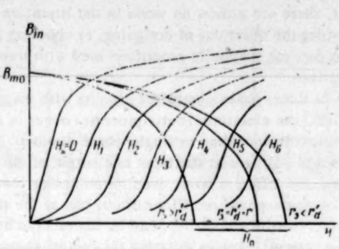

Fig. 3. Working trajectories of a magnetic amplifier with a counter-emf.

In charging storage batteries, principally starter batteries, there is a significantly large voltage drop from their emf, caused by internal impedances, so that E U_m ≈ ≈ 1. In schemes for controlling the rotational speed of motor armatures, there can be, as a function of its magnitude, $0 \leq E/U_m \leq 1$.

If the voltage drop across a magnetic amplifier is greater than the voltage drop across the input (the magnetic amplifier is operating on the upper portion of the magnetic characteristics) (Fig. 3), then $r_e < r'_d$.

The method just presented for obtaining the desired characteristic is convenient in those cases when the supply voltage and the load parameters are invariant.

When the load parameters vary, it is convenient to give different values to the resistance r_e and the current I, and to compute the value of H corresponding to them from (19), and the value of B_m from the formula

$$B_m = \frac{\sqrt{U^2 - I^2(r_e + r_{ma})^2}}{4.44 f w_\sim S}. \tag{20}$$

By conjoining the thus obtained function $B_m = f(H)$ with the characteristics $B_m = f(H, H_=)$, we can find the magnetic amplifier characteristics being sought.

In many cases, the magnetic amplifier operates with H = const. Such modes of amplifier operation occur, for example, in charging starter storage batteries, in controlling the rotational velocity of a motor armature with constant torque, etc.

In order to obtain the characteristic of a saturated reactor magnetic amplifier, providing a constancy of charging current, it is necessary to know the law of variation of the voltage across the terminals of the storage battery as a function of the charging time for I = const, i.e., it is necessary to have the function $U_d = f(t)$ or $E = f(t)$ and the internal resistance r.

Magnetic Amplifier Operation with Three-Phase Rectifier Bridge

Three-phase rectifier schemes are widely used in technology, chiefly in power rectification stands. However, there are almost no works in the literature which consider the questions of designing, or choosing the parameters for, the magnetic amplifiers used with three-phase rectifiers.

In three-phase controlled circuits with magnetic amplifiers, the electromagnetic processes occur in a more complex manner than in single-phase circuits. The currents and voltages at the input and output of the rectifier bridge are different here, even for an active load.

A three-phase rectifier circuit, just as the single-phase circuits considered earlier, can be represented by an equivalent circuit. For calculating the circuit elements, it is convenient to represent a three-phase rectifier circuit by a Y-network. With this, the transfiguration must be so effected that, in the equivalent Y-network, the same linear voltages and currents occur as in the rectifier circuit, while the same power as before acts on the load.

With an active load, the power of one phase of the equivalent Y-network, P_p, equals

$$P_p = U_p I \tag{21a}$$

or

$$P_p = I^2 r_p , \tag{21b}$$

where r_p is the phase resistance of the equivalent Y-network.

In a circuit with an active load, the rectified voltage ordinarily equals

$$U_d = I_d r_d , \tag{22}$$

where r_d is the active load impedance.

By setting $U = U_p$ in (3), and by substituting (2), (3), and (22) in (21a) and (21b), we get

$$P_p = I_d^2 \frac{r}{\beta_u \beta_i} \tag{23a}$$

$$P_p = I_d^2 \frac{r_p}{\beta_i^2} . \tag{23b}$$

Equating (23a) and (23b), we obtain, finally,

$$r_p = \frac{\beta_i}{\beta_u} r_d . \tag{24}$$

Expression (24) is the condition for the transfiguration of a three-phase rectifier circuit to an equivalent Y-network with the resistance of each phase equal to r_p. This expression is analogous to Expression (16) for single-phase rectifier circuits.

Figure 4 shows the three-phase rectifier bridge circuit with an active load (a) and the equivalent Y-network corresponding to this circuit (b). An analogous Y-network is also equivalent to a three-phase circuit with zero output. The difference is solely in the magnitude of phase resistance r_p, determined by the coefficients β_i and β_u.

The values of the coefficients β_i and β_u for a three-phase rectifier bridge circuit operating on an active load are given in Table 1.

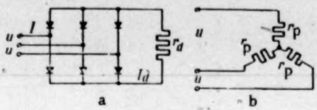

Fig. 4.

TABLE 1

Mode of rectifier operation	β_i	β_u
Sinusoidal voltage on rectifier input	1.227	2.12
Sinusoidal current on rectifier input	1.35	2.34

For other forms of load (counter-emf and active-inductive load), the coefficients β_i and β_u are given in [1, 6, 7].

Figure 5 shows the circuit of a three-phase rectifier with a magnetic amplifier and an active load (a) and the equivalent Y-network (b) (for the purposes of simplification, the functional dependence of the magnetic amplifier's induction on current is not shown in Fig. 5b).

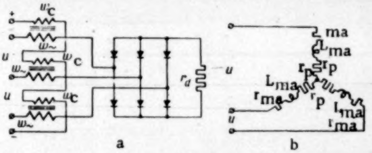

Fig. 5.

The following equation is valid for the fundamental harmonics of voltage and current for each phase of the equivalent Y-network [with the same assumptions as for (17)]:

$$U_L^2 + I^2 (r_p + r_{ma})^2 = U_p^2 . \tag{25}$$

In designing three-phase circuits, one frequently has to do with linear voltage sources. By taking this into account, and by expressing the voltage and current in terms of magnetic induction and magnetic field strength, according to (19), after some uncomplicated transformations, we obtain

$$\frac{3B_m^2}{B_{m0}^2} + \frac{3H^2}{H_0^2} = 1. \tag{26}$$

For the substituting of (19) in (25), it is assumed that U is the linear source voltage and that $r_e = r_p$.

As with (18), (26) is the equation of an ellipse which, when joined to the characteristics $B_m = f(H, H_=)$, allows one to obtain easily the desired magnetic amplifier characteristics.

The coefficients β_I and β_u are different for the modes of sinusoidal current and sinusoidal voltage on the rectifier input. However, the ratios of the coefficients, β_I/β_u for each of these modes are almost identical, being equal to 0.579 for the mode of sinusoidal voltage, and to 0.577 for the mode of sinusoidal current.

Sinusoidal voltage at the rectifier input occurs only for $B_m = 0$. But, $B_m \neq 0$ always for magnetic amplifier operation. Therefore, in computing the magnetic amplifier characteristics $H = f(H_=)$, the ratio $r_p = 0.577 r_d$ should be used.

If it is required to determine the load characteristics $H_d = f(H_=)$, then it is necessary to multiply the ordinates of the curves $H = f(H_=)$ by the coefficient β_I.

For variations of the load parameters or of the line voltage U, it is convenient to compute the magnetic induction B_m by the formula

$$B_m = \frac{\sqrt{U^2 - 3I^2(r_p + r_{ma})^2}}{\sqrt{3} \cdot 4.44 f w_{\sim} S}. \qquad (27)$$

For operation of the rectifier on a counter-emf, the equivalent Y-network in accordance with (11a), will have a form analogous to that shown in Fig. 4. The only difference will be that, in this case,

$$r_p = \frac{\beta_I}{\beta_u} r_d'. \qquad (28)$$

For operation of a three-phase rectifier on a counter-emf, the same ratio is retained between the fundamental harmonic of the input voltage and the dc component of the output voltage as for a purely active impedance, i.e., for charging storage batteries with rectified current, the coefficients β_u given in Table 1 are valid. Also retained is the ratio between the fundamental harmonic of input current and the dc component of the output current [1]. As for an active load, we consider that $r_p = 0.577 r_d'$, and r_d' is defined by (22), where $r_d = r_d'$.

Schemes for Devices for the Automatic Stabilization of Charging Current

Charging of many types of storage batteries is carried out with dc which is invariant in magnitude. In many case, the invariance in current magnitude is necessary in the charging process in order that the battery charge can be gauged. For example, the charge on acid storage batteries is determined by the density of electrolyte and voltage across the terminals, both invariant over several hours, for one and the same charging current. The charge of alkaline batteries is determined by the magnitude of the capacitance obtained by them (with an invariant charging current, the charge is here determined actually by the batteries' charging time).

In charging devices with saturated-core magnetic amplifiers, it is not difficult to implement automatic stabilization of the charging current (shown in Figs. 6 and 7).

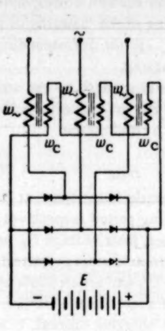

Fig. 7.

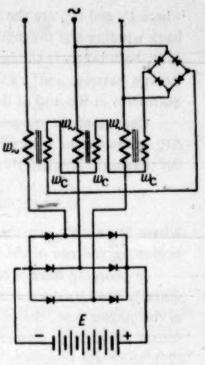

Fig. 6.

As a function of the quality of the steel and of the operational mode of the magnetic amplifier, the control winding w_c, in order to obtain a stabilized charging current, can be connected either to the terminals of the storage battery to be charged, to provide positive voltage feedback (Fig. 6), or to a source of invariable voltage, to provide constant bias (Fig. 7).

To explain the choice of one scheme or another for magnetic amplifier control, Fig. 8 shows the characteristics $B_m = f(H, H_=)$.

In the process of charging storage batteries, their voltages is changed from U_d' to U_d'' by the amount

$$\Delta U_d = U_d'' - U_d'. \qquad (29)$$

This change of voltage, in the circuit with positive feedback (cf., Fig. 6), gives rise to an increase in the magnetic amplifier's magnetizing current and, consequently, the magnetic field strength due to the current in the positive feedback winding is increased by an amount $\Delta H_= \equiv \Delta U_d$. The quantity $\Delta H_=$ is defined by the formula

$$\Delta H_= = H_='' - H_=' = \frac{\Delta U_d}{\varepsilon} \frac{w_c}{l} = (I_='' - I_=') \frac{w_c}{l}, \qquad (30)$$

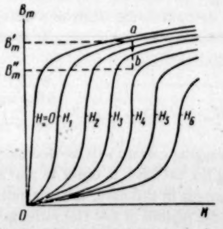

Fig. 8. Working trajectories of a magnetic amplifier used in charging devices.

where $I'_=$ and $H'_=$ are the magnetizing current of the feedback winding and magnetic field strength corresponding to it, both taken at the beginning of the charging of the storage battery, and $''_=$ and $H''_=$ are the corresponding quantities at the end of the charging.

Change of the magnetic field strength by the amount $\Delta H_=$ gives rise to a decrease in the magnetic induction in the magnetic amplifier's cores by an amount

$$\Delta B_m = B'_m - B''_m, \qquad (31)$$

Where B'_m and B''_m are the magentic inductions at the beginning and end of the charging period respectively.

In charging storage batteries, their voltage U_d ordinarily changes considerably (in acid storage batteries of the starter type, the voltage U''_d can reach 135% of its initial value U'_d). However, in accordance with (20) or (27), to obtain constancy of the charging current, it is necessary to decrease insignificantly the magnetic induction in the magnetic amplifier's cores. Therefore, the magnetic amplifier must operate in the saturated region of the characteristic $B_m = f(H, H_=)$ so that, with an increase in voltage U_d, the relative growth in the magnetic field strength $\Delta H_=$, induced by the positive feedback current, will be larger than the relative decrease in magnetic induction ΔB_m. In Fig. 8, the working trajectories of the magnetic amplifier are shown by the dashed lines between points a and b.

To obtain a charging current which is invariant in magnitude, it is necessary to choose such a mode of magnetic amplifier operation in which, for a variation in magnetizing magnetic field strength defined by (30), the magnetic induction must be changed by the amount ΔB_m, computed in accordance with (20) or (27) and (31). This mode of magnetic amplifier operation, providing automatic stabilization of the charging current, we express by the equation

$$(H''_= - H'_=)_{H=\text{const}} = \frac{\Delta U_d}{r_c}\frac{w_c}{l}, \qquad (32a)$$

where $(H''_= - H'_=)_{H=\text{const}}$ are the limits of variation of the magnetizing strength on the family of characteristics $B_m = f(H, H_=)$ for variation of the magnetic induction, computed from (20) or (27), from B'_m to B''_m.

The right member of (32a) is the increment of magnetic field strength as the result of a change in voltage of the storage battery in accordance with (29).

If

$$(H''_= - H'_=)_{H=\text{const}} > \frac{\Delta U_d}{r_c}\frac{u_c}{l}, \qquad (32b)$$

then the charging current will be decreased in the process of charging the battery. In order to provide a constant charging current in this case, the magnetic amplifier must operate in the regions of low field strength H or high field strength $H_=$, i.e., the trajectory must be shifted either to the left, or down, or down and to the left simultaneously.

$$(H''_= - H'_=)_{H=\text{const}} < \frac{\Delta U_d}{r_c}\frac{w_c}{l}, \qquad (32c)$$

then the charging current will be increased in the process of charging the battery. In order to provide here a constant charging current, the magnetic amplifier must operate in the regions of large field strength H and low field strength $H_=$, i.e., the trajectory must be shifted either to the right, or up, or up and to the right simultaneously.

Charging devices in which stabilization of charging current was provided by the choice of the proper mode of magnetic amplifier operation were considered in [3, 4].

To decrease the dimensions and weight of the power magnetic amplifiers used in charging devices, it is ordinarily recommended that one use cold-rolled steel such as, for example, É320, É330, É370. These brands of steel differ from transformer steel, not only by their large values of magnetic saturation induction, but also by the steepness of the slope of the characteristics, particularly in the case when toroidal cores prepared from strips are used [8].

If the characteristics $B_m = f(H, H_=)$ of the magnetic amplifiers used are almost vertical in their unsaturated portions then, to provide constancy of charging current, it suffices to provide a constant bias using, for this, small-size germanium diodes of type DG-Ts (Fig. 7). Connecting a battery in the bias circuit can permit the elimination of the effect of oscillations in the supply voltage U on the magnitude of the charging current. Since the magnetic induction B_m changes within narrow limits during the battery charging process, then this method allows the implementation of a completely satisfactory stabilization of charging current.

Example of the Determination of the Basic Parameters of a Saturated Reactor Magnetic Amplifier

We earlier considered methods for determining the characteristics of magnetic amplifiers operating on a counter emf. We now show that, by means of the relationships already provided, we can also compute the basic parameters of a planned magnetic amplifier.

We consider the sequence of the determinations of the basic parameters of a magnetic amplifier intended for the charging of 14 starter storage batteries of type 6STÉN-140M by a current of invariable magnitude, equal to 10 amperes.

In Table 2 (the upper two rows) there are given the charging characteristics of one element of a 6STÉN-140M storage battery, 50% discharged, for charging by a 10 amp current.

The rectified voltage will equal

$$U_d = mnU_{el},$$

where m is the number of storage batteries to be charged (m = 14) and n is the number of elements in one battery (n = 6).

To determine whether or not it is possible to charge the given quantity of storage batteries, one must com-

TABLE 2

Circuit parameters	Time, in hours						
	0	1	2	4	6	8	10
Charging current I_d amperes	10	10	10	10	10	10	10
Voltage on a storage battery element, volts	2.1	2.17	2.2	2.23	2.34	2.59	2.59
Rectified voltage, volts	176.4	182	185	187	196.4	217.5	217.5
Equivalent phase resistance r_p, ohms	10.18	10.5	10.68	10.8	11.33	12.54	12.54
$B_m = f(t)$	. . .	. . .	. . .	. . .	. . .	. . .	. . .

pute $U_{d\ max}$. For this, it is necessary to know the maximum possible voltage on one element, $U_{el\ max}$. For starter batteries, ordinarily $U_{el\ max} \leq 2.7$ v. Then, $U_{d\ max} = 226.8$ v.

According to (3) and the data of Table 1, in the example under consideration, if the voltage drop in the rectifier is neglected, the rectified voltage can equal

$$U_d = \beta_u U_p = (2.12 - 2.34) \frac{220}{\sqrt{3}} = 269 - 297 \text{ v.}$$

With the given relationships of the possible rectified voltage and the maximum possible voltage on the storage batteries, we decide that charging will occur with an approximately sinusoidal voltage on the rectifier bridge's input. But since $B_m \neq 0$ with this, then the equivalent phase resistance will be defined by the relationship

$$r_p = 0.577 \frac{U_d}{10}.$$

The results of computing r_p are given in Table 2.

The current I on the rectifier input, according to (2), will equal 8.15 amp.

In (27), which relates the given parameters with the magnetic amplifier's parameters, there are still four unknown quantities: B_m, $w_\sim$, S and r_{ma}. The active impedance of winding $w_\sim$ is very small and, for a preliminary estimate of the parameters, it may be neglected.

When positive voltage feedback is used, constancy of charging current can be attained only when the magnetic amplifier operates on the saturated portion of characteristics $B_m = f(H, H_=)$. Therefore, the magnitude of B_m can be given for a well-known brand of steel. By being given the magnitude of S as well, we can compute the number of turns of winding $w_\sim$.

In order that the initially chosen values of $w_\sim$ and S correspond closely to the actual magnitudes, we can use the following assumptions.

For the initial and final moments of storage battery charging, the following relationships are valid:

$$U^2 = U'^2_L + I^2 r'^2_p, \qquad U'_L = 4.44 f w_\sim S B'_m \cdot 10^{-8},$$

$$U^2 = U''^2_L + I^2 r''^2_p, \qquad U''_L = 4.44 f w_\sim S B''_m \cdot 10^{-8},$$

$$H' = H'' = H = \frac{I w_\sim}{l}.$$

The quantities with one prime (') relate to the beginning of the charging period of the storage battery, while those with two primes relate to the period's end. The resistances r_{ma} are ignored here, since we are making only a preliminary choice of parameters.

By transforming these equations, we obtain a function for the determination of the volume of steel

$$V = \frac{I^2 \sqrt{r''^2_p - r'^2_p}}{4.44 f H \cdot 10^{-8} \sqrt{B'^2_m - B''^2_m}}.$$

Due to the increase of voltage on the storage batteries to provide I = const, the magnetic induction B_m must be decreased. This decrease in induction is ordinarily insignificant in the charging of starter storage batteries. By taking this into account, and by selecting the magnetic induction B_m, one can compute the value of the square root $\sqrt{B'^2_m - B''^2_m}$.

By being given the magnitude of the magnetic field strength H for the selected type of steel, we can approximately determine the core volume.

If the invariance of the charging current is to be provided by biasing, then the chosen magnitude of H must correspond to the vertical segments of the steel's magnetic characteristics.

The expression given for the volume of steel can facilitate to a significant degree the determination of the magnetic amplifier parameters if one uses, for example, standard three-leg laminas [9]. From the known volume V one can choose the type of lamina and, from this, one can select l and S. From the known value of S, one can approximately determine the number of turns of winding $w_\sim$ by the formula

$$w_\sim = \frac{I \sqrt{r''^2_p - r'^2_p}}{4.44 f S \cdot 10^{-8} \sqrt{B'^2_m - B''^2_m}}.$$

From the number of turns found for winding $w_\sim$, one can approximately gauge the resistance r_{ma}, for which it is necessary to be given the current density and to compute the mean length of the turns.

In thus computing approximately the basic parameters of the magnetic amplifier, it is necessary to determine the law of variation of variation of magnetic induction $B_m = f(t)$ in accordance with (27) and to conjoin the function thus obtained for H = const with the characteristics $B_m = f(H, H_{=})$. The results of the computation of $B_m = f(t)$ can be found in Table 2.

The choice of the required mode of magnetic amplifier operation to provide I_d = const was presented in a previous section.

Limitations on the size of this paper prevent us from giving here the entire design of the magnetic amplifier.

CONCLUSIONS

The transfiguration suggested of one-phase and three-phase rectifier bridges to equivalent loads permits the use of the simplest, most graphic and sufficiently accurate graphicoanalytic method of designing saturated reactor magnetic amplifiers.

In this paper we have shown the simplest methods of stabilizing charging current, which are attained by the proper choice of operating mode of the magnetic amplifier.

LITERATURE CITED

[1] V. G. Komar, Operation of Semiconductor Rectifiers in Control Circuits Theory and Design [in Russian] (Gosénergoizdat, 1952).

[2] K. N. Borisov, "Speed control of dc motors by means of chokes and semiconductors," Élektrichestvo No. 2 (1957).

[3] I. I. Ratrauz and V. A. Belous, "Contactless charging devices," Élektrichestvo No. 12 (1949).

[4] A.G. Zdrok, "The use of ac and semiconductor rectifiers in autotractor technology," Avtomobilnar i Traktornaya Promyshlen.) No. 10 (1956).

[5] M. A. Rozenblat, Magnetic Amplifiers [in Russian] (Izd. Sovetskoe Radio, 1956).

[6] V. L. Inosov and V. E. Krutikova, "Calculating the modes of heavy rectifiers with account taken of their internal impedance," Research Papers, 3 [in Russian] (Inst. Élektrotekh. AN USSR, 1949).

[7] I. S. Kurdiani and O. K. Khomeriki, "Operation of three-phase rectifier supplied from transformer current," Élektrichestvo No. 3 (1954).

[8] O. I. Aven, "Magnetic alloys for magnetic amplifier cores and their curves of simultaneous magnetization by constant and variable fields," Avtomatika i Telemekhanika 17 No. 4 (1956).*

[9] V. Yu. Roginskii, Semiconductor Rectifiers [in Russian] (Gosénergoizdat, second edition, 1957).

---

* See English translation.

10

ON THE SIMULATION OF LINEAR SYSTEMS WITH n STATIONARY RANDOM INPUT PROCESSES WITHOUT THE USE OF RANDOM FUNCTION GENERATORS

Ya. Shilkhanek

(Pardubice, Czechoslovakia)

Translated from Avtomatika i Telemekhanika Vol. 21, No. 5, pp. 652-654, May, 1960
Original article submitted January 12, 1960

A method is described for determining the mean value of the square of the output quantity of a linear system with n stationary random input processes by means of a simulating device without the use of random function generators. This method is a generalization to systems with n inputs of the method described in [2].

In solving various problems in the domain of regulation and automatic control, one frequently has to deal with the problem of determining the average value of the square of the output quantity of a system with n stationary random processes at the system's inputs. We shall assume that the input processes are stationary and ergodic, and that their spectral densities (proper and mutual) are rational fractional functions of the complex frequency s.

Posing of the Problem

We denote by y(t) the output quantity of the linear system under consideration. The mean value of the square of y(t) is defined by the relationship

$$\overline{y^2} = \lim_{t\to\infty} \frac{1}{t} \int_0^t [y(\tau)]^2 d\tau. \tag{1}$$

A generator of n stationary random processes with given proper and mutual spectral densities was described in [1]. On the basis of this generator we can construct a block schematic for determining the mean value of the square of the system's output quantity (Fig. 1). On this block schematic, $Q_1, Q_2, \ldots, Q_n$ are the noncorrelated generators of white noise, Sh are shaping filters, S_n is the given linear system with n inputs, Sq is a squaring device, I is an integrator, $x_1(t), x_2(t), \ldots, x_n(t)$ are the random input processes of system S_n, and y(t) is the system's output process.

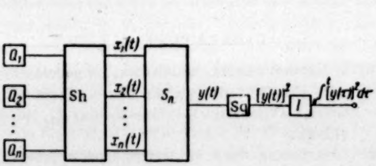

Fig. 1.

For sufficiently large t, one can determine the mean value of the square of y(t) from the integrator's output quantity in accordance with (1). With this, it is necessary to use n generators of noncorrelated white noise. These generators must be quite accurate and stable.

A method was described in [2], applicable to linear systems with one stationary random input process, for determining the mean value of the square of the output quantity by means of a simulating device, eliminating the necessity of using white noise generators. This method is based on the possibility of generating an input random process with a known spectral density by means of a white noise generator and a linear shaping filter Sh (the determination of whose transfer function is described in [1, 2,]).

We denote by W(t) the impulsive response of the series-connected shaping filter Sh and the given linear system S_1. Based on known relationships, we obtain

$$\overline{y^2} = \int_0^\infty [W(\tau)]^2 d\tau. \tag{2}$$

The block schematic shown on Fig. 2 follows from this. In this case, the input of the shaping filter has applied to it, not white noise, but a unit pulse function (a Dirac function). With increasing t, the integrator's output quantity tends to the quantity $\overline{y^2}$.

The superiority of this method is primarily that the white noise generator is excluded from the solving block schematic. The linear system is acted upon by a precisely defined function of time, which increases the accuracy of the determination of the quantity $\overline{y^2}$. Below we give a generalization of this method for a linear system S_n with n stationary random process at the system's inputs.

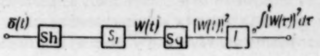

Fig. 2.

Solution of the Problem

The correlation function of the output quantity of a linear system with n stationary random processes at the inputs is defined [2] by the relationship.

$$\varphi_{yy}(\tau) = \sum_{m=1}^{n} \sum_{k=1}^{n} \int_{0}^{\infty} -$$

$$- \left[W_m(\tau_1) \int_{0}^{\infty} W_k(\tau_2)\, \varphi_{mk}(\tau - \tau_2 + \tau_1)\, d\tau_2 \right] d\tau_1, \tag{3}$$

where $\varphi_{mk}(\tau)$ is the mutual correlation (cross-correlation) function of the mth and kth random processes at the input, $W_i(\tau)$ is the system's impulsive response to the ith input and $\varphi_{yy}(\tau)$ is the correlation function of the system's output quantity.

We use (3) to determine the magnitude of $\overline{y^2}$. Since the series connection of the shaping filters Sh and the system S_n is a linear system with n inputs then, in our case, $W_i(\tau)$ will be the impulsive response to the ith input of shaping filters Sh at the output of the system S_n. The function $\varphi_{mk}(\tau)$ (the correlation functions of the random processes at the inputs of shaping filters Sh) are defined by the equations

$$\begin{aligned} \varphi_{mk}(\tau) &= \delta(\tau) \quad \text{for} \quad m = k, \\ \varphi_{mk}(\tau) &= 0 \quad \text{for} \quad m \neq k. \end{aligned} \tag{4}$$

By substituting (4) in (3), for $\tau = 0$, we obtain the quantity $\overline{y^2}$ in the form

$$\overline{y^2} = \varphi_{yy}(0) = \sum_{i=1}^{n} \int_{0}^{\infty} [W_i(\tau)]^2\, d\tau. \tag{5}$$

We denote by $\overline{y_i^2}$

$$\overline{y_i^2} = \int_{0}^{\infty} [W_i(\tau)]^2\, d\tau, \tag{6}$$

i.e., the mean value of the square of the output quantity y when the inputs of the shaping filters are acted upon by only one white noise generator Q_i.

Then, from (5), we get

$$\overline{y^2} = \sum_{i=1}^{n} \overline{y_i^2}. \tag{7}$$

Consequently, each value of $\overline{y_i^2}$ [cf., (6)] can be determined by the method described in [2].

Thus, the mean value of the square $\overline{y^2}$ of the output quantity of linear system S_n with n stationary random input processes can be obtained at the output of the block schematic shown on Fig. 3. At the inputs of shaping filters Sh there act, at the individual moments of time T_i, unit pulse functions $\delta(t - T_i)$. The moments T_i (i = 1, 2, . . . , n) must be so determined that, at these moments, the entire system is found in a virtual resting state. The integrator I sums the values of $\overline{y^2}$ step by step in accordance with (7), such that, for $t > \max\{T_1, T_2, \ldots, T_n\}$, its output quantity tends to the value $\overline{y^2}$.

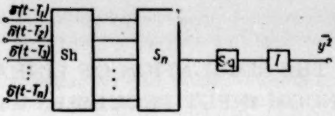

Fig. 3.

It is well known, from the methods of solving problems on simulating devices (analog computers), that the unit pulse functions can be replaced by the introduction of the proper initial conditions.

CONCLUSIONS

In the solution of various practical problems, it is necessary to determine the mean value of the square of the output quality of a linear system S_n at the n inputs of which there act n stationary random processes with known spectral densities in the form of rational-fractional functions of the complex frequency s. This problem can be solved by using the block schematic shown in Fig. 1.

For a system S_1 with one stationary random process at the input, a method is described in [2] which eliminates the use of a random process generator. In the present paper, this method was generalized to an arbitrary linear system S_n with n inputs, acted upon by n stationary random processes with known proper and mutual spectral densities.

The block schematic for the analog computer computations consists, in addition to the given linear system, of shaping filters (their transfer functions are determined by the very simple methods described in [1]) a squaring device and an integrator (Fig. 3). At the inputs of the shaping filters appear, not white noise, but unit pulse functions. With this, the mean value of the square $\overline{y^2}$ is obtained at the integrator's output.

The advantage of this method of computing the quantity $\overline{y^2}$ is, above all, that random function generators are eliminated. Since the entire system is acted upon, not by random processes, but by accurately defined functions of time [the pulse functions $\delta(\tau)$], one can expect a greater accuracy in determining the desired quantity $\overline{y^2}$.

LITERATURE CITED

[1] I. Matyash and Ya. Shilkhanek, "A generator of random processes with a given matrix of spectral densities," Avtomatika i Telemekhanika 21, No. 1 (1960).

[2] J. H. Laning and R. H. Batten, Random Processes in Automatic Control [Russian translation] (IL, 1958).

INFORMATION

BUREAU OF THE PRESIDIUM OF THE ACADEMY OF SCIENCES OF THE USSR

Decision of Feb. 12, 1960, Number 134, Moscow

On the Decision of the Conference on the Theory of Invariance and its Application to Automatic Devices of October 20, 1958 (Kiev)

After hearing the communication of the chairman A. A. Dorodnitsyn, of the commission of the Presidium of the AN SSSR on the decision of the Conference on the Theory of Invariance and its Application to Automatic Devices, of Oct. 20, 1958 (in Kiev), the Bureau of the Presidium of the Academy of Science of the USSR has decided:

1. To endorse the conclusions of the commission of the Presidium of the AN SSSR on the decision of the Conference on the Theory of Invariance and its Application to Automatic Devices, of Oct. 20, 1958 (in Kiev) the Appendix).

2. To publish the conclusions of the commission in the journal Avtomatika i Telemekhanika (Automation and Remote Control).

Vice-President of the
Academy of Science, USSR
Academician A. V. Topchiev

Chief Scientific Secretary
Presidium of the Academy of
Science, USSR
Corresponding Member AN SSSR
E. K. Fedorov

APPENDIX TO THE DECISION OF THE BUREAU OF THE PRESIDIUM AN SSSR OF FEBRUARY 12, 1960, Number 134

Conclusions of the Commission in Connection with the Discussion on the Theory of Invariance

The commission, consisting of Academician A. A. Dorodnitsyn, Academician AN Ukrainian SSR A. Yu. Ishlinskii and Corresponding Member AN SSSR B. N. Petrov, designated on October 28, 1958 by the vice president of the AN SSSR, Academician A. V. Topchiev, in considering the decisions of the Kiev Conference on the Theory of Invariance and Its Application to Automatic Devices (Oct. 20, 1958), the decisions of the Presidium of the Academy of Science of the USSR of April 1, 1941, Section 5, the conclusions of the commission of the Presidium of the Academy of Science of the USSR for discussion and judging the work of Professor G. V. Shchipanov, "Autocontrolled systems with several degrees of freedom," the work of Prof. G. V. Shchipanov itself, and certain materials in the discussion of the work of G. V. Shchipanov, established the following.

In the journal Avtomatika i Telemekhanika (Automation and Remote Control) No. 1 (1939) there was published the paper of Prof. G.V. Shchipanov, "Autocontrolled systems with several degrees of freedom". This paper gave rise to wide discussion, the materials of which were published in a number of journals.

By decision of the Presidium of the Academy of Science of the USSR, taken on March 4, 1940, a commission was created to discuss and judge the work of Prof. G. V. Shchipanov, "Autocontrolled systems with several degrees of freedom ," this commission consisting of Vice-President of the AN SSSR Academician O. Yu. Shmidt, Academician S. A. Chaplygin, S. L. Sobolev, N. E. Kochin, and Corresponding Member AN SSSR N. G. Bruevich.

The commission's conclusions were discussed at the April 1, 1941 session of the Presidium of the AN SSSR, at which time the decision was taken to take the commision's conclusions under consideration, to publish them, and to consider the work of the commision as finished.

The commission's conclusions contained the dissenting opinions of Academicians V. S. Kulebakin and N. N. Luzin which considered necessary further research into the conclusions of Section 2, in which the estimate of the work of G. V. Shchipanov was contained.

In the following years, a number of works were published which, in some degree or other, treated the questions of compensation or invariance (the works of Academician

N. N. Luzin, Academician V. S. Kulebakin, A. G. Ivakhnenko , B. N. Petrov, G. M. Ulanov, and others).

On October 16-20, 1958, in Kiev, there was held the Conference on the Theory of Invariance and Its Application to Automatic Devices, convened by the Engineering Section of the AN Ukr SSR, the Kiev City Seminar and the Electrical Engineering Institute of the Ukr SSR, in which scientific workers from Moscow, Leningrad, Kiev and other cities of the Soviet Union participated.

At the Kiev Conference, a decision (resolution) was taken, noting the necessity of developing methods of disturbance compensation and the principle of invariance, in which it was stated, in Section 7:

"7. In view of the fact that the decision of the Presidium of the Academy of Science of the USSR on April 1, 1941 concerning the assertions of the conclusions of the special commission on the work of G. V. Shchipanov delayed development of the theory and practice of constructing automatic systems using compensation of disturbing stimuli and various invariance principles and does not make possible the proper and necessary progress in this important area of automation today, we ask the Presidium of the Academy of Science of the USSR to reconsider its decision as concerns the erroneous conclusions of the aforementioned commission."

As a result of the consideration of all the material cited above, we can draw the following conclusions:

1. The conclusions of the aforementioned commission to discuss and judge the work of Prof. G. V. Shchipanov, taken into consideration and published by the Presidium of the Academy of Science of the USSR, must be considered correct as concerns the first point and the first paragraph of the second point, in which it is stated that:

"1. The commission considers that questions of control theory have undoubtedly tremendous importance in the matter of the development of our national economy and the strengthening of the defense of our country, and must be worked out in the Institute for Automation and Remote Control of the Academy of Science of the USSR.

2. The work of Prof. G. V. Shchipanov under consideration, "Autocontrolled systems with several degrees of freedom," contains a whole series of incorrect and unfounded assertions."

Indeed, G. V. Shchipanov's work did contain incorrect and unfounded assertions. Among these assertions were the author's conclusions that, if the compensation condition held, then an ideal and universal controller was obtained; that the construction of regulators which did not satisfy the theorems presented in the paper must be considered as unsuitable; that with the compensation condition met, and for zero initial conditions, a free component appears, etc.

As is clear from the test and diagrams of G. V. Shchipanov's paper, he considered controllers based on the principle of deviation without additional direct or indirect stimuli proportional to the disturbance f(t) acting on the object of control, and he attempted to use, for the synthesis of such controllers, the condition of complete compensation while, in this case, it is impossible to use the condition of complete compensation.

2. However, the commission's conclusion (second paragraph of the second point) that the basic error in Prof. G. V. Shchipanov's paper is the "compensation condition", which leads mathematically to absurd conclusions and which does not correspond at all to actually realizable controllers, contains itself an erroneous conclusion, in that it is far too general a statement.

The basic error of G. V. Shchipanov consisted, not in the formulation of this condition, as was asserted in the commission's conclusions (on the contrary, this was his fundamental result!), but in the application of the compensation condition to the design of a class of control systems which does not permit its use.

As was shown by subsequent investigations, including those in Proceedings of the Kiev Conference on Invariance Theory, "the compensation condition" or the "invariance condition" can be used for designing a number of types of automatic control systems, for example, combined systems, with stimulus by deviation and by disturbance, interconnected automatic control systems for several quantities, and also several types of dynamic systems which do not come under the heading of automatic control systems, for example, bridge systems, complex electric networks, gyroscopic devices, etc.

Thus, the "compensation condition", or the "invariance condition" formulated by Prof. G. V. Shchipanov was a new design relationship which can be successfully used for designing a definite class of dynamic systems.

3. The aforementioned inaccuracy in the formulation of the commission's conclusions, and the absence of constructive criticisms in them, led, in some cases, to incorrect judgments on works in automatic control, even when the compensation condition was used correctly in them, which could not render possible development in this direction. Therefore, the commission considers it advantageous to publish, in one of the technical journals an expanded paper devoted to the prospective applications of the invariance principle, and which would cite the cases when it is advantageous to use this principle and when its use is inadmissible.

At the same time, the commission considers it necessary to note the imperfect editing of the decision of the Kiev Conference on the Theory of Invariance and its Application to Automatic Devices, from which one might gather the impression that the works of G. V. Shchipanov did not contain errors.

Commission Members
A. A. Dorodnytsin,
A. Yu. Ishlinskii,
B. N. Petrov.

THE APPROACHING FIRST CONGRESS OF THE INTERNATIONAL FEDERATION OF AUTOMATIC CONTROL

Translated from Avtomatika i Telemekhanika, Vol. 21, No. 6, pp. 657-658, June, 1960

In June of this year, the First Congress of the International Federation of Automatic Control (IFAC) will convene in Moscow. The coming Congress is a great event in world science in the area of automatic control, one recognized as exerting an influence on the development of automation in all countries.

Automation, one of the most important phenomena of our time, puts into practice the most daring dreams of many generations of mankind. Automation opens up new horizons for various branches of industry; the theory of automatic control approaches many scientific disciplines, with the raising of many problems regarding control, and modifies in principle many notions in science and technology which prevailed 10 to 15 years ago.

In recent years scientists have been faced with the most complex scientific problems of automatic control. It is difficult to overestimate the significance of these problems. Success in working them out will create the basis of rapid growth of technical progress.

It is clear that if the scientists and engineers of all countries will work in close accord on the problems of automatic control, the necessary results will be obtained very much sooner and at less expense. Such international collaboration in the field of research on automatic control is natural and necessary. Collaboration in automation is a demand of our times. Our country has made its choice; we are for the uniting of the efforts of the scientists and engineers of different countries, we are for collaboration, for close contacts of Soviet and foreign specialists in automation.

Even in 1956, Soviet scientists, along with those of other countries, were taking the initiative in this field by founding the International Federation of Automatic Control (IFAC). The formation and establishment of the IFAC has resulted in a condition of creative scientific and commercial collaboration.

The Executive Council of the IFAC, with Dr. G. Chesnut (USA) as its chairman, which was elected in September, 1957, at the First General Assembly in Paris, performed a great and very useful work. It set down the life principle of the new international scientific organization.

The Second General Assembly of IFAC was held in Chicago in September, 1959. It approved the new, improved rules and regulations, endorsed the draft of organization of the First Congress prepared by the Soviet National Committee, and heard a series of special reports.

The General Assembly elected the new staff of the Executive Council and a new President, Professor A. M. Letov, representative of the National Committee on Automative Control of the USSR.

The activity of the Federation proceeds in a condition of close scientific and commercial collaboration. To strengthen the exchange of scientific information between the national organizations of the IFAC at the present time, scientific-technical committees have been formed on theory, the technical resources of automation, on applications, terminology, education, and bibliography.

An important aspect of the activity of the IFAC is the conducting of international congresses on automation. The preparation and organization of the First Congress of the IFAC, entrusted to the National Committee of the Soviet Union, developed with the active participation of almost all the national organizations of the IFAC. In the total preparatory work a new contribution is made to the international collaboration of scientists. Reports totalling 285 were submitted for scientific consideration; they can be classified into three groups.

The reports of the first group were concerned with current problems of the theory of continuous and discrete systems of automatic control, the theory of structures and the construction of signals, stochastic, and special mathematic problems. Much attention was allotted to the theory of optimal and self-adjusting systems. A description of experimental methods of research was given in a series of reports.

Reports of the second group were concerned with the theory and experience in constructing elements of control systems, programming and computing equipment, control machines and systems of automatic control. There were reports explaining special problems in the construction of logical and digital elements and their use in digital machines.

The third group of reports tell of the experience of automation in various branches of industry — machine building, metallurgy, chemistry, energetics, petroleum production, and so on. Much attention is given to problems in the application of digital computing technique for the control of complex technological processes.

It is expected that in June of this year a considerable number of eminent specialists in the field of automation from various countries will meet in Moscow. They will be able to exchange current ideas, scientific engineering problems and the methods of solving them. This will significantly expand the scientific and business contacts of Soviet specialists with their foreign colleagues.

For more comprehensive discussion of the reports presented to the Congress, the texts of the reports were sent beforehand to the participants, which should promote at the Congress a broad scientific discussion of the most important problems of automation. This discussion may evoke independent scientific interest. It will give the participants in the Congress the possibility of profoundly discussing with the authors of reports and other specialists the problems which interest them. Discussion is a manifestation of the creative form of contacts within the framework of the IFAC which enables exposing "white spots in the field of the theory of automatic control, posing new scientific problems, defining the limits of application of the various methods of solving theoretical or applied problems. Soviet scientists and engineers whose work has won universal recognition are preparing with great interest for the Congress and for discussion at the Congress of actual problems of automatic control.

Soviet specialists working in the field of automation will receive in their own country a considerable number of foreign colleagues. They are doing everything they can to assure that this reception will be friendly and mutually advantageous.

The development of scientific contacts between scientists and engineers of different countries which will result from the Congress will undoubtedly have an important value for the further strengthening of peace and friendship between nations.

A MESSAGE FROM THE PRESIDENT OF THE IFAC

Translated from Avtomatika i Telemekhanika, Vol. 21, No. 6, pp. 659-660, June, 1960

The occasion of the First Congress of the International Federation of Automatic Control (IFAC) is a primary event in the life of specialists in automation throughout the world.

It is expected that a very large number of eminent specialists from 30 countries will gather in Moscow in the summer of 1960 and will be able to discuss current ideas, scientific and engineering problems arising in automatics, and the methods of solving them. The principal importance of this event is that the coming Congress, like the earlier assemblies of IFAC, will demonstrate the potential possibilities of science and the acceptability for all of the form of organization of the IFAC, in which the need for cooperation, for a living exchange of scientific ideas and scientific results, is vitally important and inescapable.

The first Congress of the IFAC is a serious event of international significance, destined to exert a notable influence on the development of automation throughout the world; this explains the enormous interest in the Congress on the part of scientists, engineers, and business circles of the various countries.

The first task of IFAC is to conduct this Congress on the highest scientific and engineering level.

The Congress is being conducted with the motto: to theory – practical applicability; to technical resources – maximum reliability; to applications – the greatest effectiveness. It expresses the clear thought of the central administration regarding the creative activity of scientists and engineers throughout the world who have in mind enriching the world with products of material security. The conditions necessary for conducting the Congress have been created.

More than 280 scientific papers are to be discussed. The more active the discussion of the reports, the better IFAC will fulfill its first task. The Organizing Committee of the Congress is enlisting about 100 scientists and engineers from different countries in the posts of section chairmen of the session. They should not only know the reports well and comment on the addresses, but also foresee the possible development of discussion as regards both various aspects of the reports, and the long-range development and application of the ideas they contain.

Discussion at the Congress will be a development of the highest form of scientific contacts within the framework of the IFAC, for which we are striving so much. The IFAC has developed excellent prospects, for future scientific contacts, and in other directions.

The Executive Council of IFAC has formed scientific-technical committees which are beginning work in the following areas:

1. Theory
2. Technical resources
3. Applications of automation
4. Terminology and designations
5. Education
6. Bibliography

The basic task of the committees is to effect the international exchange of scientific information in the field of automation among the member countries of the IFAC.

Scientific connections of the IFAC with other, related international federations are also being developed.

At the present time the IFAC includes the most eminent organizations in the area of automation from 23 countries: Austria, Belgium, Great Britain, the Hungarian People's Republic, Denmark, India, Israel, Italy, the Chinese People's Republic, the Netherlands, Norway, the Polish People's Republic, the Rumanian People's Republic, the USSR, the USA, Turkey, France, Finland, Czechoslovakia, Sweden, Switzerland, Yugoslavia, and Japan.

It is expected that a number of new countries will join the IFAC in the near future.

It is a pleasure for me to mention here that a spirit of excellent, close scientific and business collaboration prevails in our international society, and that this has been shown above all by the fact that in all questions that have arisen in the IFAC, a complete and general agreement has always been reached.

All our meetings which have been held in Germany, France, Switzerland, Italy, and America have taken place with the warm hospitality of the national organizations of the IFAC and their active participation.

The spirit of collaboration in the IFAC is expressed likewise by the fact that a reciprocal exchange of books is developing among the various national organizations of the IFAC, and likewise the visitation of scientific institutions and automated enterprises. Such an exchange of visits and books is of great mutual benefit.

It is to be hoped that the spirit ot collaboration will grow and be strengthened even more during the First Congress of the IFAC.

The National Committee of the Soviet Union has developed a broad program of action in preparation for the Congress, the realization of which is a contribution of the utmost importance to the strengthening and growth of the IFAC.

The spirit of collaboration in the IFAC will serve the strengthening of peace throughout the world.

A. Letov, President of the IFAC

ANALYTICAL CONTROLLER DESIGN. III

A. M. Letov

Moscow

Translated from Avtomatika i Telemekhanika, Vol. 21, No. 6, pp. 661-665, June, 1960

A solution is given of the variational problem of an optimally controlled system when account is taken of servomotor speed limitations.

1. Servomotor. Speed Limitations

In the present paper we shall study the case of analytical controller design when limitations ou servomotor speed are taken into account, a problem which was touched on slightly in [1, 2]. Let us pose the problem. We consider a closed autocontrolled system in which the disturbed motion is given by the equations

$$g_k = \dot{\eta}_k - \left(\sum_\alpha b_{k\alpha}\eta_\alpha + m_k\xi\right) = 0 \quad (k = 1, \ldots, n), \quad \dot{\xi} = f(\sigma) \tag{1.1}$$

Here, the η_k are the coordinates, and the $b_{k\alpha}$ are constant parameters of the object of control, while ξ is the coordinate, and the m_k are parameters of the controlling organ. The function $f(\sigma)$ is the subject of our search.

By basing ourselves on well-known attempts [3]*, we shall assume that $f(\sigma)$ lies in functions of class A', for which the following relationships hold:

$$\sigma f(\sigma) > 0, \quad \sigma \neq 0, \quad \left(\frac{df}{d\sigma}\right)_{\sigma=0} > 0. \tag{1.2}$$

The argument of the function, $\sigma = \sigma(\eta_1, \ldots, \eta_n, \xi)$ is also to be determined.

As the criterion of optimality, we consider the functional

$$I[f(\sigma)] = \int_0^\sigma (V + \dot{\xi}^2)\, dt, \tag{1.3}$$

where V is a positive-definite function of the form

$$V = \sum_k a_k\eta_k^2 + c\xi^2. \tag{1.4}$$

We consider the natural boundary conditions:

$$\begin{gathered}\eta_1(0) = \eta_{10}, \ldots, \ \eta_n(0) = \eta_{n0}, \ \xi(0) = \xi_0, \\ \eta_1(\infty) = \ldots = \eta_n(\infty) = \xi(\infty) = 0.\end{gathered} \tag{1.5}$$

We shall search for those continuous functions ξ, $\eta_1, \ldots, \eta_n$ of class C_1 which, while satisfying (1.1) and boundary conditions (1.5), minimize the functional in (1.3). Equations (1.1) are defined in the open region $N(\xi, \eta_1, \ldots, \eta_n)$, so that the problem just formulated is an ordinary Lagrange variational problem, the procedures for whose solution are well known.

To obtain the equations of the variational problem, we set

$$H = V + f^2(\sigma) + \lambda[\xi - f(\sigma)] + \sum \lambda_k g_k. \tag{1.6}$$

We then write the partial derivatives of the function H:

$$\begin{aligned}&\frac{\partial H}{\partial\dot{\eta}_k} = \lambda_k, \quad &&\frac{\partial H}{\partial\eta_k} = 2a_k\eta_k - \sum_\alpha \lambda_\alpha b_{\alpha k},\\ &\frac{\partial H}{\partial\dot{\xi}} = \lambda, \quad &&\frac{\partial H}{\partial\xi} = 2c\xi - \sum_\alpha m_\alpha\lambda_\alpha,\\ &\frac{\partial H}{\partial\dot{\sigma}} = 0, \quad &&\frac{\partial H}{\partial\sigma} = [2f(\sigma) - \lambda]\frac{\partial f}{\partial\sigma}.\end{aligned}$$

The equations sought have the form

$$\begin{gathered}\dot{\eta}_k = \sum_\alpha b_{k\alpha}\eta_\alpha + m_k\xi, \quad \dot{\xi} = f(\sigma),\\ \dot{\lambda}_k = -\sum_\alpha b_{\alpha k}\lambda_\alpha + 2a_k\eta_k \\ \dot{\lambda} = 2c\xi - \sum_k \lambda_k m_k,\\ 0 = [2f(\sigma) - \lambda]\frac{\partial f}{\partial\sigma} \qquad (k = 1, \ldots, n).\end{gathered} \tag{1.7}$$

2. Solution Abutting the Optimal Curve's Left End

We shall study the solution of the problem for the two cases presented by the last equation of (1.7).

We consider the first case:

$$\frac{\partial f}{\partial\sigma} = 0. \tag{2.1}$$

---

* In autocontrol systems such as (1.1), the function σ describes the control law, and depends on $\eta_1, \ldots, \eta_n, \xi$.

If we are considering class A' functions, then there exists a positive number σ_* such that, from (2.1), we find

$$f(\sigma) = \pm \bar{f}, \quad |\sigma| \geqslant \sigma_*. \tag{2.2}$$

Thus, the controller equation is defined everywhere for $|\sigma| \geq \sigma_*$, although the number σ_* itself is still unknown.

Let

$$\Delta(\rho) = |b_{k\alpha} - \rho\delta_{k\alpha}| \tag{2.3}$$

be the determinant system (1.1) for $m_k = 0$. Then Solution (2.2) of system (1.1) is written in the following form:

$$\begin{gathered} \eta_k = \sum_{s=1}^{n} \Delta_k(\rho_s) C_s e^{\rho_s t} + M_k + N_k t, \\ \xi = \bar{C} \pm \bar{f}t, \\ \lambda_k = \sum_{s=1}^{n} \bar{\Delta}(-\rho_s) \bar{D}_s e^{-\rho_s t} + \varphi_k(t), \\ \lambda = \bar{D} + \psi(t) \end{gathered} \tag{2.4}$$

Here, ρ_k are simple roots of the equation $\Delta(\rho) = 0$, while $-\rho_k$ are simple roots of the equation

$$\bar{\Delta}(\rho) = |-b_{\alpha k} - \rho\delta_{\alpha k}| = 0; \tag{2.5}$$

$M_k + N_k t$, $\varphi_k(t)$, $\psi(t)$ are the corresponding particular solutions arising from the appearance of the line integral for the function ξ; Δ_k are the minors of the determinant in (2.3) and $\bar{\Delta}_k$ are the minors of the determinant in (2.5) corresponding to the elements with ordinal number k in the first row; $\bar{C}_1, \ldots, \bar{C}_n, \bar{C}, \bar{D}, \bar{D}_1, \ldots, \bar{D}_n$ are the $2n + 2$ arbitrary constants. We call the function defined by (2.4) a solution abutting the left (initial) end of the optimal curve ($t = 0$).

This solution will be necessary only for the verification that the boundary conditions hold.

3. Solution Abutting the Optimal Curve's Right End

We now consider the second case presented by the last of Eqs. (1.7)

$$2f(\sigma) = \lambda \tag{3.1}$$

System (1.7) becomes linear with constant coefficients:

$$\begin{gathered} \dot{\eta}_k = \sum_\alpha b_{k\alpha}\eta_\alpha + m_k\xi, \\ 2\ddot{\xi} = 2c\xi - \sum_k m_k\lambda_k, \\ \dot{\lambda}_k = -\sum_\alpha b_{\alpha k}\lambda_\alpha + 2a_k\eta_k \qquad (k = 1, \ldots, n) \end{gathered} \tag{3.2}$$

Let

$$\nabla(\mu) = \left|\begin{array}{l} b_{11} - \mu, \ldots \quad b_{1n}, \; . \; m_1 \ldots\ldots, 0 \ldots\ldots, 0 \\ \cdots\cdots\cdots\cdots\cdots\cdots\cdots\cdots\cdots\cdots \\ b_{n1}, \ldots\ldots, b_{nn} - \mu m_n, \quad \ldots 0 \ldots\ldots, \bar{0} \\ 0, \ldots\ldots, 0, \ldots, 2c, -2\mu^2, -m_1, \ldots, -m_n \\ 2a_1, \ldots\ldots, 0, \; . \; 0, \ldots\ldots -b_{11} - \mu, \; ., -b_{n1} \\ \cdots\cdots\cdots\cdots\cdots\cdots\cdots\cdots\cdots\cdots \\ 0, \ldots\ldots, 2a_n, \; . \; 0, \ldots\ldots -b_{1n}, \ldots, -b_{nn} - \mu \end{array}\right| \tag{3.3}$$

be the determinant of the system. It is easily proven that, if $\mu_1, \ldots, \mu_n$ are simple roots of the equation $\nabla(\mu) = 0$, then $-\mu_1, \ldots, -\mu_n$ will also be simple roots of this equation. For the proof of this assertion, it suffices to execute the following operations:

1) write the determinant $\nabla(-\mu)$,

2) transpose the middle row downwards,

3) transpose the first n rows downwards,

4) in the determinant thus formed, transpose the middle column to the right, making it the last column,

5) transpose the first n columns to the right.

As the result of these operations, we obtain the determinant

$$\nabla(-\mu) = \left|\begin{array}{l} -b_{11} + \mu, \ldots, -b_{n1}, \quad 0, \quad 2a_1, \ldots, \quad 0 \\ \cdots\cdots\cdots\cdots\cdots\cdots\cdots\cdots\cdots\cdots \\ -b_{1n}, \ldots, \quad -b_{nn} + \mu, \quad 0, \quad 0, \ldots, \quad 2a_n \\ -m_1, \ldots\ldots, -m_n, \quad 2c - 2\mu^2, \; 0, \ldots, \quad 0 \\ 0, \ldots, \quad 0, \quad m_1, \; b_{11} + \mu, \ldots, \; b_{1n} \\ \cdots\cdots\cdots\cdots\cdots\cdots\cdots\cdots\cdots\cdots \\ 0, \ldots, \quad 0, \quad m_n, \; b_{n1}, \ldots, \; b_{nn} + \mu \end{array}\right|$$

Now, in order to convince ourselves of the validity of our assertion, it suffices to:

a) take out the minus signs in the first n columns and make them rows;

b) multiply the last n rows by -1 and make them columns.

If, with such transpositions, the column numbers become row numbers and conversely, we obtain, after their termination, the following identity:

$$\nabla(\mu) = \nabla(-\mu). \tag{3.4}$$

To complete the argument, we recall the possibility of so numbering the roots that the following condition holds:

$$\operatorname{Re}\mu_k \leqslant 0 \quad (k = 1, \dots n+1). \tag{3.5}$$

Then, taking the conditions at infinity into account, we write the solution of Eqs. (3.2) in the following form:

$$\begin{aligned}\eta_k &= \sum_{s=1}^{n+1} \Delta_k(\mu_s) c_s e^{\mu_s t},\\ \xi &= \sum_{s=1}^{n+1} \Delta_{n+1}(\mu_s) c_s e^{\mu_s t},\\ \lambda &= 2\sum_{s=1}^{n+1} \mu_s \Delta_{n+1}(\mu_s) c_s e^{\mu_s t},\\ \lambda_k &= \sum_{s=1}^{n+1} \Delta_{n+1+k}(\mu_s) c_s e^{\mu_s t}.\end{aligned} \tag{3.6}$$

Here, the Δ_r are the minors of determinant (3.3) with respect to the elements of r of the first row, and the c_r are constants of integration.

To obtain the controller's equation for the open region, it suffices to take the first n + 2 rows of formulas (3.6) and to eliminate time. This equation has the form

$$\begin{vmatrix} \Delta_1(\mu_1), & \dots, & \Delta_1(\mu_{n+1}), & \eta_1 \\ \dots & \dots & \dots & \dots \\ \Delta_n(\mu_1), & \dots, & \Delta_n(\mu_{n+1}), & \eta_n \\ \Delta_{n+1}(\mu_1), & \dots, & \Delta_n(\mu_{n+1}), & \xi \\ \mu_1\Delta_{n+1}(\mu_1), & \dots, & \mu_{n+1}\Delta(\mu_{n+1}), & \dot{\xi} \end{vmatrix} = 0. \tag{3.7}$$

After expanding the determinant, we find

$$\dot{\xi} = \sum_{\alpha=1}^{n} p_\alpha \eta_\alpha - r\xi \tag{3.8}$$

which is a linear equation with constant coefficients.

We must now convince ourselves of the possibility of determining the arbitrary constants of integration. Formulas (2.4) and (3.6) contain 3n + 3 constants of integration. For their determination we have the n + 1 initial conditions and the 2n + 2 continuity conditions for the functions ξ, $\eta_1, \dots, \eta_n$, $\lambda_1, \dots, \lambda_n$, λ at the point σ_*, and also the continuity condition for the function $f(\sigma)$ which we are seeking. We now show how to find this function and the constant σ_* simultaneously.

Let

$$\frac{1}{h}\left(\sum_{\alpha=1}^{n} p_\alpha \eta_\alpha - r\xi\right) = \sigma, \tag{3.9}$$

where h is some positive constant.

Equation (3.8) gives

$$\dot{\xi} = h\sigma. \tag{3.10}$$

To determine the magnitude of σ_* we find

$$h\sigma_* = \bar{f}. \tag{3.11}$$

Thus, the final form of the controller equation is

$$\dot{\xi} = \begin{cases} +\bar{f} & \text{for } \sigma \geqslant \sigma_*,\\ h\sigma & \text{for } |\sigma| < \sigma_*,\\ -\bar{f} & \text{for } \sigma \leqslant \sigma_*. \end{cases} \tag{3.12}$$

4. Two Problems

What has been presented allows us to formulate two problems. The first of them consists of the following. Given that linear system (1.1), (3.9), (3.10) is stable for any deviations. Consequently, nonlinear optimal system (1.1), (3.9), (3.12) is stable at least for any disturbances with respect to σ which satisfy the inequality $|\sigma| \leq \sigma_*$. By virtue of the continuity property of the region of attraction, this system is extended to the limits $|\sigma| = \sigma_*$. It is required to determine the boundaries of the region of attraction.

Second problem: We consider the functional in (1.3), and remove the term ξ^2 from it. Equations (1.7) of the variational problem then give the solution $f(\sigma) = \bar{f}\operatorname{sign}\sigma$. This solution is compatible with the Weierstrass-Erdmann conditions. It is required to determine the construction of the switching function $\sigma = \sigma(\eta_1, \dots, \eta_n, \xi)$.

5. Example

In the case n = 1, $b_1 = b$, $m_1 = m$, $a_1 = a$, we have the characteristic equation

$$\mu^4 - (b^2 + c)\mu^2 + am^2 + cb^2 = 0, \tag{5.1}$$

and the controller equation in the open region is written in the form

$$\dot{\xi} = -\frac{(\mu_1 - b)(\mu_2 - b)}{m}\eta + (\mu_1 + \mu_2 - b)\xi. \quad (5.2)$$

This equation coincides with Eq. (5.4) which was found in [1, 2].

We easily convince ourselves that, in the general case, Eq. (3.8) coincides exactly with Eq. (4.5) of work [1], which was found for an open region, and with Eq. (3.9) of work [2] for regions bounded with respect to the angle of deviation of the controlling organ.

From this there derives the interesting conclusion that, everywhere in the open region, the formula for the optimal controller is the same, and is determined only by the functional adopted as the criterion.

As in work [2], the question as to the stability of system (1.1), (3.12) must be considered separately.

The author is deeply grateful to N. N. Krasovskii for his very useful remarks and advice in regard to the problem considered here.

LITERATURE CITED

1. A. M. Letov, "Analytical controller design. I", Avtomatika i Telemekhanika 21, 4 (1960).†
2. A. M. Letov, "Analytical controller design. II", Avtomatika i Telemekhanika 21, 5 (1960).†
3. A. M. Letov, Stability of Nonlinear Controlled Systems [in Russian] (Gostekhizdat, 1955).

---

† See English translation.

INVESTIGATION OF PROBABILITY STABILITY USING EXAMPLE OF AUTOMATIC CONTROL OF AIRCRAFT COURSE

V. S. Novoselov

Leningrad

Translated from Avtomatika i Telemekhanika, Vol. 21, No. 6, pp. 666-673, June, 1960

Definitions are given for weak and strong probability stability of undisturbed motion. The concept of weak stability is a variation, and something of a generalization, of the definition of stability with respect to upper limits of dispersion [1]. The definition of strong stability is close to the concepts of probability stability given in [2-5]. With the example of aircraft course stabilization by means of an autopilot with a constant speed servomotor, the attempt is made to construct a methodology for the investigation of automatic control and regulation systems as regards their probability stability.

1. Let the motion of an automatic regulation or control system be defined by differential equations with random parameters and by random disturbing forces which we shall call, in their totality, random factors.

In the absence of random factors, the system's motion will be called undisturbed. We consider the random process $\{x_i(t)\}$ $(i = 1, 2, \ldots, n)$ of deviations from undisturbed motion by the system, and the n-dimensional band of width ϵ.

We denote by $\tau(\epsilon, T)$ the length of time during which, in a total time interval of duration T, some selected realization of the random process lies within the ϵ-band, i.e., $|x_i(t)| \leq \epsilon$ for $0 \leq t \leq T$.

The relative time spent by the given realization in the ϵ-band during time interval T equals

$$\nu(\epsilon, T) = \tau(\epsilon, T)/T.$$

Since the occurrence of some realization or another is a random phenomenon, then $\nu(\epsilon, T)$ is also a random variable.

Let there exist two positive numbers $Q_1 < 1$ and $Q_2 \leq 1$ such that

$$P\{\nu(\varepsilon, T) > Q_1\} > Q_2, \qquad (1.1)$$

where the symbol P denotes the probability of the event cited within the braces. In this case, we shall say that the random process $\{x_i\}$, during time T, is found in the ϵ-band with relative time Q_1 and with a probability not less than Q_2.

If the following relationship holds:

$$P\{\nu(\varepsilon, T) = 1\} > Q \quad (0 < Q < 1), \qquad (1.2)$$

than the random process $\{x_i\}$ during time interval T lies completely within the ϵ-band with a probability not less than Q.

The quantities ϵ, Q_1, Q_2 and Q give a graphic quantitative estimate in the probabilistic sense of the stability of undisturbed motion during the finite time interval T.

The following definitions of probability stability of undisturbed motion can be put forth.

We call an undisturbed motion weakly probabilistically stable with respect to the admissible set of random factors if, for all $\epsilon > 0$ and for any positive numbers arbitrarily close to unity $Q_1 < 1$, $Q_2 \leq 1$, there exists a subset of random factors for which Relationship (1.2) holds for infinitely large T.

We call an undisturbed motion strongly probabilistically stable with respect to the admissible set of random factors if, for all $\epsilon > 0$ and for a positive number $Q \leq 1$ which is arbitrarily close to unity, there exists a subset of random factors for which relationship (1.2) holds for infinitely large T.

As follows from the definitions, the property of an undisturbed motion to be weakly or strongly probabilistically stable is related to the concept of admissible random factors. A motion which is stable for some admissible random factors may be unstable for another set of them. The adoption of one or another set of admissible random factors will make concrete the concepts of stability just introduced.

Theorem 1. If the process $\{x_i\}$ has zero mathematical expectation and, for all $\delta > 0$, there exists a subset of random factors for which $\tilde{\sigma}_i < \delta$, where $\tilde{\sigma}_i$ is the time average of the dispersion of the process $\{x_i\}$, then the undisturbed motion is weakly probabilistically stable.

We give proof of this theorem, without pretending, however, to complete mathematical rigor.

For the random process $\{x_i(t)\}$ $(i = 1, 2, \ldots, n)$, let there exist a continuous distribution function

$$F(\xi_i, t) = P\{x_i \leqslant \xi_i, t\}.$$

We introduce the random function

$$\varphi(\varepsilon, t) = \begin{cases} 1, \text{ if } \ |x_i| \leqslant \varepsilon, \\ 0, \text{ if, for at least one subscript } j \ |x_j| > \varepsilon, \end{cases}$$

Functions of this type are used in many works [6-8]. For $\nu(\epsilon, T)$ we will have

$$\nu(\varepsilon, T) = \frac{1}{T}\int_0^T \varphi(\varepsilon, t)\,dt.$$

We set up the Chebyshev inequality

$$P\{\mu(\varepsilon, T) \geqslant 1 - Q_1\} \leqslant \frac{M[\mu(\varepsilon, T)]}{1 - Q_1}, \quad (1.3)$$

where M is the symbol for mathematical expectation and $\mu(\epsilon, T(= 1 - \nu(\epsilon, T)(0 < Q_1 < 1)$. We have

$$M[\nu(\varepsilon, T)] = \frac{1}{T}\int_0^T M[\varphi(\varepsilon, t)]\,dt =$$

$$\frac{1}{T}\int_0^T P\{|x_i| \leqslant \varepsilon, t\}\,dt. \quad (1.4)$$

where the symbol ~ denotes an average over the infinite time interval.

Since

$$\widetilde{P}\{|x_i| \leqslant \varepsilon\} > \widetilde{F}(\varepsilon) - \widetilde{F}(-\varepsilon),$$

On the basis of formulas (1.3) and (1.4), we obtain an estimate of the relative time $\nu(\epsilon)$ spent by the process in the ϵ-band during the course of an infinite interval of time:

$$P\{\nu(\varepsilon) > Q_1\} \geqslant \frac{\widetilde{P}\{|x_i| \leqslant \varepsilon\} - Q_1}{1 - Q_1},$$

where $\widetilde{F}(\epsilon)$ and $\widetilde{F}(-\epsilon)$ denote the average distribution function, taken for the values $\xi_i = \epsilon$ and $\xi_i = -\epsilon$ ($i = 1, 2, \ldots, n$) respectively, we then find that

$$P\{\nu(\varepsilon) > Q_1\} > \frac{\widetilde{F}(\varepsilon) - \widetilde{F}(-\varepsilon) - Q_1}{1 - Q_1}.$$

In the case of stationary processes, the probability functions do not depend on time, so that we shall have

$$\widetilde{P}\{|x_i| \leqslant \varepsilon\} = P\{|x_i| \leqslant \varepsilon, 0\};\ \widetilde{F}(\varepsilon) = F(\varepsilon, 0),\ \widetilde{F}(-\varepsilon) = F(-\varepsilon, 0).$$

For the dispersion of a random process with zero mathematical expectation, we have the obvious estimate

$$\sigma_i^2(t) \geqslant \varepsilon^2 P_i(\varepsilon, t),$$

where ϵ is an arbitrarily small positive number. Moreover,

$$P_i(\varepsilon, t) = P\{|x_i| \geqslant \varepsilon, -\infty < x_j < \infty\} \quad (j = 1, 2\ldots, i-1, i+1, \ldots, n).$$

We therefore obtain

$$P\{|x_i| < \varepsilon, t\} \geqslant 1 - \frac{1}{\varepsilon^2}\sum_{i=1}^{n} \sigma_i^2(t).$$

By taking the time average, we find that

$$\widetilde{F}(\varepsilon) - \widetilde{F}(-\varepsilon) > 1 - \frac{1}{\varepsilon^2}\sum_{i=1}^{n} \widetilde{\sigma}_i^2.$$

By virtue of Formula (1.5), we shall have

$$P\{\nu(\varepsilon) \geqslant Q_1\} > 1 - \frac{\sum_{i=1}^{n} \widetilde{\sigma}_i^2}{\varepsilon^2(1 - Q_1)}.$$

Therefore, the random process being considered, during an infinite segment of time, will find itself in the ϵ-band for relative time Q_1 with probability Q_2, these quantities satisfying the relationships

$$Q_2 = 1 - \frac{n\sigma^2}{\varepsilon^2(1 - Q_1)}, \quad \widetilde{\sigma}_i \leqslant \sigma. \quad (1.6)$$

From whence it follows that the undisturbed motion will be weakly probabilistically stable if the time average of the dispersion can be made arbitrarily small. Indeed, for any Q_1 and Q_2 which are arbitrarily close to unity, there exists a sufficiently small σ which satisfies relationships (1.6).

Theorem 1 is thereby proven.

We note that, for stationary processes, the dispersions do not depend on time, so that $\widetilde{\sigma}_i = \sigma_i(0)$.

Let an automatically controlled system be described by the equations

$$\frac{dx_i}{dt} = X_i(x_1, x_2, \ldots, x_n, t) + f_i(t) \quad (i = 1, 2, \ldots, n) \quad (1.7)$$

with random functions $f_i(t)$ and random initial data x_i^0.

We shall study the behavior of the process $\{x_i\}$ for small-size random factors $f_i(t)$ and x_i^0, i.e., for arbitrarily small $\alpha > 0$ and $\beta > 0$ and numbers $A > 0$ and $B > 0$ arbitrarily close to unity in the relationships

$$P\{|f_i(t)| < \alpha\} > A, \quad P\{|x_i^0| < \beta\} > B. \quad (1.8)$$

With such a choice of the random factors, the following theorem is valid.

Theorem 2. If the null solution of system (1.7) is stable for constantly acting disturbances [9], then it will be strongly probabilistically stable with respect to the upper limits of the disturbing functions and the initial data.

To find sufficient conditions for strong probability stability, both for linear and nonlinear control systems, one can use the method of constructing A. M. Lyapunov's functions [9] if the conditions of the corresponding Lyapunov theorems hold for a sufficiently large number of realizations.

It is necessary to mention that stability for constantly acting disturbances is not always decisive in establishing strong probability stability. It can happen that the solution of system (1.7) may turn out to be Lyapunov-stable for some functions $f_i(t)$ and unstable for others. If the probability of finding the realizations $\{f_i(t)\}$ in the first of these sets can be assumed to be sufficiently great, then the solution of system (1.7) will possess strong stability. The bandwidth ϵ can be made arbitrarily small by the proper choice of initial data.

We consider the system of linear differential equations

$$\frac{dx_i}{dt} = \sum_{j=1}^{n} a_{ij}x_j + f_i(t).$$

As is well known [10], the solution of this system is given in the form

$$\left\| \begin{matrix} x_1 \\ x_2 \\ \cdot \\ \cdot \\ \cdot \\ x_n \end{matrix} \right\| = X(t) \left\| \begin{matrix} x_1^0 \\ x_2^0 \\ \cdot \\ \cdot \\ \cdot \\ x_n^0 \end{matrix} \right\| + \int_0^t X_1(t, u) \left\| \begin{matrix} f_1(u) \\ f_2(u) \\ \cdot \\ \cdot \\ \cdot \\ f_n(u) \end{matrix} \right\| du \qquad (1.9)$$

Here, $X(t)$ is the normal fundamental matrix solution of the homogeneous system.and $X_1(t, u) = X(t)X^{-1}(u)$, where $X^{-1}(u)$ is the inverse matrix of $X(u)$.

If, for definite values of α and β, values of A and B satisfying inequalities (1.8) be known, then from formula (1.9), one can determine the quantities $\epsilon > 0$ and $Q > 0$ such that the random process $\{x_i\}$ will be found in the ϵ-band for any time interval T.

The necessary and sufficient condition for stability of a linear system for constantly acting disturbances has the form

$$\int_0^\infty |x_{ij}^1(t, u)|\, du < \infty. \qquad (1.10)$$

where the x_{ij}^1 are elements of the matrix $X_1(t, u)$.

The correlation matrix of the solution of the system of linear differential equations equals [11].

$$R(t, \tau) = X(t+\tau)\, r_1 \overline{X}(t) + \int_0^{t+\tau} du_1 \int_0^t X_1(t+\tau, u_1)\, r_2(u_1, u_2)\, \overline{X}_1(t, u_2)\, du_2, \qquad (1.11)$$

where r_1 is the correlation matrix of the original data, $r_2(u_1, u_2)$ is the correlation matrix of the input process; a superscript bar denotes the conjugate of the function. Let a_{ij} = const and let the roots of the characteristic equation have negative real parts; then, by transforming the equation to canonical variables, one can convince oneself that condition (1.10) holds.

In this case, for all $\mu > 0$, one can find $\nu_1 > 0$ and $\nu_2 > 0$ such that, for $|r_{ij}^1| < \nu_1$ and $|r_{ij}^2| < \nu_2$, we obtain $|R_{ij}(t, \tau)| < \mu$. Here, we have denoted by r_{ij}^1, r_{ij}^2 and R_{ij} the elements of the correlation matrices r_1, r_2 and R, respectively. Further, we have $\sigma_i = R_{ii}(t, 0)$ and, consequently, $\tilde{\sigma}_i < \mu$. From whence, based on Theorem 1, we are led to the proof of the following theorem:

Theorem 3. If the roots of the characteristic equation of a system of linear differential equations with constant coefficients have negative real parts, then its solution, for null initial data and disturbing functions, equal to $M[f_i(t)]$, is weakly probabilistically stable with respect to the upper bounds of the dispersions of the input process and the initial data.

For definite ν_1 and ν_2, one can determine from formula (1.11) the upper bound of the dispersion of the random process deviations of the disturbed motion from the undisturbed. After this, for selected ϵ and Q_1, one easily finds from (1.6) the definite probability of finding this process in the ϵ-band for relative time Q_1 over an infinite interval.

2. We illustrate the results of Section 1 by the example of a system of automatic aircraft course control by means of an autopilot.

With certain simplifying assumptions, the equations of the controlled system are written in the form [12-13]

$$\ddot{\varphi} + M\dot{\varphi} = -N\eta,\ \dot{\eta} = F(\psi),\ \ \psi = \varphi + \beta\dot{\varphi} - \frac{1}{a}\eta. \qquad (2.1)$$

Here, φ is the aircraft's yaw angle, η is the angle of rudder rotation, M and N are constants characterizing, respectively, the aircraft's natural damping and the effectiveness of the rudder device. ψ is the argument of the servomotor, β is the coefficient of artificial damping, $1/a$ is the feedback coefficient. All coefficients in these equations are positive. The servomotor characteristic $F(\psi)$ has the form

$$F(\psi) = \begin{cases} K & \text{for} \quad \psi > \psi_0 \\ 0 & \text{for} \quad |\psi| \leqslant \psi_0 \\ -K & \text{for} \quad \psi < -\psi_0, \end{cases} \qquad (2.2)$$

where $K > 0$ is the servomotor's constant speed, $2\psi_0 > 0$ is the width of the symmetric insensitivity zone.

Let the aircraft's flight, the direction of motion of which is controlled by the autopilot, occur in air layers, the density of which is a random variable. We shall therefore set $M = m\gamma$ and $N = n\gamma$. Here, m and n are positive constants, γ is the air density, taking the form of a piecewise constant random variable.

We introduce the following notation, which is convenient for the problem under consideration [13]:

$$x_1 = \frac{M^2}{N}\dot{\varphi} + M\eta, \quad x_2 = -M\eta,$$

$$x_3 = \frac{M^2}{N\beta}\psi = \frac{M^2}{N}\left(\frac{\varphi}{\beta} + \dot{\varphi} - \frac{\eta}{a\beta}\right), \qquad t' = Mt$$

and the dimensionless coefficients

$$\alpha = \frac{1}{\beta M}, \qquad r = \frac{M}{a\beta N},$$

$$F(\psi) = F\left(\frac{N\beta}{M^2}x_3\right) = F'(x_3).$$

By taking the derivatives with respect to t' of x_1, x_2, and x_3, we get, by virtue of (2.1),

$$\frac{dx_1}{dt'} = -x_1 + F'(x_3), \qquad \frac{dx_2}{dt'} = -F'(x_3),$$
$$\frac{dx_3}{dt'} = (\alpha - 1)x_1 + \alpha x_2 - rF'(x_3). \tag{2.3}$$

The derivative of the positive-definite function

$$V = \frac{|\alpha - 1|}{2}x_1^2 + \frac{\alpha}{2}x_2^2 + \int_0^{x_3} F'(x_3)\,dx_3,$$

computed with account taken of system (2.3), has the form

$$\frac{dV}{dt'} = -|\alpha - 1|x_1^2 + (\alpha - 1 + |\alpha - 1|)x_1F'(x_3) - rF'^2(x_3).$$

We obtain from this dV/dt < 0 if the following condition holds:

$$M\left(\frac{M}{a} + N\beta\right) - N > 0. \tag{2.4}$$

Condition (2.4) is equivalent to the inequality

$$\gamma > \gamma_1, \quad \gamma_1 = \frac{an}{m(m + an\beta)}.$$

The density of air can be considered bounded, so that we find such a sufficiently large number γ_2 that, with probability equal to unity, we get $\gamma < \gamma_2$.

Let the probability be larger than some number Q' that there appear a realization for which, during the entire time of motion, $\gamma_1 < \gamma < \gamma_2$. We denote by l_ϵ the least value of the function $V(x_1, x_2, x_3; \gamma)$ on the set for which $\gamma_1 \leq \gamma \leq \gamma_2$; one of the coordinates x_i is equal in absolute magnitude to ϵ; the remaining ones are less than or equal to ϵ.

Let there be known a quantity Q" such that

$$P\{|x_i^0| < \delta\} > Q'', \tag{2.5}$$

where δ will be less than ϵ, and is defined by the condition

$$\int_0^{\delta} F'(x_3)\,dx_3 + \frac{\alpha}{2}\delta^2 + \frac{|\alpha - 1|}{2}\delta^2 < l_\epsilon$$

for any α which satisfies the inequality

$$\frac{1}{\beta m\gamma_2} \leqslant \alpha \leqslant \frac{1}{\beta m\gamma_1}.$$

By assuming that the choice of initial data and the inhomogeneity of the atmosphere are statistically independent events, we obtain, by virtue of the well-known Lyapunov theorem on stability of motion [9], the expression

$$P\{\nu(\varepsilon) = 1\} > Q,$$

where

$$Q = Q' \cdot Q''. \tag{2.6}$$

Therefore, the random process of deviations of direction of motion of the aircraft from the given course is found completely in the ϵ-band with probability Q.

If the aforementioned events are dependent, then Q" in formula (2.6) must be replaced by the conditional probability of the event defined by formula (2.5), given that the event characterized by the formula $\gamma_1 < \gamma < \gamma_2$ has occurred.

Let $\gamma^* = M[\gamma]$ satisfy the condition $\gamma_1 < \gamma^* < \gamma_2$, which is equivalent to the meeting of condition (2.4) in the absence of random factors. It should be remarked that condition (2.4) is essential, since [12] it will be necessary and sufficient for the Lyapunov stability of the null solution of system (2.1).

In considering the density γ, differing slightly, probabilistically, from γ^*, we arrive at the following conclusion, based on our previous consideration. The aircraft motion with zero initial data and with atmospheric density γ^* is strongly probabilistically stable with respect to the upper bounds of the initial data and to the differences $\gamma - \gamma^*$.

We now turn to the consideration of weak probabilistic stability of the aircraft's course.

We shall assume that the aircraft is acted upon by random gusts of wind, shock waves and other stimuli whose effect on aircraft yaw may be taken into account by the introduction of the random function $f(t)$ in the right member of the first equation of system (2.1). This function equals the ratio of the torque induced by these stimuli to the aircraft's moment of inertia with respect to the yaw axis. We shall also assume that the necessary probabilistic characteristics of the one-dimensional random process $f(t)$ are given.

For action of the disturbance $f(t)$, let the nonlinear element with characteristic given by (2.2) admit the statistical linearization [14]

$$F(\psi) = k_0 M[\psi] + k_1(\psi - M[\psi]), k_0 = \text{const}, k_1 = \text{const}.$$

With this, the coefficient k_1 for the nonlinear characteristic of (2.2) is greater than zero.

The mathematical expectations $M[\varphi]$, $M[\dot{\varphi}]$, $M[\psi]$, and $M[\eta]$ will satisfy system (2.1) if, in the right number of the first equation, one adds the function of time $M[f(t)]$ and, in the right member of the second equation, one replaces the existing function by $k_0 M[\psi]$.

The random process of deviations of the aircraft's motion from the mathematical expectation is defined by the equations

$$\begin{gathered}\ddot{\varphi}' + M\dot{\varphi}' = -N\eta' + f'(t),\\ \dot{\eta}' = k_1\psi',\\ \psi' = \varphi' + \beta\dot{\varphi}' - \frac{1}{a}\eta',\end{gathered} \qquad (2.7)$$

where the primes denote the differences of the corresponding variables from their mathematical expectations.

For the case under consideration, we introduce the notation

$$x_1 = \varphi', \quad x_2 = \dot{\varphi}', \quad x_3 = \eta'.$$

Then, system (2.7) takes the form

$$\frac{dx_1}{dt} = x_2, \quad \frac{dx_2}{dt} = -Mx_2 - Nx_3 + f'(t),$$
$$\frac{dx_3}{dt} = k_1\left(x_1 + \beta x_2 - \frac{1}{a}x_3\right).$$

We find the characteristic equation for the homogeneous system:

$$\lambda^3 + \left(M + \frac{k_1}{a}\right)\lambda^2 + k_1\left(\frac{M}{a} + N\beta\right)\lambda + k_1 N = 0. \qquad (2.8)$$

The coefficients of the third-degree polynomial in (2.8) are positive. Therefore, if the following condition (the second Hurwitz condition) is met:

$$\left(M + \frac{k_1}{a}\right)\left(\frac{M}{a} + N\beta\right) - N > 0 \qquad (2.9)$$

the roots of characteristic Eq. (2.8) have negative real parts.

Relationship (2.9) holds for any positive k_1 if the coefficients of (2.1) satisfy condition (2.4).

On the basis of Theorem 3, we are led to the following conclusion. If condition (2.4) is met, then the undisturbed motion ($M[\varphi]$, $M[\dot{\varphi}]$, $M[\psi]$ and $M[\eta]$) is weakly probabilistically stable with respect to the upper boundaries of the dispersion of the disturbing torque and of the initial data.

We note that, for $M[f(t)] = 0$, the null solution $\varphi = \dot{\varphi} = \psi = \eta = 0$ will be undisturbed.

LITERATURE CITED

1. N. D. Moiseev, "On the probabilistic treatment of the concepts of 'stability of motion'," Uch. Zap. Rostovsk. n/D Gos. Univ. 18, 3 (1953).
2. N. D. Moiseev, "On Lyapunov probability stability", Doklady Akad. Nauk SSSR No. 5 (1936).
3. N. D. Moiseev, "Über stabilitäts Wahrscheinlichkeitsrechnung," Mathematische Zeitschrift 42 (1937).
4. V. V. Stepanov, "On the definition of probability stability," Doklady Akad. Nauk SSSR No. 8 (1938).
5. I. I. Vorovich, "On the stability of motion for random disturbances," Izvest. AN SSSR, Ser. Matemat. 20, 1 (1956).
6. Yu. V. Linnik and A. P. Khusu, "Mathematical-statistical description of surface irregularities for grinding," Inzh. Sborn. 20 (1954).
7. A. P. Khusu, "On certain functionals given on surfaces, which arise in engineering," Vestn. LGU No. 1 (1948).
8. A. P. Vorob'ev, "Some investigations of ship roll by methods of probability theory," Uch. Zap. Leningr. Gos. Univ. No. 217 (Mekhanika, 1957).
9. N. G. Chetaev, Stability of Motion [in Russian] (Gostekhizdat, 1955).
10. V. V. Nemytskii and V. V. Stepanov, Qualitative Theory of Differential Equations [in Russian] (Gostekhizdat, 1949).
11. Yu. V. Linnik and V. S. Novoselov, "Random disturbances or regular gyroscope precession," Prikl. Matem. i Mekh. 17, 3 (1953).
12. A. A. Andronov and N. N. Bautin, "Theory of course stabilization of neutral aircraft with constant servomotor speed autopilots," Izvest. AN SSSR Otd. Tekhn. Nauk 3, 6 (1955).
13. A. A. Fel'dbaum, Introduction to the Theory of Nonlinear Circuits [in Russian] (Gosénergoizdat, 1948).
14. I. E. Kazakov, "Approximate probabilistic analysis of operational accuracy of essentially nonlinear automatic systems," Avtomatika i Telemekhanika 17, 5 (1956).*

---

*See English translation.

THE PROBLEM OF SHAPING FILTERS AND OPTIMAL LINEAR SYSTEMS

Yu. P. Leonov

Moscow

Translated from Avtomatika i Telemekhanika, Vol. 21, No. 6, pp. 674-681, June, 1960

It is shown that, under sufficiently general conditions, a nonstationary random process can be formed from "white noise" by means of linear filters. The weight functions of the shaping filters are determined.

1. Posing of the Problem

Given a random function Y(t) ($-\infty < t < +\infty$) which is stationary "white noise" with mathematical expectation $M[Y] = 0$, correlation function $k_y(u) = \delta(u)$ and spectral density function $G(\omega) = 1/2\pi$. It is necessary to show that a nonstationary random function X(t), with $M[X] = 0$, ($0 < t < T$) may, under certain conditions, be presented in the form

$$X = A_x Y \tag{1}$$

where the operator A_x is defined if the function X(t) is given.*

In work [1], expression (1) is called the integral canonical representation of the random function X(t). The problem posed here is also called the problem of constructing a shaping filter.

We shall also consider here the inverse problem of presenting the "white noise" Y(t) in terms of X(t). In this case,

$$Y = A_x^{-1} X. \tag{2}$$

2. Solution of the Problem

Let Y(t) ($-\infty < t < +\infty$) be a stationary random function with correlation function $k_y(u) = \delta(u)$ and spectral density function $G(\omega) = 1/2\pi$ ($-\infty < \omega < +\infty$). The function Y(t) is frequently called "white noise", since it contains all frequencies with identical dispersion density.

It is well known [1] that a random function Z(t) can be presented as a series (canonical expansion)

$$Z(t) = \sum_{k=1}^{\infty} B_k z_k(t), \tag{3}$$

where the random variables satisfy the conditions

$$M[B_j B_i] = \delta_{ji} D_j = \begin{cases} D_j & \text{for} \quad j = i \\ 0 & \text{for} \quad j \neq i \end{cases} \tag{4}$$

and the $z_k(t)$ are some regular (nonrandom) functions [1].

In order that series (3) converge in the mean† to the function Z(t), according to the basic lemma of correlation theory [2], it is necessary and sufficient that the series

$$k_z(t_1, t_2) = \sum_{k=1}^{\infty} D_k^z z_k(t_1) z_k(t_2) \tag{5}$$

converge to the correlation function in the usual sense. With this, the definition of convergence in the mean is meaningful only for random functions with finite dispersion

To solve the basic problem, it is necessary for us to present the function Y(t) in the form of (3). We therefore, consider this problem first. In order to represent the function Y(t) by the series of (3), it is necessary to introduc a new concept of convergence. Convergence in the mean can obviously not be used, since the function Y(t) has infinite dispersion. Specifically, we shall say that the random function $U_n(t)$, as a function now of the parameter n, converges weakly in the mean to the random function U(t) if there exists, in the mean-square sense, the limit of the following integral as $n \to \infty$:

$$a_n(T) = \int_0^T R(t)\, U_n(t)\, dt, \tag{6}$$

where R(t) is an arbitrary "sufficiently smooth"‡ random function, uncorrelated with $U_n(t)$, and such that

$$\int_{-\infty}^{\infty} k_R^2(t, t)\, dt < \infty.$$

The random variable of (6) is basically identical to the generalized random function introduced in [4, 5]. The only difference is that here, as the space of the basic functions, we have choosen the space of random functions while, in [4, 5], the space of nonrandom functions was considered.

---

* For stationary random processes, such a representation is well known (cf., for example, [3]).

† Convergence in the mean is defined by the condition

$$\lim_{n\to\infty} M\left[Z(t) - \sum_{k=1}^{n} B_k z_k(t)\right]^2 = 0.$$

‡ It is assumed that the random function R(t) has a bounded dispersion, is continuous in the mean, and has the necessary number of continuous stochastic derivatives.

Below, we extend the results of correlation theory [2] to generalized random functions. Such an extension is carried out here, since it is lacking in [4, 5].

According to the basic lemma of correlation theory, it is necessary and sufficient for the convergence of (6) that there exist the limit, in the ordinary sense, of the numbers

$$p_{n,n'} = M\,\{a_n,\ a_{n'}\}$$

independently of which sequences $\underline{n}$ and n' run through as n, n' → ∞.

Thus, it is necessary and sufficient that there exist the limit of the numbers

$$p_{n,n'} = \int_0^T\!\!\int_0^T k_R(t_1,\ t_2)\, M\,\{U_n(t_1)\, U_{n'}(t_2)\}\, dt_1 dt_2 \qquad (7)$$

independently of which sequences $\underline{n}$ and n' run through as n, n' → ∞.

We now consider the function $U_n(t)$, defined by the formula

$$U_n(t) = \sum_{k=1}^{n} C_k y_k(t), \qquad (8)$$

where the random variables C_k satisfy the condition

$$M\,\{C_\mu C_\nu\} = \delta_{\nu\mu} N^2 \qquad (9)$$

and $\{y_k\}$'s an arbitrary system of orthonormal functions on the interval (−∞, + ∞), complete in L_2. We then obtain, for the numbers $p_{n,\,n'}$:

$$p_{n,n'} = N^2 \int_0^T\!\!\int_0^T k_R(t_1,\ t_2) \sum_{k=1}^{\min(n,n')} y_k(t_1)\, y_k(t_2)\, dt_1 dt_2. \qquad (10)$$

The numbers $p_{n,\,n'}$, defined by (6), converge in the mean. Indeed,

$$p_{n,n'} = N^2 \int_0^T \sum_{k=1}^{\min(n,n')} \eta_k(t_1)\, y_k(t_1)\, dt_1, \qquad (10a)$$

where $\eta_k = (k_R,\ y_k)$ are the Fourier coefficients of the function $k_R(t_1,\ t_2)$. By virtue of the fact that $k_R \in L_2$** and that the system of functions $\{y_k\}$ is complete in L_2, the sum of the integrand of (10a) converges in the mean as n → ∞ to the function $k_R(t_1,\ t_2)$. With these conditions, we obtain the following for p_∞:

$$p_\infty = N^2 \int_0^T k_R(t,\ t)\, dt. \qquad (11)$$

But formally, on the other hand, we have

$$N^2 \int_0^T\!\!\int_0^T k_R(t_1,\ t_2)\, \delta(t_1 - t_2)\, dt_1 dt_2 = N^2 \int_0^T k_R(t,\ t)\, dt = p_\infty.$$

Thus, the series $N^2 \sum_{k=1}^{\infty} y_k(t_1) y_k(t_2)$, which, formally, is the correlation function of the random function

$$Y(t) = \sum_{k=1}^{\infty} C_k y_k(t), \qquad (12)$$

possesses the properties of a delta-function.

Consequently, it may be said that the random function Y, defined by the series of (12), converges weakly in the mean to white noise.

We now turn to the basic problem. We present the white noise Y(t) by the series in (12), with the assumption that $\{y_k\}$ is a system of orthonormalized functions which is complete in L_2. We then determine the random variables C_k in (12) from the formula

$$C_k = \frac{V_k}{\sqrt{D_k}}, \qquad (13)$$

where the random variables V_k are the coefficients in the expansion of random function X(t) in a series of the form of (3):

$$X(t) = \sum_{k=1}^{\infty} V_k x_k(t) \qquad (14)$$

and $D_k = M[V_k]^2$.

We now consider the linear operator

$$AY = \int_{-\infty}^{+\infty} w_x(t,\ \tau)\, Y(\tau)\, d\tau, \qquad (15)$$

where the weight function is defined by the series

$$w_x(t,\ \tau) = \sum_{k=1}^{\infty} \sqrt{D_k}\, x_k(t)\, y_k(\tau). \qquad (16)$$

The functions $x_k(t)$ are the same as in (14). Then, from (12), (13), (15), and (16), we get

$$AY = \int_{-\infty}^{+\infty} w_x(t,\ \tau)\, Y(\tau)\, d\tau = \sum_{k=1}^{\infty} V_k x_k(t) \qquad (17)$$

and, consequently, we have

$$X = AY = \int_{-\infty}^{+\infty} w_x(t,\ \tau)\, Y(\tau)\, d\tau. \qquad (18)$$

** This follows from the condition

$$\int_{-\infty}^{+\infty} k_R^2(t,\ t)\, dt < \infty.$$

where the integral is taken in the mean, and $w_x(t, \tau)$ is defined by formula (16).

We note that (17) is a generalized random function $X(w_x)$ in the sense of [4, 5] (the notation is the same as in work [5]). Giving the function $w_x(t, \tau)$ is equivalent to defining the space of the basic functions, depending on a continuously varying parameter $\underline{t}$ (the usual functions from the space of basic functions depend on a discretely varying parameter). The necessary requirements on the function $w_x(t, \tau)$ are determined by the finitude of the dispersion of the random function $X(t)$.

The functions $w_x(t, \tau)$ and $Y(\tau)$ in (17) can be defined in infinitely many ways. For this, it suffices to use any other expansion of the function $X(t)$ in a series of the form of (14). As is well known [1], it is always possible to do this.

We also note that if the "white noise" $Y(t)$ is so chosen that (18) holds, then there exists one, and only one, function $w_x(t, \tau)$.

Indeed, if it be assumed that, for one $X(t)$, there exist two functions w_1 and w_2, then from (18), we obtain

$$\int_{-\infty}^{+\infty} \{w_1(t, \tau) - w_2(t, \tau)\}\, Y(\tau)\, d\tau \equiv 0. \qquad (19)$$

By virtue of the completeness of the system of functions $\{y_k\}$, this identity is possible only if $w_1 = w_2$.

After the problem of (1) is solved, there is no difficulty in solving that of (2).

Indeed, we consider the linear operator

$$A_x^{-1}X = \int_{-\infty}^{+\infty} w_x^{-1}(t, \tau)\, X(\tau)\, d\tau, \qquad (20)$$

where the weight function is defined by the series

$$w_x^{-1}(t, \tau) = \sum_{k=1}^{\infty} \frac{y_k(t) a_k(\tau)}{\sqrt{D_k}}, \qquad (21)$$

the functions $a_k(t)$ satisfy the conditions

$$(a_j,\ x_i) = \delta_{ji} \qquad (22)$$

and $\{y_k\}$ is an arbitrary system of orthonormal functions which is complete in L_2.

From (20), (21), and (22) we obtain

$$Y = A_x^{-1}X = \sum_{k=1}^{\infty} \frac{V_k}{\sqrt{D_k}}\, y_k(t). \qquad (23)$$

On the basis of what has been previously stated, the series in (23) converges weakly in the mean to white noise. Consequently, we have

$$Y(t) = \int_{-\infty}^{+\infty} w_x^{-1}(t, \tau)\, X(\tau)\, d\tau, \qquad (24)$$

where the function $w_x^{-1}(t, \tau)$ is defined by relationship (21). Thus, we have obtained the solutions to the problems of (1) and (2).

However, it is sometimes important to know which functional Hilbert space H_B it is in, whose metric, the series of (21), converges to the function $w_x^{-1}(t, \tau)$, and whether, in general, such a space exists. It is obvious that the function $w_x^{-1}(t, \tau)$ itself will also lie in the space H_B since, by definition, it is a complete space.

We now determine the space H_B. We compute the scalar product of any two functions $w_1(t, t_1)$ and $w_2(t, t_2)$ in H_B by the formula

$$(w_1, w_2)_B = \iiint k(t_1, t_2)\, w_1(t, t_1)\, w_2(t, t_2)\, dt_1 dt_2 dt, \qquad (25)$$

where $k(t_1, t_2)$ has the form

$$k(t_1,\ t_2) = \sum_{k=1}^{\infty} D_k^2\, x_k(t_1)\, x_k(t_2). \qquad (26)$$

The domain of integration in (25) is defined as $t, t_1, t_2 \in T$. For simplicity of notation, the limits of integration will always be omitted. The coefficients D_k and the functions $x_k(t)$ in (26) are, respectively, the dispersions of the random variables V_k and the coordinate functions of expansion (14) of the random function $X(t)$. The series in the right member of (26) converges to the function $k(t_1, t_2)$ since the following series converges:††

$$k_x(t_1,\ t_2) = \sum_{k=1}^{\infty} D_k x_k(t_1)\, x_k(t_2). \qquad (27)$$

It is also obvious that the function $k(t_1, t_2)$ is symmetric and positive-definite. As follows from (25), the square of the norm of a function $w(t, \tau)$ in space H_B is defined by the formula

---

†† Indeed, if series (14) converges in the mean to random function $X(t)$ then, in accordance with the basic lemma, series (27) must converge to $k_x(t_1, t_2)$. Consequently, the positive series $\sum_{k=1}^{\infty} D_k$ must converge, and $D_k \to 0$ for $k \to \infty$.

Thus, the series $\sum_{k=1}^{\infty} D_k^2$ is dominated by the convergent series $\sum_{k=1}^{\infty} D_k$ and, consequently, from the convergence of series (27) for any $t_1, t_2 \in T$ follows the convergence of series (25) for the same $t_1, t_2 \in T$.

$$\|w\|_B^2 = \iiint k(t_1, t_2)\, w(t, t_1)\, w(t, t_2)\, dt_1\, dt_2\, dt. \quad (28)$$

It is easily verified that the norm thus defined, by virtue of all symmetry and positive-definiteness of function $k(t_1, t_2)$, satisfies all the necessary axioms for norms.

We now define the functional Hilbert space H_B as a linear set of continuous functions which is closed in the sense of the metric introduced by (28).

We now prove that series (21) converges to the function $w_x^{-1}(t,\tau)$ in the metric of space H_B. For this, we find the square of the norm of a segment of series (21):

$$\left\| \sum_{k=n}^{n+m} \frac{y_k(t) a_k(\tau)}{\sqrt{D_k}} \right\|_B^2 = \sum_{k=n}^{n+m} D_k. \quad (29)$$

Since the series $\sum_{k=1}^{\infty} D_k$ converges, then the sum in the right member of (29) tends to zero as $n \to \infty$. It follows, thus, that series (21) converges in the metric of space H_B and, consequently, the existence of the space in which the function $w_x^{-1}(t,\tau)$ lies is proven. However, it is possible to construct, not just one, but a nondenumerable set of spaces H_B^l in whose metrics series (21) converges. It suffices for this, for example, to substitute for the function $k(t_1, t_2)$ in formulas (26) and (28) the functions

$$k_l(t_1, t_2) = \sum_{k=1}^{\infty} D_k^l x_k(t_1) x_k(t_2) \quad (l = 2, 3, 4, \ldots,). \quad (30)$$

Space H_B is obtained for $l = 2$. In particular cases, it may turn out that function $w_x^{-1}(t,\tau)$ lies in subspace of H_B, for example L_2, or even the set of C of continuous functions. With this, $C \subset L_2 \subset H_B$.

3. Application of Representations (1) and (2) to Optimal Linear System Theory

The problem of determining an optimal linear operator B consists of the following. It is necessary to approximate in the very best way to a given random function Z(t) by a random function BX [an operator on X(t)] by observing the random function $X(\tau)$ on the interval $(-\infty, t)$. It is assumed with this that $M[X] = M[Z] = 0$. The optimal operator B obviously lies in the class of linear operators, namely,

$$\Gamma(t) = BX = \int_{-\infty}^{t} w^*(t, \tau)\, X(\tau)\, d\tau, \quad (31)$$

where $w^*(t,\tau)$ is the weight function corresponding to the optimal operator. The closeness of the function $\Gamma(t)$ to Z(t) is defined by the mean square error

$$M\{\Gamma(t) - Z(t)\}^2. \quad (32)$$

An operator B^* which provides a minimum mean square error is considered to be optimal. It can be shown [1] that the optimal weight function must satisfy an integral equation of the form

$$\int_{-\infty}^{t} w(t, \tau)\, k_x(u, \tau)\, d\tau = k_{xz}(t, u) \quad (-\infty < u < t), \quad (33)$$

where $k_x(t_1, t_2)$ and $k_{zx}(t_1, t_2)$ are, respectively, the autocorrelation function of X(t) and the cross correlation function of X(t) and Z(t), which are assumed to be known.

Here we considered only one variant of the optimal system problem. Other variants lead to integral equations analogous to (33). We therefore limit ourselves to a consideration of the solution of Eq. (33). To solve Eq. (33), we must first make one remark, which is a simple corollary to the results of Section 2.

Let there be given the weight function $\omega(t,\tau)$ of an arbitrary linear system.

It may always be assumed that this linear system forms, from some white noise,

$$Y(t) = \sum_{k=1}^{\infty} \frac{F_k}{\sqrt{D_{F_k}}} y_k(t),$$

at its input, a random function P(t) of the form

$$P(t) = \sum_{k=1}^{\infty} F_k b_k(t).$$

According to (16), the weight function $\omega(t,\tau)$ must have the form

$$\omega(t, \tau) = \sum_{k=1}^{\infty} \sqrt{D_{F_k}}\, b_k(t)\, y_k(\tau) = \sum_{k=1}^{\infty} \eta_k(t)\, y_k(\tau), \quad (34)$$

Then, the weight function $\omega^{-1}(t,\tau)$ of the inverse operator, in accordance with (21), is written in the form

$$\omega^{-1}(t, \tau) = \sum_{k=1}^{\infty} \frac{y_k(t)\, d_k(\tau)}{\sqrt{D_{F_k}}} = \sum_{k=1}^{\infty} y_k(t)\, \zeta_k(\tau), \quad (35)$$

where the functions $b_k(t)$ and $d_k(t)$ satisfy the biorthogonality condition

$$(b_j, d_i) = \delta_{ji}. \quad (36)$$

On the basis of the remark just made, the solution of Eq. (33), if it exists, is determined in an elementary way. Indeed, we present the function $k_x(u, \tau)$, the weight function of the linear operator in Eq. (33), by the series

$$k_x(u, \tau) = \sum_{k=1}^{\infty} \eta_k(u) y_k(\tau), \tag{37}$$

where $\eta_k = (k_x, y_k)$ and $\{y_k\}$ is any complete system of orthonormalized functions in L_2. Then, in accordance with the previous remark, the weight function of the inverse operator has the form

$$k_x^{-1}(\tau, u) = \sum_{1}^{\infty} y_k(\tau) \zeta_k(u). \tag{38}$$

By applying the inverse operator to both members of Eq. (33) and by taking (38) into account, we obtain the solution in the form

$$w^*(t, \tau) = \sum_{k=1}^{\infty} y_k(\tau) \int k_{zx}(t, u) \zeta_k(u)\, du. \tag{39}$$

If we use the expansion of the correlation function in a series such as (5), we then obtain

$$k_x(u, \tau) = \sum_{k=1}^{\infty} D_k x_k(u) x_k(\tau)$$

and, for the inverse operator,

$$k_x^{-1}(\tau, u) = \sum_{k=1}^{\infty} \frac{a_k(\tau) a_k(u)}{D_k}.$$

Then, for the weight function of the optimal operator, we get

$$w^*(t, \tau) = \sum_{k=1}^{\infty} \frac{a_k(\tau)}{D_k} \int k_{zx}(t, u) a_k(u)\, du. \tag{40}$$

If we use the expansion of the correlation function in a series with respect to orthonormalized eigenfunctions, we obtain

$$k_x(u, \tau) = \sum_{k=1}^{\infty} D_k \psi_k(u) \psi_k(\tau),$$

where D_k and $\psi_k(t)$ are, respectively, the eigenvalues and eigenfunctions of the equation

$$\int k_x(u, \tau) \psi(\tau)\, d\tau = D\psi(u). \tag{41}$$

Formula (39) is then written in the form

$$w^*(t, \tau) = \sum_{k=1}^{\infty} \frac{1}{D_k} \psi_k(\tau) \int k_{zx}(t, u) \psi_k(u)\, du. \tag{42}$$

Results (40) and (42) were obtained in [1].

The author thanks V. S. Pugachev and A. M. Yaglom for reviewing the manuscript and for their valuable remarks.

LITERATURE CITED

1. V. S. Pugachev, Theory of Random Functions and its Application to Automatic Control Problems [in Russian] (Gostekhizdat, 1957).
2. A. Blanc-Lapierre and R. Forte, Théorie des fonctions aléatoires (Paris, 1953).
3. A. M. Yaglom, "Introduction to the theory of stationary random functions," Uspekhi Matem. Nauk 7, 5 (1952).
4. I. M. Gel'fand, "Generalized random processes," Doklady Akad. Nauk SSSR 100, 5 (1955).
5. K. Ito, "Stationary random distributions," Mem. College Sci. Univ. Kyoto, Ser. A. 28 (1953).

THE OPTIMAL CONTROL OF SYSTEMS WITH DISTRIBUTED PARAMETERS

A. G. Butkovskii and A. Ya. Lerner

Moscow

Translated from Avtomatika i Telemekhanika, Vol. 21, No. 6, pp. 682-691, June, 1960

The paper poses the problem of the optimal control of systems with distributed parameters for certain classes of objects described by systems of first-order partial differential equations and by the heat conduction equation. The solution is adduced for one optimal control problem for an object described by a first-order partial differential equation, and the functional block schematic is given for an optimal control system for objects of this type.

The recently developed optimal system theory allowed new approaches to the solution of the control problem to be developed. The posing of the problem, in all the generally known works on optimal control theory, derived from the tendency to take into account limiting conditions imposed on the controlling stimuli and on the coordinates of the given portions of systems described by systems of ordinary differential equations (for example, [1-4]).

The solutions of these problems can be based on L. S. Pontryagin's maximum principle [3-7], R. Bellman's dynamic programming method [8], or on the use of isosurfaces in phase space [9, 10]. However, in many engineering applications, one has to do with objects with spatially distributed parameters which are impossible to replace by delay lines. This can give rise to the circumstance that the controlling stimuli can be applied to various points or regions of the distributed system or to the position that the control problem is the attainment of a given distribution of object states.

The optimal control problems for such objects cannot be solved by a direct employment of the well-known methods, and require a new approach to their posing and to their solution.

1. Posing of the Problem

We shall consider systems with distributed parameters which are described by partial differential equations.

Many objects of control can be described by systems of first-order partial differential equations:

$$\frac{\partial Q_i}{\partial t} = f_i\Big(x,\ t,\ Q_1 \ldots, Q_n,\ \frac{\partial Q_1}{\partial x}, \ldots \qquad (1)$$

$$\ldots, \frac{\partial Q_n}{\partial x},\ u_1, \ldots, u_k,\ v_{k+1}, \ldots, v_r,\ w_{r+1}, \ldots, w_s\Big)$$

$$(i = 1, 2, \ldots n),$$

where $Q_i = Q_i(x, t)$ $(i = 1, \ldots, n)$ are functions of the two arguments x and t, defined in the rectangle $l_0 \leq x \leq l_1$, $t_0 \leq t \leq t_1$ and characterizing the object's state; $u_j = u_j(t)$ $(j = 1, 2, \ldots, k)$ are controlling functions of the variable t, constrained by the condition

$$F(u_1, \ldots, u_k) \leqslant C. \qquad (2)$$

Here, F is some given functional, and C is a constant.

Further, $v_j = v_j(x, t)$ $(j = k + 1, \ldots, r)$ are controlling functions of two variables, constrained by the conditions

$$\left|\frac{\partial^{\gamma+\delta} v_j}{\partial x^{\gamma}\partial t^{\delta}}\right| \leqslant A_j, \qquad (3)$$

where γ and δ depend on j, $w_j = w_j(x)$ $(j = r + 1, \ldots, s)$ are controlling functions of one variable x, constrained by the condition

$$\left|\frac{d^{\alpha} w_j(x)}{dx}\right| \leqslant B_j, \qquad (4)$$

where α depends on j.

In the given case, we can formulate three optimal control problems.

I. To vary the controlling stimuli u_j, v_j, w_j $(j = 1, \ldots, s)$ constrained by conditions (2), (3), (4), so that, with initial conditions

$$Q_i(x,\ t_0) = Q_{in}(x) \qquad (5)$$

and boundary conditions

$$Q_i(l_0,\ t) = Q_{i0}(t)$$

some functional

$$I = I\left(x,\ t,\ Q_i, \frac{\partial Q_i}{\partial x}, \frac{\partial Q_j}{\partial t}, u_j, v_j, w_j\right)$$

$$(i = 1, \ldots, n;\ j = 1, \ldots, s) \qquad (6)$$

will be minimized. Here, Q_i, u_j, v_j, w_j are vectors with the corresponding coordinates.

II. To vary u_j, v_j, w_j $(j = 1, 2, \ldots, s)$ so that a function of the type of (6), for fixed values of x lying on the segment $[l_0, l_1]$ (for example, for $x = l_1$), attains its minimum value.

III. Finally, to vary u_j, v_j, w_j $(j = 1, 2, \ldots, s)$ so that a functional of the type of (6), for fixed values of t lying on the segment $[t_0, t_1]$, attains its minimum value.

This is the problem with "free ends," i.e., in the case when no limitations are imposed on the functions $Q_i = Q_i(x, t)$ for $t = t_1$ $(i = 1, 2, \ldots, n)$. However, it is meaningful in some cases to require that the state functions $Q_i = Q_i(x, t)$ $(i = 1, 2, \ldots, n)$ differ in some known sense from certain given functions $Q_i^* = Q_i^*(x)$ by a magnitude not exceeding a permissible deviation ϵ. In other words, it is necessary to require that the vector function $Q = Q(x, t) = (Q_1(x,t), \ldots, Q_n(x, t))$, for $t = t_1$, lie in some given ϵ-neighborhood of the vector function $Q^* = Q^*(x) = (Q_1^*(x), \ldots, Q_n^*(x))$, i.e., that the following condition holds:

$$\max |Q_i^*(x) - Q_i(x, t_1)| \leqslant \epsilon \qquad (l_0 \leqslant x \leqslant l_1,\ i = 1, 2, \ldots n). \tag{7}$$

In connection with this, one might also pose the problem: to vary the controlling stimuli u_j, v_j, w_j $(j = 1, 2, \ldots, s)$ so that there shall be minimized, in some sense, the deviation of the vector function $Q(x, t)$ from a given vector function $Q^*(x)$ for a fixed time t_1, for example, to attain

$$\min \max |Q_i^*(x) - Q_i(x, t_1)| \qquad (l_0 \leqslant x \leqslant l_1,\quad i = 1, 2, \ldots, n). \tag{8}$$

Many controlled objects are described by partial differential equations of second and higher orders. Here, we shall consider one of the fundamental problems of mathematical physics, namely, the heat conduction equation. We first consider the one-dimensional heat conduction equation in the simplest case:

$$\frac{\partial Q}{\partial t} = a \frac{\partial^2 Q}{\partial x^2} + g(x, t, u_1(t)) \tag{9}$$

with initial conditions

$$Q(x, t_0) = Q_0(x) \tag{10}$$

and boundary conditions

$$\left.\frac{\partial Q}{\partial x}\right|_{x=l_0} + \beta_0(l_0, t) = \psi_1(t, u_2(t)), \qquad \left.\frac{\partial Q}{\partial x}\right|_{x=l_1} + \beta_1(l_1, t) = \psi(t_3, u_3(t)). \tag{11}$$

Here, g, ψ_1 and ψ_2 are given functions of their arguments; a, β_0 and β_1 are coefficients which, in the general case, depend on x, t and $Q(x, t)$; $Q = Q(x, t)$ is a function of the two arguments x and t, defined in the region $l_0 \leq x \leq l_1$, $t_0 \leq t \leq t_1$ and characterizing the state of the controlled object, and $u_1(t)$, $u_2(t)$ and $u_3(t)$ are controlling functions constrained by conditions (2) for $k = 3$.

The optimal control problem for such objects can consist of the determination of the law of variation of the controlling stimuli $u_1(t)$, $u_2(t)$, and $u_3(t)$, constrained by conditions of the type of (2), for which the functional

$$I = I\left(t, x, Q, \frac{\partial Q}{\partial x}, \frac{\partial Q}{\partial t}, u_1, u_2, u_3\right) \tag{12}$$

attains its minimum value. In other cases, instead of minimizing functional (12) with the same conditions (2), it is necessary to choose the controlling stimuli so that functional (12) will be minimized but, for fixed x from $[l_0, l_1]$ or for fixed t from $[t_0, t_1]$.

Additional conditions, analogous to condition (7) can be imposed on the function $Q = Q(x,t)$, i.e., the function $Q = Q(x, t)$, at time $t = t_1$, must lie in some given ϵ-neighborhood of a given function $Q^* = Q^*(x)$, for example,

$$\max |Q^*(x) - Q(x, t_1)| \leqslant \epsilon \quad (l_0 \leqslant x \leqslant l_1). \tag{13}$$

An analogous problem can be posed for a three-dimensional object, described, for example, by the heat conduction equation

$$\frac{\partial Q}{\partial t} = a\left(\frac{\partial^2 Q}{\partial x^2} + \frac{\partial^2 Q}{\partial y^2} + \frac{\partial^2 Q}{\partial z^2}\right) + \nu_1 \frac{\partial Q}{\partial x} + \nu_2 \frac{\partial Q}{\partial y} + \nu_3 \frac{\partial Q}{\partial z} + g(P, t, u_1, \ldots, u_k) \tag{14}$$

with initial condition

$$Q(P, 0) = Q_0(P) \tag{14'}$$

and boundary condition

$$\left.\frac{\partial Q}{\partial n}\right|_{\Gamma} + \beta Q\Big|_{\Gamma} = \psi(P, t, u_{k+1}, \ldots, u_r)\Big|_{\Gamma}. \tag{15}$$

Here, P is a point of the body D bounded by surface Γ; n is the external normal; a, ν_1, ν_2, ν_3, β are given functions of the point P and time t; g and ψ are given functions of their arguments. Limitations of the type of (2) are imposed on the controlling stimuli $u_1, \ldots, u_r$.

It might be important here to solve the problem of finding such controlling stimuli which, in conjunction with limitations (2), will give the functional

$$I = I(P, t, Q(P, t); u_1, \ldots, u_r) \tag{16}$$

its minimum value.

With this there may still be imposed the further condition that the function $Q = Q(P, t)$ for $t = t_1$ be found in some ϵ-neighborhood of a given function $Q^*(P)$, for example, that the following condition hold:

$$\max_{P\in D} |Q^*(P) - Q(P, t_1)| \leqslant \varepsilon. \qquad (17)$$

Here there might also arise the problem: to so vary the controlling stimuli $u_1, \ldots, u_r$ that the deviation of the function $Q(P, t_1)$ from the given function $Q^*(P)$ is minimal in some sense — for example, that during time $t = t_1 - t_0$ the following integral be a minimum:

$$\iiint_D [Q^*(P) - Q(P, t_1)]^2\, dP.$$

Moreover, the following problem is also of interest: to determine those controlling stimuli $u_1, \ldots, u_r$ so that the functional of (16) will attain a minimum, where the point $P \in \Gamma' \subset \Gamma$, where Γ' is some definite part of the boundary.

It is necessary to mention that here, as in the case when the object is described by equations of the type of (1), the controlling functions may depend, not only on time t, but also on the spatial coordinates x, x and y, or x, y, z, or only on the space coordinates.

A large number of engineering problems, related to the creation of optimal control systems for objects with distributed parameters, lead to the mathematical problems which we have just enumerated.

Such objects, for example, are flow-through furnaces for the heating or thermal processing of materials. If, with this, we are limited to the accuracy of solution which the theory of regular regimens [11] can give, then objects of this type can be described by first-order partial differential equations of the type of (1). In this case, the limitations of (2) flow from the limitations on range of variation of the controlling stimuli, limitations on their speed of variation, etc. Limitations (3) and (4) are imposed on spatially distributed controlling actions as occur, for example, in velocity heating furnaces, deriving from the impossibility of practical implementation in the furnaces of temperature fields with very high gradients. For such objects, functional (6) to be minimized might stand for the time to compensate disturbing stimuli, the mean square deviation of the material's temperature at the furnace output from a given temperature, etc. As disturbing stimuli here, there might be adduced variations of temperature at the input to the furnace (or in one of its zones), variations in the tempo at which the material is fed through the furnace, variations in thickness of the layer of material to be heated. Introducing the quantity Q, which characterizes the material's state, as a vector rather than a scalar, is due to the fact that the requirements on the processing might include, not one, but several indicators, such as, for example, temperature, chemical constitution, crystal structure, etc.

The problem of optimizing a thick body in a flow-through or chamber furnace leads to a posing of the problem wherein the object is described by second-order partial differential equations, such as (9). It might be necessary here to attain a given temperature distribution, in minimal time or with minimal expenditure of energy [functional (12)], in the body to be heated, or to guarantee that the nonuniformity of heating does not exceed some given magnitude.

It is with such types of problems that one has to deal in creating automatic control systems for a broad class of frequently occurring practical production processes. In addition to the aforementioned heating and thermal flow-through and chamber furnaces, this class of objects includes rotating kilns for sintering free-flowing materials, continuous dessicators for ribbon and free-flowing materials, blast and open-hearth furnaces, ribbon-sintering furnaces, machines for continuous plating, etc.

2. Example of an Object with Distributed Parameters

For a certain class of objects, such as continuous furnaces for heating "fine" billets, heat exchangers, and many others, the equations describing the process can be reduced to first-order partial differential equations.

We consider, for example, the one-sided heating of a "fine" lamina (Biot criterion, $Bi \leq 0.25$) which (Fig. 1) moves through the furnace of length L with a velocity of $\nu = \nu(t) \geq 0$ for $0 \leq t \leq T$. We use the notation: thermal capacity of the metal is c, the specific weight is γ, the lamina thickness is s, the heat transfer coefficient to the metal in the given range of temperature variation is α.

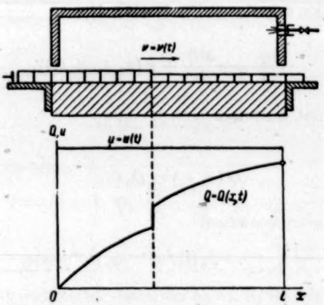

Fig. 1. Single zone flow-through heating furnace. $Q = Q(x, t)$ is the metal temperature as a function of the coordinate x and the time t; u(t) is the furnace temperature as the controlling stimulus; $\nu = \nu(t)$ is the speed at which the metal passes through the furnace.

We assume that the temperature of the furnace's working space (Fig. 1) is the same at all points and that, for $0 \leq t \leq T$, the following limitation is imposed on it:

$$u_1 \leqslant u(t) \leqslant u_2, \tag{18}$$

where u_1 and u_2 are, respectively, the upper and lower admissible or attainable limits of temperature variation of the furnace's working space.

With the aforementioned assumptions taken into account, one can write the equation of the metal heating process in the furnace in the form

$$a\frac{\partial Q}{\partial t} + av\frac{\partial Q}{\partial x} + Q - u = 0. \tag{19}$$

Here, $Q = Q(x, t)$ is the metal temperature at point $\underline{x}$ at time $\underline{t}$; $a = c\gamma s/\alpha$ is the coefficient characterizing the metal's thermal properties. We shall assume that this coefficient depends only on the quantity

$$\xi = x - \int_0^t \nu(p)\,dp.$$

In the case of radiant heat transfer, this equation can be considered the same as an equation in increments.

The initial conditions have the form

$$Q(x,\ 0) = Q_0(x),\ 0 \leqslant x \leqslant L,$$

where $Q_0(x)$ is a given function.

The boundary conditions have the form

$$Q(0,\ t) = 0,\ 0 \leqslant t \leqslant T.$$

In Eq. (19) we carry out the nondegenerate change of variables given by the formulas

$$x = \xi + \int_0^\tau \nu(p)\,dp, \quad t = \tau. \tag{20}$$

The inverse transformation has the form

$$\xi = x - \int_0^t \nu(p)\,dp, \quad \tau = t. \tag{21}$$

After the change of variables, Eq. (19) takes the form

$$a(\xi)\frac{\partial Q(\xi,\ \tau)}{\partial \tau} + Q(\xi,\ \tau) = u(\tau). \tag{22}$$

In this equation, the term with the partial derivative with respect to ξ drops out. By solving this equation for fixed ξ and, thereafter, transforming back to the original variables by means of Formulas (21), we get

$$Q(x,\ t) = e^{-\frac{t}{a}}\left[Q_0\left(x - \int_0^t \nu(p)\,dp\right) + \right. \tag{23}$$
$$\left. + \frac{1}{a}\int_0^t u(p)\,e^{\frac{p}{a}}\,dp\right],$$

where Q_0 and $\underline{a}$ are given functions of the single argument $\xi = x - \int_0^t \nu(p)\,dp$.

3. Optimal Control of Systems with Distributed Parameters

For many objects described by equations of the type of (19), the optimal control problem amounts to finding controlling stimuli, constrained by a condition $u_1 \leq u(t) \leq u_2$ for $0 \leq t \leq T$, such that the functional

$$I = \int_0^T [Q_g - Q(L,\ t)]^2\,dt \tag{24}$$

attains its minimum value. Here, Q_g is some given function of time $\underline{t}$ or is a constant.

For the continuous furnace of the example of Section 2, this requirement signifies the requirement that the mean square deviation of the metal's temperature at the furnace output from a given temperature be minimized.

By setting $x = L$ in formula (23) and substituting in (24), we get

$$I = \int_0^T \left[Q_g - e^{-\frac{t}{a}}Q_0\left(L - \int_0^t \nu(p)\,dp\right) - \right. \tag{25}$$
$$\left. - \frac{1}{a}e^{-\frac{t}{a}}\int_0^t u(p)\,e^{\frac{p}{a}}\,dp\right]^2 dt.$$

With the notation

$$\Theta(t) = Q_g - e^{-\frac{t}{a}}Q_0\left(L - \int_0^t \nu(p)\,dp\right).$$

Expression (25) can be written in the following equivalent form:

$$I = \int_0^T [Q(t) - \Delta(t)]^2\,dt, \tag{26}$$

where $\Delta(t)$ is defined by the equation

$$a\Delta'(t) + \Delta(t) = u(t) \text{ for } \Delta(0) = 0.$$

Here, the optimal control u = u(t) can be found by means of L. S. Pontryagin's maximum principle [6].

The function H has the form

$$H = \psi_0 [\theta(t) - \Delta(t)]^2 - \frac{1}{a}\psi_1 \Delta(t) + \frac{1}{a}\psi_1 u(t), \tag{27}$$

where ψ_0 = const < 0, and ψ_1 satisfies the equation

$$\dot{\psi}_1 = 2[\theta(t) - \Delta(t)]\psi_0 + \frac{1}{a}\psi_1. \tag{28}$$

We determine from (28) that

$$\psi_1(t) = e^{\frac{t}{a}}\left\{C + \int_0^t [\theta(p) - \Delta(p)] e^{-\frac{p}{a}} dp\right\}, \tag{29}$$

where C is an arbitrary constant.

The maximum of the function H is attained for

$$u(t) = \begin{cases} u_2, & \text{if} \quad \psi_1 > 0, \\ u_1, & \text{if} \quad \psi_1 < 0. \end{cases}$$

However, based on the maximum principle, it is impossible to find an optimal control u = u(t) in the case when $\psi_1(t) \equiv 0$ on some segment of the extremals. Such segments, following Rozonoér ([12], Pt. II), we shall call singular. On singular segments, function H does not depend on u, and the control u = u(t) with the condition $u_1 \leq u(t) \leq u_2$ must be so chosen that

$$\theta(t) - \Delta(t) \equiv 0. \tag{30}$$

We assume that condition (30) is met on the portions of the optimal process for $0 \leq t \leq t_1$ and $t_2 \leq t \leq T$. Then, in accordance with [12], Pt. I, in the conditions of problems with "free ends," it is necessary to have $\psi_1(T) = 0$. From this we find that, in expression (29), the constant C equals zero and that, during the course of the optimal process, the following condition must hold:

$$\int_0^T [\theta(t) - \Delta(t)] e^{-\frac{p}{a}} dp = \int_{t_1}^{t_2} [\theta(t) - \Delta(t)] e^{-\frac{p}{a}} dp = 0. \tag{31}$$

Thus, the optimal control has the form

$$u(t) = \begin{cases} u_1 & \text{for} \quad \int_0^t [\theta(p) - \Delta(p)] e^{-\frac{p}{a}} dp > 0, \\ u_2 & \text{for} \quad \int_0^t [\theta(p) - \Delta(p)] e^{-\frac{p}{a}} dp < 0. \end{cases} \tag{32}$$

We now assume that it is necessary to smooth, in some optimum way in the sense of minimizing the functional of (24), step disturbances in the coefficient a. The function a = a(ξ) has the form*

$$a = a(\xi) = \begin{cases} a_1 & \text{for} \quad \xi \leqslant 0, \\ a_2 & \text{for} \quad \xi > 0, \end{cases}$$

where a_1 and a_2 are constants and $\xi = x - \int_0^t \nu(p)\,dp$.

In this case, θ(t), at some moment of time t', $t_1 \leq t' \leq t_2$, will have a jump. Then, in accordance with (32), the optimal control corresponds to the maintenance of u during the interval (t_1, t_2) at one of the limiting levels, the choice of which depends on whether the coefficient a decreased or increased.

The moment t_1 at which there occurs the transition from the singular segment to the nonsingular one is defined by condition (31). The optimal process thus obtained is shown in Fig. 2.

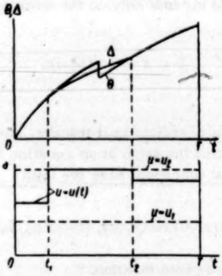

Fig. 2. Optimal process for a disturbance in the coefficient a.

We now determine the optimal control u = u(t) on the singular segments where condition (30) holds. For this, we multiply both members of expression (30) by $ae^{t/a}$ and differentiate them with respect to t. Then, if the function $Q_0(x)_t$ is differentiable with respect to t, we obtain for $0 \leqslant L - \int_0^t \nu(p)\,dp \leqslant L$,

$$u(t) = Q_g + a\nu(t) e^{-\frac{t}{a}} Q_0'\left(L - \int_0^t \nu(p)\,dp\right), \tag{33}$$

where

$$a = \begin{cases} a_1 & \text{for} \quad t \in [0, t_1], \\ a_2 & \text{for} \quad t \in [t_2, T]. \end{cases}$$

---

* This corresponds to a variation in thickness of the billets fed to the continuous furnace.

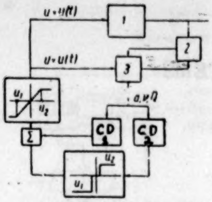

Fig. 3. Block schematic for the optimal control system for an object with distributed parameters. R is a three-position relay: u_1, 0, u_2 as a function of the signal $\delta a = a_2 - a_1$. 1 is the object, 2 is the optimizer, 3 is a model of the object.

It is obvious that condition (33) will also be sufficient for the holding of condition (30). Thus, expression (33) gives the sought-for control on the singular segments of the optimal trajectory.

Implementation of the optimal control process we have found may be achieved, for example, by means of the system whose block schematic is shown on Fig. 3. As is obvious from formulas (31) and (33), it is necessary, for the implementation of the optimal process, to have the function $Q_0 = Q_0(x)$, the coefficient a, and the velocity function $\nu = \nu(t)$.

These data can be obtained from a model of the object, the parameters of which are tuned automatically by means of the optimizer. The initial data, obtained from the model, are fed to computing devices CD1 and CD2. Device CD1 determines the moments for the initial transition from the singular portion of the trajectory to the nonsingular one, and from the nonsingular one to the singular one. With this, there is first opened, and then closed, a key which passes the sign of the increment of coefficient a which is subject to the disturbance. Relay element R has the output values u_2 or u_1 as a function of the sign of the increment of a. Device CD2, using the initial data in correspondence with formula (33), determines the value of controlling parameter u = u(t).

SUMMARY

1. In automating objects with distributed parameters, it is necessary, in seeking an optimal control, to go to a variational problem of a new type, formulated in Section 1 of the present work.

2. The standard works on optimal control theory do not directly give a general method for solving the problem posed here.

3. The characteristic special features of the objects of control considered here are: the presence of both lumped and spatially distributed controlling stimuli and the limitations associated with them, which are imposed, not only on the time derivatives of the controlling stimuli, but also on their derivatives with respect to the spatial coordinates and their combinations. It is an essential point that these controlling stimuli can enter, not only into the equations of the process, but also into the boundary conditions.

4. Control of the objects of the type considered may be directed towards the achievement, either of a minimal deviation of the object's state from a given one, or to a given distribution of object states with certain conditions being met. There becomes very important, with this, the question of the attainability of the given states.

5. In the present paper we cited one of the ways in which the problem posed here can be reduced to a problem which can be solved by means of L. S. Pontryagin's maximum principle.

6. For the optimal control of the objects considered, the control system must contain a sufficiently large operational memory in which there can be stored the disturbing and controlling stimuli for a quite prolonged period of object operation.

LITERATURE CITED

1. A. A. Fel'dbaum, "Optimal processes in automatic control systems," Avtomat. i Telemekh. 14, 5 (1953).
2. A. Ya. Lerner, "Improving the dynamic properties of automatic compensators by means of nonlinear connections," Avtomat. i Telemekh. 13, 2 and 4 (1952).
3. V. G. Boltyanskii, R. V. Gamkrelidze, and L. S. Pontryagin, "On the theory of optimal processes," Doklady Akad. Nauk SSSR 110, 1 (1956).
4. R. V. Gamkrelidze, "Optimally fast processes with phase coordinate limitations," Doklady Akad. Nauk SSSR 124, 3 (1959).
5. L. S. Pontryagin, "Optimal control processes," Uspekhi Matem. Nauk 14, 1 85 (1959).
6. R. V. Gamkrelidze, "On the general theory of optimal processes," Doklady Akad. Nauk SSSR 123, 2 (1958).
7. V. G. Boltyanskii, "The maximum principle in optimal process theory," Doklady Akad. Nauk SSSR 119, 6 (1958).
8. R. Bellman, Dynamic Programming(Princeton University Press, Princeton, New Jersey, 1957).
9. A. Ya. Lerner, "On the limiting speed of action of automatic control systems," Avtomat. i Telemekh. 15, 5 (1954).
10. E. A. Rozenman, "On optimal transient responses in systems with limited power," Avtomat. i Telemekh. 18, 6 (1957).†
11. G. M. Kondrat'ev, Heat Measurements [in Russian] (Mashgiz, 1957).
12. L. I. Rozonoér, "L. S. Pontryagin's maximum principle in optimal system theory," Avtomat. i Telemekh. 20, 10-12 (1959).†

---

† See English translation.

THEORY OF CERTAIN INDIRECT CONTROL SYSTEMS WITH SEVERAL ESSENTIAL NONLINEARITIES

R. A. Nelepin

Leningrad

Translated from Avtomatika i Telemekhanika, Vol. 21, No. 6, pp. 692-705, June, 1960

In various domains of technology there are employed single-pulse systems for controlling pressure, level, temperature, speed, etc., with hydraulic, electromechanical or pneumatic amplifiers. The presence of moving parts and linkages in the controllers gives rise to the appearance of dry friction, free play, etc., that is, to factors which occasion essential nonlinearities of the characteristics. As shown both by theoretical investigations and by practical experience, these nonlinearities frequently have a decisive effect on dynamics.

One of the first works devoted to the analysis of the dynamics of nonlinear systems of indirect control is Léauté's classic work [1]. The most significant results in this direction were obtained by A. A. Andronov and his coworkers ([2, 3] and others). These, and many other, investigations explained the influence, principally, of one or another nonlinearity individually. In actual conditions, there are usually several characteristic nonlinearities. The problem thus arises of singling out systems with standard complexes of essential nonlinearities and, on the basis of an analysis of their dynamics, of constructing nomograms or tables which might facilitate the design and adjustment of these systems. The solution of this problem, despite the significant number of investigations, remains in its initial stages [4].

Below, we consider the simplest systems with account taken of nonlinearities of the types of hysteresis loops, dead zones and saturation. Each of these nonlinearities is given a physical interpretation, but other factors can be reduced to them.

The System to Be Considered

For the disturbed motion of the indirect control schemes [5, 6] to be considered, we have:

the equation of the object of control

$$T_a\dot{\varphi} + k\varphi = \mu; \tag{1}$$

the equation of the measurer and valve, with account taken of Coulomb friction in the valve

$$\gamma\eta + b\,\mathrm{sign}\,\dot{\eta} = \varphi + \delta\mu \begin{cases}\text{for} & \dot{\eta} \neq 0\\ \text{for} & \dot{\eta} = 0,\end{cases} \tag{2}$$

$$\text{but } |\gamma\eta - \varphi - \delta\mu| = b,$$

$$\eta = \text{const} \quad \text{for } |\gamma\eta - \varphi - \delta\mu| < b;$$

the equation of the servomotor with a dead zone and power limitations

$$\begin{aligned} T_s\dot{\mu} - c\,\mathrm{sign}\,\eta &= -\eta \quad \text{for} \quad c < |\eta| < c_1\\ \dot{\mu} &= 0 \quad\quad \text{for} \quad |\eta| \leqslant c,\\ \dot{\mu} &= \text{const for} \quad |\eta| \geqslant c_1. \end{aligned} \tag{3}$$

As $c_1 \to \infty$, we have, from (3), the equation of a proportional control servomotor with a dead zone:

$$\begin{aligned} T_s\dot{\mu} - c\,\mathrm{sign}\,\eta &= -\eta \quad \text{for} \quad |\eta| > c,\\ \dot{\mu} &= 0 \quad \text{for} \quad |\eta| \leqslant c. \end{aligned} \tag{4}$$

As $c_1 \to c$ and $(c_1 - c)/T_s = 1/T_C = \text{const}$, we obtain the equation of a constant speed servomotor with a dead zone:

$$\begin{aligned} T_s\mu - c\,\mathrm{sign}\,\eta &= -c_1\,\mathrm{sign}\,\eta \quad \text{for} \quad |\eta| > c,\\ \dot{\mu} &= 0 \quad \text{for} \quad |\eta| \leqslant c, \end{aligned} \tag{5}$$

Here, φ, η, μ are dimensionless coordinates of the object, the valve and the servomotor (the measurer's coordinate is eliminated by means of the valve equation); T_a and T_s are the time constants of the object and servomotor, respectively; k is the self-alignment coefficient; γ is the measurer's nonuniformity coefficient; δ is the feedback factor; b and c are the insensitivity coefficients of the valve and servomotor, respectively; c_1 is the value of coordinate η for which $\dot{\mu}$ attains its greatest magnitude.

We shall consider all the coefficients in Eqs. (1)-(5) to be constant, while of them, in particular cases, b, c, k and δ may be zero, and, moreover, k and δ can be less than zero. For $\delta = 0$, we have a controller without feedback.

As an example, Fig. 1 shows the schemes of controllers whose dynamics, with well-known assumptions, are described by the equations just given. Some of the controllers with such schemes are obtained from the I. I. Polzunov TsKTI, the F. É. Dzerzhinskii VTI, the A. N. Krylov TsNII (SSSR), the English Kent and Bailey companies, the German Askania Company (controllers with jet pipes) and others. It is important to mention that the most widely used schemes in practice of those cited are the controller schemes with feedback of Fig. 1, b and c, in which the measurer and valve are rigidly

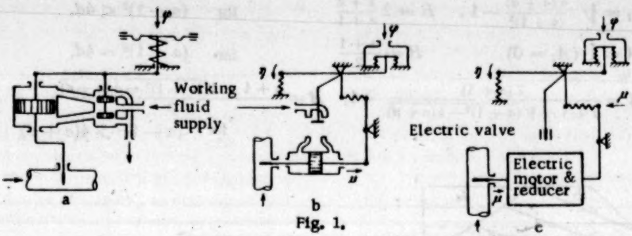

Fig. 1.

connected, and the frictional forces in these elements are inseparable. For such schemes, the foregoing equations take into account the dry friction in all the elements – in the measurer, valve and servomotor.

Method of Investigation

For the investigation of the aforementioned systems, the concept of phase space is applicable, this concept having achieved great popularity in control theory, both in the USSR and other countries, after the well-known works of A. A. Andronov and his school.

We note the specific peculiar features of constructing the phase images of the systems with which we are dealing. First, these systems are piecewise linear, which allows us to obtain the equations of the phase trajectories in the usual form. In considering spaces composed of regions with different trajectories, the concept of virtual singular points is useful [7]. Second, in the three-dimensional phase spaces of the systems under investigation, the trajectories are laid out on a definite form of oriented plane, which permits the investigation of the projections of such spaces on one plane; to eliminate nonsingle-valuedness we employ multisheeted phase surfaces [8, 9] which are analogous to the Riemann surfaces in the theory of functions of a complex variable.

The representation in phase space of a topological map leads, in essential points, to quantitative results by means of the method of point transformations of Poincaré – Brauer – Birkhoff – Andronov. We note that the presence of the Kronecker function in [2] allows the representative point to move only in definite directions on parts of the segments of the characteristics of the equivalent nonlinear link $\dot{\mu} = f(\varphi + \delta\mu)$. We denote these as the basic directions. As the basic directions of the remaining segments, we shall understand such directions in which the representative point can move in its cyclical circuit of the designated characteristic. If the point does not move in a basic direction, then it will either move during a finite time only in basic directions, or fall on a resting segment (or at infinity), without completing an oscillation. Therefore, for an employment of the method of point transformations, it suffices to take into account only those portions of the phase surface sheets which correspond to the aforementioned basic directions which allow one to obtain a simplified multisheet surface with linked (joined) phase trajectories immediately.

Parameter Space of the Systems Considered

For system (1)-(3), the regions corresponding to the different types of motion are located in the space of parameters

$$a = \frac{\delta T'_a}{\gamma k T_s} \gtrless 0, \quad d = \frac{T_a}{\gamma k^2 T_s} > 0 \ (\text{for} \ k > 0),$$

$$d_1 = \frac{T_a}{\gamma k^2 T_s} > 0 \ (\text{for} \ k < 0), \quad G = \frac{\gamma c}{b} \geqslant 0$$

and are defined in the following way. In the region for which $a > -1$, $a + d > 0$, i.e., $\delta T_a + \gamma k T_s > 0$, $1 + \delta k > 0$, $k > 0$ (we call it region I), there lies surface T whose coordinates are determined, after elimination of the parameter V_1, from the equations

$$F_1(V_1) = F(V_1), \quad \left(\frac{\partial F_1}{\partial V}\right)_{V_1} = \left(\frac{\partial F}{\partial V}\right)_{V_1}, \tag{6}$$

where

$$F_1 = G\left(B \ln \frac{B}{B-V} - V\right) + \begin{cases} \sqrt{1 + A_1^2}\exp\left(\frac{1}{A_1} \operatorname{arc\,tg} A_1\right) & \text{for} \quad (a-1)^2 < 4d, \\ e & \text{for} \quad (a-1)^2 = 4d, \\ \exp\left(\frac{A}{A-1} \ln A\right) & \text{for} \quad (a-1)^2 > 4d, \end{cases}$$

$$F = \begin{cases} \sqrt{A_1^2 + (V-1)^2} \exp\left(-\frac{1}{A_1} \operatorname{arc\,tg} \frac{A_1}{V-1}\right) & \text{for} \quad (a-1)^2 < 4d, \\ (V-1)\exp\frac{1}{1-V} & \text{for} \quad (a-1)^2 = 4d, \\ (V-1)\exp\left(\frac{A}{1-A} \ln \frac{V-1}{V-A}\right) & \text{for} \quad (a-1)^2 > 4d, \end{cases}$$

$$A_1 = \sqrt{\frac{4(a+d)}{(a+1)^2} - 1}, \quad B = 2\frac{a+d}{a+1} \qquad \text{for} \quad (a-1)^2 < 4d,$$

$$A = 1 \ (A_1 = 0), \qquad B = \frac{a+1}{2} \qquad \text{for} \quad (a-1)^2 = 4d,$$

$$A = \frac{2(a+1)}{a+1-\sqrt{(a+1)^2 - 4(a+d)}} - 1, \quad B = \frac{a+1+\sqrt{(a+1)^2 - 4(a+d)}}{2}$$

$$\text{for} \quad (a-1)^2 > 4(a+d)$$

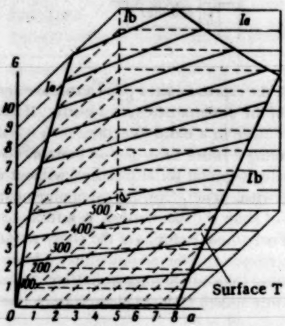

Fig. 2.

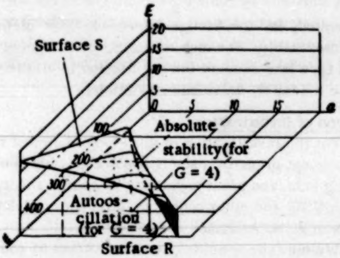

Fig. 3.

Surface T, part of which is shown on Fig. 2, divides region I into the subregions of absolute stability Ia and of rigid autooscillation mode Ib. In subregion Ia lie the points for which $d < d^0$ (for $a = a^0$ = const, $G = G^0$ = const), where a^0, d^0 and G^0 are the coordinates of surface T. For $G = 0$ (i.e., $c = 0$), subregion Ib degenerates to the region of soft autooscillation mode and, for $G = \infty$ (i.e., $b = 0$), disappears entirely due to the coalescence of surface T and the plane $a = -1$.

In the absence of a dead zone of the servomotor ($c = 0$), the boundary of stability coincides with that found previously in [3], and is defined by the trace of surface T on the plane $G = 0$ passing through the points $a = -1$, $d = 1$, and $a = 0$, $d = 3.04$. The remaining regions of the space being considered are of lesser practical interest; without giving the formulas for them, we fall back on Table 1, in which the case $c_1 = \infty$ is referred to system (1)-(3).

For system (1), (2), (4), the corresponding regions are constructed in the space of parameters a, d, d_1, G, $E = b/\gamma\,(c_1 - c) \geq 0$. If the point lies in the aforementioned subregion Ib, the given system, for $G > 0$, can be absolutely stable or autooscillatory (rigid mode). The parameter values on the boundary between stability and autooscillations in subregion Ib are determined by eliminating parameter V_2 from the system

$$F_1(V_2) = F(V_2), \quad \left(\frac{\partial F_1}{\partial V}\right)_{V_2} > \left(\frac{\partial F}{\partial V}\right)_{V_2},$$

$$E = \begin{cases} \dfrac{B}{2(1+A_1^2)}\left(B \ln \dfrac{B}{B-V_2} - V_2\right) & \text{for} \quad (a-1)^2 < 4d, \\ \dfrac{B}{2}\left(B \ln \dfrac{B}{B-V_2} - V_2\right) & \text{for} \quad (a-1)^2 = 4d, \\ \dfrac{B}{2A}\left(B \ln \dfrac{B}{B-V_2} - V_2\right) & \text{for} \quad (a-1)^2 > 4d. \end{cases} \tag{7}$$

When $V_2 = V_1$, the inequality in (7) becomes an equality. Stability corresponds to values of $E > E^0$ (for $a = a^0$ = const, $d = d^0$ = const, $G = G^0$ = const), where a^0, d^0, G^0 and E^0 are defined in accordance with (7). For fixed G, the parameter space of system (1), (2), (4) for region I can be constructed in the coordinates a, d, E. With this, the region of autooscillation will be bounded by the plane $E = 0$, the cylindrical surface R and by some surface S (Fig. 3). An increase in G leads to a decrease in the region of autooscillation. A number of the com-

TABLE 1

Form nonlin. considered		Character of poss. syst. motions in reg. of param. values			
Values of nonlin. parameters	Name of nonlin.	I $a > -1$ $a + d > 0$ (for $k > 0$)	II $a < -1$ $a + d > 0$ (for $k > 0$)	III $a < -1$ $a + d_1 > 0$ (for $k < 0$)	IV 1) $a + d < 0$ (for $k > 0$) or 2) $a + d_1 < 0$ (for $k < 0$) or 3) $a + d_1 > 0$ $a > -1$(for $k < 0$)
$c_1 = \infty$ $c = 0$ $b = 0$	Linear system	Abs. stability	Abs. instability	Abs. stability	Abs. instability
$c_1 \neq \infty$ $c = 0$ $b = 0$	Saturation nonlinearity	Absolute stability	Autooscillation (soft mode)	Stability bounded instab. "in the large"	Absolute instability
$c_1 = \infty$ $c \neq 0$ $b = 0$	Servomotor dead zone	Absolute stability	Stab., bounded instab. "in the large"	Autooscillation (soft mode)	Instability
$c_1 = \infty$ $c = 0$ $b \neq 0$	Coulomb friction in valve	Abs. stability or autooscillations (soft mode)	Absolute instability	Autooscillations (soft mode)	Absolute instability
$c_1 \neq \infty$ $c = 0$ $b \neq 0$	Satur. nonlin., Coulomb fric. in the valve	Abs. stability or autooscillations (soft mode)	Autooscillations (soft mode)	Autoosc. (soft mode) bounded instab. "in the large"	Absolute instability
$c_1 = \infty$ $c \neq 0$ $b \neq 0$	Coulomb fric. in valve and servom. dead zone	Abs. stability or autooscillations (rigid mode)	Stab. bounded instability "in the large"	Autooscillations (soft mode)	Instability
$c_1 \neq \infty$ $c \neq 0$ $b \neq 0$	Satur. nonlin., Coulomb fric. in valve and servom. dead zone	Abs. stability or autooscillations (rigid mode)	Autooscillations (rigid mode) or abs. stability	Autooscillations (soft mode), bounded instab. "in the large" or abs. instab.	Instability

TABLE 2

G=0	*a*	0,000	1,000	2,148	3,867	6,472	8,180	11,01
	d	3,045	4,441	5,905	7,977	10,98	12,89	16,05
	E	∞	∞	∞	∞	∞	∞	∞
	a	14,90	25,02	55,48	106,0	156,3	206,4	256,8
	d	20,21	30,92	63,50	114,2	164,9	215,4	266,3
	E	∞	∞	∞	∞	∞	∞	∞
	a	306,8	356,9	407,1	507,2	1008	1508	2008
	d	316,6	366,9	417,5	517.7	1020	1520	2022
	E	∞	∞	∞	∞	∞	∞	∞
G=0,2	*a*	1,054	3,992	6,679	10,75	13,28	13,42	13,45
	d	9,857	16,26	22,80	32,40	39,19	38,53	38,61
	E	5,158	9,411	13,83	20,36	24,35	24,57	24,62
	a	13,27	16,34	23,90	31,68	39,67	55,51	87,21
	d	39,80	45,31	62,18	79,19	97,04	113,6	200,6
	E	25,45	29,24	40,92	52,82	65,18	89,33	137,6
	a	165,6	244,6	322.4	635,0	947,1	1260	1571
	d	368,2	538,4	703,1	1368	2030	2692	3352
	E	255,5	374,8	491,1	959,4	1426	1894	2359
G=1,0	*a*	0,9120	4,337	9,561	15,17	25,68	29,01	29,22
	d	22,85	47,29	81,06	115,5	166,7	198,4	199,1
	E	2,026	4,702	8,456	12,33	18,09	21,42	21,74
	a	29,36	30,45	35,50	51,21	66,48	84,20	117,3
	d	200,5	206,9	236,4	327,4	420,4	515,7	703,1
	E	21,88	22,62	25,95	36,25	47,73	57,62	78,94
	a	183,6	347,6	512,6	675,5	1329	1982	2635
	d	1077	1989	2913	3810	7429	$11,04\cdot10^3$	$14,65\cdot10^3$
	E	121,4	225,3	330,4	432,9	845,5	1258	1669
G=2,0	*a*	0,1526	2,138	7,707	16,19	25,32	39,14	47,73
	d	33,39	61,85	129,7	223,9	321,0	464,5	552,0
	E	0,9529	2,038	4,631	8,376	12,19	17,86	21,32
	a	48,28	50,08	58,31	83,83	110,3	137,3	119,1
	d	557,4	576,0	659,6	915,5	1175	1444	1971
	E	21,56	22,29	25,58	35,72	46,09	56,74	77,73
	a	298,6	564,8	832,7	1096	2158	3216	4278
	d	3022	5590	8192	$10,71\cdot10^3$	$20,92\cdot10^3$	$31,05\cdot10^3$	$41,26\cdot10^3$
	E	119,5	221,7	325,1	426,0	833,6	1235	1644
G=3,0	*a*	0,6062	3,353	11,04	22,75	35,38	54,43	66,99
	d	65,54	119,8	251,5	435,4	626,6	905,8	1089
	E	0,9683	2,048	4,662	8,329	12,19	17,78	21,49
	a	69,55	80,91	116,0	152,9	190,0	264,2	412,4
	d	1125	1288	1785	2305	2824	3856	5909
	E	22,20	25,51	35,48	45,97	56,53	77,23	118,7
	a	781,1	1148	1515	2981	4443	5908	7364
	d	$10,98\cdot10^3$	$15,99\cdot10^3$	$21,02\cdot10^3$	$41,05\cdot10^3$	$60,95\cdot10^3$	$80,94\cdot10^3$	$100,7\cdot10^3$
	E	221,4	322,3	424,3	828,6	1232	1636	2035
G=4,0	*a*	1,056	4,563	14,37	29,30	45,44	69,65	85,53
	d	105,7	196,6	413,6	716,8	1033	1490	1788
	E	0,9743	2,054	4,663	8,345	12,19	17,74	21,35
	a	88,88	103,4	148,3	195,3	242,4	336,9	525,6
	d	1850	2123	2948	3805	4652	6353	9728
	E	22,13	25,42	35,54	46,07	56,28	76,97	118,2
	a	996,0	1466	1932	3796	5667	7532	9397
	d	$18,11\cdot10^3$	$26,48\cdot10^3$	$34,71\cdot10^3$	$67,56\cdot10^3$	$100,7\cdot10^3$	$133,8\cdot10^3$	$166,6\cdot10^3$
	E	220,6	323,4	423,8	824,2	1232	1634	2038

TABLE 2 (continued)

$G=5,0$	a	1,507	5,760	17,70	35,84	55,52	85,10	104,6
	d	157,2	291,2	616,1	1067	1542	2231	2682
	E	0,9797	2,054	4,674	8,337	12,24	17,86	21,56
	a	108,4	126,0	180,8	237,6	234,8	411,0	639,4
	d	2764	3165	4409	5675	6934	9536	$14,53\cdot 10^3$
	E	22,19	25,48	35,62	46,06	56,25	77,77	118,3
	a	1208	1779	2345	4602	6880	9148	$11,41\cdot 10^3$
	d	$26,88\cdot 10^3$	$39,35\cdot 10^3$	$51,60\cdot 10^3$	$100,3\cdot 10^3$	$149,9\cdot 10^3$	$199,1\cdot 10^3$	$248,0\cdot 10^3$
	E	219,3	320,6	419,8	822,5	1228	1630	2031
$G=6,0$	a	1,952	6,968	21,06	42,24	65,40	100,5	122,0
	d	218,1	405,7	860,7	1477	2139	3117	3700
	E	0,9748	2,044	4,703	8,251	12,16	17,92	21,32
	a	123,1	123,3	128,2	148,5	212,7	279,6	347,5
	d	3727	3729	3881	4412	6130	7893	9690
	E	21,41	21,45	22,40	25,44	35,53	45,98	56,40
	a	483,0	752,0	1420	2097	2763	5418	8104
	d	$13,24\cdot 10^3$	$20,22\cdot 10^3$	$37,40\cdot 10^3$	$55,08\cdot 10^3$	$72,12\cdot 10^3$	$140,0\cdot 10^3$	$209,4\cdot 10^3$
	E	77,20	117,9	218,0	322,9	422,5	818,0	1224
$G=7,0$	a	0,0112	2,392	8,148	24,37	48,83	75,40	115,6
	d	160,0	288,0	535,8	1142	1969	2843	4136
	E	0,4305	0,9713	2,038	4,697	8,297	12,15	17,87
	a	141,8	148,1	170,3	244,9	323,8	399,0	553,9
	d	4958	5184	5818	8151	$10,62\cdot 10^3$	$12,83\cdot 10^3$	$17,48\cdot 10^3$
	E	21,36	22,37	25,40	35,54	46,67	56,00	76,33
	a	867,0	1643	2411	3180	6254	9319	$12,45\cdot 10^3$
	d	$26,99\cdot 10^3$	$50,29\cdot 10^3$	$73,13\cdot 10^3$	$95,99\cdot 10^3$	$187,4\cdot 10^3$	$278,3\cdot 10^3$	$373,0\cdot 10^3$
	E	119,2	222,2	322,5	422,5	823,0	1223	1636
$G=8,0$	a	0,1451	2,850	9,431	27,99	55,30	85,41	130,8
	d	205,1	371,5	697,8	1495	2520	3648	5296
	E	0,4313	0,9826	2,092	4,821	8,265	12,16	17,82
	a	160,8	166,6	193,2	275,6	364,3	450,2	626,5
	d	6383	6617	7505	$10,35\cdot 10^3$	$13,49\cdot 10^3$	$16,38\cdot 10^3$	$22,44\cdot 10^3$
	E	21,60	22,17	25,36	34,98	46,13	55,55	76,37
	a	978,3	1849	2723	3590	7060	$10,52\cdot 10^3$	$14,00\cdot 10^3$
	d	$34,49\cdot 10^3$	$63,94\cdot 10^3$	$93,66\cdot 10^3$	$122,8\cdot 10^3$	$239,8\cdot 10^3$	$356,1\cdot 10^3$	$473,8\cdot 10^3$
	E	117,3	218,6	319,4	418,5	825,8	1227	1628
$G=9,0$	a	0,2777	3,290	10,62	31,01	61,93	95,20	145,2
	d	255,0	461,3	867,0	1826	3156	4523	6531
	E	0,4289	0,9762	2,079	4,697	8,323	12,09	17,50
	a	176,8	187,5	215,8	307,4	405,5	503,9	702,2
	d	7723	8340	9378	$12,91\cdot 10^3$	$16,75\cdot 10^3$	$20,56\cdot 10^3$	$28,27\cdot 10^3$
	E	20,95	22,40	25,34	34,92	45,40	56,05	77,47
	a	1091	2058	3034	3997	7870	$11,74\cdot 10^3$	$15,59\cdot 10^3$
	d	$43,03\cdot 10^3$	$79,42\cdot 10^3$	$116,6\cdot 10^3$	$152,7\cdot 10^3$	$298,9\cdot 10^3$	$444,6\cdot 10^3$	$589,0\cdot 10^3$
	E	118,4	216,0	322,0	421,5	821,5	1220	1615
$G=10,0$	a	0,4121	3,722	11,80	33,92	68,43	106,1	160,5
	d	310,7	559,4	1054	2177	3849	5630	7986
	E	0,4281	0,9861	2,067	4,634	8,308	12,42	17,56
	a	198,6	205,1	239,0	341,2	447,0	554,6	773,4
	d	9765	9988	$11,52\cdot 10^3$	$15,92\cdot 10^3$	$20,38\cdot 10^3$	$24,96\cdot 10^3$	$34,36\cdot 10^3$
	E	21,74	22,13	25,66	35,73	44,93	55,60	76,97
	a	1212	2266	3352	4421	8701	$12,96\cdot 10^3$	$17,21\cdot 10^3$
	d	$53,20\cdot 10^3$	$96,52\cdot 10^3$	$142,7\cdot 10^3$	$187,3\cdot 10^3$	$366,2\cdot 10^3$	$543,0\cdot 10^3$	$720,0\cdot 10^3$
	E	120,0	215,5	323,5	423,5	826,0	1223	1621

TABLE 3

$G = 0,2$	$a=0$	d	100	200	300	400	500
		E	220,4	459,6	698,8	943,4	1187
	$a=5$	d	100	200	300	400	500
		E	209,2	448,2	689,0	931,4	1176
	$a=10$	d	100	200	300	400	500
		E	197,0	437,1	678,8	921,8	1165
	$a=15$	d	100	200	300	400	500
		E	183,7	421,2	665,4	909,8	1154
	$a=25$	d	100	200	300	400	500
		E	154,7	397,6	640,4	886,1	1131
	$a=50$	d	500	1000	1500	2000	2500
		E	1070	2296	3527	4762	5995
	$a=100$	d	500	1000	1500	2000	2500
		E	936,8	2174	3407	4644	5883
	$a=200$	d	500	1000	1500	2000	2500
		E	589,5	1904	3151	4409	5637
	$a=300$	d	1000	1500	2000	2500	3000
		E	1601	2881	4131	5378	6612
	$a=400$	d	1000	1500	2000	2500	3000
		E	1218	2584	3853	5104	6352
	$a=500$	d	1000	1500	2000	2500	3000
		E	0	2256	3562	4828	6084
	$a=2,5\cdot 10^3$	d	$50\cdot 10^3$	$110\cdot 11^3$	$150\cdot 10^3$	$200\cdot 10^3$	$250\cdot 10^3$
		E	$117,9\cdot 10^3$	$242,3\cdot 10^3$	$367,1\cdot 10^3$	$492,1\cdot 10^3$	$616,4\cdot 10^3$
	$a=5\cdot 10^3$	d	$50\cdot 10^3$	$100\cdot 10^3$	$150\cdot 10^3$	$200\cdot 10^3$	$250\cdot 10^3$
		E	$111,5\cdot 10^3$	$236,1\cdot 10^3$	$361,0\cdot 10^3$	$485,2\cdot 10^3$	$609,7\cdot 10^3$
	$a=10\cdot 10^3$	d	$50\cdot 10^3$	$100\cdot 10^3$	$150\cdot 10^3$	$200\cdot 10^3$	$250\cdot 10^3$
		E	$91,08\cdot 10^3$	$223,1\cdot 10^3$	$347,9\cdot 10^3$	$472,0\cdot 10^3$	$597,4\cdot 10^3$
	$a=15\cdot 10^3$	d	$50\cdot 10^3$	$100\cdot 10^3$	$150\cdot 10^3$	$200\cdot 10^3$	$250\cdot 10^3$
		E	$83,16\cdot 10^3$	$208,8\cdot 10^3$	$334,5\cdot 10^3$	$459,8\cdot 10^3$	$585,4\cdot 10^3$
$G = 1,0$	$a=0$	d	100	200	300	400	500
		E	31,99	69,09	106,8	144,9	183,1
	$a=5$	d	100	200	300	400	500
		E	26,59	64,29	102,2	140,4	178,7
	$a=10$	d	100	200	300	400	500
		E	19,34	58,98	97,36	135,7	174,2
	$a=15$	d	100	200	300	400	500
		E	0	53,14	92,08	131,3	169,3
	$a=25$	d	100	200	300	400	500
		E	0	37,74	80,39	120,3	159,3
	$a=50$	d	500	1000	1500	2000	2500
		E	129,7	329,8	525,3	721,4	917,7
	$a=100$	d	500	1000	1500	2000	2500
		E	0	271,4	473,6	672,3	868,9
	$a=200$	d	1000	1500	2000	2500	3000
		E	0	343,2	560,0	761,4	959,5
	$a=300$	d	1000	1500	2000	2500	3000
		E	0	0	403,2	633,7	845,4
	$a=400$	d	1000	1500	2000	2500	3000
		E	0	0	0	455,3	703,9
	$a=500$	d	1000	1500	2000	2500	3000
		E	0	0	0	0	499,8
	$a=2,5\cdot 10^3$	d	$50\cdot 10^3$	$100\cdot 10,^3$	$150\cdot 10^3$	$200\cdot 10^3$	$250\cdot 10^3$
		E	$17,34\cdot 10^3$	$37,29\cdot 10^3$	$57,24\cdot 10^3$	$77,19\cdot 10^3$	$97,05\cdot 10^3$
	$a=5\cdot 10^3$	d	$50\cdot 10^3$	$100\cdot 10^3$	$150\cdot 10^3$	$200\cdot 10^3$	$250\cdot 10^3$
		E	$14,48\cdot 10^3$	$36,77\cdot 10^3$	$54,77\cdot 10^3$	$74,72\cdot 10^3$	$94,64\cdot 10^3$

TABLE 3 (continued)

$G=1.0$	$a=10\cdot 10^3$	d	$50\cdot 10^3$	$100\cdot 10^3$	$150\cdot 10^3$	$200\cdot 10^3$	$250\cdot 10^3$
		E	0	$29{,}00\cdot 10^3$	$49{,}47\cdot 10^3$	$69{,}58\cdot 10^3$	$89{,}71\cdot 10^3$
	$a=15\cdot 10^3$	d	$50\cdot 10^3$	$100\cdot 10^3$	$150\cdot 10^3$	$200\cdot 10^3$	$250\cdot 10^3$
		E	0	$21{,}40\cdot 10^3$	$43{,}50\cdot 10^3$	$64{,}12\cdot 10^3$	$84{,}39\cdot 10^3$
$G=2{,}0$	$a=0$	d	100	200	300	400	500
		E	9,938	22,94	36,30	49,83	63,49
	$a=5$	d	100	200	300	400	500
		E	4,487	19,39	32,98	46,63	60,36
	$a=10$	d	100	200	300	400	500
		E	0	14,90	29,28	43,14	57,12
	$a=25$	d	100	200	300	400	500
		E	0	0	0	30,32	45,57
	$a=50$	d	1000	1500	2000	2500	3000
		E	98,28	170,6	242,2	313,4	384,9
	$a=100$	d	1000	1500	2000	2500	3000
		E	0	130,0	205,6	278,9	351,8
	$a=200$	d	1000	1500	2000	2500	3000
		E	0	0	0	190,0	268,7
	$a=2{,}5\cdot 10^3$	d	$50\cdot 10^3$	$100\cdot 10^3$	$150\cdot 10^3$	$200\cdot 10^3$	$250\cdot 10^3$
		E	$5{,}493\cdot 10^3$	$12{,}85\cdot 10^3$	$20{,}15\cdot 10^3$	$27{,}42\cdot 10^3$	$34{,}72\cdot 10^3$
	$a=5\cdot 10^3$	d	$50\cdot 10^3$	$100\cdot 10^3$	$150\cdot 10^3$	$200\cdot 10^3$	$250\cdot 10^3$
		E	$2{,}778\cdot 10^3$	$11{,}03\cdot 10^3$	$18{,}45\cdot 10^3$	$25{,}77\cdot 10^3$	$33{,}07\cdot 10^3$
	$a=10\cdot 10^3$	d	$50\cdot 10^3$	$100\cdot 10^3$	$150\cdot 10^3$	$200\cdot 10^3$	$250\cdot 10^3$
		E	0	$5{,}594\cdot 10^3$	$14{,}49\cdot 10^3$	$22{,}10\cdot 10^3$	$29{,}55\cdot 10^3$
	$a=15\cdot 10^3$	d	$50\cdot 10^3$	$100\cdot 10^3$	$150\cdot 10^3$	$200\cdot 10^3$	$250\cdot 10^3$
		E	0	0	$8{,}431\cdot 10^3$	$17{,}77\cdot 10^3$	$25{,}64\cdot 10^3$
$G=3{,}0$	$a=0$	d	100	200	300	400	500
		E	4,195	10,71	17,39	24,24	31,16
	$a=5$	d	100	200	300	400	500
		E	0	7,554	14,67	21,66	28,67
	$a=10$	d	100	200	300	400	500
		E	0	0	11,26	18,72	25,95
	$a=25$	d	100	200	300	400	500
		E	0	0	0	0	14,30
	$a=50$	d	1000	1500	2000	2500	3000
		E	37,09	76,54	113,9	147,0	187,9
	$a=200$	d	1000	1500	2000	2500	3000
		E	0	0	0	0	59,40
	$a=2{,}5\cdot 10^3$	d	$50\cdot 10^3$	$100\cdot 10^3$	$150\cdot 10^3$	$200\cdot 10^3$	$250\cdot 10^3$
		E	$2{,}352\cdot 10^3$	$6{,}250\cdot 10^3$	$10{,}06\cdot 10^3$	$13{,}84\cdot 10^3$	$17{,}64\cdot 10^3$
	$a=5\cdot 10^3$	d	$50\cdot 10^3$	$100\cdot 10^3$	$150\cdot 10^3$	$200\cdot 10^3$	$250\cdot 10^3$
		E	0	$4{,}731\cdot 10^3$	$8{,}701\cdot 10^3$	$12{,}54\cdot 10^3$	$16{,}36\cdot 10^3$
	$a=10\cdot 10^3$	d	$50\cdot 10^3$	$100\cdot 10^3$	150.10^3	$200\cdot 10^3$	$250\cdot 10^3$
		E	0	0	$5{,}011\cdot 10^3$	$9{,}510\cdot 10^3$	$13{,}53\cdot 10^3$
	$a=15\cdot 10^3$	d	$50\cdot 10^3$	$100\cdot 10^3$	$150\cdot 10^3$	$200\cdot 10^3$	$250\cdot 10^3$
		E	0	0	0	0	$10{,}01\cdot 10^3$
$G=4{,}0$	$a=0$	d	100	200	300	400	500
		E	1,918	5,776	9,754	13,83	17,97
	$a=5$	d	100	200	300	400	500
		E	0	0	7,311	11,60	15,84
	$a=10$	d	100	200	300	400	500
		E	0	0	0	8,825	13,42
	$a=50$	d	1000	1500	2000	2500	3000
		E	0	38,22	61,90	84,80	107,5
	$a=2{,}5\cdot 10^3$	d	$50\cdot 10^3$	$100\cdot 10^3$	$150\cdot 10^3$	$200\cdot 10^3$	$250\cdot 10^3$
		E	$1{,}048\cdot 10^3$	$3{,}555\cdot 10^3$	$5{,}905\cdot 10^3$	$8{,}226\cdot 10^3$	$10{,}55\cdot 10^3$

TABLE 3 (continued)

$G=4,0$	$a=5\cdot10^3$	d	$50\cdot10^3$	$100\cdot10^3$	$150\cdot10^3$	$200\cdot10^3$	$250\cdot10^3$
		E	0	$2,135\cdot10^3$	$4,745\cdot10^3$	$7,148\cdot10^3$	$9,503\cdot10^3$
	$a=10\cdot10^3$	d	$50\cdot10^3$	$100\cdot10^3$	$150\cdot10^3$	$200\cdot10^3$	$250\cdot10^3$
		E	0	0	0	$4,298\cdot10^3$	$7,039\cdot10^3$
$G=5,0$	$a=0$	d	100	200	300	400	500
		E	0	3,363	5,977	8,644	11,38
	$a=5$	d	100	200	300	400	500
		E	0	0	3,494	6,599	9,476
	$a=50$	d	1000	1500	2000	2500	3000
		E	0	14,01	36,03	51,71	67,04
	$a=2,5\cdot10^3$	d	$50\cdot10^3$	$100\cdot10^3$	$150\cdot10^3$	$200\cdot10^3$	$250\cdot10^3$
		E	0	$2,212\cdot10^3$	$3,816\cdot10^3$	$5,382\cdot10^3$	$6,961\cdot10^3$
	$a=5\cdot10^3$	d	$50\cdot10^3$	$100\cdot10^3$	$150\cdot10^3$	$200\cdot10^3$	$250\cdot10^3$
		E	0	0	$2,771\cdot10^3$	$4,441\cdot10^3$	$6,051\cdot10^3$
$G=6,0$	$a=0$	d	100	200	300	400	500
		E	0	2,010	3,853	5,712	7,618
	$a=5$	d	100	200	300	400	500
		E	0	0	0	3,730	5,887
	$a=50$	d	1000	1500	2000	2500	3000
		E	0	0	20,79	32,94	44,18
	$a=2,5\cdot10^3$	d	$50\cdot10^3$	$100\cdot11^3$	$150\cdot10^3$	$200\cdot10^3$	$250\cdot10^3$
		E	0	$1,440\cdot10^3$	$2,611\cdot10^3$	$3,749\cdot10^3$	$4,891\cdot10^3$
	$a=5\cdot10^3$	d	$50\cdot10^3$	$100\cdot10^3$	$150\cdot10^3$	$200\cdot10^3$	$250\cdot10^3$
		E	0	0	$1,630\cdot10^3$	$2,907\cdot10^3$	$4,087\cdot10^3$
$G=7,0$	$a=0$	d	1000	1500	2000	2500	3000
		E	12,72	20,32	28,08	35,95	43,80
	$a=50$	d	1000	1500	2000	2500	3000
		E	0	0	0	21,66	29,96
	$a=2,5\cdot10^3$	d	$50\cdot10^3$	$100\cdot10^3$	$150\cdot10^3$	$200\cdot10^3$	$250\cdot10^3$
		E	0	$0,9578\cdot10^3$	$1,866\cdot10^3$	$2,732\cdot10^3$	$3,594\cdot10^3$
$G=8,0$	$a=0$	d	1000	1500	2000	2500	3000
		E	9,490	15,36	21,32	27,40	33,54
	$a=50$	d	1000	1500	2000	2500	3000
		E	0	0	0	12,67	20,43
	$a=2,5\cdot10^3$	d	$50\cdot10^3$	$100\cdot10^3$	$150\cdot10^3$	$200\cdot10^3$	$250\cdot10^3$
		E	0	$0,6344\cdot10^3$	$1,374\cdot10^3$	$2,049\cdot10^3$	$2,736\cdot10^3$
$G=9,0$	$a=0$	d	1000	1500	2000	2500	3000
		E	7,240	11,87	16,62	21,42	26,32
	$a=50$	d	1000	1500	2000	2500	3000
		E	0	0	0	0	13,49
	$a=2,5\cdot10^3$	d	$50\cdot10^3$	$100\cdot10^3$	$150\cdot10^3$	$200\cdot10^3$	$250\cdot10^3$
		E	0	$0,3726\cdot10^3$	$1,031\cdot10^3$	$1,582\cdot10^3$	$2,133\cdot10^3$
$G=10,0$	$a=0$	d	1000	1500	2000	2500	3000
		E	5,620	9,408	13,26	17,24	21,09
	$a=50$	d	1000	1500	2000	2500	3000
		E	0	0	0	0	8,134
	$a=2,5\cdot10^3$	d	$50\cdot10^3$	$100\cdot10^3$	$150\cdot10^3$	$200\cdot10^3$	$250\cdot10^3$
		E	0	0	$0,7817\cdot10^3$	$1,244\cdot10^3$	$1,692\cdot10^3$

puted values of the coordinates of surface R are given in Table 2, and those for surface S, in Table 3. The values of parameter E in Table 2 are given for the points of contact of surfaces R and S. Surface T consists of the traces of surface R on the plane $E = 0$, so that Table 1 also contains the boundary values of the parameters for the previous system (1)-(3). For $G = 0$ in subregion Ib, the system (1), (2), (4), will always be autooscillatory (soft mode). With no feedback in the controller ($\delta = 0$), the boundary of stability is defined by the traces of surfaces R and S on the plane $a = 0$, and coincides with that constructed previously in [2]. The behavior of the system in the other regions is clear from Table 1, where the case $c_1 \neq \infty$ (i.e., $E \neq 0$) has been referred to system (1), (2), (4). We note that in region IV, for $k > 0$, $c > 0$, for some initial conditions there is a subregion of attraction of the rest segment. This last remark also applies to system (1)-(3).

In the previously cited cases of rigid modes of autooscillation, the threshold values of the initial deviations, bounding the subregions of stability of systems (1)-(3) and (1), (2), (4) "in the small," may be expressed by the formulas

$$\varphi(0)+\delta\mu(0)=b+\gamma c+\begin{cases}\dfrac{2b\left(1+A_1^2\right)}{B\left(B\ln\dfrac{B}{B-V_2}-V_2\right)} & \text{for}\quad (a-1)^2<4d,\\[2ex] \dfrac{2b}{B\left(B\ln\dfrac{B}{B-V_2}-V_2\right)} & \text{for}\quad (a-1)^2=4d,\\[2ex] \dfrac{2bA}{B\left(B\ln\dfrac{B}{B-V_2}-V_2\right)} & \text{for}\quad (a-1)^2>4d,\end{cases}$$

$$\dot\varphi(0)+\delta\dot\mu(0)=0, \tag{8}$$

where the parameter V_2 is defined by the first equation and inequality in (7).

For $k = 0$, the systems under consideration are autooscillatory only if $\delta > 0$ and $b \neq 0$.

From the spaces constructed it follows that the Coulomb friction in the valve has a negative effect on stability. The servomotor's dead zone and the saturation nonlinearity affect stability positively for stable objects ($k > 0$) and negatively for unstable objects ($k < 0$). On the whole, the effect of the nonlinearities treated here is so significant that, due to them, an absolutely stable linear system may become absolutely unstable, and conversely. In the most important region practically, $k > 0$, $\delta > 0$, the dependence of the boundary of stability on the magnitude of the Coulomb friction and on the magnitude of the saturation nonlinearity parameter c_1 is only observed when several nonlinearities are taken into account jointly. In this region, the deleterious influence on stability of the Coulomb friction in the valve can be compensated by an increase in the servomotor's dead zone, or by limiting its maximum power. These stability requirements are in conflict with requirements for rapidity of system response. Increasing the stability margin at the cost of increasing δ is contrary to the requirement on static accuracy. It is therefore advantageous to have quantities estimates.

For relay system (1), (2), (5), the parameter space was previously constructed in [3]. It follows, from a comparison of the stability boundaries of these three systems, that the region of stability of system (1)-(3) is bounded upon the introduction of a saturation nonlinearity; with a transition from system (1), (2), (4) to a relay system, no increase in the region of stability occurs.

Other Questions of Dynamics

In analyzing a system by our designated method, the "amplitudes" of autooscillations are defined by the coordinates of the stable fixed points of the corresponding point transformations, and the periods of autooscillations are defined by the sums of the times spent by the representative point on the segments of the trajectories making up closed cycles. Thus, for system (1)-(3), in subregion Ib, the "amplitude" of the autooscillation $x_n = (\varphi + \delta\mu)_{\max}$ is expressed by formulas (8) with V_3 replacing V_2 in them, where the parameter V_3 is determined from the system

$$F_1(V_3)=F(V_3),\quad \left(\frac{\partial F_1}{\partial V}\right)_{V_3}<\left(\frac{\partial F}{\partial V}\right)_{V_3}. \tag{9}$$

With this, the period of autooscillation, for example, for $(a-1)^2 > 4d$, will be

$$T_{\mathrm{p}}=\frac{2T_a}{k}\left[\frac{A}{B(A-1)}\ln A\,\frac{V_3-1}{V_3-A}+\frac{A/B\,\dfrac{2b}{x_{\mathrm{p}}-b-\gamma c}+V_3}{B}+\right.$$
$$\left.+\ln\frac{(V_3-A)\exp\left(\dfrac{1}{1-A}\ln\dfrac{V_3-1}{V_3-A}\right)}{(V_3-A)\exp\left(\dfrac{1}{1-A}\ln\dfrac{V_3-1}{V_3-A}\right)-\dfrac{A}{B}\,\dfrac{2\gamma c}{x_{\mathrm{p}}-b-\gamma c}}\right] \tag{10}$$

Autooscillations are ordinarily not the working modes of the systems being considered, so that we shall not give all the corresponding formulas here. But, for $k = 0$, $\delta > 0$, $b > 0$, all three systems are autooscillatory, and may be used as stabilization systems of certain processes only under the condition that the maximum deviation $\varphi_{\max}$ of the controlled quantity be small in the autooscillatory mode. In this case, the relative "amplitudes"

of the autooscillation $\Phi = (\varphi_{\max} - \gamma c_1)/\gamma(c_1 - c)$, defining the value of $\varphi_{\max}$, are expressed by the formulas:
for system (1)-(3)

$$\Phi_1 = E + E\frac{1-2h}{E^*} - 1, \tag{11}$$

for system (1), (2), (4),

$$\begin{aligned} \Phi_2 &= E + 2h\left(\frac{U_p^2}{4} - 1\right) \quad \text{for} \quad E > E^*, \\ \Phi_2 &\equiv \Phi_1 \qquad\qquad\qquad\quad \text{for} \quad E < E^*, \end{aligned} \tag{12}$$

for system (1), (2), (5),

$$\Phi_3 = \frac{E^2}{8h} - 1. \tag{13}$$

Here, $h = a^2/4d$; E^* and U_p are defined by the equations

$$(L)_{U=0,\, E=E^*} = 0, \quad (L)_{U=U_p} = 0,$$

$$L = \sqrt{A_1^2 + \left[\sqrt{U^2 + 4E(1 + A_1^2)} - 1\right]^2} \exp\left[-\frac{1}{A_1} \operatorname{arc\,tg} \frac{A_1}{\sqrt{U^2 + 4E(1 + A_1^2)} - 1} - \right.$$

$$\left. - \sqrt{A_1 + (U + 1)^2} \exp\left(\frac{1}{A_1} \operatorname{arc\,tg} \frac{A_1}{U + 1}\right) \right. \qquad \text{for} \quad h < 1,$$

$$L = \left(\sqrt{U^2 + 4E} - 1\right) \exp\left(-\frac{1}{\sqrt{U^2 + 4E} - 1}\right) - (U + 1) \exp \frac{1}{U + 1} \quad \text{for} \quad h = 1,$$

$$L = \left(\sqrt{U^2 + 4AE} - 1\right) \exp\left(\frac{A}{1 - A} \ln \frac{\sqrt{U^2 + 4AE} - 1}{\sqrt{U^2 + 4AE} - A}\right) -$$

$$- (U + 1) \exp\left(\frac{A}{A - 1} \ln \frac{U + A}{U + 1}\right) \quad \text{for} \quad h > 1,$$

where, in accordance with our previous notation,

$$A_1 = \sqrt{\frac{1}{h} - 1}, \quad A = \frac{1 + \sqrt{1 - 1/h}}{1 - \sqrt{1 - 1/h}}.$$

Formulas (11)-(13) isolate, in coordinates E, h, the regions for which one of the inequality signs $\Phi_1 \gtrless \Phi_3$, $\Phi_2 \gtrless \Phi_3$, is valid, and it follows from them, that systems (1)-(3) and (1), (2), (4), when compared with system (1), (2), (5) in terms of the magnitude of Φ, gain with a decrease in h and an increase in E, and lose for the inverse changes of the parameters.

Analysis of phase spaces permits one to establish the conditions for monotonic (without overshoot) flow of the transient response. We note that the region of monotonicity of System (1)-(3) is broadened upon the introduction of a saturation nonlinearity. For system (1), (2), (4), the region in which the transient response, with initial conditions $-\infty < \varphi(0) + \delta\mu(0) < \infty$, $\dot{\varphi}(0) + \delta\dot{\mu}(0) = 0$, occurs without overshoot and which lies in parameter space inside the region of stability, is defined by the inequalities

$$\sqrt{A_1^2 + (B - 1)^2} \exp\left(-\frac{1}{A_1} \operatorname{arc\,tg} \frac{A_1}{B - 1}\right) \leqslant \frac{2(1 + A_1^2)}{B} GE \quad \text{for} \quad (a - 1)^2 < 4d,$$

$$B \leqslant 1 + \frac{2}{B} GE \exp \frac{1}{B - 1} \quad \text{for} \quad (a - 1)^2 = 4d,$$

$$B \leqslant A + \frac{2A}{B} GE \exp\left(\frac{1}{A - 1} \ln \frac{B - 1}{B - A}\right) \quad \text{for} \quad (a - 1)^2 > 4d.$$

Practical Applications of the Theory

An important assumption in the theory presented is the neglect of inertial forces in the controlling devices. However, as was shown by experimental investigation of a number of control schemes for naval steam energy stands, this assumption was justified in the corresponding cases (low inertia measuring system, hydraulic piston servomotor).

As an example of the use of the results presented, we determine the magnitude of the feedback factor necessary for stabilizing the steam pressure regulator [10] of the A. N. Krylov TsNII system, one of which was demonstrated at the All-Union Industrial Exhibition in 1957. For this example, it was determined that: $T_a = 60$ seconds; $k = 0.25$; $\gamma = 0.03$; $T_s = 40$ seconds; $c = 0.2$; $b = 0.001$; $c_1 = 0.9$; i.e., $a = 200\delta$; $d = 800$; $G = 6$; $E = = 0.0476$. From the tables we find that, for stability, the adjustment must provide $\delta > 0.09$, which is borne out by practical testing.

The data given are applied in an analogous way to some other practical problems.

LITERATURE CITED

1. H. Léauté, "Mémoire sur les oscillations à longues périodes dans les machines actionées par des moteurs hydrauliques," Journal de l'Ecole polytechnique 55 (1885).
2. A. A. Andronov, N. N. Bautin, and G. S. Gorelik, "Autooscillations of the simplest schemes containing automatic variable pitch screws," Doklady Akad. Nauk SSSR, Nov. Ser. 47, 4 (1945).
3. A. A. Andronov and N. N. Bautin, "On the effect of Coulomb friction in valves on the indirect control process," Izvest. AN SSSR, Otd. Tekhn. N. No. 7 (1955).
4. V. V. Petrov and G. M. Ulanov, "On the status and problems of the study of dynamics of nonlinear automatic control systems by means of phase space, and on the questions of their dynamic accuracy," Session of the AN SSSR on the Scientific problems of Automating Production [in Russian] (Izd. AN SSSR, 1957) 2.
5. V. V. Solodovnikov (ed.), Automatic Control Fundamentals.1 [in Russian] (Mashgiz, 1954).
6. E. P. Popov, Dynamics of Automatic Control Systems [in Russian] (Gostekhizdat, 1954).
7. R. E. Kalman, Physical and Mathematical Mechanisms of Instability in Nonlinear Automatic Control Systems, Trans. ASME 79, No. 3 (1957).
8. V. V. Kazakevich, "Multiple systems and the simplest dynamic models of time," Doklady Akad. Nauk SSSR, Nov. Ser. 24, 4 (1950).
9. V. V. Petrov and G. M. Ulanov, "Theory of the two simplest relay systems of automatic control," Avtomat. i Telemekh. 11, 5 (1950).
10. M. Sh. Shifrin, Control of Naval Boiler Aggregates [in Russian] (Sudpromgiz, 1957).

ON THE THEORY OF OSCILLATIONS OF QUASI-LINEAR SYSTEMS WITH CONSTANT LAGS

S. N. Shimanov

Sverdlovsk

Translated from Avtomatika i Telemekhanika, Vol. 21, No. 6, pp. 706-709, June, 1960

The conditions are given for the existence and stability of almost periodic oscillations in quasi-linear systems with time delays.

The problem of studying the conditions for the appearance of autooscillations, and also forced oscillations, in control systems is of significant interest. The study of oscillations in control systems described by ordinary differential equations was the subject-matter of works by B. V. Bulgakov [1], A. M. Letov [2], A. I. Lur'e [3], M. A. Aizerman, Ya. Z. Tsypkin, and others. In particular, very effective use was made in the works cited of the method of small parameters in the study of oscillations in certain controlled systems.

It is of interest to develop the method of small parameters in the direction of its use in the study of the appearance and stability of periodic and almost periodic modes in nonlinear control systems. The present paper presents the author's results in the theory of almost periodic oscillations in general quasi-linear systems with constant lags.

The method of N. N. Bogolyubov [4] is used in this work. The paper is a development of results obtained by I. G. Malkin [5] in solving the problem of the existence of almost periodic modes in quasi-linear systems whose motions are described by ordinary differential equations.

In clearing up the question of stability, the methods of A. M. Lyapunov, developed in the works of N. G. Chetaev [6], N. N. Krasovskii [7], and others, turned out to be very useful.

1. We consider a system whose motions are described by a set of differential-difference equations of the form

$$\frac{dx_s(t)}{dt} = a_{s1}x_1(t) + \ldots + a_{sn}x_n(t) + b_{s1}x_1(t-\tau) + \ldots + b_{sn}x_n(t-\tau) + f_s(t) + \mu F_s[t;\ x_1(t), \ldots, x_n(t);\ x_1(t-\tau), \ldots, x_n(t-\tau);\ \mu] \quad (s = 1, \ldots, n) \tag{1}$$

Here, a_{si}, b_{si} are constant coefficients; τ is a constant which characterizes the temporal delay; $f_s(t)$ are finite trigonometric sums; $F_s(t, x_1, \ldots, x_n, x'_1, \ldots, x'_n, \mu)$ are polynomials in $x_1, \ldots, x_n, x'_1, \ldots, x'_n$ and trigonometric finite sums in t with frequencies which do not depend on the variables x, x', and μ is a small parameter on which the coefficients of the F_s depend analytically; $[x'_1 = x_1(t-\tau), \ldots, x'_n = x_n(t-\tau)]$.

We consider the characteristic equation

$$\Delta(\lambda) \equiv |a_{si} - \delta_{si}\lambda + b_{si}\exp(-\lambda\tau)| = 0. \tag{2}$$

Theorem 1. If Eq. (2) has no roots on the imaginary axis of the λ plane, then system (1) admits a unique almost periodic solution $x_s^*(t, \mu)$ for sufficiently small $|\mu|$.

The proof of this theorem is carried out by the method of successive approximations on the basis of the following lemma.

Lemma 1. We consider the system of linear differential-difference equations

$$\frac{dx_s(t)}{dt} = a_{s1}x_1(t) + \ldots + a_{sn}x_n(t) + b_{s1}x_1(t-\tau) + \ldots + b_{sn}x_n(t-\tau) + f_s(t) \quad (s = 1, \ldots, n). \tag{3}$$

This system is obtained from (1) for $\mu = 0$.

If characteristic Eq. (2) has no roots on the imaginary axis of the λ plane, then Eq. (3) admits one, and only one, almost periodic solution $x_s^*(t)$, and this solution has the estimate

$$|x_s^*(t)| < AM, \tag{4}$$

where A does not depend on the f_s, and is determined only by the coefficients a, b and the lag τ.

We construct the solution $x_s^*(t)$ by Bückner's method in the following way. Let $\Delta_{jk}(i\lambda)$ be the cofactor of the element in the kth column and jth row of the matrix $\|\Delta(i\lambda)\|$. We introduce the notation $\Gamma_{kj}(i\lambda) = \Delta_{jk}(i\lambda)/\Delta(i\lambda)$.

Let
$$K_{js}(t) = \frac{1}{2\pi}\int_{-\infty}^{+\infty} e^{i\lambda t}\Gamma_{js}(i\lambda)\,d\lambda.$$

It can be shown that the integral

$$\int_{-\infty}^{+\infty} |K_{js}(t)|\,dt \tag{5}$$

has a finite value.

Then the almost periodic solution of system (3) is determined by the formulas

$$x_s^* = \sum_{j=1}^{n}\int_{-\infty}^{+\infty} f_j(\xi)\,K_{sj}(\xi - t)\,d\xi \equiv \sum_{j=1}^{n}\int_{-\infty}^{+\infty} f_j(t+\xi)\,K_{sj}(\xi)\,d\xi \quad (s = 1, \ldots, n).$$

From this expression, for the solutions x_s^*, with account taken of (5), the estimate of (4) is rapidly obtained.

In the course of the proof of convergence of the successive approximations for the almost periodic solution of system (1), a rough estimate is obtained for the region of existence of an almost periodic solution in terms of the parameter μ.

Theorem 2. If all the roots of Eq. (2) have negative real parts, then the solution $x_s^*(t, \mu)$ of system (1) will be asymptotically stable for $t \to +\infty$ and for sufficiently small, by modulus, initial functions, characterizing the disturbance μ for sufficiently small $|\mu|$.

2. We consider the case when, among the roots of Eq. (2), there are m purely imaginary ones: $\omega_1 i, \omega_2 i, \ldots, \omega_m i$. We assume that to these roots there will correspond m periodic solutions $\varphi_{s1}, \varphi_{s2}, \ldots, \varphi_{sm}$ of homogeneous system (3). The periods of these solutions will be, respectively: $2\pi/|\omega_1|, \ldots, 2\pi/|\omega_m|$. In case some of the ω equal zero, the periods of the solutions will be arbitrary, and we shall take them as equal to, for example, 2π. We assume that $\omega_m \neq 0$.

We again consider system (3), in which we shall assume the $f_s(t)$ to be arbitrary, almost periodic functions.

Lemma 2. We consider the auxiliary system

$$\begin{aligned}\frac{dx_s(t)}{dt} &= a_{s1}x_1(t) + \ldots + a_{sn}x_n(t) + b_{s1}x_1(t-\tau) + \ldots + b_{sn}x_n(t-\tau) + \\ &+ f_s(t) + \varphi_{s1}W_1(t) + \ldots + \varphi_{sm}W_m(t) \quad (s = 1 \ldots, n)\end{aligned} \tag{6}$$

No matter what the almost periodic functions $f_s(t)$, it is always possible to construct almost periodic functions $W_1, \ldots, W_m$ with frequencies whose moduli do not exceed 2ϵ (ϵ is an arbitrarily small positive number) such that system (6) will admit an almost periodic solution of the form

$$x_s^* = M_1\varphi_{s1} + \ldots + M_m\varphi_{sm} + \varphi_s(t), \tag{7}$$

where $M_1, \ldots, M_m$ are arbitrary constants, and $\varphi_s(t)$ is an almost periodic function. The functions $\varphi_s(t)$ will be completely uniquely defined if it is required that, for example, frequencies equal to the frequencies $\omega_1, \ldots, \omega_m$ not enter in φ_n. The functions φ_s admit estimates of the type of (4).

Lemma 3. We consider an auxiliary system of the form

$$\begin{aligned}\frac{dx_s(t)}{dt} &= a_{s1}x_1(t) + \ldots + a_{sn}x_n + b_{s1}x_1(t-\tau) + \ldots + b_{sn}x_n(t-\tau) + f_s(t) + \\ &+ \mu F_s[t, x_1(t), \ldots, x_n(t-\tau), \mu] + \varphi_{s1}W_1 + \ldots + \varphi_{sm}W_m \quad (s = 1, \ldots, n).\end{aligned} \tag{8}$$

System (8) permits almost periodic solutions of the form

$$x_s^*(t, M_1, \ldots, M_m, \mu) = \varphi_{s1}M_1 + \ldots + \varphi_{sm}M_m + \varphi_s + \mu\bar{x}_s^*(t, M, \mu) \quad (s = 1, \ldots, n). \tag{9}$$

where $M_1, \ldots, M_m$ are arbitrary parameters, defined in some neighborhood of the point $\bar{M}_1, \ldots, \bar{M}_m$, $\mu = 0$, and the $\bar{x}_s^*$ are analytical functions of the parameters $M_1, \ldots, M_m$, in the neighborhood of the point $\bar{M}_1, \ldots, \bar{M}_m$, $\mu = 0$.

With respect to t, the function x_s^* is almost periodic. Solution (9) exists for completely determined functions $W_1, \ldots, W_m$ with low frequencies, less than some 2ϵ, and are analytic with respect to the parameters $M_1, \ldots, M_m$ and μ in the neighborhood of the same point $\overline{M}_1, \ldots, \overline{M}_m, 0$. With our assumptions as to F_s and as to the polynomials $\underline{x}$, the point $\overline{M}_1, \ldots, \overline{M}_m$ is arbitrary.

The proof is carried out on the basis of Lemma 2 by the method of successive approximations.

The lemma generalizes a result of the author [8] obtained earlier for ordinary equations and functions F_s which are periodic in $\underline{t}$.

3. We assume that we have found the almost periodic solutions of auxiliary system (8) and the corresponding slowly varying functions $W_1, \ldots, W_m$. We note that, for the sequel, it suffices to find, for example, only several terms in the series expansions of these functions in powers of μ.

Thanks to the fact that the F_s are assumed to be polynomials in $\underline{x}$ and finite trigonometric sums in $\underline{t}$, it is always possible to choose a number ϵ sufficiently small that the functions W_i will have the expressions

$$W_i \equiv \mu Q_i(M_1, \ldots, M_m) + \\ + \mu^2 W_i'(t, M_1, \ldots, M_m, \mu) \quad (i = 1, \ldots, m),$$

where the Q_i are determined in the following manner.

Let $\psi_{s1}, \ldots, \psi_{sm}$ be periodic solutions of the linear homogeneous system "adjoint" to system (3):

$$\frac{dx_s(t)}{dt} = -a_{1s}x_1(t) - \ldots - \\ - a_{ns}x_n(t) - b_{1s}x_1(t+\tau) - \ldots - b_{ns}x_n(t+\tau).$$

Let $\lim\limits_{t \to +\infty} (1/t) \int\limits_0^t \sum\limits_{s=1}^n \varphi_{sj} \psi_{sk} \, dt = d_{jk}$. It can be shown that $|d_{jk}| \neq 0$. Then

$$d_{j1}Q_1 + \ldots + d_{mj}Q_m + P_j = 0 \quad (j = 1, \ldots, m),$$

where

$$P_j \equiv \lim_{t \to +\infty} \frac{1}{t} \int\limits_0^t \sum_{s=1}^n F_s[t, x_1^0(t), \ldots, \\ x_n^0(t), x_1^0(t-\tau), \ldots, x_n^0(t-\tau), 0] \, \psi_{sj}(t) \, dt. \\ (j = 1, \ldots, m).$$

In the last expression,

$$x_s^0 = M_1\varphi_{s1} + \ldots + M_m\varphi_{sm} + \varphi_s \quad (s = 1, \ldots, n)$$

are solutions of system (1) with $\mu = 0$.

Theorem 3. Let the system of equations

$$P_j(M_1, \ldots, M_m) = 0 \quad (j = 1, \ldots, m) \qquad (10)$$

admit the solutions $M_j = \overline{M}_j$, and let system (1), for $\mu = 0$, admit almost periodic solutions.

If the equation

$$\left| \frac{\partial (P_j(\overline{M}))}{\partial \overline{M}_k} - \delta_{jk}\lambda \right| = 0 \qquad (11)$$

has roots with negative real parts, and the roots of (2), not lying on the imaginary axis, have negative real parts, then system (1) has an almost periodic solution in a sufficiently small region $|\mu| \leq \mu^*$, asymptotically stable for $t \to \infty$ and initial disturbances of sufficiently small moduli. This solution, to a first approximation, is defined by the formulas

$$x_s = \overline{M}_1\varphi_{s1} + \\ + \ldots + \overline{M}_m\varphi_{sm} + \varphi_s(t) \quad (s = 1, \ldots, n). \qquad (12)$$

SUMMARY

It was shown in this work that, for quasi-linear systems with time delays, it is possible to establish the conditions for existence and stability of almost periodic motions analogous to the well-known conditions for systems described by ordinary differential equations.

LITERATURE CITED

1. B. V. Bulgakov, Oscillations [in Russian] (Gostekhizdat, 1954).
2. A. M. Letov, "On the autopilot problem," Vestnik Moskovskogo Universiteta No. 1 (1946).
3. A. I. Lur'e, Some Nonlinear Problems in Automatic Control Theory [in Russian] (Gostekhizdat, 1951).
4. N. N. Bogolyubov and Yu. A. Mitropol'skii, Asymptotic Methods in Nonlinear Oscillations Theory [in Russian] (Fizmatgiz, 1958).
5. I. G. Malkin, Certain Problems in Nonlinear Oscillation Theory [in Russian] (Gostekhizdat, 1956).
6. N. G. Chetaev, Stability of Motion [in Russian] (Gostekhizdat, 1956).
7. N. N. Krasovskii, "On the use of Lyapunov's second method for equations with time delays," Prikl. Matem. i Mekh. 20, 4 (1956).
8. S. N. Shimanov, "Oscillations of quasi-linear systems with nonanalytic characteristic nonlinearities," Prikl. Matem. i Mekh. 21, 3 (1957).

TRANSIENT RESPONSES IN CONTROL SYSTEMS WITH LAGS

Z. Sh. Blokh

Moscow

Translated from Avtomatika i Telemekhanika, Vol. 21, No. 6, pp. 710-719, June, 1960

A method is given for constructing the transient response in systems with lags. Transfer functions are found for systems with lags, where these lags may be in the forward circuit, in the basic feedback path and in auxiliary feedback paths. For the transient response under consideration, an integral equation is set up and solved, its solution being given in the form of a series which converges absolutely and uniformly on any given finite interval of time.

Estimates of overshoot and control time (duration of the transient response) are given, based on the parameters of the real and imaginary frequency characteristics of the system with lags.

Relationships are derived which permit one to compare different integral criteria of control quality for systems with, and without, lags.

1. Representation and Construction of the Transient Response

We consider a model of a control circuit with a lag (Fig. 1), where $\Phi(z)$ is the link's transfer function when the lag is not taken into account, and θ is the lag time which, in the sequel, we shall take to be constant. By assuming that, to construct the representation function $\varphi_{\text{out}}(t)$, we should take into account the initial function $\varphi^{*}_{\text{in}}(t)$, given in the interval $-\theta \leq t \leq 0$, which precedes the initial moment of time,* we may write

$$L[\varphi_{\text{out}}(t)] = \Phi(z)e^{-\theta z}L[\varphi_{\text{in}}(t)] + \Phi(z)\varepsilon(\theta, z), \quad (1)$$

where L is the symbol of the Laplace transform,

$$\varepsilon(\theta, z) = e^{-\theta z}\int\limits_{-\theta}^{0}\varphi^{*}_{\text{in}}(t)e^{-zt}\,dt.$$

Formula (1) shows that, for nonzero initial functions, the representation of the transient response output signal consists of two terms, whereby the effect of the initial functions can be taken into account independently by assuming that, at the input of the ordinary link with transfer function $\Phi(z)$, there acts an external disturbance, given by the representation $\varepsilon(\theta, z)$. By taking this circumstance into account, we shall henceforth consider a standard representation of the transient response in a closed linear control system with lags (Fig. 2) in the form

$$W(z) = \frac{W_0(z)e^{-\theta_1 z}}{1 + W_k(z)e^{-\theta_2 z}}, \quad (2)$$

where $W_0(z) = \Phi_1(z)L[\varphi_{\text{in}}(t)]$, $W_k(z) = \Phi_1(z)\Phi_2(z)$, $\theta_2 = \theta_1 + \theta_3$. It is assumed with this that the functions $\Phi_1(z)$ and $\Phi_2(z)$ must take into account the lags in the auxiliary feedback paths in those cases when this is necessary.

In work [2], for representations of the type given in (2), there is given a method of constructing the transient response based on the expansion of W(z) in an infinite series in powers of $W_k(z)$ which converges for $|W_k(z)| < 1$, i.e., for small values of the gains.

It is preferable to give a method of constructing the transient response which does not entail the investigation of convergences of an infinite series. Directly from formula (2) we obtain

$$W(z) = W_0(z)e^{-\theta_1 z} - W(z)W_k(z)e^{-\theta_2 z}. \quad (3)$$

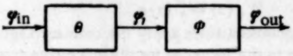

Fig. 1.

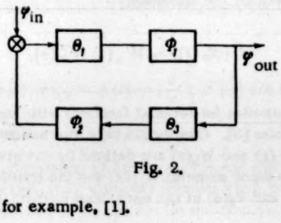

Fig. 2.

---

*Cf., for example, [1].

By applying the convolution and lag theorems [3] to expression (3), we obtain an integral equation for the transient response being sought:

$$\varphi_{out}(t) = \tag{4}$$

$$= \varphi_0(t-\theta_1) - \int_0^t \varphi_{out}(\tau)\varphi_k(t-\theta_2-\tau)\,d\tau,$$

where $\varphi_{out}(t)$, $\varphi_0(t)$, and $\varphi_k(t)$ are the time domain functions corresponding to the transforms W(z), $W_0(z)$, and $W_k(z)$. The solution of Eq. (4) is written in the form of a series:

$$\varphi_{out}(t) = \varphi_0(t-\theta_1) - \varphi_1(t-\theta_1-\theta_2) +$$

$$+ \varphi_2(t-\theta_1-2\theta_2) - \ldots + \tag{5}$$

$$+ (-1)^n \varphi_n(t-\theta_1-n\theta_2),$$

which converges absolutely and uniformly in t on any finite interval of time. The sufficient conditions which are imposed on the initial function $\varphi_0(t)$ and the kernel $\varphi_k(t)$ of integral Eq. (4) amount, as is well known [4], to the holding of the conditions

$$|\varphi_0(t)| < Ae^{at}, \quad |\varphi_k(t)| < Be^{bt},$$

where A, B, a, b are positive constants.

In computing by formula (5), it must be taken into account that all the functions entering into it, $\varphi_m(t-\theta_1-m\theta_2)$ (m = 0, 1, 2, . . . n), equal zero for negative values of the argument. This important circumstance allows one to find the values of $\varphi_{out}(t)$ exactly for any previously given finite interval of time t which, at the same time, can be considered as an approximation for a large interval.

To construct the time domain functions entering into formula (5), we take into account that the transform of any of them,

$$L[\varphi_m(t-\theta_1-m\theta_2)] = \tag{6}$$

$$= W_0(z) W_k^m(z) e^{-(\theta_1+m\theta_2)t},$$

is easily obtained if we apply the ordinary Laplace transformation to the formulas for the successive determinations of the $\varphi_m(t-\theta_1-m\theta_2)$ by integral Eq. (4). In practice, the problem reduces to the determination of the functions $\varphi^*_m(t)$, given by the transforms

$$L[\varphi^*_m(t)] = W_0(z) W_k^m(z), \tag{7}$$

from the formulas for rational fractions with known multiple poles [3]. One should take into account with this that $W_0(z)$ and $W_k(z)$ are defined by the given transform of the input stimulus $W_{in}(z)$ and the transfer functions $\Phi_1(z)$ and $\Phi_2(z)$ of the open-loop circuits (Fig. 2).

As an example of the application of the formulas we have derived, we construct the transient response for the representation

$$W(z) = \frac{ke^{-\theta z}}{z[(T_1z+1)(T_2z+1)+ke^{-\theta z}]}.$$

Since

$$\lim_{z\to\infty} zW(z) = \varphi_{out}(0) = 0,$$

we shall find it preferable to consider the transform of the transient response's velocity,

$$L\varphi'_{out}(t) = zW(z) = \frac{ke^{-\theta z}}{(T_1z+1)(T_2z+1)+ke^{-\theta z}}.$$

In accordance with our notation $\theta_1 = \theta_2 = \theta$,

$$W_0(z) = W_k(z) = \frac{k}{(T_1z+1)(T_2z+1)}.$$

The transforms of the successive functions, in accordance with formula (7), are found from the expression

$$L[\varphi^*_m(t)] =$$

$$= \frac{k^{m+1}}{(T_1z+1)^{m+1}(T_2z+1)^{m+1}} \quad (m = 0, 1, 2, \ldots, n). \tag{8}$$

Since

$$L^{-1}\left[\frac{1}{(T_kz+1)^{m+1}}\right] = \frac{t^m e^{-\frac{t}{T_k}}}{T_k^{m+1}m!} \quad (k = 1, 2),$$

then all the functions given by the transforms of (8) are defined by the convolution formula

$$\ddot{\varphi}_m(t) = \frac{k^{m+1}e^{-\frac{t}{T_2}}}{(m!)^2(T_1T_2)^{m+1}}\int_0^t \tau^m(t-\tau)^m e^{-\left(\frac{\tau}{T_1}-\frac{\tau}{T_2}\right)}d\tau.$$

Consequently,

$$\dot{\varphi}_m(t) = \tag{9}$$

$$\frac{k^{m+1}}{(m!)^2(T_1T_2)^{m+1}}\int_0^t e^{-\frac{t}{T_2}}dt\int_0^t \tau^m(t-\tau)^m e^{-\left(\frac{\tau}{T_1}-\frac{\tau}{T_2}\right)}d\tau.$$

The solution being sought is written in the form

$$\varphi_{out}(t) = \varphi_0(t-\theta) - \varphi_1(t-2\theta) + \ldots +$$

$$+ (-1)^{n-1}\varphi_n(t-n\theta),$$

where all the functions φ^*_m are computed from formula (9).

For representations of more general types, the method just presented for constructing the transient responses leads to arduous computations, particularly when the gains are large.

2. Frequency Characteristics of Systems with Lags

By taking into account that, in representation (2), the factor $e^{-\theta_1 z}$ leads only to a shift of the corresponding time domain characteristic by the amount θ_1, we shall find it more advantageous in the sequel to consider the following function as the representation of a transient response with lags:

$$W(z) = \frac{W_0(z)}{1 + W_k(z)\, e^{-\theta z}}. \tag{10}$$

As will be shown later, the frequency characteristics corresponding to representation (10) ordinarily have a finite number of points of intersection with the frequency axis, and do not differ essentially in their main features from the analogous characteristics of systems without lags. This allows us to carry over to systems with lags the estimating methods which have been previously developed for systems without lags (5, 6, 7).

If all the poles of representation (10) lie in the left half-plane, then the abscissa of convergence of the integral

$$W(z) = \int_0^\infty \varphi(t)\, e^{-zt}\, dt,$$

is $\sigma < 0$, and we can set $z = i\omega$ in it. Then,

$$W(i\omega) = S(\omega) + iQ(\omega) = \int_0^\infty \varphi(t)\, e^{-i\omega t}\, dt.$$

Consequently,

$$S(\omega) = \int_0^\infty \varphi(t) \cos \omega t\, dt. \tag{11}$$

$$Q(\omega) = -\int_0^\infty \varphi(t) \sin \omega t\, dt. \tag{12}$$

The functions $S(\omega)$ and $\varphi(t)$, $Q(\omega)$ and $\varphi(t)$ are Fourier transform pairs. Based on their duality property [8], one can write

$$\varphi(t) = \frac{2}{\pi} \int_0^\infty S(\omega) \cos t\omega\, d\omega, \tag{13}$$

$$\varphi(t) = -\frac{2}{\pi} \int_0^\infty Q(\omega) \sin t\omega\, d\omega. \tag{14}$$

If representation (10) has a simple pole at the origin:

$$W(z) = \frac{\Phi(z)}{z},$$

we then set

$$\Phi(i\omega) = R(\omega) + iI(\omega)$$

and find the transient response corresponding to W(z) from the convolution formula, taking into account that the transient response for $\Phi(z)$ is determined from formulas (13) and (14):

$$\varphi(t) = \frac{2}{\pi} \int_0^t \int_0^\infty R(\omega)\, 1(t-\tau) \cos \tau\omega\, d\omega\, d\tau.$$

By changing the order of integration, we get

$$\varphi(t) = \frac{2}{\pi} \int_0^\infty \frac{R(\omega)}{\omega} \sin t\omega\, d\omega. \tag{15}$$

Analogously,

$$\begin{aligned} \varphi(t) &= -\frac{2}{\pi} \int_0^t \int_0^\infty I(\omega)\, 1(t-\tau) \sin \tau\omega\, d\omega\, d\tau = \\ &= \frac{2}{\pi} \int_0^\infty \frac{I(\omega)}{\omega} \cos t\omega\, d\omega - \frac{2}{\pi} \int_0^\infty \frac{I(\omega)}{\omega}\, d\omega. \end{aligned} \tag{16}$$

Since the first of these integrals equals zero for $t \to \infty$, then

$$\varphi(\infty) = \varphi_v = -\frac{2}{\pi} \int_0^\infty \frac{I(\omega)}{\omega}\, d\omega = \frac{2}{\pi} \int_0^\infty S(\omega)\, d\omega, \tag{17}$$

where

$$S(\omega) = -\frac{I(\omega)}{\omega}, \tag{18}$$

and φ_s is the steady-state value of the output coordinate.

Consequently,

$$\varphi(t) = -\frac{2}{\pi} \int_0^\infty S(\omega) \cos t\omega\, d\omega + \varphi_v. \tag{19}$$

By shifting the origin of coordinate, we shall henceforth consider as the transient response the time domain function

$$\psi(t) = \varphi_v - \varphi(t) = \frac{2}{\pi} \int_0^\infty S(\omega) \cos t\omega\, d\omega. \tag{20}$$

A comparison of formulas (13) and (20) shows that the function $S(\omega)$, given by formula (18), is the frequency characteristic of the system for the transient response $\psi(t)$.

3. Some Properties of the Frequency Characteristics W(z)

We limit our consideration to the case when the representation has a simple pole at the origin. Since, for linear systems and a broad class of disturbing actions $W_0(z)$ and $W_k(z)$ are rational fractions, then, by introducing the following notation into formula (10):

$$zW_0(z) = \frac{d_0(z)}{d_1(z)}, \quad W_k(z) = \frac{d_2(z)}{d_3(z)},$$

$$D_0(z) = d_0(z)\,d_3(z),$$

$$D_1(z) = d_1(z)\,d_3(z), \quad D_2(z) = d_1(z)\,d_2(z),$$

where $d_k(z)$ and $D_k(z)$ are polynomials in z, we present the function $\Phi(z)$, for $z = i\omega$, in the form

$$\Phi(i\omega) = \frac{D_0(i\omega)}{D_1(i\omega) + D_2(i\omega)\,e^{-i\theta\omega}} = R(\omega) + iI(\omega).$$

By setting $D_k(i\omega) = x_k + iy_k$ $(k = 0, 1, 2)$, we get

$$R(\omega) = \frac{Ax_0 + By_0}{A^2 + B^2},$$

$$I(\omega) = \frac{Ay_0 - Bx_0}{A^2 + B^2},$$

$$A = x_1 + x_2\cos\theta\omega + y_2\sin\theta\omega,$$

$$B = y_1 + y_2\cos\theta\omega - x_2\sin\theta\omega.$$

The zeros of the frequency characteristics $R(\omega)$ and $I(\omega)$ are defined, respectively, by the roots of the transcendental equations:

$$\begin{gathered} x_0x_1 + y_0y_1 + (x_0x_2 + y_0y_2)\cos\theta\omega + \\ + (x_0y_0 - y_0x_2)\sin\theta\omega = 0, \\ y_0x_1 - x_0y_1 + (y_0x_2 - x_0y_2)\cos\theta\omega + \\ + (y_0y_2 + x_0x_2)\sin\theta\omega = 0. \end{gathered} \tag{21}$$

Let the stimulus $\varphi_{in}(t) = 1(t)$ be applied to the measuring device, and let $W_k(z) = zW_0(z)$. Then $D_0(z) = D_2(z)$ and Eqs. (21) for $R(\omega)$ and $I(\omega)$ are rewritten in the form, respectively,

$$\cos\theta\omega = -\frac{x_1x_2 + y_1y_2}{x_2^2 + y_2^2}, \quad \sin\theta\omega = \frac{y_1x_2 - x_1y_2}{x_2^2 + y_2^2}. \tag{22}$$

Let the polynomials $D_2(z)$ and $D_1(z)$ be of degrees m and n, respectively, where $m \leq n$. Then, a detailed analysis of formulas (22) leads to the following results.

The frequency characteristic $R(\omega)$ has a finite number of points of intersection with the ω axis for $m < n-1$, independently of the system parameters and the lag θ. For $m \geq n-1$, the number of points of intersection with the ω axis will be finite only if the following inequality holds:

$$\lim_{\omega\to\infty}\left|\frac{x_1x_2 + y_1y_2}{x_2^2 + y_2^2}\right| > 1. \tag{23}$$

Frequency characteristic $I(\omega)$, and with it frequency characteristic $S(\omega)$, has a finite number of points of intersection with the ω axis for $m < n$ independently of the system parameters and the lag θ. Since the case $m = n$ is not possible for $\varphi(0) = 0$, the characteristics $I(\omega)$ and $S(\omega)$, for sufficiently large ω, do not change sign, and tend to zero for $\omega \to \infty$. The same behavior occurs for characteristic $R(\omega)$ for $m < n-1$ or, if inequality (23) holds, for $m < n$. Consequently, for the particular case being investigated, one can neglect the high-frequency parts of the characteristics $R(\omega)$, $I(\omega)$ and $S(\omega)$ and can estimate the errors thus introduced by means of the formulas derived in [5, 6], for characteristics without lags. For the characteristics of systems with lags we thereby establish the concept of the essential interval of frequency on which they should be constructed. Thus, for example, considering $S(\omega) > 0$, for definiteness, in the high-frequency interval $\omega_c \leq \omega \leq \infty$, and by then discarding this segment of the characteristic, we obtain, by using the results of [6], the following estimate of the transient response error:

$$|\Delta\psi| \leqslant \psi(0) - \frac{2}{\pi}F, \tag{24}$$

where F is the area bounded by the frequency characteristic $S(\omega)$ in the chosen essential interval of frequency $0 \leq \omega \leq \omega_c$, $\psi(0) = \varphi_s$. Since φ_s is easily computed from the given representation of the transient response, then formula (24) allows the essential frequency interval (by area) to be so chosen that the error in the transient response will not exceed the previously given quantity $|\Delta\psi|$.

4. Estimate of Overshoot and Control Time

To determine overshoot and control time from frequency characteristics, we construct these latter from a large number of computed ordinates in the essential frequency interval, and then replace them by the sum of standard characteristics for which the formulas of the corresponding transient responses have been previously obtained. After this, one computes the ordinates of the transient response being investigated and, from the curve thus constructed, one fins the overshoot and the control time. If one takes as standards the natural frequency characteristics of simple systems without lags, then the constructions and computations involved in estimating overshoot and control time are significantly simplified [7]. We limit ourselves to the consideration of just two standard cases, referring the reader to the literature [7] for a more complete analysis. As standards, we shall choose the frequency characteristics corresponding to the representation

$$W(z) = \frac{b_1 z + a_2}{z(z^2 + a_1 z + a_2)}. \tag{25}$$

By setting z = iω in (25) we obtain, for zW(z),

$$R(\omega) = \frac{c_2\omega^2 + c_4}{\omega^4 + d_2\omega^2 + c_4}, \tag{26}$$

where $c_2 = a_1b_1 - a_2$, $c_4 = a_2^2$, $d_2 = a_1^2 - 2a_2$ are three new essential parameters of characteristic R(ω) by which it is completely defined. Among the various possible types of curves for R(ω), we consider in detail the characteristic which is nonnegative in the essential frequency interval (Fig. 3). Let the characteristic R(ω) of the system with lags under investigation be nonnegative in the essential interval $0 \leq \omega \leq \omega_2$ and have one maximum $R = R_1$ for $\omega = \omega_1$. We choose the parameters c_2, c_4 and d_2 such that the characteristic of the system with lags shall coincide with that given by (26) in the three points for $\omega = 0$, $\omega = \omega_1$ and $\omega = \omega_2$ (Fig. 3). Since, by (26), R(0) = = 1, then coincidence of the ordinates at the point ω = 0 is attained by a simple change of scale for the investigated characteristic of the system with lags. After this, the parameters being constructed are determined from the system of equations

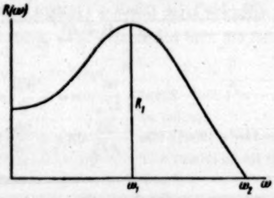

Fig. 3.

$$R_1 = \frac{c_2\omega_1^2 + c_4}{\omega_1^4 + d_2\omega_1^2 + c_4} = \frac{c_2}{2\omega_1^2 + d_2}, \tag{27}$$

$$c_2\omega_2 + c_4 = 0$$

by the formulas

$$c_2 = \frac{R_1\omega_1^4}{\omega_2^2(1 - R_1)}, \quad c_4 = \frac{R_1\omega_1^4}{R_1 - 1}, \tag{28}$$

$$d_2 = \frac{\omega_1^4}{\omega_2^2(1 - R_1)} - 2\omega_1^2.$$

We then compute the initial parameters:

$$a_2 = \sqrt{c_4}, \quad a_1 = \sqrt{d_2 + 2a_2}, \quad b_1 = \frac{a_2 + c_2}{a_1}. \tag{29}$$

By the formulas derived in [9], the quantities just found permit one to compute the overshoot and control time exactly for the transient response corresponding to the representation of (25).

We now give the computational scheme:

$$\Delta\phi = \sqrt{\frac{F(-b_1)}{a_2}}\, e^{-\frac{\alpha}{\beta}\gamma}, \tag{30}$$

$$\operatorname{tg}\gamma = -\frac{\beta b_1}{a_2 - \alpha b_1}, \quad e^{\alpha T} = s\sqrt{\frac{F(-b_1)}{a_2}}.$$

In the formulas just given, $\Delta\psi$ is the overshoot, T is the control time, s is a parameter defining the zone of admissible deviations (s = 10 to 20), $2\alpha = a_1$, $\beta = \sqrt{a_2 - \alpha^2}$, $F(-b_1) = b_1^2 - a_1b_1 + a_2$.

As an example, we estimate the quality of control in a static system with lags by setting, in the representation of (10),

$$W_k(z) = zW_0(z) = \frac{k(T_1z + 1)}{(T_2z + 1)(T_3z + 1)}$$

and by taking $T_1 = 0.1$ second, $T_2 = 1$ second, $T_3 = 0.2$ second, k = 4.

By using the method developed in [2], we can determine that the system is stable if the lag time is θ < 0.48 second. For the following computations, we take θ = 0.3 second.

The closed system's real frequency characteristic is

$$R(\omega) = \frac{(400 + 4\omega^2)\cos\theta\omega + 100 - 8\omega^2}{A^2 + B^2}, \tag{31}$$

where $A = 5 - \omega^2 - 20\cos\theta\omega + 2\omega\sin\theta\omega$, $B = 6\omega + 2\omega\cos\theta\omega - 20\sin\theta\omega$.

The points of intersection of characteristic R(ω) with the ω axis are defined by the equation

$$\cos\theta\omega = \frac{2\omega^2 - 25}{\omega^2 + 100},$$

which has the sole real solution $\omega_2 = 4.7$.

In addition, we find from formula (31) that R(0) = 0.8 and $R_1 = 1.7$ for ω = 4 at the maximum point. We change the scale of the axis of ordinates, setting R(0) = 1, R_1 = = 2.12. Then, by formulas (28) and (29), we find: $a_1 = 2$, α = 1.3, $a_2 = 22$, $b_1 = 0.069$, $\beta^2 = 21.6$. By substituting

TABLE 1

k	1.6	1.2	1.0	0.8	T_i	5	4	3	2
S_0	8	6	5	4	S_0	8.0	6.4	4.8	3.2
ω_2	0.54	0.64	0.74	0.82	ω_2	0.54	0.54	0.57	0.6
ω_1	0.27	0.32	0.37	0.41	ω_1	0.27	0.27	0.285	0.3
S_1	1.05	1	0.97	0.95	S_1	1.05	1.25	1.7	2.0

these values in formulas (30), we obtain: $\tan\gamma = -0.0145$, $\gamma = \pi - 0.01 = 3.13$, $\Delta\psi = 0.64$, $T = 4.6$ seconds for $s = 20$. From the exact curve of the transient response, constructed by the method presented in Section 1 to verify our example, $\Delta\psi = 0.6$ (with the scales of the variables taken into account), which differs little from the estimated value. In astatic systems with variable loads, $\varphi_s = 0$, and formulas (18) to (30) cannot be applied. For such systems, one may take as standard the frequency characteristics corresponding to the representation

$$W(z) = \frac{b_1}{z^2 + a_1 z + a_2}.$$

By setting $z = i\omega$, we obtain, for the real frequency characteristic,

$$S(\omega) = \frac{b_1(a_2 - \omega^2)}{(a_2 - \omega^2)^2 + a_1^2\omega^2}. \qquad (32)$$

The three essential parameters b_1, a_1 and a_2 of the characteristic of (32) are defined by the ordinates in three chosen points of the analogous characteristic of the system with lags under investigation as a function of its behavior. If it be required that the characteristics coincide for $\omega = 0$, $\omega = \omega_1$ and $\omega = \omega_2$ for $S(\omega_2) = 0$, then the parameters being sought are determined from the formulas

$$a_2 = \omega_2^2,\ b_1 = S_0 a_2 = S_0\omega_2^2,\ a_1^2 = \frac{S_0\omega_2^2(\omega_2^2 - \omega_1^2) - S_1(\omega_2^2 - \omega_1^2)^2}{S_1\omega_1^2}, \qquad (33)$$

where S_0 and S_1 are the ordinates of the investigated system's frequency characteristic at the points $\omega = 0$ and $\omega = \omega_1$, respectively.

As an example of the use of formulas (33), we take the analysis of the control quality of concentrating sulfur dioxide (SO_2) for an external disturbance $\varphi_{in} = 1(t)$ applied to the object of control. With some simplifying assumptions, we give the basic functions entering into the representation of (2):

$$W_0(z) = \frac{k_1k_2k_3}{z(T_1z+1)(T_2z+1)(T_3z+1)},$$

$$W_k(z) = \frac{(T_iz+1)k_1k_2k_3k_6k_8}{(T_1z+1)(T_2z+1)(T_3z+1)(T_6z+1)(T_8z+1)kT_iz} \qquad (34)$$

In the sequel, we shall measure time in minutes, taking into account the corresponding scale changes in representation of the transient response. Taking the controller adjustment parameters T_i and k as variables, we present the analysis for the following values of the remaining system parameters: $\theta_1 = 0.25$ minutes, $\theta_2 = 1$ minute, $T_1 = 0.25$ minutes, $T_2 = 0.5$ minutes, $T_3 = 0.33$ minutes, $T_8 = 0.25$ minutes, $T_6 = 1$ minute, $k_1k_2k_3 = 1$, $k_6k_8 = 1$.

By substituting the parameters' numerical values in formulas (34) and discarding the factor $e^{-0.25z}$, the effect of which is taken into account by shifting the time domain characteristic by $\theta = 0.25$ minutes, we obtain

$$W(z) = \frac{24(z+1)(z+4)}{z(z+4)^2(z+3)(z+2)(z+1) + \frac{96}{k}\left(z + \frac{1}{T_i}\right)e^{-z}}.$$

By setting $z = i\omega$ in this representation, we find that

$$W(i\omega) = \frac{(96-24\omega^2)A + 120\omega B + i[1200A - B(96-24\omega^2)]}{A^2+B^2},$$

where

$$A = -\omega^6 + 75\omega^4 - 224\omega^2 + \frac{96}{kT_i}\cos\omega + \frac{96\omega}{k}\sin\omega,$$

$$B = -14\omega^5 - 190\omega^3 + 96\omega - \frac{96}{kT_i}\sin\omega + \frac{96\omega}{k}\cos\omega.$$

We separate out, for the further computations, the real frequency characteristic

$$S(\omega) = \frac{(96-24\omega^2)A + 120\omega B}{A^2+B^2}. \qquad (35)$$

Analysis of stability, carried out in [2], showed that the system is stable in the following range of parameter variations: $1.8 \le T_i \le 5$, $0.8 \le k \le 1.6$.

Since, within the given limits of parameter variation, the characteristics $S(\omega)$, found from formula (35), do not increase in the interval $0 \le \omega \le \omega_2$, then, for the subsequent estimates, we took $\omega_2 = 2\omega_1$. The values of the ordinates of $S(\omega_k)$, computed from formula (35) for $T_i = 5$ in the range $0.8 \le k \le 1.6$, and for $k = 1.6$ in the range $2 \le T_i \le 5$, are given in Table 1.

Substitution of the values thus found into formulas (33) allowed the computation of a_1, a_2 and b_1 for the accepted values of controller adjustment, T_i and k. After this, the greatest deviation of the controlled coordinate, and the control time, were computed by the

TABLE 2

k	1.6	1.2	1.0	0.8	T_1	5	4	3	2
ψ max	0.83	0.85	0.89	0.87	ψ max	0.83	0.82	0.85	0.82
T	19	14	11	8.3	T	19	15	10.3	7.4

formulas derived in [9]. If $a_1^2-4a_2 > 0$, then

$$\psi_{\max}=S_0\omega_2 e^{-\alpha t_{el}},\ t_{el}=\frac{1}{\alpha^2-\omega_2^2}\ln\frac{\alpha+\sqrt{\alpha^2-\omega_2^2}}{\omega_2}, \quad (36)$$

where $2\alpha = a_1$. The control time T was defined by the transcendental equation

$$\frac{S_0\omega_2^2}{2\sqrt{\alpha^2-\omega_2^2}}\left(e^{-z_1T}-e^{-z_2T}\right)=\frac{1}{s} \quad (37)$$

for $s = 10$, $z_1 = \alpha - \sqrt{\alpha^2-\omega_2^2}$, $z_2 = \alpha + \sqrt{\alpha^2-\omega_2^2}$.

If $z_2 \gg z_1$, we may then use the following formula for the determination of the control time:

$$T\approx\frac{1}{z_1}\ln\frac{sS_n\omega_2^2}{2\sqrt{\alpha^2-\omega_2^2}}. \quad (38)$$

In the case $a_1^2-4a_2 < 0$, the greatest deviation, and the control time, were determined from the formulas

$$\psi_{\max}=S_0\omega_2 e^{-\frac{\alpha}{\beta}\gamma}, \quad \operatorname{tg}\gamma=\frac{\beta}{\alpha}, \quad (39)$$

$$T=\frac{1}{\alpha}\ln\left(sS_0\omega_2\right),$$

where $2\alpha = a_1$, $\beta^2 = \omega_2^2-\alpha^2$. The results of all these computations are given in Table 2.

Analysis of the results obtained shows that the isodrome controller time T_1 and the parameter k, corresponding to the range of the throttled controller, have very little influence on the greatest deviation of the controlled parameter. The control time is essentially decreased by decreases in T_1 and k. The optimal adjustment of the controller corresponds to the lowest values of k and T_1 which are compatible with the stability requirements. Verification of the computations made by more exact methods showed that the deviations of the estimated values from the more exact ones did not go beyond the limits of computational accuracy.

LITERATURE CITED

1. A. D. Myshkis, Linear Differential Equations with Lagged Arguments [in Russian] (Gostekhizdat, 1951).
2. Ya. Z. Tsypkin, "Systems with lagging feedback," Tr. NISO No. 24 (1947).
3. M. F. Gardner and D. L. Barnes, Transients in Linear Systems [Russian translation] (Gostekhizdat, 1949).
4. V. I. Smirnov, Course in Higher Mathematics. 4 [in Russian] (Gostekhizdat, 1951).
5. Z. Sh. Blokh, "Certain estimates of control quality from frequency characteristics," Avtomat. i Telemekh. 16, No. 3 (1955).
6. Z. Sh. Blokh, "Some properties of automatic control systems' frequency characteristics," Izvest. AN SSSR, Otd. Tekhn. N. No. 2 (1956).
7. Z. Sh. Blokh, "On the computation of overshoot and control time from the basic parameters of the frequency characteristics," Nauchn. Tr. Moskovsk. Lesotekhnicheskogo Inst. No. 8 (1958).
8. E. C. Titchmarsh, Introduction to the Theory of Fourier Integrals [Russian translation] (Gostekhizdat, 1948).
9. Z. Sh. Blokh, Dynamics of Linear Automatic Machine Control Systems [in Russian] (Gostekhizdat, 1952).

LYAPUNOV FUNCTIONS FOR RELAY CONTROL SYSTEMS

Yu. I. Alimov

Sverdlovsk

Translated from Avtomatika i Telemekhanika, Vol. 21, No. 6, pp. 720-728, June, 1960

The idea of a trajectory is introduced, and the stability in the large is investigated of the equilibrium state of one class of relay control systems.

1. In many cases, the dynamic properties of automatic-control relay systems are well described by a mathematical model consisting of a combination of a linear part having a transfer function

$$W(p) = \frac{\sigma(p)}{y(p)} = \frac{b_n p^{n-1} + b_{n-1} p^{n-2} + \cdots + b_1}{a_{n+1} p^n + a_n p^{n-1} + \cdots + a_1} k_p \qquad (1)$$

$$(a_1, \ldots, a_{n+1}, b_1, \ldots, b_n = \mathrm{const}, b_1, a_{n+1}, k_p > 0)$$

and a relay element without a zone of insensitivity having the characteristic form $y = \varphi(\sigma)$.

In actual fact, both the input $\sigma(t)$ and the output $\varphi(\sigma(t))$ of any real unit approximating such a relay element (a kinematic couple with dry friction, an amplifier with a small zone of linearity, a relay, etc.) are continuous functions of the time. If the coordinate $\sigma(t)$ passes rapidly through its threshold value $\sigma = 0$, the function $\varphi(\sigma)$ can be assumed to be discontinuous, and we can set $\varphi(\sigma) = \operatorname{sign}\sigma$, for example. Such an idealization becomes unsatisfactory for the investigation of those relay systems (sliding and partially sliding regimes, motion with stops [1-4]) for which $\sigma(t)$ remains for long periods of time near to its change-over value. The continuous character of the function $\varphi(\sigma)$ is taken into account most simply in the description of such motions by the Coulomb characteristic:

$$y = \varphi(\sigma) = \begin{cases} -(1-\varphi_0) & \text{for } \sigma < 0, \\ \xi & \text{for } \sigma = 0, \\ +(1+\varphi_0) & \text{for } \sigma > 0, \end{cases} \qquad (2)$$

where $\varphi_0 = \mathrm{const}$, $|\varphi_0| < 1$, and ξ can be any number from the interval $[-(1-\varphi_0), 1+\varphi_0]$, and with $\xi = \xi(t)$ expressed as in [3], so that the equations (1)-(2) for $y(t) = \varphi(0) = \xi(t)$ are compatible with the equality $\sigma(t) = 0$.

In order to derive and investigate the phase space of the system (1)-(2), we write its equations in the normal Cauchy form

$$\dot{\mathbf{x}} = \mathbf{A}\mathbf{x} + \mathbf{b}\varphi(\sigma), \quad \sigma = \mathbf{k}'\mathbf{x}, \qquad (3)$$

using for brevity of notation the usual vector-matrix notation of [5]: **A** is a square matrix, and **x**, **b**, and **k** are n-dimensional column matrices. The prime indicates the transpose of a matrix, so that, according to the rule for multiplying matrices ([5], p. 14) $\mathbf{k}'\mathbf{x}$ is a scalar, and $\mathbf{k}\mathbf{b}'$ is a square matrix. The transformation of the equations (1)-(2) to the normal form is particularly simple, and yields

$$\begin{aligned} \dot{x}_k &= x_{k+1} \quad (k = 1, \ldots, n-1), \\ \dot{x}_n &= -a_{n+1}^{-1}\left(\sum_{i=1}^{n} a_i x_i + k_p \varphi(\sigma)\right), \\ \sigma &= \sum_{i=1}^{n} b_i x_i. \end{aligned} \qquad (4)$$

In several works (for example, see [1]) the trajectories of the system (2)-(3) have been considered close to a certain periodic motion with simple switching conditions, and in [6], close to the origin. In [1, 3, and 4] sliding regimes of relay systems were investigated in detail. Many authors have laid out the whole **x** phase space of the system (2)-(3) in trajectories for n = 2, 3. This is done below for any n under the assumption that

$$a_{n+1}^{-1} k_p b_n = -\mathbf{k}'\mathbf{b} > 0 \qquad (5)$$

(the case

$$b_n = 0, \quad b_{n-1} > 0 \qquad (6)$$

was considered in [7], the violation of the conditions (5)-(6) is connected [1, 6] with the loss of stability). The second Lyapunov method is applied to the dynamic system obtained. Effective algorithms are obtained for deriving a wide class of sufficient conditions for stability in the large of the equilibrium of the system (2)-(3) with a stable or unstable linear part. The stability criteria given in this paper are expressed in terms of the coefficien of the transfer function (1), but the method of constructing the Lyapunov functions is described in invariant form, and it can be applied in obtaining criteria expressed in terms of the elements of the matrices **A**, **b**, and **k** in the usual form. In the case

$$\operatorname{Re}\lambda_i < 0 \quad (i = 1, \ldots, n), \tag{7}$$

where λ_i are the roots of the equation det $(\mathbf{A} - \lambda\mathbf{E}) = 0$, the Lyapunov functions are obtained by the interlacing method, and can be used to estimate the control time. The case

$$\lambda_1 = 0,\ \operatorname{Re}\lambda_k < 0 \quad (k = 2, \ldots, n). \tag{8}$$

is also discussed briefly.

It should be mentioned that the unsymmetric characteristic (2) must also be considered [1] in the investigation of systems

$$\dot{\mathbf{z}} = \mathbf{A}\mathbf{z} + \mathbf{b}\varphi\ (\mathbf{k}'\,\mathbf{z}),\quad \varphi(\sigma) = \begin{cases} -1 & \text{for } \sigma < 0, \\ +1 & \text{for } \sigma > 0 \end{cases} \tag{9}$$

with a symmetric relay link when, for example, in the case (7) we are investigating the effect of a discontinuous external action:

$$\sigma(t) = \mathbf{k}'\,\mathbf{z}(t) + \mathbf{1}(t)\,\sigma_0, \tag{10}$$

and in the case (8) for motion with a linear input:

$$\sigma(t) = \mathbf{k}' z(t) + \mathbf{1}(t)\,(\sigma_0 + \sigma_1 t). \tag{11}$$

The system (9)-(10) and (11) reduces to the form (2)-(3) by a nonsingular linear transformation of the coordinates **z**. The value of φ_0 is determined here from the parameters σ_0 and σ_1 of the external disturbance.

2. We denote by $\mathbf{x}_+(\mathbf{x}^0, t)$, and $\mathbf{x}_-(\mathbf{x}^0, t)$ the trajectories of the systems

$$\dot{\mathbf{x}} = \mathbf{f}_+(\mathbf{x}) = \mathbf{A}\mathbf{x} + \mathbf{b}\,(1 + \varphi_0), \tag{12}$$

$$\dot{\mathbf{x}} = \mathbf{f}_-(\mathbf{x}) = \mathbf{A}\mathbf{x} - \mathbf{b}\,(1 - \varphi_0), \tag{13}$$

passing for t = 0 through the point $\mathbf{x}^0$ of the space **x**. For the investigation of the system (2)-(3) and (7), it is convenient to write Equations (12) and (13) in the form

$$\dot{\mathbf{x}}_+ = \mathbf{A}\mathbf{x}_+,\ \mathbf{x}_+ = \mathbf{x} + \mathbf{A}^{-1}\mathbf{b}\,(1 + \varphi_0), \tag{12'}$$

$$\dot{\mathbf{x}}_- = \mathbf{A}\mathbf{x}\ ,\ \mathbf{x}\ = \mathbf{x} - \mathbf{A}^{-1}\mathbf{b}\,(1 - \varphi_0). \tag{13'}$$

We denote by $\dot{\sigma}_+(\mathbf{x})$ and $\dot{\sigma}_-(\mathbf{x})$ the derivatives with respect to time of the function $\sigma(\mathbf{x}) = \mathbf{k}'\mathbf{x}$ according to the systems (12) and (13). Thus,

$$\sigma_+(\mathbf{x}) = \mathbf{k}'\mathbf{A}\mathbf{x} + \mathbf{k}'\mathbf{b}\,(1 + \sigma_0),$$

$$\dot{\sigma}_-(\mathbf{x}) = \mathbf{k}'\mathbf{A}\mathbf{x} - \mathbf{k}'\mathbf{b}\,(1 - \varphi_0),$$

and, according to (5), we have

$$\dot{\sigma}_+(\mathbf{x}) < \dot{\sigma}_-(\mathbf{x}). \tag{14}$$

Using the method in [1-4, 6, 7], we give the determination of the trajectory $\mathbf{x}(\mathbf{x}^0, t)$ of system (2)-(3) satisfying the condition (5).

(a) In the space $\sigma(\mathbf{x}) > 0$ $(\sigma(\mathbf{x}) < 0)$ we assume that $\mathbf{x}(\mathbf{x}^0, t) = \mathbf{x}_+(\mathbf{x}^0, t)$. $(\mathbf{x}(\mathbf{x}^0, t) = \mathbf{x}_-(\mathbf{x}^0, t))$.

(b) At any point $\mathbf{q}_1$ of the set $\sigma(\mathbf{x}) = 0$, $\dot{\sigma}_+(\mathbf{x})\,\dot{\sigma}_-(\mathbf{x}) > 0$, representing two half-planes $(\mathbf{k}'\mathbf{b})^{-1}\,\mathbf{k}'\mathbf{A}\mathbf{x} < -(1 + \varphi_0)$, $\mathbf{k}'\mathbf{x} = 0$ and $(\mathbf{k}'\mathbf{b})^{-1}\mathbf{k}'\mathbf{A}\mathbf{x} > (1 - \varphi_0)$, $\mathbf{k}'\mathbf{x} = 0$, the trajectories $\mathbf{x}_+(\mathbf{q}_1, t)$, $\mathbf{x}_-(\mathbf{q}_1, t)$ intersect the switching surface $\sigma(\mathbf{x}) = 0$ in the same direction. We determine $\mathbf{x}(\mathbf{q}_1, t)$ by linking continuously at $\mathbf{q}_1$ those half-trajectories $\mathbf{x}_+(\mathbf{q}_1, t)$ and $\mathbf{x}_-(\mathbf{q}_1, t)$ which lie close to $\mathbf{q}_1$ in the regions $\sigma(\mathbf{x}) > 0$ and $\sigma(\mathbf{x}) < 0$, respectively.

(c) According to (14), at every point $\mathbf{q}_0$ of the set $\sigma = 0$, $\dot{\sigma}_+(\mathbf{x})\,\dot{\sigma}_-(\mathbf{x}) < 0$ the trajectories $\mathbf{x}_+(\mathbf{q}_0, t)$, and $\mathbf{x}_-(\mathbf{q}_0, t)$ intersect the surface $\sigma(\mathbf{x}) = 0$ in the same direction. In accord with what was said in Sec. 1, we will assume that in the set consisting of the zone

$$(1 - \varphi_0) > (\mathbf{k}'\mathbf{b})^{-1}\mathbf{k}'\mathbf{A}\mathbf{x} > -(1 + \varphi_0),\ \mathbf{k}'\mathbf{x} = 0, \tag{15}$$

the representative point of the system (2)-(3) moves according to the equations

$$\dot{\mathbf{x}} = \mathbf{A}\mathbf{x} + \mathbf{b}\varphi\ (0) = \mathbf{A}\mathbf{x} + \mathbf{b}\xi(t). \tag{16}$$

where $\xi(t)$ is chosen so that the derivative with respect to time $\dot{\sigma}_0(\mathbf{x})$ of the function $\sigma(\mathbf{x})$ obtained as in (16), satisfies the equality

$$\dot{\sigma}_0(\mathbf{x}) = \mathbf{k}'\mathbf{A}\mathbf{x}(t) + \mathbf{k}'\mathbf{b}\xi(t) = 0. \tag{17}$$

If we combine (16) and (17), we obtain

$$\sigma(\mathbf{x}) = \mathbf{k}'\mathbf{x} = 0,$$

$$\dot{\mathbf{x}} = \mathbf{f}_0(\mathbf{x}) = \mathbf{B}\mathbf{x},\ \mathbf{B} = \mathbf{A} - (\mathbf{k}'\mathbf{b})^{-1}\mathbf{b}\mathbf{k}'\mathbf{A}. \tag{18}$$

Various forms of the scalar representation of (18) are given in [1, 3, and 4]. For trajectories of the system (18) we will use the notation $\mathbf{x}_0(\mathbf{x}^0, t)$.

(d) We consider finally the boundary $\sigma(\mathbf{x}) = 0$, $\dot{\sigma}_+(\mathbf{x})\,\dot{\sigma}_-(\mathbf{x}) = 0$ of the zone (15) of the sliding regime, represented by the two hyperlines

$$\mathbf{k}'\mathbf{x} = 0,\ \dot{\sigma}_+(\mathbf{x}) = \mathbf{k}'\mathbf{A}\mathbf{x} + \mathbf{k}'\mathbf{b}\,(1 + \varphi_0) = 0 \tag{19}$$

and

$$\mathbf{k}'\mathbf{x} = 0,\ \dot{\sigma}_-(\mathbf{x}) = \mathbf{k}'\mathbf{A}\mathbf{x} - \mathbf{k}'\mathbf{b}\,(1 - \varphi_0) = 0. \tag{20}$$

According to (12), (13), (14), and (18), for all the points q_+ and q_-, belonging, respectively, to the straight lines (19) and (20), the relations

$$\mathbf{f}_+(\mathbf{q}_+) = \mathbf{f}_0(\mathbf{q}_+),\ \ \mathbf{f}_-(\mathbf{q}_-) = \mathbf{f}_0(\mathbf{q}_-), \tag{21}$$

and

$$\dot{\sigma}_-(\mathbf{q}_+) > 0,\ \ \dot{\sigma}_+(\mathbf{q}_-) < 0, \tag{22}$$

are valid, so that, for example, for the straight line (19), we have

$$\frac{d^m}{dt^m}[\sigma_+(\mathbf{q}_+)]_+ = \frac{d^m}{dt^m}[\dot{\sigma}_+(\mathbf{q}_+)]_0,\ \ m \geqslant 1, \tag{23}$$

where $\frac{d^m}{dt^m}[\dot{\sigma}_+(\mathbf{q}_+)]_+$ and $\frac{d^m}{dt^m}[\dot{\sigma}_+(\mathbf{q}_+)]_0$ are the derivatives of order m with respect to the time of the function $\dot{\sigma}_+(\mathbf{x})$, evaluated at the point $\mathbf{q}_+$ by (12) and (18). It is evident from (23) that in a sufficiently small neighborhood of the point $\mathbf{q}_+$ the positive half-trajectories $\mathbf{x}_+(\mathbf{q}_+, t)$, and $\mathbf{x}_0(\mathbf{q}_+, t)$ lie simultaneously either in the region $\dot{\sigma}_+(\mathbf{x}) \geqslant 0$, or in the region $\dot{\sigma}(\mathbf{x}) < 0$. In this neighborhood for t > 0, in the first case of the similar location of the trajectories $\mathbf{x}_+(\mathbf{q}_+, t)$, and $\mathbf{x}_0(\mathbf{q}_+, t)$, we set $\mathbf{x}(\mathbf{q}_+, t) = \mathbf{x}_+(\mathbf{p}_+, t)$; in the second $\mathbf{x}(\mathbf{q}_+, t) = \mathbf{x}_0(\mathbf{q}_+, t)$. The positive half-trajectory $\mathbf{x}(\mathbf{p}_+, t)$ will be unique since, according to (22), the trajectories $\mathbf{x}_-(\mathbf{q}_+, t)$ for t > 0 start in the half-space $\sigma(\mathbf{x}) < 0$. The straight line (20) can be considered similarly.

3. The solution $\mathbf{x}(\mathbf{x}^0, t)$ of the system (2)-(3), determined as above, is also a generalized solution of this system in the sense of the definition of A. F. Filippov [8].

(We mention that the essence of A. F. Filippov's definition is precisely the definition of the discontinuous right-hand sides, including infinite valued functions, continuous in the same sense as the characteristic (2)). The fact that the solution $\mathbf{x}(\mathbf{x}^0, t)$ can be continued for t → + ∞, its uniqueness, and the property $\mathbf{x}((\mathbf{x}^0, t_1), t_2) = \mathbf{x}(\mathbf{x}^0, t_1 + t_2)$ for t ≥ 0 are obvious; the continuity relative to $\mathbf{x}^0$ and t can easily be proved by using (21).

Thus, for the reflection of $\mathbf{x}(\mathbf{x}^0, t)$ for t ≥ 0, we can apply all the results of the general theory of dynamic systems [9], and this, in turn, makes it possible to use a series of results formulated for classical systems of differential equations, but permitting obvious generalizations to abstract dynamic systems – for example, the theorems of E. A. Barbashin and N. N. Krasovskii [10] concerning stability in the large.

4. We will form the Lyapunov function V(x) for the system (2)-(3) and (5) in the case (7) by linking on the surface $\sigma(\mathbf{x}) = 0$ the Lyapunov functions

$$V_+(\mathbf{x}) = \mathbf{x}_+\mathbf{H}\mathbf{x}_+,\ \ \mathbf{x}_+ = \mathbf{x} + \mathbf{A}^{-1}\mathbf{b}(1 + \varphi_0), \tag{24}$$

$$V_-(\mathbf{x}) = \mathbf{x}_-\mathbf{H}\mathbf{x}_-,\ \ \mathbf{x}_- = \mathbf{x} - \mathbf{A}^{-1}\mathbf{b}(1 - \varphi_0) \tag{25}$$

(H is a symmetric matrix of the nth order) for the systems (12') and (13'), respectively:

$$V(\mathbf{x}) = \begin{cases} V_+(\mathbf{x}) - V_+(0) & \text{for } \sigma(\mathbf{x}) \geqslant 0, \\ V_-(\mathbf{x}) - V_-(0) & \text{for } \sigma(\mathbf{x}) \leqslant 0. \end{cases} \tag{26}$$

The continuity of V(x) is ensured if $V_+(\mathbf{x})$ and $V_-(\mathbf{x})$ are chosen so that the equality

$$V_+(\mathbf{x}) - V_+(0) = V_-(\mathbf{x}) - V_-(0) \text{ for}$$
$$\sigma(\mathbf{x}) = \mathbf{x}'\mathbf{k} = 0. \tag{27}$$

holds. Since the relation $V_+(\mathbf{x}) - V_+(0) = V_-(\mathbf{x}) - V_-(0)$ is equivalent to $\mathbf{x}'\mathbf{H}\mathbf{A}^{-1}\mathbf{b} = 0$, the condition (27) used in the linking can be written in the form

$$\mathbf{H}\mathbf{A}^{-1}\mathbf{b} = \mu\mathbf{k}\ \ (\mu = \text{const} \neq 0). \tag{28}$$

It is evident from the relation

$$V(\mathbf{x}) = \mathbf{x}'\mathbf{H}\mathbf{x} + 2\mu\sigma\cdot\varphi(\sigma), \tag{29}$$

that follows from (26) and (28), that if the function $\mathbf{x}'\mathbf{H}\mathbf{x}$ satisfying condition (28) is positive-definite, then the function V(x) will also be positive-definite for μ > 0.

For any solution $\mathbf{x}(\mathbf{x}^0, t)$ everywhere except possibly at points of intersection of $\mathbf{x}(\mathbf{x}^0, t)$ with the surface $\sigma(\mathbf{x}) = 0$, the derivative $\dot{V}(\mathbf{x})$ with respect to time of the function (29) along $\mathbf{x}(\mathbf{x}^0, t)$ exists and satisfies the relations

$$\dot{V}(\mathbf{x}) = \begin{cases} \dot{V}_+(\mathbf{x}) & \text{for } \sigma(\mathbf{x}) > 0, \\ \dot{V}_-(\mathbf{x}) & \text{for } \sigma(\mathbf{x}) < 0, \\ \dot{V}_0(\mathbf{x}) & \text{for } \sigma(\mathbf{x}) = 0,\ \dot{\sigma}_+(\mathbf{x})\cdot\dot{\sigma}_-(\mathbf{x}) < 0, \end{cases} \tag{30}$$

where $\dot{V}_+(\mathbf{x}) = \mathbf{x}_+'(\mathbf{H}\mathbf{A} + \mathbf{A}'\mathbf{H})\mathbf{x}_+$ and $\dot{V}_-(\mathbf{x}) = \mathbf{x}_-'(\mathbf{H}\mathbf{A} + \mathbf{A}'\mathbf{H})\mathbf{x}_-$ are the derivatives with respect to time of the functions $V_+(\mathbf{x})$ and $\dot{V}_-(\mathbf{x})$ according to (12') and (13'), and $\dot{V}_0(\mathbf{x}) = \mathbf{x}'(\mathbf{H}\mathbf{B} + \mathbf{B}'\mathbf{H})\mathbf{x}$ is the derivative with respect to time of the function (29) according to (18).

Let the form $-\mathbf{x}'\mathbf{G}\mathbf{x}$ (G is a symmetric matrix of the nth order) be positive-definite. Then when the condition (7) is satisfied, there exists one, and only one, form $x'Hx$, related to $x'Gx$ by

$$G = HA + A'H, \tag{31}$$

where the form $x'Hx$ is positive-definite (A. M. Lyapunov). It is evident, in addition, that the function $V_+(x)$ or the function $V_-(x)$ will be negative everywhere, except at the point x_+^0, where $x_+ = x_+^0 + A^{-1}b(1 + \varphi_0) = 0$, or the point x_-^0, where $x_- = x_-^0 - A^{-1}b(1 - \varphi_0) = 0$). If

$$a_1^{-1}k_p b_1 = k'A^{-1}b > 0, \tag{32}$$

corresponding to negative feedback in the system (1)-(2), then $\sigma(x_+^0) < 0$ and $\sigma(x_-^0) > 0$, so that

$$\begin{aligned} \dot{V}_+(x) &< 0 \quad \text{for} \quad \sigma(x) \geqslant 0, \\ \dot{V}_-(x) &< 0 \quad \text{for} \quad \sigma(x) \leqslant 0. \end{aligned} \tag{33}$$

If the inequalities (33) are satisfied, the function $V(x)$ decreases along any trajectory $x(x^0, t)$, while the point representing the system (2)-(3) moves according to Equations (12) or (13). It remains to show that $V(x)$ also decreases for motion according to (18). We now turn to the proof of this fact, and formulate the final results in the following theorem:

Theorem I. If the conditions (5), (7), and (32) are satisfied for the system (2)-(3), and if there exists a negative-definite form $x'Gx = x'(HA + A'H)x$, satisfying (28), then the equilibrium solution $x = 0$ of this system is asymptotically stable in the large.

In accordance with the equality $H = GA^{-1} - A'HA^{-1}$ we write the relation

$$Hbk'A = GA^{-1}bk'A - A'HA^{-1}bk'A. \tag{34}$$

Further, according to the linking conditions (28) we have

$$A'HA^{-1}bk'A = \mu A'kk'A. \tag{35}$$

If we substitute (34) and (35) in the expression

$$\begin{aligned} \dot{V}_0(x) &= x'(HB + B'H)x = \\ &= x'(G - (b'k)^{-1}(Hbk'A + A'kbH))x, \end{aligned}$$

we obtain the identity

$$\dot{V}_0(x) = f_0'(x)A'^{-1}GA^{-1}f_0(x),$$

from which it follows that $\dot{V}_0(x)$ is zero only at points x_0 of the set $f_0(x) = 0$. This set and the surface $\sigma(x) = 0$ have only one common point – the origin 0.

Actually, we have [see (16)-(18)], the equality

$$f_0(x) = Ax + b\xi,$$

so that $x_0 = -\xi A^{-1}b$. According to (32) the relation $\sigma(x_0) = -\xi k'A^{-1} \cdot b = 0$ can hold only for $\xi = 0$, i.e., only at the point 0. At the remaining points of the surface $\sigma(x) = 0$, the function $\dot{V}_0(x)$ is negative.

Thus, when the conditions of Theorem I are satisfied, the infinitely large positive-definite function (29) strictly decreases along any nonzero trajectory $x(x^0, t)$. The system (2)-(3) will satisfy all the essential conditions of Theorem I of [10].

We have reduced the investigation of the equilibrium stability of the system (2)-(3) in the case considered to a study of conditions that are sufficient for the compatibility of the equality (28) and the Sylvester criterion for the sign-definiteness of the form $x'Gx$. The limitation (5) appears [7] to be a necessary condition for this compatibility. It is now clear, that in its final part, the method of obtaining the Lyapunov functions is a modification of the method of I. G. Malkin [2] (p. 163), [11, 12], of investigating absolute stability.

5. Let it be possible to choose a negative-definite form $x'Gx = x'(HA + A'H)x$, satisfying (28). If we use the results in [5], p. 251, and consider a pencil of forms

$$x'Gx + \nu \cdot x'Hx, \tag{36}$$

we obtain the inequality

$$\nu_1 x'Hx \leqslant -x'Gx \leqslant \nu_n x'Hx, \tag{37}$$

where ν_1 and ν_n are the least and greatest roots of the characteristic equation of the pencil (36), respectively. From (37) we obtain

$$\nu_1 \cdot V(x) \leqslant -\dot{V}(x) \leqslant \nu_n \cdot V(x) \tag{38}$$

for the rate of change $\dot{V}(x)$ of the function (29) for the motion by using (12) and (13).

For the forms $x'Hx$ and $\dot{V}_0(x) = x'(HB + B'H)x$ on the surface $k'x = 0$ the relation

$$x'Hx = V(x), \quad \nu_1^0 x'Hx \leqslant -\dot{V}_0(x) \leqslant \nu_{n-1}^0 x'Hx, \tag{39}$$

holds, where ν_1^0, ν_{n-1}^0 are the smallest and largest roots, respectively, of the characteristic equation of the form $x^{0\prime}(HB + B'H)^0 x^0 + \nu^0 x^{0\prime} H^0 x^0$, obtained from the pencil

$$x'(HB + B'H)x + \nu x'Hx$$

on applying the relation $k'x = 0$.

The time taken for the distance $r^2 = V(x)$, from a representative point of the system (2)-(3) to the origin, to decrease from the value r_1 to the value r_2, can be given its coarsest estimate by using the inequalities (38) and (39) in a way similar to that in [13] for a linear system. The frequency method [14] is applied to calculate the roots $\nu_1, \nu_n, \nu_1^0, \nu_{n-1}^0$.

6. We now consider the case when the equations of motion of the relay system considered above have the form (2) and (4), i.e., when they are actually given in the form (1)-(2), which is the most common in control theory. The relation (31) between the matrix $\mathbf{G} = -\|\beta_{ij}\|_1^n$ and $\mathbf{H} = \|\alpha_{ij}\|_1^n$ (the abbreviated notation is borrowed from [5]) and the condition (28) for $\mu = k_p$ can be written

$$\beta_{ij} = a_{n+1}^{-1}(\alpha_{in}a_j + \alpha_{jn}a_i) - \\ - \alpha_{ji-1} - \alpha_{ij-1}\,(b_0 = \alpha_{i0} = \alpha_{0i} = 0), \tag{40}$$

$$\alpha_{1k} = a_1 b_k \quad (k = 1, \ldots, n), \tag{41}$$

and the Lyapunov function (29) takes the form

$$V(\mathbf{x}) = \sum_{i,\,j=1}^{n} \alpha_{ij} x_i x_j + 2k_p \varphi(\sigma)\sigma. \tag{42}$$

The investigation of the conditions under which the form $-\mathbf{x}'\mathrm{G}\mathbf{x} = \sum\limits_{i,\,j=1}^{n} \beta_{ij} x_i x_j$, which satisfies the conditions (40) and (41), can be positive-definite is more convenient if it is reduced to a consideration not of the matrix $\|\beta_{ij}\|_1^n$, but of the matrix $\|\gamma_{ij}\|_1^n$ congruent to it [5] (p. 240), for which

$$\begin{aligned} &\gamma_{11} = \beta_{11}, \quad \gamma_{i1} = \gamma_{1i} = \beta_{i1} - \beta_{11} a_i, \\ &\gamma_{ij} = \gamma_{ji} = \beta_{ij} - \beta_{i1} a_j - \beta_{1j} a_i + \beta_{11} a_i a_j, \end{aligned} \tag{43}$$

since the quantities γ_{ij} can be expressed more simply in terms of α than the quantities β_{ij}.

A relatively uncomplicated calculation shows that the components of α satisfy condition (41) if, and only if, the components of γ satisfy

$$\gamma_{11} = 2a_{n+1}^{-1} b_n, \quad \gamma_{kk} = \\ = 2\Big(B_{kn} + \sum_{r=0}^{k-3} (-1)^r \gamma_{k+r+1,\,k-r-1}\Big) \\ (k = 2, \ldots, n), \tag{44}$$

where

$$B_{kn} = b_{k-1} a_k - \\ - \sum_{r=0}^{k-2} (-1)^r (b_{k+r} a_{k-r-1} + b_{k-r-2} a_{k+r+1}), \tag{45}$$

$$b_{n+l} = a_{n+l+1} = \alpha_{i,\,n+l} = \gamma_{n+l+1,\,i} = 0,$$

$$\gamma_{n+1,\,i} = -\gamma_{1i} a_{n+1} \quad (l \geqslant 1).$$

We now denote by D_n the determinant of the matrix $\|\gamma_{ij}\|_1^n$, and write Theorem I in a concrete form.

Theorem II. If the elements of the determinant D_n satisfy the relations (44) and (45), and if the quantities γ_{ij} $(i \neq j)$ can be chosen so that all the diagonal minors D_{kn} of the determinant D_n are positive, then the equilibrium state of the system (1)-(2) is asymptotically stable as a whole if its linear part is asymptotically stable for $b_n > 0$.

7. If the condition (8) is satisfied, then the Lyapunov function for the system (2), (4) can be taken to have the form

$$V(\mathbf{x}) = \sum_{i,\,j=2}^{n} \alpha_{ij} x_i x_j + 2k_p \varphi(\sigma)\sigma, \tag{46}$$

obtained from (41) and (42) for $a_1 \to 0$. By calculations and reasoning similar to that in Sec. 4, and with the derivative of $V(\mathbf{x}(\mathbf{x}^0, t))$ [2, 11, 12] taken as the n-variable form,

$$x_1' = \varphi(\sigma), \quad x_k' = x_k \quad (k = 2, \ldots, n).$$

it is easy to show that Theorem II is valid in this case. The construction of the Lyapunov function, however, loses its elegant geometric interpretation. The stability criteria obtained from Theorem II with the assumption (7) tend for $a_1 \to 0$ to a sufficient condition for stability of the system (2), (4) when its linear part is neutral for one coordinate. We note here that these criteria, for $b_n \to 0$, tend to the stability criteria obtained in [7] for $b_n = 0$.

The method of obtaining Lyapunov functions proposed in 4 and 6 thus becomes, for $a_1 \to 0$, an extension of the method of L. G. Malkin to relay systems.

Below (in 8 and 9 we obtain the minimum limitations for n = 3, 4 stability criteria which can be obtained by using Theorem II. These criteria are equivalent to the stability conditions that follow from the theorem of A. I. Lur'e as given by A. M. Letov in [2] (p. 124). Consequently, the assumption [11] that I. G. Malkin's method will give more precise stability conditions than the Lur'e algorithm for control systems with one nonlinear link is, generally speaking, not justified. This method is, however, [2, 12] suitable for obtaining simplified criteria for the stability of systems of high order (n ≥ 5). In Sec. 10 of the present paper, an effective algorithm is proposed for obtaining such criteria.

8. For n = 3 the determinant D_n has the form

$$D_3 = \begin{vmatrix} 2a_4^{-1} b_3 & \gamma_{12} & \gamma_{13} \\ \gamma_{21} & 2B_{23} & \gamma_{23} \\ \gamma_{31} & \gamma_{32} & 2(B_{33} - a_4\gamma_{12}) \end{vmatrix} \tag{47}$$

The simultaneous validity of the inequalities

$$B_{23} > 0. \quad B_{33} - a_4\gamma_{12} > 0, \qquad D_{22} = 4a_4^{-1}b_3B_{23} - \gamma_{12}^2 > 0 \tag{48}$$

is a necessary condition that all the principal minors of the determinant (47) be positive. For $\gamma_{13} = \gamma_{23} = 0$ this condition is also sufficient.

From (48) we obtain the relation

$$\gamma_{12} < a_4^{-1} B_{33},$$

$$-2\sqrt{a_4^{-1} b_3B_{23}} < \gamma_{12} < -2\sqrt{a_4^{-1} b_3B_{23}}$$

and this can be used to obtain necessary and sufficient conditions for the solvability of (48) for γ_{12}:

$$B_{23} = b_1a_2 - b_2a_1 > 0, \qquad B_{33} = b_2a_3 - b_3a_2 - b_1a_4 > -2\sqrt{b_3a_4B_{23}}. \tag{49}$$

According to Theorem II, the conditions (49) are sufficient for the stability in the large of the system (2), (4) that we are considering.

9. For n = 4

$$D_4 = \begin{vmatrix} 2a_5^{-1}b_4 & \gamma_{12} & \gamma_{13} & \gamma_{14} \\ \gamma_{21} & 2B_{24} & \gamma_{23} & \gamma_{24} \\ \gamma_{31} & \gamma_{32} & 2(B_{34} + \gamma_{24}) & \gamma_{34} \\ \gamma_{41} & \gamma_{42} & \gamma_{43} & 2(B_{44} - a_5\gamma_{13}) \end{vmatrix} \tag{50}$$

The simultaneous validity of the inequalities

$$B_{24} > 0, \quad 4a_5^{-1} b_4(B_{34} + \gamma_{24}) - \gamma_{13}^2 > 0, \qquad 4B_{24}(B_{44} - a_5\gamma_{13}) - \gamma_{24}^2 > 0 \tag{51}$$

is a necessary condition that all the principal minors of the determinant (50) be positive. For $\gamma_{12} = \gamma_{14} = \gamma_{23} = \gamma_{34} = 0$, if

$$D_{24} = 4a_5^{-1} b_4B_{24}, \quad D_{34} = 2B_{24}(4a_5^{-1} b_4(B_{34} + \gamma_{24}) - \gamma_{13}^2).$$
$$D_{44} = [4B_{24}(B_{44} - a_4\gamma_{13}) - \gamma_{24}^2]\,[4a_5^{-1} \cdot b_4(B_{34} + \gamma_{24}) - \gamma_{13}^2].$$

this condition also appears to be sufficient. If we use the results of [15] (p. 95), we arrive at the following necessary and sufficient conditions for the solvability of the inequality (51) for γ_{13} and γ_{24}:

$$B_{24} > 0, \tag{52}$$

$$M^3 + N^3 - M^2N^2 - \frac{9}{8}MN + \frac{27}{956} > 0, \tag{53}$$

where

$$M = 0.25\, B_{44}B_{24}^{-\frac{1}{3}}b_4^{-\frac{2}{3}}a_5^{\frac{2}{3}}, \tag{54}$$

$$N = 0.24\, B_{34}B_{24}^{-\frac{2}{3}}b_4^{-\frac{1}{3}}a_5^{\frac{1}{3}}.$$

According to Theorem II, the conditions (52)-(54) are sufficient for stability in the large for the system (2), (4).

10. For $n \geq 5$, the most precise criteria that can be obtained from Theorem II involve calculations that make them practically inapplicable in their general form. In order to obtain simplified stability criteria, the method can be recommended of insisting that only one or two elements γ_{ij} $(i \neq j)$ be exactly equal to zero, and of reducing the condition that the main minors of the determinant D_n be positive to inequalities similar to the relations (46) and (51).

Thus, for example, the simple inequalities

$$B_{55} + \gamma_{53} + a_6\gamma_{12} > 0. \quad 4a_6^{-1} b_5B_{25} - \gamma_{12}^2 > 0, \qquad 4B_{35}B_{45} - \gamma_{53}^2 > 0 \tag{55}$$

are obtained for n = 5, when the values of the elements γ_{12} and γ_{35} of the determinant D_5 are left as variable quantities. Calculations similar to those in 8, applied to the system (55), yield the criteria

$$B_{25}, \quad B_{35}, \quad B_{45} > 0,$$

$$B_{55} > -2(\sqrt{B_{34}B_{45}} + \sqrt{a_6b_5B_{25}})$$

for the stability of the relay system considered. If we do not assume that the elements γ_{24} and γ_{53} are equal to zero, we obtain

$$D_5 = 2a_6^{-1}b_5 \begin{vmatrix} 2B_{25} & 0 & \gamma_{24} & 0 \\ 0 & 2(B_{35} + \gamma_{24}) & 0 & \gamma_{35} \\ \gamma_{24} & 0 & 2(B_{45} + \gamma_{53}) & 0 \\ 0 & \gamma_{53} & 0 & 2B_{55} \end{vmatrix}.$$

The reasoning applied in 9 leads to stability conditions given by the relations $B_{25} > 0$, $B_{55} > 0$, and (53), where $M = 0.25\, B_{25}^{-1/3} B_{35}B_{55}^{-2/3}$, $N = 0.25\, B_{25}^{-2/3}B_{45}B_{55}^{-1/3}$.

In conclusion, we note that the very simple stability criterion

$$B_{kn} > 0$$

can be obtained from Theorem II for any $n \geq 2$, if we set $\gamma_{ij} = 0$, for $i \neq j$, in the determinant D_n.

The author wishes to thank E. A. Barbashin for his guidance and help in the work involved in preparing the present paper.

LITERATURE CITED

1. Ya. Z. Tsypkin, The Theory of Automatic Control Relay Systems [in Russian] (Moscow-Leningrad, 1955).
2. A. M Letov, The Stability of Nonlinear Control Systems [in Russian] (Gostekhizdat, Moscow-Leningrad, 1955).
3. Yu. I. Neimark, "Sliding and periodic regimes of a

relay system," Trudy GIFTI i Radiofakul'teta GGU 30 (1956).

4. Yu. V. Dolgolenko, The Sliding Regime in Relay Systems of Direct Control [in Russian] Author's Abstract: Dissertation (Leningrad, 1955).
5. F. R. Gantmakher, Matrix Theory [in Russian] (Gostekhizdat, Moscow-Leningrad, 1953).
6. D. V. Anosov, "The stability of equilibrium positions of relay systems," Avtomat. i Telemekh. 20, 2 (1959).*
7. Yu. I. Alimov, "Stability in the large of an equilibrium state of relay control systems," Izv. Vysshei Shk., Radiofizika 2, 6 (1959).
8. A. F. Filippov, "Differential equations with piecewise-continuous right-hand sides," Uspekhi Matem. Nauk 13, 4, 217 (1958).
9. V. V. Stepanov and V. V. Nemytskii, Qualitative Differential Equation Theory [in Russian] (Gostekhizdat, Moscow-Leningrad, 1949).
10. E. A. Barbashin and N. N. Krasovskii, "The stability of motion in the large," Doklady Akad. Nauk SSSR 86, 3 (1952).
11. I. G. Malkin, "The theory of stability of control systems," Prikl. Matem. i Mekh. 15, 1 (1951).
12. A. K. Bedel'baev, "Some simplified stability criteria," Avtomatika i Telemekhanika 20, 6 (1959).*
13. N. G. Chetaev, "The choice of stability parameters in mechanical systems," Prikl. Matem. i Mekh. 15, 3 (1951).
14. E. I. Baranchuk, "The application of certain methods from the theory of automatic control to the analysis of the stability of nonlinear systems," Nauchn. Dokl. Vysshei Shkoly, Elektromekhanika i Avtomatika No. 1 (1959).
15. A. I. Lur'e, Some Nonlinear Problems in the Theory of Automatic Control (Gostekhizdat, 1951).

---

*See English translation.

THE APPLICATION OF THE METHOD OF SMALL PARAMETERS IN THE INVESTIGATION OF SYSTEMS OF AUTOMATIC CONTROL WITH DELAY

Yu. A. Ryabov

Moscow

Translated from Avtomatika i Telemekhanika, Vol. 21, No. 6, pp. 729-739, June, 1960

A method of investigation of systems of automatic regulation (SAR) with retardation is presented, based on the consideration of retardation as a small parameter and the application of the Lyapunov-Poincaré method of small parameters. The case is considered of a SAR expressed as a linear equation with constant coefficients and with a single constant retardation.

In many problems of automatic control, the delay is small and plays the role of a type of interference causing a distortion in that "undisturbed" process which would occur in the absence of any delay. It is therefore completely natural in such problems to consider the delay as a small parameter, and to attempt to apply the Poincaré-Lyapunov method of small parameters. One method of investigation of automatic control systems with delay is to seek the solution of the relevant differential equations by using successive approximations, with the first approximation taken to be the solution of these equations with a zero delay. We will consider here linear equations with constant coefficients and a single constant delay, although this method can also be used with known restrictions in the case of equations with variable coefficients with delay, and also in the case of quasi-linear equations.

1. In the general case, the equations we will consider have the form

$$\dot{x}_s(t) = \sum_{j=1}^{n} [a_{sj} x_j(t) + b_{sj} x_j(t-\mu)] \quad (s = 1, \ldots, n), \tag{1}$$

where a_{sj} and b_{sj} are constant coefficients and μ is the constant delay.

Let the functions $x_1^{(0)}, \ldots, x_n^{(0)}$ form a solution of the system (1) for $\mu = 0$ (we will call this solution undisturbed) and for the initial conditions $x_s(0) = x_{s0}$ ($t = 0$ being the initial instant of time). If we rewrite (1) in the form

$$\dot{x}_s(t) = \sum_{j=1}^{n} \bar{a}_{sj} x_j(t) + \sum_{j=1}^{n} b_{sj} [x_j(t-\mu) - x_j(t)], \quad \bar{a}_{sj} = a_{sj} + b_{sj}, \tag{2}$$

then we can consider the difference $x_j(t-\mu) - x_j(t)$ in these equations as a type of nonlinearity depending on the small parameter μ and becoming zero for $\mu = 0$. Then for obtaining the solution of the system (2), it is natural to consider the method that is applied in the theory of differential equations with small parameters (see, for example, [1]). If we take $x_s^{(0)}$ for the zeroth approximation, then, for the first approximation, we use $x_s^{(1)}$, $s = 1, \ldots, n$, which is the solution of the system

$$\dot{x}_s(t) = \sum_{j=1}^{n} \bar{a}_{sj} x_j^{(1)}(t) + \sum_{j=1}^{n} b_{sj} [x_j^{(0)}(t-\mu) - x_j^{0}(t)], \tag{3}$$

for the same initial conditions $x_s^{(1)}(0) = x_{s0}$. Since the functions $x_j^{(0)}(t)$ are already known, then the differences $x_j^{(0)}(t-\mu) - x_j^{(0)}(t)$ are known functions of t and the delay μ, where μ plays the part of a parameter. The equations (3) are ordinary linear inhomogeneous equations. Their solutions, defined uniquely for all $-\infty < t < \infty$, are obtained in the form $x_s^{(1)} = x_s + \bar{x}_s^{(1)}$, where the functions $\bar{x}_s^{(1)} = \bar{x}_s^{(1)}(t, \mu)$ become zero for $t = 0$ or $\mu = 0$. The second approximation $x_s^{(2)}$ is obtained in a similar way as the solution of the inhomogeneous linear system

$$\dot{x}_s^{(2)}(t) = \sum_{j=1}^{n} \bar{a}_{sj} x_j^{(2)}(t) + \sum_{j=1}^{n} b_{sj} [x_j^{(1)}(t-\mu) - x_j^{(1)}(t)] \tag{4}$$

with the initial conditions $x_s^{(2)}(0) = x_{s0}$. As a result we obtain $x_s^{(2)} = x_s^{(0)} + \bar{x}_s^{(1)} + \bar{x}_s^{(2)}$, where the functions $\bar{x}_s^{(2)} = \bar{x}_s^{(2)}(t, \mu)$ are of the second order of smallness relative to μ, (and so on. For the kth approximation we obtain $x_s^{(k)} = x_s^{(0)} + \bar{x}_s^{(1)} + \ldots + \bar{x}_s^{k}$. In the limit (for $k \to \infty$) the solution of the system (1) can be written as a series:

$$x_s = x_s^{(0)} + \sum_{k=1}^{\infty} \bar{x}_s^{(k)} \quad (s = 1, \ldots, n), \tag{5}$$

where the functions $\bar{x}_s^{(m)}$, $m = 1, 2, \ldots$ are of order m relative to μ. Each term of this series is a function that is analytic in $\underline{t}$ and μ for $-\infty < t < \infty$ and any finite μ. It can be shown, that, if μ does not exceed a certain bound μ_0 which depends on the coefficients of the system (1), then the series (5) is convergent and is uniformly convergent relative to $\underline{t}$ in any finite interval of $\underline{t}$. The sum of this series for $\mu < \mu_0$ is consequently an analytic function of $\underline{t}$, and the above iteration process, in all cases when μ is sufficiently small, can be used to obtain a solution of the equations (1) in $-\infty < t < \infty$ having continuous derivatives of all orders at every point and satisfying the given initial conditions $x_s(0) = x_{s0}$.

2. It follows from the general theory of differential equations with delay that the solution of the system (1) depends not only on the initial values x_{s0} of the functions sought at the initial instant of time $t = 0$, but also on the so-called initial functions $\varphi_1, \ldots, \varphi_n$. The functions $x_1, \ldots, x_n$ are set equal to the respective initial functions in the interval $-\mu \leq t < 0$. These initial functions express the "previous history" or the "hereditary properties" of the dynamic system being considered that is described by the equations (1). The solution obtained by our proposed method is uniquely determined by a single set of initial values x_{s0}. This solution does not exhibit the so-called "hereditary properties," and is only one particular solution among the infinite number of solutions determined by the same initial conditions but with different initial functions. The question arises of the position of this solution of the system (1) among the other solutions.

We will consider as an example the equation

$$\dot{x}(t) = ax(t-\mu), \tag{6}$$

where $\underline{a}$ is a positive number, and we denote by $\psi(t)$ the solution of this equation corresponding to some initial function $\varphi(t)$ that is defined, continuous, and bounded for $-\mu \leq t < 0$. By using the "step" method we obtain successively the values of $\psi(t)$ in each of the intervals $[t_{k-1}, t_k]$, $t_k = k\mu$, $k = 1, 2, \ldots$ As is known (see [2], for example), we can be sure that the function $\psi(t)$ will possess in the interval $t_{k-1} \leq t < t_k$ continuous derivatives up to and including the $(k-1)$th order, and a continuous $\underline{k}$th derivative in the interval $t_{k-1} \leq t < t_k$. It is therefore possible to express this function in the interval $t_{k-1} \leq t \leq t_k$ in the form of a Taylor series with a remainder as

$$\psi(t) = \psi_k + \bar{t}\dot{\psi}_k + \ldots + \frac{\bar{t}^{k-1}}{(k-1)!}\psi_k^{(k-1)} + \frac{\bar{t}^k}{k!}\psi^{(k)}(\theta_k), \tag{7}$$

where $\bar{t} = t - t_k$, $\psi_k = \psi(t_k)$, $\psi_k^{(\sigma)} = \psi^{(\sigma)}(t_k)$, $\sigma = 1, 2, \ldots, k-1$, $t_{k-1} < \theta_k < t_k$, where $\psi^{(k)}(\theta_k) = a^k\varphi(\bar{\theta})$, $\mu < \bar{\theta} < 0$. Moreover, by using the condition of continuity of the derivatives of the function $\psi(t)$ at $t = t_k$ up to and including the $(k-1)$th order (derivatives from the left, of course), we arrive at the following relations between the values of the function $\psi(t)$ at the points $t = t_k$, $t = t_{k-1}$ and its derivatives at the point $t = t_{k-1}$:

$$\begin{aligned} u_0 &= \psi_k - \mu a u_0 + \frac{\mu^2}{2} a u_1 - \ldots + (-1)^{k-1}\frac{\mu^{k-1}}{(k-1)!} a u_{k-1} + \delta_k, \\ u_1 &= a u_0 - \mu a u_1 + \ldots + (-1)^{k-2}\frac{\mu^{k-2}}{(k-2)!} a u_{k-2} + \delta_{k-1}, \\ &\ldots\ldots\ldots\ldots\ldots\ldots\ldots\ldots\ldots\ldots\ldots\ldots\ldots\ldots \\ u_{k-1} &= a u_{k-2} + \delta_1, \end{aligned} \tag{8}$$

where $u_j = \psi^{(j)}(t_{k-1})$, $j = 1, \ldots, k-1$, $u_0 = \psi(t_{k-1})$, $\delta_\sigma = (-1)^\sigma a^k \mu^\sigma/\sigma!\ \varphi(\theta_\sigma)$, $-\mu < \theta_\sigma < 0$.

These equations are linear algebraic equations in $u_0, \ldots, u_{k-1}$. If we solve them for $u_0, \ldots, u_{k-1}$, and then express $\dot{\psi}_k, \ddot{\psi}_k, \ldots$ by the formulas $\dot{\psi}_k = au_0$, $\ddot{\psi}_k = au_1, \ldots$ and substitute these expressions in (7), we obtain $\psi(t)$ in the interval $t_{k-1} \leq t \leq t_k$ in the form $\psi(t) = \tilde{\psi}_k(t) + \Delta\psi_k(t)$, where the function $\tilde{\psi}_k(t)$ corresponds to the solution of Equations (8) for $\delta_1 = \ldots = \delta_k = 0$, and the function $\Delta\psi_k(t)$ depends linearly on $\delta_1, \ldots, \delta_k$ and is of the order $\underline{k}$ relative to μ. Thus,

$$\Delta\psi_2(t) = \bar{t}\,\frac{\delta_2}{A} + \frac{\bar{t}^2}{2}a^2\varphi(\bar{\theta}_2),\ \Delta\psi_3(t) =$$

$$= \bar{t}\left(\frac{\mu^2}{2}\delta_2 + A\delta_3\right)\frac{1}{\Delta_2} + \frac{\bar{t}^2}{2}(A\delta_2 + \delta_3)\frac{1}{\Delta_2} + \frac{\bar{t}^3}{3!}a^3\varphi(\bar{\theta}_3),$$

where $A = 1 + \mu a/a$, $\Delta_2 = A^2 - \mu^2/2$, and the arguments $\bar{\theta}_2, \bar{\theta}_3$ of the function φ are in the interval $(-\mu, 0)$. If $|\varphi(t)| \leq \gamma$, then we can obtain the inequality

$$|\Delta\psi_2(t)| \leqslant \frac{|a\mu|^2}{2}\left(1 + \frac{\mu}{|A|}\right)\gamma,\ |\Delta\psi_3(t)| \leqslant$$

$$\leqslant \frac{|a\mu|^3}{3!}\left[1 + \left(2\mu^2 + \frac{5}{2}|A|\mu\right)\frac{1}{\Delta_2}\right]\gamma$$

$$t_1 \leqslant t < t_2, \quad t_2 \leqslant t < t_3$$

and similar formulas for $\Delta\psi_4, \Delta\psi_5, \ldots$. These inequalities show that for small values of μ, or, more correctly, for small values of the product $|a|\mu$, the functions $\Delta\psi_k$ decrease very rapidly in absolute value for increasing k. For all values of k we have $|\Delta\psi_k(t)| \le Q_k(\mu)\gamma$, where $Q_k(\mu)$ is of order k relative to μ.

We will now consider the solution $\overline{x}(t, t_k)$ of Eq. (6) obtained by the method of iterations for the initial condition $x(t_k) = \psi_k$. Since this solution has continuous derivatives of any order at $t = t_k$, a relation similar to (7) and (8) can be obtained for it. As a result, we find that, in the interval $t_{k-1} \le t < t_k$,

$$\overline{x}(t, t_k) = \widetilde{\psi}_k(t) + \Delta\overline{x}_k(t),$$

where the function $\Delta\overline{x}_k(t)$ consists of terms of order k and higher relative to μ for $t_{k-1} \le t < t_k$. For the difference between the functions $\overline{x}(t, t_k)$ and $\psi_k(t)$ in this interval, we obtain the inequality

$$|\psi(t) - \overline{x}(t, t_k)| \leqslant |\Delta\psi_k(t)| + |\Delta\overline{x}_k(t)|.$$

For values of μ for which the solution $\overline{x}(t, t_k)$ exists and for all values of t, we have $\lim\limits_{k\to\infty} \Delta\overline{x}_k = 0$. This is clear from the fact that if we expand $\overline{x}(t, t_k)$ in a double series of powers of $t - t_k$ and μ, then $\Delta\overline{x}_k$ is part of the remainder term of this series. It can be shown that for these values of μ we have $\lim\limits_{k\to\infty} Q_k(\mu) = 0$, so that $\Delta\psi_k \to 0$, and also $|\psi(t) - \overline{x}(t, t_k)| \to 0$ for $k \to \infty$.

If we denote by $\varphi_k(t)$ and $\overline{\varphi}_k(t)$ functions given in the interval $t_{k-1} \le t < t_k$, and coinciding in this interval with $\psi(t)$ and $\overline{x}(t, t_k)$, respectively, then these functions can be considered as initial functions determining the solution $\psi(t)$ and $\overline{x}(t, t_k)$ for $t > t_k$. Since the difference $\varphi_k(t) - \overline{\varphi}_k(t)$ tends to zero for $k \to \infty$, and in view of the continuous dependence of the solutions of differential equations with delay on the initial functions, the solution $\psi(t)$ will be a more accurate approximation to the solution $\overline{x}(t, t_k)$ for $t > t_k$, for larger t_k. The following theorem can be proved rigorously.

Let two arbitrary positive numbers ϵ and L be given, where ϵ can be as small as we wish and L can be as large as we wish. Then, in every case, if $\mu < 1/(|a|e)$, there is an instant of time T such that if $t_* > T$, then in the interval $[t_*, t_* + L]$, where $t_* > T$, the inequality $|\psi(t) - \overline{x}(t, t_k)| \le \epsilon$, will hold where $\psi(t)$ is the solution of Equation (6) determined by the initial function $\varphi(t)$, and $x(t, t_k)$ is the solution of this equation obtained by the method described above for the initial condition $x|_{t=t_k} = \psi(t_*)$. The time T depends on ϵ, a, μ, and on the upper limit of the absolute value of $\varphi(t)$.

This theorem can easily be extended to cover the case of the equation

$$\dot{x}(t) = ax(t) + bx(t-\mu),$$

where a, b, μ are constants, and also the case of the system

$$\dot{x}_s(t) = a_{s1}x_1(t-\mu) + \ldots + a_{sn}x_n(t-\mu) \qquad (s = 1, \ldots, n), \tag{8*}$$

where $a_{s\sigma}$ and μ are constant. In the latter case the theorem holds if $\mu < 1/(|\overline{\lambda}|e)$, where $\overline{\lambda}$ is the root of the characteristic equation with the largest absolute value for $\mu = 0$. In the general case of a system of type (1), we have not proved this theorem rigorously, but it is evident that it is valid.

Thus, in all cases of equations with a delay of a certain type, when the delay is sufficiently small, a phenomenon takes place that can be called the relaxation of "heredity," i.e., the weakening of the influence of the "heredity" with time.

In fact, let us consider a dynamic system described by the equations (1). Because of the dependence of the solution of these equations on the initial functions, the state of the system at any instant of time $t > 0$ will depend not only on its state of the system at any instant $t = 0$, but also, on its state in the preceding interval of time from $t = -\mu$ to $t = 0$. We will consider a certain instant t_*, that is sufficiently far from the origin, and will assume that the state of the system at this instant is fixed. Then, in view of the above-stated theorem, the state of the system for a reasonably large interval of time beginning with t_* will depend mainly on its state at the instant of time $t = t_*$, and can be adequately predicted. The influence of the state of the system in the interval of time preceding t_* becomes smaller as the time t_* becomes larger. The behavior of the system in this case corresponds to a certain extent to a so-called Markoff process.

The question is very intersting as to whether this phenomenon also occurs for systems described by more complex equations with delay—for example, in the case of variable coefficients with delay, and in the case of nonlinear systems.

On the basis of what has been said, the solutions obtained by the proposed method can be called "limiting" solutions. For linear systems of the type (1) when the above-stated theorem holds, it can be proven that certain characteristics of the asymptotic behavior are the same (for $t \to \infty$) for the limiting solutions and for any solution of the system corresponding to arbitrary initial functions. Thus, it can be shown that if the functions $x_1, \ldots, x_n$ in the "limiting" solution constructed for any initial conditions $x_s(0) = x_{s0}$ tend to zero for $t \to \infty$, then any solution of the system (1) has the same property. Also, if the initial conditions are such that the functions $x_1, \ldots, x_n$ in the "limiting" solution increase without limit in absolute value, then, for arbitrary initial functions (if they are not specially chosen – a case that will be considered below), the functions $x_1, \ldots, x_n$ in the corresponding solution also increase without limit (in absolute value). If all the roots of the characteristic equation for the system (1) for $\mu = 0$ have negative real parts, and if μ does not exceed a certain bound μ_0, then the functions $x_1, \ldots, x_n$ in any "limiting" solution tend to zero as $t \to \infty$, and so do the solutions for arbitrary initial functions. In other words, the zero solution of the system (1) possesses asymptotic stability both for $\mu = 0$ and for $\mu < \bar{\mu}$, and this property does not depend either on the initial conditions or on the initial functions. If, among the roots $\lambda_1, \ldots, \lambda_n$ of the characteristic equation, there are roots with positive real parts, then the zero solution ceases to be stable both for $\mu = 0$ and for any other value of μ. This conclusion concerning the equivalence in a certain sense of the solutions of a system of the type (1) for $\mu = 0$ and $\mu \neq 0$ agrees with the results of [3]. Nothing that has been said in this section contradicts the results of A. D. Myshkis ([4], §§ 11, 23) on the classification of solutions of equations with delay. Let us assume, for example, that all the roots $\lambda_1, \ldots, \lambda_n$ of the characteristic equation for the system (1) for $\mu = 0$ have negative real parts. Then, according to this classification, all the solutions can be separated for sufficiently small μ into two categories: 1) the weakly damped solutions, tending to zero not more rapidly than $e^{\rho t}$, where ρ is the least of the absolute values of the real parts of the roots $\lambda_1, \ldots \lambda_n$; 2) the strongly damped solutions, tending to zero as rapidly as we please according to the law $e^{\alpha t}$, where $\alpha \to -\infty$ for $\mu \to 0$. If the solution of the system (1) is sought by using Euler's method in the form of exponential functions $x_s = c_s e^{\lambda t}$, then the solutions of the first type correspond to those roots of the characteristic equation

$$\| a + be^{-\lambda\mu} - E\lambda \| = 0, \qquad (9)$$

of the system (1) that, for $\mu \to 0$, tend to the corresponding roots $\lambda_1, \ldots, \lambda_n$ of the characteristic equation $\| a + b - E\lambda \| = 0$. The solutions of the second type correspond to those complex roots $\alpha \pm \beta_i$ of Equation (9) for which $\alpha \to -\infty$ for $\mu \to 0$. For arbitrary initial functions we obtain a solution that can be represented as some combination of the two types of solution. The terms corresponding to solutions of the second type decrease very rapidly, and, after a relatively short time interval starting at the initial instant, they cease to influence the further behavior of the solution, which is thereafter determined by the main terms corresponding to a combination of solutions of the first type. The "limiting" solution corresponds to this latter combination of solutions of the first type.

If among the roots $\lambda_1, \ldots, \lambda_n$ there are roots with positive real parts, then for arbitrary initial functions we obtain a solution in which the functions $x_1, \ldots, x_n$ increase in absolute value without limit. It is, of course, possible to choose the initial functions in such a way that they correspond to solutions of the form $x_s = c_s e^{\alpha t} \cos \beta t$ or to a combination of such solutions, where $\alpha + \beta i$ is a root of Equation (9) that is discontinuous for $\mu = 0$, i.e., $\alpha \to -\infty$ for $\mu \to 0$. In other words, for the zero solution of the system (1) for sufficiently small μ, as for $\mu = 0$, the so-called stability condition is satisfied.

3. We will consider a system of equations arising in a problem on the stabilization of a rocket relative to its yaw angle γ by an automatic pilot with rigid inverse coupling, and a delay μ in the argument of the controlling parameter of the rudder mechanism:

$$\ddot{\gamma}(t) + b_1 \dot{\gamma}(t) + b_3 \delta(t) = 0, \quad \delta(t) + \delta(t) = \sigma(t - \mu), \quad \sigma(t) = p_1 \gamma(t) + p_2 \gamma(t). \qquad (10)$$

Here b_1 and b_3 are positive constant coefficients characterizing the object being controlled, and p_1 and p_2 are positive constant parameters of the regulator. Since the regulator does not act until $\gamma = \dot{\gamma} = 0$, and then $\delta = 0$, the initial functions must be assumed to be zero, i.e., we set $\sigma = 0$ for $-\mu \leq t < 0$, and the initial values are $\gamma(0) = \gamma_0$, $\dot{\gamma}(0) = \dot{\gamma}_0$, $\delta(0) = 0$.

We will give the formulas that can be used in the iteration method to construct the "limiting" solution $\bar{\gamma}(t, t_0)$ of this system for the arbitrary initial conditions $\gamma(t_0) = \gamma_0$, $\dot{\gamma}(t_0) = \dot{\gamma}_0$, $\delta(t_0) = \delta_0$. Here we are interested only in the regulated coordinate γ, and so we transform the system (10) into a single equation for γ:

$$\dddot{\gamma}(t) + (1 + b_1)\ddot{\gamma}(t) + b_1\dot{\gamma}(t) + b_3[p_1\gamma(t - \mu) + p_2\dot{\gamma}(t - \mu)] = 0. \qquad (10^*)$$

If we set $\mu = 0$ and assume for simplicity that $t_0 = 0$, then we obtain the "undisturbed" solution $\gamma^{(0)}(t)$ of this equation in the form

$$\gamma^{(0)} = A_1 e^{\lambda t} + (A_2 \cos \omega t + A_3 \sin \omega t) e^{at}, \qquad (11)$$

where

$$A_1 = \frac{1}{s}[\ddot{\gamma}_0 - 2a\dot{\gamma}_0 + (a^2 + \omega^2)\gamma_0],$$

$$A_2 = \frac{1}{s}[-\ddot{\gamma}_0 + 2a\dot{\gamma}_0 + (\lambda^2 - 2a\lambda)\gamma_0],$$

$$A_3 = \frac{1}{\omega^2 s}[(a - \lambda)\ddot{\gamma}_0 + (\lambda^2 + \omega^2 - a^2)\dot{\gamma}_0 + \lambda(a^2 - \omega^2 - a\lambda)\gamma_0], \quad s = (a - \lambda)^2 + \omega^2.$$

Here λ, a ± iω are the roots of the characteristic equation for the system (10) for $\mu = 0$:

$$k^3 + (1 + b_1)k^2 + (b_1 + b_3p_2)k + b_3p_1 = 0. \quad (12)$$

This equation has one real root and two complex (or purely imaginary) roots. Our main interest, of course, is to find the region of values of the coefficients of the system, for which λ and a are negative, i.e., the region of asymptotic stability of the zero solution of the system (10) for $\mu = 0$.

The first approximation of the "limiting" solution is obtained in the form $\gamma^{(1)} = \gamma^{(0)} + \bar{\gamma}^{(1)}$, where $\bar{\gamma}^{(1)}$ is the solution of the linear homogeneous equation

$$\dddot{\bar{\gamma}}^{(1)} + (1 + b_1)\ddot{\bar{\gamma}}^{(2)} + (b_1 + b_3p_2)\dot{\bar{\gamma}}^{(1)} + b_3p_1\bar{\gamma}^{(1)} = \\ = -b_3p_1[\gamma^{(0)}(t-\mu) - \gamma^{(0)}(t)] - b_3p_2[\dot{\bar{\gamma}}^{(0)}(t-\mu) - \\ - \gamma^{(0)}(t)]$$

for zero initial conditions. This solution is found from the formula

$$\bar{\gamma}^{(1)} = \frac{b_3}{s}\int_0^t f(t-\tau)[p_1\Delta\gamma^{(0)}(\tau) + p_2\Delta\dot{\gamma}^{(0)}(\tau)]\,d\tau, \quad (13)$$

where

$$\Delta\gamma^{(0)}(t) = \gamma^{(0)}(t-\mu) - \gamma^{(0)}(t),$$

$$\Delta\dot{\gamma}^{(0)}(t) = \frac{d}{dt}\Delta\gamma^{(0)}(t),$$

$$f(t) = -e^{\lambda t} + \left(\cos\omega t + \frac{\lambda - a}{\omega}\sin\omega t\right).$$

The function $\Delta\gamma^{(0)}$ can be written according to (11) in the form

$$\Delta\gamma^{(0)}(t) = A_1\chi_1e^{\lambda t} + [(A_2\chi_2 - A_3\chi_3)\cos\omega t + \\ + (A_2\chi_3 + A_3\chi_2)\sin\omega t]e^{at}, \quad (14)$$

where the quantities $\chi_1 = e^{-\lambda\mu} - 1$, $\chi_2 = e^{-a\mu}\cos\omega\mu - 1$, $\chi_3 = e^{-a\mu}\sin\omega\mu$ are of the first order relative to μ. If we differentiate this equation with respect to t, we obtain $\Delta\dot{\gamma}^{(0)}(t)$.

A calculation leads to the formula

$$\bar{\gamma}^{(1)} = (M_1^{(1)} + M_2^{(1)}t)e^{\lambda t} + \\ + [(N_1^{(1)} + N_2^{(1)}t)\cos\omega t + \\ + (L_1^{(1)} + L_2^{(1)}t)\sin\omega t]e^{at}, \quad (15)$$

where

$$M_2^{(1)} = -\chi_1\frac{A_1b_3}{s}(p_1 + p_2\lambda), \quad N_2^{(1)} = \frac{1}{2}(l_2A_2 + l_3A_3),$$

$$L_2^{(1)} = \frac{1}{2}(-l_3A_2 + l_2A_3).$$

$$M_1^{(1)} = \frac{2(a-\lambda)}{s}M_2^{(1)} - \frac{2\omega}{s}L_2^{(1)},$$

$$L_1^{(1)} = \frac{(\lambda-a)^2 - \omega^2}{\omega s}M_2^{(1)} - \frac{1}{\omega}N_2^{(1)} + \frac{2(\lambda-a)}{s}L_2^{(1)}.$$

$$l_2 = \frac{b_3}{s}[(p_1 + p_2a)\bar{\chi}_2 + p_2\omega\bar{\chi}_3],$$

$$l_3 = \frac{b_3}{s}[p_2\omega\bar{\chi}_3 + (p_1 + p_2a)\bar{\chi}_2],$$

$$\bar{\chi}_2 = \chi_2 - \frac{\lambda - a}{\omega}\chi_3, \quad \bar{\chi}_3 = \chi_3 - \frac{\lambda + a}{\omega}\chi_2.$$

All the approximations can be obtained similarly in the form

$$\gamma^{(k)} = \gamma^{(0)} + \bar{\gamma}^{(1)} + \ldots + \bar{\gamma}^{(k)},$$

where

$$\bar{\gamma}^{(m)} = M_m(t)e^{\lambda t} + [N_m(t)\cos\omega t + \\ + L_m(t)\sin\omega t]e^{at} \quad (16)$$

and M_m, N_m, and L_m are polynomials in t of degree m with constant coefficients of order m relative to μ. It can be shown that when $\lambda < 0$, $a < 0$, and $|\lambda| > |a|$, the sequence $\{\gamma^{(k)}\}$ converges for any finite value of t, if $\mu^2e^{-\lambda\mu} < 1/e \approx 0.368$.

An investigation of this "limiting" solution shows directly that if the "undisturbed" solution $\gamma^{(0)}$ tends to zero for $t \to \infty$, then the function $\bar{\gamma}(t, t_0)$ will have this property for all values of μ that do not exceed a certain value. From what has been said in Section 2, it follows that in this case all solutions of the system (10) also tend to zero for $t \to \infty$. We thus arrive at an estimate of the limiting value of μ for which the delay does not destroy the asymptotic stability of the control process that occurs for $\mu = 0$.

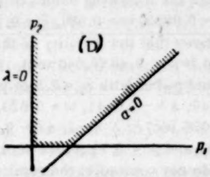

The region of stability D of the zero solution of the system (10) for $\mu = 0$ in the plane of the control parameters p_1 and p_2 has the form shown in the sketch. On the left boundary of this region (taking $p_1 = 0$) we have $\lambda = 0$ and $a = -0.525$, while on the right boundary [where $p_2 = 1/(1 + b_1)p_1 - b_1/b_3$] we have $\lambda = -(1 + b_1)$ and $a = 0$. As ω increases, the frequency increases like $\sqrt{p_2}$. It is of interest to investigate the stability near the right boundary of the region D where a is small in absolute value in comparison with λ and where the delay can serve as a disturbance in a system of undamped oscillations. We will not give the derivation, but will give an approximate estimate which is easily obtained in the case $a < 0$, $\lambda < 0$ for the difference $\Delta \bar{\gamma}(t) = \bar{\gamma}(t, t_0) - \gamma^{(0)}(t) = \sum_{k=1}^{\infty} \bar{\gamma}^{(k)}(t)$. For "undisturbed" systems depending on the delay μ, this estimate has the form

$$|\Delta \bar{\gamma}(t)| \leqslant \sqrt{A_2^2 + A_3^2}\,[e^{(q+a)t} - e^{at}], \qquad (17)$$

where A_2 and A_3 are the coefficients in the "undisturbed" solution $\gamma^{(0)}$; and the value of q, with precision up to terms of the first order relative to μ, is equal to $q = \mu\bar{q}$, where

$$\bar{q} = \frac{b_3}{2\omega}\sqrt{\frac{a^2+\omega^2}{(a-\lambda)^2+\omega^2}[p_1^2 + 2p_1p_2a + p_2^2(a^2+\omega^2)]}. \qquad (18)$$

Although the inequality (17) is not exact, it is, however, completely satisfactory for all practical purposes, and calculations show that it is actually valid for all t. It follows from this inequality that if μ is small enough, then $q + a < 0$, i.e.,

$$\mu < \frac{|a|}{\bar{q}}, \qquad (19)$$

$\Delta \bar{\gamma}(t) \to 0$ for $t \to \infty$, and the stability of the control process is ensured.

The inequality (19) is convenient because of the fact that it directly gives an approximate limit of the delay for which the control process retains its stability.

Let us set, for example, $b_1 = 0.05$, $b_3 = 0.15$, $p_2 = 3$ and $p_2 = 2$, where the unit of time is 0.1 sec. These values correspond to a system that can be realized in practice, and yield the following values of the parameters: $\lambda = -0.871$, $a = -0.0893$, $\omega = 0.580$, $\bar{q} = 0.192$. The inequality (19) shows that the stability of the control process is ensured if $\mu < 0.46$ (0.046 sec). For the same values of b_1, b_3 and p_2, but with $p_1 = 2.5$ or $p_1 = 3$, we obtain: $\lambda = -0.942$, $a = -0.0541$, $\omega = 0.629$, $\bar{q} = 0.208$ and $\mu < 0.26$ (0.026 sec) or $\lambda = -1$, $a = -0.025$, $\omega = 0.670$, $\bar{q} = 0.221$ and $\mu < 0.11$ (0.011 sec), respectively. These estimates do not contradict the results obtained by modelling the system (10) on the ÉMU-8 modelling apparatus.

If μ has a value such that the inequality (19) is not satisfied, then the control process cannot be stable, and, as calculations show, $\gamma(t)$ increases with t. Thus, if μ is given, it then follows from (18) that for a fixed p_2 the values of p_1 for which the process is stable are bounded on the right by some number p_1^* lying inside the region D, and for a fixed p_1 the values of p_2 are bounded above by some number p_2^*. These results do not contradict those of other authors who have considered systems of the type (10) (for example, see [5]), but the condition (19) is in our opinion more convenient in practical applications.

In the investigation of the system (10) it is essential to have an estimate of the rate of damping of the controlled coordinate $\gamma(t)$, i.e., to solve the problem of the quality of the regulation. If this problem is solved for the system (10) for $\mu = 0$, then, by using the inequality (17), we can estimate the dependence on the time of the magnitude of the disturbances caused by a delay, and also solve the problem of finding the quality of control in the case $\mu \neq 0$. It should be mentioned that the factor $\sqrt{A_2^2 + A_3^2}$ in formula (18) is comparable in value to the initial value γ_0. The function $f(t) = e^{(q+a)t} - e^{at}$ thus determines approximately the amount of "disturbance" due to γ_0. For example, if $b_1 = 0.05$, $b_3 = 0.15$, $p_1 = 2.5$, $p_2 = 3$ and $\mu = 0.1$ (0.01 sec), the maximum of the function $f(t)$ is attained for $t = 23.6$ (2.36 sec), and the value of this maximum is approximately 0.18, and we can conclude that this "disturbance" is not greater than about 20% of γ_0. In this case the delay has a relatively small effect on the quality of control. For the same coefficients, however, but with $\mu = 0.2$, we find that $\max f(t) \approx 0.51$ (for $t = 3.6$ sec) and that for $t = 10$ sec we have $f \approx 0.30$. Consequently, the "disturbances" are so large, that even though the values of the coefficients lie inside the region of stability of the process for $\mu = 0.2$, the quality of the control is unsatisfactory: the damping of the oscillations of the coordinate $\gamma(t)$ is too slow, due to the influence of the delay.

If it is necessary to investigate the character of the regulation process and the character of the "disturbances" in more detail, then we must obtain an approximate solution by using the method described in Section 2. For example, let $b_1 = 0.05$, $b_3 = 0.15$, $p_1 = 2.5$, $p_2 = 3$, $\gamma_0 = 1$, $\dot{\gamma}_0 = 0$, $\delta_0 = 0$, and $\mu = 0.1$, and let the unit of time be 0.1 sec. If we use the "step" method, we find that in the interval $0 \leq t \leq t_1 = \mu$ the function $\gamma(t)$ can be obtained from the equation $\dddot{\gamma} + 1.05\ddot{\gamma} + 0.05\dot{\gamma} = 0$ with the initial conditions $\gamma_0 = 1$, $\dot{\gamma}_0 = \ddot{\gamma}_0 = 0$. Therefore, $\gamma(t) \equiv 1$.

In the interval $t_1 \leq t \leq t_2 = 2\mu$, the function $\gamma(t)$ satisfies the equation

$$\dddot{\gamma} + 1.05\ddot{\gamma} + 0.05\dot{\gamma} + 0.375 = 0$$

and the initial conditions $\gamma_0 = 1$, $\dot{\gamma}_0 = \ddot{\gamma}_0 = 0$, so that

$$\gamma(t) = 1 - \frac{15}{38}(1 - e^{-(t-t_1)}) + \frac{3000}{19}(1 - e^{-0.05(t-t_1)}) - 7.5(t - t_1). \qquad (20)$$

We now obtain the "limiting" solution $\bar{\gamma}(t, t_2)$ of the equation (10) and choose the instant of time $t = t_2$ as the initial time with the initial conditions defined by (20). With an error of less than 0.0001 we obtain $\gamma_0 = 0.9999$, $\dot{\gamma}_0 = -0.0018$, $\ddot{\gamma}_0 = -0.0356$.

The calculation of the functions $\gamma^{(0)}$, $\bar{\gamma}^{(1)}$, and $\bar{\gamma}^{(2)}$ yields

$$\gamma^{(0)}(t) = 0.306\, e^{\lambda\bar{t}} + (0.694 \cos\omega\bar{t} + 0.516 \sin\omega\bar{t})\, e^{a\bar{t}}.$$

$$\bar{\gamma}^{(1)}(t) = (-0.00773 + 0.00125\,\bar{t})\, e^{\bar{\lambda} t} + $$

$$+ [(0.00773 + 0.0156\,\bar{t}) \cos\omega\bar{t} +$$

$$+ (0.0193 + 0.00904\,\bar{t}) \sin\omega\bar{t}]\, e^{a\bar{t}},$$

$$\bar{\gamma}^{(2)}(t) = (-0.000263 - 0.0000760\,\bar{t} + 0.00000254\,\bar{t}^2)\, e^{\lambda\bar{t}} +$$

$$[(0.000263 - 0.000070\,\bar{t} + 0.000172\,\bar{t}^2) \cos\omega\bar{t} + (0.000173 +$$

$$+ 0.000278\,\bar{t} + 0.000075\,\bar{t}^2) \sin\omega\bar{t}]\, e^{a\bar{t}},$$

where $\bar{t} = t - t_2$, $\lambda = -0.9419$, $a = -0.05407$, $\omega = 0.6287$, and the coefficients are given with an accuracy of one-half the value of the last figure. With an error of less than 0.005 for all values of t, we can write the second approximation to $\bar{\gamma}(t, t_2)$ in the form

$$\bar{\gamma}(t, t_2) = \gamma^{(0)} - 0.008\, e^{\lambda t} + [(0.008 + 0.0155\,\bar{t} + $$

$$+ 0.00017\,\bar{t}^2) \cos\omega\bar{t} + \tag{21}$$

$$+ (-0.019 + 0.0093\,\bar{t} + 0.00008\,\bar{t}^2) \sin\omega\bar{t}]\, e^{a\bar{t}}.$$

It is not difficult to see that the predominant part in each function is played, as in the case of the functions $\bar{\gamma}^{(1)}$ and $\bar{\gamma}^{(2)}$, by the terms of the highest degree in t in the coefficients of $e^{at}\cos\omega\bar{t}$ and $e^{at}\sin\omega\bar{t}$ (in the function $\bar{\gamma}^{(1)}$ these terms attain a value of approximately 0.12 in absolute value, while the remaining terms do not exceed 0.03 in absolute value; in the function $\bar{\gamma}^{(2)}$ these terms reach 0.035 in absolute value, while all the remaining terms are not larger than 0.0026). In the function $\bar{\gamma}^{(3)}$ these terms are

$$(0.00000125 \cos\omega\bar{t} + 0.00000037 \cdot \sin\omega\bar{t})\, \bar{t}^3 e^{a\bar{t}}$$

and do not exceed 0.001 for any t. In $\bar{\gamma}^{(4)}$ these terms are only one-fifth as large, etc., so that if we want to calculate $\bar{\gamma}(t, t_2)$ with an accuracy of 1%, we can limit our calculation to the second approximation.

We now estimate the error committed in using the "limiting" solution $\bar{\gamma}(t, t_2)$ to represent the exact solution $\gamma(t)$ for $t \geq t_2$. In order to do this, we compare the function $\gamma(t)$ in the interval $t_1 \leq t < t_2$, represented by the formula (20), with the function $\bar{\gamma}(t, t_2)$ in the same interval. It is convenient to write both these functions in the form of a Taylor's series of powers of $t - t_2$ with a remainder. For $\gamma(t)$ we obtain

$$\gamma(t) = \gamma_0 + \dot{\gamma}_0\bar{t} + \frac{\ddot{\gamma}_0}{2}\bar{t}^2 - 0.05627\,\bar{t}^3 + 0.01476\,\bar{t}^4 -$$

$$- 0.00328\,\bar{t}^5 + \Delta_1, \tag{22}$$

where $|\Delta_1(t)| < 0.00055\,(\bar{t} + \mu)$, $\bar{t} = t - t_2$ and γ_0, $\dot{\gamma}_0$, $\ddot{\gamma}_0$ are the values of the function $\gamma(t)$ and its derivatives at the instant $t = t_2$, calculated by using the expression (20). For the second approximation (21) of the "limiting" solution, we obtain

$$\bar{\gamma}(t, t_2) = \gamma_0 + \dot{\gamma}_0\bar{t} + \frac{\ddot{\gamma}_0}{2}\bar{t} - 0.05626\,\bar{t}^3 +$$

$$+ 0.01484\,\bar{t}^4 - 0.00127\,\bar{t}^5 + \Delta_2, \tag{22*}$$

where $|\Delta_2(t)| < 0.00045\,\bar{t}^6$. The difference between the expressions for the function is

$$\gamma(t) - \bar{\gamma}(t, t_2) = -0.00001\,\bar{t}^3 - 0.00008\,\bar{t}^4 - 0.00201\,\bar{t}^5$$

where $|\Delta_3(t)| < 0.00055\,(\bar{t} + \mu)^6 + 0.00045\,\bar{t}^6$. The difference between the corresponding expressions for the function $\sigma = p_1\gamma + p_2\dot{\gamma}$ is

$$\Delta\sigma(t) = \sigma(t) - \bar{\sigma}(t, t_2) = -0.00009\,\bar{t}^2 - 0.00098\,\bar{t}^3 -$$

$$- 0.003\,\bar{t}^4 - 0.0005\,\bar{t}^5 \quad \epsilon. \tag{23}$$

where $|\epsilon| < 2 \cdot 10^{-7}$. It follows from this last formula that $|\Delta\sigma(t)| < 5.1 \cdot 10^{-6}$. We should mention that the coefficients in (22*), written with an accuracy of 0.00001, do not vary if the function $\bar{\gamma}^{(2)}$, is left out, and this is, of course, also true for the functions $\bar{\gamma}^{(3)}$, $\bar{\gamma}^{(4)}$, etc. We can therefore assume that formula (23) is valid not only for the second approximation, but also for the "limiting" solution itself.

We must therefore compare two solutions of the equation (10*) for $t \geq t_2$ for which the functions $\sigma(t)$ and $\bar{\sigma}(t, t_2)$ (which play the part of initial functions and are given in the interval $t_2 - \mu \leq t < t_2$) differ from one another by not more than $5.1 \cdot 10^{-6}$. It is not difficult to establish that, in all cases for any $t \geq t_2$, these two solutions will not differ from one another by more than this amount. The solution $\bar{\gamma}(t, t_2)$ has an accuracy that is more than that needed in practice. The influence of "heredity" on the solution $\gamma(t)$ as early as for $t = t_2 = 0.02$ sec has practically vanished.

We mention that the accuracy would be completely satisfactory if the "limiting" solution were calculated directly for the initial conditions of the problem $\gamma_0 = 1$, $\dot{\gamma}_0 = \ddot{\gamma}_0 = 0$. In other words, the control process described by the system of equations (10) is approximated sufficiently well by the solution obtained by the iteration method, if only the initial values of the problem $\gamma_0 = 1$, $\gamma_0 = \delta_0 = 0$ are used, and without taking into account the initial functions.

It can be established from formula (21) that the "disturbance" related to μ does not exceed 0.15, i.e., 15% of the initial value γ_0. It should be mentioned that a more detailed investigation of the "disturbances" leads to approximately the same estimate as that obtained by using the approximate formula (18).

I feel that I must express my thanks to A. M. Letov, who suggested to me the problem of calculating the role of the initial functions, or the "heredity," in systems of automatic control, and whose advice, in the course of several discussions of the problem, was very helpful.

LITERATURE CITED

1. I. G. Malkin, Certain Problems in the Theory of Nonlinear Vibrations [in Russian] (Gostekhizdat, 1956).
2. L. É. Él'sgol'ts, "Approximate methods of integrating differential-difference equations," Uspekhi Matem. Nauk 8, 4 (1953).
3. Chin Yuan-shun, Liu Jing-ching, and Wang Lian, Science Record, New Ser., 2, No. 4 (1958).
4. A. D. Myshkis, Linear Differential Equations with a Delayed Argument [in Russian] (Gostekhizdat, 1951).
5. M. E. Salukvadze, "The influence of certain typical nonlinearities on the adjustment of an automatic pilot," Avtomat. i Telemekh. 20, No. 5 (1959).*

---

*See English translation.

THE APPLICATION OF LYAPUNOV'S METHOD TO PROBLEMS IN THE STABILITY OF SYSTEMS WITH DELAY

B. S. Razumikhin

Moscow

Translated from Avtomatika i Telemekhanika, Vol. 21, No. 6, pp. 740-748, June, 1960

We consider the application of the direct Lyapunov method to problems in the stability of systems with delay. Certain criteria are given for the stability and asymptotic stability of such systems. The possibility is shown of applying quadratic forms in stability problems in a first approximation, and estimates are proposed for the perturbations.

One of the important problems attracting the attention of many scientific workers is the stability problem for systems with delay.

Any automatic control system is in some measure a system with delay, and the influence of this delay on the stability must be ascertained. The influence of even small delays can be very significant, for example, in systems with transitional high-frequency vibration processes. The scientific development of the last three decades has shown that the most effective and universal method of investigating stability is the direct Lyapunov method. There is therefore a natural tendency to derive methods for investigating the stability of systems with delay based on the ideas of the Lyapunov theory of the stability of motion.

1. Definitions and Statement of Problem

We consider the system of differential equations

$$\frac{dx_i}{dt} = X_i\,[t;\ x_1(t-\tau),\ \ldots,\ x_n(t-\tau)] \qquad (i = 1, \ldots, n), \tag{1}$$

where $X_i[t;\ x_1(t-\tau),\ \ldots,\ x_n(t-\tau)]$ is a functional that is continuous and bounded in the region $t \geq t_0$, $|x_j| < H$ ($j = 1, \ldots, n$) and satisfies the condition $X_i(t;\ 0, \ldots, 0) = 0$. For a given t, the value of the functional X_i is determined by the values of the function $x_1(t-\tau), \ldots, x_n(t-\tau)$ of τ in the intervals $0 \leq \tau \leq h_1(t), \ldots, 0 \leq \tau \leq h_n(t)$. The functions $h_1(t), \ldots, h_n(t)$ are assumed to be positive and bounded, i.e., $0 \leq h_j(t) \leq h$ ($j = 1, \ldots, n$) for $0 \leq t < \infty$.

Definition 1. The functional $X_i[t;\ x_1(t-\tau), \ldots, x_n(t-\tau)]$ is called continuous, if, for any arbitrarily small $\epsilon > 0$, there exists a positive number $\delta(\epsilon, t_0) > 0$ such that

$$|X_i\,[t;\ x_1^{(1)}(t-\tau),\ \ldots,\ x_n^{(1)}(t-\tau)] - X_i\,[t;\ x_1^{(2)}(t-\tau),\ \ldots,\ x_n^{(2)}(t-\tau)]| < \varepsilon$$
$$\text{for}\quad \|x^{(1)} - x^{(2)}\| \leqslant \delta,$$

where

$$\|x\| = \sup \|x_j(t-\tau)\| \ \text{for}\ \ 0 \leqslant \tau \leqslant h_j(t) \quad (j = 1, \ldots, n).$$

If δ can be chosen independently of t_0, the functional is called uniformly continuous.

Definition 2. The solution $x_1(t) = 0, \ldots, x_n(t) = 0$ of the system (1) is stable, if, for every $t_0 > 0$ and $\epsilon > 0$, we can find a number $\delta(\epsilon, t_0)$ such that from the condition $\|x(t_0-\tau)\| \leq (\epsilon, t_0)$ follows $|\overline{x}(t)| < \epsilon$ for any $t > t_0$. Here, and in what follows, $\|x(t_0-\tau)\| = \sup\{|x_j(t_0-\tau)|\}$ for $0 \leq \tau \leq h_j(t_0)$, $|\overline{x}_j(t)| = \sup\{|x_j(t)|\}$ for $t > t_0$.

If the number δ is independent of t_0, then the stability is called uniform.

Definition 3. If, for the conditions stated in definition 2, there exists a positive number δ_1 such that from the condition $\|x(t_0-\tau)\| < \delta_1$ it follows that $\lim\limits_{t\to\infty} |\overline{x}(t)| = 0$, then the undisturbed motion $x_1 = \ldots = x_n = 0$ is called asymptotically stable.

Definition 4. The functional $U[t;\ x_1(t-\tau), \ldots, x_n(t-\tau)]$ is called sign-definite, if there exists a continuous function $\varphi(r)$, satisfying the conditions $\varphi(0) = 0$, $\varphi(r) > 0$ for $r \neq 0$, and such that in the region where the inequalities $t \geq T$, $|x_j(t)| < H$ are satisfied where T is a sufficiently large, and H a sufficiently small, positive number, then either $U[t;\ x_1(t-\tau), \ldots, x_n(t-\tau)] \geq \varphi(|x(t)|)$, or $U[t;\ x_1(t-\tau), \ldots, x_n(t-\tau)] \leq -\varphi(|x(t)|)$. In the first case the functional is positive-definite; in the second, negative-definite.

A pecularity of the Lyapunov method in its application to stability problems for systems of the type (1) is that either the Lyapunov function is replaced by a functional [*], the derivative of which, in view of (1), is also a functional, or the functional is the derivative of an ordinary Lyapunov function in view of (1). The minimal class of curves, on which these functionals must satisfy the conditions of the Lyapunov theorem, are the set of solutions of the system of equations for the disturbed motion which correspond to the chosen system of initial functions. In stability problems a knowledge of the solutions is not assumed, and therefore a basic problem is the selection of those classes of curves on which the fulfilling of the conditions of Lyapunov's theorem ensures the stability of the undisturbed motion.

The present work has the object of showing that Lyapunov's V-function method can be effectively applied in stability problems for systems with delay. Here the class of functions mentioned above is determined by the Lyapunov functions themselves.

2. Stability Theorems

We will consider functions $V(t; x_1, \ldots, x_n)$ that are continuous, that have bounded continuous, partial derivatives, and that are sign-definite in the region $t \geq t_0, |x_j| < H$ $(j = 1, \ldots, n)$. Because of (1) the derivative of such a function represents the continuous functional

$$U[t; x_1(t-\tau), \ldots, x_n(t-\tau)] =$$

$$= \frac{\partial V}{\partial t} + \sum_{k=1}^{n} \frac{\partial V}{\partial x_k} X_k[t; x_1(t-\tau), \ldots, x_n(t-\tau)]. \quad (2)$$

The functional (2) evidently also has a meaning when it is expressed on a set of curves which are not integral curves of the system (1). In what follows we will consider a functional formally defined by the relation (2) on a set of continuous curves $\{y_1(t), \ldots, y_n(t)\}$ that contains not only integral curves of the system (1). A sufficient condition for the stability of undisturbed motion of the system considered is given by the following theorem.

Theorem 1. If for the disturbed-motion equations (1) there exists a positive-definite function $V(t; x_1, \ldots, x_n)$, whose derivative $dV/dt = U[t; x_1(t-\tau)]$, by the above equations, is such that for every $t \geq t_0$ the functional $U[t; y_1(t-\tau), \ldots, y_n(t-\tau)]$ is negative or identically zero on the set of continuous functions $\{y_1(\sigma), \ldots, y_n(\sigma)\}$, satisfying the condition $V[\sigma; y_1(\sigma), \ldots, y_n(\sigma)] \leq V[t; y_1(t), \ldots, y_n(t)]$ for $\sigma < t$, then the undisturbed motion is stable.

In the proof of this theorem we use a theorem on the continuous dependence of the solutions of the system (1) on the initial functions, according to which, for any number $c > 0$ as small as we please and any number $T > t_0 + h$, a positive number $\delta(c, T)$ can be found such that the condition $\| x(t_0-\tau) \| \leq \delta(c, T)$ (see definition 2) for all t in the interval (t_0, T) ensures the validity of the inequality $V[t; x_1(t), \ldots, x_n(t)] \leq c$. The fact that the inequality $V[t; x_1(t), \ldots, x_n(t)] \leq c$ holds for all $t \geq t_0$ follows from the conditions of the theorem.

The criterion for asymptotic stability is obtained from the following theorem.

Theorem 2. If, for the conditions of Theorem 1, the function $V(t; x_1, \ldots, x_n)$ admits an infinitely small upper limit, and the function $U[t; y_1(t-\tau), \ldots, y_n(t-\tau)]$ is negative-definite, then the undisturbed motion is asymptotically stable.

The proof of this theorem is based on the estimate obtained for the functional U along all the solutions of the system (1) satisfying the conditions $V[t; x_1(t), \ldots, x_n(t)] = c$, i.e., on the relation

$$V(\sigma, x_1(\sigma), \ldots, x_n(\sigma)) \leqslant c \quad \text{for } \sigma \leqslant t,$$

where c is any arbitrarily small positive number.

Theorems 1 and 2 give sufficient conditions for stability and asymptotic stability, regardless of the size of the delay. These conditions are close to being necessary for large values of the delay. It is a more important fact that Theorems 1 and 2 determine the boundary set of curves on which the functional dV/dt must be of a constant sign or sign-definite. These conditions are expressed by the inequality

$$V[\sigma, x_1(\sigma), \ldots, x_n(\sigma)] \leqslant$$

$$\leqslant V[t; x_1(t), \ldots, x_n(t)] \quad \text{for} \quad t-h \leqslant \sigma \leqslant t \quad (3)$$

and are needed for obtaining other stability criteria.

Less stringent stability conditions can be obtained by excluding from the set of continuous lines satisfying condition (3) those which in view of the system (1) do not yield solutions. In this case, it is possible to obtain stability criteria as the criteria for the sign-definiteness of the functional U on the curves obtained from one or other of the estimates of solutions satisfying condition (3).

We will consider one of the possible methods of obtaining such stability criteria. Let

---

[*] See the results of N. N. Krasovskii in [1].

$$S_i^{(1)}(t; c) = \sup | X_i [\sigma; y_1(\sigma - \tau), \dots, y_n(\sigma - \tau)] | \quad (i = 1, \dots, n)$$

on the set of continuous curves satisfying the conditions

$$V(t; y_1(t), \dots, y_n(t)) = c, \quad V(\sigma; y_1(\sigma), \dots, y_n(\sigma)) \leqslant c \quad \text{for} \quad t - h \leqslant \sigma \leqslant t$$

It follows from the system (1) that the inequalities

$$| x_i(t') - x_i(t'') | \leqslant S_i^{(1)}(t; c) | t' - t'' |. \quad (i = 1, \dots, n) \tag{4}$$
$$\text{for} \quad t - h \leqslant t' \leqslant t, \ t - h \leqslant t'' \leqslant t.$$

must hold.

It is not difficult, in addition to this, to prove the validity of the following criterion.

Theorem 3. If, for the equations of the disturbed motion (1), there exists a positive-definite function $V(t; x_1, \dots, x_n)$ having an infinitely small upper limit, and a positive number $\overline{c}$ such that the derivative of the function V determines the functional $dV/dt = U$ by using the system (1) where this functional is negative-definite along every curve $(y_1(t), \dots, y_n(t))$ satisfying the conditions $V[t; y_1(t), \dots, y_n(t)] = c$, $V[\sigma; y_1(\sigma), \dots, y_n(\sigma)] \leq c$ for $\sigma \leq t \geq t_0$, $| x_i(t'') | \leq S_i^{(1)}(t; c) | t' - t'' | \quad (i = 1, \dots, n)$ for $t - h \leq t' \leq t \geq t_0$, $t - h \leq t'' \leq t \geq t_0$, then the undisturbed motion is asymptotically stable.

This criterion involves the delay, and yields the possibility of estimating its influence on the stability. Better precision in the stability criterion can be obtained by replacing the functions $S_i^{(1)}(t; c)$ by the functions $S_i^{(2)}(t; c)$ defined by the condition $S_i^{(2)}(t; c) = \sup | X_i [\sigma_i; y_1(\sigma - \tau), \dots, y_n \times (\sigma - \tau)] |$ on the set of curves $\{y_1(\sigma), \dots, y_n(\sigma)\}$ satisfying the conditions of Theorem 3. Further methods of improving the criteria are obvious. The effectiveness of the method proposed can be shown by many examples considered in [2]. We will give some simple examples:

1. The region of stability of the trivial solution of the equation

$$\frac{dx}{dt} = -ax(t) - bx(t - \tau),$$

determined by the Lyapunov method, is shown in Fig. 1.

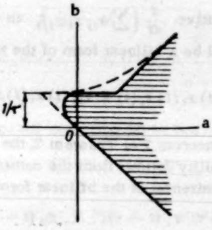

Fig. 1.

The broken line shows the limit of the region of stability, obtained from the accurate solution.

2. The trivial solution of the equation

$$\frac{dx}{dt} = -\int_{t-h}^{t} x(\zeta)\, d\zeta$$

is stable if $h \leq \pi/\sqrt{2} \approx 2.24$. If we apply the Lyapunov V-function theorem, we obtain the condition $h \leq 2$.

Thus, in the case of a system with delay, the Lyapunov method is an effective and universal method of investigating stability.

3. Stability According to the First Approximation to Systems With Delay

In stability problems relative to the first approximation for general systems, quadratic forms have found a wide application as Lyapunov functions. Quadratic forms have just as wide an application in stability problems of systems with delay.

We will consider the system of differential equations for disturbed motion,

$$\frac{dx_i}{dt} = F_i [t; x_1(t), \dots, x_n(t), x_1(t - \tau), \dots, x_n(t - \tau)], \tag{5}$$

where the F_i are holomorphic functions of the variables $x_1(t), \dots, x_n(t)$, $x_1(t - \tau), \dots, x_n(t - \tau)$, satisfying the condition $F_i(t; 0, \dots, 0) = 0 \ (i = 1, \dots, n)$, with τ a constant.

If we use the notation $p_{ij}(t) = \partial F_i / \partial x_j$, $q_{ij} = \partial F_i / \partial x_j(t - \tau)$, then, for $x_1(t) = \dots = x_n(t) = x_1(t - \tau) = \dots = x_n(t - \tau) = 0$, we obtain the system of equations

$$\frac{dx_i}{dt} = \sum_{j=1}^{n} [p_{ij}(t) x_j(t) + q_{ij}(t) x_j(t - \tau)] \tag{6}$$
$$(i = 1, \dots, n)$$

For a system of the type (6) we can look for a Lyapunov function in the form of a sign-definite quadratic form $V = \sum_{i,\, j=1}^{n} \alpha_{ij}(t) x_i x_j$. As a Lyapunov function for (6), we can take, in particular, the quadratic form that is a Lyapunov function for the usual system:

$$\frac{dx_i}{dt} = \sum_{j=1}^{n} [p_{ij}(t) + q_{ij}(t)] x_j \quad (i = 1, \ldots, n). \tag{7}$$

which is obtained from (6) for $\tau = 0$ and is obtained by some one of the known methods.

The derivative $\frac{d}{dt}\left(\sum \alpha_{ij} x_i x_j\right)$, in view of the system (6), will be a bilinear form of the type

$$\frac{dV}{dt} \sum_{i,\, j=1}^{n} [b_{ij}(t) x_i(t) x_j(t) + c_{ij}(t) x_i(t) x_j(t-\tau)]. \tag{8}$$

By using Theorem 1 or Theorem 2, the stability or asymptotic stability follows from the constancy of sign or the sign-definiteness of the bilinear form (8) if

$$V[t-\tau;\ x_1(t-\tau), \ldots, x_n(t-\tau)] \leqslant$$
$$\leqslant V[t;\ x_1(t), \ldots, x_n(t)]. \tag{9}$$

For these conditions the bilinear form (8) can be majorized by a quadratic form, and the stability conditions can be obtained from a known inequality of Sylvester. The proposed method can also be used to obtain an estimate for the disturbances, to determine the degree of stability (quality criteria), and to solve the stability problem for a finite interval of time.

The majorant of the bilinear form (8) can be obtained in the following ways:

First method. The quadratic form majorizing the bilinear form dV/dt can be obtained as the solution of the problem of maximizing the function (8) under the condition (9). This problem can be solved by applying the Lagrange method of undetermined parameters. Then, if we use a known inequality for quadratic forms, obtained by using their canonical representation, we obtain the following inequality for the bilinear form (8):

$$\sum_{i,\, j=1}^{n} [\beta_{ij}(t) + \delta_{ij}\sqrt{h'(t)}]\, \zeta_i(t) \zeta_j(t) \geqslant \frac{dV}{dt} \geqslant$$
$$\geqslant \sum_{i,\, j=1}^{n} [\beta_{ij}(t) + \delta_{ij}\sqrt{h''(t)}]\, \zeta_i(t) \zeta_j(t), \tag{10}$$

where ζ_i is the canonical variable, $\beta_{ij}(t)$, $h'(t)$ and $h''(t)$ are linear combinations of the coefficients of the system of equations for the disturbed motion and the coefficients of the quadratic form V are $\delta_{ij} = 1$ for $i = j$, $\delta_{ij} = 0$ for $i \neq j$.

On the basis of the inequality (10), the asymptotic stability of the trivial solution of system (6) for any value of the delay $\tau > 0$ follows from the positive-definite quadratic form V and the negative-definite quadratic form

$$\sum_{i,\, j=1}^{n} [\beta_{ij}(t) + \delta_{ij}\sqrt{h'(t)}]\, \zeta_i(t) \zeta_j(t). \tag{11}$$

Second method. This method of obtaining a majorant for the bilinear form dV/dt can be used to estimate the influence of the size of the delay on the stability of the undisturbed motion.

It is obvious that the expression (8) for dV/dt can be written in the form

$$\frac{dV}{dt} = \sum_{i,\, j=1}^{n} \{[b_{ij}(t) + c_{ij}(t)]\, x_i(t) x_j(t) + c_{ij}(t) x_i(t) [x_j(t-\tau) - x_j(t)]\}. \tag{12}$$

A known formula due to Lagrange then yields

$$x_j(t-\tau) - x_j(t) = -\tau \dot{x}_j(\sigma_j), \tag{13}$$

where $\sigma_j = t - \theta_j \tau$, $0 < \theta_j < 1$.

If we substitute (13) in (12) and replace $\dot{x}_j$ by the right-hand side of the corresponding equation from the system (6), we obtain

$$\frac{dV}{dt} = \sum_{i,\, j=1}^{n} \Big\{[b_{ij}(t) + c_{ij}(t)]\, x_i(t) x_j(t) - \tag{14}$$
$$-\tau \Big[x_i(t) c_{ij}(t) \sum_{s=1}^{n} \big(p_{js}(\sigma_j) x_s(\sigma_j) + q_{js}(\sigma_j) x_s(\sigma_j - \tau)\big)\Big]\Big\}.$$

A multilinear form is obtained for dV/dt, and the condition for asymptotic stability will be the negative-definiteness of this form for the condition (3). If we transform to canonical variables $y_1, \ldots, y_n$, in which $V = \sum_{i=1}^{n} y_i^2$, we obtain conditions that are equivalent, in the case considered, to the condition (3):

$$\sum_{i=1}^{n} y_i^2(\sigma_j) < \sum_{i=1}^{n} y_i^2(t), \tag{15}$$
$$\sum_{i=1}^{n} y_i^2(\sigma_j - \tau) < \sum_{i=1}^{n} y_i^2(t) \quad (j = 1, \ldots, n).$$

The majorant for dV/dt can be obtained here by replacing the conditions (15) by the less stringent conditions

$$|y_i(\sigma_j)| \leqslant \sqrt{\sum_{i=1}^{n} y_i^2(t)},$$

$$|y_i(\sigma_j - \tau)| \leqslant \sqrt{\sum_{i=1}^{n} y_i^2(t)}. \tag{16}$$

If we substitute (16) in (14), we obtain, after some simple transformations, the inequality

$$\frac{dV}{dt} < \sum_{i,\, j=1}^{n} [a_{ij}(t) + \delta_{ij}\, \tau\omega(t;\tau)]\, y_i y_j, \tag{17}$$

where δ_{ij} is the Kroneker delta, and $\omega(t;\tau)$ is a known function of the coefficients of the system (6), of the coefficients of the quadratic form V, and of the magnitude of the delay τ.

The asymptotic stability criterion is obtained from the Sylvester conditions for the right-hand side of the inequality (17) to be negative.

4. Estimates of the Disturbances

The desired estimate cannot be directly obtained from the inequalities (10) or (17), since these inequalities were obtained by using condition (3) which is not satisfied by the estimate obtained in this way. We therefore start from the assumption that the desired estimate has the form

$$V \leqslant V_0 \exp \int_{t_0}^{t} \lambda(t)\, dt. \tag{18}$$

From this inequality follows the condition

$$V[t-\tau;\, x_1(t-\tau), \ldots, x_n(t-\tau)] \leqslant$$

$$\leqslant V[t;\, x_1(t), \ldots, x_n(t)] \exp \int_{t-\tau}^{t} -\lambda(t)\, dt, \tag{19}$$

which must replace condition (3) in the reasoning in Sec. 3.

If we use the notation $\varphi(t) = \exp \int_{t-\tau}^{t} -\lambda(t)\, dt$ and repeat the calculation in Sec. 3, we obtain for dV/dt the inequality, to replace (10),

$$\sum_{i,\, j=1}^{n} [\beta_{ij}(t) + \delta_{ij} \sqrt{\varphi(t)\, h'(t)}]\, \zeta_i \zeta_j \geqslant \frac{dV}{dt} \geqslant \sum_{i,\, j=1}^{n} [\beta_{ij}(t) + \delta_{ij} \sqrt{\varphi(t)\, h''(t)}]\, \zeta_i \zeta_j \tag{20}$$

or the inequality, to replace (17),

$$\frac{dV}{dt} < \sum_{i,\, j=1}^{n} \{a_{ij}(t) +$$

$$+ \delta_{ij}\, [\omega_1(t;\tau) \sqrt{\varphi(t)} + \omega_2(t,\tau) \sqrt{\psi(t)}]\, \tau\}\, y_i y_j, \tag{21}$$

where $\omega_1(t;\tau)$ and $\omega_2(t;\tau)$ are known functions of the same arguments occurring in the functions $\omega_1(t;\tau)$ [(17)] and

$$\psi(t) = \exp \int_{t-2\tau}^{t} -\lambda(t)\, dt.$$

In addition, in the case of the inequality (20), the function $\lambda(t)$ must not be less than the largest root of the equation

$$\det \| \beta_{ij}(t) + \delta_{ij} [\sqrt{\varphi(t)\, h'(t)} - \lambda] \| = 0. \tag{22}$$

In the case of the inequality (21), the function $\lambda(t)$ must be not less than the largest of the roots of the equation

$$\det \| a_{ij}(t) + \delta_{ij}\, \{\tau\, [\omega_1(t;\tau) \sqrt{\varphi(t)} +$$

$$+ \omega_2(t;\tau) \sqrt{\psi(t)}] - \lambda\} \| = 0. \tag{23}$$

We now obtain the inequality for determining the function $\lambda(t)$:
in the first case –

$$\lambda(t) \geqslant \bar{\mu}(t) - \sqrt{h'(t)} \exp \left[-\frac{1}{2} \int_{t-\tau}^{t} \lambda(t)\, dt \right], \tag{24}$$

in the second case –

$$\lambda(t) \geqslant \bar{\mu}(t) - \tau \left[\omega_1(t;\tau) \exp \frac{1}{2} \int_{t-\tau}^{t} - \right.$$

$$\left. -\lambda(t)\, dt + \omega_2(t;\tau)\, \exp \frac{1}{2} \int_{t-2\tau}^{t} -\lambda(t) dt \right]. \tag{25}$$

In both cases $\bar{\mu}(t)$ is the largest root of the equation

$$\det \| a_{ij}(t) - \delta_{ij}\, \mu \| = 0. \tag{26}$$

For determining the function $\lambda(t)$, we can now apply the known method of successive approximations.

EXAMPLES

The value of Lyapunov's direct method lies in the fact that at the present time it is difficult to find stability problems where the application of this method is doubtful. The results given below of the solution of particular problems are of an illustrative character, since these problems can be solved by other methods, and a comparison can be made of the results of the various methods of solution.

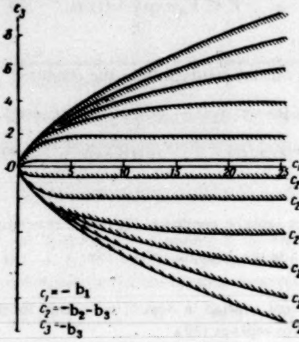

Fig. 2.

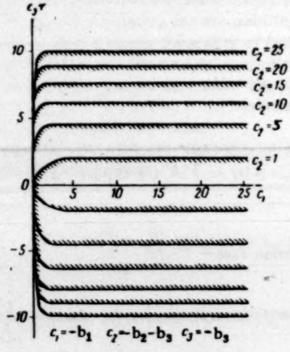

Fig. 3.

1. In Fig. 2 and Fig. 3 are shown the stability regions in the coefficient space for the equations of disturbed motion for the stability problem of a control system described by the differential equations

$$\frac{dx_1}{dt} = b_1x_1(t) + b_2x_2(t) + b_3x_2(t-\tau),$$
$$\frac{dx_2}{dt} = x_1(t). \tag{27}$$

The Lyapunov function for the given problem is taken to be the quadratic form $V = \alpha_{11}x_1^2 + 2\alpha_{12}x_1x_2 + \alpha_{22}x_2^2$, which satisfies the equation

$$\frac{dV}{dx_1}[b_1x_1 + (b_2+b_3)x_2] + \frac{\partial V}{\partial x_2}\cdot x_1 = -x_1^2 - x_2^2. \tag{28}$$

The corresponding stability regions, shown in Fig. 2 and Fig. 3, were obtained by using Sylvester's conditions for the sign-definiteness of the majorant of the bilinear form dV/dt obtained by the first and second methods given in Sec. 3.

2. In Fig. 4 we give the results of calculating the permissible delay in an automatic pilot, if the airplane is to be longitudinally stable. The equations for the disturbances in the motion of a plane with an automatic pilot in the case considered have the form

$$\frac{dx_1}{dt} = p_{11}x_1(t) + p_{12}x_2(t) + p_{13}x_3(t-\tau),$$
$$\frac{dx_2}{dt} = x_1(t), \tag{29}$$
$$\frac{dx_3}{dt} = p_{31}x_1(t) + p_{32}x_2(t).$$

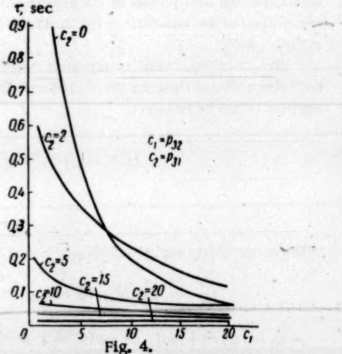

Fig. 4.

The Lyapunov function in this example is also taken to be the quadratic form $V = \alpha_{11}x_1^2 + 2\alpha_{12}x_1x_2 + \alpha_{22}x_2^2 + 2\alpha_{23}x_2x_3 + \alpha_{33}x_3^2$, which satisfies the equation

$$\frac{\partial V}{\partial x_1}(p_{11}x_1 + p_{12}x_2 + p_{13}x_3) + \frac{\partial V}{\partial x_2}x_1 + \\ + \frac{\partial V}{\partial x_3}(p_{31}x_1 + p_{32}x_2) = -(x_1^2 + x_2^2 + x_3^2). \tag{30}$$

The majorant for ∂V/∂t is obtained by using the second method in Sec. 3.

The results of the calculation show that the fact that the system is highly stable for $\tau = 0$ does not guarantee its stability in the presence of delay.

LITERATURE CITED

1. N. N. Krasovskii, Some Problems in The Theory of the Stability of Motion [in Russian] (Fizmatgiz, 1959).
2. B. S. Razumikhin, The Application of the Lyapunov Method in Certain Problems of Motion Stability: Doctoral Dissertation (Inst. Mekhaniki, Akad. Nauk SSSR, 1958).

SOME QUESTIONS CONCERNING COORDINATED CONTROL SYSTEMS

E. M. Syuzyumova

Moscow

Translated from Avtomatika i Telemekhanika, Vol. 21, No. 6, pp. 749-760, June, 1960

A theorem concerning inverse transfer matrices is considered, which can be used to formulate the conditions of static independence of the control of several variables in a short form. Also considered are the conditions for dynamic independence of several nonlinear coordinated control systems.

1. The Theorem of Control Inverse Transfer Matrices

In the works of L. N. Voznesenskii [1, 2], there appears a theory of autonomous or independent control of several coordinated variables. In these works a general method is given for the determination of the transfer functions of control couplings. In designing control systems with several controlled variables, in particular, control systems for central power station turbines, we can apply the theorem proven below, which states that the matrix of machine couplings is the inverse of the matrix of control couplings. This theorem can be used not only for the simple determination of the transfer functions of the control couplings, but also for an easy verification of the correctness of the results obtained. We will prove this theorem as applied to an example of the control of three coordinated variables.

The equations for the control system will be assumed to be:

the equations for the machine (relative to the original equilibrium position)

$$\begin{aligned} T_{a1}\dot{\psi}_1 + c_{11}\mu_1 + c_{12}\mu_2 + c_{13}\mu_3 &= \lambda_1, \\ T_{a2}\dot{\psi}_2 + c_{21}\mu_1 + c_{22}\mu_2 + c_{23}\mu_3 &= \lambda_2, \\ T_{a3}\dot{\psi}_3 + c_{31}\mu_1 + c_{32}\mu_2 + c_{33}\mu_3 &= \lambda_3. \end{aligned} \qquad (1)$$

the equations for the servomotors in the case of one amplification stage

$$\begin{aligned} T_{s1}\dot{\mu}_1 + \mu_1 - (d_{11}\eta_1 + d_{12}\eta_2 + d_{13}\eta_3) &= 0, \\ T_{s2}\dot{\mu}_2 + \mu_2 - (d_{21}\eta_1 + d_{22}\eta_2 + d_{23}\eta_3) &= 0, \\ T_{s3}\dot{\mu}_3 + \mu_3 - (d_{31}\eta_1 + d_{32}\mu_2 + d_{33}\eta_3) &= 0. \end{aligned} \qquad (2)$$

In the equations (1) we have used the relative variables $\psi_n = \Delta q_n/\delta_n q_{n0} = \varphi_n/\delta_n$ for the machine, where φ_n is the usual relative machine variable. This is done in order to eliminate the nonuniformities δ_1, δ_2, and δ_3.

If we use the fact that for ideal regulators $\eta_1 = \psi_1$, $\mu_2 = \psi_2$, and $\eta_3 = \psi_3$, we can rewrite (2) in the form

$$\begin{aligned} T_{s1}\dot{\mu}_1 + \mu_1 - (d_{11}\psi_1 + d_{12}\psi_2 + d_{13}\psi_3) &= 0, \\ T_{s2}\dot{\mu}_2 + \mu_2 - (d_{21}\psi_1 + d_{22}\psi_2 + d_{13}\psi_3) &= 0, \\ T_{s3}\dot{\mu}_3 + \mu_3 - (d_{31}\psi_1 + d_{32}\psi_2 + d_{33}\psi_3) &= 0. \end{aligned} \qquad (3)$$

The coupling coefficients c_{ik} in the equations (1) are for the internal machine coupling, while d_{ik} in Eq. (3) are for the external control coupling.

The problem of realizing statically independent control reduces to that of finding the values of the regulator-to-servomotor transfer functions d_{ik} for which the external control couplings disconnect the internal couplings of the machine. This problem has often been solved for special cases, and it has been solved in general form by L. N. Voznesenskii. In the most concise form this problem can be stated as the briefest theorem of inverse transfer matrices: the matrix $\| d_{ik} \|$ of the control couplings transfer functions that ensure static independence is the inverse of the matrix $\| c_{ik} \|$ of the internal machine couplings.

For the proof, we apply to the three machine variables in turn the following three systems of unit loads:

$$\begin{aligned} &1)\ \lambda_1 = 1,\ \lambda_2 = \lambda_3 = 0; \\ &2)\ \lambda_2 = 1,\ \lambda_1 = \lambda_3 = 0; \\ &3)\ \lambda_3 = 1,\ \lambda_1 = \lambda_2 = 0. \end{aligned} \qquad (4)$$

For statically independent control, the static conditions for the first case must be

$$\begin{aligned} &1)\ \eta_1 = \psi_1 = \lambda_1 = 1, \\ &\eta_2 = \psi_2 = \lambda_2 = 0,\ \eta_3 = \psi_3 = \lambda_3 = 0. \end{aligned} \qquad (5)$$

Similarly, in the second and third cases,

$$2)\ \eta_2 = 1,\ \eta_1 = \eta_3 = 0;$$

$$3)\ \eta_3 = 1,\ \eta_1 = \eta_2 = 0.$$

Static displacements of the servomotors are determined by the substitution of (5) in (3):

$$\begin{aligned} &1)\ \mu_1 = d_{11},\quad \mu_2 = d_{21},\quad \mu_3 = d_{31}; \\ &2)\ \mu_1 = d_{12};\quad \mu_2 = d_{22},\quad \mu_3 = d_{32}; \\ &3)\ \mu_1 = \mu_{13},\quad \mu_2 = d_{23},\quad \mu_3 = d_{33}. \end{aligned} \qquad (6)$$

If we substitute (4) and (6) in (1), we obtain the static conditions for the first case:

$$
\begin{aligned}
1)\ & c_{11} d_{11} + c_{12} d_{21} + c_{13} d_{31} = 1, \\
& c_{21} d_{11} + c_{22} d_{21} + c_{23} d_{31} = 0, \\
& c_{31} d_{11} + c_{32} d_{21} + c_{33} d_{31} = 0.
\end{aligned}
\tag{7}
$$

Thus,

$$
d_{11} = \frac{C_{11}}{\Delta_c}, \quad d_{21} = \frac{C_{12}}{\Delta_c}, \quad d_{31} = \frac{C_{13}}{\Delta_c}, \tag{8}
$$

where Δ_c is the matrix determinant of $\| c \|$, and C_{ik} is its cofactor. Similarly, for the second and the third case, we obtain:

$$
2)\ d_{12} = \frac{C_{21}}{\Delta_c}, \quad d_{22} = \frac{C_{22}}{\Delta_c}, \quad d_{23} = \frac{C_{32}}{\Delta_c};
$$

$$
3)\ d_{13} = \frac{C_{31}}{\Delta_c}, \quad d_{23} = \frac{C_{32}}{\Delta_c}, \quad d_{33} = \frac{C_{33}}{\Delta_c}.
$$

We now note that, in the system (7), the subscripts of each term $c_{ik} d_{ki}$ are such that the subscripts ki of the unknown quantities are in the opposite order to the subscripts ik of the coefficients c_{ik}. Thus, the general expression for the transfer function d_{ik} can be written in the form $d_{ik} = C_{ik}/\Delta_c$. The matrix $\| c_{ik} \|$ is thus adjoint to the matrix $\| d_{ik} \|$. It follows from this by a known theorem from matrix theory that $\| d_{ik} \| = \| c_{ik} \|^{-1}$. The theorem is thus proven.

As a consequence of this theorem we have $| d_{ik} | = | c_{ik} |^{-1}$, or, in other notation, $\Delta d = \Delta c^{-1}$. This result yields the shortest method of checking whether the control transfer functions correspond to the integral machine couplings.

We will demonstrate the application of the theorem to the classic example for this problem, i.e., the problem of regulating a two-point extraction power station turbine by the application of the theory of independent control [1, 2].

We introduce the following notation: ω, p_1, and p_2 are the controlled variables; ω_0, p_{10}, and p_{20} are the nominal values of these variables; N_1, N_2, and N_3 are the powers of the three sections of the turbine; N_{10}, N_{20}, and N_{30} are the maximum powers of the three sections; D_1, D_2, and D_3 are the values of steam flow through the three sections; D_{10}, D_{20}, and D_{30} are the maximum steam flow through the sections; D_{I} and D_{II} are steam flow through separators; N_0, $D_{\mathrm{I}0}$, and $D_{\mathrm{II}0}$ are the nominal electric and heat loads of the turbine; V_1 and V_2 are the volumes of the separators; γ_1 and γ_2 are the specific weights of the steam in the separators.

We write the equations for the machine in terms of absolute variables:

$$
\begin{aligned}
J\omega \frac{d\omega}{dt} &= N_1 + N_2 + N_3 - N_{\text{gen}} \\
V_1 \frac{d\gamma_1}{dt} &= D_1 - D_2 - D_{\mathrm{I}}, \\
V_2 \frac{d\gamma_2}{dt} &= D_2 - D_3 - D_{\mathrm{II}}.
\end{aligned}
\tag{9}
$$

We shall rewrite these equations in terms of relative variables:

$$
\begin{aligned}
T_{a1} \dot{\psi}_1 + c_{11}\mu_1 + c_{12}\mu_2 + c_{13}\mu_3 &= 0, \\
T_{a2} \dot{\psi}_2 + c_{21}\mu_1 + c_{22}\mu_2 \phantom{{}+ c_{13}\mu_3} &= 0, \\
T_{a3} \dot{\psi}_3 \phantom{{}+ c_{21}\mu_1} + c_{32}\mu_2 + c_{33}\mu_3 &= 0,
\end{aligned}
\tag{10}
$$

where $\psi_1 = \Delta\omega/\delta_1\omega_0$, $\psi_2 = \Delta p_1/\delta_2 p_{10}$, $\psi_3 = \Delta p_2/\delta_3 p_{20}$.

The coefficients c_{ik} are given by

$$
\| c_{ik} \| = \left\| \begin{matrix} c_{11} & c_{12} & c_{13} \\ c_{21} & c_{22} & 0 \\ 0 & c_{32} & c_{33} \end{matrix} \right\| = \left\| \begin{matrix} \frac{N_{10}}{N_0} & \frac{N_{20}}{N_0} & \frac{N_{30}}{N_0} \\ \frac{D_{10}}{D_{\mathrm{I}0}} & -\frac{D_{20}}{D_{\mathrm{I}0}} & 0 \\ 0 & \frac{D_{20}}{D_{\mathrm{I}0}} & -\frac{D_{30}}{D_{\mathrm{II}0}} \end{matrix} \right\| \tag{11}
$$

The matrix $\| d_{ik} \|$ of the control transfer functions is uniquely defined by the inverse matrix theorem $\| d_{ik} \| = \| c_{ik} \|^{-1}$, and

$$
\Delta_c = \frac{N_{10}}{N_0} \frac{D_{20}}{D_{\mathrm{I}0}} \frac{D_{30}}{D_{\mathrm{II}0}} + \frac{D_{10}}{D_{\mathrm{I}0}} \frac{D_{20}}{D_{\mathrm{II}0}} \frac{N_3}{N_0} + \frac{D_{10}}{D_{\mathrm{I}0}} \frac{N_{20}}{N_0} \frac{D_{30}}{D_{\mathrm{II}0}},
$$

$$
\begin{gathered}
d_{11} = \frac{C_{11}}{\Delta_c} = \frac{\frac{D_{20}}{D_{\mathrm{I}0}} \frac{D_{30}}{D_{\mathrm{II}0}}}{\Delta_c}, \\
d_{12} = \frac{C_{21}}{\Delta_c} = \frac{\frac{N_{20}}{N_0} \frac{D_{30}}{D_{\mathrm{II}0}} + \frac{N_{30}}{N_0} \frac{D_{20}}{D_{\mathrm{II}0}}}{\Delta_c}, \\
d_{13} = \frac{C_{13}}{\Delta_c} = \frac{\frac{N_{30}}{N_0} \frac{D_{20}}{D_{\mathrm{I}0}}}{\Delta_c}; \\
d_{21} = \frac{C_{12}}{\Delta_c} = \frac{\frac{D_{10}}{D_{\mathrm{I}0}} \frac{D_{30}}{D_{\mathrm{II}0}}}{\Delta_c}, \\
d_{22} = \frac{C_{22}}{\Delta_c} = -\frac{\frac{N_{10}}{N_0} \frac{D_{30}}{D_{\mathrm{II}0}}}{\Delta_c}, \quad d_{23} = \frac{C_{32}}{\Delta_c} = -\frac{\frac{N_{30}}{N_0} \frac{D_{10}}{D_{\mathrm{I}0}}}{\Delta_c}.
\end{gathered}
\tag{12}
$$

As is to be expected, these more simply expressed values of the transfer functions coincide with those obtained by I. N. Voznesenskii [2, 3]. What is new here is the compact form of the entire derivation in the form of the inverse matrix theorem, and also the consequent possibility of thoroughly verifying the final result by using the relation $\Delta d \times \Delta c = 1$.

It is obvious from the proof of the theorem that only after the transformation to the relative coordinates ψ

are the matrices $\|c\|$ and $\|d\|$ related by the inverse matrix theorem. The matrices $\|i\|$ and $\|k\|$ [2, 3], reduced in [2], with respect to nonrelative variables, do not satisfy the inverse matrix theorem. The reason for the transformation to relative variables is thus made clear.

For the APT-12, one of the two-point extraction turbines produced in this country, with parameters $t_0 = 435°C$, $p_0 = 35$ atm, $p_1 = 10$ atm, $p_2 = 1.2$ atm, $p_k = 0.05$ atm, the flows through the sections are $D_{10} = 130{,}000$ kg/hr, $D_{20} = 80{,}000$ kg/hr, and $D_{30} = 40{,}000$ kg/hr.

The heat drops used are:

$H_1\eta_1 = 55$ kcal/kg, $H_2\eta_2 = 93$ kcal/kg, $H_3\eta_3 = 81$ kcal/kg.

The maximum powers of the sections are

$$N_{10} = \frac{D_{10}H_1\eta_1}{860} = 8320 \text{ kw} \qquad N_{20} = \frac{D_{20}H_2\eta_2}{860} = 8650 \text{ kw}$$

$$N_{30} = \frac{D_{30}H_3\eta_3}{860} = 3770 \text{ kw}$$

The nominal loads are

$$N_0 = 12{,}000 \text{ kw}, \; D_{I0} = 50{,}000 \text{ kg/hr},$$
$$D_{II0} = 40{,}000 \text{ kg/hr}$$

The coefficients c, obtained by using the formulas (11), are

$$c_{11} = 0.69, \quad c_{12} = 0.72, \quad c_{13} = 0.31,$$
$$c_{21} = 2.6, \quad c_{22} = -1.6, \quad c_{23} = 0.0,$$
$$c_{31} = 0.0, \quad c_{32} = 2.0, \quad c_{33} = -1.0$$
$$\text{and } \triangle_c = 4.581.$$

The coefficients d, calculated from formula (12), are

$$d_{11} = 0.35, \quad d_{12} = 0.293, \quad d_{13} = 0.108,$$
$$d_{21} = 0.568, \quad d_{22} = -0.151, \quad d_{23} = 0.176,$$
$$d_{31} = 1.135, \quad d_{32} = -0.31, \quad d_{33} = -0.65$$
$$\text{and } \triangle_d = 0.218.$$

Thus, $\Delta d \times \Delta c = 1$.

The fact that the product $\Delta d \Delta c$ is equal to one verifies the results of the calculation.

2. The Dynamic Independence of Certain Nonlinear Coordinated Control Systems

A. Possible methods for the control of central power station turbines

The central problem of contemporary turbine control is to find methods of increasing the rapidity of action of control systems without a corresponding increase in oil-pump capacities and a further expansion of the oil-systems. The importance of this problem is shown on the one hand by the continual decrease in the time of acceleration of the turbine rotors and the growth in the control forces with the consequent increase in the operating volumes of the servomotors and, on the other hand, by the impossibility of any further development in the oil-system, which has already grown in some cases to abnormal proportions.

The importance of the problem of increasing the rapidity of action is greatest for the turbines in central power stations, where oil pumps with limited capacity are called on to ensure the supply for a complex control system which, for a two-point extraction turbine, contains three main servomotors, and where all the difficulties are consequently increased. The conditions of dynamic independence demand the maintenance of equality of the time for the three servomotors [2]. If the operating volume for each servomotor is 10 dm^3, and the time for each servomotor is 0.25 sec (which is usual for condensing turbines), then the oil-pump capacity needed to supply only the main servomotors amounts to 430 m^3/hr, and this is practically unattainable.

In uncoordinated control of two-point extraction turbines, the problem is made easier by the fact that the control of the pressures, in the separators—in particular, of the pressure in the second separator—can be rather slow, and the second and third servomotor times can be rather large (Fig. 1a_1). In coupled independent autonomous control, the times of all three servomotors must be equal (Fig. 1a_3). This is the condition for dynamic independence. As was shown in detail by P. E. Boloban in [4], the working of statically independent systems is not significantly worsened by using servomotors with essentially different times, which are used in the case of uncoordinated control (Fig. 1a_2). It is shown [4] that such control is sufficiently stable. The mutual disturbances of the variables also reach significant values. The best results are obtained with a solution due to A. V. Shcheglyaev (Fig. 1b_2). Here servomotors with different times are also used, but the supply of oil to the servomotors is limited, not by the opening in the valves, but by different diaphragms in the supply lines, the servomotors being identical. This leads to nonlinearity of the servomotors. We will compare the possible systems of coordinated control using the same over-all oil supply $Q_{x\,\max}$. In systems with three different servomotors, this quantity is

$$Q_{x\,\max} = \frac{V_1}{T_{s1}} + \frac{V_2}{T_{s2}} + \frac{V_3}{T_{s3}}.$$

In systems with identical servomotors (Fig. 1a_3, b_3), we have $Q'_{x\,\max} = 1/T_s\,(V_1 + V_2 + V_3)$. In order to satisfy the condition $Q_{x\,\max} = Q'_{x\,\max}$, we must have

$$\frac{V_1}{T_{s1}} + \frac{V_2}{T_{s2}} + \frac{V_3}{T_{s3}} = \frac{1}{T_s}\,(V_1 + V_2 + V_3).$$

Assuming all the servomotors identical, i.e., $V_1 + V_2 = V_3$, we obtain

$$\frac{1}{T_{s1}} + \frac{1}{T_{s2}} + \frac{1}{T_{s3}} = \frac{3}{T_s}.$$

In Fig. 1a_2 we have taken the following relation between the servomotor times: $T_{s1} : T_{s2} : T_{s3} = 1:3:9$.

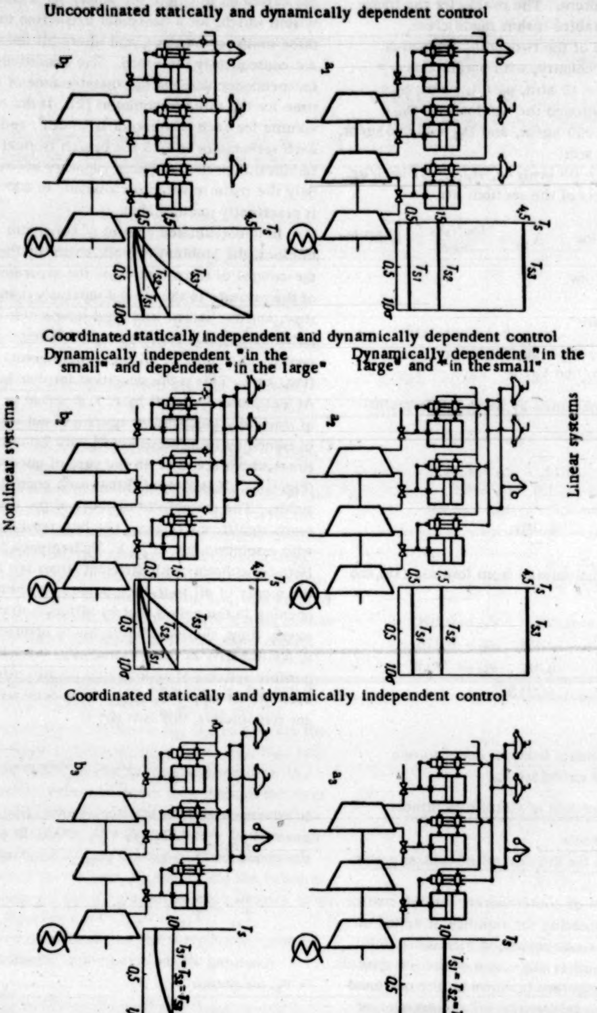

Uncoordinated statically and dynamically dependent control
Coordinated statically independent and dynamically dependent control
Dynamically independent "in the small" and dependent "in the large"
Dynamically dependent "in the large" and "in the small"
Coordinated statically and dynamically independent control
Nonlinear systems
Linear systems
a_1
b_1
a_2
b_2
a_3
b_3
T_s
T_{s1}
T_{s2}
T_{s3}
$T_{s1}=T_{s2}=T_{s3}$
0,5
1,5
4,5
10
10σ

Fig. 1. Possible method of control of central power station turbines.

In addition $1/T_{s1} + 1/3T_{s1} + 1/9T_{s1} = 3/T_{s1}$ or $13/9\,T_{s1} = 3 \cdot 1/T_s$; $T_{s1} = 13/27\,T_s$. If we take the times T_s for the identical servomotors in the system in Fig. 1 to be 1 sec, then $T_{s1} = 13/27$ sec ≈ 0.5 sec, $T_{s2} = 3T_{s1} \approx 1.5$ sec, $T_{s3} \approx 4.5$ sec. These relations are shown in Fig. 1.

Thus, even a very large difference in the servomotor times – in the ratio of 1 : 3 : 9 – with the same maximum oil supply, leads to a decrease in the time of the first servomotor of only 50% (0.5 sec instead of 1.0 sec). However, the time for the third servomotor increases to 4.5 times its value. These results are very unsatisfactory, and we are forced to look for other solutions to the problem.

In A. V. Shcheglyaev's method (Fig. $1b_2$) a higher oil-pump output was used than in the first method (Fig $1a_2$). Moreover, A. V. Shcheglyaev's systems, from the point of view of stability, are dynamically independent, since for small oscillations (small σ) their servomotor times are equal. Deviations from dynamic independence occur only for large disturbances, and in this case they are significantly large.

Dynamic independence "in the small" and "in the large" in a nonlinear system in which the rapidity of action approximates that for a system with instantaneous servomotor action, is attained in the method of control proposed by the author and described below. In this method, a common diaphragm in the supply lines of the main servomotors is used.

B. Coordinated control with a common diaphragm in the supply lines of the main servomotors

Let all three main servomotors of a central power station turbine have identical performances (i.e., identical times, identical operating volumes, and identical valves), and let the total calculated operating sections of all three valves be connected to the common main line supplying all three servomotors, in the shape of a diaphragm (Fig. $1b_3$), the valve cross sections being as great as possible within the permissible limits of construction. Since in this case the pressures ahead of all three servomotors (the pressure beyond the diaphragm) are the same, the times of all three servomotors are the same at any given instant of time. These times will vary, however, as functions of the total opening of all three valves $\Sigma\sigma + \sigma_1 + \sigma_2 + \sigma_3$, and the system is consequently dynamically nonlinear.

The necessary and sufficient condition for dynamical independence in a nonlinear system, as given by I. N. Voznesenskii, is the equality of the servomotor times. The conditions for dynamic independence of nonlinear systems have not yet been considered in general. It can be proven, however, that in the case of such nonlinear systems, where the servomotor times are functions of μ, η, and $\sigma = \eta - \mu$, the equality of the times of the corresponding servomotors at every instant of time will also be the condition of dynamic independence. The mode of variation of the times as functions of $\Sigma\sigma_x = \sigma_{1x} + \sigma_{2x} + \sigma_{3x}$ is shown in Fig. 2a for various values of the ratio $\alpha = R_3/R_0$, where R_3 is the total resistance of the fully open valves ($\Sigma\sigma = 3$) of all three servomotors ($R_3 = 1/9\,R_1$), R_0 is the resistance of the diaphragm, T_{s0} is the time of servomotor for fully open values and no diaphragm, and $T_{sx\,\max}$ is the value of T_{sx} for fully open valves ($\sigma_1 = \sigma_2 = \sigma_3 = 1$). A decrease in α brings the control conditions closer to those of instantaneous operation of the servomotors. The smaller α, the greater the extent to which the diaphragm becomes the only resistance limiting the discharge, since downstream from the valve, there only remain functions of the diaphragm activation, i.e., of limiting the discharge through it.

In Fig. 2b the dependence of the speed of the servomotor and of the oil discharge on $\Sigma\sigma$ is shown for various

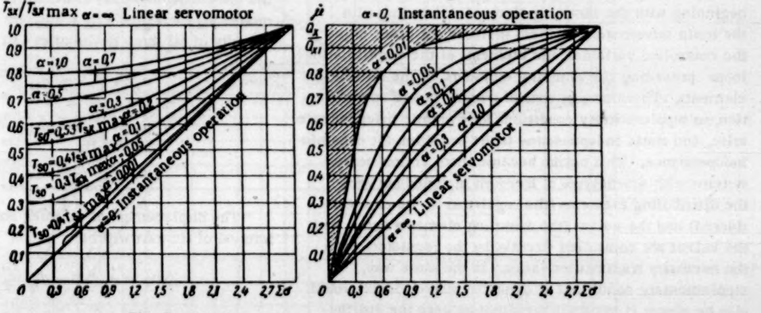

Fig. 2. Nonlinear servomotor characteristics.

$$a - T_{sx} = T_{s0}\sqrt{\frac{(\Sigma\sigma)^2 + 18\alpha}{18\alpha}}, \quad T_{sx}\max = T_{s0}\sqrt{\frac{1 + 2\alpha}{2\alpha}};\ b - \dot{\mu} = \frac{\sigma}{T_{sx}},\ Q_x = \dot{\mu} Q_{x1}$$

values of α. The shaded area represents the unused capacity of the oil pump for $\alpha = 0.01$. The calculation of the relations shown in Fig. 2 was carried out for a constant maximum oil discharge.

The advantages of nonlinear control with a common diaphragm, as found in the VTI system, are demonstrated by the investigation of the transfer process in an APT-12 turbine.

C. The dynamic independence of systems with nonlinear servomotors with a common diaphragm in the supply feed line.

It is known that the condition for static independence is the static linearity of the machine and static linearity of the coupling system, i.e., the constancy of all the transfer functions. L. N. Voznesenskii has shown that the condition for dynamic independence in a linear system is the equality of the servomotor times. This condition is obtained under the assumption not only of static, but also of dynamic linearity, i.e., the constancy of the dynamic parameters – the times of the machine and of the servomotors. In connection with the proposed nonlinear solution, in which the servomotor times, although they are equal one to the other at any instant of time, all vary as functions of the sum $\sigma_1 + \sigma_2 + \sigma_3$, the question arises as to whether dynamic independence can exist in such a dynamically nonlinear system, and under what conditions. In order to answer this question, it is necessary to consider the question of dynamic independence in its general form.

It should be noted that the conditions of dynamic independence have been obtained up to the present time [2, 3] from a consideration of the combined system of equations of a closed-loop system. This leads to unnecessary complication. All the conditions of dynamic independence are localized in series open-loop servosystems, and the appearance of these systems in control with power amplification involves these supplementary conditions. Not all of the amplification loop of each of the separate systems enters these systems, but only a part, beginning with the summing element and ending with the main servomotor. In them there do not occur either the controlled variables, the elements of the amplification loops preceding the summing elements, or the distribution elements. Therefore, in control without power amplification, no supplementary conditions for dynamic independence arise, and static independence is the condition for dynamic independence. This occurs because there are no servosystems with new degrees of freedom included between the distributing elements (the regulators in the case considered) and the valves (the summing elements here), and the valves are controlled directly by the regulators with the necessary transmission ratios. In the same way, supplementary conditions of dynamic independence would also be absent if the main servomotors were the distributing elements. This method, although theoretically ideal, is unsuitable in practice, since it leads to an excessively large weight of the lever coupling mechanism.

With the appearance of control with power amplification of servosystems, which are included between the distributing elements (not coinciding with the main servomotors) and the valves, only one supplementary condition must arise – the servosystems must be arranged so that the valves are controlled as before in accordance with the necessary transmission ratios. When this condition is satisfied, the undistorted transfer of pulses from the regulators to the servomotors is ensured for the same assigned ratios when new degrees of freedom—servomotors of the follow-up systems – are introduced. We will consider the conditions of such an undistorted transfer.

Let η_1, η_2, η_3 be the pulse-distributing elements, and μ_1, μ_2, μ_3 be the pulse-summing elements. In the consideration of the general case, we will assume that η_1, η_2, and η_3 are, respectively, the arbitrary functions $\varphi_1(t)$, $\varphi_2(t)$, and $\varphi_3(t)$ of the time.

The equations for μ_1, μ_2, and μ_3 are

$$\begin{aligned} T_{s1}\dot{\mu}_1 + \mu_1 - (d_{11}\eta_1 + d_{12}\eta_2 + d_{13}\eta_3) &= 0, \\ T_{s2}\dot{\mu}_2 + \mu_2 - (d_{21}\eta_1 + d_{22}\eta_2 + d_{23}\eta_3) &= 0, \\ T_{s3}\dot{\mu}_3 + \mu_3 - (d_{31}\eta_1 + d_{32}\eta_2 + d_{33}\eta_3) &= 0. \end{aligned} \tag{13}$$

The times T_s are here the above-mentioned function of $\Sigma\sigma$. Let any of the regulators, for example η_1, suffer a very small displacement. This causes valve displacements

$$\begin{aligned} \Delta\sigma_1 &= d_{11}\Delta\eta_1, \\ \Delta\sigma_2 &= d_{21}\Delta\eta_1, \\ \Delta\sigma_3 &= d_{31}\Delta\eta_1. \end{aligned} \tag{14}$$

For very small variations of $\Delta\eta_1$, and correspondingly small values of $\Delta\sigma_1$, $\Delta\sigma_2$, and $\Delta\sigma_3$, we can assume that the pressure beyond the diaphragm is constant. Since the pressure in front of all three servomotors is identical and equal to the pressure behind the common diaphragm, the instantaneous values of the times of all three servomotors $T_{s1x} = T_{s2x} = T_{s3x} = T_{sx}$, are also identical. The velocity of all three servomotors will be

$$\begin{aligned} \dot{\mu}_1 &= \frac{\Delta\sigma_1}{T_{sx}} = d_{11}\frac{\Delta\eta_1}{T_{sx}}, \\ \dot{\mu}_2 &= \frac{\Delta\sigma_2}{T_{sx}} = d_{21}\frac{\Delta\eta_1}{T_{sx}}, \\ \dot{\mu}_3 &= \frac{\Delta\sigma_3}{T_{sx}} = d_{31}\frac{\Delta\eta_1}{T_{sx}}. \end{aligned} \tag{15}$$

The displacement of all three servomotors during the interval of time Δt will be

$$\begin{aligned} \Delta\mu_1 &= \dot{\mu}_1\Delta t = d_{11}\frac{\Delta\eta_1\Delta t}{T_{sx}}, \\ \Delta\mu_2 &= \dot{\mu}_2\Delta t = d_{21}\frac{\Delta\eta_1\Delta t}{T_{sx}}, \\ \Delta\mu_3 &= \dot{\mu}_3\Delta t = d_{31}\frac{\Delta\eta_1\Delta t}{T_{sx}}. \end{aligned} \tag{16}$$

In each small interval of time, the displacement of the servomotors will have the ratios $\Delta\mu_2/\Delta\mu_1 = d_{21}/d_{11} = j_{21}$, $\Delta\mu_3/\Delta\mu_1 = d_{31}/d_{11} = j_{31}$, and this ensures the dynamic independence. The displacements μ_1, μ_2, and μ_3 of the servomotors for the regulator control input η_1, in a finite interval of time expressed in terms of the same ratios, are obtained by integrating the relations (16):

$$\begin{aligned} \mu_1 &= \int \dot{\mu}_1 dt = d_{11} \int \frac{\eta_1}{T_{sx}} dt, \\ \mu_2 &= \int \dot{\mu}_2 dt = d_{21} \int \frac{\eta_1}{T_{sx}} dt, \qquad (17) \\ \mu_3 &= \int \dot{\mu}_3 dt = d_{31} \int \frac{\eta_1}{T_{sx}} dt. \end{aligned}$$

The equality of the times of all three servomotors at every instant of time is thus a sufficient condition for dynamic independence. The times do not have to be constant, but can be arbitrary functions of μ and η, i.e., the system can be dynamically nonlinear.

A system with a common diaphragm in the supply line satisfies these conditions. This system is nonlinear, and in it $T_{s1} = T_{s2} = T_{s3} = f(\Sigma\sigma)$; it is, however, dynamically independent of the equality of the servomotor times, and is the most direct and radical solution of the problem of dynamic independence. If the supply of oil to the servomotors is limited by the maximum capacity of the pump, this system permits operation with partially open servomotors with significantly smaller times than in the case of fully open servomotors. In this system, the constancy of the sum of the velocities of all three servomotors is ensured, while the separate velocities are determined by the transfer functions. This has, in general, the same advantages as operation in parallel. Thanks to the constancy of the velocity sum, the peaks in the amount of oil necessary for one servomotor are covered by the smaller amounts necessary for the others. This also guarantees the greatest possible operating speed for a given pump capacity, if the dynamic independence is strictly preserved.

D. Transient processes in central power plant turbines

If the stability conditions of a certain nonlinear system could be investigated analytically in closed form, then the transient processes occurring in it could be determined only by numerical integration at the present time. The accuracy of such an integration was verified by comparison with the analytic solution.

In Fig. 3 is shown the transient process in a system of coordinated control of a two-point extraction turbine with nonlinear servomotors. The continuous curve shows the process for the times of the main servomotors $T_{s1\,max} = T_{s2\,max} = T_{s3\,max} = 1$ sec. The curve is not drawn for the nominal electric load drop ($\lambda = 1$) ($N_0 = 12{,}000$ kw), since this load was beyond the limits of independent control, but for the maximum electric load within the limits of independence ($\lambda = 0.88$).

The equations of the machine in this case are

$$\begin{aligned} T_{a1}\dot{\psi}_1 + c_{11}\mu_1 + c_{12}\mu_2 + c_{13}\mu_3 &= 0; \\ T_{a2}\dot{\psi}_2 + c_{21}\mu_1 + c_{22}\mu_2 + c_{23}\mu_3 &= 0; \\ T_{a3}\dot{\psi}_3 + c_{31}\mu_1 + c_{32}\mu_2 + c_{33}\mu_3 &= 0. \end{aligned}$$

The equations of the regulators (ideal) are

$$\eta_1 = \psi_1; \ \eta_2 = \psi_2; \ \eta_3 = \psi_3.$$

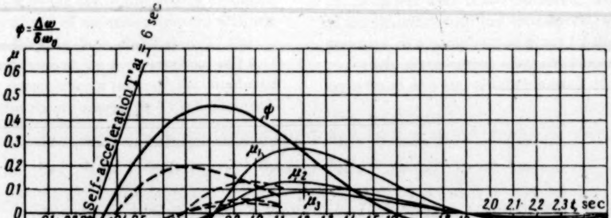

Fig. 3. The transient process in the control system of a two-point extraction turbine with nonlinear servomotors.

The servomotor equations:

$$T_{s1}\dot{\mu}_1 + \mu_1 - (d_{11}\eta_1 + d_{12}\eta_2 + d_{13}\eta_3) = 0;$$
$$T_{s2}\dot{\mu}_2 + \mu_2 - (d_{21}\eta_1 + d_{22}\eta_2 + d_{23}\eta_3) = 0;$$
$$T_{s3}\dot{\mu}_3 + \mu_3 - (d_{31}\eta_1 + d_{32}\eta_2 + d_{33}\eta_3) = 0.$$

The numerical values of the coefficients c_{ik}:

$$c_{11} = 0.69,\quad c_{12} = 0.72,\quad c_{13} = 0.31,$$
$$c_{12} = 2.6,\quad c_{22} = -1.6,\quad c_{23} = 0,$$
$$c_{13} = 0,\quad c_{32} = 2.0,\quad c_{33} = -1.0.$$

The numerical values of the coefficients d_{ik}:

$$d_{11} = 0.35,\quad d_{12} = 0.293,\quad d_{13} = 0.108,$$
$$d_{21} = 0.563,\quad d_{22} = -0.151,\quad d_{23} = 0.176,$$
$$d_{31} = 1.135,\quad d_{32} = -0.31,\quad d_{33} = -0.165.$$

The times of the machine:

$$T_{a1} = \delta_1 T'_{a1} = 0.05\cdot 6 = 0.3 \text{ sec},$$
$$T_{a2} = \delta_2 T'_{a2} \approx 0.1\cdot 1.95 \approx 0.2 \text{ sec},$$
$$T_{a3} = \delta_3 T'_{a3} \approx 0.2\cdot 1.95 \approx 0.4 \text{ sec}.$$

The transient process in Fig. 3 shows a strict static and dynamic independence of control in this nonlinear system. Because of the application of servomotors with large nonlinearities ($\alpha = 0.05$) which were similar to servomotors with constant velocity, the overshoot of the number of revolutions was $\Delta\psi = 0.45$ or, in absolute values, $\Delta n = \Delta\psi\delta\omega_0 = 67.5$ rpm. For $T_{a1} = 6$ sec and $T_{s\,max} = 1.0$ sec, i.e., for the maximum pump output $Q_{x\,max} = 91$ m^3/hr, such an overshoot is evidence of quick response.

The broken curves in Fig. 3 show the drop of the same load for $T_{s\,max} = 0.65$ sec, which corresponds to $Q_{x\,max} = 120$ m^3/hr. These values were also taken in the VTI project. To them corresponds a dynamic overshoot of the number of revolutions less than 1%.

In the coordinated control of several variables, there are therefore nonlinear systems that use the capacity of the oil-pump reasonably fully, and which, relative to the use of this capacity, are close to systems with instantaneous servomotor actuation. Static and dynamic independence are maintained in such systems of coordinated control. It must be assumed that in the coordinated control of several variables, nonlinear systems must be used in solving the problems that arise.

LITERATURE CITED

1. L. N. Voznesenskii, "The question of the choice of a control system for central power station turbines," Coll: The Soviet Energy System (Leningrad, 1934).
2. L. N. Voznesenskii, "The regulation of machines with a large number of controlled parameters," Avtomat. i Telemekh. No. 4-5 (1938).
3. V. E. Solovei, "Control of steam turbines with two-point steam extraction," Avtomat. i Telemekh. No. 2 (1939).
4. P. E. Boloban, An Investigation of the Dynamic Properties of Statically Independent Control Systems for Turbines with Two-Point Steam Extraction. Dissertation, VTI (1951).

ON THE PRINCIPLES OF SYNTHESIZING AUTOMATIC SYSTEMS WITH MANY CONTROLLED QUANTITIES

P. I. Chinaev

Kiev

Translated from Avtomatika i Telemekhanika, Vol. 21, No. 6, pp. 761-771, June, 1960

The paper suggests principles for synthesizing systems with many controlled variables. The basic mathematical relationships for combined-type automatic systems are derived in matrix form.

It is shown that the use of the principles of physical realizability, invariance, and optimality permit one to select a controller's operator coefficients (elements of matrices B and C) for multiloop systems.

Solution of the problem of the complex automation of production is inseparably related to the development of methods for synthesizing systems with many controlled quantities.

The widespread use of complicated systems for the simultaneous control of several physical quantities is a result of the tendency to get the greatest energy or most economical output from the employment of complicated objects (plants).

It is convenient, in analyzing and synthesizing systems with many variables, to use matrix and operational calculi. The use of matrix calculus allows one to give the solution of the synthesis and analysis problems compactly and elegantly.

The importance of the use of the matrix calculus for analysis and synthesis of multiloop systems was first asserted, in our country, by V. S. Kulebakin [1] and N. N. Luzin [2] and, abroad, by A. Boksenbom and R. Hood [3]. Matrix methods were successfully employed in automatic control theory abroad by Ts'ien Süeh-sen [4], M. Colomb and E. Usdin [5], R. I. Kavanagh [6], and, in our country, by M. V. Meerov [7], P. V. Bromberg [8], E. I. Baranchuk [9], and others.

We now formulate the synthesis problem for systems with many controlled quantities. Let there be a complicated plant, i.e., a plant in which there flow many processes which are subject to control. We denote by $x_1, x_2, \ldots, x_n$ the plant's output coordinates. These physical quantities characterize the plant's state. In the general case, two types of stimuli act on the plant. On the one hand, there are the external, uncontrolled, stimuli $f_1, f_2, \ldots f_n$ which disturb the desirable state of the plant and, on the other, the so-called controlling (regulated) stimuli $y_1, y_2, \ldots, y_n$ by means of which the disturbed state is reconstituted. With account taken of the nomenclature just introduced, we can present the structure of a complicated plant by the scheme of Fig. 1.

Each of the output controlled coordinates x_i can be considered as a linear combination of the input quantities:

$$
\begin{aligned}
x_1 &= a_{11}y_1 + a_{12}y_2 + \ldots + a_{1n}y_n + h_{11}f_1 + h_{12}f_2 + \ldots + h_{1n}f_n, \\
x_2 &= a_{21}y_1 + a_{22}y_2 + \ldots + a_{2n}y_n + h_{21}f_1 + h_{22}f_2 + \ldots + h_{2n}f_n, \\
&\cdots\cdots\cdots\cdots\cdots\cdots\cdots\cdots\cdots\cdots\cdots\cdots \\
x_n &= a_{n1}y_1 + a_{n2}y_2 + \ldots + a_{nn}y_n + h_{n1}f_1 + h_{n2}f_2 + \ldots + h_{nn}f_n.
\end{aligned}
\tag{1}
$$

The quantities a_{ij} and h_{rk} are polynomials in the operator $D = d/dt$ of degree not higher than the second. They reflect the effect of the input quantities y_i and f_i on the corresponding output quantities.

By using matrix notation, we can write (1) in the form

$$X = AY_{\text{ob}} + HF,$$

where

$$X = \left\| \begin{matrix} x_1 \\ x_2 \\ \vdots \\ x_n \end{matrix} \right\|, \quad Y = \left\| \begin{matrix} y_1 \\ y_2 \\ \vdots \\ y_n \end{matrix} \right\|, \quad F = \left\| \begin{matrix} f_1 \\ f_2 \\ \vdots \\ f_n \end{matrix} \right\|, \quad A = \left\| \begin{matrix} a_{11}a_{12} \ldots a_{1n} \\ a_{21}a_{22} \ldots a_{2n} \\ \cdots\cdots \\ a_{n1}a_{n2} \ldots a_{nn} \end{matrix} \right\|, \quad H = \left\| \begin{matrix} h_{11}h_{12} \ldots h_{1n} \\ h_{21}h_{22} \ldots h_{2n} \\ \cdots\cdots \\ h_{n1}h_{n2} \ldots h_{nn} \end{matrix} \right\|$$

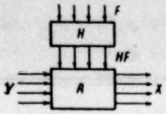

Fig. 1. Block schematic of an object with many parameters. A is an operator matrix whose elements characterize the object's natural motions; H is an operator matrix whose elements characterize the transformation of the external stimuli F to the form X with account taken of A; X, Y, F are column matrices whose elements are the coordinates, respectively, of the controlled (x_i), controlling (y_i) and disturbing (f_i) quantities.

Since the quantities f_i vary arbitrarily, one should then expect that, for a definite initial state of the plant and unchanged values of y_i (for an unchanged position of the controlling organs), the x_i will vary arbitrarily.

The attempt to obtain a desirable character of the variations of quantities x_i leads either to an auxiliary transformation of matrix A or to such a preliminary variation of the inputs y_i that, with the previous matrix A, a desirable variation of the x_i will be obtained. Intervention in the structure of matrix A is undesirable, since the plant ordinarily presents itself as an invariable system element.

Consequently, there remains one possibility, namely, to introduce controlling stimuli (the coordinates y_i) by such laws that the resulting x_i will be desirable. In other words, instead of the plant matrix A, one must find a system matrix W which includes A ($A \subset W$) such that the previous inputs y_i and f_i will result in a desirable temporal variation of the quantities x_i.

We denote the controller matrices by B and C. Then, the controlling action of the controller on the plant can be written in the form

$$Y_{reg} = BF + CX, \tag{2}$$

where

$$B = \left\| \begin{matrix} b_{11} b_{12} \dots b_{1n} \\ b_{21} b_{22} \dots b_{2n} \\ \cdot\ \cdot\ \cdot\ \cdot\ \cdot\ \cdot \\ b_{n1} b_{n2} \dots b_{nn} \end{matrix} \right\|, \quad C = \left\| \begin{matrix} c_{11} c_{12} \dots c_{1n} \\ c_{21} c_{22} \dots c_{2n} \\ \cdot\ \cdot\ \cdot\ \cdot\ \cdot\ \cdot \\ c_{n1} c_{n2} \dots c_{nn} \end{matrix} \right\|$$

The comparison condition for the required controlling stimulus of the object (plant) Y_{ob} and the intended Y_{reg} is

$$Y = Y_{ob} = -Y_{reg} \tag{3}$$

which is simultaneously the condition for a closed system.

Therefore, the definitive equations for the complicated plant can be written in the form

$$X = AY + HF, \quad Y = -BF - CX. \tag{4}$$

By multiplying the second equation on the left by matrix A and then substituting into the first equation, we obtain

$$X = -ABF - ACX + HF$$

or

$$(E + AC)X = (H - AB)F,$$

where

$$E = \left\| \begin{matrix} 1\ 0 \dots 0 \\ 0\ 1 \dots 0 \\ \cdot\ \cdot\ \cdot \\ 0\ 0 \dots 1 \end{matrix} \right\|$$

Equation (4) is the generalization of an ordinary differential equation for a single-loop automatic system to the case of a multiloop system of the combined type (Fig. 2).

For a multiloop servosystem (Fig. 3), Eq. (4) will have the form

$$(E + AC)X = ACG \tag{5}$$

or

$$(E + AC)X = ACG + HF.$$

For a multiloop stabilization system ($B \equiv O$) (Fig. 4):

$$(E + AC)X = HF. \tag{6}$$

All our further discussion will have to do with systems of the combined type.

If the inverse matrix $(E + AC)^{-1}$ exists, then

$$X = (E + AC)^{-1}(H - AB)F$$

or

$$X = WF,$$

where

$$W = (E + AC)^{-1}(H - AB). \tag{7}$$

From the synthesis point of view, the matrices A, H, F, and X are given, and the matrices B and C are unknown.

Since there are two unknowns and only one equation, it is necessary to find an additional condition relating the coefficients of matrices A, B, C, H, F, and X. Such conditions can be found on the basis of the following principles: the principle of realizability, the principle of invariance, and the principle of optimality.

We first explain the essential points of these principles, and then go on to show how it is practical to use them for obtaining the required additional relationships between B, C, A, H, F, and X.

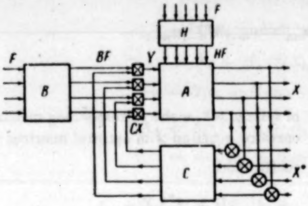

Fig. 2. Block schematic of a multiloop combined system. A, H, F, X, Y are the same as in Fig. 1; B is an operator matrix whose elements implement the transformation of F to Y (the controller matrix for disturbances); C is an operator matrix whose elements implement the transformation of the deviations X to CX (controller matrix for deviations); X^0 is a column matrix whose elements are the nominal output coordinates CX. ⊠ is the symbol for summation of the controlling stimuli; ⊗ is the symbol for summation of the output coordinates and their nominal values.

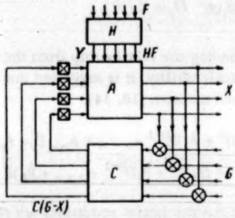

Fig. 3. Block schematic of a multiloop servosystem. A, H, C, X, Y, F are the same as in Figs. 1 and 2; G is a column matrix whose elements are the coordinates of the controlling actions on the system.

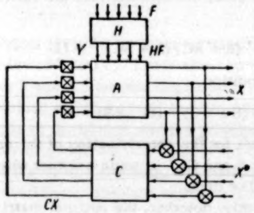

Fig. 4. Block schematic of a multiloop stabilization system. A, H, C, X, Y, X^0 are the same as on Fig. 2.

We turn first to the principle of realizability. In creating a controller, the designer must be certain that it is possible to realize such a controller. First, there must be certainty that the controller is capable of functioning in general and, second, there must be certainty that the controller can operate within given limits under the conditions of physical realizability (conditions of stability, speed limitations, overload limitations).

From the mathematical point of view, the realizability condition is equivalent to the existence of the inverse matrix $(E+AC)^{-1}$. To find the inverse matrix, we can use the efficient methods of matrix theory [10, 11]. Thus, for example, the bordering method [12] is very convenient. According to this method, the nth-order inverse matrix $M_n^{-1} = (E+AC)^{-1}$ is found in terms of the (n-1)th-order inverse matrix M_{n-1}^{-1} and the coefficients of the original matrix M_n:

$$M_n^{-1} = \left\| \begin{matrix} M_{n-1}^{-1} + \dfrac{M_{n-1}^{-1} u_{n-1} v_{n-1} M_{n-1}^{-1}}{\alpha_n}; & -\dfrac{M_{n-1} u_{n-1}}{\alpha_n} \\ -\dfrac{v_{n-1} M_{n-1}^{-1}}{\alpha_n}, & \dfrac{1}{\alpha_n} \end{matrix} \right\|. \tag{8}$$

Here, u_{n-1} and v_{n-1} are (n-1)th-order columns and rows in the original matrix:

$$M_n = (E + AC) = \left\| \begin{matrix} m_{11} m_{12} \dots m_{1n} \\ m_{21} m_{22} \dots m_{2n} \\ \dots\dots\dots\dots \\ m_{n1} m_{n2} \dots m_{nn} \end{matrix} \right\|;$$

$$u_{n-1} = \left\| \begin{matrix} m_{1n} \\ m_{2n} \\ \vdots \\ m_{n-1,\,n} \end{matrix} \right\|, \quad \begin{matrix} v_{n-1} = [m_{n1} m_{n2} \ldots m_{n,\,n-1}], \\ \\ \alpha_n = m_{nn} - v_{n-1} M_{n-1}^{-1} u_{n-1}. \end{matrix} \tag{9}$$

The synthesis problem is easily solved if one has prior knowledge of the optimal matrix – the transformer of system W* or the corresponding matrix W* of the operator equation with optimal matrices – with the coefficients

$$\begin{gathered} (A_0^{\bullet} D^n + A_1^{\bullet} D^{n-1} + A_2^{\bullet} D^{n-2} + \ldots + A_{n-1}^{\bullet} D + A_n^{\bullet}) X = \\ = (B_0^{\bullet} D^n + B_1^{\bullet} D^{n-1} + \ldots + B_n^{\bullet}) F, \\ (A_0^{\bullet},\ A_1^{\bullet}, \ldots,\ A_n^{\bullet},\ B_0^{\bullet},\ B_1^{\bullet}, \ldots,\ B_n^{\bullet} \text{ do not depend on } \ D = d/dt). \end{gathered}$$

In this case, the condition for the existence of the solution X

$$(E + AC)(E + AC)^{-1} = l E \tag{10}$$

and the condition

$$(E + AC)^{-1} (H - AB) = W^{*}$$

are sufficient for the determination of the coefficients of matrices B and C; l is some constant which does not depend on D = d/dt.

Frequently, however, the optimal matrix W* is not known. Besides, the mathematical solution X may not lie within the same limits as those given by technological conditions (the conditions of physical realizability).

For finding the relationship from the condition of physical realizability, it is suggested that one use the equivalence theorem [13, 14]. If

$$\begin{gathered} (A_0 D^n + A_1 D^{n-1} + \ldots + A_{n-1} D + A_n) X = \\ = (B_0 D^n + B_1 D^{n-1} + \ldots + B_n) F \end{gathered} \tag{10'}$$

and F ≡ E, but the initial conditions are $(D^i X)_0 \equiv 0$, then it is equivalent to seek the solution for the equation

$$(A_0 D^n + A_1 D^{n-1} + \ldots + A_{n-1} D + A_n) X = 0$$

with the initial conditions which satisfy the following system of inhomogeneous algebraic equations:

$$\begin{aligned} A_0 X_0 + 0 (DX)_0 + \ldots + 0 (D^{n-1} X)_0 &= -B_0, \\ A_1 X_0 + A_0 (DX)_0 + \ldots + 0 (D^{n-1} X)_0 &= -B_1, \\ \ldots\ldots\ldots\ldots\ldots\ldots\ldots\ldots &\ \ldots\ldots\ldots\ldots \\ A_{n-1} X_0 + A_{n-2} (DX)_0 + \ldots + A_0 (D^{n-1} X)_0 &= -B_{n-1}. \end{aligned} \tag{11}$$

In conditions (11), $X_0 = X_0(-0)$.

For the compensation of jumps in the external disturbance F ≡ E, it is necessary, in addition, to give the initial value of the solution

$$X(+0) = -A_n^{-1} B_n. \tag{12}$$

Conditions (11) can be extended to the more general law of variation f [15], specifically,

$$f_i(t) = \sum_{k=0}^{m} [f_{ki}(t) - f_{k-1,\,i}(t)]\, E(t - k\tau_i) \quad (i = 1, 2, \ldots, n), \tag{13}$$

where E(t) is a unit step function, m is the number of segments of the linear approximation of $f(t)$, and τ is the length of these segments.

The representation of any analytic function in the form of (13) is given in [16].

If, instead of $f_1(t)$ and $E(t - k\tau_1)$, we consider the matrices, then the expression

$$F = \sum_{k=0}^{m} [f_{ki}(t) - f_{k-1,\,i}(t)]\, E(t - k\tau) \tag{14}$$

is an approximate expansion of the arbitrary vector function F(t) in terms of unit step disturbances. Then, the equivalent initial conditions will be found as the solution of the following system of inhomogeneous equations:

$$
\begin{gathered}
A_0X_0 + 0\,(DX)_0 + \ldots + 0\,(D^{n-1}X)_0 = \\
= -B_0\sigma_0 + B_1\sigma_1 - B_2\sigma_2 + \ldots + (-1)^{s+1}B_s\sigma_s, \\
A_1X_0 + A_0\,(DX_0) + \ldots + 0\,(D^{n-1}X)_0 = \\
= -B_1\sigma_0 + B_3\sigma_2 - B_3\sigma_2 + \ldots + (-1)^{s+1}B_{s+1}\sigma_s, \\
A_2X_0 + A_1\,(DX)_0 + A_0\,(D^2X)_0 + \ldots + 0\,(D^{n-1}X)_0 = \\
= -B_2\sigma_0 + B_3\sigma_1 - \ldots + (-1)^{s+1}B_{s+2}\sigma_s, \\
\ldots\ldots\ldots\ldots\ldots\ldots\ldots\ldots\ldots\ldots \\
A_{n-2}X_0 + A_{n-3}\,(DX)_0 + \ldots + A_0\,(D^{n-2}X)_0 + 0\,(D^{n-1}X)_0 = \\
= -B_{n-2}\sigma_0 + B_{n-1}\sigma_1 - B_n\sigma_2, \\
A_{n-1}X_0 + A_{n-3}\,(DX)_0 + \ldots + A_0\,(D^{n-1}X)_0 = -B_{n-1}\sigma_0 + B_n\sigma_1, \\
X(+0) = -A_n^{-1}B_n\sigma_0,
\end{gathered}
\tag{15}
$$

where

$$\sigma_s = \frac{\tau^s}{s!}\sum_{k=0}^{m} k^s\,(f_k - f_{k-1}) \quad (s = 0, 1, 2, \ldots, r).$$

It ordinarily suffices to limit oneself to the case when r = 2. In addition to conditions (15), the following conditions, defining the accuracy ϵ of the equivalent substitution, must be observed:

$$
\begin{gathered}
-B_0\sigma_1 + B_1\sigma_2 + \ldots + (-1)^sB_{s-1}\sigma_s \leqslant \varepsilon_1, \\
B_0\sigma_2 - B_1\sigma_3 + \ldots + (-1)^sB_{s-2}\sigma_s \leqslant \varepsilon_2, \\
\ldots\ldots\ldots\ldots\ldots\ldots\ldots\ldots \\
(-1)^{s-1}B_0\sigma_{s-1} + (-1)^sB_1\sigma_s \leqslant \varepsilon_{s-1}, \\
(-1)^sB_0\sigma_s \leqslant \varepsilon_s.
\end{gathered}
\tag{16}
$$

Each of the quantities $\epsilon_1, \epsilon_2, \ldots, \epsilon_s$ must be chosen less than the quantity ϵ, which depends on the initial equation and on the form of $f(t)$.

Thus, thanks to (15), one can, with the condition that $|E + AC| \neq 0$, establish the relationships between the initial conditions of the solution $(D^{(i)}X)_0$ (i = 0, 1, . . . , n−1) and the coefficient matrices $A_0, A_1, \ldots, A_{n-1}$ and $B_0, B_1, \ldots, B_{n-1}$ or, what amounts to the same thing, between the elements of the known and unknown matrices, A, B, C, and H.

For brevity, we write the equivalence conditions (15) in the form

$$(D^{(i)}X)_0 = \Phi_i\,(A, B, C, H, \sigma) \tag{17}$$
$$(i = 0, 1, 2, \ldots, n-1).$$

By the conditions of physical realizability, the initial values X_0 and their derivatives $(D^{(i)}X)_0$ (i = 1, 2, . . . , n−1) are bounded (for example, the accelerations are bounded by conditions of reliability, etc.):

$$\Phi_i\,(A, B, C, H, \sigma) \leq N_i. \tag{18}$$

Conditions (18) can be taken as auxiliary limitations on the choice of B and C. Limitations on the coefficients of matrices B and C from the condition of required quality can be obtained on the basis of the two other principles: the principle of invariance and the principle of optimality. We consider in detail the principle of invariance [17].

Following V. S. Kulebakin, we shall distinguish two forms of invariance: absolute and selective (autonomous) [18].

In the first case, the controlled quantity X will be unchanged under any arbitrary stimuli $F(f_1, f_2, \ldots, f_n)$. This means that

$$H - AB \equiv 0. \tag{19}$$

Equation (19) can hold if

1) H ≡ 0, AB ≡ 0,
2) (H − AB) ≡ 0.

The condition H ≡ 0 means that F is not applied directly to the plant.

The condition that AB ≡ 0 holds if

$$
\begin{gathered}
a_{11}b_{1p} + a_{12}b_{2p} + \cdots + a_{1n}b_{np} = 0, \\
a_{21}b_{1p} + a_{22}b_{2p} + \cdots + a_{2n}b_{np} = 0, \\
\ldots\ldots\ldots\ldots\ldots\ldots\ldots \\
a_{n1}b_{1p} + a_{n2}b_{2p} + \cdots + a_{nn}b_{np} = 0
\end{gathered}
$$

for all p = 1, 2, . . . , n.

For $|A| \neq 0$, all the $b_{ij} = 0$, i.e., the controller is also insulated from the external disturbances (the trivial case).

The case when $|A| = 0$ gives the possibility of obtaining a system which is invariant with respect to F for $b_{ij} \neq 0$.

If the determinant $|A|$ of the plant matrix equals zero, this means that there is a linear relationship between the rows (or columns). But, since a relationship of the rows (or columns) corresponds to a relationship between the processes in the plant, then this latter fact means that there is the possibility of an internal compensation of the external disturbances (by virtue of the properties of the plant itself).

It is possible to create a complicated plant in which each natural process is exactly simulated. Then, the rows of the determinant $|A|$ will always be proportional. The model (simulated processes) can be so constructed that the processes in it will flow significantly faster than in the natural plant. Therefore, before the plant reacts to changes of the external conditions, there will be developed, thanks to the speed of the model, the necessary reconstitution of the stimuli to the plant to compensate the applied disturbances, so that the plant's state, characterized by the coordinates $x_i(t)$, can remain unchanged. However, with this, the stimuli do not act directly on the plant ($H \equiv 0$).

Case 2 refers to the generally known case of external disturbance compensation [17].

A controller with matrix B must be so chosen that the following conditions are met:

$$\begin{aligned} &a_{11}b_{1p} + a_{12}b_{2p} + \cdots + a_{1n}b_{np} = h_{1p}, \\ &a_{21}b_{1p} + a_{22}b_{2p} + \cdots + a_{2n}b_{np} = h_{2p}, \\ &\cdot\ \cdot\ \cdot\ \cdot\ \cdot\ \cdot\ \cdot\ \cdot\ \cdot\ \cdot\ \cdot\ \cdot\ \cdot\ \cdot\ \cdot\ \cdot\ \cdot \\ &a_{n1}b_{1p} + a_{n2}b_{2p} + \cdots + a_{nn}b_{np} = h_{np} \quad (p = 1, 2, \ldots n). \end{aligned} \tag{20}$$

From this, with the condition $|A| \neq 0$, there are determined all the elements of the projected controller B which measures the external disturbances. The elements of controller C (which measures the deviations of controlled quantity X) are found from condition (10). The case of invariance considered above refers to the case when there is no a priori information as to F. It is obtained by means of controllers B and C, both by direct measurements (by controller B) and by indirect (by controller C) (by means of a preliminary deviation of the controlled quantity).

The choice of the controller parameters on the basis of the invariance principle can be significantly eased if there is information as to F. For example, if it is known that F is the solution of some homogeneous equation $K(D)F = 0$, where $K(D)$ — the Kulebakin operator [13] — enters into operator Eq. (10).

From this there follows the practical approach to setting up auxiliary limitations on the coefficients of matrices A, B, C, and H.

From the known F there is found the K(D) representation (or the corresponding matrix K). The right member of Eq. (4) or Eq. (10) takes the form

$$(H - AB) = KL \tag{21}$$

or

$$\begin{aligned} &B_0D^n + B_1D^{n-1} + \ldots + B_{n-1}D + B_n = \\ &= K(D)(L_0D^m + L_1D^{m-1} + \ldots + L_m). \end{aligned} \tag{22}$$

The matrix L or the operator L(D) are so chosen that the order of matrix KL will equal the order of the original matrix (H − AB). If the operator K(D) has order n then, obviously, L = constant, and the matrix L can be taken as a diagonal matrix with constant coefficients.

Finally, one may use the criterion of absolute invariance, presented in [18].

As applied to system (4), this takes the form: the necessary and sufficient condition that the system's first unknown function x_1 be independent of any analytic function f_1 consists in the identical vanishing of the minor Δ_{11}.

Consequently, each of the unknown x_i will be invariant with respect to f_i if the corresponding minors Δ_{ii} equal zero identically. By equating these minors Δ_{ii} to zero, we obtain the additional limitations on the coefficients of matrices B and C.

The condition of absolute invariance is implemented with difficulty, so that one frequently limits oneself to the condition of selective invariance. In [4] and [19] this was formulated as the criterion of autonomy. In almost all systems with many variables, there is a reciprocal effect on the control loops via the plant. These so-called natural connections, caused by the interactions between the physical processes, can have an adverse effect on the dyanmic properties of the system as a whole.

Selective invariance supposes that each system output x_i reacts only to "its" input f_i. Mathematically, this means that the system's matrix operator W must have the diagonal form. As was shown in works [2, 10, 11], any nonsingular matrix operator W can be transformed to the Hermite triangular form by being multiplied left or right by some matrix S. The matrix S possesses the property that its determinant is not identically zero and does not depend on D = d/dt. By successively carrying out elementary transformations on the rows, we can take the matrix W to the form where all the elements below the diagonal are zero, and if we apply, to the already transformed matrix, a succession of elementary operations on the columns, we shall finally obtain a matrix with only its diagonal elements different from zero.

Thus, we present the original matrix W in the form

$$W = SE(D)T. \tag{23}$$

Matrices S and T are called transforming matrices. They are triangular matrices whose determinants do not equal zero and do not depend on D.

The diagonal elements of the matrix E(D) are defined by the following formulas:

$$e_{11} = \frac{\Delta_n(D)}{\Delta_{n-1}(D)}, \quad e_{22} = \frac{\Delta_{n-1}(D)}{\Delta_{n-2}(D)}, \ldots, e_{nn} = \frac{\Delta_1(D)}{\Delta_0} = \Delta_1(D). \tag{24}$$

where Δ_r is the greatest common divisor of the rth-order minors.

If we impose the requirement that all nondiagonal elements of matrices S and T be zero, then this will mean the holding of the criterion of selective invariance. The criterion of autonomy [4] flows from this as a particular case.

By writing matrix Eq. (23) in expanded form:

$$\begin{Vmatrix} w_{11} w_{12} \dots w_{1n} \\ w_{21} w_{22} \dots w_{2n} \\ \dots\dots \\ \dots\dots \\ w_{n1} w_{n2} \dots w_{nn} \end{Vmatrix} = \begin{Vmatrix} s_{11} s_{12} \dots s_{1n} \\ 0 \; s_{22} \dots s_{2n} \\ 0 \; 0 \dots\dots \\ \dots\dots \\ 0 \; 0 \dots s_{nn} \end{Vmatrix} \begin{Vmatrix} e_{11} \; 0 \dots 0 \\ 0 \; e_{22} \dots 0 \\ \dots\dots \\ \dots\dots \\ 0 \; 0 \dots e_{nn} \end{Vmatrix} \begin{Vmatrix} \tau_{11} \; 0 \dots 0 \\ \tau_{21} \tau_{22} \dots 0 \\ \dots\dots \\ \dots\dots \\ \tau_{n1} \tau_{n2} \dots \tau_{nn} \end{Vmatrix}, \qquad (25)$$

and by carrying out the multiplications on the right side, and then setting up the equations $w_{ij} = s_{ij} e_{ij} \tau_{ji}$ of the matrix elements, we obtain the additional necessary conditions for determining B and C.

If, further, the requirements are also imposed that all the s_{ij} ($j \neq i$) and τ_{kr} ($k \neq r$) equal zero, then this will also mean the possibility of autonomous control.

Finally, we consider the third principle – the principle of optimality.

The fact of the matter is that one does not succeed in establishing an explicit relationship between the desirable variations of the x_i and the coefficients of matrices A_i and B_i ($i = 0, 1, \dots, n$). Therefore, the optimality condition denotes the best approximation of the solution X being sought to some optimal X^*, chosen from the condition of least dynamic error and least duration of the transient response in the integral sense. As a criterion of optimality, one can take the minimum mean square error for the multiloop system $\overline{\epsilon^2} = \min$. This case was considered in detail in [5, 9]. This last method requires that $F(f_1, \dots, f_n)$ be considered as stationary random functions of time.

We consider optimality in the integral sense. We place on X the additional requirement of 2n-fold differentiability. We write the system of n homogeneous equations for X:

$$\begin{gathered} XA_0D^{(n)}X + XA_1D^{(n-1)}X + \dots + XA_{n-1}DX + XA_nX = 0, \\ DXA_0D^{(n)}X + DXA_1D^{(n-1)}X + \dots + DXA_{n-1}DX + DXA_nX = 0, \\ \dots\dots\dots\dots\dots\dots\dots\dots \\ D^{(n-1)}XA_0D^{(n)}X + D^{(n-1)}XA_1D^{(n-1)}X + \dots + D^{(n-1)}XA_{n-1}DXA_nX = 0. \end{gathered} \qquad (26)$$

We consider the homogeneous equation $A_0D^{(n)}X + A_1D^{(n-1)}X + \dots + A_{n-1}DX + A_n = 0$ instead of the original Eq. (10'), so that, on the basis of the equivalence theorem, we can obtain a close solution from the left member of (10') if the initial conditions are taken to be nonzero (equivalent) [cf. (15)].

By integrating this system by parts between the limits of zero and infinity, we obtain a new inhomogeneous system of scalar equations where, as the variables, we consider the integral estimates [20] of the form

$$I_0 = \int_0^\infty (X)^2 dt, \quad I_1 = \int_0^\infty (DX)^2 dt, \dots, \quad I_{n-1} = \int_0^\infty (D^{(n-1)} X)^2 dt.$$

This system establishes the connections I_i ($i = 0, 1, \dots, n-1$) among the equivalent initial conditions $(D^iX)_0$ ($i = 0, 1, \dots, n-1$), the boundary conditions (at infinity) $(D^{(i)}X)_\infty$ ($i = 0, 1, \dots, n-1$), and the matrix coefficient A_i, B_i ($i = 0, 1, \dots, n-1$) or, what amounts to the same thing, the coefficients of matrices A, B, C, H and σ.

Since $(D^{(i)}X)_0$, in its turn, is also expressed in terms of A, B, C, H, and σ (17), and all the $(D^{(i)}X)_\infty = 0$ ($i = 1, 2, \dots, n-1$) (condition for a stable process) and $(X)_\infty$ is given as the new steady-state condition of the system from the static calculations of the system, then Eqs. (26), after integration, can be put in the form

$$\begin{Vmatrix} A_n & -A_{n-2} \dots 0 \\ 0 & A_{n-1} \dots 0 \\ 0 & -A_n \dots 0 \\ \dots & \dots -A_0 \\ 0 & 0 \quad A_1 \end{Vmatrix} \times \begin{Vmatrix} I_0 \\ I_1 \\ \vdots \\ I_{n-1} \end{Vmatrix} = \begin{Vmatrix} G(A, B, C, H, \sigma) \end{Vmatrix} \qquad (27)$$

The determinant of the characteristic matrix is $|E + AC| \neq 0$ (by the Hurwitz condition), so that system (27) is solvable for the I_l. If we now impose on the I_l or on their combinations the requirement that they have minimal value [20-22], we then obtain the relationship sought for the choice of the coefficients for the controllers of the multiloop system.

Let $I_l = I_l(A, B, C, H, \sigma)$. We set up the linear combinations of the integral estimates:

$$\int_0^\infty [\alpha_{0l}(X)^2 + \alpha_{1l}(T_1DX)^2 + \dots + \alpha_{r-1,\,l}(T_{r-1}^{r-1}D^{(r-1)}X)^2]\,dt = \psi_l(A, B, C, H, \sigma) \quad (l = 0, 1, 2, \dots, r). \tag{28}$$

Then the minimum of the functionals will be found by solving the Euler-Lagrange equations.

The parameters A, B^*, C^*, H, σ which satisfy the optimality condition

$$\min \psi_l\ (A, B, C, H, \sigma), \tag{29}$$

will also be sought.

Thus, based on the use of the three principles presented for the synthesis of automatic systems with many variables, we obtain relationships from which we find the optimal coefficients of the controller matrices B and C:

the realizability condition

$$(E + AC)(E + AC)^{-1} = lE,$$

the condition of physical realizability

$$(D^{(i)}X)_0 = \Phi_i(A, B, C, H, \sigma) \leq N_i,$$

the Kulebakin invariance condition

$$(H - AB) = KL,$$

the absolute invariance condition

$$\Delta_{ii} = 0,\ H \equiv 0,\ AB \equiv 0,\ (H - AB) = 0, \tag{30}$$

the selective invariance condition (autonomy criterion)

$$w = SE(D)T,\ s_{ij} = r_{ij} = 0\ (i \neq j),$$

the optimality condition

$$(E + AC)^{-1}(H - AB) = W^*,$$

the optimality condition by the mean square estimate

$$\bar{\varepsilon}^2 = \min,$$

the optimality condition in the integral sense

$$\psi_l\ (A, B, C, H, \sigma) = \min.$$

For systems with many variables, satisfying these relationships presents large computational difficulties. However, if they are reduced to programs for high-speed computers, which permit a large number of computations to be made, then the problem of synthesizing systems with many variables will be solved without a great deal of work.

LITERATURE CITED

1. V. S. Kulebakin, Foreword to the paper of N. N. Luzin, "On the study of the matrix theory of differential equations," Avtomat. i Telemekh. No. 5 (1940).
2. N. N. Luzin, "On the study of the matrix theory of differential equations," Avtomat. i Telemekh., No. 5 (1940).
3. A. S. Boksenbom and R. Hood, General Algebraic Method to Control Analysis of Complex Engine Types. NACA, Rep. 980 (1950).
4. Ts'ien Süeh-sen Engineering Cybernetics [Russian translation] (IL, 1956).
5. M. Colomb and E. Usdin, A Theory of Multidimensional Servosystems, J. Franklin Inst. 253, 1 (1952).
6. R. L. Kavanagh, The Application of Matrix Methods to Multivariable Control Systems, J. Franklin Inst. 262, No. 5 (1956).
7. M. V. Meerov, Structural Synthesis of High-Accuracy Automatic Control Systems [in Russian] (Fizmatgiz, 1959).
8. P. V. Bromberg, Stability and Autooscillations of Sampled-Data Systems [in Russian] (Oborongiz, 1953).
9. E. L. Baranchuk, "On the theory of multidimensional servosystems," Proceedings of the Second All-Union Conference on Automatic Control Theory [in Russian] (Izd. AN SSSR, 1955) 1.
10. R. A. Frazer, W. J. Duncan, and A. R. Collar, Matrix Theory and its Applications to Differential Equations and Dynamics [Russian translation] (IL, 1950).
11. F. R. Gantmakher, Matrix Theory [in Russian] (Gostekhizdat, 1953).
12. V. N. Faddeeva, Computational Methods of Linear Algebra [in Russian] (Gostekhizdat, 1950).
13. P. I. Chinaev, "On the conditions for the equivalent replacement of transfer functions by the operator K(D) representation," Doklady Akad. Nauk SSSR 126, 3 (1959).
14. P. I. Chinaev, "On the question of synthesizing linear connected control systems," Proceedings of the Conference on Invariance Theory and its Applications [in Russian] (Izd. AN USSR, 1959).
15. P. I. Chinaev, "On one method of determining the transient component of motion of automatic systems with arbitrary disturbances," Izv. AN SSSR, Otd. Tekhn. Nauk, Ser. Énergetika i Avtomatika No. 4 (1959).

16. Ya. Z. Tsypkin, Transient and Steady-State Processes in Sampled-Data Circuits [in Russian] (Gosénergoizdat, 1951).

17. V. S. Kulebakin, "On the applicability of the principle of absolute invariance to physically real systems," Doklady Akad. Nauk SSSR 60, 2 (1948).

18. N. N. Luzin and P. I. Kuznetsov, "On absolute invariance and invariance to within ϵ in the theory of differential equations, "Doklady Akad. Nauk SSSR 51, 4 (1946).

19. I. N. Voznesenskii, "On the question of choosing a control scheme for turbine generators," Collected Papers on Soviet Energy Plants [in Russian] (1934) 6.

20. A. A. Fel'dbaum, "Investigation of the dynamics of automatic control systems by the method of a generalized integral criterion," Élektrichestvo No. 7 (1951).

21. A. A. Krasovskii, "Integral estimates and the choice of parameters for automatic control systems," Fundamentals of Automatic Control Theory, edited by V. V. Solodovnikov [in Russian] (Mashgiz, 1954).

22. O. M. Kryzhanovskii, "On numerical integral criteria of optimality of control processes," [in Ukrainian] Dopovidi AN USSR No. 3 (1953).

A METHOD FOR OBTAINING TRANSFER FUNCTIONS OF AUTOMATIC CONTROL SYSTEMS OPERATING ON ALTERNATING CURRENT

N. P. Vlasov

Gor'kii

Translated from Avtomatika i Telemekhanika, Vol. 21, No. 6, pp. 772-778, June, 1960

A general method is suggested for obtaining transfer functions of automatic control systems operating on ac, where the systems are described by linear differential equations with periodic coefficients. The limitations which are thereby imposed on the systems are established. The transfer functions are obtained for several devices, and methods for simplifying them are cited.

In systems operating on ac, the amplitude-modulated oscillations obtained in the modulator pass along the control loop and are applied to a phase detector which separates out the modulating function.

Thus far, the literature has contained no method that would apply without limitation to all systems operating on ac which are described by linear differential equations with periodic coefficients. Below, we present a method which allows the problem posed to be solved.

1. Transfer Function of a Linear Passive Quadripole Connected between an Ideal Modulator and an Ideal Phase Detector

We consider a segment of circuitry (Fig. 1) consisting of an ideal modulator M, a linear passive quadripole and an ideal phase detector D.

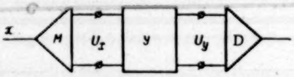

Fig. 1.

Let x(t) be the function at the input of the ideal modulator, which multiplies x(t) by $\cos(\omega_0 t + \varphi)$. At the modulator output we obtain

$$u_x(t) = x(t)\cos(\omega_0 t + \varphi). \qquad (1)$$

Let $u_y(t)$ be the function at the linear quadripole's output and the ideal phase detector's input. The ideal phase detector multiplies the function $u_y(t)$ by $\cos(\omega_0 t + \psi)$. At the phase detector's output we shall have

$$u_g(t) = u_y(t)\cos(\omega_0 t + \psi). \qquad (2)$$

Equations (1) and (2) can be considered as linear equations with periodic coefficients. The quadripole in the circuit is linear and, consequently, is described by linear differential equations. Thus, the entire system under consideration is described by linear differential equations with periodic coefficients.

The Laplace transform of the quadripole's equation has the form

$$U_y(p) = Y(p)\,U_x(p). \qquad (3)$$

Here, Y(p) is the quadripole's transfer function.

The transforms of Eqs. (1) and (2) are

$$U_x(p) = \tfrac{1}{2}[X(p - j\omega_0)e^{j\varphi} + X(p + j\omega_0)e^{-j\varphi}], \qquad (4)$$

$$U_g(p) = \tfrac{1}{2}[U_y(p - j\omega_0)e^{j\psi} + U_y(p + j\omega_0)e^{-j\psi}]. \qquad (5)$$

By substituting $U_x(p)$ from Eq. (4) in Eq. (3), and then substituting $U_y(p)$ from Eq. (3) in Eq. (5), we obtain the following expression for the Laplace transform $U_g(p)$:

$$\begin{aligned} U_g(p) = \frac{1}{4}\{Y(p - j\omega_0)e^{j\psi}[X(p - j2\omega_0)e^{j\varphi} + \\ + X(p)e^{-j\varphi}] + Y(p + j\omega_0)e^{-j\psi}[X(p)e^{j\varphi} + \\ + X(p + j2\omega_0)e^{-j\varphi}]\}. \end{aligned} \qquad (6)$$

The terms $X(p-j2\omega_0)$ and $X(p + j2\omega_0)$ are the transforms of the function x(t), modulated at twice the carrier frequency. We shall assume that the phase detector contains low-frequency filters which do not pass oscillations modulated at twice the carrier frequency. We therefore discard these terms, and rewrite Eq. (6) in the form

$$\begin{aligned} U_g(p) = \frac{1}{4}[Y(p - j\omega_0)e^{j(\psi-\varphi)} + \\ + Y(p + j\omega_0)e^{-j(\psi-\varphi)}]\,X(p). \end{aligned} \qquad (7)$$

We now formulate the conditions whose holding permits the terms $X(p-j2\omega_0)$ and $X(p + j2\omega_0)$ to be discarded.

Let the function Y(p) be represented as the quotient of polynomials

$$Y(p) = \frac{F_1(p)}{F_2(p)}.$$

We shall assume that the polynomials $F_1(p)$ and $F_2(p)$ have no common factors, and that the degree of polynomial $F_2(p)$ is not lower than the degree of polynomial $F_1(p)$. Then, if none of the complex conjugate roots of polynomial $F_2(p)$ has a frequency close, or equal, to the carrier frequency, the aforementioned terms may be discarded.

For the transfer function of the segment of circuitry under consideration, we shall have

$$Y_g(p) = \frac{U_g(p)}{X(p)} = \frac{1}{4}[Y(p - j\omega_0)e^{j(\psi-\varphi)} + \\ + Y(p + j\omega_0)e^{-j(\psi-\varphi)}]. \quad (8)$$

We note that $Y_g(p)$ is a function of the operator p with real coefficients, since it is the sum of two complex conjugate expressions.

We now change the argument of the function $Y_g(p)$ to $S = p/\omega_0$, and we set $\psi - \varphi - \delta$. Then,

$$Y_g(s) = \tfrac{1}{4}[Y(s - j)e^{j\delta} + Y(s + j)e^{-j\delta}]. \quad (9)$$

The transfer function defined by Eqs. (8) and (9) depends, in the general case, on the frequency of the generator which supplies the modulator and the phase detector. Let the quadripole be designed to operate for some definite carrier frequency ω_0, while the generator supplying the modulator and the phase detector has the frequency ω_g. In this case, the transfer function of the series of links of Fig. 1, instead of (8), is given by

$$Y_g(p) = \frac{1}{4}[Y(p - j\omega_g)e^{j(\psi-\varphi)} + \\ + Y(p + j\omega_g)e^{-j(\psi-\varphi)}]. \quad (10)$$

We introduce the parameter $\lambda = \omega_g/\omega_0$.

By making the transition to the operator s in Eq. (10), we obtain, instead of (9), the transfer function

$$Y_g(s, \lambda) = \tfrac{1}{4}[Y(s - j\lambda)e^{j\delta} + Y(s + j\lambda)e^{-j\delta}]. \quad (11)$$

Formula (11) allows one to establish how the transfer function changes as the carrier and generator frequencies move apart.

2. Application of Formulas (8)-(11) to a Differentiating Quadripole, and Some Deductions from the Theory

In ac servosystems, the quadripole whose circuit is shown on Fig. 2 is used as a differentiating loop. The transfer function of such a quadripole can be written in the following way (bearing in mind that the filters on Fig. 2 are symmetric):

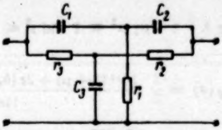

Fig. 2.

$$Y(p) = \frac{p^2 + k_1\omega_0 p + \omega_0^2}{p^2 + k_2\omega_0 p + \omega_0^2} \quad (12)$$

In order to obtain from Y(p) the transfer function for the modulating oscillation, we use the formulas for the approximate transformation of (12):

$$\frac{1}{2p}(p^2 + \omega_0^2) = p'. \quad (13)$$

By using formula (13), we obtain the following expression for the transfer function of the differentiating quadripole's modulating oscillation:

$$Y' = \frac{2p' + k_1\omega_0}{2p' + k_2\omega_0} = \frac{2s' + k_1}{2s' + k_2}. \quad (14)$$

For such a quadripole, we find the transfer function $Y_g(s)$ by means of formula (9):

$$Y_g(s) = \frac{[s^2(s^2+4) + s(k_1+k_2)(s^2+2) + k_1k_2(s^2+1)]\cos\delta + s^2(k_2-k_1)\sin\delta}{2[s^2(s^2+4) + 2sk_2(s^2+2) + k_2^2(s^2+1)]}. \quad (15)$$

We set $s^2 \ll 1$. The meaning of this inequality is very simple. It is known, from Laplace transform theory, that there exists a certain region of values of the parameter p on the complex variable plane for which there is a one-to-one correspondence between the original time domain function and its transform. The inequality $s^2 \ll 1$ isolates, in this region, some subregion in which the approximate function $Y_g(s)$ can be used. For $\delta = 0$, this approximate function has the form

$$Y_g(s) = \frac{1}{2}\frac{(2s + k_1)}{(2s + k_2)}. \quad (16)$$

The function $Y_g(s)$ coincides to within a factor of 1/2 with (14). The factor 1/2 is the transfer factor of an ideal modulator and an ideal phase detector.

We now compute the differentiating quadripole's transfer function for deviations of the carrier from the generator frequency.

By using formula (11), we obtain

$$Y_g(s) = \frac{1}{2}\frac{[c + s(k_1 + k_2)(s^2 + \lambda^2 + 1) + k_1k_2(s^2 + \lambda^2)]\cos\delta + (k_2 - k_1)\lambda(s^2 + \lambda^2 - 1)\sin\delta}{[c + 2sk_2(s^2 + \lambda^2 + 1) + k_2^2(s^2 + \lambda^2)]}, \tag{17}$$

where

$$c = s^2(s^2 + 2\lambda^2 + 2) + (\lambda^2 - 1)^2.$$

By setting $\lambda = 1 + \mu$, $\mu^2 \ll 1$ and $s^2 \ll 1$, we find the approximate transfer function

$$Y_g(s) = \frac{1}{2}\frac{[4s^2(1 + \mu) + 2s(k_1 + k_2)(1 + \mu) + k_1k_2(1 + 2\mu)]\cos\delta + 2(k_2 - k_1)\mu\sin\upsilon}{[4s^2(1 + \mu) + 4sk_2(1 + \mu) + k_2^2(1 + 2\mu)]}. \tag{18}$$

Computations showed that, for $s \le 0.3$, the transfer functions computed by formulas (15) and (16) were sufficiently close.

Analogous results were provided by calculations with formulas (17) and (18) for $\mu = \pm 0.1$. The curves constructed from formulas (17) and (18) are analogous to those given in [1].

With certain assumptions [3], the following function is found at the Selsyn modulator's output:

$$u_x(t) = U_m\left[x(t)\cos(\omega_0 t + \psi) + \frac{1}{\omega_0}\frac{dx}{dt}\sin(\omega_0 t + \varphi)\right]. \tag{19}$$

For the transfer function of the circuit segment consisting of a modulator, a linear quadripole and a phase detector, we obtain

$$Y_g(s) = \frac{U_m}{4} j[(s - j)Y(s - j)e^{j\delta} - (s + j)Y(s + j)e^{-j\delta}]. \tag{20}$$

Let the quadripole in the circuit under consideration be inertialess with gain $Y(s) = k_0$. We may then write

$$Y_g(s) = \frac{U_m}{2} k_0(\cos\delta + s\sin\delta). \tag{21}$$

In this case, for the proper choice of phase angles φ and ψ, the circuit under consideration is equivalent to a differentiating link [3].

We derive still one more conclusion from the results obtained.

In the circuit segment between the modulator and the phase detector, let there be connected in series two directed links, with transfer functions $Y_1(p)$ and $Y_2(p)$. By using the method presented, we obtain the transfer function for the modulating oscillation in the form

$$Y_g(s) = \frac{1}{4}[Y_1(s - j)Y_2(s - j)e^{j\delta} + Y_1(s + j)Y_2(s + j)e^{-j\delta}]. \tag{22}$$

Suppose the transfer functions Y'_1 and Y'_2 for both links can be found by a transformation using operation (13). If one forms the function $Y' = Y'_1Y'_2$, this function will obviously not be equivalent to function (22). Since it is necessary to have modulators and phase detectors in servo and automatic control systems operating on ac, it is then obviously impossible to seek the circuit's transfer function for the modulating oscillation by transforming each link separately in accordance with formula (13); the circuit as a whole must be transformed.

3. Servosystem with a Two-Phase Asynchronous Motor

We now consider a servosystem in which the phase detector is a two-phase asynchronous motor. We find the system's transfer function, and answer the question as to whether it is possible to transform the circuit links con-

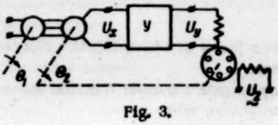

Fig. 3.

nected in the control loop separately from the phase detector, the asynchronous motor. This is frequently the method employed in investigating this system. The servosystem's schematic is shown in Fig. 3. We now write the system's equations:

the equation of the differential

$$\theta_1 - \theta_2 = x(t), \tag{23}$$

the equation of the ideal modulator

$$u_x(t) = x(t)U_m \cos(\omega_0 t + \varphi), \tag{24}$$

the transformed equation of the quadripole

$$U_y(p) = Y(p)U_x(p), \tag{25}$$

the equation of motor rotation

$$J\frac{d^2\theta_2}{dt^2} = M_e(t) - M_r(t), \tag{26}$$

where

$$M_e(t) = \frac{1}{r}\left[\psi_a u_2 - \psi_b u_y - \frac{d\theta_2}{dt}(\psi_b^2 + \psi_a^2)\right]. \tag{27}$$

Here, ψ_a and ψ_b are the stator winding flux linkages, $\underline{r}$ is the rotor resistance, $u_y = d\psi_a/dt$, $u_2 = d\psi_b/dt$;

$$u_2 = U_{2m} \sin(\omega_0 t + \psi), \tag{28}$$

is the voltage on the stator's second winding.

We assume that

$$M_r(t) = k\, d\theta_2/dt. \tag{29}$$

We also assume, as is frequently done, that

$$\psi_a^2 \ll \psi_b^2$$

and discard the ψ_a^2 in the right member of Eq. (27). Then, Eqs. (23)-(26) which describe the scheme will be linear equations with periodic coefficients. Equation (25) is written for the Laplace transformed equation. We apply the Laplace transform to the other equations just enumerated. By solving the transformed equations for $\Theta_2(p)$ and then discarding the terms for twice the carrier frequency, we obtain the following expression for the transfer function, written in terms of the operator $\underline{s}$:

$$\frac{\theta_2(s)}{X(s)} = \frac{1}{T_2 s(T_1 s + 1)}\left[\frac{s - j2}{s - j}Y(s - j)e^{j\delta} + \frac{s + j2}{s + j}Y(s + j)e^{-j\delta}\right]. \tag{30}$$

Here, T_1 and T_2 are dimensionless constants.

Let the quadripole in the circuit be inertialess, with gain k_0. Then, instead of (30), we shall have

$$\frac{\theta_2(s)}{X(s)} = \frac{2k_0[(s^2 + 2)\cos\delta + s\sin\delta]}{T_2 s(T_1 s + 1)(s^2 + 1)}. \tag{31}$$

In the system considered, the asynchronous motor is the sole link with an operator transfer factor. A formula analogous to (31) was obtained by I. M. Sadovskii [4].

The transfer function is simplified still further if we set $\delta = 0$ and $s^2 \ll 1$.

Then,

$$\frac{\theta_2(s)}{X(s)} = \frac{4k_0}{T_2 s(T_1 s + 1)}. \tag{32}$$

In this form, the transfer function of the asynchronous motor is used in many works (for example, in [5]).

It follows from expressions (30) and (31) that it is impossible to present the system's transfer function as the product of the transfer functions of the quadripole and the asynchronous two-phase motor.

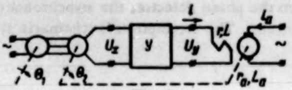

Fig. 4.

4. Servosystem with a Single-Phase Commutator Motor

1. Control is effected on the side of the excitation winding (Fig. 4). Such a system was investigated by E. I. Chernov, and the transfer function was obtained for it by means of a very cumbersome mathematical apparatus (integration by means of infinite series) with rigid limitations (the action of unit input functions and a simplified transfer function of the differentiating quadripole were considered) [6]. We now write the system's equations. As the equations for the differential, modulator and quadripole, we use Eqs. (23), (24) and (25), respectively.

The equation of the excitation winding circuit is

$$u_y(t) = ir + L\frac{di}{dt}, \tag{33}$$

the equation of the armature circuit

$$u(t) = i_a r_a + L_a \frac{di_a}{dt} + Ci\frac{d\Theta_2}{dt}, \tag{34}$$

the equation of armature rotation

$$J\frac{d^2\Theta_2}{dt^2} = Cii - M_r(t). \tag{35}$$

It was assumed in [6] that the two last terms in the right member of Eq. (34) are small. We shall make the assumption that the last term, which makes the equation nonlinear, is small. With this condition, if u(t) is a sinusoidal function of time, then $i_a(t)$ is also a sinusoidal function.

We set

$$i_a = I_m \cos(\omega_0 t + \psi) \tag{36}$$

and take Eq. (29) for $M_r(t)$.

By transferring to the transforms of these equations and then solving them for $\Theta_2(p)$, dropping the terms modulated by twice the carrier frequency, we obtain the following equation for the transfer function:

$$\frac{\Theta_2(s)}{X(s)} = \frac{1}{T_2 s\,(T_1 s + 1)}\left[\frac{Y(s - j)\,e^{j\delta}}{1 + T_a(s - j)} = \frac{Y(s + j)\,e^{-j\delta}}{1 + T\ \ (s + j)}\right]. \tag{37}$$

Here T_1, T_2 and T_a are dimensionless constants.

No limitations are placed on either the signal or the quadripole's transfer function in formula (37).

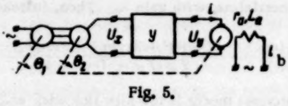

Fig. 5.

2. System with control on the armature side (Fig. 5). We again make use of Eqs. (23)-(25), and we write the motor equations as follows:

the equation of the armature circuit

$$u_y(t) = ir_a + L_a\frac{di}{dt} + Ci_b\frac{d\Theta_2}{dt}, \tag{38}$$

the equation of armature rotation

$$J\frac{d^2\Theta_2}{dt^2} = Ci_b i - M_r(t). \tag{39}$$

We take

$$i_b = I_m \cos(\omega_0 t + \psi), \tag{40}$$

and we use Eq. (29) for $M_r(t)$.

By transferring to the transforms of these equations and then solving them for $\Theta_2(p)$, dropping the terms modulated by twice the carrier frequency, we obtain the following expression for the transfer function:

$$\frac{\Theta_2(s)}{X(s)} = \frac{1}{2}\,\frac{Y(s-j)\,[T_a(s+j)+1]\,e^{j\delta} + Y(s+j)\,[T_a(s-j)+1]\,e^{-j\delta}}{T_k s\,\{k_m(T_m s+1)\,[(T_a s+1)^2 + T_a^2] + T_a s + 1\}}. \tag{41}$$

There is no difficulty in obtaining the transfer function for servosystems with feedback, for systems stabilized by differentiating quadripoles, etc. The necessary condition remains the linearity of the equations which describe the system.

SUMMARY

1. The method presented permits one to obtain the transfer functions for servosystems and automatic control systems operating on ac, for circuit configurations of any degree of complexity. These functions can be investigated by the methods used in the investigation of dc systems. The systems must be described by linear differential equations with periodic coefficients.

2. The method makes it possible to establish the limitations which must be imposed on the circuit configuration in order that, for the investigation, one might discard the terms modulated by twice the carrier frequency, such terms arising in systems of this nature.

3. The transfer functions for the discrepancies of the carrier and generator frequencies are obtained.

4. It was shown that the transfer functions obtained by this method can be simplified by using the inequality $s^2 \ll 1$.

5. The method can be used for investigating mixed systems in which only part of the links operate on ac.

LITERATURE CITED

1. N. Z. Litvin-Sedov (ed.), Correcting Circuits in Automation: Collection [Russian translation](IL, 1954).
2. H. M. James, N. B. Nichols and R. S. Phillips, Theory of Servomechanisms [Russian translation] (IL, 1951).
3. D. Morris, "Theoretical and experimental methods of analyzing envelopes of modulated signals in ac servosystems," Automatic Control (collected papers of the Conference at Cranfield, 1951) [Russian translation] (IL, 1959).
4. I. M. Sadovskii, "Asynchronous servomotors as control system elements," Automat. i Telemekh. 13, 1 (1952).
5. A. A. Fel'dbaum, Electrical Systems of Automatic Control [in Russian] (Oborongiz, 1957).
6. E. L. Chernov, "Investigation of low-power ac servomechanisms," Avtomat. i Telemekh. 13, 1 (1952).

DETERMINATION OF DYNAMIC CHARACTERISTICS OF CHEMICAL ENGINEERING APPARATUS AS WELL AS THE RELEVANT CRITERIA OF PERSISTENCE AND CONTROLLABILITY

B. N. Devyatov

Novosibirsk

Translated from Avtomatika i Telemekhanika, Vol. 21, No. 6, pp. 779-790, June, 1960

Nonstationary processes in moving media are considered from the point of view of the control problem for a broad class of technological apparatus operating on the counterflow principle.

The criteria of persistence and controllability of continuous processes in moving media are defined with the aim of explaining their dependence on the apparatus parameters and mode of operation.

INTRODUCTION

Until now, in the design of technological apparatus no investigation was ordinarily made of the stability of the chosen mode of operation or of the possibilities of controlling it.

In some cases, the very simplest controller provides sufficient accuracy of process flow, while sometimes this cannot be provided by a very complicated and expensive controller. Sometimes, the cost of the controller can exceed the cost of the plant itself.

Today, the automation of chemical engineering apparatus entails controllers which, as a rule, are designed for a preexisting plant, and any changes in the plant to improve stability or controllability become either impossible or extremely difficult. In many cases, the operation of new technological systems is impossible without automatic control.

In connection with what has just been said, it becomes very important to study the plant as a basic link in the automatic control system. The problems of optimal parameters of the plant and of the controller must be solved simultaneously and compatibly. The general posing of the problem was given by V. S. Kulebakin at the Second All-Union Conference on Automatic Control [1].

It is from this point of view that the present paper solves the problem of analyzing the persistence and controllability of processes in the widely used apparatus of chemical technology.

For widely used types of engineering continuous-flow apparatus, a characteristic of the processes is the interaction of the media along the entire path of their motion by the principle of direct flow or, even more frequently, by the counterflow principle. Therefore, in considering the questions of control of continuous processes, one must solve the general nonstationary problem of the interaction processes of the moving media in these apparatus.

As apparatus of this type we have: heat exchangers, absorbers, scrubbers, extractors, fractionating columns, roasting ovens, etc. In all of these devices, the speed of interaction of the moving media is basically determined by the difference in concentration at their boundary surfaces, analogous to the circumstance that heat transmission is basically determined by the temperature difference of the interacting media.

In the present work, the problem is considered in terms of the example of implementing a process by the counterflow method, although the corresponding results can also be obtained for the case of direct flow.

I. Basic Equations of Nonstationary Processes of Moving Media Interaction in Engineering Apparatus

1. We consider heat exchangers with thin walls [2, 3] and, simultaneously, apparatus with diffusion processes (absorbers, scrubbers, extractors, etc.) without taking account of the thermal effect of the reactions in them.

Let u(x, t) and v(x, t) be the relative temperatures* (or, for other apparatus, the corresponding concentrations) of the moving media, where x is the coordinate of the apparatus cross section, measured in the direction of motion of medium u.

If, in the course of time t, the ideally mixed fluid portions touch one another along some boundary surface with thermal resistance or, as the case may be, with diffusion resistance, then

$$\frac{du}{dt} = k_1(v-u), \qquad \frac{dv}{dt} = k_2(u-v),$$

where k_1 and k_2 are positive constants. With these conditions, we easily convince ourselves, by the use of the concept of a function's complete differential, that the general equations for the interaction of moving media,

---

[*] For the unit of measurement of u and v we take the value u(0, 0) in the transient response and, as the zero of measurement, we take the value v(l, 0), where l is the length of the apparatus.

in the case of counterflow† have the form

$$\frac{\partial u}{\partial t} + w_1 \frac{\partial u}{\partial x} = k_1 (v - u), \qquad \frac{\partial v}{\partial t} - w_2 \frac{\partial u}{\partial x} = \\ = k_2 (u - v). \tag{1}$$

With this, $k_1 = kp/s_1c_1\gamma_1$ for heat exchangers. Here, k is the heat transmission factor, p is the perimeter of the lateral cross section of the surface separating the media, s_1 is the area of the lateral cross section of the first medium, c_1 is heat capacity, γ_1 is specific weight, w_1 and w_2 are the absolute values of the linear velocities of the moving media and k_2 is the corresponding coefficient for the second medium.

Obviously, for other apparatus, certain of these constants are replaced by others which express the analogous laws of diffusion.

The solutions of these equations will depend on the initial and the boundary conditions

$$u(x, 0) = u(x), \; v(x, 0) = v(x);$$

for direct flow

$$u(0, t) = \varphi_1(t), \; v(0, t) = \psi_1(t)$$

for counterflow

$$u(0, t) = \varphi_2(t), \; v(l , t) = \psi_2(t).$$

With the methods of operational calculus, the problem can be conveniently solved for any initial and boundary conditions for either direct flow or counterflow.

2. We now consider the more general case of heat exchangers, namely, heat exchangers with thick walls.

In the transient mode we shall take into account the thermal capacity of the walls separating the two media, ignoring, with this, the heat flux along the walls and the transient responses in the directions of the walls' lateral cross sections.

In the given case, the equations for counterflow have the form [4]

$$\begin{aligned} &\frac{\partial T_1}{\partial t} + \frac{\partial T_1}{\partial x} w_1 = k_1(T - T_1), && T_1 = T_1(x, t), \\ &\frac{\partial T}{\partial t} = k_2 (T_1 - T) + k_3 (T_2 - T), && T = T(x, t), \\ &\frac{\partial T_2}{\partial t} - \frac{\partial T_2}{\partial x} w_2 = k_4 (T - T_2), && T_2 = T_2(x, t), \end{aligned} \tag{2}$$

where k_1, k_2, k_3 and k_4 are constants; T, T_1, and T_2 are the temperatures of the walls and the moving media at cross section x in relative units.

3. Further, with account taken of the walls' thermal capacity and of the distribution of heat along the walls, the equations of the nonstationary heat exchange assume the form

$$\begin{aligned} &\frac{\partial T_1}{\partial t} + \frac{\partial T_1}{\partial x} w_1 = k_1 (T - T_1), \\ &\frac{\partial T}{\partial t} - a \frac{\partial^2 T}{\partial x^2} = k_2 (T_1 - T) + k_3 (T_2 - T), \\ &\frac{\partial T_2}{\partial t} - \frac{\partial T_2}{\partial x} w_2 = k_4 (T - T_2). \end{aligned} \tag{3}$$

With this, a is a constant which corresponds to the heat distribution along the walls.

4. If one considers general Eqs. (1) for the nonstationary processes in moving media as applied to apparatus in which chemical reactions occur, then one can obtain a generalization of these equations when account is taken of the reactions' thermal effects. With this, the question is considered only in a first approximation (the problem is linearized).

In the general case, the equations of the nonstationary processes take the form

$$\begin{aligned} &\frac{\partial u}{\partial t} + \frac{\partial u}{\partial x} w_1 = \alpha_1 u + \beta_1 v + \gamma_1 T_1 + \delta_1 T_2, \\ &\frac{\partial v}{\partial t} - \frac{\partial v}{\partial x} w_2 = \alpha_2 u + \beta_2 v + \gamma_2 T_1 + \delta_2 T_2, \\ &\frac{\partial T_1}{\partial t} + \frac{\partial T_1}{\partial x} w_1 = \alpha_3 u + \beta_3 v + \gamma_3 T_1 + \delta_3 T_2, \\ &\frac{\partial T_2}{\partial t} - \frac{\partial T_2}{\partial x} w_2 = \alpha_4 u + \beta_4 v + \gamma_4 T_1 + \delta_4 T_2, \end{aligned} \tag{4}$$

where u, v, T_1 and T_2 are indices of concentration and temperature in their proper relative units; α_i, β_i, γ_i, δ_i ($i = 1, 2, 3, 4$) are constants of the linear approximation.

If the reaction in the apparatus occurs in a diffusion region, then with account taken of the thermal effect in a first approximation, these equations, in the particular case, take the simpler form

$$\begin{aligned} &\frac{\partial u}{\partial t} + \frac{\partial u}{\partial x} w_1 = k_1 (v - u) + m_1 v + m_2 T_2, \\ &\frac{\partial v}{\partial t} - \frac{\partial v}{\partial x} w_2 = k_2 (u - v) - m_3 v - m_4 T_2, \\ &\frac{\partial T_1}{\partial t} + \frac{\partial T_1}{\partial x} w_1 = a_1 (T_2 - T_1), \\ &\frac{\partial T_2}{\partial t} - \frac{\partial T_2}{\partial x} w_2 = a_2 (T_1 - T_2) + \\ &+ a_3 [k_2 (u - v) - m_3 v - m_4 T_2], \end{aligned} \tag{5}$$

where k_i, a_i ($i = 1, 2$) and m_j ($j = 1, 2, 3, 4$) are the corresponding constants. Small changes in the k_i are compensated approximately by the proper choice of the m_j.

II. Equations of Stationary Processes of Moving Media Interaction in Engineering Apparatus

Under the conditions of a stationary mode of operation, the basic system of partial differential equations obtained becomes a system of ordinary differential equations. The solutions are obtained in an elementary manner in the form of linear combinations of characteristic (eigen) functions, and depend on the roots of the corresponding characteristic equations.

1. For the case corresponding to the general Eqs. (1), we get

$$w_1 = \frac{du}{dx} = k_1(v - u); \quad w_2 \frac{dv}{dx} = k_2(v - u).$$

---

† In the given case, and in the sequel, the equations for direct flow processes are obtained by replacing w_2 by $-w_2$.

The characteristic equation has the form

$$\lambda^2 - \left(\frac{k_2}{w_2} - \frac{k_1}{w_1}\right)\lambda = 0.$$

2. For the second case, that of general Eqs. (2), with account taken of the walls' thermal capacity, the steady-state equations are simplified, and assume a form analogous to the foregoing:

$$w_1 \frac{dT_1}{dx} = \bar{k}_1 (T_2 - T_1), \quad w_2 \frac{dT_2}{dx} = \bar{k}_2 (T_2 - T_1),$$

$$\lambda^2 - \left(\frac{\bar{k}_2}{w_2} - \frac{\bar{k}_1}{w_1}\right)\lambda = 0,$$

where

$$\bar{k}_1 = \frac{k_1 k_3}{k_2 + k_3}, \qquad \bar{k}_2 = \frac{k_2 k_4}{k_2 + k_3}.$$

In the conditions of the steady state, this corresponds completely to the physical meaning of the assumptions made earlier.

3. For the steady state of a heat exchanger when account is taken of heat flux along the walls, one obtains from general Eqs. (3) a system of ordinary differential equations which leads to a fourth-degree characteristic equation. With this, one of the roots equals zero, while the remaining three roots are found from the third-degree equation

$$\lambda^3 + \left(\frac{k_1}{w_1} - \frac{k_4}{w_2}\right)\lambda^2 - \left(\frac{k_3}{a} + \frac{k_1 k_4}{w_1 w_2} + \frac{k_2}{a}\right)\lambda + $$
$$+ \left(\frac{k_2 k_4}{a w_2} - \frac{k_1 k_3}{a w_1}\right) = 0.$$

4. In the remaining two cases, one obtains the corresponding fourth-degree characteristic equations.

III. Determination of the Transient Responses from the Basic Equations of Moving Media Interaction in Apparatus for the Case of Counterflow

Using the methods of operational calculus, one can easily solve the problem for direct flow and for counterflow for various methods of disturbing the steady state. In practice, these disturbances might be disturbances in concentration (or temperature), in the velocities of the moving media, and also in the volume of reagent applied to the input of the apparatus. Obtaining exact solutions for the most general equations is arduous. In those cases when such solutions can be found in general form, they are inconvenient, due to the complicated structure and the unwieldiness of the expressions.

It is convenient to carry out the analysis of quality of transient responses by operator methods, using as a basis their approximate representation by means of a series expansion of the transforms, as this was done in the monographs of A. V. Lykov [5] for the classical problem of heat conduction in nonmoving media. Such a choice of the approximate solution corresponds completely to the method of small disturbances which, in many cases, can be made basic to the investigation of transient responses from the point of view of the control problem.

However, while retaining coincidence of the approximate and exact curves of the transient response in the neighborhood of the initial point, we can also achieve their complete coincidence at the end point – in the steady state. With this, we employ an exponential law for the approximate solution‡ with the proper choice of the undefined coefficients in accordance with two conditions:

a) a common point and a common tangent with the curve of the exact solution at the beginning of the process;

b) a common asymptote as t → ∞.

The solution has the form

$$u\,\Big|\text{ or }\; T_1\Big| = \begin{cases} 0 & \text{for } t < \tau \\ \varphi(t-\tau) & \text{for } t > \tau,\; \varphi(t) = \end{cases}$$
$$= m - ne^{-rt}, \tag{6}$$

where τ is the lag time, and m, n and r are determined in correspondence with conditions a) and b) for the given form of basic equations and the method of disturbing the steady state.

We consider some examples.

1. The transient response of the first medium at the apparatus output for a unit step disturbance of its concentration (or temperature) at the input. In the descriptions of the transient responses we shall introduce dimensionless complex parameters and, as the unit of time, we choose $(\tau_1 + \tau_2)/2$ $(\tau_1 = l/w_1,\ \tau_2 = l/w_2)$.

By assuming zero initial conditions, we find the expression for the curve of the transient response in the form of (6) with the corresponding relationships for m, n and r, while taking $\tau = 2/(1 + (w_1/w_2))$.

For general Eqs. (1), we get

$$m - n = e^{-2\alpha}, \quad nr \doteq 2\alpha\beta e^{-2\alpha}, \quad m =$$
$$= \frac{(\alpha - \beta)\, e^{2(\beta-\alpha)}}{\alpha - \beta\, e^{2(\beta-\alpha)}}.$$

Here, the two dimensionless complex parameters are

$$\alpha = \frac{lk_1}{2w_1}, \quad \beta = \frac{lk_2}{2w_2}.$$

For general Eqs. (2) we get

$$m - n = e^{-2\left(1+\frac{k_2}{k_3}\right)\alpha}, \quad nr =$$
$$= 2\alpha^2\left(1 + \frac{k_2}{k_3}\right)\left(\frac{k_2}{k_1} + \frac{\beta}{\alpha}\frac{k_3}{k_4}\right) e^{-2\left(1+\frac{k_2}{k_3}\right)\alpha},$$
$$m = \frac{(\alpha - \beta)\, e^{2(\beta-\alpha)}}{\alpha - \beta e^{2(\beta-\alpha)}},$$

where there are now four dimensionless parameters which,. in the given case, have the form

---

‡ In the first approximation, the exponential law is generally characteristic of processes flowing at the expense, as it were, of a loss of activity. This is attested by theoretical considerations and much experimental data.

$$\alpha = \frac{\bar{k}_1 l}{2w_1}, \quad \beta = \frac{\bar{k}_2 l}{2w_2}, \quad \frac{k_2}{k_3}, \quad \frac{k_3}{k_4}.$$

Note: With the given method of disturbing the steady state, the sole case of general equations of the form of (3) requires special consideration, since the curve of the transient response will have a break at time $t = 2/(1 + (w_1/w_2))$.

For general Eqs. (4), the quantity m, as in the previous cases, is simply determined from the conditions for the new steady state, while n and r are determined from the following relationships:

$$m - n = \frac{1}{2}\left(1 + \frac{1}{k}\right)\varepsilon_1 + \frac{1}{2}\left(1 - \frac{1}{k}\right)\varepsilon_2, \quad nr =$$
$$= \left(1 + \frac{1}{k}\right)\frac{l^2(\beta_1\alpha_2 + \delta_1\alpha_4)}{4w_1w_2} \times \left(\varepsilon_1 - \frac{1-k}{1+k}\varepsilon_2\right) -$$
$$- \frac{(1-k^2)}{2k^2}\frac{l}{2w_2}\left(\frac{\beta_1\alpha_2 + \delta_1\alpha_4 - \beta_2\gamma_2 - \delta_2\gamma_4}{\alpha_1 - \gamma_3} - \frac{\beta_2\alpha_2 + \delta_2\alpha_4}{2\alpha_3} -\right.$$
$$\left. - \frac{\beta_1\gamma_2 + \delta_1\gamma_4}{2\gamma_1}\right)(\varepsilon_1 - \varepsilon_2),$$

where

$$\varepsilon_1 = \exp\frac{[(1+k)\alpha_1 + (1-k)\gamma_3]\,l}{2w_1},$$
$$\varepsilon_2 = \exp\frac{[(1-k)\alpha_1 + (1+k)\gamma_3]\,l}{2w_1},$$
$$k = \sqrt{1 + \frac{4\gamma_1\alpha_3}{(\alpha_1 - \gamma_3)^2}}.$$

With this, the dimensionless complex parameters are introduced in correspondence with the structure of the expressions found.

For Eqs. (5), a particular case of (4), the corresponding relationships for m, n and r have the form

$$m - n = e^{-2\alpha}, \quad nr = e^{-2\alpha}\, 2\beta(\alpha + \alpha_{11} + \alpha_{23}),$$

where the following four dimensionless parameters have been introduced:

$$\alpha = \frac{lk_1}{2w_1}, \quad \beta = \frac{lk_2}{2w_2}, \quad \alpha_{11} = \frac{lm_1}{2w_1}, \quad \alpha_{2.3} = \frac{lm_2a_3}{2w_1}.$$

2. Transient response of the first medium at the output for a step disturbance of its linear velocity from w_1 to w_1 instantaneously over the entire length of the apparatus.

The question posed is meaningful basically for heat exchange apparatus. For the initial conditions, we take the condition of stationary (steady) apparatus mode of operation.

Despite the fact that, in the given case, the problem is nonlinear, the corresponding values of m, n and r will be easily computed for all three forms of the basic equations, (1), (2) and (3). With this, we always have $\tau = 0$, $m - n = 0$, where m is defined from the conditions of the new steady state for each case. Thus, for example, for the simplest general equations, (1) and (2), we obtain

$$r = \frac{\alpha e^{2(\beta-\alpha)}}{m\,[\beta e^{2(\beta-\alpha)} - \alpha]}\frac{w_1}{w_1}\left(1 + \frac{w_1}{w_2}\right)(\beta - \alpha)$$

for the proper expressions for α and β for each case.

3. Transient response of the first medium at the output for a step variation of the volume of reagent applied at the input while the concentration and linear velocity are maintained.** Such a posing of the problem is meaningful for all the apparatus considered, not just for heat exchangers. As before, we take the steady-state conditions to be the initial conditions.

As in the previous case, the problem is nonlinear but, for Eqs. (1), also leads to a simple solution, which can be extended as well to the more complicated Eqs. (4) and (5).

The results of the theoretical analysis of the transient responses in moving media are found to be in correspondence with the existing experimental data, obtained both under laboratory conditions and in factories. The theoretical and experimental curves of the transient responses, as well as for individual data — obtained in parallel experiments — are in good agreement.

As an illustration, Fig. 1 shows the theoretical (1) and experimental (2) curves for the transient responses in the case of Eqs. (1) for a step disturbance of the temperature of one of the media.

IV. Transfer Functions and Block Schematics of Engineering Apparatus as Objects of Control (Plants)

On the basis of Eqs. (1)-(5) of nonstationary processes in engineering apparatus, one can find the corresponding transfer functions, and construct the block schematics. With this, one can find either exact or approximate expressions for the transfer functions.

In particular, when we have to do with basic Eqs. (2) or (1), for the case of counterflow, we obtain the block schematic shown in Fig. 2.

Here,

$$K_{11}(p) = \frac{U_{\text{out}}(p)}{U_{\text{in}}(p)} \quad \text{for } V_{\text{in}} = 0;$$

$$K_{22}(p) = \frac{V_{\text{out}}(p)}{V_{\text{in}}(p)} \quad \text{for } U_{\text{in}} = 0.$$

$$K_{12}(p) = \frac{V_{\text{out}}(p)}{U_{\text{in}}(p)} \quad \text{for } V_{\text{in}} = 0;$$

$$K_{21}(p) = \frac{U_{\text{out}}(p)}{V_{\text{in}}(p)} \quad \text{for } U_{\text{in}} = 0.$$

If, as the unit of time, we take $(\tau_1 + \tau_2)/2$, letting $q = p(\tau_1 + \tau_2)/2$, then the exact expressions for the transfer functions will have the form††

** From which one immediately can obtain the solution of the problem with the condition that the volume and the concentration of the reagent applied at the input simultaneously change by jumps.

†† For the case of general Eqs. (1), all the expressions given below are considered in the limit as $\alpha_2, \alpha_3 \to \infty$.

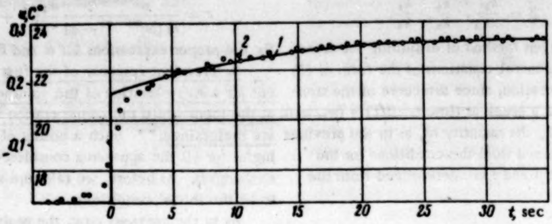

Fig. 1.

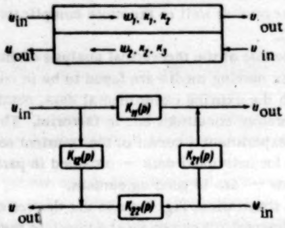

Fig. 2.

$$K_{11}(q) = e^{A(q)} W(q), \quad K_{22}(q) = e^{-A(q)} W(q)$$

$$K_{12}(q) = 2\beta \frac{(1 + qT_2)(1 + qT_3)}{1 + qT_{23}} \frac{\operatorname{sh} B(q)}{B(q)} W(q),$$

$$K_{21}(q) = 2\beta \frac{w_2}{w_1} \frac{1}{1 + qT_{23}} \frac{\operatorname{sh} B(q)}{B(q)} W(q),$$

where

$$W(q) = \frac{1}{\operatorname{ch} B(q) + \frac{C(q)}{B(q)} \operatorname{sh} B(q)},$$

$$B(q) = \sqrt{C^2(q) - 4\alpha\beta \frac{(1 + qT_2)(1 + qT_3)}{(1 + qT_{23})^2}},$$

$$A(q) = q \frac{\frac{w_1}{w_2} - 1}{\frac{w_1}{w_2} + 1} + \beta \frac{1 + qT_2}{1 + qT_{23}} - \alpha \frac{1 + qT_3}{1 + qT_{23}},$$

$$C(q) = q + \beta \frac{1 + qT_2}{1 + qT_{23}} + \alpha \frac{1 + qT_3}{1 + qT_{23}},$$

$$T_2 = \frac{2}{1 + \frac{w_1}{w_2}} \frac{1}{\alpha_2}, \quad T_3 = \frac{2}{1 + \frac{w_1}{w_2}} \frac{1}{\alpha_3}, \quad T_{23} = \frac{2}{1 + \frac{w_1}{w_2}} \frac{1}{\alpha_2 + \alpha_3}.$$

There are thus five dimensionless complex parameters in the transfer functions obtained: α, β, w_1/w_2, $\alpha_2 = l k_2/2w_1$, $\alpha_3 = l k_3/2w_1$.

The approximate representation of transfer function K_{11}, found from the corresponding expression for the transient response (6) has the form

$$\overline{K}_{11}(q) = m \frac{1 + q \frac{m - n}{m} \frac{1}{r}}{1 + q \frac{1}{r}} \exp\left(-q \frac{2}{1 + \frac{w_1}{w_2}}\right).$$

An analogous expression is obtained for $\overline{K}_{22}$ by considering transient response (6) for the other medium.

From the approximateexpressions $\overline{K}_{11}$ and $\overline{K}_{22}$ for basic Eqs. (1), (2), (4), and (5), one can easily observe the dependence of these transfer functions on the parameters and operating mode of the apparatus.

V. Definition of the Universal Characteristics of Persistence and Controllability for the Class of Apparatus Operating on the Counterflow Principle

From the theoretically obtained expressions (1) for the transient responses, one can find the characteristics of persistence and controllability of processes in engineering apparatus.

The persistence criterion S is introduced as a generalization of the plant's time constant [3]. The persistence S is defined as the magnitude of the area included between the curve of the transient response and the horizontal line corresponding to the value of the new steady state (Fig. 3). In accordance with this definition, $S = \int_0^\infty [1 - \bar{u}(t)]dt$ ‡‡

where $\overline{u}(t)$ is the expression for the transient response at the output of the apparatus (for the temperature or concentration of the reagent, respectively).

With respect to the ease of controlling a process, the positive effect of persistence, and the adverse effect of lag are well known. Consequently, as the controllability criterion R for the mode of apparatus operation, one can take the relative magnitude of the persistence (as compared with the magnitude of the lag time) $R = S/\tau$.

By thus defining the persistence and controllability of a process (S and R), we can find their general expressions for all the cases considered of basic equations and disturbing actions.

With this, using relationship (6), we find that

$$S = \frac{1}{m} \int_0^\infty n e^{-rt} dt = \frac{n}{rm}.$$

---

‡‡ In the particular cases, which arise frequently in technology, when the expression for the transient response has the form $y = 1 - \exp(-t/T_a)$, we obtain $S = T_a$, where T_a is the plant's time constant.

In case of a dependency of the transient response on the initial conditions, the quantity S is even more meaningful, since it characterizes the persistence of the given initial steady state of apparatus operation. In the determination of the analytic expressions for the persistence and controllability characteristics in each case, the dimensionless complex parameters of the apparatus and its operating mode are introduced in the proper fashion.

We note that, in a control process, an action on the first medium is frequently effected by means of the second medium. Consequently, in defining controllability, it is reasonable to also take into account the other lag time by using the arithmetic mean $\tau = (\tau_1 + \tau_2)/2$. If, moreover, τ is taken as unity, then R = S.

We adduce several examples:

1. For disturbances of concentration (or, respectively, of temperature), we get:

a) for the case of general Eqs. (1),

$$S = R = \frac{e^{-2\alpha}}{2\alpha\beta} \frac{[(\alpha-\beta)e^{2\beta} + \beta e^{2(\beta-\alpha)} - \alpha]^2}{[\alpha - \beta e^{2(\beta-\alpha)}](\alpha-\beta)e^{2(\beta-\alpha)}}, \qquad (7)$$

b) for the case of general Eqs. (2),

$$S = R = \frac{n^2}{2m} \frac{\frac{k_1}{k_2}}{\left(1 + \frac{k_2}{k_3}\right)^2 \alpha^2 e^{-2\left(1+\frac{k_3}{k_4}\right)\alpha} \left[1 + \frac{\beta}{\alpha} \frac{k_1}{k_2} \frac{k_3}{k_4}\right]}$$

where

$$m = \frac{(\alpha-\beta)\, e^{2(\beta-\alpha)}}{\alpha - \beta\, e^{2(\beta-\alpha)}}, \quad n = m - e^{-2\left(1+\frac{k_3}{k_4}\right)\alpha}.$$

2. With disturbances of velocity of the first medium, we obtain, for Eqs. (1) and (2),

$$S = \frac{(\bar{\alpha}-\beta)\ {}^{2(\beta-\bar{\alpha})}}{\bar{\alpha} - \beta e^{2(\beta-\bar{\alpha})}} \frac{[\beta e^{2(\beta-\alpha)} - \alpha]}{\alpha e^{2(\beta-\alpha)}} \frac{1}{\beta-\alpha} \frac{1}{1 + \frac{w_1}{w_2}} \frac{w_1}{\bar{w}_1},$$

where, in the case of Eqs. (1),

$$\alpha = \frac{lk_1}{2w_1}, \quad \beta = \frac{lk_2}{2w_2}, \quad \bar{\alpha} = \frac{lk_1}{2\bar{w}_1},$$

and, in the case of Eqs. (2),

$$\alpha = \frac{l\bar{k}_1}{2w_1}, \quad \beta = \frac{l\bar{k}_2}{2w_2}, \quad \bar{\alpha} = \frac{l\bar{k}_1}{2\bar{w}_1},$$

From the persistence and controllability characteristics, obtained in their general form and qua criteria, one can easily carry out their analytical and graphical analysis.

As an example, Fig. 4 shows the controllability curves $R(\beta)$ for various values of α and for fixed values of the remaining parameters ($k_1/k_2 = k_2/k_3 = 0.5$, $k_3/k_4 = 2$). Fig. 5 gives the curves $R(\beta)$ under the condition that there be maintained the given process completeness[***] P = 1 – m, m = 0.8 for k_3/k_4 = 0.5; 1; 2; 5 ($k_1/k_2 = 0.5$, $k_2/k_3 = 1$). The condition that a definite completeness of the process be given is a standard practical requirement.

In all cases, just as in those of the examples given (cf. Figs. 4 and 5), one can graphically give a comparative estimate of persistence and controllability of processes as functions of the parameters and operating modes of the apparatus. With this, one can immediately take into account any additional condition relating the possible variations of these parameters. In the example given (Fig. 5), such a condition was the specification of a definite process completeness.

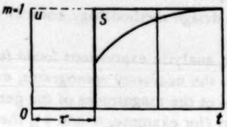

Fig. 3.

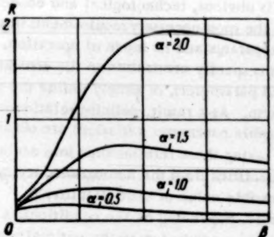

Fig. 4.

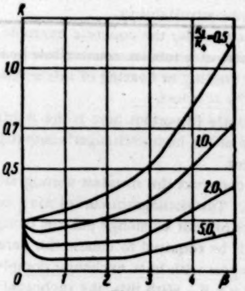

Fig. 5.

The domains of variation of α, β and other parameters for various apparatus can be established from concrete industrial data in each individual case. After this, if necessary, one can easily extend the corresponding graphs

---

[***] As the process completeness P, one takes the relative change of the input quantity after its passage through the apparatus, i.e.,

$$P = (u_{in} - u_{out})/u_{in} = 1 - m.$$

from the general analytic expressions for persistence and controllability of the process.

From the existing experimental data on heat exchangers, the values of α and β are found to lie within the limits shown on the graphs. In particular, a heat exchanger was tested in almost the conditions of actual practice, giving the figures $\alpha \approx 1.2$, $\beta \approx 0.6$, $\alpha \approx 0.85$, $\beta \approx 0.5$.

VI. Design Methodology. Example

By using the results obtained for the choice of the optimal parameters of engineering apparatus, we can take into account the requirement that the controllability be as good as possible.

The proper design methodology consists of the following:

1. From the analytic expressions found for R, one easily constructs the necessary nomograms, expressing the relationships of the magnitudes of the generalized plant parameters (for example, α and β), the process completeness P and the controllability R.†††

2. As is obvious, technological and economic conditions fix the most necessary requirements imposed on the concrete apparatus and its mode of operation. These requirements specify constraints on the erstwhile free, generalized parameters, or simply define the values of some of them. As a result, definite relationships connecting the possible parameter variations are obtained.

3. By taking these relationships into account, we choose the free quantities from the nomograms, trying for the greatest possible value of controllability R.

As a rule, depending on the conditions, a compromise solution must be adopted as to the optimal plant parameters with respect to process completeness, apparatus economy and controllability.

We now consider the concrete example of choosing the parameters of a tubular counterflow heat exchanger, used for the cooling or heating of salt solutions before they enter the reactors.

Particularly important here is the stabilization of the temperature at the heat exchanger's output prior to entry into the reactor.

1. We construct the simplest nomogram from expression (7). The nomogram curves must correspond to equal values of heat exchange process completeness.

2. Let it be required to choose the parameters for two heat exchangers with heat exchange completeness of P = = 0.1 and P = 0.6. With this, the technical data dictates that, in both cases, the generalized parameter β must be chosen only within the limits $0.6 \leq \beta \leq 1.2$.‡‡‡ With this, in accordance with expression (7), with large values of process completeness P, the magnitude of R increases sharply as β increases, and, for small values of P, it remains almost unchanged.

3. By considering the variation of the plant's controllability R on the interval (0.6; 1.2), either by nomogram or by formula (7), we arrive at the following conclusions:

a) in the given interval of variation of β, magnitude of the controllability R remains almost unchanged for the first heat exchanger. Therefore, the choice of β does not affect the plant's controlling properties[1] and, in this respect, can be made arbitrary.

b) for the second heat exchanger, the magnitude of R varies significantly in the given interval. In the given case, it is advantageous to choose the limiting value of $\beta = 1.2$, so as to provide the largest controllability of the process. It is desirable to make such a choice of β even in the case when this entails some insignificant deterioration of the other characteristics of the heat exchanger.

SUMMARY

1. The nonstationary problem of the interaction of moving media in engineering apparatus was considered.

2. A method was obtained for finding an approximate analytic expression for the transient responses in the commonest case of motion of media by the counterflow principle.

3. The characteristics of process persistence and controllability were obtained, in general form and qua criteria, for the broadest class of engineering apparatus operating on this counterflow principle. These characteristics have simple analytical expressions in elementary functions, and depend on a minimal number of dimensionless complex parameters, which provides ease and availability of the engineering designs.

4. Thus, possibilities were disclosed for the study of the dependence of some transient response or another on changes in system parameters for a wide class of engineering apparatus. The apparatus characteristics thus found are necessary for the solution of two problems which are important in practice: a) for the design of apparatus for an optimal steady-state operating mode with account taken of the indices of stability of this mode; b) for the simultaneous and compatible design of controller and plant.

LITERATURE CITED

1. V. S. Kulebakin, "On the basic problems and methods of increasing the quality of automatically controlled systems," Proceedings of the Second All-Union Conference on Automatic Control Theory [in Russian] (AN SSSR, 1955) 2.

---

††† A special work [6] is devoted to the construction of such nomograms. The nomograms therein given eliminate the necessity of constructing the corresponding curves in each concrete case.

‡‡‡ After the definitive choice of β, one can determine the corresponding value of α, and from this find the diameter and number of the tubular heat exchanger's internal tubes.

[1] By the concept "controlling properties" we have in mind the properties rendering possible the attainment of the best control quality (for example, a large persistence and a small lag).

2. B. N. Devyatov, "Transient responses of continuously acting heat exchangers," Doklady Akad. Nauk SSSR 90, 5 (1953).
3. B. N. Devyatov, "Definition of the characteristics of persistence and controllability of engineering apparatus in connection with the problem of optimal plant and controller parameters," Izvest. Akad. Nauk SSSR, Otd. Tekhn. No. 5 (1958).
4. B. N. Devyatov, "Transient responses of continuously acting heat exchangers with thick walls," Doklady Akad. Nauk SSSR 130, 1 (1960).
5. A. V. Lykov, Heat Conduction of Nonstationary Processes [in Russian] (Gosénergoizdat, 1948).
6. B. N. Devyatov and Yu. N. Kornev, "Determination of controllability of counterflowing heat exchanging apparatus," Collection: Proceedings of the Institute of Automation and Electrometrics of the SO AN SSSR [in Russian] (1960) No. 2 (in press).

AUTOMATIC CONTROL OF THE TURBINE DRILLING PROCESS BY MEANS OF ADAPTIVE SYSTEMS

M. G. Éskin

Moscow

Translated from Avtomatika i Telemekhanika, Vol. 21, No. 6, pp. 791-805, June, 1960

The paper considers automatic control devices, used for choosing optimal parameter ratios under changes in the external conditions of turbine drilling.

Results are adduced from the development of control schemes with respect to two parameters and of extremal type schemes wherein account is taken of the pecularities associated with the specific object of control.

An extremal device, based principally on discrete elements, is described. A semiautomatic control scheme is provided, the basis of the scheme being a scan of the technological process over a wide range of parameter variation.

The problem of automating the control of the turbine drilling process of oil and gas wells is the choice and maintenance of the optimal values of two parameters: the axial force P on the gouge and the rotational speed n of the gouge under variations in drilling conditions. With the turbine method of drilling, there is ordinarily implemented operational control only of the quantity P in the limits of 5 to 35 tons, by changes in the weight of the column of drilling pipe which gives rise to the axial force on the gouge. The turbine has the so-called "soft" characteristic, so that, with increasing axial force P, the velocity n of gouge rotation can be varied within the limits of 1200 to 1400 rpm. The partial derivative $\partial n/\partial P$ depends on the properties of the rock being drilled and on the state of the gouge.

An automatic control device is used to choose the optimal parameter ratios by adjusting the system parameters as the external drilling conditions change.

Automatic Control in Terms of One Parameter

The control system includes an automatic controller of one parameter as one of its elements. In addition to this, a one-parameter automatic controller has independen applications.

In the sequel we shall use the notation: Q is the difference between the total weight of the column of tubing Q_0 and the force Q_1 at the upper end of the column, V_s is the velocity supplied to the column's upper end and V_d is the drilling speed.

In the steady state, and with no friction, $P = Q$ and $V_d = V_s$.

Ordinary controllers maintain the value of Q, given by a setting Q_c. The magnitude of Q_c is varied by the control device or by a driller, manually.

Figure 1 shows the functional schematic of the type AVÉ automatic controller.

The force Q is measured by a transducer — a spring element, transforming force to a selsyn's angle of rotation. The angle of rotation of a second selsyn is a given setting. The difference between the angles of the transducer and setting selsyns, transformed to an ac signal, is applied to the input of an electronic amplifier; the power is then amplified by a rotary amplifier and applied to the excitation winding of a generator which supplies the dc executive motor. This motor implements the supply of the drilling instrument. Due to this, the forces P and Q are varied until such time as the difference between the angles of the transducer and setting selsyns becomes close to zero.

In the AVÉ scheme there are, not two, but four selsyns, which give the capability for both manual and mechanized (for automatic control) introduction of the settings.

Both rigid and flexible stabilizing connections are provided in the system.

Type AVÉ automatic controller was tested under industrial conditions. The tests showed that the AVÉ provides the required static and dynamic indices for the existing changes in drilling conditions, including drilling speeds close to zero. Today, design work is proceeding for several modifications of type AVÉ controllers for different drilling stands.

Automatic Control in Terms of Two Parameters

The drilling process is still insufficiently studied, which renders difficult the determination of the best law of automatic control. The development of automatic control devices proceeds step-by-step in parallel with the development of the technology.

Each of the devices developed, being based on definite technological assumptions, verifies in its turn the correctness of these assumptions. It is this wherein consists the complexity of solving the problems of optimal control and optimal technology.

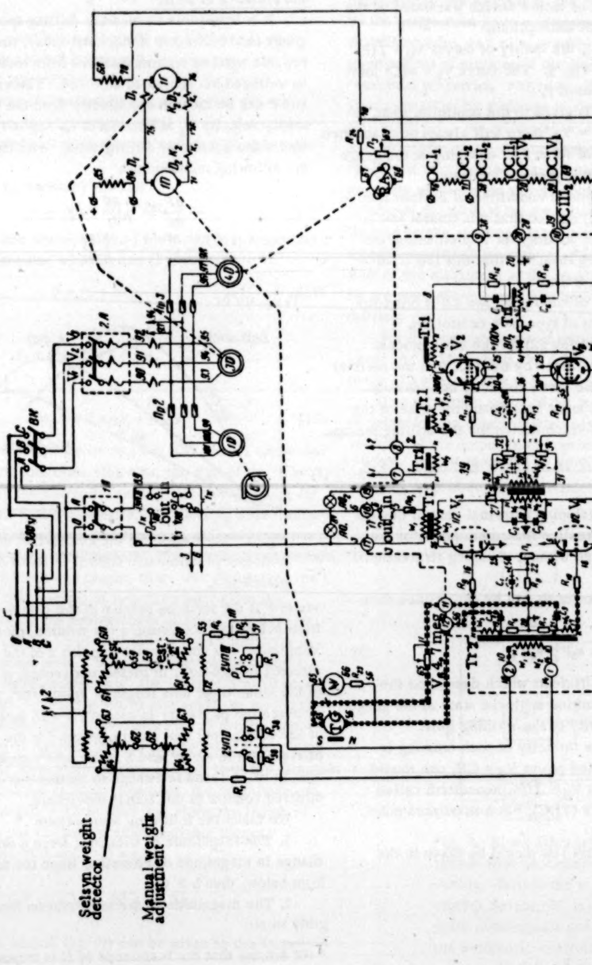
Selsyn weight detector
Manual weight adjustment
-300V
250V
100V
OCI1
OCII1
OCIII1
OCIV
Tr1
V1
V2
V3
V4
out
in
mes
est.

Fig. 1.

The simplest system providing variation of axial force P when drilling conditions change is a device for maintaining a given relationship

$$V_s = \varphi(Q). \tag{1}$$

In a particular case, this relationship has the form

$$k_1V_s + k_2Q = C, \tag{2}$$

where k_1 and k_2 are given coefficients, and C is a value given by the setting.

The development of such a device was based on the following technological assumptions.

For different rocks, the family of curves $V_d = f(P)$ has the form shown in Fig. 2. The curve $V_s = \varphi(Q)$ joins points of optimal values of P.

If control law (1) is given to the controller, then, in the steady state for $V_s = V_d$, there will always be established a definite value of axial force P_{oi}, changing as the gouge enters rocks of different degrees of hardness.

Testing, under industrial conditions, of devices implementing control law (2) showed that this control law is unsuitable, with turbine drilling, for implementing the basic process of crushing rock, but that this law is advantageous for working wells.

Today, capability of control by law (2) is provided in several modifications of type AVE controllers.

The unsuitability of law (2) for the basic process of turbine drilling is explained by the fact that the optimal points P_{oi}, V_{oi} cannot be given correctly beforehand, since it is impossible to know beforehand the state of the gouge and other factors which determine the drilling process.

Automatic Control in Terms of Extremal Values. Technological Premises

The purpose of developing extremal control devices (ECD) for drilling is to realize maximum power of the turbine drill on the gouge without changing its rotational speed.

The turbine drill power N_1 can be determined from the formula

$$N_1 = k_3P - k_4P^2, \tag{3}$$

where k_3 and k_4 are coefficients which depend on the physical design of the turbine drill, the state of the gouge, the properties and quantity of the washing fluid.

Considering that the intensity of rock crushing is proportional to the applied power $V_d = CN$, one should assume that the function $V_d = f(P)$, henceforth called the turbine drilling curve (TDC), has a maximum point, at which $\partial V_d/\partial P = 0$.

Therefore, the control law should be taken in the form

$$\frac{\partial V_d}{\partial P} = \delta \quad (\delta \geqslant 0). \tag{4}$$

In some cases, the control system, for $\delta < 0$, is made unstable. Therefore, δ should be chosen with some margin of error. Details on this will be given below.

Turbine drilling curves $V_d = f(P)$ and $N = Pn = f_1(P)$, taken off experimentally,* essentially confirmed the assumptions made.

On Control System Structures in Connection with the Pecularities of Measurement of the Quantities and with the Presence of Noise

It is impossible to measure drilling speed V_d and gouge load P directly since, until today, the problem of reliable wireless communications from locus of drilling to wellhead has remained unsolved. The values of V_d and P can be measured indirectly from the values of the supply velocity V_s and the force Q_1 applied at the upper end of the column of drilling tube. With this, we use the following relationships:

$$-\frac{\partial F}{\partial x} = q\,\frac{\partial V}{\partial t} - qg \pm h, \tag{5}$$

$$-\frac{\partial V}{\partial x} = -\frac{1}{k}\,\frac{\partial F}{\partial t}, \tag{6}$$

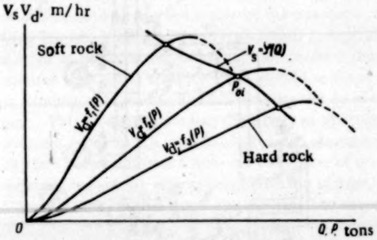

Fig. 2. Illustration for the elucidation of the principle of automatic control in terms of two parameters.

where F is the force on point x of the column, directed from below and compressing the column, measured in kilograms, V is the velocity of point x of the column, directed from below, in meters per second, q is the mass of the column per unit length in kg·sec²/m², g is the acceleration of gravity in m/sec², k = ES is the rigidity of the column per unit length, where E is the modulus of elasticity in kg/m² and S is the tube's cross-sectional area in m², h is the resistance to motion per unit length, directed counter to the actual movement.

We make the following assumptions:

1. The magnitude of frictional force h does not change in magnitude or direction; since the tube is moved from below, then h > 0.

2. The magnitude of the acceleration force is negligibly small:

---

*We assume that the magnitude of N is proportional to N_1.

$$q\frac{\partial V}{\partial t} \ll qg - h. \tag{7}$$

For the determination of the subsurface parameters V_d and P from the surface parameters V_s and Q_1, we obtain the following simplified expressions:

$$P = (qg - h)\,l - Q_1, \tag{8}$$

$$V_d = -\frac{l}{k}\,\frac{\partial P}{\partial t} + V_s. \tag{9}$$

Here, V_d and P are simply V and F for $x = l$, and V_s and $-Q_1$ are V and F for $x = 0$.

For $h \ll qg$, we have $P = Q$.

The limits of applicability of assumption (7) were determined on an electromechanical model of a turbine drill, connected to actual elements of an AVÉ automatic controller.

If force Q_1 varies by the law

$$Q_1 = Q_{1_0} - \alpha t, \tag{10}$$

where Q_{1_0} is the initial value of force and α is a constant; then, in accordance with (8) and (9), we get

$$P = P_0 + \alpha t, \tag{11}$$

where

$$P_0 = (qg - h)\,l - Q_{1_0}$$

and

$$V_d = -l\alpha / k + V_s. \tag{12}$$

On the model, reproducing Eqs. (5) and (6) connected to actual AVÉ controller elements, the sign of the velocity introduced by the controller setting was changed and, for various α and l, the quantities P, V_d and V_s were oscillographed. Graphs constructed from Eqs. (11) and (12) were laid on these same oscillograms. Then, from a comparison of the oscillograms and graphs, there was determined the time t from the moment of switching settings to the moment at which the replacement of Eqs. (5) and (6) by Eqs. (8) and (9) no longer entailed a significant error in the measurement of V_s. This time depends on α and l and, for $l < 2000$ meters, is of the order of 3 to 10 seconds.

The basic assumption (which may entail an essential error) is the assumption of the constancy of the frictional force h. If it is assumed that all the points of the column are translated from below during drilling, then the direction of force h does not change. However, the magnitude of h can be changed, both in time and along the length of the column, due to random unaccountable causes.

From Eqs. (11) and (12) we get

$$\Delta P = \alpha \Delta t, \quad \Delta V_d = \Delta V_s.$$

Whence control law (4) can be given in the form

$$\delta = \frac{\Delta V_s}{\alpha \Delta t}, \tag{4'}$$

where the increment ΔV_s is chosen for α = const on the interval of time Δt, and $\delta \geq 0$ is a given quantity.

Averaging in the Choice of Values of ΔV_s and Δt

In the limit, the quantity $\Delta V_s/\Delta t$ is the acceleration of shaft sinking but, for its reliable determination, the quantities ΔV_s and Δt must have finite values. This is explained by the following: the process of rock crushing by the gouge must have a discrete character; the column of drilling tube, as a rule, is subject to oscillations due to pulsations of pressure of the wash fluid and also due to resonance properties. Moreover, the sinking of the column is accompanied by a change in the frictional force on the well walls (cf., the relationships shown below on Figs. 12 and 13). This makes the measurement on instantaneous speed and acceleration inapplicable, and creates the necessity of averaging the measured quantities. The minimum duration of the interval of measurement is limited by the aforementioned sources of noise, by the signal's maximum frequency, which is determined by the shift of the maximum as the rock's drill resistance changes, by the state of the gouge and by other conditions of drilling.

For the test specimen of the control devices, we chose $\Delta t \approx 10$ seconds, for $\Delta P = 1$ to 2.5 tons, and a range of variation of $P \approx 5$ to 35 tons.

The minimum value of ΔP is limited by the dispersion of points for the determination of ΔV_d, and by the small velocity of the output in the optimum zone.

The maximum value of ΔP is limited by the admissible amplitude of oscillation in the optimum zone.

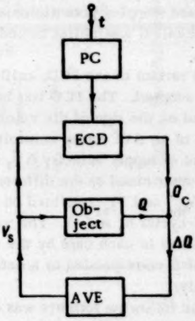

Fig. 3. Block schematic of a system with an extremal control device. ECD is the extremal control device, PC is the program commutator and AVÉ is the automatic controller.

Basic Schemes of Extremal Control Devices (ECD)

When averaging over a lengthy time interval (~ 10 seconds) is employed, it is necessary to stabilize the load on the gouge during this interval. Therefore, the system with the ECD was connected in a two-loop scheme (Fig. 3).

The first loop is a high-speed control system, used for stabilizing the load on the gouge. This loop comprises a servosystem in which the quantity Q, equal to P in the steady state, follows the given value of the setting Q_c. This loop is implemented by analog elements.

The second loop is a slow-acting, but accurate system used for the implementation of the control law $\partial V_d/\partial P = \delta$ by controlling the controller setting. This loop is implemented, in whole or in part, by discrete (digital) elements.

In the development of the ECD, the methods adopted for measuring the supply velocity V_s were to measure the increment of supply ΔS during a calibrated time interval Δt, or to measure the time increment Δt for a calibrated supply interval ΔS. Various ECD schemes were analyzed in correspondence with these methods. The simplest were the relay ECD systems. In these schemes, only two positions were provided for the organ for introducing the setting Q_c as a function of the sign.

Two variants of the relay schemes were developed, one with variations in the magnitude of setting Q_c, and the other with changes in sign of the velocity of introducing the setting Q_c.

ECD Circuit Elements and Physical Construction

In the first variant of the ECD, calibrated supply intervals were adopted. The ECD was built of basically analog electromechanical elements [2, 3] and acted on the settings of a type AN-1 electropneumatic controller by means of a pulsed stepping potentiometer. The design of the electromechanical assemblies turned out to be very complicated.

In the second variant of the ECD, calibrated time intervals Δt were adopted. The ECD was built of digital elements and acted on the sign of the velocity of introducing the setting of an AVÉ rotary controller.

The increment of supply velocity ΔV_s on the interval Δt [cf., (4')] was determined as the difference of the supply velocities $V_{s_{bi}}$ and $V_{s_{ai}}$, defined on the two measurement half-cycles bi and ai. The velocity of supply was determined in each case by the number of pulses, each of which corresponded to a definite small magnitude of supply.

As a result, the following formula was obtained for the increment of supply velocity:

$$\Delta V_{s_i} = V_{s_{bi}} - V_{s_{ai}} = \frac{n_{bi} - n_{ai}}{\Delta t} \gamma, \qquad (13)$$

where γ is a proportionality factor relating magnitude of supply to number of pulses.

The measurement half-cycles begin after that moment of time when Eqs. (8) and (9) become valid.

For pulse addition, reversible counters were used. To determine the sign of the difference $\Delta V_s/\alpha\Delta t - \delta$, [cf., (4')], a nominal quantity of pulses n_N were introduced into the counter. Let $n_N = \alpha\Delta t^2\delta/\gamma$. By substituting n_N and Δ_{si} in (4'), we obtain the algebraic sum

$$\sum n = n_{bi} - n \quad - n_N, \qquad (14)$$

whose sign definesthe sign of the expression $\Delta V_s/\alpha\Delta t - \delta$.

For $\delta = 0$, the scheme operates in the following manner. Let the setting be increased, and let $\partial Q_c/\partial t = = \alpha > 0$. Increasing Q_c leads to an increase of Q and P.

The measurement half-cycle begins at time t_1. During the first half-cycle, $t_2 - t_1 = \Delta t$, there occurs subtraction followed by storage of the negative number of pulses $-n_{ai}$. During the second half-cycle $t_3 - t_2 = \Delta t$, there occurs the addition of n_{bi} followed by reading of the difference $\Delta n_i = n_{bi} - n_{ai}$. As a function of the sign of the difference Δn_i there is not carried out (for a positive sign) or there is carried out (for a negative sign) a switching of the sign of the velocity of introducing the setting.

For operation by the law $\partial V_d/\partial P = \delta$, where $\delta > 0$, after the first half-cycle there is introduced the nominal quantity of pulses ± n_N.

The basic element of the scheme is the reversible counter, which does reading, storage and subtraction of pulses in accordance with the commands obtained from the program commutator (Fig. 4).

The assembly for setting introduction consists of a selsyn driven at a slow rotational speed by a dc motor via a reducer.

The program commutator consists of disks rotated by a synchronous motor via a reducer.

The reversible counter is a ten-place electron-tube counter. It has the built-in capability of being switched to subtraction and addition, as well as the capability of having a nominal number of pulses n_N introduced into it.

The pulse transducer consists of a selsyn, rectifier, and flip-flop with total feedback used for pulse shaping. Each rotation of the selsyn corresponds to an advance of the upper end of the drill column by a fraction of a millimeter.

Figures 5 and 6 show exterior views of the assemblies of the extremal device.

Testing and Directions of Further Improvement of the ECD Scheme

Testing of the extremal devices was carried out on the turbine drilling model and under industrial conditions, with drilling being carried out at depths up to 2000 meters.

For the tests, at the lower end of the model drilling tube column, there was simulated the turbine drilling curve (TDC) of the extremal type, close to a sinusoid within the limits of 0 to π. In addition, there was simulated dry friction, applied to several points of the drill column.

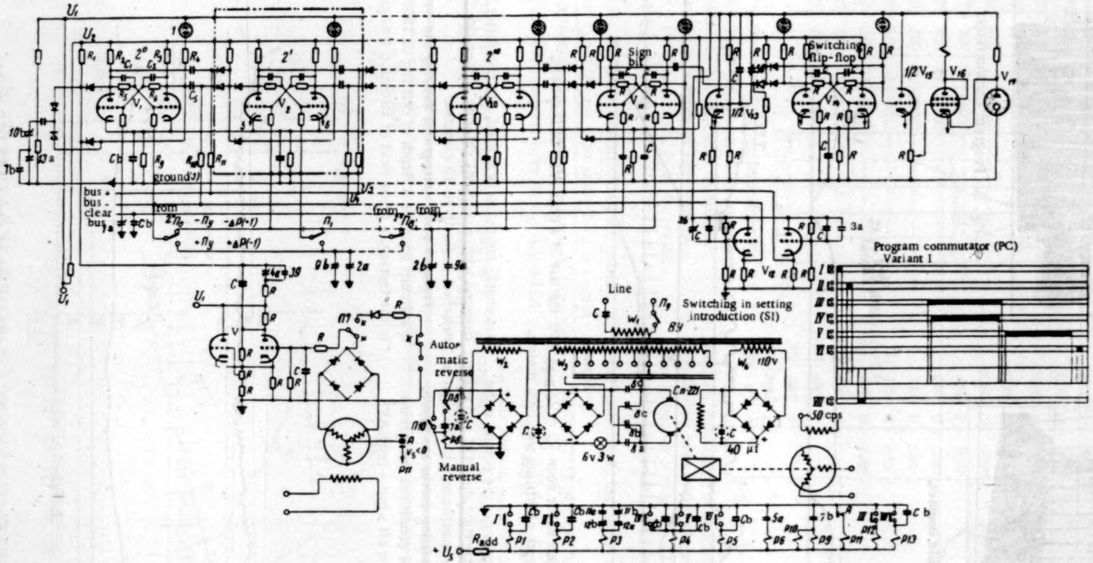
U_1
U_2
2^0
$2'$
$2''$
Sign bit
Switching flip-flop
$1/2\,V_{13}$
$1/2\,V_{15}$
V_{16}
V_{17}
ground(3)
bus +
bus -
clear bus
from
Program commutator (PC)
Variant I
Line
Switching in setting introduction (SI)
Automatic reverse
Manual reverse
W_1
W_2
W_3
W_4
110 v
6 v 3 w
40 μf
50 cps
R_{add}
$+U_s$

Fig. 4. Functional schematic of an ECD built of digital elements.

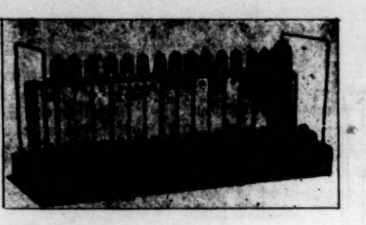

Fig. 5. Reversible counter.

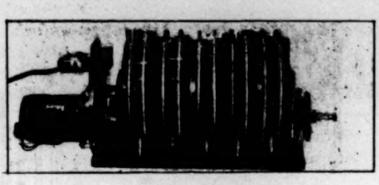

Fig. 6. Program commutator.

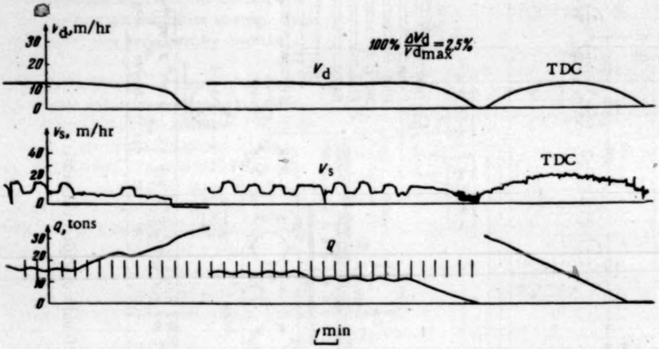

Fig. 7. Output in the zone $V_d = V_{d\ max}$ with the use of a type ATB ECD system. A model. Depth of drilling was 1000 meters.

Figure 7 shows the cartograms of the output at the maximum to the left, and to the right, the TDC and auto-oscillations in the zone of the maximum. At the right of this same figure, the turbine drilling curves are shown.

In testing under industrial conditions the turbine drilling curves were first taken off when a type AVÉ automatic controller was used, the controller setting being changed with a constant velocity. Then the ECD was switched in for 10 to 20 minutes.

Figure 8 gives cartograms showing the output in the maximum zone for a depth of drilling of 1950 meters. In the testing, a great deal of attention was given to the

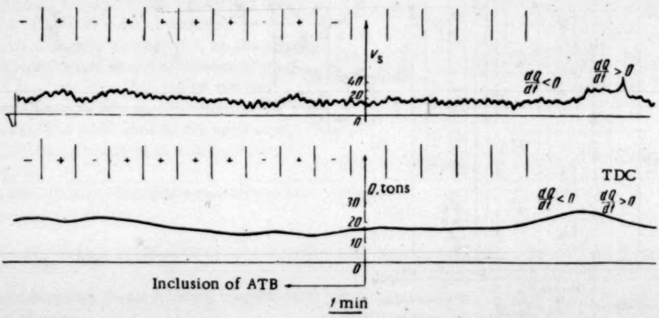

Fig. 8. Output in the zone $V_d = V_{d\ max}$ with the use of a type ATB ECD system. Industrial testing. Depth of drilling was 1950 meters (V_s in meters/hour).

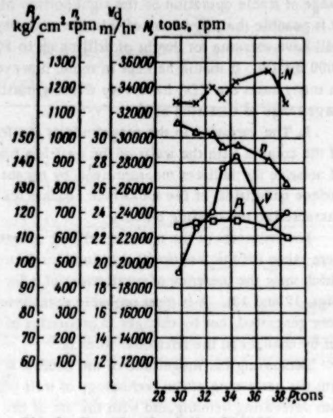

Fig. 9. Functional relationships V_d, n, N = f(P), constructed from averaged values of the data from industrial testing at a depth of 1670 meters, N = Pn in tons rpm, P_I is the pressure of the wash fluid.

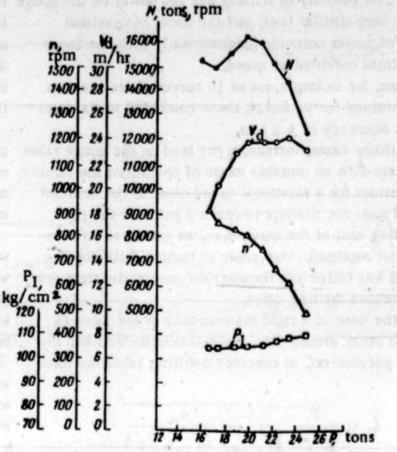

Fig. 10. Functional relationships V_d, n = f(P), constructed from averaged values of the data from industrial testing at a depth of 1900 meters. P_I is the pressure of the wash fluid.

taking off, under industrial conditions, of the turbine drilling curves V_d = f(P), and their study from the point of view of determining the extremal character of the TDC, and the extent of their monotonicity on the individual segments [4].

To this end, an instrument was developed for measuring the rotational velocity of the turbine drill, and transmitting the results of the measurement to the surface.

Figures 9-11 give the functional relationships of V, n, N = f(P, t).

On the basis of the investigation and testing of the two ECD designs, one may draw several conclusions and map out plans for the further perfecting of ECD for turbine drilling:

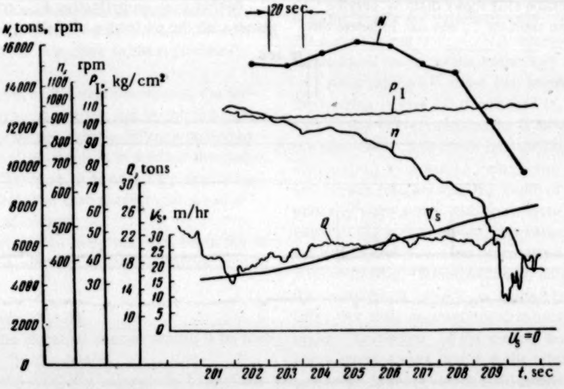

Fig. 11. Portions of the cartograms with recordings of the current values of Q, V_s and n corresponding to Fig. 10.

1. The velocity of drilling and the power on the gouge vary by very similar laws, and the zones of maximal choice of power coincide fundamentally with the zones of maximal mechanical speed.

Thus, for example, out of 10 curves where maxima were obtained for V_s and N, these coincided in six cases with an accuracy of ± 2 tons.

In many cases, increasing the load on the gouge takes the system into an unstable mode of operation; the turbine drill subsides for a rotational speed close to the nominal one, and does not manage to reach a point on the right descending arm of the curve–i.e., an extremal relationship is not attained. One cause of turbine drill stopping is that it has fallen into the unstable zone on the right arm of the turbine drilling curve.

In the case of a rigid maintenance of the force Q_1, and with other assumptions, the relationship between the critical parameters, as concerns stability, takes the form [5]

$$l_c < \frac{T}{\sqrt{\frac{q}{k}}} \sqrt{\frac{n_c}{n_{fr}\left(1 - 2\frac{n_c}{n_{fr}}\right)}} \tag{15}$$

$$\operatorname{arc\,tg} \frac{1}{c_1\sqrt{qk}} \sqrt{\frac{1}{n_{fr}n_c\left(1 - 2\frac{n_c}{n_{fr}}\right)}}.$$

Here, l_c and n_c are the critical values of the tube column length and the turbine drill's speed of rotation, n_{fr} is the turbine drill's free-running speed, T is the turbine drill's time constant, and c_1 is a coefficient defining the rock's resistance to drilling.

This result was obtained by use of the method of Chebotarev, which was developed by him for the analysis of the stability of quasi-polynomials.

Analysis of expression (15) shows that, by varying the turbine drill's time constant T, one can increase the range of stable operation on the right portion of the TDC; it is possible that, by virtue of this, the majority of TDC will have extrema for depths of drilling up to 2000 to 3000 meters. It should be kept in mind, however, that in many cases the TDC have very slanting portions in a large range of variation of P.

2. The variation in the magnitude of the friction h of the column with the walls of the well is a basic source of noise in the indirect measurement, by means of the surface quantities, of the subsurface quantities which characterize the drilling process.

For estimates of the noise in drilling operations, there were taken off the functional relationships Q, n = $f(t)$, which show the presence of oscillations of n for Q = const (Figs. 12 and 13). It is most probable that these oscillations were generated, not by changes in properties of the rock, but by changes in the frictional force h.

Decreasing the magnitude of the friction h is connected with the perfecting of the technology of well pipe laying: with decreasing bending, and with the use of the proper wash fluids. One of the effective methods of decreasing h must be to rotate the tube column with low velocities.

It should be considered that, for vertical wells with drilling depths up to 2500 to 3000 meters, and with the proper technological operating mode, the noise engendered by the forces h will basically be less than the signal level.

3. An extremal device for drilling must be based on the computation of averaged values of velocity. The averaging time can be about 10 to 20 seconds and, in the future, must be made more precise. This makes it necessary to construct two-loop systems, similar to those described above.

4. To shorten the operation cycle of an ECD and to decrease the output time in the maximum zone, a fast-acting operative control system is of great value.

Further work on perfecting ECD must proceed together with the perfecting of drilling technology, partic-

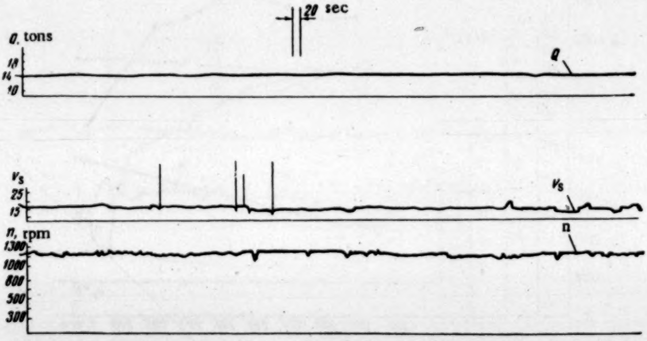

Fig. 12. Cartogram portions with recording of the current values of Q, n and V_s for Q ≈ const. V_s in meters per hour. Operational drilling. Depth of 1750 meters. Wash fluid was water.

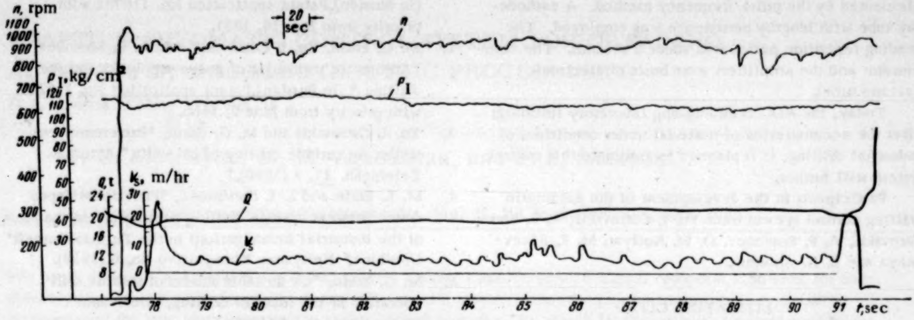

Fig. 13. Cartogram portions with recording of the current values of Q, n and V_s for Q ≈ const. Operational drilling. Depth of 2000 meters. Wash fluid was clay mortar.

ularly as it has to do with decreasing frictional noise, and increasing the zone of stable turbine drilling operation.

Under these conditions, the problem of creating a reliable extremal device for turbine drilling for vertical wells of depths of 2500 to 3000 meters, devices based on the designs developed, is a completely realistic task.

Turbine drill control by maximum mechanical velocity, using surface parameters, has still a limited use.

When the depth of drilling is increased beyond 2500 to 3000 meters, the frictional forces between the column and the well walls will increase significantly. This is particularly essential for wells with bends. This can lead to the appearance of errors in measuring the velocity of drilling, as a result of which the monotonic form of the individual segments of the turbine drilling curve will be disrupted, i.e., the curve will have several false maxima.

As the depth of drilling increases, the zone of stable turbine drill control constricts, and the probability is increased that the turbine drill will stop until the turbine drilling curve makes the transition to the right-hand descending portion.

In addition, to this, as the depth increases, the predominant role begins to be played, not by the mechanical speed of drilling, but by the quantity of rock drilled by one gouge, since the time required to replace the gouge increases sharply. Therefore, it is necessary to place a more complicated criterion than mechanical speed of drilling at the basis of control.

The reasons enumerated impelled us to begin the development of a new device for automatic drilling control (ADC).

Principles of ADC Construction

The defect in the extremal control system is its scan of the process curve "in the small".

At the basis of the ADC is a compulsory scan of the process "in the large". As applied to drilling, the scan is carried out within the limits of variation of the load on the gouge from the minimum to the maximum, whereby the entire turbine drilling curve is taken off and stored.

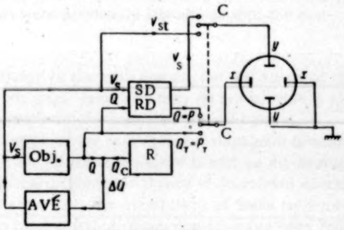

Fig. 14.

The structural block schematic of the semiautomaton ADC is shown on Fig. 14. By means of an automatic data transmitter the quantity Q and, correspondingly, the load P on the gouge are varied linearly. The storage device SD stores the curve $V_s = f(Q)$ corresponding, under the assumptions made, to the curve $V_d = f(P)$.

After taking off of the first information (data) curve, the reading device RD is switched in, and periodically repeats the curve, reproducing it on the screen of a cathode-ray tube CRT. The curve thus obtained is analyzed by a driller (i.e., by a human being), using special nomograms which take into account the depth of drilling and the partially worn gouge and, from these data, the optimal value of P_{0i} is determined, this value being then set by the driller, and thereafter maintained automatically by the AVE controller. Simultaneously, current information as to the quantities P_{0i} and V_s is applied to the plates of the CRT. For this, commutator C is used. Prolonged and major deviations of the current information from the curve attest to the fact that the information has become obsolete. In this case, the old information is erased, and the process is repeated from the beginning.

In a test specimen, the storage and reading devices were made with magnetic tape. Recording was implemented by the pulse-frequency method. A cathode-ray tube with lengthy persistence was employed. The reading repetition period was about 2 seconds. The commutator and the amplifiers were built of electronic vacuum tubes.

Today, the ADC is undergoing laboratory finishing; after the accumulation of material under conditions of industrial drilling, it is planned to automate this control system still further.

Participants in the development of the automatic drilling control system were Yu. I. Ostrovskii, A. S. Bondarevskii, A. P. Sosenkov, O. M. Kotlyar, M. R. Kraevskaya and B. N. Anokhin.

LITERATURE CITED

1. M. G. Éskin, "Automatic device for supplying the gouge at the locus of drilling for turbine drilling" [in Russian], Patent application No. 110782 with priority from Jan. 16, 1951.
2. M. G. Éskin, Yu. I. Ostrovskii and A. P. Sosenkov, "Automatic controller of gouge supply for turbine drilling" [in Russian], Patent application No. 118273 with priority from June 2, 1955.
3. Yu. I. Ostrovskii and M. G. Éskin, "Extremum controller for turbine drilling of oil wells," Avtomat. i Telemekh. 17, 9 (1956).†
4. M. E. Éskin and E. I. Romanova, "Functional dependence between turbine drilling parameters on the basis of the industrial investigations in the Tuimazaburneft' Combine," Neftyanoe Khozyaistvo No. 6 (1958).
5. M. G. Eskin, "On unstable modes of turbine drill operation at the locus of drilling," Neftyanoe Khozyaistvo, No. 6 (1959).

---

† See English translation.

ADAPTIVE AUTOMATIC CONTROL SYSTEM FOR OBTAINING ALUMINUM BY THE ELECTROLYTIC PROCESS USING A COMPUTING DEVICE

É. P. Sarkisyan, M. M. Agababyan, and P. S. Saakyan

Erevan

Translated from Avtomatika i Telemekhanika, Vol. 21, No. 6, pp. 806-811, June, 1960

The paper describes an adaptive automatic control system, constructed with digital computer elements, for the electrolytic process for obtaining aluminum. The control system causes the process to minimize a variable component of the cost, depending on the technological process. The search for the optimal mode is carried out in terms of one variable, namely, the position of the anode.

The control system also includes several systems for stabilizing parameters, whose setting is automatically varied as the conditions of the process change. The optimal settings were previously introduced into the controlling device's memory.

The modern industrial method of obtaining aluminum is the electrolysis of fused cryolite-alumina. In the electrolysis process, aluminum is produced at the cathode and, at the carbon anode, oxygen which, at high electrolysis temperatures, forms carbon monoxide and carbon dioxide with the carbon anode.

In theory, Faraday's law states that, in the electrolysis of fused cryolite-alumina, 0.336 g of aluminum should be produced per hour at the cathode when a current of 1 amp is used. In practice, in industrial baths embodying the current level of technological proficiency, the production of aluminum is 12 to 15% less than the theoretical value. This is due to a number of reasons, above all, to the metal solubility in the fused electrolyte and its being borne to the anode by the diffusion, convection and circulation of the electrolyte with the reverse formation of aluminum oxide.

As the result of many years of investigation and industrial use of aluminum baths, it has been established that the basic process indices – productivity and specific expenditure of electric energy – are influenced by the current density, the distance between electrodes, the temperature of the electrolyte, the concentration of alumina, the cryolite ratio, the form of the electrolyzer, the levels of electrolyte and metal in the bath, etc. These parameters change during the electrolysis process.

The control of the technological processes in present-day aluminum baths is effected manually, on the basis of rough measurements and subjective analysis which depends on the experience and individual proficiency of the operator.

It should be mentioned that in industry there are individual schemes designed to maintain constant just one of the parameters, while the others assume arbitrary values. These are automatic stabilization schemes for the voltage in the bath, and for the resistance of the interelectrode gap. However, they do not provide a solution to the problem of automatic process control.

In spite of the fact that the aluminum industry has existed for a long time, there is still no all-embracing, scientifically grounded theory of aluminum electrometallurgy, i.e., the electrolysis of fused cryolite-alumina, and no mathematical dependencies have been found between the output as a function of current, the specific expenditure of electric energy and the various parameters which determine the process under industrial conditions.

Today, obtaining mathematical relationships between the parameters of processes which occur in complicated physicochemical, electrodynamic and thermal conditions, on the sole basis of theoretical investigations, is tremendously difficult and unrealistic. The existing process of electrolysis of fused cryolite-alumina belongs to those technological processes in which such indices as productivity and specific expenditure of electric energy depend on many interrelated variable parameters, and are not found in a single-valued relationship with any one of them for arbitrary values of the remaining ones.

Consequently, the automatic control of the process of fused cryolite-alumina electrolysis can be implemented only on the basis of an analysis of the process indices, namely, the output as a function of current, and the specific expenditure of electric energy.

With the aims of increasing the efficiency of the process and of freeing the maintenance personnel from working in an atmosphere of noxious gases, there was developed an adaptive automatic control system for the electrolysis process which uses a computing device, the essence of which is described below.

The system is based on the following assumptions. The electrolysis bath is considered as an insulated thermodynamical system; the series current, the alumina concentration and the composition of electrolyte in the bath are stabilized. The bath has a new design which permits complete collection of the output gases and a continuous supply of alumina. A single-period oscillation of anode motion is implemented. By the use of a computer there is carried out an automatic search for the optimal anode position, corresponding to the least value of that portion of the aluminum cost which depends on the state of flow of the process. Under definite conditions, forcing external stimuli are applied to the system and, on the basis of an analysis of the results of the process' reaction to the external stimuli, a search is automatically carried out for the optimal process conditions.

Stabilization of alumina concentration and electrolyte composition is introduced for the purpose of providing a uniform course of the process.

Stabilization of the series current is necessary to eliminate the effect on the bath's operating mode of a disturbed operating mode in the other, series-connected baths, and also to eliminate oscillations, deleterious for the electrolysis process, of the metal and disturbances of the correspondence between the form of the anode base and the surface of the liquid metal and, consequently, a nonuniform distribution of current in the electrolyte and in the anode base.

Thus, the sole advantageous and practically admissible controlling factor for the automatic search for an optimal process turned out to be just the displacement of the anode which, in the system developed, is used as the external forcing stimulus on the system.

The following requirements were imposed on the aluminum electrolyzer which was to operate in the adaptive system for automatic process control:

1) hermetic sealing, permitting complete removal of the output gases without losses and the rarefaction of atmospheric air, which is a necessary condition for the continuous determination of the indices of the process;

2) a continuous supply of alumina and fluorine salts.

At the Kanakerskii Aluminum Plant, there was developed, installed and subjected to industrial testing, an electrolyzer satisfying the requirements of automation. As the criterion of optimality of process flow there was chosen the degree of approximation to the least value of variable component of aluminum cost C_v, which depends on the course of the technological process and mirrors the variation of cost of electric energy and anode mass expended to obtain one ton of aluminum.

Figure 1 shows the block schematic for the adaptive system of automatic process control for the electrolysis of fused cryolite-alumina. According to this scheme, to the controlling device, via analog-to-digital converted AD, the values of the variable process parameters from the electrolyzer transducers are applied and, from the control console (desk), the values of the constant coefficient and stabilized parameters.

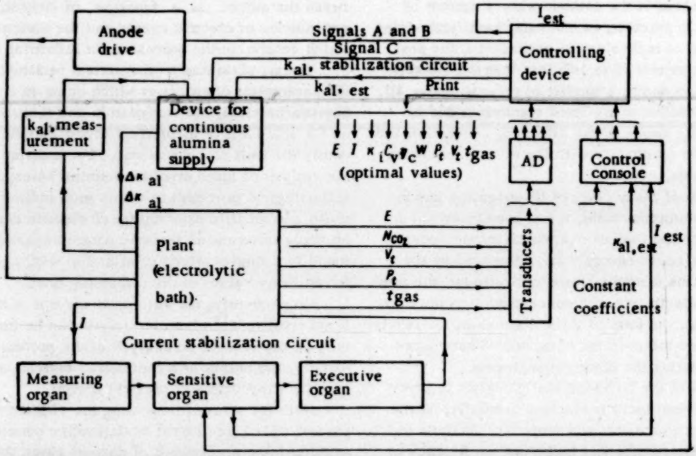
Anode drive
Signals A and B
Signal C
k_{al}, stabilization circuit
k_{al}, est
Print
I_{est}
Controlling device
k_{al}, measurement
Device for continuous alumina supply
E I κ_i C_v η_c W P_t V_t t_{gas}
(optimal values)
AD
Control console
$\Delta\kappa_{al}$
$\Delta\kappa_{al}$
Plant (electrolytic bath)
E
N_{CO_2}
V_t
P_t
t_{gas}
Transducers
$\kappa_{al,est}$
I_{est}
Constant coefficients
I
Current stabilization circuit
Measuring organ
Sensitive organ
Executive organ

Fig. 1. Block schematic of the adaptive system of automatic process control for the electrolysis of fused cryolite-alumina. E is the voltage on the bath, I is the series current, N_{CO_2} is the percentage content of CO_2 in the output gases, P_t is the pressure of the output gases, V_t is the volume of the output gases, t_{gas} is the temperature of the output gases, Δk_{al} is a batch of alumina, Δk_{cr} is a batch of cryolite, k_{al} is alumina concentration, k_{cr} is cryolite concentration, A is raise, B is lower and C is supply alumina.

As a result of an analysis of the applied data, the control device sends a control signal to the automated electric anode drive scheme, this signal being necessary for the search for the optimal anode position. The controlling device prints out the process indices and parameters, both for the optimal anode positions and for the intervals between them.

The automated electric anode drive in the developed system provides automatic step-wise raising or lowering of the anode upon receipt of pulses from the controlling device, with the capability of regulating the magnitude of the translation step and of automatic lowering of the anode as metal is removed from the bath.

During the period of discharging metal from the bath, performed every three days and lasting only several minutes, the control device is switched out of the control system. Since variations in the temperature of the ambient medium have great influence on the mode of bath operation, the most advantageous sets of stabilizing parameter values are introduced into the controlling device for various values of the ambient medium temperature. When the temperature of the ambient medium reaches a definite value, the controlling device automatically supplies the stabilization circuit with the best values of the corresponding settings.

The system must provide stabilization of alumina concentration, which requires continuous measurement of alumina concentration whose practical implementation poses great difficulties. In connection with this, the controlling device, in addition to the functions already mentioned, is also used for the maintenance of alumina concentration constancy by determining the moment when a definite batch is spent and is sending a signal to the supply device to supply the electrolyzer with the corresponding new batch of alumina.

Figure 2 shows the functional block schematic of the controlling device, expressing the following two groups of operational modes: a) periodically repeating, and b) continuous.

The following modes appertain to the periodically repeating ones:

1. Determination of the direction of search for the optimal anode position.
2. Search for the optimal position.
3. Repetitive computation of the indices of the process in the optimal anode position followed by their print-out, and the print-out of the values of the variable parameters corresponding to the optimal anode position.
4. Periodic computation, after a definite interval of time following the establishment of an optimal anode position, of the quantity C_v and a comparison of it with the value of $C_{v.o}$ in the optimal position.

The following modes of operation are the continuous ones:

1. Generation of signals to supply the established batch of alumina to the electrolyzer bath.
2. Transmitting the proper settings to the series current and alumina concentration circuits upon changes in ambient medium temperature. It should be mentioned that the computation of the variable component of aluminum cost C_v must be performed with a very high accuracy, with an error not greater than 0.1%. This requirement is dictated both by economic considerations, and by the capabilities of technological implementation of the search for the optimal anode position under the technological conditions of the electrolysis process.

The requirements of high computational accuracy, the necessity of performing the operations of storage (memory), many logical operations, etc., led to the construction of the controlling device on the principles of electronic digital computers. The stability of the system is thus known to be guaranteed both for the control algorithm and for the conditions under which the search for the optimal anode position is carried out.

The output as a function of current, η_c, will increase only up to a definite point as the interelectrode distance increases, after which it begins to decrease monotonically. Consequently, the value of C_v connected with the voltage on the bath and the formula for output as a function of current given in the functional block schematic (Fig. 2), will have a least value for just one anode position. According to the search algorithm, when the anode is sufficiently close to the optimal position, no signal is sent to the anode drive, and anode motion is cut off, thus eliminating the possibility of anode oscillations about its optimal position.

The quality of the search which, in the system under consideration is characterized by the closeness of the anode to the optimal position, depends on the size of the anode translation step, and can be improved only by an experimental selection of the most successful size of the translation step, the capability of changing which has been built into a circuit of the automated anode drive.

In conclusion, it should be mentioned that the implementation and introduction into practice of the system described here, which differs radically from all previously existing automation systems, are connected with the achievement of greater economic efficiency. The yearly economy due to increased output of metal without an additional utilization of electric energy and also to the decreased expenditure for wages with complete automation of process control, at the Kanakerskii Aluminum Plant alone, constitutes some 10 to 15 million rubles a year for the capital outlays of less than one year.

Economy will be obtained also by simplification of the ventilation system and a decreased cost of ventilation.

The introduction into practice of the system described will also lead to the freeing of human beings from hard and unhealthful conditions, to an improvement of the atmospheric purity of the factories and the populated areas around the factories, and to a solution of the problem

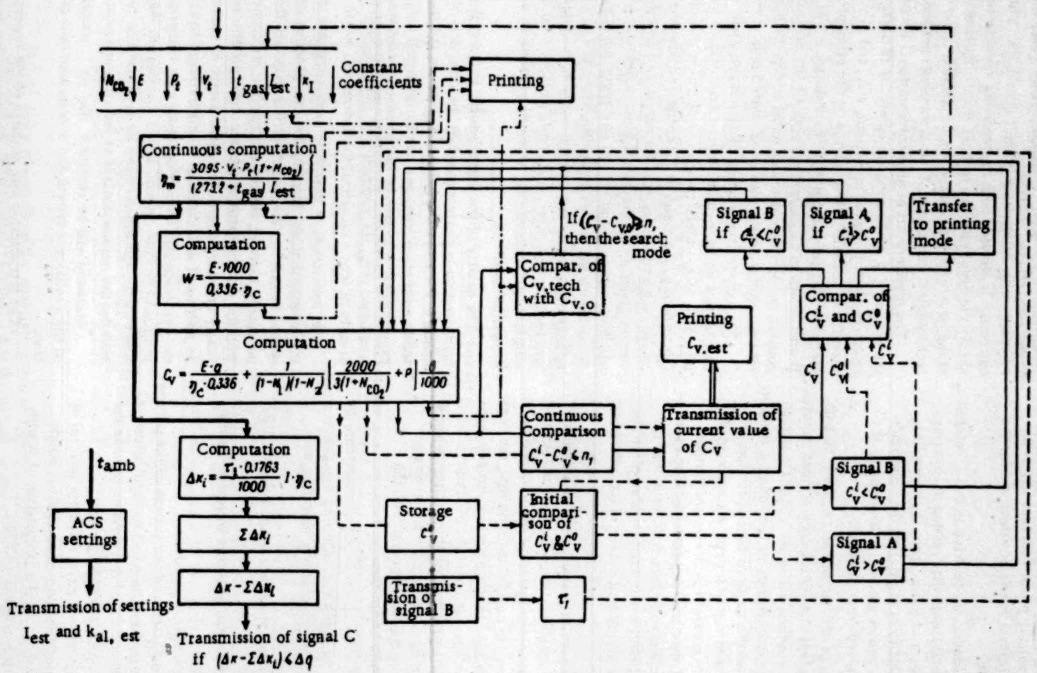
Constant coefficients
N_{CO_2} E P_t V_t t_{gas} I_{est} κ_I
Printing
Continuous computation
$\eta_m = \frac{3095 \cdot V_t \cdot P_t (1+N_{CO_2})}{(273.2+t_{gas}) I_{est}}$
Computation
$W = \frac{E \cdot 1000}{0.336 \cdot \eta_C}$
Computation
$C_V = \frac{E \cdot q}{\eta_C \cdot 0.336} + \frac{1}{(1-N_1)(1-N_2)} \left[\frac{2000}{3(1+N_{CO_2})} + P\right] \frac{\theta}{1000}$
If $(C_V - C_{V.0}) > n$, then the search mode
Compar. of $C_{V.tech}$ with $C_{V.o}$
Signal B if $C^i_V < C^0_V$
Signal A if $C^i_V > C^0_V$
Transfer to printing mode
Compar. of C^i_V and C^0_V
Printing $C_{V.est}$
C^i_V C^{0i}_V C^i_V
Continuous Comparison $C^i_V - C^0_V \leq n_1$
Transmission of current value of C_V
t_{amb}
ACS settings
Transmission of settings I_{est} and $k_{al,\, est}$
Computation $\Delta\kappa_i = \frac{\tau_1 \cdot 0.1763}{1000} I \cdot \eta_C$
$\Sigma \Delta\kappa_i$
$\Delta\kappa - \Sigma\Delta\kappa_i$
Transmission of signal C if $(\Delta\kappa - \Sigma\Delta\kappa_i) \leq \Delta q$
Storage C^0_V
Initial comparison of C^i_V & C^0_V
Signal B $C^i_V < C^0_V$
Signal A $C^i_V > C^0_V$
Transmission of signal B
τ_1

Fig. 2. Functional block schematic of the controlling device. ------- denotes the mode of determining the direction of search, ———— denotes the search mode, —·—·—· denotes printing, ━━━━ denotes the continuous mode; ACS stands for Automatic Control System, C^0_V and C^i_V denote the previous and following values of the variable component of cost, respectively, τ_1 is a delay line, n is the zone of permissible deviations of cost.

of complete recovery and utilization of the noxious gases and sprays.

The system developed opens up the possibility of a profounder study of the technological process and a gathering of the experimental data whose statistical processing allows a mathematical description to be given of a complicated process. This enables one to determine the future paths and prospective development of electrolysis technology, to implement more accurate and economical designing of aluminum electrolyzers and to execute further perfecting of their physical design.

USE OF ELECTROTHERMAL ISODROME DEVICES FOR THE INTERCONNECTED CONTROL OF PRODUCTION PROCESSES

G. M. Fialko

Sverdlovsk

Translated from Avtomatika i Telemekhanika, Vol. 21, No. 6, pp. 812-820, June, 1960

A method is considered for the implementation of autonomous isodrome control of complicated plants by means of electrothermal devices, not requiring the complication of the controller's measuring elements. These devices are connected as identical electrothermal isodrome controllers, and differ only by the method of their connection in the control loop.

A method is described for determining the parameters of such devices, starting from the autonomy conditions, and the results are given of an experimental verification of separated and interconnected control schemes on a simulation device.

Complicated controlled plants frequently contain several controlled parameters, each of which depends on several controlling actions. Since the effect of the individually acting controllers in such objects is to worsen the quality of the control process, this leads to the necessity of using interconnected control, an advanced form of which is the autonomous control scheme suggested by I. N. Voznesenskii [1, 2].

Ordinarily, in autonomous control schemes, the communication signal between controllers is formed in the measuring elements of the leading controllers. In the general case of isodrome control, when the isodrome times are not equal among themselves, it is required, for the realization of these communications, to complicate the controller's measuring element, and to introduce a communication link allowing the derivatives of the controlled parameter to be obtained [3].

The necessity of complicating the circuit of the controller's measuring element in order to realize communication crossovers creates definite difficulty in implementing schemes for interconnected control of complex plants, since very frequently the measuring portion of a controller is simultaneously used for the purposes of automatic inspection. Moreover, the use of this communication signal is connected with the addition of a delay to the control circuit, a delay which is ordinarily attributable to the controller transducer. It is therefore of interest to use, for communications between controllers, signals which are not from the transducers, but from other elements of the control circuit.

In the present work we show the possibility of realizing autonomous control of technological processes by means of communications from the executive mechanisms of the leading controllers.

1. Determination of the Parameters of the Crossover Controller Communication Elements

We consider a plant with three controlled parameters, on each of which all the controlling elements have an effect. A skeleton scheme of this complicated control system is shown on Fig. 1. In addition to the signal of the measuring element and isodrome of its own loop, there is applied to the amplifying element of each controller a communication signal from the remaining two controllers. These external signals are applied from the

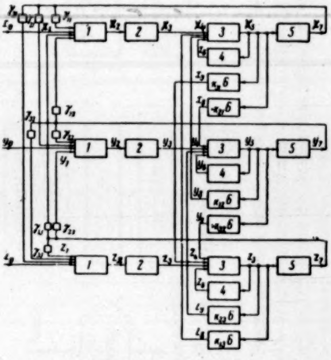

Fig. 1. Skeleton scheme of interconnected control of a plant with three controlled parameters. 1 is the plant, 2 is a measuring element, 3 is an amplifier, 4 is an isodrome, 5 is an executive mechanism with a controlling organ and 6 is a crossover communication device.

link whose input is connected to the inputs of the executive mechanisms of the leading controllers. The equations of the individual loops of the scheme of Fig. 1 can be given in the following form:

$$
\begin{aligned}
x_1 &= \gamma_{11}x_7+\gamma_{12}y_7+\gamma_{13}z_7+x_0,\\
x_2 &= A_1x_1,\\
x_3 &= A_2x_2,\\
x_4 &= x_3-x_6+y_8+z_8,\\
x_5 &= A_3x_4,\\
x_6 &= A_4x_5,\\
x_7 &= A_5x_5,\\
y_1 &= \gamma_{21}x_7+\gamma_{22}y_7+\gamma_{23}z_7+y_0,\\
y_2 &= B_1y_1,\\
y_3 &= B_2y_2,\\
y_4 &= y_3-y_6+x_8+z_9, \qquad (1)\\
y_5 &= B_3y_4,\\
y_6 &= B_4y_5,\\
y_7 &= B_5y_5,\\
z_1 &= \gamma_{31}x_7+\gamma_{32}y_7+\gamma_{33}z_7+z_0,\\
z_2 &= C_1z_1,\\
z_3 &= C_2z_2,\\
z_4 &= z_3-z_6+x_9+y_9,\\
z_5 &= C_3z_4,\\
z_6 &= C_4z_5,\\
z_7 &= C_5z_5,
\end{aligned}
$$

Here, x_2, y_2, z_2 are the controlled parameters, x_7, y_7, z_7 are the controlling actions, x_0, y_0, z_0 are the external disturbances, γ_{ij} (i, j = 1, 2, 3) are known coefficients of the plant which take into account the influence of the controlling elements on the controlled parameters. We denote by A_1, B_1, C_1 the operators of the individual objects of control, whose forms depend on the properties of these objects. The operators of the remaining links of the control circuit equal

$$
\begin{aligned}
&A_2=a_2,\ \ A_3=a_3,\ \ A_4=\frac{a_4}{1+pT_{I1}},\ \ A_5=\frac{a_5}{pT_{c1}},\\
&B_2=b_2,\ \ B_3=b_3,\ \ B_4=\frac{b_4}{1+pT_{I2}},\ \ B_5=\frac{b_5}{pT_{c2}}, \quad (2)\\
&C_2=c_2,\ \ C_3=c_3,\ \ C_4=\frac{c_4}{1+pT_{I3}},\ \ C_5=\frac{c_5}{pT_{c3}}.
\end{aligned}
$$

The equations of the communication devices have the form

$$
\begin{aligned}
&x_8=K_{21}x_5,\ \ x_9=K_{31}x_5,\ \ y_8=K_{12}y_5,\\
&y_9=K_{32}y_5,\ \ z_8=K_{13}z_5,\ \ z_9=K_{23}z_5, \qquad (3)
\end{aligned}
$$

where K_{12}, K_{13}, K_{21}, K_{23}, K_{31}, K_{32} are unknown operators of the communication devices which must be determined. We obtain the following system of equations from (1) and (3):

$$
\begin{aligned}
x_5 &= A_3x_4=A_0(x_3+K_{12}y_5+K_{13}z_5),\\
y_5 &= B_3y_4=B_0(y_3+K_{21}x_5+K_{23}z_5), \qquad (4)\\
z_5 &= C_3z_4=C_0(z_3+K_{31}x_5+K_{32}y_5),
\end{aligned}
$$

where

$$A_0=\frac{A_3}{1+A_3A_4},\quad B_0=\frac{B_3}{1+B_3B_4},\quad C_0=\frac{C_3}{1+C_3C_4}, \quad (4')$$

System (4) can be put in the form

$$
\begin{aligned}
Ax_5-K_{21}y_5-K_{13}z_5 &= x_3,\\
-K_{21}x_5+By_5-K_{23}z_5 &= y_3, \qquad (5)\\
-K_{31}x_5-K_{32}y_5+Cz_5 &= z_3,
\end{aligned}
$$

where

$$A=A_0^{-1},\ B=B_0^{-1},\ C=C_0^{-1}. \qquad (5')$$

We obtain the following expressions from (5) for x_5, y_5, z_5:

$$
\begin{aligned}
x_5 &= \frac{1}{\Delta}(D_1x_3+D_2y_3+D_3z_3),\\
y_5 &= \frac{1}{\Delta}(D_4x_3+D_5y_3+D_6z_3), \qquad (6)\\
z_5 &= \frac{1}{\Delta}(D_7x_3+D_8y_3+D_9z_3),
\end{aligned}
$$

where, by Δ, we denote the determinant of system (5), equal to

$$\Delta=\begin{vmatrix} A & -K_{12} & -K_{13}\\ -K_{21} & B & -K_{23}\\ -K_{31} & -K_{32} & C \end{vmatrix}, \qquad (7)$$

and, by $D_1, \ldots, D_9$, we denote its cofactors, equal to

$$
\begin{aligned}
&D_1=BC-K_{32}K_{23},\quad D_2=K_{12}C+K_{32}K_{13},\\
&D_3=K_{12}K_{23}+BK_{13},\ D_4=K_{21}C+K_{31}K_{23},\\
&\qquad\qquad\qquad\qquad\qquad\qquad\qquad\qquad (8)\\
&D_5=AC-K_{31}K_{13},\quad D_6=AK_{23}-K_{21}K_{13},\\
&D_7=K_{21}K_{32}+BK_{31},\ D_8=AK_{32}+K_{31}K_{12},\\
&D_9=AB-K_{21}K_{12}.
\end{aligned}
$$

We note that for system (5) to have a solution, it is necessary that its determinant not equal zero:

$$\Delta \neq 0. \tag{9}$$

From (1) and (6) we get

$$\begin{aligned} x_7 &= \frac{1}{\Delta} A_5 (D_1 x_3 + D_2 y_3 + D_3 z_3), \\ y_7 &= \frac{1}{\Delta} B_5 (D_4 x_3 + D_5 y_3 + D_6 z_3), \\ z_7 &= \frac{1}{\Delta} C_5 (D_7 x_3 + D_8 y_3 + D_9 z_3). \end{aligned} \tag{10}$$

Taking into account the expressions for the controlling parameters, we obtain, from (1) and (10), the following relationships for the controlled parameters:

$$\begin{aligned} x_2 &= A_1 \left\{ \frac{1}{\Delta} [(M_1 D_1 + M_2 D_4 + M_3 D_7) x_3 + (M_1 D_2 + M_2 D_5 + M_3 D_8) y_3 + \right. \\ &\qquad \left. + (M_1 D_3 + M_2 D_6 + M_3 D_9) z_3] + x_0 \right\}, \\ y_2 &= B_1 \left\{ \frac{1}{\Delta} [(M_4 D_1 + M_5 D_4 + M_6 D_7) x_3 + (M_4 D_2 + M_5 D_5 + M_6 D_8) y_3 + \right. \\ &\qquad \left. + (M_4 D_3 + M_5 D_6 + M_6 D_9) z_3] + y_0 \right\}, \\ z_2 &= C_1 \left\{ \frac{1}{\Delta} [(M_7 D_1 + M_8 D_4 + M_9 D_7) x_3 + (M_7 D_2 + M_8 D_5 + M_9 D_8) y_3 + \right. \\ &\qquad \left. + (M_7 D_3 + M_8 D_6 + M_9 D_9) z_3] + z_0 \right\}, \end{aligned} \tag{11}$$

with the notation

$$\begin{gathered} M_1 = \gamma_{11} A_5, \ M_2 = \gamma_{12} B_5, \ M_3 = \gamma_{13} C_5, \ M_4 = \gamma_{21} A_5, \ M_5 = \gamma_{22} B_5, \\ M_6 = \gamma_{23} C_5, \ M_7 = \gamma_{31} A_5, \ M_8 = \gamma_{32} B_5, \ M_9 = \gamma_{33} C_5. \end{gathered} \tag{12}$$

We obtain the following autonomy conditions from (11):

$$\begin{aligned} M_1 D_2 + M_2 D_5 + M_3 D_8 &= 0, \\ M_1 D_3 + M_2 D_6 + M_3 D_9 &= 0, \\ M_4 D_1 + M_5 D_4 + M_6 D_7 &= 0, \\ M_4 D_3 + M_5 D_6 + M_6 D_9 &= 0, \\ M_7 D_1 + M_8 D_4 + M_9 L_7 &= 0, \\ M_7 D_2 + M_8 D_5 + M_9 D_8 &= 0. \end{aligned} \tag{13}$$

In accordance with (8), the communication operators being sought, K_{12}, K_{13}, K_{21}, K_{23}, K_{31}, K_{32}, enter into the expressions for D_1-D_9. We consider a method of determining these operators, starting from the autonomy conditions. These autonomy conditions (13) can be given in the following form:

$$\begin{gathered} \Delta_1 = \begin{vmatrix} A & -K_{12} & -K_{13} \\ M_1 & M_2 & M_3 \\ -K_{31} & -K_{32} & C \end{vmatrix} = 0, \\ \Delta_2 = \begin{vmatrix} A & -K_{12} & -K_{13} \\ -K_{21} & B & -K_{23} \\ M_1 & M_2 & M_3 \end{vmatrix} = 0, \\ \Delta_3 = \begin{vmatrix} M_4 & M_5 & M_6 \\ -K_{21} & B & -K_{23} \\ -K_{31} & -K_{32} & C \end{vmatrix} = 0, \\ \Delta_4 = \begin{vmatrix} A & -K_{12} & -K_{13} \\ -K_{21} & B & -K_{23} \\ M_4 & M_5 & M_6 \end{vmatrix} = 0, \\ \Delta_5 = \begin{vmatrix} M_7 & M_8 & M_9 \\ -K_{21} & B & -K_{23} \\ -K_{31} & -K_{32} & C \end{vmatrix} = 0, \\ \Delta_6 = \begin{vmatrix} A & -K_{12} & -K_{13} \\ M_7 & M_8 & M_9 \\ -K_{31} & -K_{32} & C \end{vmatrix} = 0. \end{gathered} \tag{14}$$

We consider determinants Δ_1 and Δ_2, which have two identical rows in common. It is well known that the condition for a third-order determinant to equal zero is the equality, or proportionality, of the elements of two of its rows or columns [4]. On the strength of this property, we obtain the following relationship between the common rows of these two determinants*:

$$\frac{A}{M_1} = -\frac{K_{12}}{M_2} = -\frac{K_{13}}{M_3}. \tag{15}$$

From (15) we obtain the values of the operators:

$$K_{12} = -A \frac{M_2}{M_1}, \quad K_{13} = -A \frac{M_3}{M_1}. \tag{15'}$$

By an analogous consideration of determinant pairs Δ_3, Δ_4 and Δ_5, Δ_6, we get

$$K_{21} = -B \frac{M_4}{M_5}, \quad K_{23} = -B \frac{M_6}{M_5}, \tag{16}$$

$$K_{32} = -C \frac{M_8}{M_9}, \quad K_{31} = -C \frac{M_7}{M_9}. \tag{17}$$

By using the expressions obtained for the communication operators between the controllers, we can show that the requirement that the determinant of system (5) not equal zero reduces to the meeting of the condition

---

*This solution is unique, since the proportionality of the other rows in determinants Δ_1 and Δ_2 leads to a zero value for the determinant of system (5), which contradicts (9).

$$\begin{vmatrix} \gamma_{11} & \gamma_{12} & \gamma_{13} \\ \gamma_{21} & \gamma_{22} & \gamma_{23} \\ \gamma_{31} & \gamma_{32} & \gamma_{33} \end{vmatrix} \neq 0. \qquad (18)$$

This condition is usually met in actual objects of control (plants).

By substituing the values of A, B, C and $M_1, \ldots, M_9$ from (5') and (12) in (15'), (16) and (17), we get

$$K_{21} = -\frac{\gamma_{21}}{\gamma_{22}} \frac{a_5 T_{c2}(1 + b_3 b_4)}{T_{c1} b_5 b_3} \frac{(1 + pT'_{I2})}{(1 + pT_{I2})},$$

$$K_{31} = -\frac{\gamma_{31}}{\gamma_{33}} \frac{a_5 T_{c3}(1 + c_3 c_4)}{T_{c1} c_5 c_3} \frac{(1 + pT'_{I3})}{(1 + pT_{I3})},$$

$$K_{12} = -\frac{\gamma_{12}}{\gamma_{11}} \frac{b_5 T_{c1}(1 + a_3 a_4)}{T_{c2} a_5 a_3} \frac{(1 + pT'_{I1})}{(1 + pT_{I1})},$$

$$K_{32} = -\frac{\gamma_{32}}{\gamma_{33}} \frac{b_5 T_{c3}(1 + c_3 c_4)}{T_{c2} c_5 c_3} \frac{(1 + pT'_{I3})}{(1 + pT_{I3})}, \qquad (19)$$

$$K_{13} = -\frac{\gamma_{13}}{\gamma_{11}} \frac{c_5 T_{c1}(1 + a_3 a_4)}{T_{c3} a_5 a_3} \frac{(1 + pT'_{I1})}{(1 + pT_{I1})},$$

$$K_{23} = -\frac{\gamma_{23}}{\gamma_{22}} \frac{c_5 T_{c2}(1 + b_3 b_4)}{T_{c3} b_5 b_3} \frac{(1 + pT'_{I2})}{(1 + pT_{I2})},$$

where

$$T'_{I1} = \frac{T_{I1}}{1 + a_3 a_4}, \; T'_{I2} = \frac{T_{I2}}{1 + b_3 b_4}, \; T'_{I3} = \frac{T_{I3}}{1 + c_3 c_4}. \qquad (20)$$

The following relationships usually hold in isodrome controllers of production processes:

$$a_3 a_4 > 1, \; b_3 b_4 > 1, \; c_3 c_4 > 1;$$

$$T_{Ij} \geqslant (10 - 100)\, T'_{Ij}. \qquad (21)$$

By taking (21) into account, we can present the communication operators in the form

$$K_{21} = -\frac{\gamma_{21}}{\gamma_{22}} \frac{a_5}{T_{c1}} \frac{T_{c2}}{b_5} \frac{b_4}{1 + pT_{I2}},$$

$$K_{31} = -\frac{\gamma_{31}}{\gamma_{33}} \frac{a_5}{T_{c1}} \frac{T_{c3}}{c_5} \frac{c_4}{1 + pT_{I3}},$$

$$K_{12} = -\frac{\gamma_{12}}{\gamma_{11}} \frac{b_5}{T_{c2}} \frac{T_{c1}}{a_5} \frac{a_4}{1 + pT_{I1}}, \qquad (22)$$

$$K_{32} = -\frac{\gamma_{32}}{\gamma_{33}} \frac{b_5}{T_{c2}} \frac{T_{c3}}{c_5} \frac{c_4}{1 + pT_{I3}}$$

$$K_{13} = -\frac{\gamma_{13}}{\gamma_{11}} \frac{c_5}{T_{c3}} \frac{T_{c1}}{a_5} \frac{a_4}{1 + pT_{I1}},$$

$$K_{23} = -\frac{\gamma_{23}}{\gamma_{22}} \frac{c_5}{T_{c3}} \frac{T_{c2}}{b_5} \frac{b_4}{1 + pT_{I2}}. \qquad (22)\ \text{(cont.)}$$

From (22) one easily deduces the structure of the communication operators for plants with n controlled parameters:

$$K_{ji} = -\frac{\gamma_{ji}}{\gamma_{jj}} \frac{E_{5i}}{E_{5j}} E_{4j}, \qquad (23)$$

where E_4 and E_5 denote, respectively, the isodrome operators and the operators for the controlling organ with an executive mechanism for the individual controllers.†

The communication operators of (22) can be realized by electrothermal devices of the isodrome type whose heater windings are connected in the output circuit of the leading controller's amplifier, and whose thermocouples are connected at the input of the driven controller's measuring element. The time constant of this communication device must equal the isodrome time of the driven controller, and the transfer factor of this link depends solely on the ratios of the parameters of the two control contours: driven and driving.

The method described for the realization of the connections (communications) between the controllers in order to obtain autonomous control allows one to eliminate the delays of the driven controllers' measuring elements, and to increase the dynamic control accuracy. Realization of these communications by means of electrothermal isodromes with even tuning of the isodrome times [5] is particularly valuable for the autonomous control of inertial plants.‡

2. Experimental Verification on a Simulator of the Interconnected Control Scheme

For the purpose of verifying the effectiveness of the method suggested for realizing connections in interconnected control schemes, an experimental investigation was carried out on a simulator for systems of individual and of interconnected control. In its technological features, the simulator is a model of one of the portions of the drying-absorbing section of a plant for sulfuric acid production by the contact process.

Figure 2 shows the block schematic of the simulator. To monohydrate absorber I, with a closed sprinkling cycle, there is applied acid Q_1 with concentration S_1 and acid Q_2 with concentration S_2. To tower II, there is fed monohydrate Q_4 of concentration S_3, and water Q_6. Dried acid, of quantity Q_2 and concentration S_2, is applied to pump V in supply tank III and, from there, to absorber I. The continuous separation of the process output is realized by flows Q_5 and Q_7.

---

† The validity of formula (23) was also verified by the author for a plant with the number n = 4 of controller parameters.

‡ For isodrome times up to 500 seconds, autonomy can also be realized by the dynamic connections of the VTI system [6].

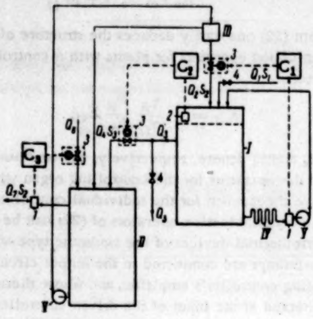

Fig. 2. Block schematic of the simulator. I is the absorber, II is the tower, III is the supply tank, IV is the cooler, V is the pump, C_1 and C_3 are the controllers of acid concentration, C_2 is the controller of acid level; 1 is the concentration measuring transducer, 2 is the level measuring transducer, 3 is the controlling valve with executive mechanisms, 4 is the disturbing organ.

In this simulator, there was an automatic maintenance of constant concentration S_3 and acid level H in absorber I, and acid concentration S_2 in tower II. Acid level in this tower was kept constant by an overflow drain.

With individual operation of the controllers, controller C_1 of monohydrate concentration controls the quantity of dried acid Q_2 applied to absorber I, monohydrate level controller C_2 controls the quantity of monohydrate Q_4 applied to drying tower II, and controller of dried acid concentration C_3 controls the amount of water Q_6 applied to the drying tower II. For the dynamics of the controlled parameters, the following differential equations are valid:

$$\begin{aligned}\Delta S_3 &= A_1(\alpha_1\Delta S_2 + \alpha_2\Delta Q_2 + \alpha_3\Delta Q_1),\\ \Delta H_1 &= B_1(\Delta Q_1 + \Delta Q_2 - \Delta Q_4 - \Delta Q_5), \qquad (24)\\ \Delta S_2 &= C_1(\alpha_4\Delta Q_4 + \alpha_5\Delta S_3 + \alpha_6\Delta Q_6),\end{aligned}$$

where

$$A_1 = \frac{e^{-p\tau_1}}{1+pT_1}, \quad B_1 = \frac{1}{pF}, \quad C_1 = \frac{e^{-p\tau_2}}{1+pT_2},$$

$$\alpha_1 = \frac{Q_2^\circ}{Q_3^\circ}, \quad \alpha_2 = \frac{Q_1^\circ(S_2^\circ - S_1^\circ)}{(Q_3^\circ)^2}, \quad \alpha_3 = \frac{Q_2^\circ(S_1^\circ - S_2^\circ)}{(Q_3^\circ)^2}, \qquad (24')$$

$$\alpha_4 = \frac{Q_6^\circ S_3^\circ}{(Q_4^\circ + Q_6^\circ)^2}, \quad \alpha_5 = \frac{Q_4^\circ}{Q_4^\circ + Q_6^\circ}, \quad \alpha_6 = \frac{Q_4^\circ S_3^\circ}{(Q_4^\circ + Q_6^\circ)^2}.$$

Here, we have adopted the following notation: p is the differentiation operator, T_1 and T_2 are the time constants, respectively, of absorber I and tower II; τ_1, τ_2 and τ_3 are the lags of the controlled parameters; F is the image surface of the acid in tower II. A superscript of zero denotes the corresponding quantity in the system's equilibrium state.

Analysis of the right members of Eqs. (24) shows that the deviation ΔS_3 from the actual variations of ΔS_2, as well as the deviation ΔS_2 from the actual variations of ΔS_3, are less than the changes of these controlled parameters from other disturbances. By neglecting these influences in the given investigation, we obtain the following equations for the simulator inputs in general form:

$$x_1 = \gamma_{11}x_7 + x_0, \; y_1 = \gamma_{21}x_7 + \gamma_{22}y_7 + y_0, \qquad (25)$$
$$z_1 = \gamma_{32}y_7 + \gamma_{33}z_7 + z_0,$$

where x_1, y_1, z_1 are the plant's inputs, x_7, y_7, z_7 are the controlling flows, $\gamma_{11} = \alpha_2$, $\gamma_{21} = 1$, $\gamma_{22} = -1$, $\gamma_{32} = \alpha_4$, $\gamma_{33} = \alpha_6$, $x_0 = \alpha_3\Delta Q_1$, $y_0 = \Delta Q_1 - \Delta Q_5$ and $z_0 = 0$.

The apparatus used on the actual plant was set up on the simulator. All controllers were electrical with electrothermal isodromes and with constant servomotor speeds. The optimal parameters (internal connections) of the individual controllers were determined from the conditions that the transient responses have damping degree $\psi = 0.8$ and minimal squared deviation of the controlled parameter [7]. The simulator parameters are given in Table 1.

The operators of the electrothermal devices of the controllers' crossover communications were calculated by the methodology presented previously.

According to (22), with account taken of the coefficient matrix of the simulator and the parameters of the individual control circuits, we have

$$K_{12} = 0, \quad K_{13} = 0, \quad K_{21} = 6.05\,\frac{1 + 0.191\,p}{1 + 2.1\,p}, \qquad (26)$$
$$K_{23} = 0, \quad K_{31} = 0, \quad K_{32} = 60.5\,\frac{1 + 0.277\,p}{1 + 3.6\,p}.$$

The actual controller connections were realized by electrothermal isodromes whose operators were equal to

$$K_{21} = \frac{6.05}{1 + 2.1\,p}, \quad K_{32} = \frac{57.5}{1 + 3.5\,p}. \qquad (27)$$

The method of testing was the following: Two forms of external disturbances were communicated to the simulator: a) the quantity of acid Q_1 applied to absorber I was varied; b) the quantity of acid Q_5 withdrawn "from stock" was varied. These disturbances were communicated to the simulator both for individual operation of the controllers and for the interconnected control scheme. The results of the tests are given in Table 2.

The simulator tests show that, with interconnected control, the dynamic deviations of all the controlled parameters were less by 20% than those with individual control. The same verification of an interconnected con-

TABLE 1

Controller	Plant parameters				Controller parameters							
	τ, min	T_a, min	$\frac{\tau}{T_a}$	a_1, $\frac{\% H_2SO_4}{1/min}$ (cm/1/min)	a_2, $\frac{mv}{\% H_2SO_4}$ (mv/cm)	a_3, mv^{-1}	a_4, mv	a_5, 1/min	T_c, min	T_I, min	$\frac{T_I}{T_a}$	K_0
Concentration controller of absorber I	0.8	8.4	0.094	−0.23	18.9	6.0	12.3	1.47	0.27	3.5	0.42	15.9
Level controller of absorber I	0.2	6.42	0.0312	21.9	0.393	1.62	5.75	1.63	0.284	1.97	0.314	50
Concentration controller of tower II	1.9	3.65	0.52	0.076	48.6	0.42	28.6	2.18	0.57	3.65	1.0	1.66

TABLE 2

	Individual control		Interconnected control		
	mean parameter value	mean deviation (δ_1)	mean parameter value	mean deviation (δ_2)	$\frac{\delta_2 \cdot 100}{\delta_1}$
Concentration controller of absorber I	0.65% H_2SO_4	0.0076% H_2SO_4	0.65% H_2SO_4	0.00628% H_2SO_4	82.6
Level controller of absorber I	33.6 cm	0.5 cm	33.7 cm	0.4 cm	80.0
Concentration controller of tower II	0.275% H_2SO_4	0.021% H_2SO_4	0.276% H_2SO_4	0.0169% H_2SO_4	80.5

trolled assembly under production conditions in a chemical plant showed a decrease in dynamic deviations of the controlled parameters of 33%.

SUMMARY

The paper demonstrated the possibility of obtaining autonomy in interconnected control schemes for technological processes by means of simple electrothermal devices analogous, in their physical design, to electrothermal isodromes. The initial data for determining the parameters of these devices are the parameters of the leading and driven controllers. The paper gives the method for determining these parameters. An experimental verification of the method suggested for realizing crossover communication on a simulator showed the capabilities of increasing dynamic control accuracy. The advantages of this method of realizing autonomy in interconnected control schemes for technological processes are:

a) simplicity of introducing autonomous or interconnected control in individually acting controllers;

b) no necessity to complicate the controllers' measuring elements;

c) capability of obtaining large time constants, which is particularly important for inertial plants;

d) simplicity of physical design and reliability of operation.

These advantages allow one to recommend the introduction of electrothermal communication devices in autonomous control systems.

LITERATURE CITED

1. L. N. Voznesenskii, "On the question of choosing a control scheme for turbine generators," Towards a Soviet Energy System [in Russian] (Gosénergoizdat, 1934).
2. L. N. Voznesenskii, "On the control of machines with large numbers of controlled parameters," Avtomat. i Telemekh. No. 4 and 5 (1938).
3. G. M. Fialko and D. L. Mil'man, "Controllers for the interconnected control of acid concentration and level in the drying-absorbing sections of plants for the production of sulfuric acid by the contact process," Tr. UNIKhIM No. 3 (1955).
4. A. K. Sushkevich, Fundamentals of Higher Algebra [in Russian] (OGIZ, 1941).
5. G. M. Fialko and L. A. Kostromitin, "Electrothermal isodrome with tuned isodrome time," Patent application No. 768557, Aug. 13, 1949.

6. V. D. Mironov and E. P. Stefani, Electronic Automatic Controllers of Thermal Processes [in Russian] (Gosénergoizdat, 1955).

7. G. M Fialko, "Simulation and computation of optimal parameters of an automatic control system in chemical industry," Proceedings of the Second All-Union Conference on Automatic Control Theory [in Russian] (Izd. AN SSSR, 1955) 2.

CONTROL OF CHEMICAL PRODUCTION PROCESSES BY INDICATORS OF PRODUCT QUALITY

V. V. Aronovich, I. A. Anisimov, M. I. Lyudmirskii, and R. S. Patushinskaya

Moscow

Translated from Avtomatika i Telemekhanika, Vol. 21, No. 6, pp. 821-832, June, 1960

As applied to chemical production, automatic control, in the overwhelming majority of the cases, reduces to stabilization of the processes by maintaining the constancy of indirect parameters: temperature, pressure, discharge, level, etc. Such control satisfies the requirements of a given yield and quality of the end product only under the condition that the composition and quality of the raw material are constant. If these conditions are disturbed, the necessity arises of manually resetting the data transmitter mechanisms of the majority of controllers. More complete automation of a process can be achieved only by control in accordance with the indicators determining the quality (composition) of the selected intermediate and end products. With this, the task of process optimization still rests with the operator. The transition to complete automation can be made if the optimization is implemented automatically.

Below we provide several examples of control by qualitative indicators.

A typical process in chemical industry is continuous fractionating. The requirements of obtaining fractionating products of a strictly given composition, with a simultaneous intensification of the process and an increase in its economy, can be fulfilled only with complete automation of the fractionating column. The use of automation is the more important when the components to be separated have boiling points which are close together, and when there is withdrawal of intermediate fractions.

In this case, a beneficial effect can be achieved with cascaded control with the simultaneous use of quality (composition) controllers of the end and intermediate products.

As is well known, for stable operation of any fractionating column, it is necessary to have an equality of the material and heat flows entering and leaving the column. With this, the consumption of heat for separation must be minimal. Moreover, for the withdrawal of distillate, vat residue and intermediate fractions with a minimum of admixtures, it is necessary to maintain a definite form of the composition distribution curve along the height of the column.

We consider a scheme for the automation of a fractionating column as applied to the rectification of alcohol (Fig. 1). In the initial product which is to be rectified, the constitution by weight is 48% ethyl alcohol, 50% water and 2% higher alcohols. The rectification task is to obtain a distillate whose weight composition must be 89-90% ethyl alcohol and not more than 0.1% higher alcohols, with a vat residue (fusel water)* containing no more than 0.01% ethyl alcohol, and intermediate fractions containing 10-12% higher alcohols.

The scheme can also be recommended for the separation of other mixtures.

To control the supply of raw material (the intermediate product of the low-boiling fraction), discharge controller D is used, its setting being established by the production personnel as a function of the presence of raw material and the required productivity of the column.

For the control of the composition of the vat product (fusel water) and the composition of the intermediate fractions – the higher alcohols – three-stage assembly K_{fw} is used. The first stage of the control assembly acts on the valve installed on the steam supply line from the boiler. The rate of steam discharge is established automatically from the output quantity of the second stage which measures the temperature in the steam area of the column's fifth plate. The dependence of the amount of higher alcohols accumulated in their tap-off zones (the third, fourth, fifth and sixth plates) on the temperature in the steam area of the fifth plate (this temperature equals 96 to 98°C) has been theoretically established and experimentally verified. In its turn, the assignment of the temperature is automatically established from the output quantity of the transducer measuring the alcohol loss in the fusel water (third stage).

Operation of controlling assembly K_{fw} proceeds in the following manner: The controller's temperature data transmitter on the fifth plate is set to its least value, the controller's alcohol loss data transmitter is set for minimal

---

*"Fusel water" ("fuzel'naya voda") is apparently the Russian term for the mixture of fusel oil and water left as residue after distillation of the alcohol [Publisher's note].

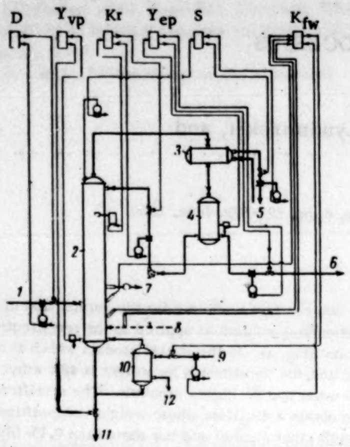

Fig. 1. Schematic of an automated alcohol fractionating column. 1) Intermediate product of low-boiling fraction, 2) column, 3) condenser, 4) storage tank, 5) cooling water, 6) rectified alcohol, 7) fraction of higher alcohols, 8) saturated water vapor (for measuring losses), 9) heating steam, 10) boiler, 11) fusel water (vat product), 12) steam condensate.

loss. If the actual loss turns out to be greater than the admissible value, the temperature assignment is automatically changed, increasing the assigned temperature value on the fifth plate. As a result, the application of steam to the "concentrated" vat product is increased.

The three-stage controller just described makes it possible to control the contents of the vat product and the intermediate fractions by controlling the application of steam as a function of the changes of two parameters, and by establishing the required tap-off of the intermediate fractions. The presence of this cascaded controller virtually eliminates the disturbing stimuli which arise due to oscillations in steam pressure. As a result of its operation, the assembly automatically expends a minimal quantity of steam; a further decrease in steam supply leads to an increased loss of alcohol in the tapped-off fusel water. Withdrawal of the intermediate fractions occurs from the zone of maximum concentration.

For the control of the required composition of the final product (the distillate), cascaded control is also used. Two-stage controller Kr consists of a controller of reflux discharge which acts on the end product return valve. The assignment of reflux discharge is automatically established by the end product composition transducer. This transducer is installed on the tenth plate from the top where, for an insignificant change in composition, there occurs the greatest change in the transducer's output quantity.

The equality of the thermal flows entering and leaving the fractionating column is maintained by the elasticity of the steam in the column by means of two-stage control assembly S, consisting of a discharge controller which acts on the supply of cooling water. The assignment of the discharge is automatically established from the pressure transducer. The balance of the material flows is maintained by level controller Y_{vp} in the vat column, acting on the withdrawal of the vat product. In addition, control is provided for the withdrawal of distillate from the tower by end product controller Y_{ep}.

With the use of the control system just described, the column operates completely automatically. If the operator has increased the supply of raw material for rectification, then, in the column, there will be a decrease in temperature (thanks to the introduction of the additional quantity of raw material), the temperature controller of the three-stage controller operates, and the assignment of steam supply to the column vat is increased. As a result of the increased supply of steam, the pressure in the column is raised. With this, the pressure transducer of controller S changes the assignment of water discharge, increasing the supply, i.e., the supply of steam and water will be put into correspondence with the increased load. The withdrawal of distillate and vat product is also increased automatically. With the introduction of an additional quantity of raw material into the column, the concentration of alcohol on the plates is increased. With the action of the rectificate composition transducer, the supply of reflux is decreased, the level in capacity of the end product is increased, and withdrawal of rectificate is increased. With an increase in raw material supply, there is also an automatic increase in the withdrawal of the higher alcohol fractions. Obviously, the scheme will operate analogously if there is an increase in alcohol content of the raw material supplied.

To implement the scheme just described, there were developed special quality indicator transducers for determining rectificate, vat product and higher alcohol fractions composition.

The operation of the instrument for distillate composition is based on a comparison of the buoyancies of the vapors of standard fluids and the vapors found in the column. The standard fluid fills a hull whose inner surface is a bellows: the hull is mounted in the column. The pressure difference experienced by the bellows is transmitted, via a special frictionless gasket, to the pneumatic compensation system. The pressure of the compensating air is proportional to the difference in buoyancy, i.e., to the composition of the vapor at the corresponding point of the column. The instrument can be used for binary mixtures. For multicomponent mixtures, the instrument is useful only in the case when the content of all the com-

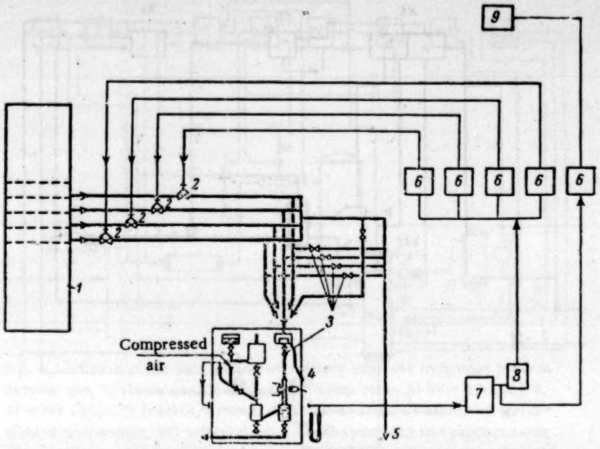

Fig. 2. Schematic of the instrument for measuring concentration of the higher alcohols. 1) Column, 2) valve membrane, 3) stopcock, 4) photoelement with lamp, 5) higher alcohol fraction, 6) storage device, 7) pressure measurer, 8) controlling block, 9) concentration measurer.

ponents (apart from the investigated ones) remains invariant.

The transducer for determining the composition of the vat product (the instrument for determining the loss of alcohol in the fusel water) works on the basis of the phenomenon that the boiling temperatures of the pure high-boiling component and the vat residue are different. If, in the vat area of the fractionating column, there is introduced an insignificant amount of saturated water vapor (high-boiling component), then, from the magnitude of temperature difference between the steam just introduced and the steam already existing in the column, one can determine the content of the highly volatile component (alcohol). For this, the pressure of the introduced steam must equal the pressure in the column, for which the delivery of the steam is implemented via a valve and the condensation chamber. The temperature difference is measured by resistance thermometers (200 ohms) in conjunction with a standard electronic bridge scaled for one-ohm impedance differences. Thermometers are installed in the condensation chamber and in the column vat.

The instrument for determining the composition of higher alcohols operates periodically with a cycle of 5 to 6 minutes on the principle of stratification of the higher alcohols in a saturated solution of sodium chloride (Fig. 2). The command instrument (a timer) every five minutes automatically extracts a specimen of definite volume from the corresponding plate and mixes it with a proportioned volume of sodium chloride solution. After mixing, stratification occurs; the higher alcohols, being lighter, are distributed higher. Thanks to the choice of the proper dyes, the layer of higher alcohols is sharply distinguished by its color. Compressed air, automatically supplied after stratification, forces the mixture into a measuring container where a device with a photoelement reacts to the passage of the plane of stratification of the higher alcohols from the remaining components of the solution. With this, there is ascertained, and stored, the air pressure, which is proportional to the volume occupied by the higher alcohols. The stored pressure acts on the controlling valve installed at the outlet from this plate. Simultaneously with the storing of the pressure, there occurs a decantation of the fluid from the instrument and the withdrawal of a specimen from another plate. A cycle during which there is established the necessary withdrawal from the four tables occupies from 20 to 25 minutes. Moreover, the instrument determines and fixes the mean content of the higher alcohols in the common collector, so that a full cycle takes about 30 minutes. Since the redistribution of the higher alcohols occurs slowly, cyclical operation with a 30-minute period is fully justifiable.

The control system just described was implemented at one of the factories and operated successfully for more than a year and a half. As the result of its introduction, the expenditure of steam and water per ton of raw material was decreased by approximately 4 to 5%, the productivity of the aggregate was increased by 5%, disruptions of the technological regimen were eliminated, and, in particular,

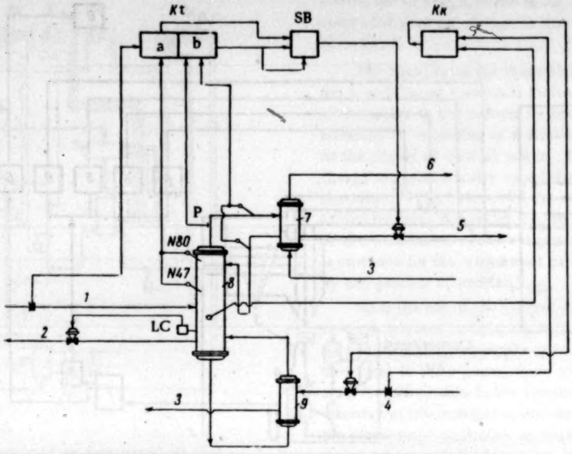

Fig. 3. Schematic of an automated column for hydrocarbon separation. 1) Ethane-ethylene group, 2) ethane fraction, 3) propane-propylene fluid, 4) gaseous propane-propylene, 5) ethylene fraction, 6) propane-propylene vapor to the compressor, 7) condenser, 8) column, 9) boiler.

there was a decrease in the losses of alcohol in the fusel water.

On the same principles there was constructed a control system by quality indicators for another fractionating process, intended for the separation of hydrocarbon mixtures (Fig. 3).

The rectifier is supplied with an ethane-ethylene fraction with an admixture of methane and propylene. The fraction has a nonconstant composition. The distillate withdrawn is the ethylene fraction with a minimal content, while the vat product is the ethane fraction with a minimal ethylene content. The pressure in the column is 22 kg/cm^2.

The column vat control assembly Kk, consisting of a heat carrier discharge controller and a vat composition transducer, varies the supply of heat carrier to the column.

Column top controller Kt, consisting of the ethylene fraction (distillate) discharge controller and the distillate composition transducer, varies the withdrawal of the distillate.

Equality of the flows of entering and withdrawn materials is maintained by level controller LC, acting on the withdrawal of ethane. Equality of heat flows is controlled by pressure transducer P, acting on controller Kt and then on the withdrawal of ethylene.

The quality of the upper product (the distillate) is determined by the temperature difference between two points fastening parts of the column. For different disturbing stimuli, worsening the distillate composition, an increase in the content of ethane in the ethylene occurs more intensively on the lower plates, i.e., "contraction" of the column begins, leading to an increase in the temperature difference. Conversely, with an increase in saturation of the column by ethylene, a decrease in the temperature difference occurs. It should be mentioned that pressure oscillations in the column have little effect on the magnitude of the temperature difference. The temperature difference is determined by resistance thermometers in conjunction with one type EMD instrument, calibrated for a measurement range of 0 to 5°C (the range of temperature differences). Experimental results have established that the most characteristic points are plates 47 and 80. The output quantity of the temperature difference instrument changes the assignment on the ethylene withdrawal controller. In view of the large capacity of the column and the large magnitude of the transient and transfer lags in the scheme, there were introduced additional correcting pulses as functions of the speed of variation of the magnitude of the load on the column, i.e., as functions of the speed of variation of the fundamental disturbing stimulus. These pulses are formed by means of a lead block and the controlling block and, in conjunction with the pulses for the temperature difference between plates 47 and 80, act on the assignment of the ethylene withdrawal controller (assembly a). It should be taken into account that, when a mixture containing methane is supplied to the column, the instrument for the temperature difference between plates 47 and 80 begins to

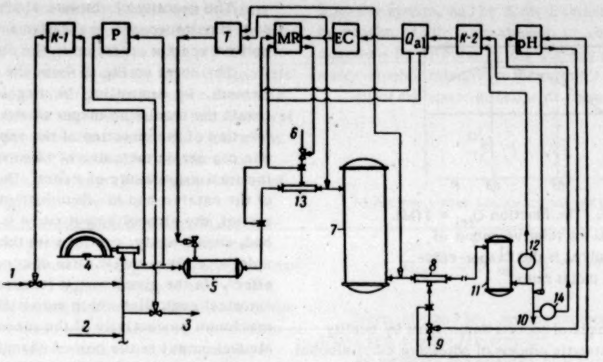

Fig. 4. Scheme of the automation of a direct ethylene hydration process. 1) Fresh gas, 2) return gas, 3) exhaust, 4) compressor, 5) heat exchanger, 6) water vapor, 7) reactor, 8) neutralization T-bend, 9) alkalized water-alcohol condensate, 10) water-alcohol condensate, 11) end product tank, 12) specific gravity transducer, 13) mixing T-bend, 14) concentration pH transducer.

give incorrect indications; the presence of methane also worsens the conditions for condensation of ethylene in the dephlegmator, which leads to an increase of pressure in the column. In view of the impossibility of condensing methane due to the absence of a supply of a freezing agent, it is drawn out from the column together with the ethylene fraction, i.e., the withdrawals from the column are increased apart from the dependency on the saturation status of the ethylene. To determine the methane content in the ethylene fraction, there is used the temperature difference of the phlegm and the upper part of the column, which is increased by the presence of methane. However, the indication of temperature difference can also be increased without the appearance of methane (for example, for a decrease in the amount of phlegm). Therefore, it is necessary to change the ethylene withdrawal controller assignment as a function of the temperature difference between the phlegm and the top of the column only with the condition that there has been a simultaneous rise in the pressure in the column. For this, the pulses from the instruments (transducer for the temperature difference between the phlegm and the top of the column, and the pressure transducer) are applied to the right side of controller Kt (assembly b) and, if a definite magnitude is reached, act on the switching block SB, thereby connecting the data transmitter for the ethylene withdrawal controller with the output from the transducer for the temperature difference between the phlegm and the top of the column (or of the pressure).

Thus, with normal column operation, the assignment of the ethylene withdrawal controller is established as a function of the quality of the upper product, with corrections for the speed of change of the load, and for the appearance of methane in the column, as a function of the methane content with a simultaneous increase of pressure in the column.

Equality of the quantities of heat entering and leaving the column is controlled by controller Kt from signals applied from pressure transducer P.

As the transducer for end product composition, a recording chromothermograph is used. So that the chromothermograph could be used as a controller, a special attachment was developed [2] which implements the following functions: fixing of the ethylene's peak amplitude on the chromatogram, which approximately corresponds to its concentration, by volume, in the end product; 2) transformation of the peak amplitude to a proportional magnitude of compressed air pressure (within the limits of 0 to 1 atm); 3) storing this air pressure until the results of the subsequent analysis are obtained.

The attachment consists of a ratchet mechanism with a rheostat transducer, and electromagnetic relay and a type ÉMD electronic balanced bridge; the attachment's operation is controlled by a timer.

As a function of the ethylene content in the end product, the output quantity (pressure) of the controlling chromothermograph attachment is changed; this pressure is applied to the data transmitter of the heat carrier (propane-propylene vapors) discharge in the fractionating column boilers.

The system just described, installed in one of the synthetic alcohol factories, turned out to be workable, and a prolonged industrial test is currently in progress.

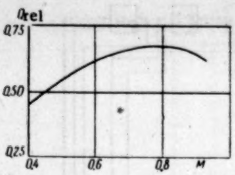

Fig. 5. The function $Q_{rel} = f(M)$. Q_{rel} is the relative output of alcohol, M is the "vapor-ethylene" molar ratio.

The next example of process automation by quality indicators is the catalytic process of obtaining ethyl alcohol by the direct hydration of ethylene (Fig. 4).

Concentrated ethylene with an admixture of ethane and methane (the forward gas) is mixed with the gas which did not react in the reactor (the return gas) and is supplied, via a system of heat exchangers, to an adiabatic reactor. After entry into the reactor, the gas is diluted in a given ratio by live steam in the mixing T-bend. In the reactor, at a definite temperature, there occurs the catalytic transformation of the steam-gas mixture to ethyl alcohol. The unreacted gas is separated in separators, is mixed with concentrated ethylene and applied to the compressor intake, where it is compressed and then is recirculated through the system.

Used as the catalyst is phosphoric acid on a solid carrier, with part of the acid being carried off by the gases, so that the steam-gas mixture leaving the reactor is subjected to neutralization by the alkalized water-alcohol condensate. After neutralization, the water-alcohol condensate is separated from the steam-gas mixture in the system of separators, after which it is directed to the fractionating column for fixing.

The activity of the catalyst used drops during a definite period of use, so that the necessity of replacing it arises, and therefore, the process of obtaining alcohol by the direct hydration method is carried on periodically.

The systems, used in the majority of factories, of controlling individual unconnected parameters (temperature and pressure before the reactor, steam-ethylene ratio, etc.) do not provide the maintenance of an optimal operating mode, for which one attains the maximum output of alcohol per ton of ethylene fed through with a minimal expenditure of water vapor.

For optimization of the process, an automation scheme was suggested which is based on the existence of an empirical relationship between the quantity of absolute alcohol obtained from direct hydration systems and the molar ratio of steam vapor to the circulating ethylene (Fig. 5). This relationship was obtained in NII synthetic alcohols on a reactor model, and was reinforced by further theoretical investigations.

The quantity of absolute alcohol is that quantitative, and, simultaneously, qualitative indicator which defines optimal reactor operation in the direct hydration system.

The curve on Fig. 5 shows the presence of an extremum. By controlling the magnitude of M, one can obtain the maximum output of alcohol whereby, as a function of the direction of the approach to the extremum, one can obtain the value of M corresponding to the minimal expenditure of steam. Due to the change of state of the catalyst and the disturbances of the process parameters, the alcohol output curve is continuously shifted, and, consequently, control with the aim of maintaining a definite given molar ratio does not give the necessary effect. In the given case, it is more effective to use an extremal controller which automatically maintains the maximum productivity of the reactor in terms of absolute alcohol output as the cost of changing the molar ratio.

The quantity of absolute alcohol obtained also depends on the reactor temperature, in that an increase in the reaction temperature causes the transformation of the ethylene to proceed more intensively and, consequently, increases the output of alcohol, but, with this, the catalyst is depleted; and there is a corresponding shortening of its useful life. Depletion of the catalyst is characterized by the temperature in the lower portion of the reactor, while the degree of transformation of the ethylene is characterized by the temperature in the reactor's upper portion. The temperature in the reactor's upper portion must increase as a function of the time of catalyst operation. In practice, there exists a temperature range inside of which there occurs a resetting of the data transmitter every four or five days. With an increase of temperature in the reactor's lower portion, the assignment for its upper portion must necessarily be decreased.

The automation scheme must also provide for control of the pressure and concentration of the ethylene applied to the reactor. In addition, it is necessary to control the intake of alkalized water-alcohol condensate in the neutralization T-bend, with the aim of maintaining a constant alkalinity (pH value) of the mixture obtained in the reactor.

In correspondence with all this, the scheme proposed for automating the process of direct ethylene hydration (Fig. 4) contains the following elements.

Controller MR, maintaining the molar "steam-ethylene" ratio and acting on the valve for the steam supply to the mixing T-bend. To the assignment chamber of controller MR there is applied the output coordinate of extremal controller EC. To the input of controller EC there is applied a signal from the assembly measuring the output of (obtained) absolute alcohol Q. Concentration measurer K-2 is intended for the introduction of corrections to the indications of assembly Q_{al}.

In actual production, there occur changes in the supply of ethylene and, from this, oscillations in the obtaining of absolute alcohol. As a result, with the presence of lags in the system, there occurs a "false" translation of the extremal controller which, essentially, increases the time necessary for finding an optimum of the process. In some intervals of time, the changes in ethylene supply occur more frequently than the time necessary for the automatic determination of an optimum. To create more favorable operating conditions for the extremal controller, there was adopted, as the quantity to be optimized, the ratio of the quantity of absolute alcohol obtained to the quantity of circulating ethylene, i.e., the aggregate's productivity of alcohol per ton of circulated ethylene.

Two-pulse temperature controller T is used for controlling the reactor temperature by acting on the steam supply valve feeding the heat exchanger. The temperature assignment for the reactor's upper portion is set by hand from the graphs. Over an entire run, the magnitude of the assignment is changed three or four times; for deviations of the temperature in the lower portion from the assigned value, there is an automatic correction made of the magnitude of the assignment for the reactor's upper portion. Controller T consists of two electronic potentiometers whose output signals are applied to the controlling block.

Pressure controller D, consisting of standard measuring elements, acts on the valve installed on the gas "exhaust" line.

Ethylene concentration controller K-1 varies the supply of the forward gas in the circulation system. An infrared gas analyzer, based on the selectivity of the absorption effect of hydrocarbon gases in the infrared portion of the spectrum, is used as the controller's transducer.

Control of the hydrogen-ion concentration in the water-alcohol condensate is effected by an electronic pH meter with a pneumatic output, in conjunction with highly alkaline electrodes. Maintenance of the pH of the concentration is implemented by changes in the quantity of the alkalized water-alcohol condensate introduced into the neutralization T-bend. In connection with the circumstance that the proper temperature must be given to the alkalized condensate, a two-pulse pH controller is used after the neutralization T-bend, i.e., there is a temperature correction introduced.

To implement the control scheme, it is necessary to measure continuously the quantity of absolute alcohol obtained from the hydration system. Direct measurement of the quantity of water-alcohol condensate, with its subsequent concentration correction, fails to give the requisite effect because of the liquid's high temperature. Moreover, a variable quantity of alcohol is continuously introduced into the hydration system in the form of the alkalized water-alcohol condensate.

To determine the absolute quantity of alcohol, one can use an equation obtained from a consideration of the balance of the water introduced into the reactor and the water contained in the water-alcohol condensate after the reactor. If we denote by W the weight in tons of the water vapor introduced into the reactor, then this same weight of water will be obtained at the tank's output. Denoting by W_{al} the weight in tons of absolute alcohol obtained from the system, and by K the fractional concentration, by weight, of this same alcohol, we obtain the following equations for calculating the quantity of water in the water-alcohol mixture at the system's output:

a) for the water mixed with alcohol

$$\frac{W_{al}}{K}(1-K);$$

b) for the water necessary for obtaining the alcohol

$$\frac{M_w}{M_{al}}W_{al}=\frac{18}{46}W_{al}=0.39\,W_{al}.$$

Here, M_w and M_{al} are the molecular weights of water and alcohol, respectively.

By equating the quantity of water vapor used with the water in the water-alcohol mixture, we obtain

$$W_{vap}=\frac{W_{al}}{K}(1-K)+0.39\,W_{al};\qquad(1)$$

or, after transformation,

$$W_{al}=\frac{W_{vap}K}{1-1.61K}.\qquad(2)$$

In view of the absence of a device for automatically solving Eq. (2), it can be transformed to a multinomial. For this, we expand expression (2) in a series of powers of the difference $\Delta K = K - K_a$, where $K_a = 0.105$ is the actual mean concentration by weight.

By using Taylor's formula, and limiting ourselves to the first two terms, we obtain

$$W_{al}=0.1122\,W_{vap}+1.14\,W_{vap}\Delta K.\qquad(3)$$

By substituting, in the second term of Eq. (3), the mean expenditure of steam, equal to 11.25 tons/hour, we get

$$W_{al}=0.1122\,W_{vap}+12.74\Delta K.\qquad(4)$$

Automatic solution of Eq. (4) can be implemented by pneumatic adding elements of the MAUS system. Pneumatic signals are applied to the adder from the steam expenditure and from concentration measurer K. The concentration of the water-alcohol condensate is determined from the specific gravity for constant temperature, with the condition that the hydrogen-ion concentration, the pH, be maintained constant.

In the measurement of the discharges of ethylene and steam and the concentration of the water-alcohol condensate, there occur momentary oscillations of these quantities, so that there arise synchronous distortions of the value of the quantity to be optimized. To eliminate these distortions, the values of concentration and steam and ethylene discharges are averaged by means of integrators which permit the determination of total value over a definite interval of time, i.e., a quantity proportional to the average value of the measured parameter during that same interval of time. An integrator consists of an aperiodic link with positive feedback and an adding link. The aperiodic link is a series connection, of a variable pneumatic impedance (a throttle), and a pneumatic capacitance; the link's gain can be changed by changing the throttle opening.

For the automatic determinations of the quantity of absolute alcohol obtained and of the quantity to be optimized, it is necessary to take into account that the changes in the discharges of the circulating gas and water vapor applied to the mixing T-bend occur at the beginning of the technological scheme of the process, whereas the measurement of water-alcohol condensate concentration occurs at the end. Lag time, determined experimentally, is about 8 to 10 minutes. Therefore, in the measurement and control systems, there is introduced a time shift between the application of signals from the ethylene and steam discharge transducers and the alcohol concentration transducer. For this there are used pneumatic devices, developed in the IAT AN SSSR [3], which permit the storage of the discrete quantities put out by the integrators.

In the scheme used for integration with account taken of a time shift (Fig. 6), it is provided that the output pressures from the discharge meters for ethylene DT-2 and for steam DT-1, and from concentration determination element K-2, are applied to the corresponding integrators with 10-minute integration times. The integrated value of concentration from integrator IN-3 is applied directly to the device for discharge measurement DM, and the results of the integrations of the ethylene and steam discharges are applied from integrators IN-1 and IN-2 to storage devices S-2 and S-4. The integrated values are retained in these storage elements for 10 minutes, and are then transmitted to elements S-5 and S-6, whence, with a 10-minute shift with respect to the integral value of the concentration, they are applied from S-5 to the RB block, and from S-6 to the DM block. After transmission of the stored values to the second set of storage elements, the first set is cleared for reception of the new integral values.

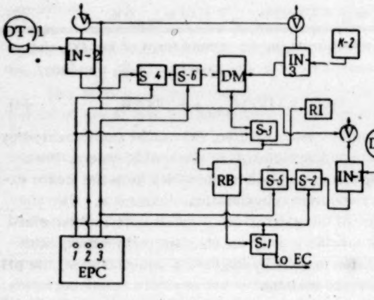

Fig. 6. Integration scheme with a time shift. V is a valve; DT-1 and DT-2 are the discharge transducers for steam and ethylene, respectively; IN-1, IN-2, IN-3 are integrators; S-1, S-2, S-3, S-4, S-5 and S-6 are storage devices; DM is the measurer of absolute alcohol discharge; RI is the recording instrument; RB is the ratio block; EC is the extremal controller; EPC is the electropneumatic command instrument.

The twinning of the storage elements is designed to eliminate oscillations of the integrated values during the switching period. Each 10.5 minutes valves V are opened automatically, and the pneumatic capacitors are discharged into the atmosphere, i.e., the integrated value is cleared to zero. After closure of valves K, the integrators are again prepared for new integrations. All switching operations are carried out by the electropneumatic command instrument EPC in accordance with a given graph.

As the extremal controller in the proposed scheme, it was suggested that one use a type ÉPR pneumatic series controller with a stored maximum. However, in connection with the complexity of the control problem, it turned out to be necessary to introduce the following changes:

1. On the curve of the function "relative output of alcohol – molar ratio" (Fig. 5), there does not in practice exist a clearly expressed extremum point and, consequently, it is impossible to use a controller with storage of the maximum, since a controller of this type will transfer to this maximum. In the case given here, it is necessary to provide a comparison of each succeeding value, not with the maximum value, but with the preceding one (to use a controller of the step type).

2. Experimental data, taken off from an operating hydration system, showed that during a system run there occurs a continuous shift of the maximum in arbitrary directions, so that a working point lying on the curve's left arm actually falls on its right side, which leads to a sharp increase in steam discharge to the mixer for one and the same output of alcohol. Therefore, such an extremal control system is necessary for which the approach to the extremum, for any direction of its translation, is always carried out on the side of the least discharge of steam (a controller with nonreturn to the maximum).

3. Since the quantity to be optimized is applied discretely to the optimizer and does not change during a 10-minute period, the output pressure from controller EC will continuously change, attaining an inadmissible magnitude. It is necessary to provide a limitation on the time of change of the output pressure.

4. The "steam-ethylene" ratio varies only within definite limits, given by the technological regulations, since it is necessary to establish a limit on the pressure at the controller's output.

In the scheme described, the transition to a step-type controller was implemented by installing a block for the comparison of the last magnitude p_{last} with the previous one p_{prev}. This block is so adjusted that a change in direction of the controller's output pressure (reverse) occurs, not only when $p_{last} < p_{prev}$, but also for $p_{last} \leq \leq p_{prev} + \Delta p$, where Δp is a previously given small pressure.

The simultaneous installation of two comparison blocks (last magnitude with the maximal and with the preceding magnitudes) and logical elements for conjunction and disjunction permitted the implementation of approach to the maximum from the side of the least expenditure of steam. The limitations introduced into the controller were implemented by means of a signalling relay and logical disjunction elements, and the step-function output from the controller was achieved by installing a pneumatic interruptor, controlled by command instrument EPC.

Use of this scheme permitted the transition to a completely automatically controlled direct ethylene hydration aggregate. Preliminary tests showed the capability of essentially increasing the output of alcohol. The use of the automation scheme turned out to be particularly effective at the ends of the system's runs — output was increased by 15 to 25%; the increase in alcohol output at the beginning of the run was about 5 to 8%. The figures just cited were obtained by integrating the curves of alcohol output at the beginning and end of runs with the control system switched in, and switched out. It was simultaneously found that the optimal magnitude of the "steam-ethylene" molar ratio is lower than that established by the chart of the technological regimen. Thus, for the optimal recommended molar ratio M = 0.75, the actual M, found by the extremal controller, was about 0.65 to 0.68. The transition to the lower ratio gives a significant economy of steam without simultaneously shortening the useful life of the catalyst.

Testing on the efficiency of use of the entire system continues.

SUMMARY

1. The workability was verified, for several typical processes, of an automatic control system using instruments for quality indicators.

2. The possibility was proven of completely automatic control of these processes for variable quality and quantity of raw materials.

3. Special quality transducers were developed which provide an accuracy in measuring product composition on the order of 0.1%.

4. The possibility was demonstrated of creating quality transducers from standard measuring elements connected in logical schemes.

LITERATURE CITED

1. V. V. Aronovich and L. A. Anisimov, "Quality indicator controllers of the fractionating process," Vestnik Tekhicheskoi i Ékonomicheskoi Informatsii Goskhimkomiteta No. 6 (1958).

2. M. L. Lyudmirskii, "Controlling attachment to a chromatograph," Vestnik Tekhnicheskoi i Ékonomicheskoi Informatsii Goskhimkomiteta No. 5 (1959).

3. T. K. Berends and A. A. Tal', "Pneumatic calculating devices. Automation of chemical production," Collected Papers [in Russian] (Izd. Goskhimkomiteta, 1959) 4.

DEVELOPMENT OF APPARATUS FOR THE AUTOMATIC CONTROL OF BOILER AGGREGATES

V. D. Mironov

Moscow

Translated from Avtomatika i Telemekhanika, Vol. 21, No. 6, pp. 833-839, June, 1960

The principles of constructing electronic sampled-data systems of automatic control are presented.

A VTI contact controller system is considered. The path is pointed out for the further improvement of sampled-data control systems.

The development of the means of automatic control of boiler aggregates engaged the attention of many specialists in the Soviet Union more than 30 years ago. The first serious successes were obtained in the direction of developing hydraulic control systems with jet amplifiers.* There were constructed trial specimens of various electrical systems, including photoelectronic,† induction-electronic‡ and also those based on the use of a contact measuring instrument (including a controller with a "falling arc").** Work on automation of boiler aggregates was broadly developed after 1945. The basis for this was the aforementioned hydraulic control system, controller systems with "falling arcs" and the newly developed "electromechanical" control systems† which were used as standards in all new boiler aggregates. Further efforts, directed toward the development of more highly perfected controllers, led to the development of an "electronic" system** which by degrees displaced the other designs and is today the standard for the new powerful stands.

We now turn to the consideration of modern electronic automatic control systems. The following principles underlie the systems' construction: parallelism of inspection and control, electrical methods of action, sampled-data character of the executive mechanisms' control. Prolonged, massive industrial testing of electronic controllers verified the correctness of the choice of these principles, which were also retained for the succeeding perfected electronic systems.

1. The Principle of Parallelism

Common to all the developed means of automatic boiler aggregate control considered is the principle of parallel action of the automation and inspection devices.

In a number of branches of industry, a different system of inspection and control has been used until now, a system in which the automatic controller is connected in series with the secondary inspection instrument (the so-called "instrument" system). In this variant, a disturbance of the function of the inspection instrument leads to a complete disruption of the control system as a whole.

With parallel action of independent inspection and control systems (in the so-called "apparatus" type systems), the reliability is significantly improved. In this case, one arm is completely subsidiary to the second. The probability of disturbance of the automatic control arm is significantly lower here, since a fewer number of simpler elements are included in it. Increased reliability is furthered by the specialization of the functions of the control and inspection systems, which reduces the technical requirements imposed on the apparatus of each system separately, and leads to a simplification of the apparatus.

2. Electrical Methods of Action

Latterly, the development of control systems for boiler aggregates has confidently followed the path of using electrical means.

The use of electric energy for implementing the functions of signal transmission from measuring elements to the controller and beyond, to the executive mechanism—for purposes of amplifying signals, transforming them, forming the control laws—allowed one to unify homogeneous elements independently of the purpose of the controller, virtually removing limitations on the physical placement of the elements.

The use of electric energy removes the need to impose requirements on the qualitative state of the carriers of auxiliary energy, requirements which arise, for example, in hydraulic and pneumatic systems, and which lead to the necessity of employing additional equipment.

The capability of employing sensitive, low-inertia measuring elements possessing, as a rule, little energy, provides a high quality in the automatic controllers. The use of such elements presupposes the presence of high-gain amplifiers in the controller, since the controller's output element – the executive mechanism – must possess great mechanical energy. This requirement is easily met by certain electrical (for example, electronic) amplifiers which, at the same time, have little inherent inertia. The use of electronic amplifiers simultaneously opens up broad possibilities of introducing simple elements into the controllers for shaping the control laws.

---

* Developed by the "Teploavtomat" Plant.

† Developed by the Central Boiler-Turbine Institute (TsKTI).

‡ Developed by the All-Union Electrical Engineering Institute (VEI).

** Developed by the All-Union Heat Engineering Institute (VTI).

One has succeeded in building a controller in which high reliability of operation is joined with diversity of function, universality – with simplicity of manufacture, the convenience of adjustments collected on one panel of the calibrating organ – with stability of the adjustment parameters, a significant range of variation of these parameters with a high sensitivity and significant controller output power.

3. Block Schematics

A large role in the development of a control system is played by the choice of the optimal block schematic for the controller. In particular, it is of interest to compare the three characteristic schemes shown on Fig. 1.

The scheme of Fig. 1a assumes the presence of amplifier 2, acting on an astatic executive mechanism and feedback device 4, forming the device's control law, which shunts the amplifier and the executive mechanism. The capability of remote control of the executive mechanism is provided by means of device 5.

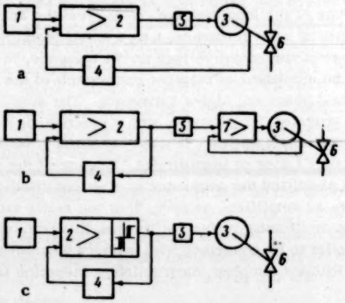

Fig. 1. Controller block schematics. a) A feedback path shunts the amplifier and an astatic executive mechanism, b) the feedback path shunts only the amplifier, while the astatic executive mechanism is transformed to a static one by the use of an auxiliary amplifier, c) the feedback loop shunts an amplifier with a relay characteristic; the executive mechanism is astatic with a constant velocity, 1) a transducer, 2) an amplifier, 3) an executive mechanism, 4) a feedback device, 5) a remote control organ, 6) a controlling organ, 7) an auxiliary amplifier.

In the scheme of Fig. 1b, forming of the control law is implemented by feedback device 4†† in a loop which shunts only amplifier 2. A system is formed which forms the control law in the form of an electric voltage (current) which is then processed by static executive mechanism 3. Since the output quantity generated by the forming device (properly speaking, by the controller) carries insignificant energy, auxiliary amplifier 7 has to be introduced into the executive mechanism. The ordinarily used astatic executive mechanism is transformed to a static one (i.e., to a servosystem) by shunting it, together with the additional amplifier, by a static feedback path.

In the scheme of Fig. 1c, an amplifier with a relay (trigger) characteristic is used, which also permits formation of the control law within the limits of controller 2 proper, but without the necessity of shunting the executive mechanism by a feedback circuit (as in the scheme of Fig. 1a), and without the necessity of using a second amplifier (as in the scheme of Fig. 1b). In contradistinction to the first two variants, however, there is now the specific requirement imposed here that the executive mechanism possess a constant speed. A comparison of the block schematics from the point of view of satisfying the basic requirements of their use – reliability of operation, implementation of the given control law, convenience of adjustment, maintenance, etc. – leads to the following conclusions.

The greatest reliability of operation can be achieved with a controller constructed in accordance with the scheme of Fig. 1c. The scheme of Fig. 1a is complicated by the presence of the external feedback path, disturbance of which leads to a sharp translation of the controlling organ. The scheme of Fig. 1b is complicated by the presence of the second amplifier and the second feedback circuit; disturbance of the forward path from the controller to the executive mechanism in this case leads to a sharp displacement of the controlling organ. The transition from remote to automatic control of the executive mechanism in the schemes of Figs. 1 b and 1 c also, as a rule, gives rise to sharp displacements of the controlling organ.

Implementation of the given control law may be executed with somewhat greater accuracy in the scheme of Fig. 1b, and, particularly, in the scheme of Fig. 1a. However, when the controlling organ reaches an extreme position here, there occurs a disruption of the control law, as a result of which the controlled quantity experiences a significant deviation after the return of the controlling organ to the range of control.

In all cases, one may achieve approximately equivalent convenience of adjustment and maintenance.

The cost of the apparatus turns out to be approximately equivalent for the variants of Fig. 1a and 1c, and is higher for the variant of Fig. 1b. In cases when it is necessary for one controller to control several identically displaced controlling organs, the cost of the variant constructed according to the scheme of Fig. 1b may turn out to be comparable to, and even less than, the cost for the other two variants. However, this advantage is accompanied by the defects that arise when the controlling organ, having reached an "end" position, returns to the range of control.

---

†† Formation of the control law can also be carried out in the amplifier's "forward" path without the use of feedback, but this entails great difficulty in its realization.

4. Electronic Controllers of the VTI System

With account taken of the considerations presented earlier, there was developed a reasonable universal electronic control system put in production in 1951. As the basic variant of this system, the structural scheme of Fig. 1c was realized, developed in more detail in the skeleton scheme of Fig. 2. The primary instruments 1, 2 and 3 measure the necessary quantities. The primary instruments provide, at their outputs, a dc or ac current proportional to the measured quantity. Signals from the primary instruments are applied to the electronic controlling instrument EC, containing a measuring device, an amplifier and a feedback device. In measuring device 5 there is implemented algebraic summation of the signals of the primary instruments and from manual data transmitter 4. The total voltage $\underline{x}$ from the measuring device is applied to amplifier 6. The output signal $\underline{y}$ is fed to feedback device 7, shunting the amplifier, and is also directed to the external circuit. In the executive circuit there are provided: switch 8 from automatic to remote control, remote control key 9, final amplifier (magnetic starter) 10, and executive mechanism 11 with shaft position indicator 12. The lower portion of Fig. 2 shows how the controller (connected in the PI and PID modes) processes a unit step of the input quantity $\underline{x}$.

In a complete electronic system there are provided diverse primary instruments (transducers) checking temperature, pressure, pressure drops, mechanical translations, ac current strength, oxygen content in gases, etc., the corresponding controlling instruments, executive mechanisms and auxiliary elements. Different combinations of instruments permit the implementation of simple and of complex (including connected) schemes for the realization of different control laws, etc..

Figure 3 shows a simplified schematic of one of the most widely distributed combinations, namely, a type EC-III (ER-III) electronic controlling instrument permitting simultaneous connection of from one to three primary instruments with induction transformers and acting on one executive mechanism. Controllers of this type are used, for example, for the automation of boiler aggregate supply, for controlling the ratios of steam-air and heat-air, for controlling evacuation of the fire boxes, etc.

The controller's measuring device contains the power supply for the three induction transformers and a potentiometer, filling the role of a manual data transmitter. Together with the transformer supplying its winding, each induction transformer forms an equilibrium bridge in the diagonal of which a voltage divider is connected, enabling the necessary fraction of the signal from the given transducer to be used. The data transmitter circuit forms an analogous bridge as well.

The algebraic sum of the voltages from the transducers (zero in the steady state) is applied to the electronic device which contains an input transformer and a two-stage balancing phase-selective amplifier with a relay output, shunted by a negative feedback path of RC elements.

The amplifier is supplied with a variable anode voltage. Its first stage is connected in a parallel scheme and is distinguished by the presence of a capacitor which shunts the anode load resistor. From the output of the first stage is obtained a smoothed dc voltage whose sign depends on the phase of the input voltage. This gives the amplifier the property of noise resistance, i.e., a small functional dependence of the output voltage on the presence, in the signal to be amplified, of reactive components of the fundamental phase and higher harmonics. The amplifier normally operates, for example, with a reactive signal at its input whose amplitude is some ten times greater than the controller's zone of insensitivity. The use of the given amplifier permitted the avoidance of a serious disadvantage of ordinary ac amplifiers, namely, their too facile saturability for small noise levels. In its turn, this permitted the controller to be connected with primary instruments provided with the simplest, most reliable, induction trans-

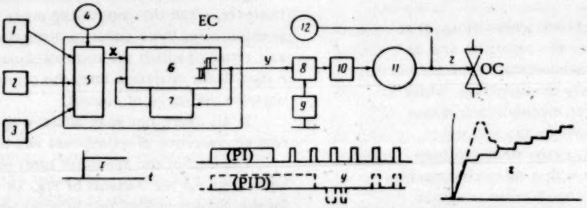

Fig. 2. Skeleton scheme of an electronic controller. 1, 2, and 3) primary instruments (transducers), 4) data transmitter, 5) measuring device, 6) amplifier, 7) feedback device, 8) operation mode switch, 9) remote control key, 10) magnetic starter, 11) executive mechanism, 12) shaft position indicator.

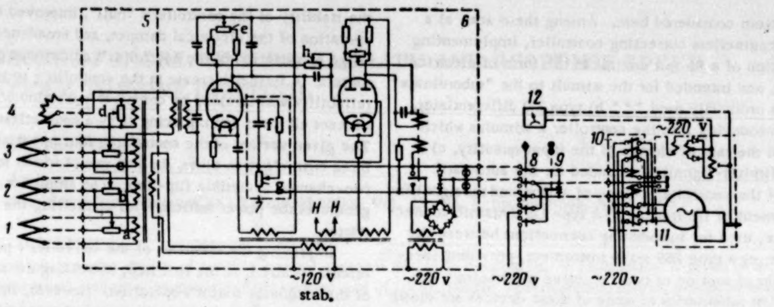
5
6
e
i
h
12
4
d
3
2
1
a
f
g
7
H H
10
~220 v
8
9
11
~120 v
stab.
~220 v
~220 v
~220 v

Fig. 3. Simplified schematic of electronic controller EC-III. Adjustment organs: a, b, c) sensitivity transducers, d) measuring device zero corrector, e) amplifier zero corrector, f) replaceable "isodrome time" resistor, g) "communication speed", h) "damper", i) "insensitivity zone". The remaining nomenclature corresponds to that of Fig. 2.

formers which produce signals with noise of the character cited.

There is an electric damper connected between the first and second stages by means of which the deleterious effect of pulsations of the quantity to be controlled, which are observed in some cases, may be eliminated.

The second stage is also a balancing scheme. In the diagonal of the bridge formed by the two triodes of the second vacuum tube and by two load impedances, there is connected a divider which supplies the controlling winding of the reversible polarized relay, shunted by a capacitor to eliminate contact vibrations. An additional improvement in the operating conditions of the relay's contacts, plus the provision of a loop-type characteristic of the relay element, is attained by the use of a second winding, the so-called "holding" winding, which conducts current during the periods of contact making, and also by the use of an arc-arresting device, namely, semiconducting rectifiers shunting the external load. The relay contacts control the transmission of current pulses from the auxiliary rectifier in the external circuit to the signal lamps, and also to the feedback device.

The feedback device consists of one or two (in other controller modifications) series-connected RC networks, supplied by a regulated fraction of the output voltage pulse. The output voltage of this device is applied to the floating grid of the amplifier's first-stage vacuum tube.

The controller's external circuit contains a reversible three-phase magnetic starter which directly controls the motor of the executive mechanism. Capability of remote control has been provided.

The executive mechanism is a three-phase asynchronous motor with a two-stage reducer. The physical design of the mechanism includes a brake for decreasing the effect of "run-out", a hand wheel for manual (local) control, a single-pole terminal switch and a rheostat transducer for remote indications of the output shaft position. Modifications of the mechanism provide output torques of 25 and 100 kg for a shaft rotation of 90° in 30 seconds.

Depending on the modifications of the feedback device, the controller, under definite conditions, approximately implements P-, PI or PID ‡‡ control laws with a wide range of tuning parameter adjustments.

In addition to the basic devices already cited, the complete apparatus contains a group of auxiliary instruments which extend the technical capabilities of the

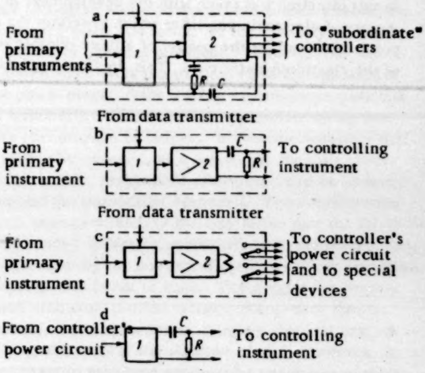
a
From primary instruments
1
2
To "subordinate" controllers
R
C
From data transmitter
b
From primary instrument
1
2
C
R
To controlling instrument
From data transmitter
c
From primary instrument
1
2
To controller's power circuit and to special devices
d
From controller's power circuit
1
C
R
To controlling instrument

Fig. 4. Skeleton schematics of certain auxiliary devices of the electronic control scheme. a) Type ĖKR contactless correcting controller, b) type ĖD differentiator, c) type ĖOS limiter-signaller, d) type DS dynamic connection device, 1) measuring device, 2) amplifier.

---

‡‡ Translator's note: The foregoing letters stand for: Proportional, Integral and Derivative.

control system considered here. Among these are: a) a type ÉKR contactless correcting controller, implementing the formation of a PI-law control in the form of electrical quantities, and intended for the stimuli to the "subordinate" controllers ordinarily used,[***] b) type ÉD differentiator, used for introducing into the controller a stimulus which depends on the rate of change of the input quantity, c) a type ÉOS limiter-signaller, intended for the automatic limiting of the controller's range of action and the signalling of the moment of limitation, d) a type DS dynamic connection device, used for introducing connections between the controllers, e) a type ÉSP servo instrument, providing identity of paths of motion of two executive mechanisms, etc. The skeleton schematics of some of these devices are shown in Fig. 4.

5. Further Development of Electronic Control Systems

Prolonged use tests of more than ten thousand electronic controllers permitted their weak points to be made manifest. About 90% of all the cases of disrupted normal controller functioning were due to failures of the controlling instrument amplifier's output element — polarized relay RP-5. The remaing 10% of the failures were almost uniformly distributed between the magnetic starter and the executive mechanism. An insignificant number of failures occurred in the remaining elements.

Further perfecting of the apparatus for electronic automation was executed in several stages.

The first problem was to increase the reliability of performance of the polarized relay. An important step in this direction was taken with the development of a new variety of electronic amplifier which generates the output power necessary for the control of a more reliable relay of the electromagnetic type. This, by the way, increased the stability of the controller's "null", improved the operation of the electrical damper, and broadened the range of variation of the controller's adjustment parameters. A further increase in the controlling instrument's reliability was attained by completely eliminating the contact element and replacing it by a contactless one. The given variant of the controlling instrument contains three twin electron tubes, the last two of which form the two-channel reversible flip-flop. The amplifier directly generates the power sufficient for controlling the magnetic starter.

Improving the elements of the controller's power circuit entailed, as the first step, increasing the reliability of the magnetic starter's operation. However, its replacement by contactless elements — terminal magnetic amplifiers — provides a real gain only when this is simultaneously accompanied by a radical change in the physical design of the executive mechanism, which must require moderate electric power and must possess low inherent inertia.

The development of such an executive mechanism led to the creation of several models of electromechanical and electrohydraulic types. All of them operate in conjunction with fast-acting, one-stage terminal magnetic amplifiers, process sufficiently well-defined pulses of duration greater than 0.1 second, are self-braking, and are equipped with organs for remote and local control.

The combination of flip-flop controlling instrument with terminal magnetic amplifier plus "sampled-data" executive mechanism forms a high-reliability control system which answers to the various requirements of automation in energetics and in other branches of industry.

[***] This corresponds to element 2 in the previously considered scheme of Fig. 1b.

METHODS OF INCREASING RELIABILITY AND RESPONSE SPEED OF STEAM TURBINE CONTROL

V. N. Veller

Moscow

Translated from Avtomatika i Telemekhanika, Vol. 21, No. 6, pp. 840-848, June, 1960

The question as to the choice of reliable control element design is considered. A description is given of a hydrodynamical scheme for steam turbine control and of its elements: self-centering piston, pump, accelerator, etc.

The reliability of operation of an automatic control system and its individual assemblies essentially determines the possibility of automating some object or another. Indeed, automation is called upon to replace human labor by the more accurate "labor" of an automaton. But, with unreliable means of automation, the labor of the machine operator is frequently replaced by the more highly specialized labor of the automata maintenance men, which makes the automation of the given process meaningless.

However, the concept itself of "reliability of automata operation" is not accurately defined.

The reliability of automata operation and automatic control system operation depends basically on the dynamic properties of the automaton or system, on the reliability of the physical design and on the quality of the manufacture and choice of the materials.

In this paper, the attempt is made to establish criteria which would allow comparisons of automata designs in terms of their reliability. With this, questions of dynamic properties, quality of manufacture and quality of materials are excluded from consideration because, first of all, a large number of works are devoted to these questions and, secondly, it is desired to give special prominence to the necessity of creating reliable physical designs of automatic devices.

By the reliability of operation of some mechanism or another is understood its trouble-free use. It is necessary to establish some criteria which would allow the provision of the possible occurrence of troubles due to faults in the automaton's physical design. Without such criteria, comparisons of designs in terms of their reliability would require many years of testing of the competing designs. And even under these conditions the comparison would be rendered difficult due to troubles in the automata for reasons indirectly related to their physical design (technological errors, faulty maintenance, etc.).

If one analyzes the statistics of control system troubles, then one can turn one's attention to the disturbances in similar physical assemblies. Such assemblies are joints, springs, membranes, contacts, radio tubes, etc.

The assemblies enumerated have one common idiosyncrasy – the causes of failure accumulate in them. In the course of time, joints wear. Springs under high tension break from fatigue. Membranes, just as springs, break from fatigue. Contacts burn out. In radio tubes, emission ceases, etc. The designer's problem in using these elements consists in this, that he must create for them such operating conditions that disruptions of their normal functioning will be completely eliminated or put off for the longest possible time. When, for random causes, difficult operating conditions arise, the disruptions occur in precisely these most vulnerable assemblies.

On many of the turbines of old design produced by the Leningrad Metal Factory, there is used a relatively little-turned speed controller. In the majority of cases, this controller operates sufficiently reliably. But cases are known when increases in rotor vibration appeared in three power plants. This loading circumstance gave rise to a systematic breakdown of the controller spring due to the phenomenon of fatigue. It became necessary that the springs be changed, as a preventive measure, once in four months. Many more examples could be adduced to support the proposition advanced. The consideration of such examples leads to the conclusion that the reliability of any control system as, moreover, with any mechanism, is determined by the number of elements whose operation depends on the factor of time. The greater the number of such elements, the less reliable the control system. Certainly, it is impossible to compare physical designs solely on the basis of the numbers of such elements. It is necessary to take into account the conditions of their operation as well. Improvement of these conditions permits the reliability of such elements, and of the system as a whole, to be increased.

The reliability criterion just formulated allows one not only to estimate the quality of the physical design, but also makes it possible to choose the most reasonable methods of improving it, and allows one to avoid creating designs which, while new, give no practical increase in reliability.

In this paper we present methods for increasing reliability and speed of response of steam turbine control systems. The selection and development of these methods is based on the reliability criterion suggested. Thus, the contents of this paper are, as it were, the working out of an example of the use of the given criterion for creating rational control systems. Although the paper is devoted to a particular question, its results also have a more general value.

I. A Reasonable System of Steam Turbine Control — a Hydrodynamical One

The multiformity of physical designs of control system assemblies for steam turbines is determined, to a significant degree, by patent restrictions and by the preferences evolved by different designers for various requirements. One group consider principally engineering sophistication, another considers compactness, a third, convenience of maintenance, etc. A consequence of such a diversity of approaches is the difficulty of choosing a best solution. We shall make the attempt to analyze the existing speed controller designs on the basis of the reliability criterion.

The physical designs of the ordinary centrifugal controllers with hinge joints are insufficiently reliable due to wear of the joints. This is supported by the fact that, in repairing turbines, it is necessary, as a rule, to overhaul the hinge joints. An increase of reliability is attained by eliminating the hinge joints, i.e., by making the transition to unjointed controllers. This path was taken by Westinghouse, Allis-Chalmers and also in the developments of MĒI, the Stalin LMZ, and many other factories and organizations.

But it is impossible to separate the physical design of the controller from the other assemblies of the control system. A unified approach to the solution of the problem always gives better results.

In many contemporary control systems for steam turbines, oiled servomotors are used. Consequently, the reliability of the control system depends on the reliability of the oil supply. The most reliable drive for the oil pumps is the drive from the turbine's principal shaft (such a drive is received by the entire turbine works). With this, the operation of the pump depends on the number of rotations of the aggregate, which permits the pump to be used, in the given case, as a sampled-data transducer of the speed controller.

Oiled servomotors, as a rule, are controlled by cylindrical valves. If a cylindrical valve is used as a piston, receiving pressure impulses from the pump, then a control system with one amplifier will consist of a pump, a valve, and a servomotor. All these elements are necessarily independent of the type of control system and, consequently, no matter what speed regulator might be used (mechanical, electrical, etc.), it would be an extra link of the scheme. Naturally, the removal of excess links always increases system reliability, if, with this, no deterioration of control quality ensues.

Such a control system was used by Westinghouse, Sultser and Simmonds-Shukkert, and by the Kirovskii Plant in the USSR, which supports the correctness of the logical deduction just made. However, all the aforementioned factories subsequently turned from such simple control schemes. An analysis of the results of operation of these systems under working conditions shows that the basic reasons for the troubles in their functioning are:

1) increase of insensitivity of the spring-loaded piston-valve;
2) oil pressure pulsations at the pump's output;
3) unsatisfactory form of the pump's characteristics.

The example just considered shows that the reliability criterion suggested is necessary but not sufficient. It was emphasized earlier that its use permitted the choice of the theoretically most reliable control system, but this sytem must, in addition, possess high sensitivity, accuracy and speed of response. However, this criterion permits us to mark out the path to perfecting a control system. If it is assumed that the basic functional schematic of a control scheme is correctly chosen, then the path to its further development is also clear. In the case under consideration, the chosen scheme becomes workable if, without lowering reliability and complicating the scheme, one succeeds in eliminating the observed causes of trouble. We present methods below which permit the problem thus posed to be solved, thanks to which the simple control scheme created turned out to be completely workable.

1. Use of a self-centering piston. The previously known methods of increasing the sensitivity of piston mechanisms turned out to be inapplicable in the given case. With the use of an intermittent piston, static friction is replaced by kinetic friction, but this reduces the friction coefficient by no more than a factor of two, which is inadequate for contemporary requirements on the quality of controller operation. The use of rotating pistons reduces the friction coefficient by a large factor, but when the piston is loaded by a steel spring, it forces a significant loading on the supporting bearings, reducing the reliability of the piston mechanism.

The problem was solved by the creation of a self-centering piston [1, 2].

On the outer surface of such a piston two series of notches are made (Fig. 1). In each notch (I, II, III and IV) liquid is supplied from the delivery cavity via a specially drilled aperture f_0 of small diameter. From the notches, the liquid flows via the gap between the piston and the cylinder. To prevent the fluid from falling from the delivery cavity into the notches, there is provided on the piston's surface, in addition to drill-hole f_0, a drain gutter a, from which the fluid is directed to the reduced pressure cavity by a longitudinal drain of relatively large cross-sectional area.

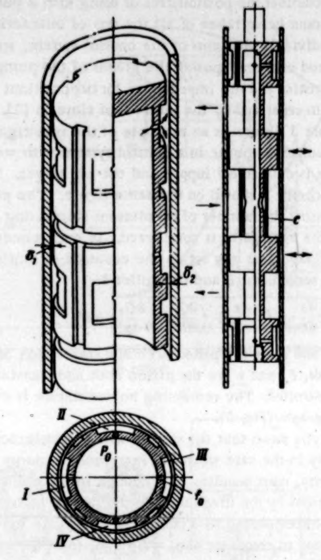

Fig. 1. Self-centering piston.

If external forces press the piston to the cylinder wall, then, in notch I, positioned on the side of the lesser gap δ_1, the pressure P_1 is increased, so that the resistance to the flow of liquid from the notch is increased. In notch III, on the opposite side, the liquid pressure falls due to the decrease of the resistance to flow through the enlarged gap δ_2. A pressure difference, $P_I - P_{III}$ appears which, in overcoming the action of the external forces, tends to return the piston to a coaxial position with respect to the cylinder. The maximum pressure difference will occur when the piston touches the cylinder wall. In this case, in the notch on the side of the null gap, virtually the full fluid pressure P_0 will exist and, on the opposite side, the minimum possible (corresponding to the maximum gap δ). Under these conditions of fluid supply to notch I, the pressure in it will be close to P_0 by virtue of the fact that gap δ_1 equals zero. Consequently, the pressure difference will be larger, the lower the pressure P_{III} in notch III. It is therefore necessary to attain a decrease in resistance to the flow of fluid from the notch, and to prevent fall of fluid from the delivery cavity to the notch apart from drill-hole f_0.

The fluid pressure in any notch is determined from the relationship

$$\frac{P}{P_0} = \frac{B}{P_0}\left[\sqrt{1 + 2\frac{P_0}{B}} - 1\right], \tag{1}$$

where P is the pressure in the centering notch, and P_0 is the pressure in the delivery cavity,

$$2B = \left[\frac{12\mu f_0}{\delta^3\left(\frac{l}{m} + \frac{l}{m_1} + \frac{2b}{L_{av}}\right)\sqrt{1,12\rho}}\right]^2. \tag{2}$$

In expression (2), μ is the dynamic coefficient of viscosity, in kg·sec/m²; f_0 is the area of the delivery drill-hole in m²; δ is the gap between cylinder wall and piston at the locus of the notch in meters; ρ is the fluid density in kg·sec²/m⁴; l/m, l/m_1 and $2b/L_{av}$ are the ratios of width of leakage flow to the length of the path to the reduced pressure cavity.

Experimental verification [3] supported the high efficiency of such a method of decreasing the friction coefficient.

The special feature of this method is that it can be used for any medium — liquid or gas.

2. Pulsations of oil pressure at the pump's output. A study of the operation of hydrodynamical control under working conditions showed that the pressure at the pump's output pulsates independently of the changes in number of rotations. With this, the period of the oscillations of pressure is so great that the piston taking the pressure and, following it, the principal servomotor, are able to follow the changes in pressure.

A detailed study of this question [4] showed that the causes of the pulsations are vortex formations in the oil

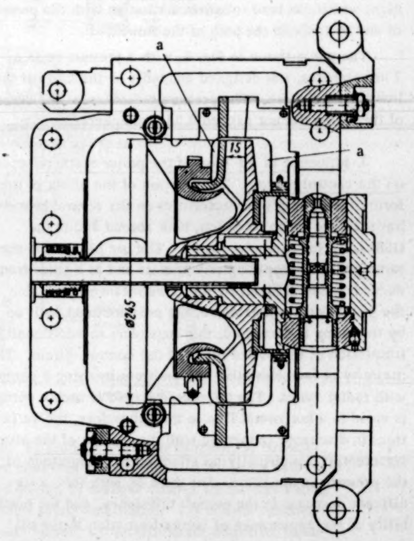

Fig. 2. Oil pump.

flow. Discovery of the reasons for the pulsations permitted the development of measures to eliminate them.

To eliminate vortex formation before input to the wheel, a well-streamlined input chamber is used (Fig. 2). Then, before the input to the vane channel itself, there is employed a directing apparatus with radial vanes. To eliminate the effect of leakage from the lateral chambers on the entering oil flow, there was used a special hooked form of packing. Such a packing squeezes the leakage flow to the lateral disk wall and eliminates its effect on the basic flow. The use of such a form allows the use of packing with relatively large radial gaps, which increases the reliability of operation of the pump, the disk of which is fitted directly onto the turbine shaft.

Vortex formation in the vane channel of the pump is reduced with a decrease in angle of attack. We therefore adopted an angle of attack no greater than 3 to 6°.

Disturbances of the flow at the pump's output can arise due to the action of parasitic flows in the pump's lateral chambers a (cf., Fig. 2). To eliminate this effect, it is more advantageous to use a directing vane apparatus at the pump's output, and not the helices which are the most widely disseminated in contemporary pumps. The vane directing apparatus has an advantage over the helix also in the respect that it eliminates the possibility of vortex formation at the output of the directing apparatus. For this, it is only necessary to have a sufficiently free chamber on it and, correspondingly, a small velocity of flow. In a helix, the velocity of flow is comparatively high, which can lead to vortex formation with the presence of any obstacle in the path of the flow.

The pump shown in Fig. 2, with a pressure head of 7 atmospheres, was designed and built on the basis of the investigation given. The pressure pulsations at the output of this pump did not exceed 0.03 atmospheres.

3. Influence of the form of the pump characteristics on the control process. The question of the effect of the form of the pump's characteristics on the control process has received much attention, both abroad and in the USSR (cf., for example, [5, 6]). The use of one and the same pump for supplying servomotors and as a pulse transducer is made difficult by the circumstance that, when the piston servomotors move, the pressure head built up by the pump is decreased; this engenders an additional translation of the pulsed organ of the control system. The majority of factories solve this problem by using a pump with radial vanes. The QP characteristic of such a pump is close to a horizontal line so that, therefore, the variations in discharge connected with the motion of the piston servomotors has virtually no effect on the magnitude of the pressure at the pump. But there is, with this, a significant decrease in the pump's efficiency, and the possibility of the appearance of vortex formation in the oil flow. We therefore used only pumps with vanes curved contrary to the direction of circumferential velocity.

To consider the possibilities of using such a pump, with account being taken of all the sets of interactions of the individual elements of the control system, we used the method of superimposing the graphs of the pump characteristics and the impedances for two positions for the system separated by the interval of time Δt [7].

Figure 3 illustrates an example of the investigation of the transient response in a control system with servomotors, a two-sided oil supply and cut-off valves. The control scheme is shown on the same figure. The process of decreasing the number of revolutions (increasing the load on the aggregate) is considered. In correspondence with the graphs, we can set up the equation of motion of piston servomotor 3 and controller 1:

$$F_S \frac{dz}{dt} = F_C \frac{dx}{dt} + \left(\frac{\partial Q_1}{\partial p} + \frac{\partial Q_2}{\partial p}\right) \Delta P_2 , \qquad (3)$$

where F_S and z are the piston area and translation of the servomotor, F_C and x are the piston area and translation of the controller. The remaining nomenclature is clear from the graph (Fig. 3).

Analysis shows that the system will be dynamically stable only in the case when the increment of pump productivity, corresponding to a change in the number of revolutions by the magnitude of the degree of nonuniformity (corresponding to a change of aggregate load from free-running to complete) $\Delta p_2 = \Delta p_{max}$, must be greater than the expenditure (in liters per second) of the oil applied to the servomotor for maximum raising of the valve. In [7] a detailed analysis of four variants of the control scheme was given.

If, as the principal servomotors, one uses servomotors with circulating valves (the Brown-Bovary system), then it is most advantageous to use valves with double throttling [8] in which not only the supply, but also the drainage, of oil is throttled. In these valves the aperture profile can be so chosen that, for slow motion of the valve, the pressure of the fluid in the line between the apertures will change for an unchanged discharge of oil via the valve. With this, there will be the least effect of servomotor motion on pressure pulses.

In other systems we recommend the use of a pump with two disks, wherein one is used for supplying the servomotors, and the other as a pulse transducer. In this case there is virtually no action of the servomotor on the pressure pulse.

4. Two-injector oil supply scheme. A centrifugal pump does not possess the property of automatic intake, i.e., upon rarefaction in the intake housing and the entry of air into it, the supply of fluid from the pump ceases.

To increase the reliability of operation of a centrifugal pump, various auxiliary devices are used, providing a tributary at the input to the pump. Using the reliability criterion, we chose an injector method of creating a tributary at the pump's input (Fig. 4). The injector has no moving parts and therefore, as a mechanism, is very reliable. This method was suggested and developed by the

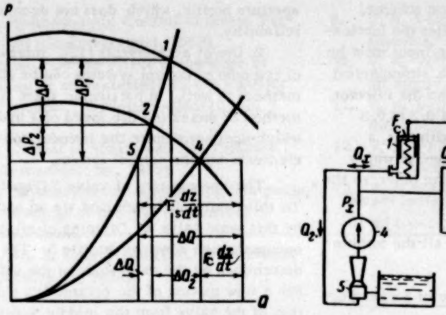
P
1
2
3
4
5
6
ΔP
ΔP_1
ΔP_2
$F_s dt$
dz
ΔQ
ΔQ_1
ΔQ_2
$F_c \frac{dz}{dt}$
Q
F_c
Q_I
Q_{II}
P_2
Q_2
F_s
Q_n

Fig. 3. Effect of servomotor piston motion on impulse pressure. 1) Piston controller, 2) valve, 3) servomotor, 4) pump, 5) injector, 6) constant throttle.

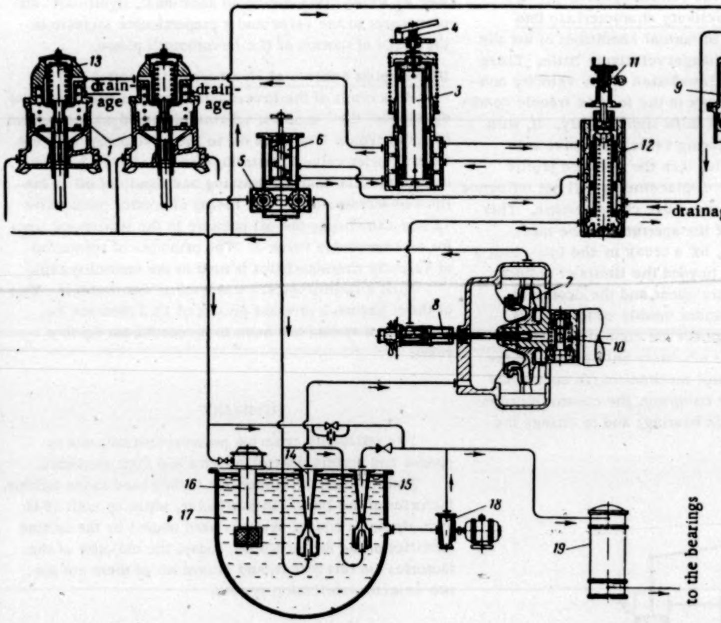
1
2
3
4
5
6
7
8
9
10
11
12
13
14
15
16
17
18
19
drainage
drainage
drainage
drainage
to the bearings

Fig. 4. Simplest schematic of a hydrodynamic control scheme. 1) Throttle valve servomotor, 2) cut-off valve servomotor, 3) piston controller-valve, 4) mechanism for checking velocity of automaton for safe increase of rotations, 5) spherical reverse valve, 6) filter, 7) oil pump, 8) manual control for cut-off valve, 9) intermediate amplifier for the cut-off valve drive, 10) velocity safety automaton, 11) control mechanism, 12) valve control mechanism for the controlling and cut-off valves, 13) intermediate amplifier servomotor for the throttled valve drive, 14) injector support, 15) injector lubricating point, 16) auxiliary turbopump, 17) oil reservoir, 18) spare pump with an electric drive, 19) oil cooler.

Westinghouse Company. In the Westinghouse scheme, the tributary injector simultaneously supplies the lubrication system. Therefore, the pressure at the input must be chosen rather high (on the order of 1 to 1.5 atmospheres) which increases the expenditure of power on the injector. For reliable pump operation, a tributary of 0.2 to 0.3 atmospheres is sufficient. In connection with this, a scheme with two injectors was suggested, one of which supplies oil to the lubrication system and the other, to the input of the pump (Fig. 4). With such a scheme, the expenditure of power on the oil supply is decreased by 15 to 25% [9, 10]. Such schemes are used by all the turbine factories in the USSR.

II. Methods of Increasing Speed of Response of Steam Turbine Control Systems

An increase in speed of response without a decrease in reliability can be obtained only with the condition that the use of new methods does not require the introduction of additional elements to the control system.

1. Separation of the velocity characteristic into static and dynamic [11]. In normal conditions of use the frequency of the ac line changes relatively little. There is a correspondingly small translation of the velocity controller's clutch. With a break in the load (a trouble condition), the controller's clutch shifts significantly. If, with a servomotor with a circulating valve, the valve axle bearing is made immovable, then the aperture profile beyond the limits of small displacements will not influence the form and curvature of the static characteristic. This ordinarily closed portion of the aperture can be made sufficiently wide, and then, for a break in the load, with a displacement of the valve beyond the limits of ordinary oscillations, a large aperture opens, and the degree of nonuniformity of control (under trouble conditions) is sharply decreased, which speeds the control process.

In the given case, it is necessary only to change the physical design of the control mechanism (in controllers made by the Brown-Bovary company, the control mechanism includes the valve axle bearing) and to change the aperture profile, which does not decrease the system's reliability.

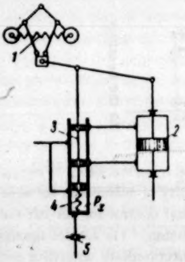

Fig. 5. Accelerator.

2. Use of accelerators [12]. Increases in the speed of response of control systems can be obtained by other methods as well. In particular, there is suggested a method of increasing the speed of a hydraulic servomotor which does not require the introduction of additional elements into the control system.

The lower cavity of valve 3 (Fig. 5) is made closed. To this cavity oil is supplied via an aperture controlled by this same valve 3. Draining of oil from the cavity occurs through constant throttle 5. The pressure P_x is determined by the magnitude of the valve displacement. For a slow motion of the controller's clutch, the deviation of the valve from the middle position is small, so that the action of the accelerator has a small effect on the deviation of the valve. For a rapid motion of the clutch, the deviation of the valve from the center position will be large, and there will be a corresponding increase of pressure P_x, which gives rise to an additional, significant displacement of the valve and a proportionate increase in the speed of motion of the servomotor's piston.

III. Simplest Scheme of Hydrodynamic Control [13]

As a result of the investigation carried out, there was developed the simplest scheme of hydrodynamic control (Fig. 4). Pump 7 supplies oil to the servomotors and, via filter 5 under valve 3, is spring-loaded. Valve 3 of the double throttle controls draining and supply of oil in the lines of servomotor 13. By means of control mechanism 12 one can change the oil pressure in the servomotor lines for an immovable valve 3. The principle of separation of velocity characteristics is used in the control system.

Such a control system was used on four turbines. Two of them had back pressure powers of 12.3 thousand kw. The control system has been in successful use for four years.

SUMMARY

The reliability criterion presented permits one to choose and perfect control systems and their elements.

The methods developed are widely used in the turbine factories of the USSR. In particular, while up until 1941 hydrodynamic control systems were unused by the turbine factories of the Soviet Union, today, the majority of the factories use this system, and almost all of them use the two-injector lubrication system.

LITERATURE CITED

1. V. N. Veller, Patent No. 68029 (1942).
2. V. N. Veller and A. A. Zhuravleva, "A self-centering piston," Teploenergetika No. 3 (1954).
3. V. N. Veller and A. A. Zhuravleva, "Comparative investigation of pistons," Teploenergetika No. 2 (1958

4. V. N. Veller, Hydrodynamic Control of Steam Turbines [in Russian] (Gosénergoizdat, 1953).
5. V. M. Taranenko, "On the effect of the slope of the pump-controller characteristic on the stability of the control process," Kotloturbostroenie No. 7 (1952).
6. L. I. Kirillov, Control of Steam and Gas Turbines [in Russian] (Gosénergoizdat, 1952).
7. V. N. Veller, "Hydrodynamic control with one pump," Collected Proceedings of the VTI [in Russian] (Gosénergoizdat, 1959).
8. L. I. Kirillov, Kh. F. Ketov, and O. A. Pyzh, Patent No. 33963 (January 31, 1934).
9. V. N. Veller, "Comparative analysis of oil supply schemes," Izvest. VTI No. 11 (1948).
10. V. N. Veller, "Two-injector scheme of steam turbine oil supply," Elektricheskie Stantsii No. 9 (1957).
11. V. N. Veller, "Separation of velocity characteristics into static and dynamic," Izvest. VTI No. 3 (1941).
12. V. N. Veller, "The use of accelerators in steam turbine control systems," Teploénergetika No. 9 (1957).
13. V. N. Veller, A. A. Zhuravleva, and V. L. Podgaevskii, "A simple scheme of hydrodynamic control," Élektricheskie Stantsii No. 7 (1958).

COMPLEX AUTOMATION OF AN OPEN-HEARTH FURNACE WITH GAS HEATING

M. M. Gordon

Sverdlovsk

Translated from Avtomatika i Telemekhanika, Vol. 21, No. 6, pp. 849-856, June, 1960

A system is described for the automatic control of an open-hearth furnace's thermal operating mode. The system consists of eight control loops connected via the plant. The questions of measuring several controlling parameters are considered.

The paper discusses the attempt to automate open-hearth furnace No. 14 of the Nizhne-Tagil'skii Metallurgical Combine.* The furnace has a capacity of 380 tons, and is fired by coke and blast-furnace gases. For the torch candling coal tar or anthracene oil are used, while oxygen is used for the intensification of the combustion process. There is today no boiler-reclaimer furnace.

This paper deals with the automation only of the furnace's thermal operating modes; stimuli to the physicochemical processes occurring in the tank are not taken into account.

In the development of the automation scheme, the following basic idiosyncrasies of the open-hearth process were taken into account. In the automation of an open-hearth furnace it is impossible to select the combustion and thermal loads on the basis of some previously worked-out program, since the furnace properties continuously change during the course of the run; the scheme itself must choose the regimen which is optimal at the given moment. To shorten the duration of the smelting process (the blow) it is desirable to maximize the thermal load on the furnace. In the existing furnace designs this entails an increase in thermal efficiency. However, an increase in the thermal load is limited by the following factors:

1. The temperature of the regenerator's crown and upper checkered brickwork must not be higher than a limit due to the durability of the refractory material.
2. There must be provided complete combustion of the fuel in the working area.
3. Driving out of the flame from the working area must be limited, both by the magnitude of the heat losses, and by the durability of the front wall.

Measurements

For normal operation of a system for open-hearth furnace automation, it is necessary to measure, correctly and reliably, the aforementioned parameters on which limitations are imposed. Most important also are the questions of the dynamics of the measurement process. Use of the ordinary methods of measurement turned out to be inapplicable for furnace automation, except for the method for measuring the temperature of the regenerators' upper checkered brickwork by means of radiation pyrometers with electronic potentiometers. Use of these radiation pyrometers for measuring the crown temperature turned out to be impossible. Lengthy experience shows that it is impossible to provide reliable usage of this measurement in connection with the frequent slagging of the tuyere apertures, the formation of "icycles" in the pyrometer's field of vision, and in connection with the distortions due to tongues of flame reaching into the pyrometer's field of vision.

A significantly more reliable crown temperature measurement was successfully provided by the subcrown photopyrometer of the Central Laboratory for Automation of the Ministry of Construction of the RSFSR (Russian Soviet Federated Socialist Republic). The basic part of this instrument is an antimony-cesium vacuum photoelement installed in a water-cooled tuyere inside the furnace's working space directly under the crown. The photoelement's peep hole has a diameter of 0.9 mm and is continuously blown off by compressed air. The disturbances connected with obstructions of the peep hole, icicle formation and flame effects are virtually nonexistent here.

The measurement of pressure under the crown under conditions of actual use is implemented with sufficient reliability. The enclosed devices can operate without overhaul or cleaning for periods of several months.

In [1] doubts were expressed as to whether it were possible to consider the pressure under the crown as a quantity characterizing the gas outflow and brick loosening action from the furnace's working space. Contradicting this, the attempt to employ automation on furnace No. 14 showed that this quantity quite accurately characterizes the pressure regimen in the working space and that, therefore, the scheme should not be complicated by the introduction of auxiliary pulses for controlling gas outflow and brick loosening.

---

*The work on the complex automation of an open-hearth furnace was carried on jointly by the All-Union Research Institute for Metallurgical Heat Engineering (under the direction of V. N. Timofeev and G. L. Shirokov), the industrial-engineering enterprises of the Uralmetallurgavtomatik (under the direction of M. M. Gordon and B. G. Gutner) and by the Nizhne-Tagil'skii Metallurgical Combine (under the direction of G. A. Petrov and L. N. Mikhailov).

Type RDM-35 compensation bell recorder-controller, heretofore used for controlling the pressure under the crown, turned out to be unfit. The controller's sensitive element must react to pressure changes with maximal speed. In addition, it must filter out the pulsations of pressure engendered by the irregularities of the combustion process. The period of the pressure pulsations connected with the irregularities of the combustion process is about 3 to 4 seconds. The impulse tube, together with the measuring instrument (the sensitive element) constitutes an oscillatory link. It is important to match the parameters of the impulse tube with those of the measuring instrument such that the period of the free oscillations of the sensitive element plus the impulse tube is about 6 to 7 seconds. This can be achieved by using a membrane sensitive element and a large-diameter impulse tube ($1\frac{1}{2}$ to 2 inches), for a length of line of some tens of meters. From the point of view of filtering out the pulsations, an installation of the instrument too close to the furnace is undesirable. A corresponding instrument with a membrane sensitive element was constructed at the Nizhne-Tagil'skii Metallurgical Combine. For the inspection of incompleteness of combustion, it is necessary to carry out a continuous analysis of the flue gases. The difficulty of this measurement is widely known. For an open-hearth furnace, the problem is solved in the following way. The intake points are positioned on the air regenerators, close to the damstone walls between the slag chamber and the regenerator, i.e., where the flue gases are sufficiently well mixed. The flue gas to be analyzed is drawn off by means of a steam ejector pump. The mixture of gas and steam is sprinkled with water, causing the steam to condense, and the moisture thus formed is removed by means of a two-stage centrifugal separator. The dried and cleaned sample, under a pressure of several hundred millimeters of water column, is applied to a type MGK-348 magnetic gas analyzer transducer, which analyzes the specimen for oxygen content. The air-cooled enclosed tuyere in the regenerator crown is periodically (for each dumping) blown off by steam, thus preventing it from clogging. The transport time for the gas specimen from the ejector pump to the gas analyzer transducer is about 15 to 17 seconds for an impulse line some 45 to 50 meters in length. The diameter of the impulse tube is one-half inch.

Two gas analyzers are installed on the furnace, for the right and left sides of the furnace separately. The moving system of the gas analyzers' secondary instruments are switched in only when the sample flue gases flow around the corresponding transducer. Switching in of the moving systems is implemented with a delay of two minutes after the beginning of dumping. Thanks to this, the gas analyzer does not record the transient combustion mode associated with the reversing of the furnace. In the control process, it is always that gas analyzer around whose transducer the flue gases flow that participates.

Another essentially new measuring instrument is a design of the Uralmetallurgavtomatik, a pulsed ultrasonic discharge meter for coal tar and anthracene oil. The instrument is not subject to clogging, since there is no place in it where the fluid would be stationary and where, therefore, there could accumulate sludge settling from the fluid. There are no moving parts in the instrument's transducer.

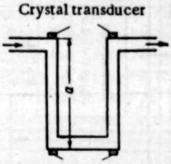

Fig. 1.

The instrument's basic element (its transducer, which is found in the coal tar conduit) is a U-shaped channel drilled in the metallic body (Fig. 1). On the front ends of the transducer's tube there are installed piezoelectric crystals, capable of transforming ultrasonic oscillations to electric waves and vice versa. Two of the crystals are transducers of the ultrasonic vibrations, and two of them are receivers.

A pulse sent by the crystal transducer arrives at the crystal receiver after the time $T = a/c$, where $\underline{a}$ is the distance between the crystals and $\underline{c}$ is the velocity of sound in the fluid. The ultrasonic pulse received is transformed to an electric voltage, amplified and applied to the crystal transducer, which sends the following ultrasonic pulse, etc. This method, as is known from the literature [2], provides temperature error compensation.

If the fluid is moving with velocity $\underline{v}$, then the intervals between pulses in the two channels of the transducer will be different. In one case, this interval will equal $T_1 = a/(c + v)$ and, in the other, $T_2 = a/(c-v)$.

Consequently, the pulse trains in the two transducer channels will have different frequencies. In the first case, this frequency will equal

$$f_1 = (c + v)/a;$$

in the second,

$$f_2 = (c-v)/a.$$

The difference of these frequencies

$$f_1 - f_2 = f_d = 2v/a$$

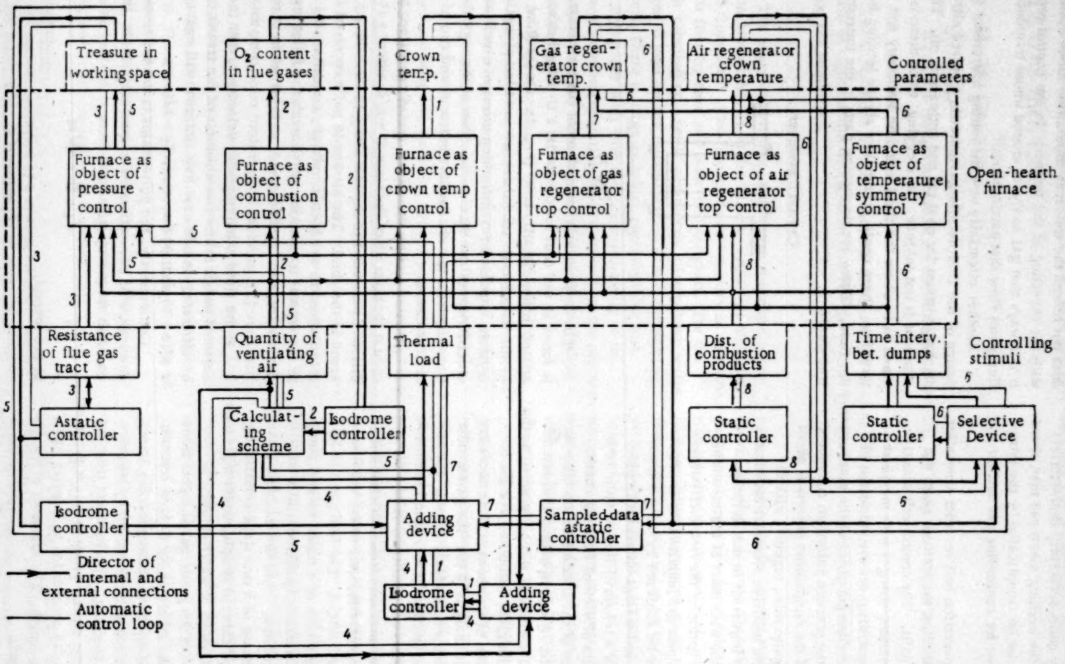
Treasure in working space
O₂ content in flue gases
Crown temp.
Gas regenerator crown temp.
Air regenerator crown temperature
Controlled parameters
Furnace as object of pressure control
Furnace as object of combustion control
Furnace as object of crown temp control
Furnace as object of gas regenerator top control
Furnace as object of air regenerator top control
Furnace as object of temperature symmetry control
Open-hearth furnace
Resistance of flue gas tract
Quantity of ventilating air
Thermal load
Dist. of combustion products
Time interv. bet. dumps
Controlling stimuli
Astatic controller
Calculating scheme
Isodrome controller
Static controller
Static controller
Selective Device
Isodrome controller
Adding device
Sampled-data astatic controller
Isodrome controller
Adding device
Director of internal and external connections
Automatic control loop
1
2
3
4
5
6
7
8

Fig. 2. Simplified block schematic of the open-hearth furnace's automatic control scheme. 1) Direction of internal and external connections, 2) automatic control loops.

depends only on the speed of the fluid and does not depend on the velocity of sound. With this, the result of the measurement does not depend on the temperature. Thus, the frequency f_d is a measure of the discharge rate.

The instrument's electronic scheme isolates the frequency f_d and transforms it to a dc voltage proportional to this frequency. The dc voltage is applied to the electric potentiometer, graduated in discharge units.

The transducer's U-shaped design permitted the channel diameter to be made sufficiently small, so that the instrument can measure small discharges of fluid. The range of the instrument's scale is zero to 1000 kg/hour. The fact that both transducer channels are drilled in one metallic body provides virtual equality of temperature in the channels even in the absence of discharge. This is important for the stability of the instrument's null.

Automatic Control

A simplified block schematic of the automatic control scheme for the open-hearth furnace's thermal regimen is shown in Fig. 2. The individual loops of this multiloop system are denoted on the figure by the numbers appended to the lines.

The control process proceeds in the following manner: in the filling period, when the temperature of the crown of the working space and the upper checkered brickwork of the regenerators is low, and there is no production of gases in the vat, pressure control in the working space is implemented by the rotation of the flue gas damper with a vertical axis, which controls the hydraulic jet of the astatic controller (control loop 3). The oxygen content on the checkered brickwork of the air regenerators at this time ordinarily does not fall below the given magnitude (6%), and the quantity of ventilating air is determined by the pneumatic computing scheme in correspondence with the quantity and caloricity of the fuel applied to the furnace. The computing scheme applies ventilating air with a coefficient of excess of $\alpha = 1.1$ before oxygen deduction. The thermal load is maximal at this time. The assigned value of oxygen concentration – 6 % – was determined empirically. In this case, on the gas checkered brickwork where there is virtually no outflow air, there is no CO in the flue gases.

If there is, in the charge, an uncovered oil waste, then the percentage of oxygen in the flue gases begins to decrease even during the course of charging. In this case, the gas analyzer, acting on a type IP-130 isodrome controller (control loop 2) corrects the operation of the computing scheme and adds air so that the assigned percentage of oxygen in the flue gases will be maintained. With this, the flue gas damper moves closer to an open state.

During the pig iron priming, the gas analyzer so increases the supply of air that the flue gas damper is opened completely. Then control of the furnace working space pressure enters into play by changing the thermal load, i.e., by changing the discharge of coke oven gas and, consequently, of air. This control is implemented by a type 04 isodrome controller (control loop 5). This controller acts on the adding device which controls the thermal load data transmitter, i.e., the discharge of coke oven gas. The discharge of blast-furnace gas remains constant during the entire smelting run, the resin is applied after draining of the slag from the furnace, and its discharge remains constant until the end of the smelting run. The discharge of oxygen is given by a steel mill hand.

With vigorous action in the vat, the amount of gas escaping from the boiling metal becomes so large, ordinarily, that the ventilator is completely filled, and the oxygen content in the combustion products remains low. In this case, when the computing scheme, as corrected by the gas analysis, requires more air than the ventilator can give (with account taken of the oxygen applied to the furnace), then operation of control loop 4 begins. The special differential manometer of this loop (not shown on the figure), which reacts only to drops greater than the corresponding full ventilator load, begins, by means of type IP-130 isodrome controller, to act on the adding device controlling the data transmitter of the coke gas controller. As a result, the thermal load is decreased. In this case, the discharge of ventilating air always remains maximal, and the discharge of coke oven gas is reduced to a very small amount or even to zero.

As the generation of gas from the vat decreases, the limiting actions concerned with incompleteness of combustion (loop 4) and working space pressure (loop 5) begin to weaken, and the thermal load is increased. However, there is a simultaneous increase in the crown temperature. The rising of this temperature leads to the formation of an input signal to loop 1, the action of which also limits the thermal load down to the end of the smelting run. This limitation is implemented by means of the adding device, common to loops 1 and 4, via a type IP-130 isodrome controller, the one which acts to limit the thermal load as a function of combustion incompleteness. In case of overheating of both gas checkered brickworks, control loop 7 can also limit the thermal load. This loop works on the principle of sampled-data control.

For stable operation of the entire system, it is necessary to match the speeds of action of the individual loops. The fastest system is that which controls the pressure in the working space by means of the flue gas damper. The time of a complete damper rotation is 10 seconds. Pressure control by means of thermal load variation is somewhat slower since there are several delays in the control loop from the pneumatic computing scheme. Still slower is the system for correcting air supply as the result of gas analysis; the time of the double isodrome controller, i.e., the time during which the executive mechanism duplicates its traverse due to astatic stimuli, is about one minute. Finally, the slowest control systems are those for thermal load as a function of crown temperature and incompleteness of combustion. The doubled time here is about 2 minutes.

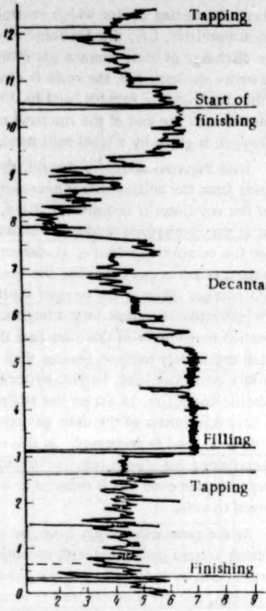

Fig. 3. Discharge of coke oven gas during a smelting run (scale is 0 – 10,000 m³/hour).

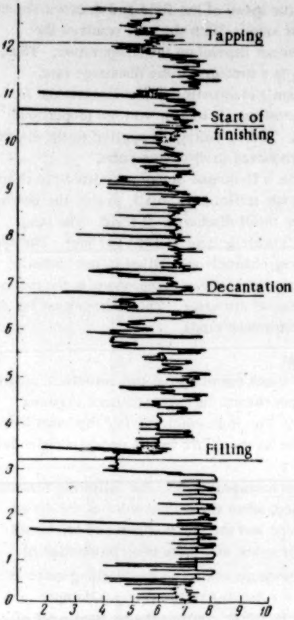

Fig. 4. Air discharge during a smelting run (scale is 0 – 50,000 m³/hour).

Only slightly related with the control loops just enumerated are the assemblies for controlling the upper temperatures of the air and gas checkered brickworks and for automatic dumping. These receive pulses from an integral time relay which operates with alternating pulses as functions of upper temperatures of the air and gas checkered brickworks. The alternation occurs each 20 seconds.

The integral time relay is a static controller of the temperature symmetry of the upper checkered brickworks of the regenerators (control loop 6). By means of temperature measurements of the top of the air checkered brickwork, control is effected by the damper's static distribution law. If the temperature approaches the assigned magnitude, than this damper begins to be throttled (control loop 8). Thanks to this, the quantity of flue gases passing through the air checkered brickworks is decreased, and their temperature begins to rise.

If the temperature of one of the gas checkered brickworks approaches the limiting magnitude, the command to dump is applied sooner than would be done by the integral relay, apart from the static controller. If the temperature of both gas checkered brickworks approaches the limiting value, there begins the discontinuous decrease of the thermal load by the action of control loop 7, as was discussed earlier.

Figure 3 is a diagram of coke oven gas expenditure during one smelting run. It is clear that, during the time of violent vat operation (from 7:30 to 9:00), the discharge of gas falls almost to zero, then increases somewhat and, in the last period of the run, during the finishing period, again decreases (on Fig. 3, from 10:00 to 12:00). The diagram of air expenditure has a completely different form (cf. Fig. 4). During the period of violent boiling, when the discharge of coke oven gas is small, the expenditure of air is very large, which is also provided by the combustion of the carbon monoxide released from the boiling metal at this time. With this, the flue gas temperature, during the entire smelting run, oscillates within virtually constant limits (Fig. 5). This oscillation is related to the reversal of the flame, and must not be eliminated by the system of automation.

It is not necessary to change the adjustment of the scheme during the furnace run. As the properties of the furnace worsen, there is an automatic change in the significance of the individual control loops. Thus, for example, as the draft worsens, there is a decrease in the operating time of the controller which controls the pressure rotating the damper and an increase in the operating time of the controller which limits the load as a function of the pressure in the furnace's working space.

Complete combustion of the carbon monoxide released from the vat, and the maintenance of the maximum thermal load admissible at each moment, provide a lowering of the specific expenditure of the nominal fuel with a simultaneous increase in productivity of the furnace. A comparison of smelting runs made with, and without, inclusion of the automation scheme showed that furnace productivity, thanks to automation, increased with a simultaneous lowering of the specific discharge of the nominal fuel.

It is also obvious that, with automatically controlled operating modes, the furnace's strength must be increased thanks to lesser temperature oscillations inside the refractory surface. However, the automated furnace is operating today only on its second operating period, so that it is impossible to make quantitative deductions as to the effect of the introduction of automation on length of service life.

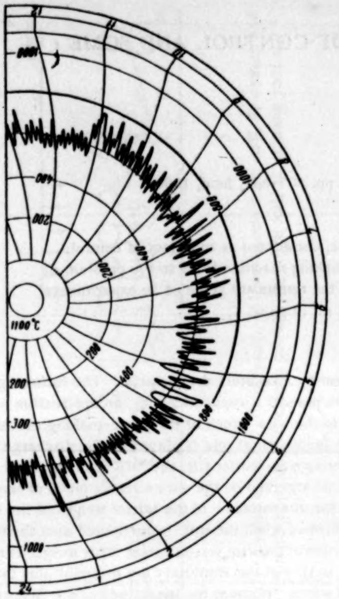

Fig. 5. Flue gas temperature in the course of a smelting run.

LITERATURE CITED

1. M. M. Kotrovskii and V. S. Kostogryzov, Automatic Control of the Thermal Processes in Metallurgical Production [in Russian] (Metallurgizdat, 1952).
2. D. Kritz, "Ultrasonic Flowmeter," Instruments and Automation No. 11 (1955).

A PAPER-MAKING MACHINE AS AN OBJECT OF CONTROL AND SOME WAYS TOWARD ITS COMPLEX AUTOMATION

A. S. Shamson

Leningrad

Translated from Avtomatika i Telemekhanika, Vol. 21, No. 6, pp. 857-866, June, 1960

The statistical and dynamic characteristics of a paper-making machine, considered as an object of control, are determined. It is shown that the complex automation of a paper-making machine leads to the problem of autonomous control. Possible ways to realize autonomy are cited, and the results are given of an experimental investigation of a system for automatically controlling the weight of 1 m^2 of paper.

Contemporary schemes for automating paper-making provide for control of its basic technological variables, but the interrelationships of these variables via the controlled object are not taken into account in the schemes put forth. Automation at such a level may be defined as partial, since it does not exclude the mutual influences of the controlled quantities in the object's dynamic regimen.

With the intensification of the production process which accompanies the increase of speed of paper sheet up to 500 to 600 m/min, partial automation cannot provide normal use of a paper-making machine. Under these conditions, effective control of the latter is only possible with complex automation, which must not only provide automatic control of all the basic portions of the process, but must also take into account the interrelationships of the corresponding controlled quantities.

The problem of complex automation requires a different approach, new in principle, to construction of automatic control systems for the productive flow. Such an approach assumes first of all, the development of a method for investigating and describing a paper-making machine as an object of control. This question, as is well known, has not yet been considered in the literature. The data obtained may be used for the exposition of the principles of constructing an automatable complex, and also for the development of the technical means for realizing it. The present paper is devoted to these questions.

1. Method of Investigation

Figure 1 shows a simplified schematic of the paper-making machine. The high-concentration stuff from the machine stuff chest is supplied to the supply tank. From there, the stuff is directed to the mixing pump in a suction pipe which also supplies recycled water. With the mixing, low-concentration stuff is formed, which is then supplied to the head box via the washing and screening equipment. At this step of the process, the fundamental role is played by the maintenance of the constancy of the concentration which determines the content of the paper sheet by absolutely dry material. The following step in the process is connected with the application of the stuff to the wire screen of the paper-making machine. Here, the fundamental role is played by the discharge of stuff through the outlet slit, the "slice" of the head box. On this discharge and on the wire screen's speed of motion, depends the magnitude of the initial weight of the layer which is formed when the stuff is distributed over the registering portion of the wire screen table. This weight is made up of the weight of the absolutely dry material plus the weight of water. Whereas the magnitude of the first of these weight components depends principally on the regimen of the preceding steps in the technological process, on all the following steps only removal of water occurs, and virtually no change in the content of absolutely dry material occurs. This underlines the possibility of using, to derive the differential equations of the object of control, the equations of its material balance with respect to each of the aforementioned weight components.

The values of the coefficient of the differential equations can be obtained analytically by means of the paper-making machine's static characteristics. Such characteristics must be given in the form of mathematical relationships, expressing the basic indicators of the regimen at the individual portions of the process as functions of the operative variable technological factors. For this in individual cases, for example, for the drying part, it turns out to be impossible to obtain the static characteristics in a form convenient for calculation. This latter circumstance imposes definite limitations on the analytic method of investigating a paper-making machine as an object of control, and requires that experimental methods be used.

2. Derivation of the Equations of the Object of Control's Dynamics

The material balance equations of the paper-making machine with respect to the absolutely dry material and with respect to moisture content have the forms, respectively,

$$G_d - G_s - G_w = 0, \qquad (1)$$

where G_d is the specific weight of discharge of the absolutely dry material when filled, G_s is the same, but in the mixing device with the paper stuff, G_w the same, but in the mixing device with recycled water;

$$G_0 W_0 - q_r - q_{su} - q_p - q_D - G_0 W_k = 0, \tag{2}$$

where G_0 is the initial weight of the layer formed when the stuff is distributed on the screen, in g/m², W_0 is the moisture content of the stuff applied to the screen, W_k is the moisture content of the finished paper, q_r, q_{su}, q_p, and q_D are the dessication speeds with 1 m² on, respectively, the registering part, the suction cabinet and the couch roll, the pressing and the drying portions.

The material balance equations, when expressed in terms of finite increments, take the form

$$\frac{dG}{dt} = C^{*}\Delta G_s + G_s \Delta C^{*} - C\Delta G_d - G_d \Delta C, \tag{3}$$

where G is the content of absolutely dry material in 1 m² of finished paper, C* is the concentration of stuff in the machine stuff chest and C is the concentration of stuff in the head box;

$$\frac{dW_k}{dt} = W_0 \Delta G_0 + G_0 \Delta W_0 - \Delta q_r - \Delta q_{su} - \Delta q_p - \Delta q_D - W_k \Delta G_0 - G_0 \Delta W_k. \tag{4}$$

The terms of Eqs. (3) and (4) can be expressed in terms of the static characteristics, obtained from an analysis of the physical features of the process, estimates of the interactions of the material fluxes, and mathematical processing of the regularities already known in the theory of paper production [1]. By carrying out the corresponding substitutions, and then going over to relative quantities, we obtain

$$\begin{gathered}
(A_{111}s + A_{110})x_1 + (A_{131}s + A_{130})x_3 + A_{141}sx_4 = \\
= B_{110}\mu_1(t-\tau') + f_1(t-\tau'), \\
-(A_{211}s + A_{210})x_1(t-\tau'') + (A_{222}s^2 + A_{221}s + A_{220}) \\
x_2 - A_{230}x_3(t-\tau'') + \\
+ A_{240}x_4(t-\tau'') + A_{250}x_5' = \\
= B_{220}\mu_2(t-\tau_1) + f_2(t-\tau_1), \\
-A_{310}x_1 + (A_{331}s + A_{330})x_3 = \\
= \mu_3(t-\tau'), \quad A_{440}x_4 = \mu_4, \quad A_{551}sx_5 = \mu_5;
\end{gathered} \tag{5}$$

where x_1, x_2, x_3, x_4, x_5 are the relative values of the controlled quantities of the weight of 1 m², the moisture content of the paper, the discharge of stuff from the head box when filled, speed of the wire screen's motion and pressing pressure, respectively; μ_1, μ_2, μ_3, μ_4, μ_5 are the relative values of the controlling actions applied, respectively, by the stuff valve on the suction side of the mixing pump, the valve on the steam trunks to the drying portion, the valve on the supply trunk taking stuff from

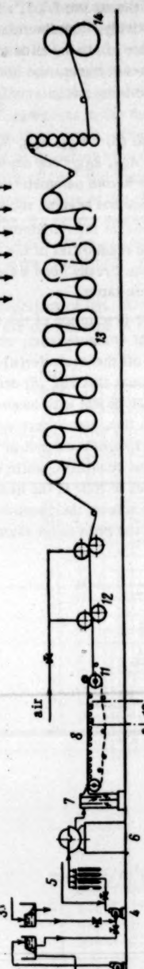

Fig. 1. 1) Machine stuff chest, 2) high-concentration stuff, 3) recycled water, 4) mixing pump, 5) low-concentration stuff, 6) washing and screening equipment, 7) head box, 8) wire screen table, 9) registering portion, 10) suction portion, 11) couch roll, 12) pressing portion, 13) drying portion, 14) calenders.

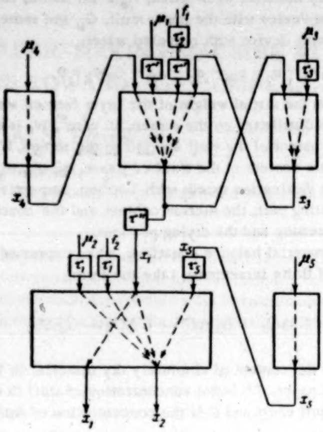

Fig. 2.

the mixing pump to the head box, the controlling organs in the electric drive system and in the system of press roller clamps; f_1 and f_2 are the relative values of the disturbing actions related, respectively, to changes in the parameters of the stuff and the steam; τ', τ'', τ_1 and τ_2 are the "pure" lags, respectively, from the mixing pump to the "slice" of the head box, from the slice to the calender machine, in the steam trunks, and from the machine stuff chest to the mixing pump; s = d/dt is the differentiation operator.

The coefficients of Eqs. (5) – A_{111}, A_{110}, A_{131}, A_{130}, A_{141}, A_{310}, A_{331}, A_{330}, A_{440}, A_{580}, B_{110} – are expressed in simple ways in terms of the known parameters of the technological process. There has been no success in obtaining analogous expressions for the remaining coefficients, since, for this, one must use regularities of the processes in the drying portion. As has already been stated, it is difficult to make use of these latter.

Data for the exhaustive description of the object of control gives its temporal characteristics, obtained experimentally. In taking off the characteristics cited, it should be taken into account that Eqs. (5) define the paper-making machine as an object with interrelated controlled quantities. With this, part of such quantities (the weight of 1 m² and the moisture content of the paper) constitute the object's output quantities, while the other part (concentration and level of stuff in the head box, speed of motion of the wire screen, the vacuum in the suction devices, pressure of the press roller clamps, etc.)

Form of channel	Structure of channel	Sign of controling action	Object's transfer function
Principal internal channel	$\mu_1 \to x_1$	$-\mu_1$	$\frac{k}{(s+a)} e^{-(\tau'+\tau'')s}$
	$\mu_2 \to x_2$	$+\mu_2$	$-\frac{k_1}{(s+a_1)(s+b_1)} e^{-\tau_1 s}$
	$\mu_2 \to x_2$	$-\mu_2$	$-\frac{k_2}{(s+a_2)(s+b_2)} e^{-\tau_1 s}$
One-sided internal channel	$\mu_4 \to x_4 \to x_1$	$-\mu_4$	$-ke^{-\tau''s}$;
	$\mu_4 \to x_4 \to x_2$	$-\mu_4$	$-\frac{k}{(s+a)(s+b)} e^{-\tau''s}$
	$\mu_4 \to x_4 \to x_1$	$+\mu_4$	$-\frac{k_1 s}{(s+a)(s+b)} - k_2 e^{-\tau''s}$
	$\mu_4 \to x_4 \to x_2$	$+\mu_4$	$-\frac{k_1 s}{(s+a_1)(s+b_1)} - -\frac{k_2}{(s+a_2)(s+b_2)} e^{-\tau''s}$
	$\mu_3 \to x_3 \to x_2$	$+\mu_3$	$\frac{k}{(s+a)(s+b)} e^{-\tau''s}$
Two-sided (cross-over) internal channel	$\mu_1 \to x_1 \to x_2$	$+\mu_1$	$\frac{k}{(s+a)(s+b)} e^{-(\tau'+\tau'')s}$
	$\mu_2 \to x_2 \to x_1$	$+\mu_2$	$\frac{k_1}{(s+a_1)(s+b_1)} e^{-\tau_1 s}$
	$\mu_2 \to x_2 \to x_1$	$-\mu_2$	$\frac{k_2}{(s+a_2)(s+b_2)} e^{-\tau_1 s}$
	$\mu_3 \to x_3 \to x_1$	$+\mu_3$	$\frac{ks}{(s+a)(s+b)} e^{-\tau''s}$

relate to the individual portions of the process and, for the object as a whole, can be considered as input stimuli. The structural schematic of the object of control is shown on Fig. 2. In correspondence with such a scheme, the temporal characteristics (run curves) were obtained by applying disturbances in the form of unit steps from each of the controlling organs. The object's reaction was determined as its output by a simultaneous measurement of the weight of 1 m² and the moisture content of the finished paper. Some of the characteristics obtained are shown on Fig. 3. On the basis of the results obtained, the transfer functions of the various channels of the object of control were established. These data are given in the table.

A comparison of Eqs. (5) with the tabulated data attests to the coincidence of the qualitative features of the process obtained by a theoretical analysis and those established experimentally. This is also attested to by the quantitative estimates of object dynamics from Eqs. (5). Figs. 3a, c and d show, together with the experimental run curves, the temporal characteristics obtained by calculation.*

3. Determination of Object's Dynamic Characteristics from Data on Normal Use

The methods considered for the experimental investigation of the object of control are inapplicable to high-speed paper-making machines. In this case, the applica-

---

* The characteristics were obtained for paper-making machine No. 3 of the Krasnyi Kursant (Red Student) Plant.

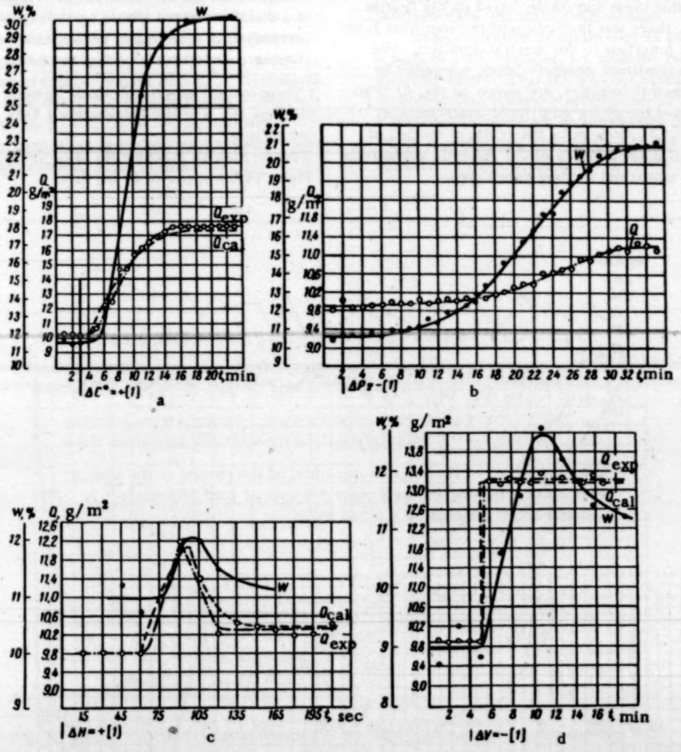

Fig. 3. Curves of a run of the object of control. Q is the weight of 1 m² of paper, W is the paper's moisture content, ΔC* is the unit step of concentration, ΔP is the unit step of drying steam pressure, ΔH is the unit step of level in the head box, ΔV is the unit step of velocity of wire screen motion.

tion of disturbing stimuli to the object's input leads to a significant disruption of the process. Moreover, random uncontrolled disturbances, whose effect is tremendously difficult to eliminate, essentially limit the accuracy of the measurements of object reaction.

In view of this, the possibilities of determining the dynamic characteristics of a paper-making machine by the statistical processing of its normal use data were studied. In correspondence with the theory of the method expounded in [2, 3], we obtained simultaneous recordings of the variable process quantities by the channel "concentration of stuff in the machine stuff chest – weight of 1 m^2 of finished paper" (Fig. 4).† In this case, the paper-making machine is considered as a linear object with one input and one output. After processing the curves obtained on a mechanical correlator, we obtained the autocorrelation function $R(\tau)$ of the input signal (Fig. 5a) and the cross-correlation function $C(\tau)$ of the input and output processes (Fig. 5b). On this same correlator, based on the Fourier transformation, there was implemented the transition from the correlation functions to the spectral densities. The object's phase-amplitude characteristics, computed by dividing the spectral densities, are shown on Fig. 6. This same figure shows the phase-amplitude characteristics of another object,‡ obtained by the ordinary method of an experimental determination of the dynamic characteristics and by the statistical method considered.

4. Certain Principles of Complex Automation of Paper-Making Machines

Results of the investigation of the dynamic properties define the paper-making machine as an object of control with interrelated controlled quantities. For the automatic control of such objects, one should create the conditions for which it is possible to control each controlled quantity independently of the others. It is known that such a problem is solvable on the basis of the principle of autonomous control. The realization of this principle is possible by two routes:

1) dissection of a multiconnected control system into a series of dynamically independent systems;

2) provision of high control quality of the individual quantities by constructing optimal processes in the separate systems.

The first of these methods is known as the method of connected control, since it provides dynamic dissection of a multiconnected system by introducing artificial compensating connections between the controllers. Design of these connections is carried out on the basis of a dia-

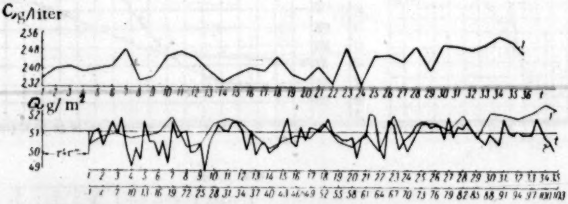

Fig. 4. Recording of the variable quantities of the process in the channel "concentration in machine stuff chest – weight of 1 m^2 of paper": 1 is concentration, 2 is weight of 1 m^2 of paper.

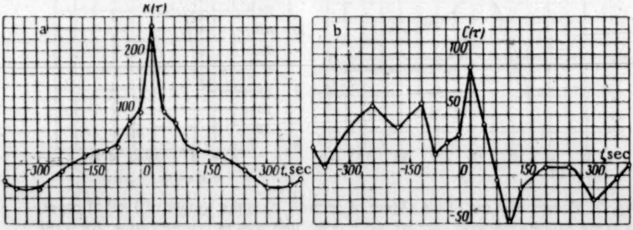

Fig. 5.

---

† These recordings were obtained by using paper-making machine No. 5 of the Balakhninskii TsBK at a speed of 400 m/min.

‡ Paper-making machine No. 3 of the Krasnyi Kursant Plant, with a speed of 50 m/min.

gonalization of the basic matrix of the transfer functions of the closed-loop control systems of the interrelated quantities [4, 5].

For the compensating connections for the automation of a paper-making machine, the following relationships were obtained:

$$D_{12}(s) = -\frac{M_{11}(s)}{M_{12}(s)} D_{22}(s), \tag{6}$$

$$D_{21}(s) = -\frac{M_{22}(s)}{M_{21}(s)} D_{11}(s), \tag{7}$$

$$D_{13}(s) = \frac{M_{13}(s) M_{22}(s) - M_{12}(s) M_{23}(s)}{M_{11}(s) M_{22}(s) - M_{12}(s) M_{21}(s)} D_{33}(s), \tag{8}$$

$$D_{23}(s) = \frac{M_{11}(s) M_{23}(s) - M_{21}(s) M_{13}(s)}{M_{11}(s) M_{22}(s) - M_{12}(s) M_{21}(s)} D_{33}(s), \tag{9}$$

where $M_{11}(s)$, $M_{22}(s)$, $M_{12}(s)$, $M_{21}(s)$, $M_{13}(s)$ and $M_{23}(s)$ are the transfer functions of the object for the channels, respectively: "concentration – weight of 1 m^2," "steam pressure – moisture content," "concentration – moisture content," "steam pressure – weight of 1 m^2," "concentration – level in head box," "level in head box – moisture content"; $D_{11}(s)$, $D_{22}(s)$ and $D_{33}(s)$ are the transfer functions of the controllers in the separate systems – weight of 1 m^2, moisture content, level in head box.

The second of these methods cited is based on the unbounded increase in the gains of the separate systems with the condition that their stability be retained [6]. Although this method provides absolute autonomy of the processes in certain ideal cases, its use is possible, since a large part of the separate systems of the complex automated paper-making machine can possess partial autonomy.

In the study of the dynamic properties of the object of control, it was established that, of all the technological connections of the controlled quantities, the most powerful connections were those in which the weight of 1 m^2 of paper participated. It was on the basis of this that there arose the possibility of solving the problem under consideration by constructing an optimal process only in the system for the automatic control of the weight of 1 m^2 of paper sheet. The difficulties which ensue with this in view of the object's high inertia, and the significant delays in passing signals through it, are overcome in the case of sampled-data (discontinuous) control.

As the criterion of optimality in the control of the weight of 1 m^2 of paper, we took the minimum of the dynamic errors. This leads to the requirement that the control system possess a given order of astatism and have a transient response which terminates in minimal time. These requirements are realized in the system whose discrete transfer function has the form

$$K^{*}(z) = \frac{b_0 z^{-(l-l_1)} + b_1 z^{-(l-l_1+1)} + \cdots + b_{l_1} z^{-l_1}}{a_0 + a_1 z^{-1} + a_2 z^{-2} + \cdots + a_l z^{-l}}; \quad l_1 \leqslant l, \quad z = e^{sT}, \tag{10}$$

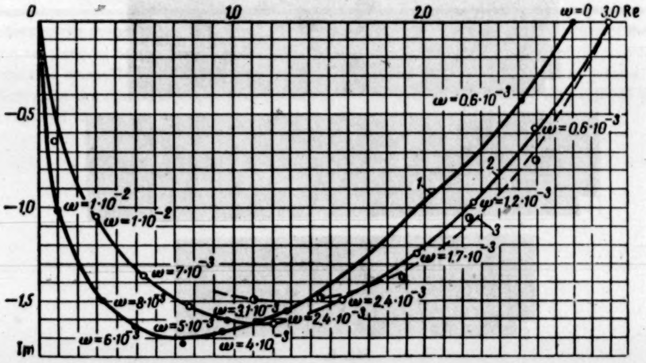

Fig. 6. Phase-amplitude characteristics of the object of control for the channel "concentration in machine stuff chest – weight of 1 m^2 of paper" (without discounting lags): 1 is from the correlation functions for paper-making machine No. 5 of the Balakhninskii TsBK, 2 is from the run curves for machine No. 3 of the Krasnyi Kursant Plant, 3 is from the correlation functions for the same machine.

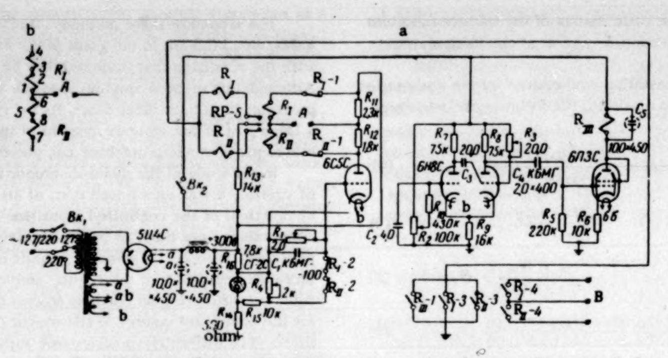

b
a
R_I
R_{II}
A
RP-5
R_I-1
R_{II}-1
R_{11} 2.3к
R_{12} 1.8к
R_{13} 14к
6C5C
Вк₂
Вк₁
5Ц4С
~127/220
+300В
7.8к
СГ2С
C_1 КБМГ-100В
R_I-2
R_{II}-2
R_4 2к
R_{15} 10к
R_{14} 570 ohm
10.0×450
10.0×450
R_7 75к
R_8 75к
R_3 200
6Н8С
C_3
C_4 КБМГ 20×400
6П3С
R_{III}
C_5
100×450
C_2 4.0
R_2 100к
430к
R_9 16к
R_5 220к
R_6 10к
R_{III}-1
R_I-3
R_{II}-3
R_I-4
R_{II}-4
B

Fig. 7. a) Scheme of the sampled-data element. A is the controlling signal, B is the correction pulse, R_I, R_{II} and R_{III} are type RPN (U1720213) relays; b) scheme for connecting the windings of relay RP-5 (U1722025).

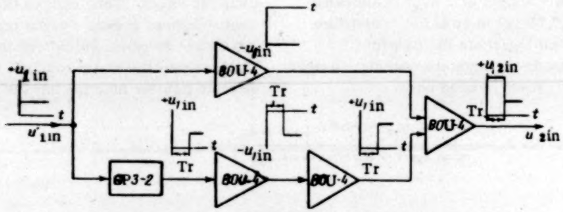

$+u_{1in}$
u'_{1in}
$-u_{1in}$
BOU-4
Tr
t
$+u_{2in}$
u_{2in}
GP3-2

Fig. 8.

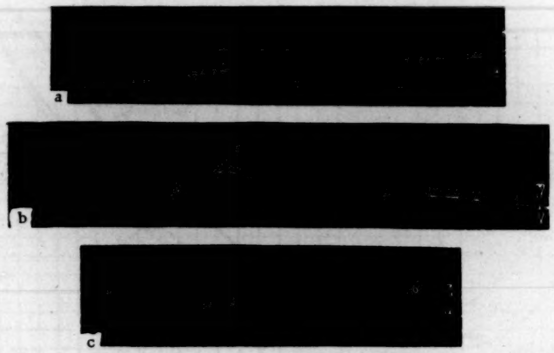

Fig. 9.

if the following conditions[**] hold:

$$a_0 + a_1 + a_2 + \cdots + a_l = b_0 + b_1 + b_2 + \cdots + b_{l_1},$$
$$b_0 + b_1 + b_2 + \cdots + b_{l_1} = 1 \qquad (11)$$

The practical realization of conditions (11), as was shown in work [7], requires the introduction of a correcting circuit containing a system of sampled-data filters or a digital computing device.

In conclusion, we consider one of the variants of the solution proposed for the problem.

5. Optimal System for the Automatic Control of the Weight of 1 m^2 of Paper Sheet

In the system for the automatic control of the weight of 1 m^2 of paper, there was used a discrete controller. This controller contains a sampled-data element providing width modulation of the sequence of error signals [8]. The schematic of such a sampled-data element is shown in Fig. 7. The correction circuit, connected in series, was assembled from blocks of analog computer MPT-9 and constant lag block BPZ-2 (Fig. 8). The MPT-9 simulator also provided the realization of a model of the object (the channel "concentration of stuff – weight of 1 m^2 of finished paper"). The results of an experiment performed on the model thus obtained for the control system are shown on Fig. 9, where one can see the object's run curve (a), the control process in the system without the correction circuit (b), and the process in the corrected system (c). As is clear, the speed of response and the accuracy are close to their limiting values,[††] which allows us to consider the automatic control system under consideration for controlling the weight of 1 m^2 of paper as an optimal system.

SUMMARY

1. The data of the theoretical analysis described a paper-making machine as an object of control with several interrelated controlled quantities.

2. To determine the dynamic properties of such an object, it is required to use the theoretical method proposed, in conjunction with the well-known methods of experimental investigation.

3. Consideration of a paper-making machine as a complex to be automated is related to the solution of the autonomous control problem. In a first approximation, this problem can be solved by the optimization of the process in the system for the automatic control of the weight of 1 m^2 of paper.

LITERATURE CITED

1. A. S. Shamson, "Certain characteristics of a paper-making machine to be automated," Bumazhnava Promyshlennost' No. 3 (1959).
2. L. G. Henderson and C. J. Pengilley, "The Experimental Determination of System Transfer Functions from Normal Operating Data," J. Brit. IRE 18, No. 3 (1958).
3. V. V. Solodovnikov and A. S. Uskov, "Frequency methods of determining the dynamic characteristics of objects of automatic control from data of their normal use," Avtomat. i Telemekh. 20, 12 (1959).[‡‡]
4. A. S. Boksenbom and R. Hood, General Algebraic Method Applied to Control Analysis of Complex Engine Types, NACA TR, 980 (1950).
5. B. V. Il'in, "On the Choice of a Reasonable Automatic Control Scheme: Dissertation [in Russian] (LÉTI Ul'yanov (Lenin) 1958).
6. M. V. Meerov, "On the autonomy of multiconnected systems, stable for an unlimited increase in static accuracy," Avtomat. i Telemekh. 17, 5 (1956).[‡‡]
7. Ya. Z. Tsypkin, "Correction of sampled-data regulation and control systems," Avtomat. i Telemekh. 18, 2 (1957).[‡‡]
8. A. S. Shamson, Patent No. 126356, with priority to Jan. 19, 1959.

[**] For controlling signals in the form of unit steps.

[††] We have in mind the values of the maximum deviation (y_{max}) and the duration of the transient response (t_{tra}) which can be obtained in an automatic control system of the type considered with infinite gain.

[‡‡] See English translation.

AUTOMATION AND CENTRALIZATION OF A COPPER MINE

V. V. Kryuchkov
Moscow

Translated from Avtomatika i Telemekhanika, Vol. 21, No. 6, pp. 867-876, June, 1960

The paper describes the set of measures adopted for the automation and centralization of the technological processes executed in the pits of one of the large mines in the USSR with subterranean extraction of the ore, the Degtyarskii Copper Mine.

The Degtyarskii Copper Mine is the oldest mining enterprise, comprised of several underground pits, thoroughly reconstructed during the years of the first Five-Year Plans. The copper ore of the Degtyarskii mine is processed on the nearby large concentration plants and copper smelters.

The set of measures adopted, and the experimental design and research work implemented, and to be implemented, at this mine aroused the justified interest of many other mining enterprises. The experience here was successsfully extended to analogous shafts and mines of nonferrous and ferrous metallurgy.

Employment was found at the mine for the devices of a developed modern centralization of the pit, a signalling, centralization and blocking system (SCB) with high-frequency communications of the transport dispatcher with the electric locomotive engineers, devices for high-frequency and low-frequency (conductor) production communications between the general works dispatcher and the work divisions (the so-called system of loudspeaker annoucements, calls and conversations), devices for the centralized control of electric locomotives at the sites of loading and unloading ore. Also automated were the skip hoist machines, a device for hoisting empty rock dumps, control for the shaft top cager mechanism, transfer of trucks in the cages, compressors, furnace, ventilation, pumping stands, and many other shaft devices.

Devices were developed for the automatic weighing of trucks with ore in transit, inspection of the state of the steel cables of the hoisting machines, various systems of remote control devices, while sharply decreasing the requirements on the cable shops.

The mine pits were equipped with television in the devices for centralization and control of truck hoist machines, instruments using radioactive isotopes for the inspection of ore level in ore chutes and bins, temperature inspection devices using semiconductors, etc.

Parallel with the solution of the questions of automation and centralization of the mine, there was executed significant work on the mechanization and dissemination of new technological processes of extracting and transporting ore.

Pit Centralization

A modern mining enterprise is equipped with complicated machines, mechanisms and devices, the majority of which are included in a unitary technological process — the extraction and transportation of minerals — so that on their concordant operation depends the production of the entire mine as a whole. It is in connection with this that centralized control of pit mines has particular importance today.

With the introduction of the centralized system, the dispatcher of the Degtyarskii Copper Mine pits obtained the capability of continuously inspecting:

1) number of ore-laden skips,
2) number of trucks unloaded on dumpers, by level;
3) ore level in bins, by level
4) operation of the machines for transportation crushing conversion,
5) quantity of rocks taken from the pits,
6) number of trucks let down into the pits from the scaffolding,
7) operation of the cage hoists,
8) expenditure of compressed air and water, by level,
9) magnitude of insulation impedance in the 380 volt lines,
10) pressure of compressed air and water in one of the most typical levels,
11) lowering of pit top-cager temperature below +2°C,
12) operation of the automated water-draining equipment.

At the dispatcher's disposal there are various means of control and, in particular, a widely ramified communication system with all the productive divisions.

One of the basic devices of centralized communication is the announcement call and conversation system, implementable by means of high-frequency apparatus using the trolley lines of the electric locomotives' contact network. The given communications system is intended for powerful loudspeaker announcements at the various production divisions as to preparations for use of explosives, possible accidents, and also for inquiry by the dispatcher

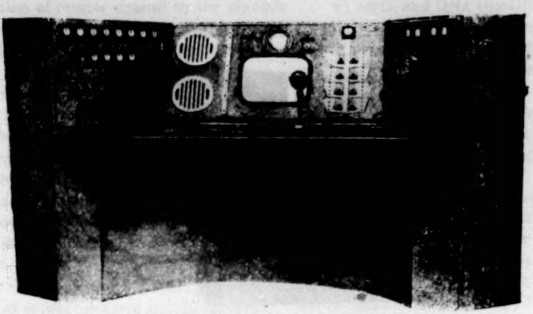

Fig. 1. Over-all view of the central control desk.

as to individual workers located in the production divisions. The apparatus allows the dispatcher to be called from any division where he may be and for conversations to be held with him.

The loudspeakers are used for announcements or for calling workers to the apparatus. After the call, the conversation with the dispatcher is conducted by the usual microtelephone, and the loudspeakers are automatically switched off.

With workers serving in the hoist cages, the dispatcher is connected by means of semiconductor apparatus of the production loudspeaker communications system.

For observation of the mine yards and the receiving areas there is provided a multicamera industrial television setup with five transmitting cameras. By means of a special commutator, the dispatcher can switch any of the five cameras to his viewing screen.

At the objects of observation there are established the transmitting cameras which permit the implementation of remote aiming, optimal focusing, diaphragming and change of objects.

Figure 1 shows an over-all view of the central control desk of the pit "Kapital'naya 2". The central control desk is located in a special room on one of the pit levels. On the desk's left-hand panel there are counters for the numbers of trucks unloaded in bins, by level, quantity of rock extracted, etc., and the equipment for the dispatcher's high-frequency announcement, call and conversation communications system.

On the front panel there is marked a mnemonic scheme of the hoist cages, controls for inspecting bin loading, by level, and instruments for inspecting the number of loaded skips. On the same panel is the closed-circuit television viewing screen.

On the desk's right-hand panel there are instruments for inspecting the magnitude of insulation of the low-voltage 380 volt lines, for inspecting pressure and expenditure of water and compressed air. Here is installed a four-party telephone intercom device, by means of which the dispatcher is connected with the works' switchboard and also with the works' superintendent.

A special cabinet was installed for accomodating the dispatcher's television system receiver, the electric power supply, the relay circuits and the recording instruments.

All the information at the dispatcher's desk is transmitted by means of a contactless remote control system.

Two types of remote control and signalling systems were used.

1. A contactless cyclical teletransmission system based on magnetic elements with rectangular hysteresis loops and on filamentless thyratrons, with time separation of the channels. This system was developed by the Institute of Automation and Remote Control of the Academy of Sciences of the USSR.

The system permits a virtually unlimited increase in the number of channels, requires no special power supplies, can be used not only for inspection but also for controlling mechanisms. The system is sufficiently fast-acting.

2. A system of ferrite-transistor cells, also with time separation of channels, based on circuit elements developed by the Central Research Institute for Complex Automation.

Part of the over-all centralization system is the centralization of underground transportation. The transportation dispatcher is near the pit dispatcher's room and, with his own desk and by means of an SCB system, can inspect movements of the rolling stock, by mining operation, can change signal arms by remote control, can establish routes and can inspect the positions of signal arms and the states of signal lights.

High-Frequency Communications with Electric Locomotives

The transportation dispatcher has at his disposal high-frequency (HF) communications with the moving electric locomotives. These communications are implemented by the electric locomotive contact network.

The introduction of dispatcher communication with the electric locomotive engineers immediately improved the transportation operations, significantly increased the safety of motion and use of the rolling stock. High-fre-

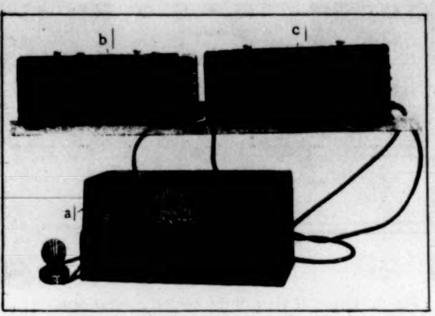

Fig. 2. Dispatcher equipment for high-frequency communication with the electric locomotives. a is the calling block, b is the receiver-transmitter, c is the power supply.

quency communication of the transportation dispatcher with the moving electric locomotives is firmly entrenched in the pit regimen. Electric locomotives without high-frequency communications are considered dangerous, and cannot be placed on the line.

HF communications with the electric locomotives consists of the dispatcher's and the "subscriber's" assemblies. The dispatcher's assembly is a receiver-transmitter HF set with selective calling of the out-stations. The assembly (Fig. 2) consists of three blocks: the calling block a, the receiver-transmitter b and the power supply c.

The calling block, with the microphone, is installed at the dispatcher's desk. All the controls are placed on the calling block's front panel. Here are located a loudspeaker, 15 calling buttons, the stop button, a button for switching in the local telephone network and the lamp signals. To call any out-station, the dispatcher pushes the corresponding call button; this switches in the receiver-transmitter and the audio-frequency call generator. Depending on the ordinal number of the button pressed, a voltage of one of 15 fixed calling frequencies is generated in the line, modulating the transmitter's carrier frequency. After the signal denoting that the called out-station has switched in, the sending of the call is automatically stopped, and the communication line is set up for the ensuing conversation.

Obtaining a call signal, the out-station worker converses with the dispatcher without himself doing any switching. After termination of the conversation, the dispatcher presses the "stop" button, thus switching his transmitter, his assembly and that of the out-station to the "waiting" mode.

The out-station assembly (Fig. 3) consists of a receiver-transmitter with a built-in loudspeaker, a power supply and a microphone with a signal lamp and a call button. The signal lamp is lit when the dispatcher's transmitter is switched in, and shows that the dispatcher is busy. The given communications system is connected into the local telephone network, and the dispatcher can authorize conversations from any electric locomotive with subscribers of the local telephone network.

Remote Control by Electric Locomotives at the Ore Loading and Unloading Sites

An urgent problem was the introduction of a system of remote control by the mine's electric locomotives at the sites of ore loading and unloading. Indeed, the transfer of the functions of chute drawer and tipper to the electric locomotive engineers permitted an increase in the productivity of work, a shortening of the time to load an ore truck, an increase in the effective capacity of the switching yard and the freeing of a large number of workers who had been occupied at the chutes and dumpers.

The system of remote control from the electric locomotives makes it possible for the electric locomotive's engineer to carry out all the operations for loading and unloading directly at the chutes and dumpers and to control the movement of the rolling stock from a stationary control desk.

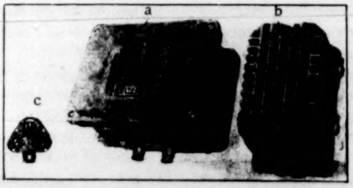

Fig. 3. Out-station assembly of the high-frequency electric locomotive communications system. a is the receiver-transmitter, b is the power supply, c is the microphone.

For the implementation of remote control by the electric locomotives, the corresponding portions of the trolleys are insulated from the remainder of the contact network and form the zone of remote control. The voltage on the contact conductors of this zone are applied via the contactor of the command block. In the power circuit on the electric locomotive are connected the contactors of the receiving device's reverser. One of the contactors, "forward", with ordinary control, is mechanically held in the switched-in position, maintaining the normal supply scheme of the electric locomotive's motor. I₁. the remote control mode, the mechanical holding of the electric locomotive with the contactor is removed.

Upon the command "forward", the full voltage of the contact network is applied to the insulated trolley segment, providing inclusion of the "forward" contactor in the electric locomotive's receiving device.

Upon the command "backward", the voltage on the insulated trolley segment is momentarily applied (during 0.2 seconds) through a current-limiting resistor, which is thereafter shunted, and the insulated trolley segment is immediately connected into the contact network. This provides inclusion of the "backward" contactor in the electric locomotive's receiving device, and a change in the direction of motion.

The command "stop" switches the insulated segment of the trolley out of the contact network.

The scheme of remote control from the electric locomotives provides:

a) the capability of the electric locomotive's engineer to switch, from his cab, the electric locomotive onto remote control, which is implemented from a stationary contro desk;

b) remote control of the electric locomotive's motion "forward" and "backward";

c) automatic cessation of electric locomotive remote control upon transmission of the command "stop";

d) stopping of the electric locomotive if it accidentally leaves the controllable segment;

e) voice and light signalling as to the motion of the remotely controlled electric locomotive;

f) automatic repetition of the transmitted command upon accidental momentary separation of the pantograph from the trolley conductor;

g) uninterrupted motion in the loading or unloading zone of a normally controlled electric locomotive;

h) impossibility of passing control signals to neighboring portions.

The following devices enter into the set of apparatus for remote control from electric locomotives at the loci of ore loading and unloading:

Control apparatus installed in the hauling gear right at the chutes or dumpers, and serving for the application of the commands "forward", "backward" and "stop" by means of a special lever, inserted by the engineer in the apparatus frame.

Command blocks, installed at the beginning of the cross-over or at the chutes, and serving for the transmission of the commands obtained from the control apparatus to the electric locomotives' receiving blocks, and for switching in the power voltage to the insulated trolley sections.

Receiving blocks, installed in the electric locomotives and intended for the connecting of its motor in accordance with the received commands, and also for stopping the electric locomotive if it accidentally leaves the remote control zone.

Auxiliary electromechanical braking devices, installed on the electric locomotive motors, and serving for the automatic braking of the electric locomotives upon receipt of the command "stop" and also for accidental departures of the electric locomotives from the remote control zone. The braking device consists of a brake disk on the motor shaft, a braking tape and a braking magnet.

The remote control scheme can also embody other means of automatic braking: electrohydraulic or electropneumatic.

Automation of Shaft Ventilation Doors

To improve ventilation of the mining works, and also to increase the capacity of the haulage lines in the mine, the shaft ventilation doors were automated.

Fig. 4. Over-all view of the shaft's automatic ventilation door.

The automation of the process of opening and closing the doors permitted the freeing of a significant number of workers who had been occupied in the maintenance of the ventilation doors.

In addition to the economy realized by freeing the service personnel, the use of automatic shaft doors significantly improved the operating conditions of underground transportation and provided safe operation in their servicing. The ventilation doors were provided with electric drives, as being the most reliable, economical and most readily amenable to automation. The over-all view of a door is given in Fig. 4.

The ventilation door automation scheme provides for automatic opening of the door as an electric locomotive or a truck approaches, and the automatic closing of the door after passage of all the rolling stock, signalling of door position to the dispatcher's SCB desk, elimination of collisions of electric locomotives with closed doors by taking voltage off the trolley segments on either side of the door, the impossibility of opening the door when rolling stock approaches from both sides simultaneously, switching of a yellow signal light to red upon approach of rolling stock in the contrary direction, acoustical announcement to people of the contrary rolling stock as to the closed door, impossibility of closing the door while rolling stock is situated in it.

Automatic Weighing of Ore Trucks in Transit

For the inspection of the amount of rock extracted, equipment for the automatic weighing of trucks in transit was developed. With this, the weighing of trucks does not require uncoupling of the rolling stock or any other operations connected with the use of manual labor. Such a weighing scheme significantly increases the productivity of the electric locomotives, the turnover of the truck yards, and frees the majority of the service personnel. Moreover, it eliminates the possibility of erroneous recording.

To automate the process of weighing ore trucks in transit, use was made of the method of weighing by means of measuring the bending of a rail from the action of the truck's weight on it. Foil tension impedances were used as the transducers by means of which the rail bending is measured.

The equipment for weighing an ore truck in transit consists of three basic assemblies: a) a weighing portion with tension impedance weight transducers; b) path transducers; c) recording instrument.

For weighing, the weighing portion is cut out from the rail path. The weight transducer with foil tension impedances is welded to the rails. Switching in of the electrical scheme is implemented by pedal-type path transducers, installed before and after the weighing segment.

The recording instrument (Fig. 5) is an electronic self-recording bridge with a built-in mechanism for adding the weights of all the ore passing over the segment, or for weighing the empty and loaded trucks separately, and a device for automatically setting the measuring scheme to zero before the weighing of each set of rolling stock.

The weighing block schematic is shown in Fig. 6. The weight transducers are welded to the ends and bases of the measurement rails and operate on expansion and compression. The tension impedances installed in these transducers are connected in a bridge circuit. The use of all four arms of the bridge for measurement increases the sensitivity of the measuring scheme and provides temperature compensation for it. In the diagonals of the measuring scheme two slide wires are connected: the first one operational, the second one designed for automatic zero adjustment before the weighing of each set of rolling stock.

The equipment for the automatic weighing of pit trucks in transit provides: a) weighing of trucks with an accuracy of ± 2.5% when moving with speeds up to

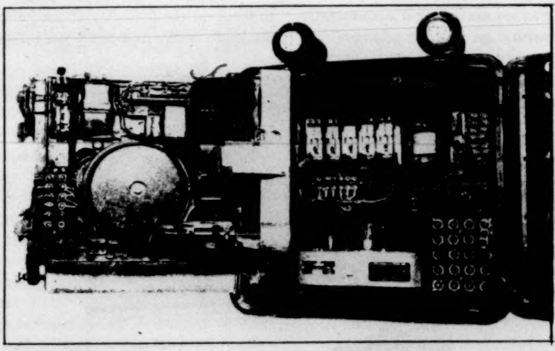

Fig. 5. Recording instrument for automatic truck weighing (with opened hood).

5 km/hour; b) automatic elimination from the total weight of a truck of an average tare weight; c) weighing of empty and loaded trucks separately; d) automatic summation of the weight of all ore passing over the weighing segment; e) recording on a strip diagram of the weight of each truck individually; f) weighing of the rolling stock without including the weight of the electric locomotive.

The given equipment was designed for heavy-duty operation in mine conditions.

Automatic and Remote Control of the Mechanisms of Shaft Top Cagers and Truck Exchange at the Loading Platforms

Control of the shaft top cager mechanisms at all the levels is exercised by one person, the so-called "cager", since complex automation and remote control of the shaft top cager mechanisms was carried out at the mine. With this, all the top cager mechanisms – hammers, detents, grids – are outfitted with pneumatic drives and are controlled either remotely, by the engineer of the hoist machine, or from a stationary desk on the level, or automatically. Control of operation of these mechanisms, is executed by the cager who, as needed, moves from one level to another, and carries out all the work for the receipt and output of loads.

As means of control, the cager is given a new system of shaft top cager signalling with loudspeaker communications and with high-frequency connections with the moving cages. All the technological processes from loading the trucks with rock to unloading them at the receiving platforms have been automated. For this end, the whole complex of mechanisms was developed and modernized.

An over-all view of the equipment is shown in Fig. 7. The operation of the equipment occurs in the following fashion. A truck with rock is pushed from the cage by means of a pneumatic plunger, after which it is clamped by the plunger and fed to the dumper. In the dumper it is automatically stopped and then unloaded. After halting of the dumper, the stopper is removed and the truck is pushed by a pneumatic plunger and moves along a slope to the top cager again.

At the mine, the following measures have also been taken:

Complete automation of the skip hoists, operating by a motor-generator system. The starting impulse for the skip hoist is given from the measuring hopper, after which all operation of the hoist proceeds automatically.

Automation of the principle water draining apparatus, which provides reliability of pump operation, and frees the service personnel.

On the surface, there has been complex automation of the compressor stands, the furnace stands, the rock dumps. The principal ventilation equipment has been subjected to remote control.

The automated mine equipment is supplied with built-in temperature protection of electric motors from winding-overheating and of mechanisms from bearing-overheating.

For the temperature protection of motors and mechanism bearings, use was made of thermal transducers in the form of semiconducting thermal impedances (thermistors), satisfactorily solving the problem of protection of unattended aggregates from overheating.

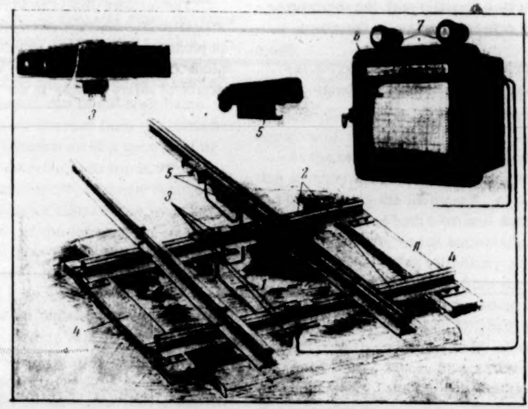

Fig. 6. Block schematic of automatic truck weighing in transit: 1) weighing section of track rail; 2) measuring rails; 3) weight transducer; 4) concrete foundations; 5) path transducers; 6) recording instrument; 7) counter for adding weights of all ore passing over segment.

Fig. 7. Over-all view of the automated equipment for exchanging trucks and loading at the dumper.

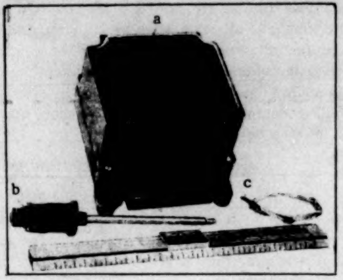

Fig. 8. Apparatus for temperature protection of motors. a is the relay block, b is the transducer for motor protection, c is the transducer for bearing protection.

The action of the apparatus is based on the capability of certain types of thermistors to sharply, by a factor of one hundred, decrease their resistance when the ambient temperature rises above a definite limit. This limit can be regulated by the magnitude of the voltage applied to the thermistors. Miniature thermistors, properly encased (Fig. 8), are inserted in the windings of electric motors, or in mechanism bearings, and a relay winding is connected in series with the thermistor. The relay operates for a sharp decrease in thermistor resistance.

The thermal transducer for bearing protection is a metallic sleeve, screwed into the body of the bearing, with a built-in thermistor, while the thermal transducer for insertion in electric motor windings is executed in the form of a flexible plastic tube with a thermistor fixed in its end.

The relay has a switch setting which allows the temperature of relay operation to be established between the limits of 80 to 110°C in steps of 10°C.

The totality of all the work in this direction permitted a significant reduction in service personnel, an increase in productivity of the mechanisms and in the general productivity of labor, and also the guarantee of a high degree of safety of work in the mine.

USE OF ELECTRONIC COMPUTERS FOR BESSEMER PROCESS AUTOMATION

V. M. Glushkov, L. N. Dashevskii, and A. I. Nikitin

Kiev

Translated from Avtomatika i Telemekhanika, Vol. 21, No. 6, pp. 877-883, June, 1960

1. Introduction

Automatic inspection and control of the Bessemer process makes it possible to obtain steel of a given carbon content with a significantly smaller number and duration of blows.

Implementation of automatic inspection and control of steel was possible after a great deal of experimental work, carried out by the Dneprodzerzhinskii Evening Metallurgical Institute and by the Dzerzhinskii works on the analysis of existing nonautomatic methods of inspecting Bessemer smelting processes and on the development of new methods, amenable to automation on the basis of the employment of high-speed electronic digital computers.

The complexity in the development of inspection methods useful for automation results from the following factors.

The speed at which the process flows virtually eliminates the possibility of carrying out chemical analysis of the metal during the course of the smelting, analysis which would give the most valuable and accurate data for establishing the time for tipping the converter with a given carbon content. At the same time, the same speed of process flow poses very narrow limits within which the converter's tipping (pouring) time can deviate.

Photoelectric transducers not equipped with special cooling devices are positioned, due to the high flame temperatures, at a significant distance from the converter, which is the cause of the appearance of a great deal of noise which distorts the transducer indications. To this is conjoined the great nonuniformity of flame luminosity at different points, and at different times at the same point, which also lowers the value of the information obtained from photoelectric transducers.

The enumerated factors make it difficult to obtain the original experimental data for determining the time of converter pouring. The difficulties in principle are consequences of the circumstance that very many physical and chemical factors influence the speed at which the process flows and, consequently, the time of converter pouring, factors such as, for example, the initial content of carbon and silicon in the pig iron, the number of smelts on a given bottom, the velocity of air blowing, the temperature regimen of the smelter and other factors. To take the influence of the foregoing factors into consideration is difficult for the following two reasons.

1. The physical and chemical processes which specify the dependence of the time of pouring on the factors mentioned have not been completely studied, and we have this dependence only in the form of experimental (very numerous, to be sure) tables and graphs, containing a quite significant number of errors.

2. Taking the aforementioned factors into account can only be done at the time of, or immediately before, the beginning of the smelting run itself, since only at this time are the necessary initial data at hand, for example, information as to the consumption of air, the serial number of the smelting run, etc.

Thus, all the difficulties mentioned can be generalized as follows: For an accurate determination of the time for ending a blow, it is required to process and take into account very rapidly a large quantity of data, each component of which individually can be obtained only with significant random errors.

2. Posing of the Problem. Information Sources

The problem is thus posed: It is required to develop a system which permits cessation of blowing of rail steel with carbon content within the limits of 0.48 to 0.58%.

If we take into account the speed of carbon burn-out, equal to 0.007 to 0.008% per second, we find that the moment of converter tilting must be predicted with an accuracy of ± 5 seconds.

As the result of a theoretical and practical investigation of many methods of inspecting the Bessemer process and determining the moment τ_t of tilting the converter, methods suggested both here and abroad, we adopted the following methods, which are maximally satisfactory due to their relatively high reliability and practicality.

1. Determination of τ_t from the amount of air blown through the converter. This method is based on the fact that the quantity of carbon "burned-out" of the pig iron depends directly on the quantity of air blown through the converter. Thus, τ_t can be predicted from the initial carbon content of the pig iron and the integral expenditure of air through the converter. The reliability of this method is lowered because not all the oxygen in the air enters into reaction with the pig iron's carbon, and part of it is lost with the exhaust gases.

2. Determination of τ_t from a W-diagram. Empirical investigations showed that, if one establishes transducers

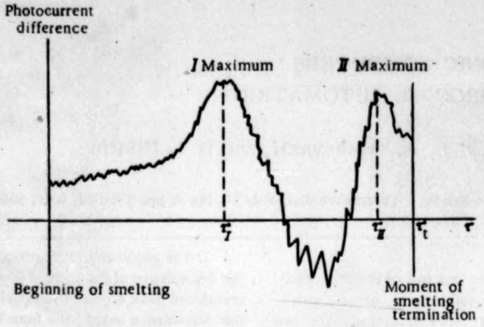

Fig. 1.

which record the converter flame's illumination in two different nonintersecting spectral regions (for example, infrared and yellow), then the difference of currents of these transducers from one smelting operation to another gives a characteristic curve recalling an inverted letter W (Fig. 1). With this, the termination of the smelting operation coincides in time with the dropping off of the curve from maximum II, and can be computed, to a good approximation, from the formulas:

$$\tau_t = \tau_{II} + 50 \text{ sec or } \tau_t = \tau_I + \tau'.$$

Here, τ_I and τ_{II} are the moments at which the maxima appear on the W-diagram, and τ' is some time (8 to 10 minutes) which depends on the temperature of the metal. Physically, the method is based on the circumstance that the time until maximum I, the so-called "blow period" has a large dispersion and is not subject to any accurate estimate, while the processes in the converter after the appearance of maximum I, coinciding with the beginning of intensive combustion of CO, are more determinate, and the time of smelting termination can be predicted.

The reliability of the method is lowered because of the strong noise superimposed on the photoelectric transducer signals.

3. Determination of τ_t from the metal's temperature. The temperature of the metal directly influences the speed at which the chemical processes in the converter t into account gives both direct and indirect data as to the time of smelting termination.

4. Determination of τ_t from the transparency of the flame. It has been empirically established that, a short time before smelting termination, a powerful formation of powder begins on the surface of the metal, thanks to which the flame's transparency drops sharply, after which, with the cessation of the dust formation, it again increases. The moment of minimum transparency is related to the moment of smelting termination, and gives still another "reference point" for determining the latter. The reliability of the method also drops because of the strong noise superimposed on the signal for determination of the flame's transparency.

5. Determination of τ_t on the basis of statistical data for a large number of smelting runs. With this, one takes into account the large amount of attendant factors such as, for example, ordinal number of the lining, original manganese content of the pig iron, as well as original content of silicon, carbon, etc.

3. Method of Processing Information

Prediction of the moment τ_t of smelting termination on the basis of the information obtained from all the previously described sources is implemented by using the methods of mathematical statistics. There is today no exact analytic description of the process.

The reliability of each of the aforementioned methods, while all are of the same order of magnitude, still differs in amount from one to the next. With this there arise two possibilites of using the information obtained from the transducers: a) choose the most reliable method and compute τ_t on its basis; b) attempt to take into account the information given by all the aforementioned methods.

We found it advantageous to take the second path. With this, we start from the natural assumption that the errors of physically independent methods are so distributed that they partially compensate one another, i.e., that the mean square error in determining τ_t as the weighted average of the times determined by each of the individual methods is less than the mean square error in predicting τ_t on the basis of one of the methods, even the most reliable.

Thus, it is proposed to compute τ_t by the formula

$$\tau_t = \frac{\sum n_i^2 \tau_i}{\sum n_i^2},$$

where the τ_i are the times computed on the basis of each of the individual methods and the n_i are the weights, which depend on the reliability of each method.

With this, the reliability of the method is understood in two senses. First, as the general reliability, inversely proportional to the mean square deviation of the values of τ_t determined by this method from the true value of τ_t. Second, as the particular reliability, depending on the signal-to-noise ratio, and varying from one smelting operation to the next. The fact of the matter is that, as shown by a preliminary investigation by means of self-recorders, the "quality" curves (signal-to-noise ratio) obtained from signals of one and the same transducer changed for different reasons, where the presence of heightened noise is clear even at the beginning of a smelting run, and may be discounted by a corresponding change of the weight coefficients n_i.

It is clear that a huge increase in the number of methods for determining τ_t, while not giving a significant decrease in the mean square error, significantly increases the complexity of the apparatus, and is thus inefficient.

4. Stages of the Work

With all that has been stated taken into account, the work on automating the Bessemer process was divided into two stages.

The first stage was the development of an information (data-gathering) device and its establishment at the Dzerzhinskii Works and its use in the mill conditions with automatic attachment to the transducers and with automati starting and stopping.

The second stage was the development of a controlling digital machine.

It was proposed that the following ensue from the use of the information device.

1. A definitive determination of the basic parameters of the controlling machine (memory size, speed of action, type of input device).

2. Determination of the coefficients for the statistical relationships, to be subsequently introduced into a passive memory of the controlling machine.

3. Determination of the weights n_i characterizing the reliability of the individual methods of determining τ_t.

4. Definitive determination of the methodology of smoothing the transducer signals so as to isolate the useful information.

5. Verification of the reliability of the automatic operation of the electronic digital computer in factory conditions, and specification of the design pecularities of such a machine (heat protection, screening, etc.).

5. Digital Recording Device

In accordance with the stated plan of work, a digital recording device (DRD) was developed at the Computing Center of the AN USSR.

We now consider its scheme of operation.

During converter blowing, the DRD takes in, and records, signals from four photoelectric transducers and an air consumption meter.

Recording of the photoelectric transducer signals is implemented serially, with the recording of the signal from one transducer taking 0.1 seconds. Thus, receipt of a signal from each photoelectric transducer occurs once in each 0.4 seconds. The signals from each photoelectric transducer are transformed to a digital code in the memory of the DRD. Provision is made in the DRD for the primordial processing of the data obtained as the result of transformation of the transducer signals.

If one considers a transducer signal as the realization of a nonstationary random process consisting of the superposition of a determinate process $F(\tau)$ and a random stationary process $\Phi(\tau)$, then the processing carried out in the DRD corresponds to the smoothing of such a process by the method of moving averages. It amounts to this, that what is printed out is not each value obtained as the result of transforming the transducer signal, but the arithmetic average of the values over some interval (the averaging interval).

This method is the most suitable in the given case since the carrier curves $F(\tau)$ assume the most diverse forms from smelting run to smelting run, and their approximation by means of some analytic expression or another is very troublesome. The possibility is not excluded that, as a result of processing the data obtained from use of the DRD, there will be recommended other methods of smoothing random nonstationary processes.

As a result of preliminary investigations, it was found, that, for the existing amplitudes and correlation function of $\Phi(\tau)$, the optimal value of the averaging interval lies between 4 and 12 seconds (optimal in the sense of obtaining the least mean square error in determining the maximum of $F(\tau)$). In accordance with this, the capability of changing the interval of averaging within these limits was provided in the DRD. The definitive determination of the optimal size of the interval of averaging is one of the basic problems which must be solved as a result of using the DRD.

The signals from the air expenditure meter are taken in by the DRD as they are sent and transformed in the machine's memory to a code corresponding to the numerical value of the quantity of air blown through the converter from the beginning of the smelting run up to the given moment.

Printing of these values is carried out simultaneously with the printing of the averaged values of the parameters obtained from the photoelectric transducers.

The operation of the DRD is strictly cyclic. With the value of the averaging interval $\bar{\tau}$ established prior to the beginning of blowing, each printing (not counting the values of the total expenditure of air) corresponds to the averaged value of some parameter, assigned to the midpoint of this interval.

Thus, to determine the time τ to which some printed parameter value appertains, we can use the formula

$$\tau = (n-1)\bar{\tau} + \frac{\bar{\tau}}{2} = \left(n - \frac{1}{2}\right)\bar{\tau},$$

where n is the ordinal number of the print-out from the beginning of the smelting run.

With this, the absolute error in the determination of τ does not exceed ± 0.2 seconds for a duration of the smelting run not greater than 20 minutes.

In the lacunae between blowings (for several seconds until converter charging), the DRD records the signals from the individual photoelectric transducer,* averages the digital values of the parameter thus obtained during one averaging interval, and prints this averaged value. The averaging interval chosen for DRD operation during blowing can differ from the interval chosen for DRD operation in the periods between blows.

The magnitudes of the input signals from the photoelectric transducers are transformed in the DRD to binary code with a relative error of ± 0.5% of the maximum value of the transformed signals. This corresponds to obtaining codes with seven correct, and one doubtful, bits.

Printing of the averaged parameter values of the DRD is executed in the decimal system, with two correct decimal places and a five or a zero in the least significant place, which corresponds to the same relative error of ± 0.5%.

The capability has been built into the DRD of introduction of signal scale factors, the aim being to obtain numerical output values in the ordinarily accepted units of brightness or temperature.

The indication of quantity of blown air is printed in the form of a four-digit number, where the maximum value of the most significant digit is 3. This corresponds to a relative error not exceeding ± 0.1% of the upper limit of the scale, whereby the expenditure transducer can be so constructed that the results are obtained in normal cubic meters.

Conditions of DRD use. The DRD is supplied from a three-phase ac line of 380/220 volts. Preliminary stabilization of the line voltage is provided by means of ferroresonant stabilizers.

The power drawn from the line by the DRD does not exceed 1.5 kw. The DRD is designed to operate with forced internal ventilation. The DRD's ventilation stream must have the following parameters: rate of expenditure is 900 cubic meters per hour, temperature is 10 to 15°C, pressure is 60 mm of water. With internal ventilation which meets these specifications, the DRD can operate reliably when situated in the normal temperature regimen of Bessemer operation.

The DRD is not hermetically sealed against dust.

After completion of the complex adjustment of the DRD in conjunction with the transducers, it is intended that it operate normally, with switching in and out of devices connected to the converter mechanism, without attendance by the DRD maintenance personnel during a shift. Between shifts, cleaning and checking of the DRD by engineers will be necessary.

Physical design and basic elements of the DRD. Physically, the DRD is a metal cabinet measuring 1.8 × × 1.4 × 0.5 meters, comprised of the electronic part of the DRD and the power supply. The cabinet is attached to cables with metallic pedestals measuring 0.1 × 0.5 × × 0.5 meters for a numeric printing device.

The control console is placed on the cabinet's front panel.

For the basic standard elements in the DRD we used flip-flops, amplifiers and cathode followers, developed at the Computing Center of the AN USSR on the basis of the analogous elements used in the high-speed electronic computer "Kiev". These elements provide high reliability of DRD operation. These standard elements were built as metal plug-in units, measuring 150 × 90 × 35 mm.

Standardization and rapid replacement of the blocks provided for easy use and repair of the DRD.

Type RP, RSM, and RS electromagnetic relays were used for switching transducer channels and for controlling the numeric printing device.

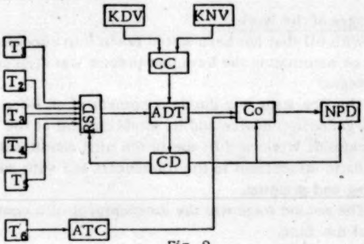

Fig. 2.

The block schematic of the DRD is shown in Fig. 2. Signals from the five photoelectric transducers T_1-T_5 are applied to relay switching device RSD which connects them in turn to the input of analog-to-digital transformer ADT. The codes formed in the analog-to-digital transformer are transmitted to counting device Co which forms the arithmetic average of the numerical values of the signals received during one averaging interval.

The counting device is thus the DRD's flip-flop memory, storing information from all transducers and transmitting it, at the end of the averaging interval, to numeric printing device NPD.

Transformation of the transducers' analog signals is implemented in the ADT by eight cycle pulses supplied by the central control block CC. The cycle pulses are the basic time markers, synchronizing directly or indirectly the entire operation of the machine, including the definition of duration of the averaging interval, the duration of the printing period, etc.

The signal of transformation conclusion is sent by the analog-to-digital transformer to control device CD which, after each transformation, signals switching of the RSD relays. The control device keeps count of the recorded points, and sends a signal when the averaging interval terminates.

---

* For example, a transducer recording the lining's temperature.

Signals from air expenditure meter T_6, via air transducer control unit ATC, are applied to the counting device. Signals arriving from T_6 during the printing period are stored in the ATC and, at the termination of printing, are then added into the counting device.

The DRD block schematic just described, as well as the devices used in the DRD together with the flip-flops and the relay switching gear, correspond fully to the specific purpose of the DRD: the recording of weak signals with a comparatively slow speed of action.

The DRD was installed in the Dzerzhinskii Works in March, 1960.

Today, the data obtained from the DRD, together with data obtained on the basis of chemical analyses of pig iron and steel specimens, is being subjected to mathematical processing, and the program for the controlling machine is being written.

NEW METHOD AND UNIVERSAL MEASURING DEVICE FOR ACTIVE INSPECTION ON METAL-CUTTING MACHINES

G. L. Perfil'ev

Sverdlovsk

Translated from Avtomatika i Telemekhanika, Vol. 21, No. 6, pp. 884-891, June, 1960

The use of active inspection is one of the most important directions in the automation of control of high-accuracy technological processes in machine building. Broad use of active inspection is limited by the lack of industrial output of active control instruments which are sufficiently universal to satisfy the very diverse requirements of their installation on machine stands which differ in purpose, type and physical design.

An urgent, and the most pressing, problem today is the development of a unified design of a measuring device, or, at least, its basic and common components, and the organization of their production by the instrument building industry. The principal such component is that for reading off the dimensions of a piece during the course of its technological processing. It must transform the measured quantity to an electrical output quantity. The physical design of such a component (assembly) must be sufficiently universal so that it might be used in diverse machine stands.

The electrical parameter generated by such an assembly must be proportional only to the changes in dimension of the piece, and must not depend on the speed and direction of the piece's motion.

The production of a unified measuring assembly of such a type by the instrument building industry would provide the most rapid and massive use of active inspection of piece dimensions. The price of the instruments produced would be incomparably lower, and the quality higher, as compared with the price and quality of the instruments designed and produced today for the individual needs of different factories and organizations which are instrument users. The assemblies for attaching the measuring device, and the assemblies for mounting it on different machine stands, can also be mass-produced by the instrument building factories, but in view of their heterogeneity and relative simplicity, it would be most efficient to develop standard plans and to print albums of blueprints for their manufacture in the instrument shops of the user factories.

This paper presents the results of work carried out by the author in the S. M. Kirov Ural Polytechnic Institute on the creation of a universal measuring assembly for active inspection, namely, a vibrating-contact transducer-dimension-recorder.

Existing methods and instruments for active inspection of measuring pieces in the process of their fabrication on machine stands do not provide the necessary accuracy and reliability of inspection, require frequent adjustments and are insufficiently universal, which inhibits their widespread introduction into production automation.

The principal feature of existing devices is the use of the method of following the dimensional changes of a piece by means of a probe sliding along its surface with large contact forces and with a lever transfer mechanism to the indicating instrument. Replacement of the mechanical indicating instrument (minimeter, pointer-type indicator) by high-sensitivity electric, pneumatic and other transducers complicates the physical design of the measuring device, but cannot eliminate the inadequacies inherent in mechanical transmission and sliding probes or the measurment errors which thus arise.

Attempts to employ, for active inspection, measuring devices without mechanical probing but based on contactless methods of transforming variations in piece dimensions to some parameter or other (air pressure, reluctance, capacitance, photoelectric or radiation effects) have not found use. This is explained by the specific features of the inspection conditions on machine stands where pieces of different metals are processed with different speeds in different conditions of the ambient medium, with cuttings of different dimensions where access to the cutting zone is difficult and where there are other factors which prevent one from obtaining a single-valued change of the enumerated output parameters of the measuring device for a dimensional change of the pieces.

It is obvious that a universal instrument for active inspection of dimensions must be constructed on the basis of other, new, measurement principles, without the transmission of the measured translation by an inertial level mechanism.

Such a new solution, different in principle from the older ones, is the method of measuring by means of a vibrating probe. In measurements by this method, the surface of the piece to be worked on the stand is contacted by a vibrating tip. The tip is placed at the end of a flat spring, the other end of which is fastened to the frame of a special transducer. The spring's free end is given a harmonic oscillatory motion by an electromagnet.

The vibrating probe is tuned to a natural frequency of 100 cps. The electromagnet, supplied by current at the industrial frequency, synchronously vibrates the probe and maintains its oscillation.

The amplitude of the tip's oscillation is always kept significantly greater than the surplus on the piece, the magnitude of whose removal it is desired to measure during the working process. The transducer's frame is so installed that the oscillations of the measuring tip are limited by its contiguity with the piece's surface.

At the beginning of processing, when the surplus has still not been taken off, the amplitude of the tip's oscillations is minimal. As the surplus is successively removed, the amplitude will increase in proportion to the magnitude of change of the piece's dimensions.

Consequently, the magnitude of the change in amplitude of the probe's oscillations will, in this case, define the amount of surplus removed from the piece.

There exist many methods of remote measurement of amplitude magnitude. The simplest, and at the same time very accurate, of these is electrical, when the oscillatory system is rigidly connected with the armature of a miniature magnetoelectric vibrogenerator.

If the armature oscillations occur with constant frequency, then the magnitude of the voltage of the induced current will be proportional only to the magnitude of the amplitude. By measuring the vibrogenerator's voltage by a voltmeter, the scale of which is calibrated in millimeters, one can determine remotely the magnitude of change of the piece's dimensions in the process of its working.

The vibrating probe eliminates sliding of the measuring tip along the surface of the moving piece, since it touches the piece for only very short intervals of time (of the order of microseconds), approaching it each time in a direction perpendicular to the surface to be measured.

Since the piece is moved, each contact with it is made at a new point of its surface. In completing 100 oscillations a second, the tip makes the same number of measurements at different points on the piece. The quantity obtained as the result of each measurement will be transformed to the corresponding amplitude of the induced ac voltage. By means of an electrical scheme and the choice of a measuring instrument with the necessary frequency of natural oscillation of its moving system, one can average, within wide limits, the results of measurements over time. For a vibrating probe, the speed and direction of the piece's motion in the plane perpendicular to the line of measurement are indifferent, and do not affect the results of the measurements. Oscillations of the tip with amplitudes greater than the surplus allow it to get over sharp humps on the surface of the piece and irregularities, even for comparatively large speeds of motion, make it possible to measure pieces with surface discontinuities (bushings and shafts with key and splined grooves), and introduces the instrument into apertures to be ground together with the abrasive wheel, all without having recourse to special devices which are required by almost all the active inspection devices in existence.

The flexible connection of the transducer with the surface of the piece protects the transducer from disruptions of calibration from random mechanical shocks experienced by the tip.

The electrical connection of the transducer with the sensitive measuring instrument allows the implementation of remote measurement, permits any increase in magnitude of the translation which depends only on the relationship of transducer power and measuring device sensitivity, allows the measurement results to be averaged, and, finally, makes it easy to obtain a current pulse for introducing commands of the executive mechanism controlling the machine stand. The generator principle of transforming mechanical parameters to electrical ones is the most reliable, simple and stable, since it requires no auxiliary apparatus in the form of stabilizers, electronic amplifiers, etc. Use of this principle simplifies the installation and use of the instrument. The transducer, hooked up to the indicating instrument, is a complete aggregate, always prepared for action and not requiring a new calibration when the object to be measured is changed.

The magnitude of the contact force of the vibrating tip at the moment when it touches the surface of the piece does not exceed 1 to 3 grams and, for a narrow range of measurement (for example, for measuring microirregularities), may be reduced to tenths of a gram. The smallness of the contact force is explained by the fact that each successive contact, after the first, of the probe with the piece occurs at the moment when the speed of the probe's motion is minimal and, in its turn, is determined only by the magnitude of the impulse obtained by the probe from the synchronous swinging electromagnet during one half-period.

After a great deal of design and investigative work, and testing of transducers on various machine stands, there was developed a type of universal transducer, whose dimensions were satisfactory for its mounting on different stands, with high sensitivity, indication stability, uniformity of scale for requirements of piece inspection during the working process for the operations of external and internal grinding of cylindrical pieces, plane grinding, turning, boring, honing.

Figure 1 shows the over-all view of the transducer, and Fig. 2 shows its kinematic and electric scheme. In the frame of the transducer, which is a cylinder of diameter about 30 mm and length about 100 mm, two electromagnets are placed. On one end of their face surfaces one end of the plane spring is rigidly fastened. The other end of the spring is attached to the transducer's moving system which has two extensions, one of which is the probe with a tip which makes contact with the piece, the other of which passes through the center of the cylindrical frame and is attached to the armatures of the two electromagnets. The electromagnet positioned closer to the plane

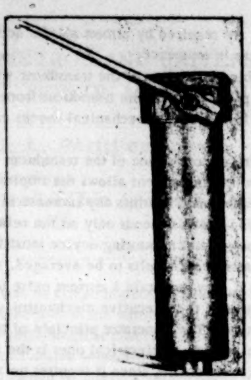

Fig. 1. Exterior view of the universal vibrocontact transducer with rotatable probe.

spring serves to swing the probe. It is supplied from the industrial ac line.

The second electromagnet is the winding of the generator, positioned on the casing attached to the transducer frame, wtih an aperture in the central portion. In this aperture, the armature, consisting of a lamina of transformer steel, can oscillate freely.

At a very small distance from the armature end are placed two constant Alnico magnets, a closed magnetic circuit surrounding the generator winding. Oscillations of the armature before the poles of different polarity induce changes in the magnetic field strength in the armature and induce an electric current in its winding whose voltage is proportional to the speed of these changes.

The speed of the armature's pole piece during its free oscillations varies sinusoidally. Passing through the interpolar distance, the armature has its maximum velocity, while at the limiting positions this velocity equals zero. The ac current induced in the winding has the same correct sinusoidal form. With the oscillations of the transducer's moving system limited by contact of the tip with the piece at the moment of its boundary position, the sinusoidal character of the induced emf is not changed. This allows one to obtain a scale with uniform and stable scale divisions.

Large frictional losses, excessive power of the swinging electromagnet, a very largerange of limitation of the probe amplitude in comparison with the amplitude of its free oscillations, all these lead to a distortion of the curve's form and, correspondingly, to nonuniformity in the scale divisions and instability of instrument graduation.

Figure 3 shows an oscillogram taken off for the operation of a normally adjusted transducer. The two traces here, with a common null position, are the voltage curves of the generator and of the 50 cps supply for the swinging electromagnet. On the oscillogram has been photographed the processes of switching in and out of electromagnet swing. The swing of the transducer's moving system up to its maximum amplitude (0.7 mm) occurs in the course of 8 to 10 periods, i.e., during a time of about 0.2 seconds. After switching off of the electromagnet swings, the oscillations are smoothly damped at the same frequency, which shows the correct-

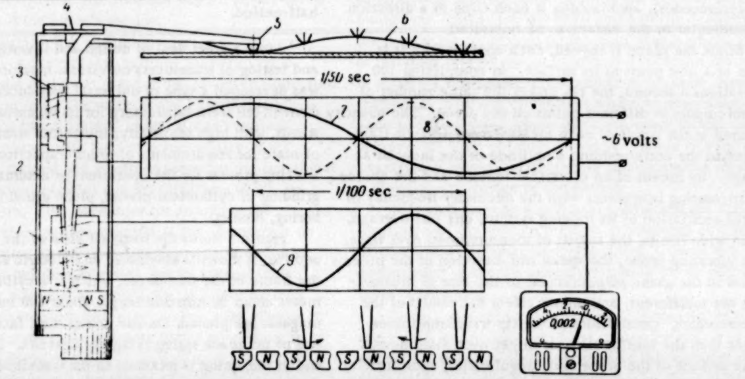

Fig. 2. Kinematic and electric scheme of the vibrocontact transducer. 1) Generator; 2) central connection of moving system; 3) swinging electromagnet; 4) flat spring; 5) probe with a tip; 6) curve of tip's position; 7) curve of electromagnet's voltage; 8) curve of the tip's speed of motion; 9) curve of generator's emf.

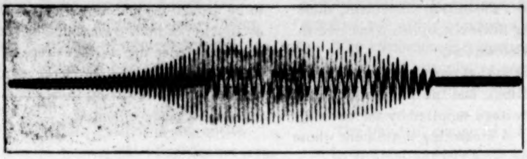

Fig. 3.

ness of the tuning of the moving system's natural frequency, and the smallness of the frictional losses.

All that has been said earlier is necessary to take into account only in the development of a new physical design of the transducer. A correctly designed and adjusted transducer, in conjunction with its measuring instrument, provides stability of graduation under any conditions, and requires no surveillance or new graduation during its use. As measuring instruments, one can use magneto-electric millivoltmeters or microammeters of any type. The choice of some measuring instrument or another is determined by its dimensions, required class of accuracy, convenience, reliability and conditions of use. As a function of the chosen type of measuring instrument, one designs the winding of the generator in which the emf is induced. The best operation of the measuring instrument is provided in the case when the generator's internal impedance equals the impedance of the external circuit of rectifiers and measuring instrument chassis. The use of a magneto-electric instrument stems from the requirements of high sensitivity, uniformity of scale divisions and low power drain. The most appropriate type of instrument for factory conditions, as concerns electrical data, is a type M-24 microammeter with a scale up to 100 microamperes.

Figure 4 shows a measuring device assembly. The scale of the instrument has been replaced by a new one, calibrated from the transducer, allowing one to read off directly changes in the dimensions in fractions of a millimeter.

The limited size of the electric measuring instrument's scale does not permit full use to be made of the broad range of dimension measurement possessed by the transducer when the maximum amplitude of its tip's oscillations is 0.7 mm, or to obtain the micron accuracy thus provided. Shunting of the measuring instrument, or introducing an additional resistance increases the range of measurement, but with a simultaneous increase in the scale division. For active inspection it is most efficient to use the limited scale of the measuring instrument for reading with the greatest accuracy and clarity only at the limits of the approach of the piece's dimensions to the given ones. For this purpose, the measuring instrument's movable system is clamped, by a stretched spiral filament, to an arrester of pointer motion which is positioned at the zero scale division, and is so designed that its deviations from the rest position occur for three- or four-fold values of the maximum current stated on the scale. The measuring instrument's winding can bear such an increase in current without danger.

By changing the magnitude of the stretch on the pointer filament at the zero rest position, one succeeds, while still retaining high sensitivity, in changing the absolute magnitude of the range of measurement. When taking off a large surplus with the vibration transducer, this allows one to obtain higher sensitivity of the measuring instrument only when the piece's dimensions approximate to the nominal ones. The rest of the time, the instrument's pointer will press against the stop to the left of the zero division.

Experience showed that, for an assembled vibrocontact transducer, it is desirable to produce microammeters with adjustable preliminary stressing of the movable system, allowing one most simply to use the entire range of transducer measurement in the limits of 0.1 to 0.7 mm, with the smallest scale division being 2 microns. The transducer supply is taken from the ac line via a small-power transformer which steps the voltage down to 6 volts. The transducer draws about 0.2 watts of power. Oscillations of the line voltage up to 30% do not affect the results of measurement.

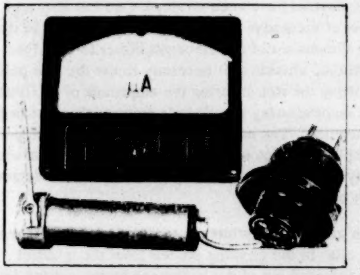

Fig. 4. Measuring device assembly, consisting of a universal vibrocontact transducer and a microammeter with rectifiers mounted in the chassis and with a transformer for the transducer supply from the 220 volt line.

In addition to the basic, most simple, scheme of connecting a transducer to a measuring instrument, there was developed a measuring device with two transducers, connected in a compensation circuit.

The nub of this device is that one transducer directly measures the piece dimensions, and the voltage generated by it is compared with a voltage supplied by the second, compensating, transducer. A measuring instrument whose zero scale division is in the center of the scale is so connected that, for equality of the voltages of both transducers, its pointer is established at the zero division. The amplitude of oscillation of the compensating transducer's probe is limited by a micrometric device. The adjustment of the measuring device is implemented by a preliminary processing of the first workpiece. By regulating the position of the working transducer with respect to the piece, one establishes the amplitude of oscillation of the working transducer at a somewhat higher quantity than the surplus on the piece. Thereafter, by means of the micrometric devices, the amplitudes of the compensating transducer are regulated until the zero position of the measuring instrument's pointer is reached, indicating that, in the given case, the nominal dimension has been reached. After this, a new piece, clamped in the stand, is worked until its dimensions reach the nominal value or lie within the admissible limits stated on the measuring instrument's scale.

The compensation scheme makes it possible to carry out remote electrical tuning of the measuring instrument, to use the measuring instrument without preliminary stressing of the movable system on the stop, to permit the working transducer to operate with any amplitudes, to switch the measuring instrument to different scale divisions by shunting it by different resistances and, thus, to follow the dimensions from the beginning of surplus removal. By connecting, instead of the measuring instrument, a high-sensitivity relay or an electronic device with an analogous action, one can send impulses to control the stand when the piece dimensions established by the micrometric devices have been attained. One can also send any number of successive pulses to control the machine stand as the dimensions of the piece get closer to the given dimensions, wherein it is necessary to use the first pulse for shifting the stop limiting the amplitude of oscillation of the compensating transducer's probe to the next degree of dimension. The use of such a measuring device permits the implementation of program control by servo drives, both by time and by previously given dimension degrees (orders of magnitude).

In measuring apertures by the single-contact scheme, errors arise in the grinding process from the mandrel being squeezed out of the workpiece by the cutting forces. Installation of a second, compensation, transducer in which the amplitude of probe oscillations is accurately limited by the ground surface of the face plate, as shown in Fig. 5, allows these errors to be compensated automatically. Squeezing out of the mandrel from the ring to be ground engenders a decrease in the amplitude of oscillation of both transducers by one and the same amount. Since the voltages tapped off from the transducers are connected, after rectification, in series opposition, the resulting indication of the measuring instrument is not changed.

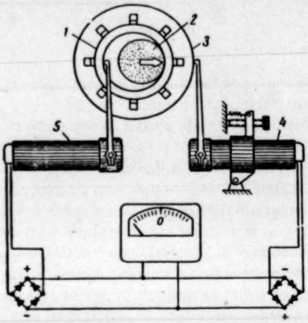

Fig. 5. Scheme of a measuring device with two transducers for measuring aperture diameters with automatic compensation of errors from the mandrel being squeezed out of the workpiece by the cutting forces. 1) Ring to be ground; 2) abrasive wheel; 3) face plate; 4) compensating transducer with the controlling device; 5) working transducer.

When the hole to be ground has been ground to the given dimension, the voltages of both transducers are compared and the pointer of the measuring instrument is established at the zero division at the center of the scale. Adjustment for the given dimension of the hole is implemented by shifting the compensation transducer by means of a screw, changing the transducers's position with respect to the face plate's cylindrical surface.

On the basis of a vibrocontact transducer, one easily solves the problem of building an automatically compensated measuring and controlling instrument with a large angular scale. The compensating voltage is taken off from the transducer whose amplitude of probe oscillation is limited by the profile of a cam positioned on the axis bearing the measuring instrument's pointer. The cam and the pointer are turned by a servo motor supplied by the amplified error emf of the working and compensation transducers (i.e., by the amplified voltage difference).

The advantages of such an auto-compensated device over the analogous devices with wire potentiometers are the absence of dc supply sources and normal elements, the decrease of the servo motor power to a very low magnitude, since the rotation of a profile cam requires virtually no force apart from that of overcoming the friction in its supporting miniature bearings.

The low power of the servo motor allows the number of amplification stages in the mismatch amplifier to be decreased, and decreases the dimensions of the entire instrument. On the basis of a universal vibrocontact transducer, there were designed, built and tested instruments for inspecting hole diameters in a grinding operation in one section, inspecting deep, large-diameter holes along the entire length, for inspecting hole diameters in discontinuous surfaces in one section, diameters of smooth and ground shafts over the entire length, trunnion diameters from 3 to 8 mm with tolerances of 4 microns, diameters of shafts on universal precision lathes, for the inspection of deep holes for honing over the entire length.

In all these experiments, the universal vibrocontact transducer devices operated without failures, providing stability of results, high sensitivity and lack of temperament with respect to operating conditions in strong jets of cooling fluid (water and kerosene). The transducer operated reliably in difficult dusty conditions with dry grinding and with various size chips on the lathe.

The vibrocontact transducer satisfactorily solved the problem posed, namely, to create a unified design for the basic assembly for the measuring devices of active inspection.

The physical design of the transducer is quite compact and is completely sealed hermetically. The probe, free to rotate by 360 degrees is provided with a hard-fused tip and makes it possible to implement measurement of opened surfaces and holes. The transducer's sensitivity and small contact force allow measurements to be made with micron accuracy.

Adjustment of the transducers during their assembly provided identity of their sensitivities, allowing interchangeability of transducers and measuring instruments. The transducer can be used for visual inspection in the working process, for active inspection in automated inspection, for implementing feedback of actual dimensions in machine stands with program control, for feeding dimension information to computing devices and as the controlling organ in automatic following and copying systems.

QUESTIONS OF STABILITY OF OPERATION OF CLOSED (OR LENGTHY) SCHEMES CONSTRUCTED OF CERTAIN TYPES OF LOGICAL ELEMENTS

I. Gashkovets and N. P. Vasil'eva

Prague, Moscow

Translated from Avtomatika i Telemekhanika, Vol. 21, No. 6, pp. 892-901, June, 1960

The requirements on the "input-output" characteristics of logical elements are developed for providing stable operation of rings or lengthy circuits of these elements. Conditions are derived which are necessary for obtaining characteristics of this nature for schemes consisting of identical logical repeaters or identical inverters.

1. Stability Conditions for Closed Circuit Operation

It is well known [1] that, to obtain stable operation of ring circuits consisting of identical logical elements (for example, ring counters, shift registers, or dynamic memory flip-flops), it is necessary that the "input-output" characteristic of the open-loop ring have the form shown on Fig. 1, i.e., for input signals less than some critical magnitude the characteristic should fall below the line 0-I and, for signals larger than the critical value, should lie above the line 0-I. Thus, the characteristic must have three segments:

first segment, lying below the line 0-I, on which $du_{out}/du_{in} < 1$;

second segment on which $du_{out}/du_{in} > 1$;

third segment, lying above the line 0-I, on which $du_{out}/du_{in} < 1$.

A characteristic of this type will always have two stable points of intersection (near 0 and I) with the line 0-I representing the geometric locus of points on which the input equals the output, i.e., with the characteristic of the closed system. These points are the two stable states of the closed system for zero and for complete outputs.

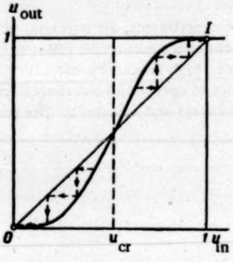

Fig. 1.

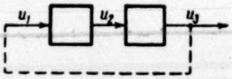

Fig. 2.

If the circuit is a long open circuit of logical elements, then, for proper operation of such a circuit it is also necessary that signals less than some critical signal u_{cr} be damped in it, and that signals greater than this critical value pass without damping.

Obviously, the conditions for proper operation of such a scheme coincide with the stability conditions for a ring circuit which, in this sense, is equivalent to an open-loop scheme with an infinite number of elements.

For ring circuits constructed of asynchronous or single-cycle elements, it is necessary that each element of the circuit have a characteristic such as that shown in Fig. 1, since the minimal number of elements forming a ring circuit equals one.

In two-cycle schemes, the minimal number of elements forming a closed ring equals two. Therefore, to obtain stable operation of a closed scheme consisting of identical elements, it is mandatory that each element have the input-output characteristic such as that of Fig. 1, but that the total input-output characteristic of two series-connected elements have the form defined above.

Below we shall consider only two-cycle systems of elements, in which a closed-loop scheme must always contain an even number of elements.

We consider what requirements must be placed on the characteristics of each element in order that two series-connected elements (Fig. 2) in a closed-loop circuit operate stably.

Ring circuits are ordinarily constructed either of repeaters or of inverters.

Repeaters. Fig. 3 shows three types of repeater characteristics (curves 1, 2 and 3). Series-connection of two identical repeaters with characteristics of this type does not permit one to obtain an over-all input-output characteristic with two stable states as on Fig. 1. This is easily explained by refering to Fig. 4. A series-connection of two repeaters with characteristics of different types, such as curves 2 and 3 of Fig. 3 allows one to obtain an over-all input-output characteristic with two stable states (Fig. 5). But, to construct a ring circuit of such elements, it is necessary to have two types of repeaters, which is usually inconvenient.

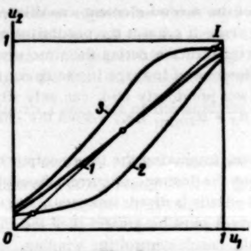

Fig. 3.

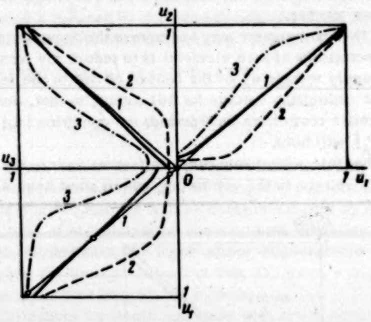

Fig. 4.

Thus, if the ring circuit must be constructed of identical repeaters, it is necessary that each repeater have an input-output characteristic of a form similar to the form of the characteristic of Fig. 1.

Inverters. To obtain stable operation of a closed-loop scheme consisting of inverters, it is sufficient if the characteristic of each inverter element has the form shown in Fig. 6 a and b by the solid lines. Then, with a series connection of two elements, the over-all input-output characteristic will possess two stable states for closed-loop operation (the solid lines in Fig. 6 c).

If the inverter has a characteristic similar to that shown by the dashed lines in Fig. 6 a, then a closed-loop scheme of such inverters will not be stable (Fig. 6c, the dashed line).

2. Analysis of Repeater Operation

We consider, from the point of view of stability of operation, logical elements constructed on the principle of single-core fast-acting Ramey amplifiers.

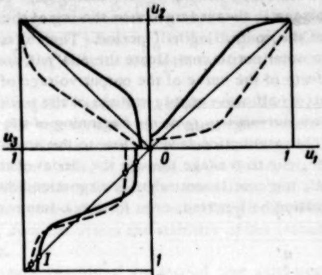

Fig. 5.

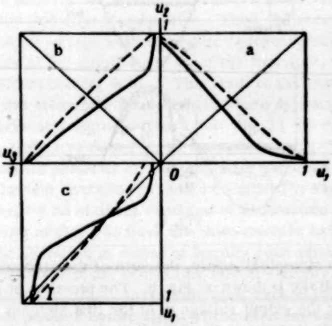

Fig. 6.

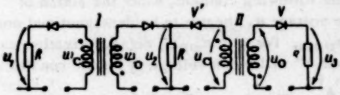

Fig. 7.

The scheme of a circuit segment of two such logical elements is shown in Fig. 7. The voltages are so chosen that

$$u_A = -u_B = \frac{w_o}{w_c} u'_A = \frac{w_o}{w_c} u'_B.$$

Conditions for stable operation for signals close to the maximum. In cores made of material with a rectangular hysteresis loop, the actual ratio B_r/B_s is always less than unity. This leads to a small phase shift between currents and voltages, both in the working and in the controlling circuits of the cores. However, for those parameter relationships which occur for normal operation of logical elements, the lag of the leading edge for the output voltage is always larger than the lag of the beginning of the controlling half-period. Therefore, in the sequel, in order not to complicate the analysis, we assume that the form of the curve of the output voltage of each element is a half-wave supply voltage of the working circuit with cut-off $\alpha_{2\min}$ at the beginning of the half-period. This assumption is very close to the actual facts since, due to leakage through the diodes of the working circuit, the core is somewhat demagnetized during the controlling half-period, even for a maximum controlling signal.

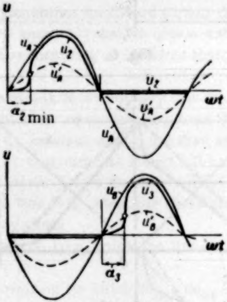

Fig. 8.

For a sinusoidal supply, the form of the element's output voltage is shown in Fig. 8. The presence of a cut-off in the output voltage u_2 of the first element leads to a further increase in the cut-off angle of the output voltage u_3 of the following element. This is explained by the fact that, at the beginning of the controlling half-period, the following element, under the action of reference voltage u_A, begins to be demagnetized until "time" $\alpha_{2\min}$. For $\omega t = \alpha_{2\min}$, demagnetization ceases, since diode V' will block voltage u_2 for the condition that $|u_2| \geq |u'_A|$.

After this, the magnetic flux in the core during this half-period still cannot return to the original saturated state, since the diode remains cut-off.

Therefore, at the beginning of the working half-period of the second element, the magnetic induction of its core is less than B_r by an amount corresponding to the demagnetizing action of voltage u'_A in the interval $0 < \omega t < \alpha_{2\min}$.

Consequently, output voltage u_3 will have a cut-off angle α_3 with $\alpha_3 > \alpha_{2\min}$.

Thanks to this, the element's input-output characteristic, controlled from the output of the same element independently of the ratio of the numbers of turns, w_c and w_o, will lie below the line 0-1 (Fig. 1).

It is impossible to eliminate this phenomenon by increasing the amplitude of controlling voltage u_2, since an increase in the amplitude of the controlling voltage only increases the voltage drop, cutting off diode V'. Therefore, an increase of the ratio of the voltage supplying the operating circuit u_A to the voltage u'_A supplying the controlling circuit, which can be achieved by increasing the ratio w_o/w_c, gives nothing in this sense.

The presence of leakage in the controlling circuit diode V', of the second element can dilute this phenomenon somewhat, since it creates the possibility of returning the flux to the initial state during the time when $u_2 > u'_A$.

The presence of leakage in the operating (working) circuit, as was previously said, can only strengthen the inequality $\alpha_3 > \alpha_{2\min}$, i.e., worsen the characteristic (Fig. 9).

However, improving the input-output characteristic by increasing the leakage of current through diode V' of the control circuit is disadvantageous, since the diode's leakage current must be greater than the magnetization current of the core's controlling winding, and this sharply decreases the number of admissible input diodes of the circuit, which are used to obtain logical functions of one kind or another.

The most correct way to improve the input-output characteristics of such elements is to reduce the form of the supply voltage u'_A of the control circuit to the form of the controlling voltage for full output, so that, during the entire controlling half-period, the condition $|u_2| \geq$ $\geq |u'_A|$ will hold.

For this, with a sinusoidal half-wave source, the supply voltage in the controlling circuit must have a

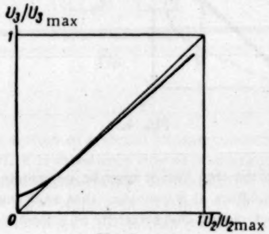

Fig. 9.

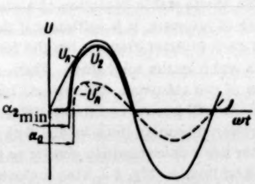

Fig. 10.

cutoff α_0 in the controlling half-period equal to, or greater than, the quantity $\alpha_{2\min}$, as shown in Fig. 10.

For such a form of supply voltage of the control circuit, the element's input-output characteristic for $\alpha_0 = \alpha_{2\min}$ will have the form of curve 1 in Fig. 11.

If the cut-off angle α_0 of the control circuit's supply voltage is chosen greater than $\alpha_{2\min}$ then, for control signals for which $\alpha_{2\min} < \alpha_2 < \alpha_0$, the core will generally not be demagnetized, and the output voltage will be complete (the upper horizontal portion of the characteristic (in Fig. 12). For control signals for which $\alpha_2 > \alpha_0$, the core is partially demagnetized and the output is decreased (the sloping portion of characteristic 1 in Fig. 12).

An increase in the minimum magnitude of the output voltage gives rise to a decrease of the quantity $\int_0^{\pi} u'_A d\omega t$ due to cutoff. This decrease can be compensated by increasing the amplitude of u'_A but, with this, there occurs opening of diode V in the operating circuit during the controlling half-period which loads the control circuit. The core is demagnetized under the action of voltage u_C, applied to the control winding, this voltage being less than voltage u'_A by the amount of the voltage drop across resistance R induced by the demagnetizing current and the transformation from the working circuit.

If the voltage u'_A is chosen so that

$$\frac{1}{\omega w_y}\int_{\alpha_0}^{\pi} u_y \, d\omega t = 2\Phi_s,$$

then, in the controlling half-period without a signal, the core's magnetic polarity will be completely reversed and its free-running voltage will be determined only by the magnitude of magnetization current in the operating half-period. In this case, the input-output characteristic will have the form of curve 2 in Fig. 11, for $\alpha_0 = \alpha_{2\min}$, and of curve 2 on Fig. 12, for $\alpha_0 > \alpha_{2\min}$.

Conditions for stable operation with small signals. Further increase of the amplitude of the control circuit's supply voltage leads to the consequence that, in the controlling half-period, the second core is saturated for $\omega t < \pi$.

With the previously considered conditions in the second core's controlling half-period — the first core's working half-period — after the demagnetizing voltage u'_A begins to act, i.e., for $\omega t > \alpha_0$, the second core is demagnetized more rapidly than the first is magnetized, since the first core is magnetized under the action of voltage $u_A - R[i_{\mu o} + w_o(i_{\mu o} + i_T)/w_C]$, and the second core is demagnetized under the action of voltage $u_B - i_T R = -u_A - i_T R$, where $i_{\mu o}$ is the magnetization current of the operating circuit, and i_T is the transformation current.

After negative saturation of the second core, at time $\omega t = \alpha_M$ (for signals close to zero), magnetization of the first core continues under the action of voltage $u_A - u'_A$. It can be shown that, at the end of the half-period, the first core has returned to its original state, i.e., that the saturation of the second core in its controlling half-period, for $\alpha_M < \pi$, does not affect the stability of the circuit's operation.

Demagnetization of the second core until negative saturation in the controlling half-period occurs for signals for which the cut-off angle $\alpha_2 \geq \alpha_M$ since, under the action of such signals, the second core's control circuit is disconnected after its saturation. Thus, the second core's output voltage will equal zero independently of the magnitude of the cutoff angle α_2 of the first core, with the condition that $\alpha_2 \geq \alpha_M$. This leads to the consequence that, in the element's characteristic, there appears a lower horizontal segment (curve 3 in Fig. 11 for $\alpha_0 = \alpha_{2\min}$ and curve 3 in Fig. 12 for $\alpha_0 > \alpha_{2\min}$). This characteristic possesses all the properties necessary for stable element operation in closed circuits(Cf., Fig. 1).

Thus, for an element executed in accordance with the scheme of Fig. 7 to have the characteristic necessary for stable operation in closed or lengthy open circuits, it is necessary that the controlling circuit's supply voltage have cut-off α_0 whose magnitude must exceed the minimum possible cutoff $\alpha_{2\min}$ of the element's output voltage induced by incomplete rectangularity of the core material. The amplitude of this voltage must be chosen from the condition

$$\frac{1}{\omega w_C}\int_{\alpha_0}^{\alpha_M} u_C \, d\omega t = 2\Phi_s,$$

where $\alpha_M < \pi$.

The choice of the voltage u'_A from this condition always entails that the voltage transformed from the

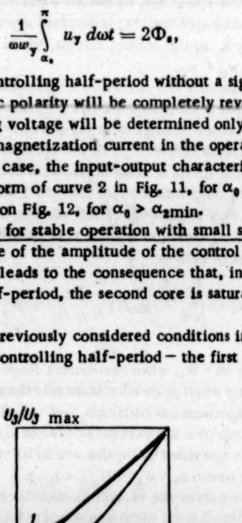

Fig. 11.

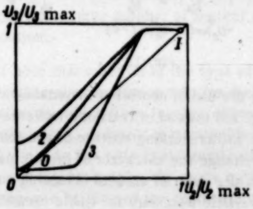

Fig. 12.

element's controlling circuit to its working circuit is higher than the working circuit's supply voltage u_B and opens diode V of the working circuit.

In order to avoid this, one can either open the element's working circuit in the controlling half-period or increase the supply voltage of the element's working circuit in the controlling half-period. The first is achieved by connecting in the element's circuit, instead of resistance R, a nonlinear resistance in the form of a diode, opened in the working circuit only during the working half-period (Fig. 13) by means of auxiliary voltages u''_A and u''_B, properly phased.

The second can be achieved by using a special supply source [2] or by the circuit of Fig. 14 which allows one to obtain a larger half-wave supply voltage for the working circuit in the controlling half-period than in the working half-period, so that the following relationship holds during the course of the controlling half-period

$$u_B = -u_A \geqslant u'_A \frac{w_0}{w_c}.$$

Returning now to the logical elements of the scheme of Fig. 13, we note that the operation of the elements of the scheme of Fig. 13 differs from the operation of the elements of Fig. 7's scheme only in that, instead of resistor R, there is a nonlinear resistance (a diode, controlled by voltage u''_A or u''_B) which is close to zero during magnetic polarity reversal of the core and, after saturation of the cores, increases sharply and limits the current. Thanks to this, the elements of the scheme of Fig. 13 have lower losses in the active impedances of the windings and the forward impedances of the diodes which, in our previous considerations, we neglected. This decrease of losses in the elements permits an increase in the number of elements which can be connected at the output of each element, which is very important in complicated logical schemes. An increase in the operating voltage in the controlling half-periods in the scheme of Fig. 7 leads to the same advantage.

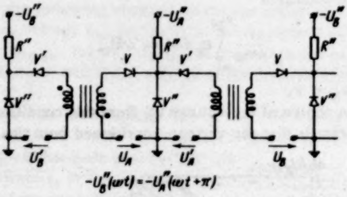

Fig. 13.

However, the use of nonlinear impedance V'' (the scheme of Fig. 13) instead of resistor R (scheme of Fig. 7) or an increase in the working voltage of the scheme of Fig. 7 do not change the character of the element's operation from the point of view of obtaining an input-output characteristic necessary for stable element operation in closed circuits. Therefore, the conditions for stable operation remain the same as those obtained for the scheme of Fig. 7.

3. Analysis of Repeater Operation with a Simplified Source of Supply

We consider still another form of logical element based on the Ramey scheme (Fig. 15). This scheme differs from that of Fig. 7 in that it has one and the same source of supply for the working and the controlling circuits, which would correspond to a choice of $u_A = u'_A$ in the scheme of Fig. 7.

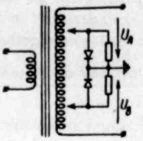

Fig. 14.

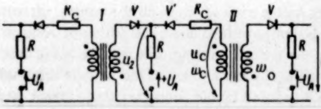

Fig. 15.

We now show that, to obtain a stable characteristic for the scheme of Fig. 15, it is necessary to connect a resistance R_C in the control circuit, while simultaneously choosing $w_C < w_O$.

We consider the operation of element II in the absence of an output from element I (i.e., for a null signal). We assume that the voltage drop across resistor R from the magnetization current $i_{\mu O}$ of the operating circuit of element I is small in comparison with voltage u_A.

Then, magnetization of element I will occur almost from the very beginning, of the working half-period, i.e., as soon as u_A becomes greater than zero (Fig. 16), under the action of voltage

$$u_2 = (u_A - i_{\mu O} R) \frac{R_C}{R + R_C} \approx u_A \frac{R_C}{R + R_C}.$$

With $\omega t = \alpha_0$, when the current flowing through the controlling winding of core II attains the magnitude of the demagnetization current $i_{\mu C}$ of core II, i.e., the quantity $u_A/(R + R_C)$ becomes equal to $i_{\mu C}$, core II begins to be demagnetized under the action of voltage $u_C = -u_2 + i_{\mu C} R_C$, where $u_2 = u_A - R(i_{\mu O} + i_{\mu C})$.

The diode of the second element's operating circuit remains cut off until the inequality $|u_C| w_O/w_C < |u_A|$ no longer holds. After the advent of the inequaltiy $|u_C| w_O/w_C \geq |u_A|$ (for $\omega t > \alpha_1$), this diode is opened and the transformation current appears which is added to the current $i_{\mu C}$, and demagnetization occurs under the action of the voltage $u_C = -u_2 + (i_{\mu C} + i_T)R_C$, where $u_2 = u_A - -R(i_{\mu O} + i_{\mu C} + i_T)$.

After voltage u_A passes through its maximum, all these phenomena repeat in the reverse order: For $\omega t = \alpha_1'$ diode V is cut off and transformation ceases, then demagnetization of core II ceases for $\omega t = \alpha_M$.

To meet the conditions for obtaining a stable input-output element characteristic, it is necessary, first, to choose the magnitudes of R and R_C so that the current of the second element's control circuit, approximately equal, until the beginning of its magnetic polarity reversal, to the quantity $u_A/(R + R_C)$, attain the magnitude $i_{\mu O}$ for $\omega t = \alpha_0$, where $\alpha_0 > \alpha_{2\min}$ ($\alpha_{2\min}$ is the minimum cut-off angle of total output voltage, defined by the nonrectangularity of the core material's hysteresis loop and the working circuit diode's current leakage). Second, the ratio of number of turns w_O/w_C must be so chosen that the equality

$$\frac{1}{w_O}\int_0^{\pi} u_2\, d\omega t = \frac{1}{w_C}\int_{\alpha_0}^{\alpha_M} u_C\, d\omega t,$$

holds, i.e., that the core be demagnetized during the controlling half-period by the same amount as the core in the working half-period is magnetized.

From Fig. 16, it is easily explained that, for small control signals for which $\alpha_2 > \alpha_M$, the output voltage of element II will be determined only by the voltage drop from current $i_{\mu O}$, i.e., the element's input-output characteristic will have a lower horizontal portion (Fig. 17). Analogously, for control signals for which $0 < \alpha_2 < \alpha_0$, i.e., for signals less than the full output signal, the output voltage of element II will equal the maximum, i.e., the input-output characteristic will have an upper horizontal segment (Fig. 17).

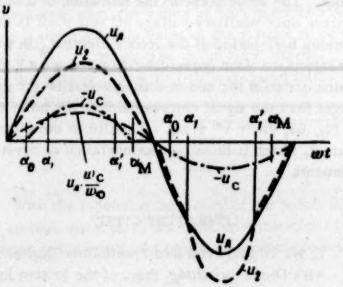

Fig. 16.

Thus, the scheme of Fig. 15 possesses a stable input-output characteristic for correctly chosen parameters when it operates from an ordinary ac supply source without use of a device creating a cut-off in the controlling half-period of controlling supply voltage. This is the virtue of the scheme of Fig. 15. The presence of transformation current in the element's controlling half-period is a disadvantage of the scheme, since it increases losses in the element and decreases the number of elements it is possible to connect to the output of each element. To eliminate this disadvantage, one can increase the amplitude of the working voltage in the controlling half-period if one uses a special asymmetric supply source (Fig. 14) with two output voltages and a common current.

When a supply source with one output voltage is used, this is not possible.

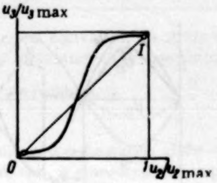

Fig. 17.

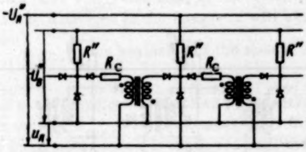

Fig. 18.

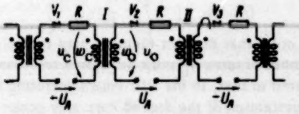

Fig. 19.

In that case, in the circuit of Fig. 15, instead of resistor R, one can use the same diode with an auxiliary voltage as in the scheme of Fig. 13. The scheme thus obtained (Fig. 18) has a stable characteristic without a special cut-off in the supply circuit of the element's control winding and has sufficiently small losses, i.e., permits the control of a large number of logical elements connected to the output.

We note that schemes of the type of Figs. 10 and 13 possess stable characteristics only for such forms of supply voltage curves which have leading edges with finite slopes (as, for example, sinusoids or trapezoids with sloping leading edges). Only in this case is automatic cut-off obtained. With a rectangular supply, the angle α_0 will equal zero, and automatic holding of the condition $0 < \alpha_2 < \alpha_0$ is impossible.

4. Analysis of Inverter Operation

Figure 19 shows a circuit segment consisting of two logical elements, namely inverters.

It was shown earlier that, for stable operation of closed inverter circuits, it suffices that each element have an input-output characteristic of the form shown by the solid line in Fig. 6a, i.e., the output voltage must be close to zero for signals which do not attain the maximum value.

We now consider the conditions which must hold in the circuit of Fig. 19 in order to obtain such a characteristic.

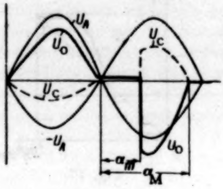

Fig. 20.

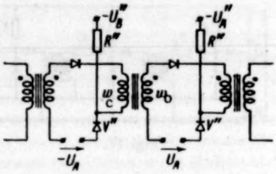

Fig. 21.

In order that the first element may control the second, the number of turns w_c must be chosen less than w_o. This is required so that, in the first core's operating half-period, demagnetization of the second core may occur only after termination of the first core's magnetization. For a magnetized core, its control circuit is always open in the working half-period, since the voltage transformed in the control circuit for a magnetized core is always less than the supply voltage (since $w_c < w_o$).

For demagnetization of the second element's core in its controlling half-period, i.e., after saturation of the first element's core, the voltage transformed in the second element's working circuit can exceed the element's supply voltage u_A. In this case, diode V_3 will be opened, and a transformation current arises. However, the ampere-turns induced in the third element by this current will not suffice for demagnetizing this element's core.

In order that the second element's output voltage reach zero for control by an incomplete signal from the first element, it is necessary that demagnetization of the second element's core in its controlling half-period occur more rapidly than its magnetization in the operating half-period (Fig. 20). This can be achieved by choosing the ratio of the number of turns by starting from the condition

$$\frac{1}{\omega w_c}\int_{\alpha_m}^{\alpha_M} u_c\, d\omega t = \frac{1}{\omega w_o}\int_0^{\pi} u_o\, d\omega t = 2\Phi_s,$$

where $u_c = u_A - (i_{\mu c} + i_T)R$ and $\alpha_m < \alpha_{2\min}$.

For equal speeds of magnetic polarity reversal in the controlling and operating half-periods, an input-output characteristic of the form of that shown in Fig. 6a, cannot be obtained.

The presence of transformation current for core demagnetization increases the element's power requirements, i.e., decreases the number of logical schemes that can be hung on the element's output. Transformation may be obviated by using an aysmmetric supply source (Fig. 14).

Figure 21 shows an inverter scheme not requiring an asymmetric voltage supply, in which resistor R is replaced by a controllable nonlinear impedance, namely, a diode. The diode prevents the formation of transformation current since auxiliary voltage u_A'' cuts it off in the nonworking half-period of the second element. In addition, for saturation of the cores of the first and second elements, which occurs at the end of demagnetization for signals larger than the signal corresponding to the point of inflection of Fig. 6a, diode V'' is cut off and limits the elements' current, which is important for operation on several logical elements.

LITERATURE CITED

1. E. W. Hogue, Saturable Transformer Digital Amplifier with Diode Switching, Proc. of the Eastern Joint Computer Conference (Dec. 10-12, 1956).
2. M. A. Boyarchenkov and N. P. Vasil'eva, Fast-Acting Magnetic Amplifiers [in Russian] (Gosénergoizdat, 1958).

ON ONE METHOD OF CONSTRUCTING ANALOG-TO-DIGITAL TRANSFORMERS

A. K. Zavolokin and G. I. Kurakhtanov

Moscow

Translated from Avtomatika i Telemekhanika, Vol. 21, No. 6, pp. 902-906, June, 1960

A method is suggested for constructing a transformer of voltage to its numerical equivalent, the method being based on a preliminary transformation of the input quantity to proportionate time intervals by integration.

A block schematic of the transformer and an analysis of its operation are provided.

For the transformation of voltages to their digital (numerical) equivalents, wide use has been made of devices in which the continuous (analog) quantity is first transformed to a time interval proportionate to it. During this interval, pulses with a constant repetition rate pass through a concidence scheme and are accumulated in a counter. At the end of the interval, the number staticized in the counter unambiguously characterizes the value of the transformed voltage.

The time intervals of the proper lengths are ordinarily obtained as the result of a comparison of the voltage to be transformed with a sawtooth voltage. The interval commences when the sawtooth passes through zero. The interval ends when the values of both quantities coincide. Thus, if the maximum value of the voltage to be transformed, $U_{\max}$, corresponds to the time interval $T_{\max}$, then the following interval will correspond to the current value of voltage U

$$T = \frac{T_{\max}}{U_{\max}} U. \tag{1}$$

With the repetition frequency of the pulses filling the counter equal to f, the number N staticized in the counter as the result of a transformation cycle equals

$$N = fT \tag{2}$$

or, by taking Eq. (1) into account,

$$N = \frac{fT_{\max}}{U_{\max}} U. \tag{3}$$

It is obvious that, with such a method of transformation the numerical equivalent is proportional to the instantaneou value possessed by the voltage to be transformed at the end of the interval.

Processing of the time interval by means of the method just described is now the generally accepted procedure. However, another method, with no less advantageous conditions, is possible for the implementation of the preliminary transformation of the analog quantity to a time interval. It amounts to the implementation of the preliminary transformation in two steps by an integrato Initially, the voltage U is integrated during a strictly defined time $T_{\max}$ such that, at the end of the first cycle, the value staticized in the integrator will equal $\int_0^{T_{\max}} U dt.$ At the beginning of the second cycle, the input of the integrator is supplied by a generator of reference voltage $U_{\max}$ with the opposite sign from that of U. The integration process is continued until the total quantit becomes equal to zero which is characterized by the expression

$$\int_0^{T_{\max}} U dt - \int_0^{T} U_{\max} dt = 0 \tag{4}$$

or

$$\int_0^{T_{\max}} U dt = U_{\max} T, \tag{5}$$

where T is the time of the second cycle.

The left member of (5) can be expressed in terms of the average value U_{av} of the voltage during time $T_{\max}$, namely,

$$\int_0^{T_{\max}} U dt = U_{av} T_{\max}. \tag{6}$$

From (5) and (6) we can define

$$T = \frac{T_{\max}}{U_{\max}} U_{av} \tag{7}$$

If, during the duration of the second cycle, we pass pulses through a coincidence scheme at the counter's input then, on the basis of (2) and (7), we obtain the following numerical equivalent, staticized in the counter

$$N = \frac{fT_{\max}}{U_{\max}}U_{\mathrm{av}} \tag{8}$$

It is clear from this last expression that, with this method of developing the time interval, the numerical equivalent corresponds, not to the instantaneous value of the voltage at the end of the interval (as occurs when a sawtooth voltage generator is used), but to its average value over the fixed time interval $T_{\max}$.

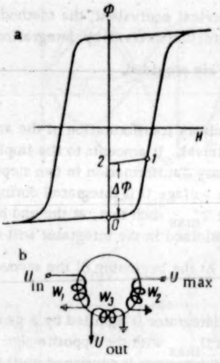

Fig. 1. Magnetic element and its hysteresis loop.

A voltage transformer constructed on the basis of the method just described can be obtained quite simply if, as the integrator, one uses a magnetic element whose core material has a rectangular hysteresis loop. As is well known, when a voltage pulse u(t) is applied to the magnetic element's input, the magnetic flux in the core changes by the amount ΔΦ. This means that, if the core's magnetic state corresponds to point 0 (Cf., Fig. 1a) then, under the stimulus of the pulse, the core transfers to the state characterized by point 2. Such a transition is executed along the portion 0-1-2 of the hysteresis loop. With this, the magnetic flux changes by the amount

$$\Delta\Phi = \int_0^t u(t)\,dt. \tag{9}$$

In the particular case when u(t) is a rectangular pulse of height U_{in} and duration $T_{\max}$, the change in flux will equal

$$\Delta\Phi = U_{\mathrm{in}}T_{\max} \tag{10}$$

We now consider the inverse problem. Let it be known beforehand that the core is found in state 2. Some rectangular pulse of height $U_{\max}$ is applied to the magnetic element's winding, taking the core to the zero state. It is required to determine the time T during which the core makes the transition to this state. With (10) taken into account, the solution of this problem leads to the expression

$$T = U_{\mathrm{in}}\frac{T_{\max}}{U_{\max}}. \tag{11}$$

In the more common case, when the magnetic element has two windings with number of turns equal to W_1 and W_2 (Cf., Fig. 1b), Eq. (11) takes the form

$$T = U_{\mathrm{in}}\frac{W_2T_{\max}}{W_1U_{\max}}. \tag{12}$$

It follows from expressions (9)-(12) that, if there is applied to winding W_1 of the magnetic element, which has already been established in the zero state, a rectangular voltage pulse of fixed duration $T_{\max}$ and unknown amplitude U_{in}, and if, during a certain time, a voltage pulse of opposite polarity of sufficient duration and with accurately fixed amplitude $U_{\max}$ is applied to winding W_2 then, at output winding W_3, there will appear a rectangular pulse U_{out} whose duration is proportional to the magnitude of the input voltage U_{in}. This has been shown quite well experimentally. In particular, for the practical implementation of the transformer, the integrating elements were subjected to a special investigation, these elements having cores which were formed of five Perminvar rings (strip thickness 10 mm, number of turns 16, height of one ring 6 mm, mean diameter 8 mm). With this, the maximum duration of the output pulse was 1000 microseconds. The output pulse duration was measured with an error not exceeding 2 microseconds, and the error in measuring the input voltage did not exceed 0.2%. As a result of the experimental investigation, it was established that the deviation of the relationship T = F(U_{in}) from linearity did not exceed the errors in measurement.

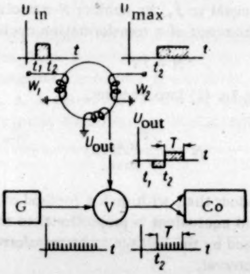

Fig. 2. Block schematic for explaining the transformer's principle of operation.

If the signal U_{out} is used to control the valve V (Fig. 2) through which the pulses from generator G pass, to be staticized in counter Co, then the number accumulated in the counter during the time of application of the output pulse will be proportional to the magnitude of the voltage U_{in}. The principle of operation of such a device is clear from Fig. 2, and requires no further explanation.

If one relates the magnitude of the interval $T_{\max}$ to the repetition rate of the pulses applied to the counter input, then one can automatically compensate errors arising because of instability of the pulse frequency or instability of the value of $T_{\max}$. It should be mentioned that such compensation is difficult to implement in transformers based on the comparison of the voltage to transformed with a sawtooth voltage.

In the transformer under consideration, these errors can be completely compensated by means of matching shift registers, as follows from an analysis of the block schematic shown in Fig. 3 and, in its general features, explaining the device's principle of operation.

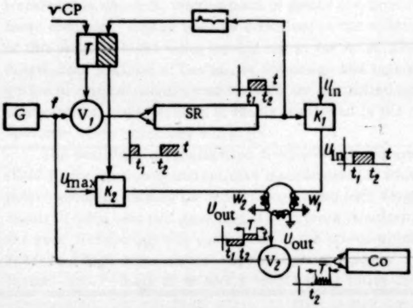

Fig. 3. Block schematic of a transformer with two counters.

At the beginning of operation, trigger (flip-flop) T is established in such a state that valve V_1 is closed and key K_2 is open. A current sufficient to establish the core in the zero position flows through winding W_2 of the magnetic element. After the advent of a clearing pulse (CP) the trigger transfers to its second stable state, opening V_1 and closing K_2. Staticizing of pulses of frequency f transpires in the shift register (SR). At time t_1, the final flip-flop of the shift register operates, opening key K_1. This key will remain open until time t_2, when the last flip-flop of the shift register again transfers to the zero state. During the interval $T_{\max} = t_2 - t_1$, a current, induced by voltage U_{in} and changing the core's magnetic state, passes through key K_1 and winding W_1. It is obvious with this that

$$T_{\max} = \frac{2^{m-1}}{f}, \tag{13}$$

where $\underline{m}$ is the number of stages of the shift register.

At time t_2, key K_1 is closed and trigger T is transferred to its initial state, closing V_1 and opening K_2, by means of a pulse obtained after differentiation of the trailing edge of the shift register's output signal (the differentiating circuit is shown by the rectangles with the representations of the two heteropolar pulses; the hatched pulses are not used). The core is transferred to the zero state by the current induced by the voltage $U_{\max}$. With this, a rectangular signal U_{out} of duration T is put out from the output winding, opening valve V_2. Pulses of frequency f pass through V_2 and are accumulated in the counter (Co). The relationship between the number N staticized in the counter and the magnitude of the voltage U_{in} can be determined by solving Eqs. (2), (12), and (13) simultaneously, giving the expression

$$N = U_{\mathrm{n}} \frac{2^{m-1} W_2}{U_{\max} W_1}. \tag{14}$$

It is clear from this last equation that the value of the numerical equivalent is proportional to the voltage U_{in} to be transformed, and depends neither on the pulse repetition frequency f nor on the absolute value of the time interval T.

A more detailed analysis of the transformer just considered shows that the shift register and the accumulating counter can be combined. This is illustrated by the block schematic of Fig. 4. Its difference from the block schematic of Fig. 3 is that valve V_1, via a discrimination scheme, shown conventionally by the diodes D_1 and D_2, is controlled both by trigger T and by output pulse U_{out}. With this, the requirement for a special counter disappears.

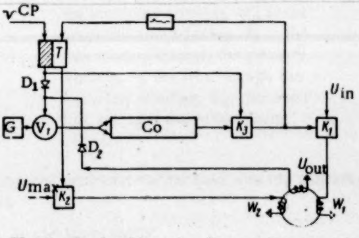

Fig. 4. Block schematic of a transformer with one counter.

The operating cycle of a device constructed in accordance with the scheme of Fig. 4 is executed in two stages. In the first stage, there occurs a change in the core's magnetic state under the action of voltage U_{in} which is completely analogous to the first stage of the scheme described above. It is easily seen that, at the moment when the first stage terminates (at the moment when a negative pulse is applied to trigger T), all the flip-flops of the shift register are in the zero state. At the termination of the first stage, key K_3 is closed and K_2 is opened. The magnetic element is returned to the zero state, thanks to which an output pulse U_{out} of the proper polarity is put out, opening valve V_1. Through V_1 there pass pulses to be staticized in the flip-flops of the shift register, acting now as an accumulating counter. Thanks to lock-out key K_3 (which can be opened only after the advent of a clear pulse CP), for any number written in the counter, key K_1 will be closed during the course of the entire second stage, which is a necessary condition for correct operation.

The principle cited was verified experimentally on practical devices, which were tubeless transformers to the proper binary equivalents. Among its virtues are the simplicity of the practical schemes, ease of implementation completely by semiconducting elements, absence of rigid requirements on stability of pulse repetition frequency f and transformation interval T.

NEW ELECTROMAGNETIC EXECUTIVE ORGANS FOR AUTOMATIC CONTROL SYSTEMS

A. M. Bamdas, V. A. Kulinich, V. A. Somov, V. A. Suchkov, S. V. Shapiro, A. O. Schmidt , and Ku Shên-ku

Gor'kii

Translated from Avtomatika i Telemekhanika, Vol. 21, No. 6, pp. 907-917, June, 1960

Brief descriptions are given of new electromagnetic executive organs – original transformers controlled by shunt magnetization. The operating principles of such transformers with feedback are given. A new group of three-phase transformers is described, as well as original automatic devices for transforming single-phase current to three- or two-phase.

There is a very pressing problem in the creation, for automatic control systems, of executive organs without transferrable contacts, moving parts or power electronic-ionic elements. One of the new directions in the solution of this problem is the work, carried out in the A. A. Zhdanov Polytechnic Institute of Gor'kii, in the design and investigation of original transformers* which are controlled by changing the magnetization of shunts positioned in the apertures of the secondary windings.

The new shunt magnetization controlled transformers (SMCT) are more economical than transformers [1] with power windings located on different cores and with magnetic shunts divided into two parts (Fig. 1). In these transformers, the poor electromagnetic connection of the power windings leads to a high utilization of copper and a low power factor. The leakage in an SMCT is relatively lower and, consequently, the weight of active material is also lower. An SMCT is more economical, more compact and lighter than a set-up with power magnetic amplifiers – with saturable reactors – in those cases when a transformer is necessary to connect the supply line with the load. Today, SMCTs are used by a number of enterprises in the USSR in various automatic devices, for example, in voltage and current stabilizers, in controlled rectifier machines, in transformers of numbers of phases, in program control apparatus, etc. The SMCTs in use have powers of 0.1 to 150 kv-a; a single-phase SMCT is being developed with a power of 5600 kva-a.

The domain of application of the SMCTs can still not be accurately defined, due to the short span of time elapsed since their development. They will probably find further application as executive organs of automatic voltage controllers in those cases when reliability and compactness are decisive in the choice of the power elements.

This paper basically contains information on various SMCT systems. A significant part of it reflects work carried out in 1959 and not yet published; data on work executed somewhat earlier have already appeared in print [2].

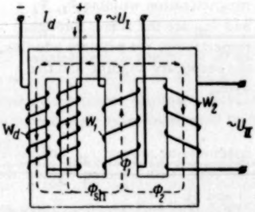

Fig. 1. Scheme of a transformer with smooth voltage control. W_1 is the primary winding , W_2 is the secondary winding, W_d is the magnetization winding, Φ_1 is the flux running through the primary winding, Φ_2 the flux through the secondary winding, Φ_{sh} the shunt flux and I_d is the magnetizing current.

1. Single-Phase SMCT

We consider two basic physical designs of single-phase SMCTs. The first was developed for controllers with thorough control, the second is advantageous, principally, for executive elements of various stabilizers.

In the first design (Fig. 2), core 1, on which primary winding W_1 is placed, and core 2, together with the corresponding portions of the frame, constitute the basic magnetic circuit. Cores 3 and 4 are the magnetic shunt, divided into two portions. On these cores are placed identical windings W_d, connected in opposition and sup-

---

* A. M. Bamdas and V. A. Somov, Patent application No. 110770, Committee on Patents, USSR.

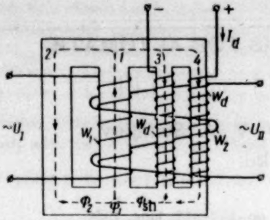

Fig. 2. Scheme of a transformer with a magnetized shunt positioned in the secondary winding's aperture: 1 and 2 are the cores of the basic magnetic circuit, 3 and 4 are the cores of the magnetic shunt, W_1 is the primary winding, W_2 is the secondary winding, W_d is the magnetization winding, Φ_1, Φ_2 and Φ_{sh} are the fluxes through, respectively, the primary winding, the secondary winding and the shunt.

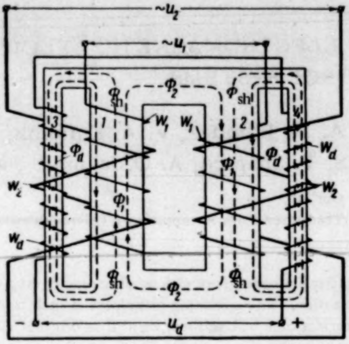

Fig. 3. SMCT scheme for voltage control within narrow limits. 1 and 2 are the cores of the basic magnetic circuit, 3 and 4 are the cores of the magnetic shunt, W_1, W_2 and W_d are the primary, secondary and magnetization windings respectively, Φ_2 is the basic flux, Φ_{sh} is the shunt flux (variable) and Φ_d is the shunt flux (constant).

plied by dc magnetizing current I_d. Secondary winding W_2 encompasses core 1 with winding W_1 and the magnetic shunt (cores 3 and 4).

The variable magnetic fluxes Φ_{sh} and Φ_1 have contrary directions. By taking this into account, we obtain the magnitude of the flux Φ_2 through the secondary winding from the equation (in symbolic form)

$$\dot{\Phi}_2 = \dot{\Phi}_1 - \dot{\Phi}_{sh}.$$

Obviously, control of current I_d and the variations of flux Φ_{sh} connected with this permit the implementation of smooth control of secondary voltage U_{II}. For an invariant primary voltage, the greatest value of U_{II} is obtained for the greatest current I_d; in this operating mode, there is almost complete expulsion of variable flux from the shunt.

To a certain extent, the SMCT is a development of a well-known system of a controlled transformer with a movable magnetic shunt [3] in the aperture of the power winding. Indeed, the magnetization shunt in the SMCT is analogous in its effect to a displacement of part of itself (i.e., to an increase of the air gap between the shunt and the basic magnetic circuit).

In the second design, shown in Fig. 3, both basic cores 1 and 2 are used for the locus of winding W_1. In comparison with the first design, the expenditure of copper for the magnetization windings is considerably less here.

Cores 3 and 4, symmetrically positioned at the sides of the basic cores are, in conjunction with the corresponding portions of the frame, the magnetic shunts. On these cores are placed the magnetization windings, connected in series opposition. The secondary circuit consists of the two W_2 windings.

The constant magnetic flux Φ_d, induced by current I_d, is completed by cores 1 and 2 of the basic magnetic circuit.

We now characterize certain of the SMCT parameters.

1. The power factor of the SMCT primary circuit during the control process for a constant active load varies within approximately the same limits as the power factor for machines consisting of transformers with series-connected saturable reactors.

2. For an invariable I_d, the SMCT load characteristic is a falling one. Automatic control of current I_d permits an artificial characteristic of any form to be obtained.

3. The power dissipated in the dc circuit of an SMCT without feedback is approximately twice the value of the loss in the primary winding's copper.

4. With account taken of the magnetization losses, the efficiency of the prepared specimens of SMCTs, with power from 1 to 50 kv-a, lies between the limits of 0.85 to 0.95 for a normal load.

5. The form of the SMCT's secondary voltage curve changes during the control process. For a nominal I_d, the curve is practically a sinusoid; for the least value of I_d, the distortion coefficient for the prepared specimens amounted to 30 to 35%.

6. The gains and time constants of SMCTs have values of the same orders of magnitude as the saturable reactors of the corresponding power.

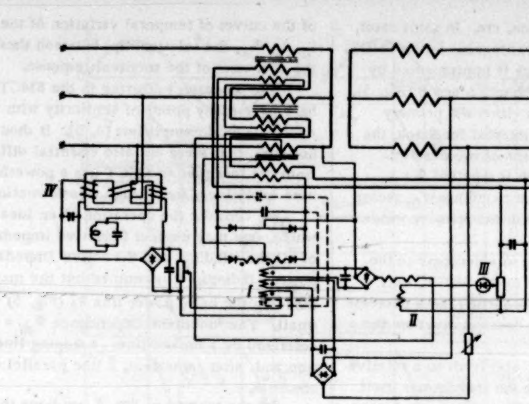

Fig. 4. Automatic control device for an electric drive with voltage stabilization and with current cutoff. I) and II) saturable reactors of the control scheme, III) stabilitron, IV) ferroresonant stabilizer.

7. Oscillations of the line frequency, just as for saturable reactors, have an insignificant effect on the SMCT properties.

8. The expenditure of active materials for an SMCT depends on its physical design, the depth of control and the character of the load. For an SMCT (Fig. 2) with control of U_{II} from zero to the nominal value, approximately, the expenditure of steel is greater than for an ordinary transformer by a factor of 1.8 to 1.9, while the expenditure of copper is greater by a factor of 2.2 to 2.5. In an SMCT (Fig. 3) intended for use as the executive organ of a voltage stabilizer, operating for deviations of the primary voltage within the limits of ± 12% from the nominal value, the expenditure of steel, in comparison with ordinary transformers, is higher by 30 to 35% and the expenditure of copper is higher by 45 to 50%.

The control schemes for automatic devices with SMCTs do not differ in principle from those used in devices with saturable reactors.

Figure 4 gives the scheme for the automatic control of an electric drive with voltage stabilization and with a sharp current cutoff; with overloading, a special device, cutting in a stabilitron, sharply lowers the secondary voltage.

2. Single-Phase SMCT With Feedback

In SMCTs, as in saturable reactors, the magnetization shunt can also be implemented by several individual circuits [4, 5, 6], and here also it is possible to have feed-

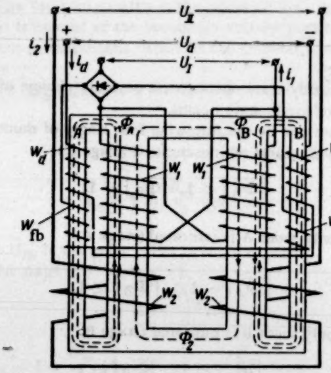

Fig. 5. SMCT scheme with external feedback.

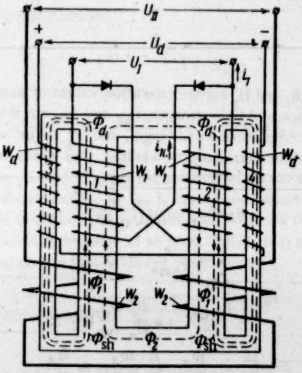

Fig. 6. SMCT scheme with internal feedback.

back windings, initial magnetization, etc. In some cases, the introduction of feedback is advantageous for an SMCT.

Here, external current feedback is implemented by auxiliary windings W_{fb}, located on shunts A and B (Fig. 5), and a rectifier bridge connected in either the primary or secondary winding circuit. For internal feedback, the SMCT's primary winding must consist of two parallel-connected halves W_1, each of which is supplied via a diode (Fig. 6). In this case, auxiliary windings W_{fb} shown in Fig. 5 could be amalgamated with the primary windings W_1.

Use of external feedback leads to a decrease in the power of the control signal applied to the SMCT, i.e., to an increase in the gain and, consequently, to a decrease in weight of the control block, but does not decrease the weight of the SMCT itself.

Internal feedback in an SMCT also leads to a relative decrease in the weight of copper in the transformer itself by approximately 15%. The expenditure of copper for the primary circuit of an SMCT with internal feedback increases by approximately 50% due to the fact that current flow in any of the W_1 windings only during a half a period and due to the decrease in the power factor. On the other hand, as was shown by investigations, the weight of the magnetization winding is decreased by a factor of from 5 to 8. We now give several parameters of an SMCT with internal feedback, the transformer power being 1.33 kv-a: weight of winding copper 21 kg, weight of steel 23 kg, dimensions 416 × 152 × 270 mm. The transformer was designed for explosion-proof usage.

3. Certain Elements of the Theory of Operation of a Single-Phase SMCT

We now give a mathematical analysis of the operation of an SMCT which will allow us to determine the form of the curves of temporal variation of the quantities i_1, i_2, i_d, u_2, Φ_A, the relationships between these quantities and the character of the transient response.

The processes occurring in the SMCT designs considered here have many points of similarity with those in single-cycle magnetic amplifiers [4, 5]. It should be mentioned, however, that there are also essential differences stemming from the fact that an SMCT has a powerful magnetic flux used exclusively for voltage transformation.

We consider the operation of an ideal SMCT, in which, one may neglect inductive impedance, dissipation of all the windings and the active impedances of the power windings. It is assumed that the magnetizing force inducing the basic power flux Φ_2 (Fig. 5) is negligibly small. The functional dependence $\Phi_{sh} = f(B_{sh})$ is characterized by a broken line: a sloping line until saturation and, after saturation, a line parallel to the axis of abscissas.

For the scheme of Fig. 5, we have the following basic equations of the ideal SMCT:

$$\bar{u}_1 = \bar{i}_1 \bar{R}_L + \frac{d}{d\tau}(\bar{\Phi}_A - \bar{\Phi}_B), \tag{1}$$

$$\bar{u}_d = \bar{i}_1 \bar{R}_d + \frac{d}{d\tau}(\bar{\Phi}_A + \bar{\Phi}_B), \tag{2}$$

$$\bar{i}_d + \bar{i}_1(1 \pm K_{fb}) = \bar{i}_A, \tag{3}$$

$$\bar{i}_d - \bar{i}_1(1 \mp K_{fb}) = \bar{i}_B, \tag{4}$$

where $\tau = \omega t$ and $K_{fb} = W_{fb}/W_1$.

The quantities $\bar{u}_1$, $\bar{u}_d$, $\bar{I}_d$, $\bar{R}_d$, $\bar{R}_L$, $\bar{\Phi}_A$, $\bar{\Phi}_B$, $\bar{I}_1$, $\bar{I}_A$, $\bar{I}_B$ are given in relative units, the base values adopted being

$$\Phi_{bas} = B_s Q_{sh}\ U_{bas} = \omega W_k \Phi_{bas} \cdot 10^{-8},\ I_{bas} = \frac{H_s l_{sh}}{W_k},$$

$$R_{bas} = \frac{U_{bas}}{I_{bas}} = \omega \frac{B_s}{H_s} \frac{Q_{sh}}{l_{sh}} W_k^2 \cdot 10^{-8},$$

where B_s and H_s are the saturation values of magnetic induction and field strength, Q_{sh} and l_{sh} are the shunt's active cross section and length, and W_k is the number of turns of the corresponding winding. For example,

$$u_1 = \frac{u_1}{\omega W_1 B_s Q_{sh} \cdot 10^{-8}},$$

$$\bar{i}_d = \frac{i_d}{I_{basd}} = \frac{i_d W_d}{H_s l_{sh}},$$

$$\bar{R}_L = \frac{R_L}{R_{bas\,2}} = \frac{R_L}{\omega \frac{B_s}{H_s} \frac{Q_{sh}}{l_{sh}} W_2^2 \cdot 10^{-8}},$$

$$\bar{\Phi}_A = \frac{\Phi_A}{\Phi_{bas}} = \frac{\Phi_A}{B_s Q_{sh}} = \frac{B_A}{B_s}.$$

In steady-state operation, a periodic change of the shunt's magnetic state occurs.

There can be the following four stages of shunt states:

1) both shunts are unsaturated (stage C)

$$|\bar{\Phi}_A| < 1,\ |\bar{\Phi}_B| < 1;$$

2) only shunt A is saturated (stage A)

$$|\bar{\Phi}_A| = 1,\ |\bar{\Phi}_B| < 1;$$

3) only shunt B is saturated (stage B)

$$|\bar{\Phi}_A| < 1,\ |\bar{\Phi}_B| = 1;$$

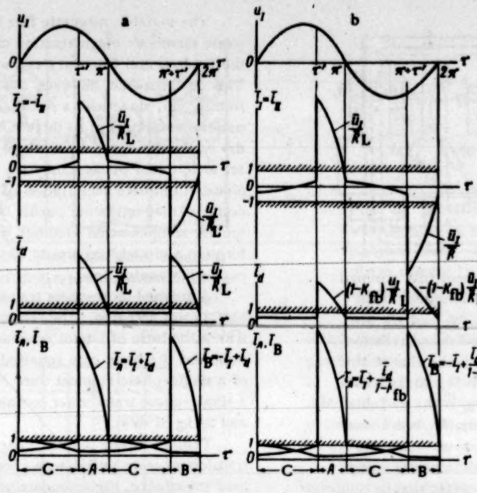

Fig. 7. Curves of the temporal variation of $\bar{i}_1$, $\bar{i}_2$, $\bar{i}_d$, $\bar{i}_A$, $\bar{i}_B$ during one period (the cycle C-A-C-B-C): a) without feedback ($K_{fb} = 0$) and b) with feedback ($K_{fb} = 0.5$).

4) both shunts are saturated (stage H)

$$|\bar{\Phi}_A| = 1, \quad |\bar{\Phi}_B| = 1.$$

As a function of the magnitude of the primary voltage and the magnetizing current, the following cycles of stages are possible during a period: 1) C-C, 2) C-A-C-B-C, 3) C-H-C-H-C, 4) C-H-A-C-H-B-C, 5) H-H.

The most interesting is the cycle C-A-C-B, since only with it is control of the secondary voltage possible. For this, the instantaneous values of the currents $\bar{i}_1$ and $\bar{i}_d$ equal:

for stage C C($0 < \tau < \tau'$)

$$\bar{i}_1 = -\frac{\bar{U}_m}{2}\cos\tau + \frac{\bar{U}_m}{4}(1+\cos\tau'),$$

$$\bar{i}_d = 1 + \frac{\bar{U}_m}{4}(\cos\tau' - 1),$$

where $\bar{U}_m$ is the peak value in relative units;

for stage A($\tau' < \tau < \pi$)

$$\bar{i}_1 = \frac{\bar{U}_m}{\bar{R}_L}\sin\tau,$$

$$\bar{i}_d = 1 + \frac{\bar{U}_m}{\bar{R}_L}(1-K_{fb})\sin\tau + \frac{\bar{U}_m}{\bar{R}_L}(\cos\tau' - 1),$$

where τ' is the moment when stage C is replaced by stage A. These expressions are obtained from the condition that $\bar{R}_L < 0.1$. It can also be shown that

$$\cos\tau' = \pi\frac{\bar{I}_d - 1}{\bar{U}_m}\bar{R}_L - 1,$$

where $\bar{I}_d = \bar{U}_d/\bar{R}_d$. The average value of load current over one half-period equals

$$\bar{I}_{1.\,av} = (\bar{I}_d + a + 1)\frac{1}{1-K_{fb}},$$

where

$$a = \frac{\bar{U}_m}{2\pi}(1 + \tau' - \pi + \sin\tau' + \pi\cos\tau'). \tag{5}$$

Figure 7a and b, gives the theoretical curves of the changes in currents $\bar{i}_d$, $\bar{i}_1$, $\bar{i}_A$, $\bar{i}_B$ during one period in the absence of feedback ($K_{fb} = 0$) and with feedback ($K_{fb} = 0.5$). For the transient response in an ideal SMCT, it is not difficult to obtain the following expressions:

$$\bar{I}_d = \bar{I}_{d,\,av} + \frac{\pi}{2}\frac{\bar{R}_L}{\bar{R}_d}\frac{1}{1-K_{fb}}\frac{d\bar{I}_{d,\,av}}{d\tau},$$

$$\bar{I}_d\frac{1}{1-K_{fb}} = \bar{I}_{1.\,av} + \frac{\pi}{2}\frac{\bar{R}_L}{\bar{R}_d}\frac{1}{1-K_{fb}}\frac{d\bar{I}_{1.\,av}}{d\tau}.$$

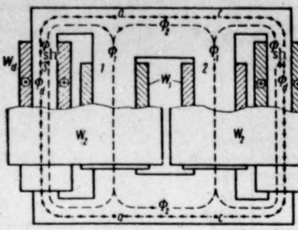

Fig. 8. Single-phase element of a grouped transformer with matched magnetization winding connections. W_1, W_2 and W_d are the primary, secondary and magnetization windings respectively, Φ_1 is the flux in the primary winding, Φ_2 is the flux linked with the secondary winding, Φ_{sh} is the variable flux of the magnetic shunts, Φ_d is the constant magnetization flux, 1 and 2 are the cores of the basic magnetic circuit, 3 and 4 are the cores of the magnetic shunts.

From whence it follows that an ideal SMCT, just as an ideal magnetic amplifier, is a first-order aperiodic link with time constant

$$T = \frac{\pi}{2}\frac{\bar{R}_L}{\bar{R}_d}\frac{1}{1-K_{fb}}. \tag{6}$$

4. Grouped Three-Phase SMCTs

In previous publications [2] there were described three-phase variants of the SMCT. We now communicate information on a grouped transformer, developed by the authors, with three individual single-phase SMCTs of a new type (Fig. 8). The grouped transformers are intended for the smooth control of three-phase voltage for symmetrical phase loads, for example, for supplying rectifier stands. Voltage control, as in the SMCT of Fig. 3, is implemented by changes in current I_d flowing through the series-connected magnetization windings W_d.

In the new single-phase SMCT, both windings W_d are so connected that the constant magnetization flux Φ_d virtually doesn't flow through cores 1 and 2 of the basic magnetic circuit, but is closed only through the loop formed by the cores of the shunts and the frame. It is necessary for this that the currents I_d be directed in windings W_d as shown in Fig. 8.

It is easily concluded that the basic cores of the new variant of the SMCT must have a smaller cross-sectional area than in the case of the design shown in Fig. 3. Thanks to this, there is also a relative decrease in the expenditure of the active materials – copper and steel.

In designs of SMCT intended for profound voltage control, higher than 50%, the economy in copper weight amounts to 20%.

The variable magnetic flux induces, in the single-phase element's magnetization circuit, a resulting emf at the fundamental frequency and with higher harmonics. This circumstance, however, is admissible for a grouped transformer, since with a series connection of the magnetization circuits of its three component elements and the symmetric load, the emf's of the fundamental harmonics are annihilated because they are equal and 120° out of phase. Complete annihilation of the variable emf in a common magnetization circuit is given by the use of special compensation windings, placed on the shunts and forming a closed loop around which the currents at the higher harmonics flow.

A grouped three-phase transformer of this type with SMCTs was prepared. The test specimen had a power of 6 kv-a, the ratio of lateral cross-sectional areas of the shunt and the basic core equalled 0.83. The dimensions of a single-phase element were 355 × 120 × 335 mm, with a single-phase transformer containing 21 kg of copper and 22 kg of steel.

Testing showed that the characteristics of the grouped transformer were satisfactory. For a constant nominal load impedance, the secondary voltage was varied within the limits of 22 to 100%. For nominal values of load and current I_{d_N}, the value of cos φ was 0.93, and the efficiency in this case, with losses, in the magnetization winding taken into account, was 91%.

The form of the curve of line voltage U_2 depends on the magnitude of the load impedance and on the relative value of the magnetization current. For their nominal values, the distortion in the curve's form was small.

5. Static Transformers of Numbers of Phases with SMCTs

A common fault in the executive organs of static devices serving for the transformation of single-phase current to three-phase or two-phase is that variations in the load parameters, as well as the supply net regimen, lead to the appearance of asymmetries in the multiphase system of voltages obtained. If we take, as the criterion for judging the operation of a transforming device, the asymmetry coefficient of this system of voltages, we obtain the following expressions for the transformer of single-phase voltage to three-phase (Fig. 9a) and to two-phase (Fig. 9b):

$$\dot{\varepsilon}_U = \frac{\dot{U}_2}{\dot{U}_1} = \frac{2g - \frac{1}{\sqrt{3}}(b_L + b_C) - j\,(2b + b_L - b_C)}{2g + \frac{1}{\sqrt{3}}(b_L + b_C) - j\,(2b + b_L - b_C)}, \tag{7}$$

$$\dot{\varepsilon}_U = \frac{\dot{U}_2}{\dot{U}_1} = \frac{(g - b - b_L) - j\,(g + b - b_C)}{(g - b + b_L) + j\,(g - b + b_C)}, \tag{8}$$

where g is the active component of conductance of one phase of the load, b is the reactive component of conductance of one phase of the load, b_L and b_C are the inductive and capacitive conductances of the transformer arms.

Figure 10 shows, for a transformer of single-phase to three-phase current, the characteristic $\epsilon = f(S/S_L)$, com-

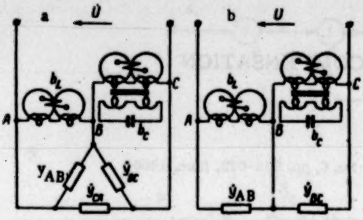

Fig. 9. Basic functional transformer schemes. a) transformer of single-phase current to three-phase, b) transformer of single-phase to two-phase current.

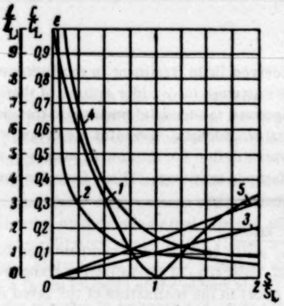

Fig. 10. Transformer device characteristics. 1) Curve of asymmetry coefficient variation; 2) relative change of induction for cos φ = 1; 3) relative change of capacitance for cos φ = 1; 4) relative change of induction for cos φ = 0.8; 5) relative change of capacitance for cos φ = 0.8.

puted for the relative variation of apparent power of the active-inductive load with cos φ = 0.8, from which it follows that, as the apparent power deviates from its nominal value, the asymmetry of the voltage system rapidly increases (curve 1) and goes beyond the limit of the admissible value of ϵ = 5%. An analogous phenomenon also occurs in the transformer of single-phase current to two-phase. With variations in the line frequency, there also occurs a rapid increase in asymmetry of the multi-phase voltage systems.

As shown by analysis, to stabilize the symmetry of a multi-phase voltage system, it is required to control the parameters of the elements of the executive organ – the transformer device. Curves 2-5 of Fig. 10 show what relative values must be possessed by the inductance and capacitance of the arms of a transformer of single-phase to three-phase current for variations of the relative values of apparent load power and for different values of its power factor.

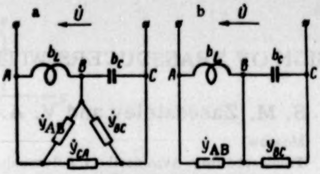

Fig. 11. Modified transformer schemes with symmetry stabilization of the multiphase systems. a) Transformer of single-phase current to three-phase; b) transformer of single-phase current to two-phase.

Variation of parameters can be implemented automatically† if the elements of the executive organ are constructed of controllable devices. Such elements might be saturable reactors or SMCTs.

Figure 11 shows modifications of the circuits given previously which allow them to be transformed to controller executive organs of transformers of numbers of phases with automatic stabilization of secondary voltage symmetry. In the transformer whose circuit is shown on Fig. 11a, a saturable reactor is used as the inductive arm. In the capacitive arm, control of the reactive power of the condenser battery is implemented by varying the voltage on its terminals, thanks to its connection via an SMCT.

The scheme of Fig. 11b, is a modification of the transformer of single-phase current to two-phase.

Test results for a trial device of 1.5 kv-a power showed that the value of the asymmetry coefficient is less than 5% for a fourfold change in the impedance of the load circuit and a change in the power factor between the limits of unity and 0.6. These results were also obtained for changes in voltage and frequency of the supply line within ± 20%.

In conclusion we note that the executive organs – transformers with automatic stabilization of output voltage symmetry – can be constructed for significant output power.

LITERATURE CITED

1. English patent, class 38/IV, No. 031124, 1934.
2. A. M. Bamdas, V. A. Somov, and A. O. Schmidt, Transformers and Stabilizers Controlled by Shunt Magnetization [in Russian] (Gosénergoizdat, 1959).
3. B. E. Paton and V. K. Lebedev, Elements of Designing AC Circuits and Apparatus for Arc Welding [in Russian] (Izd. AN USSR, 1953).
4. M. A. Rozenblat, Magnetic Amplifiers [in Russian] (Izd. Sovetskoe Radio, 1956).
5. G. F. Storm, Magnetic Amplifiers [Russian translation] (IL, 1957).
6. V. A. Geiger, Magnetic Amplifier Circuits [in Russian] (Gosénergoizdat, 1959).

---

† A. M. Bandas and V. A. Kulinich, Patent application No. 120594, Committee on Patents, USSR.

DESIGN OF TRANSDUCERS WITH FORCE COMPENSATION

S. M. Zasedatelev and V. A. Rukhadze

Moscow

Translated from Avtomatika i Telemekhanika, Vol. 21, No. 6, pp. 918-928, June, 1960

The paper considers questions in the design of pneumatic transducers and dc electrical transducers based on the principle of force compensation. Considerations are adduced as to the choice of the instruments' functional schematics and physical designs. The causes are established for the appearance of instrument errors: nonlinearity errors in the transformation of a measured parameter to an output signal, sensitivity thresholds, temperature errors, and errors from changes in the static pressure of the medium. Computational formulas are provided, and recommendations are given for decreasing the magnitude of the errors.

INTRODUCTION

In the design of industrial instruments, ever greater use is being made of the force compensation method, the essence of which is that an input signal to be measured is transformed by the instrument's sensitive element to a force, and this force is equalized (compensated) by a force developed in the instrument at the cost of some energy from an external source. The equalizing force is proportional to the instrument's output signal. Thus, the input quantity is transformed to an output signal.

In those cases when both the input quantity and the output signal of the instrument are transformed to forces simply and without significant errors, the use of force compensation allows one to obtain small values of error, in particular, those components of the error which are engendered by changes in the ambient conditions and by imperfections and instability of the instrument's individual elements. Therefore, despite some complexity of the instrument's physical design, devices using force compensation have been widely employed for measuring, and transforming to compressed air pressure or to dc force, such quantities as pressure, pressure drop, density, level of liquid, and temperature. Force compensation has also been widely used in pneumatic and electrical transformers, automatic controllers and calculating devices.

In the development of such devices, it should be kept in mind that, in addition to reliability, stability of operation, simplicity of maintenance and low cost — mandatory properties for industrial instruments — the functional scheme and the physical construction must provide the capability of actually attaining the good static and dynamic accuracy which are the basic virtues of force compensation.

Creation of high-accuracy instruments is significantly facilitated if one knows the dependence of the various components of error on the instrument's physical (design) parameters and if one could compute, if only approximately, the probable magnitude of the error. Questions of design and construction of instruments with force compensation have received little treatment in the literature. Here, we make the attempt to consider certain of these questions as they appertain to industrial pneumatic transducers and dc electrical transducers. Formulas are given, without derivations, which define the instrument accuracy as a function of the design parameters. These formulas can be used for instrument design.

1. Basic Errors

The static error of force compensation instruments is made up, basically, of the following components:

1. Errors in the realization of the given functional relationship of the output signal to the quantity to be measured. Since this relationship must be a linear one in the majority of cases, these ordinarily are called nonlinearity errors.

2. The error caused by friction losses in mechanisms and hysteresis losses in elastic elements and magnetic systems. It determines the threshold of sensitivity and the variation.

3. Temperature errors, expressing themselves in a shift of the range of the output signal and in changes in the magnitude of this range as the instrument's temperature changes. The second component of these errors in compensation transducers is ordinarily significantly less than the first.

4. An error from changes in the static pressure of the medium to be measured. It occurs at points where the force arising from the sensitive element is derived from the medium to be measured in the atmosphere via an elastic discriminating element, and when a change in static pressure gives rise to a change in the force on the sensitive element (for example, in the case when fluid level is measured by a float).

5. Errors from changes of the supply source parameters (pressure of the air supplied to the instrument, electrical line voltage).

6. Errors from "aging" of the instrument's elements leading to changes of the instrument's indications with the

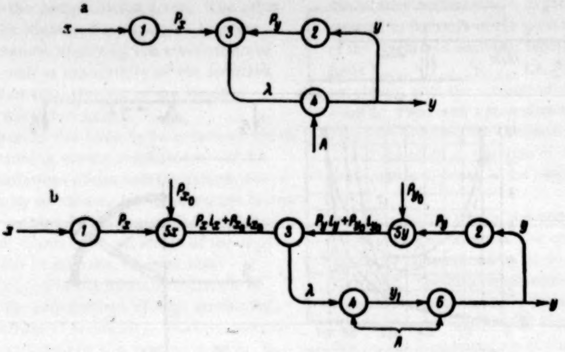

Fig. 1.

passage of time. Although this error component can be eliminated by periodic calibration of the instrument, its appearance, under actual conditions of use, should always be considered possible.

A dynamic error appears in the form of pulsations of the output signal and a displacement of its average magnitude which arise both from external jars and vibrations and from auto-oscillatory modes in the closed compensation system. Moreover, a dynamic error can appear in the form of a lag in changes of the output signal after changes in the quantity to be measured, or in the form of distortions of amplitude, phase or form of the output signal for a periodic change of the quantity to be measured.

2. Choice of Instrument Scheme

Compensation measurement of forces can, in a first approximation, be presented by the following functional schematic (Fig. 1a). The quantity x to be measured is transformed by sensitive element 1 to the force P_x which is compared with force P_y of compensation element 2, proportional to the output signal y.

The difference of these forces disturbes the equilibrium of movable system 3 and creates a translation λ of it. This latter is applied to an equilibrium indicator — transformer 4, which also generates the output quantity y, obtaining energy A from an external source.

To any range of variation of the quantity to be measured there must correspond a definite range of variation of the output signal. In the scheme being considered, this correspondence is defined only by the parameters of the sensitive and the compensation elements. For this there is frequently used a lever transfer mechanism with a definite transfer ratio i. On the schematic (Fig. 1b), this mechanism is denoted by 5x and 5y. Since the physical design of such instruments is already relatively complex in itself, it is ordinarily considered worthwhile to introduce some additional complication in the form of a mechanism with a variable (adjustable) transfer ratio, permitting the transducer to be tuned for different ranges of variation of the quantity to be measured for some adopted standard range of the output signal. To the mechanism there are also applied the constant (adjustable) forces P_{x_0} and P_{y_0}, introduced for the formation of the nonzero range of variation of the measured and output quantities.

As a rule, to increase the output signal's power, the output quantity y is not taken off directly from the equilibrium indicator — transformer 4, but from power amplifier 6 which, obtaining some quantity y_1 from the indicator, amplifies its power and transforms it to the quantity y.

The functional schematic and the physical configuration of the transfer mechanism and, in particular, the mechanism for adjusting the transfer ratio, determine to a large extent the physical design of the entire instrument.

In the majority of industrial instruments, a two-lever mechanism (Fig. 2a) is used in which the force P_x to be measured creates a torque on one lever, while the compensating force P_y creates a torque on the other. The transfer ratio is determined by the position of the connection 1, executed in the form of a shaft or a slider, transmitting force from one lever to the other. Curve i in Fig. 2b shows the transfer ratio $i = a/(l - a)$ as a function of the connection position. The curve s_i characterizes the so-called tuning sensitivity $s_i = (di/l)/(da/l) = l^2/a(l - a)$ which is relatively small for middle positions of the connection and increases sharply as the connection is shifted toward the bearings. From the curve for i^2 one can determine the complete change of the transfer ratio for identical limiting positions of the slider on both sides of the middle position.

The "one-lever" scheme (Fig. 2c) used in many instruments has the same tuning characteristic as the two-lever one.

The majority of such mechanisms are designed for changes of the transfer ratio by a factor of from 6 to 10. Greater variations of the transfer ratio are rarely employed since they render difficult the tuning of the necessary

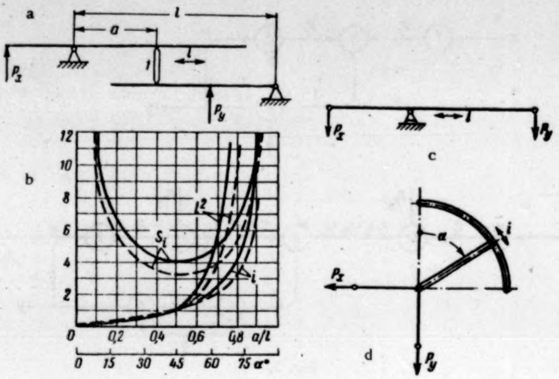

Fig. 2.

range, and lower the stability of instrument operation for slider positions close to the bearings where the sensitivity of the tuning is too great.

Comparatively recently, use began to be made of the so-called "vector" mechanism (Fig. 2d), consisting of three shafts hinged together. Two shafts, transmitting the forces P_x and P_y are at right angles to each other. The end of the third shaft is hinged to the frame of the instrument. Change of the angle α at which this shaft is established is implemented by the tuning of the mechanism's transfer ratio. The sensitivity of tuning of this mechanism, $s_i = \pi/\sin 2\alpha$, in the ordinarily used middle region, is less than in the lever schemes. The curves s_i, $\underline{i}$ and i^2 for this mechanism are given by the dashed lines in Fig. 2b.

Tuning of the transfer ratio is sometimes implemented also by shifting the compensation element, by replacing it or by changing the transfer ratios of auxiliary levers. Such rough (step-wise) tuning, in connection with a smooth tuning, allows one instrument to be used, in wide range of variation of forces, which is an undeniable advantage in use. However, this may decrease the accuracy due to the difficulty of creating a mechanism which is sufficiently sensitive for small measured forces and, at the same time, is strong and reliable in measuring large forces.

In choosing the mechanism scheme, great importance inheres in the positioning of the equilibrium indicator. In existing instruments it is placed either before the tuning mechanism in the sensitive element or after this mechanism in the compensation element. As applied to a two-lever mechanism, these variants of indicator positioning are shown in Fig. 3a and b.

The second variant is more convenient to build, since it allows implementation of the equilibrium indicator, compensation element and other assemblies to be joined in one device with a lever for receiving forces from the transfer mechanism. This device is easily unified and a single physical realization of it can be used for different instruments: manometers, differential manometers, level meters, hardness meters, thermometers and others, so long as the parameter to be measured is transformed to a force of a definite magnitude. The entire range of forces generated by the sensitive elements of different instruments may be transformed to the output signals of a small number of standard size devices of this type.

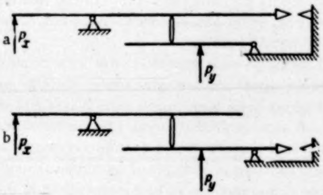

Fig. 3.

The first variant gives a physical design which is less convenient for unification, since here the equilibrium indicator is directly, ordinarily via a lever, connected with the sensitive element. The advantage of this scheme amounts to this, that inreturning the range of forces to be measured, the sensitive element keeps invariant its position which it was given when the instrument was regulated. This manifests itself favorably in the accuracy when there are changes in static pressure and when there are oscillations of the ambient temperature. Moreover, it is easier here to obtain small translations of the sensitive element, which also makes the instrument capable of high accuracy in its operation.

It is necessary to bear in mind that all actual instruments implement force compensation only with some approximation, since only a part of the force to be measured is equalized by the compensation force. The other part of the force to be measured is expended in overcoming various resistances hindering the translations of the moving system, such as the rigidity of the sensitive and compensation elements, rigidity of the flexible bearings, as well as frictional forces.

Naturally, the part of the force to be measured which is expended in overcoming elastic impedances will be decreased as the translations of the moving system decrease. In the majority of modern instruments, use is made of high-sensitivity equilibrium indicators and amplifiers which provide a total operational excursion of the equilibrium indicator of tens of microns, or even less.

Of course, the choice of equilibrium indicator is subject, not only to the requirement of high sensitivity, but also to considerations of reliability, stability, simplicity, and low reaction forces on the moving system. In penumatic instruments, nozzle-flapper type transformers are used almost exclusively while, in electrical instruments, induction, capacitance, contact and other types of transformers are used.

The choice of the basic dimensions of the transfer mechanism, the sensitive and the compensation elements, is determined by the necessity of obtaining a given accuracy, by the magnitude of the forces to be measured, and by requirements for small dimensions.

From the point of view of accuracy, apparently, it is advantageous to have large forces developed by the sensitive element: the larger these forces, the less will be the deleterious effect of rigidity of the elastic elements, frictional forces and additional forces giving rise to errors with changes in the medium's static pressure.

3. Nonlinearity Error

This error is made up of the nonlinearities of the transformations to forces of the quantity to be measured and the output signal, and the nonlinearities which occur in compensation.

The nonlinearity created by the sensitive elements is small as a rule, since these are hardly translated at all under conditions of force compensation. No nonlinearities at all arise from such devices as buoys, bells, and other forms of sensitive elements of fluid differential manometers. In practice, the nonlinearities created by tubular manometric springs and bellows are negligible.

Noticeable nonlinearities can appear upon changes in the effective areas of membranes, in particular, elastic ones. For example, let the effect area f vary proportionately to the pressure p by the function $f = f_0 (1 + np)$, where f_0 is the effective area of the unloaded membrane and the product of the pressure p by the coefficient n represents the relative change of effective area with changes in pressure, since $np = (f - f_0)/f_0$. Then, the force $P = pf$ on the membrane will depend nonlinearly (quadratically) on changes of pressure. By comparing it with a linear change of force with pressure $P^* = pf_{max}$, where $f_{max} = f_0 (1 + np_{max})$ and defining, as is usually done, the relative nonlinearity η of force as a function of pressure as the ratio of the greatest difference $(P^* - P)_{max}$ of the linear and nonlinear functions to the maximum force $P_{max} = f_{max} p_{max}$, i.e., as $\eta = (P^* - P)_{max}/P_{max}$, we obtain, after the corresponding transformations, $\eta = np/4$. Thus, with a proportionate change of effective area with pressure, the nonlinearity of the force equals 1/4 of the relative variation of the effective area of the manometric element in the given range of pressure variation.

The nonlinearity of the compensation elements of penumatic transducers can be compensated to a certain extent by the nonlinearity of the manometric sensitive elements. The magnetoelectric force mechanisms of electrical transducers have the same character of nonlinearity as the manometric elements. Here, the nonlinearity is a consequence of changes in induction of the magnetic field due to the magnetizing or demagnetizing action of the compensation current, which is particularly marked for large currents. Ferrodynamic compensation elements can also provide a significant nonlinearity.

The nonlinearity in the compensation of forces is a consequence of the conjunction of the nonlinearity of the equilibrium indicators' characteristics and the previously noted incompleteness of compensation when part of the force to be compensated is expended in overcoming the resistance of flexible elements. If we denote this part of the force P_x to be measured by P_z, we can then express the relative nonlinearity $\eta = \eta_{P_x - P_y}$ of the force to be measured to a compensating force as $\eta_{P_x - P_y} = \xi \eta_{\lambda - y}$, where $\xi = P_z/P_x$ is the coefficient of noncompensation and $\eta_{\lambda - y}$ is the nonlinearity of the equilibrium indicator; the nonlinearity of the compensating element is not taken into account here.

The functional relationship of the nonlinearities and the design parameters of the instrument can be considered in greater detail by setting up the equilibrium equation of the moving system. For this, by means of the transfer ratios i_x and i_y, we relate the force P_x to be measured and the compensating force P_y to the equilibrium indicator. We then relate to this same place the total force $T = \sum_n k_n \lambda_n i_n$, generated by the flexible elements with rigidities k_n and translations λ_n. It is also necessary to take into account the additional forces $Q_x = \sum_{n_x} k_{n_x} \delta_{n_x} i_{n_x}$ and $Q_y = \sum_{n_y} k_{n_y} \delta_{n_y} i_{n_y}$ of the flexible elements, from the sensitive element up to the equilibrium indicator and from the equilibrium indicator up to the compensation element, these forces arising due to the deformations δ_n of the instrument mechanism. We then obtain

$$P_x i_x - Q_x = P_y i_y - Q_y + T$$

or

$$P_x i_x - \sum_{n_x} k_{n_x} \delta_{n_x} i_{n_x} =$$

$$P_y i_y - \sum_{n_y} k_{n_y} \delta_{n_y} i_{n_y} + \sum_n k_n \lambda_n i_n.$$

We introduce the relationship between the translations λ and the output signal $\underline{y}$ for a concrete equilibrium indicator and amplifier, obtained by computations or selected experimentally, in the form, for example,

$$\lambda = \alpha_1 y + \alpha_2 y^2 + \alpha_3 y^3$$

and we then compute the magnitude of the deformations δ of the mechanism. Then, by assuming a linear relation between the output signals and the compensation forces, we can obtain an equation of the form

$$P_x = a_1 P_y + a_2 P_y^2 + a_3 P_y^3.$$

Investigation of the nonlinearity of this functional dependency shows that, to decrease it, one should choose the largest possible linear working segment of the equilibrium indicator's characteristic, should decrease the magnitude of its total excursion λ_{max}, should decrease in every way the rigidity of the flexible elements (sensitive and compensation flexible bearings, elastic output) and, conversely, should increase the rigidity of the levers and connections of the moving system and the instrument frame.

4. Sensitivity Threshold

Friction in the bearing of the moving system can give a significant increase to the sensitivity threshold. In view of the small translations of the mechanism, it is advantageous to use flexible bearings, for example, in the form of cruciform belt supports. Knife and ball bearings, although simpler physically, can be sources of significant friction, particularly when the manufacture and mounting are of inadequate quality.

Large frictional forces arise at the place of contact of the slider of the range regulator and the levers, and these are particularly noticeable in instruments with small forces to be measured. Therefore, from the point of view of frictional losses in the connections between the levers, it is preferable to employ flexible belting, despite the great complexity of its fabrication and of instrument calibration.

Serious attention must be given to the construction of the connection of the mechanism with the sensitive and compensation elements. From the point of view of minimal frictional losses, a rigid attachment is the best. But, in the majority of cases, such a solution leads to a significant increase in rigidity, so that flexible connections are more frequently used. It is also necessary to bear in mind that significant additional translations of the moving system can appear if the belting connection is only a little twisted and there has not been, with this, sufficient preparatory tightening.

In view of the smallness of the working translations of the moving system, hysteresis of the flexible elements is negligible in practice. However, with significant deviations of the moving system from the equilibrium position, for example, for overloaded instruments, the variations can attain significant magnitudes.

If one relates to the equilibrium indicator, and adds, all the forces P^0 which must be applied to each element of the instrument in order to eliminate hysteresis corresponding to the total possible excursion of the moving system, then one can calculate the instrument's sensitivity threshold η^0 as the ratio of this total related hysteresis force $\sum_n P_n^0 i_n$ to the total force $P_{x_{max}}$ to be measured, also related to the equilibrium indicator

$$\eta_i^0 = \frac{\sum_n P_n^0 i_n}{P_{x\,\max} i_x}.$$

Ferrodynamic force mechanisms have large values of hysteresis. The most radical measure in the fight to overcome these is to choose materials with small magnetic losses and to prepare the magnetic systems of thin sheet material or sintered powders.

5. Temperature Error

Just as the nonlinearity error, this error is made up of the errors of the sensitive element, the compensation element, and the error of the force-equilizing mechanism.

Temperature changes of the manometric elements lead to changes in their effective areas, which can lead to force changes which are very noticeable when elastic nonmetallic membranes are used. Therefore, serious attention should be given to the temperature stability of the effective area of such membranes.

In differential manometric transducers there have been used complicated physical designs of the sensitive elements, protected from overloads, consisting of two and more membranes with liquid charges. Increase of liquid pressure due to its expansion from temperature rises can be the cause of large temperature errors, and sometimes such devices have special temperature compensators.

Noticeable errors can be generated by magnetoelectric, electromagnetic and ferrodynamic mechanisms due to temperature variations, of magnetic induction and magnetic permeability. Here too, thermal compensators are frequently used.

Temperature variations in the dimensions of the mechanism assembly with rigidity present gives a component $\eta_\lambda{}^t$ of the temperature error which can be computed from the formula

$$\eta_{i\lambda}^t = \xi \frac{\Delta\lambda_t}{\lambda_{max}},$$

where $\Delta\lambda_t$ is the calculated magnitude of the temperature excursion of the equilibrium indicator, λ_{max} is the total working excursion of the equilibrium indicator and ξ is the noncompensation coefficient.

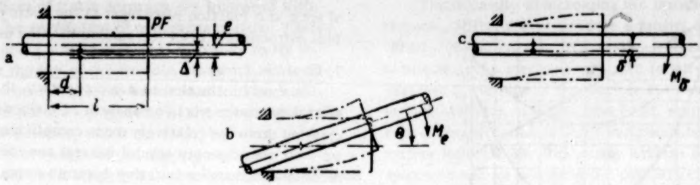

Fig. 4.

Temperature variations of the modulus of elasticity of the flexible elements lead to the appearance of temperature errors due to changes in the strain forces of these elements. The relative error per degree change in temperature is calculated as the ratio of the algebraic sum of the temperature changes of the forces of the elastic elements, referred to the equilibrium indicator, $\sum_n \gamma_n P_n i_n$, to the total force $P_{x_{\max}}$ to be measured, i.e.,

$$\eta'_\gamma = \frac{\sum_n \gamma_n P_n i_n}{P_{x_{\max}} i_x}.$$

Here, γ_n are the temperature coefficients of the moduli of elasticity of the individual flexible elements.

One should not lose sight of the possibility of temperature errors arising due to nonuniform heating of the different parts of the instrument and to their deformation by, for example, one-sided heating close to a heat source. For protection against this, it is advantageous to provide the instrument casing with a layer of heat insulation and to use coverings for it with low absorption coefficients.

For the first heating-cooling cycles of the instrument there is not infrequently observed an irreversible shift of the range due to relaxation forces and the associated deformations of the various assemblies. The most radical method of combating this is to remove the overstrained and temperature-mechanically-aged assemblies and components of the transducer. This is a most desirable measure to take, since it renders possible the improvement of the instrument's stability of operation in the course of time, and this index of accuracy of instrument operation is one of the most important of its use characteristics.

It is necessary to mention that the temperature error is the most difficult to eliminate because of the incomplete homogeneity of properties of the materials employed. With the necessity of obtaining small temperature errors, adjustable temperature compensation elements have been introduced (for example, in the equilibrium indicator) although temperature calibration of the instrument is entailed by this.

6. Errors from Changes in the Medium's Static Pressure

Derivation of the sensitive element's force from the medium to be measured is implemented, in the majority of compensation differential manometers, level meters and hardness meters, by means of a pivoting lever with compression of a bellows or a membrane. Despite the complexity of its physical design, a bellows derivation device is more frequently used, in view of its significantly lower rigidity.

The error of bellows extraction due to changes in the medium's static pressure is related both to the imperfections of its fabrication (which may be corrected by calibration) and with the unavoidable deformations of the extraction components with instrument operation; this part of the error cannot be eliminated by calibration, but can be lessened by the proper choice of the design parameters of the extraction device.

Among the first group of causes is noncoincidence of the line of action of the resultant pressure force on the bellows head with the center of vibration of the lever and the bellows' torsion axis. With this, a torque acts on the lever which is propotional to the static pressure; it also gives rise to an instrument error.

The various design methods of compensating this torque by instrument calibration must be implemented by at least one of the following kinematic operations:

1. Translation of the lever's center of rotation with respect to its axis by the amount Δ (Fig. 4a), which decreases the initial eccentricity.
2. Rotation of the lever, together with the bellows head, by the angle θ (Fig. 4b) which creates, by virtue of the torsion of the bellows, a torque M_θ, proportional to the static pressure.
3. Displacement of the extraction lever together with the bellows head and the bearings (Fig. 4c). With this, as in the previous case, there appears a torque M_δ proportional to the static pressure. The torques $M_\theta + M_\delta$ can compensate the torque giving rise to the instrument error.

Their magnitudes, determined by the methods of strength of materials, can be computed from the formulas

$$M_\theta = pFlm_\theta\theta \text{ and } M_\delta = pFm_\delta\delta.$$

Here, p is the medium's static pressure, F is the effective area, and l is the length of the extraction bellows, and

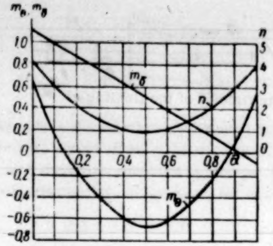

Fig. 5.

the coefficients

$$m_\theta = \frac{2}{15}(1 - 9\alpha + 9\alpha^2)$$

and

$$m_\delta = \frac{11 - 12\alpha}{10}, \text{ where } \alpha = \frac{a}{l}$$

(Fig. 4a). The functional relationship of m_θ and m_δ on the position of the bearings along the length of the bellows is given in Fig. 5, which provides a representation of the effectiveness of these calibration steps.

The second group of causes of errors from static pressure results from a displacement of the extraction lever's center of rotation with respect to the line of action of the pressure's resultant force on the bellows head due to the deformations of the lever, bearings and instrument frame under the action of the static pressure and the force to be measured, and also to changes in the extraction unit's rigidity as the magnitude of the static pressure changes.

The rigidity k of the bellows extractor as a function of the torque necessary to rotate the extraction lever to the angle θ can be determined by the formula

$$k = \frac{M}{\theta} = \frac{B}{l}n = 2pFlm_\theta,$$

where B is the flexion rigidity of the bellows, p is the medium's static pressure (considered to be positive if it acts on the outside of the bellows) and the coefficient $n = 4(1 - 3\alpha - 3\alpha^2)$, just as the previously introduced coefficient m_θ, depends on the placement of the bearings along the length of the bellows. The graphs of these coefficients show (Fig. 5) that, for $\alpha \approx 0.127$ and $\alpha \approx 0.873$, the extractor rigidity does not depend on the static pressure but, with such positions of the bearings, the rigidity is approximately 2.7 times greater than the minimum rigidity, corresponding to a position of the bearings in the center of the bellows. Therefore, the definitive position of the bearings is established with account being taken of the admissible magnitude of the extractor rigidity.

A membrane extractor has an analogous character of error as a function of changes in the static pressure. This extractor has been less studied than the bellows type.

7. Dynamic Errors

In contradistinction to static accuracy, the computation of dynamic errors and analysis of methods of decreasing them are relatively more complicated, and here we shall consider only several general considerations and recommendations for lowering dynamic errors.

Very small translations of the moving system provide the transducer with faster acting force compensation than in noncompensation instruments. However, a closed compensation system, with significant inertia of the moving system and with high sensitivity of the equilibrium indicator and amplifier, acting practically like a relay for oscillations of the moving system, operates, as a rule, in an auto-oscillatory mode.

To eliminate oscillations, relatively powerful dampers are frequently used (due to the small velocities of motion of the moving system). In many of the most recent differential manometer models, damping is implemented in the sensitive element with a fluid charge serving simultaneously to protect this element from overheating. Since excessive damping lowers the instrument's speed of response, the damper must have a controllable degree of damping. This control is necessary in view of the fact that the frequency of the natural oscillations of the moving system and the natural damping change strongly with changes in the range of the quantity to be measured, and as functions of variations in the density and viscosity of the medium to be measured, the dimensions of the impact conduits, the temperature of the instrument, etc.

Recently, to decrease dynamic errors, there have been used stabilizing devices, permitting the introduction in the output signal and the compensation force of components proportional to the integral and the derivative (with respect to time) of the difference of the measured and the compensating forces. The additional complexity of the instrument occasioned by this is repaid by the capability for a significant improvement of the dynamic characteristics.

In developing the physical design of these instruments, one should take into account, the necessity for equalizing all the moving elements. In addition to decreasing the effect of external shocks and vibrations, this makes the instrument less sensitive to slants, and allows the transducer to be established in an arbitrary position.

In designing the frame, it is desirable to make provisions for mounting the transducer on shock absorbers, which might be necessary in case of particularly heavy vibration conditions.

SUMMARY

The course of development of schemes and physical designs of instruments with force compensation, and the foregoing considerations as to their accuracy, allow the following remarks to be made.

The indices of static accuracy are improved with decreases in the coefficient of noncompensation. Therefore, in designing instruments, it is necessary to try to decrease the rigidity of the flexible elements and to increase the forces (torques) to be measured. The instrument's frame and the components of the mechanism must be as rigid as possible, which must not, however, lead to an increase in weight of the moving elements.

One of the basic directions in the development of force compensation devices must be the improvement of their stability of operation for prolonged use and in conditions of changing ambient temperatures.

The necessity of increasing the instruments' speed of response, will probably produce a further tendency to decrease dimensions and, principally, weight of the moving elements of the mechanism, which requires a corresponding decrease in rigidity of the flexible elements and an increase in their stability. On the other hand, seemingly, one should expect complication of force compensation schemes by various stabilizing and auxiliary devices both for improving dynamics and for widening the possibilites of using these instruments for solving functional dependencies in logical inspection and control schemes.

FORCED PERIODIC MOTION OF A HYDRAULIC ACTUATING MECHANISM WITH A POSITIONAL LOAD

V. A. Khokhlov

Moscow

Translated from Avtomatika i Telemekhanika, Vol. 21, No. 6, pp. 929-933, June, 1960

In this paper we investigate the forced periodic motion of the piston of a hydraulic actuating mechanism, throttle controlled (slide valve), with a positional load. We determine the transient process of the mechanism during sinusoidal slide valve motion. The effect of fluid compression is estimated.

It is well known that throttle (slide valve) controlled hydraulic actuating mechanisms, in the absence of external loads, can to a high degree of accuracy, be approximated by integrating sections. However, if loading is taken into account, excluding dry friction, the motion of the piston is described by a nonlinear equation [1].

In this paper we investigate the forced motion of the piston under positional (spring) loading

$$P = kx, \tag{1}$$

where P is the load (force) applied to the piston, x is the coordinate of motion of the piston relative to its average position and k is the "stiffness" of the load.

A schematic of the mechanism is shown in Fig. 1 where 1 denotes the controlling four-chambered valve, 2 is the piston and 3 is the spring representing the load.

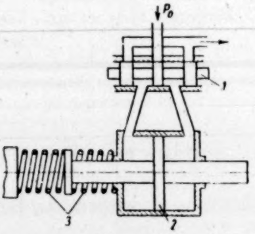

Fig. 1.

In this paper, we have made the following assumptions: there is no leakage, the coefficient of loss of the fluid in the valve chambers and the pressure p_0 in the main pressure chamber are constant. The initial overlaps or gaps in the slide valve are equal to zero and the valve openings are rectangular.

INITIAL EQUATION

Let us consider first the motion of a hydraulic actuating mechanism with an incompressible working fluid. As a result of the presence of a nonholonomic relation between the piston and the slide valve, the motion of the mechanism cannot be determined by only one force equation, for example, in d'Alembert's form. In writing the equation of motion it is necessary to take into account the equality of the forces. We will assume as a basic condition in writing the equation that the flow of the fluid is continuous. For a hydraulically actuated mechanism with a four-chambered sliding valve the condition of continuous flow for the assumptions which we have made can be presented in the form [1]

$$\frac{dx}{dt} = k_v \sqrt{1 - \frac{\Delta p}{p_0} \operatorname{sign} \rho}\, \rho, \tag{2}$$

where k_v is the steepness of the velocity characteristic at no load, ρ is the displacement of the slide valve from the average position, Δp is the pressure drop in the working cylinders due to the applied load, sign ρ is the sign of the direction of the displacement of the slide valve from the mean position (the plus sign corresponds to the movement of the slide valve to the right, Fig. 1).

Force equation (1) may be written in the form

$$\Delta p = \frac{kx}{F}, \tag{3}$$

where F is the effective area of the piston.

Substituting (3) into (2) we get the equation of motion of a hydraulic actuating mechanism in the open loop condition

$$\frac{dx}{dt} = k_v \sqrt{1 - \frac{kx}{Fp_0} \operatorname{sign} \rho}\, \rho. \tag{4}$$

In this paper we examine the forced motion of the piston due to the sinusoidal motion of the slide valve $\rho = \rho^* \sin \omega t$. The initial equation for the analysis of the mechanism takes the form

$$\frac{dx}{dt} = k_v \sqrt{1 - \frac{kx}{Fp_0} \operatorname{sign} \sin \omega t}\, \rho^* \sin \omega t. \tag{5}$$

THE REACTION OF THE PISTON TO THE SINUSOIDAL MOTION OF THE SLIDE VALVE

The reaction of the unloaded piston of a hydraulic actuating mechanism to the sinusoidal motion of the slide valve is determined by the integral equation (5) for k = 0.

For zero initial conditions

$$x=\frac{k_v\rho^*}{\omega}(1-\cos\omega t). \qquad (6)$$

In order to determine the reaction of the loaded piston ($k \neq 0$) we will write equation (5) in the form

$$\frac{dx}{\sqrt{1-\frac{kx}{Fp_0}\operatorname{sign}\sin\omega t}}=k_v\rho^*\sin\omega t\,dt. \qquad (7)$$

This equation can be integrated over intervals of ωt which are integral multiples of π inasmuch as the sign of the motion of the slide valve, sign sin ωt is constant within each interval.

Integrating equation (7) over the first interval ($0 < \omega t = \varphi_1 < \pi$) for sign sin $\omega t = +1$ we get

$$\frac{2Fp_0}{k}\sqrt{1-\frac{kx}{Fp_0}}+c_{11}=\frac{k_v\rho^*}{\omega}\cos\omega t. \qquad (7a)$$

For zero initial conditions $c_{11}=\frac{k_v\rho^*}{\omega}-\frac{2Fp_0}{k}$,

in this case

$$x=\frac{k_v\rho^*}{\omega}(1-\cos\varphi_1)-\frac{k_v^2\rho^{*2}k}{4Fp_0\omega^2}(1-\cos\varphi_1)^2. \qquad (8)$$

Performing successive integrations of equation (7) over the successive intervals, in each of which sign sin ωt is constant and applying the method of matching to determine the initial conditions in each of the successive intervals we can find a general expression for the reaction of the piston

$$x=-\Big[x_{i-1}-\frac{k_v\rho^*}{\omega}\sqrt{1+\frac{kx_{i-1}}{Fp_0}}\,(1-\cos\varphi_1)+\frac{k_v^2\rho^{*2}k}{4Fp_0\omega^2}(1-\cos\varphi_1)^2\Big]\operatorname{sign}\sin\varphi_i. \qquad (9)$$

where i = 1, 2, 3, . . . , is the interval number for integral values of π.

TRANSITIONAL PROCESS FOR POSITIVE POSITIONAL LOADING

The transitional process for positive positional loading is completely characterized by three parameters: the greatest piston displacement, the amplitude of the oscillations that are set up, and their duration.

The greatest piston displacement for k > 0 may be found from equation (8) if we substitute $\varphi_1 = \pi$;

$$x_1=\frac{k_v\rho^*}{\omega}\left(2-\frac{k_v\rho^*}{\omega}\frac{k}{Fp_0}\right). \qquad (10)$$

Thus, the greatest displacement of the piston will exceed that at no-load by

$$\Delta x_1=\left(\frac{k_v\rho^*}{\omega}\right)^2\frac{k}{Fp_0}. \qquad (10a)$$

Let us find the ratio between the amplitude of the slide valve displacement and its oscillation frequency $\varkappa = \rho^*/\omega$ during which the pressure developed by the liquid becomes equal to the positional loading during the furthest displacement of the piston. For this condition $x_1 = Fp_0/k$ and equation (10) takes the form

$$\frac{Fp_0}{k}=k_v\varkappa\left(2-k_v\varkappa\frac{k}{Fp_0}\right). \qquad (10b)$$

Solving this equation for $\varkappa$, we get

$$\varkappa=\frac{\rho^*}{\omega}=\frac{Fp_0}{k_vk}. \qquad (10c)$$

Thus, we see that a throttle-controlled hydraulic actuating mechanism with sinusoidal slide valve displacement and positional loading will have the mode of operation of the move only for the condition

$$\frac{\rho^*}{\omega}<\frac{Fp_0}{k_vk}. \qquad (10d)$$

We can find the amplitude of the resulting piston oscillations x^* from equation (9) if we let x = 0 for $\cos\varphi_1 = 0$. For this case

$$x^*-\sqrt{1+\frac{kx^*}{Fp_0}}\frac{k_v\rho^*}{\omega}+\frac{k_v^2\rho^{*2}k}{4Fp_0\omega^2}=0. \qquad (10e)$$

Solving this equation for x^* we find the amplitude of the resulting piston oscillations

$$|x^*|=k_v\frac{\rho^*}{\omega}\left(1-\frac{kk_v}{4Fp_0}\frac{\rho^*}{\omega}\right).$$

Thus, for the established mode of operation the phase shift between the motion of the piston under positional loading and the motion of the slide valve is $-\pi/2$, this corresponds to the phase shift for the unloaded actuating mechanism. The amplitude characteristic is a function of the ratio of the valve displacement to the frequency of the introduced signal ρ^*/ω and depends upon the parameters of the mechanism: the area F, pressure p_0, steepness of the velocity characteristic at no-load k_v and the load stiffness k.

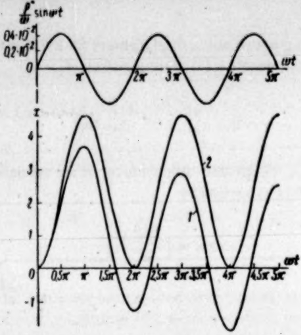

Fig. 2.

The determination of the duration of the transitional process is difficult in the general form. Therefore, it may be found by orientation from the character of the changes in the small deviations x_1 of the piston as computed from equation (9).

As an example of the application of the results which have been obtained, we show in Fig. 2 the transitional process in the motion of the piston of the hydraulic actuating mechanism having the following dimensions and parameters: $F = 44\ \text{cm}^2$, $\rho_0 = 50\ \text{kg/cm}^2$, $k_v = 530\ \text{sec}^{-1}$ and $k = 400$ kg/cm. The transitional process (curve 1) has been plotted for the case in which the piston load during the maximum piston displacement is $\frac{2}{3}\rho_0 F$; this corresponds to $\rho^*/\omega = 0.42 \times 10^{-2}$ cm · sec. We also show in Fig. 2 the transitional process for an unloaded piston for the same excitation (curve 2).

ESTIMATION OF THE EFFECT OF FLUID COMPRESSION

Before we evaluate the effect of the compressibility of the fluid enclosed in the force cylinder upon the motion of the piston we will find the dependence of the motion of the cylinder upon changes in the applied force P_0 (Fig. 3a). In the figure Δx denotes the displacement of the cylinder due to the action of the force ΔP and l_0 is the depth of the fluid column in the cylinder.

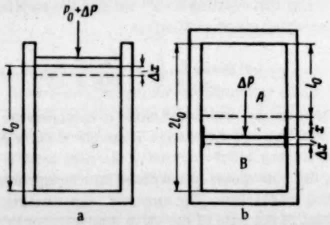

Fig. 3. Diagram of the force cylinder. a) a) one sided, b) two sided

Assuming that the cylinder and the piston have absolute stiffness and that there are no losses, we may write

$$\gamma_0 V_0 = \gamma_1 V_1,$$

where γ_0, V_0 are the specific gravity and initial volume of the fluid under pressure due to the applied force P_0; γ_1, V_1 are the specific gravity and volume of the fluid after the applied force P_0 has been increased by ΔP.

Since $V_1 = V_0$ and $\Delta V = F\Delta x$, we get

$$\Delta x = \frac{V_0(\gamma_1 - \gamma_0)}{F\gamma_1}.$$

We may write the following expression for the specific gravity of the fluid*

$$\gamma_1 = \gamma_0 + k_\gamma \frac{\Delta P}{F},$$

where k_γ is a coefficient of proportionality. We may now write

$$\Delta x = \frac{k_\gamma V_0 \Delta P}{\left(\gamma_0 + k_\gamma \frac{\Delta P}{F}\right) F^2}. \tag{11}$$

The above equation shows that the piston displacement is proportional to the applied force and depends upon the change in the specific gravity of the fluid due to this force.

Let us evaluate the influence of the second factor. Comparing equations (11) and (6) in [2] we notice that $\dfrac{\gamma_0 + k_\gamma \frac{\Delta P}{F}}{k_\gamma} = G -$ is the modulus of volume elasticity (bulk modulus).

The modulus of elasticity of the working fluid in the hydraulic system over the range of pressure changes of up to 200-300 kg/cm² is practically constant. Then, $k_\gamma = \Delta P/F$ in equation (11) is very close to zero and the specific gravity of the fluid may be considered constant in magnitude, i.e., $\gamma_1 = \gamma_0$. Under these conditions equation (11) may be written in the form

$$\Delta x = \frac{V_0 \Delta p}{FG} = \frac{l_0 \Delta P}{FG}. \tag{11a}$$

The above analysis shows that if we take into account the losses in the compressible fluid passing through the slot in the valve we can make use of the equations for incompressible fluids. With this in mind we will represent the hydraulic actuating mechanism by means of the schematic of Fig. 4. Here 1 is a spring imitating the stiffness of the applied load, 2 is a spring imitating the stiffness of the fluid, x_1 is the displacement of the fluid cross-section in the vicinity of the boundary walls of the force cylinder (in cross sections I and II).

---

* According to [2] this equation is correct for the case where the applied force does not produce a pressure of more than (20-30) × 10^3 kg/cm³ in the fluid.

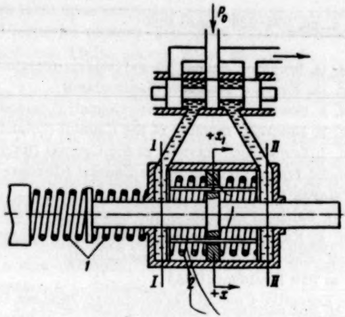

Fig. 4. Equivalent schematic of a hydraulic actuating mechanism which takes into consideration the compression of the working fluid.

We will find the change in stiffness of the fluid enclosed in the force cylinder (Fig. 3b) and the displacement of the piston due to the action of the applied force ΔP. Examining the work of the actuating mechanism only for the actuator we note that the fluid in chambers A and B, Fig. 3b, will always be under excess pressure and the applied load, acting on the piston, does not create a pressure drop exceeding the pressure in the main pressure chamber. Therefore, the pressure in the working cylinder cannot fall below zero (excess). Therefore, the stiffness of the fluid in the cylinders, according to equation (11a) may be represented in the form

$$k_{f\ A,B} = \frac{FG}{l_0 + x}.$$

Therefore, the total stiffness k_f is the sum of k_{fA} + k_{fB}:

$$k_f \quad \frac{2l_0GF}{l_0^2 - x^2}.$$

The piston displacement under the action of the applied force ΔP is

$$\Delta x = \frac{l_0^2 - x^2}{2l_0GF}\,\Delta P. \tag{11b}$$

Let us now examine the equations of motion of an actuating mechanism, taking into consideration the compressibility of the fluid.

According to the equivalent schematic of the mechanism (Fig. 4) the motion of the piston is determined by three equations:

(1) the force equation (3)

(2) the equation of flow through the slide valve (2), using the new designations this equation takes the form

$$\frac{dx_1}{dt} = k_v \sqrt{1 - \frac{\Delta p}{p_0}\,\mathrm{sign}\,\rho}\ \rho;$$

(3) the equation connecting the pressure drop, due to the load in the working chambers, with the relative piston displacement; this equation according to (11b) is of the form

$$kx = \frac{2l_0GF}{l_0^2 - x^2}(x_1 - x). \tag{12}$$

The simultaneous solution of the indicated equations gives us the equation

$$\frac{kl_0^2 + 2l_0GF - 3kx^2}{2l_0GF}\,\frac{dx}{dt} = k_v \sqrt{1 - \frac{kx}{p_0}\,\mathrm{sign}\,\rho}\ \rho. \tag{13}$$

For $\rho = \rho^* \sin \omega t$ equation (13) may be integrated in a similar manner to equation (7).

Neglecting the changes in the stiffness of the liquid during the motion of the piston,† we get

$$\frac{dx}{dt} = \frac{2GF}{kl_0 + 2GF} k_v \sqrt{1 - \frac{kx}{p_0}\,\mathrm{sign}\,\rho}\ \rho. \tag{14}$$

Comparing the above equation with equation (4) obtained in the analysis of the motion of an actuating mechanism with an incompressible fluid we note that the right sides of the equations differ only by a constant multiplier $2GF/kl_0 + 2GF$. This multiplier, for $kl_0 \ll 2GF$, a condition which as a rule exists in practice, is close to unity. Therefore, the compressibility of the fluid in the force cylinder has a relatively small effect upon the motion of a piston with only one positional load.

LITERATURE CITED

1. V. A. Khokhlov, "The analysis of the motion of a loaded hydraulic actuating mechanism with feedback," Avtomat. i Telemekh. 18, 9 (1957).‡
2. M. Kornfel'd, Elasticity and Strength of Fluids [in Russian] (Gostekhizdat, 1951).

---

† Under this condition the deviation of the curve for the transitional piston process from the curve computed without taking into consideration the compressibility of the fluid will exceed the deviation obtained from the solution of equation (13).

‡ See English translation.

INFORMATION

INTERNATIONAL FEDERATION OF AUTOMATIC CONTROL (IFAC) AND ITS FIRST CONGRESS

Translated from Avtomatika i Telemekhanika, Vol. 21, No. 6, pp. 934-937, June, 1960

I. Brief History of its Development

The question of forming the International Federation of Automatic Control was first brought up in September, 1956, during the International Congress of Automatic Regulation in Heidelberg (West Germany).

The initiating group of scientists and engineers from among the participants in the Congress, at a special meeting, adopted a resolution signed by 26 representatives of various countries, among them representatives of the USSR, in which the formation of the International Federation of Automatic Control was approved.

It was pointed out in the resolution that the IFAC is created for the purpose: 1) of promoting the exchange of scientific information in the area of automatic control between the member-countries and 2) of organizing international congresses of automatics.

At the same meeting a preparatory committee was elected to compose a draft of rules and regulations of the IFAC and call a first organizational meeting of representatives of the interested countries, a General Assembly.

The First General Assembly of the IFAC, held in September, 1957, in Paris, approved the code of rules of the IFAC and elected the managing organ of the Federation, the Executive Council, consisting of 11 members and headed by G. Chestnut (USA), the president of the IFAC.

The General Assembly decided to call the First Congress of the IFAC in Moscow in 1960.

The Executive Council of the IFAC of the first staff did great work in the organizational strengthening of the Federation. Six special scientific-technical committees were created by it for the development of the international exchange of scientific information in the field of automatics. The Executive Council also established the Advisory Committee of the IFAC.

The Second General Assembly was called in September, 1959, in Chicago. It approved a new code of rules of the Federation and the draft of the scientific program of the First Congress of the IFAC, worked out by the Soviet Union's National Committee of Automatic Control [see Avtomat. i Telemekh. 22, 1 (1959)].*

In accordance with the Code of Rules of the General Assembly a new staff of the Executive Council was elected, as well as a new president of the IFAC, Professor A. M. Letov, a representative of the USSR.

The Executive Council now includes the following:

Prof. A. M. Letov, President (USSR)
Prof. E. Gereke, First Vice-President (Switzerland)
Prof. O. Benedict, Second Vice-President (Belgium)
Prof. M. Kyueno, Treasurer (Switzerland)
Prof. J. Howells, member of the Council (England)
Prof. P. Nowacki, member of the Council (Poland)
Prof. J. Evangelisti, member of the Council (Italy)
Prof. Ed Trnka, member of the Council (Czechoslovakia)
Dr. H. Balchen, member of the Council (Norway)
Prof. K. Kaneshige, member of the Council (Japan)
Dr. G. Chestnut, member of the Council as Past President (USA)

The Executive Council has designated Professor D. Eckman (USA) as chairman of the Advisory Comitteee and Dr. J. Loeb (France) as vice-chairman, Dr. G. Ruppel (West Germany) as honorary secretary of the IFAC and Professor V. Broid (France) as honorary editor of the "IFAC Bulletin."

The chairman of the scientific-technical committees of the IFAC are: Committee on Theory – Academician B. N. Petrov (USSR), Committee on Technical Resources – Dr. D. Boromissa (Hungary), Committee on the Utilization of Automatics – Dr. D. Moseley (USA), Committee on Education – Prof. A. Marino (Italy), Committee on Terminology and Designations – Prof. E. Gereke (Switzerland), Committee on Bibliography – Prof. V. Oppelt (West Germany).

The Second General Assembly noted the great work performed by the Executive Council of the first staff and issued a special resolution expressing appreciation to Dr. G. Chestnut and certain other workers in the IFAC for their contribution to the creation of the Federation. A resolution to hold the Second Congress of the IFAC in Switzerland in 1963 was adopted at the Assembly.

In the preceding period the activity of the IFAC was devoted primarily to preparations for the First Congress of the Federation.

In all, 23 countries are represented by their national organizations in the IFAC, and this number includes a majority of the countries most advanced in industrial respects.

On January 1, 1960 the IFAC became a member of the International Council of Scientific and Technical Societies.

II. The Soviet Union's National Committee of Automatic Control

The Soviet Union is represented in IFAC by its National Committee of Automatic Control, formed in the

---

*See English translation.

Academy of Sciences of the USSR. The representative of the National Committee of the USSR is Academician V. A. Trapeznikov.

The National Committee unites the most eminent specialists of the Soviet Union in automatics and in its work leans upon territorial groups formed in scientific and industrial centers: Leningrad, Kiev, Novosibirsk, Sverdlovsk, Tbilis, Erevan, Baku, and Ivanov.

A number of scientific-technical committees have been formed in the Soviet Union's National Committee of Automatic Control:

1) On the theory of automatic regulation and control — chairman, Prof. Ya. Z. Tsipkin; vice-chairman, Prof. A. A. Krasovskii; scientific secretary, A. N. Korolev, Candidate in Technical Sciences (C. T. S.).

2) On technical resources of automatics and remote control — chairman, Prof. B. S. Sotskov (Corresp. member); vice-chairman, D. I. Ageikin, C.T. S.; scientific secretary, I. E. Dekabrun, C.T.S.

3) On automatic electrical operation and its application to electrical machinery — chairman, Prof. M. G. Chilikin; vice-chairman, Prof. I. I. Petrov; scientific secretary, A. A. Sirotin, C.T.S.

4) On the automation of continuous productive processes in the metallurigcal, chemical, energy and other fields of industry — chairman, E. L. Stefani, C.T.S.; vice-chairman, A. Ya. Lerner, D.T.S.; scientific secretary, C. P. Khlebnikov, Engineer.

5) On the automation of productive processes in machine building — chairman Academician V. I. Dikushin; vice-chairman, Academician I. I. Artobolevskii; scientific secretary, V. M. Raskatov, Engineer.

6) On the automation of productive process in agriculture — chairman, Academician VASKhNIL I. A. Budzko; vice-chairman, N. N. Levykin, C.T.S.; scientific secretary, K. M. Poyarkov, Engineer.

7) On terminology — chairman, M. A. Gavrilov; vice-chairman, A. V. Khramoi, C.T.S.; scientific secretary, E. V. Babicheva, Engineer.

The Soviet Union's National Committee of Automatic Control gave its assent to the Executive Committee of the IFAC to hold the First International Congress of the Federation in Moscow, and, consequently, assumes responsibility for the organization of that Congress.

III. The First Congress of the IFAC

The First Congress of the IFAC will be held June 27 to July 7, 1960 on the premises of Moscow University on Lenin Heights.

An organizing committee has been formed to carry out the practical work in preparing for the Congress: Academician V. A. Trapeznikov (chairman), Academician, B. N. Petrov (vice-chairman), V. V. Karibskii, Engineer (vice-chairman), B. N. Naumov, C.T.S. (vice-chairman) and N. O. Biryukov, C.T.S. (scientific secretary).

The organizing committee is performing much preparatory work, with the active support of the national organization-members of the IFAC. Great interest in the coming Congress is observed on the part of specialists of many countries of the world. A great number of reports have been submitted to the organizing committee, from 21 countries, and from them 285 reports have been selected.

The reports selected for presentation to the Congress are distributed by country as follows:

Austria	5	Canada	1	France	9
England	28	China	6	West Germany	15
Belgium	4	Norway	3	Czechoslovakia	5
Hungary	5	Poland	11	Switzerland	1
E. Germany	3	Rumania	6	Sweden	1
India	1	USSR	81	Yugoslavia	2
Italy	7	USA	73	Japan	18

The reports have been divided into three groups:

I. Theory of automatic regulation and control.

II. Technical resources of automatics and remote control.

III. Applications of automatics.

Within each of these groups the reports have been subdivided according to related scientific indications into separate sections. The ten sections of Group I included 143 reports, the five sections of Group II include 56, and the six sections of Group III include 86 reports. Simultaneous work of up to 11 sections is provided for.

The following is an enumeration of the sections of the Congress, with an indication of the number of reports pertaining to them.

I. 1. Theory of continuous linear systems — 23
I. 2. Theory of continuous nonlinear systems — 14
I. 3. Theory of discrete systems — 25
I. 4. Stochastic problems — 18
I. 5. Theory of optimal systems — 12
I. 6. Theory of self-adjusting systems — 20
I. 7. Theory of structures and the construction of signals — 7
I. 8. Special mathematical problems — 13
I. 9. Modeling and experimental methods of investigation — 11
II. 1. Electrical and magnetic elements of systems of regulation — 9
II. 2. Electrical computing and modeling equipment, programming elements and machines — 10
II. 3. Counters, elements and systems of automatic control and remote control of productive processes — 8
II. 4. Pneumatic means of automatics and calculating technique — 11
II. 5. Instruments and equipment of automatic control — 18
III. 1. Automation of machine building—10
III. 2. Automation of energy systems — 24

- III. 3. Automation of the chemical and petroleum processing industry – 8
- III. 4. Automated electrical operation and electrical machines – 12
- III. 5. Automation of metallurgical processes – 17
- III. 6. Unclassified problems – 9

An additional six reports were presented to combined sessions of some sections of Group III.

The names of the sections give a complete enough representation of the subject of the accepted reports. A characteristic feature should be noted – the great attention devoted in the reports to the application of computer technique for the control of complicated forms of technological processes, including the control of nuclear processes, the application of optimal, extreme and self-adjusting systems.

On the whole the reports contain very valuable scientific information which sheds light on the experience and the level of knowledge attained in the area of automatics, and creates the basis for scientific discussion of the most important current problems of automatics.

The reports were prepared in conformance with the motto: to theory – practical applicability; to technical resources – maximum reliability; to applications – the greatest effectiveness.

The publication of the reports in the form of brochures in the Russian and English languages enables all the participants in the Congress to share more fruitfully in the scientific discussion, since they will have become acquainted with the contents of the reports.

In the future the papers of the Congress will be published in a separate issue which can be purchased by any one who wishes to purchase it.

Besides the sectional sessions, two plenary sessions are included in the program of the Congress. At the first of these a report by Academician V. A. Trapeznikov on the basic tasks of contemporary automatics will be heard and discussed, and in the final session the work of the Congress will be summed up.

Within the framework of the Congress there will be organized an international exhibition of books and journals on questions of automatics, an exhibit of instruments and equipment of automatics and telemechanics based on new principles, and also a demonstration of scientific and popularized scientific films on automatics and telemechanics.

During the period of the Congress it is proposed to conduct a series of lectures on current problems of automatics by eminent foreign scientists for the Soviet community.

The program of the Congress provides for visits of its participants to cultural and to more than 30 scientific and educational institutions and industrial enterprises in Moscow, Leningrad, and Kiev.

The participants in the technical excursions will become acquainted with the work done in the Soviet Union in the creation and utilization of various systems of automatic regulation and control, its resources in computing and measuring techniques, remote and telemechanical systems, automated lines and automated industrial production, machine tools with program control, and also with the state of higher education in educational institutions.

During the working period of the Congress there will be a session of the leaders of the IFAC organs, the Executive Council and the scientific-technical committees, which have to consider a series of questions regarding the current activities of the Federation and its plans for the future.

IV. General Schedule of the Congress

June 24 – Sessions of the Executive Council and the scientific-technical committees of the IFAC
June 25 – General Assembly of the IFAC; sessions of the scientific-technical committees of the IFAC
June 27 – morning – official opening of the Congress of the IFAC, plenary session
June 27 – evening – sectional sessions
June 28 to July 1 – sectional sessions and technical excursions in Moscow
July 2 – morning – plenary session
July 2 – evening – session of the Executive Council of the IFAC
July 3 to July 7 – technical excursions in Moscow, Leningrad, and Kiev

The Moscow International Congress of Automatic Control, as the First Congress of the IFAC, is destined to play an important role in the matter of strengthening international scientific contacts between specialists in this field of science, which is the basis for the development of one of the fundamental and very perspective directions of new technique.

N. O. Biryukov

ESTIMATING THE MEAN SQUARE DEVIATION FROM A GIVEN TRAJECTORY

E. A. Barbashin

Sverdlovsk

Translated from Avtomatika i Telemekhanika, Vol. 21, No. 7, pp. 941-950, July, 1960
Original article submitted March 19, 1960

New methods for estimating the mean square deviation from a given trajectory are given. The estimates obtained provide a method of choosing the external influences so that this mean square value will be small. Conditions are given for the existence of motion exactly over a given trajectory.

We consider the system of differential equations

$$\frac{dx_i}{dt} = \sum_{k=1}^{n} a_{ik}(t)\, x_k + \sum_{k=1}^{m} b_{ik} u_k(t) \quad (i = 1, 2, \ldots, n;\ m \leqslant n). \tag{1}$$

Here b_{ik} are constants, $u_k(t)$ scalar functions which we shall call control functions, and $a_{ik}(t)$ continuous functions of time. The system may be written in the following matrix form:

$$\frac{d\mathbf{x}}{dt} = \mathbf{A}(t)\,\mathbf{x} + \sum_{k=1}^{m} \mathbf{b}_k u_k(t), \tag{2}$$

where the vectors $\mathbf{b}_k(b_{1k}, b_{2k}, \ldots, b_{nk})$ will be assumed to be linearly independent.

Suppose for $t_0 \leq t \leq t_0 + T$ we have given a curve $x_i = f_i(t)$ $(i = 1, 2, \ldots, n)$, or, in vector form, $\mathbf{x} = \mathbf{f}(t)$. It is required to find a system of control functions $u_k(t)$ for which the solution $x_i(t)$ of system (1), with initial conditions $x_i(t_0) = f_i(t_0)$, will coincide with the given functions $x_i = f_i(t)$ for $t_0 \leq t \leq t_0 + T$. In other words, it is required to choose the control functions so that the given trajectory will be realized.

From the theory of dynamic programming it is clear that for $m < n$ this problem need not even have a solution. In this case [1, 2] there remains the question of choosing a system of control functions which will yield the best approximation to the given trajectory. However, it should be noted that even in the simplest case, when one attempts to guarantee a minimum of the mean square deviation from a given trajectory, the existent methods [2, 3] lead to solving boundary value problems for systems of ordinary differential equations, in which the form of the system changes when the functions $f_i(t)$ change.

Ya. N. Roitenberg [4], following an idea of A. Ya. Lerner, indicated another approach to solving the problem: he described a method of constructing piecewise constant control functions guaranteeing that the trajectory $\mathbf{x} = \mathbf{x}(t)$ of Equation (2) intersects the given trajectory $\mathbf{x} = \mathbf{f}(t)$ at prescribed moments of time $t_0, t_1, \ldots, t_r$ in the interval $[t_0, t_0 + T]$. However, this method of solution may prove to be unsatisfactory in many cases for the simple reason that small perturbations in the control functions found in this manner lead to the loss of the property for which they were constructed; i.e., the perturbed trajectory of Equation (2) may not intersect the given trajectory at a single moment of time in the given interval.

In this paper, following the first of the two directions indicated for solving the problem, we give up the aim of making the deviation a minimum, preferring to indicate an approach whereby the deviation may simply be made small. We assume that the deviation $\|\mathbf{z}\|$ of the quantity of interest to us may be associated with the deviation $\|\mathbf{y}\|$ of another quantity by means of the inequality

$$\|\mathbf{z}\| \leqslant A\,\|\mathbf{y}\|, \tag{3}$$

and assume that the minimum $\|\mathbf{y}\|$ is easily found. In this case, one may replace the problem of finding $\min\|\mathbf{z}\|$ by the problem of finding $\min\|\mathbf{y}\|$. Since these are different problems, we obtain a somewhat worse approximation, which, however, may prove to be accurate in practice. Such an approach to the problem decreases significantly the calculational difficulties, since the method, while still leading to the solution of a system of ordinary differential equations, may be carried through once and for all for a given matrix $\mathbf{A}(t)$, and is suitable when the given trajectory $\mathbf{f}(t)$ is varied, as well as when the control vectors $\mathbf{b}_i$ are. This solution admits a simple geometrical interpretation; consequently, it may be modelled, in the sense that a simple calculational analog device, using continuously varying parameters, may be employed in place of complicated digital computers to solve the problem.

In this paper the question of estimating the mean square value of the deviation is considered; the question of estimating the maximum deviation will be taken up in a succeeding paper.

1. Estimate for the Mean Square Deviation

In Equation (2) we introduce the change of variables $\mathbf{z} = \mathbf{x} - \mathbf{f}(t)$ and obtain the new equation

$$\mathbf{z} = \mathbf{A}(t)\,\mathbf{z} + \sum_{k=1}^{m} \mathbf{b}_k u_k(t) + \mathbf{A}(t)\,\mathbf{f}(t) - \dot{\mathbf{f}}(t). \tag{4}$$

With the aim in mind of estimating the solution to Equation (4) determined by the initial condition $\mathbf{z}(t_0) = 0$, and for simplicity, setting $t_0 = 0$ in all that follows, we write the solution $\mathbf{z}(t)$ according to Cauchy's formula ([5], page 172)

$$\mathbf{z}(t) = \int_0^t \mathbf{F}(t)\,\mathbf{F}^{-1}(\tau)\left[\sum_{k=1}^{m} \mathbf{b}_k u_k(\tau) + \right. \\ \left. + \mathbf{A}(\tau)\,\mathbf{f}(\tau) - \dot{\mathbf{f}}(\tau)\right] d\tau. \tag{5}$$

Here $\mathbf{F}(t)$ is the fundamental matrix satisfying the equation

$$\mathbf{F}(t) = \mathbf{A}(t)\,\mathbf{F}(t),$$

$\mathbf{F}^{-1}(t)$ being the inverse matrix.

Introducing the notation

$$\mathbf{y}(t) = \sum_{k=1}^{m} \mathbf{b}_k u_k(t) + \mathbf{A}(t)\,\mathbf{f}(t) - \dot{\mathbf{f}}(t), \tag{6}$$

we obtain

$$\mathbf{z}(t) = \int_0^t \mathbf{F}(t)\,\mathbf{F}^{-1}(\tau)\,\mathbf{y}(\tau)\,d\tau. \tag{7}$$

Theorem 1. There exists a least positive constant L such that

$$\|\mathbf{z}\| = \left[\int_0^T \sum_{i=1}^{n} z_i^2(t)\,dt\right]^{1/2} \leqslant L\left[\int_0^T \sum_{i=1}^{n} y_i^2(t)\,dt\right]^{1/2}. \tag{8}$$

The number L may be found from the formula

$$L^2 = \int_0^T \sum_{i=1}^{n} x_i^2(t)\,dt, \tag{9}$$

where the functions $x_i(t)$ satisfy the system of equations

$$\begin{aligned} \dot{x}_i &= \sum_{k=1}^{n} a_{ik}(t)\,x_k - \frac{p_i}{\lambda}, \\ \dot{p}_i &= -\sum_{k=1}^{n} a_{ki}(t)\,p_k + x_i \quad (i = 1, 2, \ldots, n) \end{aligned} \tag{10}$$

under the boundary conditions

$$\begin{gathered} x_i(0) = 0; \quad p_i(T) = 0; \\ \int_0^T \sum_{i=1}^{n} p_i^2(t)\,dt = \lambda^2 \quad (i = 1, 2, \ldots, n). \end{gathered} \tag{11}$$

The number L is also equal to the largest value of λ for which the boundary value problem (10)-(11) is solvable.

However, the solution of the boundary value problem (10)-(11) may entail considerable difficulty; therefore, we shall present a convenient method of estimating the number L.

Theorem 2. The inequality $L \leq L_1$, holds, where

$$L_1^2 = \int_0^T\int_0^t \sum_{i,k=1}^{n} w_{ik}^2(t, \tau)\,d\tau\,dt. \tag{12}$$

Here $w_{ik}(t,\tau)$ designate the elements of the matrix $\mathbf{F}(t)\mathbf{F}^{-1}(\tau)$. We note that, if $\mathbf{A}$ is a constant matrix, then $\mathbf{F}(t)\mathbf{F}^{-1}(\tau) = \mathbf{F}(t-\tau)$.

2. Choice of the Control Functions

After L or L_1 is found by some means or another, in order to obtain the most accurate estimate of the mean square deviation, it is necessary to choose the control functions so that the quantity

$$\|\mathbf{y}\| = \left(\int_0^T \sum_{i=1}^{n} y_i^2(t)\,dt\right)^{1/2}$$

is a minimum. For convenience we use the notation

$$\mathbf{r}(t) = \dot{\mathbf{f}}(t) - \mathbf{A}(t)\,\mathbf{f}(t).$$

The problem consists in choosing for each value t such values $u_1(t), u_2(t), \ldots, u_m(t)$, which will guarantee the value of the quantity $\|\mathbf{y}\|$ to be a minimum. But the quantity $\|\mathbf{y}\|$ will be minimal if, and only if, for each value t in the interval $[0, T]$, the quantity

$$|\mathbf{y}(t)| = \left|\sum_{i=1}^{m} \mathbf{b}_i u_i(t) - \mathbf{r}(t)\right|$$

is also minimal. Here $|\mathbf{y}(t)|$ denotes the length of the vector $\mathbf{y}(t)$.

We consider now the hyperplane Q spanned by the vectors $\mathbf{b}_1, \mathbf{b}_2, \ldots, \mathbf{b}_m$. It is clear that the magnitude $|\mathbf{y}(t)|$ determines the distance from the point A, whose radius-vector is $\mathbf{r}(t)$, to some point B with radius-vector $\sum_{i=1}^{m} \mathbf{b}_i u_i(t)$, lying on the plane Q.

Thus, $|\mathbf{y}(t)|$ will be the least for the given t, if the number $u_i(t)$ is chosen so that the point B is the projection of the point A onto the plane Q, that is so that $|\mathbf{y}(t)|$ will be the distance from the point A to the plane Q.

According to [6] (page 205), we have

$$AB^2 = \frac{\Gamma(\mathbf{b}_1, \mathbf{b}_2, \ldots, \mathbf{b}_m, \mathbf{r}(t))}{\Gamma(\mathbf{b}_1, \mathbf{b}_2, \ldots, \mathbf{b}_m)}, \qquad (13)$$

where

$$\Gamma(\mathbf{b}_1, \mathbf{b}_2, \ldots, \mathbf{b}_m, \mathbf{r}(t)) =$$

$$= \begin{vmatrix} (\mathbf{b}_1, \mathbf{b}_1)(\mathbf{b}_1, \mathbf{b}_2) \cdots (\mathbf{b}_1, \mathbf{b}_m)(\mathbf{b}_1, \mathbf{r}(t)) \\ \cdots\cdots\cdots\cdots\cdots\cdots\cdots\cdots \\ (\mathbf{b}_m, \mathbf{b}_1)(\mathbf{b}_m, \mathbf{b}_2) \cdots (\mathbf{b}_m, \mathbf{b}_m)(\mathbf{b}_m, \mathbf{r}(t)) \\ (\mathbf{r}(t), \mathbf{b}_1)(\mathbf{r}(t), \mathbf{b}_2) \cdots (\mathbf{r}(t), \mathbf{b}_m)(\mathbf{r}(t), \mathbf{r}(t)) \end{vmatrix}$$

and

$$\Gamma(\mathbf{b}_1, \mathbf{b}_2, \ldots, \mathbf{b}_m) =$$

$$= \begin{vmatrix} (\mathbf{b}_1, \mathbf{b}_1)(\mathbf{b}_1, \mathbf{b}_2) \cdots (\mathbf{b}_1, \mathbf{b}_m) \\ \cdots\cdots\cdots\cdots\cdots \\ (\mathbf{b}_m, \mathbf{b}_1)(\mathbf{b}_m, \mathbf{b}_2) \cdots (\mathbf{b}_m, \mathbf{b}_m) \end{vmatrix}$$

is Gramme determinant, $(\mathbf{b}_i, \mathbf{b}_k)$ denoting the scalar product. Since the vectors $\mathbf{b}_1, \mathbf{b}_2, \ldots, \mathbf{b}_m$ are linearly independent, $\Gamma(\mathbf{b}_1, \mathbf{b}_2, \ldots, \mathbf{b}_m) \neq 0$.

Let $u_1(t), \ldots, u_m(t)$ be chosen to minimize $|\mathbf{y}(t)|$; then

$$(\mathbf{y}(t), \mathbf{b}_k) = \left(\sum_{i=1}^{m} \mathbf{b}_i u_i(t) - \mathbf{r}(t), \mathbf{b}_k\right) = 0$$

$(k = 1, 2, \ldots, m)$, since the vector $\mathbf{y}(t)$ is orthogonal to all of the vectors $\mathbf{b}_k$.

To determine $u_i(t)$, we have the system of equations

$$\sum_{i=1}^{m} (\mathbf{b}_k, \mathbf{b}_i)\, u_i(t) = (\mathbf{r}(t), \mathbf{b}_k) \quad (k = 1, 2, \ldots, m). \; (14)$$

The determinant of this system is equal to $\Gamma(\mathbf{b}_1, \mathbf{b}_2, \ldots, \mathbf{b}_m)$ and therefore is different from zero.

Denoting $H^2 = \min \int_0^T |\mathbf{y}(t)|^2\, dt$, according to (13), we have

$$H^2 = \frac{1}{\Gamma(\mathbf{b}_1, \mathbf{b}_2, \ldots, \mathbf{b}_m)} \int_0^T \Gamma(\mathbf{b}_1, \mathbf{b}_2, \ldots, \mathbf{b}_m, \mathbf{r}(t))\, dt. \qquad (15)$$

These formulas take on a particularly simple form if the system of vectors $\mathbf{b}_1, \mathbf{b}_2, \ldots, \mathbf{b}_m$ is orthogonal, i.e., if $(\mathbf{b}_i, \mathbf{b}_k) = 0$ for $i \neq k$ and $(\mathbf{b}_i, \mathbf{b}_i) = 1$. In this case, we have $u_i(t) = (\mathbf{r}(t), \mathbf{b}_i)$ $(i = 1, 2, \ldots, m)$:

$$H^2 = \int_0^T \mathbf{r}^2(t)\, dt - \sum_{i=1}^{m} \int_0^T (\mathbf{r}(t), \mathbf{b}_i)^2\, dt. \qquad (15')$$

If there is only one control function, then

$$u(t) = \frac{(\mathbf{r}(t), \mathbf{b})}{|\mathbf{b}|^2}$$

and

$$H^2 = \int_0^T \mathbf{r}^2(t)\, dt - \frac{1}{|\mathbf{b}|^2} \int_0^T (\mathbf{r}(t), \mathbf{b})^2\, dt. \qquad (15'')$$

Formula (15) indicates that the exact realization of the given trajectory is possible only if, at each moment of time,

$$\Gamma(\mathbf{b}_1, \mathbf{b}_2, \ldots, \mathbf{b}_m, \mathbf{r}(t)) = 0. \qquad (16)$$

Equation (16) means that the curve $z = \mathbf{r}(t)$ lies in the plane spanned by the vectors $\mathbf{b}_1, \mathbf{b}_2, \ldots, \mathbf{b}_m$.

Otherwise, the solvability conditions for the system $\sum_{i=1}^{m} \mathbf{b}_i u_i(t) - \mathbf{r}(t) = 0$ could be formulated in purely algebraic language ([7], page 40).

3. Choice of the Optimal System of Control Vectors

Having found H, we obtain the formula $\|\mathbf{z}\| \leq LH$ for estimating the mean square deviation. If the quantity H is large, then, in order to decrease $\|\mathbf{z}\|$ one must enlarge the collection of control functions. If, however, the set of control functions may not be enlarged, then in certain problems, for a given trajectory $\mathbf{x} = \mathbf{f}(t)$, one may always choose an optimal system of control vectors $\mathbf{b}_1, \mathbf{b}_2, \ldots, \mathbf{b}_m$, i.e., a system guaranteeing a minimal value for H.

We consider the matrix $C = \{c_{ik}\}$, where $c_{ik} = \int_0^T r_i(t)\, r_k(t)\, dt$ and $r_i(t)$ are the projections of the vector $\mathbf{r}(t)$. The eigenvalues of this matrix are nonnegative. We arrange them in increasing order:

$$\lambda_1 \geqslant \lambda_2 \geqslant \cdots \geqslant \lambda_n \geqslant 0.$$

To each eigenvalue λ_k there corresponds at least one eigenvector $\mathbf{b}_k$; it is known ([6], page 20) that it is possible to orthonormalize a system of eigenvectors. Thus, we obtain an orthogonal system of eigenvector for the matrix $\mathbf{C}$.

Theorem 3. The orthonormal system of eigenvectors $\mathbf{b}_1, \mathbf{b}_2, \ldots, \mathbf{b}_m$ of the matrix $\mathbf{C}$ is an optimal system of control vectors, in that, if the system of control functions is taken according to (14), then

$$H^2 = \int_0^T \mathbf{r}^2(t)\,dt - \sum_{i=1}^{m} \lambda_i = \sum_{k=m+1}^{n} \lambda_k. \qquad (17)$$

We note now that the exact realization of the trajectory by choosing an optimal system of control functions and control vectors may be attained for $m < n$ only if

$$\lambda_{m+1} = \lambda_{m+2} = \ldots = \lambda_n = 0$$

But this means that the equation

$$D(\lambda) = \begin{vmatrix} c_{11} - \lambda, & c_{12}, & \cdots & c_{1n} \\ \cdot & \cdot & \cdot & \cdot \\ c_{n1}, & c_{n2}, & \cdots & , c_{nn} - \lambda \end{vmatrix} = 0$$

has a zero root of multiplicity $n-m$. The conditions of existence of such a root have the form $D(0) = D'(0) = \ldots = D^{(n-m+1)}(0) = 0$. Geometrically, these conditions mean that the curve $z = r(t)$ lies in an m-dimensional linear subspace of the space $(z_1, z_2, \ldots, z_n)$.

To calculate H^2 from formula (17), it is necessary to know the roots $\lambda_{m+1}, \ldots, \lambda_n$. It is known ([10], page 80) that

$$H^2 = \frac{1}{2\pi i} \int_R z \frac{D'(z)}{D(z)}\,dz, \qquad (17')$$

where R is any contour in the complex plane enclosing only the indicated roots of the equation $D(\lambda) = 0$. In particular, R may be taken as the circle of radius ϵ and center at the origin, if it is known that $\lambda_{m+1} < \epsilon < \lambda_m$. To determine a minimal set of control functions allowing one to attain a trajectory with prescribed accuracy, it is useful to use the reasoning in [10], page 79, or any other known method (for example, the method of Sturm) for determining the number of roots of the equation $D(\lambda) = 0$, in the interval $(0, \epsilon)$. If this number is equal to l, then $n-l$ control functions and $n-l$ control vectors may be chosen so that the inequality $H^2 < \epsilon l$ will hold. The best estimate of the accuracy of the approximation in this case provides formula (17') again. In each case, it is useful to remember that the approximation using m control functions will be most accurate when the coefficients of the powers of λ not surpassing the degree $m-n$ in the equation $D(\lambda) = 0$ are small in absolute value.

APPENDIX

Proof of Theorem 1. It is easy to see that

$$L^2 = \max \int_0^T \sum_{k=1}^{n} z_k^2(t)\,dt$$

under the condition that $\int_0^T \sum_{k=1}^{n} y_k^2(t)\,dt = 1$.

We shall solve this variational problem on the basis of Pontryagin's maximum principle and the method of paper [3]. According to [3], one should introduce supplementary variables

$$x_i = z_i \text{ for } i = 1, 2, \ldots, n,$$
$$x_{n+1} = \int_0^t \sum_{k=1}^{n} x_k^2(t)\,dt, \quad x_{n+2} = \int_0^t \sum_{k=1}^{n} y_i^2(t)\,dt$$

and write the corresponding Hamiltonian system

$$\dot{x}_i = \sum_{k=1}^{n} a_{ik}(t)\,x_k + y_i, \quad \dot{x}_{n+1} = \sum_{k=1}^{n} x_k^2, \quad \dot{x}_{n+2} = \sum_{k=1}^{n} y_k^2,$$

$$\dot{p}_i = -\sum_{k=1}^{n} a_{ki}(t)\,p_k - 2p_{n+1}x_i, \quad \dot{p}_{n+1} =$$

$$= 0, \quad \dot{p}_{n+2} = 0 \quad (i = 1, 2, \ldots, n). \qquad (18)$$

We shall seek $\max x_{n+1}(T)$ under the condition that $x_{n+2}(T) = 1$. According to [3], it is necessary to construct the Hamiltonian function

$$H = \sum_{i,k=1}^{n} a_{ik}p_i x_k + \sum_{i=1}^{n} p_i y_i + p_{n+1} \sum_{k=1}^{n} x_k^2 + p_{n+2} \sum_{k=1}^{n} y_k^2.$$

The maximum principle tells us that y_i should be chosen so that H is a minimum. The condition of H being minimal takes the form

$$2p_{n+2}y_i + p_i = 0 \quad (i = 1, 2, \ldots, n).$$

Bearing in mind the boundary conditions for the system (18): $x_i(0) = 0$, $p_i(T) = 0$ for $i = 1, 2, \ldots, n$, $p_{n+1}(T) = -\frac{1}{2}$, $p_{n+2}(T) = \lambda/2$, $x_{n+2}(T) = 1$, we have

$$p_{n+1}(t) = -\frac{1}{2}, \quad p_{n+2} = \frac{\lambda}{2} \text{ and } y_i(t) = -\frac{p_i(t)}{\lambda}.$$

The essential portion of system (18) may now be rewritten in the form

$$\dot{x}_i = \sum_{k=1}^{n} a_{ik}x_k - \frac{p_i}{\lambda}, \quad \dot{p}_i =$$

$$= -\sum_{k=1}^{n} a_{ki}p_k + x_i \quad (i = 1, 2, \ldots, n). \qquad (19)$$

This system must be solved under the conditions

$$x_i(0) = 0, \ p_i(T) = 0 \ (i = 1, 2, \ldots, n);$$

$$x_{n+2}(T) = \frac{1}{\lambda^2} \int_0^T \sum_{k=1}^{n} p_k^2(t)\, dt = 1. \tag{20}$$

We show now that $L^2 = \lambda$, where λ is the largest eigenvalue for which the boundary problem (19)-(20) has a solution. For this purpose, writing the system (19) in matrix form,

$$\dot{\mathbf{x}} = \mathbf{A}(t)\mathbf{x} - \frac{\mathbf{p}}{\lambda}, \ \dot{\mathbf{p}} = -\mathbf{A}^*(t)\mathbf{p} + \mathbf{x}$$

[here $\mathbf{A}^*(t)$ denotes the matrix conjugate to $\mathbf{A}(t)$], we take the scalar product of the first equation with $\mathbf{p}$, and of the second with $\mathbf{x}$. Adding the resulting equations, we obtain

$$(\dot{\mathbf{x}}, \mathbf{p}) + (\dot{\mathbf{p}}, \mathbf{x}) = (\mathbf{A}(t)\mathbf{x}, \mathbf{p}) - (\mathbf{A}^*(t)\mathbf{p}, \mathbf{x}) - \frac{\mathbf{p}^2}{\lambda} + \mathbf{x}^2.$$

Integrating from 0 to T, and remembering the relation

$$(\mathbf{A}(t)\mathbf{x}, \mathbf{p}) = (\mathbf{x}, \mathbf{A}^*(t)\mathbf{p}),$$

we obtain

$$(\mathbf{x}, \mathbf{p})\big|_0^T = \int_0^T \mathbf{x}^2 dt - \frac{1}{\lambda}\int_0^T \mathbf{p}^2 dt$$

or

$$L^2 = \lambda,$$

since, by virtue of condition (20),

$$(\mathbf{x}(t), \mathbf{p}(t))\big|_0^T = 0, \ \int_0^T \mathbf{p}^2(t)\, dt = \lambda^2.$$

We now turn to some remarks on the connection between our considerations and the simplest concepts of functional analysis ([9], page 114). Formula (7) defines a linear operator W taking the vector function $\mathbf{y}$ of the Hilbert space $L_{2n}(0,T)$ into a function of the same space. The operator W is bounded and has norm L which will now be found. The adjoint operator W^* has the form [2]

$$W^*\mathbf{y} = \int_t^T (\mathbf{F}^*(t))^{-1}\mathbf{F}^*(\tau)\,\mathbf{y}(\tau)\, d\tau; \tag{21}$$

the inverse operators W^{-1}, $(W^*)^{-1}$ are given by the formulas

$$W^{-1}\mathbf{z} = \dot{\mathbf{z}} - A(t)\,\mathbf{z}, \ (W^*)^{-1}\mathbf{z} = -\dot{\mathbf{z}} - \mathbf{A}^*(t)\,\mathbf{z} \tag{22}$$

If we introduce the notation

$$[\mathbf{y}, \mathbf{z}] = \int_0^T (\mathbf{y}(t)\,\mathbf{z}(t))\, dt,$$

then, of course,

$$[W\mathbf{y}, \mathbf{z}] = [\mathbf{y}, W^*\mathbf{z}].$$

The variational problem which has been solved is the problem of finding the maximum of the functional

$$I = [W\mathbf{y}, W\mathbf{y}] - \lambda[\mathbf{y}, \mathbf{y}] = [W^*W\mathbf{y}, \mathbf{y}] - \lambda[\mathbf{y}, \mathbf{y}].$$

The variation δI is found by the formula

$$\delta I = 2[W^*W\mathbf{y}, \delta\mathbf{y}] - 2\lambda[\mathbf{y}, \delta\mathbf{y}].$$

Since $\delta I = 0$, it follows that $W^*W\mathbf{y} - \lambda\mathbf{y} = 0$, or

$$\int_t^T \int_0^\alpha (\mathbf{F}(\alpha)\mathbf{F}^{-1}(t))^*\mathbf{F}(\alpha)\mathbf{F}^{-1}(\tau)\,\mathbf{y}(\tau)\, d\tau\, d\alpha - \lambda\mathbf{y} = 0. \tag{23}$$

Thus, the value $\lambda = L^2$ of interest to us is the largest eigenvalue of the operator W^*W. Equation (23) is an integral equation. Using formula (22), it is easy to go from it to the differential equation

$$\mathbf{y} - \lambda W^{-1}W^{*\,-1}\mathbf{y} = 0,$$

which, written in detail, assumes the form

$$\frac{d}{dt}\left(\frac{d\mathbf{y}}{dt} + \mathbf{A}^*(t)\,\mathbf{y}\right) - \mathbf{A}(t)\left(\frac{d\mathbf{y}}{dt} + \mathbf{A}^*(t)\,\mathbf{y}\right) + \frac{\mathbf{y}}{\lambda} = 0. \tag{23 }$$

This equation should be considered together with the easily deduced conditions $d\mathbf{y}/dt + \mathbf{A}^*(t)\mathbf{y} = 0$ at $t = 0$, $\mathbf{y}(T) = 0$, and also the condition $\int_0^T \mathbf{y}^2(t)\, dt = 1$.

The substitution of the variables $d\mathbf{y}/dt + \mathbf{A}^*(t)\mathbf{y} = -\mathbf{x}/\lambda$, $\mathbf{p} = -\lambda y$ into Equation (23') again leads to the boundary value problem (19)-(20). However, the purpose of our remarks is not to rederive conditions (19)-(20), but to indicate the applicability of direct methods in the search for L^2. One of such methods is, for example, the method of steepest descent ([9], page 541).

Proof of Theorem 2. We have $\|\mathbf{z}\|^2 = \int_0^T z_k^2(t)\,dt$.

Since

$$z_i(t) = \sum_{k=1}^{n} \int_0^t w_{ik}(t, \tau)\, y_k(\tau)\, d\tau,$$

then

$$\|\mathbf{z}\|^2 = \int_0^T \sum_{i=1}^{n} \Big[\int_0^t \sum_{k=1}^{n} w_{ik}(t, \tau)\, y_k(\tau)\, d\tau\Big]^2 dt \leq$$

$$\leq \int_0^T \sum_{i=1}^{n} \left[\int_0^t \sqrt{\sum_{k=1}^{n} w_{ik}^2(t, \tau) \sum_{k=1}^{n} y_k^2(\tau)}\, d\tau\right]^2 dt.$$

Using the Bunyakovskii-Schwartz inequality ([8], page 242), we obtain

$$\|\mathbf{z}\|^2 \leqslant \int_0^T \sum_{i=1}^{n} \int_0^t \sum_{k=1}^{n} w_{ik}^2(t, \tau)\, d\tau \int_0^t \sum_{k=1}^{n} y_k^2(\tau)\, d\tau\, dt.$$

When t in the second integral is replaced by T, the inequality is only strengthened. The inequality

$$\|\mathbf{z}\|^2 \leqslant \|\mathbf{y}\|^2 \int_0^T \int_0^t \sum_{i,\,k=1}^{n} w_{ik}^2(t, \tau)\, d\tau\, dt$$

gives the required result.

Proof of Theorem 3. Since the quadratic form

$$I(\beta_i) = \sum_{i,\,k=1}^{n} c_{ik}\beta_i\beta_k = \int_0^T \Big(\sum_{k=1}^{n} \beta_k r_k(t)\Big)^2 dt \qquad (24)$$

is positive-definite, its eigenvalues, that is, the eigenvalues of the matrix **C**, will be nonnegative. If the system of vectors $\mathbf{b}_1, \mathbf{b}_2, \ldots, \mathbf{b}_m$ is orthonormal, then according to formula (15'), we have

$$H^2 = \int_0^T \mathbf{r}^2(t)\, dt - \sum_{k=1}^{m} (\mathbf{b}_k, \mathbf{r}(t))^2 dt.$$

It is necessary to choose the system of vectors in such a manner that the sum $\sum_{k=1}^{m} \int_0^T (\mathbf{b}_k, \mathbf{r}(t))^2 dt$ will be the largest possible. Consider the first term of this sum:

$$I_1 = \int_0^T (\mathbf{b}_1, \mathbf{r}(t))^2\, dt = \sum_{i,\,k=1}^{n} \int_0^T r_i(t)\, r_k(t)\, dt\, b_{1i} b_{1k} =$$

$$= \sum_{i,\,k=1}^{n} c_{ik} b_{1i} b_{1k} = I(b_{1i}).$$

Here b_{1k} are the projections of the vector $\mathbf{b}_1$. The problem reduces to finding the maximum of the quadratic form $I(b_{1i})$ under the condition $\sum_{i=1}^{n} b_{1i}^2 = 1$.

It is known ([8], page 28), that this maximum is equal to the largest eigenvalue λ_1, and is attained for the eigenvector $\mathbf{b}_1$ corresponding to this number. To satisfy the condition that the succeeding term

$$I_2 = \int_0^T (\mathbf{b}_2, \mathbf{r}(t))\, dt = I(b_{2i})$$

be a maximum under the subsidiary conditions $(\mathbf{b}_1, \mathbf{b}_2) = 0$, $\mathbf{b}_2^2 = 1$, it is necessary to take $\mathbf{b}_2$ as the eigenvector corresponding to the eigenvalue λ_2. According to the extremal theory of quadratic forms ([8], page 28) the maximum I_2 will be equal to λ_2. If $\lambda_1 = \lambda_2$, then for $\mathbf{b}_2$ one should choose, among the infinite set of eigenvectors of the multiple root λ_1, a vector which is orthogonal to $\mathbf{b}_1$. Proceeding analogously, we obtain the complete solution to the problem.

Since $\int_0^T \mathbf{r}^2(t)\, dt = \sum_{i=1}^{n} c_{ii} = \sum_{i=1}^{n} \lambda_i$ is an invariant quadratic form I, formula (17) is obvious.

Example. We consider the system

$$\dot{x}_1 = x_2 + b_1 u(t), \quad \dot{x}_2 = -x_1 + b_2 u(t) \qquad (25)$$

and attempt to find u(t) so that the solution of this system is realized by motion along the trajectory $x_1 = t - 1$, $x_2 = t + 1$ for $0 \leq t \leq 1$.

First, we calculate L_1 (Theorem 2). The fundamental matrix for the system (25) has the form

$$\mathbf{F}(t) = \begin{Vmatrix} \cos t, & \sin t \\ -\sin t, & \cos t \end{Vmatrix}$$

from which

$$\mathbf{F}(t)\,\mathbf{F}^{-1}(\tau) = \mathbf{F}(t - \tau) = \begin{Vmatrix} \cos(t-\tau), & \sin(t-\tau) \\ -\sin(t-\tau), & \cos(t-\tau) \end{Vmatrix}.$$

Thus, formula (12) yields

$$L_1 = T = 1.$$

We introduce the change of variables $z_1 = x - t + 1$, $z_2 = y - t + 1$ into the system (25). The new system takes the form

$$\dot{z}_1 = z_2 + b_1 u + t, \quad \dot{z}_2 = -z_1 + b_2 u - t. \qquad (26)$$

We obtain $r_1(t) = -t$ and $r_2(t) = t$. If $b_1^2 + b_2^2 = 1$, then formula (15") gives

$$u(t) = (b_2 - b_1)\,t, \quad H^2 = \frac{2 - (b_2 - b_1)^2}{3}. \qquad (27)$$

Thus,

$$\|z\| \leqslant L_1 H = \left(\frac{2 - (b_2 - b_1)^2}{3}\right)^{1/2}.$$

We now attempt to find a vector $\mathbf{b}(b_1, b_2)$ so that the approximation will be the most accurate. First, we calculate the elements of the matrix $\mathbf{C}$, entering into Theorem 2. As a result, we obtain

$$c_{11} = \frac{1}{3}, \quad c_{12} = c_{22} = -\frac{1}{3}.$$

The characteristic equation of the matrix is $\lambda^2 - \frac{2}{3}\lambda = 0$, from which $\lambda_1 = \frac{2}{3}$, $\lambda_2 = 0$. According to Theorem 3, the control vector $\mathbf{b}$ may be chosen so that $H = 0$, and then the trajectory will be realized exactly. The vector $\mathbf{b}$ we are seeking should be the eigenvector of the matrix $\mathbf{C}$, corresponding to the value $\lambda_1 = 2/3$.

To determine b_1 and b_2, we have the system

$$c_{11}b_1 + c_{12}b_2 = \lambda_1 b_1,$$
$$c_{21}b_1 + c_{22}b_2 = \lambda_1 b_2, \quad b_1^2 + b_2^2 = 1,$$

from which we find $b_1 = -\sqrt{2}/2$, $b_2 = \sqrt{2}/2$. From formula (27) it follows that $u(t) = \sqrt{2}\,t$. Otherwise, the optimal values of b_1 and b_2 may be found immediately from formula (27).

LITERATURE CITED

1. R. Bellman, "Notes on control processes. 1. On the minimum of maximum deviation," Quart. Appl. Math. 14 (1957).
2. R. Bellman, Some Aspects of the Mathematical Theory of Control Processes, Rand Corporation (1958) chap. 4.
3. L. I. Rozonoér, "The L. S. Pontryagin maximum principle in the theory of optimal systems. II", Avtomatika i Telemekhanika 20, 11 (1959).*
4. Ya. N. Roitenberg, "Some problems in the Theory of dynamic programming," Prikl. Matem. i Mekh. 23, 4 (1959).
5. V. V. Nemytskii and V. V. Stepanov, Qualitative Theory of Differential Equations [in Russian] (Gostekhizdat, 1949).
6. F. R. Gantmakher, Theory of Matrices [in Russian] (Gostekhizdat, 1953).
7. V. I. Smirnov, Course in Higher Mathematics [in Russian] (Gostekhizdat, 1949) vol. 3, part 1.
8. R. Courant and D. Hilbert, Methods of Mathematical Physics [Russian translation] (Gostekhizdat, (1933) vol. 1.
9. L. V. Kantorovich and G. N. Akilov, Functional Analysis in Normed Spaces [in Russian] (Fizmatgiz, 1959).
10. M. A. Lavrent'ev and B. V. Shabat, Methods of the Theory of Functions of a Complex Variable [in Russian] (Gostekhizdat, 1951).

---

* See English translation.

INVESTIGATION OF THE PERIODIC BEHAVIOR OF RELAY SYSTEMS WITH EXTREMUM REGULATION

I. S. Morosanov

Moscow

Translated from Avtomatika i Telemekhanika, Vol. 21, No. 7, pp 951-957, July, 1960

Original article submitted December 12, 1959

On the basis of the approximate calculation of the periodic behavior of relay systems with extremum regulation (RSÉR) [5], we have determined the areas within which self-oscillations exist in such systems for linear object units of any kind. We have also considered some methods for stabilizing these systems (at high frequencies).

At the present time, we are acquainted with two types of relay systems with extremum regulation (RSÉR), those in which the quantitative output magnitude of the object is tied (or fixed), and those in which it is floating with respect to the circuit extremum level (Figs. 1a and 1b).

In systems with a fixed level, the quantization is determined only by means of increments in the forbidden direction,* the first increment being exactly computed with respect to the extremum [1]. In systems with floating regulation, the quantization is determined by taking into account increments occurring in both directions, the starting point being determined by the initial conditions and independent of the extremum position [2, 3, 4].

We have carried out below a comparative analysis of these systems in terms of the index of periodic behavior, which is a basic characteristic of SÉR.

1. Computation of the Parameters of the Periodic Behavior

We will assume that in RSÉR with a floating grid the quantization of the level of the initial conditions is chosen so that the extremum of the statistical characteristic of the object coincides with one of the quantization levels. Then we may use the same model (Fig. 2) in the determination of the index of the periodic behavior of both systems. We will make use of the method of balancing of harmonics in the same form that was outlined in paper [5] for application to extremum systems. From the known frequency characteristics for the linear links $K_1(j\omega)$ and $K_2(j\omega)$, and the system $K_0(j\omega)$, we get the equivalent frequency characteristic of the extremum system (Fig. 3):

$$K(j\omega) = K_0^2\left(j\frac{\omega}{2}\right) K_1^2\left(j\frac{\omega}{2}\right) K_2(j\omega)\, e^{j\frac{\pi}{2}}. \qquad (1)$$

The amplitude Y_1 and the oscillation frequency ω are outputs for the object and are associated with the parameters of the extremum regulator $\varkappa$ (which is quantized in steps corresponding to the level) and the coefficient of amplification k_p by means of the following relations:

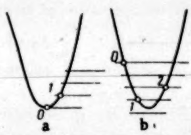

Fig. 1.

$$Y_1 = \frac{8k_p^2\, k}{\pi^3} \left| K(j\omega) \right|, \qquad (2)$$

$$\varkappa = \frac{8k_p^2\, k}{\pi^3} \left| K(j\omega) \right| f(\alpha), \qquad (3)$$

where $f(\alpha) = 1 + \sin\alpha$ for RSÉR with an extremum index based upon the deviation (increment), and $f(\alpha) \approx 2\alpha/\omega$, for RSÉR with an extremum indicator based upon the integral of the deviation, and the supplementary angle with respect to π of the phase difference of the first harmonic of the expansion of the periodic sequences at the input and output of the regulator. The angle α is measured as shown in Fig. 3.

If, in a system with a floating grid, the statistical quantization of the extremum does not coincide with either quantization level, the amplitude of the system oscillations will be larger, and the oscillation frequency will be lower, than that obtained from Equations (2) and (3). This is due to the fact that the factual magnitude of the increment, as computed with respect to the extremum, exceeds $\varkappa$ by $0 \leq \Delta\varkappa < \varkappa$; this is determined from the initial conditions.

---

* We will call increments in the forbidden, or the allowed, direction increments in the output magnitude corresponding to their distance from, or their closeness to, the extremum.

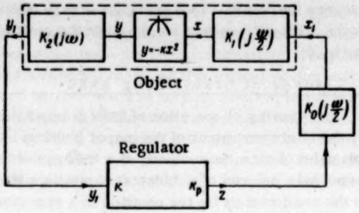

Fig. 2.

Paper [5] has determined the regions in which periodic solutions for the RSÉR studied in this article exist, and has shown that they satisfy the necessary conditions for stable self-oscillation. The sufficient conditions for stable self-oscillation of RSÉR are unknown. Papers [3, 6] show the possibility of the existence of complex periodic operation, due to multiple switches, over a period.

2. Regions within Which Simple Self-Oscillations Exist for RSÉR

Let us determine the regions within which simple self-oscillations exist.

Let us make use of the conditions existing during the time of switchover in the system [5] (Fig. 4):

$$Y_1 \cos(\omega t_\varkappa - \theta) - Y_1 = -\varkappa, \tag{4}$$

where

$$t_\varkappa = \frac{1}{\omega}\left(\alpha + \frac{\pi}{2} + \theta\right) \tag{5}$$

is the switchover time, Y_1 and θ are the modulus and phase of the equivalent frequency characteristics of system (1).

It is obvious that simple self-oscillations exist if $2Y_1 > \kappa > Y_1$, i.e., $Y_1 > Y_1 \cos(\omega t_\kappa - \theta) > 0$; therefore

$$\frac{\pi}{2} > \alpha > 0. \tag{6}$$

Thus, the boundary of the region in which simple self-oscillations exist is determined by the frequency ω_0, which corresponds to the point K(jω) [(1)], lying on the negative real semiaxis ($\alpha = 0$, Fig. 3).

In systems whose extremum indicator is the integral of the increment, the conditions at the switchover time are given by

$$\int\limits_{\theta/\omega}^{t_\varkappa} [Y_1 \cos(\omega t - \theta) - Y_1]\, dt = -\varkappa. \tag{7}$$

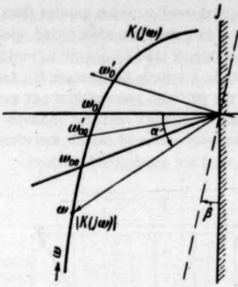

Fig. 3.

For this case, the limiting conditions for the existence of self-oscillations are given by

$$\int\limits_{\theta/\omega}^{t_\varkappa} [Y_1 \cos(\omega t - \theta) - Y_1]\, dt = \int\limits_{t_\varkappa}^{t} [Y_1 \cos(\omega t - \theta) - Y_1 \cos(\omega t_\varkappa - \theta)]\, dt, \tag{8}$$

where t is determined by the first maximum of the integral in the right side of Equation (8).

Substituting the value of t_κ from (5), we get

$$Y_1 \int\limits_0^{\frac{1}{\omega}\left(\frac{\pi}{2}+\alpha\right)} [\cos\omega t - 1]\, dt = Y_1 \int\limits_{\frac{1}{\omega}\left(\frac{\pi}{2}+\alpha\right)}^{\frac{1}{\omega}\left(\frac{3\pi}{2}-\alpha\right)} \left[\cos\omega t - \cos\left(\frac{\pi}{2}+\alpha\right)\right] dt. \tag{9}$$

From this we get the following equation for α:

$$\cos\alpha - \left(\frac{\pi - 2\alpha}{3}\right)\sin\alpha = \frac{\pi/2 + \alpha}{3}, \tag{10}$$

which for $0 < \alpha < 2\pi$, has the solution $\alpha = 0.367$. This means that the region for which simple self-oscillations exist for this system is determined by the frequency ω_{00}, for which the phase of $K(j\omega) = -(\pi - 0.367)$ (Fig. 3).

An effort to realize operation at frequencies above the indicated boundary leads to the appearance of re-

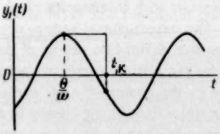

Fig. 4.

peated switchovers in the system. when the deviations from the extremum reach a value greater than 2 quantized steps. As a result, in RSÉR based upon simple increments, increments lead to complex (multiple) oscillations, while, in a system based upon the integral of the increment, the periodic process does not even become established. Complex periodic behavior differs sharply from the harmonic, and cannot, therefore, be analyzed by means of the established method.

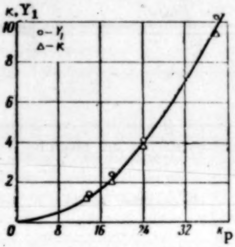

Fig. 5.

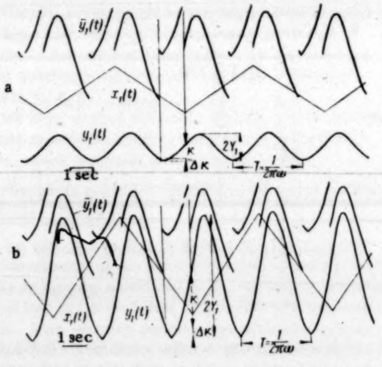

Fig. 6. $\overline{y}_1(t)$ – quantized with respect to the level of $y_1(t)$.

For increases in the case of RSÉR with floating grid quantization, pictures were taken during experiments of periodic processes with frequencies close to the boundary frequency. The experimental system consisted of an actual operator and object in a set-up of the type MN-8. The output for the critical mode of operation ($\alpha = 0$) was realized by the choice of κ for several fixed values of k_p, the initial values being chosen so that the statistical extremum was close to one of the quantization levels. Comparison of the computed and experimental data (Fig. 5) shows a sufficiently satisfactory agreement between the results. Two examples of self-oscillation at the critical frequency are shown in the oscillograms in Fig. 6.

3. Means of Stabilizing RSÉR

The quality of operation of RSÉR is usually evaluated by the minimum values of the output hunting. From this point of view, the synthesis of a RSÉR, in which we do not take account of accidental excitations, is subject to the requirements for the creation of a system with a maximum self-oscillation frequency. The critical self-oscillation frequency in RSÉR may be basically increased if we prevent repeated switchovers in the system. In order to do this, for example, we open (or disconnect) the system for a short time when the output exceeds two quantization levels (with respect to the extremum value) [1]. However, this procedure requires a preliminary knowledge of the self-oscillation frequency, which may not always be available. For example, in some cases, the same regulator must, without resetting, alternately regulate an entire series of objects, all the objects having the same structure, but each linear unit having a different time constant and having extremum statistical characteristics of different curvature.

The prevention of repeated false switchovers in RSÉR without first narrowing the self-adjustment region

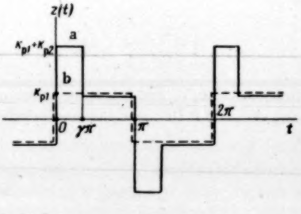

Fig. 7.

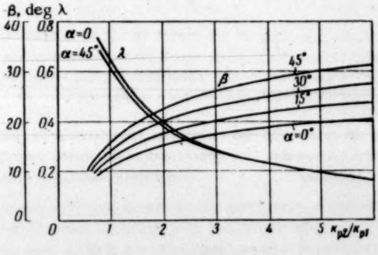

Fig. 8.

of the system is accomplished by the use of a special logical device which either permits or forbids switchover, depending upon the previous situation. The structure and manner of realizing this logical device will be discussed below. We wish to note at once, however, that such a solution is useful only for a system with a floating grid which is quantized with respect to a level, since it is only in such a system that we can have a definite regulation process both before and after a passage through an extremum.

The region within which simple self-oscillations exist widens in this case to $\alpha = -0.339$ for RSÉR with an extremum indicator based upon the deviation, and to $\alpha = 0.168$ for an extremum indicator based upon the integral of the deviations (Fig. 3, ω_0' and ω_{00}', respectively).

Further widening of the region in which self-oscillations exist for RSÉR may be obtained with the aid of so-called pulse stabilization, as outlined in the appendix of the articles on the usual operation of relay systems in papers [7, 8]. In contrast to [8], where a precise computation of the stabilization effect is made, we will make use of the approximate method of evaluating the effect, using as the basis of our computations the method of balancing the harmonics. In essence, harmonic stabilization consists in forcing the system to move in the direction of the extremum after a change in sign is obtained during scanning. This occurs due to a previous mutilation in the series of regular pulses $z(t)$ at the regulator output, as shown in Fig. 7a. It is obvious that the first harmonic of the series in Fig. 7a leads the first harmonic of the series in Fig. 7b by a phase angle β. This leads us to the following method for determining the indices of periodic operation of the stabilized system: we use a method of computation which is similar to that outlined in Section 1, but we use a system of coordinates which is rotated by an angle β in the direction of the phase lead (Fig. 3).

The parameter γ – the relative duration of the corrective pulse – must, for the above-outlined reasons, be independent of the self-oscillation frequency; this can only be realized in systems with floating grid quantization. Actually, in order to obtain a corrective pulse in such a system after the passage through the extremum, we can make use of the fixation times of the allowed increments. For example, for RSÉR, due to the fact that $(1-\gamma)\pi$ of the half-period $z(t)$ is equal to $(\omega t_K - \theta)$ of period $\varphi_1(t)$, we get

$$\gamma = 0.75 - \frac{\alpha}{2\pi}. \quad (11)$$

Having determined γ, we can compute β as the difference in the phase angles of the first harmonics in the expansion of the series shown in Fig. 7.

In Fig. 8 we show the family of β curves as functions of the relative values of the corrective impulse k_{p2}/k_{p1} (Fig. 7); the parameter of this family of curves is α. In Fig. 7, we also plot the curves for $\lambda < 1$, where λ is the transmission coefficient; we must take the value of λ into account in the regulatory circuit in order to maintain the same coefficient of amplification as for the unstabilized system.

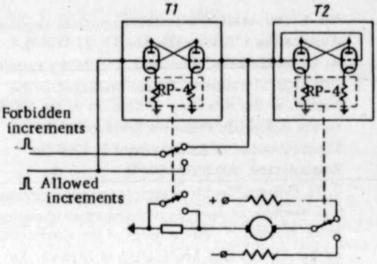

Fig. 9.

Let us examine the circuit of Fig. 9, which permits us to utilize both methods of increasing the self-oscillation frequency in RSÉR. At the input to the circuit, we apply the fixation impulses of the forbidden and allowed increments. The trigger T2 (with one symmetrical output) represents the output relay as in any extremum relay regulator. Trigger T1 (with two outputs) fulfills the following logical functions: 1) it forbids every second fixation pulse of the forbidden increment if it was not preceded by a fixation pulse of the allowed increment; 2) it permits a third fixation pulse of the forbidden increment even if an increment of the allowed fixation has not been received. As we can see from the circuit, the logical operation of the trigger T1 corresponds exactly to the requirement for the formation of a corrective pulse during pulse stabilization. In this manner, the circuit described above prevents repeated switchovers, maintains the system within the extremum region during false switchovers prior to the time that the extremum is reached, and generates a regular series of pulses, shown in Fig. 7a, independently of the absolute values of the self-oscillation frequencies of the system.

SUMMARY

1. The limits of the region within which simple self-oscillations exist in relay SÉR for object units of any type have been determined.
2. We propose that, in order to increase the self-oscillation, use be made of corrective pulses and of measures which prevent repeated switchovers. The given circuit for the concrete realization of these methods for increasing the frequency is independent of the absolute value of the self-oscillation frequency.

3. We have shown that RSER with floating level grid quantization possess a more elastic structure, in the sense that they are more "self-regulating" under conditions in which the parameters of the regulated object change.

LITERATURE CITED

1. Yu. I. Ostrovskii, "Pneumatic extremum-regulator," Avtomatika i Telemekhanika 18, 11 (1957).†
2. A. G. Ivakhnenko, "Automatic regulatory systems with logical elements," Paper presented at the Session of the Academy of Science of the USSR on the Scientific Problems Involved in the Mechanization of Industry held in 1956 [in Russian] (Izd. AN SSSR, 1957).
3. L. N. Fitsner, "On the principles of construction and methods of analysis of some types of extremum systems," Proceedings of the Conference on the Theory and Application of Discrete Automatic Systems [in Russian] (Izd. AN SSSR, 1960).
4. V. V. Kazakevich, R. V. Kornilov, and N. G. Khristoforov, "Electronic extremum regulators," Proceedings of the Conference on the Theory and Application of Discrete Automatic Systems [in Russian] (Izd. AN SSSR, 1960).
5. L. S. Morosanov, "Computation of stable behavior in systems with extremum regulation with independent hunting," Proceedings of the Conference on the Theory and Application of Discrete Automatic Systems [in Russian] (Izd. AN SSSR, 1960).
6. V. V. Kazakevich, Theory of an Ideal Model of Extremum Regulation, Avtomatika i Telemekhanika 21, 3 (1960).†
7. Ya. Z. Tsypkin, "Stabilization of automatic regulation relay systems," Convegno sui problemi dell' automatismo (Conference on Automation Problems), Milan. 1 (Consiglio Nazionale Delle Ricerche, Rome, 1958).
8. N. A. Korolev, "Pulse stabilization of automatic regulation relay systems," Avtomatika i Telemekhanika 18, 5 (1957).†

---

† See English translation.

CONTINUOUS EXTREMUM CONTROL SYSTEMS IN THE PRESENCE OF RANDOM NOISE

A. A. Pervozvanskii

Leningrad

Translated from Avtomatika i Telemekhanika, Vol. 21, No. 7, pp 958-963, July, 1960
Original article submitted December 14, 1959

The dynamics of one class of continuous systems of extremum control is investigated. The drift in the position of the extremum, and also the high frequency interference, are regarded as random functions of time.

The extremum control systems are viewed as working on the principle of proportional search. In contrast to discrete systems, the trial pulse is separated from the working action not in time but in the range of frequencies used. Such devices were first described in the book [1], where first attempts were also made to analyze their dynamic behavior, and also to provide qualitative estimates on the impact of random noise.

The block diagram of an extremum system of this type is shown in Fig. 1. The generator of the trial pulses delivers them in the form of a periodic function of time (it is usually either a sine or a square wave). The trial pulse is fed to the controlled object. As shown later, the amplitude of the fundamental harmonic component at the output of the controlled system is approximately proportional to the magnitude of the rate of change of the characteristic (that is, to the derivative of the function representing the dependence of the output on the input).

The magnitude of the indicated amplitude and, thus, of the rate of change obtained with the aid of a demodulator, can be regarded as an error signal of a typical control system; by using a controller the error is made to approach zero, i.e., to bring the system to the extremum point.

Thus, if the value of the rate of change is found:

$$k(x) = \frac{df}{dx},$$

then the motion of the control unit can be performed in accordance with the equation

$$\frac{dx}{dt} = \alpha k(x),$$

where $\alpha > 0$ when the search is for a maximum, but $\alpha < 0$ when it is for a minimum.

In view of the formulated conditions, the time constant $\dfrac{1}{\left|\alpha \dfrac{dk}{dx}\right|}$ should be much less than the period $2\pi/\omega_0$ of the trial pulses.

It was already shown in [1] that, when designing an extremum system, the very nature of the problem demands that two kinds of changes in output (or input) of the system which are not under control be taken into account: a) a slow drift — a gradual change of the characteristic, which includes the slipping away of the extremum point to be followed by the controller, and b) high-frequency disturbances.

If the former type is regarded as a useful signal (as the term is used in the theory of optimum filters), and if the controller is adjusted accordingly to provide optimum performance, the latter appears to be just interference in the controller which should be filtered out.

There is usually a frequency band between the frequencies of the drift and of the noise which, on the whole, is free from the uncontrollable changes. It seems natural that use should be made of this range in generating trial pulses. In actual practice, however, the band may be fairly narrow, and we shall see that the frequency thus selected for the trial signals will not be distinct enough from the frequencies of the useful signal and, in consequence, not distinct enough from the working frequencies of the controller, which is inadmissible.

In view of the above difficulties, objections were raised in [1] against such systems being widely used for practical purposes. Nevertheless, the basis of the working of an extremum controller, as described above, has some very important good points, the fundamental one being the comparative ease with which the search for an extremum dependent on several coordinates, when the working action is continuous (in time), can be realized (see, for example, its mathematical analysis in [2]). It is very important, therefore, from the practical point of view to be able to find an answer to the question as to whether the bandwidth of the testing signals is in fact limited only to the frequency band which is noise-free. When the noise is of a random character (this case is of particular interest as the noise localized at one frequency does not cause the above-mentioned difficulties), it should not, if properly filtered, exert a decisive influence on the working of the system even when the frequency of the trial pulses is definitely within the noise band.

Let us examine an object such that the extremum of its characteristic is searched for changes only in one coordinate. Its idealized block-diagram given in Fig. 2a contains a linear dynamic input with transfer function $\bar{K}_1(p)$ $(p \equiv \frac{d}{dt})$, a nonlinear static element with characteristic $y = f(x)$ which has a single extremum in the considered range, and the linear dynamic output with transfer function $K_2(p)$.

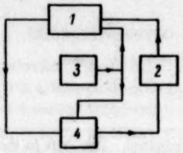

Fig. 1. 1) Object, 2) control unit, 3) generator of the trial pulses, 4) demodulator.

We assume that some external disturbances which it is not possible to control are acting both on the input (Z_1) and on the output (Z_2) of the object. Each disturbance is thought to consist of two components:

$$Z_1 = Z_{10} + Z_{11}, \qquad Z_2 = Z_{20} + Z_{21}, \tag{1}$$

where the 0 subscript denotes the components which correspond to the slow drift (useful signal), the subscript 1 denotes the component corresponding to interference.*

The components Z_{11} and Z_{21} can be represented in the form (see, for example, [3])

$$Z_{11} = A_1 \sin \omega_0 t + B_1 \cos \omega_0 t,$$
$$Z_{21} = A_2 \sin \omega_0 t + B_2 \cos \omega_0 t, \tag{2}$$

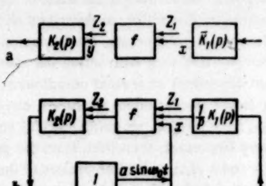

Fig. 2. 1) Generator of trial pulses, 2) phase-shifter, 3) demodulator.

where ω_0 is the frequency of the trial pulses; A_1, B_1, A_2, B_2 are slowly varying random functions (compared with $\sin \omega_0 t$) uncorrelated to one another (or to Z_{10} or Z_{20}).

A signal proportional to the displacement of the workpiece (the working signal) and the trial disturbance $\underline{a} \sin \omega_0 t$ from the generator of the trial signals act on the input of the object. To simplify the matter, it is assumed that the trial pulse excites the input of the nonlinear block $\underline{x}$. The transfer function of the workpiece is represented as $1/p\, \bar{\bar{K}}_1(p)$, where the operator $\bar{\bar{K}}_1(p)$ characterizes the dynamics of the operating device, as well as the characteristics of the auxiliary compensating networks. The latter, though not indispensable, are introduced in order to improve the dynamic properties of the system as a whole.

The output y_1 of the object is fed to the demodulating device to determine the amplitude of the fundamental harmonic of the output signal.

An ideal demodulator operating on the basis of the relation

$$x_1 = b\,\frac{\omega_0}{\pi} \int_0^{\frac{2\pi}{\omega_0}+t} y_1 \sin(\omega_0 t + \varphi)\, dt, \tag{3}$$

is considered where the phase difference φ is introduced by means of a phase-shifter, the lag being due to the passing of the testing signal through the object, that is,

$$\varphi \approx \operatorname{Arg} K_2(j\omega_0). \tag{4}$$

Other types of demodulating devices can be analyzed; for example, a device with synchronous filters [1, 2] where the product of the output and the testing signals $y_1 b \sin(\omega_0 t + \varphi)$ is fed through a filter. However, with sufficiently efficient filtering of the higher harmonics, there is basically no fundamental difference between the latter device and the ideal demodulator.

With the assumptions as above, we show in Fig. 2b the whole scheme of the extremum control system; for the sake of simplicity, the notation $K_1(p) = \bar{K}_1(p)\,\bar{\bar{K}}_1(p)$ was introduced.

We now proceed to analyze the scheme. We expand the expression for the signal at the output of the nonlinear member:

$$y = f(x + Z_1 + a \sin \omega_0 t) + Z_2$$

into a Taylor's series about the point $x + Z_{10}$:

$$y = Z_2 + f(x + Z_{10}) +$$
$$+ f'(x + Z_{10})\,[(A + a) \sin \omega_0 t + B_1 \cos \omega_0 t] + \ldots \tag{5}$$

---

*It is obvious that the component Z_{20} (the drift either up or down of the characteristic) provides no useful information.

As the ideal demodulation takes place in successive members, it is possible from the start to retain in the formula for y only the terms with the fundamental frequency (with an accuracy up to the terms containing derivatives of the order higher than two). We thus obtain

$$y^{*} = A_2 \sin\omega_0 t + B_2 \cos\omega_0 t +$$

$$f'(x + Z_{10})\,[(A_1 + a)\sin\omega_0 t + B_1 \cos\omega_0 t].$$

Should f(x) be a second-degree parabola

$$f(x) = -\frac{x^2}{2},$$

then

$$f'(x) = -x \tag{6}$$

and the quantity y^{*} proves linearly dependent on x.

We shall write down the transformation of the signal y^{*} after it has passed through the linear part of the characteristic of the object. We represent y^{*} as

$$\begin{aligned} y^{*} &= [A_2 + f'(x + Z_{10})(A_1 + a)]\sin\omega_0 t + \\ &+ [B_2 + f'(x + Z_{10}) B_1]\cos\omega\, t = \\ &= A_y \sin\omega_0 t + B_y \cos\omega_0 t. \end{aligned} \tag{7}$$

When a linear differential operator operates on the product of a harmonic function of time and an arbitrary function u(t),† we can write the result as

$$\begin{aligned} K_2(p)\,[u(t)\sin\omega_0 t] &= \sin\omega_0 t K_{21}(p)\,u(t) + \\ &+ \cos\omega_0 t K_{22}(p)\,u(t), \\ K_2(p)\,[u(t)\cos\omega_0 t] &= \cos\omega_0 t K_{21}(p)\,u(t) - \\ &- \sin\omega_0 t K_{22}(p)\,u(t), \end{aligned} \tag{8}$$

where

$$K_{21}(p) = \operatorname{Re} K_2(p + j\omega_0),$$

$$K_{22}(p) = \operatorname{Im} K_2(p + j\omega_0).$$

Hence,

$$\begin{aligned} y_1 &= \sin\omega_0 t\,[K_{21}(p)\,A_y - K_{22}(p)\,B_y] + \\ &+ \cos\omega_0 t\,[K_{22}(p)\,A_y + K_{21}(p)\,B_y] \end{aligned} \tag{9}$$

(only the fundamental frequency components are kept).

In view of the fact that the amplitude changes little within a period, we obtain, at the output of the demodulator,

$$\begin{aligned} x_1 = b\,\{&[\cos\varphi K_{21}(p) + \sin\varphi K_{22}(p)]\,[A_2 + \\ &+ f'(x + Z_{10})(A_1 + a)] + \\ &+ [\sin\varphi K_{21}(p) - \cos\varphi K_{22}(p)]\,[B_2 + \\ &+ f'(x + Z_{10})\,B_1]\}. \end{aligned} \tag{10}$$

The equation of the closed-loop system, dependent on the "tracking error" $\epsilon = x + Z_{10}$, takes the form

$$\begin{aligned} \varepsilon - \frac{b}{p} K_1(p)\,\{&[\cos\varphi K_{21}(p) + \\ &+ \sin\varphi K_{22}(p)]\,[A_2 + f'(\varepsilon)(A_1 + a)] + \\ &+ [\sin\varphi K_{21}(p) - \cos\varphi K_{22}(p)]\,[B_2 + \\ &+ f'(\varepsilon)\,B']\} = Z_{10}. \end{aligned} \tag{11}$$

The obtained equation is nonlinear. Furthermore, when $A_1, B_1 \neq 0$, its coefficients are random functions of time; it proves impossible to analyze the equation in a general case.

We shall not consider (11) further (unless the high-frequency noise at the input of the object is absent). We shall then have to deal with an equation describing a system equivalent to a system which consists of one linear part and one nonlinear element $f'(\epsilon)$.

This can be investigated for arbitrary f(x) by the method of statistical linearization (see, for example, [4]).

Let $M\{Z_{10}\} = M\{Z_{22}\} = 0$; then also $M\{\epsilon\} = 0$, and $f'(\epsilon)$ is approximately equal to $f'(\epsilon) = k(\sigma_\epsilon)\epsilon$, where $k(\sigma_\varepsilon) = \frac{2}{\sigma_\varepsilon^2}\int_0^\infty f'(\varepsilon)\,\varepsilon\psi(\varepsilon)\,d\varepsilon$, and $\psi(\epsilon) = \frac{1}{2\pi\sigma_\varepsilon}\exp\left(-\frac{\varepsilon^2}{2\sigma_\varepsilon^2}\right)$ is the probability density of ϵ (it is assumed that ϵ has a Gaussian distribution).

Equation (11) takes the form

$$\begin{aligned} \Big\{1 - \frac{ab}{p} K(\sigma_\varepsilon) K_1(p)\,&[\cos\varphi\,(K_{21}(p) - \\ &- K_{22}(p)) + \sin\varphi\,(K_{21}(p) + K_{22}(p))]\Big\}\,\varepsilon = \\ = Z_{10} + \frac{b}{p} K_1(p)\,&[(\cos\varphi K_{21}(p) + \sin\varphi K_{22}(p))\,A_2 + \\ &+ (\sin\varphi K_{21}(p) - \cos\varphi K_{22}(p))\,B_2] \end{aligned} \tag{12}$$

or

$$\Phi(p)\,\varepsilon = Z_{10} + \Phi_1(p)\,A_2 +$$

$$+ \Phi_2(p)\,B_2.$$

---

† The above rules can be easily derived by using the Leibnitz formula.

One can obtain a formula for the variance of ϵ by regarding the above as a linear equation

$$\sigma_\epsilon^2 = \frac{1}{2\pi}\int_{-\infty}^{\infty}\left\{\frac{S_0(\omega)}{|\Phi(j\omega)|^2} + \right.$$

$$\left. + \frac{S_2(\omega)\left[|\Phi_1(j\omega)|^2 + |\Phi_2(j\omega)|^2\right]}{|\Phi(j\omega)|^2}\right\} d\omega, \tag{13}$$

where $S_0(\omega)$ is the spectral density of Z_{10}, and $S_2(\omega) = S_{A2}(\omega) = S_{B2}(\omega)$ are the spectral densities of the "amplitudes" of high-frequency noise.

When the expression $S_{Z2}(\omega)$ for the spectrum of the noise itself is at one's disposal, $S_2(\omega)$ is evaluated with the aid of the formula [3]

$$S_2(\omega) =$$

$$= \frac{2}{\pi}\int_0^{\infty}\cos\omega\tau\, d\tau \int_0^{\infty} S_{Z_2}(\omega)\cos(\omega - \omega_0)\,\tau\, d\omega \tag{14}$$

We also notice that (13) can be simplified by making use of the formula

$$|\Phi_1(j\omega)|^2 + |\Phi_2(j\omega)|^2 = \{|K_{21}(j\omega)|^2 +$$

$$+ |K_{22}(j\omega)|^2\}\frac{b^2}{\omega^2}|K_1(j\omega)|^2. \tag{15}$$

which can easily be obtained.

The integrals on the right-hand side of (13) have been tabulated (see, for example, [4]), and their values expressed‡ directly in terms of the coefficients of the transfer functions $K_1(p)$ and $K_2(p)$, the parameters which determine the spectral densities of the external disturbances, as well as by the linearization coefficient $k(\sigma_\epsilon)$. When the integration has been performed, we see that (13) becomes an equation in σ_ϵ which usually is solved graphically.

When f(x) represents the equation of the second-degree parabola, $f(x) = -x^2/2$, then Equation (11) becomes linear $[k(\sigma_\epsilon) \equiv -1]$.

If the quantity $1/T = ab$ is introduced (which actually gives the gain coefficient of the controlling device), it is then obvious that $\sigma_\epsilon^2 = c_0 + c_1(1/a^2)$, where c_0 and c_1 are independent of the choice of the amplitude a of the testing signal.

It is advisable that the selection of the optimum value of a be in accordance with the condition for the minimum total error Δ, which can be given, for example, by the expression

$$\Delta = a + 2\sigma_\epsilon,$$

that is, in the form of a sum of systematic deviations due to the trial disturbance and of random deviations due to disturbances not under control. **

As the first approximation, we have

$$a_{\text{opt}} = \sqrt[4]{4c_1}\,.$$

Some examples of the evaluation of systems are now given:

1. Let

$$K_1(p) = \frac{1}{T_1p + 1}, \quad K_2(p) = 1, \quad \varphi = 0,$$

$$S_0(\omega) = \frac{\sigma_0^2 2T_0}{T_0^2\omega^2 + 1}, \quad S_2(\omega) = T_a\sigma_a^2.$$

Then

$$\sigma_\epsilon^2 = \sigma_0^2\frac{T_0(T_1 + T_0)}{T_0^2 + T(T_1 + T_0)} + \sigma_a^2\frac{T_a}{2a^2T^2},$$

$$a_{\text{opt}} \approx \sqrt[4]{\frac{2T_a}{a^2T^2}\sigma_a^2}\,.$$

2. Let $K_1(p) = 1$, $K_2(p) = \dfrac{1}{T_2p + 1}$, $\varphi = \operatorname{Arg} K_2(f\omega)$.

The external acting forces are given by the same expression as in the first example.

Then

$$\sigma_\epsilon^2 = \sigma_0^2\frac{T_c}{T_0}\frac{2T_2^2c^4 + 2T_2T_0c^2 + 2T_2T_c + TT_0}{T_2^2c^6 + T_2T_0c^4 + TT_0c + T^2} +$$

$$+ \sigma_a^2\frac{cT_a}{2a^2T}\frac{2T_2c^3 + T}{T_2c^3 + T},$$

where

$$c = \cos\varphi = \frac{1}{\sqrt{1 + T_2^2\omega^2}}.$$

The condition $\omega \ll \omega_0$ was used in the calculations. Then [whatever the order of $K_2(p)$] $K_{21}(j\omega)$ and $K_{22}(j\omega)$ can be represented by the formulas of the type $(a_0j\omega + a_1)/(b_0j\omega + b_1)$, that is, only the terms linear in ω are retained in the numerator as well as in the denominator.

It is obvious that the methods described here can also be applied to analyze a more involved case, viz., to find the extremum of a function of several variables, in particular, when the construction of autocontrolled systems by the methods given in [2] is technically feasible. They are also useful, at least in principle, to synthesize the optimum compensating filters when the properties of the object and the external acting forces are given.

---

‡It is advisable to assume in the calculations that, within the range of realizable frequencies, $\omega \ll \omega_0$.

**But if one starts with the supposition that the quantity given is the coefficient b, then the optimum value of the amplitude a becomes different. In the examples given below, it is obvious that $a_{\text{opt}} = 0$ $(T = \infty)$. This conclusion is in agreement with the one reached in [5, 6] for the case of a simpler discrete system where the magnitudes of the working and of the trial steps were assumed equal or proportional.

LITERATURE CITED

1. Ch'ien Hsüeh-sên, Technical Cybernetics [Russian translation] (IL, 1956).
2. A. A. Krasovskii, "The dynamics of continuous systems of extremum control based on the gradient method," Izd. Akad. Nauk SSSR, Otdel. Tech. Nauk, Avtomatika i Énergetika No. 3 (1959).
3. B. R. Levin, Theory of Random Processes with Applications to Radio (Izd. Sovetskoe Radio, 1957).
4. A. A. Fel'dbaum, "Steady-state processes in a simple discrete extremal system with random noise present," Avtomat. i Telemekh. 20, 8 (1959).††
5. A. A. Pervozvanskii, "Application of Markov chains to the evaluation of steady-state errors in extremum regulators," Izv. Akad. Nauk, Otdel. Tech. Nauk No. 3 (1960).

---

††See English translation.

INVESTIGATION OF A SERVOSYSTEM WITH AN ELECTROMAGNETIC INDUCTION CLUTCH WHICH OPERATES WITH LOW-NULL CURRENTS

P. F. Klubnikin

Moscow

Translated from Avtomatika i Telemekhanika, Vol. 21, No. 7, pp 964-972, July, 1960
Original article submitted November 18, 1959

In this article, we analyze a servosystem where a reversive electromagnetic induction clutch which operates with low null currents is used. A method of increasing the stability margin of such a system is considered. The experimental results are also given.

At the present time, reversive electromagnetic clutch drives are used to an ever-increasing extent in automatic control systems [1]. The reasons for this are that their design is simple and that they have good dynamic properties. For instance, a clutch drive has a minimum number of parts in the system, a minimum weight per given output power, it can be linked in a simple manner with a semiconductor amplifier, etc.

It is known [1] that, for the normal operation of an automatic control system which has an induction clutch drive, so-called null currents, which must not fall below a certain given magnitude, are transmitted through the clutch control windings. An attempt to reduce the null currents leads to unstable operation of the system, since, apart from other effects, the drive characteristics become nonlinear.

In servosystems, the presence of large null currents in the clutch control windings results in superfluous energy losses, which cause the heating of parts. Therefore, it is desirable to reduce the null currents to a minimum. In this article, we shall investigate a servosystem with an induction clutch operating with low null currents. We shall also explore the possibility of increasing the system stability margin.

1. Operational Characteristics of a Servosystem with Small Clutch Null Currents

On the basis of the clutch motion equations [1], for the servosystem illustrated in Fig. 1, we have the following system of equations:

$$
\begin{gathered}
\mathrm{I}\,\frac{d\theta}{dt} = M_{\mathrm{to}} - M_l\\
M_{\mathrm{to}} = C_0\,[(B_1^2 - B_2^2)\,n_0 - \theta\,(B_1^2 + B_2^2)],\\
F_1\left(B_1,\ \frac{dB_1}{dt},\ \ldots,\ i_1,\ \frac{di_1}{dt},\ \ldots\right) = 0,\\
F_2\left(B_2,\ \frac{dB_2}{dt},\ \ldots,\ i_2,\ \frac{di_2}{dt},\ \ldots\right) = 0,\\
T_1\frac{di_1}{dt} + i_1 = k_{\mathrm{a}}\varphi'(\varepsilon) + i_0,
\end{gathered}
$$

$$
\begin{gathered}
T_2\frac{di_2}{dt} + i_2 = k_{\mathrm{a}}\varphi'(-\varepsilon) + i_0,\\
\varepsilon = k_{\mathrm{T}}\,(E - \theta),
\end{gathered}
\tag{1}
$$

where θ is the angular velocity of the clutch output shaft, I is the clutch rotor moment of inertia, M_{to} is the clutch shaft torque, M_l is the loading moment, C_0 is the proportionality coefficient [1], B_1 and B_2 are the values of magnetic induction in the air gaps of the first and the second electromagnet, respectively, i_1 and i_2 are the currents in the control windings, T_1 and T_2 are the coefficients which depend on the control windings inductance, k_{a} is the amplifier amplification factor, i_0 is the null current intensity in the control windings, ε is the amplifier input voltage, E is the voltage supplied to the system input, and n_0 is the turning speed of the clutch electromagnets.

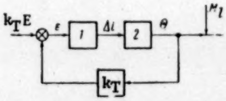

Fig. 1. 1) Amplifier; 2) clutch drive.

If we neglect the magnetic flux rise time with respect to the current, i.e., if we substitute the $B_1 = f_1(i_1)$ and $B_2 = f_2(i_2)$ functions for the third and the fourth equations in system (1), then, considering that there is only an inertial load at the system output, Equations (1) can be written in the following form:

$$
\begin{gathered}
I_1\frac{d\theta}{dt} = M_1 - M_2 - \frac{\theta}{n_0}(M_1 + M_2),\quad M = f(i),\\
T_1\frac{di_1}{dt} + i_1 = k_{\mathrm{a}}\varphi'(\varepsilon) + i_0\quad (i_1 > 0)\\
T_2\frac{di_2}{dt} + i_2 = k_{\mathrm{a}}\varphi'(-\varepsilon) + i_0\quad (i_2 > 0),\ \varepsilon = k_{\mathrm{T}}(E - \theta).
\end{gathered}
\tag{2}
$$

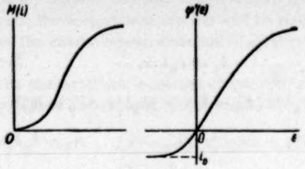

Fig. 2.

Here $I_1 = I + I_l r^2$, I_l is the load moment of inertia, r is the reductor gear ratio, and M_1 and M_2 are the moments acting on the rotor due to the first and the second electromagnets.

The approximate shape of the $M = f(i)$ and $i = \varphi'(\epsilon)$ functions is shown in Fig. 2.

We shall denote: $M_1 - M_2 = f_1(\Delta i)$, and $M_1 + M_2 = f_2(\Delta i)$, where $\Delta i = i_1 - i_2$. The approximate shapes of the $f_1(\Delta i)$ and $f_2(\Delta i)$ functions are shown in Fig. 3.

Then, assuming that $T_{1,2}$ = const, after elementary transformations (2), we obtain

$$\frac{I_1}{f_2(\Delta i)}\frac{d\theta}{dt} + 0 = n_0 \frac{f_1(\Delta i)}{f_2(\Delta i)},$$

$$T_1 T_2 \frac{d^2 \Delta i}{dt^2} + (T_1 + T_2)\frac{d\Delta i}{dt} + \Delta i =$$

$$= k_a \varphi(\varepsilon) + k_a \frac{T_1 + T_2}{2}\frac{d\varphi(\varepsilon)}{dt} + k_a \frac{T_2 - T_1}{2}\frac{d\varphi''(\varepsilon)}{dt},$$

$$\varepsilon = k_T (E - \theta), \qquad (3)$$

where

$$\varphi(\varepsilon) = \varphi'(\varepsilon) - \varphi'(-\varepsilon), \quad \varphi''(\varepsilon) = \varphi'(\varepsilon) + \varphi'(-\varepsilon).$$

Thus, a servosystem of the simplest form with small null currents in the clutch control windings is described by a nonlinear system of equations with variable coefficients (3). It is important to note that the coefficient in front of the derivative θ in the first equation of system (3) changes considerably if Δi varies.

Its maximum value is equal to $T_{max} = \frac{I_1 n_0}{2M_0(i_0)}$, i.e., it is completely determined by the null current i_0 magnitude. For instance, for $i_0 \to 0$, $T_{max} \to \infty$. In the latter case, the system of equations (1) assumes the form

$$I\frac{d\theta}{dt} = M_{to} - M_l$$

$$M_I = C_0 (n_0 - 0) B^2 \text{ sign } \varepsilon,$$

$$F\left(B, \frac{dB}{dt}, \ldots, i, \frac{di}{dt}, \ldots\right) = 0,$$

$$T_1 \frac{di_1}{dt} + i_1 = k_a \varphi(\varepsilon) \quad \left(\text{for } \frac{d\varepsilon}{dt} > 0\right),$$

$$T_2 \frac{di_2}{dt} + i_2 = k_a \varphi(\varepsilon) \quad \left(\text{for } \frac{d\varepsilon}{dt} < 0\right),$$

$$\varepsilon = k_T (E - 0). \qquad (4)$$

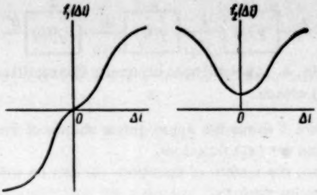

Fig. 3.

The analysis of this system of equations is more complicated than the analysis of system (3).

Practice shows that the basic problem which has to be solved if the clutch is to operate with small null currents is the problem of securing the system stability.

The investigation of the servosystem stability by using Equations (3) or (4) is a rather complicated problem. An attempt to solve this equation by introducing a number of simplifying assumptions leads to contradiction with regard to the results obtained in experimental investigation of such systems.

In connection with the above-mentioned, one important fact should be emphasized. It is not at all necessary to reduce the null currents to zero.

Energy balance calculations show that the losses due to small null currents (for instance, constituting 10 to 15% of the maximum currents) are very small and entirely admissible even in servosystems. On the other hand, a reduction of null currents to zero complicates the system stabilization and its design to a considerable extent, since the more complicated system of Equations (4) has to be investigated in this case.

Finally, by using the general motion stability theory it is also in this case possible, in principle, to select system parameters for which the system is stable; however, large amplification factors cannot be thereby secured and, consequently, the system accuracy will be low.

Let us consider one of the methods for increasing the system stability margin for small null currents – the method of compensating the nonlinear characteristics.

2. The Method of Increasing the System Stability Margin for Small Null Currents

Let us introduce an additional inertialess link with the characteristic $\varphi^*(\epsilon_1)$ in the servosystem chain, as is shown in Fig. 4. Let the $\varphi^*(\epsilon_1)$ function be such that the following condition is satisfied:

$$0 = n_0 F\{k_a \varphi[\varphi^*(\varepsilon_1)]\} = n_0 a \varepsilon_1, \qquad (5)$$

where

$$F(\Delta i) = \frac{f_1(\Delta i)}{f_2(\Delta i)}.$$

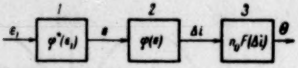

Fig. 4. 1) Nonlinear element; 2) amplifier; 3) clutch.

Figure 5 shows the approximate shapes of the $\varphi(\epsilon)$, $F(\Delta i)$, and $\varphi^*(\epsilon_1)$ functions.

Then, the system of Equations (3) can be written in the following form*:

$$\frac{T_1}{f_2(\Delta i)}\frac{d\theta}{dt} + \theta = n_0F(\Delta i),$$

$$T_1T_2\frac{d^2\Delta i}{dt^2} + (T_1 + T_2)\frac{d\Delta i}{dt} + \Delta i =$$

$$= k_a\varphi_1(\varepsilon_1) + k_a\frac{T_1 + T_2}{2}\frac{d\varphi_1(\varepsilon_1)}{dt},$$

$$\varepsilon_1 = k_T(E - \theta), \tag{6}$$

where $\varphi_1(\epsilon_1) = \varphi[\varphi^*(\epsilon_1)]$.

The system of Equations(6) differs from the system (3) by the form of the current difference Δi vs. error curve.

We shall investigate the stability of a servosystem with an additional link in the case where condition (5) is satisfied.

By expanding the $F(\Delta i)$ and $\varphi_1(\epsilon_1)$ functions into the power series

$$F(\Delta i) =$$

$$= k_2\Delta i + k_3\Delta i^2 + k_4\Delta i^3 + \ldots \quad \varphi_1(\varepsilon_1) =$$

$$= k_1\varepsilon_1 + \alpha\varepsilon_1^2 + \alpha_2\varepsilon_1^3 + .$$

and by substituting them in (6) while neglecting the fourth and the subsequent terms, we obtain

$$T^*(\Delta i)\frac{d0}{dt} + \theta = n_0k_2\Delta i + n_0k_3\Delta i^2 + n_0k_4\Delta i^3,$$

$$T_1T_2\frac{d^2\Delta i}{dt^2} + (T_1 + T_2)\frac{d\Delta i}{dt} + \Delta i =$$

$$= k_ak_1\varepsilon_1 + k_a\alpha\varepsilon_1^2 + k_a\alpha_1\varepsilon_1^3 + \tag{7}$$

$$+ k_a\frac{T_1 + T_2}{2}(k_1 + 2\alpha\varepsilon_1 + 3\alpha_1\varepsilon_1^2)\frac{d\varepsilon_1}{dt},$$

$$\varepsilon_1 = k_T(E - \theta),$$

where $T^*(\Delta i) = I_1n_0/f_2(\Delta i)$.

Let us apply to the system a constant action E_0. Then, according to (7), the equations for the servosystem stimulated motion will be of the following form:

$$T^*(\Delta i)\frac{d\theta}{dt} + 0 = B_1\Delta i + B_2\Delta i^2 + B_3\Delta i^3,$$

$$T_1T_2\frac{d^2\Delta i}{dt^2} + (T_1 + T_2)\frac{d\Delta i}{dt} + \Delta i =$$

$$= -A_10 + A_20^2 - A_30^3 -$$

$$- A_4\frac{d\theta}{dt} + A_5\frac{d\theta^2}{dt} - A_6\frac{d\theta^3}{dt}, \tag{8}$$

where

$$A_1 = k_ak_1k_T +$$

$$+ 2k_ak_T^2\alpha(E_0 - \theta_0) + 3k_ak_T^3\alpha_1(E_0 - \theta_0)^2,$$

$$A_2 = k_ak_T^2\alpha + 3k_ak_T^3\alpha_1(E_0 - \theta_0), \quad A_3 = k_ak_T^3\alpha_1,$$

$$A_4 = A_1\frac{T_1 + T_2}{2},$$

$$A_5 = A_2\frac{T_1 + T_2}{2}, \quad A_6 = A_3\frac{T_1 + T_2}{2},$$

$$B_1 = n_0k_2 + 2n_0k_3\Delta i_0 + 3n_0k_4\Delta i_0^2,$$

$$B_2 = n_0k_3 + 3n_0k_4\Delta i_0, \quad B_3 = n_0k_4.$$

Here, θ_0 and Δi_0 are the respective steady-state values of the angular velocity and the current difference at the system output,or the particular solutions of (8).

The $T^*(\Delta i)$ function can be well approximated by the relation

$$T^*(\Delta i) = \frac{T_0 + \alpha_2\Delta i^2}{1 + \alpha_3\Delta i^2},$$

where T_0, α_2, and α_3 are constant coefficients.

In stability investigation, we shall use the methods of the Lyapunov general theory of motion stability [3].

Let us consider the first approximation of the system of Equations (8). After reduction to the normal Cauchy form, we obtain:

$$\frac{dx}{dt} = z, \quad \frac{dy}{dt} = \frac{B_1}{T_0}x - \frac{1}{T_0}y,$$

$$\frac{dz}{dt} = -\left(\frac{1}{T_1T_2} + \frac{A_4B_1}{T_0T_1T_2}\right)x + \tag{9}$$

$$+ \left(\frac{A_4}{T_0T_1T_2} - \frac{A_1}{T_1T_2}\right)y - \frac{T_1 + T_2}{T_1T_2}z.$$

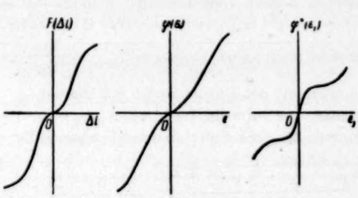

Fig. 5.

---

*In order to simplify calculations, the last term of the second equation in (3) is assumed to be equal to zero, since the magnitudes of T_1 and T_2 differ little from each other, and $d\varphi(\epsilon)/dt >> d\varphi^*(\epsilon)/dt$. It can be shown that the retention of this term would not affect the results to be obtained later.

where x = Δi and y = θ.

On the basis of one of the well-known Lyapunov theorems, the servosystem motion will be stable if all roots of the characteristic equation of system (9) are negative.

The characteristic equation of the first-approximation system of equations is of the form

$$a_0p^3 + a_1p^2 + a_2p + a_3 = 0,$$

where

$$a_0 = T_0T_1T_2,\quad a_1 = T_1T_2 + T_0T_1 + T_0T_2,$$

$$a_2 = T_0 + T_1 + T_2 + A_1B_1\frac{T_1+T_2}{2},$$

$$a_3 = 1 + A_1B_1.$$

All roots of the characteristic equation will be negative if

$$\begin{gathered} 2a_1^2 - 6a_0a_2 > 0, \\ a_1^2a_2 + 3a_0a_1a_3 - 6a_0a_2^2 > 0. \end{gathered} \tag{10}$$

By substituting the values of the characteristic equation coefficients in(10), we obtain

$$\begin{gathered} (T_1T_2 + T_0T_1 + T_0T_2)^2 - 3T_0T_1T_2\left[T_0 + T_1 + T_2 + \frac{1}{2}(T_1+T_2)A_1B_1\right] > 0, \\ (T_1T_2 + T_0T_1 + T_0T_2)^2\left[T_0 + T_1 + T_2 + \frac{1}{2}(T_1+T_2)A_1B_1\right] + 3T_0T_1T_2(T_1T_2 + \\ + T_0T_1 + T_0T_2)(1 + A_1B_1) - 6T_0T_1T_2\left[T_0 + T_1 + T_2 + \frac{1}{2}(T_1+T_2)A_1B_1\right]^2 > 0. \end{gathered} \tag{11}$$

An analysis of inequalities (11) shows that the A_1B_1 product must be a sufficiently small quantity (positive or negative) if these inequalities are to be satisfied. For instance, for $T_0 = 0.15$, $T_1 = 0.05$, and $T_2 = 0.01$, the system will be stable if the product A_1B_1 value lies in the $-3 < A_1B_1 < 1$ interval.

We shall determine the conditions for the smallness of the A_1B_1 value by developing the expression for this product:

$$\begin{gathered} A_1B_1 = \\ = k_a k_1 k_2 k_\text{T} n_0 + k_a k_1 k_\text{T}(2n_0k_3\Delta i_0 + 3n_0k_4\Delta i_0^2) + \\ + 2\alpha k_a k_\text{T}^2(E_0 - \theta_0)(k_2n_0 + 2n_0k_3\Delta i_0 + 3n_0k_4\Delta i_0^2) + \\ + 3\alpha_1 k_a k_\text{T}^3(E_0 - \theta_0)^2(k_2n_0 + 2n_0k_3\Delta i_0 + 3n_0k_4\Delta i_0^2). \end{gathered} \tag{12}$$

It is obvious from expression (12) that the value of A_1B_1 can be small only if the α and α_1 coefficients are negative. Actually, the values of Δi_0 and $E_0-\theta_0$ are positive.† The k_3 coefficient is also positive, which can be readily demonstrated if we consider the character of the F(Δi) function (Fig. 5). The k_4 coefficient can be negative; however, it has a small value. Therefore, the terms in brackets in (12) in the operating range of Δi variations are positive. The first term in (12), which represents the amplification factor of an open linearized system for $E_0 = 0$, has a comparatively large value (it is usually equal to 500-1000 and over). Consequently, the value of the A_1B_1 product can be reduced only by considering the last two terms in (12) for negative values of α and α_1,‡ i.e., only if the $\varphi^*(\epsilon_1)$ function is defined.

It can be readily shown that the necessary form of the $\varphi^*(\epsilon_1)$ function, for which the α coefficient is negative, can be obtained by satisfying condition (5). The condition (5) will be called the condition for the linear compensation of the clutch static characteristic.

Actually, it can be seen from Fig. 5 that the series obtained by expanding the $\varphi^*(\epsilon_1)$ function must have a negative sign in front of the second term, i.e.,

$$\varphi^*(\varepsilon_1) = r_1\varepsilon_1 - r_2\varepsilon_1^2 + \ldots. \tag{13}$$

This follows also from the manner of composing the $\varphi^*(\epsilon_1)$ function, which can be written in the following form:

$$\dot{\varphi}_1(\varepsilon_1) = \varepsilon_{12} + \left[\varepsilon(\theta_1) - \frac{\theta_1}{n_0 a}\right],$$

where θ_1 is the fixed value of the θ(ε) function, and ϵ_{12} is the corresponding value of ε.

Then, by writing the function which approximates the amplifier characteristic in the form

$$\varphi(\varepsilon) = k_{a_1}\varepsilon + k_{y_2}\varepsilon^2 + \ldots$$

and substituting here the value of ε from (13), we obtain

$$\begin{gathered} \varphi_1(\varepsilon_1) = \\ = k_{a_1}r_1\varepsilon_1 - (k_{a_1}r_2 - k_{a_2}r_1^2)\varepsilon_1^2 - 2k_{a_2}r_1r_2\varepsilon_1^3 + \ldots. \end{gathered} \tag{14}$$

---

†Obviously, due to the symmetry of the clutch characteristics for a negative signal at the system input, this remains valid if Equations (8) are composed with respect to the negative increment.

‡The α_1 coefficient can also be positive. This depends on the actual system parameter values.

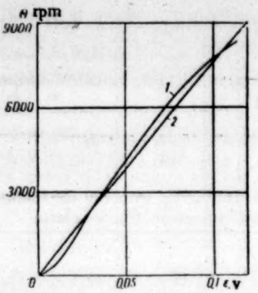

Fig. 6.

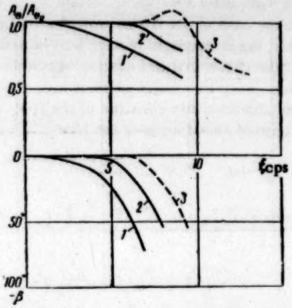

Fig. 7.

Under the condition where $k_{a1}r_2 > k_a r_1^2$, which can always be satisfied, the signs in front of the second and the third terms in series (14), which correspond to terms with α and α_1, are negative.

Thus, it follows from the above that a linear compensation of the clutch static characteristic provides the possibility of increasing the stability margin of a servosystem with a clutch operating with small null currents. This is confirmed by experiments, the results of which are presented below.

3. Experimental Results

The experiments were performed with a drive which had the following parameters: rotor radius: 26 mm; rotor thickness: 0.5 mm; rotor moment of inertia: $I = 0.07$ g·cm·sec²; maximum ampere-turns in the control winding: 550 a. t.; the number of poles in the spider: 6; angular velocity of electromagnet poles: $n_0 = 11,800$ rpm; the maximum output shaft torque: $M_{to} \approx 3$ kg·cm; the maximum output shaft power: 100 w.

The clutch operation was regulated by means of an electronic amplifier (the maximum control current: 100 ma). In order to simplify the experiments, the $\varphi^*(\epsilon_1)$ function was reproduced by means of a standard KNB nonlinear electronic unit.

It should be noted that the practical realization of the $\varphi^*(\epsilon_1)$ function in the system does not require a special unit; it can be secured by using nonlinear resistors, for instance, thyrites, which are connected to the input of the amplifier which controls the clutch. This is especially easy to arrange in the case where amplifiers based on semiconductor elements are used.

Figure 6 shows the dependences of the clutch output shaft speed on the amplifier voltage (1) before and (2) after compensation of the characteristic for $i_0 = 0.08 i_{max}$.

Figure 7 shows the frequency characteristics of a closed system (the relative amplitude A_θ/A_{θ_0}, where A_{θ_0} is the input voltage amplitude and A_θ is the velocity amplitude at the system output, and the phase β) for $i_0 = 0.08 i_{max}$ when the nonlinear element is absent (curves 1) and when the nonlinear element is present (curves 2). For the sake of comparison, system characteristics for normal (large) null currents $i_0 = 0.32 i_{max}$ (curves 3) are shown by dotted lines in the same figure. In all cases, the $k = k_a k_1 k_2 k_T n_0$ coefficient was chosen in such a manner that the system was stable for any input signals; it was equal to 36.4, 118, and 1500, respectively. The frequency characteristics were plotted for the large input signal $\theta_0 = 0.5\theta_{max} = 4710$ rpm.

It is obvious from Fig. 7 that the application of linear compensation of the clutch characteristics makes it possible to increase the system stability margin and, consequently, to increase its accuracy for small null currents.

As was to be expected on the basis of the above theoretical investigation, experiments showed that, for small null currents, the system stability is disturbed only when a voltage E is supplied to the system input, and it depends only on the magnitude of this voltage (i.e., on the value of $A_1 B_1$). This causes the appearance of self-oscillations in the control currents which lead to their simultaneous rise. This is illustrated by the oscillograms shown in Fig. 8.

The oscillations which appear in the system if its stability is disturbed are of a complicated character, and they should be studied separately.

It should be noted that the system efficiency is not affected if it is unstable in the above sense; however, the energy loss arising in this causes rapid heating in clutch drives with a power of over 100 w, and, therefore, unstable system operating conditions are inadmissible.

SUMMARY

1. A servosystem where a drive with a reversive electromagnetic induction clutch which operates with small null currents [$i = (0.02\text{-}0.08)i_{max}$] is used is described by a system of nonlinear differential equations with variable constants. The over-all amplification factor of a linearized system for which a stable system

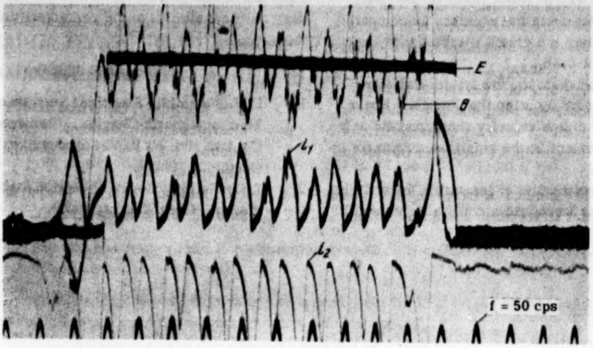

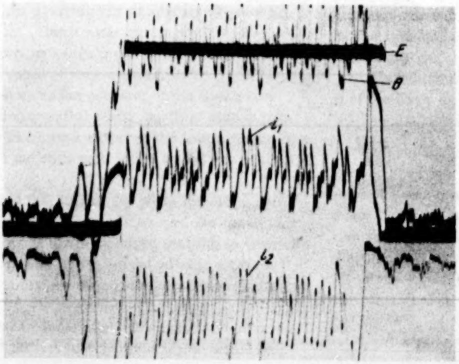

Fig. 8.

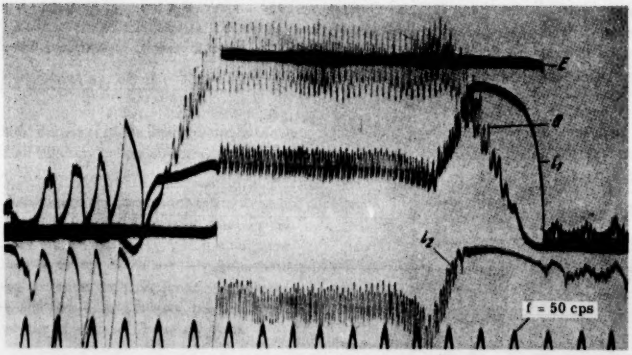

operation is possible will be much lower in this case, which leads to a lower operation accuracy in comparison with a system where the clutch operates with large null currents [$i = (0.2-0.3)i_{max}$].

2. For small null currents, the system stability margin can be increased by using the described linear compensation of the clutch velocity characteristic or by using a nonlinear element in the amplifier circuit (or in the amplifier itself).

3. The described method of increasing the stability margin of a nonlinear servosystem could also be used in other automatic control systems if the characteristics of their units are similar to the characteristics described in this article.

LITERATURE CITED

1. P. F. Klubnikin, Electrical Servomechanisms with Electromagnetic Clutches. Elements of Automatic Control. Ed. by V. V. Solodovnikov [in Russian] (Mashgiz, 1958) 2.
2. I. G. Malkin, Theory of Motion Stability [in Russian] (Gostekhizdat, 1952).

THE MAXIMUM DYNAMIC CHARACTERISTIC VALUES OF SERVOMECHANISM COMPONENTS OF SERVOSYSTEMS. I

G. A. Nadzhafova

Moscow

Translated from Avtomatika i Telemekhanika, Vol. 21, No. 7, pp 973-981, July, 1960
Original article submitted April 1, 1960

The problem of the shortest transient process in electrical servosystems is considered. An electric dc servomechanism with independent excitation is investigated.

The maximum dynamic characteristic values of systems with limited values of the torque, the angular velocity, and the voltage supplied to the servomechanism are determined.

The operation speed of servosystems is mainly determined by the dynamic characteristics of powered servomechanisms. The limitations imposed on the coordinates of servomechanisms do not permit an arbitrary increase in the speed of servosystems.

We shall consider the problem of the maximum possible operation speed of electrical final elements in servosystems with limited values of the motor torque, the motor rpm, and the voltage supplied to the motor armature.

It is assumed that, under the given operating conditions, the motor heating does not exceed the maximum allowable values. It is also assumed that the servomechanism is controlled by changing the voltage which is supplied to the armature circuit for a constant excitation flux.

We shall try to determine the maximum operation speed of electrical servomechanisms which would be compatible with the limitations imposed on the system. These evaluations will make it possible to verify the maximum possible operation speed of a servosystem or to select a final mechanism on the basis of the technological requirements imposed on the servosystem.

1. Equation of Motion of the Servomechanism

The schematic diagram of the servosystem is shown in Fig. 1. We shall investigate the power-controlled electric motor.

In order to investigate the servomechanism dynamic characteristics, we must know the equation relating the monitoring quantity – the voltage U_A – to the output shaft rotation angle α_2 or α_1. If we neglect the armature reaction, the eddy currents, the inductance in the motor armature circuit, and some other factors, the equation of the motor armature circuit will be of the form

$$U_A - E_{mot} = I_A R_A, \qquad (1)$$

where $E_{mot} = k_e \Phi \omega_1$ is the motor counter-emf, I_A is the armature current, R_A is the armature winding resistance, k_e is a constant coefficient, and Φ is the motor excitation flux.

The equation of motion of the electric motor shaft is of the form

$$I\frac{d\omega_1}{dt} = M_{mot} - M_L \quad \text{or} \quad I\frac{d^2\alpha_1}{dt^2} = M_{mot} - M_L, \qquad (2)$$

where I is the motor and load moment of inertia, reduced to the motor shaft, $M_{mot} = k_m \Phi I_A$ is the motor torque, M_L is the load moment, reduced to the motor shaft, and k_m is a constaht coefficient.

From Eqs. (1) and (2), we obtain the equation for the controlled servomechanism in the following form:

$$I\frac{d^2\alpha_1}{dt^2} + \frac{k_e k_m \Phi^2}{R_A}\frac{d\alpha_1}{dt} = \frac{k_m \Phi}{R_A} U_A - M_L. \qquad (3)$$

In order to generalize the obtained results, we shall represent Eq. (3) in a system of dimensionless coordinates by introducing the following relative quantities: $\alpha_1 - \alpha_{ass}/\alpha_{bas} = x$ is the deviation of the motor shaft rotation angle from the assigned value, $\omega_1 - \omega_{ass}/\omega_{bas} =$

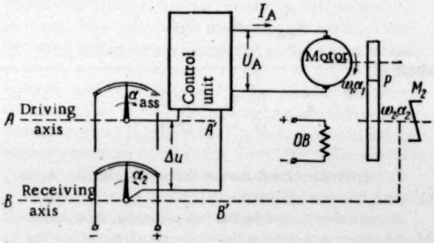

Fig. 1.

= y is the deviation of the motor angular velocity from the assigned value, $U_A/U_{A\,bas} = u$ is the control voltage, $I_A/I_{A\,bas} = i_A$ is the armature current, $I_L/I_{A\,bas} = i_L$ is the load current ($I_L = M_L/k_m\Phi$), $\omega_{ass}/\omega_{bas} = \varphi$ is the rate of change in the driving action α_{ass}, and $t/T_{bas} = \tau$ is the dimensionless time.

For the basic quantities, we shall use: the nominal voltage, the short-circuit motor current, the boundary velocity, and the drive electromechanical and angular constants, which are equal to

$$T_{bas} = \frac{I_{bas}}{k_m\Phi I_{A\,bas}} = \frac{GD^2}{375}\frac{n_0}{M_{sc}}, \quad \alpha_{bas} = T_{bas}\omega_{bas}.$$

Let us write the equations of motion (3) and (2) for the accepted type of driving actions in terms of dimensionless quantities:

$$\frac{d^2x}{d\tau^2} + \frac{dx}{d\tau} = u - i_L - \varphi, \tag{4}$$

$$\frac{d^2x}{d\tau^2} = i_A - i_L, \quad \frac{dx}{d\tau} = y. \tag{5}$$

The considered types of driving actions are given below.

2. Characteristics of Loads, Driving Actions, and Restrictions

In the majority of cases, servosystems are either not loaded with the static resistance moment, when they have to overcome only the load inertia forces, or they are loaded with resistance moments, which are due either to the overbalancing load or to dry friction forces.

In connection with this, in the first part of this paper, we shall consider the inertial forces ($I \neq 0$ and $M_L = 0$) and the constant resistance moment ($I \neq 0$ and M_L = const) as loads reduced to the motor shaft.

The behavior of a system loaded with inertial forces and the dry friction moment ($I \neq 0$ and $M_L = M_T \sin\omega$) will be investigated in the second part of this article.

For the driving actions, we shall use the actions defined by a class of reproducible functions of the following form:

$$\alpha_{ass} = A_0 + A_1 t,$$

where

$$A_0 = \begin{cases} 0 & \text{or} \quad t < 0, \\ 1 & \text{or} \quad t \geqslant 0. \end{cases}$$

In particular cases, one of the coefficients – A_0 or A_1 – can be equal to zero.

As was mentioned in the introduction, in the considered servomechanism, the basic restrictions are the restrictions with respect to the moment, velocity, and voltage, i.e., the following conditions hold:

$$\left|\frac{d^2x}{d\tau^2}\right| \leqslant i_{ma}, \quad \left|\frac{dx}{d\tau}\right| \leqslant y_{ma}, \quad |u| \leqslant u_{ma}.$$

The above coordinate restrictions are interlinked by the servomechanism mechanical characteristic (Fig. 2). As can be seen from the mechanical characteristic equation

$$\omega_1 = \frac{U_A}{k_e\Phi} - M\frac{R_A}{k_e k_m\Phi^2},$$

the torque developed by the motor, the motor angular velocity, and the armature voltage are closely related by the static dependence $\omega_1 = f(M, U_A)$. Therefore, the mechanical characteristic is limited by a certain polygon, which contains the region of maximum allowable values of these quantities. The corresponding sides of this polygon of maximum allowable values limit either the maximum moment (i_{ma}), or the moment (i_{ma}) and voltage (u_{ma}), or the moment (i_{ma}), the voltage (u_{ma}), and the angular velocity (y_{ma}). In dependence on operating conditions, either $d^2x/d\tau^2$, or $d^2x/d\tau^2$ and $dx/d\tau$ and $d^2x/d\tau^2$ and u, or $d^2x/d\tau^2$, u, and $dx/d\tau$ will be limited. The regions of possible operating conditions for the case where $i_L = 0$ and $\varphi = 0$ are shown in Fig. 3.

With regard to the requirements for the optimum conditions in a control process where the maximum operating speed is to be attained, it is necessary to ensure that one of the restricted coordinates is maintained at its maximum value during particular motion stages [1, 2].

3. Equations of Isochrone Regions

In order to determine the maximum capabilities of servomechanisms with regard to their operation speed, it is necessary to establish relations between the initial mismatch values and the optimum transient process times, during which the mismatches are reduced to zero.

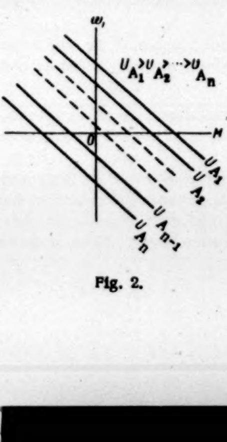

Fig. 2.

For this purpose, it is convenient to use the method of isochrones, which was first used by A. Ya. Lerner in the investigation of optimum systems [3]. The isochrones represent the totality of initial states of a dynamic system from which it passes into an assigned state in the minimum possible time for an optimum control law.

For plotting the region of isochrones, it is necessary to integrate Eq. (4) and to reverse the direction of time τ readings, while the time at which the transient process is completed is taken as the initial time. For the accepted reading direction, the time $\beta = \tau_* - \tau$, where $\tau_* = \beta_*$ is the transient process time (the isochrone time).

If only the motor torque is limited, the isochrone region equation is of the form

$$x_0 = \mp \frac{i_{ma}}{4}\beta_*^2 - \frac{y_0}{2}\beta_* \pm \frac{1}{4i_{ma}}\left(i_L - \frac{y_0}{\beta_*}\right)^2\beta_*^2. \qquad (6)$$

In this equation, x_0 is the initial mismatch between the servosystem receiving and driving axes, y_0 is the initial mismatch between the angular velocities of the receiving and the driving axes, β_* is the isochrone time [i.e., the transient process time during which the servosystem, under optimum control conditions, passes from the initial state, which is determined by the tracing point (x_0, y_0) on the (x, y) phase plane, to the assigned state, namely, to the state defined by the point with the coordinates $(x = 0, y = 0)$, i_{ma} is the maximum allowable motor current, which is proportional to the maximum torque value, and i_L is the load current due to the constant resistance moment.

If the motor torque and angular velocity are limited, the isochrones are described by the equation

$$x_0 = \pm y_{ma}\beta_* \pm \frac{y_{ma}^2}{2(i_{ma} \pm i_L)} \pm \frac{(y_{ma} \mp y_0)^2}{2(i_{ma} \mp i_L)}. \qquad (7)$$

In this equation, y_{ma} is the maximum value of the servomechanism velocity.

If the motor torque and the voltage supplied to the armature circuit are limited, the isochrone equation will be of the following form:

$$x_0 = (\varphi \mp u_{ma} + i_L)\,\beta_* \mp \frac{y^2}{2(i_{ma} \pm i_L)} \pm \frac{(y_0 \mp y_x)^2}{2(i_{ma} \mp i_L)} - \frac{(\varphi \mp u_{ma} \mp i_{ma})\,y}{i_{ma} \pm i_L} \mp y_0, \qquad (8)$$

where u_{ma} is the maximum armature voltage, y_x is the velocity for which the maximum voltage is attained, and $\underline{y}$ is the present velocity on the mechanical characteristic portion which corresponds to $u = u_{ma}$. In order to determine Eq. (8), the present value of velocity $\underline{y}$ must be expressed in terms of y_0. For this, we use the expressions for the connection times β_1 and β_2, where β_1 is the braking time, and β_2 is the sum of the time β_1 and the motion time $\Delta\beta$ for the constant maximum voltage:

$$\beta_1 = \frac{y}{i_{ma} \pm i_L}, \qquad \beta_2 = \beta_* \pm \frac{y_0 - y_x}{i_{ma} \mp i_L},$$

$$\Delta\beta = \ln \frac{i_{ma} \mp i_L}{u_{ma} \mp \varphi - y \mp i_L}, \quad \beta_2 = \beta_1 + \Delta\beta.$$

In dependence on the initial system state (x_0, y_0), a well-defined time β_1 must be secured for a given isochrone time. In connection with this, there is, on the one hand, a well-defined relation between y_0 and $\underline{y}$ and, consequently, between β_1 and β_2, on the other hand. By using the values $y \geq y_x$, we plot the $\beta_1 = \varphi_1(y)$ and $\Delta\beta = \varphi_2(y)$ curves. For every given $\underline{y}$, we find the corresponding β_2 and, consequently, the value of y_0.

If the motor torque, voltage, and angular velocity are limited, the isochrone is described by the equation

$$x_0 = \mp y_{ma}(\beta_* - 1) \mp \frac{(y_x \mp y_0)(u_{ma} \mp \varphi - y_{ma} \mp i_L)}{i_{ma} \mp i_L} \mp (u_{ma} \mp \varphi - y_{ma} \mp i_L) \ln \frac{i_{ma} \mp i_L}{u_{ma} \mp \varphi - y_{ma} \mp i_L} \pm \frac{y_L^2}{2(i_{ma} \pm i_L)} \pm \frac{(y_x \mp y_0)^2}{2(i_{ma} \mp i_L)} - y_0. \qquad (9)$$

The isochrones consist of closed curves composed of two branches, which are described by the above equations, and of lines corresponding to the restriction of the system coordinates.

In order to plot the isochrone regions, we must determine the limits of the servomechanism operating conditions.

4. Determination of the Operating Condition Limits

The servomechanism operating conditions differ from each other with respect to the number of restrictions imposed on the system coordinates. In our case, we shall consider the regions corresponding to operating conditions with restrictions pertaining only to the moment, restrictions with respect to the moment and velocity, restrictions with respect to the moment and voltage, and restrictions with respect to the moment, voltage, and velocity (Fig. 3). For plotting the isochrone regions in correspondence to the operating condition regions, it is necessary to use well-defined isochrone equations by choosing from (6)-(9) the equation corresponding to the given operating conditions.

The limits of the servomechanism operating conditions are determined in dependence on the isochrone time β_*. However, the determinations with respect to time are necessary, but not sufficient, conditions.

Within limits of the found time determinations, it is necessary to provide determinations with respect to the initial conditions.

If, according to the motor operating conditions, no restrictions are imposed on voltage and angular velocity, the regime characterized by restrictions only with respect to the moment will apply for any β_*. The isochrones corresponding to this case, plotted according to Eq. (6), are shown in Fig. 4.

If the working mechanism imposes a certain given restriction on the motor speed, while no restrictions with respect to voltage are present, two regimes are possible. For $\beta_* < \beta_{*li}$, there will be only one restriction with respect to the moment; for $\beta_* > \beta_{*li}$, two restrictions are possible. The isochrone limiting time is determined by the expression

$$\beta_{*li} = \frac{y_{ma}}{i_{ma} + i_L}. \tag{10}$$

In order to find the equation for the regime limit, we shall determine β_*, assuming that the system motion corresponds to the limiting case, i.e., although the system attains the maximum speed, the braking begins at the moment when this speed is attained. In this,

$$\beta_* = \mp \frac{y_0}{i_{ma} \mp i_L} + \frac{2y_{ma} i_{ma}}{i_{ma}^2 - i_L^2}. \tag{11}$$

By using Eqs. (7) and (11), we find the regime limits:

$$x_0 = \pm \frac{y_0^2}{2(i_{ma} \mp i_L)} \mp \frac{2y_{ma}^2 i_{ma}^2}{(i_{ma} \pm i_L)^2 (i_{ma} \mp i_L)} \pm \frac{y_{ma}^2 i_{ma}}{(i_{ma} \pm i_L)^2}. \tag{12}$$

Figure 5 represents the division of the phase plane into regions with respect to the character of the optimum process phase trajectory when restrictions with respect to the moment and speed are present.

In the region represented by the shaded area A, the phase trajectories are limited only with respect to the moment. The isochrones for the initial conditions valid for this region are found from Eq. (6), and, for initial conditions valid outside this region, Eq. (7), which takes into account the restriction with respect to speed, holds. Figure 5 shows examples of isochrones corresponding to different operating conditions.

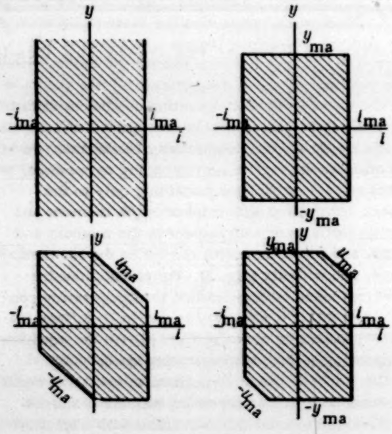

Fig. 3. Regions of motion restrictions.

In the case where a definite restriction is imposed not only on the moment, but also on the motor speed and voltage, three kinds of operating conditions should be distinguished, namely, the regime characterized by a restriction only with respect to the moment, the regime with moment and voltage restrictions, and, finally, the regime where all three coordinates are limited.

In correspondence with the above-mentioned, there are two isochrone limiting time values β_{*li_1} and β_{*li_2}.

If

$$\beta_* < \beta_{*li_1} = \frac{y_x}{i_{ma} + i_L}, \tag{13}$$

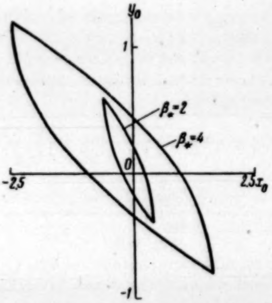

Fig. 4. Isochrones for the case where only the motor torque is limited (i_{ma} = 0.25; i_L = 0.05).

we have a regime with restrictions only with respect to the moment, and, if

$$\beta_{*1i_1} < \beta_* < \beta_{*1i_2} = \beta_{*1i_1} + \Delta\beta_{\max}, \qquad (14)$$

where $\Delta\beta_{\max} = \ln \dfrac{i_{ma} + i_L}{u_{ma} - \varphi - y_{ma} + i_L}$, we have regimes with restriction only with respect to the moment, as well as with restrictions with respect to the moment and voltage. In this case, a regime with all three kinds of restrictions will not be present.

If $\beta_* > \beta_{*1i_2}$, all three kinds of operating conditions will be present.

In the case under consideration, the phase plane is divided by two boundary curves into regions corresponding to the above operating conditions.

The equation of the boundary curve which separates the region where only the moment is restricted from the region where both the moment and the voltage are restricted (speed restrictions are not present) is determined in a similar manner. In this, the isochrone time β_*, which corresponds to the limiting case, is expressed by the relation

$$\beta_* = \frac{y_x}{i_{ma} \mp i_L} \mp \frac{y_0 \mp y_x}{i_{ma} \mp i_L}. \qquad (15)$$

The operating conditions boundary is determined by the equation

$$x_0 = \mp \frac{y_x^2}{2(i_{ma} \pm i_L)} \pm \frac{y_0^2 - y_x^2}{2(i_{ma} \mp i_L)}. \qquad (16)$$

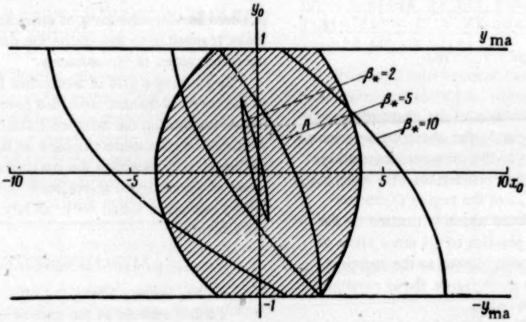

Fig. 5. Isochrones and boundary lines for the case of moment and speed restrictions ($i_{ma} = 0.25$; $i_L = 0.05$; $\varphi = 0$; $y_{ma} = 1.0$).

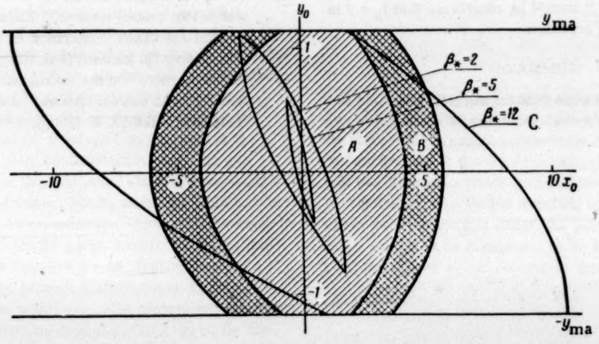

Fig. 6. Isochrones and boundary curves in the case of restrictions with respect to the moment, voltage, and speed ($i_{ma} = 0.25$; $i_L = 0.05$; $\varphi = 0$; $u_{ma} = 1.25$; $y_x = 1.0$; $y_{ma} = 1.15$).

The equation of the boundary curve which separates the region where the moment and the voltage are restricted from the region where the moment, the voltage, and the speed are restricted is obtained by eliminating the limiting isochrone time which is expressed by the relation

$$\beta_{*} = \frac{y_{\mathrm{ma}}}{i_{\mathrm{ma}} \pm i_{\mathrm{L}}} + \ln \frac{i_{\mathrm{ma}} \mp i_{\mathrm{L}}}{u_{\mathrm{ma}} - y_{\mathrm{ma}} \mp \varphi \mp i_{\mathrm{L}}} + \frac{u_{\mathrm{ma}} \mp y_0 \mp \varphi - i_{\mathrm{ma}}}{i_{\mathrm{ma}} \mp i_{\mathrm{L}}}. \qquad (17)$$

The regime boundary to be found is described by the equation

$$x_0 = \pm (y_{\mathrm{ma}} \mp y_0) \mp \frac{y^2_{\mathrm{ma}}}{2\,(i_{\mathrm{ma}} \pm i_{\mathrm{L}})} \pm \frac{(y_0 \mp y_x)\,(u_{\mathrm{ma}} \mp \varphi \mp i_{\mathrm{L}})}{i_{\mathrm{ma}} \mp i_{\mathrm{L}}} \pm$$
$$\pm \frac{(y_0 \mp y_x)^2}{2\,(i_{\mathrm{ma}} \mp i_{\mathrm{L}})} \pm (\varphi \mp v_{\mathrm{ma}} + i_{\mathrm{L}}) \ln \frac{i_{\mathrm{ma}} \mp i_{\mathrm{L}}}{u_{\mathrm{ma}} - y_{\mathrm{ma}} \mp \varphi \mp i_{\mathrm{L}}}, \qquad (18)$$

where

$$y_x = u_{\mathrm{ma}} - \varphi - i_{\mathrm{ma}}.$$

Figure 6 shows the division of the phase plane into regions. In the shaded area A, the phase trajectories are limited only with respect to the moment, the doubly shaded area B corresponds to restrictions with respect to the moment and voltage, and the region C, encompassing the unshaded band which is limited by the maximum speed values, pertains to all three kinds of restriction – restrictions with respect to the moment, voltage, and speed. The same figure shows examples of isochrones for all three cases.

The asymmetry in the regions of isochrones and regime boundaries which are shown in Figs. 4, 5, and 6 is a consequence of the effect of the load current i_{L}, which is due to the overbalancing load. If the load current is absent, it should be considered that $i_{\mathrm{L}} = 0$ in the corresponding equations.

SUMMARY

The obtained equations for the isochrones and regime boundaries for different cases of operation of powered servomechanisms of electrical servosystems make it possible to determine the maximum possible operation speed of servosystems.

By plotting a grid of isochrones for different values of the servomechanism and load parameters when the region containing the assigned initial mismatches and technical requirements imposed on the system is known, we are able to ascertain the maximum possible operation speed of the designed servosystem or to select a suitable final mechanism which will satisfy the technical requirements.

LITERATURE CITED

1. A. Ya. Lerner, "Design of high-speed automatic control systems in the case of limited values of the controlled device coordinates," Transactions of the Second All-Union Conference on Automatic Control Theory [in Russian] (Izd. AN SSSR, 1955) 2.
2. A. A. Fel'dbaum "On the synthesis of optimum automatic control systems," Transactions of the Second All-Union Conference on Automatic Control Theory [in Russian] (Izd. AN SSSR, 1955) 2.
3. A. Ya. Lerner, "On the maximum operation speed of automatic control systems," Avtomatika i Telemekhanika 15, 6 (1954).

CALCULATION OF STATIC CHARACTERISTICS OF "NOZZLE-BAFFLE" ELEMENTS

E. A. Andreeva

Moscow

Translated from Avtomatikai Telemekhanika, Vol. 21, No. 7,
pp 982-996, July, 1960
Original article submitted March 7, 1960

This article presents a calculation method for plotting the static discharge and power characteristics of a "nozzle-baffle" element for compressible and incompressible viscous fluids.

One of the basic elements in pneumatic and hydraulic automation is the "nozzle-baffle" throttle (Fig. 1). The operation of this element is determined by its static characteristics: by the discharge characteristic, i.e., the dependence of the working fluid mass G which is discharged through the throttle on pressure p_0, before the baffle, on pressure p_e at the radius of the nozzle end-face, and on distance h between the nozzle and the baffle, and by the power characteristic, i.e., the dependence of the force F which is generated by the jet action on the baffle on the same parameters p_0, p_e, and h.

In developing a calculation method for plotting the static characteristics, it is necessary to distinguish between two cases: a) when the element is used in hydraulic devices, which means that the working medium is a viscous incompressible liquid, and b) when the element is used in pneumatic devices, when it can be considered that the working medium is an ideal viscous gas.

In the first case, the method of plotting the static discharge $G=G(p_0, p_e, h)$ and power $F=F(p_0, p_e, h)$ characteristics of the "nozzle-baffle" element can be obtained by solving the hydrodynamic problem of the steady-state flow of a viscous incompressible liquid in the radial gap which is formed by the nozzle end-face and the baffle plate surface. In this, the pressure distribution along the radius r of the gap has to be found.

In the second case, the method for plotting the characteristics can be developed on the basis of the equation for the pressure distribution along the gap radius as found for the first case, which applies to an infinitely small volume $2\pi hdr$, where the fluid can be considered to be incompressible. After this, the equation is integrated for the entire volume by taking into account the state equation for an ideal gas and, as a result, we find the pressure distribution of an ideal viscous gas in the radial gap. The present article investigates a calculation method of plotting the static discharge and power characteristics of a "nozzle-baffle" element for a viscous incompressible and a viscous compressible fluid. Brief information on this work has been published in [6] and [9].

1. THE CASE OF A VISCOUS INCOMPRESSIBLE LIQUID

Formulation of the Problem of Steady-State Flow of a Viscous Incompressible Liquid in a Radial Gap

By taking into account the axial symmetry of the flow under consideration, which makes it convenient to use a cylindrical coordinate system (r, z), this problem is reduced to determining the pressure field $p=p(r, z)$. The system of equations which consists of the continuity equation

$$\frac{\partial v_r}{\partial r} + \frac{v_r}{r} + \frac{\partial v_z}{\partial z} = 0 \qquad (1)$$

and the Navier-Stokes equations

$$v_r \frac{\partial v_r}{\partial r} - v_z \frac{\partial v_r}{\partial z} = -\frac{1}{\rho}\frac{\partial p}{\partial r} + \nu\left(\frac{\partial^2 v_r}{\partial r^2} + \frac{\partial^2 v_r}{\partial z^2} + \frac{1}{r}\frac{\partial v_r}{\partial r} - \frac{v_r}{r^2}\right), \qquad (2)$$

$$v_r \frac{\partial v_z}{\partial r} + v_z \frac{\partial v_z}{\partial z} = -\frac{1}{\rho}\frac{\partial p}{\partial z} + \nu\left(\frac{\partial^2 v_z}{\partial r^2} + \frac{\partial^2 v_z}{\partial z^2} + \frac{1}{r}\frac{\partial v_z}{\partial z}\right), \qquad (3)$$

is the basic system of equations to be used in the solution of this problem. In these equations, v_r and v_z are the radial and the axial components of the velocity vector (cm/sec), ρ is the liquid density (kg·sec²/cm⁴), and ν is the kinematic viscosity coefficient (cm²/sec).

Since we shall further consider only those cases where the distance h is small, the pressure under the baffle plate can be considered to be independent of the axial coordinate z, i.e., it can be assumed that

$$\frac{\partial p}{\partial r} = \frac{dp}{dr}.$$

For this, Eqs. (1), (2), and (3) form a closed system:

$$\frac{\partial v_r}{\partial r} + \frac{v_r}{r} + \frac{\partial v_r}{\partial z} = 0, \qquad (4)$$

$$v_r \frac{\partial v_r}{\partial r} + v_z \frac{\partial v_r}{\partial z} = -\frac{1}{\rho}\frac{dp}{dr} + $$

$$+ \nu\left(\frac{\partial^2 v_r}{\partial r^2} + \frac{\partial^2 v_r}{\partial z^2} + \frac{1}{r}\frac{\partial v_r}{\partial r} - \frac{v_r}{r^2}\right), \qquad (5)$$

the solution of which, with the consideration of the boundary conditions

$$\begin{aligned} v_r(r, 0) &= 0, \qquad v_z(r, 0) = 0, \\ v_r(r, h) &= 0, \qquad v_z(r, h) = 0, \end{aligned} \qquad (6)$$

$$p(r_e) = p_e, \qquad (7)$$

$$\int_0^h v_r dz = \frac{Q}{2\pi r}, \qquad (8)$$

where Q is the volumetric liquid discharge (cm³/sec), yields the pressure distribution $p = p(r)$ in which we are interested and, besides, the velocity fields $v_r = v_r(r, z)$ and $v_z = v_z(r, z)$.

By using the concept of the stream function $\psi = \psi(r, z)$, which, by definition, must transform the continuity equation (4) into an identity, the system of equations (4) and (5) and the corresponding boundary conditions (6)-(8) can be conveniently represented in the form of the equation which determines the stream function:

$$\frac{\partial\psi}{\partial z}\left(\frac{\partial^3\psi}{\partial z^2 \partial r} - \frac{2}{r}\frac{\partial^2\psi}{\partial z^2}\right) - \left(\frac{\partial\psi}{\partial r}\right)\left(\frac{\partial^3\psi}{\partial z^3}\right) =$$

$$= r\nu\left(\frac{\partial^4\psi}{\partial z^4} + \frac{\partial^4\psi}{\partial z^2 \partial r^2} - \frac{1}{r}\frac{\partial^3\psi}{\partial z^2 \partial r}\right), \qquad (9)$$

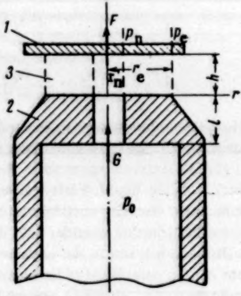

Fig. 1. Diagram of the "nozzle-baffle" element. 1) Baffle; 2) nozzle; 3) radial gap; r_n is the nozzle radius, and r_e is the end-face radius; p_n is the pressure at the nozzle radius, and p_e is the pressure after throttling.

the relations which determine the velocity fields with respect to the stream function:

$$v_r = \frac{1}{r}\frac{\partial\psi}{\partial z}, \qquad v_z = -\frac{1}{r}\frac{\partial\psi}{\partial r}, \qquad (10)$$

and the equation which determines the pressure field with respect to the velocity fields:

$$\frac{1}{\rho}\frac{dp}{dr} = -v_r\frac{\partial v_r}{\partial r} - v_z\frac{\partial v_r}{\partial r} +$$

$$+ \nu\left(\frac{\partial^2 v_r}{\partial z^2} + \frac{\partial^2 v_r}{\partial z^2} + \frac{1}{r}\frac{\partial v_r}{\partial r} - \frac{v_r}{r^2}\right). \qquad (11)$$

In solving Eq. (9) by taking into account relations (10), it is necessary to consider the boundary conditions (6) and (8), and in integrating Eq. (11), condition (7) must be taken into account.

Thus, after integrating Eq. (9) and taking into account (10) and (11), we shall obtain the velocity field under the baffle plate and the pressure distribution in the radial gap.

Analysis of Some Known Solutions

Before obtaining the general solution of the problem, let us determine to what extent the solutions obtained for certain coarse approximations correspond to the actual conditions.

If we assume that the liquid is not viscous ($\nu = 0$), we shall obtain the Bernoulli integral as the solution of Eqs. (2) and (3):

$$\frac{p}{\rho} + \frac{v_r^2}{2} = \frac{p_e}{\rho} + \frac{v_{r_e}^2}{2}.$$

where

$$v_r = \frac{G}{2\pi r h \rho}, \qquad v_{r_e} = \frac{Q}{2\pi r_e h \rho}.$$

For this, the pressure field in criterion form will be

$$B - B_e = -12.5A^2(\alpha^2 - 1), \qquad (13)^*$$

where

$$B = \frac{p h^4 \rho}{\mu^2 r_e^2 \cdot 10^2}, \quad B_e = \frac{p_e h^4 \rho}{\mu^2 r_e^2 \cdot 10^2},$$

$$A = \frac{Gh}{\pi\mu r_e^2 \cdot 10^2}, \quad \alpha = \frac{r_e}{r};$$

p is the pressure under the baffle plate at the radius r (kg/cm²), p_e is the pressure at the nozzle end-face radius (kg/cm²), μ is the dynamic viscosity coefficient (kg·sec/cm²), r_e is the nozzle end-face radius (cm), h is the gap between the nozzle and the baffle (cm), r is the present radius (cm), and G is the mass discharged (kg·sec/cm).

---

* As in Russian [Publisher's note].

If we neglect the inertia terms in Eqs. (2) and (3), but consider that the liquid is viscous, the pressure field will be of the form

$$B - B_e = 6A \ln \alpha. \quad (14)$$

This relation is given in [2].

Paper [3] provides the approximate solution of the system of equations (1)-(3):

$$B - B_e = 6A \ln \alpha - 12.5A^2 (\alpha^2 - 1). \quad (15)$$

Paper [4] provides the equation for the pressure distribution in the radial gap:

$$B - B_e = 6A \ln \alpha - 19.3A^2 (\alpha^2 - 1), \quad (16)$$

which represents a linear combination of approximate solutions (13) and (14), and secures a parabolic radial velocity component distribution in the axial direction. This assumption determines the coefficient in front of the term that characterizes the pressure field in the case where viscosity is neglected.

In Fig. 2, all the above solutions are compared with each other and with the experimantal data borrowed from [4].

Curves 1, 2, 4, and 3 correspond to solutions (13), (14), (15), and (16), respectively. The solid lines pertain to divergent flow, and the dotted lines pertain to convergent flow. The points mark the experimental data which were processed in terms of the same criteria; the white and black points correspond to divergent and convergent flows, respectively. The experiments were performed with a nozzle with $r_n = 0.384$ cm and $r_e = 5.24$ cm. Water was used as the working liquid. Divergent flow was investigated for the gap h = 0.0367 cm between the nozzle and the baffle plate, the discharge Q = 36.4 cm^3/sec, and the temperature t = 12°C, while the dynamic viscosity coefficient was $\mu = 0.0124$ g/cm · sec. Convergent flow was investigated for h = 0.0356 cm, Q = 9.61 cm^3/sec, t = 14°C, and $\mu = 0.0117$ g/cm · sec.

An analysis of the diagrams in Fig. 2 makes it possible to draw the following conclusions:

1. Solutions (13) and (14) do not accurately represent the actual pressure distribution pattern; curves 1 and 2, which correspond to these solutions, do not even qualitatively agree with experimental data.

2. Solution (15) reflects the pressure distribution pattern more accurately, but the corresponding curve 4 still deviates to a great extent from the experimental curve.

3. Equation (16) yields a pressure distribution which is in good agreement with the experimental distribution for divergent flow (solid curve 3), while the correspondence is less accurate for convergent flow (dotted line 3). However, this equation, since it is a semiempirical equation, is not rigorously defined, and, therefore, we cannot be sure that it will agree well with experimental data under different conditions.

Therefore, it became necessary to find a more rigorous solution of this problem.

Determination of the Stream Function and of the Velocity Field

By using the same procedure as in [1], we shall assume that the stream function can be represented as the series

$$\psi(r, z) = \sum_{k=1}^{\infty} \frac{a_k(z)}{r^{k-1}}. \quad (17)$$

By substituting (17) in Eq. (9) and in relations (10), after some transformations, we obtain

$$-\frac{2}{r^2} a_1' a_1'' - \sum_{i=1}^{\infty} \frac{2}{r^{i+2}} \sum_{k=1}^{i+1} a_k' a_{i-k+2}'' -$$

$$-\sum_{i=1}^{\infty} \frac{1}{r^{i+2}} \Big[\sum_{k=1}^{1} (i - k + 1) (a_k' a_{i-k+2}'' -$$

$$- a_k''' a_{i-k+2}) \Big] =$$

$$= \nu \left[\sum_{i=1}^{\infty} \frac{i(i+2)}{r^{i+2}} a_{i+1}'' + \frac{a_1^{IV}}{r^0} + \frac{a_2^{IV}}{r} + \frac{a_3^{IV}}{r^2} + \sum_{i=1}^{\infty} \frac{a_{i+3}^{IV}}{r^{i+2}} \right], \quad (18)$$

$$v_r = \sum_{k=1}^{\infty} \frac{a_k'(z)}{r^k}, \quad v_z = \sum_{k=1}^{\infty} \frac{a_k(z)}{r^{k+1}} (k - 1). \quad (19)$$

By now equating in (18) the coefficients in front of terms with equal powers of r, we shall obtain the following system of ordinary differential equations with respect to the $a_k = a_k(z)$ function:

$$a_1^{IV} = 0,$$

$$a_2^{IV} = 0,$$

$$a_3^{IV} = -\frac{2}{\nu} a_1' a_1'',$$

$$\cdots\cdots\cdots \quad (20)$$

$$a_{i+3}^{IV} = -\frac{2}{\nu} \sum_{j=1}^{i+1} a_j' a_{i-j+2}'' - \frac{1}{\nu} \sum_{j=1}^{i} (i - j + 1)$$

$$(a_j' a_{i-j+2}'' - a_j''' a_{i-j+2}) - i(i+2) a_{i+1}''$$

$$(i = 1, \ldots, \infty).$$

By integrating these equations, the $a_k = a_k(z)$ functions are determined with an accuracy equal to that of the arbitrary constants. The substitution of these functions in (19) makes it possible to determine the velocity distribution after finding the arbitrary constants by using conditions (6) and (8).

By using the notation

$$V_z = \frac{v_z}{6v_0\zeta(1-\zeta)} \frac{35}{\mathrm{Re}} \left(\frac{r}{h}\right)^2 \frac{1}{\zeta},$$

$$V_r = \left[\frac{v_r}{6v_0\zeta(1-\zeta)} - 1\right] \frac{35}{\mathrm{Re}} \frac{r}{h}, \qquad (21)$$

$$= \frac{z}{h}, \quad \mathrm{Re} = \frac{v_0 h}{\nu}, \quad v_0 = \frac{Q}{2\pi r h}$$

and noting that the functions $a_k = 0$ for even values of k, the found velocity distribution law can be represented in the following form:

in the first approximation (k = 1)

$$V_z = 0, \qquad V_r = 0; \qquad (22)$$

in the second approximation (k = 3)

$$V_z = (1-\zeta)(1-2\zeta)(\zeta^2-\zeta-1),$$
$$V_r = 7\left(\zeta^4 - 12\zeta^3 + \frac{7}{2}\zeta^2 - \frac{7}{2}\zeta - \frac{1}{7}\right); \qquad (23)$$

in the third approximation (k = 5)

$$V_z = (1-\zeta)(1-2\zeta)(\zeta^2-\zeta-1) + \left(\frac{h}{r}\right)^2 \frac{1}{1-\zeta} \times$$
$$\times \left(\frac{4}{9}\zeta^7 - 2\zeta^6 + \frac{8}{3}\zeta^5 - \frac{12}{5}\zeta^3 + \frac{4}{3}\zeta^2 + \frac{256}{15}\zeta - \frac{16}{5}\right) -$$
$$- \mathrm{Re}\frac{h}{r}\frac{1}{1-\zeta}\left(\frac{32}{35}\zeta^9 - \frac{16}{5}\zeta^8 + \frac{19}{3}\zeta^7 - \frac{9}{2}\zeta^6 -\right.$$
$$\left. - \frac{48}{35}\zeta^5 + \frac{17}{5}\zeta^4 - \frac{6}{5}\zeta^3 - \frac{26}{231}\zeta + \frac{53}{770}\right), \qquad (24)$$

$$V_r = 7\left(\zeta^4 - 2\zeta^3 + \frac{1}{2}\zeta^2 + \frac{1}{2}\zeta - \frac{1}{7}\right) + \left(\frac{h}{r}\right)^2 \times$$
$$\times \frac{1}{1-\zeta}\left(\zeta^7 - 4\zeta^6 + \frac{14}{3}\zeta^5 - 3\zeta^3 + \frac{4}{3}\zeta^2 + \frac{64}{5}\zeta - \frac{8}{5}\right) -$$
$$- \mathrm{Re}\frac{h}{r}\frac{1}{1-\zeta}\left(\frac{8}{5}\zeta^9 - 8\zeta^8 + \frac{57}{4}\zeta^7 - 9\zeta^6 -\right.$$
$$\left. - \frac{12}{5}\zeta^5 + \frac{51}{10}\zeta^4 - \frac{3}{2}\zeta^3 - \frac{13}{154}\zeta + \frac{53}{1540}\right)$$

The Pressure Field

By substituting now the expressions (22), (23), and (24) in Eq. (11)† and by integrating it while taking into account (7), we obtain the pressure distribution:

in the first approximation

$$p - p_e = \frac{7G\mu}{\pi\rho h^3} \ln\frac{r_e}{r} + 0.125\frac{G^2}{\pi^2\rho h^3}\left(\frac{1}{r_e^2} - \frac{1}{r^2}\right) \qquad (25)$$

and in the criterion form

$$B - B_e = 6A\ln\alpha - 12.5A^2(\alpha^2 - 1); \qquad (26)$$

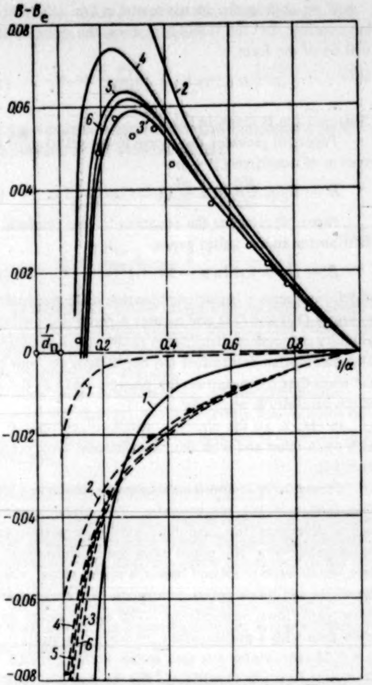

Fig. 2. Pressure distribution along the baffle plate radius. $B-B_e = (p-p_e)\cdot h^4 \rho/\mu^2 r_e^2 \cdot 10^{-2}$ is the dimensionless pressure drop.

in the second approximation

$$p - p_e = \frac{6G\mu}{\pi\rho h^3} \ln\frac{r_e}{r} + 0.1678\frac{G^2}{\pi^2\rho h^2}\left(\frac{1}{r_e^2} - \frac{1}{r^2}\right) \qquad (27)$$

and in the criterion form

$$B - B_e = 6A\ln\alpha - 16.78A^2(\alpha^2 - 1); \qquad (28)$$

in the third approximation

$$p - p_e = \frac{6G\mu}{\pi\rho h^3} \ln\frac{r_e}{r} + 0.1678\frac{G^2}{\pi^2\rho h^2}\left(\frac{1}{r_e^2} - \frac{1}{r^2}\right) +$$
$$+ 0.001425\frac{G^3}{\pi^3\rho}\left(\frac{1}{r_e^4} - \frac{1}{r^4}\right) +$$
$$+ 0.0003675\frac{G^3}{\pi^3\rho h\mu}\left(\frac{1}{r_e^4} - \frac{1}{r^4}\right) \qquad (29)$$

---

† It should be noted that, here, the $v_z = v_z(r, z)$ and $v_r = v_z(r, z)$ functions which are represented by a finite number of terms of the series are substituted in (11), which leads to contradiction: dp/dr depends on z. In order to eliminate this contradiction, averaging with respect to z is used.

and in the criterion form

$$B - B_e = 6A \ln \alpha - 16.78A^2(\alpha^2 - 1) - \tag{30}$$
$$- 0.142A^2\beta^2(\alpha^4 - 1) - 3.67A^3(\alpha^4 - 1),$$

where $\beta = h/r_e$.

Figure 2 shows a comparison between the obtained pressure distribution relations (26), (28), and (30) and experimental data. It is obvious from the comparison that Eqs. (26), (28), and (30) (curves 4, 5, and 6 correspond to these equations in Fig. 2) define pressure distributions which are the closer to the experimental distribution, the larger the number of terms of the series that are taken into account. For convergent flow, these equations provide a better agreement with experimental data than Eq. (16).

Thus, Eqs. (26), (28), and (30) for the pressure distribution under the baffle plate, which are obtained by solving the hydrodynamic problem and which are in good agreement with experimental data, can be used for calculating the pressure distribution as well as for determining the static discharge and power characteristics. It is obvious from Fig. 2 that the third approximation (curve 6) provides only an insignificant improvement in accuracy in comparison with the second approximation (curve 5), but it yields an equation which is much more complicated for use in calculations. Therefore, for determining the pressure field as well as the discharge and the power characteristics, it is advisable to use the second approximation (28).

The Discharge Characteristics

If we consider that the liquid flowing through the nozzle is not viscous, this will permit us to express the pressure p_n at the nozzle radius in terms of pressure p_0 before the baffle and in terms of discharge G. In this case,

$$p_n = p_0 - \frac{\rho}{2} \bar{v}_{r_n}^2, \tag{31}$$

where

$$\bar{v}_{r_n} = \frac{1}{h}\int_0^h v_{r_n}\,dz = \frac{G}{2\pi r_n h\rho}. \tag{32}$$

With this, Eq. (31) in the criterion form will be

$$B_n - B_0 \doteq -12.5A^2\alpha_n^2 \tag{33}$$

where

$$B_c = \frac{p_n h^4 \rho}{\mu^2 r_e^2\, 10^2}, \quad B_0 = \frac{p_0 h^4 \rho}{\mu^2 r_e^2 \cdot 10^2}, \quad \alpha_n = \frac{r_e}{r_n}. \tag{34}$$

By applying now Eqs. (26), (28), and (30) to the point $r = r_n$, i.e., by substituting in them $\alpha = \alpha_n$ and $B = B_n$ and eliminating B_n from them according to Eq. (33), we shall obtain the following discharge characteristics of the "nozzle-baffle" element:

In the first approximation

$$B_0 - B_e = 6A \ln \alpha_n + 12.5A^2, \tag{35}$$

in the second approximation

$$B_0 - B_e = 6A \ln \alpha_n + (16.78 - 4.28\alpha_n^2)A^2, \tag{36}$$

in the third approximation

$$B_0 - B_e = 6A \ln \alpha_n + (16.78 - 4.28\alpha_n^2)A^2 -$$
$$- 0.142A^2\beta^2(\alpha_n^4 - 1) - 3.67A^3(\alpha_n^4 - 1). \tag{37}$$

If we take into account the viscosity of the liquid flowing through the nozzle, the discharge characteristic in the second approximation will be of the form

$$B_0 - B_e = 6A \ln \alpha_n + 8\frac{A}{\varkappa_n} +$$
$$+ (16.78 - 29.28\alpha_n^2 + 50\alpha_n^4\beta), \quad \varkappa_n = \frac{r_n^4}{h^3}, \tag{38}$$

where l is the nozzle length (cm).

Figure 3 shows the family of discharge characteristic curves (36) with respect to α_n, which are plotted in terms of criteria that do not contain the nozzle parameters:

$$A^* = \frac{G}{\pi\mu h \cdot 10^2}, \quad B^* = \frac{ph^2\rho}{\mu^2 \cdot 10^{12}}.$$

It is obvious from the figure that the curves intersect and that they have pressure drop values for which discharge does not occur at all. However, neither of these conditions can actually be realized. The contradiction can be explained by the fact that a finite number of terms of the series were used and that the liquid flow losses in the $0 \le r \le r_n$ region were not taken into account. This contradiction limits the regions where the solutions are valid in the following manner:

for $\alpha_n < 1.98$

$$A_{\lim} = \frac{4.09 - 6\ln\alpha_n}{(16.78 - 4.28\alpha_n^2)},$$

and for $1.98 < \alpha_n < 1.98^2$

$$A_{\lim} = \frac{6\ln 1.98^2 - 6\ln\alpha_n}{4.28(1.98^4 - \alpha_n^2)}.$$

Figure 4 shows a comparison between the discharge characteristics for different gaps h between the nozzle and the baffle, calculated according to the second-approximation equation (38), and experimental data which were processed in terms of the same criteria. The theoretical curves are shown by solid lines, and the experimental curves are represented by solid lines with points. The experimental data, which were borrowed

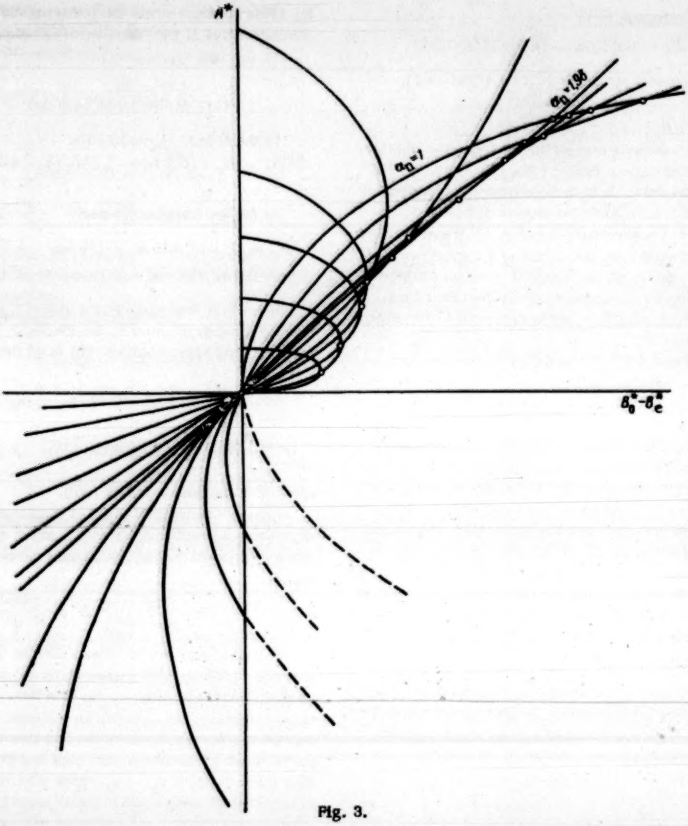

Fig. 3.

from [5], were obtained for a nozzle with $d_n = 0.6$ mm and $d_e = 0.95$ mm, where the working liquid was AMG-10 oil at $t = 50°C$ with the density $\rho = 8.66 \times 10^{-7}$ kg · sec² per cm⁴, and the dynamic viscosity coefficient $\mu = 8.66 \times 10^{-8}$ kg · sec/cm².

It is obvious from the comparison that a good quantitative agreement is secured for numbers $A \leq 2$ and $B - B_e \leq 30$, while, for numbers $A > 2$ and $B - B_e > 30$, a good qualitative agreement and an insufficient quantitative agreement is obtained. This unsatisfactory quantitative agreement can be explained by the fact that the solution was obtained for laminar flow and that the discharge A values exceed the maximum value.

The Power Characteristic

Equations (26), (28), and (30) express the law of pressure distribution under the baffle plate in those cases where $r_n \leq r \leq r_e$. Moreover, the pressure at the baffle center, where $r = 0$, can be considered to be known, since, here, $p = p_0$.

Let us assume that the pressure between the points $r = 0$ and $r = r_n$ is linearly distributed, i.e.,

$$p = p_0 - \frac{p_0 - p_n}{r_n} r. \qquad (39)$$

Thus, the pressure distribution over the entire baffle surface is known.

After integration, we obtain the following power characteristics of the "nozzle-baffle" element:

in the first approximation

$$D = 3A\,(\alpha_n^2 - 1) + 12.5A^2\alpha_n^2\left(\frac{1}{3} - 2\ln\alpha_n\right); \qquad (40)$$

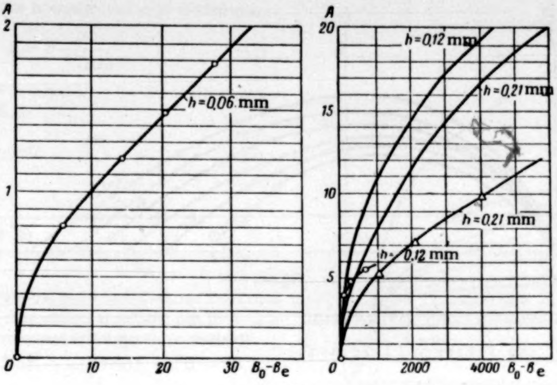

Fig. 4.

in the second approximation

$$D=3A(\alpha_n^2-1)+16.78A^2\alpha_n^2(0.248-2\ln\alpha_n); \tag{41}$$

in the third approximation

$$D=3A(\alpha_n^2-1)+16.78A^2\alpha_n^2(0.248-2\ln\alpha_n)-\\ -14.28A^2\beta^2(1-\alpha_n^2)_2-3.675A^3(1-\alpha_n^2)^2, \tag{42}$$

where

$$D=\frac{Fh^4\rho}{\pi\mu^2r_e^2r_n^2 10^2}.$$

Figure 5 shows the family of power characteristic curves (41) with respect to α_n, which are expressed in terms of the criteria

$$D^*=\frac{F\rho}{\pi\mu^2\cdot 10^2},\quad B_0^*=\frac{p_0h^2\rho}{\mu^2\cdot 10^2},\quad B_e^*=\frac{p_eh^2\rho}{\mu^2\cdot 10^2}.$$

It is obvious from the figure that:

1) If r_e/h = const, for an increase in α_n, the derivative $\left.\frac{dD^*}{d(B_0^*-B_e^*)}\right|_{(B_0^*-B_e^*)=0}$ decreases, i.e., if r_n decreases for the same pressure drop value Δp at the "nozzle-baffle" throttle, the force becomes smaller;

2) If α_n = const, h = const, and Δp = const, while r_e increases, $\left.\frac{dD^*}{d(B_0^*-B_e^*)}\right|_{(B_0^*-B_e^*)=0}$ becomes larger, and the force increases, i.e., if r_n and r_e increase by the same amount, the force becomes larger;

3) If r_n = const, h = const, and Δp = const, while r_e increases, it can be readily shown that $\left.\frac{dD^*}{d(B_0^*-B_e^*)}\right|_{B_0^*-B_e^*=0}$ increases, i.e., the force becomes larger;

4) If r_e = const and h = const, the larger α_n, i.e., the smaller r_n, the smaller the Δp values for which the force becomes negative;

5) If α_n = const and h = const, the larger r_e and r_n, the larger the Δp values for which the force becomes negative;

6) If r_n = const and h = const, the larger r_e, the larger the Δp values for which the force becomes negative.

Thus, by solving the system of hydrodynamic equations for an incompressible viscous liquid, we have obtained the following characteristics:

1) the pressure field under the baffle

$$B-B_e=6A\ln\alpha-16.78(\alpha^2-1)A^2, \tag{43}$$

2) the discharge characteristic

$$B_0-B_e=6A\ln\alpha_n+(16.78-4.28\alpha_n^2)A^2, \tag{44}$$

3) the power characteristic

$$D=3A(\alpha_n^2-1)+\\+16.78A^2\alpha_n^2(0.248-2\ln\alpha_n). \tag{45}$$

Consequently, if we know the pressure drop B_0-B_e at the "nozzle-baffle" throttle and the nozzle parameters α_n, we can find the discharge A from Eq. (44), and, if we know A, we can determine the force D by using (45) and the pressure field $B-B_e$ under the baffle by using (43). The obtained results are valid only for laminar flow.

If the "nozzle-baffle" element is used in pneumatic devices, where the working fluid is air, the pressure field and the discharge and power characteristics for an ideal viscous gas must be obtained. For calculating the pressure field of a viscous compressible fluid, we shall use the pressure distribution obtained for a viscous incompressible fluid and applied to an infinitely small region.

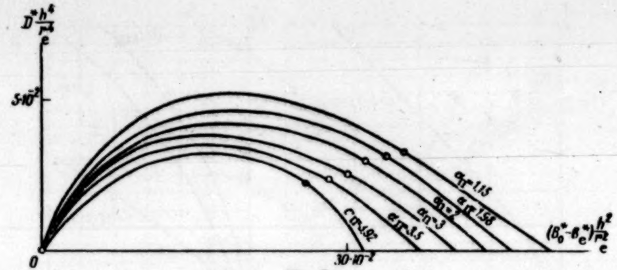

Fig. 5.

2. THE CASE OF A VISCOUS COMPRESSIBLE FLUID

Determination of the Pressure Field under the Baffle

By using relation (28), we shall write the expression for the pressure drop dp for an infinitely small element with the radius dr, where the liquid can be considered to be incompressible, i.e., where ρ = const:

$$dp = -\frac{6G\mu}{\pi h^3\rho}\ln\frac{r+dr}{r} - 0.1678\frac{G^2}{\pi^2h^2\rho}\left[\frac{1}{(r+dr)^2}-\frac{1}{r^2}\right]. \qquad (46)$$

By expanding ln (r + dr)/r into a power series with respect to dr, and by neglecting small quantities of the second order, we obtain

$$dp = -\frac{6G\mu}{\pi h^3\rho}\frac{dr}{r} + 2\cdot0.1678\frac{G^2dr}{\pi^2h^2r^3\rho}. \qquad (47)$$

If we consider the fluid to be an ideal gas and assume that the flow is polytropic, we obtain

$$\rho = \rho^*\left(\frac{p}{p_{atm}}\right)^{1/n}, \qquad (48)$$

where n is the polytrope exponent, and ρ^* is the density at atmospheric pressure p_{atm}.

If we substitute relation (48) in relation (47) and integrate the obtained expression, we shall find the pressure distribution along the radius, which will have the following form when expressed in terms of criterion numbers:

$$B^{\frac{n+1}{n}} - B_e^{\frac{n+1}{n}} = \frac{n+1}{n}[6A\ln\alpha - 16{,}78A^2(\alpha^2-1)]\,B_{atm}^{\frac{1}{n}} \qquad (49)$$

where

$$B = \frac{ph^4\rho^*}{\mu^2r_e^2\cdot10^2}, \quad B_e = \frac{p_eh^4\rho^*}{\mu^2r_e^2\cdot10^2},$$

$$B_{atm} = \frac{p_{atm}h^4\rho^*}{\mu^2r_e^2\cdot10^2}, \quad A = \frac{Gh}{\pi\mu r_e^2\cdot10^2}, \quad \alpha = \frac{r_e}{r}.$$

If the process is isothermic, i.e., n = 1, the pressure distribution along the radius will be

$$B^2 - B_e^2 = 2[6A\ln\alpha - 16.78A^2(\alpha^2-1)]\,B_{atm}. \qquad (50)$$

An approximate solution of the system of hydrodynamic equations for a viscous compressible fluid has been obtained in [7], which is here presented in terms of the same criteria numbers:

$$B^{\frac{n+1}{n}} - B_e^{\frac{n+1}{n}} = \frac{n+1}{n}[6A\ln\alpha - 21A^2(\alpha^2-1)]\,B_{atm}^{\frac{1}{n}} \qquad (51)$$

The Discharge Characteristic

If the fluid flowing through the nozzle is considered to be compressible, but not viscous, then, by means of the St. Venant–Wenzel equation, we can express the pressure p_n at the nozzle radius in terms of the pressure p_0 in front of the baffle and the discharge G:

$$\frac{n-1}{n}\left[B_0^{\frac{n-1}{n}} - B_n^{\frac{n-1}{n}}\right] = 12.5\frac{B_{atm}^{\frac{1}{n}}}{B_n^{2/n}}\alpha_n^2$$

where

$$B_0 = \frac{p_0h^4\rho^*}{\mu^2r_e^2\,10^2}, \quad B_c = \frac{p_nh^4\rho^*}{\mu^2r_e^2\cdot10^2}. \qquad (52)$$

By applying relation (49) to the point r = r_n, i.e., assuming that $\alpha = \alpha_n$ and B = B_n in this relation, and by using relation (52), we shall obtain the discharge characteristic for a polytropic fluid outflow from the "nozzle-baffle" element:

$$\frac{n-1}{n}\left[B_0^{\frac{n-1}{n}} - B_n^{\frac{n-1}{n}}\right] = 12.5A^2\alpha_n^2\frac{B_{atm}^{1/n}}{B_n^{2/n}},$$

$$B_n^{\frac{n+1}{n}} - B_e^{\frac{n+1}{n}} = \frac{n+1}{n}[6A\ln\alpha_n - 16.78A^2(\alpha_n^2-1)]\,B_{atm}^{1/n}. \qquad (53)$$

If the fluid outflow is considered to be isothermic,

$$\rho = p\frac{\rho^*}{p_{\text{atm}}}. \tag{54}$$

By substituting this relation in the Bernoulli equation for a compressible fluid:

$$\int_{p_0}^{p_{\text{n}}} \frac{p_{\text{atm}}}{\rho^*}\frac{dp}{p} + \frac{\bar{v}^2_{r_{\text{n}}}}{2} = 0, \tag{55}$$

where

$$\bar{v}_{r_{\text{n}}} = \frac{1}{h}\int_0^h v_{r_{\text{n}}}\,dz = \frac{Gp_{\text{atm}}}{2\pi r_{\text{n}} h p_{\text{n}} \rho^*},$$

and by integrating the obtained expression, we shall find the relation between the pressure p_n at the nozzle radius and the pressure p_0 in front of the baffle:

$$\ln\frac{B_0}{B_{\text{n}}} = 12.5A^2\alpha_{\text{n}}\frac{B_{\text{atm}}}{B^2_{\text{n}}}. \tag{56}$$

If we apply relation (49) to the point $r = r_n$ and use relation (56), we obtain the discharge characteristic for an isothermic outflow from the "nozzle-baffle" element:

$$B_0 = \\ = \sqrt{B^2_{\text{c}} + 2[6A\ln\alpha_{\text{n}} - 16.78A^2(\alpha^2_{\text{n}} - 1)]\,B_{\text{atm}}} \times \\ \times \exp\frac{12.5A^2\alpha^2_{\text{c}}B_{\text{atm}}}{B^2_{\text{e}} + 2[6A\ln\alpha_{\text{n}} - 16.78A^2(\alpha^2_{\text{n}} - 1)]\,B_{\text{atm}}}. \tag{57}$$

Figure 6 shows a comparison between the discharge characteristics calculated according to Eq. (57), which are represented by a solid line, and experimental data for different distances between the nozzle and the baffle plate, which are plotted as solid lines with points. The experimental data, which were taken from [8], were obtained for a nozzle with $r_n = 0.613$ mm and $r_e = 1.61$ mm. The working fluid was air, for which $\rho^* = 11.8 \times 10^{-10}$ kg·sec²/cm⁴, $\mu = 1.845 \times 10^{-10}$ kg·sec/cm², $t = 20°$C, and $p_{\text{atm}} = 746$ mm Hg.

It is obvious from relation (57) that, for a certain value of A, the expression

$$B^2_{\text{e}} + 2[6A\ln\alpha_{\text{n}} - 16.78A^2(\alpha^2_{\text{n}} - 1)]\,B_{\text{atm}}$$

becomes equal to zero, and B_0 becomes indeterminate. If we develop this indeterminacy, we find that $B_0 \to \infty$ for

$$B^2_{\text{e}} + 2[6A\ln\alpha_{\text{n}} - 16.78A^2(\alpha^2_{\text{n}} - 1)]\,B_{\text{atm}} \to 0.$$

Consequently, the calculated discharge characteristics will have asymptotes, whose equation will be

$$B^2_{\text{e}} + 2[6A\ln\alpha_{\text{n}} - 16.78A^2(\alpha^2_{\text{n}} - 1)]\,B_{\text{atm}} = 0. \tag{58}$$

It can be seen from Fig. 6 that the theoretical characteristics are qualitatively in good agreement with experimental data, while their quantitative agreement is not satisfactory. The quantitative disagreement becomes greater with an increase in the gap h between the nozzle and the baffle. The correction for the theoretical characteristic, which is obtained by taking into account the viscosity of the fluid flowing through the nozzle, is negligibly small and does not reduce the disagreement between the theoretical and experimental curves. Consequently, the quantitative disagreement can be explained by the fact that the outflow becomes turbulent, while the turbulence increases with an increase in the gap h between the nozzle and the baffle, and also by the fact that the discharge values exceed the maximum value.

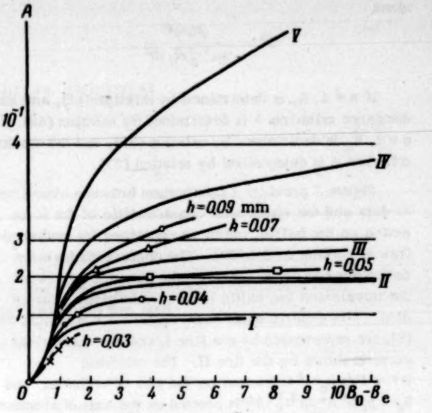

Fig. 6. Dependence of the discharge of a viscous compressible fluid through the "nozzle-baffle" throttle on the pressure drop at the throttle for different gaps between the nozzle and the baffle plate.

The Power Characteristic

Relation (49) describes the pressure distribution along the end-face radius for $r_n \leq r \leq r_e$. Moreover, it is assumed that, for $0 \leq r \leq r_n$, the pressure changes according to the equation

$$p = p_0 - \frac{p_0 - p_{\text{n}}}{r_{\text{n}}}\,r. \tag{59}$$

Thus, the pressure distribution law for the entire baffle plate surface is known. By integration over the surface, we obtain the power characteristics of the "nozzle-baffle" element for a viscous compressible fluid:

$$D = \frac{1}{3}B_0 + \frac{2}{3}B_{\text{n}} - B_{\text{e}} + \left(\frac{B_{\text{atm}}}{B_{\text{e}}}\right)^{\frac{1}{n}} \\ (12A - 4\cdot 16.78A^2)\left(\frac{1}{6}\alpha^2_{\text{n}} + \frac{1}{3\alpha_{\text{n}}} - \frac{1}{2}\right), \tag{60}$$

where

$$D = \frac{Fh^4\rho^*}{\pi\mu^2 r_e^2 r_n^2 10^2} \cdot$$

If $n \neq 1$, B_n is determined by relation (52), and the discharge criterion A is determined by relation (53). If $n = 1$, B_n is determined by relation (56), and the discharge criterion A is determined by relation (57).

Figure 7 provides a comparison between experimental data and the calculated characteristic of the force action on the baffle, which was obtained for isothermic flow according to Eq. (60). The characteristics were determined in dependence on the distance h between the nozzle and the baffle for a certain given pressure drop. The experimental data, which were borrowed from [8], are represented by the line I, and the theoretical curve is shown by the line II. The criterion $D^* = F/\pi p_e r_n^2$ is plotted on the axis of ordinates, and $B_e = p_e h^4 \rho^* / \mu^2 r_e^2 \cdot 10^2$ is plotted on the axis of abscissas. The experiments and calculations were performed for air for $r_n = 0.5$ mm, $\alpha_n = 4.45$, $p_0 - p_e = 0.5$ kg/cm², $\mu = 1.845 \times 10^{-10}$ kg·sec/cm², and $\rho^* = 11.8 \times 10^{-10}$ kg·sec²/cm⁴.

It is obvious from the figure that, also in this case, a good qualitative agreement is observed, while the results do not agree quantitatively, which also indicates that the flow is turbulent and that the discharge A values exceed the maximum values.

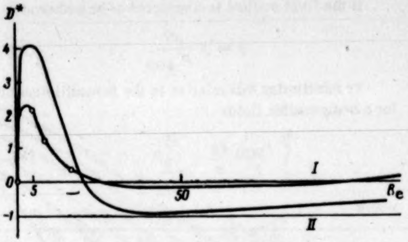

Fig. 7. Dependence of the force acting on the baffle plate from the side of the viscous compressible fluid stream on the gap between the nozzle and the baffle.

SUMMARY

1. The pressure field under the baffle plate and the discharge and the power characteristics of a "nozzle-baffle" element for a compressible and an incompressible viscous liquid flow were obtained.
2. The applicability limits for the theoretical discharge characteristic were established.
3. The theoretical characteristics for an incompressible fluid were compared with experimental data. A good agreement was observed for Reynolds numbers smaller than 800. For Reynolds numbers larger than 800, a good qualitative agreement was observed, while the quantitative correspondence was not satisfactory.
4. We compared the theoretical characteristics for a compressible fluid with experimental data, and it was found that a good qualitative agreement exists even in the region of discharge A values which exceed the maximum value.
5. We investigated the influence of the nozzle parameters r_n and r_e on the discharge and the power characteristics.

LITERATURE CITED

1. N. A. Slezkin, "Viscous liquid flow in a cone and between two cones," Matematicheskii Sbornik 42, 1 (1935).
2. T. M. Bashta, Aircraft Hydraulic Drives and Units [in Russian] (Oborongiz, 1951).
3. N. P. Shumskii, "Results of experimental and theoretical investigations of control devices of the 'nozzle-baffle' type," Systems, Devices, and Elements in Pneumatic and Hydraulic Automation [in Russian] (Izd. AN SSSR, 1959).
4. J. H. McGinn, "Observations on the radial flow of water between fixed parallel plates," Appl. Scient. Res. A. 5, 4 (1955).
5. I. M. Krassov and B. G. Turbin, "Dynamic effect of flow in a 'nozzle-baffle' hydraulic amplifier," Avtomatika i Telemekhanika 20, 12 (1959).‡
6. E. A. Andreeva, "Calculation of static characteristics of the 'nozzle-baffle' element," Systems, Devices, and Elements in Pneumatic and Hydraulic Automation [in Russian] (Izd. AN SSSR, 1959).
7. M. Raymond Comolet, "Nombre de Reynolds critique d'un écoulement visqueux, radial divergent entre deux plans parallèles," L'Academie des sciences, Paris, Comptes rendus 244, 11 (Fevrier, 1957).
8. V. N. Dmitriev, Experimental and Theoretical Investigation of a Pneumatic Relay of the "Nozzle-Baffle" Type: Dissertation for the Degree of Candidate of Technical Sciences (Institute Avtomatiki i Telemekhaniki AN SSSR, 1955).
9. E. A. Andreeva, "Calculation of static characteristics of a pneumatic 'nozzle-baffle' element," Problems in Pneumatic and Hydraulic Automation [in Russian] (Izd. AN SSSR, 1960).

‡See English translation.

DYNAMIC CHARACTERISTICS OF A "JET AMPLIFIER – SERVOMECHANISM" SYSTEM

B. D. Kosharskii

Khar'kov

Translated from Avtomatika i Telemekhanika, Vol. 21, No. 7,
pp. 997-1006, July, 1960
Original article submitted December 30, 1959

The structural layouts and the basic dynamic characteristics of a linearized "jet amplifier – servomechanism" system are investigated for the cases where single- and two-stage amplifiers are used.

Theoretical and experimental frequency characteristics are given.

The aim of the present article is to determine the basic dynamic characteristics of a linearized "jet amplifier – servomechanism" system for the parameter interval which is encountered in industrial devices.

Figure 1 shows the schematic and the structural layouts of elements in a "single-stage amplifier – servomechanism" system. The presence of a velocity feedback section in this layout is determined by the fact that, when the servomechanism is immobile, the pressure drop in the receiving nozzles of the nozzle plate differs from the pressure drop behind the receiving nozzles when the servomechanism piston moves. The hydraulic phenomena which occur in this case have been considered in detail in [1].

The jet tube motion is generally described by the differential equation*

$$\frac{1}{L_{\mathrm{jt}}}\left(\mathrm{I}_{\mathrm{jt}}\frac{d^2\sigma_{\mathrm{j}}}{dt^2}+H_{\mathrm{jt}}\frac{d\sigma_{\mathrm{j}}}{dt}+M_{\mathrm{jt}}\sigma_{\mathrm{j}}\right)=M_{\mathrm{c}}, \tag{1}$$

where I_{jt} is the moment of inertia of the jet amplifier kinematic system, equal to 2×10^{-3} kg·cm·sec², H_{jt} is the coefficient of viscous friction, which arises due to the fact that the jet tube end is immersed in the amplifier oil tank (on the basis of our experimental data, which are given in [2], the value of H_{jt} depends on the input signal frequency ω and is equal to $1.1 \times 10^{-3}\sqrt{\omega}$ kg·cm·sec), M_{c} is the control moment which is applied to the jet tube, $M_{\mathrm{c\,max}} = 35 \times 10^{-3}$ kg·cm, σ_{j} is the linear deviation of the jet tube end with respect to its equilibrium position, $\sigma_{\mathrm{j\,max}} = 0.15$ cm, L_{jt} is the jet tube length from the rotation axis to the outlet section of the conical endpiece, equal to 16.6 cm, and M_{jt} is the moment due to the mass of statically unbalanced elements of the amplifier kinematic system which is reduced to the jet tube and is equal to 2×10^{-3} kg · cm.

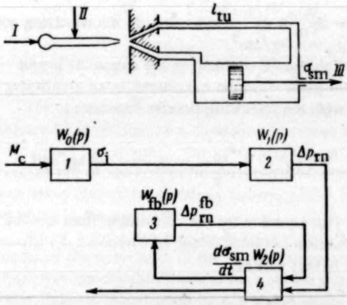

Fig. 1. I) Working agent feed; II) control moment; III) to regulating unit; 1) jet tube; 2) nozzle plate; 3) velocity feedback; 4) connecting lines and servomotor.

The transfer function of the first element in the structural layout – the jet tube – will be written in the following form:

$$W_0(p)=\frac{\sigma_{\mathrm{j}}}{M_{\mathrm{c}}}=\frac{k_0}{T_1^2p^2+T_2p+1}, \tag{2}$$

where

$$k_0=L_{\mathrm{jt}}/M_{\mathrm{jt}},\quad T_1^2=\mathrm{I}_{\mathrm{jt}}/M_{\mathrm{jt}},\quad T_2=H_{\mathrm{jt}}/M_{\mathrm{jt}}.$$

---

* This equation is somewhat different from the similar equation given in [2], since a combination of a jet tube with two springs can be considered as a particular case, which is encountered only in certain types of regulators.

With the numerical values, this equation will be

$$W_0(p) = \frac{8200}{p^2 + 0.54\sqrt{\omega}\, p + 1}.$$

In order to obtain the over-all jet amplifier characteristic, it is necessary to consider the equation which characterizes the pressure variation in the receiving nozzles when the jet tube is deflected. This dependence, which has been considered in [1], has a rather complicated form; however, it can be considered as linear if we assume with a certain degree of accuracy that the oil does not move in the receiving nozzles. According to the obtained experimental data, this characteristic remains unchanged in a wide range of the working medium pressure values at the jet tube inlet (p_{jc} = 3-20 kg/cm²) and is described by the equation

$$\Delta p_{rn} = 0.8 p_{jc} \frac{\sigma_j}{\sigma_{j\,max}}, \qquad (3)$$

where Δp_{rn} is the pressure drop in the receiving nozzles, and p_{jc} = 8 kg/cm².

The second element in the structural layout – the nozzle plate – can be considered as an amplifying section with the following transfer function:

$$W_1(p) = \frac{\Delta p_{rn}}{\sigma_j} = k_1 = 42.8 \text{ kg/cm}^3. \qquad (4)$$

The equation for the connecting lines and the servomechanism (without taking into account dry friction and pure delay) will be:

$$m_t \frac{d^2\sigma_{sm}}{dt^2} + h_t \frac{d\sigma_{sm}}{dt} = \Delta p_{rn} \quad F_{sm}, \qquad (5)$$

where $m_t = m_{pl} + m_o$; m_{pl} is the servomechanism piston mass and the reduced mass of all kinematic system links connected to the piston, approximately equal to 0.11-0.13 kg·sec²/cm, and m_o is the mass of the working liquid in the servomechanism cylinder and connecting lines, which is reduced to the piston; $h_t = h_{pl} + h_{cy} + h_{tu}$ is the coefficient which characterizes the magnitude of viscous friction of the servomechanism mobile parts and of the working liquid in the cylinder and the connecting lines.

The magnitude of $h_{pl} + h_{cy} < 0.0005$ kg·sec/cm, and can be neglected in practice. Moreover, the following notation was used in Eq. (5): σ_{sm} is the servomechanism piston stroke ($\sigma_{sm\,max}$ = 20 cm), and F_{sm} is the servomechanism piston surface area, equal to 50.2 cm².

According to [3], the value of m_o is determined from the equation

$$m_o = F_{sm} \frac{\gamma_o}{g} \left[\sigma_{sm\,max} + l_{tu} \left(\frac{d_{sm}}{d_{tu}} \right)^2 \right], \qquad (6)$$

where l_{tu} is the over-all length of the connecting lines from the amplifier to the servomechanism (cm), equal to double the route length L, d_{tu} is the connecting lines diameter, equal to 1 cm, and γ_o is the oil specific weight, equal to 0.0009 kg/cm³.

With the numerical values, $m_o = 0.0009 + 0.003\, l_{tu}$ kg·sec²/cm.

Consequently,

$$m_t = 0.13 + 0.003\, l_{tu}. \qquad (7)$$

On the basis of Poiseuille's law, since the working liquid flow in the connecting lines is laminar, we can write

$$h_t \approx h_{tu} = 8\pi\mu\, l_{tu\,e} \left(\frac{d_{sm}}{d_{tu}} \right)^4, \qquad (8)$$

where $l_{tu\,e}$ is the equivalent length of the connecting lines, where all local resistances are taken into account, and μ is the dynamic viscosity coefficient of the working liquid – transformer oil – for γ_o = 0.0009 kg/cm³ and a viscosity of 2°E, equal to $\mu = 12 \times 10^{-8}$ kgsec/cm².

In numerical form, $h_t = 0.0124\, l_{tu\,e}$ kg·sec/cm².

Equation (5) does not reflect the characteristics of the section under consideration with sufficient accuracy, since it does not take into account the effect of "pure delay", which is determined by the acceleration time τ_a in the channel and the pressure propagation time τ_p in the line.

The total "pure delay" time (without taking into account the elasticity of the connecting lines) is determined from the expression

$$\tau = \tau_a + \tau_p = \frac{\gamma_o d_{tu}^2}{32 g\mu} + \frac{l_{tu}}{\lambda_o}, \qquad (9)$$

where λ_o is the pressure propagation rate in the connecting oil line, equal to 12×10^4 cm/sec.

In numerical form, $\tau = 0.239 + l_{tu}/(12 \times 10^4)$.

If we consider the delay, instead of Eq. (5), we shall write

$$\left(\frac{m_t}{F_{sm}} p + \frac{h_t}{F_{sm}} p \right) \sigma_{sm} = \Delta p_{rn} \quad e^{-p\tau}. \qquad (10)$$

The section transfer function will be

$$W_2(p) = \frac{\sigma_{sm}}{\Delta p_{rn}} = \frac{e^{-p\tau}}{(T_3^2 p^2 + T_4 p)\, k_2} \qquad (11)$$

where $k_2 T_3^2 = m_t/F_{sm}$ and $k_2 T_4 = h_t/F_{sm}$.

If, for the case under consideration, we conventionally assume that $l_{tu\,e} \approx 1.2\, l_{tu}$† and consider that the

---

† The actual value of the $l_{tu\,e}$ depends on the device operating conditions and has to be accurately determined in each individual case.

k_2 coefficient is a proportionality factor, numerically equal to unity, we obtain

$$T_3^2 = (25 + 0.6 l_{tu}) \cdot 10^{-4} \frac{\text{kg} \cdot \text{sec}^2}{\text{cm}^3},$$

$$T_4 = 3 \cdot 10^{-4} l_{tu} \frac{\text{kg} \cdot \text{sec}}{\text{cm}^3}.$$

According to [1], the velocity feedback equation will be

$$\Delta p_{rn}^{fb} = -0.92 \frac{\gamma_0 k_a}{g F_{rn}} \frac{d\sigma_{sm}}{dt} \times$$

$$\times \left[2 \left(\sum_{i=0}^{i=m} \Delta F_{ri} v_{aFi} + \sum_{j=n}^{j=s} \Delta F_{rj} v_{aFj} \right) - \right.$$

$$\left. - k_a \frac{d\sigma_{sm}}{dt} \left(\sum_{i=0}^{i=m} \Delta F_{ri} - \sum_{j=n}^{j=s} \Delta F_{rj} \right) \right], \qquad (12)$$

where F_{rn} is the receiving nozzle surface area, equal to 0.27 cm², $k_a = F_{sm}/F_{rn} \cos \beta$ (β is the receiving nozzle tilt angle with respect to the jet tube axis; for $\beta = 0° 30'$, $k_a = 180$), ΔF_{ri} and ΔF_{rj} are the elementary receiving nozzle surface areas covered by the jet (the index i pertains to a nozzle completely covered with the jet, and the index j pertains to a nozzle partially covered by the jet)‡, and v_{aFi} and v_{aFj} are the average jet velocities at the elementary area ΔF_r.

The absolute value of the second term of the expression in square brackets in (12) is smaller than the first term value 25- to 60-fold, and it can be neglected. Therefore, instead of Eq. (12), we can write

$$\Delta p_{rn}^{fb} \approx -1.84 \frac{k_a \gamma_0}{g F_{rn}}$$

$$\left(\sum_{i=0}^{i=m} \Delta F_{ri} v_{aFi} + \sum_{j=n}^{j=s} \Delta F_{rj} v_{aFj} \right) \frac{d\sigma_{sm}}{dt}.$$

If the jet tube is in the middle position, the quantity in parentheses is equal to $F_{rn} v_{aF\,av}$, where $v_{aF\,av}$ is the average jet velocity at the transition section (for $p_{jc} = 8$ kg/cm², $v_{aF\,av} = 780$ cm/sec).

The expression in parentheses can be replaced by a simpler relation:

$$\sum_{i=0}^{i=m} \Delta F_{ri} v_{aFi} + \sum_{j=n}^{j=s} \Delta F_{rj} v_{aFj} \approx k_c F_{rn} v_{r\,av}$$

where k_j varies from 1.5 to 2.0 in dependence on the jet tube deflection; we assume that $k_j \approx 1.75$.

The velocity feedback equation, in its final form, will be

$$\Delta p_{rn}^{fb} = -1.84 \frac{k_a k_j \gamma_0 v_{aF\,av}}{g} \frac{d\sigma_{sm}}{dt}. \qquad (13)$$

The velocity feedback transfer function will be determined by the expression

$$W_{fb}(p) = \frac{\Delta p_{rn}^{fb}}{\sigma_{sm}} = -k_{fb} T_5 p, \qquad (14)$$

where

$$k_{fb} T_5 = 1.84 \frac{k_a k_j \gamma_0 v_{aF\,av}}{g} = 0.42 \frac{\text{kg} \cdot \text{sec}}{\text{cm}^3}.$$

The transfer function of the entire "single-stage amplifier – servomechanism" system will be

$$W_{am}(p) = \frac{\sigma_{sm}}{M_c} = \frac{W_0(p) W_1(p) W_2(p)}{1 - W_2(p) W_{fb}(p)} = \qquad (15)$$

$$= \frac{k_0 k_1 e^{-p\tau}}{p (T_1^2 p^2 + T_2 p + 1)(k_2 T_3^2 p + k_2 T_4 + k_{fb} T_5 e^{-p\tau})}.$$

The performed calculations show that expression (15) can be simplified to a considerable extent for low input signal frequencies. The corresponding values of $W_{am}(p)$ and of the system frequency characteristic parameters (determined with an accuracy of ~ 5%) are given in the Appendix.

Figure 2 shows the amplitude (a) and the phase (b) frequency characteristics of the "single-stage amplifier – servomechanism" system for a servomechanism piston diameter equal to 80 mm, a piston stroke of 200 mm, and for connecting line lengths equal to $l_{tu} = 10$-100 m (which corresponds to a distance of 5-50 m from the regulator to the servomechanism).

In order to verify the calculation formulas, we processed the oscillograms obtained in testing a "single-stage amplifier – servomechanism" system. In the tests, the jet tube was rigidly connected to a mechanical generator of sinusoidal oscillations, i.e., the σ_j coordinate was subjected to forced sinusoidal oscillations.

In this case, instead of Eq. (15), the following equation is used for describing the system transfer function:

$$W_{am}^*(p) = \frac{\sigma_{sm}}{\sigma_{sm}} = \frac{k_0^* k_1 e^{-p\tau}}{p (k_2 T_3^2 p + k_2 T_4 + k_{fb} T_5 e^{-p\tau})},$$

where $k_0^* = 1$.

As can be seen from Fig. 3, the agreement between the theoretical values and the experimental data (white points) is entirely satisfactory.

---

‡This has been treated in detail in [1].

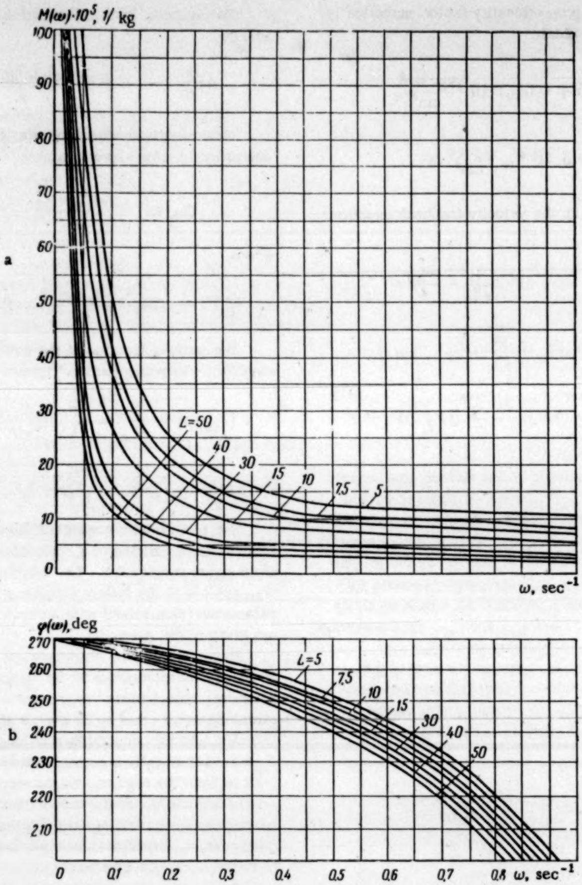

Fig. 2.

The "two-stage amplifier–servomechanism" system (Fig. 4) operates with different working medium pressures in the jet and the gate valve stages (p_{jc} = = 8 kg/cm^2 and p_{vs} = 12-15 kg/cm^2).

Since, in the first amplification stage, the receiving nozzles are directly built into the gate valve piston, which follows the jet tube displacement, this element can be considered as a closed circuit with a feedback coefficient equal to unity [2].

Considering that the oil flow velocity in the gate valve receiving nozzles is slight and can be neglected, the open-circuit equation of motion will be written thus:

$$m_v \frac{d^2\sigma_v}{dt^2} + h_v \frac{d\sigma_v}{dt} = k_1 p_{jc} \frac{\sigma_c}{\sigma_{j\,max}} F_{dv}, \quad (16)$$

where m_v is the mass of the gate valve parts and of the working liquid in the valve which is reduced to the piston and is approximately equal to 0.0002 kg ·sec^2/cm, h_v is the coefficient characterizing the mag-

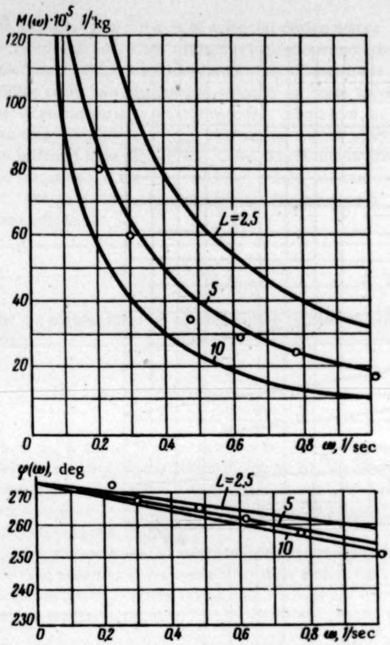

Fig. 3. The amplitude and the phase frequency characteristics of a "single-stage amplifier – servomechanism" system.

nitude of viscous friction in the gate valve element (it is assumed that $h_v = 0.03$ kg·sec/cm), F_{dv} is the surface area of the small driving piston, equal to 12.6 cm², and σ_v is the gate valve linear displacement.

Equation (16) can be written in the following form:

$$(T_{3.1}^2 p^2 + T_{4.1} p)\,\sigma_v = \sigma_j, \qquad (17)$$

where

$$T_{3.1}^2 = \frac{m_v \sigma_{j\,\max}}{k_1 p_{jc} F_{dv}} = 3.7\cdot 10^{-7}\ \text{sec}^2,$$

$$T_{4.1} = \frac{h_v \sigma_{j\,\max}}{k_1 p_{jc} F_{dv}} = 0.5\cdot 10^{-4}\ \text{sec}.$$

The open-circuit transfer function will be

$$W_{1.1}^{*}(p) = \frac{\sigma_v}{\sigma_j} = \frac{1}{T_{3.1}^2 p^2 + T_{4.1} p} \qquad (18)$$

The transfer function of the gate valve element is determined by the expression

$$W_{1.1}(p) = \frac{W_{1.1}^{*}(p)}{1 + W_{1.1}^{*}(p)} = \frac{1}{T_{3.1}^2 p^2 + T_{4.1} p + 1}. \qquad (19)$$

The values of the $T_{3.1}$ and $T_{4.1}$ time constants mainly depend on the gate valve device design.

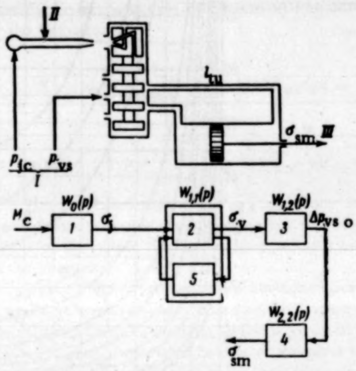

Fig. 4. Schematic diagram and the structural layout of a "two-stage amplifier – servomechanism" system. I), II), and III) same designation as in Fig. 1; 1) jet tube; 2) driving gate valve; 3) driven gate valve; 4) connecting lines and servomotors; 5) rigid feedback.

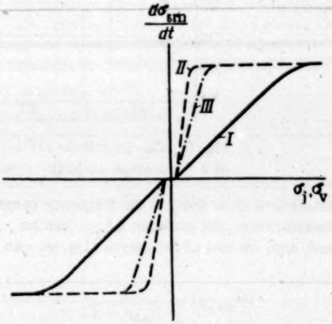

Fig. 5. Characteristics of single- and two-stage amplifiers. I) For a single- or two-stage amplifier if additional triangular bypass openings are provided in the gate valve; II) for a two-stage amplifier with rectangular bypass openings in the gate valve; III) for a two-stage amplifier with round bypass openings.

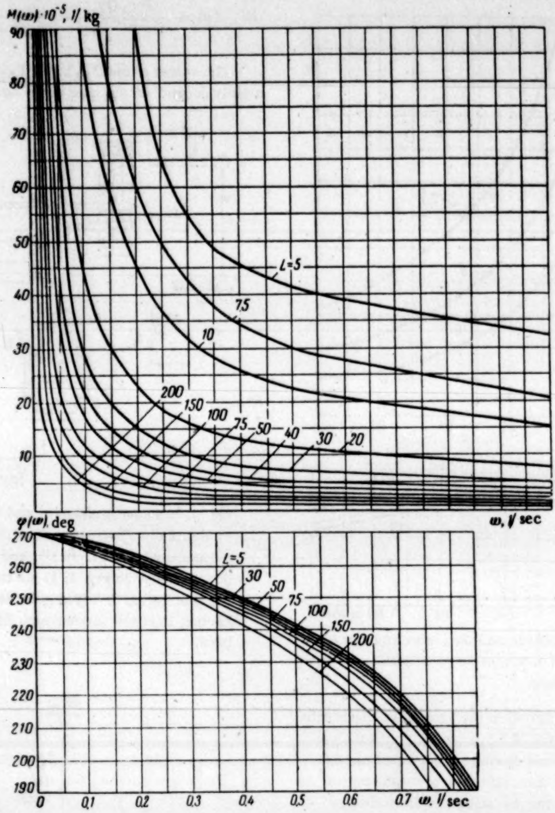

Fig. 6. The amplitude M(ω) and the phase $\varphi(\omega)$ frequency characteristics of a "two-stage amplifier – servomechanism" system.

Calculations show that, in the frequency range under consideration, the quantity $T^2_{3.1}$ can be neglected, and, instead of expression (19), we can write

$$W_{1.1}(p) = \frac{1}{T_{4.1}p + 1}. \qquad (20)$$

Thus, the transfer function of the first amplification stage in a two-stage amplifier will be

$$W_{1\,\mathrm{am}}(p) = W_0(p)\,W_{1.1}(p) = \qquad (21)$$

$$= \frac{k_0}{(T_1^2p^2 + T_2p + 1)(T_{4.1}p + 1)}.$$

One of the basic advantages of "single-stage amplifier – servomechanism" systems which are used in hydraulic regulators, is a small insensitivity zone and a considerable length of the linear portion of the curve which characterizes the dependence of the servomechanism piston velocity on the input signal magnitude (Fig. 5). In many cases, the fulfillment of this condition is indispensable if a satisfactory regulation quality is to be secured.**

Experiments show that, in two-stage amplifiers, the above-mentioned dependence is similar to the dependence for single-stage amplifiers only in the case where

---

** For instance, in the case where two-pulse feed regulators for boiler units with hydraulic feedback are used.

the amplifier gate valve is of a special design and is provided with additional triangular bypass openings. In other cases, which are illustrated in Fig. 5, the linear portion of the servomechanism velocity vs. gate valve displacement curve is greatly reduced. Therefore, in two-stage amplifiers, $\sigma_{j\,max}$ can assume values which are different from those given above, which would affect the magnitude of the $T_{3.1}$ and $T_{4.1}$ time constants.

The gate valve element equation for the second stage will be

$$\Delta p_{vs\,o} = k_2 p_{vs} \frac{\sigma_v}{\sigma_{j\,max}}, \qquad (22)$$

and the transfer function will be written in the following form:

$$W_{1.2}(p) = \frac{\Delta p_{vs\,o}}{\sigma_v} = \frac{k_2 p_{vs}}{\sigma_{j\,max}} = k_2', \qquad (23)$$

where p_{vs} is the oil pressure at the second amplification stage inlet, $\Delta p_{vs\,o}$ is the pressure drop in the connecting lines at the second stage outlet, and k_2 is a coefficient which depends on the design of the pistons and the driven gate valve bypass openings.

For the numerical values, $W_{1.2}$ (p) = 64 kg/cm^3.

The equation of the connecting lines and of the servomechanism (without taking into account dry friction) will be similar to Eq. (10):

$$m_t \frac{d^2 \sigma_{sm}}{dt^2} + h_t \frac{d\sigma_{sm}}{dt} = \Delta p_{vs\,o} \; F_{sm} e^{-p\tau}, \qquad (24)$$

However, m_t, h_t, F_{sm}, σ_{sm}, and τ can assume values which are different from those given above, since, in the case of two-stage amplifiers, different servomechanism types can be used and, correspondingly, the dimensions of the connecting lines can be different.

The section transfer function will be

$$W_{2.2}(p) = \frac{\sigma_{sm}}{\Delta p_{vs\,o}} = \frac{e^{-p\tau}}{p(T_{3.2}^2 p + T_{4.2})}, \qquad (25)$$

where $T_{3.2}^2 = m_t/F_{sm}$ and $T_{4.2} = h_t/F_{sm}$.

The over-all transfer function of the "two-stage amplifier – servomechanism" system will be determined by the expression

$$W_{oaa}(p) = W_{1\,am}(p)\, W_{1.2}(p)\, W_{2.2}(p) = \frac{k_0 k_2' e^{-p\tau}}{p(T_1^2 p^2 + T_2 p + 1)(T_{4.1} p + 1)(T_{3.2}^2 p + T_{4.2})}. \qquad (26)$$

The simplified values of $W_{oa\,a}$(p) for low input signal frequencies and the corresponding parameter values of the system frequency characteristics are given in the Appendix.

Figure 6 shows the frequency characteristics of a "two-stage amplifier – servomechanism" system (for the amplifier static characteristic which is given in Fig. 5, curve 1), where a servomechanism of the same type with a piston diameter of 80 mm and a maximum stroke of 200 mm for a route length of up to 200 m (i.e., for $l_{tu} \leq 400$ m) is used.

LITERATURE CITED

1. B. D. Kosharskii, "Some problems in the design of hydraulic jet amplifiers", Avtomatika i Telemekhanika 17, 7 (1956).††
2. S. Z. Dushkas, and S. L. Cahn, "Analysis of some hydraulic components used in regulators and servomechanisms," Trans. ASME 74, 4 (May, 1952).
3. M. M. Gordon, Calculation of Automatic Control Devices for Thermal Processes [in Russian] (Metallurgizdat, 1956).

---

†† See English translation.

System	Input signal frequency, cps	Simplifications used	System transfer function $W_{\text{am}}(p) = \frac{\varphi_{\text{sm}}}{M_{\text{C}}}$	Frequency characteristics	Values of the frequency characteristic parameters
Single-stage amplifier – servomechanism	$\omega > 0.3$	The transfer function and the frequency characteristic parameters are reduced with respect to theoretical dependences	$\frac{k_0 k_1 e^{-p\tau}}{p(T_1^2 p^2 + T_2 p + 1)(k_2 T_3^2 p + k_2 T_4 + k_{\text{fb}} T_5 e^{-p\tau})}$	Amplitude $M_{\text{am}}(\omega) = \frac{k_0 k_1}{\sqrt{R^2 + S^2}}$ Phase	$R = k_2 T_1^2 T_3^2 \omega^4 - k_{\text{fb}} T_1^2 T_5 \omega^3 \sin \omega\tau -$ $- (k_2 T_3^2 + k_2 T_2 T_4 + k_{\text{fb}} T_2 T_5 \cos \omega\tau)\,\omega^2 +$ $+ k_{\text{fb}} T_5 \omega \sin \omega\tau$ $S = (k_2 T_2 T_3^2 + k_2 T_1^2 T_4 +$ $+ k_{\text{fb}} T_1^2 T_5 \cos \omega\tau)\omega^3 - k_{\text{fb}} T_2 T_5 \omega^2 \sin \omega\tau -$ $- (k_2 T_4 + k_{\text{fb}} T_5 \cos \omega\tau)\,\omega$
	$\omega = 0.05 - 0.3$	The transfer function is defined with respect to theoretical dependences, and the frequency characteristic parameters are reduced with respect to the simplified expressions	$\frac{k_0 k_1 e^{-p\tau}}{p(T_1 p^2 + T_2 p + 1)(k_2 T_3^2 p + k_2 T_4 + k_{\text{fb}} T_5 e^{-p\tau})}$	$\varphi_{\text{am}}(\omega) = \operatorname{arctg} \frac{S \cos \omega\tau - R \sin \omega\tau}{R \cos \omega\tau + S \sin \omega\tau}$	$R = -(k_2 T_3^2 + k_2 T_2 T_4 + k_{\text{fb}} T_2 T_5 \cos \omega\tau)\,\omega^2 +$ $+ k_{\text{fb}} T_5 \omega \sin \omega\tau$ $S = (k_2 T_1^2 T_4 + k_{\text{fb}} T_1^2 T_5 \cos \omega\tau)\,\omega^3 -$ $- (k_2 T_4 + k_{\text{fb}} T_5 \cos \omega\tau)\,\omega$
	$\omega < 0.15$	The transfer function and the frequency characteristic parameters are reduced with respect to the simplified expressions	$\frac{k_0 k_1 e^{-p\tau}}{p(k_2 T_3^2 p + k_2 T_4 + k_{\text{fb}} T_5 e^{-p\tau})}$		$R = k_{\text{fb}} T_5 \omega \sin \omega\tau$ $S = -\omega (k_2 T_4 + k_{\text{fb}} T_5 \cos \omega\tau)$
Two-stage amplifier – servomechanisms	$\omega > 0.5$	The transfer function and the frequency characteristic parameters are defined with respect to theoretical dependences	$\frac{k_0 k_2 e^{-p\tau}}{p(T_1^2 p^2 + T_2 p + 1)(T_{4.1} p + 1)(T_{3.2}^2 p + T_{4.2})}$	Amplitude $M_{\text{am}}(\omega) = \frac{k_0 k_2'}{\sqrt{R_1^2 + S_1^2}}$ Phase	$R_1 = (T_2 T_{3.2}^2 T_{4.1} + T_1^2 T_{3.2}^2 + T_1^2 T_{4.1} T_{4.2})\,\omega^4 -$ $- (T_{3.2}^2 + T_{4.1} T_{4.2} + T_2 T_{4.2})\,\omega^2$ $S_1 = T_1^2 T_{3.2}^2 T_{4.1} \omega^5 - (T_{3.2}^2 T_{4.1} + T_2 T_{3.2}^2 +$ $+ T_2 T_{4.1} T_{4.2} + T_1^2 T_{4.2})\,\omega^3 + T_{4.2}\omega$
	$\omega = 0.15 - 0.5$		$\frac{k_0 k_2' e^{-p\tau}}{p(T_1^2 p^2 + T_2 p + 1)(T_{3.2}^2 p + T_{4.2})}$	$\varphi_{\text{oaa}}(\omega) =$ $= \operatorname{arctg} \frac{-(S_1 \cos \omega\tau + R_1 \sin \omega\tau)}{R_1 \cos \omega\tau - S_1 \sin \omega\tau}$	$R_1 = T_1^2 T_{3.2}^2 \omega^4 - (T_{3.2}^2 + T_2 T_{4.2})\,\omega^2$ $S_1 = -(T_2 T_{3.2}^2 + T_1^2 T_{4.2})\,\omega^3 + T_{4.2}\omega$
	$\omega < 0.15$	The transfer function and the frequency characteristic parameters are defined with respect to the simplified expressions			$R_1 = -(T_{3.2}^2 + T_2 T_{4.2})\omega^2$ $S_1 = -(T_2 T_{3.2}^2 + T_1^2 T_{4.2})\,\omega^3 + T_{4.2}\omega$

DETERMINATION OF MAXIMUM ERROR OF A BINARY MULTIPLIER

Yang Hsi-zeng

Peiping

Translated from Avtomatika i Telemekhanika, Vol. 21, No. 7,
pp. 1007-1014, July, 1960
Original article submitted September 30, 1959

A digital integrator scheme based on a binary multiplier is considered with analysis of its error due to fluctuations in the frequency of output pulses. A formula is derived for the maximum value of this error.

There is, at present, a wide field of application for digital integrators in digital differential analyzers, as well as in specialized computing devices. The accuracy of their work, however, has not until now been investigated [1, 2]. One type of error is considered in the present paper, namely, of a digital integrator based on binary multipliers [3], the error being due to fluctuations in the frequency of its output pulses. The outline of a digital integrator based on binary multipliers is shown in Fig. 1. The input and output pulses of the integrator are shown in Fig. 2.

The pulses f enter the binary counters $C_0, C_1, \ldots, C_n$. At the output of each digital place of the counter, pulse series with frequencies $f \cdot 2^{-1}, \ldots, f \cdot 2^{-n}$ were obtained. These pulses proceed to the gates $B_0, B_1, \ldots, B_n$, controlled by the corresponding digital places of the register. All the outputs of the gates are combined and fed to the output of the integrator. When "1" is retained in a given digital place, then the corresponding gate is open.

The number of pulses at the output of the integrator during time T is equal to

$$y = Tf \sum_{k=1}^{n} k_k \cdot 2_n^{-k},$$

where k_i is the coefficient of the corresponding power of 2 in the binary representation of the number which is in the register; k_i are either = 0 or = 1.

We put into this formula $x = \sum_{k=1}^{n} k_k \cdot 2^{-k}$.; this is the binary representation of the number in the register, and $T = \sum_{0}^{N} \Delta t$ (where $\Delta t = 1/f$) is the time period of travelling of the input pulses. We obtain as a result

$$y = f \sum_{0}^{N} x\Delta t \approx f \int_{0}^{T} xdt. \qquad (1)$$

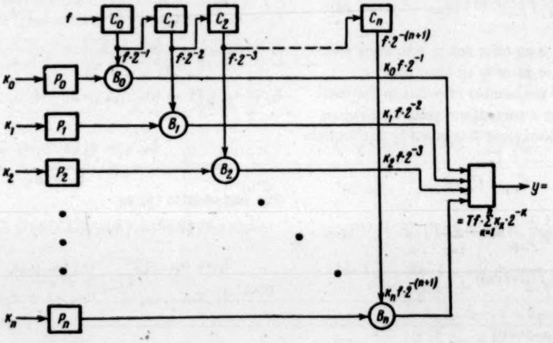

Fig. 1.

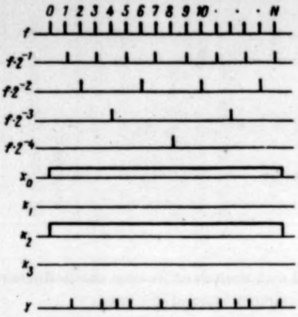

Fig. 2.

1. Maximum Frequency Fluctuation of an Integrator

The number of pulses at the output of a sum circuit within the time interval T is equal to [4]

$$C_{\mathrm{FI}} = \sum_{i=0}^{n} \left[Tf \cdot 2^{i-(n+1)} + \frac{1}{2} \right]_{\mathrm{i.p.}} k_i. \quad (2)$$

The subscript "i.p." denotes here that the integral part of the expression in square brackets should be taken. The time T can be expressed by the number N of pulses entering the counter C:

$$T = (a_0 \cdot 2^0 + a_1 \cdot 2^1 + \ldots + a_n \cdot 2^n) \frac{1}{f} = \frac{N}{f} \cdot (3)$$

Should the number of pulses, which is determined by the code in the register, be distributed uniformly within the time interval $2^{n+1}/f$, then the number of pulses through the sum circuit would be equal to

$$C_{\mathrm{u}} = \sum_{i=0}^{n} Tf \cdot 2^{i-(n+1)} k_i. \quad (4)$$

In this case there is no error due to frequency fluctuation, that is, the integrator is an ideal one.

The difference in the number of pulses in the ideal integrator and one with a nonuniform pulse distribution at an arbitrary moment of time T is given by the formula

$$D = C_{\mathrm{FI}} - C_{\mathrm{u}} =$$

$$\sum_{i=0}^{n} \left[Tf \cdot 2^{i-(n+1)} + \frac{1}{2} \right]_{\mathrm{i.p.}} k_i - \sum_{i=0}^{n} Tf \cdot 2^{i-(n+1)} k_i =$$

$$= \sum_{i=0}^{n} \left\{ \left[Tf \cdot 2^{i-(n+1)} + \frac{1}{2} \right]_{\mathrm{i.p.}} - \right.$$

$$\left. - Tf \cdot 2^{i-(n+1)} \right\} k_i = \sum_{i=0}^{n} \delta_i. \quad (5)$$

The above difference gives the error of an actual integrator as compared with the ideal one.

By substituting (3) into (5) and bearing in mind that $\sum_{n=2}^{n} \left[\frac{1}{2} + a_i 2^{-p} \right]_{\mathrm{i.p.}} = 0$, one can express (5) as follows:

$$\delta_0 = \frac{1}{2} k_0$$

$$[a_n - (a_{n-1} \cdot 2^{-1} + a_{n-2} \cdot 2^{-2} + \ldots + a_0 \cdot 2^{-n})],$$

$$\delta_1 = \frac{1}{2} k_1 [a_{n-1} - (a_{n-2} \cdot 2^{-1} + \ldots + a_0 \cdot 2^{1-n})],$$

$$\cdots\cdots\cdots\cdots\cdots\cdots\cdots\cdots$$

$$\delta_k = \frac{1}{2} k_k [a_{n-k} - (a_{n-(k+1)} \cdot 2^{-1} + \ldots + a_0 \cdot 2^{k-n})],$$

$$\cdots\cdots\cdots\cdots\cdots\cdots\cdots\cdots$$

$$\delta_{n-1} = \frac{1}{2} k_{n-1} [a_1 - a_0 \cdot 2^{-1}], \quad (6)$$

$$\delta_n = \frac{1}{2} k_n a_0.$$

2. Positive Error Due to Frequency Fluctuations

As seen from (6), in order to obtain the maximum positive magnitude of D, it is necessary that the following be satisfied:

$$k_i = 0 \ \text{ for } \ a_{n-i} = 0, \quad k_i = 1 \ \text{ for } \ a_{n-i} = 1.$$

Were it not so, either some positive terms would be lost ($k_i = 0$ when $a_{n-i} = 1$), or negative ones added ($k_i = 1$ when $a_{n-i} = 0$), from the terms in the expression (6) for the error.

In view of the fact that in (6) k and a are two-valued variables, one can express the necessary condition for obtaining the maximum positive value of D in the form

$$k_i = a_{n-i}. \quad (7)$$

We substitute (7) into (5) and, denoting $2\delta_i$ by ξ_i, we obtain

$$\xi_0 = a_n [1 - (a_{n-1} \cdot 2^{-1} + a_{n-2} 2^{-2} + \ldots + a_0 \cdot 2^{-n})],$$

$$\xi_1 = a_{n-1} [1 - (a_{n-2} \cdot 2^{-1} + \ldots + a_0 \cdot 2^{1-n})].$$

$$\cdots\cdots\cdots\cdots\cdots\cdots\cdots\cdots$$

$$\xi_k = a_{n-k} [1 - (a_{n-(k+1)} \cdot 2^{-1} + \ldots + a_0 \cdot 2^{k-n})],$$

$$\cdots\cdots\cdots\cdots\cdots\cdots\cdots\cdots$$

$$\xi_{n-1} = a_1 (1 - a_0 \cdot 2^{-1}), \quad (8)$$

$$\xi_n = a_0.$$

One can rewrite (8) as

$$\xi_0 = a_n [2^{-n} + (\bar{a}_{n-1} \cdot 2^{-1} + \ldots + \bar{a}_0 \cdot 2^{-n})],$$

$$\xi_k = a_{n-k} [2^{k-n} + (\bar{a}_{n-(k+1)} \cdot 2^{-1} + \quad (9)$$

$$+ a_{n-(k+2)} \cdot 2^{-2} + \ldots + \bar{a}_0 \cdot 2^{k-n})],$$

$$\cdots\cdots\cdots\cdots\cdots\cdots\cdots\cdots$$

$$\xi_{n-1} = a_1 (2^{-1} - \bar{a}_0 \cdot 2^{-1}), \quad \xi_n = a_0$$

or

$$\xi_0 = \frac{a_n}{2^n}(1 + \bar{a}_0 \cdot 2^0 + \bar{a}_1 \cdot 2^1 + \ldots + \bar{a}_{n-1} \cdot 2^{n-1}),$$

$$\xi_1 = \frac{a_{n-1}}{2^{n-1}}(1 + \bar{a}_0 \cdot 2^0 + \bar{a}_1 \cdot 2^1 + \ldots + \bar{a}_{n-2} \cdot 2^{n-2}),$$

$$\ldots\ldots\ldots\ldots\ldots\ldots\ldots\ldots\ldots\ldots$$

$$\xi_k = \frac{a_{n-k}}{2^{n-k}}(1 + \bar{a}_0 \cdot 2^0 + {}$$

$$+ \quad \bar{a}_1 \cdot 2^1 + \ldots + \bar{a}_{n-(k+1)} \cdot 2^{n-(k+1)}),$$

$$\ldots\ldots\ldots\ldots\ldots\ldots\ldots\ldots\ldots\ldots$$

$$\xi_{n-1} = \frac{a_1}{2^1}(1 + \bar{a}_0), \tag{10}$$

$$\xi_n = \frac{a_0}{2^0}$$

and

$$\Delta_n = 2D = \sum_{p=0}^{n} \frac{a_p}{2^p}\left[1 + \sum_{s=1}^{p} \bar{a}_{s-1} \cdot 2^{s-1}\right] = \sum_{p=0}^{n} \xi_p, \tag{11}$$

where the bar over a letter denotes the complement of the given two-valued variable, that is, $\bar{a}_{n-1} = 1 - a_{n-1}$.

As seen from (11), the error Δ_n consists of n + 1 component terms ξ_p (p assumes the values from 0 to n). It is convenient to write (10) and (11) in terms of the digits "1" and "0". We denote the terms of error which are present when $a_i = 1$ by the symbol "1". Inversely, the terms of the error which are absent when $a_i = 0$ are denoted by the symbol "0". Now the a_i, which equal 1 or 0, appear as coefficients of the corresponding power of 2 of the number T.

It can be shown that taking the complement of all the terms ξ_p of the error in (11), except ξ_0 and ξ_n which are in the state "1" (present), will not change the magnitude of the error Δ.

Proof. Taking the complements of $a_1, \ldots, a_{n-1}$ (a_0 and a_n remain "1") we obtain

$$\Delta_n = \frac{a_0}{2^0} + \frac{\bar{a}_1}{2^1}(1 + \bar{a}_0) + \frac{\bar{a}_2}{2^2}(1 + \bar{a}_0 + a_1 \cdot 2^1) + \ldots$$

$$\ldots + \frac{\bar{a}_p}{2^p}(1 + \bar{a}_0 + a_1 \cdot 2^1 + \ldots + a_{p-1} \cdot 2^{p-1}) + \ldots$$

$$\ldots + \frac{a_n}{2^n}(1 + \bar{a}_0 + a_1 \cdot 2^1 + \ldots + a_{n-2} 2^{n-1}). \tag{12}$$

Subtracting (12) from (11) and taking into account that

$$a_i \bar{a}_j - \bar{a}_i a_j = a_i + \bar{a}_j - 1, \tag{13}$$

one can show that

$$\Delta_n - \Delta_n' = 0 \quad \text{or} \quad \Delta_n = \Delta_n'. \tag{14}$$

3. Maximum Positive Error

The maximum positive error is attained when all the even terms $\xi_0, \xi_2, \ldots \xi_{2p}$ of the error are present, and all the odd terms $\xi_1, \xi_3, \ldots, \xi_{2p-1}$ are absent.

Proof. We rewrite (11), putting now $a_i = 1$ for even i and equal 0 for odd i:

$$\Delta_{pM} = 1, 0, 1, \ldots, 0, 1, 0, 1, 0, 1, \ldots, 0, 1. \tag{15}$$

It is being taken as valid that with the terms ξ_0 and ξ_n always present, and all even terms present, and all odd ones absent in the terms $\xi_{2p-1}, \ldots, \xi_{n-1}$, whatever the combination of presences and absences of the remaining terms $\xi_1, \xi_2, \ldots, \xi_{2p-2}$, the error

$$\Delta_1 = 1, \xi_1, \xi_2, \ldots, \xi_{2p-3}, \xi_{2p-2}, 0, 1, 0, 1, \ldots, 0, 1 \tag{16}$$

never exceeds Δ_{pM}, that is, $\Delta_1 \leq \Delta_{pM}$.

The inequality can be verified by putting p = 1, 2, 3, ...

We shall show now that the above assumption remains valid when instead of $\xi_1, \xi_2, \ldots, \xi_{2p-2}$ we take $\xi_1, \xi_2, \ldots, \xi_{2p}$, in other words, that for the error

$$\Delta_2 = 1, \xi_1, \xi_2, \ldots, \xi_{2p-3}, \xi_{2p-2}, \xi_{2p-2}, \xi_{2p} 0, 1, \ldots, 0, 1 \tag{17}$$

the inequality $\Delta_2 \leq \Delta_{pM}$ is valid.

The change from (16) to (17) involves the appearance of two new terms ξ_{2p-2} and ξ_{2p}, and they can take any form, depending on their presence or absence. Four combinations are altogether possible: 0, 0; 1,1; 1,0; 0,1.

Each case corresponding to a respective combination is considered separately:

a) ξ_{2p-1} and ξ_{2p} are absent (0, 0). Then

$$\Delta_3 = 1, \xi_1, \xi_2, \ldots, \xi_{2p-3}, \xi_{2p-2}, 0, 0, 0, 1, 0, \ldots, 0, 1. \tag{18}$$

We find the difference

$$\Delta_1 - \Delta_3 = \frac{1}{2^{2p}}\left(1 + \sum_{s=1}^{2(p-1)} \bar{a}_s 2^s + 2^{2p-1}\right) -$$

$$- 2^{2p} \sum_{s=p+1}^{n/2} \frac{1}{2^{2s}} =$$

$$= \frac{1}{6} + \frac{1}{2^{2p}}\left(1 + \sum_{s=1}^{2(p-1)} \bar{a}_s 2^s\right) + \frac{1}{3}\frac{1}{2^{n-2p}} > 0.$$

Hence,

$$\Delta_3 < \Delta_1 \leqslant \Delta_{pM}$$

b) ξ_{2p-1} and ξ_{2p} are present (1,1). Then

$$\Delta_4 = 1, \xi_1, \xi_2, \ldots, \xi_{2p-3}, \xi_{2p-2},$$

$$1, 1, 0, 1, \ldots, 0, 1, 0, 1. \tag{19}$$

Taking the complements of all the terms in (19), except of ξ_0 and ξ_n, we obtain the expression

$$\Delta_4' = 1, \bar{\xi}_1, \bar{\xi}_2, \ldots, \bar{\xi}_{2p-3}, \bar{\xi}_{2p-2},$$
$$0, 0, 1, 0, \ldots, 1, 0, 1, 1. \tag{20}$$

Taking the complements of $\xi_1, \ldots, \xi_{2p-2}$ in (16), but leaving the remaining terms as they are, we obtain the expression

$$\Delta_1'' = 1, \bar{\xi}_1, \bar{\xi}_2, \ldots, \bar{\xi}_{2p-3}, \bar{\xi}_{2p-2},$$
$$0, 1, 0, 1, \ldots, 0, 1, 0, 1. \tag{21}$$

We form the difference

$$\Delta_1'' - \Delta_4' = \sum_{k=p}^{n/2} \frac{1}{2^{2k}}\Big[1 + \sum_{s=0}^{2(k-1)} a_s 2^s + \sum_{s=k}^{n/2} 2^{2s-1}\Big] -$$
$$-\Big\{\sum_{k=p}^{n/2-1} \frac{1}{2^{2k+1}}\Big[1 + \sum_{s=0}^{2k-2} a_s 2^s + \sum_{s=k}^{n/2-1} 2^s + 2^{2k-1}\Big] +$$
$$+\frac{1}{2^n}\Big[1 + \sum_{s=0}^{2p-2} a_s 2^s + \sum_{s=p}^{n/2-1} 2^{2s} + 2^{2p-1}\Big]\Big\} =$$
$$= \frac{1}{6} - \frac{1}{3}\,\frac{1}{2^{n-2p+1}} + \frac{1}{3}\Big[1 + \sum_{s=0}^{2p-2} a_s 2^s\Big]\Big[\frac{2}{2^{2p}} - \frac{1}{2^n}\Big] > 0$$

or $\Delta_4' < \Delta_1''$.

It follows from the proof given in Section 2 that $\Delta_4' = \Delta_4$. In addition, we know that $\Delta_1'' \leq \Delta_{pM}$. Thus, $\Delta_{pM} \geq \Delta_1'' > \Delta_4' = \Delta_4$ and, therefore, $\Delta_4 < \Delta_{pM}$.

c) ξ_{2p-1} is present, ξ_{2p} absent (1,0). Then

$$\Delta_5 = 1, \xi_1, \xi_2, \ldots, \xi_{2p-3}, \xi_{2p-2},$$
$$1, 0, 0, 1, \ldots, 0, 1. \tag{22}$$

Taking the complements of all the terms in (22) except of ξ_0 and ξ_n, we obtain the expression

$$\Delta_5' = 1, \bar{\xi}_1, \bar{\xi}_2, \ldots, \bar{\xi}_{2p-3}, \bar{\xi}_{2p-2},$$
$$0, 1, 1, 0, 1, 0, \ldots, 1, 0, 1, 1. \tag{23}$$

Subtracting (23) from (21), we obtain

$$\Delta_1'' - \Delta_5' = \sum_{k=p}^{n/2} \frac{1}{2^{2k}}\Big[1 + \sum_{s=0}^{2k-2} a_s 2^s + \sum_{s=k}^{n/2} 2^{2s-1}\Big] -$$
$$-\Big\{\sum_{k=p}^{n/2-1} \frac{1}{2^{2k+1}}\Big[1 + \sum_{s=0}^{2k-2} a_s 2^s + \sum_{k+1}^{n/2-1} 2^{2s} + 2^{2k-1}\Big] +$$
$$+\frac{1}{2^{2p}}\Big[1 + \sum_{s=0}^{2p-2} a_s 2^s + 2^{2p-1}\Big] + \frac{1}{2^n}\Big[1 + \sum_{s=0}^{2p-2} 2^{2s} +$$
$$+ 2^{2p-1}\Big]\Big\} = \frac{1}{3}\Big[\frac{1}{2} + \frac{5}{6}\,\frac{1}{2^{n-2p}} -$$
$$-\Big(1 + \sum_{s=0}^{2p-2} a_s 2^s\Big)\Big(\frac{1}{2^{2p}} + \frac{1}{2^{n-1}}\Big)\Big] > 0,$$

as

$$1 + \sum_{s=0}^{2p-2} a_s 2^s < 2^{2p-1}.$$

It follows from the relations $\Delta_5' = \Delta_5$ and $\Delta_1'' = \Delta_{pM}$ that $\Delta_{pM} \geq \Delta_1'' > \Delta_5' = \Delta_5$ and, consequently, $\Delta_5 < \Delta_{pM}$.

d) ξ_{2p-1} absent, ξ_{2p} present (0,1). In this case, we obtain

$$\Delta_6 = 1, \xi_1, \xi_2, \ldots, \xi_{2p-3}, \xi_{2p-2},$$
$$0, 1, 0, 1, \ldots, 0, 1, \tag{24}$$

that is, $\Delta_6 = \Delta_1$ [see (16)].

We have proved in this way that for any combination of presences and absences of the terms $\xi_1, \xi_2, \ldots, \xi_{2p}$

$$\Delta_2 \leqslant \Delta_{pM}.$$

This method can be generalized for an arbitrary number of terms, from ξ_1 to ξ_{n-1}. Therefore, for any combination of presences and absences of $\xi_1, \ldots, \xi_{n-1}$, we always have $\Delta_7 \leq \Delta_{pM}$, where

$$\Delta_7 = 1, \xi_1, \xi_2, \ldots \xi_{2p-3}, \xi_{2p-2},$$
$$\xi_{2p-1}, \xi_{2p}, \xi_{2p+1}, \ldots, \xi_{n-1}, \xi_n. \tag{25}$$

The magnitude of the maximum positive error can be evaluated from the formula

$$\Delta_{pM} = \frac{1}{2}\Big[\sum_{p=0}^{n/2} \frac{1}{2^{2p}}\Big(1 + \sum_{s=1}^{p} 2^{2s-1}\Big) +$$
$$+\ r\,\frac{1}{2^{n+1}}\Big(1 + \sum_{1}^{n/2} 2^{2s-1}\Big)\Big] =$$
$$= \frac{1}{6}\Big\{n + \frac{1}{3}\Big[10 + (-1)^{r+1}\frac{1}{2^n}\Big]\Big\},$$

where $r = 1$ if $\underline{n}$ is odd and $r = 0$ if $\underline{n}$ is even.

It follows from the proof in Section 2 that the maximum error appears twice for even $\underline{n}$ in the operation of an integrator:

1) when the number of input pulses and the value of the number appearing in the register are $\sum_{p=0}^{n/2} 2^{n-2p}$, as shown above;

2) when the number of input pulses and the value of the number in the register are $2^n + \sum_{p=0}^{n/2-1} 2^{n-2p-1} + 1$.

With $\underline{n}$ odd, the maximum positive error also appears twice in the process of the integrator operation:

1) when the number of input pulses and the value of the number of the register are $\sum_{p=0}^{(n-1)/2} 2^{(n-1)-2p} + 2^n$;

2) when the number of input pulses and the value of

the number of the register are $\sum_{p=0}^{n/2-1} 2^{n-2p}+1.$

4. Maximum Negative Error

In order that the maximum negative error be attained, it is necessary, as seen from (6) that the conditions be established: $k_1 = 0$ where $a_{n-1} = 1$, but $k_1 = 1$ when $a_{n-1} = 0$, that is $k_k = \bar{a}_{n-k}$.

The expression for the negative error assumes the form

$$\Delta_{n}=\sum_{p=0}^{n} \mu_p = \sum_{p=0}^{n} \frac{\bar{a}_p}{2^p}\left(1+\sum_{s=1}^{p} a_{s-1}2^{s-1}\right).$$

It can be shown, as in the case of the positive error, that taking the complements of all the terms μ_p of the error, except the fixed μ_0 and μ_n which have the state "1" (they are present), does not change the value of the error Δ_n.

To determine the maximum negative error, the same method as for the positive error is used, and we obtain an expression for the maximum negative error:

$$\Delta_{n.M}= \frac{1}{2}\left\{\sum_{k=0}^{n/2}\frac{1}{2^{2p}}\left(1+\sum_{1}^{k}2^{2s-1}\right)+r\frac{1}{2^{n+1}} \times\right.$$
$$\left.\times\left(1+\sum_{1}^{n/2}2^{2s-1}\right)\right\}=\frac{1}{6}\left\{n+\frac{1}{3}\left[10+(-1)^{r+1}\frac{1}{2^n}\right]\right\},$$

where $r = 1$ for odd n and $r = 0$ for even n.

The error $\Delta_{n.M}$ appears twice when n is even:

1) when the number of input pulses is $\frac{1}{3}(2^{n+1}+1)$,

and the value of the number in the register is $\sum_{p=0}^{n/2} 2^{n-2p}$;

2) when the number of input pulses is $\frac{1}{3}(2^n-1)$,

and the value of the number in the register is $2^n +$
$+\sum_{p=0}^{n/2-1} 2^{n-2p-1}+1.$

It also appears twice when n is odd:

1) when the number of input pulses is $\frac{1}{3}(2^{n+1}-1)$,

and the value of the number in the register is $2^n +$
$+\sum_{p=0}^{(n-1)/2} 2^{(n-1)-2p}$;

2) when the number of input pulses is $\frac{1}{3}(2^n+1)$, and the value of the number in the register is

$$\sum_{p=0}^{n/2-1} 2^{n-2p}+1.$$

SUMMARY

1. If n is even, the integration error is maximum when the values of the function under the integration sign are either $\sum_{p=0}^{n/2} 2^{n-2p}$ or $2^n+\sum_{p=0}^{n/2-1} 2^{n-2p-1}+1$,

2. If n is odd, the integration error is maximum when the values of the function under the integration sign are either $2^n+\sum_{p=0}^{(n-1)/2} 2^{(n-1)-2p}$ or $\sum_{p=0}^{n/2-1} 2^{n-2p}+1$,

3. The maximum integration error increases with the increasing number of members of the integrator.

4. The obtained formula may be applied to evaluate the maximum error of a system with several integrators used for solving equations.

In conclusion, the author wishes to express his sincere thanks to V. V. Karibskii for his assistance in the preparation of this paper.

LITERATURE CITED

1. R. E. Sprague, "Fundamental concepts of the differential analyzer method of computation," Math. Tables and Other Aids to Compute, 37 (1952).
2. Lundh Yngvar, "Digital technique for small computation," J. Brit. Inst. Radio Engrs, 19, 1 (January, 1959).
3. A. A. Voronov and G. N. Sokolov, "A device for programming curves of second order, based on a digital integrator," Avtomat. i Telemekh. 20, 2 (1959).*
4. V. V. Karibskii, "On the error of a linear interpolator for digital programming control," Avtomat. i Telemekh. 20, 6 (1959).*

---

* See English translation.

EXPONENTIAL CONVERTERS WITH A LOGARITHMIC TRANSFORMATION LAW

A. I. Novikov

Moscow

Translated from Avtomatika i Telemekhanika, Vol. 21, No. 7,
pp. 1015-1025, July, 1960
Original article submitted January 19, 1960

Exponential converters with a logarithmic transformation law are considered. The basic equations which characterize the operation of converters are given. The errors are analyzed. Various converter variants are studied.

INTRODUCTION

As a rule, a linear relation between the measured and the received parameter values is required in remote-measurement systems. This is explained by the fact that the taking and interpolation of readings can be conveniently performed on a linear scale, that the quantities to be measured can be added at the receiving end, and that the absolute error within the range can remain constant. A linear relation is usually secured by the application of linear converters.

A linear relation between the measured and the received parameters can be secured not only by means of linear converters. Let there be a converter, which we shall call a functional converter, where the parameter x to be measured is transformed into the analog y according to the equation

$$y = f(x). \tag{1}$$

Let us assume that x, in turn, is a function of λ and that it changes according to the law

$$x = \varphi(\lambda). \tag{2}$$

Then the transformed function, which is to be transmitted through the communication channel, will be

$$y = f[\varphi(\lambda)]. \tag{3}$$

Assume that the receiver contains a device whose characteristic is an inverse function with respect to the converter characteristic:

$$z = f^{-1}(y). \tag{4}$$

We shall call this device an inverse functional converter. Then, at the output of this converter, the received signal will be equal to the transmitted quantity $\varphi(\lambda)$:

$$z = f^{-1}\{f[\varphi(\lambda)]\} = \varphi(\lambda). \tag{5}$$

Thus, the relation between the transmitted $\varphi(\lambda)$ and the received z parameters will be linear, although the transformed parameter y changes nonlinearly in dependence on $\varphi(\lambda)$. The linear converter would constitute a particular case of the functional converter.

Certain types of functional converters secure a sufficiently high transformation stability, and they have simple circuits. The exponential converters which are considered below belong to this type.

Basic Relations

In an exponential converter with a logarithmic transformation law, the voltage, which changes according to the $Ee^{-t/\tau}$ or the $E[1-e^{-t/\tau}]$ law, is compared with the data transmitter voltage.

The converter consists of a bridge circuit (Fig. 1).

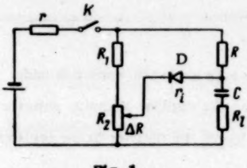

Fig. 1.

A resistor R_1 and a potentiometric data transmitter R_2 are connected to one branch of the bridge, and the resistor R and capacitor C are connected to the other branch. A diode D is provided in the bridge diagonal between the data transmitter R_2 slider and capacitor C. A rectangular voltage is periodically supplied to the bridge by means of key K (Fig. 2a).

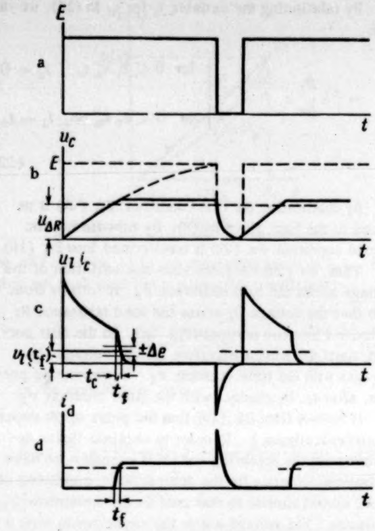

Fig. 2.

In this, the voltage across capacitor C will rise in the manner shown in Fig. 2b, and the current through the capacitor will change according to the diagram in Fig. 2c.

At the comparison time t_c, when the voltage across the capacitor attains the value $U_{\Delta R}$, the diode will be unlocked. The character of the diode current variation is shown in Fig. 2d.

After the time t_c, the voltage across the capacitor will remain constant up to the video pulse end, since the unlocked diode resistance $r_1 \ll R$. The moment of comparison and its corresponding time t_c can be fixed with respect to the change in the diode circuit current i_d (Fig. 2d) and with respect to the change in the capacitor circuit current i_c or the voltage U_l across the load resistance R_l (Fig. 2c).

Let us determine the effect of the circuit parameters on the pulse width t_c and the trailing edge duration t_f (Fig. 2c). The values of t_c and t_f will be determined with respect to variations of the voltage across the resistance R_l, because this method is the simplest.

The equivalent circuit of a converter in the state preceding the comparison moment is shown in Fig. 3. The equations are of the following form:

$$\frac{E}{p} = i_1(r + R_1 + R_2) - i_2(R_1 + R_2), \tag{6}$$

$$0 = -i_1(R_1 + R_2) + i_2\left(R_1 + R_2 + R + R_l + \frac{1}{Cp}\right).$$

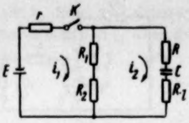

Fig. 3.

By solving these equations, we shall find the voltage across the capacitor:

$$U_C = Ek\left(1 - e^{-\frac{t_1}{CR_0}}\right), \tag{7}$$

the voltage across the load resistance R_l:

$$U_l = Ek\frac{R_l}{R_0}e^{-\frac{t_1}{CR_0}}, \tag{8}$$

the voltage at the data transmitter R_2 slider:

$$U_{\Delta R} = Ek\frac{\Delta R}{R_1 + R_2}\left(1 - \frac{rk}{R_0}e^{-\frac{t_1}{CR_0}}\right), \tag{9}$$

where

$$k = \frac{R_1 + R_2}{R_1 + R_2 + r}, \tag{10}$$

$$R_0 = R + R_l + rk, \tag{11}$$

and ΔR is the resistance between the data transmitter R_2 slider and the ground.

The present time t_1 changes within the $0 \le t_1 \le t_c$ interval. The pulse width t_c is determined by the equation

$$U_c + U_l = U_{\Delta R} + \Delta E, \tag{12}$$

where ΔE is the diode unlocking voltage.

The reduced expressions yield the equation

$$t_c = CR_0 \ln \frac{m + q(1 - \lambda n)}{1 - \lambda n - \frac{\Delta E}{Ek}}, \tag{13}$$

where

$$m = \frac{R}{R_0},\ q = \frac{rk}{R_0},\ n = \frac{R_2}{R_1 + R_2},\ \lambda = \frac{\Delta R}{R_2}.$$

The parameter λ to be transmitted will change within the interval

$$\lambda_{\min} \leqslant \lambda \leqslant 1,$$

where

$$\lambda_{\min} = \frac{R_l}{(R + R_l)n}. \tag{14}$$

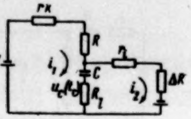

Fig. 4.

For determining the trailing edge duration t_f, we shall use an equivalent circuit (Fig. 4) which corresponds to the converter state after the comparison time t_c. The following assumptions were made with regard to this circuit: the current in the R_1R_2 circuit is assumed to be constant after the comparison time t_c, since $R \gg R_1 + R_2$; the diode internal resistance is constant and equal to r_i after unlocking.

The circuit shown in Fig. 4 is described by the equations

$$\frac{Ek - U_C(t_c)}{p} = i_1\left(R + R_l + rk + \frac{1}{Cp}\right) + i_2\left(R_l + \frac{1}{Cp}\right),$$
$$\frac{U_C(t_c) - U_{\Delta R}(t_c)}{p} = -i_1\left(R_l + \frac{1}{Cp}\right) + i_2\left(r_i + \Delta R + R_l + \frac{1}{Cp}\right), \tag{15}$$

where $U_C(t_c)$ and $U_{\Delta R}(t_c)$ are the voltage across the capacitor,and at the data transmitter slider,at the comparison time t_c, respectively.

By using Eq. (15), we shall determine the voltage $U_l(t_2)$ across the load resistance R_l and the current $i_2(t_2)$ which is transmitted through the diode after the comparison time t_c (Fig. 2, c and d):

$$U_l(t_2) = Ek\frac{R_l}{R_0}e^{-\frac{t_c}{\tau_1}}e^{-\frac{t_2}{\tau_2}}, \tag{16}$$

$$i_2(t_2) = \frac{Ek_1}{R_0}e^{-\frac{t_c}{\tau_1}}(1 - e^{-\frac{t_2}{\tau_2}}), \tag{17}$$

where

$$\tau_1 = CR_0, \tag{18}$$

$$\tau_2 = C\left[R_l + \frac{(R + rk)(r_i + \Delta R)}{R + rk + r_i + \Delta R}\right], \tag{19}$$

$$k_1 = \frac{k(R + rk)}{R + rk + r_i + \Delta R}. \tag{20}$$

From (16) we find the trailing edge duration:

$$t_f = \tau_2 \ln \frac{Ek}{U_l(t_f)} \frac{R_l}{R_0} e^{-\frac{t_c}{\tau_1}}. \tag{21}$$

In Eq. (21), $U_l(t_f)$ is the voltage at the level of which the trailing edge duration t_f is read.

By substituting the variable t_1 for t_c in (16), we obtain

$$U_l = Ek\frac{R_l}{R_0}e^{-\frac{t_1}{\tau_1}}e^{-\frac{t_2}{\tau_2}} \left| \begin{array}{l} \text{for } 0 \leqslant t_1 \leqslant t_c, \quad t_2 = 0, \\ \text{for } 0 < t_2 \leqslant \infty, \; t_1 = t_c. \end{array} \right. \tag{22}$$

By substituting the first condition, Eq. (22) is reduced to the form given by (8); by substituting the second condition, Eq. (22) is transformed into Eq. (16).

Thus, Eq. (22) fully describes the variation of the voltage across the load resistance R_l. It follows from (22) that the voltage U_l across the load resistance R_l is divided into two portions (Fig. 2c). In the first portion, until the comparison time t_c, the voltage U_l changes with the time constant τ_1. In the second portion, after t_c, U_l changes with the time constant τ_2.

It follows from Eq. (13) that the pulse width depends logarithmically on λ. In order to obtain a linear dependence at the receiving end, it is necessary to have an inverse converter for the demodulator, consisting of an RC circuit similar to that used in the transmitter converter. The voltage across the capacitor in such a converter must change in step and according to the same law as in the converter capacitor, i.e.,

$$U(t) = E(1 - e^{-\frac{t_1}{\tau_1}}). \tag{23}$$

By substituting (13) in (23), we obtain

$$U(\lambda) = E\left[1 - \frac{1 - \lambda n - \frac{\Delta E}{Ek}}{m + q(1 - \lambda n)}\right]. \tag{24}$$

It follows from (24) that U(λ) changes nonlinearly in dependence on λ (Fig. 5). The nonlinearity is due to the presence of the resistance r in the converter (Fig. 1), as a result of which the voltage across the data transmitter R_2 changes nonlinearly throughout the range, as follows from Eq. (9).

In the case where $r = 0$ or $r \ll R$, the dependence of U(λ) on λ will be linear:

$$U(\lambda) = E\left(b + \frac{n}{m}\lambda\right), \tag{25}$$

where

$$b = 1 - \frac{1 - \frac{\Delta E}{Ek}}{m} \approx 0. \tag{26}$$

We shall define the degree of nonlinearity of U(λ) in expression (24) by the ratio of the maximum deflec-

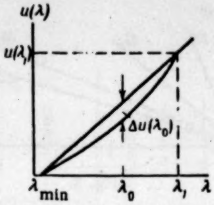

Fig. 5.

tion $\Delta U(\lambda_0)$ (Fig. 5) to the maximum value $U(\lambda_1)$, which we shall call the nonlinearity coefficient:

$$\beta = \frac{\Delta U\,(\lambda_0)}{U\,(\lambda_1)}. \tag{27}$$

In the considered case,

$$\beta = \frac{\lambda_0 - \lambda_{\min}}{1 - \lambda_{\min}} - h\left[1 - \frac{1 - \lambda n}{m + q\,(1 - \lambda_0 n)}\right], \tag{28}$$

where

$$\lambda_0 = \frac{m + q}{nq} - \frac{1}{nq}\sqrt{hnm\,(1 - \lambda_{\min})}, \tag{29}$$

$$h = \frac{1}{1 - \dfrac{1 - n}{m + q\,(1 - n)}}. \tag{30}$$

Converter Errors

From Eq. (13), it follows that the pulse width t_c depends on the feed voltage E. The reduced error due to variations of the feed voltage E is equal to

$$\delta_{\Delta E} = \frac{\Delta t}{t_{c\max}} = \frac{\ln\dfrac{1 - \lambda n - \dfrac{\Delta E}{E'k}}{1 - \lambda n - \dfrac{\Delta E}{Ek}}}{\ln\dfrac{m + q\,(1 - n)}{1 - n - \dfrac{\Delta E}{Ek}}}, \tag{31}$$

where $E' = E \pm \delta E$.

Figure 6, a and b, shows the calculated U_l curves which illustrate the variation of t_c when the feed voltage E changes twofold.

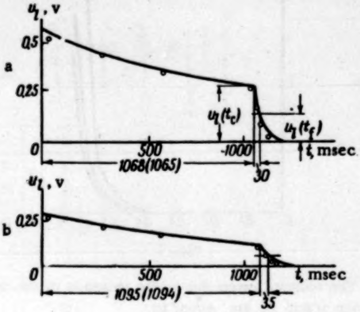

Fig. 6.

The calculation results are given in Table 1.

The calculations were performed according to Eq. (22) for the circuit shown in Fig. 1, where the measured parameters had the following values: R_1 = 692 ohm, $\Delta R_2 = R_2$ = 700 ohm, R = 74,460 ohm, R_n = 818 ohm, r_i = = 870 ohm, r = 0, C = 20.4 μf, ΔE = 0.35 v.

For a feed voltage of E = 50 v, the comparison time t_c = 1068 msec, and for E = 25 v, t_c = 1095 msec.

The experimental curves are marked by points in Fig. 6. The experimentally obtained values of t_c are in brackets. As follows from Fig. 6, a and b, the theoretical and experimental curves practically coincide.

In calculating the diode bias, ΔE is obtained from the condition

$$r_i = \frac{\Delta E}{i_d} = (3 - 4)\,R_0. \tag{32}$$

For silicon D-202 diodes, ΔE = 0.35 v. The characteristics of three specimens of D-202 diodes are given in Fig. 7.

The accuracy in reading the pulse width t_c is determined by the magnitude of the pulse trailing edge t_f and by the operation threshold magnitude ± Δe (Fig.

TABLE 1

E=50			E=25		
t_1, sec	t_2, sec	U_l, v	t_1, sec	t_2, sec	U_l, v
0	0	0.543	0	0	0.271
0.3	0	0.447	0.3	0	0.223
0.6	0	0.367	0.6	0	0.183
1.068	0	0.271	1.094	0	0.133
1.068	0.02	0.179	1.094	0.02	0.088
1,068	0.04	0.118	1.094	0.04	0.058
1.068	0.08	0.051	1.094	0.08	0.025
1.068	0.12	0.022	1.094	0.12	0.011

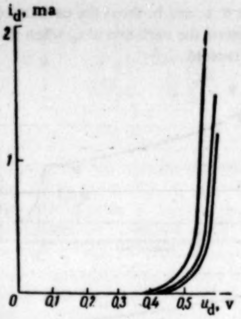

Fig. 7.

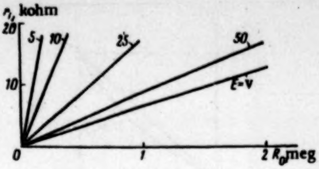

Fig. 8.

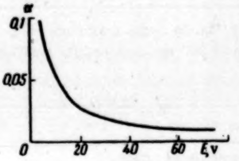

Fig. 9.

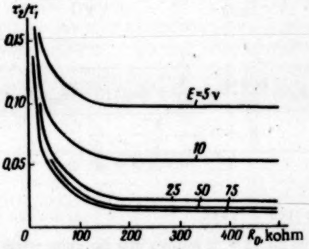

Fig. 10.

2c). The reduced errors due to the presence of the trailing edge t_f and Δe are equal to

$$\delta_{\Delta t}=\frac{\tau_2}{\tau_1}\frac{\ln\frac{Ek}{U_l(t_f)}\frac{R_l}{R_0}e^{-\frac{t_c}{\tau_1}}}{\ln\frac{m+q(1-n)}{1-n-\frac{\Delta E}{Ek}}}, \tag{33}$$

$$\delta_{\Delta e}=\frac{\tau_2}{\tau_1}\frac{\ln\left(1\pm\frac{\Delta e}{U_l(t_f)}\right)}{\ln\frac{m+q(1-n)}{1-n-\frac{\Delta E}{Ek}}} \tag{34}$$

respectively.

It follows from (33) and (34) that the errors $\delta_{\Delta t}$ and $\delta_{\Delta e}$ depend on the relation

$$\frac{\tau_2}{\tau_1}=\left[R_l+\frac{(R+rk)(r_i+\Delta R)}{R+rk+r_i+\Delta R}\right]\frac{1}{R_0}\approx\alpha+\frac{R_l+\Delta R_2}{R_0}, \tag{35}$$

since

$$r_i+\Delta R\ll R+rk.$$

For a fixed feed voltage E, it can be considered that

$$\alpha=\frac{r_i}{R_0}=\mathrm{const}, \tag{36}$$

since the diode internal resistance r_i changes almost linearly with a change in R_0 (Fig. 8).

The dependence of α on E for silicon D-202 diodes is shown in Fig. 9. The variation of τ_2/τ_1 in dependence on R_0 is given in Fig. 10. From expression (35) and the diagrams in Fig. 10, it follows that τ_2/τ_1 is independent of the capacitance value and is directly proportional to ΔR and R_l and inversely proportional to E and R_0. Thus, in order to reduce the trailing edge duration t_f and the $\delta_{\Delta t}$ and $\delta_{\Delta e}$ errors, it is necessary to reduce R_l and ΔR and to increase the feed voltage E and the resistance R. The change in the trailing edge duration t_f when the feed voltage E changes twofold can be seen in Fig. 6, a and b. The increase in t_f with an increase in the $\frac{R_l+\Delta R}{R_0}$ ratio if τ_1 remains constant and $\alpha = 0.012$ can be seen in the voltage U_l oscillograms, which are shown in Fig. 11. The duration t_f in Figs. 6 and 11 is read at the $U_l(t_f) = 0.5\,U_l(t_c)$ level.

Converter Circuits

Table 2 provides circuits and equations for some other converters.

In circuit No. 1, when the key K is closed, capacitor C is quickly charged to voltage E. During discharge, the voltage across capacitor C, which varies exponentially, is compared with the voltage $U_{\Delta R}$ across the data transmitter.

TABLE 2

Circuit No.	Circuit	Character of operation	Pulse width	Reduced error due to changes in E	Reduced error due to the presence of trailing edge t_f	Reduced error due to the presence of operation threshold ±Δe	Remark
1	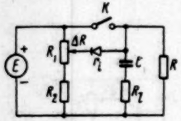	Discharge	$t_c = R_0 C \ln \frac{m}{1 - n\lambda - \frac{\Delta E}{E}}$	$\delta_{\Delta E} = \frac{\ln \frac{1 - n\lambda - \frac{\Delta E}{E'}}{1 - n\lambda - \frac{\Delta E}{E}}}{\ln \frac{m}{1 - n - \frac{\Delta E}{E}}}$	$\delta_{\Delta t} = \frac{\tau_2}{\tau_1} \frac{\ln \frac{E \frac{R_l}{R_0} e^{\frac{t_c}{\tau_1}}}{U_0}}{\ln \frac{m}{1 - n - \frac{\Delta E}{E}}}$	$\delta_{\Delta e} = \frac{\tau_2}{\tau_1} \frac{\ln \left(1 \pm \frac{\Delta e}{U_0}\right)}{\ln \frac{m}{1 - n - \frac{\Delta E}{E}}}$	$R_0 = R + R_l$ $m = \frac{R}{R_0}$, $n = \frac{R_1}{R_1 + R_2}$, $\lambda = \frac{\Delta R}{R_1}$, $\tau_2 = R_l + r_l + \Delta R_0$. $\Delta R_0 = \frac{\Delta R_1 (R_1 + R_2 - \Delta R_1)}{R_1 + R_2}$
2	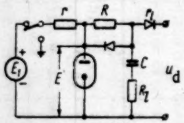	Charge	$t_c = R_0 C \ln \frac{m}{1 - n\lambda - \frac{\Delta E}{E}}$				$R_0 = R + R_l$ $m = \frac{R}{R_0}$, $n = \frac{U_{d\,max}}{E}$, $\lambda = \frac{U_d}{U_{d\,max}}$, $\tau_2 = R_l + r_l$

TABLE 2 (Continued)

Circuit No.	Circuit	Character of operation	Pulse width	Reduced error due to changes in E	Reduced error due to the presence of trailing edge t_f	Reduced error due to the presence of operation threshold $\pm\Delta e$	Remark
3	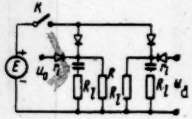 K E u_0 η R_l R R_l η R_l u_d	Discharge	$t_0 = R_0 C \ln \frac{1-\frac{\Delta E}{U_0}}{\lambda-\frac{\Delta E}{U_0}}$	—	—	—	$\lambda = \frac{U_d}{U_0}$, $R_0 = R + R_l$
4	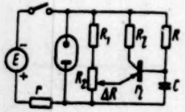 E r R_1 R_2 R R_2 ΔR η C	Charge	$t_0 = RC \ln \frac{1}{1-n\lambda-\frac{\Delta E}{E_0}}$	$\delta_{\Delta E} = \frac{\ln \frac{1-n\lambda-\frac{\Delta E}{E'}}{1-n\lambda-\frac{\Delta E}{E}}}{\ln \frac{1}{1-n-\frac{\Delta E}{E}}}$	$\delta_{\Delta t} = \frac{\tau_2}{\tau_1} \frac{\ln \frac{i_d}{i_d - i_f}}{\ln \frac{1}{1-n-\frac{\Delta E}{E}}}$	$\delta_{\Delta e} = \frac{\tau_2}{\tau_1} \frac{\ln\left(1 \pm \frac{\Delta i}{i_d - i_f}\right)}{\ln \frac{1}{1-n-\frac{\Delta E}{E}}}$	$n = \frac{R_1}{R_1 + R_2}$, $\lambda = \frac{\Delta R}{R_2}$, $i_d = \frac{Ek_1}{R} e^{-\frac{t_2}{\tau_2}}$, $k_1 = \frac{R}{R+r_1+\Delta R}$

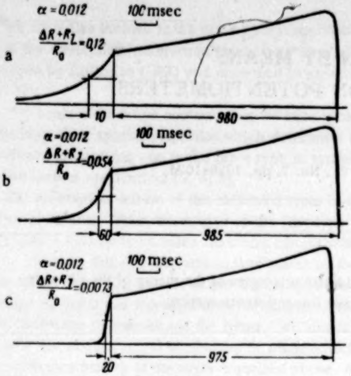

Fig. 11.

If such a converter is used in a remote-measurement system, the voltage in the inverse converter will change linearly with λ:

$$U(\lambda) = E\left(b_1 + \frac{n}{m}\lambda\right), \tag{37}$$

where

$$b_1 = \left(1 - \frac{\Delta E}{E}\right)\frac{1}{m} \approx 0.$$

This constitutes the difference in principle between this converter and the one considered above.

In a number of cases, the converter can be conveniently controlled by supplying a voltage to the diode input. Such converters are described in Table 2; they are based on circuits Nos. 2 and 3.

The pulse width t_c in circuit No. 2 directly depends on the feed voltage, and therefore, a stabilivolt is provided at the converter input. In contrast to circuit No. 2, circuit No. 3 does not require stabilized voltage. Its principle of operation is clear from Fig. 12. The voltage U(t) changes exponentially, and is compared with two steady voltages U_0 and U_d. The pulse width between t_0 and t_d does not depend on the exponential voltage amplitude:

$$t_c = t_d - t_0 = CR \ln \frac{U_0}{U_d}.$$

If U_0 is fixed and U_d changes in correspondence with the parameter to be measured, the pulse width t_c will change according to the logarithmic law.

In circuit No. 3, when key K is closed, the capacitors in the RC cells, which have equal time constants, are charged to voltage E. After the key is opened, the capacitors discharge through the resistor R. The comparison time of the U_C and U_0 voltages in one RC cell is the beginning of reading the pulse width t_C, and the U_C and U_d comparison time in the other RC cell is the end of this pulse reading.

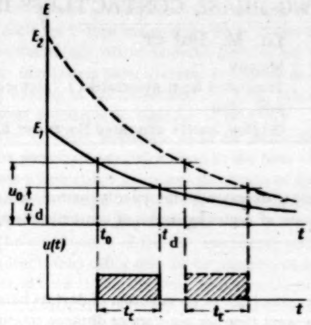

Fig. 12.

As was mentioned above, the comparison time in the converter can be fixed not only with respect to the change in the voltage across the resistance R_l, but also with respect to changes in the diode circuit current i_d. Such a circuit is shown in Table 2 (No. 4). The fixing of t_c with respect to the i_d current has a number of advantages. A transistor, which acts as an amplifier at the same time, is used as the comparing element.

The front duration t_f in such a circuit is reduced by eliminating the resistance R_l [see Eqs. (19) and (35)]. However, in the construction of such circuits, it is necessary to use stable silicon transistors, which have large emitter-base and emitter-collector reverse resistances, affected only slightly by temperature and voltage variations.

The described converters can be used in the construction of remote-measurement, remote-signalization, and remote-control systems.

LITERATURE CITED

1. A. I. Novikov, "Exponential time-pulse converters," Avtomatika i Telemekhanika 18, 8 (1957).*
2. V. A. Il'in and A. I. Novikov, "New principles in the construction of remote-measurement systems with time-pulse and pulse-width modulation," Avtomatika i Telemekhanika 19, 8 (1958).*
3. V. A. Il'in, "Principles of the design of contactless remote-control systems with exponential converters," Avtomatika i Telemekhanika 20, 4 (1959).*
4. V. A. Il'in, A. I. Novikov, S. V. Polyanskii, and E. Ya. Karasik, "The VST-1 time-pulse remote-measurement system," Byull. Tekhn.-Ekonom. Inform. 8 (1959).

---

*See English translation.

TRANSFORMER DISTANCE TRANSMISSION BY MEANS OF TWO PHASE CONTACTLESS INDUCTION POTENTIOMETERS

Yu. M. Pul'er

Moscow

Translated from Avtomatika i Telemekhanika, Vol. 21, No. 7, pp. 1026-1034,
July, 1960
Original article submitted November 5, 1959

In this paper we examine the circuit construction, operation and basic principles of the theory of the distance transmission of angles by means of contactless two-phase inductive linear potentiometers.

The principles of construction of devices being used at the present time for transformer distance transmission are based upon the application of inductive selsyn elements, which in their method of construction represent, as we know, two-and three-phase machines of the asynchronous type, behaving as transformers and in no way differing in principles from sine-cosine rotary transformers.

Contactless selsyn-transformers, whose construction is likewise based upon the principles of electrical machinery, have found wide application. Of the known types of contactless selsyns, we wish first of all to point out the construction of the type of [1, 2].* In this, a series of extremely successful constructional solutions has been found for the magnetic circuit of a machine which ensures the necessary changes in the flux linkages between the stationary exciting ring winding and the stator winding which is of the customary type used in electrical machines. We also wish to point out the second type of known construction, the properties of which consist of a varying constructive displacement between two stages, the input (or output) transformer and the portion similar to an electrical machine. The first stage consists of either a ring transformer, which ensures a flux linkage between its movable and stationary windings which does not change with changes in the rotor position [3, 5], or of an electrical machinery stage of the sine-cosine rotary transformer type, proposed in [6].

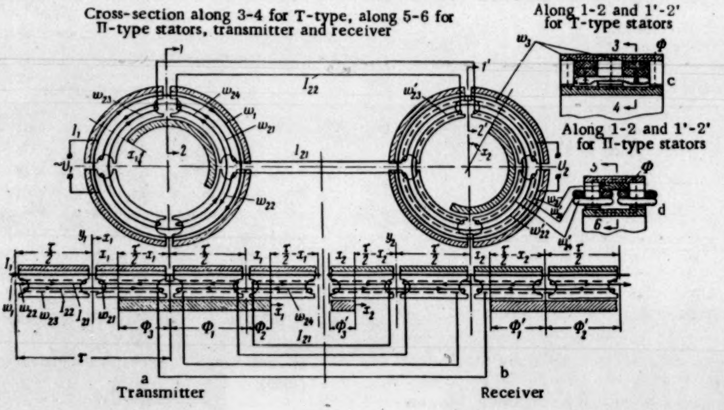
Cross-section along 3-4 for T-type, along 5-6 for Π-type stators, transmitter and receiver
Along 1-2 and 1'-2' for T-type stators
Along 1-2 and 1'-2' for Π-type stators
w_3
3
4
5
6
Φ
c
d
1
1'
2
2'
l_{22}
l_{21}
l_1
w_{23}
w_{24}
w_1
w_{21}
w_{22}
w'_{23}
w'_{22}
w'_{24}
x_1
x_2
$\sim U_1$
U_2
y_1
y_2
$\frac{\tau}{2}$
$\frac{\tau}{2}-x_1$
$\frac{\tau}{2}-x_2$
Φ_3
Φ_1
Φ_2
Φ'_3
Φ'_1
Φ'_2
τ
a
Transmitter
b
Receiver

Fig. 1.

---

*These constructions have been widely applied, mainly in inductive operation; however, in many cases, they may be used successfully in transformer operation, with the limitations pointed out in [5].

We may also include in the same group the construction of the contactless transformerlike selsyn ("Sinchrotel") developed by Kollsman (USA) and described in survey paper [7].

The contactless selsyn constructions we have mentioned have their special properties, which determine the expediency of applying one or the other type in systems used for various applications [2, 4, 5].

The contactless selsyns of the indicated types have a series of defects. Thus, the selsyns of the first type [1, 2] have a relatively complex magnetic circuit with double air gaps; this imposes certain limitations on their use as transformers [5]. Selsyns of the second type are two-stage devices; this increases their weight, the number of clearance tolerances, and the losses. We should also note the technological difficulties of manufacturing close-tolerance selsyns of the types described above, and especially the difficulties in manufacturing the close-tolerance rotors. This circumstance limits the possibility of constructing miniature selsyns.

We will show below that if we place, on the stator, a linear inductive potentiometer having a range of ±90° [8], in which the second pair of coils is displaced by 90° with respect to the first pair, the apparatus acquires properties which are analogous to the properties of a selsyn transformer. This analogy consists of the fact that, with the aid of such two-phase inductive potentiometers, there appears another possible construction for a transformer for distance transmission of angular position. Since contactless instruments are of the greatest practical interest, in the present paper we will examine transmission systems using contactless, two-phase, inductive potentiometers. These potentiometers, which do not involve two-stage transformations, are distinguished by their ease of manufacture and can be made to extremely small tolerances.

1. Description of the Construction of Two-Phase Induction Contactless Potentiometer-Selsyns (TIP)

The construction of a TIP-transmitter and receiver, connected in a distance transmission circuit, is shown in Fig. 1.

As we see from Fig. 1, a and b, the stators of the TIP transmitter and receiver differ from the contactless induction potentiometer [8], having the well-known construction described above, because it is single-phase and the former have a two-phase winding consisting of two pairs of coils w_{21}, w_{22}, and w_{23}, w_{24} mutually displaced by 90°. Each of these coils covers the central part of the stator for a T-type stator (Fig. 1a) or the lateral part (one or both) for a Π-type stator (Fig. 1d).

Each pair of coils (for example, w_{21} and w_{22}) forming one phase, is interconnected so that the directions of the emf's or currents are opposing.

If we make use of the generally accepted selsyn terminology, then the two-phase transmitter winding consisting of two pairs of coils w_{21}, w_{22} and w_{23}, w_{24} (Fig. 1a) and the receiver coils w'_{21}, w'_{22} and w'_{23}, w'_{24} (Fig. 1b) form synchronized windings.

The circular (or ring) winding, consisting of two circular coils for T-type stators (Fig. 1b), or of one coil for Π-type stators (Fig. 1d), remains the same as for an inductive contactless potentiometer and serves as the exciting winding in the transmitter, w_1 (Fig. 1a), and as the signal winding in the receiver, w_3 (Fig. 1b)

The TIP rotor represents, as in the contactless induction potentiometer [8], a plate in the form of a semicylinder which closes the magnetic circuit of the stator over an arc of length τ (or 180°), forming in all its positions an even air gap of length δ.

The construction of the TIP transmitter and receiver is identical; they differ only in the dimensions and the number of turns in the winding. In particular, the receiver synchronizing windings can have a higher resistance than those of the transmitter, so as to lower the necessary transmitter power, while the higher-resistance signal winding will increase the magnitude of the difference signal.

The stator magnetic circuit may be either a T- or a Π-type (Fig. 1, c and d).

2. Principles Behind Remote Transmission by Means of Two-Phase Induction Potentiometers

The circuit of Fig. 1[†] shows the transmitter and receiver connections for a remote transmission system. We can see from the circuit that, for a current in the transmitter ring winding w_1 due to the ac voltage U_1 when the transmitter rotor is in its mean position (Fig. 1a), i.e., for $x_1 = 0$, the total transformation emf and the current I_{22} in the coils w_{23} and w_{24} is zero; but for this rotor position, the total transformation emf is a maximum for coils w_{21} and w_{22}, since coil w_{21} is placed into a position where the flux linkages with the exciting ring winding w_1 are a maximum.

If, in this position of the transmitter rotor ($x_1 = 0$), the receiver rotor were also rotated by $\tau/2$, for example, to the right with respect to the first position (considering that the transmitter and receiver axes y_1 and y_2 are parallel), then in this rotor position the voltage U across signal winding $w_3 = 0$. This is due to the fact that for $x_1 = 0$ the coils w'_{23} and w'_{24} of one phase of the transmitter are deenergized. In this case, as we can see from Fig. 1b, when the receiver rotor is displaced by $\tau/2$ from the transmitter rotor, i.e., for $x_2 \big|_{x_1 = 0} = \tau/2$ (or 90°), the w_3 winding has no flux

---

[†] The four-conductor connection (Fig. 1) can be replaced by a three-conductor connection by combining two conductors in one of the two pairs of conductors (with current I_{21} or I_{22}).

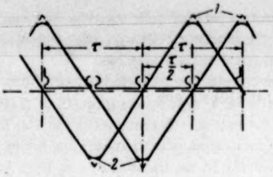

Fig. 2.

linkages with the coils w'_{21} and w'_{22} which are included in the opposite phase. For the indicated rotor position, $U_2 = 0$.

We can, on the basis of the same reasoning, see from the circuits of Fig. 1,a and b, that U_2 will also be zero for every $\tau/2$ (or 90°) shift of the transmitter rotor if we preserve the mutual 90° rotor displacement. We prove below that the synchronized state of the system $U_2 = 0$ will occur for a mutual perpendicular displacement of the transmitter and receiver over a whole revolution. We should point out that for the given distance transmission system, as in the known transformer transmission systems, the position of agreement between the transmitter and receiver corresponds to null values of voltage across the receiver signal winding which is connected to the input of the servo-drive amplifier.

We wish, first of all, to indicate that, if it follows from strictly linear dependence curves that dependence of the output voltage upon the rotor position for each winding is synchronized for $-\tau/2 \leq x_1 \leq \tau/2$ and $\tau/2 \leq x_1 \leq 3\tau/2$, then, at the points which determine the boundaries of these intervals, there will theoretically be a break in the continuity of the indicated curves (Fig. 2, curve 1). However, in the actually constructed device, due to the continuity of the field the linear portions are connected by a continuous curve in the region of the maximum or the minimum (Fig. 2, curve 2).

The continuity of the characteristics ensures a stable state in the position of agreement between the transmitter and receiver in those rotor positions which correspond to the regions in the vicinity of the maximum and minimum points.

Let us first examine analytically the operation of the distance transmission system over the interval $0 < x_1 < \tau/2$ corresponding to the linear part of the ideal theoretical synchronizing winding output voltage characteristic at no-load.

On the basis of the distance transmission circuit construction (Fig. 1) and the scanner construction in the TIP transmitter and receiver (Fig. 1, a and b), and making use of the designations for the currents, fluxes, and displacements indicated in the diagram, we can write the system of equations for the magnetic fluxes in the transmitter and receiver. While writing these equations, we may neglect the leakage fluxes and also the boundary effects, i.e., we will consider that the specific magnetic conductivity along the gap G_0 = const over the range 0 to $\tau/2$. The behavior of the system for rotor positions corresponding to the neglected zones of the synchronous winding output voltage, and also for arbitrarily large differences, will be examined later.

Taking into account the symmetry of the transmitter and receiver windings (for the transmitter: $w_{21} = w_{22} = w_{23} = w_{24} = w_2$; for the receiver: $w'_{21} = w'_{22} = w'_{23} = w'_{24} = w'_2$), we can write the following equations: for the transmitter

$$\dot{\Phi}_1 = [\dot{I}_1 w_1 - (\dot{I}_{21} w_2 + \dot{I}_{22} w_2)]\, G_0 \frac{\tau}{2}, \tag{1}$$

$$\dot{\Phi}_3 = [\dot{I}_1 w_1 - (\dot{I}_{21} w_2 - \dot{I}_{22} w_2)]\, G_0 \left(\frac{\tau}{2} - x_1\right), \tag{2}$$

$$\dot{\Phi}_2 = [\dot{I}_1 w_1 + (\dot{I}_{21} w_2 - \dot{I}_{22} w_2)]\, G_0 x_1; \tag{3}$$

for the receiver

$$\dot{\Phi}'_1 = -(\dot{I}_{21} w'_2 + \dot{I}_{22} w'_2)\, G_0 \left(\frac{\tau}{2} - x_2\right), \tag{4}$$

$$\dot{\Phi}'_2 = (\dot{I}_{21} w'_2 - \dot{I}_{22} w'_2)\, G_0 \frac{\tau}{2}, \tag{5}$$

$$\dot{\Phi}'_3 = (\dot{I}_{21} w'_2 + \dot{I}_{22} w'_2)\, G_0 x_2. \tag{6}$$

In addition, we have for the transmitter primary winding w_1 the relationship

$$\dot{U}_1 = j\omega 10^{-8} w_1 [\dot{\Phi}_1 + \dot{\Phi}_2 + \dot{\Phi}_3] + \dot{I}_1 Z_{1s}, \tag{7}$$

and for the receiver signal winding w_2,

$$\dot{U}_2 = j\omega 10^{-8} w_3 [\dot{\Phi}'_1 + \dot{\Phi}'_3 + \dot{\Phi}'_2]. \tag{8}$$

The emf of the transmitter synchronizing windings, using the current direction shown in Fig. 1a, is determined by the equations

$$E_{21} = j\omega 10^{-8} w_2 [\dot{\Phi}_1 + \dot{\Phi}_3 - \dot{\Phi}_2],$$

$$E_{22} = j\omega 10^{-8} w_2 [\dot{\Phi}_1 + \dot{\Phi}_2 - \dot{\Phi}_3].$$

For the counter-emf in the receiver synchronizing windings, using the current directions shown in Fig. 1b, the actual equations are

$$E'_{21} = -j\omega 10^{-8} [-\dot{\Phi}'_1 + \dot{\Phi}'_2 + \dot{\Phi}'_3],$$

$$\dot{E}_{22} = -j\omega 10^{-8} [\dot{\Phi}'_1 + \dot{\Phi}'_2 - \dot{\Phi}'_3].$$

The equations for the currents in the synchronizing windings are

$$\dot{E}_{21} + \dot{E}'_{21} = j\omega 10^{-8} w_2 \times$$

$$\times [(\dot{\Phi}_1 + \dot{\Phi}_3 - \dot{\Phi}_2) - (-\dot{\Phi}'_1 + \dot{\Phi}'_3 + \dot{\Phi}'_2)] =$$

$$= \dot{I}_{21} Z_{21s}, \tag{9}$$

$$E_{22} + \dot{E}'_{22} = j\omega 10^{-8} w_2 \times$$

$$\times [(\dot{\Phi}_1 + \dot{\Phi}_2 - \dot{\Phi}_3) - (\dot{\Phi}'_1 + \dot{\Phi}'_2 - \dot{\Phi}'_3)] = \dot{I}_{22} Z_{22s}. \tag{10}$$

The system of 10 equations in 10 unknowns which we have written down is easily solved if we make the substitutions given below.

Removing the parentheses in Equations (1)-(3) and performing the indicated additions, we get for the transmitter currents

$$\dot{\Phi}_1 + \dot{\Phi}_2 + \dot{\Phi}_3 = \tag{11}$$

$$= 2\dot{I}_1 w_1 G_0 \frac{\tau}{2} - 2\dot{I}_{21} w_2 C \left(\frac{\tau}{2} - x_1\right) - 2\dot{I}_{22} w_2 G_0 x_1,$$

$$\dot{\Phi}_1 + \dot{\Phi}_3 - \dot{\Phi}_2 = 2\dot{I}_1 w_1 G_0 \left(\frac{\tau}{2} - x_1\right) - 2\dot{I}_{21} w_2 G_0 \frac{\tau}{2} \tag{12}$$

$$\dot{\Phi}_1 + \dot{\Phi}_2 - \dot{\Phi}_3 = 2\dot{I}_1 w_1 G_0 x_1 - 2\dot{I}_{22} w_2 G_0 \frac{\tau}{2}. \tag{13}$$

Removing the parentheses in Equations (4)-(6) and performing the indicated additions, we get for the receiver currents

$$\dot{\Phi}'_1 + \dot{\Phi}'_2 + \dot{\Phi}'_3 = -2\dot{I}_{22} w'_2 G_0 \left(\frac{\tau}{2} - x_2\right) +$$

$$+ 2\dot{I}_{21} w'_2 G_0 x_2, \tag{14}$$

$$-\dot{\Phi}'_1 + \dot{\Phi}'_2 + \dot{\Phi}'_3 = 2\dot{I}_{21} w'_2 G_0 \frac{\tau}{2}, \tag{15}$$

$$-\dot{\Phi}'_1 - \dot{\Phi}'_2 + \dot{\Phi}'_3 = 2\dot{I}_{22} w'_2 G \frac{\tau}{2}, \tag{16}$$

Taking into account the symmetry of the transmitter and receiver synchronizing windings, the total leakage resistance of the two winding contours of the synchronizing system equals $Z_{21s} = Z_{22s} = Z_{2s}$, where Z_{2s} is total leakage resistance of each of the two contours of the synchronizing windings, through which the currents $\dot{I}_{21}$ and $\dot{I}_{22}$ flow.

Substituting (11) in (7), (12) and (15) in (9), and (13) and (16) in (10), we get

$$2j\omega 10^{-8} w_2 \left[\dot{I}_1 w_1 G_0 \left(\frac{\tau}{2} - x_1\right) - \dot{I}_{21}(w_2 + w'_2) G_0 \frac{\tau}{2}\right] =$$

$$= \dot{I}_{21} Z_{2s}, \tag{17}$$

$$2j\omega 10^{-8} w_2 \left[\dot{I}_1 w_1 G_0 x_1 - \dot{I}_{22}(w_2 + w'_2) G_0 \frac{\tau}{2}\right] =$$

$$= \dot{I}_{22} Z_{2s}, \tag{18}$$

$$2j\omega 10^{-8} w_2 \left[\dot{I} w_1 G_0 \frac{\tau}{2} - \dot{I}_{21} w_2 G_0 \left(\frac{\tau}{2} - x_1\right) - \dot{I}_{22} w_2 G_0 x_1\right] =$$

$$= \dot{u}_1 - \dot{I}_1 Z_{1s}, \tag{19}$$

where z_{1s} is the total leakage resistance of the exciting windings.‡

From Equations (17) and (18) we get the relations between the primary and secondary currents :

$$\dot{I}_{21} = \frac{2j\omega 10^{-8} w_2 \dot{I}_1 w_1 G_0 \left(\frac{\tau}{2} - x_1\right)}{Z_{2s} + j\omega 10^{-8} w_2 G_0 \tau (w_2 + w'_2)}. \tag{20}$$

$$\dot{I}_{22} = \frac{2j\omega 10^{-8} w_2 \dot{I}_1 w_1 G_0 x_1}{Z_{2s} + j\omega 10^{-8} w_2 G_0 \tau (w_2 + w'_2)}. \tag{21}$$

Let $j\omega 10^{-8} w_2 G_0 \tau (w_2 + w_2) = a$; after substituting (20) and (21) in (19), we get

$$\dot{U}_1 = j\omega 10^{-8} w_1^2 G_0 \tau \dot{I}_1 \times$$

$$\times \left\{1 \frac{4j\omega 10^{-8} w_2 G_0 \tau}{Z_{2s} + a} \frac{1}{\tau^2} \left[\left(\frac{\tau}{2} - x_1\right)^2 + x_1^2\right]\right\} + \dot{I}_1 Z_{1s}. \tag{22}$$

If we let $j\omega 10^{-8} w_1^2 G_0 \tau = jx_0$, then $j\omega 10^{-8} w_2^2 G_0 \tau = = jx_0 \frac{w_2^2}{w_1^2}$. Let $\frac{w_2}{w_1} = k_{21}$, $\frac{w'_2}{w'_1} = k_{23}$. Then

$$\dot{U}_1 = jx_0 \dot{I}_1 \times$$

$$\times \left\{1 \frac{4jx_0 k_{21}^2}{Z_{2s} + jx_0 (k_{21}^2 + k_{23}^2)} \left[\frac{1}{4} \frac{2x_1}{\tau}\left(1 - \frac{x_1}{\tau}\right)\right]\right\} +$$

$$+ \dot{I}_1 Z_{1s}.$$

Then primary current I_1 is determined by the equation

$$\dot{I}_1 = \frac{\dot{U}_1}{jx_0 \left\{1 - \frac{4jx_0 k_{21}^2}{Z_{2s} + jx_0 (k_{21}^2 + k_{23}^2)} \left[\frac{1}{4} - \frac{2x_1}{\tau}\left(1 - \frac{x_1}{\tau}\right)\right]\right\} + Z_{1s}}.$$

---

‡ In the given investigation we neglect, in order to simplify the discussion, the differential leakage of the contactless induction potentiometer [8] and consider that Z_{1s} and Z_{2s} are independent of the rotor position.

Note that formula (23) shows that the primary current is independent of x_2, i.e., of the position of the receiver rotor. Substituting (14) in (8), we get, for the signal voltage $\dot{U}_2$ across the w_3 receiver winding (Fig. 1),

$$\dot{U}_2 = j\omega 10^{-8} w_3 \left[-2\dot{I}_{22} w_2' \left(\frac{\tau}{2} - x_2 \right) + 2\dot{I}_{21} w_2' x_2 \right] G_0 \tag{24}$$

or, substituting (20) and (21),

$$\dot{U}_2 = \frac{2\,(j\omega)^2 10^{-8} w_3 10^{-8} w_2' G_2^2}{(Z_{2s} + a)} \frac{\tau^2}{\tau^2} \frac{w_3}{w_3} \left[-\left(\frac{\tau}{2} - x_2 \right) x_1 + \left(\frac{\tau}{2} - x_1 \right) x_2 \right].$$

Making use of (22) and (23), we get

$$\dot{U}_2 = \dot{U}_1 \frac{2jx_0 \frac{w_3^2}{w_1^2} \frac{w_2}{w_1}}{Z_{2s} + jx_0 (k_{21}^2 + k_{23}^2)} \frac{\frac{w_2'}{w_3} \frac{1}{\tau^2} \left[-\left(\frac{\tau}{2} - x_2 \right) x_1 + \left(\frac{\tau}{2} - x_1 \right) x_2 \right]}{\left\{ 1 - \frac{4jx_0 k_{21}^2}{Z_{2s} + jx_0 (k_{21}^2 + k_{23}^2)} \left[\frac{1}{4} - \frac{2x_1}{4} \left(1 - \frac{x_1}{\tau} \right) \right] \right\} + \frac{Z_{1s}}{jx_0}} \tag{25}$$

or

$$\dot{U}_2 = \dot{U}_1 \frac{jx_0 \frac{w_3^2}{w_1^2} \frac{w_2}{w_1} \frac{w_2'}{w_3}}{Z_{2s} + jx_0 (k_{21}^2 + k_{23}^2)} \frac{\frac{1}{\tau} (x_2 - x_1)}{\left[1 - \frac{4jx_0 k_{21}^2 \left| \frac{1}{4} - \frac{2x_1}{\tau} \left(1 - \frac{x_1}{\tau} \right) \right]}{Z_{2s} + jx_0 (k_{21}^2 + k_{23}^2)} \right] + \frac{Z_{1s}}{jx_0}}. \tag{26}$$

Thus, it follows from the expression for the signal voltage $\dot{U}_2$ (Equation 26) that the latter (if we neglect the stipulated changes in the denominator term) is proportional to the angular difference between the transmitter rotor for $0 < x_1 < \tau/2$ and the receiver rotor for $0 < x_2 < \tau/2$.

In the position in which the transmitter and the receiver agree, their rotors are in a mutually perpendicular position.

We wish also to underline the fact that, for the case where several TIP receivers operate in parallel from one transmitter, there is no mutual interaction between them during mutual disagreement due to the fact that the synchronizing currents $\dot{I}_{21}$ and $\dot{I}_{22}$ according to (20) and (21), are independent of the receiver rotors.

Now let us examine the operation of the system for all other possible positions of the transmitter rotor, and, therefore, also for difference angles of large $\pm\,\tau/2$, including the regions where the secondary current (or voltage) characteristics bend over.

In order to do this, we will make use of formulas (20) and (21). In the actual construction, the functions $\dot{I}_{21}$ and $\dot{I}_{22}$ [formulas (20) and (21)] do not have a discontinuity at $x_1 = \tau/2$ but change continuously (the discontinuity occurs only for the case of ideal linearity). In order to analyze the system for rotor positions in the vicinity of the points of theoretical discontinuity, and also for differences in position involving these points, the rational periodic functions $\dot{I}_{21}$ and $\dot{I}_{22}$ are approximated by sinusoids. As a result, the currents $\dot{I}_{21}$ and $\dot{I}_{22}$ take the form

$$\dot{I}_{21} = k_1 \sin \frac{\pi}{\tau} \left(\frac{\tau}{2} - x_1 \right), \quad \dot{I}_{22} = k_1 \cos \frac{\pi}{\tau} x_1, \tag{27}$$

where

$$k_1 = \frac{jx_0 \frac{w_2}{w_1} \dot{I}_1 G_0 \tau}{Z_{2s} + jx_0 \frac{w_2}{w_1}}.$$

Here $\dot{I}_1$ is determined from (23); if we take into consideration the small change in the denominator, we can assume, in the given case, that $\dot{I}_1$ is independent of x_1.

The indicated substitution corresponds to the fact that in (26) the function $G_0\,(\tau/2 - x_1)$ is replaced by $G_0\tau\ \sin \pi/\tau\ (\tau/2 - x_1) = G_0\tau\ \cos(\pi/\tau)x_1$, and the function $G_0\,x_1/\tau$, by $G_0\tau\ \sin(\pi/\tau)x_1$. Analogously, $G_0(\tau/2 - x_1)$ is replaced by $G_0\tau\ \sin \pi/\tau\ (\tau/2 - x_2) = G_0\,\tau\ \cos (\pi/\tau)\,x_2$ and the function $G_0\,x_2/\tau$, by $G_0\tau\ \sin(\pi/\tau)\ x_2$.

Substituting in the expression for the signal voltage (24) the currents I_{21} and $\dot{I}_{22}$, taking into account the approximation introduced in formula (26) and bearing in mind the substitution (27) resulting from the latter, we get the following expression for the signal voltage:

$$\dot{U}_2 = k_2 \left[-\sin \frac{\pi}{\tau} \left(\frac{\tau}{2} - x_2 \right) \sin \frac{\pi}{\tau} x_1 + \right.$$
$$\left. + \sin \frac{\pi}{\tau} \left(\frac{\tau}{2} - x_1 \right) \sin \frac{\pi}{\tau} x_2 \right] = k_2 \sin \frac{\pi}{\tau} (x_1 - x_2). \tag{28}$$

Here k_2. taking account of the substitution (22), will be determined by the formula

$$k_2 = \frac{jx_0 \frac{w_3}{w_1} \frac{w_2 w_2}{w_1^2} \dot{I}_1}{\frac{Z_{2e}}{jx_0} + (k_{21}^2 + k_{23}^2)} . \tag{29}$$

In (29), as well as in (27), we can practically neglect the insignificant variation in the current $\dot{I}_1$ due to the location of the transmitter rotor x_1 [see (23)] and consider that $k_2 \approx$ const.

Equation (28) determines the character of the changes in the receiver signal voltage for transmitter and receiver corresponding to arbitrarily large differences, and also to zones of theoretical discontinuity of the curves of the synchronizing currents $\dot{I}_{21}$ and $\dot{I}_{22}$.

As we see from (28), the voltage undergoes practically the same type of changes with changes in rotor position and with differences in position between the two rotors as in transformer distance transmission for the known types of selsyns of the electrical machine type.

However, as indicated above, formulas (26) and (28) have been obtained for idealized cases, the first for the triangular, and the second for the sinusoidal, form of these characteristics.

In the actual construction, characteristics (20) and (21) are close to triangles with rounded tops and are periodic, continuous functions. Therefore, a more rigorous analysis of an analogous system for any range of differences in the positions of transmitter and receiver and for all matching positions over an entire revolution will be obtained if we represent the characteristics in (20) and (21) in the form of trigonometric series.

Therefore, we must consider that formula (29) is true only for the basic harmonics of functions (20) and (21). Therefore,

$$U_2 = kU_1 \Big[\sum_{n=1,3,5,\ldots} A_2(n) \sin n\left(\frac{\tau}{2} - x_2\right) \times \times \sum_{1,3,5,\ldots} A_1(n) \sin n \frac{\pi}{\tau} x_1 + + \sum_{1,3,5,\ldots} A_1(n) \sin n\left(\frac{\tau}{2} - x_1\right) \sum_{1,3,5,\ldots} A_2(n) \sin n \frac{\pi}{\tau} x_2 \Big]. \tag{30}$$

is a more rigorous expression for the signal voltage of the system.

SUMMARY

1. The method of distance transmission by means of two-phase induction potentiometers, which we have examined in this paper, ensures circular tracking having only one stable position for the case in which the transmitter and rotor positions agree.

2. The transmitter and receiver of the distance transmission system considered in this article are elements with single-stage transformation. They are easy to construct and may be built to very small tolerances.

3. The absence of receiver reaction due to changes in its rotor position permits us to operate several receivers in parallel from one transmitter; in the process, the indication of each receiver is automatically brought into agreement with the transmitted signal. This is of basic importance in complex systems in which centralized transmitters operate a great many receivers.

The basic distance transmission properties of contactless two-phase potentiometers which have been examined in this paper permit us to recommend this device for use in automatic installations.

LITERATURE CITED

1. A. G. Iosif'yan, and D. V. Svecharnik, Selsyns [in Russian] (Gosénergoizdat, 1942).
2. D. V. Svecharnik, Distance Transmission [in Russian] (Gosénergoizdat, 1959).
3. Terman Patent DRP No. 162740, Beckman Patent DRP No. 405156.
4. D. P. Mkrtchyan and V. V. Khrushchev, Single-Phase Selsyns [in Russian] (Sudpromgiz, 1957).
5. Yu. M. Pul'er, "Contactless sine-cosine rotational transformer-selsyns," Élektrichestvo 1 (1958).
6. I. M. Sadovskii, Author's Certificate No. 56183 and 65902.
7. E. Widermuth, "Inductive distance transmission systems and their building blocks," Feinwerktechnik 62, 10 (1958).
8. Yu. M. Pul'er, "Inductive linear potentiometers," Avtomatika i Telemekhanika 17, 7 (1956).**

** See English translation.

CONTACTLESS SEMICONDUCTOR SWITCHING ELEMENTS

E. V. Miller

Leningrad

Translated from Avtomatika i Telemekhanika, Vol. 21, No. 7, pp. 1035-1045,
July, 1960
Original article submitted December 28, 1959

Contactless switching element circuits developed to replace relays in automatic control systems are discussed, and also the calculation of these elements. An example is given of their use in a typical automated system.

Many different types of contactless devices which replace this or that relay have been built in recent years both in the USSR and abroad. Such devices have a practically unlimited service life, and do not require any servicing while in use.

The replacement of contact devices with contactless ones is especially important in those automatic control systems which operate in the presence of dust and dirt- for example, in metallurgical plants, ore-concentration factories, flour mills, etc. In the foreign press, there are communications about the development of entire automated systems using contactless switching elements (so-called logic elements), built from semiconductors and rectangular loop magnetic elements.

Only the systems which use semiconductors are discussed in this article.

Elements of switching circuits with contacts are shown in Fig. 1; they may be called "and," "or," "not," and "command," according to the functions they perform.

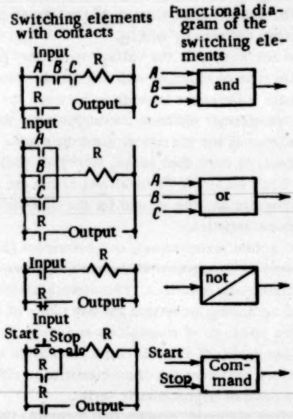

Fig. 1. Basic elements of switching circuits.

The existing semiconductor "and," "or," and "not" circuits may be divided into three basic groups:

1) using diodes only
2) using transistors only
3) using both diodes and transducers

Diode circuits are presented, for example, in [5] and [6]. They are very simple and cheap, but when several elements are connected to operate one after the other, a large number of separate power supplies of different amplitude are required; therefore, they are not suitable for the system being developed.

Transistor circuits [3, 5, 6] can be subdivided into two subgroups: a) with series, and b) with parallel connection of the transistors. Like the diode circuits, the series-connected transistor circuits require a separate power supply for each input. Moreover, when elements with series-connected transistors are used, the assembly of a number of elements into a common automatic control circuit becomes very complex.

Elements with parallel-connected transistors permit the use of one power supply for any number of elements in the automated circuit, and are easily assembled into any kind of circuit.

Combined diode-transistor circuits, depending on their use, can be cheaper than transistor circuits (when their use reduces the number of transistors required). By using parallel-connected transistors, it is possible to obtain a system of elements for which only one power supply is required, and these elements will easily combine into various circuits. The "command" ("memory") element is built only from transistors.

The industrial electrification faculty of the remote Northwest Polytechnic Institute (SZPI), as a result of research, developed a system of contactless switching elements using typical semiconductor diodes and transistors. The features of the system developed which differ from existing circuits are:

a) the possibility of simple combination of the

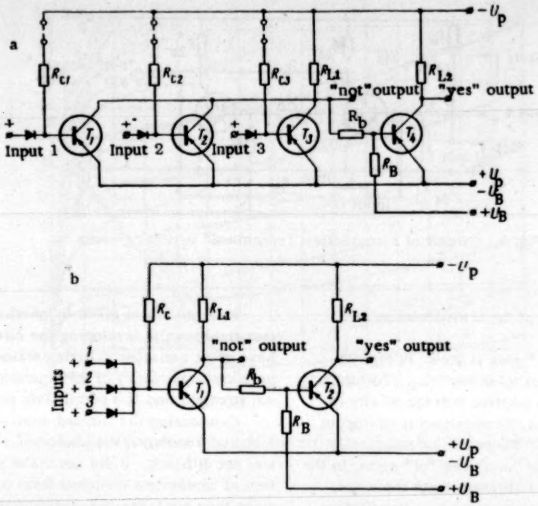

Fig. 2. Circuits of contactless switching elements: a) "and" gate, b) "or" gate.

contactless elements developed for the assembly of different automated switching circuits;

b) the operation of the elements is almost independent of the ambient temperature up to 50°C; this is ensured by the use of bias on all elements, and by a suitable choice of the transistor operating modes;

c) the absence of a separate "not" element, and the construction of "and," "or," and "command" elements with two outputs, "yes" and "not"; this reduces the total number of elements required by automatic control circuits.

The input signal to an element can come from any sort of transducer which gives a small voltage (thermocouple, photocell, induction switch), or from switching apparatus with contacts. Moreover, the outputs from the elements can excite the inputs of other contactless elements, or of amplifiers. The separate elements of the circuits developed are described below.

A contactless "and" gate which gives two outputs, "yes" and "not," is depicted in Fig. 2a. The input transistors T_1, T_2, and T_3 have a common load resistance R_{L1}, and their bases are connected through resistances R_{C1}, R_{C2}, and R_{C3} to the negative terminal of the power supply. In this case, all three transistors are on in the absence of input signals, a current flows through resistance R_{L1} and the collector-to-emitter voltage of T_1, T_2, and T_3 is a fraction of a volt. A load resistance R_{L2} is wired into the collector circuit of output transistor T_4, and its base is connected to the common collector terminal of the input transistors through a voltage divider consisting of resistances R_b and R_B. Hence, if one of the transistors T_1, T_2, or T_3 is on, the base current of T_4 will be positive (for a suitable relation between R_b and R_B), and the collector current of T_4 will be very small. Therefore, the potential at the "yes" output point will differ little from the potential at point $-U_p$, and will be almost equal to the $+U_p$ potential at the "not" output point. If a positive signal is impressed on the base of one of the input transistors, it will be cut off, but the "yes" and "not" output potentials will not change, due to the other two transistors, which are still on. If a positive voltage is simultaneously impressed on all the input transistors, they will all be cut off, no current will flow through R_{L1}, a negative base current will arise in T_4, and this will cause it to turn on. In this manner, the "yes" and "not" output voltages will change places: the potential on the first will be nearly $+U_p$, and the second will be nearly $-U_p$.

There is a resistance R_B fed from a low voltage supply U_B to eliminate the effect of the ambient temperature, and the heating of the transistors themselves, on the output voltages. The temperature has practically no effect on the operation of the gate, if U_B and R_B are correctly chosen.

Semiconductor diodes are provided to eliminate the effect of the element currents on the primary transducers,

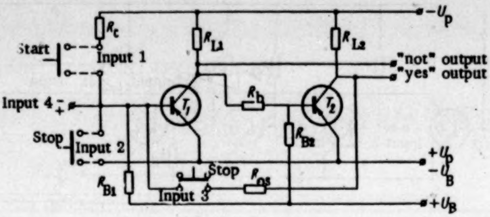

Fig. 3. Circuit of a contactless "command" switching element.

and to prevent interaction of the transducers on one another.

The circuit of the "or" gate is shown in Fig. 2b. Here there is only one input transistor – T_1. To turn it on, it is sufficient to put a positive voltage on any of the three inputs. Otherwise, its operation is analogous to that of the "and" gate. There can be practically any number of inputs to the "and" and "or" gates; in the first gate, this requires an additional input transistor, diode, and resistance R_c; in the second, it is sufficient to add only an input diode.

The described operation of the "and" and "or" gates can occur with input signals from contact or contactless transducers. If one or more inputs of the "and" gate must be connected to the outputs of other contactless elements, then one or more straps (shown by dots in Fig. 2a) must be removed from the R_c resistances, and the free ends of these resistors are considered as inputs.

The "or" gate, intended for operation with other elements, must be built analogously to an "and" gate, but the R_c resistances in this case must be connected not to $-U_p$, but to $+U_p$ (the input transistors will be on in the absence of input signals). In this case, the input of each of the transistors must be not positive, but negative, and correspondingly, the "yes" and "not" outputs change places.

The circuit of a "command" element, wired like a fixed bias trigger, is shown in Fig. 3.[*] Transistor T_1 is cut off when there are no input signals, and T_2 is on; this is ensured by appropriate relations between the individual resistances in the circuit. When a negative pulse is impressed on input 4, or when the "start" button connected to input 1 is pressed, transistor T_1 turns on, and T_2 is cut off. The cut-off condition of T_2 ensures that a base current will flow into T_1 through resistance R_{os}. Thus, when the negative pulse is removed from input 4 (or the "start" button is released), T_1 remains on, and T_2 remains cut off. In order to restore T_1 to cut-off and to turn T_2 on, one need only feed a positive pulse to input 4 (or press the normally open "stop" switch in input 2, or the normally closed switch in input 3).

Preference was given to junction, over point-contact, transistors in developing the circuits, since the latter have great variation in their parameters, a large temperature dependency of their parameters, less mechanical strength, and less permissible power dissipation.

Considering the limited number of types of manufactured transistors, the choice of a junction transistor was not difficult. It did not make sense to build a system of contactless elements from power transistors, since they are large and would require much power, as well as heat sinks. It was better to select small transistors, but with very small transistors, the base current is comparable with leakage and possible noise currents. Hence, it was desirable to choose transistors with base currents not less than one-tenth of a milliampere. Moreover, it was desirable to use hermetically sealed transistors for protection against dust and humidity. Therefore, the most suitable domestically manufactured transistors are the P-13, P-14, and P-15 series. The P-13A has the largest current amplification factor of all these, and thus permits the connecting of the largest number of other elements to its output. Thus, it was used in the elements developed.

It should be noted that silicon transistors are suitable for operation at higher temperatures than germanium, and, when they are manufactured on a large scale, it will become very desirable to use them for automated systems which operate at temperatures higher than 50°C.

The determination of the parameters of the "and" and "or" gates essentially leads to the choice of the voltages U_p and U_B, and the resistances R_c, R_B, R_b, and R_L. The output characteristics of the P-13A transistor are needed for the computation of these parameters. These characteristics, taken for one typical sample of this transistor, are shown in Fig. 4 at temperatures of 20°C (solid lines), and 50°C (dotted lines). A load line for the resistance R_L is drawn on the characteristic for a certain voltage U_p. The mode must be chosen so that the load line will intersect the characteristic at the

---

[*] In the U.S., this circuit is also known as a binary memory, or "flip-flop" [Publisher's note].

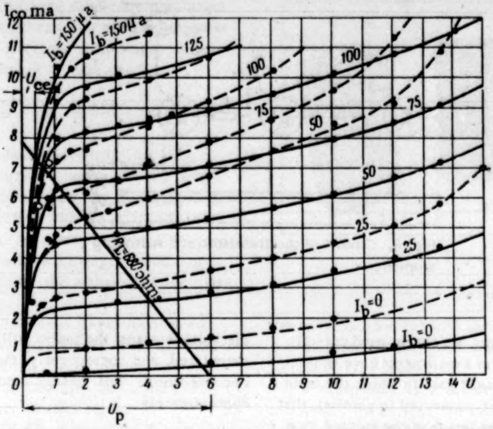

Fig. 4. Experimental output characteristics of the P-13A transistor.

knee of the curve, so as to make the collector current depend almost entirely on the load resistance R_L. It can be seen from this condition that increasing voltage U_p causes a large current stability against fluctuations of this voltage, the temperature, and the base current. On the other hand, a long service life of the element is desirable, and this is ensured by lowering the voltage. According to the manufacturer's data on the P-13A transistor, the limiting voltage for a common emitter circuit is 10 volts, so U_p was set at 6 volts to increase the reliability.

The load resistance, ignoring the voltage drop across the conducting transistor, is determined from the relation

$$R_L \geqslant \frac{U_p}{I_{me}}.$$

The maximum emitter current $I_{me} = 10$ ma. The resistance $R_L = 680$ ohms in the circuits. Hence, the collector current will be approximately

$$I_{co} = \frac{U_p}{R_L} = 8.9\,\text{ma}.$$

Drawing the load line corresponding to resistance R_L (Fig. 4), it can be seen that the base current I_b must be not less than 125-150 μa, so that the load will fall on the knee of the output characteristic. Setting $I_b = 200\ \mu$a for reserve, and neglecting the voltage drop between emitter and base, we find the resistance

$$R_c \quad \frac{U_p}{I_b} = \frac{6}{200\cdot 10^{-6}} = 30\,000\ \text{ohms}.$$

The resistance R_b is chosen with input transistors T_1, T_2, and T_3 cutoff for the "and" gate (or input transistor T_1 of the "or" gate). In this case, the base current which will ensure that the output transistor T_4 is on in the "and" gate (or T_2 in the "or" gate) must also be $I_b = 200\ \mu$a. This will give the sum

$$R_L + R_b \approx \frac{U_p}{I_b} = \frac{6\cdot 10^6}{200} = 30{,}000\ \text{ohms}.$$

Since the resistance R_L found earlier is small in comparison to R_b, it can be neglected, and the resistance R_b can be made 30000 ohms for standardization. The bias voltage amplitude U_B must be greater than the voltage U_{ce} (see Fig. 4) to ensure a positive potential on the base of the cut-off transistor T_2 of the "or" gate. The latter is not more than 0.3 volt for different samples of the P-13A transistor, with a resistance R_c = = 30000 ohms, using characteristics taken at +50°C. Therefore, U_B must be on the order of 0.6 volt.

The inequality

$$\frac{U_{ce} + U_B}{R_b + R_B} R_B < U_B,$$

must be satisfied so that a positive potential will be ensured on the base of the cut-off transistor T_2; from this,

$$R_B < \frac{U_B R_b}{U_{ce}}.$$

For the assumed values of U_B, U_{ce}, and R_b,

$$R_B < \frac{0.6\cdot 30\,000}{0.3}, \quad R_B < 60\,000\ \text{ohms}.$$

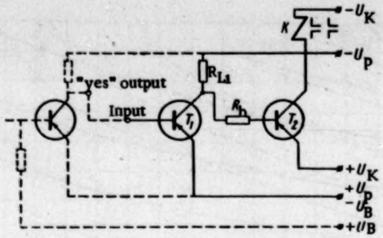

Fig. 5. Circuit of the transistorized switching amplifier.

Making R_B = 56000 ohms, we obtain good cut-off of the output transistor T_2, as experiments have shown.

It is evident, for the "and" gate in which the input transistors T_1, T_2, and T_3 are connected in parallel, that the voltage drop U_{ce} will be less than the voltage drop across one transistor. Therefore, the same values of U_B and R_B will ensure even better temperature compensation.

Any diodes which have a reverse voltage greater than U_p, and current rating greater than I_b, can be used as input diodes. In particular, any of the DGTs-type diodes are suitable. The only other calculation needed for the "command" element is the determination of the resistances for the potentiometer, which comes from the formula [1]

$$R_B \leqslant \frac{U_B}{I_{cb_{\max}}},$$

$$R_{os} \leqslant \left(\frac{\beta_{\min}}{1 + \beta \frac{U_B}{U_p} \frac{R_L}{R_B}} - 1 \right) R_L; \; R_b = R_{os}.$$

The amplitude of I_{cb} at 20°C is 30μa, according to the manufacturer's data for the P-13A transistor. We find that

$$I_{cb_{\max}} = I_{cb_{20^\circ}} \cdot 2^{\frac{t_{\max}-20}{10}} = 30 \cdot 2^{\frac{50-20}{10}} = 240 \ \mu a.$$

The minimum amplification factor of the P-13A transistor may be on the order of $\beta_{\min}$ = 25. Then

$$R_B \leqslant \frac{0.6}{240 \cdot 10^{-6}}; \quad R_B \leqslant 2500 \text{ ohms},$$

$$R_{os} \leqslant \left(\frac{25}{1 + 25 \frac{0{,}6 \cdot 680}{6 \cdot 2500}} - 1 \right) 680;$$

$$R_{os} \leqslant 10\,000 \text{ ohms}.$$

When several inputs are connected to the output of one "and" or "or" gate (with the output transistor on), the voltage across the inputs will be even lower than calculated, and consequently, the operation will not become worse. The voltage across the inputs will be approximately

$$U_{in} = \frac{U_p}{R_L + R_{in}} R_{in},$$

with the output transistor cut off, where R_{in} is the resistance of all n input circuits.

Since $R_{in} = R_c/n$, then, by setting n = 10 (which is sufficient for the majority of the circuits encountered in practice), we get R_{in} = 30000/10 = 3000 ohms. Then

$$U_{in} = \frac{U_p}{680 + 3000} \cdot 3000 = 0.81 \, U_p.$$

Consequently, each input current will be 0.81 I_b = 162 μa. Since the calculated base current, I_b = 200 μa, was chosen with a reserve (instead of 125 to 150 μa), the drop to 162 μa will not make the system operation worse.

It should be noted that the transistors manufactured at present have a large variation in their parameters and characteristics. Therefore, the characteristics of each transistor must be taken into account when such circuits are built.

The elements which are constructed from the P-13A low power junction transistor have a very small output current which is not sufficient to control the coils of the power relays. Hence, amplifiers must be used to increase the power, and they may be transistor or magnetic. The first type is cheaper, lighter, and smaller in size. Therefore, it follows logically to give it preference. The circuit of such an amplifier of the utmost simplicity is shown in Fig. 5. The amplifier uses two transistors T_1 and T_2 (type P4B). The transistor shown in the circuit with dotted lines is the output transistor of the contactless element. The amplifier works as a phase inverter, as does the contactless element itself. The coil of relay K is the load resistance of T_2; this relay must operate at a voltage $U_K \leq 70$ volts (since this is the maximum voltage rating of the transistor). The maximum power rating (P_{max}) of the P4B transistor with a heat sink is 25 watts. The load power in this case can be

$$P_L \leqslant 4P_{max}\sqrt{iP_L} \leqslant 100 \text{ watts.}$$

An amplifier with a P4B output transistor can, in this way, control the coils of dc series KP-500 relays up to the fifth size, inclusive (operating at voltages up to 70 volts), or series KTP relays with dc magnetic systems. More powerful transistors (for example, type P207) can be used to control relay coils with larger current requirements; this may require the addition of one more amplification stage.

The load power of the output stages mentioned corresponds to ambient temperatures up to 30°C, with the use of a suitable heat sink. For smaller heat sinks or ambient temperatures higher than 30°C, the P4B transistors can control only smaller relays.

For standardization, the first transistor T_1 is also a P4B. The resistance R_{L1} is chosen on the basis of the base current of T_1, with a signal impressed on the amplifier input from the output of any of the elements. This current will be

$$I_{b1} = \frac{U_p}{R_L} = \frac{6}{680} \cdot 10^3 = 8.9 \text{ ma.}$$

We find from the output characteristic of the P4B transistor (which is not shown in the article, but appears in handbooks) that the collector current I_{co1} must be ≈ 75 ma so that the voltage U_{ce} will not be more than 1 volt, if the current $I_{b1} = 8.9$ ma.

The resistance

$$R_{L1} = \frac{U_p - U_{ce}}{I_{co1}} = \frac{6-1}{75 \cdot 10^{-3}} = 68 \text{ ohms.}$$

In finding the necessary base current of T_2, the load resistance of the coil of the fifth size series KP-500 relay must be taken into account; R_K is 70.5 ohms at a voltage of 55 volts. A current

$$I_{K2} = \frac{U_K - U_{ce}}{R_K} = \frac{55-1}{70.5} = 0.77 \text{ amp.}$$

corresponds to such a resistance (assuming $U_{ce} = 1$ volt).

The base current I_{b2} must be ≥ 50 ma so that U_{ce} will not be more than 1 volt.

If the collector of T_1 is directly connected to the base of T_2, the base current of T_2 will be $I_{b2} = I_{K1} = 75$ ma with T_1 cut off.

Since this current is larger than necessary, more reliable operation of the amplifier is assured.

An external view of a contactless "command" element (2 units in one case) is shown in Fig. 6; (a) with the cover on, and (b) with the cover off. The initial construction was done with standard cases and sockets for the IR-type relay.

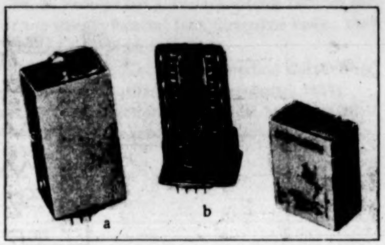

Fig. 6.

A commonly used circuit for controlling the machinery for moving and locking the cross-slide of a powerful metal turning lathe (a) and an analogous circuit using contactless elements (b) is shown in Fig. 7.

The control circuits for the motor which moves the cross-slide up and down and the motor which clamps and unclamps the cross-slide by means of a special lever-screw device are shown in Fig. 7a. Relays UR and DR control the slide motion motor, and CC and UC control the clamp – unclamp motor. In order to move the cross-slide upwards, one presses the appropriate button, and the intermediate relay 1 IR is energized. This relay first turns on the unclamp relay UC. When the unclamping process is completed, limit switch LS opens, the unclamping is stopped, and the cross-slide begins to move. After the "up" button is released, or URS opens when maximum travel is reached, relay 1 IR and the coil of the UR are deenergized, and the upward movement ceases. Simultaneously, the clamp relay CC is energized. Clamping of the cross-slide ceases when the overload relay OR operates; its coil is connected in the main circuit of the clamp motor. The operation is analogous for downward motion.

A block diagram of the same device with contactless elements is shown in Fig. 7b. Only the input and output elements are shown in it. All outputs without designations are "yes" outputs. "Not" and other outputs are indicated by appropriate labels.

When the "up" switch is pressed, input signals are fed to the "and/not" element, the "or" gate, and the "and" gate. The connection of an input signal to the "and/not" element removes the signal from the input of the "and$_1$" gate in the circuit of the CC coil, and so the latter cannot be energized. A signal is fed from the "or" gate to the "and$_2$" gate. A second input to it comes from the "and$_3$" gate with a "yes" output. Hence, the UC coil is powered through amplifier A_2, and begins to unclamp the cross-slide. When the slide is unclamped,

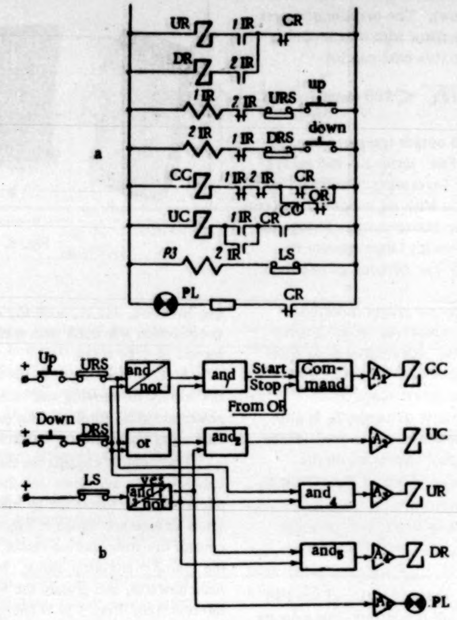

Fig. 7.

the limit switch LS opens, the "and$_3$" gate does not give a "yes" output, and consequently, there will be no output signal from the "and$_2$" gate. The UC coil is deenergized. The removal of the input signal from the "and$_3$" gate will cause its "not" output to cease, and as a result, the UR coil is energized through "and$_4$" and amplifier A_3 (one of the inputs to "and$_4$" comes from the "up" switch, which is still pressed). When the "up" switch is released, a second input signal will be impressed on "and$_1$" (the first being present from the opening of LS), and consequently, a "start" pulse will be sent to "command." As a result of this, the CC coil of the clamp motor will be energized through amplifier A_1. Clamping of the cross-slide is begun. It will continue until the OR relay operates; this feeds a "stop" pulse to the "command" element, thus deenergizing the CC coil, and causing the clamping of the slide to stop. Pilot lamp PL (as in the circuit of Fig. 7a) lights when the slide is unclamped. In the circuit being discussed (Fig. 7b), push button switches, limit switches with contacts, and the contacts of the overload relay are shown as input transducers. Replacing these with contactless elements, if necessary, does not cause any special difficulties. Induction switches can be used as connecting and tracking devices; they can have very small dimensions, since the input signals are of such low power. Contactless relays, which operate from a comparison of voltage drops in the main current circuit with a reference, can be used instead of current-operated contact relays.

The circuit being considered has a relatively small number of relays, and only illustrates the principle of using the elements developed. They can be used with considerably more effectiveness in circuits with a larger number of relays.

The dimensions and weight of equipment which uses the contactless elements described is significantly less than of that using contact relays. The service life is determined by the service life of the transistors and diodes which, according to existing preliminary data, may be years if the operating modes are correctly chosen.

LITERATURE CITED

1. Semiconductor Electronics [in Russian] (Gosenergoizdat, 1959).

2. N. I. Chistyakov (ed.), Transistor Electronics and Apparatus Construction [in Russian](Oborongiz, 1959)

3. V. V. Pavlov (ed.), Transistors in Protective Relays, Measuring Instruments, and Telemechanics for Energy-Generating Systems [Russian translation] (Gosénergoizdat, 1958).

4. Ya. A. Fedotov (ed.), Semiconductor Devices and Their Use [in Russian] (Izd. Sovetskoe Radio, 1957 (2nd ed.), 1958 (3rd ed.)).

5. F. V. Maiorov, Electronic Numerical Calculating Machines [in Russian] (Gosénergoizdat, 1957).

6. A. I. Kitov, Electronic Numerical Machines [in Russian] (Izd. Sovetskoe Radio, 1956).

CALCULATION AND CONSTRUCTION OF INDUCTION CLUTCHES

M. S. Mirenskii

Moscow

Translated from Avtomatika i Telemekhanika, Vol. 21, No. 7, pp. 1046-1056, July, 1960

Original article submitted February 24, 1960

The construction of an induction clutch is described; it is simpler to make and more reliable in use than induction clutches described earlier in the literature. A calculation of a hollow rotor is made; it is based on experimental data which confirm the possibility of considering the hollow rotor as a squirrel cage consisting of a finite number of bars. The effective flux, torque, and geometric dimensions of the basic clutch parts are also calculated.

Recently, induction clutches have found use in automatic apparatus where they are intended to operate in servosystems as low-inertia controllable drives. These clutches work on a principle analogous to that of the asynchronous slipping clutches [1]. The operating principle and constructional diagram of the clutch are given in [2]. Induction clutches do not differ in their dynamic properties from two-phase motors with hollow rotors, and are better than dc motors. Their advantage is that powerful magnets, electromagnets, or electronic amplifiers are not required for controlling them.

1. Description of the New Clutch Construction

The clutch being examined in this article is separated into two halves in order to simplify the construction and also to increase the reliability in use. Each half (Fig. 1) consists of a motor 1, star-wheel 2, hollow rotor 3, control winding 4, and stationary flux path 5. Two clutches working on a common gear box must be used so that reverse is possible. The theoretical kinematic diagram of the clutch combination is shown in Fig. 2. To accomplish reverse, the clutches could be combined as shown in Fig. 3. One motor serves as the drive for both clutches in this scheme; it is linked to them through a gear box. However, it can be affirmed that the use of a separate squirrel cage induction motor to drive the second clutch simplifies the construction and makes it more applicable for operation in servosystems, since the insufficiently reliable and noisy element – the second gear box – is eliminated by doing this. The clutch whose constructional diagram is shown in Fig. 1 is simpler to make and more reliable in use

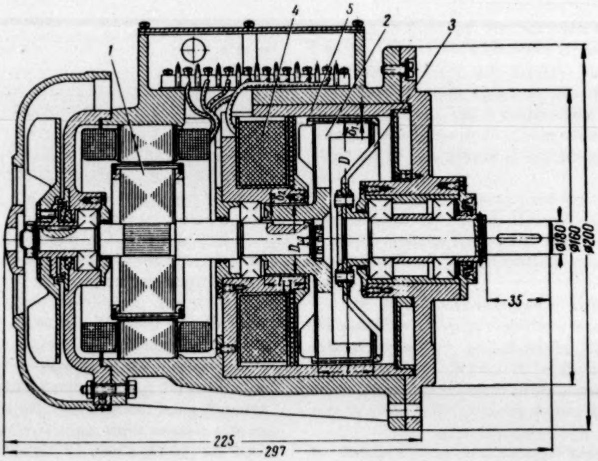

Fig. 1.

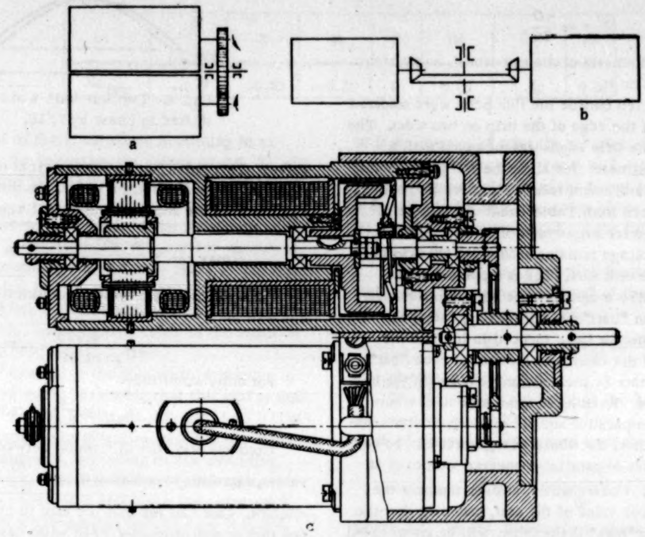

Fig. 2. Combination of the two halves of the clutch with a gear box. a) Using spur gears, b) using bevel gears, c) actual construction of the type of combination shown in a).

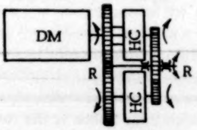

Fig. 3. Diagram showing two half-clutches connected to operate from one drive motor. DM – drive motor, HC – half-clutch, R – gear box.

than the clutch described in [2]. If the double clutch breaks down, it is replaced by another double clutch; in case of failure in a system consisting of two half-clutches, only one of its halves is replaced.

2. Calculation of Induction Clutches

Calculations of induction clutches done in the literature, particularly in [2], are based on speculative conclusions, and therefore, the correctness of the calculated formulas is not always confirmed by a check on the finished clutches. This author has succeeded in devising a method for calculating induction clutches, based on data obtained as results of specially designed experiments; the calculation is analogous to that for electrical machines. One must be able to determine the amplitude of the emf induced in the hollow rotor, the flux magnitude generated by the control winding, and finally, the ohmic resistance of the rotor, in order to calculate the geometric dimensions of the individual elements of the clutch. Therefore, a description of the experiments which permit one to find the comparatively simple solution of the problems enumerated above is presented below.

Data of the Experimental Investigation of the Hollow Rotor

The hollow rotor, as will be shown below, can be considered as a squirrel cage, in which the distance between bars is very small. The following experiments performed by the author serve as the basis for this statement. A strip of copper foil with a width equal to the axial length of a tooth of the star-wheel is fastened along the inner surface of the stationary flux path within which the star-wheel rotates. The length L of this strip is changed from experiment to experiment, beginning from the full length 12τ of the circumference of the internal bore of the flux path, and passing through a series of values equal to 6τ, 2τ, τ, $\tau/2$, $\tau/4$, $\tau/18$, and $\tau/36$. In the last experiment, a thin wire was used as the strip.

Assuming the tooth width is τ, and the teeth are equally spaced with gap τ, we can write

$$\tau = \frac{\pi D}{2z},$$

where D is the diameter of the star-wheel, and z is the number of teeth on it.

Two wires, led outside the flux path, were soldered to the middle of the edge of the strip on two sides. The voltage across the strip edges was measured with a vacuum tube voltmeter for all of the foil sizes listed above. The measurement results are given in Table 1.

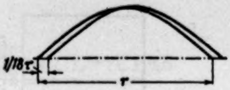

Fig. 4. Two sine half-waves, shifted in phase by τ/18.

It can be seen from Table 1 that the voltage remains unchanged for strip widths of 2τ and above. Likewise, the voltage remains unchanged for strip sizes, from $\tau/18$ to the thin wire. Let us suppose that the hollow rotor is like a squirrel cage with infinitesimal distance between "bars". Consequently, each "bar" has its own electromotive force induced in it. The harmonic curves of the change in the emf of each "bar" are shifted in phase by the solid angle between the bars being considered. Keeping in mind that all the bars are connected in parallel and are spatially shifted relative to one another, the whole arrangement can be considered as a series of parallel-connected sources of an alternating emf. Consequently, at each moment the total instantaneous value of the emf, assuming that the resistance of the "bars" is the same, will be equal to [4]

$$\sum\nolimits_{\text{inst}} = \frac{e_1 + e_2 + \cdots e_n}{n}, \qquad (1)$$

where e is the instantaneous value of the emf in a given bar at a given time, and n is the number of parallel-connected emf's or "bars". If any emf in one or more bars has a negative value at a given time, its amplitude in expression (1) is written with a minus sign. Hence, the measured emf's shown in Table 1 are the total emf of sources connected in parallel and shifted in phase. However, starting with the thin wire and up to the strip which is $\tau/18$ wide, the amplitude of the emf remains the same. In this parallel connection, the phase shift caused by the spatial shift of the infinitely thin conductors does not cause a noticeable change in the total emf, if the angle is less than a certain value. This may be seen by constructing two arbitrary harmonic curves shifted in phase, let us say, by $\tau/18$, or 10 electrical degrees. Let us assume that the emf in each conductor is sinusoidal. Then, for the two curves shown in Fig. 4, and shifted by $\tau/18$ or 10 electrical degrees, relative to one another, it can be said that one of these curves varies as $\sin \omega t$, and the other as $\sin(\omega t - 10)$. The amplitude is set as unity in both cases. The amplitude of the resultant curve will be defined at the intersection of these curves. This point lies at 95 electrical degrees for the first, and 85 for the second curve. In this case, the amplitude of the resultant curve will equal

$$E_{\text{max res}} = \frac{\sin 95° + \sin 85°}{2} = 0.996.$$

Consequently, the effective value of the resultant emf will be

$$E_{\text{eff}} = \frac{0.996}{1.41} = 0.706.$$

For unity amplitude,

$$E_{\text{eff}} = \frac{1}{1.41} = 0.709.$$

Consequently, the difference between the effective values, expressed in percent, will equal $\frac{(0.709 - 0.706) \cdot 100}{0.709} = 0.38\%$. One can see that the emf in the thin conductor and that in the conductor $\tau/18$ wide can be considered equal. This is confirmed by experiment (see Table 1). It can be considered, on the basis of what has been said, that the number of "bars" in a hollow rotor is

$$n_z = \frac{2\tau z}{\frac{1}{18}\tau} = 36z.$$

The optimum number of teeth is z = 6 for all clutches, regardless of their power and speed. In this case, the number of "bars" $n_z = 216$.

As can be seen from Table 1, the measured voltage decreases according to the degree to which the circumferential strip length is increased. An emf is induced in the "bars" of the strip which is equal in length to the circumference of the hollow rotor; this emf is equal to the emf measured in the strip or thin conductor. We will assume that the emf in the "bar" is sinusoidal, as before. During one-half of the period corresponding to τ, 18 harmonic curves which vary sinusoidally as $\sin(\omega t - \varphi)$ are induced, and are shifted by $\varphi = 10$ electrical degrees relative to one another. In this case, the total emf at each instant can be determined from expression (1). All these harmonic curves are expressed by the functions: $\sin(\omega t - 0)$, $\sin(\omega t - 10)$, $\sin(\omega t - 20)$, . . . , $\sin(\omega t - 180)$, respectively.

TABLE 1

L	12τ	6τ	2τ	τ	$\frac{1}{2}\tau$	$\frac{1}{4}\tau$	$\frac{1}{18}\tau$	$\frac{1}{36}\tau$	Thin wire
U, v	0.068	0.068	0.068	0.133	0.158	0.172	0.175	0.175	0.175

TABLE 2

ωt	0	30	60	90	120	150	180
Σe_{inst}	−0.6	−0.52	−0.30	0	0.30	0.52	0.6

The results of the summations according to expression (1) for the instantaneous values $\omega t = 0, 30, 60, 90, 120, 150$, and 180 electrical degrees are presented in Table 2.

As can be seen from Table 2, the amplitude of the resultant curve is defined at $\omega t = 0$ and 180 electrical degrees. The amplitude of the total curve is thus equal to $e_{max\ res} = 0.6\ e_{max}$, where e_{max} is the amplitude of one curve which varies sinusoidally as $\sin(\omega t - \varphi)$.

Consequently, the effective value of the resultant emf is $e_{eff\ res} = 0.415\ e_{max}$.

The emf measured in the thin wire, according to Table 1, is 0.175 volts. Assuming that this emf is sinusoidal, we find that its amplitude is $0.175 \cdot 1.41 = 0.247$ volts. Consequently, the effective value of the resultant emf for 18 components, according to the preceding, will equal $e_{eff\ res} = 0.247 \cdot 0.425 = 0.105$ volts.

The voltage measured across the strip of width τ, corresponding to a half-period, will be $e_{eff} = 0.133$ volts, according to Table 1.

Keeping in mind that the emf in the thin wire does not in fact change sinusoidally, but according to the curve shown in Fig. 5, it can be acknowledged that the measurements approach calculated data rather closely. All this confirms the correctness of the assumption that the hollow rotor can be considered as a squirrel cage which consists of a definite number of "bars" shorted at their ends by cylindrical strips lying beyond the limits of the teeth on the star-wheel.

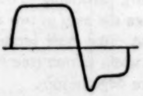

Fig. 5. Oscillogram of the change in the emf in a thin wire, and in a conductor $\tau/18$ wide.

3. Calculation of the emf in One "Bar" of the Rotor

An emf is induced in a rotor "bar" in the same manner as in high-frequency induction machines. A description of the mechanism of inducing the emf and the method of calculating it is given in [3], where the amplitude of the induced emf is determined from the formula

$$E_{eff} = 2k_b W f \Phi_a \cdot 10^{-8}\ \text{volts}.$$

Here, k_b is a coefficient of the instantaneous emf curve equal to approximately 1.15, according to [3]; W is the number of turns (in our case, W = 0.5); f is the frequency of the current, equal to $f = nz/60$ in our case; n is the angular velocity of the motor in rpm; $\Phi_a = \Phi_z - \Phi_g$ is the effective value of the flux.

In the last expression, Φ_z is the flux of one tooth, and Φ_g is the gap flux.

Consequently, the expression for the electromotive force, as it pertains to the "bars" of the rotor and the six-pronged star, takes the form

$$E_{eff} = 11.5n\Phi_a \cdot 10^{-10}\ \text{volts}. \quad (2)$$

Calculating the Flux Φ_a

The flux Φ_a is calculated on the basis of the following considerations. The over-all flux generated by the teeth of the star is determined from the formula

$$\Phi_{ov} = \frac{0.4\pi AW_\delta}{R_{ov}}$$

where AW_δ are the ampere-turns which generate the flux in the air gap, and R_{ov} is the reluctance of the air gaps. The flux path has two gaps: δ_1 – between the star-wheel and the flux path, and δ_2 – between the hub of the star-wheel and the flux path (see Fig. 1).

Therefore,

$$R_{ov} = R_1 + R_2,$$

$$R_1 = \frac{\delta_1 k_\delta}{S} = \frac{2\delta_1 k_\delta}{\pi Dl}, \quad R_2 = \frac{\delta_2}{\pi D_H l_H}.$$

Here R_1 is the reluctance of the main air gap; R_2 is the reluctance of the air gap between the hub of the star-wheel and the flux path; S – the cross section of the teeth on the star-wheel, reckoned from the inner diameter of the wheel; D – the inner diameter of the wheel, in cm; l – the axial length of a star-wheel tooth, in cm; D_H – the diameter of the wheel hub; l_H – the hub length over the part adjacent to the stationary portion of the flux path, in cm (see Fig. 1); k_δ – the Carter coefficient, which accounts for the fact that the wheel is toothed, and is determined from the formula

$$k_\delta = \frac{t + 10\delta_1}{b + 10\delta_1}.$$

In the last expression, $t = \pi D/6$; $b = \pi D/12$.

Consequently,

$$R_{ov} = \frac{2\delta_1 D_H l_H k_\delta + \delta_2 Dl}{\pi Dl D_H l_H}$$

whence

$$\Phi_{ov} = \frac{1{,}26 \cdot 0.85 AW \pi Dl D_H l_H}{2\delta_1 D_H l_H + \delta_2 Dl},$$

where AW are the ampere-turns which generate the flux Φ_{ov} in the air gap and in the steel flux path.

The coefficient 0.85 in the last formula takes into account that approximately 85% of the ampere-turns are effective in generating the flux in the air gap.

The flux in one tooth is

$$\Phi_z = \frac{\Phi_{ov}}{6} = \frac{0.56AWDlD_H l_H}{2\delta_1 D_H l_H k_\delta + \delta_2 Dl}.$$

The flux Φ_g generated in one gap is determined from the following expressions [5]:

$$\Phi_g = 1.55AWl \lg \frac{\delta_1 k_\delta + \frac{\pi m}{4}}{\delta_1 k_\delta},$$

where m = π D/12 is the gap width.

One can therefore write

$$\Phi_a = \Phi_z - \Phi_g =$$

$$= \frac{0.56AWDlD_H l_H}{2\delta_1 D_H l_H k_\delta + \delta_2 Dl} - 1.55AWl \lg \frac{\delta_1 k_\delta + \frac{\pi m}{4}}{\delta_1 k_\delta}. \quad (3)$$

The amplitudes of the emf's induced in the thin wires of two finished clutches, and the calculated values of the emf's from formulas (2) and (3), were compared in order to check how closely the calculated values approach reality. The results of the comparisons are given in Table 3.

As can be seen, the values computed from formulas (2) and (3) are sufficiently accurate for practical use.

5. Calculating the Ohmic Resistance of the Rotor "Bars"

The computation of the rotor resistance is analogous to that for a squirrel cage. As is known [6], the phase resistance of a squirrel cage is

$$r_{rot} = r_b + \frac{2r_K}{c^2}, \quad (4a)$$

where r_b is the resistance of a squirrel cage bar; $2r_K/c^2$ is the resistance of the part of the short-circuiting ring which contacts the "bar". The "bar" resistance of a hollow rotor is

$$r_b = \frac{\rho l}{S},$$

where ρ is the resistivity of the rotor metal; l – the "bar" length in meters, taken as the axial length of the star-wheel; $S = \frac{\pi D\Delta}{n_z}$ – the cross-sectional area of the bar in mm²; D – the rotor diameter in mm, and Δ – the wall thickness of the hollow cylindrical rotor in mm.

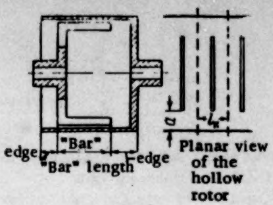

Fig. 6.

The resistivity ρ must be chosen on the basis of the expected overheating temperature of the rotor being planned. For aluminum at an overheating temperature of 100°C, ρ = 0.035, and for duralumin at 150°C, ρ = = 0.07.

Consequently,

$$r_b = \frac{6.9 \cdot 10^{-2} \rho l}{D \cdot \Delta}. \quad (4b)$$

There are no so-called short-circuiting rings in the hollow rotor, but the edges of the rotor which protrude beyond the limits of the star-wheel (as shown in Fig. 6), can be considered as short-circuiting rings. Therefore, the resistance r_K in the expression $2r_K/c^2$ for the edge of the hollow rotor included between the axes of two adjacent "bars" is determined analogously to r_b:

$$r_K = \frac{\rho l_K}{S_K},$$

where $l_K = \frac{\pi D}{n_z} = 14.5 \cdot 10^{-6}$ D is the length of the protruding edge (in mm), pertaining to one bar, equal to the distance between the axes of two adjacent "bars" (see Fig. 6); $S_K = a\Delta$ – the cross section of the edge in mm²; a – the edge width in mm (see Fig. 6); Δ – the wall thickness of the edge in mm.

Consequently,

$$r_K = \frac{14.5 \cdot 10^{-6} D\rho}{a \cdot \Delta}.$$

The quantity c^2 in the expression $2r_K/c^2$ is determined from the formula [6]

TABLE 3

Clutch power, watts	Emf measured in a wire equal to the tooth length, volts	Emf computed from formulas (2) and (3)	Error, %
50	0.04	0.047	17.5
500	0.175	0.190	8.5

TABLE 4

Clutch power, watts	Rotor material	Dimensions					Emf in a bar τ/18 wide, volts	Drive motor shaft power during clutch engagement, watts	Rotor bar resistance		Error, %
		ρ	a, mm	l, mm	D, mm	Δ, mm			calculated, ohms	from experimental data, ohms	
5	Aluminum	$35\cdot10^{-3}$	2	12	42.6	0.4	$14\cdot10^{-3}$	14.2	$3.5\cdot10^{-3}$	$3.29\cdot10^{-3}$	−6.5
20	"	"	4	14	68.6	0.4	$35\cdot10^{-3}$	81	$2.71\cdot10^{-3}$	$3.28\cdot10^{-3}$	+176
50	"	"	4	9	78.6	0.4	$47\cdot10^{-3}$	190	$2.42\cdot10^{-3}$	$2.51\cdot10^{-3}$	+3.
300	Duralumin	$7\cdot10^{-2}$	8.5	30	105.5	0.75	$195\cdot10^{-3}$	630	$0.30\cdot10^{-3}$	$0.3\cdot10^{-3}$	0
500	"		6.5	45	96.5	0.75	$190\cdot10^{-3}$	1520	$0.43\cdot10^{-3}$	$0.51\cdot10^{-3}$	+19

Note: The values of ρ are given for a 50 watt clutch with an overheating temperature of 100°C; the overheating temperature is 150°C for clutch powers greater than 50 watts.

$$c = 2\sin\frac{\pi p}{n_z} = 2\sin\frac{180.6}{216} = 0.174,$$

where p is the number of pairs of poles. In our case, p is equal to the number of teeth, that is, $p = z = 6$. Thus, $c = 0.174$ and

$$\frac{2r_K}{c^2} = \frac{9.66\cdot10^{-4}\rho D}{a\Delta}. \qquad (4c)$$

The total phase resistance of the rotor, that is, the "bar" resistance of the hollow rotor and the parts of the rotor edge in contact with them, is found by substituting the values from (4b) and (4c) in (4a):

$$r_{\rm rot} = \frac{6.9\cdot10^{-3}\rho\,(al + 1.4\cdot10^{-3}D^2)}{Da\Delta}. \qquad 4d)$$

The method shown for determining the ohmic resistance of the rotor "bars" can be checked experimentally. Keeping in mind that the motor shaft power is entirely dissipated in heat as the clutch is engaged, we can write

$$P_{\rm mo} = M_{\rm st}\, n_{\rm mo}\, 1.025\cdot10^{-5} = \frac{n_z E^2_{\rm eff}}{r_{\rm rot}}, \qquad (5)$$

where $P_{\rm mo}$ is the shaft power of the motor during clutch engagement, $M_{\rm st}$ is the starting torque of the clutch, and $n_{\rm mo}$ is the motor speed during clutch engagement. Thus,

$$r_{\rm rot} = \frac{n_z E^2_{\rm eff}}{P_{\rm mo}}.$$

Data obtained from finished clutches are compared in Table 4; this permits one to compute the ohmic resistance of a rotor "bar" from formula (4) and from the experimental data as used in formula (5).

6. Calculating the Clutch Torque

During engagement to the motor shaft, a torque is applied equal to the starting torque of the clutch. Consequently, one can write, on the basis of expression (5),

$$M_{\rm st} = \frac{n_z E^2_{\rm eff}\, 10^5}{r_{\rm rot}\, n_{\rm mo}\, 1.025} = \frac{211\cdot E^2_{\rm eff}\, 10^5}{r_{\rm rot}\, n_{\rm mo}}. \qquad (6)$$

Substituting the value for $r_{\rm rot}$ from (4) and for $E_{\rm eff}$ from (2) in expression (6), we get

$$M_{\rm st} = \frac{4n_{\rm mo}\Phi_a\, Da\,\Delta\cdot10^{-20}}{\rho\,(al + 1.4\cdot10^{-3}D^2)}. \qquad (7)$$

The expression for the flux can be put in the form

$$\Phi = \tau l B$$

where $\tau = \frac{\pi D}{2z}$, l is the tooth length of the star-wheel in cm, and B is the flux density in gauss.

For the six-pronged star, $\tau = 0.261\,D$ (D in mm), and one can write

$$\Phi = 0.261\,DlB. \qquad (8)$$

Substituting Φ from (8) in expression (7), we get

$$M_{\mathrm{st}} = \frac{27.2\cdot 10^{-12}\, n_{\mathrm{mo}} D^3 l^2 B^2 a \Delta}{p\,(al + 1.4\cdot 10^{-2} D^2)}. \qquad (9)$$

Since the torque developed by the hollow rotor is caused by the rotor slipping with respect to the rotating star-wheel, the general expression for the clutch torque can be put in the following form:

$$M_{\mathrm{c}} = \frac{27.2\cdot 10^{-12}\, n_{\mathrm{n}}\, s D^3 l^2 B^2 a \Delta}{p\,(al + 1.4\cdot 10^{-2} D^2)}, \qquad (10)$$

where $s = \frac{n_w - n_{rot}}{n_w}$ is the slip of the hollow rotor with respect to the star-wheel, n_w is the speed of the wheel, and n_{rot} is the rotor speed.

It can be seen by comparing expressions (9) and (10) that the torque is proportional to the slip, if the flux and speed of the motor change very slightly. Consequently, the characteristics $s = f(M)$, or $n = f(M)$ will vary linearly. In reality, the clutches actually made have an $n = f(M)$ characteristic which is not strictly linear. But to simplify the solution of the problems concerning induction clutches, one can assume that this characteristic is linear. Consequently, the characteristic $n = f(P_{ms})$, where P_{ms} is the power at the clutch shaft in watts, will be parabolic. The maximum power developed by the clutch (the apex of the parabola) will be developed when slip $s = 0.5$.

7. Calculating the Geometric Dimensions of the Clutch

The determination of the basic dimensions of the main clutch parts is based on expressions (9) and (10). One must also consider what dimensions are desirable from a standpoint of construction. The values n_{mo}, B, a, and Δ in expressions (9) and (10) must be determined from a number of variables, keeping the following considerations in mind:

a. Increasing the motor speed reduces the clutch and motor size, and also reduces the exciting ampere-turns. However, the noise of the clutch at higher speeds becomes significant, and the requirements on dynamic balancing of its rotating parts become more stringent.

b. In choosing the flux density B in the air gap, one must simultaneously check the degree of saturation in the individual parts of the flux path (in the root of a star-wheel tooth, in the hub, and in the cavity of the stationary flux path).

c. The values of a and Δ can be selected on the basis of the data shown in Table 5, for clutches planned to operate at high frequency (400 cps).

TABLE 5

Power range, watts	5–50	60–100	125–300	500–1000
a, mm	3	4–5	5–7	8–10
Δ, mm	0.4	0.55	0.75	1.00

d. The most favorable ratio of D to 1 is determined from computations using a number of variables.

8. Calculating the Clutch Excitation

In calculating the clutch excitation, one must take into account the ampere-turns necessary for the two air gaps and for the steel flux path. The general expression is written in the form

$$\Sigma AW = AW_{sf} + AW_{\delta_1} + AW_{\delta_2},$$

where ΣAW are the total ampere-turns, AW_{sf} – the ampere-turns of the steel flux path, AW_{δ_1} – the ampere-turns of the main air gap, and AW_{δ_2} – the ampere-turns of the air gap between the star-wheel hub and the stationary flux path.

The method of calculating the ampere-turns is shown in various references (see, for example, [6]). In connection with this, one should keep in mind that the flux of the star-wheel goes only in one direction, and therefore, formula (6-5) in [6] takes the form

$$F_\delta = 0.8 B_\delta \delta.$$

9. Calculating the Drive Motor Power

It was shown above that the clutch develops maximum power when the slip $s = 0.5$. Consequently, the drive motor must develop a power of $P_{mo} = 2P_{mp}$, where P_{mp} is the maximum power of the clutch. This means that the nominal power of the motor must be twice the nominal (maximum) clutch power. The overload rating of the drive motor is determined from the following calculation. The starting torque of the clutch, as was shown above, is found from the relation $M_{st} = 2M_{nom}$, where M_{nom} is the nominal clutch torque.

It follows from the preceding that the drive motor speed during clutch engagement is thus equal to $n_{mo} \approx 2n_{NS}$, where n_{NS} is the nominal speed of the clutch.

Consequently, the motor must develop the power

$$P_{mo} = 2n_{NS}\, 2M_{NS} \cdot 1.025 \cdot 10^{-5} \approx 4P_{NS}$$

as the clutch is engaged.

This means that the motor must develop a maximum power which is twice its nominal power.

Note: The motor slip was not taken into account in the calculations which have been made. Moreover, it has been assumed that the mechanical characteristic of the clutch, $n_c = f(M_c)$, is linear.

LITERATURE CITED

1. V. S. Sharov, Slipping Clutches [in Russian] (Gosénergoizdat, 1958).
2. V. V. Solodovnikov (ed.), Fundamentals of Automatic Control [in Russian] (Mashgiz, 1959) vol. 2, chap. 1.

3. A. E. Alekseev, "High frequency machines," Electrical Machine Construction [in Russian] (NTOE Press, 1930).
4. A. S. Kasatkin and M. A. Perekalin, Electrotechnology [in Russian] (Gosénergoizdat, 1955).
5. K. Schmidt, Fortschritte im Bau von Mittel und Hochfrequenzmaschinen (ETZ, 1928).
6. P. S. Sergeev (ed.), Design of Electrical Machines [in Russian] (Gosénergoizdat, 1950).

EFFECT OF MAGNETIZATION IRREGULARITY ON THE STATIC CHARACTERISTICS OF CORES. II

G. D. Kozlov

Moscow

Translated from Avtomatika i Telemekhanika, Vol. 21, No. 7, pp. 1057-1072,
July, 1960
Original article submitted November 25, 1959

The effect of magnetization irregularity on the static characteristics of cores is considered. Characteristics obtained by experiment and by calculation are compared. Some recommendations concerning the selection of geometric relations of a divided magnetic circuit are given.

The present paper is devoted to further studies of the magnetization irregularity effect on the core static characteristics. In [1-3], the irregularity in core magnetization was considered for a toroidal magnetic circuit and for a hysteresis loop in the shape of a parallelogram. In this, the slope of the "horizontal" portions of the hysteresis loop was not taken into account (the angle $\delta = 0$). The characteristics of materials used in practice actually have a certain slope in the saturation region (the angle $\delta \neq 0$), which has to be taken into account. This is especially important in analyzing the operation of a divided magnetic circuit.

In the present paper, we shall consider the magnetization irregularity effect on the core characteristics in the case where the material hysteresis loops are of the shape shown in Fig. 1. The dependence of the magnetic characteristics of a core with a divided magnetic circuit on its dimensions and the location of the magnetizing winding will also be considered.

For the sake of simplicity, the effect of the core magnetization irregularity will be analyzed for a toroidal shape of the magnetic circuit.

1. Toroidal Magnetic Circuit

In order to determine the $B = f(F)$ magnetic characteristics of the core when the material hysteresis loops have the shape shown in Fig. 1, it is first necessary to find a mathematical expression for individual branches of hysteresis loops in the $b = f(h)$ form [3].

Mathematically, individual hysteresis loop branches can be represented in the following manner:

The Ultimate Hysteresis Loop

Rising branch

$$b = \frac{2b_p}{h_s - h_p}\left(h - \frac{h_s + h_p}{2}\right) + \operatorname{tg}\delta\,\frac{h_s + h_p}{h_s - h_p}(h - h_p), \quad (1)$$

descending branch

$$b = \frac{2b_p}{h_s - h_p}\left(h + \frac{h_s + h_p}{2}\right) + \operatorname{tg}\delta\,\frac{h_s + h_p}{h_s - h_p}(h + h_p); \quad (2)$$

positive saturation

$$b = b_p + \operatorname{tg}\delta\,(h + h_p), \quad (3)$$

negative saturation

$$b = -b_p + \operatorname{tg}\delta\,(h - h_p). \quad (4)$$

Here, $\operatorname{tg}\delta = \frac{b_s - b_p}{h_s - h_p} = \frac{b_r - b_p}{h_p}$ is the slope of the saturation and maximum magnetization branches of the hysteresis loops.

Symmetric Hysteresis Loop Cycles

Rising branch

$$b = \frac{b_p}{h_s - h_p}[(2h - h_м) - h_p] + \operatorname{tg}\delta\,\frac{h_s + h_p}{h_s - h_p}h - \operatorname{tg}\delta\,\frac{h_м + h_p}{h_s - h_p}h_p, \quad (5)$$

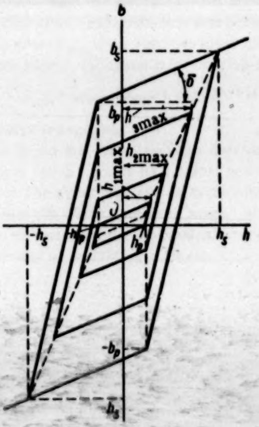

Fig. 1.

descending branch

$$b=\frac{b_p}{h_s-h_p}[(2h+h_{\text{м}})+h_p]+\operatorname{tg}\delta\,\frac{h_s+h_p}{h_s-h_p}h+\operatorname{tg}\delta\frac{h_{\text{м}}+h_p}{h_s-h_p}h_p\,; \tag{6}$$

positive magnetization

$$b=\frac{b_p}{h_s-h_p}(h_{\text{м}}-h_p)+\operatorname{tg}\delta\,\frac{h_{\text{м}}-h_p}{h_s-h_p}h_p+\operatorname{tg}\delta\,h, \tag{7}$$

negative magnetization

$$b=-\frac{b_p}{h_s-h_p}(h_{\text{м}}-h_p)-\operatorname{tg}\delta\,\frac{h_{\text{м}}-h_p}{h_s-h_p}h_p+\operatorname{tg}\delta\,h. \tag{8}$$

By substituting $h = h_M$ in Eqs. (5) and (6) or (7) and (8), we can determine the loci of the peaks of symmetric hysteresis loop cycles:

$$b=\frac{b_p}{h_s-h_p}(h_{\text{м}}-h_p)+\frac{\operatorname{tg}\delta}{h_s-h_p}(h_s h_{\text{м}}-h_p^2). \tag{9}$$

For $h_M \geq h_s$ values, the material magnetization is reversed with respect to the ultimate hysteresis loop. For this, the maximum induction values are determined by the h_M value, and they lie on the straight line

$$b=b_p+\operatorname{tg}\delta\,(h_{\text{м}}+h_p). \tag{10}$$

For field strength values $h_M \leq h_p$, the material magnetization will not be reversed with respect to the symmetric hysteresis loops; in this case, the maximum induction values will lie on the straight line

$$b = h_M \operatorname{tg}\delta. \tag{11}$$

However, individual layers of the core material will have different field strengths for the same magnetization ampere-turns. Therefore, for determining the total change in the $B = f(F)$ core induction, Eqs. (1)-(11) should be reduced to the $b = f(F)$ form and then substituted in Eq. (8) [3]:

$$B=\frac{1}{R_{\text{н}}-R_{\text{в}}}\int\limits_{R_{\text{в}}}^{R_{\text{н}}} b\,dR. \tag{11a}$$

The transformed Eqs. (1)-(11) will assume the following forms, respectively:

Ultimate Hysteresis Loop

Rising branch

$$b=\frac{2b_p}{F_s-F_p}\left(F\frac{R_{\text{н}}}{R}-\frac{F_s+F_p}{2}\right)+\operatorname{tg}\delta\frac{F_s+F_p}{F_s-F_p}\left(F\frac{R_{\text{в}}}{R}-F_p\right), \tag{12}$$

descending branch

$$b=\frac{2b_p}{F_s-F_p}\left(F\frac{R_{\text{н}}}{R}+\frac{F_s+F_p}{2}\right)+\operatorname{tg}\delta\frac{F_s+F_p}{F_s-F_p}\left(F\frac{R_{\text{в}}}{R}+F_p\right); \tag{13}$$

positive saturation

$$b=b_p+\operatorname{tg}\delta\left(F\frac{R_{\text{н}}}{R}+F_p\right), \tag{14}$$

negative saturation

$$b=-b_p+\operatorname{tg}\delta\left(F\frac{R_{\text{н}}}{R}-F_p\right). \tag{15}$$

Symmetric Hysteresis Loop Cycles

Rising branch

$$b=\frac{b_p}{F_s-F_p}\left[(2F-F_{\text{м}})\frac{R_{\text{н}}}{R}-F_p\right]+\operatorname{tg}\delta\left[\frac{F_s+F_p}{F_s-F_p}F\frac{R_{\text{н}}}{R}-\frac{F_p}{F_s-P_p}\left(F_{\text{м}}\frac{R_{\text{н}}}{R}-F_p\right)\right] \tag{16}$$

descending branch

$$b=\frac{b_p}{F_s-F_p}\left[(2F+F_{\text{м}})\frac{R_{\text{н}}}{R}+F_p\right]+\operatorname{tg}\delta\left[\frac{F_s+F_p}{F_s-F_p}F\frac{R_{\text{н}}}{R}+\frac{F_p}{F_s-F_p}\left(F_{\text{м}}\frac{R_{\text{н}}}{R}-F_p\right)\right]; \tag{17}$$

positive magnetization

$$b-\frac{b_p}{F_s+F_p}\left(F_{\text{м}}\frac{R_{\text{в}}}{R}-F_p\right)+\operatorname{tg}\delta\left[F\frac{R_{\text{н}}}{R}+\frac{F_p}{F_s-F_p}\left(F_{\text{м}}\frac{R_{\text{в}}}{R}-F_p\right)\right], \tag{18}$$

negative magnetization

$$b=-\frac{b_p}{F_s-F_p}\left(F_{\text{м}}\frac{R_{\text{в}}}{R}-F_p\right)+\operatorname{tg}\delta\left[F\frac{R_{\text{в}}}{R}-\frac{F_p}{F_s-F_p}\left(F_{\text{м}}\frac{R_{\text{в}}}{R}-F_p\right)\right]. \tag{19}$$

In order to find the "normal magnetization curve," Eqs. (9)-(11) must be reduced to the following form:

$$b=\frac{b_p}{F_s-F_p}\left[F_{\text{м}}\frac{R_{\text{в}}}{R}-F_p\right]+$$

$$+\frac{\operatorname{tg}\delta}{F_s-F_p}\left[F_s F_{\text{м}}\frac{R_{\text{в}}}{R}-F_p^2\right], \qquad (20)$$

$$b=b_p+\operatorname{tg}\delta\left[F_{\text{м}}\frac{R_{\text{в}}}{R}+F_p\right], \qquad (21)$$

$$b=\operatorname{tg}\delta\, F_{\text{м}}\frac{R_{\text{в}}}{R}. \qquad (22)$$

In this case, we shall assume that $\operatorname{tg}\delta = \frac{b_s - b_p}{F_s - F_p} = \frac{b_r - b_p}{F_p}$ determines the saturation line slope for the internal layer of the core material ($R = R_B$). For this, the core dimensions are so chosen that the inequality

$$\alpha < \beta \qquad (23)$$

is satisfied (case 1 [3]).

Here, $\beta = h_s/h_p = F_s/F_p$ is the coefficient which characterizes the magnetic material.

In dependence on the maximum value F_M of magnetization ampere-turns, the alternating magnetization of the core will take place under different conditions. Three shapes of symmetric alternating magnetization loops can be distinguished: 1) for the $F_p < F_M \leq \alpha F_p$ values, 2) for the $\alpha F_p < F_M \leq F_s$ values, and 3) for the $F_s < F_M \lesssim \alpha F_s$ values.

The derivations of analytical expressions describing the total change in the core induction $B = f(F)$ for different alternating magnetization conditions are given in the Appendix. By using these equations, we determined the family of symmetric alternating magnetization loops and the normal magnetization curve for the $b_p = 1$, $b_s = 1.4$, $\alpha = 2$, and $\beta = 4$ values; the results are given in Fig. 2. In plotting the calculated characteristics, the relative quantity F/F_p was laid off on the axis of abscissas. In this, the maximum value of magnetization ampere-turns was chosen in such a manner that $F_M/F_p = \alpha$ for the first type of symmetric alternating magnetization loops, $F_M/F_p = \beta$ for loops of the second type, and $F_M/F_p = \alpha\beta$ for loops of the third type.

For the sake of comparison, Fig. 3 shows the family of symmetric alternating magnetization loops, obtained experimentally for a core made of the 50 NP material, the dimensions of which are given in Table 1.

Figure 4 shows the $B = f(F)$ dependence of the ultimate alternating magnetization loop and the "normal magnetization curve" (dotted line), which were plotted separately with respect to the known material parameters h_p, h_s, b_p, and b_s.

From the plotting in Fig. 4, it is obvious that the intersections of the continuations of linear portions of the "normal magnetization curve" with the coordinate

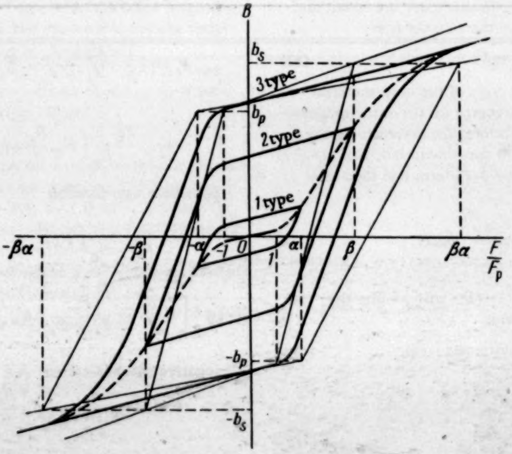

Fig. 2.

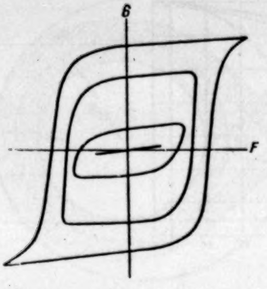

Fig. 3.

axes and with each other make it possible to determine the values of b_s, b_r, $F_s(\alpha - 1)/\ln\alpha$, and $F_p(\alpha - 1)/\ln\alpha$—by means of which all parameters of the magnetic material can be determined if the value of α is known.

Thus, if the material hysteresis loop is known, then, for certain given dimensions of the toroidal core, it is possible to plot the family of the core alternating magnetization loops and the "normal magnetization curve." Conversely, by means of simple geometric constructions and calculations, the magnetic material parameters h_p, h_s, b_p, and b_s can be determined with respect to the available experimental "normal magnetization curve."

Let us consider the order of determining these parameters with respect to the experimental "normal magnetization curve."

1) We plot the experimental dependence $U_{av} = f(F)$ for a core whose dimensions are known. Here, U_{av} is the average voltage over a half-period, and F are the magnetization ampere-turns for a sinusoidal current.

Since the value of U_{av} is proportional to B_{max}, it can be considered that the $U_{av} = f(F)$ dependence is proportional to $B_{max} = f(F)$.

2) The "normal magnetization curve" $B_{max} = f(F)$, which is obtained experimentally, is plotted in a coordinate system. Then, by continuing the linear portions of the "normal magnetization curve" until they intersect the coordinates and each other, we obtain the X, Y, and Z intersection points (Fig. 4). It is obvious from the plot that the magnitude of OY corresponds to the b_r value; the projection of OZ on the axis of ordinates corresponds to the b_s value; the projection of OZ on the axis of abscissas corresponds to the $F_s(\alpha - 1)/\ln\alpha$ value; and the projection of OX on the axis of abscissas corresponds to the $F_p(\alpha - 1)/\ln\alpha$ value. Hence, since the value of α is known, we determine the F_p, F_s, $\mathrm{tg}\delta = (b_s - b_r)/F_s$, and $b_p = b_r - \mathrm{tg}\delta\, F_p$ values, and we find the material parameters h_p, h_s, b_p, and b_s.

3) By substituting the found values in Eqs. (38)-(42) (see Appendix), we can calculate the "normal magnetization curve." Moreover, by plotting the theoretical curve in the same coordinate system as the experimental curve, we can estimate the accuracy in determining the magnetic material parameters.

Figure 5 shows the experimental (solid lines) and the theoretical (dotted lines) normal magnetization curves for different cores, the data of which are given in Table 1.

A comparison of characteristics obtained by experiment and by calculation (Fig. 5) shows that, if the material hysteresis loops are represented in the shape

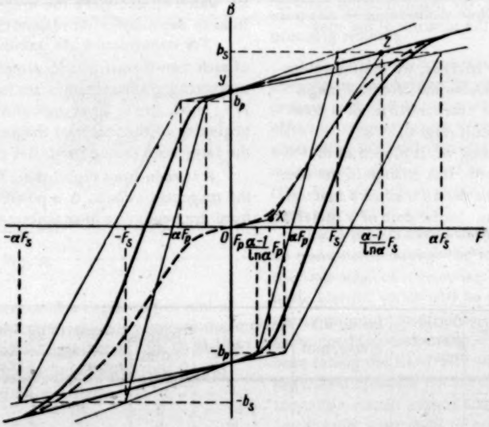

Fig. 4.

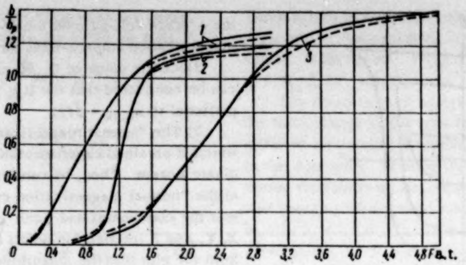

Fig. 5.

of parallelograms, where the slope of "horizontal" portions and the effect of the core magnetization irregularity are taken into account, it is possible to obtain theoretical relations which analytically describe the static core characteristics. For practical purposes, the agreement between the theoretical and experimental characteristics is satisfactory.

2. The Divided Magnetic Circuit

The operation principle of devices with divided magnetic circuits is actually based on the irregularity in magnetizing the magnetic circuit along different closed magnetic loops. Therefore, in analyzing the magnetization process in such a magnetic circuit, it is necessary to analyze the irregular magnetization in separate connecting links as well as in the entire magnetic circuit. In this case, the $\Phi_{max} = f(F)$ dependence can be conveniently used for the magnetic regime characteristics of the magnetic circuit.

In divided magnetic circuits, the connecting link magnetic conditions are determined not only by the magnetic circuit dimensions, the magnetization ampere-turns, and by F, but also by the location of the magnetizing winding.

In order to simplify the analysis, we shall consider a two-hole transfluxor in studying the effect of magnetization irregularity on the characteristics of a core with a divided magnetic circuit (Fig. 6).

If the magnetizing winding $W_\sim$ is placed at the connecting link I, the magnetic flux change in the connecting links II and III can be determined as a function of magnetizing ampere-turns. In the case of a material with the hysteresis loop shown in Fig. 1, the magnetization reversal in the magnetic circuit will first take place around the large hole in the volume which is in contact through link II and then around both holes in the volume which is in contact through link III. The magnetization reversal through link II takes place in the toroidal volume, and the magnetization reversal through link III occurs in a somewhat extended volume, whose shape is similar to a transmission belt. In order to simplify the analysis, the extended volume can be reduced to a toroidal volume without changing either the outside or the inside perimeter lengths l_{o2} and l_{i2}, or the volume cross section. The analysis of magnetization reversal processes in toroidal volumes can be entirely replaced by an analysis of these processes in equivalent toroidal cores. Therefore, all the conclusions concerning the magnetization irregularity in toroidal cores (see [3] and Section 1 of the present paper) are applicable to toroidal volumes. Fig. 7 shows the experimental magnetic characteristics $\Phi_{max} = f(F)$ of connecting links II and III, which characterize the magnetic flux changes in the links in dependence on magnetizing ampere-turns.

For convenience in comparing the characteristics of such transfluxors and for simplifying the analysis, magnetizing ampere-turns are represented in relative F/F_p units, where F_p is the value of ampere-turns at the beginning of the material magnetization reversal around the large hole (along the I-II-I path).

It is seen from Fig. 7 that, for suitable dimensions of the magnetic circuit, it is possible to determine beforehand the beginning of magnetization reversal in con-

TABLE 1

Curve No.	Material type	Outside diameter, mm	Inside diameter, mm	Ratio of core radii, α	Height, mm	Magnetizing winding, turns	Measuring winding, turns
1	Ferrite	13	7.8	1.67	3	20	250
2	50NP	27.8	20	1.39	5	20	130
3	KhVP	39.2	28.2	1.39	10	40	120

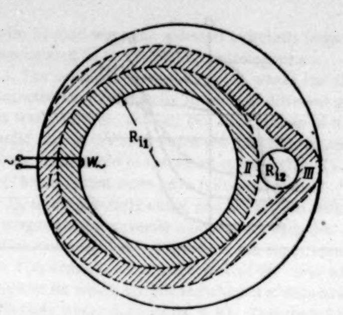

Fig. 6.

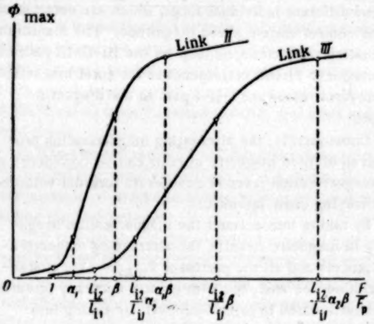

Fig. 7.

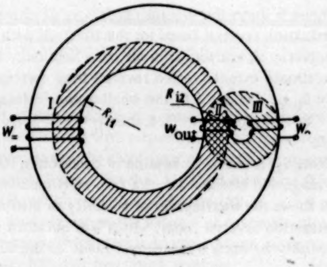

Fig. 8.

necting link III with respect to the beginning or end of magnetization reversal in link II. If it is required that the magnetization reversal in connecting link III begins after the end of magnetization reversal in link II, the following inequality must be satisfied:

$$\beta \leqslant \frac{l_{i2}}{l_{o1}}, \tag{24}$$

where l_{i2} is the inside perimeter of the "extended" volume (magnetization reversal along the I-III-I path), and l_{o1} is the outside perimeter of the toroidal volume (magnetization reversal along the I-II-I path).

Consequently, in this case, the magnetization reversal in the connecting link will occur successively, moving from one connecting link to another as the magnitude F of the magnetizing ampere-turns increases.

It should be noted here that inequality (24) must be satisfied if a reliable "magnetic decoupling" between individual magnetic circuit components is to be secured (which is necessary in almost all devices where divided magnetic circuits are used). By selecting suitable magnetic circuit dimensions, it is also possible to vary the slope of $\Phi_{max} = f(F)$ characteristics, and, for certain materials (for a sufficiently small value of the β coefficient), an equal slope of the $\Phi_{max} = f(F)$ characteristics can be obtained for different links in the magnetic circuit. This, in turn, will make it possible to obtain voltage pulses of identical shapes.

If the slopes of the $\Phi_{max} = f(F)$ characteristics are to be identical, the following relation must be satisfied:

$$\alpha_2\beta + \frac{1}{\alpha_1\beta} = 2. \tag{25}$$

Here, $\alpha_2 = l_{o2}/l_{i2}$ is the ratio of the outside perimeter to the inside perimeter (alternating magnetization along the I-III-I path), and $\alpha_1 = l_{o1}/l_{i1}$ is the ratio of the outside toroidal volume perimeter to the inside perimeter (alternating magnetization along the I-II-I path), where l_{i1} is the toroidal volume perimeter (alternating magnetization along the I-II-I path).

The devices where the principle of successive magnetization of links in a divided magnetic circuit is used can be successfully applied in distributing and blocking systems.

All the above-mentioned concerning magnetization irregularity can be used in considering the operation of devices with divided magnetic circuits. In studying the effect of magnetization irregularity on the device characteristics, we shall consider the example of a two-hole transfluxor, which is used as a controllable transformer (Fig. 8). We shall describe the operation principle of such a device [4 and 5].

Let a preliminary current pulse of large amplitude be transmitted through the winding $W_=$. This will cause the saturation of connecting links II and III in the magnetic circuit, which will be preserved also after the termination of the preliminary current pulse. Under these conditions, the magnetic flux around the smaller hole (along the III-II-III path) will not change, since, regardless of where the field is directed, a part of the magnetic circuit path is already saturated. Due to the insufficient magnitude of magnetizing ampere-turns, the magnetic flux around the large hole (along the

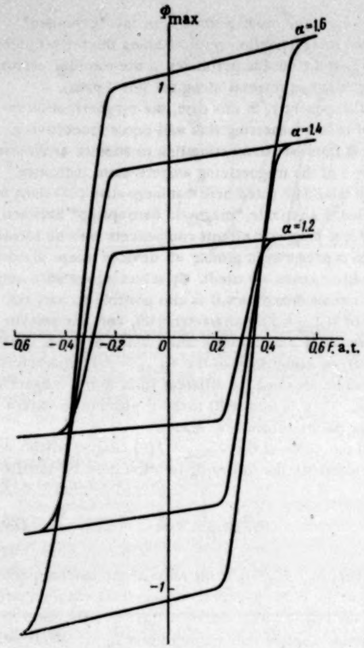

Fig. 9.

III-I-III path) will not change, either. Consequently, no voltage will appear at the W_{out} winding.

If a control current pulse is now transmitted through the $W_=$ winding, in the direction opposite to the blocking direction, the magnetization reversal in the magnetic circuit will take place around the large hole (along the I-II-I path) in the opposite direction. Under these magnetizing conditions, the magnetization reversal can now take place around the smaller hole (along the III-II-III path). As a result, a voltage, the magnitude of which is proportional to the amplitude of the control current pulse, arises at the W_{out} winding. This mutual dependence can be explained in the following manner: when the magnetization reversal in the magnetic circuit takes place around the large hole (along the I-II-I path), the magnetic polarity of connecting link II is reversed completely or partially by the control current pulse in dependence on its magnitude. This determines the larger or smaller reversal volume magnetization round the smaller hole (along the III-II-III path).

The alternating magnetization of the magnetic circuit in volumes around the smaller hole (along the III-II-III path) follows the ultimate hysteresis loop,

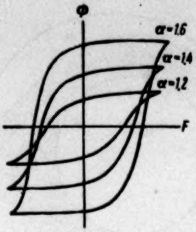

Fig. 10.

while the alternating magnetization of the magnetic circuit around the large hole (along the I-II-I path) follows different individual loops, which are determined by the control current phase magnitude. The maximum alternating magnetization loop for the III-II-III path in the magnetic circuit corresponds to the total magnetization reversal along the I-II-I path in the magnetic circuit.

Consequently, the alternating magnetization processes in divided magnetic circuits can be considered as the magnetization reversal in separate toroidal volumes with varying cross sections.

By taking into account the magnetization irregularity in magnetic circuits, the alternating magnetization process and all the pertinent $\Phi_{max} = f(F)$ characteristics can be analyzed with greater accuracy (greater than that secured in [5]). Moreover, by taking into account the effect of magnetization irregularity on the static characteristics, these characteristics can be calculated with an accuracy sufficient for practical purposes.

Figure 9 shows the theoretical family of ultimate magnetization reversal loops for the III-II-III path in the magnetic circuit for different cross sections. The large ultimate magnetization reversal loop corresponds to $S_{II} = S_{max}$ and $\alpha = 1.6$; the smaller ones correspond to $S_{II} = 2/3\ S_{max}$ and $\alpha = 1.4$, and $S_{II} = 1/3\ S_{max}$ and $\alpha = 1.2$.

Here, S_{II} is the cross section of connecting link II in the magnetic circuit. For the sake of comparison, Fig. 10 shows the oscillogram of a family of ultimate magnetization reversal loops, which was obtained experimentally by using a transfluxor made of the 65NP material.

SUMMARY

1. The representation of the material hysteresis loops in the shape of parallelograms (Fig. 1) is justified since the mutual agreement of the "normal magnetization curves" obtained by calculation and by experiment can be used for practical purposes.

2. The method of determining the core induction as the $B = f(F)$ function of magnetizing ampere-turns

can also be used when the material hysteresis loops are not represented in the shape of parallelograms.

3. The conclusions reached in [3], where the effect of magnetization irregularity in cores of different geometry was taken into account (for three values of α), are valid also in the case where the material hysteresis loops are represented in the above manner (Fig. 1).

4. Since actual cores have finite dimensions ($\alpha > 1$), in all practical cases, one has to deal with the core magnetization reversal loop, and not with the material hysteresis loop. Therefore, the experimental $U_{av} = f(F)$ dependence must be plotted for cores with dimensions for which the plotted characteristics have considerable linear portions ($\alpha < \beta$). This makes it easier to determine the material magnetic parameters (h_p, h_s, b_p, and b_s).

5. The magnetization reversal in a divided magnetic circuit can be conveniently represented as the material magnetization reversal in separate volumes. The magnetization reversal processes in toroidal volumes are identical to magnetization reversal processes in toroidal cores.

6. The determination of all magnetic characteristics of a divided magnetic circuit can be reduced to the determination of magnetic characteristics of the corresponding toroidal volumes.

7. If inequality (24) for a divided magnetic circuit is satisfied, the magnetic circuit dimensions are characterized in such a manner, that the magnetization reversal in one of the sections begins only after the magnetization reversal ends in the other. Thus, if this inequality is satisfied, a considerable "magnetic decoupling" for separate magnetization reversal loops is secured.

APPENDIX

a) Ultimate Magnetization Reversal Loop ($F_s < F_M \lesssim \alpha F_s$)

Let us first consider the conditions for the core magnetization reversal with respect to the ultimate loop, which pertains to the third type of symmetric magnetization reversal loops. For this, we shall substitute (12)-(15) in Eq. (8), which was borrowed from [3].

In dependence on the value F of magnetization ampere-turns, the ultimate magnetization reversal loop will have different functional sections.

1st Section. For $-F_M \le F \le F_p$,

$$B_1 = \frac{1}{R_H - R_B}\int\limits_{R_B}^{R_H}\left[-b_p + \operatorname{tg}\delta\left(F\frac{R_B}{R} - F_p\right)\right]dR.$$

By solving this equation, we obtain

$$B_1 = -b_p + \operatorname{tg}\delta\left[\frac{\ln\alpha}{\alpha-1}F - F_p\right]. \qquad (26)$$

2nd Section. For $F_p \le F \le \alpha F_p$,

$$B_2 = \frac{1}{R_H - R_B}\left\{\int\limits_{R_B}^{R}\left[\frac{2b_p}{F_s - F_p}\left(F\frac{R_B}{R} - \frac{F_s + F_p}{2}\right) + \right.\right.$$

$$\left. + \operatorname{tg}\delta\frac{F_s + F_p}{F_s - F_p}\left(F\frac{R_B}{R} - F_p\right)\right]dR +$$

$$\left. + \int\limits_{R}^{R_H}\left[-b_p + \operatorname{tg}\delta\left(F\frac{R_B}{R} - F_p\right)\right]dR\right\},$$

where $R = R_B\, F/F_p$.

By solving this equation, we obtain

$$B_2 = \frac{1}{\alpha-1}\frac{b_p}{F_s - F_p}\left[2F\left(\ln\frac{F}{F_p} - 1\right) - \right.$$

$$\left. - F_s(\alpha - 1) + F_p(\alpha + 1)\right] +$$

$$+ \frac{1}{\alpha-1}\frac{\operatorname{tg}\delta}{F_s - F_p}\left[2FF_p\left(\ln\frac{F}{F_p} - 1\right) + \right. \qquad (27)$$

$$\left. F(F_s - F_p)\ln\alpha + F_p^2(\alpha + 1) - F_sF_p(\alpha - 1)\right].$$

3rd Section. For $\alpha F_p \le F \le F_s$,

$$B_3 = \frac{1}{R_H - R_B}\int\limits_{R_B}^{R_H}\left[\frac{2b_p}{F_s - F_p}\left(F\frac{R_B}{R} - \frac{F_s + F_p}{2}\right) + \right.$$

$$\left. + \operatorname{tg}\delta\frac{F_s + F_p}{F_s - F_p}\left(F\frac{R_B}{R} - F_p\right)\right]dR.$$

By solving this equation, we obtain

$$B_3 = \frac{b_p}{F_s - F_p}\left[\frac{\ln\alpha}{\alpha-1}2F - (F_s + F_p)\right] +$$

$$+ \operatorname{tg}\delta\frac{F_s + F_p}{F_s - F_p}\left[\frac{\ln\alpha}{\alpha-1}F - F_p\right]. \qquad (28)$$

4th Section. For $F_s \le F \le \alpha F_s$,

$$B_4 = \frac{1}{R_H - R_B}\left\{\int\limits_{R_B}^{R}\left[b_p + \operatorname{tg}\delta\left(F\frac{R_B}{R} + F_p\right)\right]dR + \right.$$

$$+ \int\limits_{R}^{R_H}\left[\frac{2b_p}{F_s - F_p}\left(F\frac{R_B}{R} - \frac{F_s + F_p}{2}\right) + \right.$$

$$\left.\left. + \operatorname{tg}\delta\frac{F_s + F_p}{F_s - F_p}\left(F\frac{R_B}{R} - F_p\right)\right]dR\right\},$$

where $R = R_B\, F/F_s$.

By solving this equation, we obtain

$$B_4=\frac{1}{\alpha-1}\frac{b_p}{F_s-F_p}\Big[2F\left(1+\ln\frac{\alpha F_s}{F}\right)-$$
$$-F_s(\alpha+1)-F_p(\alpha-1)\Big]+ \qquad (29)$$
$$+\frac{1}{\alpha-1}\frac{\operatorname{tg}\delta}{F_s-F_p}\Big[2FF_p\left(1-\ln\frac{F}{F_s}\right)+$$
$$+F(F_s+F_p)\ln\alpha-F_p^2(\alpha-1)-F_sF_p(\alpha+1)\Big].$$

5th Section. For $\alpha F_s \le F \le F_M$.

$$B_5=\frac{1}{R_{\text{н}}-R_{\text{в}}}\int\limits_{R_{\text{в}}}^{R_{\text{н}}}\left[b_p+\operatorname{tg}\delta\left(F\frac{R_{\text{в}}}{R}+F_p\right)\right]dR.$$

By solving this equation, we obtain

$$B_5=b_p+\operatorname{tg}\delta\left[\frac{\ln\alpha}{\alpha-1}F+F_p\right]. \qquad (30)$$

The mathematical expression for the descending branch of the ultimate magnetization reversal loop is determined in a similar manner.

b) Second Type of Symmetric Magnetization Reversal Loops ($\alpha F_p < F_M \le F_s$).

For studying this type of magnetization reversal loops, we shall substitute Eqs. (16)-(19) in Eq. (8), which was borrowed from [3]. In dependence on the value F of magnetization ampere-turns, this type of magnetization reversal will have different functional sections.

1st Section. For $-F_M \le F \le F_p$.

$$B_1=\frac{1}{R_{\text{н}}-R_{\text{в}}}\int\limits_{R_{\text{в}}}^{R_{\text{н}}}\left\{-\frac{b_p}{F_s-F_p}\left(F_{\text{м}}\frac{R_{\text{в}}}{R}-F_p\right)+\right.$$
$$\left.+\operatorname{tg}\delta\left[F\frac{R_{\text{в}}}{R}-\frac{F_p}{F_s-F_p}\left(F_{\text{м}}\frac{R_{\text{в}}}{R}-F_p\right)\right]\right\}dR.$$

After solving this equation, we shall have

$$B_1=-\frac{b_p}{F_s-F_p}\left[\frac{\ln\alpha}{\alpha-1}F_{\text{м}}-F_p\right]+$$
$$+\operatorname{tg}\delta\left[\frac{\ln\alpha}{\alpha-1}F-\frac{F_p}{F_s-F_p}\left(\frac{\ln\alpha}{\alpha-1}F_{\text{м}}-F_p\right)\right]. \qquad (31)$$

2nd Section. For $F_p \le F \le \alpha F_p$.

$$B_2=\frac{1}{R_{\text{н}}-R_{\text{в}}}\int\limits_{R_{\text{в}}}^{R}\left\{\frac{b_p}{F_s-F_p}\left[(2F-F_{\text{м}})\frac{R_{\text{в}}}{R}-F_p\right]+\right.$$
$$+\operatorname{tg}\delta\left[\frac{F_s+F_p}{F_s-F_p}F\frac{R_{\text{в}}}{R}-\frac{F_p}{F_s-F_p}\left(F_{\text{м}}\frac{R_{\text{в}}}{R}+F_p\right)+\right.$$
$$+\frac{1}{R_{\text{н}}-R_{\text{в}}}\int\limits_{R}^{R_{\text{н}}}\left\{-\frac{b_p}{F_s-F_p}\left(F_{\text{м}}\frac{R_{\text{в}}}{R}-F_p\right)+\right.$$
$$\left.+\operatorname{tg}\delta\left[F\frac{R_{\text{в}}}{R}-\frac{F_p}{F_s-F_p}\left(F_{\text{м}}\frac{R_{\text{в}}}{R}-F_p\right)\right]\right\}dR,$$

where $R = R_BF/F_p$.

By solving this equation, we obtain

$$B_2=\frac{1}{\alpha-1}\frac{b_p}{F_s-F_p}\Big[2F\left(\ln\frac{F}{F_p}-1\right)-$$
$$-F_{\text{м}}\ln\alpha+F_p(\alpha+1)\Big]+$$
$$+\frac{\operatorname{tg}\delta}{\alpha-1}\frac{1}{F_s-F_p}\Big[F(F_s-F_p)\ln\alpha+ \qquad (32)$$
$$+2F\left(\ln\frac{F}{F_p}-1\right)-F_{\text{м}}F_p\ln\alpha+F^2_p(\alpha+1)\Big].$$

3rd Section. For $\alpha F_p \le F \le F_M$.

$$B_3=\frac{1}{R_{\text{н}}-R_{\text{в}}}\int\limits_{R_{\text{в}}}^{R_{\text{н}}}\left\{\frac{b_p}{F_s-F_p}\left[(2F-F_{\text{м}})\frac{R_{\text{в}}}{R}-F_p\right]+\right.$$
$$\left.+\operatorname{tg}\delta\left[\frac{F_s+F_p}{F_s-F_p}F\frac{R_{\text{в}}}{R}-\frac{F_p}{F_s-F_p}\left(F_{\text{м}}\frac{R_{\text{в}}}{R}+F_p\right)\right]\right\}dR.$$

By solving this equation, we obtain

$$B_3=\frac{b_p}{F_s-F_p}\left[\frac{\ln\alpha}{\alpha-1}(2F-F_{\text{м}})-F_p\right]+ \qquad (33)$$
$$+\operatorname{tg}\delta\left[\frac{F_s+F_p}{F_s-F_p}\frac{\ln\alpha}{\alpha-1}F-\frac{F_p}{F_s-F_p}\left(\frac{\ln\alpha}{\alpha-1}F_{\text{м}}+F_p\right)\right].$$

4th Section. For $-F_p \le F \le F_M$.

$$B_4=\frac{1}{R_{\text{н}}-R_{\text{в}}}\int\limits_{R_{\text{в}}}^{R_{\text{н}}}\left\{\frac{b_p}{F_s-F_p}\left(F_{\text{м}}\frac{R_{\text{в}}}{R}-F_p\right)+\right.$$
$$\left.+\operatorname{tg}\delta\left[F\frac{R_{\text{в}}}{R}+\frac{F_p}{F_s-F_p}\left(F_{\text{м}}\frac{R_{\text{в}}}{R}-F_p\right)\right]\right\}dR.$$

After solving this equation, we obtain

$$B_4=\frac{b_p}{F_s-F_p}\left[\frac{\ln\alpha}{\alpha-1}F_{\text{м}}-F_p\right]+ \qquad (34)$$
$$+\operatorname{tg}\delta\left[\frac{\ln\alpha}{\alpha-1}F+\frac{F_p}{F_s-F_p}\left(\frac{\ln\alpha}{\alpha-1}F_{\text{м}}-F_p\right)\right]$$

The mathematical expression for the descending branch of this type of symmetric magnetization reversal loops is determined in a similar manner.

c) First Type of Symmetric Magnetization Reversal Loops ($F_p < F_M \le \alpha F_p$).

In order to determine the $B = f(F)$ dependence for this type of magnetization reversal loops, we shall substitute Eqs. (16)-(19) in Eq. (8), which was borrowed from [3]. In dependence on the values F of magnetizing ampere-turns, the symmetric magnetization reversal loops will have different functional sections.

1st Section. For $-F_M \le F \le F_p$,

$$B_1 = \frac{1}{R_{\text{н}} - R_{\text{в}}} \int\limits_{R}^{R_1} \left\{ -\frac{b_p}{F_s - F_p}\left[F_{\text{м}} \frac{R_{\text{в}}}{R} - F_p\right] + \right.$$

$$\left. + \operatorname{tg}\delta\left[F\frac{R_{\text{в}}}{R} - \frac{F_p}{F_s - F_p}\left(F_{\text{м}}\frac{R_{\text{в}}}{R} - F_p\right)\right]\right\} dR +$$

$$+ \frac{1}{R_{\text{н}} - R_{\text{в}}} \int\limits_{R_1}^{R_{\text{н}}} \operatorname{tg}\delta\, F\, \frac{R_{\text{в}}}{R}\, dR,$$

where $R_1 = R_B F_M / F_p$.

By solving this equation, we obtain

$$B_1 = -\frac{1}{\alpha - 1}\frac{b_p}{F_s - F_p}\left[F_{\text{м}}\left(\ln\frac{F_{\text{м}}}{F_p} - 1\right) + F_p\right] +$$

$$+ \frac{\operatorname{tg}\delta}{\alpha - 1}\left\{F \ln\alpha - \frac{F_p}{F_s - F_p}\left[F_{\text{м}}\left(\ln\frac{F_{\text{м}}}{F_p} - 1\right) + F_p\right]\right\}. \tag{35}$$

2nd Section. For $F_p \le F \le F_M$,

$$B_2 = \frac{1}{R_{\text{н}} - R_{\text{в}}}\int\limits_{R_{\text{в}}}^{R}\left\{\frac{b_p}{F_s - F_p}\left[(2F - F_{\text{м}})\frac{R_{\text{в}}}{R} - F_p\right] + \right.$$

$$\left. + \operatorname{tg}\delta\left[\frac{F_s + F_p}{F_s - F_p} F \frac{R_{\text{в}}}{R} - \frac{F_p}{F_s - F_p}\left(F_{\text{м}}\frac{R_{\text{в}}}{R} + F_p\right)\right]\right\} dR +$$

$$+ \frac{1}{R_{\text{н}} - R_{\text{в}}}\int\limits_{R}^{R_1}\left\{-\frac{b_p}{F_s - F_p}\left[F_{\text{м}}\frac{R_{\text{в}}}{R} - F_p\right] + \operatorname{tg}\delta\left[F\frac{R_{\text{в}}}{R} - \right.\right.$$

$$\left.\left. - \frac{F_p}{F_s - F_p}\left(F_{\text{м}}\frac{R_{\text{в}}}{R} - F_p\right)\right]\right\} dR + \frac{1}{R_{\text{н}} - R_{\text{в}}}\int\limits_{R_1}^{R_{\text{н}}} \operatorname{tg}\delta\, F \frac{R_{\text{в}}}{R}\, dR,$$

where $R = R_B F/F_p$, $R_1 = R_B F_M / F_p$.

After solving this equation, we obtain

$$B_2 = \frac{1}{\alpha - 1}\frac{b_p}{F_s - F_p}\left[2F\left(\ln\frac{F}{F_p} - 1\right) + \right.$$

$$\left. + F_{\text{м}}\left(1 - \ln\frac{F_{\text{м}}}{F_p}\right) + F_p\right] +$$

$$+ \frac{\operatorname{tg}\delta}{\alpha - 1}\frac{1}{F_s - F_p}\left[F\left(F_s - F_p\right)\ln\alpha + \right. \tag{36}$$

$$\left. + 2FF_p\left(\ln\frac{F}{F_p} - 1\right) + F_{\text{м}}\left(1 + \ln\frac{F_{\text{м}}}{F_p}\right)F_p + F_p^2\right]$$

3rd Section. For $-F_p \le F \le F_M$,

$$B_3 = \frac{1}{R_{\text{н}} - R_{\text{в}}}\int\limits_{R_{\text{в}}}^{R_1}\left\{\frac{b_p}{F_s - F_p}\left[F_{\text{м}}\frac{R_{\text{в}}}{R} - F_p\right] + \right.$$

$$\left. + \operatorname{tg}\delta\left[F\frac{R_{\text{в}}}{R} + \frac{F_p}{F_s - F_p}\left(F_{\text{м}}\frac{R_{\text{в}}}{R} - F_p\right)\right]\right\} dR +$$

$$+ \frac{1}{R_{\text{н}} - R_{\text{в}}}\int\limits_{R_1}^{R_{\text{н}}} \operatorname{tg}\delta\, F\frac{R_{\text{в}}}{R}\, dR,$$

where $R_1 = R_B F_M / F_p$.

By solving this equation, we obtain

$$B_3 = \frac{1}{\alpha - 1}\frac{b_p}{F_s - F_p}\left[F_{\text{м}}\left(\ln\frac{F_{\text{м}}}{F_p} - 1\right) + F_p\right] + \frac{\operatorname{tg}\delta}{\alpha - 1}\left\{F\ln\alpha + \right.$$

$$\left. + \frac{F_p}{F_s - F_p}\left[F_{\text{м}}\left(\ln\frac{F_{\text{м}}}{F_p} - 1\right) + F_p\right]\right\}. \tag{37}$$

The mathematical expression for the descending branch of this type of symmetric magnetization reversal loops is determined in a similar manner.

d) Normal Magnetization Curve

For determining the mathematical expressions for the "normal magnetization curve, Eqs. (20)-(22) must be substituted in Eq. (8) from [3]. In dependence on the value of F_M, the "normal magnetization curve" will have functional sections.

Zero Section. For $0 \le F_M \le F_p$,

$$B_0 \max = \frac{1}{R_{\text{н}} - R_{\text{в}}}\int\limits_{R_{\text{в}}}^{R_{\text{н}}} \operatorname{tg}\delta\, F_{\text{м}}\frac{R_{\text{в}}}{R}\, dR.$$

By solving this equation, we obtain

$$B_0 \max = \operatorname{tg}\delta\,\frac{\ln\alpha}{\alpha - 1}\, F_{\text{м}}. \tag{38}$$

1st Section. For $F_p \le F_M \le \alpha F_p$,

$$B_1 \max = \frac{1}{R_{\text{н}} - R_{\text{в}}}\left\{\int\limits_{R_{\text{в}}}^{R}\left[\frac{b_p}{F_s - F_p}\left(F_{\text{м}}\frac{R_{\text{в}}}{R} - F_p\right) + \right.\right.$$

$$\left.\left. + \frac{\operatorname{tg}\delta}{F_s - F_p}\left(F_s F_{\text{м}}\frac{R_{\text{в}}}{R} - F_p^2\right)\right] dR + \int\limits_{R}^{R_{\text{н}}} \operatorname{tg}\delta\, F_{\text{м}}\frac{R_{\text{в}}}{R}\, dR\right\},$$

where $R = R_B F_M / F_p$.

By solving this equation, we obtain

$$B_1 \max = \frac{1}{\alpha - 1}\frac{b_p}{F_s - F_p}\left[F_{\text{м}}\left(\ln\frac{F_{\text{м}}}{F_p} - 1\right) + F_p\right] +$$

$$+ \frac{1}{\alpha - 1}\frac{\operatorname{tg}\delta}{F_s - F_p}\left[F_{\text{м}}F_p\left(\ln\frac{F_{\text{м}}}{F_p} - 1\right) + F_{\text{м}}(F_s - F_p)\ln\alpha + F_p^2\right]. \tag{39}$$

2nd Section. For $\alpha F_p \le F_M \le F_s$,

$$B_2 \max = \frac{1}{R_{\text{н}} - R_{\text{в}}}\int\limits_{R_{\text{г}}}^{R_{\text{н}}}\left[\frac{b_p}{F_s - F_p}\left(F_{\text{м}}\frac{R_{\text{в}}}{R} - F_p\right) + \right.$$

$$+\frac{\operatorname{tg}\delta}{F_s-F_p}\left(F_sF_{\text{M}}\frac{R_{\text{B}}}{R}-F_p^2\right)\right]dR.$$

By solving this equation, we obtain

$$B_{2}\max=\frac{b_p}{F_s-F_p}\left[\frac{\ln\alpha}{\alpha-1}F_{\text{M}}-F_p\right]+ \qquad (40)$$

$$+\frac{\operatorname{tg}\delta}{F_s-F_p}\left[\frac{\ln\alpha}{\alpha-1}F_sF_{\text{M}}-F_p^2\right].$$

3rd Section. For $F_s \le F_M \le \alpha F_s$.

$$B_{3\max}=\frac{1}{R_{\text{H}}-R_{\text{B}}}\left\{\int\limits_{R_{\text{B}}}^{R}\left[b_p+\operatorname{tg}\delta\left(F_{\text{M}}\frac{R_{\text{B}}}{R}+F_p\right]dR+\right.\right.$$

$$+\int\limits_{R}^{R_{\text{H}}}\left[\frac{b_p}{F_s-F_p}\left(F_{\text{M}}\frac{R_{\text{B}}}{R}-F_p\right)+\right.$$

$$\left.\left.+\frac{\operatorname{tg}\delta}{F_s-F_p}\left(F_sF_{\text{M}}\frac{R_{\text{B}}}{R}-F_p^2\right)\right]dR\right\},$$

where $R = R_BF_M/F_s$.

By solving this equation, we obtain

$$B_{3}\max=\frac{1}{\alpha-1}\frac{b_p}{F_s-F_p}\times \qquad (41)$$

$$\times\left[F_{\text{M}}\left(1+\ln\frac{\alpha F_s}{F_{\text{M}}}\right)-F_s-F_p(\alpha-1)\right]+\frac{1}{\alpha-1}\frac{\operatorname{tg}\delta}{F_s-F_p}\times$$

$$\times\left[F_{\text{M}}\left(F_s-F_p\right)\ln\alpha+F_{\text{M}}F_p\left(1+\ln\frac{\alpha F_s}{F_{\text{M}}}\right)-F_sF_{\text{M}}-F_p^2(\alpha-1)\right].$$

4th Section. For $\alpha F_s \le F_M$.

$$B_{4}\max=\frac{1}{R_{\text{H}}-R_{\text{B}}}\int\limits_{R_{\text{B}}}^{R_{\text{H}}}\left[b_p+\operatorname{tg}\delta\left(F_{\text{M}}\frac{R_{\text{B}}}{R}+F_p\right)\right]dR.$$

By solving this equation, we obtain

$$B_{4}\max=b_p+\operatorname{tg}\delta\left[\frac{\ln\alpha}{\alpha-1}F_{\text{M}}+F_p\right]. \qquad (42)$$

LITERATURE CITED

1. R. W. Roberts and R. J. Van Nice, "Influence of ID/OD ratio on static and dynamic properties of toroidal cores," Trans. AIME 74, pt. 1 (1955).
2. M. A. Rozenblat, "Dependence of static characteristics of toroidal cores on their dimensions," Avtomatika i Telemekhanika 19, 8 (1958).*
3. G. D. Kozlov, "Effect of magnetization irregularity on the static characteristics of cores," Avtomatika i Telemekhanika 21, 1 (1960).*
4. J. A. Rajchman, and A. W. Lo, "The transfluxor," Proc. IRE 44 (March, 1956).
5. H. W. Abbott and J. J. Suran, "Multihole ferrite core configurations and applications," Proc. IRE 45 (August, 1957).

---

*See English translation.

A TRANSISTORIZED MAGNETIC AMPLIFIER*

R. A. Lipman and M. V. Ol'shvang

Moscow

Translated from Avtomatika i Telemekhanika, Vol. 21, No. 7, pp. 1073-1083, July, 1960

Original article submitted December 18, 1959

This article deals with a transistorized magnetic amplifier, which works as a continuously controlled switch and is based on a pulse-width modulated relaxation-oscillator. The theoretical analysis of the circuit is provided, and experimental results are quoted.

When a transistor (T) is operated as a switch, it becomes possible to make it much more efficient, i.e., to raise the ratio between the power dissipated in the load and that in the transistor. Thus, the output power of the transistor amplifier can be greatly increased.

The switching operation of the transistor is widely used in amplifiers with a continuous input – output characteristic, as well as in purely relay circuits. In the former case, the transistor is periodically switched, and the continuous variation of the mean value of the output power is attained by changing the relative duration of the open-circuited condition of the transistor (in a manner similar to a thyratron or relay-contact amplifier with a continuous control).

There are many circuits which provide a continuously controlled switching operation of the transistor [1-7 and others]. In the majority of them, the control of power transistors is accomplished by means of some type of pulse-width modulation, which transforms the variations in the signal strength into aproportional change in the relative duration of the pulse.

The special characteristic of the circuit proposed by Morgan [7] is the combination of the functions of a power amplifier with those of a pulse-width modulator. Moreover, the power transistor which controls the power in the load also serves as an amplifier for the oscillator with the pulse-width modulation.

The Morgan circuit (Fig. 1a) is based on a blocking-oscillator with a series overloading transformer. The feedback transformer (FBT) has a working winding w_o which is connected in series with the load impedance R_l and L_l, a return winding w_r which is connected in parallel with the emitter-collector circuit through a large building-out resistor R_b (a small resistor r_b serves to supply the bias for the emitter) and a feedback winding w_f connected in the base circuit. When the feedback current i_f is positive (Fig. 1a), the transistor is conducting, and the feedback circuit is completed through the emitter circuit of T (rectifier B_c is then blocked). When $i_f < 0$, the transistor becomes blocked, and the feedback circuit is completed through rectifier B_c and the adjustable resistor R_c.

Windings w_o and w_r have only a few turns; moreover, the resistance of the feedback circuit (both for the conducting and blocked conditions of the transistor), which is connected to windings w_o and w_r, is considerably smaller than resistances R_l and R_b. Hence, the FBT works as a current transformer, i.e., the value of the collector current i_{co} and of the return current i_r are practically independent of the feedback resistance. The value of that resistance only affects the speed of the inductance variations in the core of the FBT.

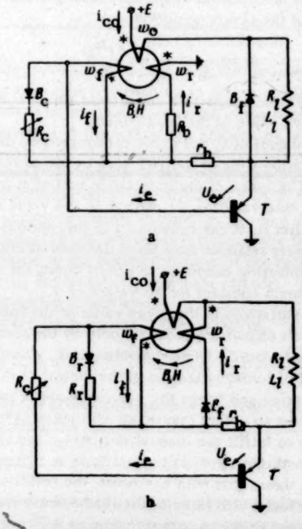

Fig. 1.

***From a paper read at the All-Union Seminar on Magnetic Components in Automation and Computers on October 13, 1959.**

Under certain conditions the circuit in Fig. 1a becomes self-oscillating. The oscillations are discontinuous, each cycle consisting of two distinct periods: a) a period when the transistor is completely conducting (both junctions being biased in the forward direction), the load voltage is near to that of the supply, the return current approaches zero, and the speed of the inductance variations in the core of the FBT is positive and is determined by the value of the load current; b) a period when the transistor is blocked (both junctions are biased in the reversed direction), the voltage across the load and the collector current approach zero, the return current is maximum and the speed of the inductance variations of the FBT core are negative and are determined by the value of the return current and of resistance R_c. The transition from one period to the other is caused by the saturation of the core and is short compared with the period of oscillations.

Moreover, owing to the existence of the feedback rectifier B_f, which shunts the load during the reversing period, the mean value of the load current I_l will equal, irrespectively of the value of L_l,

$$I_l = \frac{E}{R_l}\,\frac{t_o}{t_o + t_r} = \frac{E}{R_l}\gamma, \tag{1}$$

where t_o is the duration of the operation period, t_r the duration of the reversing period, and

$$\gamma = \frac{t_o}{t_o + t_r} = \frac{I_l R_l}{E} \tag{1a}$$

is the transistor conduction coefficient which is equal to the relative value of the load current.

The values of t_o and t_r are determined by the remagnetization time of the FBT core in the corresponding period. The speed of the inductance variation in the operating interval does not depend on the value of R_c (the rectifier B_c is not conducting in this period). Hence, with a purely resistive load, when the load current is equal in the conducting condition to E/R_l = const, the value of t_o will remain constant for all values of γ.

The variations in the mean value of the load current in Morgan's circuit are provided only by the changes in the reversing time. When the value of R_c is increased, the speed of remagnetization of the core rises in the reversing period, and hence, the value of t_r decreases.†

In order to obtain maximum efficiency ($\gamma \approx 1$), it is necessary to fulfill the inequality $t_r \ll t_o$; and in the unloaded condition ($\gamma \ll 1$) inequality $t_r \gg t_o$ must hold. It can be shown that with t_o = const, the reversing time variation factor is related to the load current variations factor k_I and to the maximum value of the conduction coefficient γ_{max} by means of the following equation:

$$\frac{t_{r\,max}}{t_{r\,min}} = k_I\,\frac{1 - \gamma_{max}/k_I}{1 - \gamma_{max}}. \tag{2}$$

For instance, for $k_I = 10$ and $\gamma_{max} = 0.9$, it is necessary to provide a $t_{r\,max}/t_{r\,min} \approx 90$, i.e., the adjustable core remagnetization factor must be considerably larger than the load current variations factor.

From (1) and the condition that t_o = const, it follows that the range of the oscillating frequency f variations will be equal to

$$\frac{f_{max}}{f_{min}} = k_I = \frac{I_{l\,max}}{I_{l\,max}}. \tag{3}$$

The large variation ranges of the adjustable remagnetization time and the oscillation frequency are the important defects of the circuit in Fig. 1a, which lead to the impossibility of obtaining a large amplifier output-current variations factor. The above defect becomes worse with an inductive load. For a constant base circuit resistance, the core remagnetization time with a nonconducting transistor is in the first approximation inversely proportional to the mean value of the load current during the operation period. Providing the time constant of the load is sufficiently large, the mean value of the current i_l for time t_o is close to the mean value of the load current I_l for the whole cycle.

Thus, for an inductive impedance load, the duration of the operational period will no longer remain constant, but will change approximately in inverse proportion to the mean value of the load current:

$$t_o \equiv \frac{1}{I_l}. \tag{4}$$

From (4) and (1) we obtain the following expressions for the reversing time variation factor and the self-oscillation frequency:

$$\frac{t_{r\,max}}{t_{r\,min}} = k_I^2\,\frac{1 - \gamma_{max}/k_I}{1 - \gamma_{max}}, \tag{2a}$$

$$\frac{f_{max}}{f_{min}} = k_I^2. \tag{3a}$$

For instance, in order to obtain $k_I = 10$ and $\gamma_{max} = 0.9$, it is necessary to make $t_{r\,max}/t_{r\,min} \approx 900$ and $f_{max}/f_{min} = 100$, which it is impossible to attain in practice.

The above defect can be overcome if Morgan's circuit is altered as shown in Fig. 1b. The difference between the circuits of Figs. 1a and 1b consists of the following: The control of the speed of core remagnetization is attained in the operation interval (with a conducting transistor); for this purpose the adjustable resistance R_c is connected in the base circuit in series with the feedback winding. Moreover, the demagnetization of the core in the reversing interval is accomplished by means of the load current which flows through the reversed rectifier; for this purpose the return winding is connected in series with the reversed rectifier B_f.

---

† A photovaristor, magnetic amplifier, etc., can be used as a controlled resistance R_c.

Thus, a decrease in the adjustable resistance R_c leads to a slowing down of the core remagnetization in the operation period, and hence, to a rise in t_o. Moreover, the load current increases. The rise in the load current automatically leads to a decrease in time t_r, since current i_r, which remagnetizes the core, is equal to the load current in the reversing interval. Thus, although the control signal affects directly only the duration t_o of the transistor's conducting condition, the circuit automatically changes the duration t_r of the nonconducting condition. Moreover, for a rising t_o the value of t_r decreases, and vice versa.

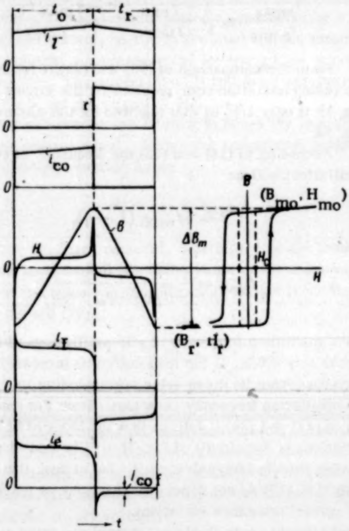

Fig. 2.

In order to obtain quantitative relations, let us examine the working of the circuit in Fig. 1b under the condition that the time constant of the load is sufficiently large compared with the period of oscillations. Moreover, let us assume that the current during this period remains practically constant (the instantaneous and mean values of the current coincide).

Diagrams of the changes in variables of Fig. 1b circuit are shown in Fig. 2. During the operation period, the transistor is conducting and the return current is zero (rectifier B_f is nonconducting), the collector current is equal to that of the load, the feedback current is positive and runs through the adjustable resistance R_c and the base of the transistor (rectifier B_r is nonconducting). The value of the feedback current, which is the same as that of the base, is obtained from equation

$$i_f = i_e = I_f \frac{w_o}{w_f} - \frac{Hl_m}{w_f} > \frac{I_l}{\beta}, \qquad (5)$$

where H is the field strength in the core, l_m is the length of the mean line of force, β is the current gain coefficient of the transistor for $U_{co} = 0$ and $i_{co} = I_l$. The fulfillment of inequality (5) provides a conducting condition for the transistor. The speed of the core inductance variations is determined by the expression

$$w_f S_c \frac{dB}{dt} = i_f (R_r + r_e + r_f + r_b), \qquad (6)$$

where S_c is the cross-sectional area, r_e the emitter-base impedance of a conducting transistor, r_f the resistance of the feedback winding, and r_b the biasing resistance.

The inductance of the core increases with a speed determined by the expression (6), and its magnetic condition varies according to the rising portion of the hysteresis loop (Fig. 2). When the core becomes saturated, the field strength rises rapidly, and the feedback current decreases according to (5). When the field strength reaches a certain value

$$H = H_{mo} = \frac{I_l w_o}{l_m}\left(1 - \frac{w_f}{\beta w_o}\right), \qquad (7)$$

inequality (5) no longer holds, i.e., the transistor passes from the saturated condition to an active condition. This leads to an avalanche decrease in the base current (see Appendix); at the end of this process, the transistor becomes blocked, the voltage across the load drops almost to zero, the current in the load is completed through the reversed rectifier B_f and the return winding ($i_r = I_l$), and the feedback current changes its sign and flows through circuit B_r, R_r (a small portion of the feedback current equal to the reversed current of the collector junction I_{cr} branches off to the base circuit). Thus, the reversing period is initiated.

The feedback current is then equal to

$$i_f = -i_r \frac{w_r}{w_f} - \frac{Hl_m}{w_f} = -I_l \frac{w_r}{w_f} - \frac{Hl_m}{w_f}, \qquad (8)$$

and the speed of the inductance variations is determined from the equation

$$w_f S_c \frac{dB}{dt} = i_f (R_r + r_f + r_r) \approx i_f R_f < 0, \qquad (9)$$

where r_r is the forward resistance of the rectifier B_r ($r_f + r_r \ll R_r$). The emitter receives a negative voltage

$$U_e = -\left(I_l \frac{w_r}{w_f} + \frac{Hl_m}{w_f}\right) R_r + I_l r_b < 0, \qquad (10)$$

thus ensuring a blocking of the transistor in the reversing period.

The inductance of the core decreases with a speed determined by the expression (9), and its magnetic condition changes according to the descending portion of the hysteresis loop (Fig. 2). When the core becomes saturated in the negative direction, the field strength rises rapidly, and the value of the voltage (10) which blocks the transistor decreases (H < 0).

When the field strength reaches the value

$$H = H_{mr} = -\frac{I_l w_r}{l_m}\left(1 - \frac{r_b w_o}{R_r w_r}\right), \tag{11}$$

inequality (10) no longer holds, and the transistor passes to an active state. This produces an avalanche breakdown of the transistor (see Appendix) and at the end of the process, an operational period is again reestablished.

Let us determine the values of t_r and t_o and the frequency of self-oscillations. By integrating Equation (9) in conjunction with (8) in the limits of B_{mo} and B_{mr}, we obtain:

$$t_r = \frac{1}{R_r}\left(\frac{w_f^2 \Delta\Phi_m + QR_r}{I_l w_r - H_c l_m}\right), \tag{12}$$

where $\Delta\Phi_m = S_c(B_{mo} - B_{mr}) = S_c \Delta B_m$ is the full variation of the flux in the core and H_c is the coercive force of the static hysteresis loop, and

$$Q = l_m \int_0^{t_r} (H - H_c)\,dt = Q(\Delta\Phi_m) \tag{13}$$

is the so-called switching coefficient of the core.

Normally, $H_c l_m \ll I_l w_r$; moreover,

$$t_r \approx \frac{1}{I_l}\left(\frac{w_f^2 \Delta\Phi_m + QR_r}{R_r w_r}\right). \tag{12a}$$

For magnetic materials with a high degree of saturation, the values of B_{mo} and B_{mr} depend to a small degree only on H_{mo} and H_{mr}; it is therefore possible to consider approximately that $\Delta\Phi_m$ and Q do not depend on the load current and are determined only by the dimensions and the material of the core. Moreover, the reversing time will, according to (12a), change inversely proportionately to the load current.

From (1) and (12a) we can obtain the following expressions for t_r and t_o:

$$t_r = \frac{(w_f^2 \Delta\Phi_m + QR_r)\, R_l}{w_r E R_r}\,\frac{1}{\gamma}, \tag{14}$$

$$t_o = \frac{(w_f^2 \Delta\Phi_m + QR_r)\, R_l}{w_r E R_r}\,\frac{1}{1-\gamma}. \tag{15}$$

It follows from (15) that variation of the core remagnetization controlled time factor in the circuit of Fig. 1b is equal to

$$\frac{t_{p\,max}}{t_{p\,min}} = \frac{1-\gamma_{min}}{1-\gamma_{max}} = \frac{1-\gamma_{max}/k_I}{1-\gamma_{max}}. \tag{16}$$

From the comparison of (26) and (2a), it follows that the remagnetization time required for the circuit in Fig. 1b is only $1/k_I^2$ of that required for the circuit of Fig. 1a.

According to (14) and (15), the frequency of self-oscillations will be

$$f = 4 f_{max}\gamma(1-\gamma), \tag{17}$$

where

$$f_{max} = \frac{w_r R_r E}{4R_l(w_f^2 \Delta\Phi_m + QR_r)} \tag{18}$$

is the maximum frequency of self-oscillations which occurs at $\gamma = 0.5$. If the load current is increased or decreased from its mean value corresponding to $\gamma = 0.5$, the oscillation frequency decreases. From the comparison of (17) and (3a), it follows that the range of frequency variations in the circuit of Fig. 1b will be considerably smaller than in Morgan's circuit. Let us note that relations (14)-(17) do not depend on the value or nature of the control resistance variations.

Different controllable resistances can serve as R_c. Fig. 3 shows an amplifier circuit, of the type found in

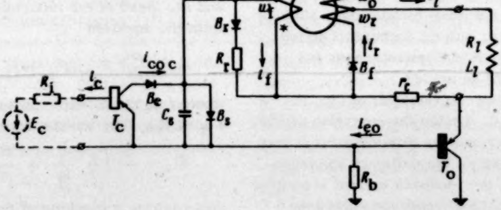

Fig. 3.

Fig. 1b, in which a transistor T_c is used as the controlled variable R_c. Rectifier B_e prevents the blocking of the operational transistor T_o by the control signal. The shunting rectifier B_s provides a path for the return current of the collector junction of the operational transistor T_o during the reversing period. The capacitance C_s improves the switching conditions and raises the stability of the oscillations. Resistor R_b provides a small initial positive bias for the operational transistor, thus helping the starting of oscillations (providing conditions of "soft" self-excitation).

The control signal (source of emf E_c with an internal resistance R_i) is fed to the input of the controlling transistor. A rising control signal decreases the static output resistance of T_c thus leading to an increase in the duration of the operational period t_o, and hence, to a rise in the load current. A rise in the load current automatically involves a decrease in the reversing time according to (12a). Equations (14)-(17) and the diagrams in Fig. 2 hold for the circuit of Fig. 3.

Let us examine the relation between the load current and the control signal. During the operational period, the following equation holds:

$$i_f = i_{eo} = i_{coc}. \qquad (19)$$

The feedback current is determined by the load current according to (5); if the value of the magnetizing current is neglected, the following relation is obtained from (5) and (19):

$$I_l = \frac{w_f}{w_b} I_{eo} = \frac{w_f}{w_o} I_{coc} \qquad (20)$$

Thus, in the above circuit there is a close relation between the load and the collector currents in the controlling transistor, which is determined by the transformation coefficient of the FBT and does not depend on the characteristics of the transistors, the resistance of the load, or the supply voltage.

The relation between the collector current of the controlling transistor and the controlling signal is determined by the T_c transistor characteristic. If the collector reaction is neglected, the following relation will hold:

$$I_{co\,c} = \varphi_1(E_c, R_i) \qquad (21)$$

or

$$I_{co\,c} = \varphi_2(I_c). \qquad (21a)$$

Equations (20) and (21) determine the transmission characteristic of the amplifier as a whole. This characteristic is a reproduction of the controlling transistor characteristic with its current gain amplified by a factor of $n = w_f/w_o$, and it does not depend on the values of E or R_l. A limitation is placed on the value of n by inequality (5), and the following condition must be observed for its fulfillment:

$$n = \frac{w_f}{w_b} < \beta_o \qquad (22)$$

i.e., the resulting current gain cannot exceed the products $\beta_c\beta_o$ (β_c and β_o are the current gains of transistors T_c and T_o).

Below we give the experimentally obtained characteristics of an amplifier assembled according to the diagram of Fig. 3.

Its circuit parameters are: core OL 14/17 – 3.5 – 0.05-79NM, $w_o = w_r = 20$, $w_f = 300$, $R_r = 60$ ohms, $r_b = 0.4$ ohms, $R_b = 100$ kilohms, $c_s = 0.02$ μf, T_o – P4B, T_c – P201, B_f – D303, B_b, B_s, and B_r – D7B.

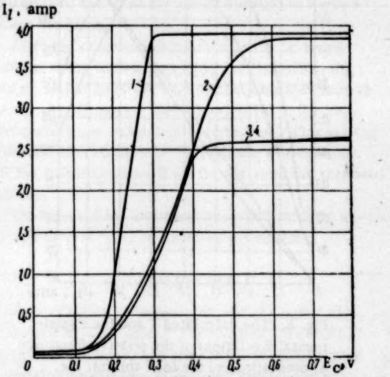

Fig. 4. Relation between the load current and the control signal emf. 1) R_l = 10 ohms, E = 45 v, R_i = 0; 2) R_l = 10 ohms, E = 45 v, R_i = 50 ohms; 3) R_l = 10 ohms, E = 30 v, R_i = 50 ohms; 4) R_l = 15 ohms, E = 45 v, R_i = 50 ohms. For all the curves, the value of L_l varies in the range of 0.2 to 8 h.

Figure 4 shows the relation between the load current and the control signal emf for various values of the supply voltage, the load resistance, and the internal resistance of the signal source. Over the operating portion of the characteristic, the load current is practically independent of the values of E and R_l, thus confirming the theoretical considerations. The power gain over the linear portion of the characteristics of curves 2, 3, and 4 is equal to $4R_lR_i(\Delta I_l/\Delta E_c)^2 = 3\cdot10^5$. The current ratio amounts to $k_I \approx 40$-50.

Figure 5 compares the calculated [from formula (17)], with the experimentally obtained, relation between the relative oscillation frequency and the load current. The experimental value of f_{max} = 1600 cps, and the value calculated from Eq. (18) is 2000 cps ($\Delta\Phi_m \approx 0.7\cdot10^{-5}$ v · sec, $Q \approx 0.5\cdot10^{-3}$ amp · sec). The maximum of the experimental characteristic 2 is displaced with respect to that of the calculated characteristic 1 in the direction of the lower currents. This is probably due to the fact that, by decreasing the load current, the value of $\Delta\Phi_m$ is slightly reduced, and hence, the value of f/f_{max} is increased. Due to this change, the range of the oscillation frequency variations becomes smaller than the calculated value. For instance, when the load current is changed from 4 to 0.4 amp ($k_I = 10$) the value of f varies only by a factor of 2. The switching time of the power transistor amounted to 20-40 μsec.

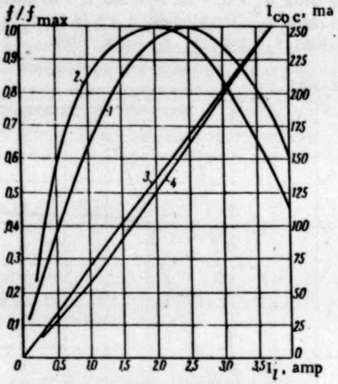

Fig. 5. The calculated 1 and the experimental 2 relations of the relative frequency of oscillations to the load current; the calculated 3 and the experimental 4 relations of the collector current of the controlling transistor to the load current.

Figure 5 shows the calculated and experimental relations of the mean collector current over time t_o of the controlling transistor to the load current, a relation which confirms expression (20). The experimental value of $I_{co\,c}$ was determined as the mean value of the current over one cycle divided by γ.

Figure 6 provides the over-all characteristic for various ambient temperatures and several samples of transistors T_o. The curves confirm the independence of the load current from the characteristic of the operating transistor, and show the relatively small effect of temperature on the curve $I_l = I_l(I_c)$.

It follows from the examination of Fig. 6a that variation of the ambient temperature in the range of -60°C to + 55°C is equivalent to a change in the emf of the input signal of $\Delta E_c \approx 0.25$ v. If the amplifier is used in a closed-loop control system, it is easy to provide conditions which would make the effect of this variation insignificant with respect to the accuracy of the system's operation. Let us assume, for instance, that the input of the amplifier receives a control signal from a measuring element of a voltage regulator, and that it is required to make the error of regulation due to the temperature drift of the amplifier less than 1% (± 0.5%) when the temperature varies in the range of - 60°C to + 55°C. In order to fulfill this requirement, it is obviously sufficient to make the sensitivity of the measuring device equal 0.25 v per 1% of the measured voltage. Such a sensitivity is possessed, for instance, by a measuring element consisting of a nonlinear bridge circuit with two reference diodes of the D813 type.

It is important to note that normal operating conditions and the measuring range of the output variable in the amplifier of Fig. 3 are preserved over a wide range of ambient temperatures.

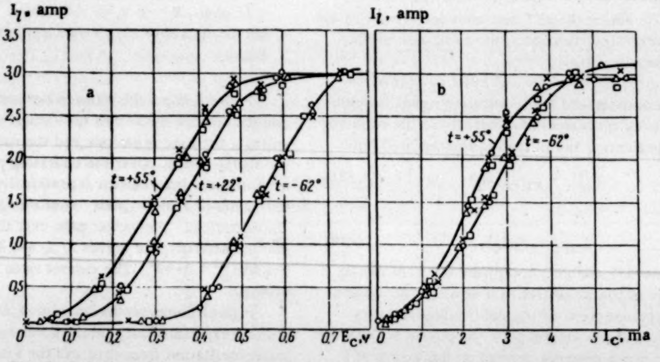

Fig. 6. Relation of the load current to the control signal emf a and to the control current b for various ambient temperatures; the experimental points correspond to various samples of transistors. E = 40 v, R_l = 10.5 ohms, R_i = 70 ohms.

On the basis of the results thus obtained, it is possible to make the following conclusions on the advantages of the Fig. 1b circuit (Fig. 3) as compared with Morgan's circuit:

1. Under similar conditions the Fig. 1b circuit requires a much smaller range of variations in the duration of the controlled core remagnetization time and a smaller variation of the frequency of oscillations. These factors raise considerably the stability of operation and provide a far larger ratio of load current variations.

2. The maximum oscillation frequency occurs in the circuit of Fig. 1b at $I_l \approx 0.5\,E/R_l$, and not at $I_l \approx E/R_l$, which is the maximum for the Fig. 1a circuit. Thus, the mean power loss in the transistor is decreased.

3. The over-all characteristic of the Fig. 3 circuit is stable with respect to supply voltage and load resistance variations.

APPENDIX

After the saturation of the core and the passing of the transistor to an active condition (see Fig. 1b circuit), the following equations will hold for small increments of the variables:

$$\begin{gathered}
\Delta i_{co} w_o - \Delta i_r w_r - \Delta i_f w_f = \Delta H l_m \\
\Delta i_{co} = -\Delta i_r \ (i_{co} + i_r = I_l = \mathrm{const}), \\
\Delta i_e = \Delta i_f = \frac{w_f S_c}{R_f} \frac{d\Delta B}{dt}, \\
\Delta B = \mu_S \Delta H, \\
\tau_\beta \frac{di_{co}}{dt} + \Delta i_{co} = \beta \Delta i_e .
\end{gathered} \qquad \text{(A1)}$$

where R_f is the impedance of the transistor base circuit, τ_β is the time constant of transistor T, μ_S is the permittivity of the "saturated" core.

Solving the family of equations (A1) with respect to the increment of the base current, we have

$$\Delta i_e \{p^2 \tau_\mu \tau_\beta - p\,[(b-1)\,\tau_\mu - \tau_\beta] + 1\} = 0, \qquad \text{(A2)}$$

where

$$\tau_\mu = \frac{w_0^2 S_c \mu_S}{R_f l_m}, \quad b = \frac{\beta\,(w_o + w_r)}{w_f}, \quad p \equiv \frac{d}{dt}. \qquad \text{(A3)}$$

The solution of (A2) with initial conditions of $\Delta i_e(0) = 0$ and $(d\Delta i_e/dt)(0) = \epsilon$ gives

$$\Delta i_e = \frac{\epsilon}{p_1 - p_2} (e^{p_1 t} - e^{p_2 t}). \qquad \text{(A4)}$$

where p_1 and p_2 are the roots of the characteristic equation which corresponds to equation (A2). If condition

$$b = \beta \frac{w_p + w_r}{w_f} > 1 + \frac{\tau_\beta}{\tau_\mu}, \qquad \text{(A5)}$$

is fulfilled, both roots p_1 and p_2 will have a positive real component, and the measuring of the current will be unstable.

After the saturation of the core in the operating period at the instant when inequality (5) no longer holds, the speed of the base current variations is negative ($\epsilon < 0$). At that instant an avalanche decrease in the base current expressed by relation (A4) will therefore begin if condition (A5) is fulfilled. This process will continue until the transistor passes from an active to a blocked condition.

After the saturation of the core in the reversing condition at the instant inequality (10) is broken, the speed of variations of the base current becomes positive ($\epsilon > 0$). At this instant an avalanche rise in the base current will begin according to expression (A4), providing condition (A5) is fulfilled. This process will continue until the transistor passes from the active to the saturated condition.

Thus, providing condition (A5) is fulfilled, the circuit will be in a state of sustained oscillations.

LITERATURE CITED

1. H. W. Collins, "Magnetic Amplifier Control of Switching Transistors," Trans. AIME 75 (1959).
2. V. G. Konstantinov, "A transistorized amplifier for controlling dynamo excitation" Vestnik Élektropromyshlennosti 1 (1959).
3. Yu. A. Konev, Functional pulse converters," Collection: Transistor Instruments and Their Application [in Russian] (Izd. Sovetskoe Radio, 1958).
4. O. A. Kossov, "Operation of a semiconductor switch with various load characteristics," Élektrichestvo 5 (1959).
5. O. A. Kossov, "Crystal-magnetic amplifier," Avtomat. i Telemekh. 20, 7 (1959).‡
6. L. L. Setyukov and N. N. Rukovishnikov, "Transistorized power amplifiers. Scientific papers at high schools," Radiotekhnika i Élektronika 3 (1958).
7. R. E. Morgan, "A new control amplifier using a saturable current transformer and a switching transistor," Communication and Electronics 39 (1958).

---

‡ See English translation.

A NEW METHOD OF SPECTRAL MEASUREMENTS BY MEANS OF PHOTOSENSITIVE LAYERS

W. Lueck

Berlin

Translated from Avtomatika i Telemekhanika, Vol. 21, No. 7, pp. 1084-1087, July, 1960

Original article submitted July 10, 1959

Spectral measurements in the regions of visible and infrared radiation involve certain difficulties in the case where the amounts of the radiation energy to be measured are small. This problem arises when it becomes necessary to measure the intensity of a narrow frequency band, since the radiated power

$$J_{oa} = \int_{\lambda_1}^{\lambda_2} I_\lambda \, d\lambda$$

decreases as the band narrows. For instance, if interference filters are used for selection [1], the radiated power values can be extremely small (of the order of 10^{-10} w).

Along with vacuum thermoelements [2], different types of photocells, photoresistors, and phototransistors are used as sensing elements. The sensitivity of photoeffect elements is much higher than the sensitivity of vacuum thermoelements. For instance, the sensitivity of a vacuum thermoelement is approximately 30 v/w, and the sensitivity of a mass-produced PbS photoresistor is 150 v/w (for ideal blackbody radiation at 300°). In many cases, this ratio will be of the order of 1:100 in favor of photoconductors.

Figure 1 shows the spectral distribution curves for the relative sensitivity of some known photocell materials. This figure indicates that the spectral characteristics lie in the wavelength region extending from x-ray radiation to infrared radiation (approximately 10 μ).

All these photocell materials are strongly affected by temperature as well as aging. If they are placed in thermostats, direct measurements become very complicated.

Figure 2 indicates the sharp drop in the sensitivity of lead sulfide photoresistors with temperature changes [3].

Moreover, the spectral properties change also with

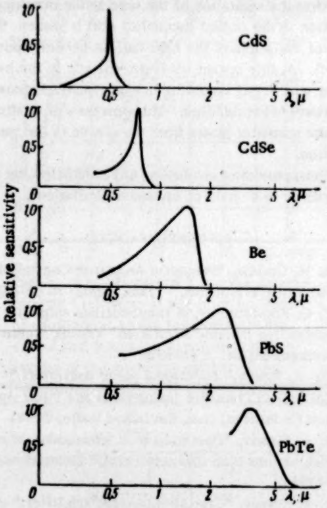

Fig. 1. Spectral distribution of the sensitivity of some sensitive layers (photoresistors).

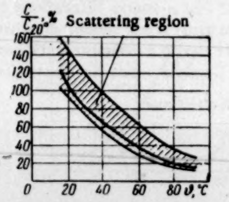

Fig. 2. Temperature dependence of the sensitivity of PbS layers.

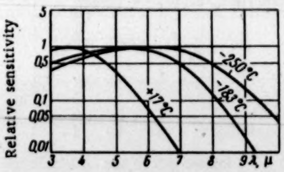

Fig. 3. Temperature dependence of the spectral sensitivity of PbTe layers.

the cell temperature, as can be seen in Fig. 3, where the spectral sensitivity distribution of lead telluride resistors is shown [4].

Therefore, in order to eliminate the "subjective" errors of photocells, compensation methods, where the measurements are compared with measurements of known steady radiation sources, are used. The comparison is performed by alternating screening of the photocell from the measured and the standard radiation by means of rotating mirrors or disks with openings, as well as by means of oscillating diaphragms [5]. Figs. 4 and 5 show examples of such comparison methods, where mechanical diaphragming is used. Along with the presence of mechanical rotating parts, the above methods have an additional disadvantage, which consists in the fact that the "standard radiation source" device must be modified for compensation, which makes it often difficult to obtain reproducible results.

A method of eliminating the above deficiencies is proposed below [6]. According to this method, the photocell is irradiated by a variable light flux, and the indicator amplifier transconductance is regulated with respect to the alternating component of the cell current or voltage. This measurement method has the advantage that the measurements are performed directly and without compensation. Moreover, the receiver (photocell) receives a bias voltage due to the steady component of the variable light flux, as a result of which the noise level is exceeded and the receiver sensitivity is increased.

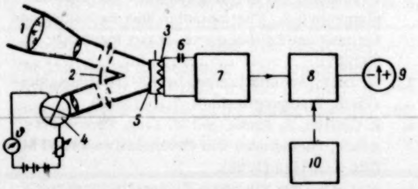

Fig. 4. Block diagram of the arrangement for temperature measurements with TMR-2000. 1) To the measurement object; 2) diaphragm which oscillates at 50 cps; 3) photoresistors; 4) comparison lamp; 5) slit diaphragm; 6) capacitor; 7) ac voltage amplifier; 8) discriminator; 9) deviation indicator; 10) line voltage.

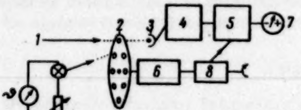

Fig. 5. Operation principle of a milliscope (Hartman and Braun). 1) To the measurement object; 2) rotating disk with openings; 3) photocell or photoconductor; 4) ac voltage amplifier; 5) discriminator; 6) motor; 7) deviation indicator; 8) generator.

The operation principle is clear from Fig. 6. Along with the $J_x(\lambda)$ radiation to be measured, light of variable intensity, which consists of the steady $\mathcal{J}_k(\lambda)$ and the variable $\mathcal{J}_k(\lambda)$ components, is incident on the photosensitive layer. The photoconductor resistance changes in accordance with the spectral sensitivity distribution characteristic, and the sum of these variations is transformed into current and voltage variations. By $\epsilon(\lambda)$, we shall designate the slope of the $dU_a/dJ(\lambda)$ transformation function, where U_a is the output voltage variation, and $J(\lambda)$ is the variation of radiation in dependence on the wavelength for a certain given cell voltage and a given external resistance. Then the external resistance voltage u_a will be determined by the expression

$$u_a = \varepsilon(\lambda)\,[J_x(\lambda) + J_k(\lambda) + \mathcal{J}_k(\lambda) + J_0],$$

where J_0 is the very small photoconductor dark current.

If, for instance, by means of a spectral filter placed in front of the photosensitive layer, the wavelength range is reduced to such an extent that the frequency dependence ϵ, J_x, and J_k can be neglected, the resulting voltage u_a will be found from the equation

$$u_a = \varepsilon\,(J_0 + J_k + J_x) + \varepsilon\mathcal{J}_k,$$

where the first term on the right-hand side of the equation corresponds to the steady component, and the second term corresponds to the variable component; while ϵ is the sensitivity, dependent on temperature and aging, whose influence on the measurement results must be eliminated.

Since the magnitude of $\mathcal{J}_k$ is constant, the variable component of the photocell current is the measure of this sensitivity. The variable and the steady voltage components can be readily separated. Both components can be now separately amplified, and the amplification factor of the steady-component amplifier can be varied while keeping it inversely proportional to the variable-component magnitude, so that the steady-component amplification will be

$$v_{=} = \frac{v_{\max}}{v\varepsilon\mathcal{J}_k} = \frac{v_0}{\varepsilon}.$$

Consequently, a voltage which is independent of the

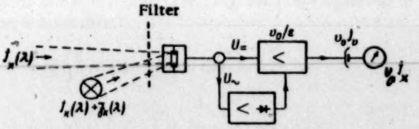

Fig. 6. Principle of radiation measurement with automatic sensitivity regulation.

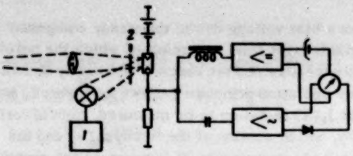

Fig. 7. Operation principle of a pyrometer for the radiation portion in automatic sensitivity regulation. 1) Constant-amplitude ac current; 2) filter.

cell sensitivity will appear at the steady-component amplifier output:

$$u_A = \frac{v_0}{\varepsilon}(\varepsilon J_0 + \varepsilon J_k + \varepsilon J_x) = v_0 J_v + v_0 J_x,$$

where

$$\varepsilon J_0 + \varepsilon J_k = \varepsilon J_v.$$

This voltage depends only on the intensity J_x of the radiation to be measured. The bias voltage $v_0 J_v$ can be compensated electrically.

The radiation to be measured, which is focused by a lens or a concave mirror, is directed to a lead sulfide photoresistor through a monochromatic light filter.

With respect to the transmission frequency and the bandwidth, the light filter is selected in such a manner that the radiation component of the greatest intensity is received. Moreover, the following condition is imposed on the light filter: the change in the characteristic of the PbS spectral sensitivity distribution due to changes in the surrounding temperature and aging must not disturb the validity of the above dependences as a result of the difference between the radiator and the variable light source spectra. Thus, the variable light flux of constant amplitude falls on the PbS photoresistor after passing through the same light filter through which the light flux to be measured passes.

For instance, an incandescent lamp with low thermal inertia, which is fed through a commutator or is supplied an ac current of constant magnitude, can be used as the constant-amplitude light source.

The shape of the variable light flux vs. time curve is not of great importance; however, it must be stable. In selecting the frequency, it should be ensured that the rise and attenuation times of the photoresistor be of the order of 10^{-4}-10^{-5} sec. The maximum frequency is basically determined by the variable light flux source, while the optimum value for the amplifier is 50 cps.

The resulting cell voltage is divided into the steady and variable components by means of a choke and a capacitor; both these components are then separately supplied to amplifiers with negative feedback. The output power of the amplifiers is so chosen as to make it possible to use measuring instruments with crossed coils, which are excited by the rectified variable component. The $v_0 J_v$ steady component is compensated by the stabilized bias voltage.

LITERATURE CITED

1. H. Günzler, Farbgläser und Metallinterferenzfilter, Feingerätetechnik 10 (1956).
2. G. Kortüm, Zur Leistungsfähigkeit der Thermoelemente bzw. Thermosäulen über Bedeutung und Messung der Zeitkonstante, Jenaer Rundschau 2, 3 (1957).
3. W. Lück, Automatisierung bei HF-Erwärmungsprozessen, Fertigungstechnik 7, 10 (1957).
4. P. Görlich, A. Krohs, and W. Lang, Photowiderstande, Photodioden und Phototransistoren, ATM, J394-1-J394-3 (1958).
5. W. Lück, Über ein neues Temperaturmessgerät, Der Industriebetrieb 2, 17-21 (1957).
6. WP, 42 i/40 406.

LETTERS TO THE EDITOR

AN ERROR IN THE ARTICLE "EFFECT OF FLUCTUATIONS ON THE SIMPLEST PARAMETRIC SYSTEMS" BY V. I. TIKHONOV (AVTOMATIKA I TELEMEKHANIKA, VOL. 19, NO. 8, 1958)

I. A. Bol'shakov

Translated from Avtomatika i Telemekhanika, Vol. 21, No. 7, pp. 1088-1089, July, 1960

The article by V. I. Tikhonov is devoted to the interesting problem of the effect of fluctuations on parametric systems, which has been treated in a number of important contributions. Therefore, the conclusions reached in the article deserve the most careful study. However, this study shows that the basic results presented in the article are not correct, which is due to errors in calculation.

The errors begin with the expression for $\vartheta_2(j\alpha, j)$ on page 718, where the $2\alpha\sigma_1\sigma_2$ factor instead of $2\alpha\sigma_2\sigma_\xi(t, u)$ should be in the front of the integral in the last part of the equation. This can be shown by considering Eq. (5), where, instead of $\sigma_\mu\sigma_\nu R_{\mu\nu}$, the mutual central moment of the quantities $\alpha\eta(u)$ and $\int\limits_u^t \xi(x_2)\,dx_2$, which is equal to

$$\alpha\sigma_1\sigma_1\int\limits_u^t R_{12}(u-x_2)\,dx_2.$$

should be substituted.

Similar errors in calculating the mutual moments are found in Eqs. (12), (13), and (14). As a result, the equations for example No. 2 on page 721, beginning with the equation directly following (16), are incorrect. Actually, the output dispersion y(t) is of the following form:

$$\sigma^2 = \\ = y_0^2\exp\left\{-2m_1(t-t_0)+2\sigma_1^2\int\limits_0^{t-t_0}(t-t_0-s)\,R_1(s)\,ds\right\}\times \\ \times\left[\exp\left\{2\sigma_1^2\int\limits_0^{t-t_0}(t-t_0-s)\,R_1(s)\,ds\right\}-1\right].$$

This dispersion does not tend to infinity in every case when t increases, which follows from the results described in the article, which the author admitted to be unusual. On the contrary, the dispersion of output fluctuations tends to zero if the following condition is satisfied:

$$m_1 - 2\sigma_1^2\int\limits_0^\infty R_1(s)\,ds > 0. \qquad (1)$$

As is shown by calculations for actual electronic devices which are subject to fluctuations, condition (1) is not always satisfied in these devices. Small parametric effects always occur - for instance, in electronic servosystems; however, this never leads to an infinite root-mean-square error. Therefore, the "physical explanation", whereby the author attempted to substantiate the obtained incorrect result, is obviously not valid.

ANSWER TO I. A. BOL'SHAKOV

My article (Avtomatika i Telemekhanika, No. 8, 1958, p. 716) contains a calculation error. It can be readily corrected. For this, all the σ_ζ factors in front of the integrals in Eqs. (8), (12), (13), (14), and (18) (regardless of the argument) should be replaced by σ_1, and Eq. (9) must be written thus:

$$m(t) = y_0\exp\left[-m_1(t-t_0)+\frac{1}{2}\sigma_1^2\int\limits_{t_0}^{t}\int\limits_{t_0}^{t}R_1(x_2-x_1)\,dx_1\,dx_2\right]+ \\ +\int\limits_{t_0}^{t}\left[m_2-\sigma_1\sigma_2\int\limits_u^t R_{12}(u-x_2)\,dx_2\right]\exp\left[-m_1(t-u)+\frac{1}{2}\sigma_1^2\int\limits_u^t\int\limits_u^t R_1(x_2-x_1)\,dx_1\,dx_2\right]du.$$

The error does not affect the results in the first and the third examples. In the second example, the system will be stable with respect to dispersion if the following inequality is satisfied:

$$m_1 - 2\sigma_1^2 \int_0^\infty R(s)\,ds > 0.$$

If we introduce the correlation time $\xi(t)$ for a random process

$$\tau_k = \int_0^\infty R(s)\,ds,$$

this equation can be written as

$$m_1 > 2\sigma_1^2 \tau_k. \qquad \text{(I)}$$

As a rule, the correlation time τ_k is a positive quantity, and dispersion σ_1^2 is also basically a positive quantity. Therefore, if (I) is satisfied, also inequality (16) is automatically satisfied:

$$m_1 > \sigma_1^2 \tau_k.$$

Consequently, if (I) is satisfied, the system is statistically stable (i.e., stable with respect to the average value and dispersion). If the inverse inequality is satisfied, the system is unstable. For this case, the physical explanation given on page 722 holds. Therefore, we cannot entirely agree with L. A. Bol'shakov's remarks.

V. I. Tikhonov

DISCUSSION

ON THE BOOK "ELEMENTS OF STRUCTURAL SYNTHESIS OF RELAY CONTROL CIRCUITS" BY V. N. ROGINSKII

(AN SSSR PRESS, MOSCOW 1959; 168 pages)

V. I. Shestakov

Translated from Avtomatika i Telemekhanika, Vol. 21, No. 7, pp. 1090-1094, July, 1960

Although the development of methods for the mathematical analysis, synthesis, and simplification of relay circuits is of great importance for automation and remote control, communications, and computer techniques, no textbook or monograph which would be devoted to the latest results in the theory of relay circuits is yet available in Russian. The monograph, Theory of Relay-Contact Circuits, by M. A. Gavrilov, which was published in 1950 in a small edition, has become a bibliographic rarity.

It is understandable that the numerous specialists engaged in the construction of automatic devices in different branches of technology greeted with interest the book, Elements of Structural Synthesis of Relay Control Circuits, by V. N. Roginskii.

However, in no way does this book justify the readers' expectations. The contemporary state of the relay circuit theory and the basic trends in its development have been outlined in the book, not only in an insufficiently thorough and substantial manner, but even essentially incorrectly. In particular, the relation between the theory of relay-contact (r-c) circuits and the theory of contactless relay circuits is incorrectly defined. It is stated in the book that the "theory of relay-contact circuits is applied to an ever-increasing extent also to relay circuits with contactless elements" (p. 13). However, as is well known, r-c circuits constitute only one of the particular variants of relay circuits, and, therefore, the theory of r-c circuits cannot be generally applied to any relay circuits. At the present time, there is a fast-developing general theory of relay circuits — the theory of logic networks, which can also be applied to r-c and to contactless relay circuits. The book does not even mention the existence of this theory.

It is not mentioned, either, that the theory of r-c circuits, to the synthesis of which the book is devoted, is not so important now as it was 10-15 years ago, and that the methods of synthesis of contactless relay circuits—where electron tube, semiconductor, and magnetic switching elements are used—are becoming more important.

The book under discussion is not a textbook or a monograph, but a compilation of the author's papers on the theory of synthesis of r-c circuits, which were published in 1954-1959 in various scientific journals and collections. The introduction defines the main tasks in electrocommunication and the main problems in its automation, and it contains a brief historical outline of the development and the contemporary state of the structural synthesis theory of relay and, mainly, r-c circuits. However, as was indicated above, this outline is not satisfactorily presented.

Chapters 1-4 present the basic postulates of the theory of r-c circuits, various methods of describing their structure and operating conditions, the basic problems in the synthesis of sequential circuits, and the algebraic transformations of contact circuits. The basic operations and principles of logic algebra (Boolean algebra) and their schematic interpretation are given in this chapter. Chapters 5 and 6 describe some methods for the transformation and simplification of contact circuits. Special attention is paid to the method based on the so-called "consideration of unused combinations." Chapter 7 considers in detail the graphic method of contact circuit synthesis. Chapters 8 and 9 present the theory of the synthesis of mixed Π-type r-c circuits, which has been proposed earlier by the author; chapter 10 is devoted to the theory of the synthesis of r-c circuits with capacitors. The book ends with chapter 11, which very briefly describes a machine for the synthesi of contact (1, k)-poles, an apparatus developed by the author in 1956 in collaboration with A. A. Arkhangel'skaya and V. G. Lazarev.

The book does not contain a summary which would briefly and concisely formulate the results obtained by the author, which is especially conspicuous, since there is nowhere in the book a clear distinction between the author's own results and the well-known results contributed by other authors.

It should be also noted that those branches of r-c circuit theory to which the author has contributed are treated in least detail in the book. The papers which are the closest to the author's own contributions with respect to the subject and content are either not mentioned at all in the text or are insufficiently treated. Thus, for instance, little is said about the papers concerning the methods for the minimization of the expressions for the Boolean functions and of the corresponding circuits, which are based on the use of adjacent constituents. Neither does the book contain even a brief survey of the work on the theory of circuits with elements with finite admittances, although chapters 8 and 9 present a synthesis theory for a particular case of such circuits – the so-called "mixed relay" circuits of the Π-type—which has been proposed by the author.

The author does not mention anywhere in the book that the idea of using the so-called "unused combinations," i.e., the combinations which, according to the synthesis conditions, cannot occur in the operation of the circuit to be synthesized, is not new. Neither does the author mention the fact that the terms "unused states" and "indifferent states," which he uses, are simply Russian translations of the English terms "unused output combinations" and "don't care combinations," respectively, and that the first of these terms is equivalent to the term "invalid combinations." However, these terms were used in English literature concerning the theory of relay circuits in exactly the same sense as the Russian synonyms which the author used even before the publication of his first paper in this field: "Consideration of unused combinations in the synthesis of relay-contact circuits" (Avtomatika i Telemekhanika, Vol. 15, No. 3, 1954).

While repeatedly applying Boolean algebra to valve elements, the author does not consider it necessary to mention the fact that the possibility of such application was first demonstrated by M. A. Gavrilov in his paper "Relay-contact circuits with valve elements" (Izvest. Akad. Nauk SSSR, Otd. Tech. Nauk, No. 2, 1945). This article is not even mentioned in the bibliography.

In the same manner, when introducing on page 19 a new symbol $A \times B$ for the harmonic addition operation $A \cdot B$, the author does not mention that this operation has been known for a long time: it was first applied more than twenty years ago in the theory of electrical and, in particular, relay circuits.

The limited space does not permit us to adduce a number of other examples of such peculiarities in presentation, due to which a reader who is not sufficiently familiar with the literature concerning the theory of relay circuits can receive an impression that many of the already known results are new, and that they have been obtained by the author of the book.

Actually, the book contains only a small number of results contributed exclusively by its author, and this apparently explains the manner in which the state of those sections of the r-c circuit theory to which the author's own results relate is presented.

The author's work, which is presented in chapters 5 and 6, does not contain new results concerning the essence of contact circuit minimization. Actually, this was not the author's intention, as can be seen from the footnote on page 70: "The aim of the present work is the finding of suitable expressions for the subsequent transition to the circuit, and not the determination of minimum forms."

The idea of the graphic method for the synthesis of contact circuits, which is presented in chapter 7, does not belong exclusively to the author of the book. This method was proposed in 1955 by G. N. Povarov for the synthesis of symmetric and quasi-symmetric circuits. V. N. Roginskii later showed that every circuit can be considered as quasi-symmetric if weights 2^{i-1} are added to relays with the numbers $i = 1, 2, \ldots, n$ and if the numbers of combinations for which a certain given circuit must be closed are taken as the working numbers of the relay circuit. This is actually the only contribution of V. N. Roginskii to the development of this method.

Only chapters 8 and 9 contain a theory which is based on ideas belonging exclusively to the author of the book. These chapters describe the results of three papers that were published by the author in 1957, where he attempted to put forward a theory of the synthesis of Π-type mixed relay circuits, i.e., of such r-c circuits where the contact circuits can be connected in parallel, as well as in series, to the relay windings and to certain additional resistances of finite magnitude. However, this attempt was entirely unsuccessful, and the theory proposed by the author is far from satisfactory in the physical and mathematical sense, and is totally unsuitable for practical use.

The main principle of this theory is based on the assumption of dividing the synthesis of the relay circuits into two stages: the stage of determining the circuit structure and the stage of the electrotechnical calculation of its elements. The author assumes that the structure of a Π-type mixed r-c circuit can be determined if only the "orders of admittance" of its elements are known. In order to designate that a certain dipole has a finite admittance G of the same, lower, or higher order in comparison with that of relay A, the author uses the symbols $G_{=A}$, $G_{<A}$, and $G_{>A}$, respectively, which he defines in the following manner: $G_{=A}$, if the relay A operation is not disturbed either for a series or a parallel connection of G to A, and $G_{<A}$ (or $G_{>A}$) if the operation of relay A is disturbed only for a series (or parallel) connection of G to A.

The author considers that the case where the operation of relay A is disturbed for a series, as well as a parallel, connection to G is possible, but of no practical importance.

The basic deficiency of the above determination is the dependence of the order of admittance on the voltage applied to the circuit and on the internal resistance of its source.

It can be readily shown through simple examples that, by changing the magnitude of the emf E and of the internal resistance R_E of its source, we can obtain any order of the admittance G for a dipole which has a constant resistance R, for instance, equal to the resistance R_A of the relay A winding. Let V_A and i_A be the minimum voltage and current sufficient for reliable operation of relay A, and i_a and i_b be the respective currents through the relay A winding when it is connected in series and in parallel to a dipole with the resistance R equal to the resistance R_A.

By simple calculations, using only Kirchhoff's laws, we obtain

1) $i_a < i_A$ and $i_b > i_A$, i.e., $G_{<A}$ for $V_A < E < 2V_A$ and $R_E = 0$;

2) $i_a > i_A$ and $i_b > i_A$, i.e., $G_{=A}$ for $E > 2V_A$ and $R_E = 0$;

3) $i_a \geq i_A$ and $i_b < i_A$, i.e., $G_{>A}$ for $E \geq 6V_A$ and $R_E = 4R_A$;

4) $i_a = i_b < i_A$, i.e., relay A will not operate when it is connected either in series or in parallel to the resistance R for $E = 2V_A$ and $R_E = R_A$.

It is perfectly obvious that similar results will be obtained in the general case, where $R \neq R_A$, when the voltage drop in the considered circuits connecting the relay A winding to the resistance R plays the role of the emf E.

The dependence of the order of admittance on voltage does not permit us to determine the order of admittance of all elements of the circuit to be synthesized before we begin its synthesis, since various switchings will occur during the circuit operation process, as a result of which some of the relays will be interconnected in a different way than before. Due to this, the voltage distribution among the circuit elements will change, and this, in turn, can cause a change in the beforehand-determined orders of admittance of the circuit elements. The orders of admittance of the circuit elements for different closing and dropout combinations of all relays in the circuit can be determined only after the circuit structure is known, and the electrotechnical calculation of the circuit parameters is performed.

Thus, the author's basic idea of the possibility of dividing the synthesis of a Π-type mixed r-c circuit into two stages is illusory.

The main reason for the fallacy of the proposed synthesis theory consists in the fact that the author attempted to operate only with admittances, while ignoring the well-known physical fact that the operation of an electromagnetic relay is determined by the current passing through its windings, and that the current in circuits with finite admittances depends equally on the circuit admittance, as well as on the voltage applied to the circuit. In other words, the main reason for the fallacy of this theory is the attempt to ignore Kirchhoff's laws for electrical circuits.

This theory is unsatisfactory also from a mathematical point of view, due to the large number of fundamental mathematical and logical errors and the fact that many determinations are not satisfactory and, in some cases, nonexistent.

We shall first mention the statements which are obviously incorrect. One of such statements is, for instance, the statement contained in the following phrase (my emphasis): "We shall also assume that the admittance and parameter values of relays are chosen in such a manner that if a finite number of admittances of the same order are connected in parallel or in series, the over-all admittance will be of the same order, i.e.,

$$A + B_{=A} + \cdots + K_{=A} = (A + B + \cdots + K)_{=A},$$
$$A \cdot B_{=A} \cdot \cdots \cdot K_{=A} = (A \cdot B \cdot \cdots \cdot K)_{=A}. \quad (8.11'')$$

Generally speaking, this statement is not valid for any order determination, since it contradicts the basic axiom of finite quantities — the Archimedes axiom.

Expression (8.10) contains a printing error, which becomes obvious if we compare it with expression (8.7). If we eliminate this error by reversing one of the signs > and <, we obtain the following statements: if $A_{>B}$ and $B_{>A}$, the circuit cannot be realized; if $A_{<B}$ and $B_{<A}$, the circuit cannot be realized.

The fallacy of these statements can be readily demonstrated by adducing examples of circuits for which the $A_{>B}$ and $B_{>A}$ relations, as well as the $A_{<B}$ and $B_{<A}$ relations, are satisfied. The first of these relations holds for circuits in the above-considered example for the case (3) if relay B, which is identical to relay A, is used as dipole B with the resistance $R = R_A$. The second of these relations is satisfied for circuits of the case (1) in the same example, by the same substitution of relay B for dipole B.

Conditions (8.7) do not follow from determinations of the order of admittance, and, generally speaking, they are not satisfied, since the $B_{=A}$, $B_{<A}$, and $B_{>A}$ relations and the $A_{=B}$, $A_{>B}$, and $A_{<B}$ relations are independent of each other.

All the above reasoning on the orders of admittance apply under the assumption that the term "admittance" is used in the generally accepted sense, i.e., that it denotes the quantity reciprocal to impedance. However, in the symbols $G_{=A}$, $G_{<A}$, and $G_{>A}$, the sign G designates the so-called "structural admittance," which the author determined only for two values of ordinary admittance: for the 0 and ∞ values. According to the determination given on page 20 in the book, the structural admittance G is equal to 0 and 1, while the corresponding ordinary admittance Y is equal to 0 and ∞, respectively. The structural admittance G, which corresponds to the Y values lying between 0 and ∞, is not determined anywhere in the book. Therefore, it is impossible to tell what is the structural admittance G of a dipole which has a certain admittance Y (for instance, admittance Y = 1 mho) and, conversely, if a dipole structural admittance not equal to 0 and 1 is given, it is impossible to tell what is the ordinary admittance Y of such a dipole.

In the same manner, the operations that the author denotes by symbols $G_1 + G_2$, $G_1 \cdot G_2$, and $\bar{G}$ are not defined for finite admittance values. Throughout the book up to chapter 8, these operations are applied only for the values of structural admittances G_1 and G_2 equal to 0 and 1. For these values, the operation symbols "+,"

"." and "–" are used in the sense of Boolean operation symbols: for addition, multiplication, and negation (complementing to 1), respectively. For structural admittances not equal to 0 and 1, these operations do not pertain to Boolean algebra operations. In this case, they represent isomorphic operations for ordinary addition, harmonic addition, and inversion – the basic algebraic operations for dipole circuits of the A-type (or of the Π-type in the presently adopted terminology) – the existence of which is not mentioned in the book, although the papers where they are described are contained in the bibliography at the end of the book. By not mentioning the existence of this algebra, the author loses the possibility of offering any isomorphic presentation of the basic operations of this algebra, and, therefore, leaves the $G_1 + G_2$, $G_1 \cdot G_2$, and $\bar{G}$ symbols without any algebraic definition. Therefore, all the formulas where the algebraic signs "+", ".", and "–" are encountered between the structural admittance symbols which are not equal to 0 and 1 are devoid of any algebraic sense.

Neither are the $G_{=A}$, $G_{<A}$, and $G_{>A}$ symbols defined mathematically – which is anyway essentially impossible, unless the structural admittance G is defined.

Due to the fact that the symbols of basic operations and relations are not defined and that no concrete relation exists between structural and ordinary admittances, the entire theory presented in chapters 8 and 9 is devoid of any mathematical sense and cannot be used for any calculations of admittance values.

There are no logical proofs for any statements in the book or in the papers published earlier by the author and presented in the book. A number of formulas are given without derivations and proofs. Because of this, it happens that some formulas in the book are either incorrect or contradictory. Thus, for instance, the author states that "the law of commutativity is valid for an equivalence

$$\frac{a}{b} = \frac{b}{a}" \qquad (5.8)$$

and, at the same time, considers that the equality $\overline{\left(\frac{a}{b}\right)} = \frac{\bar{a}}{\bar{b}}$ holds. The last equality, however, is incompatible with equality (5.8), since it can be readily shown that the inversion operation is nondistributive with respect to any commutative operation of Boolean algebra.

The equivalence symbol $\frac{a}{b}$ is not rigorously defined. Not only in the author's different papers, but also in different places in the same paragraph – § 3 in chapter 5 – this symbol has a different meaning. By loose reasoning, the author finally arrives at the following expression for symbol $\frac{a}{b}$ by means of Boolean algebra operations:

$$\frac{a}{b} = ab + (a + b)\,\omega = ab\bar{\omega} + (a + b)\,\omega, \qquad (5.11)$$

where ω is any expression of this algebra. Equation (5.11) satisfies, as can be readily shown, only the following Boolean functions of the two arguments a and b: ab, a, b, and a + b. Only the first and the last of these functions are symmetric, so that the author's statement that formula (5.8) holds for equivalences is, generally speaking, incorrect.

It would be possible to quote other examples of internal contradictions in the equivalence calculations presented in the book.

The book contains many formulas, but they not actually used for calculations. There are almost no calculations which would be complete and without omissions.

In conclusion, it should be noted that an absence of logic is noticeable not only in the presentation of theory, but also in the composition of the book. For instance, problems in the synthesis of sequential circuits are considered in chapter 3, and the algebraic transformations which are used for their synthesis are presented in chapter 4. The methods for describing the structure and the operating conditions of r-c circuits are treated in chapter 2, while these methods are based on the use of the algebraic apparatus presented in chapters 4 and 5. The graphic method for the synthesis of contact circuits is considered in chapter 7, and the machine for the synthesis of contact circuits according to this method is described in chapter 11. Between these naturally connected chapters, the author has for some reason inserted chapters treating r-c circuits with finite admittances, i.e., circuits, the synthesis of which cannot be secured either by the graphic method described in chapter 7 or, even less, by the machine for synthesis which is described in chapter 11. Another example showing that subjects which naturally follow each other are contained in different parts of the book are the general problems in the synthesis of sequential circuits and the synthesis of sequential circuits with capacitors. These closely related subjects are considered in chapters 3 and 10, and the intermediate chapters contain material which is only indirectly connected with these circuits.

Only an absence of proper scientific criticism can explain the publication of this book, which does not contain anything new in comparison with the papers published earlier by the author, is full of mathematical and logical errors, and also presents a false picture of the contemporary state and development trends of the theory of relay circuits, reproducing almost without changes the physically and mathematically unsubstantiated theory of the synthesis of Π-type mixed relay circuits.

REPLY TO V. I. SHESTAKOV'S CRITICAL REVIEW OF THE BOOK "ELEMENTS OF STRUCTURAL SYNTHESIS OF RELAY CONTROL CIRCUITS " BY V. N. ROGINSKII

V. N. Roginskii

Translated from Avtomatika i Telemekhanika, Vol. 21, No. 7, pp. 1094-1098, July, 1960

The book under discussion is devoted to the presentation of problems connected with the structure of relay circuits. The book provides methods which the author thinks can be recommended in engineering practice, while most attention was paid to the design of the simplest circuits possible. All the methods presented in the book have been tested in practice by the author, by the team with which he works, and in a number of scientific and design organizations. For the purposes of clarifying these methods, some elements of the theory of contact and relay circuits have been presented in the book.

The book does not pretend to deal with all aspects of the theory of relay circuits, which is obvious from its title: "Elements . . . ." Moreover, only the synthesis of a narrow class of relay circuits is considered – the class of control circuits, the characteristics of which are described in the introduction. The number of branches of the modern theory of relay circuits which were not included in the book could be considerably enlarged in comparison with those V. I. Shestakov mentioned in his note.

It cannot be said that the theory of relay-contact circuits is presently of lesser importance than 10-15 years ago, since the number of relays and relay circuits which are developed and produced by the industry increases every year. Just now, when relay devices are used in enormous quantities in many fields of the national economy, the problem of the design of efficient circuits is most important. Experience shows that the application of theoretical methods (in particular, also methods presented in the book) will make it possible to simplify the existing circuits and to reduce the number of their elements sometimes by one-third. The present-day importance of this problem is emphasized by an ever-increasing number of papers in this field (including papers by V. I. Shestakov). The appearance of new elements and new theories, which also have to be developed, is another matter. I do not propose to contest their importance, but it seems to me that they cannot be set off against each other. In my opinion, the general trend of development in the nearest future is the formation of a general theory for the design of discrete action circuits, which is mentioned in the introduction. It is possible that the statement, that the theory of relay-contact circuits is applied to an ever-increasing extent to relay circuits with contactless elements, cannot be taken as completely true, but it can be hardly understood as a statement that this theory can be applied to *any* relay circuit (emphasis supplied by V. I. Shestakov).

Also, the book is not an historical treatise, and, therefore, it is not necessary at all to specify who was the first to use the multiplication sign for denoting consecutive connection, who was the first to analyze circuits with valve elements, who derived the formula for the calculation of admittances connected in series ("harmonic addition") and when, etc. With regard to the questions raised in the critical note, it can be said that the book contains references to papers by M. A. Gavrilov on circuits with valve elements (pages 9-10 and 28) and also to papers dealing with the problem of circuits with finite admittance elements by V. I. Shestakov, M. A. Gavrilov, and other authors (page 10).

In the same manner, there is no need to mention the translations of particular terms into foreign languages in the book.

I took the stand that the simplification of contact circuits by using so-called "unused combinations" was well known, and I did not undertake historical research in order to establish priority in this field. In my first paper concerning this problem (Avtomatika i Telemekhanika, Vol. 15, No. 3, 1954), to which, in particular, V. I. Shestakov refers, it was stated in the first paragraph: "A possible way of simplifying the circuit is, *as is known*, the consideration of those combinations which are not encountered in the operation of the circuit." The author's role is defined with sufficient clarity in the book, where it is said that ". . . a system for describing such combinations by means of connection tables and formulas, and methods for applying the conditions to circuits by taking into account the indifferent combinations, which have been developed by the author, are given" (page 11). I do not think that even readers unfamiliar with literature concerning the theory of relay circuits can draw the conclusion that all the material in the book is the author's contribution.

The book does not contain a consideration of basic problems in minimization, as V. I. Shestakov rightly notes. At the present time, minimization denotes the determination of minimum normal forms of Boolean functions, which does not always provide the possibility of obtaining a Π-type contact dipole circuit with a minimum number of contacts, especially if unused combinations are present. Experience shows that in many (and, for a large number of relays, in the majority of) cases, H-type circuits are simpler for solutions which do not correspond to the minimum forms. In the same manner, the minimization of individual circuits does not provide the possibility of designing circuits with an over-all minimum number of contacts by combining these circuits into a single network (even for Π-type). Therefore, in practical application, the introduction of the minimization concept (in the above sense) can be even disadvantageous, since, in designing, the impression can be formed that a "minimum" circuit is secured, while a circuit with an even smaller number of contacts can be obtained if nonminimum solutions are used for individual circuits. Since, at the present time, there is no method for the design and determination of actually minimum circuits, the book provides recommendations for the design of circuits with the greatest degree of contact unification, which approaches the minimum conditions. Therefore, "minimization" has not been treated in the book, and individual minimization methods are used only for simplifying the writing of structural formulas.

At the same time, contact multipoles with a number of contacts close to the minimum, when simplifications due to indifferent combinations are automatically taken into account, can be designed by using the graphic method presented in chapter 7.

If the history of the development of this method is to be presented, one has to begin, on the one hand, with papers by M. A. Gavrilov and C. E. Shannon, which deal with the connection of multipoles, and then pass to cascade methods and methods for the design of symmetric circuits, which have been developed by G. N. Povarov (they are presented in the first part of the chapter), and, on the other hand, with papers dealing with unused combinations. In the graphic method, all operations are performed with three-valued functions, for which the concepts of "symmetry" and, even more so, "quasi-symmetry" are not defined (and, possibly, cannot be defined). This method provides possibilities (circuits with "direct lead-outs" and the consideration of unused combinations) which the above-mentioned methods do not have. In fact, the application of the graphic method principles to the G. N. Povarov method (i.e., to two-value logic) made it possible to demonstrate that all functions (two-valued, and not three-valued) are quasi-symmetrical in the sense defined by G. N. Povarov.

Another way of securing simpler circuits, is, as is known, the use of parametric dependences in the circuits, i.e., the design of such circuits where the operation of individual relays depends not only on whether the circuit is closed or open, but also on the current intensity in the closed circuit. Such circuits were designed and operated before the theory of relay circuits appeared, in the same way as contact circuits were designed and modified for a long time before C. E. Shannon and V. I. Shestakov formulated the basic principles of the theory of such circuits. Thus, the "idea" of these circuits does not belong to the author of the book, but rather has existed a long time, and individual papers devoted to this question are available in literature. The book provides only a certain generalization of the experience gained and the definitions of rules for transforming circuits with parametric dependences for certain restrictions, which are mentioned below.

The statement that " the assumption of the possibility of dividing the synthesis process into two stages — the determination of the circuit structure and the electrical calculation of its parameters — is illusory" can be explained only by the author's total unfamiliarity with the practice of designing relay circuits and calculating their parameters.

It is awkward to talk about such truisms in an academic journal, but, since much space has been devoted to this question in the review, I shall take the liberty to dwell on it.

The division of circuit design into two interlinked stages is a necessary sequential process which is the result of long-standing experience, and only correct solutions in both stages can secure an efficient circuit. The calculation of elements can be performed only after the structure is determined, but, in composing the structure, the capabilities of relays must be taken into account.

Let us consider the simplest case, where ordinary electromagnetic relays without parametric dependences are used and where, from the structural point of view, it is only necessary that the series circuit be closed and the shunting circuit open for the relays to operate. If, for instance, it is required that relay X operate only when button A is pressed, one of the possible solutions of the circuit structure will be the series connection of the button closing contact to the relay winding, i.e., a circuit with the structural formula aX. However, even for such a circuit, the relay will operate in the required manner only if all the circuit parameters are accurately calculated (including the voltages and the current source impedances). If the calculations are erroneous, the relay may not operate, or it may "burn" and become unusable when the contact closes. A different structure can also be considered: $\bar{a} + X$. For such a circuit, elements with different parameters are required. However, if the structure is wrongly chosen — if, for instance, an opening, instead of a closing contact is installed in the above circuit (i.e., if the $\bar{a}X$ circuit is chosen) — the calculation of circuit parameters will not help, and the circuit will operate in accordance with the assigned conditions.

In view of the necessity for such order, it is possible to talk about the interaction between individual elements in the circuit without first determining their parameters during the structural synthesis stage.

In a contact circuit with only two combinations – open and closed – the concept of the circuit operation coincides with the concept of its admittance: 0 or ∞ (or 0 and 1 in theory). For relay circuits, such single-value correspondence between the circuit admittance and the operation of the circuit relays does not exist, and, as V. I. Shestakov rightly remarks, the operation of relays in the circuit depends on many factors, including the voltage applied. In order to take into account the influence of all circuit parameters on the operation of relays, the concept of the circuit admittance and the concept of a relay circuit operation are separated in the book, in the first place. The concept of the circuit equivalence with respect to operation is introduced. In order to express the effect of the admittances included in the circuit on the relay operation, we introduced the concept of the "order of admittance," which "does not characterize the absolute admittance (or impedance) value, but the effect of this admittance on the operation of relays in the circuit, i.e., which pertains to the actual circuit parameters and the voltage supplied to it" (page 121). Thus, the critic's statement that an attempt has been made to operate solely with "admittances" is entirely incomprehensible.

It should be remarked that the concept of the "order of admittance" characterizes the influence of different impedances on the operation of relays for certain given methods of connecting these impedances to the relay windings. Therefore, it is entirely senseless to talk either about the "magnitude" of the order, or about any well-defined correspondence between the "orders of admittance" and admittance values expressed, for instance, in mho. Since these concepts, although denoted by the same term, refer to different physical properties ("admittance" is the property of an element, and its magnitude is the reciprocal of impedance, while the "order of admittance" is the effect of this element on another in a given circuit), there is not, and cannot be, any well-defined relation between them.

In the examples given in the review, reference is made not to the order, but to the value of admittance ("the term 'admittance' is used in the generally accepted sense," as the author of the note states), and, therefore, the reasoning in the note does not essentially apply to the material presented in the book, which only confirms the absence of the above-mentioned relation.

Thus, there is a misunderstanding in this case, which is caused by the confusion in using the terms. Perhaps a term not including the term "admittance" should be found for the characteristic of the interaction of elements with finite admittance. I chose this term in order to characterize the influence which a finite admittance exerts on the relays of the circuit. Thus, for instance, an element with a "lower order of admittance" in the circuit affects the operation of the corresponding relay as a break in the circuit (very small admittance), although, with respect to the absolute value, the admittance of this element can be equal to the relay admittance.

Let us now consider the parametric interaction of relays in the circuit. Consider a circuit with two relays, where they are connected in series or in parallel during the operation process. In both cases, in dependence on the circuit parameters (including voltage), it can happen that: 1) both relays operate; 2) only the first relay operates; 3) only the second relay operates; 4) neither of the relays operates. Thus, for the same structure and in dependence on the parameters, sixteen circuits with different modes of operation can be obtained. Therefore, in the stage of structural synthesis of a circuit with parametric dependences, it should be indicated how the relays are to operate if they are connected in parallel or in series. From all the possible combinations, I selected the three combinations which are most important in practice, and I introduced the $A_{=B}$, $A_{>B}$, and $A_{<B}$ symbols, which indicate how these relays must operate. The existing methods for the design of relays make it possible to select parameters for which the relay will operate in correspondence with the assigned conditions (as is confirmed by examples given in the critical review). Formulas (8.7) and (8.11) are conditions which are imposed on the relays and which limit the group of the circuits under consideration, and not "statements," as V. I. Shestakov described them. As statements, they are "generally speaking, incorrect." Besides, it is difficult to find a theory for which it could not be said that its postulates and assumptions are "generally speaking, incorrect." In particular, the equivalences $aa\ldots a = a$, and $a + \bar{a} = 1$ in the theory of contact circuits, and some other equivalences are valid only for ideal contacts, and they are "generally speaking, incorrect." However, this in no way belittles the significance of the entire theory.

The author of the note was right in noticing the printing error in expression (8.10), which should be corrected to read: "if $A_{>B}$ and $B_{>A}$ (or $A_{<B}$ and $B_{<A}$), the circuit cannot be realized."

However, the statement in the review that this relation is inaccurate is not correct. Actually, if the circuit contains two relays, $A_{<B}$ and $B_{<A}$, which are connected, for instance, in series, the relation $A_{<B}$ indicates that, if the circuit is closed, relay A must operate and relay B must not operate, and the $B_{<A}$ relation indicates that relay B must operate and relay A must not operate, i.e., both conditions are incompatible, and the realization of such a circuit is an impossibility.

The "+" and "." symbols in chapters 8 and 9 correspond, as in the case of contact circuits, to parallel and series connection, and the symbol "–" is determined by expressions (8.19) and (8.20) (page 125).

The symbols used make it possible to transform circuits containing not only contacts, but also relay windings and resistors, and to obtain circuits which are equivalent to the relays contained in the circuit with respect to operation, and not to determine the electrical admittance of these circuits. Therefore, these operations cannot be compared with operations of the "algebra of dipole circuits of the A-type."

Thus, it is obvious that the mathematical and logical "errors" cited by V. I. Shestakov, either do not exist or are based on a conscious or unconscious confusion with regard to the concepts, "admittance value" and "order of admittance," which, as was indicated, pertain to different physical quantities.

In another place in the review, inaccuracies and contradictions in operations with equivalences are indicated.

The equivalence symbol a/b[*] is used in those cases where the given conditions are satisfied by several solutions (circuits) which are characterized by the inequality (5.10), from which all particular solutions can be found by using formula (5.11). In particular, a/b indicates that, for the given conditions, b can be substituted for a, and conversely, in the formula (circuit). The commutativity of the a/b symbol is obvious from (5.10) and (5.11).

As regards the supposedly incorrect equality $\overline{(a/b)} = \bar{a}/\bar{b}$, which is the only one indicated in the critical review, its proof is so elementary that I did not consider it necessary to provide it in the book. However, since V. I. Shestakov raised this question, I shall give the derivation. We start, for instance, with expression (5.11), and we write

$$\frac{a}{b} = ab + \omega(a + b);$$

$$\frac{\bar{a}}{\bar{b}} = \bar{a}\bar{b} + \omega'(\bar{a} + \bar{b}).$$

By inverting the first of these expressions, we obtain

$$\overline{\left(\frac{a}{b}\right)} = \overline{ab + \omega(a + b)} = (\bar{a} + \bar{b})(\bar{\omega} + \bar{a}\bar{b}) =$$

$$= \bar{\omega}(\bar{a} + \bar{b}) + \bar{a}\bar{b}(\bar{a} + \bar{b}) = \bar{\omega}(\bar{a} + \bar{b}) + \bar{a}\bar{b} = \frac{\bar{a}}{\bar{b}}.$$

The other relations with equivalences can be verified in a similar manner. Therefore, it is hard to understand what is meant by other examples of "internal contradictions in equivalence calculations presented in the book" which are mentioned in the review.

In conclusion, it should be noted that V. I. Shestakov's remark on the absence of "proper scientific criticism" is completely devoid of substance. The material presented in the book was the subject of many reports and discussions at various conferences and seminars. In particular, V. I. Shestakov twice came forward with his "criticism" (at the All-Union Conference on the Theory of Relay-Actuated Devices in 1957, and at the Session of the Scientific Council of the Moscow Electrotechnical Institute of Communications in 1959); however, he was not supported by the specialists who were present. I am also familiar with V. I. Shestakov's several negative references to the manuscripts of my papers. However, the above papers were published after they passed due criticism and discussion. Finally, V. I. Shestakov could have organized the discussion of these papers in the seminar which he heads.

In conclusion, we can say the following:

1. V. I. Shestakov's critical review presents the content of the book, as well as the individual theories, in an incorrect and tendentious manner. The only correct remark pertains to the printing error in formula (8.10).

2. In presenting the problem of transforming relay circuits, V. I. Shestakov, in spite of what is said in the book, treats the concept of the "order of admittance," which pertains to the conditions of relay operation in the circuit, as the "admittance value" and the assumptions used as "statements." Thus, all that has been said with respect to this question in the review does not pertain to my book. Moreover, the review indicates that its author is completely unfamiliar with practical methods for the calculation of relay circuit electrical parameters.

3. Neither does V. I. Shestakov's statement that the inversion operation is nondistributive with respect to any commutative Boolean algebra operation (emphasis supplied by V. I. Shestakov) pertain to the material in the book, since the "equivalence" a/b is not a Boolean operation, but a conventional way of writing the fact that the circuit x in question, which satisfies the given conditions, can have two values: x = a and x = b, which is analogous to the way of writing the general solution of the equation $y^2 = a$ in the form $y = \pm\sqrt{a}$. It is true that the difference here consists in this: that, for contact circuits, the above fact results in a number of other particular values, which are determined by formula (5.11).

---

[*] With regard to this theory, A. A. Lyapunov writes: "The methods of taking into account the so-called 'unused combinations,' which have been developed by V. N. Roginskii, who proposed a suitable algebraic tool (for the transformation of equivalences), also played an important role" (Mathematics in the USSR During the Last Forty Years [in Russian] (Fizmatgiz, 1959, Vol. 1, p. 872).

ERRATUM

Vol. 21, No. 2, pp. 114-116, October, 1960

The article by A. A. Fel'dbaum published in Avtomatika i Telemekhanika, No. 2, contains errors in final derivations. In the corrected form, some of the equations in this article should be written thus:

$$L_{jk} = \delta_{jk}\,\alpha_k^2\sigma^2 + (\gamma_j\gamma_k + \gamma_j B_k + \gamma_k B_j + B_k B_j) + \\ + \sum_{\nu=1}^{m} [(\gamma_j + B_j) A_{k\nu} + (\gamma_k + B_k) A_{j\nu}]\,\xi_\nu + \sum_{\mu,\,\nu=1}^{m} A_{k\nu} A_{j\mu}\,\xi_\mu\,\xi_\nu. \tag{37}$$

$$I_{jk,\,n+1} = \delta_{jk}\,\alpha_k^2\sigma^2 + (\gamma_j\gamma_k + \gamma_j B_k + \gamma_k B_j + B_j B_k) + \\ + \sum_{\nu=1}^{m} [(\gamma_j + B_j) A_{k\nu} + (\gamma_k + B_k) A_{j\nu}]\,J_{\nu,\,n} + \sum_{\mu,\,\nu=1}^{m} A_{k\nu} A_{j\mu}\,I_{\mu\nu,\,n}. \tag{38}$$

$$I_{jk} = \delta_{jk}\,\alpha_k^2\sigma^2 + (\gamma_j\gamma_k + \gamma_j B_k + \gamma_k B_j + B_j B_k) + \sum_{\nu=1}^{m} [(\gamma_j + B_j) A_{k\nu} + (\gamma_k + B_k) A_{j\nu}]\,J_\nu + \\ + \sum_{\mu,\,\nu=1}^{m} A_{k\nu} A_{j\mu}\,I_{\mu,\,\nu} \qquad (j,\,k = 1, \ldots, m). \tag{43}$$

Further, in Eqs. (49), (52), and (53), the coefficient "4" in one of the terms should be replaced by "2." With this, Eq. (55) can be reduced to the following form:

$$e = \left(A_0 - \frac{\delta}{4}\right)^2 + \left(\frac{\delta}{k}\right)^2 \frac{1}{\left(4 - \frac{8}{A_0}\right)^2} + \left(\frac{k}{A_0}\right)^2 \frac{1}{1 - \left(1 - 4k + \frac{k\delta}{A_0}\right)^2}.$$

BLANK
PAGE

THE MECHANIZATION AND AUTOMATION OF PRODUCTION - THE GENERAL LINE OF DEVELOPMENT OF INDUSTRY

Results of the June Plenum of the Central Committee of the Communist Party of the Soviet Union

On July 13 - 16, 1960, a Plenum of the Central Committee of the Communist Party of the Soviet Union was held, at which great attention was devoted to problems in the automation of industry.

The Plenum summed up the work of industry and transportation done in the year and a half since the Twenty-first Congress of the Communist Party of the Soviet Union. The basic conclusion of the Plenum was that the grand program for the creation of the material and technical basis of Communism adopted by the Twenty-first Congress of the Communist Party of the Soviet Union is being successfully accomplished.

Work upon the introduction of progressive technological processes, on the mechanization and automation of industry, the general line of development of industry, is expanding.

Technological progress in all branches of the national economy is inseparably connected with success in Soviet sciences. In the area of automatic control our science has substantial attainments and, in a number of directions, is outstripping the science of more developed capitalistic countries. As a result of the theoretical and experimental work of Soviet scientists, there have been successful planning and building of many complex systems of automation and remote control, the automatic control systems of cosmic rockets, for example, which assure precise escape of artificial satellites of the earth and sun into assigned trajectories, or automatic control systems for atomic reactors, metallurgical and other complex aggregates.

All these tasks can be solved only on the basis of development of the theory of automatic control and the creation of automatic systems of high quality.

Soviet scientists have put forward a number of new ideas which already have found application in the techniques of automatic control. Results have been obtained which lay a basis for the theory of discrete automatic systems and represent a fundamental contribution to the theory of automatic control, including relay, impulse and digital systems of automation, which are extensively applied in engineering. A number of the principles revealed, to which automatic systems are subject, and also the methods developed for the investigation and calculation of these systems, are being extensively utilized by scientific research and experimental design organizations in creating systems of automatic control. Important results have been obtained in the area of nonlinear systems of control, the theory of combined and self-contained systems, and in the theory of invariability. A beginning has been made in the development of automation in the designing of technical equipment. A firm theoretical foundation has been created for the building of optimal and self-adjusting systems of automatic control which establish the most rapid and economical system of flow of a technological process. New principles of research have been worked out regarding semiconductors, magnets and pneumatic elements for the building of reliable automatic systems.

The First Congress of the International Federation on Automatic Control has been held with great success. More than a thousand scientists and specialists participated in it, including more than seven hundred delegates from foreign countries.

The reports presented to the Congress, and the discussions which revolved about them, showed that Soviet scientists are working in the most up-to-date directions in automation. Many very eminent foreign scientists unanimously noted the high level of Soviet science in the area of automation.

It should be mentioned, however, that, side by side with great success of our scientists in the field of automation, the mechanization and automation of production are still being accomplished slowly. The Plenum of the Central Committee of the Communist Party of the Soviet Union emphasized that solving the fundamental problem of the current Seven-Year Plan – to gain the maximum amount of time in the peaceful competition of socialism with capitalism – is possible only through a universal raising of the tempo of technical progress, and on one basis – increase in the productivity of labor.

The July Plenum of the Central Committee of the Communist Party of the Soviet Union bound the Party, the Soviet and economic organizations to work out and put into effect measures directed toward the most rapid introduction into production of the attainments of science and technique, toward the creation and utilization of the output of the most improved machines, equipment and apparatus for complex mechanization and automation of productive processes.

Decisive importance in accelerating the tempo of technical progress lies in advancing the growth of machine-tool construction, the expansion of production and raising the technical level of machines, apparatus, instruments and means of mechanization and automation. In the light of these tasks, in spite of the success obtained, it is impossible to be satisfied with the condition of scientific research in the area of automation. It is necessary to expand by several times the front of scientific research, both as regards problems whose solution will permit obtaining in the very near future a great economic effect, and as regards long-range problems of the growth of automation many years from now.

It is necessary to expand much more extensively the fundamental theoretical and research work, without which a valuable solution of the problems of automation is unthinkable.

It is necessary to put into effect more rapidly the practice, recommended by the Plenum of the Central Committee of the Communist Party of the Soviet Union, of cooperative creative participation of scholars, engineer-technologists, designers, builders, and factory workers in the creation of progressive technological processes and new technique in all stages of their development from laboratory investigation to introduction into production.

In recent years there has been a substantial change in the character of the problems facing science in the area of automation. Present-day complex systems of automatic control can no longer be built on the basis of mere engineering intuition or of experience. Without guiding principles based on profound theoretical assumptions, it is impossible to determine the most advantageous structures for control systems. Therefore, it is necessary to accelerate the elimination of gaps in the theory of automatic control by concentrating our efforts on the solution of the main problems, such as problems in the creation of new control systems by complex aggregates with an abundance of elements and connections between them.

Side by side with the further development of essential divisions in the theory of automatic control, special attention should be devoted to the creation of a theory of self-adjusting systems and systems of optimiization and a theory of modeling and the algorithmization of technological processes.

It is necessary to develop the method and apparatus for automatic investigation of technological and industrial processes as the objects of automation.

It is necessary to have considerable strengthening of research work on raising the reliability of control apparatus. In the area of problems in the building of technical means of automation, this task is a decisive one, since, if there will be no automatic equipment of high reliability, the tasks of building completely automated productive complexes can not be solved in practice.

The resolution of the Plenum of the Central Committee of the Communist Party of the Soviet Union, "On the course of fulfillment of decisions of the Twenty-first Congress of the Communist Party of the Soviet Union regarding development of industry and transport, the introduction of the latest attainments of science and technique into production," has an exceptionally important significance for the creation of the material and technical basis of communism in our country.

Soviet specialists in automation are applying every effort, all their knowledge, intelligence, and energy to bring to life the historic decision of our Party regarding further acceleration of the building of a communist society.

AUTOMATIC OPERATING MODE OPTIMIZATION OF A CLASS OF SYSTEMS WITH RESPECT TO STATISTICAL PERFORMANCE CRITERIA*

S. A. Doganovskii

Moscow

Translated from Avtomatika i Telemekhanika, Vol. 21, No. 8, pp. 1105-1114,
August, 1960
Original article submitted March 22, 1960

This article is concerned with problems in automatic optimization of the operating mode of a system subject to random disturbances. The design of a computer whose operation is based on assigned performance criteria is substantiated. Results obtained in investigating the optimization process are given.

1. Formulation of the Problem

One of the most important problems in complex automation consists in securing such a control of industrial devices that they operate under the most advantageous (optimum) conditions. This problem is now being solved, due to the widespread introduction of various modern computer devices in control systems and the provision of self-adjusting automatic control systems.

As is known [1], automatic optimization systems, which select the system optimum operating mode, represent an important class of self-adjusting systems.

The optimum operating mode of a system is determined in correspondence with the performance criterion, which is assigned beforehand on the basis of technological requirements imposed on the quantity to be optimized in concrete problems of industrial process (device) control. The formulation of the required and the most suitable performance criterion is, in each case, a separate, and, quite often, a very complicated problem.

In a number of industrial systems to be controlled, where random disturbances play an important role, it is advisable to accept a certain average value for the deviation of the quantity x to be controlled as the performance criterion φ, for instance,

$$\int |x(t)|\,dt, \int [x(t)]^2\,dt, \int x(t-\tau)\ F(t)\,dt$$

or the sum of averaged values of the system variables x_i, for instance,

$$\sum_{i=1}^{n} \alpha_i \int |x_i(t)|\,dt,\ \ \sum_{i=1}^{n} \alpha_i \int [x_i(t)]^2\,dt,$$

$$\sum_{j=1}^{m} \sum_{i=1}^{n} \int F_j(t)\,x_i(t-\tau)\,dt$$

or

$$\int \alpha_i \sum_{i=1}^{n} |x_i(t)|\,dt,\ \int \alpha_i \sum_{i=1}^{n} [x_i(t)]^2 dt,$$

$$\int \sum_{j=1}^{m} \sum_{i=1}^{n} F_j(t)\,x_i(t-\tau) dt,$$

where α_i are certain weighting factors of the system, and F_j are disturbances acting on the system. Hereafter, the optimization of the system operating mode will designate the minimization of the φ quantity, which is determined on the basis of an accepted performance criterion.

Such statistical processing of data on the process (system to be controlled) state must be performed by the computer, which we shall call the unit for forming the quantity to be minimized† (UFQM) [4]. The UFQM output signal φ determines the variable (or a number of such variables φ_i) to be minimized in the process of optimizing the system operating mode. Then the φ_i quantities, together with the values H_i of the restrictions for the entire system which are to be taken into account [2], are fed to the inputs of an automatic optimizer, which searches for the necessary system parameters Z_i for which the minimization of the UFQM output signal is secured.

---

* The basic principles used in this article were discussed on June 10, 1959 at the IAT AN SSSR (Institute of Automation and Remote Control, Academy of Sciences, USSR) seminar on the theory of optimum, self-adjusting, and interdependent automatic control systems.

† In the particular case of correction with respect to the minimum of the mutual correlation function, the forming of φ is performed by a correlator-type computer.

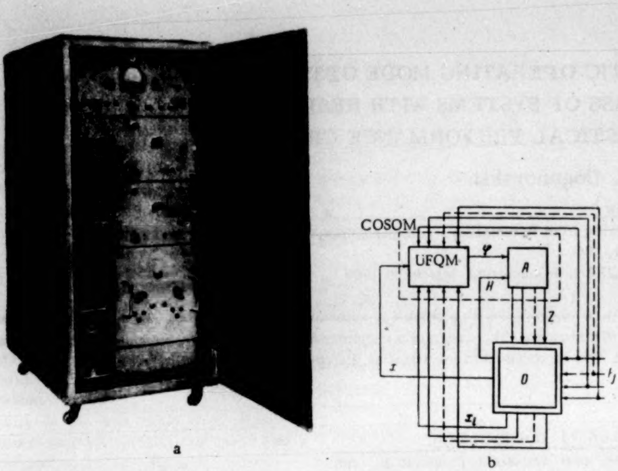

a

b

Fig. 1.

The control device of such an automatic control system, which was developed at IAT AN SSSR during the years 1957-1959, was designated as the computer for optimizing the system operating mode (COSOM) (Fig. 1a). The automatic control system, the block diagram of which is shown in Fig. 1b, has the following characteristics. In the first place, the formation of the control signal φ_1 is here effected after preliminary statistical processing of the system state data, which is secured by UFQM. Therefore, the effect of random factors (disturbances) acting on the optimizer A, which is the basic component in the control of the system, is considerably reduced. In the second place, the quantity to be minimized is not the controlled variable $\underline{x}$ itself, but the quantity φ, which is formed on the basis of the performance criterion, which determines the optimum operating mode of the system. Therefore, the system characteristic with respect to φ is always at the optimum, even in the case where the characteristics of the system to be controlled are linear. Papers [2, 3, 4] are devoted to problems in the design of such a class of automatic control systems.

The main purpose of the present paper is the investigation of the process of the system's approach to its optimum operating mode under the action of random disturbances. In the general case, the process of the system motion as represented in Fig. 1b is an unsteady-state process even in the case of steady-state random disturbances F_i.

The consideration will be restricted here solely to the case where the system operating mode is searched for with respect to one variable of the system to be controlled, without taking into account possible restrictions of the control system variables with respect to the integral of the square of the controlled variable $\underline{x}$ for a steady-state random input disturbance F. The case of the asymptotically steady-state (quasi-steady-state) process of the system motion is considered. The obtained results are then rendered more accurate by estimation of errors to be found, which is connected with the limitation of the UFQM averaging time interval in actual self-adjusting systems.

2. Equations of the System and the Investigation Method

For an illustration of the method used in investigating the system whose diagram is shown in Fig. 1b, consider an actual system O', which is a system for compensating disturbances F, acting at its input (Fig. 2). The structural diagram of such a system is typical for control systems which respond to disturbances [5, 6]. Here, disturbance F is fed directly to one of the inputs of the system O to be controlled and, moreover, to its second input through compensating device k_0. The adjustment of the compensating device secures compensation of disturbance F at the output of the system to be controlled, i.e., in such a system, conditions under which the controlled variable $\underline{x}$ is independent (invariant) of disturbance F can be secured. If the characteristics of the system to be controlled change and, consequently, if the conditions for the controlled variable invariance are disturbed, COSOM must act, in the general case, on the parameter of the linear, as well as the nonlinear section of the compensating device, thereby correcting its operation. This correction of the compensating device parameters is performed in accordance with the beforehand-assigned performance criterion on the basis of statistical processing of the system state data. The tuning of the compensating device is completed after the conditions for the controlled variable invariance are satisfied, i.e., after the system optimum operating mode has been secured. Thus, in the system shown in Fig. 2, the conditions for the controlled variable invariance are automatically secured by COSOM, which leads to the most advantageous (optimum) operating mode of the entire system.

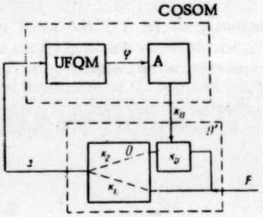

Fig. 2.

Let us consider the case where the system to be controlled is an inertialess linear system whose channels have transfer coefficients k_1 and k_2, respectively, and the compensating device is an amplifier with a variable amplification factor k_0.

For the performance criterion of the system optimum operating mode, we shall take the well-known criterion of minimum root-mean-square error (RMSE). In practice, it is more suitable to take the minimum of the controlled variable mean square, i.e.,

$$\varphi = \lim_{T\to\infty} \frac{1}{T}\int_0^T [x(t)]^2 dt. \tag{1}$$

Let us consider the search for the system optimum operating mode without taking into account the restrictions imposed on the system variables for the class of steady-state random input disturbances F with the spectral density $S_F(\omega)$. The system control device, COSOM, operates in the following manner [4]. Let there be a certain initial value of the amplification factor $k_0(0)$ of the compensating device for which the invariance conditions in the system are not satisfied, i.e., $k_0(0) \neq k_1/k_2$. Consequently, there will be random deviations of the controlled variable x(t) at the system output. At the beginning, COSOM forms the φ_1 quantity in UFQM according to the assigned performance criterion (1) and memorizes φ_1. Then COSOM assigns a trial step by changing the amplification factor $k_0(0)$ of the compensating device by Δk_0; in this, the $\varphi = \varphi_1 + \Delta\varphi$ quantity is formed again, and the quantity $\Delta\varphi$ is determined, which is fed to the input of the final (integrating) optimizer device, and which changes the amplification factor k_0 of the compensating device.

For the shaping of φ signals, UFQM is provided with a generating unit, which is used as a quadrator, and an averaging unit, which consists of a pulse filter. The latter represents an integrator with the cancellation of readings after integration time T. The necessary division of the integration result by T is secured by a suitable choice of the integrator scale factor.

From a practical point of view, φ cannot be determined over an infinite integration time interval. Therefore, the determination quantity φ^* [7], which is given by the following expression, is formed in UFQM:

$$\varphi^* = \frac{1}{T}\int_0^T [x(t)]^2 dt. \tag{2}$$

Assuming that the formed signals φ and φ^* are close to each other, we arrive at the system asymptotic steady-state operating mode. Then the φ quantity can be expressed in terms of the spectral density $S_F(\omega)$ of the input disturbance by the relation

$$\varphi \approx \frac{1}{\pi}\int_0^\infty S_F(\omega)\,|K(j\omega)|^2\,d\omega, \tag{3}$$

where $|K(j\omega)|$ is the modulus of the transfer coefficient of the system to be controlled.

For the case of an inertialess linear system, expression (3) will be written in the following form:

$$\varphi = \frac{1}{\pi}\int_0^\infty S_F(\omega)(k_1 - k_2k_0)^2\,d\omega = D(k_1 - k_2k_0)^2, \tag{4}$$

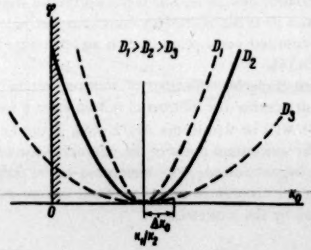

Fig. 3.

where D designates the input disturbance dispersion

$$D = \frac{1}{\pi}\int_0^\infty S_F(\omega)\,d\omega. \qquad (5)$$

Since φ is the quantity to be minimized in the system, Eq. (4) determines the system characteristic as the object of optimum (extremal) control (Fig. 3). The amplification factor k_0 of the compensating device is the argument of this characteristic, and the transfer coefficients k_1 and k_2 of the system to be controlled and the dispersion D of the input disturbance are the parameters of the characteristic. A change in the system parameters will cause a shift of the characteristic extremum with respect to the k_0 axis and will change the slope of its branches. The minimum of the φ quantity will be secured for a given value of the compensating device amplification factor k_0 for which the following condition for the controlled variable invariance is satisfied:

$$k_0 = \frac{k_1}{k_2}. \qquad (6)$$

For $k_1 > 0$ and $k_2 > 0$, k_0 cannot be determined by values in the left half-plane in Fig. 3, which is marked by the shaded boundary of the region where changes of the compensating device amplification factor are allowable.

Figure 3 also shows the magnitude of the trial step Δk_0, which is assigned by the automatic optimizer in searching for the necessary value of the amplification factor k_0 which will satisfy Eq. (6). Thus, the formation of the quantity φ to be minimized on the basis of a given performance criterion makes it possible to reduce the linear system O characteristic to the extremal value (Fig. 3).

Figure 4 illustrates the structure of a system subject to extremal control with the characteristic of Fig. 3.

Here, K_1, K_2, K_3, and K_4 are contacts of the optimizer control device A, MD is the optimizer memory device, and ID is the optimizer final (integrating) device. A detailed description of such an optimizer system is given in [4].

Let us find the equations of motion for the system and determine the number of search steps n for which the system will be within the $\Delta k_0/2$ zone in the neighborhood of the extremum point of the characteristic of the system to be controlled. The increment in the output voltage of the automatic optimizer final device will be determined by the expression

$$\delta z_i = \frac{k_{\mathrm{fd}}}{RC}\int_0^{T_{\mathrm{os}}} \Delta\varphi_i\,dt = \frac{k_{\mathrm{fd}}}{RC}T_{\mathrm{os}}\,\Delta\varphi_i, \qquad (7)$$

where $\Delta\varphi_i$ is the function increment at the ith point, T_{os} is the optimizer operating step time, k_{fd} is the scale factor of the optimizer final device, RC is the time constant of the optimizer final device, and z_i is the output voltage of the optimizer final device.

By substituting in Eq. (4)

$$k_1 - k_2 k_0 = z, \qquad (8)$$

we obtain the following expression for the characteristic of the system to be controlled:

$$\varphi = Dz^2.$$

Consequently, for small values of Δz,

$$\Delta\varphi = 2z_i D\Delta z. \qquad (10)$$

By substituting in Eq. (7) the value of $\Delta\varphi_i$ from Eq. (10), we obtain the equation for the output voltage increment in the optimizer final device:

$$\delta z_i = \frac{k_{\mathrm{fd}}}{RC}T_{\mathrm{os}}\,2Dz_i\Delta z = \theta z_i = BDz_i, \qquad (11)$$

where

$$B = 2\frac{k_{\mathrm{fd}}}{RC}T_{\mathrm{os}}\,\Delta z. \qquad (12)$$

As it is assumed that the disturbance F which acts on the system belongs to the class of steady-state random disturbances, the quantity D is constant and, consequently, θ is also a constant quantity.

Starting with the initial value of $k_0(0)$, the values of δz_i will be determined by expressions of the following form:

$$\begin{aligned}\delta z_i &= \theta z_i = \theta(z_{i-1} - \delta z_{i-1}) = \\ &= \theta[z_0(1-\theta)^{i-1} - \theta z_0(1-\theta)^{i-1}] = \\ &= \theta z_0(1-\theta)^i.\end{aligned} \qquad (13)$$

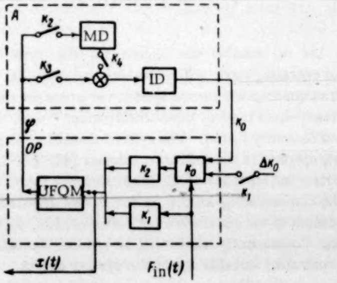

Fig. 4

and the value of z_n will be determined by the expression

$$z_n = z_0 (1 - \theta)^n. \tag{14}$$

By solving simultaneously Eqs. (8) and (14), we obtain the equation

$$k_1 - k_2 k_0 [n] = [k_1 - k_2 k_0 (0)] (1 - \theta)^n = \\ = \left[\frac{k_1}{k_2} - k_0 (0) \right] (1 - \theta)^n k_2. \tag{15}$$

By solving Eq. (15) with respect to $k_0[n]$, we find the system equation of motion as a function of the number of steps in searching for the required value of the compensating device amplification factor:

$$k_0 [n] = \frac{k_1}{k_2} [1 - (1 - \theta)^n] + k_0 (0) [1 - \theta]^n. \tag{16}$$

From a consideration of the system equation of motion in the adjustment of the required amplification factor value (16), it follows that the following inequality has to be satisfied if the scanning process is to be convergent:

$$| 1 - \theta | < 1, \tag{17}$$

i.e.,

$$\theta < 2. \tag{18}$$

Figure 5 shows the diagrams of the system motion during the adjustment of the required value of the compensating device amplification factor k_0 as functions of the argument n for jumplike changes in the k_1/k_2 parameters of the system to be controlled.

Until now, our point of departure was the assumption that the dispersion D was formally determined by averaging the square values of input disturbances F of the system to be controlled over an infinite observation interval ($T \to \infty$). However, the integration time interval is always finite in practice, and it is convenient to make it as small as possible, because, in the first place, the actual integrator circuits are imperfect and their errors increase with time, and, in the second place, a reduction of the scanning time is thereby achieved. Therefore, for steady-state random input disturbances, the magnitude of dispersion (D_T), produced over the finite interval T, will also be a random quantity, which will fluctuate about its average value D, which is determined for an infinite integration time interval.

The degree of approximation of D by the D_T function can be characterized by the magnitude of the mean square deviation of these functions:

$$\sigma_D^2 = M [(D_T - D)^2], \tag{19}$$

where M is the sign of mathematical expectation, or[‡]

$$\sigma_D^2 = \frac{2}{T^2} \int_0^T (T - \tau) 2R^2 (\tau) d\tau, \tag{20}$$

where

$$R (\tau) = M [F (t) F (t + \tau)].$$

Thus, if we know the input disturbance autocorrelation function $R(\tau)$, we can determine σ_D^2.

Since the input disturbance spectral density $S_F(\omega)$ is connected with the autocorrelation function by Fourier transformation, we obtain the following expression:

$$\sigma_D^2 = \frac{4}{T^2} \int_0^T (T - \tau) \left[\frac{1}{\pi} \int_0^\infty S_F (\omega) \cos \omega\tau \, d\omega \right]^2 d\tau. \tag{21}$$

Let us consider a case often encountered in practice, where the spectral density of the input disturbance F is of the following form:

$$S_F (\omega) = \frac{S_0}{1 + \omega^2 T_0^2}. \tag{22}$$

Then the equation for determining the root-mean-square error σ_D will be written thus:

$$\sigma_D = \frac{2S_0}{\pi T} \sqrt{\int_0^T (T - \tau) \left[\int_0^\infty \frac{\cos \omega\tau}{1 + \omega^2 T_0^2} d\omega \right]^2 d\tau}. \tag{23}$$

The integral in square brackets in expression (23) can be determined as:

$$\int_0^\infty \frac{\cos \omega\tau}{1 + \omega^2 T_0^2} d\omega = \frac{\pi}{2T_0} e^{-\frac{\tau}{T_0}}. \tag{24}$$

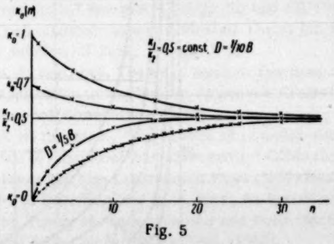

Fig. 5

[‡] A normal probability distribution of the F(t) function is assumed.

By substituting (24) in (23), after suitable transformations, we obtain the equation

$$\sigma_D = \frac{S_0}{T_0}\psi\left(\frac{T}{T_0}\right), \tag{25}$$

where

$$\psi\left(\frac{T}{T_0}\right) = \frac{1}{\sqrt{2}}\sqrt{\frac{e^{-2T/T_0}-1}{2\left(\frac{T}{T_0}\right)^2} + \frac{1}{\frac{T}{T_0}}}. \tag{26}$$

Expressions (25) and (26) indicate that the root-mean-square error tends to zero for T→ ∞. By assigning the maximum allowable value σ_{Dma}, S_0, and T_0, we find the required value of the integration time T by using the inequality

$$\sigma_D = \frac{S_0}{T_0}\psi\left(\frac{T}{T_0}\right) \leqslant \sigma_{D\,\mathrm{ma}}. \tag{27}$$

The graph of the $\psi(T/T_0)$ function is shown in Fig. 6.

Let us now determine the number of search steps for which the system falls within the $\Delta k_0/2$ zone in the neighborhood of the extremum point of the system characteristic.

From Eqs. (13) and (14), we find

$$z_0(1-\theta)^n = \frac{\Delta z}{2}. \tag{28}$$

The number of search steps for which the system falls within the $\Delta k_0/2$ zone is determined from Eqs. (28) and (12):

$$n = \frac{\ln\frac{\Delta z}{2z_0}}{\ln(1-BD)} = \frac{\ln\frac{\Delta k_0}{2[k_0(0)-k_1/k_2]}}{\ln(1-BD)} = \frac{\ln\frac{1}{C}}{\ln(1-BD)}, \tag{29}$$

where

$$C = \frac{k_0(0)-k_1/k_2}{\Delta k_0/2}. \tag{30}$$

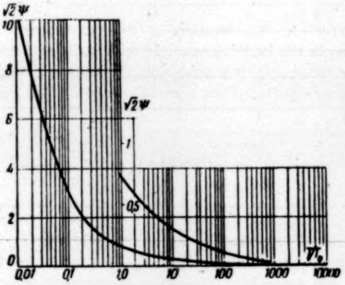

Fig. 6

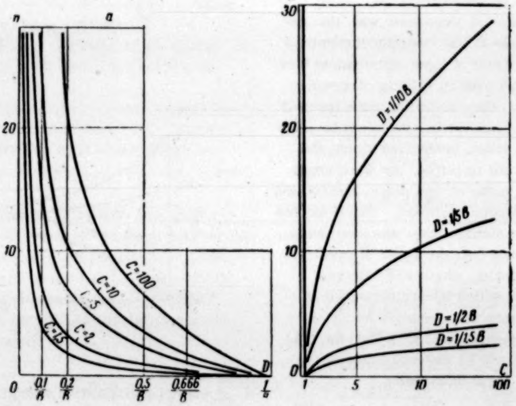

Fig. 7

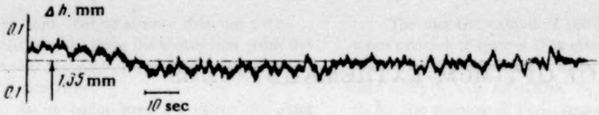

Fig. 8

Figure 7 shows the graphs plotted with respect to Eq. (29), which indicate the effect of quantities B, C, and D on the number of steps required in searching for the system optimum operating mode. The quantity C shows how many trial steps $\Delta k_0/2$ are contained in the interval between the initial and the required (for securing the extremum) values of the compensating device amplification factor k_0; it is determined by the assigned value of Δk_0, which is the initial deviation of the compensating device amplification factor from the required value, and it does not depend on D_T fluctuations. Since, as was mentioned above (Fig. 3), changes in D_T cause changes in the slope of the system characteristic branches, the number of search steps for which the system motion will settle in the neighborhood of the extremum point will also fluctuate about its average value M[n].

The mathematical expectation of n, which is, as can be seen from Eq. (29), a nonlinear function of D_T, will be determined by the expression

$$M[n] = \ln \frac{1}{C} \int_{-\infty}^{\infty} \frac{p(D_T)}{\ln(1-BD_T)} dD_T. \qquad (31)$$

Here, $p(D_T)$ is the probability density of the random quantity D_T.

The above investigation is theoretically valid for the case of an asymptotically steady-state process of the system motion toward its optimum operating mode. Nevertheless, the investigation method considered is applicable to a number of practical problems.

As an example, Fig. 8 shows a typical oscillogram of thickness fluctuations of a metal strip at the input of a continuous-operation cold-rolling mill [8]. By using Eqs. (19) - (27), a preliminary statistical processing of data in this oscillogram will make it possible to find the necessary averaging time T of the UFQM integrating device, to determine the COSOM parameters with respect to Eqs. (29) - (31), and to determine the necessary number of search steps in designing a self-adjusting system for the automatic control of the strip thickness in continuous-operation cold-rolling mills [4].

SUMMARY

1. Automatic optimization systems, including the computer for optimizing the system operating mode (COSOM), represent a new and promising direction in the development of modern high-quality automatic control systems. They can be used in various branches of technology, for instance, for the optimum control of welding conditions in electric tube-welding mills, for the control of the strip thickness in continuous-operation cold-rolling mills, in designing self-adjusting autopilots, etc.

2. The performed investigation of the self-adjustment process in systems of this class makes it possible, in a number of practical cases, to determine the necessary number of steps in the search for the optimum operating mode and to determine the parameters of individual COSOM units.

The author extends his thanks to A. A. Fel'dbaum for his valuable advice in the completion of this work, and to Yu. P. Leonov for his discussion of the obtained results.

LITERATURE CITED

1. A. A. Fel'dbaum, Computers in Automatic Systems [in Russian] (Fizmatgiz, 1959).
2. A. A. Fel'dbaum, "Automatic optimizer," Avtomat. i Telemekh. 19, No. 8 (1958).**
3. A. B. Chelyustkin and V. A. Ivanov, "A self-adjusting system for the automatic control of welding conditions in electric pipe-welding mills," Élektrichestvo No. 2 (1960).
4. S. A. Doganovskii, "Automatic adjustment of compensator parameters in disturbance-response control systems," Avtomatika i Telemekhanika 20, No. 8 (1959).**
5. V. S. Kulebakin, "On the applicability of the absolute invariance principle in actual physical systems," Doklady Akad. Nauk SSSR 60, No. 2 (1948).
6. B. N. Petrov, "On the applicability of invariance conditions," Proceedings of the Second All-Union Conference of Automatic Control Theory [in Russian] (Izd.AN SSSR, 1955) Vol. 2.
7. V. S. Pugachev, Theory of Random Functions and Its Application to Problems in Automatic Control [in Russian] (Gostekhizdat, 1957).
8. N. N. Druzhinin, "Application of complex automation to continuous-operation mills," Collection: Heavy Machine Construction News (1958) Nos. 7-8.
9. W. B. Davenport and W. L. Root, An Introduction to the Theory of Random Signals and Noise (McGraw-Hill Book Company, New York, 1958).

** See English translation.

TWO TYPES OF OPTIMUM-EXTREMAL SYSTEMS

L. N. Fitsner

Moscow

Translated from Avtomatika i Telemekhanika, Vol. 21, No. 8, pp. 1115-1121,
August, 1960
Original article submitted March 22, 1960

The design of the two simplest types of extremal systems with inertial linear units is considered.

In the system of the first type, the scanning process is completed in the minimum time for assigned restrictions of the variable of the system to be controlled. In the system of the second type, the scanning process takes place for a minimum value of the dynamic error integral. The diagram of the optimum control equipment and the results of experimental investigations of the systems are provided.

1. Introduction

Systems which are designed for the automatic determination of the input in any industrial device for which its output, which depends on the input value, assumes either the minimum or the maximum value are presently used to an ever-increasing extent. Such systems are called extremal systems.

In [1], it was shown that extremal systems belong to a separate class of automatic control systems, being conceptually different from most other such systems. At the same time, extremal and (other) automatic control systems have many characteristics in common. Therefore, in developing the theory of extremal systems, it is often possible to use certain principles and methods of the more developed theory of automatic control systems.

The present paper is concerned with the design of optimum extremal systems with respect to quickness of response and the integral value of the dynamic error.

It is assumed that the scanning process for finding the extremum points occurs in an inertial system with a limited value of one of its variables. For automatic control systems with optimum quickness of response, this problem and its solution are known [2, 3].

The basic results obtained in these papers can also be used in designing extremal systems with the optimum quickness of response.

In designing optimum extremal systems, a number of restrictions are imposed on the characteristics of the system where the scanning is to be effected. It is assumed that no random disturbances affect this system during the scanning process and that the system output quantity y is related to its input quantity x by a parabolic dependence of the following form:

$$y = a(x-b)^2 + c. \qquad (1)$$

Quantities c and b can assume different values during the scanning process. The a coefficient is assumed to be constant, although, for certain more complicated control systems, this restriction may not be introduced. It is assumed that b can change only stepwise in the system to be controlled.

As a rule, the characteristics of actual industrial systems differ from those used in this paper, and, therefore in certain cases, for instance, when random disturbances of large magnitude are present in the system to be controlled, the extremal system may be inoperative. The characteristics of the system to be controlled are usually approximations of the above-indicated characteristics, and, therefore, the extremal systems under consideration will be only approximations of the optimum systems. However, even in these cases, although the control system described below is not actually an optimum system, it will still be possible to reduce the scanning time for finding the extremum, as well as the integral dynamic error of the extremal system.

We shall assume that the system to be controlled, where the scanning takes place, consists of two units: the linear inertial and the nonlinear inertialess units. The linear unit consists of two integrating elements, which are connected in series. The linear unit input is restricted with respect to its modulus. The nonlinear unit of the system is described by Eq. (1). We shall consider the case where it is possible to measure the rate of change in the linear unit output and, as a result of this measurement, obtain, for instance, a voltage proportional to this rate.

2. Extremal System with Optimum Quickness of Response

The structural diagram of the extremal system is shown in Fig. 1. The system consists of the scanning object O and the control equipment CE. We shall consider the case where the system input quantity x_2 is limited with respect to its modulus: $|x_2| \leq E$. Let the coordinate origin be chosen in such a manner that b = 0 corresponds to the extremum of y at a certain instant of time, which is taken for zero. Let us assume that, for $t \geq 0$, the value of x will deviate from the extremum point by b. It is required that the system find the extremum point in the minimum time.

In this case, the deviation from the extremum point can be determined by the equation

$$b = \frac{1}{2a}\frac{dy}{dx}. \tag{2}$$

It is known [2, 3] that, in an automatic control system which controls a system that includes two integrating elements and has an input quantity whose modulus is restricted, the deviation is eliminated in the minimum time for the following control conditions:

$$x_2 = \begin{cases} +E \text{ for } & x_1|x_1| + \frac{2xa_1E}{a_2} > 0, \\ -E \text{ for } & x_1|x_1| + \frac{2xa_1E}{a_2} < 0. \end{cases} \tag{3}$$

Here, E designates the maximum allowable value of x_2.

This control condition can be used in designing an extremal system with optimum quickness of response. In an extremal system, it is first of all necessary to reduce most effectively the value of x_1 when the system moves in the wrong direction. This operation must be effected at definite times while the system moves in the correct direction, in order to prevent the transition of the extremum point due to the presence of integrating elements in the system. In order to determine the switching time, according to (3), it is necessary to know the value of x_1 and the deviation of x from the extremum point, which is given by (2).

Let us express b in the following form:

$$b = \frac{1}{2a}\frac{dy}{dx} = \frac{1}{2a}\frac{dy}{dt}\cdot\frac{dx}{dt} = \frac{1}{2a\,x_1}\frac{dy}{dt}. \tag{4}$$

Hence, by taking into account (3), the control conditions for the extremal system can be written thus:

$$x_2 = \begin{cases} +E, \text{when } |x_1^3|\frac{aa_2}{Ea_1} + \frac{dy}{dt} > 0 \text{ for } & x_1 < 0 \\ \quad\text{and } |x_1^3|\frac{aa_2}{Ea_1} + \frac{dy}{dt} < 0 \text{ for } & x_1 > 0, \\ -E, \text{when } |x_1^3|\frac{aa_2}{Ea_1} + \frac{dy}{dt} > 0 \text{ for } & x_1 > 0 \\ \quad\text{and } |x_1^3|\frac{aa_2}{Ea_1} + \frac{dy}{dt} < 0 \text{ for } & x_1 < 0 \end{cases} \tag{5}$$

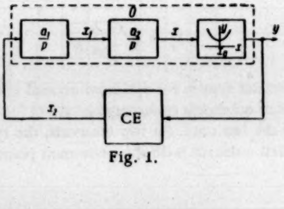

Fig. 1.

The electric circuit of the equipment securing optimum control of system O is given in Fig. 2. The equipment includes a polarized relay P_2, a two-coil polarized relay P_1, a dc amplifier A_1 [4], with diodes D_1 and D_2 for the shaping of $|x_1|$, and a differentiator, which is based on an amplifier A_2. For obtaining the $|x_1^3(aa_2/Ea_1)|$ term, a carborundum resistor T with a nearly third-power voltampere characteristic is used [5]. The characteristic of the nonlinear resistor T can be brought closer to a third-power characteristic by means of resistor R_3. If the output y of the system to be controlled changes slowly, difficulties are encountered in obtaining the dy/dt derivative. The output signal y usually contains high-frequency disturbances, which are intensified by the differentiator and which suppress the main signal proportional to the derivative. Therefore, instead of the derivative, it is advisable to determine the increments

$$\Delta y = y_1 - y_2 \tag{6}$$

for equal time intervals

$$\Delta t = t_1 - t_2. \tag{7}$$

In determining Δy, it is necessary to calculate the small difference between two large voltages and also to memorize the voltage over the Δt period. This problem was solved by means of a capacitor circuit [6].

3. Extremal System with the Minimum Integral Dynamic Error

The following quantity will be designated as the integral dynamic scanning error:

$$I = \int_0^T (y - y_e)\,dt. \tag{8}$$

Here, T is the scanning time, and y_e is the extremal value of y.

According to (1),

$$y_e = c. \tag{9}$$

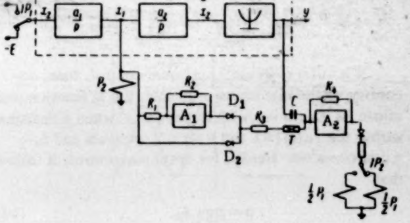

Fig. 2.

By substituting (1) and (9) in (8), we obtain

$$I = \int_0^T a\,(x-b)^2\,dt. \tag{10}$$

For the system considered above (Fig. 1), we shall first find the control conditions for which the error will be at the minimum:

$$I = I_{\min}\,.$$

In automatic control systems, the $I_{\min}$ quantity corresponds to the minimum value of the integral of the quadratic dynamic error.

We shall use L. S. Pontryagin's maximum principle [7]. We shall substitute the functions and write the system equation in terms of symbols used in [7]:

$$I = \bar{x}_0 \quad a\,(x-b)^2 = \bar{x}_1^2,$$

$$\sqrt{a}\,a_2 x_1 = \bar{x}_2, \quad a_1 a_2 \sqrt{a}\,x_2 = u.$$

As a result, we obtain

$$\begin{gathered} \bar{x}_0 = \int_0^T \bar{x}_1^2\,dt = \int_0^T f^0\,dt, \quad \bar{x}_1^2 = f^0, \\ \dot{\bar{x}}_1 = \bar{x}_2 = f^1, \quad \dot{\bar{x}}_2 = u\,(t) = f^2. \end{gathered} \tag{11}$$

By using the L. S. Pontryagin maximum principle, we shall write the equations for the $\psi_0 = \psi_0(t)$, $\psi_1 = \psi_1(t)$, and $\psi_2 = \psi_2(t)$ functions:

$$\begin{gathered} \dot{\psi}_i = -\sum_{\alpha=0}^{2} \frac{\partial f^\alpha}{\partial \bar{x}_i}\,\psi_\alpha \qquad (i = 0,\ 1,\ 2), \\ \psi_0 = 0, \quad \dot{\psi}_1 = -2\bar{x}_1\psi_0, \quad \dot{\psi}_2 = -\psi_1. \end{gathered} \tag{12}$$

The function $H = H(\bar{x}_0, \bar{x}_1, \bar{x}_2, \psi_0, \psi_1, \psi_2, u)$ is of the following form:

$$H = \psi_0 f^0 + \psi_1 f^1 + \psi_2 f^2 = \psi_0 \bar{x}_1^2 + \psi_1 \bar{x}_2 + \psi_2 u. \tag{13}$$

If $u = u(t)$ represents optimum control, then, according to the maximum principle, the H function must attain its maximum with respect to $\underline{u}$, when $\underline{u}$ changes within the $|u(t)| \leq 1$ and $0 \leq t \leq T$ intervals and $\psi_0 = \text{const} = -a^2 \leq 0$. Hence, for optimum control, it follows that

$$u = \operatorname{sign} \psi_2. \tag{14}$$

Thus, the totality of optimum trajectories must satisfy the following system of equations:

$$\dot{\bar{x}}_1 = \bar{x}_2, \quad \dot{\bar{x}}_2 = \operatorname{sign} \psi_2, \quad \dot{\psi}_1 = 2a^2 x_1, \quad \dot{\psi}_2 = -\psi_1. \tag{15}$$

Thus, in order to secure $I_{\min}$, as well as the minimum scanning time, the system input whose modulus is restricted must assume either the $x_2 = +E$ or $x_2 = -E$ value.

Let us consider the motion system in two intervals corresponding to $x_2 = +E$ and $x_2 = -E$. The velocity at the beginning of the first interval and at the end of the second interval is assumed to be equal to zero. In this case, the motion times for the first (t_1) and the second (t_2) intervals are equal to each other:

$$t_1 = t_2\,. \tag{16}$$

The dynamic error is

$$\begin{gathered} I = a\int_0^{t_1} \left(\frac{a_1 a_2 E t^2}{2} - b\right)^2 dt + \\ + a\int_0^{t_1} \left(\frac{a_1 a_2 E t_1^2}{2} - b + a_1 a_2 E t_1 t - \frac{a_1 a_2 E t^2}{2}\right)^2 dt = \\ = \frac{23}{30} a_1^2 a_2^2 a E^2 t_1^5 - 2 a_1 a_2 a E b t_1^3 + 2b^2 a t_1. \end{gathered} \tag{17}$$

Let us determine t_1 for which $I = I_{\min}$. By finding the partial derivative of I with respect to t_1 from Eq. (17),

$$\frac{23}{6} a_1^2 a_2^2 E^2 t_1^4 - 6 a_1 a_2 E b t_1^2 + 2b^2 = 0 \tag{18}$$

we obtain

$$t_1 = 1.04 \sqrt{\frac{b}{a_1 a_2 E}}\,. \tag{19}$$

By substituting (19) in (17), we obtain

$$I_{\min} = \frac{0.772\,ab^2\sqrt{b}}{\sqrt{a_1 a_2 E}}\,. \tag{20}$$

It should be noted that, according to [2],

$$t_1^* = \sqrt{\frac{b}{a_1 a_2 E}} \tag{21}$$

for a similar system for optimum control conditions with respect to quickness of response.

In the last case, for two intervals, the system operation will coincide with the extremum point.

From a comparison between (19) and (21), it is obvious that, for control conditions securing a minimum value of the dynamic error integral, the retarding time is shorter than for optimum control conditions with respect to time. Consequently, the system must first pass the extremum point, then change direction of motion, and again pass through the extremum point from the other side, etc.

We shall demonstrate that the system motion during the intervals following the two considered above hardly affects the value of the dynamic error integral.

From (19) and (21), we find

$$t_1 = 1.04\, t_1^{*}. \tag{22}$$

The system transition beyond the extremum point is

$$\Delta b = (1.04t_1)^2 a_1 a_2 E - t_1^2 a_1 a_2 E = 0.08 a_1 a_2 E t_1^2. \tag{23}$$

By using (20), we find the ratio of $I^{*}_{\min} = I_{\min}(\Delta b)$ to $I_{\min} = I_{\min}(b)$:

$$\frac{I^{*}_{\min}}{I_{\min}} = 0.002. \tag{24}$$

The $I^{*}_{\min}$ quantity can be neglected. Fig. 3 shows the dependence of αI on βt_1, where

$$\alpha = \sqrt{\frac{a_1 a_2 E}{a^2 b^b}}, \tag{25}$$

$$\beta = \sqrt{\frac{a_1 a_2 E}{b}}. \tag{26}$$

It is obvious from the graph that, for equal α and β, the dynamic error integral I_{oqr} for a system with optimum quickness of response [which corresponds to $t_1\beta = 1$ according to (21)] differs little from its minimum value, which corresponds to $t_1\beta = 1.04$ according to (20).

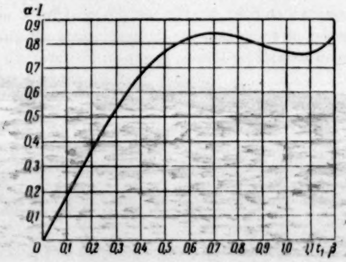

Fig. 3

By substituting (21) in (17), we find

$$I_{oqr} = 0.778\,\alpha. \tag{27}$$

According to (20),

$$I_{\min} = 0.772\,\alpha. \tag{28}$$

Let us denote the ratio of $I_{\min}$ to I_{oqr} by δ. From (27) and (28), we obtain

$$\delta\,\% = \frac{I_{\min}}{I_{oqr}} = 99.23\,\%. \tag{29}$$

Thus, the considered extremal systems, the one with the optimum quickness of response and the one with the minimum value of the dynamic error integral, are close to each other and they have practically the same control equipment.

4. Experimental Investigation Results

The above optimum control scheme for an extremal system was experimentally investigated by means of an electronic simulating device. The quadratic characteristic of the nonlinear part of the model simulating the system to be controlled was reproduced by means of a carborundum resistor [5]. The oscillogram in Fig. 4 shows two scanning processes. In the first section, for $t < t_1$, the scanning was effected for the open carborundum resistor circuit [the term $\left[\left|x_1^3\right|\frac{aa_2}{Ea_1}\right]$ was not included in control conditions (5)]. The scanning system did not find the extremum point, and the amplitude of the system oscillations increased.

For $t = t_1$, the $|x_1^3|\frac{aa_2}{Ea_1}$ term was introduced in the control program, and the system attained the extremum point in the minimum time and performed small oscillations about this point.

We also investigated the optimum scanning process in an extremal system whose inertial part consisted of an inertial element with the time constant T and the amplification factor a_1 and an integrating element with the coefficient a_2, which were connected in series. The optimum conditions for controlling a regulating system with such an inertial part have been considered in [8].

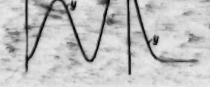

Fig. 4

For the experimental system, these conditions can be written in the following form by taking into account (4):

$$x_2 = \begin{cases} +E, \text{ when } & 2aa_2T\left[\left|x_1^2 + a_1Ex_1\ln\left(\left|\frac{x_1}{a_1E}\right|+1\right)\right|\right] + \frac{dy}{dt} > 0, \text{ for } x_1 < 0 \\ \quad \text{and} & 2aa_2T\left[\left|x_1^2 + a_1Ex_1\ln\left(\left|\frac{x_1}{a_1E}\right|+1\right)\right|\right] + \frac{dy}{dt} < 0, \text{ for } x_1 > 0 \\ -E, \text{ when } & 2aa_2T\left[\left|x_1^2 + a_1Ex_1\ln\left(\left|\frac{x_1}{a_1E}\right|+1\right)\right|\right] + \frac{dy}{dt} > 0, \text{ for } x_1 > 0 \\ \quad \text{and} & 2aa_2T\left[\left|x_1^2 + a_1Ex_1\ln\left(\left|\frac{x_1}{a_1E}\right|+1\right)\right|\right] + \frac{dy}{dt} < 0, \text{ for } x_1 < 0 \end{cases} \qquad (30)$$

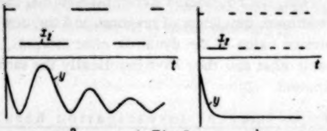

a Fig. 5 b

The oscillogram of the scanning process in an extremal system where nonlinear velocity feedback was not present in the control equipment is shown in Fig. 5a. The oscillogram of the scanning process in the same system with the optimum control conditions (30) is shown in Fig. 5b.

As in the above-considered case, the system was able to find the extremum point in the minimum time (for a given restriction of x_2), and it performed small oscillations about this point.

K. B. Norkin and V. A. Yakovlev collaborated in the experimental investigation of this system.

LITERATURE CITED

1. A. A. Fel'dbaum, Basic Trends in the Development of Computers for Automatic Systems, Report to the Session of the Academy of Sciences, USSR, on Scientific Problems in Industrial Automation [in Russian] (Izd. AN SSSR, 1957).
2. A. A. Fel'dbaum, "The simplest relay systems in automatic control," Avtomat. i Telemekh. 10, No. 4 (1949).
3. A. Ya. Lerner, "Improvement of dynamic properties of automatic compensators by means of nonlinear couplings," Avtomat. i Telemekh. 13, Nos. 2 and 4 (1952).
4. B. Ya. Kogan, Electronic Simulation Devices and Their Application in the Investigation of Automatic Control Systems [in Russian] (Fizmatizdat, 1959).
5. V. V. Pasynkov, Nonlinear Semiconductor Resistors (in Russian) (Leningradskii dom nauchno-tekhnicheskoi propagandy, Inst. Polyprovodnikov, AN SSSR, 1957).
6. L. N. Fitsner. A Device for Voltage Differentiation, Author's Certificate No. 119015 (1958).
7. R. V. Gamkrelidze, "On the general theory of optimum processes," Doklady Akad. Nauk SSSR 123, No. 2 (1958).
8. L. N. Fitsner, "Selection of Power Units of Optimum Automatic Control Systems," Avtomat. i Telemekh. 19, No. 12 (1958).*

---

* See English translation.

ON A PROBLEM OF OPTIMUM CONTROL

I. A. Litovchenko

Moscow

Translated from Avtomatika i Telemekhanika, Vol. 21, No. 8, pp. 1122-1133,
August, 1960
Original article submitted December 16, 1959

The problem of optimization (in the specified meaning of the term) is considered in tracking a trajectory of a body in accordance with the rule of proportional search [1]. The control function related to the position of the direction control is given on an interval of the real axis. The method of parametric representation of the control function [2, 3] is used in solving the problem; this enables one to use the methods of classical calculus of variations. The optimum control is found and its sufficient conditions are analyzed.

1. Statement of the Variational Problem in the General Case

The equations of motion of a point A* attacking goal B† in accordance with the rule of proportional search, are as follows [1]:

$$\rho\dot{\Phi}_c = v_c \sin(\varphi_c - \Phi_c) - v \sin(\varphi - \Phi_c),$$

$$\dot{\varphi} = \xi(t)\,\dot{\Phi}_c, \tag{1.1}$$

$$\dot{\rho} = v_c \cos(\varphi_c - \Phi_c) - v \cos(\varphi - \Phi_c),$$

where ρ is the distance from the point A to the goal B; φ is the climbing angle of the trajectory of point A; φ_C is the trajectory angle of the goal B (φ_C = const) – putting $\varphi_C > 0$ does not reduce the generality of the case; Φ_C is the sighting angle (Fig. 1); v and v_C are the magnitudes of the velocities of the point A and the goal B, respectively (they are assumed constant, and $v_C < v$); $\xi(t)$ is the control function connected with the autopilot and with the position of the direction control.

When $\rho < 0$, i.e., when $v_C \sin(\varphi_C - \Phi_C) - v \sin(\varphi - \Phi_C) = 0$, it is the case of the so-called "tracking triangle," i.e., a relationship between φ and Φ_C such that it ensures the interception of the goal. At the initial moment of time $t^{(1)} \varphi^{(1)} = \varphi(t^{(1)})$ and $\Phi_C^{(1)} = \Phi_C(t^{(1)})$ do not usually satisfy the above relation, and thus arises the optimum (in the specified meaning) control problem of getting point A on the tracking triangle.

We shall regard the following as the optimum trajectory. If at the initial moment of time the tracking triangle occurs, then $\dot{\Phi}_C = 0$, i.e., the tracking line does not change its direction in space and $\Phi_C = \Phi_C^{(1)} \equiv \text{const}$ $\left(\int_{t^{(1)}}^{t} \dot{\Phi}_c\,dt = 0\right)$. Otherwise, we have $\dot{\Phi}_C \neq 0$ and the tracking line turns the angle $|\Phi_C^{(2)} - \Phi_C^{(1)}|$ [this is a monotonic change in the angle Φ_C, as can be seen from the first equation (1.1)]. The less $|\Phi_C^{(2)} - \Phi_C^{(1)}|$ becomes, the nearer is the transition path of point A to the path $\dot{\Phi}_C = 0$, i.e., to the tracking triangle whose occurrence ensures (within the limits of the proposed problem) a mathematically precise interception. It is proposed‡ that the equation bringing point A from its initial state to the tracking triangle be called an optimum one if $L = \left|\int_{t^{(1)}}^{t^{(2)}} \dot{\Phi}_c\,dt\right|$ attains its minimum value: $\min L = \min|\Phi_C^{(2)} - \Phi_C^{(1)}|$, this $\min|\Phi_C^{(2)} - \Phi_C^{(1)}|$ being equivalent to $\min \Phi_C^{(2)}$ ($\dot{\Phi}_C > 0$) or $\max \Phi_C^{(2)}$ ($\dot{\Phi}_C < 0$).

The trajectory corresponding to a controlling optimum (in the above meaning) will be called an optimum path.

Note. $\Phi_C^{(2)} = \Phi_C(t^{(2)})$, where $t^{(2)}$ is the moment of time either of the point A entering the tracking triangle, or of intercepting the goal B.

We introduce the notation $\Phi_C = x_1$, $\varphi = x_2$, $\rho/\rho^{(1)} = x_3$, $\rho^{(1)} = \rho(t^{(1)}) = \text{const}$. A parametric representation of $\xi(t)$ is introduced as done by Miele [2, 3]. We represent $\xi(t)$ as a smooth function of a new controlling parameter p satisfying the following conditions:

$$\xi = 0 \quad \text{when} \quad -\infty < p \leqslant p_1,$$

$$\xi = 1 \quad \text{when} \quad p_2 \leqslant p < +\infty,$$

$$\xi = \xi(p) \text{when} \quad p_1 \leqslant p \leqslant p_2$$

(a single-valued transformation).

---

* Subsequently, we shall understand by "point A" the center of gravity of the controlling body A. The equations of motion of the body about its center of gravity (about the point A) are not considered.

† The goal B is understood to be a body.

‡ The criterion of optimum control was introduced by B. V. Shirokorad.

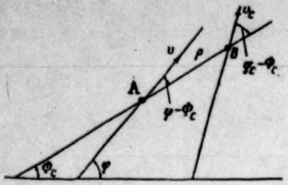

Fig. 1.

Due to this representation, the role of the control function is taken over by p. Owing to the way the function is introduced, one is able to apply the methods of classical calculus of variations to find the optimum solution.

It should be noted that the Miele method does not pretend to be unique. In the last few years Soviet and foreign research workers [4-8] have submitted quite effective methods of finding optimum processes in systems with restrictions. The Miele method, however, is especially suitable, as it permits reduction of the problem with restrictions to Meyer's problem, and thus allows application of the full apparatus of the classical calculus of variations.

The simultaneous equations (1.1) are now written in the form

$$\dot{x}_1 = \frac{1}{x_3 p^{(1)}}\left[v_c \sin(\varphi_c - x_1) - v \sin(x_2 - x_1)\right],$$

$$\dot{x}_2 = \frac{\xi(p)}{x_3 p^{(1)}}\left[v_c \sin(\varphi_c - x_1) - v \sin(x_2 - x_1)\right], \qquad (1.2)$$

$$\dot{x}_3 = \frac{1}{p^{(1)}}\left[v_c \cos(\varphi_c - x_1) - v \cos(x_2 - x_1)\right],$$

where $\xi = \xi[p(t)]$.

The boundary conditions are:
At $t = t^{(1)}$, $x_1^{(1)}$, $x_2^{(1)}$, $x_3^{(1)}$ are given;
At $t = t^{(2)}$ we have

$$v_c \sin(\varphi_c - x_1^{(2)}) - v \sin(x_2^{(2)} - x_1^{(2)}) = 0, \qquad (1.3)$$

$$x_3^{(2)} < 0$$

($t^{(2)}$ is not known).

Meyer's variational problem [9] can be stated in the following way.

Within the class of functions $x_1(t)$, $x_2(t)$, $x_3(t)$, $p(t)$, satisfying the equations of motion (1.2), and the boundary conditions (1.3), a system of functions is to be determined such that it minimizes $|x_1^{(2)} - x_1^{(1)}|$.

The solution is sought within the class of sectionally smooth functions x_1, x_2, and x_3; the function p(t) may have discontinuities of the first kind. We shall call the path as given by x_1, x_2, x_3 and p admissible when x_1, x_2, x_3 and p satisfy all the conditions of the Meyer's problem. A control program corresponding to an admissible path shall be called admissible. We shall consider one particular case prior to solving the general case.

2. A Particular Case

We assume that $|\varphi_c - x_1|$ and $|x_2 - x_1|$ are small (for example, not exceeding 10°); this is often encountered in practice. Now the simultaneous equations (1.2) and the boundary conditions (1.3) can be expressed in the following way:

$$\dot{x}_1 = ax_1 - bx_2 + c, \quad \dot{x}_2 = (ax_1 - bx_2 + c)\xi(p),$$
$$\dot{x}_3 = \frac{v_c - v}{p^{(1)}}, \quad x_3 = 1 - \frac{v - v_c}{p^{(1)}}t, \qquad (2.1)$$

$$a = \frac{v - v_c}{x_3 p^{(1)}} > 0, \quad b = \frac{v}{x_3 p^{(1)}} > 0, \quad c = \frac{v_c \varphi_c}{x_3 p^{(1)}} > 0,$$

or

$$a = \frac{v - v_c}{p^{(1)} - (v - v_c)\,t}, \qquad b = \frac{v}{p^{(1)} - (v - v_c)\,t},$$
$$c = \frac{v_c \varphi_c}{p^{(1)} - (v - v_c)\,t}. \qquad (2.2)$$

The boundary conditions are:
At $t = t^{(1)}$ $x_1^{(1)}$, $x_2^{(1)}$ are given;
At $t = t^{(2)}$

$$\tilde{a}x_1^{(2)} - \tilde{b}x_2^{(2)} + \tilde{c} = 0 \qquad (2.3)$$
$$(\tilde{a} = ax_3 p^{(1)}, \quad \tilde{b} = bx_3 p^{(1)}, \quad \tilde{c} = cx_3 p^{(1)}).$$

We introduce the notation $\Phi \equiv \tilde{a}x_1 - \tilde{b}x_2 + \tilde{c}$. The Meyer's variational problem, as applied to this particular case of the simultaneous equations (2.1), can be described in the following way. In the class of functions $x_1(t)$, $x_2(t)$, $p(t)$ satisfying the equations of motion (2.2) together with the boundary conditions (2.3) a system of functions is to be found minimizing $|x_1^{(2)} - x_1^{(1)}|$.

In order to solve this, we introduce Lagrange's function:

$$F = \lambda_1[ax_1 - bx_2 + c - \dot{x}_1] +$$
$$+ \lambda_2[\xi(p)(ax_1 - bx_2 + c) - \dot{x}_2]. \qquad (2.4)$$

Euler's equations take the form

$$a\lambda_1 + a\xi(p)\lambda_2 + \dot{\lambda}_1 = 0,$$
$$a\lambda_1 + b\xi(p)\lambda_2 - \dot{\lambda}_2 = 0, \qquad (2.5)$$
$$\lambda_2(ax_1 - bx_2 + c)\frac{d\xi}{dp} = 0.$$

From the last Euler equation of the (2.5) system it can be seen that the optimum path (when it does exist) may consist of three branches: a) $d\xi/dp = 0$ $(\lambda_2 \neq 0)$, i.e., $\xi = 0$ and $\xi = 1$ (two branches); b) $\lambda_2 = 0$ $(d\xi/dp \neq 0)$, i.e., the controlling function ξ is not constant($ax_1 - bx_2 + c \neq 0$ as the tracking triangle does not occur).

We shall deal first with the case of $\lambda_2 = 0(d\xi/dp \neq 0)$. It follows from the equations (2,5) that when $\lambda_2 = 0$ then also $\lambda_1 = 0$. But both the Lagrange multipliers λ_1 and λ_2 cannot vanish simultaneously [9] at any point of the interval $(t^{(1)}, t^{(2)})$ as it would eventually be inconsistent with the boundary conditions (2.3) being independent. This means that a curve with a variable ξ, and such that $\lambda_2 = 0$, does not exist. Therefore, a possible optimum trajectory consists of two branches: $\xi = 0$, $\xi = 1(d\xi/dp = 0)$.

We shall now show that the branch $\xi = 0$ does not satisfy the boundary condition at the upper end. As assumed, the initial point is in the region of $\Phi \neq 0$ (the tracking triangle not increasing).

It should be $\Phi^{(2)} = 0$ for an admissible path at $t = t^{(2)}$. Consequently, if, say, $\Phi^{(1)} > 0$ then Φ must, in the course of time, decrease (not necessarily monotonically). How this function changes in time during motion along a trajectory of the simultaneous equations (2,1) can be found by taking the derivative of Φ with respect to time; due to the equations of motion (2,1), the latter is obtained as

$$\frac{d\Phi}{dt} = \tilde{a}\dot{x}_1 - \tilde{b}\dot{x}_2 = \frac{(\widetilde{ab}\xi)(\tilde{a}x_1 - \tilde{b}x_2 + \tilde{c})}{x_3\rho^{(1)}} = \frac{\tilde{a} - \tilde{b}\xi}{x_3\rho^{(1)}}\Phi.$$

When $\xi = 0$ we have $\frac{d\Phi}{dt} = \frac{\tilde{a}}{x_3\rho^{(1)}}\Phi$ As $\tilde{a} > 0(\tilde{a} = v - v_c)$. $x^3\rho^{(1)} > 0$, the sign of $d\Phi/dt\,(\xi = 0)$ agrees with the sign of Φ. Therefore, if $\Phi^{(1)} > 0$ in the case of motion along the path with the control $\xi = 0$, the function Φ must increase monotonically, but if $\Phi^{(1)} < 0$ it decreases monotonically. This shows that the branch $\xi = 0$ cannot satisfy the boundary condition at the upper end.

When $\xi = 1$ we have $\frac{d\Phi}{dt} = \frac{\tilde{a} - \tilde{b}}{x_3\rho^{(1)}}\Phi = -\frac{v_c}{x_3\rho^{(1)}}\Phi$.

Consequently, $d\Phi/dt\,(\xi = 1)$ is opposite in sign to Φ, i.e., the branch $\xi = 1$ could be a solution of the boundary problem.

We shall show that the branch $\xi = 1$ is actually an optimum one, i.e., gives the min $|x_1^{(2)} - x_1^{(1)}|$. In the system of equations (2.1) we shall take x_2 as the independent variable (we shall show later that this is permissible). Then the simultaneous equations (2.1) reduce to a single equation:

$$\frac{dx_1}{dx_2} = \frac{1}{\xi(x_2)}, \quad 0 \leqslant \xi(x_2) \leqslant 1. \qquad (2.6)$$

We shall determine the admissible displacements in the (x_2, x_1) plane as those which are not consistent with (2.1) or (2.6) [10]. Let I represent the point corresponding to the initial moment of time $t^{(1)}$ (Fig. 2). We shall now determine where the point could be displaced during the subsequent time interval $t^{(1)} + \Delta t$.

It follows from (2.6) that $1 \leq (dx_1/dx_2) \leq +\infty$. The representative point can therefore at the time $t^{(1)} + \Delta t$ be found only in the region bounded by the straight lines $(dx_1/dx_2) = +\infty$ and $(dx_1/dx_2) = 1$, i.e., in the zones A' or A" (Fig. 2). B is clearly the prohibited zone.

We draw the straight line $\tilde{a}x_1^{(2)} - \tilde{b}x_2^{(2)} + \tilde{c} = 0$ in the plane (x_2, x_1), on which the representative point at the time moment $t^{(2)}$ (Fig. 3) should lie. The gradient of the straight line is $\frac{\tilde{b}}{\tilde{a}} = \frac{v}{v - v_c} > 1$, as $v > v_c$. There are three possible positions of the initial point I with respect to the straight line $\Phi^{(2)} = 0$:

1) the initial point is below the straight line $\Phi^{(2)} = 0$; therefore, $\Phi^{(1)} < 0$,

2) the initial point is above the straight line $\Phi^{(2)} = 0$; therefore, $\Phi^{(1)} > 0$,

3) the initial point is on the straight line $\Phi^{(2)} = 0$, i.e., $\Phi^{(1)} = 0$ also and thus, the tracking triangle conditions take place straightaway, with no transition process. This case of course, need not be considered.

We now return to the first two cases.

1. The point I_1 is below the straight line $\Phi^{(2)} = 0$, i.e., in the region of $\Phi < 0$. It follows from equations (2.1):

$$\dot{x}_1 = \frac{1}{x_3\rho^{(1)}}\Phi, \qquad \dot{x}_2 = \frac{1}{x_3\rho^{(1)}}\xi\Phi. \qquad (2,7)$$

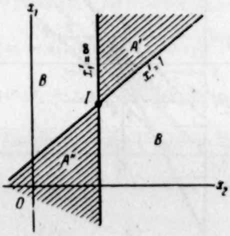

Fig. 2.

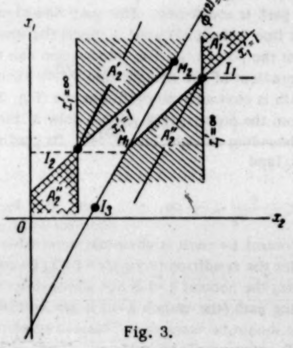

Fig. 3.

As $x_3\rho^{(1)} \geq 0$, and $\xi \geq 0$, then below the line $\Phi^{(2)}=0$, x_1 and x_2 are monotonically decreasing functions of time. This makes it possible to take x_2 instead of time t as an independent variable, and also turns the zone A'_1 into a prohibited one, as displacements consistent with the equations of motion (2.1) and (2.6) are found in the zone A_1^{*} (Fig. 3).

This confirms the existence of an optimum trajectory in the case under consideration. It will consist of a straight line I_1M_1 ($\xi=1$) until the latter intersects the straight line $\Phi^{(2)}=0$ at the point M_1. The intersection occurs because the gradient of the boundary line $\Phi^{(2)}=0$ exceeds unity. The optimum character of this trajectory is obvious (Fig. 3). From the point I_1 (Fig. 3) we draw a straight line parallel to the boundary line $\Phi^{(1)}=0$. Its gradient is $v/(v-v_c)$. It was assumed that $0 < v_c < v$; hence $1 < v/(v-v_c) < +\infty$. If the control $\xi=$ const takes place (the path consists of one branch) it is obvious that the admissible controls must satisfy the conditions

$$\frac{v-v_c}{v} < \xi \leqslant 1, \qquad \xi = \text{const}. \tag{2.8}$$

Thus, the control $\xi=0$ (if this one occurs only) proves not admissible. The corresponding path (the branch $\xi=0$) must, therefore, be discarded. This is in agreement with the result obtained analytically. In addition, $\xi=0$ signifies that the body A is not controlled. Disregarding the exceptional case when it is directed toward the goal already at the initial moment of time (the tracking triangle has occurred), we can draw the conclusion that an uncontrolled body A cannot intercept the goal B.

2. The initial point I_2 is above the straight line $\Phi^{(2)}=0$, i.e., in the region of $\Phi>0$. The equations (2.1) indicate that in this region x_1 and x_2 increase monotonically with time; thus, the zone A_2^{*} becomes prohibited, and the displacements consistent with the equations (2.6) and (2.1) are in the zone A_1^{*}. The existence of the optimum path is confirmed. This path runs along the straight line I_2M_2 ($\xi=1$) until it meets the straight line $\Phi^{(2)}=0$ at the point M_2. The intersection can take place as the gradient of the straight line $\Phi^{(2)}=0$ exceeds unity. This path is obviously an optimum one (Fig. 3).

From the point I_2 (Fig. 3), we draw a line parallel to the bounding straight line $\Phi^{(2)}=0$. Its gradient is $v/(v-v_c)$ and

$$1 < \frac{v}{v-v_c} < +\infty, \qquad \text{as} \quad 0 < v_c < v.$$

A control $\xi=$ const is obviously admissible provided it satisfies the condition $(v-v_c)/v < \xi \leq 1$ ($\xi=$ const). Therefore, the control $\xi=0$ is not admissible. The corresponding path (the branch $\xi=0$) is not admissible either and should be discarded. This is in agreement with the result obtained analytically.

__Note.__ The equations (2.1) are valid in the region $|\varphi_c - x_1| \leq 10°$, $|x_2 - x_1| \leq 10°$, i.e., within and on the perimeter of the parallelogram A'B'E'D' shown in Fig. 4. The center of the parallelogram lies on the bounding straight line $\Phi^{(2)}=0$ ($x_1^{(2)}=\varphi_c$ and $x_2^{(2)}=\varphi_c$ satisfy the equation $\Phi^{(2)}=0$). It is obvious that the solution of the variational problem is possible when the initial points lie either in the region ABD (when $\Phi^{(1)}>0$) or in DBE (when $\Phi^{(1)}<0$) (AB∥A'B', DE∥D'E', ∠BAD=π/4).

It would be interesting to find the time $t^{(2)}$ of entry on the tracking triangle under the optimum control $\xi=1$. When $\xi=1$, the equations (2.1) can be integrated. We write the optimum curve equations in the form:

$$x_1 = M_1\left(\frac{\rho}{\rho^{(1)}}\right)^{\frac{v_c}{v-v_c}} + N_1,$$

$$x_2 = M_2\left(\frac{\rho}{\rho^{(1)}}\right)^{\frac{v_c}{v-v_c}} + N_2, \tag{2.9}$$

$$M_1 = M_2 = \frac{1}{v_c}\left[(v_c - v)\,x_1^{(1)} + v x_2^{(1)} - \varphi_c v_c\right],$$

$$N_1 = \frac{1}{v_c}\left[v\left(x_1^{(1)} - x_2^{(1)}\right)\right] + \varphi_c v_c],$$

$$N_2 = \frac{1}{v_c}\left[(v - v_c)\left(x_1^{(1)} - x_2^{(2)}\right) + \varphi_c v_c\right]. \tag{2.10}$$

As the optimum path satisfies the boundary conditions, one is able to find $t^{(2)}$, the time of entry on the straight line $\Phi^{(2)}=0$. We have

$$(\tilde{a} - \tilde{b})\,M_1\left(\frac{\rho^{(2)}}{\rho^{(1)}}\right)^{\frac{v_c}{v-v_c}} + \tilde{a}N_1 - \tilde{b}N_2 + \tilde{c} = 0$$

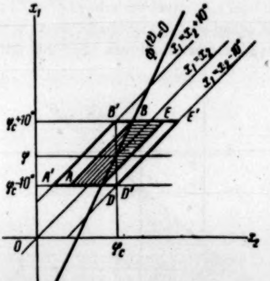

Fig. 4.

or, taking into account the expressions for $\tilde{\mathfrak{A}}$, $\tilde{\mathfrak{B}}$ and $\tilde{\mathfrak{C}}$,

$$-v_c M_1\left(\frac{\rho^{(2)}}{\rho^{(1)}}\right)^{\frac{v_c}{v-v_c}} + (v-v_c)N_1 - vN_2 + \varphi_c v_c = 0. \tag{2,11}$$

It is easy to show that $(v-v_c)N_1 - vN_2 + \varphi_c v_c \equiv 0$ for any $x_1^{(1)}$ and $x_2^{(1)}$ from the region where the equations (2.1) are valid. Then it follows from (2.11) that

$$M_1\left(\frac{\rho^{(2)}}{\rho^{(1)}}\right)^{\frac{v_c}{v-v_c}} = 0.$$

We shall distinguish two cases:

a) $M_1 = 0$, $\rho^{(2)} \neq 0$. But $M_1 = -(\Phi^{(1)}/v_c)$; therefore, the vanishing of M_1 denotes that already at the initial moment of time $t^{(1)}$, the tracking triangle occurs, which is contrary to our assumption.

b) $M_1 \neq 0$, $\rho^{(2)} = 0$. Then $t^{(2)}$ is equal to the time t_p of intercepting goal R; the latter time can be obtained from the equation $\rho = \rho^{(1)} - (v-v_c)t$ for $\rho = 0$ as

$t_d = \rho^{(1)}/(v-v_c)$; therefore, $t^{(2)} = t_p = \rho^{(1)}/(v-v_c)$.

3. General Case

We now proceed to the equations (1.2) and the general variational problem. There are the same stages in solving it as in the case considered previously. The Lagrange function F becomes

$$\begin{aligned} F = {} & \lambda_1\left\{-\dot{x}_1 + \frac{1}{x_3\rho^{(1)}}[v_c\sin(\varphi_c - x_1) - v\sin(x_2 - x_1)]\right\} + \\ & + \lambda_2\left\{-\dot{x}_2 + \frac{\xi(p)}{x_3\rho^{(1)}}[v_c\sin(\varphi_c - x_1) - v\sin(x_2 - x_1)]\right\} + \\ & + \lambda_3\left\{-\dot{x}_3 + \frac{1}{\rho^{(1)}}[v_c\cos(\varphi_c - x_1) - v\cos(x_2 - x_1)]\right\}. \end{aligned} \tag{3.1}$$

The Euler equations are

$$\begin{aligned} & \frac{\lambda_1}{x_3}[v\cos(x_2 - x_1) - v\cos(\varphi_c - x_1)] + \\ & + \frac{\lambda_2\xi(p)}{x_3}[v\cos(x_2 - x_1) - v_c\cos(\varphi_c - x_1)] + \\ & + \lambda_3[v_c\sin(\varphi_c - x_1) - v\sin(x_2 - x_1)] + \dot{\lambda}_1\rho^{(1)} = 0, \\ & -\lambda_1\frac{v}{x_3}\cos(x_2 - x_1) - \lambda_2\frac{v\xi(p)}{x_3}\cos(x_2 - x_1) + \\ & + \lambda_3 v\sin(x_2 - x_1) + \dot{\lambda}_2\rho^{(1)} = 0, \\ & \frac{\lambda_1}{x_3^2}[v\sin(x_2 - x_1) - v_c\sin(\varphi_c - x_1)] - \\ & - \lambda_2\frac{\xi(p)}{x_3^2}[v_c\sin(\varphi_c - x_1) - \\ & - v\sin(x_2 - x_1)] + \dot{\lambda}_3\rho^{(1)} = 0, \\ & \frac{\lambda_2}{x_3}\frac{d\xi}{dp}[v_c\sin(\varphi_c - x_1) - v\sin(x_2 - x_1)] = 0. \end{aligned} \tag{3,2}$$

The last of the Euler equations (3.2) shows that the theoretically possible optimum trajectory may consist of three branches:

a) $(d\xi/dp) = 0$, $(\lambda_2 \neq 0)$, $\xi = 0$, $\xi = 1$.

b) $\lambda_2 = 0$, $d\xi/dp \neq 0$, i.e., ξ is not constant [$v_c\sin(\varphi_c - x_1) - v\sin(x_2 - x_1) \neq 0$, as the tracking triangle does not occur in accordance with our assumptions]. The branch with variable ξ satisfies the following simultaneous equations obtained from (3. 2) by putting $\lambda_2 = 0$.

$$\begin{aligned} & \frac{\lambda_1}{x_3}[v\cos(x_2 - x_1) - v_c\cos(\varphi_c - x_1)] + \\ & + \lambda_3[v_c\sin(\varphi_c - x_1) - \\ & - v\sin(x_2 - x_1)] + \dot{\lambda}_1\rho^{(1)} = 0, \\ & -\lambda_1\frac{v}{x_3}\cos(x_2 - x_1) + \lambda_3 v\sin(x_2 - x_1) = 0, \\ & \frac{\lambda_1}{x_3^2}[v\sin(x_2 - x_1) - v_c\sin(\varphi_c - x_1)] + \dot{\lambda}_3\rho^{(1)} = 0. \end{aligned} \tag{3.3}$$

The function F of (3,1) obviously does not depend on time; thus, Euler's equations (3.2) have the following first integral:

$$\lambda_1\dot{x}_1 + \lambda_2\dot{x}_2 + \lambda_3\dot{x}_3 = C = \text{const}.$$

To determine the constant C of the first integral, it is necessary to consider the transversality conditions [9] which easily provide that $C \equiv 0$ (the function $|x_1^{(2)} - x_1^{(1)}|$ to be minimized does not depend on $t^{(2)}$, i.e., the variational problem is time-independent). Making use of equations of motion (1.2) we write the first integral in the form:

$$\begin{aligned} & \frac{\lambda_1}{x_3}[v_c\sin(\varphi_c - x_1) - v\sin(x_2 - x_1)] + \\ & + \lambda_2\xi(p)[v_c\sin(\varphi_c - x_1) \\ & - v\sin(x_2 - x_1)] + \\ & + \lambda_3[v_c\cos(\varphi_c - x_1) - v\cos(x_2 - x_1)] = 0. \end{aligned} \tag{3.4}$$

When $\lambda_2 = 0$ we have

$$\begin{aligned} & \frac{\lambda_1}{x_3}[v_c\sin(\varphi_c - x_1) - v\sin(x_2 - x_1)] + \\ & + \lambda_3[v_c\cos(\varphi_c - x_1) - v\cos(x_2 - x_1)] = 0. \end{aligned} \tag{3.5}$$

From the second equation in (3,3) and from (3.5), the relation between x_1 and x_2 is found which must take place when ξ is not constant:

$$\operatorname{tg}(x_2 - x_1) = -\frac{v_c \cos(\varphi_c - x_1) - v\cos(x_2 - x_1)}{v_c \sin(\varphi_c - x_1) - v\sin(x_2 - x_1)}. \tag{3.6}$$

Here $v_c \sin(\varphi_c - x_1) - v\sin(x_2 - x_1) \neq 0$, as the tracking triangle does not occur; in addition, λ_1 and λ_3 cannot vanish simultaneously on the curve with variable ξ, because when $\lambda_1 = 0$, it follows from the equations (3.3) that also $\lambda_3 = 0$. But the Lagrange multipliers cannot vanish simultaneously [9] (on the branch with variable ξ we have $\lambda_2 = 0$) at any point of the interval $(t^{(1)}, t^{(2)})$.

From the equations (3.6) we obtain the relationship:

$$\cos(\varphi_c - x_2) = \frac{v}{v_c} > 1. \tag{3.7}$$

The inconsistent relation (3 7) was obtained as a result of the assumption that there is a curve with variable ξ ($\lambda_2 = 0$). There are no branches, therefore, when the controlling function is variable. The theoretically possible optimum control is $\xi = 0$ and $\xi = 1$, i.e., the same as in the particular case above.

Further, it is necessary to clarify as to whether the controls $\xi = 0$ and $\xi = 1$ are admissible, i.e., whether the corresponding paths satisfy the boundary conditions. It is obvious that both paths ($\xi = 0$ and $\xi = 1$) pass through the initial point. We introduce the notation:

$$v_c \sin(\varphi_c - x_1) - v\sin(x_2 - x_1) \equiv G,$$

$$G_1^{(2)} = G(t^{(2)}), \quad G^{(1)} = G(t^{(1)}) \tag{3.7'}$$

(according to our assumption $G^{(1)} \neq 0$). An admissible trajectory should have

$$G^{(2)} = 0, \quad \dot{x}_3^{(2)} < 0, \tag{3.8}$$

at $t = t^{(2)}$, and if, say, $G^{(1)} > 0$, then the function G will finally decrease along the path (but not necessarily monotonically). To study how the function G varies with time, its derivative with respect to time is considered, and in view of the equations of motion (1.2) we obtain

$$\frac{dG}{dt} = \frac{d}{dt}[v_c \sin(\varphi_c - x_1) - v\sin(x_2 - x_1)] =$$

$$= -v_c \cos(\varphi_c - x_1)\dot{x}_1 -$$

$$- v\cos(x_2 - x_1)(\dot{x}_2 - \dot{x}_1).$$

But $\dot{x}_2 = 0$ when $\xi = 0$; thus

$$\left(\frac{dG}{dt}\right)_{\xi=0} = -(\dot{x}_1 \dot{x}_3 \rho^{(1)})_{\xi=0} = -\left(\frac{G\dot{x}_3}{x_3}\right)_{\xi=0}, \tag{3.9}$$

and $\dot{x}_1 = \dot{x}_2$ when $\xi = 1$; hence

$$\left(\frac{dG}{dt}\right)_{\xi=1} = -[\dot{x}_1 v_c \cos(\varphi_c - x_1)]_{\xi=1} =$$

$$= -\left[\frac{G v_c \cos(\varphi_c - x_1)}{x_3 \rho^{(1)}}\right]_{\xi=1} \tag{3.9'}$$

$(G)_{\xi=0}$, $((G)_{\xi=1})$ denotes that the function G is taken on the path with control $\xi = 0$ ($\xi = 1$).

We consider the condition (3.9) when $\xi = 0$. It indicates that the path with the control $\xi = 0$ can satisfy the first boundary condition in (3.8) ($G^{(2)} = 0$) in the region $\dot{x}_3 > 0$ only. Therefore, the second boundary condition in (3.8) ($\dot{x}_3^{(2)} < 0$) cannot be satisfied. The branch $\xi = 0$ thus proves inadmissible and must be discarded. The corresponding physical meaning is the trajectory of an uncontrolled body A. It is obvious that if the body A is not directed at $t = t^{(1)}$ toward the meeting point (the tracking triangle does not occur) then the further motion along the path with $\xi = 0$ cannot take it to the goal B.

The condition (3.9') when $\xi = 1$ shows that the path with the control $\xi = 1$ can intersect $G^{(2)} = 0$ at $t = t^{(2)}$ only in the region where $\cos(\varphi_c - x_1) > 0$. The significance of this condition will be explained later. But it can already be said now that it is not a very severe one and that it can be satisfied.

We shall show that the path $\xi = 1$ is actually an optimum one. We consider all the admissible displacements in the plane (x_2, x_1) [i.e, the displacements which are not inconsistent with the equation of motion (1.2)]. This was certainly possible in the simpler cases of the simultaneous equations (2,1) or (2 8).

In the general case, the possibility of such a consideration is determined by the following facts. First, by studying the Euler equations (3.2) it was found that such a curve does not exist when the control function ξ is not constant ($d\xi/dp \neq 0$). In an unfavorable case when $\lambda_2 = 0$ one could obtain a relation between x_1, x_2, and x_3 which would be fulfilled on the curve with a variable control function ξ. Then it would be necessary to consider all the admissible displacements in the space of the variables x_1, x_2, x_3, and this would make it rather involved.

Secondly, the first boundary condition at the upper end $G_1^{(2)} = 0$ is independent of $x_3^{(2)}$. The function x_3 depends only on x_1 and x_2 and the other boundary condition $\dot{x}_3^{(2)} < 0$ can, therefore, be investigated in the plane of (x_2, x_1) only. In the initial condition, a vital role is only played by the initial values of the functions x_1 and x_2 (this is indicated by the physical aspect of the problem). All this enables one to consider admissible displacements in the plane (x_2, x_1) which are given by the first two equations in the system (1.2), the equation $dx_1/dx_2 = 1/\xi\,(x_2)$ on condition that $0 \leq \xi\,(x_2) \leq 1$. It is reasonable to refer our discussion to the square of side 2π, its center coinciding with the origin (Fig. 5); x_1 and x_2 being angles, one can consider $x_1 + 2k\pi$ as coinciding with x_1, and $x_2 + 2m\pi$ with x_2 ($\underline{k}$ and $\underline{m}$ are integers). The boundary branch $G^{(2)} = 0$ (3.7') has three branches in the square: $G_1^{(2)} = 0$, $G_2^{(2)} = 0$, $G_3^{(2)} = 0$ (Fig. 5). The branches are in fact arcs of some periodic curve with period equal to $2\sqrt{2}\pi$ along the appropriate axis. The straight line $x_1 = x_2$ which is cut by $G_1^{(2)} = 0$ at the points (φ_C, φ_C) and $(-\pi/2-\varphi_C, -\pi/2-\varphi_C)$ serves as the axis of $G_1^{(2)} = 0$. The width of the belt (along axis Ox_2) containing $G_1^{(2)} = 0$ is $2 \arcsin(v_C/v)$. The other two branches $G_2^{(2)} = 0$ and $G_3^{(2)} = 0$ "meander" around the straight lines $x_1 = x_2 + \pi$ and $x_1 = x_2 - \pi$. We denote the region between $G_2^{(2)} = 0$ and $G_1^{(2)} = 0$ by Δ_{12}, and the region between $G_3^{(2)} = 0$ and $G_1^{(2)} = 0$ by Δ_{13}, the region above $G_2^{(2)} = 0$ by Δ_2, and the region below $G_3^{(2)} = 0$ by Δ_3.

The function G is positive in the regions Δ_{12} and Δ_3, and negative in Δ_{13} and Δ_2. In addition, the curves $\dot{x}_3 = 0$ are also shown in Fig. 5, i.e., the curves $v_C \cos(\varphi_C - x_1) - v \cos(x_2 - x_1) = 0$. We introduce the notation $v_C \cos(\varphi_C - x_1) - v \cos(x_2 - x_1) \equiv_b$ /// The curve $g = 0$ has four branches in the square of side 2π:

$$g_1 = 0, \quad g_2 = 0, \quad g_3 = 0, \quad g_4 = 0.$$

Notation: δ_{12} is the region between $g_1 = 0$ and $g_2 = 0$, δ_{24} the region between $g_2 = 0$ and $g_4 = 0$, δ_{13} the region between $g_1 = 0$ and $g_3 = 0$, δ_3 the region above $g_3 = 0$, δ_4 the region below $g_4 = 0$. We notice that $\dot{x}_3 > 0$ in the regions δ_{13} and δ_{24}, and $\dot{x}_3 < 0$ in the regions δ_{12}, δ_3, and δ_4.

The tangents to g_1 and g_2 are drawn at the point $x_1 = \varphi_C$ (their gradients are unity). The strip between the two tangents parallel to the straight lines $x_1 = x_2$ has the width equal to $2 \arccos(v_C/v)$ (if measured along Ox_2). When $v_C < (\sqrt{2}/2)v$ (usually there is $v_C \leq \frac{1}{2}v$) we have in the I part $\arcsin(v_C/v) < \arccos(v_C/v)$; therefore, the strip embracing the branch $\xi = 1$ lies entirely within the region δ_{12} ($\dot{x}_3 < 0$). An analogous approach will show, on the contrary, that the branches $G_2^{(2)} = 0$ and $G_3^{(2)} = 0$ are submerged in the region of $\dot{x}_3 > 0$. Thus the paths which at $t = t^{(2)}$ are located on those branches are not admissible as obviously $\dot{x}_3^{(2)}$ is positive, i.e., the second boundary condition (3.8) ($\dot{x}_3^{(2)} < 0$) is not satisfied. Thus the solutions of the boundary problem can only be represented by the paths crossing the curve $\overline{G}_1^{(2)} = 0$ at some $t = t^{(2)}$, the entire one lying in the region δ_{12} ($\dot{x}_3 < 0$).

We denote the strip containing the curve $G_1^{(2)} = 0$ by $\Delta_{G_1^{(2)}}$, the strip containing the curve $G_2^{(2)} = 0$ by $\Delta_{G_2^{(2)}}$ and the strip containing the curve $G_3^{(2)}$ by $\Delta_{G_3^{(2)}}$.

We now determine the admissible displacements in the plane (x_2, x_1) [10]. The admissible displacements are located in the regions Δ_{12} and Δ_3 — both within and on the boundary of the angle formed by the rays $x_1' = 1$ and $x_1' = \infty$ (the angle opening upward as in these regions on the function $G > 0$); in the regions Δ_{13} and Δ_2, inside and on the boundary of the angle formed by the rays $x_1' = 1$ and $x_1' = \infty$ (the angle now opening downward as in these regions the function $G < 0$).

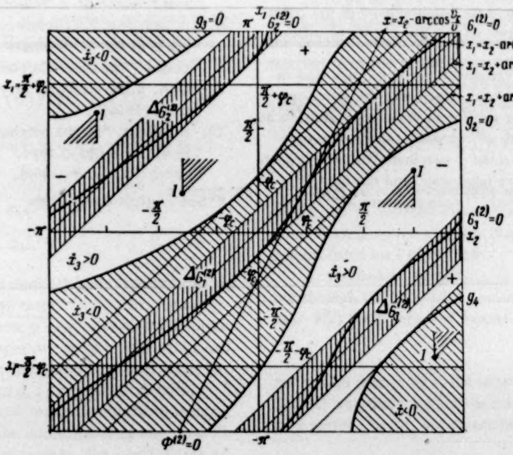

Fig. 5. $\varphi_c = \frac{\pi}{4}$, $v_c = \frac{1}{3}v$

Further, we shall consider various positions of the initial point I in the square with side 2π (Fig. 5). The variational problem admits no solution for all the points I not in $\Delta_{G_1^{(2)}}$, as no path starting from such an initial point can be admissible: none satisfies all the boundary conditions (3.8). Now let $I \in \Delta_{G_1^{(2)}}$. All the admissible trajectories starting from I must stay in $\Delta_{G_1^{(2)}}$, otherwise they would cease to be admissible. First it is obvious that the trajectory $\xi = 0$ is not admissible for any point I, as it stops neither on the curve $G_2^{(2)} = 0$ nor on $G_3^{(2)} = 0$ in the region of $\dot{x}_3 > 0$, i.e., the second boundary condition of (3.8) is not satisfied; secondly, if $I \in \Delta_{G_1^{(2)}}$, the branch $\xi = 1$ is admissible and gives min (max) $x_1^{(2)}$. When the point I approaches the boundary of the region $\Delta_{G_1^{(2)}}$, the region containing the admissible paths shrinks and in the limit (I is on the boundary of $\Delta_{G_1^{(2)}}$) it degenerates into the line $\xi = 1$.

Notes. a) Straight lines $x_1 = \varphi_c + (\pi/2)$ and $x_1 = -\varphi_c - (\pi/2)$ are drawn in Fig. 5. In the region between these straight lines $\cos(\varphi_c - x_1) > 0$. It is demonstrated in Fig. 5 that in the region of $\cos(\varphi_c - x_1) < 0$ the path $\xi = 1$ cannot cross $G_1^{(2)} = 0$. Such an intersection is only possible in the region of $\cos(\varphi_c - x_1) > 0$.

b) The tangent to the curve $G_1^{(2)} = 0$ at the point (φ_c, φ_c) has a gradient equal to $x_1' = [v/(v - v_c)]$ and also $x_1'' = 0$, i.e., the point (φ_c, φ_c) is a point of inflection. Coming back to the particular case in section 2 we notice that $\Phi^{(2)} = 0$ has the gradient $[v/(v - v_1)]$ and that it passes through the point (φ_c, φ_c). The equations (2.1) are thus valid exactly in the neighborhood of the point (φ_c, φ_c) where the curve $G_1^{(2)} = 0$ has a point of inflection.

c) The general variational problem, as stated in section 1, can also be formulated (with the same optimum requirement) for a different boundary condition at the upper end, namely: $\rho^{(2)} = 0$ when $t = t^{(2)}$. The optimum path will now consist of two branches: the branch where the control $\xi = 1$ takes over, and the branch $x_1 = x_1^{(TR)} = \text{const}$, $x_2 = x_2^{(TR)} = \text{const}$, where $x_1^{(TR)}$ and $x_2^{(TR)}$ satisfy the tracking triangle formula, i.e., the conditions $v_c \sin(\varphi_c - x_1^{(TR)}) - v \sin(x_2^{(TR)} - x_1^{(TR)}) = 0$, $\dot{x}_3 < 0$. The optimum character of this trajectory is obvious as the control $\xi = 1$ gives min (max) $x_1^{(TR)}$, and x_1 does not vary when the tracking triangle condition is satisfied. In addition, both branches can also be obtained from the Euler equations (3.2).

In conclusion the author wishes to express his thanks to B. V. Shirokorad and A. M. Letov for formulating the problem and constant advice given during the work.

LITERATURE CITED

1. A. S. Lokk, Missile Control [in Russian] (GITTL, 1957).
2. A. Miele, "An extension of the theory of the optimum burning program for the level flight of a rocket-powered aircraft," Journal of the Aeronautical Sciences Vol. 24, No. 12 (1957).
3. A. Miele, "Optimum burning program as related to aerodynamic heating for a missile traversing the atmosphere of the earth," [Russian translation] (Proc. Eighth International Astronautical Congress (Barcelona, 1957); cf. Voprosy raket. tech., No. 4 (1958).
4. L. S. Pontryagin, "Optimum control processes," Usp. Matem. Nauk 14, No. 1 (85) (1959).
5. R. V. Gamkrelidze, "On the general theory of optimum processes," Doklady AN SSSR 123, No. 2 (1958).
6. R. V. Gamkrelidze, "Optimum high-speed processes with restraints in phase coordinates," Doklady AN SSSR 125, No. 3 (1959).
7. N. N. Krasovskii, "On the theory of optimum control," Avtomat. i Telemekh. 18, No. 11 (1957).[**]
8. R. Bellman, J. Glicksberg, and O. Gross, Some Aspects of the Mathematical Theory of Control Processes (The Rand Corporation, January 16, 1958).
9. G. A. Bliss, Calculus of Variations [Russian translation] (1950).
10. A. Miele, "Flight mechanics and variational problems of a linear type," J. of the Aerospace Sciences 25, No. 9 (1958).

[**] See English translation.

ON THE STABILITY OF THE PERIODIC MOTION OF PIECEWISE LINEAR AUTOMATIC CONTROL SYSTEMS

K. K. Belya

Moscow

Translated from Avtomatika i Telemekhanika, Vol. 21, No. 8, pp. 1134-1140,
August, 1960
Original article submitted January 28, 1960

The stability of periodic motions of piecewise linear automatic control systems is investigated on the basis of the resulting equation L(D)z = −K(D) f(z) + F(t).

1. Considered in [1] is a dynamic system described by the equations

$$\dot{z}_i = \sum_{j=1}^{n} a_{ij} z_j + \lambda_i f(z_1) + F_i(t) \quad (i = 1, 2, \ldots, n), \tag{1}$$

where a_{ij}, λ_i are given numbers (some of them are actually zero), $F_i(t)$ is a periodic function of time having the total period T (in particular a constant number, which may be even zero), $f(z_1)$ is a given piecewise linear function. The same reference gives a method for constructing the linear approximation equations permitting solution of the problem of the stability of a periodic solution $\tilde{z}_i(t)$ of the given system.

In the determination of the periodic solutions of the system (1) it is customary to start from the resulting equation [2,3,4]

$$L(D) z_1 = -K(D) f(z_1) + F(t), \tag{2}$$

where F(t) is a periodic function of time having the period T, and

$$L(D) = a_0 D^n + a_1 D^{n-1} + \ldots + a_n,$$
$$K(D) = b_0 D^n + b_1 D^{n-1} + \ldots + b_n \tag{3}$$

are linear differential operators (D is the symbol for the generalized derivative with respect to time). Usually, the degree m of the operator polynomial K(D) is lower than the degree n of the operator polynomial L(D), and, consequently, some of the first coefficients of K(D) in (3), i.e., $b_0, b_1, \ldots, b_{n-m-1}$ are equal to zero.

Equation (2) is obtained immediately from system (1) after eliminating all the coordinates z_i and their derivatives, except z_1. Consequently, the coefficients $a_0, a_1, \ldots, a_n, b_{n-m}, b_{n-m+1}, \ldots, b_n$ of the polynomials (3) depend only upon a_{ij} and λ_i. It is even easier to write equation (2) if the transfer function of the linear part of the control system is known:

$$W(p) = \frac{K(p)}{L(p)}.$$

The polynomials (3) are here the denominator and the numerator of the transfer function of the linear part, respectively.

The periodic solutions of equation (3) are obtained in the form $\tilde{z}_1(t)$ or $f[\tilde{z}_1(t)]$. In order to solve the problem of the stability of the periodic solutions $\tilde{z}_1$, $f(\tilde{z}_1)$, according to [1], one must use the reverse transformation, namely, express all the coordinates $\tilde{z}_i$ through $\tilde{z}_1$, and then introduce the linear approximation equation.

Here we suggest another method for constructing the linear approximation and a direct method for solving the problem of the stability of the periodic solution $\tilde{z}_1$, starting from the resulting equation (2).

2. Therefore, let us consider an automatic control system described by the equation

$$L(D) z = -K(D) f(z) + F(t). \tag{4}$$

Let $\tilde{z}$ be a known periodic solution of equation (4), which can be ascribed either to an external periodic force F(t), or to the dynamic properties of the nonlinear system itself for F(t) ≡ const.

Let us denote by $\tau_1, \tau_2, \ldots, \tau_l$ the times of passing through the links of the piecewise linear characteristic $f(\tilde{z})$ for a period of motion T, where $T = \sum_{j=1}^{l} \tau_j$; let us also denote by t_j the instants when the coordinates $\tilde{z}$, $f(\tilde{z})$ and their derivatives may be discontinuous within a period, i.e., t_j are determined by the formulas

$$t_j = \sum_{i=1}^{j} \tau_i \quad (j = 1, 2, \ldots, l).$$

where $t_l = T$. The subscripts of τ and t are always in correspondence with the order in which they are met, both in one and in the other direction during the period of motion, and not with the geometrical sequence of the joints.

If $x(t)$ is a sufficiently small deviation of the perturbed motion $z(t)$ of the system under study from the known (unperturbed) motion $\tilde{z}(t)$, i.e.,

$$x(t) = z(t) - \tilde{z}(t),$$

this deviation is determined by the equation

$$L(D)\,x(t) = -K(D)\{x(t)\,[D_z f(z)]_{z=\tilde{z}}\}, \quad (5)$$

where $[D_z f(z)]_{z=\tilde{z}}$ is the generalized derivative of the function $f(z)$ with respect to its argument z for $z=\tilde{z}$. If one takes

$$f(z) = k_j z + \gamma_j,$$

one finds

$$\begin{aligned}[D_z f(z)]_{z=\tilde{z}} &= \\ = \sum_{\nu=0}^{\infty}\sum_{j=1}^{l} \Big\{k_j\,[\mathbf{1}(t-\nu T-t_{j-1}) &- \\ - \mathbf{1}(t-\nu T-t_j)] + \frac{\Delta f_j}{\dot{\tilde{z}}(t_j)}\,\delta(t-\nu T-t_j)\Big\}&,\end{aligned} \quad (6)$$

where $\mathbf{1}(t)$ is the unitary function of Heaviside, $\delta(t)$ is the Dirac momentum function, and Δf_j denotes a discontinuity of the characteristic $[f(z)]_{z=\tilde{z}}$ at the time $t=\nu T+t_j$, i.e.,

$$\begin{aligned}\Delta f_j &= f[\tilde{z}(\nu T+t_j+0)] - \\ &- f[\tilde{z}(\nu T+t_j-0)] = \\ &= f[\tilde{z}(t_j+0)] - f[\tilde{z}(t_j-0)] = \\ &= (k_{j+1}-k_j)\,\tilde{z}(t_j) + \gamma_{j+1} - \gamma_j.\end{aligned} \quad (7)$$

Formulas (6) and (7) are effective only when $\tilde{z}(t)$ is a continuous function of time. As is well known, this condition is fulfilled for $m \le n-1$.

As to the derivative $\dot{\tilde{z}}(t)$, it has discontinuities of the first order in the points of discontinuity of $[f(z)]_{z=\tilde{z}}$. Consequently, for these points one must replace t_j in formula (6) either by t_j-0 or by t_j+0. In the following we shall always use t_j+0, i.e., we shall consider the right-hand value $\dot{\tilde{z}}(t_j+0)$.

The product $x(t)[D_z f(z)]_{z=\tilde{z}}$ will be written in the form

$$x(t)[D_z f(z)]_{z=\tilde{z}} = \sum_{\nu=0}^{\infty}\sum_{j=1}^{l}\Big[k_j x_{\nu j}(t) + \\ + \frac{\Delta f_i}{\dot{\tilde{z}}(t_j+0)}\,x(\nu T+t_j+0)\,\delta(t-\nu T-t_j)\Big], \quad (8)$$

where

$$\begin{aligned}x_{\nu j}(t) = x(t) \quad &\text{for} \quad \nu T+t_{j-1} < t < \nu T+t_j, \\ x_{\nu j}(t) = 0 \quad &\text{for} \quad \nu T < t < \nu T+t_{j-1} \\ &\text{and} \quad \nu T+t_j < t < \nu T+T.\end{aligned} \quad (9)$$

If (8) is introduced into (5), we get

$$L(D)\,x(t) = -K(D)\Big\{\sum_{\nu=0}^{\infty}\sum_{j=1}^{l}\Big[k_j x_{\nu j}(t) + \\ + \frac{\Delta f_j}{\dot{\tilde{z}}(t_j+0)}\,x(\nu T+t_j+0)\,\delta(t-\nu T-t_j)\Big]\Big\}. \quad (10)$$

Let us show that equation (10) is really a linear approximation in the sense of Lyapunov, and that, therefore, it can serve for deciding whether the periodic solution $\tilde{z}(t)$ is stable or not.

It was shown in [5,6] that the linear approximation for solving the problem of the stability of a periodic solution of the system (1) has the form

$$Dx_i = \sum_{j=1}^{n} a_{ij}x_j + \lambda_i\,[D_z f(z)]_{z=\tilde{z}}\,x_1 \quad (i=1,2,\ldots,n). \quad (11)$$

As has been done on system (1), where, by eliminating all the z_i's except z_1, and by replacing z_1 by z, we got the resulting equation (2), system (11) can give the linear approximation (10) corresponding to the resulting equation (2).

In fact, if $x_2, x_3, \ldots, x_n$ are eliminated from (11) and x_1 is denoted by x, and if the expansion (8) is taken into account, the actual linear approximation of (11) takes just the form (10). After all, equation (10) is nothing but another way of writing the linear approximation (11). Consequently, equation (10) solves the problem of the stability of periodic solution $\tilde{z}(t)$ of the resulting equation (2), similarly to a well-known theorem by Lyapunov: if the zero solution $x(t)=0$ of the linear approximation (10) is asymptotically stable, then also the periodic solution $\tilde{z}(t)$ is asymptotically stable.

3. On the basis of (9), for each period of motion, i.e., for $\nu T < t \le \nu T+T$, (10) gives the equations

$$[L(p) + k_j K(p)]\,x(t) = 0, \\ p \equiv \frac{d}{dt} \quad (j=1,2,\ldots,l), \quad (12)$$

which describe the perturbate process in the given interval of time, except for the discrete points $\nu T+t_j$. In these points the deviation $x(t)$ and its derivatives lose the discontinuities $\Delta x_{\nu j}^{(k)}$, which are determined by the system of equations (see the Appendix):

$$0 = -\Delta f_j\,\frac{b_0}{\dot{\tilde{z}}(t_j+0)}\,x(\nu T+t_j+0),$$

$$(a_0 + k_jb_0)\,\Delta x_{\nu j} = -\,\Delta k_jb_0x\,(\nu T + t_j + 0) - $$
$$-\,\Delta f_j\,\frac{b_1}{\dot{z}\,(t_j + 0)}\,x\,(\nu T + t_j + 0),$$

$$(a_0 + k_jb_0)\,\Delta x_{\nu j} + (a_1 + k_jb_1)\,\Delta x_{\nu j} = \tag{13}$$
$$= -\,\Delta k_j\,[b_0x'\,(\nu T + t_j + 0) + b_1x\,(\nu T + t_j + 0)] - \Delta f_j\,\frac{b_2}{\dot{z}\,(t_j + 0)}\,x\,(\nu T + t_j + 0),$$
$$\cdots\cdots\cdots\cdots\cdots\cdots\cdots\cdots\cdots$$
$$(a_0 + k_jb_0)\,\Delta x_{\nu j}^{(n-1)} + \cdots + (a_{n-1}k_jb_{n-1})\,\Delta x_{\nu j} =$$
$$= -\Delta k_j\,[b_0x^{(n-1)}\,(\nu T + t_j + 0) + \cdots + b_{n-1}x\,(\nu T + t_j + 0)] -$$
$$-\Delta f_j\,\frac{b_n}{\dot{z}\,(t_j + 0)}\,x\,(\nu T + t_1 + 0),$$

where we have used the notation $\Delta k_j = k_{j+1} - k_j$.

The first equation of (13) means that the coefficient b_0 must be equal to zero, as has already been mentioned. The other $\underline{n}$ equations of (13) are a system of linear equations which can be solved with respect to the jumps $\Delta x_{\nu j}$, $\Delta x'_{\nu j}$, . . . , $\Delta x_{\nu j}^{(n-1)}$.

Let us write the corresponding solution in matrix form

$$\Delta X_j = A_jX\,(\nu T + t_j + 0), \tag{14}$$

where

$$\Delta X_j = \left\|\begin{matrix}\Delta x_{\nu j}\\ \Delta x'_{\nu j}\\ \cdot\\ \cdot\\ \Delta x_{\nu j}^{(n-1)}\end{matrix}\right\|, \quad X\,(t) = \left\|\begin{matrix}x\,(t)\\ x'\,(t)\\ \cdot\\ \cdot\\ x^{(n-1)}\,(t)\end{matrix}\right\|,$$

$$A_j = \left\|\begin{matrix}0 & 0 & 0 & 0 & \dots & 0 & 0\\ \alpha_{j1} + \beta_{j1} & 0 & 0 & 0 & \dots & 0 & 0\\ \alpha_{j2} + \beta_{j2} & \alpha_{j1} & 0 & 0 & & 0 & 0\\ \alpha_{j3} + \beta_{j3} & \alpha_{j2} & \alpha_{j1} & 0 & \dots & 0 & 0\\ \cdots & \cdots & \cdots & \cdots & \cdots & \cdots & \cdots\\ \alpha_{j,\,n-1} + \beta_{j,\,n-1} & \alpha_{j,\,n-2} & \alpha_{j,\,n-3} & \alpha_{j,\,n-4} & \dots & \beta_{j1} & 0\end{matrix}\right\|. \tag{15}$$

The elements of α_{jn}, β_{jn} of the matrix (15) are obtained from the recurrent formulas

$$\alpha_{jn} = -\,\frac{b_n}{a_0}\,\Delta k_j - \sum_{i=1}^{n-1}\frac{a_{n-i} + k_jb_{n-i}}{a_0}\,\alpha_{ji},$$

$$\beta_{jn} = -\,\frac{b_{n+1}}{a_0}\,\frac{\Delta f_j}{\dot{z}\,(t_j)} - \sum_{i=1}^{n-1}\frac{a_{n-i} + k_jb_{n-i}}{a_0}\,\beta_{ji},$$

where

$$\alpha_{j1} = -\,\frac{b_1}{a_0}\,\Delta k_j, \quad \beta_{j1} = -\,\frac{b_2}{a_0}\,\frac{\Delta f_j}{\tilde{z}\,(t_j)}\,.$$

Equations (12) and (14), taken together, are equivalent to equation (10), and represent another form of the linear approximation when x(t) is varied. On the basis of these equations, the determination of the variation of x(t) is reduced to a storing of the solutions of (12) taking into account the jumps (14) in the interval of a period.

4. After integration of the linear approximation (12), (14) in a period of motion, i.e., for $\nu T < t \le \nu T + T$, we get

$$X\,(\nu T + T) = UX\,(\nu T), \tag{16}$$

where U is a square matrix.

Let us determine the matrix U.

Let $x_j(t)$ be a solution of the equation

$$[L\,(p) + k_jK\,(p)]\,x\,(t) = 0.$$

Let us write this solution in the form

$$x_j\,(t) = \sum_{i=1}^{n} e^{\lambda_{ij}t}\,C_{ji}, \tag{17}$$

where λ_{ji} are the roots of the characteristic equation

$$L\,(\lambda_j) + k_jK\,(\lambda_j) = 0.$$

(case of simple roots) and the C_{ji}'s are integration constants.

From (17) we can build the matrix

$$X(\nu T + t_{j-1} + \bar{t}) = X_j(\bar{t}) = M_j(\bar{t})\, C_j, \tag{18}$$

where

$$M_j(\bar{t}) = \left\| \begin{matrix} e^{\lambda_{j1}\bar{t}} & e^{\lambda_{j2}\bar{t}} & \dots & e^{\lambda_{jn}\bar{t}} \\ \lambda_{j1}e^{\lambda_{j1}\bar{t}} & \lambda_{j1}e^{\lambda_{j2}\bar{t}} & \dots & \lambda_{jn}e^{\lambda_{jn}\bar{t}} \\ \dots & \dots & \dots & \dots \\ \lambda_{j1}^{n-1}e^{\lambda_{j1}\bar{t}} & \lambda_{j2}^{n-1}e^{\lambda_{j2}\bar{t}} & \dots & \lambda_{jn}^{n-1}e^{\lambda_{jn}\bar{t}} \end{matrix} \right\| \qquad C_j = \left\| \begin{matrix} C_{j1} \\ C_{j2} \\ \vdots \\ C_{jn} \end{matrix} \right\|.$$

The integration constants are determined by the equation

$$C_j = M_j^{-1}(0)\, X(\nu T + t_{j-1} + 0). \tag{19}$$

On the other hand, if we store the solution (18) for two successive intervals j − 1 and j, we get

$$X(\nu T + t_{j-1} + 0) = M_{j-1}(\tau_{j-1})\, C_{j-1} + \Delta X_{j-1}$$

or, taking (14) into account

$$X(\nu T + t_{j-1} + 0) = (E - A_{j-1})^{-1} M_{j-1}(\tau_{j-1})\, C_{j-1}, \tag{20}$$

where E denotes the unit matrix.

If (20) is introduced in (19), we get the recurrent formula for the integration constants

$$C_j = M_j^{-1}(0)\, B_{j-1}^{-1} M_{j-1}(\tau_{j-1})\, C_{j-1}, \tag{21}$$

where B_{j-1} is a nonsingular triangular matrix

$$B_{j-1} = E - A_{j-1}.$$

Taking into account the fact that, according to (19),

$$C_1 = M_1^{-1}(0)\, X(\nu T + 0),$$

formula (21) can be written in the form

$$C_j = U_j X(\nu T + 0), \tag{22}$$

where

$$U_j = M_j^{-1}(0) \prod_{n=1}^{j-1} B_{j-n}^{-1} M_{j-n}(\tau_{j-n})\, M_{j-n}^{-1}(0) \tag{23}$$

$$(j = 2, \dots, l + 1).$$

The product of the matrix under the sign Π is made to the right with n increasing. Here, $M_{l+1}^{-1}(0)$ can be replaced by $M_1^{-1}(T)$.

For $j = l + 1$ and $\bar{t} = 0$, formulas (18) and (22) give

$$X(\nu T + T + 0) = M_{l+1}(0)\, C_{l+1} =$$

$$= M_{l+1}(0)\, U_{l+1} X(\nu T + 0),$$

whence, according to (16), we get

$$U = M_{l+1}(0)\, U_{l+1}(0)$$

or, taking (23) into account,

$$U = \prod_{n=l}^{l} B_{l-n+1}^{-1} M_{j-n+1}(\tau_{j-n+1})\, M_{j-n+1}^{-1}(0). \tag{24}$$

Formula (24) gives the matrix U of transformation (16).

5. It is well known that the zero solution of equation (10) is asymptotically stable, i.e., the variation x(t) and all its derivatives down to the (n − 1)th derivative tend to zero when the time increases beyond any limit if the characteristic numbers of the matrix U of transformation (16)(i.e., the roots of the characteristic equation of the linear approximation

$$\det(U - \rho E) = 0, \tag{25}$$

where E = the unit matrix, ρ = a scalar parameter) all lie within the unit circle in the plane of the roots.

In this case, the periodic motion $\mathfrak{Z}(t)$ is asymptotically stable.

Reference [6] showed that in the autonomous discontinuous case the periodic motion is stable also when one of the roots of the characteristic equation (25) is equal to unity, provided all the other roots are less than one in modulus. But if only one of the roots of the characteristic equation (25) has a modulus greater than unity, the corresponding periodic motion is unstable (this is a theorem analogous to that of Andronov and Vitt).

APPENDIX

Let us substitute in equation (10)

$$D^q x(t) = p^q x(t) + \sum_{\nu=0}^{\infty} \sum_{j=1}^{l} [\Delta x_{\nu j} \delta^{(q-1)} (t - \nu T - t_j) + \cdots + \Delta x_{\nu j}^{(q-1)} \delta (t - \nu T - t_j)],$$

$$D^q \left[\sum_{\nu=0}^{\infty} \sum_{j=1}^{l} k_j x_{\nu j}(t)\right] = k_j p^q x(t) + \sum_{\nu=0}^{\infty} \sum_{j=1}^{l} (\Delta [k_j x(t)] \delta^{(q-1)} (t - \nu T - t_j) + \cdots +$$

$$+ \Delta [k_j x(t)]^{(q-1)} \delta (t - \nu T - t_j)), \quad \left(p \equiv \frac{d}{dt}\right),$$

where

$$\Delta [k_j x(t)]^{(k)} = k_{j+1} x^{(k)} (\nu T + t_j + 0) - k_j x^{(k)} (\nu T + t_j - 0) =$$

$$= k_{j+1} x^{(k)} (\nu T + t_j + 0) - k_j [x^{(k)} (\nu T + t_j + 0) - \Delta x_{\nu j}^{(k)}] =$$

$$= x^{(k)} (\nu T + t_j + 0) \Delta k_j + k_j \Delta x_{\nu j}^{(k)}$$

and

$$D^q \left[\sum_{\nu=0}^{\infty} \sum_{j=1}^{l} \frac{\Delta f_1}{\dot{z}(t_j + 0)} x(\nu T + t_j + 0) \delta (t - \nu T - t_j)\right] =$$

$$= \sum_{\nu=0}^{\infty} \sum_{j=1}^{l} \frac{\Delta f_j}{\dot{z}(t_j + 0)} x(\nu T + t_j + 0) \delta^{(q)} (t - \nu T - t_j).$$

Then let us equate the coefficients of $\underline{p}$ and $\delta^{(q)}$. As a result of this operation, we get equation (12) and, correspondingly, for each of the discontinuity points $t = \nu T + t_j$, we obtain the equations

$$0 = -\Delta f_j \frac{b_0}{\dot{z}(t_j + 0)},$$

$$a_0 \Delta x_{\nu j} = -b_0 [\Delta k_j x(\nu T + t_j + 0) + k_j \Delta x_{\nu j}] - \Delta f_j \frac{b_1}{\dot{z}(t_j + 0)} x(\nu T + t_j + 0),$$

$$a_0 \Delta x'_{\nu j} + a_1 \Delta x_{\nu j} = -b_0 [\Delta k_j x'(\nu T + t_j + 0) + k_j \Delta x'_{\nu j}] - b_1 [\Delta k_j x(\nu T + t_j + 0) + k_j \Delta x_{\nu j}] -$$

$$- \Delta f_j \frac{b_2}{\dot{z}(t_j + 0)} x(\nu T + t_j + 0),$$

. . . .

$$a_0 \Delta x_{\nu j}^{(n-1)} + \cdots + a_{n-1} \Delta x_{\nu j} = -b_0 [\Delta k_j x^{(n-1)} (\nu T + t_j + 0) + k_j \Delta x_{\nu j}^{(n-1)}] - \cdots -$$

$$- b_{n-1} [\Delta k_j x(\nu T + t_j + 0) + k_j \Delta x_{\nu j}] - \Delta f_j \frac{b_n}{\dot{z}(t_j + 0)} x(\nu T + t_j + 0)].$$

By combining the terms of these equations according to the discontinuities $\Delta x_{\nu j}^{(q)}$, we get system (13).

LITERATURE CITED

1. M. A. Aizerman and F. R. Gantmakher, "Concerning the stability of periodic conditions in nonlinear systems with a piecewise linear characteristic," Avtomat. i Telemekh. 19, No. 6 (1958).*
2. M. A. Aizerman and F. R. Gantmakher, "Determination of the periodic conditions in systems with a piecewise linear characteristic, consisting of joints parallel to two given straight lines," Avtomat. i Telemekh. 18, Nos. 2 and 3 (1957).*
3. L. A. Gusev, "Determination of the periodic conditions of automatic control systems with a nonlinear element with a piecewise linear characteristic," Avtomat. i Telemekh 19, No. 10 (1958).*
4. K. K. Belya, "On self-oscillatory conditions arising in nonlinear automatic control systems with a nonsensitive region, a gap, or a limitation in modulus," Tr. VVIA, No. 713 (1959).
5. M. A. Aizerman and F. R. Gantmakher, "Stability, according to the linear approximation, of the periodic solution of a system of differenital equations with discontinuous right-hand members," Prikl. Matem. i Mekh. 21, No. 5 (1957).
6. M. A. Aizerman and F. R. Gantmakher, "The stability of periodic motions," Prikl. Matem. i Mekh. 22, No. 6 (1958).

---

* See English translation.

REDUCED EQUIVALENT AMPLIFICATION FACTOR OF A NONLINEAR ELEMENT IN THE PRESENCE OF NOISE

B. D. Kislov

Moscow

Translated from Avtomatika i Telemekhanika, Vol. 21, No. 8, pp. 1141-1148,
August, 1960
Original article submitted February 29, 1960

The reduced equivalent amplification factor of a nonlinear element in the presence of noise is found; it is suggested that it be used in studies of periodic modes in self-oscillating automatic control systems when high-frequency noise effects them.

Let us examine an automatic control system composed of a linear and a nonlinear part, and described by equations

$$\sum_{i=0}^{n} a_i \frac{d^i X}{dt^i} = \sum_{j=0}^{m} b_j \frac{d^j Y}{dt^j}, \qquad (1)$$

$$Y = f_{\text{н}}(Z), \qquad (2)$$

$$Z(t) = X(t) + X_{\Pi}(t), \qquad (3)$$

where (1) and (2) are the equations for the linear part of the system and the nonlinear inertialess part, respectively.

A vibratory signal, or noise in the form of a periodic disturbance $X_{\Pi}(t)$, whose frequency spectrum lies beyond the pass band of the linear part of the system, ω_c, acts on the input of the nonlinear element; according to equation (3), the output function X(t) also acts on this element. Later, we shall examine the case when $X_{\Pi}(t)$ is a random function.

We will be interested in the periodic oscillations of X(t), whose frequencies lie between $\omega_c > \omega > (\omega_c/2)$ (ω_c is the cutoff frequency of the linear part of the system). In this case, X(t) can be represented as a harmonic function of the type

$$X(t) = A\cos\omega t, \qquad (4)$$

where A and ω are the amplitude and frequency, respectively, of self-oscillation X. The oscillations of X can be determined by the harmonic-balance method, and the presence of noise is reflected only in the form of an equation for the conditional equivalent amplification factor of the nonlinear element. This equivalent amplification factor will depend on the type of nonlinear element, the amplitude and frequency of the unknown periodic oscillations, the shape of the disturbance, and also on the phase shift between the disturbance and the unknown periodic oscillations. When the frequency of $X_{\Pi}(t)$ is high, the effect of the phase shift between the functions $A\cos\omega t$ and $X_{\Pi}(t)$ and their frequency shift is not very great, and one can introduce the concept of an average (reduced) equivalent amplification factor.

The function Z(t) may be either periodic or almost periodic, but in either case, the first harmonic amplitude of $X_{\Pi}(t)$ is nearly A at high frequency.

We will assume that the frequency spectrum of disturbance $X_{\Pi}(t)$ is large enough so that A can be taken as the first harmonic amplitude of the function Z(t).

Let us approximate the function $X_{\Pi}(t)$ by a step function $\overline{X}_{\Pi}(t)$ (Fig. 1a). Then expression (3) for Z(t) takes the form

$$Z(t) = \overline{Z}(t) = A\cos\omega t + \overline{X}_{\Pi}(t). \qquad (5)$$

The function $\overline{X}_{\Pi}(t)$ during period τ can be represented as the sum of n rectangular pulses, with width Δt and height Π_i ($i = 1, 2, 3, \ldots, n$), equal to the ordinates of the steps of function $X_{\Pi}(t)$ in the time interval $\Delta t(i-1) < t < i\Delta t$. The function $\overline{X}_{\Pi}(t)$ can be represented as a series

$$\overline{X}_{\Pi}(t) = \sum_{i=1}^{n} \delta X_{\Pi_i}(t), \qquad (6)$$

for an infinite time interval; the series consists of impulses

$$\delta X_{\Pi_i}(t) = \begin{cases} 0 \text{ for } & (i-1)\Delta t + \beta\tau \geqslant t \geqslant i\Delta t + \beta\tau, \\ \Pi_i \text{ for } & (i-1)\Delta t + \beta\tau < t < i\Delta t + \beta\tau \end{cases} \tag{7}$$

Here $\underline{i}$ is the ordinal number of the impulses of (7), and of the pulse of $\overline{X}_{\Pi}(t)$, as shown in Fig. 1a and 1b; $\beta = 1, 2, 3, \ldots, \infty$ is the period number of $\overline{X}_{\Pi}(t)$. In the function $\overline{Z}(t)$, $A \cos \omega t$ can also be represented as a series which consists of $\underline{n}$ periodic impulses $\delta X_i(t)$ $(i = 1, 2, 3, \ldots, n)$

$$A \cos \omega t = \sum_{i=1}^{n} \delta X_i(t), \tag{8}$$

where

$$\delta X_i(t) = \begin{cases} 0 & \text{for } (i-1)\Delta t + \beta\tau \geqslant t \geqslant i\Delta t + \beta\tau, \\ A \cos \omega t & \text{for } (i-1)\Delta t + \beta\tau < t < i\Delta t + \beta\tau. \end{cases} \tag{9}$$

Just as for the function $\delta X_{\Pi_i}(t)$, an infinite number of values for $\beta = 1, 2, 3, \ldots, \infty$ is assumed for each value of $\underline{i}$.

As can be seen from expression (9) and Fig. 1c, the impulses of $\delta X_i(t)$, in contrast to those of $\delta X_{\Pi_i}(t)$, are not rectangular.

In case the ratio $T/\tau = \gamma$ is an integral number, the period of the functions $\delta X_i(t)$ is equal to T, and each of the functions $\delta X_i(t)$ contains γ pulses during period T. If γ is not an integral number, the period of the functions will equal cT, where $\underline{c}$ is the least integer for which the product $c\gamma$ is also integral.

The impulses of $\delta X_i(t)$, like those of $\delta X_{\Pi_i}(t)$, will follow one another at intervals τ, and will be concurrent when indices $\underline{i}$ and β are identical (Figs. 1b, 1c, and 1d). In this case,

$$\delta Z_i(t) = \delta X_i(t) + \delta X_{\Pi_i}(t) \quad (i = 1, 2, 3, \ldots\, n) \tag{10}$$

are impulse functions defined by expressions:

$$\delta Z_i(t) = \begin{cases} 0 & \text{for } (i-1)\Delta t + \beta\tau \geqslant t \geqslant i\Delta t + \beta\tau, \\ A \cos \omega t + X_{\Pi} & \text{for } (i-1)\Delta t + \beta\tau < t < i\Delta t + \beta\tau, \end{cases} \tag{11}$$

and the sum of all functions $\delta Z_i(t)$ $(i = 1, 2, 3, \ldots, n)$ gives $\overline{Z}(t)$, i.e.,

$$\overline{Z}(t) = A \cos \omega t + \overline{X}_{\Pi}(t) = \sum_{i=1}^{n} \delta Z_i(t). \tag{12}$$

Let us write expression (10) in the form

$$\delta Z_i(t) = (A \cos \omega t + \Pi_i)_{(i-1)\Delta t + \beta\tau < t < i\Delta t + \beta\tau}, \tag{13}$$

where Π_i is a constant equal to the height of the $\underline{i}$th impulse of $\overline{X}_{\Pi}(t)$ during the time being considered, which depends on $\underline{i}$ and β (Fig. 1).

Let us shift $\overline{X}_{\Pi}(t)$ in expression (12) relative to itself by an amount equal to $k\Delta t$, where $k = 0, 1, 2, \ldots, (n-1)$.

Then expression (12) takes the form

$$\overline{Z}_k(t) = A \cos \omega t + \overline{X}_{\Pi}(t - k\Delta t) = \\ = \sum_{i=1}^{n} (A \cos \omega t + \Pi_i)_{(i+k-1)\Delta t + \beta\tau < t < i(i+k)\Delta t + \beta\tau}. \tag{14}$$

We will define the reduced equivalent amplification factor of the nonlinear element as the ratio of the first harmonics of the functions, expressed as Fourier series, at the output and input of the nonlinear element.

In this case, the equivalent amplification factor is defined by the expression

$$J_k = \frac{2}{TA} \int_0^T Y_k \cos \omega t \, dt + j \frac{2}{TA} \int_0^T Y_k \sin \omega t dt, \tag{15}$$

where

$$Y_k = f_{\text{н}}(Z_k) = \\ = f_{\text{н}} \left[\sum_{i=1}^{n} (A \cos \omega t + \Pi_i)_{(i+k-1)\Delta t + \beta\tau < t < (i+k)\Delta t + \beta\tau} \right]. \tag{16}$$

Since any phase shift of $\overline{X}_{\Pi}(t)$ with respect to $A \cos \omega t$ is equally probable, and has little effect on the equivalent amplification factor if $X_{\Pi}(t)$ is high frequency, we will define the mean equivalent amplification factor as the arithmetic mean

$$J_{\text{av}} = \frac{1}{n} \sum_{k=0}^{n-1} J_k \tag{17}$$

for time shifts of $\overline{X}_\Pi(t)$ by $k\Delta t$ as k changes from 0 to $n-1$. Putting expressions (15) and (16) in formula (17) in place of I_k, we get

$$I_{\text{av}}=\frac{2}{TA}\int_0^T\frac{1}{n}\sum_{k=0}^{n-1}f_{\text{н}}\left[\sum_{i=1}^{n}A\cos\omega t+\right.$$

$$\left.+\Pi_i)_{(i+k-1)\Delta t+\beta\tau<t<(i+k)\Delta t+\beta\tau}\right]\cos\omega t\,dt+$$

$$+j\frac{2}{TA}\int_0^T\frac{1}{n}\sum_{k=0}^{n}f_{\text{н}}\left[\sum_{i=1}^{n}(A\cos\omega t+\right. \tag{18}$$

$$\left.+\Pi_i)_{(i+k-1)\Delta t+\beta\tau<t<(i+k)\Delta t+\beta\tau}\right]\sin\omega t\,dt.$$

after transformations.

Since series (14) is formed by adjacent pulses of (13), the relation

$$Y_k=f_{\text{н}}\left[\sum_{i=1}^{n}A(\cos\omega t+\right.$$

$$\left.+\Pi_i)_{(i+k-1)\Delta t+\beta\tau<t<(i+k)\Delta t+\beta\tau}\right]= \tag{19}$$

$$=\sum_{i=1}^{n}f_{\text{н}}[(A\cos\omega t+\Pi_i)_{(i+k-1)\Delta t+\beta\tau<t<(i+k)\Delta t+\beta\tau}].$$

is justified.

Analogously, one can write

$$\sum_{k=0}^{n-1}f_{\text{н}}[(A\cos\omega t+\Pi_i)_{(i+k-1)\Delta t+\beta\tau<t<(i+k)\Delta t+\beta\tau}]=$$

$$=f_{\text{н}}\left[\sum_{k=0}^{n-1}(A\cos\omega t+\Pi_i)_{(i+k-1)\Delta t+\beta\tau<t<(i+k)\Delta t+\beta\tau}\right]=$$

$$=f_{\text{н}}(A\cos\omega t+\Pi_i). \tag{20}$$

On the basis of (19) and (20), expression (18) can be put in the form

$$I_{\text{av}}=\frac{1}{n}\sum_{i=1}^{n}\left\{\frac{2}{TA}\int_0^T f_{\text{н}}(A\cos\omega t+\Pi_i)\cos\omega t\,dt+\right.$$

$$\left.+j\frac{2}{TA}\int_0^T f_{\text{н}}(A\cos\omega t+\Pi_i)\sin\omega t\,dt\right\}, \tag{21}$$

or

$$I_{\text{av}}=\frac{1}{n}\sum_{i=1}^{n}I(A,\Pi_i), \tag{22}$$

where

$$I(A,\Pi_i)=$$

$$=\frac{2}{TA}\int_0^T f_{\text{н}}(Z_{\Pi_i})\cos\omega t\,dt+j\frac{2}{TA}\int_0^T f_{\text{н}}(Z_{\Pi_i})\sin\omega t\,dt, \tag{23}$$

$$Z_{\Pi_i}=A\cos\omega t+\Pi_i. \tag{24}$$

In this case, $I(A,\Pi_i)$ is the equivalent amplification factor of the nonlinear element, calculated under the condition that the function $Z=Z_{\Pi_i}(t)$ at the output of the nonlinear element is defined by expression (24).

Let us assume that $X_\Pi(t)$ is approximated in such a manner that it has different heights m during period τ and that their amplitudes are equal to

$$\Pi_q(q=1,2,3,\ldots,m).$$

The term Δt_q will denote the sum of time intervals Δt long, which occur in one period τ, during which the function $X_\Pi(t)$ assumes the value Π_q.

Then, saying that $n=\tau/\Delta t$, expression (22) will be written as

$$I_{\text{av}}=\sum_{q=1}^{m}\frac{\Delta t_q}{\tau}I(A,\Pi_q), \tag{25}$$

where Π_q can equal zero for one of the values $q=1,2,3,\ldots,m$.

If $f_H(Z)$ has even symmetry, and the term $\overline{X}_\Pi(t)$ in $\overline{Z}(t)$ has such a form that for every value of $\Pi_i>0$ during a period there is a $\Pi_i<0$ of equal absolute magnitude, one can easily see that expression (25) assumes the form

$$I_{\text{av}}=\sum_{q=1}^{\sigma}2\frac{\Delta t_q}{\tau}I(A,\Pi_q). \tag{26}$$

Here the value of q corresponds to the sections where $\Pi_q\geq 0$ or $\Pi_q\leq 0$ for the function $X_\Pi(t)$; $\sigma=(m/2)$ for even m and $\sigma=(m+1)/2$ for odd m.

The q for which Π_q is zero (m odd) is taken when Δt_q is at half-amplitude during period τ. The period of the function $\overline{X}_\Pi(t)$ was broken into n equal parts in determining the mean equivalent amplification factor; time shifts of $\overline{X}_\Pi(t)$ by $k\Delta t$ were considered, where $k=0,1,2,3,\ldots,(n-1)$ (n values in all).

Let us divide Δt into λ equal parts, so the period τ will be divided into $n\lambda$ equal parts. We will define the reduced mean equivalent amplification factor I_{av} for such time shifts of the function

$$X_\Pi[t-k\Delta t-(e/\lambda)\Delta t],$$

where a series of intermediate values e = 0, 1, 2, ..., $\lambda-1$ are assumed at each value k = 0, 1, 2, ..., (n−1).

Since expression (25) does not depend on the phase shift of $\overline{X}_\Pi(t)$, one can easily see that the expression for the unknown mean equivalent amplification factor will be the same as (25).

As $\lambda \to \infty$, the expression for I_{av} is defined as the mathematical expectation, since any phase shift of $\overline{X}_\Pi(t)$ is equally probable. Therefore, the equivalent amplification factors developed above may be considered not only as the arithmetic mean of all possible discrete initial phase shifts of $\overline{X}_\Pi(t)$, but as the mathematical expectation also.

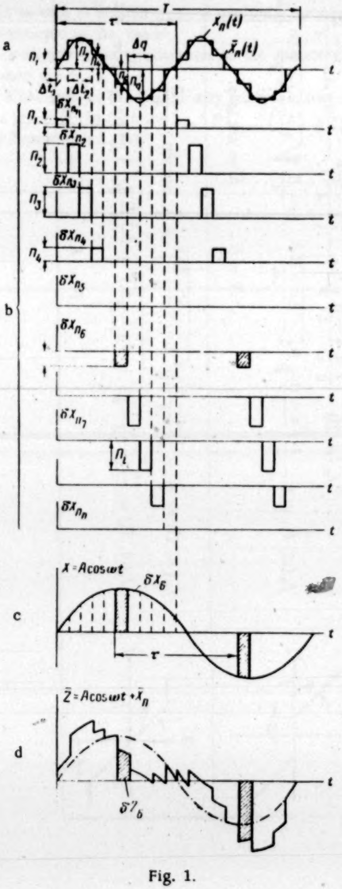

Fig. 1.

In order to get the expression for the mean equivalent amplification factor for a continuous function, Δt must be made to approach zero as a limit in formulas (25) and (26). The expression $(\Delta t_q/\tau)$ appears in (25) and (26); it depends on the value of Π_q, and is a discrete function.

As $\Delta t \to 0$, $n \to \infty$, $\Pi_q \to \Pi$, and the ratio $\Delta t_q/\tau$ tends toward a continuous function:

$$(\Delta t_q/\tau) \to W(\Pi)\,d\Pi.$$

In this case, expression (25) assumes the form

$$I_{av} = \frac{2}{TA}\int_{-\infty}^{+\infty} W(\Pi)\,d\Pi\int_{0}^{T} f_{\text{н}}(A\cos\omega t+\Pi)\cos\omega t\,dt + \tag{27}$$

$$+\,j\,\frac{2}{TA}\int_{-\infty}^{+\infty} W(\Pi)\,d\Pi\int_{0}^{T} f_{\text{н}}(A\cos\omega t+\Pi)\sin\omega t\,dt.$$

It follows from the formulas obtained that the reduced equivalent amplification factor does not depend on the frequency of the noise, but is determined by its form. Hence, W(Π) can be treated as the probability density that the function $X_\Pi(t)$ assumes the value Π during a period. Therefore, if a random stationary process, whose frequency spectrum lies beyond the the pass band of the system, is considered to be the noise, then the formula obtained would hold, but the probability density W(Π) in this case must be preliminarily computed from the given random process.

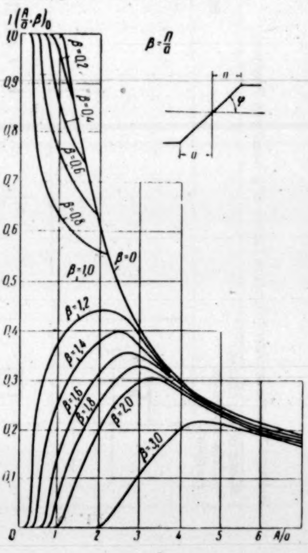

Fig. 2.

Reduced Equivalent Amplification Factor of a Nonlinear Element

Shape of the characteristic nonlinear element	Formulas for $I_0(A, \Pi)$ and N
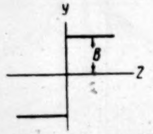	$I_0(A, \Pi) = \frac{4}{\pi}\frac{1}{A}\sqrt{1-\left(\frac{\Pi}{A}\right)^2},$ $N = B.$
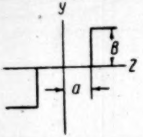	$I_0(A, \Pi) = \frac{2}{\pi}\frac{a}{A}\sqrt{1-\left(\frac{a-\Pi}{A}\right)^2}$ for $(A-\Pi) < a,$ $I_0(A, \Pi) = \frac{2}{\pi}\frac{a}{A}\left[\sqrt{1-\left(\frac{a-\Pi}{A}\right)^2}+\sqrt{1-\left(\frac{a+\Pi}{A}\right)^2}\right]$ for $(A-\Pi) > a;$ $N = B/a.$
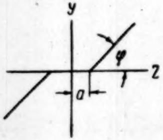	$I_0(A, \Pi) = \frac{1}{2}\frac{1}{\pi}\frac{a-\Pi}{A}\sqrt{1-\left(\frac{a-\Pi}{A}\right)^2}-\frac{1}{\pi}\arcsin\frac{a-\Pi}{A}$ for $(A-\Pi) < a,$ $I_0(A, \Pi) = 1-\frac{1}{\pi}\Bigl[\frac{a-\Pi}{A}\sqrt{1-\left(\frac{a-\Pi}{A}\right)^2}+\frac{a+\Pi}{A}\sqrt{1-\left(\frac{a+\Pi}{A}\right)^2}+\arcsin\frac{a-\Pi}{A}+\arcsin\frac{a-\Pi}{A}$ for $(A-\Pi) > a;$ $N = K, \qquad K = \operatorname{arc\,tg}\varphi.$
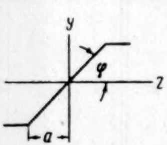	$I_0(A, \Pi) = \frac{1}{2}+\frac{1}{\pi}\frac{a-\Pi}{A}\sqrt{1-\left(\frac{a-\Pi}{A}\right)^2}+\frac{1}{\pi}\arcsin\frac{a-\Pi}{A}$ for $(A-\Pi) < a,$ $I_0(A, \Pi) = \frac{1}{\pi}\left[\frac{a-\Pi}{A}\sqrt{1-\left(\frac{a-\Pi}{A}\right)^2}+\frac{a+\Pi}{A}\sqrt{1-\left(\frac{a+\Pi}{A}\right)^2}+\arcsin\frac{a-\Pi}{A}+\arcsin\frac{a-\Pi}{A}\right]$ for $(A-\Pi) > a;$ $N = K, \qquad K = \operatorname{arc\,tg}\varphi.$

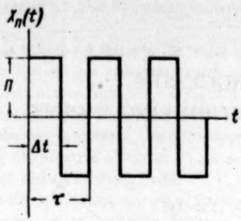

Fig. 3.

Elementary terms of the type $I(A, \Pi_q) = NI_0(A, \Pi_q)$ appear in formulas (25) and (26); expressions for these, which pertain to certain types of nonlinear elements, are presented in the Table.

It is convenient to characterize the quantity Π_q by the ratio $\beta = \Pi_q/a$.

When systems are graphically analyzed, one can use a graph of the function $I_{av} = NI_{0av} = f(A)$, whose form depends on $\lambda_\Pi(t)$.

The graphs can easily be obtained for any type of step disturbance $\overline{X}_\Pi(t)$ or random function, whose probability density is approximated by discrete functions, by means of a family of curves of $I_0(A/a)$, plotted for elementary terms, where $\beta = \beta_1, \beta_2, \beta_3, \ldots = \text{const}$.

One of these families, plotted for the case when the nonlinear element has the characteristics of a linear amplifier over a limited range, is shown in Fig. 2.

When $X_\Pi(t)$ is shaped as in Fig. 3, where τ is the period, Π the height, Δt the step width of X_Π, $I_{0av} = I_0$, these families are coincident with the families of I_{0av} at $\beta = \beta_1, \beta_2, \beta_3, \ldots = \text{const}$.

We will get one curve for the dependence of the mean equivalent amplification factor of the nonlinear element for a given disturbance.

The analysis of stable self-oscillation in a disturbed system is done by means of a graph of the disturbance and a graph of the linear part of the system in the same manner as for an analysis of system stability without perturbation.

ON THE CONTROL OF CERTAIN INDUSTRIAL PROCESSES BY MEANS OF MINIMUM CHANGES OF THE CONTROLLING INPUTS

I. A. Burovoi and S. V. Emel'yanov

Moscow

Translated from Avtomatika i Telemekhanika, Vol. 21, No. 8, pp. 1149-1157,
August, 1960
Original article submitted July 14, 1959

The problem of developing automatic control systems which ensure the required transient response with minimum change of the controlling inputs, necessary only for compensating for disturbances (without measuring the latter), is discussed.

It is shown that this problem can be solved by using automatic control systems which have a variable structure.

A nonlinear industrial electrical regulator with a variable structure, which has been developed, is described as an example of one of the many practical solutions of the stated problem.

In the control of certain continuous industrial processes with interrelated parameters, the best technical and economic features are achieved when the controlling inputs need only be changed, in accordance with the static characteristics of the systems, enough to compensate for disturbances. We will call these changes of the controlling inputs minimum.

In the use of existing industrial regulators, it is, in principle, possible to have transients for which the changes of the controlling inputs will not exceed those necessary to compensate for disturbances. However, these modes are realized only for very small amplification factors in the control circuit, and this causes a large dynamic error and increases the control time. The transient response of systems having delay is especially bad when the above-mentioned limitations on the magnitude of the controlling inputs are imposed.

Hence, a contradiction arises between technological requirements and the dynamics of control in the use of existing industrial regulators for a number of systems; for technological reasons, it is best to minimize the given value of the controlled parameter by means of minimum changes of the controlling inputs, but the error will be maximum when the change of controlling input is minimum, according to the conditions of the dynamics of control.

It is for this reason that it is necessary to devise automatic control systems which ensure the required quality of control for minimum changes of the controlling inputs, necessary only for compensating for disturbances in the static modes (without measuring the latter).

Let us clarify the necessity for stating such a problem by a series of technological examples.

When the hot mass does not burn completely in firing in the boiling layer, it is best to control the temperature of the boiling layer by changing the consumption of air (the draft), both from a transmission coefficient standpoint, and from a standpoint of the dynamic characteristics of the process.

However, a change in the draft also strongly affects the hydrodynamics of the boiling layer. This effect is especially strong in the treatment of polydispersed materials obtained in industry; the range of change in the draft is extremely small for these materials.

Stable "boiling" cannot be achieved if the draft velocity is low. Stable boiling occurs when the efflux of small fractions reaches 30–50% of the load.

If the draft is further increased, the efflux of small particles from the boiling layer increases sharply, and at a certain time its quality begins to get worse.

The air draft at which the quality of the small particles which are carried off begins to get worse corresponds to the ultimate (maximum) productive capacity of the apparatus (furnace); the most intensive (stable) boiling is also ensured at this draft.

Any change in the draft will either lead to a reduction in the yield of the furnace and intensity of boiling, or will cause the quality of the small particles being borne off to worsen. In view of this, it is clear how important it is to ensure that disturbances are compensated for by minimum changes in the draft, in the operation of an automatic system which controls the temperature of the boiling layer.

In controlling the boiling-layer temperature when the hot mass burns completely (firing of zinc concentrates, pyrites, etc.), the changes of the controlling flow (load) which are necessary for a stable temperature in static modes does not exceed ±5–8%. In this case, the fluctuation in the concentration of SO_2 in the burned gases occuring in the sulfuric acid industry should not exceed ±0.3–0.6%, which is completely permissible.

The most important thing in the reliable use of straight-flow evaporative elements, which are used to control the heat output from the boiling layer, is to have a mode in which the changes in the aqueous lead of the element are minimum, since it is known that straight-flow evaporative elements do not work well when the load changes sharply [1,2].

In controlling the temperature of flame-heated, reflective, Martin, rotary, and other furnaces, it is best to minimize the changes in fuel and air consumption [3]. It is known that the greater the change in the consumption of fuel and air, the more the hydraulic mode of the furnace deviates from optimum. This causes the thermodynamic performance to become worse, and complicates the operation of the control system because of a displacement of the flame root with respect to the pulse-selection points.

One could give analogous examples from a number of other technological processes – controlling the discharge density of classifiers with minimum fluctuations in the pulp speed in the classifiers, controlling the superheat of steam with minimum variations in the consumption of the injected water, etc.

The problem stated was successfully solved by the development of a new regulator which was based on the theory of nonlinear automatic control systems with variable structure [4–7].

Let us examine a very simple automatic control system as an example illustrating the synthesis of a nonlinear control law which ensures the necessary change in the structure of the regulator; this system is described by a nonlinear differential equation of the second order. The block diagram is shown in Fig. 1a.

Without the nonlinear device which changes the structure of the closed loop, the control system is described by the following linear differential equations:

equation of the controlled object:

$$T_a\dot{x} + px = -\mu + f(t); \qquad (1)$$

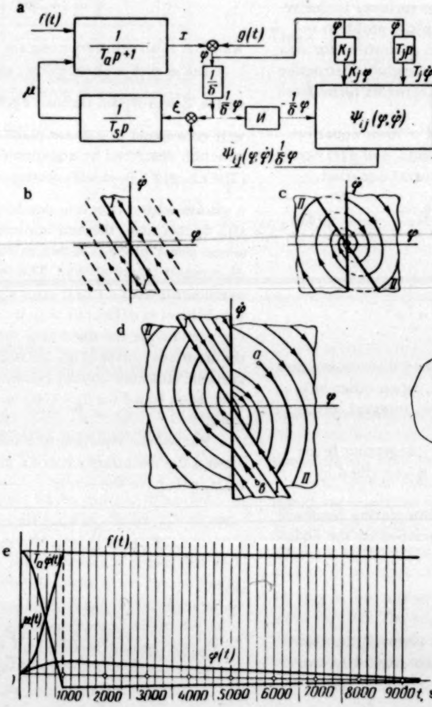
a
f(t)
1
T_ap+1
x
g(t)
φ
1
δ
μ
1
T_sp
ε
$\frac{1}{\delta}\varphi$
И
$\frac{1}{\delta}\varphi$
φ
φ
K_j
T_jp
$K_j\varphi$
$T_j\dot{\varphi}$
$\Psi_{ij}(\varphi,\dot{\varphi})$
$\Psi_{ij}(\varphi,\dot{\varphi})\frac{1}{\delta}\varphi$
b
$\dot{\varphi}$
I
φ
c
$\dot{\varphi}$
II
φ
II
d
$\dot{\varphi}$
II
a
φ
б
II
e
f(t)
$T_a\varphi(t)$
μ(t)
φ(t)
1
1000
2000
3000
4000
5000
6000
7000
8000
9000
t, sec

Fig. 1.

equation of the master element:

$$x - g(t) = \varphi, \tag{2}$$

equation of the astatic regulator:

$$T_s \dot{\mu} = \frac{1}{\delta} \varphi. \tag{3}$$

Here x is the relative change in the coordinates being controlled, φ is the relative change in the error signal, μ is the relative movement of the controlling mechanism, f(t) is the disturbing input, g(t) is the master input, T_a/ρ is the time constant of the controlled object, $1/\rho$ is the static-transmission coefficient of the object, T_s is the integration constant of the astatic regulator, and $1/\delta$ is the static-transmission coefficient of the sensing device.

Let us synthesize the nonlinear control law of the linear automatic control system being examined, with changes of the controlling inputs minimized. We will use the method of multileafed phase surfaces to derive this nonlinear control law [8]. Then the problem reduces to one of constructing a phase portrait of the nonlinear system, which reflects the succession of structure changes necessary to meet the requirements formulated above.

Eliminating the variables x and μ from equations (1), (2), and (3), and setting f(t) = const, and g(t) = const, we get a second order linear differential equation

$$\ddot{\varphi} + 2b\dot{\varphi} + \omega_0^2 \varphi = 0, \tag{4}$$

where

$$2b = \frac{\rho}{T_a}, \quad \omega_0^2 = \frac{1}{T_a T_s \delta}.$$

Three quite easily realizable system structures are possible for a given object structure, when other influences on the control law (derivative, integral, etc.) are absent.

1. The object is in a negative integrating feedback loop. In this case, the system is described by equation (4).
2. The object is in a positive integrating feedback loop. In this case, the system is described by the equation

$$\ddot{\varphi} + 2b\dot{\varphi} - \omega_0^2 \varphi = 0. \tag{5}$$

3. The system is opened at the error signal channel. In this case, the equation for the control system has the form

$$\ddot{\varphi} + 2b\dot{\varphi} = 0. \tag{6}$$

Eliminating time from equations (4), (5), and (6), we get an image of the control process on phase planes $\dot{\varphi}$ and φ.

It can be shown that only the two system structures described by equations (4) and (6) need be used to realize the control process with the restrictions imposed earlier. In this case, the relation between coefficients 2b and ω_0^2 in equation (4) is chosen so that the process will be oscillatory.

The phase plane for equation (4) will be filled by a family of spirals (Fig. 1c). The equation for the spirals will take the form:

$$(\dot{\varphi} + b\varphi)^2 + \omega_1^2 \varphi = C \exp\left[\frac{2b}{\omega_1}\left(\alpha + \operatorname{arctg} \frac{\dot{\varphi} + b\varphi}{\omega_1 \varphi}\right)\right], \tag{7}$$

where $\omega_1 = \sqrt{\omega_0^1 - b^2}$, and C is an arbitrary constant.

The phase plane for equation (6) will be filled by a family of straight lines (Fig. 1b), whose equation is:

$$\dot{\varphi} = -2b\varphi + A, \tag{8}$$

where A is an arbitrary constant.

Let us plot a phase plane, so that if $(T_j\dot{\varphi} + K_j\varphi)\varphi \leq 0$, where T_j and K_j are defined by the ratio $2b = (K_j/T_j)$, it will correspond to a phase plane of a system with a structure described by equation (6) (leaf I), and if $(T_j\dot{\varphi} + K_j\varphi)\varphi > 0$, it will correspond to a phase plane of a system with a structure described by equation (4) (leaf II). In this case, the new nonlinear control system, whose phase plane is shown in Fig. 1d, meets all the requirements stated above. The process goes on without overcontrol with a small error signal φ. The controlling mechanism is deflected only by an amount necessary to compensate for the disturbing input. This follows from the transient curves (Fig. 1e) occurring in the finished variable-structure control system. The control processes have been found for $T_a = 7000$ sec, $T_s = 50$ sec, and $\rho = 1$.

Hence, the equation of a nonlinear regulator, which ensures the necessary structure change during the transient, will have the form:

$$T_s \dot{\mu} = \frac{1}{\delta}\varphi - \Psi_{ij}(\varphi, \dot{\varphi}) \frac{1}{\delta}\varphi, \tag{9}$$

where

$$\Psi_{ji}(\varphi, \varphi) = \begin{cases} 0 & \text{for} \quad (T_j\dot{\varphi} + K_j\varphi)\varphi > 0 \\ 1 & \text{for} \quad (T_j\dot{\varphi} + K_j\varphi)\varphi \leqslant 0 \end{cases}$$

Let us compare the properties of this nonlinear system with those of a linear control system based on the

IR - 130 isodromic industrial regulator and consisting of the static and astatic parts with transfer functions K_{st} and $1/T_s p$, respectively.

By means of simple transformations, the IR-130 regulator can be made into an integral regulator with derivative action (Fig. 2a). The derivative coefficient T is related to the constants of the static and astatic parts by the relation $T = T_s K_{st}$.

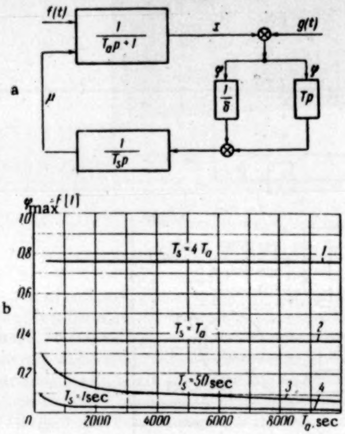

Fig. 2

The comparison is made for systems which operate as stabilizers; consequently, the maximum dynamic error is the main index of comparison.

The parameters of these automatic control systems are chosen so that they will not have overshoot, and so that the movement of the controlling mechanism will be minimized. Since the coefficients ρ and δ are set equal to unity, the coefficient in the linear variation must not exceed unity, on the basis of the restrictions imposed on the movement of the controlling mechanism.

Since the transient is not oscillatory, the integration constant of the regulator T_s is related to the time constant of the object T_a by the equation:

$$T_s = \frac{4}{\delta(\rho + K_{st})^2} T_a. \tag{10}$$

The maximum error for the linear system is found from the formula

$$\varphi_{max} = \dot{\varphi}_0 \sqrt{T_a T_s \delta \exp\left[\frac{2(\rho + K_{st}) T_s \delta}{\sqrt{|4T_a - (\rho + K_{st})^2 T_s \delta|\, T_s \delta}} \rightarrow\right.}$$

$$\left. \rightarrow \sqrt{\left(\operatorname{arc\,tg} \frac{(\rho + K_{st}) T_s \delta}{\sqrt{|4T_a - (\rho + K_{st})^2 T_s \delta|\, T_s \delta}} - \frac{\pi}{2}\right)}\right], \tag{11}$$

and for the nonlinear system from the formula

$$\varphi_{max} = \dot{\varphi}_0 \sqrt{T_a T_s \delta \exp\left[\frac{2\rho T_s \delta}{\sqrt{(4T_a - \rho^2 T_s \delta) T_s \delta}} \left(\operatorname{arc\,tg} \frac{\rho T_s \delta}{\sqrt{(4T_a - \rho^2 T_s \delta) T_s \delta}} - \frac{\pi}{2}\right)\right]}, \tag{12}$$

where $\dot{\varphi}_0 = f(t)/T_a$.

The formulas were derived by means of point transformation, by reflecting the $+\dot{\varphi}$ half-line into the $+\varphi$ half-line.

Graphs of the dynamic error for an object without (1), and with (2), differentiation are shown in Fig. 2b; the derivative action was chosen so as to result in the least values of φ_{max} for minimum movement of the controlling mechanism. Curves for an object with a nonlinear regulator are shown also in Fig. 2b for $T_s = 50$ sec (3), and $T_s = 1$ sec (4).

A comparison of the results obtained shows that in a system with nonlinear correction, the error can be made adequately small as the rapidity of regulator response is increased, in contrast to a linear system, where the error magnitude is constant for different values of T_a. Such a response cannot be achieved in a linear system, since T_s is related to T_a by formula (10). Moreover, the error in a linear system decreases as the time constant of the object increases.

It is difficult to obtain "pure" (undistorted) differentiation for the formulation of a nonlinear control law as applied to slowly occurring processes. In making a linear actuating mechanism, special linearizing elements are built into the regulator; in particular, thermoelements are used in the IR - 130 regulator. Therefore, it would appear wise to build such apparatus by using a nonlinear regulator with a variable structure, in which it would be possible to eliminate the derivative and linearizing elements of the actuating mechanism. The circuit of a regulator which has been developed is shown in Fig. 3, and an over-all view of the experimental model in Fig. 4. The regulator consists of logic circuits, incorporating a constant-velocity integral link, which ensures, in conjunction with relays P_1, P_2, P_3, P_4, P_5, and P_6, the necessary structure change of the system during the transient. The regulator includes a constant-velocity integrating actuating mechanism.

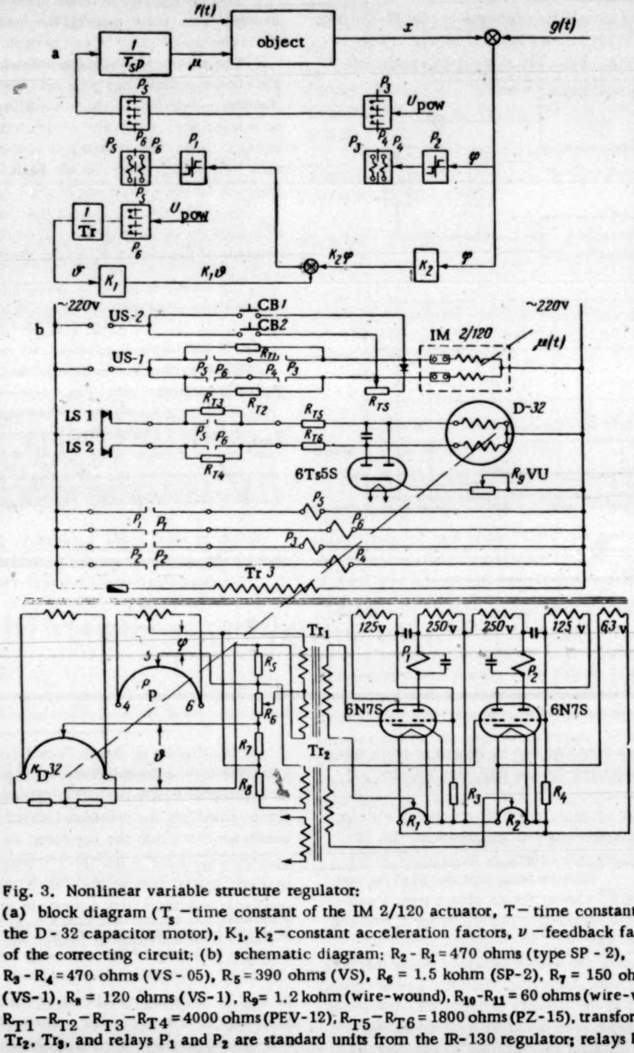
a
f(t)
object
x
g(t)
1/T_sp
μ
P5
P3
U pow
P6
P4
P1
P2
φ
1/Tr
K2φ
K2
ϑ
K1
K1ϑ
b
~220v
US-2
CB1
CB2
US-1
IM 2/120
μ(t)
RT1
RT2
RT3
RT4
RT5
RT6
LS 1
LS 2
D-32
6Ts5S
R9 VU
Tr 3
Tr1
Tr2
P
K D32
R5
R6
R7
R8
125v
250v
125v
63v
6N7S
6N7S
R1
R2
R3
R4

Fig. 3. Nonlinear variable structure regulator:
(a) block diagram (T_s —time constant of the IM 2/120 actuator, T — time constant of the D-32 capacitor motor), K_1, K_2—constant acceleration factors, ν—feedback factor of the correcting circuit; (b) schematic diagram: $R_2 - R_1 = 470$ ohms (type SP-2), $R_3 - R_4 = 470$ ohms (VS-05), $R_5 = 390$ ohms (VS), $R_6 = 1.5$ kohm (SP-2), $R_7 = 150$ ohms (VS-1), $R_8 = 120$ ohms (VS-1), $R_9 = 1.2$ kohm (wire-wound), $R_{10} - R_{11} = 60$ ohms (wire-wound), $R_{T1} - R_{T2} - R_{T3} - R_{T4} = 4000$ ohms (PEV-12), $R_{T5} - R_{T6} = 1800$ ohms (PZ-15), transformers Tr_1, Tr_2, Tr_3, and relays P_1 and P_2 are standard units from the IR-130 regulator; relays P_3, P_4, P_5, and P_6 are type RPT-100; CB 1 and CB 2 are control buttons; US-1, and US-2 are universal switch gangs, LS 1 and LS 2 are limit switches.

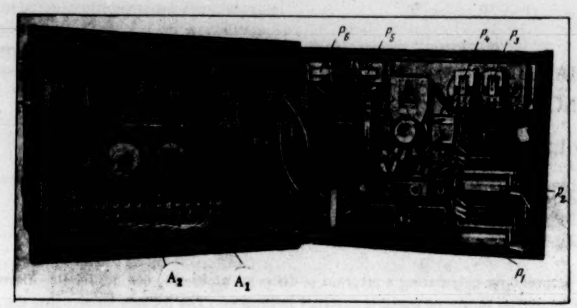

Fig. 4. Over-all view of the nonlinear regulator. A_1—adjusting knob for the T coefficient; A_2—adjusting knob for the K_1 and K_2 factors; P_1 and P_2 are the error channel and correcting loop channel relays; P_3, P_4, P_5, and P_6 are type RPT - 10 relays.

The experimental data obtained on the transients showed that the regulator ensures a high control quality of stable objects without delay, and of objects having a relatively small delay, with minimum changes in the controlling inputs, which are practically equal to the amounts necessary to compensate for disturbances.

If significant delay is present in the object, the structure of the logic networks, and also other system characteristics, are chosen in accordance with the dynamic properties of the object.

The regulator successfully passed industrial tests and is being used experimentally. The test results permit one to predict that this type of regulator will find use in the automation of continuous industrial processes in which control should be accomplished with minimum changes in the controlling inputs, because of technological reasons, and also in cases where high static and dynamic control accuracy must be ensured without introducing derivatives of the parameter being controlled into the control law.

A theoretical analysis of a nonlinear regulator with variable structure, which was actually built, is an independent problem and will be considered separately.

The electrical type of nonlinear variable-structure regulator, which was described above, is one of many possible constructions based on the principle being considered, namely, a method for construction systems which ensure a high control quality with minimum changes in the controlling inputs. This principle may also be applied to pneumatic, hydraulic, as well as other electrical apparatus.

M. S. Lodyseva and O. P. Zelentsov took part in this work.

LITERATURE CITED

1. I. A. Burovoi, "On the automatic control of firing in the boiling layer," Tsvetnye Metally, No. 3(1955).
2. I. A. Burovoi, Automating Firing Processes in the Boiling Layer, from the collection on the automation of industrial processes, 3rd edition [in Russian] (Tsiintsvetmet, 1958).
3. I. A. Burovoi, Yu. A. Bykhovskii, I. I. Zaberezhnyi. and I. M. Rafalovich, Experience in the Automation of Flame Reflecting and Refining Copper Smelting Furnaces [in Russian] (Metallurgizdat, 1953).
4. Ya. Z. Tsypkin, Theory of Automatic Control Relay Systems [in Russian] (Gostekhizdat, 1955).
5. A. M. Letov, "Conditionally stable controlled systems (concerning one class of optimum controlled systems)," Avtomat. i Telemekh. 18, 7 (1957). *
6. S. V. Emel'yanov, "A method for deriving complex control laws, using only the error signal, or the factor being controlled and its first derivative," Avtomat. i Telemekh. 18, 10 (1957).*
7. I. Flügge-Lotz and C. F. Taylor, Synthesis of a Nonlinear Control System. Trans. IRE. PGAC-1 (May, 1956).
8. V. V. Petrov and G. M. Ulanov, "The theory of two very simple control systems," Avtomat. i Telemekh. 11, 5 (1950).

---

*See English translation.

SERVOMECHANISM-COMPENSATION BY USING DISCRETE CALCULATING DEVICES

L. I. Volgin and L. I. Smolyar

Moscow

Translated from Avtomatika i Telemekhanika, Vol. 21, No. 8, pp. 1158-1164,
August, 1960
Original article submitted January 11, 1960

A method is proposed for calculating a program of discrete calculating devices for linear servomechanisms, based on the use of statistical results on possible external influences. The method ensures that the systems obtained will satisfy the "roughness" condition in the presence of unstable elements in the control circuit.

Special importance has recently been attached to methods of calculation of automatic control systems and elements, based on the theory of stationary processes. A significant contribution to the development of these methods has been made by the Soviet scientists A. Ya. Khinchin [1] and A. N. Kolmogorov [2]. There is a good description of the theory in a publication by A. M. Yaglom [3].

The application of the theory of stationary processes in technology was initiated by N. Wiener. Wiener's investigations in [4] played an important part in the development of practical methods of designing selective and smoothing filters, which are important component parts of many automatic systems. Statistical methods in the designing of various technical devices have recently been developed in the works of V. V. Solodovnikov [5], V. S. Pugachev [6], Ya. Z. Tsypkin [7], L. T. Kuzin [8], and others.

Calculating devices of the discrete type (pulse filters and digital machines) have recently been used in various technical systems. In the present work we will consider the problem of the synthesis of servomechanisms containing such devices. A peculiarity of this problem lies in the fact that only part of the system is synthesized — the correcting element supplied by the discrete calculating device, while the object of the control is given. It is necessary, in the synthesis of the correcting element to the object, to consider the possibility of destroying the "roughness" of the system by a divergence between the parameters of the correction link and the controlled object, which leads to the accumulation of errors and instability.

For systems with a stably controlled object, the problem of synthesizing a discrete calculating device, and taking into consideration the "roughness" condition, was solved by S. Chang [9]. Here we will solve the problem for the control of an arbitrary object, stable or unstable. In contrast with Chang's method, which involves laborious calculation, the proposed solution is based on applying the method of equations involving polynomials developed in [10]. The solution of these equations is not a mathematically difficult operation, and can be completely carried out by hand. The problem we consider reduces to a system of two equations of this type. A method of solving these equations involving polynomials is given in the Appendix.

1. Some Results from the Theory of Discrete Stationary Processes

The results that we give here are available in one form or another in [3, 4, 7, 8, 9]. The various authors have, however, used different operational methods. The method used here also differs somewhat from those used previously.

We will use the delay operator z as the basic operator, where this operator is related to the differentiation operator p and the delay interval T by the equation $z = \exp(-pT)$. The use of the physically realizable operator $\exp(-pT)$ instead of $\exp(pT)$ simplifies the description and design of the dynamic systems.

A stationary discrete process will be a sequence of random variables $X = \{x_i\}$ $(i = -\infty, \ldots, +\infty)$, possessing the following properties:

1. the mean value of the random variable x_i does not depend on the subscript i, and for simplicity we will assume that this mean value is zero;
2. the correlation coefficient of the random variables x_i and x_{i+k} depends only on the difference k between the subscripts; we denote it by

$$\psi(k) = \overline{x_i x_{i+k}} \quad (k = -\infty, \ldots, +\infty).$$

The quantity $\psi(0) = \overline{x_i^2}$ is called the dispersion of the stationary discrete process.

The double infinite z-representation of the sequence of these coefficients will be called the correlation-representation of the process

$$\Psi(z) = \sum_{k=-\infty}^{+\infty} \psi(k) z^k. \quad (1)$$

Since the correlation coefficients are even functions of k, the correlation-representation of the process possesses the symmetry property relative to the unit circle described by the relation

$$\Psi(z) = \Psi(z^{-1}). \tag{2}$$

A sufficient condition for the convergence of the series (1) is

$$\left|\frac{\psi(k+1)}{\psi(k)}\right| \leqslant l < 1 \qquad (k > M). \tag{3}$$

If this condition is satisfied, then the function $\Psi(z)$ is analytic in the ring

$$1 - \delta < |z| < 1 + \delta \quad (\delta > 0)$$

and (1) is the Laurent expansion of the function in this ring. The correlation coefficients $\psi(k)$ can be expressed in terms of $\Psi(z)$ as the coefficients of this Laurent expansion

$$\psi(k) = \frac{1}{2\pi j} \oint\limits_{|z|=1} z^{-k}\Psi(z)\frac{dz}{z}. \tag{4}$$

We will limit ourselves to the consideration of processes with correlation-representations that are rational functions of z.

The following method is proposed for obtaining the correlation-representation in terms of the sequence of correlation coefficients. We first of all sum the part of the series (1) with nonnegative powers

$$\Psi_+(z) = \sum_{k=0}^{\infty} \psi(k) z^k. \tag{5}$$

Condition (3) ensures that this series can be summed for all $|z| < 1 + \delta$. We obtain as a result a rational function in the form

$$\Psi_+(z) = \frac{K(z)}{U^+(z)}, \tag{6}$$

where $K(z)$ and $U^+(z)$ are polynomials in z, and the polynomial $U^+(z)$ has no zeros inside the unit circle. The part of the series (1) with negative powers of k

$$\Psi_-(z) = \sum_{k=1}^{\infty} \psi(k) z^{-k} \tag{7}$$

can be obtained from the part with nonnegative powers from the relation

$$\Psi_-(z) = \Psi_+(z^{-1}) - \psi(0).$$

It is also a rational function of z

$$\Psi_-(z) = \frac{Q(z)}{U^-(z)}, \tag{8}$$

where $Q(z)$ and $U^-(z)$ are polynomials in z, and the polynomial $U^-(z)$ has no zeros outside the unit circle.

The function $\Psi(z)$ is obtained as the sum of (6) and (8)

$$\Psi(z) = \Psi_-(z) + \Psi_+(z). \tag{9}$$

This function can be reduced to the form

$$\Psi(z) = \frac{I(z)}{U(z)}, \tag{10}$$

where $I(z)$ and $U(z)$ are polynomials in z.

The factorization of this function

$$\Psi(z) = \Psi^+(z)\Psi^-(z) \tag{11}$$

is carried out by factorizing its numerator and denominator:

$$I(z) = I^+(z) I^-(z), \tag{12}$$

$$U(z) = U^+(z) U^-(z). \tag{13}$$

We introduce the notation

$$\Psi^+(z) = \frac{I^+(z)}{U^+(z)}, \quad \Psi^-(z) = \frac{I^-(z)}{U^-(z)}. \tag{14}$$

For the addition of statistically independent processes, the correlation-representation of the sum will be equal to the sum of the correlation-representations of the two components.

When a stationary discrete process passes through a stable system with transfer function $H(z)$, the output is also a stationary process with correlation-representation [9]:

$$\Psi_y(z) = H(z) H(z^{-1}) \Psi_x(z). \tag{15}$$

2. Statement of the Problem

We will consider a servomechanism with a discrete calculating device having the transfer function

$$H(z) = \frac{W(z)G(z)}{1 + W(z)G(z)}, \tag{16}$$

where G(z)=[P(z)/R(z)] is the transfer function of the given part of the system, W(z)=[C(z)/D(z)] is the linear program of the discrete calculating device, and P(z), R(z), C(z), and D(z) are polynomials in z.

The input of the servomechanism is the sum of two processes — the useful signal S(z) and the disturbance N(z)

$$X(z) = S(z) + N(z). \tag{17}$$

The program of the discrete calculating device must be chosen so that the output of the system

$$Y(z) = H(z)\,X(z) \tag{18}$$

reproduces as well as possible the given function of the useful signal

$$V(z) = \Lambda(z)\,S(z). \tag{19}$$

The operator Λ(z) characterizes tracking or tracking with lead

$$\Lambda(z) = z^{-\lambda} \quad (\lambda = 0, 1, 2, \ldots). \tag{20}$$

We will assume that the signal and the disturbance are stationary statistically independent processes with zero means and the given correlation coefficients

$$\psi_s(k) = \overline{s_i s_{i+k}},\ \psi_N(k) = \overline{n_i n_{i+k}}. \tag{21}$$

We construct the correlation-representations of these processes, and factorize them:

$$\Psi_s(z) = \frac{I_s^+(z)\,I_s^-(z)}{U_s^+(z)\,U_s^-(z)}, \qquad \Psi_N(z) = \frac{I_N^+(z)\,I_N^-(z)}{U_N^+(z)\,U_N^-(z)}. \tag{22}$$

We calculate the correlation-representation of the sum of these processes and factorize it:

$$\Psi_x(z) = \Psi_s(z) + \Psi_N(z) = \frac{I_x^+(z)\,I_x^-(z)}{U_s^+(z)\,U_s^-(z)\,U_N^+(z)\,U_N^-(z)}. \tag{23}$$

The polynomials $U_s(z)$ and $U_N(z)$ are assumed to have no common factors

$$(U_s, U_N) = 1. \tag{24}$$

The error of the system is the difference between the actual and the desired signal at the output. The representation of the error signal has the form

$$E = Y - V = H(S + N) - \Lambda S = (H - \Lambda)S + HN. \tag{25}$$

If we take into account the statistical independence of the signal and the disturbance, and use the rule (15), we obtain the correlation-representation of the error

$$\Psi_e = (H - \Lambda)(\hat{H} - \hat{\lambda})\Psi_s + H\hat{H}\Psi_N, \tag{26}$$

where for brevity we have used the notation $H = H(z^{-1})$, $\hat{\Lambda} = \Lambda(z^{-1})$.

As a measure of the quality of the system, we take the dispersion of the error $J = \psi_e(0)$, which is obtained as the zeroth coefficient of the Laurent expansion of $\Psi_e(z)$ and which is equal to

$$J = \frac{1}{2\pi j} \oint\limits_{|z|=1} \Psi_e(z)\,\frac{dz}{z}. \tag{27}$$

In choosing the program for the discrete calculating device, it is necessary to ensure that the following conditions are satisfied:

1. The synthesized system must be stable; this means that the function H(z) must have no poles in the region $|z| \leq 1$.
2. The program of the discrete calculating device must be physically realizable; this means that the function W(z) must not have a pole for z = 0.
3. The "roughness" condition must be taken into account in the synthesis of the system, i.e., the condition that the reduction of the zeros and poles of H(z) located in the region $|z| < 1$ must be excluded.
4. The synthesized system must be optimal, i.e., a minimum condition must be satisfied for the dispersion of the error

$$\delta J = \frac{1}{2\pi j} \oint\limits_{|z|=1} \delta\Psi_e(z)\,\frac{dz}{z}. \tag{28}$$

In the following section, we give an algorithm for choosing W(z) so that it satisfies these conditions.

3. Algorithm for Choosing a Program for a Discrete Calculating System

The algorithm is as follows:

1. Factorize the polynomials P(z) and R(z)

$$P = P^+P^-, \quad R = R^+R^-. \tag{29}$$

2. Form the system of polynomial equations

$$U_N^+P^-\theta + R^-\Phi = I_x^+, \tag{30}$$

$$z^\lambda I_x^- P^-\theta + U_s^+\Pi = I_s U_N^-. \tag{31}$$

We solve this system for the unknown polynomials θ, Φ, and Π, taking into consideration the condition of physical realizability $\Phi(0) \neq 0$ (see the Appendix to this paper and the Appendix to [10]).

We then choose a solution in which the lowest power of θ occurs.

3. We find the program for the discrete calculating device from the formula

$$W = \frac{U_N^+ R^+ \theta}{P^+ \Phi}. \tag{32}$$

We will show that the above algorithm yields a solution that satisfies all the stated conditions. If we substitute (32) in (16) and use (30), we obtain

$$H = \frac{U_N^+ P^- \theta}{I_x^+}. \tag{33}$$

The expression (33), obtained without reduction of the zeros or poles in $|z| < 1$, satisfies the "roughness" condition. Since I_x^+ has no zeros for $|z| \leq 1$, the system obtained is stable.

The condition $W(0) < \infty$ for physical realizability is satisfied by the method of solution of the polynomial equations. It remains to prove that the system is optimal.

We find for the variation of the correlation-representation of the error (26) the expression

$$\delta\Psi_e = (H\Psi_x - \Lambda\Psi_s)\,\delta\hat{H} + (\hat{H}\Psi_x - \hat{\Lambda}\Psi_s)\,\delta H.$$

We now calculate the integrals of each of the terms of this expression

$$\Gamma_1 = \oint\limits_{|z|=1} (H\Psi_x - \Lambda\Psi_s)\,\delta\hat{H}\,\frac{dz}{z},$$

$$\Gamma_2 = \oint\limits_{|z|=1} (\hat{H}\Psi_x - \hat{\Lambda}\Psi_s)\,\delta H\,\frac{dz}{z}.$$

It should first of all be noted that the second integral is reduced to the first by the substitution $u = z^{-1}$. Thus, to prove that the system is optimal, it is sufficient to prove that $\Gamma_1 = 0$. If we substitute in Γ_1 the expressions in (20), (22), (23), and (33), we obtain

$$\Gamma_1 = \oint\limits_{|z|=1} \frac{z^\lambda I_x^- P^- \theta - I_s U_N^-}{z^\lambda U_s^+ U_s^- U_N^-}\,\delta\hat{H}\,\frac{dz}{z}.$$

Using (31), we can write this expression in the form

$$\Gamma_1 = -\oint\limits_{|z|=1} \frac{\Pi}{z^\lambda U_s^- U_N^-}\,\delta\hat{H}\,\frac{dz}{z}.$$

The value of this integral is equal to the sum of the residues of the integrand at its poles outside the unit circle. This function, however, has no poles for $|z| > 1$, and so $\Gamma_1 = 0$. The validity of the algorithm is thus proved.

In the case when the given part of the system is stable

$$R^- = 1, \tag{34}$$

the calculation of a program for a discrete correcting device is somewhat simpler. In this case, condition (30) imposes no limitations on θ. Therefore, when θ has been obtained from equation (31), it can be substituted in (30) and the corresponding Φ can be calculated. The program $W(z)$ is thus obtained more quickly in this case.

SUMMARY

The condition that the "roughness" of the system be maintained, when calculating devices are introduced into it, has a serious effect on the method of calculation of the system. The theory shows that the introduction of calculating elements in servomechanisms can, in all cases, be used to obtain optimal systems, satisfying the "roughness" condition, but in the case of unstable objects of control, the system will not be as good as in the case of stable objects of control. The control program for unstable objects also turns out to be more complicated. In order to obtain a high-quality servosystem, it is desirable first of all to make the object being controlled stable at the expense of supplementary internal coupling. In those cases where the introduction of this coupling is impossible, we can have recourse to stabilizing and optimizing the system by a discrete calculating device.

APPENDIX

The solution of the system of polynomial equations can be reduced to the solution of one polynomial equation. Assume that there are two equations:

$$A_1X + M_1Y_1 = B_1, \tag{I}$$

$$A_2X + M_2Y_2 = B_2 \tag{II}$$

in the unknown polynomials X, Y_1, Y_2. We will assume that the polynomials M_1 and M_2 have no common factors

$$(M_1, M_2) = 1.$$

We will show that this system is equivalent to the "combined" system

$$(A_1M_2 + A_2M_1)\,X + M_1M_2Y = (B_1M_2 + B_2M_1). \tag{III}$$

This equation is obtained by reducing the original equations to the same modulus $M = M_1M_2$ and then adding them. We denote Y by the sum of Y_1 and Y_2.

It is clear that every solution of the original equations will be a solution of the combined equation. We will show that the converse is also true: every solution of the combined equation is a solution of the original equations. In order to do this, we write equation (III) in the form

$$(A_1X - B_1) M_2 + (A_2X - B_2) M_1 = -M_1M_2Y.$$

Since the right-hand side of this equation is divisible by M_1, and the second term on the left-hand side is also divisible by M_1, then the same is true of the first term on the left-hand side. But, since M_1 and M_2 are relatively prime, then $(A_1X - B)$ must be divisible by M_1. We thus obtain (I). Equation (II) is obtained in a similar way. Thus the equations (I) and (II) follow from (III), which means that a solution of (III) will also be a solution of (I) and (II).

LITERATURE CITED

1. A. Ya. Khichin, "The theory of the correlation of stationary stochastic processes,"* Usp. Matem. Nauk, No. 5 (1938).
2. A. N. Kolmogorov, The Interpolation and Extrapolation of Stationary Random Sequences [in Russian] (Izd. AN SSSR, Math. Ser., 1941).
3. A. M. Yaglom, "An introduction to the theory of stationary random functions,"* Usp. Matem. Nauk 7, No. 5 (1952).
4. N. Wiener, The Extrapolation, Interpolation and Smoothing of Stationary Time Series (Wiley, New York, 1949).
5. V. V. Solodovnikov, Introduction of the Statistical Dynamics of Automatic Control Systems [in Russian] (Gostekhizdat, 1952).
6. V. S. Pugachev, The Theory of Random Processes and Its Application to Problems of Automatic Control [in Russian] (Gostekhizdat, 1957).
7. Ya. Z. Tsypkin, The Theory of Pulse Systems [in Russian] (Gostekhizdat, 1958).
8. L. T. Kuzin, Certain Questions Concerning the Synthesis of Pulse Servomechanisms for Stationary Random Influences, in the collection "Automatic Control and Calculation Technique," edited by V. V. Solodovnikov [in Russian] (Mashgiz, 1958).
9. S. S. L. Chang, "Statistical design theory for strictly digital sampled-data systems" Transactions of AIEE 76, part I (1957).
10. L. N. Volgin, " A method of synthesis of linear pulse systems of automatic control according to dynamic criteria," Avtomat. i Telemekh. 20, No. 10 (1959).*

---

*See English translation.

DIGITAL COMPUTATION ELEMENTS, BASED ON THE PRINCIPAL OF INTEGRATING VOLTAGE PULSES

E. K. Yuferova

Moscow

Translated from Avtomatika i Telemekhanika, Vol. 21, No. 8, pp. 1165-1172,
August, 1960
Original article submitted November 24, 1959

Two digital devices, based on the principle of integrating voltage pulses, are considered.

At the present time, in addition to digital computers based completly on the application of devices using crystal semiconductors, there are also many computers using a combination of the latter with magnetic elements with cores having rectangular hystersis loops (ferrotransistor elements).

One of the directions being taken in the development of ferrotransistor elements is toward the creation of junctions and elements based on the principle of integrating voltage pulses. The principle of integrating voltage pulses by using saturated magnetic cores has been known for a long time. It has been applied in designing magnetic amplifiers, pulse transformers, and other similar devices.

In digital technique, the first development of elements based on this principle was relatively recent [1, 2].

We will describe briefly the basis of this method.

If the input of an R-L electric circuit with a saturated magnetic core (Fig. 1a) consists of pulses of arbitrary form from a voltage pulse generator with low internal resistance, and if the energy of a single pulse is not sufficient to cause a complete magnetic pole reversal of the core, then the magnetic state of the core-material will vary by steps, and change from a state of negative magnetic saturation to the opposite state of positive magnetic saturation. In this case the core accumulates or integrates the pulses arriving at its input coil (Fig. 1b).

If it is assumed that the operating resistance R of a circuit containing saturated magnetic cores is so small that it can be neglected, and that all the voltage U is available for magnetic pole reversal of the core, then, starting from the equality

$$U = e = W_i \frac{d\Phi}{dt},$$

we can obtain known expressions for the variation of the induction ΔB due to one voltage pulse, and for the maximum number, n, of pulses that can be accumulated in the integrating core:

$$\Delta B = \frac{\int_0^{t_p} U\,dt}{W_i S}, \qquad n = \frac{2B_s W_i S}{\int_0^{t_p} U\,dt}$$

Here W_i is the number of turns in the integrating coil, Φ and B_s are the current, and the residual induction of the core-material, B_m is the maximum induction of the core-material, e the emf arriving at the coil, S the cross section of the core, and t_p the duration of the pulse.

It is evident, from the approximate expression for the maximum number of pulses that can be accumulated by the integrating core, that this number is given in terms of the amplitude and duration of the pulses, the number of turns in the integrating coil, the cross section of the core, and the residual induction of the core-material.

A more accurate and complete expression for the number of pulses accumulated in the integrating core can be obtained from the expression for the energy communicated to the core during its pole reversal. For a review of the essential principles and basic properties of elements constructed on these principles, however, this question need not be considered.

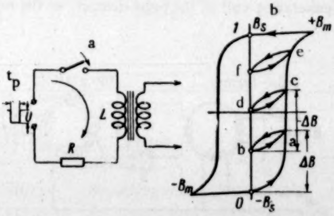

Fig. 1. (a) Electric circuit with saturated magnetic core; (b) hystersis loop for the core-material.

Up to the present time, there have been investigations of two types of elements based on integrating voltage pulses. The first type is based on the accumulation in the integrating core of a definite, previously given number of pulses, and the subsequent delivery of a signal to the output when the integration has been completed. These elements are called pulse-accumulators or integrators. They can be widely applied as frequency-dividers, calculators, decipherers, and linear relays. The second type is characterized by being able to receive an input of not more than three pulses, and, depending on the number accumulated, yielding different output signals. This type of element is used in the adders in arithmetic devices applied in building digital computers.

1. Voltage Pulse Accumulators or Integrators

We show in Fig. 2 a circuit diagram of an integrator, which explains the principle of its operation. A similar scheme, using material in the form of a ribbon, was first proposed in 1955 in [1]. We will describe briefly the principle of operation of the integrator. It consists of two basic parts: a pulse-former and an integrating element. The action of the pulse-formers is to generate pulses of constant area (in the time-emf plane) for admissible variations in the parameters of the device and in the conditions in the surrounding medium.

The purpose of the integrating element is to accumulate a definite number of pulses, to switch the circuits (from the integrating circuit to the regeneration circuit), return the core to its original state of magnetic saturation, and transmit an output signal with energy equal to the sum of the energy absorbed by the core during the accumulation period.

In Fig. 3 and Fig. 4 we show the two most common integrating circuits.

Certain modifications are possible in the integrators: the introduction of a bias in a return circuit to a battery or condenser, an automatic bias on the regeneration coil (Fig. 3; 1, 2, and 3 respectively), and finally, the latter possibility with minimal resistance in the integrating circuit (Fig. 4).

The notation in Figs. 3 and 4 is as follows: W_g is the generating coil of the pulse-former, W_r the regeneration coil of the pulse-former, W_k the feedback coil, W_a and W_s are pulse-former output coils, W_i is the integrating coil of the integrating element, W_{re} the regeneration coil of the integrating element, W_o and W_p are the feedback windings for the integrating and regenerating circuits respectively, W_h is the output winding of the integrator, R_{in} the resistance in the circuit-base of the pulse-former, R_{re} the resistance in the regeneration circuit of the pulse-former, R_b is the circuit-base of the integrating element, R_i the resistance in the integrating circuit, R_e the negative-feedback resistance in the pulse-former emitter-circuit triode.

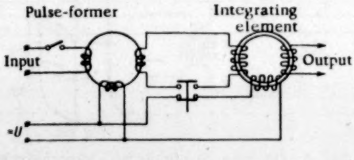

Fig. 2.

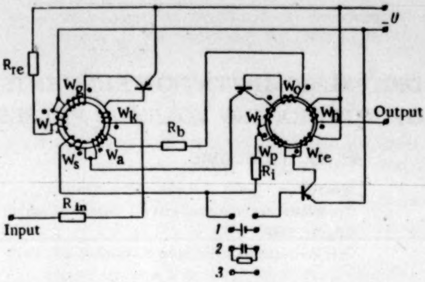

Fig. 3. General circuit diagram of an integrator.

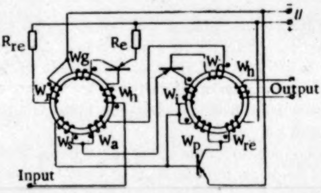

Fig. 4. General circuit diagram of an integrator with minimum resistance in the integrating circuit.

All the integrator circuits used ferrite cores of type FP-7A and FP-7C and the triodes P13, P14, P15, and P16.

In practice, a large number of pulses can be accumulated in a single integrating core. The number depends on the parameters of the signal generated by the pulse-former, and on the properties and dimensions of the integrating element.

Under laboratory conditions, we have been able to accumulate up to 120 pulses in one element with a core of mark FP-7 ferrite 9 mm in diameter. However, when the reliability of operation of the element is considered, and imperfections in the ferrite and the triodes are taken

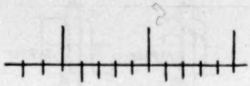

Fig. 5. FP-7C, 5 mm diameter
$W_i = 20$

into account, the number of pulses that can be accumulated in practice is limited.

Figure 5 shows an oscillogram of the pulses in the output coils of integrators accumulating 5 pulses.

At the present time, standard integrators are designed that can accumulate 5 and 10 pulses, the cores of these integrators having a diameter of 5 mm and being made of FP-7C ferrite. Their nominal collector voltage is15 v, with a permitted variation of ± 20-25% from the nominal value.

Several independently operating accumulators can be connected in series. In this way a large capacity can be attained with a relatively small number of pulse-counters. Each stage of such a counter works from the output pulses of the previous stage. The pulse-formers of the integrators are transitional elements between the stages. Each stage can be regulated by varying the resistance in the base of the triode in its integrating circuit. Several such counters were constructed and tested.

As an example we mention a four-stage adjustable counter capable of counting 600, 400, and 200 pulses. The second stage of this counter was adjustable for the accumulation of 6, 4, or 2 voltage pulses. The first, third, and fourth stages were not adjustable, and could accumulate 10, 5, and 2 pulses, respectively. The whole counter operated stably in a range of collector voltages from 11 to 22 v with a nominal value of 15 v.

We will now discuss the advantages and disadvantages of these integrators.

A basic and indisputable advantage is their economy in the number of elements needed in their construction —cores, triodes, and resistances. For example, a 65536 frequency divider can be easily constructed by using four integrators in series, where each of the stages divides the frequency by 16. For this, it is necessary to have only 8 cores made of material with a rectangular hysteresis loop, 12 triodes, and 12 resistances. To carry out the same operation using triggers, 16 double stages are needed, and 32 ferrite cores, 32 triodes, and 32 resistances would be required with this method.

A second advantage of the integrators is the absence of generators of powerful variable pulses. Each integrating stage in a counter made up of integrators operates independently, using only the output pulses from the previous stage. The number of stages of such a counter can be made as large as we wish.

One of the disadvantages of the integrators is the high rejection rate of triodes. Triodes must be rejected in connection with both their collector current and the value of their input and contact resistance in switching operations. A second disadvantage is the length of the delay between the input and output signals. When multi-stage counters are used, this delay must always be taken into account.

2. Adders

We will consider the essential basis of a method of constructing adders, using a principle of integrating voltage pulses proposed in 1958 [3].

In Fig. 6 are shown the main elements of the adder —the integrating magnetic element and the selecting circuits. The object of the integrating magnetic element is to add the items arriving at the input. Depending on the number of pulses arriving, the polarity of the core of the integrating element is reversed through a partial cycle to one of three possible states: a, b, or c (Fig. 7). The quantities to be added can arrive at the input of the adder simultaneously or displaced in time, but they must arrive at the integrating element before the arrival of the calculating signal. This signal produces a magnetic pole reversal to the original state of magnetic saturation, and at the same time causes pulses accumulated in the integrating element to be added together. This calculation can be carried out in two ways: by three consecutive voltage pulses, the action of each of which is equivalent to the action of one recorded pulse (Fig. 8a), or by the action on the core of a single powerful current pulse (Fig. 8b).

Here the emf e arriving at the integrating-element output-coil will be proportional to the magnitude $\Delta\Phi$ of the variation of the current in the core.

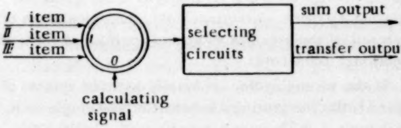

Fig. 6.

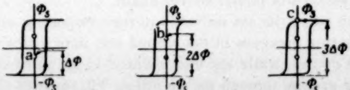

Recording of 1 voltage pulse

Recording of 2 voltage pulses

Recording of 3 voltage pulses

Fig. 7.

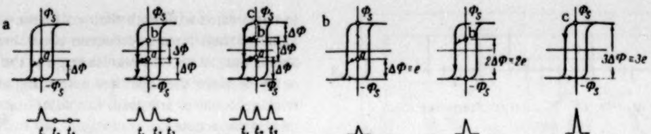

Record of one unit | Record of two units | Record of three units | Record of one unit | Record of two units | Record of three units

Fig. 8. The calculation of information recorded in an integrating core: (a) Three successive voltage pulses; (b) A powerful current pulse.

Depending on the method of calculation used, adders can be four-cycle or two-cycle. Both these types record the incoming signal in one cycle, but the calculation is carried out in one cycle in one of them, and in three cycles in the other.

One or other time-sequence of pulses (in the case of a four-cycle adder), or a single pulse of a definite amplitude (in the case of a two-cycle adder), arrive at the input of the selecting circuits. The task of these selecting circuits is to distribute the results of the summation arriving from the integrating element into the adder-sum and adder-transfer channels, and then to record the results and transfer the corresponding values to the adder-sum and adder-transfer outputs.

We will consider two types of adder, a four-cycle and a two-cycle.

In Fig. 9 we show the block-diagram of one of the possible variants of four-cycle adders. In the integrating magnetic element there is a Y1 amplifier, and a strictly saturated magnetic core. The selecting circuits contain a Y2 amplifier with divided outputs and two cores for the intermediate storage of information.

The adder operates in the following way. In the first cycle, with a system of pulses I, the information passing through the input amplifier is recorded in the integrating element. Simultaneously, the calculation of the result of the previous addition is performed from the selection-circuit cores.

In the second cycle, cophasally with the system of pulses II, the integrating element counts a single unit, and records it in the sum magnetic core. In the case when a single unit is recorded in the third and fourth operation cycles of the adder, there will be no signal at the output of the magnetic element. The unit recorded in the sum-core B appears in the output of the adder-sum when a system I of pulses arrives again.

When two units are recorded in the integrating core, their counting proceeds in the second and third adder operational cycles, while the unit counted in the third cycle, after passing through the amplifier Y2, reverses the magnetic polarity of the transfer-core A and returns the sum-core B to its original zero state. In this case, with the arrival of a system I of pulses, a signal appears at the output of the adder-transfer.

Finally, in the case of the additon of three units in the integrating magnetic element, the counting of the third unit and its transcription on the sum-core occur in the fourth operational cycle of the adder. In this case a system I of pulses will produce signals at both the sum- and the transfer-output. This type of four-cycle adder is the most economical from the point of view of the number of elements needed for it. A disadvantage of all four-cycle adders is their slowness of operation.

In Fig. 10, we show one possible block-diagram for a four-cycle adder. Its selecting circuit consists of three triodes and three cores. Counting in the integrating element proceeds in one cycle by a current pulse. A signal of completely definite amplitude will be obtained at the output, and this signal will depend on the sum of the pulses arriving at the adder-input (Fig. 8b). The selecting circuits of the adder perform an amplitude separation of the pulse arriving at their inputs. This is done by the

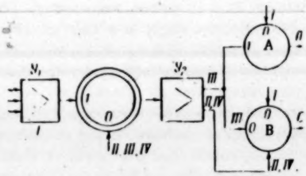

Fig. 9.

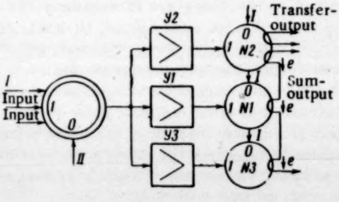

Fig. 10.

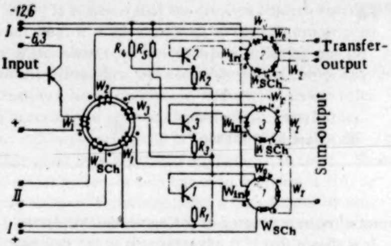

Fig. 11.

choice of the corresponding bias values for the amplifiers Y1, Y2, and Y3. The quantity counted by the integrating element and selected by the amplifiers is recorded in the corresponding sum- or transfer-core.

In Fig. 11 is shown the principle of the electric circuit of a two-cycle adder. It consists of four FP-7C ferrite cores 4 mm in diameter, and four P14, P15, or P16 triodes. The adder operates at a frequency of 50-100 kc. The signal-noise ratio (for the noise, we have taken the signal at the adder-sum output for the addition of two units arriving at the input) was not less than 10.

As an example, we show in Fig. 12 oscillograms of signals at the output of the adder-sum for the addition in the latter of one (a), two (b), and three (c) units. Temperature experiments were carried out both for separate adders, and for adders in series. Stability of operation was checked for a series of temperatures differing by 10° C. The collector voltage was also varied within limits varying by ± 20% from its nominal value.

The experiments gave very satisfactory results, and it was found that the adder operated stably in a range of temperatures from −40 to +55° C, and for variations of the collector voltage from 20% below to 27% above the nominal value.

The main advantage of adders constructed on the principle of integrating voltage pulses, as in the integrators considered earlier, is the small numbers of elements needed in their construction. Adders with three inputs and two outputs can be built with three or four cores and the same number of triodes. They are simple to construct, reliable, and permit a sufficiently great variation from their normal operating regime. The frequency of operation of the adders, and consequently their rate of operation, can be significantly increased.

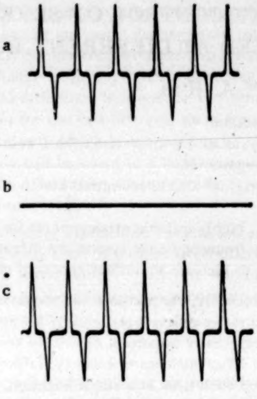

Fig. 12.

In conclusion, we should say that magnetic elements built on the principle of integrating voltage pulses would appear to have good future prospects in applications both as integrators and as adders. They can be widely applied both in calculating devices and in various designs of automatic control and remote control mechanisms.

LITERATURE CITED

1. Pittman G. F., "A high-accuracy static Time delay device utilizing transistors " AJEE Transactions, P. I, Communication and Electronics 74 (March, 1955).
2. Van Nice R. J. and Lyman R. C., "A predetermined scaler utilizing transistors and magnetic cores," Proceedings of the National Electronics Conference, 11, (Oct., 3, 4, 5, 1955).
3. A. K. Zavolokin and E. K. Yuferova, Method of Summation, Doctor's Certificate No. 117040.

REMOTE CONTROL OF SEVERAL OBJECTS LOCATED AT DIFFERENT PLACES

V. A. Il'in

Moscow

Translated from Avtomatika i Telemekhanika, Vol. 21, No. 8, pp. 1173-1180,
August, 1960
Original article submitted March 11, 1960

New, highly reliable arrangements for selection and control of objects located at different remote places by a binary frequency code system are discussed in this paper. It is shown that it is advantageous to use two-section filters to increase the effectiveness of channel utilization when the frequency method of selection is employed.

Until recently, the methods and technical means of remote control were developed mainly for applications to large and especially important objects in power systems and certain other branches of industry, said objects being concentrated each time at a single location.

Now, after introduction of more perfect automatic control methods of production processes, the problem has arisen of controlling from a distance a great number of relatively small operational units carrying out certain functions at different places; as, for instance, to control objects distributed along pipelines, railroad tracks, a canal, etc.; objects located at various distant points distributed over the wide area of an oil refinery, a gas production plant, a large factory, an irrigation system, etc.; or objects distributed throughout the great underground space of a mine.

The volume of work connected with development of remote control of such multiple objects dispersed in area (if for nothing else than their great quantity) will in the future exceed by tenfold or better the work connected with remote control of objects "concentrated" (lumped) in a single location.

At present, remote control has already been introduced at several thousand points of oil-well operations, and a great amount of development work is in process on remote control of multiple or dispersed objects in the petroleum and gas industries, in mines, factories, city public utilities, etc.

When relatively large concentrated objects in electric power stations or substations are remotely controlled, a control sending or dispatching point (DP) is connected with each of the points to which the control commands are executed ("Execution Points," (EP) by one or several communications lines. When disperse objects are remotely controlled, each communication line is utilized for transmission of information concerning several "executing" objects, which are connected to the line at various points; the number of such points may be very large. This increases the effectiveness of the communication line's utilization, and is the main distinction of remote control systems for disperse objects in comparison with systems for objects concentrated in one place.

It is, therefore, natural that rational methods of information transmission between the dispatch point and disperse control objects may differ substantially from transmission methods between the DP and concentrated control objects.

"Execution" points (where the controlled operation is carried out) usually work automatically without any attending personnel, and, therefore, much higher demands must be made of them with respect to dependability. It is even advantageous to introduce a somewhat higher or additional complexity into the apparatus at the dispatching end, in exchange for a simplification, and increased reliability, of the remotely controlled arrangements at the execution points. Thus, it is advantageous to employ simple and highly reliable completely automatic arrangements for operation selection at the EP, while using, in many cases, a system of interrogation by choice or a cyclical scanning system, controlled to run at a predetermined sequence, for transmission of the remote measurement results and of alarm signals. This makes it possible, when remote measurement data and alarm signals are transmitted back from the EP to the DP, not to accompany them by the address of the EP, which considerably simplifies the coding arrangement at the EP.

Interrogration of the objects is carried out either at the choice of the dispatcher, automatically, according to a predetermined program, or may be started up by a signal from the EP indicating a change in the regime of one of the objects. The latter signal is a common one to all execution points (indicating an accident, a breakdown, or other trouble at any point). The period of interrogation or scanning cycle must be much smaller (at least by several times) than the time needed for the particular technological process to reach equilibrium; the scanning cycle may be from a few seconds to ten minutes, or even more. However, needless decrease of the cycle period can lead to a widening of the frequency band needed for transmission, to an unjustified acceleration of the remote control system's operation, and to a lowering of the stability with respect to interferences.

In [3] it is shown that for disperse objects distributed over an area, it is advantageous to use communication lines of the cluster (or bunch) type. In laying out the communication lines, all execution points comprised in the remote control system are arranged in groups (clusters) according to certain characteristics or arbitrary rules, and each such group is connected with the dispatcher point by a separate communication line. There is an optimum for the number of such groups if it is necessary to have, simultaneously, a high degree of structural reliability and relatively short lengths of communication lines.

In [4] it is shown that to increase the reliability of a remote control system, the execution points must be connected in parallel to the communication line, just as in power distribution and broadcasting over wire networks the subscribers are connected in parallel.

1. Selection of Objects When Using a Dual-Frequency Code

In [5] several call systems for making connections with disperse objects, using a single frequency assigned to each particular object, were compared to each other. Some frequency selectors which operate by means of electrical L-C resonant circuits without making or breaking of contacts were offered in that paper. Such contactless frequency selectors are of considerable interest with respect to comparatively simple systems of remote control having a relatively small number of execution points (up to 12–24) in a bunch, with communication lines of 15–30 km in length, and with several objects of remotely controlled actions and of remote measurements on call at every EP. At the present time, there are already in operation several thousand execution points at oil wells equipped with such remote controls using single-frequency selector systems. Frequency selector systems with electrical L-C networks are beginning to be employed in other fields of industry as well.

When remote control is provided for pipelines, gas-distribution systems, irrigation systems, and similar enterprises of the national economy, the necessity of connecting many execution points to a common communication line arises and, additionally, in a number of cases, of operating numerous objects at each execution point. In these applications, operation over considerably greater distances is also required.

Presently existing contactless devices for selection and switching-on of a controlled object, such as those of the tuned-frequency type, those of the exponential-transformer type [6], and those of the magnetic type with cores having a rectangular hysteresis loop (RHL), are all about equal to each other with respect to reliability and complexity. Thus, each RHL cell [2], as well as each tuned-frequency relay (including the electric circuit associated with it) [5], consists of a transformer with ferromagnetic core, of condensers, and of diodes or transistors. However, in some circuits employed with the RHL cells, no condensers are used. For the same output power, the over-all dimensions and other characteristics of the RHL and tuned-frequency systems are about equal. The substantial difference between the two systems lies in the fact that for the first RHL cell there are only two operational states in which it can possibly be, while the frequency relay can be tuned to a large number of frequencies and can be in two different states at each of its operational frequencies.

The number of all feasible discrete-selection indexes for a frequency relay is $\underline{n}$ times larger than for an RHL cell, where $\underline{n}$ is the number of discrete working frequencies available in the transmission band when single-frequency selection is used.

Contactless selectors using a dual-frequency code differ still more from the other devices: the number of possible states of such a selector (or decoder) to which it can be adjusted is $n(n-1)$ times larger than for a single device using RHL, while with respect to complexity it is about equivalent to two single-frequency relays with their associated electric circuits. This makes it possible to carry out the selection of an equally large number of disperse objects by a substantially simpler contactless arrangement.

It should also be taken into account that when the signal level is limited, stability of transmission against interference is much better with frequency diversification used for multiplexing than with time separation, and that in connections by wire lines and in many others the permissible signal level actually is limited.

Selectors (decoders) based on tuned-frequency elements are not the only devices which can secure the simplest and most dependable solutions of these problems.

For selection of disperse objects it is advantageous to employ arrangements using elements which are able to be in numerous diverse states (providing numerous characteristic indexes for selection). Frequency selectors have such properties, but exponential transformers with time separation of signals also have them [6].

When stability against interference is of importance, the methods used must also be compared with respect to this property.

As a result of investigations carried out at the Institute for Automation and Remote Control of the Academy of Sciences of the USSR, schemes of dual-frequency codes were suggested and developed in which damage to any one of the components cannot cause a wrong selection or execution of a wrong command signal, but produces – in the worst case – only a precautionary refusal to execute any command.

One such scheme is presented in Fig. 1. In this scheme, no local power supply is required. Two frequencies, f_1 and f_2, are transmitted consecutively from the dispatch point.

A voltage divider stepdown transformer decreases the effects of the line on two series resonance circuits L_1C_1 and L_2C_2.

The first circuit is tuned to frequency f_1, the second to f_2. When frequency f_1 is transmitted, capacitor C is charged by way of the diode preceding it up to a voltage u, at which the energy ($cu^2/2$) is sufficient to operate relay P. The emitter-collector resistance of the transistor in the other circuit is then sufficiently high.

When the second oscillation of frequency f_2 is transmitted, the output voltage of the second circuit is applied either directly or through a diode to the emitter-base terminals of the transistor, and opens it up for operation of the relay: specifically, capacitor C is discharged through the transistor and the discharge current going through the relay coil causes the armature to make or break contact. The relay may be automatically locked in, when this is needed. The results proved definitely that, when the reverse sequence occurs (first frequency f_2, then f_1), or where damage occurs to any of the components, false operation of the relay does not take place.

The number of objects N available for selection is determined by the code formula:

$$N = n(n-1),$$

where n is the number of discrete resonance frequencies into which the available frequency band can be subdivided for use as remote control channels without any substantial interference occurring between adjoining frequency channels.

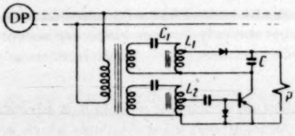

Fig. 1. Circuit diagram for control-object selection without local power supply, using a dual-frequencies code.

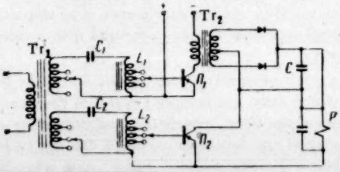

Fig. 2. Object-selection circuit by codes of dual frequencies with amplifier.

Thus, for instance, when the frequency band available is 300 to 3000 cps, inductances, having cores of a silicon-iron-aluminum alloy (similar to the one known in the U.S.A. under the trade name of "Sendust") are used, n = 10 to 20.

This scheme can also be used when the control signals are transmitted by radio. The above code formula determines the number of selections available, all operating on a single carrier frequency; the receivers may be different.

The time t needed to charge condenser C to a potential equal to 90% of the ultimate value is obtained when $R_3 \gg Z_K$ and $Z_K \gg R_d$ [1], by means of the formula:

$$t = 5n_1^2 \cdot CZ_K,$$

where $Z_K = Q\omega L_1$ is the equivalent total resistance of the circuit, n_1 — the transformation ratio of the autotransformer, R_d — the resistance of the diode, and R_3 — the emitter-collector resistance of the transistor in the nonconductive state. Parameters are chosen so that t is equal to 0.3 to 1.5 sec.

The discharge time constant τ of the condenser C through the transistor while the relay is being operated is

$$\tau \approx C(R_p + R_K),$$

where R_p is the resistance of the relay and R_K — the emitter-collector resistance of the transistor (in the high conductivity state).

The energy needed to actuate the relay is

$$W \geqslant \frac{E_p^2}{R_p} t_c,$$

where E_p is the voltage needed for causing the relay to operate, t_c — the time it takes the relay to operate.

On the basis that the condition $\tau \geq k_1 t_c$ where $k_1 = 1.5$ to 2.0 is fulfilled, we have:

$$C \geqslant \frac{k_1 t_c}{R_p + R_K}.$$

The potential E_c on the condenser at which the relay will operate (disregarding losses in the condenser) can be expressed as follows:

$$E_c \geqslant E_p \frac{R_p + R_K}{R_p}.$$

The same resonant circuits L_1C_1 and L_2C_2 can be utilized also for selection and control of a second object by means of transmitting the frequencies in inverse order (first f_2, then f_1). This decreases the average number of resonant circuits per control object to one; it is accomplished by addition to the scheme represented in Fig. 1 of a second transistor, one or more diodes, another condenser C, and a second relay. Such a scheme was used in one of the control systems developed by the Institute for Automation and Remote Control of the Academy of Sciences of the USSR [IAT].

In the scheme of Fig. 1, the energy for charging of condenser C is derived from the first tuned circuit, and in consequence, a higher audiovoltage must be transmitted over the line. To remove this shortcoming, an amplifier is added at the output from the first tuned circuit. One such scheme is represented in Fig. 2.

In distinction from Fig. 1, here the output voltage of frequency f_1 from transistor Π_1 is applied through transformer T_{r_2} to a pair of halfwave rectifiers, the output from which is connected to condenser C. The oscillation of frequency f_1, transmitted from the dispatch point, only opens the transistor. This permits keeping the amplitudes of the control frequencies transmitted over the line at a lower level.

The distant operational-control units at the execution points may differ from the control units that serve for selection of the control objects, in that they are provided with an additional resonant circuit of frequency f_3 and another transistor, connected in a manner similar to that of the L_2C_2 circuit and transistor Π_2.

In that case the distant control command, "switch on," is transmitted by a combination of frequencies f_1 and f_2, but the command, "switch off" —by consecutive sending of frequencies f_1 and f_3.

It is thus obvious that damage of any component of the diagrams shown in Fig. 1 and Fig. 2 or opening of any of the circuit connections can result only in a preventative noncompliance (rejection) but not to a false selection or execution of a false command.

2. Two-Section Filters

The L-C resonant circuit as a means for frequency selection is distinguished by the highest simplicity; however, it has relatively low selectivity for off-frequencies far from resonance, i.e., when there is large frequency separation such that

$$Q^2\left(\frac{f}{f_0}-\frac{f_0}{f}\right)^2 \gg 1,$$

where $Q=(\omega L/R)$ is the figure of merit of the circuit.

To decrease the interaction between the tuned relays and the resonant circuits, it is necessary to make the interspace between adjoining resonant frequencies several times larger than the bandpass width of the circuit. The utilization of the available frequency range then becomes very ineffective.

Consequently, it is advantageous to use resonance circuits in those cases where the available frequency band is wide enough to accommodate the entire control system in question, with something left to spare. This usually is the case when one is concerned with relatively simple control systems, where the problem of economy in the transmission of the control signals is not of prime importance.

High efficiency of transmission-channel utilization is achieved by the use of multisection (iterative) bandfilters having high attentuation in the nonpass regions. And the higher the requirements for attenuation in the nonpass regions are, the more iterated sections the bandpass filter must have.

In a number of cases it is advantageous to use the standard four- or six-section filters of voice-frequency

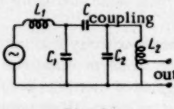

Fig. 3.

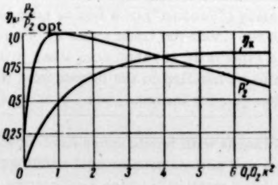

Fig. 4.

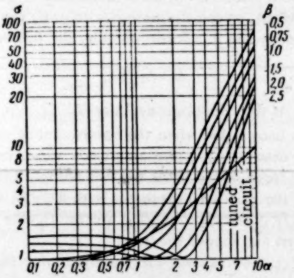

Fig. 5.

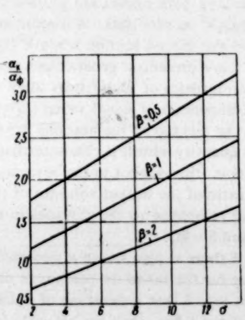

Fig. 6.

telegraphy, which are produced commercially as components of systems for multiplexing of telegraph channels.

Increase of attenuation in the nonpassing regions is accompanied by decrease of efficiency and increase of attenuation in the passing range of the filter. Therefore, for many remote control systems, a reasonable compromise must be found between a single-section filter and a complex filter having a great many inductances and capacitances.

For the remote control of disperse objects, a good solution of this problem is provided by the two-section filters which are widely used in radio circuits: they make it possible to increase the number of frequency relays in a given frequency band several times with respect to the number of relays feasible when resonant circuits are used. When a relative attenuation between adjoining operational frequencies of the order of 2 nepers (which is equivalent to a factor of about 7) is permissible, such filters are in no way inferior to more complex filters.

Two-section filters can be installed to replace resonant L-C circuits without substantial change in the operations of the system, and their design and adjustment are distinguished by simplicity [7].

The circuit diagram of a two-section filter adapted to replace a resonant circuit arrangement is shown in Fig. 3. When, in this diagram, $C_1 = C_2 = C$, the coefficient of coupling k is determined by the formula:

$$k = \frac{C_c}{C}.$$

where C_c is the coupling capacitance.

It is known that when the coefficient of coupling k is larger than $(1/\sqrt{Q_1Q_2})$ the amplitude versus frequency-response curve of the filter has two humps, and that the width of the pass band increases with $k^2Q_1Q_2$, where $Q_1 = (\omega L_1/R_1)$ and $Q_2 = (\omega L_2/R_2)$ are the figures of merit of the first and second sections.

In Fig. 4 two curves are presented: one showing the power P_2 in the second section, and the second the efficiency η_K of the entire filter (exclusive of the associated tuned relay); both curves are plotted versus the quantities $Q_1Q_2k^2$ as abscissas. A maximum of power is transferred to the second section when $k^2Q_1Q_2 = 1$.

In Fig. 5 are presented generalized amplitude-frequency characteristics of such filters when the two sections have components of equal value ($L_1 = L_2$, $C_1 = C_2$, $Q_1 = Q_2 = Q$). In this figure the abscissa $\alpha = Q[(f/f_0) - (f_0/f)]$ represents a quantity which is characteristic of the "off-tune" condition with respect to the resonance frequency f_0, σ is the ratio of the output voltages of the filter or of the circuit at resonance to the voltages in the "off-tune" condition, and $\beta = kQ$.

In Fig. 5 there is also shown a generalized characteristic curve for the tuned-to-resonance circuit. It is evident from Fig. 5 that a decrease of β increases the selectivity of the filter when the off-tune frequency is far away from the resonant frequency; it is therefore advantageous to choose for the tuned relays $\beta < 1$.

Let us compare the properties of the resonant circuit scheme and the two-section filter scheme with respect to their use for selection and operation of control objects. We assume that technical requirements make it necessary to have at the adjoining frequency an attenuation which is at least 10 times that of the frequency in operation. The horizontal line $\sigma = 10$ on Fig. 5 corresponds to this condition. For $\sigma = 10$ the resonant circuit scheme requires an off-tune value of $\alpha = 10$, while the two-section filter secures the same $\sigma = 10$ at $\alpha = 3.6$ and $\beta = 0.5$; i.e., with the two-section filter about 1/3 of the interspace between adjoining operational frequencies is needed.

It should be noted that the attenuation of a two-section filter increases much more rapidly with the distance from the resonance frequency than that of the tuned circuit. It the attenuation of the tuned circuit increases in proportion to the first power of the off-tune characteristic α, then the attenuation of the two-section filter increases nearly in proportion to the second power of this quantity.

When β is decreased below 0.5, the qualifications of the two-section filter for selection of control objects improve only insignificantly, while the transmitted power and the efficiency decrease sharply.

In Fig. 6 are shown three curves expressing the ratio (α_K/α_Φ) as a function of σ for various values of β. Here α_K is the off-tune value of the tuned circuit, and α_Φ the off-tune value of the filter. The curves of Fig. 6 show how many times greater the interspaces between adjoining operational frequencies must be when tuned circuits are used than when filters are used, to obtain equal differences of attenuation σ between adjoining operational frequencies.

The load can be connected into the second section of the filter in the same way as into the output of a single-section tuned circuit, and the design computations are also the same. The same is true for the input connections.

To obtain higher sensitivity it is necessary to employ, in both the filter and tuned-to-resonance circuits, inductances with high figures of merit $Q = (\omega L/R)$. At present, in the audiofrequencies range, these requirements are met by inductances having a core of an aluminum silicon-iron alloy ("Sendust") or a ferrite core (such as the one known under the trade name of "Ferrocart"). The former are especially advantageous when relatively high power has to be handled in the output from the tuned circuit or filter (as, for instance, when a neutral relay is used).

Inductances with ferrite cores have smaller over-all dimensions and permit simpler coil windings; therefore, they may have relatively wider applications. The neutral relay in the output from a tuned circuit or bandpass filter is usually connected by way of a transistor amplifier.

LITERATURE CITED

1. L. S. Gutkin, Conversion of Superhigh-Frequencies and Detection [in Russian] (Gosenergoizdat, 1953).
2. V. A. Zhozhikashvili and K. G. Mityushkin, Contactless Devices of Telecontrol-Telesignalization (TU-TS) [in Russian], Branch office of VINITI, project 26, 1957.
3. V. A. Il'in, "Selection of communication channels design for distant control systems," Avtomat. i Telemekh. 18, No. 7 (1957).*
4. V. A. Il'in, "Schemes for connection of multiple control objects located at different places to a communications line," Avtomat. i Telemekh. 21, No. 4 (1960).*
5. V. A. Il'in and K. P. Kurdyukov, "Frequency methods for remote control of objects located at different places," Avtomat. i Telemekh. 19, No. 2 (1958).*
6. V. A. Il'in, "Principles for design of remote control systems using exponential converters," Avtomat. i Telemekh. 20, No. 4 (1959).*
7. A. A. Kolosov, Resonance Systems and Tuned Amplifiers [in Russian] (Svyazisdat, 1949).

---

*See English translation.

ANALYSIS OF NOISE IN A 0.4/6 kv POWER NETWORK

L. B. Venchkovskii

Moscow

Translated from Avtomatika i Telemekhanika, Vol. 21, No. 8, pp. 1181-1187,
August, 1960
Original article submitted March 10, 1960

The results of the study of the noise in an 0.4/6 kv oilfield powder network at 150 cps to 100 kc are given. Experimental data is analyzed statistically and approximate formulas for the functions of the pulse noise amplitude distribution found.

Side by side with the utilization of high-tension power lines of hundreds of kilovolts for communication and remote-control purposes, greater attention has been paid in recent years to low-voltage power networks of 0.4 – 35 kv. The interest they have aroused is due, first, to the great extent and branching of these networks and, secondly, to their sufficiently high reliability. The use of power lines for communication and remote-control purposes provides in many cases considerable saving in equipment, owing to the elimination of separate communication channels.

The superposition of remote-control channels over power lines meets in practice with many difficulties, which are connected with the simultaneous transmission over the line of a commercial frequency voltage, and with a large attenuation as compared with normal transmission channels. The high attenuation of the power lines is due to nonhomegeneity and branchings, as well as to the large number of loads which shunt the line. It is only natural that under such conditions the adoption of these lines for high-quality communication channels becomes too expensive and complicated. Moreover, the difficulty of installing highly reliable remote-control systems over these lines is due to their high noise level, produced by switching and various electrical devices.

Recently, several organizations studied the parameters of 0.4-35 kv networks and found that it was possible to install communication and remote-control channels over such lines. Work in this sphere has been carried out in mining and agriculture. The main attention in these investigations was paid to the measurement of attenuation and input impedances of lines, and the least attention was devoted to noise, whose levels were estimated approximately. The knowledge of the nature and level of noise, however, is one of the conditions for a correct design of a communications system and, especially, of a remote-control system.

The constantly growing interest in using power networks for remote-control channels and the absence of sufficient data on the noise in these lines, made it necessary to carry out a fuller investigation of the nature of noise in power networks. In the present work, we give some of the results of such investigations carried out on a 0.4/6 kv oilfield power network.

1. Noise in an Oilfield Power Network

A 0.4/6 kv power network of one of the oilfields in the Groznyi area was chosen as the subject for investigations. The construction of the network is sufficiently typical for a system with distributed objects. The 6 kv open wire (sometimes cable) lines connect a 35/6 kv step-down substation to distributing transformers. In addition to the 6/35 and 6/0.4 kv transformers, powerful induction motors for compressors and boring installations can also be connected to the 6 kv line. Each transformer point has several radially distributed 380 v lines for supplying groups of 15-30 kw induction motors of the rocker platforms. Welding equipment is also fed from the low-voltage network. The 6 kv lines are usually several km long, and the 380 v lines, several hundred meters. Both the high-and low-voltage lines work in a star connection with an ungrounded neutral line. The noise in these lines was studied on a phase-to-phase basis.

The above construction of a power network is also typical for other industrial establishments, such as mines, large factories, chemical combines, etc.

The investigation of noise in power networks, like that of any other communication or remote-control channel, consists in the first place in determining the nature of the noise, and then measuring its frequency and amplitude characteristics. Both the qualitative and quantitative noise characteristics must be studied over a wide range of frequencies for several fixed bandwidths of the receiving devices, normally with a simultaneous measurement of the attenuation and the input impedance of the lines.

The noise type, which later determines the methods of measuring the noise amplitude and frequency charac-

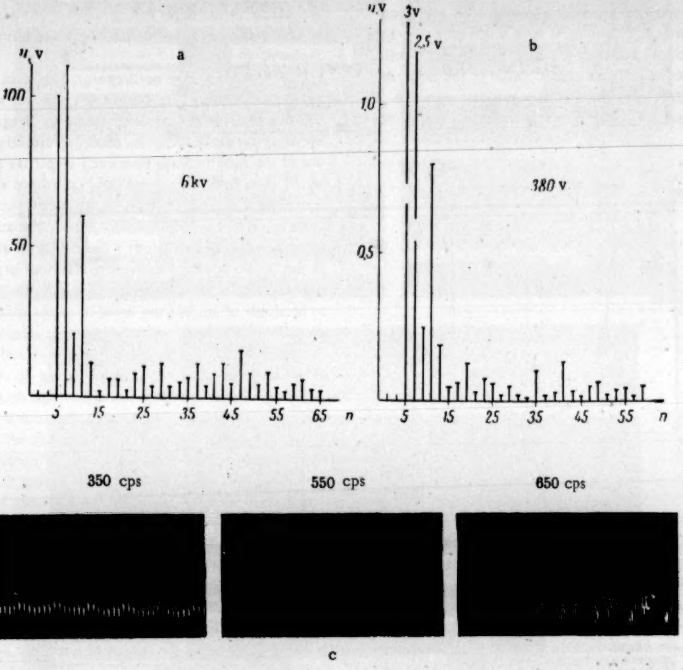

Fig. 1. Harmonic components of 50 cps.

teristics, can be conveniently determined from an oscillogram of the noise. The recording of the noise can, for instance, be made with a loop oscilloscope whose vibrators are connected to the output of a selective device. When operating with a multiloop oscilloscope,it becomes possible to record noise from several receivers with different bandwidths and at different frequencies. This is important for comparing noise at various frequencies for a transient condition in the line.

Noise was measured in the range of 150 cps to 100 kc. A preliminary recording of the noise on an eight-loop oscilloscope type MPO-2 revealed several bands with noise of different types. In the lower frequency part of the range (up to 5-10 kc),the high noise level is due to the harmonics of the commercial frequency of 50 cps. The level of this noise can be measured in effective values directly at the output of narrow-band devices. Fig. 1 shows a discrete noise spectrum in this range for a 6 kv (a) and a 380 v (b) network. The level of harmonics was measured by means of a selective voltmeter RVS-253. It will be seen from the drawing that, owing to the three-phase construction of the line, only odd harmonics are present in the network (n is the number of the harmonic). The relative level of harmonics with respect to the line voltage is lower in the high- than in the low-voltage network. Repeated measurements of the harmonic voltages at different times of the day,and in various parts of the network,showed that the level of separate harmonics can vary by 20-50%, but that the nature of their distribution remains unchanged. The study of the oscillograms of separate harmonics showed that,with the rise in the order of the harmonic and an increase in the bandwidth of the measuring device,the sinusoidal shape of the harmonic becomes distorted,owing to the pulsation of adjacent components (Fig. 1c).

If the measuring frequency is raised above 5 kc,and the bandwidth increased, the received noise acquires a fluctuating nature. The amplitude probability density distribution of this noise approaches the normal law (in the bandwidth of the order of several kilocycles). This range extends from 5 to 30 kc. It should be noted, however, that,from 15 kc up,in addition to the fluctuation noise,there appear occasional noise pulses, whose overshoots exceed considerably the level of the fluctuation noise. The noise level in this range can be measured directly by means of a normal tube voltmeter type LV-9 connected to the output of a selecting device. It will then read the root-mean-square value of the noise decreased by 10%. Obviously, in this measurement the level of occasional noise pulses is not taken into account.

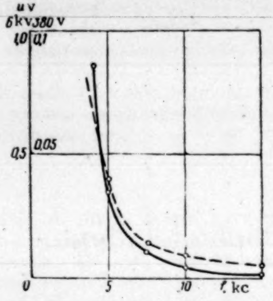

Fig. 2.

Fig. 2 shows the curves of the rms values of the fluctuation noise in the range of 5-15 kc for the 380 v network (dotted line), and for the 6 kv network (full line) at a bandwidth of 2 kc.

From 30-35 kc up to several hundred kc, with a sufficiently wide bandwidth (about 10 kc), the noise acquires a pulse nature both in the high-and low-voltage networks (Fig. 3a and b). Obviously, the boundary between the two ranges is nominal.

The study of the oscillograms of pulse noise in this range led to the establishment of a synchronous relationship between the appearance of the overshoots and the voltage of the network. The noise pulses have a repetition frequency of 100 cps. Owing to the three-phase construction of the line, the pulses which correspond to the other two phases appear attenuated to 1/2 or 1/3 of the value of the main pulses. At much less frequent intervals, single pulses or groups of pulses appear, which are not synchronized with the frequency of the network. They are due to switching phenomena in the line. Tests have shown that such a noise structure is peculiar not only to oilfield networks, but also to networks of mines and industrial establishments, i.e., to networks with a large number of electrical installations, which are simultaneously connected to the mains.

The oscillographic investigation of the noise has also shown the nature of the noise due to separate sources, and the simultaneous recording of calibrating signals provided a scale for their measurement.

The main source of noise in the 380 v network is due to welding, and therefore, the noise due to the operation of welding equipment was investigated with particular care. The study of the oscillograms revealed that the nature of the noise during welding remains the same as before the welding, but its amplitude increases by a factor of 20-30.

Fig. 3a shows an oscillogram of noise in a 380 v network at 45 kc. The gain of the receiver was reduced to 1/10 when recording noise during welding. The top oscillogram shows the noise recorded directly at the output of the intermediate frequency amplifier with a bandwidth of $\Delta f = 200$ cps, and the bottom one shows the recording of the noise envelope at the output of the amplifier with a bandwidth of $\Delta f = 2$ kc. The amplitudes of separate noise overshoots at a bandwidth of about 10 kc in the 30-60 kc range amount to fractions of a volt during welding. The noise spectrum during welding extends to hundreds of kc, but the level of noises drops rapidly with frequency, owing to a sharp rise in attenuation.

High level of pulse noise in the 6 kv and the 380 v networks is also caused by the switching-in of heavy 500 kw motors. It will be seen from the drawing that, during the starting of the motor, a characteristic sequence of 100 cps pulses appears. The switching-off of the same motor leads to a short splash of noise of considerable amplitude. Value of the overshoots during the transient period of motor operation is 20-50 times larger than during its steady-state running, and amounts to several tenths of a volt at frequencies between 30 and 50 kc in a bandwidth of about 10 kc.

The recording of noise during the switching-in of the motor was carried out simultaneously on two frequencies. The top oscillogram in Fig. 3c shows noise recorded at 60 kc at the output of a straight amplifier with a bandwidth of 10 kc. The middle oscillogram represents the recording of noise at 120 kc directly at the output of the intermediate frequency amplifier with a bandwidth of 200 cps and, finally, the bottom one represents the recording of the envelope of this noise at the output of the amplifier with a bandwidth of 2 kc.

It is convenient to estimate the value of noise pulses by the number of pulses which exceed a given level per unit of time. By counting the number of pulses which exceed various levels, it is possible to plot the amplitude characteristic of pulse noise in the network at a given frequency. For this purpose, a stepped device with a controllable level of operation is connected to the output of the constant bandwidth selective receiver. The counting of pulses which exceed a given level can be carried out either by means of compact counters working on cold-cathode thyratrons, or by measuring the mean repetition frequency of the pulses. The amplitude characteristic can also be determined from the oscillograms of the pulse noise.

The frequency characteristic of the noise level variations can be plotted on the basis of a family of amplitude characteristics whose parameter is the frequency. Fig. 4 shows curves of the variations of pulse noise level with respect to frequency for 380 v networks

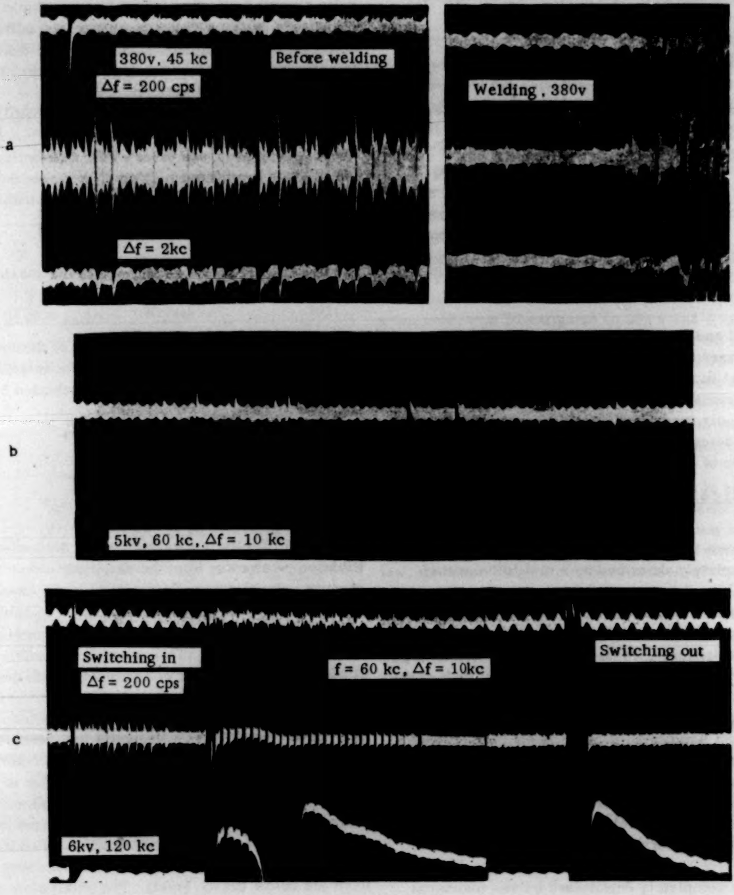

Fig. 3. Oscillograms of pulse noise: a) in the 380 v network, b) in the 6 kv network, c) when connecting and disconnecting a motor in the 6 kv network.

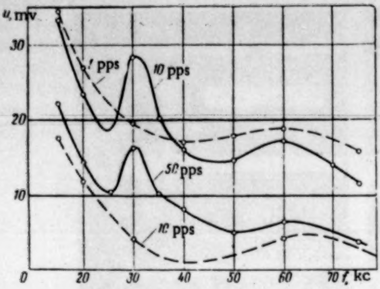

Fig. 4.

(dotted line) and for 6 kv networks (full line). The curve parameter consists of the number of pulses which exceed a given level in a unit of time. The bumps in the curve are due to resonance phenomena in the line. For other lines, resonances may occur at other frequencies; however, the characteristic of all these curves consists in the reduction of the noise level with a rising frequency.

2. Statistical Characteristic of Pulse Noise

It is known that a random process such as the pulse noise is completely described by a multidimensional distribution law. In practice, however, it is possible to use simpler statistical characteristics. In the first instance, it is possible to find the distribution of the overshoot noise amplitudes, which is fairly fully represented by a single-dimensional function of the amplitude probability density distribution. This characteristic also provides the most objective means for comparing the results of various noise level measurements in the channel, and makes it possible to evaluate their interference for various transmission methods of the signal.

The problem of the statistical analysis of the measurement results amounts to finding the type of distribution law which corresponds to the data obtained. The most simple and best known is the normal distribution, which is completely determined by two numerical parameters: the mean value and the root-mean-square deviation. Hence, in the case of asymmetrical distributions, one aims at finding a function f(x) which will transform the given distribution into a normal one. This means that, irrespective of the type of distribution of $\underline{x}$, the distribution of the converting function f(x) is normal. Such a conversion is of practical interest, since the distribution of the converting function f (x) is fully determined by the root-mean-square deviation σ and the mean value $\overline{f(x)}$.

The amplitude characteristics of the pulse noise in the 380 v and 6 kv networks, and the data obtained from the statistical analysis of the oscillograms of pulse noise, give reasons to believe that the distribution of pulse amplitudes is represented by logarithmic-normal distribution laws. This means that the logarithm of the random value $\underline{x}$ is distributed according to the normal law (the converting function is f (x) = log x). The density of distribution has the form

$$p(\log x) = \frac{1}{\sqrt{2\pi}\,\sigma} \exp\left[-\frac{(\log x - \log a)^2}{2\sigma^2}\right], \quad (1)$$

where log a is the mean value of the distribution of log x. Since log a is the median of the logarithmic-normal distribution, $\underline{a}$ must correspond to the median in the distribution of $\underline{x}$. It can be shown that

$$\bar{x} = a \cdot 10^{\frac{\sigma^2}{2M}}$$

and the abscissa, which corresponds to the maximum distribution density value (mode),

$$x_{\max} = a \cdot 10^{-\frac{\sigma^2}{M}},$$

where M = log e = 0.4343. The values of the median, the mode, and mean distribution of $\underline{x}$ are related to the parameters of the transformed distribution by the formulas

$$\log x_{\max} = \log a - 2.3\,\sigma^2, \quad (2)$$

$$\log x_{0.5} = \log a, \quad (3)$$

$$\log \bar{x} = \log a + 1.15\,\sigma^2. \quad (4)$$

The difficulty in determining the theoretical distribution parameters from the amplitude characteristics of pulse noise is due to the presence in the channel of a fluctuation noise level, which is small as compared with the pulse noise, and the existence of internal receiving device noises. This makes it impossible to count at zero level the number of overshoots which are only due to pulse noise. Nevertheless, it is possible to assume, owing to the difference in the levels of fluctuation and pulse noise (the difference increases with rising frequency), that a large part of the amplitude characteristic in the region of large amplitudes is entirely due to pulse noise. The distribution in that part of the amplitude characteristic after logarithmic transformation can be regarded as a truncated normal distribution with an unknown cut-off level x_0 (it is unknown how many pulses there are below the x_0 level). The parameters of the

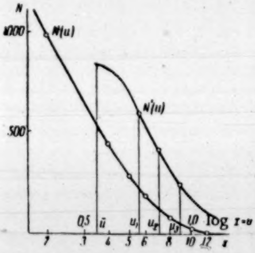

Fig. 5. Amplitude characteristic of pulse noise.

full distribution can be determined either from the tables or from three arbitrary points of the empirical probability density distribution curve of the number of overshoots N'(u) (Fig. 5) taken from the formulas

$$\overline{\log x} = \bar{u} = \frac{u_3^2 - (B+1)\,u_2^2 + Bu_1^2}{2\,[u_3 - (B+1)\,u_2 + Bu_1]}, \tag{5}$$

$$\sigma = \sqrt{\frac{(u_3 - \bar{u})^2 - (u_2 - \bar{u})^2}{2 \ln \frac{N'(u_2)}{N'(u_3)}}} = \sqrt{\frac{(u_3 - \bar{u})^2 - (u_1 - u)^2}{2 \ln \frac{N'(u_1)}{N'(u_2)}}}, \tag{6}$$

where $u_i = \log x_i$, $N'(u_i)$ is the value of the probability density at point u_i, and

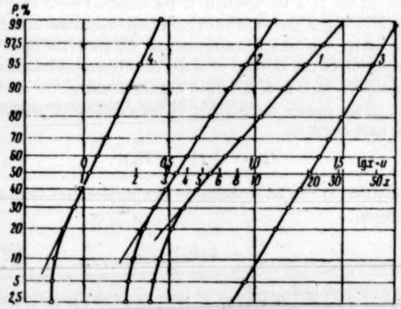

Fig. 6. Diagram of the distribution of pulse noise amplitudes. 1) 380 v network, f = 35 kc ($\bar{u}$ = 0.75, σ = 0.35); 2) 380v network, f = 50 kc ($\bar{u}$ = 0.55, σ = 0.26); 3) 380v network, f = 70 kc ($\bar{u}$ = 1.31, σ = 0.255); 4) 6 kv cable network, f = 115 kc ($\bar{u}$ = 0.03, σ = 0.17).

$$B = \ln \frac{N'(u_2)}{N'(u_3)} \Big/ \ln \frac{N'(u_1)}{N'(u_2)}. \tag{7}$$

It will be seen from formulas (5) - (7) that the determination of the parameters of the converted distribution is obtained by means of the ratio of $N'(u_i)$ values; hence, it is not necessary to normalize the curve N'(u), and the scale along the y axis can be arbitrary.

The normal distribution law was checked by plotting the distribution function points on special probability paper (Fig. 6) on which a normal distribution curve is represented by a straight line. The method of straightened curves[1] provides a fairly accurate indication of even the smallest deviation from the normal distribution law. Some 20 amplitude characteristics of pulse noise were investigated in 380 v and 6 kv power networks in the range above 30 kc. In all the cases, a good approximation to the logarithmic-normal law was obtained for the range of the large amplitude overshoots. Fig. 6 shows several straightened-out distribution diagrams. The deviation from straight lines in the region of small amplitudes is due to the appearance of overshoots caused by fluctuation noise.

The above research makes it possible to arrive at the conclusion that the amplitude characteristics of pulse noise in 380 v and 6 kv power networks are correctly approximated by a logarithmic-normal distribution law, for whose complete definition it is sufficient to know only two numerical parameters. The knowledge of the distribution parameters simplifies considerably the measurement of noise and the comparison and design of noiseproof communication and remote-control systems for power networks.

The author wishes to express his gratitude to G. A. Shastova for her continual interest in the work, and to V. A. Zakharov for his assistance in testing.

LITERATURE CITED

1. A. Hald, Mathematical Statistics with a Technical Supplement [Russian translation] (IL, 1956).

DESIGNING CIRCUITS WHICH CONTAIN CORES WITH RECTANGULAR HYSTERESIS LOOP CHARACTERISTICS

V. F. Belyavskii and Yu. M. Shamaev

Moscow

Translated from Avtomatika i Telemekhanika, Vol. 21, No. 8, pp. 1188-1197,
August, 1960
Original article submitted September 19, 1959

The application of the dynamic characteristics of ferrite cores which have rectangular hysteresis loops, for designing electromagnetic circuits, is described. A formula for the transient process in an electromagnetic circuit of known parameters is given. The parameters of a complex circuit with ferrite cores, which provide the required working conditions, are determined. Experimental results obtained in checking the above technique are cited.

1. Introduction

Modern high-speed devices employed in automation and computers use circuits which contain ferrite cores with rectangular hysteresis loops on a wide scale. The cores of these devices work under conditions of dynamic remagnetization which take microseconds or fractions of a microsecond. Contrary to the static conditions for which the behavior of a ferromagnetic core can be represented by the characteristic B = B(H), there is no similar characteristic for dynamic conditions, if the law of variation of the magnetic field H(t) or B(t) is not known.

The determination of the dynamic characteristic which represents the behavior of a ferromagnetic core under the effect of an arbitrary pulse is the main problem for any computation of the above electromagnetic circuits.

Physical processes occurring in dynamic remagnetization can be accounted for by means of generalized electrodynamic factors such as eddy currents and magnetic viscosity. In ferrite cores magnetic viscosity is the determining factor, since the low conductivity of the core materials practically eliminates any eddy currents.

The laboratory of the Theoretical Foundations of Electrical Technology Department of the Moscow Electrotechnical Institute derived – on the basis of experimental, and at a later date, theoretical investigations of dynamic remagnetization of ferrite cores with rectangular hysteresis loops – an equation which represents the behavior of ferrite when it is arbitrarily remagnetized in [1-3]:

$$\frac{dB}{dt} = \frac{\delta}{2}\left(2B_s - B_r - B_{\text{н}}\right) \left[1 - \left(\frac{2B - B_r - B_{\text{н}}}{2B_s - B_r - B_{\text{н}}}\right)^2\right](H - H_{\text{st}}), \tag{1}$$

where B, B_H, B_r, and B_s are the magnetic inductions at instant t, respectively, the initial, residual and saturated inductions; H is the strength of the external field at instant t; H_{st} is the field strength of B_{st} = B on the static hysteresis loop which corresponds to the initial magnetic condition of the ferrite; δ is the coefficient of magnetic viscosity, which is determined experimentally.

If we denote the position of the center of a particular half-cycle as

$$B_{\text{C}} = \frac{1}{2}\left(B_r + B_{\text{н}}\right), \tag{2}$$

equation (1) can be represented in a differential form as follows:

$$\frac{dB}{dt} = \delta\left(B_s - B_{\text{C}}\right) \left[1 - \left(\frac{B - B_{\text{C}}}{B_s - B_{\text{C}}}\right)^2\right](H - H_{\text{st}}) = r(B)(H - H_{\text{st}}) \tag{3}$$

or in an integral form

$$Q = Q(B) = \int_0^t (H - H_{\text{st}})\, dt = \frac{1}{\delta}\left(\tanh^{-1}\frac{B - B_{\text{C}}}{B_s - B_{\text{C}}} - \tanh^{-1}\frac{B_{\text{н}} - B_{\text{C}}}{B_s - B_{\text{C}}}\right). \tag{4}$$

The left-hand side of the latter expression by analogy with mechanical terminology can be called the intensity pulse of the effective field. Under the intensity of the effective field, we understand the excess of the external field strengh H over the field strength H_{st} on the corresponding static hysteresis loop at B = B_{st}.

Equations (3) and (4) represent the dynamic properties of the ferrite cores and confirm sufficiently well the experimental characteristics of remagnetizations of the ferrite cores, starting with pulse fields which exceed the coercive force by a factor of 2 [3]. The value of δ at room temperature is approximately equal for different ferrites under both complete and partial remagnetization conditions:

$$\delta \approx (6-7)\,10^{6}\ \text{cm/coul}$$

Of the many problems encountered in the calculations of electromagnetic circuits, we shall only discuss two: the calculation of the transient process in the circuit with known parameters and the determination of the parameters of a complex circuit with ferrite cores, which provides the required condition of operation.

The solution of these problems is made by means of the above dynamic characteristics of a ferrite core.

2. Calculation of a Transient Process in a Circuit Which Contains a Toroidal Ferrite Core

Let us first determine the voltage pulse across the winding of a core in the most simple case, when the core has one winding with a number of turns w_1 in which current i_1 (t) is flowing. The geometrical dimensions of the core are also known (and hence the length of the mean line of force l and the cross section S) as well as its magnetic properties (H_0, B_r, B_s) and its initial magnetic condition B_H.

In the absence of skin effect and stray fields, the magnetic field strength and induction in a ferrite core can be represented as mean values:

$$H = H_{\mathrm{m}} = \frac{\Sigma i_k w_k}{l}, \tag{5}$$

$$B = B_{\mathrm{m}} = \frac{\int\limits_0^t u_k\,dt}{w_k S} + B_{\text{н}}. \tag{6}$$

Let us replace, in our calculations, the actual static hysteresis loop of the core by a rectangular one with a coercive force

$$H_0 = \frac{1}{\tau}\int\limits_0^{\tau} H_{\mathrm{st}}\,dt, \tag{7}$$

where τ is the time of nominal remagnetization.

From expression (4) it follows directly that

$$\frac{B - B_{\mathrm{c}}}{B_s - B_{\mathrm{c}}} = \mathrm{th}\left[\delta Q(t) + \tanh^{-1}\frac{B_{\text{н}} - B_{\mathrm{c}}}{B_s - B_{\mathrm{c}}}\right]. \tag{8}$$

By substituting (8) in equation (3) we obtain an expression for the voltage pulse across the winding of the core:

$$u_1(t) = w_1 S\frac{dB}{dt} = \frac{w_1 S\delta\,(B_s - B_{\mathrm{c}})\,[H(t) - H_0]}{\mathrm{ch}^2\left[\delta Q(t) + \tanh^{-1}\frac{B_{\text{н}} - B_{\mathrm{c}}}{B_s - B_{\mathrm{c}}}\right]}. \tag{9}$$

The field strength H (t) in the core is completely determined by the current i_1 (t) under the above conditions, and therefore the voltage pulse can be calculated.

Let us now examine the case when the ferrite core N has another winding with w_2 turns loaded by an effective resistance R_2 (Fig. 1a). Now the strength of the magnetic field H(t) in the core will be determined by an algebraic sum of the field strengths established by the known currents i_1 (t) in winding w_1 and the unknown current i_2 (t) in winding w_2.

In order to calculate the voltage pulses u_1 (t) and u_2 (t) across both the windings of the core, let us first refer the parameters of the electromagnetic circuit to the material of the core. Such a change-over involves the following recalculation of values: the voltages are multiplied by a coefficient of the type $1/w_k S$, the currents are multiplied by a coefficient w_k/l and the resistances by $l/w_k^2 S$. The dynamic condition equation (3) makes it possible to represent the ferrite core in the form of an equivalent circuit, in which a nonlinear resistance r(B) is connected in parallel with the source of the static field strength H_0. The complete equivalent circuit of the above core is shown in Fig. 1b.

Let us replace the parallel connected resistances r(B) and r_2 by a single resistance R(B) and let us calculate the voltage pulse u_1(t) for a certain equivalent core N_e, which has only one winding with a number of turns w_1 in which a known current i_1(t) is flowing (Fig. 1c). The dynamic characteristic of core N_e is easily found from

$$Q_{\mathrm{e}}(B) = Q(B) + \frac{w_2^2}{R_2}\frac{S}{l}(B - B_{\text{н}}) = Q(B) + Q_r. \tag{10}$$

If core N had several output windings with effective resistances, the second term of the right-hand side of expression (10) would consist of the appropriate sum.

Further determination of the voltage pulse u_1(t) can be conducted more conveniently by a graphical method, since in order to obtain the analytical relation $dB/dt = f(t)$ it is necessary to solve the transcendental equation (10) We determine the value of H_1(t) for known values of w_1, l and i_1(t) and plot the curve for

$$Q_{\mathrm{c}}(t) = \int\limits_0^t (H_1 - H_0)\,dt = Q_{\mathrm{e}}(t). \tag{11}$$

By a simple addition of the ordinates of the dynamic characteristic Q(B) of the core and of the straight line Q_r, we find the characteristic of Q_e(B). From the relationships Q_e(t) and Q_e(B) thus obtained, we find graphically the relation B(t). The further calculation of the voltage pulse u_1 (t) is carried out from the formula:

$$u_1(t) = \frac{r(B)\,r_2}{r(B) + r_2}(H_1 - H_0)\,w_1 S, \tag{12}$$

into which are inserted values of H_1 and B obtained for a definite value of t from the curves of the relation of the above values to time.

The electromagnetic circuit with the voltage pulse source is transformed to the cases examined above by converting the source of voltage to a source of current. This statement is made clear by Fig. 2.

The nonlinear nature of the effective resistance of the input or output circuit of the core provides further difficulties, which can be resolved by methods for the solution of nonlinear equations. Similar difficulties are encountered when the input (output) impedances of the core windings are inductive or capacitive.

Figure 3 shows the voltage pulses $u_1(t)$ for various laws of the variation of the magnetizing current $i_1(t)$ and various initial conditions of B_H of a ferrite core BT-2 with dimensions $D \times d \times h = 4.85 \times 2.84 \times 1.44$ mm^3 and magnetic characteristics: B_r = 2200 gauss, B_s = 2500 gauss, $\delta = 6.35 \cdot 10^6$ cm/coul, H_0 = 0.8 amp/cm. Curve 1 corresponds to $H_m = i_1 w_1 / l$ = 2.8 amp/cm = const and $B_H = -B_r$; curve 2 corresponds to H_m = 2.8 amp/cm = const and $B_H = 0$; curve 3 was obtained for a linearly rising current $i_1 = k_1 t$ (k_1 = 8.9 amp/μsec and $B_H = -B_r$; curve 4 was obtained for the effect ($B_H = -B_r$) of a transcendental current pulse on the ferrite core, with the current rising up to the value of i_m = 0.9 amp = const according to the same linear law $i_1 = k_1 t$.

The voltage pulses were calculated from formula (9) for $w_1 = 5$, $w_2 = 3$, and $R_2 = \infty$.

Figure 4 shows the oscillograms of the magnetizing current $i_1(t)$ and voltage $u_2(t)$ for the corresponding windings of the same core, both for open-circuit and loaded conditions, with an effective resistance R_2. In the initial condition (t = 0) the core is characterized by induction $B_H = -B_r$. Curves 1 and 2 were plotted for $R_2 = \infty$; curve 3 for R_2 = 50 ohms; curve 4 for R_2 = 10 ohms. Points show the calculation results. Figures with dashes refer to voltage oscillograms.

3. Determining the Parameters of Electro-Magnetic Circuits Which Contain Several Ferrite Cores

In the controlling and logical elements of computers, circuits with ferrite cores are used. The basic problem in designing these circuits consists in determining the winding data for the selected cores, the values of resistances in coupling circuits, and the required magnetizing pulse - which would provide the operation of the device for the given conditions.

Let us show how it is possible to solve the above problem by means of the dynamic characteristic of the core.

For a concrete example let us examine the widely used circuit of a shift register, constructed with transformer elements (the ferrite core operates as a transformer). Figure 5a shows a circuit of a two-phase shift register and Figure 5b and c that of a three-phase register. The parameters of all the cores and coupling circuits are the same. The operating (clock) pulses i_{T1}, i_{T2} and i_{T3} have similar values but arrive at the input windings of the cores at different times, establishing negative field strengths. In the initial position all the cores of the

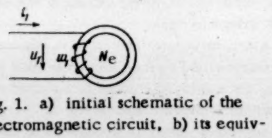

Fig. 1. a) initial schematic of the electromagnetic circuit, b) its equivalent alent circuit, c) a circuit with an equivalent core.

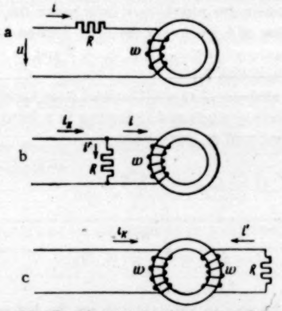

Fig. 2. a) initial schematic of the electromagnetic circuit with a voltage source, b) transformation of the voltage source into a current source $i_k = u/R$, c) equivalent circuit.

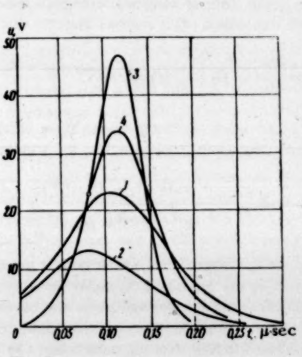

Fig. 3

registers are in the condition of a negative remanent induction $-B_r$. The operation of the clock pulses does not affect the magnetic condition of the cores. Let us now assume that at the input of core 1 there appears a pulse which can remagnetize this core to a value of $+B_r$. It is obvious that the remagnetization of the first core will not affect the remaining cores of the register, since a flow of current in the coupling loop between cores 1 and 2 is prevented by the rectifying element (diode). The next instant, under the effect of the clock pulse i_{T1}, the first core will be remagnetized to its initial condition ($-B_r$), and the current produced by this action in the coupling loop between cores 1 and 2 will remagnetize core 2 into condition $+B_r$. Under the effect of pulse i_{T_2} the unit information which corresponds to induction $+B_r$ is shifted to the third core. In this process currents arise both in the coupling loop between the second and the third cores (forward movement of information) and between the second and first cores (reversed movement of information). In the two-phase register (Fig. 5a) the reversed current produces a certain change in the condition of the first core.

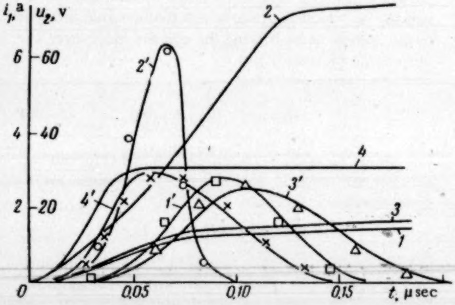

Fig. 4

In the three-phase register the magnetic condition of the first core is not altered because the clock pulse is applied simultaneously to cores 2 and 1 (Fig. 5b), thus keeping the first core in condition $-B_r$, or because pulse i_{T1} overlaps in time pulse i_{T2} (Fig. 5c), thus keeping core I in condition $-B_r$ when the second core is being remagnetized.

Since the condition of work of all the links (stages) is the same, the designing of the register can be based on a single link. One link consists of two cores connected by their coupling circuit, and its computation consists in analyzing the operating conditions of the circuit, i.e., of the forward and reversed movement of the information pulses. Providing all the link parameters are the same, the consideration of only one condition of a circuit consisting of three cores 1, 2 and 3 will lead to the same results.

For the sake of simplicity let us neglect the different resistances of the diode for different currents and represent the impedance of the coupling circuits by means of the effective resistances:

$$r = R + R_e. \qquad (13)$$

Let us first examine the operation of a two-phase shift-register link. Let it be necessary according to the operating condition of the register to transmit unit information from the second core to the third in time τ, and let us assume that at the same time a variation in the condition of the first core of $\Delta B = b2B_r$ is permissible. The calculation is made for the condition of a simultaneous remagnetization of all the three cores. For a complete remagnetization of the second and third cores by the value of the induction change $\approx 2B_r$, it is necessary to apply to them a field-strength pulse equal to

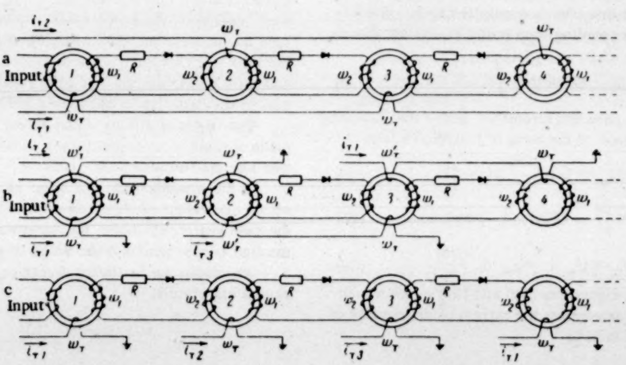

Fig. 5. Schematic of magnetic shift registers consisting of transformer elements: a) two-phase register; b and c) three-phase registers.

$$Q_w = Q(2B_r) + H_0\tau = S_w + H_0\tau, \qquad (14)$$

where S_w is the value of the effective field-strength pulse for complete remagnetization, given by equation (4) for $B_H = -B_r$ and $B = +B_r$. The value of S_w is usually called the coefficient of remagnetization.

The value of the variation of the inductance ΔB in the first core corresponds to a pulse of

$$Q(b) = q(b) S_w + h(b) H_0\tau. \qquad (15)$$

Here q(b) is the dynamic characteristic (4) in relative values and

$$h(b) = \frac{1}{b2B_r H_0} \int\limits_{-B_r}^{-B_r + b2B_r} H_{st} \, dB \qquad (16)$$

is the mean value of the mean strength of the static field for partial remagnetization (in relative values).

The value of the clock field-strength pulse for time τ can be represented by the expression:

$$Q_\tau = \frac{w_\tau}{l} \int\limits_0^\tau i_\tau \, dt = \frac{(i_\tau)_{cp} w_\tau}{l} \tau. \qquad (17)$$

Let us denote the ratio of the number of turns in the coupling loop $n = w_1/w_2$, and let us refer all the values which characterize the condition of the link to the second core. The field-strength pulse Q_w which provides in time τ a variation of induction in core 3 of $2B_r$ is multiplied by w_1/w_2 when it is referred to an equivalent circuit of the link (Fig. 6a); i.e., it is multiplied by n and the variation in induction by w_2/w_1, i.e., by 1/n. The referred admittance of the coupling circuit of cores 2 and 3 will then assume the form:

$$G = gw_1^2 \frac{S}{l} = gw_2^2 \frac{S}{l} n^2. \qquad (18)$$

The field-strength pulse Q(b) in the preceding coupling loop is multiplied by 1/n when it is referred to the equivalent circuit, and the induction variation $b\,2B_r$ occurring in the first core is multiplied by n. The admittance of this coupling loop in the equivalent circuit is equal to

$$G' = gw_2^2 \frac{S}{l}. \qquad (19)$$

From the equivalent circuit we derive the following obvious expressions on the basis of Kirchhoff's laws

$$nQ_w = G'n^2 \frac{2B_r}{n}(n-1), \qquad (20)$$

$$\frac{Q(b)}{n} = G' 2B_r (1 - bn), \qquad (21)$$

$$Q_\tau = Q_w + nQ_w + \frac{Q(b)}{n}. \qquad (22)$$

Combining expressions (20) and (22) we obtain an equation which determines the ratio n of the number of turns as a function of b:

$$n^2 - \frac{1}{b}\left(1 - \frac{Q(b)}{Q_w}\right) n - \frac{1}{b} \frac{Q(b)}{Q_w} = 0. \qquad (23)$$

Expression (22) assumes after transformation the form:

$$\frac{Q_\tau}{Q_w} = \frac{n-b}{n-1} n. \qquad (24)$$

Thus the controlling factor in determining the winding data of cores and the magnetizing clock pulse for two-phase registers with one diode is the variation of the induction due to the reverse movement of the information pulse.

For the above conditions we find the value:

$$gw_2^2 = \frac{Q_w l}{S2B_r(n-1)}. \qquad (25)$$

The value of one of the quantities, for instance w_2, depends on the value adopted for the other quantity, g. Let us assume that the impedance of the coupling loop is known. Under these conditions we find w_2 from (25). Now it remains to determine the value of the building-out resistance R which it is necessary to connect in series with the selected diode. Experimental investigations of diodes show that their direct resistance under pulse conditions can be represented by an effective resistance R_e which in practice has single-value relations to the current pulse flowing through the diode over a given time interval [4], i.e.,

$$R_e = f\left(\int\limits_0^\tau i\,dt\right) = f(q). \qquad (26)$$

Since, by taking expressions (23) and (29) into account, the value of the current pulse q can be assumed to be known

$$q = gw_2 S2B_r(n-1), \qquad (27)$$

it is possible to find the value of R_e from the characteristic of R_e (q), and then find the value of the building-out resistor R in the coupling circuit.

If the difference in the equivalent resistances of the diodes is taken into account, the value of n as determined from equation (23) is decreased. Other factors, however, such as the simultaneous remagnetization of the cores increase n. This holds sufficiently well for the second and third cores, but the rise of the magnetic induction in the first core is completed before the other two.

The opposite effects of the above two phenomena make it possible to neglect them in the first approximation and use formulas (23) - (25).

In the separate link of a three-phase register, whose equivalent circuit is shown in Fig. 6b, contrary to the case examined above, the variation of induction in the first core is zero and the value of pulse Q is unknown.

We obtain the following design expression from the equivalent circuit:

$$\frac{Q_\tau}{Q_w} = 1 + n + \frac{1}{n-1}, \qquad (28)$$

$$gw_2^2 = \frac{Q_w l}{S2B_r(n-1)}. \qquad (29)$$

The ratio $Q_T/Q_W = f(n)$ has a minimum at n = 2. Hence expressions (28) and (29) take the form:

$$Q_\tau = 4Q_w, \tag{30}$$

$$gw_2^2 = \frac{Q_w l}{S2B_r}. \tag{31}$$

Thus the parameters of a three-phase register circuit are calculated from the minimum of the field strength pulse for time τ.

Expression (30) determines the full value of the magnetizing pulse only in the first circuit (Fig. 5b). In the second circuit (Fig. 5c) this expression determines only that part of the pulse which is produced by the generator during time τ. The full value of the symmetrical magnetizing pulse, whose duration is twice as great as τ, is equal to 8 Q_W.

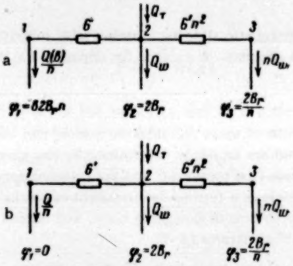

Fig. 6. Equivalent circuit for calculating parameters of a register link: a) for a two-phase register, b) for a three-phase register.

Let us note that in the coupling loops during time τ for n = 2 there flow equal current pulses, and hence the equivalent resistances of the diodes can also be considered equal.

Methods of integral calculations are also applicable to other circuits with ferrite cores, which perform different functions in digital computers [5, 6].

3. Conclusions

It follows from the above that by means of equations (3) and (4) it is possible to evaluate circuits with ferrite cores for different pulse effect.

The oscillograms of the pulse voltages (Fig. 4) appended to the article and the experimental checking of model ferrite-diode circuits designed on the basis of the theoretical considerations showed that the computations were sufficiently accurate. As compared with the experimental data, the calculation error does not exceed 10 - 20%.

LITERATURE CITED

1. Yu. M. Shamaev, G. F. Lisitsyn, and A. I. Pirogov, "Methods and results of measurements of static and dynamic characteristics of ferrites with rectangular hysteresis loops," Scientific Reports of Higher Schools, Electromechanics and Automation section, No. 3 (1958).
2. Yu. M. Shamaev, V. L. Dyatlov, and A. I. Pirogov, "Dynamic characteristics of ferrites," Scientific Reports of Higher Schools, Electromechanics and Automation section, No. 1 (1959).
3. Yu. M. Shamaev, A. I. Pirogov and V. F. Belyavskii, "Pulse remagnetization of ferrites with rectangular hysteresis loops," Engineering and Physical Journal. Proceedings of the 3rd All-Union Conference on Ferrites (1959).
4. F. E. Pashukanis, "Consideration of the inertia of crystal diodes in designing pulse devices," Scientific Reports of Higher Schools, Radiotechnical and Electronic section, No. 2 (1959).
5. V. F. Belyavskii and Yu. M. Shamaev, "Application of equations of the dynamic condition of ferromagnetic cores with rectangular hysteresis loops for calculating pulse circuits," Scientific Reports of Higher Schools, Electromechanical and Automation section, No. 1 (1959).
6. V. F. Belyavskii and Yu. M. Shamaev, "Calculation of stable state conditions of operation of pulse circuits which contain ferrites with rectangular hysteresis loops," Engineering and Physical Journal. Proceedings of the 3rd All-Union Conference on Ferrites (1959).

ON CHOOSING THE OPTIMUM NUMBER OF POLE PAIRS AND THE MAIN DIMENSIONS OF ELECTROMAGNETIC SLIPPING CLUTCHES WITH MASSIVE STEEL ARMATURES

A. D. Posdeev

Ul'yanovsk

Translated from Avtomatika i Telemekhanika, Vol. 21, No. 8, pp. 1198-1205,
August, 1960
Original article submitted February 29, 1960

The relations for the optimum number of pole pairs of electromagnetic slipping clutches with massive steel armatures are found. The change in permeability is taken into account. A method for choosing the main dimensions of the clutch is described.

Electromagnetic slipping clutches (e.s.c.) and brakes with massive steel armatures find ever wider use in drives for automatically controlling speed [1] and torque [2], to provide smooth engagement and braking, and for obtaining stable slipping speeds in drives with asynchronous motors [3], as loading devices for bench tests, etc. Among their advantages are simplicity of construction, low consumption of nonferrous metal, low cost, ease of control, and the ability to dissipate a large amount of heat in the armature.

The methods which have been developed for determining the main dimensions D, l_δ and the optimum number of pole pairs, p_0, of an e.s.c. with a massive steel armature [4, 5], are based on relations derived on the assumption that the permeability of the armature material, μ, does not change. In these methods, there is a certain arbitrariness in choosing μ, and this leads to different results in calculations (see example below).

The design formulas for determining p_0, D and l_δ presented in this paper take into account the change in permeability as the magnetic field strength changes. The results of these formulas do not depend on the choice of μ, and are uniquely determined by the given technical conditions (the torque M, and the relative speed n_s). This article is a further development of works published on the problems of designing e.s.c. and brakes with massive steel armatures [4-7].

1. Optimum Number of Pole Pairs

The expressions for the maximum torque M_k and critical speed n_{sk} of an e.s.c. with a massive steel armature and poles of alternating polarity, and also the equation for the mechanical characteristic, considering the change in μ, are derived in [7]:

$$M_k = \frac{(i_1w_1)^2 \mu_0 p D l_\delta^n \sin\left(\frac{t}{\tau}\frac{\pi}{2}\right)}{55{,}2\, k_{ad} k_2 \delta (1+\varkappa)(1+\sin\varphi)}, \tag{1}$$

$$n_{sk} = \left[\frac{\sqrt{2}(1+\sin\varphi)}{i_1w_1}\right]^{\frac{n-1}{n}} \frac{115\delta^2 (1+\varkappa)^2 p^{\frac{7n+1}{n}} k_2^n K \zeta_\rho}{\mu_0^2 k_1^4 (Dk_{ad})^{\frac{n+1}{n}} D^2 \sin^2\left(\frac{t}{\tau}\frac{\pi}{2}\right)}, \tag{2}$$

$$\frac{n_s}{n_{sk}} = \frac{\left[1+\sin\varphi - \frac{M}{M_k}\sin\varphi \pm \sqrt{\left(1+\sin\varphi - \frac{M}{M_k}\sin\varphi\right)^2 - \left(\frac{M}{M_k}\right)^2}\right]^{\frac{3n+1}{2n}}}{\left(\frac{M}{M_k}\right)^2} \tag{3}$$

Here M_k is in kg·m; n_{sk} – rpm; i_1w_1 are the ampere-turns of the excitation winding, in amps; p is the number of pole pairs; D, and l_δ are the diameter and length of the machine along the air gap, m; δ – the air gap, m; t/τ – ratio of the designed pole width to pole spacing; k_{ad} is the reaction coefficient of the armature along the longitudinal axis; ζ_ρ – the design value of armature material resistivity, considering the edge effect ohm·m; K is a coefficient in the equation of a parabola $B_m = KH_m^{\frac{1}{n}}$, which approximates the basic magnetization curve [8]; k_1 and k_2 are coefficients which depend on the exponent n [6], and can be set equal to $k_1 = 0.845$, and $k_2 = 0.87$ for ferromagnetic materials, taking hysteresis into account; $\varkappa$ is a coefficient equal to the ratio of the drop in mmf in the steel inductor, F_c, to the mmf in the air gap, F_δ;

$$\sin\varphi = \sqrt{\frac{n+1}{3n+1}}.$$

In the given relations, one should assume that

$$t/\tau = 1,\ k_{ad} = \frac{\pi}{4},\ i_1 w_1 = \frac{\pi}{4} F_1,$$

for e.s.c. with nondistinct poles, where F_1 is the mmf of the excitation winding, per pair of poles. The relations given in [5] follow from (1), (2), and (3) in the particular case when $n = 1$ [μ = const].

The numerical coefficient in the formula for M_k, as further analysis will show, should be approximately 53.6; this takes into account the loss in the armature from the higher flux harmonics in the air gap.

As the relative speed is increased from zero to n_{sk}, the reaction mmf of the armature, F_2, grows, and F_δ decreases. It can be shown, that in the extreme

$$F_\delta (1 + \varkappa) = F_2 k_{ad} = \frac{i_1 w_1}{\sqrt{2(1+\sin\varphi)}} \approx 0{,}56\, i_1 w_1. \quad (4)$$

The change in the mmf's F_δ and F_2 as a function of speed obeys the following rules:

$$\lambda = \frac{F_\delta (1+\varkappa)}{i_1 w_1} = \frac{B_\delta}{B_{\delta\,\max}} = \frac{M/M_k}{\sqrt{2(1+\sin\varphi)}\left[\left(\frac{M}{M_k}\right)^2 \frac{n_s}{n_{sk}}\right]^{\frac{n}{3n+1}}}, \quad (5)$$

$$0 = \frac{F_2 k_{ad}}{i_1 w_1} = \frac{\left[\left(\frac{M}{M_k}\right)^2 \frac{n_s}{n_{sk}}\right]^{\frac{n}{3n+1}}}{\sqrt{2(1+\sin\varphi)}}. \quad (6)$$

Here, B_δ is the flux density in the air gap of the e.s.c., which results after the field in the gap is brought to a pole generated by the excitation winding, webers/m^2; $B_{\delta\,\max}$ is the maximum flux density in the gap for a given $i_1 w_1$ corresponding to $n_s = 0$.

Curves of λ and θ as a function of M/M_k for the stable region of the mechanical characteristic, where $0 \leqslant n_s \leqslant n_{sk}$ are shown in Fig. 1.

The flux density under a pole, $B_{z\delta}$, is approximately twice as much as the variable component of the flux density in the gap, B_δ, for induction clutches, since $B_{z\delta} = 2 B_\delta k_n$, where k_n = 1.05 to 1.1 [4]. Moreover, $\frac{t}{\tau} \approx 1$, and $k_{ad} \approx 0{,}785$. for the clutches mentioned.

Taking these relations into account, and doing a calculation analogous to that done in [7], we can get the expressions:

$$M_k = \frac{(i_1 w_1)^2 \mu_0 p D l}{55{,}2 \cdot 0{,}785 \cdot 2 k_2 k_n\, \delta (1+\varkappa)(1+\sin\varphi)}, \quad (7)$$

$$n_{sk} = \left[\frac{\sqrt{2(1+\sin\varphi)}}{i_1 w_1}\right]^{\frac{n-1}{n}} \frac{115\delta^2 (1+\varkappa)^2 p^{\frac{2n+1}{n}} k_2^2 K \zeta \rho (2k_n)^2}{\mu_0^2 k_1^4 (0{,}785 D)^{\frac{n+1}{n}} D^2}. \quad (8)$$

Hence, the maximum torque of an induction clutch, for an identical number of excitation ampere turns, is approximately half as much as for clutches with poles of alternate polarity, and the critical speed is four times as great. It should be mentioned that the above-mentioned facts are justified for nonsaturated machines with the same κ. In iron-clad inductors, κ can be greater than in induction clutches, as a result of the large leakage flux, and this, of course, somewhat alters the quantitative relations obtained, as they pertain to induction clutches.

The effect of p on the mechanical characteristics of the clutch is seen in Fig. 2, where the mechanical characteristics for a nonsaturated inductor (κ = const) are plotted in relative units (the values of M_{k1} and n_{sk1} when $p = p_1$ are taken as references) for different values of p but with the other parameters remaining the same, and the excitation remaining unchanged. Figure 2 shows that as p decreases in the region of low slip, the torque increases, but becomes less when n_s is large.

Thus, if, for example, the given operating speed lies to the left of point A (Fig. 2.), the value $p = p_1/1.5$ is preferred over $p = p_1$. If the given n_s lies to the left of point C, then $p = 0.5p_1$ is preferable . In the zone from C to A, the optimum number of pole pairs is $p = p_1/1.5$, for the given three values. Consequently, a certain value of p, for which the torque will be greatest, will correspond to each speed n_s. Physically, the increase in the torque when the slip is small and p decreases is explained by the increase in the penetration depth of the field, and consequently, by a lowering of the electrical resistance of the armature. The decrease in the torque, when the slip is large and p lessens, occurs because of an increase in the demagnetizing effect of the armature reaction.

In order to determine the optimum number of pole

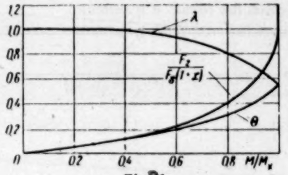

Fig. 1.

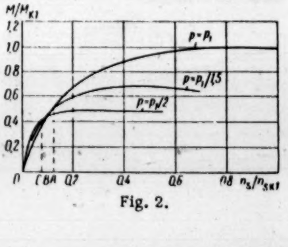

Fig. 2.

pairs, relations are used which associate the magnetic quantities (the first harmonic of the field strength at the surface, H_{mx0}, and the flux density in the gap) with the torque M and the speed n_s:

$$\sqrt{\mu_{ste}^{(1m)}}H_{mx0} = \frac{0{,}187 B_\delta D \sin\left(\frac{t}{\tau}\frac{\pi}{2}\right) k_1^2}{k_2}\sqrt{\frac{n_s}{p\zeta\rho}} \qquad (9)$$

(here $\mu_{ste}^{(1m)}$ is the permeability determined from the basic magnetization curve when $H = H_{mx0}$),

$$l_\delta = \frac{13{,}4 M k_2}{D^2 H_{mx0} B_\delta \sin\left(\frac{t}{\tau}\frac{\pi}{2}\right)},^{*} \qquad (10)$$

and also from the balance-of-mmf's equation which follows from the vector diagram of the e.s.c. [7]:

$$(i_1 w_1)^2 = F_\delta^2 (1 + \varkappa)^2 + k_{ad}^2 F_2^2 + 2F_\delta (1 + \varkappa) F_2 k_{ad} \sin\varphi. \qquad (11)$$

In expression (11), we get

$$F_\delta = B_\delta \frac{2\delta}{\mu_0}, \qquad (12)$$

for clutches with poles of alternate polarity; for induction clutches:

$$F_\delta = B_{2\delta}\frac{2\delta}{\mu_0} = \frac{4B_\delta k_n}{\mu_0}; \qquad (13)$$

$$F_2 = \frac{D}{p} H_{mx0}. \qquad (14)$$

We will also consider the relation

$$\mu_{ste}^{(1m)} = K H_{mx0}^{\left(\frac{1}{n} - 1\right)} \qquad (15)$$

Eliminating B_δ and H_{mx0} from equations (9), (10), (12), and (14), and putting the values obtained for F_δ and F_2 into (11), and then examining the function M = = f(p), which results, at the extremes, we can get a value of p_0 at which the torque is maximum.

For clutches with poles of alternate polarity,

$$p_0 = \left\{ A \left[\frac{i_1 w_1}{\sqrt{2(1 + \sin\varphi)}}\right]^{\frac{n-1}{n}} \cdot \frac{\mu_0^2 k_1^4 (k_{ad} D)^{\frac{n+1}{n}} D^2 \sin^2\left(\frac{t}{\tau}\frac{\pi}{2}\right) n_s}{115\delta^2 (1 + \varkappa)^2 k_2^2 K \zeta\rho}\right\}^{\frac{n}{2n+1}}. \qquad (16)$$

For induction clutches,

$$p_0 = \left\{ A \left[\frac{i_1 w_1}{\sqrt{2(1 + \sin\varphi)}}\right]^{\frac{n-1}{n}} \cdot \frac{\mu_0^2 k_1^4 (0.785 D)^{\frac{n+1}{n}} D^2 n_s}{115 (2k_n)^2 \delta^2 (1 + \varkappa)^2 k_2^2 K \zeta\rho}\right\}^{\frac{n}{2n+1}}. \qquad (16')$$

Here,

$$A = C^2 \left[\frac{2(1 - \sin\varphi)}{C^2 - 1 + 2C\sin\varphi}\right]^{\frac{n-1}{2n}};$$

$$C = \frac{\sqrt{(n+1)(3n+1)} + \sqrt{19n^2 + 8n + 1}}{2n}.$$

The dependence of A on the exponent, n, of the parabola which approximates the actual function, is shown in Fig. 3. Since the steel used for making the armature has n = 7 − 12, one can set A equal to 5, on the average.

Comparing expression (16) for p_0 with (2) for the critical speed n_{sk}, we find that the coefficient A is the ratio of the speed at which (for the given $p = p_0$) the torque is greatest (in comparison with any other value of p) to the critical speed when $p = p_0$. Since A = 5, the maximum torque (which is the best operating point on the mechanical characteristic) occurs when $n_s \approx 0.2 n_{sk}$, and this gives $M/M_k \approx 0.7$. The computation for μ = const gives the best point when $n_s = 0.0607 n_{sk}$ (A = 16.5), and this corresponds to $M/M_k = 0.59$.

When the clutch is designed, the excitation ampere-turns $i_1 w_1$ are initially unknown, and hence it is best to select them on the basis of the flux density in the air gap at no-load

$$i_1 w_1 = B_{\delta\max}\frac{2\delta(1 + \varkappa)}{\mu_0}. \qquad (17)$$

In the determination of the main dimensions D and l_δ, some nominal value of B_δ is ordinarily given as the flux density in the air gap. The relation between B_δ and $B_{\delta\max}$ is given by the curve $\lambda = f(M/M_k)$ in Fig. 1. The armature reaction mmf is low up to $M/M_k = 0.7$, and the decrease in the flux density in the air gap is not more than 12% of that at no-load. Therefore $B_{\delta\max} = (1.0-1.14)B_\delta$ depending on the given M_H/M_K.

One further thing should be mentioned. If the overload ability, $M_H/M_K = 0.7$, meets technical requirements, then n_{sH} should be substituted directly in the expression for p_0. If M_H/M_K must be less than 0.7, then the quantity ϵn_{sH} should be used in (16), where

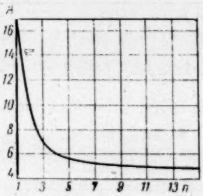

Fig. 3.

---

[*] In the given expression, the numerical coefficient, 13.4, takes into account the loss in the armature due to the higher harmonics of the flux density in the gap, whereas in [7], this coefficient, equal to 13.8, is derived without considering the latter.

$$\varepsilon = \frac{n_s / n_{sH} \text{ for } M / M_K = 0{,}7}{n_{sH} / n_{sK} \text{ for a given } M_H / M_K} \approx$$

$$\approx \frac{0{,}2}{n_{sH} / n_{sK} \text{ for a given } M_H / M_K}.$$

The ratio n_{sH} / n_{sK} for a given M_H / M_K is determined from the mechanical characteristic (3). The curves given in [7] may be used for this purpose; they are plotted for various values of n, as a function of the given (3).

Considering all this, we finally obtain:

a)
$$p_0 = \left\{ A \left[\frac{B_\delta 2\delta (1 + \varkappa)}{\lambda \mu_0 \sqrt{2 (1 + \sin \varphi)}} \right]^{\frac{n-1}{n}} \cdot \right. \tag{18}$$

$$\left. \cdot \frac{\mu_0^2 k_1^4 (k_{ad} D)^{\frac{n+1}{n}} D^2 \sin^2 \left(\frac{t}{\tau} \frac{\pi}{2} \right) \varepsilon n_{sH}}{115 \delta^2 (1 + \varkappa)^2 k_2^2 K \zeta \rho} \right\}^{\frac{n}{2n+1}},$$

for a clutch with poles of alternate polarity, and

b)
$$p_0 = \left\{ A \left[\frac{B_\delta 2\delta (1 + \varkappa)}{\lambda \mu_0 \sqrt{2 (1 + \sin \varphi)}} \right]^{\frac{n-1}{n}} \right. \tag{18'}$$

$$\left. \cdot \frac{\mu_0^2 k_1^4 (0{,}785\, D)^{\frac{n+1}{n}} D^2 \varepsilon n_{sH}}{115 (2k_n)^2 \delta^2 (1 + \varkappa)^2 k_2^2 K \zeta \rho} \right\}^{\frac{n}{2n+1}}.$$

for an induction clutch.

2. The Procedure for Determining the Main Dimensions

On the basis of the information given above, the following procedure is recommended for determining the main dimensions of an e.s.c. with a massive armature, for given values of M_H and n_{sH}.

1. The quantities D and δ are chosen according to the practical demands of construction, and p_0 is determined. One can assume that $B_\delta = 0.6 - 0.7$ webers per m^2, and $t/\tau = 0.6 - 0.75$ for an iron-clad inductor. The drop in the mmf in the steel, F_C, is evaluated while the steel is in an oriented state. Computations on actually constructed clutches show that on the average, $\kappa = 0.5 - 1.0$. The basic recommendations are given in [4] for induction clutches.

2. The curve $\sqrt{\mu} H = f(H)$. is plotted from the basic magnetization curve of the material chosen.

3. The quantity $\sqrt{\mu_{ste}^{(1m)}} H_{mx0}$ is computed from formula (9), and H_{mx0} is found from the curve:

$$\sqrt{\mu} H = f(H)$$

4. The quantity l_δ is determined from (10).

5. The excitation ampere turns $i_1 w_1$ are found from (11), or can be found more accurately by the method given in [6].

Later, the geometric dimensions of the inductor are made more precise, and a verifying calculation is made, according to the method described in [6]. The dimensions D and l_δ, which are determined from electromagnetic conditions, must be large enough to dissipate the heat caused by the losses in the anchor and excitation winding of the clutch. Since the heat transfer coefficient and the permissible overheating of different parts of the machine depend on a number of physical and constructional considerations, the problem of calculating D and l_δ from thermal conditions is very difficult. Therefore, we recommend that experimental data on the determination of the permissible heat load, Δp_s, per unit area of the armature surface along the air gap, be used.

In Fig. 4, curves are shown of Δp_s as a function of the linear velocity of the armature; they were plotted from the data of a number of studies on clutches with an external armature and air cooling. Curve 1 (for an armature with a smooth external surface) and curve 2 (for an armature with cooling fins) are plotted from the data of the ENIMS [11], and curve 3 was plotted from data of the Stromag firm [10] for clutches with longitudinal channels along the external surface of the armature. These clutches take an intermediate position between clutches with a smooth armature and clutches with an armature having cooling fins, insofar as their ability to dissipate heat is concerned. Curve 3 also takes an intermediate position between the ENIMS curves. Experimental dependencies of

$$D^2 l_\delta = f\left(\frac{P}{n}\right)$$

are presented in [9] for different power ratings of the actuating mechanisms; these dependencies are plotted

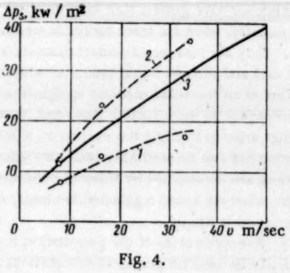

Fig. 4.

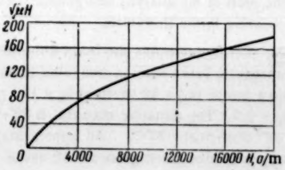

Fig. 5.

for the case of loss dissipation by the armature when the speed regulation is close. The relation

$$\frac{\Delta p_s \max}{v_y} \approx \left(0.65 - 1.30 \right) \frac{\text{kw} \cdot \text{sec}}{\text{m}^3}.$$

can be obtained from them.

It follows from curve 3 of Fig. 4 that

$$\frac{\Delta p_s}{v_y} \approx (0.8 - 1.43) \frac{\text{kw} \cdot \text{sec}}{\text{m}^3}.$$

Hence, the experimental data presented mutually agree, and the curves in Fig. 4 can be recommended for direct calculations.

3. Conclusions

1. The formulas presented for determining the optimum number of pole pairs and the main dimensions of electromagnetic slipping clutches with massive steel armatures were derived from relations in which the change in permeability, μ, as the magnetic field strength in the anchor changes was taken into account. The correctness of these relations is confirmed by experimental studies [6, 7].

2. When p_0, D, and l_δ are found from relations based on the assumption that μ is constant [4, 5], the results depend on the average value of μ selected. The method presented in this article gives a unique solution for given values of $(M_H, n_{sH}, M_H/M_K)$, and the data obtained occupy an intermediate position in relation to the results obtained from the method explained in [5] (see example below).

3. It has been theoretically established that induction clutches have greater size than clutches of alternate polarity, when the same torque is transmitted by each. They are best used in small diameters (D = 10 to 15 cm) and with an inside inductor, when the leakage flux of an iron-clad inductor is significantly large in comparison to the effective flux, and, moreover, difficulties arise in locating the excitation winding. Induction clutches can be profitably used also when the dimensions are determined by thermal conditions (for example, when the speed regulation is close), since their construction is simple.

4. Average values of the permissible thermal load which can be used for practical calculations are presented on the basis of the analysis and generalization of data appearing in the literature.

Example. Let us determine the main dimensions of an electromagnetic brake with an iron-clad inductor which develops a torque M_H = 28 kg-m at n_s = 120 rpm and M_H/M_k = 0.7. The armature material is ST-20L, $\rho = 0.16 \cdot 10^{-4}$ ohm-m at 20°C. An approximation of the basic magnetization curve gives n = 10 and K = 0.675. The coefficient ζ is determined from [12]. We will take $\zeta = 1.7$ as a first approximation, and an armature temperature of 120°C. Then $\zeta\rho_{oes} = \zeta\rho(1 + \alpha\Delta t) = 0.408 \times 10^{-6}$ ohm-m. The curve $\sqrt{\mu}\,H = f(H)$, plotted on the basis of the magnetization curve, is shown in Fig. 5.

We will assume that

$$D = 0{,}4\ \text{m},\ \delta = 1{,}0\text{mm},\ t/\tau = 0{,}7;\ B_\delta = 0{,}65\ \text{webers/m}^2;\ \varkappa = 0{,}5.$$

We find that $k_{ad} = 0{,}85;\ \lambda = 0{,}88;\ \sin\varphi = 0{,}595;\ \varepsilon = 1;\ \sin\left(\frac{t}{\tau}\frac{\pi}{2}\right) = 0{,}89.$

Moreover, we will consider that

$$A = 5;\ k_1 = 0{,}845;\ k_2 = 0{,}87;\ \mu_0 = 1{,}256 \cdot 10^{-6}\ \text{h/m}.$$

We find the optimum number of pole pairs from (18): p = 11.2.

We will use p = 12. We find from (9) that

$$\sqrt{\mu_{sle}^{(1m)}}\, H_{mx0} = 175 \sqrt{\frac{\text{h}}{\text{m}}}\ a/\text{m}$$

We get H_{mx0} = 17500 a/m from the curve $\sqrt{\mu}\,H = f(H)$. From formula (10), we determine that l_δ = 0.2 m. Ultimately, the geometrical dimensions of the inductor are determined and a confirming calculation is made.

For comparison, we will compute p_0 according to T. A. Glazenko's method [5]. There is a parameter

$$K = \frac{D^2}{4\delta_\varepsilon} \sqrt{\frac{\gamma\mu_0}{\mu}\,\omega_s} = \frac{165}{\sqrt{\mu}}.$$

Consequently, K depends on the chosen value of the relative permeability. If one assumes that μ = 1000, as in the examples of [5], then K = 5.22 and p_0 = 6.

This average value of μ has no real basis. For example, in our case μ_e = 95.5 at the surface. If μ = 150 is taken as an average value, then K = 13.5, which gives p_0 = 12.

Let us determine the main dimensions D and l_δ by V. S. Sharov's method for p = 12 from the relation presented in [4] on page 18:

$$D^3 l_\delta = \frac{M p \sqrt{\mu\rho} \cdot 10^{18}}{7.1 \cdot B_{1m}^2 \sqrt{f_s}\, k_T},\ \text{cm}^3.$$

Here, [μ] is in h/cm. It follows that we take $\rho = 0.24 \cdot 10^{-4}$ ohm-cm, for our case:

$$B_{1m} \approx \frac{4}{\pi} \sin\left(\frac{t}{\tau}\frac{\pi}{2}\right) B_\delta = 0.737\ \frac{\text{webers}}{\text{m}^2} = 7370\ \text{gauss}$$

$$f_s = \frac{p n_s}{60} = 24\ \text{cps}.$$

$$k_T = 1.2\ ([4],\ \text{page } 77).$$

$$D^3 l_\delta = 7.3 \cdot 10^8 \sqrt{\mu}.$$

In determining μ, V. S. Sharov recommends either that one assumes the value $B_\Delta = (14 - 16)\cdot10^3$ gauss for the average magnetic flux density in the active layer, and finds μ at this B_Δ from the magnetization curve ([4], pages 22, 76, 88), or that one is given B_{z0} as the flux density at the surface of the armature ([4], pages 43, 61).

We will use the first method.

For a B_Δ equal to 14000 gauss, one can find that $\mu = 0.76\cdot10^{-5}$ h/cm from the magnetization curve for ST-20L, and $D^2 l_\delta = 20.1\cdot10^5$ cm^3. When D = 40 cm, $l_\delta = 31$ cm.

If $B_\Delta = 16000$ gauss, then

$$\mu = 0{,}296\cdot10^{-5};\ D^2 l_\delta = 12{,}5\cdot10^5\,\text{cm}^3,\ l_\delta = 19{,}5\ \text{cm}.$$

Thus the results of the methods mentioned depend substantially on the value of μ which is chosen.

LITERATURE CITED

1. Ya. B. Rozman, Series PMS Drive with an Asynchronous Slipping Clutch and Centrifugal Speed Regulator, Guide Material on the Electrification of Metal Turning Lathes [in Russian] (ÉNIMS, 1957).
2. The Use of Induction Clutches in Wire-drawing Machines, Express-Information [in Russian], T. M. 1863, 1864(1956).[Reference from Werkstatt und Betrieb, 2 (1956).]
3. H. J. Rathbun, "Eddy-current brake equipped valve controller, which regulates the brake excitation," Application and Industry, No. 7, (1955).
4. V. S. Sharov, Electromagnetic Slipping Clutches [in Russian] (Gosénergoizdat, 1958).
5. T. A. Glazenko, "Some problems in designing asynchronous clutches with monolithic armatures," Avtomat.i Telemekh. 19, 8 (1958). †
6. A. D. Pozdeev, "Computation of the mechanical characteristics of an electromagnetic slipping clutch with a massive steel armature," News of the Technical School for Electromechanics [in Russian] (1958).
7. A. D. Pozdeev, "Maximum torque and critical speed of an electromagnetic slipping clutch with a massive steel armature," Trudy Kharkovskogo Politekhnicheskogo Instituta im. V. I. Lenina 20, 1st ed. (1959).
8. L. R. Neiman, Surface Effect in Ferromagnetic Bodies [in Russian] (Gosénergoizdat, 1949).
9. W. J. Gibbs, "Theory and design of Eddy-current slipping clutches," Beama Journal (1946).
10. Induction Clutches — Catalog of the Stromag Firm (Federated German Republic).
11. Asynchronous Clutches for Transmitting Torque up to 2 kg-m [in Russian], Technical Report of the ÉNIMS (1952).
12. G. L. Areshyan, A Method of Computing the Edge Effect, from the collection of scientific works of the Erevanskii Polytechnic Institute [in Russian] No. 5, (1954).

---

† See English translation.

CONTACTLESS MAGNETIC TIME RELAYS*

N. M. Tishchenko

Moscow

Translated from Avtomatika i Telemekhanika, Vol. 21, No. 8, pp. 1206-1217,
August, 1960
Original article submitted December 31, 1959

Time relays which use the inertial properties of magnetic amplifiers are examined. It is known that under certain conditions, time relays with ashort-circuited network possess asatisfactorily high stability of operating time. An appoximate design method is presented for this type of relay.

Contactless magnetic time relays are one of the varieties of magnetic amplifiers which operate linearly and generate a given time delay from the moment a signal is received until the relay operates.

The inertial properties of magnetic amplifiers are utilized in contactless magnetic time relays. Ordinarily, in using magnetic amplifiers, one attempts to lower their inertia as much as possible, since it is known that this is one of their greatest deficiencies, but special measures are taken to increase it in contactless magnetic time relays.

It is known that the time characteristics of contactless magnetic relays depend substantially on the feedback coefficient, the amplitudes of the control and bias currents, and the circuit connection of the ac winding. By using these factors, the delay time of ordinary contactless magnetic relays can be sharply increased (see, for example [1-4]). However, the length and especially the stability of the operating time of such devices is not always satisfactory, and this forces one to take special measures to increase the inertia of contactless magnetic relays. The following things are most frequently done to accomplish this:

1) increase the inertia of the controlling network; this is done by connecting additional inductances, capacitances, thermistors, etc. (Fig. 1a, 1b, 1c);

2) variable negative feedback (Fig. 1d, 1e, 1f)

3) short-circuited winding (Fig. 1g).

Without going into detail on relays of the first type, we will note that the connection of additional elements

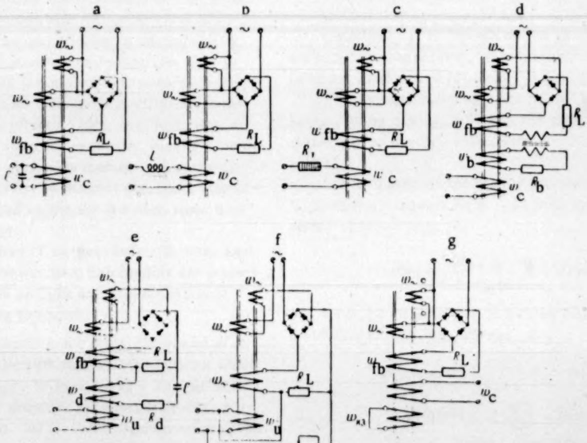

Fig. 1.

---

* The work was reported at the All-union Conference on Magnetic Elements of Automation, Telemechanics, and Computer Technique, November 29, 1957.

in the controlling circuit means an increase in the control power, and also in the size and weight.

Here it is appropriate to mention a circuit suggested by V. N. Tkachev and S. V. Solntsev (Fig. 2a). The relay is activated by breaking contacts K_1 and K_2. When this is done, the operating point moves from A to B (Fig. 2b), and then, as the capacitor charges, the current in the control winding drops to zero, and the relay operates.

The investigations of those authors have shown that the instability of the relay operating time does not exceed 0.7% for a 10% change in the line voltage, and 6.8% for a temperature change from +70 to -50°C. It should be mentioned, however, that the capacitance, C, is 15 μf for an operating time of 3.24 seconds.

Time relays using the transient in a variable negative feedback network have been examined in a number of papers, including those of I. B. Negnevitskii and I. S. Mikadze [6, 8].

We will note that besides such advantages of these relays as relatively large time delay, and the possibility of controlling the operating time over wide limits without significantly increasing the control power, there are also important disadvantages. In the first rank of these, one should mention the necessity of using high value capacitances (hundreds of microfarads for operating times of 5 to 10 seconds) or powerful differentiating transformers, which means a significant increase in size and weight. One should also mention the substantial dependence of the operating time on the line voltage fluctuations and control current fluctuations [6].

I. S. Mikadze suggested that the variable feedback signal be amplified by an additional magnetic amplifier in order to eliminate these disadvantages; this naturally complicates the circuit a great deal.

1. A Contactless Magnetic Time Relay with a Short-Circuited Winding

Contactless magnetic time relays with short-circuited windings are very simple and reliable, and at the same time have small dimensions. However, the maximum time delay, and especially its stability, as a rule, is not high for relays of this type, and this limits their use.

Practice has shown that time relays of this type can be successfully used when stability requirements are comparatively stringent, provided the delay time is relatively small and special measures are taken for stabilization. Thus, for example, the relay developed by N. A. Polyakova [7] ensures a time stability of ± 5% for a line voltage change of ± 10%, when the operating time is controllable from 5 to 10 seconds.

The greatest error of the relay developed in the ITM Electric Model Shop and the VT of the Academy of Sciences, USSR [3], is 7% for an operating time of 3 to 20 seconds, and a supply voltage change between 190 and 240 volts (nominally, 220 volts).

It should be noted, however, that the signal source voltage for this relay was stabilized by a special stabilizer. The greatest operating time instability of the relay was caused by temperature change. Unfortunately, no data on operating-time temperature stability were given in [3,7].

Let us examine the time relay whose circuit is shown in Fig. 3. The saturable reactor for this relay was made from alloy 79NM toroid cores, 42/30 mm in diameter, and 3 mm thick.

Two windings, which were meant to increase the relay inertia, were wound on the saturable reactor, as well as the control, feedback, and bias windings. One of these windings (w_{k32}) was wound with 1 mm diameter wire and was short-circuited, and the other (w_{k31}) was wound with relatively thin wire and was shorted through a wire-wound rheostat, R_4, which permits one to control the operating time of the relay from 0.2 to 0.5 seconds.

The rectifier bridge was assembled from type DGTs-24 germanium diodes. A small-sized type RSM-2 relay was used as an actuating relay. Resistance R_1 in the control circuit, and R_3 in the bias circuit serve for regulation. Resistance R_2 was made from copper wire, and is intended to compensate for temperature. The temperature stabilization of the bias circuit is ensured by the fact that the bias winding is wound with Constantan wire.

The results of the experimental investigation of the operating time stability of dozens of relays is given in the Table.

The static characteristics of the time relay being studied are shown in Figs. 4, 5, and 6; they were taken

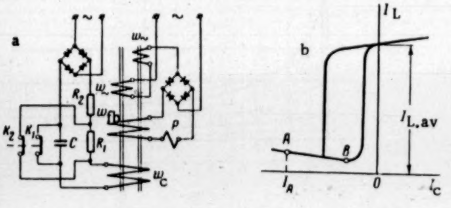

Fig. 2.

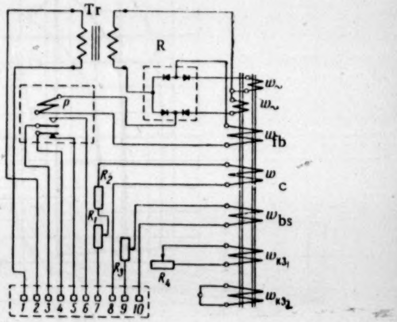

Fig. 3.

TABLE

Test conditions	Greatest relay operating time change, in % of its nominal value	
	t = 0.5	t = 0.3
Change of supply voltage (40 volts, 1000 cps) by ±2 volts	1,9	2,7
Temperature change from +20 to + 70°C	6	6,8
Temperature change from + 20 to − 50°C	6	3,5

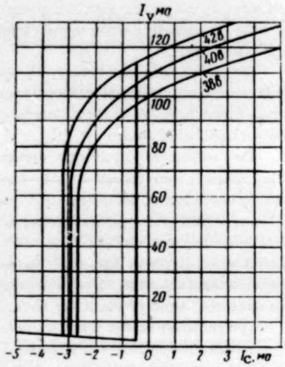

Fig. 4.

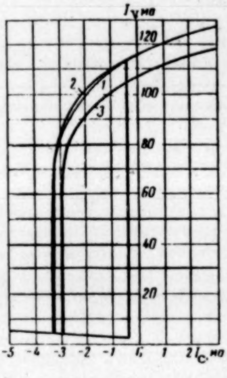

Fig. 5. 1) f = 1000 cps, U = 40 v; 2) f = 1010 cps, U = 40 v; 3) f = =990 cps, U = 39 v.

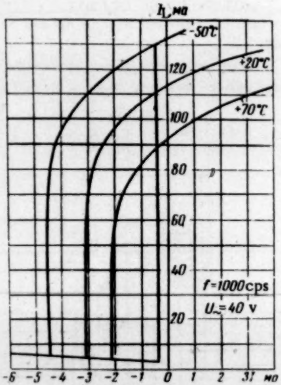

Fig. 6.

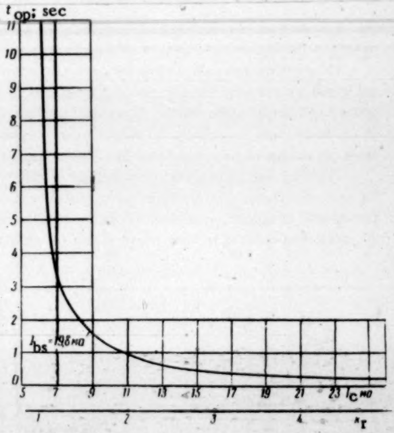

Fig. 7.

at various voltages and frequencies of the source, and also at different temperatures. These characteristics were taken with the bias circuit open.

The dependence of the operating time of the relay on the control current is shown in Fig. 7, as is also the reserve factor $k_r = I_c/I_{op}$; the bias current was held constant. One's attention is drawn to the fact that as I_c, and consequently k_r, grows, the dependence of the operating time on these quantities drops sharply.

The dependence of the operating time on the bias current is given in Fig. 8, and the dependence of operating time on control current is given in Fig. 9 for different resistances connected to the w_{ks1} winding.

The weight of the entire apparatus together with the actuating relay is 420 grams. The dimensions are 55 × 80 × 72 mm.

2. Methods for Raising the Stability of the Relay Operating Time

It is evident that it is essential to ensure the stability of the relay static characteristics, primarily the pull-in current, in order to increase the operating time stability. Since the pull-in current is somewhat more stable than the drop-out current, it is essential that a contactless magnetic relay with normally open contacts be used.

The basic way of stabilizing the static characteristics is to select the operating mode of the magnetic amplifier so that it approaches the ideal amplifier [9, 11]. As is known, the latter is achieved when the following two conditions are met [9, 10, 11].

1) The total resistance of the load circuit, ΣR_L, must be substantially less than the inductive reactance of the ac winding, X_{ch}, in the no-load state. This condition will hold if $X_{ch} = (160-200)\, \Sigma R_L$.

2) The semiconductor rectifiers must be designed so that the reverse currents will be negligibly small, that is, $K_R \approx 1/k_f$. Here K_R is the rectification coefficient, and k_f is the form factor. The latter conditions ordinarily occur when the reverse voltage on the rectifiers is significantly less than the maximum permissible rating.

If the above conditions are met, the necessary stability of the relay operating current without bias is ensured (see Figs. 4-6).

The stability of the operating current often drops when bias is introduced, and one is obliged to take special measures to improve it, for example, stabilization of the bias voltage, temperature compensation of the bias circuit, etc. [1, 2].

Stabilization of the operating current against supply voltage changes can be accomplished with automatic bias, that is, bias supplied by a rectified current from the same source which feeds the ac relay circuit.

As is known [1-3], the operating time stability of a contactless magnetic relay increases substantially as the operating current reserve factor increases (Fig. 7). However, the increase in the reserve factor is limited by the power of the signal source, and by the relay properties.

The choice of the feedback coefficient, K_{fb}, is equally important for the operating time stability of a contactless magnetic relay.

It is known that the relay operating time sharply increases when K_{fb} is nearly unity, but at the same time, the instability both of the contactless relay static characteristic and of its operating (and drop-out) time also increases. The choice of the parameters of the short-circuited winding is very important. Indeed, the

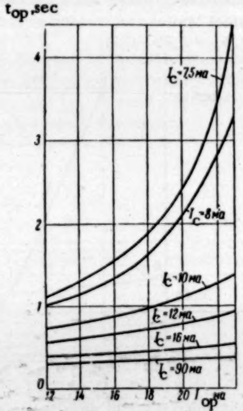

Fig. 8.

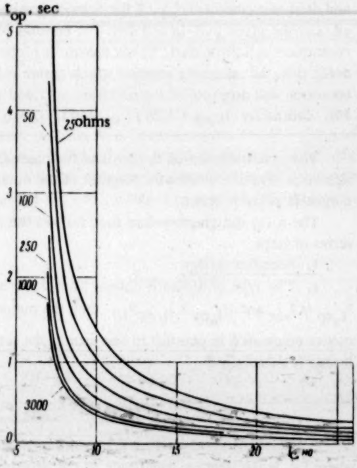

Fig. 9.

temperature instability of the relay operating time is determined to a significant degree by the temperature instability of the resistance of this winding. It is not possible to make this winding from alloys with a low temperature coefficient of resistance because of the high resistivity. Therefore, the winding resistance must be made as low as possible. This can be done by increasing the wire diameter. It is evident that better utilization of the winding window is ensured as the wire diameter is increased, because the copper fill factor, k_{cu}, becomes large.

3. Design of a Time Relay

An approximate method for designing a contactless magnetic time relay with a short-circuited winding is presented below.

The design procedure takes the following basic steps:

a) select the actuating relay (repeater-relay),

b) plot the static characteristic of the contactless magnetic relay

c) design the contactless relay from its static characteristic, taking into account the operating time,

d) design the mechanical construction of the saturable reactor.

Ordinarily, the given quantities in the design of a contactless magnetic relay are: relay operating time, t_{op}, the number of contacts on the actuating relay and their basic characteristics, power source frequency, f, pull-in current, I_{op}, drop-out current, I_{do}, and the ambient temperature change $\theta_1 - \theta_2$.

In choosing an actuating relay, one should be guided toward a relay with the least winding resistance compatible with minimum operating power.

Starting with the operating (pull-in) current, $I_{r,op}$ and drop-out current, $I_{r,od}$ of the actuating relay selected, and the given pull-in and drop-out currents of the contactless relay, its static characteristic is plotted. In doing this, the necessary reserves which ensure reliable operation and drop-out of the relay are provided (Fig. 10). Ordinarily, $I_{L,op} = 1.25\ I_{r,op}$ and $I_{L,do} = 0.75 \times \times I_{r,do}$.

The bias is chosen on the basis of the preceding design steps, and the schematic diagram of the contactless magnetic relay is drawn.

The relay design procedure then follows the next series of steps.

1. Rectifier Design

a. The type of diodes is chosen from the quantities $I_{L,op} \approx I_{sat}$ and $U_{L,op} = I_{L,op} R_L$; then the number of diodes connected in parallel in one arm of the rectifying bridge is determined

$$n = \frac{I_{L,op}}{2I_{DC}}, \qquad (1)$$

where I_{dc} is the average amplitude of the permissible dc of one diode at maximum ambient temperature.

The number of diodes connected in series in one arm of the rectifying bridge is found:

$$m = \frac{1{,}57\, I_{L,op} R_L}{U_{rv}}, \qquad (2)$$

where U_{rv} is the amplitude of the reverse voltage on one rectifying element which is permissible at the maximum ambient temperature.

b. The resistance of a bridge diode is found:

$$R_d = 2m\left(\frac{R_{df}}{n} + \frac{U_{th}}{I_{L,op}}\right), \qquad (3)$$

where R_{df} is the differential diode resistance in the forward direction, and U_{th} is the threshold diode voltage in the forward direction [10, 11].

2. Calculating the Parameters of the Saturable Reactor

a. The inductive reactance of the saturable reactor without excitation is found:

$$X_{ch} = (160 - 200)\,[(1.2 - 1{,}4)\,R_L + R_d]. \qquad (4)$$

b. The necessary power supply voltage is computed:

$$U_c = 1.11\ I_{L,op}\,[(1.2 - 1{,}4)\,R_L + R_d]. \qquad (5)$$

c. The volume of steel in the flux path is calculated:†

$$V_{st} = 2\,\frac{U_c^2\,\mu_d \cdot 10^7}{f B_m^2 k_{st} X_{ch}}, \qquad (6)$$

where μ_d is the differential permeability for the alternating component of the flux [10], B_m is the design value of flux density, gauss; and k_{st} is the packing factor of the steel laminations making up the flux path (ordinarily, $k_{st} = 0.85 - 0.9$).

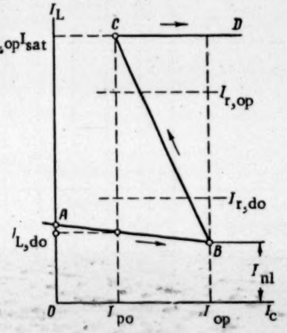

Fig. 10.

---

† The formula is derived in the Appendix.

One of the existing types of flux paths, for which V_{st} is greater than or equal to the value calculated from (6) is chosen.

d. Then the number of turns in the ac windings is computed: ‡

$$W_\sim = \frac{1.125\, B_m X_{ch}\, l_{st}}{\mu_d U_c}. \tag{7}$$

For a series connection of the ac windings, $W_\sim = 2w_\sim$, and for a parallel connection $W_\sim = w_\sim$. Here, $w_\sim$ is the number of turns on one core.

e. The number of turns in the feedback winding is found:

$$w_{fb} = (0.505 - 0.525)\, W_\sim \tag{8}$$

for high-permeability permalloy alloys; and

$$w_{fb} = (0.525 - 0.65)\, W_\sim. \tag{9}$$

for transformer steel flux paths, and also for high permeability alloys having an air gap.

f. The no-load current is computed:

$$I_{nl} = \frac{U_c}{1.11\, X_{ch}}. \tag{10}$$

g. The number of turns in the control winding is found:

$$w_c = \left(w_{fb} - \frac{W_\sim}{2}\right) \frac{I_{L,op} - I_{nl}}{|I_{op} - I_{dc}|} =$$

$$= W_\sim (K_{fb} - 1)\, \frac{I_{L,cp} - I_{nl}}{\Delta}, \tag{11}$$

where Δ is the width of the relay characteristic.

h. The no-load current corresponding to the given values of I_{op} and I_{do} is calculated from the $I_{L,do}$ of the actuating relay which was chosen:

$$I_{nl_2} = I_{L,do} - \frac{|I_{op} - I_{do}|\, w_c}{\frac{W_\sim}{2} + w_{fb}}. \tag{12}$$

If I_{nl} is greater than I_{nl_2}, a new value of X_{ch} is computed:

$$X_{ch} = \frac{U_c}{1.11\, I_{nl_2}}. \tag{13}$$

Then a new value of V_{st} is computed, a new flux path is selected, and the number of turns in the ac, feedback, and control windings are recalculated.

j. The ampere-turns of the bias winding are found [2]:

$$I_{bs} w_{bs} = I_{op} w_c - I_{nl}\, w_{fb} \tag{14}$$

Having been given I_{bs} or w_{bs}, we find the second factor.

k. The diameter of the winding wires is calculated: ac winding

$$d_\sim = 1.13 \sqrt{\frac{I_{L,op}}{j}}\, C, \tag{15}$$

where C = 1 for series connection, and C = ½ for parallel, control winding

$$d_c = 1.13 \sqrt{\frac{I_c}{j}}. \tag{16}$$

The diameters of the wires in the feedback, d_{fb}, and bias, d_{bs}, windings are computed analogously.

l. The area of the winding window, which is occupied by the ac, feedback, control, and bias windings, is found:

$$Q_0 = \frac{w_\sim d_\sim^2 + w_{fb} d_{fb}^2 + w_c d_c^2 + w_{bs} d_{bs}^2}{k_{cu}}, \tag{17}$$

where k_{cu} is the copper-fill factor (ordinarily, $k_{cu} = 0.2 - 0.3$).

3. Designing the Short-Circuited Winding

Starting from the given operating time, the area of the winding window occupied by the short-circuited coil is determined: • •

$$Q_{os} = \frac{t_{op}(K_{fb} - 1)}{\ln \frac{I_c - I_{op}}{I_c - I_{do}}}\, \frac{\rho\, l_{st}\, l_{cu}\, 10^6}{\mu Q_{st}\, k_{st}\, k_{cu}} - Q_{oc}, \tag{18}$$

where ρ is the resistivity of copper (0.0175 ohm·mm² per m); l_{cu} is the average length of the wire in the winding, cm; μ is the differential permeability for the magnetic field of the control signal (a method for determining μ is given in [1]),

$$K_{fb} = \frac{2w_{fb}}{W_\sim}, \tag{19}$$

$$Q_{oc} = \frac{w_c d_c^2}{k_{cu}}. \tag{20}$$

---

‡ The formula is derived in the Appendix.

• • The formula is derived in the Appendix.

Then the total window area occupied by all the windings, including the short-circuited one, is found. When this is done, an additional window area Q_b is provided to pass the reel of the winding machine:

$$Q_{o\Sigma} = Q_o + Q_{os} + Q_b. \qquad (21)$$

If the value of $Q_{o\Sigma}$ which is obtained exceeds the winding window area of the flux path chosen earlier, a flux path with a larger window is chosen, and the saturable reactor must be redesigned.

If the area $Q_{o\Sigma}$ is less than or equal to the winding window area of the chosen flux path, the number of turns in the short-circuited winding is found from the formula,

$$w_s = \frac{k_{cu} Q_{os}}{d_s^2}. \qquad (22)$$

The wire diameter, d_s, is made as large as possible.

4. Constructional Design of the Saturable Reactor

The constructional design problem is one of determining the size of the winding window necessary to contain all the windings and insulating layers, and comparing it with the window of the type of flux path chosen. For toroidal reactors, the external diameter of the saturable reactor and its height are determined in addition to this. A constructional design of a saturable reactor is given in [11].

APPENDIX

1. Derivation of formula (6):

$$X_{ch} = \omega L = 2\pi f \frac{0{,}4\,\pi W_{\sim}^2 Q_{st} k_{st} \mu_d}{2 l_{st} \cdot 10^8}, \qquad (I)$$

$$U_c = 4{,}44\, f W_{\sim} B_m Q_{st} k_{st} \cdot 10^{-8} \qquad (II)$$

Squaring both sides of equation (II), and solving for $W_{\sim}^2$, we get

$$W_{\sim}^2 = \frac{U_c^2 \cdot 10^{16}}{(4{,}44\, f B_m Q_{st} k_{st})^2}. \qquad (III)$$

Substituting (III) into (I), we find

$$X_{ch} = \frac{0{,}4\,\pi^2 f Q_{st} k_{st} \mu_d}{l_{st} \cdot 10^8} \, \frac{U_c^2 \cdot 10^{16}}{(4{,}44\, f B_m Q_{st} k_{st})^2}. \qquad (IV)$$

Taking into account that $V_{st} = Q_s l_{st}$, we find

$$V_{st} = 2\,\frac{U_c^2 \mu_d \cdot 10^7}{f B_m^2 k_{st} X_{ch}}.$$

after simple transformations.

2. Derivation of formula (7). Solving equation (II) for Q_{st}, and substituting it into (I), we get

$$X_{ch} = \frac{0.1\,\pi^2 W_{\sim} \mu_d U_c}{1{,}11\, l_{st} B_m}, \qquad (V)$$

whence

$$W_{\sim} = \frac{1.125\, B_m X_{ch} l_{st}}{\mu_d U_c}.$$

3. Derivation of formula (18).

Ignoring the delay in the ac circuit, one can write

$$\frac{\tau}{1 - K_{fb}} \frac{di_c}{dt} + i_c = \frac{U_c}{R_c}, \qquad (VI)$$

for an idealized amplifier [1], where τ is the time constant of the magnetic amplifier control circuit with the feedback loop open.

Taking the short-circuited winding into account [1]

$$\tau = \tau_c \left(1 + \frac{w_s^2 R_c}{w_c^2 R_s}\right), \qquad (VII)$$

where R_s is the resistance of the short-circuited winding, and R_c is the resistance of the control winding.

As is known,

$$\tau_c = \frac{L_c}{R_c} = \frac{0.4\,\pi w_c^2 Q_{st} k_{st} \mu}{l_{st} \cdot 10^8} : \frac{4 w_c}{10^2} \frac{l_{cu} \rho}{\pi d_c^2}. \qquad (VIII)$$

We get

$$\tau_c = \frac{\pi^2}{10^7} \frac{\mu}{\rho} \frac{Q_{st} k_{st}}{l_{st} l_{cu}} w_c d_c^2. \qquad (IX)$$

$$\frac{w_s^2 R_c}{w_c^2 R_s} = \frac{w_s^2}{w_c^2} \frac{4 w_c l_{cu} \rho}{10^2 \pi d_c^2} \frac{10^2 \pi d_s^2}{4 w_s l_{cu} \rho} \qquad (X)$$

from this,after simple transformations, or

$$\frac{w_s^2 R_c}{w_c^2 R_s} = \frac{w_s d_s^2}{w_c d_c^2} = \frac{Q_{os}}{Q_{oc}}. \qquad (XI)$$

Taking equations (IX-XI) into account, we will rewrite formula (VII) in the form

$$\tau = \frac{\pi^2}{10^7} \frac{\mu}{\rho} \frac{Q_{st} k_{st} k_{cu}}{l_{st} l_{cu}} Q_{oc} \left(1 + \frac{Q_{os}}{Q_{oc}}\right)$$

or

$$\tau = \frac{\mu}{10^6 \rho} \frac{Q_{st} k_{st} k_{cu}}{l_{st} l_{cu}} (Q_{oc} + Q_{os}). \qquad \text{(XII)}$$

Integrating equation (VI), and considering that $i_c = I_{op}$ when $t = t_1$ and $i_c = I_{do}$ when $t = t_2$, we get [1]

$$t_{op} = \frac{\tau}{K_{fb} - 1} \ln \frac{I_c - I_{op}}{I_c - I_{do}} \qquad \text{(XIII)}$$

Substituting the value of τ from equation (XII), we find that

$$t_{op} = \frac{\mu Q_{st} k_{st} k_{cu}}{10^6 \rho l_{st} l_{cu}} \frac{Q_{oc} + Q_{os}}{K_{fb} - 1} \ln \frac{I_c - I_{op}}{I_c - I_{do}},$$

whence

$$Q_{os} = t_{op} \frac{(K_{fb} - 1) \rho l_{st} l_{cu} 10^6}{\mu Q_{st} k_{st} k_{cu} \ln \frac{I_c - I_{op}}{I_c - I_{do}}} - Q_{oc}$$

LITERATURE CITED

1. M. A. Rozenblat, Magnetic Amplifiers [in Russian] (Sovetskoe Radio, 1956).
2. M. A. Rozenblat and S. A. Dokhman, "Contactless magnetic relays," Avtomat.i Telemekh.15, No. 1 (1954).
3. L. I. Gutenmakher,V. V. Bardizh, and M. L. Avrukh, Contactless Automatic Systems [in Russian] (Izd. AN SSSR, 1950).
4. A. S. Tulin, "Experience in factory designing of contactless relays," [in Russian] (Izd. AN SSSR, 1951).
5. V. V. Bardizh, "Some elements of contactless automation," Transactions of the Conference on Contactless Automation [in Russian] (Izd. AN SSSR, 1951).
6. I. S. Mikadze and I. B. Negnevitskii, "Contactless magnetic time relays," Transactions of the Moscow Energetics Institute, 14th ed. [in Russian] (Gosénergoizdat, 1953).
7. N. A. Polyakova, "The protection of electric-arc steel-smelting furnaces from short-circuits and overloads," Thesis submitted for the Degree of Technical Science Candidate [in Russian] MEI, 1954.
8. I. S. Mikadze, "Contactless magnetic time relays," Thesis submitted for the Degree of Technical Science Candidate [in Russian] (MEI, 1952).
9. N. M. Tishchenko, "Characteristics of magnetic amplifiers with feedback," Avtomat.i Telemekh., 17, No. 6 (1956). ††
10. N. M. Tishchenko, "Approximate analytic expressions for the characteristics of reactor magnetic amplifiers without feedback," Avtomat.i Telemekh. 15, No. 2 (1954).
11. N. M. Tishchenko, "Contactless magnetic relays," in Guide to the Design of Elements and Systems of Automation (in Russian), edited by B. N. Petrov, 3rd ed. (Oborongiz, 1959).

---

†† See English translation.

DETERMINATION OF PARAMETERS OF COMBINED LINEAR CONTROL SYSTEMS

V. Ya. Rotach

Moscow

Translated from Avtomatika i Telemekhanika, Vol. 21, No. 8, pp. 1218-1223,
August, 1960
Original article submitted April 25, 1960

This article presents a method for determining the parameters of linear combined control systems and servosystems with respect to the transfer loci of the system to be controlled, the analytical expression of which can be unknown.

The application of the disturbance-compensation principle makes it possible to increase to a considerable extent the accuracy of the operation of automatic control systems, and, in particular cases, even to secure the complete independence (invariance) of the controlled variable with respect to measured disturbances [1]. In contrast to ordinary systems (Fig. 1a), besides deviations of the controlled variable, one or several additional disturbances, suitably transformed in the introducing devices, are fed to the regular input in combined control systems (Fig. 1b). As in the case of ordinary systems, the aim in the design of combined systems is the determination of the regulator and the disturbance introducing device parameters for which the system sacrifices the performance specifications. In this, the practical realization of the obtained transfer functions must be as simple as possible.

The control systems in Fig. 1a and b can be formally transformed into the system shown in Fig. 1c, where the disturbances are reduced to a single control input. It can be readily shown that the controlled variable $\underline{x}$ in this system will change in exactly the same way as in the system in Fig. 1a, if the transfer function of the filter through which the disturbance is transmitted before it is introduced in the system as an additional control input in the following form:

$$W_f(p) = \frac{W_{sd}(p)}{W_{sc}(p)\,W_r(p)}. \tag{1}$$

For the combined system in Fig. 1b, the filter-transfer function is determined by the equation,

$$W_f(p) = \frac{W_{sd}(p)}{W_{sc}(p)\,W_r(p)} - W_i(p). \tag{2}$$

In connection with this, the controlled variable in the systems given in Fig. 1a and b can be represented by the following general expression:

$$x = \Phi(p)\left[x_y + W_{f1}(p)\,x_{i1} + \cdots + W_{fk}(p)\,x_{\text{вк}} + \cdots\right], \tag{3}$$

where

$$\Phi(p) = \frac{W_{sc}(p)\,W_r(p)}{1 + W_{sc}(p)\,W_r(p)}$$

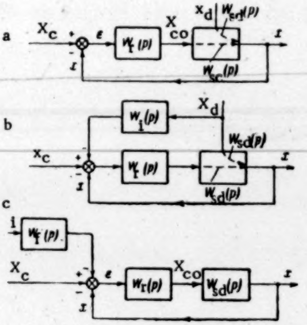

Fig. 1. Structural diagrams of control systems. x_c) Command; x_d) disturbance; x_{co}) control input; x) controlled variable; ϵ) deviation; W_{sc} (p) and W_{sd} (p) are the transfer functions of the system to be controlled with respect to the control and disturbance inputs, respectively; W_r (p) is the regulator transfer function; W_i (p) is the transfer function of the disturbance introducing device; and W_f (p) is the filter-transfer function.

is the servosystem transfer function with respect to the control input, and $W_{fk}(p)$ is the k-th disturbance filter-transfer function.

The more accurately the controlled variable responds to the control input and the lesser its response to disturbances, the better the performance of the control system. From this point of view, the part of the control system in Fig. 1c which is characterized by the transfer function $\Phi(p)$ must transmit the control input x_y with as little distortion as possible.

The output quantities of disturbance filters can be considered as interferences imposed on the useful control signal by the disturbances. Therefore, in adjusting the system, one should find such a filter-transfer function for which the best filtration of disturbances in the range of frequencies which are readily transmitted by the servosystem is secured. This condition is given by the expression,

$$|W_f(i\omega)| = \min, \tag{4}$$

i.e., the system response to disturbances decreases as the deviation from zero of the filter frequency response decreases in the frequency range from $\omega = 0$ to the cutoff frequency $\omega = \omega_{co}$ of the servosystem, which can be found from the frequency response curve $|\Phi(i\omega)|$ (Fig. 2.)

The endeavor to satisfy optimum performance conditions (4) must not result in a reduction of the servosystem stability margin, which can be estimated with respect to the fluctuation characteristic,

$$\frac{|\Phi(i\omega_r)|}{|\Phi(i0)|} \leq M_{ma}. \tag{5}$$

Here, $|\Phi(i0)|$ and $|\Phi(i\omega_r)|$ are the frequency response values for the servosystem at zero and resonance ω_r frequencies (Fig. 2), and M_{ma} is the maximum allowable value of the fluctuation characteristic (usually $M_{ma} = 1.4$-2).

The introduction of additional disturbances in the system shown in Fig. 1b does not affect the system stability, since the number of closed loops in the system does not increase, and the disturbance-introducing devices do not enter the existing loops. This fact makes it possible to vary the filter-transfer function by changing the transfer function of the disturbance-introducing device without causing the system to lose its stability. Consequently, the design of a combined system can be divided into two stages.

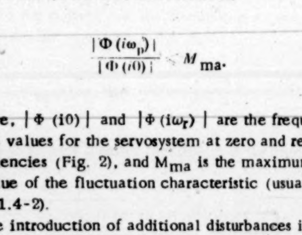

Fig. 2. Frequency response curve of the servosystem.

1. The regulator is adjusted under the assumption that the system operates only in response to the controlled variable deviation. This is necessary because it is impossible to introduce additional effects from all disturbances in the system.

2. The transfer function of the introducing devices is determined with respect to condition (4).

The first-stage calculation is performed in the usual manner [2 and 3]. By taking into account Eq. (2), the optimum performance condition (4) is rewritten in the following manner:

$$\left| \frac{W_{sd}(i\omega)}{W_{sc}(i\omega)\, W_r(i\omega)} - W_i(i\omega) \right| = \min. \tag{6}$$

In the particular case, where it is possible to secure the following form of the introducing-device transfer function

$$W_{ii}(p) = \frac{W_i(p)}{W_{sc}(p)\, W_r(p)}, \tag{7}$$

the controlled variable is not at all affected by the disturbance. It should be noted that in order to satisfy the absolute invariance conditions, the transfer function of the introducing device must coincide with the transfer function (1) of the filter in a system which responds only to controlled variable deviations.

In actual automatic control systems, it is usually difficult to satisfy the absolute invariance conditions, since the technical realization of the introducing-device transfer function, which is necessary for satisfying the above conditions, is either difficult or physically impossible.

In this case, one should select a simple introducing device, the transfer function of which, in a certain sense, would deviate as little as possible from the transfer function of an ideal introducing device. In order to solve this problem, in particular, we can use the simplest approximation method, the interpolation method, according to which it is necessary that the functions to be approximated coincide in several points assigned beforehand. In practice, in order that condition (4) is sufficiently well satisfied, it is usually sufficient that the transfer loci $W_i(i\omega)$ and $W_{ii}(i\omega)$:

$$W_i(i0) = W_{ii}(i0) = \frac{W_{sd}(i0)}{W_{sc}(i0)\, W_r(i0)},$$

$$W_i(i\omega_r) = W_{ii}(i\omega_r) = \frac{W_{sd}(i\omega_r)}{W_{sc}(i\omega_r)\, W_r(i\omega_r)} \tag{8}$$

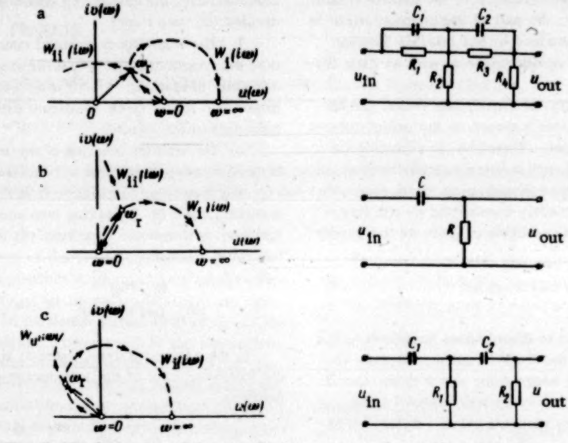
a
$iv(\omega)$
$W_{1i}(i\omega)$
$W_{i}(i\omega)$
ω_r
$u(\omega)$
0
$\omega=0$
$\omega=\infty$
b
$iv(\omega)$
$W_{1i}(i\omega)$
$W_{i}(i\omega)$
ω_r
$u(\omega)$
$\omega=0$
$\omega=\infty$
c
$iv(\omega)$
$W_{u}(i\omega)$
$W_{i}(i\omega)$
ω_r
$u(\omega)$
$\omega=0$
$\omega=\infty$
C_1
C_2
R_1
R_2
R_3
R_4
u_{in}
u_{out}
C
R
u_{in}
u_{out}
C_1
C_2
R_1
R_2
u_{in}
u_{out}

Fig. 3. Configuration of the transfer locus vectors for an ideal introducing device and a circuit of passive electric fourpoles for securing approximate invariance.

$$\text{a} - W_{i}(p) = k_{i}\,\frac{T_2'^2p^2 + T_1'p + 1}{T_2^2p^2 + T_1p + 1},$$

$$\text{b} - W_{i}(p) = k_{i}\,\frac{Tp}{Tp + 1},$$

$$\text{c} - W_{i}(p) = k_{i}\,\frac{T_2^2p^2}{T_2^2p^2 + T_1p + 1}$$

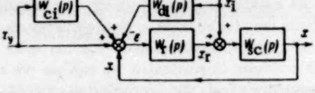
$W_{ci}(p)$
$W_{di}(p)$
x_i
x_y
+
+
$-\varepsilon$
+
+
$W_r(p)$
x_r
$W_{sc}(p)$
x
-x

Fig. 4. Structural diagram of a combined system with an additional control signal input.

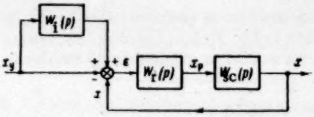
$W_i(p)$
x_y
+
+
ε
-
x
$W_r(p)$
x_p
$W_{sc}(p)$
x

Fig. 5.

coincide for the zero and resonance frequencies of the system.

The above conditions can be realized by means of relatively simple devices. Figure 3 shows several most typical configurations of the W_{ii} $(i\omega)$ locus vectors for $\omega = 0$ and $\omega = \omega_r$. The same Figure also shows examples of passive electric fourpoles for which conditions (8) can be realized for each of these cases.

The tuning conditions for a combined system with additional control input can be found in a similar manner (Fig. 4). The mismatching in this system is determined by the equation

$$\varepsilon = x_y - x = \Phi(p)\left[\frac{1}{W_{sc}(p)\,W_r(p)} - W_i(p)\right] x_y, \quad (9)$$

and, therefore, the optimum performance condition is written in the following manner:

$$\frac{1}{W_{sc}(p)\,W_r(p)} - W_{ii}(p) = \min. \quad (10)$$

The considered method for determining combined system parameters can also be extended to the design of autonomous control systems with several interdependent variables.

Example of Calculation

An automatic control system has two additional inputs: a disturbance and a control input (Fig. 5). The transfer functions of the system, to be controlled with respect to the control and the disturbance inputs, are determined by the equation:

$$W_{sc}(p) = W_{sd}(p) = \frac{1}{p^2 + 3p + 1}.$$

The regulator transfer function is of the form:

$$W_r(p) = k_r\left(1 + \frac{1}{T_{re}p}\right),$$

where k_r and T_{re} are the transfer coefficient and the reset time, respectively.

The calculation of the regulator tuning, performed by means of the method described in [3] for $M_{ma} = 1.62$, yielded the following results:

$$k_{r\,opt} = 11, \quad T_{re\,opt} = 1.5\,\text{min}, \quad \omega_p = 2.8 \ \text{min}^{-1}.$$

1. Determination of the transfer function of the disturbance-introducing device. By substituting in Eq. (7) the expressions for the transfer functions of the system to be controlled and the regulator, we obtain:

$$W_{dii}(p) = 0.091\,\frac{1.5_p}{1.5\,p + 1},$$

i.e., the actual differentiating element makes it possible to satisfy the absolute invariance conditions for the controlled variable with respect to disturbance.

2. Determination of the transfer function of the control input introducing device. In correspondence with Eq. (7), the transfer function of the introducing device,

$$W_{cii}(p) = 0{,}136\,\frac{p^3 + 3p^2 + p}{1{,}5\,p + 1}$$

for which the absolute invariance conditions are satisfied, cannot be physically realized.

The vector

$$\frac{1}{W(i\omega_r)} = 0{,}935e^{i142{,}6^\circ}$$

is in the second quadrant of the complex plane, and, therefore, for approximate invariance, an introducing device of the type shown in Fig. 3c must be chosen. If $C_1/C_2 = 2$ in this system, the maximum ratio of time constants T_2/T_1 will be equal to 0.41. In this case, the numerical values of the transfer coefficient k_i and of the time constants T_2 and T_1 are determined from the equations

$$\operatorname{tg}\varphi_i(\omega_r) = \frac{T_1\omega_r}{1 - T_1^2\omega_r^2},$$

$$A_n(\omega)_r = \frac{T_2^2\omega_r^2}{\sqrt{(1 - T_2^2\omega_r^2)^2 + T_1^2\omega_r^2}},$$

which yields

$$k_i = 12.9; \quad T_1 = 0.252; \quad T_2 = 0.104.$$

Figure 6 shows the variation of the controlled variable in a combined system for the adjustment found and a unit-step input. For the sake of comparison, this Figure also shows the variation of the controlled variable under

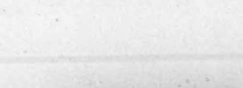

Fig. 6

the same conditions, where, however, no additional control signal input is provided (dotted line).

LITERATURE CITED

1. V. S. Kulebakin, "Basic problems in improving the performance of automatic control systems and methods for their solution," Transactions of the Second All-Union Conference on Automatic Control Theory [in Russian] (Izd. AN SSSR, 1955) Vol. 11.
2. E. G. Dudnikov, Elements of the Automatic Control of Thermal Processes [in Russian] (Gosénergoizdat, 1956).
3. V. Ya. Rotach, "Calculation of the adjustment of industrial automatic regulators with respect to the control system dynamic characteristics," Tr. Moskovskogo Énergeticheskogo Instituta (1957) Vol. 29.

HYDRAULIC SERVOMOTOR MOTION IN AUTOMATIC CONTROL SYSTEMS WITH A JET AMPLIFIER

V. I. Gol'traf

Leningrad

Translated from Avtomatika i Telemekhanika, Vol. 21, No. 8, pp. 1224-1227, August, 1960
Original article submitted March 7, 1960

The equation for the hydraulic servomotor in automatic control systems with a jet amplifier is derived. Experimental data derived in verifying the obtained result are provided.

A hydraulic servomotor, which is controlled by a jet amplifier, is used as the final mechanism in many automatic control systems. Various designs of amplifiers with a flapper or a jet pipe as mobile elements are used.

In certain systems, a reset device is provided in one of the piping branches connecting the servomotor to the amplifier. As the working liquid moves through the throttle of the reset device, a pressure drop arises across its membrane causing the membrane to displace. Thus, a considerable number of control systems are designed according to the scheme shown in Fig. 1.

We shall determine the equations of motion of the servomotor in such automatic control systems.

Every jet amplifier design is characterized by a well-defined static dependence of the mobile element position on the pressure drop in the receiving nozzles. This dependence is such that a deflection ΔS of the flapper or the jet tube from the equilibrium position that does not exceed a certain given value ΔS_0 causes an almost proportional increase in the pressure drop ΔP between the receiving nozzles of the jet amplifier.

Consider the system shown in Fig. 2. We shall neglect the effect of external loads on the servomotor motion, the friction in the servomotor, its unbalanced state, the inertia of the servomotor mobile parts, and water leaks in the servomotor, as is often done in deriving the equations for a servomotor which is controlled by a cut-off valve. Assuming that the water flow in the piping connecting the amplifier to the servomotor is turbulent, we obtain the following expression for the pressure drops, which are measured by pressure gauges,

$$\Delta P_{\text{м}} = \left(\zeta_s + \frac{\lambda l}{d}\right)\frac{\gamma v^2}{2g} + \Delta P_i, \qquad (1)$$

where ζ_s is the resistance coefficient of the servomotor throttle, λ is the linear resistance coefficient, l is the piping length, d is the inside diameter of the piping, γ is the working liquid specific weight, g is the acceleration due to gravity, v is the water flow velocity in the piping, and ΔP_i is the pressure drop across the reset-device membrane.

From the equation of continuity, it follows that the water flow through any piping section is equal to the volume traversed by the piston in unit time.

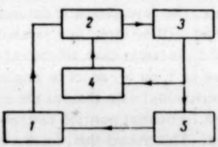

Fig. 1. (1) System to be controlled; (2) measuring component; (3) amplifier; (4) reset device; (5) servomotor.

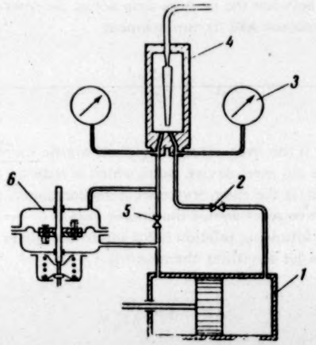

Fig. 2. (1) Servomotor; (2) servomotor throttle; (3) pressure gauge; (4) amplifier; (5) reset-device throttle; (6) reset device.

Consequently,

$$v = \frac{m_s' F_s}{f}, \qquad (2)$$

where m_s' is the servomotor piston velocity, F_s is the active surface area of the servomotor piston, and f is the inside cross-sectional area of the piping.

From (1) and (2), it follows:

$$\Delta P_M = \frac{\gamma}{2g}\left(\zeta_s + \frac{\lambda l}{d}\right)\left(\frac{F_s}{f}\right)^2 (m_s')^2 + \Delta P_i. \qquad (3)$$

For the servomotor motion, $\Delta P_M < \Delta P$ always holds.

In this case, it can be considered that the $\Delta P - \Delta P_M$ difference is equal to the pressure loss in the amplifier receiving nozzles, which is a quadratic function of the servomotor velocity, i.e.,

$$\Delta P - \Delta P_M = \zeta_p \frac{\gamma (m_s')^2}{2g}, \qquad (4)$$

where ζ_s is the resistance coefficient of the amplifier receiving nozzles.

This condition will always be satisfied if we assume that the ζ_p coefficient is not constant, but depends on a given manner on the parameters that define the state of the system in Fig. 2. Such parameters are obviously the position ΔS of the jet pipe, the static pressure drop ΔP, and the liquid flow resistances which are determined by the servosystem design. If we neglect the inertia of mobile parts in the reset device, the friction in it, and the initial tension in its spring, the effect of which is felt only for very small deviations of the mobile element from its neutral position, we can establish a well-defined relation between the pressure drop across the reset-device membrane and its displacement:

$$\Delta P_i = \frac{c_i \Delta m_i}{F_i}, \qquad (5)$$

where c_i is the over-all rigidity of all elastic elements acting on the reset-device stem, which is reduced to the stem, Δm_i is the reset-device-stem displacement, and F_i is the active reset-device membrane area.

The following relation holds within the linear interval of the jet amplifier characteristic:

$$\Delta P = \Delta P_0 \frac{\Delta S}{\Delta S_0}, \qquad (6)$$

where ΔP_0 is the static pressure drop between the receiving nozzles, which corresponds to the mobile element deflection ΔS_0.

By taking into account (3), (5), and (6), equation (4) can be rewritten thus:

$$\frac{\Delta P_0}{\Delta S_0}\Delta S - \frac{c_i \Delta m_i}{F_i} = \frac{(m_s')^2 F_s^2 \gamma}{2g}\left(\frac{\zeta_p}{F_s^2} + \frac{\zeta_s}{f^2} + \frac{\lambda l}{d f^2}\right). \qquad (7)$$

By introducing relative coordinates,

$$\sigma = \frac{\Delta S}{\Delta S_0}, \qquad \mu = \frac{\Delta m_s}{m_s}, \qquad \xi = \frac{\Delta m_i}{m_i},$$

where Δm_s is the servomotor displacement, m_s is the maximum servomotor stroke, and m_i is the maximum stroke of the reset device stem, we obtain:

$$\Delta P_0 \sigma - \frac{c_i m_i}{F_i}\xi = \frac{F_s^2 \gamma m_s^2}{2g}\left(\frac{\zeta_p}{F_s^2} + \frac{\zeta_s}{f^2} + \frac{\lambda l}{d f^2}\right)\mu'^2. \qquad (8)$$

Finally, by using (8), the servomotor equation in the considered case can be written in the following form:

$$\mu' = \operatorname{sign}(\sigma - \rho\xi)\,\frac{\sqrt{|\sigma - \rho\xi|}}{T_s}, \qquad (9)$$

where

$$\rho = \frac{c_i m_i}{F_i \Delta P_0}, \qquad T_s = F_s m_s \sqrt{\frac{\gamma}{2g\Delta P_0}\left(\frac{\zeta_p}{F_s^2} + \frac{\zeta_s}{f^2} + \frac{\lambda l}{d f^2}\right)}.$$

When σ changes from 0 to 1, T_s does not remain constant. This is explained by the fact that the expression determining T_s contains the ζ_p coefficient, which, as was established experimentally, basically depends on σ. As the jet amplifier mobile element moves from the neutral to the extreme position, the change in T_s is determined by the ratio of ζ_p to the over-all resistance coefficient over the path traveled by the working liquid. If the ζ_p coefficient constitutes only an insignificant part of the over-all resistance coefficient ζ, it can be considered that $T_s = \text{const}$ throughout the entire range of the relative coordinate σ variation.

In this case, the dependence of the servomotor velocity μ' on $\sigma - \rho\xi$ will be close to a parabolic dependence. If the value of ζ_p is larger than all the other resistances, the dependence of T_s on σ cannot be neglected. It follows from experimental data that, as the mobile element deflection from its neutral position increases, the value of ζ_p decreases. This means that, for $\sigma = 0$, the value of T_s will be at the maximum. Due to this, the deviation from linearity of the $\mu' = f(\sigma - \rho\xi)$ characteristic will be less pronounced.

This deduction can be confirmed experimentally. Figures 3 and 4 show the results obtained in experimental verification of a system which differs from that in Fig. 2 by the fact that it does not contain the reset device 6 with throttle 5 (i.e., the equation $\rho\xi = 0$ holds).

During the tests, the jet-tube deflections did not exceed the ΔS_0 value. In the case shown in Fig. 3, there was practically no resistance in the servomotor throttle. Due to this, the time for the servomotor displacement through the distance m_s was 19 sec for the maximum jet-pipe deflection. It follows from the above graph that the servomotor motion can be sufficiently accurately described by the equation

$$\mu' = \frac{\sigma}{T_s}, \qquad (10)$$

where $T_s = \text{const}$.

In the second case (Fig. 4), there was a considerable resistance to the liquid flow from the amplifier to the servomotor, due to which the minimum time for the servomotor displacement through distance m_s was 160 sec. In the given case, the servomotor motion can be sufficiently accurately described by the equation

$$\mu' = \operatorname{sign} \sigma \, \frac{\sqrt{|\sigma|}}{T_s}, \qquad (11)$$

where $T_s = \text{const}$.

Thus, in investigating the dynamics of an automatic control system with a hydraulic servomotor which is driven by a jet amplifier, the servomotor equation should be written in the form given by (9).

The T_s coefficient in this equation generally depends on the relative coordinate σ, the pressure drop ΔP_0 between the nozzles, which corresponds to the mobile element displacement ΔS_0, and the flow resistance of the working liquid. This dependence must be determined experimentally for every individual jet amplifier type.

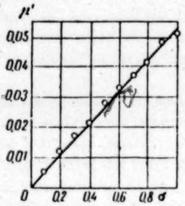

Fig. 3.

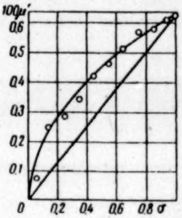

Fig. 4.

BLANK
PAGE

RESULTS OF THE FIRST CONGRESS OF THE INTERNATIONAL FEDERATION OF AUTOMATIC CONTROL (IFAC)

Translated from Avtomatika i Telemekhanika, Vol. 21, No. 9, pp. 1229-1239,
September, 1960

The sessions of the IFAC First Congress, which was prepared and organized by the National Committee of the Soviet Union for Automatic Control, were held from June 27 to July 2 on the premises of the Lomonosov Moscow State University. The Congress was a very important event in the history of automatic-control development. Its import can be judged by the following figures. The number of participants at the Congress included 1190 delegates from 29 countries, and almost as many guests. During the sessions of the 21 Congress sections, 270 reports were heard and discussed; over 400 statements were pronounced in the discussions of these reports.

The Congress was opened by the address of the IFAC president, Prof. A. M. Letov, on June 27 at the first plenum. The IFAC past-president, G. Chestnut, welcomed the Congress delegates in his speech at this session. The first Vice-President of the Council of Ministers of the USSR, Comrade A. N. Kosygin addressed the Congress delegates in the name of the Soviet Government. The Congress delegates were greeted by the President of the Academy of Sciences USSR, Academician A. N. Nesmeyanov, Prof. E. Gerecke (Switzerland), Prof. R. Oldenburger (USA), and Comrade Wu Juyen (Chinese People's Republic).

In his closing address at the first plenum, the president of the National Committee of the Soviet Union for Automatic Control, Academician V. A. Trapeznikov, read the report "Automation and Mankind."

The subsequent work of the Congress took place during the sessions of different sections. The problems in automatic-control theory were considered in nine sections; five sections were devoted to problems in providing the technological basis of automation; the work in six sections concerned the problems in applying automation theory and technology in automating industrial processes; one section was devoted to general problems pertaining to automatic control as a scientificotechnical branch of science.

The closing plenum was held on June 2. During this session, the following persons surveyed the scientificotechnical problems discussed at the Congress: the president of the IFAC Scientificotechnical Committee on Theory, Academician B. N. Petrov (USSR), the president of the IFAC Scientificotechnical Committee on Automation Technology, Prof. G. Boromiss (Hungary), and the president of the IFAC Scientificotechnical Committee on Practical Application, Prof. D. Mosley (USA). The president of the IFAC Consulting Committee, Prof. D, Eckman (USA), made an announcement concerning the activities of this committee. The president of the IFAC Scientificotechnical Committee on Terminology, Prof. E. Gerecke (Switzerland), dwelled on the problems in the work of this committee. The Congress was closed by the final address of the IFAC president, Prof. A. M. Letov.

SURVEY OF THE SCIENTIFICOTECHNICAL PROBLEMS CONSIDERED AT THE CONGRESS*

Automatic-Control Theory

The theory of automatic control was treated in 139 reports. The reports themselves as well as the ensuing discussions were a vivid demonstration of the high level attained in the development of the theory of automatic control, which is based on a widespread use of rigorous mathematical methods and is concerned with the solution of basic problems in the analysis and synthesis of modern automation systems.

Theoretical problems were discussed in the work of nine sections.

Twenty-three reports were discussed in the Section dealing with the Theory of Continuous Linear Systems. Reports devoted to problems in the invariance theory and the theory of multiple feedback and autonomous control systems created the greatest interest and the liveliest discussions. The discussion of these problems showed that, at the present time, the theory provides the basic principles for the design of automation sys-

* This survey was compiled from the above-mentioned reviewing reports by the three presidents of the IFAC Scientificotechnical Committees: Academician B. N. Petrov (USSR, Committee on Theory), Prof. G. Boromiss (Hungary, Committee on Technology), and Prof. D. Mosley (USA, Committee on Practical Application). This survey does not review the work of the Section for General Problems in Automatic Control (terminology, training of specialists, etc.).

tems which respond little to undesirable disturbances and accurately follow the control inputs.

In the work of this Section, much attention was paid to the analysis of multiple feedback control systems and general methods for their synthesis, methods for improving the dynamic properties of control systems with one and several controlled parameters, and also problems in the theory of systems with lag elements.

A number of reports were devoted to improved and generalized methods for determining the stability and the performance of automatic-control systems.

Fourteen reports were discussed in the work of the Section dealing with the Theory of Continuous Nonlinear Systems. Exact as well as approximate methods for the investigation of such systems were surveyed.

A number of reports were concerned with the development of the describing-function method. It was shown that this method, which gained widespread use in engineering practice, can be extended, in matrix representation, to the case of multiperiod oscillations, subharmonic and superharmonic resonance phenomena, oscillation synchronization, and parametric amplification. An approach to the solution of some problems in the synthesis of nonlinear systems subject to random disturbances, based on a combination of the describing-function and the statistical-linearization methods, was indicated.

It was also shown that, by using different variants of the describing-function method, it is possible to study the effect of the limited power of feed sources in control systems and to find conditions for suppressing self-oscillations by external periodic inputs, and to determine the conditions for suppressing self-oscillations in systems with backlash. One of the reports presented a variant of the describing-function method where Nichols loci are used.

Two points of view were expressed in the discussion on the application of the describing-function method. One of them states that, regardless of the extreme effectiveness of the describing-function method, it should be used with a certain caution, since the fact that no self-oscillations are detected by means of this method does not confirm the absence of any complex periodic motions in a system. According to the other point of view, the simple and efficient describing-function method yields accurate results in practically all problems encountered in practice, and can be developed so that it yields subharmonic solutions.

Besides the above problems, the following problems were considered in this Section: effect of programmed variation of the regulator gain on the control performance, problems in calculating the static characteristics of complex nonlinear systems, and a new method for calculating the integral quadratic criterion of nonlinear systems.

In the Section dealing with the Theory of Discrete Systems, twenty-five reports were discussed; problems in the theory of relay (off-on), sampled-data, and digital automation systems were considered. Along with problems in the analysis and synthesis of discrete systems intended for the solution of ordinary control problems, much attention was paid to problems in designing optimum and self-adjusting discrete systems.

The reports devoted to the theory of relay systems presented exact and approximate methods for the analysis of subharmonic oscillations, as well as methods for the design of relay systems with optimum quickness of response which are subject to random disturbances.

Reports relating to the theory of sampled-data systems were the most numerous in this Section. A survey of mathematical methods for the investigation of such systems was presented; among the problems discussed were those encountered in the design of multimode and multiple feedback sampled-data systems, problems in the design of sampled-data systems with variable parameters, methods for statistical calculation of sampled-data systems, and methods for investigating nonlinear sampled-data systems. The problems in the design of optimum and self-adjusting sampled-data systems whose structure comprises feedback with respect to the performance criterion were also considered. A number of reports were devoted to the theory of relay sampled-data (digital) systems. The simplest systems of this type were analyzed by using the phase-plane method and by introducing lags with random variation. The recently developed branches of the theory of digital automatic systems, including the determination of the effect of quantization with respect to a certain level, methods for determining periodic modes, the synthesis of systems with lag compensation, and the synthesis of optimum systems, were presented. The liveliest discussion developed with regard to problems in the application of digital computers in sampled-data control systems and the application of the phase-space and operator methods in investigating sampled-data systems. The necessity for developing methods for the analysis and synthesis of nonlinear sampled-data systems and sampled-data systems subject to random disturbances was emphasized in the discussion.

Eighteen reports were discussed in the work of the Section dealing with Stochastic Problems. One of the main problems in this field is that of the statistical analysis and synthesis of nonlinear systems. Three different trends in work on this group of statistical automation problems became apparent through the reports and the ensuing discussions. The first trend pertains to the category of problems which include the development and generalization of the statistical-linearization method and its application, as well as the formulation of an exact theory for a given class of nonlinear systems, which would be based on the theory of Markov's random processes, and the development of methods for the synthesis of systems which can be reduced to linear systems. During the discussions great interest on the part of scientists from different countries was shown in the statistical-linearization method, which is conceptually close to the harmonic linearization method and the deterministic theory of nonlinear systems. In addition to what was said in the course of the discussions regarding the application of the Markov theory of random processes in the analysis of automatic systems, Soviet scientists reported a number of interesting results which were not known outside of our country before. In the discussion concerning problems in the statistical theory of nonlinear systems capable of reduction to linear systems, a number of interesting results, promising successful application in the design of self-adjusting and self-optimizing systems, were announced.

The second trend pertains to problems in the theory of statistical synthesis of linear systems. The discussion revealed the appearance in this field of two new competitive approaches in the USA which have been well developed in the papers of American as well as Soviet scientists. These two approaches are the application of the dynamic programming method for the determination of the optimum program for the controlling section of a system and the development of methods for the direct determination of differential or difference equations of optimum systems.

The third trend pertains to problems in finding the algorithms of optimum systems. It was demonstrated in the discussion that the majority of problems in detecting and processing information in the presence of noise and random disturbances can be considered from a unique point of view and solved by a unique theoretical method.

In addition to the reports and the discussion concerning the above three basic trends, the work in this Section also included the discussion of problems in experimental determination of characteristics of control systems and systems to be controlled, as well as of statistical characteristics of random processes, problems in statistical calculation of linear systems, problems in determining errors in the conversion of continuous information into discrete information, as well as problems in applying the information-theory methods to the determination of the transmission capacity of automatic systems and their components.

Twelve reports were discussed in the Section dealing with the Theory of Optimum Systems; general methods for investigating optimization problems, as well as the results obtained in solving individual problems, were considered. The general methods for the investigation of optimum systems are mainly connected with the development of methods for the solution of nonclassical variation problems. The report dealing with these problems was devoted to the maximum principle and the theory of optimum automatic-control systems and aroused great interest and a lively discussion. The participants in the discussion remarked that this principle provides a powerful tool for the investigation of nonlinear optimization systems, while the restrictions imposed on the control functions are of a general nature; at present, it is one of the most general principles, thus making it possible to solve a large number of problems by means of it.

Much attention was paid to problems met in the synthesis of optimum systems. The inverse time methods and methods for construction of isosurfaces in the system phase space, both of which are based on the application of the maximum principle, were discussed. Practical examples of system synthesis performed by the above-mentioned methods were given.

The connection between the maximum principle and the dynamic programming method was analyzed during the discussion. It was noted that the dynamic programming method, when applied to optimum control problems, yields functional equations which are closely related to the maximum principle equations. However, it was indicated that the application of the dynamic programming method involves considerable calculation difficulties.

Great interest was exhibited in the formulation and solution of some problems in optimum control of systems with distributed parameters (which are described by partial differential equations), as well as of general and particular problems in the theory of optimum linear-control systems.

Twenty reports were presented to the Section dealing with the Theory of Self-Adjusting Systems. The items discussed in this Section were biological and mechanical systems capable of adaptation to changing conditions, with the aim of securing such an interaction between the system to be controlled and the surrounding medium, for which, in a given sense, the optimum state of the system to be controlled is secured. Systems where adaptation is secured by automatic scanning as well as by changing the system state with respect to an open-loop or closed-loop cycle (without automatic scanning) were considered.

Problems in the following branches of the theory of automatic control were considered: the statistical theory of automatic optimization systems, dynamics of self-adjusting systems, bioelectric control, the study of characteristics of physiological control systems, and the theory of self-adjusting autopilots.

Interesting reports were presented on the theory and application of computers for the approximate determination of characteristics of systems subject to automatic and self-adjusting control.

The reports concerning problems in biological cybernetics brought about an especially lively discussion, which showed that Soviet, Yugoslav, and American scientists contributed much to the development of principles for the design of systems in many ways similar to living organisms. Six reports were devoted to the results obtained in studying biological self-adapting systems. The results obtained by a group of scientists in studying problems of bioelectric control attracted deserved attention; these results make it possible to use biocurrents in a living organism for the control of artificial organs supplanting the lost ones.

At present, the methods and procedures used in automatic-control theory are applied in the investigation of biological systems to an ever-increasing extent. This trend in cybernetics, which is beginning to yield interesting results, was reflected in the reports and in the ensuing discussions. It should be noted that the discussion in the work of this Section was perhaps the liveliest, indicating the especially great interest of the scientific world in this important and promising direction of the automatic-control theory.

It was indicated in a number of reports and in the following discussions that it was necessary to investigate and develop self-adjusting systems capable of operating under conditions of rapid drift of characteristics and parameters of the systems to be controlled. These problems are closely connected with problems in the stability of the self-adjustment process, and, therefore, the importance of exact mathematical formulation of stability conditions in self-adjusting systems was repeatedly emphasized in the discussions.

Seven reports were discussed in the Section dealing with the Theory of Structures and Signal Flow Diagrams. A number of important problems in the theory of relay devices and the theory of signal flow diagrams were discussed; these problems included: development of methods for the synthesis of relay devices and problems in the design of relay structures with assigned reliability; problems in the application of a new logic language for the description of discrete time sequences; problems in the mechanization of the analysis and synthesis of relay devices; problems in noise stability and the efficiency of information transfer in remote measurement systems. However, due to the fact that no reports from a number of eminent scientists from abroad working in this field, scientists from the USA in particular, were submitted to the Section, many other important problems in the modern theory of structures and the theory of signal flow diagrams were not discussed. This gap was partially filled by scientists from the Soviet Union and abroad, who took part in the discussion.

Considering that the structural theory of relay devices is one of the important branches of the modern automatic-control theory, it was planned to hold in the nearest future a special symposium on the theory of relay devices and related scientific fields.

The discussion in the Section dealing with Special Mathematical Problems comprised thirteen reports pertaining to three special mathematical problems in automatic-control theory.

The first problem pertains to the determination and investigation of steady-state conditions in automatic control systems which are described by differential equations with continuous right-hand sides.

A number of important aspects of this problem were treated in the reports: a more rigorous and exact mathematical definition of the steady-state conditions concept was given; the results obtained in investigating the dependence of the periodic solutions of a system of differential equations on its parameters were described.

The second problem pertains to the investigation of nonlinear systems with discontinuous characteristics. With regard to these systems, problems in determining steady-state conditions were discussed.

The third problem pertains to the stability of automatic-control systems. The main problems treated in the reports,and in the lively discussion they gave rise to,pertain to the further development of methods of determining stability by using the second Lyapunov method.

Eleven reports were discussed in the Section dealing with Simulation and Experimental Investigation Methods. The application of simulation methods,where not only analog, but also digital and analog-digital (combined) devices are used for the investigation and design of complex control systems,is a separate and important problem.

The solution of this group of problems will help in mechanizing certain human mental processes and considerably increase their efficiency. By using simulation methods, the experimental techniques are rendered more accurate and prerequisites for a more efficient use of equipment for the testing of actual systems are secured. The development of equipment and methods for digital simulation was widely reflected in the reports and the ensuing discussion; with regard to programmed-control systems, new methods for the reproduction of second-order curves by means of digital computers were proposed. The application of combined digital-analog computers (in particular, for the reproduction of nuclear reactor kinetics) was also considered.

It was noted that, besides improving the accuracy, the application of digital-simulation methods considerably increases the maximum allowable range in which the variables change.

A method which was proposed for the solution of partial differential equations by means of electronic models aroused great interest; this method is based on the connection between the equations to be solved and the processes which appear in practical circuits subject to random disturbances.

One of the reports mentioned the development of an original simulating device which operates with high-frequency alternating current and which consists of passive circuits combined with follow-up multiplier systems; this device has a relatively high accuracy and is reversible, which considerably enlarges its scope.

It was noted in the discussion that the new ideas in the application of electronic models for the optimization of the performance of systems used for the automatic control of industrial processes offer great opportunities for the design of optimum systems, as well as for obtaining more accurate information on the systems to be controlled.

Automation and Remote-Control Technology

Fifty-five of the reports submitted to the Congress were devoted to problems in construction, investigation, and design of automation and remote-control equipment. These reports were discussed at the sessions of five Sections.

Nine reports were discussed in the Section dealing with Electric and Magnetic Components of Control Systems. Problems in the theory of magnetic amplifiers (three reports) were most thoroughly treated. A detailed theoretical analysis of the effect of dynamic properties of magnetic cores in the presence of eddy currents and magnetic viscosity on the characteristics of the basic magnetic amplifier types was presented for the first time in one of these reports. These results make it possible to determine the theoretical characteristics of different amplifier types and to find ways for their improvement.

Moreover, among the problems considered in the work of this Section were problems in the design of logic elements and their use in control circuits; problems pertaining to measurement methods; and problems in the design and investigation of some special electric automation devices (photoresistors and quick-action step motors).

In the report devoted to logic components, attention was drawn to the fact that a system of logic elements can be without a special memory component, since, in the design of circuits requiring the application of such a component, one can use standard logic components and circuit feedbacks.

Ten reports were discussed in the Section dealing with Electrical Computers and Simulating Devices and Programming Machines and Components. According to their character, the problems considered in these reports can be divided into three groups.

The first group was dealt with in reports devoted to problems in the design of new computers. The following items were considered in these reports: the design of a new computer for algebraic functions of a complex variable; the design of a synthesizer in the shape of a nonuniform electronic lag line; the design of a discretely acting computer of the electric-grid type intended for the solution of unsteady-state field equations. Also among the items discussed was a system for the control of industrial processes containing a correcting computer having a remote measurement selector for centralized control. (A ternary code is used in the selector of this computer.) Finally, this group included a report on the application of automatic optimizers for automatic synthesis and the solution of variation problems.

The reports of the second group related to computers for the automation of industrial processes. The SKZhAT electronic digital computer, designed for the control of such processes as chemical synthesis, distillation, and blast-furnace processes, belongs to this class of computers.

The reports of the third group treated problems in the improvement of computer components. There was a communication on the automatic zero stabilization in operating amplifiers, for which a number of circuits for reducing the zero drift were proposed and a comparative evaluation of different circuits was given. The problem of the design of nonlinear computer units, based on semiconductor resistors made of silicon carbide, was discussed. A report devoted to the logical synthesis of functional generators was read.

The reports and the ensuing discussion showed the great importance of computer techniques in the solution of modern problems in automatic control.

Eight reports were discussed in the Section dealing with Data Transmitters, Components, and Automation and Remote-Control Systems for Industrial Processes. The main trends in the development of remote control and measurement techniques were discussed in the reports presented to this Section. In the field of remote measurement, the main development trend consists in the application of contactless digital and code-pulse systems; in the field of remote control of a large number of distributed systems, this trend can also be reduced to the application of contactless equipment. In the work of this Section, much attention was paid to problems in the operational accuracy and reliability of remote measurement and control systems. Among the items discussed were performance criteria for remote control systems based on different characteristics, such as the specific signal content index, the information transfer quality index, the information channel utilization factor, and the technical efficiency.

Ten reports were discussed in the Section dealing with Pneumatic Devices in Automation and Computer Techniques. Problems in the design of the following pneumatic and hydraulic automation components were considered: pneumatic throttles of the nozzle-flapper type which control devices having jet pipes, servovalves with discharge feedback, and long lines which connect the control valve to the drive. Moreover, there was a report on the general principles of the theory and design of pneumatic automation elements. This generalized report aroused great interest and a lively discussion.

Among the reports presented to this Section, the most interesting were those devoted to the development of pneumatic equipment designed for mathematical and logic operations. It was shown that pneumatic devices can be used successfully for the realization of analogous simulating devices and that the most diverse relay circuits for algebraic and time logic functions can be constructed.

A report containing an analysis of the dynamics of the copying machine hydraulic drive and a report devoted to the investigation of automatic-control systems for complex hydrodynamic machines aroused great interest. A report considering problems of the dynamic suspension of machine parts in a viscous liquid brought about a lively discussion.

Eighteen reports, divisible into three groups, were discussed in the Section dealing with Automatic-Control Equipment and Devices.

Sensing elements were considered in the reports of the first group. The results obtained in the development of a thermomagnetic compensation gas analyzer to be used for the accurate measurement of high oxygen concentrations were discussed. The application of radioactive isotopes in automatic-control systems for mining extraction and sinking machines was demonstrated.

The reports of the sec[illegible]e devoted to improved measurem[illegible]

Methods for the automation of sampling and chemical analysis and for the automation of measurements in plotting the dynamic characteristics of nuclear reactors were considered. A report presenting a method for determination of the hunting angle of the earth's satellites by means of a gyroscope and by means of devices using nuclear radiation was discussed.

The third group of reports was devoted to the results achieved in the design of individual intrument parts. These achievements include, for instance, the production of components with a higher temperature stability and a method for determining optimum vibrations, which exclude the effect of Coulomb friction.

Application of Theory and Technology for the Automation of Industrial Processes

Problems in practical application of the automation theory and technology were treated in sixty-seven reports. These reports were discussed at the sessions of six Sections.

Ten reports were discussed in the Section concerned with Automation of Machine Construction. In the work of this Section, most attention was paid to problems in the design and practical realization of automatic-control systems for different machines. These problems comprised the selection of the simplest and most efficient devices for recording different types of information; the selection of computer and programming devices; the determination of the optimum operating conditions for a given machine. The groups of problems considered in the work of this Section encompassed the main trends in the development of programmed control techniques for machine tools, as well as a number of special problems connected with the operational reliability of machine tools.

In the discussion following the reading of reports, it was noted that digital-control methods play an especially important role in machine construction.

Twenty-two reports were discussed in the Section occupied with the Automation of Power Systems.

An analysis of the reports submitted to this Section indicates that a number of new and important scientific and practical results have been achieved. The most important are the following: Equations which determine the main characteristics of the most important power-generating systems to be controlled (boiler units, nuclear reactors, and heat exchangers) have been derived. Experimental data characterizing the properties of typical systems to be controlled (industrial furnaces, power-generating devices, etc.) have been obtained. New criteria for the optimum operating conditions of systems to be controlled, which take into account the effect of the controlled variable deviations and of changes in the energy carrier flow on the efficiency of devices, have been proposed. A number of original schemes for the automation of the most important systems to be controlled (boiler units, nuclear reactors, metallurgical furnaces, and fractionating columns) have been described. New views have been expressed on the principles of operating mode optimization to be applied to controlled systems, and first attempts have been made to determine the scope of different types of self-adjusting systems. Specifications for the characteristics and parameters of certain systems to be controlled, based on control conditions, have been formulated and substantiated.

Nevertheless, the discussion showed that, at the present time, no substantial progress toward solving the following important problems in industrial automation has been achieved: general principles for the design of automatic-control systems for complex industrial combines have not yet been formulated, and methods for improving the operational reliability of automatic-control systems have yet to be devised.

Eight reports were presented to the Section concerned with Automation in the Chemical and Oil-Refining Industries. The main attention in the work of this Section was centered on two problems. The first pertained to the determination of dynamic properties of systems to be controlled in the chemical industry, and the second problem involved the application of computers for the analysis, calculation, and control of technological processes. The considerable number of reports devoted to the study of dynamics of systems to be controlled and the animated discussion called forth by them convincingly prove that the development of computer techniques does not lessen the importance of determining the dynamic properties of systems to be controlled in analytical form. The study of characteristics of systems to be controlled still remains one of the most important stages in designing complex automation systems.

However, the problems encountered in the application of computers to automatic-control systems for technological processes were considered only in their most general form, indicating that computer techniques have not yet been introduced in industrial automation on a large scale.

In the reports and the discussion, attention was drawn to the necessity of directing efforts toward the solution of the following important problems: determination of dynamic properties of systems to be controlled and of entire technological chains; development of optimization algorithms for technological processes; establishment of efficiency criteria for a justified application of computers and the development of general principles of complex automation.

Ten reports were discussed in the Section dealing with Automated Electric Drives and Electrical Machines. The greatest interest was aroused by problems met in seeking new methods for accelerating transient processes in automated electric drive systems, problems in the design of new components and devices, and methods for the synthesis of nonlinear automated drive systems.

The reports and the discussion emphasized the necessity for a further development and a more widespread application of methods for the analysis and synthesis of automated drive systems with optimum quickness of response, the necessity for a more widespread application of computers in systems for the control of electrical drives, the need for devising new compact and reliable automation components and devices, and the necessity of developing improved measuring instruments of high accuracy.

Thirteen reports were discussed in the Section occupied with Automation of Metallurgical Processes. Among the problems discussed were the determination of static and dynamic characteristics of systems to be controlled, problems met in the design of new automatic control systems for complex metallurgical units, and problems in the design of new, improved components for automation systems. Equations were adduced which fairly accurately described the static and dynamic properties of a number of important metallurgical devices (rolling mills, boiling-layer furnaces, heating wells, etc.); a large number of pertinent experimental data also were given.

It was announced that new control systems, based on self-adjustment principles and the extensive use of computer techniques, were developed and tested in industry. Methods for the complex automation of individual units and of entire shops and plants, where process optimization requirements, determined by a number of technological and efficiency specifications are taken into account, were outlined in these papers. Information was provided on the development of new original and efficient components in automatic-control systems for industrial processes (electron-optical equipment for the measurement of dimensions and rate of rollings, pneumatic meters with vane-shaped profiles, thermoelements, etc.).

The discussion that developed in the work of this Section showed that, for the further development of automation in metallurgy, it will be necessary to devise methods for the mathematical description of characteristics of systems to be controlled, to develop unique principles for the design of automatic-control systems, and to establish performance criteria for automatic-control systems to be used in complex metallurgical devices. It was also indicated that methods of automatic control with respect to disturbances, statistical methods for determining disturbances acting on a system, and self-adjusting systems for devices whose operating mode is optimized by means of models should be developed and utilized on a larger scale; that it is necessary to further improve and increase the reliability of components in automatic-control systems for metallurgical devices, which is especially pertinent to data transmitters, final mechanisms and regulating components, since they operate under heavy-duty conditions in metallurgical plants.

Four reports were discussed in the Section dealing with Unclassified Problems. The greatest interest was shown in reports devoted to problems in control and regulation in the cement and sugar industries. It was remarked in the discussion that these reports contain many valuable results obtained in the field of automation in sugar refining and cement production; however, it was also noted that the complex processes occurring in blast furnaces have not been thoroughly analyzed in developing automatic-control systems to be used in the cement industry.

In conclusion, it should be noted that the numerous discussions which developed during the work of the Congress were entirely businesslike, that they contained a great deal of well-meant criticism, and that, consequently, they were fruitful.

The work of the Congress, the slogan of which was "The theory should be widely applicable, the technology should have the maximum reliability, and the automation systems should be highly efficient," showed that this slogan very accurately characterizes the modern trends in automatic-control development.

DUAL-CONTROL THEORY. I

A. A. Fel'dbaum

Moscow

Translated from Avtomatika i Telemekhanika, Vol. 21, No. 9, pp. 1240-1249,
September, 1960
Original article submitted March 23, 1960

Some fundamental problems in communication theory and control theory are compared. The problem of designing an optimum (in the statistical sense) closed-loop dual-control system, is formulated. Its solution, as well as examples and some generalizations, will be given in parts II, III, and IV.

Introduction

A general block diagram of signal transmission, as investigated in communication theory is shown in Fig. 1. The transmitted signal x^* proceeds from the transmitting device A to the communication channel H^*. The mixing of signal and interference (noise) h^* now takes place. The resultant signal y^* represents a mixture of the transmitted signal and the interference. The resultant signal proceeds to the input of receiver B. The optimum receiver problem consists in obtaining the signal $\underline{x}$ at its output, such that it is, in a specified sense, closest to the transmitted signal x^* or to some transformation of the signal x^*. The mathematical side of the problems related to such systems has been the subject of important investigations by A. N. Kolmogorov [1], N. Wiener [2], C. E. Shannon [3], and A. Wald [4]. This type of system was investigated in the works on communication theory by V. A. Kotel'nikov [5], D. Middleton, D. Van Meter [6], and others. The cited works differ in their various approaches to the problem, but are all basically concerned with the investigation of the scheme represented by the block diagram in Fig. 1. The results obtained in the above-cited works, and in particular the Kolmogorov-Wiener theory, have proved useful in formulating the statistical theory of automatic-control systems. This theory has been expounded in the books of V. S. Pugachev [7], J. H. Laning, Jr., and R. H. Battin [8], and others. The fullest consideration has been given to the theory of linear systems. If a system is linear, then whatever the closed-loop system, it is easy to obtain an open-loop system equivalent to it. That is why the automatic-control systems, which, as a rule, are closed-loop systems, enable one to use the scheme as in Fig. 1, provided that the system is linear. Some complications and difficulties arise when the interference does not appear at the input of the system, but at the input of the controlled object – the latter being inside the closed-loop network. This also creates difficulties which are not, however, of a fundamental nature. More serious difficulties arise due to the bounds to which the power of the system's signals are subjected. The problem becomes more involved when the controlled object is nonlinear or it is required that an optimum control system, which often proves to be nonlinear, is designed. It is not always possible to proceed from an open nonlinear system to an equivalent closed-loop one; furthermore, this is an extremely involved process. In such a case, the open-loop scheme depicted in Fig. 1 cannot be used in practice. A number of attempts have been made to reduce approximately nonlinear systems to equivalent linear ones (see, for example, the paper of I. E. Kazakov [9]). Such studies are of considerable practical value but do not, in their present state, provide a means of estimating how close the obtained approximation is to the true solution; neither do they enable one to synthesize the optimum system.

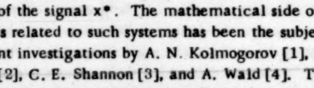

Fig. 1.

In order to be able to solve optimum problems of the control theory, a fundamentally different approach is required. Firstly, a different block diagram replacing that depicted in Fig. 1 is needed. Before selecting a common scheme to be used in automatic-control theory, it seems advisable to have a preliminary survey of certain basic concepts of the theory.

Figure 2, a shows the controlled object B with $\underline{x}$ as its output, $\underline{u}$ as the controller, and $\underline{z}$ as the disturbance (interference). When the system has several inputs and outputs, one can regard $\underline{x}$, $\underline{u}$, and $\underline{z}$ as vector quantities.

The output $\underline{x}$ depends on $\underline{u}$ and $\underline{z}$. This dependence can be described either by a linear or a nonlinear operator, and in a particular case of memoryless systems, only by a function. The interference $\underline{z}$ is generally a function of time. Thus, since a change in the system's characteristics can be considered a particular result of interference (e.g., the parametric effect), then hereafter everything in the system's characteristics that changes with time will be attributed to interference. If, for example, x depends on u as in

$$x = [a_0 + f_0(t)]\,u^2 + [a_1 + f_1(t)]\,u + a_2 + f_2(t). \quad (1)$$

then the vector

$$z = \{z_0,\, z_1,\, z_2\},$$
$$z_0 = f_0(t),\ \ z_1 = f_1(t),\ \ z_2 = f_2(t) \quad (2)$$

gives the interference or disturbance, and the formula

$$x = [a_0 + z_0]\,u^2 + [a_1 + z_1]\,u + a_2 + z_2 \quad (3)$$

represents a particular operator.

If the object has memory and if, for example, its motion can be described by a differential equation of the nth order, then its state is considered as one of the characteristics of the object as described by the value of the vector x in the n-dimensional phase space.

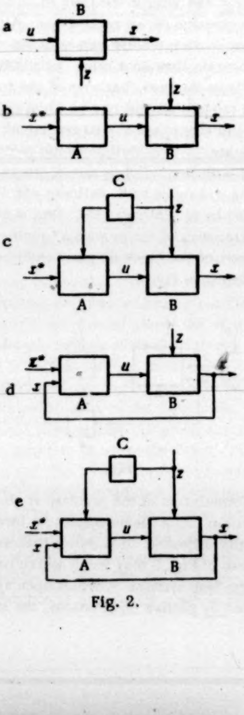

Fig. 2.

Complete information about a system thus consists of information about its operator, interference (noise), and the state of the system. The controlling device may be given and is considered as known. The open-loop systems are automatic-control systems of a simple type. A block diagram of an open-loop system is shown in Fig. 2, b and is of the same character as the one given in Fig. 1. The exciting quantity x* enters the input of the regulating member A, determining how the output quantity x should vary. The output u of the regulating device enters the input of the object B under control. The output x of the controlled object B does not proceed in this case to the regulating member A.

The required rule of change in x can only be implemented when full information about the controlled system is available, i.e., when its operator and state x are known, at least at the initial moment of time, as well as the interference z. The latter should be known a priori at all moments of time, including future moments. The required rule of change in x must be one of the admissible ones, such that it can be implemented for the given class of initial states of the system and for a class of controlling motions u staying within acceptable bounds.

The above conditions, and, in particular, the a priori full knowledge of the controlled system, cannot be satisfied in practice. This is why an accurate implementation of the required control rule cannot be obtained. Sometimes the interference z is not known a priori, but it is possible to measure it with a device C (see Fig. 2, c) and to introduce the outcome of the measurement into the controlling member A. One can then find in the latter the required controlling rule u. Such a scheme is also an open-loop one. But the scheme depicted in Fig. 2, c differs in some ways from the scheme with complete a priori information about the system, as now future magnitudes of the interference z remain unknown. Because of this, the exact implementation of the required rule of variation of the controlling quantity x is not always feasible.

When the state x of the system is not known, then, generally speaking, it is not possible to implement the required rule of the change in x. To be able to attain the required variation in x, or one near to it, a feedback network is needed to feed the output quantity x to the input of the controlling member A (see Fig. 2, d). Having compared x and x*, the controlling member generates the regulating action u, bringing x to its required value. The block diagram of Fig. 2, d is a closed-loop scheme, and is of the utmost importance in the automatic-control theory.

A closed-loop network offers far-reaching possibilities not available in an open-loop system. For example, it may be possible for a class of objects B of control to obtain a process x close to the one required even when the interference z remains unknown and incapable of measurement. Let, for example, the interference z, together with the controlling action u, be applied at the input of the controlled object B, the latter representing an inertia member. If the quantity $x^* = x$ is to be attained, the regulating member can be implemented in the form of an amplifier of high gain $k >> 1$, the difference $x^* - x$ being sent to its input.

It is not difficult to see that the requirement $x^* = x$ will be satisfied approximately, whatever the continuously varying interference z, provided k is sufficiently high and the bounds of variability of u are such that the interference z can be compensated by u.

This principle of neutralizing the interference can be generalized and applied to cases considerably more involved, combining the system's accuracy with its stability. A detailed analysis of the applicability of this principle was carried out by M. V. Meerov in his monograph [10].

When the interference z can be measured, it is possible to implement a combined system (see Fig. 2, e) of measurement of the state of the controlled system x as well as of its interference. Such systems are of considerable practical value. We shall not, however, concern ourselves with them but shall limit the study to the "pure" type of closed-loop systems, considering them as being of primary importance.

The input quantity x^* may be previously unknown; usually, neither do we have any prior knowledge of the interference z. Consequently, these processes become random, and, in a favorable case, the a priori information is limited to our knowledge of their statistical characteristics. Such processes may be regarded as belonging to a class of curves $x^*(\lambda)$ and $z(\mu)$ where λ and μ are parameter vectors $(\lambda_1, \ldots, \lambda_q)$ and $(\mu_1, \ldots, \mu_m)$, respectively, with their probability distributions either known or unknown.

In communication channels connecting the blocks of a system, the errors of measurement or noise can be regarded as subsidiary random processes as well, with either known or unknown characteristics. Thus, the analysis of a control system and the synthesis of the regulating member can be regarded as problems of a statistical nature. The problem should be solved for an over-all block diagram in which all the above features of an automatic-control system are reflected. Such a block diagram is depicted in Fig. 3; it is the subject of the present paper as well as that of further papers in this series.

The input quantity x^* proceeds to the input of the controlling member A through channel H^* where it becomes mixed with noise h^*. Thus, the quantity y^* entering the input of A is generally not equal to the actual value of the input quantity x^*. There also exists a class of systems with the external input x^* altogether absent. Generally speaking, however, it cannot be neglected. A similar mixing takes place of the state x of controlled object B and noise h in channel H; quantity y entering A will not, as a rule, be equal to x. The regulating action u proceeds next from A to controlled object B having previously passed through channel G where it was mixed with noise g. The quantity v proceeding to the controlled object is not, as a rule, equal to u.

Dual Control

One cannot neutralize, in a general case, the interference z by a regulation u if the interference z is not known. Its direct measurement is not, as a matter of fact, often possible. In such a case, an open-loop system is useless. But the closed system in Fig. 3 shows how z can be indirectly determined by measuring the input and the output, in and out of object B, by studying its characteristics. The input of controlling member A enters both the input v and the output x of the object or, in any case, the quantities u and y related to v and x. The examination of the quantities u and y provides information on the characteristics of object B. It should be understood that this information is never complete, as the noises g and h render an exact measurement of B's characteristics impossible; if the actual form of the object's operator is not known either, a full determination of its characteristics would not be possible even in the absence of noise, unless the determination time is infinitely great. The lack of complete information on the disturbance z can assume the form of an a posteriori probability distribution of its parameters. Although the latter does not provide precise values of the parameters, it is more accurate than an a priori distribution, as the former reflects the real character of the interference.

If the random process can be measured directly, one is able eventually to specify its statistical characteristics more accurately. The method which provides such improvement with the aid of dynamic programming was discussed in examples by R. Bellman and R. Kalaba [11, 12] and also by M. Freimer [13]. One is able to find the characteristics of the process x^* more accurately in the open part of the block diagram in Fig. 3, or in a similar scheme in Fig. 1.

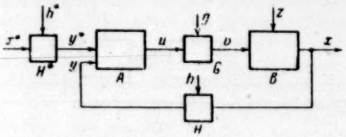

Fig. 3.

This formulation of the problem is characteristic for an open system. In a closed system its formulation becomes totally different. It is shown that some processes in the system of Fig. 3 may occur which have no counterpart in open-loop systems. Whereas open systems can only be studied by passive observations, the study may develop into an active one in closed systems. In order to improve the investigation one may vary the signals u (or v) which act on the controlled object B. The object is, as it were, "reconnoitered" by signals of an enquiring character whose purpose it is to promote a more rapid and more accurate study of the object's characteristics and of the methods of controlling it.

However, the controlling movements are necessary not only to study or to *learn* the characteristics of the object or the ways of controlling it, but also to implement the regulation, to *direct* the object to the required state. Thus, the controlling effects in the general block diagram in Fig. 3 must be twofold: they must, to a certain extent, be *investigating* as well as *directing*.

The control whose regulating effects are of this twofold character will in the sequel be called *dual control*; the papers in the present series will be devoted to the theory of dual control.

Dual control is particularly useful and even indispensible in cases where the operator and the interference z in the object B are complex, and the object is thus distinguished either by its complexity or by the variability of its characteristics. Some typical examples of systems with dual control are to be found in automatic search systems, in particular, in automatic optimization systems (see, for example, [14 and 15]). In these systems, the investigating or "trial" part can usually be separated easily from thecontrolling or "operating" part of the signal, either by the difference in their frequency ranges or because they interweave in time. Such a separation, however, need not always take place; an effect can be twofold in character by virtue of being partly diagnostic and partly regulating.

Thus, in dual-control systems, there is a conflict between the two sides of the controlling process, the investigational and the directional. An efficient control can only be effected by a well-timed action on the object. A delayed action weakens the control process. But the control can only be effective when the properties of the object are sufficiently well known; one needs, however, more time to become familiar with them. A too "hasty" controlling member will carry out the operational movement without making proper use of the results of trial investigations performed on the object. A too "cautious" system will bide its time unnecessarily long and process the received information without directing the object to its required state at the right time. In each case, the control process may not prove the best one and may not even prove to be up to the mark. Our problem is to find out, one way or another, which combination of these two sides of the regulation would prove to be most suitable. The operations must be so selected as to maximize a criterion of the control's quality.

As shown above, the incomplete information about the object will be expressed by the presence of the probability distributions of potentially possible characteristics of the object. The regulating member compares, as it were, the various hypotheses on the object, with probability of its occurrence being attached to each hypothesis. These probabilities vary with time. There may be a control method such that the most probable hypothesis will always be selected and, therefore, assuming that it is valid, the optimum control method will be attained. Such a control system is not generally optimum in the absolute meaning of the word as the complete information on the object has not been utilized. The probability distribution of the different hypotheses extracted from the experiments is distorted as the probability 1 was ascribed to one of them and the probability 0 to others. A better control method will be one whereby the probabilities of all the hypotheses would be taken into account.

The probability distribution of hypotheses will vary with time, the higher probabilities concentrating more and more in the region of those hypotheses which approach the true characteristics of the object. The pace of concentration and, therefore, the success of the subsequent regulating movements, depends on the character of the preceding regulating movements, on how well they have "sounded" the object. Thus, two factors should be taken into account by the controlling member which decides the specific amount of regulating movement at any given moment of time:

(a) The loss occurring in the value of the quality criterion due to the fact that the outcome of the operation at a given moment, and at subsequent moments of time, will cause a deviation of the object either from the required state or from the best attainable one. The average value of this loss shall be called the *action risk*.

(b) The loss occurring in the value of the quality criterion due to the fact that the magnitude of the controlling action has not proved the best to obtain information on the characteristics of the object; in view of this, the subsequent actions will not be the best posssible ones either. The average value of this loss shall be called the *investigation risk*.

It will be shown that for a certain class of systems, the total risk will be equal to the sum of the action and investigation risks.

All systems of automatic search (see [14]) are characterized by trial actions. Dual control, therefore, is applicable to all systems of automatic search and, in particular, to automatic optimization systems. It can also be applied to other types of closed-loop systems which do not belong to the automatic search class at all. To illustrate the difference between the two types of dual-control systems, a few examples will be given.

Figure 4,a shows a system which operates as follows: the main regulating member A implements the control of object B, either in an open- or in a closed-loop network (the closed one is indicated by a dashed line). The

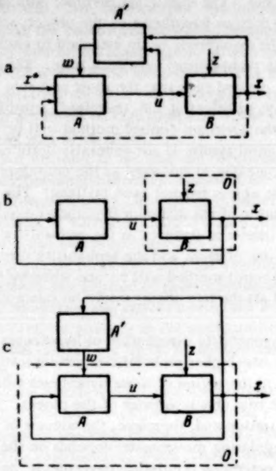

Fig. 4.

regulating movements u are of the investigational and action type simultaneously. The quantities u and x, from the input and the output of object B, respectively, enter an additional controlling member A'. The latter receives the characteristics of object B from the results of the investigations; subsequently, in accordance with an algorithm given in advance and fed into the device from outside, the parameters of controlling member A are so computed that its controlling action is optimal. Having the results of the computation, the additional regulating action w establishes the computed optimum parameters in the main controlling member A. This process may repeat itself periodically.

Such systems contain investigational movements; however, the automatic search is absent. The parameters of member A are established, not via automatic search, but from an algorithm given in advance, from a function of the determined characteristics of object B. There is no investigational component in the operation w. The channel w is not usually found in a closed network, as the change in the coefficients of A has no effect on the coefficients of B.

A block diagram of an automatic optimization system is presented in Fig. 4,b. Here the action u is dual in character, investigating object B as well as directing it to its optimum mode of action. The latter corresponds to an extremum of quantity Q dependent on x. The optimum mode is found by means of automatic search. The latter is conducted in such a way that the information received from the investigating action u and from the output x of the system is analyzed in controlling member A. This permits determination of the regulating part of the same action u on the same object B whose input and output were investigated, so that the same quantity x which was being investigated can be changed in the right direction.

The combination of the investigating and directing operations has, so far, not constituted the whole search, but only one of its distinct features. There is no search in the system depicted in Fig. 4,a; it takes place, however, in the system of automatic optimization shown in Fig. 4,b. But both systems are of the dual-control type.

In Fig. 4,b the controlled object is inside a dashed rectangle denoted by O. In this case, it does not differ from object B. The dual control, however, can also be applied to control the entire automatic system, considered as a complex object. For example, in Fig. 4,c the complex object O inside the dashed rectangle comprises the controlling member A and the object B of control. The auxiliary controlling member A' investigates the process x and, with the aid of the controlling process w, can vary the algorithm of regulation implemented by member A. The w processes are twofold in character. The investigation of changes in the algorithm of member A and their effect on the process x results in regulating processes w, bringing the algorithm of member A to such a form that the process x will either prove admissible, favorable, or optimum, depending for what purpose the system will be used. Here an automatic search takes place in the closed network of processes $w \to x \to u$.

Statement of the Synthesis Problem of an Optimum System of Dual Control

The problem of designing an optimum, in the specified meaning of the word, controlling member A, as shown in Fig. 3, is formulated below. It is advisable when formulating the problem to make use of certain concepts of the theory of games and of A. Wald's [4] theory of statistical decisions (see D. Blackwell and M. A. Girshick [16], and also Chow [17]). In solving the variational problem as stated later in the present series of papers, use is made of the concepts of R. Bellman's dynamic programming (see, for example, [18]). In the subsequent parts of this series, the mathematical exposition may appear somewhat cumbersome but is actually quite simple. The main contents of the papers deals with further development of the concepts of automatic control briefly described above.

Consider the scheme presented in Fig. 3. The following limitations of the statement of the problem are introduced.

1) A discrete-continuous system is investigated in which the time but not the level is quantized. All magnitudes occurring in the system are considered at discrete moments of time $t = 0, 1, 2, \ldots, n$ only. Any

magnitude at the sth moment of time will carry the index s. Thus, the considered quantities are x^*_s, x_s, y_s, v_s, g_s, etc.

Such limitation enables one to simplify the computation. Moreover, in many cases this actually occurs. The transition to the continuous time can in some cases be accomplished in an intuitive manner by making the time interval between the discrete values approach zero (see Part III). One meets with considerable difficulties in more fully examining the passage to the limit.

2) The time interval, or the number of cycles n within which the process is being investigated, is assumed to be a fixed constant. In certain cases no major difficulties arise when proceeding to the limit with $n \to \infty$. A wider generalization relating to a variable number n of cycles not known beforehand would be of interest, but will not be tackled in the present paper.

3) A Bayesian problem, in which a priori densities of random variables are given, is considered. Other formulations, for example, minimax, are also of considerable interest, but far more difficult to solve. This problem could also be formulated in relation to the concept of the so-called "inductive probability" (see, for example, the paper of L. S. Schwartz, B. Harris, and A. Hauptschein [19]).

We assume that h^*_s, h_s, g_s, are sequences of independent random variables with identical distribution densities $P(h^*_s)$, $P(h_s)$, $P(g_s)$. Further, let $z_s = z(s, \mu)$, and $x^*_s = x(s, \lambda)$ where μ and λ are random parameter vectors with coordinates μ_i and λ_i, respectively:

$$\mu = (\mu_1, \ldots, \mu_m), \qquad \lambda = (\lambda_1, \ldots, \lambda_q). \tag{4}$$

The a priori probability densities $P(\mu)$ and $P(\lambda^*)$ are given.

4) The object B is assumed to be memoryless; in other words, the values x_s of its output depend only on the values of the input quantities z_s and v_s at the same moment of time:

$$x_s = F_0(z_s, v_s). \tag{5}$$

The functions F_0 and z_s are assumed to be finite and single-valued, continuous and differentiable.

A generalization relating to objects with memory and with x_s depending on x_r, z_r, v_r $(r < s)$ will be given in Part IV. It should be pointed out that memoryless objects are of great practical value. Namely, if the input data (initial conditions or values of parameters) are given for a certain model, and one is able to carry out experiments using this model and also to register the results, then such an object becomes equivalent to a memoryless one.

5) A simple criterion W of quality is introduced.

Let the partial loss function corresponding to the sth time moment be of the form

$$W_s = W(s, x_s, x^*_s). \tag{6}$$

Moreover, let the total loss function W for the total time be equal to the sum of partial loss functions (such a criterion shall be called a simple one):

$$W = \sum_{s=0}^{s=n} W(s, x^*_s, x_s). \tag{7}$$

The smaller the mathematical expectation of W, the better is the system. It shall be called optimum when its average risk R (i.e., the mathematical expectation M of the quantity W) is minimal. The amount of risk is given by the formula

$$R = M\{W\} = \tag{8}$$
$$= M\left\{\sum_{s=0}^{s=n} W(s, x^*_s, x_s)\right\} = \sum_{s=0}^{s=n} M\{W_s\} = \sum_{s=0}^{s=n} R_s.$$

Each $R_s = M\{W_s\}$ will be called a partial risk due to the sth cycle.

There may be many types of simple criteria, for example,

$$W_s = \alpha(s)[x_s - x^*_s]^2. \tag{9}$$

Criteria of practical importance need not always be simple, and generalizations relating to other criteria would therefore be of interest.

The formulation of the optimum strategy problem in terms of risks is not the only one in existence. There exist a number of studies in which closed systems are investigated from the point of view of the information theory (see, for example, R. L. Dobrushin's paper [20]). As the primary aim of a control system does not lie in transmitting information but in designing required processes, the formulation of the problem in the language of statistical decisions fits in better with the intrinsic nature of the problem.

6) All the quantities occurring in the sth cycle will be regarded as scalar. Our object, therefore, has only a single input v and a single output x. The exposition becomes more involved with generalizations relating to objects with several inputs and outputs (see Part IV).

7) We assume that the manner by which the signal and the noise are combined in H*, H, or G blocks is

known and invariable, and that the blocks are memoryless. Thus,

$$v = v(u, g),$$
$$y^* = y^*(h^*, x^*),\qquad (10)$$
$$y = y(h, x).$$

Therefore, the conditional probabilities $P(y^*|x^*)$ and $P(y|x)$ and $P(v|u)$ make sense.

8) We assume that the controlling member A generally possesses a memory and that, moreover, for the sake of generality, the algorithm of its action is a random one, i.e., the part A exhibits random strategy.

We introduce the vectors $(0 \leq s \leq n)$:

$$\begin{aligned} \mathbf{u}_s &= (u_0, u_1, \ldots, u_s), \\ \mathbf{y}^*_s &= (y^*_0, y^*_1, \ldots, y^*_s), \qquad (11) \\ \mathbf{y}_s &= (y_0, y_1, \ldots, y_s). \end{aligned}$$

The controlling member can now be characterized by the probability densities

$$P_s(u_s) = \Gamma_s(u_s, \mathbf{u}_{s-1}, \mathbf{y}^*_s, \mathbf{y}_{s-1}) \qquad (0 \leqslant s \leqslant n). \quad (12)$$

The problem consists in finding a sequence of functions F_s such that the average risk R (see [8]) becomes minimal.

LITERATURE CITED

1. A. N. Kolmogorov "Interpolation and extrapolation of stationary random sequences," Izvest. AN SSSR Ser. Matem. 5, 1 (1941).
2. N. Wiener, Extrapolation, Interpolation, and Smoothing of Stationary Time Series (J. Wiley and Sons, New York, 1949).
3. C. E. Shannon, "A mathematical theory of communication," Bell System Techn. J. 27, 3 (1948).
4. A. Wald, Statistical Decision Functions (J. Wiley and Sons, New York; Chapman and Hall, London, 1950).
5. V. A. Kotel'nikov, Theory of Potential Noise Stability [in Russian] (Gosénergoizdat, 1956).
6. D. Van Meter and D. Middleton, Modern Statistical Approaches to Reception in Communication Theory. Trans. IRE, IT-4 (Sept., 1954).
7. V. S. Pugachev, Theory of Random Functions and Its Applications to Automatic Control [in Russian] (Gostekhizdat, 1957).
8. J. H. Laning, Jr. and R. H. Battin, Random Processes in Automatic Control (McGraw-Hill, New York, 1956).
9. I. E. Kazakov, "An approximate statistical analysis of accuracy of essentially nonlinear systems," Avtomat. i Telemekh. 17, 5 (1956).*
10. M. V. Meerov, The Synthesis of Networks of Automatic Control Systems of High Accuracy [in Russian] (Fizmatgiz, 1959).
11. R. Bellman and R. Kalaba, On Communication Processes Involving Learning and Random Duration. IRE National Convention Record , Part 4 (1959).
12. R. Bellman and R. Kalaba, On Adaptive Control Processes. IRE National Convention Record, Part 4 (1959).
13. M. Freimar, A Dynamic Programming Approach to Adaptive Control Processes. IRE National Convention Record, Part 4 (1959).
14. A. A. Fel'dbaum, Computers in Automatic Systems [in Russian] (Fizmatgiz, 1959).
15. A. A. Fel'dbaum, Problems of statistical theory of automatic optimization, Proc. of the 1st. International Congress of Automatic Control (IFAC) [in Russian] (Moscow, 1960).
16. D. Blackwell and M. A. Girshick, Theory of Games and Statistical Decisions [Russian translation] (IL, 1959).
17. C. K. Chow, An Optimum Character Recognition System Using Decision Functions. IRE Trans. EC-6 , No. 4 (1957).
18. R. Bellman, "Dynamic programming and stochastic control processes," Information and Control 1, 3 (Sept., 1958).
19. L. S. Schwartz, B. Harris, and A. Hauptschein, Information Rate from the Viewpoint of Inductive Probability. IRE National Convention Record, Part 4 (1959).
20. R. L. Dobrushin, "Transmission of information in channels with feedback," Teor. Ver. i ee Prim. 3, 4 (1958).

---

*See English translation.

PARAMETRIC PHENOMENA IN THE SIMPLEST CONTINUOUS EXTREMAL CONTROL SYSTEMS

V. S. Baranova and A. A. Pervozvanskii

Leningrad

Translated from Avtomatika i Telemekhanika, Vol. 21, No. 3, pp. 1250-1253,
September, 1960
Original article submitted March 14, 1960

This article presents an analysis of a continuous control system where the extremum of the characteristic of an inertialess system to be controlled is searched for and maintained in the presence of intensive random noise in the frequency band which includes the frequency of the periodic trial input. The stability conditions for this system are determined.

The spectrum of uncontrolled external signals acting on an extremal control system usually contains a low-frequency band, which is determined by the drift of elements in the system, and a low-frequency band determined by noise. Between these bands lies a frequency band which is almost free from noise. However, this third band may be insufficiently broad to serve for assigning the frequency of trial inputs [1, 2]. Therefore, the case wherein the trial input frequency lies within the noise band is of especial interest. However, if we assume that the high-frequency noise appears only at the output of the system to be controlled, no basic difficulties are encountered in analyzing the equations of the closed-loop system [2]. For a controlled system whose characteristic is given by a quadratic parabola, the control system is described by linear equations with constant coefficients. For an arbitrary characteristic, the problem of determining the main deviation of the system operating conditions from the extremum can also be solved by using the statistical linearization method. However, if high-frequency noise appears at the system input, the coefficients in the equation for the closed-loop system become random functions of time. The investigation of such equations is a complicated task.

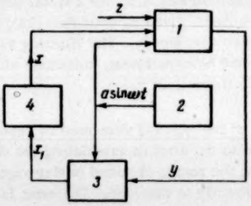

1) System to be controlled; 2) generator of trial oscillations; 3) demodulator; 4) final mechanism.

An inertialess system of the simplest form with high-frequency noise at the input of the system to be controlled is considered below. The block diagram of this system is given in the figure.

If the characteristic of the system to be controlled is given by the quadratic parabola $y = -x^2$, the system operation will be described by the following equations:

1) The equation of the system to be controlled,

$$y = -(x + a\sin\omega t + z)^2,$$

where $\underline{a}$ sin ωt is the trial input, and $\underline{z}$ is the noise;

2) the demodulator equation,

$$x_1 = \frac{b\omega}{2\pi}\int_t^{\frac{2\pi}{\omega}+t} y\sin\omega t\,dt; \tag{1}$$

3) the final mechanism equation,

$$x - x_0 = \int_0^t x_1\,dt.$$

We shall limit our consideration to the case wherein the spectrum z(t) of the normal random noise has a narrow band and the noise can, consequently, be represented in the form

$$z(t) = A(t)\sin\omega t + C(t)\cos\omega t. \tag{2}$$

Here, A(t) and C(t) are slowly changing (in comparison with the trial input) random processes. By taking into account condition (2), system (1) is reduced [2] to the equation

$$\frac{dx}{dt} + b[a + A(t)]x = 0 \tag{3}$$

or

$$\frac{dx}{dt} + \xi(t)\,x = 0\,^{*}, \qquad (4)$$

while

$$m_\xi = b\,(a + m_A), \quad B_\xi(\tau) = b^2 B_A(\tau), \qquad (5)$$

where m_A, B_A, m_ξ, and B_ξ are the mathematical expectations and the autocorrelation functions of the A(t) and ξ (t) processes, respectively.

Thus, the presence of high-frequency noise at the input of the system to be controlled causes the appearance of a parameter which changes in random fashion in time in the equation which determines the variable x of the control mechanism. According to this method [3], after correcting the error contained therein, we shall obtain the following equations for the mathematical expectation and dispersion:

$$m_x(t) = x_0 \exp\left\{-\left[m_\xi - \int_0^{t-t_0} B_\xi(\tau)\,d\tau\right](t-t_0)\right\} \times$$

$$\times \exp\left[-\int_0^{t-t_0} \tau B_\xi(\tau)\,d\tau\right], \qquad (6)$$

$$\sigma_x^2(t) = x_0^2 \exp\left\{-2\left[m_\xi - 2\int_0^{t-t_0} B_\xi(\tau)\,d\tau\right](t-t_0)\right\} \times$$

$$\times \exp\left[-4\int_0^{t-t_0} \tau B_\xi(\tau)\,d\tau\right] -$$

$$- x_0^2 \exp\left\{-2\left[m_\xi - \int_0^{t-t_0} B_\xi(\tau)\,d\tau\right](t-t_0)\right\} \times$$

$$\times \exp\left[-2\int_0^{t-t_0} \tau B_\xi(\tau)\,d\tau\right]. \qquad (7)$$

Here, $x = x_0$ for $t = t_0$.

The values of m_x and σ_x for $t \to \infty$ obviously depend on the sign in front of the quantities:

$$\lambda = m_\xi - \int_0^\infty B_\xi(\tau)\,d\tau, \quad \mu = m_\xi - 2\int_0^\infty B_\xi(\tau)\,d\tau. \ (8)$$

Since $T = \int_0^\infty B_\xi(\tau)\,d\tau > 0$ and $\mu = \lambda - T$, the following variants can be realized:

I. $\lambda > 0, \ \mu > 0$;
II. $\lambda > 0, \ \mu = 0$;
III. $\lambda > 0, \ \mu < 0$; (9)
IV. $\lambda = 0, \ \mu < 0$;
V. $\lambda < 0, \ \mu < 0$.

In this connection, the following cases can occur under steady-state conditions:

I. $m_x(\infty) = 0$, $\sigma_x^2(\infty) = 0$ for any initial conditions;

II. $m_x(\infty) = 0$ for any initial condition, and

$$\sigma_x^2(\infty) = x_0^2 \exp\left[-4\int_0^\infty \tau B_\xi(\tau)\,d\tau\right];$$

III. $m_x(\infty) = 0$ for any initial condition; for $x_0 \neq 0$, $\sigma_x^2(t)$ increases boundlessly with time or, in other words, the system is unstable with respect to dispersion;

IV. $m_x(\infty) = x_0 \exp[-\int_0^\infty \tau B_\xi(\tau)\,d\tau]$, and the system is unstable with respect to dispersion;

V. The system is unstable with respect to the average value as well as with respect to dispersion.

Hence, it is obvious that the dispersion is limited under steady-state conditions if $\mu \geq 0$. For a system described by Eq. (3), this condition is of the following form:

$$b\,(a + m_A) - 2b^2 \int_0^\infty B_A(\tau)\,d\tau \geqslant 0 \qquad (10)$$

or, for b > 0,

$$a \geqslant 2b\tau_A \sigma_A^2 - m_A. \qquad (11)$$

Here, $\sigma_A^2 = B_A(0)$ is the dispersion of the random process A(t), and $\tau_A = [1/B_A(0)]\int_0^\infty B_A(\tau)\,d\tau$ is the time of the correlation process A(t).

These conclusions were verified by experiment.† For b = 1, Eq. (3) was reproduced by means of an electronic simulating device. The random noise was secured by a low-frequency noise generator. In this, the correlation time was $\tau_A = 0.25$ sec, and $\sigma_A^2 = 8$ v.

A decrease in the a parameter, which corresponded to the amplitude of trial oscillations, led to "stability" losses. In this, as was to be expected from relation (7), which was written for Eq. (3), the "stability" disturbance took place aperiodically, i.e., for a small deviation from the a = 4 limit, given by condition (11), the dispersion σ_x^2 changed very slowly. The limiting value itself, which was found by experiment, coincided almost exactly with the theoretical value.

---

[*] Equations of the type (4) were used in paper [3]. However, due to the error in calculating the characteristic function, the results obtained in this paper could not be used directly in this case. The error in [3] was detected by V. I. Osorin in the reference journal Mekhanika 10, 11232 (1959).

[†] E. P. Gil'bo performed the experiment.

Thus, the stability loss in scanning and in maintaining the extremum, caused by the presence of high-frequency noise at the input of the system to be controlled, is entirely possible. This limits the possible amplitudes of trial oscillations and, consequently, the maximum allowable scanning loss.

Regardless of the simplicity of the problem as formulated at the outset, its investigation made it possible to obtain a definite physical result which can be applied to all continuous extremal systems operating in accordance with the gradient method. It consists in the fact that the consideration of random noises leads to the necessity of a more complicated approach to the stability problem in such systems than was used, for instance, in [4], where the entire problem was reduced to the investigation of linear systems with constant coefficients.

If the noise level at the input of the system to be controlled is high, the following of the extremum may be impossible due to the noise parametric action.

LITERATURE CITED

1. Ch'ien Hsüeh-sên, Technical Cybernetics [Russian translation] (IL, 1956).
2. A. A. Pervozvanskii, "Continuous extremal control systems with random noise," Avtomat. i Telemekh. 21, 7 (1960).‡
3. V. I. Tikhonov, "Effect of fluctuations on the simplest parametric systems," Avtomat. i Telemekh. 19, 8 (1958).‡
4. A. A. Krasovskii, "Dynamics of continuous extremal control systems which are based on the gradient method," Izvest. Akad. Nauk SSSR, Otdel. Tekh. Nauk. Avtomat. i Énergetika No. 3 (1959).

---

‡ See English translation.

EFFECT OF FLUCTUATIONS ON EXTREMAL RELAY SYSTEMS UNDER SELF-OSCILLATION CONDITIONS

I. S. Morosanov

Moscow

Translated from Avtomatika i Telemekhanika, Vol. 21, No. 9, pp. 1254-1263,
September, 1960
Original article submitted March 16, 1960

This article presents an analysis of extremal relay control systems under self-oscillation conditions with fluctuations at the regulator input. A method of statistical linearization of such systems, based on the reduction of external random disturbances to parametric action on the regulator, is proposed. This method makes it possible to obtain an expression for the equivalent gain in the form of a random step function of time according to the describing-function method. The average value of this function is taken as the statistically equivalent transfer coefficient of the nonlinear component.

This method can be applied to ordinary nonlinear self-oscillation systems.

In extremal relay systems (ERCS), the self-oscillation mode is the operating mode. Under operating conditions, an actual system is usually subject to the action of external random disturbances. The present work analyzes the behavior of ERCS under self-oscillation conditions, when $\xi(t)$ fluctuations are applied to the regulator, input. The investigation is based on the statistical-linearization method in conjunction with the describing-function method applied in the form developed for extremal systems in [1].

The use of the statistical-linearization method [2] in the investigation of systems allowing stable self-oscillation states was first proposed in [3]. In [2] and [3], by operating with the first moments of random functions, the linear (equivalent in the probability sense) relation between the input and output moments of the function at the input and output of the nonlinear component is determined on the basis of a certain criterion, while, in [3], this is achieved by using the describing-function method. This method cannot be applied to extremal relay systems. This is due to the fact that, for random disturbances at the extremal regulator input, the parameter of this regulator (the relay threshold) becomes a function of the instantaneous value of the external random disturbance. Therefore, for nonlinearities of this type, the consideration cannot be limited to the random function moments at the regulator input.

Another statistical-linearization method is proposed in the present paper. It is based on a nonlinear reduction of the random function to a form suitable for introducing the regulator fluctuating parameter in the expression for the equivalent gain of the nonlinear element, which is obtained according to the describing-function method. Thus, if, in [3], the equivalent coefficient is obtained as a function of the first moments of the external random disturbance, here it represents a random function of time. Its average value is found with respect to the distribution density of the determined fluctuating parameter function.

The results obtained in investigating ERCS in accordance with the above-mentioned idea for the system linearization are given below.•

1. Formulation of the Problem and the Method of Solution

Let $\xi(t)$ represent a steady-state normal random process with zero average value and intensity σ_ξ, which is smaller than the amplitude Y of self-oscillations in the system, and let the basic components of the fluctuation spectrum $\xi(t)$ be comparable to the frequency ω of self-oscillations. Such a statement of the problem is of practical value since the high-frequency fluctuation components can always be suppressed by means of a weak filter in the control circuit without affecting the dynamic properties of the system.

As is known, ERCS have two basically nonlinear inertialess components. In approximating the static characteristic $y = f_1(x)$ of the system to be controlled by a quadratic parabola, due to the smallness of σ_ξ the system to be controlled can be represented in the form of a linear element with the equivalent transfer locus

---

• In connection with another problem, a statistical-linearization method, conceptually close to the method mentioned above and based on different physical assumptions, was proposed by A. A. Pervozvanskii in [8].

$K(j\omega)$ in investigating self-oscillations [1]. The second nonlinear component —the controlling device with $z = f_2(y)$— has the ratchet-relay characteristic [4] shown in Fig. 1.

This characteristic can be described by the expression

$$z = \begin{cases} \pm k_p & \text{for } y \lesseqgtr 0, \quad \dot{y} > 0; \\ \pm k_p & \text{for } y + \kappa_1 > 0, \\ \mp k_p & \text{for } y + \kappa_1 < 0, \end{cases} \Big\} \ \dot{y} < 0. \qquad (1)$$

Here, k_p is the relay gain (the choice of the sign sequence depends on the initial conditions) and $\kappa_1 = \kappa - y^*$ is the regulator fluctuating parameter, which is expressed in terms of κ (quantization step of the output quantity with respect to level) and y^*, which depends on the system type.

Let the input quantity of the control device be expressed by the sum

$$y = Y \sin \omega t + \xi(t). \qquad (2)$$

Then

$$y^* = Y + \xi(t)_{t=\frac{\pi}{2\omega}} \qquad (3)$$

for ERCS with a floating quantization grid, and

$$y^* = [Y \sin \omega t + \xi(t)]_{\max} \qquad (3a)$$

for ERCS with a fixed grid of the output quantity quantization with respect to level in the system to be controlled [5]. According to (1), we shall write the condition for the pertinent switching moment in the system:

$$y(t_n) + \varkappa_1(t_n) = 0. \qquad (4)$$

By substituting (2) in (4), we can reduce the random component $\xi(t)$ of the control device input to the fluctuating parameter κ_1 and thus represent the effect of an external random disturbance on the system only in the form of a parametric action on the regulator.

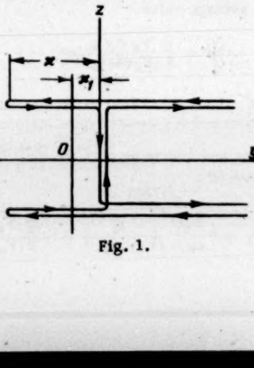

Fig. 1.

Since the actuation phase β of the relay enters the expression for the relay regulator equivalent gain, the fluctuating parameter of this regulator can be conveniently transformed into the fluctuating actuation phase $\delta\beta$ of the relay for a regulator sinusoidal input. As is shown below, the final results can thus be geometrically interpreted in a clear manner. Thus, the second stage in solving the stated problem consists in the nonlinear transformation of the relay parameter random function into the random function $\delta\beta$, with the ultimate aim of determining the distribution density of the new random parameter $\delta\beta$.

Assuming that $\delta\beta = \text{const} \neq 0$ during the period T of the regular input first harmonic, the equivalent gain $S(Y, \delta\beta)$ for the given period can be obtained. It should be noted that this operation is valid if the self-oscillations in the system are settled within a time interval which is less than the period T. As is shown below, in ERCS this is practically always the case.

In the final stage, the average value $\overline{S(Y, \delta\beta)}$ is determined, after which, by plotting the graphic solution in the usual form given by the describing-function method, we can find the average values of the self-oscillation regime characteristics in ERCS when the above $\xi(t)$ fluctuations act at the regulator input.

2. Distribution of the ERCS Relay Actuation Phase under Self-Oscillation Conditions in the Presence of Fluctuations

We shall first find the static characteristics of the phase distribution for an ERCS with a floating grid of output quantization with respect to level.

The phase distribution will be expressed in terms of angles ωt, where ω is the periodic regime frequency at the output of the extremal system to be controlled.

In the absence of fluctuations, the relay actuation phase β_0 will be determined by the moment when the $Y_0 \sin \omega_0 t$ signal intersects a certain level κ, which is measured from the Y_0 value, i.e.,

$$Y_0 \sin \beta_0 = \varkappa - Y_0, \qquad (5)$$

where [5] $Y < \kappa \leq 2Y$.

For a random external input, considering that the $\xi(t)$ fluctuations enter the control signal linearly, we shall seek the phase β^* of the sinusoidal component at the moment when the $\xi(t_2) + Y_0 \sin \beta^*$ signal intersects the level measured from $Y_0 + \xi(t_1)$:

$$\xi(t_2)_{t_2=\frac{\beta^*}{\omega}} + Y_0 \sin \beta^* = \varkappa - [Y_0 + \xi(t_1)]. \qquad (6)$$

By eliminating (5) from (6), we obtain

$$Y_0 (\sin \beta^* - \sin \beta_0) + \xi(t_1) + \xi(t_2) = 0. \qquad (7)$$

In order to determine the statistical characteristics of the random function $\delta\beta$ according to Eq. (7), we shall use the solution which has been proposed in [6].

Let us define more accurately the above restrictions which have been imposed on $\xi(t)$. We shall consider that $\xi(t)$ is a centered function with a Gaussian distribution and the autocorrelation function $\sigma_\xi^2 R(\tau)$, where

$$\sigma_\xi < Y \tag{8}$$

and the correlation time

$$\overline{\frac{\beta^* - \beta_0}{\omega}} < \tau_k < \frac{\pi}{2\omega} \tag{9}$$

throughout the entire working range of the frequencies ω.

Condition (9) permits us to consider that the first intersection, the one in which we are interested, is also the only one; this condition also determines the independence of the $\xi(t_1)$ and $\xi(t_2)$ values of the random function $\xi(t)$.

Under the assumption that the fluctuations are small, we shall introduce a small parameter μ, by denoting in correspondence with (9):

$$\xi(t_1) + \xi(t_2) = \zeta(t_2) = \mu\zeta^*\left(\frac{\beta^*}{\omega_0}\right), \tag{10}$$

and we write the initial equation (7) in the form

$$Y_0(\sin\beta^* - \sin\beta_0) + \mu\zeta^*\left(\frac{\beta^*}{\omega_0}\right) = 0. \tag{11}$$

According to [6], we shall seek the solution of this equation in the form of a power series of μ

$$\beta^* = \beta_0 + \mu\beta_1 + \mu^2\beta_2 + \dots \tag{12}$$

By substituting β^* in (11), we obtain

$$Y_0\{\sin(\beta_0 + \mu\beta_1 + \mu^2\beta_2 + \dots) -$$

$$- \sin\beta_0\} + \mu\zeta^*\left[\frac{1}{\omega_0}(\beta_0 + \mu\beta_1 + \mu^2\beta_2 + \dots)\right] = 0.$$

We expand the functions of the β^* variable in a Taylor series with respect to β_0:

$$Y_0\Big\{(\mu\beta_1 + \mu^2\beta_2 + \dots)\cos\beta_0 -$$

$$- \frac{1}{2}(\mu\beta_1 + \mu^2\beta_2 + \dots)^2 \sin\beta_0 + \dots\Big\} + \mu\zeta^*\left(\frac{\beta_0}{\omega_0}\right) +$$

$$+ \frac{\mu}{\omega_0}\zeta^{*\prime}\left(\frac{\beta_0}{\omega_0}\right)\left[\frac{1}{\omega_0}(\mu\beta_1 + \mu^2\beta_2 + \dots)\right] + \dots = 0.$$

By equating the coefficients in front of the equal powers of the μ parameter, we arrive at the following system of equations:

$$\beta_1 Y_0 \cos\beta_0 + \zeta^*\left(\frac{\beta_0}{\omega_0}\right) = 0,$$

$$\beta_2 Y_0 \cos\beta_0 - \beta_1^2 \frac{1}{2} Y_0 \sin\beta_0 + \beta_1 \frac{1}{\omega_0^2}\zeta^{*\prime}\left(\frac{\beta_0}{\omega_0}\right) = 0,$$

. . . .

whence we find the successive approximations for $0 < \beta_0 \leq (\pi/2)$ (the region wherein self-oscillations exist [5]):

$$\beta_1 = -\frac{\zeta^*\left(\frac{\beta_0}{\omega_0}\right)}{Y_0\cos\beta_0},$$

$$\beta_2 = \frac{\zeta^*\left(\frac{\beta_0}{\omega_0}\right)\zeta^{*\prime}\left(\frac{\beta_0}{\omega_0}\right)}{\omega_0^2 Y_0^2 \cos^2\beta_0} + \frac{1}{2}\frac{\zeta^{*2}\left(\frac{\beta_0}{\omega_0}\right) Y_0 \sin\beta_0}{(Y_0\cos\beta_0)^3}.$$

Consequently, the solution of Eq. (11) with an accuracy to μ^2 can be represented by the expression

$$\beta^* - \beta_0 = \delta\beta = -\mu\frac{\zeta^*\left(\frac{\beta_0}{\omega_0}\right)}{Y_c\cos\beta_0} +$$

$$+ \mu^2\left\{\frac{\zeta^*\left(\frac{\beta_0}{\omega_0}\right)\zeta^{*\prime}\left(\frac{\beta_0}{\omega_0}\right)}{(\omega_0 Y_0\cos\beta_0)^2} + \frac{1}{2}\frac{\zeta^{*2} Y_0\sin\beta_0}{(Y_0\cos\beta_0)^3}\right\}. \tag{13}$$

According to (10), due to the independence of $\xi(t_1)$ and $\xi(t_2)$ and the steady-state property of $\zeta(t)$, we finally write (13) in the form

$$\delta\beta = -\frac{\zeta}{Y_0\cos\beta_0} + \frac{\zeta\zeta'}{(\omega_0 Y\cos\beta_0)^2} + \frac{1}{2}\frac{\zeta^2 Y_0\sin\beta_0}{(Y_0\cos\beta_0)^3}. \tag{14}$$

The $\delta\beta(t)$ function has a physical meaning only for instants of time t_n which coincide with the times of observing the β^* phase of the first harmonic of the regular input, and it is equal to $\delta\beta(t_n)$ for any instant of time within the $t_n \leq t < t_{n+1}$ interval.

Let us find some values of the statistical characteristic $\delta\beta$. By averaging (14) with respect to t_n, we obtain the following average value:

$$\overline{\delta\beta} = \frac{1}{2}\frac{Y_0\sin\beta_0}{(Y_0\cos\beta_0)^3}\sigma_\zeta^2, \tag{15}$$

where $\sigma_\zeta^2 = 2\sigma_\xi^2$, since, according to the condition $\xi^2 = 0$, $\overline{\xi\xi'} = 0$.

By squaring and averaging (14), we shall find [6] the dispersion of $\delta\beta$:

$$D(\delta\beta) =$$

$$= \frac{\sigma_\zeta^2}{(Y_0\cos\beta_c)^2} + \left(\frac{\omega_\zeta}{\omega_0}\right)^2\frac{\sigma_\zeta^4}{(Y_0\cos\beta_0)^4} + \frac{\sigma_\zeta^4(Y_0\sin\beta_0)^2}{2(Y_0\cos\beta_0)^6},$$

where $\omega_{\zeta}^{2} = -(d^{2}R/d\tau^{2})_{\tau=0}$ denotes the root-mean-square value of the frequency of the energy spectrum of fluctuations ζ. If condition (8) is satisfied, we can use only the first term in the above equation:

$$D(\delta\beta) = \frac{\sigma_{\zeta}^{2}}{Y_{0}^{2}} \frac{1}{\cos^{2}\beta_{0}}. \qquad (16)$$

The characteristic function $\delta\beta$ serves for determining† [6] the distribution density $w(\delta\beta)$:

$$w(\delta\beta) = \left[1 - \delta\beta\frac{\sin\beta_{0}}{\cos\beta_{0}} + \right.$$

$$\left. + (\delta\beta)^{3}\frac{Y_{0}^{2}}{2\sigma_{\zeta}^{2}} \sin\beta_{0}\cos\beta_{0}\right] \frac{Y_{0}}{\sigma_{\zeta}} \frac{\cos\beta_{0}}{\sqrt{2\pi}} e^{-\frac{(\delta\beta)^{2}}{2\sigma_{\zeta}^{2}} Y_{0}^{2}\cos^{2}\beta_{0}}$$

or, by taking into account the smallness of σ_{ζ},

$$w(\delta\beta) = (1 - \delta\beta \operatorname{tg}\beta_{0}) \frac{Y_{0}}{\sigma_{\zeta}} \frac{\cos\beta_{0}}{\sqrt{2\pi}} e^{-\frac{1}{2}\left(\frac{\delta\beta}{\sigma_{\zeta}}\right)^{2} Y_{0}^{2}\cos^{2}\beta_{0}} \qquad (17)$$

For ERCS having a fixed quantization grid, the calculation of the same statistical characteristics of the relay actuation phase distribution $\Delta\beta$ is considerably more complicated. Therefore, we shall calculate only the average value $\overline{\Delta\beta}$ for this case.

By analogy with (7) and on the basis of (3a), we obtain the initial equation in the following form:

$$Y_{0}(\sin\beta^{*} - \sin\beta_{0}) +$$

$$+ [Y_{0}\sin\omega_{0}t_{1} + \xi(t_{1})]_{\max} + \xi(t_{2}) - 0. \qquad (18)$$

After denoting $s = Y_{0}\sin\beta_{0}$ and $\eta = [Y_{0}\sin\omega_{0}t + \xi(t)]_{\max}$, we shall use solution (14) for $\zeta = \xi + \eta$:

$$\Delta\beta = \frac{\xi + \eta}{s'} + \frac{(\xi + \eta)(\xi' + \eta')}{\omega_{0}^{2}s'^{2}} - \frac{s''(\xi + \eta)^{2}}{2s'^{3}}.$$

Hence, for $\overline{\xi} = 0$ and $\overline{\xi'} = 0$, and mutually independent values of ξ, ξ', η, and η', we obtain:

$$\overline{\Delta\beta} = -\frac{\overline{\eta}}{s'} - \left[\frac{s''\sigma_{\xi}^{2}}{2s'^{3}} + \frac{s''\overline{\eta^{2}}}{2s'^{3}}\right], \qquad (19)$$

i.e., the problem of determining $\overline{\Delta\beta}$ is reduced to the determination of $\overline{\eta}$ and $\overline{\eta}^{2}$.

We shall determine η as

$$\eta = s(\gamma + \delta\gamma) - s(\gamma) + \xi\left(\frac{\gamma + \delta\gamma}{\omega_{0}}\right), \qquad (20)$$

where γ corresponds to the extremum of s, and $\delta\gamma$ is determined from the condition

$$s'(\gamma + \delta\gamma) + \xi'\left(\frac{\gamma + \delta\gamma}{\omega_{0}}\right) = 0. \qquad (21)$$

Then

$$\overline{\eta} = \overline{s(\gamma + \delta\gamma)} - s(\gamma) = \overline{s(\delta\gamma)}, \qquad (22)$$

$$\overline{\eta^{2}} = \overline{[s(\delta\gamma) + \xi(\gamma + \delta\gamma)]^{2}} = \overline{s^{2}(\delta\gamma)} + \sigma_{\xi}^{2}, \qquad (23)$$

since $s(\delta\gamma)$ is a function of ξ', i.e., it is independent of ξ.

Thus, having determined, as before, the distribution density δ_{γ} from solution (21), we can calculate $\overline{\eta}$ and $\overline{\eta^{2}}$ and, consequently, also $\overline{\Delta\beta}$. In the final form,

$$\overline{\Delta\beta} = \frac{\sigma_{\xi}}{Y_{0}^{2}} \frac{\sin\beta_{0}}{\cos^{3}\beta_{0}} - \left(\frac{\omega_{\xi}}{\omega_{0}}\right)^{2} \frac{\sigma_{\xi}^{2}}{2Y_{0}^{2}} \frac{1}{\cos\beta_{0}}$$

or

$$\overline{\Delta\beta} = \overline{\delta\beta} - \left(\frac{\omega_{\xi}}{\omega_{0}}\right)^{2} \frac{\sigma_{\xi}^{2}}{2Y_{0}^{2}} \frac{1}{\cos\beta_{0}} \qquad (24)$$

The determination of higher statistical characteristics $\Delta\beta$ involves considerable difficulties in calculation and requires the knowledge of higher $\xi(t)$ moments.

3. Determination of the ERCS Regulator Equivalent Gain in the Case of Parametric Random Action

We shall determine the time t_{ss} necessary for the self-oscillations to reach the steady-state in an ERCS with respect to the self-oscillation period T in the system. From the condition for the existence of self-oscillations in ERCS [5], it follows that $T > T_{cr} = (2\pi/\omega_{cr})$, where ω_{cr} is the maximum value of the self-oscillation frequency, which is determined by the equation

$$2\theta_{1}\left(\frac{\omega_{cr}}{2}\right) + \theta_{2}(\omega_{cr}) = \frac{\pi}{2}. \qquad (25)$$

Here, θ_{1} and θ_{2} are the phase responses of linear factors in the equivalent diagram of the extremal system to be controlled before and after the nonlinear static characteristic, respectively.

In the majority of cases of practical interest, the inertial portion of the system to be controlled can be represented by a connection in series of first-order factors. In this, the transient process time can be approximately determined with respect to the interval ω_p, where the real part of the transfer locus of the system inertial portion is positive:

---

† By taking only the first term in the expansion of the characteristic function $\overline{e^{jv\delta\beta}}$ with respect to $\delta\beta$.

$$\theta_1(\omega_p) + \theta_2(\omega_p) = \frac{\pi}{2}. \tag{26}$$

For any number of first-order factors,

$$t_{ss} < \frac{2\pi}{\omega_p}.$$

From a comparison between (25) and (26), it follows that ω_{cr} is always smaller than ω_p, i.e.,

$$t_{ss} < \frac{2\pi}{\omega_p} < \frac{2\pi}{\omega_{cr}} < T. \tag{27}$$

Thus, it can be said that self-oscillations in ERCS attain the steady-state in a time which is less than one period in all cases of practical interest. This fact makes it possible to determine, by using the describing function method, the equivalent complex gain $S(Y, \delta\beta)$ of the control device as a function of $\delta\beta(t_n)$, assuming that $\delta\beta = \text{const}$ during the averaging period $t_{n+1} - t_n$. In this, $S(Y, \delta\beta)$ will always represent a random step function of time instants t_n. If we know the $\delta\beta$ distribution, we can determine the average value of the $S(Y, \delta\beta)$ function.

For ERCS of the type under discussion, $S(Y, \delta\beta)$ in exponential form for $\delta\beta \neq 0$ is expressed by [1]

$$S(Y, \delta\beta) = \frac{4k_p}{\pi Y_0} e^{j(\beta_0 + \delta\beta)}$$

or, for $\beta_0 = \pi - \alpha_0$[1] and $\delta\beta = \delta\alpha$, by

$$\frac{1}{S(Y, \delta\alpha)} = N(Y, \delta\alpha) = -\frac{\pi Y_0}{4k_p} e^{j(\alpha_0 - \delta\alpha)}. \tag{28}$$

The average value is given by

$$\overline{N(Y, \delta\alpha)} = \int_{-\infty}^{\infty} N(Y, \delta\alpha)\, w(\delta\alpha)\, d(\delta\alpha). \tag{29}$$

After substituting in (29) the expressions for the integrands from (28) and (17) and after integration (see [7]), we obtain

$$\overline{N(Y, \delta\alpha)} = \frac{\pi Y_0}{4k_p} e^{j\alpha_0}\left[1 + j2\frac{\sigma_\xi^2}{Y_0^2}\frac{\sin\alpha_0}{\cos^3\alpha_0}\right] e^{-\frac{\sigma_\xi^2}{Y_0^2\cos^2\alpha_0}}. \tag{30}$$

We shall expand $\exp(-\sigma_\xi^2/Y_0^2\cos^2\alpha_0)$ in a power series of $(\sigma_\xi^2/Y_0^2\cos^2\alpha_0)$ and, by using only the linear approximation, we shall reduce (30) to the form:

$$\overline{N(Y, \delta\alpha)} = N(Y, 0) + \overline{\delta N(Y, \delta\alpha)}, \tag{31}$$

where $N(Y, 0) = (-\pi Y_0/4k_{cr})e^{j\alpha_0}$ is the inverse of the equivalent gain in the absence of a random parametric action, and $\overline{\delta N(Y, \delta\alpha)}$ is the average value of the correction brought forth by fluctuations.

By developing the $N(Y, 0)$ and $\delta N(Y, \delta\alpha)$ expressions for $\alpha_0 = \arcsin[(\varkappa - Y_0)/Y_0]$[1], after simple transformations we finally obtain the following expression suitable for graphic construction:

$$N(Y, 0) = -\frac{\pi}{4k_p}\left[\sqrt{2\varkappa Y_0 - \varkappa^2} + j(\varkappa - Y_0)\right], \tag{32}$$

$$\overline{\delta N(Y, \delta\alpha)} = \frac{\pi\sigma_\xi^2}{4k_p}\left[\frac{(\varkappa - Y_0)^2 + Y_0^2}{\sqrt{(2\varkappa Y_0 - \varkappa^2)^3}} - j\frac{(\varkappa - Y_0)}{\sqrt{(2\varkappa Y_0 - \varkappa^2)^3}}\right]. \tag{33}$$

The conditions for the existence of periodic solutions in the system are determined by the equation

$$K(j\omega) = N(Y, 0) + \overline{\delta N(Y, \delta\alpha)}, \tag{34}$$

where $K(j\omega)$ is the equivalent transfer locus of the extremal system to be controlled [1]. The graphic construction in Fig. 2 gives an example of the fulfillment of condition (34) as a result of which the average values of the self-oscillation frequency and amplitude in the system are determined.

As was indicated above, for ERCS with a fixed quantization grid, the derivation of the expression for the distribution density $\Delta\beta$ is difficult, and the final solution of the problem cannot be obtained. We shall limit our analysis here to the following qualitative considerations.

Consider the expression for the average deviation of the relay actuation phase,

$$\overline{\Delta\beta} = \overline{\Delta\alpha} = \overline{\delta\alpha} - \frac{\sigma_\xi^2}{2Y^2}\frac{\omega_\xi^2}{\omega_0^2}\frac{1}{\cos\alpha_0} \tag{35}$$

Let us introduce the $R(\tau) = e^{-(\beta^2/4)\tau^2}\cos\overline{\omega}\tau$ function.

Then,

$$\omega_\xi^2 = -\left(\frac{d^2R}{d\tau^2}\right)_{\tau=0} = \overline{\omega}^2 + \frac{\beta^2}{2}, \tag{36}$$

where $\overline{\omega}$, as is known, denotes the average value of the fluctuation energy spectrum frequency, and β denotes the average spectrum width.

Expression (35), together with (36), indicates that $\overline{\Delta\alpha} < \overline{\delta\alpha}$ always holds and that, for some values of ω_ξ^2,

$\overline{\Delta\alpha}$ can change its sign. This means that for random external disturbances applied to the regulator input of an ERCS having a fixed quantization grid, the self-oscillation frequency for a given σ_ξ is lower than in the preceding system and that, if $\overline{\Delta\alpha} \lessgtr 0$, it can be even lower than the self-oscillation frequency ω_0 of an undisturbed system.

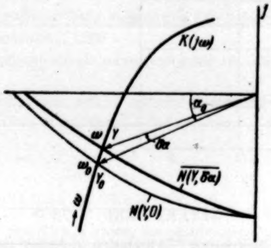

Fig. 2.

4. Certain Generalizations and Comparative Characteristics of the Statistical-Linearization Method under Consideration

The statistical-linearization method which has been considered in application to ERCS can be even more readily applied to ordinary self-oscillation systems having relay characteristics of any type if, naturally, the restrictions imposed on $\xi(t)$ are maintained. Since a random external disturbance $\xi(t)$ applied to the relay component input in a self-oscillation system is always reduced to the random distribution of the relay-actuation phase, the equivalent gain $S(Y, \delta\alpha)$ of a nonlinear element can be found as a step function with a random amplitude distribution according to the usual rules of the describing-function method.

The average value of $\overline{S(Y, \delta\alpha)}$ is determined once and for all with respect to the found expression for distribution (17); this determination is reduced to the calculation of integrals of the type

$$\int_{-\infty}^{\infty} e^{-hx^2-jax} x^n dx = j^n \frac{d^n\left(e^{-a^2/4h}\right)}{da^n}, \tag{37}$$

which are calculated according to the method indicated in [7].

For instance, let us find the $\overline{S(Y, \delta\alpha)}$ expression for a relay with the insensitivity zone 2a. As is known, in this case,

$$S(Y, 0) = \frac{4}{\pi Y}\cos\alpha, \tag{38}$$

where $\alpha = \arcsin(a/Y)$, and the relay gain k_p is assumed to be equal to unity for the sake of simplicity.

Then

$$S(Y, \delta\alpha) = \frac{4}{\pi Y}\cos(\alpha + \delta\alpha)$$

and

$$\overline{S(Y, \delta\alpha)} = \int_{-\infty}^{\infty} S(Y, \delta\alpha)\, w(\delta\alpha)\, d(\delta\alpha), \tag{39}$$

where

$$w(\delta\alpha) = (1 - \delta\alpha\,\mathrm{tg}\,\alpha)\frac{Y}{\sigma}\frac{\cos\alpha}{\sqrt{2\pi}} e^{-\frac{1}{2}\left(\frac{\delta\alpha}{\sigma}\right)^2 Y^2\cos^2\alpha}$$

[see (17)].

Let us consider some particular cases.

1. Let a = 0 (the relay has no insensitivity zone). For this case, we obtain

$$S(Y, \delta\alpha) = \frac{4}{\pi Y}\cos\delta\alpha, \tag{40}$$

$$w(\delta\alpha) = \frac{1}{\sqrt{2\pi}}\frac{Y}{\sigma} e^{-\frac{1}{2}\left(\frac{\delta\alpha}{\sigma}\right)^2 Y^2}, \tag{41}$$

i.e., we obtain a Gaussian distribution.

By calculating the integral (39) for a = 0, we obtain

$$\overline{S(Y, \delta\alpha)} = \frac{4}{\pi Y} e^{-\frac{\sigma^2}{2Y^2}} = \frac{4}{\pi Y} e^{-\frac{1}{4\beta^2}}, \tag{42}$$

where $\beta = (Y/\sqrt{2}\sigma)$.

2. For $a \neq 0$, the $w(\delta\alpha)$ distribution is nonsymmetrical, leading to a complex expression for $\overline{S(Y, \delta\alpha)}$. Omitting the intermediate derivation steps, we shall write the result obtained in calculating integral (39) in the following form:

$$\overline{S(Y, \delta\alpha)} = \frac{4}{\pi Y}\cos\alpha\, e^{-\frac{1}{4\beta^2\cos^2\alpha}} - (\mathrm{tg}\,\alpha + j)\frac{1}{2\beta^2}\frac{\mathrm{tg}\,\alpha}{\cos\alpha} e^{-\frac{1}{4\beta^2\cos^2\alpha}}. \tag{43}$$

The second term in the right-hand side of Eq. (43) is due to the $w(\delta\alpha)$ terms which distort the symmetric $\delta\alpha$ distribution.

Let us compare the obtained expressions for $\overline{S(Y, \delta\alpha)}$ with the results given in [3] for the same nonlinearity types.

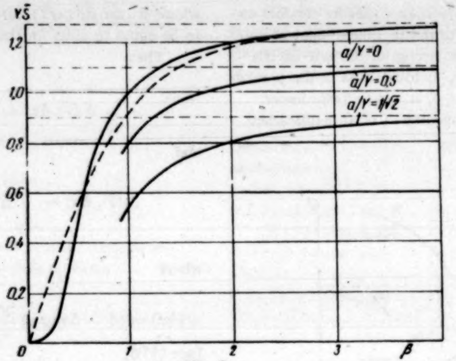

Fig. 3.

Figure 3 shows the $Y\overline{S(Y, \delta\alpha)}$ dependence plotted as a function of the $\beta = Y/\sqrt{2}\sigma$ parameter according to Eq. (42) and the curve, shown by the dotted line, plotted for the same case according to the equation given in [3]. The same diagram shows the $Y\overline{S}(Y, \delta\alpha)$ curves for $a/Y = 0.5$ and $a/Y = 1/\sqrt{2}$, which were obtained according to Eq. (43) without taking into account the distortion of the symmetry of $w(\delta\alpha)$. Similar dependences based on equations used in [3] are not provided here, since, for $\sigma \to 0$, one can use only a finite number of terms of the double infinite series, which expresses the equivalent gain value in this case in expanding the indeterminacies for their calculation.

A comparison of characteristics for a relay without an insensitivity zone (Fig. 3) shows that both static-linearization methods yield approximately equal results, at least in the region of small values (in correspondence with the assumptions of the method proposed). The expression $\overline{S(Y, \delta\alpha)}$ which was found here was given in unexpanded form and not in the form of an infinite series as in [3], thereby considerably reducing the amount of work involved in calculation. In conclusion, it should be noted that the statistical linearization method used in [3] cannot reveal the presence of a complex component in the expression for the equivalent gain for a relay with an insensitivity zone, which is important, for instance, in analyzing the stability of periodic regimes.

LITERATURE CITED

1. I. S. Morosanov, "Calculation of steady-state conditions in extremal control systems with independent scanning," Transactions of the Conference on the Theory and Application of Discrete Automatic Systems [in Russian] (Izd. AN SSSR, 1960).
2. I. E. Kazakov, "Approximate probability analysis of the operational accuracy of essentially nonlinear automatic systems," Avtomat. i Telemekh. 17, 5 (1956).‡
3. A. A. Pervozvanskii, "An approximate method for the investigation of self-oscillation systems in the presence of random disturbances," Izvest. Akad. Nauk SSSR, Otdel. Tekh. Nauk, 3 (1958).
4. I. S. Morosanov, "Extremal control methods," Avtomat. i Telemekh. 18, 11 (1957).‡
5. I. S. Morosanov, "Investigation of periodic operating conditions in extremal relay control systems," Avtomat. i Telemekh. 21, 7 (1960).‡
6. R. L. Stratonovich, Selected Problems in the Theory of Fluctuations in Radio Engineering [in Russian] (Izd. Sovetskoe Radio, 1960).
7. V. I. Bunimovich, Fluctuation Processes in Radio Receivers [in Russian] (Izd. Sovetskoe Radio, 1951).
8. A. A. Pervozvanskii, "Self-oscillation systems in the presence of slowly changing external disturbances," Izvest Akad. Nauk SSSR, Otdel. Tekh. Nauk, Mekhanika i Mashinostroenie, 1 (1959).

---

‡See English translation.

EXTREMAL CONTROL BY THE METHOD OF RANDOM SCANNING

L. A. Rastrigin

Moscow

Translated from Avtomatika i Telemekhanika, Vol. 21, No. 9, pp. 1264-1271,
September, 1960
Original article submitted April 18, 1960

The present article describes a method of random scanning in application to problems in extremal control of multiparameter systems. A device which realizes this method is described.

1. Formulation of the Problem

In the majority of cases, the problems encountered in the synthesis of self-adjusting systems, which are currently gaining widespread use, are reduced to the optimization of a certain performance function Q of these systems, i.e., to the search for conditions which secure the minimum value Q^* of this function.

Let Q be a function of the parameters $x_1, x_2, \dots, x_n$,

$$Q = Q(x_1, x_2, \dots, x_n), \qquad (1)$$

while Q^* is the smallest of all possible values of this function:

$$Q^* = Q(x_1^*, \dots, x_n^*) \leqslant Q(x_1, \dots, x_n) \qquad (2)$$
$$(-\infty < x_i < \infty,\ i = 1, \dots, n).$$

It is necessary to find values of the $x_1^*, x_2^*, \dots, x_n^*$ parameters for which the Q function is minimized, i.e., values which satisfy expression (2).

It is obvious that in order to solve this problem it is necessary to ascertain the existence of at least one minimum of the performance function. The number of minima is, however, not limited. It will be shown below that the proposed scanning system discriminates between the values of the minima and statistically tends to secure the smallest of these minima.

At present, there are several automatic optimization methods, i.e., methods of searching for the optimizing series of parameters $x_1^*, \dots, x_n^*$. From among these methods, the method of alternating parameter changes (the Gauss-Zeidel method), the gradient method, and the method of quickest triggering (the Kantorovich method) should be mentioned. These methods have been applied and are presently used in a large number of automatic optimization systems (see, for instance, [1]).

The scanning organized in correspondence with the above methods has the character of predetermined scanning, i.e., of scanning where the changes in the $x_1, x_2, \dots, x_n$ parameters are rigorously predetermined by the type of function Q and the organization of the selected scanning method.

However, predetermined scanning is not the only possible method. W. R. Ashby [2] came forward with his idea of random scanning, which was used as the basis of the present paper.

2. The Random Scanning Method

In terms of the control theory, Ashby's idea can be represented in the following manner.

Assume that the system to be controlled can exist in a certain multiplicity set $P = \{\overline{p}\}$ of states, finite or infinite. In this case, the system is considered to be adjusted if it is in one of the states contained in the multiplicity subset $P^* \subset P$. The only requirement imposed on this multiplicity subset is that it be of equal power to the multiplicity set P.

Thus, the problem of the adjustment of the system to be controlled is reduced to the selection of a method and organization of searching for one of the $\overline{p}^*$ elements of the multiplicity set P^* among all possible elements $\overline{p}$ in the multiplicity set P. Ashby suggested that $\overline{p}^*$ be sought not with respect to a given rule, as in the case of predetermined scanning, but by means of random selections to be performed by a "selection amplifier" [3].

Ashby's selection amplifier operates in the following manner (see Fig. 1). A certain state $\overline{p}$, selected at random, is communicated to the system to be controlled SC by means of a generator of random events, GRE, which secures a regime of random selections from the source of all possible states SS, i.e., from the multiplicity set P. In this, the selector unit SU, after receiving information on the reaction of the controlled system to the variant supplied by GRE, either sends a command to GRE to produce the next random selection in the case of $\bar{p} \neq \bar{p}^*$ or, in the case of $\bar{p} = \bar{p}^*$, disconnects GRE and thereby locks the system in this state.

It is obvious that, in operation with respect to such commands, the selection unit will screen out the $\bar{p} \neq \bar{p}^*$ states until it finds, by chance, the required state, which it will preserve continuously until any external or internal factors transfer the system from this state into another $\bar{p} \neq \bar{p}^*$ state. After this, the above-considered mode of random searching for the state $\bar{p}^*$ will again become operative. W. R. Ashby's well-known homeostat operates on the basis of this principle [2 and 3].

It should be noted that Ashby's system is characterized by three specific features: it has a source of all possibilities (the multiplicity set P of elements), a device securing a regime of random selections from a general totality P (generator of random events), and a device which supplies the criterion according to which the required element is selected in the system to be controlled (selection unit). Another important feature is the presence of two sharply different operating conditions: the temporary, transient random scanning mode (for $\bar{p} \neq \bar{p}^*$) and the other, the stable adjusted mode (for $\bar{p} \neq \bar{p}^*$), which was to be found. It can readily be seen the the described method is essentially the realization of the trial and error method, which is widely used in practice.

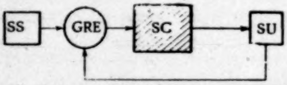

Fig. 1.

3. Application of Random Scanning to Optimization Problems

In order to apply the described random scanning to the problem of minimizing the $Q(x_1, x_2, \ldots, x_n)$ function, the "state" $\bar{p}$ of the "system to be controlled" Q must denote the velocities of its motion along the coordinates, i.e., $\bar{p} = (\dot{x}_1, \dot{x}_2, \ldots, \dot{x}_n)$, rather than its coordinates in a parametric coordinate system. It is obvious that $\bar{p}$ is the velocity vector of a point representing the state of the system to be controlled in an n-dimensional parametric space $\{x_1, x_2, \ldots, x_n\}$. Under these conditions, the control system depicted in Fig. 1 is applicable. The above-mentioned operating modes of the system are also preserved, with the exception that the system may not be immediately transferred to the Q^* state under the adjusted conditions ($\bar{p} = \bar{p}^*$) for $n > 1$; however, in this case, it will "approach" the required state, i.e., the performance function Q will have a smaller value at the end of the adjustment conditions duration than at the beginning.

As the most natural criterion for the selection of states supplied at random, we can use, for instance, the value of the derivative

$$\frac{dQ}{dt} = \frac{\partial Q}{\partial x_1} \dot{x}_1 + \ldots + \frac{\partial Q}{\partial x_n} \dot{x}_n. \tag{3}$$

If all possible states $\bar{p} = (\dot{x}_1, \dot{x}_2, \ldots, \dot{x}_n)$ which the state source SS can supply pertain to the multiplicity set P, the multiplicity set P^* must contain those states of the system to be controlled which satisfy the inequality

$$\frac{dQ}{dt} < 0, \tag{4}$$

i.e., the condition for the diminution of the performance function. This inequality represents the selection criterion. It can readily be seen that the probability that the velocity $\bar{p}$ satisfying this criterion will be selected as close to $\frac{1}{2}$, since the "quantity" $\bar{p}^* \in P^*$ is slightly less than one half of all $\bar{p} \in P$ if the hypersurfaces $Q(x_1, x_2, \ldots, x_n) = \text{const}$ in an n-dimensional parametric space are sufficiently smooth.

Thus, the algorithm of random scanning in the given case consists in the fact that the $\bar{p}$ states, which lead to $(dQ/dt) \geq 0$, are transient and are immediately replaced by other states also chosen at random. The states leading to the inequality $(dQ/dt) < 0$ are stabilized until this inequality changes its sign due to the change in the derivative. It is obvious from (3) that the change in the derivative in the fixed state, i.e., for $\bar{p} = \text{const}$, occurs due to changes in partial derivatives $(\partial Q/\partial x_i)(i = 1, 2, \ldots, n)$ during the motion of the point representing the system to be controlled in the parametric space. The transition from the adjustment value of $\bar{p}$ to another value takes place at the moment at which the derivative changes its sign, i.e., when $(dQ/dt) = 0$. It can readily be seen that, as a result of operation with respect to the indicated algorithm, the quantity Q can be reduced to its minimum value Q^* after a certain finite number of cycles in selecting $\bar{p}$.

However, the realization of such an algorithm requires the calculation of the (dQ/dt) derivative in correspondence with the selection criterion (4), which, in the end reduces the noise stability of this control system, especially for small values of the derivative modulus. Therefore, we chose a different method that did not require the calculation of the derivative and was simple and reliable, although it did reduce the response quickness in adjustment to a certain extent.

We proposed an arrangement whereby the Q value of the performance function is continuously compared with a certain level η, which changes at a constant rate $q < 0$. Let the values of Q and η coincide at the initial moment.

Then, $\eta(t) = Q_i + qt$, where Q_i is the value of the Q function at the beginning of the $\underline{i}$th stage, and $\underline{t}$ is the time.

Let us denote by $Q(\bar{p}, t)$ the performance function value at the instant of time $\underline{t}$ for the fixed rate $\bar{p}$ of changes in the system parameters. If, for the rate value $\underline{p}_i$ at the beginning of the $\underline{i}$th stage and for sufficiently small values of $t > 0$ the inequality

$$Q(\bar{p}_i, t) - \eta(t) < 0, \tag{5}$$

holds, the Q_{i+1} value of the performance function at the instant of time $t = t_i$, when the $\eta(t)$ and $Q(\bar{p}_i, t)$ values are compared again, is smaller than the Q_i value at the initial moment. At the instant of time t_i, the rate value is switched from $\bar{p}_i$ to the $\bar{p}_{i+1}$ value, and a new stage in the process is initiated.

Consequently, if inequality (5) is satisfied after the beginning of the $\underline{i}$th stage, the performance function value is smaller at the beginning of the next stage.

Thus, inequality (5) can serve as the selection criterion. Then, all values of $\bar{p}$ satisfying this inequality pertain to the multiplicity subset P^*. The $\bar{p}$ values that do not satisfy (5) are immediately rejected.

Criterion (5) does not require the calculation of the derivative, thus considerably simplifying its realization; however, it is somewhat narrower than criterion (4). Actually, inequality (5) for $t = 0$ can be written in the differential form:

$$\frac{dQ}{dt} < q. \tag{6}$$

The obtained inequality determines the selection of rate $\underline{p}$ at the initial moment. The smaller the $\underline{q}$ value, the smaller the domain of $\bar{p}$ values which satisfy this inequality. Therefore, by comparing (4) and (6), we ascertain that since $q < 0$, the domain of rate values satisfying (5) is always smaller than the domain of rate values satisfying (4).

Figure 2 shows the variation of Q for two values of $\bar{p}_i$. The thin lines in the same figure indicate η levels for different values $q_1 > q_2 > q_3$. It can readily be seen that, for $q = q_3$, the $\bar{p}_i^{(2)}$ value does not belong to P^*, while $\bar{p}_i^{(1)} \in P^*$ in the T_1 interval. With an increase in $\underline{q}$, the multiplicity set P^* becomes wider. Thus, for $q = q_1$, both rate values $p_i^{(1,2)} \in P^*$.

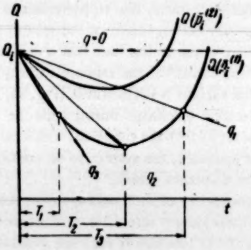

Fig. 2.

Therefore, we can consider that

$$P^* = P^*(q) \tag{7}$$

has been established.

For $q = 0$, inequalities (4) and (6) coincide, and the selection of rates at the initial moment will be equal for both criteria. However, at the switching moment, criterion (6) will yield $Q_{i+1} = Q_i$, i.e., there will be no adjustment. For large $q < 0$, the adjustment will be weak, since it follows from (5) that the $Q_i - Q_{i+1} = -qt$ difference is small, regardless of the fact that the selected rate led to $Q < Q_{i+1}$ values during the operation process (see the $q = q_3$ case for $\bar{p}_i^{(1)}$ in Fig. 2).

Thus, on the one hand, an increase in $\underline{q}$ leads to the enlargement of the multiplicity subset P^* and, on the other hand, lowers the adjustment efficiency. Therefore, there exists such a $q = q^*$ value which optimizes the considered control system with respect to adjustment speed.

The η level is essentially one of the memory organization forms where $\eta > 0$ is "memorized" instead of Q. In this case, the "memory" is shifted in time independently of the Q value until the moment at which $Q = \eta$. The presence of the $\eta - Q$ difference, the sign of which determines the device operating conditions, considerably improves its noise stability.

It should be noted that this memory form is applicable also in predetermined scanning, which is organized according to the method of alternating parameter changes or according to the quickest triggering method. In this case, there is no necessity of determining the minimum of the performance function Q in the selected direction with respect to criterion (4), and it is sufficient to introduce the described "memory" by means of the comparison signal. Such an improvement, as was shown above, considerably improves the control system noise stability, although it somewhat lowers the scanning rate.

Figure 3 shows the block diagram of a device capable of realizing extremal control by the described method of random scanning.

In this diagram, the GRE generators secure a regime of random selections from the SS source of all possible states and act on the rate of change in the parameters of the system to be controlled, SC. In this, the changing quantity Q is continuously compared with a certain signal η generated by the generator of comparison signals, GCS. The result of the $Q \gtrless \eta$ comparison determines the system operating mode, which is assigned by the control unit, CU. The operating modes are given in the table.

TABLE 1.

Operating modes	C	Q	η
preparation	$Q>\eta$	const	$c>0$
scanning	$Q<\eta$	var	$q<0$

During the preparation stage, GRE's are disconnected, and the controlled system is not excited; i.e., the tracing point is immobile and Q = const. For $Q=\eta$, the preparation operating mode is replaced by the scanning mode and during this stage the system parameters change at the constant rate $\bar{p}$, the direction and modulus of which are determined by GRE at random. At the moment when $Q=\eta$, the scanning mode is replaced by the preparation mode, etc.

It can readily be shown that the indicated device corresponds to the above-considered algorithm of random scanning with the selection criterion (5). Here, the q-parameter has a rigorously defined physical meaning: it is the rate of change in the comparison signal η under scanning conditions. It is obvious that, in the absence of hysteresis in the considered control system, the operation is possible only for

$$Q_{\min} < q. \tag{8}$$

In the opposite case, the $Q<\eta$ inequality would never be satisfied.

4. Effects of Hysteresis

It has been shown that the described device operates under two regimes: "scanning" and "preparation," and that the moment of transition from one regime to another is determined by the coincidence of Q and η signals. However, in actual devices, due to a number of causes (inertia, hysteresis of the comparison system, etc.), the switching of regimes takes place for different relations between η and Q. Thus, the moment of transition from the preparation regime to the scanning regime or the reverse is determined by the equations,

$$\eta = Q + \delta_1, \quad \eta = Q - \delta_2,$$

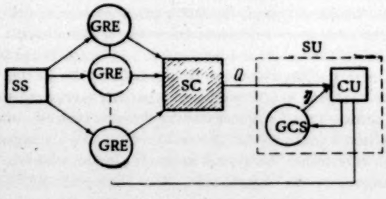

Fig. 3.

respectively, where δ_1 and δ_2 are usually sufficiently small positive quantities: $\delta_1=\delta_1(c)$ and $\delta_2=\delta_2(q, \bar{p})$.

It can readily be seen that, for disconnected GRE, i.e., for Q = const, self-oscillation conditions will arise —sawtooth oscillations of the η signal with respect to Q, where $\eta_{\max}-\eta_{\min}=\delta_1+\delta_2$.

These self-oscillations, a consequence of hysteresis in actual control systems, introduce interesting peculiarities in the device operation.

Thus, in the presence of self-oscillations, control is possible even if inequality (8) is not satisfied, i.e., if $|\bar{p}|_{\max}<|q|$. This is obvious from the graph in Fig. 4,

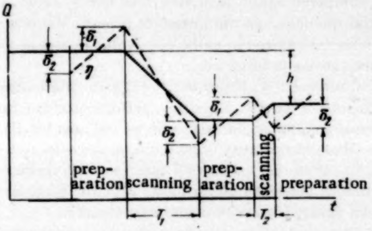

Fig. 4.

where two scanning cycles for the favorable (T_1 interval) and the unfavorable (T_2 interval) variants of the Q function variation (solid line) are shown. As a result of the action of both variants, the peformance function is reduced by h due to the fact that, in adjustment, the mutual rate of change in Q and η is less than in the unadjusted state. This leads to a change in the duration of the above regimes: $T_1 > T_2$.

Thus, as a result of hysteresis for a large $|q|$, the η signal follows the Q quantity under self-oscillation conditions, while the duration of favorable variants of Q variation ($\dot{Q}<0$) is somewhat longer than that of unfavorable variants ($\dot{Q}>0$) which ultimately leads to a systematic reduction of the performance function. Therefore, in certain cases, the deliberate introduction of hysteresis into the control system is entirely possible.

Another peculiarity due to hysteresis is the possibility of temporary derangement of the system to be controlled. This is due to the fact that a certain time is required for the "trial" of the random variant offered by a GRE. If this variant is unfavorable (Fig. 4), the Q function will be able to change during time T_2. If several such variants ($\bar{p}\neq\bar{p}^*$) are supplied, which is possible although not probable, the system to be controlled will be deranged to a certain extent.

The possibility of such derangement renders the described control system selective with respect to different minima of the Q function if such are available. Actually, after Q attained the intermediate minimum B (Fig.

5), the system will continue its motion in the neighborhood of the point B until the system, in its random motion due to the possibility of derangement, reaches the point C. From this point, the system can either return in the opposite direction or, due to the minimizing action of the described device, reach the neighborhood of the point A. In the first case, the whole process will be repeated from the beginning until the tracing point reaches point A – the smallest minimum of Q. Naturally, motion in the opposite direction, from A to B, is also possible; however, derangement variants which occur considerably less often are required in this case and, consequently, a longer time for overcoming the $h_2 > h_1$ barrier will be required. Consequently, the probability of a transition from A to B is smaller than the probability of transition from B to A. Thus, the system, being able to dwell in any region, will remain for a considerably longer time in the neighborhood of its minimum value Q^* than in any other region.

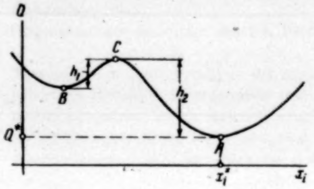

Fig. 5.

5. Experimental Verification

The possibility of optimization by the random scanning method according to the proposed scheme was checked experimentally under laboratory conditions in application to simple self-adjusting systems.

We considered the problem of the self-balancing of two independent small beam-weights which formed a system having two degrees of freedom. The beams were maintained in the horizontal position by means of leaf springs whose tension determined the deviations x_1 and x_2 from the equilibrium states of these beams. The adjustment of such a system consisted in finding the equilibrium conditions for which the deviations x_1 and x_2 of these beams were simultaneously equal to zero: $x_1 = x_2 = 0$. The adjustment of this system was performed by means of mobile weight trolleys, which were driven by two electric motors, respectively. The performance function Q of the system was realized in two variants: $Q = |x_1| + |x_2|$ and $Q = \max |x_i|$ $(i = 1, 2)$.

Thus, the problem was reduced to the minimization of the Q function, which attained its minimum $(Q^* = 0)$ only when the system was adjusted, i.e., at the moment at which both beams were in equilibrium.

The comparison signal generator consisted of a voltage divider – a rheostat which was electromechanically driven. In the first case, the selection unit was based on a three-coil polarized RP-5 relay, where $|x_1|$ and $|x_2|$ were fed to two windings, and the comparison signal η was fed to the third winding. The second variant was based on two two-coil polarized relays. The random event generator consisted of an ordinary PS-64 scaling device, to the input of which noise from a tube was supplied; when the noise was disconnected, the trigger cells were fixed in a random position which determined the motion of the weight trolleys that balanced the beams.

The performed experiments showed that:

1. Adjustment, i.e., minimization of the Q function in both variants, is possible through use of the described method.

2. The adjustment itself is independent of the rate $\underline{q}$ of signal variation η in a wide range; for different values of $\underline{q}$, only the average adjustment time changed.

3. There exists an optimum value $q = q^*$ for which the average time for the system adjustment is at the minimum, all other conditions being equal, i.e., there exists a $\underline{q}$ for which the described adjustment system is optimized with respect to quickness of response.

Another experiment was prepared for verifying the possibility of adjustment by the random scanning method in the presence of a systematic disturbance factor. For this purpose we used a beam with two trolleys, one of which moved at a constant speed, thereby introducing the disturbance, while the other was included in the above-described control system for the purpose of adjusting (balancing) this single-parameter system.

The performance function was realized in the natural way:

$$Q = |x|,$$

where $\underline{x}$ is the beam deviation from the equilibrium position. Such a device is essentially the simplest statistical follow-up system operating on the basis of the random scanning method.

Experiments showed that the performance of such a self-adjusting system is largely determined by the process speed and, consequently, by the selection of the $\underline{q}$ parameter.

SUMMARY

The proposed extremal control system, based on random scanning, can be successfully applied in automatic optimization of multiparameter systems to be controlled for any performance function, including discontinuous functions. The advantages of this system are particularly pronounced in the case of control with respect to a large number of independent or dependent parameters of the system to be controlled. Computers, which are necessary in the case of predetermined scanning, are not required in the realization of such a system, making it possible to optimize the system to be controlled with a minimum amount of equipment. The increased noise stability, secured by the application of memory in the form of reference signals, can also be used in predetermined extremal control systems.

LITERATURE CITED

1. A. A. Fel'dbaum, "An automatic optimizer," Avtomat.i Telemekh.19, 8 (1958).*
2. Ross Ashby, Design for a Brain (New York, 1952).
3. Ross Ashby, "Circuit for an amplifier of thinking ability," Collection: Automata [Russian translation] (IL, 1956).

---

*See English translation.

STABILITY OF A CONTROLLED SYSTEM WITH TWO NONLINEAR ELEMENTS

Chang Jên-wei

Moscow

Translated from Avtomatika i Telemekhanika, Vol. 21, No. 9, pp. 1272-1278, September, 1960
Original article submitted April 9, 1960

This article presents a study of the second B. V. Bulgakov problem where the nonlinearity of one of the measuring units is taken into account and a method is described for solving the stability problem, which makes it possible, on the one hand, to find acceptable regulator parameters and, on the other hand, to determine the controlled variables range, containing the coordinate origin, for which the system stability is guaranteed.

1. Formulation of the Problem

In their paper, A. M. Letov and A. I. Lur'e [1] formulated one of the most important problems in automatic control: the determination of stability criteria for controlled systems described by equations of the following form:

$$\begin{aligned}\dot{\eta}_k &= \sum_{\alpha=1}^{n} b_{k\alpha}\eta_\alpha + n_k\xi,\\ \dot{\xi} &= f(\sigma), \quad \sigma = \sum p_\alpha(\eta_\alpha) - \varphi(\xi),\end{aligned} \tag{1}$$

where $p_\alpha(\eta_\alpha)$ and $\varphi(\xi)$ are functions of the (A) class. This paper also treats the effect of various parameters characterizing nonlinear dependences on stability of systems to be controlled. The problem stated is of great practical importance. Actually, let us consider an aircraft controlled with respect to yawing by a nonlinear autopilot having rigid feedback. This autopilot has a damping gyroscope which can be described by the following equations:

$$\begin{aligned}T_s^2\ddot{\alpha} + U_s\dot{\alpha} + K_s\alpha &= \varphi_s(\bar{\sigma}),\\ \bar{\sigma} &= M\dot{\psi} + N^2\ddot{\psi},\end{aligned}$$

where α is the deviation angle of the damping gyroscope and ψ is the aircraft yaw angle. The $\varphi_s(\bar{\sigma})$ function (see Fig. 1) is of the following form:

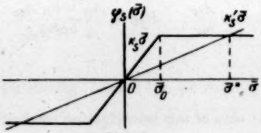

Fig. 1.

$$\varphi_s(\bar{\sigma}) = \begin{cases} k_s\bar{\sigma}_0 & \text{for} \quad \bar{\sigma} \geqslant \bar{\sigma}_0,\\ k_s\bar{\sigma} & \text{for} \quad |\bar{\sigma}| < \bar{\sigma}_0,\\ -k_s\bar{\sigma}_0 & \text{for} \quad \bar{\sigma} \leqslant -\bar{\sigma}_0. \end{cases} \tag{2}$$

The T_s^2 and U_s coefficients are usually small and, in the case where the $\varphi_s(\bar{\sigma})$ function is linear, they can be neglected [2]. Then, the equations of the aircraft motion with respect to the yaw angle can be approximately represented in the following form:

$$\begin{aligned}T^2\ddot{\psi} + U\dot{\psi} + K\psi + \mu &= 0,\\ \dot{\mu} = f^*(\sigma), \quad \sigma &= a\psi + E\alpha - \frac{1}{2}\mu,\\ \alpha = \varphi^*(\bar{\sigma}), \quad \bar{\sigma} &= M\dot{\psi} + N^2\ddot{\psi}.\end{aligned} \tag{3}$$

Here, ψ is the yaw angle, μ is the rudder deviation angle, $\varphi^*(\bar{\sigma}) = (1/K_s)\varphi_s(\bar{\sigma})$ and $f^*(\sigma)$ is the servomotor characteristic (see Fig. 2), which has the following properties:

$$\begin{aligned}\left[\frac{df^*(\sigma)}{d\sigma}\right]_{\sigma=0} &\geqslant h_0^* > 0,\\ |h_1^*\sigma| \geqslant |f^*(\sigma)| &\geqslant |h_2^*\sigma| \quad \text{for} \quad \sigma \neq 0.\end{aligned} \tag{4}$$

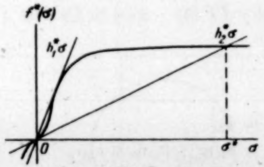

Fig. 2.

The problem of the stability of system (3) in the case where the $\varphi^*(\bar{\sigma})$ function is linear has been thoroughly investigated in [2]. The following question now arises: will the stability of system (3) deteriorate if the $\varphi^{*}(\bar\sigma)$ function is nonlinear or will it be possible to find such autopilot parameters for which this nonlinearity will not impair the stability of system (3) in comparison with the case wherein the gyroscope characteristic is linear. The purpose of the present paper is to determine the effect of the nonlinearity of $\varphi^{*}(\bar\sigma)$ on the aircraft flight stability and to find the stability criteria for the system (3). It is obvious that system (3) is a particular case of system (1).

2. General Form of the Stability Conditions

In investigating the stability of system (3), we shall use the second (direct) Lyapunov method. The Lyapunov V function is usually plotted in quadratic form, and the coefficients in the expression for $\dot V$ do not depend on the system coordinates. However, as is known, the latter condition is not compulsory. It is sometimes difficult to plot the Lyapunov function in such a way that the coefficients of the $\dot V$ form are independent of the system coordinates. Actually, if some coefficients of the $\dot V$ form depend on the system coordinates, the problem consists in finding a continuous continuum of these coordinates, which contain the coordinate origin and which lie within a certain interval (in the control range), and in selecting the remaining coefficients in such a way that the V function is actually a Lyapunov function for the given system. This method has been chosen here for solving the above problem.*

Before we start plotting any diagrams, let us reduce the initial equations (3) to the normal and dimensionless forms.

By introducing the following notation:

$$\eta_1 = \psi, \quad \eta_2 = T\frac{d\psi}{dt}, \quad t = T\tau, \quad b_{21} = -K,$$
$$b_{22} = -\frac{U}{T},$$
$$u_2 = -1, \quad p_1 = a, \quad q_1 = -\frac{N^2K}{T^2}, \tag{5}$$
$$q_2 = \left(M - \frac{N^2U}{T^2}\right)\frac{1}{T},$$
$$r = \frac{1}{l}, \quad \bar r = \frac{N^2}{T^2},$$
$$f(\sigma) = Tf^{*}(\sigma), \quad \varphi(\bar\sigma) = E\varphi^{*}(\bar\sigma),$$

we obtain:

$$\begin{aligned} \dot\eta_1 &= \eta_2, \\ \dot\eta_2 &= b_{21}\eta_1 + b_{22}\eta_2 + u_2\mu, \\ \dot\mu &= f(\sigma), \\ \dot\sigma &= p_1\eta_1 + \varphi(\sigma) - r\mu, \\ \bar\sigma &= q_1\eta_1 + q_2\eta_2 - \bar r\mu. \end{aligned} \tag{6}$$

It is obvious from Fig. 2 that, in the control range $|\sigma| \leq |\sigma^{*}|$, the entire $f^{*}(\sigma)$ function is located between two straight lines $y = h_1^{*}\sigma$ and $y = h_2^{*}\sigma$, where $h_1^{*} > h_2^{*}$. In this interval, $h(\sigma)\sigma$ can be substituted for $f(\sigma)$, where $h(\sigma) = (1/\sigma)f(\sigma)$,

$$h_1 = Th_1^{*} \geqslant h(\sigma) \geqslant Th_2^{*} = h_2,$$
$$h(0) = \lim_{\sigma\to 0}\frac{1}{\sigma}f(\sigma) = h_0 = Th_0^{*}.$$

Similarly, in the $|\bar\sigma| \leq \bar\sigma^{*}$ range, $\varphi(\bar\sigma)$ can be replaced by $k(\bar\sigma)\bar\sigma$, where

$$k(\sigma) = \frac{\varphi(\bar\sigma)}{\bar\sigma}, \quad k_1 = E\frac{k_s}{K_s} \geqslant k(\sigma) \geqslant \frac{E}{K_s}k_s' = k_2.$$

Thus, system (6) can be written in a different form:

$$\begin{aligned} \dot\eta_1 &= \eta_2, \\ \dot\eta_2 &= b_{21}\eta_1 + b_{22}\eta_2 + u_2\mu, \\ \dot\mu &= h(\sigma)\left[(p_1 + q_1k(\bar\sigma))\eta_1 + \right. \\ &\left. + q_2k(\bar\sigma)\eta_2 - (r + \bar rk(\bar\sigma))\mu\right]. \end{aligned} \tag{7}$$

We assume that system (6) remains stable after the automatic device is switched off, i.e., that all roots of the $\lambda^2 - b_{22}\lambda - b_{21} = 0$ equation have negative real parts. According to the well-known Lyapunov theorem, it is always possible to find a positive function

$$F = \tfrac{1}{2}\left(B_{11}\eta_1^2 + 2B_{12}\eta_1\eta_2 + B_{22}^2\eta_2^2\right)$$

whose sign is determined and which satisfies the equation

$$\begin{aligned} &\frac{\partial F}{\partial\eta_1}\eta_2 + \frac{\partial F}{\partial\eta_2}(b_{21}\eta_1 + b_{22}\eta_2) = \\ &= \overline{W} = -(A_{11}\eta_1^2 + 2A_{12}\eta_1\eta_2 + A_{22}\eta_2^2), \end{aligned} \tag{8}$$

where $\overline{W}$ is an assigned negative function whose sign is determined, i.e., the A_{11}, A_{12}, and A_{22} coefficients, which are not yet known, satisfy the conditions

$$A_{11} > 0, \quad A_{11}A_{22} - A_{12}^2 > 0. \tag{9}$$

From Eq. (8), the expressions for the B_{11}, B_{12}, and B_{22} coefficients can readily be found in terms of the A_{11}, A_{12}, and A_{22} coefficients:

$$\begin{aligned} B_{11} &= \frac{1}{-b_{21}b_{22}}\left[(b_{21} - b_{22}^2)A_{11} + 2b_{21}b_{22}A_{12} - b_{21}^2A_{22}\right], \\ B_{12} &= -\frac{A_{11}}{b_{21}}, \quad B_{22} = \frac{A_{11} - b_{21}A_{22}}{b_{21}b_{22}} \end{aligned} \tag{10}$$

---

* The general idea of this investigation method has been presented in a paper by V. I. Zubov [3].

Let us now consider the following positive function whose sign is determined:

$$V = F(\eta_1, \eta_2) + \frac{1}{2}\mu^2.$$

According to Eqs. (7), we find:

$$-\dot{V} = -\overline{W} - u_2B_{12}\eta_1\mu - u_2B_{22}\eta_2\mu -$$
$$- h(\sigma)\left[p_1 + q_1k(\bar{\sigma})\right]\eta_1\mu -$$
$$- q_2h(\sigma)k(\bar{\sigma})\eta_2\mu + h(\sigma)\left[r + \bar{r}k(\bar{\sigma})\right]\mu^2.$$

According to the Sylvester criterion, $\dot{V}$ will be a negative function with determined sign if the following inequality is satisfied:

$$D = \begin{vmatrix} A_{11} & A_{12} & P_1 \\ A_{12} & A_{22} & P_2 \\ P_1 & P_2 & h(\sigma)\left[r + \bar{r}k(\bar{\sigma})\right] \end{vmatrix} > 0, \qquad (11)$$

where
$$P_1 = \frac{1}{2}\left[u_2B_{12} + h(\sigma)(p_1 + q_1k(\bar{\sigma}))\right],$$
$$P_2 = \frac{1}{2}\left[u_2B_{22} + q_2h(\sigma)k(\bar{\sigma})\right].$$

According to the well-known Lyapunov theorem, system (6) will be asymptotically stable if inequalities (9) and (11) are satisfied. Inequality (11) must be satisfied for continuous continua of the σ and $\bar{\sigma}$ coordinates which fill the $|\sigma| \le \sigma^*$ and $|\bar{\sigma}| \le \bar{\sigma}^*$ regions. It is obvious from Figs. 1 and 2 that the σ^* and $\bar{\sigma}^*$ values correspond to the lower branches of the straight lines $y = h_2^*\sigma$ and $\bar{y} = k_s\bar{\sigma}$ of the nonlinear functions. Therefore, we shall henceforth consider only domains where $\underline{h}$ and $\underline{k}$ change. The extent of these domains will determine the character of the system stability. This extent obviously depends on the autopilot parameters.

3. Investigation of Stability Conditions

We shall now pass to the investigation of stability conditions for system (6). In the particular given case, we assume that $A_{12} = 0$ and $A_{11} = A_{22} > 0$ for the sake of simplicity. Inequality (9) will then always be satisfied. By expanding the determinant D, we obtain:

$$A_{22}^2h(r + \bar{r}k) - \frac{A_{22}}{4}\left[u_2B_{12} + h(p_1 + q_1k)\right]^2 -$$
$$- \frac{A_{22}}{4}\left[u_2B_{22} + q_2hk\right]^2 > 0. \qquad (12)$$

We shall denote:

$$q_2hk = x, \quad p_1h + q_1hk = y. \qquad (13)$$

By substituting (13) in (12), we obtain:

$$(x + u_2B_{22})^2 + (y + u_2B_{12})^2 < 4A_{22}h(r + \bar{r}k). \qquad (14)$$

We can readily find the expression

$$h(r + \bar{r}k) = \frac{r}{p_1}y + \left(\frac{\bar{r}}{q_2} - \frac{rq_1}{p_1q_2}\right)x = Ay + Bx,$$

where

$$A = \frac{r}{p_1}, \quad B = \frac{\bar{r}p_1 - rq_1}{p_1q_2}.$$

Inequality (14) can be written in the following form:

$$[x + (u_2B_{22} - 2A_{22}B)]^2 +$$
$$+ [y + (u_2B_{12} - 2A_{22}A)]^2 < 4A_{22}^2(A^2 + B^2) -$$
$$- 4A_{22}Bu_2B_{22} - 4A_{22}Au_2B_{12}. \qquad (15)$$

Let us substitute the expression (10) for B_{12} and B_{22} in (15) and represent it in the form:

$$(X - x_0)^2 + (Y - y_0)^2 < 4R^2, \qquad (16)$$

where

$$X = \frac{x}{A_{22}}, \quad Y = \frac{y}{A_{22}}, \quad x_0 = 2B - \frac{u_2(1 - b_{21})}{b_{21}b_{22}},$$

$$y_0 = 2A + \frac{u_2}{b_{21}}, \quad R^2 = A^2 + B^2 + C,$$

$$C = -u_2\left[\frac{(1 - b_{21})B}{b_{21}b_{22}} - \frac{A}{b_{21}}\right].$$

It is obvious that X and Y are not constant quantities in inequality (16).

It can readily be shown that, in order that inequality (16) be satisfied, it is sufficient that the following inequalities hold (see Fig. 3):

$$(x_0 - \sqrt{2}R) < X < (x_0 + \sqrt{2}R),$$

$$(y_0 - \sqrt{2}R) \leqslant Y \leqslant (y_0 + \sqrt{2}R),$$

or

$$(x_0 - \sqrt{2}R)A_{22} < q_2hk < (x_0 + \sqrt{2}R)A_{22}, \qquad (17a)$$

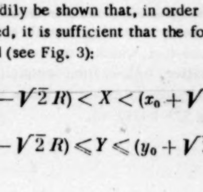

Fig. 3.

$$(y_0 - \sqrt{2}\,R)\,A_{22} \leqslant p_1h + q_1hk \leqslant (y_0 + \sqrt{2}\,R)\,A_{22}. \tag{17b}$$

In accordance with inequalities (17a) and (17b), we can find an allowable domain where h and k change and determine the effect of nonlinearity on the stability of system (6). Before this, according to the initial transformations of the coefficients, we find the expressions for R^2, x_0, and y_0:

$$R^2 = \frac{T^2(N^2al + N^2K)^2}{a^2l^2(MT^2 - N^2U)^2} + $$

$$+ \frac{T^2(N^2al + N^2K)}{alKU(MT^2 - N^2U)} + \frac{al + K}{a^2l^2K},$$

$$x_0 = \frac{2T(N^2al + N^2K)}{al(MT^2 - N^2U)} + \frac{T(1 + K)}{KU}, \quad y_0 = \frac{2}{al} + \frac{1}{K}.$$

Denoting

$$\eta = \frac{T(N^2al + N^2K)}{MT^2 - N^2U}, \quad \xi = \frac{K}{al}, \quad S = \frac{(1 + K)T}{U}. \tag{18}$$

Equations (18) include the autopilot coefficients. In the given case, it is obvious that $\xi \geq 0$ and $s \geq 0$, and the expressions for R^2, x_0, and y_0 assume the following form:

$$R^2 = \frac{1}{K^2}(\xi^2\eta^2 + S\xi\eta + \xi^2 + \xi),$$
$$x_0 = \frac{1}{K}(2\xi\eta + S), \quad y_0 = \frac{1}{K}(1 + 2\xi). \tag{19}$$

Let us find the conditions under which the inequality (12) or (16) is satisfied. According to inequality (12), it is necessary that the $h \geq m > 0$ relation holds where m is a certain finite number. Due to property (4) of the $f(\sigma)$ function, the latter inequality can always be satisfied. The $R^2 > 0$ condition, which is necessary for inequality (16) to be positive, follows from inequality (16). Let us plot the $R^2 = 0$ graphs in the (η, ξ) plane and separate the domain where $R^2 > 0$ (Fig. 4).

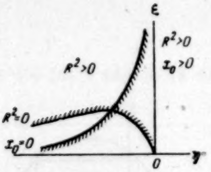

Fig. 4.

It is obvious that the $R^2 > 0$ condition is not sufficient for satisfying inequality (16) and that inequalities (17) must be considered in detail. Two cases, determined by the sign in front of q_2 —which coincides with the sign in front of η— are possible here.

1. In the case where $q_2 = (1/T^3)(MT^2 - N^2U) \geq 0$, inequality (17a) yields the condition:

$$\frac{x_0 + \sqrt{2}\,R}{x_0 - \sqrt{2}\,R} > \frac{h_1k_1}{h_2k_2} = \alpha\beta \geqslant 1, \tag{20}$$

where the quantities $\alpha = (h_1/h_2)$ and $\beta = (k_1/k_2)$ characterize the domain where h and k change.

Let us write inequality (20) in the form

$$\rho x_0 - \sqrt{2}\,R < 0, \tag{21}$$

where $\rho = \dfrac{\alpha\beta - 1}{\alpha\beta + 1} \leqslant 1.$

This inequality determines certain stability regions in the (η, ξ) plane of the autopilot parameters. The equation for the boundary of this region is $\rho x_0 - \sqrt{2}R = 0$. After substituting expression (19), this equation assumes the following form:

$$(4\rho^2 - 2)\,\xi^2\eta^2 +$$
$$+ (4\rho^2 - 2)\,S\xi\eta - 2\xi^2 - 2\xi + \rho^2S^2 = 0. \tag{22}$$

The boundaries of the stability region for different values of ρ are shown in the right (η, ξ) half-plane in Fig. 5.

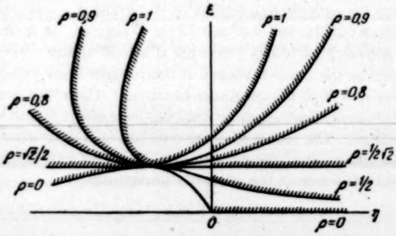

Fig. 5.

It is obvious that inequality (17a) can determine only the domain of the h and k quantities. Their maximum values are determined by inequality (17b).

Actually, inequality (17b) yields the conditions

$$\left[(y_0 - \sqrt{2}\,R) - \frac{q_1}{q_2}(x_0 - \sqrt{2}\,R)\right]\frac{A_{22}}{p_1} \leqslant$$

$$\leqslant h \leqslant \left[y_0 + \sqrt{2}\,R) - \frac{q_1}{q_2}(x_0 + \sqrt{2}\,R)\right]\frac{A_{22}}{p_1},$$

$$\frac{p_1(x_0 - \sqrt{2}\,R)}{q_2(y_0 - \sqrt{2}\,R) - q_1(x_0 - \sqrt{2}\,R)} \leqslant k \leqslant$$

$$\leqslant \frac{p_1(x_0 + \sqrt{2}\,R)}{q_2(y_0 + \sqrt{2}\,R) - q_1(x_0 + \sqrt{2}\,R)}.$$

The values of A_{22} and k have not yet been determined; suitable values of these quantities must be selected in order that the last two inequalities are satisfied.

2. In the case where $q_2 < 0$, $x_0(\eta, \xi)$ in the left (η, ξ) half-plane has different signs for different values of η and ξ, as is shown in Fig. 4. We have two cases, respectively:

for $x_0 > 0$, inequality (17a) yields the condition

$$x_0 - \sqrt{2}\,R < 0, \tag{23}$$

for $x_0 < 0$, inequality (17a) yields the condition

$$-\rho x_0 - \sqrt{2}\,R < 0, \tag{24}$$

where $\rho = \dfrac{\alpha\beta - 1}{\alpha\beta + 1} \leqslant 1.$

It can readily be shown that the equation for the boundary of the stability region, determined by inequalities (24), is of the same form as equation (22). The boundaries of the stability region for different values of ρ are shown in the left (η, ξ) half-plane in Fig. 5.

As in the preceding case, the value of k will be similarly determined by the inequality

$$\frac{(x_0 + \sqrt{2}\,R)\,p_1}{q_2(y_0 - \sqrt{2}\,R) - q_1(x_0 + \sqrt{2}\,R)} \leqslant k \leqslant$$

$$\leqslant \frac{(x_0 - \sqrt{2}\,R)\,p_1}{q_2(y_0 + \sqrt{2}\,R) - q_1(x_0 - \sqrt{2}\,R)}.$$

It is obvious from Fig. 5 that the stability region with respect to the η and ξ parameters is restricted as the value of ρ increases, i.e., as the domain wherein h and k change becomes larger. Therefore, generally speaking, the introduction of nonlinearity $\varphi(\overline{\sigma})$, which characterizes the gyroscope nonlinear property, reduces the stability of system (6). However, if, for a certain nonlinear function $\varphi(\overline{\sigma})$, corresponding, for instance, to $\rho = \rho_1$, $0 \leq \rho_1 \leq 1$, we choose the η and ξ parameters to be in the $\rho = \rho_1$ region, the nonlinearity will not affect the system stability. In this, in the region corresponding to $\rho = 1$, we can make the domain of k variations for which the system stability is guaranteed as large as we wish.

In conclusion, the author extends his thanks to A. M. Letov for his valuable advice and remarks.

LITERATURE CITED

1. A. M. Letov and A. M. Lur'e, "The state of and problems in the development of the theory of stability of automatic control systems," Transactions of the Session of the Academy of Sciences, USSR, on Scientific Problems in Industrial Automation [in Russian] (Izd. AN SSSR, 1957).
2. A. M. Letov, Stability of Nonlinear Control Systems [in Russian] (Gostekhizdat, 1955).
3. V. I. Zubov, "Certain sufficient characterisitics of the stability of a nonlinear system of differential equations," Priklad. Matem. i Mekh. 17, 4 (1953).

ON THE ACCURATE DETERMINATION OF PERIODIC REGIMES IN SECTIONALLY LINEAR AUTOMATIC CONTROL SYSTEMS*

E. N. Rozenvasser

Leningrad

Translated from Avtomatika i Telemekhanika, Vol. 21, No. 9, pp. 1279-1292,
September, 1960
Original article submitted March 14, 1960

An exact method for determining periodic regimes in arbitrary sectionally linear systems is considered. The solution of the problem is reduced to the determination of forced oscillations of a linear system with periodically changing parameters. These forced oscillations are found in an exact manner by means of a new approach, which is based on the solution of an auxiliary Fredholm integral equation of the second kind. The thus obtained periodic solution depends on the unknown times of motion along sections of nonlinear characteristics. By using this solution and the conditions for the transition from one section of the nonlinear characteristic to another, it is possible to determine the transcendental equations of periods.

1. Formulation of the Problem

By a sectionally linear control system we shall designate a system which, for certain given time intervals, is described by different systems of linear differential equations with constant or variable coefficients. In the first case, such a system will be called a steady-state system, and in the second case, it will be called an unsteady-state system.

The simplest example of sectionally linear systems is those which differ from the linear systems by the presence of nonlinear elements having sectionally linear characteristics. Various spontaneously changing cybernetic systems can be considered as the more complex of this class [1]. Until now, only steady-state sectionally linear systems were generally considered in the literature [2-5]. This problem was first studied in [2] in which a method was presented for the determination of periodic regimes by fitting the linear-system solutions corresponding to different time intervals. In so doing, the solution of the problem was always brought to the point at which a certain transcendental algebraic system of equations was composed with respect to unknown times of motion for different sections of the nonlinear characteristic ("equations of periods").

The practical application of the fitting method in the form proposed in [2] often involves difficulties due to the following reasons:

1. The period equations depend on the roots of characteristic equations of the corresponding linear systems which, if the considered system of differential equations is of a high order, precludes the possibility of expressing the obtained results in terms of initial parameters.

2. The amount of calculation involved in composition of the period equations increases markedly with an increase in the order of the initial system of differential equations.

3. This method does not make it possible to take into account the filtering properties of the linear portion of the system and to determine only a finite number of harmonics in the Fourier expansion of the periodic regime to be found.

A modified fitting method for systems with a single nonlinearity, making it posssible to write the equations of periods in terms of the initial system coefficients, was proposed in [4]. In [3], a method different from those described in [2] and [4] was used in composing the equations of periods by fitting for the case where the system contained only one nonlinearity, the characteristic of which consisted of straight lines parallel to two given lines. The method used in [3] was based on a special affine transformation of the nonlinear characteristic and could not be extended to nonlinear characteristics of a more general type.

A linear transformation making it possible to reduce the amount of calculation involved in the application of the above methods was proposed in [5].

---

* The basic results of the present paper were reported at the Seminar on Nonlinear Problems in Automatic Control Theory, held at the Institute of Automation and Remote Control, Academy of Sciences, USSR, on December 2, 1959.

In the present paper, the solution of this problem is reduced to the consideration of the Fredholm integral equation of the second kind, providing the possibility of composing the equations of periods for an arbitrary sectionally linear system. An approximate method, making it possible to use only a finite number of harmonics of the periodic regime to be found, is also described. In this, all results are expressed directly in terms of the coefficients of the initial system of differential equations.

2. Transmission of Periodic Signals through the Linear Portion of the System

Consider the differential equations

$$\dot{x}_k = \sum_{\alpha=1}^{n} b_{k\alpha} x_\alpha + F_k(t) \quad (k = 1, 2, \ldots, n), \quad (1)$$

where $b_{k\alpha}$ are constants, and $F_k(t)$ are periodic functions of the period T, which we shall consider to be sectionally continuous. It is necessary to find the periodic solutions of the system (1). This problem has been studied in detail in [6] and [7]. Another solution form, necessary for further derivations, will be given below.

Let

$$D(\lambda) = | b_{k\alpha} - \lambda \delta_{k\alpha} | \quad (2)$$

be the characteristic determinant of the system linear portion,† and let $\Delta_{k\alpha}$ be the cofactor of the element of determinant (2) which is in the kth row and in the αth column. Subsequently, it is sufficient to assume that the equation

$$D(\lambda) = 0, \quad (3)$$

the roots of which are $\lambda = \lambda_\rho$ $(\rho = 1, 2, \ldots, n)$, does not have a root equal to

$$\psi_s = \frac{2\pi i}{T} s, \quad (4)$$

where s is zero or any integer.

Under the above assumptions, the periodic solution of system (1) is uniquely defined by the equation

$$x_s^T(t) = \sum_{k=1}^{n} \int_0^T \Phi_{ks}^T(t - \tau) F_k(\tau)\, d\tau \quad (s = 1, 2, \ldots, n), \quad (5)$$

where

$$\Phi_{ks}^T(y) = -\frac{1}{T} \sum_{m=-\infty}^{\infty} \frac{\Delta_{ks}(\psi_m)}{D(\psi_m)} e^{\psi_m y} \quad (6)$$

Functions (6) can be represented in finite form. If $\lambda_\rho \neq \lambda_\alpha$ and for $\rho \neq \alpha$, we have

$$\Phi_{ks}^T(y) = \Phi_{ks}(y) = \sum_{\rho=1}^{n} \frac{\Delta_{ks}(\lambda_\rho)}{D'(\lambda_\rho)} \frac{e^{\lambda_\rho y}}{e^{\lambda_\rho T} - 1}. \quad (7)$$

For y = 0 and y = T, the sum of the series (6) is equal to

$$\Phi_{ks}^T(0) = \Phi_{ks}^T(T) = \frac{1}{2} \sum_{\rho=1}^{n} \frac{\Delta_{ks}(\lambda_\rho)}{D'(\lambda_\rho)} \operatorname{cth} \frac{\lambda_\rho T}{2} \quad \text{for} \quad 0 < y < T. \quad (8)$$

Moreover,

$$\Phi_{ks}(0) - \Phi_{ks}(T) = \delta_{ks}. \quad (9)$$

Consequently, for $k \neq s$, the $\Phi_{ks}^T(t-\tau)$ function is continuous with the square given by

$$0 \leqslant t \leqslant T, \quad 0 \leqslant \tau \leqslant T_1, \quad (10)$$

and the $\Phi_{ss}^T(t-\tau)$ functions have a discontinuity on the $t=\tau$ diagonal.

In using expression (7) in (5), it must be taken into account that, for $0 \le t \le T$, the argument $t-\tau$ of the integrand in (5) varies within the $-T \le t-\tau \le T$ interval and, in correspondence with (7),

$$\Phi_{ks}^T(t - \tau) = \begin{cases} \displaystyle\sum_{\rho=1}^{n} \frac{\Delta_{ks}(\lambda_\rho)}{D'(\lambda_\rho)} \frac{e^{\lambda_\rho (t-\tau)}}{e^{\lambda_\rho T} - 1} & \text{for} \quad 0 < t - \tau < T, \\ \displaystyle\sum_{\rho=1}^{n} \frac{\Delta_{ks}(\lambda_\rho)}{D'(\lambda_\rho)} \frac{e^{\lambda_\rho T} e^{\lambda_\rho (\tau - t)}}{e^{\lambda_\rho T} - 1} & \text{for} \quad 0 < \tau - t < T. \end{cases} \quad (11)$$

If Eq. (3) has the roots $\lambda_1, \ldots, \lambda_m$ (the multiplicities of which are $\nu_1, \nu_2, \ldots, \nu_m$), we shall have the following equation instead of (7):

$$\Phi_{ks}^T(y) = \sum_{\nu=1}^{\nu_m}{}' \sum_{\rho=1}^{m} c_{\nu,\rho}^{ks} \frac{(-1)^\nu}{(\nu-1)!} \frac{d^{\nu-1}}{(d\lambda_\rho)^{\nu-1}} \left(\frac{e^{\lambda_\rho y}}{e^{\lambda_\rho T} - 1} \right) (0 < y < T), \quad (12)$$

where the $c_{\nu,\rho}^{ks}$ quantities are coefficients in resolution into partial fractions:

$$\frac{\Delta_{ks}(\lambda)}{D(\lambda)} = \sum_{\nu=1}^{\nu_m}{}' \sum_{\rho=1}^{m}{}' \frac{c_{\nu,\rho}^{ks}}{(\lambda - \lambda_\rho)^\nu}. \quad (13)$$

Also of interest are cases of $F_k(t)$ functions with the period T as well as functions

$$F_k(t) = -F_k(t + T). \quad (14)$$

Under the above assumptions, in case (14), the periodic solution of system (1) will be written thus:

$$x_s^T(t) = \sum_{k=1}^{n} \int_0^T \Psi_{ks}^T(t - \tau) F_k(\tau)\, d\tau, \quad (15)$$

where

$$\Psi_{ks}^T(y) = -\frac{2}{T} \sum_{m=-\infty}^{\infty} \frac{\Delta_{ks}(\psi_{2m-1})}{D(\psi_{2m-1})} e^{\psi_{2m-1} y}. \quad (16)$$

---

†$\delta_{k\alpha}$ is the Kronecker symbol.

If Eq. (3) has simple roots, we also have

$$\Psi^T_{ks}(y) =$$

$$= \sum_{\rho=1}^{n} \frac{\Delta_{ks}(\lambda_\rho)}{D'(\lambda_\rho)} \frac{e^{\lambda_\rho y}}{e^{\frac{\lambda_\rho T}{2}} + 1} \quad \text{for} \quad 0 < y < \frac{T}{2},$$

$$\Psi^T_{ks}(y) = -\Psi^T_{ks}\left(y + \frac{T}{2}\right). \tag{17}$$

The case wherein Eq. (3) has multiple roots is considered in the same manner as above.

The derivation of equations contained in this paragraph is given in Appendix I.

3. Self-Oscillations of a Steady-State System Having a Single Nonlinearity

Consider the system of equations

$$\dot{x}_k = \sum_{\alpha=1}^{n} b_{k\alpha} x_\alpha + h_k f(\sigma) \qquad (k = 1, 2, \ldots, n),$$

$$\sigma = \sum_{s=1}^{n} j_s x_s, \tag{18}$$

where $b_{k\alpha}$ are the same as in (1), h_k and j_s are constants, and $f(\sigma)$ is a sectionally linear function.

We shall introduce the notation

$$H_k(\lambda) = \sum_{s=1}^{n} h_s \Delta_{sk}(\lambda), \tag{19}$$

$$M(\lambda) = -\sum_{k=1}^{n} j_k H_k(\lambda) = -\sum_{s=1}^{n} \sum_{k=1}^{n} h_s j_k \Delta_{sk}(\lambda). \tag{20}$$

We shall asume that the polynomials (20) and (3) do not have common roots. Then without restricting the generality of treatment, we can consider that, for any number T, Eq. (3) does not have roots of the form (4), which can always be secured by introducing a new nonlinear function:

$$f_1(\sigma) = f(\sigma) - c\sigma,$$

where c is a certain given number.

We shall assume that system (18) has a periodic solution of a certain period T:

$$x^T_s(t) = x^T_s(t + T) \qquad (s = 1, 2, \ldots, n),$$

$$\sigma^T(t) = \sigma^T(t + T). \tag{21}$$

Then

$$f(t) = f\left(\sigma^T(t)\right) \tag{22}$$

will also be a periodic function of the T period.

Consider the linear system

$$\dot{x}_k = \sum_{k=1}^{n} b_{k\alpha} x_\alpha + h_k f(t). \tag{23}$$

According to the above assumptions, we have a nonresonance case. In this case, the unique periodic solution of system (23) will obviously coincide with the solution (21) of system (18).

Since in the given case

$$F_k(t) = h_k f(t), \tag{24}$$

then, according to (5),

$$x^T_s(t) = \int_0^T \Phi^T_s(t - \tau) f(\tau)\, d\tau, \tag{25}$$

where

$$\Phi^T_s(y) = -\frac{1}{T} \sum_{m=-\infty}^{\infty} \frac{H_s(\psi_m)}{D(\psi_m)} e^{\psi_m y}, \tag{26}$$

and, moreover,

$$\sigma^T(t) = \int_0^T \Phi^T(t - \tau) f(\tau)\, d\tau, \tag{27}$$

where

$$\Phi^T(y) = \sum_{s=1}^{n} j_s \Phi^T_s(y) = \frac{1}{T} \sum_{m=-\infty}^{\infty} \frac{M(\psi_m)}{D(\psi_m)} e^{\psi_m y}. \tag{28}$$

Let us now consider the function (22). We shall assume that the periodic solution type (i.e., the sequence of passage over different portions of the nonlinear characteristic) is given. Then, we have

$$f(t) = a_i \sigma^T(t) + b_i \quad \text{for} \quad t_{i-1} < t < t_i$$

$$(i = 1, 2, \ldots, m), \tag{29}$$

where a_i and b_i are assigned numbers, some of which can be equal to each other; m is the over-all number of transitions from one portion of the nonlinear characteristic to another during a single period; $t_0 = 0$;

$$0 < t_1 < t_2 < \ldots < t_m = T \tag{30}$$

are unknown times which must still be determined.

Let us introduce the periodic step functions

$$A(t) = A(t+T), \quad A(t) = a_i \quad \text{for} \quad t_{i-1} < t < t_i,$$

$$B(t) = B(t+T), \quad B(t) = b_i \quad \text{for} \quad t_{i-1} < t < t_i. \tag{31}$$

Then, (29) can be rewritten thus:

$$f(t) = A(t)\,\sigma^T(t) + B(t). \tag{32}$$

By substituting this expression in (27), we obtain the integral equation

$$\sigma^T(t) =$$

$$= \int_0^T \Phi^T(t-\tau)\,A(\tau)\,\sigma^T(\tau)\,d\tau + \int_0^T \Phi^T(t-\tau)\,B(\tau)\,d\tau,$$

whose kernel

$$R_1(t,\tau) = \Phi^T(t-\tau)\,A(\tau) \tag{34}$$

and the free term

$$M(t) = \int_0^T \Phi^T(t-\tau)\,B(\tau)\,d\tau \tag{35}$$

are known functions of t_i.

We shall limit our consideration to values of t_i for which the denominator of the resolvent of kernel (34) does not become equal to zero. Then, in correspondence with the general theory [8], we can write

$$\sigma^T(t, t_1, t_2, \ldots, T) = M(t) + \int_0^T R(t,\tau)\,M(\tau)\,d\tau, \tag{36}$$

where $R(t,\tau)$ is the resolvent of kernel (34).

If

$$|R_1(t,\tau)| < \frac{1}{T},$$

the resolvent can be obtained by the method of successive approximations.

In the general case [8], the resolvent is given by the equation

$$R(t,\tau) = \frac{\sum\limits_{n=0}^{\infty} (-1)^n \frac{d_n(t,\tau)}{n!}}{\sum\limits_{n=0}^{\infty} (-1)^n \frac{d_n}{n!}}, \tag{37}$$

while

$$d_0(t,\tau) = R_1(t,\tau), \quad d_0 = 1, \tag{38}$$

and all remaining $d_n(t,\tau)$ and d_n can be successively found from the recurrent relations

$$d_{k+1} = \int_0^T d_k(\tau,\tau)\,d\tau, \tag{39}$$

$$d_n(t,\tau) = R_1(t,\tau)\,d_n - n\int_0^T R_1(t,y)\,d_{n-1}(y,\tau)\,dy. \tag{40}$$

Considering (31), (39) and (40) can be rewritten in the following form:

$$d_n(t,\tau) = d_n a_i \Phi^T(t-z) -$$

$$-n\sum_{i=1}^{m} a_i \int_{t_{i-1}}^{t_i} \Phi^T(t-y)\,d_{n-1}(y,\tau)\,dy, \quad t_{i-1} < t < t_i,$$

$$d_{n+1} = d_n \Phi^T(0) \sum_{i=1}^{m} a_i (t_i - t_{i-1}) \tag{41}$$

$$-n\sum_{i=1}^{m} a_i \int_0^T dt \int_{t_{i-1}}^{t_i} \Phi^T(t-y)\,d_{n-1}(y,t)\,dy.$$

It can be shown that

$$d_n(t,\tau) = A(\tau)\,b_n(t,\tau), \tag{42}$$

where $b_n(t,\tau)$ are continuous functions for $t \neq \tau$.

By using (42), Eq. (36) can be simplified and reduced to the form

$$\sigma^T(t, t_1, \ldots, T) =$$

$$= \int_0^T L(t,\tau)\,B(\tau)\,d\tau = \sum_{i=1}^{T} b_i \int_{t_{i-1}}^{t_i} L(t,\tau)\,d\tau, \tag{43}$$

where

$$L(t,\tau) = \frac{R(t,\tau)}{A(\tau)} \tag{44}$$

is a regular function [9].

In practical calculations, one must always take the finite number of terms in the numerator and the denominator of (37). We can derive equations which make it possible to estimate the error resulting from this procedure.

It is known [8] that

$$|d_n| \leqslant n^{\frac{n}{2}} (MT)^n,$$

$$|d_n(t,\tau)| \leqslant \frac{1}{T}(n+1)^{\frac{n+1}{2}} (MT)^{n+1},$$

where M is the maximum value of the modulus of function (34), which is found from (31), (7), and (20) in each concrete case.

Let n_0 be an integer which satisfies the condition

$$n_0 > (MTe)^2. \tag{46}$$

Then by using (45), we can derive the error estimates:

$$\left|\sum_{n=n_0}^{\infty}\frac{d_n}{n!}\right| \leqslant \sum_{n=n_0}^{\infty}\left|\frac{d_n}{n!}\right| \leqslant \frac{(MTe)^{n_0}}{\sqrt{n_0^{n_0}}}\,\frac{1}{\sqrt{n_0}-MTe},$$

$$\sum_{n=n_0}^{\infty}\left|\frac{d_n(t,\tau)}{n!}\right| \leqslant \frac{1}{T}\,\frac{(MTe)^{n_0+1}}{\sqrt{(n_0+1)^{n_0+1}}}\,\frac{1}{\sqrt{n_0+1}-MTe}. \tag{47}$$

Let us now assume that the expression for $\sigma^T(t, t_1, \ldots, T)$ has been found. Then, in order to determine the unknown times t_i, it is necessary to use conditions which determine the transition from one portion of the linear characteristic to another ("switching conditions") [10].

For instance, consider the simplest case wherein the transition takes place when the σ coordinate attains a certain given value.

Then, the following condition must be satisfied:

$$\sigma^T(t_i) = \sigma_{i\,\mathrm{ass}}, \tag{48}$$

where $\sigma_{i\,\mathrm{ass}}$ are certain assigned numbers.

By using (43), we obtain

$$\sigma^T(t_i, t_1, \ldots, t_{m-1}, T) = \sigma_{i\,\mathrm{ass}} \tag{49}$$

Expressions (49) represent the equations of periods which were to be determined. For more complex switching conditions [10], the equations of periods are composed in a similar manner.

If a computer is used for the solution of system (49), the considerations in [4] remain valid. In this, it is necessary to take into account that the periodic solutions of system (18) do not actually correspond to all systems of numbers t_i which formally satisfy Eqs. (49). It is necessary that $t_i < t_j$ for $i < j$, and that σ attains its value $\sigma_{i\,\mathrm{ass}}$ for the first time for $t = t_i$. Moreover, for physical reasons, there may be some requirements imposed on the derivative of σ, etc. [10].

Let us briefly consider the case of a symmetric periodic regime.

Let us assume that the number of transitions is $m = 2n$, and that

$$t_k - t_{k-1} = t_{k+n} - t_{k+n-1}, \quad k < n. \tag{50}$$

The nonlinear characteristic must be such that

$$a_{n+k} = a_k, \quad b_{n+k} = -b_k, \quad k < n. \tag{51}$$

We shall seek the odd periodic regime characterized by the conditions

$$x_s^T(t) = -x_s^T\left(t+\frac{T}{2}\right), \quad \sigma^T(t) = -\sigma^T\left(t+\frac{T}{2}\right). \tag{52}$$

If (50) and (51) are satisfied,

$$A(t) = A\left(t+\frac{T}{2}\right), \quad B(t) = -B\left(t+\frac{T}{2}\right), \tag{53}$$

and, consequently, by taking (52) into account,

$$f(t) = -f\left(t+\frac{T}{2}\right).$$

By using Eq. (15) and following the above reasoning, we arrive at the integral equation

$$\sigma^T(t) = \int_0^{\frac{T}{2}} \Psi^T(t-\tau)\,A(\tau)\,\sigma^T(\tau)\,d\tau + {} + \int_0^{\frac{T}{2}} \Psi(t-\tau)\,B(\tau)\,d\tau. \tag{54}$$

The solution of this equation is written analogously to (43):

$$\sigma^T\left(t, t_1, \ldots, t_{m-1}, \frac{T}{2}\right) = \int_0^{\frac{T}{2}} \overline{L}_1(t,\tau)\,B(\tau)\,d\tau. \tag{55}$$

Thus, in correspondence with (50), the number of undetermined times which have to be found is reduced by half. The equations of periods are composed as in the general case.

The derivation of equations in this paragraph is given in Appendix II.

4. Forced Oscillations of a Steady-State System Having a Single Nonlinearity

Consider a system of equations differing from (18) by the presence of a certain period T on the right-hand sides of the periodic time functions:

$$\begin{aligned} x_k &= \sum_{\alpha=1}^{n} b_{k\alpha}x_\alpha + h_k f(\sigma) + f_k(t), \qquad (k = 1, 2, \ldots, n). \\ \sigma &= \sum j_s x_s, \quad f_k(t) = f_k(t+T), \end{aligned} \tag{56}$$

We shall seek periodic solutions of the system (56) having the period T. The solution type is considered to be given beforehand. In contrast to the self-oscillation case, the initial instant of time corresponding to the periodic regime will be unknown here. We shall assume that the periodic regime (21) is determined. Then, by consideration of, instead of (56), the linear system (1), wherein

$$F_k(t) = h_k f(\sigma^T(t)) + f_k(t), \tag{57}$$

and by repeating the reasoning in the previous paragraph, we arrive at the integral equation

$$\sigma^T(t) = \int_0^T \Phi^T(t-\tau) A(\tau) \sigma^T(\tau) d\tau + \int_0^T \Phi^T(t-\tau) B(\tau) d\tau + M_1(t), \tag{58}$$

where

$$M_1(t) = \sum_{s=1}^{n} \sum_{k=1}^{n} j_s \int_0^T \Phi^T_{ks}(t-\tau) f_k(\tau) d\tau \tag{59}$$

is a known function.

By applying the superposition principle and the results of the preceding paragraph, we find

$$\sigma^T(t, t_0, \ldots, t_{m-1}) = \int_0^T L(t, \tau) B(\tau) d\tau + M_1(t) + \int_0^T L(t, \tau) A(\tau) M_1(\tau) d\tau. \tag{60}$$

By use of the switching conditions we find the equations of periods with respect to m unknowns $t_0, t_1, \ldots, t_{m-1}$.

It is known that the action of disturbances within the period T on a nonlinear system under certain conditions can cause the appearance of periodic motions within the period pT, where p is an integer ("subharmonic oscillations").

The described method can readily be applied to the case of subharmonic oscillations. Actually, the $f_k(t)$, A(t), and B(t) functions can be considered to have the pT period. Therefore, the following integral equation is valid for the σ^{pT} subharmonic oscillations:

$$\sigma^{pT}(t) = \int_0^{pT} \Phi^{pT}(t-\tau) A(\tau) \sigma^{pT}(\tau) d\tau + \int_0^{pT} \Phi^{pT}(t-\tau) B(\tau) d\tau + M_1(t), \tag{61}$$

where

$$\Phi^{pT}(y) = \frac{1}{pT} \sum_{m=-\infty}^{\infty} \frac{M\left(\frac{\psi_m}{p}\right)}{D\left(\frac{\psi_m}{p}\right)} e^{\psi_m y}. \tag{62}$$

The solution of Eq. (61) is written similarly to that of (60). By using this solution and the switching conditions, we find equations of periods for the subharmonic regime.

5. Approximate Determination of the Periodic Regime in the Form of a Trigonometric Series

Let us first consider the case of self-oscillations. In all practical calculations, we can use a finite number of terms in series (28). In this, the integral equation (33) is transformed into an equation having a degenerate kernel [8] capable of exact solution.

Actually, let

$$\tilde{\sigma}^T(t) = \int_0^T \tilde{\Phi}^T(t-\tau) A(\tau) \tilde{\sigma}^T(\tau) d\tau + \int_0^T \tilde{\Phi}^T(t-\tau) B(\tau) d\tau, \tag{63}$$

where

$$\tilde{\Phi}^T(t-\tau) = \frac{1}{T} \sum_{k=-n}^{n} \frac{M(\psi_k)}{D(\psi_k)} e^{\psi_k(t-\tau)}. \tag{64}$$

From (64) we can conclude that the solution of Eq. (63) is of the following form:

$$\tilde{\sigma}^T(t) = \sum_{i=-n}^{n} s_i e^{\psi_i t}, \tag{65}$$

where s_i are constants to be determined. By substituting (65) in (63) and equating the coefficients of equal harmonics, we obtain

$$s_i = \frac{M(\psi_i)}{D(\psi_i)} \sum_{k=-n}^{n} s_k \alpha_{i-k} + \frac{M(\psi_i)}{D(\psi_i)} \beta_i, \tag{66}$$

where

$$\alpha_k = \frac{i}{2\pi k} \sum_{s=1}^{m} a_s (e^{-\psi_k t_s} - e^{-\psi_k t_{s-1}}),$$

$$\beta_k = \frac{i}{2\pi k} \sum_{s=1}^{m} b_s (e^{-\psi_k t_s} - e^{-\psi_k t_{s-1}}) \tag{67}$$

are the coefficients of the Fourier function (31).

After solving the linear system (66), we find

$$s_i(t_1, t_2, \ldots, T) = \frac{1}{\tilde{\Delta}} \sum_{k=-n}^{n} \frac{M(\psi_k)}{D(\psi_k)} b_k \tilde{\Delta}_{ki}, \quad (68)$$

where $\tilde{\Delta}$ is the determinant of system (66):

$$\tilde{\Delta} = \left| \delta_{ks} - \frac{M(\psi_k)}{D(\psi_k)} \alpha_{k-s} \right|, \quad (69)$$

and $\tilde{\Delta}_{ki}$ are the corresponding cofactors.

By substituting (68) in (65), we find $\tilde{\sigma}^T(t, t_1, t_2, \ldots, T)$ which, together with the switching conditions, yields the system of periodic equations which was to be found. In particular, for the case (48), we have

$$\sum_{k=-n}^{n}{}' s_k(t_1, t_2, \ldots, T) e^{\psi_k t_i} = \sigma_{i\,\mathrm{ass}}$$

$$(i = 1, 2, \ldots, m). \quad (70)$$

In the case of the odd symmetric regime, the number of time unknowns will correspondingly decrease, while equations (66) will contain only quantities s_i with odd subscripts.

In the case of forced oscillations, the approximate integral equation obtained from (58) will be of the following form:

$$\tilde{\sigma}^T(t) = \int_0^T \tilde{\Phi}^T(t-\tau) A(\tau) \tilde{\sigma}^T(\tau) d\tau + \int_0^T \tilde{\Phi}^T(t-\tau) B(\tau) d\tau + M_1(t). \quad (71)$$

Its solution will be

$$\tilde{\sigma}^T(t) = M_1(t) + \sum_{i=-n}^{n} \bar{s}_i e^{\psi_i t}, \quad (72)$$

where the values of $\bar{s}_i$ are determined by the relations

$$\bar{s}_i = -m_i + \frac{1}{\tilde{\Delta}} \sum_{k=-n}^{n} \left(\frac{M(\psi_k)}{D(\psi_k)} b_k + m_k \right) \tilde{\Delta}_{ki}, \quad (73)$$

and m_i are Fourier coefficients in the expansion

$$M_1(t) = \sum_{i=-\infty}^{\infty} m_i e^{\psi_i t}. \quad (74)$$

By using (73), (72), and the switching conditions, we obtain the equations of periods.

6. The General Case of a Sectionally Linear System

Let there be a system which, for $t_{i-1} < t < t_i$, is described by the equations

$$\dot{x}_k = \sum_{\alpha=1}^{n} B^i_{k\alpha} x_\alpha + f^i_k(t)$$

$$(k = 1, 2, \ldots, n;\ i = 1, 2, \ldots, m), \quad (75)$$

where $B^i_{k\alpha}$ and f^i_k are certain given time functions.

We shall introduce the periodic functions

$$B_{k\alpha}(t) = B_{k\alpha}(t+T), \quad B_{k\alpha}(t) = B^i_{k\alpha}(t)$$

$$\text{for} \quad t_{i-1} < t < t_i,$$

$$\varphi_k(t) = \varphi_k(t+T), \quad \varphi_k(t) = f^i_k(t) \quad (76)$$

$$\text{for} \quad t_{i-1} < t < t_i.$$

Then, if the periodic regime (21) has been attained in system (75), we have

$$\dot{x}^T_k = \sum_{\alpha=1}^{n} B_{k\alpha}(t) x^T_\alpha + \varphi_k(t) \quad (k = 1, 2, \ldots, n). \quad (77)$$

After we separate the constant terms from the Fourier expansion of the $B_{k\alpha}(t)$ function, (77) will be written thus:

$$\dot{x}^T_k = \sum_{\alpha=1}^{n} \bar{b}_{k\alpha} x^T_\alpha + \sum_{\alpha=1}^{n} \bar{B}_{k\alpha}(t) x^T_\alpha + \varphi_k(t)$$

$$(k = 1, 2, \ldots, n), \quad (78)$$

where

$$\bar{b}_{k\alpha} = \frac{1}{T} \sum_{i=1}^{m} \int_{t_{i-1}}^{t_i} B^i_{k\alpha}(\tau) d\tau, \quad \bar{B}_{k\alpha}(t) = B_{k\alpha}(t) - \bar{b}_{k\alpha}. \quad (79)$$

Assuming that

$$F_k(t) = \sum_{\alpha=1}^{n} \bar{B}_{k\alpha} x^T_\alpha(t) + \varphi_k(t) \quad (k = 1, 2, \ldots, n) \quad (80)$$

and by using (5), we arrive at the Fredholm system of integral equations of the second kind:

$$x^T_s(t) = \sum_{k=1} \int_0 R_{ks}(t, \tau) x_k(\tau) d\tau + P_s(t), \quad (81)$$

where

$$R_{ks}(t, \tau) = \sum_{m=1}^{n} \Phi_{mk}^{T}(t-\tau)\,\overline{B}_{ms}(\tau), \tag{82}$$

$$P_{s}(t) = \sum_{s=1}^{n} \int_{0}^{T} \Phi_{ks}^{T}(t-\tau)\,\varphi_{k}(\tau)\,d\tau. \tag{83}$$

Here, in contrast to cases previously considered, the $\Phi_{\alpha s}^{T}$ functions depend on the unknown times t_i which, however, does not involve any difficulties in principle.

As is known [8 and 9], the system of equations (81) can be directly reduced to a single equation with arguments t and τ, which are defined within the square given by $0 \leq t \leq nT$ and $0 \leq \tau \leq nT$. Therefore, the method for solving system (77) does not differ from those described above. In particular, as in Section 5, system (77) can always be reduced to the degenerate equation.

After finding the solution

$$x_{s}^{T} = x_{s}^{T}(t,\ t_{0}, \ldots,\ T)$$

by use of the switching conditions, which can be most diverse in dependence on the design and designation of the controlled system, we arrive at the equations of periods. In particular, if we consider the system

$$x_{k} = \sum_{\alpha=1}^{n} b_{k\alpha}x_{\alpha} + h_{k}a_{i}(t)\,\sigma + b_{i}(t) \quad \text{for} \quad t_{i-1} < t < t_{i}, \tag{84}$$

instead of (56), we find that all the results obtained in Sections 3, 4, and 5 can be almost entirely applied to this system with the exception of the fact that instead of function (31), the following functions must be considered:

$$\overline{A}(t) = \overline{A}(t+T), \quad \overline{A}(t) = a_{i}(t) \quad \text{for} \quad t_{i-1} < t < t_{i},$$
$$B(t) = \overline{B}(t+T), \quad \overline{B}(t) = b_{i}(t) \quad \text{for} \quad t_{i-1} < t < t_{i}. \tag{85}$$

APPENDIX I

Derivation of Equations in Section 2

Let the Fourier expansion of the $F_k(t)$ function be of the following form:

$$F_{k}(t) = \sum_{r=-\infty}^{\infty} f_{kr}\,e^{\psi_{r}t}. \tag{86}$$

We shall seek the periodic solution of system (1) in the form of a Fourier series:

$$x_{s}^{T}(t) = \sum_{k=-\infty}^{\infty} \chi_{sk}\,e^{\psi_{k}t}. \tag{87}$$

By substituting (86) and (87) in (1) and by equating the coefficients of equal harmonics, we obtain

$$\chi_{sm} = -\sum_{k=1}^{n} \frac{f_{km}\,\Delta_{ks}(\psi_{m})}{D(\psi_{m})}. \tag{88}$$

Considering that

$$f_{km} = \frac{1}{T}\int_{0}^{T} F_{k}(\tau)\,e^{-\psi_{m}\tau}\,d\tau, \tag{89}$$

by substitution of (89)and (88) in (87) and by changing the order of summation and integration, we obtain (5).

Let us further consider the Fourier expansion of the function of the period T, which coincides with the $\Phi_{ks}(y)$ function for $0 < y < T$. We have

$$\frac{1}{T}\int_{0}^{T}\sum_{\rho=1}^{n} \frac{\Delta_{ks}(\lambda_{\rho})}{D'(\lambda_{\rho})}\,\frac{e^{\lambda_{\rho}\tau}}{e^{\lambda_{\rho}T}-1}\,e^{-\psi_{p}\tau}\,d\tau =$$
$$= \frac{1}{T}\sum_{\rho=1}^{n} \frac{\Lambda_{ks}(\lambda_{\rho})}{D'(\lambda_{\rho})}\,\frac{1}{\lambda_{\rho}-\psi_{p}} = -\frac{1}{T}\,\frac{\Delta_{ks}(\psi_{p})}{D(\psi_{p})}, \tag{90}$$

which proves Eq. (7).

Equation (12) can be proved in a similar manner if we take into account that

$$\frac{1}{(\psi_{k}-\lambda_{\rho})^{\nu}} = \frac{(-1)^{\nu}}{(\nu-1)!}\int_{0}^{T} \frac{d^{\nu-1}}{d\lambda_{\rho}^{\nu-1}}\left(\frac{e^{\lambda_{\rho}\tau}}{e^{\lambda_{\rho}T}-1}\right)e^{-\psi_{k}\tau}\,d\tau. \tag{91}$$

From (7), we further have

$$\Phi_{ks}(T) - \Phi_{ks}(0) = \sum_{\rho=1}^{n} \frac{\Delta_{ks}(\lambda_{\rho})}{D'(\lambda_{\rho})}, \tag{92}$$

whence, by taking into account the well-known equations from [11], we obtain (9).

Equation (8) can be obtained by using the following well-known property of Fourier series:

$$\Phi_{ks}^{T}(0) = \Phi_{ks}^{T}(T) = \frac{\Phi_{ks}(T) + \Phi_{ks}(0)}{2}. \tag{93}$$

Equations (15)-(17) are proved in a similar manner on the basis of the fact that, in the case (14), the Fourier expansions of the $F_k(t)$ functions will not contain even harmonics.

APPENDIX II

Proof of Equations in Section 3

The recurrent kernels for Eq. (33) will be calculated by using the equation

$$R_n(t, \tau) = \int_0^T R_1(t, y) R_{n-1}(y, \tau)\, dy. \tag{94}$$

By induction, it can be shown that

$$R_n(t, \tau) = A(\tau) L_n(t, \tau), \tag{95}$$

where

$$L_1 = \Phi^T(t-\tau), \ldots,$$

$$L_n = \sum_{i=1}^{n} a_i \int_{t_{i-1}}^{t_i} \Phi^T(t-y) L_{k-1}(y, \tau)\, dy \tag{96}$$

are continuous functions for n > 1.

Considering that $d_n(t, \tau)$ is a linear combination of $R_1, \ldots, R_n$, we obtain (42), whence, by taking into account the absolute convergence of the numerator in (37), we obtain (44). Further, by multiplying Eq.(33) by A(t), we find that the function

$$s(t) = \sigma^T(t) A(t) \tag{97}$$

satisfies the equation

$$s(t) = \int_0^T A(t) \Phi^T(t-\tau) s(\tau)\, d\tau + \int_0^T A(t) \Phi^T(t-\tau) B(\tau)\, d\tau, \tag{98}$$

whose free term is a function which can be represented by the kernel

$$N_1(t, \tau) = A(t) \Phi^T(t-\tau). \tag{99}$$

The solution of Eq. (98) can be represented in the following form:

$$s(t) = \int_0^T N(t, \tau) B(\tau)\, d\tau, \tag{100}$$

where $N(t, \tau)$ is the resolvent of kernel (99).

By direct calculation, it can be shown that the recurrent kernels N_k are equal to

$$N_k(t, \tau) = A(t) L_k(t, \tau) \tag{101}$$

and therefore

$$N(t, \tau) = A(t) L(t, \tau). \tag{102}$$

By substituting (102) and (97) in (100), we obtain (43). It now remains to prove the estimates (47). From the first of the equations (45), we have

$$s_{n_0} = \left| \sum_{k=n_0}^{\infty} d_k \right| \leqslant \sum_{k=n_0}^{\infty} \frac{k^{\frac{k}{2}}(M}{k!}. \tag{103}$$

Since, according to Stirling's formula [12],

$$n! > \left(\frac{n}{e}\right)^n, \tag{104}$$

then,

$$s_{n_0} < \sum_{k=n_0}^{\infty} \left(\frac{MTe}{\sqrt{k}}\right)^k < \sum_{k=n_0}^{\infty} \left(\frac{MTe}{\sqrt{n_0}}\right)^k. \tag{105}$$

If we assume that n_0 satisfies condition (46), then, by summing the geometric progression on the right-hand side of (105), we obtain the first of the equations (47). The residue of the numerator in (37) is estimated in a similar manner.

LITERATURE CITED

1. A. G. Ivakhnenko, Technical Cybernetics [in Russian] (GITL UkrSSR, 1959).
2. M. A. Aizerman and F. R. Gantmakher, "On the determination of periodic regimes in a nonlinear dynamic system with a sectionally linear characteristic," Priklad. Matem. i Mekh., No. 5 (1956).
3. M. A. Aizerman and F. R. Gantmakher, "Determination of periodic regimes in systems with a sectionally linear characteristic which is composed of factors that are parallel to two given straight lines," Avtomat. i Telemekh. 18, 2 and 3 (1957).‡
4. L. A. Gusev, "Determination of periodic regimes in automatic control systems containing a nonlinear element with a sectionally linear characteristic," Avtomat. i Telemekh. 19, 10 (1958).‡
5. E. N. Rozenvasser, "On the reduction of equations of a nonlinear control system to the simplest form," Avtomat. i Telemekh. 21, 1 (1960).‡
6. A. I. Lur'e, Operational Calculus [in Russian] (Gostekhizdat, 1951).
7. Ya. Z. Tsypkin, Theory of Relay Systems [in Russian] (Gostekhizdat, 1955).
8. V. I. Smirnov, Calculus Course [in Russian] (Gostekhizdat, 1951), Vol. IV.
9. I. I. Privalov, Integral Equations [in Russian] (ONTI, 1937).
10. M. A. Aizerman, Lectures on Automatic Control Theory [in Russian] (Fizmatgiz, 1958).
11. A. I. Lur'e, Certain Nonlinear Problems in Automatic Control Theory [in Russian] (Gostekhizdat, 1951).
12. G. M. Fikhtengol'ts, Differential and Integral Calculus Course [in Russian] (Gostekhizdat, 1948), Vol. II.

---

‡ See English translation.

ON THE THEORY OF TWO-CHANNEL FOLLOW-UP SYSTEMS WITH A RELAY COMPONENT IN THE AC CIRCUIT

A. A. Krasovskii

Moscow

Translated from Avtomatika i Telemekhanika, Vol. 21, No. 9, pp. 1293-1305, September, 1960
Original article submitted November 19, 1959

It is shown that the describing-function method, when applied to two-channel systems with modulation and a nonlinear element in the ac circuit, becomes an exact method for determining self-oscillations for an unbounded increase in the carrier frequency. An approximate criterion for the self-oscillation stability in such systems with a relay component is formulated. The transfer function of a system which is linearized by self-oscillations with respect to slow control inputs is determined.

In ac follow-up systems, the infralow-frequency error signal is transformed into a signal with the carrier frequency Ω, after which it is amplified and then again transformed into an infralow-frequency signal. Alternating-current follow-up systems where the infralow-frequency portion of the circuit has two channels, in particular, two identical channels and antisymmetrical cross couplings [1], are used to a considerable extent. Some automatic ac bridges [2], some follow-up hydraulic platforms, etc., belong to these systems. If the ac factors and the two-channel infralow-frequency part of the circuit are linear, such systems can be conveniently investigated by the method of complex transfer functions [1] with the application of ordinary frequency criteria for stability and performance. However, in a number of cases, two-channel relay systems with a relay element in the ac signal circuit can be recommended. A similar situation occurs in the case of considerable and unavoidable changing of the ac channel amplification factor and in a number of other cases. In such systems, the basic operating conditions are the conditions of "spatial" self-oscillations of rather high frequency and small amplitude. With respect to control inputs, which change slowly, the system behaves as a linear system due to vibrational linearization [5 and 6] by self-oscillations.

The purpose of the present article is the presentation of a relatively general method for the investigation of similar two-channel systems with a relay element in the ac circuit, as well as the analysis of certain common properties of these systems.

The method under consideration is suitable for the solution of actual technical problems.

1. Structural Diagram and the System Transfer Functions

The quantities $x_{1\,\text{in}}$ and $x_{2\,\text{in}}$ are supplied to the input of a two-channel follow-up system (Fig. 1). The output quantities $x_{1\,\text{out}}$ and $x_{2\,\text{out}}$ are subtracted from these quantities, and the following error signals are formed:

$$\varepsilon_1 = x_{1\,\text{in}} - x_{1\,\text{out}} \qquad \varepsilon_2 = x_{2\,\text{in}} - x_{2\,\text{out}}$$

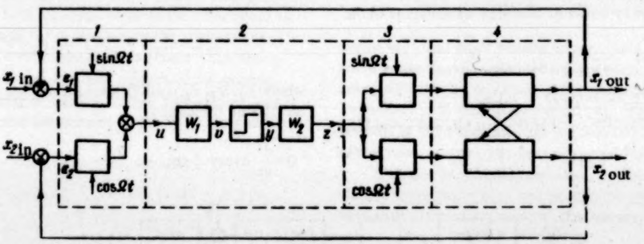

Fig. 1. General diagram of a two-channel follow-up system with a relay element in the ac circuit.

The error signals are fed to modulator 1, where they are transformed into a signal with the carrier frequency Ω:

$$u = \varepsilon_1 \sin \Omega t + \varepsilon_2 \cos \Omega t = \varepsilon \sin (\Omega t + \varphi).$$

This signal is transmitted through the first linear portion of the ac circuit, which has the transfer function* $W_1(D)$, and then through the relay element and the second linear portion, whose transfer function is $W_2(D)$.

The output signal $\underline{z}$ of the single-channel portion of the ac circuit is fed to the demodulator 3, where it is multiplied by $\sin \Omega t$ and $\cos \Omega t$. The $z \sin \Omega t$ and $z \cos \Omega t$ quantities enter the two-channel infralow-frequency part of circuit 4.

We introduce the complex quantities

$$\bar{x}_{in} = x_{1\,in} + x_{2\,in} \qquad \bar{x}_{out} = x_{1\,out} + jx_{2\,out}$$
$$\bar{z} = z \sin \Omega t + jz \cos \Omega t = jze^{-j\Omega t}, \tag{1}$$

and we write

$$\bar{\varepsilon} = \bar{x}_{in} - \bar{x}_{out} \quad \bar{x}_{out} = W(D)\,\bar{z}. \tag{2}$$

Taking into account the possible presence of antisymmetrical cross couplings in the two-channel portion of the circuit, we shall consider $W(D)$ as a complex function in the general case.

The equations of the instantaneous values of variables in the circuit single-channel portion are of the following form:

$$u = \varepsilon \sin (\Omega t + \varphi), \quad v = W_1(D)\,u,$$
$$y = f(v), \qquad z = W_2(D)\,y, \tag{3}$$

where $f(v)$ is the nonlinear factor characteristic.

The single-channel portion of the circuit consists of an ac circuit, and the variables in this circuit can be conventionally represented by complex amplitudes.

We shall assume that the variable $x = X_1 \sin \Omega t + X_2 \cos \Omega t$ has the complex "amplitude" $\bar{X}_1 = X_1 + jX_2$, which is a function of time in the general case.

In the Appendix it is shown that the complete system of equations in terms of complex variables is of the following form:

$$\bar{\varepsilon} = \bar{x}_{in} - W(D)\,\bar{z},$$
$$\bar{V} = W_1(D + j\Omega)\bar{\varepsilon},$$
$$Y_1 \sin \Omega t + Y_2 \cos \Omega t = A\,[f(V_1 \sin \Omega t + V_2 \cos \Omega t)],$$
$$\bar{z} = \frac{1}{2} W_2(D + j\Omega)\bar{Y} + \bar{z}'_g. \tag{4}$$

Here, the $A[f]$ symbol denotes the first harmonic of the almost periodic function $f(V_1 \sin \Omega t + V_2 \cos \Omega t)$. Thus, $\bar{Y} = Y_1 + jY_2$ represents the complex "amplitude" of the carrier frequency first harmonic at the nonlinear element output, to the input of which a carrier frequency signal with the complex "amplitude" $\bar{V} = V_1 + jV_2$ is supplied.

The frequency spectrum of the z'_g component begins in the vicinity of the carrier frequency Ω and then extends toward higher frequencies.

Equations (4) correspond to the structural diagram with complex transfer functions and complex variables given in Fig. 2. The following fact should be noted here. The transfer functions of the single-channel linear portions of the circuit for the envelope in the considered system with a two-channel infralow-frequency portion are obtained by the simple substitution of $D + j\Omega$ for the instantaneous values of the D operator in the transfer functions, where Ω is the carrier frequency (the factor $\frac{1}{2}$ in front of W_2 is generated by the demodulator–synchronous detector).

Such a simple rule for the formation of the transfer function for the envelope is valid only for systems with identical channels in the infralow-frequency two-channel portion of the circuit. Only in such systems can the sinusoidal as well as the cosinusoidal output signal components in the ac channel be used to the same extent. As is known [3], in ordinary ac follow-up systems with a single-channel infralow-frequency portion, the formation of the transfer function for the envelope is somewhat more complicated.

2. Steady-State Self-Oscillations

As was mentioned above, self-oscillations represent the basic operating conditions of relay systems of the class under consideration.

In order to determine steady-state self-oscillations, we shall assume that $\bar{x}_{in} = 0$, and we shall seek the solution of system (4) in the following form:

$$\bar{\varepsilon} = \bar{\varepsilon}_0 e^{j\omega_a t}, \quad \bar{V} = \bar{V}_0 e^{j\omega_a t},$$
$$\bar{z} = \bar{z}_0 e^{j\omega_a t}, \quad \bar{Y} = \bar{Y}_0 e^{j\omega_a t}, \tag{5}$$

where $\bar{\varepsilon}_0$, $\bar{V}_0$, $\bar{z}_0$, and $\bar{Y}_0$ = const, and ω_a is the self-oscillation frequency.

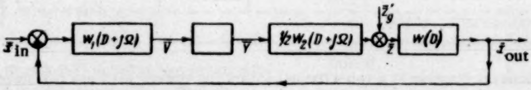

Fig. 2.

---

* $D = \frac{d}{dt}$ everywhere.

Due to the presence of the $\bar{z}'_g$ term, this is an approximate solution, and its form entirely corresponds to the describing-function method [4].

However, in application to the considered systems with a relay element in the ac circuit, the describing-function method has a special feature. This feature, which renders the describing-function method an exact method when applied to such systems, consists in the following. Here, instead of neglecting harmonics with frequencies which are multiples of the self-oscillation frequency, we neglect harmonics with frequencies which are multiples of the carrier frequency Ω or of the combined frequency $\Omega \pm \omega_a$.

Actually, for $\bar{x}_{in} = 0$, by substituting expressions (5) in equations (4), we find

$$\begin{aligned} \bar{\varepsilon}_0 &= -W(j\omega_a)\bar{z}_0, \\ \bar{V}_0 &= W_1(j\omega_a + j\Omega)\bar{\varepsilon}_0, \\ \bar{Y}_0 &= W\bar{V}_0, \\ \bar{z}_0 &= \frac{1}{2}W_2(j\omega_a + j\Omega)\bar{Y}_0 + \bar{z}'_g e^{-j\omega_a t} \end{aligned} \tag{6}$$

Here, $W_n = \frac{\bar{Y}_0}{\bar{V}_0}$ is the amplitude response of the nonlinear element, which is determined by the relation

$$\begin{gathered} Y_1 \sin\Omega t + Y_2 \cos\Omega t = Y_0 \cos(\omega_a t + \varphi_1)\sin\Omega t + \\ + Y_0 \sin(\omega_a t + \varphi_1)\cos\Omega t = Y_0 \sin(\omega_a t + \Omega t + \varphi_1) = \\ = A\{j(V_1 \sin\Omega t + V_2 \cos\Omega t)\} = A\{j[V_0 \sin(\omega_a t + \Omega t + \varphi)]\}, \\ \bar{Y}_0 = Y_0 e^{j\varphi_1}, \quad \bar{V}_0 = V_0 e^{j\varphi}. \end{gathered}$$

For a relay element without an insensitivity zone and hysteresis, which will mainly be considered below,

$$W = \frac{4a}{\pi}\,\frac{1}{V_0}, \tag{7}$$

where

$$a = \text{const.}$$

The $\bar{z}'_g e^{-j\omega_a t}$ component, the neglecting of which renders the describing-function method an approximate method, contains higher harmonics. From Eqs. (26) and (27) in the Appendix, it follows that, in the given case, the lowest frequency of these harmonics is equal either to $\Omega + \omega_a$ (the nonlinear element response is nonsymmetrical, and there is a constant component at the ac channel output) or $2(\Omega + \omega)$, while, in ordinary cases where the describing-function method is used, the lowest frequency is $2\omega_a$.

In the majority of practical cases, the carrier frequency Ω is considerably higher than the possible self-oscillation frequency. Thus, for angle-tracking systems with conical scanning, Ω is equal to $(60\pi - 200\pi)$ sec^{-1}. For ac systems with standard frequencies, Ω is equal to $(100\pi - 800\pi)$ sec^{-1}. Therefore, in the majority of cases, the $\bar{z}'_g e^{-j\omega_a t}$ component is almost completely suppressed in the two-channel portion of the circuit, which always acts as a filter for low frequencies, and the neglect of this component yields only slight inaccuracies.

Neglecting this component, we write

$$\begin{gathered} \bar{\varepsilon}_0 = -W(j\omega_a)\bar{z}_0, \quad \bar{V}_0 = W_1[j(\Omega + \omega_a)]\bar{\varepsilon}_0, \\ \bar{Y}_0 = W_n\bar{Y}_0, \quad \bar{z}_0 = \frac{1}{2}W_2[j(\Omega + \omega_a)]\bar{Y}_0. \end{gathered} \tag{8}$$

Hence,

$$\bar{V}_0 = -\frac{1}{2}W(j\omega_a)W_1[j(\Omega + \omega_a)]W_2[j(\Omega + \omega_a)]W_n\bar{V}_0$$

or

$$1 + W_1(j\omega_a)W_n = 0. \tag{9}$$

Here, the quantity

$$W_1(j\omega_a) = \frac{1}{2}W(j\omega_a)W_1[j(\Omega + \omega_a)]W_2[j(\Omega + \omega_a)]$$

can be called the over-all transfer locus of the system linear portion, and the quantity

$$W_1(D) = \frac{1}{2}W(D)W_1(D + j\Omega)W_2(D + j\Omega)$$

can be called the complex transfer function of the linear portion.

Equation (9) and the equations equivalent to it,

$$W = -W_n^{-1}, \quad W_1^{-1} = -W_n,$$

where W_1^{-1} and W_n^{-1} are the inverse loci of the linear and the nonlinear portions, respectively, whose shapes coincide with the relations of the describing function method in L. S. Gol'dfarb's form [4]. The difference consists in the expression for W_1 and the transformation of the relation into an exact equation for $\Omega \to \infty$.

It should be emphasized that, in the considered two-channel systems, where one portion of the circuit operates with alternating current, the transfer locus,

$$\begin{gathered} W_1(j\omega) = \frac{1}{2}W(j\omega)W_1(j\omega + j\Omega)\times \\ \times W_2(j\omega + j\Omega) \end{gathered}$$

is generally not symmetric with respect to the real axis (i.e., $W_l(j\omega) \neq W_l(-j\omega)$) even if there are no antisymmetrical cross couplings between identical elements in the circuit two-channel portion. Therefore, the transfer locus must be considered in the range where ω_a changes from $-\infty$ to ∞. As usual, the values of ω_a at the points of intersection between $W_l(j\omega_a)$ and W_n^{-1} (or between $W_l^{-1}(j\omega_a)$ and W_n) correspond to the frequencies of possible self-oscillations, and the $W_n = W_n(V_0)$ values at these points determine the amplitudes V_0 of possible self-oscillations (Fig. 3).

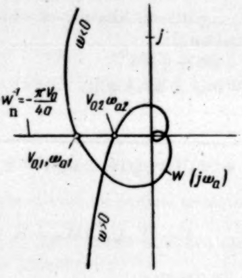

Fig. 3.

3. Stability of Self-Oscillations

In order to find the conditions for the stability of self-oscillations we shall represent them in the form

$$\bar{\varepsilon} = (\bar{\varepsilon}_0 + \overline{\Delta\varepsilon})\, e^{j\omega_a t}, \quad \bar{V} = (\bar{V}_0 + \Delta\bar{V})\, e^{j\omega_a t}, \qquad (10)$$
$$\bar{Y} = (\bar{Y}_0 + \overline{\Delta Y})\, e^{j\omega_a t}, \quad \bar{z} = (\bar{z}_0 + \overline{\Delta z})\, z^{j\omega_a t},$$

where, as above, the quantities with the "0" subscripts correspond to the amplitudes of steady-state oscillations, and the second terms on the right-hand side represent deviations. Thereafter, we shall consider the deviations to be small, i.e., we shall consider stability in Lyapunov's sense.

In order to write the equations in terms of deviations, it is necessary to establish a relation between $\overline{\Delta Y}$ and $\Delta\bar{V}$ at the relay element output and input.

For the relay element under consideration,

$$Y_1 = \frac{4}{\pi}\, a\, \frac{V_1}{V}, \qquad Y_2 = \frac{4}{\pi}\, a\, \frac{V_2}{V},$$

where

$$V = \sqrt{V_1^2 + V_2^2}.$$

Hence, with an accuracy to small higher orders, we obtain

$$\Delta Y_1 = \frac{4}{\pi}\, a \left[\frac{\Delta V_1}{V_0} - \frac{V_1}{V_0^3}(V_1\Delta V_1 + V_2\Delta V_2)\right],$$

$$\Delta Y_2 = \frac{4}{\pi}\, a \left[\frac{\Delta V_2}{V_0} - \frac{V_2}{V_0^3}(V_1\Delta V_1 + V_2\Delta V_2)\right].$$

However,

$$V_1 = V_0 \cos(\omega_a t + \varphi), \quad V_2 = V_0 \sin(\omega_a t + \varphi).$$

Therefore,

$$\overline{\Delta Y} = \Delta Y_1 + j\Delta Y_2 =$$
$$= \frac{4a}{\pi}\left\{\frac{\overline{\Delta V}}{V_0} \frac{e^{j(\omega_a t + \varphi)}}{V_0}\left[\cos(\omega_a t + \varphi)\,\Delta V_1\right.\right.$$
$$\left.\left. + \sin(\omega_a t + \varphi)\,\Delta V_2\right]\right\} = \frac{4a}{\pi V_0}\left[\overline{\Delta V} - \right.$$
$$\left. \frac{e^{2j(\omega_a t + \varphi)} + 1}{2}\,\Delta V_1 + j\,\frac{e^{2j(\omega_a t + \varphi)} - 1}{2}\,\Delta V_2\right] =$$
$$= \frac{2a}{\pi V_0}\left[\overline{\Delta V} - \overline{\Delta V}^{*} e^{2j(\omega_a t + \varphi)}\right]. \qquad (11)$$

Here, $\overline{\Delta V}^{*}$ is the complex conjugate of $\overline{\Delta V}$.

By substituting expressions (10) in (4) and considering (11), for $\bar{x}_{in} = 0$, we find

$$\overline{\Delta\varepsilon} = -W(D + j\omega_a)\,\overline{\Delta z},$$
$$\overline{\Delta V} = W_1(D + j\omega_a + j\Omega)\,\overline{\Delta\varepsilon},$$
$$\overline{\Delta z} = \frac{1}{2} W_2(D + j\omega_a + j\Omega)\,\overline{\Delta Y} + \bar{z}_g' e^{-j\omega_a t}, \qquad (12)$$
$$\overline{\Delta Y} = \frac{2a}{\pi V_0}\left[\Delta\bar{V} - \Delta\bar{V}^{*} e^{2j(\omega_a t + \varphi)}\right].$$

Thus, in the general case, the equations for the self-oscillation deviations contain a periodically changing coefficient $e^{2j(\omega_a t + \varphi)}$. If the self-oscillations vary slowly, and this is the most typical case, $\overline{\Delta V}$ and $\overline{\Delta V}^{*}$ are functions which vary slowly in comparison with $e^{2j(\omega_a t + \varphi)}$, and the effect of the second term on the right-hand side of the expression for $\overline{\Delta Y}$ can be neglected. The $\bar{z}_g' e^{j\omega_a t}$ term, which, according to what has been said above, contains higher frequencies, can be even more readily neglected.

In connection with this, the approximate equation of deviations of self-oscillations, which is obtained from Eq. (12), is of the following form:

$$\left[1 + \frac{2a}{\pi V_0} W_1(D + j\omega_a)\right]\overline{\Delta V} = 0, \qquad (13)$$

where

$$W_1(D + j\omega_a) = \frac{1}{2} W(D + j\omega_a)$$
$$W_1(D + j\omega_a + j\Omega)\, W_2(D + j\omega_a + j\Omega)$$

is the over-all transfer function of the circuit linear portion for the envelope of the self-oscillation frequency ω_a.

If we know the equation of deviations, we can use any criterion applicable to equations with complex coefficients for determining the stability conditions. By applying the Nyquist criterion, we find: if the transfer function $W_1(D)$ of the linear portion of an open-loop system does not have poles in the right half-plane, those and only those self-oscillations are stable for which the points $(\pi/2a)V_0$, j0 (V_0 is the self-oscillation amplitude) are not encompassed by the transfer locus $W_1(j\omega)$ when ω changes from $-\infty$ to ∞.

By comparing this condition with Eq. (9) for steady-state self-oscillations and the corresponding graphic plot, we readily arrive at a different formulation of the self-oscillation stability criterion for the relay system under consideration: if (-1, j0) is the intersection point between W_1 and W_n^{-1} that corresponds to the given self-oscillations, then, for a $W_1(D)$ which does not have poles in the right half-plane and if ω varies from $-\infty$ to ∞, these self-oscillations will be stable only if the transfer locus $W_1(j\omega)$ does not encompass the $(-21,\ j0)$ point, whose distance from the imaginary axis is twice as large in comparison with the first point. Thus, the self-oscillations with the ω_{a1} and ω_{a2} frequencies in Fig. 4 are unstable, and self-oscillations with the ω_{a3} and ω_{a4} frequencies are stable. Hence, it follows that self-oscillations with the largest amplitude are always stable.

It must be emphasized that the above stability criterion for self-oscillations corresponds to the approximate equation (13) and is valid insofar as this equation is valid.

Another fact should be noted. As can be seen from the above, stable self-oscillations with a positive as well as negative frequency ω_a can exist in the systems under consideration. The sign of ω_a in two-channel systems corresponds to the sense of rotation of the tracing point or to the direction of the actual three-dimensional conical motion in two-channel follow-up systems with mechanical output quantities. The frequency ω_a can have the same sign as the carrier frequency Ω, or it can be of opposite sign. In angle-tracking systems with conical scanning, the first case corresponds to the adding of the scanning and self-oscillation angular velocities, and the second case corresponds to the subtraction of these velocities. In any system of the class under consideration, the first case corresponds to the operation of the circuit single-channel portion at the combined frequency, and the second case corresponds to operation at the frequency difference.

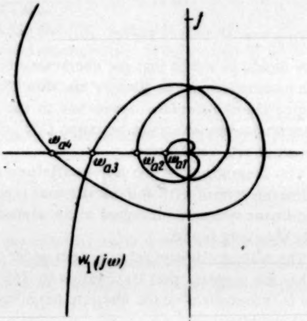

Fig. 4.

The realization of one or the other direction of self-oscillations depends on the initial phase shift in the circuit (the phase shift for $\omega_a = 0$) and the shape of $W_1(j\omega)$.

The change in the initial phase shift, produced, for instance, by changing the carrier frequency phase in the modulator, means that the entire transfer locus $W_1(j\omega)$ is rotated in the corresponding direction. In such rotation, the self-oscillations in one of the two possible directions can always be rendered unstable (see Fig. 4).

4. Reproduction of Control Inputs

With regard to the reproduction of control inputs, which change slowly in comparison with self-oscillations, the behavior of the two-channel systems under consideration is analogous to other vibrationally linearized nonlinear systems [5, 6]. For small deviations, the dynamic properties of such self-oscillation systems are close to the characteristics of linear systems.

In order to find the transfer function of a self-oscillation system with respect to the slowly changing control input $\bar{x}_{in}$, we shall write the variables in the following form:

$$\bar{\varepsilon} = \bar{\varepsilon}_0 e^{j\omega_a t} + \overline{\Delta\varepsilon},\ \bar{V} = \bar{V}_0 e^{j\omega_a t} + \overline{\Delta V},$$
$$\bar{Y} = \bar{Y}_0 e^{j\omega_a t} + \overline{\Delta Y},\quad \bar{z} = \bar{z}_0 e^{j\omega_a t} + \overline{\Delta z},$$

where the first term on the right-hand side in each expression corresponds to self-oscillations, and the second term, according to conditions, changes slowly in comparison with the first.

By substituting these expressions in equations (4), we find

$$\begin{gathered}\bar{\varepsilon}_0^{j\omega_a t} + \overline{\Delta\varepsilon} = \bar{x}_{in} - W(j\omega_a)\,\bar{z}_0 e^{j\omega_a t} - W(D)\cdot\overline{\Delta z},\\ \bar{V}_0 e^{j\omega_a t} + \overline{\Delta V} = W_1(j\Omega + j\omega_a)\,\bar{\varepsilon}_0 e^{j\omega_a t} + W_1(D + \\ + j\Omega)\,\overline{\Delta\varepsilon},\end{gathered} \tag{14}$$

$$\begin{gathered}\bar{z}_0^{j\omega_a t} + \overline{\Delta z} = \frac{1}{2} W_2(j\Omega + j\omega_a)\,\bar{Y}_0 e^{j\omega_a t} + W_2(D + \\ + j\Omega)\,\overline{\Delta Y} + \bar{z}_g';\quad Y_0 \sin(\Omega t + \omega_a t + \varphi) + \\ + \Delta Y_1 \sin\Omega t + \Delta Y_2 \cos\Omega t = A\{f\,[V_0 \sin(\Omega t + \\ + \omega_a t + \varphi) + \Delta V_1 \sin\Omega t + \Delta V_2 \cos\Omega t]\}\end{gathered} \tag{15}$$

In the considered case of a relay element with the ideal characteristic f(x) = a sign(x), the first harmonics in the expansion of the f function are expressed by the well-known equations [7]

$$f[V_0 \sin(\Omega t + \omega_a t + \varphi) + \Delta V_1 \sin \Omega t + \qquad (16)$$
$$+ \Delta V_2 \cos \Omega t] = a \operatorname{sign}[V_0 \sin(\Omega t + \omega\, t + \varphi) +$$
$$+ \Delta V \sin(\Omega t + \varphi_1)] = \frac{4a}{\pi} N \sin(\Omega t + \omega_a t + \varphi) +$$
$$+ \frac{2a}{\pi} \frac{\Delta V}{V_0} M \sin(\Omega t + \varphi_1) + \dots\dots\dots\dots,$$

where

$$\varphi_1 = \operatorname{arctg} \frac{\Delta V_2}{\Delta V_1},$$
$$N = \frac{2}{\pi} E\left(\frac{\Delta V}{V_0}\right) = 1 - \frac{1}{4}\left(\frac{\Delta V}{V_0}\right)^2 + \dots,$$
$$M = \frac{4}{\pi}\left[\frac{V_0^2}{\Delta V^2} E\left(\frac{\Delta V}{V_0}\right) - \left(\frac{V_0^2}{\Delta V^2} - 1\right) K\left(\frac{\Delta V}{V_0}\right)\right] =$$
$$= 1 + \frac{1}{8}\left(\frac{\Delta V}{V_0}\right)^2 + \dots,$$

and E and K are complete elliptic integrals of the first and the second kind, respectively.

Here, the quantities with the "0" subscript–the self-oscillation amplitudes–are always constant, and the increments ΔV, $\Delta \epsilon$, etc. change slowly or are constant.

From (15) and (16), it follows:

$$\bar{Y}_0 = \frac{4a}{\pi} N \frac{\bar{V}_0}{V_0}$$

or

$$\bar{Y}_0 = W'_n \bar{V}_0, \qquad (17)$$

where

$$W'_n = \frac{4a}{\pi} \frac{1}{V_0} N\left(\frac{\Delta V}{V_0}\right).$$

It also follows from (15) and (16) that

$$\Delta \bar{Y} = \frac{2a}{\pi} \frac{M}{V_0} \Delta \bar{V}. \qquad (18)$$

By equating the coefficients in front of $e^{j\omega_a t}$ and the slowly changing terms in equations (14) and by eliminating the intermediate variables by means of expressions (17) and (18), we find.

$$1 + W_1(j\omega_a) W'_n = 0, \qquad (19)$$

$$\bar{x}_{out} = \frac{\frac{2a}{\pi V_0} W'_1(D)}{1 + \frac{2a}{\pi V_0} W'_1(D)} \bar{x}_{in} \qquad (20)$$

Here,

$$W'_n = \frac{2a}{\pi} \frac{N}{V_0} = W_n N,$$

$$W_1 = \frac{1}{2} W(D) W_2(D + j\Omega) M W_1(D + j\Omega),$$

and $W_1(j\omega_a)$ has the previous value:

$$W'_1(j\omega_a) = \frac{1}{2} W(j\omega_a) W_1(j\Omega + j\omega_a) W_2(j\Omega + j\omega_a).$$

In the general case, for large $\frac{\Delta V}{V_0}$ deviations, the N and M quantities basically depend on these deviations.

In this, Eqs. (19) and (20) constitute a system of interdependent nonlinear equations, and the self-oscillation amplitude depends on the control input.

However, the basic system operating conditions are those conditions for which the deviations, which are caused by control inputs, are considerably smaller than the self-oscillation amplitude, i.e., $\Delta V/V_0 < 1$. Under these conditions, it can be considered that N = 1 and M = 1.

Actually, even if $\frac{\Delta V}{V_0} = 0.5$, N = 0.95 and M = 1.02. Thus, in the $0 \leq \frac{\Delta V}{V_0} \leq 0.5$ interval, the N = 1 and M = 1 equalities are satisfied very accurately. If these equalities are satisfied, Eq. (19) is transformed into the equation for steady-state self-oscillations,

$$1 + W_1(j\omega_a) W'_{\text{н}} = 0, \qquad (21)$$

which has been considered above, and Eq. (20) corresponds to the transfer function of the linear follow-up system,

$$\Phi(D) = \frac{\frac{2a}{\pi V_0} W_1(D)}{1 + \frac{2a}{\pi V_0} W_1(D)}, \qquad \bar{x}_{out} = \Phi(D) \bar{x}_{in} \qquad (22)$$

which, in the open-loop state, has the transfer function,

$$\frac{2a}{\pi V_0} W_1(D) =$$
$$= \frac{2a}{\pi V_0} \frac{1}{2} W(D) W_1(D + j\Omega) W_2(D + j\Omega).$$

It should be noted that the characteristic equation which corresponds to the transfer function (22) for slowly changing inputs coincides accurately to the $j\omega_a$ term for D with the characteristic equation (13) for the establishment of self-oscillations.

This means that, if the self-oscillations are stable, a follow-up system with self-oscillations is similar to a stable linear system with regard to the reproduction of slowly changing inputs.

The self-oscillation relay system under consideration has the property that its reaction to slow disturbances is independent of the absolute magnitude of the open-loop gain.

Actually, it follows from Eq. (9) that, if the modulus of the open-loop gain changes slowly, the self-oscillation amplitude V_0 increases in proportion to the gain:

$$W_{\text{п}}^{-1} = \frac{\pi}{4a} V_0 = -W_1(j\omega_a).$$

The $\frac{2a}{\pi V_0}$ $W_l(D)$ quantity, which enters Eq. (22), remains constant, which determines the invariability of the closed-loop system transfer function.

Here, it should be added that, if only the gain of the first factor W_1 of the circuit single-channel portion changes, which occurs often in practice, then not only is the over-all transfer function constant, but also the amplitude ϵ_0 of self-oscillations at the point of error measurement is constant (V_0 changes).

In conclusion, it should be mentioned that this method and the considered facts can be relatively simply applied to the case of a relay element with hysteresis and an insensitivity zone.

APPENDIX

It is known [8], that the transfer function for complex amplitudes (for the carrier frequency Ω envelopes) is obtained from the transfer function for instantaneous values by substituting D+jΩ for the D operator.

Thus,

$$\overline{V} = W_1(D + j\Omega)\,\overline{U}, \qquad \overline{U} = \bar{\varepsilon}. \tag{23}$$

The quantity,

$$y = f(v) = f(V_1 \sin \Omega t + V_2 \cos \Omega t),$$

where $\overline{V} = V_1 + jV_2$, can always be represented in the form

$$\begin{gathered} y = f(V_1 \sin \Omega t + V_2 \cos \Omega t) = \\ = Y^0 + Y_1 \sin \Omega t + Y_2 \cos \Omega t + \\ + \sum_{i=2}^{\infty} (Y_1^{(i)} \sin i\Omega t + Y_2^{(i)} \cos i\Omega t), \end{gathered}$$

where Y^0, Y_1, Y_2, $Y_1^{(i)}$, and $Y_2^{(i)}$ are functions of time in the general case.

In particular, if V_1, V_2 = const and the relay element has a z-shaped characteristic ($f(v) = a \operatorname{sign} v$), then

$$Y^0 = 0, \quad Y = \sqrt{Y_1^2 + Y_2^2} = \frac{4}{\pi} a,$$

$\frac{Y_1}{V_1} = \frac{Y_2}{V_2}$ (there is no phase shift in the relay element), and

$$Y_1^{(2)} = Y_2^{(2)} = 0, \quad Y^{(3)} = \sqrt{(Y_1^{(3)})^2 + (Y_2^{(3)})^2} = \frac{4}{3\pi} a,$$

$$\ldots\ldots\ldots\ldots\ldots\ldots\ldots\ldots\ldots \tag{24}$$

Thus, the relay element output can be characterized by the complex amplitude of the first harmonic $\overline{Y} = Y_1 + jY_2$ and by the complex amplitudes of higher harmonics $\overline{Y^{(i)}} = Y_1^{(i)} + jY_2^{(i)}$.

In correspondence with this, the complex amplitude of the first harmonic of the factor W_2 output will be expressed by the equation,

$$\overline{Z} = W_2(D + j\Omega)\,\overline{Y}, \tag{25}$$

and the complex amplitudes of higher harmonics of this quantity will be determined by the relations,

$$\overline{Z^{(i)}} = W_2(D + ij\Omega)\,\overline{Y^{(i)}}.$$

The instantaneous value Z of the ac channel output is equal to

$$z = Z_1 \sin \Omega t + Z_2 \cos \Omega t + z_g, \tag{26}$$

where $Z_1 + jZ_2 = \overline{Z}$, and z_g is the component corresponding to high harmonics and the component of the zero carrier frequency (if $Y^0 \neq 0$, also such a component is present).

However, according to (1) and (26),

$$\begin{gathered} \bar{z} = zje^{-j\Omega t} = (Z_1 \sin \Omega t + Z_2 \cos \Omega t + z_g)\,je^{-j\Omega t} = \\ = \frac{1}{2}(Z_1 + jZ_2) - \frac{1}{2}(Z_1 - jZ_2)\,e^{-2j\Omega t} + jz_g e^{-j\Omega t} \end{gathered}$$

or

$$\bar{z} = \frac{1}{2}\overline{Z} + \bar{z}_g'. \tag{27}$$

Here,

$$\bar{z}_g' = jz_g e^{-j\Omega t} - \frac{1}{2}(Z_1 - jZ_2)\,e^{-2j\Omega t}$$

is the component which, under steady-state conditions, has components with a frequency of the order of Ω and higher. This follows from the fact that z_g contains harmonics with double and higher frequencies. Thus, the closed systems of equations for the circuit under consideration is of the following form:

$$\begin{gathered} \bar{\varepsilon} = \bar{x}_{\text{in}} - W(D)\,\bar{z}, \\ \overline{V} = W_1(D + j\Omega)\,\bar{\varepsilon}, \\ Y_1 \sin \Omega t + Y_2 \cos \Omega t = f(V_1 \sin \Omega t + V_2 \cos \Omega t) + \sum, \\ \bar{z} = \frac{1}{2} W_2(D + j\Omega)\,\overline{Y} + \bar{z}_g', \end{gathered} \tag{28}$$

where Σ denotes higher harmonics.

Example. Consider the case where

$$W_1(D) = \text{const}, \; W_2(D) = e^{-\tau D}, \; W = \frac{1}{D(1 + TD)}.$$

This case corresponds to the inertialess first element in the ac channel (for instance, a broadband amplifier), to an element with a constant lag at the relay-element output (in particular, it can reflect the actuation time of an actual relay), and to a two-channel final element in the form of inertial and integration elements which are connected in series (for instance, electric motors).

Considering that a phase shift of the reference signal can occur in the modulator (or in the demodulator), we assume that

$$W_1^{*}(D) = \bar{k}_1.$$

where $\bar{k}_1$ is generally a complex quantity.

Thus, in the example under consideration, the overall transfer function of the linear portion is

$$W_1(D) \frac{1}{2} W(D) W_1(D + j\Omega) W_2(D + j\Omega) = \frac{1}{2} \frac{\bar{k}_1 e^{-\tau(D+j\Omega)}}{D(1+TD)} = \frac{\bar{k}e^{-\tau D}}{D(1+TD)},$$

where

$$\bar{k} = \frac{1}{2} \bar{k}_1 e^{-j\tau\Omega}.$$

For a relay element, expression (7) holds, and Eq.(9) for the self-oscillation frequencies and amplitudes assumes the following form:

$$\frac{\bar{k}e^{-j\tau\omega_a}}{j\omega_a(1 + jT\omega_a)} = -\frac{\pi V_0}{a}.$$

The corresponding graphic plot is shown in Fig. 5. The root locus portions corresponding to $\tau\omega_a > \pi$ are not shown, since the approximation of dynamic properties by means of a constant-lag element ceases to be valid in the region of frequencies higher than π/τ for a relay and many other elements.

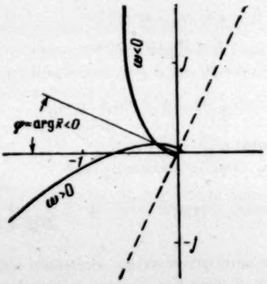

Fig. 5. Root locus of $W_1(j\omega)$ for the example under consideration.

In dependence on the $\varphi = \arg \bar{k}$ values, it is obvious that one or two self-oscillation regimes can exist in the system under consideration, which differ from each other by the magnitude and sign of ω_a (the direction of conical motion) and their amplitude.

The self-oscillation equations in terms of real quantities are of the following form:

$$\tau\omega_a + \operatorname{arc\,tg} T\omega_a = \pm \frac{\pi}{2} + \varphi.$$

$$V_0 = \frac{4ak}{\pi|\omega_a|\sqrt{1 + T^2\omega_a^2}}.$$

If $\tau = 0$, self-oscillations with finite frequency can occur only for $\varphi \neq 0$, i.e., if some cross coupling is present. Under these conditions, for $\pi/2 > \varphi > 0$, only self-oscillations with negative frequency can exist:

$$\omega_a = \frac{1}{T} \operatorname{arc\,tg}\left(\varphi - \frac{\pi}{2}\right).$$

and for $-(\pi/2) < \varphi < 0$, only self-oscillations with positive frequency can occur:

$$\omega_a = \frac{1}{T} \operatorname{arc\,tg}\left(\varphi + \frac{\pi}{2}\right).$$

As follows from the above, the self-oscillations are stable in both cases. For $T = 0$ (only integrating elements are present in the system two-channel portion):

$$\omega_a = \frac{\pm\pi/2 + \varphi}{\tau}, \quad V_0 = \frac{4ak}{\pi|\omega_a|}.$$

In this case, self-oscillations with positive as well as negative frequency can exist either for $\varphi = 0$ or $\varphi \neq 0$.

However, it follows from the above self-oscillation stability criterion that, for $\varphi > \pi/6$, only self-oscillations with negative frequency are stable, and, for $\varphi < -(\pi/6)$, only self-oscillations with positive frequency are stable.

In reproducing slowly changing control inputs, the self-oscillation system under consideration has, in accordance with (22), the following transfer function:

$$\Phi(D) = \frac{\frac{2a\bar{k}}{\pi V_0} e^{-\tau D}}{D(1+TD) + \frac{2a\bar{k}}{\pi V_0} e^{-\tau D}} \bar{x}$$

In particular, for $T = 0$, because of the relation $V_0 = \frac{4ak}{\pi|\omega|}$, the transfer function assumes the following form:

$$\Phi(D) = \frac{\frac{1}{2}|\omega_a| e^{-\tau D + j\varphi}}{D + \frac{1}{2}|\omega_a| e^{-\tau D + j\varphi}} = \frac{|\omega_a| e^{j\varphi}}{2De^{\tau D} + |\omega_a| e^{j\varphi}}$$

Here, ω_a depends only on the phase shift φ and the lag τ:

$$\omega_a = \frac{\pm\pi/2+\varphi}{\tau}.$$

Thus, the transfer function for slowly changing control inputs is invariant with respect to changes in the coefficient $\bar{k}$ modulus.

This illustrates the general aspect of the determined self-adjustment property of the considered self-oscillation systems.

LITERATURE CITED

1. A. A. Krasovskii, "On two-channel automatic control systems with antisymmetric couplings," Avtomat. i Telemekh. 18, 2 (1957).†
2. V. Yu. Kneller, "A type of ac bridges with automatic balancing by means of two parameters," Avtomat. i Telemekh. 19, 2 (1958).†
3. Correcting Circuits in Automation. Collection of articles, ed. by M. Z. Litvin-Sedoi [Russian translation] (IL, 1954).
4. L. S. Gol'dfarb, "A method for the investigation of nonlinear control systems which is based on the describing function approach." in Automatic Control Elements, ed. V. V. Solodovnikov [in Russian] (Mashgiz, 1954).
5. A. A. Krasovskii, "On the vibration method of linearization of some nonlinear systems," Avtomat. i Telemekh. 9, 1 (1948).
6. G. S. Pospelov, "Certain problems in the theory of automatic control relay systems," in Automatic Control Elements, ed. V. V. Solodovnikov [in Russian] (Mashgiz, 1954).
7. L. McCall, Elements of Servomechanism Theory [Russian translation] (IL, 1947).
8. A. A. Krasovskii, Lectures on Automation Fundamentals, Part 1: Elements of Automatic Control Systems [in Russian] (Transactions of the N. E. Zhukovskii VVIA, 1955).

† See English translation.

ON THE DYNAMIC CHARACTERISTICS OF HYDRAULIC COUPLINGS

A. M. Smirnov

Moscow

Translated from Avtomatika i Telemekhanika, Vol. 21, No. 9, pp. 1306-1310,
September, 1960
Original article submitted April 25, 1960

A method for the calculation and experimental determination of the dynamic frequency-response curves for hydraulic couplings is presented. A brief description of the equipment used in experiments and the results of the experimental determination of characteristics of some couplings are provided.

Hydraulic couplings in the shape of pipes filled with a liquid are used in automatic control systems (ACS). In designing ACS, the dynamic properties of such couplings must be taken into account. A method for the calculation and experimental determination of the dynamic frequency-response curves for hydraulic couplings is given below.

I. A. Charnyi [1] performed a theoretical investigation of the effect of piping on the accuracy of the pressure gauge which registers pressure variations. The author based his investigation on the N. E. Zhukovskii equations of the hydraulic shock theory [2], which had an additional term whereby the pressure-head loss due to friction was taken into account.

Following I. A. Charnyi [1], our theoretical investigation of the dynamic frequency response of hydraulic couplings will also be based on these equations:

$$-\frac{\partial p}{\partial x} = \rho\left(\frac{\partial v}{\partial t} + 2av\right), \qquad -\frac{\partial p}{\partial t} = K\,\frac{\partial v}{\partial x}, \tag{1}$$

$$K = \frac{K_0}{1 + \dfrac{K_0 d}{E\delta_0}}, \qquad a = \frac{16\nu}{d^2}, \tag{2}$$

where p and v are the pressure and velocity at the pipe section which is at the distance x from the origin, respectively, ρ is the liquid density, K_0 is the actual elasticity modulus of the liquid, E is Young's modulus of the first kind for the pipe material, δ_0 is the pipe wall thickness, d is the pipe inside diameter, and ν is the liquid kinematic viscosity coefficient.

The dynamic characteristics will be determined for two cases: for piping without discharge and for piping with liquid discharge.

For the first case, the boundary conditions will be written in the following form:

$$x = 0, \;\; p = p_0 e^{i\omega t}, \tag{3}$$

$$x = l, \;\; v = 0. \tag{4}$$

For the second case, considering that the discharge velocity is approximately proportional to pressure, i.e., v = Mp, we obtain the following boundary conditions:

$$x = 0, \quad p = p_0 e^{i\omega t}, \tag{5}$$

$$x = l, \quad v = Mp, \tag{6}$$

where l is the piping length, and M is the proportionality factor.

We shall consider only forced oscillations, and we shall seek partial solutions of Eq. (1) of the following form:

$$p = (A\cos nx + B\sin nx)\,e^{i\omega t}, \tag{7}$$

$$v = (C\cos nx + D\sin nx)\,e^{i\omega t}. \tag{8}$$

The values of A, B, C, D, and n are found from Eqs. (1), (7), and (8) and boundary conditions (3)-(6).

Let us consider the first case. Here, $A = p_0$, $B = p_0 \operatorname{tg} nl$, $C = \frac{i\omega}{nK} p_0 \operatorname{tg} nl$, $D = -\frac{i\omega}{nK} p_0$,

$$n = \frac{1}{c}(\omega' - ia'),$$

where $\omega' = \sqrt{\dfrac{\sqrt{\omega^4 + 4a^2\omega^2} + \omega^2}{2}}$,

$$a' = \sqrt{\frac{\sqrt{\omega^4 + 4a^2\omega^2} - \omega^2}{2}},$$

$c = \sqrt{\dfrac{K}{\rho}}$ is the sound velocity in the piping.

If a is small in comparison with ω, $a' = 0$, and $\omega' = \omega$.

By substituting the values of A, B, and n in (7), for x = l, we obtain:

$$p_l = (p_0 \cos nl + p_0 \operatorname{tg} nl \sin nl)\,e^{i\omega t}. \tag{9}$$

After transforming (9), we find

$$p_l = \frac{p_0 e^{i\omega t}}{\cos\frac{\omega' l}{c}\,\mathrm{ch}\,\frac{a' l}{c} + i\sin\frac{\omega' l}{c}\,\mathrm{sh}\,\frac{a' l}{c}}$$

or

$$p_l = p_0 A(\omega)\, e^{i[\omega t - \varphi(\omega)]}, \tag{10}$$

where

$$A(\omega) = \frac{1}{\sqrt{\mathrm{ch}^2\frac{a' l}{c} - \sin^2\frac{\omega' l}{c}}} \tag{11}$$

is the amplitude response, and

$$\varphi(\omega) = \operatorname{arc\,tg}\left(th\frac{a' l}{c}\,\mathrm{tg}\,\frac{\omega' l}{c}\right) \tag{12}$$

is the phase response.

It follows from (11) and (12) that the amplitude response A(ω) has not only one, but a number of resonance maxima for

$$\frac{\omega' l}{c} = \frac{\pi}{2} + m\pi, \tag{13}$$

where m = 0, 1, 2, . . .

Consequently, the resonance frequencies will be

$$\omega'_p = (0.5 + m)\frac{c}{2l}. \tag{14}$$

With an increase in oscillation frequency, ch $\frac{a'l}{c}$ in (11) will also increase, due to which the amplitude response will have its greatest value in the first resonance maximum. The amplitude response in the subsequent resonance maxima will gradually decrease.

Figure 1 shows the amplitude response A(ω) and the phase response φ(ω) curves, which were calculated according to Eqs. (11) and (12) for the following case:

$$l = 1000 \text{ cm}, \ \nu = 1.0 \text{ cm}^2/\text{sec}, \ \delta_0 = 0.1 \text{ cm}, \ \rho = 0.8\,\frac{\text{g sec}^2}{\text{cm}^4}, \ d = 0{,}4 \text{ cm}, \ E = 0.8\cdot 10^6 \text{ kg/cm}^2, \ K_0 = 14\,000 \text{ kg/cm}^2.$$

It is obvious from Fig. 1 that, for frequencies of up to 200 cps, the amplitude response has three resonance maxima: at frequencies of 10, 73, and 134 cps. At the resonance maxima, the phase-shift angle is equal to $\frac{\pi}{2}, \frac{3}{2}\pi, \frac{5}{2}\pi$, respectively.

For the case with liquid discharge, by using boundary conditions (5) and (6), we obtain: $A = p_0$, $n = \frac{1}{c}(\omega' - ia')$ and

$$B = p_0 \frac{\frac{i\omega}{nK}\sin nx + M\cos nx}{\frac{i\omega}{nK}\cos nx - M\sin nx}$$

By substituting the values of A, B, and n in (7), we obtain after transformations:

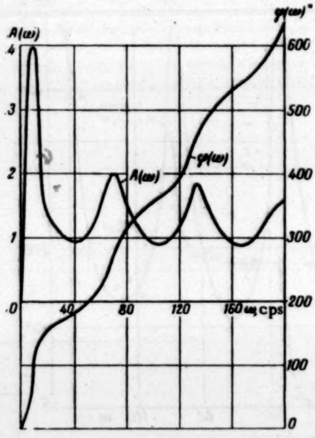

Fig. 1.

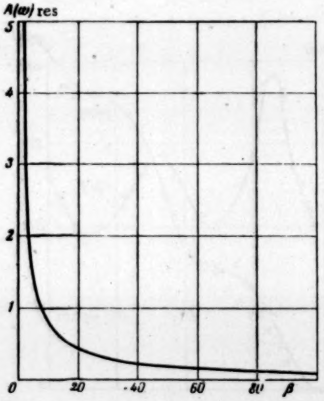

Fig. 2.

$$p_l = \frac{p_0 e^{i\omega t}}{\cos\frac{\omega' l}{c}\,\mathrm{ch}\,\frac{a' l}{c} - \beta(\omega_1 P - a_1 Q) + i\left[\sin\frac{\omega' l}{c}\,\mathrm{sh}\,\frac{a' l}{c} + \beta(\omega_1 Q - a_1 P)\right]}, \tag{15}$$

where

$$\beta = \frac{MK}{c},$$

$$a_1 = \sqrt{\frac{\sqrt{\omega^2 + 4a^2} + \omega}{2\omega}}, \quad \omega_1 = \sqrt{\frac{\sqrt{\omega^2 + 4a^2} - \omega}{2\omega}},$$

$$P = \sin\frac{\omega' l}{c}\,\mathrm{ch}\,\frac{a' l}{c}, \quad Q = \cos\frac{\omega' l}{c}\,\sin\frac{a' l}{c}.$$

If a is small in comparison with ω, $a_1=1$ and $\omega_1=0$. Thus, in the given case,

$$p_l = p_0 \frac{e^{i\omega t}}{r + iS} = p_0 A(\omega)\, e^{i[\omega t - \varphi(\omega)]}, \tag{16}$$

where the values of r and S are clear from expression (15).

The amplitude response is determined by the equation

$$A(\omega) = \frac{1}{\sqrt{r^2 + S^2}}, \tag{17}$$

and the phase response is given by the equation

$$\varphi(\omega) = \mathrm{arc\,tg}\,\frac{S}{r}. \tag{18}$$

For low-viscosity liquids (for instance, kerosene), the value of a is small. In this case, the approximate equation for $A(\omega)$ is of the following form:

$$A(\omega) = \frac{1}{\sqrt{1 - \sin^2\frac{\omega l}{c}(1 - \beta^2)}}. \tag{19}$$

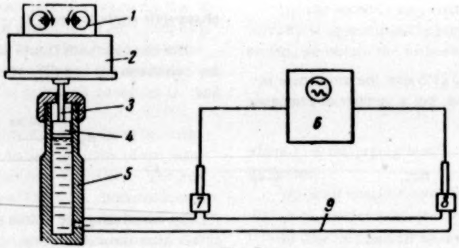

Fig. 3.

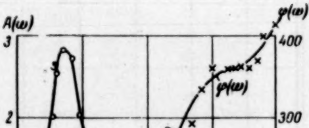

Fig. 4.

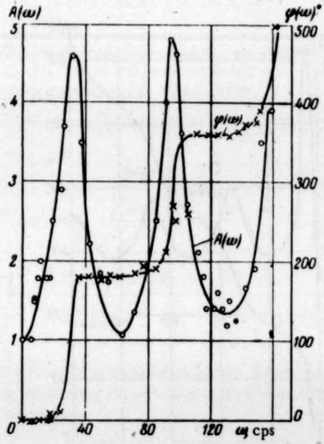

Fig. 5.

It follows from (19) that, with an increase in β, the values of $A(\omega)$ decrease. Figure 2 shows the $A(\omega)=f(\beta)$ dependence for the first resonance maximum $\frac{\omega l}{c} = \frac{\pi}{2}$, whence it can be seen that the sharpest decrease in the amplitude response occurs for $\beta = 0\text{-}8$. For $\beta > 8$, no resonance phenomena are observed with an increase in the oscillation amplitude.

The dynamic characteristics of hydraulic lines were determined by experiments where the frequency method was used [3]. The pressure oscillations at the piping inlet were secured by means of a special stand, the diagram of which is shown in Fig. 3. The stand consists of the following components: a cylinder, 5, which is filled with the liquid, a piston, 4, a rod, 3, a weight, 2, and a centrifugal vibrator, 1, which is driven by an electric motor. The rod, the weight, and the vibrator are rigidly connected to each other. Their combined weight creates a certain initial pressure in the cylinder. As the vibrator eccentric masses rotate, a harmonic disturbing force is created. By acting on weight 2, this force causes it to vibrate, due to which harmonic pressure oscillations arise in the cylinder and, consequently, in the hydraulic line 9. Centrifugal LV-500 vibrators, which were made in the Bauman MVTU, were used for this stand. A 2780-S "Orion" (Hungarian People's Rep.) two-beam pressure indicator, 6, with a piezoelectric quartz crystal was used for recording pressure oscillations at the hydraulic-line inlet and outlet. The data transmitters 7 and 8 of the pressure indicator have a high natural oscillation frequency, which attains 20 kc. Our experiments were performed in the frequency region from 0 to 160 cps. The average pressure was equal to 25-30 atm, and the total (double) amplitude varied from 6 to 20 atm.

Figures 4 and 5 show the experimental dynamic frequency-response curves for loop copper hydraulic lines with a length of 1000 cm, an inside diameter of 4 mm, and an outside diameter of 6 mm, which were filled with transformer oil (Fig. 4) and kerosene (Fig. 5). The data in Figs. 4 and 5 indicate the presence of two resonance maxima of the amplitude response. The phase-shift angle at these maxima is $\pi/2$ and $3\pi/2$. At the resonance maxima, the amplitude of pressure oscillations increases 2.8- to 4.8-fold.

For hydraulic lines filled with kerosene or transformer oil, in correspondence with Eq. (11), the frequency of the first resonance maximum for $\sin \omega l/c \approx 1$ is approximately equal to

$$\omega_p = \frac{30\,000}{l} \quad (l \text{ in cm}).$$

The frequencies of the second and the third resonance maximum will be three and five times as large, respectively. Therefore, the theoretical amplitude responses of the hydraulic lines under consideration must have resonance maxima for the 30, 90, and 150 cps frequencies, which is in good agreement with the experimental results.

Thus, the dynamic frequency-response curves for hydraulic couplings were determined theoretically and experimentally, and their flow characteristics were explained.

LITERATURE CITED

1. I. A. Charnyi, "Effect of supply pipes on the accuracy of pressure gauge readings in recording pressure pulsations," Izvest. Akad. Nauk SSSR, Otdel. Tekh. Nauk, 3 (1946).
2. N. E. Zhukovskii, Hydraulic Shock in Water Supply Pipes [in Russian] (Gostekhizdat, 1949).
3. V. V. Solodovnikov, "The frequency-response method in control theory," Avtomat. i Telemekh. 8, 2, 1947.

AN INVESTIGATION OF SOME TYPES OF MATRIX DECODERS WITH A RELAY OUTPUT

T. P. Belaya

Moscow

Translated from Avtomatika i Telemekhanika, Vol. 21, No. 9, pp. 1311-1319,
September, 1960
Original article submitted February 6, 1960

One possible approach to the analysis of matrix decoders made from semiconductor diodes and having a relay output is given.

Decoders which use unicombinational matrices (C_n^m) and which provide a defensive rejection (for any distortion of the code) are studied.

Relations for a selection network which interrelates the parameters of the output relays, matrix, and power supply voltage are derived for both continuous and pulse powering.

The industrial development of semiconductors, in particular, diodes with a large back resistance, permits one to build and use diode matrix circuits with relay output in telecontrol and telesignaling (TC–TS) apparatus.

The different types of such decoders are distinguished from one another by the object selection code (uni- or all-combinational matrices are used), by the means of generating the input (a voltage input or an input through relay contacts is used), by the switching method, and by the operating mode of the output relays.

The decoders mentioned, in contrast to the widely used matrix decoders with various kinds of trigger-circuit outputs, require rather large currents of prolonged duration, since their input resistances are relatively small.

Moreover, a significant number of parallel circuits through the forward and back resistances of diodes is formed in unicombinational matrix decoders, depending on the selected code, and this raises the requirements on the quality of the diodes, and increases the power consumed.

The matrix parameters, and sometimes the input voltages, will be different, depending on the required operating conditions and the relay parameters chosen.

Therefore, it is best to be able to evaluate this or that type of decoder beforehand, and to compute its parameters.

One possible approach to the investigation of matrix decoders with relay outputs is given in this article, and relations are derived for decoders having defense in their circuits (defensive rejection for any sort of code distortion), and which use unicombinational matrices (C_n^m), for two cases—continuous and pulse (through a capacitor) powering of the output relays.

The effect of a change in the decoder parameters and of certain external factors on the operation is also examined.

Relations for the Circuits of Unicombinational Matrices (C_n^m)

Let us examine a unicombinational matrix separately, before deriving the relations for the decoder.

A C_5^2 matrix is shown in Fig. 1; the generalized parameters for a unicombinational C_n^m matrix are designated on it. It follows from an examination of this circuit that the total number of input circuits is equal to the total number of combinational elements n; the number of output circuits is equal to the number of possible combinations of the assumed $N = C_n^m$; the number of input buses connected to one output bus is equal to the number of elements in each code m. The number of connections of one input bus to output buses s can be found from the formula $s = C_{n-1}^{m-1}$. The number of output circuits which are not connected to the given input circuit is equal to N–s.

An Investigation of Decoders with Continuous Powering of the Output Relays

Let us turn to the study of the decoder operation.

According to the equivalent diagram (Fig. 2,c) for the circuit under consideration, we can write

$$u = i\,(R_1 + R_{\text{eq}}), \tag{1}$$

where R_1 is the input resistance of the given decoder circuit, R_{eq} is the equivalent resistance of the rest of its circuits, and i is the current of the equivalent circuit.

The different operating modes of the decoder are caused by the change in the equivalent resistance R_{eq}, and current i; the resistance R_1, and applied voltage u, remain constant.

Let us explain how the change in the above-mentioned quantities is determined.

Having used the intermediate equivalent circuit (Fig. 2, b), we get

$$R_{\text{eq}} = \frac{R\ R_{\text{b}} R_{\text{p}}}{R_{\text{a}} R_{\text{b}} + R_{\text{a}} R_{\text{p}} + R_{\text{b}} R_{\text{p}}} = \frac{R_{\text{p}}}{1 + \frac{R_{\text{p}}}{R_{\text{a}}} + \frac{R_{\text{p}}}{R_{\text{b}}}}. \quad (2)$$

Resistances R_a and R_b will be equal to

$$R_{\text{a}} = (R_{\text{fd}} + R_2') \frac{1}{m}, \quad (3)$$

$$R_{\text{b}} = (R_{\text{fd}} + R_{\text{c}}) \frac{1}{n - m}. \quad (4)$$

according to the equivalent circuit of Fig. 2, a, under the condition that all elements with the same designation are identical.

Resistance R_3 in the circuit is equal to

$$R_3 = \frac{R_{\text{fd}} + R_{2(k)}}{k}.$$

The resistances R_2' and R_B, in turn, are determined from the following formulas, expressed in matrix parameters:

$$R_2' = \frac{sR_{2(m)} \left[R_{\text{rd}} + \frac{R_{\text{p}} (R_{\text{fd}} + R_{2(k)})}{k R_{\text{p}} + R_{\text{fd}} + R_{2(k)}} \right]}{R_{\text{rd}} + \frac{R_{\text{p}} (R_{\text{fd}} + R_{2(k)})}{kR_{\text{p}} + R_{\text{fd}} + R_{2(k)}} + s(s-1) R_{2(m)}} =$$

$$= \frac{1}{\frac{1}{s R_{2(m)}} + \frac{s-1}{R_{\text{rd}} + \frac{R_{\text{p}} [R_{\text{fd}} + R_{2(k)}]}{kR_{\text{p}} + R_{\text{fd}} + R_{2(k)}}}}, \quad (5)$$

$$R_{\text{c}} = \frac{1}{N - s - 4} \left[R_{\text{rd}} + \frac{R_{\text{p}} (R_{\text{fd}} + R_{2(k)})}{kR_{\text{p}} + R_{\text{fd}} + R_{2(k)}} \right], \quad (6)$$

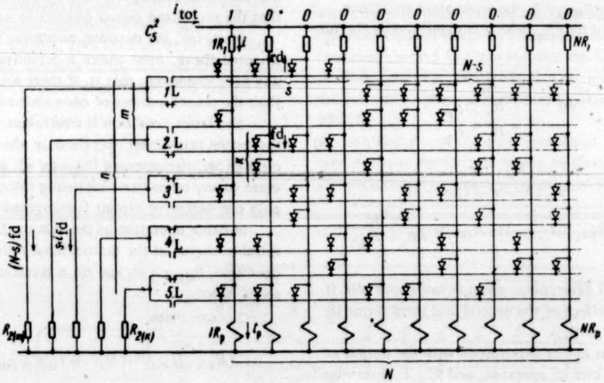

i tot
1
0
0
0
0
0
0
0
0
0
C_s^2
$1R_1$
NR_1
rd
N-s
s
1 L
2 L
3 L
4 L
5 L
m
n
k
fd
(N-s) fd
s·i fd
$R_{2(m)}$
$R_{2(k)}$
$1R_p$
i_p
NR_p
N

Fig. 1.

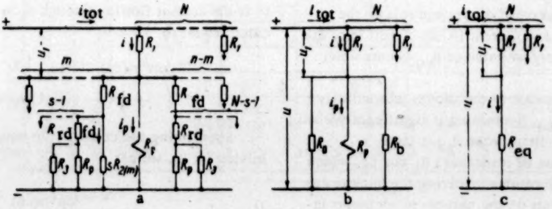

+
i tot
N
u_1
i
R_1
m
n-m
R fd
s-1
N-s-1
R rd
fd
i_p
R_p
R_3
$sR_{2(m)}$
−
a
u
R_a
R_b
b
R_{eq}
c

Fig. 2.

where R_{fd} and R_{rd} are the forward and back resistances of the diodes; R_p is the resistance of the relay coil; $R_{2(m)}$ is the value of the matrix resistance R_2 for the input circuits pertaining to the given code; $R_{2(k)}$ is the value of resistance R_2 for the defensive circuits of the matrix; k is the number of defensive circuits.

Let us find how a change in the resistance R_2 effects the equivalent resistance R_{eq}, all other quantities remaining constant. It follows from formulas (2)-(5) that the equivalent resistance will equal

$$R'_{eq} = \frac{R_p}{1 + \frac{R_p}{R'_a} + \frac{R_p}{R'_b}}, \quad (7)$$

when $R_{2(m)} = \infty$, where

$$\frac{R_p}{R'_a} = \frac{R_p m (s-1)}{R_{fd}\ (s-1) + R_{rd} + \frac{R_p (R_{fd} + R_{2(k)})}{kR_p + R_{fd} + R_{2(k)}}};$$

$$\frac{R_p}{R'_b} = \frac{R_p (N-s-1)(n-m)}{R_{fd}\ (N-s-1) + R_{rd} + \frac{R_p (R_{fd} + R_{2(k)})}{kR_p + R_{fd} + R_{2(k)}}}$$

When $R_{2(m)} = R_{2(k)} = 0$, the equivalent resistance will be designated by R''_{eq}, which is expressed by the following formula:

$$R''_{eq} = \frac{R_p}{1 + \frac{R_p}{R''_a} + \frac{R_p}{R''_b}} = \quad (8)$$

$$= \frac{R_p}{1 + \frac{R_p m}{R_{fd}} + \frac{R_p (N-s-1)(n-m)}{R_{fd}\ (N-s-1) + R_{rd} + \frac{R_p R_{fd}}{kR_p + R_{fd}}}}$$

A numerical example is given below (Appendix I) to evaluate the effect of the second and third terms in the denominator of R_{eq}.

We note that R'_{eq} is determined with the output relay of the given circuit operated, and R''_{eq} is determined when that relay is idle.

By examining the expressions introduced above, we can draw the following conclusions.

1) For a given choice of diodes and relays, the equivalent resistance and current in the circuit vary as a function of R_2. The largest value of R_{eq} occurs when $R_2 = \infty$.

2) The back resistance of the diodes substantially effects the value of R_{eq}, decreasing it significantly when R_{rd} is small, and very little when R_{rd} is large.

The absolute value of resistances R_a and R_b, which are determined from formulas involving the back resistances of diodes, depends on the number of elements in the code, the total number of elements, the number of output circuits, and the number of connections between the buses, that is, on the chosen C_n^m.

3) If it is assumed that the back resistance is sufficiently large ($R_{rd} \approx \infty$) and the matrix resistance $R_{2(m)} = \infty$, the equivalent resistance will be equal to the relay resistance, $R'_{eq} = R_p$. The resistance, $R_{2(m)} = \infty$, is characteristic for decoder inputs coming from relay contacts; in all other cases, including voltage input (if $R_{2(m)}$ is not infinite), R_{eq} will be less than the value mentioned.

4) The equivalent resistance R''_{eq} will equal

$$R''_{eq} = \frac{R_p}{1 + \frac{R_p m}{R_{fd}}},$$

for the same diode back resistance ($R_{rd} = \infty$), and for $R_{2(m)} = R_{2(k)} = 0 \left(R_a = R_{fd} \frac{1}{m}\right)$, that is, it will be significantly less than R'_{eq}.

We will derive the design formulas relating the decoder parameters to the applied voltage.

When the given voltage is applied, the decoder must ensure reliable operation of the output relay of the circuit which corresponds to the code, and must ensure that the rest of the output circuits do not operate.

Moreover, the decoder, according to the condition imposed above, must ensure a defensive rejection for any code distortion, that is, if there are more or less than the proper number of code elements m.

The latter condition is equivalent to stating that the output relay must operate only when all defensive circuits are disconnected ($R_{2(m)} = \infty$), and must not operate in any other case, including the case in which only one defensive circuit is energized.

Reliable operation of the relay will be ensured by a suitable choice of the matrix input resistance, R_1, for the condition, $R_{2(m)} = \infty$, and for a given relay pull-in reserve factor.

One can write

$$i' (R_1 + R'_{eq}) = R_1 i' + i_{op} k_{rs\,(op)} R_p = u, \quad (9)$$

for this case, where i_{op} is the operating (pull-in) current of the relay; $k_{rs(op)}$ is the pull-in reserve factor; i' is the current flowing through R_1 in the mode indicated, equal to

$$i' = i_{op} k_{rs(op)} + i_{rd}\ [(s-1)m + \\ + (N-s-1)(n-m)].$$

Substituting the current i' in equation (9), and solving for R_1, we get

$$R_1 - \frac{u - i_{op} k_{rs(op)} R_p}{i_{op} k_{rs(op)} + i_{rd}\ [m(s-1) + (n-m)(N-s-1)]}.$$

If the back resistance of the diodes is large, the second term in the denominator can be ignored, and the approximate formula

$$R_1 \approx \frac{u}{i_{op} k_{rs(op)}} - R_p.$$

can be used.

This formula, expressed in terms of the drop-out current and reset coefficient of the relay, will take the form

$$R_1 = \frac{u k_{rt}}{i_{do} k_{rs(op)}},$$

where

$$k_{rt} = \frac{i_{do}}{i_{op}}.$$

The reverse current which flows through the diodes can be found from the formula,

$$i_{rd} = \frac{u - i_{op} k_{rs(op)} (R_p + R_1)}{R_1[m(s-1)+(n-m)(N-s-1)]}.$$

By using the relations for the second operating state of the decoder (relay unoperated, where $R_{2(m)} = 0$, and $R_{rd} = \infty$, R''_{eq}), we find the forward current of the diodes. This current, $i_{fd(k)}$, depends on the number of defensive circuits formed, and can be determined from the expression

$$i_{fd(k)} = \frac{u - \frac{i_{op} k_{rt}}{k_{rs(op)}} R_1}{kR_1 + sR_2 + R_{fd}},$$

where k = 1, 2, . . . , m, . . . , n is the number of defensive circuits; the remaining designations are the same as before.

The largest current through the diodes will occur when there is one defensive circuit. It is useful to know this current in order to choose diodes correctly, so that they will not be overloaded during prolonged operation.

The power required by the matrix decoder depends on its operating mode, and a large amount of power will be required if no code is present.

This power can be determined from the formula

$$P = i_{tot} u = \frac{u^2 N}{R_1 + R''_{eq}},$$

on the basis of the equivalent circuit (Fig. 2, c), under the condition that all the circuits are identical; R''_{eq} is the equivalent resistance in the absence of code, and i_{tot} is the total current required by the decoder.

An Investigation of a Decoder with Pulse Powering of the Output Relays

A matrix decoder, whose output relays are connected through capacitors, is shown in Fig. 3.

An examination of the equivalent circuit (Fig. 4, a) shows that the given circuit has parallel circuits of two types: a) circuits which contain inductances and capacitances connected to them through the back resistances of diodes, and b) circuits which are connected through the forward resistance of diodes, and contain the resistance R_2.

An analysis of these circuits shows that the first type does not have much effect on the operation of the given circuit if the back resistance of the diodes is suf-

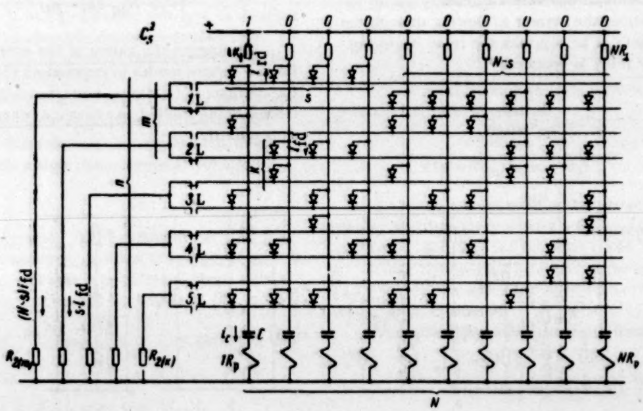

Fig. 3.

ficiently high, since the transient and steady-state current are basically determined by R_{rd}.

Therefore, all these circuits, for practical purposes, can be replaced by an equivalent resistance expressed in terms of the back resistance of a diode.

The second type of circuit contains the resistance R_2, which, as in the case examined earlier, determines the operating mode of the relay, and may change from 0 to ∞.

The circuits mentioned are shown in Fig. 4, b, where

$$R_4 = \frac{R_{rd}}{(n-m)(N-s-1)+m(s-1)}.$$

The computational equivalent circuit is shown in Fig. 4, c, where R_{eq} will assume different values which are a function of the operating mode. When $R_2 = \infty$, the equivalent resistance will equal

$$R'_{eq} = \frac{R_{rd}}{(n-m)(N-s-1)+m(s-1)} \qquad (10)$$

and when $R_2 = 0$

$$R''_{eq} = \frac{R_{fd}}{m}. \qquad (11)$$

We will derive relations for the given circuit, assuming that all quantities entering them are constant. We can write the equation

$$u = (i_c + i_1)R_1 + i_c R_p + L_p \frac{di_c}{dt} + u_c \qquad (12)$$

from the computational equivalent circuit.

In this equation, the current i_c flowing through the given circuit must not be less than the relay operating current, when the relay is operated;

$$i'_c = i_{op} k_{rs(op)}$$

but must be less than the relay drop-out current for all the remaining cases:

$$i''_c = \frac{i_{do}}{k_{rs(do)}},$$

where $k_{rs(op)} > 1$, and $k_{rs(do)} > 1$.

Manipulating equation (12) further, we obtain a second-order differential equation

$$\frac{d^2u_c}{dt^2} + \frac{R_p R + R_1}{RL_p}\frac{du_c}{dt} + \frac{1}{L_p C}u_c = u, \qquad (13)$$

where $R = \left(\frac{R_1}{R_{eq}} + 1\right)$, L_p is the inductance of the relay coil; R_p, the relay resistance; R_1, the matrix input resistance; C, the capacitance of the isolating capacitors; and u, the applied voltage.

The roots of the characteristic equation corresponding to equation (13) are

$$\alpha_{1,2} = -\frac{R_p + \frac{R_1}{R}}{2L_p} \pm \sqrt{\frac{R_p + \frac{R_1}{R}}{4L_p^2} - \frac{1}{L_p C}}. \qquad (14)$$

Integrating equation (13), we find the current through the relay and the voltage across the relay coils and capacitor:

$$u_c = \frac{uR_{eq}}{R_1 + R_{eq}}\left[1 - \frac{1}{\alpha_2 - \alpha_1}(\alpha_2 e^{\alpha_1 t} - \alpha_1 e^{\alpha_2 t})\right], \qquad (15)$$

$$i = -\frac{uR_{eq}}{(R_1 + R_{eq})L_p(\alpha_2 - \alpha_1)}(e^{\alpha_1 t} - e^{\alpha_2 t}), \qquad (16)$$

$$u_L = -\frac{uR_{eq}}{(R_1 + R_{eq})(\alpha_2 - \alpha_1)}(\alpha_1 e^{\alpha_1 t} - \alpha_2 e^{\alpha_2 t}). \qquad (17)$$

Substituting the values of the equivalent resistances for the various modes in expressions (15)-(17), we find the currents and voltages corresponding to them in the circuit being studied. A numerical example is given in Appendix II.

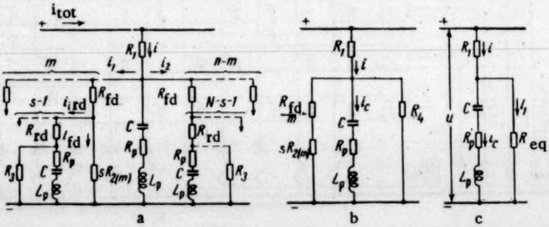

Fig. 4.

CONCLUSIONS

One can draw the following conclusions from the given analysis of the operation of the decoders mentioned above, and also from experimental work on them done by the author.

1. The choice of decoder matrix parameters (parameters of diodes, relays, etc.), and of the supply voltage for continuous and pulse powering of the latter, depends on the type of matrix ($N = C_n^m$), that is, the total number of output circuits, combinational elements, code elements, number of defensive circuits, and number of connections between the input and output circuits.

2. The operating mode of the decoder–a reliable selection of the output relay corresponding to the given code, and a defensive rejection if this code is distorted in any way–is basically determined by the matrix resistance R_2. The best results in the given two cases are obtained when this resistance changes from 0 to ∞.

3. The back resistance of the matrix diodes substantially affects the operation of the decoder output relays, and this effect increases as the total number of matrix output circuits grows.

A decrease in the diode back resistance or an increase in the total number of output circuits leads to a decrease in the relay operating reserve factor when a code is present, and in the drop-out reserve factor when no code is present, if the voltage is fixed. In a number of cases, this circumstance makes it necessary to increase the supply voltage.

4. The energy content of matrix decoders with relay output is relatively large, and is determined by the type of matrix and the output relay parameters, and also depends on the operating mode of the decoder. A large amount of power is required in the absence of code, both for continuous and for pulse-powering.

Therefore, it is best to connect this type of decoder to supplies of low power only during code reception, even if there are only an average number of output circuits (15)–(20).

Moreover, if this is done, one can lower the requirements on the permissible amplitude of diode forward current when the defensive circuits are formed, since the diodes can take a significant overload for a short time.

APPENDIX I

Numerical Example. Let us assume that a C_5^2 matrix is used in the decoder, and that it is made from type D7Zh diodes, and that type RKN telephone relays are used in the output circuits. In this case, the basic data will be

$$R_p = 1000 \text{ ohm}, R_{fd} = 10 \text{ ohm}, R_{rd} = 5\cdot 10^5 \text{ ohm}, k = 2,$$

$$N = 10,\ n = 5,\ m = 2,\ s = 4,\ N - s - 1 = 5,$$

$$R_{2(k)} = 0,\ R_{2(m)} = \infty \ (\text{for } R'_{eq}),$$

$$R_{2(k)} = R_{2(m)} = 0 \ (\text{for } R''_{eq})$$

Computations give the following results:

$$R'_{eq} = \frac{R_p}{1 + 0.011 + 0{,}03} = \frac{R_p}{1.04} = 996 \text{ ohm},$$

$$R''_{eq} = \frac{R_p}{1 + 20.0 + 0{,}03} = \frac{R_p}{201.03} = 4.97 \text{ ohm}.$$

APPENDIX II

As an example, let us find the current flowing through a relay for the case computed in Appendix I, assuming that the relay coil inductance is $L_p = 10$ h, and the capacitance C = 16 μf; all the remaining quantities are the same as in the preceding example.

The operating and drop-out currents of the relay are, respectively, $i_{op} = 20$ ma, $i_{do} = 9$ ma, $R_1 = 500$ ohms.

When the relay is operated, we get

$$R'_{eq} = \frac{R_{rd}}{(n-m)(N-s-1)+m(s-1)} =$$

$$= \frac{500\cdot 10^3}{3\cdot 5 + 2\cdot 3} = 24\cdot 10^3 \text{ ohm}$$

When the relay is idle, we get

$$R''_{eq} = \frac{R_{fd}}{m} = \frac{10}{2} = 5 \text{ ohm}.$$

Let us find the resistance R for these two cases:

$$R' = \frac{R_1}{R'_{eq}} + 1 = 1.021 \text{ ohm},$$

$$R'' = \frac{R'}{R''_{eq}} + 1 = 101 \text{ ohm}.$$

The roots of the characteristic equation for the relay in the operated state are

$$\alpha'_1 = 0,\ \alpha'_2 = -150;$$

and for the relay idle–

$$\alpha''_1 = -34.6;\ \alpha''_2 = -66.$$

The current through the relay while it is operated is found from the expression

$$i' = \frac{uR'_{eq}}{(R_1 + R'_{eq})L_p(\alpha'_2 - \alpha'_1)}\left(e^{\alpha'_1 t} - e^{\alpha'_2 t}\right) =$$

Since the second term in the parenthesis is significantly less than unity when $t = t_{op}k_{rs(op)}$, it can be neglected, and then we find that $i \approx 40$ ma.

Since the operating current of the relay is equal to $i_{op} = 20$ ma, an operating current reserve factor, $k_{rs(op)} = 2$, is ensured.

The idle relay current is found from the formula,

$$i'' = -\frac{uR''_{eq}}{(R_1 + R''_{eq})L_p(\alpha''_2 - \alpha''_1)}\left(e^{\alpha''_1 t} - e^{\alpha''_2 t}\right).$$

When $t = t_{do}$, we find that $i'' \approx 0.46$ ma, which is significantly less than the operating current.

ON THE INTERFERENCE RESISTANCE OF PULSE-TIME AND PULSE-WIDTH TELEMETERING SUBJECTED TO STRONG FLUCTUATION NOISE

N. V. Pozin

Moscow

Translated from Avtomatika i Telemekhanika, Vol. 21, No. 9, pp. 1320-1322, September, 1960
Original article submitted January 30, 1960

The possibility is discussed of raising the interference resistance of pulse-time and pulse-width telemetering by introducing a time selector into the receiver; the selector would eliminate the effect of short duration, but highly probable, errors formed by the action of fluctuation noise.

Video pulse errors are formed in the video channel of a receiver by the action of strong fluctuation noise. In general, these errors are false pulses and false spaces of different duration.*

The influence of strong fluctuation noise on the transmission of PWM and PTM telemetering is analyzed in reference [1]. It is shown that the average and mean-square errors are determined by the probabilities, P_s and P_p, of the unit errors of the space and pulse. The unit error is defined as the formation, by noise, of a false pulse or false space of duration $\Delta t = 1/W = 1/2f_c$, where $f_c = W/2$ is the cut-off frequency of the low-pass filter in the video channel, which is replaced by a band-pass filter if there is no secondary modulation before transmission.

It is assumed in [1] that the receiver is sensitive to errors of duration Δt.

Is this really necessary? It is true that an input filter with pass-band W creates the necessary conditions for passing pulses Δt wide. But the pass-band of the input filter is designed to be wide enough to pass working pulses with a sufficiently fast rise-time. If transmission stability requirements oblige one to pass pulses with a fast rise-time, this requirement does not extend to the width of those pulses.

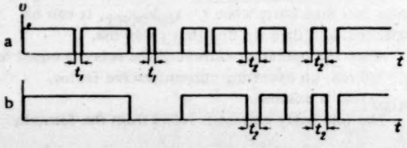

Fig. 1. Pulses in the video channel of a receiver. a) before the time selector; b) after the time selector ($t_1 < t < t_2$).

By taking special measures, such as introducing circuits in the video channel of the telemetering receiver which delay time by $\underline{t}$, and which make the receiver insensitive to short-duration errors, one can significantly increase the interference resistance of the receiver. This remark is intended to draw attention to this simple method, and to make the necessary additions to the analysis of interference resistance in reference [1], where it is assumed the main influence on the indications of the receiver is the extremely short, but highly probable, errors of unit duration, Δt.

Ideally, such a device, which can be called a time selector (filter), or duration selector, is triggered by the leading edges of the incoming pulses. Pulses are generated at the output which are time-shifted by $\underline{t}$, and which duplicate the input channel, providing it does not contain pulses or spaces shorter than $\underline{t}$. Pulses shorter than $\underline{t}$ do not trigger the device, and likewise, spaces shorter than $\underline{t}$ cannot restore it to the initial state. Thus, the time selector does not pass signals which are less in duration than some set value, $\underline{t}$ (Fig. 1).

This type of apparatus can be made in different ways. The simplest is a relay which is slow to operate and release, and which is actuated by constant amplitude pulses. In general, if there is double limiting in the video channel (Fig. 2), a low-pass filter can be used as a time selector (for instance, an integrating RC circuit), if the method of demodulation after this is such that the "piling" of the leading edges of the working pulses in the filter does not lower the measurement accuracy. If this is not so, a more complex time selector must be used†.

---

* Telemetering subjected to strong noise is ordinarily accomplished by transmission in which the rise time of the working pulses is very short. The permissible width of the leading edges in this case is of the order of the indeterminateness permissible in measuring time intervals, and distortions of the leading edges by noise can be neglected.

As is mentioned in [1], the duration of the unit error is the correlation interval of the smooth noise at the filter output, and thus the formation of unit errors can be considered independent. If the probabilities of unit errors (that is, errors of duration Δt) in a space, P_s, and pulse, P_p, are known, then the probabilities of errors which have a duration equal to the delay time, t, are found in the following manner:

$$P(t)_s = P_s^k, \text{and } P(t)_p = P_p^k \qquad (1)$$

It is certain, from the standpoint of interference resistance, that the greater the delay,

$$t = k\Delta t, \qquad (2)$$

the better—that is, the less—the error due to noise.

However, the delay cannot be too great; it is limited by the following factors.

First of all, an increase in the delay causes an increase in the minimum values of the pulses and spaces, whose duration must exceed the delay introduced by the time selector. As a result, the useful time deviation which carries information is decreased somewhat, and the telemetering accuracy is reduced, or the rapidity of response is lowered as the cycle duration is correspondingly increased. But the magnitude of these factors is not great, and it is seen that in practical devices, they do not limit the delay.

The second most important factor limiting an increase in the delay is the instability of the device which introduces this delay.

The greater the delay, the more difficult it is to meet the stability requirements. Hence, it is evident that a relatively unstable, but small, delay introduces a large error in the indications of the telemetering receiver.

A telemetering receiver insensitive to short errors of duration Δt would be of great practical value. To a lesser degree, it is also desirable to eliminate the less probable errors of duration $2\Delta t$, etc. If the duration, Δt, is comparable to the rise time of the pulse, that is, to the telemetering accuracy under conditions of strong interference, it is not difficult, in practice, to ensure a sufficiently stable delay, $t = (2-3)\Delta t$, that is, a coefficient $k = 2-3$.

In order to evaluate the interference resistance of PWM and PTM telemetering apparatus, incorporating a time selector with delay t(2) in the receiver, the probabilities P_s and P_p in the design formulas derived in [1] must be replaced by P_s^{k+1} and P_p^{k+1} respectively.

Simplified expressions for the average (δ_{av}), and mean square (δ_{ms}) reduced errors are given in the following table:‡

Method of modulation	Without delay		With delay	
	δ_{av}	δ^2_{ms}	δ_{av}	δ^2_{ms}
PWM	$\frac{P_s}{2}$	$\frac{P_s}{2Nn}$	$\frac{P_s^{k+1}}{2}$	$\frac{P_s^{k+1}(k+1)}{2Nn}$
PTM	$\frac{nP_s}{6}$	$\frac{nP_s}{12N}$	$\frac{nP_s^{k+1}}{6(k+1)}$	$\frac{nP_s^{k+1}}{12N(k+1)}$

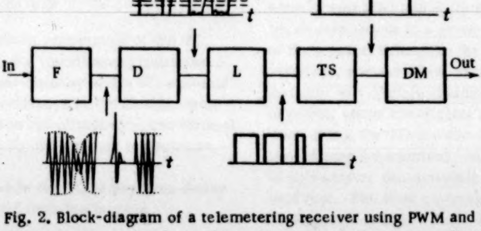

Fig. 2. Block-diagram of a telemetering receiver using PWM and a time selector. F–band-pass filter, D–amplitude detector, L–limiter, TS–time selector, DM–demodulator–this transforms pulse duration into proportional amplitudes of voltage or current.

---

† In practice, the ideal time selector is based on a scaler circuit, triggered and blocked by the respective leading edges of pulses.

‡ We must keep in mind that the formulas presented in the table do not take into account possible error at the edges of the pulses and spaces. The probability of these errors is low, but the error component due to "edge" errors will increase as the delay is increased.

SUMMARY

The introduction of duration selection in the video channel of a receiver significantly increases the interference resistance of PWM and PTM telemetering. Such a method is especially valuable in telemetering apparatus working under conditions of strong interference, since there is no strict relation between the durations of the pulse, and of the leading edge: the pass-band of the filter determines the rise time, but the duration of the shortest pulses can vary over wide limits.

The introduction of long delay, two to three times more than the duration of a unit error, Δt, is not difficult to realize, and can be used practically in all time-type telemetering apparatuses. In connection with this, it is best to examine the data of reference [1] on the comparative interference resistance characteristics of telemetering devices which use different modulation methods. Such a comparative analysis will be the subject of a special article.

LITERATURE CITED

1. N. V. Pozin, "Interference resistance of pulse-width and pulse-time telemetering subjected to strong fluctuation noise," Avtomat. i Telemekh. 20, 2, (1959).**

** See English translation.

AN APPROXIMATE CALCULATION OF THE TRANSIENTS IN A THERMISTOR CIRCUIT

N. P. Udalov

Moscow

Translated from Avtomatika i Telemekhanika, Vol. 21, No. 9, pp. 1323-1325,
September, 1960
Original article submitted February 15, 1960

A form of the differential equation for heating a thermistor by the current flowing through it is proposed; with it, one can obtain all the variables necessary for calculating the transient directly from a graph of the volt-ampere characteristic.

A graphical method of computing the transients arising in a thermistor circuit (TC) excited by a step change in the parameters which characterize the operating mode of the circuit is presented in [1], and is further developed in [2, 3]. This method has a great disadvantage: the thermal time constant, τ, whose magnitude greatly depends on temperature, enters the calculation. Assuming τ to be constant results in significant error in calculating the transients, which are accompanied by a temperature change of hundreds of degrees in the working body of the TC. This disadvantage can be eliminated by a method suggested in [4], where a form of the differential equation for the heating of a TC is given in which the thermal time constant is eliminated from the calculation. However, the solution of the problem in this case remains quite complicated.

Still another form of the differential equation is suggested below; it permits one to curtail the amount of computation significantly, and makes the calculation quite graphic.

The following form of the heating differential equation is recommended in [1] for convenience in calculating the rate of temperature change in the working body of a TC at various temperatures:

$$\frac{dT}{dt} = \frac{U_p^2 R}{H(R+r)^2} - \frac{T-T_0}{\tau}, \tag{1}$$

where T is the instantaneous temperature of the TC working body, in °K; R, the instantaneous resistance of the TC, ohms; H, the heat capacity of the TC, watt-sec//deg; r, the linear resistance in the circuit, ohms; U_p, the voltage applied to the circuit, v; τ, the thermal time constant, sec; and T_0, the ambient temperature, °K.

The power liberated in the TC at any time during the transient can be found from the formula,

$$\frac{U_p^2}{(R+r)^2} R = U'I',$$

where U' is the instantaneous voltage drop across the TC, and I' is the instantaneous current.

The time constant is defined by the expression $\tau = H/b$, where b is the dissipation coefficient. Taking this into account, we can rewrite expression (1) as

$$\frac{dT}{dt} = \frac{U'I' - b(T-T_0)}{H}$$

The product of the dissipation coefficient b and the temperature of overheating $(T-T_0)$, which appears in the above expression, is equal to the power dissipated by the TC into the surrounding medium under steady-state conditions at a temperature of the working body T, i.e.,

$$b(T - T_0) = UI,$$

where U is the voltage drop across the TC in the steady-state, and I is the steady-state current through the TC.

Consequently,

$$\frac{dT}{dt} = \frac{U'I' - UI}{H}. \tag{2}$$

Turning to the volt-ampere characteristic on which the load line $(U_p - Ir)$ is drawn (Fig. 1,a), it is easy to see that all the quantities dependent on temperature which are needed to find the TC temperature change rate can be taken directly from the figure; these are the coordinates of points K' and K, lying on the resistance line which corresponds to a given TC temperature, T. One of these points belongs to the dynamic volt-ampere characteristic, and the other, to the static. We will call the dynamic volt-ampere characteristic the geometric locus of points, whose coordinates are equal to the voltage drops across the TC and the current through it at any time during the transient. In the given case, the dynamic volt-ampere characteristic is the segment 1'-2, of the load line. The heat capacity can be found by the method suggested in [4].

Let us illustrate the technique of computing a transient by a concrete example. It is necessary to plot a curve of the current increase in a circuit consisting of a type KMT-11 TC and a linear resistance, r, connected in series. The transient arises when r is changed from r_1 = 180 kohms to r_2 = 12.65 kohms in one step. The TC is immersed in transformer oil at 20°C. The voltage, U_p, applied to the circuit is 220 v. The temperature characteristic of the TC is described by the expression $R = 0.281\,e^{\frac{4600}{T}}$, and the heat capacity, H = 2.78 mw-sec/deg. The volt-ampere characteristic of the TC, with resistance lines corresponding to eleven different temperatures, is shown in Fig. 1, a.

We begin the calculation by determining the steady-state modes of the TC before the start and after the completion of the transient. Load lines, $U_p - Ir_1$, and $U_p - Ir_2$, must be drawn for this purpose. Point 1 characterizes the state of the TC before the transient starts (R=860 kohms, T = 309°K). After the transient is completed, the state characterized by point 2 is established (R=4.4 kohms, T = 474°K).

The temperature change rates of the TC at different temperatures occuring during the transient are calculated from formula (2). For example, when T = 408° K, the point K' on the dynamic volt-ampere characteristic has the coordinates: U' = 134 v, I' = 6.2 ma, and point K on the static characteristic has coordinates U = 88 v, I = 4 ma, and consequently,

$$\frac{dT}{dt} = \frac{134\cdot 6.2 - 88\cdot 4}{2\cdot 78} = 171 \text{ deg/sec.}$$

The rates found by this method are plotted on the graph dT/dt = f(T), for the corresponding temperatures (Fig. 1, b).

Then a curve of the temperature change as a function of time is plotted (Fig. 1, c). To do this, the entire temperature change interval is divided into a series of

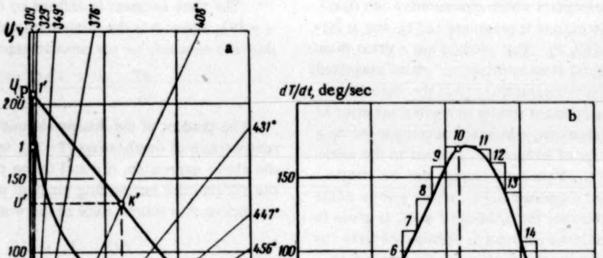

Fig. 1. An example of the calculation of a transient. a) initial volt-ampere characteristic; b) curve of the dependence of the TC working body temperature change rate on temperature; c) temperature change curve; d) current change curve.

segments, ΔT (16 parts, in the given example) within which the temperature is assumed constant, and the corresponding time intervals are computed. Thus, when the rate is $dT/dt = 9$ deg/sec, a temperature increment $\Delta T = 11$ deg (interval 1) occurs during the time $\Delta t = 11:9 = 1.22$ sec. By adding all the time intervals Δt, we construct the curve $T = f(t)$.

The construction of the curve $I = f(t)$ is clear from the drawing (Fig. 1, d).

The curve of current change obtained by calculation almost coincides with the experimental results (the dashed curve in Fig. 1, d). The experimental curve, like the initial data for the example under consideration, was taken from [5].

Transients arising as a result of a step change in the supply voltage or a change in heat-transfer conditions are calculated analogously. The volt-ampere characteristic needed for the calculation can be found analytically [6].

LITERATURE CITED

1. B. S. Sotskov, "Thermistors and their use in circuits," Avtomat. i Telemekh. 9, 1 (1948).
2. N. P. Udalov, "Transients in the simplest thermistor circuits," in Thermistors [in Russian] (Gosénergoizdat), 1959.
3. B. S. Sotskov, Fundamentals of Computation and Design of Electromechanical Elements of Automatic and Telemechanic Systems [in Russian] (VZEI, 1959).
4. I. F. Voloshin, A. S. Kasperovich, and A. G. Shashkov, Thermistors [in Russian] (Izd. AN Belo SSR, 1959).
5. A. S. Kasperovich, The Dynamic Properties of Electrical Circuits with Thermistors, Thesis submitted for the degree of Technical Science Candidate [in Russian] (Minsk, 1959).
6. N. P. Udalov, "Further notes on the calculation of thermistor characteristics," Avtomat. i Telemekh. 20, 6 (1959).*

---

*See English translation.

THE SEVENTH SCIENTIFIC-TECHNICAL CONFERENCE OF YOUNG SCHOLARS OF THE INSTITUTE OF AUTOMATION AND REMOTE CONTROL OF THE ACADEMY OF SCIENCES OF THE USSR

On March 14-16, 1960, was held the traditional (seventh) Scientific-Technical Conference of Young Scholars of the Institute of Automation and Remote Control (IARC) of the Academy of Sciences of the USSR on Problems of Automatic Control. The conference discussed the work of young scholars which was completed in 1959.

More than 400 persons participated in the work of the conference, including about 200 representatives of various organizations in Moscow and the Moscow area (scientific research institutes, institutes of higher learning, planning and design organizations, etc.).

Seventy-five reports and communications were heard, encompassing a broad range of problems of automatic control. The materials presented evoked a lively exchange of opinions.

In opening the conference the director of the Institute of Automation and Remote Control, Academician V. A. Trapeznikov, wished the young scholars success in their work and charged them to link their scientific work more closely with the practical, with the concrete needs of the national economy. At the plenary session Professor M. A. Aizerman, D. T. S., presented a report on "The scientific problem of the theory of finite automata."

At the final plenary session E. V. Voloshina and E. V. Shtil'man presented a report on "Modeling the processes of instruction." In the report they reviewed the characteristic features peculiar to the processes of instruction of animals and man, surveyed a number of automatic devices which fulfill certain functions of the human brain, and showed analogous features between certain processes in automatic systems and processes of instruction of people and animals. Between the plenary sessions, the work of the conference was done in sections:

I. Automatic control, with subsections on the theory of automatic control and systems of automatic control
II. Automatic inspection
III. Computers
IV. Elements and devices of automation and remote control
V. Statistical methods in automation
VI. Theory of relay circuits and finite automata
VII. Automated electric drive

I. Automatic Control Section

A. Subsection on the theory of automatic control

A report by V. N. Novosel'tsev was devoted to finding an expression for optional control in secondary relay-impulse systems for the case of purely relay control and for the case of relay control in the presence of a zone of insensitivity.

I. S. Morosanov discussed in his report the effect of fluctuations on relay extremal systems under auto-oscillating conditions. On the basis of evaluation the principles of harmonic and statistical linearization were assumed. The author showed that the methods of calculating statistical transfer coefficients in the form proposed by I. E. Kazakov are inapplicable in this case. But a linearization equivalent in probable meaning can be obtained in reviewing the problems of parametric effect of fluctuations. The final solution for the case of linear members of an extreme object of any order was given in graphic form. As a result, on the basis of published statistical characteristics of the fluctuations, the mean value of the frequency and amplitude of the auto-oscillations is found for a given system of extreme control.

The joint report of V. G. Gradetskii and Yu. I. Ostrovskii entitled "The operation of a system of extreme control (SEC) with memory of the extreme under noise conditions" was devoted to the problem of raising the noiseproof features of systems. The value used in the report as an index of the noiseproof feature characterizes the number of false switchings of the executive organ in a unit of time.

The task amounts to a determination of those values of the parameters of tuning of the regulator and noise filter which, at a given rate of scanning and a given loss in scanning, would provide the minimal amount of false switchings in a unit of time. This problem was solved approximately on account of its complexity. The formulas obtained have been verified by experiment.

A report by N. V. Grishko presented the results of determination of the optimal characteristics of a single extreme system during occasional functioning. The system reviewed is a natural generalization of several very noiseproof and high-grade extreme systems. The optimal characteristics are determined by varied methods by minimization of the analytical expression obtained for the mean square error through the given characteristics of the object being controlled and the characteristics produced by the extreme system.

T. G. Babunashvili devoted his report to a study of the triggering process of a regulating system containing a servomotor with a nonlinear velocity characteristic and fixed feedback. The task consisted of investigating systems with three differential first-order equations, with coefficients variable in time and one nonlinearity from the point of view of dissipativity, largely in accordance with the thinking of Kh. Masser. The author of the report determined the maximal deviations and the deviations which are determined at the end of the triggering process.

In the report of A. I. Moroz entitled "Qualitative investigation of differential equations obtained in the solution of the problem of synthesis," a method of designing regulating systems was explained. It was suggested by A. M. Letov and consisted of the fact that the equation of the regulator was defined by the task of the first integral of the system of differential equations of the object and the unknown regulator. In an occasional case the advantages and deficiencies of this method have been noted, and certain unacceptable features of the systems obtained have been disclosed. The report proposed a method of eliminating the deficiencies discovered.

A report by M. M. Simkin was devoted to the determination of periodic conditions in nonlinear impulse systems. The indicated problem is linked with a review of nonautonomous systems.

The author proposed an approximate frequency method of determining simple and complex periodic conditions in such systems.

In a report of R. P. Parsheva the problem of stability in the Lagrangian sense of transient conditions in a pentametric SAR with a single nonlinearity was discussed.

V. S. Kislyakov, in a report on "The prolonged stability of an aircraft with an automatic pilot possessing retardation," investigated the stability of short-period motion of an airplane with an automatic pilot without feedback. Disturbed movement of the system is described by third-order differential equations with constant coefficients and retardation in the characteristic of the steering gear. To determine the region of asymptotic stability as a function of retardation and adjustments of the automatic pilot, on the assumption that the characteristic of the steering gear has weak nonlinearity, the method of asymptotic approximation of N. M. Krylov and N. N. Bogolyubov was used; this was also utilized in studying the linear problem. The effect of retardation on stability of movement was explained.

In the report of B. E. Chuprun on "The formulation of a law of control of linear stable objects assuring minimal displacement of the regulating organ," a method was studied of controlling a constant-rate servomotor, in which the regulating organ deviates only to the amount needed for compensation for the displacement. It is assumed here that the form of displacement is known, but its level is not. In like manner a study was made of a case of a linear stable object of arbitrary order without and with retardation.

B. Subsection on systems of automatic control

B. B. Buyanov discussed in his report the application of the theory of systems optimal for high speed to the problem of controlling the flying shears of a rolling mill.

B. G. Volik reported on an automatic optimizer with two channels and two limitings intended to make scannings of the extreme directly on the object which has great inertness. The problem was studied with regard to the automation of chemical objects. I. N. Bocharov reported on an original instrument for photographing the distribution curve of a random value.

E. A. Rateeva reported on a three-channel optimizer for chemical production, calculated for 2-3 variables and two limiters.

In the report of V. G. Sholokhov, experimental proof was given for convergence in the process of adjusting a noise generator, by the filter-forming method, for the case of two filters, and the dependence of the time of the transitional period on the method of triggering was determined.

The report of K. B. Norkin was devoted to the problem of automatic adjustment of a transmitter's output cascade with use of a system of automatic triggering, and contained an explanation of the method of optimal selection of adjustments of the optimizator during operation with an inert object under noise conditions.

In a report of V. N. Shadrin a system of program control with frequency separation of the channels was described.

Two reports made by V. V. Karibskii and A. P. Evseeva contained data on a universal interpolator for a system of digital program control and on the automatic selection of interpolation segments for a machine with a linear interpolator.

A report by M. I. Taits described an experimental-industrial model of an instrument for automatic program installation. Reports of B. N. Andreichikov dealt with problems of the dynamic precision of machines with program control and the effects of friction and slack on the error during reverse operation.

The report of M. M. Khasanov was devoted to an analysis of the dynamic characteristics of air-conditioning equipment.

II. Automatic Inspection Section

M. V. Rybashov and I. M. Ponasenko devoted their report to a study of several circuits for the dynamic compensation of counters. The conclusions obtained were confirmed by experimental investigations on models.

V. S. Likhoninskii, in his communication "A capacitance-measuring device for digital systems of program control of productive processes," examined the operating principles of capacitance-measuring devices of the linear and rotary types for the measurement of shifts.

M. A. Prusov reported on the principles of building and designing an instrument for measuring the temperature of rotating parts. The instrument is based on utilization of turbulent currents and has a number of advantages in comparison with analogous instruments based on other principles.

The report of Yu. V. Gushchin was devoted to study of the possibility of using semiconductor crystal layers on a sulfur-cadmium base for the indication of radioactive radiations.

A. A. Kalmakov discussed in his report the possibility of using radioactive isotopes and the methods of nuclear spectroscopy for automatic control of the content of metals in alloys and products of the enrichments of ores of nonferrous metals.

V. A. Viktorov reviewed the effect of the high harmonics of a coaxial vibrator on the operation of an extremal endovibratory level indicator.

III. Computer Section

In a report by A. G. Butkovskii, "The modeling of certain objects with distributed parameters," the theoretical principles and a structural scheme are given for an electronic model of straightaway heat-treatment furnaces operating in an automatic-control system.

A. V. Shileiko, in his report on "Method of synthesis of an optimal structure of a digital model," examined problems linked with the selection of criteria of quality and method of synthesis of an optimal structure of a digital model.for which criterions of quality he assumes extreme values.

In a report of R. N. Chernyshev, "A solver amplifier with powerful output cascade," the results were given of the development of a solver amplifier, completed according to an autocompensating scheme. The amplifier has a contactless modulator on silicon diodes and a powerful output cascade.

In a report of B. A. Pereverzev entitled "Combined electromechanical assembly of an electronic modeling device" there were descriptions of the circuits, design, and basic technical data of an electromechanical unit which can operate under the conditions of a multiplier-divider, a functional converter and a coefficient buncher.

F. B. Gul'ko, in a review report entitled "High-speed electronic multiplying devices," furnished data on new electronic multiplying devices with an elevated transmission band, their characteristics, and the factors limiting high speed.

Zh. A. Novosel'tseva, in a report entitled "Controlled retardation assembly," gave the results of the development of a device for the modeling of retardation, the time of which changes in accordance with the controlling signal. The device was made for memory condensers which are switched with the help of step-by-step switches.

In a report of K. B. Norkin, "On a single method of automatic triggering of the extreme of a function of some variables," a method is given for discovering the extreme of a function which has lumps and saddles which do not require calculation of the gradient of the function.

V. A. Yakovlev, in a communication entitled "A discrete electrical differentiator," described the operating principle and design of a device for the differentiation of slowly changing voltages, which permits the calculation of the difference in voltages (from 20 mv to 2 v) at a discrete moment of time with an error not exceeding 1% of the maximum value of the scale.

V. A. Brik, in a report entitled "A digital computer for the composition of a program for the working of parts on a milling machine," discussed a device for preparing a program for the working of parts whose profiles consisted of rectilinear segments and circles. On the basis of the coordinates of the ends of the segments and the centers of the circles, the devices give the values of the linear increments of the coordinates in a binary code.

IV. Section on Elements and Devices of Automation and Remote Control

In a report of E. A. Andreeva a method was given for calculating the expense and power characteristics of a "jet-choke" element for viscous compressible and incompressible liquids.

L. A. Tenenbaum, in introducing simplified assumptions and hypotheses, derived expressions for the expense and power characteristics of a "jet-choke" element during the irregular laminar flow of a viscous incompressible liquid.

T. K. Efremova discussed pneumatic relay assemblies with temporal dependencies (guard relay, impulse starter, and impulse generator). In her report there was given a timer circuit built with these assemblies.

In a report of V. S. Matorina entitled "Magnetic output amplifiers for alternating current electromagnets," the operation of magnetic amplifiers working from the signals of magnetic logical elements was examined. Two methods of calculation for loads with high and low goodness were offered.

In M. A. Boyarchenkov's report "Standby magnetic amplifiers for direct current with increased efficiency," he analyzed the conditions for obtaining maximal power under load. New circuits of three-phase standby amplifiers and full-wave transformerless standby amplifiers were offered.

In a second report M. A. Boyarchenkov discussed the operation of a magnetic amplifier for counter emf.

N. L. Prokhorov analyzed in his report existing memory circuits for magnetic logical elements from the point of view of continuity (the memory signal during exclusion and following inclusion of the power supply current). A new continuous memory circuit was suggested.

A. L. Rozovskii, in his report entitled "A contactless code-impulse system of telemeasurement," explained the principle of construction and the solving circuits of a system built of semiconductor and magnetic elements.

In a report entitled "Contactless program-calculating device for the automation of instruments for a linecasting machine," N. V. Silaev described the circuit of such a device, based on the use of magnetic and semiconductor elements.

V. S. Serzhers reported on the possibility of constructing, from semiconductor elements, circuits of a proportional amplifier, a derivative unit, and an integrating unit for regulators for general use in industry. A typical designed assembly of units was worked out, using a printing arrangement.

B. B. Gogodevskii discussed transitional processes in electromagnetic mechanisms and the vibration of contacts. A method was given for estimating the error in calculating the dynamic characteristics of electromagnetic mechanisms.

V. Section on Statistical Methods in Automation

In a communication of L. P. Sysoev a solution was given for the problem of estimating the parameters and of detecting signals which depend nonlinearly on random parameters assumed for the background of gauss-correlated noise.

M. Yu. Gadzhiev discussed the games problem arising in the case of detection of a useful signal mixed with noise during independent change of the carrier frequency. During definite assumed interference relative to the class, formulas have been obtained for optimal composite strategy of opponents and evaluation of the game.

In a report of I. I. Paishev equipment with continuous-discrete functioning for the resolution of random functions in a canonical series was examined. Experimental results were given of the practical construction of canonical series for a definite class of random functions.

E. L. Nappel'baum communicated about the form of the optical operator for the discovery of a suitable signal on a background of normal noises with random distribution of dispersions.

The report of A. I. Teiman was devoted to problems linked with the distribution of selections of random functions. A limiting form of distribution selections was derived, and a new method offered for the evaluation of the distribution of selections of random functions for a given level.

In the communication of E. S. Kochetkov there was an examination of the problem of the construction of theoretically and practically optimal linear integral immiscible evaluations of the mathematical expectation of the correlational function of stationary random processes with continuous time. A comparison was made of the theoretically and practically optimal evaluations.

T. I. Tovstukha discussed the effect of random noise on the operation of systems of extreme control of step-by-step and sloped types. Working parameters of the system are selected from evaluations of the values of mathematical expectation and dispersions on the yield of the object of control.

In the report of V. M. Baikovskii the capacity of a channel with different-discrete modulation was determined during the absence of noise. It was shown that potentially this method of transmission has greater capacity than delta-modulation and impulse-code modulation. The connection of the rate of transmission of information during a different-discrete modulation, according to the channel with the fluctuating noises was determined from the statistics of the transferable information.

V. M. Pomažan communicated about a theoretical and experimental investigation of time systems of telemeasurement with various cycle periods and different methods of indication (with memory or integrating output devices).

VI. Section on the Theory of Relay Circuits and Finite Automata

In the report of V. D. Kazakov entitled "The shape of minimal forms of symmetrical Boolean functions of an arbitrary number of variables," it was demonstrated that the minimal sp- and ps- forms of symmetrical functions have a completely determined form and on the basis of this an account is given of a method of direct determination of the minimal forms of arbitrary symmetrical functions of n variables. Approximated estimates were given of the maximal number of minimal forms there are in an arbitrary symmetrical function of n variables.

In a report of V. P. Didenko there was an explanation of a digital method of minimization of Boolean functions with calculation of unutilizable states. The method permits rapid obtaining of partial minimal forms and can be distributed on Boolean functions with a large enough number of independent variables. An examination was also made of the method of constructing bridge structures of relay devices on the basis of partial minimal forms.

V. V. Vorsheva at the beginning of her report gave a short review of existing work on the study of circuits with real contacts. By real contacts are understood relay contacts in which there can be arbitrary changes of sequence of the interdependence of normally open and normally closed contacts of one relay or another. In the report there are an analysis and a synthesis of the circuits operating on real contacts. A method was explained for obtaining a partial minimal form giving the circuit, when realized, contacts free of competition.

T. M. Aleksandridi devoted his report to problems of the synthesis of switching circuits on the basis of two logical operations, the Schaeffer prime and the function which is double it. In the report it was proposed to realize the Schaeffer function and the function which is double it in elements operating on the principle of switching the current with transistors of type p-n-p and n-p-n respectively.

Examples were given of the construction of logical circuits made up of the elements examined.

In the report of L. A. Gusev, entitled "On minimization of the structure of finite automata," a review was given of the basic concepts of the theory of finite automata and a study made of the equivalent conversions of finite automata and the problem linked to them of minimizing the number of states of the finite automaton.

The report of O. P. Kuznetsov was devoted to a description of logical networks in which the delay times for the various elements are unequal. The author showed that the relationships determining the behavior of such networks are more complex than the known relationships occurring in each automaton. In particular, there exist autonomous logical networks, whose sequences of states are periodic.

In the report of V. D. Kazakov and V. V. Naumchenko entitled "On the realization of Boolean functions of n variables on contactless logical switches by the method of redetermination," a new approach to the minimization of relay structures was explained, consisting of the fact that a given Boolean function leads at the expense of unutilized states to an ordered (in particular, symmetrical) form, with the help of simple matrix conversions, easily mechanized. The realization of symmetrical functions can be done on the contactless models of neurons of Calberston and Makkalok-Pitts. Such a realization permitted a sharp reduction in the number of necessary elements in the circuit.

The report of A. D. Talantsev, entitled "On the use of logical-algebraic operators of transition to the analysis and synthesis of finite automata of a special type," was devoted to an examination of the logical means of synthesis and analysis of potential-impulse circuits operating under asynchronous conditions (on a nonqualitative time scale). It was shown that the procedure of integrating potential-impulse forms permits in some cases a reduction in the number of necessary logical elements by one-half or two-thirds.

VII. Section on Automated Electrical Drive

O. I. Khasaev, in his report entitled "The operation of an induction motor from a frequency converter with semiconductor triodes," presented an analytical and experimental investigation of fixed and transitional processes of an electrical impulse converter in the angle of rotation of an impulse operation with a three-stator step-by-step motor. Analytic expressions were found for the basic parameters of the converter (the angles of overlap and lead) and an analysis was given of some conditions of its operation.

In the report of V. D. Vershinin entitled "The use of the principle of invariantness in the stabilization of the speed of a direct current motor," there was an explanation of the conditions of complete invariantness during action on the voltage of a signal armature upon the current of the motor, and the possibility of it realization was shown. It was shown that the fulfillment of the conditions of complete invariantness in the actual circuit, without fail, brings upon itself instability of the system. Compensation during complete invariantness brings the system to astatism of an order equal to the number of compensated components (basic and productive) of the compelled error.

In the report of O. A. Kossov, entitled "The direct current drive with impulse semiconductor rectifiers," the economy of impulse regulation of the speed of a direct-current motor was proved in the presence of a diode shunting armature circuit, an analysis was given of the statistical characteristics of the broken system, and the effect of feedback was determined. The author presented experimental data on the test of a model of the drive with a 0.76 kw motor.

In the report of Chao Chou-lun entitled "Optimal control of cylindrical flying pruners with eccentrics," there was an examination of problems in improving the quality of SAR during introduction of feedback; criteria of the stability of a broken system were given, and the conditions for formation of autooscillations were found.

In the report of A. R. Dzhelyalov, entitled "A synchronous motor with longitudinal-transverse excitation as the object of automatic regulation," the statics of regulation during control of excitation on both axes were examined in connection with the problem of slewing of the rotor during mutual synphasing of electrical drives with a reciprocating motor. The author concluded that the control of motors is the object of automatic control, described the principles of construction of systems of automatic turning of the motor's rotor, analyzed the conditions of rotation, and also gave a qualitative characterization of those conditions.

M. Yu. Gadzhiev, F. B. Gul'ko,
A. R. Dzhelyalov, E. E. Dudnikov,
V. D. Kazakov, I. A. Litovchenko,
K. B. Norkin, and N. L. Prokhorov

BIBLIOGRAPHY

LIST OF FOREIGN WORKS PUBLISHED IN 1958 ON THE THEORY OF RELAY ACTIONS AND FINITE AUTOMATA

Translated from Avtomatika i Telemekhanika, Vol. 21, No. 9, pp. 1332-1338,
September, 1960

S. Abhyankar, "Minimal 'Sum of products of sums' expressions of Boolean function," Trans. IRE, Dec., 1958, EC-7, pp. 268-276.

A. Adám, "Dipolar electrical circuits," [in Hungarian] MTA Mat. Kut. Int. Kőzl., 1958, pp. 67-79, 207-218.

H. Arango and I. Santos, "The operation 'bridge' in Boolean algebra" [in Spanish]: Ciencia y Tec., 1958, No. 125, 168-175.

K. Aronssohn, "Calculating machines and logical circuits for cold cathode thyratrons," [in French] Onde electr., Oct., 1958, pp. 724-729.

E. K. Aschmoneit, "The electromagnetic relay as an element of the electronic circuit," [in German] Elektronik (Dtsch), 1958, 7, 8, 247-249.

D. D. Aufenkamp, "Analysis of sequential machines, II," Trans. IRE, Dec., 1958, EC-7, No. 4, 299-306.

J. Auricoste and H. L'Homme, "Magnetic logical circuits and their application in digital computers and in industrial multicycle control systems " [in French] Onde electr., March, 1958.

M. C. Badillo-Barallat, "New possibilities of trivalent logic and problems solvable by means of relays and relay circuits," [in Spanish] Calculo Autom. y Cibernetica, 1958, No. 19, 28-39, Bibl. 13.

T. G. Beatson, "Component minimization in electronic switching," Electr. Eng. (USA), 1958, 77, 3, 213.

T. G. Beatson, "Minimization of components in electronic switching circuits," Commun. and Electronics, July, 1958, 4, 283-292.

B. Beizer, "Extension of Boolean algebra for analysis of mixed switch diode circuits," Proc. IRE, 1958, 4, 779-780.

B. Beizer and S. M. Leibholz, "Designing sequential circuits," Electr. Manufact., 1958, 62, 3, 67-69, 298, 300.

C. Bellomi, "Direct horizontal unions in the algebra of variable circuits," [in Italian] Ingegneria ferroviaria, 1958, No. 2.

R. D. Berlin, "Synthesis of N-valued switching circuits," Trans. IRE, 1958, EC-7, 1, 52-56.

M. Boll, "The logic of expressions and switching," [in French] Automatisme, 1958, III, 3, 95-101.

J. Bromirski, Technika ukladów przekaznikowych, Politechnika Wroclawska, Warsaw, 1958.

D. M. Brown, "Boolean algebra: ands, ors, and nots, among other things," Amer. Math. Monthly, 1958, 65, 8, 659.

J. D. Burroughs, "A method of designing transistor switching circuits," Electr. Eng. 1958, 77, 10, 944.

J. H. Calderwood and A. Porter, "Pattern recognition in the synthesis of complex switching systems," J. Electron. Control, 1958, 4, 5, 466-480.

S. Caldwell, Switching Circuits and Logical Design, J. Wiley and Sons, N. Y., 1958.

Gh. Cartianu, S. Condrea and E. Nicolau, "Current directions of investigations in electronics and telecommunications in the Rumanian Peoples' Republic," [in Rumanian] Telecomunicatii, 1958, No. 1, 13, Bibl. 120.

P. Constantinescu, "The analysis of π and H circuits with valve elements " [in Rumanian] Studii si cercetari matematice, 1958, No. 1, 165-172.

A. H. Copeland, "Boolean algebra," Handbook of Automat. Comput. and Control, 1958, 1, 11-01-11-11.

I. Copi, C. Elgot and J. Wright, "Realization of events by logical nets," Assoc. Comput. Machinery, 1958, 5, 2, 181-196.

L. J. Corio, "Boolean algebra used to minimize selector circuits," Western Electric Engineer (USA), 11, 3, 46-48.

J. T. Culbertson, Mathematics and Logic for Digital Devices. Van Nostrand, N. Y. , 1958, pp. 10-224.

L. Dadda, "The solution of a system of Boolean equations on an electronic computer," [in Italian] La Ricerca Scientifica, 1956, No. 11, 2226-2243.

M. Diamand, "Logical circuits. Description of the principles of electronic devices," [in Spanish] Rev. telegr. Electron.(Argentina), March, 1958, 46, 545, 130-133, 149.

Walker Dickinson, "Reliability improvement by the use of multiplement switching circuits," IBM J. Res. Development, 1958, 2, 2, 142-147.

S. Iguchi, "New method of attributing the states of intermediate relays in multicontact switching circuits,"

[in Japanese] J. Inst. Electr. Commun. Engrs., Japan, 1958, 41, 4, 475-481.

G. Epstein, "Synthesis of electronic circuits for symmetric functions," Trans. IRE, 1958, EC-7, 1, 57.

F. B. Fitch, "Representation of sequential circuits in combinatory logic," Philosophy of Science, 1958, 25 4, 263-279.

"First logical machine in Hungary," Automation, May, 1958, 494-495.

B. J. Flehinger, "Reliability improvement through redundancy at various system levels," IBM J. Res. Development, 1958, No. 2, 148-158.

B. J. Flehinger, "Reliability improvement through redundancy at various system levels," IRE Nat. Conv. Rev. Rec., 1958, 6, 6, 137-151.

S. P. Frankel, "On the minimal logical complexity required for a general purpose computer," Trans. IRE, 1958, EC-7, 4, 282-285.

H. Freudenthal, Applied Mathematical Logic [in French] Paris, Gauthier-Villars, 1958, p. 57.

K. Ganzhorn, "Basic logical functions for magnetic elements," [in German] Nachr. tech. Fachber., 1959, No. 14, 14.

M. Gardner, Logic Machines and Diagrams. N. Y., 1958, 9, 157.

M. A. Gavrilov, "The states and problems of development of the structural theory of the automatic and remote control devices of relay action," [in Rumanian] Analele Romino Sovietice, 1958, XII, Series III-a, 2 (25), 21-44.

F. H. George, "Probabilistic machines," Automation Progress, 1958, 3, 1, 19-21.

R. G. Gillespie and D. D. Aufenkamp, "On the analysis of sequential machines," Trans. IRE, 1958, EC-7, 2, 119-122.

S. Ginsburg, "On the length of the smallest uniform experiment which distinguishes the terminal states of a machine," J. Assoc. Comput. Machinery, 1958, 5, 3, 266-280.

H. Z. Glattli, "Systematic deduction of logical circuits," [in German] Z. angew. Math. Phys., 1958, 9a, 3, 288-289.

A. Gonzalez del Valle, "Basic principles of the theory of circuits," [in Spanish] Calculo Autom. y Cibernetica, 1958, No. 19, 16-20.

R. Gould, "A note on contact networks for switching functions of four variables," Trans. IRE, 1958, EC-7, 3, 196-198.

M. Greniewski, "(m + n)-Element algebras and their applications to relay-contact schemas," Zastosow. Mat., 1958, IV, 142-168.

N. T. Grisamore, L. S. Rotolo and G. U. Uyehara, "Logical design using stroke function," Trans. IRE, 1958, EC-7, 3, 181-183.

J. R. Harris, "Direct-coupled transistor logic circuitry," Trans. IRE, 1958, EC-7, 1, 2-6.

R. A. Higonnet and R. A. Grea, Logical Design of Electric Circuits. McGraw-Hill, N.Y., 1958, 220 pp.

E. Hirschhorn, "Simplification of a class of Boolean function," J. Assoc. Comput. Machinery, 1958, No.1, 67-75.

D. A. Huffman, "Solvability criterion for simultaneous logical equations," Quarterly Progress Report, Research Lab. of Electronics MIT, January 15, 1958, pp.87-88.

W. S. Humphry, Jr., Switching Circuits with Computing Application. McGraw-Hill, N. Y., 1958, 264 pp.

G. Joanin, "On one of the problems relating to selector circuits," [in French] Acta Logica, 1958, No. 1, 187.

J. Jeenel, "Programs as a tool for research in system organization," IBM J. Res. Development, 1958, 2, 2, 105-122.

H. Kaltenecker, "Relay elements, logical elements and the algebra of contact circuits," [in German] Arch. techn. Messen (Dtsch). April 1958, 267, R49-R54.

S. C. Kleene, "Mathematical machines and mathematicians," Amer. Math. Monthly, 1958, 65, 8, 659.

J. Klir and L. Seidl, "Methods of analysis and synthesis of relay circuits. Part I. Methods developed abroad," [in Czechoslovakian] Slaboproudý Obzor, 1958, 19, 7, 8, 453-458, 546-550.

J. Klir and L. Seidl, "Methods of analysis and synthesis of relay circuits. Part II. Methods developed in Czechoslovakia," [in Czechoslovakian] Slaboproudý Obzor, 1958, 19, 9, 596-605.

K. Kreysa, "Mathematical method of calculating the relay circuits in servos," [in Czechoslovakian] Automatisace, 1958, No. 12, 398-404.

R. S. Ledley, "Boolean matrix equations in digital circuit design," Trans. IRE, 1958, EC-7, 2, 131-139.

R. S. Ledley, Advanced Logical Computational Methods in Digital Circuit Design. U. S. Dept. of Commerce, Nat. Bur. Standards Report N 5784, 1958, IV, 94 pp.

L. Lofgren, "Automata of high complexity and methods of increasing their reliability by redundancy," Information and Control, 1958, 1, 2, 127-147.

O. Lowenschuss, "Nonbinary switching theory," IRE Nat. Conv. Rec., Part 4, 1958, 305-317.

Chen Mao-Chao, "A magnetic core parallel adder," Trans. IRE, 1958, EC-7, 4, 262-264.

M. F. Marcovit and E. Seif, "Analytical design of resistor-coupled transistor logical circuits," Trans. IRE, 1958, EC-7, 2, 109-119.

A. A. Markov, "On the inversion complexity of a system of functions," J. Assoc. Comput. Machinery, 1958, 5, 4, 331-334.

R. A. Mathias, "Putting logic to work in designing distributed program control systems," Control Engineering, 1958, 5, 9, 139-145.

W. Mayeda, The Application of Mathematical Logic to Network Theory. Interim. Tech. Report No. 9, U. S. Army Contract DA-11-022-ORD-1983, University of Illinois, April 1958.

E. J. McCluskey, "Iterative combinational switching networks—general design considerations," Trans. IRE, 1958, EC-7, 4, 285-291.

R. F. Miller, "Formal analysis and synthesis of bilateral switching networks," Trans. IRE, 1958, EC-7, 3, 231-244.

M. R. Millet, "Microwave switching by crystal diodes," Trans. IRE, 1958, MTT-6, 3, 284-290.

Gr. C. Moisil, "The utilization of trivalent logic in the theory of automatic devices. V. P-1 circuits," [in Rumanian] V. Schemele P-1, Communicarile Acad. RPR, 1958, VIII, 1127.

Gr. C. Moisil, "On a theorem of existence in the algebraic theory of discrete automatic devices," [in French] Revue de mathématique pures et appliquées, 1958, III, 1, 1-15.

Gr. C. Moisil, "Algebraic theory of automatic devices," [in Italian] Conferenze del Seminario di Matematica dell'Universita di Bari, pp. 33-34.

Gr. C. Moisil, "Outline of the algebra of relay-contact automatic systems," [in Czechoslovakian] Zastosowania Matematyki, 1958, IV, 1, 1-27.

C. Monin, "Description and principle of the functioning of the logical commutator with one hundred positions, in operation at the Industrial Telephone Company," [in French] Bull. Soc. franc. électriciens, 1958, 8, 90, 358-366.

E. F. Morris and T. E. Wohr, "Automatic implementation of computer logic," Commun. Assoc. Comput. Machinery, 1958, 1, 5, 14-15.

F. Moskowitz, "Analysis of redundancy networks," Commun. and Electronics, Nov. 1958, 627-632.

E. Muehldorf, "Ternary relay algebra," [in German] Archiv elektr. Uebertrag. Deutsch, 1958, 12, 3, 138-148.

E. Muehldorf, "Relay circuits for trivalent logic," [in German] Archiv electr. Uebertrag., April 1958, 12, 4, 176-182.

J. S. Murphy. Basis of Digital Computers. No. 4. J. F. Rider Publ. Inc., 1958, 118-119.

A. Mullin, "Reliable stochastic sequential switching circuits," Commun. and Electronics, Nov. 1958, 606-610.

A. Mullin and W. Kellner, "A residue test for Boolean functions," Trans. Illinois State Acad. Sci., 1958, 51, 3-4, 14-19.

P. Naslin, Principles of digital computers [in French] Dunod, Paris, 1958, 224 pp.

P. Naslin, Relay circuits and multicycle devices [in French] Dunod, Paris, 1958, 229 pp.

P. Naslin, "Introduction to the theory of multicycle automatic devices," [in French] Automatisme, 1958, III, 1, 3-11; 2, 43-49; 3, 87-94; 4, 135-143; 5, 179-185; 6, 225-228; 7, 260-264.

M. Nedelcu, "On electronic circuits with relay functioning and circuits with alternating current rectifiers," [in French] Bulletin Mathématique, 2, 1, 1958, 75-94.

M. Nedelcu, "Circuits with electronic rectifiers," [in Rumanian] Comunicarile Acad. RPR, 1958, VIII, 7, 643-646.

M. Nedelcu, "Electronic circuits with relay functioning," [in Rumanian] Comunicarile Acad. RPR, 1958, VIII, 9, 893-895.

A. Nerode, "Linear automata transformations," Proc. Amer. Math. Soc., 1958, No. 9, 541-544.

D. B. Netherwood, "Logical machine design: a selected bibliography," Trans. IRE, 1958, EC-7, 2, 155-178; 3, 250.

A. F. Newell, "The design of logical circuits using transistors and square loop ferrite cores," Mullard Techn. Communs., 1958, 4, No. 34.

J. Ninomiga, "A theory of the coordinate representation of switching functions," Mem. Fac. Eng. Nagoya Univ., 1958, 10, 2, 175-190.

G. M. Philippe, "Equivalent circuits of semiconducting diodes and triodes," [in French] Revue MBLE, Jan. 1958, 1, No. 2.

M. Phister, Logical Design of Digital Computers. John Wiley and Sons, Inc., N. Y., 1958, 408 pp.

J. Piesch and H. Sequenz, "Austrian pioneers in the theory of relay circuits," [in German] Elektrotechnik und Maschinenbau 1958, 9.

A. G. Portela, "Application of logical symbols in electrical systems," [in Portuguese], Technica (Lisbon), Jan. 1958, No. 278, 253-264.

G. M. Pugmire and A. Rose, "Formulas corresponding to universal decision elements," Z. math. Logic, 1958, 4, 9.

N. S. Prywes, "Diodeless magnetic shift registers utilizing transfluxors," Trans. IRE, 1958, EC-7, 4, 316-324.

G. H. Raney, "Sequential functions," J. Assoc. Comput. Machinery, April 1958, 5, 2, 177.

L. Rieger, "On the theory of nerve networks," [in Rumanian] Aplikace Mat., 1958, 3, 4, 243-274.

R. Righi, "Switching algebra for electrical circuits with multipositional elements," [in Italian] Ingegneria Ferroviaria, 1958, 10, 881-898; 1, 1019-1030.

A. Rose, "Many-valued logical machines," Proc. Cambridge Philos. Soc., 1958, 54, 3, 307-321, bibl. 11.

A. Rose, "The use of universal decision elements as flip-flops," Z. math. Logik, 1958, 4, 169-174.

J. L. Rosenfeld, "Magnetic core pulse-switching circuits for standard packages," Trans, IRE, 1958, EC-7, 3, 223-228.

J. Roth, "Algebraic topological methods for the synthesis of switching systems. I.," Trans. Amer. Math. Soc., 1958, 88, 301-326.

N. Rouche, "Some properties of Boolean equations," Trans. IRE, 1958, EC-7, 4, 291-298.

S. Rudeanu, "The utilization of Gaulois fields in the theory of automatic devices. X. Classification of the functions of two variables" [in Rumanian], Studdi si cercetari matematice, 1958, 1, Bucharest.

A. Sageau, "Logical circuits. Principles and applications" [in French], Docaéro (Fr.) 1958, 51, 57-60.

Z. Sawicki, "The transformer realization of proposition functions," Bull. Acad. polon. sci., Serie sci. tech., 1958, VI, 2, 111-116.

A. H. Scheinman, "A numerical-graphical method for synthesizing switching circuits," Commun. and Electronics, Jan. 1958, No. 34, 687-689.

E. J. Schubert, "Matrix analysis of logical networks," Commun. and Electronics, March 1958, 10-13.

W. Semon, "Synthesis of series-parallel network switching functions," Bell System Tech. J, 1958, 37, 4, 877-898.

S. Seshu, "Theory of lineal graphs with applications in electrical engineering," Syracuse University, 1958.

C. E. Shannon, "Von Neumann's contributions to automata theory," Bull. Amer. Math. Soc., 1958, 64, 3, 123-129.

J. M. Simon, "Some aspects of the network analysis of sequence transducers," J. Franklin Inst., June 1958, 265, 439-450.

H. Soubies-Camy, "The application of logical algebra to binary digital technique," Automatisme, 1958, III, 7, 266-272; 9, 338-345; 10, 385-393; 11, 423-429.

J. J. Smith, "Relay circuit analysis—a new approach," Nuclear Engineering, 1958, 2, 22, 5-8.

A. Svoboda, "Graphical aids to minimization" [in Czech], Stroje na zpraceovani informaci, VI, Prague, 1958.

F. Svoboda, "The synthesis of relay circuits with the help of partial tests" [in Czech], Stroje na zpracovani informaci, VI, Prague, 1958, 35-53.

"Uniselector for automatic systems," Atomic World, 1958, 9, 12, 437.

J. H. Wallace, "A mechanical method for designing switching circuits," Western Electric Engineer (USA), Oct, 1958, 11, 4, 43-48.

Wang Chuan-Shan, "The realizability of tables of relay circuit wirings (in Chinese, Tse-Tung-Hua)," Automation, 1958, 1, 4, 163-171.

J. N. Warfield, "Switching circuits as topological models in discrete probability theory," Trans. IRE. 1958, EC-7, 3, 251-252.

J. N. Warfield, "A note on the reduction of switching functions," Trans. IRE, 1958, EC-7, 2, 180-181.

G. P. Weeg, "Folding of symmetric functions," Trans. IRE, 1958, EC-7, 4, 325.

F. Weitzsch, "From propositional logic to logical algebra," [in German] Electron. Rundschau (Dtsch.), 1958, 12, 5, 160-164.

M. V. Wilkes, M. A. Renwick and D. J. Wheeler, "The design of the control unit of an electronic digital computer," Proc. IEE, Part B, 1958, 105, 20, 121-128.

H. Wolpe, "Algorithm for analyzing logical statements to produce a truth function table," Communs. Assoc. Comput. Machinery, 1958, 1, 3, 4-13.

H. Zemanek, Mailüfterl—an Automatic Calculating Machine with Semiconductor Triodes Operating on the Decimal System [in German], 1958.

H. Zemanek, "The solution of equations in relay algebra " [in German], Arch. electr. Übertrag. (Dtsch.), 1958, 12, 1, 35-44.

V. D. Kazakov and O. P. Kuznetsov

AN ESTIMATE OF THE MAXIMUM DEVIATION FROM A GIVEN TRAJECTORY

E. A. Barbashin

Sverdlovsk

Translated from Avtomatika i Telemekhanika, Vol. 21, No. 10,
pp. 1341-1351, October, 1960
Original article submitted April 15, 1960

The method proposed in [1] is used to estimate the maximum deviation of motion from a given trajectory.

A method of choosing control functions and vectors is introduced for decreasing this deviation. The case of an infinite time interval is considered. The relation between the problem investigated and that of the accumulation of disturbances is studied.

We consider the system of differential equations

$$\frac{dx_i}{dt} = \sum_{k=1}^{n} a_{ik}(t)\, x_k + \sum_{k=1}^{m} b_{ik} u_k(t) \qquad (1)$$

$$(i = 1, 2, \ldots\ n, \quad m \leqslant n),$$

where $a_{ik}(t)$ are continuous functions on the interval $t_0 \le t \le t_0 + T$, and the b_{ik} are constants such that the "control" vectors $b_k(b_{1k}, b_{2k}, \ldots, b_{nk})$ $(k = 1, 2, \ldots, m)$ are linearly independent.

As in [1], we pose the problem of finding control functions $u_k(t)$, such that for $t_0 \le t \le t_0 + T$ the relation

$$x_i(t) = f_i(t) \qquad (i = 1, 2, \ldots, n) \qquad (2)$$

is satisfied, where $x_i(t)$ is the solution of the system (1) and $f_i(t)$ is a given system of functions with $x_i(t_0) = f_i(t_0)$. When $m < n$, this problem is, as a rule, insoluble, and so we try to find functions $u_k(t)$ [2] such that the expression

$$\| z \| = \max_i \max_{t_0 < t < t_0 + T} | x_i(t) - f_i(t) | \qquad (3)$$

will be a minimum.

Following the ideas of [1], we will not try to find control functions guaranteeing that the value of $\|z\|$ is exactly a minimum, but will obtain an estimate of the form

$$\|z\| \le A \|y\|,$$

where A is a constant and $\|y\|$ is the deviation from zero in some sense of another quantity y. We replace the difficult problem of finding min $\|z\|$ by the simpler problem of finding min $\|y\|$. The loss in accuracy of the approximation due to this procedure is not great for small values of $\|y\|$, while the decrease in difficulty in the numerical calculations is considerable.

In Section 1 we show that the method of choosing the control functions and vectors proposed earlier ensures a decrease, not only in the mean square value of the deviation, but also a decrease in the maximum deviation. It must be taken into consideration that the value of a control function at any given instant is chosen independently of the length of the interval over which the approximation is being carried out, and also independently of the value of this function at any other instant of time.

In Section 2, the same method of choosing the control functions [see the system (10)] is used to obtain other methods of estimating the maximum deviation. Although these other methods have no special advantages over the estimate of Theorem 1, they are of interest in several cases. In particular, Theorem 3 (and also Theorems 1 and 2) solves the problem of the accumulation of disturbances in a dynamic system. From this point of view, the results obtained are completely analagous to those obtained by B. V. Bulgakov in [3, 4]. We also note that the character of any of the three estimates of $\|z\|$ depends on the function space in which we consider y. An explanation of this phenomenon is given in the Appendix.

We consider the case T = ∞ in Section 3. It is natural to consider this case in connection with questions in the theory of stability. It is unfortunately impossible in the present paper to investigate this problem in the light of the ideas in the detailed investigation by Massera and Schäffer [5].

1. The Basic Estimate of the Maximum of the Deviation and the Choice of Control Functions

In the system (1) we make the change of variables

$$z_i = x_i - f_i(t) \qquad (i = 1, 2, \ldots, n),$$

and obtain the new system

$$\dot{z}_i = \sum_{k=1}^{n} a_{ik}(t) z_k + y_i(t) \quad (i = 1, 2, \ldots, n), \tag{4}$$

where

$$y_i(t) = \sum_{k=1}^{r} b_{ik} u_k(t) + \sum_{k=1}^{n} a_{ik}(t) f_k(t) - \dot{f}_i(t)$$
$$(i = 1, 2, \ldots, n). \tag{5}$$

The solution of the system (4) that satisfies the conditions $z_i(t_0) = 0$ is

$$z_i(t) = \int_{t_0}^{t} \sum_{k=1}^{n} w_{ik}(t, \tau) y_k(\tau) d\tau \quad (i = 1, 2, \ldots, n), \tag{6}$$

where $W_{ik}(t, \tau)$ are the elements of the fundamental matrix $\mathbf{W}(t, \tau)$ defined by the equation $d\mathbf{W}/dt = \mathbf{A}(t)\mathbf{W}$ and the condition $\mathbf{W}(\tau, \tau) = \mathbf{I}$ [$\mathbf{I}$ is the unit matrix, and $\mathbf{A}(t)$ is the matrix with its elements, coefficients $a_{ik}(t)$].

In what follows we will use the notation

$$\| z \| = \max_i \max_{t_0 < t < t_0 + T} | z_i(t) |,$$

$$y^2(t) = \sum_{i=1}^{n} y_i^2(t),$$

$$w_i^2(t, \tau) = \sum_{k=1}^{n} w_{ik}^2(t, \tau) \qquad (i = 1, 2, \ldots, n).$$

Let $y_i(t)$ be functions which are for the moment arbitrary, but such that the integral $\int_{t_0}^{t_0+T} y^2(t)\, dt$ exists.

The following theorem opens up the possibility of estimating $\| z \|$ in terms of the mean square value of the quantity $y(t)$.

Theorem 1. There exists a minimum number M, for which

$$\| z \| \leqslant M \left(\int_{t_0}^{t_0+T} y^2(\tau) d\tau \right)^{1/2}. \tag{7}$$

The number M can be obtained from the formula

$$M = \max_i \max_{t_0 < t < t_0 + T} \left(\int_{t_0}^{t} w_i^2(t, \tau) d\tau \right)^{1/2}. \tag{8}$$

If the functions $a_{ik}(t)$ are constants, then

$$M = \max_i \left(\int_{t_0}^{t_0+T} w_i^2(t_0 + T, \tau) d\tau \right)^{1/2}. \tag{9}$$

Theorem 1 evidently also solves the problem of the accumulation of disturbances when the mean square of the external forces is bounded. In fact, if

$$\int_{t_0}^{t_0+T} y^2(\tau) d\tau = L,$$

then the formula (7) gives the maximum deviation, equal to ML. From the proof of Theorem 1 given in the Appendix. it is obvious what form the functions $y_i(t)$ must take to give the maximum deviation.

It follows from Theorem 1 that $\| z \|$ can be decreased by decreasing the quantity $\| y \| = \left(\int_{t_0}^{t_0+T} y^2(\tau) d\tau \right)^{1/2}.$

The method of choosing the control functions $u_i(t)$ to ensure that $\| z \|$ is a minimum was given in Section 2 of [1]. In this paper it was shown that the control functions are determined by a system of equations of the form

$$\sum_{i=1}^{m} (\mathbf{b}_k, \mathbf{b}_i) u_i(t) = (\mathbf{r}(t), \mathbf{b}_k) \quad (k = 1, 2, \ldots, m), \tag{10}$$

where $(\mathbf{b}_k, \mathbf{b}_i)$ is the scalar product of the vectors $\mathbf{b}_k$; and $\mathbf{b}_i$, and $\mathbf{r}(t) = r_1(t), r_2(t), \ldots, r_n(t)$ are vector functions satisfying the equation

$$r_i(t) = f_i(t) - \sum_{k=1}^{n} a_{ik}(t) f_k(t) \qquad (i = 1, 2, \ldots, n). \tag{11}$$

If $u_i(t)$ is chosen according to (10), then we will have

$$y^2(t) = \sum_{i=1}^{n} y_i^2(t) = \frac{\Gamma(\mathbf{b}_1, \mathbf{b}_2, \ldots, \mathbf{b}_m, \mathbf{r}(t))}{\Gamma(\mathbf{b}_1, \mathbf{b}_2, \ldots, \mathbf{b}_m)}, \tag{12}$$

where the numerator and denominator in the fraction on the right-hand side are the Gramme determinants corresponding to the systems of vectors.

Thus, we have

$$H^2 = \|y\|^2 =$$

$$= \frac{1}{\Gamma(\mathbf{b}_1, \mathbf{b}_2, \ldots, \mathbf{b}_m)} \int_{t_0}^{t_0+T} \Gamma(\mathbf{b}_1, \mathbf{b}_2, \ldots, \mathbf{b}_m, r(t))\, dt. \tag{13}$$

It should be noted that if the functions $u_k(t)$ are chosen according to (10), then

$$\sum_{k=1}^{m} \mathbf{b}_k u_k(t) =$$

$$= \frac{1}{\Gamma(\mathbf{b}_1, \mathbf{b}_2, \ldots, \mathbf{b}_m)} \begin{vmatrix} (\mathbf{b}_1, \mathbf{b}_1) \ldots (\mathbf{b}_1, \mathbf{b}_m), & \mathbf{b}_1 \\ (\mathbf{b}_m, \mathbf{b}_1) \ldots (\mathbf{b}_m, \mathbf{b}_m), & \mathbf{b}_m \\ (\mathbf{r}, \mathbf{b}_1) \ldots (\mathbf{r}, \mathbf{b}_m), & 0 \end{vmatrix}.$$

In Section 3 of [1], a recommendation is given for the choice of the control vectors $\mathbf{b}_1, \mathbf{b}_2, \ldots, \mathbf{b}_m$, to give a minimum value for $\|y\|$ if the functions $u_k(t)$ are chosen according to (10). The choice of the control functions and the control vectors given in [1] thus contributes,not only to decreasing the mean square deviation, but also to decreasing the maximum deviation.

2. Other Estimates of $\|z\|$

In this section we give other estimates of $\|z\|$ which are independent of the estimate given in Section 1. Let $y_i(t)$ be an arbitrary function such that the integral $\int_{t_0}^{t_0+T} y(\tau)\, d\tau$ exists.

Theorem 2. The inequality

$$\|z\| \leqslant N \int_{t_0}^{t_0+T} y(\tau)\, dt \tag{14}$$

holds, where $N = \max_{i} \max_{t_0 \le t \le t_0+T_0} \max_{t_0 \le \tau \le t} w_i(t, \tau)$.

If all the eigenvalues $\lambda_i(t)$ of the matrix $\mathbf{A}(t) + \mathbf{A}^*(t)$ ($\mathbf{A}(t)$ is the matrix having the coefficients $a_{ik}(t)$ as elements, $\mathbf{A}^*(t)$ is its adjoint) are nonpositive for any value of t in the interval $t_0 \le t \le t_0 + T$, then $N = 1$, and

$$\|z\| \leqslant \int_{t_0}^{t_0+T} y(\tau)\, d\tau.$$

Formula (14) gives a new estimate of $\|z\|$. In connection with the choice of control functions, it follows from Section 2 of [1] that Theorem 2 gives no new information in choosing these functions, except that which follows from the system (10) investigated in the present paper. In fact, when the control functions are chosen according to (10), the minimum value of not only the integral $\int_{t_0}^{t_0+T} y^2(\tau)\, d\tau$, but also that of the integral $\int_{t_0}^{t_0+T} y(\tau)\, d\tau$ is ensured.

Theorem 3. There exists a least number C, such that

$$\|z\| \leqslant C \max_{t_0 < t < t_0+T} y(t). \tag{15}$$

This number is given by the formula

$$C = \max_{i} \max_{t_0 < t < t_0+T} \int_{t_0}^{t} w_i(t, \tau)\, d\tau. \tag{16}$$

If the functions $a_{ik}(t)$ are constant, then

$$C = \max_{i} \int_{t_0}^{t_0+T} w_i(t_0 + T, \tau)\, d\tau. \tag{17}$$

In addition to the basic problem, Theorem 3 also solves the problem concerning the accumulation of disturbances in the system for bounded external vector forces. If the functions $y_i(t)$ satisfy the inequality $y^2(t) = \sum_{i=1}^{n} y_i^2(t) \leqslant R^2$, then it follows from Formula (15) that $\|z\| \le RC$, while,from the proof of Theorem 3 given in the Appendix, it follows that the upper bound of RC is attained for

$$y_k(\tau) = R \frac{w_{ik}(t, \tau)}{w_i(t, \tau)},$$

where t and i are chosen so that the maximum (16) is attained. If the functions $a_{ik}(t)$ are constant, then we have

$$\|z\| \leqslant R \max_{i} \int_{t_0}^{t_0+T} w_i(t_0 + T, \tau)\, d\tau.$$

The result of the solution in the present paper and in [1] differ from that in [3] in that here the sum of the squares of the external influences $y_i(t)$ is bounded, and not each separate influence.

We now return to the main problem. Since $y_i(t) = \sum_{k=1} b_{ik} u_k(t) - r_i(t)$, where the functions $r_i(t)$ are given by Formula (11), then according to [1] $y(t) = \left(\sum_{i=1}^{n} y_i^2(t)\right)^{1/2}$ gives the distance from a point A lying on the curve $z_i = r_i(t)$ to a point B in the plane Q generated by the vectors $\mathbf{b}_1, \mathbf{b}_2, \ldots, \mathbf{b}_m$. At any given instant t, the distance AB will be a minimum if the functions $u_i(t)$ are chosen according to (10). In this case $\rho(t) = y^2(t) = AB^2$ are calculated from Formula (12),while, for the indicated choice of the control functions the quantity $\rho(t)$ will be a minimum. In order to use Theorem 3, we must calculate the greatest value of the function $\rho(t)$ for $t_0 \leq t \leq t_0+T$. This can obviously be done by elementary methods. In fact, since $\rho(t)=-[\mathbf{r}(t), \mathbf{y}(t)]$, where $\mathbf{r}(t)$ is the vector with projections $r_i(t)$ and $\mathbf{y}(t)$ is the vector with projections $y_i(t)$, we have $\rho(t)= -(\mathbf{r}, \mathbf{y})-(\mathbf{y}, \mathbf{r})$.

But, according to [6] (p. 205),

$$\mathbf{y}(t) = \frac{1}{\Gamma}\begin{vmatrix} (\mathbf{b}_1, \mathbf{b}_1), & \ldots, & (\mathbf{b}_1, \mathbf{b}_m), & \mathbf{b}_1 \\ \cdots & \cdots & \cdots & \cdots \\ (\mathbf{b}_1, \mathbf{b}_m), & \ldots, & (\mathbf{b}_m, \mathbf{b}_m), & \mathbf{b}_m \\ (\mathbf{b}_1, \mathbf{r}), & \ldots, & (\mathbf{b}_m, \mathbf{r}), & \mathbf{r} \end{vmatrix}$$

$$\mathbf{y}(t) = \frac{1}{\Gamma}\begin{vmatrix} (\mathbf{b}_1, \mathbf{b}_1), & \ldots, & (\mathbf{b}_1, \mathbf{b}_m), & \mathbf{b}_1 \\ \cdots & \cdots & \cdots & \cdots \\ (\mathbf{b}_1, \mathbf{b}_m), & \ldots, & (\mathbf{b}_m, \mathbf{b}_m), & \mathbf{b}_m \\ (\mathbf{b}_1, \dot{\mathbf{r}}), & \ldots, & (\mathbf{b}_m, \dot{\mathbf{r}}), & \dot{\mathbf{r}} \end{vmatrix} \tag{18}$$

where $\Gamma = \Gamma(\mathbf{b}_1, \mathbf{b}_2, \ldots, \mathbf{b}_m)$ is Gramme determinant for the vectors $\mathbf{b}_1, \mathbf{b}_2, \ldots, \mathbf{b}_m$.

From (18) we see that

$$(\dot{\mathbf{y}}, \mathbf{r}) =$$

$$= \frac{1}{\Gamma}\begin{vmatrix} (\mathbf{b}_1, \mathbf{b}_1), & \ldots, & (\mathbf{b}_1, \mathbf{b}_m), & (\mathbf{b}_1, \mathbf{r}) \\ \cdots & \cdots & \cdots & \cdots \\ (\mathbf{b}_1, \mathbf{b}_m), & \ldots, & (\mathbf{b}_m, \mathbf{b}_m), & (\mathbf{b}_m, \mathbf{r}) \\ (\mathbf{b}_1, \dot{\mathbf{r}}), & \ldots, & (\mathbf{b}_m, \dot{\mathbf{r}}), & (\mathbf{r}, \dot{\mathbf{r}}) \end{vmatrix} = (\dot{\mathbf{r}}, \mathbf{y}).$$

A necessary condition for a maximum is therefore

$$(\dot{\mathbf{r}}, \mathbf{y}) = 0; \tag{19}$$

and this condition is satisfied if $\dot{\mathbf{r}} = 0$, or if $\dot{\mathbf{r}}$ is orthogonal to $\mathbf{y}$. We will not consider the case $\mathbf{y} = 0$, since in this case $y^2 = \sum_{i=1}^{n} y_i^2 = 0$, and there is consequently no maximum.

To obtain a necessary condition, we introduce the parameter s, denoting the arc length of the curve $z_i = r_i(t)$. We have

$$\frac{1}{2}\frac{d\rho^2}{dt^2} = -(\ddot{\mathbf{r}}, \mathbf{y}) - (\dot{\mathbf{r}}, \dot{\mathbf{y}}) =$$

$$= -\left(\frac{d^2\mathbf{r}}{ds^2}\dot{s}^2 + \frac{d\mathbf{r}}{ds}\ddot{s}, \mathbf{y}\right) - \Gamma(\mathbf{b}_1, \mathbf{b}_2, \ldots, \mathbf{b}_m, \dot{\mathbf{r}}).$$

The equality $(\dot{\mathbf{r}}, \dot{\mathbf{y}}) = \Gamma(\mathbf{b}_1, \mathbf{b}_2, \ldots, \mathbf{b}_m, \dot{\mathbf{r}})$ is obtained directly from (18).

When we take into consideration that $\left(\frac{d\mathbf{r}}{ds}, \mathbf{y}\right) = 0$, we can write the sufficient condition for a maximum in the form

$$\left(\frac{d^2\mathbf{r}}{ds^2}, \mathbf{y}\right)\dot{s}^2 + \Gamma(\mathbf{b}_1, \mathbf{b}_2, \ldots, \mathbf{b}_m, \dot{\mathbf{r}}) > 0. \tag{20}$$

In order to find the greatest value of $\rho(t)$, we must calculate $\rho(t)$ at the points t_0 and t_0+T, and also at the maximum points, and choose the greatest value of $\rho(t)$ from these values.

3. The Approximate Trajectory in the Case T = ∞

We now consider the possibility of approximating to the given trajectory for an infinite time interval. We first of all set an upper limit to the absolute value of the elements of the fundamental matrix, and assume ([7], p. 366) that

$$|w_{ik}(t, \tau)| < Be^{-\alpha(t-\tau)}$$
$$(i = 1, 2, \ldots, n,\ k = 1, 2, \ldots, n). \tag{21}$$

This condition is equivalent to assuming that any solution of the system

$$\dot{x}_i = \sum_{k=1}^{n} a_{ik}(t)\, x_k \qquad (i = 1, 2, \ldots, n) \tag{22}$$

satisfies the inequality

$$|x_i(t)| \leqslant B\left(\sum_{k=1}^{n} x_k^2(t_0)\right)^{1/2} e^{-\alpha(t-t_0)}.$$

In fact, an arbitrary kth column $w_{1k}(t, \tau), w_{2k}(t, \tau), \ldots, w_{nk}(t, \tau)$ of the matrix $\mathbf{W}(t, \tau)$ satisfies the system (22) if $w_{ik}(\tau, \tau) = 0$ for $i \neq k$ and $w_{ii}(\tau, \tau) = 1$.

The condition (21) is always satisfied if the matrix $\mathbf{A}(t) = \|a_{ik}\|$ is constant and its eigenvalues have negative real parts.

It follows from Theorems 1, 2, and 3, that when the conditions (21) are satisfied,

$$\|z\| \leqslant B\left(\frac{n}{2\alpha}\int_{t_0}^{\infty} y^2(\tau)\, d\tau\right)^{1/2}, \tag{23}$$

$$\|z\| \leqslant B\sqrt{n}\int_{t_0}^{\infty} y(\tau)\, d\tau, \tag{24}$$

$$\|z\| \leqslant B\frac{\sqrt{n}}{\alpha}\sup_{t_0 \leqslant t < \infty} y(t). \tag{25}$$

It is obvious that in order that the solution of the system (4) be bounded, it is sufficient that one of the conditions

$$\int_{t_0}^{\infty} y^2(\tau)\, d\tau < \infty, \tag{26}$$

$$\int_{t_0}^{\infty} y(\tau)\,d\tau < \infty, \tag{27}$$

$$\sup_{t_0 < t < \infty} y(t) < \infty \tag{28}$$

be satisfied.

I. G. Malkin showed in [8] that it follows from the boundedness of all solutions of the system (2); for arbitrary $y_i(t)$ satisfying condition (28), that condition (21) is satisfied.

We now consider what conditions must be imposed on the functions $f_i(t)$ in order that the inequalities (26), (27), and (28) be satisfied when the control functions are chosen according to (10).

Since from (12) we have

$$y^2(t) = \frac{\Gamma(\mathbf{b}_1, \mathbf{b}_2, \ldots, \mathbf{b}_m, \mathbf{r}(t))}{\Gamma(\mathbf{b}_1, \mathbf{b}_2, \ldots, \mathbf{b}_m)},$$

these conditions must obviously have the form

$$\int_{t_0}^{\infty} \Gamma(\mathbf{b}_1, \mathbf{b}_2, \ldots, \mathbf{b}_m, \mathbf{r}(t))\,dt < \infty, \tag{26'}$$

$$\int_{t_0}^{\infty} \sqrt{\Gamma(\mathbf{b}_1, \mathbf{b}_2, \ldots, \mathbf{b}_m, \mathbf{r}(t))}\,dt < \infty, \tag{27'}$$

$$\sup_{t_0 < t < \infty} \Gamma(\mathbf{b}_1, \mathbf{b}_2, \ldots, \mathbf{b}_m, \mathbf{r}(t)) < \infty. \tag{28'}$$

Here the vector function $\mathbf{r}(t)$ is given by formula (11). It is also easy to show that the choice of the system of control vectors according to [1] will be possible if the condition $\int_{t_0}^{\infty} r^2(t)\,dt < \infty$ is satisfied.

Conclusions

1. The choice of control functions according to (10) makes it possible to decrease not only the mean square deviation, but also the maximum deviation.

2. The values at any given instant of time of control functions chosen according to (10) do not depend on the length of the time interval over which the approximation is being made, or on the values of the control functions at any other instant of time.

3. The choice of control functions according to (10) yields the possibility of selecting an optimal system of control vectors by using the method described in Section 3 of [1].

4. The proposed method makes it possible to avoid difficulties in numerical calculation, and permits a simple geometric interpretation and the application of modelling for the solution of the problem.

5. The proposed method is most effective for small $\min\|y\|$, and when the conditions (21) are satisfied.

APPENDIX

Proof of Theorem 1. From the relation (6) we have

$$|z_i(t)| \leqslant \int_{t_0}^{t} w_i(t, \tau)\,y(\tau)\,d\tau, \tag{29}$$

and when we use the Bunyakovskii-Schwartz inequality, we obtain

$$|z_i(t)| \leqslant \left(\int_{t_0}^{t} w_i^2(t, \tau)\,d\tau\right)^{1/2} \left(\int_{t_0}^{t} y^2(\tau)\,d\tau\right)^{1/2} \leqslant$$

$$\leqslant \left(\int_{t_0}^{t} w_i^2(t, \tau)\,d\tau\right)^{1/2} \left(\int_{t_0}^{t_0+T} y^2(\tau)\,d\tau\right)^{1/2}. \tag{30}$$

This inequality becomes an equality when the function $y_k(\tau)$ has the form

$$y_k(\tau) = \frac{w_{ik}(t, \tau)}{w_i(t, \tau)} \quad \text{for} \quad 0 \leqslant \tau \leqslant t,$$

$$y_k(\tau) = 0 \quad \text{for} \quad t \leqslant \tau \leqslant t_0 + T.$$

From (30) we obtain

$$\max_{t_0 \leqslant t \leqslant t_0+T} |z_i(t)| \leqslant \max_{t_0 \leqslant t \leqslant t_0+T} \left(\int_{t_0}^{t} w_i^2(t, \tau)\,d\tau\right)^{1/2} \left(\int_{t_0}^{t_0+T} y^2(\tau)\,d\tau\right)^{1/2},$$

from which the formulas (7) and (8) follow.

Now let $a_{ik}(t)$ be constant; we will show that $F(t, t_0) = \int_{t_0}^{t} w_i^2(t, \tau)\,d\tau$ is a monotonically increasing function of t. Actually, in this case ([9], p. 173) we have $w_{ik} = (t, \tau) = w_{ik}(t-\tau)$. If we let $t_0 < t_1 < t_2$, we can write

$$F(t_2, t_0) = \int_{t_0}^{t_2} w_i^2(t_2 - \tau)\,d\tau =$$

$$= \int_{t_0}^{t_0+t_2-t_1} w_i^2(t_2 - \tau)\,d\tau + \int_{t_0+t_2-t_1}^{t_2} w_i^2(t_2 - \tau)\,d\tau.$$

After the change of variable $\eta = \tau - t_2 + t_1$, in the second integral we have

$$F(t_2, t_0) = \int_{t_0}^{t_0+t_2-t_1} w_i^2(t_2 - \tau)\,d\tau + \int_{t_0}^{t_1} w_i^2(t_1 - \eta)\,d\eta =$$

$$= \int_{t_0}^{t_0+t_2-t_1} w_i^2(t_2 - \tau)\,d\tau + F(t_1, t_0).$$

Since the first integral is positive, we obtain the desired result.

Formula (9) follows from the fact that $F(t, t_0)$, as a monotonically increasing function, attains its maximum for $t = t_0 + T$.

We note that in the case of variable $a_{ik}(t)$, the conclusion that $F(t, t_0)$ is increasing is no longer true. Similarly, consider the equation $\dot{z} = -\tan t\, z$. The general solution of this equation is $z = c \cos t$, $w(t, \tau) = \cos t / \cos \tau$, $F(t, 0) = \int_0^t w^2(t, \tau) d\tau = \frac{1}{2} \sin 2t$. The function $F(t, 0)$ is evidently not monotonic in the interval $-\frac{\pi}{2} + \epsilon < t < \frac{\pi}{2} - \epsilon$ if ϵ is sufficiently small.

Proof of Theorem 2. We conclude from the inequality (29) that

$$|z_i(t)| \leqslant \max_{0 < \tau < t} w_i(t, \tau) \int_{t_0}^{t} y(\tau) d\tau;$$

when we increase the upper limit of integration to $t_0 + T$, we obtain

$$|z_i(t)| \leqslant \max_{t_0 < \tau < t} w_i(t, \tau) \int_{t_0}^{t_0+T} y(\tau) d\tau,$$

and (14) follows.

We now consider the case when the eigenvalues of the matrix $\mathbf{A}(t) + \mathbf{A}^*(t)$ are nonpositive for all $t \geq t_0$. In this case, the quadratic form $\sum_{i,k=1}^{n} a_{ik}(t) x_i x_k$ will also be nonpositive. It is known ([9], p. 172) that the matrix $\mathbf{W}(t, \tau)$ is equal to $F(t) F^{-1}(\tau)$, where $F(t)$ is the fundamental matrix of the system $\dot{x} = \mathbf{A}(t) x$. It is thus easy to obtain the relation

$$\frac{d\mathbf{W}}{d\tau} = -\mathbf{W}\mathbf{A}(\tau),$$

from which it follows that the rows $(w_{i1}, w_{i2}, \ldots, w_{in})$ of the matrix $\mathbf{W}(t, \tau)$ satisfy the system

$$\frac{dw_{ik}}{d\tau} = -\sum_{m=1}^{n} a_{mk}(\tau) w_{im} \qquad (k = 1, 2, \ldots, n).$$

Recalling that $w_i^2(t, \tau) = \sum_{k=1}^{n} w_{ik}^2(t, \tau)$, we have

$$\frac{d}{dt} w_i^2(t, \tau) = -2 \sum_{k=1}^{n} w_{ik} \sum_{m=1}^{n} a_{mk}(\tau) w_{im} =$$

$$= -2 \sum_{k,m=1}^{n} a_{mk}(\tau) w_{ik} w_{im} \geqslant 0,$$

according to the conditions of the theorem. Thus, $\max_{t_0 < \tau < t} w_i^2(t, \tau) = w_i^2(t, t) = 1$. It should be noted that the condition that the eigenvalues of the matrix $\mathbf{A}(t) + \mathbf{A}^*(t)$ be nonpositive can be replaced by the Sylvester criterion, or by a modification of this criterion ([6], p. 250).

Proof of Theorem 3. It follows from (29) that

$$|z_i(t)| \leqslant \int_{t_0}^{t} w_i(t, \tau) d\tau \max_{t_0 < \tau < t} y(\tau),$$

and so

$$\max_{t_0 < t < t_0+T} |z_i(t)| \leqslant \max_{t_0 < t < t_0+T} \int_{t_0}^{t} w_i(t, \tau) d\tau \max_{t_0 < \tau < t_0+T} y(\tau), \tag{31}$$

which yields

$$\|z\| \leqslant C \max_{t_0 < \tau < t_0+T} y(\tau),$$

where

$$C = \max_i \max_{t_0 < t < t_0+T} \int_{t_0}^{t} w_i(t, \tau) d\tau.$$

The fact that C is the least of the numbers satisfying the inequality follows, because the right-hand side of the inequality (31) is attained for

$$y_j(\tau) = \frac{w_{ij}(t, \tau)}{w_i(t, \tau)}.$$

Reasoning similar to that used in the proof of Theorem 1 can also be used to prove the validity of Formula (17).

Note. We will consider the relation (6) as the application of an operator $\mathbf{W}$, which transforms the vector function $y(t)$ into the vector function $z(t)$. In the present paper $z(t)$ is an element of the space $C_n(t_0, t_0 + T)$, in which the norm is defined by the formula $\|z\| = \max_i \max_{t_0 \leq t \leq t_0+T} |z_i(t)|$.

For each of the three theorems, the function $y(t)$ lies in a different space.

In the first theorem, $y(t)$ lies in the space $L_{2n}(t_0, t_0 + T)$ with the norm $\|y\| = \left(\int_{t_0}^{t_0+T} y^2(t) dt \right)^{1/2}$. In the second theorem, $y(t)$ lies in the space $L_{1n}(t_0, t_0 + T)$ with norm $\|y\| = \int_{t_0}^{t_0+T} y(t) dt$, and in the third theorem $y(t)$ lies in the space $C_n'(t_0, t_0 + T)$ with norm

$$\|y\| = \max_{t_0 < t < t_0+T} y(t).$$

In the first and third theorems we calculate the norm of the operator **W**, i.e., the least value of the number A for which the inequality $\|z\| \le A\|y\|$ is valid.

We note that the problem concerning the accumulation of disturbances in an arbitrary trajectory is essentially the problem of determining the norm of the operator **W**.

Example. We consider the system of differential equations

$$\begin{aligned} \dot{x}_1 &= -x_1 + b_1 u(t) \\ & \qquad\qquad (b_1^2 + b_2^2 = 1). \qquad (32) \\ \dot{x}_2 &= -3x_2 + b_2 u(t) \end{aligned}$$

The fundamental matrix $\mathbf{W}(t,\tau)$ of the system $\dot{x}_1 = -x_1$, $\dot{x}_2 = -3x_2$ has the form

$$\mathbf{W}(t,\tau) = \begin{vmatrix} e^{-(t-\tau)}, & 0 \\ 0 \quad , & e^{-3(t-\tau)} \end{vmatrix}.$$

Let the curve $x_1 = e^{-2t}$, $x_2 = e^{-2t}$ be given. By choosing $u(t)$, we will try to find an approximation to this curve in the interval $0 \le t \le T$. It follows from (11) that $r_1(t) = -e^{-2t}$, $r_2(t) = e^{-2t}$. The system (10) yields $u(t) = e^{-2t}(b_2 - b_1)$. By using the formulas in (12) we obtain

$$y^2(t) = e^{-4t}[2 - (b_2 - b_1)^2],$$

and from (13),

$$H^2 = \int_0^T y^2(\tau)\,d\tau = \frac{2 - (b_2 - b_1)^2}{4}(1 - e^{-4T}).$$

In order to use Theorem 1, we must calculate the number M from (9). We have

$$M_1^2 = \int_0^T e^{-2(T-\tau)}\,d\tau = \frac{1}{2}(1 - e^{-2T}),$$

$$M_2^2 = \int_0^T e^{-6(T-\tau)}\,d\tau = \frac{1}{6}(1 - e^{-6T}),$$

and so

$$M = \max\left(\sqrt{\frac{1}{2}(1 - e^{-2T})},\ \sqrt{\frac{1}{6}(1 - e^{-6T})}\right).$$

We thus have $\|z\| \le MH$, and for $T = \infty$ we have

$$\|z\| \leqslant \frac{\sqrt{2(b_2 - b_1)^2}}{2\sqrt{2}}.$$

If we now carry out the analysis according to Section 3 of [1], or if we investigate directly the result we have obtained, we can verify that for $b_1 = \sqrt{2}/2$, and $b_2 = -\sqrt{2}/2$, we can obtain an accurate representation of the given trajectory.

We now consider the method of estimation of Section 2 of the present paper. According to Theorem 2 we have $N = 1$.

On the other hand,

$$H_1 = \int_0^T y(\tau)\,d\tau =$$

$$= \int_0^T e^{-2t}\sqrt{2 - (b_2 - b_1)^2}\,dt = \frac{\sqrt{2 - (b_2 - b_1)^2}}{2}(1 - e^{-2T}).$$

From Theorem 2 we obtain

$$\|z\| \leqslant NH_1 = \frac{\sqrt{2 - (b_2 - b_1)^2}}{2}(1 - e^{-2T}).$$

and from $T = \infty$

$$\|z\| \leqslant \frac{\sqrt{2 - (b_2 - b_1)^2}}{2}.$$

In order to apply the result of the third theorem, we calculate

$$C = \max\left\{\int_0^T e^{-(T-\tau)}d\tau,\ \int_0^T e^{-3(T-\tau)}\,d\tau\right\} =$$

$$= \max\{1 - e^{-T}, \frac{1}{3}(1 - e^{-3T})\}.$$

Moreover,

$$\max_{0 \leqslant t \leqslant T} y(t) = \sqrt{2 - (b_2 - b_1)^2}.$$

Thus, according to (15), we obtain

$$\|z\| \leqslant C\sqrt{2 - (b_2 - b_1)^2}$$

and for $T = \infty$

$$\|z\| \leqslant \sqrt{2 - (b_2 - b_1)^2}.$$

As we can see, for $T = \infty$ the best estimate of $\|z\|$ is obtained from Theorem 1, and the worst from Theorem 3.

LITERATURE CITED

1. E. A. Barbashin, "An estimate of the mean square deviation from a trajectory," Avtomatika i Telemekhanika 21, No. 7 (1960).*
2. R. Bellman, "Notes on Control Process. 1. On the minimum of maximum deviation," Quarterly Appl. Math. 14 (1957).

---

[*] See English translation.

3. B. V. Bulgakov, "The accumulation of disturbances in linear oscillating systems with constant parameters," Doklady Akad. Nauk SSSR 51, No. 5 (1946).
4. B. V. Bulgakov and N. T. Kuzovkov, "The accumulation of disturbances in linear systems with variable parameters," Priklad. Matem. i Mekh. 14, No. 1 (1950).
5. J. L. Massera and J. J. Schäffer, "Linear differential equations and functional analysis," Ann. of Math. 67, No. 3 (1958).
6. F. R. Gantmakher, The Theory of Matrices [in Russian] (Gostekhizdat, 1950).
7. I. G. Malkin, The Theory of the Stability of Motion [in Russian] (Gostekhizdat, 1957).
8. I. G. Malkin, "A first approximation to stability," Coll.: Scientific Proceeding of the Kazan' Inst. of Aviation [in Russian] (1936) No. 3.
9. V. V. Nemytskii and V. V. Stepanov, The Qualitative Theory of Differential Equations [in Russian] (Gostekhizdat, 1949).

ON THE STABILITY OF AN AILERON CONTROL SYSTEM DISTURBED BY TURBULENCE

P. S. Landa and S. P. Strelkov

Moscow

Translated from Avtomatika i Telemekhanika, Vol. 21, No. 10,
pp. 1352-1364, October, 1960
Original article submitted February 22, 1960

The stable modes of an airplane wing are found with an analog computer for the case where there are no nonlinear elements in the aileron control system. It is shown that the presence in the control circuit of a gap in certain parameters leads to the excitation of hard oscillations in the system. The probability of exciting growing wing oscillations over a given period of time in which the air flow is turbulent is calculated.

An airplane wing in flight is a complex nonuniform oscillatory system with distributed parameters. An accurate solution of the wing stability problem is practically impossible, even with the help of modern computers. At present, only approximate methods are known for solving this problem to one or another degree of accuracy.

Replacement of the nonuniform distributed oscillatory system with a simplified lumped-parameter system, described by a finite number of ordinary differential equations, is the basis of all the approximate methods.

One of the most widely used replacement methods is the method of [1], which is derived from the work of Raleigh and Pitts, and has been developed further by Bubnov and Galerkin.

In the application of the Bubnov–Galerkin method to the simplest, but one of the most practically important cases, the airplane wing, in a steady flow of air, can be considered as an oscillatory system with two degrees of freedom, in which certain parameters depend on the flow velocity. This paper is devoted to a study of the oscillations and the stability of such a system when nonlinear elements and statistical influences caused by the turbulent state of the atmosphere have a substantial effect.

In the majority of works in which the flutter of a wing with an aileron is examined (see, for example, [2–4]), the system is assumed to be linear, and the aileron control stick to be either fixed or free. In actual systems, there are always nonlinear elements as a result of gaps, dry friction, etc. Therefore, it is quite interesting to analyze those cases in which the presence of these nonlinear elements cannot be overlooked because they can have a substantial effect, not only on the character of the movement, but also on the stability of the different states of movement. An example of such an effect was computed in [5].

Nonlinear flutter problems, like all problems of this type, can be solved analytically in an approximate manner by means of the harmonic linearization method (Krylov-Bogolyubov method), if it is known that nearly harmonic modes of oscillation predominate in the system. The Krylov–Bogolyubov method, as it applies to nonlinear flutter problems, is examined, for example, in [7]. The use of a mathematical analog for studying airplane wing flutter is presented in [4, 5, 6], and oscillatory systems with nonlinear hardness are examined in the latter two.

The influence of turbulence on an airplane was also examined in a number of papers (for example, in [8]). In these papers, the airplane was represented as a linear oscillatory system, and the problem was solved by the ordinary theory of stationary random processes in linear systems.

The presence of nonlinear elements in a system can lead to the appearance of periodic modes (both stable and unstable), with which linear theory cannot deal. The existence of unstable periodic modes corresponding to unstable limited cycles means that the excitation of hard oscillations in the system is possible. The latter case is especially interesting, both theoretically and practically.

In this case, the airplane can indeed fly safely only in quiet air, since dangerous oscillations of the wings cannot arise in the absence of disturbance (the system is stable in the presence of small oscillations). If random jolts, caused by atmospheric turbulence, act on the wing, dangerous growing oscillations can appear after some time. Therefore, the statistical evaluation of the probability of such oscillations arising over a given period of time is an important problem, whose solution will be presented later.

An approximate analytic solution of this problem for an airplane wing with an aileron is possible under the condition that the oscillations in the system are nearly harmonic, that is, the complex system being examined can be replaced with some equivalent oscillatory system with one degree of freedom, whose spectral characteristic approximates that of the whole system in the region of the most important frequencies. Then the Fokker-Planck equation can be used to solve the problem in a way analogous to that done in [9, 10]. However, there is quite an amount of computation even with the simplifications mentioned, and the study of the system is exceedingly complicated over the whole range of the parameters v and n, where v is the flight velocity, and n is the relative frequency of the rotary aileron oscillations. Therefore, the limits of the modes interesting to us were first determined by an analog method, and then the amplitudes of the limited cycles and the excitation probabilities were calculated for the values of the parameters obtained.

1. Basic Equations of the Bending Oscillations of a Wing with an Aileron

The Bubnov-Galerkin method gives the following equations for bending-aileron oscillations of a cantilever wing (Fig. 1):

$$M\ddot{h} + S_\beta\ddot{\beta} + M\omega_h^2 h = F_1(h, h, \beta, \dot{\beta}, v) + F_2(v, t),$$

$$S_\beta\ddot{h} + I_\beta\ddot{\beta} + I_\beta\omega_\beta^2\beta = M_1(h, \dot{h}, \beta, \dot{\beta}, v) + M_2(v, t), \tag{1}$$

where M, I_β, S_β, ω_h, and ω_β are the average parameters of the wing and aileron, respectively, characterizing the wing mass, moment of inertia and static moment of the aileron, the natural frequency of wing bending oscillations, and the natural frequency of aileron rotary oscillations, determined by the elasticity of the control levers and cables; F_1 and M_1 are the average aerodynamic force and moment acting on the wing and aileron which are moving in air with a velocity v; F_2 and M_2 are the random aerodynamic force and moment caused by the turbulent disturbances of the vertical component of flight velocity.

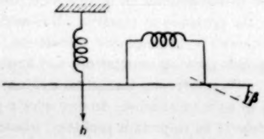

Fig. 1. Equivalent diagram of the bending oscillations of a wing with an aileron.

According to the theory based on the hypothesis of stationariness (see [11]), these aerodynamic forces and moments are expressed in the following manner:

$$F_1 = \pi\rho b^3 L\left\{-\frac{2v}{b}\frac{\dot{h}}{b} - \frac{L_a}{L}\alpha\frac{v}{b}\dot{\beta} - \frac{L_a}{L}\gamma\frac{v^2}{b^2}\beta\right\},$$

$$F_2 = 2\pi\rho L b v u,$$

$$M_1 = \pi\rho b^4 L_a\left\{-\delta\frac{v}{b}\frac{\dot{h}}{b} - \zeta\frac{v}{b}\dot{\beta} - \varepsilon\frac{v^2}{b^2}\beta\right\},$$

$$M_2 = \pi\rho b^2 L_a \delta v u,$$

where ρ is the air density at the given altitude; L, the wing span; L_a, the aileron span; b, the semichord of the wing; v, the horizontal flight velocity; u, the random vertical velocity appearing as a result of the turbulent state of the atmosphere; α, γ, δ, ζ, ϵ – coefficients which depend on the wing geometry.

The numerical values of the parameters basically correspond to the example given in [3]:

$$M = 38.3 \text{ kg};\ I_\beta = 0.0529 \text{ kgm}^2;\ S_\beta = 0.175 \text{ kgm};$$

$$\omega_h = 30 \text{ rad/sec};\quad L = 4.24 \text{ m};\quad L_a = 1{,}9 \text{ m};$$

$$b = 0.762 \text{ m};\quad \pi\rho = 3.105 \text{ kg/m}^3;\quad \alpha = 0.3458;$$

$$\gamma = 1.088;\ \delta = 0{,}007;\ \zeta = 0.0117;\ \varepsilon = 0.0104.$$

For convenience in analysis we will introduce the dimensionless coordinates, velocity and time:

$$x = \frac{h}{b},\ y = \beta,\ \bar{v} = \frac{v}{\omega_h b},\ \tau = \omega_h t.$$

Then Eq. (1) can be written in the form

$$\frac{d^2x}{d\tau^2} + x + a_{11}\bar{v}\frac{dx}{d\tau} + a_{12}\bar{v}^2 y + a_{13}\bar{v}\frac{dy}{d\tau} + a_{14}\frac{d^2y}{d\tau^2} = f_1(\tau), \quad \frac{d^2y}{d\tau^2} + n^2 y + a_{21}\bar{v}^2 y + a_{22}\bar{v}\frac{dy}{d\tau} + a_{23}\bar{v}\frac{dx}{d\tau} + a_{24}\frac{d^2x}{d\tau^2} = f_2(\tau), \tag{2}$$

where

$$n = \frac{\omega_\beta}{\omega_h},\quad f_1(\tau) = \frac{1}{\omega_h^2 bM}F_2\left(\frac{\tau}{\omega_h}\right),$$

$$f_2(\tau) = \frac{1}{\omega_h^2 I_\beta}M_2\left(\frac{\tau}{\omega_h}\right).$$

The random functions $f_1(\tau)$ and $f_2(\tau)$ can be considered stationary and normal random processes which can be characterized sufficiently by giving their spectral densities, which, in their turn, are completely determined by the spectral density of the vertical component of turbulent air velocity u.*

---

* We will neglect the effect of fluctuations in the horizontal velocity, since they are significantly less than the flight velocity.

A graph of the spatial spectrum of the turbulence, given in [8], can be used to compute the spectral density of the random quantity u. As emphasized in this work, the values of spectral density shown on the graph are very approximate, since they depend strongly on the meteorological conditions, the local terrain, and the flight altitude. For example, the intensity of the turbulence increases sharply during a storm, and may differ from the value given on the graph by orders of magnitude.

2. Basic Equations of the Bending Oscillations of a Wing with the Aileron Controlled by a Hydraulic Amplifier

The presence of special aileron control mechanisms has a substantial effect on the oscillations of the entire system. Let us examine the schematic diagram of a hydraulic amplifier aileron control as shown in Fig. 2. The dotted lines designate a parasitic feedback path between the movement of the wing and system of aileron control levers and cables, and the hydraulic amplifier. Moreover, we will assume that a gap 2 can exist in the piston valve control system of the hydraulic amplifier 1. The deflection of the piston valve is composed of the displacement given by the pilot [the "controlling input" q(t)], and some additional displacement κh, due to the parasitic feedback loop and caused by the effect of wing oscillations on the aileron control drive. For simplicity, we will consider κh to be proportional to the vertical displacement of the wing h. The quantity κ will be called the feedback coefficient.

In the analysis, we will assume that the controlling input to the piston valve is constant, or that it changes very slowly in comparison to the oscillation period of the wing. Moreover, we will assume that the feedback coefficient κ can have only two values: +1 and −1.

If we limit ourselves to the linear portion of the servomotor characteristic, the oscillations in the system containing the hydraulic amplifier, for the case when the pilot exerts no controlling action, are described by the equations

$$\frac{d^2 x}{d\tau^2} + x + a_{11}\bar{v}\frac{dx}{d\tau} + a_{12}\bar{v}^2 y + a_{13}\bar{v}\frac{dy}{d\tau} + a_{14}\frac{d^2 y}{d\tau^2} = f_1(\tau),$$

$$\frac{d^2 y}{d\tau^2} + n^2(y - a_4 z) + a_{21}\bar{v}^2 y + a_{22}\bar{v}\frac{dy}{d\tau} + a_{23}\bar{v}\frac{dx}{d\tau} + a_{24}\frac{d^2 x}{d\tau^2} = f_2(\tau), \quad \frac{dz}{d\tau} = a_3[\varphi(\varkappa x) - z]. \tag{3}$$

Here, z = r/b is the dimensionless coordinate of the servomotor shaft displacement 3, and the function $\varphi(\kappa x)$ determines the dependence between the displacements of the elements on the other side of the gap. Let us suppose that the gap size a can fluctuate within the limits a = 0−0.01. The coefficients a_3 and a_4 are, respectively, equal to 2 and 3. The remaining coefficients are determined by the parameters of the wing and aileron given above.

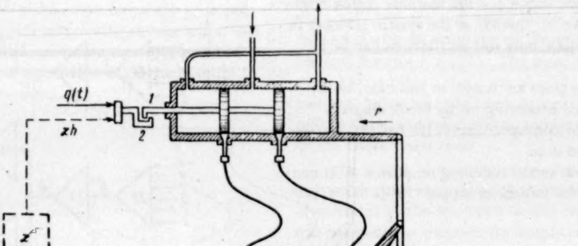

Fig. 2.

A block diagram of the system described by Eqs.(3) is shown in Fig. 3. The block with the transfer function Y(p) includes the wing and the aileron, that is, it represents an oscillatory system with two degrees of freedom; $\xi(t)$ designates the turbulent input to the system.

3. Determining the Stable Regions of the System in the Absence of Random Disturbances

As has already been shown, at first, an electronic analog of the system is studied on a type MN-7 analog computer.

In order to check the correctness of the analog, and to clarify the effect of the servomotor on system stability, a curve was taken of the dependence of the critical speed of the plane, at which flutter arises, on the relative aileron frequency n with the aileron control stick fixed. In this case, the system is described by Eqs. (2), without the terms on the right.

The stable region is located outside the curve shown in Fig. 4 by the dashed line. The results agree with the data in [2-4].

If the control stick is not fixed, the unstable region changes substantially, due to the presence of parasitic feedback in the system. We note that the concept of an unstable region independent of the oscillation amplitude has meaning only for a linear system. Therefore, let us first examine how the unstable region changes in the case when there is no gap in the aileron control system. It appears that the unstable region expands (Fig. 4, curve 1) if the feedback is positive, which corresponds to $\kappa = +1$, but if the feedback is negative ($\kappa = -1$), the system becomes more stable, and the unstable region diminishes (Fig. 4, curve 2). Insofar as the system is linear in the absence of a gap, only soft oscillations can be excited in it.

The stable regions are found, in this case, on an analog constructed according to the block diagram shown in Fig. 5, in correspondence with Eqs. (3), but the gap is set equal to zero.

The first input to the summing amplifier 2 is connected either to the integrator output 15 ($\kappa = +1$), or to the inverter output 11 ($\kappa = -1$), depending on the sign of the feedback.

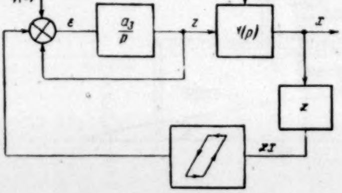

Fig. 3. Block diagram of the wing-aileron-hydraulic-amplifier system.

The presence of a gap makes it possible for hard oscillations to be excited in the system being analyzed, and for stable limited cycles to appear.

The performance of the system was studied as a function of the aileron relative frequency n for a fixed flight velocity, $\bar{v} = 0.8$. The following phenomena were observed: Soft oscillations were excited in the system when $n_1 \leq n \leq n_2$, which corresponds to an unstable region if the aileron control stick is fixed. If positive feedback existed, the oscillations grew toward infinity, but a

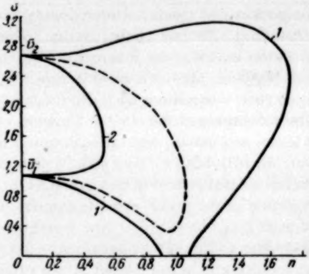

Fig. 4. Graph of the stable regions of the system.

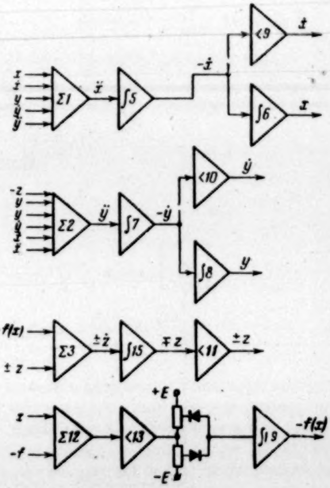

Fig. 5. Block diagram of an analog of the wing-aileron-hydraulic-amplifier system.

stable limited cycle, whose amplitude A_{xex} varied as a function of n, appeared if the feedback was negative; this is shown in Fig. 6 by the solid line. The system is stable for all other values of n, if the feedback is negative. If the feedback is positive, then for $n_1' \leq n \leq n_1$ and $n_2 \leq n \leq n_2'$, where n_1' and n_2' correspond to the limits of stability in the absence of a gap, hard oscillations are excited in the system. The dashed lines in Fig. 6 show the amplitude of the minimum initial disturbance, which must be imparted to the wing so that it can accomplish unattenuated oscillations, as a function of n.

It is evident that this quantity characterizes the amplitude of the unstable limited cycle.

4. Measuring the Probability of System Excitation in the Presence of Turbulence

The same method as in [12] was used to measure the probability of system excitation as a function of time (for given parameters and amplitude of the fluctuating disturbances). For the same set of parameters, up to fifty time intervals were measured during which the system remained unexcited. The average excitation time τ'_{av} and probability $p(\tau)$ that the system will be excited at time $\tau' \geq \tau$ were computed from these measurements.

Strictly speaking, the noise of the special generator fed to the analog must have a spectrum similar to that of the turbulence. However, the spectral components of the noise in a narrow band near the free oscillation frequency of the system play the main role in system excitation. If the free oscillation frequency did not depend on the amplitude, then it would be possible for a fixed flight velocity $\overline{V}$ and aileron frequency n to put a random input $\xi(\tau)$, with practically any spectrum, into the system being studied, providing that spectrum had the same density as the turbulence at the free oscillation frequency of the system, ω_0'.

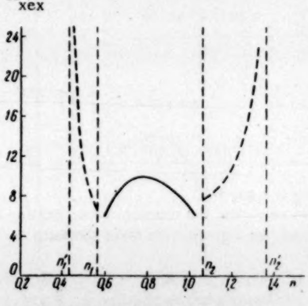

Fig. 6. Limited cycle amplitude as a function of the aileron relative frequency (experimental curves).

In reality, a weak dependence of the free oscillation frequency on the amplitude is observed in the nonlinear system being analyzed. This can be seen, for example, from Table 1, in which the oscillation frequencies measured at different wing displacements are shown for a number of values of n.

Here the following designations are introduced: $\omega(0)$ is the system oscillation frequency corresponding to very small amplitudes; $\omega(A_1)$ is the oscillation frequency near an unstable limited cycle having an amplitude A_1; $\omega(\infty)$ is the frequency corresponding to very large amplitudes.

In view of the weak dependence of the oscillation frequency on the amplitude, and, consequently, the comparatively small change in the spectral density of the noise as the amplitude varies, noise having a uniform spectrum in the region of the system operating frequency, and whose spectral density agrees with that of the actual disturbance at some average frequency $S'_{u\,av}$, can be put into the system. The amplitude of this average spectral density as a function of n is also shown in Table 1. It is evident that the spectral density of the noise fed into the system must be varied in correspondence with the data of Table 1, as the relative aileron frequency n changes. In practice, this spectral density change is accomplished in the following manner. The signal from an ultralow-frequency noise generator (see [12]) is fed into the analog through one of the amplifiers whose amplification factor is varied as n changes in correspondence with the change in spectral density. An adequately accurate relation between the amplitudes of the noise spectral density is ensured as n changes, in this way. The absolute value of the spectral density is measured with an accuracy on the order of 25% by the method described in [12]. The error in this measurement has no effect, since the absolute value of the turbulence, as has already been shown, is given very approximately, and may change substantially depending on the flight conditions.

The results of measurements of the average system excitation time are presented in Table 1 for a number of values of n; the feedback in this case is positive. It was necessary to increase the amplitude of the turbulence spectral density by a factor of four in comparison with the data of [8] so that the measurement time would not be too long. It has been shown that as n increases within the limits $n_2 \leq n \leq n_2'$, the average excitation time grows sharply, both as a result of the increase in the amplitude A_1 of the unstable limited cycle, and because of the decrease in the equivalent intensity of the turbulence. Therefore, the average excitation time in this region could be measured at only one value, n = 1.1.

It is easy to compute the probability of system excitation as a function of time from the data obtained in measuring the average time. The results of the calculations for the case when n = 0.55 are shown as a graph in

TABLE 1

n	$10^2 A_1$	$\omega(0)$	$\omega(A_1)$	$\omega(\infty)$	$10^3 S'_u$ av	τ'_{av}
0.5	2.10	0.888	0.871	0.873	5.72	180
0.55	1.44	0.892	0.892	0.891	5.56	132
1.1	1.74	1.125	1.100	1.105	3.82	334
1.2	2.20	1.188	1.123	1.155	3.53	—
1.3	3.60	1.295	1.162	1.221	3.06	—

Fig. 7. The exponential function $\exp(-\tau/\tau_{av})$ is shown by dashed lines on the same figure. It can be seen from the graph that the distribution observed does not have the exponential form predicted by theory for the excitation probability $p(\tau)$ in the case of sufficiently low noise. This difference can be explained by the fact that the noise acting on the system is high, so that the time that the mapping point spends in the phase space near the boundaries of excitation is comparable with its average dwell time in the region of the unexcited states.

One can conclude from this that the methods for theoretically computing the excitation probability, described in [9, 10] for the case of low noise, do not give accurate quantitative results. However, with the aid of these methods, one can obtain a theoretical estimate of the order of the average system excitation time, and this has practical value.

5. Theoretical Calculation of Airplane Wing Stability in the Presence of Turbulence

It has already been indicated that an analytic solution of the stability problem of a complex system affected by fluctuations is possible if certain restrictions are imposed on the system parameters, namely, oscillation in the system must be nearly harmonic. The results of studies on analogs have shown that this requirement is met sufficiently well over a wide range of change in the parameters.

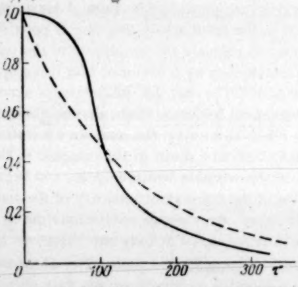

Fig. 7. Probability of system excitation for n = 0.55.

The idea of the method presented in this paper is as follows. The restriction mentioned above means that the solution of Eqs. (3) must be put in the form of almost harmonic oscillations with slowly changing amplitudes:

$$x = A\cos\omega\tau,\quad y = B\cos(\omega\tau + \varphi_1),$$

$$z = C\cos(\omega\tau + \varphi_2).$$

Then Eqs. (3) can be linearized in the ordinary manner by using the harmonic linearization method (the Krylov–Bogolyubov method). We obtain an equivalent linear set of equations as a result, and their coefficients depend on the amplitude of the wing oscillations A. In operational form, this linearized set of equations is

$$\begin{gathered}(p^2 + a_{11}\bar{v}p + 1)\,x + \\ + \;(a_{14}p^2 + a_{13}\bar{v}p + a_{12}\bar{v}^2)\,y = f_1(\tau), \\ (a_{24}p^2 + a_{23}\bar{v}p)\,x + \\ + \;(p^2 + a_{22}\bar{v}p + a_{21}\bar{v}^2 + n^2)\,y - a_4 n^2 z = f_2(\tau), \\ -a_3\varkappa C(u)\,x + (p + a_3)\,z = 0,\end{gathered} \tag{4}$$

where C(u) is determined from the function $\varphi(\kappa x) = \varphi(\kappa A\cos\omega\tau)$ expressed as a complex Fourier series:

$$\varphi(\varkappa x) = \varkappa C(u)\,x + \ldots.$$

$$u = 1 - 2\frac{a}{A},\quad C(u) = C_1(u) + jC_2(u)\,\mathrm{sign}\,\omega,$$

$$C_1(u) = \frac{1}{2} + \frac{1}{\pi}\arcsin u + \frac{1}{\pi}u\sqrt{1-u^2},$$

$$C_2(u) = \frac{1}{\pi}(u^2 - 1);$$

the term a is a gap size.

Let us now write the characteristic equation for the set obtained, for a given A; it takes the form

$$L(p) = p^5 + b_1p^4 + b_2p^3 + b_3p^2 + b_4p + b_5 = 0. \tag{5}$$

Equation (5) is an algebraic equation with complex coefficients. Since the coefficients of the equation specifically depend on the sign of ω, the roots of this equation must be complex conjugates of the form $p = -\delta(u) \pm j\omega(u)$. Therefore, one need only find the solution of Eq. (5) for positive values of ω, for example.

Let us investigate the behavior of the characteristic equation roots as a function of the relative aileron frequency $\underline{n}$ at a fixed flight velocity, $\bar{v} = 0.8$.

Let us assume that

$$p = -\delta(u) + j\omega_0 + j\omega_1(u) \tag{6}$$

for finding an approximate solution of Eq. (5); we will define ω_0 so that when $p = j\omega_0$, the modulus of $L(p)$ will be maximum. Since the system has been assumed to be narrow-band, the following inequalities must be satisfied: $\delta(u) \ll \omega_0$, and $\omega_1(u) \ll \omega_0$.

Computation and experimental data show that ω_0 differs little from unity at all values of relative aileron frequency $\underline{n}$, and at any amplitudes which are of interest to us. Therefore, we can say that $\omega_0 = 1$.

By substituting expression (6) into Eq. (5), and restricting ourselves to terms of the first order of smallness relative to δ and ω_1, we get the linear set of equations which determine $\delta(u)$ and $\omega_1(u)$.

An analysis of the behavior of the attenuation coefficient $\delta(u)$ as a function of $\underline{n}$ gives results which qualitatively agree with experimental data.

For $n_1 \leq n \leq n_2$, the system is unstable, no matter how small the amplitudes, and the oscillations jump toward infinity if there is positive feedback. However, a stable limited cycle exists if there is negative feedback. The boundaries of the unstable region, n_1 and n_2, are determined from the equation

$$\delta(u)\big|_{u=-1} = 0.$$

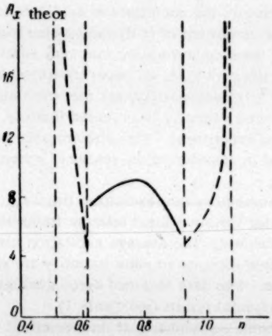

Fig. 8. Amplitude of the limited cycles as a function of relative aileron frequency (theoretical curves).

The solution of this equation gives $n_1 = 0.612$, $n_2 = 0.930$, which differs numerically somewhat from the data obtained from the analog ($n_1 = 0.565$, $n_2 = 1.06$). This difference can be explained by the inaccurate correspondence between the analog system parameters and the equation being investigated, and also by the approximateness of the theoretical calculations.

For the case of negative feedback, the amplitude of the stable limited cycle can be computed as a function of $\underline{n}$ over the range of values obtained for $\underline{n}$, by setting $\delta(u)$ equal to zero for a fixed $\underline{n}$.

The results of such a computation of the stable limited cycle amplitude are shown in the graph (Fig. 8, solid line).

The range of $\underline{n}$ over which the system will have hard excitation is determined from the equation

$$\delta(u)\big|_{u=1} = 0. \tag{7}$$

By solving this equation, one can see that hard excitation of the system is possible only if the feedback is positive, for the values of system parameters which we have chosen. It should be mentioned here that the system may have hard oscillations for other parametric values even if the feedback is negative.

The solution of Eq. (7) is $n_1' = 0.514$, $n_2' = 1.08$, for $\kappa = 1$. Consequently, the hard oscillation mode occurs when $\underline{n}$ has values which satisfy the inequalities: $n_1' \leq n \leq n_1$ and $n_2 \leq n \leq n_2'$.

Setting $\delta(u)$ equal to zero for a fixed $\underline{n}$, we can find the dependence of the unstable limited cycle amplitude A_1 on $\underline{n}$, graphically. The results of these calculations are shown on the graph (Fig. 8, dashed lines) to a scale appropriate for the experiment, and are also given in Table 2. A knowledge of the unstable limited cycle amplitude is necessary for calculating the average excitation time of the system.

The oscillations in a complex system (3) are the sum of two "natural" oscillations whose frequency and attenuation decrement are a function of amplitude. Bending oscillations of the wing predominate in one of these oscillations, and rotary oscillations of the aileron in the other. It appears that the first "natural" oscillation attenuates very slowly, whereas the second attenuates much more rapidly. Therefore, the approximately linearized oscillatory system with two degrees of freedom (4) can be replaced by a certain equivalent oscillatory system with one degree of freedom, whose oscillations are nearly the same as the bending oscillations of the wing, that is, they have the same frequency and attenuation decrement.

We get an approximate equation describing the wing oscillations as a result of this replacement:

$$(p^2 + 2\delta p + \omega^2)\,x = \omega^2 \zeta(\tau), \tag{8}$$

TABLE 2

n	$10^2 A_1$	$\omega(0)$	$\omega(A_1)$	$10^3\,\delta(0)$	$10^8 Su_{av}$	$10^7\lambda^{-1}$	τ_{av}	τ_{av}
0.55	3.23	0.95	0.93	1.24	5.17	1.05	10^{14}	$5\cdot 10^4$
0.6	1.39	0.96	0.94	0.29	5.06	0.97	1500	470
0.95	1.10	1.13	1.12	1,22	3.76	0.63	$6\cdot 10^5$	400
1.0	1.41	1.15	1.13	4.83	3.67	0.71	$2\cdot 10^{21}$	$9\cdot 10^5$
1.05	1.96	1.15	1.16	8.76	3.55	0.81	$5\cdot 10^{42}$	$4\cdot 10^{11}$

where $\zeta(\tau)$ is the equivalent noise, whose intensity depends on the amplitude of the oscillations A, in the general case.

Now the Fokker-Planck equation can be used if the noise correlation time τ_{cor} is short in comparison to the system time constant, which is about $1/\delta$, and the noise intensity is small enough so that the following conditions are met:

$$\langle\zeta\zeta^*\rangle^{1/2} \ll A_1 \ \text{for}\ \tau_{cor} \gg \frac{2\pi}{\omega}{}^{\dagger},$$

$$[\omega S(\omega)]^{1/2} \ll A_1 \ \text{for}\ \tau_{cor} < \frac{2\pi}{\omega}, \tag{9}$$

where $S(\omega)$ is half the spectral density of $\zeta(\tau)$ at the frequency ω.

Setting $x = Ae^{j(\omega\tau+\varphi)}$, $x = Aj\omega e^{j(\omega\tau+\varphi)}$ and substituting them in Eq. (8), we get a shorter equation for A in the usual manner (see [10]):

$$A = \frac{1}{2j\omega} e^{-j(\omega\tau+\varphi)} (p^2 + \omega^2)\, x =$$

$$= -A\delta(A) + \frac{1}{\lambda A} + \zeta'(\tau), \tag{10}$$

where $\zeta'(\tau)$ is the equivalent white noise having a correlation function $K(t) = 2\lambda^{-1}\,\delta(t)$, and $\lambda^{-1} = \frac{\omega^2}{4} S(\omega)$. Since the oscillation frequency depends on the amplitude, the intensity of the equivalent noise will also depend on amplitude.

The Fokker-Planck equation takes the following form in the given case:

$$\frac{\partial w}{\partial \tau} = -\frac{\partial}{\partial A}\left\{\left[-A\delta(A) + \frac{1}{\lambda A}\right] w\right\} + \frac{\partial^2}{\partial A^2}(\lambda^{-1} w). \tag{11}$$

The stationary solution of this equation corresponding to null probability flow is expressed in the following way, as can be seen by direct substitution:

$$w(A) = C_0\, A\lambda \exp\left\{-\int_a^A \lambda A\delta(A)\, dA\right\};$$

the normalizing constant C_0 is approximately equal to $\delta|_{A=0} = \delta(0)$ if the following conditions are met:

$$1/\sqrt{\lambda\delta(0)} \ll A_1,\ 1/\sqrt{K_1} \ll A_1, \tag{12}$$

where

$$K_1 = -\frac{d}{dA}[\lambda A\delta(A)]\Big|_{A=A_1}$$

It is now easy to obtain an expression for the average frequency of system transition through the excitation boundary, which is the inverse of the average excitation time, by a method analogous to the one given in [10]:

$$\gamma = \frac{1}{\lambda}\sqrt{\frac{K_1}{2\pi}}\, w(A_1) =$$

$$= \delta(0)\, A_1 \sqrt{\frac{K_1}{2\pi}} \exp\left\{-\int_0^{A_1} \lambda A\delta(A)\, dA\right\}. \tag{13}$$

Hence, a graph of $\lambda A\delta(A)$ as a function of A for different values of n must be plotted in order to compute the average excitation time of the system. Then the integral in the brackets of the exponential in (13) can be evaluated from this graph, and the value of K_1 found.

Calculations show that the equivalent noise intensity λ^{-1} depends weakly on A, the amplitude of the oscillations. Therefore, the average value of λ, which does not depend on amplitude, but is a function of n, must be used when the average excitation time of the system is computed from (13). The average noise intensities for different n are given in Table 2.

Knowing λ, the conditions of applicability of the theory [the conditions of (12)] can be checked. It appears that these conditions are met very poorly. For example, when $n = 0.55$, we have: $1/\lambda\delta(0) \approx 1/\sqrt{K_1} \approx 3\cdot 10^{-3}$, $A_1 \approx 3\cdot 10^{-2}$. Conditions (12) are met even more poorly when the noise intensity is increased fourfold, as was done in the experiment. This circumstance has already been noted in considering the results of system studies on an analog.

The average system excitation times τ_{av}, calculated from (13) for various aileron relative frequencies n, are given in Table 2. The average excitation times τ'_{av}, for a fourfold increase in noise intensity are given in the same table. The data obtained agree qualitatively with the experimental results (see Table 1).

We should remember that the numerical values of the average time obtained from theoretical calculations

---

†Here ζ^* designates the complex conjugate of ζ, and the sign < > designates a statistical average.

have meaning only as estimates of the quantities mentioned.

CONCLUSIONS

1. The presence of a parasitic positive feedback path in the control system causes the unstable region to expand. In this case, if there is a gap in the aileron control drive, the system can be excited only under definite initial conditions (in the absence of fluctuation disturbance), for certain parametric values.

2. The danger of growing oscillations of an airplane wing arises as a result of the excitation of hard oscillations in flight through turbulent air.

3. The probability of growing oscillations arising in a definite time interval depends on the intensity of the fluctuations caused by turbulent disturbance of the vertical flight velocity component, and this probability decreases sharply with a decrease in this intensity.

4. The basic role in system excitation is played by the spectral components of the turbulence near the natural bending oscillation frequency of the wing, ω_h, in other words, the amplitude of the spatial spectral density of the turbulence, $S_u'(\Omega)$, at $\Omega = \omega_h/v$.

5. The theoretical methods presented in this paper in combination with a study of the system on an analog computer permit one to get statistical estimates for the excitation time of dangerous wing oscillations as a function of the flight velocity and natural frequency of the aileron.

The authors express gratitude to R. L. Stratonovich for much valuable advice and suggestions.

LITERATURE CITED

1. E. P. Grossman, Course on the Vibration of Airplane Parts [in Russian] (Oborongiz, 1940).
2. E. P. Grossman, "Flutter" (Trudy TsAGI No. 284, 1937).
3. R. H. Scanlan and R. Rosenbaum, Introduction to the Study of Aircraft Vibration and Flutter (The MacMillan Company, New York, 1951).
4. S. P. Strelkov, and A. A. Kharlamov, "A study of the flutter of a wing with an aileron," Naucha. Dokl. Vyssh. Shkol., Fiz.-Matem. Nauki 2, No. 2 (1959).
5. D. S. Woolston, H. L. Runyan, and T. A. Byrdsong, Some Effects of System Nonlinearities in the Problem of Aircraft Flutter (NACA, TN, 1955) p.3539.
6. D. S. Woolston, H. L. Runyan, and R. E. Andrews, "An investigation of the effects of certain types of structural nonlinearities on wing and control surface flutter," J. Aero. Sci. 24, No. 1 (1957).
7. S. F. Shen, "An approximate analysis of the nonlinear flutter problem," J. Aero. Sci. 26, No. 1 (1959).
8. Yu. M. Romanovskii, and S. P. Strelkov, "Concerning the effect of atmospheric turbulence on an airplane with elastic wings at different flight velocities," Izvest. Akad. Nauk SSSR, Otdel. Tekh. Nauk, Mekh. i Mashin. No. 4 (1959).
9. R. L. Stratonovich and P. S. Landa, "The effect of noise on a generator with hard oscillations," Izv. Vuz, Radiofizika 2, No. 1 (1959).
10. P. S. Landa, "Concerning the stability of servocontrol systems in the presence of random perturbations," Avtomat. i Telemekh. 21, No. 1 (1960).‡
11. A. I. Nekrasov, The Theory of a Wing in Nonsteady-State Flow [in Russian] (Izd. AN SSSR, 1947).
12. P. S. Landa, "An analog computer study of the effect of noise on a generator with hard oscillations," Izv. Vuz, Radiofizika 2, No. 3 (1959).

---

‡ See English translation.

A VECTOR METHOD FOR CALCULATING ONE CLASS OF CONTROL SYSTEMS

S. M. Levin and L. G. Manusevich

Leningrad

Translated from Avtomatika i Telemekhanika, Vol. 21, No. 10,
pp. 1365-1374, October, 1960
Original article submitted April 18, 1960

A method for studying one class of control systems is examined. The method is based on constructing vector diagrams and finding the reflection of the parameter space on the amplitude-phase plane.

1. Statement of the Problem. Let the transfer function of an open-loop control system have the form

$$W(p) = -\frac{M(p)}{D(p)} f(p), \tag{1}$$

where f(p) is the transfer function of a group of links containing no unknown parameters,

$$\begin{gathered} M(p) = \sum_{\nu=1}^{s} m_\nu A_\nu(p) + \sum_{\lambda=1}^{r} k_\lambda B_\lambda(p) + \sum_{\nu=1}^{s} \sum_{\lambda=1}^{r} m_\nu k_\lambda C_{\lambda\nu}(p), \\ D(p) = \sum_{\nu=1}^{s} m_\nu D_\nu(p). \end{gathered} \tag{2}$$

Here m_ν and k_λ are the system parameters to be determined, and the coefficients of the polynomials $A_\nu(p)$, $B_\lambda(p)$, $C_{\lambda\nu}(p)$ and $D_\nu(p)$ depend on the parameters $l_\mu (\mu = 1, 2, \ldots, t)$ whose precise value is unknown. Let us call l_μ the "unreliable" parameters.

The transfer functions of a wide class of control systems can be reduced to the form of (1) and (2). In particular, the transfer functions of systems which are controlled by two or more physical quantities have such a form—for example, the transfer functions of airplane [1] and ship [2] control systems. In this case, the "reliable" parameters are those of the regulator, and the "unreliable" parameters are the aerodynamic and hydrodynamic coefficients.

The problem consists of determining the parameters, m_ν and k_λ, which ensure stability and the required system quality under the conditions that the "unreliable" parameters l_μ may vary between definite limits.

2. Initial Constructions. Let us first assume that the requirements on system quality are merely that the system must have a certain degree of stability [3], and let us consider the function $W(-\epsilon + i\omega)$, representing each of the terms in (2) in vector form.

Having been given an initial system of parametric values $l_\mu (\mu = 1, 2, \ldots, t)$, let us construct the following vectors for each frequency ω:

$$\overline{A_\nu}(-\varepsilon + i\omega, l_\mu) = \sum_{\gamma=1}^{n_\nu} \overline{A_\nu^\gamma}, \tag{3}$$

where $|\overline{A_\nu^\gamma}| = a_\nu^\gamma (l_\mu) R^\gamma$; $\arg \overline{A_\nu^\gamma} = \gamma\left(\varphi + \frac{\pi}{2}\right)$; a_ν^γ are the coefficients of the polynomial $A_\nu(p)$; $R =$

$= \omega \sqrt{1 + \left(\frac{\varepsilon}{\omega}\right)^2}$; $\varphi = \operatorname{arc\,tg} \frac{\varepsilon}{\omega}$; n_ν is the highest degree of the polynomial being examined.

When the parameters l_μ change, the vector $\overline{A}_\nu$ receives the increment

$$\overline{\Delta A_\nu} = \sum_{\gamma=1}^{n_\nu} \delta a_\nu^\gamma \overline{A_\nu^\gamma}, \tag{4}$$

where

$$\delta a_\nu^\gamma = \frac{a_\nu^\gamma [(l_1 + \Delta l_1), (l_2 + \Delta l_2), \ldots, (l_t + \Delta l_t)] - a_\nu^\gamma (l_1, l_2, \ldots, l_t)}{a_\nu^\gamma (l_1, l_2, \ldots, l_t)},$$

and Δl_μ is the increment of l_μ.

Considering only the linear members of δa_ν^γ expressed as a series in Δl_μ we represent δa_ν^γ in the form

$$\delta a_\nu^\gamma = \left(\frac{1}{a_\nu^\gamma}\right)_0 \sum_{\mu=1}^{t} \left(\frac{\partial a_\nu^\gamma}{\partial l_\mu}\right)_0 \Delta l_\mu. \tag{5}$$

The sign "0" indicates that the corresponding quantities are determined from the initial values of the parameters.

The vectors $\overline{B}(p)$, $\overline{C}_{\lambda\nu}(p)$, $\overline{D}_\nu(p)$ can be constructed analogously, and their increments found.

Next, having been given the initial parameters k_λ^0, m_ν^0, we construct geometric series for each frequency ω, which define the vectors $\overline{D(-\epsilon+i\omega)}$ and $\overline{-M(-\epsilon+i\omega)\, f(-\epsilon+i\omega)}$ in correspondence with formulas (2). The latter vector is derived from the vector $\overline{-M(-\epsilon+i\omega)}$ by extending it $|\overline{f(-\epsilon+i\omega)}|$ times and rotating it by an angle arg $f(-\epsilon+i\omega)$.

We will start these geometric series from point 0, and we will denote the ends by the letters D and M, respectively; we will indicate the parameters k_λ and m_ν, on which they depend, at each of the component vectors.

A change in the parameter k_λ by an amount $\delta k_\lambda = \frac{k_\lambda - k_\lambda^0}{k_\lambda^0}$ causes the vector $\overline{0M}$ to change by an amount

$$\overline{\Delta_{k_\lambda} M} = \delta k_\lambda \left[k_\lambda^0 \overline{B_\lambda}(p) + \sum_{\nu=1}^{s} k_\lambda^0 m_\nu^0 \overline{C_{\lambda\nu}}(p) \right]. \tag{6}$$

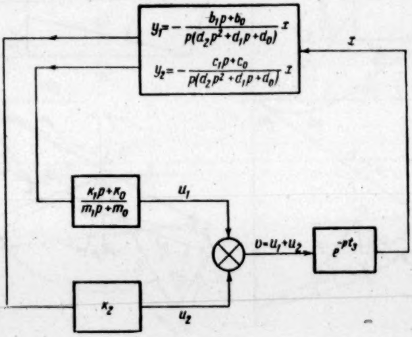
$y_1 = -\frac{b_1 p + b_0}{p(d_2 p^2 + d_1 p + d_0)} x$
$y_2 = -\frac{c_1 p + c_0}{p(d_2 p^2 + d_1 p + d_0)} x$
x
$\frac{K_1 p + K_0}{m_1 p + m_0}$
u_1
$v = u_1 + u_2$
e^{-pt_3}
K_2
u_2

Fig. 1.

Analogously, a change in m_ν causes the vectors $\overline{0D}$ and $\overline{0M}$ to change by the amounts

$$\overline{\Delta_{m_\nu} D} = \delta m_\nu \left[m_\nu^0 \overline{D_\nu(p)} \right],$$

$$\overline{\Delta_{m_\nu} M} = \delta m_\nu \left[m_\nu^0 \overline{A_\nu(p)} + \sum_{\lambda=1}^{r} k_\lambda^0 m_\nu^0 \overline{C_{\lambda\nu}(p)} \right], \tag{7}$$

respectively.

When m_ν and k_λ change simultaneously, the increment of 0M is found from the formula

$$\overline{\Delta^{\Sigma}_{k_\lambda m_\nu} M} = \overline{\Delta_{k_\lambda} M} + \overline{\Delta_{m_\nu} M} + \overline{\Delta_{k_\lambda m_\nu} M}, \tag{8}$$

where

$$\overline{\Delta_{k_\lambda m_\nu} M} = \delta k_\lambda \delta m_\nu \left[k_\lambda^0 m_\nu^0 \overline{C_{\lambda\nu}(p)} \right].$$

The vectors plotted for initial values of the parameters are enclosed in square brackets in expressions (6), (7), and (8).

Hence, a change in a parameter corresponds to a proportional change in the lengths of the vectors representing it. If the system stability does not meet requirements on system quality, the construction must be done over for $\epsilon = 0$.

It follows from (1) and the constructions described above that the ratio of the segments 0M to 0D equals the modulus of the amplitude-phase characteristic of an open-loop system (normal for $\epsilon = 0$ or expanded $\epsilon > 0$), and its argument is the angle χ between $\overline{0D}$ and $\overline{0M}$. The ratio of the lengths of M0 and MD and the angle between vectors $\overline{MD}$ and $\overline{M0}$ are equal to the modulus and argument, respectively, of the amplitude-phase characteristic of a closed-loop system with respect to the controlling input. The real part of the amplitude-phase characteristic is equal to the projection of $\overline{M0}$ along $\overline{MD}$, divided by the length of the segment MD.

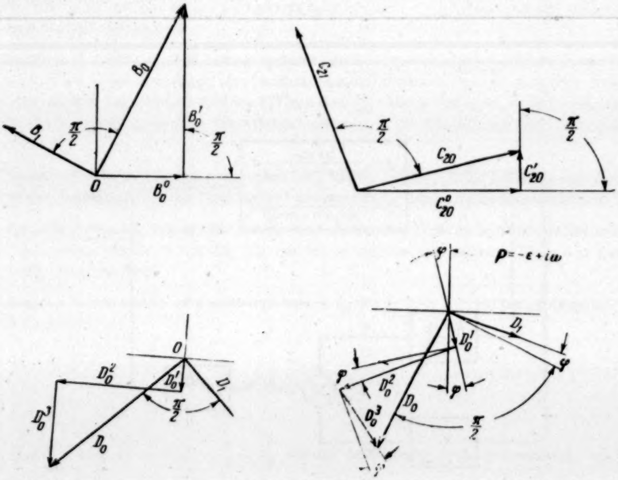

Fig. 2.

Example. Let us examine an automatic control system; the structure and transfer functions of the individual parts are shown in Fig. 1. The transfer function of this system has the form

$$W(p) = -\frac{(k_1p + k_0)(b_1p + b_0) + k_2(m_1p + m_0)(c_1p + c_0)}{p(d_3p^2 + d_2p + d_1)(m_1p + m_0)}\, e^{-pt_3}.$$

A diagram of the vectors

$$\overline{B_0(p)} = b_1p + b_0, \ \overline{B_1(p)} = \overline{pB_0(p)}, \ \overline{C_{20}(p)} = c_1p + c_0, \ \overline{C_{21}(p)} = \overline{pC_{20}(p)},$$
$$\overline{D_0(p)} = d_3p^3 + d_2p^2 + d_1p, \quad \overline{D_1(p)} = \overline{pD_0(p)},$$

where $p = i\omega$, is shown in Fig. 2. The diagram corresponds to a negative value of d_1 and to positive values of the remaining coefficients of the polynomials B(p), C(p), and D(p). A diagram of vectors $D_0(p)$ and $D_1(p)$, where $p = -\epsilon + i\omega$, is shown on the same figure for the sake of illustration. The diagram of vector $\overline{0D} = D(i\omega)$ and $\overline{0M} = -M(i\omega)e^{-i\omega t_3}$ is shown in Fig. 3 for the frequencies ω_0, ω_1, ω_2, and ω_3. Vectors $\bar{B}_0$, $\bar{B}_1$, $\overline{C}_{20}$ and $\overline{C}_{21}$ are rotated π radians in constructing the vectors $\overline{0M}$, and vectors $\overline{D}_0$ and $\overline{D}_1$ are rotated ωt_3 radians in constructing $\overline{0D}$. The amplitude-phase characteristic corresponding to this system of vectors is shown in the same figure (curve 1).

3. Analysis and Replotting of the Vector Diagrams with Fixed "Unreliable" Parameters.

We will assume that the "unreliable" parameters are fixed. Let us examine the basic methods for analyzing automatic control systems by means of vector diagrams.

1. The vector diagrams which have been plotted permit one to determine whether or not the system is stable with the given initial parameters, or whether it has a given degree of stability. This may be done on the basis of the Nyquist–Mikhailov criterion. The number of roots of the denominator with a positive real part (or with a real part greater than $-\epsilon$) may be found, for example, on the basis of the Mikhailov criterion from the be-

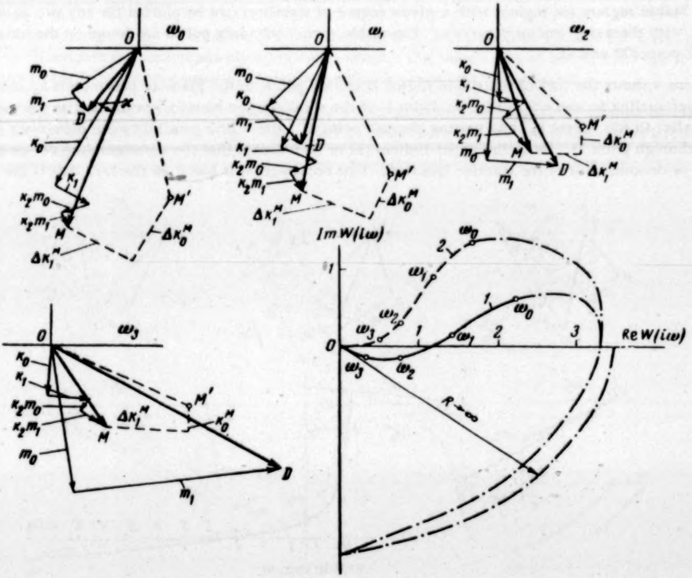

0
ω_0
m_0
m_1
D
K_0
K_1
K_2m_0
K_2m_1
M
M'
ΔK_0^M
ΔK_1^M
0
ω_1
m_0
K_0
m_1
K_1
D
K_2m_0
K_2m_1
M
M'
ΔK_0^M
ΔK_1^M
0
ω_2
K_0
K_1
K_2m_0
K_2m_1
m_0
M
M'
D
m_1
ΔK_0^M
ΔK_1^M
0
ω_3
K_0
K_1
K_2m_0
K_2m_1
m_0
M
M'
ΔK_1^M
K_0^M
D
m_1
Im W(iω)
Re W(iω)
1
2
3
0
ω_0
ω_1
ω_2
ω_3
$R \to \infty$

Fig. 3. Vector diagram and amplitude-phase characteristic of the open-loop system.

havior of vector $\overline{0D}$ Thus, the system of vectors plotted in Fig. 3 corresponds to an unstable system (the denominator of the transfer function has one root with a positive real part, since $d_1 < 0$).

2. The vector diagrams make it possible to evaluate the effect of parameters m_ν and k_λ on the shape of the amplitude-phase characteristic. Thus, for the system considered in the example, increasing k_1 at all frequencies causes angle χ to increase, that is, the argument of the amplitude-phase characteristic increases. A decrease in m_1 leads to the same result. Decreasing k_0 causes the modulus of the amplitude-phase characteristic to decrease, and a certain increase in its argument, etc.

3. The vector diagrams permit one to see the desirability of changing one or another of the parameters being examined as a group, and to determine which parameters should be changed and how, in order to shape the amplitude-phase characteristic into the desired form.

The amount of parametric change is limited, naturally, by the physical properties of each parameter. For example, the amplitude-phase characteristic of the system must be shaped so that it passes over the point (1, 0i), in order to ensure that it will be stable. The evaluations done in Section 2 permit one to determine what can be achieved, in particular, by increasing k_1 and decreasing k_0.

4. Having been given δm_ν and δk_λ on the basis of the evaluations done in Sections 2 and 3, the vectors $\overline{0D}$ and $\overline{0M}$, corresponding to a change in the parameters m_ν and k_λ, can be plotted. To do this, one need only find the increments of the respective vectors from formulas (6), (7), and (8), and plot them geometrically from points M and D. A number of such constructions must be done to find the optimum combination of parameters. Constructions corresponding to $\delta k_0 = -0.5$ and $\delta k_1 = 2$ are shown in Fig. 3 by dashed lines. Curve 2 in this figure shows the amplitude-phase characteristic of the system altered in this manner.

5. The vector diagrams plotted make it possible to decide whether it is desirable to introduce corrective links into the control system (including differentiation and integration). The introduction of such links leads to an extension and rotation of the vectors proportional to the parameters which are coefficients for the quantities being corrected. Thus, for example, the derivative of Y_2 could be introduced into Fig. 3 to increase the angle χ. This would be a vector added to point M, perpendicular to the sum of the vectors proportional to k_2.

6. Stable regions (or regions with a given degree of stability) can be plotted for any two parameters, m_ν and k_λ, with the aid of vector diagrams. The stable region boundary points are found on the basis of a coincidence of points M and D.

Figure 4 shows the loci of the stable region boundary points in the plane of parameters k_0 and m_1 for the system corresponding to curve 2 in Fig. 3. Point N of the stable region boundary is located at the intersection of a line parallel to the vector k_0^M and passing through point M', and a line parallel to the difference $\overline{m}_1^D - \overline{m}_1^M$ and passing through point D. Here, the upper indices (M or D) indicate that the corresponding vector enters the numerator or denominator of the transfer function. This construction is based on the fact that if the position of point

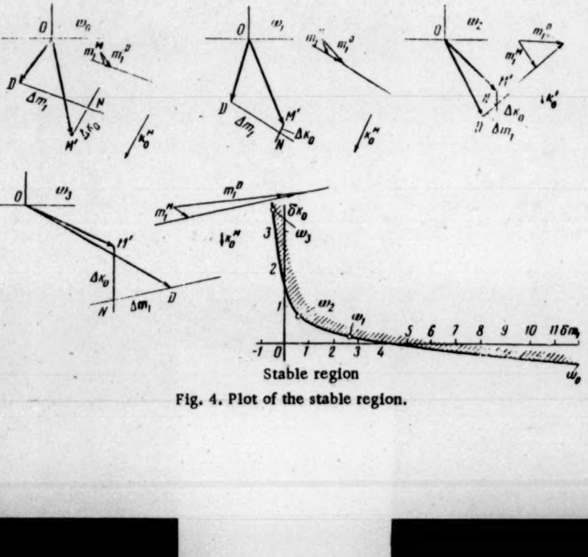

Fig. 4. Plot of the stable region.

M remains unchanged, the addition of vector $\bar{a} - \bar{b}$ to point D leads to the same change in the mutual position of points D and M as the addition of $\bar{a}$ to point D, and $\bar{b}$ to point M. The stable region in Fig. 4 is plotted on the coordinates $\delta k_0 = \Delta k_0 / k_0^0$ and $\delta m_1 = \Delta m_1 / m_1^0$, which are defined in terms of a ratio of the corresponding segments.

If both variants of the parameter enter expression (2) both linearly and in a product, then determining the stable region boundary points consists of solving a certain quadratic equation, whose coefficients are easily determined graphically (see Appendix).

7. By using vector diagrams, it is also possible to analyze control systems qualitatively by plotting the real part of the amplitude–phase characteristic of the closed-loop system with respect to the controlling input [4]. The construction consists of finding the ratio of the projection MP of vector $\overline{M0}$ on $\overline{MD}$ to the length of segment MD at each frequency ω. The effect of the system parameters on the shape of the amplitude–phase characteristic of the closed-loop system can be traced directly from the vector diagrams. A plot of the real part of the amplitude-phase characteristic of the system considered in the example is shown in Fig. 5 (curve 1). It follows from an examination of the vector diagram shown in Fig. 3 that it is sufficient to decrease m_0 in order to increase the positive region, for example. Corresponding constructions are shown in Fig. 5; the change in the position of points M, D, and P and the corresponding curve are designated by the index 2.

4. Construction of the Loci of the Ends of Vectors $\overline{0M}$ and $\overline{0D}$ as the "Unreliable" Parameters Change within Given Limits. Let the parameter l_μ assume an increment Δl_μ. Then the increment of A_0, in correspondence with (4) and (5), will equal

$$\overline{\Delta_\mu A_\nu} = \sum_{\gamma=1}^{n_\nu} \delta_\mu a_\nu^\gamma \overline{A_\nu^\gamma} \qquad \left(\delta_\mu a_\nu^\gamma = \left(\frac{1}{a_\nu^\gamma} \frac{\partial a_\nu^\gamma}{\partial l_\mu} \right)_0 \Delta l_\mu \right). \tag{9}$$

The increments $\overline{\Delta_\mu B_\lambda}$, $\overline{\Delta_\mu C_{\lambda\nu}}$ and $\overline{\Delta_\mu D_\nu}$, caused by the increment of l_μ, are found analogously. The increment of vectors $\overline{0M}$ and $\overline{0D}$, $\overline{\Delta_\mu M}$ and $\overline{\Delta_\mu D}$, can be found from expressions (2), in which A_ν, B_λ, $C_{\lambda\nu}$, and D_ν are replaced by their increments.

It is evident that a change in l_μ by an amount $n\Delta l_\mu$ corresponds to increments of $\overline{0M}$ and $\overline{0D}$ equal to $\overline{n\Delta_\mu M}$ and $\overline{n\Delta_\mu D}$. When several parameters change simultaneously, the increments of $\overline{0M}$ and $\overline{0D}$ are found as the geometric sums of the increments caused by the change in each parameter individually.

We will show how to find the correspondence between the subregion of the "unreliable" parameter space characterized by the inequalities $l'_\mu - \Delta l'_\mu \leq l_\mu \leq l'_\mu + \Delta'_\mu$ ($\mu = 1, 2, \ldots, t$) and the plane region within which the amplitude-phase characteristic can be located.

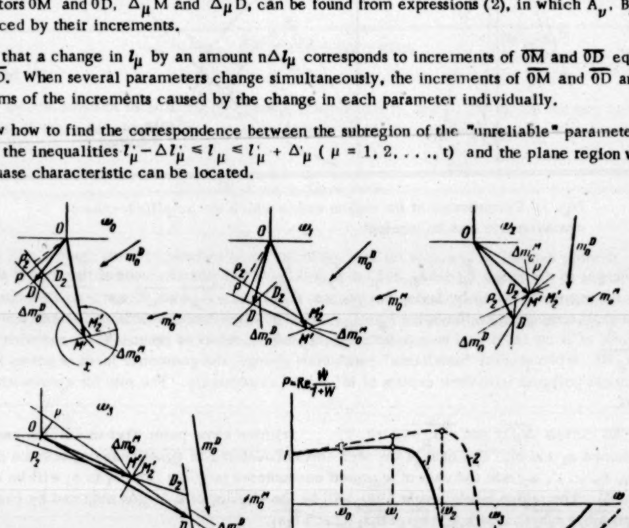

Fig. 5. Construction of the real part of the amplitude-phase characteristic of the closed-loop system.

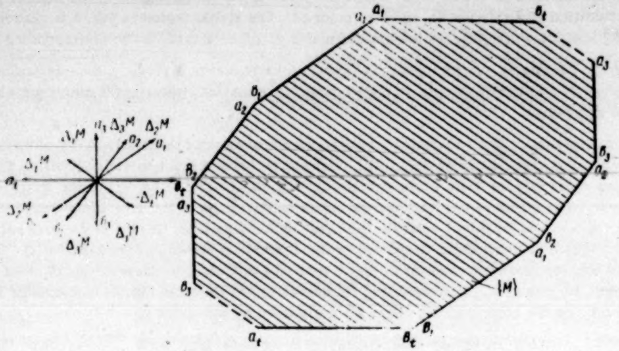

Fig. 6. Construction of the region $\{M\}$.

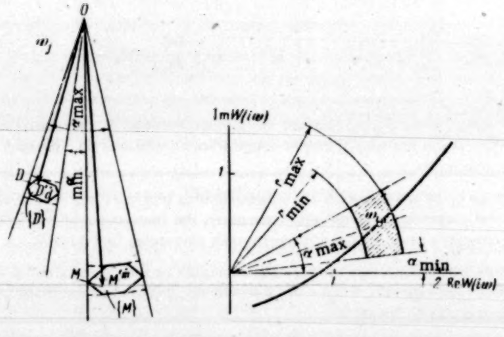

Fig. 7. Construction of the region within which the amplitude-phase characteristic can be located.

When l_μ changes in the range $\dot{l}_\mu - \Delta\dot{l}_\mu \le l_\mu \le \dot{l}_\mu + \Delta\dot{l}_\mu$, the geometric locus of the ends of the vector $\overline{0M}(\overline{0D})$ will be the segment formed by laying out vectors $\overline{\Delta_\mu M}$ and $\overline{-\Delta_\mu M}(\overline{\Delta_\mu D}$ and $\overline{-\Delta_\mu D})$ from point M(D). Here points M' and D' correspond to the value $l_\mu = \dot{l}_\mu$. When the two "unreliable" parameters ($\mu = s_1, s_2$) change, the geometric locus of point M(D) will be a parallelogram with its center at point M'(D'), and with its sides parallel to $\overline{\Delta_\mu M}(\overline{\Delta_\mu D})$. When several "unreliable" parameters change, the geometric locus of points M and D will be certain rectilineal polygons with their centers at M' and D', respectively. The rule for constructing these polygons is as follows.

We lay out the vectors $\overline{\Delta_\mu M}$ and $\overline{-\Delta_\mu M}(\mu = 1, 2, \ldots, t)$ from some point. Let us call the ends of one of the segments obtained a_1 and b_1. The ends of the segments encountered in going counterclockwise from a_1 to b_1 will be called $a_2, a_3, \ldots, a_t$, and the ends of segments encountered in going from b_1 to a_1 will be called $b_2, b_3, \ldots, b_t$ (see Fig. 6). The region being sought, $\{M\}$, will be the interior of a 2t-gon obtained by consecutively adding the vectors $\overline{a_1b_1} + \overline{a_2b_2} + \ldots + a_tb_t + \overline{b_1a_1} + \overline{b_2a_2} + \ldots + \overline{b_ta_t}$.

The region $\{D\}$ is constructed analogously.

Having constructed $\{M\}$ and $\{D\}$ at all frequencies, we shift them parallelly, so that their centers coincide with points M' and D' on the vector diagrams. We call the angle between $\overline{0d}$ and $\overline{0m}$ α, and the ratio 0m/0d will be called $\underline{r}$. The point $\underline{d}$ belongs to $\{D\}$, and point $\underline{m}$ belongs to $\{M\}$. The region within which the amplitude-phase characteristic can be located on plane W, where $\omega = \omega_j$, does not extend beyond the limits of the region characterized by the inequalities (see Fig. 7)

$$\min r(\omega_j) \leqslant |W(i\omega_j)| \leqslant \max r(\omega_j),$$
$$\min \alpha(\omega_j) \leqslant \arg W(i\omega_j) \leqslant \max \alpha(\omega_j).$$

Similar constructions can be done initially for all the given part of the "unreliable" parameter space. If the corresponding amplitude-phase characteristic location region does not provide sufficient bases for judging one or more properties of a system, the limits of this region can be made more precise by breaking up the "unreliable" parameter space into subspaces.

CONCLUSION

The method presented, based on the construction of vector diagrams, permits one to study a wide class of automatic control systems, and to solve stability and control quality problems.

The method permits one to evaluate the joint effect of both "reliable" and "unreliable" parameters on the shape of the amplitude-phase characteristic of an open-loop or closed-loop system.

The construction of vector diagrams can be used for determining the amplitude-phase characteristic of the linear part of nonlinear systems being studied, for example, by the methods given in [5, 6].

APPENDIX

Determining the Boundaries of the Stable Region in the Plane of the Parameters Entering the Numerator and Denominator Both Linearly and in the Form of a Product. Let us find a boundary point of the stable region at the frequency ω in the plane of parameters m_1 and k_1, assuming that $A_1(i\omega)$, $B_1(i\omega)$, $D_1(i\omega)$ and $C_{11}(i\omega)$ are not equal to zero [see formula (2)].

The increments of $\overline{0D}$ and $\overline{0M}$ caused by a change in these parameters can be written in the form

$$\overline{\Delta D} = \bar{h}_1 y, \quad \overline{\Delta M} = \bar{n}_1 x + \bar{h}_2 y + \bar{n}_3 xy,$$

according to (7) and (8).

Here x and y are the relative increments of k_1 and m_1, respectively, and $\bar{n}_i$ and $\bar{h}_i$ are vectors corresponding to the initial values of these parameters. The problem consists of finding values of x and y which satisfy the equality

$$\overline{0D} - \overline{0M} = \bar{n}_1 x + \bar{n}_2 y + \bar{n}_3 xy,$$

where $\bar{n}_2 = \bar{h}_2 - \bar{h}_1$.

Let us draw a line through point M parallel to $\bar{n}_1$, and lines parallel to $\bar{n}_2$ and $\bar{n}_3$ through point D. The intersection of the latter two lines with a line passing through M will be designated by the letters A and B, respectively. We will initially assume that A and B lie on one side of M (see Fig. 8). Moreover, let the directions of vectors $\bar{n}_1$, $\bar{n}_2$, and $\bar{n}_3$ be such that it is possible to go from M to D along MEFD for positive values of x and y ($\overline{ME} = \bar{n}_1 x$, $\overline{EF} = \bar{n}_3 xy$, $\overline{FD} = \bar{n}_2 y$). Since triangles ABD and AEF are similar, it follows that

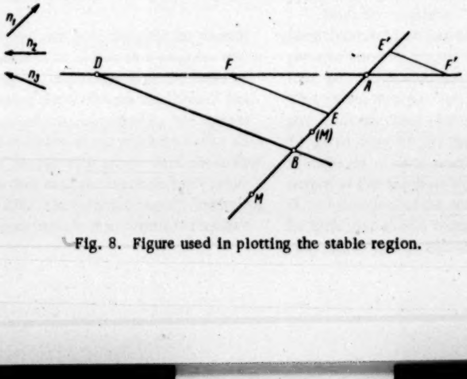

Fig. 8. Figure used in plotting the stable region.

$$\frac{b - n_1 x}{b - d} = \frac{n_3 x y}{c} = \frac{a - n_2 y}{a}, \tag{10}$$

where a, b, c, and d are equal to the lengths of AD, AM, BD, and BM, respectively.

We get Equation (11) for finding x from proportion (10):

$$x^2 + \left(\frac{c n_2}{a n_3} - \frac{d}{n_1}\right) x - \frac{b c n_2}{a n_1 n_3} = 0, \tag{11}$$

and after solving it, y is determined from the equality

$$y = a \frac{n_1 x - d}{(b - d) n_3}. \tag{12}$$

We will assume that the directions of any two of the vectors $\bar{n}_1$, $\bar{n}_2$, and $\bar{n}_3$ are opposite to those of $\overline{ME}$, $\overline{EF}$, and $\overline{FD}$. Changing the sign of the relative increments (x and y, if opposite to $\bar{n}_1$ and $\overline{ME}$, and $\bar{n}_2$ and $\overline{FD}$, or only x, if opposite to $\bar{n}_1$ and $\overline{ME}$, and $\bar{n}_3$ and $\overline{EF}$, or only y if opposite to $\bar{n}_2$ and $\overline{FD}$, and $\bar{n}_3$ and $\overline{EF}$), we arrive at the same expression for (11) and (12).

If only $\bar{n}_3$ is directed opposite to $\overline{EF}$, we get expressions differing from (11) and (12) by the sign of the quantity c, in a manner analogous to that already examined, from the similarity of triangles ABD and AE'F'. By appropriately choosing the signs of the relative increments, we can arrive at the same situation as when the directions of any one or all three of the vectors are opposite to those shown in Fig. 8.

When A and B lie on different sides of M, x and y are found from proportions differing from (10) only by the sign of d, as is clear from Fig. 8. In this case, the relative increments of m_1 and k_1 defining the system at the boundary of the stable region are found in all cases from relations (11) and (12). The quantity $c > 0$ if the directions of $\bar{n}_1$, $\bar{n}_2$, and $\bar{n}_3$ agree with the directions of $\overline{MA}$, $\overline{AD}$, and $\overline{BD}$; there are two different directions, and $c < 0$ in the remaining cases. The quantity $d > 0$ if points A and B are on one side of point M. The increment of k_1 is positive if the direction of $\bar{n}_1$ agrees with that of $\overline{MA}$; the increment of m_1 is positive if the direction of $\bar{n}_2$ agrees with that of $\overline{AD}$.

LITERATURE CITED

1. I. V. Ostoslavskii, The Aerodynamics of an Airplane [in Russian] (Oborongiz, 1957).
2. A. M. Basin, Theory of Stability on Course and Maneuverability of a Vessel [in Russian] (Gostekhizdat, 1949).
3. Ya. Z. Tsypkin and P. V. Bromberg, "On the degree of stability of linear systems," Izvest. Akad. Nauk SSSR, Otdel. Tekh. Nauk No. 12 (1945).
4. V. V. Solodovnikov, A Frequency Method for Analyzing the Quality of Automatic Control Systems [in Russian] (Mashgiz, 1950).
5. L. S. Gol'dfarb, "On certain nonlinearities in control systems," Avtomat. i Telemekh. 8, No. 5 (1947).
6. Ya. Z. Tsypkin, Theory of Automatic Control Relay Systems [in Russian] (Gostekhizdet, 1955).

CERTAIN PROBLEMS IN THE DESIGN OF MACHINES WHICH CLASSIFY OBJECTS ACCORDING TO AN IDENTIFYING FEATURE WHICH IS NOT SPECIFIED A PRIORI

É. M. Braverman

Moscow

Translated from Avtomatika i Telemekhanika, Vol. 21, No. 10,
pp. 1375-1386, October, 1959
Original article submitted February 17, 1960

The paper studies certain problems associated with the design of machines that can classify objects according to an indentifying feature which is not specified a priori. A number of general conditions are indicated for which this problem can be solved by machines with "stimulation" (machines which receive certain additional information from the operator). It is demonstrated that in a number of cases machines without stimulation can be used for the same purpose; a brief analysis is made of the capabilities of one machine of this type which has already been constructed (the "Perceptron").

1. Introduction

In designing various types of self-adaptive machines, the first problem is to design a machine that classifies input situations according to an identifying feature which is not known a priori. An example of this kind may be found in a high-speed computer which changes or formulates its program during the solution of the problem. After this machine has solved a number of problems,it will have accumulated experience which is manifested in the set of programs it has formulated. In solving a new problem the machine must first determine whether or not this problem is "similar" to some other problem it has solved previously; if this is so, then it must attempt to use a program which is already available. However, it is not known a priori which problems the machine must assume to be "similar." Thus, the experience of the machine must include not only a set of programs for solving specific problems, but also a program which is developed during the process of operation and makes it possible to separate the entire set of problems which are to be solved into classes of similar problems.

Another example is a machine designed for controlling a technological object according to a program which is not specified a priori but is developed on the basis of the actions of an operator under various conditions. But, as a rule, there is no possibility of recording the actions of the operator in the memory of the machine under all conditions that might conceivably arise—these conditions are too numerous. In that case the machine must separate the entire set of different combinations of instrument readings into classes corresponding to identical required control actions.

The basic features of the classification problem are often illustrated by the means of the following very clear example. Assume that photoelements, which act as the detectors in the machine, "scan" a certain field. The operator (human or machine) "shows" the machine geometric patterns in arbitrary sequence; these patterns have been subdivided by the operator into two classes according to some identifying feature. For example: 1) patterns located in the left and right sides of the field; 2) patterns located in the upper and lower parts of the field; 3) patterns with large and small areas; 4) squares and triangles; 5) patterns that are symmetrical relative to the horizontal and vertical axes, etc. Two situations are possible at the output of the machine (for example, the appearance of "0" or "1"). No separation of the input situations into two classes has been fed into the machine a priori. It is required that after a certain self-adaptive period the machine will be capable of producing a "1" at the output each time that the machine is shown a pattern belonging to some particular class, and of producing a "0" for the appearance of a pattern belonging to a different class.

Since the machine "does not know" a priori which identifying feature has determined the separation of the patterns into two classes by the operator, it will err at first, no matter what its algorithm for operation may be. This means that one and the same situation at the output of the machine (for example, the appearance of a "1") will arise for the appearance of patterns belonging to different classes; conversely, different situations at the output of the machine may correspond to different patterns belonging to the same class. The algorithm must be such that after a certain number of "viewings" the machine begins to operate without error, or at least in a manner where the probability of error is small. We shall assume that when a self-adaptive machine has reached this quality of operation, it has developed a "comprehension" (in the example given here, the comprehensions that are developed are "right" and "left," "upper" and "lower," etc.).

Showing another pattern to the machine corresponds to the appearance of a certain situation at the input of the machine (the excitation of certain photoelements and the nonexcitation of other photoelements). Each specific sitation at the input will sometimes be called an "object."

In the general case, the machine develops a comprehension and then converts the set of input situations into a set of output situations. In our example, the set of output situations consists of two elements (0 and 1). The machine must have a series of variable parameters for which each value completely determines the transformation law carried out by the machine. We shall call each set of specific values for these variable parameters a "state" of the machine.

Initially we shall assume that the operator feeds the machine a specific signal each time the machine commits an error (i.e., the operator feeds additional information into the machine). The state of the machine may vary according to a definite law (in the general case it is not necessarily a deterministic law), depending on the input situations and on the additional information received from the operator. Such machines shall be called "adaptive machines with stimulation."

Below we shall demonstrate that machines with stimulation are not the only class of adaptive machine. Under certain definite conditions, machines can develop comprehensions without using the additional information from the operator.

2. Certain Conditions Which Assure the Development of Comprehensions by Machines

In the general case the operator can subdivide the set of input situations into arbitrary classes (comprehensions). In principle, the machine may err until all possible objects in the given experiment have appeared, and the operator has in some way informed the machine what output situation must correspond to each possible object. But the method of "total scanning," which is the only one that can solve the problem of developing comprehensions in this general case, is inexpedient if the number of objects is sufficiently great, and if it is necessary to solve the problem in a limited time with a limited memory.

Evidently, the only method by which total scanning can be avoided is to limit a priori the set of allowed classes into which the set of objects can be subdivided by the operator.

We shall examine certain examples of the limitations which can be imposed on the allowed classes of objects and shall examine certain concepts concerning the design of machines which develop comprehensions for these limitations. For simplicity we shall assume that all possible input situations are always subdivided into three classes by the operator: a) objects corresponding to one comprehension; b) objects corresponding to a different comprehension; c) objects which do not appear in the given experiment. In other words, the machine must develop two mutually complementary comprehensions for the condition that a portion of the objects does not appear.

Example 1. Assume that the input of the machine is formed by $\underline{r}$ detectors whose state is described by the vector $(u_1, u_2, \ldots, u_r)$; assume further that $\underline{n}$ arbitrary functions of the state of the detectors are known:

$$x_i = f_i(u_1, u_2, \ldots, u_r) \quad (i = 1, 2, \ldots, n). \qquad (1)$$

Each object corresponds to a definite point with the coordinates $x_1, x_2, \ldots, x_n$ in the space $\{x\}$. We shall impose the following limitation on the allowed classes of objects. In the space $\{x\}$ it is possible to select two regions E and E' such that: a) points corresponding to objects associated with one comprehension are confined to one, and only one, region, and points corresponding to objects associated with different comprehensions are confined to different regions; b) there exists a set of hyperplanes such that the regions E and E' lie on different sides of any hyperplane in this set.

We shall turn our attention to the fact that the regions E and E' are not fixed a priori and may be different for different classes of objects.

Assume the equation for a hyperplane in $\{x\}$ is written as

$$\sigma = \sum_{i=1}^{n} \lambda_i x_i + \lambda_{n+1} = 0. \qquad (2)$$

If the hyperplane $\sigma = 0$ passes between the regions E and E', it follows that the linear function

$$\sigma = \sum_{i=1}^{n} \lambda_i x_i + \lambda_{n+1}$$

acquires positive values in one of the regions and negative values in the other region.

We shall study the $(n+1)$-dimensional space $\{\lambda\}$ with the coordinates $\lambda_1, \lambda_2, \ldots, \lambda_{n+1}$. We note that if a certain point $(\tilde{\lambda}_1, \tilde{\lambda}_2, \ldots, \tilde{\lambda}_{n+1})$ in this space defines the hyperplane

$$\sigma = \sum_{i=1}^{n} \tilde{\lambda}_i x_i + \tilde{\lambda}_{n+1} = 0$$

in the space $\{x\}$, it follows that any point in $\{\lambda\}$

lying on the straight line connecting the origin with the point $(\tilde{\lambda}_1, \tilde{\lambda}_2, \ldots, \tilde{\lambda}_{n+1})$ will define the same hyperplane. Therefore, the set of separating hyperplanes in the space $\{x\}$ will correspond to the set of straight lines in the space $\{\lambda\}$ emanating from the origin and filling a certain hypercone. The problem of developing comprehensions reduces to transferring the current value of the vector $\lambda = (\lambda_1, \lambda_2, \ldots, \lambda_{n+1})$ into the indicated hypercone. The number of errors during a series of trials (a series of "scans" of different objects) can serve as the criterion of the distance between λ and the hypercone. For example a machine classifying objects at its input for the condition that the corresponding regions E and E' can be separated by a hyperplane can operate according to the following algorithm. When a new object appears the machine determines the values of all x_i from (1) (all x_i are known functions); then the value of the linear function σ is determined for the current value $(\lambda_1, \lambda_2, \ldots, \lambda_{n+1})$, and a signal 0 or 1 appears at the output of the machine, depending of the sign of σ. From additional signals received from the operator the machine counts up the number of errors for the series of trials and alters (for example, randomly or in some other fashion) the value of $(\lambda_1, \lambda_2, \ldots, \lambda_{n+1})$; then it again determines the number of errors during the series of trials, etc., until the number of errors becomes minimal.

An algorithm of this type is the basis for a machine designed by O. Selfridge [1] and called "Pandemonium." The machine consists of several computer (or converter) stages (Fig. 1)[*]. The first stage consists of detectors D which perceive the objects. The detector outputs supply the computer devices C of the second stage that form certain functions $x_1, x_2, \ldots, x_n$ for the state of the detectors which are known a priori. The output from the ith computer device is applied to the corresponding amplifier A with a variable gain λ_i. The outputs from all the amplifiers are summed, and the sum

$$\sigma = \sum_{i=1}^{n} \lambda_i x_i$$

is applied to the decision block DB which produces 1 or 0 depending on the sign of σ. If "Pandemonium" errs, then the output applies a signal to the control unit CU. The number of errors in the operation of Pandemonium over a sufficiently long series of trials $F(\lambda_1, \lambda_2, \ldots, \lambda_n)$ is a function of the coefficients λ_i. The control unit varies λ in such a way as to minimize the number of errors during a series of trials; the variation is performed according to the method of steepest descent. Thus, the control unit is essentially an external controller with "regulating organs" $\lambda_1, \lambda_2, \ldots, \lambda_n$, that minimize the function $F(\lambda_1, \lambda_2, \ldots, \lambda_n)$.

In the example involving a machine which must classify geometric patterns projected onto the photoelement field x_i may describe the state of ith photoelement. Assume that when the photoelement is excited the corresponding coordinate acquires the value 1, and that the value 0 is acquired when it is not excited. Then the act of "showing" any pattern to the machine corresponds to a point in the space $\{x\}$ lying on one of the vertices of a unit n-dimensional hypercube (n is the number of photoelements). It is easy to see that when the machine develops such comprehensions as "left" and "right," "upper" and "lower," "large" and "small," we can find corresponding regions E and E'. However, in this space it is impossible to develop such comprehensions as a "square" or a "triangle," "a pattern symmetrical with respect to the vertical axis," and "a pattern symmetrical with respect to the horizontal axis."

Example 2. It was assumed above that only one space for performing the separation was known to us a priori. However, it is also possible to encounter the following case. Several spaces are specified (several sets of functions for the state of detectors) along with the following limitation on the allowed classes of objects: two regions E and E' having the properties indicated in the first example are found in at least one of these spaces.

The problem of developing comprehensions reduces to a search for the required vector in the spaces which are successively formed. The following condition may be used to govern the transition to trials in the next space: the absence of a variation in a certain current value of the vector λ in the sampled space such that the number of errors during the series of trials will be reduced. Since the desired variation in the vector λ must be determined each time on the basis of a finite number of steps, it follows that there may exist a certain probability that transition to trials in the next space will be performed erroneously. Thus, in the case under study the machine may develop a comprehension only with a certain probability.

As we have already noted, in our example the photoelement field cannot develop the comprehensions: a " square" and a "triangle," a "pattern symmetrical with respect to the horizontal axis, " and a "pattern symmetrical with respect to the vertical axis," if the search for the separating hyperplane is performed in a space where each coordinate corresponds to the state of one photoelement. However, it is possible to organize another space $\{x\}$ in the following fashion. Assume that the field of the photoelements forms a matrix and that the excitation of each photoelement causes the appearance of a pair of numbers (j, k) at the input of the machine; here j and k respectively denote the numbers of the row and column which locate the particular photoelement. In each row we take the excited photoelement with the smallest column number $k(j)_{\min}$ and the excited photoelement with the largest column number $k(j)_{\max}$, and then form the following half-sum for each j:

---

[*] The Pandemonium can develop several comprehensions simultaneously. In this paper we will describe a simplified Pandemonium network designed for developing just two mutually complementary comprehensions.

$$\bar{k}(j) = \frac{1}{2}\,[k(j)_{\max} + k(j)_{\min}$$

Then we find the maximum half-sum with respect to j: $\max\limits_{j} \bar{k}(j)$, and choose $f_j = \dfrac{\bar{k}(j)}{\max\limits_{j} \bar{k}(j)}$ as function of the input situation. If not a single pair of numbers with any $\tilde{j}$ appears at the input of the machine when a certain object is "shown," then we shall assume that the value of the corresponding function is $f_{\tilde{j}} = 1$.

If the photoelements form a matrix with n rows and m columns, we shall have n functions

$$f_j = \frac{\bar{k}(j)}{\max\limits_{j} \bar{k}(j)} \qquad (j = 1, 2, \ldots, n). \tag{3a}$$

Analogously, we form m functions

$$f_{n+k} = \frac{\bar{j}(k)}{\max\limits_{k} \bar{j}(k)} \qquad (k = 1, 2, \ldots, m). \tag{3b}$$

We shall study the space $\{x\}$ with the coordinates $x_i = f_i$ $(i = 1, 2, \ldots, n+m)$. In this space it is already possible to isolate patterns which are symmetrical with respect to the horizontal axis, patterns which are symmetrical with respect to the vertical axis, squares†, and triangles.

These examples demonstrate that the manner in which a machine with stimulation must operate is determined by the limitation imposed on the allowed classes of objects.‡

3. Machines Without Stimulation

Recently it has been determined that when certain additional limitations are imposed on the allowed classes of objects (these limitations are based on the statistics which govern the appearance of the object), it is possible to design machines which separate objects into classes without stimulation.

Up to now we have studied the following problem: the operator subdivides the entire set of objects into two classes; the machine, after a certain adaptive process, is required to subdivide these very objects into classes which coincide more or less exactly with the classes specified by the operator. Here we noted that the classes into which the operator subdivides the set of objects must satisfy certain limitations.

Now we shall study a different problem. A set of objects appears at the input of the machine; these objects are objectively (independently of the desires of the operator) subdivided into classes which satisfy the same limitations as those given in the preceding problem. The machine must subdivide the objects into these classes and provide the operator with information on objectively existing classes which were not known to the operator.

Both of these problems can be posed with respect to a machine without stimulation. And, although in principle the second problem is of greater interest, it is true that essentially the same machine can be used for solving both the first and second problems.

In order to clarify how either of these problems can be solved, we shall study the following simplest example. Assume that each object is made to correspond to a certain number x; assume also that on the x axis it is possible to find two nonintersecting segments $[x_1, x_2]$ and $[x_1', x_2']$ such that the numbers corresponding to objects of the same class belong to only one segment, and the numbers corresponding to objects of different classes belong to different segments.

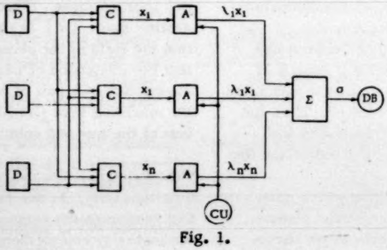

Fig. 1.

---

† It is assumed that the axes of symmetry for a square coincide with one of the rows and one of the columns of the photoelement matrix.

‡ It should be noted that the general problem of developing comprehensions is closely associated with the far more difficult problem of formulating the space proper, as well as with the problem of separating two sets in a specified space, which is treated in this paper. This problem has evidently not been posed or solved in any acceptable form as yet.

Assume further that the probability-density distribution f(x) for the appearance of objects with the coordinate x is specified. Then it is possible to establish relationships between the numbers x_1, x_2, x_1', x_2' (Fig. 2) and the properties of the probability-density function f(x), which are sufficiently general so that when the machine operates by comparing the average value $\bar{x}$ with the current value x (Fig. 3), it is capable of developing the specified comprehensions without any additional information from the operator.** This principle can be generalized to apply to multidimensional spaces.

The first to propose a self-adaptive machine without stimulation was F. Rosenblatt [2]. His machine (which he called the "Perceptron"††) operates according to a principle that differs from the one cited above. The shortcoming of the principle proposed by F. Rosenblatt is that the limitations imposed on the allowed classes of objects for which the Perceptron can operate are not natural ones and cannot be interpreted in convenient terms. However, since the Perceptron is the first constructed machine without stimulation, the subsequent sections of this paper will analyze the principle of operation of the Perceptron and certain problems in the theory of this operation.

4. The Perceptron Network‡‡

A Perceptron (Fig. 4) consists of a set of identical elements which are conditionally called neurons. A certain function x of the state of the detectors is applied to the input of each neuron at discrete instants n=0, 1, 2, . . ., corresponding to the instants at which the objects appear. Each neuron is an amplifier with a variable gain λ that changes at these same discrete instants. The increment of gain during one cycle is determined from the formula***

$$\Delta\lambda^n = \lambda^{n+1} - \lambda^n = (x^n - k\lambda^n)\,p^n, \tag{4}$$

where p is the signal produced at the output of the next Perceptron stage, and k is a certain constant. The output of the neuron at the nth instant is the quantity $\lambda^n x^n$.

All neurons are subdivided into two groups. Assume that there are l neurons in the first group and m neurons in the second group. We shall prime those quantities which refer to neurons of the second group. The variable p is the same for all neurons in one group. Thus, we obtain l + m relationships:

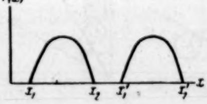

Fig. 2.

$$\Delta\lambda_i^n = (x_i^n - k_i\lambda_i^n)\,p^n \qquad (i = 1, 2, \ldots, l).$$
$$\Delta\lambda_j'^n = (x_j'^n - k_j'\lambda_j'^n)\,p'^n \qquad (j = 1, 2, \ldots, m). \tag{4a}$$

The outputs of all the neurons are summed; the outputs of the neurons in the first group are taken with a plus sign, while the neurons in the second group are taken with a minus sign. The resulting sum

$$\sigma^n = \sum_{i=1}^{l} \lambda_i^n x_i^n - \sum_{j=1}^{m} \lambda_j'^n x_j'^n$$

is applied to the input of the decision element DE at each instant; the decision element has two outputs p and p' and operates according to the law

$$p^n = \begin{cases} 1 & \sigma^n \geqslant 0 \\ 0 & \sigma^n < 0, \end{cases} \tag{4b}$$

$$p'^n = 1 - p^n.$$

Note that if the sequence of values acquired by the vector $x^n = (x_1^n, x_2^n, \ldots, x_l^n, x_1'^n, \ldots, \bar{x}_m'^n)$ and the initial value of the vector $\lambda^0 = (\lambda_1^0, \lambda_2^0, \ldots, \lambda_l^0, \lambda_1'^0, \ldots, \lambda_m'^0)$ are known, then Eqs. (4a) and (4b) completely define the value of the vector λ^n and the outputs p^n and p'^n of the decision element at all instants n = 0, 1, 2,...

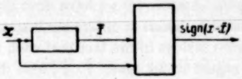

Fig. 3.

** For example, a sufficient condition is the validity of the inequalities

$$x_1\int_{x_1}^{x_2} f(x)\,dx + x_1'\int_{x_1'}^{x_2'} f(x)\,dx > x_2,$$

$$x_2\int_{x_1}^{x_2} f(x)\,dx + x_2'\int_{x_1'}^{x_2'} f(x)\,dx < x_1'.$$

Here $\int_{x_1}^{x_2} f(x)\,dx$ is the probability that an object belonging to the first class will appear, and $\int_{x_1'}^{x_2'} f(x)\,dx$ is the probability that an object belonging to the second class will appear.

†† From the English word "perception" —perception, recognition.

‡‡ The presentation of the Perceptron properties in this and subsequent sections differs from the corresponding treatment in [2].

*** Here and throughout, the superscripts n, n+1, etc., indicate a corresponding instant; they are not exponents.

We shall study the l + m)-dimensional space $\{x\}$ with the coordinates $x_1, x_2, \ldots, x_l, x'_1, \ldots, x'_m$). Each object appearing at the input corresponds to a point in $\{x\}$. At each instant the equation

$$\sigma = \sum_{i=1}^{l} \lambda_i^n x_i - \sum_{j=1}^{m} \lambda_j'^n x_j' = 0$$

specifies a hyperplane in $\{x\}$ whose directional cosines are determined by the neuron gains (i.e., by the value of the vector λ^n). Since during the process involved in the appearance of the object at the Perceptron input λ^n varies in accordance with (4a) and (4b), it follows that the hyperplane $\sigma=0$ is "rotated" in some fashion.

At each instant $\underline{n}$ the appearance of $p^n = 1$ at the Perceptron output corresponds to the appearance of an object whose coordinates lie on one side of the hyperplane; the appearance of $p'^n=1$ at the Perceptron output corresponds to the appearance of an object whose coordinates lie on the other side of the hyperplane. If, after a sufficiently large number of objects appear, the position of the hyperplane is stabilized (i.e., it merely "rocks" near a certain position), then the appearance of p=1 or p=0 at the output of the machine will determine the subdivision of the output into two classes in a more or less stable fashion; only objects whose coordinates are located in the "rocking" region will correspond first to p=1, then to p=0. Assume (as we have done throughout this paper) that the objective difference between the classes of objects resides in the fact that each class corresponds to a region in the space $\{x\}$; here these regions are governed by the limitations in Section 2. If the subdivision of objects into two classes by the Perceptron corresponds to the separation of these regions, then this will indicate that the machine has developed a comprehension.

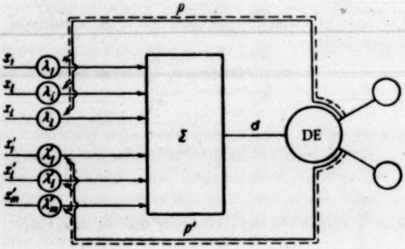

Fig. 4.

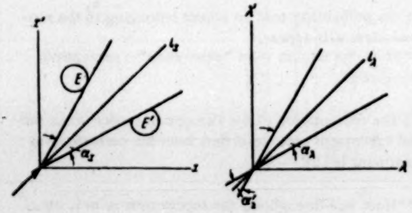

Fig. 5.

In the analysis below we shall demonstrate that the Perceptron is far from being able to develop a comprehension in this sense for all cases.

5. Certain Problems in the Theory of a Perceptron

We shall derive certain relationships which determine the process involved in the time variation of the vector λ. For simplicity we shall assume that there are two neurons with the gains λ and λ' and the inputs $\underline{x}$ and x'. However, it is obvious that if we treat x, x', λ, λ' as vectors, then the basic results remain valid.

Assume that the plane $\{x\}$ contains two regions E and E' which can be separated by the straight line l_x passing through the origin; then the set of these separating straight lines form the angle α_x (Fig. 5). As we have already noted in Section 2, each separating straight line l_x in the plane $\{\lambda\}$ corresponds to a straight line l_x passing through the origin; the set of separating lines which fills the angle α_x on the plane $\{x\}$ corresponds to the set of straight lines in the plane $\{\lambda\}$ that fills the two opposing angles α_λ and α'_λ (a "two-dimensional cone").

The problem which the machine must solve reduces to separating objects whose coordinates lie in the regions E and E'. Since all of the straight lines which separate these regions lie within the angle α_x on the plane $\{x\}$, it follows that the machine develops a comprehension only if the values of the neuron gains λ and λ' lie either solely within the angle α_λ or solely within the angle α'_λ on the plane $\{\lambda\}$ for most of the time after the adaptive process has been completed. Under these conditions the point (λ, λ') must not pass from α_λ into α'_λ (or vice versa after the adaptive process has been completed; this holds because if such a transition were to occur, the sign of σ would be changed, and on the basis of (4b) the alternate values p=1 and p=0 would correspond to the same region E (or E'); this is inadmissible.

Before we pass on to further derivations we shall study the simplest example which will show that in certain cases the Perceptron is actually capable of developing a comprehension (i.e., it is capable of performing

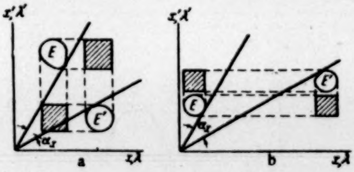

Fig. 6.

the necessary separation); it is also possible to encounter cases when the Perceptron is not capable of developing a comprehension.

Example. We shall study a Perceptron in which $k = k' = 1$. In accordance with (1), $\lambda = \tilde{x}$ and $\lambda' = \tilde{x}'$ at each instant; here $\tilde{x}$ is the x coordinate of the nearest preceding object for which $\sigma \geq 0$, and $\tilde{x}'$ is the x coordinate of the nearest preceding object for which $\sigma < 0$.

We shall superimpose the planes $\{x\}$ and $\{\lambda\}$ and shall assume for simplicity that the angle α_x is symmetrical relative to the bisectrix of the first quadrant. Then it is not difficult to see from the equation $\sigma = \lambda x - \lambda' x' = 0$ that the angle α_λ coincides with the angle α_x when the planes are superimposed (Fig. 6a). If the separation has been performed, then the point (λ, λ') must lie only in one of the shaded rectangles. It is obvious that if we shift the regions E and E' in such a way that the angles α_x and α_λ are not altered, it is possible to obtain shaded rectangles both inside and outside the angle α_λ (Fig. 6,a and b). However, if no rectangle lies inside the angle α_λ, then it is certain that separation is impossible.

We shall now continue our study of the general case. We shall assume that the sequence in which objects appear is random and that we know only the probability-density function $\varphi(x, x')$ for the appearance of an object with the coordinates (x, x'); the probability that a certain object will appear at a certain specified instant is not dependent on what has appeared previously.

Note that in this case the probabilities that the point (λ^n, λ'^n) will be shifted to the point $(\lambda^{n+1}, \lambda'^{n+1})$ depend solely on the current value of (λ^n, λ'^n) and are determined by the function $\varphi(x, x')$; i.e., the process consisting of the variation of (λ, λ') is a random Markov process.

Assume that we know how to determine $f_n(\lambda, \lambda')$ [this function is the probability-density function for (λ, λ') after n instants].

For each appearance of a new object a variation can occur either for λ only or for λ' only, since either $p = 0$ or $p = 1$ is mandatory. Therefore, only those points (λ, λ') for which either $\lambda = \tilde{\lambda}$ or $\lambda' = \tilde{\lambda}'$ can arrive at the point $(\tilde{\lambda}, \tilde{\lambda}')$ during one step. Here the point $(\lambda, \tilde{\lambda}')$ is transferred to the point $(\tilde{\lambda}, \tilde{\lambda}')$ if an object appears with the coordinates (x, x') satisfying the condition $\sigma = \lambda x - \tilde{\lambda}' x' \geq 0$ $(p = 1)$ and $x = \tilde{\lambda} - (1 - k)\lambda$; this result is valid on the basis of Eq. (4a). Analogously, the point $(\tilde{\lambda}, \lambda')$ is transferred to the point $(\tilde{\lambda}, \tilde{\lambda}')$ if an object appears with the coordinates (x, x') which satisfy the condition $\sigma = \tilde{\lambda} x - \lambda' x' < 0$ $(p = 0)$ and $x' = \tilde{\lambda}' - (1 - k')\lambda'$. The probability density for transfer from the point $(\lambda, \tilde{\lambda}')$ to the point $(\tilde{\lambda}, \tilde{\lambda}')$ is therefore equal to

$$\psi_1(\lambda, \tilde{\lambda}, \tilde{\lambda}') = \int \varphi(\tilde{\lambda} - (1 - k)\lambda, x')\, dx',$$
$$x' \tilde{\lambda}' \leqslant [\tilde{\lambda} - (1 - k)\lambda]\lambda,$$

where the integral is taken over all x' satisfying the condition

$$x' \tilde{\lambda}' \leqslant [\tilde{\lambda} - (1 - k)\lambda]\lambda.$$

The probability density for transfer from the point $(\tilde{\lambda}, \lambda')$ to the point $(\tilde{\lambda}, \tilde{\lambda}')$ is equal to

$$\psi_2(\lambda', \tilde{\lambda}, \tilde{\lambda}') = \int \varphi(x, \tilde{\lambda}' - (1 - k')\lambda')\, dx,$$
$$x\tilde{\lambda} < [\tilde{\lambda}' - (1 - k')\lambda']\lambda',$$

where the integral is taken over all x satisfying the condition

$$x\tilde{\lambda} < [\tilde{\lambda}' - (1 - k')\lambda']\lambda'.$$

The recursion relationship which determines the Markov process in the case under study is written as

$$f_{n+1}(\tilde{\lambda}, \tilde{\lambda}') = \int_{\lambda} f_n(\lambda, \tilde{\lambda}')\, \psi_1(\lambda, \tilde{\lambda}, \tilde{\lambda}')\, d\lambda + \int_{\lambda'} f_n(\tilde{\lambda}, \lambda')\, \psi_2(\lambda', \tilde{\lambda}, \tilde{\lambda}')\, d\lambda',$$

where the integrals are taken over all possible values of λ and λ', and the functions ψ_1 and ψ_2 are determined according to the expressions cited above.

The probability that the point (λ, λ') will be located within the angle α_λ after the nth instant is equal to

$$P_n((\lambda, \lambda') \in \alpha_\lambda) = \iint_{\alpha_\lambda} f_n(\lambda, \lambda')\, d\lambda\, d\lambda'. \qquad (6a)$$

The corresponding probability that the point will be located within the angle α'_λ is equal to

$$P'_n((\lambda, \lambda') \in \alpha'_\lambda) = \iint_{\alpha'_\lambda} f_n(\lambda, \lambda')\, d\lambda\, d\lambda'. \qquad (6b)$$

Here the integrals are taken over the regions belonging to the angles α_λ and α'_λ, respectively.

It is evident that the Perceptron develops the required comprehensions if after a sufficiently large number of different objects have appeared, there is established a sequence of distributions $f_n(\lambda, \lambda')$ such that either the value of P_n or the value of P'_n is close to 1 in the predominant number of cases. Quantitatively this condition can be expressed as follows: for each initial value (λ^0, λ'^0) we find a value of N such that for all $n > N$ either the inequality

$$\frac{\sum_N^n P_n}{n - N + 1} \geqslant 1 - \varepsilon, \qquad (7a)$$

or the inequality

$$\frac{\sum_N^n P'_n}{n - N + 1} \geqslant 1 - \varepsilon \qquad (7b)$$

will be satisfied.

It is possible to require that a more rigorous condition be satisfied: for each (λ^0, λ'^0) we must find an N such that for all $n > N$ we have either

$$P_n = 1 \qquad (8a)$$

or

$$P'_n = 1. \qquad (8b)$$

The validity of one of these conditions means that in the final analysis a sequence of probability-density functions $f_n(\lambda, \lambda')$ is established such that the point (λ, λ') never emerges beyond the limits of either the angle α_λ or the angle α'_λ; therefore the probability of error in the Perceptron becomes equal to zero.

It is considerably simpler to predetermine the ability of the Perceptron to satisfy one of the conditions (8a) or (8b) rather than one of the conditions (7a) or (7b). Assume that the adaptive process has been completed and that one of the conditions (8a), (8b) is satisfied. This means that the straight line $\sigma = 0$ passes rigorously between the regions E and E'. Therefore, in view of (**4a**), the value of λ can change only at those instants when $(x, x') \in E$, and that of λ', only at those instants when $(x, x') \in E'$; or conversely, the change is dependent on whether the point (λ, λ') is within the angle α_λ or within the angle α'_λ [i.e., whether condition (8a) or (8b) is satisfied]. Assume, for example, that condition (8a) is satisfied, and that λ changes in those cases when $(x, x') \in E$ (the remaining cases are treated analogously).

We shall now study only those instants $s = 0, 1, 2, \ldots$, at which an object with the coordinates (x, x') appears, instead of studying all instants; therefore, we assume that the value of λ changes. We shall choose some instant after the adaptive process has been completed as the initial instant; under these conditions the point (λ, λ') is already within the angle α_λ.

In accordance with the difference equation (4a),

$$\lambda^s = \sum_{j=0}^{s-1} (1-k)^{s-j-1} x^j + (1-k)^s \lambda^0.^{\dagger\dagger\dagger} \qquad (9)$$

The variables x^j are independent random quantities with identical probability-density functions that are equal to the conditional probability-density function for the condition $(x, x') \in E$:

$$\frac{\int\limits_E \varphi(x, x')\,dx'}{\iint\limits_E \varphi(x, x')\,dx\,dx'},$$

since the instants $s = 0, 1, 2, \ldots$ are by definition $(x, x') \in E$ at these instants.

Since λ^s is a linear function of independent random variables, it follows that

$$\overline{\lambda^s} = \sum_{j=0}^{s-1} (1-k)^{s-j-1} \overline{x^j} + (1-k)^s \lambda^0, \qquad (10)$$

where the bar above a quantity denotes mathematical expectation. The series (10) converges only for the condition $0 < k < 2$; here

$$\lim_{s\to\infty} \overline{\lambda^s} = \overline{\lambda} = \frac{1}{k}\overline{x}. \qquad (11)$$

From (9) it is also easy to derive the expression for the dispersion of the limiting probability-density function:

$$\lim_{s\to\infty} D(\lambda^s) = D(\lambda) = \frac{1}{2k-k^2} D(x). \qquad (12)$$

Thus, knowing the arrangement of the regions E and E', it is possible to find the angles α_λ and α'_λ; knowing $\varphi(x, x')$, it is possible to determine λ, $D(\lambda)$ and to estimate whether λ^s is located solely within the angle α_λ.

mate whether λ^s is located solely within the angle α_λ.

We should pay attention to the fact that the dispersion $D(x)$ in (12) is computed only for the region E. Equation (12) illustrates the part played by the feedback loops for the quantities p and p' (Fig. 4). If these relationships do not exist, then the quantity λ will change for the appearance of objects from both the region E and the region E'; the dispersion $D(x)$ will then be computed over both regions. This will cause a pronounced increase in the dispersion of the limiting distribution and will mean that the probability of the emergence of the point (λ, λ') beyond the limits of the bounded angle α_λ will have increased.

We shall now pose the following problem: the operator has a priori subdivided the objects into two classes which satisfy the limitations cited in Section 2. Is it possible always to choose the statistic involved in the appearance of the objects in such a way that the Perceptron will perform the separation conceived of by the operator?

An analysis of the Perceptron operation shows that for certain additional conditions the Perceptron is capable of performing the separation conceived of by the operator (i.e., it is able to develop the required comprehensions). However, these conditions are not obvious.

The example cited above demonstrates the possibility that there may be no statistics of object appearance for which the Perceptron can perform the required separation.

In the general case the capacity of the Perceptron for developing the required comprehensions is determined by its structure (the value of the quantity k and the specific form of the function x), by the nature of the objects which are "shown" to the machine (the arrangement of the regions E and E'), and by the statistics governing the "showing" process (the form of the probability-density function for the appearance of the objects). In order to determine this capacity a priori for a specified structure and specified "showing" statistics, it is necessary to perform a computation using formulas (5), (6), (7); this process in itself requires the use of mathematical machines.

LITERATURE CITED

1. O. G. Selfridge, Pandemonium: A Paradigm for Learning. Symposium on the Mechanization of Thought Processes (England, November, 1958).
2. F. Rosenblatt, Two Theorems of Statistical Separability in the Perceptron. Symposium on the Mechanization of Thought Processes (England, November, 1958).

[†††] Here and throughout, $(1-k)^j$ denotes the jth power of $(1-k)$.

CONTROLLING A SERVODRIVE USING ONE NULL INDICATOR WHICH PERFORMS THE FUNCTIONS OF TWO NULL INDICATORS

V. D. Vershinin

Moscow

Translated from Avtomatika i Telemekhanika, Vol. 21, No. 10,
pp. 1387-1392, October, 1960
Original article submitted April 4, 1960

The paper studies a network for summing the fine and coarse control signals; this network can be used to control a servodrive while simultaneously monitoring the accuracy of automatic tracking with only one null indicator.

In existing servodrives semiautomatic control and monitoring of the automatic tracking accuracy are achieved with two null indicators that are connected in parallel with the selsyn receivers (or other detecting elements).

The null indicators have different sensitivities with respect to the mismatch angle, and their pointers deviate in direct proportion to the envelope corresponding to the voltages from the fine and coarse detector elements:

$$\alpha_c = S\frac{U_m \sin \theta}{R_1}, \quad \alpha_f = S\frac{U_m \sin k\theta}{R_2},$$

where α_c, α_f are the deviation angles for the pointers on the null indicators for coarse and fine control, respectively; U_m is the maximum output voltage of the detector element; θ is the mismatch angle; R_1 and R_2 are the resistances in the signal-winding circuit of the null indicators; S is the slope of the characteristic for the null indicators; k is the transfer number between the detector elements for fine and coarse control.

The semiautomatic control of a servodrive using two null indicators is based on using an appropriate device (a semiautomatic control device) to achieve a constant alignment of the pointers of both null indicators with their zero positions. The basic difficulty in control of this type and in monitoring the tracking accuracy resides in the necessity for simultaneous observation of the pointers of two meters. In the analysis below we study a network for summing the fine and coarse signals; this network makes it possible to control the servodrive and to monitor the accuracy of the automatic tracking using a single null indicator.

The operation of the network (Fig. 1) is based on a nonlinear volt-ampere resistance characteristic; the fine control signal and a portion of the coarse control signal are limited by the nonlinear resistor NR formed by two solid-state rectifiers at the input of the null indicator. For a small mismatch angle the pointer of the null indicator is deflected basically by the fine control signal; for a large mismatch angle it is reflected basically by the coarse control signal. In order to avoid reverse deflection of the null indicator pointer when the phase of the fine control signal changes [i.e., when the value of the mismatch angle is in the range $\pi i/k - 2\pi i/k$ $(i = 1, 2, 3, \ldots)$], a branch with the resistor r_5 is introduced into the network. The resistor r_5 applies a voltage to the nonlinear resistance for maintaining the phase of the mismatch.

The Dependence of the Deflection Angle of the Null Indicator Pointer on the Mismatch Angle

The dependence of the deflection angle α of the null indicator pointer on the mismatch angle θ can be derived by making use of the mesh current method. In order to facilitate the derivation of this relationship, we neglect the inductive reactance of the null indicator signal winding, since it is small compared to the resistances of the loops; we shall assume that the shape of the current sinusoid (at the carrier frequency ω) is not distorted by the mismatch angle. Then

$$\begin{aligned}
U_f &= I_1(r_{i1} + r_1 + r_2 + r_3) + I_2(r_{i1} + r_1) - I_4(r_{i1} + r_1) + I_3 r_3,\\
U_f &= I_1(r_{i1} + r_1) + I_2(r_{i1} + r_1 + r) - I_4(r_{i1} + r_1),\\
U_c &= I_1 r_3 + I_3(r_{i2} + r_4 + r_3) + I_4 r_{i2},\\
U_c - U_f &= -I_1(r_{i1} + r_1) - I_2(r_{i1} + r_1) + I_3 r_{i2} + I_4(r_{i1} + r_{i2} + r_5 + r_1),
\end{aligned}$$

where r is the static resistance of the NR and is determined from the volt-ampere characteristic; r_{i1}, r_{i2} are the resistances of the output windings in the detector elements.

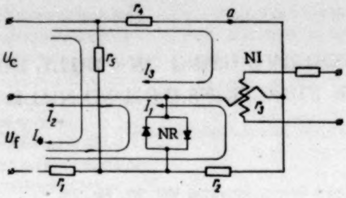

Fig. 1.

The determinant for the system of equations is

$$\Delta = \begin{vmatrix} A & C & r_3 & -C \\ C & B & 0 & -C \\ r_3 & 0 & D & r_{i2} \\ -C & -C & r_{i2} & F \end{vmatrix} = AB\,(DF - r_{i2}^2) - BFr_3^2 -$$

$$- C^2\,(AD + DF + BD - r_3^2 - r_{i2}^2 - 2r_3r_{i2}) + 2DC^3 - 2Br_3r_{i2}C,$$

where

$$A = r_{i1} + r_1 + r_2 + r_3, \qquad B = r_{i1} + r_1 + r,$$
$$C = r_{i1} + r_1, \quad D = r_{i2} + r_3 + r_4, \quad F = r_{i1} + r_{i2} + r_5 + r_1.$$

The current flowing through the signal winding of the null indicator is equal to $I = I_1 + I_3$, where $I_1 = \Delta_1/\Delta$, $I_3 = \Delta_3/\Delta$,

$$\Delta_1 = \begin{vmatrix} U_f & C & r_3 & -C \\ U_f & B & 0 & -C \\ U_c & 0 & D & r_{i2} \\ U_c - U_f & -C & r_{i2} & F \end{vmatrix} =$$

$$= U_f\,(BDF - Br_{i2}^2 - CDF + Cr_3r_{i2} + Cr_{i2}^2 - BDC + C^2D - Br_3r_{i2}) +$$
$$+ U_c\,(-Br_3F - BCr_{i2} + C^2r_{i2} + C^2r_3 + BDC - C^2D + Br_3r_{i2}),$$

$$\Delta_3 = \begin{vmatrix} A & C & U_f & -C \\ C & B & U_f & -C \\ r_3 & 0 & U_c & r_{i2} \\ -C & -C & U_c - U_f & F \end{vmatrix} =$$

$$= U_f\,(ABr_{i2} - BCr_{i2} + C^2r_{i2} - BFr_3 - ACr_{i2} + CFr_3 - C^2r_3 + BCr_3) +$$
$$+ U_c(ABF + 2C^3 - C^2B - AC^2 - C^2F - ABr_{i2} + r_3C^2 - BCr_3 + C^2r_{i2}).$$

Turning our attention to the deflection angle of the null indicator pointer instead of the current, we obtain

$$\alpha = SI, \qquad \text{or} \qquad \alpha = S\,\frac{U_f\,(Bm + N) + U_c(Bm_1 + N_1)}{Bm_2 + N_2},$$

where

$$m = DF - r_{i2}^2 - DC - r_3r_{i2} + Ar_{i2} - Cr_{i2} - Fr_3 + Cr_3,$$
$$N = -CDF + Cr_3r_{i2} + Cr_{i2}^2 + C^2D + C^2r_{i2} - ACr_{i2} + CFr_3 - C^2r_3,$$
$$m_1 = -r_3F - Cr_{i2} + DC + r_3r_{i2} + AF - C^2 - Ar_{i2} - Cr_3,$$
$$N_1 = C^2r_{i2} + C^2r_3 - C^2D + 2C^3 - AC^2 - C^2F + r_3C^2 + C^2r_{i2},$$
$$m_2 = ADF - Ar_{i2}^2 - Fr_3^2 - C^2D - 2r_3r_{i2}C,$$
$$N_2 = -C^2AD - C^2DF + C^2r_3^2 + C^2r_{i2}^2 + 2DC^3 + 2r_3r_{i2}C^2.$$

Here m_i, N_i are constant coefficients ($i = 0, 1, 2$).

The expression for the coefficient B includes r (the static resistance of the nonlinear element).

After replacing B with the expression $R_1 + r$ (where $R_1 = r_{i1} + r_1$) and replacing U_c and U_f with the expressions $U_m \sin\theta$ and $U_m \sin k\theta$, we obtain

$$\alpha = SU_{\mathrm{m}} \frac{\sin k\theta \, [(R_1 + r)\, m + N] + \sin \theta \, [(R_1 + r)\, m_1 + N_1]}{(R_1 + r)\, m_2 + N_2}\,. \tag{1}$$

This formula describes the dependence of the deflection angle of the pointer on the mismatch angle between the receiving and transmitting devices. The formula is inconvenient because it includes three variables: the mismatch angle θ, the deflection angle α of the pointer, and the static resistance r̲ of the nonlinear element.

In formulating the function $\alpha = f(\theta)$ we shall assume that the shape of the current sinusoid flowing through the movable winding of the null indicator is not distorted by the variation of the mismatch angle (or by the variation in the position of the operating point on the volt-ampere characteristic of the nonlinear element).

In order to eliminate one of the variables from the latter formula, we must determine the function $r = f_1(\theta)$ or $r = f_2(\alpha)$. Obtaining either of these functions in explicit form presents a complex mathematical problem. However, it is not mandatory to have these functions in explicit form to formulate the function $\alpha = f(\theta)$. In order to find $r = f_1(\theta)$, we shall make use of a function that expresses the current I_2 through the nonlinear resistance in terms of the mismatch angle θ:

$$I_2 = \frac{\Delta_2}{\Delta}\,,$$

where

$$\Delta_2 = \begin{vmatrix} A & U_{\mathrm{f}} & r_3 & -C \\ C & U_{\mathrm{f}} & 0 & -C \\ r_3 & U_{\mathrm{C}} & D & r_{i2} \\ -C & U_{\mathrm{C}} - U_{\mathrm{f}} & r_{i2} & F \end{vmatrix} =$$

$$= U_{\mathrm{f}}(-CDF + Cr_{i2}^2 + ADF - Ar_{i2}^2 - Fr_3^2 + C^2D + Cr_3^2 - ADC) +$$
$$+ U_{\mathrm{C}}(C^2 r_{i2} - C^2 r_3 - ACr_{i2} + CFr_3 - C^2D - Cr_3^2 + ADC - Cr_3 r_{i2}) =$$
$$= U_{\mathrm{f}}Q + U_{\mathrm{C}}w.$$

Then

$$I_2 = \frac{U_{\mathrm{f}}Q + U_{\mathrm{C}}w}{(R_1 + r)\, m_2 + N_2}\,. \tag{2}$$

As we know, the relationship between the current and voltage for nonlinear solid-state rectifiers is given by the formula

$$U_a = U_{an}\left(\frac{i_a}{I_{an}}\right)^{\beta_1},$$

where U_a, i_a are the instantaneous values of the forward voltage and current for the rectifier; U_{an}, I_{an} are the forward voltage and current for the rectifier when its class is specified [1].

Turning from the voltage to the static resistance of the rectifier in the forward direction, we obtain

$$\frac{U_a}{i_a} = \frac{U_{an}}{(I_{an})^{\beta_1}} \frac{i_a^{\beta_1}}{i_a} \quad \text{or} \quad r = M i_a^{\beta_1 - 1},$$

where

$$M = \frac{U_{an}}{(I_{an})^{\beta_1}}\,.$$

In the case under study, $I_2 = \sqrt[P]{\frac{r}{M}}$, where $P = \beta_1 - 1$. Substituting into Formula (2), we obtain

$$\sqrt[P]{\frac{r}{M}} = \frac{U_{\tau}Q + U_{\mathrm{C}}w}{(R_1 + r)\, m_2 + N_2}$$

or

$$\lambda r \sqrt[P]{r} + l \sqrt[P]{r} = U_{\mathrm{m}}(Q \sin kQ + w \sin \theta),$$

where

$$\lambda = \frac{m_2}{\sqrt[P]{M}}, \quad l = \frac{1}{\sqrt[P]{M}}(R_1 m_2 + N_2).$$

Specifying the value of r̲, we find the value of θ; then these two values are used in conjunction with Formula (1) to determine the deflection angle α of the pointer.

In Fig. 2 we have shown the dependence of the deflection angle α on the mismatch angle θ for two different cases (for a closed circuit and an open circuit at the point a in Fig. 1).

A Simplified Method for Computing the Network

In performing the computation (selecting the parameters),we assume the following parameters are known:

1. The maximum voltages applied to the detector elements, and the transfer number between detector elements.
2. The null indicator sensitivity and the resistance r_3 of the signal winding.
3. The volt-ampere characteristic of the nonlinear element.
4. The resistances of the output windings in the detector elements.
5. The mismatch angle θ within whose limits the null indicator pointer is deflected predominantly by the fine control signal.
6. The mismatch angle $\theta_2 - \theta_1$, within whose limits the pointer is deflected predominantly by the coarse control signal.
7. The deflection angles α_1 and α_2 of the pointer which correspond to the angles θ_1 and θ_2.

The angle θ_2 must be equal to the deflection angle of the pointer up to the pointer stop.

The voltage drop ΔU across the nonlinear resistance is made equal to or greater than,the null indicator voltage drop corresponding to a pointer deflection angle α_1.

The resistance r_2 is computed from the formula $r_2 = S\dfrac{\Delta U}{\alpha_1} - r_3$. The derivation of the formulas for determining the resistors r_1 and r_5 is achieved on the basis of the following conditions:

$$\frac{U_m \sin k\theta_1 - \Delta U}{r_1 + r_{t1}} + \frac{U_m \sin \theta_1 - \Delta U}{r_5 + r_{t2}} = \frac{\Delta U}{r_{\text{eq}}}, \tag{3}$$

$$\frac{U_m \sin \theta_3}{r_5 + r_{t2}} = 2\frac{U_m}{r_1 + r_{t1}}. \tag{4}$$

Formula (3) is the condition for deflection of the pointer through the angle α_1 when the mismatch angle is θ_1 (excluding the effect of the current I_3). Formula (4) is the condition for elimination of the possibility of reverse deflection of the pointer when the fine-control detector element is rotated through approximately 270° from the matched position.

In Formulas (3) and (4),

$$\theta_3 = \sim\frac{270°}{k}, \quad r_{\text{eq}} = \frac{(r_3 + r_2)\,r'}{r_2 + r_3 + r'},$$

where r' is the resistance of the nonlinear element at the knee of the volt-ampere characteristic.

After a series of simple transformations we obtain

$$r_1 = \frac{2B_1U_m - \varepsilon d r_{t1} + A_1\varepsilon}{\varepsilon d}, \quad r_5 = \frac{B_1}{d - \dfrac{A_1}{C_1}} - r_{t2},$$

where

$$A_1 = U_m \sin k\theta_1 - \Delta U, \; B_1 = U_m \sin \theta_1 - \Delta U, \; C_1 = r_1 + r_{t1},$$

$$\varepsilon = U_m \sin \theta_3, \; d = \frac{\Delta U}{r_{\text{eq}}}.$$

The resistance r_4 is obtained from the formula

$$r_4 = \frac{U_m \sin \theta_2 - U_m \sin \theta_1}{\dfrac{\alpha_2 - \alpha_1}{S}}.$$

The network described above was checked under laboratory conditions. Here the network parameters were as follows: $r_1 = 100$ kohm, $r_2 = 1$ kohm, $r_4 = 20$ kohm, $r_5 = 10$ kohm.

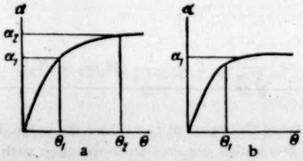

Fig. 2.

The null indicator was a ferrodynamic instrument of the type "IF-2"; the nonlinear resistance was a selenium bar of the type "AVS-18-18" with shorted outer leads (the voltage drop across it was ~1.1 v). The signals were generated by a receiving device with "SS-405" selsyns. The transfer number between the selsyns was k = 20. The deflection angle of the null indicator pointer was $\alpha_1 = \sim 25°$ and corresponded to a mismatch angle of ~3°; the deflection angle $\alpha_2 = 45°$ corresponded to the mismatch angle $\theta_2 = 12°$.

Thus,our network for summing the signals permits automatic assurance of a high sensitivity to small mismatch angles (this is the function of a fine-control null indicator) and a low sensitivity to large mismatch angles (this is the part played by a coarse-control null indicator

The fact that it is not necessary for the operator to shift his eyes from one null indicator to the other permits an improvement in the quality of semiautomatic control and makes it more convenient to monitor the accuracy of the automatic tracking. In addition, the construction of the mounting of the device is simplified, and more advantageous conditions are created for its protection from shock.

LITERATURE CITED

1. V. G. Komar, The Operation of Semiconductor Rectifiers in Control Circuits [in Russian] (Gosénergoizdat, 1952).

TAKING THE WEAK SURFACE EFFECT INTO ACCOUNT IN SWITCHING THE MAGNETIC STATE OF A FERROMAGNETIC PLATE

M. G. Vitkov

Moscow

Translated from Avtomatika i Telemekhanika, Vol. 21, No. 10,
pp. 1393-1400, October, 1960
Original article submitted March 25, 1960

The paper performs a quantitative investigation of the process involved in switching the magnetic state of sufficiently thin plane cores with rectangular hysteresis loops (for example, magnetic ribbons with a thickness of up to 3-5 μ). For thicker ribbons the qualitative picture is described. A criterion is established for the intensity of the magnetic skin effect; this criterion is a relative increase in the switching coefficient for the core. The results of the computations are compared with known experimental data on the magnetic switching of ribbon cores.

In various fields of automation and computing engineering, magnetic elements in the form of ribbon and sheet cores are widely used. Such cores are used, for example, in registers, in logic and memory cells, in decoders, etc. It is of interest to analyze the physical processes and the electrical computation method for the various types of pulsed magnetic circuits, while taking into account the effect of certain basic factors (the magnetoviscous properties of the core material, and eddy currents) which lead to closer coincidence between the computed results and the observed phenomena.

The problem of studying the effect of eddy currents for switching the magnetic state of cores with a rectangular hysteresis loop requires the solution of nonlinear differential equations.

For particular cases involving ribbon cores we use numerical integration methods [1]. The results are in good agreement with experimental data. In this paper we obtain an analytical solution of the problem. In general form such a solution may be obtained for the case of a weak surface effect, which is of special practical interest.

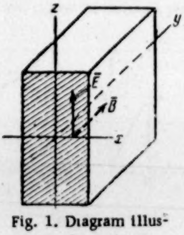

Fig. 1. Diagram illustrating the problem.

The presence of the surface effect leads to a prolongation of the magnetic switching process and to a change in its form. We derive an expression which is convenient for determining the prolongation time. The paper shows the dependence of this time on thickness and properties of the ribbon core material.

The problem is solved by the method of successive approximations used earlier for an analysis of the surface effect in ferrite ring cores. We shall cite the basic assumptions of this method and shall apply them to cores shaped in the form of a plate (Fig. 1). At the initial instant t = 0 the plate is magnetized in the direction of the y axis to an amount equal to the remanent flux density $\bar{B}_r$. The magnetic switching is performed by an external magnetic field $H = H_e(t)$ which is applied along the y axis.

The magnetic switching process in the surface layers of the plate is determined exclusively by the magnetoviscous properties of the ferromagnetic. The change in magnetic state can be expressed in terms of a pulse Q of the switching magnetic field [2]:

$$Q = \int_0^t (H - H_0)\,dt, \tag{1}$$

$$\frac{\partial B}{\partial Q} = r_{\mathrm{m}}\left(1 - \frac{B^2}{B_s^2}\right), \tag{2}$$

$$B = B_s \,\mathrm{th}\left(\frac{r_{\mathrm{m}}}{B_s}Q - \varphi\right). \tag{3}$$

Here B_s is the saturation flux density; r_{m} and H_0 are experimentally determined parameters that characterize the dynamic magnetic properties of the core material; $\varphi = \mathrm{Arth}\,\frac{B_r}{B_s}$.

For the surface layers ($H = H_e$, $Q = Q_e$),

$$Q_e = \int_0^t (H_e - H_0)\,dt.$$

The graphs corresponding to Expressions (2) and (3) are plotted in Fig. 2, where the quantities B and Q_e are given in relative units. They describe the magnetic switching process $B = B_e(t)$ in the surface layers of the plate exactly. Analogous assumptions are also the basis of the computation performed in the widely known paper [3]; however, the authors of this paper made use of a coarser approximation of expression (2) in analyzing the surface effect: $\partial B/\partial Q = \mathrm{const}$*. Such an assumption can be justified for a strong surface effect (in cores with a ribbon thickness of the order of 100 microns).

The magnetic switching in the inner layers is related to the external magnetic field pulse in a more complex fashion. It is necessary to take into account the screening effect of the eddy currents. The eddy currents induced during the magnetic switching of the plate produce an additional pulse Q_{in} for the inner layers, and thus, $Q = Q_e + Q_{\mathrm{in}}$.

In order to take the eddy currents into account we make use of the integral form of the electrodynamics equations. Assuming that in a first approximation the value of the flux density B is constant over the cross section for the case of a weak surface effect, we proceed to solve the problem in the following approximation. From the first Maxwell equation we obtain the first approximation for the intensity of the induced electric field:

$$E = x\frac{\partial B}{\partial t}.$$

The induced field is directed along the z axis. It causes eddy currents whose density J (taking the displacement currents into account) is determined by the electrical properties of the material: the conductivity σ and the permittivity ε:

$$J = x\left(\sigma + \varepsilon\varepsilon_0 \frac{\partial}{\partial t}\right)\frac{\partial B}{\partial t}.$$

The magnetic field is computed from the total-current law, while taking the boundary conditions ($H = H_e$) at the surface of the plate into account:

$$H = H_e - \frac{1}{2}(b^2 - x^2)\left(\sigma + \varepsilon\varepsilon_0 \frac{\partial}{\partial t}\right)\frac{\partial B}{\partial t},$$

where b is one-half the thickness of the plate whose magnetic state is switched.

Thus, in a first approximation the magnetic switching pulse produced by the field depends on the depth of the layer in the plate. The magnitude of the pulse can be derived on the basis of (1) by integrating the expression above for H with respect to t:

$$Q_{\mathrm{in}} = -\frac{1}{2}(b^2 - x^2)\left(\sigma + \varepsilon\varepsilon_0 \frac{\partial}{\partial t}\right)(B + B_r). \quad (4)$$

The correction for the first approximation consists of a correction proportional to the conductivity of the ferromagnetic:

$$Q_\sigma = -\frac{1}{2}(b^2 - x^2)\,\sigma(B + B_r), \quad (5)$$

and a correction which depends on the permittivity. The latter component can be written in the following form if we take (2) into account:

$$Q_\varepsilon = -\frac{1}{2}(b^2 - x^2)\,\varepsilon\varepsilon_0 r_{\mathrm{m}}\left(1 - \frac{B^2}{B_s^2}\right)(H - H_0) \quad (6)$$

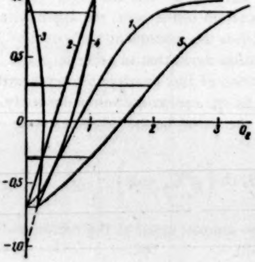

Fig. 2. Basic graphs:

$$1 - B_e = B_s\,\mathrm{th}\left(\frac{r_{\mathrm{m}}}{B_s}Q_e - \varphi\right),$$
$$2 - Q_\sigma = Q_\sigma(B),$$
$$3 - Q_\varepsilon = Q_\varepsilon(B),$$
$$4 - Q_{\mathrm{in}} = Q_\sigma + Q_\varepsilon,$$
$$5 - B = B_s\,\mathrm{th}\left\{\frac{r_{\mathrm{m}}}{B_s}(Q_e + Q_{\mathrm{in}}) - \varphi\right\}$$

---

* In terms of the notation used in [3], $\partial B/dQ \equiv f(B)$.

Thus, both corrections to the pulse are expressed as a function of the flux density B. Expression (5) in Fig. 2 corresponds to the straight line 2 whose angle with the flux density axis is proportional to the conductivity of the ferromagnetic, and increases as the layer under study is further removed from the surface of the plate. For the surface layer the angle which the straight line 2 makes with the B axis is equal to zero ($x^2 = b^2$). For the axial layer of the plate it is a maximum ($x^2 = 0$).

The graph of the function (6) is a quadratic parabola (Curve 3 in Fig. 2) which intersects the axis of ordinates at the points ±1. The maximum value of this correction increases with the intensity of the magnetic switching field. An interesting feature of this correction is its rapid tendency toward zero at the beginning and end of the magnetic switching process. This explains the fact that the effect of the permittivity on the time required for completing the magnetic switching process is weakened.

The simplicity of expressions (5) and (6) permits easy plotting of the corresponding graphs for the chosen value of x. By the same token it is easy to plot the graph of the total correction (4) for a definite value of x (Curve 4 in Fig. 2).

An important problem is the appropriate choice of the values of flux density in Formulas (4), (5), and (6). The simplest approach is to choose this value equal to the magnitude of the surface flux density $B = B_e$.

Since the magnitude of the flux density actually decreases with the depth of the layer, such a computation in a first approximation yields values of flux density that are too low. The computation will be somewhat more exact if we choose a value of flux density equal to the flux density in the axial layer for use in Formulas (4), (5), and (6). Here the result obtained in the first approximation will yield values of flux density that are too high for the individual layers.

We chose a somewhat improved form of the approximation :

$$B = B_s \operatorname{th}\left\{\frac{r_m}{B_s}[Q_e + Q_{in}(B)] - \varphi\right\},$$

which also resulted in values that were too high. In addition to achieving a certain refinement, the approximation form above simplifies the subsequent analysis substantially. The expression shows that in order to plot the graph for the variation of flux density in a layer with a specified value of x in the approximation under study, it is sufficient to shift the points on the original curve:

$$B_e = B_s \operatorname{th}\left(\frac{r_m}{B_s} Q_e - \varphi\right)$$

along the Q_e axis by an amount equal to the corresponding value of Q_{in} (Fig. 2).

The error of the approximation can easily be estimated. It does not exceed the value $50\left(\frac{B_e - B}{B_e - B_r}\right)^2$ %, where the values of the flux densities B and B_e are taken for one value of time (Fig. 2).

Figure 3 shows the corresponding computation for the case of surface effect in a thin Permalloy sheet of the type "79-NM" which was 5 μ thick. [See Appendix for "79-NM" characteristics.] In that case the surface effect is sufficiently weak, and the approximation under study assures an accuracy of approximately 10%.

The analysis of the surface effect is simplified for the case of metal ferromagnetics in which the displacement currents can be neglected, compared to the conductivity currents, right up to frequencies in the optical spectrum [4]. In that case the correction of the pulse is determined basically by the linear component of (5). This case also includes the example of a Permalloy plate cited above. The magnetic switching curves for different layers in a metallic ferromagnetic (as obtained in the approximation under study) have an interesting property. The tangents to these curves always intersect at one point lying on the straight line $B = -B_r$ (Fig. 3) when they are drawn to points with an arbitrary fixed value of flux density. A definite point corresponds to each value of flux density $B(-B_r \leq B \leq B_s)$. This property makes it possible to compute the magnetic switching rate $\partial B_x / \partial Q_e$ for a layer with the coordinate x in terms of the known function of the magnetic switching rate in the surface layer $\partial B_e / \partial Q_e$.

For a flux density B_x in the layer x,

$$\frac{\partial B_x}{\partial Q_e} = \frac{\partial B_e}{\partial Q_e}\left(1 + \frac{\partial B_e}{\partial Q_e}\frac{b^2 - x^2}{3}\sigma\right)^{-1}, \qquad (7)$$

where the quantity $\partial B_e / \partial Q_e$ is determined by substituting $B_e = B_x$ into expression (2).

In order to compare the computations above with experimental data, it is necessary to make the transition

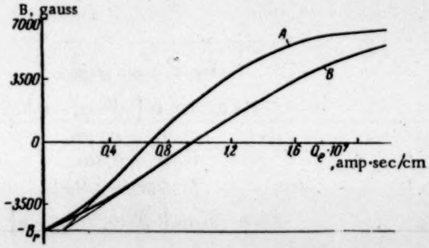

Fig. 3. Surface effect in a Permalloy ribbon. A) Magnetic switching of the surface layer; B) magnetic switching of the central layer.

to the experimentally observed average values of flux density, since the emf in the metering winding is proportional to the rate of change of the average flux density. In the approximation under study we have

$$\max\left(\frac{\partial B_{\mathrm{av}}}{\partial Q_e}\right) = \frac{r_{\mathrm{m}}}{1 + r_{\mathrm{m}}\sigma\frac{b^2}{3}}, \qquad (8)$$

with an accuracy of no less than 12.5 $(r_{\mathrm{m}}\sigma b^2)^2$%; i. e., the maximum rate of change of the average flux density is

$$\max\left(\frac{\partial B_{\mathrm{av}}}{\partial t}\right) = \frac{r_{\mathrm{m}}}{1 + r_{\mathrm{m}}\sigma\frac{b^2}{3}}(H_e - H_0). \qquad (8a)$$

The maximum value of the magnetic switching rate is achieved for an average core flux density

$$B_{\mathrm{av.m}} = -\frac{r_{\mathrm{m}}\sigma b^2 B_r}{3}\,\frac{1}{1 + r_{\mathrm{m}}\sigma\frac{b^2}{3}}. \qquad (9)$$

The approximate expressions (8) and (9) can be used for the independent determination of the parameter r_{m} from the experimental data for $(\partial B_{\mathrm{av}}/\partial Q_e)$ or $B_{\mathrm{av.\,m}}$ that are obtained when a plate made of a known metallic magnetic material is subjected to magnetic switching.

In order to check expressions (8) and (9) we make use of the results obtained from an investigation of ribbon cores made of Permalloy "79-NM" ribbon 10 and 20 μ thick [1]. The surface effect in such cores is quite pronounced. Nevertheless, as we shall demonstrate below, Formulas (8) and (9) are in good agreement with experimental results. We shall write the known characteristics for "79-NM" Permalloy:

B_s = 7000 gauss; B_r = 4900 gauss; $\sigma = 1.8 \cdot 10^4$ 1/ohm · cm.

In order to select the value of r_{m} we shall make use of the results obtained by V. L. Dyatlov, who performed an exact numerical integration for the problem. In [1] the value r_{m} = 950 ohm/cm was obtained. The results of the experiments and computations are cited in the table.

In conclusion we shall estimate the most important characteristic of ribbon cores — the duration of the magnetic switching — in the approximation used above. When there is no surface effect, this duration is determined completely by the magnetoviscous properties of the core. The theoretical duration of the magnetic switching given by expression (3) is infinite. Therefore, in practice, we use the concept of the duration required to reach a steady state at some level. We often choose the average value of the flux density over the cross section $B_{\mathrm{av}} = B_r$ as this level. The time t_r required for the magnetic switching process to reach this level is assumed to be the duration of the process. Expression (3) permits easy determination of the field pulse Q_r corresponding to this time (on the assumption that there is no surface effect):

$$Q_r = 2\frac{B_s\varphi}{r_{\mathrm{m}}}.$$

When the surface effect is present, the magnetic switching process in the core terminates at the level $B_{\mathrm{av}} = B_r$ for a field pulse which is increased by the amount $-Q_{\mathrm{in}}(B_r)$:

$$Q_{\mathrm{in}} \approx -\frac{2}{3}b^2\sigma B_r.$$

Thus, the relative increase in the pulse required for reaching completion of the magnetic switching at the specified level is

$$\frac{|Q_{\mathrm{in}}|}{Q_r} \approx \frac{b^2}{3}\,\frac{B_r}{B_s}\,\frac{r_{\mathrm{m}}\sigma}{\varphi}. \qquad (10)$$

Expression (10) determines the relative increase in the switching coefficient for the core. For magnetic switching of a core by means of rectangular current pulses (here it is possible to assume that $H_e - H_0 \approx$ const), relationship (10) also determines the relative prolongation Δt_r of the pulse. In that case,

Compared quantity	Ribbon core with thickness 2b			
	2b=10 μ		2b=20 μ	
	computed	experiment	computed	experiment
$\max\left(\frac{\partial B_{\mathrm{av}}}{\partial Q_e}\right)$, ohm/cm	400	500	140	280
$B_{\mathrm{av.m}}$, gauss	−2860	−2000	−4200	−3500

$$\frac{\Delta t_r}{t_r} \approx \frac{b^2}{3} \frac{B_r}{B_s} \frac{r_m \sigma}{\varphi}. \tag{11}$$

Expression (11) shows that the relative prolongation of the switching time due to eddy currents is in a first approximation independent of the magnetic switching rate and directly proportional to the square of the plate thickness.

For the case of ribbon cores with the parameters cited above, computation according to Formula (11) leads to the following values for the relative prolongation of the magnetic switching time: 28% for a thickness of 5 μ; 110% for a thickness of 10 μ.

These results can be used in designing magnetic elements for computer-decision units.

Expression (11) permits us to compute the allowable thickness of ribbon cores which assure the maximum rate of recording and readout of information.

The recommended plotting of the graph for the dependence of the average magnetic flux density in the core on the magnetic switching pulse can be made the basis of the electrical design for pulse networks with ribbon cores (for example, magnetic registers).

APPENDIX

We shall prove certain propositions cited in the paper.

1. We shall derive Formula (7). Assume that the curve $B_e = B_e(Q_e)$ is given. We shall study a new curve $B = B(Q_e)$ which is obtained from the first curve by shifting its points along the axis Q_e by the amount $f = f(B)$. Here $f(B)$ is a specified function of B. The curve $B(Q_e)$ is obtained by replacing the argument Q_e by the argument $Q = Q_e - f(B)$ in the curve $B_e(Q_e)$:

$$B(Q_e) = B_e[Q_e - f(B)].$$

Differentiating this equation, we obtain

$$\frac{\partial B(Q_e)}{\partial Q_e} = \frac{\partial B_e[Q_e - f(B)]}{\partial[Q_e - f(B)]} \frac{\partial[Q_e - f(B)]}{\partial Q_e}.$$

Thus,

$$\frac{\partial B}{\partial Q_e} = \left[1 - \frac{\partial f(B)}{\partial B} \frac{\partial B}{\partial Q_e}\right] \frac{\partial B_e}{\partial Q_e}\bigg|_{Q_e - f(B)}.$$

From the equation above we obtain

$$\frac{\partial B}{\partial Q_e} = \frac{\partial B_e}{\partial Q_e} \left[1 + \frac{\partial f(B)}{\partial B} \frac{\partial B_e}{\partial Q_e}\right]^{-1},$$

where the derivatives are taken for the identical fixed value $B = B_e$. The substitution $f(B) = -Q_\sigma \equiv \frac{b^2 - x^2}{2} \times$ $\times\, \sigma(B + B_r)$ leads to (7).

2. We shall show that for a weak surface effect the the flux density, averaged over the cross section of the core, is approximately equal to the flux density in a certain layer—the layer located at a distance $x = b/\sqrt{3}$ from the axis. In a linear approximation,

$$B(Q_2) = B(Q_1) + (Q_2 - Q_1)\frac{\partial B}{\partial Q},$$

where Q_1 and Q_2 are the values of the external field pulse at any instants which are sufficiently close together. Assuming $Q_1 = Q_e - Q_{in}$ and $Q_2 = Q_e$, we arrive at a convenient expression which relates the values of the flux density in the surface layer and in the layer corresponding to the specified value of the eddy current field pulse:

$$B(Q_e) = B(Q_e - Q_{in}) + Q_{in}\frac{\partial B_e}{\partial Q_e} = B_e(Q_e) + Q_{in}\frac{\partial B_e}{\partial Q_e}. \tag{12}$$

Equation (12) can easily be averaged if we keep in mind the face that only the term Q_{in}, which is proportional to $(b^2 - x^2)/2$ according to (4), is dependent on x:

$$B_{av}(Q_e) = \frac{1}{b}\int_0^B \left[B_e(Q_e) + Q_{in}\frac{\partial B_e}{\partial Q_e}\right]dx = \\ = B_e(Q_e) - \frac{b^2}{3}\left(\sigma + \varepsilon\varepsilon_0\frac{\partial}{\partial t}\right)(B_e + B_r). \tag{13}$$

Expression (13) is equal to (12) for $Q_{in} = Q_{in}(x)$ when $x = b/\sqrt{3}$; this is what we set out to prove.

Assuming $B_e = 0$ and $Q_{in} = Q_\sigma$ in (13), we arrive at the approximate expression (9).

TRANSLATOR'S APPENDIX

The characteristics of the permalloy "79-NM" are the following: thickness 0.01 mm; initial permeability μ_0 (in gauss/oe) not less than 15,000; maximum permeability μ_{max} (in gauss/oe) not less than 65,000; coercive force H_c (in oe) 0.07; saturation flux density B_s (in gauss) not less than 7,500. (See also "Characteristics of Magneto Materials for Use in Magnetic Amplifiers Operating at Audio-frequencies," Automation and Remote Control, Vol. 18, No. 10, pp. 927-933.)

LITERATURE CITED

1. V. L. Dyatlov, "Consideration of the eddy currents and viscosity for magnetic switching of ribbon cores in large fields," Nauchnye Doklady Vysshei Shkoly, Élektromekhanika i Avtomatika No. 2 (1959).
2. Yu. M. Shamaev, V. L. Dyatlov and A. I. Pirogov, "Dynamic characteristics of ferrites," Nauchnye Doklady Vysshei Shkoly, Élektromekhanika i Avtomatika No. 1 (1959).
3. T. C. Chen and A. Papoulis, "Terminal properties of magnetic cores," Proc. IRE 46, I No. 5 (1958).
4. L. Landau and E. Lifshits, Electrodynamics of Solid Media [in Russian] (Gostekhizdat, 1957).

SELECTION OF THE MOST SUITABLE CIRCUIT FOR A PHOTOELECTRIC FLUXMETER

I. G. Gutovskii

Moscow

Translated from Avtomatika i Telemekhanika, Vol. 21, No. 10,
pp. 1401-1409, October, 1960
Original article submitted March 10, 1960

This article presents the theory of photoelectric fluxmeters (PEF), i.e., amplifiers with photoelectric optical amplification. Various types of PEF with and without feedback are compared. It is shown that the greatest accuracy of integration and the greatest speed can be achieved with a PEF circuit with negative feedback with respect to the derivative with the smallest time constants in the open circuit. The proposed theory makes it possible to determine the integration accuracy in dependence on the signal shape directly with respect to the curves recorded at the output.

At the present time, the so-called photoelectric optical amplifiers (PEOA)* [1] are being used to an ever increasing extent as dc amplifiers in various measuring and automation circuits.

The principle of photoelectrical optical amplification consists in using the galvanometer of the magnetoelectric system at the input and in converting the displacement of the galvanometer light spot into voltage by means of an optical system and a photocell bridge [2].

The extremely low input noise level ($\sim10^{-9}-10^{-10}$ v) and the large amplification factor (up to 10^8 for voltage) make it possible to use PEOA in devices where ordinary electronic amplifiers cannot be utilized.

A particular example of such a device is the photoelectric fluxmeter (PEF) [3]–an integrating amplifier based on PEOA–for measuring magnetic fluxes or electric charges. The considerably greater sensitivity and accuracy, as well as a longer allowable measurement time in comparison with ordinary fluxmeters, render the PEF a valuable instrument in scientific-research work and automation.

The face that different PEF circuits are recommended in literature (see survey [3]) and a lack of comparative evaluations of their efficiency create a pressing problem, which is to be solved by theoretical analysis of the existing variants for the purpose of selecting the variant most suitable for practical application.

The PEF theory presented in this article is a development of the method described in [4], which is based on operational calculus [5].

PEF Circuits and Their Relation to Integrating Amplifier Circuits

The block diagrams of PEF are identical with the basic integrating amplifier circuits [6], which have been developed independently and mainly before the PEF circuits†.

Figure 1 shows an integrator circuit with a negative series feedback with respect to the derivative. This integrator pertains to the overwhelming majority of the PEF circuits described in literature. The wiring diagram of such PEF is given in Fig. 2 and has been described in [3] and [7]. The time constants of the amplification circuit (without taking into account the feedback) of this PEF variant are rather small [8], and, in the first approximation, this circuit can be considered as an ideal amplifier

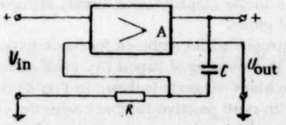

Fig. 1. Circuit of the RC-integrator with a negative series feedback.

---

* There are now greater opportunities for the application of PEOA, since the industry has started the mass production of amplifiers of this kind (F17 and F117).

† The actual differentiating circuit in the feedback loop is of no importance. For the sake of clarity, we shall use an RC circuit throughout.

The R_kC_k circuit mainly serves for ensuring stability.

The "+" and "–" signs in Figs. 1–5 conventionally indicate the presence or absence of a 180 deg phase shift of the output voltage with respect to the input voltage in the amplification circuit of the open-loop system.

with a constant amplification factor [9]. In [3] and [4], PEF of this type were called PEF of the first group.

The prototype of a PEF without feedback, which has been proposed by S. P. Kapitsa [10], has an integrating amplifier (Fig. 3). This device uses the principle of integration by means of a RC_k circuit with a decoupling amplifier A, where the usual resistance is replaced by a higher–the dynamic resistance R of the amplifier A_1 output tube. The introduction of a dynamic resistance increases the time constant $T_0 = RC_k$ of the integrating circuit and brings the operating conditions of the circuit section, which is the input section with respect to the C_k capacitor, closer to the operating conditions of the current generator. In Kapitsa's PEF, PEOA plays the role of the A_1 amplifier, and the dynamic resistance of vacuum photocells ($\rho \approx 10^9$ ohm, $T_0 \approx \rho C_k \approx 1000$ sec) plays the role of the tube dynamic resistance.

The application of negative feedback with respect to the derivative in Kapitsa's model leads to a circuit which is identical to circuits of PEF of the first group (Fig. 2), but is characterized by a larger capacitance C_k (almost by three orders of magnitude).

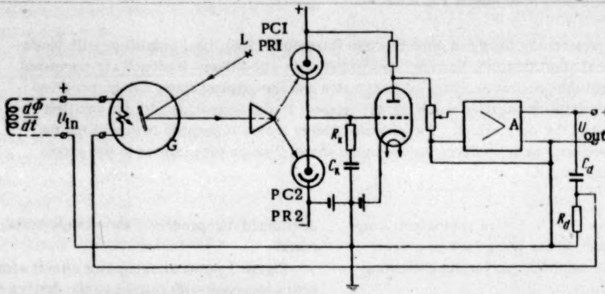

Fig. 2. PEF wiring diagram which is similar to that in Fig. 1. G) Galvanometer; L) illuminator which projects the light spot image on the photocells (PC) or the photoresistors (PR); A) electronic power amplifier; Φ) magnetic flux to be measured.

The integrating regime in the amplification circuit can also be secured by other means [11]. According to [3] and [4], we shall designate PEF with feedback and integration in the amplification circuit as fluxmeters of the second group.

PEF circuits with combined feedback have been described in a number of papers [3]. The circuit in Fig. 2 (the block diagram is shown in Fig. 1) is supplemented with rigid positive feedback with the coefficient $A_0 = r_2/(r_1 + r_2)$ (Fig. 4).

The most widely used circuit for analog computer integrators is the circuit with parallel feedback (Fig. 5). By using Kirchhoff's laws, it can be readily shown that, in contrast to the circuit in Fig. 1, the feedback of Fig. 5 does not reduce the input load current. Since this current lowers the magnetic measurement accuracy, the circuit given in Fig. 5 is not used in PEF designs.

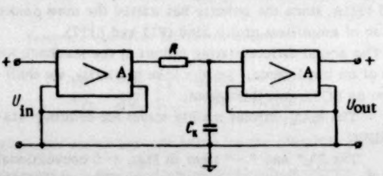

Fig. 3. Circuit of a RC-integrator using the dynamic resistance R of the amplifier A_1 output stage.

The circuit shown in Fig. 2, supplemented with positive feedback in the general case (Fig. 4), will be used as the basis hereafter. All particular circuit variants can be obtained by eliminating some of the circuit elements‡ or by changing the numerical value of individual parameters.

Basic Approximations of the PEF Theory

In the proposed PEF theory, it is assumed that all directional elements, as well as amplitude distortions and loads, are absent. In particular, it is assumed that the

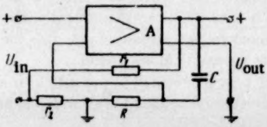

Fig. 4. Wiring diagram of a RC-integrator with combined feedback.

---

‡ Thus, for instance, Kapitsa's circuit without feedback is obtained by eliminating the feedback circuit.

connection of a measuring coil and an output instrument does not affect the PEF operation.

The conditions which the parameters of the loads to be connected must satisfy if the presented theory is to remain valid, as well as the justification of the other assumptions, will have to be treated in a separate paper.

Notation and the Basic Equations

The practical system of units is used throughout.

The electromotive force U_{in} induced in the measuring circuit or any voltage supplied to the instrument input is taken as the PEF input. The output voltage U of the amplifier A is at the same time the PEF output; f is the difference of light fluxes incident on the photocells of the photocell bridge; v is the bridge diagonal voltage; v_r is the feedback voltage; v_d is the same voltage without feedback and without taking into account the capacitor C_d leakage; t and θ are time; s is the differentiation operator.

The operator conductances (transfer functions) of the elements are given below.

1. Mirror galvanometer with an optical lever (see [11] and [12]). If we take into account the inductance of the measuring circuit,

$$W_g(s) = \frac{NS_u}{(\tau_0 s + 1)(Hs^2 + Gs + 1)}, \qquad f = W_g U_{in} \quad (1)$$

In practice, the τ_0, H, and G parameters are close to the measuring circuit time constant ($\tau_0 \approx L/R$, where L is the inductance, and R is the resistance), to $1/\omega_0^2$, and to $2\beta/\omega_0$ (ω_0 is the galvanometer natural frequency, and β is the damping coefficient), respectively. Moreover, in Eq. (1), N is the optical system conversion factor in lumens per radian; S_u is the galvanometer sensitivity in radians per volt for the chosen operating conditions.

As a rule, the galvanometer is overdamped**, and the measuring circuit inductance is neglected. Then

$$W_g(s) = \frac{NS_u}{(\tau_1 s + 1)(\tau_2 s + 1)}, \qquad (1a)$$

$$\tau_1\tau_2 = H, \qquad \tau_1 + \tau_2 = G, \qquad \tau_1 > \tau_2.$$

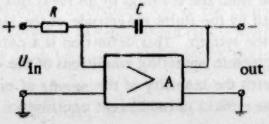

Fig. 5. Wiring diagram of a RC-integrator with parallel negative feedback.

2. Photocell bridge (vacuum photocells FE or photoresistors FS [7]). A stabilizing (correcting) R_kC_k circuit is connected to the bridge circuit:

$$W_m(s) = \alpha\rho\frac{\tau_4 s + 1}{\tau_3 s + 1}, \qquad v = W_m f. \qquad (2)$$

Here, α is the FE sensitivity (amp/lu), ρ is their dynamic resistance,

$$\tau_3 = \tau_4 + \tau_5, \qquad \tau_4 = R_k C_k, \qquad \tau_5 = \rho C_k.$$

3. Direct current amplifier (the amplifier inertness is neglected):

$$W_a = k = \text{const}, \quad U = W_a v. \qquad (3)$$

4. Differentiating element (without leakage and without taking into account the load [13]):

$$W_d(s) = \frac{\tau_d s}{\tau_d s + 1}, \qquad v_d = W_d U, \qquad (4)$$

where $\tau_d = R_d C_d$, R_d is the circuit resistance, and C_d is its capacitance.

5. The feedback operator (Fig. 4):

$$W_r(s) = W_d + \frac{R_d}{R_{du}} - A_0 = W_d - A, \qquad (5)$$

where R_{du} is the resistance of the C_d capacitor leakage, and $A_0 = r_2/(r_1 + r_2)$ is the positive feedback coefficient. Equation (5) follows from Fig. 4.

The open-circuit operator (without feedback) is obtained from (1a), (2), and (3):

$$W_0(s) = W_g W_m W_a = K_0 w_0(s), \qquad U = W_0 U_{in} \quad (6)$$

Here,

$$K_0 = S_u N\alpha\rho k = \text{const},$$

$$w_0(s) = \frac{\tau_4 s + 1}{(\tau_1 s + 1)(\tau_2 s + 1)(\tau_3 s + 1)}. \qquad (7)$$

We shall introduce the PEF constants C_{φ_0} and C_φ so that, with an accuracy to the basic errors, $\int_0 U_{in}\, d\theta = C_{\varphi_0} U$ for PEF without feedback (including PEF of the first group with an open circuit, for which the integration error exceeds $C_{\varphi_0}U$); also $\int_0^t U_{in}\, d\theta = C_\varphi U$ when feedback is present.

** This is mainly connected with the requirement for greater vibration stability of the instrument during zero adjustment (with the C_d capacitor short-circuited).

We shall also introduce the creep time constants†† T and T_r for PEF with feedback and T_0 for PEF without feedback. It will become clear later on that

$$T = K_0 C_\varphi, \qquad C_\varphi = \tau_d + C_{\varphi_0}. \tag{8}$$

$$T_r = \frac{T}{1 - AK_0}, \tag{9}$$

$$T_0 = \tau_3 + \tau_2, \tag{10}$$

$$C_{\varphi_0} = \frac{T_0}{K_0}. \tag{11}$$

By T_e, we shall denote the time interval during which integration is performed.

PEF Theory

A. PEF without Feedback

In this case, $U = W_0 U_{in}$. On the basis of (6) and (7),

$$W_0(s) = \frac{K_0}{\tau_3 s + 1} \frac{\tau_4 s + 1}{\tau_1 s + 1} \frac{1}{\tau_2 s + 1}. \tag{12}$$

If the galvanometer is overdamped, it can be considered that $\tau_2 = 0$ in the first approximation. The circuit parameters R_k and C_k can be so chosen that [10]

$$\tau_4 = \tau_1. \tag{13}$$

The first factor, to which the expression for $W_0(s)$ is now reduced, coincides with the operator of the integrating RC_k circuit with an amplifier (cf. Fig. 3; in the given case, $R = \rho + R_k$):

$$W_0(s) = \frac{K_0}{\tau_3 s + 1}. \tag{14}$$

Hence [6],

$$U = \frac{K_0}{\tau_3} \int_0^t U_{in}\, d\theta \tag{15}$$

with the error in percentages [6]

$$p = 50 \frac{T_e}{\tau_3}. \tag{16}$$

Here, τ_3 is the creep time constant.

For a more complete theory, we shall seek the relation between the observed output voltage U and the voltage U_{id} of an ideal integrator of the same sensitivity as that of the actual one under consideration. For this purpose, we shall multiply every term of the identity

$$\frac{K_0}{T_0 s} \frac{1}{W_0} \equiv \frac{1}{T_0 s} + \frac{1}{T_0 s}\left(\frac{1}{w_0} - 1\right) \tag{17}$$

by U after the preliminary transformations‡‡

$$\frac{1}{s}\left(\frac{1}{w_0} - 1\right) U = (\tau_3 + \tau_2) U +$$
$$+ \left[\frac{B_1 U'' + B_2 U' + B_3 U}{\tau_4 s + 1} + B_4 U'\right] = T_0 U + P$$

or

$$\frac{1}{s}\left(\frac{1}{w_0} - 1\right) U \approx (\tau_3 + \tau_2) U + [B_1 U'' + (B_2 + B_4) U' +$$
$$+ \tau_1 U] = T_0 U + P. \tag{18}$$

Here, P is the portion of expression (18) in square brackets,

$$B_1 = \tau_2 \tau_3 (\tau_1 - \tau_4), \qquad B_2 = (\tau_2 + \tau_3)(\tau_1 - \tau_4),$$
$$B_3 = \tau_1 - \tau_4, \; B_4 = \tau_2 \tau_3.$$

As a result, we shall find that the ideal integrator output voltage is

$$U_{id} = \frac{K_0}{T_0} \int_0^t U_{in}\, d\theta = U + \frac{\int_0^t U\, d\theta}{T_0} + \frac{P}{T_0}. \tag{19}$$

The second term in (19) is the creep, and the third term represents the error which is due to the fact that the second and the third factor in (12) differ from unity ("structural" error).

B. PEF with Series Feedback

A circuit with combined feedback represents the most general case. By substituting operators for figures in the well-known expression for the amplification factor of an amplifier with feedback, we obtain

$$W(s) = \frac{W_0}{1 + W_0 W_r}, \qquad U = W U_{in}. \tag{20}$$

---

†† Creep is the instrument reading deviation at any instant of time from the readings of an ideal integrator; it is determined by the finite magnitude of the largest time constant in the system. This definition is a natural extension to dynamic operating conditions of the concept connected with the inability of the needle of ordinary fluxmeters to remain in indifferent equilibrium if no input voltage is present.

‡‡ Transformation after the ≈ sign is valid only if $\tau_4 << 1$. For the evaluation of the error due to the $\tau_4 s + 1 \approx 1$ substitution, see [4].

By using the identity

$$\frac{1}{\tau_d s}\frac{1}{W} \equiv$$

$$\equiv 1 + \frac{1}{s}\left[\frac{1}{K_0\tau_d} + \left(\frac{1}{W_0\tau_d} - \frac{1}{K_0\tau_d}\right) + \left(\frac{W_r}{\tau_d} - s\right)\right], \tag{21}$$

we obtain, in a manner similar to that used in deriving (19) after a number of transformations [including (18)],

$$U_{\text{id}} = \frac{1}{C_\varphi}\int_0^t U_{\text{in}}\, d\theta = U + Er_1 + Er_2 + Er_3, \tag{22}$$

where

$$Er_1 = \frac{\int_0^t U d\theta}{T_r} \tag{23}$$

is the creep, and

$$Er_2 = \frac{P}{T} \tag{24}$$

is the error due to the difference between the amplification circuit and the ideal circuit (when $w_0 \equiv 1$); this error will be called the "structural" error. The quantity

$$Er_3 = \frac{\tau_d}{\tau_d + C_{\varphi_0}}\int_0^t \left(\frac{W_d}{\tau_d} U - U'\right) d\theta \approx -\tau_d U' \tag{25}$$

is the error caused by the differentiation error in the feedback circuit; this will be called the "differential" error.

C. Effect of Disturbances and Distortions

Let a disturbance, equivalent to the U_b voltage, arise at the output of the element (circuit with feedback) whose output signal U_1 is related to the input signal by the equation

$$U_1 = W_1(s)\, U_{\text{in}}.$$

By finding the equation relating U_b and U (for $U_{\text{in}} = 0$), we obtain the instrument output error

$$Er_b = U = \frac{W_2}{1 + W_0 W_r} U_b, \qquad W_1 W_2 = W_0. \tag{26}$$

The transformation

$$\frac{W_2}{1 + W_0 W_r} \equiv \frac{W_0}{1 + W_0 W_r}\frac{1}{W_1}$$

reduces the theory of disturbances to the utilization of the results obtained in Subsection B [if $(1/W_1)U_b$ is substituted for U_{in}], i.e., to a variant of Eq. (22):

$$\frac{1}{C_\varphi}\int_0^1 \left(\frac{1}{W_1} U_b\right) d\theta = Er_b + \Sigma Er, \tag{27}$$

where analogs (23)-(25) enter Σ Er after substituting Er_b for U.

Due to the possibility of zero setting between individual measurements and the limitation of the output instrument transmission band, the frequency spectra for the disturbances to be registered and for the useful signals are comparable***. Hence, $\Sigma Er \ll Er_b$ [since $\Sigma Er \ll U$ in (22)], and the term Σ Er in (27) can subsequently be neglected.

By applying transformations similar to (17) and (18) to the left-hand side of Eq. (27), we can readily obtain a sufficiently accurate expression for Er_b in developed form. In particular, for $W_1 = W_0$, it follows from (19), after substitution of U_b for U, that

$$Er_b = \frac{T_n}{T} U_b + \frac{\int_0^t U_b d\theta}{T} + \frac{P(U_b)}{T}. \tag{28}$$

The last two terms differ from (23) and (24) only by the fact that U_b was substituted for U, and, therefore, they are small simultaneously with (23) and (24) if only $U_b \le U$. For $T_e > 1$ sec, the first term is smaller than the other terms for PEF of the first group and is considerably larger for PEF of the second group. Thus, approximately,

$$\frac{\tau_3}{T} U_b < Er_b < \frac{T_e}{T} U_{b\max} \tag{29a}$$

for PEF of the first group, and

$$Er \approx \frac{\tau_3}{T} U_b \tag{29b}$$

for PEF of the second group. The right-hand side of (29a) was obtained from (28) by replacing the integral by its maximum value for $U_b = U_{b\max} = \text{const}$ and $t = T_e$, under the assumption that the basic errors are of the same order of magnitude.

Equation (27), including its variants (28), (29a), and (29b), should be considered as the initial equation for determining the parameters characterizing the quality of individual elements and of the entire instrument: the optimum sensitivity, the maximum allowable line current and the amplifier drift, the required feed stability, etc.

The amplitude distortions of the open circuit are formally equivalent to disturbances, and their effect can be taken into account by using the derived equations.

The above concerns only circuits with feedback. In circuits without feedback, the disturbance level is not lowered, which constitutes their main efficiency.

Operational Stability of PEF

The Mikhailov stability criteria [13] were found for the most general case of a circuit with combined feed-

---

*** The operation of zero setting unavoidably cuts the output signal frequency spectrum from below without discrimination between the useful signal and the disturbance; the same holds for the output instrument (for instance, a self-recorder), which can be considered as a barrier filter in the high-frequency region.

Polynomial roots (ω_2 and ω_4 are roots of the real, and ω_1, ω_3, and ω_5 are roots of the imaginary part of the characteristic equation)	Approximate expressions for the roots	General stability criteria	Stability criteria for PEF with a galvanometer under aperiodic conditions
ω_1^2	0		
ω_2^2	$\frac{1}{T_r\tau_4}$		
ω_3^2	$\frac{T}{H(\tau_3+\tau_0+\tau_d)}$	$\frac{T}{H(\tau_3+\tau_0+\tau_d)} > \frac{1}{T_r\tau_4}$	
ω_4^2	$\frac{T\tau_4+G\tau_3}{\tau_3(\tau_0+\tau_d)H}$	$\tau_4 > \frac{\tau_d+\tau_0}{1+\frac{\tau_0+\tau_d}{\tau_3}}$	$\tau_4 > \tau_d+\tau_0$
ω_5^2	$\frac{\tau_3+\tau_0+\tau_d}{\tau_3\tau_0\tau_d}$	$T < \frac{H\tau_3\frac{\tau_0+\tau_d}{\tau_4}\left(1+\frac{\tau_0}{\tau_3}\right)}{\tau_0\tau_d}$	
		$T < \frac{H\tau_3\left(1+\frac{\tau_0}{\tau_3}\right)^2}{4\tau_0\tau_d}$	$T < \frac{\tau_1\tau_2\tau_3}{4\tau_0\tau_d}$

back. The galvanometer operator was taken in the form given by (1). A variant of the Mikhailov criterion, according to which the conditions for the sequence of roots of the real and imaginary parts are found from the equation $1 + W_0(i\omega)W_r(i\omega) = 0$ (ω is the angular frequency of signal harmonics), was used. The problem is solved exactly, since it is reduced to the solution of two quadratic equations. It is sufficient to use the approximate solution (see table).

The basic stability criteria follow from the requirement that the roots be real:

$$T < \frac{\tau_3\left(1+\frac{\tau_0}{\tau_3}\right)^2}{4\tau_0\tau_d\omega_0^2}, \qquad (30)\dagger\dagger\dagger$$

and from their sequence conditions:

$$\tau_4 > \tau_d + \tau_0. \qquad (31)$$

The other conditions (not shown completely in the table) cannot be disturbed, and they do not have to be considered separately.

It follows from (30) and (31) that the measuring circuit inductance, the galvanometer natural frequency, the feedback circuit constant τ_d, and the value of T(K$_0$, accordingly restrict each other. It is also obvious that the τ_3 and τ_4 constants cannot be reduced below the determined level (30)-(31).

It should be noted that stability can be secured also if the galvanometer operates under periodic conditions and in the presence of positive feedback.

In contrast to the method used in [7], the system behavior can be determined with respect to the equations derived for the general case, and, thus, the stability margin can be determined beforehand [13].

Discussion of the Results

A. Creep and the Role of Rigid Feedback

The determination and nature of creep follow from expressions (19), (22), and (23). Assuming that the structural and differential errors are equal to zero (this is equivalent to W_0=const and $W_d = \tau_d s$), we find that creep characterizes those properties of the instrument which permit the simulation of PEF by an integrating circuit of the RC type, which is described by an equation of the type (14). The creep is caused by incomplete compensation of the input signal by the feedback signal with re-

---

††† It was indicated in [7] that the stability of PEF does not depend on the restoring moment W_m of the galvanometer tension wires. This is due to the fact that T, as well as $1/\omega_0^2$, are proportional to $1/W_m$.

spect to the derivative or its formal analog (in PEF without feedback). If additional rigid feedback is present, the input quantity compensation can be increased by using the feedback signal portion which is proportional to dU/dt. Thus, it follows from Eq. (9) that this occurs for $A > 0$ and $/ \to 1/K_0$. In this case, creep will be at the minimum. This compensation can also be reduced, which takes place for $A < 0$, for instance, due to R_{du} leakage. In this case, according to (5), creep becomes larger.

Thus, the reduction of leakage through R_{du} and the introduction of a rigid positive feedback are effective means for reducing creep.

The necessary condition for applying the other method is a sufficient smallness of amplitude distortions in the open-loop system‡‡‡. In the opposite case, due to the instability of K_0 in (9), the $0 < 1 - AK_0 = \text{const} << 1$ relation cannot be maintained throughout the entire measurement cycle.

B. Justification of Securing Integrating Conditions in the Amplification Circuit (in Circuits with Feedback)

The reduction of creep in the open circuit (in the amplification circuit), i.e., the operation of this circuit under integrating conditions (as recommended in [10] and [11]), is not justifiable.

In the first place, the expedients whereby T is augmented due to an increase in T_0 are of little effectiveness when they are not accompanied by an increase in K_0[1], since they are reduced only to an increase in $K_0\tau_d$, which is considerably smaller than T_0. This is clear from an analysis of Eqs. (8) and (11) if we take into account that the use of feedback is justified only if $C_{\varphi_0} < C_\varphi$.

Considering the effect of integration conditions in the amplification circuit on the structural error (24), we can readily see by taking into account (18) that such a regime tends to increase the error determined by the rate of change in the magnetic flux to be measured, i.e., the allowable speed of operation of PEF is reduced for a certain given accuracy (due to the increase in τ_3). At the same time, this regime sharply reduces the efficiency of feedback with respect to noise suppression [see (29a) and (29b)].

The (24) and (29a) errors are the smallest for $w_0(s) \equiv 1$. In practice, this is realized (approximately) in PEF of the first group if we provide elements with the smallest time constants in the amplification circuit, or if we correct the amplification circuit with respect to an ideal amplifier with $W_0 = \text{const}$. In this, the restrictions imposed by stability conditions must be taken into account.

C. Role of the PEF Theory in Design Calculations and in Developing Methods for Estimating the Measurement Accuracy

The given PEF theory relates in the most direct way the basic instrument errors, which are expressed in terms of the output quantity, to its parameters, eliminating the necessity of double spectral resolution, as is the case when Fourier transformation or a step function is used. This makes it easy, for instance, to calculate beforehand the allowable shape and duration of pulses for a certain assigned accuracy and parameters, or to solve any reverse problem.

SUMMARY

1. The simplest, and at the same time sufficiently perfect, PEF variant (also with the greatest operating speed) is the instrument with a negative series feedback with respect to the output derivative, and with the maximum approximation (as far as the stability conditions allow) to the ideal character of amplification in the open circuit.

2. The PEF variant with combined feedback, including rigid positive feedback, secures a considerable reduction of creep; however, it can be effectively used only in the case of sufficiently small nonlinear distortions in the amplification circuit.

3. In PEF theory, along with frequency methods, it is convenient to use the method where the basic errors are expressed in terms of integrals and derivatives of the output quantity. This method provides the simplest solution in analyzing the instrument operation, in design, and in error determination.

The method can also be useful in analyzing the operation of integrators of different types.

The author extends his thanks to S. P. Kapitsa, R. R. Kharchenko, S. G. Rabinovich, and M. I. Levin for their help in clarifying a number of principles stated in the present article.

LITERATURE CITED

1. A. N. Kasperovich, "Photoelectric amplifiers F17," Izmeritel'naya Tekh. No. 5 (1959).[2]
2. B. A. Seliber and S. G. Rabinovich, "Photocompensation dc amplifiers," Avtomat. i Telemekh. 17, No.8 (1956).[2]
3. I. G. Gutovskii, "Photoelectric fluxmeters (survey)," Izmeritel'naya Tekh. No.1 (1960).[2]
4. I. G. Gutovskii, "Photoelectric fluxmeter theory," Doklady Akad. Nauk SSSR 116, No.2 (1957).
5. Ya. Mikusinskii, Operator Calculus [Russian translation] (IL, 1956).
6. G. Korn and T. Korn, Electronic Simulating Devices [Russian translation] (IL, 1955).

---

‡‡‡ This requirement was not fulfilled in any of the proposed circuits with combined feedback [3]. It is understandable that the expected lowering of creep did not take place.

[1] This situation occurs, for instance, when T_0 increases due to an increase in C_k in the operation model in [10]. In [11], T increases proportionally with T_0 due to the simultaneous increase in the tube amplifier amplification factor. This can be brought about also without an increase in T_0.

[2] See English translation.

7. S. G. Rabinovich and A. N. Tkachenko, "On the design of photoelectric fluxmeters," Izmeritel'naya Tekh. No.5 (1959).[2]

8. R. F. Edgar, "A new photoelectric hysteresigraph," Trans. AIEE 56 (1937).

9. F. G. Brockman and W. G. Steneck, "A new automatic hysteresis curve recorder," Philips Techn. Rev. 16, No.3 (1954).

10. S. P. Kapitsa, "On photoelectric fluxmeters," Zhur. Tekh. Fiz. 25, No.7 (1955).

11. R. R. Kharchenko, Special Problems in the Dynamics of Magnetoelectric Instruments. Doctoral Dissertation (MÉI, 1956).

12. V. O. Arutyunov, Electric Measurements and Measuring Instruments [in Russian] (Gosénergoizdat, 1958).

13. A. A. Voronov, Automatic Control Fundamentals [in Russian] (Oborongiz, 1954) 2nd ed.

---

[2] See English translation.

SYNTHESIS OF CIRCUITS WHOSE OPERATION IS DESCRIBED BY BOOLEAN TIME FUNCTIONS

D. A. Pospelov

Moscow

Translated from Avtomatika i Telemekhanika, Vol. 21, No. 10,
pp. 1410-1413, October, 1960
Original article submitted May 5, 1960

This article describes methods for the synthesis of circuits whose operation can be described by means of a certain special class of time functions. The determination of this class of functions and methods for their investigation are given.

Great interest was shown lately in problems connected with the synthesis and analysis of circuits and devices whose operation can be completely described by means of a certain functional time relation between the input and output parameters. For the solution of such problems in the case where the circuit under investigation can be reduced to its equivalent trigger circuit, various methods have been proposed (see, for instance, [1], [2], and [5]). Problems in the analysis and synthesis of a certain special class of circuits, not reducible to trigger circuits, will be considered in the present article.

We shall consider the totality of sets

$$(x_1, x_2, \ldots, x_n, t), \tag{1}$$

where x_i ($i = 1, 2, \ldots, n$) can be equal to either 0 or 1, and t can assume the value of any integer from 0 to s−1, inclusively. It is obvious that the total number of different sets (1) for a certain fixed value of n is equal to $s \cdot 2^n$

Determination. A function determined by sets of the form (1), and assuming one of the two possible values 0 or 1, is called a Boolean time function.

The statement that there is a finite number of different sets (1) is equivalent to the statement that any Boolean time function can be represented in the form of a finite table.

Example 1.

x_1	x_2	t	$\varphi(x_1, x_2, t)$
0	0	0	1
0	1	0	1
1	0	0	1
1	1	0	1
0	0	1	1
0	1	1	1
1	0	1	0
1	1	1	0

$(0 \leqslant t \leqslant 1)$

Despite its "clarity of presentation," such a table determination is unsuitable in the majority of practical cases because it is cumbersome. When written in analytical form, the function under investigation is more suitable for practical work.

Consider a certain Boolean time function

$$y = \varphi(x_1, x_2, \ldots, x_n, t) \qquad (0 \leqslant t \leqslant s-1). \tag{2}$$

If t is now assigned a certain fixed value t = k where $0 \leq k \leq s-1$, function (2) assumes the form

$$y_k = \varphi_k(x_1, x_2, \ldots, x_n). \tag{3}$$

Function (3) is now an ordinary logic algebra function [2 and 6]. If we let t assume all the allowable values, we obtain the sequence of logic algebra functions

$$\varphi_0, \varphi_1, \ldots, \varphi_{s-1}. \tag{4}$$

Thus, for any Boolean time function, we can obtain a corresponding sequence of logic algebra functions.

Example 2. For the Boolean time function from example 1, we have

$$\varphi_0 = \bar{x}_1\bar{x}_2 \vee \bar{x}_1 x_2 \vee x_1\bar{x}_2 \vee x_1 x_2 = 1,$$
$$\varphi_1 = \bar{x}_1\bar{x}_2 \vee \bar{x}_1 x_2 = \bar{x}_1.$$

Let us now introduce the function τ_α, which is determined by the relation

$$\tau_\alpha = \begin{cases} 0, & t \neq \alpha \\ 1, & t = \alpha \end{cases} \qquad (0 \leqslant \alpha \leqslant s-1). \tag{5}$$

For any s−1, the following equalities hold:

$$\bigvee_{t=0}^{s-1} \tau_t = 1, \qquad \bigvee_{i \neq j} \tau_i \tau_j = 0, \tag{6}$$

which signify that at the instant of time $t = \alpha$, the τ_α function, and only τ_α, is equal to 1, while all other $\tau_i (i \neq \alpha)$ functions are equal to 0 at this moment.

By taking into account relation (5), any Boolean time function can be written in the following manner:

$$\varphi(x_1, x_2, \ldots, x_n, t) = \varphi_0\tau_0 \vee \varphi_1\tau_1 \vee \cdots \vee \varphi_{s-1}\tau_{s-1}. \tag{7}$$

Formula (7) provides means for writing any Boolean time function in convenient analytical form.

Example 3. By writing the function from example 1 in analytical form, we obtain

$$\varphi(x_1, x_2, t) = \tau_0 \vee \bar{x}_1\tau_1.$$

Determination. If in relation (7) all $\varphi_i (i=1, 2, \ldots, s-1)$ functions are represented in disjunctive (conjunctive, accordingly) perfect normal form, we shall say that the given Boolean time function is represented in a disjunctive (conjunctive) perfect normal form.

From the theory of logic algebra functions [6], it is well known that any logic algebra function can be written in one of the two perfect normal forms. This justifies us in stating that any Boolean time function can be written in one of the possible perfect normal forms.

Relation (7) and the above-formulated determination indicate that the nature of Boolean time functions is close to that of ordinary logic algebra functions. In solving problems in the analysis and synthesis of circuits whose operation is described by such functions, this makes it possible to use an apparatus similar to that already available for logic algebra functions.

One of the most important problems in the logic algebra method of circuit synthesis is the problem of minimizing the given function. In the case of Boolean time functions, this problem can be solved by using any of the methods described in [2], [4], and [6] after certain preliminary modifications. For an illustration of this statement, we shall consider the example of minimization of the Boolean time function from example 1 by means of the modified method of minimizing charts.

Example 4. The disjunctive perfect normal form for our function is

$$\varphi = (\bar{x}_1\bar{x}_2 \vee \bar{x}_1x_2 \vee x_1\bar{x}_2 \vee x_1x_2)\,\tau_0 \vee (\bar{x}_1\bar{x}_2 \vee \bar{x}_1x_2)\,\tau_1.$$

Let us apply the method of minimizing charts to this function:

$\bar{x}_1\bar{x}_2\tau_0$	$\bar{x}_1\bar{x}_2$	$\bar{x}_1\tau_0$	$\bar{x}_2\tau_0$	$\bar{x}_1$	$\cancel{\bar{x}_2}$	$\boxed{\tau_0}$
$\bar{x}_1x_2\tau_0$	$\bar{x}_1x_2$	$\bar{x}_1\tau_0$	$x_2\tau_0$	$\bar{x}_1$	$\cancel{x_2}$	$\boxed{\tau_0}$
$x_1\bar{x}_2\tau_0$	$x_1\bar{x}_2$	$x_1\tau_0$	$\bar{x}_2\tau_0$	$\cancel{x_1}$	$\cancel{\bar{x}_2}$	$\boxed{\tau_0}$
$x_1x_2\tau_0$	x_1x_2	$x_1\tau_0$	$x_2\tau_0$	$\cancel{x_1}$	$\cancel{x_2}$	$\boxed{\tau_0}$
$\bar{x}_1\bar{x}_2\tau_1$	$\bar{x}_1\bar{x}_2$	$\bar{x}_1\tau_1$	$\cancel{\bar{x}_2\tau_1}$	$\boxed{\bar{x}_1}$	$\cancel{\bar{x}_2}$	$\cancel{\tau_1}$
$\bar{x}_1x_2\tau_1$	$\bar{x}_1x_2$	$\bar{x}_1\tau_1$	$\cancel{x_2\tau_1}$	$\boxed{\bar{x}_1}$	$\cancel{x_2}$	$\cancel{\tau_1}$
~~$x_1\bar{x}_2\tau_1$~~	~~$x_1\bar{x}_2$~~	~~$x_1\tau_1$~~	~~$\bar{x}_2\tau_1$~~	~~x_1~~	~~$\bar{x}_2$~~	~~τ_1~~
~~$x_1x_2\tau_1$~~	~~x_1x_2~~	~~$x_1\tau_1$~~	~~$x_2\tau_1$~~	~~x_1~~	~~x_2~~	~~τ_1~~

According to this minimizing chart, the minimum form for our function is given by $\varphi = \bar{x}_1 \vee \tau_0$.

As can be seen from this example, the proposed minimization method makes it possible to eliminate in the given function the terms which do not depend on time, which is useful in the synthesis of time circuits. However, for large values of n or s, the corresponding minimizing charts become too cumbersome and impracical. In these cases, the method of approximate minimization can be recommended. According to this method, minimization is performed separately for all φ_i functions in expression (7). This method is especially efficient for small n and large s values.

Example 5. For the function of example 1, the approximate minimization yields the following expression:

$$\varphi = \tau_0 \vee \bar{x}_1\tau_1.$$

Determination. A Boolean time function is said to be periodic with the period q if, for any t, the following condition holds:

$$\varphi_{t+q} = \varphi_t. \tag{8}$$

It can be readily seen that any Boolean time function

$$y = \varphi(x_1, x_2, \ldots, x_n, t) \quad (0 \leqslant t \leqslant s-1)$$

can be additionally determined until a periodic function with the period $q \geq s$ is obtained. On the basis of this and relation (7), we can state that, in synthesizing any circuit whose operation is described by a certain Boolean time function, we obtain a circuit of the type shown in Fig. 1. In this circuit, switch S successively connects circuits which process the $\varphi_0, \ldots, \varphi_{s-1}$ functions. After s units of time, the cycle will be repeated. For the time unit in the operation of switch S, we can take any quantity (for instance, the physical time in which one cycle in the operation of a certain device is performed).

In such a diagramatic realization of Boolean time functions, the elimination of terms that do not contain τ_α in the function to be synthesized corresponds to the case where the circuits processing these terms are con-

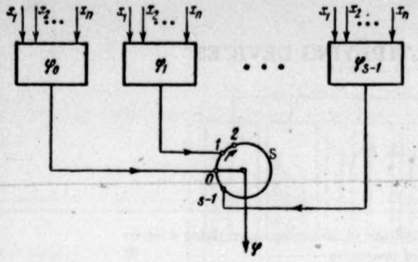

Fig. 1.

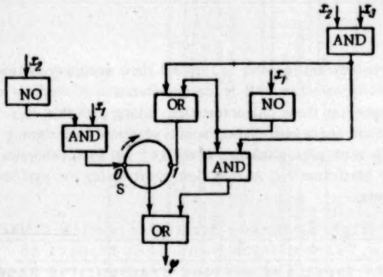

Fig. 2.

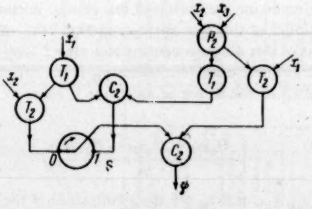

Fig. 3.

nected to the circuit output, bypassing the switch S. The presence of terms consisting only of τ_α in the function minimum form corresponds to the case where, at the instant of time $t=\alpha$, a voltage comparable to unity is supplied to the circuit output.

In conclusion, let us consider the synthesis of a circuit that processes an assigned Boolean time function.

Example 6.

x_1	x_2	x_3	t	$\varphi(x_1, x_2, x_3, t)$
0	0	0	0	0
0	0	1	0	0
0	1	0	0	0
0	1	1	0	1
1	0	0	0	1
1	0	1	0	1
1	1	0	0	0
1	1	1	0	0
0	0	0	1	1
0	0	1	1	1
0	1	0	1	1
0	1	1	1	1
1	0	0	1	0
1	0	1	1	0
1	1	0	1	0
1	1	1	1	1

The disjunctive perfect normal form for this function is

$$\varphi = (\bar{x}_1 x_2 x_3 \vee x_1 \bar{x}_2 \bar{x}_3 \vee x_1 \bar{x}_2 x_3)$$

$$\tau_0 \vee (\bar{x}_1 \bar{x}_2 \bar{x}_3 \vee \bar{x}_1 \bar{x}_2 x_3 \vee \bar{x}_1 x_2 \bar{x}_3 \vee \bar{x}_1 x_2 x_3 \vee x_1 x_2 x_3)\, \tau_1.$$

As a result of applying the method of minimizing charts, we obtain

$$\varphi = \bar{x}_1 x_2 x_3 \vee x_1 \bar{x}_2 \tau_0 \vee (\bar{x}_1 \vee x_2 x_3)\, \tau_1.$$

The corresponding functional diagram is given in Fig. 2. Its realization by means of electronic tubes yields the functional diagram shown in Fig. 3. The notation in this diagram is the same as in [4].

LITERATURE CITED

1. Yu. Ya. Bazilevskii, "Problems in the theory of logic time functions," Collection: Problems in the Theory of Mathematical Machines [in Russian] (Fizmatgiz, 1958) Vol. 1.
2. M. A. Gavrilov, Theory of Relay Contact Circuits [in Russian] (Izd. AN SSSR, 1950).
3. G. N. Povarov, "On the logical synthesis of electronic computer and control circuits," Collection: Logical Investigations [in Russian] (Izd. AN SSSR, 1959).
4. V. I. Shestakov (ed.), Synthesis of Electronic Computer and Control Circuits, [Russian translation] (IL, 1954).
5. M. L. Tsetlin, "On nonprimitive circuits," Problems in Cybernetics [in Russian] (Fizmatgiz, 1958) Vol. 1.
6. S. V. Yablonskii, "Functional constructions in k-unit logic," Trudy Matem. Inst. im. V. A. Steklov [in Russian] (Izd. AN SSSR, 1958) Vol. 51.

SURVEY AND CLASSIFICATION OF MULTIPLYING DEVICES

A. A. Maslov

Moscow

Translated from Avtomatika i Telemekhanika, Vol. 21, No. 10,
pp. 1414-1432, October, 1960
Original article submitted May 7, 1960

The paper deals with systematization of various principles of designing multiplying devices with regard to increasing their accuracy and speed of operation.

It contains some results of development of new multiplying devices carried out in the Laboratory of Analog Computers in the Institute of Automation and Remote Control of the Academy of Sciences of the USSR.

Introduction

In solving many scientific and technical problems, it is now more often necessary to use computers which perform nonlinear mathematical operations, in particular, multiplication and division.

The design of an analog multiplying (or dividing) device which would satisfy modern technological standards is a very complicated problem. This is indicated by the great diversity of the proposed principles on which the multiplication and division operations are to be based. However, regardless of the great attention paid to this problem, even the most perfect designs of multiplying devices are inferior to linear computer components with respect to the basic technical specifications, accuracy and speed.

The contradiction between the accuracy and the speed requirements, which is especially pronounced in nonlinear computer components, makes it possible to classify the multiplying devices according to the scheme given in Fig. 1. Although such a classification is somewhat arbitrary, since it is impossible to make sharp distinctions with respect to errors and the frequency passband for each group, it is very convenient in selecting the most suitable multiplying device design for a certain problem, in developing new designs, and, especially, in combining new and old designs in systems where high accuracy and good dynamic properties are required.

The classification (Fig. 1) is based on principles which make it possible to determine the limits of technical characteristics of the devices in each group. These limits are ultimately determined by the principles used in different designs, and, therefore, the diagram in Fig. 1 in many ways reflects the chart composed with respect to the characteristics determining the method of obtaining the product [1].

The aim of the present article is the systematization of the various principles used in the design of multiplying devices with respect to possibilities of their further development in order to improve their accuracy and operating speed, as well as the consideration of methods for improving these characteristics. Along with this, this article deals with certain results obtained in designing new multiplying devices at the IAT AN SSSR Laboratory for Mathematical Analog Computers during the past few years.

1. High-Accuracy Multipliers with a Narrow Transmission Band with Respect to One Input and a Broad Transmission Band with Respect to the Other Input

With respect to dynamic properties, circuits where the transfer constant changes stepwise are the most promising circuits for multipliers of this group. A circuit for a multiplier of this type is shown in Fig. 2 [2]. The upper part of this diagram consists of a closed-loop follow-up system where such admittance y_{12} is tracked that the voltage U_δ at the output of amplifier 1, equal to

$$U_\delta = \left[\frac{U_x y_{11} + U_c y_{13} - U_k y_{12}}{y_1}\right], \tag{1}$$

where y_{11}, y_{12}, and y_{13} are the admittances of the amplifier input circuit, y_1 is the admittance of the circuit parallel to the amplifier, U_x is the input signal, and U_c and U_k are constant stabilized voltages, does not exceed the absolute value of the actuation voltage $U_{\delta 0}$ of the command supply device 5. For $U_{\delta 0} y_1 \to 0$, under steady-state conditions, the admittance y_{12} is equal to

$$y_{12} = \frac{U_k y_{11}}{U_k} + \frac{U_c y_{13}}{U_k}. \tag{2}$$

In order to obtain the product, an additional admittance y_{21}, equal to y_{12}, is formed in the circuit (Fig. 2), and this admittance is commutated by means of an additional system of relay contacts or electronic switches,

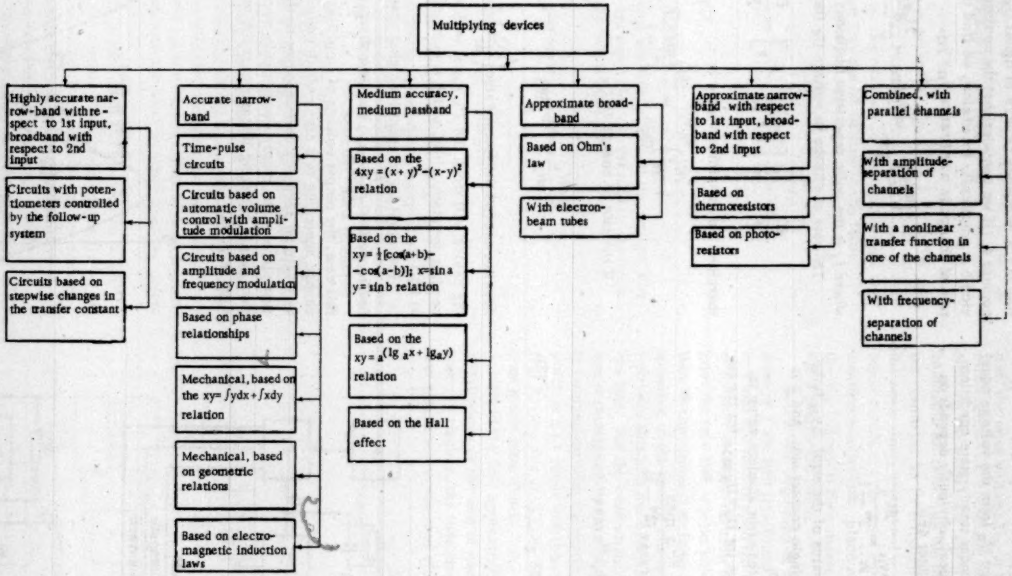
Multiplying devices
Highly accurate narrow-band with respect to 1st input, broadband with respect to 2nd input
Circuits with potentiometers controlled by the follow-up system
Circuits based on stepwise changes in the transfer constant
Accurate narrow-band
Time-pulse circuits
Circuits based on automatic volume control with amplitude modulation
Circuits based on amplitude and frequency modulation
Based on phase relationships
Mechanical, based on the $xy=\int y\,dx+\int x\,dy$ relation
Mechanical, based on geometric relations
Based on electromagnetic induction laws
Medium accuracy, medium passband
Based on the $4xy=(x+y)^2-(x-y)^2$ relation
Based on the $xy=\frac{1}{2}[\cos(a+b)-\cos(a-b)]$; $x=\sin a$ $y=\sin b$ relation
Based on the $xy=a^{(\lg_a x+\lg_a y)}$ relation
Based on the Hall effect
Approximate broadband
Based on Ohm's law
With electron-beam tubes
Approximate narrow-band with respect to 1st input, broadband with respect to 2nd input
Based on thermoresistors
Based on photoresistors
Combined, with parallel channels
With amplitude-separation of channels
With a nonlinear transfer function in one of the channels
With frequency-separation of channels

Fig. 1.

which are controlled by means of counter 4. If the binary counter 4 has a sufficiently large number of places, and if $y_{11} = y_{13} = y_2$, the voltage U_z at the output of amplifier 2 in Fig. 2 will be approximately equal to $\frac{U_x U_y}{U_k}$.

The deviation of voltage U_z from the voltage equal to the ideal product value under steady-state conditions, if all other conditions are ideal, obviously depends on the number of places in counter 4:

$$\Delta U_z = U_y \frac{\Delta y_{13}}{y_2} = \frac{2U_y}{2^n - 1},$$

where ΔU_z is the absolute value of the error, Δy_{12} is the admittance increment per single counter unit, and n is the number of binary places.

If we take the ratio of the error absolute value to the maximum output voltage for $U_y = U_{y\,max}$ for the accuracy criterion, we obtain

$$\delta U_{max} = \frac{2U_{y\,max}}{U_{z\,max}(2^n - 1)};$$

or, for $U_{x\,max} = U_{y\,max} = U_k = U_{z\,max}$,

$$\delta U_{z\,max\,1} = \frac{2}{2^n - 1}. \tag{3}$$

For a qualitative estimate of the dynamic properties of the circuit under consideration, we shall calculate the error in multiplying the sinusoidal voltage $U_x = U_{x\,max} \times \sin\omega t$ by the constant voltage $U_y = U_{y\,max}$ as a function of the frequency $f = \omega/2\pi$ of signal U_x for n places of counter 4. If we consider that the command supply device 5 is practically inertialess, we find the maximum rate of change in admittance $y_{12} = y_{21}$:

$$\left(\frac{dy_{12}}{dt}\right)_{max} = f_g \Delta y_{13} = \frac{2 f_g y_{11}}{2^n - 1},$$

where f_g is the pulse repetition frequency of generator 6.

The rate of change in voltage U_z for $U_y = \text{const}$ is

$$\frac{dU_z}{dt} = \frac{d}{dt}\left[U_y \frac{y_{12}}{y_2} - U_y\right] = \frac{U_y}{y_2}\frac{dy_{12}}{dt};$$

therefore, the maximum value is

$$\left(\frac{dU_z}{dt}\right)_{max} = \frac{2U_{x\,max} f_g}{2^n - 1}. \tag{4}$$

If the rate of change in U_x,

$$\frac{dU_x}{dt} = U_{x\,max}\,\omega \cos\omega t, \tag{5}$$

does not exceed the found value $\left(\frac{dU_z}{dt}\right)_{max}$, the multiplying device will track the U_x signal with an error not exceeding the static error, which is determined according to Eq. (3).

For signal U_x frequencies higher than the limiting frequency $f_1 = \frac{f_g}{\pi(2^n - 1)}$, the error sharply increases. In this case, the output voltage of amplifier (2) (Fig. 2) will change according to a curve which coincides with a sinusoid with an accuracy corresponding to the unit of the first place of the binary counter only over certain portions, while changing linearly over the remaining portions (Fig. 3).

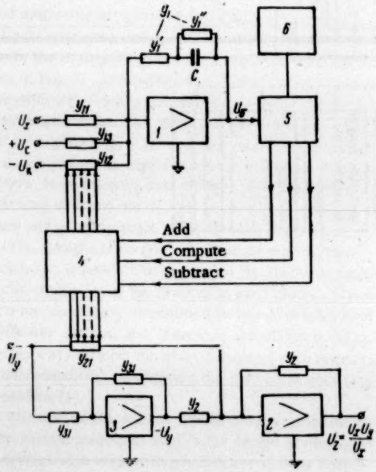

Fig. 2.

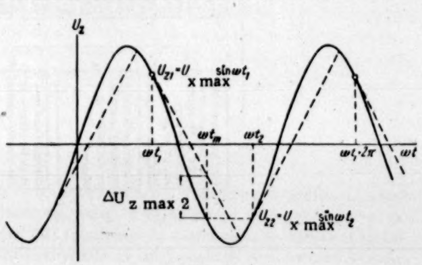

Fig. 3.

The sinusoid and the straight line begin to diverge at the instances of time $t_1+\frac{2\pi k}{\omega}$ and $t_2+\frac{2\pi k}{\omega}$, when the sinusoid slope is equal to the maximum rate of change in the output voltage.

From Eqs. (4) and (5), we find

$$\omega t_1 = \arccos\left[-\frac{2f_g}{(2^n-1)\,\omega}\right]. \qquad (6)$$

If we know t_1, the equation of the straight line issuing from the point U_{z1} can be written in the form

$$U_z = U_{z1} - \left(\frac{dU_z}{dt}\right)_{\max}(t-t_1) \qquad (7)$$

or

$$U_z = U_{x\max}\left[\sqrt{1-\frac{4f_g^2}{(2^n-1)^2\,\omega^2}} - \frac{2f_g}{2^n-1}(t-t_1)\right].$$

At the moment when the slopes of the straight line and the sinusoid are equal, for $t_m=(2\pi/\omega)-t_1$, the error is at the maximum and is equal to

$$\delta U_{z\max_2} = \frac{2f_g}{(2^n-1)\,\pi f}\arccos\frac{f_g}{(2^n-1)\,\pi f_g} - 2\sqrt{1-\frac{f_g^2}{(2^n-1)^2\,\pi^2 f^2}}. \qquad (8)$$

Figure 6 (curve a) represents the diagram of error variations $\delta U_Z(f)$ for an eleven-place binary counter, which is supplied with pulses at the repetition frequency $f_g = 1$ kc. Up to the frequency $f=f_1\approx 0.16$ cps, the error is somewhat lower than 0.1%; however, for a frequency of 3 cps, it already attains 60%.

Thus, the circuit under consideration, while securing a rather high static accuracy, has very low dynamic properties (with respect to the U_X signal), and the possibilities of improving these properties are very limited, since the binary counter filling frequency and the upper operating frequency of the switching elements which control the y_{12} and y_{21} admittances (Fig. 2) must exceed the multiplier transmission band by more than two orders of magnitude.

The dynamic properties of the circuit can be improved by using the method of place-by-place filling of the binary counter, which is sometimes used in converting a continuous quantity into a discrete quantity. A variant of the structural diagram for such a device is shown in Fig. 4. In comparison with the preceding circuit, this circuit contains an additional binary counter 8, and a command switch 4, for which a binary counter with scaling to a number of units equal to the number of places of counter 7 can also be used.

In the initial position, the command switch 4 does not transmit a pulse from generator 6 to the first place of counter 7 as usual, but to its upper nth place, whereby it is transferred from position 0 to position 1. After this, the error voltage U_δ at the output of amplifier 1 is measured by the command supply device, and, in dependence on the magnitude and sign of the error, either the command for switching the nth place to position 0 or the command for its remaining in position 1 is given. At the same time, 1 is added in the counter of the command switch 4. The next cyclic pulse from generator 6 transfers the (n−1)th place of counter 7 into position 1; the U_δ voltage is then measured again, etc., until all of the n places are filled.

Before the beginning of a new cycle, the contents of counter 7 are first transferred by a cyclic pulse to counter 8 and are then tripped out to zero. Thus, the contents of counter 8, which controls admittance y_{21}, change only after the (n + 1)th cyclic pulse from generator 6, but they change immediately by the number of units corresponding to the rate of change in signal U_x. In connection with this, also, the character of the dynamic error changes. For the case where the $U_x = U_{x\max}\sin\omega t$ voltage is multiplied by $U_y = U_{y\max}$, the increase in error in comparison with the static error begins at a frequency which is n + 1 times less than that used in the circuit in Fig. 2, i.e., at a frequency of only 0.15 cps; however, it rises much more slowly.

If, in the first approximation, we assume that the nodal points at the end of each operating cycle are accurately tracked, the maximum error will change in direct proportion to the rate of change in U_x, i.e.,

$$\delta U_{z\max} = \frac{2\pi f\,(n+1)}{f_g}. \qquad (9)$$

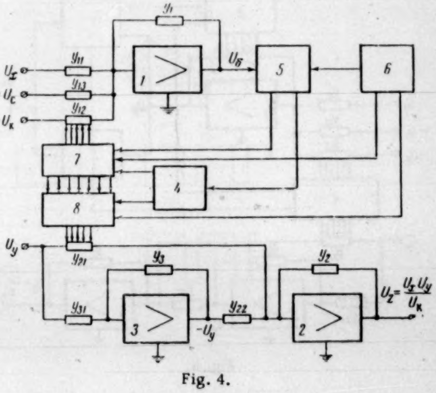

Fig. 4.

In this case, a 10% error will occur only at the 1.35 cps frequency, while in the preceding case, such an error occurred at the 0.18 cps frequency (see curve b in Fig. 6).

The deficiencies of the described method are: a considerable amount of additional equipment and more stringent requirements imposed on the transmission band of amplifier 1, which must transmit a rectangular signal with the frequency of the cyclic pulses from generator 6.

A more perfect method for increasing the operating speed of circuits where the transfer constant changes stepwise is the method of automatically changing the number of places in the counter. The essence of this method becomes clear if we consider the circuit in Fig. 2. Actually, if, for n places in the counter in this circuit, a considerable increase in the dynamic error begins with the signal U_x frequency equal to f_1, then for the (n−1)th place, this increase starts at the $2f_1$ frequency, while the error before attaining the $2f_1$ frequency also increases twofold. In the successive disconnection of lower counter places in the circuit, for U_x change rates equal to the maximum rate of change in U_z (4), the maximum dynamic error in following the sinusoidal voltage will vary in jumps at the limiting frequencies

$$f_i = \frac{f_g}{\pi (2^{n-i+1} - 1)} \quad (i = 1, 2, \ldots, n - 1).$$

In the frequency range from f_i to f_{i+1}, it will remain constant and equal to

$$\delta U_z \max = \frac{2}{2^{n-i} - 1}. \qquad (10)$$

The rate of change in voltage U_x in the circuit shown in Fig. 2 can be perhaps most suitably estimated with respect to the magnitude of the error voltage U_δ, which is demonstrated by the structural diagram shown in Fig. 5. For the disconnection of lower places in counter 4, the circuit is provided with an additional command supply device. 7, and a reversive counter 8, with a number of places securing the storage of a number of units equal to the number of places to be disconnected.

The command supply device 7 starts to fill counter 8 when the error voltage U_δ is somewhat larger than $|2U_{\delta_0}|$, and to subtract units from it when $|U_\delta| < |U_{\delta_0}|$. For each addition of a unit to counter 8, the admittance y_1 increases twofold, and the supply of commands is switched to a higher place of counter 4.

The automatic variation of the admittance y_1 secures the correspondence between the actuation voltages of the command supply devices 5 and 7 (which remain constant during operation) and the number of places in counter 4 (Fig. 5).

The described method ensures the multiplication of the sinusoidal signal U_x by a constant quantity at $f_g = 1$ kc and n = 11, with an error less than 6.4% at frequencies of up to 10 cps, and with an error of less than 12.8% at frequencies of up to 20 cps, etc. (Fig. 6c). Moreover, the application of this method does not involve more stringent requirements for the quality of amplifier 1, and the use of two multiplace counters is not necessary.

Finally, another way of improving dynamic properties of the circuit in Fig. 2 is the use of the time-pulse interpolation effect [2].

When the circuit in Fig. 2 operates under self-oscillation conditions, and the number contained in the binary counter alternately increases or decreases by unity, the $y_{12} = y_{21}$ admittances change linearly, and not in steps, as functions of U_x; therefore, the over-all number of counter places can be reduced without diminishing the accuracy. However, in this case, pulsations with the fre-

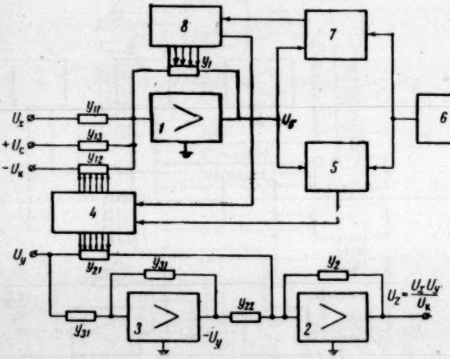

Fig. 5.

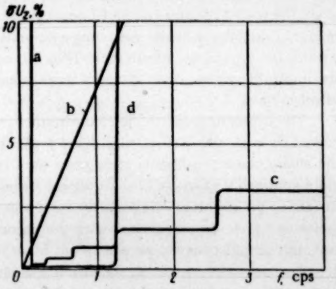

Fig. 6.

quency of self-oscillations whose amplitude sharply increases with a decrease in the number of places arise at the device output; therefore, the possibilities of broadening the transmission band by this method are limited. The frequency-response curve of the circuit in Fig. 2 under self-oscillation conditions for $n = 8$ and $f_g = 1$ kc is shown in Fig. 6d.

2. Accurate Narrow-Band Multipliers

The most effective method for eliminating the influence of intrinsic tube parameters in linear decision elements is the application of circuits with deep negative feedback.

Multipliers based on the negative feedback principle also secure a comparatively high accuracy; however, at the present time, the application of this principle is possible only in circuits where the output signals are first transformed into the amplitude or duty ratio of rectangular oscillations [14 and 13], in circuits where different methods of signal modulation by sinusoidal voltage are used [14 and 22], and also in certain circuits with special electron-beam tubes [56 and 61].

As a rule, in replacing input voltages by signals of different shapes and higher frequencies, the production of final results requires also reverse transformation, which necessitates the use of detectors, frequency or phase discriminators, circuits for producing the average voltage, etc; therefore, the transmission band of multipliers with preliminary transformation of signals is essentially limited to the region of audio-frequencies and, in many cases, to regions of considerably lower frequencies.

Up to now, the best technical characteristics of time-pulse devices have been secured by using circuits with stabilized electronic keys [7], for which, according to the data provided by the authors, the accuracy was 0.1% for a transmission band of up to 200 cps. However, such circuits are extremely complicated, and they require a large number of decision amplifiers. In connection with this, an investigation with the aim of finding ways for improving the quality of time-pulse devices by using simpler means has been conducted at the Institute of Automation and Remote Control, Academy of Sciences, USSR. Figure 7a shows the block diagram of a multiplier with combined connection of time-pulse dividers. The structure of this circuit is similar to the circuit proposed by A. A. Fel'dbaum and A. I. Manukhin [6]; however, the electronic keys are connected simultaneously to the input circuits and to the circuits parallel to amplifiers 1 and 2. The upper part of the circuit in Fig. 7a consists of a closed-loop follow-up system where the factor U_x is transformed into relative operation times of keys K_1 and K_2. Trigger Tr is switched from one steady state to another with a frequency equal to the frequency f_{sg} of sawtooth oscillations. The relation between times t_1 and t_2 (Fig. 7b) for each of the trigger states depends linearly on voltage U_1, due to changes in the duration of the total $U_1 + U_{sg}$ voltage, which is smaller than the trigger switching voltage U_{s1}, and larger than U_{s2}.

The keys are controlled by the trigger in phase opposition in such a manner that, when key K_1 is open, K_2 is closed, and conversely. The average value of the U_{k2} voltage at the key K_2 output, to which voltage U_0 is supplied, is proportional to its relative open-state time $\alpha = t_1/T$ (Fig. 7b), i.e., $U_{k2\,av} = -U_0\alpha$. Correspondingly, $U_{k1\,av} = U_x(1-\alpha)$.

For a sufficiently large amplification factor of amplifier 1, such a voltage U_1 is obtained at its output that

$$\frac{U_x(1-\alpha)}{R_1 + R_{f1}} = -\frac{U_0\alpha}{R_2 + R_{f2}}$$

or

$$\frac{\alpha}{1-\alpha} = U_x\frac{R_2 + R_{f2}}{U_0(R_1 + R_{f1})}. \qquad (11)$$

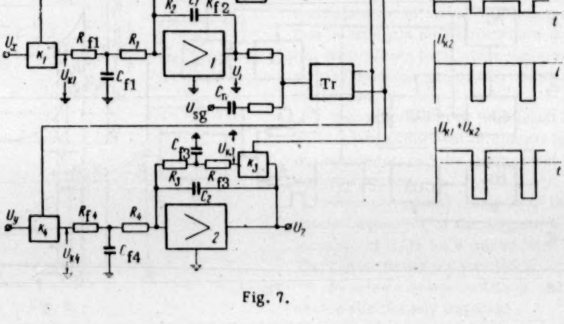

Fig. 7.

For the lower portion of the circuit, the following relation holds;

$$U_z = -\frac{\alpha}{1-\alpha} U_y \frac{R_{f1} + R_1}{R_{f2} + R_2}.$$

By substituting here the $\frac{\alpha}{1-\alpha}$ value from (11),we have

$$U_z = -\frac{U_x U_y}{U_0}.$$

Instead of obtaining the duty ratio ξ of rectangular pulses, which is usually determined by the equation $\xi = \frac{t_1 - t_2}{T}$, the voltage U_x is here transformed into the value of the fraction $\frac{\alpha}{1-\alpha} = \frac{t_1}{t_2}$. If the range in which the duty ratio ξ changes is limited by definition by a number less than 1, the fraction $\frac{\alpha}{1-\alpha}$ can change from zero to infinity. In practice, the duty ratio maximum value $\xi_{\max}$ is limited by a number less than 1, and the value of the fraction $\frac{\alpha}{1-\alpha}$ is limited by a finite quantity, since the time (Fig. 7b) cannot change smoothly if it becomes smaller than the sum of the leading and trailing trigger front times $t_l + t_t$. If t_l and t_t are given, $\xi_{\max}$ will linearly decrease with an increase in the sawtooth oscillation frequency f_{sg}, since

$$\xi = \frac{t_{1\max} - t_{2\min}}{T} = 1 - 2t_{2\min} f_{sg} \qquad (12)$$

and the upper limit of changes in $\frac{\alpha}{1-\alpha}$ is related to the f_{sg} frequency by the equation

$$\left(\frac{\alpha}{1-\alpha}\right)_{\max} = \frac{1}{t_{2\min} f_{sg}} - 1. \qquad (13)$$

By comparing (12) and (13), we can readily see that the value of $\left(\frac{\alpha}{1-\alpha}\right)_{\max}$ can be chosen to be considerably greater greater than $\xi_{\max}$ for a large f_{sg} frequency. For equal product scales, this makes it possible to reduce the transfer constant of the output decision amplifier, by means of which the error caused by the keys can be considerably reduced. If the f_{sg} frequency is increased, filters for a broader transmission band can be designed. The simultaneous connection of filters in input circuits and circuits parallel to amplifiers 1 and 2 (Fig. 7) also contributes to the improvement of the circuit dynamic properties due to the forcing action of filters R_{f2}, C_{f2}, R_2, and R_{f3}, C_{f3}, R_3.

An experimental check of the mock-up of a multiplier circuit with combined connection of pulse dividers, which was based on ÉMU-8 decision amplifiers, indicated the possibility of securing the following characteristics after careful circuit adjustment:

1) a maximum static error of 0.2 v if the factor voltages U_x and U_y and the output voltages U_z change in the interval from 0 to 100 v;

2) drift of less than 40 mv over a period of 10 min when $U_y = 100$ v is multiplied by $U_x = 0$;

3) a drift of not more than 70 mv over a period of 10 min when $U_x = 100$ v is multiplied by $U_y = 0$;

4) a drop in the amplitude response in both channels of not less than 5% for a frequency of up to 400 cps and for a commutation frequency of 10 kc.

The wiring diagram of the mock-up is not given here, since it was constructed only for checking the possibility of realizing the advantages of the considered structural scheme.

As another example, we shall consider the logarithmic time-pulse multiplier. The block diagram of the device for the case of single-quadrant multiplication is shown in Fig. 8a. Here, the transformation of the U_x, U_y, and U_z voltages into relative durations of rectangular pulses at the output of triggers Tr1 and Tr2 is secured by comparing them with exponentially changing voltages.

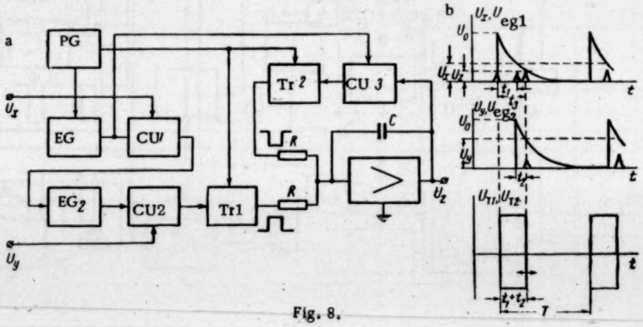

Fig. 8.

The pulse generator PG switches triggers Tr1 and Tr2 and actuates the exponential voltage generator EG1 whose output voltage $U_0e^{-t/\tau}$ is compared with the U_x voltage by the comparison unit CU1. At the moment when these two voltages are equal, which occurs after the time $t_1 = -\tau \ln \frac{U_x}{U_0}$, a pulse which triggers EG2 appears at the CU1 output. A pulse at the CU2 output, which returns the Tr1 trigger into the initial position, appears after the time $t_2 = -\tau \ln \frac{U_y}{U_0}$.

The duration of the positive pulse at the Tr1 output is equal to the sum of the times $t_1 + t_2 = -\tau \ln \frac{U_xU_y}{U_0}$.

A pulse of negative polarity with an amplitude equal to the amplitude of the pulse supplied by trigger Tr1 is tapped off the output of trigger Tr2; therefore, the U_z voltage at the amplifier output is such that its duration is $t_3 = t_1 + t_2$.

Since $t_3 = -\tau \ln \frac{U_z}{U_0}$, $U_z = \frac{U_xU_y}{U_0}$.

If multiplication in four quadrants has to be secured, all circuit units have to be doubled and adapted for work with negative voltages.

The ease with which one can switch over to division operations and the considerable simplification in the case of the multiplication of several voltages constitute the advantages of this circuit.

With regard to accuracy, this circuit occupies a middle position between closed-loop and open-loop devices. With respect to open-loop circuits, the error of which usually exceeds 1%, the gain in accuracy is obtained by replacing the sawtooth voltage by an exponential voltage, which can be secured with very high accuracy.

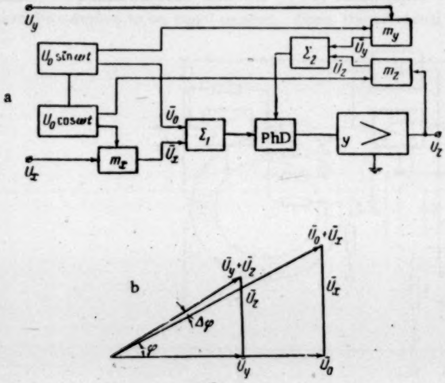

Fig. 9.

As in other time-pulse devices, the transmission band remains lower than the frequency of PG cyclic pulses by more than one order of magnitude.

An experimental check of the multiplier mock-up, which was constructed in accordance with the structural diagram and where standard elements used in computer units were utilized, yielded the following characteristics:

1) The accuracy was 0.5% with respect to a maximum output voltage of 100 v;

2) the frequency response remained horizontal for from zero to 20 cps for a commutation frequency of 1 kc.

As a rule, circuits based on different methods of signal modulation [14-22] are considerably more complicated than time-pulse circuits; however, due to the possibility of selecting a frequency of sinusoidal carrier oscillations which is considerably higher than the frequency of rectangular oscillations (from 100 to 1000 kc), these circuits have a broad transmission band (up to 1-10 kc). Attempts further to increase the carrier oscillation frequency lead to a sharp deterioration of accuracy, since the mutual influence of individual units becomes more pronounced. The design of, and comparison between, different variants of such circuits are given in [17] and [18].

Figure 9 shows a simplified variant of a multiplier circuit with amplitude modulation of signals; the circuit operating principle is based on phase relationships. Two high-frequency voltages with a phase shift of 90 deg are modulated by voltages U_x, U_y, and U_z by means of modulators m_x, m_y, and m_z.

The phase of the vector sum of voltages $\bar{U}_0 = U_0 \sin \omega t$ and $\bar{U}_x = m_xU_0 \cos \omega t$ is compared by the phase detector PhD with the phase of the vector sum $\bar{U}_y + \bar{U}_z = m_yU_0 \times \sin \omega t + m_zU_0 \cos \omega t$ (Fig. 9b). If the phases of these two sums do not coincide, an error voltage, which causes the output voltage to change until it assumes a magnitude proportional to the product of U_x and U_y, arises at the amplifier input.

With respect to accuracy and operating speed, such a circuit does not have any advantages over other devices with signal modulation, but it is considerably simpler and less expensive than the latter, and it secures a direct multiplication of factors with alternating signs. The fact that no stringent requirements are imposed on the amplifier transmission band, since the amplifier amplifies the already detected signal, also constitutes an advantage of this circuit.

The deficiencies of this circuit are the necessity for an accurate adjustment of circuits in the m_x, m_y, and m_z modulators and the requirement for a high carrier frequency stability.

An experimental mock-up of the multiplier constructed according to the diagram in Fig. 2 secured an accuracy of 0.5% for a transmission band of up to 5 kc. The carrier frequency was 465 kc.

By using a quartz oscillator, the device accuracy can be additionally improved.

3. Medium-Accuracy Multipliers with a Medium Transmission Band

This group comprises indirect-action multipliers, where the multiplication operation is replaced by summation and functional conversion operations [23-50], and multipliers based on the Hall effect in semiconductors [52 and 55].

The possibility of improving the accuracy of indirect-action circuits is limited by difficulties involved in constructing accurate nonlinear converters. Up to now, the best results (0.5-1%) were obtained with circuits based on the principle of sectionally linear approximation. The transmission band of indirect-action devices is limited by the parasitic parameters of functional converter elements. By using special corrective circuits, it can be brought up to a few tens and, in individual cases, even to a few hundreds of kilocycles [27, 37, and 38].

In circuits where the Hall effect in semiconductors is used, an accuracy of 0.3-1% can be secured for a transmission band from 1 to 10 kc [52-55].

Multiplier circuits with quadratic functional converters are most widely used at the present time, which is explained by their relative simplicity and the possibility of application for solving a relatively large number of problems.

The following circuit types are used for squaring: diode circuits [25, 28, 30, 31, 35, 36, 37, and 39], nonlinear semiconductor resistors of the thyrite or willemite type [32, 34, 46, 47, 48, 50, and 51], circuits with sawtooth voltage detection [23, 24, 33, and 42], electron-beam functional converters, etc. The quadratic sections of the volt-ampere characteristics of semiconductor or vacuum diodes, the quadratic dependence of the anode current on the grid voltage in three-electrode tubes [25, 29, 43, and 44], etc. can also be used.

Different variants of multiplier circuits based on quadrators as well as surveys of these circuits with indications of past and possible future improvements, have been sufficiently treated in literature (see, for instance, [1]), and, therefore, we shall not consider them here.

In logarithmic multipliers [15, 63, and 65], the product is obtained as a result of finding the antilogarithm of the sum of logarithms of the input quantities. Such devices are usually constructed according to the diagram shown in Fig. 10. The determination of antilogarithms is here secured by connecting the logarithmic functional converter +ln to the circuit parallel to the decision amplifier. Voltages U_a and U_b are added to the U_x and U_y factors in order to secure the multiplication of quantities with alternating signs, since the logarithms are determined only for positive argument values. In this, the U_3 voltage at the output of amplifier 3 is set in such a manner that

$$-\ln(U_a + U_x) - \ln(U_b + U_y) = \ln U_3, \tag{14}$$

i.e.,

$$U_3 = (U_a + U_x)(U_b + U_y).$$

For $U_a > |U_{x\,\max}|$ and $U_b > |U_{y\,\max}|$, all logarithms will be determined; however, in order to obtain the final result, the U_xU_b, U_yU_a, and U_aU_b components must be subtracted at the circuit output.

The character of error variations in the circuit is of theoretical interest. If we assume that all logarithmic converters have errors whose absolute values are $\Delta_{\ln}(U_x)$, $\Delta_{\ln}(U_y)$, and $\Delta_{\ln}(U_3)$, and the other operations are performed without errors, Eq. (14) should be rewritten in the following form:

$$-\ln(U_a + U_x)(U_b + U_y) =$$

$$= \ln U_3 + \ln \exp[\Delta_{\ln}(U_x) + \Delta_{\ln}(U_y) + \Delta_{\ln}(U_3)].$$

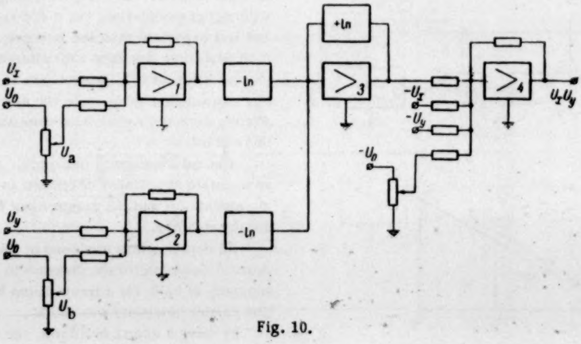

Fig. 10.

Hence,

$$U_3 = (U_a + U_x)(U_b + U_y)\exp[\Delta_{\ln}(U_x) + \Delta_{\ln}(U_y) + \Delta_{\ln}(U_3)].$$

The $\Delta_{\ln}(U_x)$, $\Delta_{\ln}(U_y)$, and $\Delta_{\ln}(U_3)$ errors are small; therefore,

$$U_3 \approx (U_a + U_x)(U_b + U_y)[1 + \Delta_{\ln}(U_x) + \Delta_{\ln}(U_y) + \Delta_{\ln}(U_3)]. \tag{15}$$

After subtracting the U_aU_b, U_aU_y, and U_bU_x components, we obtain

$$\delta(U_z) = \frac{U_{zi} - U_{za}}{U_{z\max}} = \frac{U_xU_y}{U_{z\max}}[\Delta_{\ln}(U_x) + \Delta_{\ln}(U_y) + \Delta_{\ln}(U_3)]. \tag{16}$$

Here, U_{zi} is the ideal product value, and U_{za} is the actual product value.

If we assume that the errors of functional converters are constant and equal and that they are independent of the argument values, the relative product error will be

$$\delta U_z = \frac{U_xU_y}{U_{z\max}}3\Delta_{\ln} + \frac{(U_aU_b + U_xU_b + U_yU_0)}{U_{z\max}}3\Delta_{\ln}. \tag{17}$$

Thus, the error depends linearly on the magnitude of the product itself and on each of the factors, and it contains a constant component. Physically, this is explained by the change in the transfer constant of amplifier 3, which is a consequence of connecting the amplifier to the functional converter feedback circuit.

In the case of single-quadrant multiplication, when U_x and U_y have only one sign, the U_a and U_b voltages can be assumed to be equal to zero. Then, the error will decrease with a decrease in the product value, and its maximum value will not exceed $3\Delta_{\ln}$. Actually, for small argument values, this error will be larger, since the slope of the characteristics of logarithmic converters is in this case larger, and their error sharply increases.

The considered properties of logarithmic multipliers can be used when it is necessary to maintain a higher accuracy in a certain given range of argument changes.

From among the useful properties of logarithmic devices, one should mention also the possibility of direct multiplication of several factors, division, squaring, evolution, etc. However, their widespread use is hampered by difficulties in producing simple and sufficiently accurate logarithmic functional converters.

The following property of semiconductors is used in circuits based on the Hall effect: if a semiconductor plate is placed in a magnetic field and a current is transmitted through it, an emf will arise in the plate, the direction of which will be perpendicular to the current and the magnetic flux, i.e., $E = k_1BI$.

A number of multiplier circuits based on this principle are already in existence [52 and 53]; however, best results are obtained by using closed-loop circuits, such as, for instance, the circuit shown in Fig. 11. Here, two equal elements, I and II, are placed in a magnetic flux. A steady current I_0 is transmitted through the first element. The Hall emf in the first element is compared with the voltage U_x by means of a differential amplifier, whose output voltage causes the induction in the magnetic circuit gap to change in such a manner that $k_2E_1 = k_2k_1BI_0 = U_x$, where k_1 is the Hall constant, and k_2 is the proportionality factor. Hence, $B = \frac{U_x}{k_1k_2I_0}$.

If the $\frac{R_2}{R_1} = \frac{1}{k_2}$, the U_z voltage is equal to $\frac{U_xU_y}{U_0}$. The circuit structure is the same as for other circuits with a controllable transfer constant; however, the controlled element is the variable emf.

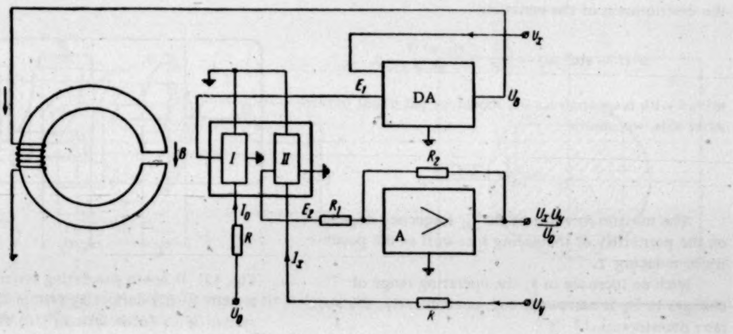

Fig. 11.

The circuit itself is purely electronic, but without the preliminary conversion of input voltages. This makes it possible to improve its dynamic properties in comparison with circuits where input voltage modulation is used; however, up to now, it was possible to secure transmission bands of only up to 10 kc. The reason for the limited possibility of broadening the transmission band in the U_X channel is the presence of the time constant $T = \frac{L}{r}$ (L is the coil inductance, and r is the coil resistance plus the differential amplifier output resistance) in the differential amplifier feedback circuit.

If the differential amplifier gain is sufficiently large, its output voltage will be related to the U_X voltage by the forcing element equation

$$U_B(p) = k_3(1 + pT)\,U_x(p). \tag{18}$$

The proportionality factor k_3 depends on the Hall constant k_1, the current I_0, the magnetic system characteristics, the differential amplifier gain with respect to the E_1 signal, etc. The enumerated factors make it possible to vary k_3 in a sufficiently wide range; therefore, we shall take its value to be equal to 1 in order that $U_B = U_x$ under steady-state conditions. Then, if U_x changes, the voltage U_B will additionally increase in proportion to the rate of change in U_x.

If the differential amplifier linearity is limited by the value of $U_{B\max}$, the maximum rate $\left(\frac{dU_x}{dt}\right)_{\max}$ can be determined by

$$pU_x(p)_{\max} = \frac{U_{B\max}}{T} - \frac{U_x(p)}{T}. \tag{19}$$

If we assume that, in the transient process, $U_{B\max}$ can exceed k times the maximum value of U_B under steady-state conditions $U_{B\,op} = U_{x\max}$ ($U_{B\max} = kU_{B\,op}$), then, for determining the limiting value of the frequency $f_{li} = \frac{\omega_{li}}{2\pi}$ of the sinusoidal signal $U_x = U_{x\max}\sin\omega t$, the discriminant of the equation

$$\omega^2(1 - \sin^2\omega t) - \left(\frac{k}{T} - \frac{\sin\omega t}{T}\right)^2 = 0,$$

solved with respect to $\sin\omega t$, should be put equal to zero. After this, we obtain

$$f_{li} = \frac{1}{2\pi T}\sqrt{k^2 - 1}. \tag{20}$$

The maximum value of the f_{li} frequency depends on the possibility of increasing k as well as the possibility of reducing T.

With an increase in k, the operating range of changes in U_B is narrowed, and, consequently, the accuracy deteriorates.

The possibility of reducing the time constant T is limited for reasons of energy, since, if the rate of change $\frac{dB}{dt}$ increases, also the power taken from the differential amplifier increases.

Work proportional to the square of induction $A = aB^2$ is used up in creating the magnetic flux. Hence, the instantaneous power is

$$\frac{dA}{dt} = 2aB\frac{dB}{dt} = U_B I_k. \tag{21}$$

For given values of induction B_{op} and $U_{B\max}$,

$$\left(\frac{dB}{dt}\right)_{\max} = \frac{U_{B\max} I_{k\max}}{2aB_{op}}. \tag{22}$$

Consequently, the possibility of increasing the circuit operating speed also by increasing $I_{k\max}$ or, which is the same, by decreasing T, is limited by the maximum amplifier power. For these reasons, multipliers based on the Hall effect have been grouped together with devices with a medium transmission band.

The accuracy of such devices is limited by instability and a considerable dependence of semiconductor properties on temperature.

At the present time Ge, Si, InSb, and InAs are used as Hall elements. Germanium and silicon elements have the largest Hall constant, and indium antimonide and indium arsenide make it possible to obtain a more powerful output. In comparison with other elements, the properties of InAs change slightly with temperature.

4. Approximate Broad-Band Multipliers

Such devices are provided with electron-beam tubes of a special design [56-61 and 66] or parametric linear circuits, where a current proportional to one factor is transmitted through a resistor which is controlled by the other factor [15].

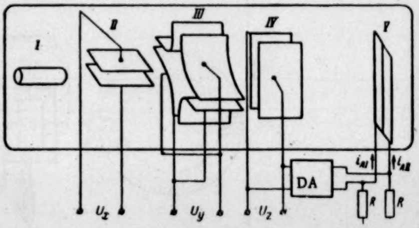

Fig. 12. I) Beam generating system; II) deflecting system 1; III) deflecting system 2; IV) deflecting system 3; V) anode system; DA) differential amplifier.

In circuits of the second type, usually the intrinsic characteristics of electron tubes are used, and, therefore, their accuracy is very low (5–10%).

A high accuracy (up to 0.5–1%) can be secured in circuits with electron-beam tubes. Here, it is extremely difficult to reduce the error, since it depends on the precision in manufacturing and assembling the tube electrodes.

As an example, Fig. 12c shows the circuit of a multiplier whose design is based on an electron-beam tube with a hyperbolic deflecting field [58]. In contrast to the uniform electrostatic field, the action of a hyperbolic field on the electronic beam is proportional, not only to the field strength, but also to the beam displacement with respect to the tube axis.

In the circuit in question, the electron beam is first deflected in the horizontal direction proportionally to the U_x voltage by means of an ordinary deflecting system, after which it enters the hyperbolic field, which is created by the factor U_y. The resulting beam deflection in the horizontal direction is proportional to the U_xU_y product, while the direction of beam deflection corresponds to the sign rule in multiplication. The hyperbolic field is created by four electrodes, whose sections with a vertical plane yields equal hyperbolic branches.

In order to obtain results in voltage form, a third deflecting system and an anode system are provided in the tube. When the beam is deflected with respect to the cut in the middle of the anode system, the equality of currents tapped off each of its halves is disturbed, and a voltage U_z, which returns the beam into its initial position, arises at the differential amplifier output. As a result, we obtain the following relation: $U_z = kU_xU_y$. According to the authors' data, the accuracy of such a device is 0.5%. The transmission band is 200 kc.

In another circuit, which is shown in Fig. 13 [56], the following well-known principle is used: an electron moving rectilinearily at the speed **V** in a magnetic field with the strength **H** is acted upon by a force equal to $\overline{\mathbf{H}} \times \overline{\mathbf{V}}$. Voltage U_x is applied to plates 1. The voltage U_y is converted into current I_k, which passes through the coil and creates the magnetic field. The greater the deflection of the beam by plates 1, the stronger the action of the magnetic field. The resulting action on the beam is proportional to the product of U_x and **H**. One-half of the screen in the tube is darkened, and, therefore, different signals are received by the photocell, in dependence on the beam position. As in the preceding case, there is a control circuit, due to which the Lorentz field, which acts on the beam electrons, is compensated by the amplifier A output voltage, which is equal to $U_z = kU_xU_y$. The error of such devices is equal to approximately 2%.

In the multiplier proposed in [60], an electron-beam tube with an ordinary electrostatic deflecting system is used. A plate, cut into four, as shown in Fig. 14, is mounted in the forward part of the tube. A current proportional to the surface area of the corresponding beam portion is tapped off each of the four plates. The currents are then summed according to the signs indicated in the figure. If the current density of the entire beam is uniform, and the factor voltages U_x and U_y are supplied to the deflecting plates, the total current will be proportional to their product, and the rule of signs will be observed. The fact that the beam cross section is not square has no importance, since the sum of segments complementing a square to form a circle is always equal to zero. The nonuniformity of the beam current density affects the device accuracy, which is low; it is equal to 3%. According to the authors' data, the transmission band is equal to 200 kc.

There is still another electron-beam tube variant [59], whose operating principle is illustrated in Fig. 15, which is intended for use in circuits with quadrators. The tube has a pair of deflecting plates, which direct a rectangular beam to a profiled parabolic screen. The beam current tapped off such a screen is proportional to the square of the voltage supplied to the plates. The beam operates with voltages of either sign, and, therefore, there is no necessity for separating the moduli in

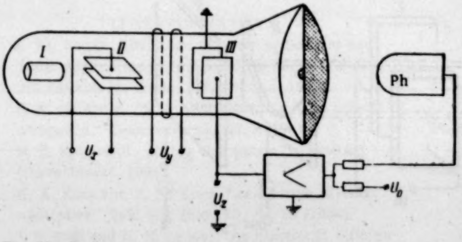

Fig. 13. I) Beam generating system; II) deflecting system 1; III) deflecting system 2; Ph) photomultiplier.

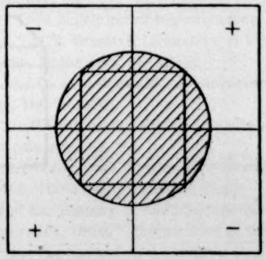

Fig. 14.

Comparative Table of Multiplier Technical Characteristics

Operating principle of the device	Static accuracy, %	Transmission band, cps
Very accurate, narrow-band with respect to one input, broad-band with respect to the other input		
Circuits with potentiometers which are controlled by a follow-up system	0.1	0.5
Circuits where the transfer constant changes stepwise	0.1	0.2
The same circuit with the application of the time-pulse interpolation method	0.1	1.2
The same circuit with place-by-place filling of the counter	0.1	1.3
The same circuit with automatic changing of the number of counter places	0.1	10
Accurate narrow-band multipliers		
Time-pulse multipliers [6]	0.4	12
Circuits with stabilized electron keys [7]	0.1	200
Logarithmic time-pulse devices	0.5	50
Time-pulse devices with combined connection of pulse dividers	0.2	400
Multipliers with amplitude modulation of input voltages [16]	0.1	10000
Multipliers based on phase relationships	1	5000
Devices of medium accuracy with a medium transmission-band		
Multipliers based on diode quadrators	0.5	10000
Multipliers based on thyrites	1	3000
Multipliers based on the Hall effect	0.5	1000
Approximate broad-band devices		
Multipliers based on Ohm's law	10	$2 \cdot 10^5$
Devices with electron-beam tubes	0.5	10^6
Combined devices with parallel channels		
Circuits with amplitude-separation of channels	0.02	100
Circuits with frequency-separation of channels	0.02	10000 and over

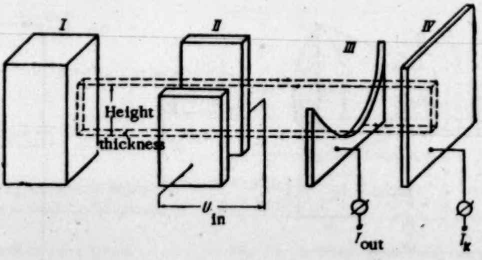

Fig. 15. I) Electron gun; II) deflecting plates; III) profiled screen; IV) collector.

using such a tube. According to the authors' data, the accuracy in squaring is 1%, and the transmission band attains several megacycles per second.

CONCLUSION

1. The above classification and survey of multipliers indicates that the use of any single principle in the design limits the maximum capabilities of these devices, either with respect to accuracy or with respect to operating speed (see Table of Technical Characteristics).

2. The considered well-known methods of increasing the operating speed of circuits where the transfer constant changes stepwise make it possible to broaden their transmission band only to a slight degree (from 0.2 to 1.3 cps). The method of automatically changing the number of binary counter places, which has been proposed here, makes it possible to improve the dynamic properties of a digital follow-up system up to 10 cps for a constant value of the product of accuracy and the transmission band.

3. In analyzing the possibilities of improving the accuracy and the operating speed of narrow-band multipliers, several new circuits have been proposed:

a) a circuit with combined connection of time-pulse dividers, which, for an accuracy of 0.2%, secures the broadening of the transmission band of time-pulse circuits to 400 cps;

b) a logarithmic time-pulse circuit, which secures an easy changeover to division operations and the possibility of direct multiplication of several factors;

c) a multiplier with signal amplitude modulation, which is based on phase relationships and which is characterized by the simplicity of its circuit and the possibility of direct four-quadrant multiplication.

On the basis of the obtained results, we can reach the conclusion that the design of a broad-band and, at the same time, accurate multiplier should not be based on any single principle, but on a combination of different circuits into a system which would make it possible to use the good dynamic properties of one principle and the high accuracy of another.

Combined multipliers will be considered in the next article [Avtomatika i Telemekhanika 21, 12 (1960)].

LITERATURE CITED

1. B. Ya. Kogan, Electronic Simulating Devices and Their Application in Investigating Automatic Control Systems [in Russian] (Fizmatgiz, 1959).
2. E. A. Goldberg, "Step multiplier in guided missile computers," Electronics 24, No. 8 (1951).
3. N. E. Kobrinskii, Analog Computers [in Russian] (Gostekhizdat, 1954).
4. G. A. Korn and T. M. Korn, "Relay time division multiplier," Rev. Sci. Instr. 25, No. 10 (1954).
5. L. S. Bruk and N. N. Lepov, "An electronic differential analyzer," Avtomat. i Telemekh. 17, No. 3 (1956).*
6. A. A. Fel'dbaum, Electrical Systems for Automatic Control [in Russian] (Oborongiz, 1957).
7. C. D. Morill and R. V. Baum, "Stabilized time division multiplier," Electronics 25, No. 12 (1952).
8. L. A. Finzi and R. A. Mathias, "An application of magnetic amplifier circuits to perform multiplication and other analytical operations," Trans. AIEE, 72 (Part I) (1953).
9. L. J. Graig, "The magnetic amplifier as analog computer component,"Proc. IRE 41, No. 10 (1953).
10. R. L. van Allen, "Four-quadrant multiplication with transistors and magnetic core," Trans. AIEE, part I--Communication and Electronics No. 21 (1955).
11. D. N. Schaefer, "A static magnetic transistor analog divider," Trans. AIEE, part I-Electronics and Communication, No. 21 (1955).
12. E. A. Goldberg, "A high-accuracy time division multiplier," RCA Rev. 13, No. 3 (1952).
13. E. Flater and K. Fränz, "Multiplicador electronica par inpulsos modulados en duracion y amplitude," Revista Telegrafica Electronica 41 (Buenos Aires, 1952).
14. M. Mehron and W. Otto, "Instantaneous electronic analog computer design," Proc. NEC No. 2 (1954).
15. Generation of Electric Oscillations of a Special Form [Russian translation], ed. by L. Yu. Blumberg and T. R. Brakhtman (Izd. Sovet-skoe Radio (1951), Vols. 1 and 2, No. 4.
16. Lukashevich, L. A., "A multiplier circuit based on the principle of double amplitude modulation," Byull. Pol'skoi Akademii Nauk, Sect. IV 3, 3 (1955).
17. Erglis, K. É., An Electronic Circuit Multiplier of Instantaneous Values of Two Alternating-Sign Voltages, Candidate's Thesis [in Russian] (MEI, 1950).
18. McCool W. A., "An AM-FM electronic analog multiplier," Proc. IRE 41, No. 10 (1953).
19. McCann G. D., Wilts C. H., and Locanthi B. N., "Electronic technique applied to analog methods of computation," Proc. IRE 37, No. 8 (1949).
20. "Computer multiplier," Proc. IRE, No. 10 (1957).
21. Locathi B. H. "A high-speed multiplier for analog computers," Electric. Eng. 69, No. 8 (1950).
22. Price R. T. M., "AM multiplier of high accuracy and wide range," MIT, Research Laboratory of Electronics, Techn. Report, No. 21 (1951).
23. Norsworthy K. H., "A simple electronic multiplier," Electronic Eng. No. 2 (1954).
24. Somerville M. J., "A circuit for analog formation of xy/Z,"Electronic Eng. 28, No. 9 (1956).
25. Vittenberg I. M., "Functional layouts of nonlinear electrical models which were developed in the Design Bureau of the Ministry of Machine and Instrument Construction, USSR," Transactions of the Second All-Union Conference on Automatic Control Theory [in Russian] (AN SSSR, 1955) Vol. 3.

26. Goff K. W. "An analog electronic correlator for acoustic measurement," J. Acoust. Soc. Am. 27, No. 2 (1955).

27. Mills R. L., "An accurate inexpensive electronic multiplier with wide dynamic range (Program of the Forty-Fifth Meeting of the Acoustical Society of America, May, 1953)," Acoust. Soc. of Am. No. 4 (1953).

28. Fitsner L. N., "A device for the multiplication of two quantities," Byull. Izobre. No. 2 (1955).

29. Holmes I. N. and Dukes M. A. "A speech-waveform correlator with magnetic tape delay and electronic multiplication," Proc. IRE, part III, No. 72 (July, 1954).

30. Pankolla H. "Ubersicht uber elektronische Multiplikationsverfahren," Messen Steuern Regeln, No. 6 (1960).

31. Trapeznikov V. A., Kogan B. Ya., Gurov V. V., and Maslov A. A., Description of the EMU-5 Electronic Mock-up [in Russian] (Inst. Telsh.- Ékonom. Inform. AN SSSR, 1956).

32. Gurov V. V., Evseev V. M., Kogan B. Ya., Maslov A. A., and Tranin F. E., Description of the EMU-8 Electronic Mock-up [in Russian] (Fil. Uses. Inst. Nauch. i Telsh. Inform. AN SSSR, 1957).

33. Maslov A. A. and Purlov Yu. G., "A universal functional converter based on the quadratic approximation principle," Avtomat. i Telemekh. 21, No. 2 (1960).

34. Kogan B. Ya., Maslov A. A., and Polonnikov D. E., "The EMU-8A electronic simulating apparatus," Vestnik Akad. Nauk SSSR, No. 7 (1958).

35. Maslov A. A., "Special diode functional converters based on semiconductor elements," Collection: Automation and Remote Control [in Russian] (Izd. AN SSSR, 1958).

36. Fitsner L. N., "A device for the multiplicauon of two quantities," Author's Certificate No. 100505 (November 25, 1952).

37. Coates H. M., "Simple square-law circuit with high frequency response," Electronic Eng. part I 29, No. 347 (1957).

38. Soltes A. S., "A wide-band square law computing amplifier," Trans. IRE, part VI 3, No. 2 (1954).

39. Fisher M. E., "The optimum design of quarter-squares, multipliers with segmented characteristics," J. Sci. Instr. 34, No. 8 (1957).

40. Keister G. L., "Square-wave analog multiplier," Transistor Circuits and Application (New York, McGraw Hill Book Co., 1957).

41. Sydnor R. L., O'Meara T. R., and Strathman J., "Analog multipliers and squarers using a multigrid modulator," Trans. IRE, EC-5, (June, 1956).

42. Pfeiffer Paul E. "A four-quadrant multiplier using triangular waves, diodes, resistors, and operational amplifiers," Trans. IRE EC-8, No. 2 (June, 1959).

43. Elias Peter, Multiplier Circuit. USA Pat. Class 235-61, No. 2741428, (April 10, 1956).

44. Stepanenko I. P., "Special uses of electronic tubes in automation and instrument construction," Collection: Progress in Electrovacuum Technology [in Russian] (Moscow – Leningrad, 1956).

45. Fisher M. E. "A wide-band analof multiplier using crystal diodes and its application to the study of a nonlinear differential equation," Electronic Eng. 29, No. 358 (1957).

46. Maslov A. A., "A multiplier – divider based on thyrites," Avtomat. i Telemekh. 18, No. 4 (1957).

47. Fitsner L. N., "A multiplier unit based on thyrites," Priborostroenie No. 4 (1956).

48. Kovach L. D., and Comley W., "An analog multiplier using thyrite," Trans. IRE EC-3, No. 2 (1954).

49. Balasanov G. N., Theoretical and Experimental Investigation of Static Power Converters with Semiconductor Resistors, Candidate's Thesis [in Russian] (IAT AN SSSR, 1954).

50. Benin V. L., "A wattmeter based on carborundum resistors," Avtomat. i Telemekh. 16, No. 2 (1955).

51. Rozenblat M. A. and Sedykh O. A., "Electrical properties and application of carborundum resistors," Avtomat. i Telemekh. 12, No. 4 (1951).

52. Chasmar R. P. "An electrical multiplier utilizing the Hall Effect in indium arsenide," Electronic Eng. 30, No. 369 (1958).

53. Lofgren Lars, "Analog multiplier based on the Hall effect," Actes. Journees Internat. Calcul Analog, Brusels, 1955 (Brussels, 1956), III-151. Discuss 115.

54. Lofgren Lars, "Analog multiplier based on the Hall effect," J. of Appl. Phys. 29, No. 2 (1958).

55. Hilsum C., "Multiplication by semiconductors," Electronic Eng. (November, 1958).

56. Deeley E. M. and Mackey D. M., "Multiplication and division by electronic-analof methods," Nature, 163, No. 4147 (1949).

57. Miller I. A., Solter A. S., and Scott R. E., "Wide-band analof function multiplier," Electronics 28, 2, 11 (1955).

58. Schmidt W., "Die Hyperbeldrore, eine Electronestrahlrohre zum multiplizeeren in Analogie-Rechen gerafen," A. omgew. Phys., No. 2, (1956).

59. Soltes A. S., "Wide-band square-law circuit element," Trans. IRE ED-2, No. 2 (April, 1955).

60. Angela E. I., "An electron - beam tube for analog multiplier," Rev. Sci. Instr. 25, No. 3 (March, 1954).

61. Cundlach F. W., "A new electron-beam multiplier with an electrostatic hyperbolic field," Journees Internat. Calcul. Analog (Brussels, 1955). Actes 1956.

62. Gurov V. V., Kogan B. Ya., Talantsev A. D., and Trapeznikov V. A., "The new electronic simula-

tion apparatus of the Institute of Automation and Remote Control, Academy of Sciences, USSR," Avtomat. i Telemekh. 17, No. 1 (1956). *

63. Davis B. E. and Swift I. H., "An analog computer technique using magnetic amplifiers," Trans. AIEE, part I – Communication and Electronics, No. 16 (Jan., 1955).

64. Breitbart (ed.) Parts and Units for Radar Stations [in Russian] (Sovetskow Radio, 1953) Part 3.

65. Burgin B. Sh., "Electrical multiplication and division and their application for measurement and control purposes," Élektrichestvo No. 9 (1958).

66. Choundhury A. K. and Nag B. R., "Analog multiplier and function generator with cathode-ray tube," Indian J. Phys. 33, (1958).

---

* See English translation.

LETTER TO THE EDITOR

J. Matyáš

Translated from Avtomatika i Telemekhanika, Vol. 21, No. 10,
pp. 1433-1434, October, 1960

In its issue No. 1 of 1960, the journal Avtomatika i Telemekhanika published the article,"On methods for the simulation of rational-fraction transfer functions without differentiating elements," by B. Ya. Kogan [1]. Before the appearance of this article, no such surveys and comparisons of different methods for the solution of this problem were available in literature. Since certain methods for the simulation of transfer functions have special advantages in various practical applications, the article by B. Ya. Kogan must be recognized as being of interest to persons engaged in solving practical problems by means of simulating devices.

At the same time, the journal Slaboproudý Obzor No. 1, 1960, published my article,"Methods for programming differential equations with constant coefficients by means of simulating devices" [2]. The above article treated also some other methods for the reproduction of programming block diagrams by means of simulating devices, which were different from those proposed in [1]. I would like to give here a brief presentation of these methods, thereby supplementing B. Ya. Kogan's article.

First, a few remarks concerning article [1].

1. The circuit in Fig. 1 [1] represents a circuit for dividing the input voltages by the coefficient a_3. Consequently, this circuit is stable for all $a_3>0$ (and not only for $a_3>1$, as was stated in [1]). For $0<a_3<1$, the resistor with the admittance a_3-1 is negative, but it can be connected to another feedback resistor. Thus, a resistor with admittance a_3 will be obtained in the feedback. For very small values of the a_3 coefficient, we shall obtain a circuit with a large amplification factor, which will be stable for all $a_3>0$. (The above circuit is unstable only for $a_3\leq 0$.) For $a_3<0$, the initial equation is multiplied by -1; for $a_3=0$, we shall obviously obtain an equation of a lower order. The case where $a_3=1$ is most often encountered in practice (generally, $a_n=1$).

2. In the method of decomposing the initial differential equation into a system of first-order equations [1], the new coefficients α_1 (see Fig. 6a and the systems of equations (15), (16), and (16a) [1]) represent the initial conditions for the pulse transfer function $w(t) = L^{-1}\{W(s)\}$ of the system under consideration, which is given by

$$\alpha_{n-k} = w^{(k-1)}(0).$$

This statement has been proved in [2].

Composition of Block Diagrams for the Programming of Rational-Fraction Functions by Means of Simulating Devices without Auxiliary Computations

Programming diagrams which contain all coefficients of the initial differential equation in nontransformed form have great advantages. In the above-mentioned article by B. Ya. Kogan, only the direct integration method and the method of combining the derivatives for $b_n=0$ have this property. The diagrams obtained as a result of using these methods are inverse (adjoint) with respect to each other.

For $m<n$, other diagrams which have this property can be obtained by various methods. All such diagrams can be completely described by means of feedbacks and couplings "which supply a forward signal." Any such diagram can be composed in a purely formal manner without any auxiliary calculations by using the following rules and conditions:

Rule 1. Any coefficient a_k on the left-hand side of the initial differential equation corresponds in the diagram to a feedback loop through n−k integrators with the open-loop feedback gain $-a_k$.

Rule 2. Any coefficient b_k on the right-hand side of the initial differential equation corresponds in the programming diagram to a loop supplying a forward signal through k integrators (passing from the system input to the system output through n−k integrators) with the gain b_k.

Condition 1. All loops supplying a forward signal must either go out from the system input (see Fig. 2 [1]) or converge to the system output (see Fig. 7 [1]).

Condition 2. Each integrator or summator in the diagram between the beginning of any feedback loop and the system output has only one input (no feedback loop or a loop supplying the forward signal must terminate in it).

Every programming block diagram set up according to rules 1 and 2,and satisfying conditions 1 and 2, represents a diagram which contains all coefficients of the initial differential equation in nontransformed form, and, conversely, any system which contains all the coefficients in nontransformed form can be composed in a purely formal manner according to the above rules and conditions.

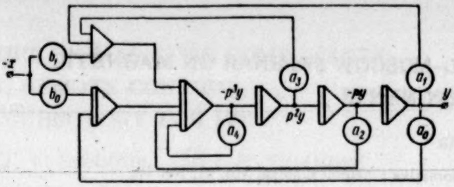

As an example, the figure shows a programming block diagram for the case where n = 5 and m = 1. (The gains of all integrators and summators are assumed to be equal to −1.)

Programming diagrams which contain all coefficients of the initial differential equation in nontransformed form have the following important advantages;

a) The programming block diagram can be obtained without any auxiliary calculations in a purely formal manner according to the above-formulated rules 1 and 2 and conditions 1 and 2.

b) The change in any coefficient of the initial equation can be effected independently of other coefficients by means of a suitable potentiometer.

c) Among these programming block diagrams, there are such diagrams which provide derivatives of the output quantity at the outputs of some of its integrators up to the n-m-1 order (see figure).

It follows from the above that programming block diagrams which contain all coefficients of the initial differential equation in nontransformed form often have important advantages over other diagrams in solving practical problems. They are described in detail in [2].

LITERATURE CITED

1. B. Ya. Kogan, "On methods for the simulation of rational-fraction transfer functions without differentiating elements," Avtomat. i Telemekh. 21, No. 1 (1960).*
2. J. Matyáš, "Programování lineárních diferenciálních rovnic s konstantními koeficienty na dif. analysátorech," Slaboproudý obzor. No. 1 (1960).

---

* See English translation.

WORK OF THE ALL-MOSCOW SEMINAR ON MAGNETIC AUTOMATION COMPONENTS

G. V. Subbotina

Translated from Avtomatika i Telemekhanika, Vol. 21, No. 10, p. 1435, October, 1960

During the first half of 1960, the All-Moscow Seminar on Magnetic Automation Components continued its work. The Seminar is being held at the Institute of Automation and Remote Control, Academy of Sciences, USSR, under the guidance of Dr. Tech. Sci. Prof. M. A. Rozenblat.

At the Seminar session which was held on February 24th, M. A. Rozenblat and G. V. Subbotina submitted a report entitled " Stability of multistage magnetic amplifiers." The report dealt with a method for determining the transfer function of a multistage summing magnetic amplifier and an investigation of stability criteria of magnetic amplifiers with internal feedback (self-magnetization) by using frequency criteria and considering the lag in load circuits. The authors showed that the obtained stability criterion makes it possible to synthesize a stable two-stage magnetic amplifier with an assigned error for a certain given gain.

In their report "Reversive dc magnetic amplifiers of greater efficiency," which was submitted on March 23rd, M. A. Boyarchenkov and M. A. Rozenblat presented the general principles for the design of highly efficient reversive amplifiers for work with dc loads. A number of new transformerless reversive amplifier circuits have been proposed.

On April 13th, N. P. Vasil'eva and I. S. Gashkovets submitted a report entitled "Stability of long circuits with logic elements," which dealt with the requirements for the "input — output" characteristics of logic elements for securing stable operation of annular or long circuits composed of identical logical repeaters or identical inverters,as well as circuits satisfying these requirements.

On April 27th, R. A. Lipman and A. I. Moskalev reported on the results of investigations of magnetic amplifiers with self-magnetization and a dc output with a circuit for voltage doubling by means of capacitors. This circuit secures a twice greater amplification with respect to voltage in comparison with the ordinarily used two-core circuits of this type. The circuit sensitivity to the feed voltage shape, which must be sinusoidal, constitutes a deficiency of this circuit.

In his report,"Magnetic transistor pulse amplifiers with dc feed,"which was submitted on May 11th, L. N. Kiselev analyzed a circuit with both magnetic amplifiers and transistors, operating under switching conditions, where the magnetic amplifier plays the role of the duty regulator. Since the magnetic amplifier represents the input stage, the transistor invertors for feeding and controlling the magnetic amplifier must secure only a power sufficient for feeding the low-power magnetic amplifier and for controlling the output stage triodes. The characteristics of a 2-kw amplifier with an output stage based on four P-207 transistors connected in parallel were given.

On May 25th, M. A. Ol'shvang reported on the development of magnetic semiconductor amplifiers with ac outputs. A magnetic amplifier is used for the first stage, and a push-pull amplifier with transistors which operate under switching conditions is used as the second stage. The semiconductor stage gain is considerably increased by providing positive feedback with respect to the load current by means of a feedback transformer. Such amplifier circuits for the control of two- and three-phase asynchronous motors,as well as a reversive circuit with a half-wave dc output,were described.

The last session of the Seminar in the first half of this year was held on June 8th. At this session, Yu. A. Avakhom submitted the report,"Control of cores with a rectangular hysteresis loop." The author proposed a new method of controlling cores for magnetic amplifiers with internal feedback with respect to the quasi-load characteristic which is close to the actual characteristic of magnetic amplifier control. The simulation of operating conditions for small and large control circuit resistances was secured by means of two different measuring circuits.

The participants at the Seminar noted that the subjects of the reports are important and of interest from the theoretical point of view, as well as for practical application. The reports were recommended for publication.

LIST OF LITERATURE ON MAGNETIC COMPONENTS FOR AUTOMATION, REMOTE CONTROL, AND COMPUTER TECHNOLOGY FOR 1959

Compiled by G. V. Subbotina and I. S. Trefilova

Translated from Avtomatika i Telemekhanika, Vol. 21, No. 10, pp. 1436-1450, October, 1960

GENERAL PROBLEMS
(Terminology, bibliography, standardization problems, etc.)

Measurement of magnetic parameters. Domestic and foreign book and periodical literature for 1955-1958; 13 titles (No. 1767). Composite Bibliographic Index of Technical Papers, 1958 (Gos. Publich. Nauchno-Tekh. SO AN SSR, Moscow, 1959) p. 171.

A. D. Nesterenko, On the Terminology in the Field of Magnetic Measurements. Problems in Magnetic Measurements (Izd. AN UkrSSR, Kiev, 1959) p. 5.

I. I. Pekker, "All-Union seminar on contactless magnetic components for automation, remote control, and computer technology, Moscow, October, 1959", Izvest. Vyssh Ucheb. Zaved., Élektromekhanika, 11, 137 (1959).

G. V. Subbotina, "Work of the All-Moscow seminar on magnetic automation components in ", Avtomat.i Telemekh. 20, 12, 1698 (1959).*

G. V. Subbotina, "List of literature on magnetic amplifiers and contactless magnetic components for 1956 (supplement)", Avtomat. i Telemekh. 20, 3, 376 (1959).*

G. V. Subbotina and I. S. Trefilova, "Magnetic components for automation, remote control, and computer technology". Annotated literature index for 1957 (Sovetskoe Radio Izd., 1959) p. 71.

G. V. Subbotina and I. S. Trefilova, "List of literature on magnetic components for automation, remote control, and computer technology for 1958 (list of domestic papers)" Avtomat. i Telemekh. 20, 9, 1902 (1959).*

Yu. P. Filimonov and M. I. Kaplan, "Literature on contactless magnetic components with a rectangular hysteresis loop", Radioélektr. Promy., 15, 55 (1959).

FERROMAGNETIC MATERIALS AND CORES

a) Magnetic Materials

V. G. Borisenko, "On suitable methods of determining the magnetic properties of cold-rolled transformer steel", Zavodskaya Lab. 25, 12, 1422 (1959)* Fig. 2, Table 3; Bibl. 4.

V. G. Vasil'ev and V. A. Zverev, "Electronic simulation of hysteresis characteristics of ferromagnetic materials", Izvest. Vyssh. Ucheb. Zaved., Élektromekhanika, 9, 3 (1959)* Bibl. 3.

V. I. Prozhzhina and N. V. Erofeeva, "On the structure of the family of symmetric hysteresis loops in ferromagnetic materials", Izvest. Akad. Nauk SSSR, Sev. Fiz. 23, 3, 304 (1959)* Fig. 2, Bibl. 5.

R. K. Kalinin', "Ratio of magnetic losses in ferrite cores with an open-loop magnetic circuit," Tr. Inst. Fiz. AN LatvSSR, 11, 73 (1959) Bibl. 8.

L. V. Kirenskii, et al., "On technical magnetization of ferromagnetic materials," Doklady Akad. Nauk SSSR 128, 2, 288 (1959) Bibl. 10.

I. Kraus, "On the problem of securing a rectangular hysteresis loop in manganese ferrites," Czechoslovak Physics Journal 9, 3, 408 (1959).

N. I. Lapkin and V. S. Mes'kin, "On the effect of high-temperature annealing on the magnetic properties of magnetically soft alloys," Izvest. Akad. Nauk SSR, Ser. Fiz. 23, 3, 280 (1959) Fig. 6, Bibl. 5.

G. Matveev and V. Khomich, "Ferrites: new magnetic materials," Radio, 8, 52 (1959).

"On the determination of the properties of electrical steel" [Résumé of the discussion in the journal Zavodskaya Laboratoriya 25, 4 (1959)] Zavodskaya Lab. 25, 12, 1415 (1959)* Bibl. 9.

A. I. Pirogov, "Effect of temperature on the magnetic reversal process in ferrite cores," Inzh. Fiz. Zhur. (Minsk, 1959).

K. A. Piskarev, "An oxide magnetic material," Author's Certificate, Class 21g, 303, No. 123259. Byull. Izobre., 20 (1959).

I. M. Puzei, "Temperature-stabilization of the magnetic properties of Permalloy," Doklady Akad. Nauk SSSR 120, 4, 768 (1958).

L. I. Rabkin, "A magnetic core", Author's Certificate, Class 21d^2, 48, 117963. Byull. Izobret. , No. 3 (1959).

L. I. Rabkin, "Certain problems in magnetic dielectrics physics," Izvest. Akad. Nauk SSSR, Ser. Fiz., 22, 10, 1276 (1958) Bibl. 6.

1

L. I. Rabkin and Z. I. Novikova, "Electrical properties of magnetic dielectrics and ferrites," Izvest. Akad. Nauk SSR, Ser. Fiz. 23, 3, 388 (1959) Fig. 15, Bibl. 2.

N. S. Siunov and V. M. Pavlinin, "Simultaneous magnetization of steel by currents of different frequency (50 and 200 cps), "Izvest. Vyssh. Ucheb. Zaved., Electromekhanika, 3, 7 (1959) Fig. 12, Bibl. 4.

L. V. Sobolev, "Voltampere characteristics and the temperature dependence of the conductivity of nickel–zinc ferrites, " Vest. Mosk. Ser. Unt., Matem., Mekhan., Astron., Fiz., Khim 1, 117 (1959) Bibl. 4.

R. V. Telesnin, T. V. Dmitrieva, and S. A. Matevosyan, "On the temperature dependence of the magnetic ductility of iron and some iron–nickel alloys," Nauchnye Doklady Vysshei Shkoy Fiz. i Matem. 5, 205 (1958) Fig. 6, Bibl. 7.

"Standard ferrite cores, " Radio, 8, 55 (1959).

Ya. S. Shvartsbart, "Magnetically soft materials produced by the Elektrostal' Plant," Collection: Magnetic Amplifiers (Mat. Nauch.–Tekh. Goveshchariya, Khar'kov, 1958 Moscow, 1959) pp. 72-77, Table 4.

b) Magnetization Processes and the Dynamic Characteristics of Ferromagnetic Materials (Losses, Eddy Currents, Viscosity, etc.)

V. V. Bardizh and V. V. Kobelev, "Calculation of magnetic reversal curves for ferrite cores," Izvest. ITM and VT AN SSSR (1959) p. 26, Fig. 15; Bibl. 3.

V. F. Belyavskii and K. M. Polivanov, "On the dynamic characteristics of ferromagnetic cores," Nauch. Doklady Vyssh. Shkol., Élektromekhanika i Avtomatika 2, 14 (1959), Fig. 12, Bibl. 12.

V. F. Belyavskii and K. M. Polivanov, "Cores made of anisotropic ferromagnetic strips," Izvest. Vyssh. Ucheb. Zaved., Élektrotekhnika, 10, 3 (1959) Bibl. 1.

V. Gaiko and I. Daniel–Sabo, "Effect of variable magnetic fields on the residual state of magnetically soft material," Czechoslovak Physics Journal 9, 1, 37 (1959) Bibl. 5.

E. I. Gurvich and E. I. Kondorskii, "Effect of microscopic inhomogeneities on the dynamic characteristics of magnetically soft alloys in weak fields," Izvest. Akad. Nauk SSSR, Ser. Fiz. 23, 3, 324 (1959) Fig. 3, Bibl. 12.

V. L. Dyatlov, "Consideration of eddy currents and viscosity in the magnetic reversal of strip cores in large fields," Nauch. Doklady Vyssh. Shkol., Élektromekhanika i Avtomatika, 2, 3 (1959) Fig. 7, Bibl. 10.

V. G. Elkin and A. I. Pirogov, "Dynamic characteristics of ferrites and their application in designing circuits with ferrite cores, " Tr. VIRTU, Minsk, No. 15 (1959).

E. I. Klepfer and G. M. Tikhomirov, "Problems in the theory of ferrite cells," Izvest. Vyssh. Ucheb. Zaved., Élektromekhanika, No. 12 (1959).

A. I. Pirogov, "Dynamics of pulse magnetic reversal in ferrites with a rectangular hysteresis loop," Collection: Tr. VTs AN SSSR (1959).

A. I. Pirogov, Pulse Magnetic Reversal in Ferrites with a Rectangular Hysteresis Loop, Candidate's Thesis (Mosk. Énerg. Inst., Moscow, 1959).

M. A. Rozenblat, "Effect of eddy currents on the characteristics of magnetic amplifiers with feedback in the case of low-resistance control circuits," Avtomat. i Telemekh. 20, 12, 1659 (1959)* Fig. 8, Bibl. 4.

N. A. Smol'kov and V. F. Belov, "Certain properties of ferrites under pulse conditions," Izvest. Akad. Nauk SSSR, Ser. Fiz. 23, 3, 357 (1959) Fig. 5, Bibl. 15.

R. V. Telesnin and E. F. Kuritsyn, "On the magnetic reversal rate in ferrites," Izvest. Akad. Nauk SSSR, Ser. Fiz. 23, 3, 352 (1959) Fig. 6, Bibl. 9.

R. V. Telesnin and A. G. Shishkov, "Effect of magnetic viscosity on the frequency characteristics of ferrites," Izvest. Akad. Nauk SSSR Ser. Fiz. 23, 3, 343 (1959) Fig. 8, Bibl. 8.

Yu. M. Shamaev, V. L. Dyatlov, and A. I. Pirogov, "Dynamic characteristics of ferrites," Nauch. Doklady Vyssh. Shkol., Élektromekhanika No. 1 (1959).

c) Core Design and Production Technology

I. S. Babayants and A. I. Ivanov, " A device for automatically maintaining a constant rotation speed of the bobbin in toroidal winding of cores." Author's Certificate, Class 21g, 1_{01}. No. 123627. Byull. Izobret., 21 (1959).

A. M. Bamdas, V. A. Somov, and A. O. Shmidt, "Certain design variants of single-phase and three-phase transformers which are controlled by shunt magnetization," Tr. Gor'kovskogo Politekhnicheskogo 15, 4, 27 (1959) Fig. 15, Bibl. 7.

N. I. Vorob'ev, "The use of enamel as insulation material between sheets in magnetic cores made of electrical strip steel," Izvest. Vysshikh Ucheb. Zaved., Élektromekhanika, 1, 125 (1959) Fig. 6, Bibl. 2.

I. K. Levochkin, "The present state of development of a new line of magnetic amplifiers with magnetic circuits made of П-shaped plates," Collection: Magnetic Amplifiers (Scientificotechnical Conference Transactions, Khar'kov, 1958; Moscow, 1959) p. 40, Fig. 5.

A. V. Netushil, "Effect of insulation thickness on the magnetic properties of foliated cores," Tr. MÉI, 30, 142 (1958).

L. I. Rabkin, "A magnetic core," Author's Certificate, Class 21g, 31_{03}, No. 120621. Byull. Izobre. 12 (1959).

B. G. Sokolov, "A line of 30- to 3000-w magnetic amplifiers with magnetic circuits consisting of three-leg plates," Collection: Magnetic Amplifiers (Scientificotechnical Conference Transactions, Khar'kov, 1958; Moscow, 1959) pp. 78-85, Fig. 4.

V. M. Kharlamov, "A method for the rejection of unsuitable magnetic materials," Author's Certificate, Class 21e, 37_{10}, No. 118902 (594056 of March 7, 1958). Byull. Izobret., 7 (1959).

T. K. Tsogoev, "An adapter to the winding device for fastening the wire end at the lead-out of components (in particular, chokes)," Author's Certificate, Class 21g, 1_{01}, No. 123626. Byull. Izobret., 21 (1959).

3. General Problems in the Theory of Nonlinear Magnetic Circuits (Calculation of Circuits with Steel Components, Ferroresonance, etc.)

L. A. Bessonov, "On the theory of oscillations in one of the ferroresonance circuits," Izvest. Vysshikh Ucheb. Zaved., Élektromekhanika, 2, 43 (1959) Fig. 12, Bibl. 2.

B. K. Bul', "Investigation of the field in the vicinity of the air gap and the calculation of permeance," Vest. Élektropromy., 9, 66 (1959).

F. F. Galteev and V. G. Morozov, "Compound ferroresonance voltage stabilizer for ac generators with permanent magnets," Nauchnye Doklady Vysshei Shkoly, Élektromekhanika i Avtomatika, 2, 151 (1959) Fig. 8, Bibl. 3.

V. P. Glukhov, "Design of a circuit consisting of a resistor and a choke with steel," Vestn. Élektropromy., 10, 42 (1959).

B. Z. Zil'berman, "Condition for the maximum accuracy of ferroresonance voltage stabilizers," Radiotekhnika 14, 4, 75 (1959).

V. D. Krochakevich, Transient Processes in Three-Phase Circuits with Rectifier Bridges. Candidate's Thesis (Lenin Komsomol Riga Aircraft-Engineering Military Academy, 1959).

M. S. Libkind and G. I. Kugushev, "Graphs for determining the harmonic composition of magnetizing currents in superimposing a steady field on a variable field," Élektrichestvo, 7, 55 (1959) Fig. 5, Bibl. 1.

E. M. Pevzner, "On the investigation of transient processes by means of dc currents in electric circuits with steel components," Izvest. Vysshikh Ucheb. Zaved., Priborostroenie, 1, 63 (1959) Fig. 1, Bibl. 1.

S. P. Pivovarov, "Design of ferroresonance voltage stabilizers," Vest. Élektroprom., 6, 60 (1959) Fig. 3, Bibl. 5.

B. A. Piontkovskii, "A ferroresonance voltage stabilizer," Author's Certificate, Class $21a^4$, 35_{14}, No. 121485. Byull. Izobret., 15 (1959).

G. M. Tikhomirov, "Representation of the hysteresis loop equation in the form of an integral with a variable upper limit," Izvest. Vysshikh Ucheb. Zaved., Élektromekhanika, 6, 3 (1959).

4. Magnetic Amplifiers, Theory, Circuits, and Design

a) Books, Monographs, and Dissertations

M. A. Boyarchenkov and M. A. Rozenblat, Fast Reversive Electric Drives with Magnetic Amplifiers (Society for the Dissemination of Political and Scientific Knowledge of the RSFSR. Dzerzhinskii Moscow NTP Institute, Moscow, 1959) p. 42.

N. P. Vasil'eva, O. A. Sedykh, and M. A. Boyarchenkov, Magnetic Amplifier Design (GÉI, Moscow—Leningrad, 1959) p. 336, Fig. 155, Bibl. 44.

N. P. Vasil'eva, Design of Magnetic Power Amplifiers. Lecture delivered as a part of the course "Electromagnetic Components and Devices" (VZÉI, Moscow, 1959) p. 46.

V. A. Geiger, Magnetic Amplifier Circuits [Russian translation from English] (GÉI, Moscow–Leningrad, 1959) Transl. by D. A. Lipman and I. I. Ratgauz, ed. by I. Ya. Lekhtman, p. 400, Fig. 154, Bibl. 548.

Li Fêng, Thermal Calculations and Investigation of the Heating of Magnetic Amplifiers with Three-Leg Cores. Candidate's Thesis (MÉI, Moscow, 1959).

A. L. Pisarev, Investigation of Steady-State Operating Conditions of Six-Choke Magnetic Amplifier Circuits with a Three-Phase Load. Candidate's Thesis (Moscow, 1959).

L. V. Safris, "A method for designing magnetic amplifiers with respect to linearized characteristics" (Central Institute for Technicoeconomic Information, Advanced Scientificotechnical and Industrial Experience, Thesis 27, No. É-59-54/24 (Moscow, 1959) p. 27

O. A. Sedykh, Problems in Selecting the Optimum Design Parameters of Magnetic Amplifiers. Candidate's Thesis (IAT AN SSSR, Moscow, 1959).

b) Single-Ended Magnetic Amplifiers

G. A. Antonov, "A differential magnetic amplifier," Author's Certificate, Class $21a^2$ 18_{08} No. 120538 (590715/24 of January 27, 1959) Byull. Izobre., 12 (1959).

V. P. Vasil'ev and N. N. Aleksandrov, "Operation of magnetic amplifiers which are controlled by means of semiconductor triodes," Sborn. Tr. Slushatelei Leningrad. Voenno-Vozdushnoi Inzh. Akad. im. A. F. Mozhaisk. 27, 138 (1959), Fig. 12, Bibl. 4.

V. S. Vysochanskii, "A single-ended magnetic amplifier with an ac output," Author's Certificate, Class $21a^2$, 18_{08}, $21e^1$, 30_{20}, No. 116921 (January 19, 1959).

N. A. Givartovskaya, "Design of a choke-coupled magnetic amplifier." Second lecture of the course "Electromagnetic components and devices" (Ugletekhizdat, Moscow, 1959) p. 20.

V. P. Glukhov, "The design of magnetic amplifiers with respect to the universal characteristics determined by physical simulation," Collection: Magnetic Amplifiers (Scientificotechnical Conference Transactions, Khar'kov, 1958, Moscow, 1959) pp. 120-130, Fig. 9.

V. P. Glukhov, "Design of a magnetic amplifier with respect to the universal characteristics obtained by physical simulation," Izvest. AN LatvSSR, 2, 51-60 (1959), Fig. 5, Bibl. 4.

V. P. Glukhov, General Theoretical Characteristics of Choke-Coupled Magnetic Amplifiers. Electrical Equipment Systems for Vehicles (Izd. AN LatvSSR, 1959) Vol. 2; Tr. Instituta Énergetiki i Élektrotekhniki AN LatvSSR, 7, 63-81 (1959).

V. P. Glukhov and É. A. Yakubaitis, "Simulation of choke-coupled magnetic amplifiers," Avtomat. i Telemekh. 20, 7, 955 (1959)*Fig. 4, Bibl. 5.

A. I. Guzenko, "Design of single-ended magnetic power amplifiers." Collection: Automatic Regulation and Control Systems (Mashgiz, Moscow, 1959) No. 97, pp. 85-96, Fig. 4, Bibl. 2.

E. D. Demidenko, "An engineering method of calculating saturation power chokes," Vest. Élektroprom., 2, 63 (1959) Fig. 5, Bibl. 3.

A. G. Zdrok, "On the design of magnetic amplifiers with active-inductive rectified loads," Élektrichestvo, 5, 25-31 (1959) Fig. 8, Bibl. 5.

N. A. Kaluzhnikov, "On the design of ac circuits of choke-coupled magnetic amplifiers with internal feedback," Avtomat. i Telemekh. 20, 5, 606 (1959)*Fig. 11, Table 1, Bibl. 8.

B. E. Kubyshin, "Problems in the linear theory of magnetic amplifiers," Sbornik Trudov Instituta Élektrotekhniki AN UkrSSR, 16, 113 (1959) Bibl. 7.

B. E. Kubyshin, "A method for calculating magnetic amplifiers on the basis of the linear theory," Sborn. Trud. Inst. Élektrotekhniki AN UkrSSR, 16, 174 (1959).

G. I. Kudryavtseva, "Certain problems in the theory and practice of fast magnetic amplifiers for follow-up systems," Transactions of the Third All-Union Conference on Automation of Industrial Processes in Machine Construction and Automated Electric Drives (Moscow, 1959).

V. S. Lerner, "Transfer functions of a magnetic amplifier for active loads," Avtomatika, AN UkrSSR, 1, 58 (1959) Fig. 4, Bibl. 11.

R. A. Lipman and I. B. Negnevitskii, "Design of single-ended magnetic amplifiers with internal feedback," Transactions of the Third All-Union Conference on Automation of Industrial Processes in Machine Construction and Automated Electric Drives (Moscow, 1959).

L. N. Lupaev and N. N. Aleksandrov, "Control of magnetic amplifiers by varying the control voltage phase," Sborn. Trud. Slushatelei Leningrad. Voenno-Vozdushnoi Inzh. Akad. im. A. F. Mozhaiskogo, 27, 158 (1959) Fig. 7b, Bibl. 3.

E. L. L'vov, "Application of the similarity theory in designing magnetic amplifiers," Nauchnye Doklady Vysshei Shkoly, Élektromekhanika i Avtomatika, 3, 119-134 (1958) Bibl. 3.

A. G. Pinchuk, "A transformer magnetic amplifier," Author's Certificate, Class $21a^2$, 18_{08}, No. 97021. Byull. Izobre., 2 (1959).

O. B. Rosenbauli, "A method for designing optimum choke-coupled magnetic amplifiers," Nauchnye Doklady Vysshei Shkoly, Élektromekhanika i Avtomatika 2, 174 (1959).

O. B. Rosenbauli and R. N. Rodin, "Design of current transformers with magnetization," Élektrichestvo, 4, 63 (1959) Fig. 12.

L. L. Samurina, "Operation of a half-wave magnetic amplifier with an active-inductive load," Izvest. Vysshikh Ucheb. Zaved., Élektromekhanika, 2, 81 (1958) Fig. 6, Table 3, Bibl. 3.

Hu Chia-yao and V. A. Shubenko, "Transient processes in magnetic amplifiers with an inductive load which is connected through a rectifier bridge," Izvest. Vysshikh Ucheb. Zaved., Élektromekhanika, 4, 84 (1959) Bibl. 94.

N. M. Yakovlev, "On the design of differential magnetic amplifiers with an ac output," Izvest. Vysshikh Ucheb. Zaved., Priborostroenie, 1, 55(1959) Bibl. 6.

N. M. Yakovlev, "Determination of the transfer function of magnetic amplifiers," Izvest. Vysshikh Ucheb. Zaved., Priborostroenie, 2, 13-21(1958) Fig. 3, Bibl. 2.

É. A. Yakubaitis and V. P. Glukhov, "Physical simulation of circuits with choke-coupled magnetic amplifiers," Izvest. AN LatvSSR, 4, 129 (1958) Fig. 2, Bibl. 5.

c) Push-Pull Magnetic Amplifiers

O. A. Kossov, "A push-pull magnetic amplifier with a dc output," Author's Certificate, Class $21a^2$, 18_{08}, No. 117345. Byull. Izobret., 2 (1959).

O. A. Kossov, "A magnetic crystal amplifier," Avotma. i Telemek. 20, 7, 988 (1959) Fig. 5, Bibl. 3.

V. E. Pankin, "A push-pull bridge magnetic amplifier," Author's Certificate, Class $21a^2$, 18_{08}, No. 122495, March 31, 1958. Byull. Izobre., 18 (1959).

M. A. Rozenblat, "A push-pull magnetic amplifier with a dc output," Author's Certificate, Class $21a^2$, 18_{08}, No. 122777, March 26, 1959. Byull. Izobre., 19 (1959).

M. A. Rozenblat and G. V. Subbotina, "Improvement of the efficiency of reversive dc magnetic amplifiers by means of transistors," Avtomat. i Telemekh. 20, 9, 1268 (1959)*Fig. 4, Bibl. 5.

O. B. Rosenbauli and R. N. Rodin, "A push-pull transformer magnetic amplifier," Author's Certificate, Class $21a^2$, 18_{08}, No. 118523 (580205 of July 9, 1957). Byull. Izobret., 6 (1959).

L. L. Samurina, "Analysis of fast push-pull magnetic amplifiers," Nauchnye Doklady Vysshei Shkoly, Élektromekhanika i Avtomatika, 3, 26 (1958) Fig. 8, Bibl. 3.

V. A. Faradzhev, "A fast reversive full-wave magnetic amplifier," Author's Certificate, Class $21a^2$, 18_{08}, No. 121817, March 8, 1958. Byull. Izobret., 16 (1959).

d) Multiphase Magnetic Amplifiers

V. V. Gorskii, "A three-phase magnetic amplifier," Author's Certificate, Class $21a^2$, 18_{08}, No. 97548. Byull. Izobret., 5 (1959).

V. A. Kulinich and A. M. Bamdas, "A device for balancing linear currents in three-phase circuits," Author's Certificate, Class $21a^2$, 43, No. 121951, January 14, 1959. Byull. Izobre., 16 (1959).

A. L. Pisarev, "Investigation of the operation of magnetic amplifiers with self-saturation for a three-phase load," Avtomat. i Telemekh. 20, 9, 1274 (1959)* Fig. 8, Bibl. 4.

A. L. Pisarev, "On the control characteristic of magnetic amplifiers operating with a three-phase load," Avtomat. i Telemekh. 20, 5, 622 (1959)*Fig. 10, Bibl. 1.

V. P. Shipillo, "A three-phase reversive magnetic amplifier," Author's Certificate, Class $21a^2$, 18_{08}, No. 121174, December 4, 1958. Byull. Izobre., 17 (1959).

e) Multistage Magnetic Amplifiers

S. I. Khmel'nik, "Functional current converter in the load of a two-stage magnetic amplifier circuit, Author's Certificate, Class $21a^2$, 18/08, No. 114548, August 21, 1958.

f) Decision Magnetic Amplifiers

V. P. Milovzorov, "Summing magnetic amplifiers," Tr. Ryazanskogo Radiotekh. Inst. 3, 95 (1958) Fig. 6, Bibl. 2.

G. I. Takhvanov, "Feedback in decision amplifiers," Tr. Ryazanskogo Radiotekh. Inst. 3, 124 (1958) Fig. 8, Bibl. 3.

MAGNETIC AMPLIFIERS, APPLICATION OF MAGNETIC AMPLIFIERS

a) General Application Problems

D. A. Alenchikov, "Development and utilization in industry of a line of magnetic amplifiers and saturation chokes," Collection: Magnetic Amplifiers (Scientificotechnical Conference Transactions, Khar'kov, 1958, Moscow, 1959) pp. 4-19, Fig. 8, Bibl. 19.

M. E. Aizenshtat, "A line of toroidal magnetic amplifiers and units with toroidal amplifiers," Collection: Magnetic Amplifiers (Scientificotechnical Conference Transactions, Khar'kov, 1958, Moscow, 1959) pp. 56-59.

B. K. Karpenko, "A nonlinear electronic amplifier for compensating the nonlinearity of rotary and magnetic amplifiers" (VINITI Branch, Moscow, 1959) p. 11; Referat. Zhur. Élektr., 4, 2947 (1960) Fig. 4.

Ya. M. Kleinman, "On the experience gained in using magnetic amplifiers in devices and equipment produced by the Yuvmetallurgavtomatika Plant," Collection: Magnetic Amplifiers (Scientificotechnical Conference Transactions, Khar'kov, 1958, Moscow, 1959) pp. 160-164, Fig. 4.

Magnetic Amplifiers. Collection of Articles Based on Scientificotechnical Conference Transactions (TsINTI of the Electrical Engineering Industry and Instrument Construction, Moscow, 1959) p. 178, Fig. 116, Bibl. 35.

M. A. Rozenblat, "Magnetic amplifiers for automatic control systems," Collection: Automatic Control and Computer Techniques (Moscow, 1959) Vol. 1, pp. 182-204, Fig. 23.

Ya. B. Rozman and V. A. Naidis, "Magnetic amplifiers as electrical components of machines and machine tools," Collection: Magnetic Amplifiers (Scientificotechnical Conference Transactions, Khar'kov, 1958, Moscow, 1959) pp. 20-27.

Ya. Yu. Solodukho, "Magnetic amplifiers in the automation of continuous-rolling mills," Collection: Magnetic Amplifiers (Scientificotechnical Conference Transactions, Khar'kov, 1958, Moscow, 1959) pp. 86-98, Fig. 12.

T. Kh. Stefanovich, "Magnetic amplifiers for automatic control systems and systems for regulating industrial electric drives," Transactions of the Third All-Union Conference on the Automation of Industrial Processes in Machine Construction and Automated Electric Drives (Moscow, 1959).

T. Kh. Stefanovich, "Magnetic amplifiers for automatic control systems and systems for regulating electric drives, " Tr. Nauchno-Issle. Inst. Élektroprom., Élektroprivod i Sreds'tva Avtomatizatsii 5, 462-476 (1959) Fig. 5.

T. Kh. Stefanovich, "Development of TUM magnetic amplifiers and complete assemblies of devices based on TUM amplifiers for industrial equipment automation," Collection: Magnetic Amplifiers (Scientificotechnical Conference Transactions, Khar'kov, 1958, Moscow, 1959) pp. 46-55, Fig. 6.

F. A. Stupel', "Problems in designing fast electromagnetic mechanisms," Tr. Khar'kovskogo Politekhnicheskogo Instituta 27, 1, 25-33 (1959) Fig. 8, Bibl. 2.

M. V. Khapatetov and M. A. Borisov, "Low-power TUM magnetic amplifiers with toroidal cores"(VINITI Branch, Advanced Scientificotechnical and Industrial Experience, Thesis 27, No. É-59-52/23 Moscow, 1959) p. 14.

É. A. Yakubaitis, "A self-oscillation synchronous oscillator with variable frequency," Choke-Coupled Magnetic Amplifiers (AN LatvSSR Press, 1959) Chap. 5, pp. 187-231, Fig. 27.

b) Application for Control of Electrical Machines

D. A. Alenchikov, " A method of calculating the characteristic of dc electric drives with choke control, which is based on using the family of external characteristics of rectifier-choke converters," Tr. Nauchno-Issle. Inst. Élektroprom., Élektroprivod i Sreds'tva Avtomatizatsii 5, 57-68 (1959) Fig. 5, Bibl. 14.

D. A. Alenchikov, "A method of calculating the characteristics of dc electric drives with choke control, which is based on using the family of external characteristics of rectifier-choke converters," Transactions of the

Third All-Union Conference on Automation of Industrial Processes in Machine Construction and on Automatic Electric Drives (Moscow, 1959).

D. A. Alenchikov, "Calculation of the static characteristics of systems with choke control," Avotmat. i Telemekh. 20, 5, 595 (1959) Fig. 10, Bibl. 5.

D. A. Alenchikov, Control of dc Motors by Means of Saturation Chokes and Semiconductor Rectifiers (TsBTI NII Élektropromyshlennosti, Moscow, 1959) p. 120.

D. A. Alenchikov and V. S. Kulebakin, "A method of calculating the characteristics of dc motors with choke control," Avtomat. i Telemekh. 20, 7, 908(1959) Fig. 5, Bibl. 4.

M. I. Aronov, "A device for automatic excitation control in dc oscillators," Author's Certificate, Class $21d^2$, 38_{20}, No. 118102. Byull. Izobre., 4 (1959).

G. M. Bider, "Application of magnetic amplifiers in automation circuits for metallurgical electric drives," Byull. Tsniichermeta, 5 (361), 54 (1959) Fig. 3.

B. S. Bochkov, L. L. Gol'dina, and L. V. Rosman, "A device for automatic unloading of synchronous machines in the case of overloads," Author's Certificate, Class 21c, 68_{01}, No. 117597. Byull. Izobret., 2 (1959).

Ya. S. Brovman, "Magnetic amplifiers with half-wave fast action in the controllable electric drive for the main motion of heavy machine tools," Collection: Magnetic Amplifiers (Scientificotechnical Conference Transactions, Khar'kov, 1958, Moscow, 1959) pp. 131–137, Fig. 9, Bibl. 5.

A. L. Vil'nyanskii, "Magnetic amplifiers as dc generators or drivers" (VINITI Branch, Advanced Scientificotechnical and Industrial Experience, Thesis 27, No. É-59-7/2, Moscow, 1959) p. 16.

V. S. Volodin, E. D. Larin, M. A. Rozenblat, and G. V. Subbotina, "A fast push-pull magnetic semiconductor amplifier for power follow-up drives," Avtomat. i Telemekh. 20, 3, 323 (1959) Fig. 12, Bibl. 5.

K. P. Garionov, "A contactless self-regulating circuit for controlling heat-powered drives with electric transmission to the moving shafts," Sborn. Leningrad. Inst. Inzh. Zheleznodorozhnogo Trans., 159, 258 (1958) Fig. 7, Bibl. 3.

L. A. Gasparyan and O. B. Rosenbauli, "A device for synchronous generator phase compounding," Author's Certificate, Class $21d^2$, 6_{01}, No. 122202, December 2, 1959. Byull. Izobret., 17 (1959).

L. A. Gasparyan, O. B. Rosenbauli, A. N. Larionov, F. F. Galteev, and T. N. Verbitskaya, "A device for regulating the voltage of synchronous generators," Author's Certificate, Class $21d^2$, 6_{01}, No. 122803, March 23, 1959. Byull. Izobret., 19 (1959).

L. V. Dranitskii, "Application of drives with magnetic amplifiers in machine tools produced by the Moscow Plant for Jig Borers," Collection: Magnetic Amplifiers (Scientificotechnical Conference Transactions, Khar'kov, 1958, Moscow, 1959) pp. 36-39, Fig. 3.

A. G. Efanov, N. G. Kozlov, and Yu. R. Reingol'd, "Results of the industrial testing of the automated dc electric drive for ÉVG-6 excavators with magnetic excitation amplifiers," Tr. Nauchn.-Issle. Inst. Élektroprom., Electric Drives and Automation Equipment 5, 283 (1959) Fig. 5.

M. N. Zaritskii, "Regulation of the automatic control system for a synchronous electric drive with choke control," Nauchnye Doklady Vysshei Shkoly, Gornoe Delo, 4, 161 (1958).

Yu. D. Kapuntsov, "A device for the control of synchronous three-phase motors," Author's Certificate, Class 21c, 59_{30}, 121838, December 7, 1958. Byull. Izobre., 16 (1959).

I. P. Kopylov, "Motors-amplifiers combining a magnetic amplifier with an electric motor," Transactions of the Third All-Union Conference on Automation of Industrial Processes in Machine Construction and Automated Electric Drives (Moscow, 1959).

I. P. Kopylov, "Motor-amplifiers for dc and ac Current," Collection: Magnetic Amplifiers (Scientificotechnical Conference Transactions, Khar'kov, 1958, Moscow, 1959) pp. 165-173, Fig. 6, Bibl. 4.

I. P. Kopylov, L. M. Polyak, and V. I. Radin, "A differential rotary amplifier with magnetization," Nauchnye Doklady Vysshei Shkoly, Élektromekhanika i Avtomatika, 1, 136 (1958) Fig. 5, Bibl. 4.

I. P. Kopylov and V. I. Radin, "An ac motor-amplifier," Élektrichestvo, 11 (1959).

O. M. Kostyuk, "An automatic voltage regulator for synchronous motors," Author's Certificate, Class $21c^2$ 57_{34}, No. 123228. Byull. Izobret., 20 (1959).

O. M. Kostyuk, "Current transformers with magnetization by dc current and particularities in their design for circuits used in automatic control of synchronous generator excitation," Sbornik Trudov Instituta Élektrotekhniki AN UkrSSR Problems in the Stability and Automation of Power Systems, 16, 135 (1959) Fig. 9, Bibl. 6.

V. S. Kulebakin and D. A. Alenchikov, "Application of saturation chokes and magnetic amplifiers in automated electric drives," Collection: Magnetic Amplifiers (Scientificotechnical Conference Transactions, Khar'kov, 1958, Moscow, 1959) pp. 60-71, Fig. 6, Bibl. 6.

A. M. Lyubavin, "A controllable electric drive with magnetic amplifiers," Tr. Nauchn.-Issle. Inst. Élektroprom., Electric Drives and Automation Equipment 5, 46 (1959) Fig. 5.

A. M. Lyubavin, "A controllable electric drive with a magnetic amplifier," Transactions of the Third All-Union Conference on Automation of Industrial Processes in Machine Construction and Automated Electric Drives (Moscow, 1959).

Kh. M. Mamisurov, "The maximum allowable number of times an asynchronous short-circuited motor can be switched on in the case of choke control," Collection: Sudovaya Élektrotekhnika i Svyaz.' 8, 19-24 (1959) Bibl. 4.

L. A. Milovidov, "Results of investigations of the static characteristics of a three-phase asynchronous electric drive system with choke control and feedback with respect to speed," Collection: Magnetic Amplifiers (Scientificotechnical Conference Transactions, Khar'kov, 1958, Moscow, 1959) pp. 138-151, Fig. 12, Bibl. 12.

L. A. Milovidov, Theoretical and Experimental Investigation of an Asynchronous Electric Drive System with Choke Control and Feedback with Respect to Speed, Candidate's Thesis (IAT AN SSSR, Moscow, 1958).

O. A. Nekrasov and A. Ya. Shikhin, "On the self-regulation of diesel locomotive generators by means of magnetic amplifiers,"Élektrichestvo, 5, 31 (1959).

M. N. Osokhin, "Power characteristics of a crane asynchronous electric drive with saturation chokes," Élektrichestvo, 12, 47-50 (1959) Fig. 2, Bibl. 3.

D. P. Pampura and B. A. Kuznetsov, "Conversion of the mechanical characteristics of asynchronous electric motors for mining shaft elevators by means of saturation chokes in the stator circuit," Izvest. Vysshikh Ucheb. Zaved., Gornoe Delo, 5, 64 (1958).

A. Ya. Petrovskii, "A line of electric drive assemblies 0.1- to 4-kw magnetic amplifiers (PMU)," Collection: Magnetic Amplifiers (Scientificotechnical Conference Transactions, Khar'kov, 1958, Moscow, 1959) pp. 28-35, Fig. 8.

A. L. Pisarev, "Application of saturation chokes and magnetic amplifiers in automated electric drives for elevators in inclined mining shafts," Collection: Magnetic Amplifiers (Scientificotechnical Conference Transactions, Khar'kov, 1958, Moscow, 1959) pp. 99-106, Fig. 5.

M. M. Rasulov, "A system for regulating the excitation of synchronous generators with magnetic amplifiers," Tr. Énerge. Inst. im. I. G. Es'man, AN AzerSSR 14, 53-68 (1959) Fig. 14, Bibl. 6.

Yu. R. Reingol'd, "Investigation of the dynamic properties of a generator-motor system with rotary and magnetic amplifiers by the method of experimental frequency characteristics," Tr. Nauchno-Issle. Inst. Élektroprom., Electric Drives and Automation Equipment 5, 29 (1959) Fig. 7, Bibl. 11.

O. B. Rosenbauli and R. N. Rodin, "A graphoanalytical method for calculating the characteristics of the choke control of asynchronous motors with a heavy Shenfer rotor," Avtomat. i Telemekh. 20, 6, 793 (1959)" Fig. 6, Bibl. 2.

O. B. Rosenbauli and R. N. Rodin, "Circuits for motor speed stabilization with three-winding transformers," Avtomat. i Telemekh. 20, 3, 318 (1959)"Fig. 3, Bibl. 1.

O. B. Rosenbauli and R. N. Rodin, "A device for the speed stabilization of three-phase asynchronous motors," Author's Certificate, Class 21c, 59_{01}, No. 118538 (586290 of November 18, 1957). Byull. Izobre., 6 (1959).

N. P. Rybalko, "A speed regulator for mining shaft elevators," Author's Certificate, Class 21c, 59_{34}, No. 117272. Byull. Izobret., 2 (1959).

V. V. Sarv, Speed-Control of Asynchronous Motors with Phase Rotors by Using Saturation Chokes in the Case of Balanced and Unbalanced Feed, Candidate's Thesis (Leningrad Institute of Electrical Engineering, 1959).

V. V. Sarv, "Speed-control of asynchronous motors by means of saturation chokes," Information Bulletin (Council of National Economy, Power Supply Management "Éstonénergo" Énergosbyt), 6, 33-39 (1959) Fig. 5.

V. V. Semenov and É.F. Stepura, "An electrohydraulic speed regulator for hydraulic turbines," Author's Certificate, Class 21c, 64_{57}, No. 123231. Byull. Izobret., 20 (1959).

O. V. Slezhanovskii, "A system of contactless control for reversive dc electric drives," Tr. Nauchn.-Issle. Inst. Élektroprom., Electric Drives and Automation Equipment 5, 79-93 (1959) Fig. 6, Bibl. 2.

M. M. Sokolov and Yu. D. Kapuntsov, "A controllable asynchronous electric drive for crane mechanisms with saturation coils," Élektrichestvo, 11 (1959) Fig. 4, Table 1, Bibl. 1.

É. F. Stepura and V. V. Semenov, "A nonlinear magnetic device for restricting the armature current in electrical machines," Author's Certificate, Class 21c, 59_{20}, No. 121837, January 16, 1959. Byull. Izobret., 16 (1959).

M.S. Ter-Mkhitarov, "Possibilities of using magnetic amplifiers in the generator excitation circuit of generator–motor systems," Collection of Scientific Papers (Perm Mining Institute), 2, 159-165 (1958).

"A device (self-operator) for the automatic control of hydroelectric power station units," Author's Certificate, Class 21c, 64_{53}, No. 120570 (589971/24 of January 15, 1958).

N. V. Sharygin, "Application of magnetic power amplifiers in high-frequency voltage-stabilization circuits of rotary generators and in infrasonic-frequency power amplifier circuits," Collection: Magnetic Amplifiers (Scientificotechnical Conference Transactions, Khar'kov, 1958, Moscow, 1959) pp. 107-112, Fig. 3.

É. A. Yakubaitis, "Static self-excitation systems with magnetic amplifiers and germanium triodes for synchronous generators operating at variable frequency," Collection: Magnetic Amplifiers (Scientificotechnical Conference Transactions, Khar'kov, 1958, Moscow, 1959) pp. 113-119, Fig. 5.

É. A. Yakubaitis and A. Z. Libman, "Railway-car electric power stations with ac generators and semiconductor rectifiers," Vest. Vses. Nauchn.-Issle. Inst. Zheleznodorozhnogo Transp., 7, 55-57 (1958) Fig. 2, Bibl. 6.

c) Application in Current and Voltage Stabilizers

L. M. Al'tshul', "An electromagnetic voltage stabilizer," Author's Certificate, Class $21d^2$, 42_{01}, No. 118104. Byull. Izobret., 4(1959).

A. M. Bamdas, V. A. Somov, and S. V. Shapiro, "New powerful ac stator stabilizers," Vest. Élektroprom., 9, 8 (1959), Fig. 5, Bibl. 4.

D. I. Bogdanov, "On the theory of voltage stabilizers with series ferroresonance," Vest. Élektroprom., 3, 53 (1959) Fig. 4, Bibl. 1.

V. S. Volodin and M. A. Rozenblat, "A stable dc voltage source with magnetic and semiconductor components," Izvest. Akad. Nauk SSSR, Otdel. Tekh. Nauk, Power Engineering and Automation, 4, 208 (1959) Fig. 4.

Yu. K. Zakharov and V. G. Nikulin, "A choke-coupled ac voltage stabilizer," Author's Certificate, Class $21d^2$, 42_{01}, No. 121182. Byull. Izobret., 14 (1959).

P. N. Loiter and E. V. Ershova, "A voltage stabilizer," Author's Certificate, Class $21d^2$, 42_{01}, No. 121850. Byull. Izobret., 16 (1959).

G. F. Neplokhov, "A device for rectified stabilization," Author's Certificate, Class $21d^2$, 42_{01}, No. 124981. Byull. Isobret., 24 (1959).

I. I. Pekker and V. V. Tsokanov, "A voltage stabilizer," Author's Certificate, Class 21c, 67_{10}, No. 124502. Byull. Izobre., 23 (1959).

S. G. Popov, "A voltage stabilizer," Author's Certificate, Class $21d^2$, 42_{01}, No. 120592. Byull. Izobret., 12 (1959).

Yu. N. Pryadilov, "Effect of load reactance on the accuracy of ac voltage stabilizers with saturation chokes," Tr. Mosk. Aviat. Tekh. Inst., 41, 47-53 (1959).

S. F. Pyatkin and P. G. Yantsev, "A contactless method for automatic stabilization of temperature in electric furnaces," Steklo i Keramika, 10, 35 (1958).

F. Sokolov, "The 28-SN-1.25 voltage stabilizer," Kinomekhanik, 6, 31 (1959).

V. P. Soskovets, "A direct-control voltage stabilizer," Vestnik Svyazi, 12, 10-11 (1959) Fig. 4.

A. S. Tofanyuk, Voltage Stabilizers (Voenizdat, Moscow, 1958) p. 83.

G. S. Finogin and A. A. Fedosin, "A current stabilizer," Author's Certificate, Class $21d^2$, 53_{02}, No. 121852, January 26, 1959. Byull. Izobret., 16 (1959).

S. V. Shapiro, "Starting stabilizers with a transformer controlled by shunt magnetization," Tr. Gor'kov. Politekh. Inst. 15, 4, 80 (1959).

d) Application in Measuring Devices

K. P. Garionov, "Multiplier circuits with magnetic amplifiers as data transmitters for voltage, power, and current in voltage self-regulation systems for diesel locomotive traction generators," Collection: Tr. Leningrad. Inst. Inzh. Zheleznodorozhnogo Transp., 159, 268 (1958) Fig. 6, Bibl. 8.

I. Ya. Kaverkin, "Two types of measuring magnetic amplifiers," Informat. Tekh. Sborn. TsBTI, 16 (145), 28 (1958) Fig. 8, Bibl. 1.

O. N. Mel'nikov, "On the application of push-pull magnetic amplifiers as components for measuring large dc current values in control systems," Élektrichestvo, 8, 36-40 (1959) Fig. 5, Bibl. 3.

A. M. Ryvkin, "A device for dc current measurements," Author's Certificate, Class 21e, 36_{01}, No. 120603 (599161/24 of May 9, 1958).

e) Other Applications

A. S. Baginskaya, "Differential protection of synchronous generators by means of current transformers with magnetization by secondary current " Izvest. Tomsk. Politekh. Inst. 94, 166 (1959), Fig. 6, Bibl. 2.

A. S. Baginskaya, "Current transformers with magnetization by secondary current for differential protection," Izvest. Tomsk. Politekh. Inst. 94, 161 (1959) Fig. 6, Bibl. 3.

I. V. Gavrilov, "Application of half-wave magnetic amplifiers in the grid control circuit of mercury rectifiers," Collection: Magnetic Amplifiers (Scientifico-technical Conference Transactions, Khar'kov, 1958, Moscow, 1959) pp. 152-159, Fig. 11.

L. S. Golubev, "A contactless device for automatic charging of storage batteries," Author's Certificate, Class 21b, 26_{02}, No. 124487. Byull. Izobret., 23 (1959).

O. I. Danilevich, "A method for starting mechanical rectifiers," Author's Certificate, Class 21g, 15_{02}, No. 121880, December 18, 1958. Byull. Izobret., 16 (1959).

Ya. A. Kantin, "A controllable transformer," Author's Certificate, Class $21d^2$, 53_{02}, No. 123602. Byull. Izobret., 21 (1959).

Yu. A. Rashkovskii, "Application of current transformers with magnetization in relay protection circuits," Tr. Khar'kov. Politekh. Inst. 27, 1, 43 (1959) Fig. 3, Bibl. 3.

MAGNETIC VOLTAGE AMPLIFIERS, MODULATORS, AND PROBES (MAGNETOMETERS)

R. Ya. Berkman and V. N. Mikhailovskii, "Measurement of variable weak magnetic low-frequency fields in geophysical prospecting," Izvest. Akad. Nauk SSSR, Ser. Geofiz., 6 (1959).

R. Ya. Berkman and V. N. Mikhailovskii, "A method for measuring variable weak low-frequency magnetic fields and its application in technology and applied physics," Avtomat. Kontrol' i Izmeritel'naya Tekh., 3 (1959).

I. G. Gol'dreer, "A converter for transforming dc signals into ac signals," Author's Certificate, Class $21d^2$, No. 124522. Byull. Izobret., 23 (1959).

K. P. Egorov and T'ung K'ai, "Magnetic modulators and the possibilities of their application in multichannel communication equipment, " Tr. Leningrad.

Élektrotekh. Inst. Svyazi.3 (36) 51 (1958) Fig. 9, Table 3, Bibl. 5.

S. P. Kolosov, "Calculation of the static characteristics of push-pull magnetic voltage amplifiers (for automatic systems)," Nauchnye Doklady Vysshei Shkoly, Élektromekhanika i Avtomatika, 2, 43 (1959) Fig. 3, Bibl. 4.

S. A. Levitan and I. B. Negnevitskii, "A magnetic modulator," Author's Certificate, Class $21d^2$, 12_{04}, No. 124521. Byull. Izobret., 23 (1959).

V. N. Mikhailovskii, B. I. Blazhkevich, R. Ya. Berkman, R. E. Martynyuk-Lototskii, Yu. I. Spektor, and E. A. Andrievskii,"z-Magnetometers with magnetic-modulation data tramsitters of the second harmonic type," Avtomat. Kontrol' i Izmeritel'naya Tekh.,3 (1959).

R. I. Yanus, L. A. Fridman, and V. I. Drozhzhina, "On the theory of differential ferroprobes with longitudinal excitation," Tr. Inst. Fiz. Metall. AN SSSR, 21, 313-326 (1959).

DISCRETE-ACTION MAGNETIC COMPONENTS

a) Books, Monographs, and Dissertations

O. V. Bachin, Possibilities of Using Transfluxors in Memory and Programming Devices (ITM and VT AN SSSR Press, 1959) p. 37.

É. D. Demin and L. A. Chinenkov, Pulse Devices with Ferrites and Semiconductors in Radio Electronics (Novosibirsk, 1959) p. 168, Fig. 98.

V. M. Doklart and G. Ya. Novik, Application of Transistor and Magnetic Components in Digital Computers (Izd. Sovetskoe Radio, 1959), p. 232.

É. I. Zarubina, "Electromagnetic lag lines with ferrite cores" (VINITI Branch, Advanced Scientifico-technical and Industrial Experience, Thesis 42, No. P-59-112/9 Moscow, 1959) p. 12.

Ya. G. Koblents, Design of Circuits and Units for Contactless ATS Magnetic Control (Svyaz'izdat, Moscow, 1959) p. 65, Fig. 30, Bibl. 12.

Ya. G. Koblents, Magnetic Commutation Fundamentals (Svyaz'izdat, Moscow, 1959) p. 58, Fig. 24, Bibl. 11.

Yu. A. Makhmudov, Exploration of the Possibility of Designing a Universal Digital Computer with Magnetic (Ferrite) Components. Candidate's Thesis (Electrical Simulation Laboratory, Academy of Sciences, USSR, 1959).

V. D. Panasenko, "Components for automatic and remote control devices," Tr. Aviats. Inzh. Akademii im. Dzerzhinskogo, Moscow, 39, 272 (1959) Table 187, Bibl. 54.

I. V. Prangishvili, Development and Investigation of Units and Assemblies of Contactless Remote Control Systems with Magnetic and Semiconductor Components. Candidate's Thesis (IAT AN SSSR, 1959).

Application of Transistor and Magnetic Components in Digital Computers. Collection of articles [Russian translation] ed. V. K. Lyubchenko and S. M. Nikulin (Sovetskoe Radio, Moscow, 1959) p. 232.

b) Application of, and Surveys Pertaining to, Discrete Components in Control Systems and Computers

Ya. A. Bedrov, "An indicator of the static state of circuits with two stable equilibrium states," Author's Certificate USSR, Class $21a^1$, 26, No. 111719, June 25, 1958.

N. P. Vasil'eva and N. L. Prokhorov, "Magnetic logical components for automatic control circuits," Avtomat. i Telemekh. 20, 12, 1647 (1959) Fig. 23, Bibl. 6.

K. Guiskii, "A linear commutator with ferrites and semiconductor triodes and a single-cycle input," Sborn. Nauchn.-Issle. Rabot Studentov Élektromekh. Fakul'teta, Leningrad Politekh. Inst., 4, 80 (1959) Fig. 5.

É. A. Demin and L. A. Chinenkov, "Semiconductor current pulse generators for the switching of commutation circuits with ferrites with a rectangular hysteresis loop," Nauchnye Doklady Vysshei Shkoy, Inzh. Radio i Elektronika, 4, 218 (1958) Fig. 12, Bibl. 3.

A. D. Drozdov, V. P. Sabadashev, and Yu. A. Vegera, " A phase-selecting device with alternating pulse current for remote control," Izvest. Vysshikh Ucheb. Zaved., Élektromekhanika, 2, 90-93 (1959) Fig. 3, Bibl. 3.

Z. S. Zorina and E. A. Shkabara, Computers Based on Ferrite Cores with Crystal Triode Control. Problems in Computer Mathematics and Technology (AN UkrSSR Press, Kiev, 1958) pp. 84-93, Fig. 9, Bibl. 5.

Yu. N. Ivenskii, Ya. A. Slepyan, and I. M. Kaplan, "Contactless end switches," Byull. Tekh.-Ékonom. Inform. Council of National Economy of the BelorusSSR, 4-5, 76 (1958).

M. I. Kaplan, "A distributor based on magnetic components," Author's Certificate, Class $21a^1$, 36, No. 123201. Byull. Izobret., 20 (1959).

Ya. G. Koblents, "Design and analysis of single-cycle magnetic logical and trigger commutation circuits," Élektrosvyaz' 3, 3, 73-81 (1959) Bibl. 8.

Ya. G. Koblents and E. I. Glaz, "Opposing ATS complex of industrial equipment based on contactless magnetic components," Élektrosvyaz' 3, 11, 58 (1959) Fig. 3, Bibl. 5.

Yu. A. Makhmudov, "A compact universal digital computer based on magnetic (ferrite) LÉM-1 components," Radiotekhnika 14, 3, 47 (1959), Fig. 1, Table 1, Bibl. 3.

K. G. Mityushkin, "The BMT-S-58 cableless remote signal device," Élektricheskie Stantsii, 8, 86 (1959) Fig. 1.

V. N. Mikhailovskii, V. N. Okhotskaya, and K. D. Nadtochii, "Contactless remote control components"

(TsITÉI Advanced Scientificotechnical and Industrial Experience, 1959), Thesis 42, No. P-59-109/8.

E. A. Nemtseva and V. P. Sabadashev, "Development of devices for the storage and circulating transmission of remote control signals with magnetic components," Collection: Nauchn. Rabot. Student. Énerget. Élektromekh. i Mekh. Fakul'tetov Novocherkasskogo Politekh. Inst.,2, 33 (1959) Fig. 7.

K. I. Petukhov, "A magnetic storage device for mining control centralization," Sbor. Leningrad. Inst. Inzh. Zheleznodorozhnogo Transp.,161, 298 (1958) Fig. 8.

I. V. Prangishvili, "Analysis of the operation of magnetic pulse components in contactless remote control devices," Avtomat. i Telemekh. 20, 4, 473 (1959) Fig. 8, Bibl. 6.

A. K. Romanov, "Operation of magnetic single-cycle shift recorders with simultaneous magnetization reversal in additional cores, " Élektrosvyaz', 10, 43 (1959), Bibl . 7.

V. P. Sabadashev and Yu. A. Vegera, "A contactless fast phase device for remote control using ac pulses," Izvest. Vysshikh Ucheb. Zaved., Élektromekhanika,2, 94 (1959) Fig. 6, Bibl. 1.

V. E. Khazatskii and V. A. Leonov, "A cyclic-action contactless commutator," Author's Certificate, Class 21c, 47_{50}, No. 121165. Byull. Izobre.,14 (1959).

c) Components Consisting of Magnetic Amplifiers with Feedback

Ya. G. Koblents, D. A. Yakovenko, and N. P. Margacheva, "A magnetic time relay," Author's Certificate, Class 21, 4/05, 21c, 68/60, No. 115510, November 29, 1958.

E. P. Krasovskii, V V. Lauér, and A. G. Shapovalenko, "An ac time relay with a magnetic amplifier," Izvest. Vysshikh Ucheb. Zaved., Énergetika, 1, 59-64 (1958) Fig. 4, Bibl. 2.

I. S. Mikadze and V. G. Kikalishvili, "A time relay with a magnetic amplifier," Tr. Tbilisskogo Nauchn. Issle. Inst. Priborostroeniya i Sredstv Avtomat. 1, 79 (Tbilisi, 1957) Fig. 6, Bibl. 2.

I. V. Prangishvili, "A contactless relay," Author's Certificate, Class 21c, 45_{01}, No. 117663. Byull. Izobret., 2 (1959).

I. I. Ratgauz, "A contactless time relay," Author's Certificate, Class 21c, 44, No. 75562. Byull. Izobret., 2 (1959).

Yu. I. Sumarokov, L. V. Shul'gin, and N. D. Sokolova, "A magnetic trigger," Author's Certificate, Class 21g, 4_{05}, No. 117666. Byull. Izobret.,2 (1959).

V. E. Khazatskii, "A magnetic trigger amplifier," Author's Certificate, Class $21a^1$, 36, No. 119892. Byull. Izobret.,10 (1959).

N. V. Khrushcheva and L. N. Bykov, "A contactless time relay," Author's Certificate, Class 21g, 4_{05}, No. 117587. Byull. Izobret.,2 (1959).

N. I. Chicherin and Yu. M. Kozlov, "A contactless three-position relay," Author's Certificate, Class $21a^1$ 27, No. 123208. Byull. Izobret.,20 (1959).

B. K. Shchukin, "A contactless relay," Author's Certificate, Class 21g, 4_{05}, No. 94434. Byull. Izobret. , 2 (1959).

d) Components with Hysteresis

V. G. Glotov and L. A. Pronin, "On the shape of the hysteresis loop of ferrite cores for memories," Vestn. Élektroprom.,7, 64 (1959) Fig. 4, Bibl. 4.

V. G. Glotov and L. A. Pronin, "Ferrites with a rectangular hysteresis loop for memories," Tr. Nauchn. Issle. Inst. Élektroprom. 4, 53-58 (1959) Fig. 5, Bibl. 5.

Yu. N. Glukhov, V. I. Zolotarevskii, M. A. Kartsev, V. P. Konstantinov, and R. P. Shidlovskii, A Ferrite Memory for 4096 Numbers. Digital Techniques and Computers (Izd. AN SSSR, 1959) pp. 5-27, Fig. 18.

L. V. Ivanov and E. N. Filinov, Control Devices for the Preparation and Adjustment of Ferrite Memories. Digital Techniques and Computers (Izd. AN SSSR, 1959) pp. 28-41, Fig. 9, Bibl. 2.

A. I. Korolev, "A contactless number code data transmitter with magnetic storage devices," Sborn. Leningrad. Inst. Inzh. Zheleznodorozhnogo Trans.,161, 292 (1958) Fig. 3.

V. R. Kulikov, "On the selection of parameters of magnetic automation components with hysteresis," Tr. Khar'kov. Politekh. Inst. 27, 1, 35 (1959) Fig. 3, Bibl. 4.

E. I. Mamonov, "A method for determining the switching time of magnetic components," Author's Certificate, Class 21e, 12, No. 124049. Byull. Izobret., 22 (1959).

A. K. Romanov, "Stability of magnetic push-pull shift recorders," Nauchnye Doklady Vysshei Shkoly, Radiotekh. i Élektron., 2, 303 (1959) Bibl. 5.

N. Ya. Matyukhin and O. V. Rosnitskii, "On the operation of ferrite cores in matrix memories," Collection: Computer Techniques (Izd. AN SSSR Moscow, 1959) pp. 119-130, Fig. 11, Bibl. 5.

L. A. Chinenkov and É. D. Demin, "A closed-loop shift recorder with magnetic components with a rectangular hysteresis loop," Author's Certificate, Class $21a^1$, 36, No. 119893. Byull. Izobret. 10 (1959).

e) Magnetic Transistor Components

É. I. Galynker, A Decimal Counter with Ferrite–Transistor Triggers. Digital Techniques and Computers (Izd. AN SSSR, 1959), pp. 183-185, Fig. 4.

M. G. Reinberg and V. A. Tret'yukhin, Ferrite–Transistor Triggers with a Single Transistor. Digital Techniques and Computers(Izd. AN SSSR, 1959) pp. 179-182, Fig. 4, Bibl. 1.

Yu. I. Serenkov and I. S. Vorontsova, "Experimental investigations of the simultaneous operation of ferrite-transistor logical cells in computer mock-ups," Nauchn.

Tekh. Informat. Byull. Leningrad. Politekh. Inst. im. M. I. Kalinina, 1, 66 (1959) Bibl. 6.

f) Ferroresonance Components

I. L. Tanatarova and V. P. Sabadashev, "Development and investigation of fast remote control devices with ferroresonance components," Collection: Nauchn. Raboty Studentov Énerget. Élektromekh. i Mekhan. Takul'tetov Novocherkasskogo Politekh. Inst., 3, 21 (1959) Fig. 9, Bibl. 2.

MAGNETIC OSCILLATORS AND FREQUENCY CONVERTERS

A. M. Bamdas and V. I. Zagryadskii, "A contactless induction frequency converter," Izvest. Vysshikh Ucheb. Zaved., Élektromekhanika, 2, 105 (1959) Fig. 3, Bibl. 14.

A. M. Bamdas and V. A. Kulinich, "Automatic balancing of a three-phase circuit feeding an active single-phase load of variable magnitude," Izvest. Vysshikh Ucheb. Zaved., Énergetika, 9, 53 (1959) Bibl. 14.

A. M. Bamdas and V. A. Kulinich, "Static converters with magnetic amplifiers for transforming single-phase currents into three-phase currents," Tr. Gor'kov. Politekh. Inst. im. Zhdanova 15, 4, 37 (1959) Fig. 6, Bibl. 13.

A. M. Bamdas and V. A. Kulinich, "A static device for transforming a single-phase system into a three-phase system," Author's Certificate, Class $21d^2$, 52, No. 120594. Byull. Izobret., 12 (1959).

K. I. Vil'pert, "A converter with semiconductor triodes for transforming dc current into ac current," Author's Certificate, Class $21d^2$, 12_{03}, No. 124520. Byull. Izobret. 23 (1959).

V. I. Zhitomirskii and E. N. Men'chukov, "A frequency divider circuit," Author's Certificate, Class $21a^4$, 48_{15}, No. 119208. Byull. Izobret., 8 (1959).

A. I. Zaitsev and Ya. V. Petrov, "A resonance three-phase frequency trebler," Izvest. Tomskogo Politekh. Inst. 97, 12 (1959), Fig. 10, Bibl. 4.

V. A. Kulinich, "Static transformation of single-phase currents into three-phase currents with balance stabilization," Izvest. Vysshikh Ucheb. Zaved., Élektromekhanika, 7, 66 (1959) Fig. 9, Bibl. 17.

Ya. V. Petrov and A. I. Zaitsev, "On the circuits of three-phase ferromagnetic frequency treblers," Izvest. Tomskogo Politekh. Inst. 97, 22 (1959) Fig. 6, Bibl. 5.

A. G. Pinchuk, "A device for frequency multiplication," Author's Certificate, Class $21d^2$, 51, No. 94694. Byull. Izobret., 1 (1959).

S. V. Pokrovskii, On the Method of Designing Static Frequency Doublers. Candidate's Thesis (MÉI, Moscow, 1959).

A. M. Pshenichnikov, "Analysis of the operation of Roer multivibrators in industrial remote measurement devices," Avtomat. i Telemekh. 20, 9, 1250-1261 (1959)* Fig. 12, Bibl. 6.

V. A. Rayushkin, "Analytical determination of idling and short-circuit regimes of frequency doublers by taking into account the higher harmonics," Tr. Khar'kov. Politekh. Inst. 27, 1, 5 (1959) Fig. 9, Bibl. 11.

L. L. Rozhanskii, "A static frequency doubler with magnetization by direct current," Tr. Khar'kov. Politekh. Inst. 27, 1, 19 (1959) Fig. 3, Bibl. 4.

A. G. Rubinshtein, D. F. Tartakovskii, and I. I. Vinshtein, "A magnetic oscillator," Author's Certificate, Class $21a^4$, 13, No. 122782, February 7, 1959. Byull. Izobret., 19 (1959).

A. B. Flerov and V. P. Sabadashev, "Investigation of extrinsic characteristics of magnetic frequency treblers," Collection: Nauchnye Raboty Studentov Énerget. Élektromekh. i Mekhani. Fakul'tetov Novocherkasskogo Politekh. Inst., 3, 41-50 (1959), Fig. 9, Bibl. 4.

L. A. Chinenkov and É. A. Demin, "Frequency dividers with ferrites and semiconductor triodes," Élektrosvyaz' 6, 6, 11 (1959) Bibl. 8.

V. I. Shchitnikov, "A method for dividing the pulse repetition frequency," Author's Certificate, Class $21a^1$, 36, No. 124003, Byull. Izobret., 22 (1959).

MAGNETIC MEASUREMENTS AND METHODS FOR TESTING MAGNETIC COMPONENTS

Yu. A. Avakh, "A new method for controlling magnetic amplifiers," Nauchnye Doklady Vysshei Shkoly, Mashinostroenie i Priborostroenie, 2, 175-182 (1959).

Yu. A. Avakh, "A device for testing magnetic amplifiers which are controlled by direct current," Author's Certificate, Class 21e, 36_{10}, No. 121874, December 18, 1958. Byull. Izobret., 16 (1959).

O. N. Al'tgauzen and N. A. Semenova, "On the method of measuring the magnetic properties of electrical steel in weak and medium fields," Zavodskaya Lab. 25, 4, 426-428 (1959)* Fig. 3, Bibl. 4.

"Methods and equipment for inspecting ferrite toroidal cores with respect to their magnetic properties," 1953-1957, 14 titles (01 No. 1301), Novo. Zarubezhnoi Radioélekt. VNT MO SSSR, 7, 32 (April, 1959)

R. Kh. Bal'yan, V. I. Laletin, and I. V. Trofimov, "A method for demagnetizing the cores of pulse transformers," Radiotekhnika 14, 8, 40 (1959) Fig. 2, Bibl. 2.

R. Kh. Bal'yan, V. I. Laletin, and I. V. Trofimov, "A device for demagnetizing the cores of pulse transformers," Author's Certificate, Class $21d^2$, 12_{02}, No. 121501. Byull. Izobret., 15 (1959).

A. A. Bondar', "A method for dividing losses in magnetic cores," Author's Certificate, Class 21e, 12, No. 123249. Byull. Izobret., 20 (1959).

G. Kh. Vyal'yamyaé, "A device for determining the magnetic properties of ferromagnetic materials," Author's Certificate, Class 21e, 12, No. 123607. Byull. Izobret., 21 (1959).

L. N. Gertsiger, "The IMI-2 magnetic induction meter," Priborostroenie, 5, 27 (1959).

K. K. Gomoyunov, "A method for determining the magnetic properties of ferromagnetic cores," Author's Certificate, Class 21e, 12, No. 119249. Byull. Izobret., 8 (1959).

G. L. Gornshtein and M.M. Leshchines, "The problem of measuring magnetic induction in electrical steel in a magnetic field of 10 at/cm," Zavodskaya Lab. 25, 12, 1427 (1959)*Fig. 1, Table 2, Bibl. 2.

V. V. Druzhinin, "On the shape of specimens for determining the magnetic characteristics of electrical steel," Zavodskaya Lab. 25, 4, 429 (1959)*Fig. 2, Table 5.

V. V. Druzhinin, Yu. E. Zubov, A. A. Kozhurov, and R. I. Yanus, "A device for magnetic and electrical investigation of whole electrical steel sheets," Author's Certificate, No. 118903, March 7, 1959.

V. V. Druzhinin and I. P. Kudryavtsev, "On the quantitative determination of texture in cold-rolled transformer steel, " Zavodskaya Lab. 25, 12, 1425 (1959)*Fig. 3, Bibl. 4.

E. L. Kantor, "Inspection of the basic ferromagnetic characteristics of toroidal cores in mass production," Priborostroenie, 11, 21 (1959).

V. P. Karpenko, Possibilities of Using T-Circuits for Magnetic Measurements, Magnetic Measurement Problems(Izd. AN UkrSSR, Kiev, 1959) pp. 105-119, Fig. 11, Bibl. 4.

V. P. Karpenko, A Calorimetric Method of Measuring Losses in Ferromagnetic Materials. Magnetic Measurement Problems (Izd. AN UkrSSR, Kiev, 1959) pp. 96-104, Fig. 2, Bibl. 5.

I. I. Kifer, "Magnetic measurement methods and equipment," Zavodskaya Lab. 25, 4, 423-425 (1959).*

I. I. Kifer and V. U. Marguleva, "On the oscillographic method of testing magnetically soft materials," Zavodsk. Lab. 25, 4, 434(1959)*Fig. 3, Table 4, Bibl. 3.

B. E. Kubyshin, Determination of the Permeability of Substances in Variable Fields. Magnetic Measurement Problems (Izd. AN UkrSSR, Kiev, 1959) pp. 6-19 Fig. 5, Bibl. 3.

E. D. Mamontov, "A method for measuring the permeability of closed-loop cores in variable magnetic fields," Author's Certificate, Class 21e, 37_{10}, No. 122548, January 17, 1959. Byull. Izobret., 18 (1959).

V. M. Mezhenin, "A new device for testing magnetic amplifiers" (VINITI Branch, Moscow, 1959) p. 11, Ref. Zh. Élektrotekh., 4, 2947 (1960).

V. I. Molotkov, "A method for determining the hysteresis loop of ferromagnetic materials," Author's Certificate, Class 21e, 37_{10}, No. 123620. Byull. Izobret., 21 (1959).

A. D. Nesterenko, The Use of Balancing Circuits for Testing Magnetically Soft Materials in Steady Magnetic Fields. Magnetic Measurement Problems. (AN Izd. Ukr. SSR, Kiev, 1959) pp. 53-61, Fig. 8, Bibl. 5.

V. F. Petrochenko, "Separation of losses in steel by the method of two different frequencies in the case of constant losses due to eddy currents," Magnetic Measurement Problems (Izd. AN UkrSSR Kiev, 1959) pp. 45-52, Table 2, Bibl. 6.

L. I. Rabkin, E. V. Ébanoidze, Z. A. Isaeva, and N. P. Goryachev, "A method of testing ferrites," Author's Certificate, Class 21e, 37_{10}, No.119935. Byull. Izobret., 10 (1959).

I. M. Rozhanovskii, "Magnetic characteristics of electrical steels in variable magnetic fields," Magnetic Measurement Problems (Izd. AN UkrSSR, Kiev, 1959) pp. 20-32, Fig. 14, Table 4.

I. M. Rozhanovskii, "Recommended methods for separating losses in electrical steels," Magnetic Measurement Problems (Izd. AN UkrSSR, Kiev, 1959) pp. 33-44, Fig. 4, Table 2, Bibl. 8.

A. A. Roitman, "On magnetic tests of cold-rolled textured electrical steel," Zavodskaya Lab. 25, 4, 433 (1959).*

N. M. Rudnyi, A. Z. Veksler, and I. F. Kobyakov, "A stabilized sinusoidal current source for checking electrical measuring instruments," Collection of Reports on Scientific Investigations Performed in the Institutes of Measures and Measuring Instruments of the Council of Ministers of the Standartgiz, Moscow–Leningrad, 3, 77 (1959), Report No. 288.

N. A. Semenova and O. N. Al'tgauzen, "On the method of determining magnetic properties in the Epstein apparatus," Zavodskaya Lab. 25, 12, 1418 (1959)* Fig. 3, Bibl. 5.

O. P. Sidorov, "A device for measuring hysteresis losses in ferromagnetic materials," Author's Certificate, Class 21e, 37_{10}, No. 119262. Byull. Izobret., 8 (1959).

E. K. Ul'yanova, "A device for determining the pulse characteristics of ferrite cores," Tr. Nauchn. Issle. Inst. Élektropro. 4, 59 (1959) Fig. 3.

E. N. Chechurina, "Peculiarities in testing ferromagnetic materials in the case of simultaneous magnetization in steady and variable fields," Tr. VNIIM: Investigations in the Field of Electrical Measurements, Standartgiz, Moscow–Leningrad, 38 (98), 126-135 (1959) Fig. 7, Table 4, Bibl. 7.

N. G. Chernysheva, "On methods of determining the properties of electrical steel, " Zavodskaya Lab. 25, 4, 437 (1959).*

E. T. Chernyshev, E. N. Chechurina, N. G. Chernysheva, and I. A. Oralova, "Development of methods and equipment for testing normal magnetic material specimens at frequencies over 1000 cps in the 10,000-gauss induction range," Collection of Reports on Scientific Investigations performed in the Institutes of the Committee for the Council of Ministers of the Standards, Measures, and Measuring Instruments USSR (Standartgiz, Moscow–Leningrad, 1959), No. 3, p. 77, Report No. 289.

Yu. M. Shamaev, F. G. Lisitsyn, and A. I. Pirogov, "Measurement method and the results obtained in measuring the static and dynamic characteristics of ferrites with a rectangular hysteresis loop," Nauchnye Doklady Vysshei Shkoly, Élektromekhanika i Avtomatika, 3, 3 (1958), Fig. 16, Bibl. 7.

R. I. Yanus, Certain Problems in the Theory and Techniques of Magnetic Measurements. Author's Abst. of Ph. D. Dissertation (UF AN SSSR, Sverdlovsk, 1959).

R. I. Yanus, "On nondestructive methods for testing electrical sheet steel," Zavodskaya Lab. 25, 12, 1421-1422 (1959)* Bibl. 9.

R. I. Yanus and Yu. A. Vdovin, "A method for determining the magnetic properties of electrical steel," Author's Certificate, Class 21e, 37_{10}, No. 124547. Byull. Izobret., 23 (1959).

R. I. Yanus, V. V. Kubarev, Yu. A. Vdovin, and I. P. Kolpakov, "An automatic device for sorting electrical steel sheets," Zavodskaya Lab. 25, 4, 480 (1959).*

R. I. Yanus and T. M. Senkevich, "A simple electromagnetic device for thickness measurement," Tr. Inst. Fiz. Metallov AN SSSR, 21, 131 (1959).

BLANK
PAGE

DUAL CONTROL THEORY. II

A. A. Fel'dbaum

Moscow

Translated from Avtomatika i Telemekhanika, Vol. 21, No. 11,
pp. 1453-1464 , November, 1960
Original article submitted March 23, 1960

Basic formulas are derived and the optimum control algorithm is determined in the general case, first for an open-loop and then for a closed-loop nonlinear system of dual control [1].

Similarities and differences between the solutions for open and closed systems are indicated.

1. Derivation of the Risk Formula in Open-Loop Systems

We start first by deriving the formulas for an open system shown in Fig. 1. This is done to demonstrate certain methods which have led to the obtained results; also to compare certain characteristics of the open and closed systems. The open system is basically more simple than the closed one, and this makes the derivation of the formulas easier in the former case.

The problem is stated as follows [1]: all quantities are functions of discrete time at the time moments 0, 1, ..., s, ..., n, where n is fixed. The input is

$$x_s^* = x_s^*(s, \boldsymbol{\lambda}), \tag{1}$$

where $\boldsymbol{\lambda}$ is the parameter vector

$$\boldsymbol{\lambda} = (\lambda_1, \ldots, \lambda_q) \tag{2}$$

with an a priori probability density $P_0(\boldsymbol{\lambda}) = P(\boldsymbol{\lambda})$. The input x^* becomes mixed with noise h^* in the channel or system H^*, at whose output y^* is obtained. Statistical properties of the noise, and the method of combining the signal and the noise in H^* are known. Consequently the conditional probability $P(y_s^*/x_s^*)$ is also known, being identical for all s , as the probability density $P(h_s^*)$ of the noise is assumed as not varying with s*.

The characteristic of the controlled object B is given by the formula

$$x_s = F_0(z_s, v_s), \tag{3}$$

where F_0 is a known function, and

$$z_s = z_s(s, \boldsymbol{\mu}), \tag{4}$$

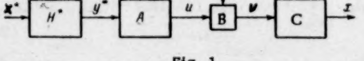

Fig. 1

in which $\boldsymbol{\mu}$ is the parameter vector

$$\boldsymbol{\mu} = (\mu_1, \mu_2, \ldots, \mu_m) \tag{5}$$

with given a priori probability density $P_0(\boldsymbol{\mu}) = P(\boldsymbol{\mu})$. The quantity v_s is obtained at the output of the channel G, in which quantity u_s is mixed in a known manner with the noise g_s, whose probability density $P(g_s)$ does not vary with s. Thus, the conditional probability density $P(v_s \mid u_s)$ is also known. It is now required to find such a sequence of probability densities $\Gamma_s(u_s \mid \mathbf{y}_{s-1}^*)$, that the average risk, that is, the mathematical expectation of the quantity

$$W = \sum_{s=0}^{s=n} W_s(s, x_s^*, x_s), \tag{6}$$

will be minimum.

Therefore, the minimum of the quantity

$$R = M\{W\} = \sum_{s=0}^{s=n} M\{W_s\} = \sum_{s=0}^{s=n} R_s \tag{7}$$

is required. The function Γ_s is the required algorithm of the controlling member A.

Further notation is introduced. Let $P(x_s \mid u_s)$ be the conditional probability density of x_s with given u_s. This function can be computed from the formulas (3) and (4), when the probability density $P(\boldsymbol{\mu})$ is known. In addition, let $P(\mathbf{y}_{s-1}^* \mid \mathbf{x}_{s-1}^*)$ be the conditional probability density of the vector

$$\mathbf{y}_{s-1}^* = (y_0^*, y_1^*, \ldots, y_{s-1}^*) \tag{8}$$

when the vector

$$\mathbf{x}_{s-1}^* = (x_0^*, x_1^*, \ldots, x_{s-1}^*) \tag{9}$$

is known.

It follows from the properties of the channel H^* that

$$P(\mathbf{y}_{s-1}^* \mid \mathbf{x}_{s-1}^*) = \prod_{i=0}^{i=s-1} P(y_i^* \mid x_i^*). \tag{10}$$

---

* All external noises are regarded as independent.

The vector $\mathbf{x}^*_{s-1}$ depends on s and $\boldsymbol{\lambda}$, and therefore $P(\mathbf{y}^*_{s-1} | \mathbf{x}^*_{s-1})$ depends also on s and $\boldsymbol{\lambda}$.

We denote by $\Omega(x_s, v_s, u_s, \mathbf{y}^*_{s-1})$ the region of variation of the parameters $x_s, v_s, u_s, \mathbf{y}^*_{s-1}$. An infinitely small element of this region is denoted by

$$d\Omega(x_s, v_s, u_s, \mathbf{y}^*_{s-1}) = dx_s\, dv_s\, du_s\, dy^*_0 \ldots dy^*_{s-1} \quad (11)$$

At first we shall write down the expression for the conditional partial risk r_s at the sth moment, understanding by the latter the magnitude of the risk R_s when the vector $\mathbf{x}^*_s$ is kept fixed or, what amounts to the same, when the vector $\boldsymbol{\lambda}$ remains fixed. Then

$$r_s = M\{W_s | \mathbf{x}^*_s\} =$$

$$= \int\limits_{\Omega(x_s, v_s, u_s, y^*_{s-1})} W_s(s, x^*_s, x_s) P(x_s | v_s) \times$$

$$\times P(v_s | u_s) \Gamma_s(u_s | \mathbf{y}^*_{s-1}) \quad (12)$$

$$P(\mathbf{y}^*_{s-1} | \mathbf{x}^*_{s-1})\, d\Omega(x_s, v_s, u_s, \mathbf{y}^*_{s-1}).$$

Let $\Omega(\boldsymbol{\lambda})$ be the region of variation of the vector $\boldsymbol{\lambda}$ and $d\Omega(\boldsymbol{\lambda})$ an infinitely small element of it. The partial risk R_s is given by the formula

$$R_s = \int\limits_{\Omega(\lambda)} r_s P(\boldsymbol{\lambda})\, d\Omega(\boldsymbol{\lambda}) =$$

$$= \int\limits_{\Omega(x_s, u_s, r_s, y^*_{s-1}, \lambda)} W_s(s, x^*_s, x_s) P(x_s | v_s) \times$$

$$\times P(v_s | u_s) \Gamma_s(u_s | \mathbf{y}^*_{s-1}) P(\mathbf{y}_{s-1} | \mathbf{x}^*_{s-1})$$

$$P(\boldsymbol{\lambda})\, d\Omega(x_s, u_s, v_s, \mathbf{y}_{s-1}, \boldsymbol{\lambda}) =$$

$$= \int\limits_{\Omega(x_s, u_s, v_s, y_{s-1})} P(x_s | v_s) P(v_s | u_s) \Gamma_s(u_s | \mathbf{y}^*_{s-1})$$

$$\Big\{ \int\limits_{\Omega(\lambda)} W_s[s, x^*_s(s, \boldsymbol{\lambda}), x_s] \times$$

$$\times P(\mathbf{y}^*_{s-1} | \mathbf{x}^*_{s-1}) P(\boldsymbol{\lambda})\, d\Omega(\boldsymbol{\lambda}) \Big\}\, d\Omega(x_s, u_s, v_s, \mathbf{y}^*_{s-1}). \quad (13)$$

The expression in the braces represents an integral over the region $\Omega(\boldsymbol{\lambda})$, as W_s and $P(\mathbf{y}^*_{s-1} | \mathbf{x}^*_{s-1})$ generally depend on $\boldsymbol{\lambda}$. Having performed the integration, we obtain a function ρ_s in the braces depending on x_s, s, $\mathbf{y}^*_{s-1}$. The dependence on s is shown in the index s, and therefore one can write

$$\rho_s = \rho_s(x_s, \mathbf{y}^*_{s-1}) = \int\limits_{\Omega(\lambda)} W_s[s, x^*_s(s, \boldsymbol{\lambda}), x_s] \cdot$$

$$\cdot P(\mathbf{y}^*_{s-1} | \mathbf{x}^*_{s-1}) P(\boldsymbol{\lambda})\, d\Omega(\boldsymbol{\lambda}). \quad (14)$$

Then

$$R_s = \int\limits_{\Omega(x_s, v_s, u_s, y^*_{s-1})} P(x_s | v_s) P(v_s | u_s) \Gamma_s(u_s | \mathbf{y}^*_{s-1}) \times$$

$$\times \rho_s(x_s, \mathbf{y}^*_{s-1})\, d\Omega(x_s, v_s, u_s, \mathbf{y}^*_{s-1}). \quad (15)$$

From (7) the total risk R is determined from the expression

$$R = \sum_{s=0}^{s=n} R_s = \sum_{s=0}^{s=n} \int\limits_{\Omega(x_s, v_s, u_s, y^*_{s-1})} P(x_s | v_s) P(v_s | u_s) \times$$

$$\times \Gamma_s(u_s | \mathbf{y}^*_{s-1}) \rho_s(x_s, \mathbf{y}^*_{s-1})\, d\Omega(x_s, v_s, u_s, \mathbf{y}^*_{s-1}). \quad (16)$$

The functions Γ_s are to be selected in such a way that the value of R is a minimum.

2. Determination of Optimum Strategy for Open-Loop Systems

It can be seen from the formula (16) that the selection of functions Γ_s for fixed s only affects the component R_s corresponding to the sth time moment. In this way the total risk is identical with action risk and one is allowed to select Γ_s such that it minimizes a single R_s in (15). As the function Γ_s represents probability density, we have

$$\int\limits_{\Omega(u_s)} \Gamma_s(u_s)\, d\Omega(u_s) = 1. \quad (17)$$

The expression for R(s) is rewritten as follows:

$$R_s = \int\limits_{\Omega(u_s, y^*_{s-1})} \Gamma_s(u_s | \mathbf{y}^*_{s-1}) \Big\{ \int\limits_{\Omega(x_s, v_s)} P(x_s | v_s) P(v_s | u_s) \times$$

$$\times \rho_s(x_s, \mathbf{y}^*_{s-1})\, d\Omega(x_s, v_s) \Big\}\, d\Omega(u_s, \mathbf{y}^*_{s-1}). \quad (18)$$

The integral in the braces represents a function of u_s and $\mathbf{y}^*_{s-1}$ which we shall denote by $\xi_s(u_s, \mathbf{y}^*_{s-1})$, that is,

$$\xi_s(u_s, \mathbf{y}^*_{s-1}) =$$

$$= \int\limits_{\Omega(x_s, v_s)} P(x_s | v_s) P(v_s | u_s) \rho_s(x_s, \mathbf{y}^*_{s-1})\, d\Omega(x_s, v_s). \quad (19)$$

Then

$$R_s = \int\limits_{\Omega(y^*_{s-1})} I(\mathbf{y}^*_{s-1})\, d\Omega(\mathbf{y}^*_{s-1}),$$

where

$$I(\mathbf{y}^*_{s-1}) = \int\limits_{\Omega(u_s)} \Gamma_s(u_s | \mathbf{y}^*_{s-1}) \xi_s(u_s, \mathbf{y}^*_{s-1})\, d\Omega(u_s) =$$

$$= (\xi_s)_{\mathrm{av}} \int\limits_{\Omega(u_s)} \Gamma_s(u_s | \mathbf{y}^*_{s-1})\, d\Omega(u_s) = (\xi_s)_{\mathrm{av}} \geqslant (\xi_s)_{\mathrm{min}}. \quad (20)$$

One can take the average value $(\xi_s)_{\mathrm{av}}$ outside the integration in accordance with the integral mean value theorem. The function Γ_s represents probability density and hence its integral over the region $\Omega(u_s)$ equals unity.

It follows from the expression (20) that a minimum value of $I(\mathbf{y}^*_{s-1})$ is $(\xi_s)_{\min}$. It is not difficult to show that I attains this value if the function Γ_s is chosen accordingly. In fact, let u^*_s be the value of u_s corresponding to the minimum (for instance, the least of all local minima) of the function $\xi_s(u_s)$ in the region $\Omega(u_s)$. We assume that such a value exists either within or on the boundary of the region.

Consider the function

$$\Gamma_s(u_s) = \delta(u_s - u^*_s), \tag{21}$$

where δ is the unit impulse function (otherwise Dirac's δ-function). Formula (21) provides the optimum algorithm of the member A, as substituting (21) into the left-hand side of (20) and using a well-known property of δ-function, we find

$$\begin{aligned} I &= \int\limits_{\Omega(u_s)} \Gamma_s(u_s \mid \mathbf{y}^*_{s-1})\, \xi_s(u_s, \mathbf{y}^*_{s-1})\, d\Omega(u_s) = \\ &= \int\limits_{\Omega(u_s)} \delta(u_s - u^*_s)\, \xi_s(u_s, \mathbf{y}^*_{s-1})\, d\Omega(u_s) = \\ &= \xi_s(u^*_s) = \min_{u_s \in \Omega(u_s)} \xi_s(u_s) = (I)_{\min}. \end{aligned} \tag{22}$$

The minimum values of I for each $\mathbf{y}^*_{s-1}$ provide also the minimum of R_s.

Thus, the optimum strategy, as seen from the formula (21), does not prove random but regular. The value of u_s should be taken as equal to a u^*_s. As seen from the formula (20), the value u^*_s which minimizes the function $\xi_s(u_s, \mathbf{y}^*_{s-1})$ depends on $\mathbf{y}^*_{s-1}$. In other words, as

$$\xi_s(u^*_s, \mathbf{y}^*_{s-1}) = \min, \tag{23}$$

the quantity u^*_s is a function of $\mathbf{y}^*_{s-1}$:

$$u^*_s = u^*_s(\mathbf{y}^*_{s-1}). \tag{24}$$

This makes also the function Γ_s in the formula (21) depend on $\mathbf{y}^*_{s-1}$:

$$\Gamma_s = \delta(u_s - u^*_s) = \delta[u_s - u^*_s(\mathbf{y}^*_{s-1})]. \tag{25}$$

Thus, the optimum strategy proves regular; it is determined in the general case from all the preceding values of y^*_i ($i = 0, \ldots, s-1$). It should be shown that the regularity of the optimum decisions occurs in a wide group of problems in Wald's general theory of statistical decisions.

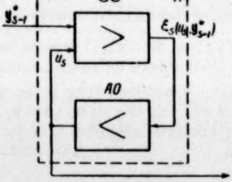

Fig. 2

The integral $\xi_s(u_s, \mathbf{y}^*_{s-1})$ can be evaluated with the aid of a computer CO (Fig. 2). The block diagram of the optimum controlling member can then be represented as shown in Fig. 2. The automatic optimizer AO selects a value u_s such that ξ_s becomes least. This value is now sent to the output of the block A. Were it possible to determine the value of u^*_s analytically as a function of $\mathbf{y}^*_{s-1}$, the block A could be constructed differently. However, the formula for $\xi_s(u_s, \mathbf{y}^*_{s-1})$ is as a rule most difficult to obtain explicitly and that is why the computer CO must perform automatically the integrations with respect to x_s and v_s, as shown in the formula (18). In this way the minimization of the integral ξ_s can be achieved directly.

3. Derivation of Risk Formula for Closed-Loop Systems

Consider now a block diagram of a closed system shown in Fig. 3. In order to simplify the exposition we neglect the interference h^* in the channel H^* (see, for example, Fig. 1 or Fig. 3 of [1]); x^* is thus assumed known. It was shown previously how the interference h^* should be taken into consideration, and should such a need arise, this can be done without any real difficulties. Our notation remains the same. In addition, there is also the feedback channel H with interference h_s which has a constant in time density distribution $P(h_s)$.

The way in which the signal and noise combine in the channel H is given and the conditional probability density $P(y_s \mid x_s)$ can therefore be found, and consequently the conditional probability density

$$P(\mathbf{y}_s \mid \mathbf{x}_s) = \prod_{i=0}^{i=s} P(y_s \mid x_s). \tag{26}$$

In a closed system it is necessary to take into account also the vectors

$$\begin{aligned} \mathbf{x}^*_s &= (x^*_0, x^*_1, \ldots, x^*_s), \\ \mathbf{y}_s &= (y_0, y_1, \ldots, y_s), \\ \mathbf{u}_s &= (u_0, u_1, \ldots, u_s), \\ \mathbf{v}_s &= (v_0, v_1, \ldots, v_s), \\ \mathbf{x}_s &= (x_0, x_1, \ldots, x_s). \end{aligned} \tag{27}$$

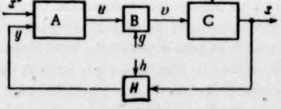

Fig. 3

The determination of the optimum controlling member A is reducible to the determination of its strategy, random in the general case, ensuring the minimizing of the risk R. The function $\Gamma_s(u_s \mid \mathbf{x}_s^*, \mathbf{y}_{s-1}, \mathbf{u}_{s-1})$, is assumed to represent random strategy, that is, the conditional probability density of u_s when the vectors $\mathbf{x}_s^*$, $\mathbf{y}_{s-1}$, and $\mathbf{u}_{s-1}$ remain fixed. Now Γ_s is a function of $\mathbf{x}_s^*$, $\mathbf{y}_{s-1}$, and $\mathbf{u}_s$.

First we shall write down the expression for the conditional partial risk r_s and we shall now understand by it the risk R_s when all the preceding motions of the system A are known, that is, when the vectors $\mathbf{x}_s^*$, $\mathbf{y}_{s-1}$, and $\mathbf{u}_{s-1}$ are fixed. Thus,

$$r_s = M\{W_s \mid \mathbf{x}_s^*, \mathbf{y}_{s-1}, \mathbf{u}_{s-1}\} =$$

$$= \int\limits_{\Omega(x_s, v_s, u_s)} W_s(s, x_s^*, x_s) P_s(x_s \mid v_s) \times$$

$$\times P(v_s \mid u_s) \Gamma_s(u_s \mid \mathbf{x}_s^*, \mathbf{y}_{s-1}, \mathbf{u}_{s-1}) \, d\Omega(x_s, v_s, u_s). \tag{28}$$

In this formula $P_s(x_s \mid v_s)$ is understood to represent the conditional probability density of the output x from the object B when its input v is known; as shown below, this probability need not be the same for different s.

If one considers the values of r_s corresponding to different trials of the system, then generally speaking the vectors $\mathbf{u}_{s-1}$ and $\mathbf{y}_{s-1}$, not known beforehand, can for different trials assume different values. Therefore, in computing the average partial risk R_s it is necessary, when averaging r_s, to take into account the joint probability distributions $P(\mathbf{u}_{s-1}, \mathbf{y}_{s-1})$ of the vectors $\mathbf{u}_{s-1}$ and $\mathbf{y}_{s-1}$, which in the general case are not statistically independent of one another. Thus,

$$R_s = M\{r_s\} =$$

$$= \int\limits_{\Omega(x_s, v_s, u_s, y_{s-1})} W_s(s, x_s^*, x_s) P_s(x_s \mid v_s) P(v_s \mid u_s) \times$$

$$\times \Gamma_s(u_s \mid \mathbf{x}_{s-1}^*, \mathbf{u}_{s-1}, \mathbf{y}_{s-1}) P(\mathbf{u}_{s-1}, \mathbf{y}_{s-1})$$

$$d\Omega(x_s, v_s, \mathbf{u}_s, \mathbf{y}_{s-1}). \tag{29}$$

The values of the quantities u_i and y_i ($i = 0, \ldots, s-1$) are memorized in the controlling member A. Thus the input and the output of B are known — admittedly not exactly, but with some error due to the presence of g and h, the input and the output interference respectively. This knowledge enables one to obtain a more accurate probability density of the parameter vector $\boldsymbol{\mu}$ on which in turn depends the interference z_s acting on the object B. The better $\boldsymbol{\mu}$ is known, the more fully determined is the method of regulating the object. One can derive a Bayesian formula in order to determine the a posteriori probability density of vector $\boldsymbol{\mu}$ in the sth beat. Consider the probability density[†] $P(\boldsymbol{\mu}, \mathbf{u}_{s-1}, \mathbf{y}_{s-1})$ of a joint event consisting in a simultaneous occurrence of the vectors $\boldsymbol{\mu}$, $\mathbf{u}_{s-1}$ and $\mathbf{y}_{s-1}$. Let $P(\mathbf{u}_{s-1}, \mathbf{y}_{s-1} \mid \boldsymbol{\mu})$ be the conditional joint probability density of the vectors $\mathbf{u}_{s-1}$ and $\mathbf{y}_{s-1}$ when $\boldsymbol{\mu}$ is kept fixed and $P(\boldsymbol{\mu} \mid \mathbf{u}_{s-1}, \mathbf{y}_{s-1})$ is the conditional probability density of $\boldsymbol{\mu}$ when the vectors $\mathbf{u}_{s-1}$ and $\mathbf{y}_{s-1}$ are fixed. The latter is the required a posteriori probability density of the vector $\boldsymbol{\mu}$. Then, of course,

$$P(\boldsymbol{\mu}, \mathbf{u}_{s-1}, \mathbf{y}_{s-1}) = P(\mathbf{u}_{s-1}, \mathbf{y}_{s-1} \mid \boldsymbol{\mu}) P(\boldsymbol{\mu}) =$$

$$P(\boldsymbol{\mu} \mid \mathbf{u}_{s-1}, \mathbf{y}_{s-1}) P(\mathbf{u}_{s-1}, \mathbf{y}_{s-1}). \tag{30}$$

$P(\boldsymbol{\mu})$ denotes the a priori probability density of vector $\boldsymbol{\mu}$. Hence the formula is obtained giving the a posteriori probability density of vector $\boldsymbol{\mu}$:

$$P(\boldsymbol{\mu} \mid \mathbf{u}_{s-1}, \mathbf{y}_{s-1}) = \frac{P(\boldsymbol{\mu}) P(\mathbf{u}_{s-1}, \mathbf{y}_{s-1} \mid \boldsymbol{\mu})}{P(\mathbf{u}_{s-1}, \mathbf{y}_{s-1})} =$$

$$= \frac{P(\boldsymbol{\mu}) P(\mathbf{u}_{s-1}, \mathbf{y}_{s-1} \mid \boldsymbol{\mu})}{\int\limits_{\Omega(\boldsymbol{\mu})} P(\mathbf{u}_{s-1}, \mathbf{y}_{s-1} \mid \boldsymbol{\mu}) P(\boldsymbol{\mu}) \, d\Omega(\boldsymbol{\mu})}. \tag{31}$$

In the latter formula $\Omega(\boldsymbol{\mu})$ denotes the range of variability of vector $\boldsymbol{\mu}$ and $d\Omega(\boldsymbol{\mu})$ its infinitely small element.

In formula (31) a special role is played by the likelihood function $P(\mathbf{u}_{s-1}, \mathbf{y}_{s-1} \mid \boldsymbol{\mu})$. The probability densities of quantities are called likelihood functions when the vector $\boldsymbol{\mu}$, whose values are subject to hypothesis testing, is kept fixed. We obtain the likelihood function for the closed-loop system shown in Fig. 3. Obviously, we have

$$P(\mathbf{u}_{s-1}, \mathbf{y}_{s-1} \mid \boldsymbol{\mu}) = P(u_0, y_0 \mid \boldsymbol{\mu}) P(u_1, y_1 \mid \boldsymbol{\mu}, u_0, y_0) \times$$

$$\times P(u_2, y_2 \mid \boldsymbol{\mu}, \mathbf{u}_1, \mathbf{y}_1) \ldots P(u_{s-1}, y_{s-1} \mid \boldsymbol{\mu}, \mathbf{u}_{s-2}, \mathbf{y}_{s-2}). \tag{32}$$

A typical factor on the right-hand side is a probability density

$$P(u_i, y_i \mid \boldsymbol{\mu}, \mathbf{u}_{i-1}, \mathbf{y}_{i-1}) =$$

$$= P(y_i \mid \boldsymbol{\mu}, u_i, \mathbf{u}_{i-1}, \mathbf{y}_{i-1}) P(u_i \mid \boldsymbol{\mu}, \mathbf{u}_{i-1}, \mathbf{y}_{i-1}) =$$

$$= P(y_i \mid \boldsymbol{\mu}, i, u_i) P(u_i \mid \boldsymbol{\mu}, \mathbf{u}_{i-1}, \mathbf{y}_{i-1}) =$$

$$= P(y_i \mid \boldsymbol{\mu}, i, u_i) \Gamma_i(u_i \mid \mathbf{u}_{i-1}, \mathbf{y}_{i-1}). \tag{33}$$

Thus $P(y_i \mid \boldsymbol{\mu}, u_i, \mathbf{u}_{i-1}, \mathbf{y}_{i-1})$ depends neither on $\mathbf{u}_{i-1}$ nor on $\mathbf{y}_{i-1}$, but only on $\boldsymbol{\mu}$, on the beat index i and on the value of u_i. In addition, $P(u_i \mid \boldsymbol{\mu}, \mathbf{u}_{i-1}, \mathbf{y}_{i-1})$ does not depend on $\boldsymbol{\mu}$ but only on $\mathbf{u}_{i-1}$ and $\mathbf{y}_{i-1}$ and this is precisely the stochastic algorithm Γ_i of the controlling member A.

[†] In a number of subsequent formulas the dependence of the probability density on $\mathbf{x}_s^*$ is not stated explicitly but it is always implied.

By substituting the expression (33) into (32) we find that

$$P(\mathbf{u}_{s-1}, \mathbf{y}_{s-1} \mid \mu) = \Big[\prod_{i=0}^{s-1} P(y_i \mid \mu, i, u_i)\Big]$$

$$\Big[\prod_{i=1}^{s-1} \Gamma_i(u_i \mid \mathbf{u}_{i-1}, \mathbf{y}_{i-1})\Big] P_0(u_0). \tag{34}$$

Here $P_0(u_0)$ is the initial probability density of $\underline{u}$ which also should be given.

Now one is able to substitute the likelihood function obtained in (34) into the a posteriori probability density formula (31). We obtain

$$P_s(\mu) = P(\mu \mid \mathbf{u}_{s-1}, \mathbf{y}_{s-1}) =$$

$$P(\mu) \frac{\Big[\prod_{i=0}^{s-1} P(y_i \mid \mu, i, u_i)\Big] \prod_{i=0}^{s-1} \Gamma_i}{P(\mathbf{u}_{s-1}, \mathbf{y}_{s-1})}. \tag{35}$$

In the above formula the following notation has been introduced:

$$\Gamma_0 = P_0(u_0). \tag{36}$$

Knowing the a posteriori probability density $P_s(\mu)$ one is able to determine more precisely the expression of the probability density $P_s(x_s \mid v_s)$ which appears in the formula (29). From the formulas (3) and (4) we find that

$$x_s = F_0(z_s, v_s) = F(s, \mu, v_s). \tag{37}$$

The quantities $\underline{s}$ and v_s which appear in the function F are parameters. This formula enables one to find the conditional probability density $P_s(x_s \mid v_s)$ when $P_s(\mu)$ is known.

Since

$$\int_{(\Omega v_s)} P_s(x_s \mid v_s) P(v_s \mid u_s)\, d\Omega(v_s) = P_s(x_s \mid u_s) =$$

$$= \int_{\Omega(\mu)} P(x_s \mid \mu, u_s) P_s(\mu)\, d\Omega(\mu), \tag{38}$$

the expression (29) giving R_s can be re-written in the following way:

$$R_s = \int_{\Omega(x_s, \mathbf{u}_s, \mathbf{y}_{s-1})} W_s(s, x_s^*, x_s)$$

$$\Big[\int_{\Omega(v_s)} P_s(x_s \mid v_s) P(v_s \mid u_s)\, d\Omega(v_s)\Big] \times$$

$$\times\, \Gamma_s(u_s \mid \mathbf{x}_{s-1}^*, \mathbf{u}_{s-1}, \mathbf{y}_{s-1})$$

$$P(\mathbf{u}_{s-1}, \mathbf{y}_{s-1})\, d\Omega(x_s, \mathbf{u}_s, \mathbf{y}_{s-1}) =$$

$$= \int_{\Omega(x_s, \mu, \mathbf{u}_s, \mathbf{y}_{s-1})} W_s(s, x_s^*, x_s) P(x_s \mid \mu, u_s)$$

$$P_s(\mu) \Gamma_s(u_s \mid \mathbf{x}_{s-1}^*, \mathbf{u}_{s-1}, \mathbf{y}_{s-1}) \times$$

$$\times\, P(\mathbf{u}_{s-1}, \mathbf{y}_{s-1})\, d\Omega(x_s, \mu, \mathbf{u}_s, \mathbf{y}_{s-1}). \tag{39}$$

Substituting the formula (35) for $P_s(\mu)$ and cancelling $P(\mathbf{u}_{s-1}, \mathbf{y}_{s-1})$ we obtain

$$R_s = \int_{\Omega(x_s, \mu, \mathbf{u}_s, \mathbf{y}_{s-1})} W_s(s, x_s^*, x_s) P(x_s \mid \mu, u_s) P(\mu) \times$$

$$\times \prod_{i=0}^{s-1} P(y_i \mid \mu, i, u_i) \prod_{i=0}^{s} \Gamma_i\, d\Omega(x_s, \mu, \mathbf{u}_s, \mathbf{y}_{s-1}). \tag{40}$$

The total risk is given by

$$R = \sum_{s=0}^{s=n} R_s = \sum_{s=0}^{s=n} \int_{\Omega(x_s, \mu, \mathbf{u}_s, \mathbf{y}_{s-1})}$$

$$W_s(s, x_s^*, x_s) P(x_s \mid \mu, u_s) P(\mu) \times$$

$$\times \prod_{i=0}^{s-1} P(y_i \mid \mu, i, u_i) \prod_{i=0}^{s} \Gamma_i\, d\Omega(x_s, \mu, \mathbf{u}_s, \mathbf{y}_{s-1}). \tag{41}$$

Let us compare the expressions (16) and (41) of risks in open and closed systems. In the formula (16) only the $\underline{s}$th component R_s was influenced by the function Γ_s; the total risk associated with Γ_s was exclusively an action risk. In the formula (41), however, the function Γ_s influenced not only the term R_s (action risk) but also all the other components R_i where i > s. As regards Γ_s, the sum $\sum_{i=s+1}^{n} R_i$ represents the investigation risk. In fact, the selection of Γ_s influences the character of the process in the subsequent beats, as it causes either a better or a worse investigation of the characteristics of the object B; the latter amounts to the determination of the probability density $P_s(\mu)$. Thus the total risk regarded as a function of Γ_s ($0 \le s \le n$) represents the sum of the action risk and the investigation risk. As regards Γ_n only a single action risk occurs.

When the object B has memory the selection of Γ_s influences not only R_s but also the terms R_i when i > s even when the additional investigation of the object B has not taken place (see Paper IV in this series). Consequently, in this case the action risk is expressed by a more involved formula, and the interconnection between the action and the investigation risks proves also to be more involved.

4. Determination of Optimum Strategy in Closed Systems

It is required to select the functions Γ_i in the formula (41) such that the risk R be minimum. As Γ_i represents probability densities they must satisfy the condition (17).

To be able to select Γ_n we consider the last component R_n of R:

$$R_n = \int_{\Omega(x_n, \mu, \mathbf{u}_n, \mathbf{y}_{n-1})}$$

$$W_n(n, x_n^*, x_n) P(x_n \mid \mu, u_n) P(\mu) \times$$

$$\times \prod_{i=0}^{n-1} P(y_i \mid \mu, i; u_i) \prod_{i=0}^{n-1} \Gamma_i \Gamma_n\, d\Omega(x_n, \mu, \mathbf{u}_n, \mathbf{y}_{n-1}). \tag{42}$$

We assume that $\Gamma_0, \ldots, \Gamma_{n-1}$ are given, and only Γ_n is to be selected such that R_n becomes minimum provided a constraint as in (17) is satisfied:

$$\int\limits_{\Omega(u_n)} \Gamma_n(u_n, \mathbf{u}_{n-1}, \mathbf{y}_{n-1})\, d\Omega(u_n) = 1. \qquad (43)$$

In order to simplify the expression (42), put

$$\alpha_n = \alpha_n(\mathbf{u}_n, \mathbf{y}_{n-1}) =$$

$$= \int\limits_{\Omega(x_n, \boldsymbol{\mu})} W_n(n, x_n, x_n^*)\, P(x_n \mid \boldsymbol{\mu}, u_n)$$

$$P(\boldsymbol{\mu}) \prod_{i=0}^{n-1} P(y_i \mid \boldsymbol{\mu}, i, u_i)\, d\Omega(x_n, \boldsymbol{\mu}). \qquad (44)$$

Further, put

$$\beta_k = \prod_{i=0}^{k} \Gamma_k; \qquad (45)$$

then

$$R_n = \int\limits_{\Omega(u_n, \mathbf{u}_{n-1}, \mathbf{y}_{n-1})}$$

$$\alpha_n(u_n, \mathbf{u}_{n-1}, \mathbf{y}_{n-1})\, \beta_{n-1} \Gamma_n\, d\Omega(\mathbf{u}_n, \mathbf{y}_{n-1}) =$$

$$= \int\limits_{\Omega(\mathbf{u}_{n-1}, \mathbf{y}_{n-1})} \beta_{n-1} \varkappa_n(\mathbf{u}_{n-1}, \mathbf{y}_{n-1})\, d\Omega(\mathbf{u}_{n-1}, \mathbf{y}_{n-1}), \qquad (46)$$

where

$$\varkappa_n(\mathbf{u}_{n-1}, \mathbf{y}_{n-1}) =$$

$$\int\limits_{\Omega(u_n)} \alpha_n(u_n, \mathbf{u}_{n-1}, \mathbf{y}_{n-1})\, \Gamma_n(u_n, \mathbf{u}_{n-1}, \mathbf{y}_{n-1})\, d\Omega(u_n). \qquad (47)$$

If the Γ_n is selected such that for any set of vectors $\mathbf{u}_{n-1}$ and $\mathbf{y}_{n-1}$ the quantity κ_n^* remains least, then the integral (46) will also be minimum (bearing in mind that the quantity β_{n-1} is assumed known. By regarding the vectors $\mathbf{u}_{n-1}$ and $\mathbf{y}_{n-1}$ in the formulas (44) and (47) as parameters, one is able to find a value u_n^* such that the function α_n is minimum. We put

$$\gamma_n^* = \alpha_n(u_n^*, \mathbf{u}_{n-1}, \mathbf{y}_{n-1}) = \min_{u_n \in \Omega(u_n)} \alpha_n(u_n, \mathbf{u}_{n-1}, \mathbf{y}_{n-1}). \qquad (48)$$

The quantity u_n^*, of course, depends on $\mathbf{u}_{n-1}$ and $\mathbf{y}_{n-1}$:

$$u_n^* = u_n^*(\mathbf{u}_{n-1}, \mathbf{y}_{n-1}). \qquad (49)$$

Then the optimum function Γ_n satisfying the condition (43) is

$$\Gamma_n(u_n, \mathbf{u}_{n-1}, \mathbf{y}_{n-1}) = \delta(u_n - u_n^*), \qquad (50)$$

because in this case

$$\varkappa_n = \alpha_n(u_n^*, \mathbf{u}_{n-1}, \mathbf{y}_{n-1}) = (\alpha_n)_{\min} = (\varkappa_n)_{\min}. \qquad (51)$$

This follows from the considerations similar to those given above when the conditions (19), (20), and (21) were derived.

Now the optimum function Γ_{n-1} will be determined. Consider the sum of the last two terms R_{n-1} and R_n. First of all, we introduce the function

$$\alpha_k = \alpha_k(u_k, \mathbf{u}_{k-1}, \mathbf{y}_{k-1}) =$$

$$\int\limits_{\Omega(x_k, \boldsymbol{\mu})} W_k(k, x_k^*, x_k)\, P(x_k \mid \boldsymbol{\mu}, u_k) \times$$

$$\times P(\boldsymbol{\mu}) \prod_{i=0}^{k-1} P(y_i \mid \boldsymbol{\mu}, i, u_i)\, d\Omega(x_k, \boldsymbol{\mu}) \qquad (0 \leqslant k \leqslant n). \qquad (52)$$

There the expression $\prod_{i=0}^{k-1} P(y_i \mid \boldsymbol{\mu}, i, u_i)$ equals unity when $k = 0$.

Now the sum of the last two terms becomes

$$S_{n-1} = R_{n-1} + R_n =$$

$$= \int\limits_{\Omega(\mathbf{u}_{n-1}, \mathbf{y}_{n-2})} \alpha_{n-1} \beta_{n-1}\, d\Omega(\mathbf{u}_{n-1}, \mathbf{y}_{n-2}) +$$

$$+ \int\limits_{\Omega(\mathbf{u}_n, \mathbf{y}_{n-1})} \alpha_n \beta_n\, d\Omega(\mathbf{u}_n, \mathbf{y}_{n-1}). \qquad (53)$$

When $i \leq n-2$, the Γ_i are assumed to be known and Γ_n is always selected in accordance with the formula (50). Then

$$S_{n-1} = \int\limits_{\Omega(\mathbf{u}_{n-2}, \mathbf{y}_{n-2})} \beta_{n-2} \Bigg\{ \int\limits_{\Omega(u_{n-1})} \Gamma_{n-1} \alpha_{n-1}\, d\Omega(u_{n-1}) +$$

$$+ \int\limits_{\Omega(u_{n-1}, y_{n-1})} \Gamma_{n-1} \alpha_n(u_n^*, \mathbf{u}_{n-1}, \mathbf{y}_{n-1})\, d\Omega(u_{n-1}, y_{n-1}) \Bigg\}. \qquad (54)$$

This quantity is least when the expression within the braces is least; we write the latter in full as

$$\varkappa_{n-1}(\mathbf{u}_{n-2}, \mathbf{y}_{n-2}) =$$

$$= \int\limits_{\Omega(u_{n-1})} \Bigg\{ \Gamma_{n-1} \alpha_{n-1} + \int\limits_{\Omega(y_{n-1})}$$

$$\Gamma_{n-1} \alpha_n(u_n^*, \mathbf{u}_{n-1}, \mathbf{y}_{n-1})\, d\Omega(y_{n-1}) \Bigg\}\, d\Omega(u_{n-1}) =$$

$$= \int\limits_{\Omega(u_{n-1})} \Gamma_{n-1}(u_{n-1}, \mathbf{u}_{n-2}, \mathbf{y}_{n-2}) \times$$

$$\times \Bigg\{ \alpha_{n-1} + \int\limits_{\Omega(y_{n-1})}$$

$$\alpha_n(u_n^*, \mathbf{u}_{n-1}, \mathbf{y}_{n-1})\, d\Omega(y_{n-1}) \Bigg\}\, d\Omega(u_{n-1}). \qquad (55)$$

Now consider the function

$$\gamma_{n-1} = \gamma_{n-1}(\mathbf{u}_{n-1}, \mathbf{y}_{n-2}) = \alpha_{n-1} +$$

$$+ \int\limits_{\Omega(y_{n-1})} \alpha_n(u_n^*, \mathbf{u}_{n-1}, \mathbf{y}_{n-1})\, d\Omega(y_{n-1}). \qquad (56)$$

We find the value u_{n-1}^* which is the minimum value of this function. This value obviously depends on $\mathbf{u}_{n-2}$ and $\mathbf{y}_{n-2}$:

$$u_{n-1}^* = u_{n-1}^*(\mathbf{u}_{n-2}, \mathbf{y}_{n-2}). \qquad (57)$$

Then the most suitable function Γ_{n-1} such that it ensures the minimum of κ_{n-1} and satisfies the condition (17) will be

$$\Gamma_{n-1}(u_{n-1}, \mathbf{u}_{n-2}, \mathbf{y}_{n-2}) = \delta(u_{n-1} - u^{*}_{n-1}). \quad (58)$$

By applying analogous arguments one can determine the whole sequence of the functions Γ_i using the following procedure.

We introduce the function

$$\gamma_{n-k} = \alpha_{n-k} + \int\limits_{\Omega(y_{n-k})} \gamma_{n-k+1}(u^{*}_{n-k+1}, \mathbf{u}_{n-k}, \mathbf{y}_{n-k})\, d\Omega(y_{n-k}), \quad (59)$$

where $\gamma_n = \alpha_n$. Let the minimum of γ_{n-k} over u_{n-k} be denoted by γ^{*}_{n-k}:

$$\gamma^{*}_{n-k} = (\gamma_{n-k})_{u_{n-k}=u^{*}_{n-k}} =$$

$$= \min_{u_{n-k}\in\Omega(u_{n-k})} \gamma_{n-k}(u_{n-k}; \mathbf{u}_{n-k-1}, \mathbf{y}_{n-k-1});$$

$$u^{*}_{n-k} = u^{*}_{n-k}(\mathbf{u}_{n-k-1}; \mathbf{y}_{n-k-1}). \quad (60)$$

Then the optimum function Γ^{*}_{n-k} is given by the formula

$$\Gamma^{*}_{n-k} = \delta(u_{n-k} - u^{*}_{n-k}), \quad (61)$$

where δ is the unit impulse function. Then

$$(S_{n-k})_{\min} = \Big(\sum_{i=0}^{i=k} R_{n-i}\Big)_{\min} =$$

$$= \int\limits_{\Omega(\mathbf{u}_{n-k-1}, \mathbf{y}_{n-k-1})} \beta_{n-k-1}\gamma^{*}_{n-k}\, d\Omega(\mathbf{u}_{n-k-1}, \mathbf{y}_{n-k-1}). \quad (62)$$

In this way Γ_i are determined when $i = n, n-1, \ldots, 1$. As far as the determination of $\Gamma_0 = P_0(u_0)$ is concerned, this function may be given beforehand and then no selection is required. If the best Γ_0 can be chosen, the selection takes place in accordance with the procedure shown above. When $k = n-1$ we arrive at the formula

$$(S_1)_{\min} = \int\limits_{\Omega(u_0, y_0)} P_0(u_0)\gamma^{*}_1(u_0, y_0)\, d\Omega(u_0, y_0). \quad (63)$$

The total risk therefore when all Γ_i $(i = 1, \ldots, n)$ are optimal, is expressed by the formula

$$R = R_0 + (S_1)_{\min} =$$

$$= \int\limits_{\Omega(x_0, \mu, u_0)} W_0(0, x^{*}_0, x_0) P(x_0 \mid \mu, u_0) \times$$

$$\times P(\mu) P_0(u_0)\, d\Omega(x_0, \mu, u_0) +$$

$$+ \int\limits_{\Omega(u_0, y_0)} P_0(u_0)\gamma^{*}_1(u_0, y_0)\, d\Omega(u_0, y_0) =$$

$$= \int\limits_{\Omega(u_0)} P_0(u_0)\Big[\alpha_0(u_0) +$$

$$+ \int\limits_{\Omega(y_0)} \gamma^{*}_1(u_0, y_0)\, d\Omega(y_0)\Big] d\Omega(u_0), \quad (64)$$

where

$$\alpha_0 = \alpha_0(u_0) =$$

$$= \int\limits_{\Omega(x_0, \mu)} W_0(0, x^{*}_0, x_0) P(x_0 \mid \mu, u_0) P(\mu)\, d\Omega(x_0, \mu). \quad (65)$$

We put

$$\gamma_0 = \gamma_0(u_0) = \alpha_0(u_0) + \int\limits_{\Omega(y_0)} \gamma^{*}_1(u_0, y_0)\, d\Omega(y_0). \quad (66)$$

It can be seen from the formula (64) that the quantity R becomes minimum when

$$\Gamma_0 = P_0(u_0) = \Gamma^{*}_0 = \delta(u_0 - u^{*}_0), \quad (67)$$

where the value u^{*}_0 makes the function $\gamma(u_0)$ minimum.

The value u^{*}_0 is dependent on the a priori probabilities, also generally on the given data, but not on observations which are not available at the initial moment of time.

Thus in the case of a closed system as well, the optimum strategy proves to be not random but a regular one. This conclusion is naturally valid within the bounds of the limitations accepted when formulating this theory.

The determination of sequence of functions γ_{n-k} may prove rather tedious in actual examples if electronic computers are not used. Even so, it has only been possible so far to solve only relatively simple problems in which the memory capacity necessary to memorize the functions is not too great.

The obtained system with the optimum control algorithm Γ^{*}_i is, generally speaking, a dual control system in which the u_i serve not only as directing but also as investigating operations. In the absence of investigation, the probability density $P_s(\mu)$ would remain equal to $P_0(\mu)$ and the investigation risk would be null.

It may happen that in a particular case of a dual control system the process of investigating the object proceeds in the same way, no matter what the values of the regulating operations within the admissible bandwidth; what is only required is that the regulating operations take place. Such a system (an example is given in the next paper) is called neutral. In a neutral system the investigation risk is independent of the quantity u_i, but $P_s(\mu)$ is not identical with $P_0(\mu)$ but varies with s.

LITERATURE CITED

1. A. A. Fel'dbaum, "Theory of dual control. I," Avtomat. i Telemekh. 21, No. 9 (1960).‡

---

‡See English translation.

THE DYNAMICS OF SELF-ADAPTIVE SYSTEMS WITH EXTREMAL CONTINUOUS ADJUSTMENT OF THE COMPENSATING NETWORK IN THE PRESENCE OF RANDOM DISTURBANCES

I. E. Kazakov

Moscow

Translated from Avtomatika i Telemekhanika, Vol. 21, No. 11,
pp. 1465-1474, November, 1960
Original article submitted May 28, 1960

The problem is considered of estimating the accuracy of self-adaptive systems with extremal continuous adjustment of the compensating network parameters, where this adjustment is made by using the gradient method, and variable controlling signals, variable object parameters, and random disturbances are considered.

1. Formulation of the Problem

The development and application of self-adaptive systems gives rise to problems in the probability-theoretic analysis of these systems under the influence of random disturbances. The solution of these problems can be used as a basis for the synthesis and design of the systems. The statistical theory of self-adaptive systems is in its initial stage of development. At the present time, known results have been obtained in the theory of discrete (step) systems of extremal control. The mean error of control and the optimal size of the steps have been determined for such systems in the case of random disturbances of particular types. This work has appeared in several papers. The main directions of these investigations are well described in [1-4].

The statistical dynamics of self-adaptive systems with continuous operation have not yet been sufficiently studied. Moreover, the design of such systems is of practical interest because of the simplicity of their construction. From the probability-theoretic investigations devoted to this type of self-adaptive system, we particularly note the works [1, 5, 6], in which the problem we are considering has been formulated in connection with systems of continuous operation. In [7] the dynamics are investigated of systems with continuous operation that use the gradient method. Also, in [8], the analysis is carried out of a particular case of a system of extremal continuous control, operating in the presence of random disturbances.

In the present work, we consider the problem of analyzing the accuracy of a self-adaptive system with continuous extremal adjustment of the compensating network parameters, where adjustment is obtained by the gradient method in relation to the variation of the external controlling signals and the parameters of the controlled object.

An automatic self-adaptive system with extremal adjustment of the compensating network parameters is essentially a system of automatic synthesis of a compensating network with a given structure. Such a system must ensure the adjustment of the compensating network parameters, such that an extremum is maintained in some index of the performance of the control process. The block diagram of such a linear system is shown in Fig. 1. It consists of a main control network and an auxiliary network for the automatic adjustment of the compensating apparatus. The structure of the compensating network is given, and the parameters of this network depend on the adjustment.

The main control network consists of the object of the control together with the control apparatus and the compensating network. The object and the control apparatus have $\underline{m}$ variable parameters $y_1, \ldots, y_m$ and are characterized by the linear operator $\Phi_R(y_1, \ldots, y_m, p)$, where $p = d/dt$. The compensating device includes $\underline{n}$ adjustable parameters $x_1, \ldots, x_n$ and can also be characterized by a linear operator $\Phi_k(x_1, \ldots, x_n, p)$. To the control system is fed the useful control signal $Z(t)$ of an arbitrary unknown form, and the random disturbance $X(t)$. The function $Z(t)$ is smooth, and varies slowly in comparison with the processes in the main control circuit.

The equations describing the operation of the main control network shown in Fig. 1 are

$$\begin{gathered} Y = \Phi_R(y_1, \ldots, y_m, p)\,V, \\ V = \Phi_k(x_1, \ldots, x_n, p)\,[\Delta + X], \\ \Delta = Z - Y \end{gathered} \tag{1}$$

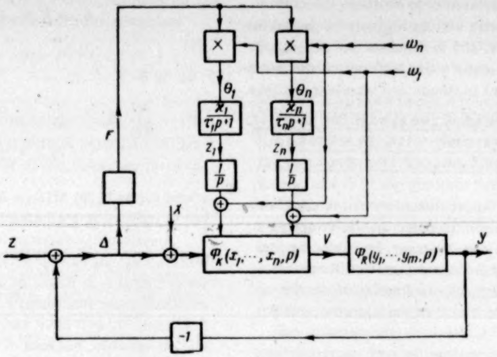
×
×
w_n
w_1
θ_1
θ_n
$\frac{\varkappa_1}{\tau_1 p+1}$
$\frac{\varkappa_n}{\tau_n p+1}$
z_1
z_n
$\frac{1}{p}$
$\frac{1}{p}$
F
X
Z
Δ
V
y
$\varphi_k(x_1, \cdots, x_n, p)$
$\varphi_k(y_1, \cdots y_m, p)$
-1

Fig. 1. Block diagram of a self-adaptive continuous system.

The auxiliary networks include a functional device for determining the control performance index F, a device for determining the extremum of the control performance index, and elements that ensure the adjustment of the parameters according to the signals $z_1, \ldots, z_n$. The form of the auxiliary networks for the extremal adjustment depend on the method used in determining the extremum of the control process performance index. This control performance index is a functional of the parameters of the objects of control and the compensating device, and also of the characteristics of the controlling signals and the disturbances.

One of the general methods of obtaining the extremal adjustment is to determine the gradient of the functional in the space of the parameters $x_1, x_2, \ldots, x_n$ and to arrange to have the adjustment of these parameters in the direction of this gradient. The method of estimating the control performance index depends on the type of problem and on the form of the disturbances experienced by the system.

When the controlling signal Z(t) and the parameters of the object $y_1, \ldots, y_m$ vary slowly, and consequently the processes in the device that adjust the compensating network parameters are slow relative to the processes in the main network, and when the random disturbance X(t) is a stationary random function, wide application is found in systems of automatic control of estimating the control process performance by the mean square of the control error. The functional-characterized network for obtaining an estimate of the performance of the control process consists, in this case, of a multiplying block for obtaining the square of the control error $\Delta = Z - Y$ and a device for calculating the mathematical expectation of the square of the error. It is, however, difficult in practice to construct a device that will obtain the mean square error Δ. It is simpler to carry out the averaging operation by using an inertial link with time constant T, which guarantees accurate averaging.

The equations for such a functional-characterized device are

$$U = \Delta^2, \quad (Tp + 1)\, F = U. \qquad (2)$$

Further auxiliary networks contain synchronous detectors which include multipliers for calculating the product of the signal F and the test signals (i=1, 2, ..., n) and the subsequent filters and inertial links for averaging the product signals Fw_i. At the output of the synchronous detectors, signals are obtained containing quantities that are proportional to the gradient components of the functional F with respect to the parameters x_i ($i = 1, \ldots, n$). The test signals are also fed directly to the adjustable parameter network. For continuous adjustment of the compensating network parameters, the rates of change of the parameters x_i ($i = 1, 2, \ldots, n$) are proportional to the measured components of the gradient, and the equations of the adjusting network are

$$\begin{aligned} \theta_i &= Fw_i, && (3)\\ (\tau_i p + 1)\, z_i &= -\varkappa_i \theta_i, &&\\ px_i &= z_i + pw_i && (i = 1, 2, \ldots, n), \end{aligned}$$

where the quantities τ_i are the time constants of the filters.

The test signals w_i ($i = 1, 2, \ldots, n$) for determining the components of the gradient of F can be both sinusoidal harmonics and random, unrelated signals. When regular test signals are used, their frequency must be chosen sufficiently low, so that the signals will pass through the filter of the functional-characterized network forming the quantity F. If random test signals are used, they must possess a sufficiently low frequency spectrum.

It is obvious that the time constants satisfy the relations $\tau_i > T$ ($i = 1, 2, \ldots, n$). The system of equations (1-3) completely describes the operation of a self-adaptive system. The problem is to estimate the control error Δ in the system with various regimes for the adjustment of the parameters, and to estimate the adjustment network parameters κ_1 and τ_1 that will ensure the necessary accuracy of control in steady and transient regimes.

2. The Approximate Equations for Linear Self-Adaptive Systems with Extremal Continuous Adjustment of the Compensating Networks

The direct use of the nonlinear system of equations (1-3) for solving the problems posed above is very difficult. These problems can, however, be solved by methods from random function transformation theory. In order to apply these methods, we first transform the equations. In the neighborhood of the extreme values of the variables x_{i0} ($i = 1, 2, \ldots, n$), the operator corresponding to the compensating network can be written

$$\Phi_k(x_1, \ldots, x_n, p) = \Phi_k(x_{10}, \ldots, x_{n0}, p) + \sum_{\nu=1}^{n} u_\nu b_\nu(p) + \ldots, \qquad (4)$$

where

$$b_\nu(p) = \left[\frac{\partial \Phi_k(x_i, p)}{\partial x_\nu}\right]_{x_i = x_{i0}} \quad (\nu = 1, 2, \ldots, n);$$

x_{i0} are the values of the variables x_i for which the functional F attains its extremum, and $u_\nu = x_\nu - x_{\nu 0}$ are the variations of the parameters from their extremum values.

We write the variables occurring in the equations (1) and (2) in the form

$$Y = Y_0 + \sum_{i=1}^{n} Y_i, \qquad (5)$$

$$V = V_0 + \sum_{i=1}^{n} V_i, \quad \Delta = \Delta_0 + \sum_{i=1}^{n} \Delta_i,$$

$$U = U_0 + \sum_{i=1}^{n} \frac{\partial U}{\partial \Delta} \Delta_i, \quad F = F_0 + \sum_{i=1}^{n} F_i,$$

where the zero subscript indicates values of the variables corresponding to the regime of operation for optimal values of the parameters $x_i = x_{i0}$ ($i = 1, 2, \ldots, n$). The components Y_i, V_i, Δ_i, F_i are the variations of the variables for deviations of the ith parameter x_i from its nominal value. If we use the expressions (4) and (5), and limit ourselves to small quantities of the first order relative to the variations of the parameters and the variables corresponding to these parameters, we obtain the following system of equations for determining the variations in the variables:

$$Y_i = \Phi_R(y_1, \ldots, y_m, p) V_i, \qquad (6)$$

$$(Tp + 1) F_i = U_i,$$

$$V_i = \Phi_k(x_{10}, \ldots, x_{n0}, p) \Delta_i + c_i u_i,$$

$$\theta_i = F_0 w_i + \sum_{k=1}^{n} F_k w_i,$$

$$\Delta_i = -Y_i, \qquad (\tau_i p + 1) z_i = -\varkappa_i \theta_i,$$

$$U_i = \frac{\partial U}{\partial \Delta_i} \Delta_i, \qquad p u_i = z_i + p w_i - p x_{i0}$$

$$(i = 1, 2, \ldots, n),$$

where $c_i(t) = b_i(p)\, M[\Delta_0 + X]$ ($i = 1, 2, \ldots, n$), the symbol M indicating mathematical expectation.

A system of equations for determining the variables Y_0, V_0, Δ_0 can be obtained from the equations (1) for $x_i = x_{i0}$ ($i = 1, 2, \ldots, n$). In the neighborhood of the extremum, the functional F, and consequently, the functional U, will have zero linear terms relative to the ith variable, because of the conditions for an extremum. Therefore in determining the value of $\partial U / \partial \Delta_i$ we must take into account the quadratic term. As a result, the value of $\partial U / \partial \Delta_i$ will be obtained from the equality

$$\frac{\partial U}{\partial \Delta_i} = \sum_{j=1}^{n} \Delta_j \quad (i = 1, 2, \ldots, n). \qquad (7)$$

In the general case, the investigation of the accuracy of control and the accuracy of adjustment of the compensating network parameters is therefore reduced to the integration of the system of equations (1) for $x_i = x_{i0}$ and the integration of the system of equations (6) with the conditions (7) and the subsequent calculation of the probability characteristics of the control error Δ. It should be noted that the analysis of these equations does not present any difficulty in principle for arbitrarily rapidly varying parameters, or, therefore, for any operating regime of the system.

In the practically important type of case when the processes in the parameter adjustment network are slow compared with those in the main network, the system of equations (6) can be simplified. In this case, after the main network has been operating for a certain time, the variations $u_i = x_i - x_{i0}$ ($i = 1, 2, \ldots, n$) can be considered as constant parameters. The network equations then take the form

$$(Tp + 1)(\tau_i p + 1) z_i = -\varkappa_i w_i^2 \sum_{j=1}^{n} b_{ij} u_j - \varkappa_i \varphi_i,$$

$$p u_i = z_i + p w_i - p x_{i0}, \quad (i = 1, 2, \ldots, n), \qquad (8)$$

where

$$\varphi_i = U_0 w_i + \sum_{k, j=1}^{n} b_{kj} [u_k u_j + u_j w_k + u_k w_j + w_k w_j] w_i - w_i^2 \sum_{j=1}^{n} b_{ij} u_j$$

$$(i = 1, 2, \ldots, n),$$

$$b_{kj} = a_k a_j \quad (k, j = 1, 2, \ldots, n), \qquad (8')$$

$$a_k = \int_0^\infty g_{\Delta_k}(t, \tau)\, c_k(\tau)\, d\tau \quad (k = 1, 2, \ldots, n).$$

The quantity $g_{\Delta_k}(t, \tau)$ is a weight function for the output Δ_k, where this output satisfies the equations

$$\begin{aligned} Y_i &= \Phi_R(y_1, \ldots, y_m, p)\, V_i, \\ V_i &= \Phi_k(x_{10}, \ldots, x_{n0}, p)\, \Delta_i + \delta(t - \tau), \\ \Delta_i &= -Y_i, \end{aligned} \tag{9}$$

where $\delta(t - \tau)$ is the delta function.

In order to obtain the system of equations (8) from the equations (6) we use one of the equations from the system (1) for $x_i = x_{i0}$:

$$(Tp + 1)\, F_0 = U_0. \tag{10}$$

In the case we are considering, the system of equations (8) can be used for the analysis of the accuracy of adjustment of the parameters x_i ($i = 1, 2, \ldots, n$), and for the calculation of the mathematical expectation m_{u_i} and the mean square of the deviations of the quantities u_i. These accuracy estimates for the adjustment can be applied in the choice of the optimal values of the amplification coefficients κ_i and the time constants τ_i and T, and also for the choice of the test signal amplitudes w_i.

The final calculation of the mathematical expectancy of the control accuracy for a self-adaptive system is made by using the formula

$$m_\Delta = m_{\Delta_0} + \sum_{i=1}^{n} a_i m_{u_i}, \tag{11}$$

where m_{Δ_0} is the mathematical expectation of the control error for the optimal values of the parameters $x_i = x_{i0}$, and m_{u_i} is the mathematical expectation of the parameter adjustment errors $u_i = x_i - x_{i0}$.

The standard deviation of the control error is calculated from the formula

$$D_\Delta = D_{\Delta_0} + 2 \sum_{i=1}^{n} a_i K_{\Delta_0 \Delta_i} + \sum_{i=1}^{n} \sum_{j=1}^{n} a_i a_j K_{\Delta_i \Delta_j}, \tag{12}$$

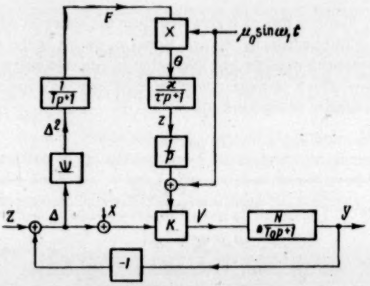

Fig. 2. Self-adaptive system with continuous extremal adjustment of the compensating network amplification coefficient.

where D_{Δ_0} is the standard deviation of the control error Δ_0 for optimal values of the parameters $x_i = x_{i0}$; $K_{\Delta_0 \Delta_i}$, $K_{\Delta_i \Delta_j}$ are the correlation coefficients of the random components of the control error.

3. An Application of the Theory

We will take as an example to illustrate the application of the theory, a system with one adjustable parameter in the compensating network – its amplification k, and with the gradient determined by the synchronous detector method [11]. Fig. 2 shows a block diagram of such a system. The control error $\Delta = Z - Y$ is squared and the square averaged in a filter with time constant T. A second filter with time constant τ is used to average the periodic signal of the multiplier of the synchronous detector.

Let the random disturbance X be a stationary random function, let the control input $Z = z_0 = \text{const}$, and let the parameters of the object of control N and T_0 vary slowly with respect to time (relative to the processes in the main control network).

On the basis of Fig. 2, the equations of the main control network are

$$(T_0 p + 1)\, Y = Nk\,[\Delta + X], \quad \Delta = Z - Y. \tag{13}$$

If we note that $m_x = 0$, then for the mathematical expectation and the standard deviation of the control error, we have the expressions

$$m_\Delta = \frac{z_0}{1 + Nk}, \tag{14}$$

$$\sigma_\Delta^2 = \int_0^\infty \left| \frac{Nk}{Ti\omega + 1 + Nk} \right|^2 G_x(\omega)\, d\omega. \tag{15}$$

For $G_X(\omega) = G_0 = \text{const}$, corresponding to a disturbance X in the form of white sound, formula (15) yields the expression

$$\sigma_\Delta^2 = \frac{\pi N^2 G_0 k^2}{2(1 + Nk)\, T_0} \tag{16}$$

for the standard deviation.

If we recall that the performance of the control process is measured by the expression $F = m_\Delta^2 + \sigma_\Delta^2$ we find that the extremal value k can be obtained from the condition

$$\frac{d}{dt}\,[m_\Delta^2 + \sigma_\Delta^2]_{k=k_0} = 0, \tag{17}$$

where m_Δ and σ_Δ^2 are given by the expressions in (14) and (16).

The equation determining the extremal value k_0 in the given case is

$$\pi N^3 G_0 k_0^3 + \pi N^2 G_0 3 k_0^2 + \pi N G_0 2 k_0 - 4 T_0 z_0 = 0. \tag{18}$$

Equation (18) is best solved graphically, when the functions N(t) and $T_0(t)$ are given. The result yields the optimal value of the amplification factor $k_0(t)$ of the compensating network.

The complete set of equations for the adjustment network in the case we are considering is obtained as the special case of the equations (2) and (3) for one adjustable parameter.

Because of the slowness of the processes in the adjustment network, the approximate equations of the type (8) for the adjusting network are

$$(Tp + 1)(\tau p + 1)z = \tag{19}$$

$$= -\varkappa w^2 a^2 u - \varkappa\varphi, \quad pu = z + pw - pk_0.$$

If we neglect small quantities of the third order, then on the basis of the expression (8') the disturbing function φ satisfies the relation

$$\varphi = U_0 w, \tag{20}$$

where $U_0 = \Delta_0^2$ is the square of the control error for $k=k_0$.

Since we have assumed that the variation of the variables N, T_0, k_0 is slow compared with the processes in the main network, the coefficient $\underline{a}$ is given by the expression

$$a = -\frac{Nz_0}{(1 + Nk_0)^2}\left[1 - \exp\left(-\frac{1 + Nk_0}{T_0}\,t\right)\right].$$

For the analysis of the system of equations (19) and (20) that follows, we must first of all transform the expression (20) by applying the method of statistical linearization to the quadrator [10]. Since the quadrator has an even-symmetric characteristic, we must apply the statistical linearization method in the form [10]

$$U_0 = \Delta_0^2 = f_0 + k_1\Delta_0^0,$$

where $f_0 = m^2_{\Delta_0} + \sigma^2_{\Delta_0}$ is the mathematical expectation of the function U_0; Δ_0^0 the random component of Δ_0 having a zero mathematical expectation; and $k_1 = 2m_{\Delta_0}$ is the statistical amplification coefficient of this random component.

We now use the system of equations (19), apply the method of statistical linearization [10] to the quadrator to obtain the mathematical expectation of the adjustment error m_u, and obtain the system of linear equations

$$(Tp + 1)(\tau p + 1)z =$$

$$= -\varkappa w^2 a^2 m_u - \varkappa w\,[m^2_{\Delta_0} + \sigma^2_{\Delta_0}], \tag{21}$$

$$pm_u = z + pw - pk_0.$$

Since the time constants T and τ of the filters are such that the variables m_u, m_{Δ_0}, σ_{Δ_0} can be assumed to vary slowly with the processes occurring in the filters, then the system of equations (21) reduces to the following equation for m_u:

$$pm_u + \varkappa b_1 m_u = -pk_0 + pw - \varkappa b_2\,[m^2_{\Delta_0} + \sigma^2_{\Delta_0}]. \tag{22}$$

Here

$$b_1 = \int_0^t g_2(t, \tau)\,w^2(\tau)a^2(\tau)\,d\tau,$$

$$b_2 = \int_0^t g_2(t, \tau)\,w(\tau)\,d\tau,$$

where $g_2(t, \tau)$ is a weighting function for the left-hand side of the first equation of the system (21).

The quantities b_1 and b_2 are mean values of the variables a^2w^2 and $\underline{w}$, and are obtained by using two filters in the adjustment network. The quantity b_2 is close to zero, while $b_1 \approx$ const. The solution of equation (22) can be used to obtain the function

$$m_u(t) =$$

$$= m_u(0)\,e^{-\varkappa b_1 t} + \int_0^t e^{-\varkappa b_1(t-\tau)}\,[\dot{w}(\tau) - \dot{k}_0(\tau)]\,d\tau.$$

In particular, for the test signal $w = \mu_0 \sin\omega_1 t$, we obtain

$$m_u = -\frac{\dot{k}_0}{\varkappa b_1} + \frac{\mu_0}{\sqrt{1 + \dfrac{\varkappa^2 b_1^2}{\omega_1^2}}}\sin\omega_1 t. \tag{23}$$

For finding the random component of the adjustment error u^0 (superscript "0" denotes the centralized random function), we obtain from the system (19) the equation

$$(Tp + 1)(\tau p + 1)\,z^0 = \tag{24}$$

$$= -\varkappa w^2 a^2 u^0 - \varkappa w 2m_{\Delta_0}\Delta_0^0, \quad pu^0 = z^0.$$

The system of equations (24) is linear with variable coefficients, and can be solved by using linear-theory methods. However, if we take into consideration what was said about the system of equations (21), the system (24) can also be written as

$$pu^0 + \varkappa b_1 u^0 = \tag{25}$$

$$= -z_1^0, \quad (\tau p + 1)(Tp + 1)\,z_1^0 = 2\varkappa m_{\Delta_0} w\Delta_0^0.$$

The function Δ_0^0 is a stationary random function with a spectral distribution

$$G_{\Delta_0}(\omega) = \frac{k_0^2 N^2}{T_0^2\omega^2 + (1 + k_0 N)^2}\,G_0.$$

The function z_1^0 is obtained from the function Δ_0^0 by multiplication by the test signal $\mu_0 \sin\omega_1 t$ in the synchronous detector and averaging in two stationary filters; z_1^0 is a stationary random function with a spectral density of the form [9]

$$G_{z_1}(\omega) =$$

$$G_{\Delta_0}(\omega)\left\{\frac{\varkappa^2 m^2_{\Delta_0}\mu_0^2}{(T + \tau)^2(\omega + \omega_1)^2 + [1 - T\tau(\omega + \omega_1)^2]^2} + \right.$$

$$\left. + \frac{\varkappa^2 m^2_{\Delta_0}\mu_0^2}{(T + \tau)^2(\omega - \omega_1)^2 + [1 - T\tau(\omega - \omega_1)^2]^2}\right\}. \tag{26}$$

The solution of the first equation of the system (25) can be used to determine the quantity $u^0(t)$ and the standard deviation from the expression

$$D_{u}(t) = G_0 k_0^2 N^2 \varkappa^2 m_{\Delta_0}^2 \mu_0^2 \int_0^t e^{-\varkappa b_1 t_1} dt_1 \int_0^t e^{-\varkappa b_1 t_2} k_{z_1} (t - t_2 + t_1)\, dt_2, \qquad (27)$$

where

$$k_{z_1}(\tau) = \int_0^\infty g_{z_1}(\omega) \cos \omega\tau \, d\omega,$$

$$g_{z_1}(\omega) = \frac{1}{T_0^2 \omega^2 + [1 + N k_0]^2} \left\{ \frac{1}{(T + \tau)^2 (\omega + \omega_1)^2 + [1 - T\tau (\omega + \omega_1)^2]^2} + \right.$$

$$\left. + \frac{1}{(T + \tau)^2 (\omega - \omega_1)^2 + [1 - T\tau (\omega - \omega_1)^2]^2} \right\}.$$

In a steady state the standard deviation D_u can be obtained by calculating the integral

$$D_u = G_0 k_0^2 N^2 \varkappa^2 m_{\Delta_0}^2 \mu_0^2 \int_0^\infty g_{z_1}(\omega) \frac{1}{\varkappa^2 b_1^2 + \omega^2} d\omega. \quad (28)$$

Moreover, by analyzing the initial second moment of the adjustment error for various values of the parameters κ and τ, we can choose their optimal values to correspond to the minimum of

$$m_{u\,\max}^2 + D_u = \left(\frac{\mu_0}{\sqrt{1 + \frac{\varkappa^2 b_1^2}{\omega_1^2}}} - \frac{k_0}{\varkappa b_1} \right)^2 + \qquad (29)$$

$$+ \frac{G_0 k_0^2 N^2 \varkappa^2 z_0^2 \mu_0^2}{(1 + k_0 N)^2} \int_0^\infty g_{z_1}(\omega) \frac{1}{\varkappa^2 b_1^2 + \omega^2} d\omega.$$

The optimal values of the parameters κ and τ of the adjustment network depend on the level of the spectral density G_0 of the random disturbance, on the size of the useful control signal z_0, and also on the size of the amplification coefficients of the object N and the correlation network k_0.

The parameters of the adjusting network can thus only be chosen to be optimal for definite calculated conditions.

It can be seen from the expression (29) that the adjustment error depends greatly on the test signal amplitude. For fixed values of the parameters κ and τ, the error in the adjustment of the amplification coefficient of the compensating network for varying external conditions is obtained for a steady regime from formulas (23) and (28).

We now obtain the mathematical expectation of the deviation in the estimation of the accuracy of control in the form $m_{\Delta_1} = a m_u$. The standard deviation of the accuracy of control is calculated from the formula

$$D_{\Delta_1} = a^2 D_u.$$

According to the formulas (11) and (12), the accuracy of control in the case of a self-adaptive system is calculated from the expressions

$$m_\Delta = m_{\Delta_0} + m_{\Delta_1}, \quad D_\Delta = D_{\Delta_0} + D_{\Delta_1} + 2K_{\Delta_0\Delta_1},$$

where $K_{\Delta_0\Delta_1}$ is the correlation moment for the steady regime, equal to

$$K_{\Delta_0\Delta_1} = \int_0^\infty G_{\Delta_0}(\omega) \left| \frac{\varkappa m_{\Delta_0} \mu_0}{\varkappa b_1 + i\omega} \right.$$

$$\left[\frac{e^{i\omega_1}}{-T\tau(\omega + \omega_1)^2 + (T + \tau)\, i\,(\omega + \omega_1) + 1} + \right.$$

$$\left. \left. + \frac{e^{-i\omega}}{-T\tau(\omega - \omega_1)^2 + (T + \tau)\, i\,(\omega - \omega_1) + 1} \right] \right| d\omega,$$

and

$$D_{\Delta_0} = \frac{\pi N G_0 k_0^2}{2(1 + k_0 N) T_0}.$$

LITERATURE CITED

1. Chien Hsüeh-hsien, Technical Cybernetics [Russian translation] (IL, 1956).
2. A. A. Fel'dbaum, The Influence of Random Factors on Processes of Automatic Scanning. The Theory and Application of Discrete Automatic Systems. Transactions of the 1958 conference, edited by Ya. Z. Tsypkin [in Russian] (Izd. AN SSSR, 1960).
3. A. A. Fel'dbaum, "Steady processes in the simplest discrete extremal system in the presence of random disturbances," Avtomat. i Telemekh. 20, No. 8 (1959).*
4. A. A. Fel'dbaum, "The statistical theory of the gradient method of automatic optimization in the case of an object with a quadratic characteristic," Avtomat. i Telemekh. 21, No. 2 (1960).*
5. V. M. Kuntsevich, "The investigation of a system of extremal control in the presence of random disturbances," Izvest. Akad. Nauk SSSR, Otdel. Tekh. Nauk, Énergetika i Avtomatika No. 1 (1960).
6. A. P. Roberts, "Self-optimizing systems for a certain class of randomly varying inputs," Trans. Soc. Instrum. Technology 11, No. 3 (1959).
7. A. A. Krasovskii, "The dynamics of continuous systems of extremal control based on the gradient method," Izvest. Akad. Nauk SSSR, Otdel. Tekh. Nauk, Énergetika i Avtomatika, No. 3 (1959).
8. A. A. Pervozvanskii, "Continuous systems of extremal control in the presence of random disturbances," Avtomat. i Telemekh. 21, No. 7 (1960).*

9. V. S. Pugachev, The Theory of Random Functions and Their Application to Problems of Automatic Control [in Russian](Gostekhizdat, 1958).

10. I. E. Kazakov, "An Approximate Probability Analysis of the Accuracy of Operation of Essentially Nonlinear Systems," Avtomat. i Telemekh. 17, No. 5 (1956).*

11. I. E. Kazakov, The Accuracy of Self-Adaptive Systems with Extremal Continuous Adjustment of the Compensating Network. [in Russian] Zhukovskii Collection of Scientific Works VVIA (1960).

---

* See English translation.

THE STABILITY OF A CERTAIN NONLINEAR CONTROLLED SYSTEM

Chang Jên-wei

Moscow

Translated from Avtomatika i Telemekhanika, Vol. 21, No. 11,
pp. 1475-1480, November, 1960
Original article submitted May 3, 1960

A method is analyzed for solving the problem of determining the stability of a certain system in which the controlled object has a nonlinear characteristic for large initial perturbations.

1. Statement of the Problem

The stability of a controlled system with a nonlinear actuating mechanism was studied in [1, 2, 3]. In these papers the perturbed movement of the controlled object was described by linear differential equations on the basis of linear object characteristics or by linearization. As we know, the form of the equations for perturbed motion of a controlled system depends on the conditions of the specific problem. We shall study the horizontal flight of a controlled aircraft at a constant velocity. In this case the equations for perturbed motion are of the following form:

$$\begin{gathered} T^2\ddot{\psi} + U\dot{\psi} + K(\beta) + \mu = 0, \\ \dot{\psi} - \dot{\beta} - n\beta = 0, \\ \mu = f(\sigma), \quad \sigma = a\psi + E\dot{\psi} + G^2\ddot{\psi} - \frac{1}{l}\mu . \end{gathered} \tag{1}$$

Here ψ is the yawing angle; β is the slip angle; μ is the deviation angle of the steering wheel; $f(\sigma)$ is the nonlinear characteristic of the servomotor and belongs to functions of class A or A' [2]. The function $K(\beta)$, which characterizes the lateral stability moment, is essentially nonlinear (Figs. 1, 2).

A problem of this type was investigated for the general case of sufficiently small perturbations in a monograph by A. M. Letov [2]. Letov proved the theorem on the stability (in a first approximation) of an automatic control system with an essentially nonlinear actuator. But if we do not limit our analysis to movement near the origin, then it is necessary to take into account the effect of a change in the sign of the function $K(\beta)$. In other words, in that case we cannot linearize the first equation of the system (1).

At present a general method for solving this type of problem does not yet exist. In this paper we study one particular method for analyzing the stability of the system (1) and demonstrate that the known Lyapunov methods can be extended to a control system with a nonlinear object.

2. Investigation of the Stability in the General Case

In order to investigate the stability of the system (1) we make use of the second Lyapunov method. Before formulating the Lyapunov function we shall reduce the original equations of system (1) to dimensionless form. From Fig. 1 it is evident that the nonlinear function $K(\beta)$ can be replaced approximately by the function $k\beta + m\beta^3$, where $\underline{k}$ and $\underline{m}$ have opposite signs. Fig. 1 corresponds to $k>0$, $m<0$, and Fig. 2 corresponds to $k<0$, $m>0$.

Introducing the new variables $\eta_1 = \psi$, $\eta_2 = T\frac{d\psi}{dt}$, $\eta_3 = \beta$ and $t = T\tau$, we obtain

$$\begin{aligned} \dot{\eta}_1 &= \eta_2, \\ \dot{\eta}_2 &= a_{21}\eta_1 + a_{22}\eta_2 + a_{23}\eta_3 + m_2\eta_3^3 + n_2\sigma, \\ \dot{\eta}_3 &= \eta_2 + a_{33}\eta_3, \\ \dot{\sigma} &= q_1\eta_1 + q_2\eta_2 + q_3\eta_3 + \bar{q}_2\eta_2\eta_3^2 + \bar{q}_3\eta_3^3 - \gamma\sigma - sf(\sigma), \end{aligned} \tag{2}$$

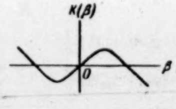

Fig. 1.

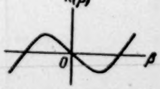

Fig. 2.

where

$$a_{21} = \frac{-alT^2}{T^2 + lG^2}, \quad a_{22} = \frac{-T(U + lE)}{T^2 + lG^2},$$

$$a_{23} = \frac{-kT^2}{T^2 + lG^2}, \quad a_{33} = -nT,$$

$$m_2 = -\frac{mT^2}{T^2 + lG^2},$$

$$n_2 = \frac{lT^2}{T^2 + lG^2}, \quad q_1 = \frac{al(UG^2 - ET^2)}{T(T^2 + lG^2)},$$

$$q_2 = a - \frac{kG^2}{T^2} + \frac{|U + lE|(UG^2 - ET^2)}{T^2(T^2 + lG^2)},$$

$$q_3 = \frac{nkG^2}{T} + \frac{k(UG^2 - ET^2)}{T(T^2 + lG^2)},$$

$$\bar{q}_2 = \frac{-mG^2}{T^2}, \quad \bar{q}_3 = \frac{nmG^2}{T} + \frac{m(UG^2 - ET^2)}{T(T^2 + lG^2)},$$

$$\gamma = \frac{l(UG^2 - ET^2)}{T(T^2 + lG^2)},$$

$$s = \frac{T^2 + lG^2}{lG^2} s, \quad f(\sigma) = h\sigma + \varphi(\sigma), \quad \varphi(\sigma) \geqslant 0.$$

We shall assume that the characteristic equation

$$D(\lambda) = \begin{vmatrix} -\lambda & 1 & 0 \\ a_{21} & a_{22} - \lambda & a_{23} \\ 0 & 1 & a_{33} - \lambda \end{vmatrix} = 0 \qquad (3)$$

has roots restricted to negative real parts. Under these conditions the following inequalities must be satisfied on the basis of the Routh-Hurwitz criterion:

$$a_{22} + a_{33} < 0, \; a_{21}a_{33} > 0,$$
$$(a_{22} + a_{33})(a_{22}a_{33} - a_{21} - a_{23}) + a_{21}a_{33} < 0. \qquad (4)$$

Then, according to the Lyapunov theorem there exists a positive-definite quadratic form $F = \frac{1}{2} \sum_{i,k=1}^{3} B_{ik}\eta_i\eta_k$, whose derivative satisfies the relationship

$$\frac{\partial F}{\partial \eta_1}\eta_2 + \frac{\partial F}{\partial \eta_2}(a_{21}\eta_1 + a_{22}\eta_2 + a_{23}\eta_3) + \qquad (5)$$
$$+ \frac{\partial F}{\partial \eta_3}(\eta_2 + a_{33}\eta_3) = -A(\eta_1^2 + \eta_2^2 + \eta_3^2),$$

where A is a specified positive constant number.

From Eq. (5) we can find the unknown coefficients β_{ik} which are expressed in terms of $a_{21}, a_{22}, a_{23}, a_{33}$, and A.

We shall study the function

$$V = F(\eta_1, \eta_2, \eta_3) + \frac{1}{2}\sigma^2$$

and shall formulate its total time derivative. In view of (2), we shall have

$$-\dot{V} = -\frac{\partial F}{\partial \eta_1}\eta_2 -$$
$$- \frac{\partial F}{\partial \eta_2}(a_{21}\eta_1 + a_{22}\eta_2 + a_{23}\eta_3 + m_2\eta_3^2 + n_2\sigma) -$$
$$- \frac{\partial F}{\partial \eta_3}(\eta_2 + a_{33}\eta_3) -$$
$$\sigma[q_1\eta_1 + q_2\eta_2 + q_3\eta_3 + \bar{q}_2\eta_2\eta_3^2 + \bar{q}_3\eta_3^2 - \gamma\sigma - sf(\sigma)].$$

Denoting η_3^2 by η and making use of relationship (5), we rewrite $-\dot{V}$ in the following form:

$$-\dot{V} = \frac{1}{2}A\eta_1^2 + \frac{1}{2}A\eta_2^2 + \left(\frac{1}{2}A - m_2B_{23}\eta\right)\eta_3^2 -$$
$$-(m_2B_{12}\eta)\eta_1\eta_3 - (m_2B_{22}\eta)\eta_2\eta_3 + \frac{1}{2}A(\eta_1^2 + \eta_2^2 + \eta_3^2) -$$
$$-(q_1 + n_2B_{12})\sigma\eta_1 - (q_2 + n_2B_{22} + \bar{q}_2\eta)\sigma\eta_3 -$$
$$-(q_3 + n_2B_{23} + \bar{q}_3\eta)\sigma\eta_3 + \gamma\sigma^2 + sh\sigma^2 + s\varphi(\sigma)\sigma.$$

This expression can be treated as the sum of two quadratic forms relative to η_1, η_2, η_3, and σ, whose coefficients depend on η. In order to find the sufficient conditions for stability of the system (2) we formulate the following two determinants:

$$D_1 = \begin{vmatrix} \frac{1}{2}A & 0 & \frac{1}{2}m_2B_{12}\eta \\ 0 & \frac{1}{2}A & \frac{1}{2}m_2B_{23}\eta \\ \frac{1}{2}m_2B_{12}\eta & \frac{1}{2}m_2B_{22}\eta & \frac{1}{2}(A - m_2B_{23}\eta) \end{vmatrix},$$

$$D_2 = \begin{vmatrix} \frac{1}{2}A & 0 & 0 & \frac{1}{2}(q_1 + n_2B_{12}) \\ 0 & \frac{1}{2}A & 0 & \frac{1}{2}(q_2 + n_2B_{22} + \bar{q}_2\eta) \\ 0 & 0 & \frac{1}{2}A & \frac{1}{2}(q_3 + n_2B_{23} + \bar{q}_3\eta) \\ \frac{1}{2}(q_1 + n_2B_{12}) & \frac{1}{2}(q_2 + n_2B_{22} + \bar{q}_2\eta) & \frac{1}{2}(q_1 + n_2B_{23} + \bar{q}_3\eta) & \gamma + sh \end{vmatrix}$$

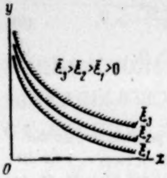

Fig. 3.

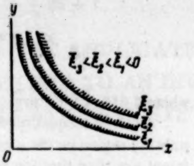

Fig. 4.

Expanding them, we obtain

$$D_1 = A^2 + B_1\eta + C_1\eta^2,$$

$$D_2 = A^2(\gamma + sh) + A_2 + B_2\eta + C_2\eta^2, \tag{6}$$

where the coefficients B_1, C_1, A_2, B_2, C_2 can be found easily.

If the inequalities $D_1 > 0$, $D_2 > 0$ had been valid for any value of η, then in accordance with the Silvester criterion the form for $-\dot{V}$ would have been definitely negative in the entire space (η_1, η_2, η_3, σ); therefore the system (2) would have been asymptotically stable as a whole. Since the coefficients of the polynomials (6) may be negative, the inequalities $D_1 > 0$, $D_2 > 0$ are satisfied only for a certain finite set of values η.

Basing ourselves on this fact, we use the Lyapunov theorem to state that if the inequalities $D_1 > 0$, $D_2 > 0$ are valid for values of η which belong to a certain unbroken continuum $[0, \bar{\eta}]$ containing the origin, then the system (2) will be asymptotically stable for any initial perturbations of η_1, η_2, and σ and for initial perturbations of η_3 such that its absolute values do not exceed $\sqrt{\bar{\eta}}$. The existence of such an $\bar{\eta} > 0$ is guaranteed if $A^2(\gamma + sh) + A_1 > 0$, since in view of the continuity condition it is possible to find a limiting value $\bar{\eta} < \eta^*$ such that over the semi-interval $[0, \eta^*]$ the inequalities $D_1 > 0$, $D_2 > 0$ are valid. It is evident that $\eta^* = \min(\eta^{(1)}, \eta^{(2)})$, where $\eta^{(1)}$ and $\eta^{(2)}$ are the first roots of the equations $D_1 = 0$, $D_2 = 0$ on the semi-axis $(0, +\infty)$.

3. Investigating the Stability Conditions

We now proceed to a detailed study of the applicability of the inequalities $D_1 > 0$, $D_2 > 0$. For simplicity we assume that $n = 0$, $G^2 = 0$, and $f(\sigma)$ belong to the class A' [2]. Then $\eta_1 = \eta_3$ and the system (2) will be written as

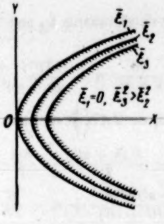

Fig. 5.

$$\begin{aligned}
\dot{\eta}_1 &= \eta_2, \\
\dot{\eta}_2 &= a_{21}\eta_1 + a_{22}\eta_2 + m_2\eta_1^3 + n_2\sigma, \\
\dot{\sigma} &= q_1\eta_1 + q_2\eta_2 + q\eta_1^3 - \gamma\sigma - sf(\sigma),
\end{aligned} \tag{7}$$

where

$$a_{21} = -(k + al), \quad a_{22} = \frac{-(U + lE)}{T},$$

$$m_2 = -m, \ n_2 = l,$$

$$q_1 = \frac{-E}{T}(k + al),$$

$$q_2 = a - \frac{E}{T^2}(U + lE), \quad q = \frac{-Em}{T},$$

$$\gamma = \frac{-El}{T},$$

$$s = \frac{1}{l}, \quad f(\sigma) = h\sigma + \varphi(\sigma), \quad h > 0, \quad \varphi(\sigma) \geqslant 0.$$

In that case the determinants D_1, D_2 are written as

$$D_1 = \begin{vmatrix} \frac{1}{2}A + m_2B_{12}\eta & \frac{1}{2}mB_{22}\eta \\ \frac{1}{2}mB_{22}\eta & \frac{1}{2}A \end{vmatrix},$$

$$D_2 = \begin{vmatrix} \frac{1}{2}A & 0 & \frac{1}{2}(B_{12}l + q_1 + q\eta) \\ 0 & \frac{1}{2}A & \frac{1}{2}(B_{22}l + q_2) \\ \frac{1}{2}(B_{12}l + q_1 + q\eta) & \frac{1}{2}(B_{22}l + q_2) & \frac{h}{l} + \gamma \end{vmatrix},$$

where B_{12}, B_{22} are expressed in terms of A by the following formulas:

$$B_{12}=\frac{A}{k+al}, \quad B_{22}=\frac{T(1+k+al)A}{(k+al)(U+lE)}.$$

Expanding the determinants D_1 and D_2 we obtain

$$D_1=\frac{A}{4}\left[1+\frac{2m}{k+al}\eta-\frac{m^2T^2(1+k+al)^2}{(k+al)^2(U+lE)^2}\eta^2\right],$$

$$D_2=2A^2\left(\frac{h}{l}+\gamma\right)-$$

$$-A\left[\frac{lA}{k+al}-\frac{E(k+al)}{T}-\frac{Em}{T}\eta\right]^2-$$

$$-A\left[\frac{(1+k+al)lTA}{(k+al)(U+lE)}+a-\frac{E}{T^2}(U+lE)\right]^2.$$

We introduce the substitutions

$$k+al=x, \quad \frac{U+lE}{T}=y,$$

$$\frac{hT}{l^2E}-1=z, \quad m\eta=\xi,$$

$$2x^2z=X, \quad \frac{x}{y}(1+x)-y+\frac{aT}{E}=Y$$

and select the as yet undefined constant A in the form

$$A=\frac{(k+al)^2E}{lT}.$$

Making use of these substitutions, we write the sufficient conditions $D_1>0$, $D_2>0$ for stability of the system (7) in the following form:

$$1+2\xi\frac{1}{x}-\frac{\xi^2(1+x)^2}{x^2y^2}>0, \tag{8}$$

$$X-Y^2-\xi^2>0. \tag{9}$$

where $\xi\in[0,\bar{\xi}]$, $\bar{\xi}=m\bar{\eta}$.

Based on inequality (8), it is possible to plot the stability region on the plane of parameters x, y for different specified limiting values $\bar{\xi}=m\bar{\eta}$ (Figs. 3, 4). Analogously, inequality (9) determines the boundaries of the stability region on the X, Y plane for various values of $\bar{\xi}=m\bar{\eta}$ (Fig. 5).

Inequalities (8), (9) must be satisfied simultaneously for different values of $\bar{\xi}=m\bar{\eta}$. In view of continuity and for an appropriate selection of the parameters a, l, E, and h, such a requirement may be satisfied.

In conclusion the author expresses his appreciation to A. M. Letov for a number of valuable suggestions and remarks.

LITERATURE CITED

1. A. I. Lur'e, Certain Nonlinear Problems in Automatic Control Theory [in Russian](Gostekhizdat, 1951).
2. A. M. Letov, Stability of Nonlinear Control Systems [in Russian] (Gostekhizdat, 1955).
3. I. G. Malkin, "On stability theory for controlled systems," Priklad. Mat. i Mekh. No. 1 (1951).

FOUNDATIONS FOR THE APPLICATION OF THE HARMONIC LINEARIZATION METHOD TO AN INVESTIGATION OF PERIODIC OSCILLATIONS IN SYSTEMS WITH LAG*

V. S. Kislyakov

Moscow

Translated from Avtomatika i Telemekhanika Vol. 21, No. 11,
pp. 1481-1489, November, 1960
Original article submitted April 18, 1960

The paper studies the problems of applying the harmonic linearization method (Krylov and Bogolyubov [1, 2]) to an investigation of periodic oscillations in control systems with lag that are described by linear nth order differential equations with a lagging argument.

In [3] a number of specific examples involving the application of the asymptotic methods developed by N. M. Krylov and N. N. Bogolyubov for investigating periodic oscillations in both linear and nonlinear control systems with lag are studied without rigorous mathematical foundations. The essence of the asymptotic methods was reduced to finding the solution for the equation under study in the form of the sum of its particular solutions expanded into formal series in the small parameter ϵ. For the case where a nonlinear equation was investigated the so-called "generating" solution was determined first (i.e., a periodic solution of an ordinary linear differential equation with a lagging argument, which is derived from the nonlinear equation for $\epsilon = 0$). For this purpose it is quite natural to begin with an attempt at applying asymptotic methods (the method of harmonic linearization) in the investigation of periodic oscillations in linear systems with lag. Our present paper is devoted to precisely this subject.

1. Assume that a controlled system with lag is described by ordinary linear differential nth order equations with constant coefficients and a lagging argument:

$$L[y(t)] \equiv y^{(n)}(t) + \sum_{\nu=1}^{n} [a_\nu y^{(n-\nu)}(t) + b_\nu y^{(n-\nu)}(t-\tau_\nu)] = 0, \tag{1}$$

where L is a linear differential operator; a_ν, b_ν are constant real coefficients, and τ_ν are real positive constants which characterize the time lag.

Such an equation was investigated in detail in [4-7] and in other papers. Schmidt [5] studied an equation of the type (1) and demonstrated that if a) the solution y(t) is continuous, together with its first n derivatives, over the entire real axis, and b) for $t \to \pm\infty$ the function y(t) does not increase more rapidly than $c|t|^\alpha$ (α, $c > 0$ are constants), then the nature of the solution for Eq. (1) depends on the existence of real zeros for the transcendental characteristic function defined by the equation

$$l(\omega) = (j\omega)^n + \sum_{\nu=1}^{n} [a_\nu (j\omega)^{n-\nu} + b_\nu (j\omega)^{n-\nu} e^{-j\tau_\nu\omega}]. \tag{2}$$

Schmidt also demonstrated that the function $l(\omega)$ has a finite number of real zeros and proved the following theorem: if $l(\omega)$ contains exactly m real zeros† ($m > 0$), then a) the homogeneous differential equation (1) has m linearly independent particular solutions, and b) any solution y(t) which for $t \to \pm\infty$ does not increase more rapidly than $c|t|^\alpha$ can be written as the sum

$$y(t) = \sum_{k=1}^{m} \alpha_k y_k(t), \tag{3}$$

where α_k are arbitrary constants and $y_k(t)$ are those particular solutions that are contained in any series $y_1(t)$, $y_2(t)$, . . . , $y_m(t)$ which includes functions of the form $\exp(j\lambda t)$, $t\exp(j\lambda' t)$, $t^2\exp(j\lambda'' t)$, . . . ; here λ, λ', and λ'' respectively denote all simple, all double, and all triple (etc.) real zeros of the function $l(\omega)$.

2. One of the possible Krylov-Bogolyubov methods, which is called the harmonic linearization method in automatic control theory, can be reduced to the following when applied to nth order equations of the form (1). Equation (1) is replaced by an ordinary linear nth order differential equation of the following form, which has no lag in its argument:

---

* Paper presented November 19, 1959 at the Seminar on Differential-Difference Equations Held in the Lomonosov Moscow State University.

† We mean ω_1, ω_2, . . . , ω_m.

$$y^{(n)}(t) + \frac{1}{1+c_1}\sum_{\nu=1}^{n} c_{\nu+1} y^{(n-\nu)}(t) = 0, \tag{4}$$

where c_ν ($\nu = 1, 2, \ldots, n$) are the coefficients to be determined. In order to determine the coefficients c_ν we assume formally that

$$y(t) = A\cos\omega t, \tag{5}$$

in accordance with the Krylov-Bogolyubov asymptotic methods [2].

Differentiating Eq. (5) $\underline{n}$ times with respect to $\underline{t}$, we obtain

$$\begin{aligned} \dot{y}(t) &= -A\omega\sin\omega t,\\ \ddot{y}(t) &= -A\omega^2\cos\omega t,\\ \dddot{y}(t) &= A\omega^3\sin\omega t,\\ &\ldots\ldots\ldots\ldots \end{aligned} \tag{6}$$

Substituting the values of $y(t)$ and its $\underline{n}$ first derivatives from Eq. (5) and (6) into (1) and (4), we set the coefficients of the sines, cosines, and corresponding powers of ω equal to one another. As a result we obtain

$$\begin{aligned} c_1 &= -\frac{b_1}{\omega}\sin\omega\tau_1,\\ c_2 &= a_1 + b_1\cos\omega\tau_1 - \frac{b_2}{\omega}\sin\omega\tau_2,\\ &\ldots\ldots\ldots\ldots\ldots\ldots\\ c_n &= a_{n-1} + b_{n-1}\cos\omega\tau_{n-1} - \frac{b_n}{\omega}\cos\omega\tau_n,\\ c_{n+1} &= a_n + b_n\cos\omega\tau_n. \end{aligned} \tag{7}$$

Thus the linear differential $\underline{n}$th order equation, with periodic solutions of the form (5) that are common to the differential-difference equation (1), will be

$$L^*[y(t)] \equiv \left(1 - \frac{b_1}{\omega}\sin\omega\tau_1\right) y^{(n)}(t) + \sum_{\nu=1}^{n-1}\left(a_\nu + b_\nu\cos\omega\tau_\nu - \frac{b_{\nu+1}}{\omega}\sin\omega\tau_{\nu+1}\right)\times \tag{8}$$

$$\times\, y^{(n-\nu)}(t) + (a_n + b_n\cos\omega\tau_n)\, y(t) = 0,$$

where L^* is a linear differential operator.

Applying the Euler method [4], consisting of the substitution

$$y(t) = e^{\lambda t}, \tag{9}$$

to Eq. (1) and (8), we obtain the characteristic equations for (1):

$$F(\lambda) \equiv \lambda^n + \sum_{\nu=1}^{n}\left[a_\nu\lambda^{n-\nu} + b_\nu\lambda^{n-\nu}e^{-\lambda\tau_\nu}\right] = 0 \tag{10}$$

and (8):

$$F^*(\lambda) \equiv \left(1 - \frac{b_1}{\omega}\sin\omega\tau_1\right)\lambda^n +$$

$$+ \sum_{\nu=1}^{n-1}\left[\left(a_\nu + b_\nu\cos\omega\tau_\nu - \frac{b_{\nu+1}}{\omega}\sin\omega\tau_{\nu+1}\right)\lambda^{n-\nu}\right]$$

$$+ a_n + b_n\cos\omega\tau_n = 0, \tag{11}$$

respectively; here F and F^* are characteristic functions corresponding to the operators L and L^*.

3. We shall prove a number of theorems by means of which we can clarify the possibility of applying the Krylov-Bogolyubov asymptotic methods to an investigation of periodic oscillations in controlled systems with lag. It is assumed that the controlled system can be described by $\underline{n}$th order linear differential equations with constant coefficients and a lagging argument.

Theorem 1. Assume the characteristic equations for the linear differential equations (1) and (8) have purely imaginary roots. Then the characteristic functions $F(j\omega)$ and $F^*(j\omega)$ have an equal number of identical real zeros‡ which determine the periodic solutions of Eq. (1) and (8).

Proof. We know that for the existence of periodic solutions of a linear differential equation (even one with a lagging argument [5]) it is necessary and sufficient that its corresponding characteristic equation have purely imaginary roots.

Assuming $\lambda = j\omega$, we obtain

$$F(j\omega) \equiv (j\omega)^n + \sum_{\nu=1}^{n}\left[a_\nu(j\omega)^{n-\nu}\right.$$

$$\left. + b_\nu(j\omega)^{n-\nu}e^{-j\tau_\nu\omega}\right] = 0, \tag{12}$$

$$F^*(j\omega) \equiv \left(1 - \frac{b_1}{\omega}\sin\omega\tau_1\right)(j\omega)^n +$$

$$+ \sum_{\nu=1}^{n-1}\left[\left(a_\nu + b_\nu\cos\omega\tau_\nu - \frac{b_{\nu+1}}{\omega}\sin\omega\tau_{\nu+1}\right)(j\omega)^{n-\nu}\right]$$

$$+ a_n + b_n\cos\omega\tau_n = 0. \tag{13}$$

Using the Euler formulas $\exp(-j\omega\tau_n) = \cos\omega\tau_n - j\sin\omega\tau_n$, it is easy to see that Expression (13) can be transformed to

$$F^*(j\omega) \equiv$$

$$\equiv (j\omega)^n + \sum_{\nu=1}^{n}\left[\left(a_\nu + b_\nu e^{-j\tau_\nu\omega}\right)(j\omega)^{n-\nu}\right] = 0. \tag{14}$$

---

‡We mean the roots $\omega_1, \omega_2, \ldots$

From this it follows that for ω equal to the zeros of the characteristic functions we have $F(j\omega) = F^*(j\omega) = l(\omega)$.

Based on the results cited by Schmidt [5], it can be stated that the characteristic functions $F(j\omega)$ and $F^*(j\omega)$ have the same number of identically equal real zeros which determine the periodic solutions of Eq. (1) and (8). Thus we have proved the theorem.

Theorem 2. Assume the periodic solutions of Eq.(1) are determined by the initial functions $\varphi^{(r)}(t)$ $(r = 0, 1, \ldots, 2m-1)$ specified over the initial set E_{t_0} consisting of the points on the time segment $t_0-\tau \le t \le t_0$; assume further that for $t = t_0 = 0$ these functions have the value $\varphi^{(r)}(t_0)$. Now assume that the characteristic functions $F(j\omega)$ and $F^*(j\omega)$ have m real zeros. Then the differential equation (8) has periodic solutions of the form $y_k(t) = \beta_{2k-1}\sin\omega_k t + \beta_{2k}\cos\omega_k t$ $(k = 1, 2, \ldots, m)$ [where β_{2k-1}, β_{2k} are arbitrary constants, ω_k are the real roots of the characteristic functions $F(j\omega)$ (or $F^*(j\omega)$)] which are common to Eq. (1), provided that the arbitrary constants β_{2k-1}, β_{2k} of the periodic solutions for (8) are identically equal to the arbitrary constants of the periodic solutions for (1).

Proof. In order to determine the arbitrary constants β_{2k-1}, β_{2k} of the periodic solutions for (1) (the quasipolynomial of these constants has m real zeros) it proves sufficient to specify the numerical values of the initial function $\varphi(t)$ and its (2m−1)th derivative at the point $t = t_0$.

From the Schmidt Theorem it follows that any solution $y(t)$ of the differential equation (1) (which satisfies the conditions assumed in the theorem) can be written in the form of the sum

$$y(t) = \sum_{k=1}^{m} y_k(t). \tag{15}$$

In accordance with Theorem 2, $y_k(t) \equiv \overline{y}_k(t)$ $(k = 1, 2, \ldots, m)$ where $\overline{y}_k(t)$ are those particular solutions which are determined by the real zeros of the characteristic function $F^*(j\omega)$. Here the arbitrary constants β_{2k-1}, β_{2k} can easily be determined from the solution of algebraic equations which is obtained if Eq. (15) is differentiated (2m−1) times with respect to t, and the resulting expressions are set equal to the numerical values of the initial function $\varphi(t_0)$ and its (2m−1) derivatives for $t = t_0 = 0$. Thus Eq. (8) has periodic solutions

$$y(t) = \beta_{2k-1}\sin\omega_k t + \beta_{2k}\cos\omega_k t \qquad (k = 1, \ldots, m) \tag{16}$$

that are common to Eq. (1).

Thus the theorem has been proved.

Theorem 3. The sum of the particular solutions for Eq. (1),

$$y(t) = \sum_{k=1}^{m} (\beta_{2k-1}\cos\omega_k t + \beta_{2k}\sin\omega_k t), \tag{17}$$

(each of these solutions is found using the Krylov-Bogolyubov asymptotic method) satisfies the differential-difference equation (1).

Proof. The statement of the theorem stems from the fact that the particular solutions of (1) that are found using the asymptotic methods coincide exactly with the particular periodic solutions of that equation. The sum of the latter is also a solution of the differential-difference equation on the basis of the Schmidt Theorem cited above. The theorem has been proved.

In 1959 the paper by A. Khalanai [11] was published; this paper provided the foundations of the averaging method as applied to systems of quasilinear differential equations with a lagging argument. It proved the theorem (analogous to the corresponding theorem formulated by N. M. Bogolyubov [12] for systems of differential equations without lag) stating that the error in determining the periodic solution of the averaged system is small compared to error in the periodic solution of the original system of differential equations with a lagging argument. It should be noted that the theorem formulated by A. Khalanai was proved for a system of differential equations with a lagging argument reduced to standard form [2]. However, differential equations with a lagging argument can be reduced to standard form by substitution of variables only for the case where the linear terms in the system do not contain lag. Thus in the general case the problem of reducing a system of differential equations with a lagging argument to standard form should be considered still unsolved. Such reduction is obviously complicated (even when we seek only periodic oscillations) by the fact that the second order differential equation with a lagging argument which describes the periodic oscillatory mode may have two proper frequencies (this is in contrast to an ordinary differential equation and was demonstrated above). This result also follows from [13].

4. We shall study the equality between the periodic solutions for nth order equations of the form (1) with a lagging argument and periodic solutions of ordinary differential equations of the 2m-th order. We shall assume that an ordinary linear equation of the 2m-th order has periodic solutions equal to those of an nth order differential equation with a lagging argument if: a) the characteristic equations corresponding to the differential equations with and without lag in the argument have equal purely imaginary roots; b) the periodic solutions are determined by equal arbitrary constants; c) the original equations are satisfied for any combination of periodic solutions of the form

$$y(t) = \beta_1 \sin\omega_1 t + \beta_2\cos\omega_1 t + \beta_3\sin\omega_2 t + \\ + \beta_4\cos\omega_2 t + \cdots + \beta_{2m-1}\sin\omega_m t + \beta_{2m}\cos\omega_m t.$$

We shall prove a number of theorems which can be used to provide the foundation for postulating equality between the periodic solutions of differential equations with a lagging argument (1) and the periodic solutions of equations without lag.

Theorem 4. If the quasipolynomial $F(j\omega)$ of the linear differential nth order equation (1) has m real roots, then: a) the characteristic equation for the ordinary linear differential equation which has purely imaginary roots equal to those of Eq. (1) is of degree $2m$; b) its corresponding differential equation is of order $2m$.

Proof. From the general theory of linear differential equations it is known that the maximum number of linearly independent solutions of a linear differential equation is equal to its order. It is also known that if the characteristic equation has $2m$ purely imaginary roots, then the roots can only be conjugate pairs. Therefore the characteristic equation for a linear differential equation without lag that has purely imaginary roots equal to the characteristic equation for the linear differential equation (1) will have the degree $2m$; the differential equation that corresponds to it will have the order $2m$. The theorem has been proved.

From Theorem 1 it follows directly that the characteristic quasipolynomial $F(j\omega)$ has a finite number of real roots. Assume that the number of purely imaginary zeros of the quasipolynomial $F(j\omega)$ is equal to m. Then from Theorem 4 it follows that the characteristic equation for a linear differential equation with no lag and periodic solutions identically equal to the solutions of the equation with a lagging argument is of degree $2m$. We are confronted with the problem of how to determine the coefficients of this characteristic equation. We know that between the coefficients of the algebraic equation

$$\lambda^{2m} + a_1\lambda^{2m-1} + \ldots + a_{2m} = 0 \tag{18}$$

and its roots $\lambda_1, \lambda_2, \ldots, \lambda_{2m}$ there is the following relationship:

$$\begin{gathered}
\lambda_1 + \lambda_2 + \ldots + \lambda_{2m} = \sum_{i=1}^{2m} \lambda_i = -a_1, \\
\lambda_1\lambda_2 + \lambda_1\lambda_3 + \ldots + \lambda_{2m-1}\lambda_{2m} = \sum_{\substack{i,\,j=1\\(i<j)}}^{2m} \lambda_i\lambda_j = a_2, \\
\lambda_1\lambda_2\lambda_3 + \lambda_1\lambda_2\lambda_4 + \ldots + \lambda_{2m-2}\lambda_{2m-1}\lambda_{2m} = \\
= \sum_{\substack{i,\,j,\,k=1\\(i<j<k)}}^{2m} \lambda_i\lambda_j\lambda_k = -a_3, \\
\ldots\ldots\ldots\ldots\ldots\ldots\ldots\ldots\ldots\ldots \\
\lambda_1\lambda_2\ldots\lambda_{2m} = (-1)^{2m}a_{2m}.
\end{gathered} \tag{19}$$

Thus if we know the purely imaginary roots of the characteristic equation for the linear differential equation (1),

$$\lambda_1 = +j\omega_1,\ \lambda_2 = -j\omega_1, \ldots,$$
$$\lambda_{2m-1} = +j\omega_m,\ \lambda_{2m} = -j\omega_m,$$

then it is always possible to determine the coefficients of the characteristic equation in unique fashion; thus it is possible to determine the coefficients of an ordinary linear $2m$-th order differential equation in the form

$$\begin{gathered}
y^{(2m)}(t) + a_1y^{(2m-1)}(t) + \\
+ a_2y^{(2m-2)}(t) + \ldots + a_{2m}y(t) = 0.
\end{gathered} \tag{20}$$

Here it is easy to show that the coefficients $a_1, a_3, a_5, \ldots$ for the odd-order derivatives will always be equal to zero.

Theorem 5. Assume the periodic solutions of Eq. (1) are determined by the initial functions $\varphi^{(r)}(t)$ ($r = 0, 1, \ldots, 2m-1$) specified over the initial set E_{t_0}; assume further that for $t = t_0 = 0$ these functions have the values $\varphi^{(r)}(t_0)$, and the periodic solutions of Eq. (20) are determined by the initial conditions for $t = t_0 = 0$, $y_0^{(r)}$ ($r = 0, 1, \ldots, 2m-1$). Now assume the characteristic equations corresponding to the differential equations (1) and (20) have $2m$ equal purely imaginary roots. Then for $\varphi^{(r)}(t_0) \equiv y_0^{(r)}$ ($r = 0, 1, \ldots, 2m-1$) the differential equations (1) and (20) have equal particular periodic solutions $y_k(t)$, and any solution $y(t)$ can be written in the form of the sum

$$y(t) = \sum_{k=1}^{m} y_k(t),$$

where $y_k(t)$ are those particular solutions which correspond to the purely imaginary roots of the characteristic equations.

Proof. The equality between the particular periodic solutions $y_k(t)$ for Eq. (1) and (20) follows directly from the equality between the purely imaginary roots of the characteristic equations and the equality between the arbitrary constants determined from identical initial conditions. The second postulate in the theorem for Eq. (1) stems from the Schmidt Theorem; for Eq. (20) it stems from the determination of its coefficients. The theorem is proved.

5. As an example that illustrates the theorems proved above, we shall study the equation**

$$\ddot{y}(t) - 2y\left(t - \frac{\pi}{2}\right) + 3y(t) = 0, \tag{21}$$

whose periodic solutions are determined by the initial functions $\varphi^{(r)}(t)$ ($r = 0, 1, 2, 3$) that have the values $\varphi^{(r)}(t_0)$ for $t = t_0 = 0$.

**Equation (21) was presented to the author for solution by A. M. Zverkin in the course of discussing this paper at the Seminar on Differential-Difference Equations in the Lomonosov Moscow State University.

The quasipolynomial corresponding to Eq. (21),

$$E(\lambda) \equiv \lambda^2 - 2\lambda e^{-\frac{\pi}{2}\lambda} + 3 = 0,$$

has purely imaginary roots $\lambda = \pm j$, $\lambda = \pm 3j$ (this can easily be determined by direct substitution); the periodic solution of Eq. (21) corresponding to these roots is written as

$$y(t) = \beta_1 \sin t + \beta_2 \cos t + \\ + \beta_3 \sin 3t + \beta_4 \cos 3t.$$

We shall make use of the Krylov-Bogolyubov asymptotic method for determining the periodic solutions of Eq. (21). For this purpose we transform Eq. (21) to the form

$$\left(1 + \frac{2\sin\frac{\pi}{2}\omega}{\omega}\right)\ddot{y}(t) - 2\cos\frac{\pi}{2}\omega\dot{y}(t) + \\ + 3y(t) = 0. \tag{22}$$

The corresponding characteristic equation will be

$$F^{*}(\lambda) \equiv \left(1 + \frac{2\sin\frac{\pi}{2}\omega}{\omega}\right)\lambda^2 - 2\cos\frac{\pi}{2}\omega\lambda + \\ + 3 = 0. \tag{23}$$

In order for the differential equation (22) to have periodic solutions it is necessary and sufficient that $\lambda = j\omega$. Substituting $\lambda = j\omega$ into (23) and separating real and imaginary parts, we obtain

$$2\omega\cos\frac{\pi}{2}\omega = 0, -\omega^2\left(1 + \frac{2\sin\frac{\pi}{2}\omega}{\omega}\right) + 3 = 0. \tag{24}$$

From the simultaneous solution of Eq. (24) we find $\omega = 1$; $\omega = 3$. Thus $\lambda = \pm j$, $\lambda = \pm 3j$, and the example does not contradict Theorem 1. The periodic solutions of Eq. (22) corresponding to the particular values of ω are

$$y(t) = \beta_1 \sin t + \\ + \beta_2 \cos t, \quad y(t) = \beta_3 \sin 3t + \beta_4 \cos 3t. \tag{25}$$

The arbitrary constants in expression (25) are determined from the solution of the algebraic equations

$$\varphi(t_0) = \beta_2 + \beta_4, \quad \dot{\varphi}(t_0) = \beta_1 + 3\beta_3, \\ \ddot{\varphi}(t_0) = -\beta_2 - 9\beta_4, \; \dddot{\varphi}(t_0) = -\beta_1 - 27\beta_3 \tag{26}$$

and will be equal to

$$\beta_1 = \frac{9\dot{\varphi}(t_0) + \ddot{\varphi}(t_0)}{8}, \qquad \beta_2 = \frac{9\varphi(t_0) + \ddot{\varphi}(t_0)}{8}, \\ \beta_3 = -\frac{\dot{\varphi}(t_0) + \dddot{\varphi}(t_0)}{24}, \qquad \beta_4 = -\frac{\varphi(t_0) + \ddot{\varphi}(t_0)}{8}, \tag{27}$$

respectively.

Thus Eq. (21) and (22) have general periodic solutions of the form (25). The results which we have obtained do not contradict Theorem 2. It is easy to see that any solution y(t) that equals the sum of particular periodic solutions $y(t) = \beta_1 \sin t + \beta_2 \cos t + \beta_3 \sin 3t + \beta_4 \cos 3t$ satisfies Eq. (21). The latter does not contradict Theorem 3.

Further, the ordinary linear differential equation whose characteristic equation has the purely imaginary roots $\lambda_{1,2} = \pm j$, $\lambda_{3,4} = \pm 3j$ and whose coefficients are determined from formulas (19) is written as follows:

$$\ddddot{y}(t) + 10\ddot{y}(t) + 9y(t) = 0 \tag{28}$$

(the form above can easily be verified). The order of Eq. (28) is $2m = 4$. The latter result does not contradict Theorem 4. Assume the periodic solutions of Eq. (28) are determined by the initial conditions for $t = t_0 = 0$, $y_0^{(r)} \equiv \varphi^{(r)}(t_0)$ $(r = 0, 1, 2, 3)$. Then the general solution of Eq. (28) will be

$$y(t) = \beta_1 \sin t + \beta_2 \cos t + \beta_3 \sin 3t + \beta_4 \cos 3t,$$

in which the arbitrary constants β_1, β_2, β_3, β_4 are determined from the solution of the algebraic equation (26). This result does not contradict Theorem 5.

The author considers it his duty to express his sincere appreciation to all participants of the Seminar on Differential-Difference Equations in the Lomonosov Moscow State University conducted under the supervision of L. É. Él'sgol'ts, who took an active part in discussing this paper and helped substantially in the formulation of the paper.

LITERATURE CITED

1. N. M. Krylov and N. N. Bogolyubov, Introduction to Nonlinear Mechanics [in Russian] (Izd. AN Ukr SSR, 1937).
2. N. N. Bogolyubov and Yu. A. Mitropol'skii, Asymptotic Methods in the Theory of Nonlinear Oscillations [in Russian] (Fizmatgiz, 1958).
3. V. S. Kislyakov, "Application of the method of asymptotic Krylov-Bogolyubov approximations to the investigation of systems with lag," Avtomat. i Telemekh. 21, No. 4 (1960).††
4. L. É. Él'sgol'ts, Qualitative Methods in Mathematical Analysis [in Russian] (Gostekhizdat, 1955).
5. E. Schmidt, "Uber eine Klasse linearer funktionaler Differentialgleichungen," Math. Ann. 70 (1911).
6. E. Hilb, "Zur Theorie der linearen funktionalen Differentialgleichungen," Math. Ann. 77 (1917).
7. A. F. Leont'ev, "Differential-difference equations," Matematicheskii Sbornik 24 (16), No. 3 (1949).
8. A. D. Myshkis, "General theory of differential equations with a lagging argument," Uspekhi Mat. Nauk 4, No. 5 (1949).

9. A. D. Myshkis, Linear Differential Equations with a Lagging Argument [in Russian] (Gostekhizdat, 1951).
10. V. V. Stepanov, Course in Differential Equations [in Russian] (Gostekhizdat, 1953).
11. A. Khalanai, "Averaging method for systems of differential equations with a lagging argument," Revue de mathematiques pures et appliquees 4, No. 3 (1959).
12. M. A. Krasovskii and S. G. Krein, "On the averaging principle in nonlinear mechanics," Uspekhi Mat. Nauk 10, No. 3 (65) (1955).
13. L. É. Él'sgol'ts, "Certain properties of the periodic solutions for linear and quasilinear differential equations with deviating arguments," Vestnik Moskovskovo Universiteta No. 5 (1959).

†† See English translation.

EQUIVALENT TRANSFORMATIONS OF SEQUENTIAL MACHINES

A. Sh. Blokh

Minsk

Translated from Avtomatika i Telemekhanika, Vol. 21, No. 11,
pp. 1490-1496, November, 1960
Original article submitted May 7, 1960

The paper defines certain equivalent transformations of sequential machines and the corresponding structures of the machines.

1. The Structure of a Sequential Machine

We specify the sequential machine A (in abbreviated notation s.m. A) which is defined by the system of functions

$$s = f_1(q), \quad q' = f_2(x, q)$$

$$0 \leqslant s \leqslant m_s, \quad 1 \leqslant x \leqslant m_x, \quad 1 \leqslant q \leqslant m_q). \qquad (\bullet)$$

The values $\underline{x}$ are called input values; $\underline{s}$ are called output values; $\underline{q}$ are called numbers of states (or in abbreviated form x, s, q states). The time is varied in discrete fashion, and the values x, s, q vary only at the discrete instants of time $t_1, t_2, \ldots$ The "prime" denotes the state of the s.m. at the next instant.

By specifying the series of input values $x_1, x_2, \ldots, x_n$ at the instants $t_1, t_2, \ldots, t_n$ and the initial state q_0, we shall obtain the series of output values $s_1, s_2, \ldots, s_n$. The two series $x_1, x_2, \ldots, x_n$ and $s_1, s_2, \ldots, s_n$ are called an experiment of length $\underline{n}$. Two experiments are equal if both their input and output series are equal.

For a fixed input value $\underline{x}$ the equation $q' = f_2(x, q)$ defines a certain transformation of states $\underline{q}$ (i.e., it defines a certain generalized substitution a_x of the elements $\underline{q}$). We shall denote the operator for this substitution by the symbol A_x, and shall write the equation $q' = f_2(x, q)$ as $q' = A_x q$. Such a notation is sometimes more convenient. We depict the substitution a_x graphically as follows: a) we mark m_q points that are numbered $1, 2, \ldots, m_q$; b) the transition from the preceding state $\underline{q}$ to the next state q' is indicated by an arrow directed from q to q' (Fig. 1).

The graphical representation of the substitution, which indicates the corresponding value of $\underline{s}$ near $\underline{q}$, is called the structure of the substitution. The structures of all substitutions a_x form the structure [1] of s.m. A (Fig. 2). The structure of an s.m. defines it completely.

Discrete (digital) automatic systems are specified in various ways. But for synthesis of such systems we specify them in the form of s.m. (cf., for example, [3]). Depending on the method used for this transition, various s.m. are obtained.

Thus the same digital automatic system can be described by different pairs of functions (•). Thus we are confronted with the problem of choosing the optimum (in a certain sense) s.m. for synthesizing the specified digital automatic system.

2. Equivalent Transformations of Sequential Machines

Two s.m. A and B are called equivalent if for any experiment in machine A it is possible to indicate an equal experiment in machine B and vice versa. The transition from s.m. A to an equivalent s.m. B is called an equivalent transformation of s.m. A to s.m. B; we shall write this transformation as follows; $B = \alpha A$ where α denotes the transformation operator. The simplest operator α is the operator for the enumeration of states when each state $\underline{q}$ is assigned a different number in such a way that different numbers $\underline{q}$ correspond to different new numbers. We shall assume that such an enumeration does not alter the structure of the s.m. However, note that a different numbering of states $\underline{q}$ leads to a different realization; therefore a successful choice of the numbering for $\underline{q}$ can lead to a structurally simpler automatic system.

Since all equivalent s.m. perform an identical manipulation of the input data we encounter the problem of choosing an s.m. which will satisfy the specified conditions in optimum fashion (in particular, such a condition as the smallest number of different states). In order to achieve such a choice there must be a reserve

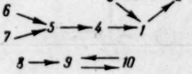

Fig. 1

of definite basic equivalent transformations. Below we shall indicate certain elementary transformations, but they are insufficient for transferring each s.m. into any equivalent s.m. The problem involving the completeness of the set of basic equivalent transformations will be studied in a different paper.

3. Terminology and Notation

The set of states q_i having the property that for a given q_i it is possible to indicate a natural number r_i for which $A_x^{r_i} q_i = q_i$ is defined as the center of the substitution a_x. The sub-sets of the center which are invariant relative to A_x are called kernels of the substitution. If the equation $A_x q = q_1$ does not have a solution, then the element q_1 is called the extreme element of the substitution. The chain $q_0, q_1 = A_x q_0, \dots, q_\nu = A_x^\nu q_0$ is called a trunk of the substitution a_x with a beginning q_0 (the extreme element) and an end q_ν; the set of trunks with one end q_ν is called a tree with the base q_ν.

Figure 1 shows the graphical representation of the substitution. The elements 1, 2, 3, and 9, 10 form two kernels. The two kernels form a center. The elements 6, 7, 8 are extreme elements.

The two trunks 7, 5 and 6, 5 form a tree. In turn, the tree forms the trunks 7, 5, 4, and 6, 5, 4.

We shall denote an experiment by the letter $\mathscr{E}$. If we desire to indicate that the experiment $\mathscr{E}$ leads to the state $\underline{q}$, begins with the state $\underline{q}$, or contains $\underline{q}$ in the middle, we write $\mathscr{E}_q$, $q\mathscr{E}$, $\mathscr{E}_1 q \mathscr{E}_2$, respectively. If the experiment $q_1 \mathscr{E} q_2$ exists, then q_1 is called the state which precedes q_2, and q_2 is called the state which follows q_1.

4. Identification of Equivalent States

If the experiments $q_1\mathscr{E}$ and $q_2\mathscr{E}$ are equal, then q_1, q_2 are called equivalent states relative to the experiment $\mathscr{E}$. If q_1, q_2 are equivalent for any $\mathscr{E}$, then q_1 and q_2 are called equivalent states and are denoted by $q_1 \sim q_2$. For the experimenter the states q_1 and q_2 are indistinguishable. It is evident that

1° if $q_i \sim q_j$, then $q_j \sim q_i$;
2° if $q_i \sim q_j$ and $q_j \sim q_\nu$, then $q_i \sim q_\nu$;
3° if $q_i \sim q_j$, then for any x we have $A_x q_i \sim A_x q_j$.

Therefore, the set of states can be subdivided into classes $Q_1, Q_2, \dots, Q_p$ of equivalent states. We shall not study classes consisting of one element. The structure of the s.m. determines those equivalent transformations which can be performed on them. Therefore, we shall study the structure of a s.m. when there are equivalent states. Since the structure of a s.m. is formed by the structures of a substitution, it is sufficient to study the structure of an individual substitution.

Assume $P_1, P_2, \dots, P_r$ are classes of equivalent states located on a given trunk with a kernel. We shall introduce the set $M = P_1 + P_2 + \dots + P_r$. Let $q_1 \in M$ denote the element preceding all the remaining elements of M on the specified trunk. If M is contained only in the kernel, then q_1 can be any element in M.

Assume $q_\alpha = A_x^\alpha q_1$ is the first equivalent state following q_1. Then from the property 3° it follows that $A_x q_\alpha \sim A_x q_1$, etc. There the function $s = f_1(q)$ will be a periodic function, beginning with q_1, on the given trunk. Here the number of elements in the kernel is divisible

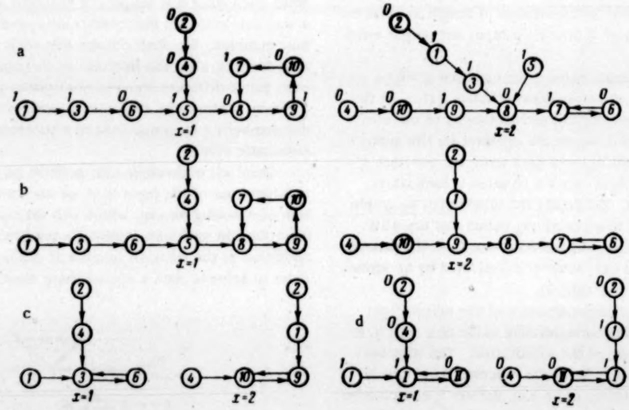

Fig. 2

by the period. If the equivalent states are located on different trunks of the substitution, then $f_1(q)$ acquire equal values over segments of the equivalent states. By identifying equivalent states of s.m.A we obtain (cf. Moore [2]) the s.m.B which is equivalent to the original one. Such a transition consists of the following: in the substitution a_x we retain one of the periods $f_1(q)$ which forms a new kernel; the equivalent portions located on different trunks are joined.

Example (Fig. 2). In machine A we have two classes of equivalent states: $Q_1 \{3, 5, 7, 9\}$, $Q_2 \{6, 8, 10\}$. The transition from A to B is achieved as follows. In the substitution a_2 we join the equivalent states 3, 5, 9 on different trunks with a common base; we leave the states which are not included in the classes Q_1 and Q_2, and one period later we replace the designations of the elements included in the period with the designation of the corresponding class. In Fig. 2, b, c, d we have shown the stages of the transition. The transition to equivalent machines by identifying equivalent states reduces the number of states. A machine without equivalent states is called a simple machine. In the analysis below we shall study only simple machines.

The indicated structure of an s.m. when equivalent states are present can serve as the necessary identifying feature for detecting equivalent states. But note that if $Q_1, Q_2, \ldots, Q_r$ are classes of equivalent states relative to each substitution, then this does not yet mean that they will be classes of equivalent states. For example (Fig. 3) the states 1, 3 are equivalent with respect to each substitution, but 1 is not equivalent to 3. In order to verify this it is sufficient to study two experiments:

s	1	0	1	0
q	1	2	1	2
x	1	2	2	1

s	1	0	1	1
q	3	4	5	3
x	1	2	2	1

5. Annulment of Regular Sub-Sets

Assume the state $\underline{q}$ of s.m.A has the following property: for any experiment with the initial state $\underline{q}$ there is an equal experiment in A. The question arises as to whether this state $\underline{q}$ can be discarded. But if we discard the state $\underline{q}$ then the structure of the machine is disrupted since the states preceding $\underline{q}$ will not have a next state. Therefore the annulment of one state $\underline{q}$ involves the annulment of all preceding states. We shall formulate this more precisely. The sub-set R of the set of states in s.m.A is called regular if together with $q \in R$ all the preceding $\underline{q}$ also belong to R, and if for an experiment with its initial state in $\underline{R}$ there is an equal experiment with its initial state not in R.

Theorem 1. The annulment of regular sub-sets transforms an s.m. into an equivalent one (cf. Appendix).

Example. We shall study machines A (Fig. 4a) and B (Fig. 4b).

It is evident that A ~ B. In order to verify this it is sufficient to check state 5. For experiments δ_1 beginning with x = 1 the state 5 ~ 1; for experiments δ_2 beginning with x = 2 the state 5 ~ 4. The transition from A to B is achieved by discarding the state 5 rather than by identifying equivalent states.

6. Partial Enumeration

As we have already noted, enumeration is an equivalent transformation. We shall now determine the structure required for s.m.A in order to ensure that the enumeration of states over less than all substitutions will be an equivalent transformation.

The states $q_1, q_2, \ldots, q_r$ which are such that from the presence of just experiment δq_i, it follows that there exist $\underline{r}$ equal experiments δq_ν ($\nu = 1, 2, \ldots, r$), are called similar states.

Theorem 2. If the states $q_1, q_2, \ldots, q_r$ are similar, then any permutation $q_1, q_2, \ldots, q_r$ in any substitution of s.m.A transforms A to the equivalent s.m.B for which $q_1, q_2, \ldots, q_r$ remain similar (for the proof, cf. Appendix).

Example. We shall study machine A (Fig. 5a). Machine A does not contain equivalent states and regular parts. It would seem that it is impossible to reduce the number of states. Note, however, that the states 1, 3 are similar. Interchanging the positions of states 1, 3 in the substitution a_2, we make the transition to the equiv-

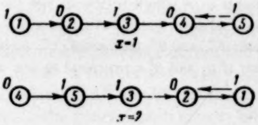

Fig. 3

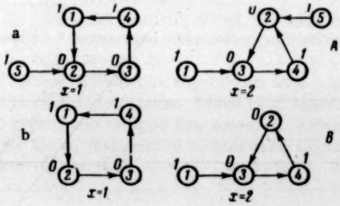

Fig. 4

alent machine B (Fig. 5b). In machine B the state 3 can be discarded. We obtain D ~ A with a smaller number of states (Fig. 5c). As we can see, the simplification was achieved at the expense of the possibility of enumerating the states in one substitution.

The machine is called "simplest" if for each initial state there is an experiment which distinguishes this state from others. If there is just one substitution in the machine for which there are no equivalent states relative to the substitution, then the machine is simplest. For the simplest s.m.A the sufficient condition formulated in Theorem 2 for the equivalence of partial enumeration is also necessary; this flows from Theorem 3 (for proof, cf. Appendix).

Theorem 3. We specify the simplest machines Π_1 and Π_2. Assume $q_1 \to q_2 \to \ldots \to q_r \to q_1$ is one of the cycles for the operator β. If the machines $A = \Pi_1 + \Pi_2$ and $B = \beta\Pi_1 + \Pi_2$ are equivalent, then the elements $q_1, q_2, \ldots, q_r$ are similar.

7. The Search for Equivalent Transformations

The structural properties of s.m. studied above make it possible to find equivalent transformations involving identification and annulment of regular subsets, and partial enumeration. The corollaries of Theorem 4 and its proof cited in the Appendix can facilitate the search for equivalent transformations considerably.

Theorem 4. If in the simple s.m.A there is just one state q_0 such that for any experiment $q_0\delta$ there is an equal experiment $q_0^1\delta$ in the simple s.m.B (where q_0^1 can be different for different experiments $q_0\delta$), then there are identical submachines A^* and B^* in s.m.A and s.m.B.

The theorem is proven in two stages. First we find the states $q_1 \in A$ and $q_1^1 \in B$ which correspond to one another for any experiment δ. Then it is demonstrated that the states in A which follow q_1 and the states in B which follow q_1^1 form identical structures for the two submachines A^* and B^* (for proof, cf. Appendix). Note merely that if q_1 and q_1^1 correspond to one another for any δ, then the state $A_x q_1$ corresponds to the state $B_x q_1^1$ for any δ. Therefore, such corresponding states q_1 and q_1^1 must be sought for in the kernels of the substitutions.

Assume that in s.m.A there is a substitution whose center consists of one kernel. In that case any state in this kernel can be chosen as q_1. All states following q_1 form the submachine A^*. Therefore an investigation of the possibility of applying equivalent transformations to s.m.A must be performed among states which are not included in submachine A^*.

Assume now that s.m.A has no substitutions whose centers consist of one kernel. Without undertaking a more detailed study of the problem, we shall say that it is not possible to accurately indicate which kernel of the substitution a_x contains the state q_1. In that case we formulate the submachines A_ν^* ($\nu = 1, 2, \ldots, r$; $r \le k$) (certain of these submachines may coincide or may be contained in one another) for each of the k kernels of some one substitution a_x.

It is necessary to perform investigations of the possibility of applying equivalent transformations to s.m.A among those states of A which are not included in submachine A_1^*; then we investigate the states of A which are not included in A_2^*, etc.

Let us restate the fact that these conclusions apply to simple s.m. (i.e., to machines without equivalent states).

APPENDIX

Proof of Theorem 1. If the experiment δ begins with $q \,\bar{\in}\, R$, then it does not contain states in R in view of the regularity of R. Therefore, in machine B the same experiment δ corresponds to this experiment. If the experiment δ begins with the state $q_1 \in R$, then according to the condition of the theorem there exists $q_2 \,\bar{\in}\, R$, and $q_2 \sim q_1$ relative to δ. Therefore, in machine B the specified experiment with the initial state q_1 must correspond to an equal experiment with the initial state q_2.

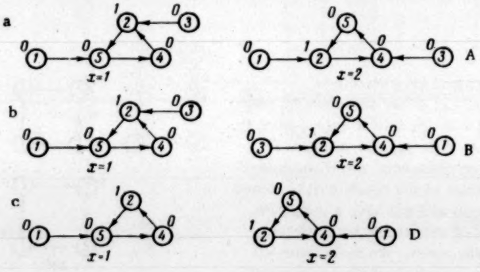

Fig. 5

Proof of Theorem 2. A portion of the substitutions of an s.m. forms the structure of a certain machine Π_1, and the remaining portion of the substitutions forms the structure of another submachine Π_2. We shall represent the original s.m. with the sum of these submachines.

Assume $A = \Pi_1 + \Pi_2$, $B = \beta\Pi_1 + \Pi_2$, where β is the transposition of similar elements q_1, q_2. We shall not only prove that the theorem is satisfied, but we shall also demonstrate that for equal corresponding experiments δ_A and δ_B the last states are identical. For experiments δ_A of length 1 the theorem is obvious, since these δ_A can serve as the experiment δ_B. Assume the theorem and the corollary are valid for experiments of length $l < m$. We shall prove that for this case the theorem is valid for experiments of length m. The experiment δ_A is written in the form $L_1 q_\alpha q_\gamma$.

We shall study two cases.

A. Assume q_α coincides with q_1 or q_2, and q_α separates Π_2 from Π_1; i.e., the next-to-last input value x_α belongs to Π_2, and the last value x_γ belongs to Π_1. In order to be specific we shall assume $q_\alpha = q_1$. We shall formulate the experiment δ_B, which is equal to $L_1 q_1 q_\gamma$, in the following manner. In machine A we take the experiment $\delta_1' q_2$ equal to $\delta_1 q_1$. For machine B we take the experiment $\delta_1'' q_2$ (which is of length $m-1$) to be equal to $\delta_1' q_2$. Continuing it by means of the input value x_γ, we obtain the experiment $\delta_1'' q_2 q_\gamma$ which is equal to $\delta_1 q_1 q_\gamma$.

B. If the conditions for case "A" are not satisfied, then the formulation of δ_B is simplified. On the basis of $\delta_1 q_\alpha$ we formulate an equal $\delta_1'' q_\alpha$ in B and continue it one step to $\delta_1' q_\alpha q_\gamma$ using the input value x_γ. Thus we have proven Theorem 2.

Proof of Theorem 3. We have the arbitrary experiment $\delta_A q_1$. We shall continue it in the machine Π_2 using the experiment δ_1 (i.e., we take the input values of δ_1 from Π_2) which distinguishes the state q_1. For the experiment $\delta_A q_1 \delta_1$ we can indicate an equal experiment $\delta_B q^1 \delta_1$ in the machine B which is equivalent to A. But since L_1 distinguishes the state q_1 in Π_2, we have $q^1 = q_1$.

Thus in B there is an experiment $\delta_B q_1$ equal to $\delta_A q_1$. We shall now continue the experiment $\delta_A q_1$ by means of the experiment δ_2 in the machine Π_1 which distinguishes the state q_1. The experiment $\delta_A q_1 L_2$ has an equal experiment $\delta_B q^1 \delta_2$ in the machine B. But δ_2 distinguishes q_1 in Π_1. Therefore q^1 must be that state which became q_1; i.e., $q^1 = q_r$.

Thus, we have the experiment $\delta_B q_r$ which is equal to $\delta_A q_1$. We shall now take the experiment $\delta_B q_r$. Reasoning analogously, we find that for $\delta_B q_r$ there is an equal experiment $\delta_A q_r$. Therefore, having $\delta_A q_1$, we obtain an equal experiment $\delta_A q_r$. Reasoning analogously with respect to $\delta_A q_r$, we obtain an equal experiment $\delta_A q_{r-1}$, etc. Therefore we immediately have r equal to the experiments

$$\delta_A q_1, \ \delta_A q_2, \ \ldots, \ \delta_A q_r.$$

Proof of Theorem 4. We shall take an arbitrary experiment $q_0 \delta_0$ in the machine A. For the machine B there is a set Q of states q_0^i such that $q_0^i \delta_0$ are equal to $q_0 \delta_0$. When the experiment δ_0 is extended the set Q will be decreased; however, due to the condition in the theorem the set will not be vacant. Since the set Q is finite it is possible to find a continuation of $q_0 \delta_1$ such that the corresponding set Q_0 will not be diminished for any continuation of it.

Assume the experiment $q_0 \delta_1$ ends with the state q_1 and that equal experiments in B end with the state q_1^i ($i = 1, 2, \ldots, k$). Any experiment $q_1 \delta$ in the machine A has k equal experiments $q_1 \delta$ in the machine B. In order to verify this it is sufficient to study the experiments $q_1 \delta$ and $q_1^i \delta$ as continuations of the experiments $q_0 \delta_1$ and $q_0^i \delta_1$. Since the experiments $q_1^i \delta$ are equal, we find that q_1^i ($i = 1, 2, \ldots, k$) are equivalent states of the machine B; this contradicts the simplicity condition for machine B. Therefore the set Q_0 consists of one element q_0^1. Thus, the state q_1 corresponds not to k states but only to one state q_1^1 for any experiment δ. But if q_1, q_1^1 correspond to one another for any experiment, then the states following them (as parts of equivalent experiments $q_1 \delta$ and $q_1^1 \delta$) will also correspond to one another. From the simplicity condition for the machines A and B it follows that the correspondence will be mutually single-valued.

Assume that the states following q_1 form the set A^*, and that the states following q_1^1 form the set B^*. We shall show that A^* and B^* are identical sequential machines. Assume $q_2 \in A^*$ and $q_2^1 \in B^*$ correspond. Then from equality of the experiments $q_2 \delta q_3$ and $q_2^1 \delta q_3^1$ and the simplicity of the machines A and B it follows that q_3 and q_3^1 also correspond. Thus we find that the mutually single-valued correspondence established between the states A^* and B^* is maintained for any experiment. Therefore the machines A^* and B^* are identical.

Corollary. If the machine A is closely coupled and is equivalent to B, then A is identical to a part of B. In fact, for closely coupled machines A^* coincides with A.

LITERATURE CITED

1. A. Sh. Blokh, "On problems solved by sequential machines," Problems in Cybernetics [in Russian] (Fizmatgiz, 1960) No. 3.
2. E. F. Moore, Speculative Experiments with Sequential Machines. Automatons, Edited by E. Shannon and J. McCarthy [Russian translation] (IL, 1956).
3. A. Sh. Blokh, "Synthesis of contact-relay networks," Doklady Akad. Nauk SSSR 117, No. 4 (1957).

THE THEORY OF A MAGNETIC MODULATOR WITH CROSSED FIELDS AND A FUNDAMENTAL FREQUENCY OUTPUT

F. I. Kerbnikov

Moscow

Translated from Avtomatika i Telemekhanika Vol. 21, No. 11,
pp. 1497-1502, November, 1960
Original article submitted April 9, 1960

A theory is provided for the operation of a magnetic modulator with crossed fields and a periodically changing inductance of the control winding. The basic conclusions arrived at in the work are confirmed experimentally.

Paper [1] provides the theory and design of a magnetic modulator with mutually perpendicular fields and a fundamental frequency output for an ideal case when under the effect of the current in the excitation winding W_1 (Fig. 1), the inductance of the control winding W_c varies periodically between the values L_{max} and $L_{min} = 0$. In fact, a modulator with a 1000-2000 ferrocart core has a ratio of inductance L_{max} to L_{min} amounting to 4-5 owing to the limited power of the source and nonuniform cross section of the core for the exciting flux, thus leaving some of the core sections unsaturated. Hence, the operation of a magnetic modulator with finite variations of the control winding W_c inductance is of considerable interest.

Let us examine a steady state condition in a control circuit with the signal source connected and a rectangular wave modulating current supplied, for instance, by a magnetic transitron generator through a large resistor.

Let us find the relation between the amplitude of the first harmonic voltage at the output of the modulator and the ratio $L_{max}/L_{min} = m$ for a signal voltage E.

Figure 2a shows the characteristic variations with time of the excitation current i_1; Fig. 2b, those of the inductance L of winding W_c; and Fig. 2c, d, those of i_c flowing through the winding. At instant $t = 0$ the inductance of the control winding rises instantaneously from L_{min} to L_{max}. It is known that with the change in the inductance the value of the flux linkage ψ cannot change immediately (otherwise the control circuit would have an infinitely large emf induced in it [2]). Hence, if we denote by I_{2k} the value of the current in winding W_c of inductance L_{min} before the instantaneous change, the value of current I_{10} at the end of the instantaneous change of the inductance to L_{max} will be represented by

$$\psi(0) = I_{2k}L_{min} = I_{10}L_{max} = \text{const}, \tag{1}$$

i.e., the current in the control winding will decrease in an inverse proportion to the inductance of the winding:

$$\frac{I_{2k}}{I_{10}} = \frac{L_{max}}{L_{min}} = m. \tag{2}$$

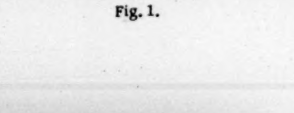

Fig. 1.

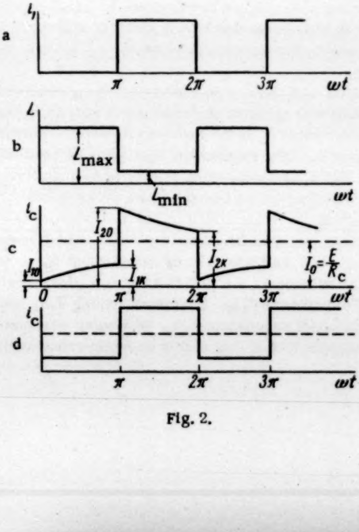

Fig. 2.

After current i_C drops to the value of I_{10} at $t = 0$ it will begin to rise exponentially with a time constant of τ:

$$i_{C1} = I_{10} + (I_0 - I_{10})\left(1 - e^{-\frac{t}{\tau}}\right), \quad 0 \leqslant \omega t \leqslant \pi, \tag{3}$$

where

$$\tau = \frac{L_{\max}}{R_C}, \quad R_C = R_0 + R_1, \quad L_{\max} = \frac{0{,}4\pi W_C^2 \mu_0 S}{l \cdot 10^8}$$

and $I_0 = E/R_C$ is the direct current component in the control circuit at the steady state condition.

At the instant $t = \pi/\omega$ the inductance of the control winding is reduced instantaneously to $L_{\min}$; the control current, which has by then reached the value of I_{1k}, instantaneously rises to I_{20} and then falls exponentially with a time constant of $\tau_1 = \tau/m$:

$$i_{C2} = I_{20} + (I_0 - I_{20})\left[1 - e^{-\frac{m}{\tau}\left(t - \frac{\pi}{\omega}\right)}\right], \quad \pi \leqslant \omega t \leqslant 2\pi. \tag{4}$$

In a steady state at $t = 2\pi/\omega$, the control current $i_C = I_{2k}$.

It is obvious that by similarity with equation (2) it is possible to represent the ratio of currents I_{1k} and I_{20} at the beginning and end of the instantaneous variations of the inductance from $L_{\max}$ to $L_{\min}$ by

$$\frac{I_{20}}{I_{1k}} = \frac{L_{\max}}{L_{\min}} = m. \tag{5}$$

By inserting in equations (3) and (4) respectively the values of $t = \pi/\omega$ and $t = 2\pi/\omega$ we obtain for currents I_{1k} and I_{2k} the expressions

$$I_{1k} = I_{10} + (I_0 - I_{10})\left(1 - e^{-\frac{\pi}{\omega\tau}}\right), \tag{6}$$

$$I_{2k} = I_{20} + (I_0 - I_{20})\left(1 - e^{-\frac{\pi m}{\omega\tau}}\right). \tag{7}$$

By solving equations (2), (5), (6), and (7) with respect to I_{10} and I_{20} we obtain

$$I_{10} = I_0 K, \tag{8}$$

$$I_{20} = I_0 K_1, \tag{9}$$

where

$$K = \frac{1 - e^{-\frac{\pi m}{\omega\tau}} + me^{-\frac{\pi m}{\omega\tau}} - me^{-\frac{\pi(m+1)}{\omega\tau}}}{m\left[1 - e^{-\frac{\pi(m+1)}{\omega\tau}}\right]},$$

$$K_1 = \frac{m - me^{-\frac{\pi}{\omega\tau}} + e^{-\frac{\pi}{\omega\tau}} - e^{-\frac{\pi(m+1)}{\omega\tau}}}{1 - e^{-\frac{\pi(m+1)}{\omega\tau}}}.$$

By inserting the values of I_{10} and I_{20} in equations (3) and (4) we have

$$i_{C1} = I_0 - I_0 e^{-\frac{t}{\tau}}(1 - K), \quad 0 \leqslant \omega t \leqslant 2\pi, \tag{10}$$

$$i_{C2} = I_0 - I_0 e^{-\frac{tm}{\tau}}(1 - K_1), \quad \pi \leqslant \omega t \leqslant 2\pi. \tag{11}$$

For a voltage at the output of the modulator with a small internal impedance of the signal source we have

$$u_{H1} = i_{C1} R_1 = I_0 R_1 - I_0 R_1 (1 - K)\, e^{-\frac{t}{\tau}}, \quad 0 \leqslant \omega t \leqslant \pi, \tag{12}$$

$$u_{H2} = i_{C2} R_1 = I_0 R_1 - I_0 R_1 (1 - K_1)\, e^{-\frac{tm}{\tau}}, \quad \pi \leqslant \omega t \leqslant 2\pi. \tag{13}$$

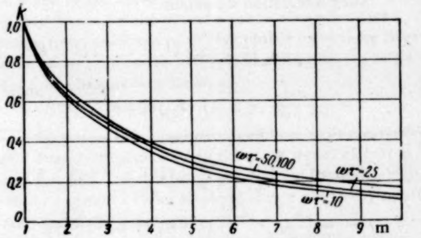

Fig. 3.

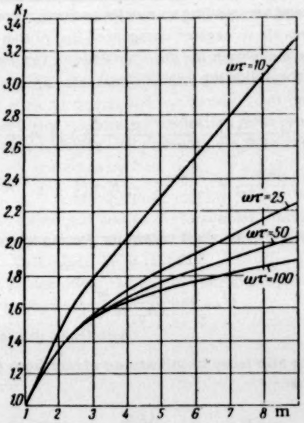

Fig. 4.

Table 1

Core number	D_{ext}, mm	D_{int}, mm	μ_0, gauss/oe	B_s, gauss	H_c, oe	T_k, °C	Cross section for the longitudinal flux, cm²
1	29.4	17.6	1200	2400	0.1	120	0.68
2	29.4	17.6	2260	2000	0.1	80	0.68

The amplitude of the first harmonic of the output voltage is

$$U_{1m} = \sqrt{U_{1a}^2 + U_{1b}^2},$$

where

$$U_{1a} = \frac{1}{\pi}\int_0^{2\pi} u_n \sin \omega t \, d\omega t,$$

$$U_{1b} = \frac{1}{\pi}\int_0^{2\pi} u_n \cos \omega t \, d\omega t.$$

After integration we obtain

$$U_{1a} = -\frac{ER_1}{\pi R_c}\Big[\frac{\omega^2\tau^2}{1+\omega^2\tau^2}\big(1+e^{-\frac{\pi}{\omega\tau}}\big)(1-K) - \frac{\omega^2\tau^2}{m^2+\omega^2\tau^2}e^{-\frac{\pi m}{\omega\tau}}(1-K_1)\big(1+e^{-\frac{\pi m}{\omega\tau}}\big)\Big].$$

$$U_{1b} = -\frac{ER_1}{\pi R_c}\Big[\frac{\omega\tau}{1+\omega^2\tau^2}\big(1+e^{-\frac{\pi}{\omega\tau}}\big)(1-K) - \frac{\omega\tau}{m^2+\omega^2\tau^2}e^{-\frac{\pi m}{\omega\tau}}(1-K_1)\big(1+e^{-\frac{\pi m}{\omega\tau}}\big)\Big].$$

Voltage U_{1m} rises monotonically with an increasing m and $\omega\tau$, tending to a definite limit. For $\omega\tau > 10$ it is possible to neglect component U_{1b} of the output voltage and obtain for the amplitude of the first harmonic the following expression:

$$U_{1m} = \frac{ER_1}{\pi R_c}\Big[\frac{\omega^2\tau^2}{1+\omega^2\tau^2}(1-K)\big(1+e^{-\frac{\pi}{\omega\tau}}\big) - \frac{\omega^2\tau^2}{m^2+\omega^2\tau^2}e^{-\frac{\pi m}{\omega\tau}}(1-K_1)\big(1+e^{-\frac{\pi m}{\omega\tau}}\big)\Big]. \tag{14}$$

If $\omega\tau \to \infty$, we shall obtain for the modulator output voltage

$$U_{1m} = \frac{4ER_1}{\pi R_c}\,\frac{m}{m+1}. \tag{15}$$

If m also tends to infinity we obtain from (15) the expression

$$U_{1m} = U_{1m\,\max} = \frac{4ER_1}{\pi R_c} = 1.27E\,\frac{R_1}{R_c}. \tag{16}$$

Let us note that for $\omega\tau \to \infty$ and $m \to \infty$ the coefficient $K \to 0$ and $K_1 \to 2$. This limiting operating condition of the modulator corresponds to a square wave current in the control winding (Fig. 2d), whose amplitude is twice the direct component $I_0 = E/R_c$ of the current. In fact, the magnetic energy stored in the longitudinal field of the modulator for $L = L_{max}$ is completely dissipated in the load in the following interval, when $L = L_{min}$, thus doubling the load current compared with the direct component of the current in the steady state.

Figures 3 and 4 show the relations of coefficients K and K_1 to m for $\omega\tau$ values of 10, 25, 50, and 100. It will be seen that K is relatively independent of $\omega\tau$.

The relation of the first harmonic amplitude to m, calculated from formula (14) for various values of $\omega\tau$, is shown in Fig. 5. It will be seen that with a decreasing m and $\omega\tau$ the amplitude of the first harmonic voltage at the output decreases, but even for $\omega\tau = 25$ and $m = 5$ it remains equal to half its maximum possible value, and it is only 25% below U_{1m} which corresponds to $\omega\tau \to \infty$.

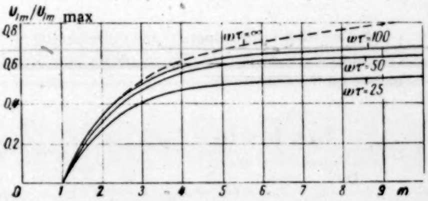

Fig.5

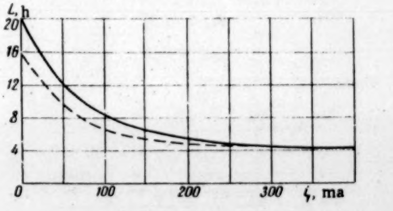

Fig.6

Table 2.

$\omega\tau$	R_c, (ohms)	m								Note
		2		3		4		5		
		calc.	expt.	calc.	expt.	calc.	expt.	calc.	expt.	
50	2000	0.4	0.4	0.61	0.6	0.71	0.7			Modulator with core No. 1
100	1000	0.43	0.42	0.63	0.6	0.74	0.72			
60	2000	0.4	0.4	0.61	0.6	0.72	0.7	0.76	0.74	Modulator with core No. 2
120	1000	0.43	0.42	0.63	0.63	0.75	0.74	0.83	0.83	

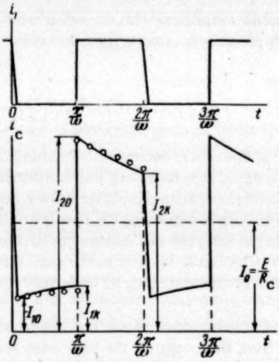

Fig.7

Tests of several modulators with two different types of cores, whose characteristics are given in Table 1, have fully confirmed the theoretical conclusions obtained above.

Figure 6 shows the experimentally obtained characteristic variations in the inductance of the control winding ($W_c = 2800$ turns, $R_0 = 200$) of the modulator with cores No. 1 and No. 2 when the excitation circuit ($W_1 = 200$ turns) is fed by a direct current. These characteristics were used for calculating the transfer constants of the modulator when excited with a square-wave current.

Table 2 gives the computed and experimental values of the transfer constant U_{1m}/E for the above modulators at 1000 cps for various values of $\omega\tau$ and m.

It should be noted that not only the transfer constants but also the curves of the experimental and theoretical current i_c variations in the control winding coincide. For instance, Fig. 7 shows an oscillogram of the excitation current i_1 and the control circuit current i_c for $\omega\tau = 50$ and $m = 5$. The points shown on the curve $i_c = f(t)$ have been calculated from formulas (10) and (11) for the above values of $\omega\tau$ and m, for which $I_{10} = 0.3I_0$, $I_{20} = 1.7I_0$, $I_{1k} = 0.34I_0$, and $I_{2k} = 1.5I_0$. It will be seen that the shape of the curve for the current in the control winding, and hence for the output voltage, does not differ greatly from the shape of the excitation current for large values of $\omega\tau$, and in the half-period corresponding to $L = L_{max}$ it changes very little.

CONCLUSIONS

The theory of a magnetic modulator with a periodically changing inductance in the input signal circuit has been derived. It has been shown that a sufficiently high transfer constant can be obtained with a relatively small variation of the inductance.

For this purpose it is necessary to make the maximum value of $\omega\tau$ in the input circuit of the modulator sufficiently high ($\omega\tau \geq 25$). Under this condition the shape of the output voltage wave resembles closely that of the excitation current.

The basic conclusions hold both for modulators with mutually perpendicular fields and for those of the same type but with the signal and excitation fields connected in parallel, since a parallel excitation field produced by a half-wave rectifier will also vary the inductance of winding W_c periodically from L_{max} to L_{min}.

LITERATURE CITED

1. F. I. Kerbnikov and M. A. Rozenblat, "Magnetic modulators with transverse excitation," Avtomat. i Telemekh. 19, 9 (1958).*
2. M. A. Rozenblat, Magnetic Amplifiers [in Russian] (Izd. Sovetskoe Radio, 1956).

---

* See English translation.

REVERSIVE (DUODIRECTIONAL*) MAGNETIC DC AMPLIFIERS OF INCREASED EFFICIENCY

M. A. Boyarchenkov and M. A. Rozenblat

Moscow

Translated from Avtomatika i Telemekhanika, Vol. 21, No. 11,
pp. 1503-1513, November, 1960
(Presented at the All-Moscow seminar on contactless magnetic components,
March 23, 1960)
Original article submitted April 9, 1960

The conditions for obtaining increased efficiency of reversive magnetic amplifiers with dc output are determined. New circuits for reversive amplifiers satisfying these conditions are presented; among these are some that have increased efficiency without using transformers.

Introduction

The use of dynamoelectric amplifiers in automatic control systems presents numerous difficulties; the most substantial of these difficulties are their lack of dependability in operation, the fact that they are complicated to adjust, their need of periodic maintenance, etc. Therefore, a tendency has lately developed to replace dynamoelectric amplifiers by magnetic amplifiers. The use of magnetic amplifiers makes it possible to create control systems which require almost no adjustment, and which are distinguished by high technical and economic merits. In the creation of such systems, a considerable part is played by the right choice of the magnetic amplifier, by the correct approach to the design of the system, and by the using of advantageous design data.

Any reversive full-wave magnetic amplifier is composed of two, or, in the general case, of several half-cycle (half-wave) amplifiers.

There are two basic principles which may be used in the design of full-wave, two-semicycle amplifiers: the principle of summation of voltages obtained at the outputs of the semicycle amplifiers and the principle of summation of the output currents. A scheme based on the first principle is shown diagrammatically in Fig. 1. In this scheme, separate resistors R_b serve as load resistances for each of the two amplifiers. To obtain a maximum of power in the output when this scheme is used, the total common load resistance R_H must be equal to $\sqrt{2}\,R_b$. Amplifiers built according to this principle have very low efficiency; therefore, their application is limited to the area of low output power [1].

The diagram of a scheme based on algebraic summation of currents is shown in Fig. 2. When the signal is applied to the control winding, the current in the output of one of the component amplifiers is increased; in the output of the other, decreased. To obtain maximum power output, it is necessary that the output current of the second component amplifier have a minimum value when the output current of the first is at a maximum. To achieve this, the two component half-wave amplifiers must be made to work in the combined full-wave amplifier in the same way as when they operate separately.

Direct subtraction of the two direct currents obtained from the output of the half-wave amplifiers is impossible because of the mutual interaction between the two amplifiers when they are connected with each other as shown. Usually this interaction is decreased by insertion of ballast resistances R_b (shown in Fig. 2 in dotted lines). But these ballast resistances greatly decrease the efficiency. Instead of ballast resistances, control valves can be used in this scheme [2]. In our paper reversive amplifiers are reviewed which do not contain such valves.

Basic Principles for Design of More Efficient Reversive Magnetic Amplifiers

Let us discuss the character of the interaction of the two amplifiers in Fig. 2 in more detail. To present a clearer picture of the conditions, we shall assume that

---

* In the original Russian and in the author's abstract in English, the term "reversive" is used. Inasmuch as this term is unfamiliar in the USA, it has been replaced in the title by "duodirectional," which is the shortest equivalent term for this concept accepted in authoritative texts of the English-speaking world; see, e.g., Magnetic-Amplifier Circuits by William A. Geyger, 2d edit., McGraw-Hill, New York, 1957, p.77. In the text, however, the word "reversive" has been kept as the shorter of the two terms [Publisher's note].

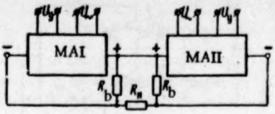

Fig. 1.

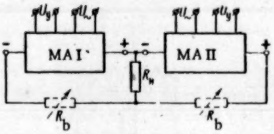

Fig. 2.

for the half-wave amplifications single-core magnetic amplifiers are used; a circuit diagram of these is shown in Fig. 3. As will be made evident in the forthcoming discussion, this amplification scheme serves as the basic element for construction of more complex schemes of magnetic amplifiers. Before going to the examination of the basic circuits for connection of half-wave amplifiers into reversive combinations for dc amplification, let us point out some specific features in the operation of the scheme of Fig. 3 which must be taken into consideration in the design of such reversive amplifiers.

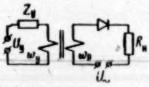

Fig. 3.

Let us assume that the core in the device of Fig. 3 has a rectangular hysteresis loop (Fig. 4). In order to obtain the lowest possible value of the load current in this scheme—$I_{\text{load min}}$—it is necessary as a rule to have the following condition fulfilled:

$$\int_0^{T/2} u\,dt \leqslant (B_s - B_y)\, w_p S, \tag{1}$$

where $\underline{u}$ is the voltage applied during the active (output contributing) half-period to the operational winding w_p; B_y, the value of the magnetic induction in the core at the end of the control half-period (at the start of the active half-period); B_s, the induction at saturation; and T, the period of the supply voltage. In the specific case when $B_y = -B_s$, condition (1) assumes the following form:

$$\int_0^{T/2} u\,dt \leqslant 2 w_p S B_s. \tag{2}$$

When condition (1) is fulfilled, the core either does not reach the saturation state at all, or reaches it only at the end of the active half-period when $\omega t = \pi$. When condition (1) is not fulfilled, then the induction of the core becomes equal to the saturation value B_s at some moment during the active half-period which is determined by the expression

$$\omega t = \alpha = \arccos\left[1 - \frac{\omega (B_s - B_y)}{U_m} w_p S\right] < \pi. \tag{3}$$

During the time interval when $\alpha \leq \omega t \leq \pi$ there will be a current $i = u/R$ going through the load, where R is the complete resistance of the load circuit. In formula (3) U_m is the amplitude value of the supply voltage, and $\omega = 2\pi f$, its angular frequency. In the half-period scheme of Fig. 3 by itself there is no difficulty whatsoever in fulfilling conditions (1) or (2), and in obtaining a high ratio of high to low load current values. However, when two or more half-wave amplifiers of Fig. 3 are combined into a reversive scheme, condition (1) is usually violated, because of an increase of the left side of the inequality, and/or because of a decrease of the right side.

An increase of the left part of inequality (1) takes place as a result of a redistribution of voltage in the windings of the reversive scheme which are in the active state during a given half-wave period. A decrease of the right side is caused by a redistribution of voltage in the active circuit while it is in the control exercising half-period.

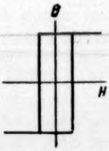

Fig. 4.

Let us illustrate the nature of the voltage redistributions and the consequences thereof by discussing, for example, these phenomena in the most simple full-wave magnetic amplifiers (Fig. 5). Let us examine first the scheme of Fig. 5a, which represents a differential connection of two half-wave amplifiers the active half-periods of which are shifted in phase by a half-period. The instantaneous polarities of the supply voltage for the separate amplifiers are shown in the figure by asterisks. When no signal current is present, the following current relationship is in effect:

$$i_1(t) = -\, i_2\left(t \pm \frac{T}{2}\right) \tag{4}$$

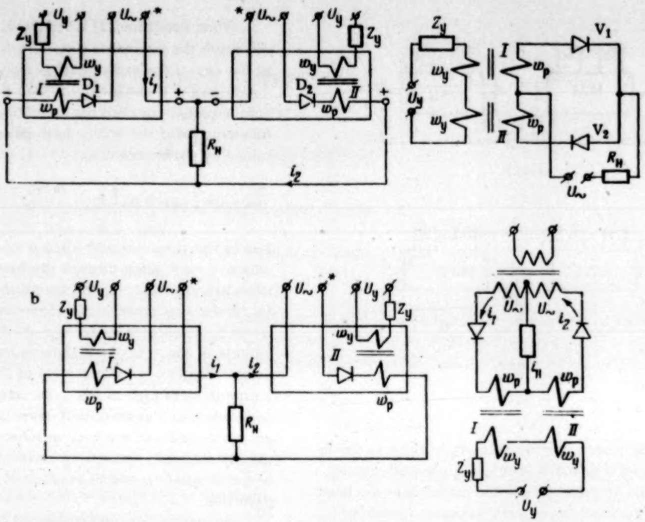

Fig. 5.

and the dc component is absent from the output load. Let us assume now that to the amplifier input a current signal I_y is applied which is of such magnitude and polarity that core II is saturated during the entire active half-period, and the current $i_2 = u/R$ is flowing. In order to obtain the maximum intensity of current in the output from the amplifier, the current i_1 must have the least possible value, that is, the core I must not get saturated before the end of its working half-period. This can be achieved only if, during the control half-period, an induction B_y will be established which will satisfy inequality (1). However, in the scheme of Fig. 5a, this condition cannot be fulfilled. Indeed, if core II, during its active half-period, is saturated, then only a small part of the supply voltage will be applied to rectifier valve V_1 which is equal to

$$u_{\text{rev}} = u - i_2 R_{\text{н}} = i_2 (R_0 + R_{\text{в}}), \qquad (5)$$

where R_0 and R_B are the resistances of the winding w_p and of the rectifier valve in the forward direction.

This voltage determines the highest rate of change of the magnetic induction in core I that can possibly be produced by the signal I_y during the control half-period; indeed, when the condition

$$w_p S \frac{dB_I}{dt} \geqslant u_{\text{rev}} \qquad (6)$$

is reached, valve V_1 becomes conducting, and the circuit loop formed by the valves and operational (active) w_p, which has a rather low total resistance, practically shortcircuits the control winding w_y of core I, because of the transformer coupling between the windings w_y and w_p of core I.

The largest possible change of induction in core I during the control half-period is

$$\Delta B = B_s - B_y \approx \frac{1}{w_p S} \int_0^{T/2} u_{\text{rev}} dt = \qquad (7)$$

$$= \frac{U_{\text{av}} \left(1 - \dfrac{R_{\text{н}}}{R_{\text{н}} + R_0 + R_{\text{в}}}\right)}{2 f w_p S},$$

where U_{av} is the average value of the supply voltage and f—its frequency.

Thus, B_y for core I will differ but little from B_s, and during the next half-period the mean value of current i_1 will differ only very little from the mean value of current i_2, regardless of the magnitude of the signal. Because of this, the maximum value of the constant component of the load current in the scheme of Fig. 5a will be much smaller than for the nonreversive half-wave scheme of Fig. 3 by itself.

Let us now consider the scheme of Fig. 5b. Here, in distinction from scheme 5a, the operational periods for the two cores are not shifted in time, but coincide. Let us assume that the magnitude and the polarity of the signals are such, that at the end of the control half-period we have induction $B_{yI} = -B_s$ in core I, and in core II the induction $B_{yII} = +B_s$. During the entire operational half-period core II is saturated, and to the operational winding w_p of core I the following voltage is applied:

$$u_2 = u + [u - i_2(R_0 + R_{\text{н}})] \approx 2u. \qquad (8)$$

Therefore, to comply with condition (1) or (2), for the scheme of Fig. 5b a supply voltage must be chosen which is one-half of the one used for the scheme of Fig. 3. Otherwise, core I also would reach the saturation stage approximately in the middle of its operational half-period, and this would lead to appearance of a considerable i_1 current, which, going through the valves and the w_p windings, can be much larger than the load current i_H.

Thus, we come to the conclusion that in order to keep the working conditions of a half-wave amplifier unaltered when connecting it with other similar amplifiers into a reversive scheme, we must remove the effect of the load voltage upon the operation of the half-wave amplifier which must have a minimum of output current at the time. This effect can be avoided by the use of the well-known bridge scheme (Fig. 6) of subtraction of the output currents from two half-wave amplifiers. The device is built up from four controlled rectifying amplifier elements. As such, single-core half-wave magnetic amplifiers such as shown in Fig. 3 may be used, or any known combinations of part cycle amplifiers, such as two-half-wave or multiphase amplifiers. Let the assembly be so arranged that the rectified current in the output of elements B_1 and B_1' increases, and the rectified current in the output of elements B_2 and B_2' decreases when the control signal is in action. The presence of ballast resistance R_b which is equal in value to the load resistance R_H prevents redistribution of voltage when the signal is on. Indeed, the voltage drops across R_b and R_H are applied to B_2 and B_2' with opposite polarities. This results in the fact that the operating conditions of elements B_2 and B_2', when included in this combined operation system, remain practically the same as when they are used separately. Therefore, the current in the output of these elements can actually reach minimum values at the proper time, and thus assure maximum output in the load circuit of the assembly. In distinction from the scheme of Fig. 2, the system of Fig. 6 has a much higher efficiency, which reaches 50% in the absence of losses in the windings and in the rectifiers.

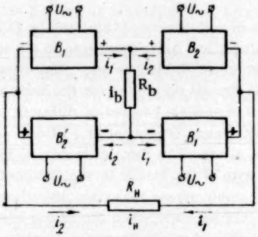

Fig. 6.

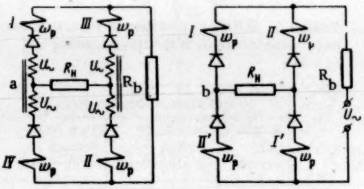

Fig. 7.

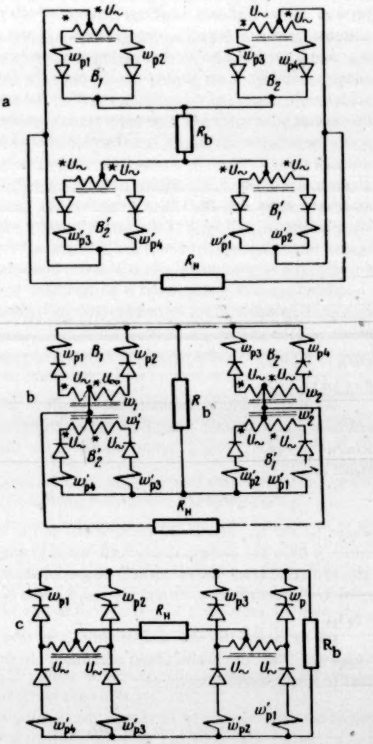

Fig. 8.

If in the system of Fig. 6 each of the four elements B_1, B_1^{*}, B_2, and B_2^{*} consists of a single-core amplifier (Fig. 3), then the assembly is the well known bridge scheme of reversive full-wave amplification by means of half-wave components (Fig. 7a). The scheme of Fig. 7a may easily be simplified by using a common source of power supply (Fig. 7b) and employing two amplifiers instead of four; the latter is possible since the cores I and II and the cores III and IV work in identical regimes, and it is therefore possible to have only two cores with two operational windings on each core, and connect the four windings in the bridge scheme (Fig. 7b). This is possible to do in every full-wave scheme built up from any half-wave elements.

When, for instance, the component magnetic amplifiers (controlled rectifying elements) in Fig. 6 consist of twin half-period devices with center tap connections, we have the amplifier scheme of Fig. 8a. And this scheme also can be simplified by the use of common cores for pairs of two operational windings through which the same currents must pass (as e.g., the windings w_{p1} and w_{p1}^{*}, and w_{p2} and w_{p2}^{*}), and also by decreasing the number of secondary windings of the supply transformer; the latter is achieved by means of connecting together the points in the circuit which are at equal potentials. For this purpose, the scheme of Fig. 8a is redrawn as shown in Fig. 8b, wherein those ends of the secondary windings which at a given moment are at a positive potential are shown by asterisks. From Fig. 8b it is evident that the two secondary windings w_1 and w_1, and the two secondary windings w_2 and w_2^{*} can be replaced each by a single winding. As a result, the scheme of Fig. 8a is transformed into Fig. 8c.†

Other magnetic amplifiers with reversive or duodirectional operation may be constructed in a similar manner.

Dependence of Efficiency upon Various Factors

We shall examine the basic factors which affect the efficiency of magnetic amplifiers built according to the scheme of Fig. 6. The dc power output in the load is equal to

$$P_{\text{н}} = I_{\text{н}}^2 R_{\text{н}} = (I_{10} - I_{20})^2 R_{\text{н}}, \tag{9}$$

where I_{10} and I_{20} are the dc components of the output currents from the corresponding half-wave amplifiers. The effective (root-mean-square) values of these currents are respectively $I_1 = k_{f1} I_{10}$, $I_2 = k_{f2} I_{20}$, and $I_{H\,eff} = k_f I_H$.

Let us assume for the sake of simplicity that $k_{f1} = k_{f2} = k_f$. Then the entire power consumed in the circuit is approximately equal to

$$P_c = (I_1 + I_2)^2 R_b + (I_1 - I_2)^2 R_{\text{н}} + I_1^2 2R + I_2^2 2R, \tag{10}$$

where R is the resistance of one operational winding together with the valve connected in series with it. From (9) and (10) we find the following expression for the efficiency of the amplifier:

$$\eta = \frac{P_{\text{н}}}{P_c} = \frac{(I_1 - I_2)^2 R_{\text{н}}}{k_f^2 [(I_1 + I_2)^2 R_b + (I_1 - I_2)^3 R_{\text{н}} + (I_1^2 + I_2^2) 2R]}. \tag{11}$$

We introduce the following denotations: 1) the ratio of the currents in the windings of the two half-wave amplifiers $k = I_1/I_2$, and 2) the ratio of the resistance of one operational winding and the valve associated with it to the load resistance $m = R/R_H$. After introduction of these denotations into (11) and assuming that $R_b = R_H$, we have

$$\eta = \frac{\left(1 - \frac{1}{k}\right)^2}{2k_f^2 (1 + m) \left(1 + \frac{1}{k^2}\right)}. \tag{12}$$

Values of efficiencies calculated by (12) for various reversive amplifiers built according to the scheme of Fig. 6 are given in Table 1 below. The efficiency data in this table are all computed for the same resistances ratio m = 0.1, but for a number of different current ratios k of the half-wave component amplifiers. The data in Table 1 are arranged in three columns: a) for the case when each arm of the bridge in Fig. 6 contains a single half-period single-phase magnetic amplifier according to Fig. 7; b) for the case when the bridge arms are made up of twin half-period single-phase amplifiers according to Fig. 8; and c) for the case of three-phase half-period amplifiers according to Figs. 9 and 10 in the bridge arms.

TABLE 1. Efficiency values of reversive magnetic amplifiers with resistive loading and m = 0.1

k	Amplifier in bridge arms		
	Single half-period	Two half-periods single-phase	Two half-periods three-phase
	$k_f = 1.57$	$k_f = 1.11$	$k_f \approx 1.00$
5	0.11	0.23	0.28
10	0.15	0.30	0.36
20	0.17	0.33	0.41
∞	0.19	0.37	0.46

---

† It should be emphasized that the output leads from the transformers in the schemes of Fig. 8 are connected to center taps of the secondary windings, and that in both halves of the secondary windings on either side of the center taps there are always equal potentials $U_{\sim}$.

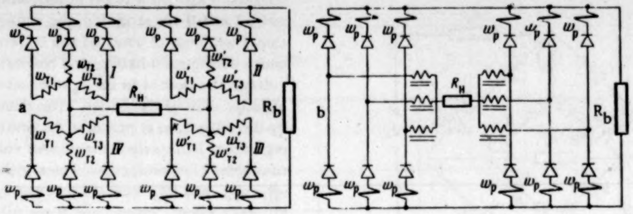

Fig. 9.

The values for k_f given in the table all correspond to the maximum value of the load current and to a currents ratio $k=\infty$.

Reversive schemes of magnetic amplifiers using three-phase elements can be built on the same principles as those described above. In Fig. 9a a scheme of a reversive amplifier is shown which is composed of a three-core magnetic amplifier with internal feedback. Comparing Figs. 9a and 9b, it is evident that by combining each two secondary transformer windings of Fig. 9a designated by the same symbols w_{T1}, w_{T2}, etc., a simplified version of the scheme (Fig. 9b) is obtained. For correct operation of the amplifier, the voltages across the transformer windings w_{T1}, w_{T2}, and w_{T3} must be shifted in phase by 180° with respect to the voltages of the corresponding transformer windings w'_{T1}, w'_{T2}, and w'_{T3}. The entire amplifier is built on six cores. If the three-core amplifier in the scheme of Fig. 9 is replaced by a three-phase bridge magnetic amplifier composed of six cores, the result is the scheme shown in Fig. 10 [3].

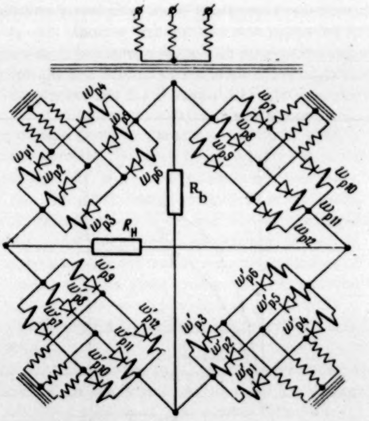

Fig. 10.

Two-half-period Schemes of Reversive Magnetic Amplifiers of High Efficiency Without Transformers

In the schemes of Figs. 8, 9, and 10, a supply transformer with a power rating exceeding 2-3 times the load power (see Table 2) is an inevitable part of the device.

However, utilizing the principles for designing reversive amplifier schemes stated above, it is possible to construct schemes of two-half-period reversive amplifiers without the use of supply transformers. It would appear that such an amplifier could be constructed by combining two single-half-period reversive amplifiers built according to the scheme of Fig. 7b and delivering during alternating half-periods their outputs to a common load. One of the feasible schemes of such a combination of single-half-period amplifiers is shown in Fig. 11a. In this scheme a common ballast resistance $R_0=R_H$ is connected in series with the power supply. However, this scheme is inoperative, for this addition of resistance R_0 eliminates the redistribution of the supply voltage during the active half-period only in the w_p windings of an unsaturated core after saturation of one of the other cores. However, if one of the cores (for instance, I) is saturated during the entire working half-period, then the reverse supply voltage on the valves connected in series with the operational windings of another core (IV), which is at the time in the control half-period, will be close to zero; and that will be so, specifically, also for the core which, for efficient operation, should have a minimum of current in its windings at that time. As was pointed out above, this lowering of the reverse voltage on the valves leads to a considerable increase of the current through the operational windings in the next active half-period of operation; and thus the current in the output load is considerably lowered.

Better operational characteristics are obtained by a two-half-period reversive scheme suggested by the authors which is shown in Fig. 11b.

As pointed out above, to be sure of high efficiency in any reversive magnetic amplifier, the following two conditions must be fulfilled: 1) saturation of one or several cores during a half-period must not lead to an increase of the voltage applied to the terminals of the

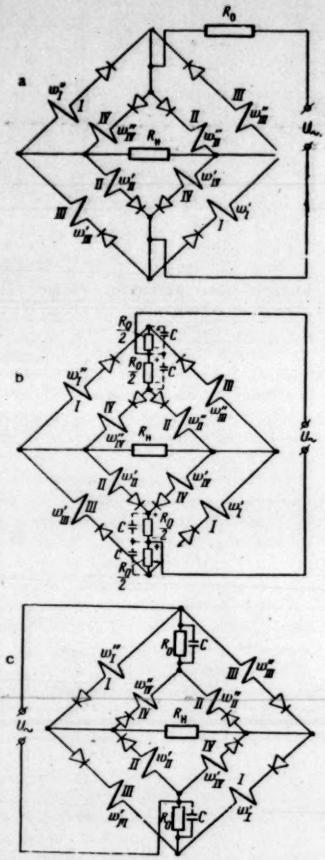

Fig. 11.

operational windings of the unsaturated cores during that half-period; 2) presence of a signal at the input of the amplifier, and, hence, of a voltage in the output load must not lead to a decrease of the reverse voltage on the valves in the regulatory half-period.

Satisfaction of both above conditions is achieved in the scheme of Fig. 11b by adding, prior to the entrance of the supply voltage to each of the two apexes of the two bridges of Fig. 11a, a resistance $R_0/2$ and a capacitance C in parallel with each of these resistors. The value of R_0 is chosen to be equal to one-half of the load resistance R_H. As a result of this, when, for instance, cores I and II are saturated, the voltages on the operational windings of cores III and IV remain unaltered, because during each half-period one-half of the supply voltage is absorbed in the R_0 resistances connected at opposite ends of the bridge. The shunting of the resistors by the capacitors C produces the result that during the regulatory half-periods the reverse voltages on the valves, connected, for instance, in series with windings w_{III}, w_{III}'', w_{IV}', and w_{IV}'', also are practically not decreased at all, even when cores I and II are fully saturated during the working half-period. The magnitude of capacitance C is not critical; it may be chosen to equal $C \approx (1-2)/(R_0 f)$, where f is the frequency of the supply voltage. Electrolytic condensers may be used for this purpose, since, first, the voltages across the resistors $R_0/2$ are of constant polarity as shown in Fig. 11b, and, second, leakage currents in the condensers have no substantial effect on the operation of the amplifier.

A warning, however, must be given against the choice of condensers of capacitance values so high that the voltage across them during the entire period of the supply voltage will practically be equal to the full amplitude variation of voltage across R_0 at $C = 0$: for, since the voltage across the condensers is subtracted from the supply voltage, with such very high capacitances an output voltage from the amplifier is observed which is somewhat lower than the maximum possible.

In place of the scheme of Fig. 11b, the scheme of Fig. 11c can also be used, which makes it possible to satisfy the above indicated condition with fewer resistors and condensers. This scheme, however, has the drawback that the reverse voltage on the valves may reach higher values than in scheme 11b. Let us assume, for example, that the magnitude and polarity of the signals is such that cores I and II are completely saturated during the respective working half-periods. The peak inverse voltages on the valves connected in series will then be $\frac{1}{2} U_m$ for the scheme of Fig. 11b, and U_m for the scheme of Fig. 11c, where U_m is the value of the supply voltage amplitude.

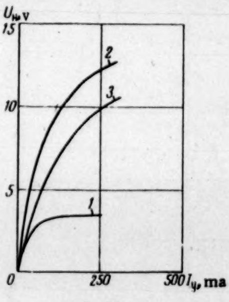

Fig. 12.

TABLE 2

Scheme of:	$\frac{U_p}{U_H}$	$\frac{I_p}{I_H}$	$\frac{P_{core}}{P_H}$	$n_c \frac{P_{core}}{P_H}$	$\frac{U_B}{U_H}$	$\frac{I_B}{I_H}$	$\frac{P_B}{P_H}$	$n_B \frac{P_B}{P_H}$	$\frac{P_{tr}}{P_H}$	η_{max}
Fig. 8	1.11	0.78	1.74	6.94	3.14	0.78	2.45	19.6	2.96	0.406
Fig. 9	0.855	0.59	1	6	2.1	0.59	1.24	14.9	2.74	0.5
Fig. 10	0.37	0.82	0.43	5.15	1.05	0.58	0.61	14.6	2.1	0.5

A consideration of the actual working conditions will decide which of the above schemes is the most advantageous in every specific case.

In Fig. 12, characteristic curves are given for amplifiers constructed according to the scheme of Fig. 11a (curve 1), according to the scheme of 11b with ripple-smoothening condensers (curve 2), and according to the same scheme without ripple-smoothening (curve 3). The differences in characteristics evident in Fig. 12 will become still larger when there is an opposing emf or an inductance in the amplifier output load.

Experimental comparisons of the proposed schemes with all other known schemes of reversive half-period amplifiers with dc output have shown that the proposed schemes not only make it possible to operate without a power transformer, but also have the highest efficiency, which approaches 0.4 when losses in windings and valves are small.

Comparison of Various Schemes

Selection of one or the other scheme of a reversive magnetic amplifier for application in a specific control system must be made after all the technical and economic aspects of the feasible modifications have been discussed and the most advantageous decided upon.

We present above in Table 2 a number of data, characteristic of the operation of our schemes shown in Figs. 8, 9, and 10. The testing of these schemes was carried out with purely ohmic resistances in the loads; the remanent inductance of the operational windings and the leakage inductances of the transformer as well as losses in the windings and valves were neglected in these experiments. All data given in this table are relative—with reference to the average values of the amplifier output characteristics I_H (current), U_H (voltage), and P_H (power).

The rated core power P_{core}, given in the table, is the product of the maximum rms values of the voltage in the operating winding U_p, the current through it I_p, and the number of operating windings n on the core. The rated rectifier power P_B is understood to equal the product of the peak inverse voltage U_B at the valve with the maximum rms value of the current I_B through the valve.

In the above table n_c designates the number of cores, and n_B the number of valves used in the scheme. P_{tr} is the rated power of the transformer.

CONCLUSIONS

On the basis of our investigation the following conclusions can be drawn:

1) For construction of reversive (duodirectional) schemes of magnetic amplifiers with dc output operating with higher efficiencies, it is advantageous to use a scheme based on subtraction of currents of nonreversive amplifiers.

2) To obtain increased efficiency in these schemes the following conditions must be fulfilled:

a) saturation of one or of several cores must not lead to increase of the voltage at the terminals of the working windings of any of the nonsaturated cores during the working half-period;

b) the voltage on the load must not produce a decrease of the inverse (rectifier) valve voltage during the control half-period.

3) Fulfillment of condition 2) can be assured by connection of half-wave amplifiers into the bridge scheme of Fig. 6.

4) To obtain higher efficiency, it is necessary in addition to fulfillment of conditions 2) to assure a high ratio of high to low current in the working windings of the nonreversive amplifiers and small pulsations in the rectified current. Therefore, all other conditions being equal, reversive amplifiers using three-phase current have the highest efficiency.

5) In this paper new schemes for reversive magnetic amplifiers with dc outputs without the use of transformers have been proposed; they satisfy conditions 2) and have high efficiencies.

LITERATURE CITED

1. M. A. Rozenblat, Magnetic Amplifiers [in Russian] (Izd. Sovetskoe Radio, 1960).

2. M. A. Rozenblat and G. V. Subbotina, "Increase of efficiency in reversive magnetic amplifier by means of transistors," Avtomat. i Telemekh. 20, No. 9 (1959)‡

3. S. S. Roizen, "Application of magnetic amplifiers in electric transmissions," Byull. Tyazhpromélektroproekta, No. 3 (1957).

---

‡ See English translation.

APPLICATION OF TRANSISTORS IN CIRCUITS OF VIBRATIONAL VOLTAGE REGULATORS

A. G. Zdrok

Moscow

Translated from Avtomatika i Telemekhanika, Vol. 21, No. 11
pp. 1514-1524, November, 1960
Original article submitted May 6, 1960

Electrical circuits are reviewed in which transistors and two position vibrators are used for voltage regulation of dc generators. Arrangements are presented which provide increase of the armatures frequency of vibration, as well as schemes using additional transformers or choke coils to secure better performance of the regulator at elevated ambient temperatures. Results of experimental investigations are given.

Vibratory electromagnetic relays and regulators have found wide application in various technical fields [1]; for instance, voltage regulation of modern dc and ac generators of automobiles is carried out exclusively by means of vibrating regulators [2].

A serious shortcoming of vibratory regulators is the presence of a continuously vibrating switching system which all the time breaks and makes contacts to open and close an inductive current-carrying electrical circuit.

It is known that the wearing out of contacts is due to mechanical, chemical, and electrical phenomena. The greatest wear is caused by electrical phenomena occurring when an arc is produced during the breaking of contacts. However, when the current in the circuit of the contacts is lower than 0.05-0.06 amp, and the voltage applied to them is less than the breakdown voltage of the air gap at the contact, then there is practically no erosion taking place when contacts are broken [1]. Such conditions for operation of contacts can be obtained by various schemes using semiconductors.

In the present paper, electrical regulation schemes are reviewed which use transistors and two-position vibrators for control of dc generators.

1. Simplest Circuits for Voltage Regulation

A number of schemes for voltage regulation of dc generators in which transistors and vibratory elements are employed were reviewed in [3]. The vibrators reviewed there consist of nonsymmetrical polarized two-position relays (one of the two contact positions being "predominant").

In actual operations two-position vibrational regulators having one pair of normally closed contacts proved the most dependable; our manufacturing industry has become quite familiar with the production techniques of such regulators. Therefore, it is most advantageous in schemes employing transistors also to use vibrational regulators with one pair of contacts.

One of the feasible schemes for voltage regulation by means of a vibratory device in combination with a transistor is shown in Fig. 1. In this figure, OB is the excitation winding of a generator, and OO and K are the

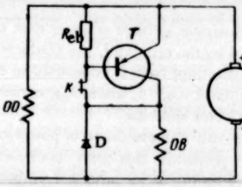

Fig. 1.

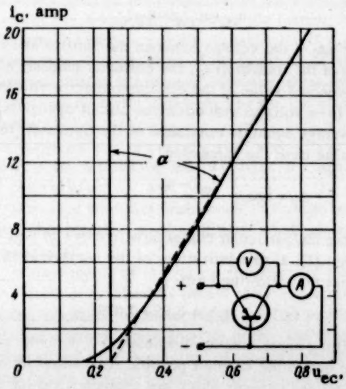

Fig. 2.

energizing coil and the contacts of the vibrator. R_{eb} is a resistance connected as shown between the emitter and base electrodes of transistor T which serves the purpose of decreasing the potential difference between these electrodes when contacts K are broken. Semiconductor diode D serves to eliminate the effect of the self-induction emf in the generator's excitation winding upon the operation of the transistor; see [4] and [5]. The generator excitation winding is in our figure connected in the collector loop of transistor T. However, it may be connected instead in the emitter circuit. The power being broken by the separation of the contacts is the same in both cases; therefore, in general, both of these methods of connection of the excitation winding are of equal value.

However, in single conductor systems it is more advantageous to have the generator excitation winding in the emitter circuit of the transistor: in this case, if the generator minus pole is connected to the housing, it will not be necessary to insulate the transistor housing from the generator housing. In this way the generator housing may be utilized as a thermal sink to carry away the heat from the transistor. Such schemes will be discussed below.

The scheme of Fig. 1 operates in the following manner.

When the generator voltage is lower than the one to be maintained by the regulator, the contacts K are closed, and the transistor base is connected to the collector. We then have $u_{cb} = 0$, where u_{cb} is the voltage between the collector and base.

In Fig. 2 the volt-ampere curve of power transistor P208 at $u_{cb}=0$ is presented; this curve can be expressed with an accuracy sufficient for practical purposes by the formula

$$u_{ec} = u_{T0} + R_T i_c, \tag{1}$$

where u_{ec} is the voltage between the emitter and collector of the transistor; i_c, the collector current; u_{T0}, the projected value of the emitter-collector voltage at $i_c = 0$ (e-c voltage with collector circuit open). R_T is the average dynamic resistance of the transistor, for which we have the expression

$$R_T = \operatorname{tg}\alpha = \frac{u_{ec} - u_{T0}}{i_c}.$$

For the particular characteristic curve of Fig. 2, expression (1), after substitutions of the numerical values, assumes the following form:

$$u_{ec} = 0.25 + 0.029\, i_c.$$

Using approximation formula (1) it becomes possible to obtain the simplest possible expressions for the voltages and currents which are characteristic for the processes taking place in the schemes under discussion. For example, when self-excitation takes place in the generator, the voltage generated u_G is balanced by the sum of the voltage drops in the transistor and in the excitation winding; that is, we have

$$u_G = u_{ec} + i_B r_B, \tag{2}$$

where r_B and i_B are respectively the resistance of and the current in the excitation winding.

Considering that $i_B = i_c$ (Fig. 1), and substituting (1) and (2), we obtain the following expression for the generator excitation current:

$$i_B = \frac{u_G - u_{T0}}{r_B + R_T}. \tag{3}$$

When the generator voltage u_G reaches the standard output value, contacts K are opened. Then we have $u_{eb} \approx 0$, since the base is usually connected with the emitter by a resistance R_{eb} of low ohmage. In order to obtain simple relationships, let us assume that the inductances of the excitation winding of the generator and of the vibrator energizing coil are constant, and that the resistance of the transistor in the reverse direction is infinite. Then for our scheme in its present condition the following equation will be valid:

$$L_B \frac{di_B}{dt} + i_B r_B + u_D = 0, \tag{4}$$

where u_D is the potential drop across the rectifier diode D, L_B—the inductance of the generator excitation winding.

Since in this state the resistance of the transistor is considerably higher than that of the diode which is now in the forward conductance state, it is possible to consider that as a first approximation the extra current caused by the closing of passage through the transistor is going through the diode loop, and that

$$i_B \approx i_D. \tag{5}$$

Vibrating voltage regulators usually have high ratios of release currents to holding current reaching up to 0.95. By the time the next contact make is due, the current in the diode usually has not had time to go down to zero. Therefore, the volt-ampere curve of the shunting diode may be expressed, with accuracy sufficient for practical purposes, by an experimental formula similar to (1), which is as follows:

$$u_D = u_{D0} + i_D R_D. \tag{6}$$

Solving equation (4) for the generator excitation current i_B, taking into account (1), (5), and (6), we obtain the following formula for the excitation current during the time when the regulator contacts are open:

$$i_B = i_{B0} e^{-\frac{r_B + R_D}{L_B} t} - \frac{u_{D0}}{r_B + R_D}\left(1 - e^{-\frac{r_B + R_D}{L_B} t}\right), \tag{7}$$

where i_{B0} is the magnitude of the generator excitation current at the moment of opening of the contacts.

Expression (7) makes it possible in a relatively simple way to obtain an approximate estimate of the average value of the diode current, and to choose the proper type of diode. To do this it is sufficient to substitute into (7) the value of i_D from (5). Also the time interval must be known during which the contacts remain open, and the vibration frequency. Then for the average value of the diode current I_D the following formula is obtained:

$$I_D = \frac{f_c L_n}{r_n + R_D} \left[\left(i_{n0} + \frac{u_{D0}}{r_n + R_D} \right) \left(1 - e^{-\frac{r_n + R_D}{L_n} t_p} \right) - \frac{u_{D0}}{L_n} t_p \right], \quad (8)$$

where f_c is the frequency of vibration of the contacts, and t_p is the time the contacts are open during a cycle.

By the use of a shunting semiconductor diode not only is the proper operation of the transistor under the prevailing conditions of back and forth switching secured, but also the appearance of excessive voltage between the emitter and collector is excluded.

When the contacts are open, the generator voltage u_G and the voltage across the diode are of the same polarity; consequently

$$u_{ec} = u_G + u_D. \quad (9)$$

Solving equations (6), (7), and (9) simultaneously, we obtain an expression for the voltage u_{ec} between the emitter and collector of the transistor at the time when contacts K are open:

$$u_{ec} = u_G + u_{D0} + R_D \left[i_{n0} e^{-\frac{r_n + R_D}{L_n} t} - \frac{u_{D0}}{r_n + R_D} \left(1 - e^{-\frac{r_n + R_D}{L_n}} \right) \right]. \quad (10)$$

The product of R_D with the expression in the brackets can amount to only a few percent of the voltage to be regulated. The same is true for the voltage u_{D0}. Therefore, one may consider that in schemes where the excitation windings are shunted by a semiconductor diode, the voltage between emitter and collector is approximately equal to the voltage of the generator which is being regulated. The larger the resistance of the diode circuit loop, the higher is the emitter to collector voltage.

Formulas (9) and (10) make it possible to estimate the maximum voltage that can be expected on the transistor in this application, and accordingly to choose the proper transistor for it.

When a shunting diode is not present at the moment the contacts are opened, the voltage across the transistor may exceed the regulation voltage of the generator u_G by a factor of several times [3].

It is the resistance R_{eb} connected between the emitter and the base (Fig. 1) which determines the potential difference between the emitter and base when the contacts K are open. Thus, the resistance of the transistor in the nonconducting state is determined by the value of resistance R_{eb}.

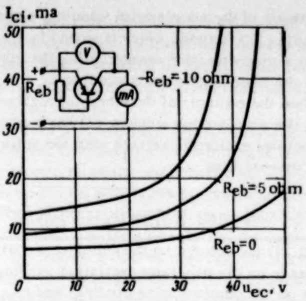

Fig. 3.

In Fig. 3 are presented volt-ampere curves of transistor P208 for various values of resistance R_{eb} to illustrate the effect of the shunting resistance upon the transistor resistance in its nonconducting phase. I_{ci} in Fig. 3 is the initial collector current. The characteristic curves of Fig. 3 were taken at an ambient temperature of 50°C. The measurements were made after a two-hour warmup of the transistor. The surface area of the heat sink, which was made of aluminum, was 750 cm^2.

Voltage regulator schemes such as those shown in Fig. 1 have two substantial shortcomings: 1) Relatively low speed of the regulation process, and large fluctuations in the voltage being regulated, both of these being due to the low frequency of armature vibrations; and 2) the current through the contacts and the resistance of the transistor in its closed (nonconducting) condition are both determined by the magnitude of the shunting resistance R_{eb}; the lower R_{eb}, the larger the current that is interrupted by breaking of the contacts; but if R_{eb} is increased, then the resistance of the transistor in its blocked condition is lowered. However, these shortcomings can be easily eliminated by the use of special schemes.

2. Methods for Raising the Working Frequency in Voltage Regulators by Means of Transistors

Increased vibration frequencies in voltage regulators are obtained by the use of additional windings and resistances (Fig. 4).

In the scheme of Fig. 4a the frequency of the armature vibrations is raised by means of an acceleration winding YO which is connected in parallel with the generator excitation winding OB; in this and in the following schemes the beginnings of windings are indicated in the figures by points. In order to compensate for the lowering of the resultant magnetic force with increasing speed of rotation of the generator armature, caused by the presence of the acceleration winding, a compensating winding KO is added which is wound in a sense to produce a magnetization counteracting the magnetization by the basic acceleration winding.

When the contacts of the vibratory regulator are closed, the acceleration winding YO has applied to it the generator excitation voltage with the voltage on KO added; thus we have

$$u_{y} = u_{\text{в}} + u_{C} = (r_{\text{в}} + r_{C})i_{\text{в}}, \qquad (11)$$

where u_Y is the voltage on the acceleration winding; u_B, the voltage on the generator excitation winding; u_C, the voltage on the compensating winding; and r_C, the resistance of the compensating winding.

When contacts K are open, the excitation winding is shortcircuited by the diode: the voltage on the acceleration winding then is equal to the potential drop across the diode. When the contacts are broken, the voltage on winding YO is decreased abruptly by

$$\Delta u_{y} = (r_{\text{в}} + r_{C})\, i_{\text{в}} - u_{D}. \qquad (12)$$

The change of current through winding YO can be expressed by the following simple formula (neglecting the mutual effects of windings OO and OY):

$$i_{y} = \frac{(r_{\text{в}} + r_{C})i_{\text{в}}}{r_{y}} e^{-\frac{r_{y}}{L_{y}}t} - \frac{u_{D}}{r_{y}}\left(1 - e^{-\frac{r_{y}}{L_{y}}t}\right), \qquad (13)$$

where r_Y and L_Y are the resistance and inductance of the acceleration winding.

It follows from expression (13) that at the instant

$$t_{0} = \frac{L_{y}}{r_{y}} \ln\left[1 + \frac{(r_{\text{в}} + r_{C})i_{\text{в}}}{u_{D}}\right] \qquad (14)$$

the current in the acceleration winding changes its direction: when $0 \leq t \leq t_0$ the resultant magnetizing force is equal to the sum of the magnetizing forces produced by the principal and acceleration windings, and when $t > t_0$ —to their difference.

Consequently, when the contacts are opened, the resulting magnetizing force of the regulator windings is substantially decreased, which leads to a considerable demagnetization of the vibrator core, and this in turn brings about a faster closure of the contacts [remember that the vibrator being of the "normally closed" type, the contact "make" is mostly caused by spring action on the armature opposed to the magnetic action— Translator].

If the "make" of the contacts occurs at time t_p after the preceding break, acceleration winding YO will have at that moment the voltage u_Y applied to it, and the current in this winding will begin to rise; this change will take place according to the following expression:

$$i_{y} = \frac{(r_{\text{в}} + r_{C})i_{\text{в}}}{r_{y}}\left(1 - e^{-\frac{r_{y}}{L_{y}}(t_{p}+t)}\right) + \\ + \frac{u_{D}}{r_{y}}\left(e^{-\frac{r_{y}}{L_{y}}t} - e^{-\frac{r_{y}}{L_{y}}(t_{p}+t)}\right) \qquad (15)$$

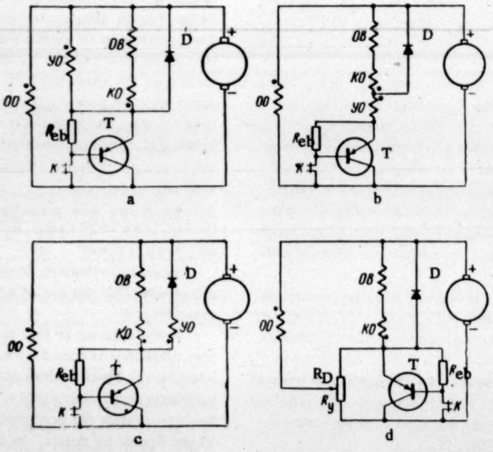

Fig. 4. Scheme of voltage regulation with acceleration of vibration of the regulator armature.

The increasing current in the acceleration winding will speed up the occurrence of the "break" of the vibrator contacts.

In the circuit of Fig. 4b acceleration is achieved by a winding YO connected in series with the emitter of the transistor. When the contacts are closed, the current in this winding is determined by the expression

$$i_y = i_B e^{-\frac{R}{L}t} - \frac{u_{T0}}{R}\left(1 - e^{-\frac{R}{L}t}\right), \tag{16}$$

where i_B is the excitation current when the contacts are closed,

$R = r_B + R_T + r_Y + r_C$, and $L = L_B + L_Y + L_C$;

here r_Y, r_C, L_Y, and L_C are the resistances and inductances of the acceleration winding and of the compensating winding, connected now in series.

The volt-ampere curve of the transistor in this case is again represented by formula (1).

When the contacts K are opened, the generator excitation current is substantially going only by way of the diode circuit, while the winding YO is practically currentless. Thus, the magnetizing force of the regulator winding is diminished, and thereby conditions for faster closing of the contacts are created.

The frequency of the regulator armature's vibrations can be raised also by connecting an acceleration winding in series with the shunting diode (Fig. 4c). The acceleration winding YO is connected in opposition to the principal regulator winding OO. In the circuit of Fig. 4a the winding YO must be of high resistance, in the circuits of Figs. 4b and 4c—of low resistance.

In Fig. 4d a circuit for voltage regulation of a generator is presented, in which a frequency increase of the vibrator armature is obtained by means of an additional "acceleration resistor" R_Y with another resistor R_D connected in series with it.

The entire resistance $(R_Y + R_D)$ is connected in shunt to the transistor, and the principal winding of the vibrator is now connected to the tap between R_Y and R_O, instead of to the minus pole of the generator armature as before. The magnitude of the shunting resistance $(R_Y + R_D)$ is determined by the excursions of the excitation current in the process of the voltage regulation of the generator. In voltage regulators used in automobiles, the R_Y part of the auxiliary resistance serves not only for purposes of acceleration but also as a heat sink for the principal regulator winding OO.

The voltage applied to the principal vibrator winding when the contacts are closed is almost equal to the generator voltage. The voltage across the shunting resistance $(R_Y + R_D)$ when the contacts are broken is determined by (9) and (10) above. The voltage on the vibrator winding OO is then equal to

$$u_0 = u_{ec}\frac{R_D}{R_y + R_D} - u_D. \tag{17}$$

Obviously, the smaller R_D, the smaller the voltage on the OO winding at the moment the contacts are broken, and the faster the falling off of the current in it takes place. When $R_D = 0$ the accelerating action of the OO winding in the scheme of Fig. 4d is similar to that of Fig. 4a.

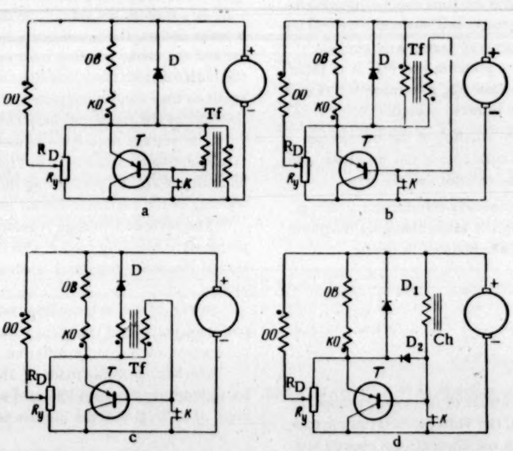

Fig. 5. Scheme of voltage regulation with an additional blocking circuit.

However, these schemes are not altogether equivalent to each other: in the scheme of Fig. 4d closing and opening of the contacts is affected by changes in the magnetizing force of only winding OO, while in the scheme of Fig. 4a both windings OO and YO are having an effect. Also, the magnetizing force produced in the OO winding varies only within relatively small limits in the process of regulation. The latter property is also shared by the schemes of Figs. 4b and 4c.

The scheme using an additional acceleration resistance has, in comparison with the schemes using additional windings for acceleration, also the advantage that less space for accommodation of the windings is needed. This makes it possible to decrease the size of the regulator magnetic system and to save on copper.

An analysis of this kind of scheme for raising the vibration frequency of the regulator armature is given in [2].

In the schemes of Fig. 4 discussed above the generator excitation winding was connected in the emitter circuit of the transistor. However, in all these schemes the excitation winding may be just as well connected in the collector circuit, as was shown in Fig. 1.

3. Voltage Regulation Schemes with an Additional Blocking Circuit

In the voltage regulation schemes of Figs. 1 and 4, the current load on the vibrator contacts is much lower than in the ordinary regulators used at the present time. However, depending upon the magnitude of the R_{eb} resistance, the currents being interrupted by the contacts can still be of considerable magnitude.

Using additional blocking circuits it is possible practically to eliminate the currents depending upon the presence of the R_{eb} resistance, and, consequently, to unload the contacts still more and practically exclude erosion. Such schemes are presented on Fig. 5; in these schemes instead of the resistor R_{eb} a transformer Tf or a choke coil Ch is used in suitable places.

In Fig. 5a the primary winding of the transformer connects the emitter and collector of the transistor, and the secondary winding, the emitter and the base.

If the primary and secondary transformer windings w_1 and w_2 are traversed by the same changing magnetic flux, the following emf's are induced in them:

$$e_1 = -w_1 \frac{d\Phi}{dt}, \qquad e_2 = -w_2 \frac{d\Phi}{dt};$$

from this it follows that

$$\frac{e_1}{e_2} = \frac{w_1}{w_2}.$$

Consequently, if the effect of the voltage drops in the windings is neglected, the voltage variations across the emitter and base when the contacts are opened and closed will be of the same character as those across the emitter and collector. When contacts K are closed the voltage on the primary winding is determined by the transistor volt-ampere curve of Fig. 2; it is equal to the emitter-collector voltage corresponding to the collector voltage $u_c = 0$. When the contacts are open the voltage on the primary transformer winding is determined by formulas (9) and (10). The voltages applied between the emitter and base will be similar in shape. When contacts K are open, the positive pole of the potential, produced by the emf induced in the secondary transformer winding, will be applied to the base, the negative—to the emitter. In this way passage of current through the transistor is reliably blocked. In the scheme of Fig. 5a the primary and secondary transformer windings must be of high ohmage.

The scheme of Fig. 5b works in a similar manner. Here the primary transformer winding is connected in parallel to the generator excitation winding. In Fig. 5c a voltage regulation scheme is shown having a low ohmage primary transformer winding connected in series with the diode. If the variation of the voltage drop across the diode with current is neglected, the shape of the voltage induced in the secondary winding will be the same as that induced in the scheme of Fig. 5a. In the scheme of Fig. 5d, a positive potential on the transistor base relative to the emitter is secured by the use of choke coil Ch connected between the plus pole of the generator and the transistor base.

In order for the induced emf to last longer, the time constant of the choke circuit must be increased. This is easily accomplished by connecting another semiconductor diode D_2 in parallel with the choke. In the scheme of Fig. 5d, the diode D_2 serves also to limit the magnitude of the applied signal.

To decrease the power handled by the contacts when a break occurs, the secondary windings of the transformers and the choke winding must be of high ohmage: if the currents from these windings are made sufficiently small so they can be neglected, then there will be only the load of the transistor base current on the contacts.

The voltage regulation schemes with a supplementary blocking circuit shown in Figs. 5a, 5b, and 5c can be realized also by connecting the generator excitation winding in the collector circuit loop of the transistor.

The reviewed voltage regulation schemes with supplementary blocking circuit also insure dependable operation of the entire regulator at elevated ambient temperatures.

In Fig. 6[*] the relationships between the emitter-collector voltage of transistor P208 and the collector output current are given for different emitter-base voltages.

The heat sink was made of aluminum, the active heat absorbing area was $750\ cm^2$ at an ambient temperature of 85°C; this is the highest permissible ambient

---

[*] The curves of Fig. 6 are for the same transistor specimen as those of Fig. 3.

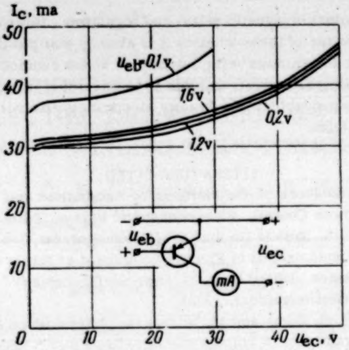

Fig. 6.

temperature when the collector of the transistor is loaded to the maximum rated power output. The voltages between the emitter and base were applied from a source which had a constant output resistance.

With increase of positive potential on the base relative to the emitter, the collector current first decreases. At a potential between 0.2 and 1.2 v the collector current reaches a minimum. With further increase of positive potential on the base, the collector current somewhat increases. Hence, when P 208 type transistors are used, the transformer or choke must be so chosen, that positive potentials within the indicated limits are provided on the transistor base when the contacts are open. Base emitter potentials close to those required can be obtained by including in all these schemes an additional germanium or silicon diode in the emitter-base circuit in a manner similar to Fig. 5d.

4. Some Results of Experimental Investigations

To illustrate the processes taking place in some of the schemes for voltage regulation described in this paper and to confirm some of the mathematical relationships given, a number of voltage and current oscillograms are given below in Figs. 7 and 8; these oscillograms were taken on a dc generator with a power output of 1500 w at a rated voltage of 28 v, controlled by a regulator consisting of a vibrator in combination with a transistor. The minimum speed of revolutions of the generator armature at the rated voltage and at full load was 1550 rpm with the generator still cold. A transistor of the P4A type was connected in series with the excitation winding which had a resistance of 8 ohms; a VG-10 valve was in parallel with the excitation winding; the load on the generator consisted of a storage battery which was being charged at a current of 15 amp. To increase the speed of the regulator operation an acceleration resistance $R_Y \approx 0.14\ R_D$ was connected in the circuit.

Figures 7a and 7b represent oscillograms of the generator voltage u_G, of the emitter-collector voltage u_{ec}, of the emitter-base voltage u_{eb}, and of the collector current i_c of the transistor. The potential difference u_{eb} when the transistor is passing current is shown above the zero line, the blocking u_{eb} potential—below the zero line.

These oscillograms illustrate the operation of the scheme shown in Fig. 5a at n = 1500 rpm. The average value of the generator excitation current was 1.43 amp, the generator voltage was 28.2 v. To obtain the blocking voltage u_{eb}, an interstage transformer from a Rodina-47 receiving set was used. The scales of the u_G and u_{ec} voltages on the oscillograms were the same. The u_{eb} voltages are shown on a magnified scale.

The emitter-collector voltage u_{ec} is here approximately equal to the generator voltage u_G; thus relationships (9) and (10) are confirmed. The shape of the u_{eb} voltage variations is approximately the same as that of the u_{ec} variations; the slight differences observed between these two are due to deviations of the vibrator natural frequencies.

The other schemes work in a similar manner.

Figure 8 shows oscillograms of current i_D, and also of voltages u_G and u_{eb}, illustrating the blocking of the transistor by means of a choke coil according to the scheme of Fig. 5d. The primary winding of an interstage transformer from a Rodina-47 receiver-set was used as a choke coil. The emitter-base part of the transistor was shunted by a semiconductor diode of type DG-Ts24 in order to limit the blocking signal.

CONCLUSIONS

At present the industry of our country has mastered the production of germanium transistors for currents up

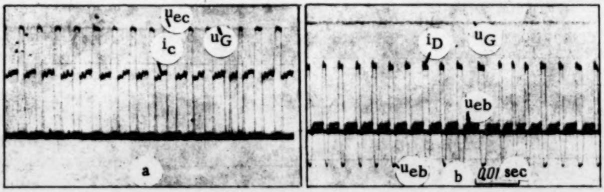

Fig. 7. Oscillograms of voltage and currents illustrating the operation of the circuit of Fig. 5a.

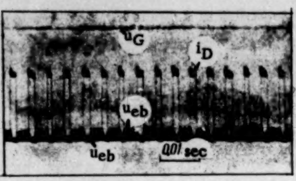

Fig. 8. Oscillograms of u_{eb} and i_D illustrating the operation of the circuit of Fig. 5d.

to 25 amp [6]. By means of the above described schemes it is possible when regulating the voltage of generators with excitation currents to 25 amp to have at the vibrator contacts being broken currents of only 0.3 to 0.8 amp.

The great majority of automobile generators have excitation currents of 1.5–3.0 amp. When vibratory regulators in combination with transistors are used on these generators, the current broken by the vibrator contacts will be from 0.03 to 0.09 amp.

By combined use of vibratory electromagnetic regulators and of transistors it will be possible to avoid erosion of contacts.

The schemes reviewed here by no means exhaust the many feasible combinations of transistors with vibratory electromagnetic relays and regulators. However, by the use of these schemes it is already now possible to lower the currents being interrupted at the contacts to a considerable extent, and thus to considerably increase the dependability of vibratory electromagnetic voltage regulators.

LITERATURE CITED

1. Handbook on the Elements of Automation and Remote Control. Electromagnetic Relays. Edited by B. S. Sotskov [in Russian] (Gosénergoizdat, 1958).
2. Fundamentals of Electric Equipment of Planes and Autos. Edited by A. N. Larionov [in Russian] (Gosénergoizdat, 1955).
3. A. G. Zdrok and M. N. Fesenko, "Application of transistors in voltage regulation schemes," Vestnik Élektropromyshlennosti No. 9 (1958).
4. V. G. Konstantinov, "Transistor amplifier for excitation control of electrical machines," Vestnik Élektropromyshlennosti No. 1 (1959).
5. O. A. Kossov, "Operation of a semiconductor switch with loads of different nature," Élektrichestvo No. 5 (1959).
6. A. V. Krasilov, A. B. Polyanov, and E. S. Saltykova, "A powerful germanium transistor," Élektrichestvo No. 1 (1959).

DESIGNING CIRCUITS FOR STABILIZING COMPOUND ELECTRIC DRIVES WHICH USE A SPECIAL THREE-WINDING TRANSFORMER

O. B. Rosenbauli and R. N. Rodin

Moscow

Translated from Avtomatika i Telemekhanika, Vol. 21, No. 11,
pp. 1525-1535, November, 1960
Original article submitted April 22, 1959

A method is presented for computing the parameters of circuits for stabilizing the speed of compound dc and ac drives using a special three-winding transformer. A graphical method for plotting the circuit characteristics of the drive stabilizer is given; the non-linearity of the magnetization curve of the three-winding transformer core is taken into account.

The methods presented are illustrated by an example in which the parameters and characteristics of a stabilization circuit are given; the circuit controls a dc drive powered from the ac line through a rectifier.

Circuits using a special three-winding transformer for stabilizing the speed of dc and ac motors have found contemporary use [1]. Such circuits have a number of important advantages. In particular, they permit one to realize feedback compensating for perturbations with a single device, to decrease the weight of active materials in the controlling device, to simplify the adjustment of the system, and to decrease the variety and number of circuit elements. The advantages of such circuits permit them to be widely used in a number of dc and ac electric drive systems. The correct choice of the stabilizing circuit parameters is important in designing such systems. At present, problems related to the computation of such stabilizing systems have not been dealt with in periodical literature. This article presents a method for computing the parameters of circuits for stabilizing the speed of dc motors with a choke regulator connected to the ac line through a rectifier, and three-phase motors with a Shenfer rotor; a method for calculating the characteristics of the three-winding transformer used in the speed stabilizer of the drive is also presented.

1. Designing a Three-winding Transformer for a DC Motor Speed Stabilizer

A three-winding transformer is used as the compounding element in the circuit for controlling and stabilizing the speed of a dc motor shown in Fig. 1. It can be seen from this circuit that the load current $I_{\sim}$ flows through the current winding of the transformer; the voltage winding in series with an additional resistance R_d is connected to the supply voltage $U_{\sim}$, and the secondary winding feeds the stabilizing winding of the controlling device through a rectifier. It was shown in [1] that the expression for the current in the secondary circuit of such a transformer, I_2, is

$$I_2 = k(U_{\sim} - k_1 I_{\sim}), \tag{1}$$

where

$$k = \frac{W_2}{W_u \sqrt{(R_1' + R_2)^2 + \left(\frac{R_2 R_1'}{X_m'}\right)^2}}, \quad k_1 = \frac{W_i R_1}{W_u},$$

if the voltage and current windings are connected opposing.

Here W_i is the number of turns in the current winding of the transformer; W_u the number of turns in the voltage winding; W_2 the number of turns in the secondary winding; R_1' the resistance of the voltage winding referred to the secondary winding; X'_m the inductive reactance of the magnetizing circuit referred to the secondary; and R_2, the resistance of the secondary circuit $R_2 = r_2 + R_L$.

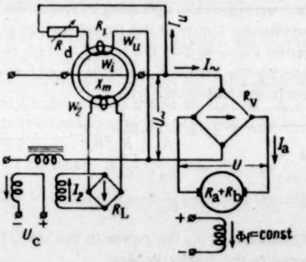

Fig. 1.

The expression for the rotary shaft speed of the motor connected to the supply through a rectifier is

$$n = \frac{U_{\sim} - I_{\sim} R_e}{c_n}, \tag{2}$$

where

$$R_e = \frac{k_i}{k_u}(R_r + R_a + R_b), \quad c_n = \frac{c\Phi_f}{k_u}.$$

Here R_r is the rectifier resistance, R_a and R_b are the resistances of the motor armature and brushes, respectively, k_i and k_u are rectifier coefficients for current and voltage, Φ_f is the motor field winding flux, and *c* is a constant.

Comparing equations (1) and (2), we can conclude that the three-winding transformer is a static speed transducer when the condition

$$\frac{W_i R_1}{W_u} = R_e = \text{const} \tag{2a}$$

is met.

The initial data for designing the compounding transformer are the parameters of the rectifier, motor, and transformer load. It will be assumed that the currents and voltages in the transformer are nearly sinusoidal in all operating modes of the stabilizing system, and that the rectifier resistance and coefficient are constant. Such assumptions are fully justified, since the transformer operates over a linear portion of the core magnetization curve. As was noted in [1], k_u varies over a small range. Therefore, by setting k_u at some value within this range, it can be considered constant with sufficient accuracy. It will be further assumed that the load resistance R_L is significantly greater than the secondary winding resistance, and that the effect of the magnetizing circuit is negligibly small ($X_m \approx \infty$). The assumptions mentioned are justified by the good agreement between the computed and experimentally found transformer parameters. It is recommended that a toroid core made of a high-permeability material (type NP-50, NP-65, etc.) be used for the flux path of the transformers in order to diminish the leakage flux and eddy current losses in the steel.

We will keep the operating range of the transformer within the limits of the linear portion of the magnetization curve so that the signal will be undistorted. Considering the assumptions made, equation (1) can be written in the following form:

$$I_2 = \frac{K_w E_n}{R_2 + K_w^2 R_1}, \tag{3}$$

where

$$E_n = c_n n, \tag{4}$$

$$K_w = \frac{W_2}{W_u}. \tag{5}$$

Considering (3), the power in the load, P_L, can be expressed in the following way:

$$P_L = \frac{K_w^2 E_n^2 R_2}{(R_2 + K_w^2 R_1)^2}. \tag{6}$$

Let us find the condition of maximum power transfer to the load by the transformer. To do this, we will find the greatest maximum of the function $P_L = f(K_w^2, R_2)$:

$$\frac{\partial P_L}{\partial R_2} = (R_2 + K_w^2 R_1)^2 - 2R_2(R_2 + K_w^2 R_1) = 0,$$

whence

$$R_2 = R_1 K_w^2, \tag{7}$$

and

$$\frac{\partial P_L}{\partial (K_w^2)} =$$

$$= (R_2 + K_w^2 R_1)^2 - 2K_w^2(R_2 + K_w^2 R_1) R_1 = 0,$$

whence

$$K_w^2 = \frac{R_2}{R_1}. \tag{8}$$

It can thus be seen from equations (6)-(8) that the greatest maximum condition for function $P_L = f(K_w^2, R_2)$ is expressed by the equation

$$R_1 = \frac{E_n^2}{4P_L}. \tag{9}$$

It can be shown, by using the initial set of transformer equations given in [1], that the expression for the current in the voltage winding is

$$I_u' = \frac{U_{\sim}' + I_{\sim}' R_2}{R_1' + R_2}, \tag{10}$$

in which the apostrophes denote that the corresponding quantities are referred to the secondary winding.

Solving equations (5) and (10) together in terms of I_u, $U_{\sim}$, $I_{\sim}$ we get a final equation for the current in the voltage winding:

$$I_u = \frac{U_{\sim} + I_{\sim} R_e}{2R_1}. \tag{11}$$

The voltage across the voltage winding of the transformer can be expressed by the following equation:

$$U_v = 4.44 f W_u B_m a b k_{ff} 10^{-8}, \tag{12}$$

where B_m is the effective flux density in the transformer core; *a* and *b* are the dimensions of the sides of the core cross section; and k_{ff} is the core fill-factor.

Taking (8) into account, the solution of (12) for the product of the sides of the flux path cross section assumes the form

$$ab = \frac{\sqrt{P_L R_1}\, 10^8}{4.44 f B_m k_{ff} W_u}. \tag{13}$$

Keeping equalities (3) and (8) in mind, the expression for the ampere-turns of the secondary winding can be written in the following manner:

$$I_2 W_2 = \frac{E_n W_i}{2R_e}. \tag{14}$$

If q, Δ, and k_f are the wire cross section, current density, and fill-factor of the flux path window for the various windings, and D_0 is the diameter of this window the joint solution of equation (14) and the window fill equation:

$$\frac{\pi(D_{av} - a)^2}{4} = \tag{15}$$

$$= \frac{q_i W_i 10^{-2}}{k_{fi}} + \frac{q_u W_u 10^{-2}}{k_{fu}} + \frac{q_2 W_2 10^{-2}}{k_{f2}} + \frac{\pi D_0^2}{4}$$

gives the expression for the average diameter of the toroidal flux path:

$$D_{\text{av}} = a + \sqrt{\frac{4I_1W_i10^{-2}}{\pi\Delta_i k_{fi}} + \frac{4I_uW_u10^{-2}}{\pi\Delta_u k_{fu}} + \frac{2E_nW_i10^{-2}}{\Delta_2 R_e \pi k_{f_2}} + D_0^2}. \tag{16}$$

Hence the average line length is

$$l_{\text{av}} = \pi\left(a + \sqrt{\frac{4I_1W_i10^{-2}}{\pi\Delta_i k_{f1}} + \frac{4I_uW_u10^{-2}}{\pi\Delta_u k_{fu}} + \frac{2E_nW_i10^{-2}}{\Delta_2 R_e \pi k_{f_2}} + D_0^2}\right). \tag{17}$$

The amount of additional resistance in the voltage winding circuit can be found from the equation

$$R_{\text{d}} = R_1 - \frac{\rho l_{\text{vu}} W_u}{q_u} 10^{-2}, \tag{18}$$

where

$$l_{\text{vu}} = 2a + 2b + 4\lambda_u = 2\left(a + b + 2\frac{q_uW_u10^{-2}}{l_{\text{av}}k_{\text{fu}}}\right);$$

λ_u is the thickness of the voltage winding cross section and ρ is the resistivity of the winding wire.

The expression for the resistance of the secondary winding is

$$r_2 = \frac{\rho l_{\text{v2}} W_2}{q_2} 10^{-2}, \tag{19}$$

where

$$l_{\text{v2}} = 2a + 2b + 8\lambda_u + 4\lambda_2 =$$

$$= 2\left(a + b + 4\frac{q_uW_u}{l_{\text{av}}k_{\text{fu}}}10^{-2} + 2\frac{q_2W_2}{l_{\text{av}}k_{\text{f}_2}}10^{-2}\right)$$

(λ_2 is the thickness of the secondary winding cross section).

The weight of the copper in the transformer is

$$G_{\text{M}} = \frac{\gamma_{\text{M}}}{\rho}\left[\frac{I_i^2 r_i}{\Delta_i^2} + \frac{I_u^2 R_u}{\Delta_u^2} + \frac{I_2^2 r_2}{\Delta_2^2}\right] \tag{20}$$

(here γ_{M} is the specific gravity of the copper).

The total weight of the transformer is determined by the sum of the weights of copper and steel:

$$G_{\text{tot}} = G_{\text{M}} + V_{\text{st}}\gamma_{\text{st}}, \tag{21}$$

where γ_{st} is the specific gravity of the core material, and V_{st} is the volume of steel in the core:

$$V_{\text{st}} = abl_{\text{av}}k_{\text{ff}}. \tag{22}$$

This method for designing a transformer is illustrated by an example given at the end of this article.

2. Designing a Three-winding Transformer for Stabilizing the Speed of an AC Motor

Three-winding transformers are used as compounding elements in circuits for stabilizing the speed of a three-phase motor with a Shenfer rotor, and a two-phase motor with a thin-walled rotor, which are shown in Figs. 2a and 2b. These transformers are built like the transformer shown in the circuit of Fig. 1, except that an additional inductive reactance X_I is connected in the circuit of the voltage windings; X_I is a choke with an air gap.

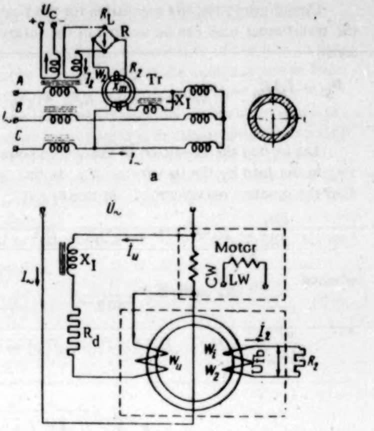

a

b

Fig. 2. CW – motor control winding, LW – motor line winding, U_{fb} – feedback voltage.

It has been shown in [1] that if the current and voltage windings are connected opposing, and $X_I' = (R_1' \sin\varphi)/\cos\varphi$, the expression for the current in the secondary circuit is

$$I_2 = k_2U_\sim - I_\sim k_3. \tag{23}$$

Using the designations mentioned above, we get the following expressions for the coefficients k_2 and k_3 when $X_m = \infty$:

$$k_2 = \frac{K_w}{\sqrt{(R_1K_w^2 + R_2)^2 + X_I^2K_w^4}},$$

$$k_3 = \frac{\dfrac{R_1W_i}{W_u\cos\varphi}}{\sqrt{(R_1K_w^2 + R_2)^2 + X_I^2K_w^4}}.$$

Here φ is the phase angle between the current in winding W_i and the voltage across W_u.

For the circuit shown in Fig. 2a $\varphi = \varphi_L - 30°$ (see Fig. 3), and for the circuit shown in Fig. 2b $\varphi_L = \varphi$, where φ_L is the phase angle between the load current and the voltage.

We will designate the expression $U_\sim = \dfrac{I_\sim R_1W_i}{\cos\varphi W_u}$ by the letter A and write equation (23) in the following form:

$$I_2 = \frac{K_wA}{\sqrt{(R_1K_w^2 + R_2)^2 + R_1^2K_w^4\operatorname{tg}^2\varphi}}. \tag{24}$$

Considering (24), the expression for the power in the transformer load can be written in the following form:

$$P_L = I_2{}^2 R_2 = \frac{K_w{}^2 A^2 R_2}{(R_1 K_w{}^2 + R_2)^2 + R_1{}^2 K_w{}^4 \operatorname{tg}^2 \varphi} \cdot \quad (25)$$

Let us find the condition of maximum power transfer to the load by the transformer. To do this, we will find the greatest maximum of function $P_L = f(K_w^2, R_2)$:

$$\frac{\partial P_L}{\partial R_2} = R_1{}^2 K_w{}^4 (1 + \operatorname{tg}^2 \varphi) - R_2{}^2 = 0,$$

whence

$$R_2 = R_1 K_w{}^2 \frac{1}{\cos\varphi}, \quad (25a)$$

and

$$\frac{\partial P_L}{\partial (K_w{}^2)} = R_2{}^2 - R_1{}^2 K_w{}^4 (1 + \operatorname{tg}^2 \varphi) = 0,$$

whence

$$R_2 = R_1 K_w{}^2 \frac{1}{\cos\varphi}. \quad (25b)$$

It can thus be seen from equations (25a) and (25b) that the greatest maximum of $P_L = f(K_w^2, R_2)$ is expressed by the equation

$$K_w = \sqrt{\frac{R_2}{R_1} \cos\varphi}. \quad (26)$$

The joint solution of equations (25) and (26) gives the following expression for the resistance of the voltage winding:

$$R_1 = \frac{A^2 \cos\varphi}{2P_L (1 + \cos\varphi)}. \quad (27)$$

Using the initial set of transformer equations given in [1], it can be shown that the expression for the current in the voltage winding circuit is

$$I_u = \frac{K_w \sqrt{U_\sim{}^2 K_w{}^2 + 2U_\sim \frac{W_2}{W_u} I_\sim R_2 \frac{W_i}{W_2} \cos\varphi + I_\sim{}^2 R_2{}^2 \left(\frac{W_i}{W_2}\right)^2}}{\sqrt{(R_2 + R_1 K_w)^2 + R_1{}^2 \operatorname{tg}^2 \varphi K_w{}^4}}. \quad (28)$$

The voltage across the voltage winding can be found from the following dependence:

$$U_v = 4.44\, f W_u B_m abk_{ff}\, 10^{-8}. \quad (29)$$

Considering (26), the solution of (29) for the product of the sides of the flux path cross section is

$$ab = \frac{\sqrt{\frac{P_L R_1}{\cos\varphi}}\, 10^8}{4.44 f B_m k_{ff} W_u}. \quad (30)$$

If $n_{mo} = 0$, then I_2 must also be 0. Consequently, equation (24) can be written thus:

$$U_\sim = cI_\sim, \quad (31)$$

where

$$c = \frac{R_1 W_i}{W_u \cos\varphi}. \quad (32)$$

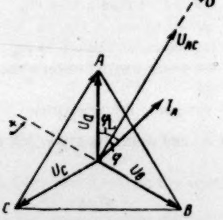

Fig. 3.

Hence, the transformer design consists of the following series of steps:

1. Using equations (27) and (31), we find $\underline{c}$ and R_1 under starting conditions. The quantity A is determined from conditions when the motor is running steadily at its nominal rpm.

2. We find K_w by using equation (26).

3. Having been given a series of values for W_i, we find the corresponding values of W_u from (32), and knowing K_w, we then find W_2.

4. Using (24) and (28), we find the currents in the secondary and voltage winding circuits.

5. Using (30), we find the transformer flux path cross section for the values of W_u obtained in step 3.

6. Choosing a flux path with a square cross section and expressing the wire cross section in terms of a permissible current and current density, we find the diameter and average line of the flux path from (15).

7. Using (18), we find the value of the additional resistance.

8. We find the copper weight and total weight of the transformer from (20) and (21) for the various values of W_i assumed in step 3.

9. The last step is to construct a graph of the total transformer weight as a function of the number of turns in the current winding. We then find the number of turns W_i which gives the minimum total weight, and we take all the parameters computed above which correspond to this W_i.

The graph $G_{tot} = f(W_i)$ is shown in Fig. 4 for a transformer operating as in Fig. 2b, with the following initial data: $I_\sim$ = 0.25 amp; $U_\sim$ = 50 v; U_{tr} = 25 v; $\cos\varphi_L$ = 0.5; P_L = 1 w; R_L = 1000 ohm; I_2 = 0.033 amp.

The transformer core material is 50NP.

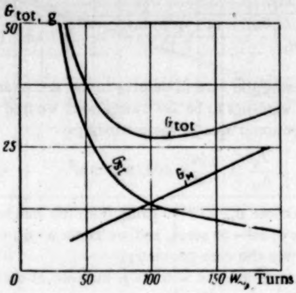

Fig. 4.

3. Computing the Transformer Characteristics

The change in the permeability of the iron in the core must be accounted for if the accuracy of the calculations of the three-winding transformer characteristics is to be increased. Using the equivalent circuit of a transformer operating in a dc motor speed stabilizing circuit (Fig. 5), we find the load current by the equivalent generator method. The linear inductance in the voltage winding circuit must be taken into account in the calculation.

If it is assumed that $\dot I_\sim' = I_\sim'(\cos\varphi_L - j\sin\varphi_L)$, the expression

$$\dot I_0 = \frac{U_\sim' + I_\sim' R_2(\cos\varphi_L - j\sin\varphi_L)}{R_1' + R_2} \qquad (33)$$

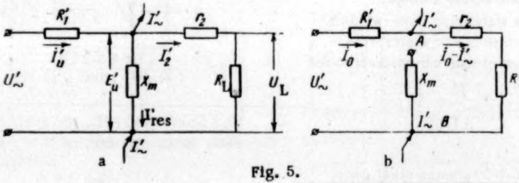

Fig. 5.

is justified for the current $\dot I_0$ (see the circuit of Fig.5b), whence

$$U_{AB} = U_\sim' - \dot I_0 R_1' = \qquad (34)$$

$$= U_\sim' - \frac{[U_\sim' + (I_\sim'\cos\varphi_L - jI_\sim'\sin\varphi_L) R_2] R_1'}{R_1' + R_2}.$$

When $\cos\varphi_L = 1$, equation (34)takes the form

$$U_{AB} = U_\sim' - \frac{U_\sim' + I_\sim' R_2}{R_1' + R_2}. \qquad (35)$$

The resistance of the equivalent circuit with respect to terminals AB is equal to

$$R_{AB} = \frac{R_1' R_2}{R_1' + R_2}. \qquad (36)$$

Fig. 6 shows an equivalent diagram of the transformer, consisting of a source U_{AB}, linear resistance R_{AB}, and non-linear reactance X_m connected in series. The current in this circuit is found from the formula

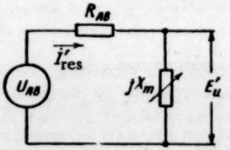

Fig. 6.

$$\dot I_{res} = \frac{\dot U_{AB}}{R_{AB} + jX_m}. \qquad (37)$$

If the transformer parameters are known, and a number of values $I_\sim'$ are given, the voltages corresponding to them, U_{AB}, can be found. We will solve equation (37) graphically. Both axes will be given identical voltage scales (Fig. 7). We will plot the voltage E_u– the voltage across the non-linear reactance X_m–along the ordinate, and the voltage across R_{AB} will be plotted along the abscissa. We draw a number of circles with radius U_{AB}, centered at the origin. Each such

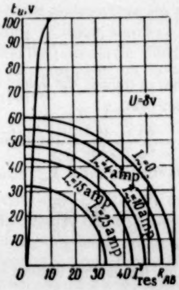

Fig. 7.

circle corresponds to definite values of the voltage $U_\sim'$ and current $I_\sim'$. If the magnetization curve of the steel core is also plotted on these coordinates, using the equations

$$E_u' = 4.44\ fW_2B_mSk_{ff}\ 10^{-8}, \qquad (38)$$

$$H_ml_{av} = \sqrt{2}\cdot 0.4\pi I_{res}'W_2, \qquad (39)$$

the points where this curve intersects the circles will be operating points for the transformer. Having a family of curves $E_u' = f(U_{res}'R_{AB})$ for $U_\sim$ = const , and $E_u' = f(I_{res}'R_{AB})$ for $I_\sim$ = const , we find the required dependencies $I_2 = f(U_\sim)$ and $I_2 = f(I_\sim)$. The function $I_2 = f(U_\sim)$ for $I_\sim$ = const is analogous to the function $n = f(U_\sim)$ for a drive with a constant load torque on the motor shaft. The function $I_2 = f(I_\sim)$ for $U_\sim$ = const is analogous to the mechanical characteristic of the drive, $n = f(M)$, for a constant supply voltage.

Example 1. Design of a stabilizing three-winding transformer for a "supply-rectifier — dc motor" system. The drive speed as a function of load current is expressed by the equation

$$n = \frac{U_\sim - R_eI_\sim}{c_n} = \frac{U_\sim - 0.15I_\sim}{3.7\cdot 10^{-3}}. \qquad \text{(ex. 1)}$$

The nominal load current $I_\sim$ = 20 amp; nominal shaft speed n = 3000 rpm; transformer power rating P_L=2 watts (U_2 = 80 v, I_2 = 0.025 amp). Core material is 50 NP.

Considering the size of the load current ($I_\sim$=20 amp), it is best, for technical reasons, to make the transformer with a one-turn current winding (W_i = 1). The area occupied by the current winding must be chosen on the basis of an appropriate value of D_0.

1. The supply voltage is found from expression (2), using the nominal values of $I_\sim$ and n:

$$U_\sim = c_nn + I_\sim R_e =$$

$$= 3.7\cdot 10^{-3}\cdot 3000 + 20\cdot 0.15 = 14.1 \text{ v.} \qquad \text{(ex.2)}$$

2. The circuit resistance of the voltage winding is found from (9):

$$R_1 = \frac{(c_nn)^2}{4P_L} = \frac{(3.7\cdot 10^{-3}\cdot 3000)^2}{4\cdot 2} = 15.2 \text{ ohms.} \qquad \text{(ex. 3)}$$

3. The number of turns in the voltage winding, according to equation (2a), is

$$W_u = \frac{R_1}{R_e} = \frac{14.1}{0.15} = 101 \text{ turns.} \qquad \text{(ex. 4)}$$

4. The transformation ratio K_w equals

$$K_w = \sqrt{\frac{R_L}{R_1}} = \sqrt{\frac{3200}{15.2}} = 14.5 \qquad \text{(ex. 5)}$$

according to (8).

5. We compute the number of turns in the secondary winding from (5):

$$W_2 = K_wW_u = 14.5\cdot 101 = 1470 \text{ turns.} \qquad \text{(ex. 6)}$$

6. The current in the voltage winding circuit is found from (11):

$$I_u = \frac{U_\sim + I_\sim R_e}{2R_1} = \frac{14.1 + 20\cdot 0.15}{2\cdot 15.2} = 0.562 \text{ amp.} \qquad \text{(ex. 7)}$$

7. Choosing the current density in the secondary and voltage windings to be Δ = 3 amp/mm², we find the wire cross-sectional area of these windings:

$$q_u = \frac{I_u}{\Delta_u} = \frac{0.562}{3} = 0.1842 \text{ mm}^2. \qquad \text{(ex. 8)}$$

8. We choose B_m = 12000 gauss from the magnetization curve of NP-50 steel, and we make a = b in order to optimize the core geometry.

9. In correspondence with (30), the side of the toroid flux path cross section is

$$a = b = \sqrt{\frac{10^8\sqrt{P_LR_1}}{4.44fB_mk_{ff}W_u}} =$$

$$= \sqrt{\frac{10^8\sqrt{2\cdot 15.2}}{4.44\cdot 400\cdot 12000\cdot 0.43\cdot 101}} = 0.77 \text{ cm.} \qquad \text{(ex. 9)}$$

10. According to (32), the average diameter of the flux path, for D_0 = 10 mm, is

$$D_{av} = a +$$

$$+ \sqrt{\frac{4I_uW_u10^{-2}}{\pi\Delta_uk_{fu}} + \frac{2E_nW_i10^{-2}}{\pi R_e\Delta_2k_{f2}} + D_0^2} = 0.77 +$$

$$+ \sqrt{\frac{4\cdot 0.562\cdot 101\cdot 10^{-2}}{3.14\cdot 0.3\cdot 3} + \frac{2\cdot 3.7\cdot 10^{-3}\cdot 3000\cdot 10^{-2}}{3.14\cdot 0.15\cdot 0.3\cdot 3} + 1} =$$

$$= 2.3 \text{ cm.} \qquad \text{(ex. 10)}$$

11. The length of the average toroid line, l_{av}, is found from (33):

$$l_{av} = \pi D_{cav} = 3.14\cdot 2.3 = 7.24 \text{ cm.} \qquad \text{(ex. 11)}$$

12. The volume of the flux path is

$$V_{st} = a^2l_{av}k_{ff} = (0.75)^2\cdot 7.24\cdot 0.43 = 1.85 \text{ cm}^3. \qquad \text{(ex. 12)}$$

13. The average length of a turn in the voltage winding is found from the equation

$$l_{vu} = 4\left(a + \frac{q_uW_u10^{-2}}{k_{fu}l_{av}}\right) =$$

$$= 4\left(0.77 + \frac{0.1842\cdot 101\cdot 10^{-2}}{0.3\cdot 7.24}\right) = 3.34 \text{ cm.} \qquad \text{(ex. 13)}$$

14. The additional resistance is

$$R_d = R_1 - \frac{\rho l_{vu}W_u}{q_u}10^{-2} = 15.2 -$$

$$- \frac{3.34\cdot 101}{57\cdot 0.1842}10^{-2} = 14.882 \text{ ohms.} \qquad \text{(ex. 14)}$$

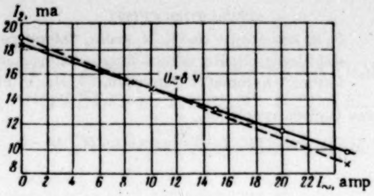

Fig. 8.

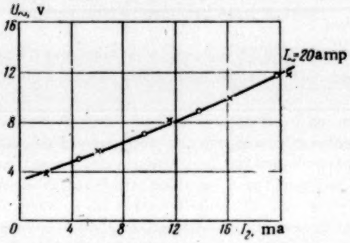

Fig. 9.

15. The average length of the secondary winding is found from the equation

$$l_{v2} = 4\left(a + 2\frac{q_u W_u 10^{-2}}{l_{av} k_{fu}} + \frac{q_2 W_2 10^{-2}}{l_{av} k_{f2}}\right) = 4$$

$$= \left(0.77 + 2\frac{0.1842 \cdot 101 \cdot 10^{-2}}{7.24 \cdot 0.3} + \frac{0.0081 \cdot 1470 \cdot 10^{-2}}{7.24 \cdot 0.3}\right) = 3.98 \text{ cm.}$$

(ex. 15)

16. The secondary winding resistance equals

$$r_2 = \frac{\rho l_{v2} W_2}{q_2} 10^{-2} = \frac{3.98 \cdot 1470}{57 \cdot 0.0081} 10^{-2} = 128 \text{ ohms.} \quad \text{(ex. 16)}$$

17. We use the well-known formula

$$G_M = \frac{\gamma_M}{\rho}\left[\frac{I_u{}^2 R_u}{\Delta_u{}^2} + \frac{I_2{}^2 r_2}{\Delta_2{}^2}\right] =$$

$$= 8.9 \cdot 57\left[\frac{(0.562)^2 \cdot 0.318}{3^2} + \frac{(0.025)^2 \cdot 128}{3^2}\right] = 10.1 \text{ g}$$

(ex. 17)

to find the weight of the copper.

18. The total transformer weight is equal to

$$G_{tr} = G_M + \gamma_{st} V_{st} = 10.1 + 8.2 \cdot 1.85 = 25.2 \text{ g.} \quad \text{(ex. 18)}$$

Example 2. Graphical computation of the characteristic $U_\sim = f(I_2)$ and $I_2 = f(I_\sim)$ for the three-winding transformer whose parameters were found in Example 1. The circuit parameters are R_1 = 15.2 ohms; R_2 = 3200 ohms; W_1 = 1; W_u = 101; W_2 = 1470; r_2 = 128 ohms.

1. Let us determine the equivalent values of resistances, currents, and voltages:

$$R_1' = R_1\left(\frac{W_2}{W_u}\right)^2 = 15.2\left(\frac{1470}{101}\right)^2 = 3240 \text{ ohm,}$$

$$I_\sim' = I_\sim \frac{W_1}{W_2} = \frac{I_1}{1470},$$

$$U_\sim' = U_\sim \frac{W_2}{W_u} = U_\sim \frac{1470}{101}.$$

(ex. 19)

2. Having been given a series of values for $I_\sim$, we will find the equivalent currents. The results are shown in Table 1.

Table 1

$I_\sim$, amp	0	2	4	6	10	15	20	25
$I'_\sim$, ma	0	1.36	2.72	4.07	6.8	10.2	13.6	17

3. Having been given a series of values for $U_\sim$, we find the equivalent voltages. The results are shown in Table 2.

Table 2

$U_\sim$, v	2	6	8	12	16
$U'_\sim$, v	29.1	87.2	116.4	174.5	232.5

Table 3

$I_\sim$, amp	0	4	10	15	25
U_{AB}, v	60.1	55	48.2	43.4	32.1

4. Using equation (36), we find R_{AB}:

$$R_{AB} = \frac{R_1' R_2}{R_1' + R_2} = \frac{3240 \cdot 3338}{3240 + 3338} = 1625 \text{ ohm.} \quad \text{(ex. 20)}$$

5. Using equations (38) and (39), we plot the magnetization curve of the 50NP core material on the coordinates E_u' and $I'_{res}R_{AB}$. The curve obtained for the transformer core is shown in Fig. 7.

6. We find the U_{AB} corresponding to the different $I_\sim'$ found in step 2, for each $U_\sim$ assumed in step 3. The results of these computations are given in Table 3 for $U_\sim$ = 8 volts.

Fig. 7 shows the construction for finding the transformer operating points on the plane $E_u' = f(I'_{res}R_{AB})$. Using the expression

$$I_2 = E_u' / R_2, \quad \text{(ex. 21)}$$

where

$$R_2 = R_L + r_2, \quad \text{(ex. 22)}$$

we find the dependence $I_2 = f(I_\sim)$ (cf. Fig. 8). The function $I_2 = f(I_\sim)$, observed experimentally with a transformer made according to the design data of Example 1, is shown also in Fig. 8 (circles denote the calculated curve, and crosses show the experimental one). We find the dependence $U_\sim = f(I_2)$ for $I_\sim$ = const from analogous constructions for other values of $U_{\sim}$. Fig. 9 shows $U_{\sim} = f(I_2)$ for $I_{\sim} = 20$ amp. This figure also shows the function $U_{\sim} = f(I_2)$ observed experimentally with the transformer previously mentioned.

The good agreement between the calculated and experimentally observed characteristics shows that the assumptions made above are justified in the design of a three-winding transformer.

LITERATURE CITED

1. O. B. Rosenbauli and R. N. Rodin, "Motor speed stabilizing circuits using a three-winding transformer," Avtomat. i Telemekh. 20, No. 3(1959).*

---

* See English translation.

AN APPROXIMATE DETERMINATION OF JET REACTION IN A "NOZZLE-FLAPPER" HYDRAULIC AMPLIFIER

I. M. Krassov, L. I. Radovskii, and B. G. Turbin

Moscow

Translated from Avtomatika i Telemekhanika, Vol. 21, No. 11,
pp. 1536-1538, November, 1960
Original article submitted April 9, 1960

A method is presented for computing the approximate magnitude of the force with which a jet of working fluid, issuing from a nozzle, affects the flapper. The results obtained are compared to experimental data.

In nozzle-flapper hydraulic amplifiers [1] the jet of working fluid issuing from the nozzle acts as a force upon the flapper. The magnitude of this hydro-dynamic force (let us call it the jet reaction) is an important factor in choosing the control element for the amplifier, and in analyzing the joint operation of the control element and amplifier.

In recent years, a number of experimental and theoretical works concerned with the study of the interaction between the jet and flapper have been completed [2-4]. This paper presents a method for calculating approximately the jet reaction; it agrees well with the experimental results given in [4].

One can consider that the jet reaction is composed of three forces:

A. Force N_1, which varies with the mass flow rate of working fluid issuing from the nozzle. This component can be found from the expression

$$N_1 = m\,(V_c - V_H), \tag{1}$$

where V_c is the projection of the working fluid velocity at the point of exit from the nozzle along an axis perpendicular to the plane of the flapper, V_H is the projection of the working fluid velocity at discharge [over the area of the nozzle end-face of external radius $r_H = d_H/2$ (see figure)] along an axis perpendicular to the plane of the flapper, and $\underline{m}$ is the mass flow per second issuing from the nozzle.

Setting the velocity of the discharge equal to zero ($V_H = 0$), and assuming that

$$m = Q\rho, \quad V_c = \frac{Q}{F}, \quad F = \frac{\pi d_c^2}{4}, \tag{2}$$

where Q is the volume rate of working fluid discharged through the nozzle, ρ is the density of the working fluid, F is the sectional area of the nozzle end-face, and d_c is the nozzle diameter, we get

$$N_1 = \frac{4\rho Q^2}{\pi d_c^2}. \tag{3}$$

B. The force generated by the pressure of the working fluid on the nozzle end-face area; it equals

$$N_2 = \frac{\pi d_c^2}{4} p_c, \tag{4}$$

where p_c is the working fluid pressure at the nozzle end-face (in atmospheres, gauge).

The pressure p_c is assumed to be identical over the entire area of the nozzle end-face.

C. The force exerted by the working fluid pressure in the gap between the end of the nozzle and the flapper. This third component can be represented in the form

$$N_3 = 2\pi \int_{r_c}^{r_H} p_r r\,dr, \tag{5}$$

where $\underline{r}$ is the flow radius of the nozzle end, r_c is the nozzle radius, r_H is the external radius of the nozzle end and p_r is the working fluid pressure in gap between the nozzle end and the flapper, over a radius $\underline{r}$.

If we assume that the pressure p_r over the end-face radius varies linearly from p_c to 0, that is,

$$p_r = p_c\left(1 - \frac{r}{r_H}\right), \tag{6}$$

then we get

$$N_3 = \pi p_c\left(\frac{d_H^2 - d_c^2}{4} - \frac{d_H^3 - d_c^3}{6 d_H}\right). \tag{7}$$

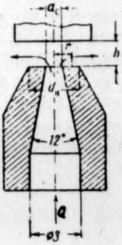

h, mm	p_1, kg/cm²	μ	N, G	N_e, G	$[N-N_e]$, G
0.15	10	0.717	96	95	1
0.20	10	0.667	101	100	1
0.25	10	0.670	109	115	6
0.15	20	0.700	191	190	1
0.20	20	0.647	200	220	20
0.20	30	0.675	303	300	3
0.25	30	0.638	321	320	1
0.15	40	0.637	375	375	—
0.20	40	0.664	400	400	—
0.25	40	0.644	429	420	9

The jet reaction, being the sum of the three components mentioned above, will equal

$$N = \frac{4\rho Q^2}{\pi d_c^2} + \frac{\pi}{6}\left(\frac{d_H^2}{2} + \frac{d_c^3}{d_H}\right) p_c. \tag{8}$$

The formula for volume discharge rate through the nozzle is

$$Q = \mu_c \frac{\pi d_c^2}{4} \sqrt{\frac{2}{\rho}(p_1 - p_c)}, \tag{9}$$

where p_1 is the pressure in the receiver, and μ_c is the inherent discharge rate factor of the nozzle (without the flapper); we find from this that

$$p_c = p_1 - \frac{8\rho Q^2}{\pi^2 d_c^4 \mu_c^2}. \tag{10}$$

In this case,

$$N = \frac{4\rho Q^2}{\pi d_c^2} + \tag{11}$$

$$+ \frac{\pi}{6}\left(\frac{d_H^2}{2} + \frac{d_c^3}{d_H}\right)\left(p_1 - \frac{8\rho Q^2}{\pi^2 d_c^4 \mu_c^2}\right).$$

If the discharge is into the atmosphere, Q can be written in the form

$$Q = \mu \pi d_c h \sqrt{\frac{2}{\rho} p_1}, \tag{12}$$

where μ is the discharge rate factor of the nozzle and flapper combined, and h is the gap between the nozzle and the flapper.

Expressions (11) and (12) enable one to find the jet reaction N, if the parameters d_c, d_H, μ_c, μ, h and p_1 are known. The supply pressure p_0 can be substituted for pressure p_1, since they are statically related.

The calculated values N of the jet reaction were compared with experimental data N_e for a nozzle of the first type with diameters $d_c = 1$ mm, and $d_H = 1.35$ mm [4], working in AMG-10 oil at a temperature of 50-55°C. Expressions (11) and (12) give

$$N = [8.03(\mu h)^2 + 0.00865]\, p_1 \tag{13}$$

for a nozzle with these dimensions, and an experimentally determined $\mu_c = 0.9$.

The values of discharge rate factor μ for the nozzle and flapper combination which were used for computing the jet reaction from formula (13) were taken from reference [5]. The calculated results and experimental data are given in the table.

A comparison of the calculated and experimental values of jet reaction given in the table shows satisfactory agreement. Hence the method being considered can be recommended as an approximate determination of the force on a flapper, if the amplifier parameters approximate those given in [4].

CONCLUSIONS

1. Computational formulas are given which permit one to calculate the approximate force on a flapper as liquid flows around it.
2. It is shown that calculated and experimentally found values of the force on a flapper agree.

LITERATURE CITED

1. I. M. Krassov, Hydraulic Amplifiers [in Russian] (Gosénergoizdat, 1959).
2. V. N. Dmitriev and A. G. Shashkov, "The effect of a jet on a flapper in pneumatic and hydraulic controlling apparatus of the 'nozzle - flapper' type," Avtomat. i Telemekh. 17, No. 6 (1956).*
3. E. A. Andreeva, "On computing the static characteristics of a 'nozzle-flapper' element," Pneumatic and Hydraulic Control Systems, Apparatus, and Elements [in Russian] (Izd. AN SSSR, 1959).
4. I. M. Krassov and B. G. Turbin, "Jet effect in a 'nozzle-flapper' hydraulic amplifier," Avtomat. i Telemekh. 20, No. 12 (1959).*
5. I. M. Krassov and B. G. Turbin, "Volume rate factors of a 'nozzle-flapper' hydraulic throttle," The Automation of Industrial Processes [in Russian] (Izd. AN SSSR, 1960) 3rd ed.

---

* See English translation.

DETERMINING THE EFFECT OF REGULAR SIGNAL DYNAMICS IN THE STATISTICAL LINEARIZATION METHOD

M. I. Gusev

Kalinin

Translated from Avtomatika i Telemekhanika, Vol. 21, No. 11,
pp. 1539-1546, November, 1960
Original article submitted May 19, 1960

The paper studies the effect of the dynamics of a deterministic function on the transfer coefficient for fluctuations when regular and random functions pass simultaneously through a nonlinearity.

1. Statement of the Problem

In analyzing the operational precision of both linear and nonlinear dynamic systems, many engineering computations treat only the first probability moments of random functions. The approximate statistical linearization theory [1, 2] which is based on these engineering requirements has made it possible to perform fruitful investigations of nonlinear systems; these investigations have exposed very interesting system properties which are both harmful and useful from the point of view of engineering practice. According to statistical linearization theory, two functions are considered statistically equivalent if they have identical first and second moments when a specified distribution law governs their arguments. Here, the first or second statistical linearization method is used to determine the transfer coefficients of a nonlinear element: K_0 is the transfer coefficient for the useful signal, and K_1 is the transfer coefficient for fluctuations.

In many engineering problems, the value of the mathematical expectation for the random perturbation varies insignificantly, whereas the useful signal varies relatively rapidly. Therefore, it is natural to consider the dynamics of the useful signal in computing the coefficients K_0 and K_1. In this regard it is of interest to study [3] which provides a method for taking into account the dynamics of the useful signal. Using this method, we derive analytical expressions which make it possible to determine how the transfer coefficient for the fluctuations is affected both by the parameters of the distribution law for the random process and by certain parameters which characterize the dynamics of the regular component.

2. Determining the Transfer Coefficient of a Nonlinear Element for Fluctuations while taking into account the Dynamics of the Regular Signal

We shall assume that the nonlinearity described by the functional relationship $v = f(v_0)$, where v_0 is the input and v is the output, is subjected to three components $v_0 = \beta + x + y$, where β is the constant component which contains the practically constant mathematical expectation of the random perturbation; x is the random component which has a zero mathematical expectation, and y is any regular signal. If K is the equivalent transfer coefficient of the nonlinear element for fluctuations, and k is the transfer coefficient for the useful signal, then the instantaneous value of the difference

$$x_d = f\,(\beta + x + y) - (Kx + ky) \qquad (1)$$

is caused by the neglect of the higher harmonics and a certain constant component λ at the output of the nonlinearity. The instantaneous value of the difference x_d is a function of x and y whose properties are characterized by the distribution laws $q(x)$ and $p(y)$ respectively. The criterion which we shall choose for selecting the optimal value of the equivalent transfer coefficient will be the minimum mean-square error for the instantaneous difference x_d. Then the problem of finding the equivalent transfer coefficient reduces to finding the minimum for the expression

$$M = \int_{-\infty}^{\infty}\int_{-\infty}^{\infty} x_d^2\, q\,(x)\, p\,(y)\, dxdy. \qquad (2)$$

With respect to the distribution function $p(y)$ we must note the following. Assume that the useful signal varies according to a sinusoidal law $y = a \sin \xi$, and that each of the possible values of y in the limits $-a$ to $+a$ corresponds to an innumerable set of values ξ:

$$\xi_k = \frac{\pi k}{\omega} + \frac{(-1)^k}{\omega} \arcsin \frac{y}{a} \qquad (k = 0,\ \pm 1,\ \pm 2\ \ldots). \qquad (3)$$

From this we treat ξ in accordance with [4] as a certain random quantity; we find

$$p(y) = \begin{cases} \dfrac{1}{\omega a\sqrt{1-\left(\frac{y}{a}\right)^2}} \displaystyle\sum_{k=-\infty}^{\infty} \omega\left[\frac{\pi k}{\omega} + \frac{(-1)^k}{\omega} \arcsin \frac{y}{a}\right], & |y| < a, \\ 0 & |y| > a. \end{cases} \tag{4}$$

Assume now that the quantity ξ is uniformly distributed over the interval $-\pi \leq \xi \leq +\pi$; then in the infinite sum (4) only two terms corresponding to $k = 0$ and $k = 1$ will be nonzero. Then $p(y)$ can be written in simpler form:

$$p(y) = \begin{cases} \dfrac{1}{\pi a\sqrt{1-\left(\frac{y}{a}\right)^2}}, & |y| < a, \\ 0, & |y| > a. \end{cases} \tag{5}$$

In this case the distribution function $p(y)$ will characterize the dynamic properties of the regular signal y which is studied jointly with the random process x that is characterized by its distribution function; thus $p(y)$ will, so to speak, itself become random, since the phase of the regular signal is actually distributed uniformly over the interval $-\pi \leq \xi \leq +\pi$ when this signal is treated jointly with the random signal.

Taking the above into account and performing the minimization of expression (2) with respect to K, we obtain the following result after simple computations if we assume that the random signal is distributed normally:

$$K = \frac{1}{\overline{x^2}} \int_{-\infty}^{\infty}\int_{-\infty}^{\infty} xf(\beta + x + y)\, q(x)\, p(y)\, dx dy, \tag{6}$$

where $\overline{x^2}$ is the mean-square value of the input signal x.

For the purposes of further computation we shall modify the expression for K somewhat. Assume that a constant component γ acts at the input of the nonlinear element instead of the random signal x; then the constant component of the output signal is written as

$$g(\gamma) = \int_{-\infty}^{\infty} f(\gamma + \beta + y)\, p(y)\, dy. \tag{7}$$

Now expression (7) shall be treated as a certain fictitious nonlinearity whose input is subjected to the random signal x; then,

$$K_x = \frac{1}{\overline{x^2}} \int_{-\infty}^{\infty} xg(x)\, q(x)\, dx. \tag{8}$$

Substituting Eq. (8) into Eq. (7), we obtain an expression for the equivalent transfer coefficient which coincides with (6). Such a treatment permits us not only to simplify the analytical computations but also experimentally to determine the fictitious nonlinearities by studying the effect of the regular signal on the original nonlinearity. It is convenient to perform the analytical computation of the fictitious nonlinearities and the equivalent transfer coefficients K_x by representing the nonlinearities in terms of "choppers" [5]; the expression for the nonlinearities are shown in Table 1. The results obtained by computing the fictitious nonlinearities and the values of K_x are cited in Table 2. Figure 1 shows the normalized transfer coefficients K_{x_1} and K_{x_3} for fluctuations in the cases of a relay element and an element with "negative overlaps" (cf. third characteristic from top in Table 1) when a constant component, noise and a sinusoidal signal act on these elements. The graph shows the strong effect of the normalized regular signal proper and the constant component normalized to the amplitude of the regular signal; the constant component shifts the value of the transfer coefficient into the negative region for $\eta = 1$ and $\zeta \approx 1{,}2$.

For a relay element with a dead band that is subjected to the same three components the transfer coefficient K_{x_2} also passes into the negative region (Fig. 2). Figure 3 shows the values of the transfer coefficient K_{x_4} for fluctuations in the case of a linear element with a dead band; Fig. 4 shows the transfer coefficient K_{x_5} for fluctuations in the case of a limiter that is subjected to a constant component, a sinusoidal signal, and noise with a Gaussian distribution. From the figures the strong effect of the dynamics of the regular component on the equivalent transfer coefficient is evident.

3. On the Possibility of Generalizing the Effect of the Dynamics of an Arbitrary Signal on the Transfer Coefficient for Fluctuations

In closed-loop control systems the form of the processes can be described with sufficient accuracy by the expression $y = Ce^{-ax} \sin \Omega x$. In order to estimate the effect of a signal having such a form we expand this expression into a Fourier series:

Table 1. Analytical Expression for Inertialess Nonlinearities

Shape of the characteristic	Mathematical expression in terms of "choppers"
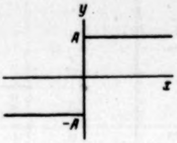	$y = A\frac{\lvert x\rvert}{x}$
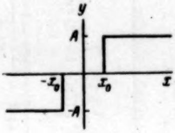	$y = \frac{1}{2}A\left[\frac{\lvert x+x_0\rvert}{x+x_0} + \frac{\lvert x-x_0\rvert}{x-x_0}\right]$
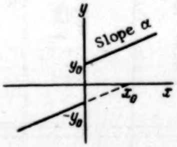	$y = \alpha\left(x + x_0\frac{\lvert x\rvert}{x}\right)$
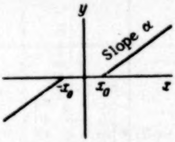	$y = \alpha\left[x - \frac{1}{2}\lvert x+x_0\rvert + \frac{1}{2}\lvert x-x_0\rvert\right]$
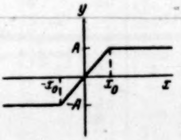	$y = \frac{1}{4}\Big\{2\alpha x + \lvert\alpha x + A\rvert - \lvert\alpha x - A\rvert +$ $+ (2A - \lvert\alpha x + A\rvert - \lvert\alpha x - A\rvert)\frac{\lvert x\rvert}{x}\Big\}$

$$y = \frac{a_0}{2} + a_1\cos\omega x + \ldots + a_n\cos n\omega x + b_1\sin\omega x + \ldots + b_n\sin n\omega x,$$

where

$$\begin{aligned} a_k = \frac{C}{T}\Bigg\{&\frac{\Omega - k\omega}{\alpha^2 + (\Omega - k\omega)^2} + \frac{\Omega + k\omega}{\alpha^2 + (\Omega + k\omega)^2} - \\ &- \frac{e^{-\alpha T}[\alpha\sin(\Omega - k\omega)T + (\Omega - k\omega)\cos(\Omega - k\omega)T]}{\alpha^2 + (\Omega - k\omega)^2} - \\ &- \frac{e^{-\alpha T}[\alpha\sin(\Omega + k\omega)T + (\Omega + k\omega)\cos(\Omega + k\omega)T]}{\alpha^2 + (\Omega + k\omega)^2}\Bigg\} \end{aligned}$$

$$\begin{aligned} b_k = \frac{C}{T}\Bigg\{&\frac{\alpha}{\alpha^2 + (\Omega - k\omega)^2} + \frac{\alpha}{\alpha^2 + (\Omega + k\omega)^2} + \\ &+ \frac{e^{-\alpha T}[(\Omega - k\omega)\sin(\Omega - k\omega)T - \alpha\cos(\Omega - k\omega)T]}{\alpha^2 + (\Omega - k\omega)^2} + \\ &+ \frac{e^{-\alpha T}[(\Omega + k\omega)\sin(\Omega + k\omega)T - \alpha\cos(\Omega + k\omega)T]}{\alpha^2 + (\Omega + k\omega)^2}\Bigg\}. \end{aligned}$$

Table 2. Values of the Effective Nonlinear Characteristic and the Effective Transfer Coefficient

Shape of the characteristic	$g(\gamma)$	K_x
Relay element	$\frac{2A}{\pi}\arcsin\frac{\gamma+\beta}{a}$	$\frac{4\zeta^2\xi}{\sqrt{2\pi^3}}\int\limits_0^1(2x-1-\eta)\arcsin(2x-1)e^{\frac{-\zeta^2(2x-1-\eta)^2}{2}}dx$
Relay element with dead band $V=\frac{x_0}{a}$	$\frac{A}{\pi}\left(\arcsin\frac{\gamma+\beta+x_0}{a}+\arcsin\frac{\gamma-\beta-x_0}{a}\right)$	$\frac{2\zeta^2\xi}{\sqrt{2\pi^3}}\left\{\int\limits_0^1(2x-1-\eta-V)\arcsin(2x-1)\times\right.$ $\times\exp\left[\frac{-\zeta^2(2x-1-\eta-V)^2}{2}\right]dx+\int\limits_0^1(2x-1-\eta+V)\times$ $\left.\times\arcsin(2x-1)\exp\left[\frac{-\zeta^2(2x-1-\eta+V)^2}{2}\right]dx\right\}$
Element with "negative overlaps"	$\alpha(\gamma+\beta)+\frac{2ax_0}{\pi}\arcsin\frac{\gamma+\beta}{a}$	$\alpha\left\{1+\frac{4\zeta^2\xi}{\sqrt{2\pi^3}}V\int\limits_0^1(2x-1-\eta)\arcsin(2x-1)\times\right.$ $\left.\times\exp\left[-\frac{\zeta^2(2x-1-\eta)^2}{2}\right]dx\right\}$

Table 2 (cont'd)

Shape of the characteristic	$g(\gamma)$	K_x
Linear element with dead band $V = \frac{x_0}{a}$	$\alpha(\gamma+\beta) - \frac{\alpha x_0}{\pi}\left(\arcsin\frac{\gamma+\beta+x_0}{2} + \arcsin\frac{\gamma+\beta-x_0}{a}\right) -$ $-\frac{1}{2}\left[\frac{2\alpha(\gamma+\beta)}{\pi}\arcsin\frac{\gamma+\beta+x_0}{a} +\right.$ $\left. + \frac{2\alpha a}{\pi}\sqrt{1-\left(\frac{\gamma+\beta+x_0}{a}\right)^2}\right] +$ $+\frac{1}{2}\left[\frac{2\alpha(\gamma+\beta)}{\pi}\arcsin\frac{\gamma+\beta-x_0}{a} +\right.$ $\left. + \frac{2\alpha a}{\pi}\sqrt{1-\left(\frac{\gamma+\beta-x_0}{a}\right)^2}\right]$	$\alpha\left\{-1 - \frac{2\zeta^3}{\sqrt{2\pi^3}}\int_0^1 (2x-1-\eta-V)(2x-1) \times\right.$ $\times \arcsin(2x-1)\exp\left[-\frac{\zeta^2}{2}(2x-1-\eta-V)^2\right]dx -$ $-\frac{2\zeta^3}{\sqrt{2\pi^3}}\int_0^1 (2x-1)(2x-1-\eta+V) \times$ $\times \arcsin(2x-1)\exp\left[\frac{-\zeta^2(2x-1-\eta+V)^2}{2}\right]dx +$ $+\frac{2\zeta^3}{\sqrt{2\pi^3}}\int_0^1 \sqrt{1-(2x-1)^2}\left[(2x-1-\eta+V) \times\right.$ $\times \exp\left[-\frac{\zeta^2}{2}(2x-1-\eta+V)^2\right] - (2x-1-\eta-V) \times$ $\left.\left. \times \exp\left[-\frac{\zeta^2}{2}(2x-1-\eta-V)^2\right]\right]dx\right\}$
Limiter $V = \frac{x_0}{a}$	$\alpha(\gamma+\beta) + \frac{\alpha}{2\pi}(\gamma+\beta+x_0)\arcsin\frac{\gamma+\beta+x_0}{a} +$ $+\frac{a\alpha}{2\pi}\sqrt{1-\left(\frac{\gamma+\beta+x_0}{a}\right)^2} - \frac{\alpha}{2\pi}(\gamma+\beta-x_0) \times$ $\times \arcsin\frac{\gamma+\beta-x_0}{a} - \frac{a\alpha}{2\pi}\sqrt{1-\left(\frac{\gamma+\beta-x_0}{a}\right)^2} +$	$\alpha\left\{\frac{1}{2} + \frac{1}{\sqrt{2\pi^3}}\zeta^3\int_0^1 (2x-1-\eta-V) \times\right.$ $\times \left[(2x-1)\arcsin(2x-1) + \sqrt{1-(2x-1)^2}\right] \times$ $\times \exp\left[-\frac{\zeta^2}{2}(2x-1-\eta-V)^2\right]dx - \frac{1}{\sqrt{2\pi^3}}\zeta^3\int_0^1 (2x-1-\eta+V) \times$

Table 2 (cont'd)

Shape of the characteristic	$g(\gamma)$	K_x
	$+\frac{A}{\pi}\arcsin\frac{\gamma+\beta}{a}+\frac{a}{2}\Bigl[\frac{\gamma+\beta+x_0}{\pi}\arcsin\frac{\gamma+\beta+x_0}{a}-$ $-\frac{\gamma+\beta+x_0}{2}\pi+\frac{a}{\pi}\sqrt{1-\left(\frac{\gamma+\beta+x_0}{a}\right)^2}-$ $-\frac{\gamma+\beta+x_0}{\pi}\arcsin\frac{\gamma+\beta}{a}+\frac{a}{\pi}\sqrt{1-\left(\frac{\gamma+\beta}{a}\right)^2}+$ $+\frac{a}{2\pi}\Bigl[(\gamma+\beta-x_0)\arcsin\frac{\gamma-\beta}{a}-\frac{\gamma+\beta-x_0}{2}\pi+$ $+a\sqrt{1-\left(\frac{\gamma+\beta}{a}\right)^2}-a\sqrt{1-\left(\frac{\gamma+\beta-x_0}{a}\right)^2}-$ $-(\gamma+\beta-x_0)\arcsin\left(\frac{\gamma+\beta-x_0}{a}\right)\Bigr]$	$\times\left[(2x-1)\arcsin(2x-1)+\sqrt{1-(2x-1)^2}\right]\times$ $\times\exp\Bigl[-\frac{\zeta^2}{2}(2x-1-\eta+V)^2\;dx+\frac{2}{\sqrt{2\pi^3}}\zeta^3V\times$ $\times\int_0^1(2x-1-\eta-V)\Bigl[(2x-1)\arcsin(2x-1)-\frac{2x-1}{2}\pi+$ $+\sqrt{1-(2x-1)^2}-\sqrt{1-(2x-1-V)^2}-$ $-(2x-1)\arcsin(2x-1-V)\Bigr]\times$ $\times\exp\left[-\frac{1}{2}\zeta^2(2x-1-\eta-V)^2\right]dx+\frac{1}{\sqrt{2\pi^3}}\zeta^3\int_0^1(2x-1-\eta)\times$ $\times\Bigl[(2x-1-V)\arcsin(2x-1)-\frac{(2x-1-V)}{2}\pi+$ $+\sqrt{1-(2x-1)^2}-\sqrt{1-(2x-1-V)^2}-$ $-(2x-1-V)\arcsin(2x-1-V)\Bigr]\times$ $\times\exp\left[-\frac{1}{2}\zeta^2(2x-1-\eta)^2\right]dx\Bigr\}$

Note: For simplicity in performing the computations we have introduced the following substitutions in the table and in the graphs: $\xi = A/\sigma$: $\zeta = a/\sigma$; $\eta = \beta/a$; $V = x_0/a$

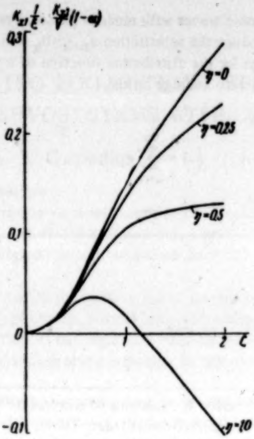

Fig. 1.

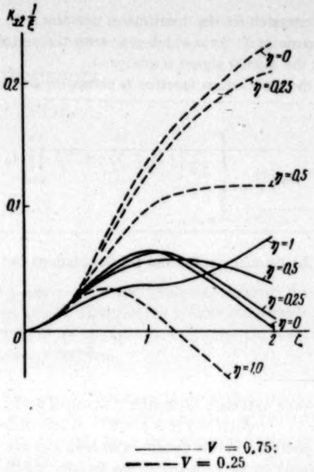

Fig. 2.

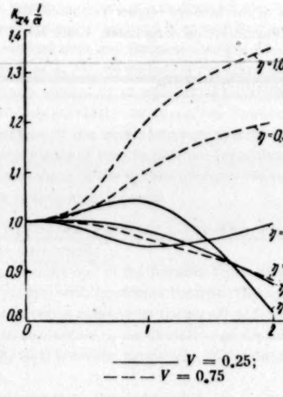

Fig. 3.

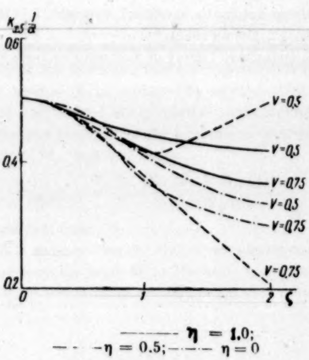

Fig. 4.

The expression for the coefficients contains still another parameter $T = 2\pi\omega$ which represents the period over which the regular signal is analyzed.

In [4] the distribution function is computed for the sum of harmonic waves with random phases. For our case we introduce the substitution $a_{n+k} = b_k$ and obtain the expression for the distribution function of a regular signal with a zero average value:

$$W_{12n}(x) = \begin{cases} \frac{1}{2A}\left[1 + 2\sum_{r=1}^{\infty} \cos\frac{\pi r x}{A} \prod_{k=1}^{2n} I_0\left(\frac{a_k \pi r}{A}\right)\right], & |x| < A, \quad \left(A = \sum_{k=1}^{2n} a_k\right). \\ 0 & |x| > A, \end{cases}$$

Then the transfer coefficient for fluctuations can be written as

$$K_x = \frac{1}{\bar{x}^2} \int_{-\infty}^{\infty} \int_{-\infty}^{\infty} x f\left(x + \frac{a_0}{2} + \beta + y\right) p(x) W_{12n}(y)\, dx dy.$$

Thus when necessary (although it involves great difficulties in computation) it is possible to determine the effect produced by the dynamics of such a rather complex signal on the behavior of the transfer coefficients for fluctuations.

In conclusion it is necessary to note the substantial effect produced by the constant signal and the dynamics of the regular signal on the behavior of the transfer coefficient for fluctuations; this underscores the necessity of exercising great care when using statistical linearization methods.

LITERATURE CITED

1. I. E. Kazakov, "Approximate probability analysis of the operational precision of essentially nonlinear automatic systems," Avtomat. i Telemekh. 17, No. 5 (1956).*
2. V. S. Pugachev, Theory of Random Functions and its Application to Problems in Automatic Control [in Russian] (Gostekhizdat, 1957).
3. M. I. Somerville and D. P. Atherton, "Multigain representation for a single-valued nonlinearity with several inputs, and the evaluation of their equivalent gains by cursor method," Proc. IEE, Part C, No. 8 (1958).
4. B. R. Levin, Theory of Random Processes and Its Application in Radio-Engineering [in Russian] (Izd. Sovetskoe Radio, 1957).
5. L. L. Ivanov, On the Solution of a Problem with Functions That Have Discontinuous Derivatives or Discontinuities, Collection of Scientific Papers of the Moscow Higher Technical School [in Russian] (Gosénergoizdat, 1958) No. 87.

---

* See English translation.

PLOTTING LOGARITHMIC FREQUENCY RESPONSES FOR SERVOSYSTEMS WITH COMBINED CONTROL

A. I. Guzenko

Moscow

Translated from Avtomatika i Telemekhanika, Vol. 21, No. 11,
pp. 1547-1553, November, 1960
Original article submitted April 21, 1960

The paper studies the substitution of an equivalent servosystem for a servosystem with combined control; the equivalent system has control only with respect to deviation, and its transfer function has a form convenient for application of the logarithm frequency response method. Nomograms are cited which facilitate the plotting of logarithmic frequency responses for the elements in the equivalent servosystem.

A substantial improvement in the dynamic properties of automatic control systems is possible when combined control methods are used; in such methods control relative to the basic perturbations acting on the system is combined with control relative to deviation [1-5].

In [6] the possibility of computing servosystems with combined control by the logarithmic frequency response method was demonstrated. This paper developed a convenient method for plotting the logarithmic frequency responses for a servosystem with combined control while taking the perturbation signal into account only in the low-frequency region.

In this paper we develop a method for plotting the logarithmic frequency responses of servosystems with combined control over any frequency range. This method is based, as in [6], on replacing the servosystem with combined control by an equivalent servosystem with control solely relative to deviation. However, the transfer function of the equivalent servosystem is given a form which makes it easy to plot the logarithmic frequency responses of the system over any frequency range when nomograms are used.

1. The Transfer Function for the Equivalent Servosystem

Figure 1 shows one of the possible block diagrams for a servosystem with combined control. This system incorporates control relative to the signal g(t) in addition to control relative to the deviation of the controlled quantity x(t) from the magnitude of the control signal g(t).

To establish the relationship of the quantities $\epsilon(t)$, y(t), and x(t) in the system to the signal g(t), the transforms of the differential equations can be written in the following form:

$$\begin{aligned} \varepsilon(p) &= g(p) - x(p), \\ y(p) &= \varepsilon(p) W_1(p) + g(p) W_g(p), \\ x(p) &= y(p) W_2(p). \end{aligned} \qquad (1)$$

The transfer functions of the system for the error $\epsilon(p)$ and for the controlled quantity x(p) relative to the signal g(t) are given by the following expressions on the basis of (1):

$$\begin{aligned} \Phi_{\varepsilon.g}(p) &= \frac{1 - W_2(p) W_g(p)}{1 + W_1(p) W_2(p)}, \\ \Phi_{x.g}(p) &= \frac{W_2(p)[W_1(p) + W_g(p)]}{1 + W_1(p) W_2(p)}. \end{aligned} \qquad (2)$$

Formulas (2) can be written as

$$\begin{aligned} \Phi_{\varepsilon.g}(p) &= \left[1 + \frac{W_2(p)[W_1(p) + W_g(p)]}{1 - W_2(p) W_g(p)}\right]^{-1}, \\ \Phi_{x.g}(p) &= \frac{W_2(p)[W_1(p) + W_g(p)]}{1 - W_2(p) W_g(p)} \times \\ &\times \left[1 + \frac{W_2(p)[W_1(p) + W_g(p)]}{1 - W_2(p) W_g(p)}\right]^{-1}. \end{aligned} \qquad (3)$$

From this it follows that a servosystem with combined control can be replaced by an equivalent servosystem with control solely relative to the deviation. The transfer function for the equivalent open-loop servosystem, $W_{\text{eq.}}(p)$, is equal to

$$W_{\text{eq.}}(p) = \frac{W_2(p)[W_1(p) + W_g(p)]}{1 - W_2(p) W_g(p)}, \qquad (4)$$

as is evident from (3).

It is evident that the equivalent servosystem is formed from the same basic elements $W_1(p)$, $W_2(p)$, and $W_g(p)$ which make up the system with combined

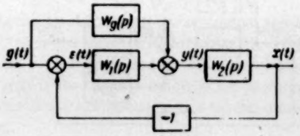

Fig. 1

control. The element $W_g(t)$ in the combined system which performs control relative to the signal forms a direct positive coupling circuit with the element $W_1(p)$, and forms a positive feedback loop with the element $W_2(p)$. Figure 2 shows the block diagram obtained in accordance with (4) for a servosystem with combined control that is equivalent to the block diagram in Fig. 1.

The transfer function of the equivalent servosystem (4) can be written differently:

$$W_{eq.}(p) = \frac{W_2(p)\,W_g(p)}{1 - W_2(p)\,W_g(p)}\left[1 + \frac{W_1(p)}{W_g(p)}\right]. \qquad (5)$$

This amounts to representing the equivalent servosystem in the form of a serial connection of the element with the transfer function $W_1(p)/W_g(p)$ that is connected by positive direct unity coupling, and the element with the transfer function $W_2(p)\,W_g(p)$ that is connected by unity positive feedback. The block diagram of the equivalent servosystem (5) is shown in Fig. 3.

We denote the transfer function of elements with positive direct unity coupling by $F_{1\,dir.}(p)$ and the transfer function of elements with unity positive feedback by $F_{1fb}(p)$; i.e., we write

$$F_{1dir.}(p) = 1 + \frac{W_1(p)}{W_g(p)}, \qquad F_{1fb}(p) = \frac{W_2(p)\,W_g(p)}{1 - W_2(p)\,W_g(p)}. \qquad (6)$$

Then

$$W_{eq.}(p) = F_{1dir}(p)\,F_{1fb}(p). \qquad (7)$$

From the above it is evident that the systems in Fig. 1 and Fig. 3 are dynamically equivalent. The subsequent analysis therefore consists of studying the dynamic properties of the system (7). For this purpose it is necessary to plot the frequency response of the system in Fig. 3 for open-loop conditions after first plotting the frequency response of the elements with transfer functions of the form

$$F_{1dir.}(p) = 1 + W(p), \qquad F_{1fb}(p) = \frac{W(p)}{1 - W(p)}. \qquad (8)$$

2. Plotting the Logarithmic Frequency Responses for an Element with the Transfer Function $F_{dir.} = W'(p) + W''(p)$

We shall study the more general problem of plotting logarithmic frequency responses for an element with the transfer function

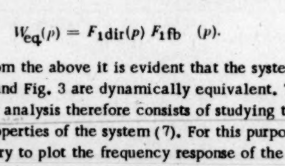

Fig. 2

$$F_{dir.}(p) = W'(p) + W''(p). \qquad (9)$$

To do this the amplitude-phase characteristics for elements with transfer functions $W'(p)$ and $W''(p)$ are written as

$$W'(j\omega) = H'(\omega)\,e^{j\theta'(\omega)}, \qquad W''(j\omega) = H''(\omega)\,e^{j\theta''(\omega)}. \qquad (10)$$

Therefore

$$W(j\omega) = H(\omega)\,e^{j\theta(\omega)} = H'(\omega)\,e^{j\theta'(\omega)} + H''(\omega)\,e^{j\theta''(\omega)}, \qquad (11)$$

where $W(j\omega) = F_{dir.}(j\omega)$, or

$$\frac{H(\omega)}{H'(\omega)}\,e^{j[\theta(\omega)-\theta'(\omega)]} = 1 + \frac{H''(\omega)}{H'(\omega)}\cos[\theta''(\omega) - \theta'(\omega)] + j\,\frac{H''(\omega)}{H'(\omega)}\sin[\theta''(\omega) - \theta'(\omega)]. \qquad (12)$$

Equation (12) makes it possible to use the known $[H''(\omega) - H'(\omega)]$db and $[\theta''(\omega) - \theta'(\omega)]^\circ$ to plot the nomograms for the geometric loci of the amplitudes $(H - H')$db and phases $[\theta(\omega) - \theta'(\omega)]^\circ$; these, in turn, are used to plot the logarithmic amplitude (H, db) and phase (θ°) responses for the element with the transfer function (9).

In [7] we plotted the nomograms for the geometric loci of the values for the amplitude $A(\omega)$ and phase $\varphi(\omega)$ characteristics for a closed-loop system:

$$\Phi(j\omega) = A(\omega)\,e^{j\varphi(\omega)} \qquad (13)$$

from the values of the amplitude $H_{ol}(\omega)$ and phase $\theta_{ol}(\omega)$ characteristics of the open-loop system (Fig. 4):

$$W_{ol}(j\omega) = H_{ol}(\omega)\,e^{j\theta_{ol}(\omega)} \qquad (14)$$

The relationship between the amplitude-phase responses of the closed-loop $\Phi(j\omega)$ and open-loop $W_{ol}(j\omega)$ systems:

$$\Phi(j\omega) = \frac{W_{ol}(j\omega)}{1 + W_{ol}(j\omega)} \qquad (15)$$

can be written as

$$\frac{1}{A(\omega)}\,e^{j\varphi(\omega)} = 1 + \frac{1}{H_{ol}(\omega)}\cos\theta_{ol}(\omega) - j\,\frac{1}{H_{ol}(\omega)}\sin\theta_{ol}(\omega) \qquad (16)$$

on the basis of (13) and (14).

Comparing Eq. (12) with Eq. (16), we find that for the condition

$$\begin{aligned} [H(\omega) - H'(\omega)]\,\text{db} &= -A(\omega)\,\text{db}, \\ \pm[\theta(\omega) - \theta'(\omega)]^\circ &= \mp\varphi(\omega)^\circ, \\ [H''(\omega) - H'(\omega)]\,\text{db} &= -(H_{ol})\,\text{db}, \\ \pm[\theta''(\omega) - \theta'(\omega)]^\circ &= \mp\theta_{ol}(\omega)^\circ \end{aligned} \qquad (17)$$

the nomograms plotted for determining the values of the amplitude and phase responses of the closed-loop

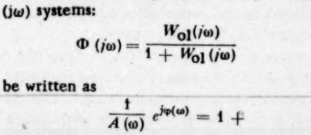

Fig. 3

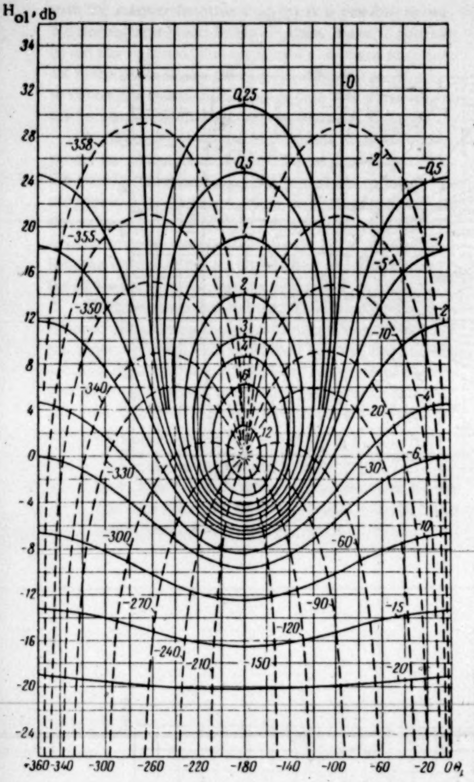

Fig. 4

system from the values of the amplitude and phase responses of the open-loop system can be used for determining the amplitude difference (H'' – H') db and the phase difference (θ – θ')°.

Figure 5 shows the nomograms for the geometric loci used to determine the difference between the values of the amplitude (H – H') db and phase (θ – θ')° characteristics for the elements with the amplitude-phase responses W(jω) and W'(jω) from the difference between the values of the amplitude (H'' – H') db and phase (θ'' – θ')° characteristics for the elements with the amplitude-phase responses W''(jω) and W'(jω); this is done on the basis of the nomogram in Fig. 4 and conditions (17). If, as is the case in the example under study, W'(jω) = 1 (i.e., H'(ω) = 0 db and θ'(ω) = 0°), then Eq. (17) is written as

$$H(\omega) = -A(\omega), \quad \pm\theta(\omega) = \mp\varphi(\omega), \qquad (18)$$
$$H''(\omega) = -H_{ol}(\omega), \quad \pm\theta''(\omega) = \mp\theta_{ol}(\omega);$$

i.e., the nomogram shown in Fig. 5 makes it possible immediately to determine the amplitude-frequency and phase-frequency responses for the system element that is connected by direct positive unity coupling.

3. Plotting the Logarithmic Frequency Responses for an Element with the Transfer Function $F_{1fb}(p) = W(p)/[1-W(p)]$

Assuming $F_{1fb}(j\omega) = B(\omega)e^{j\beta(\omega)}$,

$$W(j\omega) = H(j\omega)e^{j\theta(\omega)}, \qquad (19)$$

and the amplitude-phase response of the element with the transfer function $F_{1fb}(p) = W(p)/[1 + W(p)]$ is

$$\frac{1}{B(\omega)}e^{j\beta(\omega)} = -1 + \qquad (20)$$
$$+\frac{1}{H(\omega)}\cos\theta(\omega) - j\frac{1}{H(\omega)}\sin\theta(\omega).$$

Equation (20) makes it possible to plot the nomograms for the geometric loci of the amplitude (B, db) and phase (β°) from known H, db, and θ°; then it is possible to plot the logarithmic amplitude and phase responses for the element with the transfer function $F_{1fb}(p) = W(p)/[1 + W(p)]$.

Comparing Eq. (16) and Eq. (20), we verify the fact that for the conditions

$$B(\omega) = A(\omega), \quad \beta^\circ = (180 + \varphi)^\circ \qquad (21)$$
$$H(\omega) = H_{ol}(\omega), \quad \theta^\circ = (180 + \theta_{ol})^\circ$$

the nomograms plotted from Eq. (16) and (20) are identical.

On the basis of the nomogram in Fig. 4 and conditions (21) Figure 6 shows the nomograms for the geometric loci of the values for the amplitude (B, db) and phase (β°) responses of the element with the amplitude-phase response $F_{1fb}(j\omega)$ as a function of the values for the amplitude (H, db) and phase (θ°) responses of the element with the amplitude-phase response W(jω).

Conclusions

1. In order to plot the logarithmic frequency responses of a servosystem with combined control that is achieved by introducing coupling relative to the control signal (Fig. 1), the block diagram of the equivalent servosystem with control only with respect to deviation must be represented as shown in Fig. 3. In that case the transfer function of the equivalent open-loop servosystem is

$$W_{eq}(p) = F_{1dir.}(p)\,F_{1fb}(p),$$

where

$$F_{1dir.}(p) = 1 + \frac{W_1(p)}{W_g(p)},$$

$$F_{1fb}(p) = \frac{W_2(p)\,W_g(p)}{1 - W_2(p)\,W_g(p)}.$$

$W_g(p)$ is the transfer function for control signal coupling; $W_1(p)$ is the transfer function for the servosystem elements encompassed by the control-signal coupling; $W_2(p)$ is the transfer function for servosystem elements which are not encompassed by the control-signal coupling.

2. In order to plot the logarithmic frequency responses for the elements of an equivalent servosystem

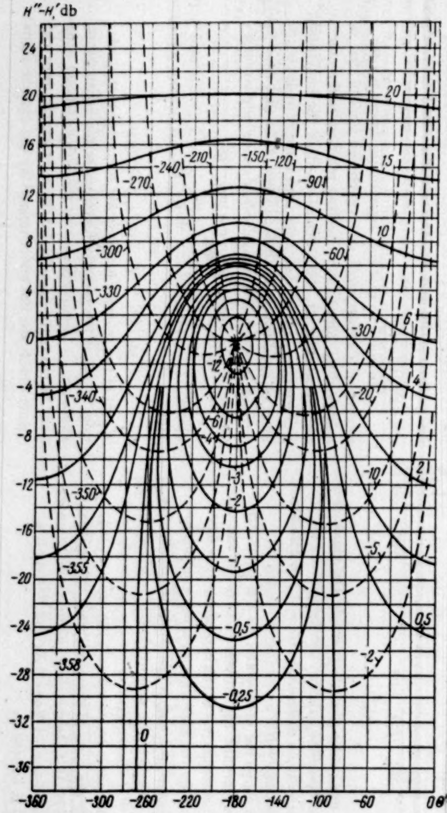
H''-H,' db
24
20
16
12
8
4
0
-4
-8
-12
-16
-20
-24
-28
-32
-36
-360
-300
-260
-220
-180
-140
-100
-60
0 θ''-θ'
20
15
10
6
4
2
1
0.5
-210
-150
-120
-240
-270
-90
-60
-300
-330
-30
-340
-20
-12
-6
-4
-3
-2
-1
-0.5
-0.25
-10
-350
-5
-355
-2
-358
0

Fig. 5

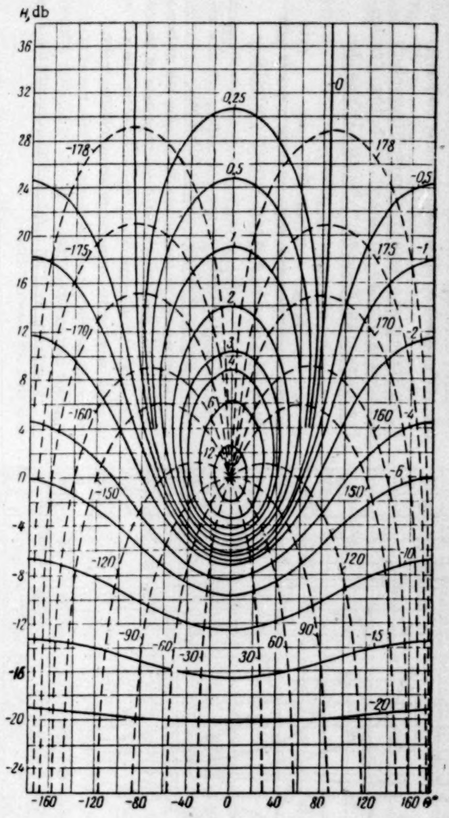
H, db
36
32
28
24
20
16
12
8
4
0
-4
-8
-12
-16
-20
-24
-160
-120
-80
-40
0
40
80
120
160 θ°
0
0.25
0.5
1
2
3
4
6
12
-178
178
-0.5
-175
175
-1
-170
170
-2
-160
160
-4
-150
150
-6
-120
120
-10
-90
-60
-30
30
60
90
-15
-20

Fig. 6

with the transfer function $F_{1dir}(p)$ it is possible to use the nomograms given in Fig. 5; these make it possible to use the values of the amplitude and phase responses for elements with the transfer function $W_1(p)/W_g(p)$ to obtain the values of the amplitude and phase responses for elements with the transfer function $F_{1dir}(p)$.

3. In order to plot the logarithmic frequency responses for elements of the equivalent servosystem with the transfer function $F_{1fb}(p)$ it is possible to use the nomograms shown in Fig. 6; these make it possible to use the values of the amplitude and phase responses for elements with the transfer function $W_2(p)W_g(p)$ to obtain the values of the amplitude and phase responses for elements with the transfer function $F_{1fb}(p)$.

4. The nomograms in Figs. 5 and 6 can be used not only for plotting the logarithmic frequency responses of servosystems with combined control, but also for plotting the logarithmic frequency responses of elements forming a circuit with direct positive coupling (the nomograms in Fig. 5) and with positive feedback (the nomograms in Fig. 6).

LITERATURE CITED

1. V. S. Kulebakin, "On the applicability of the invariance principle in real physical systems," Doklady Akad. Nauk SSSR 60, No. 2 (1948).
2. G. M. Ulanov, "Automatic control systems and servosystems which operate on open-loop and closed-loop cycles; the invariance principle," Doklady Akad. Nauk SSSR 96, No. 5 (1954).
3. V. S. Kulebakin, On Basic Problems and Methods in Improving the Performance of Automatic Control Systems, Transactions of the Second All-Union Conference on Automatic Control Theory [in Russian] (Izd. AN SSSR, 1953).
4. B. N. Petrov and G. M. Ulanov, Problems in the Theory of Combined Control, Scientific-Engineering Problems of Automatic Electric Drives [in Russian] (Izd. AN SSSR, 1957).
5. A. G. Ivakhnenko, "On methods for eliminating the steady-state error component in automatic control systems," Doklady Akad. Nauk SSSR 77, No. 6 (1952).
6. V. A. Besekerskii and S. M. Fedorov, Design of Combined-Control Servosystems Using the Method of Logarithmic Frequency Responses, Scientific-Engineering Information on Instrumentation [in Russian] (1957) No. 4.
7. G. Chestnat and R. Maier, Design and Computation of Servosystems and Control Systems [in Russian] (Gosenergoizdat, 1959) Part I.

ON SYNTHESIZING CONTROL PROGRAMS IN SYSTEMS THAT INCLUDE A DIGITAL COMPUTER

P. F. Klubnikin

Moscow

Translated from Avtomatika i Telemekhanika, Vol. 21, No. 11,
pp. 1554-1559, November, 1960
Original article submitted May 23, 1960

The paper studies the use of the specified transfer function of the closed-loop system to synthesize the control program of a digital machine which operates in the closed-loop of an automatic control system.

At present automatic control systems which include a digital machine (DM) are widely used in industry. Such systems have a number of advantages over conventional systems [1]; in particular, they make it possible to design control systems with new properties, such as the selection of the optimum mode of operation, the ability to operate in self-adaptive fashion, etc. Moreover, systems including DM have a number of features which require special synthesis methods.

By treating DM as a special kind of pulse element it is possible to use the Ya. Z. Tsypkin theory of pulse systems [2] in order to compute systems that include DM. However, the problems of synthesizing a control program while taking into account the realization of that program in the DM have as yet been treated only cursorily in literature.

Experience in applying DM to automatic control systems shows that in realizing the control program the program volume (in the sense of the number of arithmetic operations and "memory" cells in the machine) is of great significance. This fact must certainly be taken into account for synthesis.

Another important problem in synthesizing the control program is the program stability. Notwithstanding the fact that the stability requirement for the control program in a DM operating in the closed loop of a system has not been considered mandatory by certain authors, experiment shows that an unstable control program is inadequate.

This paper studies the problem of synthesizing the control program for specified performance of the closed-loop system while taking into account the program realization features indicated above.

Synthesis of the Control Program

We shall study the synthesis of the control program for a system whose block diagram is shown in Fig. 1. The devices for conversion of analog quantities to digital quantities and vice versa are referred to the controlled object in the closed loop.

Assume the object is characterized by the transfer function (in the sense of a Laplace transform)

$$W_H(p) = \frac{N(p)}{M(p)},$$

where N(p) and M(p) are polynomials, $M(p) = 0$ may have one zero root*, and the degree of N(p) is lower than the degree of M(p).

Assuming that the DM computes the control signal during a time $T = \text{const}$ (T is the time required for computation cycle) and assuming that a mandatory condition is the presence of a converter at the output of the DM fixing the output quantity of the DM over the time required for the cycle, we obtain

$$W_H^*(p) = \sum_{\nu=1}^{k} C_\nu \frac{e^{-Tp}}{e^{-Tp_\nu} - e^{-Tp}}, \qquad (1)$$

where

$$C_\nu = \frac{N(Tp_\nu)(1 - e^{Tp_\nu})}{M'(Tp_\nu)\,Tp_\nu}, \qquad M'(p) = \frac{d}{dp} M(p).$$

In accordance with [3] we use the substitution $e^{-Tp} = z$ and write the transformation (1) as

$$W_H^*(z) = \frac{a_k z^k + a_{k-1} z^{k-1} + \ldots + a_1 z}{b_k z^k + b_{k-1} z^{k-1} + \ldots + b_1 z + b_0}, \qquad (2)$$

where a_j and b_j are coefficients that depend on C_ν and $d_\nu = e^{-Tp_\nu}$.

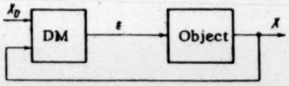

Fig. 1

---

* This is the case which is most often encountered in practice.

Note that (in contrast to the well-known z transform tables) expression (2) takes into account the fixing of the DM output (i.e., it takes into account the term $(1 - e^{-Tp})/p$); therefore the use of (2) simplifies the computations which are required for synthesis of the control program.

Note that the zeros and poles of the rational fraction $\frac{1}{z} W^{*}_{H}(z)$ are located outside of the unit circle on the z plane, provided only that the zeros and poles of the transfer function $W_H(p)$ for the object belong to the left half-plane of the plane p. This fact, as we shall see below, facilitates synthesis of a stable control program for specified performance of the closed-loop system.

As we know [3], the control program of the DM can be represented by the transfer function

$$W_{M} = (z) \frac{A_n z^n + A_{n-1} z^{n-1} + \ldots + A_1 z + A_0}{B_n z^n + B_{n-1} z^{n-1} + \ldots + B_1 z + B_0}, \tag{3}$$

where A_k and B_k are the coefficients to be selected in the synthesis of the control program.

The synthesis of a stable control program (3) is performed for a specified transfer function $W_{sp.}(z)$ of the closed-loop system; this transfer function is selected on the basis of the requirements imposed on the system and the nature of the specified input X_0 (its rate of change, the presence of random noise). It may be written as

$$W_{sp.}(z) = \Gamma_1 z + \Gamma_2 z^2 + \Gamma_3 z^3 + \ldots + \Gamma_m z^m \tag{4}$$

or

$$W_{sp.}(z) = \frac{g_1 z + g_2 z^2 + g_3 z^3 + \ldots + g_l z^l}{g'_0 + g'_1 z + g'_2 z^2 + \ldots + g'_{l+m} z^{l+m}}. \tag{5}$$

Note that in the first case (4) the system has a so-called infinite degree of stability and a finite transient response time equal to Tm. It is evident that the condition for first order astatism in the system will be

$$\Gamma_1 + \Gamma_2 + \Gamma_3 + \ldots \Gamma_m = 1. \tag{6}$$

For higher order astatism it is necessary that (4) contain $(1 - z)$ to the appropriate power as a multiplier.

In the second case, for which $W_{sp.}(z)$ is written in the form (5), it is necessary that the roots of the denominator in (5) have a modulus greater than unity in order to assure stability of the closed-loop system.

In the analysis we shall assume that the transfer function of the closed-loop system is specified in the form (4) or (5).

By analogy with [4] we subdivide the control program into a series of elements each of which is defined by its transfer function (Fig. 2). However, in contrast to [4], we choose the transfer functions of the elements $D_1(z)$ and $D_3(z)$ in the form

$$D_1(z) = W_3(z),\quad D_3(z) = \frac{W_{sp}(z)}{W_H(z)}. \tag{7}$$

Then it follows from a study of the block diagram in Fig. 2 that the transfer function for the closed-loop system is equal to the specified transfer function; i.e., we obtain

$$X^{*} = W_{sp}(z) X^{*}_{0}.$$

The transfer function $D_2(z)$ may be taken in simplest form, and its coefficients are chosen from the conditions of proper stability and stability for the closed loop of the system (Fig. 2). In other words, the transfer function is chosen so that the roots of the equation

$$1 + D_2(z) W_H(z) = 0$$

will have a modulus exceeding unity. For example, sometimes choosing $D_2(z)$ in the form

$$D_2(z) = \frac{a_{11} z + a_{10}}{b_{11} z + b_{10}}, \tag{8}$$

where $\left|\frac{b_{10}}{b_{11}}\right| > 1$, makes it possible to satisfy these conditions.

The resulting control program (Fig. 2) is stable; to verify this it is sufficient to demonstrate the stability of the program corresponding to the element $D_3(z)$. This is very simple to do; in fact, substituting expression (2) into (7), we obtain

$$D_3(z) = \frac{(\Gamma_1 + \Gamma_2 z + \Gamma_3 z^2 + \ldots + \Gamma_m z^{m-1})(b_k z^k + b_{h-1} z^{k-1} + \ldots + b_1 z + b_0)}{a_k z^{k-1} + a_{k-1} z^{k-2} + \ldots + a_2 z + a_1}.$$

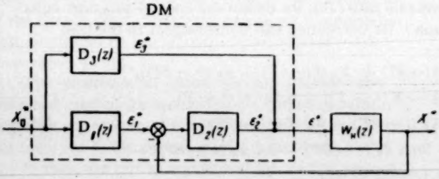

Fig. 2

The stability derives from the fact that the zeros in the denominator coincide with the zeros of $W_H(z)/z$ and lie outside the unit circle. It is evident that the stable control program for the system in Fig. 2 can be written as

$$\varepsilon^{*}_{1} = D_1(z) X^{*}_{0},\quad \varepsilon^{*}_{cl} = D_3(z) X^{*}_{0}, \tag{9}$$

$$\varepsilon^{*}_{2} = D_2(z)(\varepsilon^{*}_{1} - X^{*}),\quad \varepsilon^{*} = \varepsilon^{*}_{2} + \varepsilon^{*}_{cl}.$$

The transfer function of the control program (3) will then consist of two transfer functions:

$$\varepsilon^{*} = W_{1M}(z)\,X_0^{*} - D_2(z)\,X^{*},$$

where

$$W_{1M}(z) = D_1(z)\,D_2(z) + D_3(z).$$

Taking (2), (4), (7), and (8) into account, we write the control program (9) in the form of the difference equations

$$\begin{aligned}
\varepsilon_1(t) &= \Gamma_1 X_0(t-T) + \Gamma_2 X_0(t-2T) + \ldots + \Gamma m X_0(t-mT),\\
\varepsilon_2(t) &= \frac{a_{10}}{b_{10}}[\varepsilon_1(t) - X(t)] + \frac{a_{11}}{b_{10}}[\varepsilon_1(t-T) - X(t-T)] - \frac{b_{11}}{b_{10}}\varepsilon_2(t-T),\\
\varepsilon_3(t) &= C_0 X_0(t) + C_1 X_0(t-T) + C_2 X_0(t-2T) + \ldots + C_i X_0[t-(m+k-1)T] -\\
&\quad - \frac{a_2}{a_1}\varepsilon_3(t-T) - \frac{a_3}{a_1}\varepsilon_3(t-2T) - \ldots - \frac{a_k}{a_1}\varepsilon_3[t-(k-1)T],\\
\varepsilon(t) &= \varepsilon_2(t) + \varepsilon_3(t).
\end{aligned} \tag{10}$$

Here the values of the quantities in each current computation cycle are represented in terms of a function of the argument (t), and the values of the quantities in the preceding nth cycle are given in terms of functions of the argument (t − nT):

$$C_0 = \frac{1}{a_1}\Gamma_1 b_0,$$

$$C_1 = \frac{1}{a_1}(\Gamma_1 b_1 + \Gamma_2 b_0),$$

$$C_2 = \frac{1}{a_1}(\Gamma_1 b_2 + \Gamma_2 b_1 + \Gamma_3 b_0),$$

$$\ldots\ldots\ldots\ldots\ldots\ldots$$

$$C_i = \frac{1}{a_1}\Gamma_m b_k.$$

It is obvious that it is not difficult to formulate the program for computing the control signal in the DM using Eq. (10); under these conditions the program volume is small.

Experimental Results

In order to illustrate the above we shall study an example of synthesizing the control program for the DM of a system (Fig. 1) for the case where the object has the transfer function:

$$W_M(p) = \frac{k(T_1 p + 1)}{p(T_2 p + 1)(T_3^2 p^2 + 2\xi T_3 p + 1)}, \tag{11}$$

where

$$k = 0.0091;\ T_1 = 1.085\ \text{sec},\ T_2 = 2\xi T_3 = 0.05;$$
$$T_3^2 = 0.0205\ \text{sec}^2.$$

Then for a computing-cycle time T = 0.1 sec we use (1) and (11) to obtain

$$\begin{aligned}
W_H(z) &= \frac{a_4 z^4 + a_3 z^3 + a_2 z^2 + a_1 z}{(1-z)(e^{-\frac{T}{T_2}} - z)(z^2 + k_1 z + k_0)} =\\
&= \frac{a_4 z^4 + a_3 z^3 + a_2 z^2 + a_1 z}{b_4 z^4 + b_3 z^3 + b_2 z^2 + b_1 z + b_0},
\end{aligned} \tag{12}$$

where $a_1 = 0.0625$; $a_2 = -0.045$; $a_3 = 0.00571$; $a_4 = 0.00771$; $b_0 = 9.9$; $b_1 = -24.75$; $b_2 = 24.39$; $b_3 = -10.54$; $b_4 = 1$; $k_0 = 1.277$; $k_1 = -1.747$.

We shall choose the transfer function for the closed-loop system as

$$W_{sp}(z) = \Gamma_1 z + \Gamma_2 z^2 + \Gamma_3 z^3 + \Gamma_4 z^4 + \Gamma_5 z^5, \tag{13}$$

where

$$\Gamma_1 = \Gamma_2 = \Gamma_3 = \Gamma_4 = \Gamma_5 = 0.2. \tag{14}$$

A check of the stability for the closed loop of the system (Fig. 2) shows that the transfer function $D_2(z)$ can be written as the fraction (8). Here the roots of the equation

$$1 + D_2(z)\,W_H(z) = 0 \tag{15}$$

have a modulus greater than unity for $a_{10} = 1$; $a_{11} = e^{-T/T_2} = 7.8$; $b_{10} = 0.123$; $b_{11} = -0.053$.

Substituting the values of the coefficients in (12) and (13) into (10), we obtain the control-program equation for computing the control signal in the DM:

$$\begin{aligned}
\varepsilon_1(t) &= 0.2\,[X_0(t-T) + X_0(t-2T) + X_0(t-3T) + X_0(t-4T) + X_0(t-5T)],\\
\varepsilon_2(t) &= 8.13\,[\varepsilon_1(t) - X(t)] + 63.5\,[\varepsilon_1(t-T) - X(t-T)] + 0.42\,\varepsilon_2(t-T),\\
\varepsilon_3(t) &= 31.7\,X_0(t) - 47.5\,X_0(t-T) + 30.5\,X_0(t-2T) - 3.2\,X_0(t-3T) -\\
&\quad -31.7\,X_0(t-5T) + 47.5\,X_0(t-6T) - 30.5\,X_0(t-7T) + 3.2\,X_0(t-8T) +\\
&\quad + 0.72\varepsilon_3(t-T) - 0.091\,\varepsilon_3(t-2T) - 0.123\varepsilon_3(t-3T),\\
\varepsilon(t) &= \varepsilon_2(t) + \varepsilon_3(t).
\end{aligned} \tag{16}$$

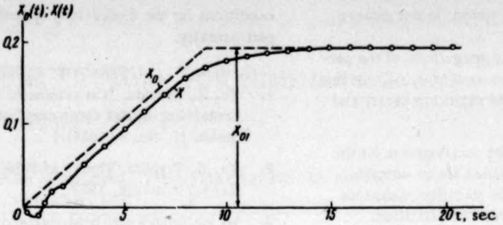

Fig. 3

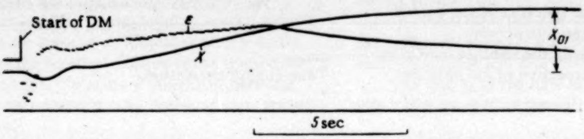

Fig. 4

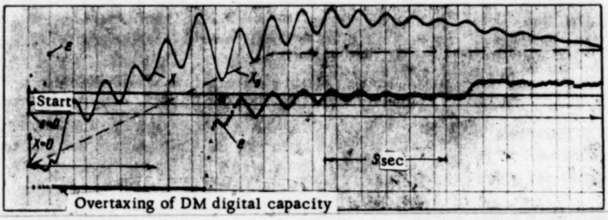

Fig. 5

Figure 3 shows the graph for the control process in the closed-loop system. The control signals were computed from Eq. (16). In performing the experiment we used a specialized high-speed DM which performed the computations during a time equal to a portion of the cycle $T = 0.1$ sec. We ensured a constant cycle by using a special control network.

From the graph in Fig. 3 it is evident that in accordance with (15) the system has first order astatism and has a velocity gain of approximately 4 $\sec^{-1}$. The segment in Fig. 3 corresponding to the initial operation of the system after it has been energized is especially well illustrated on the typical control process oscillogram shown in Fig. 4.

The experimental results not only illustrate the described method for synthesizing a control program; they also are of special interest in clarifying the specifics involved in the operation of a system with a DM.

In fact, the initial segment of the control process is usually not taken into account in theoretical papers dealing with systems incorporating a DM. This was evidently the reason for previous underestimation of the stability conditions for the control program.

The indicated segment is not a transient response in the general sense of automatic control theory; it arises due to an absence of information in the "memory" of the machine concerning the values of the input and the output quantities over the preceding cycles $X_0(t-hT)$, $X_1(t-hT)$, ... (where $h = 1, 2, ..., n$), etc., during the initial period of operation for the system. (Incidentally, experiment shows that the process corresponding to the initial segment may also occur when information is lost in the machine due to random failures.) As a result, the input of the object will be subjected to a perturbation (Fig. 3) whose form is determined by the "transfer function of the control program" [in the general case (5)] or by the difference equations (12).

If the control program is stable, then the magnitude of the indicated perturbation decreases; after n cycles, where n is the number of preceding cycles which are used in the program (in our case eight, Fig. 4), it becomes equal to zero. After that the conventional transient response begins in the system in accordance with (6).

For an unstable program the magnitude of the perturbation increases with each subsequent cycle, and this leads to an overtaxing of the DM digital capacity and cessation of operation.

The above is verified by the oscillograms for the control process (cf. Fig. 5) obtained for an unstable control program even though the stability conditions for the closed-loop system proper were satisfied.

Conclusions

We have analyzed a simple method for synthesizing a control program for specified performance of a closed-loop system when the specifics of the control-program realization are taken into account.

The necessity of satisfying the stability conditions for the control program irrespective of the stability conditions for the closed-loop system was verified experimentally.

LITERATURE CITED

1. Ya. Z. Tsypkin, "On automatic control systems containing digital computers," Avtomat. i Telemekh. 17, No. 8 (1956).†

2. Ya. Z. Tsypkin, Theory of Pulse Systems [in Russian] (Fizmatgiz, 1958).

3. W. K. Zinvill and I. M. Salzer, "Analysis of control systems involving digital computers," Proc. IRE No. 7 (1953).

4. J. Tou, "Digital compensation for control and simulation," Proc. IRE 45, No. 9 (1957).

---

† See English translation.

A VACUUM-TUBE NETWORK FOR SUMMING SIGNALS

V. D. Vershinin

Moscow

Translated from Avtomatika i Telemekhanika, Vol. 21, No. 11,
pp. 1560-62, November, 1960
Original article submitted May 24, 1960

In servodrives two channels are often used for transmitting signals. The coarse and fine control signals are summed at the input of an amplifier after a definite matching of the receiver relative to the transmitter has been carried out. There are a number of networks for performing this summation by means of neon lamps, transformers, etc.

Figure 1 suggests a simpler and more reliable network for summing such signals.

The principle governing the operation of the network is the following: a bias voltage corresponding to the operating point on the transfer characteristic is applied to one grid of a dual triode, and a negative bias voltage with a magnitude equal to or greater than the cutoff voltage for the tube is applied to the other grid.

We shall derive the expression for the summed ac component of plate voltage as a function of the mismatch angle of the receiver relative to the transmitter.

The receiver produces modulated fine and coarse control signals which can be written as

$$U_c = U_m \sin\theta \sin\omega t,$$
$$U_f = U_m \sin k\theta \sin\omega t,$$

where U_c, U_f are the coarse and fine signals produced by the detectors; U_m is the amplitude of the voltage tapped off from the detectors; θ is the mismatch angle between the transmitter and the receiver; ω is the carrier frequency in $\sec^{-1}$; $\underline{k}$ is the transfer number between the coarse and fine control detectors.

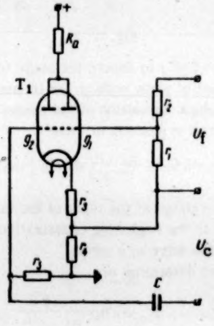

Fig. 1

The grid g_2 of the tube is subjected to a voltage which is phase-shifted through an angle

$$\varphi = \operatorname{arc\,tg} \frac{x_c}{r_5 + r_{i2} + r_4}$$

and has a magnitude equal to

$$U'_c = U_m m \sin\theta \sin(\omega t - \varphi) - U_{\text{bias2}}, \qquad (1)$$

where

$$m = \frac{r_4 + r_5}{\sqrt{(r_{i2} + r_5 + r_4)^2 + x_c^2}},$$

r_{i2} is the internal resistance of the coarse-control detector; $U_{\text{bias 2}}$ is the bias voltage at the second grid and is determined by the voltage drop across the resistors r_3 and r_4.

The first grid g_1 is subjected to a voltage equal to

$$U'_f = U_{\max} n \sin k\theta \sin\omega t - U_{\text{bias1}}, \qquad (2)$$

where

$$n = \frac{r_1}{r_1 + r_2 + r_{i1}};$$

$U_{\text{bias 1}}$ is the bias voltage at the first grid and is determined by the voltage drop across the resistor r_3.

After the signals have been amplified, the plate voltage will be

$$U_a = \mu_1 (U_m n \sin k\theta \sin\omega t - U_{\text{bias1}}) + \\ + \mu_2 [U_m m \sin\theta \sin(\omega t - \varphi) - U_{\text{bias2}}], \qquad (3)$$

where μ_1, μ_2 are the gains for the two arms of the tube.

Figure 2 shows the waveshapes of the currents in the left and right halves of the tubes, as well as the waveshape of the over-all plate current for a constant mismatch angle; the figure corresponds to the case where the voltages U'_f and U'_c are in phase opposition. The curve abcd bounds the ordinates for the instantaneous value of the current in the right half of the tube; the curve $\underline{e}$ bounds the ordinates of the current in the left half of the tube, and the curve abfd bounds the ordinates of the resultant current.

If we approximate the transfer characteristics of the tube by a straight line, then we shall have a constant identical gain for both halves of the tube. In that case the ac component of plate voltage (its effective value) ΔU_a will be given by the following formula when the phase shift angle φ is neglected:

$$\Delta u_a = \mu\,(U'_m \sin k\theta + U''_m \sin\theta), \qquad (4)$$

where $U'_m = \frac{U_m n}{\sqrt{2}}$ is the effective value of the voltage at the grid g_1 arriving from the fine-control detector; U''_m is the effective value of the ac voltage component at the grid g_1, corresponding to operation of the left half of the tube.

The graph of the ac component of the plate current as a function of the mismatch angle θ is shown in Fig. 3.

If we design a network with a deep dip Δu_1 (this can be achieved by increasing the coefficient n), it follows that when the drive compensates for a large mismatch angle at the controller output, a smaller voltage will correspond to this mismatch angle range ($k\theta$ = 360° to 180°); this will cause braking of the controlled object.

This fact can be used in certain servodrives (drives which have a high overthrust speed, etc.) in order to reduce the compensation of large mismatch angles; i.e., the rate at which the controlled object arrives at the matched position is reduced.

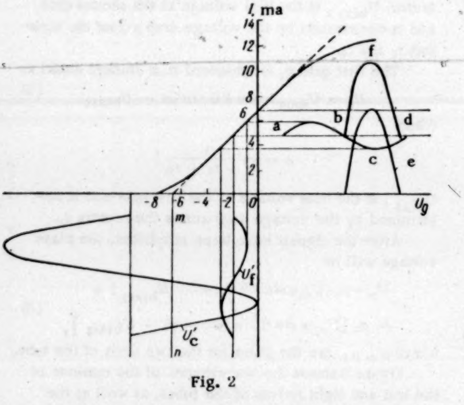

Fig. 2

The bias voltage at the first grid g_1 of the tube and the plate load resistance are chosen from the operating conditions of the amplifier based on the fine-control voltage; their computation is performed on the basis of the requirements imposed on the amplifier. The bias voltage at the second grid g_2 is determined by the required range over which operation must be based solely on the fine-control voltage and the tube cutoff voltage. The range over which the amplifier (drive) is operated by the fine-control signal only (θ_1) is somewhat greater than the required operational precision of the drive:

$$U_{\text{bias}2} = U_{co} + U_1, \quad U_1 = U_m m \sin\theta_1 \sin(\omega t - \varphi),$$

where U_{co} is the cutoff voltage of the tube and is determined from the transfer characteristic.

The resistors r_3 and r_4 (Fig. 1) are related by the following expressions:

$$\frac{r_3}{r_3 + r_4} = \frac{U_{\text{bias}1}}{U_{\text{bias}2}} \quad I_a (r_3 + r_4 + r_i + r_a) = U_a.$$

Here I_a is the dc component of the plate current, and r_i is the plate resistance of the tube.

From these relationships we obtain

$$r_4 = \left(\frac{U_a}{I_a} - r_i - r_a\right)\left(1 - \frac{U_{\text{bias}1}}{U_{\text{bias}2}}\right),$$

$$r_3 = r_4 \frac{U_{\text{bias}1}}{U_{\text{bias}2}} \left(1 - \frac{U_{\text{bias}1}}{U_{\text{bias}2}}\right)^{-1}.$$

The capacitor C (Fig. 1) which blocks dc current from the coarse-control detector coil must have a maximum capacitance in order to reduce the phase shift angle φ and increase the coefficient m; however, its magnitude is limited by physical size (in practice it can be equal to 2 μ f). The resistance r_5 is determined from the grid current conditions. In choosing the parameters of the network it is important to know the data for the voltage divider consisting of the resistors r_1 and r_2.

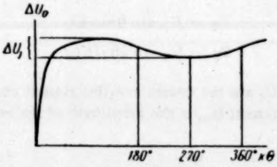

Fig. 3

Using $k\theta_2$ (≈ 270°) to denote the angle for which the ac component of plate voltage has its maximum dip (Fig. 3) due to phase opposition of the coarse and fine control voltages, it is possible to write

$$\mu\left(U''_m \sin\theta_2 - U_m \frac{n}{\sqrt{2}} \sin k\theta_2\right) = \Delta u,$$

where Δu is the voltage at the input of the last stage and corresponds to the beginning of saturation in the amplifier or in the drive as a whole.

From this we determine n:

$$n = (\Delta u + \mu U''_m \sin\theta_2) \frac{\sqrt{2}}{\mu U_m \sin k\theta_2}.$$

In designing and checking the network we use the following parameters: T is a dual "6N7S" triode;* r_1 = = 27 kohm; r_2 = 1 meg; r_3 = 1 kohm; r_4 = 4 kohm; r_5 = = 27 kohm; r_a = 20 kohm; C = 2μf.

The signals at the grids of the tube were supplied from "SS-405" selsyns, and the transfer number between selsyns was 20.

Notwithstanding its simplicity, the network analyzed above not only sums signals but also amplifies them.

---

* The specifications for the "6N7S" tube are: $\underline{E}_f$ = 6.3 v, $\underline{I}_f$ = 0.8 amp, $\underline{E}_p$ = + 300 v, $\underline{I}_p$ = 3.5 ma, $\underline{E}_{c_1}$ = −6 v, $\underline{g}_m$ = 1600 μmho, $\underline{r}_p$ = 22 k, $\underline{R}_L$ = 16 k, $\underline{P}_p$ = 6 w, $\underline{P}_{out}$ = = 4.2 w [Publisher's note].

BLANK
PAGE

DETERMINING THE TRANSFER FUNCTIONS FOR CERTAIN SYSTEMS WITH VARYING PARAMETERS

B. E. Rudnitskii
(Leningrad)

Translated from Avtomatika i Telemekhanika, Vol. 21, No. 12, pp. 1565-1575,
December, 1960
Original article submitted May 23, 1960

The paper presents a method for determining the transfer functions of systems that are described by ordinary differential equations of high order with variable coefficients, provided that the coefficients of the equations can be represented by polynomials.

INTRODUCTION

The frequency method for analyzing systems with varying parameters is based on the concept of transfer functions Y(t, p) for such systems; these depend on time t, in contrast to the transfer functions for systems with constant parameters.

We shall study a dynamic system which is described by the following n-th order differential equation with variable coefficients:

$$\sum_{k=0}^{n} a_k(t)\frac{d^k x_{\text{out}}(t)}{dt^k} = \sum_{k=0}^{m} b_k(t)\frac{d^k x_{\text{in}}(t)}{dt^k}, \tag{1}$$

where $x_{\text{in}}(t)$ and $x_{\text{out}}(t)$ are the input and output quantities of the system, respectively; $a_k(t)$ and $b_k(t)$ are time-varying coefficients.

Equation (1) can be written as follows:

$$N(t, D)\, x_{\text{out}}(t) = M(t, D)\, x_{\text{in}}(t), \tag{2}$$

where $D = d/dt$ is the differential operator, and N(t, D) and M(t, D) are operators for the left and right sides of equation (1), respectively. As demonstrated in [1], the transfer function for the system described by Eq. (1) is a particular solution of the differential equation

$$\sum_{k=0}^{n}\frac{1}{k!}\frac{\partial^k N(t, p)}{\partial p^k}\frac{\partial^k Y(t, p)}{\partial t^k} = M(t, p), \tag{3}$$

where Y(t, p) is the transfer function for the system under study; the functions N(t, p) and M(t, p) are obtained from the operators N(t, D) and M(t, D), respectively, by substituting the complex quantity p for the differentiation operator D. In equation (3) the quantity t is the independent variable, and p is the parameter.

The frequency method can assure an appreciable reduction in the amount of computations compared to methods involving direct solution of the differential equations for systems with varying parameters when system stability is estimated or when the response of the system to regular or random perturbations is studied. Under these conditions, it is a very important fact that the transfer function Y(t, p) of a system with varying parameters is independent of the nature of the input perturbation. Moreover, determining the nature of the response of the system to a certain random perturbation when the frequency method is used, does not require repeated solutions for various values of the random perturbation function; this is in contrast to methods based on an empirical solution of the differential equation for the system.

In many practical cases for which other methods of analysis cause serious difficulties the frequency method makes it possible to derive the solution in convenient form (cf. below). Usually, the basic difficulties which arise on applying the frequency method to the analysis of systems with varying parameters are associated with determining the transfer function Y(t, p). The solution of Eq. (3) in general form is a problem that is no less complex than solving Eq. (2), since Eq. (3) is of the same order as (2) and its coefficients depend both on the argument t and on the parameter p. For an approximate solution of Eq. (3) for aperiodic variation of the coefficients $a_k(t)$ and $b_k(t)$ it is possible to make use of the Zadeh method [2]. Under these conditions the solution is obtained in the form of a series that converges for a sufficiently slow variation of the parameters. The basic shortcoming of this method is that it cannot be applied for a rapid variation of the parameters.

In practice, we often encounter cases where the coefficients $a_k(t)$ and $b_k(t)$ of Eq. (1) are represented by polynomials, or when these coefficients can be approximated by appropriate polynomials with a sufficient accuracy for the purposes of computation. We shall study certain possibilities for the solution of Eq. (3) if the coefficients $a_k(t)$ and $b_k(t)$ are of the form

$$a_k(t) = \sum_{l=0}^{q} a_{k,l}\, t^l, \quad b_k(t) = \sum_{l=0}^{s} b_{k,l}\, t^l.$$

In contrast to the Zadeh method, the results cited below can be applied for rapid variation of the parameters as well.

1. CERTAIN RELATIONSHIPS FOR THE TRANSFER FUNCTION OF A SYSTEM WHOSE EQUATION HAS COEFFICIENTS THAT CAN BE REPRESENTED BY POLYNOMIALS

If the coefficients $a_k(t)$ and $b_k(t)$ of Eq. (1) are represented by polynomials, then the functions N(t, p) and M(t, p) in Eq. (3) are polynomials in the variables t and p:

$$N(t, p) = \sum_{k=0}^{n} \Big(\sum_{l=0}^{q} a_{k,l}\, t^l\Big) p^k, \quad M(t, p) = \sum_{k=0}^{m} \Big(\sum_{l=0}^{s} b_{k,l}\, t^l\Big) p^k. \tag{4}$$

The following particular case of Eq. (3) will be of special interest:

$$\sum_{k=0}^{n} \frac{1}{k!} \frac{\partial^k N(t, p)}{\partial p^k} \frac{\partial^k Y(t, p)}{\partial t^k} = 1. \tag{5}$$

Theorem 1. If $Y_1(t, p)$ is a solution of Eq. (5), then the function

$$Y(t, p) = \sum_{v=0}^{s} \frac{1}{v!} \frac{\partial^v M(t, p)}{\partial t^v} \frac{\partial^v Y_1(t, p)}{\partial p^v} \tag{6}$$

is a solution of Eq. (3).

We can demonstrate the validity of the theorem by the direct substitution of (6) into (3).

Theorem 2. There exists a solution Y(t, p) of Eq. (5) which is a solution of the equation

$$\frac{1}{q!} \frac{\partial^q N(t, p)}{\partial t^q} \frac{\partial^q Y(t, p)}{\partial p^q} + \frac{1}{(q-1)!} \frac{\partial^{q-1} N(t, p)}{\partial t^{q-1}} \frac{\partial^{q-1} Y(t, p)}{\partial p^{q-1}} + \ldots \\ \cdots + N(t, p)\, Y(t, p) = 1. \tag{7}$$

Proof. Assume for the time being that Y(t, p) is some solution of Eq. (5). We shall formulate the function

$$u(t,\ p)=\sum_{v=0}^{q}\frac{1}{v!}\frac{\partial^{v}N(t,\ p)}{\partial t^{v}}\frac{\partial^{v}Y(t,\ p)}{\partial p^{v}}. \tag{8}$$

According to theorem 1, the function u satisfies the equation

$$\sum_{k=0}^{n}\frac{1}{k!}\frac{\partial^{k}N(t,\ p)}{\partial p^{k}}\frac{\partial^{k}u(t,\ p)}{\partial t^{k}}=N(t,p). \tag{9}$$

Its solution is the function u ≡ 1. The initial conditions for the function u will be the following:*

$$u(0,\ p)=1,\qquad \frac{\partial^{k}u(0,\ p)}{\partial p^{k}}=0\quad(k=1,\ 2,\ldots,\ n-1). \tag{10}$$

We shall find the initial conditions which must be satisfied by the function Y(t, p). From relationships (10) we have

$$u(0,\ p)=\sum_{v=0}^{q}\frac{1}{v!}\frac{\partial^{v}N(0,p)}{\partial t^{v}}\frac{\partial^{v}Y(0,\ p)}{\partial p^{v}}\equiv 1, \tag{11}$$

$$\frac{\partial^{k}u(0,\ p)}{\partial t^{k}}=\sum_{v=0}^{q}\frac{1}{v!}\sum_{l=0}^{k}C_{k}^{l}\frac{\partial^{v+l}N(0,\ p)}{\partial t^{v+l}}\frac{\partial^{v+k-l}Y(0,\ p)}{\partial p^{v}\partial t^{k-l}}\equiv 0. \tag{12}$$

Condition (11) makes it possible to determine Y(0, p) by solving a q-th order differential equation relative to Y(0, p). Substituting Y(0, p) and its derivatives with respect to p into condition (12) for k = 1, we obtain the equation for ∂Y(0, p)/∂t. From this equation we find ∂Y(0, p)/∂t. Then we find $\partial^2 Y(0,p)/\partial t^2$ in analogous fashion from condition (12) for k = 2, etc. Thus, we obtain the initial conditions for Eq. (5). Solving this equation for these initial conditions, we obtain a function Y(t, p) which is such that the function u defined according to formula (8) will satisfy Eq. (9) for the initial conditions (10). Then u ≡ 1. Therefore, the function Y(t, p) is a solution of Eq. (7). The theorem has been proven.

Systems having equations with coefficients that are first and second degree polynomials are of special practical interest. We shall dwell in more detail on the solution of Eq. (7) for such systems.

2. THE TRANSFER FUNCTION WHEN THE COEFFICIENT N(t, p) IN EQ. (3) IS LINEAR WITH RESPECT TO THE VARIABLE t.

In that case Eq. (7) is written as

$$\frac{\partial N(t,\ p)}{\partial t}\frac{\partial Y_{1}(t,\ p)}{\partial p}+N(t,\ p)\,Y_{1}(t,\ p)=1, \tag{13}$$

where

$$N(t,\ p)=\sum_{k=0}^{n}a_{k,0}\,p^{k}+t\sum_{k=0}^{n}a_{k,1}\,p^{k}=A(p)+tB(p).$$

---

* Here and throughout $\frac{\partial^{k}u(0,\ p)}{\partial t^{k}}$ denotes $\left.\frac{\partial^{k}u(t,\ p)}{\partial t^{k}}\right|_{t=0}$. Analogously,

$$\frac{\partial^{k}Y(0,\ p)}{\partial p^{k}}=\left.\frac{\partial^{k}Y(t,\ p)}{\partial p^{k}}\right|_{t=0},\qquad \frac{\partial^{k}N(0,\ p)}{\partial t^{k}}=\left.\frac{\partial^{k}N(t,\ p)}{\partial t^{k}}\right|_{t=0}.$$

Solving Eq. (13), we obtain

$$Y_1(t, p) = \exp\left(-tp - \int \frac{A(p)}{B(p)}dp\right)\left[\int_{p_0}^{p} \frac{1}{B(p)} \exp\left(tp + \int \frac{A(p)}{B(p)}dp\right)dp + C(t)\right]. \tag{14}$$

We are interested only in those solutions of $Y_1(t,p)$ which satisfy Eq. (5). This imposes a certain condition on the function $C(t)$. As shown in section I of the Appendix, the function $C(t)$ must satisfy the following equation:

$$\sum_{k=0}^{n}(a_{k,0} + a_{k,1}t)\frac{d^kC(t)}{dt^k} = e^{tp_0}\exp\left(\int \frac{A(p)}{B(p)}dp\right)\Big|_{p=p_0}. \tag{15}$$

Thus, in order for the solution (14) of Eq. (13) to satisfy Eq. (5) it is necessary and sufficient that the function $C(t)$ satisfy Eq. (15).

Remark. If the solution of Eq. (5) is found according to this theorem, then the solution of Eq. (3) will be found according to theorem 1.

3. THE TRANSFER FUNCTION FOR THE CASE WHERE THE COEFFICIENT N(t,p) OF EQ. (3) IS A POLYNOMIAL OF THE SECOND DEGREE IN t.

In that case Eq. (7) is written as

$$\frac{1}{2!}\frac{\partial^2 N(t, p)}{\partial t^2}\frac{\partial^2 Y_1(t, p)}{\partial p^2} + \frac{\partial N(t, p)}{\partial t}\frac{\partial Y_1(t, p)}{\partial p} + N(t, p)Y_1(t, p) = 1, \tag{16}$$

where

$$N(t, p) = \sum_{k=0}^{n} a_{k,0}\,p^k + t\sum_{k=0}^{n} a_{k,1}\,p^k + t^2\sum_{k=0}^{n} a_{k,2}\,p^k = A(p) + tB(p) + t^2D(p).$$

We shall apply the Lemma cited in section II of the Appendix to Eq. (16). In the case under study,

$$d = d(t, p) = \frac{A(p)}{D(p)} + t\frac{B(p)}{D(p)} + t^2, \quad b = b(t, p) = \frac{B(p)}{D(p)} + 2t,$$

$$f = f(t, p) = \frac{1}{D(p)},$$

$$b^2(t, p) = \frac{B^2(p)}{D^2(p)} + 4t\frac{B(p)}{D(p)} + 4t^2, \quad \frac{db(t, p)}{dp} = \frac{\frac{dB(p)}{dp}D(p) - B(p)\frac{dD(p)}{dp}}{D^2(p)},$$

$$\varphi(t, p) = \frac{A(p)}{D(p)} + t\frac{B(p)}{D(p)} + t^2 - \frac{1}{4}\frac{B^2(p)}{D^2(p)} - t\frac{B(p)}{D(p)} - t^2 +$$

$$+ \frac{B(p)\frac{dD(p)}{dp} - D(p)\frac{dB(p)}{dp}}{2D^2(p)} =$$

$$= \frac{A(p)}{D(p)} - \frac{1}{4}\frac{B^2(p)}{D^2(p)} + \frac{B(p)\frac{dD(p)}{dp} - D(p)\frac{dB(p)}{dp}}{2D^2(p)} = \varphi(p).$$

Thus, the following postulate is valid: if in Eq. (16) the function $N(t,p)$ is a polynomial of the second degree in t, then the solution of Eq. (16) can be written as

$$Y_1(t, p) = \exp\Big(-tp - \frac{1}{2}\int \frac{B(p)}{D(p)}\,dp - \int g(p)\,dp\Big)\Big\{\int_{p_0}^{p} \exp\Big(2\int g(p)\,dp\Big) \times \tag{17}$$

$$\times \Big[\int_{p_0}^{p} \frac{1}{D(p)} \exp\Big(tp + \frac{1}{2}\int \frac{B(p)}{D(p)}\,dp - \int g(p)\,dp\Big)dp + C_1(t)\Big]dp + C_2(t)\Big\},$$

where g(p) satisfies the equation

$$\frac{d}{dp} g(p) = g^2(p) + \varphi(p) \tag{18}$$

or

$$Y_1(t, p) = \gamma(p) \exp\Big(-tp - \frac{1}{2}\int \frac{B(p)}{D(p)}\,dp\Big) \times$$

$$\times \Big\{\int_{p_0}^{p} \frac{1}{\gamma^2(p)}\Big[\int_{p_0}^{p} \frac{\gamma(p)}{D(p)} \exp\Big(tp + \frac{1}{2}\int \frac{B(p)}{D(p)}\,dp\Big)dp + C_1(t)\Big]dp + C_2(t)\Big\}, \tag{19}$$

where $\gamma(p)$ satisfies the equation

$$\frac{d^2}{dp^2}\gamma(p) + \varphi(p)\gamma(p) = 0. \tag{20}$$

As shown in section III of the Appendix, the function $C_1(t)$ in expression (17) or (19) can be chosen arbitrarily – for example: $C_1(t) = C_1 = \text{const}$; the function $C_2(t)$ satisfies the equation

$$\sum_{k=0}^{n} (a_{k,0} + a_{k,1}t + a_{k,2}t^2)\frac{d^k}{dt^k} C_2(t) = e^{tp_0}\frac{1}{F_3(p_0)}, \tag{21}$$

where

$$F_3(p) = \exp\Big(-\frac{1}{2}\int \frac{B(p)}{D(p)}\,dp - \int g(p)\,dp\Big) = \gamma(p)\exp\Big(-\frac{1}{2}\int \frac{B(p)}{D(p)}\,dp\Big).$$

Thus, in finding the transfer function from the second order equation (16) for a certain specific value of time $t = T$ it is necessary to satisfy only one initial condition which determines the value of the function $C_2(t)|_{t=T}$. This condition can usually be established on the basis of physical concepts: for example, from a study of the limits $\lim_{p\to\infty} Y(t, p)$ or $\lim_{p\to 0} Y(t, p)$.

The function Y(t, p) which satisfies Eq. (3), is defined in terms of the function $Y_1(t, p)$ in accordance with theorem 1.

4. ON THE TRANSFER FUNCTION FOR THE CASE WHERE THE COEFFICIENT N(t, p) IN EQ. (3) IS A POLYNOMIAL OF DEGREE q IN t.

If the coefficient N(t, p) in Eq. (3) is a polynomial of degree q in t, then it can be shown that the solution of Eq. (5) under these conditions can be written as

$$Y_1(t, p) = e^{-tp} F_{q+1}(p)\Big\{\int_{p_0}^{p} F_q(p)\Big[\int_{p_0}^{p} F_{q-1}(p)\ldots\Big(\int_{p_0}^{p} e^{tp}F_1(p)\,dp + C_1(t)\Big)dp + \tag{22}$$

$$+ C_2(t)\Big]dp + \ldots + C_{q-1}(t)\Big\}dp + C_q(t),$$

where the function $C_q(t)$ satisfies the equation

$$\sum_{k=0}^{n}\Big(\sum_{l=0}^{q} a_{k,l}\, t^l\Big)\frac{d^k}{dt^k}C_q(t)=\frac{e^{tp_0}}{F_{q+1}(p_0)},$$

and the functions $C_{q-1}(t), \ldots, C_1(t)$ are arbitrary.

Thus, in finding the transfer function $Y(t, p)$ from the q-th order equation (5) for a certain specific value of time $t = T$ only one initial condition besides the dependence on the order of Eq. (5) must be satisfied; this condition determines the value of the function $C_q(t)|_{t = T}$ in expression (22).

5. EXAMPLES

We shall study examples which illustrate the application of the method presented above.

Example 1. We shall determine the mean-square value $\sigma(t)$ of the signal at the output of the system shown in Fig. 1 that is subjected to a random input perturbation with the spectral density $S_{in}(\omega) = S_0 = \text{const}$ for $t \gg T_{s.s.}$ [$S(\omega) = 2\int\limits_0^\infty R_{in}(\tau)\cos\omega\tau d\tau$; $R_{in}(\tau)$ is the correlation function for the random input perturbation, $R_{in}(\tau) = S_0\delta(\tau)$, $\delta(\tau)$ is a unit pulse function, and $T_{s.s.}$ is the time required for the system to reach a steady state.

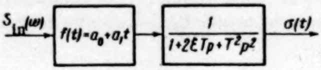

Fig. 1.

By applying theorem 1, we shall obtain the following expression for the transfer function $Y(t, p)$ of the system shown in Fig. 1:

$$Y(t, p)=\frac{a_0+a_1t}{1+2\xi Tp+T^2p^2}+a_1\frac{d}{dp}\left[\frac{1}{1+2\xi Tp+T^2p^2}\right]$$

or

$$Y(t, p)=\frac{a_0+a_1t-2\xi Ta_1+[(a_0+a_1t)\,2\xi T-2T^2a_1]\,p+(a_0+a_1t)\,T^2p^2}{(1+2\xi Tp+T^2p^2)^2}.$$

Making use of the latter expression, we find the mean-square value for the random signal at the output of the system for $t \gg T_{s.s.}$:

$$\sigma^2(t)=\frac{S_0}{2\pi}\int\limits_{-\infty}^{\infty}|Y(t, j\omega)|^2d\omega=$$

$$=\frac{S_0}{8\xi^3T}\,[2\,(a_0+a_1t)^2\,\xi^2-(a_0+a_1t)\,a_12\xi T\,(1+2\xi^2)+a_1^2T^2\,(1+\xi^2+4\xi^4)].$$

Example 2. We shall find the spectral density $S_{out}(t, \omega)$ of the signal $x_{out}(t)$ at the output of the system shown in Fig. 2 for the instant time $t = a_0/a_1$, if $\xi = 0.55$, $T = 0.6$ sec, and the input signal $x_{in}(t)$ has a spectral density $S_{in}(\omega)$.

The relationship between the quantities $x_{in}(t)$ and $x_{out}(t)$ is determined from the equation

$$T^2\left(\frac{a_0}{a_1}-t\right)\frac{d^3x_{\text{out}}(t)}{dt^3}+2\xi T\left(\frac{a_0}{a_1}-t\right)\frac{d^2x_{\text{out}}(t)}{dt^2}+$$
$$+\left(\frac{a_0}{a_1}-t\right)\frac{dx_{\text{out}}(t)}{dt}+x_{\text{out}}(t)=x_{\text{in}}(t).$$

Thus, for the example under study,

$$N(t,p)=T^2\left(\frac{a_0}{a_1}-t\right)p^3+2\xi T\left(\frac{a_0}{a_1}-t\right)p^2+\left(\frac{a_0}{a_1}-t\right)p+1,$$

$$A(p)=1+\frac{a_0}{a_1}p\,(1+2\xi Tp+T^2p^2),$$
$$B(p)=-p\,(1+2\xi Tp+T^2p^2),\quad M(t,p)=1.$$

From formula (14) we obtain the following result after performing the transformations for $t = a_0/a_1$:

$$Y\left(\frac{a_0}{a_1},p\right)=1-\frac{Cp}{\sqrt{1+2\xi Tp+T^2p^2}}\exp\left(-\frac{\xi}{\sqrt{1-\xi^2}}\operatorname{arc\,tg}\frac{\xi+Tp}{\sqrt{1-\xi^2}}\right).$$

The constant C is found from the obvious condition

$$\lim_{p\to\infty}Y\left(\frac{a_0}{a_1},p\right)\to 0.$$

We obtain

$$C=T\exp\left(\frac{\pi}{2}\frac{\xi}{\sqrt{1-\xi^2}}\right).$$

Thus, we finally obtain

$$Y\left(\frac{a_0}{a_1},p\right)=1-\frac{pT\exp\left(\frac{\pi}{2}\frac{\xi}{\sqrt{1-\xi^2}}\right)}{\sqrt{1+2\xi Tp+T^2p^2}}\exp\left(-\frac{\xi}{\sqrt{1-\xi^2}}\operatorname{arc\,tg}\frac{\xi+Tp}{\sqrt{1-\xi^2}}\right)$$

and the spectral density $S_{\text{out}}(t = a_0/a_1, \omega)$ is determined from the expression

$$S_{\text{out}}\left(\frac{a_0}{a_1},\omega\right)=S_{\text{in}}(\omega)\left|Y\left(\frac{a_0}{a_1},j\omega\right)\right|^2.$$

Figure 3 shows the graph of the function $S_{\text{out}}(\frac{a_0}{a_1},\omega)/S_{\text{in}}(\omega)$ for the assumed values of the parameters ξ and T.

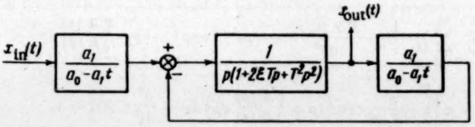

Fig. 2.

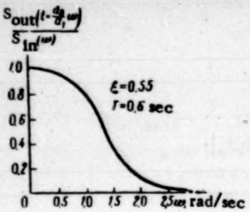

Fig. 3.

CONCLUSION

The paper has cited the relationships in the region of the variable **p** which determine the transfer function Y (t, p) of a system with varying parameters if the coefficients in its equation can be represented by polynomials (theorems 1 and 2). These relationships make it possible to obtain the transfer functions of the systems in general form for linear variation of the coefficients in their equations, as well as in certain particular cases when the variation of the coefficients is governed by a parabolic law.

In the general case, the use of theorems 1 and 2, instead of Eq. (3) for determining the transfer function of a system with varying parameters is expedient when the condition $q < n$ is satisfied (where q is the degree of the polynomial coefficients $a_k(t)$ in the left-hand side of the equation for the system, and n is the order of the equation), since under these conditions the order of the differential equation for the transfer function is reduced.

Using the proposed method, it is possible to determine the transfer function for the series connection of inertialess sections with polynomial gain-variation laws and sections (systems) with constant parameters (the latter may have varying parameters).

The method presented for determining the transfer functions is applicable for rapid variation of the parameters when the use of the well-known Zadeh method is impossible.

The author expresses his appreciation to N. A. Lebedev for a number of valuable suggestions made during the course of writing this paper.

APPENDIX

I. We shall prove that in expression (14) the function C (t) must satisfy Eq. (15). We have

$$\frac{\partial^k Y_1(t,\,p)}{\partial t^k} = \sum_{v=0}^{k} C_k^v (-p)^{k-v} \exp\left(-tp - \int \frac{A(p)}{B(p)}dp\right) \times$$
$$\times \left[\int_{p_0}^{p} \frac{p^v}{B(p)} \exp\left(tp + \int \frac{A(p)}{B(p)}dp\right)dp + \frac{d^v}{dt^v} C(t)\right]. \tag{23}$$

Substituting this expression into Eq. (5), we obtain

$$\sum_{k=0}^{n} \frac{1}{k!} \frac{\partial^k N(t,\,p)}{\partial p^k} \sum_{v=0}^{n} C_k^v (-p)^{k-v} \exp\left(-tp - \int \frac{A(p)}{B(p)}dp\right) \times$$
$$\times \left[\int_{p_0}^{p} \frac{p^v}{B(p)} \exp\left(tp + \int \frac{A(p)}{B(p)}dp\right)dp + \frac{d^v}{dt^v} C(t)\right] = 1$$

or

$$\sum_{v=0}^{n} \sum_{k=v}^{n} \frac{1}{(k-v)!} \frac{\partial^k N(t,\,p)}{\partial p^k} (-p)^{k-v} \exp\left(-tp - \int \frac{A(p)}{B(p)}dp\right) \times$$
$$\times \left[\int_{p_0}^{p} \frac{p^v}{v!B(p)} \exp\left(tp + \int \frac{A(p)}{B(p)}dp\right)dp + \frac{d^v}{dt^v} C(t)\right] = 1,$$

or

$$\sum_{v=0}^{n}{}' \frac{\partial^{v} N(t, p)}{\partial p^{v}}\Big|_{p=0} \exp\left(-tp - \int \frac{A(p)}{B(p)}\, dp\right) \times$$

$$\times \left[\int_{p_0}^{p} \frac{1}{v!B}\frac{{}^{v}}{(p)} \exp\left(tp + \int \frac{A(p)}{B(p)}\, dp\right) dp + \frac{d^{v}}{dt^{v}} C(t)\right] = 1,$$

or

$$\int_{p_0}^{p} \frac{1}{B(p)} \exp\left(tp + \int \frac{A(p)}{B(p)} dp\right) \sum_{v=0}^{n} \frac{1}{v!} \frac{\partial^{v} N(t, p)}{\partial p^{v}}\Big|_{p=0} p^{v} dp +$$

$$+ \sum_{v=0}^{n} \frac{1}{v!} \frac{\partial^{v} N(t, p)}{\partial p^{v}}\Big|_{p=0} \frac{d^{v}}{dt^{v}} C(t) = \exp\left(tp + \int \frac{A(p)}{B(p)} dp\right),$$

or

$$\int_{p_0}^{p} \exp\left(tp + \int \frac{A(p)}{B(p)} dp\right) \frac{A(p) + tB(p)}{B(p)}\, dp +$$

$$+ \sum_{v=0}^{n} \frac{1}{v!} \frac{\partial^{v} N(t, p)}{\partial p^{v}}\Big|_{p=0} \frac{d^{v}}{dt^{v}} C(t) = \exp\left(tp + \int \frac{A(p)}{B(p)} dp\right),$$

and, finally,

$$\sum_{k=0}^{n} \frac{1}{k!} \frac{\partial^{k} N(t, p)}{\partial p^{k}}\Big|_{p=0} \frac{d^{k}}{dt^{k}} C(t) = \exp(tp_0) \exp\left(\int \frac{A(p)}{B(p)} dp\right)\Big|_{p=p_0},$$

where

$$\frac{1}{k!} \frac{\partial^{k} N(t, p)}{\partial p^{k}}\Big|_{p=0} = a_{k,0} + a_{k,1} t.$$

Thus, in expression (14) the function C(t) satisfies Eq. (15).

II. It is possible to formulate the following Lemma which we shall cite without proof.

Lemma. The solution of the equation

$$\frac{d^2}{dt^2} y(t) + b(t) \frac{d}{dt} y(t) + d(t) y(t) = f(t) \tag{24}$$

can be written as

$$y(t) = \exp\left(-\frac{1}{2}\int b(t)\, dt - \int g(t) dt\right) \left\{\int_{t_0}^{t} \exp\left(2\int g(t)\, dt\right) \times\right.$$

$$\left. \times \left[\int_{t_0}^{t} f(t) \exp\left(\frac{1}{2}\int b(t)\, dt - \int g(t) dt\right) dt + C_1\right] dt + C_2\right\}, \tag{25}$$

where the function g(t) satisfies the equation

$$\frac{d}{dt} g(t) = g^2(t) + \varphi(t), \tag{26}$$

and

$$\varphi(t) = d(t) - \frac{1}{4} b^2(t) - \frac{1}{2} \frac{db(t)}{dt}.$$

or

$$y(t) = \gamma(t) \exp\left(-\frac{1}{2}\int b(t)\,dt\right) \times$$
$$\times \left\{\int\limits_{t_0}^{t} \frac{1}{\gamma^2(t)}\left[\int\limits_{t_0}^{t} f(t)\,\gamma(t) \exp\left(\frac{1}{2}\int b(t)\,dt\right)dt + C_1\right] dt + C_2\right\}, \tag{27}$$

where the function $\gamma(t)$ satisfies the equation

$$\frac{d^2}{dt^2}\gamma(t) + \varphi(t)\,\gamma(t) = 0. \tag{28}$$

III. We shall find the conditions which the functions $C_1(t)$ and $C_2(t)$ must satisfy in expressions (17) or (19). We have

$$\frac{\partial^k Y_1(t, p)}{\partial t^k} = \sum_{v=0}^{n} C_k^v (-p)^{k-v} e^{-tp} F_3(p) \times$$
$$\times \left\{\int\limits_{p_0}^{p} F_2(p)\left[\int\limits_{p_0}^{p} p^v e^{tp} F_1(p)\,dp + \frac{d^v}{dt^v} C_1(t)\right] dp + \frac{d^v}{dt^v} C_2(t)\right\},$$

where

$$F_1(p) = \frac{\exp\left(\frac{1}{2}\int \frac{B(p)}{D(p)}\,dp - \int g(p)\,dp\right)}{D(p)} = \frac{\gamma(p)}{D(p)} \exp\left(\frac{1}{2}\int \frac{B(p)}{D(p)}\,dp\right),$$
$$F_2(p) = \exp\left(2\int g(p)\,dp\right) = \frac{1}{\gamma^2(p)},$$
$$F_3(p) = \exp\left(-\frac{1}{2}\int \frac{B(p)}{D(p)}\,dp - \int g(p)\,dp\right) = \gamma(p) \exp\left(-\frac{1}{2}\int \frac{B(p)}{D(p)}\,dp\right).$$

Substituting the latter expression into Eq. (5), we obtain

$$\sum_{k=0}^{n} \frac{1}{k!} \frac{\partial^k N(t, p)}{\partial p^k} \sum_{v=0}^{k} C_k^v (-p)^{k-v} e^{-tp} F_3(p) \times$$
$$\times \left\{\int\limits_{p_0}^{p} F_2(p)\left[\int\limits_{p_0}^{p} p^v e^{tp} F_1(p)\,dp + \frac{d^v}{dt^v} C_1(t)\right]dp + \frac{d^v}{dt^v} C_2(t)\right\} = 1,$$

or

$$\sum_{v=0}^{n} \sum_{k=v}^{n} \frac{1}{(k-v)!} \frac{\partial^k N(t, p)}{\partial p^k} (-p)^{k-v} e^{-tp} F_3(p) \times$$
$$\times \left\{\int\limits_{p_0}^{p} F_2(p)\left[\int\limits_{p_0}^{p} \frac{p^v}{v!} e^{tp} F_1(p)\,dp + \frac{d^v}{dt^v} C_1(t)\right] dp + \frac{d^v}{dt^v} C_2(t)\right\} = 1,$$

or

$$\sum_{v=0}^{n} \frac{\partial^v N(t,p)}{\partial p^v}\bigg|_{p=0} e^{-tp} F_3(p) \times$$

$$\times \left\{ \int_{p_0}^{p} F_2(p) \left[\int_{p_0}^{p} \frac{p^v}{v!} e^{tp} F_1(p)\, dp + \frac{d^v}{dt^v} C_1(t) \right] dp + \frac{d^v}{dt^v} C_2(t) \right\} = 1.$$

or

$$\int_{p_0}^{p} F_2(p) \left[\int_{p_0}^{p} e^{tp} F_1(p) \sum_{v=0}^{n} \frac{1}{v!} \frac{\partial^v N(t,p)}{\partial p^v}\bigg|_{p=0} p^v dp + \right.$$

$$\left. + \sum_{v=0}^{n} \frac{1}{v!} \frac{\partial^v N(t,p)}{\partial p^v}\bigg|_{p=0} \frac{d^v}{dt^v} C_1(t) \right] dp + \sum_{v=0}^{n} \frac{1}{v!} \frac{\partial^v N(t,p)}{\partial p^v}\bigg|_{p=0} \frac{d^v}{dt^v} C_2(t) = \frac{e^{tp}}{F_3(p)},$$

or

$$\int_{p_0}^{p} F_2(p) \left[\int_{p_0}^{p} e^{tp} F_1(p) \frac{A(p) + tB(p) + t^2 D(p)}{D(p)}\, dp \right] dp +$$

$$+ \int_{p_0}^{p} F_2(p)\, dp \sum_{v=0}^{n} \frac{1}{v!} \frac{\partial^v N(t,p)}{\partial p^v}\bigg|_{p=0} C_1(t) +$$

$$+ \sum_{v=0}^{n} \frac{1}{v!} \frac{\partial^v N(t,p)}{\partial p^v}\bigg|_{p=0} \frac{d^v}{dt^v} C_2(t) = \frac{e^{tp}}{F_3(p)},$$

or, finally,

$$\sum_{k=0}^{n} \frac{1}{k!} \frac{\partial^k N(t,p)}{\partial p^k}\bigg|_{p=0} \frac{d^k}{dt^k} C_2(t) = \frac{e^{tp_0}}{F_3(p_0)},$$

where

$$\frac{1}{k!} \frac{\partial^k N(t,p)}{\partial p^k}\bigg|_{p=0} = a_{k,0} + a_{k,1} t + a_{k,2} t^2.$$

Thus, we have established the following fact: if in Eq. (5) the function $N(t,p)$ is a polynomial of second degree in $\underline{t}$, then the function $Y_1(t,p)$ defined by formulas (17) or (19) satisfies Eq. (5) for the condition that the function $C_2(t)$ satisfies Eq. (21).

In accordance with the above, the function $C_1(t)$ can be chosen arbitrarily in expressions (17) and (19); for example, $C_1(t) = C_1 = \text{const}$.

SUMMARY

There is explained a method of determination of transfer functions of systems described by common high-order differential equations with variable coefficients when these coefficients are polynomials.

LITERATURE CITED

1. A. I. Lur'e, Operational Calculus [in Russian] (Gostekhizdat, 1951).
2. L. A. Zadeh, "Frequency analysis of circuits with varying parameters", Proc. IRE, 38, No. 3 (1950).

ON METHODS FOR REALIZING A FINITE AUTOMATON WHOSE CYCLICAL NATURE IS DETERMINED BY THE VARIATION OF THE INPUT STATE

M. A. Aizerman, L. A. Gusev, L. I. Rozonoer, I. M. Smirnova,
and A. A. Tal'
(Moscow)

Translated from Avtomatika i Telemekhanika, Vol. 21, No. 12,
pp. 1576-1594, December, 1960
Original article submitted May 24, 1960

The paper studies three methods for an economical (in the sense of the number of states) realization of a finite automaton specified by an equation (table) and operating in a cyclic manner determined by the variations in the states of its inputs.

The methods differ as a function of the quantity of information arriving at the input of the automaton. The first method (the Huffman method) is used when the minimum information (information solely on the state of the input at the given instant) is available; the second method presupposes that additional information on the instants at which the input states change is supplied to the automaton; the third method is used when information on the state of the input at both the given instant and at a certain preceding instant is supplied to the automaton.

It is demonstrated that under conditions where the third method is used it is possible to achieve the most economical automaton.

1. A FINITE AUTOMATON AND A SEQUENTIAL MACHINE

In [1, 2] a finite automaton is defined as a dynamic system whose behavior at specified instants of time (cycles) 1, 2, . . . , p is determined by the equation

$$\varkappa(p) = F[\varkappa(p-1),\ \rho(p-1)], \tag{1}$$

where $\varkappa(p)$ and $\rho(p)$ are variables which acquire values from specified finite alphabets $\{\varkappa\}$ and $\{\rho\}$ (the alphabet $\{\varkappa\}$ contains $\underline{k}$ symbols, and the alphabet $\{\rho\}$ contains r symbols); $F(\varkappa, \rho)$ is a single-valued function.

The basic table for the automaton in [1, 2] was defined as the table (cf. Table 1) in which each column was assigned a definite value $\rho(p-1)$, and each row was assigned a definite value $\varkappa(p-1)$; the corresponding value of $\varkappa(p)$, determined on the basis of (1), is written in the square located at the intersection of any row and column.

The output of the automaton was made to correspond to the variable λ which acquired values from the alphabet $\{\lambda\}$ containing $\underline{l}$ symbols. This variable was defined by the equation

$$\lambda(p) = \Phi[\varkappa(p)], \tag{2}$$

which in [1, 2] was called the equation for the output converter.

TABLE 1

	ρ_1	ρ_2	$\cdots$	ρ_r
$\varkappa_1$	$\varkappa_3$	$\varkappa_2$	$\cdots$	$\varkappa_7$
$\varkappa_2$	$\varkappa_1$	$\varkappa_r$	$\cdots$	$\varkappa_2$
$\vdots$	$\vdots$	$\vdots$	$\cdots$	$\vdots$
$\varkappa_k$	$\varkappa_4$	$\varkappa_2$	$\cdots$	$\varkappa_2$

We shall now make two remarks concerning these concepts.

1. By introducing the new variable μ, Eq. (1) can be written as

$$\varkappa(p) = \mu(p-1), \quad \mu(p) = F[\varkappa(p), \rho(p)]. \tag{3}$$

If we eliminate μ from (3), then we immediately obtain Eq. (1). But, if we eliminate $\varkappa$ from (3), then we obtain

$$\mu(p) = F[\mu(p-1), \rho(p)]. \tag{4}$$

Therefore, it is natural to apply the term "finite automaton" to dynamic systems whose behavior is described by Eq. (4); i.e., it is applied in the general case in the system of equations (3).

2. It is natural to study output converters of a more general type

$$\lambda(p) = \Psi[\varkappa(p), \rho(p)], \tag{5}$$

instead of (2).

A converter of the type

$$\lambda(p) = \Phi[\mu(p), \rho(p)] \tag{5'}$$

can be treated as a particular case of (5), since if we take (3) into account we obtain the relationship

$$\lambda(p) = \Phi\{F[\varkappa(p), \rho(p)], \rho(p)\},$$

instead of (5'); this latter relationship does not differ from (5). Note that for the same reason a converter of the type

$$\lambda(p) = \Phi[\varkappa(p), \mu(p), \rho(p)]$$

is also no more general than the converter (5).

We shall treat Eq. (3) and (5) jointly. A dynamic system which is described by the system of equations (3) + (5) is often a sequential machine. We shall also make use of this term henceforth.*

Since Eq. (2) is a particular case of Eq. (5), the concept "sequential machine" includes the concept "finite automaton." But, on the other hand, there exists the following theorem which demonstrates that a sequential machine "cannot do" any more than a finite automaton with an output converter (cf. also thereom 1 in [4]).

Theorem. Each sequential machine M can be made to correspond to a finite automaton A with an output converter in such a way that for any initial state of machine M we find an initial state of automaton A which for any input sequence results in an output sequence of automaton A for all p ≥ 1that reproduces the output sequence of machine M with a lag of one cycle. Conversely, each automaton A with an output converter can be made to correspond to a sequential machine M in such a way that for any initial state of automaton A there can be found an initial state of machine M which for any input sequence will cause the output sequence of the machine M to reproduce the output sequence of automaton A with a lead of one cycle for all p ≥ 0 (cf. proof of the theorem in Appendix I).

If the problem is to clarify what a sequential machine and a finite automaton "can do," then in view of the proven theorem cited above there is no need to analyze them separately. But these concepts are not equivalent in the sense that for the performance of the same "task" a sequential machine may require a smaller number of states than the corresponding finite automaton. This fact is essential for us, since in this paper we shall study precisely the problem of minimizing the number of states.

---

* In [3] the term "sequential machine" denotes a system which is described by Eq. (1) + (2); i.e., in our terminology it is a finite automaton with an output converter.

2. STATEMENT OF THE PROBLEM

The system of equations (3) + (5) contains four variables: λ, μ, $\varkappa$, and ρ. If two of them ($\varkappa$ and μ) can be eliminated from the system in such a way that the remaining variables (λ and ρ) are related to an expression of the form

$$\lambda(p) = F_1[\lambda(p-1), \rho(p)] \tag{6}$$

or

$$\lambda(p) = F_2[\lambda(p-1), \rho(p-1)], \tag{6'}$$

then this means that the sequential machine (3) + (5) will again form an automaton* whose states are coded using the symbols $\{\lambda\}$. Of course, such an elimination of variables is far from being possible in all cases, and thus a sequential machine does not always realize a finite automaton.

In this paper we study only sequential machines which will realize a finite automaton (6); the finite automaton must be such that its operational cycles 1, 2, ... , p are determined in a single-valued manner by the instants at which the input state changes. It is precisely with this case that we must deal when we design contact-relay networks.** It is assumed that the basic table for the automaton (6) is given. The purpose of this paper is to study various methods for realizing this basic table using a sequential machine, and for determining a minimum number of states which the sequential machine must have for various realizations when it operates in accordance with the specified table.

The methods for realizing the specified automaton are separated in accordance with the volume of information concerning the state of the input which is "communicated" to the automaton from the outside.

The minimum information on the input which must be introduced into the automaton is information on the state of the input at a specified instant (i.e., the symbol $\rho(p)$). When only this information is available, the realization of the automaton on the basis of delay elements (cf. for example, [1, 2]) cannot be achieved directly, since in order to control the delay elements certain additional information on the onset of a cycle must be introduced into these elements; i.e., information of the change of the input state (a signal from a "clock"***). In that case it is possible to use the method described in [2] for constructing an automaton operating in cycles that coincide with the input change from another automaton which operatores on "fast" cycles that are determined by subdividing the time axis into intervals that are small compared to the intervals $\rho(p)$ over which the inputs change. For simplicity in presentation we shall assume that the "fast" cycling is uniform. The problem then reduces to studying the scheme shown in Fig. 1. In this scheme A (the broken line) denotes a specified automaton that operates in cycles over which the inputs are changed; F denotes a "fast" automaton operating over "fast" cycles that are not in any way associated with $\rho(p)$; Conv. is the output converter. In other words, a specified finite automaton (6) is realized from a sequential machine (4) + (5) under conditions where the cycling of automaton (4) is assumed to be "fast" and in no way related to the instants ρ (p) at which the changes occur. The problem consists of determining the minimum number of states for automaton F, its basic table, and the table for the converter Conv. from the specified basic table for automaton A.

---

*The basic table for such an automaton is also of the form shown for Table 1; however, the symbol λ is written throughout in place of $\varkappa$.

**If we have in mind a contact-relay network, then ρ denotes the state of the input contacts, and λ denotes the states of the output circuits (the actuating relays). The basic table specifies the states of the output circuits as a function of their preceding states and of their inputs; the number of automaton states (this is the quantity of interest to us) then predetermines the number of secondary relays which the corresponding multicycle relay network must contain. The cycling is determined by the changes of the input states if each operation occurs at the instant that the state of the input contacts of the network changes.

***It is assumed that such a "clock" can be artificial.

In section 3, we demonstrate how this problem is solved by the Huffman method [5].

In section 4, it is assumed that information on the instants ρ (p) at which the changes occur* is fed to the automaton from outside in addition to the symbols proper.

When such information on the input is available, automaton A can be realized directly by using delay elements. It is demonstrated that the number of states under these conditions can be made less than when realization is achieved according to the scheme shown in Fig. 1.

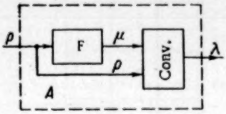

Fig. 1.

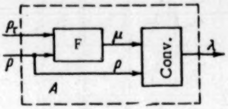

Fig. 2.

In section 5, we study the case where information on the input states ρ (p) and ρ_τ (p) at the specified instant and τ sec before, respectively, is introduced continuously into the automaton; here τ is the time interval between cycles of the "fast" automaton (Fig. 2). It is demonstrated that in this case, the number of required states for automaton F may not only be substantially reduced, but can be in a certain definite sense reduced to a limitingly small number. This means that no other measures (in particular, no further increase in the input information) can realize an automaton F with a small number of internal states.

3. THE RELIZATION OF AUTOMATON A ON THE BASIS OF USING THE STABLE STATES OF THE "FAST" AUTOMATON F

Assume that the basic table for automaton A is specified and that it is required to realize this automaton according to the scheme in Fig. 1. As a specific example of the basic table for this automaton A being synthesized, we shall study Table 2.

We shall count the number of different symbols in the alphabet $\{\lambda\}$ in some column of the table under study. We shall denote this number by a_j (the values of a_j for Table 2 are written out in its lower row) and shall determine $\alpha = \sum_{j=1}^{r} \alpha_j$ (for the case of Table 2 we have $\alpha = 10$).

Now we shall formulate a new table containing r columns (corresponding to the r inputs $\rho_1, \rho_2, \ldots, \rho_r$) and α rows. In each of the columns of the new table we write all of the different symbols λ which are encountered in the corresponding column of the original table; we write them in such a way that in each row of the new table we have written one and only one value of λ (Table 3 is filled in accordance with Table 2).

We shall study some row in the new table (for example, the fourth row from the top in Table 3). In the square of this row corresponding to input ρ_2 we have written the value λ_2. Returning to the original table (Table 2) we find the symbols located in those squares of λ, which correspond to the remaining inputs (in this particular case, ρ_1 and ρ_3). In our examples, it is λ_6 in the column ρ_1, and λ_3 in the column ρ_3. In Table 3 we write the subscripts for these λ in the fourth row which is under study; i.e., we write the number 6 in the square corresponding to ρ_1, and the number 3 in the square corresponding to ρ_3 (Table 4). Proceding in the same fashion in each row of Table 3, we fill all of its squares (Table 5).

---

[*] For example, there is an individual input filament which may be in one of two states; these states change only when ρ (p) changes.

TABLE 2

	ρ_1	ρ_2	ρ_3
λ_1	λ_5	λ_2	λ_3
λ_2	λ_6	λ_4	λ_3
λ_3	λ_6	λ_2	λ_6
λ_4	λ_5	λ_3	λ_3
λ_5	λ_7	λ_2	λ_1
λ_6	λ_7	λ_5	λ_1
λ_7	λ_5	λ_3	λ_6
α_j	3	4	3

TABLE 3

ρ_1	ρ_2	ρ_3
λ_5		
λ_6		
λ_7		
	λ_2	
	λ_4	
	λ_3	
	λ_5	
		λ_3
		λ_6
		λ_1

For the purpose of more efficiently isolating those squares in Table 5, in which the symbols λ_i, are written rather than the subscripts, the symbols are placed in parentheses.

The table in its new form (Table 5) represents merely a different form of notation for the original Table 2 and coincides with the "table of transfers" (the flow-table) introduced by Huffman [5].

Any basic table for a specified automaton can be reformulated in accordance with the flow table in a manner which is completely analogous to that described above using the example of Table 2 and Table 5. Further analysis leading to the solution of the problem which we have posed follows from the results of [5] and is further demonstrated using the example of Table 5.

We shall assign the corresponding symbol from the alphabet $\{\mu\}$ to each row of the flow table; we shall write it in at the left (Table 5). We shall study any column in Table 5 as the basic table for an autonomous automaton that has ten states denotes by the symbols μ_i (i = 1, . . . , 10). Of these states the stable ones are those which correspond to the squares containing symbols in parentheses. The numbers in the remaining squares are treated as indications of the stable state to which the autonomous automaton is transferred during one cycle. As an example, Fig. 3 shows the graphs for the three autonomous automatons (for ρ_1, ρ_2, and ρ_3) that correspond to Table 5.

Now we shall study the automaton F which operates in arbitrary but sufficiently rapid cyclical manner* and realizes these graphs. The basic table for automaton F is immediately restored from the flow table, and, for example, for the case shown in Fig. 3 (i.e., Table 5) it has the form shown in Table 6.

Finally, we shall formulate the converter Conv. which makes each value μ_i correspond to the value λ_j which was written into the row μ_i in the flow table. For the case of Table 5 this converter is determined in accordance with Table 7.

---

*It is required only that the time between two cycles of automaton F be less than the time between any two changes in the value of ρ.

TABLE 4

ρ_1	ρ_2	ρ_3
λ_5		
λ_6		
λ_7		
6	λ_2	3
	λ_4	
	λ_3	
	λ_5	
		λ_3
		λ_6
		λ_1

TABLE 5

	ρ_1	ρ_2	ρ_3
μ_1	(λ_5)	2	1
μ_2	(λ_6)	5	1
μ_3	(λ_7)	3	6
μ_4	6	(λ_2)	3
μ_5	5	(λ_4)	3
μ_6	6	(λ_3)	6
μ_7	7	(λ_5)	1
μ_8	6	2	(λ_3)
μ_9	7	5	(λ_6)
μ_{10}	5	2	(λ_1)

TABLE 6

	ρ_1	ρ_2	ρ_3
μ_1	μ_1	μ_4	μ_{10}
μ_2	μ_2	μ_7	μ_{10}
μ_3	μ_3	μ_6	μ_9
μ_4	μ_2	μ_4	μ_8
μ_5	μ_1	μ_5	μ_8
μ_6	μ_2	μ_6	μ_9
μ_7	μ_3	μ_7	μ_{10}
μ_8	μ_2	μ_4	μ_8
μ_9	μ_3	μ_7	μ_9
μ_{10}	μ_1	μ_4	μ_{10}

We shall use the scheme in Fig. 4 to formulate a sequential machine from automaton F (this machine has a basic table given by Table 6) and the converter Conv. (the converter is based on Table 7).

If the readout unit reads out the symbols ρ and λ only the instants $t_1 + \tau$, $t_2 + \tau$, . . . , $t_p + \tau$, where t_1, t_2, . . . , t_p are the instants at which the input changes (these instants determine the cycling) and τ is the duration of a cycle in the "fast" automaton F, then these values of ρ and λ are related to each other by the original Table 2; thus automaton A is realized.

We shall now turn from the scheme of Fig. 4, to the scheme shown in Fig. 1; i.e., we shall apply not only μ but also ρ to the input of the converter.

Using the scheme in Fig. 1, it is possible to construct not merely one but a set of sequential machines which realize the specified automaton A. They differ from one another both in terms of the automaton F and in terms of their converters Conv. Among this set of sequential machines we find minimal machines; i.e., we find those in which automaton F has the smallest number of states. We already know one sequential machine in this set (it was formulated above from the scheme in Fig. 4 and is a particular case of the scheme shown in Fig. 1); generally speaking, however, this machine is not minimal. We are required to find a minimal sequential machine.

TABLE 7

μ	μ_1	μ_2	μ_3	μ_4	μ_5	μ_6	μ_7	μ_8	μ_9	μ_{10}
λ	λ_5	λ_6	λ_7	λ_2	λ_4	λ_3	λ_5	λ_3	λ_6	λ_1

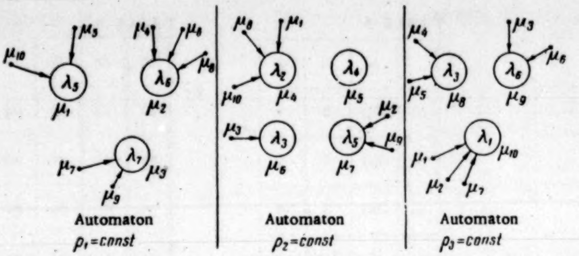

Automaton $\rho_1 = const$ Automaton $\rho_2 = const$ Automaton $\rho_3 = const$

Fig. 3.

Two sequentail machines B and C shall be called equivalent (cf. [6]) if for each state b̲ of machine B there is found at least one state c̲ in machine C (and conversely, for each state c' of the machine C there is found a state b' of the machine B) which is such that for any identical input sequences the machines will produce identical output sequences beginning with the initial states b, c or b', c'. If the state b under study can be made to correspond to several states c̲, then we shall combine these states into a group {c}. It is directly evident that states combined into a group {c} are equivalent in the sense that for any input sequence the output sequence of machine C is independent of the state in the group {c} which is chosen as the initial state.

By studying all the states b̲ in the machine B in sequence, we subdivide all the states for the machine C into non-intersecting groups of equivalent states.

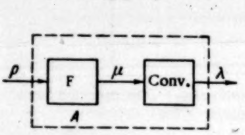

Fig. 4.

Obviously, it may occur that several states b̲ correspond to one and the same group of states {c}. Then these states b̲ form a group of equivalent states for machine B. If only one state b̲ corresponds to the group of states {c}, then we shall say that this state b̲ forms a group consisting of one element.

From the above it is evident that even though equivalent sequential machines B and C have a different number of states, these states are subdivided into an identical number of paired equivalent groups. This number of groups is an invariant; i.e., it does not change for transition from one machine to any other equivalent machine.

The invariant number can be determined from a study of any single sequential machine in the given set by combining all of its equivalent states into groups. Each group cannot contain less than one state. Therefore, it is clear that if among a set of equivalent sequential machines there were to be found a sequential machine in which each group contained only one state, then this would be the sequential machine with the minimum possible number of states in the given set.

As we have already stated, in this paper we are treating only those sequential machines which realize a finite automaton.

The states which can be established in the automaton after any change in the input are fully defined by one row in the flow table (Table 5). Assume now that the flow table contains several rows with identical numbers in identical columns.* Then it is easy to see that the states corresponding to these rows are equivalent.

In fact, due to the effect produced by any input these states make the transition into exactly the same new state; this is true because in each column of the table there cannot appear two different circles with identical symbols. Therefore, all subsequent changes of the inputs lead to one and the same sequence of changes in state; this, in turn causes the appearance of identical output sequences.

---

*For squares which do not contain (λ_j) the number written in the square is assumed to represent the subscript j̲.

Conversely, the states μ_k and μ_s are certainly not equivalent if the corresponding rows of the table contain different numbers even in one column.

Now we examine the flow table, isolate all the coincident rows, and replace each group of coincident rows with one row containing the same numbers. Under these conditions all the symbols (λ_j) which are encountered even in one of the coincident rows are retained in the single row which replaces the coincident rows. Thus, for example, in Table 5, the coincident fourth and eighth rows

μ_4	6	(λ_2)	3
μ_8	6	2	(λ_3)

are replaced by the row

μ_4	6	(λ_2)	(λ_3)

,

and the first and tenth coincident rows

μ_1	(λ_5)	2	1
μ_{10}	5	2	(λ_1)

are replaced by the row

μ_1	(λ_5)	2	(λ_1)

.

After combining all coincident rows and numbering them, we replace Table 5 with Table 8.

The flow table in which all possible substitutions of this kind are made is called the minimal flow table. Assume that it contains β rows. From the above it follows that it determines a sequential machine that is equivalent to the specified automaton and in which each group contains only one state. This is the sought for minimal sequential machine.

From the minimal flow table we immediately restore the original table for the automaton F and the converter. For the example above these correspond to Tables 9 and 10, respectively, (the dashes in Table 10 denote that the contents of the corresponding squares have no significance for the operation of the sequential machine).

Automaton F can now be formulated by the methods of aggregation from any appropriate set of elements. When the relay method of realization is used, we require at least s_0 secondary relays, where s_0 is the minimum number satisfying the inequality

$$2^{s_0} \geq \beta.$$

In order to avoid "competition" between elements, the number of relays must be increased. When the $(2s_0 + 1)$-realization developed by Huffman [5] is used for this purpose we require $2s_0 + 1$ relays.

4. THE REALIZATION OF AUTOMATON A USING DELAY ELEMENTS

Assume now that in addition to the information on the instantaneous value ρ of the automaton input we have a special device ("a clock") which signals the onset of a cycle of automaton A. In this case, for which the cyclical operation is determined by any change in the input state, this means that we have additional information available on the fact that the symbol ρ changed at the input of the automaton.

When such additional information is present there is no longer any need to construct automaton A (whose cyclical operation is determined by the instants at which the input states change) using the "fast" automaton F. In that case automaton A can be constructed directly from elements operating in the required cyclical manner; this can be done using aggregation methods for constructing automaton A from any complete set in the manner described in [1]. If, for example, the automaton is constructed from a complete set consisting of delay elements and logic converters, then the additional information on the change on the input is applied to all the delay elements. In realizing the automaton according to the method described in [1] it will have l states, where l is the number of rows in the basic table being realized (in our example this is Table 2). Sometimes $l < \beta$, and then such a construction of automaton A is more economical than that described in section 2 involving its construction from a "fast" automaton F. But, it is also possible that $l > \beta$; in these cases the realization of the automaton described in [1] is less economical than its realization from automaton F.

Note, however, that in [1] no limitations were imposed on the sequences $\rho(t)$ which could be applied to the input of the automaton.

In the case under study here, for which the cyclical operation is determined solely by the instants at which the symbol ρ changes, the choice of the input sequences $\rho(t)$ is limited by the fact that one and the same symbol cannot be repeated twice in succession in the input sequence. Thus, for example, the sequence

Cycle	1	2	3	4	5	...
ρ	ρ_1	ρ_7	ρ_3	ρ_6	ρ_6	...

cannot occur, since the fifth cycle cannot arise as long as the symbol ρ_6 is not replaced by another symbol.

The limitation which this condition imposes on the possible input sequence makes it possible to use elements operating in the required cyclical manner to construct an automaton A which realizes the specified basic table and has less than l states. Below we shall demonstrate that for such a realization we require no more than β (and often substantially less) states.

We shall use R to denote the set of all input sequences $\rho(t)$ which satisfy the limitation indicated above. Now the problem can be formulated as follows. Assume that we have specified the basic table for automaton A with states and inputs taken from the alphabets $\{\lambda\}$ and $\{\rho\}$, respectively. It is required to construct a sequential machine B.

$$\begin{aligned} \varkappa(p) &= \mu(p-1), \\ \mu(p) &= F[\varkappa(p), \rho(p)], \\ \lambda(p) &= \Phi[\varkappa(p), \rho(p)], \end{aligned} \tag{7}$$

such that for all sequences belonging to the set R it will realize the table for automaton A and have the minimum possible number of states s. In other words, it is required to find the minimal sequential machine from the class of sequential machines which are equivalent relative to the set R and realize the basic table of the automaton.*

In order to solve this problem we shall use the specified basic tables of the realized automaton A to formulate the corresponding flow table (for the example under study this is Table 5); then we modify this flow table in the following manner.

1. In all squares containing just numbers [and not symbols (λ_j)] we write the additional symbol μ indicating the state into which the system transfers due to the flow table. Thus, for example, in row μ_4 and column ρ_1 we write the additional symbol μ_2 along with the number 6, since in this column the symbol λ_6 in parentheses is located in row μ_2. As a result we obtain Table 11 instead of Table 5.

2. After that we eliminate all symbols corresponding to stable states from the flow table; i.e., we eliminate all the symbols λ_i in parentheses. The squares in which these symbols were written are left empty.

3. In the entire table we replace the symbols μ by the symbols $\varkappa$ while retaining the subscripts. As a result of this we obtain Table 12 instead of Table 5.

In contrast to the flow table which describes the operation of the machine

---

* Here we shall call two sequential machines B and C equivalent relative to the set of input sequences R if each state of machine B can be made to correspond to a state of machine C (and conversely); thus, when any two corresponding states are assumed to be the initial states, machines B and C respond to any identical input sequences belonging to the set R by producing identical output sequences $\lambda(t)$ (cf. [7]).

TABLE 8

	ρ_1	ρ_2	ρ_3
μ_1	(λ_5)	2	(λ_1)
μ_2	(λ_6)	5	1
μ_3	(λ_7)	3	6
μ_4	6	(λ_2)	(λ_3)
μ_5	5	(λ_4)	3
μ_6	6	(λ_3)	6
μ_7	7	(λ_5)	1
μ_8	7	5	(λ_6)

TABLE 9

	ρ_1	ρ_2	ρ_3
μ_1	μ_1	μ_4	μ_1
μ_2	μ_2	μ_7	μ_1
μ_3	μ_3	μ_6	μ_8
μ_4	μ_2	μ_4	μ_4
μ_5	μ_1	μ_5	μ_4
μ_6	μ_2	μ_6	μ_8
μ_7	μ_3	μ_7	μ_1
μ_8	μ_3	μ_7	μ_8

TABLE 10

	ρ_1	ρ_2	ρ_3
μ_1	λ_5	—	λ_1
μ_2	λ_6	—	—
μ_3	λ_7	—	—
μ_4	—	λ_2	λ_3
μ_5	—	λ_4	—
μ_6	—	λ_3	—
μ_7	—	λ_5	—
μ_8	—	—	λ_6

$$\mu(p) = F[\mu(p-1),\ \rho(p)], \qquad \lambda(p) = \Phi[\mu(p),\ \rho(p)],$$

the reformulated Table 12 describes the operation of the machine

$$\varkappa(p) = F[\varkappa(p-1),\ \rho(p-1)], \qquad \lambda(p) = \Phi[\varkappa(p),\ \rho(p)].$$

In view of the reformulated flow table the states of the machine can be subdivided into non-intersecting groups corresponding to the symbols $\varkappa_i$; these groups may appear for one another input symbol ρ_j. Thus, for example, according to Table 12 the input ρ_1 corresponds to the group of states $G_1\{\varkappa_1, \varkappa_2, \varkappa_3\}$, the input ρ_2 corresponds to the group $G_2\{\varkappa_4, \varkappa_5, \varkappa_6, \varkappa_7\}$, and the input ρ_3 corresponds to the group $G_3\{\varkappa_8, \varkappa_9, \varkappa_{10}\}$. But, in view of the limitation imposed on the class of possible input sequences, two identical input symbols cannot be encountered in succession. Therefore, if the machine is in one of the states in group G_i, then the symbol ρ_i cannot appear at the input.

It is precisely for this reason that the squares corresponding to states in the group G_i are left unfilled in the column ρ_i of the reformulated flow table. In determining the sequence $\varkappa(t)$ from the specified sequence $\rho(t)$ it is never necessary to know the contents of those squares, provided only that the input sequence of symbols ρ belongs to the set R (i.e., if it does not contain repeating symbols). Therefore, these empty squares can be filled quite arbitrarily.

The states of the machine can be called equivalent relative to the set of input sequences R if a machine having these states as initial states responds with identical output sequences to identical input sequences in the set R.

The problem of constructing a minimal machine reduces to the problem of combining states that are equivalent relative to R. However, the problem of matching states in machines for which the set of input sequences is bounded involves essential peculiarities in comparison to the analogous problem in the preceding section (cf. [7]). We shall study any two rows in Table 12 and compare them; we shall pay attention only to the output symbols and shall take into account the fact that we can write an arbitrary symbol in the empty squares. We shall say that two rows coincide if we can fill the empty squares in such a way that the squares in identical columns contain identical symbols $\varkappa$.

TABLE 11

	ρ_1	ρ_2	ρ_3
μ_1	(λ_5)	$\mu_4, 2$	$\mu_{10}, 1$
μ_2	(λ_6)	$\mu_7, 5$	$\mu_{10}, 1$
μ_3	(λ_7)	$\mu_8, 3$	$\mu_9, 6$
μ_4	$\mu_2, 6$	(λ_2)	$\mu_8, 3$
μ_5	$\mu_1, 5$	(λ_4)	$\mu_8, 3$
μ_6	$\mu_2, 6$	(λ_3)	$\mu_9, 6$
μ_7	$\mu_3, 7$	(λ_5)	$\mu_{10}, 1$
μ_8	$\mu_2, 6$	$\mu_4, 2$	(λ_2)
μ_9	$\mu_3, 7$	$\mu_7, 5$	(λ_6)
μ_{10}	$\mu_1, 5$	$\mu_4, 2$	(λ_1)

TABLE 12

	ρ_1	ρ_2	ρ_3
$\varkappa_1$		$\varkappa_4, 2$	$\varkappa_{10}, 1$
$\varkappa_2$		$\varkappa_7, 5$	$\varkappa_{10}, 1$
$\varkappa_3$		$\varkappa_8, 3$	$\varkappa_9, 6$
$\varkappa_4$	$\varkappa_2, 6$		$\varkappa_8, 3$
$\varkappa_5$	$\varkappa_1, 5$		$\varkappa_8, 3$
$\varkappa_6$	$\varkappa_2, 6$		$\varkappa_9, 6$
$\varkappa_7$	$\varkappa_3, 7$		$\varkappa_{10}, 1$
$\varkappa_8$	$\varkappa_2, 6$	$\varkappa_4, 2$	
$\varkappa_9$	$\varkappa_3, 7$	$\varkappa_7, 5$	
$\varkappa_{10}$	$\varkappa_1, 5$	$\varkappa_4, 2$	

If two rows coincide, then it follows immediately from the definition of "states equivalent relative to R" that the symbols $\varkappa$ written in these rows corresponds to non-equivalent states. Such rows cannot be made to coincide. Examples of such rows are 1 and 3, 4 and 10, etc., in Table 12.

However, if two rows coincide, then we obtain identical output subscripts in each column if the empty squares are appropriately filled. In view of the definition, the symbols $\varkappa$ used in these rows correspond to states that are equivalent to R.

Thus, in Table 12, for example, such states are $\varkappa_1$ and $\varkappa_{10}$ (the first and tenth rows, respectively), $\varkappa_1$ and $\varkappa_7$, $\varkappa_2$ and $\varkappa_7$, $\varkappa_2$, and $\varkappa_9$, etc.

Note, however, that if we combine the first and seventh rows, it follows that after that, the first row can no longer be combined with the tenth row, nor can the second row be combined with the seventh. Thus, the compression of the table on the basis of combining a number of rows can be achieved in more than one fashion, and the limiting compression is achieved by examining the various possible entries in the emtpy squares.

Under these conditions the compressed table with the minimal possible number of rows may not be the only such table. Thus, in the example cited above, (Table 12) four different combinations of states are possible which lead to the same minimal number (five) of rows:

I. $\{\varkappa_1, \varkappa_8\}$, $\{\varkappa_2, \varkappa_7, \varkappa_9\}$, $\{\varkappa_3, \varkappa_6\}$, $\{\varkappa_4\}$, $\{\varkappa_5, \varkappa_{10}\}$;
II. $\{\varkappa_1, \varkappa_{10}\}$, $\{\varkappa_2, \varkappa_7, \varkappa_9\}$, $\{\varkappa_3, \varkappa_6\}$, $\{\varkappa_4, \varkappa_8\}$, $\{\varkappa_5\}$;
III. $\{\varkappa_1\}$, $\{\varkappa_2, \varkappa_7, \varkappa_9\}$, $\{\varkappa_3, \varkappa_6\}$, $\{\varkappa_4, \varkappa_8\}$, $\{\varkappa_5, \varkappa_{10}\}$;
IV. $\{\varkappa_1, \varkappa_7\}$, $\{\varkappa_2, \varkappa_9\}$, $\{\varkappa_3, \varkappa_6\}$, $\{\varkappa_4, \varkappa_8\}$, $\{\varkappa_5, \varkappa_{10}\}$.

The result obtained from the combination of rows in Table 12 corresponding to the first variant is shown in Table 13. A dash in a square of the table denotes that for the state $\varkappa_4$ the input ρ_2 cannot appear, and thus the contents of this square do not play a part. The fact that Table 12 cannot be compressed to a number of rows less than five can easily be detected from the fact that among the states $\varkappa_1, \varkappa_2, \varkappa_3, \varkappa_4, \varkappa_5$ there is not a single pair of equivalent states.

Assume that we have been able to compress the table down to γ rows. After that we use the table to restore the table for the automaton (we shall call it automaton A^*) and the converter Conv. in exactly the same way as was done at the end of the preceding section (for our example cf. Tables 14 and 15, respectively).

TABLE 13

	ρ_1	ρ_2	ρ_3
$\varkappa_1$	$\varkappa_2$, 6	$\varkappa_4$, 2	$\varkappa_5$, 1
$\varkappa_2$	$\varkappa_3$, 7	$\varkappa_2$, 5	$\varkappa_5$, 1
$\varkappa_3$	$\varkappa_2$, 6	$\varkappa_3$, 3	$\varkappa_3$, 6
$\varkappa_4$	$\varkappa_2$, 6	—	$\varkappa_1$, 3
$\varkappa_5$	$\varkappa_1$, 5	$\varkappa_4$, 2	$\varkappa_1$, 3

TABLE 14

	ρ_1	ρ_2	ρ_3
$\varkappa_1$	$\varkappa_2$	$\varkappa_4$	$\varkappa_5$
$\varkappa_2$	$\varkappa_3$	$\varkappa_2$	$\varkappa_5$
$\varkappa_3$	$\varkappa_2$	$\varkappa_3$	$\varkappa_3$
$\varkappa_4$	$\varkappa_2$	—	$\varkappa_1$
$\varkappa_5$	$\varkappa_1$	$\varkappa_4$	$\varkappa_1$

TABLE 15

	ρ_1	ρ_2	ρ_3
$\varkappa_1$	λ_6	λ_2	λ_1
$\varkappa_2$	λ_7	λ_5	λ_1
$\varkappa_3$	λ_6	λ_3	λ_6
$\varkappa_4$	λ_6	—	λ_3
$\varkappa_5$	λ_5	λ_2	λ_3

A sequential machine constructed according to the scheme shown in Fig. 1 but incorporating automaton A^* instead of the "fast" automaton F realizes the specified automaton A. But now the automaton A^* which contains the constructed machine, no longer operatres with fast cycles (i.e., it does not operate with stable states); rather it operates with the cycles of automaton A (i.e., in cycles determined by changes in the input state). Automaton A^* can therefore be realized from any complete set of elements (for example, it can be constructed from elements which cause a one-cycle delay and instantaneous converters). Automaton A^* has γ states under these conditions.

It is obvious that $\gamma \leq \beta$, since in particular it is possible to fill the empty squares in such a way that the reformulated table coincides with the original (unmodified) flow table. It is also obvious that $\gamma \leq l$, since a realization with l states is always possible as was indicated at the beginning of the section.

On the basis of the above it is possible to determine how to use the additional information concerning the instants at which the input changes introduced into the automaton for the purpose of reducing the number of states; we can also determine how the realization of the automaton from elements operating in the same cyclical manner (for example, using delay elements) is often more advantageous than realizing the automaton from elements operating with "fast" cycles (with stable states).

In Appendix II we demonstrate the relationship between the algorithm cited in this section for compressing the tables and the algorithm for minimization of sequential machines with bounded input sequences [7].

5. THE FURTHER REDUCTION OF THE NUMBER OF STATES IN THE AUTOMATON ON THE BASIS OF INCREASING THE INPUT INFORMATION

We shall return to the scheme which forms automaton A from a "fast" automaton F in accordance with Fig. 1. Assume that δ is the largest number among the numbers α_j (i.e., it is the largest number of different symbols λ that are encountered in any one of the columns in the basic table). Thus, for example, in the case of Table 2, $\delta = 4$. This means that there exist an input state for which δ different symbols λ can appear at the output. But, according to the scheme in Fig. 1, this is possible only when the automaton F has at least δ

different states. Until an output converter is used in the scheme and λ is derived as a logic function of μ and ρ, the number of states of automaton F in principle cannot be made less than δ.

In realizing the automaton according to the scheme shown in Fig. 1 in section 2, we obtained the minimum number of states (which, generally speaking, may be greater than δ). Thus, in the example studied in section 2 we obtained a minimum number of states $\beta = 8$, whereas $\delta = 4$.

We shall assume now (cf. Fig. 2) that both the values ρ (p) and ρ_τ(p) are applied to the input of the automaton (i.e., the values of the input τ seconds before the specified instant are given, where τ is the duration of two"fast" cycles in automaton F).

The instantaneous values of ρ(p) and ρ_τ(p) determine the input state of the automaton. The complete input of this automaton has r^2 states. Therefore, the input alphabet should contain r^2 different symbols. However, we shall make the odd alphabet of $\underline{r}$ symbols suffice; on the other hand, each input state at the specified instant shall be assigned a pair of symbols ρ(p), ρ_τ(p) (in the indicated sequence).

Passing now to the construction of automaton A in accordance with the scheme shown in Fig. 2, we shall illustrate the reasoning above by the example studied in section 3 while keeping the general case in mind.

We shall choose the δ symbols $\mu_1, \mu_2, \ldots, \mu_\delta$. Turning to the first column in the specified basic table for automaton A, we shall assign different symbols μ_j to the different symbols λ_i which appear in that column; we shall assign identical symbols μ_j to identical symbols λ_i appearing in the column. This can always be done, since the number of different symbols λ_i in the column is no greater than δ. Now we shall turn to the second column in the table and shall perform the same operations without associating ourselves in any way with the manner in which the symbols were written in the first column. We shall proceed analogously with all the columns in the table. As a result, each square in the table will contain a symbol μ_j in addition to the symbol λ_i. As an example we cite Table 2 in section 3 with the symbols μ_j written in (Table 16).

From this table we can immediately formulate the table for the output converter in Fig. 2 (Table 17).

TABLE 16

	ρ_1	ρ_2	ρ_3
λ_1	$\lambda_5 \mu_1$	$\lambda_2 \mu_1$	$\lambda_3 \mu_1$
λ_2	$\lambda_6 \mu_2$	$\lambda_4 \mu_2$	$\lambda_3 \mu_1$
λ_3	$\lambda_6 \mu_2$	$\lambda_2 \mu_1$	$\lambda_6 \mu_2$
λ_4	$\lambda_5 \mu_1$	$\lambda_3 \mu_3$	$\lambda_3 \mu_1$
λ_5	$\lambda_7 \mu_3$	$\lambda_2 \mu_1$	$\lambda_1 \mu_3$
λ_6	$\lambda_7 \mu_3$	$\lambda_5 \mu_4$	$\lambda_1 \mu_3$
λ_7	$\lambda_5 \mu_1$	$\lambda_3 \mu_3$	$\lambda_6 \mu_2$

TABLE 17

	ρ_1	ρ_2	ρ_3
μ_1	λ_5	λ_2	λ_3
μ_2	λ_6	λ_4	λ_6
μ_3	λ_7	λ_3	λ_1
μ_4	—	λ_5	—

Here, a portion of the squares may be unfilled; this means that such combinations of ρ and μ are not encountered for the operation of the realized automaton.

The basic table for automaton F contains r^2 columns in accordance with the number of possible combinations of symbols ρ and ρ_τ (in our case the table will contain nine columns; cf. Table 18).

For example, in order to fill the square at the intersection of the row μ_3 and the column ρ_3, ρ_1 in Table 18, we find from Table 17 that the state μ_3 of the input ρ_1 is coded as the symbol λ_7 by the converter. Then from Table 16 we find that for the symbol λ_7 we establish μ_2 due to the effect of the input ρ_3. Thus, we must write μ_2 into the selected square, μ_3, ρ_3, ρ_1. Analogously, we fill all of Table 18 square-by-square. The squares con-

TABLE 18

	ρ_1			ρ_2			ρ_3		
	ρ_1	ρ_2	ρ_3	ρ_1	ρ_2	ρ_3	ρ_1	ρ_2	ρ_3
μ_1	μ_1	μ_2	μ_2	μ_1	μ_1	μ_1	μ_3	μ_1	μ_1
μ_2	μ_2	μ_1	μ_3	μ_4	μ_2	μ_4	μ_3	μ_1	μ_2
μ_3	μ_3	μ_2	μ_1	μ_3	μ_3	μ_1	μ_2	μ_2	μ_3
μ_4	—	μ_3	—	—	μ_4	—	—	μ_3	—

taining dashes denote combinations of states and inputs which cannot be encountered in the automaton for any input sequences.

The scheme shown in Fig. 2 with the converter specified by Table 17 and a "fast" automaton F corresponding to Table 18 realizes the automaton specified by Table 16 if the values of λ and ρ are written in each time during the steady state after ρ has changed.

The number of states in a sequential machine which has been constructed in this manner and realizes the automaton A is therefore equal to δ. Realization using relays can be achieved by any method; for example, a method completely analogous to the $(2s_0 + 1)$-realization developed by Huffman can be used; however, under these conditions we require not s_0 but $\underline{m}$ binary states, where $\underline{m}$ is the minimum number satisfying the inequality $2^m \geq \delta$. We shall therefore speak of the $(2m + 1)$-realization of the specified automaton.

Heretofore we assumed that ρ_τ repeats the values ρ with a lag of τ, where τ is the time between two cycles in the "fast" automaton. When realization is achieved with relays, τ is the time required for operation of the relay. Therefore, at first glance it would seem that besides competition between secondary relays we would encounter an additional problem of competition if ρ_τ repeated ρ with a lag that did not exactly coincide with the operate time for the relay. This concept is incorrect. A method of combating competition between relays [for example, Huffman's $(2s_0 + 1$-realization which becomes $(2m + 1)$-realization in our case] provides for the disconnection of all feedback loops during the steady-state period; by eliminating competition between relays the method thus eliminates competition between relays and the device that produces the signals ρ_τ.

At the beginning of this section we demonstrated that it is impossible to realize automaton A according to a scheme such that as shown in Fig. 1, no matter what additional information on the input is available if automaton F has less than δ states. Therefore within the limits of that basic scheme it is possible to produce an automaton which is more economical in terms of the number of internal states (i.e., in terms of the number of secondary relays when the relay method of realization is used). In other words, the information $\rho + \rho_\tau$ on the state of the input is at its upper limit, and a further increase in the information concerning the input is useless.

In conclusion we shall make the following remark. In comparing the three types of realization for the automaton which were described in sections 3, 4, and 5, we see that the condition $\beta \geq \gamma \geq \delta$ is always valid. In particular, in the example under study (Table 2) the required number of states prove to be equal to 8, 5, and 4, respectively.

If the information on the change in ρ which was discussed in section 4 or the information on the value of ρ which is being discussed in this section were itself to be derived from the information on the instantaneous value of ρ using auxiliary finite automata (networks containing secondary relays) then of course it would be necessary to take into account the states of these auxiliary automata as well. But this information can be introduced into the automaton by the same operator or device which is used to introduce the information on the instantaneous value of ρ; i.e., this information may be just as "external" with respect to the automaton as in ρ. If the same additional information is produced by a special device, then it is essential that this device not be included in the networks of automaton F that are encompassed with feedback loops; this device can be realized by making the input contacts more complex on the basis of completely different engineering means than those used in automaton F. Thus, if the state of any input filament is characterized by the fact that contact a is closed or open, then closure of contact b, which is coupled with contact a by a spring and is equipped with a damper, characterizes the state of that same input with a delay of τ sec. The signal denoting the fact that the input has changed can also be achieved by using purely mechanical means. In those cases, when the input signals are electrical, the information ρ_τ can be organized, for example, using capacitors. In other words, each such device is essentially an input device for the automaton; if, for example, we have relay networks in mind, the input device is no more involved in determining the number of states (or intermediate relays) than are the input or actuating relays in the network.

APPENDIX I

Proof of the theorem. Initially we shall prove the first postulate in the theorem. Assume that a sequential machine M is specified:

$$\varkappa(p) = F[\varkappa(p-1),\ \rho(p-1)], \tag{8}$$

$$\lambda(p) = \Psi[\varkappa(p),\ \rho(p)]. \tag{9}$$

We shall formulate a net (cf. [1]) consisting of two finite automata and specified by the equations

$$y(p) = \bar{F}[y(p-1),\ z(p-1)], \tag{10}$$

$$z(p) = \rho(p-1), \tag{11}$$

and shall specify the output converter

$$\chi(p) = \Psi[y(p),\ z(p)], \tag{12}$$

where the alphabets $\{y\}$ and $\{\chi\}$ coincide with the alphabets $\{\varkappa\}$ and $\{\lambda\}$, respectively. The alphabet $\{z\}$ differs from $\{\rho\}$ by the addition of one symbol z^0; the function Ψ in (12) coincides with the corresponding function in (9) in terms of all pairs of symbols in $\{\varkappa\}$ and $\{\rho\}$; it is not defined (or is arbitrarily specified) for $z = z^0$. The function $\bar{F}$ in (10) coincides with F in (8) for all combinations of symbols that do not contain z^0; for such combinations we have $\bar{F}(y, z^0) \equiv y$. The equations (10) + (11) describe a finite automaton A whose states are coded by the pair (y, z), and Eq. (12) specifies the output converter of that automaton. Each initial state $\varkappa^0$ of the sequential machine M shall be made to correspond to an initial state in automaton A which is such that

$$y(0) = \varkappa^0,\ z(0) = z^0. \tag{13}$$

For $p = 1$ it follows from (10) that $y(1) = y(0) = \varkappa^0$. For $p \geq 1$ the symbol z^0 cannot appear, and at these instants F can be replaced by F in (10); from this we have

$$y(p+1) = F[y(p),\ z(p)],\ p \geq 1. \tag{14}$$

Introducing the new variable $Y(p) \equiv y(p+1)$, $(p \geq 0)$ and taking (11) into account, it is possible to write

$$Y(p) = F[Y(p-1),\ \rho(p-1)],\ p \geq 0, \tag{15}$$

where $Y(0) = y(1) = \varkappa^0$. Equations (8), (15), and the initial conditions $\varkappa(0) = \varkappa^0$, $Y(0) = \varkappa^0$ coincide; in view of this we have

$$Y(p) \equiv \varkappa(p)$$

for any p.

But $y(p) = Y(p-1)$, whence

$$y(p) = \varkappa(p-1),\ p \geq 1. \tag{16}$$

Substituting (11) and (16) into (12) and comparing it with (9), we obtain

$$\chi(p) = \Psi[\varkappa(p-1), \rho(p-1)] = \lambda(p-1), \ p \geq 1,$$

which proves the first postulate in the theorem.

We shall prove the second postulate. Assume that the finite automaton A is specified:

$$\varkappa(p) = F[\varkappa(p-1), \rho(p-1)] \tag{17}$$

with the output converter

$$\chi(p) = \Psi[\varkappa(p)]. \tag{18}$$

We shall make this automaton correspond to the sequential machine M

$$y(p) = F[y(p-1), \rho(p-1)], \tag{19}$$

$$\lambda(p) = \Psi\{F[y(p), \rho(p)]\}, \tag{20}$$

where the alphabets $\{y\}$ and $\{\varkappa\}$ coincide. Each initial state $\varkappa^0$ of automaton A is made to correspond to the initial state $y(0) = \varkappa^0$ of the machine M. Since Eq. (17), (19), and the corresponding initial states coincide, it follows that for all $p \geq 0$ we have

$$y(p) = \varkappa(p). \tag{21}$$

Substituting (21) into (20) and taking (17) and (18) into account, we obtain

$$\lambda(p) = \Psi(F[\varkappa(p), \rho(p)]) = \Psi[\varkappa(p+1)] = \chi(p+1)$$

for all $p \geq 0$; this proves the second postulate of the theorem. Thus, the theorem is completely proved.

APPENDIX II

On the minimization of the number of states in a sequential machine when limitations are imposed on the input sequences. In order to prove that the algorithm described in section 4 for compressing tables actually leads to the minimal sequential machine, we shall relate this algorithm to the algorithm developed in [7] for minimization of sequential machines in the case of bounded input sequences.

We shall formulate the diagram of states for the sequential machine which is equivalent to the specified automaton A. This can always be done if the number of circles in the diagram of states is made to equal to the number of rows in the table for the automaton A and if the output converter is assumed identical (i.e., if it is assumed to convert the state with the number j to the output with the same number, irrespective to the input state). Assume, for example, that the table for the specified automaton A is of the form shown in Table 19 (the states are indicated by numbers).

The diagram of states for the equivalent sequential machine is shown in Fig. 5.

TABLE 19

	ρ_1	ρ_2
1	3	3
2	2	3
3	2	1

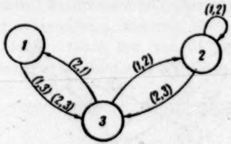

Fig. 5.

We should note one general property of the diagram of states which is formulated in this manner; the second numbers in the pairs which are written above all the arrows pointing toward each circle with the number j coincide with the number of that circle.

The matrix for the connections of the sequential machine whose diagram of states is shown in Fig. 5, is given by

$$C = \begin{array}{c} \\ 1 \\ 2 \\ 3 \end{array} \begin{array}{c} \begin{array}{ccc} 1 & 2 & 2 \end{array} \\ \left[\begin{array}{ccc} 0 & 0 & (1,3) \vee (2,3) \\ 0 & (1,2) & (2,3) \\ (2,1) & (1,2) & 0 \end{array} \right] \end{array}.$$

The following general property for the connection matrix corresponds to the property of the diagram of states mentioned above: all non-zero elements in any column of the matrix have identical second numbers (which coincide with the number of the column).

The limitations which were examined by Aufenkamp consist of the fact that not all the arrows depart from certain circles on the diagram of states; i.e., for certain states of the machine the appearance of certain input signals is not allowed. In order to make use of the Aufenkamp algorithm, it is necessary to transfer the requirement for forbidding the appearance of two successive identical inputs to the diagram of states. However, this cannot be achieved by simple erasure of certain arrows on the diagram of states, since if two or more arrows with the input numbers a_1, a_2, etc. arrive at the circle with the number $\underline{j}$, then the ability to forbid further movement from the circle $\underline{j}$ depends on which of the arrows the approach was made along. In order to avoid these difficulties we shall construct a sequential machine equivalent to A in a different manner; we shall construct it in precisely such a manner that only arrows with identical first numbers approach each circle. This can be achieved by rearranging the diagram of states for a machine which has already been constructed: each circle which is approached by $\underline{s}$ arrows with different first numbers is replaced by $\underline{s}$ circles to which only arrows with identical first numbers make an approach The second numbers of the approaching arrows remain the same. The same arrows which departed from the original circle depart from these circles. Figure 6 shows the diagram of states of Fig. 5, rearranged according to this rule. It is not difficult to see that the reconstructed sequential machine remains equivalent to the original machine since it remains equivalent to automaton A.

It is necessary to impose the required limitations on the input sequences. In order to do this, we eliminate that arrow from among the arrows departing from each circle on the diagram of states for which the first number coincides with the first number of the arrows approaching the circle. In Fig. 7 we have shown the diagram of states for Fig. 6 if the class of input sequences is bounded – two successive identical inputs are forbidden (we shall call this class R). The matrix for the connections is now given by

$$C = \begin{array}{c} \\ 1 \\ 2 \\ 3' \\ 3'' \end{array} \begin{array}{c} \begin{array}{cccc} 1 & 2 & 3' & 3'' \end{array} \\ \left[\begin{array}{cccc} 1 & 0 & (1,3) & 0 \\ 0 & 0 & 0 & (2,3) \\ (2,1) & 0 & 0 & 0 \\ 0 & (1,2) & 0 & 0 \end{array} \right] \end{array}.$$

Each column in the connection matrix for the rearranged sequential machine may contain only identical pairs.

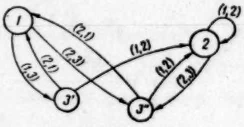

Fig. 6.

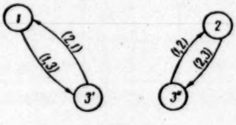

Fig. 7.

The algorithm for recognizing states that are equivalent relative to the class R for matrices of this type is substantially amplified in comparison to the general algorithm described in [7]; it reduces to the following: those rows in the matrix C corresponding to states that are equivalent relative to R form a sub-matrix of the matrix C such that two different rows cannot contain pairs that have identical first numbers and different second numbers. In our example, the states 1, and 2 or 1 and 3', or 3' and 3", or 2 and 3" are equivalent relative to R, but, states 2 and 3' or 1 and 3" are not equivalent.

Minimization reduces to replacing a group of states that are equivalent relative to R with one state. The basic difficulty resides in formulating a subdivision of all the states that are equivalent relative to R in such a way that the over-all number of groups is minimal; often this minimal number can be determined only by checking all possible variants of the subdivision.

In the simple example cited here it is immediately evident that this minimal number of groups cannot be less than two, since states 2 and 3' are not equivalent and must therefore be in a different group. But, this number is equal to two, since all states can be divided into two groups at least in the following manner: {1, 3'} and {2, 3"}.

The sufficiency of the algorithm proposed in [7] is essentially based on the fact that if the states of the machine are subdivided into equivalent groups, then there exists the symmetrical subdivision of the connection matrix required in [7]. Although the proof of this fact is not cited in [7], it is nevertheless true that the existence of such a subdivision can easily be established for a connection matrix of the type which we are studying.

The algorithm described in section 4 is a simple algorithm and a more convenient modification of the Aufenkamp algorithm.

SUMMARY

There are considered three methods of realization, which are economic from the viewpoint of number of states, of a finite automaton set by an equation (or table) and operating in a time pace regime caused by change of the input states of the automaton. The methods are distinguished by an amount of information, which defines the automaton input. The first method (Huffman method) intends minimum information, i.e., information on input state at the moment only; the second method supposes the introduction into the automaton of additional information on moments of changing input state; the third method intends introduction into the automaton of information on input state at the moment and at some preceding moment of time.

It is shown that one can get the most economic automaton using the third method.

LITERATURE CITED

1. M. A. Aizerman, L. A. Gusev, L. I. Rozonoer, I. M. Smirnova, and A. A. Tal', "Finite automata, I", Avtomatika i Telemekhanika, 21, 2 (1960).*
2. M. A. Aizerman, L. A. Gusev, L. I. Rozonoer, I. M. Smirnova, and A. A. Tal', "Finite automata, II", Avtomatika i Telemekhanika, 21, 3 (1960).*
3. E. F. Moore, "Speculative experiments with sequential machines," Symposium on Automata, edited by A. A. Liapunov [Russian translation] (Foreign Literature Press, Moscow, 1956).
4. A. Sh. Blokh, "On problems that are solved on sequential machines," Symposium on Cybernetics Problems, No. 3, Edited by A. A. Liapunov [in Russian] (Physics-Mathematics State Press, Moscow, 1960).
5. D. D. Huffman, The Synthesis of Sequential Switching Circuits, Journ. Francl. Inst. vol. 257, No. 3, 4, 1954.
6. D. D. Aufenkamp and F. E. Hon, Analysis of Sequential machines, in: Mathematics (Periodic Symposium of Translations of Foreign Papers 3: 3, 1959).
7. D. D. Aufenkamp, Analysis of Sequential machines, in: "Mathematics" (Periodic Symposium of Translations of Foreign Papers, 3: 6, 1959).

---

*See English translation.

TRANSISTORIZED RELAY NETWORKS

A. P. Suponitskii and V. D. Urin
(Moscow)

Translated from Avtomatika i Telemekhanika, Vol. 21, No. 12,
pp. 1595-1600, December, 1960
Original article submitted May 30, 1960

The paper analyzes the operation of transistorized relay networks with diode input converters. The special features of thermal stabilization in such networks are analyzed. The basic conclusions are verified experimentally.

The use of transistors in relay networks is an effective means of improving the sensitivity and lowering the power requirements in such networks. Transistorized relay networks can be operated from the control-signal source with a low power consumption. It is easy to change the settings in such networks. The networks are reliable for prolonged operation both in the "energized" and "de-energized" states. In many cases the operating conditions for such networks involve a narrow temperature range (20° ± 10°).

Most often the common-emitter transistor connection is used in relay networks.

Many relay networks compare a monitored voltage U_1 that is produced, by a detecting network, for example, with a standard voltage U_2. Each of these voltages can in the general case vary from zero to a maximum value. The monitored voltages are in many cases appreciably greater than the allowable voltage rating of the transistors. Therefore, it proves necessary to make use of such devices as, for example, a voltage divider network (Fig. 1).

These networks can be designed in two ways. In the first method the voltages are first compared and then their difference is divided down to a practical magnitude. In the other method, the monitored voltage is first divided in a definite ratio and is then compared with the set voltage. For networks which do not contain nonlinear elements both methods are equivalent. However, the second method permits simple introduction of rectifiers into the network, and these rectifiers can provide the property of diode limiting (Fig. 2). The presence of rectifiers makes three operating modes possible for the network:

1) both of the rectifiers B_1 and B_2 (as well as the transistor) are conducting;

2) the rectifier B_1 conducts, the rectifier B_2 and the transistor are cut off;

3) the rectifier B_1 is cut off, the rectifier B_2 and the transistor are conducting.

The first mode is the "working" mode. Under these conditions the operation of the network shown in Fig. 2 is fully equivalent to the operation of the network shown in Fig. 1. However, the presence of two other modes of operation for the networks shown in Fig. 2 makes it possible for us to approach the selection of parameters in a different way. It is not difficult to see that in the second mode the base current is $I_2' = 0$, and in the third mode it is $I_2' = U_2/(R_b + R_{ol})$. The network is able to protect the transistor from excessive voltages across the emitter-base junction and from overload. In the second mode of operation, this is achieved by means of the backward resistance of the rectifier B_2 (it is desirable to choose the rectifier in such a way that its backward resistance appreciably exceeds the backward resistance of the emitter-base junction). The protection of the transistor from overload in the third mode of operation is achieved by making the value of R_{ol} sufficiently large to limit the current through the transistor for the maximum value of the voltage U_2.

Since the network in Fig. 1 does not have such protective properties, the only method of limiting the current through the transistor involves lowering the sensitivity.

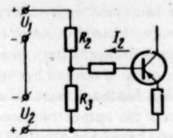

Fig. 1.

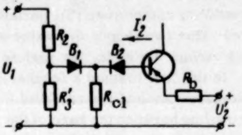

Fig. 2.

In fact, assume the parameters of the networks are chosen in such a way that the values of R_2 and R_b are identical in both cases, and $R_3 = R_3'R_{ol}/(R_3' + R_{ol})$. Then the input resistance of the networks from the U_1 side will also be the same. For the network in Fig. 1 the base current is $I_2 = (U_2 - U_1)R_3/(R_2R_3 + R_2R_b + R_3R_b)$, and for $U_2 = U_{2\max}$, $U_1 = 0$, it reaches its maximum value

$$I_{2\max} = \frac{U_{2\max}}{R_2 + R_b + \frac{R_2R_b}{R_3}}.$$

For the network in Fig. 2 operating in the third mode,

$$I'_{2\max} = \frac{U'_{2\max}}{R_{ol} + R_b},$$

where $U'_{2\max} = U_{2\max}\dfrac{R_3}{R_3 + R_2}$.

Therefore,

$$I'_{2\max} = \frac{U_{2\max}R_3}{(R_2 + R_3)(R_{ol} + R_b)} = I_{2\max}\frac{R_2R_b + R_3R_b + R_2R_3}{R_2R_b + R_3R_b + R_2R_{ol} + R_3R_{ol}}.$$

The value of R_b must be less than R_2, R_3 (since an increase in R_2, R_3, not only lowers the sensitivity but also the power consumption, and an increase in R_b basically lowers the sensitivity without having much effect on the power consumption).

It is also obvious that $R_{ol} > R_3$. Therefore, it is always true that $I'_{2\max} < I_{2\max}$. A lowering of $I_{2\max}$, (i.e., an increase in $R_2 + R_b + R_2R_b/R_3$) is possible only when the sensitivity is lowered, whereas the value of R_{ol} can be selected over wide limits for the condition that there is a corresponding variation in R_3' without worsening the sensitivity; this is true because the current I_2' depends only on the equivalent resistance $R_3 = R_3'R_{ol}/R_3' + R_{ol}$. Thus, the protective properties of the network in Fig. 2 permit a wider choice of parameters.

In performing experimental verifications (cf. below) we used the network in Fig. 2. Eliminating the rectifiers B_1 and B_2 from the network is practically equivalent to converting to the network shown in Fig. 1; if all the other parameters were to remain constant, this would cause an increase in the maximum current through the base of the input transistor (for $U_{2\max}$ and $U_1 = 0$) by a factor of approximately two (compared to the actual results); this is clearly undesirable. The use of a diode limiting network without voltage division at the input (for, $R_2 = 0$, $R_c' = \infty$) is not always possible in the problem under study. The input resistance of the network shown in Fig. 2 from the U_1 side is equal to $R_{1x} = R_2 + R_b$ (in the first mode of operation). It is assumed that the internal resistance of the source U_2 is included in the value of R_b.

Thus, a reduction in the input resistance when R_2 is removed could be compensated only by increasing R_b on the basis of a corresponding increase in the resistance of the transistor control circuit (the emitter-base resistance) in the first mode of operation for $R_2 = 0$, $R_c = R_b + R_{i1}$, where R_{i1} is the internal resistance of the source U_1. The latter result, as we shall indicate below, is undesirable.

The relationships for the network in Fig. 2 in the second and third modes of operation are derived for ideal rectifiers. The presence of a backward resistance in the rectifiers which is commensurate with the resistors R_3', R_{ol}, R_2 violates these relationships. However, the selection of the parameters is substantially affected only by the leakage of a portion of the current through the backward resistance of the rectifier B_1 in the third mode of operation. In order to compensate this phenomenon the value of R_{ol} must be increased appreciably compared to the computed value (we reduce the value of R_3'' correspondingly). The design of bistable static relay networks is possible using various methods. We studied two methods for constructing such networks from two-stage transistor amplifiers. In the first method a feedback factor equal to or greater than unity is assured because of the aggregate emitted resistance of two cascades (Fig. 3). In the second method a high feedback factor is assured because of the mutual coupling between the base of the input transistor and the collector of the output transistor (Fig. 4); this is analogous to a multivibrator circuit. The possibilities of the first of these networks have been clarified in the literature [1] where, in particular, such a network was used to obtain the maximum output power in a pulse mode of operation.

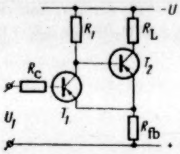

Fig. 3.

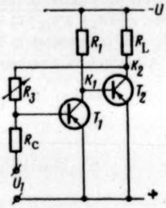

Fig. 4.

With respect to the problems under study, we found that the possibilities of using this network were limited. In accordance with [1] the relay mode of operation for the network is achieved for the condition $R_{fb} - \frac{R_c}{\beta_1\beta_2} > 0$ where R_{fb} is the feedback resistance, R_c is the normalized resistance of the control circuit. β_1 and β_2 are the values of current gain for the transistors T_1 and T_2. The supply voltage is

$$U = I_L(R_L + R_{fb}).$$

The relationships cited above show that an increase in R_c leads to an increase in R_{fb}; this, in turn, leads to an increase in the supply voltage U (for specified values of load current I_L and load resistance R_L) and also to a lowering of the efficiency of the relay networks. For a specified U, an increase in R_{fb} leads to a lowering of the output transistor gain and thus lowers the sensitivity of the over-all network.

Since the allowed voltage across the collector of the transistors is limited, the value of R_c is also limited. The limiting of R_c leads to the limiting of R_{in} since

$$R_{in} = R_c \frac{R_2 + R_b}{R_b + \frac{R_2R_3}{R_2 + R_3}} = R_c\left(1 + \frac{R_2^2}{R_b\,(R_2 + R_3) + R_2R_3}\right).$$

It should be noted that this limitation has an effect in the case where the input-signal source has a high internal resistance. The network shown in Fig. 4 is free from this limitation. The feedback factor for the netwo[illegible]ig. 4 can be found as follows.

Assume the current through the base of the input transistor has varied by the amount $+\Delta i_{b1}$. This leads to a variation in the collector current of the input transistor by the amount $+\beta_1\Delta i_{b1}$. It can be assumed that an insignificant variation of the current is accompanied by a considerably smaller variation of the potential at the point K_1 (a variation of the potential at this point corresponding to the entire working range of the current over the linear segment is equal to tenths of a volt). Therefore, it can be assumed conditionally that the potential at the point K_1 does not change. This means that the current through the base of the output transistor must vary by the amount $-\beta_1\Delta i_{b1}$, while its collector current varies by the amount $\beta_1\beta_2\Delta i_{b1}$.

If we disconnect the feedback, then the potential at the point K_2 would change by the amount $\beta_1\beta_2\Delta i_{b1}R_L$. Correspondingly, using the theorem for an equivalent generator, the current in the feedback loop would increase by the amount $+\Delta i'_{b1} = \Delta i_{b1}\beta_1\beta_2R_L/(R_3 + R_L)$ in that case. On the basis we find the feedback factor:

$$K_{fb} = \frac{\Delta i'_{b1}}{\Delta i_{b1}} = \frac{\beta_1\beta_2 R_L}{R_3 + R_L};$$

for $R_L \ll R_3$

$$K_{fb} \approx \frac{\beta_1\beta_2 R_L}{R_3}.$$

From the expression for K_{fb} it follows that the adjustment of both K_{fb} and the gain for the entire network can be achieved by varying the magnitude of R_3. The value of R_3 is bounded from below on the basis of the concepts governing the allowable current through the load when the output transistor is cut off. The condition governing a relay mode of operation $K_{fb} \geq 1$ is not related to any limitations on R_c and R_{in}.

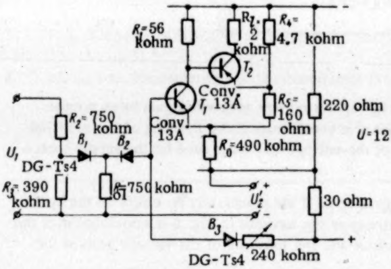

Fig. 5.

Below we cite the data for tests performed on relay networks which have the properties indicated at the beginning of the paper. The network in Fig. 5 is a development of the network shown in Fig. 3; the network in Fig. 6 is a development of the network shown in Fig. 4. In developing the relay network shown in Fig. 5 we made a number of modifications from the recommendations made in [1].

1. The supply voltage for the transistors was lowered appreciably, since operation at the maximum allowable voltage may lower the stability of the settings.

2. In order to achieve guaranteed cutoff of the output transistor we provided for automatic bias by means of a voltage divider (instead of a separate source of bias voltage between the collector of the input transistor and the base of the output transistor as proposed in [1]); this made the network simpler and more reliable.

3. The temperature stabilization of the operating point was achieved using a counter-connected diode [2]. The backward plate resistance of such a diode decreases with an increase in temperature; this increases the current in the diode circuit and compensates the increase in the initial collector current through the input transistor which accompanies an increase in temperature. Laboratory tests showed that the results were stable. This method of thermal stabilization for a variation of 20°C in the ambient temperature practically assured the maintenance of the values of the "operatc" and "release" voltages for the relays (Fig. 7, curves a). Without thermal stabilization a temperature increase of 20°C led to a shift of more than 4% of the working range for all of the relay characteristics in the direction of larger values of the control signal (Fig. 7, curves b).

A shortcoming of this method of thermal stabilization is the necessity of using two supply sources or of using a voltage divider (i.e., it is necessary to waste a portion of the power supplied from the sources). The temperature stabilization in the network shown in Fig. 6 was achieved by including a counter-connected diode with a shunt resistance in the divider circuit. This methdod is applicable both for the divider network shown in Fig. 1 and for the diode-limiting network shown in Fig. 2. In our example, a temperature variation of 20°C had practically no effect on the relay characteristic (cf. Fig. 7, curves c). Here, just as in the network shown in Fig. 5, we used automatic bias for the output transistors.

A shortcoming of this method of thermal stabilization is the fact that it can be used only with a high-resistance divider. For the examples cited above the power drawn from the source of the detected signal is twice as small in the network shown in Fig. 6 as it is in the network shown in Fig. 5. For an upper boundary of 100 v for the voltage of the measured signal, the current drawn by the network in Fig. 6 was 0.06 to 0.07 ma; the current drawn by the network in Fig. 5 was 0.13 to 0.14 ma. The loop between the operate and release voltages U_1 was equal to approximately 2 to 3 v; i.e., it corresponded to a current variation of 2 μa for the network in Fig. 6, and 3 μa for the network in Fig. 5.

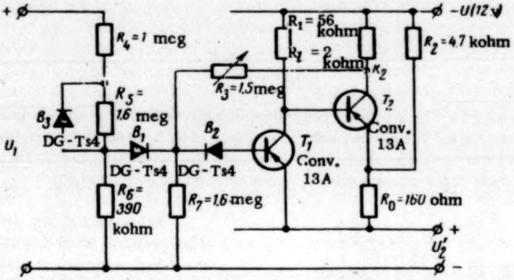

Fig. 6.

The indicated value for the loop corresponding to voltage operation was adopted to guarantee precise operation of the relays. The loop can be narrowed by a factor of several times if the filtering of the rectified voltages U, U_1, and U_2 is improved, and if the effectiveness of the voltage stabilizer used for the supply source is increased.

It should be noted that a variation of ± 10% in the magnitude of U has practically no effect on the operation of the network shown in Fig. 6. The lower current sensitivity of the network in Fig. 5 is associated with the loss of a portion of the supply voltage across the feedback resistor and the lowering of the voltage gain of the output transistor.

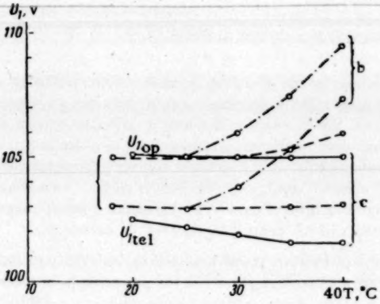

Fig. 7.

CONCLUSIONS

1. The use of a diode-limiting network which protects the transistor from overloads facilitates the selection of the parameters for the input section of a relay network and makes it possible to achieve a higher sensitivity.

2. The design of transistorized relay networks having the properties cited at the beginning of the paper is possible when various methods are used for introducing feedback. The introduction of feedback from the collector of the output transistor to the base of the input transistor offers greater possibilites than the use of a common emitter resistance, since it permits a better utilization of the transistor gains. This conclusion is of a particular nature and is applicable for the statement of the problem formulated in this particular paper.

3. The thermal stabilization of transistorized relays on the basis of using diodes as "thermistors" is fully adequate over a narrow range of temperature variation.

SUMMARY

Transistor relay circuits are considered. Operation of the said circuits with a diode inverter at the input is analyzed. The peculiarities of thermal stabilization of these circuits are studied. Main results are confirmed by an experiment.

LITERATURE CITED

1. F. L. Varpakhovskii and R. A. Lipman, "A contactless transistorized relay," Avtomatika i Telemekhanika 19, 11 (1958).*
2. M. G. Lou, Fundamentals of Semiconductor Electronics [in Russian] (Soviet Radio Press, 1958).

---

*See English translation.

A THREE-CHANNEL MULTIPLIER WITH FREQUENCY DIVISION OF THE SIGNALS

A. A. Maslov
(Moscow)

Translated from Avtomatika i Telemekhanika, Vol. 21, No. 12,
pp. 1601-1612, December, 1960
Original article submitted May 29, 1960

The paper makes a survey of multipliers of the combination type with amplitude of the channels ("coarse-fine" systems).

A new design is proposed for a multiplier with frequency division of the input signals; the properties of the device are studied, and data is cited for an experimental verification of one variant of the network based on reversive stepfinders.

An analysis of various principles for designing multipliers [1] showed that based on known principles it is not possible to design a multiplier which for a comparatively high accuracy (0.1 to 0.01%) also provides adequate dynamic properties. Certain attempts at expanding the pass band of multipliers while retaining high accuracy by making a transistion to coarse-fine systems have been undertaken by a series of authors. Thus, for example, A. A. Fel'dbaum and L. N. Fitsner developed [2] the principle of amplitude division of the channels in a multiplier (coarse-fine systems).

Several variants of multiplier networks of this type were studied in the paper by L. N. Fitsner [3]. Then G. M Petrov introduced a series of improvements into networks with amplitude division of the channels. He proposed a method for improving the dynamic properties of coarse-fine systems by introducing nonlinear transfer coefficients into one of the channels.

In all proposed networks of the combined type it was possible to achieve a static accuracy of up to 0.05% and even higher, but the pass band remained considerably lower than the frequency range of the "fine" section of the system. Thus, the basic contradiction between accuracy and speed of response in systems with amplitude division of the channels was not eliminated.

In the Institute of Automation and Remote Control of the Academy of Sciences, USSR we have for several years been developing the idea of designing computers and their elements on the basis of using parallel computing channels with frequency division of the signals.

This paper is a part of an over-all research program being conducted under the supervision of B. Ya. Kogan in this field as it applies to multiplier-divider units. This paper demonstrates that the principle of frequency division of channels makes it possible to design a multiplier with engineering characteristics that are no worse than those of linear decision elements. In order to bring out the engineering advantages of the principle of frequency division over other principles, we shall make a survey of networks with amplitude division of the channels. Then we study the engineering possibilities offered by the new block diagram for multiplier units and cite from an experimental verification of a particular variant using stepfinders.

1. COARSE-FINE MULTIPLIERS

The over-all block diagram of this type of device is shown in Fig. 1. The multiplier U_x is converted to a transfer coefficient for the elements α_1 and α_2 by the converter Conv.; this is done in such a way that $\alpha_1 = \alpha_2 =$

$= U_x^*/U_k$. The conversion of U_x into α_1 and α_2 is usually achieved using servosystems with step variations of the transfer coefficients; therefore the voltage U_x^* is equal to U_x with an accuracy of up to the error caused by the discrete nature of the converter. The error voltage $U_x - U_x^*$ is amplified by a factor K and then multiplied by U_y/U_k in the multiplying device M. The result is divided by K and is entered as one of the terms $U_{z1} = (U_x - U_x^*)/U_k$ in the adder Σ_2.

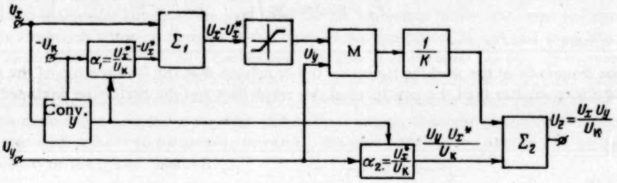

Fig. 1.

In the lower portion of the network the multiplier U_y is multiplied by $\alpha_2 = \alpha_1$; then the resulting voltage $U_{z2} = \frac{U_x^* U_y}{U_k}$ is added to U_{z1}. The total voltage is $U_z = U_{z1} + U_{z2} = \frac{U_x U_y}{U_k}$.

The static accuracy with which the production U_z can be obtained is determined by the sum of the errors of each of the terms; however, when electromechanical converters are used this error will depend basically on the error with which U_{z1} is obtained (this error is K times smaller than the error of the multiplier M).

The pass band of coarse-fine networks is usually assumed to be equal to the pass band of the coarse portion of the network, since the multiplier M is chosen with an adequate speed of response. In fact the pass band for the upper section of the network in Fig. 1 is appreciably lower than that of the multiplier M; therefore, our assertion is valid only in two cases: a) when the number of steps in the discrete section of the network is sufficiently great and turning off the upper channel leads to an insignificant increase in the dynamic error, or b) when the speed of response of the lower section of the network is several orders of magnitude smaller than the pass band of the multiplier M.

In order to clarify the effect of each of the channels on the dynamic properties of such devices, we shall study a specific example.

As our example, we shall choose the Fitsner [3] network which has the greater speed of response. The coarse section of this network (Fig. 2a) contains ten symmetrical triggers Tr1 to Tr10 with operating voltages of 0, 10, 20, . . . , 90 v. The plate circuits of the trigger tubes contain relays whose contacts change the admittances of the input circuits of the amplifiers A_1 and A_2. The relay of trigger Tr1 which operates for $U_x = 0$ switches the polarity of the voltages U_x and U_y which are applied to the network in four quadrants. The multiplier in the fine section of the network consists of a multiplying block based on thyrite resistors [4].

The number of discrete values of the controlled admittances in the network is chosen equal to ten; therefore, the accuracy of the network can be made ten times higher than the accuracy of the thyrite multiplier (i.e., 0.05 to 0.1%).

The small number of steps made it possible to both avoid using a binary counter or a stepfinder and to make the transition to a network with parallel switching of the triggers. Because of this, the speed of response for the coarse section of the network is limited only by the "operate" time of a single relay.

The dynamic error of the fine section of the network depends on the nature of the signal $K(U_x - U_x^*)$ at the output of the amplifiers A_1 and A_2. If, for example, we apply the signal $U_x = U_{x\,max} \sin \omega t$, to the input of the multiplier, then the voltage U_1 at the output of the amplifier A_1 will vary as shown in the graph in Fig. 2b. The frequency and shape of the converted voltage U_1 are variable and depend on the rate of change of the signal U_x. The relationship between the frequency f_1 of the first harmonic of U_1 and the time rate of change dU_x/dt can be expressed using the relationship

$$\frac{dU_x}{dt}\,\frac{1}{f_1} = \Delta U_T = 10 \text{ v.}$$

(Here ΔU_T is the interval between the "operate" voltages for the triggers).

For $U_x = U_{x\,max}\sin\omega t$ we obtain $U_{x\,max}\,2\pi f\cos 2\pi ft = 10 f_1$, and from this we have

$$f_1 = 20\pi f\cos 2\pi ft, \tag{1}$$

for $U_{x\,max} = 100$ v; here $f = \omega/2\pi$.

Therefore the frequency of the working signal for the condition that the fine section of the system operates must be at least 60 times smaller than the pass band of the amplifiers and the multiplier included in this section.

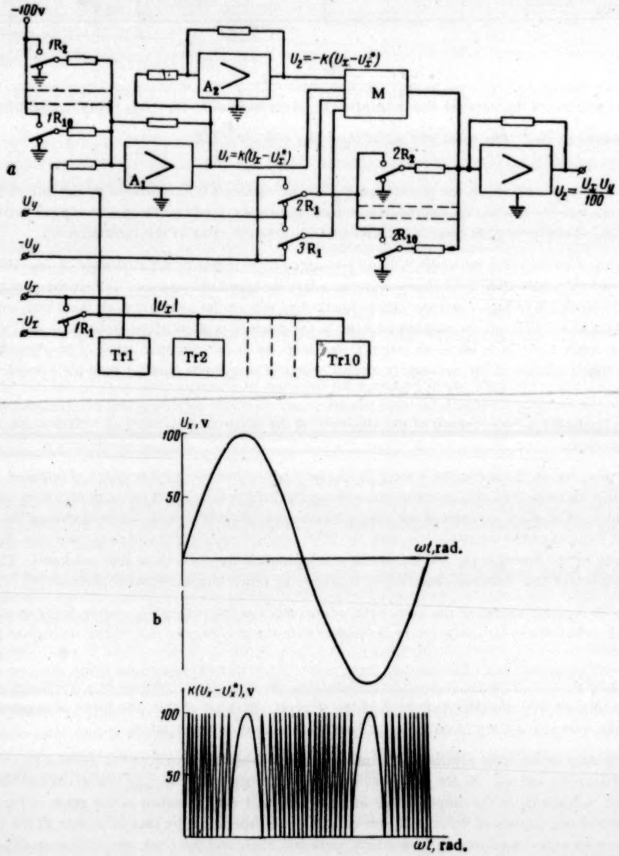

-100v
/R₂
/R₁₀
a
A₂
A₁
M
$U_2=-K(U_x-U_x^*)$
$U_1=K(U_x-U_x^*)$
U_y
$-U_y$
U_x
$-U_x$
/R₁
$|U_x|$
2R₁
3R₁
2R₂
2R₁₀
$U_z=\frac{U_x U_y}{100}$
Tr1
Tr2
Tr10
U_x, v
100
50
ωt, rad.
b
$K(U_x-U_x^*)$, v
100
50
ωt, rad.

Fig. 2.

The complex shape of the converted signal U_1 (this signal involves the presence of a large number of high-frequency harmonics with a slowly decaying amplitude) begins to have a negative effect even at very low frequencies. Usually this is manifested in the appearance of brief pulses at the output of the device at the instants that the relays commutate.

The block diagram for a multiplier with a nonlinear transfer function (this was proposed by G. M. Petrov; cf. Fig. 3) differs from the preceding network only in the arrangement of the upper channel. While the rate of change of U_x remains within the limits of the pass band for the converter Conv., the error voltage $U_x - U_x^*$ remains small and is amplified before it appears at the input of the multiplier M. In this case, the network as a whole behaves in exactly the same way as a conventional coarse-fine systems. As dU_x/dt increases, the difference $U_x - U_x^*$ also increases; however, the network continues to operate even though with a lower accuracy. When the converter ceases entirely to respond to changes in U_x (i.e., becomes equal to zero), then only the upper channel will function. This means that now the separation of functions among channels is achieved not only with respect to amplitude but also with respect to frequency; therefore, the pass band for the device will be determined by the dynamic properties of the upper channel.

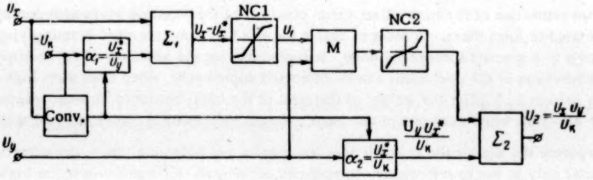
U_x
$-U_\kappa$
$\alpha_1=\frac{U_x^*}{U_y}$
Σ_1
$U_x-U_x^*$
NC1
U_1
M
NC2
Conv.
U_y
$\frac{U_y U_x^*}{U_\kappa}$
$\alpha_2=\frac{U_x^*}{U_\kappa}$
Σ_2
$U_z=\frac{U_x U_y}{U_\kappa}$

Fig. 3.

The accuracy of rhe multiplication after the lower channel has been turned off will be somewhat less than the accuracy of the multiplier M since the magnitude of the voltage at the output of the nonlinear converter NCl (Fig. 3) cannot exceed the linear range of the decision amplifier; thus the transfer coefficient for NCl corresponding to large values of $U_x - U_x^*$ must be made less than unity. Since the slope of the corresponding segment of the characteristic for NC2 must be made greater than unity, it follows that the error in the multiplication device M will be amplified.

The pass bands of the network can be assumed approximately one order of magnitude greater than the pass band of the multiplier device M. The growth of the dynamic error for the network occurs due to the appreciable expansion of the spectra for the intermediate voltages by the function generators NC1 and NC2. If, for example, $U_x = U_{x\,\max} \sin \omega t$, then the signal U_1 at the input of NC1 can be represented by the sum of the same sinusoidal signal with a smaller amplitude and a signal in the form of a trapezoid (Fig. 4). The resulting sum is approximately given by the following Fourier series:

$$U_1(t) = \left(\frac{4aU_{x\,\max}}{\pi} + bU_{x\,\max}\right) \sin \omega t + \frac{4aU_{x\,\max}}{\pi} \left(\frac{\sin 3\omega t}{3} + \frac{\sin 5\omega t}{5} + \ldots\right),$$

where a, b are proportionality coefficients.

As the frequency $f = \omega/2\pi$ increases, the higher harmonics will be suppressed more and more by the multiplying device M, and the signal at its output will approximate the shape of the sinusoidal signal. After the resulting product $U_1(t)U_y$ has been multiplied by the transfer function of NC2, the shape of the voltage U_z will be appreciably distorted (cf. Fig. 4b). Therefore, the transition to frequency division of the channels using nonlinear transfer functions does not permit full utilization of the dynamic properties of the multiplying device in the high-frequency channel. Another shortcoming of the network is the low accuracy in multiplying an ac voltage U_x by zero and by small values of U_y.

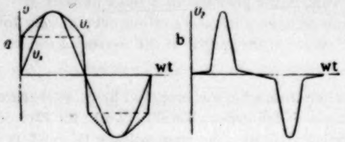

Fig. 4.

2. A THREE-CHANNEL MULTIPLIER WITH FREQUENCY DIVISION OF THE CHANNELS

In developing the network we used a very valuable quality of many multiplying devices with a controlled transfer coefficient – they are almost completely inertialess with respect to one of the channels while still assuring high accuracy.

In the block diagram of the unit under study (cf. Fig. 5) this quality is realized by subdividing each multiplier into two components: a low-frequency and a high-frequency component (i.e., $U_x = \bar{\bar{U}}_x + \tilde{U}_x$ and $U_y = \bar{\bar{U}}_y + \tilde{U}_y$). Under these conditions the products can be written as the sum of three terms:

$$U_z = U_{z1} + U_{z2} + U_{z3} = \frac{\overline{U}_x U_y + \tilde{U}_x \overline{U}_y + \tilde{U}_x \tilde{U}_y}{U_к}. \qquad (2)$$

In the first two terms one of the multipliers varies slowly, and therefore networks with controlled transfer coefficients can be used to form them. In order to obtain the third term we must use a multiplying device which assures multiplication in a specified frequency band. It is obvious that the accuracy of the multiplying device for the indicated subdivision of the operations can be increased appreciably since even when high-frequency components are present in each multiplier the weight of the error in the high-frequency channel is reduced; during periods in the over-all result when even one of the input voltages varies slowly, no error at all will be present.

In order to separate the signals the network does not require any additional units, since the converters Conv. 1 and Conv. 2 respond only to the low-frequency components of the over-all signals while the high-frequency components represent the errors of the servosystems. Each of the three channels shown in the block diagram in Fig. 5 can be detached from the system and used as an independent multiplying device. When one or two channels are detached from the network, the network still remains operable, but its engineering characteristics deteriorate.

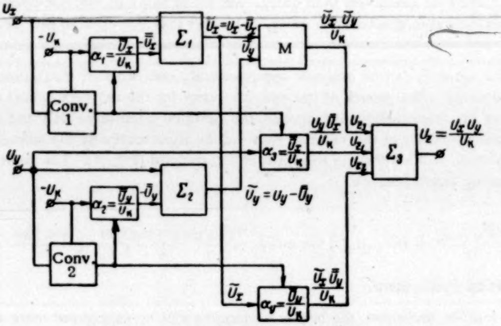
U_x
$-U_к$
$\alpha_1 = \frac{\bar{\bar{U}}_x}{U_к}$
$-\bar{\bar{U}}_x$
Σ_1
$\tilde{U}_x = U_x - \bar{\bar{U}}_x$
$\tilde{U}_y$
M
$\frac{\tilde{U}_x \tilde{U}_y}{U_к}$
Conv. 1
$\frac{U_y \bar{\bar{U}}_x}{U_к}$
$\alpha_3 = \frac{\bar{\bar{U}}_x}{U_к}$
U_{z1}
U_{z1}
U_{z2}
Σ_3
$U_z = \frac{U_x U_y}{U_к}$
U_y
$-U_к$
$\alpha_2 = \frac{\bar{\bar{U}}_y}{U_к}$
$-\bar{\bar{U}}_y$
Σ_2
$\tilde{U}_y = U_y - \bar{\bar{U}}_y$
Conv. 2
$\tilde{U}_x$
$\alpha_4 = \frac{\bar{\bar{U}}_y}{U_к}$
$\frac{\tilde{U}_x \bar{\bar{U}}_y}{U_к}$

Fig. 5.

We shall study how the accuracy and speed of response of the network are affected when various numbers of channels are used. The error due to the fact that the transfer coefficients α_1, α_2 are not identical to the transfer coefficients α_3, α_4 shall be neglected for the time being, since this error is extremely insignificant in electromechanical multiplying devices. The error in setting the magnitude of the transfer coefficients for the servosystem (this error, for example, is caused by an error in the quantization, by the dynamic error, or by other factors) is assumed to equal $\delta\alpha_s$. The error of the multiplying device M shall be assumed equal to zero when one of the multipliers $\tilde{U}_x$ or $\tilde{U}_y$ is absent;[*] the error is equal to δU_M when the voltage at the output of the multiplier M is greater than $\delta U_M U_{z\,\max}$.

When only one of the channels in the network is turned on, the network properties are quite obvious. If the network contains two electromechanical multiplying devices, then by assuming that the voltage at the output of each of the channels is equal to the sum of the ideal value of the product and the error, we can write

$$U_{z1} = \frac{U_x U_y}{U_{\text{к}}} + U_y \delta\alpha_{3s}, \ \tilde{U}_x = U_x - U_{\text{к}}\alpha_1.$$

Assuming $\alpha_1 = \alpha_{1i} + \delta\alpha_{1s}$ and $U_x - U_k\alpha_{1i} = 0$, where α_{1i} is the ideal value of α_1, we obtain $\tilde{U}_x = - U_k\delta\alpha_{1s}$.

Representing the error in the transfer coefficients α_1 through α_4 analogously, we obtain:

$$U_{z2} = \tilde{U}_x \alpha_4 = - U_y \delta\alpha_{1c} - U_{\text{к}} \delta\alpha_{1C} \delta\alpha_{4S},$$

$$U_z = U_{z1} + U_{z2} = \frac{U_x U_y}{U} - U_{\text{к}} \delta\alpha_{3C} \delta\alpha_{4S}.$$

The relative error $\delta U_z = \frac{\Delta U_z}{U_{z\,\max}}$ for $U_{z\,\max} = U_k$ is equal to

$$\delta U_z = - \delta\alpha_{3s} \delta\alpha_{4s}. \tag{3}$$

From this it follows that the errors in setting the transfer coefficients α do not add but multiply; therefore, the static accuracy is sharply improved. For example, if

$$\delta\alpha_{3s} = \delta\alpha_{4s} = 0.5\%, \ \text{then}$$
$$\delta U_z = 0.0025\%.$$

If one of the multipliers varies at such a rate that the servosystem ceases to operate (i.e., $\delta\alpha_s = 1$), then the multiplication of a slowly varying quantity by a variable quantity will be achieved with the accuracy of the operating channel.

Thus, a two-channel system incorporating two electromechanical multiplying devices assures inertialess multiplication with respect to each of the multipliers (when the other varies slowly) and permits an appreciable increase in the static accuracy.

The graphs for the variation of the error as a function of frequency for a sinusoidal signal in the case where an alternating voltage is multiplied by a slowly varying voltage and for the case where an alternating voltage is squared are shown in Figs. 6a and 6b.

In practical units the accuracy within the limits of the pass band $f_{\lim 1}$ of the servosystem proves to be less than that shown in the graphs, since in formula (3) we have not taken into account the error due to the fact that the coefficients α are not identical. If the error due to the fact that the element α_3 is not identical to the element α_1 is equal to $\delta\alpha_{3n}$, and the error due to nonidentity between the elements α_4 and α_2 is equal to $\delta\alpha_{1n}$, then the error can be determined from the expressions

$$U_{z1} = \frac{U_x U_y}{U_{\text{к}}} + U_y (\delta\alpha_{3s} + \delta\alpha_{3n}),$$

$$\tilde{U}_x = U_x - U_{\text{к}} \alpha_1 = - U_{\text{к}} \delta\alpha_{1s},$$

$$U_{z2} = \tilde{U}_x \alpha_4 = - U_y \delta\alpha_{1s} - U_{\text{к}} \delta\alpha_{1s} (\delta\alpha_{4s} + \delta\alpha_{4n}),$$

$$U_{z1} + U_{z2} = \frac{U_x U_y}{U_{\text{к}}} + U_y \delta\alpha_{3n} - U_{\text{к}} \delta\alpha_{3s} \delta\alpha_{4s} - U_{\text{к}} \delta\alpha_{3s} \delta\alpha_{4n}.$$

---

[*] In this specific network we provide for turning off the multiplying device M when one of its multipliers is small or equal to zero. The device is turned off by introducing a small dead band between M and the adder Σ_3.

From this we obtain

$$\delta U_z = -\delta\alpha_{3s}\delta\alpha_{4s} - \delta\alpha_{3s}\,\delta\alpha_{4n} + \frac{U_y}{U_{z\,\max}}\,\delta\alpha_{3n}. \tag{4}$$

The basic error must be determined by the third term in this expression; i.e., it must be determined by the nonidentity error. Therefore, there is no purpose in increasing the accuracy with which the transfer coefficients are generated. It is evident that $\delta\alpha_s$ is conveniently chosen in accordance with the accuracy requirements for alternating current. Since these requirements are usually appreciably lower than those which apply to the static accuracy, it follows that the multiplying devices in each of the channels can be simplified. In networks with binary counters, it is possible to reduce the number of stages; in networks with potentiometers it is possible to replace an amplifier with a polarized relay, etc. Just as in coarse-fine systems, it is possible to make use of stepfinders.

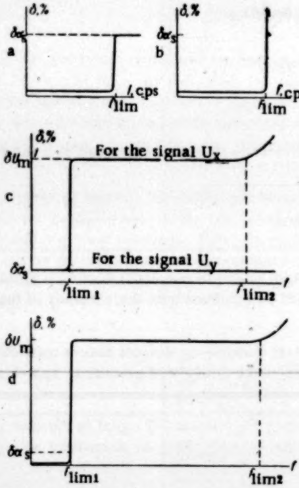

Fig. 6.

When one electromechanical and one high-frequency multiplying device are included in the network shown in Fig. 5 the multiplication is performed according to the formula $U_z = \dfrac{U_y\tilde{U}_x + U_y\overline{\overline{U}}_x}{U_k}$. The static accuracy and the dynamic error with respect to one of the inputs will be determined by the electromechanical device. As the frequency of the signal corresponding to the other multipliers increases while the first one remains constant, or in the case where an alternating voltage is multiplied by itself, the electromechanical network will operate first, followed by the high-frequency network; this procedure is the same as for a multiplying device with a nonlinear transfer function. The graph showing the variation of the error for this case is shown in Fig. 6c.

Two shortcomings of such a two-channel unit with frequency division of the signal are: in only one of the multipliers are the increased requirements imposed on the electromechanical channel and the low accuracy of multiplying the high-frequency voltage $\tilde{U}_x$ by U_y.

For the case where three channels are used in the network, all of the favorable properties of the first two variants are used.

The accuracy of multiplication by zero and by small voltages becomes very high, since the multiplying device M does not operate under these conditions. When one of the multipliers is a constant quantity, the graph for the variation of the error as a function of the frequency of the other multiplier is of the same shape as it is for a network with two electromechanical multiplying devices (Fig. 6a). The graphs for the variation of the error in the case of squaring an alternating voltage is shown in Fig. 6d.

3. A VARIANT OF A THREE-CHANNEL MULTIPLYING DEVICE WHICH USES REVERSIVE STEPFINDERS

The block diagram of the unit is shown in Fig. 7. The electromechanical multiplying devices in the low-frequency channel are designed using reversive stepfinders of the type "RShI-50/4". In each finder we use two tracks, each of which contains 50 commutator segments. The transfer coefficients for the dividers $D_1 - D_4$ can vary discretely in steps of 0.02 of the maximum value. The mismatch voltages for the servosystems $U_x - \overline{\overline{U}}_x$ and $U_y - \overline{\overline{U}}_y$ are applied to the windings of polarized relays of the type "RP-5" through two serially connected cathode

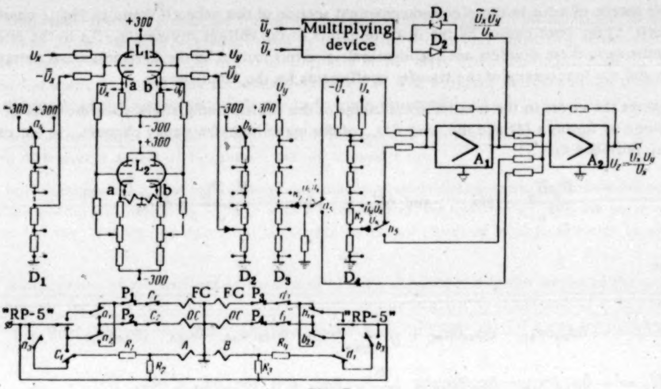

Fig. 7.

followers. When the error in one of the servosystems exceeds the quantization error, the armature of a "RP-5" is attracted to one of its contacts, and a voltage of 48 v begins to be applied to one of the electromagnets of the stepfinder. The windings of the stepfinder coils are connected through self-breaking contacts which disconnect the voltage at the instant the armature is attracted to the electromagnet; therefore, the brush of the stepfinder can be switched from commutator segment to commutator segment until the armature of the "RP-5" relay returns to the intermediate position.

The electromagnetic relays A and B (of the type "RS-13") assure operation of the network in four quadrants. When the input voltages U_x and U_y are positive the windings of these relays are de-energized; therefore, negative reference voltages are applied to the dividers D_1 and D_2, and the components $U_y\bar{\tilde{U}}_x/U_k$ and $\bar{\tilde{U}}_y\tilde{U}_x/U_k$ of the product are applied to the input of amplifier 2 through a sign-inversion amplifier 1. If, for example, the signal U_x changes sign, then as a result of the attraction of the polarized relay armature in the left side of the network to the lower contact the brushes of the stepfinder "ShI-1" are initially shifted to the zero position. Under these conditions, the contacts C_1 and C_2 which are controlled by rotor of the stepfinder are switched, the reverse-count winding is disconnected, and a voltage is applied to the winding of relay A through the resistance R_1. Relay A operates, the sign of the reference voltage across the divider D_1 changes, and the voltage from the lower contact of the polarized relay is applied to the forward-count winding FC. After the finder brush has been shifted one commutator segment in the forward direction the contact C_1 is switched to its original position, but the relay A has had time to be blocked through its contact a_3. In order to insure that the relay does not release during the time required to switch the contact C_1, its release time is somewhat retarded by a magnetizing current flowing through the resistor R_2. Then the relay A remains closed until the finder brush again returns to the zero position and the contact C_1 is switched.

The rule governing the signs is followed during the multiplication process by switching the component $\bar{\tilde{U}}_x U_y/U_k$ to the input of amplifier 2 by means of the contact a_5; the sign-converter 1 is bypassed. The second system operates analogously.

As a high-frequency channel we used diode squaring devices taken from the multiplying unit in the "EMU-5" simulator. The variable components of the multipliers U_x and U_y are taken from the outputs of cathode followers based on the tube L_1 (a "6N3P" tube; its characteristics are: $E_f = 6.3$ v, $I_f = 0.35$ amp, $E_\rho = 150$ v, $I_\rho = 7.7$ ma, $R_k = 240$ ohm, $g_m = 4900$ μmho, $r_\rho = 7.5$ k, $P_\rho = 1.5$ w).

In order that the multiplying unit in the upper channel should not create an additional error in those cases when there is no high-frequency component in one of the input voltages, a circuit consisting of two parallel silicon diodes was connected to its output. These diodes begin to pass a voltage which is above a threshold of 0.4-0.5 v; therefore if U_x or $\tilde{U}_y$ are equal to zero an error voltage lying within these limits is not passed. When $\tilde{U}_x\tilde{U}_y/U_k \neq 0$, the accuracy of the result remains practically unchanged.

The basic source of error in the electromechanical section of the network shown in Fig. 7 consists of the following factors: a) the error caused by the discrete nature of the voltage dividers $D_1 - D_4$; b) the error due to the fact that the resistors in these dividers are not identical; c) errors caused by the unsymmetrical nature of the load on the dividers and the inaccuracy of the transfer coefficients for the amplifiers.

If we neglect the errors in the transfer coefficients of the decision amplifiers, then the error of the network will be determined by formula (4) and the error δU_M of the upper high-frequency channel. In our case, the latter is equal to zero, provided that

$$\frac{\bar{U}_x \bar{U}_y}{U_H} < \delta U_M \text{ , and } \delta U_M \text{ , when } \frac{\bar{U}_x \bar{U}_y}{U_H} > \delta U_M .$$

Therefore

$$\begin{aligned} \delta U_z &= -\delta\alpha_{3s}\delta\alpha_{4s} - \delta\alpha_{3s}\delta\alpha_{4n} + \frac{U_y}{U_{z\,\max}}\delta\alpha_{3n} + \delta\alpha_{3s}\delta\alpha_{4n} + \delta U_M \quad (\delta\alpha_{3s}\delta\alpha_{4s} > \delta U_M) \\ \delta U_z &= -\delta\alpha_{3s}\delta\alpha_{4s} - \delta\alpha_{3s}\delta\alpha_{4n} + \frac{U_y}{U_{z\,\max}}\delta\alpha_{3n} + 0 \quad (\delta\alpha_{3s}\delta\alpha_{4s} < \delta U_M). \end{aligned} \tag{5}$$

The errors due to the discrete nature of the voltage dividers D_1 and D_2 were made equal to 2% in our network. The resistors were manufactured with a tolerance of 0.1%. Under these conditions the maximum possible value of the static error of the multiplying unit did not exceed 0.15%; the accuracy for multiplying high-frequency signals was not less than 1,15%.

4. THE RESULTS OF AN EXPERIMENTAL VERIFICATION OF THE MULTIPLYING UNIT

In the process of performing an experimental study of the new multiplying unit, we obtained the following characteristics.

1. The static error for input voltages of different signs. The voltages were measured by the compensation method using a normal battery element as a standard source. The results of our tests when the network operated in the first quadrant are cited in the table below. The table fixes the error voltages in volts which were computed as the differences between the calculated and measured values of the output voltage. When the network operated in the other quadrants the maximum error also did not exceed 0.1%.

U_y	U_x										
	0	10	20	30	40	50	60	70	80	90	100
0	0	0	0	0	0	0	0	0	0	0	0
10	0	—0.01	—0.03	0	0.01	0.01	0.05	0.02	0.03	—0.01	0
20	0	—0.02	—0.02	0.01	—0.01	—0.01	—0.07	—0.06	—0.04	—0.02	0.01
30	0	0.01	0.01	0	0.01	0.05	0.06	0.03	0	—0.01	—0.03
40	0	0	—0.04	—0.08	—0.04	—0.03	—0.01	—0.02	0.02	0.03	0.05
50	0	0.04	0.06	0.02	0.03	0.01	0.01	0	—0.02	—0.03	—0.01
60	0	0.01	0.03	0.05	0.02		—0.01	—0.03	—0.06	—0.03	—0.02
70	0	—0.03	—0.01	0	0.01	0.01	0.06	0.05	0.03	0	—0.01
80	0	—0.01	—0.07	—0.04	—0.03	—0.01	0	0.01	0.03	0.04	0.05
90	0	0.02	0.04	0.03	0.01	0.01	0.02	—0.01	—0.01	—0.04	—0.03
100	0	0.01	0.02	0	—0.01	—0.03	—0.07	—0.06	—0.02	0	0.01

2. The amplitude-frequency response with respect to each of the inputs for a constant second multiplier. The frequency response did not drop off within the limits of the pass band of the "EMU-8"-simulator decision amplifiers used in our mockup; i.e., it remained flat in the frequency range 0 to 10 kc for an output voltage amplitude equal to 100 v. The error in the indicated frequency range did not exceed 1%.

3. The amplitude-frequency response for squaring a sinusoidal voltage with an amplitude of 100 v. In that case, the pass band for the network was determined by the multiplying device consisting of the diode squaring unit taken from the "EMU-5"-simulator. Up to frequencies of 5 kc the error corresponding to both the dc component and the second-harmonic ac component remained less than 1%. For a fruther increase in the frequency of the input signals the shape of the output voltage began to become distorted.

4. The drift at the output of the network for multiplication of the maximum voltage of both signs by zero. The maximum drift over a period of 10 minutes did not exceed 1 mv.

5. The noise component in the out voltage. For multiplying dc voltages the pulsations did not exceed 30 mv. For multiplying an alternating voltage with a frequency of up to 10 kc by zero the noise component did not exceed 100 mv. During the operation of the stepfinders we observed brief spikes with an amplitude of up to 250 mv.

6. The oscillograms of the voltages at the output of each channel and at the output of the network as a whole were obtained for cases where a rectangular voltage was multiplied by itself and by a dc signal. The photographs taken from oscillograms of a rectangular signal with a frequency of 0.3 cps are shown in Fig. 8.

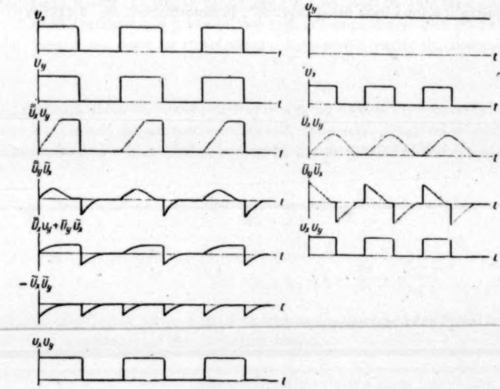

Fig. 8.

CONCLUSION

1. The author has developed a design for multiplying units of the combined type with three parallel channels and frequency division of the signals. Compared with networks using amplitude division of the signals, the new design makes it possible to assure the following advantages:

a) For an identical static accuracy (0.01 to 0.1%) the pass band of the system as a whole is extended up to the width of the pass band for the high-frequency channel.

b) It is possible to subdivide the network into individual multiplying devices without changing their circuits; here the engineering characteristics of the system are altered as a function of the number of operating channels.

c) It is possible to perform multiplication operations (even though the accuracy is lower) when one or two channels become inoperative; and this assures high reliability for the proposed unit.

d) The over-all network is distinguished by its comparative simplicity, since notwithstanding the presence of three multiplying devices each of them is subjected to less rigorous requirements than the requirements which apply when one of them is operating independently. This makes it possible to simplify the circuit for each of the channels.

2. The author has developed a variant of a three-channel network using stepfinders; experimental verification of this network proved the advantage of the new design for multiplying units.

SUMMARY

The survey of combined type of multiplying devices with amplitude-division channels is given. A new structure of a multiplying device with frequency division of input signals is proposed and its properties are considered. The data of the experimental check of a reversive step selector circuit are given.

LITERATURE CITED

1. A. A. Maslov, "Multiplying units (survey)", Avtomatika i Telemekhanika, 21, 10 (1960). *
2. A. A. Fel'dbaum and L. N. Fitsner, An Electrical Multiplying Device, Patent Application Number 104137, September 3, 1952.
3. L. N. Fitsner, "A Precision Multiplier", Avtomatika i Telemekhanika, 20, 1 (1959).
4. L. N. Fitsner, "A multiplication block using thyrites", Priborostroenie, No. 4 (1956).

---

* See English translation.

WIDE-BAND DECISION (OPERATIONAL) AMPLIFIERS

D. E. Polonnikov
(Moscow)

Translated from Avtomatika i Telemekhanika, Vol. 21, No. 12,
pp. 1613-1622, December, 1960
Original article submitted May 7, 1960

A principle is proposed for designing decision amplifiers; this principle is based on the sequential switching of stages and makes it possible to expand the pass band by approximately two orders of magnitude. A brief description is given of two types of decision amplifiers designed according to this principle. Results are cited for experimental tests which verify the theoretical propositions.

One of the basic problems which is encountered in designing analog computers (electronic simulators) is that of lowering the error with which the solution is achieved. The error involved in performing individual mathematical operations is determined to a considerable extent by the properties of the decision amplifier (in particular, by its pass band).

The complex transfer coefficient of a decision amplifier (Fig. 1) can be written as follows:

$$K(j\omega) = \frac{U_{out}}{U_{in}} = \frac{Z_2}{Z_1}\,\frac{1}{1+\dfrac{1}{K_{tr}(j\omega)}\left(1+\dfrac{Z_2}{Z_1}+\dfrac{Z_2}{Z_{in}}\right)}, \qquad (1)$$

where $K_{tr}(j\omega)$ is the transfer coefficient for an amplifier with a disconnected feedback loop, $Z_{in} = R_{in}/(1 + j\omega R_{in}C_{in})$ is the total input impedance of the amplifier proper.

The systematic relative error introduced by the amplifier is proportional to the expression

$$\left|\frac{1}{K_{tr}(j\omega)}\left(1+\frac{Z_2}{Z_1}+\frac{Z_2}{Z_{in}}\right)\right|.$$

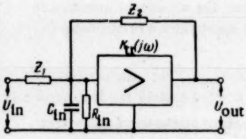

Fig. 1. Block diagram of a decision (operational) amplifier.

It is obvious that the greater the modulus of the transfer coefficient for the amplifier with an open feedback loop $|K_{tr}(j\omega)|$, and the more slowly this coefficient decreases with an increase in frequency, the smaller the error introduced by the amplifier and the more slowly this error increases with an increase in frequency.

In the majority of problems encountered in practice it is sufficient to have a high accuracy for the solution of the frequency range from zero to one kilocycle. It is not difficult to assure such a pass band for an amplifier with an open feedback loop. However, if we take into account the requirement that stability must be assured when the feedback loop is closed, the problem is seriously complicated since the decision amplifier always contains several stages of amplification and its dynamic properties are described by a high order of transfer coefficient with a large $|K_{tr}(0)|$.

In the analysis below we shall describe the principle for designing decision amplifiers which consists of the sequential connection of stages. Compared to the conventional single-circuit network, such a principle makes it possible (other conditions being equal) substantially to increase the stability margin and to expand the pass bands for the amplifier. As an example of the practical application of this principle we describe two decision amplifier networks.

1. THE PRINCIPLE OF SEQUENTIAL SWITCHING OF STAGES

Figure 2 shows the block diagram of a single-channel four-stage amplifier with an open feedback loop for high frequencies.* Its transfer coefficient can be written as follows:

$$K_{tr1} = \frac{U_{out}}{U_{in}} = \frac{K_1 K_2 K_3 K_{out}}{(1 + j\omega T_1)(1 + j\omega T_2)(1 + j\omega T_3)(1 + j\omega T_{out})}, \quad (2)$$

where K_1, K_2, K_3, K_{out} are the gains of the corresponding stages for dc operation; T_1, T_2, T_3, T_{out} are the equivalent time constants which are equal to the product of the output resistance of the corresponding stage and the total capacitance connected to its output (this includes the mounting capacitance and the input capacitance of the preceding stage). In analyzing the amplifier stability it is also necessary to take into account the transfer coefficient for the feedback circuits. But in decision amplifiers the feedback factor varies over wide limits, and therefore for convenience we shall assume that it is equal to zero; this will in no way effect the essence of the comparative analysis cited below.

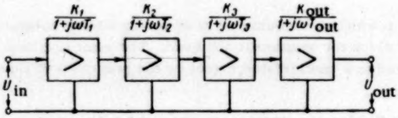
$\frac{K_1}{1+j\omega T_1}$
$\frac{K_2}{1+j\omega T_2}$
$\frac{K_3}{1+j\omega T_3}$
$\frac{K_{out}}{1+j\omega T_{out}}$
U_{in}
U_{out}

Fig. 2. Block diagram for a single-channel four-stage amplifier without feedback at high frequencies.

In order to ensure absolute stability** for the amplifier when the feedback loop is closed it is necessary that the phase (the argument) of the transfer coefficient for the open-loop circuit not exceed π for all frequencies from zero to the cutoff frequency ω_{co}. The cutoff frequency*** is defined as the frequency at which the modulus of the transfer coefficient is equal to unity; i.e., $|K_{tr}(j\omega_{co})| = 1$.

Since a dc decision amplifier as a rule is treated as a minimum-phase system, the stability requirement means that the attenuation of $|K_{tr}(j\omega)|$ must not exceed 40 db/decade in the range from zero to ω_{co}. The latter condition follows from the properties of logarithmic amplitude-frequency responses. For a constant attenuation γ expressed in decibels per frequency decade, the phase φ is determined from the approximate relationship [7]

$$\varphi = -\frac{\pi\gamma}{40}.$$

In practice a definite stability margin is required; therefore we usually choose an attenuation no greater than 33 db/decade for which the phase does not exceed 150°. In order to guarantee this condition in a four-stage amplifier it is necessary that at least two stages have time constants that are so small that the phase shift introduced by them is negligibly small right up to the cutoff frequency. It we assume that the entire circuit of the open-loop amplifier produces a phase shift no greater than 140° (an attenuation of 31 db/decade), then 10° is left for the two stages with minimal time constants. On this basis it is possible to write the conditions for a single-channel amplifier which permit us to relate the minimal time constant, the cutoff frequency and the frequency ω_{h1} at which the attenuation of $|K_{tr1}(j\omega)|$[*] begins (Fig. 3):

---

*It is assumed that one of the stages does not invert the phase.

**It is impractical to construct a conditionally stable system, since when the magnitude and form of the transfer coefficient vary, the feedback circuit of the system may prove to be unstable.

***The cutoff frequency also characterizes the pass band of the amplifier in the closed-loop state. For a transfer coefficient equal to unity the upper boundary of the pass band (at this boundary the gain decreases by 3 db) is equal to $0.3\,\omega_{co}$.

$$\frac{\omega_{co.1}}{\omega_{h1}} = 10^{\frac{20\log|K_{tr}(0)|}{\gamma}}, \tag{3}$$

$$\omega_{co.1}T_{min} \approx \frac{\tan 10^{\circ}}{2} \approx 0{,}1, \tag{4}$$

where γ is the attenuation coefficient expressed in decibels per decade (in our case 31 db/decade). Note that formula (3) is valid in the general case, irrespective of the number of channels.

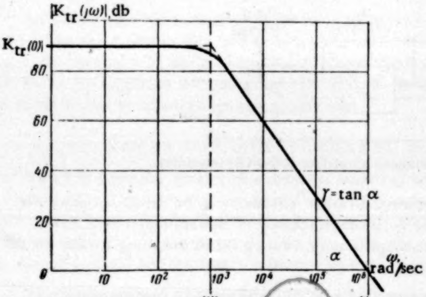

Fig. 3. Logarithmic amplitude-frequency response for the amplifier.

If the allowable error with which the operation can be performed in a definite frequency band is specified (this means that $|K_{tr1}(0)|$ and ω_{h1} are specified), then it follows from (3) and (4) that we can find the cutoff frequency and the maximum allowable T_{min}. For example, if we assume that an error of 0.1% is allowable in the range from 0 to 1000 cps, then it is necessary to choose $|K_{tr1}(0)| \leq 10^{5}$[**], $\omega_{h1} = 2\pi \cdot 10^{3}$ rad/sec, $\omega_{co1} = 10^{7}$ rad/sec and $T_{min} \leq 10^{-8}$ sec. It is extremely difficult to ensure such a small time constant for an amplifying stage in a decision amplifier. To achieve this, it would be necessary to increase the number of stages and sharply to increase the power requirements. Therefore, in conventional single-loop systems it is necessary to be satisfied either with a narrower frequency band or to increase the allowable error. If we assume that the quantity T_{min} is specified, then we find ω_{co1} and ω_{h1} by transforming (3) and (4):

$$\omega_{co1} \approx \frac{1}{10\,T_{min}}, \tag{5}$$

$$\omega_{h1} \approx \frac{1}{10T_{min}}\,10^{-\frac{20\log|K_{tr}(0)|}{\gamma}}. \tag{6}$$

For example, for $T_{min} = 0.1\ \mu$sec and $\gamma = 31$ db/decade the highest frequency $f_{h1} = \omega_{h1}/2\pi$, for which the error does not exceed 0.1% is only 100 cps.

The problem of expanding the pass band and assuring adequate stability is appreciably simplified in the network shown in Fig. 4. The input signal from the summing point is applied not only to the first stage but to all subsequent stages (the first stage provides for the possibility of summing the signals in such a way that the feedback with respect to each channel is negative). The transfer coefficient for such a four-channel network is given by the following formula:

---

[*] Here and throughout, the second subscript is used to denote the number of channels (circuits) in the network which is characterized by the specified quantity. For example, K_{tr1} is the transfer coefficient for a single-channel amplifier.

[**] The quantity $K_{tr1}(0)$ is computed for the case of operation as an adder for six inputs with the transfer coefficients 10, 5, 5.1, 1.1 and with a capacitance of up to 500 $\mu\mu$f at the summing point.

$$K_{tr4}(j\omega) = \left\{\left[\left(\frac{K_1}{1+j\omega T_1} + 1\right)\frac{K_2}{1+j\omega T_2} + 1\right]\frac{K_3}{1+j\omega T_3} + 1\right\}\frac{K_{out}}{1+j\omega T_{out}}. \tag{7}$$

If we choose

$$T_1 \gg T_2 \gg T_3 \gg T_{out}, \tag{8}$$

then as the frequency increases, the attenuation $|K_{tr4}(j\omega)|$ will first be caused by the time constant T_1 of the first stage; under these conditions the remaining time constants have practically no effect on the attenuation. The signal is amplified by all the stages. The auxiliary channels do not have any appreciable effect. But when the gain of the first stage becomes less than unity at the frequency $\omega_1 > K_1/T_1$, the signal will pass chiefly through the second channel to the second stage. The first stage together with its time constant T_1 will be switched off. At frequencies exceeding $\omega_3 > K_3/T_3$ the third stage is switched off. The signal will then pass directly to the output stage. Thus, at higher frequencies, for all practical purposes only the time constants T_{out} remains.

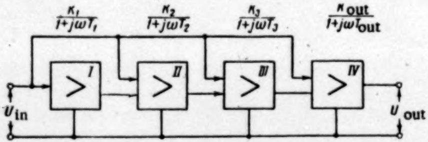
$\frac{K_1}{1+j\omega T_1}$
$\frac{K_2}{1+j\omega T_2}$
$\frac{K_3}{1+j\omega T_3}$
$\frac{K_{out}}{1+j\omega T_{out}}$
I
II
III
IV
U_{in}
U_{out}

Fig. 4. Block diagram for a multichannel amplifier at high frequencies.

Such a principle for designing a network with parallel amplification channels can be called the principle of sequential switching of stages. It is a development of the well-known method of forward signal feed in the theory of automatic control; this method was first applied to amplifiers by Deering [3] in designing a wide-band inverter (the network had two channels).

An analysis of the expression for the transfer coefficient $K_{tr4}(j\omega)$ (cf. Appendix) shows that when the following conditions are satisfied:

$$T_1 = K_1 T_2, \ T_2 = K_2 T_3, \ T_3 = K_3 T_{out}, \tag{9}$$

the attenuation at any frequencies does not exceed 20 db/decade, and the phase lag does not exceed $\pi/2$; i.e., there is a very large stability margin. In that case ω_{co4} and ω_{h4} are correspondingly equal to

$$\omega_{co.4} = \frac{K_{out}}{T_{out}} = \frac{K_{out}}{T_{min}}, \tag{10}$$

$$\omega_{h4} = \frac{1}{T_1} = \frac{1}{K_1 K_2 K_3 T_{min}}. \tag{11}$$

It can be shown (cf. Appendix) that if we specify the allowed phase shift or attenuation γ, then the time constants are approximately chosen from the following conditions:

$$T_1 = \frac{K_1 T_2}{\sqrt[3]{K_1 K_2 K_3 K_{out}}} 10^{\frac{20 \log |K_{tr}(0)|}{3\gamma}}, \tag{12}$$

$$T_2 = \frac{K_2 T_3}{\sqrt[3]{K_1 K_2 K_3 K_{out}}} 10^{\frac{20 \log |K_{tr}(0)|}{3\gamma}}, \tag{13}$$

$$T_3 = \frac{K_3 T_{\text{out}}}{\sqrt[3]{K_1 K_2 K_3 K_{\text{out}}}} \, 10^{\frac{20 \log |K_{tr}(0)|}{3\gamma}} \qquad (14)$$

Under these conditions the frequency at which the attenuation of K_{tr} begins can be increased appreciably. On the basis of (3) and (10),

$$\omega_{h4} = \omega_{co.4} 10^{\frac{-20 \log |K_{tr}(0)|}{\gamma}} = \frac{K_{\text{out}}}{T_{\text{min}}} \, 10^{\frac{-20 \log |K_{tr}(0)|}{\gamma}} \qquad (15)$$

The advantages offered by the principle of sequential switching of stages is clearly characterized by the ratios $\omega_{co4}/\omega_{co1}$ and ω_{h4}/ω_{h1} for equal T_{min} and γ:

$$\frac{\omega_{co.4}}{\omega_{co.1}} = \frac{\omega_{h4}}{\omega_{h1}} \approx 10 K_{\text{out}} \qquad (16)$$

Since it is possible to assure $K_{\text{out}} = 10$ to 50, the proposed principle makes it possible to expand the pass band by a factor of 100 to 500, and to achieve a substantial lowering of the dynamic error. For example, for $T_{\text{min}} = 10^{-7}$ sec, $\gamma = 31$ db/decade, $|K_{tr4}(0)| = 10^5$, and $K_{\text{out}} = 20$, we have $\omega_{h4} = 1.25 \cdot 10^5$ rad/sec; i.e., the error due to the amplifier will not exceed 0.1% for frequencies right up to 20 kc (for a conventional network such a small error can be achieved only up to 100 cps).

2. NETWORKS FOR MULTICHANNEL WIDE-BAND DECISION AMPLIFIERS

Figure 5 shows one variant of a decision amplifier network with sequential switching of the stages (type "MU-12"). The amplifier has four amplification channels. One is formed by the MDM* amplifier and the stages consisting of $Л_3, Л_4, Л_5$ ($Л_4, Л_5$ form a series-balanced output cathode follower); the second is formed by the capacitor C_1 and the stages $Л_1$, $Л_2$, $Л_3$, $Л_4$, $Л_5$,; the third is formed by the capacitor C_3 and the stages $Л_2$, $Л_3$, $Л_4$, $Л_5$, and the fourth is formed by the capacitors C_3 and C_5, and the stages $Л_3$, $Л_4$, $Л_5$.

The time constants of the stages, which are formed by the output resistors and capacitors of the corresponding stages (and for the MDM channel the time constant is equal to the time constant of the demodulator filter), are chosen in such a way that as the frequency increases the MDM channel is switched off first, followed by the stage $Л_2$ under these conditions the signal is amplified solely by the stage $Л_3$.

The network shown in Fig. 5 differs somewhat from the block diagram shown in Fig. 4 in that the network in Fig. 5 does not have a channel which would apply the signal directly to the output stage. Because of this the phase shift at high frequencies is greater than that produced by the ideal network due to the presence of the time constant of the stage consisting of $Л_3$. However, it is possible to make this time constant so small (due to the small input capacitance of the output cathode follower) that it begins to have an appreciable effect only at frequencies above the cutoff frequency; thus, it has no effect on stability.

In testing a mock-up of an amplifier designed according to the network shown in Fig. 5 we were able to obtain the following results.

1. The pass band (with respect to 3 db attenuation) for a transfer coefficient equal to unity, $U_{\text{out}} = 10$ v, and 50 μμf capacitors at the summing point and at the output is equal to 7 Mc.** When the capacitors are increased to 500 μμf the pass band is reduced to 0.5 Mc. For the same parameters with the exception of $U_{\text{out}} = 100$ v we obtained pass band values of 1 Mc and 100 kc, respectively.

2. The noise level at the output for a transfer coefficient equal to unity was 1 mv (in amplitude); for a transfer coefficient of a thousand it was equal to 0.5 v.

---

* The MDM amplifier consists of a modulator, a three-stage ac amplifier, and a demodulator.

** The feedback resistance and the 1 Meg input resistance were shunted by 22 μμf capacitors.

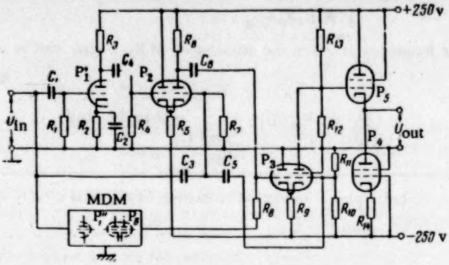
+250 v
R3
R8
C4
C8
R13
P'1
P2
C1
P5
Uin
R1
R2
C2
R4
R5
R7
R12
Uout
P4
C3
C5
P3
R11
MDM
R8
R9
R10
R14
-250 v

Fig. 5. Network for a multichannel decision amplifier ("MU-12") with a pass band of 7 Mc.

3. The null drift over a period of 8 hours was 50 μv.

Figure 6 shows a different variant of the network in which the principle of sequential switching of stages is used only partially. The signal from the summing point is applied to only the first stage ($Л'_2$, $Л_5$) in addition to the MDM channel ($Л_1$), this first stage has a wide pass band. The first stage is followed by two channels: one connects the stage to $Л'_2$, , and the second passes the signal through C_8 directly to the summing stage ($Л_3$) As the frequency increases, the second stage is switched off. The time constant for the first stage is lowered to $8 \cdot 10^{-8}$ sec due to the use of a cathode follower; the output time constant of the summing stage is also small and equals $3 \cdot 10^{-7}$ sec. Because of this it was possible to achieve an adequate stability margin for a wide pass band (cf. Fig. 8).

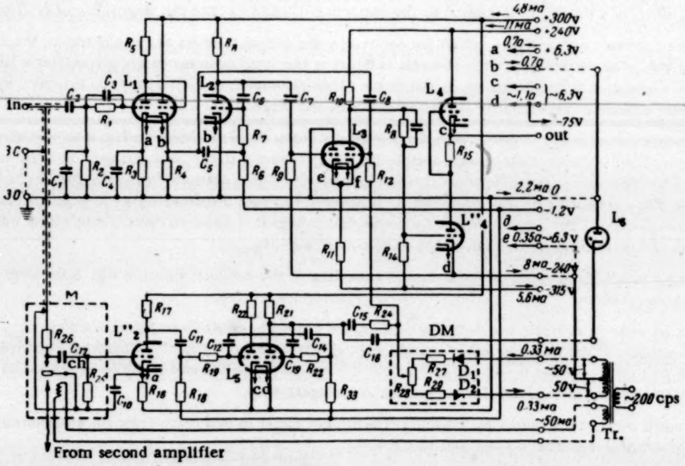
4.8ma
+300v
11ma
+240V
a 0.7a +6.3V
b 0.7a
c
d ~1.1a ~6.3V
-75V
out
In
ЗС
ЗО
C2
C3
L1
R1
R5
RA
L2
C6
C7
R10
C8
L4
R7
R8
C1
R2
C4
R3
R4
C5
R6
R9
L3
R15
a
b
e
f
c
R12
2.2ma 0
-1.2V
L''4
L6
e 0.35a ~6.3 V
R11
R14
d
8ma -240V
-315V
5.6ma
M
R17
R22
R21
C15
R24
DM
R26
C17
ch
L''2
C11
C13
C14
C16
R19
L5
C19
R22
R27
D1
R29
D2
R28
R25
C10
R16
R18
cd
R33
0.33ma
~50
50V
~200 cps
0.33ma
~50ma
Tr.
From second amplifier

Fig. 6. Network for a three-channel amplifier ("TU-10") with a pass band of 1 Mc. Ch. is a "chopper", M is a modulator, DM is a demodulator.

Note that an amplifier which is encompassed with 100% feedback is unstable. But, when the transfer coefficient for the feedback loop is taken into account (the feedback resistance and the capacitance of the summing point with respect to ground) the amplifier has an appreciable stability margin. In particular, it proved to be permissible for a capacitor up to 0.1 μf to be connected to the summing point and for a capacitor of up to 0.5 μf to be connected at the output. Thus, the capacitance of the summing point (which usually worsens stability) is used as an element in a useful corrective network in this case.

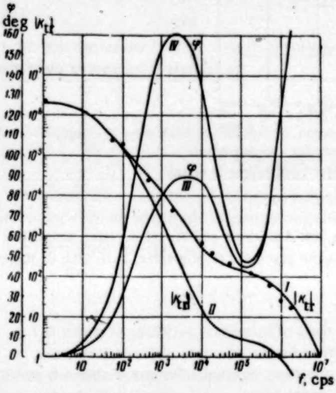

Fig. 7. The computed amplitude-frequency and phase-frequency responses for a "TU-10" amplifier with an open feedback loop. Curves I and III were taken with no corrective network. Curves II and IV were taken for the case when a corrective network was present. The points represent the experimental results.

When the ac transfer coefficient of the feedback loop must be increased (for example, in the case of a limiter or integrator), the connection of a corrective network in series with the input is provided for. Under these conditions the amplitude-frequency and phase-frequency responses acquire the form shown in Fig. 7 (curves II and IV).

The decoupling capacitors C_2, C_5, C_7, C_8 and resistors R_8, R_8, R_9, R_{12} were chosen on the basis of the requirements for assuring stability at low frequencies and satisfying the conditions governing joint operation with the MDM channel. The remaining elements in the network were chosen in such a way as to assure operation of the stages in the linear region with low plate current requirements.

Below we shall cite certain results obtained by testing a three-channel amplifier ("TU-10") which was designed according to the network shown in Fig. 6.

1. The null drift when the unit operated as a scale amplifier normalized to the input (for K = 10) was equal to ± 30 μv over a period of 8 hours.

2. The null drift when the device operated as an integrator for RC = 1 was 15 mv during 1000 sec (or 1.5 mv per 100 sec).

3. The noise at the output for a transfer coefficient equal to unity was 5 mv (the amplitude value).

4. The linear range was equal to ± 145 v for a 10 kohm load, ± 115 v for a 5 kohm load, and ± 100 v for a 2 kohm load.

5. The gain for the amplifier when the feedback loop was open was equal to (1-2) · 10^6 for dc, $8 \cdot 10^4$ at a frequency of 200 cps, 600 at a frequency of 10 kc, and 150 at a frequency of 100 kc (cf. Fig. 7).

6. The frequency at which the amplifier with a transfer coefficient of unity has an error of 0.1% was equal to 1 kc; at 10 kc and 1 Mc the errors were 1% and 30%, respectively (for $U_{out} \leq 10$ v).

The pass band (30% drop in the amplitude-frequency response) for U_{out} = 100 v, a load of 10 kohm, and a shunt capacitance of 600 μμf was 65 kc; for a shunt capacitance of 2000 μμf it was 25 kc, and for a capacitance of 0.01 μf it was 4 kc.

7. The time required to restore the working mode after amplifier overload was no greater than 3 sec.

8. The maximum allowable capacitance at the amplifier output (for a 700 μμf capacitance at the summing point) was no less than 0.25 μf (when the device operated as an amplifier or as an integrator). The maximum allowable capacitance at the summing point (for an output capacitance of 1000 μμf) was no less than 0.25 μf. Under these conditions the pulsations increased to 1 v. For the case of operation as a limiter or operation with variable resistor in the feedback loop, the maximum allowable values of capacitance at the summing point were reduced to 500 μμf for an output capacitance of up to 0.03 μf, or down to 1500 μμf for an output capacitance of up to 0.015 μf.*

---

* All of the data cited here were obtained when the last two stages (which are the main users of the power supply) were supplied from unstabilized rectifiers with pulsations of 3 v.

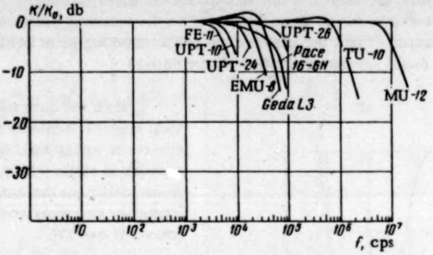

Fig. 8. Amplitude-frequency responses for various types of decision amplifiers when the transfer coefficient is equal to unity.

Figure 8 compares the amplitude-frequency responses of the best American and Soviet decision amplifiers and shows the advantages of the new amplifiers which are based on the principle of sequential switching of stages.

CONCLUSIONS

1. The proposed principle for designing of amplifiers on the basis of sequential switching of stages is a further development of the principle of parallel channels [2]; it differs for the principle of parallel channels in that the auxiliary channels are formed by elements that enter into the basic channel. Because of this it is possible to design a multichannel network with practically no need for additional parts.

2. The design of decision amplifiers according to the principle of sequential switching of stages permits us (other conditions being equal) to expand the pass band by at least two orders of magnitude while retaining the previous stability margin, or to increase the stability margin for the same pass band.

3. We have derived the conditions (12) and (14) for selecting the network time constants which assure the specified attenuation of the amplitude-frequency response; we have also established the relationship (6), (15) between the frequency range ω_h in which the specified accuracy is assured and the minimal time constant for the system.

4. Based on the principle proposed in this paper we designed two decision amplifier networks (amplifiers of the type "TU-10" and "MU-12") whose application in electronic simulators permits us substantially to lower the static and dynamic error components caused by the null drift and pass band in a decision amplifier.

APPENDIX

Analysis of the Expressions for the Transfer Coefficient of a Multiloop Network

We shall find the conditions for which the phase lag introduced by the amplifier (cf. Fig. 4) does not exceed $\pi/2$ at any frequency. For simplicity we shall study a three-stage amplifier without an output stage. The transfer coefficient will be written as follows for this case:

$$K_{\text{tr}3} = \left[\left(\frac{K_1}{1 + j\omega T_1} + 1\right)\frac{K_2}{1 + j\omega T_2} + 1\right]\frac{K_3}{1 + j\omega T_3} + 1. \tag{17}$$

Separating the real an imaginary parts, we find

$$\tan\varphi = -\frac{d}{b}\,\omega, \tag{18}$$

where

$$d = K_1K_2K_3(T_1+T_2+T_3) + K_2K_3(T_2+T_3) + K_3T_3 -$$
$$- \omega^2K_1K_2K_3T_1T_2T_3 + \omega^2K_2K_3T_1^2(T_2+T_3) + \omega^2K_3T_3(T_1^2+T_2^2) + \omega^4K_3T_1^2T_2^2T_3. \qquad (19)$$

$$b = K_1K_2K_3 + K_2K_3 + K_3 + 1 - \omega^2K_1K_2K_3(T_1T_2+T_1T_3+T_2T_3) +$$
$$+ \omega^2K_2K_3(T_1^2 - T_2T_3) + \omega^2K_3(T_1^2+T_2^2) +$$
$$\omega^2(T_1^2+T_2^2+T_3^2) - \omega^4K_2K_3T_1^2T_2T_3 + \omega^4K_3T_1^2T_2^2 + \omega^4(T_1^2T_2^2+T_1^2T_3^2+T_2^2T_3^2) + \omega^6T_1^2T_2^2T_3^2. \qquad (20)$$

In order to assure $|\varphi(\omega)| \leq \pi/2$ for any frequencies it is sufficient to have $d(\omega) \geq 0$ and $b(\omega) \geq 0$. This requirement is satisfied if we choose

$$T_1 \geq K_1T_2, \quad T_2 \geq K_2T_3. \qquad (21)$$

Analogously, we obtain the following conditions for a four-stage amplifier:

$$T_1 \geq K_1T_2,\ T_2 \geq K_2T_3,\ T_3 \geq K_3T_{out}. \qquad (22)$$

We shall determine the relationships between T_1, T_2, T_3 and T_{out} in the case where a definite attenuation γ of the logarithmic amplitude frequency response is specified for the amplifier with an open feedback loop.

Based on (3) and (10), we find

$$T_1 = \frac{1}{\omega_h} = \frac{T_{out}}{K_{out}}\, 10^{\frac{20 \log |K_{tr}(0)|}{\gamma}} \qquad (23)$$

On the other hand, the time constants must be chosen to be proportional to their gains. For the case $\gamma = 20$ db/decade this is evident from relationships (22). Therefore, we may write

$$T_1 \approx \frac{K_1}{a}T_2, \qquad T_2 \approx \frac{K_2}{a}T_3, \qquad T_3 \approx \frac{K_3}{a}T_{out}, \qquad (24)$$

where a is the unknown coefficient which must be determined.

From (24) it follows that

$$T_1 \approx \frac{K_1K_2K_3}{a^3}T_{out}. \qquad (25)$$

Eliminating T_1 from (23) and (25), we find

$$a \approx \sqrt[3]{K_1K_2K_3K_{out}} \cdot 10^{\frac{-20 \log |K_{tr}(0)|}{3\gamma}} \qquad (26)$$

Substituting the value which we have obtained for a into (24), we find the sought for relationship between the time constants which assure the attenuation γ db/decade:

$$T_1 \approx \frac{K_1T_2}{\sqrt[3]{K_1K_2K_3K_{out}}}\, 10^{\frac{20 \log |K_{tr}(0)|}{3\gamma}},$$
$$T_2 \approx \frac{K_2T_3}{\sqrt[3]{K_1K_2K_3K_{out}}}\, 10^{\frac{20 \log |K_{tr}(0)|}{3\gamma}}, \qquad (27)$$
$$T_3 \approx \frac{K_3T_{out}}{\sqrt[3]{K_1K_2K_3K_{out}}}\, 10^{\frac{20 \log |K_{tr}(0)|}{3\gamma}}.$$

SUMMARY

There is proposed a principle of designing operational amplifiers which is based on cascade successive switching off. This principle permits to enlarge the pass band on approximately two orders. Brief description of operational amplifiers of two types designed according to the proposed principle and the data of their test which confirm theoretical results are given.

LITERATURE CITED

1. P. S. T. Buckerfield, The parallel – T.D.C. Amplifier. IEE. No. 71, vol 99, Oct. 1952.
2. B. Ya. Kogan, A. A. Maslov, and D. E. Polonnikov, "Electronic simulating equipment of the type "EMU-8A", Vestnik Akad. Nauk SSSR, 7 (1958).
3. C. S. Deering, A Wide-Band Direct-Coupled Operational Amplifier. Proceedings National Simulation Conference, January 19, 20, 21, 1956.
4. G. W. Smith and R. G. Wood. Principles of Analog Computation. McGraw-Hill Book Company, Inc. 1959.
5. B. Ya. Kogan, Electronic Simulators and Their Application in the Investigation of Automatic Control Systems [in Russian] (Fizmatgiz, 1959).
6. E. A. Goldberg, Stabilization of Wide-Band Direct Current Amplifier for Zero and Gain, RCA Review, T. 11, No. 2 (1950).
7. G. W. Bode, Circuit Theory and the Design of Amplifiers with Feedback [Russian translation] (Foreign Literature Press, 1948).

THE EFFECT OF THE CHARACTERISTICS OF AN ELECTRICAL ELEMENT ON THE CHOICE OF THE PARAMETERS FOR A HYDRAULIC AMPLIFIER

I. M. Krassov, L. I. Radovskii, and B. G. Turbin
(Moscow)

Translated from Avtomatika i Telemekhanika, Vol. 21, No. 12,
pp. 1623-1626, December, 1960
Original article submitted February 24, 1960

The paper provides a basic analysis of the computation of the initial pressure in the chamber between restrictors in a hydraulic amplifier of the jet-damper type which is controlled by an electromagnetic element; the characteristics of the latter are taken into account.

Usually the basic parameters of hydraulic amplifiers designed for operation in some automatic control systems are chosen without considering the properties and special features of the elements which control the amplifiers.

In this paper we study the effect of the characteristics of an electromagnetic control element of the type "REP" [1, 2] on the choice of the initial pressure in the chamber between restrictors in a jet-damper hydraulic amplifier.

For a jet-damper amplifier (Fig. 1) the dependence of the pressure p_1 in the inter-restrictor chamber on the angle of rotation φ of the damper in a steady-state mode of operation is given by the formula

$$p_1 = \frac{\sigma^2 p_0}{\sigma^2 + a^2 (h_0 + r\varphi)^2}, \tag{1}$$

where p_0 is the supply pressure for the amplifier, h_0 is the initial gap between the nozzle and the damper, $\underline{r}$ is the radius through which the damper can be "rocked", σ is the conductivity of the constant restrictor and is equal to

$$\sigma = \mu f \sqrt{\frac{2g}{\gamma}}, \tag{2}$$

$\underline{a}$ is a quantity which characterizes the conductivity of the nozzle-damper unit and is equal to

$$a = \mu_n \pi d_n \sqrt{\frac{2g}{\gamma}}. \tag{3}$$

In expressions (2) and (3) the quantities μ and μ_n respectively denote the discharge coefficients for the restrictor and the nozzle-damper unit, f is the flow area for the restrictor orifice, d_n is the diameter of the nozzle, γ is the specific weight of the working liquid, $\underline{g}$ is the acceleration of gravity. The direction in which the angle φ is measured is shown in Fig. 1.

Formula (1) is written for the case where the gap between the nozzle and the damper is increased for small angles of rotation of the damper. The quantity a is variable, since the coefficient depends on the gap h and the Reynolds number. For a small variation of the gap this quantity can be assumed approximately constant [3] and equal to the initial gap h_0; this assumption is made here.

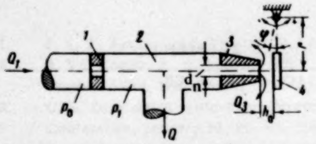

Fig. 1. Diagram illustrating the principle of a hydraulic jet-damper amplifier: 1) Nozzle with a constant flow cross section; 2) inter-restrictor chamber; 3) nozzle; 4) damper.

The achievement of high sensitivity and speed of response for the system requires that in the nominal mode of operation the amplifier must have its maximum pressure gain:

$$\left(\frac{\partial p_1}{\partial \varphi}\right)_{\varphi=0} = -\frac{2r p_{10}}{\lambda p_0} \sqrt{p_{10}(p_0 - p_{10})}, \tag{4}$$

where p_{10} is the initial steady-state value of the pressure in the chamber between restrictors,

$$p_{10} = \frac{\sigma^2 p_0}{\sigma^2 + a^2 h_0^2}, \tag{5}$$

$$\lambda = \frac{\sigma}{a}. \tag{6}$$

An analysis of the statics of just one hydraulic amplifier [4] shows that the maximum value of the pressure gain occurs for

$$p_{10} = 0.75\ p_0. \tag{7}$$

The jet of working liquid which emerges from the nozzle interacts with the damper and produces a moment M_h of the hydrodynamic forces. This moment represents the load on the control element and can be found either from tables [5] or by computation [6].

The static characteristic for the "REP" control element usually is of the form shown in Fig. 2, where $i_1, i_2, \ldots$, are the control currents; here $i_1 < i_2 < i_3 \ldots$.

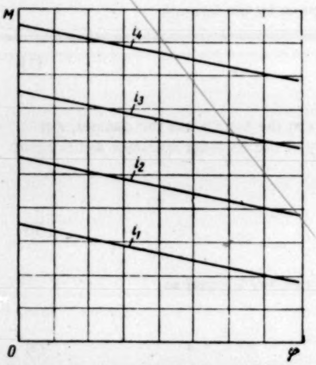

Fig. 2. Static characteristic for the electromagnetic control element.

The steady-state position of the damper is characterized by the equality of the electrical and hydrodynamic force moments:

$$M = M_h, \tag{8}$$

where M is the moment which moves the control element.

Taking into account the shape of static characteristics, we write

$$\frac{\partial M}{\partial i}\,\Delta i - \left|\frac{\partial M}{\partial \varphi}\right| \Delta\varphi = \frac{\partial M_h}{\partial \varphi}\,\Delta\varphi. \tag{9}$$

From this we obtain

$$\Delta\varphi = \frac{\dfrac{\partial M}{\partial i}}{\dfrac{\partial (M_h + |M|)}{\partial \varphi}}\,\Delta i. \tag{10}$$

Making use of (4) and (10) and taking into account the relationship

$$\left(\frac{\partial p_1}{\partial i}\right)_{\varphi=0} = \left(\frac{\partial p_1}{\partial \varphi}\right)_{\varphi=0} \left(\frac{\partial \varphi}{\partial i}\right)_{\varphi=0}, \tag{11}$$

we can write the gain of the amplifier for a nominal mode of operation for which $\varphi = 0$; we obtain an expression in the form of a current gain

$$\left(\frac{\partial p_1}{\partial i}\right)_{\varphi=0} = -\frac{2rp_{10}}{\lambda p_0}\sqrt{p_{10}(p_0 - p_{10})}\,\frac{\left(\frac{\partial M}{\partial i}\right)_{\varphi=0}}{\left|\frac{\partial M}{\partial \varphi}\right|_{\varphi=0} + \left(\frac{\partial M_r}{\partial \varphi}\right)_{\varphi=0}}. \tag{12}$$

For simplicity in notation we introduce the substitution

$$m_0 = \left(\frac{\partial M}{\partial i}\right)_{\varphi=0}, \quad n_0 = \left|\frac{\partial M}{\partial \varphi}\right|_{\varphi=0}, \quad q_0 = \left(\frac{\partial M_h}{\partial \varphi}\right)_{\varphi=0}, \tag{13}$$

where

$$m_0 = \text{const}, \quad n_0 = \text{const}. \tag{14}$$

Based on experimental data, it was established that it is possible to assume

$$q_0 = c\bar{p}_{10}, \tag{15}$$

with a sufficient degree of accuracy; here c is a constant quantity, and $\bar{p}_{10}$ is the relative pressure in the inter-restrictor chamber which is equal to

$$\bar{p}_{10} = \frac{p_{10}}{p_0}. \tag{16}$$

In addition, we introduce the substitution

$$\alpha = \frac{n_0}{c}. \tag{17}$$

Then (12) can be rewritten in the form

$$\left(\frac{\partial p_i}{\partial i}\right)_{\varphi=0} = -\frac{2rp_0}{\lambda}\bar{p}_{10}\sqrt{\bar{p}_{10}(1 - \bar{p}_{10})}\,\frac{m_0}{(\alpha + \bar{p}_{10})c}. \tag{18}$$

We determine the condition governing the existence of a maximum for the pressure gain. We formulate the equation

$$\begin{gathered}\frac{d}{d\bar{p}_{10}}\left(\frac{\partial p_1}{\partial i}\right)_{\varphi=0} = -\frac{2rp_0m_0}{\lambda(\alpha + \bar{p}_{10})c}\left[\frac{(1 - 2\bar{p}_{10})\bar{p}_{10}}{2\sqrt{\bar{p}_{10}(1 - p_{10})}} + \sqrt{\bar{p}_{10}(1 - \bar{p}_{10})}\right] + \\ + \frac{2rp_0m_0}{\lambda(\alpha + \bar{p}_{10})^2c}\left[\sqrt{\bar{p}_{10}(1 - \bar{p}_{10})}\,\bar{p}_{10}\right] = 0.\end{gathered} \tag{19}$$

After certain simplifications, Eq. (19) becomes

$$\frac{rp_0m_0}{\lambda c}\,\frac{\bar{p}_{10}\left[2\bar{p}_{10}^2 + (4\alpha - 1)\bar{p}_{10} - 3\alpha\right]}{(\alpha + \bar{p}_{10})^2\sqrt{\bar{p}_{10}(1 - p_{10})}} = 0. \tag{20}$$

Since the quantities r, $\bar{p}_0$, m_0, λ, c, α, p_{10} are positive, it follows that a solution of the equation is possible if

$$\bar{p}_{10}^2 + (2\alpha - 0.5)\bar{p}_{10} - 1{,}5\,\alpha = 0. \tag{21}$$

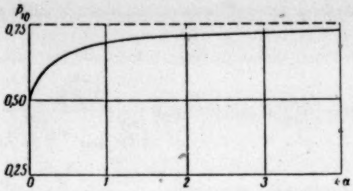

Fig. 3. Dependence of the relative pressure P_{10} on the quantity α.

From this we obtain

$$\bar{p}_{10} = \sqrt{\alpha^2 + \alpha + 0.0625} - (\alpha - 0.25). \tag{22}$$

if we take into account the fact that $\bar{p}_{10} > 0$.

Figure 3 shows the dependence of the relative pressure p_{10} on the quantity α. Examination of the curve shows that the relative pressure in the inter-restrictor chamber reaches the value 0.75 only for large values of α. For existing electromagnetic control elements and hydraulic amplifiers of the jet-damper type the value of α varies over the limits from 0.2 to 0.75; this corresponds to the initial segment of the curve $p_{10} = f(\alpha)$. For this reason it is necessary in a number of cases to take into account the effect of the control element on the operation of the hydraulic amplifier. Expression (22) makes it possible to determine the pressure p_{10} which assures the maximum pressure (or flow) gain as a function of the characteristics of the electrical control element and the characteristic of the nozzle-damper unit.

SUMMARY

There is well-grounded calculation of the initial pressure in the chamber between throttles of the hydraulic amplifier of the nozzle-flapper type which is controlled by an electromagnetic element, the characteristics of the element being taken into consideration.

LITERATURE CITED

1. Yu. M. Pul'er, "A contactless electromagnetic actuating and logometer mechanism," Priborostroenie, No. 1 (1957).
2. I. E. Dekabrun, N. P. Kozlov, and I. M. Krassov, "The dynamics of an electromagnetic control element," Avtomatika i Telemekhanika, 21, 4 (1960).*
3. I. M. Krassov and B. G. Turbin, Discharge Coefficients of a Hydraulic Jet-Damper Restrictor, Automatization of Production Processes, No. 3 (Academy of Sciences, USSR Press, 1960).
4. A. G. Shashkov, "Theory of a jet-damper control unit operating with oil," Avtomatika i Telemekhanika 17, 11 (1956).*
5. I. M Krassov and B. G. Turbin, "The force effect of a jet in a hydraulic jet-damper amplifier," Avtomatika i Telemekhanika 20, 12 (1959).*
6. I. M. Krassov, L. I. Radovskii, and B. G. Turbin, "Approximate determination of the reaction of the jet in a hydraulic amplifier," Avtomatika i Telemekhanika 21, 10 (1960).*

---

*See English translation.

8

LEV SEMENOVICH GOL'DFARB (ORBITUARY)

Translated from Avtomatika i Telemekhanika, Vol. 21, No. 12,
pp. 1627-1628, December, 1960

On October 12, 1960, an outstanding scientist and leading specialist in automation, Doctor of Sciences Professor Lev Semenovich, Gol'dfarb, died.

Soviet science has suffered a heavy loss. We have lost a magnificent scientist, talented engineer, and a splendid teacher.

Upon completing the Moscow Power Institute, L. S. Gol'dfarb, worked since 1931 in the All-Union V. I. Lenin Electrical Engineering Institute (AEI). Soon he became one of the chief participants and directors of the staff that subsequently produced a number of great specialists.

In these years Lev Semenovich developed control systems for turbogenerators, control systems for governing the operation of boilers, automatic control systems for industry, etc. Simultaneously, he was performing important theoretical work on the investigation of stability and transient responses in linearized and nonlinear systems. It was in the AEI in 1940 that he originated ideas which led him to developing a method for studying self-oscillations which has now become classical. This method has been developed and applied in books and papers on the theory and design of automatic systems; it has justifiably been named the Gol'dfarb method.

In 1941, Lev Semenovich was called to serve in the ranks of the Soviet armed services; he served in the air force until the end of the Great Patriotic War. From 1945, until his death Lev Semenovich performed major and fruitful works in the Moscow Power Institute, first as a candidate and then (after defending his doctorate dissertation in 1948) as a professor on the automation staff.

The results of the basic papers by L. S. Gol'dfarb have been published in our journal, in which he took an active part.

Lev Semenovich worked without sparing time or energy. He gave generously of his experience to the younger generation and painstakingly educated specialists in the field of automation. He achieved success in this work due to his magnificent qualtities — a love of people, a personal warmth, a lively temperament, and a clear mind.

His memory will always be carried in the hearts of all those who had the priviledge of studying under him or of working with him.

A LIST OF LITERATURE ON MATHEMATICAL SIMULATION (ANALOG COMPUTERS) FOR 1958

(Translated from: Avtomatika i Telemekhanika Vol. 21, No. 12, 1629-1652, December, 1960.

CONTENTS

A. Books
B. Proceedings of Conventions and Conferences. Information
C. General Theoretical Problems
    1. General problems
    2. Method for solving problems using simulators
    3. The accuracy of simulating devices and their elements
D. Simulators Based on Indirect Analogy
    I. Electronic devices
    II. Decision elements in electronic devices
        1. DC electronic amplifiers
        2. Decision amplifiers without vacuum tubes
        3. Integrators and differentiators
        4. Multiplier-divider units
        5. Function generators
        6. Other decision elements and auxiliary equipment
    III. Electromechanical devices
    IV. Pneumatic-hydraulic devices
    V. Specialized devices
        1. Devices for solving systems of algebraic equations. Root finders
        2. Devices for solving integral equations
        3. Correlators
        4. Various devices
E. Devices for Converting from a Digital Code to Physical Quantities and Vice Versa
F. The Use of Simulators of The Indirect Analogy Type
    I. The use of simulators for solving automatic control problems
    II. The use of simulators and their elements in aviation
    III. The use of simulators in nuclear engineering
    IV. Various applications
G. Digital Simulation
H. Bibliography

A. BOOKS

IN RUSSIAN

Belova A. I., Vitenberg I. M. and Gluzberg E. A. – A block for recording and reproducing functions (BRR) in the solution of integral equations. – Branch of the VINITI, AN SSSR, Moscow, 1958. 50 pp. with illustrations.

Bykhovskii M. L. – Fundamentals of the dynamic accuracy of electrical and mechanical networks. – AN SSSR, Moscow, 1958. 160 pp., 160 illustrations. Bibliography 89 titles. (Machinery Institute.)

Lebedev A. N. – Computer-decision units. – Mashgiz, Moscow, 1958. 378 pp., 216 illustrations. Bibliography 12 titles.

Problems in the synthesis and accuracy of complex analog devices (predominantly as they apply to mechanical computer-decision units). – AN SSSR, Moscow, 1958. 226 pp. with illustrations. (Machinery Institute.)

Problems in the theory of mathematical machines. Symposium 1. – Fizmatgiz, Moscow, 1958. 230 pp. with illustrations and tables.

IN LANGUAGES OTHER THAN RUSSIAN

Danlous-Dumesnils M. – Le calcul analogique pa

courant continu. – Paris, Dunod, 1958, 272 pp.

Karplus W. – Analog simulation. Solution of field problems. – New York, McGraw Hill, 1958, 449 pp., 241 illustrations, 21 tables.

Olson H. F. – Dynamic analogies. Ed. 2. – New York Van Nostrand, 1958, 278 pp.

Susskind A. K. ed. – Notes on analog digital conversion techniques. 2nd ed. – New York, Wiley and Sons, Inc., London, Chapman and Hall, 1958, 410 pp., ill.

Tomovic R. – Calculateurs analogiques repetifs. – Paris, Masson, 1958, 186 pp.

B. PROCEEDINGS OF CONVENTIONS AND CONFERENCES. INFORMATION

IN LANGUAGES OTHER THAN RUSSIAN

AIEE - IRE - ACM Eastern Joint Computer Conference. – Philadelphia, December 3-5, 1958. – Electr. Engng., 1958, Jan., vol. 77, No. 1, p. 73.

Analog-Rechenzentrum. – Elektro-Anz., 1958, No. 40-41. p. 383.

Association internationale pour le calcul analogique. – Rev. gen. mec., 1958, jan., an 42, No. 107, p. 50.

Central Simulation Council meeting of May 5 on nonlinear phenomena. – Instrum. and Automat., 1958, vol. 31, No. 8, pp. 1388-1390.

Computer and Automation Conference, June 2-4, 1958, University of Texas, Austin, Tex. – Instrum. and Automat., 1958, May, vol. 31, No. 5, p. 881.

Eastern Simulation Council meeting of February, 1958 at Avco. – Instrum. and Automat., 1958, vol. 31, No. 8, pp. 1385-1386.

The Electronic Computer Exhibition. National Hall, Olympia, London, Nov. 28-Dec. 4, 1958. – Process Control and Automat., 1958, Oct., vol. 5, No. 10, p. 31.

Hatcher Ch. – Nel's new computer centre. Bur. Ships J., 1958, vol. 7, No. 6, pp. 14-16.

Joint meeting of January 8 on "Interrelationship of analog and digital computers." – Instrum. and Automat., 1958, vol. 31, No. 3, pp. 487-491.

Midwestern S/C meeting of June 9 on "Cute tricks in simulation." Instrum. and Automat., 1958, vol. 31, No. 10, Pt. 1, pp. 1691-1694.

National Simulation Conference (Dallas, Texas, Oct. 23-25, 1958). – Trans. IRE, 1958, March, vol. EC-7, No. 1, p. 75.

S/C meeting of Nov. 14 on "Standard simulation circuits." – Instrum. and Automat., 1958, Jan., vol. 31, No. 1, pp. 120-122.

SE S/C meeting of September 27 on analog-digital conversion. – Instrum. and Automat., 1958, Jan., vol. 31, No. 1, pp. 119-120.

Seconde Journées Internationales de Calcul Analogique. – Strasbourg, Sept. 1, 1958. – Mesures et controle industr., 1958, fevr., an. 23, No. 249, p. 130.

Symposium on computers. (Held at the Australian Administrative Staff College MT. Eliza, Victoria, December 3-6, 1957.) – Austral. J. Instrum. Technology, 1958, Febr., vol. 14, No. 1, pp. 5-18.

Jurgen R. K. – Technical highlights of '58 Wescon. – Electronics, 1958, Nov., vol. 31, No. 45, pp. 72-75, 8 ill.

Mussard J. A. – Un centre international provisoire de calcul à Rome. – Inform. Unescu, 1958, No. 284, pp. 7-9.

WS/C and DDA Council meeting of May 5 on "Problems unique to computers of a kind." Instrum. and Automat., 1958, vol. 31, No. 7, pp. 1219-1225.

C. GENERAL THEORETICAL PROBLEMS

1. General Problems

IN RUSSIAN

Bruevich N. G. – On the problem of the inputs and outputs of complex analog units. In: Problems in the synthesis and accuracy of complex analog devices. – AN SSSR, Moscow, 1958. pp. 7-36, 29 illustrations.

Fel'dbaum. – An automatic optimizer. – Avtomatika i Telemekhanika, 19, No. 8, pp. 731-743. 9 illustrations Bibliography 6 titles (1958).

Gluzberg E. A. – On the logic possibilities of mathematical machines of the analog type. In: Problems in the theory of mathematical machines, Symposium 1. – Fizmatgiz, Moscow, 1958, pp. 135-148, 14 illustrations. Bibliography 10 titles.

Khernauér V. – Computer devices. In: Engineering techniques for automization of production processes. – Mashgiz, Moscow, 1958, pp. 112-129, 12 illustrations.

Klishov N. A. The synthesis of computer-decision units which compute implicit functions by the method of approximations. In: Problems in the synthesis and accuracy of complex analog devices. – AN SSSR, Moscow, 1958, pp. 37-51, 4 illustrations. Bibliography 5 titles.

Kuz'minok G. K. Electrical integrators and the possibilities for their application in engineering-technological computations. In: Mechanization of design and computation. – Mashgiz, Moscow-Leningrad, pp. 27-53, 5 illustrations.

Semenov V. V. Electrodynamic simulation of the hydraulic section of a hydroelectric power station. – Nauchnye Doklady Vysshei Shkoly, Energetika, No. 2, 219-230 (1958).

Shuvalov N. K. Investigating transient responses

using electronic simulators. — Sudostroenie, No. 11, 41-45, 7 illustrations. Bibliography 6 titles. (1958).

Stakhovskii, R. I. A two-channel automatic optimizer. — Avtomatika i Telemekhanika, 19, No. 8, pp. 744-756, 18 illustrations (1958). •

LANGUAGES OTHER THAN RUSSIAN

AED computer linkage. — Res. and Engng., 1958, vol. 4, No. 1, p. 27.

Analogue computation. — J. Instn. Electr. Engrs., 1958, April, vol. 4, No. 40, p. 194-197, 5 illustrations.

Bauer W. F. — Aspects of real-time simulation. — Trans. IRE, 1958, vol. EC-7, No. 2, p. 134-150.

Blackman P. F. — A computer combining analog and digital principles for complex frequency network calculations. In: Proc. Conference on Computers in Control Systems, 1957. — New York, Am. Inst. Electr. Engrs., 1958, p. 34-41, 13 illustrations. Bibliography 88 titles.

Ernst D. Die Entwicklung der Rechenmaschinen in America. — Regelungstechnik, 1958, Jg. 6, H. 3, SS. 89-92, 5 illustrations. Bibliography 30 titles.

Ferguson A. E. Analogue computers. — Austral. J. Instrum. Technol., 1958, Febr., vol. 14, No. 1, p. 19-28, 10 illustrations. Bibliography 8.

Franks R. G. E. — Maximizing control performance and economy with analog simulation. — Am. J. Instrum. Soc., 1958, vol. 5, No. 9, pp. 80-94, 9 illustrations. Bibliography 5.

Gabillard R. — Les analyseurs differentiels electroniques. — Inds. atom, 1958, vol. 2, No. 7-8, pp. 91-107.

Gait J. J. — Analogue computers and their application. — Process Control and Automat., 1958, Nov., vol. 5, No. 11, pp. 480-485, 8 illustrations Bibliography 11.

Grosch H. R. J. — The future of computing. — Ind. Engng. Chem., 1958, Nov., vol. 50, No. 11, pp. 1664-1666.

Hare R. E. and Willison W. E. — Analogue computers. — Instrum. Practice. 1958, vol. 12, No. 11, pp. 1200-1207, 13 illustrations. No. 12, pp. 1295-1303, 18 illustrations.

Henle R. A and Walsh J. L. — The application of transistors to computers. — Proc. IRE, 1958, June, Vol. 46, No. 6, pp. 1240-1254, 52 ill. Bibliography 6.

Hirst F. — History of computers. Austral. J. Instrum. Technol., 1958, Feb., vol. 14, No. 1, pp. 14-18.

Hitcheon I. C. Simulation of nonlinear field problems. — Brit. Communs. and Electronics, 1958, Feb., vol. 5, No. 2, pp. 96-99, 5 illustrations. Bibliography 7.

Kleimpeter M. —Application d'un analyseur differentiel couplé à un microreseau pour l'étude du comportement des auxiliaires d'un grand alternateur lors d'un court circuit à ses bornes. — Rev. Gen. Electr., 1958, Dec., vol. 67, No. 12, pp. 685-691.

Leondes C. T. and Nothman M. — Real-time hybrid computers for control systems. In: Proc. Conference on Computers in Control Systems, 1957. New York, Am. Inst. Electr. Engrs., 1958, pp. 88-94, 10 illustrations. Bibliography 13.

Lonergan J. P. — An introduction to the application of analogue computers. Austral. J. Instrum. Technol., 1958, vol. 14, No. 1, pp. 62-71.

Mertens H. — Prinzip und Anwendung der Analog-Rechenmaschine. — Elektronik, 1958, Mai, jg. 7, Nr. 5, SS. 130-134, 11 illustrations.

New analog-digital-analog device. — Automat. Control, 1958, vol. 8, No. 6, p. 91.

Nicolau E., Simon N., Voiculescu Ch. and Weiss A. — Elemente neliniare pentru simulatore si calculatore analogice. Realizazi experimentale. — Automat. si electron., 1958, vol. 2, No. 2, pp. 74-77.

Nothman M. H. — Combined analog-digital control system. — Electr. Manufact., 1958, vol. 61, No. 6, pp. 78-86.

Palevsky M. — Calculateurs hybrides analogiques. — Automatisme, 1958, Mars, an 3, t. 3, No. 3, pp. 115-116, 8 illustrations.

Paul R. J. A. — Analogue simulation in system design. — Control, 1958, vol. 1, Nov., No. 5, pp. 221-226, 8 illustrations; Dec., No. 6, p. 276-278, 12 illustrations. Bibliography 15.

Pieretti J. So you have a problem. A fundamental discussion of analog and digital computers and comparison of their relative advantages and disadvantages. — Manhattan Coll. Engr., 1958, vol. 15, No. 3, pp. 94, 120-121, 4 illustrations. Bibliography 4.

Rao P. V. and Krishna G. — The transformer analog computer. — Commun and Electronics, 1958, Jan., No. 34, pp. 732-738, 18 illustrations. Bibliography 14.

Rogers S. — Analog computers and computing. — Ind. Eng. Chem., 1958, Nov., vol. 50, No. 11, p. 1636-1640, 4 illustrations.

Simulation speeds research at Bell Laboratories. — Bell Labs Rec., 1958, Sept., vol. 36, No. 9, pp. 348-349, 1 ill.

Sykes R. P. A preventive maintenance program for large general purpose electronic analog computers. — IRE National Convention Rec., 1958, vol. 6, Pt. 4, pp. 191-205, append., 13 illustrations.

Szamer B. — Ueber die Entwicklung wissenschaftlicher

Rechenmaschinen. – Neue tech. Buero, 1958, Bd. 2, Nr. 10, SS. 232-234, 3 illustrations.

Thermal computers. – Mech. Engng., 1958, vol. 80, No. 5, p. 86.

Thomas G. E. – Analogue computers as design tools. – Automat. Progr., 1958, vol. 3, No. 11, pp. 415-417, 429.

Unger H. – Grundlagen elektronischer Rechenanlagen. – Werkstattstechnik und Maschinenbau, 1958, Bd. 48, Nr. 2, SS. 125A-128A, 3 illustrations.

Venning B. H. – Analogue computers as an aid to teaching. – Bull. Electr. Engng. Educ., 1958, No. 21, pp. 41-54.

West G. P. – Computer control experience gained from operation of a large combined analog digital computation system. – In: Proc. Conference on Computers in Control Systems, 1957. – New York, Am. Inst. Electr. Engrs., 1958, pp. 95-97, 4 illustrations.

West, G. P. – The role of computers in analysis and design of control systems. – Trans. IRE, 1958, vol. AC, No. 5, p. 65.

Winkler H and Gumme G. – Die Bedeutung elektronischer Analogieanlagen für den Fortschritt der Elektrotechnik. – Dtsch. Elektrotechn., 1958, Sept., Bd. 12, Nr. 9, SS. 317-324, 23 illustrations. Bibliography 10.

2. Methods for Solving Problems Using Simulators

IN RUSSIAN

Lebedev A. N. – The necessary stability conditions for mathematical simulators in solving systems of algebraic and transcendental equations with three or more unknowns by the method of choosing roots. – Izv. Vysshikh Uchebnykh Zavedenii, Priborostroenie, 1958, No. 6, pp. 38-49, 5 illustrations.

Sirazitdinov E. G. and Petrova E A. – Simulating actuating mechanisms in automatic control systems. – Izv. Vysshikh Uchebnykh Zavedenii. Priborostroenie, 1958, No. 3, pp. 63-72.

Smolov V. B. – On a certain method for simulating integro-differential functions. – Izv. Vysshikh Uchebnykh Zavedenii. Priborostroenie, 1958, No. 4, pp. 69-75, 5 illustrations.

LANGUAGES OTHER THAN RUSSIAN

Bauer W. F. – Aspects of real-time simulation. – Trans. IRE, 1958, June, vol. EC 7, No. 2, pp. 134-136.

Buehler E. – Die elektronische Nachbildung mechanischer Reibung – Regelungstechnik, 1958, Jg. 6, H. 1, SS. 14-19, 14 illustrations.

Ernst D. – Das Arbeiten mit Analogie Rechengeraeten. – Regelungstechnik, 1958, Jg. 6, H. 6, SS. 206-209, 3 illustrations. Bibliography 16.

Greenspan D – Note on analog techniques for solving two-point boundary value problems. – Rev. Sci. Instrum., 1958, Sept., vol. 29, No. 9, pp. 787 788, 1 illustration.

Herrmann H. – Aids to programming techniques for electronic analogue computers. – Abhandl. Braunschw. Wiss. Gesell., 1958, vol. 10, pp. 117-149.

Herschel R. and Kettel E. – Das Problem der Normierung bei der Anwendung von Analog-Rechenmaschinen zur Behandlung regelungstechnischer Aufgaben. – Regelungstechnik, 1958, Jg. 6, H. 11, SS. 400-405, 6 illustrations. Bibliography 6.

Horn R. E. and Honnell P. M. – Matrix programming of electronic analog computers. – Commun. and Electronics, 1958, Sept., No. 38, pp. 420-426, 11 illustrations.

Lane L. J. – A method of scaling and checking computer circuits. – Applic. and Ind., 1958, May, No. 36, pp. 67-70, 3 illustrations.

Matyas J. Vicenasobne elektricke integratory. – Slaboproudy Obzor, 1958, t. 19, No. 11, str. 758-765.

Napodobeni prubehu mechanickeho treni servomechanismo na elektronickem modelu. – Automatisace, 1958, No. 10, str. 344-345.

Nathan A. – Computing and error matrices in linear differential analyzers. – Trans. IRE, 1958, March, vol. EC-7, No. 1, pp. 32-33, ill. Bibliography.

Otterman J. – on the loop- and node-analysis approaches to the simulation of electrical networks. – Trans. IRE, 1958, Sept., vol. EC-7, No. 3 3, pp. 199-206, 10 illustrations.

Scheinman A. H. – A numerical-graphical method for synthesizing switching circuits. – Commun. and Electronics, 1958, Jan., No. 34, pp. 687-689, 7 illustrations.

Storey L. R. O. and Grierson J. K. Time-symmetric filters. I. Methods of simulation. – Electronic Engng., 1958, Oct., vol. 30, No. 368, p. 586-592, 5 illustrations. Bibliography 7.

Tomovic R. – Method of iteration and analog computation. – Ann. Assoc. Internat. Calcul. Analog., 1958, vol. 1, No. 2, pp. 60-63.

3. The Accuracy of Simulating Units and Their Elements

IN RUSSIAN

Ordanovich A.E. – The effect of nonideal characteris in integrators and adders on the operation of electronic simulators. – Nauchnye Doklady vysshei shkoly,

Fiziko-Matematicheskie Nauk. 1,155–161,1 illustrations (1958).

Problems in the synthesis and accuracy of complex analog devices (AN SSSR, Moscow, 1958. 226 pages with illustrations; Machinery Institute)

Smolov V. B. and Smirnov A. N. – Computing the accuracy of an electromechanical integrator and certain possible methods for increasing the accuracy. – Izvestiya Leningradskovo Elektrotekhnicheskovo Instituta, 1958, No. 34, pp. 34-45 3 illustrations.

Tetel'baum I. M. and Chelnokov N. N. – Increasing the accuracy with which problems can be solved on an electronic analog computer. – Transactions of the Moscow Power Institute, 27 (Gosenergoizdat, Moscow-Leningrad, 1958, pp. 259-266.)

LANGUAGES OTHER THAN RUSSIAN

Dow P. C. – An analysis of certain errors in electronic differential analyzers. Capacitor dielectric absorption. – Trans. IRE, 1958, March, vol. EC-7, No. 1, pp. 6-16, 14 illustrations. Bibliography 8.

Fixa Z. – Stanoveni presnosti analogového pocitace v cecelem oboru jeho cinnosti (Determining the accuracy of a specialized analog computer) – Stroje zpracov infirm., 1958, No. 6, pp. 153-184.

Kley A. – Einflüsse des Nullpunktfehlers und des Gitterstromes von Gleichstromverstärkern bei der Lösung linearer Differentialgleichungen mit konstanten Koeffizienten auf dem elektronischen Analogrechner. – Elektron. Rundschau, 1958, Sept., Bd. 12, No. 9, SS. 305, 8 illustrations. Bibliography 6.

Miura T. and Nagata M. – Theoretical consideration of computing errors of a slow type electronic analog computer. – Trans. IRE, 1958, Dec., vol. EC-7, No. 4, pp. 306-312, 8 illustrations, 6 tables.

Noda K. and Kurokawa K. "Estimating the error in an electrical simulator" [in Japanese with an English Abstract], Bull. Electrotechn. Lab., vol. 22, No. 3, 189-203 and 233 (1958).

Overhoff M. W. – Etude de certaines erreurs dans les calculateurs analogiques. – Ann. telecommuns, 1958, juil-août, 1958, t. 13, No. 7-8, pp. 162-168, 8 illustrations. Bibliography 6.

Petras S. – Presnost niesenia uloh na elektronickych analogovych pocitacich strojoch. (The accuracy of solving problems on electronic analog computers), Strojnoelektrotechn. casop., 1958, t. 9, No. 10, str. 602-613.

D. SIMULATING DEVICES OF THE INDIRECT ANALOGY TYPE

I. Electronic Devices

IN RUSSIAN

Kogan B. Ya., Maslov A. A. and Polonnikov D. E. – Electronic simulating equipment of the type "EMU-8A". – Vestnik Akad. Nauk, 1958, No. 7, pp. 69-74, 5 illustrations.

Petrov G. M. and Stepin V. S. – A small electronic simulator "MNM". (Central Scientific-Research Institute of Complex Automatization. Instruments and means of automatization). – Moscow, 1958. 8 pp. with illustrations.

Sitnikov O. P. and Chapunov R. P. – A dc electronic simulator. – Vestnik Vyisshei Shkoly, 1958, No. 7, p. 83.

Vitenberg I. M. – Problems of designing a high speed electrical simulator for analyzing dynamic systems. – In: Problems in the theory of mathematical machines. – Fizmatgiz, Moscow, 1958, pp. 149-166, 11 illustrations. Bibliography 14.

Vitenberg I. M. – An electronic simulator for the automatic selection of the optimal solutions of the problem for a specified system of equations. – In: Automatic control and computer engineering. – Mashgiz, Moscow, 1958. pp. 419-437, 17 illustrations.

LANGUAGES OTHER THAN RUSSIAN

Analogue computer. – Automat. Progr., 1958, vol. 3, No. 10, p. 392.

Analogue computer. – Electronic Engng, 1958, Oct., vol. 30, No. 368, p. 620.

Analogue computer. – Instrum. Rev., 1958, vol. 5, No. 59, p. 1083.

Analogue computer components. – Process Control and Automat., 1958, Jan., vol. 5, No. 1, pp. 28-29.

Analogue equipment. – Instrum. Rev., 1958, vol. 5, No. 61, p. 1169.

Analog-Rechner Type A-938. – Automatik, 1958, Bd. 3, Nr 10, S. 271.

Bevc V. – Primena elektrichih analognih sklopova u resavanju diferencijalnih jednacina. (The use of electrical simulating networks for solving differential equations) – Elektrotehn vesn., 1958, vol. 12, No. 9-10, pp. 292-295 (Yugoslavia).

Building block expansion in new analogue computer. – Automat. Control, 1958, vol. 8, No. 1, p. 45.

Calculateur analogique à 12 amplificateurs. – Mesures et contrôle industr., 1958, vol. 23, No. 256, pp. 711-713.

Camatini C., Gupido A. – La calcolatrice analogica elettronica nello studio dei probleme di regolazione automatica. – Dell inform. CGE, 1958, vol. 19, No. 1, pp. 2-15.

Choundhury A. K. and Nag B. R. – An electronic differential analyser. – Indian J. Phys., 1958, Febr.,

vol. 32, No. 2, pp. 91-108, illustrations.

Computer compresses real time by 1/3000.— Electr. Design News, 1958, vol. 3, No. 10, p. 3.

De Vos J.— Aufbau und Anwendung elektronischer Analogo-Rechner.— Werkstattstechnik und Maschinenbau, 1958, Febr., Jg. 48, H. 2, SS. 131A-132A, 4 illustrations.

Dhen W.— Aufbau und Anwendung elektronischer Analogrechner.— VDI-Berichte, 1958, Bd. 30, SS. 27-34, 10 illustrations. Bibliography 7.

Elektronikus analog szamologepek. (Electronic analog computers) — Radiotechnika, 1958, vol. 8, No. 12, pp. 357-358 (Hungary).

EMIAC-II.— E. M. I.'s analog computer.— Brit. Communs and Electronics, 1958, June, vol. 5, No. 6, pp. 444-445.

Ernst D.— Aufbau und Wirkungsweise elektronischer Analogiegerate.— Regelungstechnik, 1958, Jg. 6, H. 4, SS. 125-128, 13 illustrations; H. 5, SS. 162-167, 7 illustrations. Bibliography 6.

Ferguson A. E.— Analogue computers.— Austral. J., Instrum. Technol., 1958, Febr., vol. 14, No. 1, pp. 19-28, 10 illustrations. Bibliography 8.

Findeisen W.— Maszyny matematyczne analogowe na Wystawie "INTERKAMA 1957". (Analog Computers at the "Interkam" exhibition in 1957) — Pomiary, Automatika, Kontrola, 1958, No. 3, str. 124, 2 illustrations.

Gabillard R.— Les analyseurs differentiels electroniques.— Ind. atom., 1958, vol. 2, No. 11-12, pp. 44-58.

Gandusio G. and Guerrini F.— Calcolatrice analogica elementare per il controllo della produzione.— Strum. e automaz., 1958, vol. 6, No. 3, pp. 108-111.

Hare R. E. and Willison W. E.— Analogue computers.— Instrum. Practice, 1958, vol. 12, No. 12, pp. 1295-1303.

Henning T.— Elektroniska analoregnemaskiners oppbygging og anvendelse.— Tekn. ukebl., 1958, vol. 105, No. 2, pp. 21-28.

Jiewertz B.— Saabs elektroniska differential-analysator seda.— Tekn. tidskr., 1958, vol. 88, No. 31, pp. 773-780.

Macacu Apau.— Description of an analog computer.— J. Instrum. Control Assoc. Japan, 1958, vol. 7, No. 6, pp. 4-10.

The "Minispace" analogue computer.— Process Control and Automat., 1958, Dec., vol. 5, No. 10, pp. 417, 1 illustration.

Miura T. and Namakura T.— General description of an analog device. Hitachi Hyoron, 1958, No. 27, pp. 51-60.

Nag B. R.— An electronic differential analyser.— Indian J. Phys., 1958, Febr., vol. 32, pp. 91-108.

New analog computer speeds patching.— Control Engng., 1958, vol. 5, No. 2, p. 138.

New computer can be "tailored" to meet all needs.— Office Equipm. Ind., 1958, No. 6.

Oever M. J., ven den.— Symposium over elektronische analogon machines. De analogen rekenmaschine van de sub-afdeling der vliegtugbouwkunde der technische Hogeschool te Delft.,— Ingenieur (Nederl.), 1958, vol. 70, No. 10, pp. 029-033.

Saro analogue computer at de Havillands.— Brit. Communs. and Electronics, 1958, Feb., vol. 5, No 2, p. 116, I illustration.

Siniti Ikesawa.— An electronic simulator.— Sangyo Kikai, No. 89, pp. 25-31.

Stubbs G. S.— SADSAC: A sampled-data simulator and computer using stepping relays.— Automat. Control, 1958, Apr., vol. 8, No. 4, pp. 47-50, 6 illustrations.

Thomas E. L.— Analogue computation.— Brit. Communs and Electronics, 1958, May, vol. 5, No. 5, pp. 348-358, 14 illustrations.

Tomovic R. and Mitrovic D.— Some experiences with a repetitive differential analyser.— Bull. Inst. Nucl. Sci., 1958, vol. 8, No. 144, pp. 109-116.

U.S.A. Beckman EASE 1100 analogue computer.— Interavia Air Letter, 1958, No. 4071, p. 5.

Wechselstrom-Analogie-Rechengerät Typ IA 55.— Schweiz. Techn., 1958, Nr 2, S. 45.

Winkler H.— Methoden und Probleme der Rechenelektronik in Analogieverfahren— Technik, 1958, Jan, Bd. 13, Nr. I, SS. 6-10, 11 illustrations.

Zusatzgerät zur Nachbildung einer Zeitkonstanten für das Analogie-Rechengerät AR. 2.— Regelungstechnik, 1958, Bd. 6, Nr 9, SS. 348-349.

II. Decision Elements in Electronic Devices

1. DC Electronic Amplifiers

IN RUSSIAN

Polonnikov D. E.— The input circuits of amplifiers with contact choppers.— Avtomatika i Telemekhanika, 1958, vol. 19, No. 6, pp. 582-591, 4 illustrations. Bibliography 6.

Smolov V. B.— A decision amplifier with a differential input.— Avtomatika i Telemekhanika, vol. 19, No. 12, pp. 1145-1149.

Takhvanov G. I.— Feedback in decision amplifiers.— Transactions of the Ryazan' Radio-Engineering Institute, 1958, vol. 3, pp. 128-138, 8 illustrations.

LANGUAGES OTHER THAN RUSSIAN

Bekey G. A.— Basic components of analog computers.— 1958, Proc. Instrum. Soc. Amer. 13-th Annual

Instrum.— Automat. Confer. and Exhibit. Pt. 2.— Pittsburgh, Instrum. Soc. Amer., 1958, Part PTC 3, pp. 1-14, 16 illustrations. Bibliography 24.

Chan Go-In.— Designing dc amplifiers for electronic simulators.— Itsi Yui Shian Uzishu, 1958, No. 3, pp. 40-43 (Chinese People's Republic), no. 1, p. 198.

Chopper stabilized PC amplifiers in new desktop analogue computer.— Automat. Control, 1958, June, vol. 8, No. 6, p. 90.

Depian L. and Smith R. E.— A stabilized D-C differential transistor amplifier.— Commun. and Electronics, 1958, May, No. 36, pp. 157-159, 10 illustrations. Bibliography 8.

Hutcheon J. C.— Performance calculations for D. C. chopper amplifiers.— Electronic Engng, 1958, Aug., vol. 30, No. 366, pp. 476-480, 7 illustrations. Bibliography 7.

Kabes K. and Tikal F.— Cs. soucastky pro analogove matematicke stroje. (Czeckoslovak parts for analog computers).— Slaboproudý Obzor, 1958, sv. 19, No. 1, str. 13-19, 16 illustrations. Bibliography 12.

Klein P. E.— Doppel-Differenzier-Verstärker.— Elektronik, 1958, Bd. 7, Nr. 4, SS. 100-102, 6 illustrations.

Martin D. J.— New types of D. C. amplifier. Pt. 1. The cascade balance system.— Electronic and Radio Engr, 1958, Jan., vol. 35, new ser., No. 1, pp. 2-7, illustrations. Bibliography 7.

Maynard F. B. and Steele E. L.— A high frequency P-N-P switching transistor.— Proc. Nat. Electronics Conference 1957, vol. 13.— Chicago, Illinois, Nat. Electronics Confer., Inc., 1958, pp. 246-253, 8 illustrations. Bibliography 6.

Nitzberg R.— An improved operational amplifier.— Proc IRE, 1958, March, vol. 46, No. 3, pp. 614-615, 1 illustration.

Rao J. V.— Electronic analogue computers, 1. The adding circuit.— J. Instn. Telecommun. Engrs, 1958, vol. 4, No. 3, pp. 143-146.

Williams A. J., Eynon J. U. and Polster N. E.— Some advances in transistor modulators for precise measurement.— Proc. Nat. Electronics Conference 1957, vol. 13.— Chicago, Illinois, Nat. Electronics Conf., Inc., 1958, pp. 40-54, 10 illustrations. Bibliography 8.

2. Decision Amplifiers Without Vacuum Tubes

IN RUSSIAN

Dobrov E. V.— The effect of temperature instability of a germanium transistor modulator on the operation of a dc operational amplifier.— Priborostroenie, 1958, No. 3, pp. 12-15, 5 illustrations.

Milovzorov V. P.— Magnetic summing amplifiers.— Transactions of the Ryazan Radio-Engineering Institute, vol. 3.— Soviet Radio, 1958, pp. 95-103, 6 illustrations.

Petrov G. M. and Popov V. A.— On designing an operational amplifier using semiconductor elements.— Priborostroenie, 1958, No. 3, pp. 4-8, 12 illustrations.

Sapozhkov K. A.— Semiconductor instruments in summing decision units.— Transactions of the Ryazan Radio-Engineering Institute, vol. 3.— Soviet Radio, pp. 115-123, 5 illustrations.

LANGUAGES OTHER THAN RUSSIAN

Blecher F. H.— Transistor multiple loop feedback amplifiers.— Proc. Nat. Electronics Conf., 1957, vol. 13.— Chicago, Illinois, Nat. Electronics Conf., Inc., 1958, pp. 19-34, 10 illustrations. Bibliography 14.

Giorgis J. and Thompson C. C.— Silicon transistor performance in a chopper application.— Applic. and Ind., 1958, July, No. 37, p. 113-119, 12 illustrations. Bibliography 8.

Krause C. A. and Lowe R. R.— Design of AC computing amplifiers using transistors.— Trans. IRE, 1958, Sept., vol. EC-7, No. 3, pp. 191-195, 8 illustrations.

Schenkerman S.— Designing transistor D-C to A-C converters.— Electronics, Engng issue, 1958, Sept., vol. 31, No. 39, pp. 78-80, 3 illustrations.

3. Integrating and Differentiating Devices

Anna O.— Elektrische Integrationsverfahren.— Elektron. Rundschau, 1958, Jg. 12, Nr. 4, SS. 127-128.

Clegg J. C.— A nonlinear integrator for servomechanisms.— Applic. and Ind., 1958, March, No. 35, pp. 41-42, 5 illustrations.

Hisey B. L. and Perl E. R.— Electronic integrator with immediate digital output.— Rev. Scient. Instrum., 1958, May, vol. 29, No. 5, pp. 335-359, 6 illustrations. Bibliography 10.

Hodara H.— H-F wide-band electronic integrator design.— Electronic Industr. 1958, Oct., vol. 17, No. 10, pp. 96-100.

Integrator.— Instrum. and Automat., 1958, Nov., vol. 31, No. 11, pp. 66-68, 12 illustrations.

Johnson W.— A differentiator for a-c. computers.— Commun. and Electronics, 1958, March, No. 35, pp. 1-4, 6 illustrations. Bibliography 14.

Ranga-Rao J. V.— Electronic analogue computers. II. The integrator.— J. Instn Telecommun. Engrs, 1958, vol. 5, No. 1, pp. 33-37.

Sharp J. and Williams R. W.— An a.c. velodyne integrator.— J. Scient. Instrum., 1958, April vol. 35, No. 4, pp. 125-129, illustrations.

4. Multiplying-Dividing Devices

IN RUSSIAN

Burgin B. Sh.— Electrical multiplication and division and its application in instrumentation and control.— Elektrichestvo, 1958, No. 9, pp. 60-62, 4 illustrations.

Ismailov Sh. Yu. and Smolyarov A. M.— Load characteristics of multiplying units containing quadratic elements.— Transactions of the Ryazan' Radio-Engineering Institute, vol. 3.— Soviet Radio, 1958, pp. 34-54, 5 illustrations.

Oranskii A. M.— The application of a pulsed multiplying unit.— Transactions of the Ryazan' Radio-Engineering Institute, vol. 3.— Soviet Radio, 1958, pp. 104-114, 10 illustrations.

Steinov Gr., Derzhinskii Al. and Dmitriev M.— Electronic devices for simulating products and for dividing power functions.— Doklady Bolgarskoi Akademy Nauk, 1958, vol. 11, No. 6, pp. 465-468.

Vaisman L. V.— An electrical device for multiplication and division.— Priborostronie, 1958, No. 8, p. 16, 2 illustrations.

LANGUAGES OTHER THAN RUSSIAN

Analog multiplier.— Rev. Scient. Instrum., 1958, vol. 29, No. 12, p. 1166.

Chasmar R. P. and Cohen E.— An electrical multiplier utilizing the Hall effect in indium arsenide.— Electronic Engng., 1958, Nov., vol. 30, No 369, pp. 661-664, 5 illustrations. Bibliography 10.

Choudhury A. K. and Nag B. R.— Analogue multiplier and function generator with cathode-ray tube.— Ind. J. Phys., 1958, March, vol. 32, pp. 141-148.

Garcia Santesmaseo J. and Civot Bren A.— Multiplicador y divisor analogico a integraciones periodicas.— An. Real soc. esp. fis. y quim., 1958, A54 No. 5-6, pp. 127-138.

Hilsum C.— Multiplication by semiconductors.— Electronic Engng. 1958, Nov., vol. 30, No. 369, pp. 664-666, 7 illustrations. Bibliography 6.

Lax Ch. and Rafoeld Ph. I.— Mathematical elements for analog computers.— Instrum. and Automat., 1958, vol. 31, No. 11, pp. 1832-1833.

Laefgren L.— Analog multiplier based on the Hall effect.— J. Appl. Phys., 1958, Feb., vol. 29, No. 2, pp. 158-166, 7 illustrations. Bibliography 12.

Multiplier unit for analogue computers.— J. Scient. Instrum., 1958, vol. 35, No. 10, pp. 389.

Oxenius J.— Die Verwendung von Hall Generatoren in Analog Multiplikatoren.— Nachrichtentechn. Z., 1958, Mai, Bd. 11, Nr 5, SS. 263-268.

Riss J.— Analogova nasobicka vyuzivajici Hallova efektu. (A multiplying device which uses the Hall effect).— Sdelovaci techn., 1958, t. 6, No. 9, str. 346.

Schmid H.— A transistorized four-quadrant time-division multiplier with an accuracy of 0.1%.— Trans. IRE, 1958, vol. EC-7, No. 1, pp. 41-47.

Sideriades L. and Brunel J.— Multiplicateur de tensions pour calculatrices electroniques.— Electronique industr., 1958, No. 22, pp. 161-164.

Zeilinger K.— Wirkungsweise und Aufbau von elektromechanischen Analog-Multiplikatoren.— Elektron. Rundschau, 1958, Sept., Bd. 12, Nr. 9, SS. 307-308, 4 illustrations.

5. Function Generators

IN RUSSIAN

Ismailov Sh. Yu. and Smolyarov A. M.— The accuracy of reproducing monatomic functions using rectifier function generators.— Transactions of the Ryazan' Radio-Engineering Institute, vol. 3.— Soviet Radio, 1958, pp. 44-53, 5 illustrations. Bibliography 5.

Lebedev A. N.— Approximate simulation of certain nonlinear functions of two independent variables.— Transactions of the Ryazan' Radio-Engineering Institute, vol. 3.— Soviet Radio, 1958, pp. 74-77.

Maslov A. A.— Diode function generators of a specialized type based on semiconductor elements.— In: Automation and Remote Control.— AN SSSR, Moscow, 1958, pp. 41-48.

Maslov A. A. and Talantsev A. D.— Cathode-ray function generators based on the principle of a controlled sweep.— In: Automation and Remote Control.— AN SSSR, Moscow, 1958, pp. 49-57.

Pul'er Yu. M.— Contactless sine-cosine rotary transformer-selsyns.— Elektrichestvo, 1958, No. 1, pp. 5-9, 5 illustrations. Bibliography 6.

Rastopshin A. S.— The application of semiconductors in computer-decision instruments for the purpose of designing functional four-terminal networks.— In: The application of semiconductors in instrumentation.— Mashgiz, Moscow, 1958, pp. 83-90.

Smolov V. B.— A universal diode function generator.— Izvestiya Vysshikh Uchebnykh Zavednii, Priborostroenie, 1958, No. 5, pp. 14-18, 3 illustrations.

LANGUAGES OTHER THAN RUSSIAN

Bekey G. A.— The function generator as a basic tool for nonlinear control systems.— Automat. Control, 1958, Aug., vol. 9, No. 2, pp. 42-46, 13 illustrations.

Brown E.— The design of function generators using silicon carbide nonlinear resistors.— Electronic Engng, 1958, March, vol. 30, No. 361, pp. 154-157, illustrations.

Card programmed function generators.— Automat. Control, 1958, April, vol. 8, No. 4, p. 52.

Derzhansky A. and Stainov G.— Electronic circuit modelling a power function.— Doklady Bolgarskoi Akademy Nauk, 1958, vol. 11, No. 4, pp. 271-274, 4 illustrations.

Freudenstein F.— Four-bar function generators.— Trans. Fifth Conference on Mechanisms. (Purdue Univ. Oct. 13-14, 1958).— Cleveland, Penton Publ. Co., 1958, pp. 104-107, I illustration. Bibliography 9.

Function generation for process control simulation.— Proc. Instrum. Soc. Amer. 13th Annual Instrum.— Automat. Confer. and Exhibit, 1958, Pt. 2.— Pittsburgh, Instrum. Soc. Amer., 1958, pp. 1-23, 7 illustrations. Bibliography 24.

Function generator for two independent variables.— Instrum. Practice, 1958, July, vol. 12, No. 7; p. 769, 2 illustrations; Techn. News Bull. Nat. Bur. Standards, 1958, Apr., vol. 42, No. 4, pp. 67-70, illustrations.

Function generator uses optics.— Control Engng, 1958, vol. 5, No. 2, p. 139.

Garcia Santesmases J. and Gonzales Ibeas J.— Un Generador de functiones de diodes con modulation de señal.— An Real soc. esp. fis. y quim., 1958, vol. A54, No. 9-10, pp. 263-280.

Hellstrom M. J.— Hyperbolic analogs.— Proc. IRE, 1958, Febr., vol. 46, No. 2, p. 502, 2 illustrations.

Holbrook G. W.— Hyperbolic analogs using varistors.— Proc. IRE, 1958, vol. 46, No. 10, p. 1762.

Hybrid loop generators square root functions.— Electr. Design News, 1958, vol. 3, No. 3, pp. 22-23.

Inada Nobukazu.— A function generator.— Keisoku, J. Soc. Instrum. Technol. Japan, 1958, vol. 8, No. 10, p. 622-626.

Kelley T. J.— Multi-variable function generator.— Instrum. and Automat., 1958, Nov., vol. 31, No. 11, p. 1819, 2 illustrations.

Kovach L. D. and Comley W.— Nonlinear transfer functions with thyrite.— Trans. IRE, 1958, June, vol. EC-7, No. 2, pp. 91-97, 6 illustrations.

Lax Ch. and Rafield Ph. I.— Mathematical elements for analog computers.— Instrum. and Automat., 1958, vol. 31, No. 11, pp. 1832-1833, 5 illustrations.

Liesegang H.— Ein logaritmischer Gleichstromverstärker mit selbsttätiger Driftkompensation und kurzer Einstellzeit.— Arch. techn. Messen, 1958, Nr 268, SS. R68-R71.

Nicolau E., Simion N., Voiculescu Ch. and Weiss A.— Elemente neliniare pentru simulatore si calculatore analogica. Realizazi Esperimentale.— Automat. si electron., 1958, vol. 2, No. 2, pp. 74-77.

Revay A. W. and Ford D. J.— Design of function generators. Electric Engng., 1958, Oct., vol. 77, No. 10, pp. 927-928, 2 illustrations.

Revay A. W. and Ford D. J.— The design of function generators using short-time memory devices and nonlinear elements.— Communs. and Electronics, 1958, May, No. 36, pp. 143-152, 18 illustrations.

Schmid H.— A transistorized all-electronic cosine/sine function generator.— IRE Wescon Convent Rec., 1958, vol. 2, Pt. 4, pp. 89-107.

Scott L.— Adjustable nonlinear function generator.— Electronics, Engng ed., 1958, vol. 31, No. 27, pp. 84, 86-88.

Silverberg B.— Application techniques for arbitrary function generation.— Automat. Control, 1958, vol. 9, No. 4, pp. 17-19; No. 5, pp. 6-9, 4 illustrations.

Susini A.— Un generatore di funzione a diodi.— Elettrotechnica, 1958, Nov., vol. 45, No. 11, pp. 626-629, 11 illustrations.

Tomovich R.— New applications of an electronic function generator.— Trans. IRE, 1958, March, vol. EC-7, No. 1, pp. 48-51, 10 illustrations.

Williams R. W.— Resistance potentiometers as function generators.— Electronic Engng, 1958, Oct., vol. 30, No. 368, pp. 579-585, 23 illustrations. Bibliography 6.

Willis J.— A cathode-tube function generator.— Electronic Engng., 1958, vol. 30, No. 465, p. 458.

6. Other Decision Elements and Auxiliary Equipment

LANGUAGES OTHER THAN RUSSIAN

Douce J. L., Graduate Ph. D. and West J. C.— A magnetic-drum store for analogue computing.— Proc. Inst. Electr. Engrs, 1958, Nov., vol. 105, Pt. B., No. 24, pp. 577-580, 4 illustrations. Bibliography 11.

Gibson W. E.— Three axis flight simulator systems.— Aero-Space Engng., 1958, Aug., vol. 17, No. 8, pp. 36-39, 5 illustrations.

Hellwarth G. A.— A constant-amplitude random function generator.— Communs. and Electronics, 1958, Sept., No. 38, pp. 443-452, 15 illustrations.

Holzman E. G.— Variable transport lag simulation.— Preprint Nucl. Engng. and Sci Confer. s.a. No. 112, 27 p., illustrations.

Kozak W. S.— New job for an old method: capacitor storage used in analogue memory.— Canad. Electronics Engng., 1958, Feb., vol. 2, No. 2, pp. 38-42.

Lebrun J.— Les potentiomètres bobinés speciaux utilisés en calcul analogique.— Electronique, 1958, août 15, No. 143, pp. 33-38, 21 illustrations.

McLeod J.— Survey of recorders being used with analog computers.— Instrum. and Automat., 1958, May, vol. 31, No. 5, p. 852.

Mitchel J.— An accurate analog frequency measuring circuit.— Electr. Engng., 1958, Oct., vol. 77, No. 10, pp. 912-914, 6 illustrations.

Nestorescu D. N.— Despre stabilitatea surselor di alimentare pentru mazina analoaga de calcul.— Studiisi cercetari energ. Acad RPR, 1958, vol. 8, No. 2, pp. 304-308.

III. Electromechanical Devices

IN RUSSIAN

Baranchuk E. I.— On the theory of electromechanical differential analyzers.— Izvestiya Vysshikh Uchebnykh Zavedenii, Priborostroenie, 1958, No. 4, pp. 76-86, 4 illustrations. Bibliography 11.

Baranchuk, E. I.— On the stability and dynamic accuracy of electromechanical computer-decision units.— Izvestiya Vysshikh Uchebnykh Zavedenii, Priborostroenie, 1958, No. 2, pp. 52-62, 7 illustrations. Bibliography 7.

Gorkii V. G.— A rotary-amplifier computer.— Avtomatika i Telemekhanika, 1958, vol. 19, No. 5, pp. 448-455, 8 illustrations. Bibliography 5.

Ikhntykan A. B. and Kharkevich Yu. F.— This was achieved in a university. New means for the mechanization of mathematical computation.— Vestnik Vysshei Shkoly 1, 64-65 (1958).

LANGUAGES OTHER THAN RUSSIAN

Bell J.— An analogue computer, employing magslips and serves.— Technique, 1958, vol. 12, No. 3, pp. 20-23.

A mechanical analogue computer.— Brit. Communs. and Electronics, 1958, June, vol. 5, No. 6, p. 445, 1 illustration.

Michales G. W.— Mechanical analog computer components.— Trans. Fifth Conference on Mechanisms.— Cleveland, Penton Publ. Co., 1958, pp. 108-139, 40 illustrations. Bibliography 9.

Rogers Ch. E. and Ake J. E.— Unilog— a continuous rate computer.— ISA Journal, 1958, vol. 5, No. 2, p. 63.

Sager G.— Zum Bau der dritten deutschen Gezeitenrechenmaschine.— Feingerätetechnik, 1958, Bd. 7, Nr 12, SS. 555-559.

Zeilinger K.— Beitrag zum Aufbau einfacher Analog-Rechengerate mit elektromechanischen Bauelementen fur die Mess- und Regeltechnik.— Elektronik, 1958, Mai, Jg. 7, Nr 55, SS. 135-139, 10 illustrations. Bibliography 10.

IV. Pneumatic-Hydraulic Devices

IN RUSSIAN

Ivlichev Yu. I. and Nadzhafov E. M.— A universal pneumatic multiplier-divider unit and a unit for extracting the square root.— Avtomatika i Telemekhanika, 1958, vol. 19, No. 11, pp. 997-1009, 8 illustrations.

Kuz'manko L. V.— Slotted hydraulic integrators.— Nauchnye Doklady Vysshei Shkoly, Elektromekhanika i Avtomatika, 1958, No. 2, pp. 85-93, 3 illustrations.

V. Specialized Devices

1. Devices for Solving Systems of Algebraic Equations. Root Finders

IN RUSSIAN

Brick V. A. and Ginzburg S. A.— A computer which plots conformal representations for a power-law polynomial.— Avtomatika i Telemekhanika, 1958, vol. 19, No. 7, pp. 674-683, 6 illustrations. Bibliography 10.

Daube Ya. Ya.— A transformer analog for linear algebraic relationships.— Nauchnye Doklady Vysshei Shkoly, Energetika, 1958, No. 3, pp. 211-220, 6 illustrations. Bibliography 6.

Lebedev A. N.— On various methods for formulating a mathematical model for solving equations by the method of choosing roots.— Transactions of the Ryazan' Radio-Engineering Institute, vol. 3.— Soviet Radio, 1958, pp. 78-85, 6 illustrations.

Mikhailov N. N.— On plotting root loci for automatic control systems.— Avtomatika i Telemekhanika, 1958, vol. 19, No. 7, pp. 661-673, 9 illustrations. Bibliography 10.

Mikhailov N. N.— Electrical devices for solving algebraic equations (Survey).— Avtomatika i Telemekhanika, 1958, vol. 19, No. 5, pp. 477-490, 12 illustrations. Bibliography 24.

LANGUAGES OTHER THAN RUSSIAN

Elektrischer Analogrechner zur Ausgleichrechnung.— Vermessungstechn. Rundschau, 1958, Bd. 20, Nr 10, SS. 349-350, 1 illustration.

Hempel E.— Ueber eine elektronische Analogie-Rechenanlage zur Auflösung von linearen Gleichungssystemen.— Nachrichtentechnik, 1958, Okt., Jg. 8, H. 10, SS. 453-455, 5 illustrations.

Krishnamurthy E. V. and Ramachandran G. N.— "Lilavati" — a new analogue computer for solving linear simultaneous equations and related problems. Pt. I.— Proc. Indian Acad. Sci., 1958, Sept., vol. 48, Sect. A., No. 3, pp. 152-164, 8 illustrations. Bibliography 12.

Krishnamurthy E. V.— "Lilavati" — a new analogue computer for solving linear simultaneous equations and related problems. Pt. II. Design of model II and its application to the solution of secular equations.— Proc. Indian Acad. Sci., 1958, vol. A48, No. 5, pp. 269-283.

Lukaszewicz L.— Analizator townan algebraicznych linowych aral. (An analyzer for systems of linear algebraic equations).— Biul. zakl. aparat. mat. PAN 1958, P. L., N 5, pp. 0-19 (in Polish).

Mrkvicka J.— Elektrickenalogove stroje na reseni soustav linearnich algebraickych rovnic. (Electrical computers for solving systems of linear algebraic equations).— Stroje zpracov. inform., 1958, N 6, p. 185-208.

Nag B. R.— On the application of an electronic differential analyser for finding the roots of a polynomial.— Indian J. Phys. and Proc., 1958, May, vol. 32, No. 5, pp. 212-217, illustrations.

"Wina" network analyser.— Engineer, 1958, vol. 205, No. 5339, pp. 770-771.

2. Devices for Solving Integral Equations

IN RUSSIAN

Val'denberg Yu. S.— Computer method for solving a certain class of integral equations.— Avtomatika i Telemekhanika, 1958, vol. 19, No. 8, pp. 725-730, 2 illustrations. Bibliography 9.

Val'denberg Yu. S.— On the principles of designing an analog computer for solving integral equations. In: Automatic Control and Computer Engineering.— Mashgiz, Moscow, 1958, pp. 399-418, 6 illustrations. Bibliography 10.

Val'denberg Yu. S.— The use of a potentialoscope for realizing the iterative process in an analog computer.— Priborostroenie, 1958, No. 7, pp. 22-24, 2 illustrations. Bibliography 5.

Val'denberg Yu. S.— Development of the theory and designing a computer that solves integral equations.— Author's abstract of candidate's dissertation.— Moscow, 1958, 12 pp. (Moscow Higher Engineering School.)

Val'denberg Yu. S.— A specialized analog computer for solving integral equations.— In: Theses of the reports to the convention on computer mathematics and the application of the means of computer engineering.— Academy of Sciences, Azerbaidzhan SSR, Baku, 1958, pp. 57-58.

Vasil'ev V. G.— An automatic device for solving Volterra equations of the second kind with a kernel of the type K (t − x).— Nauchnye Doklady Vysshei Shkoly, Elektromekhnika i Avtomatika, 1958, No. 4, pp. 36-38.

LANGUAGES OTHER THAN RUSSIAN

Fisher M.— Proposed methods for the analog solution of Fredholm's integral equation.— J. Assoc. Comput. Machinery, 1958, Oct., vol. 5, No. 4, pp. 357-369. Bibliography 20.

Cabillard R.— Les analyseurs differentiels electroniques (Utilisation).— Ind. Atom., 1958, vol. 2, No. 11-12, pp. 41-58.

Zeleznikar A.— Rjesavanje nehomogenih sistema linearnih integralno-diferencijalnichjednadzhi viseg reda a konstantinim koeficijentima pomocu istommjernih elektroniskih analognih racunala. (Solutions of a system of inhomogeneous integral-differential equations of high order using dc electronic analog computers.)— Elektrotehn, vesn., 1958, vol. 12, N 5-6, pp. 177-187 (in Yugoslav, with German abstract.)

3. Correlators

IN RUSSIAN

Novikov Yu. V.— Specialized analog computer for the statistical manipulation of random processes.— In: Automatic Control and Computer Engineering.— Mashgiz, Moscow, 1958, pp. 375-398, 17 illustrations.

Samoilov A. I.— An instrument for instantaneous correlation conversion of functions.— In: Symposium of the Leningrad Institute of Railroad Transport Engineers, No. 158.— Transzheldorizdat, 1958, pp. 352-367, 6 illustrations. Bibliography 16.

LANGUAGES OTHER THAN RUSSIAN

Eddins W. T.— Sample-and-hold circuits for time correlation of analog-voltage information.— Convent. Rec. IRE, 1958, vol. 6, Rt. 5, pp. 21-24, 4 illustrations.

Shintaro Oshima, Kensuke Takashima, Katsumi Nishitor.— Reps. Electr. Commun. Labor. Nippon Telegr. and Teleph. Public Corp., 1958, May, vol. 6, No. 5, pp. 135-144, 12 illustrations.

4. Various Devices

LANGUAGES OTHER THAN RUSSIAN

Azaroff L. V.— Semiautomatic two-dimensional Fourier analog computer.— Rev. Scient. Instrum., 1958, vol. 29, No. 4, pp. 317-318.

Timbrell V.— A calculator for numerical Fourier synthesis.— J. Scient. Instrum., 1958, vol. 35, No. 9, pp. 313-318, 11 illustrations.

Tucker D. G.— An analogue computer Fourier transforms.— J. Brit. Instn Radio Engrs, 1958, Apr., vol. 18, No. 4, pp. 233-236, 2 illustrations. Bibliography 7.

Zaroodny S. L. and Leser T.— Aydar special purpose analog machine for yaev data reduction.— J. Assoc. Comput. Machinery, 1958, Jan., vol. 5, No. 1, pp. 89-99, illustrations.

Schmidt J. D., Putschi H. N. and Keonjian E.— Transistorized special purpose computer.— Proc. Nat. Electronics. Conference, vol. 13.— Chicago Nat.

Electronics Conference, Inc., 1958, pp. 624-634, 12 illustrations.

E. DEVICES FOR CONVERTING A DIGITAL CODE TO PHYSICAL QUANTITIES AND VICE VERSA

IN RUSSIAN

Anisomov B. V. and Vinogradov Yu. V.— Certain problems in the accuracy of devices which convert a voltage to a digital code with feedback.— Nauchnye Doklady Vysshei Shkoly, Mashinostroenie i Priborostroenie, 1958, No. 4, pp. 210-219.

Baltrushevich A. V.— Systems for converting a digital code into an angle of rotation or into a linear displacement.— Nauchnye Doklady Vysshei Shkoly, Elektromekhnika i Avtomatika, 1958, No. 2, pp. 59-67, 12 illustrations. Bibliography 21 (1958)

Ryzhov V. I.— Devices for converting analog quantities into codes and codes into analog quantities.— In: Automatic control and computer engineering.— Mashgiz, Moscow, 1958, pp. 243-264, 27 illustrations. Bibliography 15.

Vinogradov Yu. V.— Analyzing the accuracy of operation for a high speed device which converts a voltage into a digital code.— Author's abstract of candidate's dissertation.— Moscow, 1958, 15 pages; (Moscow Higher Engineering School).

LANGUAGES OTHER THAN RUSSIAN

Abberigi A., Bernardini C. and Quercial F.— Proposal for an analog-to-digital electronic converter suited for nuclear pulse height analysis.— Nucl. Instrum., 1958, vol. 3, No. 4, pp. 201-203, 6 illustrations.

Bauwens J. C.— Study of a digital—analogue converter.— Rev. HF, Brussels, 1958, vol. 4, No. 2, pp. 39-42.

Couleur J. F.— BIDEC, a binary—to decimal or decimal—to binary converter.— Trans. IRE, 1958, Dec., vol. EC-7, No. 4, pp. 313-316, 6 illustrations.

De Bey L. G. and Webb R. C.— A shaft position digitizer system of high precision.— IRE Nat. Convent. Rec., 1958, vol. 6, No. 5, pp. 204-210.

Digital communications for analogue computers.— Process Control and Automat., 1958, Nov., vol. 5, No. 11, pp. 498-499, 2 illustrations.

Double voltage comparison improves converter stability.— Electr. Design News, 1958, vol. 3, No. 8, pp. 14-15.

Electronic digitizer.— Automat. Progr., 1958, vol. 3, No. 5, p. 198.

Error-free analog-digital converter.— Electron Design, 1958, vol. 6, No. 14, pp. 32-33.

Fuwa Hiroshi, Kimura Iwao and Jitsukawa Taku.— An automatic calibrator for an analog-digital converter.— Bull. Electrotech. Lab., 1958, vol. 22, No. 8, pp. 583-596 and 632-633.

Fuwa Hiroshi.— Conversion of analog quantities to digital quantities. Solution performed in 1/200 seconds.— Automation, 1958, vol. 3, No. 1, pp. 44-48 (in Japanese).

Hofheimer R. W. and Perry K. E.— Digital-analog function generators.— Trans., 1958, June, vol. 1-7, No. 2, pp. 111-117, 16 illustrations, 1 table.

Ichikava — An analog-to-digital converter of the relay type.— J. Railway Engng. Res., 1958, vol. 15, No. 4, p. 180.

Ichikawa Kunihiko — A relay servosystem — an analog-to-digital converter.— Automat. Control., 1958, vol. 5, No. 4, pp. 112-120.

Kompass E. J.— What about digital transducers?— Control Engng., 1958, vol. 5, N 7, pp. 94-99.

McMillan S. H. and Sutton W. A.— A transistorized six-channel airborne digitizer.— IRE Convent. Rec., 1958, vol. 6, No. 5, pp. 26-33.

Miniaturized analog-to-digital shaft converter increases resolution, elliminates ambiguity.— Military Automat., 1958, vol. 2, No. 5, pp. 174-175.

Miura Takeo.— An analog-to-digital converter.— J. Instrum. Soc. Japan, 1958, vol. 8, No. 11, pp. 748-749.

Nakagawa Takayuki.— An analog-to-digital converter using a transistor and an iron core.— J. Appl. Phys. Japan, 1958, vol. 27, No. 4, pp. 232-235.

New analog-digital and digital-analog device.— Automat. Control, 1958, vol. 8, No. 6, p. 91.

Nottebohm H.— Ein Analog-digital-Umsetzer für Strom, Spannung, Widerstand und Kapazität.— Elektron. Rundschau, 1958, März, Nr 3, SS. 85-88, 6 illustrations.

Palevsky M.— A new approach to analog digital conversion.— Instrum. Soc. Amer. Journal, 1958, April, vol. 5, No. 4, pp. 42-44, 6 illustrations.

Palevsky M.— A solid state analog-to-digital conversion device.— IRE Nat. Convent Rec., 1958, vol. 6, Pt. 4, pp. 232-235, 4 illustrations.

Photo-electro-mechanical digitalizer.— Electron. Ind., 1958, vol. 17, No. 4, pp. 149-150, 2 illustrations.

Rosmann F.— Les convertisseurs analogiques-numeriques.— Automation, 1958, vol. 4, No. 21, pp. 141-145.

Rowe W. D.— A transistorized digital-to-analog converter.— Trans. IRE, 1958, March, vol. 1-7, No. 1, pp. 22-28, 13 illustrations.

Sawaragi Voshikazu, Akashi Haijime and Okada Tsuyoshi.— The construction and testing of an analog-to-digital-converter.— Trans. Japan. Soc. Mech. Engrs, 1958, vol. 24, No. 143, pp. 517-522

Susskind A. K.— Characteristics and appraisal of analog-digital conversion techniques.— In: Proc. Computers in Control Systems Conference, 1957.— New York, Amer. Inst. Electr. Engrs, 1958, pp. 26-29, 5 illustrations.

Togino Kazuto.— A converter which converts a digital quantity into a physical quantity.— J. Instrum. Soc. Technol. Japan, 1958, vol. 11, pp. 758-759.

Towles W. B.— Transistorized analog-digital converter.— Electronics, 1958, Aug., 1, vol. 31, No. 31, pp. 90-93, 5 illustrations.

Walton C. A.— A direct-reading printed circuit commutator for analogue-to-digital data conversion.— IBM. J. Res. and Developm., 1958, July, vol. 2, No. 3, pp. 178-192.

Willis J. and Hartley M. G.— A cathode-ray tube analogue-to-serial digital converter.— J. Sci. Instrum., 1958, June, vol. 35, No. 6, pp. 197-202, 13 illustrations.

F. THE USE OF SIMULATING DEVICES OF THE INDIRECT ANALOGY TYPE

1. The Use of Simulators for Solving Problems in Automatic Control

IN RUSSIAN

Batkov A. M.— Analysis and synthesis of linear automatic control systems using simulators.— In: Automatic control and computer engineering.— Mashgiz, Moscow, 1958, pp. 438-463, 4 illustrations. Bibliography 16.

Belyaev I. P.— Mathematical simulation of dc rotary amplifier networks.— Izvestiya Vysshikh Uchebnykh Zavedenii, Elektromekhanika, 1958, No. 1, pp. 21-34, 14 illustrations. Bibliography 8.

Efroimovich Yu. E.— A computer for controlling the operation of an arc furnace.— Elektrichestvo, 1958, No. 5, pp. 15-19, 5 illustrations.

Efroimovich Yu. E.— Simulators for remote control of electrical quantities in arc furnaces.— Elektrichestvo, 1958, No. 3, pp. 22-27, 6 illustrations. Bibliography 5.

Monastyrshin G. I.— Mathematical simulation of dry friction.— Avtomatika i Telemekhanika, 1958, vol. 19, No. 12, pp. 1091-1106, 13 illustrations. Bibliography 8.

Sirazitdinov E. G. and Petrova E. A.— Simulation of actuators in automatic control systems.— Izvestiya Vysshikh Uchebnykh Zavedenii, Priborostroenie, 1958, No. 3, p. 6, 6 illustrations. Bibliography 7.

Solodov A. V.— Statistical investigation of nonstationary processes in linear systems using inverse simulators.— Avtomatika i Telemekhanika, 1958, vol. 19, No. 4, pp. 312-324, 8 illustrations.

Velershtein R. A. and Fel'dbaum A. A.— Using an electronic simulator to design a system network which is close to optimal.— Avtomatika i Telemekhanika, 1958, vol. 19, No. 9, pp. 824-835, 14 illustrations. Bibliography 9.

LANGUAGES OTHER THAN RUSSIAN

Amber G. H. and Amber P. S.— Special purpose computers in the control of continuous processes.— Automatic Control, 1958, May, vol. 8, No. 5, pp. 43-48, illustrations.

Bigelow S. C.— The design of analog computer compensated control systems.— Applicat. and Ind., 1958, Nov., No. 39, pp. 409-415, 7 illustrations. Bibliography 11.

Black K. G. and Noorda R.— Analog computer study of wind tunnel drive.— Communs. and Electronics, 1958, Jan., No. 34, pp. 745-750, 9 illustrations. Bibliography 8.

Bradburn W. J.— Analysis of a motor speed-control system with an analog computer.— Trans. IRE, 1958, April, vol. PGIE-5, pp. 94-102, 11 illustrations.

Braun E. L. and Post G.— Systems considerations for computers in process control.— IRE Convent. Rec., 1958, vol. 6, Pt. 4, pp. 168-181, 6 illustrations.

Brown B. P.— Ground simulator studies of the effects of valve friction, stick friction, flexibility, and backlash on power control system quality-NACA, 1958, Rep. 1348, 13 p.

Chestnut H., Dabul A. and Leiby D.— Analog computer study of sampled-data systems.— In: Proc. Computers in Control Systems Conference, 1957.— New York, Amer. Inst. Electr. Engrs, 1958, pp. 71-76, 18 illustrations.

Clymer A. B.— Direct system synthesis by means of computers.— Communs. and Electronics, 1958, vol. 77, pp. 798-806.

Csordas Z.— Pneumatikus szabalyozas — modell: a korszeru folyamatszabalyozas segedeszoze.—(A pneumatic simulator — a modern means for investigating automatic control systems) — Meres es automat., 1958, vol. 6, N 2-3, pp. 84-89.

Elgerd O. I.— An analog computer study of the transient behavior and stability characteristics of serial-type digital data systems.— Communs. and Electronics, 1958, July, No. 37, pp. 358-366, 27 illustrations. Bibliography 15.

Field W. B.— Analog simulation for process design and control.— Proc. Instrum. Soc. Amer. 13th Annual Instrum. Automat. Conf. and Exhibit. Pt. 2.— Pittsburgh, Instrum. Soc. Amer., 1958, pp. 1-13, 8 illustrations, 2 tables. Bibliography 9.

Goggio E. C.— Some applications of analog-computer techniques to control system design.— Trans. IRE, April, vol. PGIE-5, pp. 70-76, 9 illustrations.

Holzman E. G.– Variable lag simulation. Preprint Nucl. Engng and Sci Conf. s.a. No. 112, 27 p., illustrations.

Petras St.– Elektronicke modelovania viacparametrovych regulacnych obvodov. (Electrical simulation of control systems with several parameters)– Strojnoelektrotechn. casop., 1958, t. 9, N 4, str. 217-230.

Prescott H. L.– Computer analyses voltage-regulator performance.– Westinghouse Engr, 1958, vol. 18, No. 3, pp. 76-79.

Prescott H. L.– Step regulator design checked on analog computer.– Electr. World, 1958, vol. 145, No. 18, pp. 56-57.

Schwartzenberg J. W.– An analog study of a high-speed recording servomechanisms.– Trans ASME, 1958, February, vol. 80, No. 2, pp. 490-496, 14 illustrations. Bibliography 6.

Straight P. E.– Effects of limiting error in feedback analysis.– J.Instrum. Soc. Amer., 1958, vol. 5, No. 5, pp. 44-49,, 11 illustrations.

Tallman G. H. and Smith O. J. M.– Analog study of dead-beat posicast control.– Trans. IRE, 1958, March, vol. PGAC-4, pp. 14-21, 10 illustrations. Bibliography 6.

Woods F. A.– Simulation of process control with an analog computer.– Industr. Engng Chem., 1958, November, vol. 50, No. 11, pp. 1627-1630, 9 illustrations.

II. The Use of Simulators and their Elements in Aviation

LANGUAGES OTHER THAN RUSSIAN

Computers and simulators.– Flight, 1958, vol. 74, No. 2590, pp. 460-461.

Controls fly trainer-almost.– Prod. Engng., 1958, July 14, vol. 29, No. 28, p. 71.

Creel H. F.– The weapons system approach to air data computing.– Aeronaut. Engng. Rev., 1958, February, vol. 17, No. 2, pp. 41-44, 50, 3 illustrations.

Dynamic simulatoring aids Short's VTOL research.– Brit. Communs and Electronics, 1958, August, vol. 5, No. 8, p. 618, 3 illustrations.

Heising C. R.– Evaluation of a turbojet control on an engine simulator.– In: Proc. Computers in Control Systems Conference, 1957.– New York, Amer. Inst. Electr. Engrs, 1958, pp. 54-57, 8 illustrations.

Hendrix G. E.– Target simulator tests beam-rider missiles.– Electronics, 1958, January 31, vol. 31, No. 5, pp. 32-35.

Hollander G. L.– Real-time airborne digital computers.– J. Instrum. Society of America, 1958, vol. 5, No. 12, pp. 26-32, 6 illustrations. Bibliography 6.

Mc Williams A. R.– An electronic brain.– Wings (S. Air U), 1958, February 17.

Nakada Y. and Scroggs S. J.– Simulation techniques in the synthesis of automatic flight-control systems.– In: Proc. Computers in Control Systems Conference, 1957.– New York, Amer. Inst. Electr. Engrs, 1958, pp. 57-59, 2 illustrations.

Schwarm E. G.– Electronic simulation for the jet age.– Aero/Space Engng., 1958, May, vol. 17, No. 5, pp. 34-37, 2 illustrations.

Simplin K. H.– Computers for simulators: A.C. or D. C.? – Flight, 1958, July 4, vol. 74, No. 2580, pp. 7-9, 5 illustrations. Bibliography 8.

III. The Use of Simulators in Nuclear Engineering

IN RUSSIAN

Chadwik G. I. and Thompson T.– Electrical simulation of the process which occurs in a reactor.–Khimiya i Khimicheskaya Tekhnologiya, 1958, No. 12, pp. 112-120, 2 illustrations.

Korolev V. V. and Sidorova I. I.– Electrical simulation of nuclear reactors.– Atomnaya Energiya, 1958, No. 1, pp. 29-43, 13 illustrations. Bibliography 27.

Leiby D. W.– The use of analog computers in designing an atomic electric power station. – Voprosy Yadernoi Energetiki, 1958, No. 4, pp. 59-72, 18 illustrations.

Toma V.– The Electronic digital computer in the institute of atomic physics of the Academy of the Roumanian People's Republic.– Byull. nauchn. inform., 1958, No. 1, pp. 121-123, (Academy of the Roumanian People's Republic, Roumanian-Soviet Scientific Institute).

LANGUAGES OTHER THAN RUSSIAN

Albrecht J.– Zur elektronischen Analogie ungedämpfter gekoppelter mechanischer Schwingungen.– Wiss. Z. Hochschule Elektrotechnik Ilmenau, 1958, Jg. 4, H I, SS. 33-39, 5 illustrations. Bibliography 11

Braffort P. and Caillet C.– Nouvelles techniques dans la simulation des centrales nucleaires.– Onde electr., 1956, août–sept., an. 38, No. 377-378, pp. 583-591, 13 illustrations. Bibliography 5.

Carteron J. M. and Deloux G.– Analog representation of heat exchange application to the simulation of heat exchangers of nuclear power plants.– In: Proc. computers in control systems conference, 1957.– New York, Amer. Inst. Electr. Engrs, 1958, pp. 48-53, 12 illustrations.

Computers in nuclear-reactor design.– J. Instn. Electr.

Engrs, 1958, May, vol. 4, No. 41, pp. 249-251.

Computer-run submarine simulator provides new dockside training.— Res. and Engng, 1958, vol. 4, No. 1, p. 43.

Electronic simulator for nuclear reactor power plants.— Engineer, 1958, December 5, vol. 206, No. 5367, p. 894.

Hanus B., Balgar J., and Mikulek M.— Elektricky analogon vymeniku tepla. (An electrical simulator for a heat-exchanger) — Slaboproudy Obzor 1958, sv. 19, No. 1, str. 36-41, 19 illustrations.

Johnson S. O., Curlee N. J. and Reihing J. V.— Simulation of hot channel boiling in water-cooled reactors.— Trans. IRE, 1958, June, vol. NS-5, No. 1, pp. 1-9, 9 illustrations.

Kourim G.— Ein elektromechanischer Reaktor —Simulatoren.— Regelungstechnik, 1958, Jg. 6, H. 5, SS. 185-188, 100 illustrations. Bibliography 9.

Kourim G.— Reaktor — Simulatoren.— Regelungstechnik, 1958, Jg. 6, H. 4, SS. 134-138, 8 illustrations. Bibliography 8.

Leiby D. W.— Analog computer study of the transient performance of a dual-cycle boiling-water-reactor nuclear power plant.— Communs and Electronics, 1958, March, No. 35, pp. 17-25, 18 illustrations. Bibliography 10.

Lynch E. E. and Waite D. P.— Steam-generator instrumentation for a nuclear power plant with analog computer verification of dynamic action.— Communs. and Electronics, 1958, November, No. 39, pp. 690-696.

Miroux J.— L'utilisation des signaux carres dans la technique des analogies electriques. Appareillage à grandes resistances pour curves rheoelectriques.— Onde electr. 1958, vol. 38, No. 375, pp. 450-457.

Nuclear reactor simulator.— Brit. Engng., 1958, vol. 40, No. 10, p. 334.

Nutter J. C.— Analogue computers in the nuclear power programme.— Instrum. Practice, 1958, January, vol. 12, No. 1, pp. 46-51, 4 illustrations. Bibliography 5.

Paul L. I. and Cox I. E. G.— Xenon-poisoning computer.— Nucleonics, 1958, vol. 16, No. 5, pp. 97-101.

Power reactor simulator.— Nuclear Engng., 1958, April, vol. 3, No. 25, p. 163.

A power reactor simulator — English electric's new model.— Nucl. Power 1958, vol. 3, No. 23, pp. 123-134.

Silks T. M. and Brondel J. O.— Analog simulation of a nuclear power plant.— Proc. Instrum. Soc. Amer. 13th Annual Instrum. Automat. Confer. and Exhibit, 1958. Pt. 2.— Pittsburgh, Instrum. Soc. Amer., 1958, Part PCT9, pp. 1-14, 12 illustrations. Bibliography 8.

Waite D. and Lynch E. E.— Computer verification of steam generator instrumentation for a nuclear power plant.— In: Proc. Computers in Control Systems Conference, 1957.— New York, Amer. Inst. Electr. Engrs, 1958, pp. 42-47, 14 illustrations.

Wilson I. and Potter R.— Analogue computers and their use in nuclear reactor safety studies.— J. Brit. Inst. Radio Engrs, 1958, February, vol. 18, No. 2, pp. 95-100, 5 illustrations.

Wilson I. and Lawrence L. A. J.— A nuclear power plant training simulator for use at Calder Hall.— J. Brit. Instn. Radio Engrs, 1958, February, vol. 18, No. 2, pp. 85-94, 9 illustrations.

Ziegler W.— Concerning a simple reactor analogue.— Nucleonik, 1958, April, vol. 1, No. 1, pp. 27-29.

IV. Various Applications

IN RUSSIAN

Gitel'man A. I.— Adjustment of the control equipment and the supply sources of gas-turbine motors using an electronic analog computer.— Energomashinostroenie, 1958, No. 10, pp. 30-34, 11 illustrations.

Golomidov I. P. and Lyubynskii E. A.— Mathematical simulation of a control system for an excavator electric drive with a compensated longitudinal-field amplifier.— Izvestiya Vysshikh Uchebnykh Zavedenii, Gornyi Zhurnal, 1958, No. 3, pp. 105-110, 3 illustrations.

Maslovskii P. M.— On the possibility of using computers in systems for the automatization of open-hearth furnaces.— Izvestiya Vysshikh Uchebnykh Zavednii, Chernye Metally, 1958, No. 5, pp. 77-88, 1 illustration.

Rotenberg R. V.— The use of electronic digital and analog computers for studying the vibrations in an automobile.— Avtomobil'naya Promyshlennost' 1958, No. 1, pp. 5-9.

Sitnik P. Kh.— Mathematical simulation of collectorless ac machines.— Izvestiya Vysshkh Uchebnykh Zavedenii, Elektromekhnika, 1958, No. 1, pp. 35-49, 8 illustrations.

Sitnik M. Kh.— Mathematical simulation of asymmetrical machines.— Izvestiya Vysshykh Uchebnykh Zavedenii, Elektromekhanika, 1958, No. 8, pp. 28-44, 14 illustrations. Bibliography 5.

Tarasov V. S., Oksenov B. E. and Butomo I. D.— The use of electronic computers for solving problems in various fields of engineering physics.— In: The Symposium: Radio physics.— Mashgiz, Moscow-Leningrad, 1958. pp. 22-240, 18 illustrations; (Leningrad Polytechnic Institute, Transactions No. 194).

Use of analog computers in shipbuilding.– Collection of abstracts of Symposium of References to foreign papers on shipbuilding, Sudpromgiz., 1958. No. 44, pp. 3-13, 11 illustrations. Bibliography 8.

Williams T., Johnson P. and Ross A.– The application of computer engineering in chemical technology.– Khimiya i Khimicheskaya Tekhnologiya, 1958, No. 7, pp. 212-233, 9 illustrations. Bibliography 53.

LANGUAGES OTHER THAN RUSSIAN

Adams J. W.– Reactor power calculator. Preprint. Nucl. Engng. Sci. Conf. s.a. No. 175, 10 p., 4 illustrations.

Analogue computer applied to inductionmotor design.– Engineering, 1958, August 8, vol. 186, No. 4822, p. 188, 2 illustrations.

An analogue computer for induction motor design.– Electr. Energy, 1958, vol. 2, No. 9, p. 362.

Analogue computer predicts radioactive fallout.– Automatic Progr. 1958, vol. 3, No. 7, pp. 254-255, 265.

Au automobile handling simulator.– Process Control and Automat., 1958, September, vol. 5, No. 9, p. 354, 1 illustration.

B. T. C. Analogue Computer.– Engineer, 1958, July 4, vol. 206, No. 5345, p. 30.

Bertein F.– Analogie électrique dans l'étude du traitement d'un lingot par la méthode de la zone fondue.– J. Phys. et Radium 1958, vol. 19, No. 12, Suppl., pp. 182-183.

Cahen F. M. and Carteron J. M.–Analog and digital computers in the French electric power production, transmission, and distribution industry.– Power Appar. and Systems, 1958, February, No. 34, pp. 1533-1538. Bibliography 17.

Corless K. G. and Aldred A. S.– An experimental electronic power system simulator.– Proc. Instn. Electr. Engrs, 1958, October, vol. 105, Pt. A, No. 23, pp. 503-511, 11 illustrations. Bibliography 19.

Designing railway springs by analogue computer.– Process Control and Automat., 1958, September, vol. 5, No. 9, pp. 378-380, 6 illustrations.

Electronic slide rule for packaging calculations.– Packaging 1958, vol. 40, No. 339, p. 64.

Fogel L. J. and Dwonzyk M.– Anticipatory display design through the use of an analog computer.– IRE Wescon Convent. Rec., 1958, vol. 2, Pt. 4, pp. 67-88.

Hálek V.–Zkusenesti z reseni hydraulickych problemu metódom elektroanalogie. (The use of the electrical simulation method for solving hydraulic problems).– Vodni hospodarstvi 1958, No. 10, pp. 297-305.

Hazel W. C.– The use of operational amplifiers in the measurements of transistor parameters.– Review of Sci. Instruments, 1958, vol. 29, No. 3, pp. 235-237.

Horgan J. D. and Pesavento J. A.– Accurate determination of capacitance by conjoining analytical and analog techniques.– Communs. and Electronics, 1958, vol. 77, pp. 397-400, illustrations. Bibliography 7.

Hornfeck A. J. and Imsland T. S.– Performance computer for steam – electric generating units.– Power Apparatus and Systems, 1958, August, No. 37, pp. 647-654, 10 illustrations. Bibliography 10.

Jespers P.– Méthode de calcul analogique de la réponse transistoire des filtres passe – bande symétriques soumis à l'application d'un signal sinusoidal de pulsation quelconque.– Ann. Assoc. Intern. Calcul. Analog., Belg. 1958, September, vol. 1, No. 2, pp. 75-83, 5 illustrations.

Karplus W. J., Bekey G. A. and Pekrul P. I.– Atmospheric diffusion of air pollutants. Analog computer study.– Industr. Engng Chem., 1958, November, vol. 50, No. 11, pp. 1657-1660, 9 illustrations. Bibliography 6.

Kennard L. J. and Nicholson C. H.– Radar simulators.– J. Brit. Inst. Radio Engrs., 1958, January, vol. 18, No. 1, pp. 17-31, 9 illustrations.

Lonegran J. P.– An introduction to the applications of analogue computers.– Austral. J. Instrum. Technology, 1958, February, vol. 14, No. 1, pp. 62-71, 7 illustrations.

Lowler E. A., Drum L. and Frank V.– Hydraulic problem solution on electronic computers.– J. Waterways and Harbors Div., Proc. Amer. Soc. Civil. Engrs, 1958, vol. 84, No. 1, pp. 1515-1-1515-38.

Meier H. P.– Die Anwendung elektronischer Rechenautomaten in der Maschinen – Industrie.– Schweiz. Bauzeitung, 1958, März 22, Jg. 76, H. 12, SS. 174-176, 3 illustrations.

Meredith J. F. and Freeman E. A.– The simulation of distributed-parameter systems with particular reference to process control problems.– Proc. Instn. Electr. Engrs, 1958, November, vol. 105, Pt. B, pp. 569-576, 13 illustrations.

Moore W. J. M., and Chen C. C.– A study of an analog computing system for an analytical plotter.– Photogrammetria, 1958-1959, vol. 15, No. 1, pp. 14-20.

Nagaraja N. S.– Fourier analysis by a general purpose electronic analogue computer.– J. Instn Telecommun. Engrs., India, 1958, vol. 4, No. 3, pp. 130-136.

Neate R. and Daecy W. J.— A simulation of melting shop operations by means of a computer.— Process control and automation, 1958, July, vol. 5, No. 7, pp. 264-272, 6 illustrations.

Noden D. A.— A balanced precision reference regulator for computer application.—IRE Convention Rec., 1958, vol. 6, Pt. 4, pp. 225-229.

Otley K. O., and Shoemaker R. F.— A voltage-sensitive switch.— Proc. IRE 1958, October, vol. 46, No. 10, pp. 1723-1730, 7 illustrations. Bibliography 36.

Phillips R. A.— Process analysis plus analog simulation yields better mill controls.— Control Engng, 1958, May, vol. 5, No. 5, pp. 113-118, 4 illustrations.

Reethof G.— Application of the analog computer to predict dynamic performance in typical hydraulic circuits.— Trans. ASME, 1958, August, vol. 80, No. 6, pp. 1299-1307, 13 illustrations. Bibliography 14.

Rogers A. E.— The analog computer its operation and use in engineering.— Proc. Instrum. Soc. Amer. 13th Annual Instrum. Automat. Confer. and Exhibit., 1958 Pt. 2.— Pittsburgh, Instrum. Soc. Amer., 1958, Part PCT2, pp. 1-14, 8 illustrations.

Steeg C. W.— Systems engineering and simulation in the military electronics industry.— Proc. Instrum. Soc. Amer. 13th Annual Instrum. Automat. Confer. and Exhibit., 1958 Pt. 2.— Pittsburgh, Instrum. Soc. Amer., 1958, part PCT10, pp. 1-14, 4 illustrations.

Tavoda O.— Zistovanie vztlakov a priesakov pomocu eleptrickej analogie. (Determining pressures and discharges using an electrical analog).—Vodohospod casop. 1958, vol. 6, No. 2, pp. 160-173, Bibliography 10.

Tenger P.— The use of radar simulators in the Royal Navy.— J. Brit. Inst. Radio Engrs 1958, January, vol. 18, No. 1, pp. 33-47, 20 illustrations.

Terrett D. S.— Applications of a general-purpose analogue computer. 2. Analogue computers in chemical engineering.— Chem. and Process Engng 1958, vol. 39, No. 12, pp. 442-445.

Thomas G. E.— Analogue computers in chemical engineering. I. General principles.— Chem. and Process Engng, 1958, vol. 30, No. 10, pp. 343-346.

Wexler H. T. and Stern R. K.— Analog computers in physical simulation.— Proc. Instrum. Soc. Amer., 13th Annual Instrum. Automat. Confer. and Exhibit., 1958, Pt. 2.— Pittsburgh, Instrum. Soc. Amer., 1958, Part PCT8, pp. 1-4, 9 illustrations.

Williams P. J.— Analog computing in the chemical and petroleum industries.— Industr. Engng. Chemistry, 1958, November, vol. 50, No. 11, pp. 1631-1635, illustrations. Bibliography 42.

Woods F. A.— Simulation of process control with an analog computer.— Industr. and Engng Chem., 1958, vol. 50, No. 11, pp. 1627-1630.

Worley Ch. W.— Analog simulation of industrial processes — 1958 Nat. Sympos. Progr. and Trends Chem. and Petrol. Instrum. Wilmington, Del. Pittsburgh Pa, Instrum. Soc. America 1958, pp. 1-17.

G. DIGITAL SIMULATION

IN RUSSIAN

Kozharskii L. A.— On a certain method for designing digital differential analyzers.— In: Problems in the theory of mathematical machines.— Moscow, Fizmatgiz, 1958, pp. 219-230, 6 illustrations. Bibliography 6.

Maiorov F. V.— Digital integrators.— In: Automatic control and digital engineering, No. 1.— Moscow, Mashgiz, 1958, pp. 240-303, 31 illustrations. Bibliography 7.

Zhidkov E. P.— Mathematical fundamentals of a digital differential analyzer.— In: Automatic control and digital engineering, No. 1.— Moscow, Mashgiz, 1958, pp. 228-239, 12 illustrations.

LANGUAGES OTHER THAN RUSSIAN

Beck R. M. and Palevsky M.— The DDA.— Instrum. and Automat., 1958, November, vol. 31, No. 11, pp. 1836-1837, 5 illustrations.

Goldman R. N.— DDA.— What is it?— Electr. Engng. 1958, July, vol. 77, No. 7, pp. 592-594, 5 illustrations.

Guzman O.— Digital moon-radar antenna programmer with analog rate signal integrator.— IRE Convent. Rec., 1958, vol. 6, Pt. 4, pp. 217-224, 11 illustrations.

Mitchell J. M. and Rugman S.— The Trice — a high speed incremental computer (New parallel digital differential analysers).— IRE, National Convent. Rec., 1958, vol. 6, Pt. 4, pp. 206-209, 9 illustrations.

Rowley G. C.— Digital differential analysers.— Brit. Communs. and Electronics 1958, December, vol. 5, No. 12, pp. 934-938, 6 illustrations. Bibliography 20.

Savastano G.— L'Analizzatore differenziale dell'universita di Napoli.— Electrotecnica, 1958, vol. 45, April, No. 4, pp. 202-212. Lugl., No. 7, pp. 354-365, 15 illustrations. Bibliography 6.

Steward M. H.— Rate limiting in incremental computes.— In: Proc. Computers in Control Systems Conference, 1957.— New York, Amer. Inst., Electr. Engrs, 1958, pp. 87-88.

Superharmonic oscillations as solutions to Duffing's equation as solved by an electronic differential analyzer.— J. Appl. Mech., 1958, June, vol. 25, No. 2, pp. 315-316.

Terao M. and Tamura K.— A semidigital process simulator.— Trans. IRE, 1958, March, vol. 1-7, No. 1, pp. 18-22, 21 illustrations.

Tootill G. C.— The incremental digital computer. (Digital differential analyzer).— Process Control and Automat., 1958, vol. 5, September, No. 9, pp. 350-354, 4 illustrations, October, No. 10, pp. 402-406, 4 illustrations. Bibliography 22.

3. Bibliography

IN RUSSIAN

Vil'dt E. O. and Landsberg R. S.— Bibliography of literature on problems of mathematical simulation (on analog computers) for 1956, Avtomatika i Telemekhanika, 1958, vol. 19, No. 5, pp. 493-506.